# Point-of-Care Ultrasound Techniques for the Small Animal Practitioner

2

Second Edition

Edited by **Gregory R. Lisciandro**

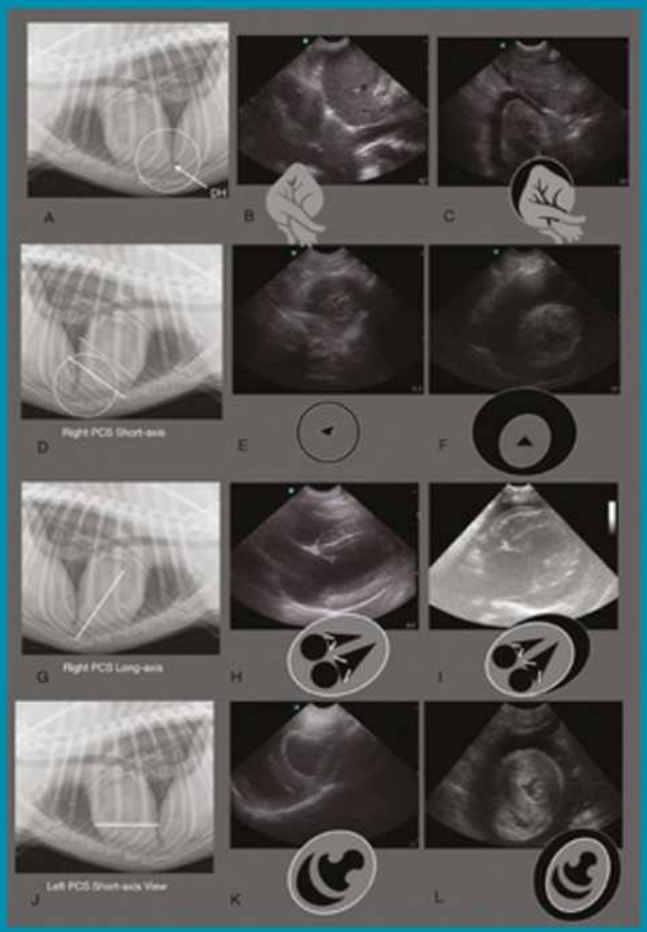

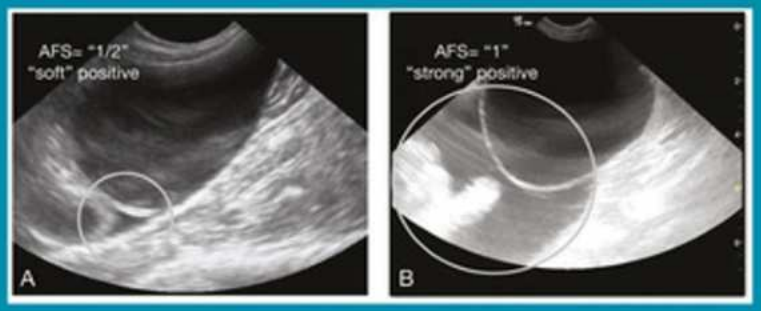


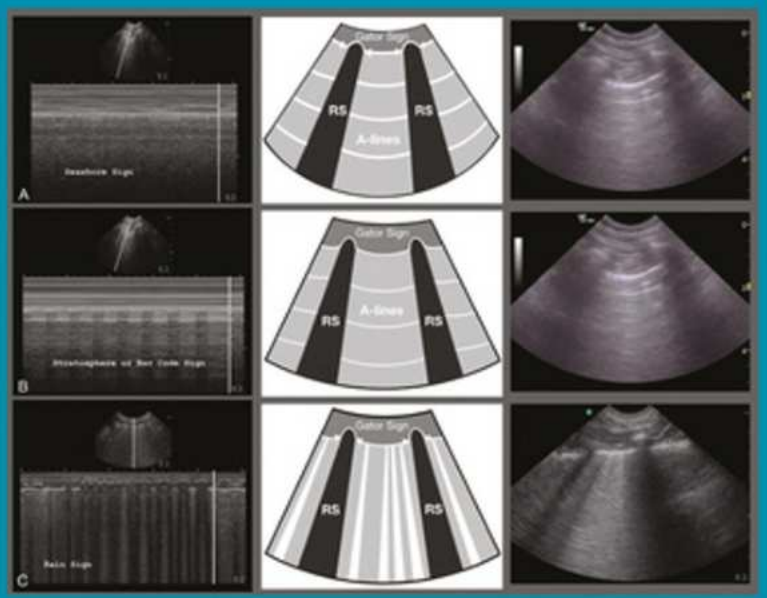


with website

WILEY Blackwell

Vetbooks.ir

# Point-of-Care Ultrasound Techniques for the Small Animal Practitioner

VetBooks.ir

Vetbooks.ir

# Point-of-Care Ultrasound Techniques for the Small Animal Practitioner

**SECOND EDITION**

Edited by

Gregory R. Lisciandro

Co-owner Hill Country Veterinary Specialists
CEO, FASTVet.com
President, International Veterinary Point-of-care Society (IVPOCUS)
Spicewood, Texas, USA

WILEY Blackwell

Vetbooks.ir

This edition first published 2021
© 2021 John Wiley & Sons, Inc.

*Edition History*
John Wiley & Sons (1e, 2014)

All rights reserved. No part of this publication may be reproduced, stored in a retrieval system, or transmitted, in any form or by any means, electronic, mechanical, photocopying, recording or otherwise, except as permitted by law. Advice on how to obtain permission to reuse material from this title is available at http://www.wiley.com/go/permissions.

The right of Gregory R. Lisciandro to be identified as the author of the editorial material in this work has been asserted in accordance with law.

*Registered Office*
John Wiley & Sons, Inc., 111 River Street, Hoboken, NJ 07030, USA

*Editorial Office*
111 River Street, Hoboken, NJ 07030, USA

For details of our global editorial offices, customer services, and more information about Wiley products visit us at www.wiley.com.

Wiley also publishes its books in a variety of electronic formats and by print-on-demand. Some content that appears in standard print versions of this book may not be available in other formats.

*Limit of Liability/Disclaimer of Warranty*
The contents of this work are intended to further general scientific research, understanding, and discussion only and are not intended and should not be relied upon as recommending or promoting scientific method, diagnosis, or treatment by physicians for any particular patient. In view of ongoing research, equipment modifications, changes in governmental regulations, and the constant flow of information relating to the use of medicines, equipment, and devices, the reader is urged to review and evaluate the information provided in the package insert or instructions for each medicine, equipment, or device for, among other things, any changes in the instructions or indication of usage and for added warnings and precautions. While the publisher and authors have used their best efforts in preparing this work, they make no representations or warranties with respect to the accuracy or completeness of the contents of this work and specifically disclaim all warranties, including without limitation any implied warranties of merchantability or fitness for a particular purpose. No warranty may be created or extended by sales representatives, written sales materials or promotional statements for this work. The fact that an organization, website, or product is referred to in this work as a citation and/or potential source of further information does not mean that the publisher and authors endorse the information or services the organization, website, or product may provide or recommendations it may make. This work is sold with the understanding that the publisher is not engaged in rendering professional services. The advice and strategies contained herein may not be suitable for your situation. You should consult with a specialist where appropriate. Further, readers should be aware that websites listed in this work may have changed or disappeared between when this work was written and when it is read. Neither the publisher nor authors shall be liable for any loss of profit or any other commercial damages, including but not limited to special, incidental, consequential, or other damages.

*Library of Congress Cataloging-in-Publication Data*

Names: Lisciandro, Gregory R., editor.
Title: Point-of-care ultrasound techniques for the small animal practitioner / edited by Gregory R. Lisciandro.
Other titles: Focused ultrasound techniques for the small animal practitioner.
Description: Second edition. | Hoboken, NJ : Wiley-Blackwell, [2020] | Preceded by Focused ultrasound techniques for the small animal practitioner / edited by Gregory R. Lisciandro. 2014. | Includes bibliographical references and index.
Identifiers: LCCN 2020000659 (print) | LCCN 2020000660 (ebook) | ISBN 9781119460985 (hardback) | ISBN 9781119460992 (adobe pdf) | ISBN 9781119461029 (epub)
Subjects: MESH: Ultrasonography–veterinary | Animal Diseases–diagnostic imaging | Point-of-Care Systems | Pets
Classification: LCC SF772.58 (print) | LCC SF772.58 (ebook) | NLM SF 772.58 | DDC 636.089/607543–dc23
LC record available at https://lccn.loc.gov/2020000659
LC ebook record available at https://lccn.loc.gov/2020000660

Cover Design: Wiley
Cover Image: © Courtesy of Gregory R. Lisciandro

Set in 10/12pt Palatino by SPi Global, Pondicherry, India

10 9 8 7 6 5 4 3 2 1

# Dedication

To my late grandparents, Sam and Bernice Long, John and Mary Lisciandro, my parents Richard and Judy, and my lovely wife Stephanie, and our four beautiful children Noah, Hannah, Sarah, and Joshua for their patience and inspiration, to all those who have believed in Global FAST, and to the good Lord for making the textbook and all its many variables fall in place to its completion.

www.VetBooks.ir

Vetbooks.ir

# Contents

List of Contributors xi

Foreword xiii

Preface xv

Acknowledgments xix

About the Companion Website xxi

**Section I: Basics of Ultrasound and Imaging 1**

1 POCUS: Introduction 3
Gregory R. Lisciandro

2 POCUS: Basic Ultrasound Physics 11
Robert M. Fulton

3 POCUS: Basic Ultrasound Artifacts 15
Robert M. Fulton

4 POCUS: Basic Ultrasound Scanning 25
Robert M. Fulton

5 POCUS: Top Ultrasound Mistakes During Global FAST 39
Gregory R. Lisciandro

**Section II: Abdomen 55**

6 POCUS: AFAST – Introduction and Image Acquisition 57
Gregory R. Lisciandro

7 POCUS: AFAST – Clinical Integration 111
Gregory R. Lisciandro

8 POCUS: Liver and Gallbladder 149
Stephanie C. Lisciandro, Jennifer M. Gambino, and Sarah Young

9 POCUS: Spleen 173
Stephanie C. Lisciandro and Sarah Young

10 POCUS: Kidney 189
Stephanie C. Lisciandro and Sarah Young

11 POCUS: Urinary Bladder 211
Stephanie C. Lisciandro and Sarah Young

12 POCUS: Gastrointestinal Tract and Pancreas 225
Søren R. Boysen and Jennifer M. Gambino

**Section III: Reproductive and Pediatric 245**

13 POCUS: Reproductive – Male 247
Robert M. Fulton

14 POCUS: Reproductive – Female 255
Robert M. Fulton

15 POCUS: Dystocia 265
Robert M. Fulton

16 POCUS: Pediatrics 271
Autumn P. Davidson and Tomas W. Baker

**Section IV: Thorax 295**

17 POCUS: TFAST – Introduction and Image Acquisition 297
Gregory R. Lisciandro

18 POCUS: TFAST – Clinical Integration 337
Gregory R. Lisciandro

19 POCUS: Heart – Introduction and Image Acquisition 389
Teresa DeFrancesco

20 POCUS: Heart - Abnormalities of Valves, Myocardium, and Great Vessels 403
Teresa DeFrancesco

21 POCUS: Heart – Pericardial Effusion and Pericardiocentesis 417
Teresa DeFrancesco

22 POCUS: Vet BLUE – Introduction and Image Acquisition 425
Gregory R. Lisciandro and Stephanie C. Lisciandro

VetBooks.ir
www.VetBooks.ir

23 POCUS: Vet BLUE – Clinical Integration 459
Gregory R. Lisciandro and Stephanie C. Lisciandro

**Section V: Vascular 509**

24 POCUS: Central Venous and Arterial Catheterization 511
Scott Chamberlin

25 POCUS: Vascular – Veins and Arteries 529
Gregory R. Lisciandro

26 POCUS: Caudal Vena Cava 541
Kris Gommeren, Elodie Darnis, and Anne-Christine Merveille

**Section VI: Ocular, Neurological, and Musculoskeletal 551**

27 POCUS: Eye 553
Jane Cho

28 POCUS: Brain – Image Acquisition 579
Cibele F. Carvalho

29 POCUS: Brain – Clinical Integration 595
Cibele F. Carvalho

30 POCUS: Nerve Blocks – Forelimb 609
Pablo E. Otero and Diego A. Portela

31 POCUS: Nerve Blocks – Pelvic Limb 619
Pablo E. Otero and Diego A. Portela

32 POCUS: Nerve Blocks – Trunk 629
Pablo E. Otero and Diego A. Portela

33 POCUS: Nerve Blocks – Neuroaxial 637
Pablo E. Otero and Diego A. Portela

34 POCUS: Musculoskeletal – Soft Tissue 647
Susanne M. Stieger-Vanegas

35 POCUS: Musculoskeletal – Bones and Joints 663
Susanne M. Stieger-Vanegas

**Section VII: Monitoring and Surveillance 683**

36 POCUS: Global FAST – Patient Monitoring and Staging 685
Gregory R. Lisciandro

VetBooks.ir

37 POCUS: Global FAST – Rapidly Detecting Treatable Forms of Shock, Advanced Life Support, and Cardiopulmonary Resuscitation 729
Gregory R. Lisciandro

38 POCUS: VetFAST-ABCDE 757
Andrea Armenise

**Section VIII: Felines and Exotic Species 775**

39 POCUS: Feline Differences – Abdomen and Thorax 777
Daniel Rodriguez and Gregory R. Lisciandro

40 POCUS: Exotic Companion Mammals 815
Sara Gardhouse and Hugues Beaufrère

41 POCUS: Marine Mammals 829
Gregory R. Lisciandro, Jennifer M. Gambino, Debra P. Moore, and Enrique Yarto

42 POCUS: Birds and Reptiles 863
Sara Gardhouse and Hugues Beaufrère

**Section IX: Ultrasound-Guided Procedures 883**

43 POCUS: Ultrasound-Guided Procedures – Abdominocentesis, Thoracocentesis, and Pericardiocentesis 885
Søren R. Boysen

44 POCUS: Ultrasound-Guided Lung and Thoracic Sampling 907
Daniel Rodriguez

**Section X: Management 919**

45 POCUS: Setting Up Successful POCUS and FAST Ultrasound Programs 921
Gregory R. Lisciandro

**Appendices** 933

I Goal-Directed Templates for Medical Records 933

II Abbreviations, Terminology and Glossary 943

III Quick References of Normal Values and Rules of Thumb 949

Index 971

# List of Contributors


**Andrea Armenise, DVM**
Director, Emergency and Intensive Care
Ospedale Veterinario Santa Fara
Bari, Italy

**Tomas W. Baker, MS**
Poundsound Consulting
Three Rivers, California, USA

**Hugues Beaufrère, DVM, PhD, Dipl. ACZM, Dipl. ABVP (Avian), Dipl. ECZM (Avian)**
Assistant Professor, Avian and Exotic Medicine
Department of Clinical Studies, Ontario Veterinary College
University of Guelph
Guelph, Ontario, Canada

**Søren R. Boysen, DVM, Dipl. ACVECC**
Professor, Veterinary Emergency and Critical Care
Department of Veterinary Clinical and Diagnostic Sciences,
Faculty of Veterinary Medicine, University of Calgary
Calgary, Alberta, Canada

**Judy Brown, DVM, Dipl. ACVECC, Illustrator**
Toronto, Canada

**Cibele F. Carvalho, DVM, MSc., PhD, Dipl. CBRV**
**CEO and Owner, NAUS**
Sao Paulo, SP, Brazil

**Scott Chamberlin, DVM, MS, Dipl. ACVECC**
First Year Graduate Veterinary Education Instructor
US Army Veterinary CorpsFort Campbell, Kentucky, USA

**Jane Cho, DVM, Dipl. ACVO**
Owner, Veterinary Eye Specialists, PLLC
Thornwood, New York, USA

**Hannah M. Cole, Illustrator**
Adkins, Texas, USA

**Elodie Darnis, DVM, DECVIM-CA (Internal Medicine)**
CHV Frégis
Arcueil, France

**Teresa DeFrancesco, DVM, Dipl. ACVIM (Cardiology), Dipl. ACVECC**
Professor, College of Veterinary Medicine
North Carolina State University
Raleigh, North Carolina, USA

**Autumn P. Davidson, DVM, MS, Dipl. ACVIM (Internal Medicine)**
Clinical Professor, School of Veterinary Medicine
University of California
Davis, California, USA

**Robert M. Fulton, DVM**
Residency Trained Theriogenology
Medical Director, Betty Baugh's Animal Clinic
Richmond, Virginia, USA

**Jennifer M. Gambino, DVM, Dipl. ACVR**
Teleradiologist Consultant
IDEXX Telemedicine Consultants
IDEXX Laboratories, Inc.
Clackamas, Oregon, USA

**Sara Gardhouse, DVM, Dipl. ACZM**
Clinical Specialist
Ontario Veterinary College
University of Guelph
Guelph, Ontario, Canada

**Kris Gommeren, DVM, MSc, PhD, Dipl. ECVECC, Dipl. ECVIM-CA**
Assistant Professor, Faculty of Veterinary Medicine
Liège University
Liège, Belgium

**Gregory R. Lisciandro, DVM, Dipl. ABVP, Dipl. ACVECC**
Co-owner Hill Country Veterinary Specialists
CEO, FASTVet.com
President, International Veterinary Point-of-care Society (IVPOCUS)
Spicewood, Texas, USA

**Stephanie C. Lisciandro, DVM, Dipl. ACVIM (Internal Medicine)**
Medical Director, Oncura Partners, LLC
Austin, Texas, USA

**Alice MacGregor Harvey, Medical Illustrator**
North Carolina State College of Veterinary Medicine
Raleigh, North Carolina, USA

**Anne-Christine Merveille, DVM, MSc, PhD, Dipl. ECVIM-CA (Cardiology)**
Assistant Professor, Faculty of Veterinary Medicine
Liège University
Liège, Belgium

**Debra P. Moore, DVM**
Assistant Clinical Professor, Mississippi State University, College of Veterinary Medicine
Institute for Marine Mammal Studies
Gulfport, Mississippi, USA

**Pablo E. Otero, MV, PhD**
Professor, Head of Anesthesiology and Pain Management Department
Facultad de Ciencias VeterinariasUniversidad de Buenos AiresBuenos Aires, Argentina

**Suji Park, Illustrator**
Englewood Cliffs, New Jersey, USA

**Diego A. Portela, MV, PhD, Dipl. ACVAA**
Assistant Professor, Anesthesiology and Pain Management
Department of Comparative, Diagnostic, and Population MedicineCollege of Veterinary MedicineUniversity of Florida
Gainesville, Florida, USA

**Daniel Rodríguez, MVZ. Esp. Dipl ACVR**
Medical Director, VETTEM México
Chapultepec, Mexico City, Mexico

**Susanne M. Stieger-Vanegas, Dr Med Vet, PhD, Dipl. ECVDI**
Associate Professor, Diagnostic Imaging
Camden Professor Radiology
Department of Clinical Sciences
Carlson College of Veterinary Medicine
Oregon State University
Corvallis, Oregon, USA

**Randi Taggart, Illustrator**
Richmond, Virginia, USA

**Enrique Yarto, MVZ, M.C.**
Centro Veterinario México-Animales Exóticos
Presidente Instituto Mexicano de Fauna Silvestre y Animales de Compañía
IMFAC, S.C.
Ciudad de México, México

**Sarah Young, DVM**
Echo Service for Pets
Ojai, California, USA

VetBooks.ir
www.VetBooks.ir

# Foreword

Vetbooks.ir

Over the past three decades, the technological miniaturization of ultrasound machines has made compact, portable ultrasound devices, ranging from pocket-sized devices to laptop-style machines, available to healthcare providers at the bedside. Healthcare providers are using ultrasound to look inside the body during their bedside evaluation of patients, which has given rise to a new field of clinical medicine called *point-of-care ultrasound*. Point-of-care ultrasound is defined as a goal-directed, bedside ultrasound examination performed by a healthcare provider to answer a specific diagnostic question or guide performance of an invasive procedure at the bedside. Providers from nearly all healthcare professions have begun to learn how to use point-of-care ultrasound, and veterinary medicine is ideally suited for integration of point-of-care ultrasound given the diverse complaints and wide range of animals that are cared for by veterinarians on a daily basis.

The first edition of this book, called *Focused Ultrasound Techniques for the Small Animal Practitioner*, was published in 2014 and described the most common focused ultrasound examinations in veterinary medicine. The first edition established a standardized approach to perform a multisystem veterinary ultrasound examination, particularly of the heart, lungs, and abdomen, and has served as a guide for veterinarians to incorporate ultrasound into their clinical practices around the world. The book has been translated into Spanish, Chinese, Greek, Japanese, and Polish, and over 2000 copies have been sold worldwide.

In this second edition, the reader experience has been enhanced in several ways. The core chapters describing the fundamental veterinary ultrasound examinations have been expanded to discuss a broader range of species, including exotic species, and a more in-depth discussion of feline species. Several new chapters have been added, including chapters on the use of ultrasound to evaluate marine mammals and zoo animals. Chapters on the nervous system describe evaluation of the brain and peripheral nerves, as well as performance of ultrasound-guided nerve blocks. The online video library has been expanded to include over 100 videos of normal and abnormal findings to supplement the book chapters.

For veterinary clinicians seeking to improve their knowledge and skills in point-of-care ultrasound, this book has evolved to become a standard reference for its high-yield chapters, online video content, and practical teaching points written by experts in the field.

*Nilam J. Soni, MD, MSc*
Associate Professor of Medicine
Department of Medicine
University of Texas Health San Antonio
San Antonio, Texas, USA

# Preface

Vetbooks.ir

POCUS is point-of-care ultrasound. Veterinary POCUS (V-POCUS), which includes FAST ultrasound examinations, is defined as a goal-directed ultrasound examination(s) performed by a veterinary healthcare provider at the point of care (cageside) to answer a specific diagnostic question(s) or guide performance of an invasive procedure(s).

The translational study from the human to the veterinary patient regarding the focused assessment with sonography for trauma (FAST) exam by Dr Søren Boysen and colleagues in 2004 was a landmark study opening the eyes of the veterinary world to the nonradiologist, noncardiologist use of ultrasound, and that the principle of FAST ultrasound, that the nonradiologist sonographer is able to recognize anechoic triangulations representing free cavitary fluid, was not only achievable but also had the potential to improve patient care and save lives.

The following year, 14 years after graduating from veterinary school, I began my residency training in emergency and critical care in San Antonio, Texas, a city supportive of military training with several bases, and thus a mecca for FAST ultrasound. At the time, my program mentor encouraged me to take on FAST ultrasound as my clinical research requirement. I balked at the idea, having failed a complete abdominal ultrasound course in 1999, six years earlier, and thus concluding that ultrasound was a skill I would never master. However, I finally agreed to read the Boysen et al. study, after which I thought: "This (FAST ultrasound) **will** improve patient care. And I only have to be able to recognize black (anechoic) triangles. I like anatomy and surgery. I **can** memorize four views. It's only four views."

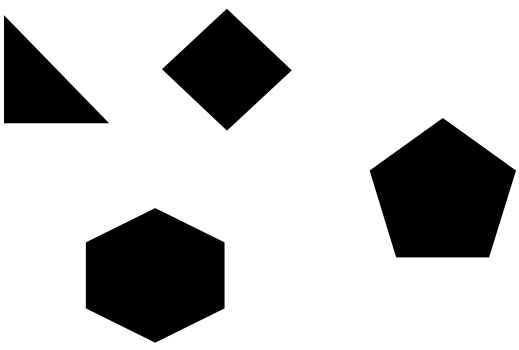

Thus, I decided that I would give ultrasound one more try. The FAST study intrigued me in the numbers of dogs with occult injury missed with traditional screening tests of physical exam, baseline blood and urine testing and radiography, but captured using FAST ultrasound. The study raised many fascinating questions, including looking past the diaphragm, adding a fluid scoring system to better categorize a positive FAST examination, and exploring the thorax with its own FAST format. Thus, my unimaginable journey began with developing AFAST, its target organ approach and its fluid scoring system; developing TFAST for pneumothorax, pleural and pericardial effusion, and its echo views for cardiac abnormalities; and most recently Vet BLUE (Veterinary Brief Lung Ultrasound Exam). Initially (2005), we combined AFAST and TFAST and referred to the study as "Combo (Combination) FAST" because we quickly realized how important it was to screen both cavities. Combining these three formats circa 2010, the study is now referred to as Global FAST and serves as an extension of the physical exam.

Now, 15 years later, the ultrasound probe is not only used by emergency veterinarians but also other nonradiologist, noncardiologist specialists as well as general practitioners. The use of ultrasound as a first-line, daily imaging modality has become commonplace globally throughout veterinary medicine, improving patient care and saving lives often by capturing disease otherwise missed with traditional work-ups without

VetBooks.ir

ultrasound and detecting complications earlier in their course. Although there may not be the published evidence, I know how much I missed on a daily basis having practiced the first 13 years of my 28-year career as a general practitioner and then followed by the first three years in emergency and critical care *without* ultrasound. Many cases from the pre-FAST era still haunt me and how I failed my patient and their families by missing conditions easily recognized with the Global FAST approach.

The objectives for POCUS and FAST examinations are to rapidly answer important clinical questions to help *rule in* and *rule out* conditions, to see your "problem" list for a more streamlined diagnostic plan; to better decide on medical versus surgical and other interventional cases; and to keep the patient alive for gold standard testing and treatment, with a better chance of survival. "Seeing" your problem list as part of your physical exam provides more evidence-based information over traditional work-up paradigm(s). Every clinical specialist, including the internist, oncologist, cardiologist, criticalist, neurologist, surgeon, anesthesiologist, ophthalmologist, dentist, and dermatologist, and the ER veterinarian and general practitioner should make learning the basics of POCUS and FAST ultrasound a core skill and first-line evaluation (extension of the physical exam) for most if not every patient. The new mantra should be "Physical examination and Global FAST!" as the starting point for every patient, providing an unbiased set of data imaging points in both cavities, the abdomen and thorax, for every veterinarian seeing clinical cases.

In my internship year at the Animal Medical Center in New York City in 1991–1992, our Intern Director, the late Dr Michael Garvey, always emphasized that we should "never send a patient out the door with something you could have easily detected by performing a good physical exam and your quick assessment tests." The day has come when the Global FAST approach should be part of your quick assessment tests. In other words, Global FAST is "an extension of your physical exam," a term coined by Rozycki and colleagues over 20 years ago. Importantly, POCUS then follows the Global FAST approach for more targeted evaluations as subsequently explained.

With POCUS examinations now being used in human and veterinary medicine on a daily basis, standardization with clear objectives is imperative not only establishing for validity and a healthy respect among our colleagues but for perfecting your skills. Recording data on goal-directed templates that demonstrate an organized, well-defined imaging protocol for answering clinically relevant questions is also key for veterinary medicine as a whole to embrace this movement. These questions must be realistically achievable, often binary, for the nonradiologist, noncardiologist sonographer. In this second edition, we have tried to make POCUS and FAST ultrasound examinations as clear as possible.

However, even with this approach, we think that caution should be exercised in how *individual* POCUS examinations are applied to patients. For example, a POCUS gallbladder examination may prove unremarkable, but if the Global FAST approach is applied to every patient as part of the *initial* evaluation process, the pericardial effusion, poor systolic function (dilated cardiomyopathy), low-grade peritonitis or small-volume hemoabdomen would *not* have been missed or delayed in its detection. In other words, the Global FAST approach should be considered your baseline imaging test with POCUS examinations considered as adjuncts. This imaging strategy prevents "satisfaction of search error" to which POCUS examinations by themselves are prone. Global FAST prevents the picking and choosing of whichever POCUS examination helps fulfill your preconceived clinical bias by providing a mandated, standardized set of imaging data points of the abdomen and thorax.

In another example, the POCUS heart provides an overview for cardiac information but is *too* focused, missing lung abnormalities and comorbidities within the patient's abdominal cavity. Through a Global FAST approach plus the *add-on* of a POCUS heart, the enlarged caudal vena cava suggesting right-sided heart congestive failure is detected, or the splenic mass or small-volume ascites is not missed, that was not even considered by the clinician but found as an unexpected comorbidity. Lastly, an unremarkable POCUS heart exam on a coughing dog, without an integrated approach with Global FAST, misses the widespread small lung nodules or the aspiration pneumonia that are *inapparent* on thoracic radiography. The "POCUS only" analogy would be similar to a selective physical examination, in which *only* the abdomen is palpated in a vomiting cat, or *only* the heart and lung ausculted in a coughing dog, or *only* the limb evaluated in a limping older dog. Most of us are aware of missing major problems when doing incomplete physical exams.

You may have or soon will have the epiphany of how powerful a tool first-line ultrasound is. The same epiphany has occurred in human medicine with similar stories of how first-line medical personnel are capturing aortic dissections in patients who have recovered and compensated, ectopic pregnancies with internal intermittent bleeding, and pulmonary thromboembolism as life-saving examples that historically would

Vetbooks.ir

have been delayed or completely missed (possibly resulting in death). Capturing these traditionally problematic life-threatening conditions is now possible on *initial* evaluation within minutes of presentation by "seeing" the problem.

In this second edition, we provide additional knowledge on what we have learned since the first edition, with more chapters and additional topics. These include additional chapters on eye and musculoskeletal exams as well as ultrasound-guided procedures, including the thoracic procedures and nerve blocks. Moreover, we devote an entire chapter to cats. We continue to push the envelope with the addition of more species including exotic companion mammals, marine mammals, birds, and reptiles. Personally, after performing thousands more exams, publishing numerous clinical studies, and through training over 1000 veterinarians in these techniques, we also share what we have learned using the Global FAST approach. We also welcome not only our previous chapter authors, who have also learned much since the first edition, but also a new set of thought-leading authors sharing their expertise in their respective chapters.

And, finally, as I prepared this second edition, reading through lists and lists of references, it became even more apparent that this paradigm change would not be possible without the many sonographers, veterinarians, residents, radiologists, and cardiologists who have painstakingly worked through untold hours of scientific research and clinical studies that have laid the foundation, for where veterinary diagnostic ultrasound is today. We extend a big thank you!

So let's get on with it. We welcome feedback by email at FASTSavesLives@gmail.com and via our Facebook page, www.facebook.com/FASTVet, or our website www.FASTVet.com. Your stories and experiences as general practitioners, emergency and critical care veterinarians, and clinical specialists are awaited. Your stories and experiences help keep the POCUS and FAST train moving forward, helping with advancements in training, perfecting imaging techniques, and their clinical applications.

# Acknowledgments

Vetbooks.ir

The following are acknowledged for their illustrative contributions: Suji Park, Englewood Cliffs, New Jersey (www.sujisuji.com); Dr Judy Brown, DVM, Dipl. ACVECC, Toronto, Canada; Hannah M. Cole, Adkins, Texas; Nancy Place, MS, Association of Medical Illustrators, San Antonio, Texas; Alice MacGregor Harvey, Medical Illustrator, North Carolina State University; and Randi Taggart, Richmond, Virginia.

Dr Karin Vomend, MVZ, Cuernavaca, Mexico, for editorial help and Dr William A. Seleen Jr, Bemus Point, New York, who read the entire manuscript and provided editing and content suggestions that helped improve the manuscript.

The entire Wiley team, including Erica Judisch, Commissioning Editor, and Jayadivya Saiprasad, Project Editor, and her staff, Holly Regan-Jones, freelance editor, for their expertise, patience, and encouragement throughout the construction and editing of the second edition, which became far bigger than originally foreseen.

The chapter authors from the United States and internationally, who not only believe in the potential for point-of-care and FAST ultrasound to make a positive impact in veterinary medicine but also generously gave their time and expertise in making this second edition possible.

Lastly, Drs Kelly Mann, DVM, DACVR, and Geoff Fosgate, DVM, PhD, DACVPM, University of Pretoria, who have helped me generously since my residency training with publishing clinical research; Dr Søren Boysen for his help, support, and friendship throughout the years; and my wife, Dr Stephanie C. Lisciandro, DVM, Dipl. ACVIM, who with her support, sacrifice, and dedication over the past decade has made it possible for me to invest the tremendous amount of time and effort needed to accomplish this task. I am forever grateful.

# About the Companion Website

Don't forget to visit the companion website for this book: www.wiley.com/go/lisciandro/ultrasound2

There you will find valuable material designed to enhance your learning, including:

- Video clips

Scan this QR code to visit the companion website.

SECTION I

# Basics of Ultrasound and Imaging

CHAPTER ONE

# POCUS: Introduction

Gregory R. Lisciandro

Vetbooks.ir

## Veterinary POCUS (V-POCUS) Defined

- *POCUS is point-of-care ultrasound.*
- *FAST is focused assessment with sonography for trauma, triage, and tracking (Lisciandro 2011).*
- *Veterinary POCUS (V-POCUS), which includes FAST examinations, is defined as a goal-directed ultrasound examination(s) performed by a healthcare provider at point of care (cageside) to answer a specific diagnostic question(s) or guide performance of an invasive procedure(s).*

We will use the acronyms POCUS and FAST throughout the textbook. It is important to read the Preface *prior to* Chapter One.

## Terminology Updates

Briefly, we will mention some of the more important changes and developments since our first edition. A more complete list of terminology and abbreviations is found in the Appendices. For a grasp of some of the basic concepts within this textbook, let's define a few things.

### The "T³" of Trauma, Triage, and Tracking

We have mostly dropped the "T³" designation that previously emphasized the "3-T approach" of applying FAST for *T*rauma, *T*riage, and *T*racking (T³), primarily because since the first edition, the T³ approach has become routine throughout North America, South America, Europe, and the Middle East in the author's experience.

### COAST³ is Out, POCUS is In

COAST³ or "cageside organ assessment with sonography for trauma (triage and tracking)" is out (similar to BOAST in human medicine) and POCUS is now the preferred mainstream term similar to what has occurred in human medicine (Rozycki et al. 2005; Lisciandro et al. 2014).

We have replaced COAST with POCUS in this second edition and advocate for POCUS (or Focused) X, or POCUS (Focused) Y, or POCUS (Focused) Z as giving better clarity to the examination and have proposed approaches to the various systems throughout this edition. The use of FoCUSED for "Focused Cardiac Ultrasound" and other confusing acronyms we hope to avoid in veterinary medicine. FoCUSED in human medicine would have been better named POCUS (or Focused Heart) Heart or POCUS (or Focused Echo) Echo. The term "Focused" as in our first edition similarly provides clarity to the examination and may be used interchangeably with specific POCUS examinations.

### FAST Survives and Continues

FAST stands for Focused Assessment with Sonography for Trauma and has been applied to the abdomen (FAST) and extended thorax (EFAST) in people (Rozycki 1998; Rozycki et al. 2001; Kirkpatrick et al. 2004). Its applications have expanded to

*Point-of-Care Ultrasound Techniques for the Small Animal Practitioner*, Second Edition. Edited by Gregory R. Lisciandro.
© 2021 John Wiley & Sons, Inc. Published 2021 by John Wiley & Sons, Inc.
Companion website: www.wiley.com/go/lisciandro/ultrasound2

nontrauma and tracking (Lisciandro 2011, 2016; McMurray et al. 2016). Problems arise in the human literature with terminology and they are not always right. For example, what exactly is EFAST? Is it a FAST *and* the thorax or *only* the thorax? What if we just do the thorax, then what FAST do we call it? Abdominal FAST (AFAST) and thoracic FAST (TFAST) give exact clarity and have been standardized and validated in published studies (Lisciandro et al. 2008, 2009; Lisciandro 2016; McMurray et al. 2016). Their acoustic windows have *exact clarity*, as does the "FAST" lung examination called Vet BLUE (Lisciandro et al. 2014, 2017).

## The Flash Exam is Not a FAST Exam

The "Flash Exam" term is applied for a general whole-cavity acoustic window approach to rapidly answer a simple binary question: is free fluid present or not in the abdominal and thoracic cavity? And now, with lung ultrasound becoming accepted among colleagues, are B-lines present or not? There is so much more to gain by using standardized acoustic windows of AFAST and TFAST (and Vet BLUE) that take about the same amount of time as the "Flash" approach. The "Flash" usually is followed by "looking around," often leading to a "satisfaction of search error" approach. Again, in the *same* amount of time, you could have done AFAST, TFAST, and Vet BLUE (Global FAST) with *standardized* acoustic windows following a protocol and gained so much more unbiased baseline patient information, while avoiding "satisfaction of search error." AFAST, TFAST, and Vet BLUE are not "Flash" exams and the terms should not be used interchangeably. We should stop teaching the "Flash" approach, just as we would not teach limited physical examinations – such as only quickly palpating the abdomen of a vomiting cat to draw clinical conclusions without looking further (Figure 1.1).

## Radiologist and Cardiologist Studies

We will refer to these studies as complete detailed abdominal ultrasound" and "complete detailed echocardiography." "Diagnostic" is a term that can be more universally applied as both a POCUS (or Focused) and FAST examination are potentially diagnostic, for example for ascites, pleural and pericardial effusion, calcaneus tendon rupture, skull fracture, a splenic mass, gallbladder mucocele, to name a few.

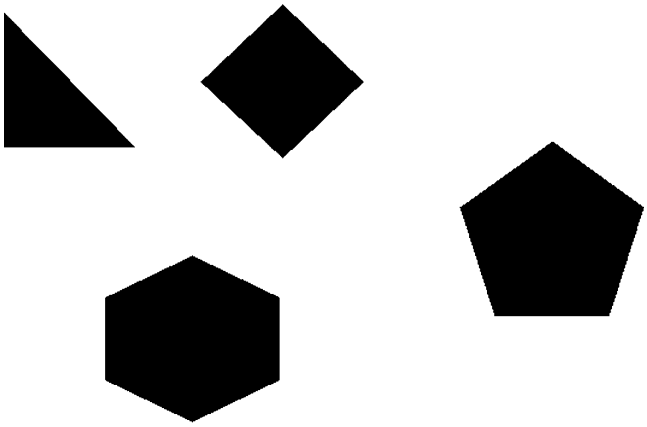

**Figure 1.1.** The premise of FAST ultrasound – anechoic triangulations are abnormal and represent free cavitary fluid. The nonradiologist can be readily trained to recognize anechoic (black) triangulations within cavities and spaces, which are abnormal in adult patients. The "Flash" exam answers a simple binary question of whether fluid is present or absent, whereas the AFAST provides more information through fluid scoring and its target organ approach, TFAST through echo views and volume status, and Vet BLUE through a regional, pattern-based approach. Courtesy of Dr Gregory Lisciandro, Hill Country Veterinary Specialists and FASTVet.com, Spicewood, TX.

## Other Terms

We have done our best to make this second edition uniform in terminology and up to date with the current consensus in both human and veterinary medicine. Some examples in which multiple terms relating to similar things are used are listed here.

The preferred term is listed first but each may be considered synonymously.

- POCUS exam and Focused exam
- sonographer and ultrasonographer
- ultrasonographically and sonographically
- color Doppler and color flow Doppler
- beam and scanning plane
- acoustic window and view
- fanning and tilting
- longitudinal and sagittal (and long axis)
- transverse (and short axis)
- orientation and plane
- probe and transducer
- curvilinear probe and microconvex probe
- B-lines and ultrasound lung rockets
- lung sliding and glide sign
- gallbladder halo sign, gallbladder halo effect, and gallbladder double rim effect

- FAST diaphragmatico-hepatic view and subxiphoid view
- acoustic coupling and probe–skin contact

We have provided a comprehensive list of abbreviations, terms, and definitions in the Appendices.

# Recording Your Findings on Goal-directed Templates

Recording data on goal-directed templates with clear objectives for answering defined clinical questions is imperative to gain the respect of our colleagues, to stay disciplined during the respective POCUS or FAST examination, to allow *post hoc* evaluation of studies, and to detect training strengths and deficiencies. Without recording your data, you cannot measure. If you cannot measure, you cannot critically study with the potential to improve. We have made great strides in Global FAST training by reevaluating our results recorded on goal-directed templates and saved video clips. A prime example is the establishment of clear tenets for the accurate TFAST diagnosis of pericardial effusion (Lisciandro 2016).

We have presented POCUS and FAST goal-directed templates and methods to efficiently save video clips for you to adapt and modify for your practice according to the types of cases you see, your practice type, and your skill level in the Appendices and Chapter 45.

# Echogenicity – Whites, Grays, and Blacks

The jargon of ultrasound can be intimidating to the novice sonographer. Clarity may be accomplished through acknowledging that *ultrasound is generally the opposite of how free fluid, air, and soft tissue appear on radiographic studies* (our brain needs to reformat itself). For example and very simplistically, air is white on ultrasound and black on radiographs. Fluid is black on ultrasound and white on radiographs. However, bone is black (shadows) on ultrasound? And white on radiographs? Or white along its proximal surface with acoustic shadowing through the far field. Now if we are losing you, hang in there. The figures help (Figures 1.2, 1.3, 1.4, 1.5). *Study them now*.

The ultrasound terms describing whites, grays, and blacks are anechoic (black), degrees of echogenicity (hypoechoic, shades of gray), and hyperechoic (white).

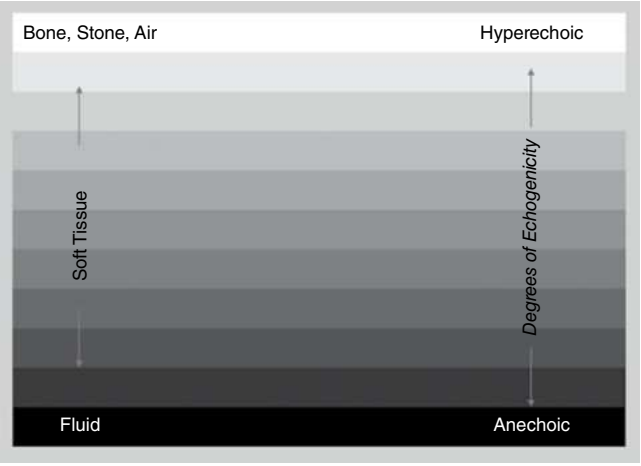


**Figure 1.2.** The figure shows the ultrasound differences in B-mode gray scale of various tissues, with bone, stone and air being most reflective of the ultrasound beam and thus portrayed as white along its surface, to soft tissues being shades of gray, to fluid which is black. Ultrasound terminology corresponds to these gray-scale colors as hyperechoic, degrees of echogenicity (hypoechoic), and anechoic. Study this chart to get the visual of what these gray-scale terms mean. Courtesy of Dr Gregory Lisciandro, Hill Country Veterinary Specialists and FASTVet.com, Spicewood, TX.

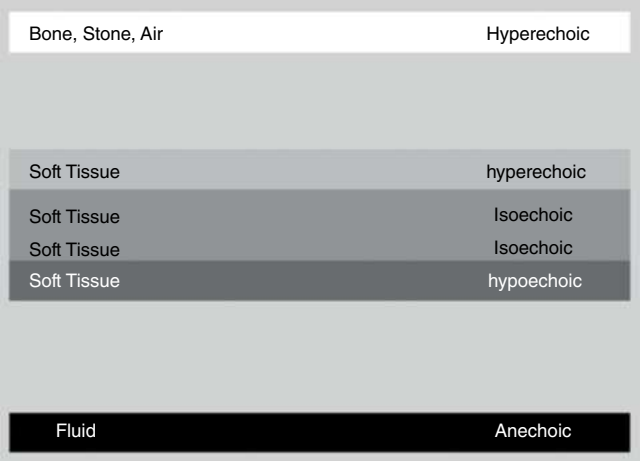


**Figure 1.3.** This figure is similar to Figure 1.2 but with some of the gray scale removed to illustrate how descriptive ultrasound terminology is used for different tissues. The soft tissue is isoechoic (same as), hyperechoic (brighter than), and hypoechoic (darker than) relative to one another. Correlate with Table 1.1 Courtesy of Dr Gregory Lisciandro, Hill Country Veterinary Specialists and FASTVet.com, Spicewood, TX.

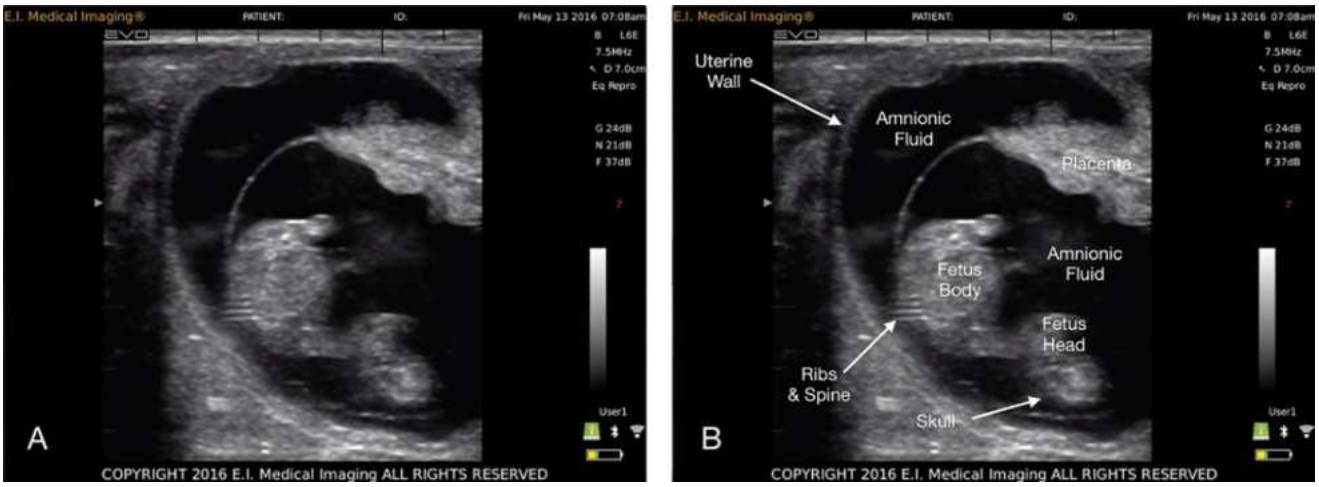


**Figure 1.4.** This figure is unlabeled and labeled for contrast of what tissue looks like in a gravid female, illustrating the different tissues and structures that correlate with concepts in Figures 1.1 and 1.2. Image used with permission from E.I. Medical, Loveland, CO, USA. www.eimedical.com

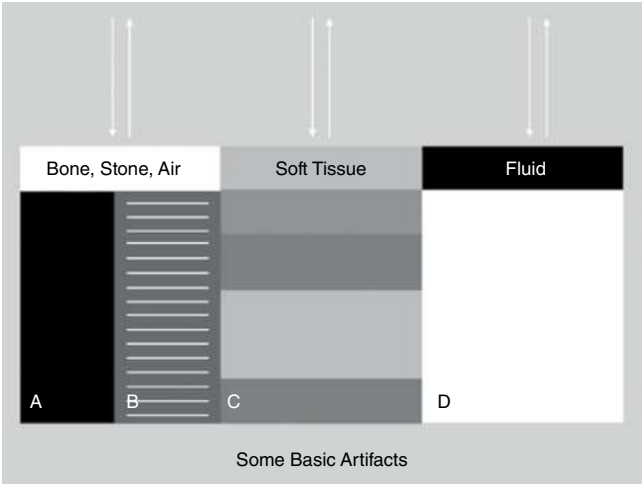


**Figure 1.5.** Ultrasound and different tissues and elements. Schematic that ties into the previous images showing various elements and the general behavior of ultrasound and its associated artifacts. The arrows represent the ultrasound beam being transmitted and returned to the transducer (probe). In (A) and (B), bone, stone, and air *reflect* because ultrasound (its echoes) does not transmit through them. As a result, they create shadowing of the beam, resulting in (A) "clean shadowing" (anechoic or black past the surface of the structure or element) or (B) "dirty shadowing," including air reverberation called A-lines (hyperechoic horizontal bars past the air). Soft tissues will absorb the ultrasound in different degrees depending on the soft tissue, thus (C) shows different degrees of echogenicity. Lastly, fluid will not absorb much of the ultrasound (echoes pass through the fluid), resulting in (D) acoustic enhancement through the far-field beyond the distal boundary of fluid, making tissues more hyperechoic (brighter) than their adjacent counterparts outside the fluid-related beam. Courtesy of Dr Gregory Lisciandro, Hill Country Veterinary Specialists and FASTVet.com, Spicewood, TX.

The terms may be used relatively between structures like "X relative to Y" and "Y relative to Z." For example, the spleen is *hyper*echoic (brighter than) to the left kidney. The liver is *hypo*echoic (darker than) to the falciform fat. The feline cortex of the kidney is isoechoic (same as) to the spleen (see Figure 1.3).

- **Anechoic (homogeneous black)**: occurs when *no ultrasound waves* are reflected back to the receiver. Thus, normal urine, normal bile, transudates, and blood all are purely anechoic (black).
- **Hypoechoic (shades of gray)**: occurs when *variable degrees of ultrasound waves* are reflected back to the transducer. Thus, the more echoes reflected back, the brighter gray the structure, and the fewer echoes, the darker the gray. Thus, all soft tissues that are not fully aerated are described relative to other distinct tissues, such that the liver is hypoechoic (darker than) relative to the spleen. Viscus organs (i.e., stomach) cannot be described this way, only their walls (i.e., stomach wall).
- **Hyperechoic (whites, bright whites)**: occurs *when all or nearly 100% of ultrasound waves* are reflected back to the transducer. Thus, bone, stone (metals), and air are strong reflectors resulting in hyperechoic (bright white) interfaces with shadowing, comet tail artifact, ring-down artifact, ultrasound lung rockets, or reverberation artifact projected *distal* to the reflective surface.
- **Isoechoic (same echogenicity)**: occurs when tissues are the same shades of gray. For example, if the liver is isoechoic to the spleen then they are the same echogenicity (same shades of gray).

# How Ultrasound Behaves Relative to Tissues and Elements

The knowledge of how ultrasound behaves relative to the structures and elements it encounters is very important. From normal tissues within the body to its various constituents (elements) of fluid, air, and mineralization, ultrasound behaves differently, causing a number of artifacts, which can be learned with diligent study, training, and practice. Foreign materials, such as plastic, metal, bone, stone, glass, and vegetative materials, also cause predictable artifacts. These artifacts will be covered in the next few chapters and throughout the textbook. It is a good idea to consider them every time you look at an image to accelerate your learning process.

Degrees of echogenicity of commonly encountered structures from hypoechoic to hyperechoic structures are listed in Table 1.1.

# Ultrasound Screen Orientation

The screen orientation should always be "head to the left and tail to the right," similar to the orientation for radiography (Figure 1.6). Thinking in this manner will help you learn the anatomy you are seeing and help you with the direction you need to go to get to the POCUS and FAST ultrasound structures of interest. The exception to this rule is that most cardiologists *reverse* the screen orientation of the heart, which is very problematic for learning image acquisition when doing a Global FAST approach. Many human institutions have rejected this approach for the noncardiologists performing POCUS and FAST examinations for the aforementioned reason.

**Table 1.1.**
Degrees of echogenicity of commonly encountered structures.

| | Structure |
|---|---|
| **Anechoic – hypoechoic (black)** | **Bile, urine** |
| | Muscle |
| Darker | Renal medulla |
| | Renal cortex |
| | Liver |
| **Shades of gray** | Fat |
| | Spleen |
| | Prostate |
| Brighter | Renal sinus |
| | Vessel walls |
| **Hyperechoic (white)** | **Bone, air, gas** |

# Directional Terms for Orientation

## *Longitudinal and Sagittal*

The term *longitudinal* refers to orientation parallel to the spine *or long axis* of the patient's body (see Figures 4.1, 4.2, 4.3). The term *sagittal* refers to the longitudinal axis of the respective deeper structure being evaluated. For example, the superficial jugular vein is imaged in longitudinal whereas the more deeply located and oblique right kidney (not parallel to the body's long axis) is imaged in sagittal planes (parallel to the right kidney's long axis). The terms are often used interchangeably (or, arguably, misused); however, by appreciating that both terms are in their own right long-axis views, directional communication between veterinarians seems to be clear by use of either term. Thus in longitudinal planes, the probe marker is directed towards the patient's head to maintain the same orientation as radiography, head to the left and tail to the right of ultrasound (and radiographic) image.

## *Transverse*

The term *transverse* refers to orientation 90° to the long axis of the structure being evaluated or the *short axis* of the patient (see Figures 4.1, 4.2, 4.3). The probe marker is turned to the left (or counterclockwise) to the patient's right side. Thus, in transverse planes, the probe marker is directed to the patient's right side to maintain the same orientation as radiography, right side on left side of ultrasound (and radiographic) image.

With that said, let's get on with Dr Fulton's chapters that will cover in more detail the physics of ultrasound, its artifacts, and various pointers on the ultrasound machine features and settings and image acquisition.

It's worth your effort and time investment to learn this core skill – POCUS and FAST improve care and save lives!

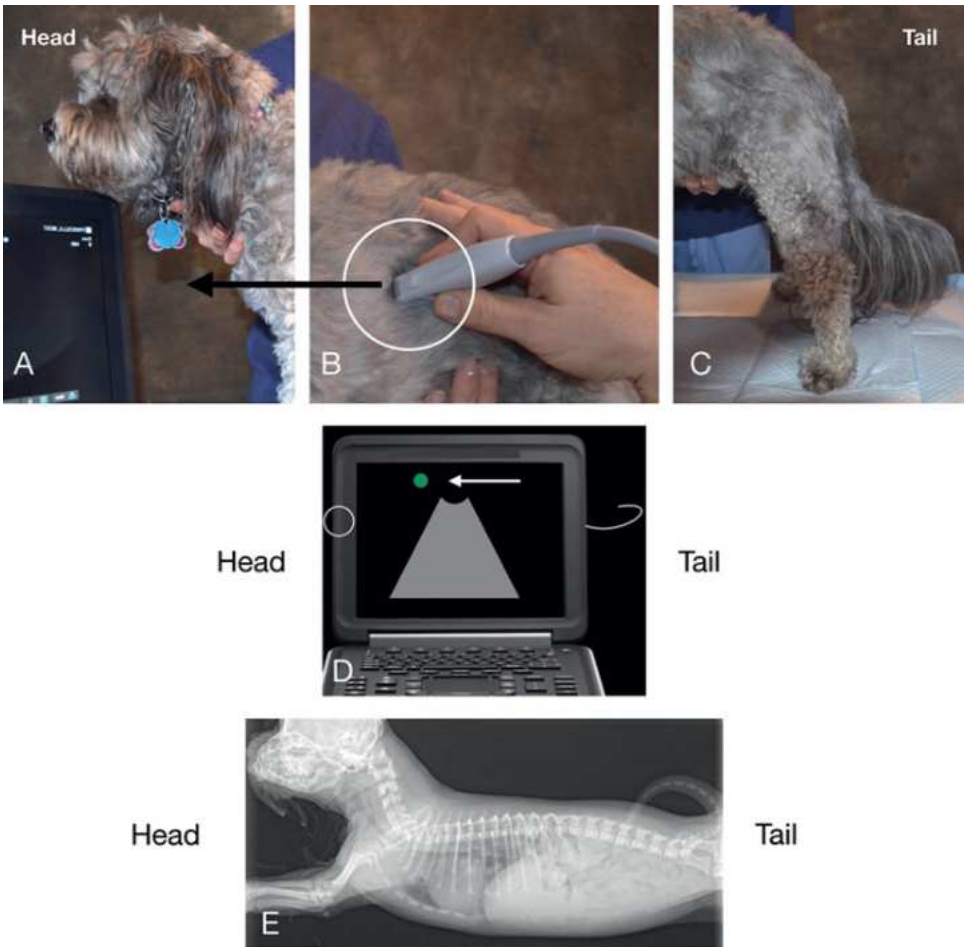


**Figure 1.6.** Longitudinal (sagittal) planes and orientation. Make the screen marker and the probe marker both consistent with "head to the left and tail to the right," which is the *same* orientation as radiography. (A) shows the head of the dog and (C) its tail. In (B), the probe is placed on the truncal area of the same dog. The white circle highlights the probe marker (can be a notch, a raised line or button, or an LED light). Every probe has its marker. In (D) is a pictorial of the ultrasound screen, and the green dot indicates the screen marker (arrow ←). Make sure that this is to the left of the screen and the probe marker is toward the head of your patient. In (E) is a radiograph showing the *same* orientation used for ultrasound, "head to the left, tail to the right." Courtesy of Dr Gregory Lisciandro, Hill Country Veterinary Specialists and FASTVet.com, Spicewood, TX.

# References

Kirkpatrick AW, Sirois M, Laupland KB, et al. 2004. Hand-held thoracic sonography for detecting post-traumatic pneumothoraces: the extended focused assessment with sonography for trauma (EFAST). *J Trauma* 57:288–295.

Lisciandro GR. 2011. Abdominal and thoracic focused assessment with sonography for trauma, triage, and monitoring in small animals. *J Vet Emerg Crit Care* 21(2): 104–122.

Lisciandro GR. 2016. The use of the diaphragmatico-hepatic (DH) views of the abdominal and thoracic focused assessment with sonography for triage (AFAST/TFAST) examinations for the detection of pericardial effusion in 24 dogs (2011–2012). *J Vet Emerg Crit Care* 26(1):125–131.

Lisciandro GR, Lagutchik MS, Mann KA, et al. 2008. Evaluation of a thoracic focused assessment with sonography for trauma (TFAST) protocol to detect pneumothorax and concurrent thoracic injury in 145 traumatized dogs. *J Vet Emerg Crit Care* 18(3):258–269.

Lisciandro GR, Lagutchik MS, Mann KA, et al. 2009. Evaluation of an abdominal fluid scoring system determined using abdominal focused assessment with sonography for trauma in 101 dogs with motor vehicle trauma. *J Vet Emerg Crit Care* 19(5):426–437.

Lisciandro GR, Fosgate GT, Fulton RM. 2014. Frequency of ultrasound lung rockets using a regionally-based lung

ultrasound examination named veterinary bedside lung ultrasound exam (Vet BLUE) in 98 dogs with normal thoracic radiographic lung findings. *Vet Rad Ultrasound* 55(3):315–322.

Lisciandro GR, Fulton RM, Fosgate GT, Mann KA. 2017. Frequency of B-lines using a regionally-based lung ultrasound examination (the Vet BLUE protocol) in 49 cats with normal thoracic radiographical lung findings. *J Vet Emerg Crit Care* 27(3):267–277.

McMurray J, Boysen S, Chalhoub S. 2016. Focused assessment with sonography in nontruamtized dogs and cats in the emegrency and critivcal care setting. *J Vet Emerg Crit Care* 26(1):64–73.

Rozycki GS. 1998. Surgeon performed US: its use in clinical practice. *Ann Surg* 228:16–28.

Rozycki GS, Ballard RB, Feliciano DV, et al. 1998. Surgeon-performed ultrasound for the assessment of truncal injuries: lessons learned from 1540 patients. *Ann Surg* 228(4):557–567.

Rozycki GS, Pennington SD, Feliciano DV. 2001. Surgeon-performed ultrasound in the critical care setting: its use as an extension of the physical examination to detect pleural effusion. *J Trauma* 50(4):636–642.

Rozycki GS, Knudson MM, Shackford SR, et al. 2005. Surgeon-performed bedside organ assessment with sonography after trauma (BOAST): a pilot study from the WTA Multicenter Group. *J Trauma* 59(6):1356–1364.

# Further Reading

Mattoon JS, Nyland TG. 2015. Fundamentals of diagnostic ultrasound. In: *Small Animal Diagnostic Ultrasound*, 3rd edition, edited by Mattoon JS, Nyland TG. St Louis: Elsevier, pp 1–49.

CHAPTER TWO

# POCUS: Basic Ultrasound Physics

Robert M. Fulton

## Introduction

Turn on the machine. Apply acoustic coupling gel. Start scanning. In the realm of the busy veterinary general practice, emergency clinic, or intensive care unit, that statement really sums up the basic use of ultrasound. Just as it is natural for us to take the stethoscope from around our neck and place it on a patient's thorax, so should be picking up the ultrasound probe and placing it on the patient. No wonder that ultrasonography has been appropriately dubbed both "an extension of the physical exam" and the "modern stethoscope" (Rozycki et al. 2001; Filly 1988). Really, one doesn't need a whole lot of instruction to start scanning; however, as for a lot of things in life, the devil is in the details. Understanding how the ultrasound image is formed (Physics), understanding inherent physical limitations (Artifacts), and knowing how to acquire the image (Technique) are the keys to acquiring and interpreting the diagnostic ultrasound image.

The focus of this and the following several chapters is a brief review of the basic physics and principles of ultrasound, including the more common problematic artifacts. For interested readers, there are more comprehensive textbooks dedicated to the physics and interpretation of ultrasound imaging (Nyland et al. 2002; Penninck 2002; Bushberg et al. 2002).

### *What POCUS Basic Ultrasound Physics Can Do*

- Provide a basic review of ultrasound physics.

### *What POCUS Basic Ultrasound Physics Cannot Do*

- Cannot provide an in-depth discussion of ultrasound physics and principles
- Cannot replace experience and knowledge of your own ultrasound machine.

### *Indications*

- All sonographers performing POCUS and FAST for a basic understanding of the physics and principles of ultrasound imaging.

## Objectives

- Provide a basic understanding of ultrasound principles to maximize accurate image interpretation.
- Provide an understanding of the fundamentals of ultrasound physics and how they relate to image formation.

## Basic Ultrasound Principles

The ultrasound machine consists of two main parts, the probe and the processor. The probe is the "brawn" and the processor the "brains" of the operation. The probe has two main functions: first, to generate a sound wave (acts as a transmitter), and second, to receive a reflected sound wave (acts as a receiver).

*Point-of-Care Ultrasound Techniques for the Small Animal Practitioner*, Second Edition. Edited by Gregory R. Lisciandro.
© 2021 John Wiley & Sons, Inc. Published 2021 by John Wiley & Sons, Inc.
Companion website: www.wiley.com/go/lisciandro/ultrasound2

The processor, located within the ultrasound unit, takes these incoming signals and turns them into a useful image.

The transmitter and receiver functions of the transducer do not occur simultaneously but rather sequentially. When placed under mechanical stress, the ceramic crystals in the transducer generate a voltage. This process, known as the piezoelectric effect, occurs during the receiving phase, which is when returning sound waves strike the transducer. When an external voltage is applied to the crystals, they exhibit the reverse phenomenon and undergo a small mechanical deformation. The subsequent release of this energy generates the ultrasound wave. This is known as the reverse piezoelectric effect. World War I saw the first practical use of the piezoelectric effect in the development of sonar using a separate sound generator and detectors (Coltrera 2010).

The sound waves generated by diagnostic ultrasound machines are typically in the 3–14 megahertz (MHz) range and are thus too high pitched to be perceived by the human ear. We can hear sounds in the range of 20 Hz (cycles/second) to 20 000 Hz. In contrast, our average canine patient hears sounds in the range of 40 Hz to 60 000 Hz. The high frequencies are in the realm of what is termed the "ultrasonic" range, basically any sound above our ability to hear and hence the name for this clinical imaging tool (Nyland et al. 2002).

The sound waves produced by the transducer penetrate the body tissues and are subject to all the rules surrounding any sound wave, including reflection, refraction, reverberation, attenuation, and impedance. The processor analyzes the transmitted signals and the returning waves, including their quantity, strength, and the time they took to return. By applying preprogrammed algorithms, the processor translates this information into a pixel, gives it an appropriate intensity (its echogenicity), and places it on the monitor screen to give us the image (sometimes being "fooled" into creating artifacts).

Between the transducer and the processor, it is easy to see why the equipment for this modality can be rather pricey. However, by using the variety of POCUS and FAST ultrasound exams outlined in this textbook, we hope that your ultrasound machine will become an asset not only with improved patient care but also with a return on investment.

## Velocity

Sound travels at specific known velocities through various materials. Remember from physics that sound travels faster though solids than through liquid or gas, and its velocity through various body tissues is known (Figure 2.1). Notice that velocity is similar through most of the soft tissues; however, current ultrasound machines cannot determine what tissues are being penetrated. Therefore, most ultrasound machines use an average velocity of 1540 m/sec for their imaging algorithms, averaging the speed of sound through fat, liver, kidney, blood, and muscle (Coltera 2010). Some newer machines allow the user to select a different constant for the specific tissue or structure they are imaging.

The first and last columns in Figure 2.1 illustrate that sound passes relatively slowly through air and relatively quickly through bone. Anyone who has picked up an ultrasound probe knows that bone (solid) or lung (air) cannot be adequately penetrated using

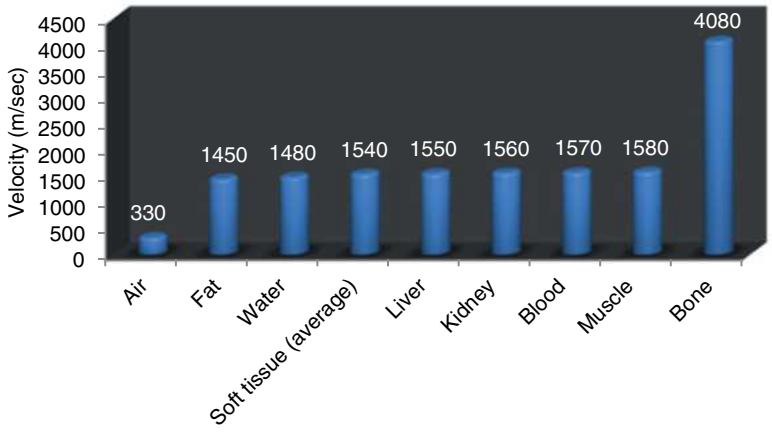


**Figure 2.1.** Velocity (m/sec) of sound through common body tissues or substances. Note the similar velocity through most soft tissues. This is the basis for using 1540 m/sec as the number in depth calculations by the ultrasound processor (Coltrera 2010).

ultrasound, thus only the surfaces of each are visible. To address this issue, the sonographer must understand the principle of acoustic impedance.

**Pearl:** Remember the saying: Ultrasound hates bone or stone and is not too fair with air.

## Acoustic Impedance

Acoustic impedance refers to the reflection and transmission characteristics of a substance. It is a measure of absorption of sound and the ratio of sound pressure at a boundary surface to the sound flux. Sound flux is flow velocity multiplied by area. If we draw an analogy to electronic circuits, acoustic impedance is like electrical resistance through a wire, sound pressure is like voltage, and flow velocity is like current. The equation that brings it all together is:

$$Z = p / v$$

where Z = acoustic impedance, p = sound pressure (or tissue density), and v = velocity (Nyland 2002).

The amplitude of a reflected sound wave is proportional to the difference in acoustic impedance between two different tissues. Air has a low impedance and bone has a high impedance when compared to soft tissue (Reef 1998) (Figure 2.2). Therefore, when a sound wave comes across a soft tissue–bone or a soft tissue–air interface (large difference in acoustic impedance), nearly all of the sound waves are strongly reflected (and a bright white echogenic line is formed at either interface). Reflection is why the sonographer cannot image through bone (solid) or lung (air) and this points up one of the most common misnomers in clinical ultrasonography: when imaging through the liver into the thorax, we term the bright, curved cranial border as the diaphragm. In reality, the diaphragm is uncommonly imaged except in bicavitary effusions. The bright white (hyperechoic), curved line is actually the strongly reflective surface of the lung (air) at the soft tissue–air boundary or interface serving as a strong reflector.

By comparing the acoustic impedance of most tissues in the body other than bone (solid) and lung (air), we see that they are very similar (there is little difference in acoustic impedance among them). This similarity makes ultrasound a great imaging tool for examining into and through soft tissues (their parenchyma). On the other hand, due to the large difference in acoustic impedance between soft tissue–air and soft tissue–bone interfaces, ultrasound is not an effective tool for examination beyond the surfaces of either aerated lung, gas-containing hollow viscus or bone (Reef 1998).

## Absorption, Scatter, and Reflection

Other ultrasound principles that affect our image include absorption, scatter, and angle of reflection. As the sound waves enter the body, some of them are absorbed by the tissues and are never reflected back to the probe. These waves are lost and do not contribute to the image. Furthermore, many of the waves are scattered by the tissues and their surface irregularities and either return to the probe (receiver) in a distorted path or do not return at all. As a result, the ultrasound waves are "misinterpreted" by the processor, and the image and its resolution are affected.

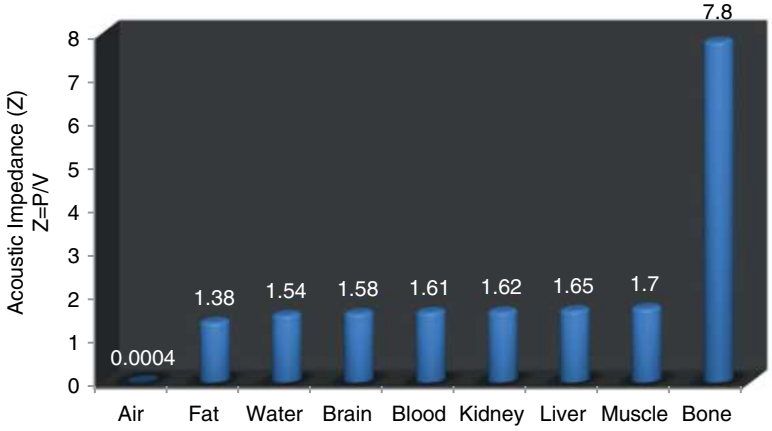


**Figure 2.2.** Acoustic impedance (106 kg/m²sec) of common body tissues or substances. This figure illustrates the degree of difference in acoustic impedance between substances that helps determine sound wave transmission. The greater the difference, the greater is reflection or loss of transmission. One can see how ultrasound is ideally suited for most soft tissue and why it is not suited for imaging bone or air-filled structures (Reef 1998).

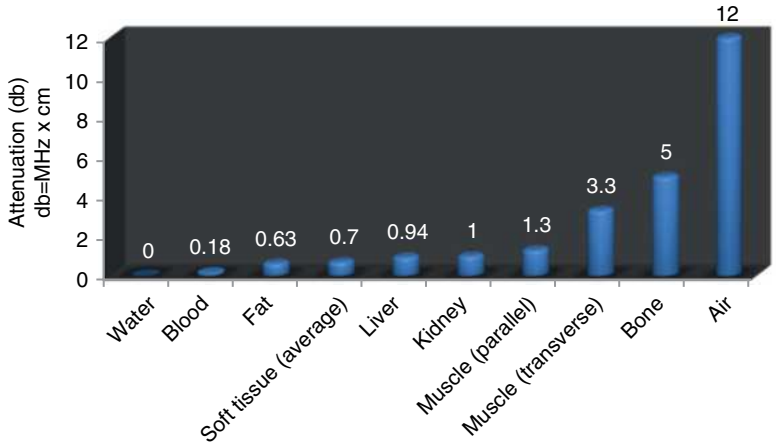


**Figure 2.3.** Attenuation (db/cm/MHz) in common tissues. Attenuation of sound energy within tissues varies with the frequency of the sound and is affected by reflection, scattering, and absorbance. Note how bone and air have the greatest attenuation values (Reef 1998).

### *Attenuation*

All sound beams lose energy, or become attenuated, during transmission through tissues; therefore, the returning sound wave is weaker than when it started. Different frequencies (MHz) are attenuated to different degrees. Because higher frequency probes send more waves per second, there is greater tissue interaction with the sound waves. This provides improved resolution but undergoes more attenuation. Low-frequency sound waves are less attenuated because of less tissue interaction, and therefore allow deeper tissue penetration. Strategies that include lowering the MHz for better penetration (depth) come at the expense of detail. Conversely, using higher frequency for more detail comes at the cost of less penetration (depth). Furthermore, high-density tissues attenuate the sound waves more than low-density tissues (Figure 2.3).

**Pearl:** The analogy of hearing a boom box from a distance can help you remember which MHz penetrates more. The bass dominates (low MHz) over higher frequencies (high MHz); thus, low MHz penetrates deeply at the expense of detail, and high MHz give better detail at the expense of penetration.

## The Final Say

By understanding the basic physical principles governing sound transmission and the limitations of the ultrasound processor, the ultrasonographer can better understand the image on the screen. Furthermore, this same knowledge is fundamental in understanding ultrasound artifacts covered in the next chapter.

## References

Bushberg JT, Seibert JA, Leidholdt EM, Boone JM. 2002. *The Essential Physics of Medical Imaging*, 2nd edition. Philadelphia: Lippincott Williams and Wilkins.

Coltera M. 2010. Ultrasound physics in a nutshell. *Otolaryngol Clin North Am* 43(6):1149–1159.

Filly RA. 1988. Ultrasound: the stethoscope of the future, alas. *Radiology* 167:400.

Nyland TG, Mattoon JS, Herrgesell EJ, et al. 2002. Physical principles, instrumentation, and safety of diagnostic ultrasound. In: *Small Animal Diagnostic Ultrasound*, 2nd edition, edited by Nyland TG, Mattoon JS. Philadelphia: WB Saunders, pp 1–18.

Penninck DG. Artifacts. In: *Small Animal Diagnostic Ultrasound*, 2nd edition, edited by Nyland TG, Mattoon JS. Philadelphia: WB Saunders, pp 19–29.

Reef V. 1998. Thoracic ultrasonography: noncardiac imaging. In: *Equine Diagnostic Ultrasound*, edited by Reef V. Philadelphia: WB Saunders, pp 187–214.

Rozycki GS, Pennington SD, Feliciano DV, et al. 2001. Surgeon-performed ultrasound in the critical care setting: its use as an extension of the physical examination to detect pleural effusion. *J Trauma* 50:636–642.

## Further Reading

Volpicelli G, Elbarbary M, Blaivas M, et al. 2012. International evidence-based recommendations for point-of-care lung ultrasound. *Intensive Care Med* 38:577–591.

CHAPTER THREE

# POCUS: Basic Ultrasound Artifacts

Robert M. Fulton

## Introduction

In this chapter, we'll look at the fundamental laws governing wave dynamics and see how ultrasound artifacts are created. Ultrasound machines rely on several physical assumptions to assign the location and intensity of each received echo. These assumptions are that the received echoes have originated from within the main ultrasound beam, an echo returns to the transducer after a single reflection, the depth of an object is directly related to the amount of time for an ultrasound pulse to return to the transducer, the speed of sound in tissue is constant (1540 m/sec), the sound beam and its echo travel in a straight path, and the acoustic energy in an ultrasound field is uniformly attenuated (Feldman et al. 2009). Artifacts may be grouped by the most important principles leading to their formation, including attenuation, velocity or propagation, and artifacts associated with multiple echoes. Many artifacts can be grouped by their association with air or fluid, making learning them easier.

### What POCUS Basic Ultrasound Artifacts Can Do

- Provide a basic understanding of how artifacts are formed to allow better interpretation of the ultrasound image.

### What POCUS Basic Ultrasound Artifacts Cannot Do

- Cannot provide an in-depth discussion of ultrasound artifacts.
- Cannot account for what artifacts your ultrasound machine's software is most biased towards.

### Indications

- Provide a basic understanding of ultrasound principles and common artifacts to maximize accurate image interpretation.

### Objectives

- Provide a basic understanding of how common ultrasound artifacts are formed to avoid image misinterpretation of artifacts for abnormalities.

## Artifacts of Attenuation: Strong Reflectors (Bone, Stone, Air)

### Shadowing, "Clean" and "Dirty"

Clean shadows and dirty shadows result from strong reflectors (bone, stone, and air). We know from differences in acoustic impedance at soft tissue–air and soft tissue–bone (stone) interfaces that most of the sound waves will be reflected, albeit in different degrees (Figures 3.1 and 3.2A).

### Bone or Stone Interface: Clean Shadowing

When the ultrasound wave strikes bone (and stone), most of the waves are reflected back so there will be an area of intense hyperechogenicity (whiteness) at the soft tissue–bone (stone) interface. Because the surface of bone is often smooth, there is little scattering or

*Point-of-Care Ultrasound Techniques for the Small Animal Practitioner*, Second Edition. Edited by Gregory R. Lisciandro.
© 2021 John Wiley & Sons, Inc. Published 2021 by John Wiley & Sons, Inc.
Companion website: www.wiley.com/go/lisciandro/ultrasound2

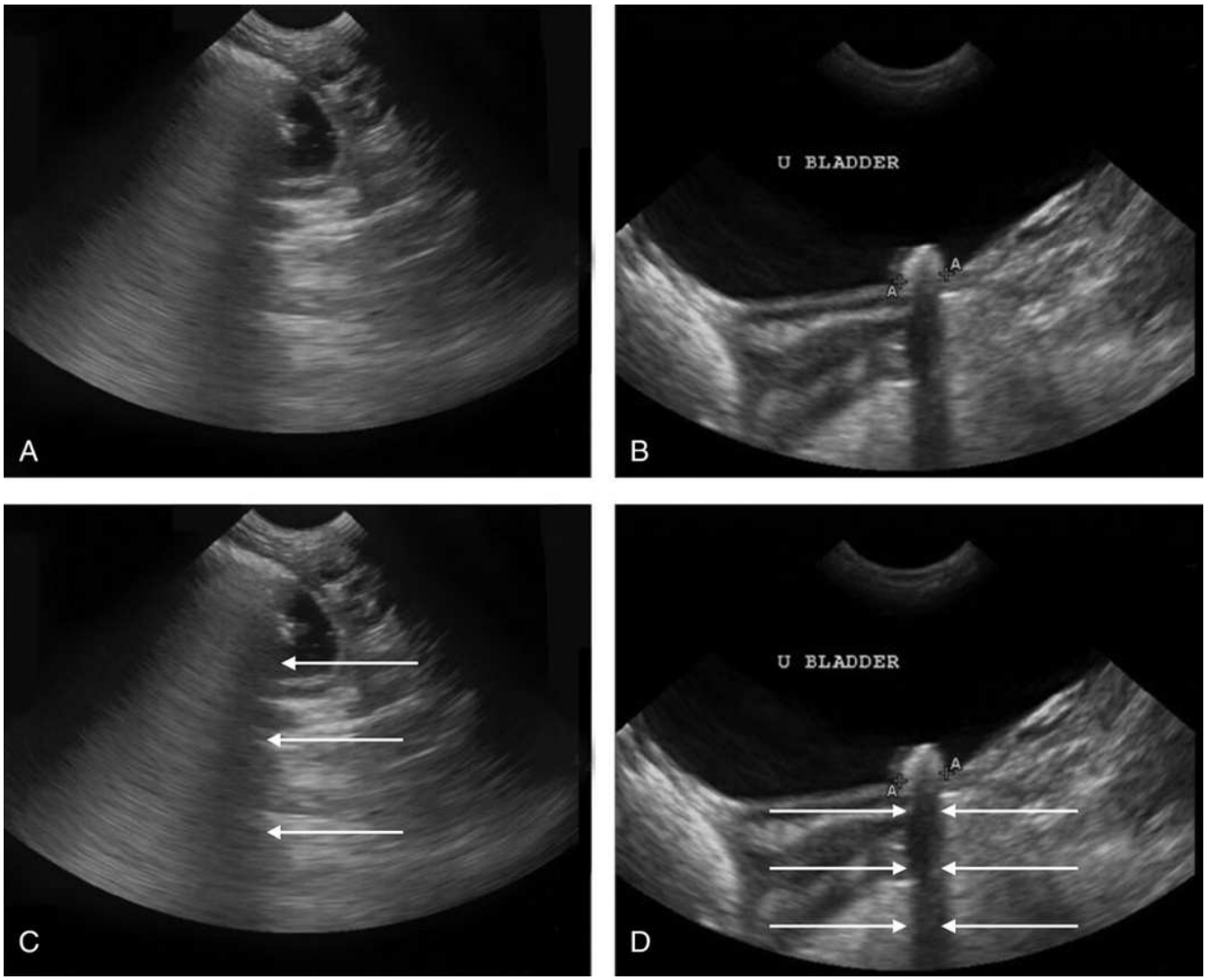


**Figure 3.1.** Dirty and clean shadowing. (A) "Dirty shadowing" created by air, a gas bubble within a fluid-filled distended loop of small bowel. "Dirty shadowing" is generated because some ultrasound waves pass through the structure. Contrast the "dirty shadowing" with the "clean shadowing" of the cystourolith (urinary bladder stone) in (B) in which all ultrasound waves are reflected back to the transducer. (B) "Clean shadowing." The smooth surface of the cystourolith (urinary bladder stone) generates the "clean shadowing" typical of bone or stone with a hyperechoic (bright white) reflective surface in the near field, completely blocking all echoes and thus resulting in an anechoic (dark or black) shadow extending from it through the far-field. In (C) and (D), the images have arrows (←) pointing out the artifact. Source: Courtesy of Dr Sarah Young, Echo Service for Pets, Ojai, California.

reverberation of the ultrasound wave and a nice, clear-cut, anechoic (blackness) "clean shadow" is produced beyond the reflector (bone or stone) (see Figure 3.1).

### *Air Interface: Dirty Shadowing*

On the other hand, soft tissue–air interfaces are more variable in their degree of reflection, with some of the ultrasound waves incompletely moving through the air-filled structure, unlike the complete reflection at bone (or stone). Thus, reverberations occur distal to the air interface, creating a "dirty shadow" (Penninck 2002) (see Figure 3.1).

## Artifacts of Attenuation: Fluid-Filled Structures

### *Edge Shadowing: Fluid-Filled Structures*

When the ultrasound waves strike the edge of a fluid-filled structure with a curved surface (its wall), such as

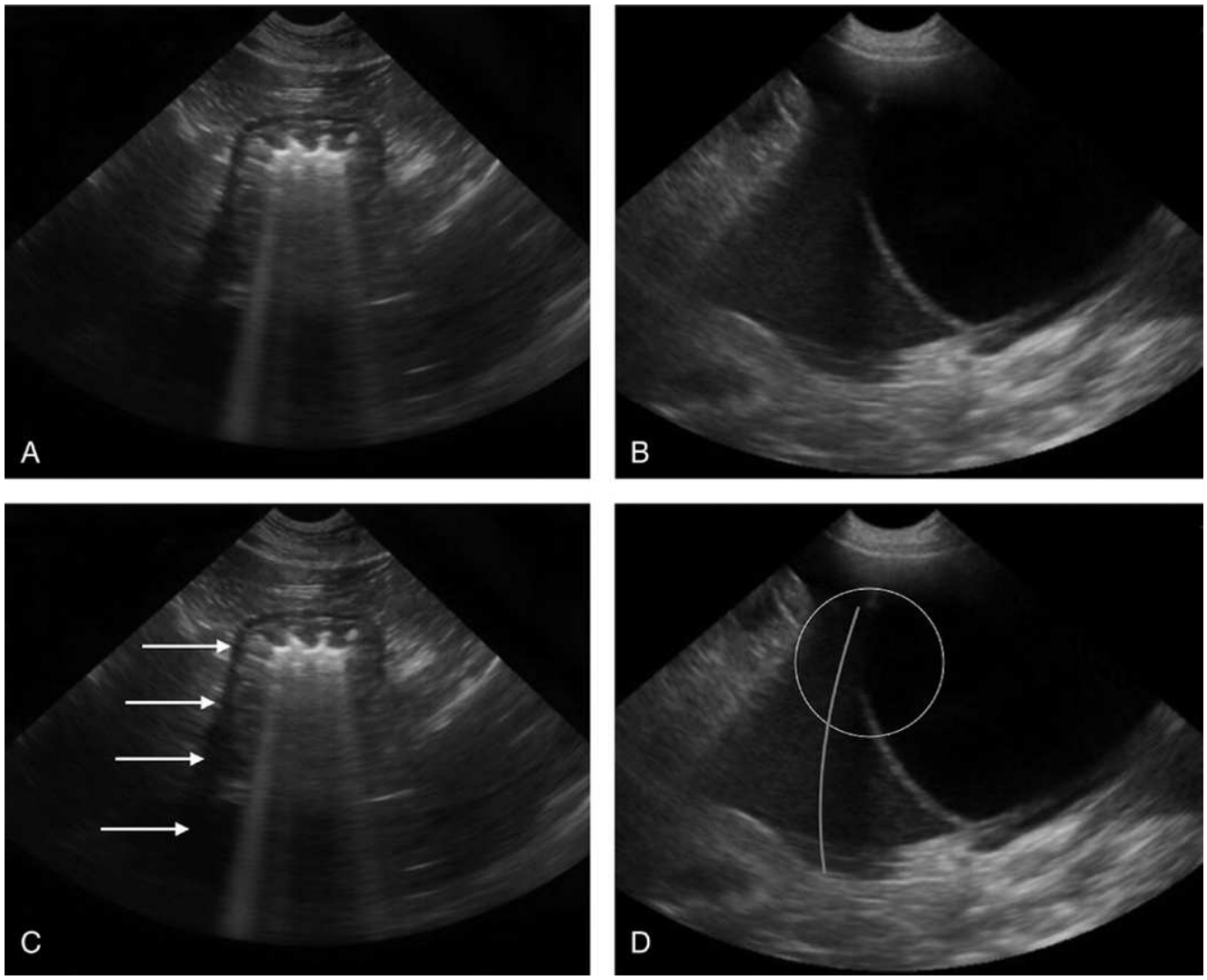


**Figure 3.2.** Edge shadowing artifact. (A) An edge shadowing artifact is seen arising from the curved edge on the left side of the stomach wall in this image, making its wall appear to extend distally as an anechoic (dark or black) line. A dirty gas shadow is also produced from gas within the stomach lumen that appears as "pseudo B-lines." (B) An edge shadowing artifact at the apex of the urinary bladder makes it falsely appear to have a rent, which can fool the hasty sonographer into thinking the free fluid is from a ruptured bladder; however, note the smooth expected normal contour of the urinary bladder. In (C) the edge shadowing artifact is outlined with arrows (←). In (D) the edge shadowing creates a false rent in the wall of the urinary bladder (*circled*) and the superimposed curved line points out the edge shadowing from the curved surface of the urinary bladder wall extending through the far-field. Source: Courtesy of Dr Sarah Young, Echo Service for Pets, Ojai, California.

the stomach wall, urinary bladder, gallbladder, eye, or cyst, ultrasound waves are reflected to a small degree and these reflected sound waves therefore do not return to the transducer. As a result, a thin hypoechoic (darker) to anechoic (black) area lateral and distal to the edge of the curved structure is formed. For example, the novice may mistake this artifact for a "rent" in the urinary bladder wall when in fact it is an artifact created by the ultrasound machine (Nyland et al. 2002) (see Figure 3.2).

## *Acoustic Enhancement: Fluid-Filled Structures*

When the sound beam passes through a fluid-filled structure, such as the gallbladder, urinary bladder, fluid-filled stomach, eye, or a cyst, ultrasound waves do not become as attenuated as the neighboring waves passing through more solid tissues to either side of the structure. Therefore, the tissues on the far side of the fluid-filled structure appear much brighter than

the neighboring tissues at the same depth. Acoustic enhancement is obvious, looking past the fluid-filled gallbladder and urinary bladder (Figure 3.3). On the other hand, by realizing how the artifact is formed, the acoustic enhancement artifact can be useful to the savvy sonographer in determining if a structure of interest is fluid filled (brighter through the far-field having acoustic enhancement) or soft tissue (lacking acoustic enhancement) (Penninck 2002) (see Figure 3.3).

# Artifacts of Velocity or Propagation

## *Mirror Artifacts: Strong Reflector (Air)*

When we image a structure that is close to a curved, strong reflector such as the diaphragm (remember this is actually the lung–air interface following the curve of the diaphragm), a sound beam can reflect off the

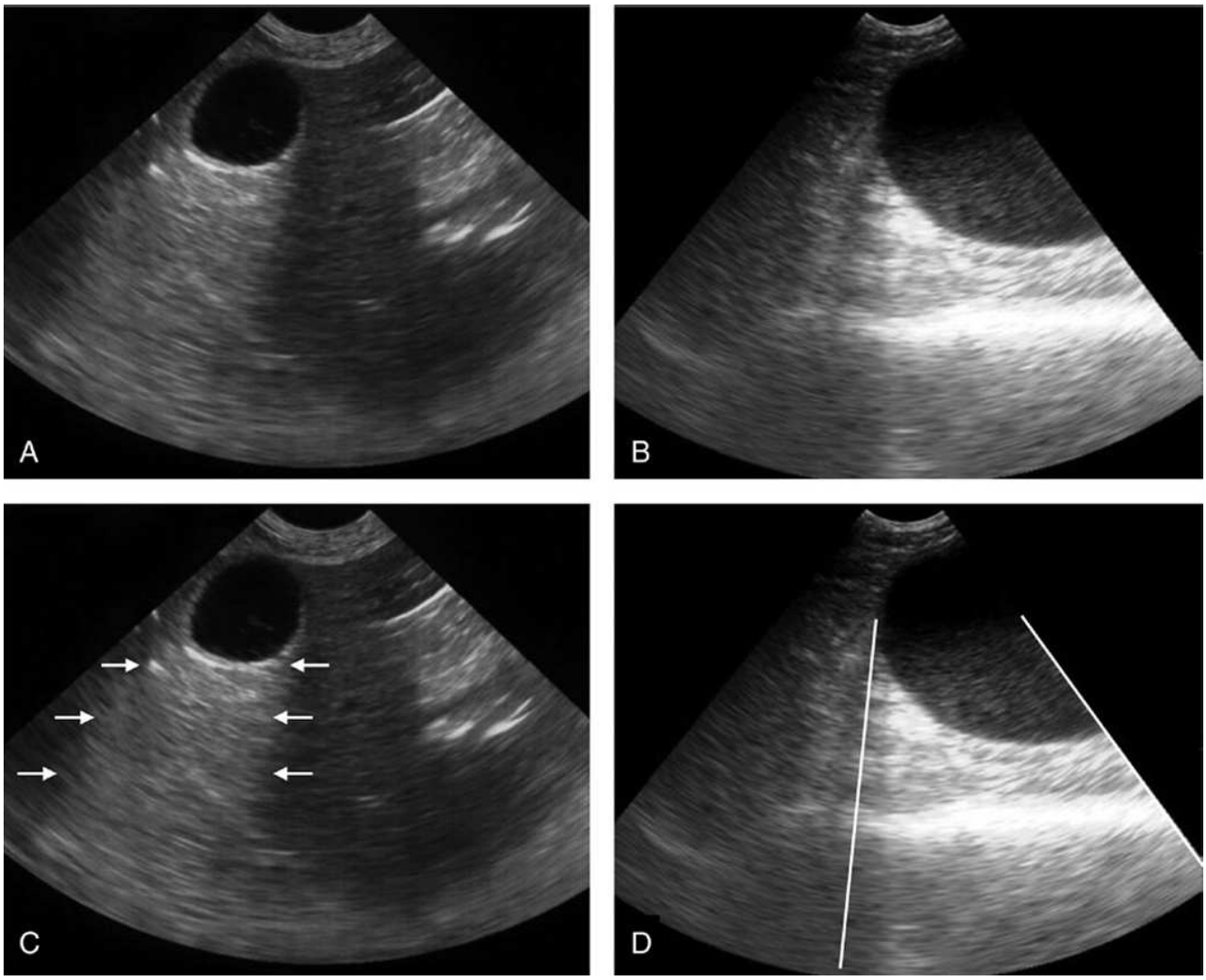


**Figure 3.3.** Acoustic enhancement artifact. Because there is less attenuation when sound moves through fluid, the area distal to a fluid-filled structure will appear hyperechoic (brighter or whiter) to the surrounding tissue. Note the hyperechoic regions distal to the gallbladder (A) and distal to the urinary bladder (B) that are outlined with arrows (←) in (C) and by white bars in (D).

curved surface, strike adjacent tissues, reflect back to the curved surface, and then reflect back to the transducer. Because the processor only uses the time it takes for the beam to return home and cannot "see" the ongoing reflections, it will be fooled into placing (mirroring) the image on the far side of the curved surface. The classic place for a mirror artifact is at the diaphragm, and the classic mistake is interpreting the artifact as a diaphragmatic hernia (Penninck 2002) (Figure 3.4).

### *Reverberation or A-Lines: Strong Reflector (Air)*

Reverberation occurs when sound encounters two highly reflective layers. The sound is bounced back and forth between the two layers before traveling back to the receiver. The probe will detect a prolonged traveling time and assume a longer traveling distance and display additional reverberated images in a deeper

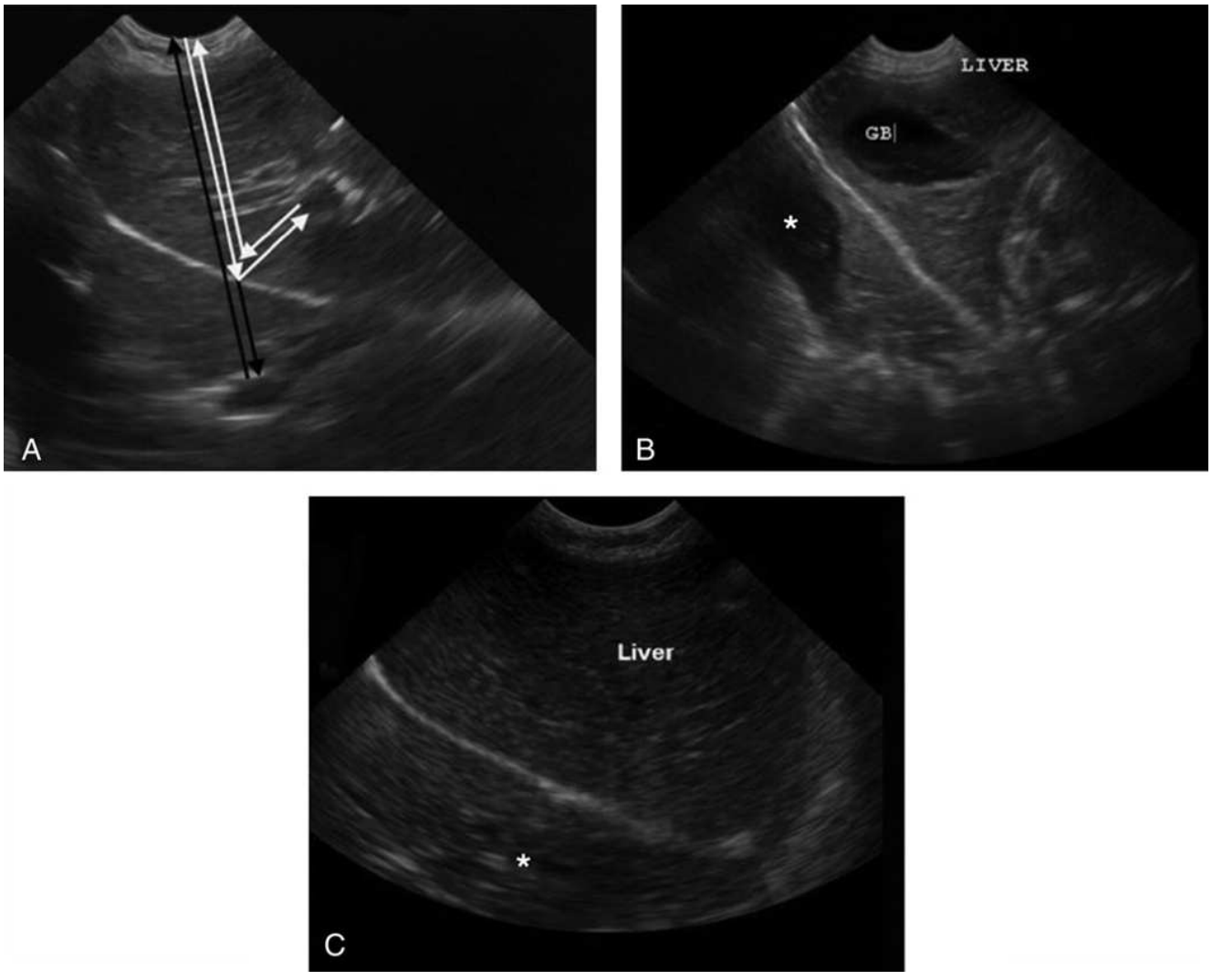


**Figure 3.4.** Mirror artifact. The gallbladder appearing to be on both sides of the diaphragm is the classic example of mirror artifact, created by a strong soft tissue–air interface. The mirror image artifact also may be generated under similar circumstances when the fluid-filled urinary bladder lies against the air-filled colon. (A) The white arrows illustrate the actual path of the sound beam reflecting off the curved lung–air interface against the diaphragm, while the black arrows illustrate the path perceived by the ultrasound processor. Note that the gallbladder falsely appears as if it is within the thorax, and should not be mistaken for a diaphragmatic hernia. (B) Mirror image artifact in which it appears that the liver and gallbladder are on both sides of the diaphragm (*). (C) Mirror image artifact in which it appears that liver (gallbladder *not* present in this view) is on both sides of the diaphragm (*). Source: Courtesy of Robert M. Fulton, DVM, Richmond, VA.

tissue layer. The reverberations can get caught in an endless loop and extend all the way to the bottom of the screen as parallel equidistant lines, referred to as A-lines (also see Chapters 22 and 23). This artifact most commonly extends beyond air-filled structures within the thorax, (e.g., lung) and within the abdomen (e.g., gastrointestinal tract), with varying width (Penninck 2002) (Figure 3.5; see also Figures 3.1 and 3.2).

### *Comet-Tail or Ring-Down Artifact: Strong Reflector (Usually Metal or Bone But Can Be Air)*

A comet-tail artifact, also called a ring-down artifact, is similar to reverberation. It is produced by the front and back of very strong reflectors with high acoustic impedance, such as metallic foreign bodies or implants,

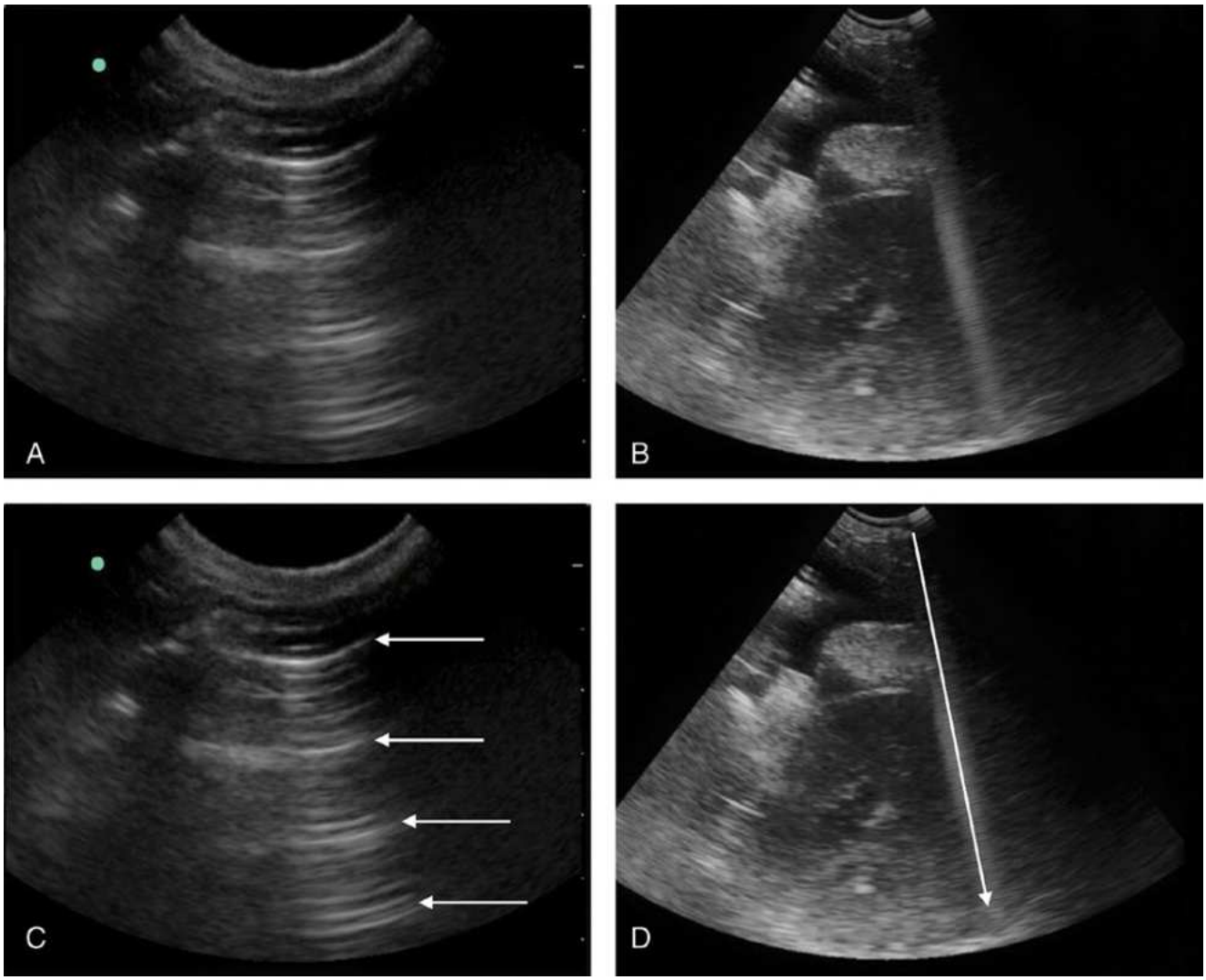


**Figure 3.5.** Reverberation artifact. (A) Reverberation artifact, also known as A-lines (think of it as "A" for air). A-lines are seen as regularly spaced parallel lines illustrated by the arrows (←) outlined in (C). The most proximal arrow in the near-field denotes the lung's surface, evident within the intercostal space between two ribs on either side (ribs [bone] creating the "clean shadowing" through the far-field). (B) The very tight and distinct band of reverberation artifact, referred to as a comet-tail or ring-down artifact, caused by sound waves reflecting off a metal needle used during abdominocentesis in the near-field. (D) The same image but with an arrow overlay to show the tight band of A-lines as the comet-tail or ring-down artifact. Any strong reflector of ultrasound waves produces this artifact that typically involves bone, stone, or metal, such as implants, needles, and foreign bodies. Source: Courtesy of Robert M. Fulton, DVM, Richmond, VA.

needles, and stylets during ultrasound-guided procedures (see also Chapters 43 and 44), or strong reflectors with very low acoustic impedance relative to their adjacent soft tissues, such as gas in the lung, gas bubbles, or gas in the bowel. The reverberations are spaced very narrowly and blend into a small band. The greater the difference between the acoustic impedance of the reflecting structure and the surrounding tissues, the greater the number of reverberation echoes (Reef 1998) (see Figure 3.5).

### *B-Lines: Strong Reflector (Air Immediately Next to Fluid)*

Ultrasound lung rockets (ULRs), more recently termed B-lines (Volpicelli et al. 2012), are vertical, narrow-based lines arising from the near-field's pulmonary–pleural line, extending to the far edge of the ultrasound screen, always obliterating A-lines, and moving "to and fro" in concert with inspiration and expiration. Although B-lines are similar to comet-tail artifacts,

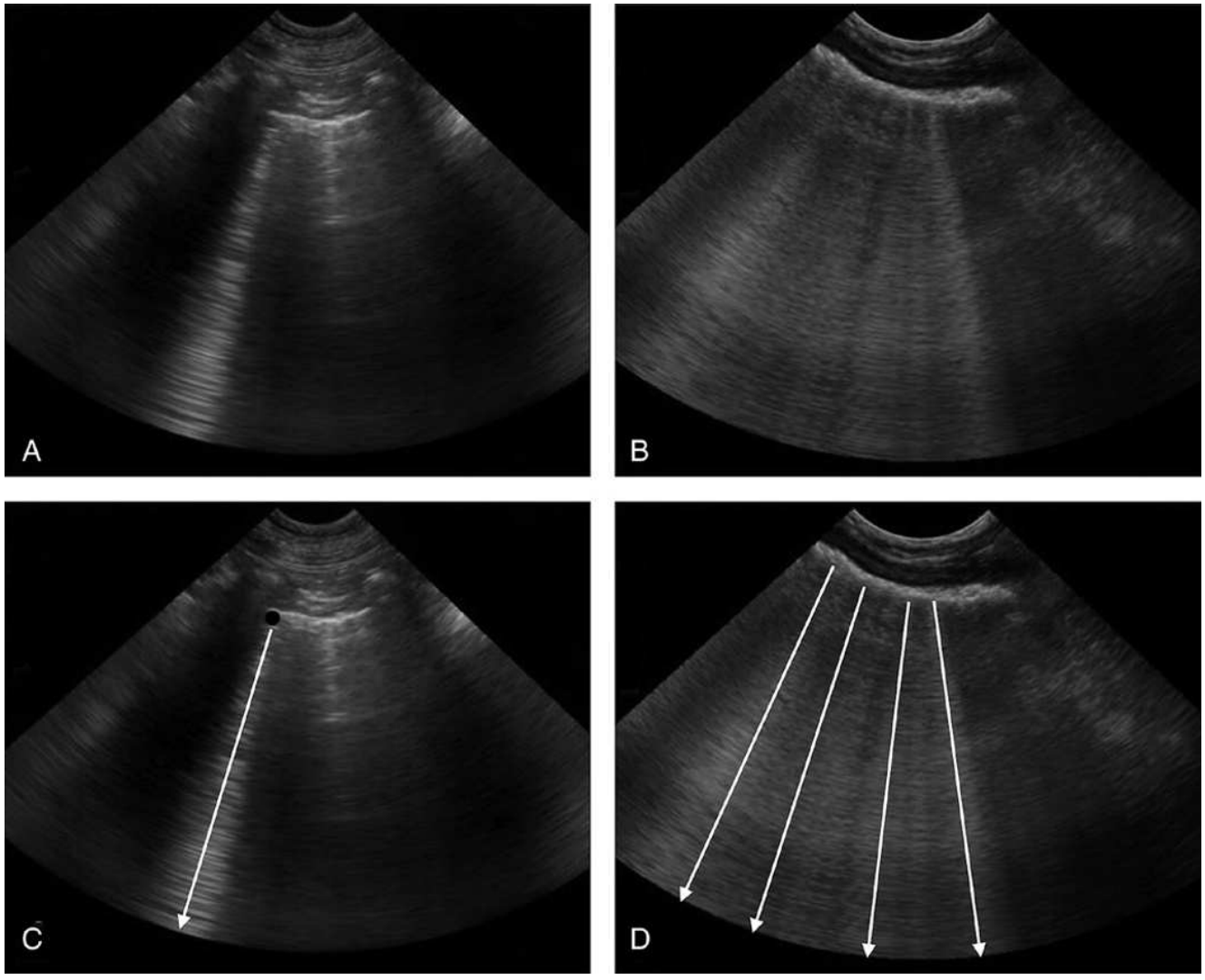


**Figure 3.6.** Pseudo B-lines. The B-line artifact begins at the lung's pleural surface and continues without loss of intensity through the far-field of the image as a hyperechoic (bright white) streak that obliterates A-lines. In real time, B-lines must oscillate with the to-and-fro motion of inspiration and expiration. Examples and descriptions are found in Chapters 22 and 23. Here, however, are pseudo B-lines. In (A), what appears to be a single B-line is in fact tightly stacked A-lines off the far side of a very small lung nodule. In (B) are multiple pseudo B-lines off the gastric wall. In (C) the nodule is indicated with a solid black circle overlay, and the arrows are over the pseudo B-line. In (D), the pseudo B-lines are indicated by the arrows (←). Source: Courtesy of Dr Gregory Lisciandro, Hill Country Veterinary Specialists and FASTVet.com, Spicewood, TX.

they are specifically created by the strong difference in impedance of air adjacent to a small amount of water and are the ultrasound near-equivalent of radiographic Kerley B lines (representing interlobar edema). Their clinical relevance is very important and explained later (see Chapters 22 and 23) (Lichtenstein and Meziere 2008; Lichtenstein et al. 2009; Lisciandro 2011; Volpicelli et al. 2012) (Figure 3.6).

# Artifacts of Multiple Echoes

## *Side-Lobe Artifact: Multiple Echoes*

We like to think of the ultrasound beam as extending from the probe in a very thin fan or rectangle, and this is exactly what the processor thinks it sees. In reality, there are smaller beams that travel laterally to the main beam.

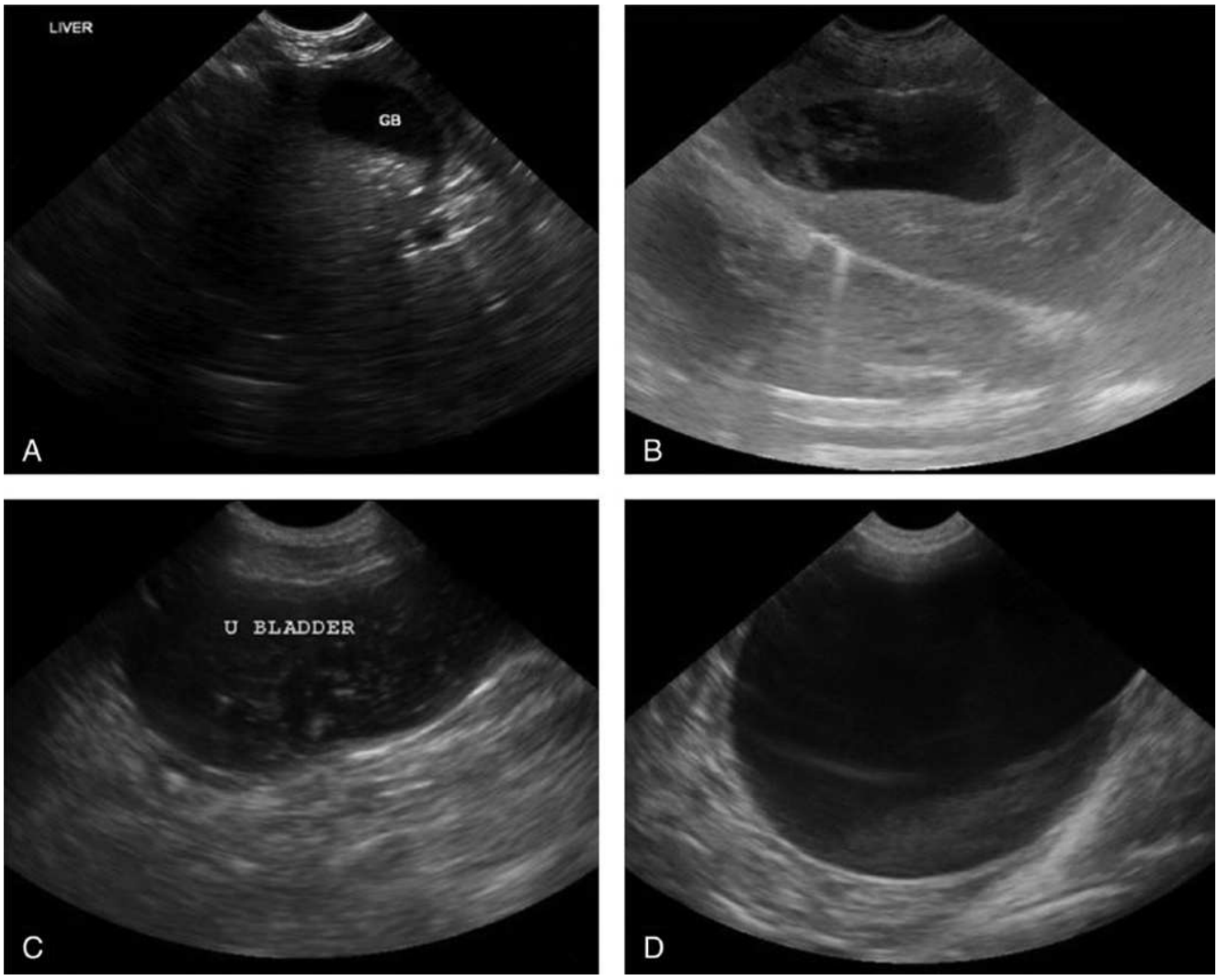


**Figure 3.7.** Sediment versus side-lobe and slice-thickness artifact. (A) Sediment will be affected by gravity and lead to a flat surface, as seen with the sludge within this gallbladder's lumen. True sediment can be stirred up by repositioning the patient or through ballottement with the ultrasound probe, whereas artifacts mimicking sediment cannot. (B) Slice-thickness and side-lobe artifacts mimic sediment in the gallbladder shown here; however, the artifact will not be altered by moving the patient's position or by ballottement. (C) True sediment in a urinary bladder with ballottement gives a snow globe appearance. (D) In contrast, the slice-thickness and side-lobe artifacts mimicking sediment shown here will fail to ballot (will not "snow globe") or change position to the gravity-dependent side of the urinary bladder when the patient is moved. Other helpful tricks that discriminate true sediment from artifact include lowering the gain and/or moving the focus cursor. Generally speaking, artifacts can be eliminated by these maneuvers, but true sediment cannot. Source: Courtesy of Robert M. Fulton, DVM, Richmond, VA.

When one of these smaller side beams is of sufficient strength and bounces off a highly reflective surface, such as the wall of the urinary bladder, it will be interpreted as coming from the main beam and the processor will place the resulting image within the main beam image, often mimicking sediment. The resulting image is usually weaker in intensity than the main image. Often, the artifact can be altered by changing probes or lowering the focal point, or lowering the gain setting – all ultrasonographic manipulations that will not remove true pathology (i.e., bladder sediment, bladder stones, etc.) (Penninck 2002) (Figure 3.7).

### *Slice-Thickness Artifact: Multiple Echoes*

Slice-thickness artifact is somewhat like the side-lobe artifact. In the gallbladder and urinary bladder in particular, this artifact mimics sludge or sediment. It occurs when part of the beam's thickness lies just outside a fluid-filled structure. These artifacts typically appear within the lumen of these structures and are somewhat hyperechoic (bright) and curved. They can be differentiated from real sediment by several methods or clues. First, gravity-dependent sediments have a flat surface whereas the artifact will be rounded. Second, by changing the position of the patient, the relative position of true sediment will change as gravity pulls it to the new lower point. Third, the sonographer can use the ultrasound probe to ballot the bladder and stir the sediment up a bit; the artifact will not yield a "snow globe" effect (sediment will) (Penninck 2002) (see Figure 3.7).

## Pearls and Pitfalls, The Final Say

By gaining a basic understanding of ultrasound physics and the common ultrasound artifacts, the nonradiologist veterinarian or veterinary sonographer can more clearly interpret the ultrasound image (Table 3.1). Always keep in mind the basic assumptions used to generate the image when scanning or viewing the ultrasound image. Your interpretive and diagnostic skills, and hence your patient, will benefit greatly.

- Knowing the basic assumptions used to generate the image leads to less misinterpretation of the ultrasound image.
- Artifacts are one of the primary pitfalls of ultrasonographic imaging.

**Table 3.1.**
Summary of common artifacts and examples.

| Name of artifact | Fluid-associated | Air-associated | Other | Common examples |
|---|---|---|---|---|
| Shadowing, clean | No | No | Bone/stone | Cystouroliths, ribs |
| Shadowing, dirty | No | Yes | Irregular/partial penetration into gas | Lung, stomach, colon, small intestine |
| Edge shadowing | No | No | Refraction off round structures | Stomach wall, gallbladder wall, urinary bladder wall |
| Acoustic enhancement | Yes | No | Decreased attenuation | Gallbladder, cysts, eye |
| Mirror image | No | Frequently | Reflection | Diaphragm/liver<br>Urinary bladder/colon |
| Reverberation A-lines | No | Yes | Typically used only in reference to lung ultrasound | Lung surface |
| Comet-tail, ring-down | No | No | Bone/stone/metal | Calculi, surgical clips, tissue mineralization |
| B-lines, also called ultrasound lung rockets (ULRs) | Yes | Yes | Air–fluid interfaces | Lung |
| Pseudo B-lines | Yes | Yes | Air–fluid interfaces (gastric luminal contents); strong soft tissue–air interfaces, i.e., lung nodules | Stomach contents, lung nodules |
| Side-lobe | Yes | No | Multiple echoes | Urinary bladder lumen, gallbladder lumen |
| Slice-thickness | Yes | No | Multiple echoes | False appearance of sludge in gallbladder, cysts |

# References

Feldman MK, Katyal, S, Blackwood MS. 2009. Ultrasound artifacts. *RadioGraphics* 29:1179–1189.

Lichtenstein DA, Meziere GA. 2008. Relevance of lung ultrasound in the diagnosis of acute respiratory failure: the BLUE protocol. *Chest* 134(1):117–125.

Lichtenstein DA, Meziere GA, Lagoueyte J, et al. 2009. A-lines and B-lines. Lung ultrasound as a bedside tool for predicting pulmonary artery occlusion pressure in the critically ill. *Chest* 136(4):1014–1020.

Lisciandro GR. 2011. Abdominal and thoracic focused assessment with sonography for trauma, triage, and monitoring in small animals. *J Vet Emerg Crit Care* 21(2):104–122.

Nyland TG, Mattoon JS, Herrgesell EJ, et al. 2002. Physical principles, instrumentation, and safety of diagnostic ultrasound. In: *Small Animal Diagnostic Ultrasound*, 2nd edition, edited by Nyland TG, Mattoon JS. Philadelphia: WB Saunders, pp 1–18.

Penninck DG. 2002. Artifacts. In: *Small Animal Diagnostic Ultrasound*, 2nd edition, edited by Nyland TG, Mattoon JS. Philadelphia: WB Saunders, pp 19–29.

Reef V. 1998. Thoracic ultrasonography: noncardiac imaging. In: *Equine Diagnostic Ultrasound*, edited by Reef V. Philadelphia: WB Saunders, pp 187–214.

Volpicelli G, Elbarbary M, Blaivas M, et al. 2012. International evidence-based recommendations for point-of-care lung ultrasound. *Intensive Care Med* 38:577–591.

CHAPTER FOUR

# POCUS: Basic Ultrasound Scanning

Robert M. Fulton

## Introduction

Ultrasound is a user-dependent imaging modality, with the quality of the image obtained directly dependent on the skill of the ultrasonographer. Many of the POCUS studies are not highly reliant on advanced skill or knowledge. Still, one *must* have a basic understanding of how to manipulate the probe and machine settings to obtain the prescribed images and optimize image quality.

### What POCUS Basic Scanning Can Do

- Provide a basic tutorial on ultrasound physics, image acquisition, and storage, and discuss basic ultrasound systematics.

### What POCUS Basic Scanning Cannot Do

- Cannot provide an in-depth tutorial on how to learn ultrasound techniques.
- Cannot replace experience and continued learning.

### Indications

- Provide a basic understanding of ultrasound principles and image acquisition, including probe type, probe manipulations and orientations, and ultrasound machine features to maximize accurate image interpretation.

### Objectives

- Provide a basic understanding of ultrasound image acquisition.
- Provide a review of basic ultrasound techniques and systematics including:
  - image planes
  - image orientation
  - probe maneuvers
  - image optimization
  - image documentation
  - basic machine selection and care.

## Understanding Features of the Ultrasound Image

### Imaging Planes

Understanding how the two-dimensional image is formed from scanning through a three-dimensional object is crucial not only to image interpretation but also communication of that information. The first piece of information is the imaging or scanning plane. The imaging plane may refer to the whole body, a part of the body (such as a leg or the head), or to a specific structure within the body, the left kidney, for instance (Figures 4.1 and 4.2).

The first of these, transverse, is any plane along the short axis of the structure being imaged.

*Point-of-Care Ultrasound Techniques for the Small Animal Practitioner*, Second Edition. Edited by Gregory R. Lisciandro.
© 2021 John Wiley & Sons, Inc. Published 2021 by John Wiley & Sons, Inc.
Companion website: www.wiley.com/go/lisciandro/ultrasound2

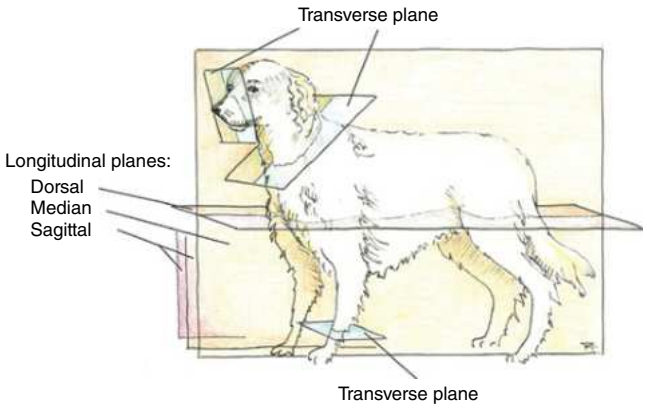


**Figure 4.1.** Longitudinal and transverse orientation shown on anatomical planes. Source: Illustration courtesy of Randi Taggart, Richmond, VA.

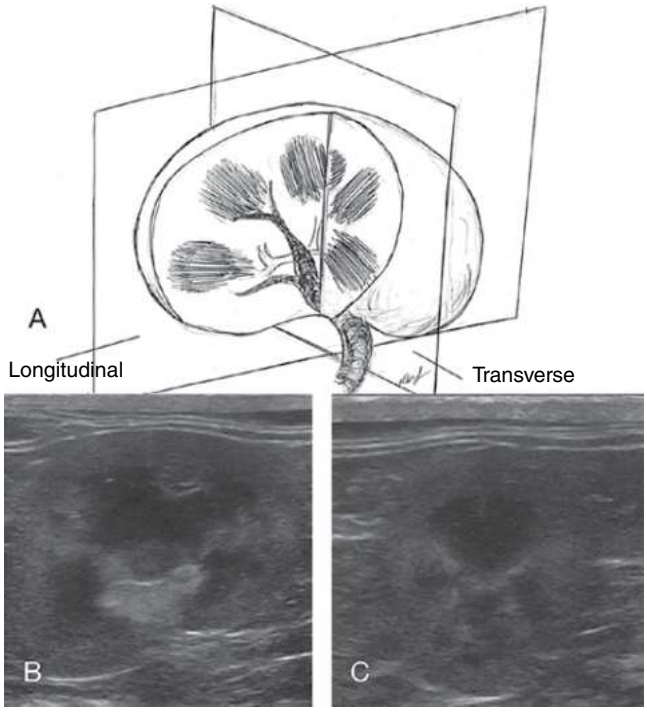


**Figure 4.2.** Examples of image planes for the kidney. In (A) the kidney is shown with longitudinal (sagittal) and transverse planes. In (B) the longitudinal (sagittal) plane is contrasted to (C) in transverse orientation on actual B-mode ultrasound images. For most nonradiologist sonographers, the kidney is more readily recognized in the longitudinal (sagittal) orientation. Source: Courtesy of Robert M. Fulton, DVM, Richmond, VA.

The second, longitudinal, is any plane that is perpendicular to the transverse plane or the long axis of the structure. Technically, the longitudinal plane has several specific types.

- *Median* – this plane splits a symmetrical structure into equal left and right halves along the long axis.
- *Sagittal or paramedian* – this plane is any plane that is parallel to the median plane. While technically incorrect, many will use *sagittal* interchangeably with *longitudinal*.
- *Dorsal* – this plane splits a structure into dorsal and ventral segments and is analogous to the coronal plane in biped scanning terminology.

Commonly, veterinary sonographers tend to talk about only two planes, transverse and longitudinal, and this suffices for most communication and image understanding (see Figures 4.1 and 4.2).

## Image Orientation

Any part of a medical record must contain the essentials of basic medical communication to have value. As veterinarians, we are taught how to communicate with each other in such a way regardless of our individual personality and training. One veterinarian can describe a lesion to another half a world away and pass along vital information. POCUS exams likewise need to have standard image orientation and recording of findings to give the study meaning.

### Ultrasonography Compared to Radiography

For standard flat film radiography, the lateral film is oriented with the patient's head to the left, and the spine or dorsum is at the top of the viewer. This is the same for either a right or left lateral image. For the ventrodorsal or dorsoventral view, the radiograph is positioned with the head pointed up, and the patient's right side toward the left-hand side of the view box.

Ultrasound follows similar conventions. When we scan from the ventral aspect, as when the patient is in dorsal recumbency, the following orientations apply.

- *Longitudinal image*: the ventrum is on the top of the screen, dorsum on the bottom. Cranial (head) is to the left and caudal (tail) is to the right, similar to lateral radiography (Figure 4.3).
- *Transverse image*: ventral and dorsal remain top and bottom, respectively, and the patient's right side is represented on the left side of the screen, and the patient's left side is represented on the right side of the screen similar to ventrodorsal radiography (see Figure 4.3).

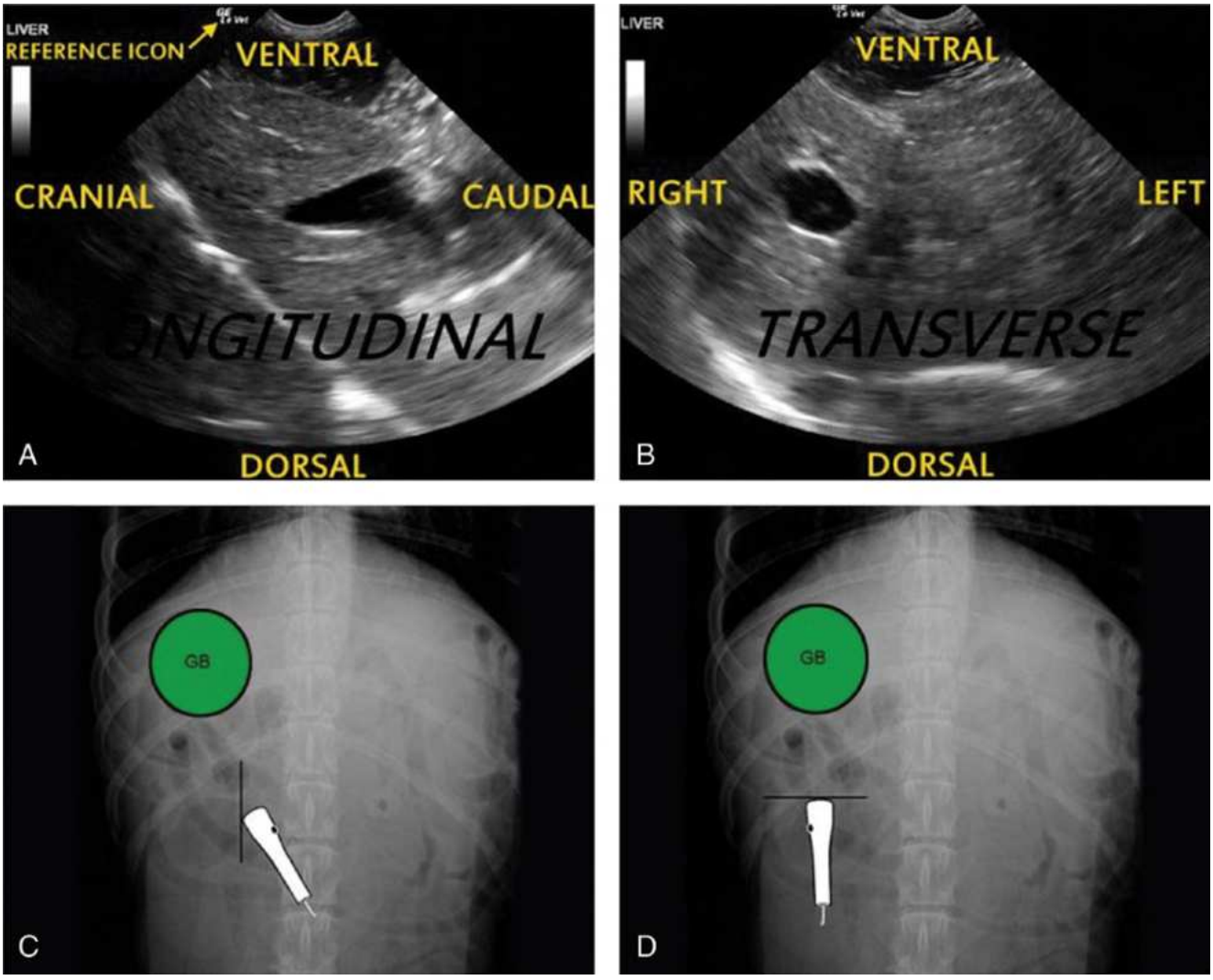


**Figure 4.3.** Standard ultrasound screen orientation, longitudinal (sagittal) and transverse. The radiograph for each orientation is located below the respective ultrasound image. Figures (A) and (C) illustrate longitudinal (or sagittal) and (B) and (D) transverse orientation with the corresponding probe position during interrogation of the liver and gallbladder via the subxiphoid region of a dog. Note that the reference icon (GELe) corresponds with the probe reference marker (dot on the probe) (labeled with arrow in (A) to the left on the ultrasound image). The best way to make standard ultrasound imaging a habit is to have the probe marker toward the head for longitudinal (or sagittal) orientation (black dot on the probe in (C) and turn (the probe head) left or counterclockwise for transverse orientation (black dot on the probe in (D) with the reference icon to the screen's left, shown at the top of the ultrasound image in (A) and (B)). If your reference icon is to the right of the ultrasound image, most ultrasound machines have a "reverse" button on their keyboard to flip the reference icon back to the standard left side (with the exception of echocardiography orientation; see Chapters 19–21).

**Pearl:** Ultrasound orientation is the same as radiography: in lateral radiography, the head is to the left and tail to the right when scanning the long axis of the patient; and in ventrodorsal radiography, the left side of the patient is on the right side of the screen when scanning the transverse axis.

This ultrasound image orientation convention is the most intuitive if the patient is positioned in dorsal recumbency with its head facing the same way the sonographer is facing with both toward the machine and its screen. Many emergent patients are not stable enough to be placed in dorsal recumbency and all FAST scans actually prescribe lateral recumbency or

sternal or standing positioning because the positioning is safer. So the sonographer may need to do some mental gymnastics at times to orient the image on the screen with the patient. What helps is thinking in terms of gravity dependent (fluid falls) and gravity nondependent (air rises) and each in terms of where the transducer is placed.

**Pearl:** When imaging, picture the gravity-dependent and gravity-nondependent regions of your patient. Keep in mind that fluid falls (gravity dependent) and air rises (gravity nondependent).

When scanning from the lateral aspect of the patient, that is, in a dorsal plane, the following conventions apply.

- *Longitudinal image*: nonrecumbent side is on top of the screen, recumbent side is on the bottom. Cranial (head) is to the left side of the screen, and caudal (tail) is to the right (see Figure 4.3).
- *Transverse image*: nonrecumbent side is still on top of the screen, recumbent side still on screen's bottom. Ventral is on the left, dorsal is on the right (see Figure 4.3).

**Pearl:** Develop the habit of having the marker toward the patient's head (longitudinal imaging) and turning left for transverse imaging to maintain proper orientation etiquette, similar to radiography.

### Probe Orientation and Reference Markers

All ultrasound probes have a reference marker to allow for proper orientation. The reference marker may be a raised dot or line molded into the plastic, or possibly a small LED light. On the image screen, there will be a symbol, often the company's logo, that corresponds with the probe's reference marker. The marker on the screen is commonly referred to as the "reference icon" (see Figure 4.3).

Sonographers should familiarize themselves with the various types of ultrasound probes (also called transducers): phased-array (also called sector), linear, and curvilinear. Furthermore, they should know that by looking at the shape of the ultrasound image, the probe is readily apparent as follows: pie-shaped pointed near-field (phased-array or sector), rectangular (linear), and pie-shaped with curved concave near-field (curvilinear) (Figure 4.4).

**Pearl:** You can tell what probe was used for the published image by looking at the image's near-field as follows: pie-shaped pointed near-field (phased-array or sector), rectangular (linear), and pie-shaped with curved concave near-field (curvilinear).

Most veterinarians are taught that when scanning the abdomen in long axis, the probe's reference marker is pointed toward the patient's head. Therefore, to maintain convention, the reference icon on the screen will also be positioned on the left-hand side of the screen (screen left = cranial, screen right = caudal). When the probe is turned into the transverse orientation, the reference marker is pointed toward the patient's right, making a counterclockwise motion ("turning left") if one views the probe from its tail or cable end (screen left = right side of patient, screen right = left side of patient). Again, the orientation is consistent with lateral and ventrodorsal radiographic orientation.

Some veterinarians are trained to orient the reference marker of the probe to be pointed caudally. Therefore, to maintain convention, the reference icon on the screen will be positioned on the right-hand side of the screen. When switching into the transverse orientation, the probe is still rotated counterclockwise. The reference marker will be pointed towards the patient's left, and the reference icon on the screen will still be on the right-hand side of the screen.

No matter which training a veterinarian has received, the image on the screen should follow proper orientation convention with the patient's head to the left (screen left is cranial) and the patient's tail to the right (screen right is caudal) as with a lateral radiograph, and the patient's right is to the left of the screen as with a ventrodorsal radiograph.

## Probe Maneuvers

There is one basic concept and six basic probe movements used in acquiring the ultrasound image. *Beginning sonographers often miss their mark because they lack structured movement of the probe when scanning*. Being able to make one type of movement at a time is essential to obtain a good image. To the casual observer, it may appear that the experienced sonographer makes free-flowing and complex moves with the probe; however, the reality is that they are simply integrating the six foundational movements *one movement at a time*.

**Pearl:** When optimizing image acquisition, a good rule of thumb is to only *perform one probe maneuver at a time*.

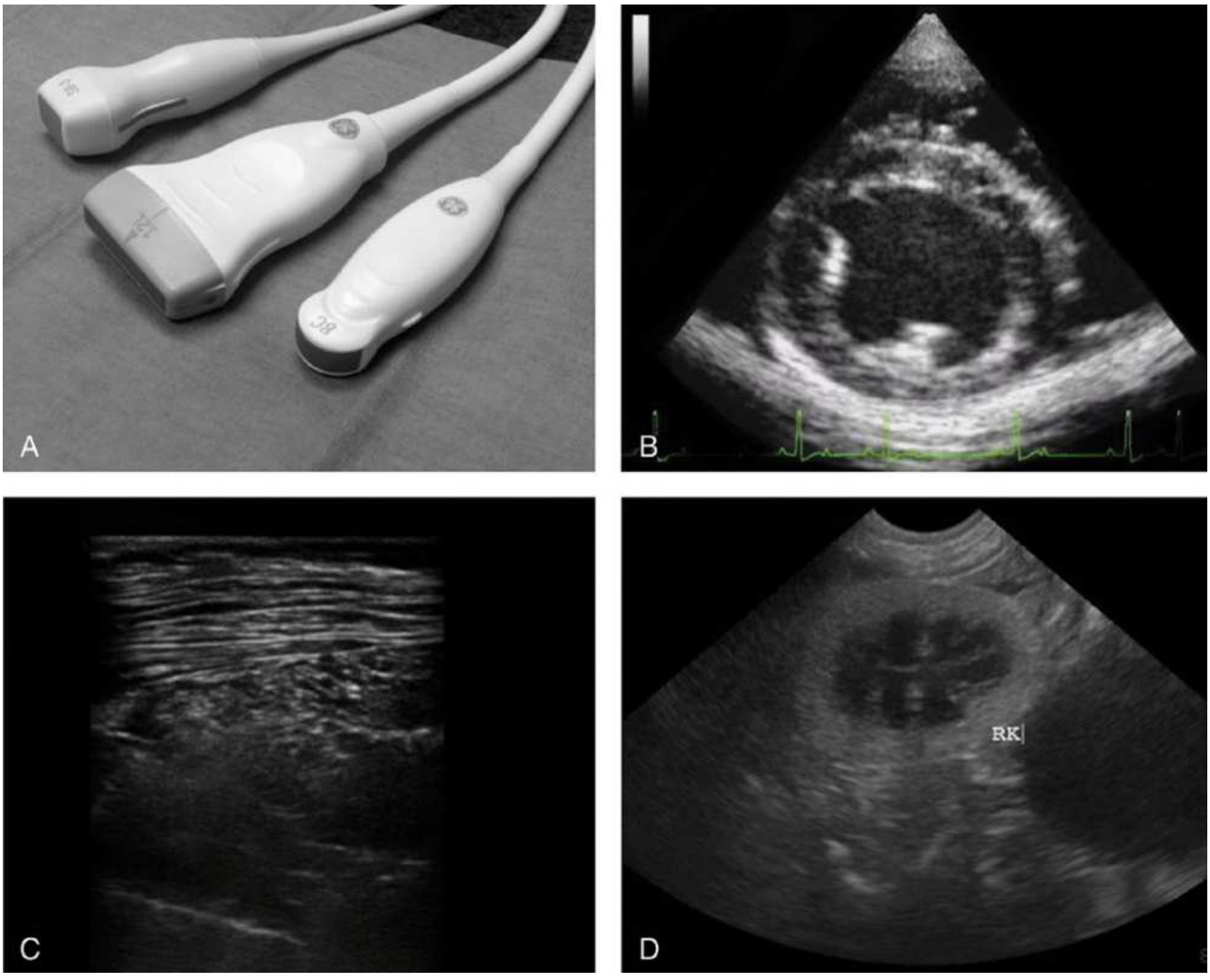


**Figure 4.4.** Electronic ultrasound probes and their characteristic B-mode images. The probe used for the ultrasound image is easily recognized by the ultrasound image's shape. From left to right in (A) are examples of the following probes (transducers): phased-array (also known as sector), linear, and curvilinear (also referred to as microconvex). A molded reference marker can be seen on all three of these probes. Other probes may use an LED light as the reference marker. The rubber probe heads (gray) represent the "footprint" or contact surface of each probe which differ between probe (transducer) types. (B) The phased-array probe ultrasound image is pie-shaped with a near-field "point." Phased-array is ideal for echocardiography because it best avoids ribs (note no rib shadow). (C) Linear probe ultrasound image with its rectangular shape. Linear is superior in detail because it sends and receives ultrasound waves 90° to the structure(s) of interest. (D) Curvilinear probe ultrasound image is pie-shaped but wide and concave in the near-field. Curvilinear (microconvex) is most commonly used by nonradiologist veterinarians because of its versatility.

Let us take a look at the one concept and the six basic or foundational probe maneuvers (Bahner et al. 2016).

## *Concept: Angle of Insonation*

This concept is very important to understand and be aware of while scanning. The angle of insonation is the angle at which the probe is held in relation to the area of interest. *It defines the angle of incidence at which the ultrasound waves strike the object*.

The clearest image is obtained when the angle of incidence is zero degrees (Figure 4.5). This results in the highest number of sound waves being reflected back to the probe. Much beyond three degrees, the

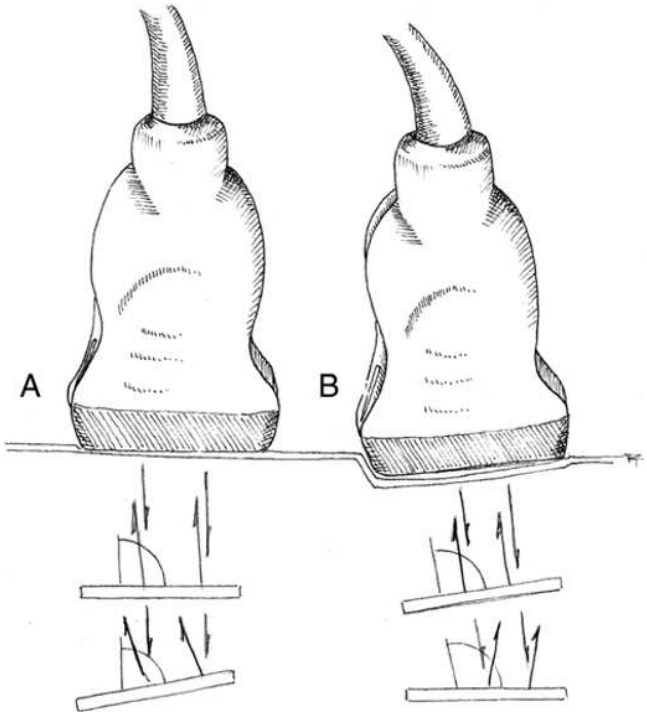


**Figure 4.5.** Angle of insonation. The angle at which the ultrasound beams strikes the organ or structure of interest is known as the angle of insonation. The best echo quality, and hence the best image quality, is achieved when the angle of insonation equals the angle of reflection. In (A), if the structure of interest is parallel to the transducer footprint, it will be best imaged. In contrast, in (B) if the area of interest is oblique then the probe must be adjusted for the optimal angle of insonation. Source: Illustration courtesy of Randi Taggart, Richmond, VA.

image quality will diminish (Bahner et al. 2016). A curvilinear probe will lead to numerous different angles of incidence with the same angle of insonation. This is one reason why curvilinear probes do not produce as detailed an image as a linear probe. While the curvilinear probe can be considered the workhorse in veterinary ultrasound, adding a linear probe to the line-up can significantly improve your images. In terms of POCUS and FAST scans, however, the more maneuverable curvilinear probes remain the most commonly prescribed.

## *Maneuvers: Basic Probe Movements and Effects on Angle of Insonation*

### Rocking (Figure 4.6)

Rocking is best visualized with a curvilinear probe, a back-and-forth movement of the probe. Imagine a rocking horse or rocking chair. The position of the probe is not moved on the patient and the angle of insonation is changed only in the longitudinal plane. The rocking movement allows an object being visualized to be in the center of the screen (Bahner et al. 2016). A simple way of determining which way to rock the probe is this: if the object in the longitudinal plane is towards the cranial side of the screen (left side), rock the probe to direct it more cranially, and conversely, if the object is towards the caudal side of the screen (right side), rock the probe to direct it more caudally. Similar motions apply when scanning in the transverse plane.

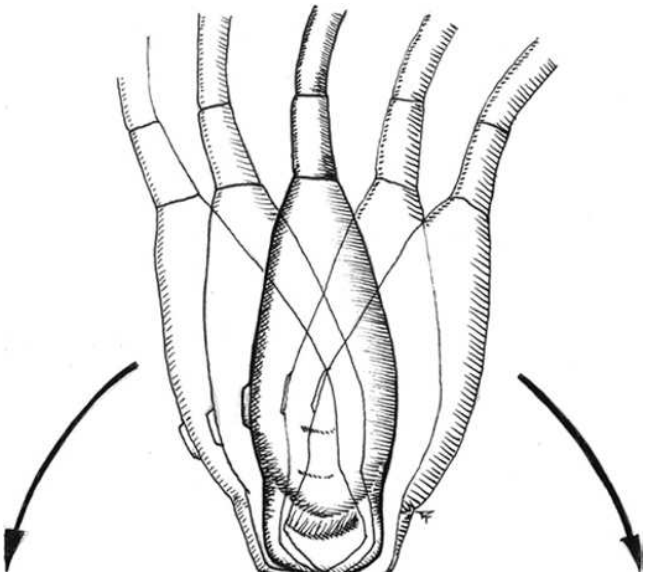

**Figure 4.6.** Rocking. The position of the probe is not moved on the patient and the angle of insonation is changed only in the longitudinal (sagittal) plane. Source: Illustration courtesy of Randi Taggart, Richmond, VA.

### Fanning (Figure 4.7)

Fanning is on the same focal point as rocking but moved in the perpendicular plane to rocking. During fanning, like rocking, the probe *stays on the same external point of* the patient, but the angle of insonation now changes in the transverse plane (side-to-side) in contrast to rocking. This motion allows for scanning a region and looking for the area of interest (Bahner et al. 2016).

### Rotating (Figure 4.8)

Rotating is another movement where the probe stays on the same external point on the patient; however, the angle of insonation is *not changed* in any plane. The probe is turned about its long axis. Picture a clock dial

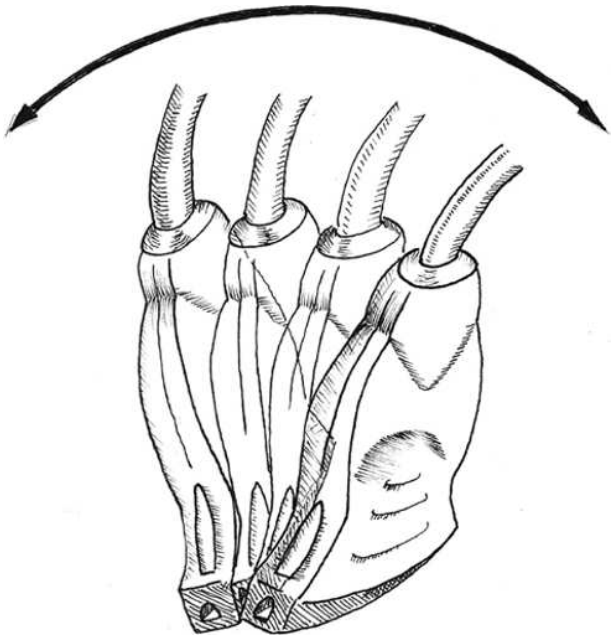

**Figure 4.7.** Fanning. The position of the probe is not moved on the patient and the angle of insonation is changed only in the transverse plane. Source: Illustration courtesy of Randi Taggart, Richmond, VA.

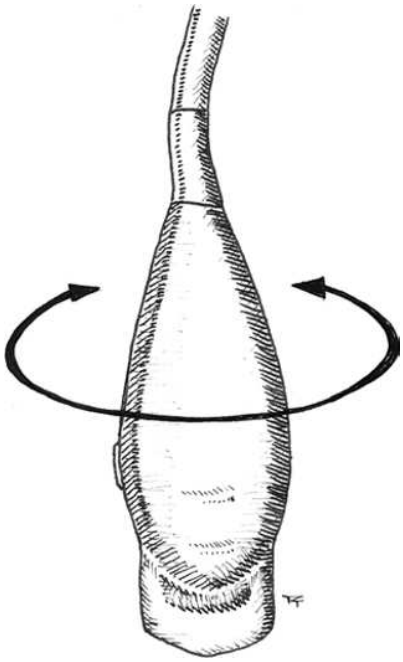

**Figure 4.8.** Rotating. The probe remains on the same focal point of the patient as with rocking and fanning. During rotating, the angle of insonation is not changed in any plane. The probe is turned about its axis in either a clockwise or a counterclockwise direction. Source: Illustration courtesy of Randi Taggart, Richmond, VA.

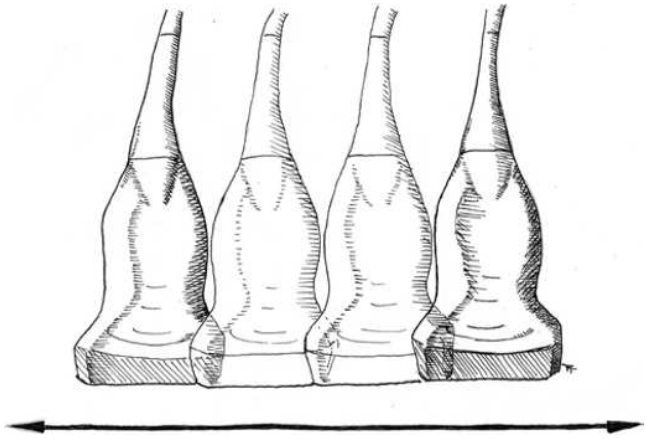

**Figure 4.9.** Sliding. The probe is moved across the body in the longitudinal axis of the patient, and the angle of insonation in relation to the patient's body is not changed. Source: Illustration courtesy of Randi Taggart, Richmond, VA.

with the probe perpendicular to the face. The probe may be rotated either clockwise or counterclockwise (Bahner et al. 2016); however, to maintain the same imaging as a ventrodorsal radiograph, rotate counterclockwise (to the left).

**Pearl:** Rocking, fanning, and rotating are on the *same fixed external point* on the patient; however, the angle of insonation is changed with rocking and fanning (but not rotating).

### Sliding (Figure 4.9)

During sliding, the angle of insonation in relation to the patient's body is *not* changed as the probe is moved across the body in the *longitudinal axis* of the patient (Bahner et al. 2016).

**Pearl:** Gradual increase in probe pressure is much better tolerated by the patient than a quick stabbing motion.

**Pearl:** Excessive pressure can push or move the area of interest out of view.

**Pearl:** There are three major reasons to use probe pressure knowing that your patient may not like the maneuver: reduce contact and air-trapping artifact, push structures out of the way, such as gas-filled small intestine, and gain more depth by moving the transducer closer to the area of interest.

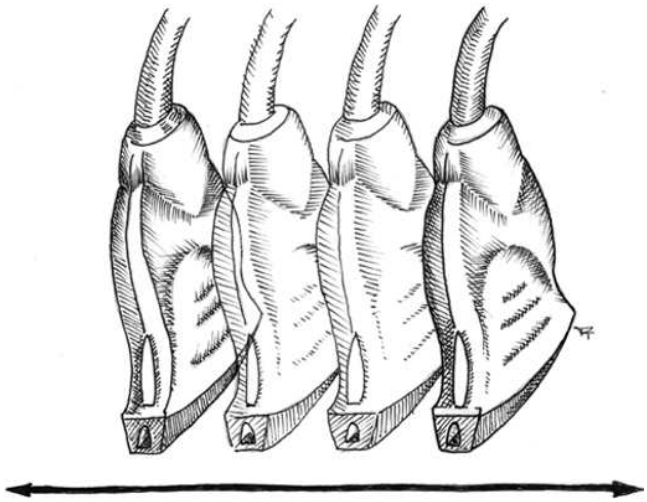

**Figure 4.10.** Sweeping. The probe is moved across the body in the transverse axis of the patient, and the angle of insonation in relation to the patient's body is not changed. Source: Illustration courtesy of Randi Taggart, Richmond, VA.

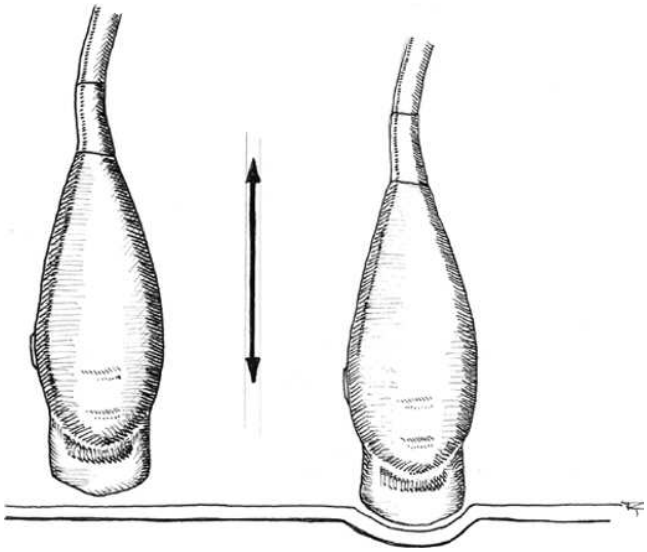

**Figure 4.11.** Pressure/Compression. Neither the probe position on the body nor its angle of insonation is changed. Rather, the probe is pushed into the body, compressing the underlying tissues. Source: Illustration courtesy of Randi Taggart, Richmond, VA.

### Sweeping (Figure 4.10)

Like sliding, during sweeping the angle of insonation in relation to the patient's body is *not* changed as the probe is moved in the *transverse axis* of the patient (Bahner et al. 2016).

### Pressure/Compression (Figure 4.11)

During pressure/compression, the probe is pressed or pushed into the body, causing compression of body tissues. The pressure/compression maneuver may help to reduce contact and air-trapping artifact, push structures out of the way, such as gas-filled small intestine, and gain more depth by moving the transducer closer to the area of interest. Uncontrolled pressure may result in moving the intended target (area of interest) out of the field of view. This effect commonly occurs with the feline spleen and kidney and at the AFAST spleno-renal (SR) view.

## Cardiac Orientation

See Chapters 17–21 for detailed information on cardiac orientation.

**Pearl:** For the POCUS and FAST ultrasound scans, begin with an intermediate setting of 8 MHz as a general rule of thumb. That being said, most chapters in this textbook provide probe frequency recommendations.

## Image Optimization: Using the "Big 4" Knobs of Depth, Gain, Frequency, and Focus

For an ultrasound image to have meaning, it must have adequate detail. The best rule of thumb is that the image should simply look "nice." This idea may be a little different from one person to another but they should all be relatively similar. Always keep in mind the angle of insonation. The ideal angle of ultrasound reflection for generating the best image is 90° on the surface of the organ of interest (see Figure 4.5). In fact, this is why linear probes, while not used by most small animal practitioners, provide superior detail when compared to curvilinear probes, which are more commonly used among small animal practitioners.

Although there are numerous buttons and knobs on the ultrasound machine that can be used to improve, or worsen, the image, the "Big 4" are depth, gain, frequency, and focus position and number. See also Chapter 5 for additional examples.

**Pearl:** Know the "Big 4" knobs: depth, gain, frequency, and focus position and number.

### Depth

When reviewing a radiograph, the clinician can become narrow-sighted by focusing on one area and not looking at the rest of the film. With ultrasound, however, the goal is to focus on one area. Adjust the depth to the area of interest. Filling up the screen with the area of interest will result in a better diagnostic ultrasound image and this strategy is used for detailed parenchymal assessment. However, during AFAST and TFAST target organs are usually reduced to 25–33% of the screen, depending on the target organ and the respective view.

Every sonographer performing ultrasound has a responsibility to know where the ultrasound scale is located; usually values are in centimeters and are displayed along the side of the machine's screen. The awareness of depth within the image is often overlooked by beginning sonographers. However, recognizing depth is of the utmost importance because what looks large on ultrasound may in fact be small. Attention to the centimeter scale on the screen also allows for eyeballing not only the depth but also the dimensions of structures in view.

### Gain

Gain is the overall brightness of the image. The ideal is not too bright and not too dark. The gain knob is the one that will adjust the overall gain setting. After first setting the overall gain, minimize dark or light bands across the screen by using the time gain compensation (TGC) knobs. These are usually sliders that adjust brightness along discrete bands across the image, although some machines have reduced the numbers of sliders to near- and far-field. The goal is to have a consistent brightness from top to bottom of the screen, in other words, gain extending through the far-field.

### Frequency

Find a happy medium between penetration and resolution. Use the highest frequency (MHz) possible yet still see as deeply as needed. The smaller the patient, the higher the frequency and the larger the patient, the lower the frequency. High MHz provides detail at the expense of penetration and low MHz provides penetration at the expense of detail. In addition to the frequency, the focus position and focus number also have a major impact on the image. Frequency is also affected by presets. Smaller parts, pediatric and smaller abdominal and cardiac presets generally increase the frequency automatically and adult and larger abdominal and cardiac presets decrease the frequency automatically.

### Focal Position and Number

The ultrasound beam has a focus position where the beams narrow to give a more detailed image at a certain depth. The beams do not converge, as we may think of light focusing on the retina, because they will again diverge beyond the focal position. The physics of this can be found in additional references (Nyland et al. 2002). Both the focus position and number of focal points can be set and adjusted by the sonographer. However, the processor can only handle a certain amount of information and by asking it to do more, it will reduce other items, normally the frame rate or how many times/second the image is refreshed. High frame rates make for a smooth image but take a lot of processing power. Low frame rates give a choppy image. Ask the processor to do more and it will respond by giving you a lower frame rate, a choppier image.

**Pearl:** For the POCUS and FAST scans, generally keep the focal point number at 1, and set the focal point's position at, or just deep to, the area of interest.

## Presets, Abdominal, Cardiac, Small Parts, etc.

Even with just these four settings, that's still a lot of knobs to be adjusting in the emergent situation. Modern ultrasound machines have a collection of imaging settings which the user may select, based upon the area of interest, such as cardiac vs abdomen vs small parts and others, and patient size, adult versus pediatric. Trying to image an abdominal structure if the machine is on the small parts preset will lead to frustration until the sonographer realizes that the preset must be changed first to be able to adjust and manipulate the Big 4 knobs.

## Alternate Imaging Tools

Up to now, we have been talking about B-mode, or standard two-dimensional, ultrasonography. A-mode has no practical bearing on the emergency scans outlined in this book and therefore will not be discussed. However, M-mode and color flow Doppler imaging are used in many of the POCUS and FAST protocols and during ultrasound-guided procedures.

### M-Mode

The "M" in M-mode stands for "motion." This mode has also been called the "ice pick" mode because it reflects a small column of ultrasound waves but follows it over time. Cardiac ultrasound is where M-mode is best known. It can be a little challenging to understand what is being displayed on the screen but using the B-mode view to show just where that "ice pick" is cutting through is helpful. M-mode is used not only for certain cardiac studies but also in certain lung and pleural space studies, vascular measurements for volume assessment, and fetal imaging. Importantly, M-mode speed may be adjusted to slow, medium, and fast, and the M-mode speed setting can significantly impact what you are attempting to interrogate, depending on the area of interest.

### Color Flow Doppler

Color flow Doppler is used in combination with B-mode ultrasonography. It allows you to see blood flow within a vessel and helps to determine the direction of that flow. Doppler is best when the flow is *parallel* with the sound beam. Color signatures are usually set up so that flow toward the probe is red – remember by "you are getting warmer" – and flow away from the probe is blue – remember by "you are getting colder" or that "blue" and "away" have the same number of letters – although this can be set on most machines to user preference. Color flow Doppler has its limitations, with low velocities and is also affected by patient movement, a phenomenon called "jumping" (see Chapter 25).

To maximize accurate image acquisition and proper interpretation, the sonographer should be familiar with settings that affect color flow Doppler (Pozniak et al. 1992). Briefly, the Big 3 are gain, pulse repetition frequency, and wall filter setting, and their effects are as follows.

- *Gain*: the overall sensitivity to flow signals.
- *Pulse repetition frequency* (also known as PRF, scale, or velocity scale): user-defined setting. Use a lower PRF with low velocities; use a higher PRF with higher velocities to correct aliasing. If too high a PRF is selected, low velocities may not be recorded, and a vessel may appear as if thrombosed (no flow); conversely, too low a PRF will lead to overlap of the signal on the image.
- *Wall filter*: removes unwanted low-velocity Doppler signals; however, if set too high, it will remove important low-velocity signals.

For more information, the reader is referred to more detailed texts (Nyland et al. 2002; Evans et al. 1989) and the machine's technical support team.

An alternate form of color flow Doppler, called power Doppler imaging (PDI), can be employed. Similar to color flow, this shows flow of fluid but at much lower velocities. The trade-off is a lack of directionality. Blood flowing at 0.5 cm/sec away from the probe will have the same color signature as blood flowing at 0.5 cm/sec toward the probe. Consider using PDI for small vessels in POCUS studies such as the optic artery and vein

**Pearl:** Color signatures are usually set up so that flow toward the probe is red and flow away from the probe is blue – remember "red is getting warmer and toward you" and "blue is away from you and getting colder" or that "away" and "blue" have the same number of letters.

**Pearl:** Color flow Doppler is optimized by understanding its settings and their effect on the image: gain, pulse repetition frequency, and wall filter setting.

## On the Horizon

### Single Crystal Probes

Single crystal probes emit a large bandwidth of sound beams instead of just one, thereby combining the benefits of high-frequency resolution and low-frequency penetration. The learning curve for imaging is generally quite different from that of traditional multicrystal ultrasound probes.

### Smartphone Applications

At the time of this writing, there are several smartphone-powered ultrasound devices approved by the Federal Drug Administration. Technology is advancing quickly and ultrasound machines may now be carried around in the healthcare provider's pocket. One must wonder what the future holds for the ease and availability of ultrasound imaging.

## Documentation of POCUS and FAST Ultrasound Examination Findings

Save and label the images. A medical record is not complete with just a written description of an image, whether that is a radiograph, an ultrasound image, computed tomography (CT), or magnetic resonance

imaging (MRI). The image must be there to back up the interpretation. Furthermore, the other imaging modalities contain information to indicate exactly where an image was obtained. For example, the radiograph has anatomical landmarks and for both CT and MRI, there is a pilot image that records where all the remaining images are obtained. For ultrasound images, there may not be any definitive markers.

An ultrasound image that makes sense to the sonographer when it was recorded may make no sense when under review two days or even two hours later. One of the most common mistakes sonographers make is not labeling their images. Label the organ or structure of interest and label your orientation as longitudinal versus transverse, if it is not evident from the image. There will be times when there are no anatomical landmarks evident on the image and labeling is your only guide (Figure 4.12).

Most ultrasound machines have some sort of body pattern that can be placed on the image with an icon to show the approximate location of the probe (see Chapter 2). Put all labels outside the image, too. Placing words across the image can potentially hide diagnostic information. If you must write across the ultrasound image, first save a picture of the unadulterated image and then save a second picture of the annotated image. Short (3–10 second) video clips can also be saved on most ultrasound machines.

For recording ultrasound findings in medical records, see suggested goal-directed templates in the respective chapters throughout the textbook.

# Ultrasound Machine and Probe Care

Not all ultrasound machines were designed for the battlefield with parts that can sustain a six-foot drop. Most were designed for the relative quiet and safety of a hospital. Ultrasound machines and their components can be easily damaged or broken by rough handling and improper use, and replacement can be costly, especially if you drop an ultrasound probe and damage its crystals. Dropping the probe is the most common cause of probe damage and machine misuse.

The second most common form of misuse involves probe head damage (Figure 4.13). There are two major forms of probe head abuse: needle damage and chemical damage. With the use of POCUS as standard of care for many invasive procedures on the human side, now fast spilling over into veterinary medicine, needle damage, in other words stabbing or catching the rubber probe head with the point of the needle, quickly leads to severe probe head damage. In the haste of the moment, the attending sonographer will often grab a bottle of isopropyl alcohol, wet down the fur with only the alcohol, and apply the probe, leading over time to chemical damage. Many ultrasound manufacturers list alcohol as an inappropriate liquid to place in direct contact with the probe head because alcohol, over time through desiccation, can cause probe head damage.

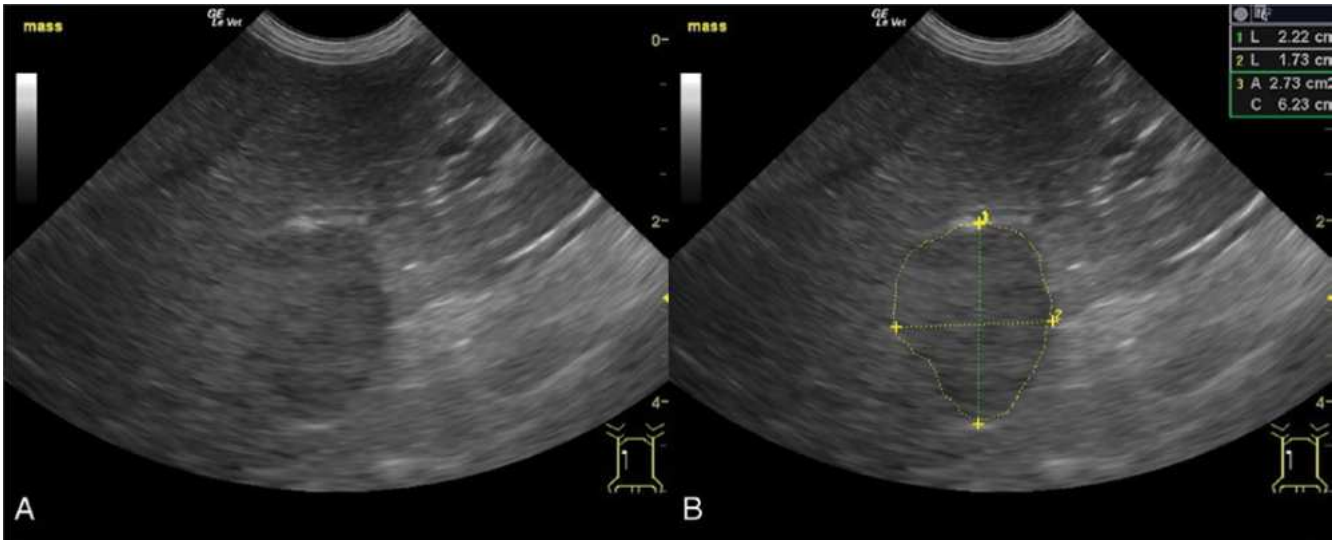


**Figure 4.12.** Labeling the image. The same image in (A) and (B) of a liver mass. The location cannot be determined by the image itself and thus the use of the body icon helps point out where the image was taken. The mass itself is circled using the various measurement features of the ultrasound machine. The measurements of the mass are displayed in the upper right of image (B). Source: Courtesy of Robert M. Fulton, DVM, Richmond, VA.

VetBooks.ir

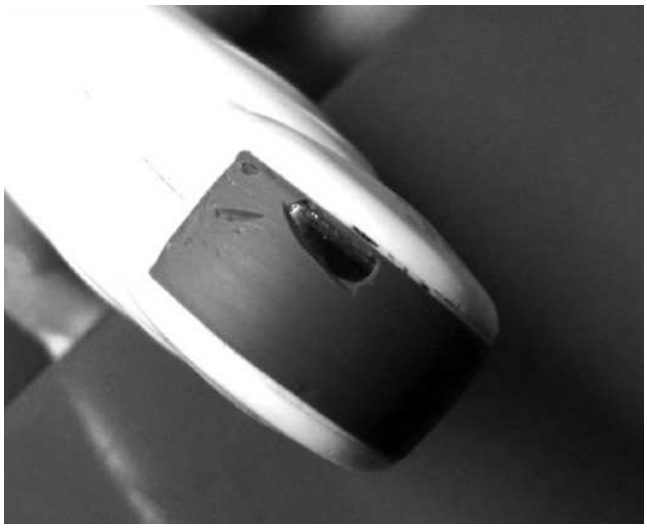

**Figure 4.13.** Probe head damage. The damage to the surface of this probe was attributed to a combination of repeated or prolonged contact with isopropyl alcohol and needle trauma. The contact layer is clearly lost over a portion of this probe, negating its ability to serve as an electrical insulator between the probe and patient. It is possible for potentially serious electric shock to occur through the damaged area. Source: Courtesy of Robert M. Fulton, DVM, Richmond, VA.

**Pearl:** Always use acoustic coupling gel on the probe head and be familiar with the guidelines provided by the ultrasound machine's manufacturer.

Importantly, it should be noted that the rubber probe head accomplishes two things. First, it acts as a coupling medium to transmit the sound wave out of the probe. Second, it is part of an electrical insulator serving as an electrical ground between the patient and the electricity being sent from the ultrasound machine to the transducer's crystals. There are currently no reports of electrocution via a damaged ultrasound probe but theoretically it's possible.

**Pearl:** Avoid probe head damage by using an acoustic coupling medium on the probe head as a barrier to alcohol, and avoid stabbing the probe head with needles during ultrasound-guided procedures.

# Deciding on an Ultrasound Machine

## *Selecting the Machine*

There are three main types of ultrasound machine: consoles, portables, and hand-helds. The console machines are big and bulky, but they have stronger processors and thus give a better image. The portables, often laptop format, are easy to move to the exam table or cage side and their image quality is constantly improving. There are several small hand-held machines now on the market. Some have adequate depth and resolution capabilities. Just make sure they don't "walk out of your clinic" or get tossed into the laundry or dropped or stepped on. It's very easy to put these hand-held devices in a lab jacket pocket and forget about them.

You may be limited to whatever you currently have in your veterinary practice, but if you are thinking of buying a new unit, consider what your main use is going to be and get the best ultrasound machine you can afford for that purpose. The axiom holds true: the better the machine, the better the image, and hence the better the diagnostic information.

## *Selecting the Probe: Linear, Curvilinear, and Phased-array*

Probes, or transducers, come in two basic types, mechanical and electronic. Mechanical probes are on many counts considered outdated but there are still some around with their working parts visibly rotating or rocking under their translucent covers. Newer ultrasounds have electronic probes as standard. Electronic probes come in various arrangements. Probes are generally described by the size and shape of their face, referred to as their "footprint," which is represented by the gray rubber probe covering (see Figure 4.13). Selecting the right probe is essential to getting good images, although there may be times when more than one probe may be appropriate for a given exam.

Three basic types of probes are used in general practice, emergency, and critical care POCUS: linear, curvilinear, and phased-array (also known as sector) (see Figure 4.4). Linear probes are typically of higher frequency and have a rectangular footprint. Curvilinear probes are arranged along a convex face and are typically of lower frequency than linear probes. A phased-array (sector) probe generates an image from an electronically steered beam in a close

VetBooks.ir

array, generating an image that comes from a point and is good for getting between ribs, such as in cardiac ultrasound. Both curvilinear and phased-array probes generate sector or pie-shaped images, narrow in the near-field and wide in the far-field. Phased-array probes are typically lower frequency. Because of their smaller footprint, "pie-shaped" image, and commonly used frequencies, curvilinear probes are generally the most versatile and ideal for POCUS and FAST studies.

Probes are generally named for the primary frequency they emit. For example, a General Electric (GE) 8C probe indicates that 8 MHz is its primary frequency and the C represents the probe's curvilinear footprint. A GE 9L probe indicates a 9 MHz primary frequency in a linear (L) probe, and a GE 7S has 7 MHz as its primary frequency in a sector (S) probe. However, modern probes are capable of emitting a range of frequencies, known as bandwidth. In choosing the best frequency, we need to go back to basics. Remember that higher frequencies are attenuated more and that means less penetration but better detail. Lower frequencies are attenuated less and that means deeper penetration but less detail. Another rule of thumb is that the smaller the patient or area of interest, the higher the frequency (MHz) versus the larger the patient or area of interest, the lower the frequency (MHz).

## Setting Up an Ultrasound Program

See Chapter 45 for additional information.

## Pearls and Pitfalls, The Final Say

In summary, these first four chapters have briefly covered some of the ultrasound basics. Other textbooks are available that go into more detail regarding ultrasound principles and artifacts, and many courses sponsored by ultrasound companies are available throughout the year to enhance learning. FASTVet.com is an online Global FAST education company. Another resource is the International Veterinary Point-of-Care Ultrasound Society's website www.IVPOCUS.org

It is important to be familiar with some of the basic principles, artifacts, and nuances associated with ultrasound as an imaging modality for your busy general practice, emergency room, or critical care unit to minimize misinterpretations. POCUS and FAST ultrasound are truly an "extension of the physical examination" and "the modern stethoscope" (Rozycki et al. 2001; Filly 1988).

So there you have it. Turn on your ultrasound machine, apply your coupling medium, and start scanning. Get POCUS and FAST and better pick your next test, more accurately treat, and better keep alive your patients for gold standard testing and treatment. POCUS and FAST save lives!

## References

Bahner DP, Blickendorf JM, Bockbrader M, et al. 2016. Language of transducer manipulation. *J Ultrasound Med* 34:183–188.

Evans DH, McDicken WN, Skidmore R, Woodcock JP. 1989. *Doppler Ultrasound: Physics, Instrumentation, and Clinical Applications*. Chichester: Wiley.

Filly RA. Ultrasound: the stethoscope of the future, alas. *Radiology* 167:400.

Nyland TG, Mattoon JS, Herrgesell EJ, et al. 2002. Physical principles, instrumentation, and safety of diagnostic ultrasound. In: *Small Animal Diagnostic Ultrasound*, 2nd edition, edited by Nyland TG, Mattoon JS. Philadelphia: WB Saunders, pp 1–18.

Pozniak MA, Zagzebski JA, Scanlan KA. 1992. Spectral and color Doppler artifacts. *Radiographics* 12:35–44.

Rozycki GS, Pennington SD, Feliciano DV, et al. 2001. Surgeon-performed ultrasound in the critical care setting: its use as an extension of the physical examination to detect pleural effusion. *J Trauma* 50:636–642.

CHAPTER FIVE

# POCUS: Top Ultrasound Mistakes During Global FAST

Gregory R. Lisciandro

## Introduction

Having trained close to 1000 veterinarians from around the world in Global FAST, AFAST, TFAST, and Vet BLUE, we have come up with our top list for image acquisition and interpretation mistakes made during Global FAST that will help synthesize the previous three excellent chapters by Dr Fulton. Whichever machine you work with, you must understand its software, how it interprets artifacts, and what its strengths and weaknesses are to gain full confidence in its imaging potential. You also need to know how to optimize image acquisition by taking advantage of external patient features and the role your hands should play. This takes time, repetition, and critical thinking during image acquisition and a sonographer who dares to use the different buttons and controls on the machine.

We strive to perform the entire Global FAST using the abdominal preset with the same curvilinear (microconvex) probe for the abdomen and thorax, including heart and lung. However, in time the sonographer may come to prefer different presets (cardiac, small parts) and probes (phased-array, linear), depending on the structure(s) of interest, the stability of the patient and the clinical questions being addressed. However, the curvilinear (microconvex) probe is absolutely acceptable for the entire Global FAST examination.

### *What POCUS Top Mistakes Can Do*

- Make the sonographer aware of the most common mistakes which occur during Global FAST image acquisition.
- Make the sonographer aware of the most common air and fluid-associated artifacts and where they commonly occur during Global FAST.
- By raising awareness of these mistakes during Global FAST, the sonographer will carry over these principles to other ultrasound studies.

### *What POCUS Top Mistakes Cannot Do*

- Cannot replace proper ultrasound training and experience.

### *Indications*

- For all sonographers performing Global FAST for a basic understanding of how to optimize image acquisition and avoid mistaking artifacts for abnormalities.

### *Objectives*

- Provide a basic understanding of Global FAST ultrasound image acquisition to help accelerate the learning process.

*Point-of-Care Ultrasound Techniques for the Small Animal Practitioner*, Second Edition. Edited by Gregory R. Lisciandro.
© 2021 John Wiley & Sons, Inc. Published 2021 by John Wiley & Sons, Inc.
Companion website: www.wiley.com/go/lisciandro/ultrasound2

- Provide a practical approach for image optimization and artifact identification as they pertain to the standardized examination of Global FAST and its 15 acoustic windows, and to help make your ultrasound interpretation more accurate.

# Image Acquisition Mistakes

## *Not Recognizing Air Trapping*

Ultrasound does not transmit through air. Air reflects your ultrasound beam from its path from the probe head to your areas of interest. Optimizing image quality relies on eliminating the phenomenon of "air trapping," especially the air trapped between the probe head and its contact with the patient's skin (Figures 5.1 and 5.2). Air trapping is potentially more problematic when not clipping hair, and hair is rarely clipped for Global FAST, AFAST (abdomen), TFAST (pleural cavity, heart, and lung), and Vet BLUE (lung). So be sure to part the hair, part the hair, part the hair! Parting the hair gets the probe in direct opposition to skin and the best image is optimized with the probe head directly on skin, with no hair in between, and with ample acoustic coupling medium. So what do we recommend?

- 70% isopropyl alcohol helps strip out air and lipids from hair follicles and is used for that reason. We use 70% isopropyl alcohol unless electrical defibrillation is anticipated (it's a burn/fire hazard in the presence of electrical current and 100% oxygen) followed by alcohol-based hand sanitizer, a brilliant trick of the trade given to me several years ago by the Mississippi State radiologist Dr Jennifer Gambino. Note that saline and water, although more gentle, lack the aforementioned properties of 70% isopropyl alcohol.
- Alcohol-based hand sanitizer is an excellent coupling medium and has advantages over both 70% isopropyl alcohol and commercially available acoustic coupling gel.

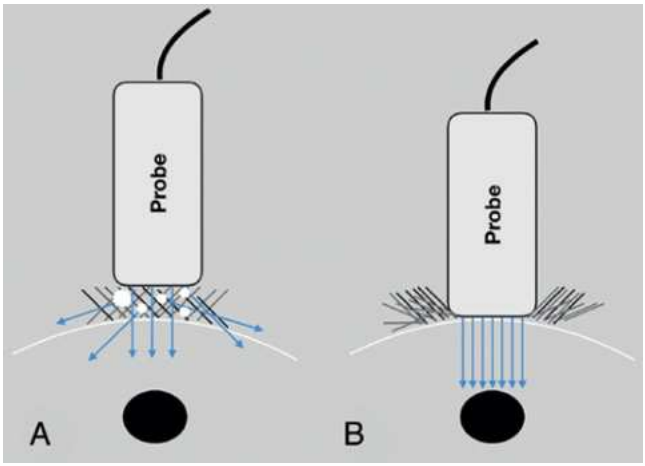


**Figure 5.2.** Air trapping. In (A) the probe head is placed on a wetted mat of fur in which air is trapped between the hairs. Air trapping attenuates the beam by its reflection and scattering of echoes (*blue arrows*) off the small pockets of air (*white circles*). In (B) the hair is parted and thus the probe head is coupled directly to the skin for best image acquisition in an unshaved patient. Note all the beam is transmitted with no reflection or scatter of echoes (*blue arrows*). Source: Courtesy of Dr Gregory Lisciandro, Hill Country Veterinary Specialists and FASTVet.com, Spicewood, TX.

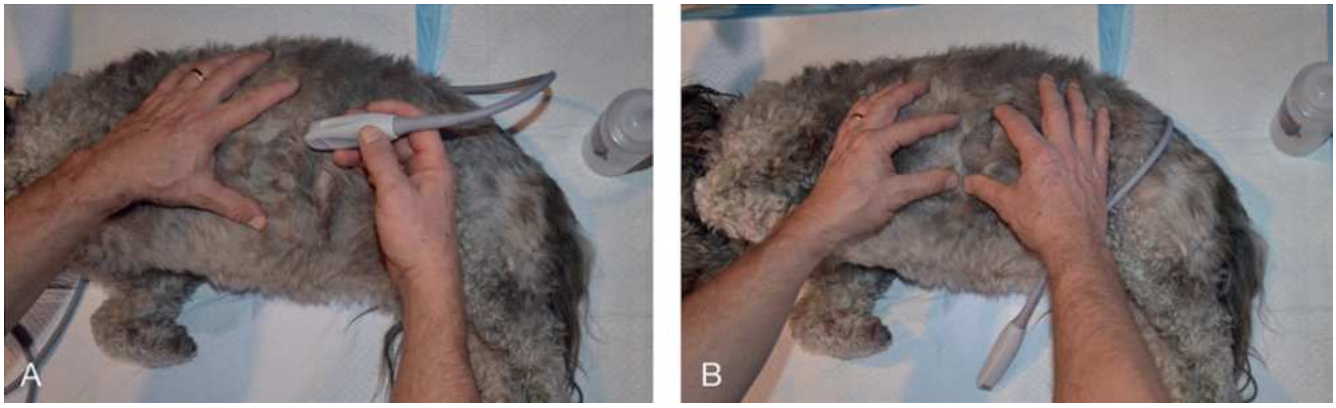


**Figure 5.1.** Wet and part the hair. In (A) the area is wetted without parting the hair. By doing so, the image will not be optimized because of all the air trapping (see Figure 5.2). In (B) the wetted hair is parted to optimize the coupling of the probe head directly to skin to produce the best image in unshaved patients. Source: Courtesy of Dr Gregory Lisciandro, Hill Country Veterinary Specialists and FASTVet.com, Spicewood, TX.

- Alcohol-based hand sanitizer when compared to 70% isopropyl alcohol is not as noxious on skin or indirectly by its fumes. The coldness associated with isopropyl alcohol is not only objectionable to your patient, but also contributes to their cooling (hypothermia) which may be detrimental for a critical patient. The fumes are also problematic for patients placed in closed environments such as an oxygen cage. My personal experience is that our patients associate the coldness with the anticipation of something painful if they have had previous blood draws and catheter placements. Try smaller volumes of 70% isopropyl alcohol and larger amounts of alcohol-based hand sanitizer.
- When compared to acoustic coupling gel, alcohol-based hand sanitizer not only wipes off your patient more readily than the gooey consistency of commercially available gel but also evaporates off the hair and skin. The final benefit is that your hands are clean after scanning!

**Pitfall:** Placing the probe on a wetted mat of hair leads to marked air trapping and poor image quality. Part the hair and get the probe head in direct opposition with the skin with an appropriate acoustic coupling medium.

**Pearl**: The alcohol-based hand sanitizer is better than 70% isopropyl alcohol because it is not noxious to the patient, either directly on the patient's skin or indirectly via fumes in closed environments. Moreover, alcohol-based hand sanitizer is not nearly as cooling as 70% alcohol, which can lead to hypothermia especially in smaller and critically ill patients.

### *Failure to Keep the Patient's Head and Ultrasound Screen in the Same Sightline*

The danger of not having the head of the patient and the ultrasound screen in the same sightline is twofold (Figure 5.3). First, if the patient decompensates or is critical, you have no idea if they are becoming distressed, cyanotic, having open-mouth breathing, etc. when you and the technician are focused on the ultrasound screen in the *opposite* direction to your patient's head. Second, by not having the patient's head and ultrasound screen in the same sightline, you and your assistant are vulnerable, leaving your face, hands, and body open to bites and scratches without defense, while focusing on the screen. And finally, spatial orientation is better learned and established even by experienced sonographers by having the machine and head of the patient in the same sightline, and you will likely be more comfortable rather than craning your neck to look at a screen in an uncomfortable direction.

### *Understanding Your Hands*

Your two hands will function differently while scanning. One is your "probe hand" (Figure 5.4). The probe hand always holds the probe and you may change which hand is your probe hand depending on where and from which side of your patient you are imaging. However, this hand's function is to work the probe. Your other hand is your "helper hand" which is used to palpate external landmarks and physically stabilize the patient or the probe on the patient, which is explained subsequently. Briefly, in standing patients, your helper hand is your "V trough" during TFAST and Vet BLUE, cupping the sternum to keep your patient from swaying (every time you lose contact, you prolong the study, which is not always in the patient's best interest) (see Figure 5.4). While performing AFAST, your helper hand is used to move less haired skin over your probe placement site for such views as the splenorenal (SR) and hepato-renal (HR) in flank areas, and the cysto-colic (CC). For TFAST recumbent views, the helper hand can lift the sternum off the table top for less weight on the probe head, which allows for finer movements and less pain because of less pressure on your patient's intercostal space. Finally, during Vet BLUE, the acoustic window you acquire may be moved together with skin, dependent on the mobility of your patient's skin, caudal and cranial over intercostal spaces at each Vet BLUE region.

### *Consistently Maintaining the Screen Orientation of Head to the Left and Tail to the Right*

When imaging in longitudinal and sagittal planes, including short- and long-axis views of the heart, maintain the head to the left and tail to the right on the screen. If the area of interest is to the left of the screen, you learn to slide or rock toward the patient's head to center the image and vice versa if to the right of the screen, slide or rock toward the patient's tail whether you are doing AFAST, TFAST or Vet BLUE (see Figure 1.6). In human medicine, physicians performing cardiac FAST and POCUS examinations will not necessarily reverse orientation, but stay consistent with all other imaging, with cranial to the left and caudal to the

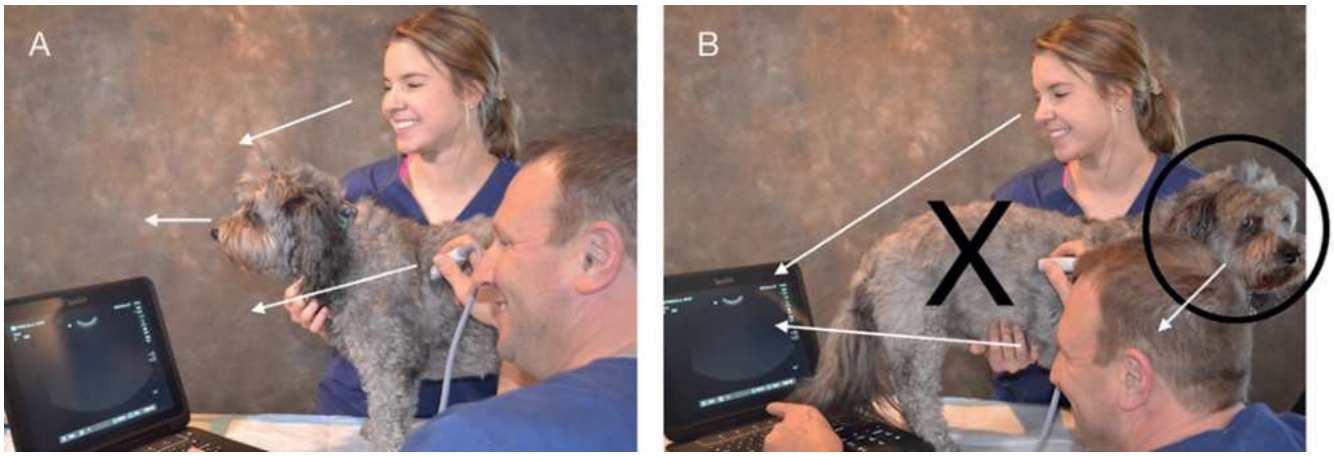


**Figure 5.3.** Best practice is the head of the patient and machine in the same sightline. In (A), the assistant, the scanner, and the patient are all facing the ultrasound screen (*arrows*). This is safest because the patient can be observed for any stress and decompensation while imaging. In (B) the head of the patient is away from the ultrasound screen. Both the assistant and scanner are focused on the screen and thus cannot readily appreciate any stress or decompensation of the patient, and cannot quickly react if the dog turns to bite them. The large "X" denotes that this is risky practice. Source: Courtesy of Dr Gregory Lisciandro, Hill Country Veterinary Specialists and FASTVet.com, Spicewood, TX.

**Figure 5.4.** The helper hand and probe hand make a difference. In (A) the helper hand moves less haired skin and can help spread the hair for optimal probe head to skin coupling. In (B) and (C) the helper hand in essence V troughs the standing patient, preventing swaying and better stabilizing the probe for maneuvering in small increments, especially important for cardiac imaging. Source: Courtesy of Dr Gregory Lisciandro, Hill Country Veterinary Specialists and FASTVet.com, Spicewood, TX.

right of the screen (Walker and Mohabir 2014). I like to call this the "rogue way" in which to capture echocardiography views, but maintaining orientation whatever the region of interest is advantageous for localizing abnormal findings, and the noncardiologist doesn't have to do any mental spatial adjustments because the cardiac ultrasound orientation is now the same as everywhere else (abdomen and lung).

## Fan, Rock Cranially, and Return for AFAST Views

As a result of work by Boysen et al. in the original FAST translational study from humans to dogs, we have simplified and standardized the probe maneuver for AFAST as "fan, rock cranially, and return to your starting point" because 397/400 views matched for detecting free intraabdominal fluid when comparing longitudinal to transverse orientation (Boysen et al. 2004). And most abdominal organ anatomy during AFAST is easier to recognize in longitudinal and sagittal planes. Consider transverse orientation as an add-on skill (Figure 5.5).

## Playing on the Short-axis and Long-axis TFAST Lines

In contrast to many echocardiography courses that begin with the long-axis cardiac views, we begin TFAST with short-axis views. Importantly, if the sonographer can grasp the "short-axis line" and "long-axis line" concept and fan the probe while *staying* on these lines, echocardiography views are learned more quickly and acquired more consistently by the noncardiologist sonographer (Figure 5.6). Without even looking at the screen, knowing you are on these TFAST

**Figure 5.6.** Short-axis and long-axis lines for echo views. If only someone had told me this back in 2005, to religiously keep the probe head parallel to the short-axis (cardiac) and long-axis (cardiac) lines while fanning, I would have gained proficiency so much faster. Trust these lines and fan while staying on them to achieve your echo views. We can tell from across the room whether or not you are successful by seeing if you are on these lines using a clockface orientation approach (see Figures 17.25 and 17.26). Wander from them and everything gets goofy. Source: Courtesy of Dr Gregory Lisciandro, Hill Country Veterinary Specialists and FASTVet.com, Spicewood, TX.

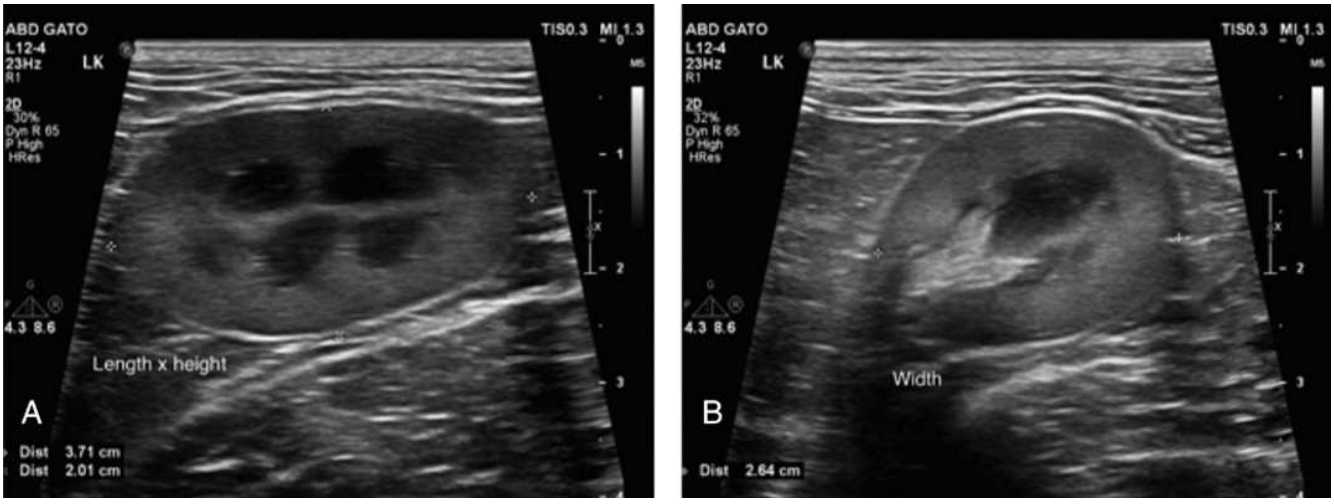


**Figure 5.5.** Anatomy generally better recognized in longitudinal (sagittal) orientation than transverse. In (A) the kidney is generally better recognized and then interrogated by fanning through longitudinal planes than in (B), showing the kidney in less recognizable transverse orientation. Source: Courtesy of Dr Daniel Rodriguez, Mexico City, Mexico.

cardiac lines will optimize success. We could literally teach you from across the room, without any screen knowledge, by just seeing whether or not you are maintaining the ultrasound beam on these lines while fanning from the apex to the base on short-axis, and from side to side on long-axis using our clockface approach (see Figures 17.25 and 17.26).

### *Failure to Maintain Probe–Skin Contact with the Patient*

Every time you lose probe–skin contact with your patient, you delay the imaging and have to reestablish your acoustic window, losing precious time and potentially increasing risk in hemodynamically fragile (and stressed) patients. There are several recommendations that involve your nonprobe "helper hand," placed into two broad categories: (1) maintaining probe–skin contact (acoustic window) by moving your patient's loose skin with the probe, and (2) maintaining probe–skin contact (acoustic window) by keeping your patient from swaying and at the same time stabilizing the probe against your patient's body.

We have found that the sonographer may take advantage of the patient's loose skin by moving the probe and skin together, and moving nearby less haired skin over the external landmark for your desired acoustic window. An example would be while doing Vet BLUE lung ultrasound, without losing probe–skin contact and your acoustic window, slide the probe together with the loose skin one intercostal space caudal and one intercostal space cranial when possible to cover the respective intercostal spaces at each respective Vet BLUE region. Another example is at the SR and HR views where the skin ventral to these views is often more sparsely haired, so your helper hand's thumb can lift or move this region dorsally over your external landmark of the costal arch and sublumbar muscles. By taking advantage of the sparsely haired area, imaging quality is markedly improved, especially in a thickly coated golden retriever, border collie or Siberian husky (see Figures 5.1 and 5.4). Another AFAST location is the CC view. Placing the probe laterally but closer to the midline where there is obvious sparsely hair coated skin markedly improves the image.

Regarding maintaining probe–skin contact, we have some pearls. First, when your patient is standing during the Global FAST approach, use your helper hand to "V trough" the patient by holding both sides of the sternum (Figure 5.7). This is especially helpful for evaluating your TFAST pericardial site (PCS) views but may also be used during Vet BLUE. Second, use your helper hand to brace your probe against the thorax or abdomen for better control of fine probe maneuvers.

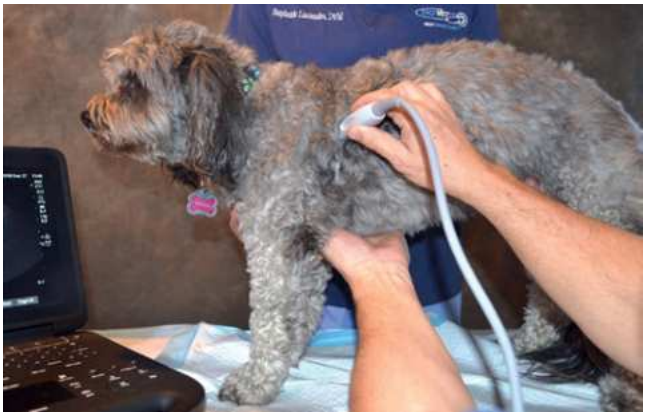

**Figure 5.7.** V trough your patient with your nonprobe helper hand. Your nonprobe helper hand is used as a V trough to keep your patient from swaying and maintaining probe to skin contact. Every time you lose contact, you potentially lose your good acoustic window and precious time. As much as possible, keep all four legs of your patient on the table. Source: Courtesy of Dr Gregory Lisciandro, Hill Country Veterinary Specialists and FASTVet.com, Spicewood, TX.

Third, as often as possible, let the patient have all four legs on the exam tabletop (see Figures 5.4 and 5.7). The only time a three-legged approach is mandatory is for the Vet BLUE cranial lung region for defining the cranial transition zone of soft tissue of the neck and then sliding caudally to image the first three intercostal spaces. Most of the time, the standing TFAST PCS views and imaging the heart may be done with all four legs on the exam table. By this approach, the patient is not swaying and feels more secure than lifting and extending a foreleg off the table. Fourth, when lifting and extending a foreleg, we lift and extend near the patient's elbow, especially for dogs. Many dogs do not like their paws being handled and associate it with the unpleasant experience of having their nails trimmed (Figure 5.8). Thus, by handling the paws, your patient becomes restless, wary, and tachycardic and may try to bite you!

## Other Probe–Skin Contact Issues

### *Not Being Aware of Drifting*

Drifting is the phenomenon of looking intensely at the ultrasound screen and not realizing that the weight of your hand and gravity has taken you to a place where

no man (or woman) has gone before – a bit of an exaggeration which will hopefully help you remember this very common mistake. The *Star Trek* phrase sounds funny but you started at the costal arch and hypaxial muscles looking for the left kidney, not realizing the probe has made it to the midline at the umbilicus (by drifting). No wonder you cannot find the left kidney! If you double-check yourself by frequently looking at the screen and then at the probe's external location on your patient, you will get to where you want to go much faster! This also occurs commonly while performing Vet BLUE in standing patients. You think you are at the Caudodorsal Vet BLUE lung region but the weight of your hand has brought you close to the Middle Vet BLUE lung region.

The best way to prevent drifting is to routinely "kickstand" out a finger that solidly touches your patient's body wall (or have another comfortable part of your hand against the patient's body wall) (Figure 5.9).

**Figure 5.8.** When extending the foreleg, don't touch the paw! Gently extend the foreleg with your helper hand placed near the elbow and away from the paw. The paw is sensitive and you may create an uncooperative patient (e.g., may bite, may become resistant to restraint, may become tachycardic) by triggering a negative response. Stay near the elbow. Shown is the acquisition of the right Vet BLUE cranial lung region view. Source: Courtesy of Dr Gregory Lisciandro, Hill Country Veterinary Specialists and FASTVet.com, Spicewood, TX.

## *Not Checking Where the Probe is Externally on the Patient*

This is really Part 2 of the previous paragraph. A few years ago, while I was performing Global FAST imaging on dolphins, the concept proved most helpful. Without goggles showing the ultrasound screen, two people were needed for imaging – one on the dock monitoring the ultrasound screen and directing the sonographer who was in the water with the dolphin, unable to see the ultrasound screen. Paying attention to external landmarks helped guide the sonographer to the AFAST target organs (and all of Global FAST) efficiently and confidently.

The same holds true with our small animal and exotic patients. Pay attention to where the probe is

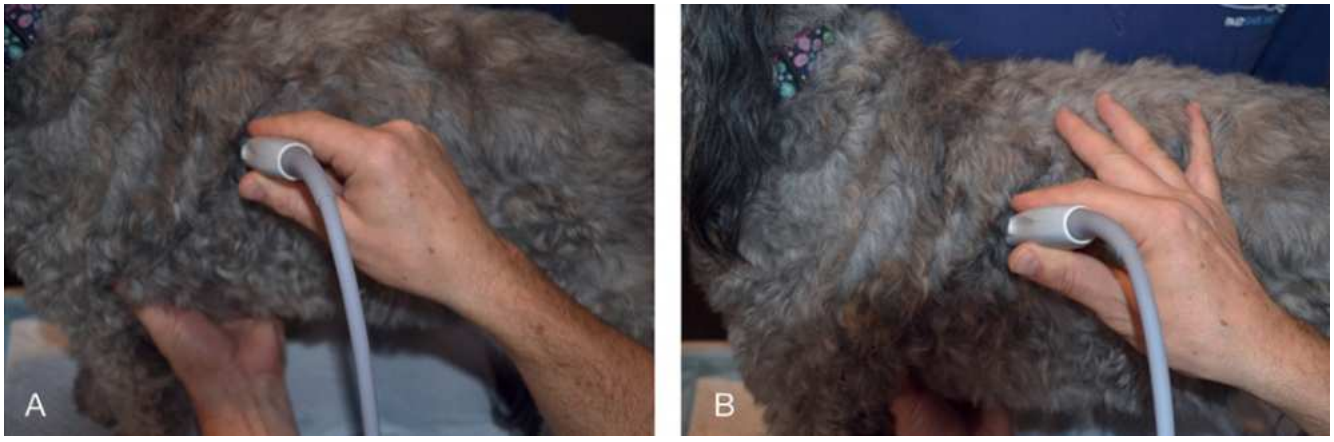


**Figure 5.9.** "Kickstand" your probe hand to prevent drifting. Having some part of your probe hand in contact with the patient will prevent drifting, which is when the sonographer is focused on the screen and unaware that the weight of their probe hand has moved the probe to a different acoustic window. In (A) the probe hand is not braced against the patient, so the sonographer is susceptible to drifting. In (B) the fingers are comfortably spread in contact with the patient's body, thus preventing drifting. Common views for drifting are especially during Vet BLUE and the least gravity-dependent SR and HR views. Source: Courtesy of Dr Gregory Lisciandro, Hill Country Veterinary Specialists and FASTVet.com, Spicewood, TX.

externally on your patient, double-checking between the ultrasound screen and the probe's external location. Look at your patient! For example, if you can't find the urinary bladder then slide toward the patient's pubis slightly off midline in lateral recumbency or along midline when standing or sternal. Some other examples – the gallbladder is right of midline in both dogs and cats so the probe has to be directed to *that side* of your patient; the TFAST chest tube site (CTS) view generally takes you to the caudodorsal transition zone, thus helping to prevent mistaking abdominal structures for lung pathology; and the kidneys are close to the caudal vena cava and aorta attached by their short renal artery and veins.

### Not Visualizing the Path of the Beam from the Probe Head

Mental visualization of success prior to a motor skill performance such as an athletic event is important and so is mentally visualizing the path of the ultrasound beam from the probe head (Figure 5.10). To get the "cardiac bump" at the diaphragmatico-hepatic (DH) view, the probe's beam must be directed toward the muscular apex of the heart which requires the probe being rocked far cranially and the beam approximating being parallel to the sternum. The AFAST CC pouch is in the most gravity-dependent region of that view so the probe should be directed toward the tabletop (when in lateral recumbency), not at the spine! Visualizing the direction in which the ultrasound beam is projecting from the probe head will contribute to your imaging success, save time, and build confidence in locating structures of interest.

### Losing Track of the Probe Orientation Marker

Make it a habit to have a finger or thumb on the probe marker or be able to clearly see the probe marker (Figure 5.11). It is easy to lose track of the probe marker without making this habitual while imaging. It not only helps with orientation but also prevents creating confusing planes through structures by the sonographer's awareness of being in longitudinal, sagittal, transverse, and short- and long-axis planes. Moreover, keep the screen orientation marker to the left so you maintain the "head to the left, tail to the right" orientation, which is the same as radiography (see Figure 1.6).

### Using More than One Probe Maneuver at a Time

One of the main rules of imaging is only performing *one probe maneuver at a time*. The five major maneuvers are rocking, fanning, rotating, sliding, sweeping and pressure/compression (see Figures 4.5–4.11). Performing only a single maneuver at a time while optimizing your image should become habitual. When you perform multiple maneuvers at the same time, you are really doodling and nothing productive typically results. This is very common with "flashing" the

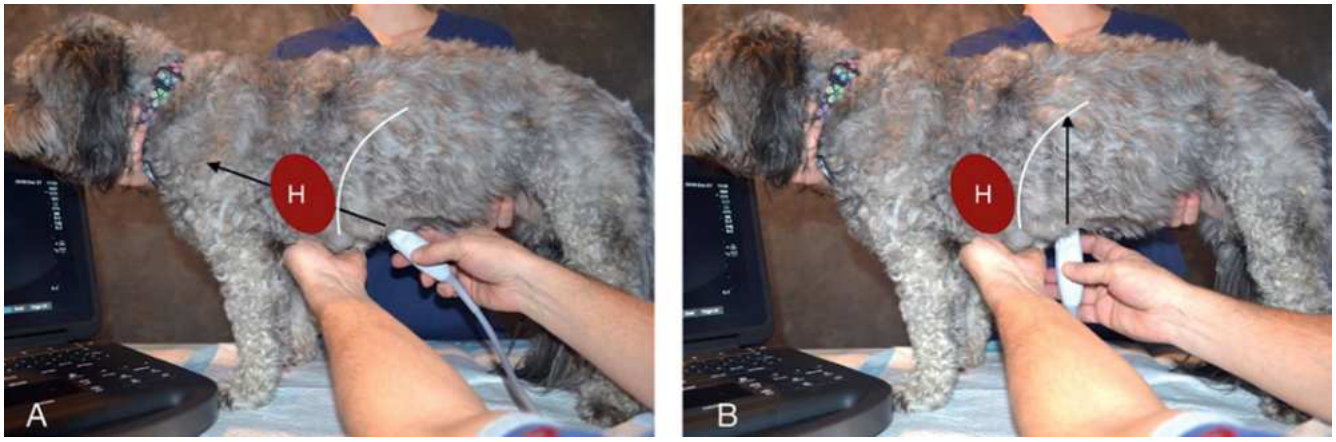


**Figure 5.10.** Paying attention to the direction of the beam. If the sonographer is to image the heart and its cardiac bump at the DH view, then the beam must be directed where the heart would be. In (A) the beam is directed in the correct direction whereas in (B) the heart will never be imaged. The "H" and red oval represent the heart; the black arrow the ultrasound beam; and the white curved line the diaphragm. Source: Courtesy of Dr Gregory Lisciandro, Hill Country Veterinary Specialists and FASTVet.com, Spicewood, TX.

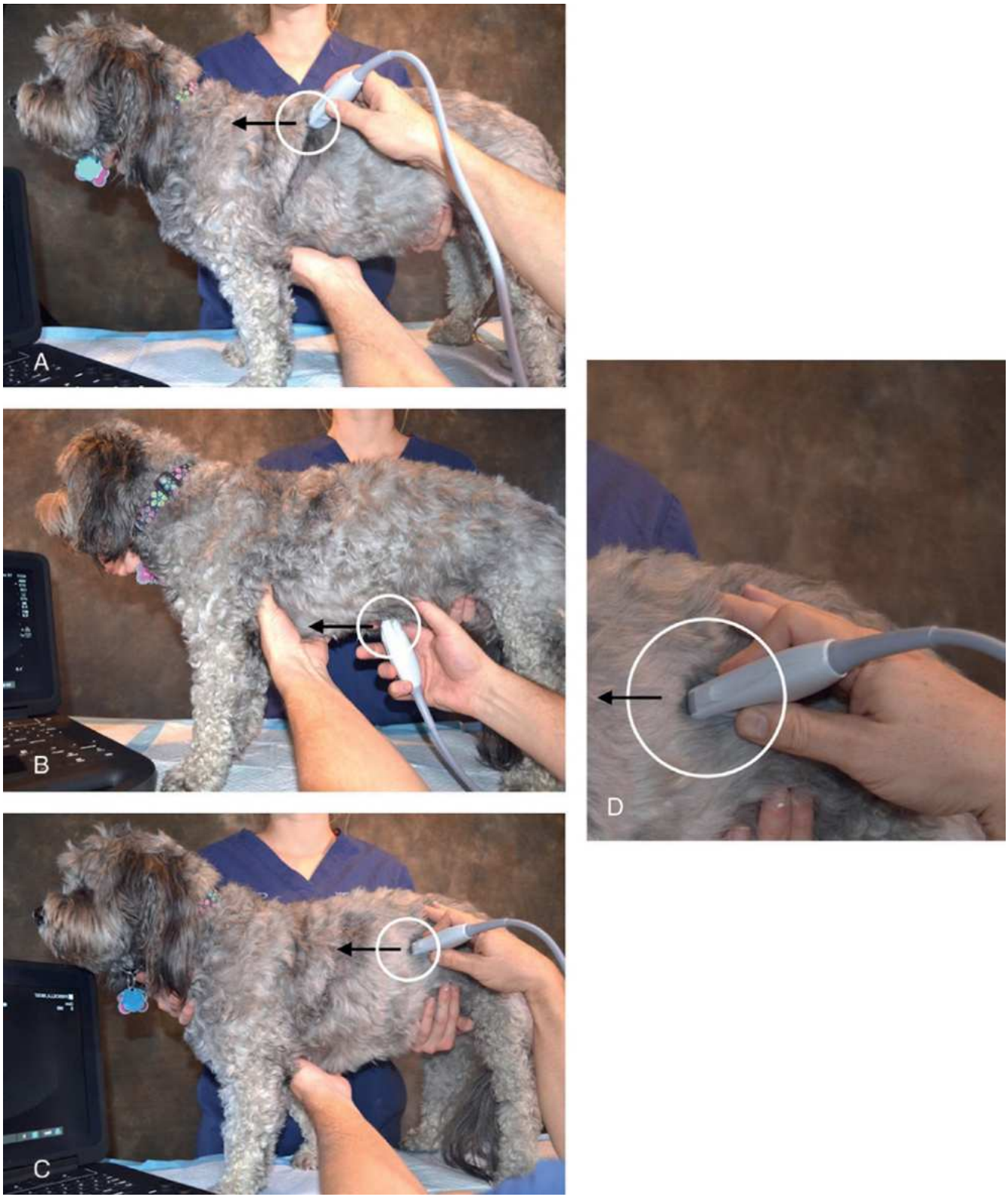


**Figure 5.11.** Be aware of the probe marker. Every probe has a marker or notch that serves as its orientation marker. Always keep track of the marker and when in longitudinal or sagittal orientation, keep it directed toward the patient's head. Getting into the habit of holding the probe with your index finger or thumb on the marker or be able to clearly see the probe marker keeps you from making mistakes and getting confused during image acquisition and interpretation. Screen orientation is also important (see Figure 1.6). Source: Courtesy of Dr Gregory Lisciandro, Hill Country Veterinary Specialists and FASTVet.com, Spicewood, TX.

abdomen, thorax, and lung (see Preface). We strongly discourage flashing but rather stick with the exact clarity of the 15 acoustic windows of Global FAST.

# Ultrasound Machine Optimization

A trouble-shooting algorithm is provided that incorporates the following major image optimization features of your machine (see Figure 5.15).

## *Failing to be Aware of the Focus Cursor*

The position of the focus cursor can have profound effects on image quality (Figure 5.12). Most sonographers are familiar with gain, and its effect on making the image brighter or darker; and frequency, lower for better imaging of the larger patient and higher for more detail and imaging the smaller patient. However, the focus cursor is often forgotten. It is usually an arrow or an icon that moves along the centimeter scale. It can be increased from one to two or three or more on some machines, but generally it's best to have only one, a single focus cursor, on your screen. Think of it as when having more focus cursors than just one, you are dividing up the energy in your ultrasound beam and the image will not be as high quality as a result.

The focus cursor should be directly across from the area or region of interest. A common mistake is moving the focus cursor to the "lung line" during Vet BLUE and then leaving the cursor in the very near-field when you then image deeper thoracic, like heart, and abdominal structures. The deeper structures will often not look good no matter what you do to the gain and frequency *until you move the focus cursor back to the center of the screen*. Conversely, you may have the focus cursor in the center of the screen while imaging abdominal and thoracic structures that may be less than optimum for lung, in which the focus cursor placed in the near-field across from the "lung line" could make a big difference in image quality (see Chapters 22 and 23). In some machines, the focus cursor actually moves on its own as depth settings are changed, and it may move to a less than optimal level within your image, so learn what your machine does to the focus cursor when you change the depth.

## *Not Paying Attention to the Centimeter Scale*

Every machine has a centimeter (cm) scale (Figure 5.13). Be familiar with where the maximum depth is on the screen, and how the marks are set up – as one hash mark every centimeter or are the hash marks every 5 mm or even every 2.5 mm? This will help you to locate the area of interest; for example, starting the FAST DH (subxiphoid) view at a depth of 5 cm even in medium-sized dogs is too superficial (shallow or magnified) and won't properly image the diaphragm and

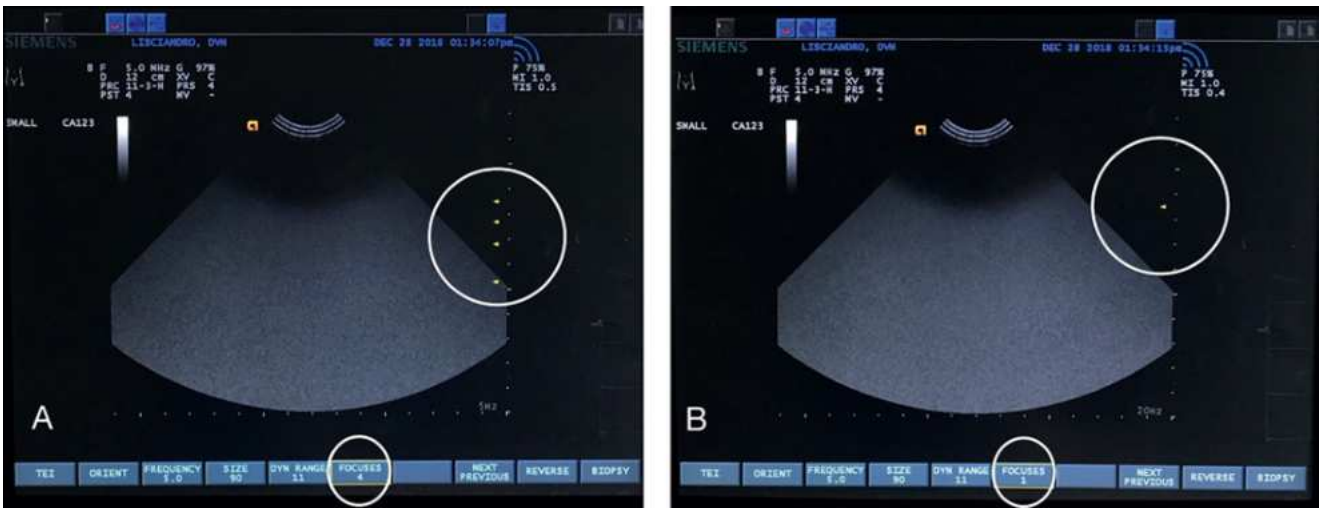


**Figure 5.12.** Focus cursor and depth. In (A) there are four focus cursors (*upper right circle*) and in (B) a single focus cursor (*upper right circle*). The best image is usually obtained by having a *single* focus cursor directly across from the area of interest so generally in the middle of the screen, unless imaging the lung in which a position directly across from the "lung line" is best. The number of focus cursors on this machine is also noted at the bottom of the screen (*circled*). Source: Courtesy of Dr Gregory Lisciandro, Hill Country Veterinary Specialists and FASTVet.com, Spicewood, TX.

**Figure 5.13.** Depth setting and the centimeter scale. The image is the same as Figure 5.12B with the focus cursor near center. The image has the centimeter scale to the right of the screen and then added numbers by the author for the depth of 12 cm. See how the hash marks correlate with 1 cm increments. Every ultrasound screen has a centimeter scale. Individual hash marks are often 1 cm (10 mm) on abdominal presets but can be every 0.5 cm (5 mm) or less. Find your cm scale and be aware of its depth scale. The screen itself has the depth (cm) and frequency (5 MHz), circled upper left and also at the screen's bottom along with number of focus cursors (1), plus other parameters noted (including the preset). Take the time to look over all the information provided on your machine's screen. Source: Courtesy of Dr Gregory Lisciandro, Hill Country Veterinary Specialists and FASTVet.com, Spicewood, TX.

gallbladder. The wise sonographer knows to start with a depth between 9 and 13 cm, get a feel for the four DH targets – diaphragm, gallbladder, cardiac bump, and caudal vena cava – and then magnify (decrease depth) once the targeted structures are identified from afar (see Chapters 6 and 7). On the other hand, lung is imaged at more shallow depths between 4 and 8 cm for smaller and larger patients, respectively.

### *Not Using the Centimeter Scale*

What looks really large on ultrasound may in fact be quite small. This is especially true with pleural effusion that looks like a lot on ultrasound but the maximum dimension is only 2 cm (or less than an inch), and merely a fissure line on the thoracic radiograph (TXR) or is missed altogether by TXR. As for masses, the seemingly large splenic mass that deforms the spleen, a serious finding, is really only 3 × 3 × 3 cm (or approximately 1¼ × 1¼ × 1¼ inches), easily missed by palpation during your physical exam and on abdominal radiography; and the lung lesion that appears so obvious is in fact a mere few millimeters (<1/3 inch) being missed or occult by thoracic radiography (and possibly CT) (Figure 5.14). Don't get me wrong, these findings may have a significant clinical bearing on your case, but a small pocket of pleural effusion in a stable case requires a calm and collected mind for decision making, and not overresponding.

## Pearls: Trouble Shooting a Poor Image

See the trouble-shooting algorithm (Figure 5.15).

- *Check your frequency*. In small dogs and cats, you can get away with higher frequencies such as 7–9 MHz; however, in large dogs (and other patients), the image will not be optimized until you lower the frequency to the 4–6 MHz range. You may have to change your preset, for example from small abdomen to medium or large abdomen, to change your frequency on some machines. Get used to looking at the frequency setting when starting to image the patient (see Figure 5.13).
- *Check your gain*. Generally, the time gain compensation (TGC) should be a gentle curve from the near-field to the far-field (Figures 5.16 and 5.17). Then, only the overall gain is used for the rest of the Global FAST ultrasound examination. However, using the TGC sliders is another strategy, depending on what level of the image needs to be brighter or darker. A common mistake when moving from AFAST and TFAST to Vet BLUE is having too much gain, in other words too bright in the near-field for lung because you needed more gain for soft tissue than lung surface imaging. Thus, the "lung line" is now too bright, lacking the contrast you need for Vet BLUE. Conversely, moving from Vet BLUE to AFAST or TFAST, you are now too dark (undergained) because the "lung line" imaging did not need as much gain as the soft tissue of abdominal and cardiac structures.
- *Check your depth*. Depending on the area of interest and the size of your patient, paying attention to the depth will help you to get where you want to go more quickly (see Figure 5.13). Generally, it's best to start with too much depth to gain an overview of what you are imaging, and to survey for recognizable landmarks prior to magnifying (decreasing the gain). And time is valuable on many fronts,

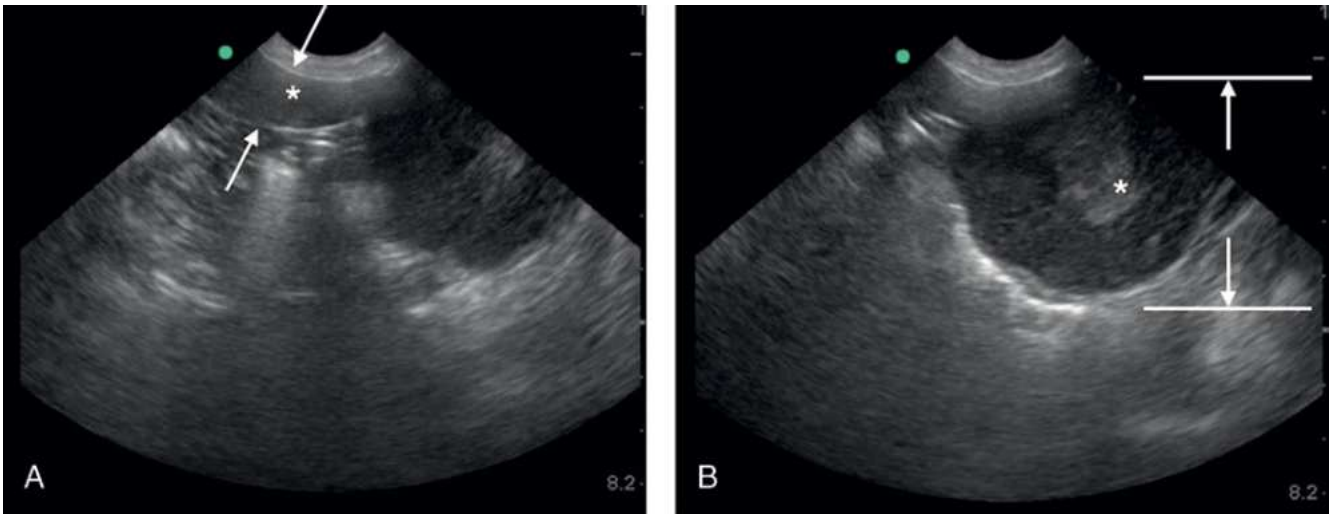


**Figure 5.14.** Splenic mass and estimating size from the centimeter scale. These images were captured during a POCUS spleen following AFAST. In (A) is the spleen (*) and arrows showing its borders. The spleen is sonographically recognized by its hyperechoic (bright white) capsule, and its splenic vessels splitting the capsule (not shown). In (B) the mass detected is eyeballed at approximately 4 × 4 cm using the centimeter scale. The mass appears large when in fact it is quite small. The finding is important and concerning because the mass *deforms* the capsule of the spleen. Source: Courtesy of Dr Gregory Lisciandro, Hill Country Veterinary Specialists and FASTVet.com, Spicewood, TX.

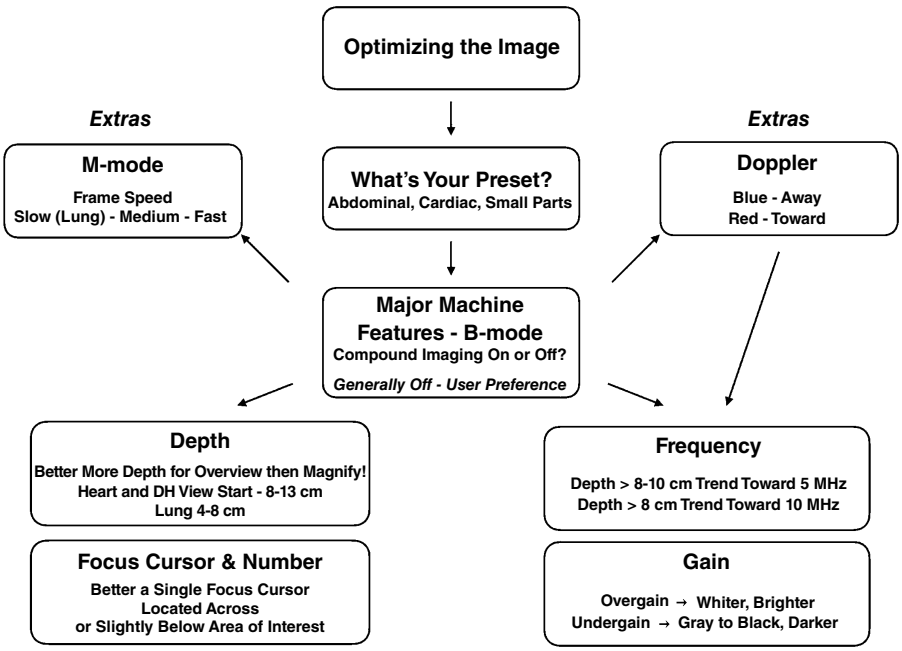


**Figure 5.15.** An algorithm for trouble shooting image acquisition with some clinical pearls and descriptors. Source: Courtesy of Dr Gregory Lisciandro, Hill Country Veterinary Specialists and FASTVet.com, Spicewood, TX.

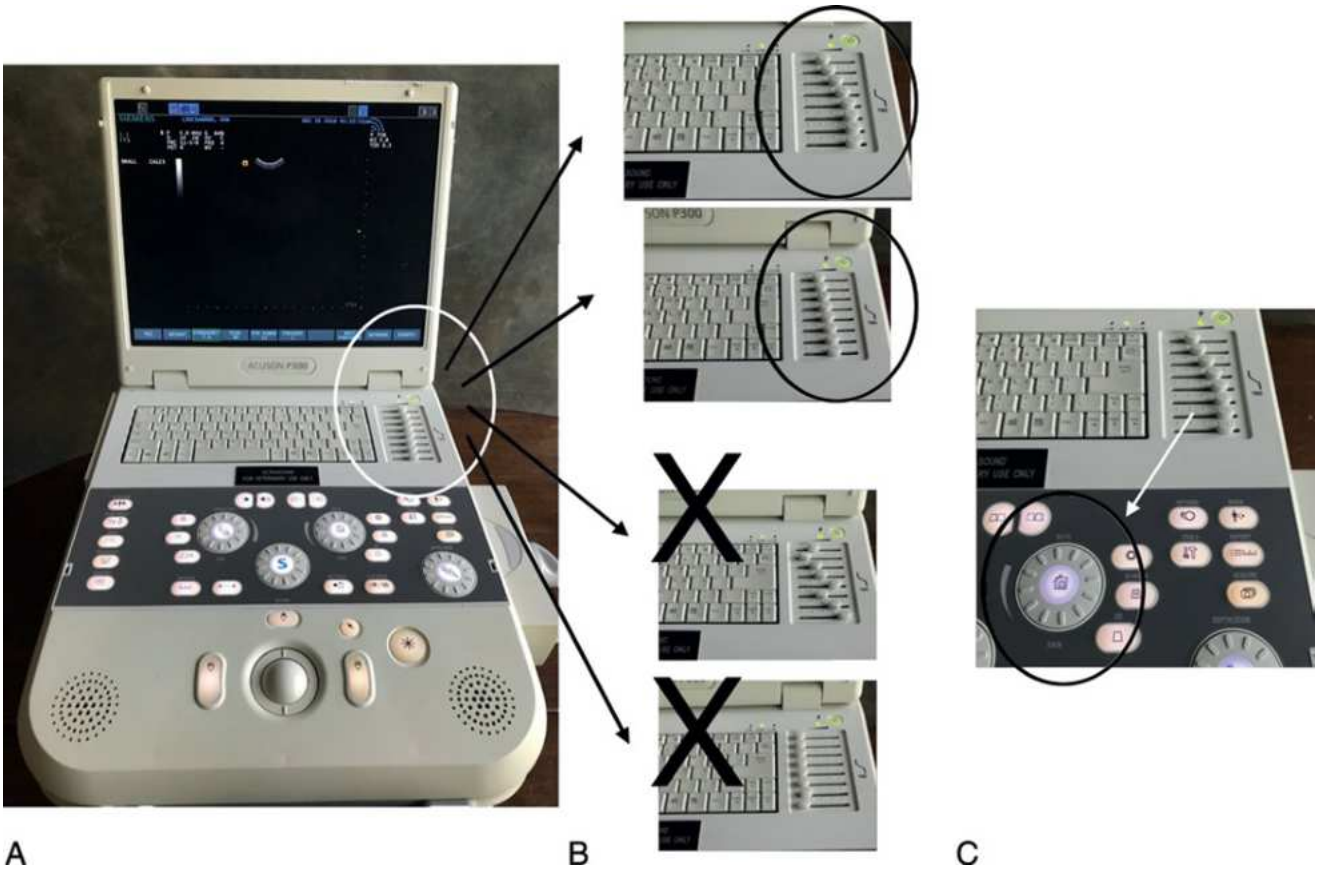


**Figure 5.16.** Time gain compensation (sliders) and the overall gain (wheel). Shown in (A) is an ultrasound machine with its keyboard and screen. The time gain compensation (TGC) is in the upper right on this keyboard. These TGC sliders can be intimidating but gain adjusts your gray scale when in B-mode. The sliders represent the different levels from the near-field to the far-field. In general, they should look like the circled upper two images in (B) and not like the lower two images (marked with an "X"). In (C) is the overall gain (circled wheel with arrow pointing to it) that may be turned clockwise and counterclockwise that alters the overall picture. If your sliders are adjusted as in (B) then you should mostly only be using the overall gain thereafter. If the image still doesn't look good then go through the trouble-shooting algorithm (see Figure 5.15). Source: Courtesy of Dr Gregory Lisciandro, Hill Country Veterinary Specialists and FASTVet.com, Spicewood, TX.

including the patience of your patient and its tolerance of your physical and chemical restraint.

- *Check the location and numbers of your focus cursor(s)*. Generally, a single focus cursor is best that is centered on the screen or directly across your area of interest.
- *Check your probe–skin contact (coupling)*. Is the probe head directly on skin? Do you have ample acoustic coupling medium?
- *Check your probe hand placement and beam direction*. Make sure that you are in the right region, using external landmarks as well as considering the direction and path of your ultrasound beam (see Figures 5.10 and 5.11).
- *Default back to original settings*. If you still cannot figure out why the image looks so wrong, push the B-mode button first and then go to presets and change to a different preset or return to the original preset, as many machines will default back to the original settings. The reality is sometimes you have no idea what you did to make everything look so bad.

See Chapter 4 for additional explanation and examples.

## Not Knowing How to Freeze and Roll the Cine Ball

You will need to know how to freeze the image on the screen. This is especially helpful when you have short-duration images of the region of interest.

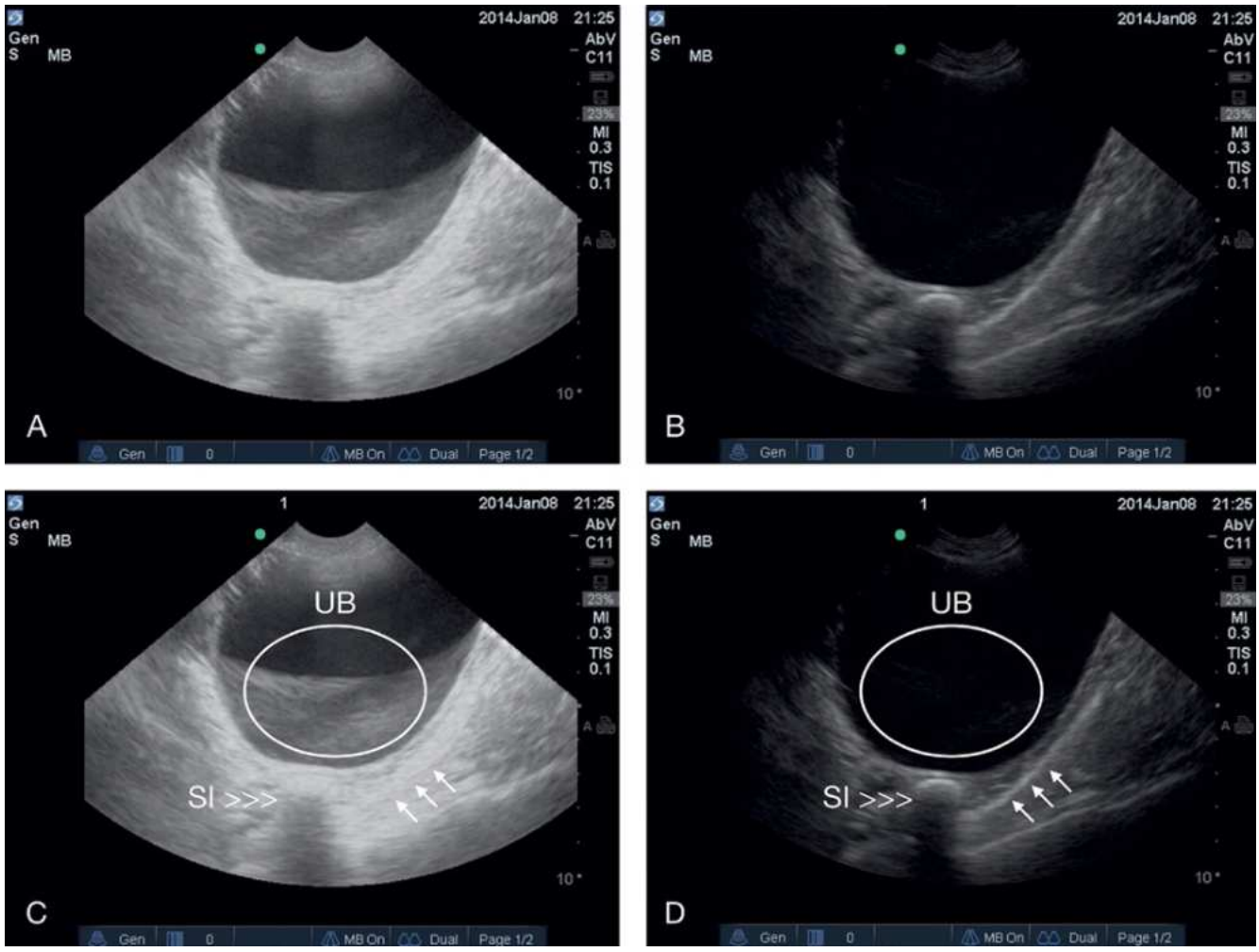


**Figure 5.17.** Slice-thickness artifact at the AFAST CC view. (A) and (B) are the same images within the same cine loop that have been extracted to show how much gain settings affect the image. In (A) is a slice-thickness artifact that is circled in (C). In (B) the gain is turned down, eliminating the artifact (true sediment would persist in gravity-dependent regions). Color flow Doppler is another technique used to look for flow (mass versus thrombus versus sediment versus artifact). (C) and (D) are labeled images of (A) and (B) respectively. Note how the loop of small intestine outside the lumen of the urinary bladder could mimic a bladder stone (cystic calculi) with a hyperechoic line (reflective air) and clean shadowing through the far-field. Note also that the screen provides a lot of information including a depth of 10 cm, an abdominal preset (Abv) in the upper right. Note, there is uniquely *no* focus cursor on machines from this manufacturer (SonoSite). Arrows indicate the body wall in the CC pouch. SI, small intestine; UB, urinary bladder. Source: Courtesy of Dr Gregory Lisciandro, Hill Country Veterinary Specialists and FASTVet.com, Spicewood, TX.

Examples include air (lung) interference of cardiac views in a panting patient, the tachycardic patient with normal higher heart rates (cats) in which the eyeball method is error prone; or you caught a quick glimpse of a structure you want to measure. Freezing the image on the screen and then rolling the cine ball through preceding frames allows you to evaluate better than in real time.

# Image Interpretation

## *Lacking Awareness of Most Common Locations for Artifacts*

In Chapter 3, Table 3.1 lists the common ultrasound artifacts and the most common locations and examples for each. Briefly, we will list here some strategies to

create better awareness of these artifacts, especially during the Global FAST approach. This leads to another major point…

Saving images is important not only for archiving patient information but for learning by reviewing studies and being able to compare to other modalities, future studies, and clinical course and outcome. For learning artifacts and how your machine interprets them, you can go through studies playing the "artifact game." For example, look at the AFAST views for mirror image artifact at the DH view on the pleural cavity side of the diaphragm, the CC view and the other side of the abdominal wall, and TFAST echo views for mirror image artifact on the far side of the pericardium. This can also be done with other artifacts in their most common locations, such as edge shadowing off the curved surface of the stomach wall, renal cortex, urinary bladder, etc.

### *Mirror Image*

This most commonly occurs at the diaphragm but the most problematic is the mirroring of the gallbladder into the thorax, especially when it's a partial mirror image. In this case, the gallbladder can mimic pleural and pericardial effusion to the hasty sonographer.

Other places for mirror image, where generally a strong air–soft tissue interface exists, are on the far side of the heart when aerated lung is in direct opposition to the pericardium, and the urinary bladder against the colon or thin body wall. See Chapter 3 for more explanation and examples.

### *Side-lobe, Slice-thickness*

This artifact occurs where there is a curve within a fluid-filled structure and is especially associated with the urinary bladder and gallbladder mimicking sediment and a mass. To differentiate artifact from sediment, consider where the gravity-dependent region is within the lumen of these structures. If "sediment" appears in nongravity-dependent regions, you should consider the possibility of artifact. Other techniques to differentiate artifact from true pathology include eliminating the artifact by turning down the gain and ballottement or changing the patient's position. Finally, some hasty sonographers will misinterpret an artifact for a mass. Simply place color flow Doppler on the suspect region for differentiation because a mass generally has pulsatile blood flow and an artifact (and thrombus) does not. See Chapter 3 for more explanation and examples.

### *Edge Shadowing*

The edge shadowing artifact is created when the ultrasound beam strikes a curved surface, creating a dark shadow that extends from that curved surface through the far-field. Edge shadowing most commonly occurs at the curved surfaces of stomach wall, renal cortex, gallbladder and urinary bladder and can be mistaken for free fluid along the stomach wall and renal cortex or defects in the wall of the gallbladder and urinary bladder, the latter especially when ascites is present on the AFAST CC view. See Chapter 3 for more explanation and examples.

## Pearls, Pitfalls, and The Final Say

The paradigm change of POCUS and FAST rests on expediting the learning process and we hope that this chapter will help accelerate your learning process by highlighting factors in a different way from other chapters in this textbook. The material in the chapter is based on training more than 1000 veterinarians in these techniques over the past 15 years as well as leading in clinical studies.

- Take the time to go through the major knobs on the machine - depth, gain (TGC and overall), focus cursor, frequency, and preset. Know where these buttons are located and play with images to get used to how to efficiently adjust their settings. Using stickers on your machine is another way to train yourself on where these buttons are located.
- Use our algorithm for trouble shooting. By doing so, you will have a way to efficiently review the most common image optimization features of your machine. *Depth, frequency, preset, focus cursor, gain (TGC and overall), probe–skin contact, direction of the beam, then default back to original settings*.
- Save images and then go through the views and play the artifact game; look through AFAST studies and see how many mirror image artifacts you see and then choose another artifact and do the same.

## References

Boysen SR, Rozanski EA, Tidwell AS, et al. 2004. Evaluation of a focused assessment with sonography for trauma protocol to detect free abdominal fluid in dogs involved in motor vehicle accidents. *J Am Vet Med Assoc* 225(8):1198–1204.

Walker C, Mohabir PK. 2014. Orientation. In: *Point-of Care Ultrasound*, edited by Soni N, Arntfield R, Koy P. Philadelphia: Elsevier Saunders, pp 25–31.

# Further Reading

Blanco P, Volpicelli G. 2016. Common pitfalls in point-of-care ultrasound: a practical guide for emergency and critical care physicians. *Crit Ultrasound J* 8(1):15.

Boivin M. 2014. Basic operation of an ultrasound machine. In: *Point-of Care Ultrasound*, edited by Soni N, Arntfield R, Koy P. Philadelphia: Elsevier Saunders, pp 32–37.

Brietkrutz R, Uddin S, Steiger H, et al. 2009. Focused echocardiography entry level: new concept of a 1-day training course. *Minerva Anesth* 75(2):285–292.

Chiem AT. 2014. Transducers. In: *Point-of Care Ultrasound*, edited by Soni N, Arntfield R, Koy P. Philadelphia: Elsevier Saunders, pp 19–24.

Goodgame B, Debesa O, Lee A, et al. 2014. Imaging artifacts. In: *Point-of Care Ultrasound*, edited by Soni N, Arntfield R, Koy P. Philadelphia: Elsevier Saunders, pp 38–48.

Hempel D, Stenger T, Campo Dell Orto M, et al. 2014. Analysis of trainees' memory after classroom presentations of didactical ultrasound courses. *Crit Ultrasound J* 6(1):10.

Hock GH, Widmer WR. 2010. Apearance of common ultrasound artifacts in conventional vs. spatial compound imaging. *Vet Radiol Ultrasound* 51(6):621–627.

Mattoon JS, Nyland TG. 2015. Fundamentals of diagnostic ultrasound. In: *Small Animal Diagnostic Ultrasound*, 3rd edition, edited by Mattoon JS and Nyland TG. St Louis: Elsevier, pp 1–49.

Mayette M, Mohabir PK. 2014. Ultrasound physics. In: *Point-of Care Ultrasound*, edited by Soni N, Arntfield R, Koy P. Philadelphia: Elsevier Saunders, pp 9–18.

SECTION II

# Abdomen

CHAPTER SIX

# POCUS: AFAST – Introduction and Image Acquisition

Gregory R. Lisciandro

## Introduction

In 2004, a focused assessment with sonography for trauma (FAST) exam was prospectively validated in traumatized dogs, translating the four acoustic windows described in human medicine (Boysen et al. 2004) (Figure 6.1). Interestingly, intraabdominal injury, more specifically hemoabdomen, was far more prevalent than previously reported with a prevalence of 38–45% versus a pre-FAST rate of 12–23% (Boysen et al. 2004).

In 2005, the original FAST examination was modified in the following ways, including renaming the study AFAST (Lisciandro et al. 2009) (Table 6.1).

- The probe was directed into the gravity-dependent regions of each acoustic window.
- The views were renamed by their target organs rather than external anatomy.
- The probe was maneuvered differently, making the major orientation longitudinal with fanning and rocking of the probe at each AFAST acoustic window *without* rotating.
- The patient was not shaved but rather the hair was parted to maximize probe–skin contact.
- A simple AFAST-applied fluid scoring system (0–4) was developed for semiquantitating volume of the effusion, with more recent modifications.
- Serial AFAST examinations were performed as standard of care for all admitted patients four hours post admission and sooner if questionable or unstable patient status.
- AFAST investigated many important clinical questions rather than a single binary question of fluid positive or negative.

The AFAST study documented that its simple abdominal fluid scoring system (0–4) reliably predicted the degree of anticipated anemia in dogs with hemoabdomen. The abdominal fluid score (AFS) differentiated lower scoring small-volume bleeders (AFS 1 and 2) from higher scoring large-volume bleeders (AFS 3 and 4). Moreover, the study answered what was implied in the original FAST study, that the historical use of radiographic abdominal serosal detail was an *unreliable test* for the presence or absence of free peritoneal fluid and its volume (Boysen et al. 2004; Lisciandro et al. 2009). In fact, 24% of dogs with normal abdominal radiographic serosal detail were AFAST positive, and 32% with decreased abdominal radiographic serosal detail were in fact AFAST negative (Lisciandro et al. 2009). Thus, in summary, not only was abdominal radiographic serosal detail *unreliable* for the presence and absence of free fluid, but abdominal serosal detail also *could not* reliably estimate the volume of free fluid present (see Figure 7.9).

The repeating of at least one more AFAST and assigning an AFS allowed the attending clinician to not only screen for the presence of free fluid that may have been missed or absent on the first AFAST examinations, but also to reassign an AFS and evaluate the urinary bladder (Lisciandro et al. 2009; Lisciandro 2011, 2012; Boysen and Lisciandro 2013). AFAST and the use of the patient's AFS were shown to be invaluable

*Point-of-Care Ultrasound Techniques for the Small Animal Practitioner*, Second Edition. Edited by Gregory R. Lisciandro.
© 2021 John Wiley & Sons, Inc. Published 2021 by John Wiley & Sons, Inc.
Companion website: www.wiley.com/go/lisciandro/ultrasound2

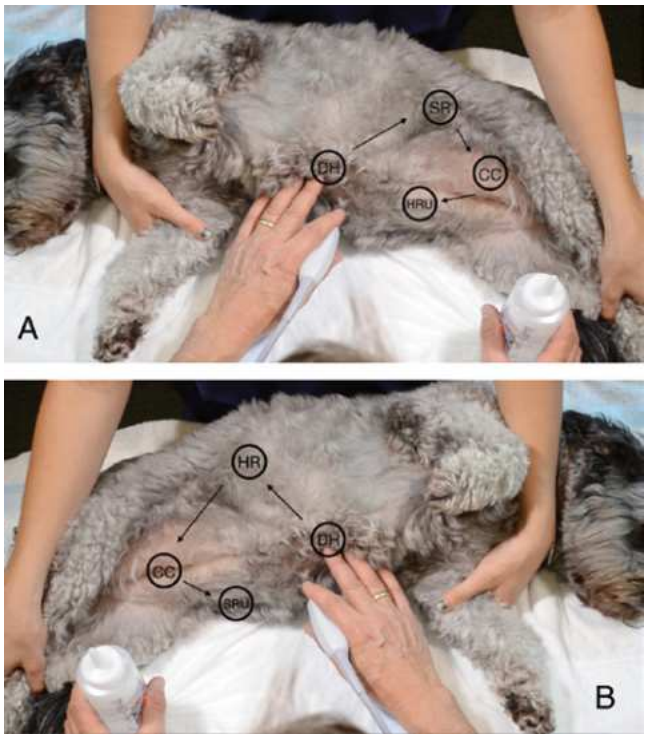


**Figure 6.1.** AFAST on a dog in right and left lateral recumbency. In (A) AFAST is shown on a dog in right lateral recumbency and in (B) left lateral recumbency. Sites are named by their target organs. The AFAST order is always the same. In right lateral, (1) DH view, (2) SR view, (3) CC view, (4) HRU view. In left lateral recumbency, (1) DH view, (2) HR view, (3) CC view, (4) SRU view. These AFAST views are part of the abdominal fluid scoring (AFS) system and the order ends at the most gravity-dependent view where abdominocentesis is likely to be performed in higher-scoring patients. Note that the 5th AFAST bonus view is not shown in these images. The AFAST views are nearly identical sonographically no matter the positioning (lateral recumbency versus standing-sternal). AFAST target organs are imaged in the same standardized manner regarding probe maneuvering with the "fan, rock (cranially) and return to your starting point" approach. Source: Reproduced with permission of Dr Gregory Lisciandro, Hill Country Veterinary Specialists and FASTVet.com, Spicewood, TX.

**Table 6.1.**
Changes in methodology from FAST to AFAST.

| Parameters | FAST (Boysen 2004) | AFAST (Lisciandro et al. 2009) |
|---|---|---|
| Shaving patient | Shaving | No shaving |
| Primary probe orientation | Longitudinal and transverse | Only longitudinal |
| Primary probe maneuver | Sliding, rotating and sweeping | Fanning and rocking |
| Main probe direction | Toward spine | Gravity-dependent pouches |
| Lateral[a] | Left | Right |
| Fluid scoring | No | Yes |
| Naming acoustic views | External locations | Target organs |
| Timing of examination (median time presentation to ultrasound examination) | Post resuscitation (median 1 hour) | Presentation and serially post resuscitation (median <5 minutes) |

[a]Lateral recumbency was a brilliant proposition, being markedly safer than dorsal recumbency (see Figure 6.5).
Source: Reproduced with permission of Dr Gregory Lisciandro, Hill Country Veterinary Specialists, FASTVet.com, Spicewood, TX.

for the detection of developing hemoabdomen (initially negative [AFS 0] turned AFAST positive [AFS 1-4]), the detection of ongoing hemorrhage (increasing fluid score), and evidence-based resolution of hemoabdomen (decreasing fluid score) (see Figure 7.9). Interestingly, the American College of Emergency Physicians has advocated the use of a serial four-hour postadmission FAST examination for all at-risk human patients since 2001 yet at the time of writing this chapter, the number one cause of death in hospitalized human trauma patients surviving traumatic brain injury during their first 48 hours of care remains ongoing, unrecognized bleeding (Bilello et al. 2011; Sobrino and Shafi 2013).

More recently, a human study showed that in people with prehospital hypotension, the only intervention that prevented the "crump factor," the phenomenon of a patient decompensating unexpectedly, was the liberal use of FAST examinations (Bilello et al. 2011). The upshot is veterinarians have a better tool, the AFAST and its applied fluid scoring system, to determine within minutes of presentation or during hospitalized care when patients are becoming unstable, to not only "see" if the patient is positive or negative for free fluid, but also the degree of bleeding (or effusion) by easily calculating the patient's AFS (0–4 scale). AFAST and AFS are the missing link to traditional trauma, triage and tracking algorithms, and by adding the target organ approach, a huge amount of clinical information is easily gained within minutes, *when minutes count*.

The comparison of the original FAST to the subsequent AFAST study is fascinating and some important differences are noted (see Table 6.1) (Boysen et al. 2004; Lisciandro et al. 2009). Remarkably, degree of trauma was very similar, including numbers of pelvic fractures and pneumothoraces

(Table 6.2), suggesting that the overall degree of trauma between studies was comparable and thus inferences may be loosely drawn (Boysen et al. 2004; Lisciandro et al. 2009).

One involves the case management and decision making for blood transfusion(s), and that knowing if the dog at triage was AFS positive affected fluid therapy administration strategies. In other words, intravenous fluid resuscitation was likely titrated more closely to low normal endpoints, such as mean arterial pressure, thus mitigating exacerbation of hemorrhage by lessening the probability of "popping the clot" and diluting clotting factors through overresuscitation in bleeding dogs (Lisciandro et al. 2009). The differences in median time from trauma to FAST/AFAST, median time presentation to FAST/AFAST (240 versus <5 minutes), and numbers of transfusions FAST/AFAST (9 versus 3) support this conclusion. AFAST was performed as part of the physical exam versus FAST, which was a second line test after initial assessment, intravenous fluid resuscitation, and blind abdominocentesis possibly to the dog's detriment by the much higher positive rate (45% versus 27%).

The original FAST study lacked a fluid scoring system, and as simple as the AFAST system is, with a range of 0–4 (AFS 0 negative all AFAST views to a maximum of four being positive for fluid at all four AFAST views), AFS provides an effective tool for decision making (see Table 7.3). This decision making, ranging from intravenous fluid resuscitation strategies to administration of blood transfusion products to the need for exploratory surgery, importantly carries the potential to improve outcome and decrease complications, as shown in people (see Chapter 7) (Blackbourne et al. 2004; Ollerton et al. 2006; Bilello et al. 2011).

Of note, dogs with pneumothorax (55%), pelvic fractures (40%), and high alanine transaminase (ALT) (>400 U/L) were also more likely to concurrently have or develop hemoabdomen detected by either their initial or serial AFAST examinations than dogs without these findings (Lisciandro et al. 2009; Lisciandro 2014c). The serial use of AFAST is helpful in determining the integrity of the urinary bladder, estimating urinary bladder volume and urine output during resuscitation (Lisciandro et al. 2009; Lisciandro 2011; Lisciandro and Fosgate 2017). Both FAST and AFAST studies documented that when the urinary bladder was imaged with an expected, smooth, rounded contour, it was unlikely to be ruptured, holding advantages over traditional means of palpation, characterization of urine post micturition, and plain radiography (Boysen et al. 2004; Lisciandro et al. 2009; Boysen and Lisciandro 2013).

More recently, a urinary bladder estimation formula for use during AFAST has been published and provides a noninvasive way to estimate urine output when serial calculations are made over time (Lisciandro and Fosgate 2017). AFAST additionally remains useful to survey for intrathoracic trauma, pleural and pericardial effusion, and lung conditions, through the acoustic

**Table 6.2.**
Comparison of FAST and AFAST in dogs.

| Parameters | FAST (Boysen et al. 2004) | AFAST (Lisciandro et al. 2009) |
|---|---|---|
| Primary presentations | 65% | 96% |
| FAST positive cases | 45% | 27% |
| Low-scoring (AFS 1 and 2) small-volume bleeders | NA | 13 |
| High-scoring (AFS 3 and 4) large-volume bleeders | NA | 14 |
| Cases of abdominocentesis prior to AFAST/FAST examination | 16 | 0 |
| Median time trauma to AFAST/FAST examination | 240 minutes | 60 minutes |
| Median time presentation to AFAST/FAST examination | 60 minutes | <5 minutes |
| | FAST was a secondary evaluation post initial resuscitation | AFAST was a first-line screening test |
| Median time for AFAST/FAST examination | 6 minutes | 3 minutes |
| | Shaved sites | No shaving |
| Pelvic fractures | 20 | 22 |
| Pneumothorax | 21 | 22 |
| Appendicular fractures | 15 | 25 |
| Diaphragmatic hernia | NA | 2 |
| Number of blood transfusions | 9 | 3 |

Source: Reproduced with permission of Dr Gregory Lisciandro, Hill Country Veterinary Specialists, FASTVet.com, Spicewood, TX.

window of the liver and gallbladder by imaging cranial to the diaphragm in every patient, dependent on patient size, coupled with depth limitations of the ultrasound machine (Boysen et al. 2004; Lisciandro et al. 2009; Lisciandro 2011, 2016a; McMurray et al. 2016).

Lastly, AFAST was never meant to be a "flash exam," meaning that it was never meant to only answer a single binary question of whether free fluid was present or absent (Table 6.3). AFAST provides much more clinical information by:

**Table 6.3.**
What clinical questions are answered using AFAST? Binary? Qualitative-quantitive?.

| | Binary | Qualitative-quantitive | [a]Sensitivity (Se)<br>[a]Specificity (Sp) |
|---|---|---|---|
| • Does the patient have free fluid in the abdominal cavity? | √<br>Yes or no | √<br>Use AFAST-applied fluid scoring system (1–4) | Se – High<br>Sp – High |
| • Does the patient have free fluid in the retroperitoneal space? | √<br>Yes or no | √<br>Trivial, mild, moderate, severe | Se – High to variable<br>Sp – High |
| • Does the patient have any obvious AFAST target organ abnormalities? | √<br>Yes or no | √ | Se – Variable, operator dependent<br>Sp – High |
| • Does the patient have pleural effusion? | √<br>Yes or no | √<br>Trivial, mild, moderate, severe via its DH view | Se – High<br>Sp – High |
| • Does the patient have pericardial effusion? | √<br>Yes or no | √<br>Trivial (<0.5 cm), nild (>0.5 and <1.0 cm), moderate (>1.0 and <2 cm), severe (>2 cm) via its DH view (Candotti and Arntfield 2015) | Se – High<br>Sp – High |
| • Does the patient have lung pathology along the pulmonary–diaphragmatic interface? | √<br>Yes or no | √<br>Vet BLUE B-line scoring<br>Vet BLUE 6 lung ultrasound signs (Lisciandro 2014b,c; Lisciandro and Fosgate 2017) | Se – Unknown, operator dependent<br>Sp – Likely high |
| • What is the patient's volume status? | √<br>Unremarkable or abnormal | √<br>Characterizing the dynamic changes in height of caudal vena cava (bounce, fluid responsive; FAT, fluid intolerant; or flat, hypovolemic) (see Figures 36.7, 36.10–36.12); coupled with hepatic venous characterization (presence or absence of the "tree trunk sign" – see Figure 36.8); and absolute maximum CVC height measurements (see Table 36.3) | [a]Hypervolemia<br>Se – Likely high<br>Sp – Likely high<br>[a]Hypovolemia<br>Se – Likely variable<br>Sp – Likely high<br>[a]Euvolemia<br>Se – Variable<br>Sp - Variable<br>[a]Integrating TFAST echo and Vet BLUE pulmonary information likely improves both Se and Sp |
| • What is the patient's urine production? | | √<br>Length (cm) × width (cm) × height (cm) × 0.625 = volume estimation (mL) | Unknown |

[a]Clinical experience, limited veterinary studies, human studies.
Source: Reproduced with permission of Dr Gregory Lisciandro, Hill Country Veterinary Specialists and FASTVet.com, Spicewood, TX.

- having a fluid scoring system
- looking cranial to the diaphragm into the thorax at the DH view for pleural and pericardial effusion and lung conditions
- examining the gallbladder wall for signs of intramural edema
- characterizing the caudal vena cava and its associated hepatic venous system
- observing the urinary bladder for its expected rounded contour and measuring it (when applicable) for bladder volume estimation and urine output
- calculating the AFS to better make sense of the volume of blood in hemorrhaging small animals
- serving as monitoring tool for any and all effusive conditions
- taking advantage of its target organ approach.

In other words, an AFAST not only provides a highly sensitive and specific means to detect intraabdominal and retroperitoneal effusions, but also serves as an abdominal soft tissue screening test for obvious target organ pathology. Patient information is acquired rapidly during AFAST (<3–4 minutes) with low patient impact (minimal restraint, no shaving) and point of care (Lisciandro et al. 2009; Lisciandro 2012, 2016a; Boysen and Lisciandro 2013; McMurray et al. 2016).

Abbreviations and terminology are listed in Table 6.4.

POCUS abdominal, thoracic, ocular, neurological, and musculoskeletal examinations are more extensively described in their respective chapters; however, the POCUS approach should always include minimally an AFAST, with its target organ approach, and AFS, and, much better, the Global FAST approach, as an extension of your physical exam for best practice. Global FAST has been advocated by the author as an extension of the physical examination for virtually any small animal patient since 2005 (Lisciandro 2011, 2012, 2014a–c, 2016a,b; Lisciandro et al. 2019), with a similar approach more recently advocated in human medicine (Lichtenstein 2010; Narasimhan et al. 2016).

## What AFAST Can Do

- Can detect free fluid in small amounts superior to physical examination and abdominal radiography and comparable to the gold standard of computed tomography (CT).
- Can detect clinically significant pleural and pericardial effusions in most cases by imaging past or cranial to the diaphragm at the AFAST DH view.
- Can detect retroperitoneal effusion when imaging at the AFAST spleno-renal (SR) and hepato-renal (HR) views and the HR5th and SR5th bonus views.
- Can anticipate degree of anemia in different patient subsets by using its easily applied abdominal fluid scoring system.
- Can be used to screen for canine anaphylaxis through the detection of sonographic striation of the gallbladder wall as the "double rim effect" or "halo effect" or "halo sign" at the AFAST DH view, referred to as the "anaphylactic gallbladder," coupled with the finding of a flat caudal vena cava (CVC) (see Figure 36.9).
- Can be used to screen for right-sided congestive heart failure through the detection of sonographic striation of the gallbladder wall as the "double rim effect" or "halo effect" or "halo sign" at the AFAST DH view, referred to as the "cardiac gallbladder," coupled with the finding of a FAT CVC (see Figure 36.7).
- Can be used to assess volume status and right-sided cardiac function by evaluating CVC size and for the presence of hepatic venous distension, the "tree trunk sign," at the AFAST DH view (see Figure 36.8).
- Can screen for concurrent target organ injury or pathology for basic soft tissue conditions of the liver, gallbladder, kidneys, urinary bladder, spleen, and gastrointestinal tract.
- Can assess urinary bladder integrity at the AFAST cysto-colic (CC) view especially when there are concerns regarding rupture in trauma cases.
- Can noninvasively estimate urinary bladder volume and thus urine output at the AFAST CC view using the formula of length (L) × width (W) × height (H) (cm) × 0.625 = estimation of urinary bladder volume (mL) (Lisciandro and Fosgate 2017).

## What AFAST Cannot Do

- Cannot sonographically characterize fluid, thus sample acquisition via abdominocentesis is required when fluid is safely accessible; and fluid analysis should be performed.
- In penetrating trauma, AFAST lacks sensitivity (in contrast to blunt trauma where it has high sensitivity) but likely is highly specific for intraabdominal and retroperitoneal injury similar to human studies (Udobi et al. 2001).
- In penetrating trauma, AFAST should *always be repeated* post resuscitation as long as necessary until assured that the patient is not a surgical candidate

**Table 6.4.**
Abbreviations and terminology. As lengthy as the list seems, the abbreviations and terminology allow for more rapid communication verbally and in medical records.

| Terminology for standardized ultrasound exams | |
|---|---|
| Abdominal FAST | AFAST |
| Thoracic FAST | TFAST |
| Veterinary Bedside Lung Ultrasound Exam | Vet BLUE |
| Global FAST | AFAST, TFAST and Vet BLUE combined as a single ultrasound examination |
| Complete Detailed Abdominal Ultrasound | |
| Complete Detailed Echocardiography | |
| Serial Examination | Repeating the standardized protocol and recording your findings. Serial examinations have also been referred to as "secondary examinations." We prefer the term "serial" (Blackbourne et al. 2004; Lisciandro et al. 2009) |
| **Ultrasound signs and characterizations used during AFAST** | |
| AFAST views:<br>DH view = diaphragmatico-hepatic view<br>SR view = spleno-renal view<br>HR view = hepato-renal view<br>CC view = cysto-colic view<br>HRU view = hepato-renal umbilical view<br>SRU view = spleno-renal umbilical view<br>HR5th bonus view = the final view of small animals when in right lateral recumbency imaging the right kidney and adjacent right liver (not part of the abdominal fluid scoring system)<br>SR5th bonus view = the final view of small animals when in left lateral recumbency imaging the left kidney and adjacent spleen (not part of the abdominal fluid scoring system) | |
| CC pouch = most gravity-dependent region where free fluid would accumulate at the CC view<br>HRU (SRU) pouch = most gravity-dependent region where free fluid would accumulate at the HRU (SRU) view<br>Pouch = most gravity-dependent region at that acoustic window | |
| Gallbladder "halo sign," also called "halo effect," "double rim effect" | Occurs with the presence of intramural gallbladder edema, recognized as sonographic striation, and supports the diagnosis of canine anaphylaxis (along with acute collapse and gastrointestinal signs and a flat CVC) versus right-sided heart failure/generalized systolic dysfunction, pericardial effusion (along with a FAT CVC) versus right-sided volume overload (FAT CVC) in collapsed, weak, hypotensive dogs (see Figures 36.7 and 36.9). There are other causes for gallbladder wall edema (see Table 7.5 and Chapter 8), however, canine anaphylaxis and heart conditions present more emergently with acute weakness or collapse in a previously healthy dog (Lisciandro 2014a) |

**Table 6.4.**
(*Continued*)

| | |
|---|---|
| Caudal vena cava (CVC) characterization by assessing maximum heights in the longitudinal orientation at the FAST DH view | 1. Bounce: expected ~35–50% dynamic respirophasic changes in CVC height during the respiratory cycle; also called a "fluid-responsive CVC"; an expected maximum height in longitudinal at the DH view is available for dogs of various weights and cats (see Tables 7.6 and 36.3 and Figures 36.9–36.12).<br>2. Flat: lacks respirophasic dynamic change (<10%) in CVC maximum height and having an abnormally *small* maximum height; also called "hypovolemic CVC" or "fluid starved CVC"; maximum heights of <0.25 cm, <0.35 cm, <0.50 cm for dogs weighing <9 kg, >9 kg, <15 kg and >15 kg, respectively (modified by Lisciandro from Darnis et al. 2018).<br>3. FAT: lacks respirophasic dynamic change (<10%) in CVC diameter during inspiration and expiration having an abnormally large maximum height (Ferrada et al. 2012a,b); also called a "fluid-intolerant CVC"; maximum heights of >1.0 cm and >1.5 cm for dogs weighing <9 kg and >9 kg, respectively (modified by Lisciandro from Darnis et al. 2018). |
| Cardiac bump | Observation at the FAST DH view where the muscular apex of the heart is beating and often indenting along the diaphragm; helps rule in and rule out pericardial effusion through presence or absence of the "racetrack sign" (Lisciandro 2014a,b, 2016a) (see Figures 7.13, 7.14 and 39.5) |
| Racetrack sign | Sign indicative of pericardial effusion at the FAST DH view through the observation of free fluid rounding the apex of the heart being contained within the pericardial sac (Lisciandro 2014a,b, 2016a) (see Figure 7.13) |
| Tree trunk sign | Observation of distended hepatic veins as they drain into a distended (FAT) caudal vena cava (abnormal finding); represents conditions impeding blood flow from the liver to the right heart, most commonly right-sided failure, pericardial effusion, and dilated cardiomyopathy (DCM), and right-sided volume overload during fluid resuscitation (Lisciandro 2014a,b; Nelson et al. 2010) (see Figure 36.8) |
| Urinary bladder volume estimation formula (mL) | Length (cm) × width (cm) × height (cm) × 0.625 (Lisciandro and Fosgate 2017) |

Source: Reproduced with permission of Dr Gregory Lisciandro, Hill Country Veterinary Specialists, FASTVet.com, Spicewood, TX.

by repeating at 2–4 hours post admission as standard of care and then continued at eight hours, 12 hours, 24 hours, two days, three days, five days, etc. post trauma at any time the patient is not doing well, for example to detect a septic abdomen or pyothorax that would otherwise be missed.

- AFAST misses peritonitis in some dehydrated and hypotensive patients, so should *always be repeated* post resuscitation and rehydration, with continued serial (repeat) exams as long as necessary until assured that the patient is not a surgical candidate.
- The AFAST AFS system is effective in cats, but cats as a species lack a large splenic blood reservoir and thus felines generally do not survive large-volume bleeds, and larger volume intraabdominal effusions are more likely to be due to uroabdomen.
- Understand that serial (repeat) exams using the Global FAST approach is an even better strategy because the thorax, heart, and lung are also surveyed.
- Cannot replace a complete detailed abdominal ultrasound.
- Cannot replace proper training.

### Indications

- All blunt and penetrating trauma cases as standard of care for screening for indirect evidence of intraabdominal and retroperitoneal injury.
- All collapsed both recovered and unrecovered cases with unexplained hypotension, tachycardia, or mentation changes.
- All anemic cases.
- All "ain't doing right" (ADR) cases.
- All postinterventional cases including intravenous fluid therapy, postsurgical cases, postpercutaneous procedures, etc. that are at risk for bleeding, infections, vascular complications.
- All peritonitis suspects, including acute abdomen, for expedient diagnosis through the detection of free fluid (and subsequent sampling, fluid analysis testing as deemed appropriate) and free air.
- Preanesthetic screening test.
- Extension of the physical exam for patients presenting once or twice a year for routine care.

### Objectives

- Be able to perform the AFAST views and apply its fluid scoring system.
- Be able to recognize basic abnormalities of the AFAST target organs in each of its views.
- Know how to assign an AFS during AFAST.
- Be able to recognize sonographic striation of the gallbladder wall, referred to as the "halo effect" or "double rim effect" or "halo sign," that can be present in both dogs and cats from different causes.
- Be able to recognize retroperitoneal free fluid and distinguish it from intraabdominal fluid.
- Know common artifacts at each AFAST view.
- Know the major pitfalls at each AFAST view.
- Know how to do a focused (POCUS) spleen examination and its importance following the completion of AFAST and after assigning an AFS.
- Understand why best practice would be to add on the Global FAST approach for all AFAST and POCUS exams (abdomen, thorax, eye, brain, musculoskeletal, etc.) to make sure that forms of peritonitis and pleuritis, presence of bleeding, and cardiac and pulmonary conditions are not being missed.

## How to Perform an AFAST Exam

### Ultrasound Settings and Probe Preferences

- Standard abdominal settings, presets, with adequate depth to be able to visualize the target organs of each AFAST view.
- Curvilinear (microconvex) probe with a range of 5–10 MHz and a maximum depth of 12–15 cm is acceptable for most dogs and cats.

### Optimizing Image Quality and Probe–Skin Contact

Hair is generally not shaved but rather parted for the best probe–skin contact with the use of isopropyl alcohol, and/or alcohol-based hand sanitizer, and/or acoustic coupling gel. The author prefers the use of minimal amounts of isopropyl alcohol to effectively part the hair followed by alcohol-based hand sanitizer. The strategy is much less noxious to your patient by minimizing the cold wetness of isopropyl alcohol and its fumes, especially when moved to an oxygen cage. Alcohol-based hand sanitizer has the added benefit of being easily wiped off and it also evaporates quickly. Isopropyl alcohol should not be used if electrical defibrillation is anticipated because it poses a burn/fire hazard. The clinician should be aware that isopropyl alcohol may cause probe head damage (see Figure 4.13).

**Pearl:** By not shaving (or limiting shaving to small acoustic windows), the cosmetic appearance of the patient is preserved (happier clients), the exam time is lessened, and imaging quality is sufficient with most newer ultrasound machines (median AFAST time <3–3.5 minutes) (Lisciandro et al. 2009; Lisciandro 2011, 2012; Boysen and Lisciandro 2013).

**Pearl:** Maximize image quality by parting the hair and getting the probe head and its acoustic coupling medium in direct contact with the patient's skin to minimize air trapping, which is your imaging enemy because ultrasound does not transmit through air. Placing the probe head on a wetted mat of hair full of trapped air will produce a poor image (see Figures 5.1 and 5.2).

**Pearl:** Hold the probe in a way that is most comfortable while being able to fan toward and away from the table top while maintaining a longitudinal (sagittal) plane in patients placed in lateral recumbency. Holding the probe like a pencil for many who have learned to scan patients in dorsal recumbency usually becomes problematic at the DH view for the caudal vena cava. Holding the probe on top and keeping the thumb on the probe marker and a finger out to prevent drifting works best.

## *Patient Positioning*

### Lateral Recumbency

Right lateral (RL) recumbency is generally preferred over left lateral (LL) recumbency for AFAST because RL recumbency is standard positioning for electrocardiographic and echocardiographic evaluation (Figures 6.2 and 6.3; see also Figure 6.1). Moreover, the left kidney (a window into the retroperitoneal space) at the AFAST SR view and the gallbladder at the DH view (by directing the probe in the gravity-dependent region or toward the tabletop) are readily imaged. RL recumbency over LL is preferred positioning for abdominocentesis because anatomically the spleen lies more on the left side of dogs and cats. LL recumbency may be used in cases in which injury prohibits RL positioning, or the right retroperitoneal space warrants imaging. In a more recent study evaluating RL versus LL recumbency, abdominal FAST time was shorter in LL recumbency and both kidneys were more reliably imaged (McMurray et al. 2016). However, this is probably due to training

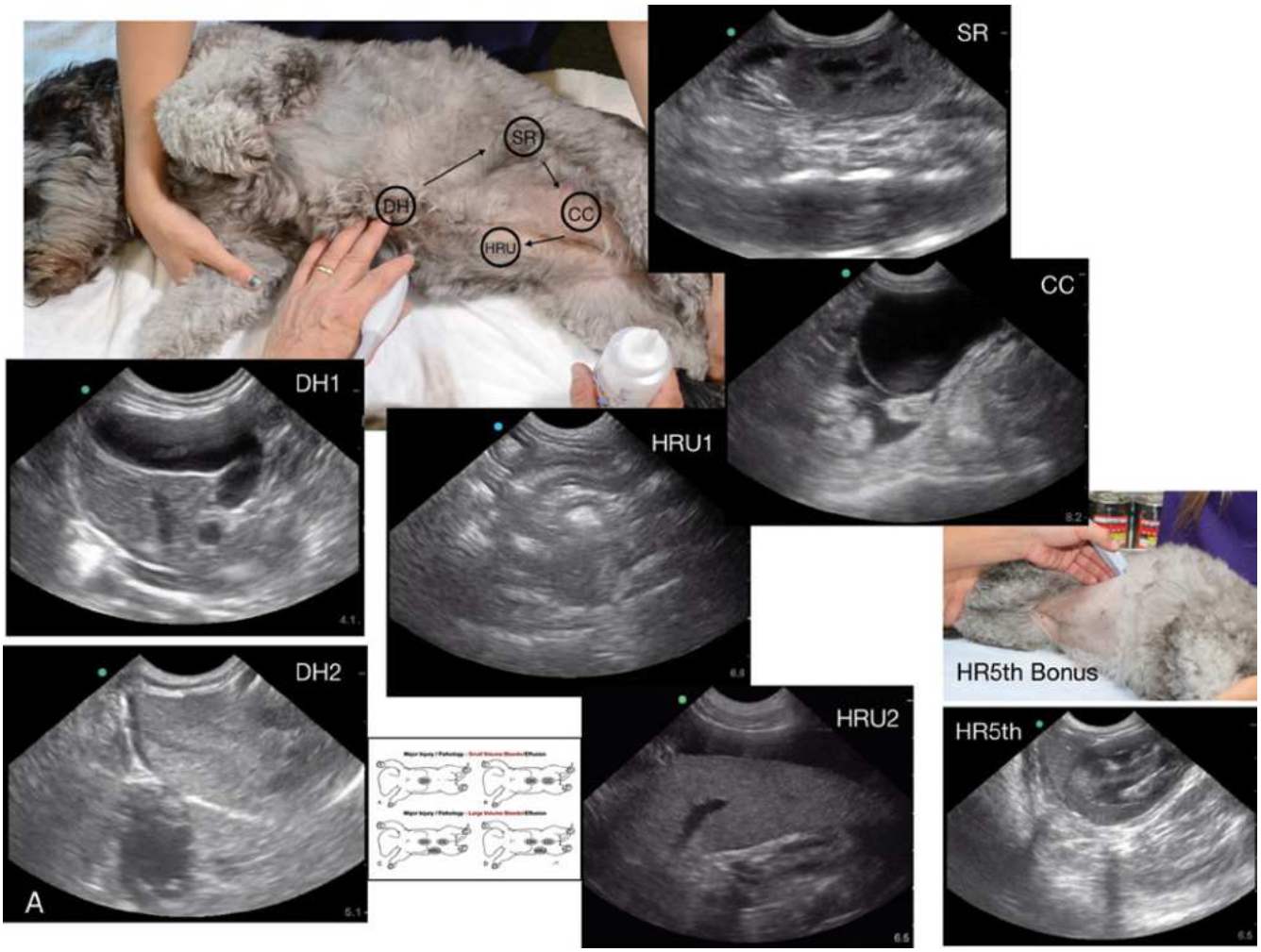


**Figure 6.2.** AFAST and its five views performed in right lateral recumbency in a dog. (A) AFAST unlabeled and (B) AFAST labeled. The order is always the same as follows: DH to SR to CC to HRU to HR5th bonus view. The final HR5th bonus view is *not* part of the abdominal fluid score. The AFAST images and their proportionality should look nearly the same regardless of positioning. DH, diaphragmatico-hepatic view; DH1, DH 1 of 2 views; DH2, DH 2 of 2 views; SR, spleno-renal view; CC, cystocolic view; HRU, hepato-renal umbilical view; HR5th, hepato-renal 5th bonus view; HRU1, 1 of 2 views; HRU2, 2 of 2 views. DIA, diaphragm; FF, free fluid; GB, gallbladder; LIV, liver; LK, left kidney; RK, right kidney; SI, small intestine. AFAST views are nearly identical no matter the positioning because the respective target organs are imaged with the same methodology. Source: Reproduced with permission of Dr Gregory Lisciandro, Hill Country Veterinary Specialists and FASTVet.com, Spicewood. TX. Illustration by Hannah M. Cole, Adkins, TX.

**Figure 6.2.** (*Continued*)

bias, as we could argue the same in RL recumbency (Lisciandro 2014a,b), and moreover, TFAST echo views are more easily acquired in RL recumbency. When combining AFAST and TFAST, RL recumbency is clearly advantageous. AFAST on a cat is shown in Chapter 39. See Chapters 17, 19, and 20 for echo views.

### Modified Lateral-Sternal

Modified lateral-sternal recumbency positioning may be used for AFAST in stressed patients by allowing the forelegs to be in sternal and moving the hindlegs together laterally (placed same side as the sonographer) (Figure 6.4). In the modified lateral-sternal positioning the AFS may be estimated because the patient isn't purely in a lateral recumbent position.

### Standing/Sternal

In respiratory-compromised patients AFAST is performed in standing or sternal knowing that the fluid scoring system is not validated in this positioning but still provides clinical information regarding the presence or absence of effusion. Whatever the AFAST options for positioning (lateral, modified lateral-sternal, standing/sternal), a negative AFS negates the need for moving the patient to lateral recumbency. Serial exams are always mandated as standard of care for a second opportunity to detect negative AFAST changing to positive, and for rescoring the patient (Lisciandro et al. 2009; Lisciandro 2011, 2014a; Boysen and Lisciandro 2013). See Chapters 36 and 37 for the most efficient ways to perform AFAST in standing-sternal positioning.

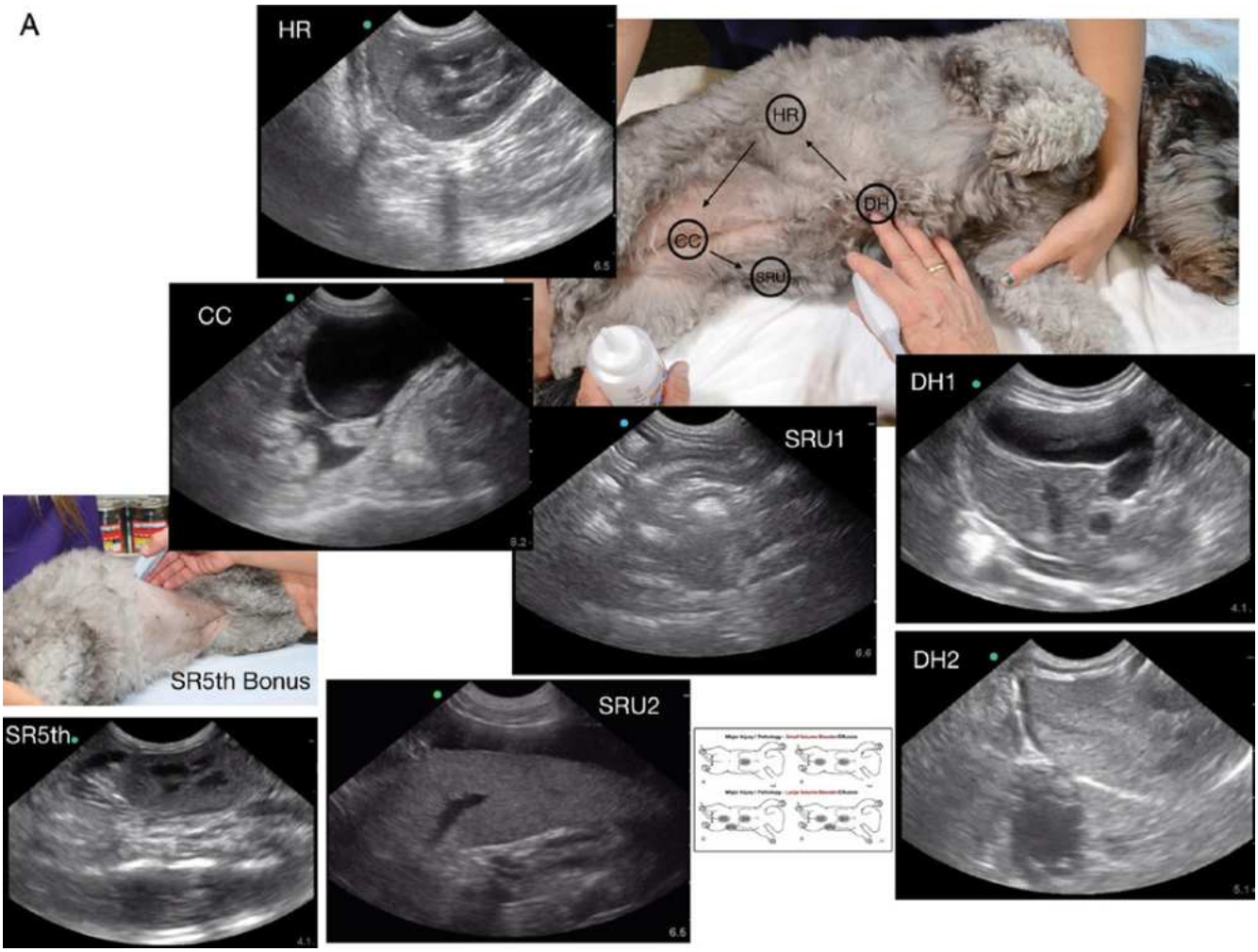


**Figure 6.3.** AFAST and its five views performed in left lateral recumbency in a dog. Shown is AFAST unlabeled in left lateral recumbency with the same images as Figure 6.2A and B. The order is analogous and always the same as follows: DH to HR to CC to SRU to SR5th bonus view. The final SR5th bonus view is *not* part of the abdominal fluid score. DH, diaphragmatico-hepatic view; DH1, DH 1 of 2 views; DH2, DH 2 of 2 views; SR, spleno-renal view; CC, cysto-colic view; HRU, hepato-renal umbilical view; HR5th, hepato-renal 5th bonus view; HRU1, 1 of 2 views; HRU2, 2 of 2 views. DIA, diaphragm; FF, free fluid; GB, gallbladder; LIV, liver; LK, left kidney; RK, right kidney; SI, small intestine. Note that the images should look identical for each AFAST view regardless of positioning (including standing/sternal, modified sternal). AFAST views are nearly identical no matter the positioning because the respective target organs are imaged with the same methodology. Source: Reproduced with permission of Dr Gregory Lisciandro, Hill Country Veterinary Specialists and FASTVet.com, Spicewood, TX. Illustration by Hannah M. Cole, Adkins, TX.

### *Considerations When Performing AFAST in Standing or Sternal Positioning*

If AFAST is negative in standing or sternal positioning, then moving the patient to lateral recumbency is unnecessary. However, if the AFAST examination is positive in standing or sternal, then move the patient to lateral recumbency (if unstable, delay until more stable) and wait for three minutes for fluid to settle before assigning an AFS (Lisciandro et al. 2009; Lisciandro 2011; Boysen and Lisciandro 2013).

When performing AFAST in standing or sternal, the sonographer must keep in mind the following points.

- As long as the AFAST is negative and the target organs are imaged at each respective view, the AFAST is complete.
- When free intraabdominal fluid is present, it will pool in different regions relative to the target organs because gravity-dependent locations differ from lateral recumbency, being at the probe head,

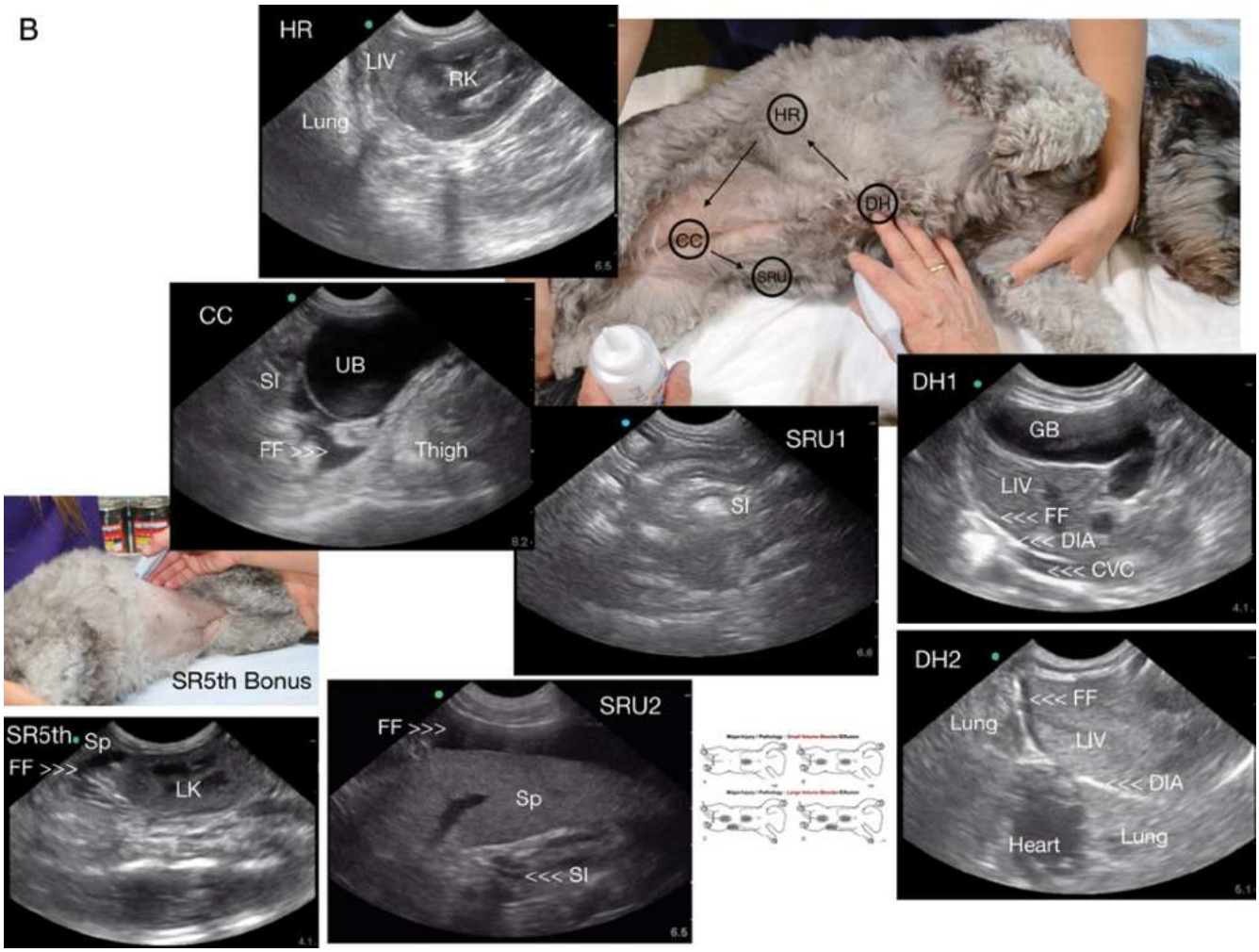


**Figure 6.3.** (*Continued*)

in the near-field, for the DH, CC, and SR/HR umbilical views.

- The gravity-dependent regions within the lumen of the gallbladder and urinary bladder also differ from lateral recumbency and the sonographer must consider the direction of the beam (its scanning plane) to best detect and interpret findings.
- The AFAST views, when performed properly, should look nearly the same *independent of positioning*.

Dorsal recumbency should never be used for AFAST (TFAST and Vet BLUE) for several reasons but most importantly because of increasing patient risk (Figure 6.5). A hemodynamically fragile patient placed in dorsal recumbency undergoes significant negative changes in ventilation and circulation, specifically venous return. Add to these respiratory and cardiovascular stresses and the increased oxygen demand in a struggling, anxious patient, and the patient risks acute and potentially catastrophic decompensation. Considering trauma, most dogs and cats have concurrent lung contusions and other thoracic-related injuries (Powell et al. 1999; Sigrist et al. 2011; Lisciandro et al. 2008) and intraabdominal bleeding (Boysen et al. 2004; Lisciandro et al. 2009). Considering nontrauma, many hypotensive triaged patients have pleural and/or pericardial effusion, and intracavitary bleeds often accompanied by anemia (McMurray et al. 2016; Lisciandro 2016a,b). Moreover, the AFS system is not validated in dorsal recumbency and only subjective terms of mild, moderate, and severe can be used (Stander et al. 2010; Sutherland-Smith et al. 2006). For clinicians who prefer performing complete detailed abdominal ultrasound in dorsal recumbency,

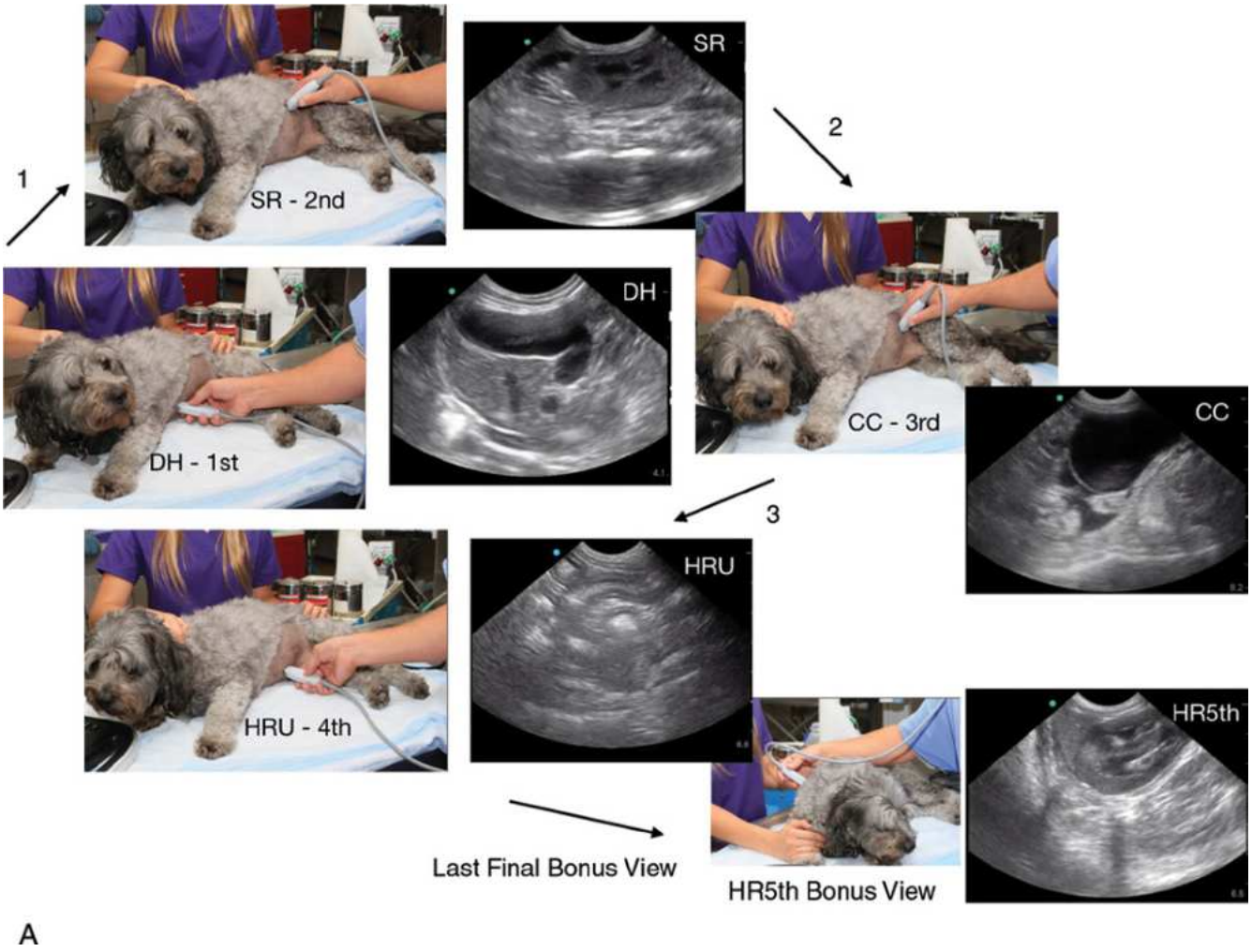


**Figure 6.4.** Modified lateral-sternal recumbency. The AFAST views are performed in the same order every time as follows: DH to SR to CC to HRU to HR5th bonus view. The final HR5th bonus view is *not* part of the abdominal fluid score.DH, diaphragmatico-hepatic view; SR, spleno-renal view; CC, cysto-colic view; HRU, hepato-renal umbilical view; HR5th, hepato-renal 5th bonus view. Note that the images should look identical for each AFAST view regardless of positioning (including standing/sternal, modified sternal). AFAST views are nearly identical no matter the positioning because the respective target organs are imaged with the same methodology. Source: Reproduced with permission of Dr Gregory Lisciandro, Hill Country Veterinary Specialists and FASTVet.com, Spicewood, TX.

perform a Global FAST *first* before moving the patient to the restraint of dorsal recumbency to best ensure patient safety.

## Naming and Order of the AFAST Views

The AFAST sites in the preferred positioning of right lateral recumbency (over left) are named according to target organs at each acoustic window and performed in clockwise order as follows: (1) DH view, (2) SR view, (3) CC view, and (4) HR umbilical (HRU) view that completes the AFAST examination and is a favorable site for abdominocentesis, being most gravity dependent (Lisciandro et al. 2009; Lisciandro 2011; Boysen and Lisciandro 2013; McMurray et al. 2016). AFAST views are shown translated onto an abdominal radiograph and CT study in Figure 6.6. The final view is the HR5th bonus view to image the right kidney and nearby liver that is not part of the AFS; the HR5th bonus view is generally performed as the final view after AFAST, TFAST, and Vet BLUE have been completed.

In LL recumbency the order is as follows: (1) DH view, (2) HR view, (3) CC view, and (4) the SR umbilical

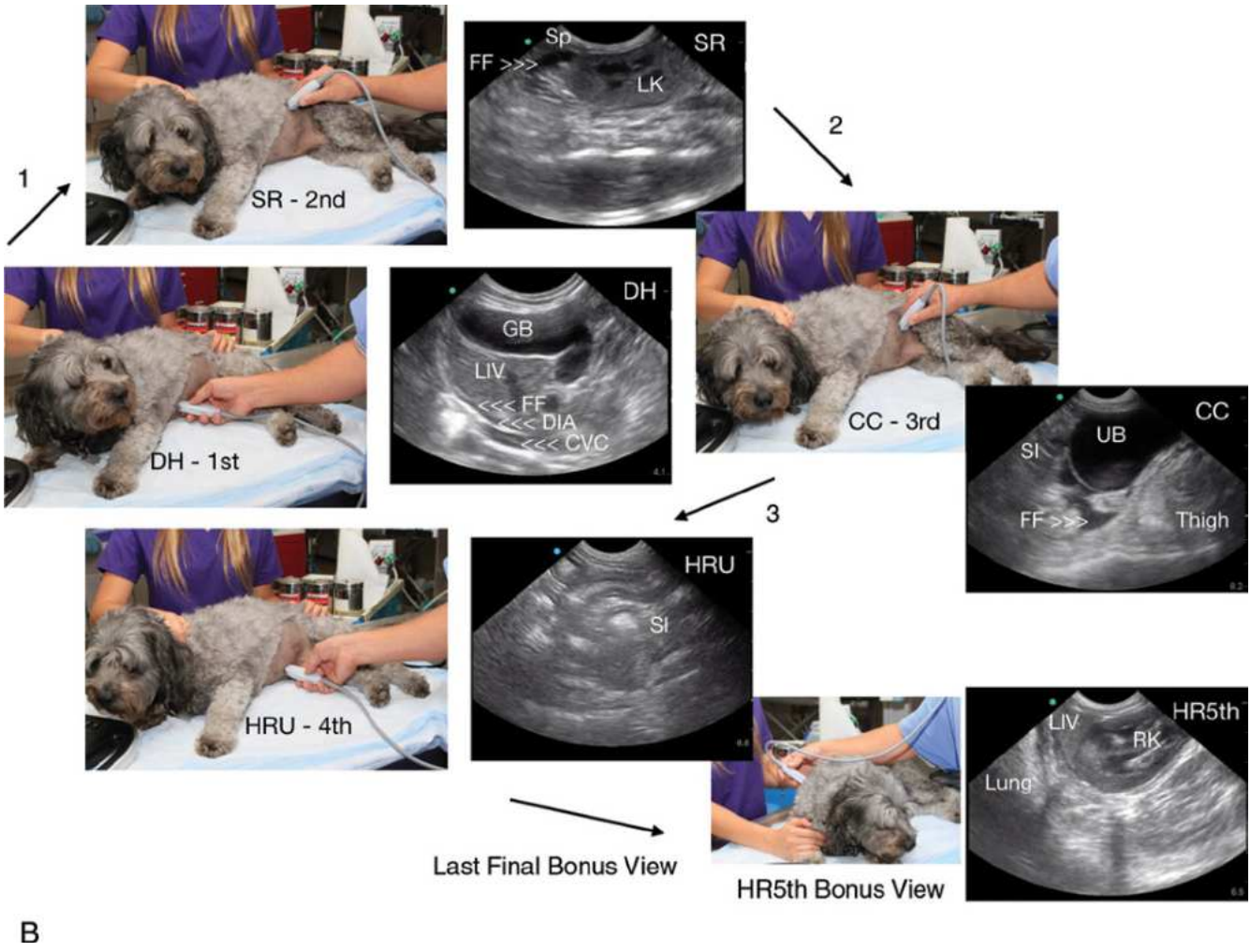


**Figure 6.4.** (*Continued*)

(SRU) view that completes the AFAST examination and is a favorable site for abdominocentesis, being most gravity dependent (see Figure 6.3). Positioning of the cat is shown in Chapter 39. The final view is the SR5th bonus view to image the left kidney and spleen and is not part of the AFS; the SR5th bonus view is generally performed as the final view after AFAST, TFAST, and Vet BLUE have been completed (Lisciandro et al. 2009; Lisciandro 2011; Boysen and Lisciandro 2013; McMurray et al. 2016).

In summary, the four primary AFAST views are part of the AFS system. The AFAST 5th bonus view (HR5th and SR5th views depending on which lateral recumbency is being used) is not part of the AFAST AFS system, but important for acquiring information for that respective retroperitoneal space and any obvious soft tissue or parenchymal abnormalities of the kidney and its adjacent liver and spleen dependent on positioning. In cats and smaller dogs when using enough depth, both kidneys are often seen through the SR (or HR) view (Lisciandro et al. 2009; Lisciandro 2011, 2012, 2014a; McMurray et al. 2016) (see Figure 6.21).

**Pearl:** By imaging using the AFAST target organ approach, sonographic anatomy is better recognized, and the sonographer is building POCUS skills on every AFAST exam, with the only pressure being the recognition of free fluid.

## Probe Maneuvering is Standardized

All AFAST acoustic views are imaged in longitudinal (sagittal) orientation with the marker of the probe always directed toward the head of the patient; with

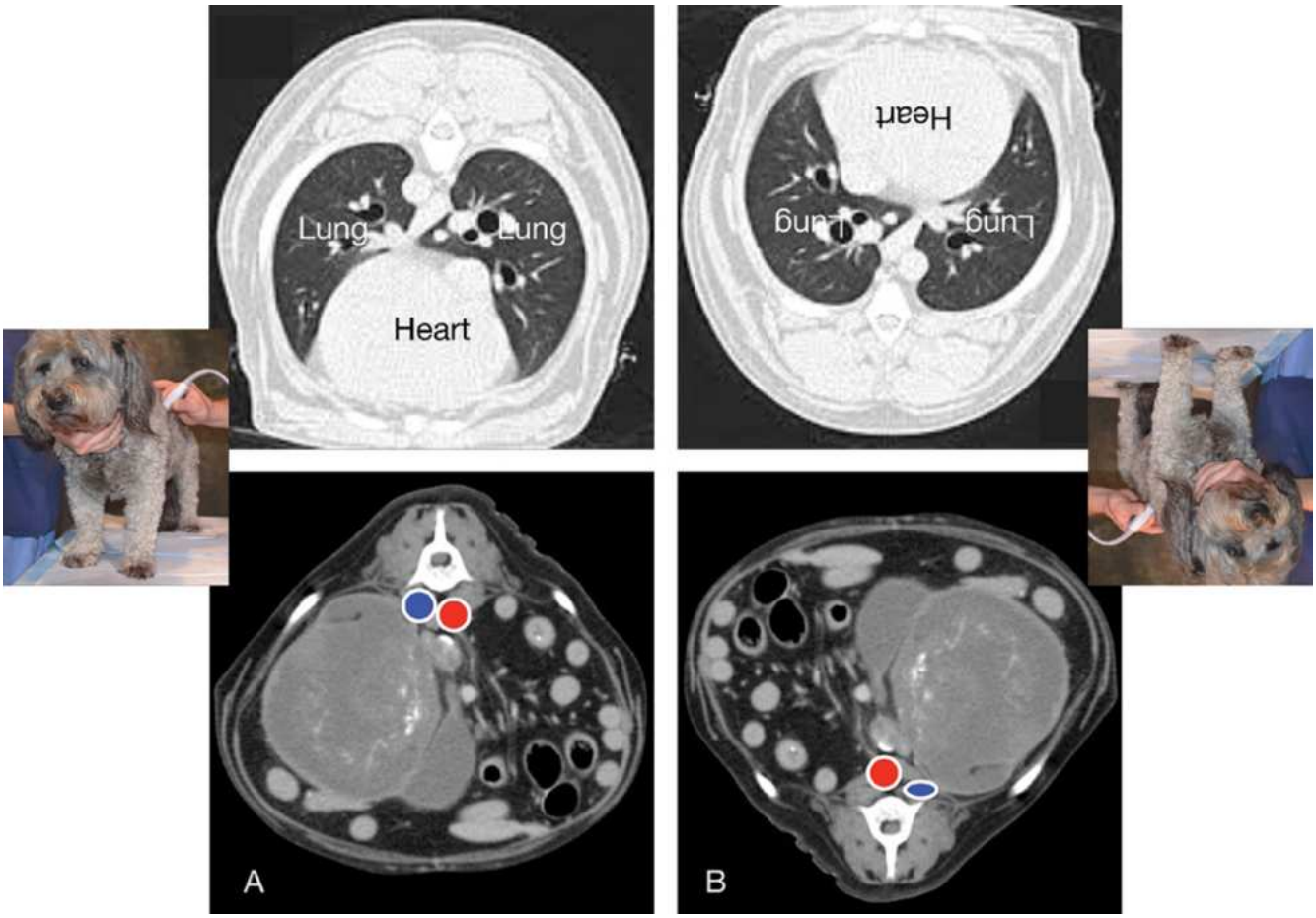


**Figure 6.5.** Never use dorsal recumbency without doing a Global FAST to assess stability. The use of dorsal recumbency on a hemodynamically fragile or unstable patient is potentially catastrophic. In (A) the computed tomography (CT) of a cross-section of the thorax and abdomen is is compared to (B) in dorsal recumbency. Ventilation is changed from (A) to (B) by moving the most aerated, least perfused, least gravity-dependent lung fields to a ventral and gravity-dependent location. Moreover, the weight of the abdominal organs against the diaphragm further adversely affects ventilation. Venous return to the heart is also markedly changed from (A) to (B) in which the CVC (*blue circle*) next to the aorta (*red circle*) becomes compressed in dorsal recumbency from the weight of the abdominal organs. In hemodynamically fragile patients, there is real risk for decompensation. Source: Reproduced with permission of Dr Gregory Lisciandro, Hill Country Veterinary Specialists and FASTVet.com, Spicewood, TX.

muscle memory, most sonographers quickly learn this repetitive probe motion. In longitudinal (sagittal) orientation target organs are more recognizable than in transverse orientation, especially for the nonradiologist sonographer (Figure 6.7). The single longitudinal (sagittal) orientation is supported by the original veterinary FAST study in which when longitudinal (sagittal) and transverse orientation were compared, they matched in 397 out of 400 views (Boysen et al. 2004). In time, rotating the probe to transverse orientation may be considered as part of each AFAST view as an add-on skill but is unnecessary.

Every AFAST view is a "fan, rock cranially, and return to your starting position" of the probe by fanning through the target organ, rocking cranially, and then returning to your starting point (see Figures 6.2, 6.3, and 6.4).

- *DH view*: Fan through the gallbladder in both directions until the gallbladder disappears in both directions, and then rock cranially to image the "cardiac bump" before returning to your starting point for one final look within the abdominal cavity.
- *SR view*: Fan through the left kidney in both directions until the left kidney disappears in both

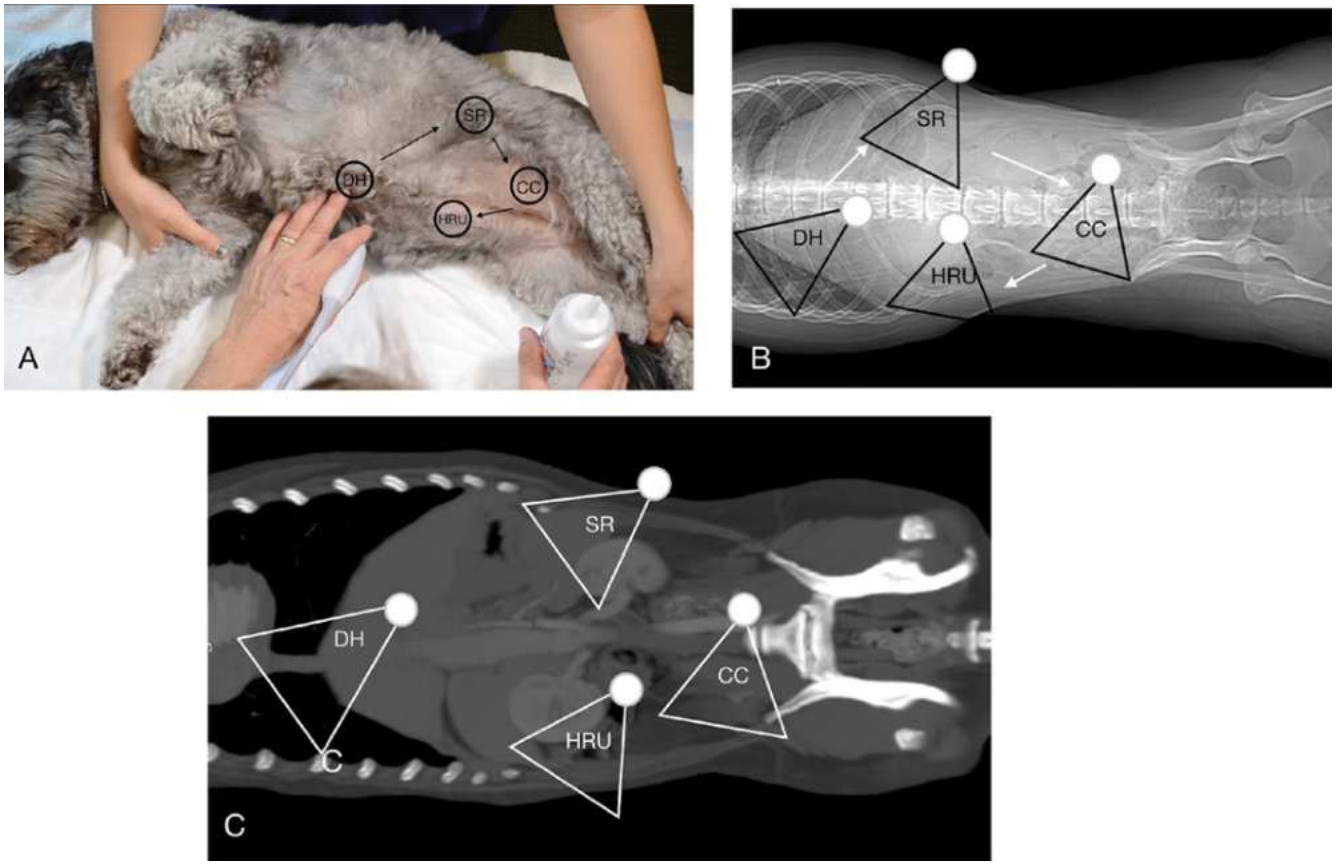


**Figure 6.6.** Correlation of AFAST acoustic windows with a dog in right lateral recumbency to an abdominal radiograph and CT. Sites are named by their target organs. In (A) the AFAST acoustic windows are labeled and correlate in (B) to a radiograph and (C) to computed tomography. The AFAST order is always the same: DH to SR to CC to HRU view. Note that the head is always to the left and tail to the right in both ultrasound and radiography. Computed tomography and radiograph courtesy of Dr Daniel Rodriguez, VETTEM, and Dr Jesús Paredes, CVM, Mexico City, Mexico. Source: Reproduced with permission of Dr Gregory Lisciandro, Hill Country Veterinary Specialists and FASTVet.com, Spicewood, TX.

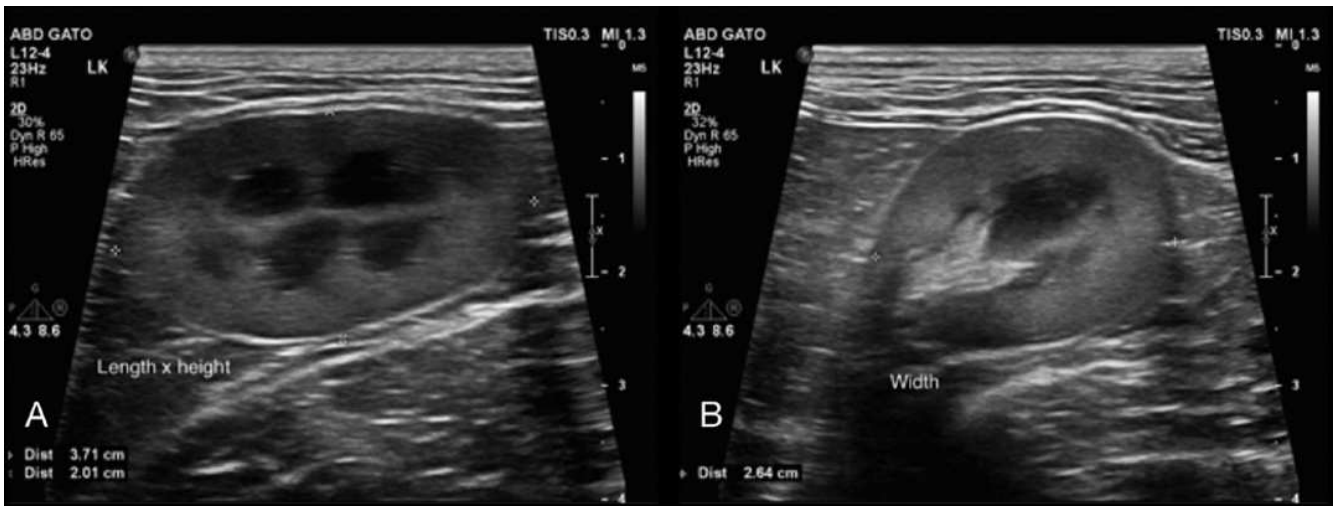


**Figure 6.7.** Longitudinal orientation for AFAST. (A) Kidney in longitudinal orientation, standard for all the AFAST views, because organs are more readily apparent in longitudinal over transverse scanning planes for most nonradiologist sonographers. (B) The same kidney as in (A) but in transverse orientation. The author keeps it simple – "fan (longitudinal planes), rock (direct the scanning plane cranial) and return to your starting point" is the AFAST mantra. Transverse orientation should be considered as an add-on AFAST skill but is unnecessary for the detection of free intraabdominal fluid (Boysen et al. 2004). Computed tomography courtesy of Dr Daniel Rodriguez, VETTEM, Mexico City, Mexico. Source: Reproduced with permission of Dr Gregory Lisciandro, Hill Country Veterinary Specialists and FASTVet.com, Spicewood, TX.

directions, and then rock cranially to image the head of the spleen (fan on it too) before returning to your starting point of the left kidney for one final look. The kidney is *retroperitoneal* and the spleen *peritoneal*. The head of the spleen is reliably imaged in both dogs and cats.

- *CC view*: Fan through the urinary bladder in both directions until the bladder disappears in both directions, and then rock cranially to image the "CC pouch", its most gravity-dependent region, and back to your starting point for one final look.
- *HRU view* (right lateral recumbency): Fan through the small bowel and spleen in both directions and then rock cranially to image the cranial abdominal region before returning to the "HRU pouch", its most gravity-dependent region, for one final look. The left kidney may be viewed with increased depth through a single HR view, especially in cats and smaller dogs (Lisciandro 2014a; McMurray et al. 2016).
- *SRU view* (left lateral recumbency): Fan through the small bowel and spleen in both directions and then rock cranially to image the cranial abdominal region before returning to the "SRU pouch", its most gravity-dependent region, for one final look. The right kidney may be viewed with increased depth through a single SR view, especially in cats and smaller dogs (Lisciandro 2014a).
- *HR5th bonus view* (right lateral recumbency): Fan through the right kidney in both directions until the right kidney disappears in both directions and then rock cranially to image the right liver lobes before returning to your starting point of the right kidney for one final look. This view is generally unnecessary if the right kidney is imaged through the SR view.
- *SR5th bonus view* (left lateral recumbency): Fan through the left kidney in both directions until the left kidney disappears in both directions and then rock cranially to image the spleen before returning to your starting point of the left kidney for one final look. This view is generally unnecessary if the left kidney is imaged through the HR view.

**Pearl:** For both those learning AFAST and experienced AFAST sonographers, only longitudinal (sagittal) orientation is necessary for the detection of free fluid at each view, with this standardization accelerating the learning process by building consistent sonographic expectations of the AFAST target organs. In time, transverse orientation may become an add-on skill but it is unnecessary.

# AFAST Diaphragmatico-Hepatic View

| Questions Asked at the DH View | |
|---|---|
| Is there any free fluid in the abdominal (peritoneal) cavity? | Yes or no |
| How much free fluid is at the DH view using the AFAST AFS system? | 0, 1/2, 1 |
| Is there any pericardial effusion? | Yes or no |
| Subjective amount? | Small (<1 cm), moderate (1–2 cm), large (>2 cm) (Candotti and Arntfield 2015)[a]<br>Must be placed into clinical context |
| Is there any pleural effusion? | Yes or no |
| Subjective amount? | Trivial, mild, moderate, severe |
| What does the pulmonary-diaphragmatic surface look like? | Unremarkable (dry lung) or abnormal |
| Are there any lung lesions along the diaphragm? | B-lines and Vet BLUE B-line scoring, shred sign, tissue sign, nodule sign, wedge sign |
| What does the gallbladder look like? | Unremarkable, halo sign (sonographic striation), abnormalities in its lumen or wall |
| What does the liver look like? | Unremarkable or abnormal |
| What do the caudal vena cava and its associated hepatic veins look like? | Unremarkable (bounce) or abnormal (FAT, flat): see Tables 7.6 and 36.3 and Figures 36.8 and 36.9 |
| Could I be mistaking an artifact or pitfall for pathology? | Know pitfalls and artifacts |

[a]The AFAST target organ approach for parenchymal abnormalities is binary using "unremarkable" or "abnormal" to capture the case for additional imaging and confirmatory testing. Over time, more interpretative skills may be gained through experience and accompanied by additional POCUS study and training.
Source: Reproduced with permission of Dr Gregory Lisciandro, Hill Country Veterinary Specialists and FASTVet.com, Spicewood, Texas.

The classic AFAST DH view is in fact part of AFAST, TFAST, and Vet BLUE because it provides a huge amount of clinical information, including structures within both the peritoneal and pleural cavities.

The DH view begins with longitudinal placement of the probe with the probe marker towards the patient's head immediately caudal to the xiphoid process.

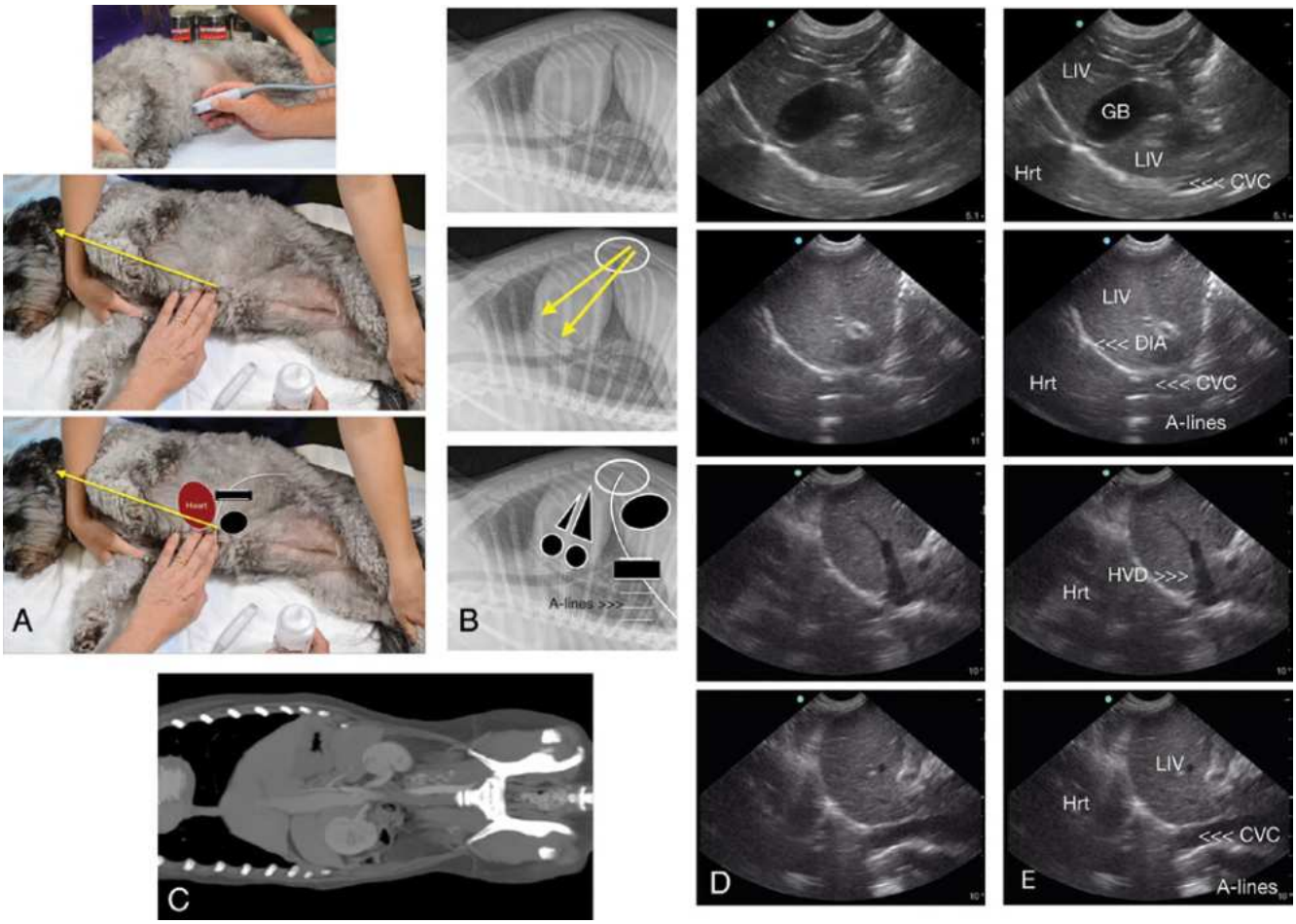


**Figure 6.8.** The DH view in a dog. In (A) is shown where the probe is placed immediately caudal to the xiphoid (*top image*) and directed cranial (*arrow*) in middle and bottom images with overlay of heart, diaphragm (*curved white line*), gallbladder (*black oval*), CVC (*black rectangle with white line as near wall and longer white line as far wall*). In (B) inverted correlating lateral thoracic radiographs in the top image, unlabeled, the middle image having arrows for direction of the ultrasound beam (scanning plane), white circle for probe placement, and bottom image with overlay of structures including the gallbladder, diaphragm, CVC, including A-lines beyond its far wall through the far-field from aerated (dry) lung, and the heart with ventricles as triangles and atria as circles. In (C) is CT for another correlation of the anatomy of the DH View. (D) and (E) are unlabeled and labeled ultrasound images of the DH view's anatomical features. Note the *consistency* of where the diaphragm is located in each of the ultrasound images. CVC, caudal vena cava; DIA, diaphragm; GB, gallbladder; Hrt, heart; HVD, hepatic venous distension; LIV, liver. Computed tomography courtesy of Dr Daniel Rodriguez, VETTEM, and Dr Jesús Paredes, CVM, Mexico City, Mexico. Source: Reproduced with permission of Dr Gregory Lisciandro, Hill Country Veterinary Specialists and FASTVet.com, Spicewood, TX.

The probe is then directed far more cranially than most sonographers expect (Figure 6.8). Depth should be adjusted so that the diaphragm courses through the distal two-thirds of the image on the screen so that the near-field is two-thirds abdomen and the far-field one-third thorax. This allows for adequate screening of both the abdomen and thorax.

The gallbladder, if not in view, is found by fanning toward the table top (when in right lateral recumbency) because of its location right of the midline in dogs and cats (further right in cats). In normalcy, the canine gallbladder is easy to find because it is generally much closer to midline than the more laterally located feline gallbladder (see Chapter 39).

The mantra for the DH view is to have a general overview of three structures – the gallbladder, "cardiac bump", and caudal vena cava – before starting the fanning, rocking, and returning. Start with a depth of 7–8 cm for cats and small dogs to 10–15 cm for medium to large dogs and then decrease depth as indicated.

Once the gallbladder is in view, then in a sequential way specifically interrogate the following.

- The abdominal cavity for free fluid by fanning through the gallbladder and adjacent liver in both directions, followed by…
- Rocking the probe toward the sternum to best image the "cardiac bump" where the muscular apex of the heart is very near or immediately against the diaphragm for pericardial effusion, and then…
- Imaging along the diaphragm for pleural effusion, and lung pathology along the pulmonary–diaphragmatic interface.

In this same plane or close by, and making sure that the probe is immediately against the xiphoid, look for the CVC as it traverses the diaphragm present in both canines and felines. The CVC is recognized by the two bright white (hyperechoic) bars that make up the near wall (short bar) and far wall (long bar) with reverberation artifact (A-lines) extending through the far-field dependent on depth and the presence of dry lung in that patient.

The steps taken during the AFAST DH view are as follows.

- The gallbladder wall and its shape should be noted and the gain adjusted based on the echogenicity of its luminal contents. In normalcy, the homogeneous anechoic (black) echogenicity of bile should approximate what would be expected for most types of free fluid.
- In dogs, the gallbladder reliably lies immediately against the diaphragm when positioned in right lateral recumbency; however, the gallbladder–diaphragm proximity is much less reliable in cats.
- When the canine gallbladder does not lie immediately against the diaphragm, liver enlargement should be suspected, and when the gallbladder is not located, the rule-out list placed into clinical context should include its rupture, its displacement (diaphragmatic herniation), or the presence of gallbladder stones, mineralization, sludge, mucoceles, and emphysematous cholecystitis.
- Once the gallbladder is recognized, fanning takes place by directing the probe away from the tabletop to the patient's left, and then by fanning toward the tabletop toward the patient's right, interrogating the adjacent liver. The feline gallbladder and biliary tract differ from dogs (see Figures 8.4 and 39.4, and Chapters 8 and 39).
- By doing so, the liver and abdominal cavity are interrogated for obvious free fluid between liver lobes and between the liver and diaphragm, and the gallbladder and liver are screened for any obvious abnormalities or sonographic deviations from normal (Figures 6.9 and 6.10).

**Pearl:** To perform the DH view consistently and effectively, while fanning through the gallbladder and liver, maintain the diaphragm in the distal two-thirds of the field of view.

**Pearl:** In low-scoring benign and pathological small-volume effusions, our research has shown the DH view as most commonly positive. These small-volume effusions are detected between the liver and diaphragm as an anechoic stripe, and between liver lobes and within the "CC pouch" as anechoic triangulations (Lisciandro et al. 2009, 2015, 2019; Hnatusko et al. 2019).

After interrogating the abdominal cavity, return to the starting point of the DH view. The probe is then rocked toward the patient's sternum, remaining on a strict longitudinal plane searching for the "cardiac bump," the reverberation of the beating heart against the diaphragm (Figure 6.11). The "cardiac bump" is used to diagnose pericardial effusion and rounded effusion, and as a single view, the "racetrack sign" (see Chapters 7, 18 and 21).

Then use the DH view as an acoustic window via the liver and gallbladder into the thorax to interrogate the pleural cavity for the presence or absence of pleural effusion, anechoic triangulated effusion, and lung along the pulmonary–diaphragmatic interface (see Chapters 7, 18, and 21).

**Pearl and Pitfall:** The "cardiac bump" is reliably imaged in dogs, but less reliable in cats because of more interposing feline lung in between the heart and diaphragm. However, most clinically relevant pericardial effusion is detected in both dogs and cats at the DH view (Lisciandro 2016a) (see Figure 6.11 and Chapter 39). Pneumothorax in either species is another reason for the inability to view the "cardiac bump."

Always look cranially past the diaphragm into your patient's thorax for pericardial effusion, pleural effusion, and deep lung pathology along the

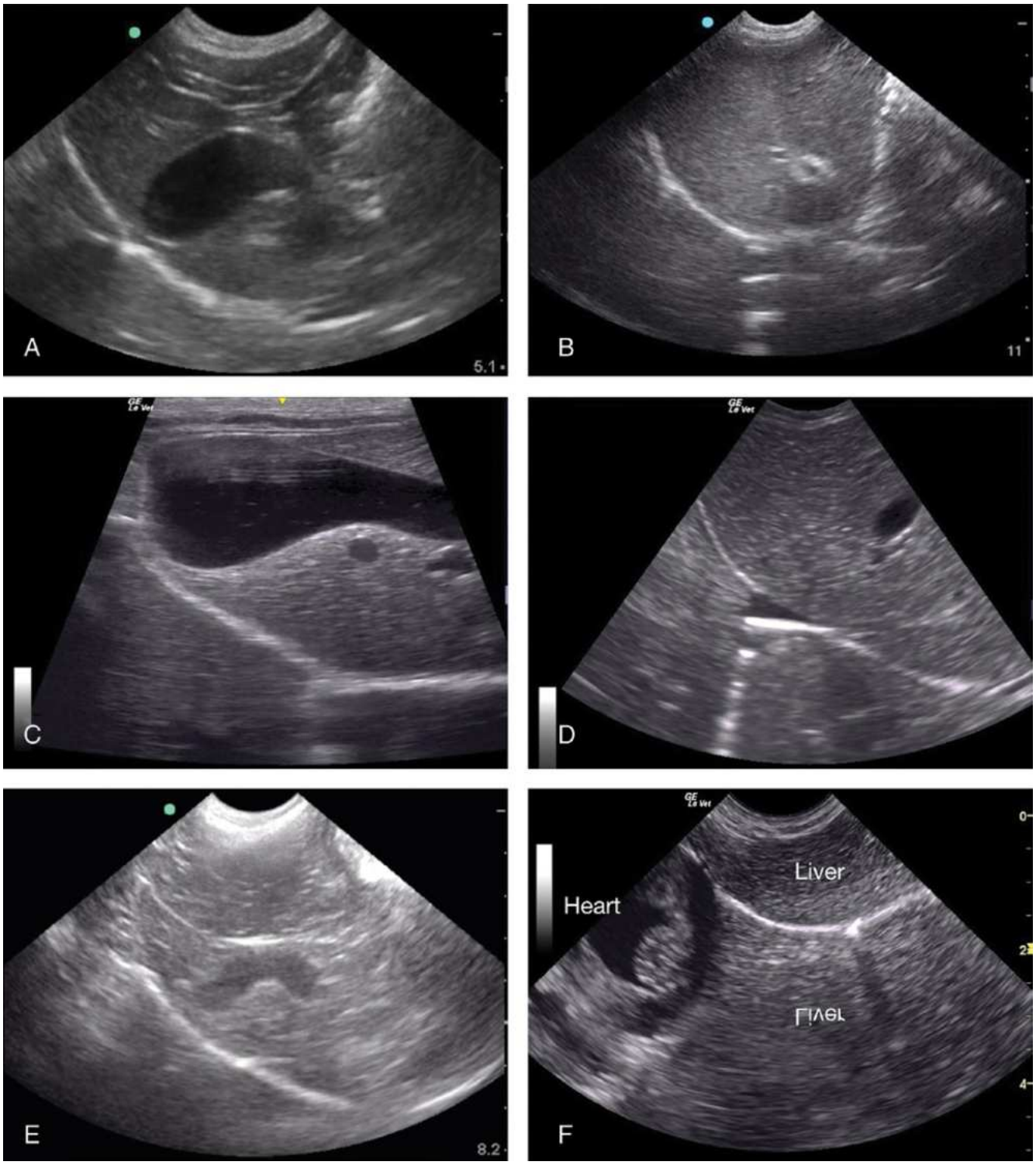


**Figure 6.9.** Images showing various anatomic features at the DH view. None of these images are positive for free fluid and only (F) is labeled. Compare these images to those labeled in Figure 6.8. In (A) the gallbladder is expected to be in close proximity to the diaphragm. Note the mirror image of the gallbladder into the thorax. In (B) the caudal vena cava is seen in the far-field as two hyperechoic bars, one as its near wall and the other as its far wall (see Figure 6.11 and Chapters 7, 26 and 36 for greater CVC detail). In (C) another image of the canine gallbladder is shown in close proximity to the diaphragm. (D) shows an anechoic triangulation formed by the CVC as it traverses the diaphragm that should not be mistaken for free fluid. A-lines are seen past the CVC's far wall due to the dry lung against the CVC. In (E) the gallbladder appears bilobed in the cat and in the near-field is robust falciform fat (see Chapter 39 for more detail). In (F) with the probe directed near parallel to the sternum, the heart ("Heart") and its left ventricle are clearly in view and may be interrogated. The liver appears homogeneous as expected and is labeled "Liver" with it mirrored on the other side of the diaphragm due to mirror image artifact common at the DH View. Note how consistent the diaphragm is within the images as a landmark for proper DH view image acquisition. Source: Reproduced with permission of Dr Gregory Lisciandro, Hill Country Veterinary Specialists and FASTVet.com, Spicewood, TX.

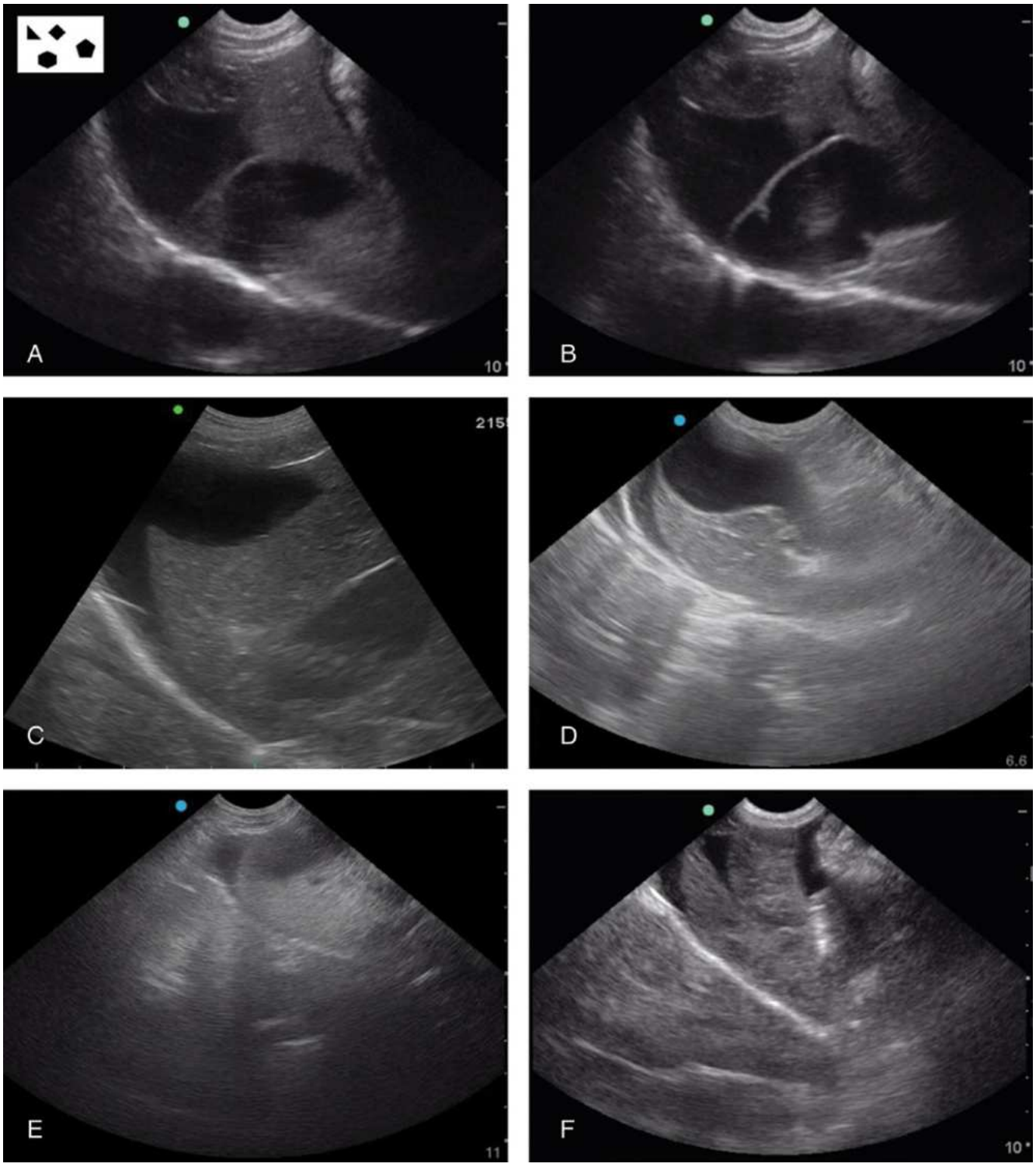


**Figure 6.10.** Variety of typical positive studies at the DH view. In (A) free fluid is apparent in the near-field to the gallbladder. In (B) similarly free fluid is in the near-field to the gallbladder. In (C) free fluid separates the liver from the diaphragm. In (D) there is a smaller abdominal effusion present separating the liver from the diaphragm. In (E) the same type of positive as in (D) is shown but with an even smaller volume. Note the probe is rocked cranial enough to get the diaphragm at the xiphoid, which is good practice for the DH view. In (F) the liver lobes are separated from one another due to the abdominal effusion. Note how consistent the diaphragm is within the images as a landmark for proper DH view image acquisition. Source: Reproduced with permission of Dr Gregory Lisciandro, Hill Country Veterinary Specialists and FASTVet.com, Spicewood, TX.

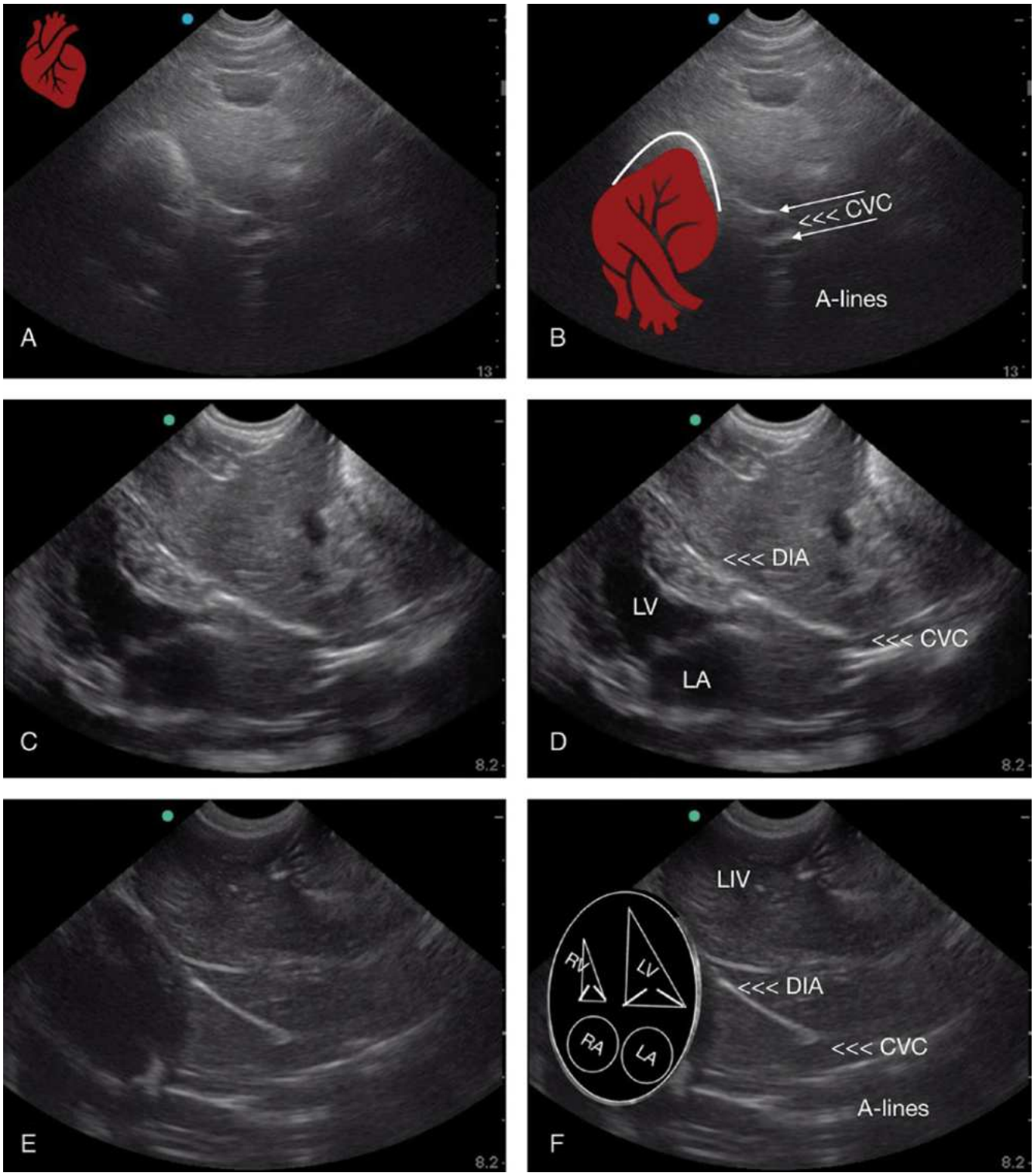


**Figure 6.11.** The "cardiac bump" at the DH view. In (A) the apex of the heart is indenting the diaphragm and in real time can be seen clearly beating against the diaphragm. In (B) a heart is superimposed to give a better idea of orientation. The arrows point out the near and far wall of the caudal vena cava (CVC). In (C) the heart is unlabeled with the left ventricle and left atrium both in view as well as the mitral valves with the same image labeled in (D) and the heart is positioned similar to the pictorial of the heart in (F). This cardiac orientation is really important to learn because the heart is generally more sonographically accessible than transthoracic TFAST pericardial site views and its echo views in respiratory distressed patients. In (E) is the unlabeled heart against the diaphragm and labeled with the addition of an overlay of the cardiac orientation in (F). Note how consistent the placement of the diaphragm is within the images as a landmark for proper DH view image acquisition. CVC, caudal vena cava; DIA, diaphragm; LA, left atrium; LIV, liver; LV, left ventricle; RA, right atrium; RV, right ventricle. Source: Reproduced with permission of Dr Gregory Lisciandro, Hill Country Veterinary Specialists and FASTVet.com, Spicewood, TX.

diaphragmatic–pulmonary interface (see Chapters 18, 22, and 23) and use TFAST pericardial site views and Vet BLUE to confirm, refute and support findings at the FAST DH view.

Following interrogation of the pleural cavity, pericardial sac, and lung along the diaphragmatic–pulmonary interface, along the same longitudinal plane of the "cardiac bump," look for the CVC, making sure depth is adequate as the CVC is the deepest structure at the DH view (Figure 6.12).

If the CVC is not seen, look for it while you rock slowly back to your starting point, making sure you are on a longitudinal plane on midline and immediately caudal to the xiphoid.

The CVC is reliably imaged with experience and should be characterized where it traverses the diaphragm, searching for the small white line in the near-field and the longer white line in the far-field paralleling one another and representing the near and far walls of the CVC, respectively. The lines that extend beyond the CVC's far wall are in fact A-lines created when aerated (dry) lung (most common) is immediately against the far wall or possibly in the presence of pneumothorax (far less common) (see Figure 6.12).

**Pearl:** Excessive probe pressure caused by pushing the probe into the patient's abdomen can distort the CVC, resulting in its flattening and false assessment (Darnis et al. 2018).

## Typical DH Positives

The classic intraabdominal positives at the DH view are usually seen while fanning away from the tabletop in the following locations: the near-field to the gallbladder, between the divisions of the liver lobes, between the liver and the diaphragm, and between the liver lobes and the falciform ligament and fat. In the near-field, the falciform ligament and fat, which can be robust even in thin cats, are typically hyperechoic (bright) in the near-field, having a coarser, brighter echotexture (hyperechoic) relative to the liver (see Figure 6.10 and Chapter 39).

The most common AFAST positive views in low-scoring AFS 1 and AFS 2 bluntly traumatized dogs and cats, clinically normal adult dogs and cats, and juvenile puppies and kittens are the nongravity-dependent DH and CC views over the most gravity-dependent HRU and SRU views (Lisciandro et al. 2009, 2015, 2019). Moreover, the umbilical HRU and SRU views are rarely the only positive view(s) among different subsets of dogs and cats (Lisciandro et al. 2009, 2015, 2019; Romero et al. 2015). Thus, pay special attention to the presence of anechoic triangles (free fluid) while fanning through liver lobes (see Figure 6.10).

## Artifacts and Pitfalls of the DH View

The DH View has many, if not all, the described ultrasound artifacts, including mirror image, acoustic enhancement, edge shadowing, side-lobe and slice-thickness (see Chapters 3 and 5). It is very important to be familiar with these common artifacts at the DH view (Figure 6.13). These same artifacts are possible at the CC view (see Figure 6.26), another AFAST view with a fluid-filled structure (DH view – gallbladder, CC view – urinary bladder).

**Pearl:** A good learning exercise is to focus on a specific artifact and then look through several DH view video clips from different patients looking for that specific artifact.

### Artifacts

#### *Mirror Image Artifact*

The DH view is the classic example for mirror image artifact, which requires a strong air–soft tissue interface such as between the lung diaphragm and liver (see Figure 6.13). As a result, the ultrasound machine's software displays the liver and its structures as mirrored into the thoracic cavity (see Chapters 3 and 5).

Common DH view mirror image artifact misinterpretations include the following.

- The liver and gallbladder mirrored into the thorax and mistaken for a diaphragmatic hernia.
- The gallbladder mirrored into the thorax and mistaken for pleural and pericardial effusion, noting that a "partial" mirroring of the gallbladder can occur.
- Ascites mirrored into the thorax can be mistaken for pleural and pericardial effusion, and liver appearing as lung, noting that a "partial" mirroring of ascites can occur.

#### *Acoustic Enhancement Artifact*

The gallbladder will make the soft tissues distal to its fluid-filled luminal contents appear much brighter (more echogenic or hyperechoic) than adjacent soft tissues, similar to what occurs with the fluid-filled urinary bladder (see Figure 6.26). Typically, the

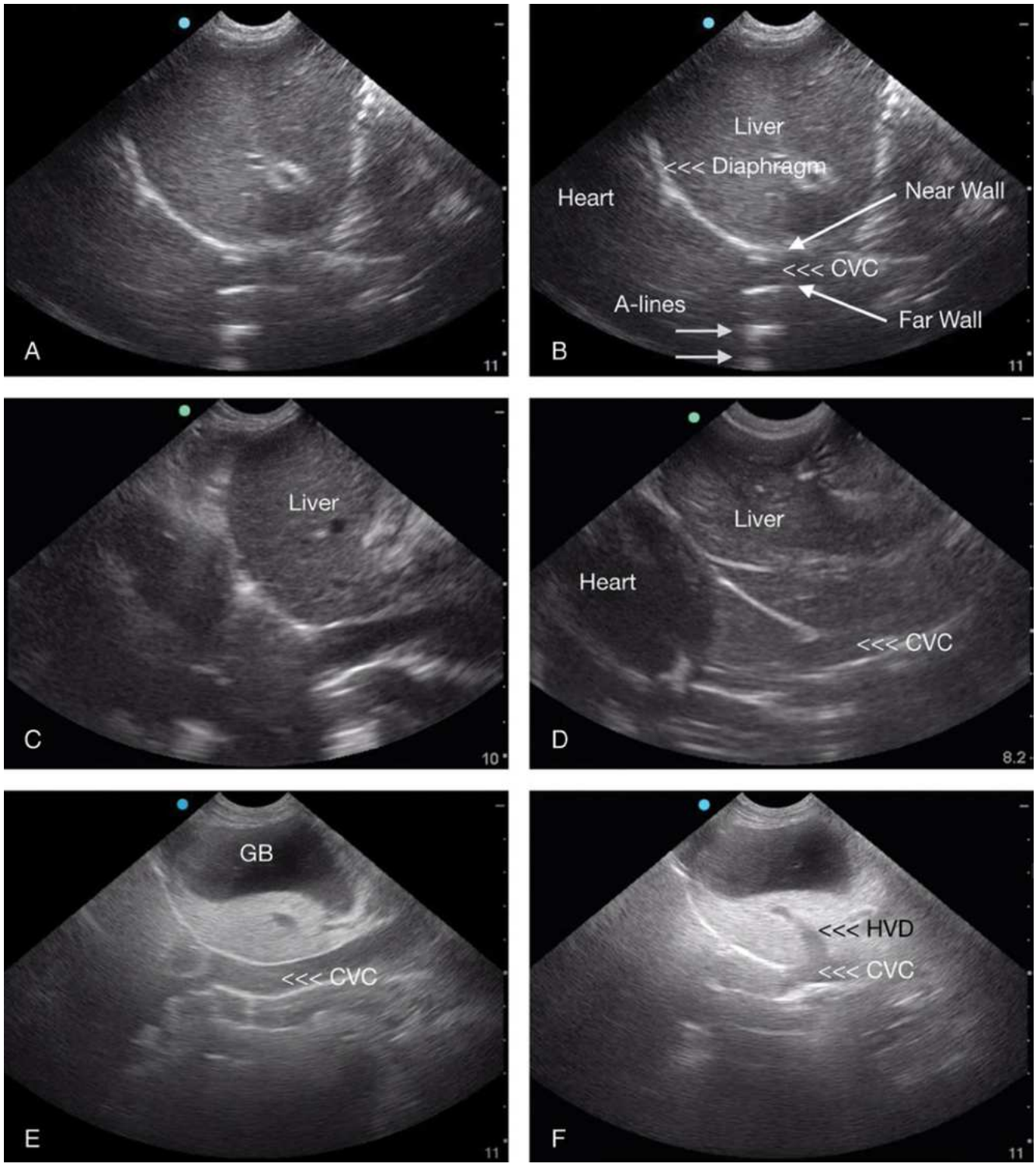


**Figure 6.12.** Variety of typical CVC images with other relevant structures. (A) Unlabeled DH view with the CVC followed by (B) labeled view of the same image. In (C) the CVC is obvious with its near and far wall and its maximum diameter, which may be eyeballed for its approximate measurement from the centimeter scale to the right of the screen. In (D) structures are labeled and similarly positioned as in (C). In (E) the CVC is distended and conspicuous due to right-sided heart failure. In (F) the DH view is fanned slightly from where in (E) the hepatic venous distension, referred to as the "tree trunk sign" (Lisciandro 2014a, 2016a), is apparent (see also Figure 36.8). Note how consistent the diaphragm is within the images as a landmark for proper DH view image acquisition. CVC, caudal vena cava; GB, gallbladder; HVD, hepatic venous distension. Source: Reproduced with permission of Dr Gregory Lisciandro, Hill Country Veterinary Specialists and FASTVet.com, Spicewood, TX.

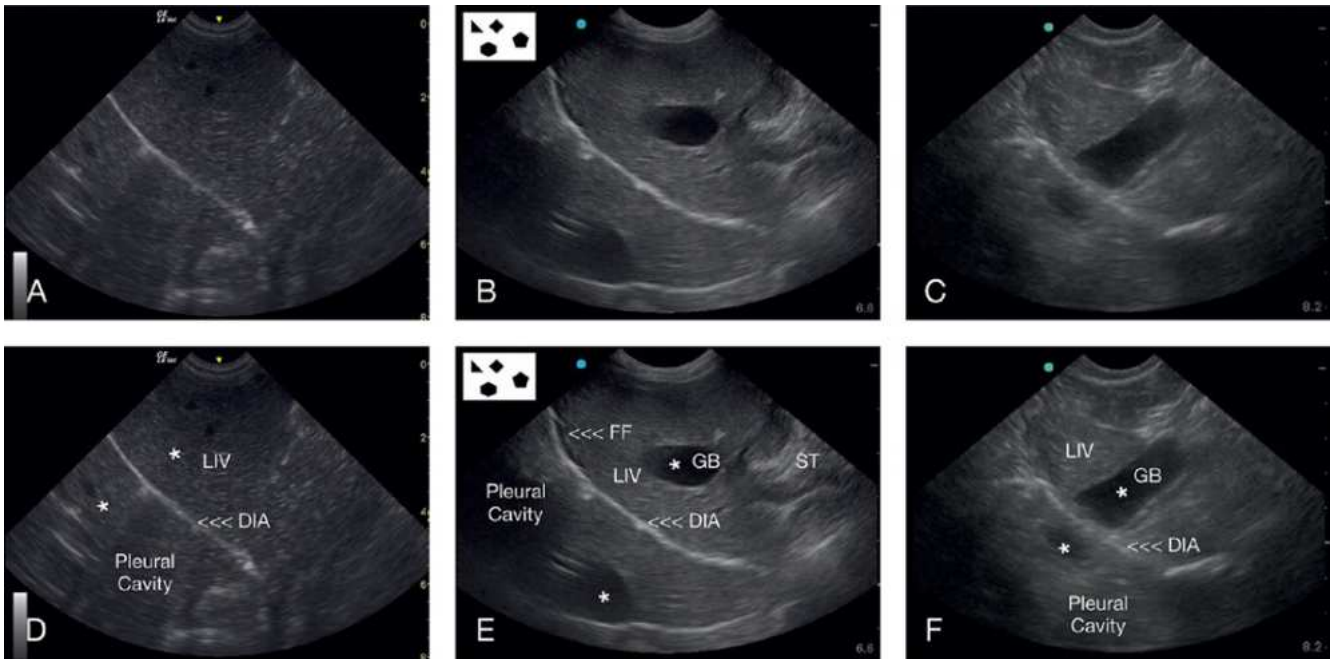


**Figure 6.13.** Mirror image artifact at the DH view. Mirror image artifact occurs wherever there is a strong soft tissue–air interface and should always be considered at the DH view. In (A) is the same image as in (D) unlabeled and labeled, respectively. The asterisks (*) show the mirroring of the liver on the other side of the diaphragm, falsely making it appear that liver is in the pleural cavity. The gallbladder is not present. In (B) is the same image as in (E) unlabeled and labeled, respectively. The asterisks (*) show the mirroring of the liver and gallbladder on the other side of the diaphragm, falsely making them appear in the pleural cavity. The mirrored gallbladder being fluid filled may be mistaken for pleural and pericardial effusion. The hepatic venous system also may be mirrored into the pleural cavity. In (C) and (F) are the last comparative images showing how the gallbladder may be partially mirrored into the pleural cavity. The question must always be asked – could I be mistaking artifact for pathology? To increase probability for a correct diagnosis, adhere to the described tenets for an accurate diagnosis of pleural and pericardial effusion (see Chapters 7, 18 and 21). Note how consistent the diaphragm is within the images as a landmark for proper DH View image acquisition. DIA, diaphragm; FF, free fluid; GB, gallbladder; LIV, liver; ST, stomach. Source: Reproduced with permission of Dr Gregory Lisciandro, Hill Country Veterinary Specialists and FASTVet.com, Spicewood, TX.

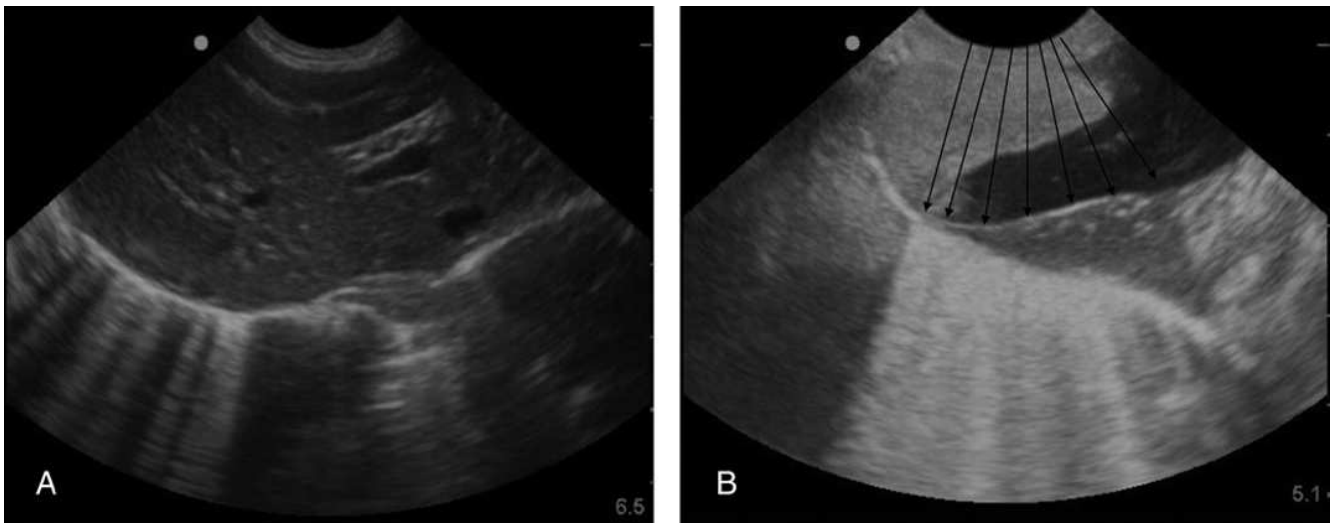


**Figure 6.14.** Showing B-lines along the pulmonary-diaphragmatic interface. Acoustic enhancement requires a fluid-filled structure, in this case at the DH view the gallbladder. In (A) multiple B-lines are obvious along the pulmonary-diaphragmatic interface. In (B) an even greater number almost coalesce along the pulmonary-diaphragmatic interface. However, and interestingly, they are in the path of the beam (its echoes) and indicated by the overlain black faint arrows on the image made more evident by acoustic enhancement artifact. Note that they are not evident to the left of the image where there is sediment and soft tissue of the liver (versus a fluid-filled gallbladder). Numbers of B-lines indicate degrees of alveolar-interstitial edema and need to be placed in clinical context with a complete Vet BLUE examination (see Chapters 22 and 23). Source: Reproduced with permission of Dr Gregory Lisciandro, Hill Country Veterinary Specialists and FASTVet.com, Spicewood, TX.

acoustic enhancement includes a brighter liver and sometimes B-lines through the far-field to the fluid-filled gallbladder (Figure 6.14) (see Chapters 3 and 5); however, when lung is truly dry, no B-lines should be seen through the acoustic enhancement, unless the lung is truly "becoming" wet (see Chapters 22 and 23).

**Pearl:** B-lines that are evident within the path of acoustic enhancement in the far-field past the gallbladder should be considered abnormal until proven otherwise and placed into clinical context unless 1–2 are seen in a giant breed. Dry lung should remain dry despite acoustic enhancement (see Figure 6.14).

### *Edge Shadowing, Side-lobe, and Slice-thickness Artifact*

These artifacts result in loss of interpretive clarity by the ultrasound machine along any luminal borders, in this case the gallbladder, thus, falsely making the gallbladder appear to contain sediment, other intraluminal abnormalities, or a mass, as well as defects along its wall similar to the urinary bladder (see Figure 6.26) (see Chapters 3 and 5).

## Pitfalls Creating False Positives

There are several fluid-filled or fluid-associated structures within the liver that the sonographer must be aware of.

### *Gallbladder and Biliary System*

When imaged in certain planes, the gallbladder and common bile duct can appear as anechoic sharp angulations like free fluid. This pitfall, misinterpreted as a false positive, is easily avoided by fanning, tracing, and connecting the gallbladder to its biliary tree (Figures 6.15 and 6.16).

### *Hepatic and Portal Veins*

The liver's venous system can appear as anechoic sharp triangulations like free fluid. The venous system as a general rule is not obvious in normalcy when patients are examined in lateral, sternal and standing positions. This false positive is easily avoided because most free fluid is not as linear as the venous system, and the venous system in most instances can be traced and seen branching (see Figure 6.12) (see Chapter 8). Color flow Doppler may be used to distinguish the venous system from free fluid but is rarely needed. Hepatic veins are differentiated from portal veins in a

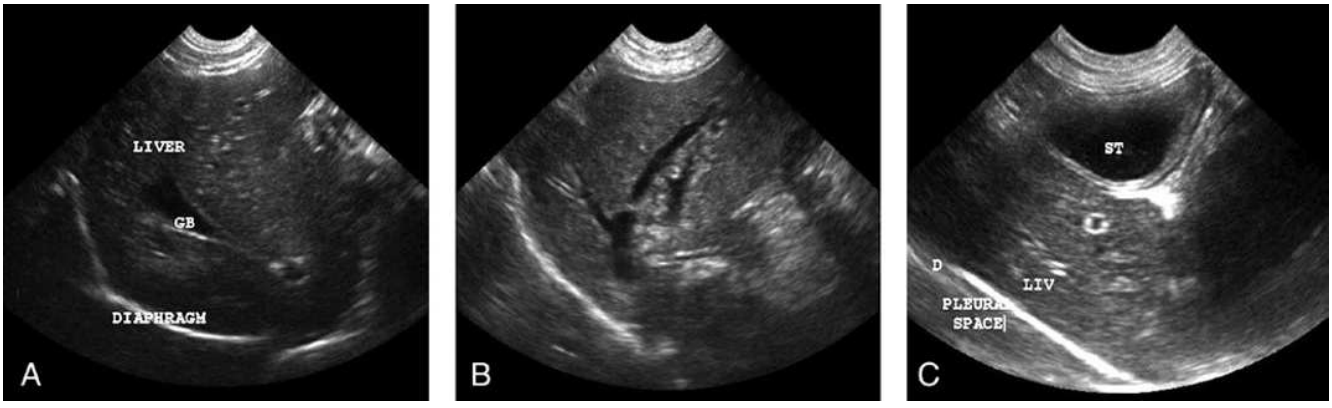


**Figure 6.15.** Pitfalls at the DH view related to the gallbladder, hepatic venous system, and stomach wall. In (A) the gallbladder (GB) appears triangulated, mimicking free fluid, but by fanning through the gallbladder in both directions, this mistake is less likely to occur. Moreover, free fluid does not have hyperechoic borders as the wall of the gallbladder does. In (B) branching of the hepatic venous system mimics free fluid. In real time and through repetition, the sonographer will get used to where fluid typically pools as well as incorporating the added information of performing the entire AFAST. In (C) the stomach is fluid filled in this patient and can mimic the gallbladder to the hasty sonographer; and its sonographically layered wall can mimic gallbladder wall edema. This area should be avoided by rocking the probe more cranial as shown in the many DH views within this chapter and Figure 5.10. GB, gallbladder; LIV, liver; ST, stomach. Source: Reproduced with permission of Dr Gregory Lisciandro, Hill Country Veterinary Specialists and FASTVet.com, Spicewood, TX.

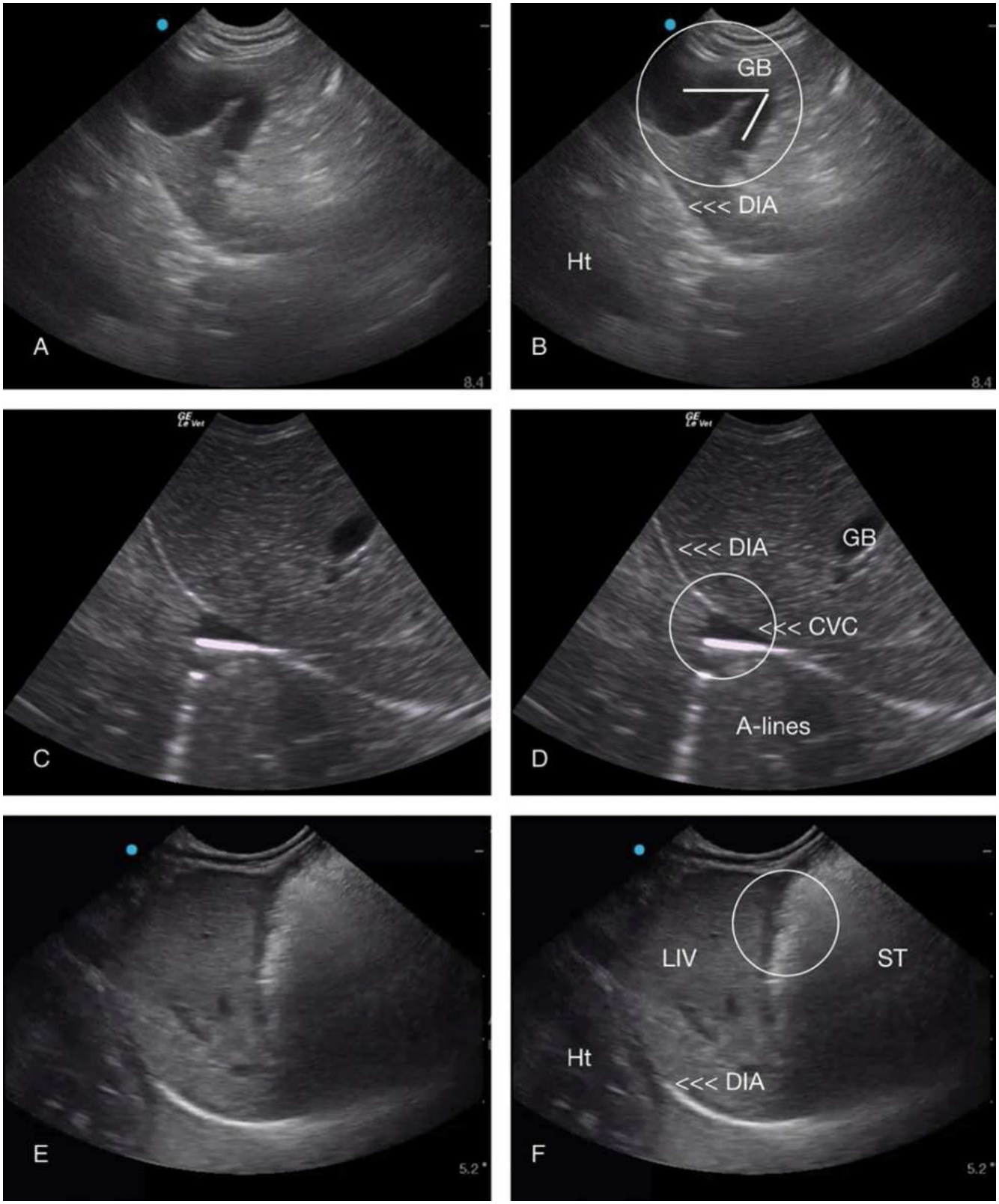


**Figure 6.16.** Additional examples of pitfalls at the DH view. (A) and (B) are the same image unlabeled and labeled. The gallbladder is bilobed, most commonly seen in cats. It appears similar to free fluid but through interrogation by fanning through the gallbladder in both directions, the rounding of the hyperechoic gallbladder wall differentiates it from free fluid. (C) and (D) are the same image unlabeled and labeled. Note the caudal vena cava (CVC) can mimic pleural effusion at the level of the diaphragm; however, the dynamic changes in CVC diameter with respiratory and cardiac cycles and its A-lines through the far-field differentiate the CVC from pleural effusion. In (E) and (F), the same image is unlabeled and labeled with a circle indicating the stomach wall that is anechoic and can mimic free fluid (and its associated edge shadowing artifact; see Figure 3.2). Note how consistent the diaphragm is within the images serving as a landmark for proper DH view image acquisition, which in and of itself (the proportionality shown) will prevent many DH view pitfalls. CVC, caudal vena cava; GB, gallbladder; LIV, liver; ST, stomach. Source: Reproduced with permission of Dr Gregory Lisciandro, Hill Country Veterinary Specialists and FASTVet.com, Spicewood, TX.

VetBooks.ir

couple of ways. First, portal veins have brighter, more echogenic (hyperechoic) walls when compared to hepatic veins and thus portal veins often appear as hyperechoic (bright white) equal [=] signs (see Chapters 8 and 39). Hepatic veins are darker walled sonographically and are generally traced as they drain into the CVC, especially when there is hepatic venous distension (see Figure 6.12F and Chapters 7, 20, and 36).

### *Caudal Vena Cava*

The CVC can mimic pleural effusion in haste, especially at the level of the diaphragm (see Figure 6.16).

### *Stomach Wall*

Typically, the sonographer should stay away from the area of the stomach during the DH view by directing the probe far cranially, striving for the proportionality shown (see Figures 6.15 and 6.16). The stomach has a sonolucent (dark or black) component to its wall, which typically appears linear in real-time imaging but can appear as an anechoic triangulation like free fluid. The stomach wall is also subject to artifacts such as edge shadowing (see Figure 3.2). The best way to avoid being confounded by the stomach is to stay further cranially when interrogating the DH view, understanding that little is gained by imaging caudally toward the stomach during an AFAST (see Figure 5.10). Free intraabdominal fluid is most commonly, easily, and accurately seen between liver lobes along the diaphragm, or between the liver and diaphragm (see Figure 6.10).

**Pearl:** Stay away from the stomach region because it is too far caudal for the DH view. Free fluid is better appreciated between the liver and diaphragm, between liver lobes more cranially along the diaphragm, and the liver and falciform fat.

### Minimizing False Negatives

Repeat AFAST serially four hours post admission as standard of care (or sooner as clinical course dictates) and routinely repeat after resuscitation and rehydration (Lisciandro et al. 2009; Lisciandro 2011; Boysen and Lisciandro 2013). The four-hour postadmission rule of thumb is supported in human medicine by the American College of Emergency Physicians (ACEP) guidelines (www.acep.org) as standard of care and has been shown to increase FAST sensitivity, improve patient management, and prevent the "crump factor" in people with hypotension (Blackbourne et al. 2004; Ollerton et al. 2006; Bilello et al. 2011). In the AFAST study, ~20% of dogs changed score on serial examination, most worsening with increasing abdominal fluid scores (Lisciandro et al. 2009).

### *Serial AFAST Examinations Increase Sensitivity*

Don't sweat questionable small pockets of free fluid. Serially repeat AFAST at least one more time four hours later (and sooner if the patient is questionable or unstable). The serial AFAST examination provides another opportunity to screen for free fluid that was absent or questionable that may now be easily seen as present (Lisciandro et al. 2009; Lisciandro 2012; Blackbourne et al. 2004), and to rescore (AFS) for worsening (increasing AFS), static (same AFS), or improving (decreasing AFS) (Lisciandro et al. 2009, 2019). Free fluid also may become safely accessible for sampling in previously lower-scoring patients, which can be hugely helpful in decision making between medical and surgical cases. Knowing whether a patient is fluid positive helps maximize fluid resuscitation (Ollerton et al. 2006).

## AFAST Spleno-Renal View

| Questions Asked at the SR (HR) View[a] | |
|---|---|
| Is there any free fluid in the abdominal (peritoneal) cavity? | Yes or no |
| How much free fluid is at the SR view using the AFAST AFS system? | 0, 1/2, 1 |
| What does the left (right when in left lateral) kidney look like?[b] | Unremarkable or abnormal |
| What does the spleen (liver when in left lateral) look like?[b] | Unremarkable or abnormal |
| Could I be misinterpreting an artifact or pitfall as pathology? | Know pitfalls and artifacts |

[a]Note that this view is the SR view in right lateral recumbency and the HR view in left lateral recumbency.
[b]It is important to know that the AFAST target-organ approach for parenchymal abnormalities is binary as "unremarkable" or "abnormal" to capture the case for additional imaging and confirmatory testing. More interpretative skills may be gained through experience, and additional ultrasound study and training.
Source: Reproduced with permission of Dr Gregory Lisciandro, Hill Country Veterinary Specialists and FASTVet.com, Spicewood, TX,

The SR view includes visualization of both the spleen (peritoneal cavity) and the left kidney (retroperitoneal space) (Figures 6.17 and 6.18).

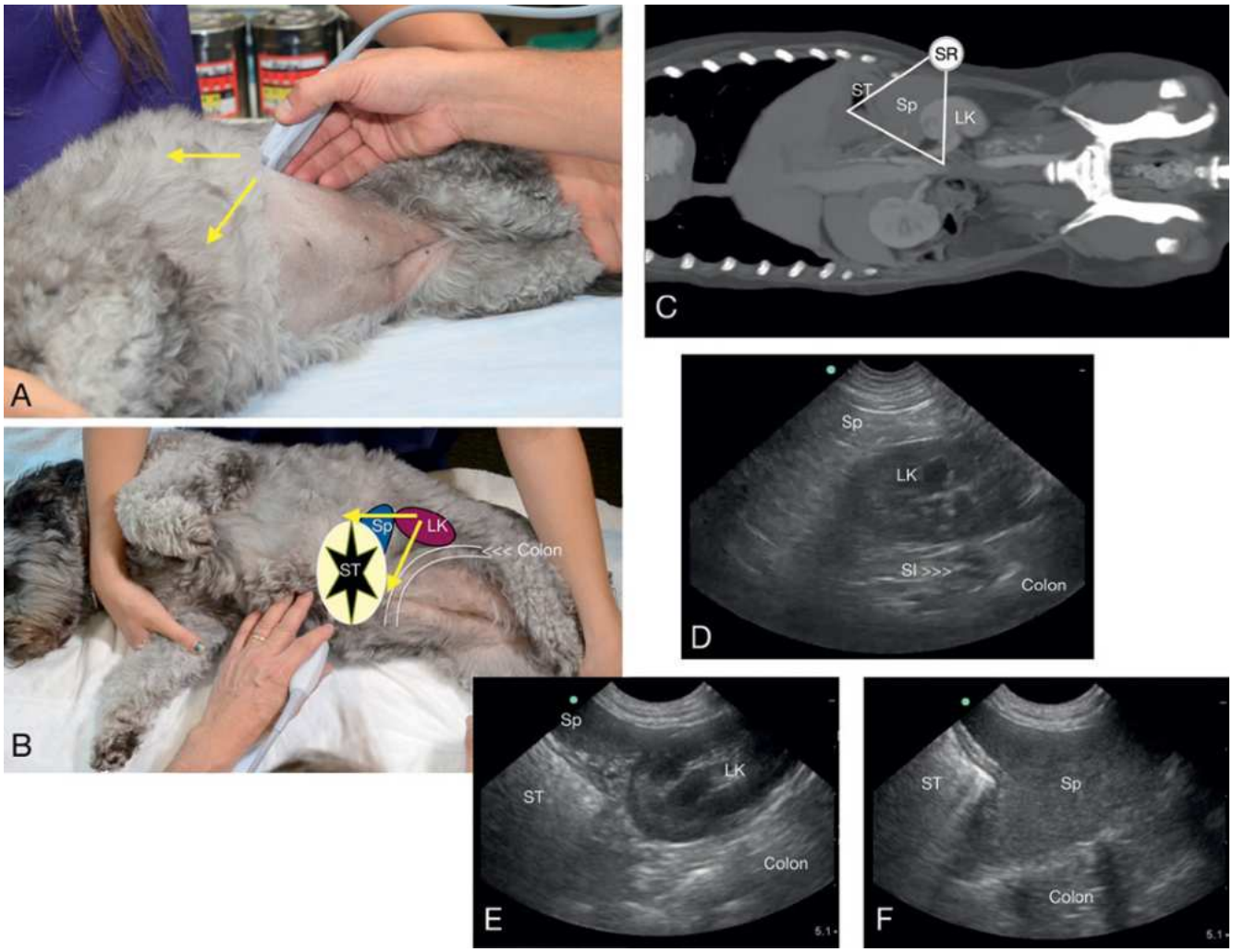


**Figure 6.17.** The SR view in a dog. In (A) is the external location where the ribs meet the hypaxial muscles dorsally, followed by (B) through (F) showing the relevant anatomy that includes the left kidney, the head of the spleen where it attaches to the greater curvature of the stomach, and the viscus often air-filled stomach cranially and colon caudally. Ultrasound cannot image past air and thus each organ causes dirty shadowing. The left kidney is retroperitoneal and the spleen is peritoneal. LK, left kidney; SI, small intestine; Sp, spleen; ST, stomach. Computed tomography courtesy of Dr Daniel Rodriguez, VETTEM, and Dr Jesús Paredes, CVM, Mexico City, Mexico. Source: Reproduced with permission of Dr Gregory Lisciandro, Hill Country Veterinary Specialists and FASTVet.com, Spicewood, TX.

The SR target organs are readily imaged in the preferred positioning of right lateral recumbency by placing the probe just caudal to the last rib and dorsally where the rib and the hypaxial muscles meet. The probe is fanned in both directions in longitudinal (sagittal) orientation, recalling that the left kidney is protected by the hypaxial muscles, and in close proximity to the great vessels because of the short renal artery and vein to the aorta and CVC, respectively.

If the left kidney is not located, the probe is rocked cranially under the costal arch and then again fanned since in most dogs the left kidney would tend to be located more cranial than caudal to your starting point.

Once the left kidney is located, it is interrogated by making it as longitudinally symmetrical as possible, and then fanning through it longitudinally (sagittal) in both directions for any free fluid and any obvious renal and perirenal pathology.

The probe is then rocked cranially to search for the head of the spleen, recalling that in dogs and cats, the spleen is reliably found because it is attached by its short gastric vessels to the greater curvature of the stomach in this region.

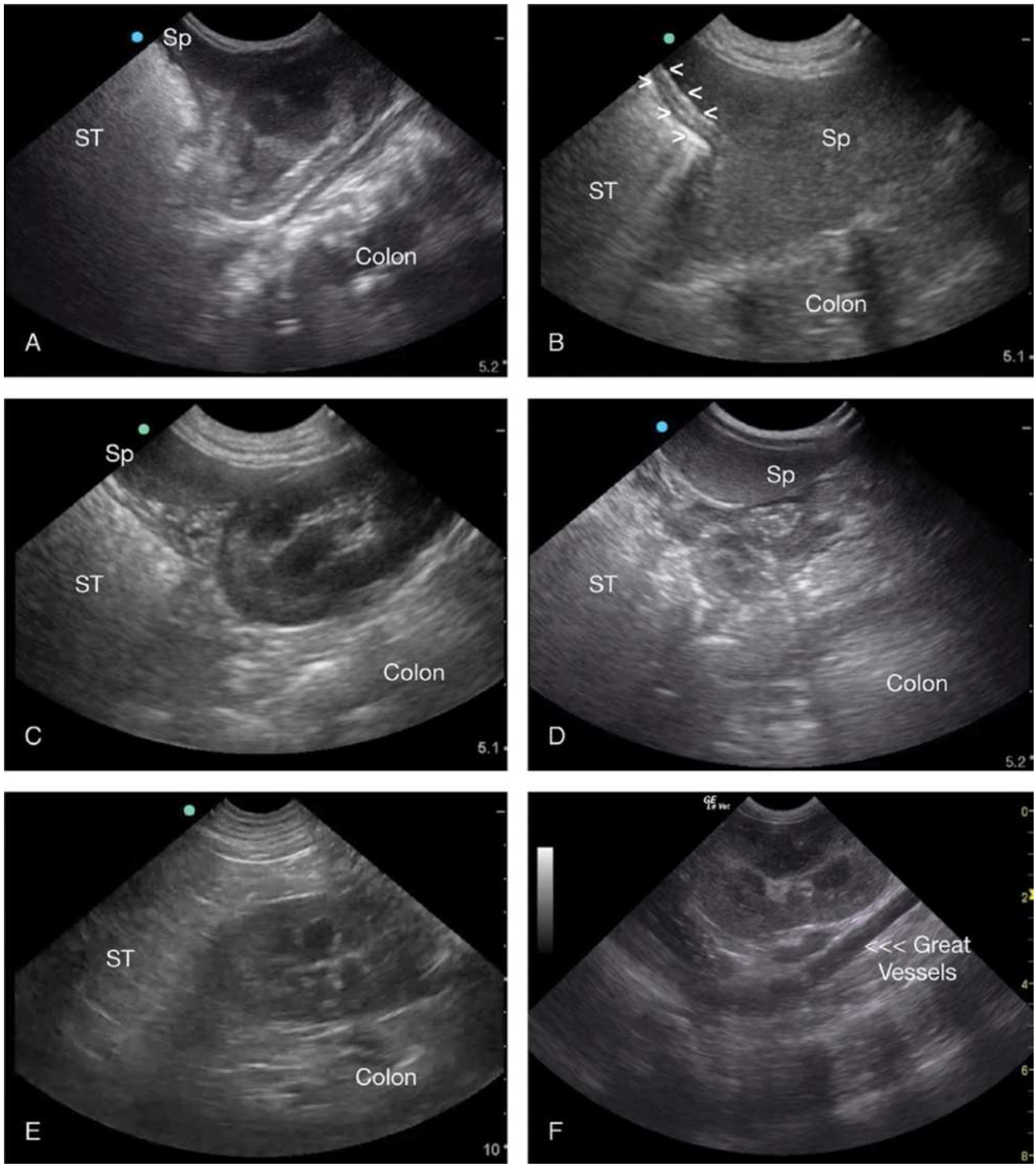


**Figure 6.18.** Examples of typical negative studies at the SR view. In (A) the air-filled stomach (ST) and the colon shadow through the far-field, giving the SR view its characteristic pie-piece of information with the head of the spleen (Sp) abutting the left kidney. In (B) the wall of the stomach is outlined (V) and a large swath of the head of the spleen is fanned and interrogated while remaining at the SR view's external location. Do not wander from this region to look for the spleen (see Focused Spleen below). In (C) is another example of the target organs of the head of the spleen and the left kidney being in view. In (D) interposing small intestine is past the spleen to the far-field ("hamburger" look of small intestine) without the left kidney target organ. (E) shows the left kidney without the spleen target organ, which will require rocking the probe cranially. In (F) are the left kidney and adjacent great vessels, keeping in mind the retroperitoneal anatomy includes the CVC, the aorta, renal artery and vein, and adrenal glands. Note the consistency in the images with their proportionality and location of the relevant SR view structures of the left kidney, spleen, stomach, and colon. Source: Reproduced with permission of Dr Gregory Lisciandro, Hill Country Veterinary Specialists and FASTVet.com, Spicewood, TX.

When free fluid is present, it is most commonly seen between the spleen and cranial left kidney, or between the cranial pole of the left kidney and the wall of the colon (Figure 6.19).

In dogs, the spleen may be used to locate the left kidney by following it caudally and medially because of its anatomical association with the left kidney, or by fanning along the great vessels since the left kidney is closely attached via its relatively short renal artery and vein. If you are having problems finding the left kidney, you have a few options.

- The spleen in dogs and cats may be used to locate the left kidney by following the spleen caudally and medially to bring you to the left kidney.
- Fan along the great vessels, paying attention to the probe's direction, recalling that the left kidney (and right) are closely attached via their respective renal artery and vein.
- Making sure that you have not drifted too far ventrally from the angle of the costal arch and hypaxial junction and into the abdomen.
- You are pushing (compression) too hard into the patient and in fact pushing the left kidney (and right) out of view.

**Pearl:** In most cats and many small dogs, both the left and right kidneys can be viewed through the single SR (or HR) view with increased depth (Figures 6.20 and 6.21).

Fanning dorsally screens for any pathology associated with the great vessels (aorta and caudal vena cava) and adrenal glands. The great vessels are common confounders and cause false positives, which are easily overcome by remembering that free fluid is rarely a linear anechoic (black) stripe(s) but rather anechoic triangulations, and thus linear anechoic stripes are more likely to be blood vessels and intestinal tract (see Figures 6.18 and 6.20). The only major exception is anechoic stripe(s) at the DH view between the liver and diaphragm (Lisciandro et al. 2015, 2019; Romero et al. 2015).

The great vessels are identified in B-mode by their shape, being linear in longitudinal and circular in transverse orientation with pulsation. Color flow Doppler may also be used to detect flow. Turning your probe transversely (turn left or counterclockwise) should change the vessel's appearance from a linear anechoic (black) rectangular shape to an anechoic (black) circle.

Retroperitoneal fluid raises the suspicion for hemorrhage, urine, and sterile and septic effusions placed into clinical context, and when found and safely accessible, fluid sampling should take place, and when inaccessible or too risky to sample, more advanced imaging is likely indicated.

- Cranial to the kidneys, origin of retroperitoneal fluid would generally include the kidneys, vertebral bodies, the great vessels and adrenal glands.
- Caudal to the kidneys, origin of retroperitoneal fluid would generally include the kidneys, ureters, vertebral bodies, and pelvis (see Figure 6.19, see also Chapters 10 and 11).

Retroperitoneal versus intraabdominal (peritoneal) fluid can be further assessed by changing patient position by moving them to a standing position and seeing if the free fluid remains in the least gravity-dependent SR view (retroperitoneal more likely), and noting that the least gravity-dependent SR view is rarely the only positive AFAST view in right lateral recumbency.

**Pearl:** Retroperitoneal fluid is not part of the AFS. Its size should be noted by its largest dimension (length, width, height) measured by either the "eyeball method" (using the centimeter scale on the ultrasound screen), or more precisely using your machine's caliper function.

### *Typical SR View Positives*

The majority of positives at the SR view are classically anechoic (black) triangles formed between the cranial pole of the kidney and colon (see Figure 6.19) and between the spleen and the cranial pole of the kidney.

### *Artifacts*

Generally, the SR view has few artifacts which are mostly colon and stomach related. The anatomy of the SR view is important to know because of the viscus organs located cranially (stomach) and caudally (transverse and descending colon). When these organs are air filled, dirty shadowing is created through the far-field, limiting imaging to a pie shape of information that includes the left kidney, head of the spleen in dogs and cats, great vessels and variably loops of small intestine (see Figures 6.17–6.19). Artifacts are described in more detail in Chapters 3 and 5.

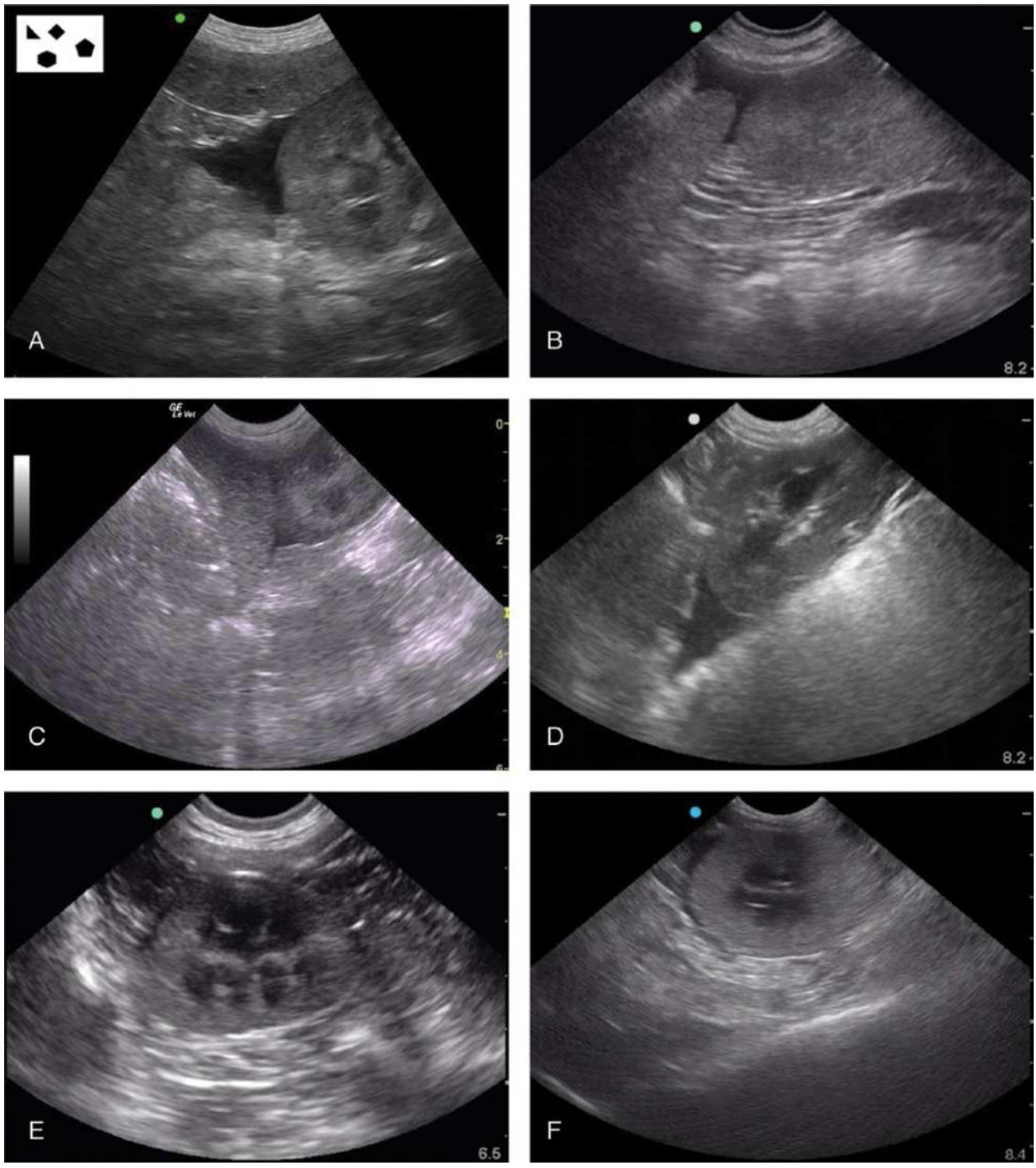


**Figure 6.19.** Examples of typical positive studies at the SR view. In (A) the spleen is in the near-field identified by its characteristic location (importance of performing the SR view the same way every time), its hyperechoic capsule, and vessels splitting its capsule. Classic triangulation between the spleen and the left kidney. In (B) is another positive with a similar location of free fluid with the triangulation outlining the spleen from the stomach (screen left) and left kidney (screen right). With fanning through the region, the left kidney is easily identified to the right of the near-field of the image. In (C) free fluid is located between the left kidney and spleen. In (D) is shown the classic triangulation off the cranial pole of the left kidney where it abuts the wall of the colon. In (E) there is some perirenal fluid to the left of the kidney that is similar to the image from another case in (F). Note differences in image quality and ultrasound machine settings making it easier or more difficult to see. Serial examinations are key when subtle findings are suspected. Moreover, the SR view is complemented by information from other AFAST views. Compare these images to the anatomy in Figures 6.17 and 6.18. Note the consistency in the images with their proportionality and location of the relevant SR view structures of the left kidney, spleen, stomach and colon. Source: Reproduced with permission of Dr Gregory Lisciandro, Hill Country Veterinary Specialists and FASTVet.com, Spicewood, TX.

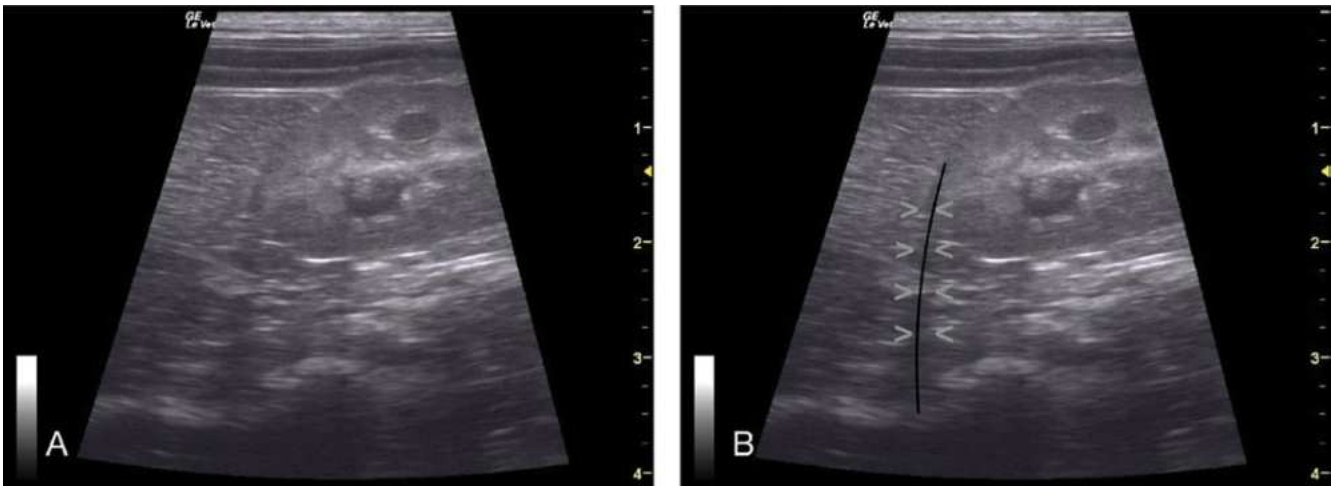


**Figure 6.20.** Edge shadowing artifact off the left kidney. (A) and (B) are the same image unlabeled and labeled for comparison. In (B) the hypoechoic linear edge shadowing artifact in (A) is outlined with (V) and with a thin black line. When free fluid is suspected off the margin of a curved surface, this artifact should always be considered as creating a false positive. Compare to Figure 6.19 (E) and (F). Source: Reproduced with permission of Dr Gregory Lisciandro, Hill Country Veterinary Specialists and FASTVet.com, Spicewood, TX.

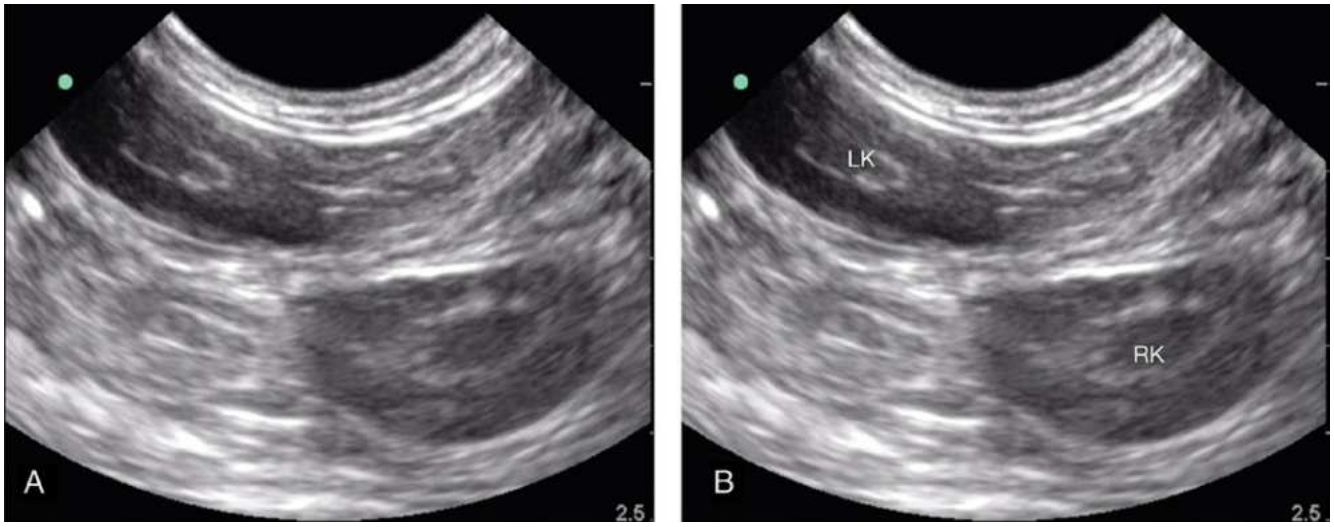


**Figure 6.21.** Both kidneys in view at the SR view. In the cat and the small dog, it is not uncommon to see both kidneys through the SR view. LK, left kidney; RK, right kidney. Source: Reproduced with permission of Dr Gregory Lisciandro, Hill Country Veterinary Specialists and FASTVet.com, Spicewood, TX.

### Air-filled Stomach

Air causes interference (ultrasound cannot image through air) cranial or to the screen's left. Study the presence of the stomach and its dirty shadowing in Figures 6.17–6.19.

### Air-filled Colon

Air causing interference is usually not problematic since dogs and cats in right lateral recumbency often have their colon (by gravity) fall adequately away from the SR view. However, it is not uncommon for the air-filled colon to dirty shadow through the far-field and is typically present caudally or to the screen's right. Study the presence of the colon and its dirty shadowing in Figures 6.17–6.19.

### False Mirror Image in Cats

Commonly in cats and less so in small dogs, both kidneys are imaged in the same field of view at the SR view. This is unlikely to be a mirror image artifact, which requires a strong air–soft tissue interface (Figure 6.22) (see Chapter 39).

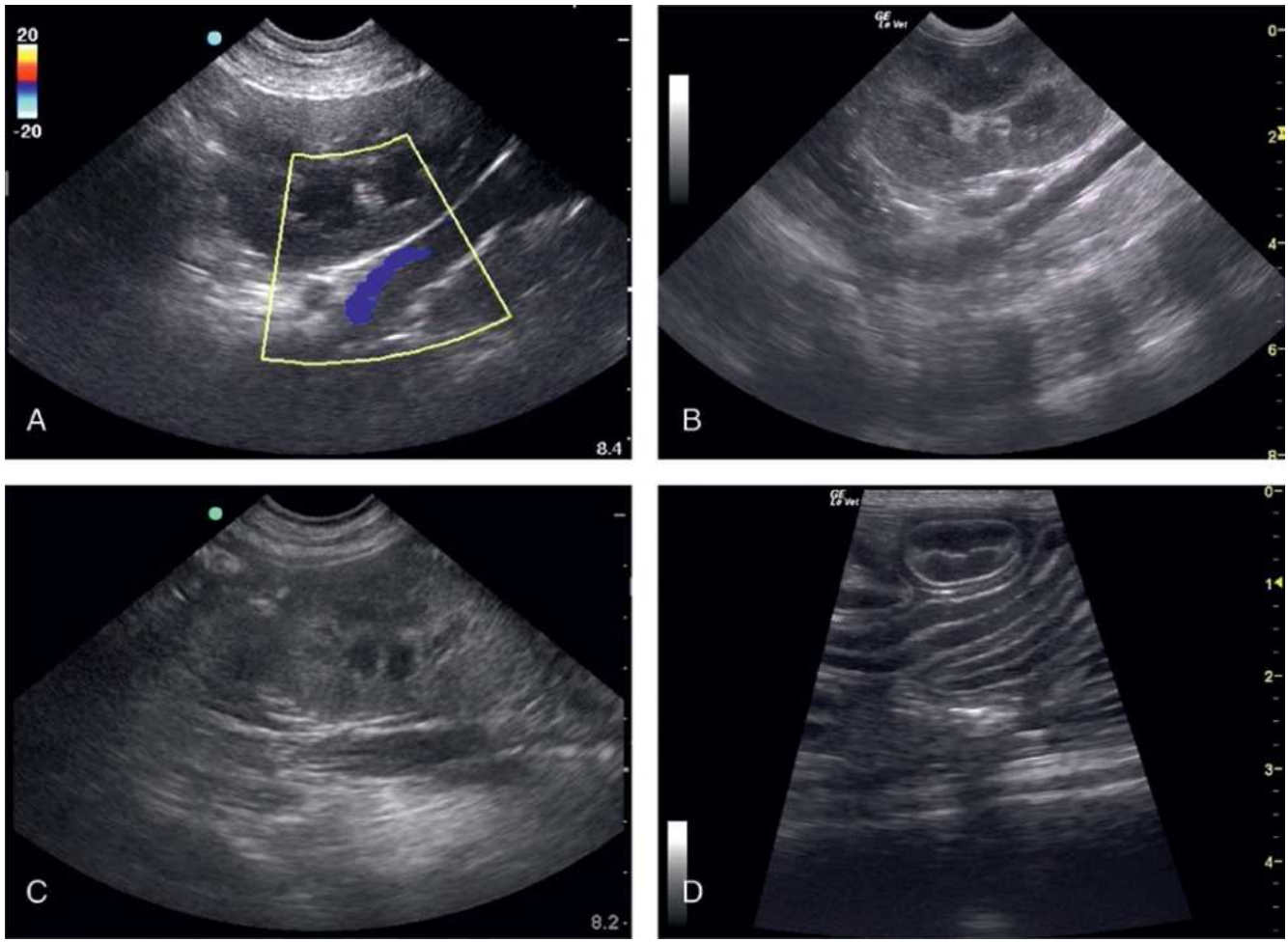


**Figure 6.22.** Pitfalls at the SR view and linear stripes are not free fluid. In (A) and (B) are similar images with color flow Doppler showing the great vessels (CVC and abdominal aorta) that are clearly linear and anechoic in B-mode in (B). In (C) it is difficult to tell if the anechoic (hypoechoic) linear stripe is great vessels or small intestine; however, when fanning as a general rule, a great vessel will be an anechoic tube with pulsation and the small intestine will have sonographically layered linear stripes as in (D). The author refers to small intestinal wall layering in transverse orientation as appearing like "hamburgers" (oval with a line through its center) and in longitudinal (sagittal) orientation as "highways" (median stripe and two shoulders of the road). Note both planes of orientation are in the image. Source: Reproduced with permission of Dr Gregory Lisciandro, Hill Country Veterinary Specialists and FASTVet.com, Spicewood, TX.

### Edge Shadowing

Any reflection of the beam (echoes) from a curved soft tissue surface will often extend a hypoechoic to anechoic line off the margin of the curved surface through the far-field. In haste, the artifact can mimic free fluid (see Figure 6.20 and Figure 3.2).

## *False Positives*

### Linear Anechoic Stripes

These rarely represent free fluid and are more likely small intestine (intraabdominal) or the great vessels (retroperitoneal). Color flow Doppler is rarely needed to differentiate between these anatomical structures and free fluid, but may be used if in B-mode the determination cannot be made using combinations of longitudinal and transverse orientations and observing for vessel pulsation (see Figure 6.22).

**Pearl:** Remember classic positives at the SR view are anechoic (black) triangles, not linear stripes.

### Retroperitoneal Fluid versus Peritoneal Fluid

The problem posed in people differs from our veterinary patients which are less obese and have a suspended (versus attached) colon. In lateral

recumbency, retroperitoneal fluid will remain static and not fall away from the field of view (see Figure 6.19). Increasing your depth will also help interrogate the two spaces, as well as considering the findings at the other AFAST views. The SR view is rarely the only positive view in intraabdominal effusions because it is the least gravity dependent. See examples in Chapter 10.

### *False Negatives*

#### Serial AFAST Examinations Increase Sensitivity

Don't sweat questionable small pockets of free fluid; stabilize the patient and do a serial (repeat) AFAST and assign an abdominal fluid score. Minimally, a second AFAST four hours later should be performed, and sooner if the patient is questionable or unstable (acep.org; Lisciandro et al. 2009; Blackbourne et al. 2004; Boysen and Lisciandro 2013).

## AFAST Cysto-Colic View

| Questions Asked at the CC View | |
|---|---|
| Is there any free fluid in the abdominal (peritoneal) cavity? | Yes or no |
| How much free fluid is at the CC view using the AFAST AFS system? | 0, 1/2, 1 |
| What does the urinary bladder look like?[a] | Unremarkable or abnormal |
| Is the patient intact reproductively?[a] | Yes or no |
| Could I be misinterpreting an artifact or pitfall as pathology? | Know pitfalls and artifacts |

[a]It is important to know that the AFAST target organ approach for parenchymal abnormalities is binary as "unremarkable" or "abnormal" to capture the case for additional imaging and confirmatory testing. More interpretative skills may be gained through experience, and additional ultrasound study and training.
Source: Reproduced with permission of Dr Gregory Lisciandro, Hill Country Veterinary Specialists and FASTVet.com, Spicewood, TX.

The classic CC view includes imaging the urinary bladder (when present) against the abdominal wall in the far-field by directing the probe externally placed dorsolateral from the midline and the scanning plane directed toward the tabletop into the most gravity-dependent pouch formed between the bladder and the gravity-dependent body wall (Figures 6.23 and 6.24). The most gravity-dependent region at the CC view is referred to as the "CC pouch" (Lisciandro 2011, 2014a; Boysen and Lisciandro 2013). The CC view is slightly a misnomer because of its target organs; only the urinary bladder is specifically imaged whereas the colon is not (Lisciandro 2014a). However, an air-filled colon will do the following.

- Obscure imaging of the "CC pouch" by dirty shadowing.
- May get between the urinary bladder and body wall, mimicking urine sediment and calculi by its dirty shadowing (see Figure 6.27 and Chapter 11).

A stool-filled colon may mimic pathology and thus a digital rectal examination and/or caudal abdominal palpation or both as part of a good physical exam can prove helpful along with additional imaging.

Place the probe dorsolateral to midline and direct toward the tabletop into the most gravity-dependent region of the CC view called the "CC pouch" where the apical urinary bladder and the abdominal wall in the far-field meet. If the urinary bladder is not in view, slide the probe toward the pubis with some fanning as needed. The process should be a slide and fan, followed by a slide and fan toward the pubis looking for the urinary bladder.

If the colon is creating dirty shadowing, then sweep the probe closer to midline while directing the ultrasound beam into the "CC pouch."

When the urinary bladder is located, then fan through it in both directions in longitudinal (sagittal) orientation with the same methodology used for the gallbladder and left kidney previously at the DH and SR views, respectively. It is very important to apply minimal probe pressure over the urinary bladder because it is easily deformed by excessive compression of the probe pushing into the patient's body wall. The sonographer can easily appreciate this "artifact" by seeing the urinary bladder appear as a "dumbbell" or its wall flattened out in the far-field against the body wall in the "CC pouch" (see Figure 6.26).

After interrogating the urinary bladder, return to your starting point by rocking back to the "CC pouch" for one final look in this most gravity-dependent region for free intraabdominal fluid.

Serial AFAST provides the opportunity to image and interrogate the urinary bladder, which is expected to fill with urine during fluid resuscitation, and if the urinary bladder is not seen then interventional and therapeutic decisions are made depending on the patient.

Urine production may be estimated using our AFAST CC formula of length (cm) × width (cm) × height (cm) × 0.625 = estimation of urinary bladder volume in milliliters (Lisciandro and Fosgate 2017). With serial measurements over time, urine output may be estimated. Excessive probe pressure will

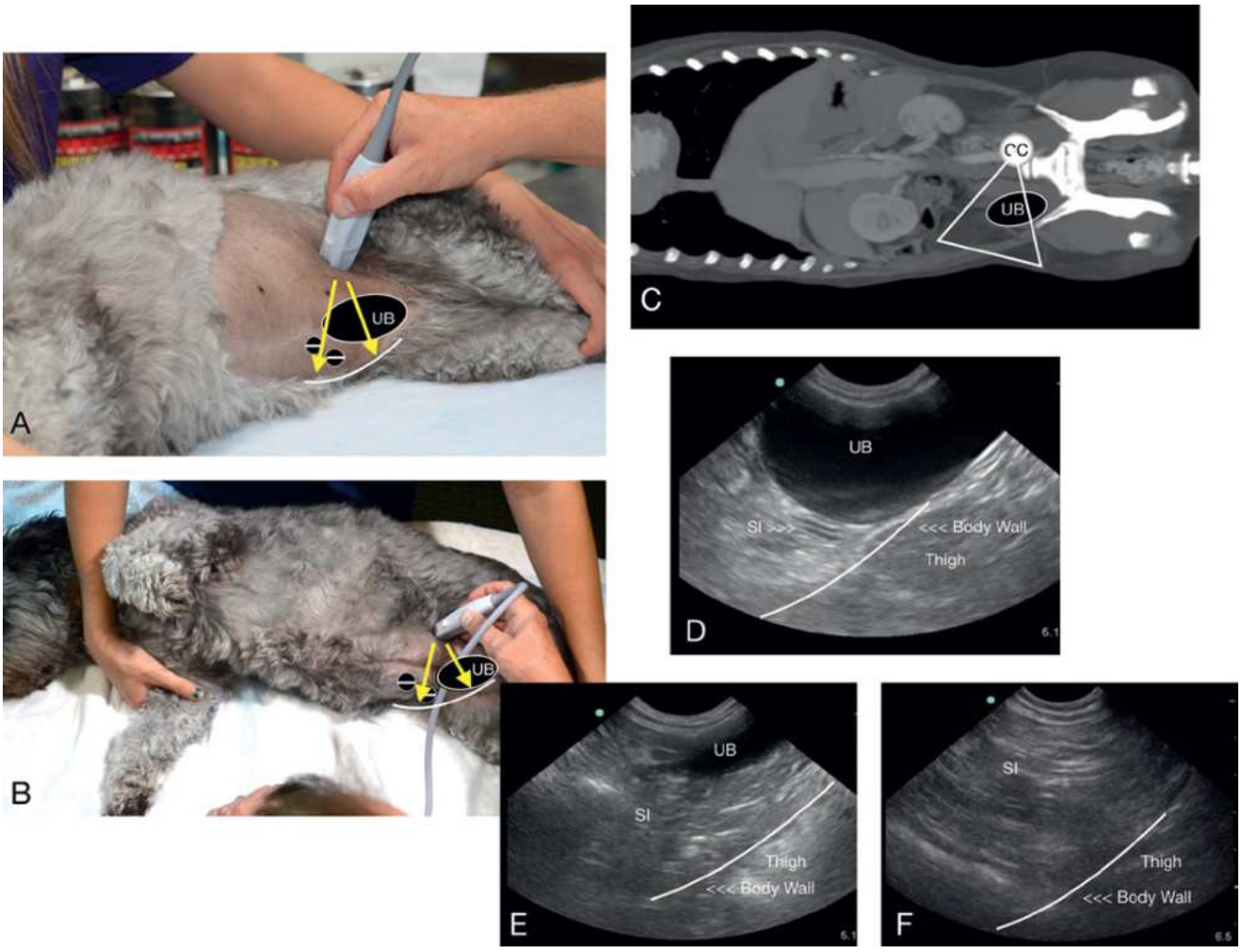


**Figure 6.23.** The CC view in a dog. In (A) the direction of the probe is shown externally dorsal to midline and directed toward the tabletop, or the most gravity-dependent region of the view. In (B) is a similar image with anatomy overlay that correlates to the CT image. The urine-filled urinary bladder serves as a recognizable landmark for the CC view and for identifying the "CC pouch" where the urinary bladder and body wall in its most gravity-dependent region are next to one another (*curved line*) as this is where free fluid would pocket. The thigh is often in view through the far-field and is screen right in (D–F). Computed tomography courtesy of Dr Daniel Rodriguez, VETTEM, and Dr Jesús Paredes, CVM, Mexico City, Mexico. Source: Reproduced with permission of Dr Gregory Lisciandro, Hill Country Veterinary Specialists and FASTVet.com, Spicewood, TX.

distort the urinary bladder, leading to erroneous measurements.

The striated rounded soft tissue structure through the far-field is often the patient's opposing thigh ("imaging ham") and not a mass. The rounded anechoic circular structures in between the urinary bladder and the thigh are often appreciated and represent the femoral artery and vein (Figure 6.25; see also Figures 6.23 and 25.8). The compression technique can determine which is the vein and which the artery in addition to the use of color flow Doppler (see Chapter 25).

**Pearl:** In blunt trauma dogs, the probability of hemoabdomen to uroabdomen has been documented in separate veterinary studies to be ~98% to ~2–4%, respectively (Boysen et al. 2004; Lisciandro et al. 2009; Simpson et al. 2009; Hoffberg et al. 2016; Grimes et al. 2018). Thus, in most canine blunt trauma cases in which the urinary bladder is not visualized, the serial AFAST examination provides a second opportunity to evaluate for the integrity of an intact urinary bladder with its expected rounded contour (Lisciandro et al. 2009). In its absence,

radiography, abdominal fluid sampling and analysis, such as comparative abdominal fluid to serum creatinine, or other more advanced imaging procedures should be considered.

**Pearl:** In cats with large-volume effusion that survive blunt trauma, the probability of a uroabdomen is much higher than a hemoabdomen because cats generally don't survive large-volume bleeds like dogs do.

## *Typical CC View Positives*

The classic CC positive view with a small-volume effusion has a small anechoic (black) triangle in the "CC pouch," between the urinary bladder apex and the body wall in the most gravity-dependent region (see Figure 6.25). Large-volume positives are usually easy to see in real time with the wafting movement of small intestines and omentum. Urinary bladder pathology such as sediment and calculi is most commonly going to be in the same most gravity-dependent view of the "CC pouch." When a mass effect is found in the urinary bladder, the best way to differentiate a thrombus from a mass is by using color flow Doppler, with a thrombus (and artifact) with no flow versus a mass with pulsatile blood flow.

**Pearl:** When a urinary bladder mass is found, differentiate through the use of color flow Doppler, with a thrombus having no flow versus a mass that will have pulsatile blood flow.

## *Artifacts*

The most relevant CC view artifacts are described below (see Figure 6.26). More detail is provided in Chapter 3.

### Acoustic Enhancement Artifact

The fluid-filled urinary bladder will make the soft tissue distal through it brighter (more echogenic), similar to what occurs with the gallbladder at the DH view. With the recommended probe positioning, the body wall will be brighter in the far-field in the "CC pouch" because of this artifact and readily seen along the body wall in the far-field deep to the urinary bladder.

### Mirror Image Artifact

The mirror image artifact requires a strong soft tissue–air interface and is most commonly observed at the DH view, the CC view (bladder mirrored on the far side of the abdominal wall) and during echo views (heart mirrored on the far side of the pericardium).

### Side-lobe and Slice-thickness Artifact

These artifacts mimic sediment and the author has even received images suggesting this artifact was a mass. Think about the artifact in terms of gravity dependency because sediment and calculi will settle into the bladder lumen and be best viewed within the "CC pouch." Lowering the gain eliminates the artifact whereas true sediment persists, and color Doppler can assess for flow (no flow = either artifact or thrombus versus flow = a mass).

### Probe Pressure Artifact

The sonographer should always be aware of the effects of probe pressure on the image. The urinary bladder is susceptible to probe pressure artifact creating misshapen appearances.

### Reverberation and Dirty Shadowing Artifact

An overlying air-filled colon will obscure the far-field, making the bladder appear in odd shapes, and if colon or small bowel gets under the bladder, either may be mistaken for sediment, calculi, and masses (see Figure 6.27) (see Chapters 3 and 11). It is a good habit to check where the probe and the beam (the scanning plane) are directed to help interpret your image (see Chapter 5).

**Pearl:** Change the position of the probe and alter the pressure of the probe on the patient (both a little more and a little less) to coax the colon out of your way or sweep toward midline while imaging in the "CC pouch" to get away from the air-filled colon.

## *False Positives*

False positives are generally not a problem at the CC view when directing the probe into the "CC pouch," the most gravity-dependent region between the urinary bladder and the body wall in the far-field. The great vessels are in the *opposite* direction, located sublumbar, which is not an imaging plane for the CC view.

If you fan dorsally into the sublumbar area, generally unnecessary during AFAST, the great vessels, female reproductive tract, and lymph nodes may become confounders because they are generally anechoic fluid-filled structures or hypoechoic structures, respectively.

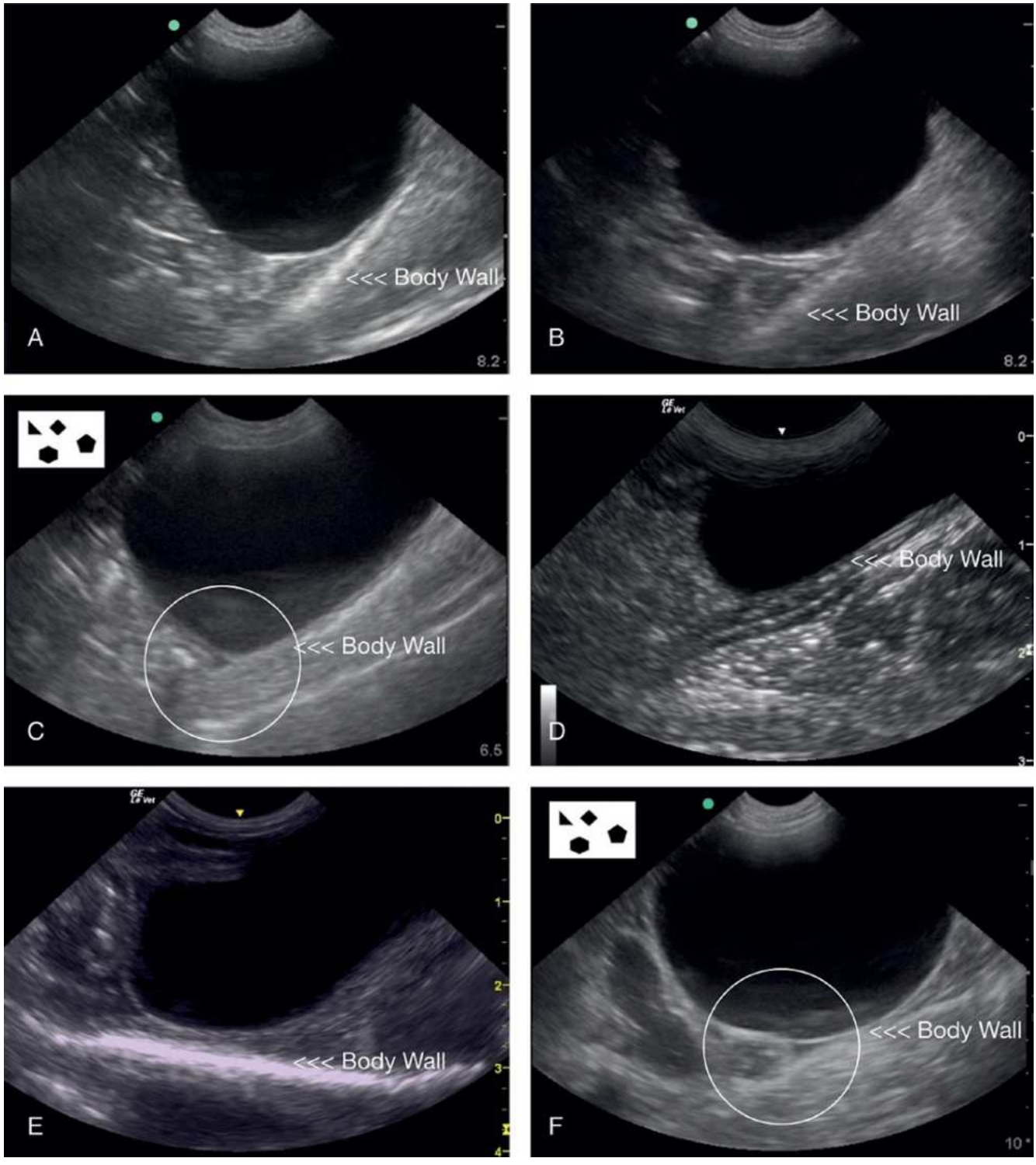


**Figure 6.24.** Examples of typical negative studies at the CC view. In all these images, note how readily recognizable is the filled urinary bladder as a landmark along with the body wall in the far-field within the "CC pouch." The "CC pouch" is very sensitive for detecting small-volume effusions as noted in (C) and (F) and the small anechoic triangulation circled, which in fact may be considered a normal finding in juvenile puppies and kittens with abdominal fluid scores of no more than 1. In fact, adult dogs and cats may also have a small amount of free fluid (<3 mm) at the CC view as the *only* positive AFAST view. The only other typical abdominal structures in these images are small intestine. Because of its facial planes and acoustic enhancement through the fluid-filled urinary bladder, the body wall is typically a hyperechoic (bright white) line. Images (A), (B), (D) and (E) are negative CC studies. Note the consistency in the images with their proportionality and location of the relevant CC view structures of the urinary bladder, "CC pouch", and body wall. Source: Reproduced with permission of Dr Gregory Lisciandro, Hill Country Veterinary Specialists and FASTVet.com, Spicewood, TX.

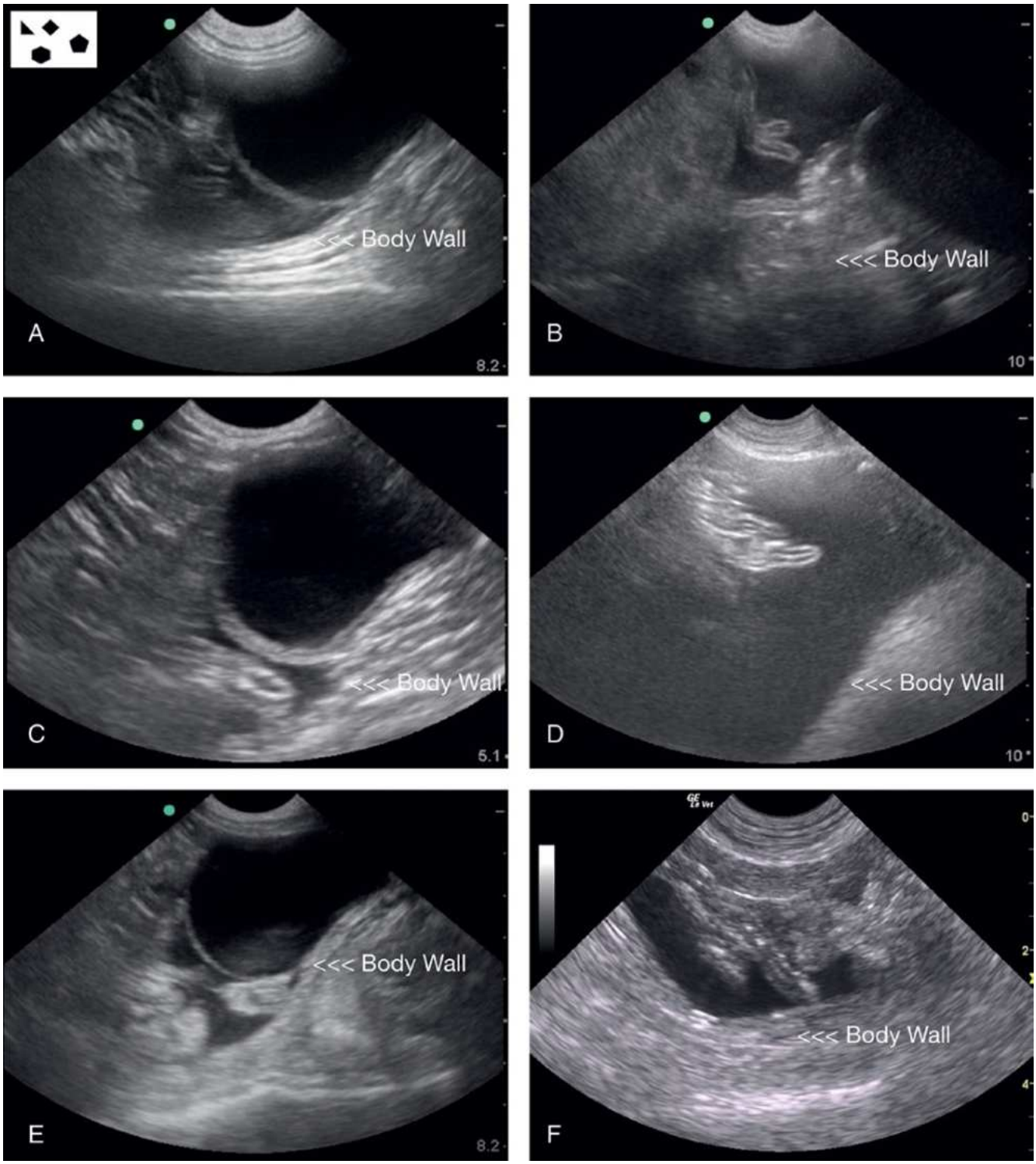


**Figure 6.25.** Examples of typical positive studies at the CC view. In (A), (C) and (E), CC view positives are shown with a urine-filled urinary bladder in contrast to images in (B), (D) and (F) in which the urinary bladder is not readily apparent as in (B) or absent in (D) and (F). The urinary bladder is likely not ruptured, as most of these patients are nontrauma cases, and the probe could be slid caudally and/or directed toward the pubis to locate a small urinary bladder. In the absence of a urinary bladder, the serial AFAST examination post resuscitation is invaluable to determine the presence of the urinary bladder and urine production. Note the consistency in the images with their proportionality and location of the relevant CC view structures of the urinary bladder, "CC pouch", and body wall. Source: Reproduced with permission of Dr Gregory Lisciandro, Hill Country Veterinary Specialists and FASTVet.com, Spicewood, TX.

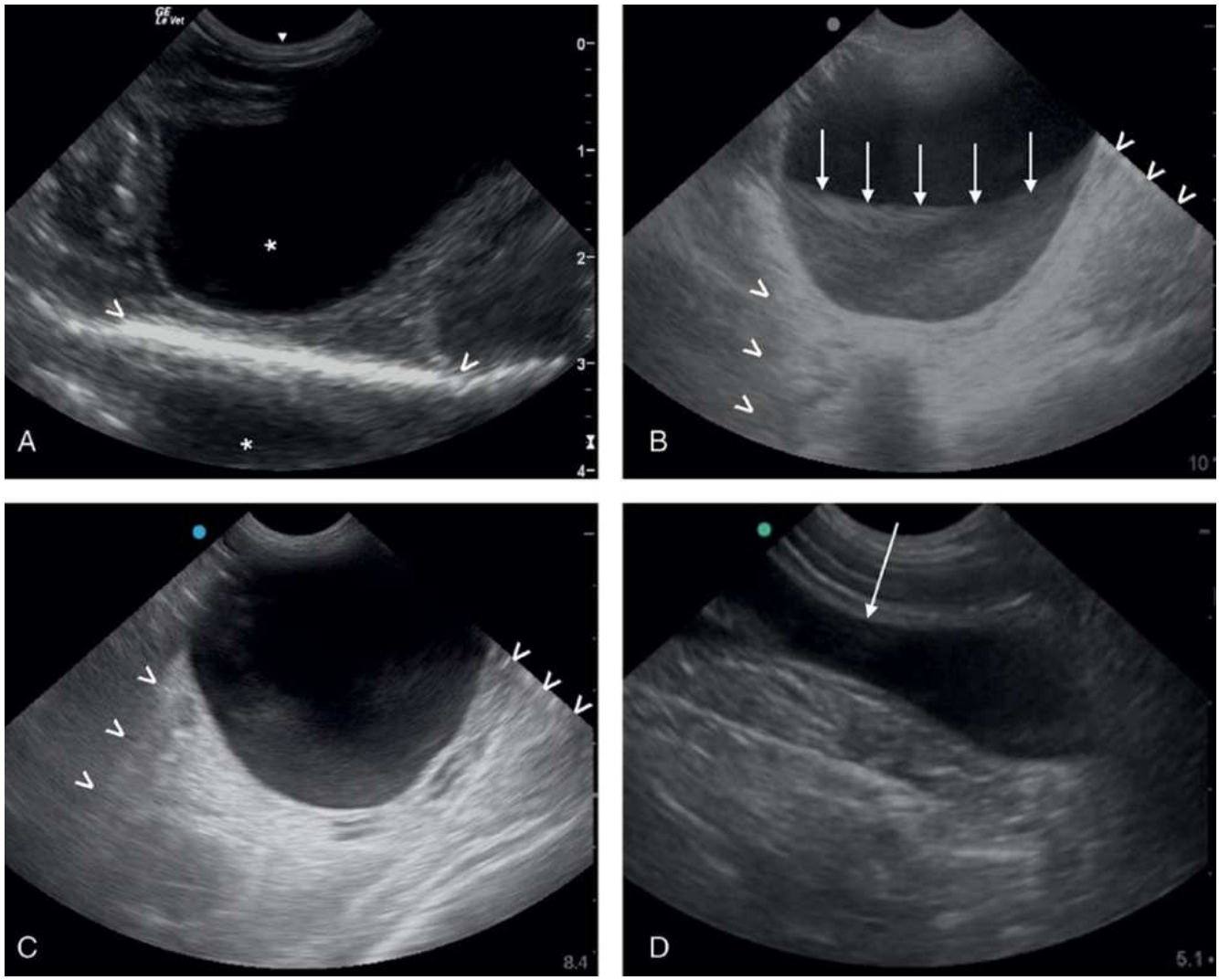


**Figure 6.26.** Relevant artifacts at the CC view. (A) A mirror image artifact is present beyond the body wall and marked with an asterisk (*). Placing the focus cursor in the center of the image and changing the angle of insonation can help eliminate mirror image. Acoustic enhancement artifact, the hyperechoic body wall, is also present through the fluid-filled urinary bladder and its cranial and caudal borders marked (V). In (B) the acoustic enhancement artifact is again marked (V). The arrows outline the borders of a slice-thickness artifact that mimics sediment. Turning down the gain will reduce the artifact whereas sediment will persist. Color flow Doppler will also demonstrate there is no flow through the artifact. In (C) is another example of acoustic enhancement artifact with marked borders (V). In (D) probe pressure deforms the shape of the urinary bladder, making it "dumbbell" or "figure 8" shaped, and is often uncomfortable for your patient. When measuring the urinary bladder for volume estimation, probe pressure will contribute to error. Source: Reproduced with permission of Dr Gregory Lisciandro, Hill Country Veterinary Specialists and FASTVet.com, Spicewood, TX.

**Pearl:** Direct the probe into the "CC pouch" as a general rule of thumb to avoid confounders.

**Pearl:** Note that in puppies and kittens <6 months of age (and even up to 9 months), many have small volumes (<3 mm maximum dimension) of anechoic free fluid (ascites) that is considered normal (Lisciandro et al. 2015, 2019; Stander et al. 2010), having AFS of 1 and 2. These juveniles are most commonly positive at the CC, SRU and DH views (Lisciandro et al. 2015, 2019; Romero et al. 2015).

### False Negatives

Don't sweat questionable small pockets of free fluid (<3 mm), by remembering the mantra of "resuscitate, rehydrate, and reevaluate" with a *serial* AFAST. Always perform at least one repeat serial AFAST four hours post admission (sooner if the patient is questionable or unstable) to avoid missing subtle or nonexistent free fluid (or other soft tissue-related pathology) on the initial AFAST that has become more obvious and substantial (Lisciandro et al. 2009).

### Abnormalities of the Urinary Bladder

The AFAST from its inception in 2005 has been a target organ approach in addition to screening for free fluid, its FAST component. With the repetitive fanning through the urinary bladder, deviations from the expected appearance of the urinary bladder are bound to be noted by the sonographer, from sediment to calculi to thrombi to masses. Some examples are shown in Figures 6.27 and 6.28 as well as some cofounders in Figure 6.29. Chapter 11 provides more detail.

## AFAST Hepato-Renal Umbilical View

| Questions Asked at the HRU (SRU) View[a] | |
|---|---|
| Is there any free fluid in the abdominal (peritoneal) cavity? | Yes or no |
| How much free fluid is at the HRU view using the AFAST AFS system? | 0, 1/2 or 1 |
| What does the small intestine look like?[b] | Unremarkable or abnormal |
| What does the spleen look like?[b] | Unremarkable or abnormal |
| Is the liver in view in the transverse plane of the umbilicus?[b] | Yes or no<br>If yes, suspect hepatomegaly |
| Is the stomach in view in the transverse plane of the umbilicus?[b] | Yes or no<br>If yes, gastric distension |
| Could I be mistaking an artifact or pitfall for pathology? | Know pitfalls and artifacts |

[a]Note that this view is the HRU view in right lateral recumbency and the SRU view in left lateral recumbency.
[b]It is important to know that the AFAST target organ approach for parenchymal abnormalities is binary as "unremarkable" or "abnormal" to capture the case for additional imaging and confirmatory testing. More interpretative skills may be gained through experience, and additional ultrasound study and training.
Source: Reproduced with permission of Dr Gregory Lisciandro, Hill Country Veterinary Specialists and FASTVet.com, Spicewood, TX.

The final AFAST view that is used for the AFS is the hepato-renal umbilical (HRU) view when the patient is in right lateral recumbency. The HRU view is imaged by placing the probe just ventral to the umbilicus while staying in the transverse plane of the umbilicus. Typically the HRU view includes loops of small intestine and often the spleen, especially in dogs. Its target organs are in reality the small intestine and spleen (Figures 6.30 and 6.31). At the level of the umbilicus, the liver and stomach should not be in view unless either is severely enlarged or distended, triggering additional imaging, such as radiography. *The liver and right kidney are not part of the HRU view*.

The probe with the marker toward the head in longitudinal (sagittal) orientation is placed just under the umbilicus and fanned through the most gravity-dependent region referred to as the "HRU pouch" (see Figure 6.30). Find evidence that you are in fact imaging intraabdominal structures such as the spleen or small intestine. In larger dogs, it is possible to be imaging through the abdominal muscles and not within the abdominal cavity.

The probe is *not* routinely run under the patient unless imaging the right kidney for the HR5th bonus view (Lisciandro et al. 2009; Lisciandro 2011).

Excessive probe pressure may cause small volumes of free fluid to move away or, in other words, to either side of the probe head and be missed.

In contrast to the previous three AFAST views, rotating the probe counterclockwise for transverse imaging at the HRU view (and SRU view when in left lateral) helps differentiate small intestinal loops from free fluid by making the small intestine in transverse or cross-section appear like "hamburgers" and in longitudinal or sagittal appear like "highways" because the small intestine consists of five ultrasonographic layers (see Figure 6.22 and Chapter 12).

When the spleen is present, use it as an acoustic window to interrogate for free fluid between its capsule and loops of small intestine.

In the first edition, this view was named the hepato-renal (HR) view and referred to as "The Big Lie" because the liver and the right kidney are not routinely examined, so neither "HR" target organ is directly scanned (Lisciandro 2014a). So we have renamed the HR view as the "HR umbilical view" to be more descriptive of where the probe is placed, and now advocate that the small intestine and spleen be its target organs.

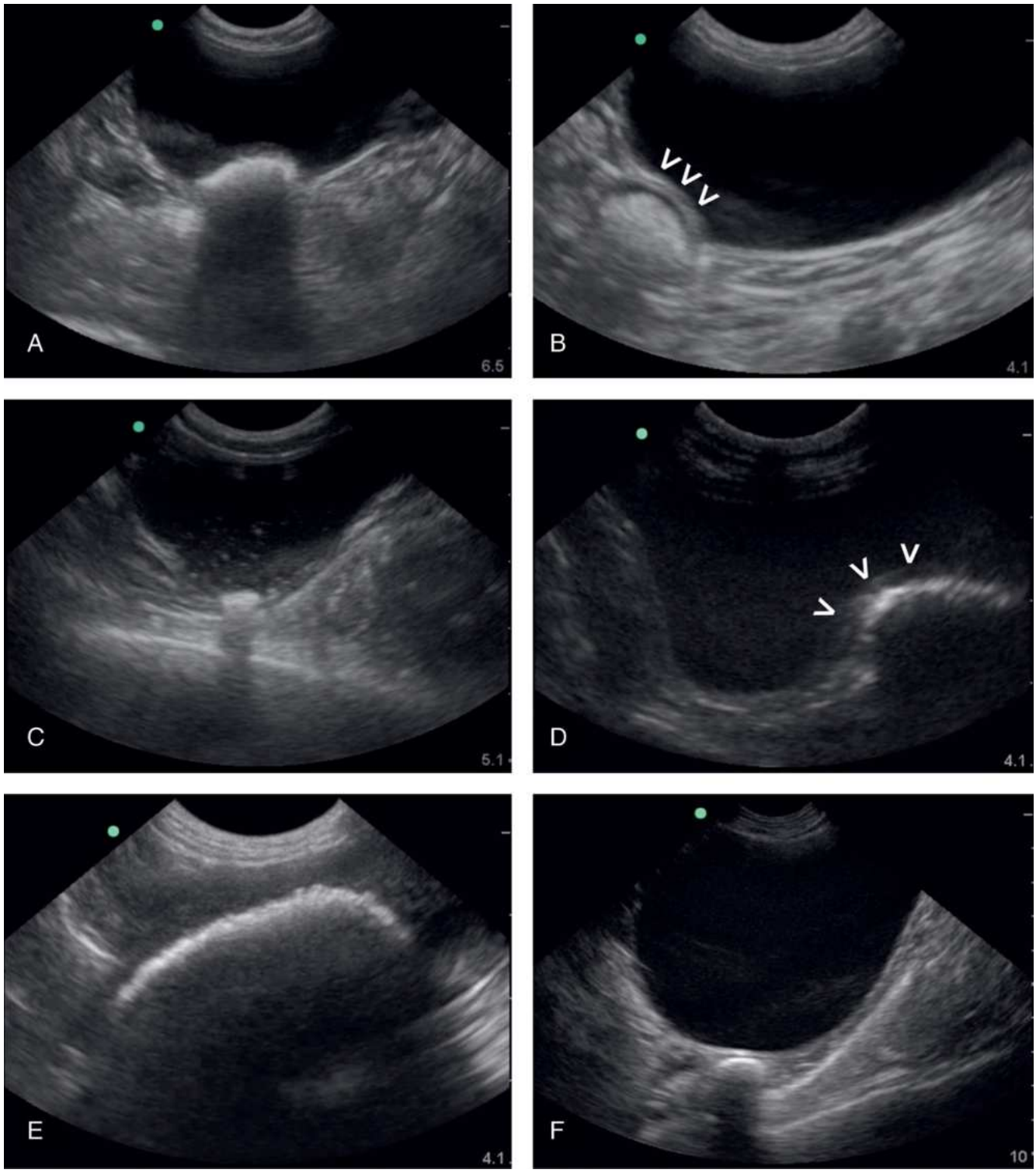


**Figure 6.27.** Calculi versus intestinal tract. The sonographer will readily appreciate deviations from the expected appearance of the urinary bladder at the CC view. In images (A), (C) and (E) bladder calculi are evident by clean shadowing through the far-field and contained within the lumen of the urinary bladder. Moreover, they should settle at the "CC pouch" where free fluid would pocket being at the CC view's most gravity-dependent region. In (B), (D) and (F) are examples of air-filled intestinal tract that mimic urinary bladder calculi illustrating how care should be taken. By examining (and magnifying) more closely, the bladder lumen can be seen to be pushed into the lumen by the loop of intestinal tract as in (B) and (D) indicated by the cursors (V). Moreover, an abdominal radiograph may be added to the diagnostic work-up. Source: Reproduced with permission of Dr Gregory Lisciandro, Hill Country Veterinary Specialists and FASTVet.com, Spicewood, TX.

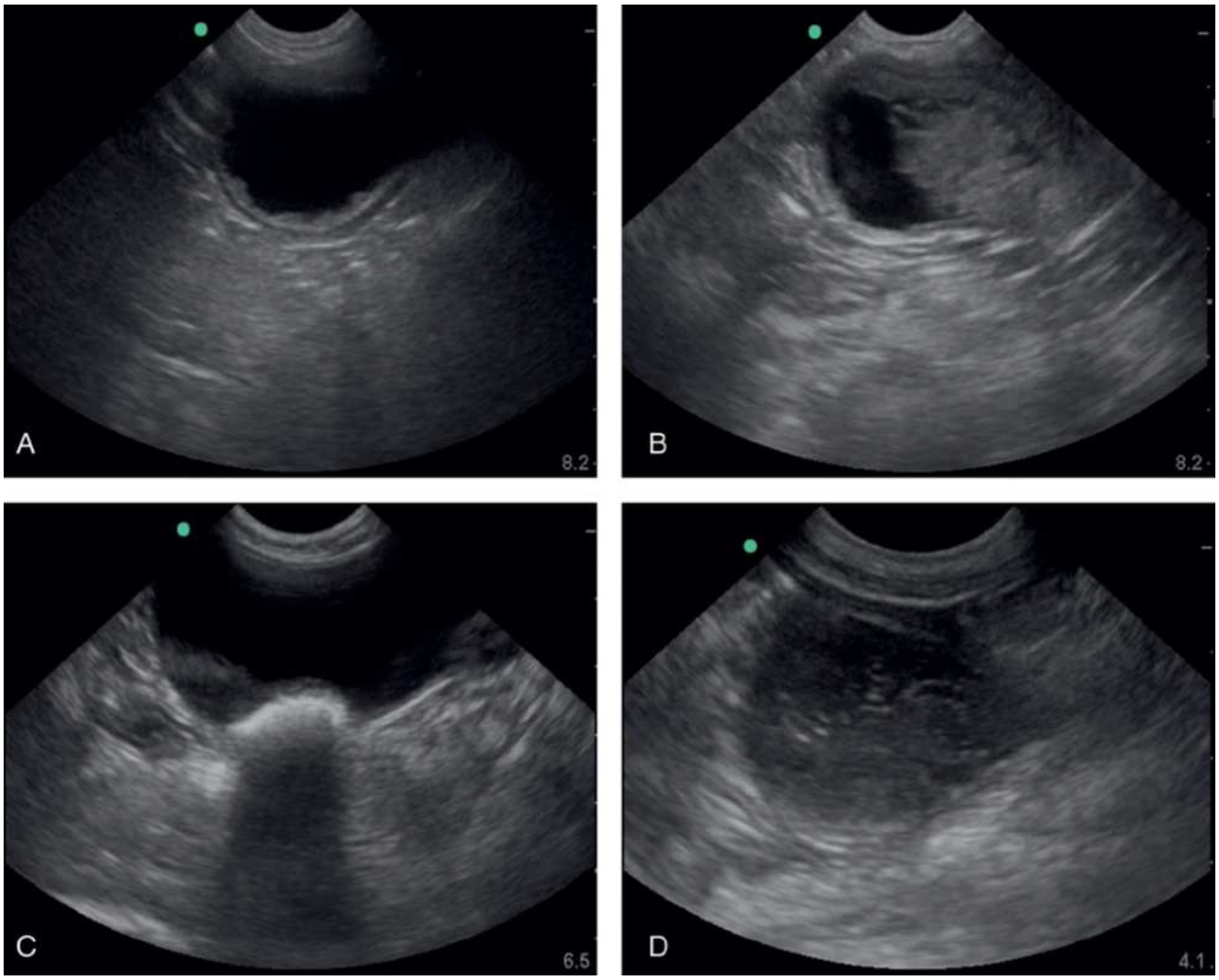


**Figure 6.28.** Various abnormal intraluminal urinary bladder findings. (A) An irregular urinary bladder wall in its apical region suggestive of chronic cystitis. (B) A soft tissue mass in the trigone region of the urinary bladder of an older female dog that was hit by a car (blunt trauma). The condition was captured and the dog diagnosed with a transitional cell carcinoma that lived with treatment for another 11 months. Color flow Doppler could be additionally applied to evaluate for blood flow (not shown). (C) Bladder calculi in a diabetic being admitted for hospitalized care. (D) A large thrombus in an older male bluntly traumatized dog. Color flow Doppler was helpful for documenting absent flow. Source: Reproduced with permission of Dr Gregory Lisciandro, Hill Country Veterinary Specialists and FASTVet.com, Spicewood, TX.

**Pitfall:** Excessive probe pressure will cause small volumes of free fluid to move away to either side of the probe head and be potentially missed.

**Pitfall:** If the probe is not directed into the abdominal cavity or lacks adequate depth then you may be imaging through planes of body wall or "imaging through bacon," as the author likes to say.

**Pearl:** The HRU view (SRU view in left lateral recumbency) is performed just ventral (right below) to the umbilicus to image the most gravity-dependent area of the laterally recumbent dog or cat.

**Pearl:** Stay longitudinal (sagittal) at all sites (DH, SR, CC) except at the HRU view where it is helpful to perform both longitudinal (fanning) and transverse (rotating to the left or counterclockwise) imaging to discriminate free fluid (anechoic black triangles) from small intestine.

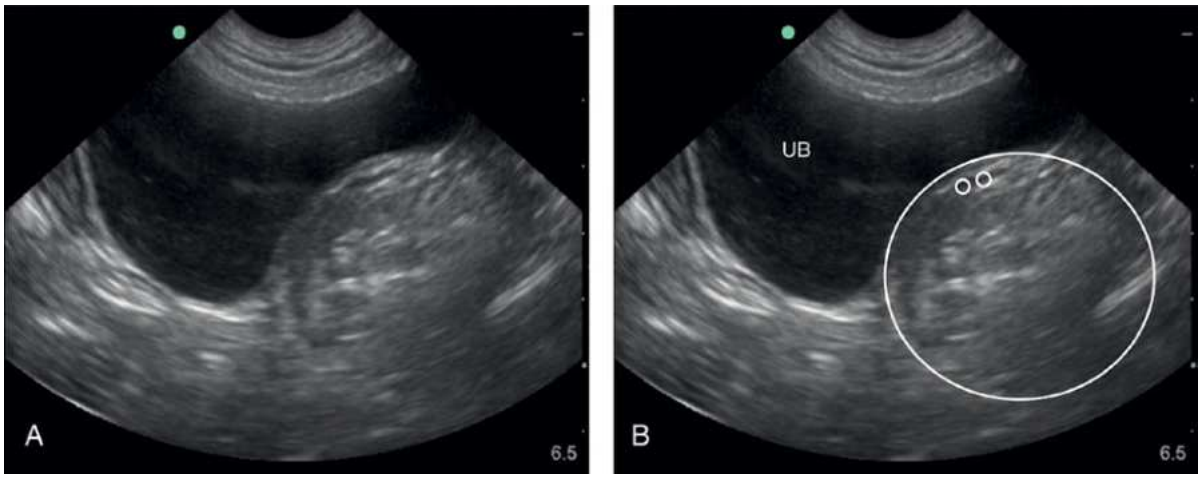


**Figure 6.29.** Pitfall of the thigh or a mass or other. In (A) and (B) are identical images unlabeled and labeled. The large circle encompasses the region of interest and its suspect origin of being the thigh muscle. The smaller circles are where typically the femoral artery and vein would be located with the patient in lateral recumbency and observing for pulsation or applying color Doppler would be helpful. The image shows how the thigh can push into the urinary bladder or stool in the colon or a caudal abdominal mass and make odd impressions when imaging the CC view with a patient in lateral recumbency. A digital rectal examination as part of a good physical examination with or without more advanced imaging is an ancillary evaluation to increase the probability of being correct. From the still B-mode image, the exact origin of the circled structure may be unclear. UB, urinary bladder. Source: Reproduced with permission of Dr Gregory Lisciandro, Hill Country Veterinary Specialists and FASTVet.com, Spicewood, TX.

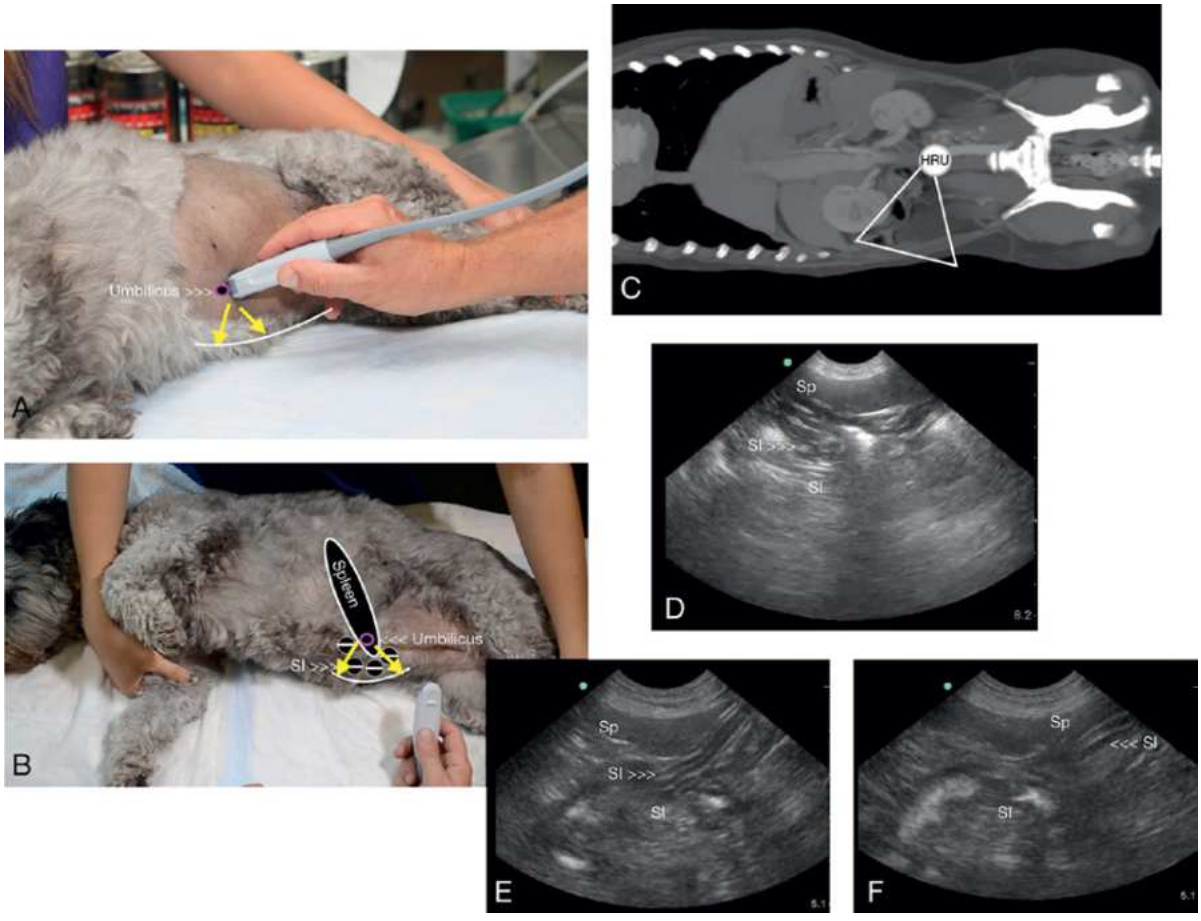


**Figure 6.30.** HRU view in a dog. In (A) and (B) the direction of the probe is shown externally ventral to midline at the level of the umbilicus with the objective to image and fan through the most gravity-dependent "HRU pouch" illustrated by the white curved line. (B) A similar image with anatomy overlay that correlates with CT image in (C). The target organs for the HRU (and SRU) view are in reality the small intestine and spleen and either or both should be recognized to confirm that you are imaging the abdominal cavity. In (D), (E) and (F) the expected sonographic images are shown. Computed tomography courtesy of Dr Daniel Rodriguez, VETTEM, and Dr Jesús Paredes, CVM, Mexico City, Mexico. Source: Reproduced with permission of Dr Gregory Lisciandro, Hill Country Veterinary Specialists and FASTVet.com, Spicewood, TX.

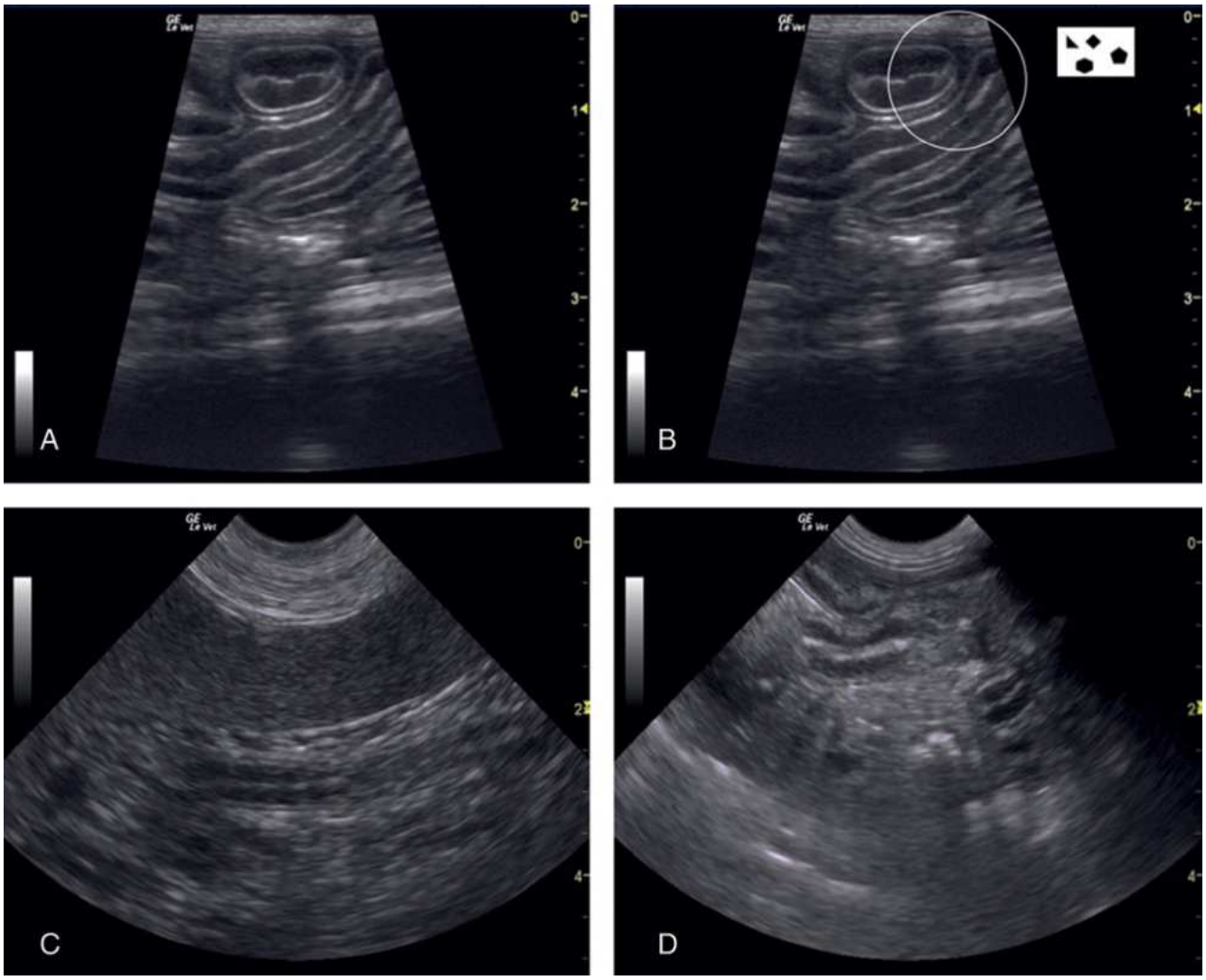


**Figure 6.31.** Examples of typical negative studies at the HRU (SRU) view. The target organs are the small intestine and spleen. By imaging either or both, the sonographer knows they are within the abdominal cavity. (A) and (B) are the same image labeled and unlabeled, showing how the small intestine in cross-section, transverse orientation, appears like "hamburgers" and in longitudinal or sagittal appears like "highways." In (B) the circle highlights an area that may or may not have a small triangulation of free fluid, illustrating the difficulty in seeing small pockets of fluids (milliliters) in between intestinal loops because of the anechoic layers of intestine. A better strategy is shown in (C) by using the spleen as an acoustic window and looking for free fluid on its far side. In (D) is another region in which soft tissue is in proximity to small intestine as a better strategy to detect small-volume effusions at this view than in (A) and (B). Source: Reproduced with permission of Dr Gregory Lisciandro, Hill Country Veterinary Specialists and FASTVet.com, Spicewood, TX.

If the right (left in left lateral recumbency) kidney needs to be imaged because of concern for retroperitoneal injury, or when hematuria exists, then the HR5th (SR5th in left lateral recumbency) bonus view should be performed. Once the four AFAST views used for the AFS are mastered, the HR5th/SR5th bonus views should be considered as an add-on skills and incorporated for all subsequent patients.

### *Typical HRU View Positives*

The HRU (SRU) view is the most gravity-dependent view in right lateral recumbency (the SRU when in left lateral recumbency) and completes the four AFAST views and the calculation of its applied fluid scoring system and assigning the AFS (see Chapter 7). The "rabbit ear sign" is typical in large-volume effusions created by small intestine and omentum

wafting in the free fluid and typical positives are shown in Figure 6.32. Furthermore, if positives were previously seen at the other less gravity-dependent AFAST views, the sonographer is already anticipating the likelihood of performing abdominocentesis at the HRU view (SRU view in left lateral recumbency).

**Pearl:** Fluid must always be characterized if safely retrievable by abdominocentesis because ultrasound cannot characterize the type of fluid based on its echogenicity.

## *False Positives*

### Gastrointestinal (GI) Tract

Small intestine and stomach may be fluid-filled or have their wall infiltrated (abnormal) in diseased states and may appear mistakenly as free fluid (see Figure 6.31).

### Midabdominal Masses

Large centrally located necrotic fluid-filled splenic, hepatic, or renal masses may be mistaken for free fluid (Figure 6.33).

### Fluid-filled Uterus

A large fluid-filled uterus in an intact female may be mistaken for free fluid (see Figure 6.33). The female reproductive tract is further addressed in Chapter 14.

**Pearl:** Consider your patient's signalment and don't mistake an enlarged uterus for free fluid.

## *False Negatives*

### Serial AFAST Increase Sensitivity

Don't sweat questionable small pockets of free fluid. Repeat the AFAST at least once four hours later (called a serial exam) as standard of care, and sooner in questionable or unstable patients (Lisciandro et al. 2009; Blackbourne et al. 2004; acep.org).

# AFAST HR5th (SR5th) Bonus View

Questions Asked at the HR5th (SR5th) Bonus View[a]

| | |
|---|---|
| Is there any free fluid in the abdominal (peritoneal) cavity? | Yes or no |
| How much free fluid is at the HR5th (SR5th) bonus view using the AFAST-applied fluid scoring system?[a] | 0, 1/2, 1<br>NOT part of the abdominal fluid scoring system |
| Is there any free fluid in the retroperitoneal space? | Yes or no<br>Trivial, mild, moderate, severe (also can measure and record its greatest dimension) |
| What does the right (#left) kidney look like?[b] | Unremarkable or abnormal |
| What does the liver (#spleen) look like?[b] | Unremarkable or abnormal |
| Could I be misinterpreting an artifact or pitfall as pathology? | Know pitfalls and artifacts |

[a]Note that this view is the HR5th bonus view in right lateral recumbency and the SR5th bonus view in left lateral recumbency, often performed with the patient standing after AFAST (and TFAST and Vet BLUE) as the last view performed.
[b]It is important to know that the AFAST target organ approach for parenchymal abnormalities is binary as "unremarkable" or "abnormal" to capture the case for additional imaging and confirmatory testing. More interpretative skills may be gained through experience, and additional ultrasound study and training.
Source: Reproduced with permission of Dr Gregory Lisciandro, Hill Country Veterinary Specialists and FASTVet.com, Spicewood, TX.

The bonus 5th view of AFAST is a bonus in that it is *not* part of the AFS system; however, it does interrogate the right (or left) retroperitoneal space more thoroughly than the SR (HR) view alone, and assesses the right liver (left liver), and right (left) kidney for soft tissue abnormalities that may otherwise be missed (Figure 6.34).

The HR5th bonus view is imaged by placing the probe at the junction of the costal arch and hypaxial muscles, identical to the SR view but with the probe directed much further cranially because the right kidney is more cranially located and obliquely positioned. In dogs, the right kidney is cupped within the renal fossa of the liver, whereas in cats it is generally separated from the liver by interposing fat (see Figure 6.34). This anatomical feature is important for

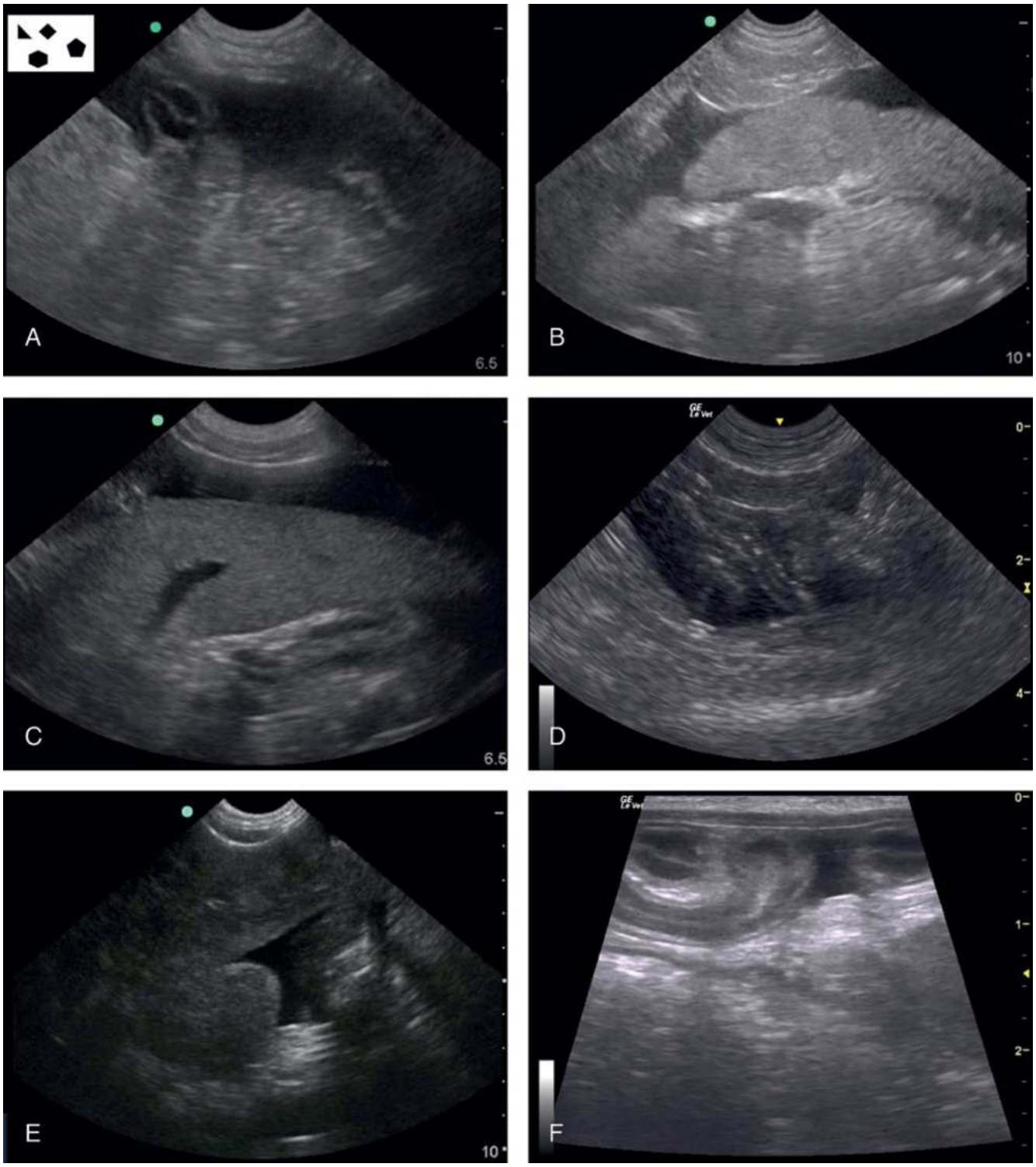


**Figure 6.32.** Examples of typical positive studies at the HRU (SRU) view. In (A) a loop of small intestine that appears like a "hamburger" is wafting in free fluid in real time and easily recognized. In (B) free fluid is outlining what appears to be the spleen. In (C) the spleen is confirmed by the finding of vessels splitting its capsule and free fluid is obvious. In (D) free fluid is seen wafting omentum and small intestine. In (E) an anechoic triangulation is obvious and lastly in (F) an anechoic triangulation, "hourglass like," is found between loops of small intestine. Source: Reproduced with permission of Dr Gregory Lisciandro, Hill Country Veterinary Specialists and FASTVet.com, Spicewood, TX.

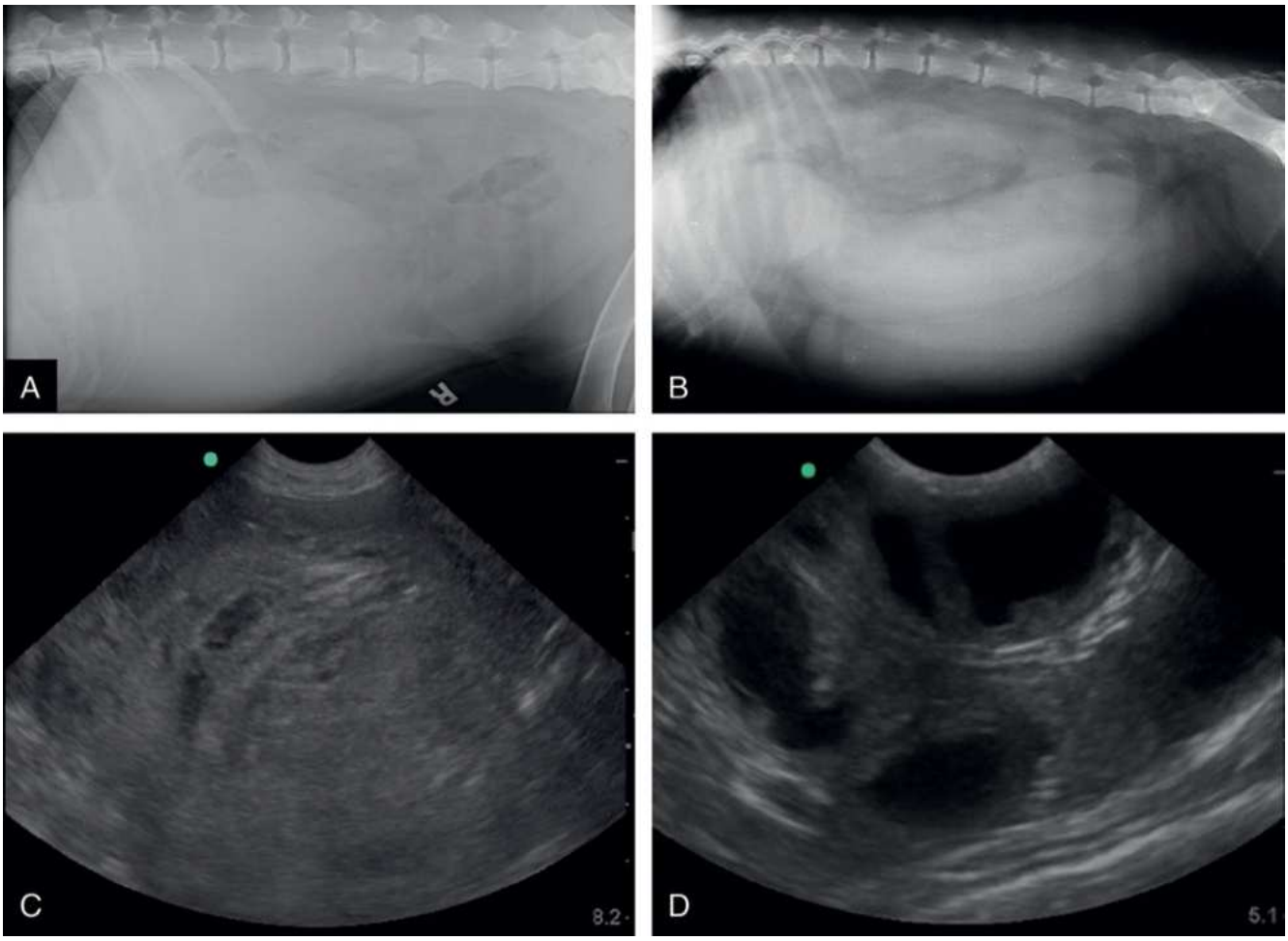


**Figure 6.33.** False positives at the HRU (SRU) view. In (A) and (C) are the abdominal radiograph and the HRU (SRU) view of a patient in which necrotic masses can have intracavitary necrosis with triangulations of fluid mimicking free fluid. Increasing your depth and sliding and sweeping your probe to add more interrogation (or adding a radiograph especially if the AFAST was performed first) is important. If the radiograph was the initial imaging test, AFAST helps differentiate free fluid from a mass or to determine that both are present. By assigning an AFS and performing abdominocentesis, fluid analysis, and cytology, decision making is expedited in most cases. (B) and (D) show an example of pyometra and how the compartmentalization of the uterus may appear like free fluid. The addition of an abdominal radiograph is complementary for best interpreting the AFAST study. Source: Reproduced with permission of Dr Gregory Lisciandro, Hill Country Veterinary Specialists and FASTVet.com, Spicewood, TX.

the sonographer because the canine right kidney is located by following and fanning the right liver caudally and dorsally. If you run out of liver caudally, then you must return to a more craniodorsal acoustic window to find the right kidney. If the costal–hypaxial muscle junction is ineffective for locating the right kidney then the probe may be moved over the 11th and 12th intercostal spaces, although rib shadowing will likely affect the imaging of the right kidney. The left kidney is independent of the liver in both dogs and cats, located more caudally, more parallel to the long axis of your patient, and generally not viewed through intercostal spaces.

The HR5th bonus view's target organs are the liver and right kidney (or left kidney and head of the spleen).

- The probe should be directed craniodorsal for the HR5th bonus view, and analogously for the SR5th bonus view.
- The author likes to find the liver and then fan through it, sliding caudally because in dogs the right kidney is cupped by the liver in its renal fossa. Thus, if you run out of liver, then you need to restart cranially within the liver again.

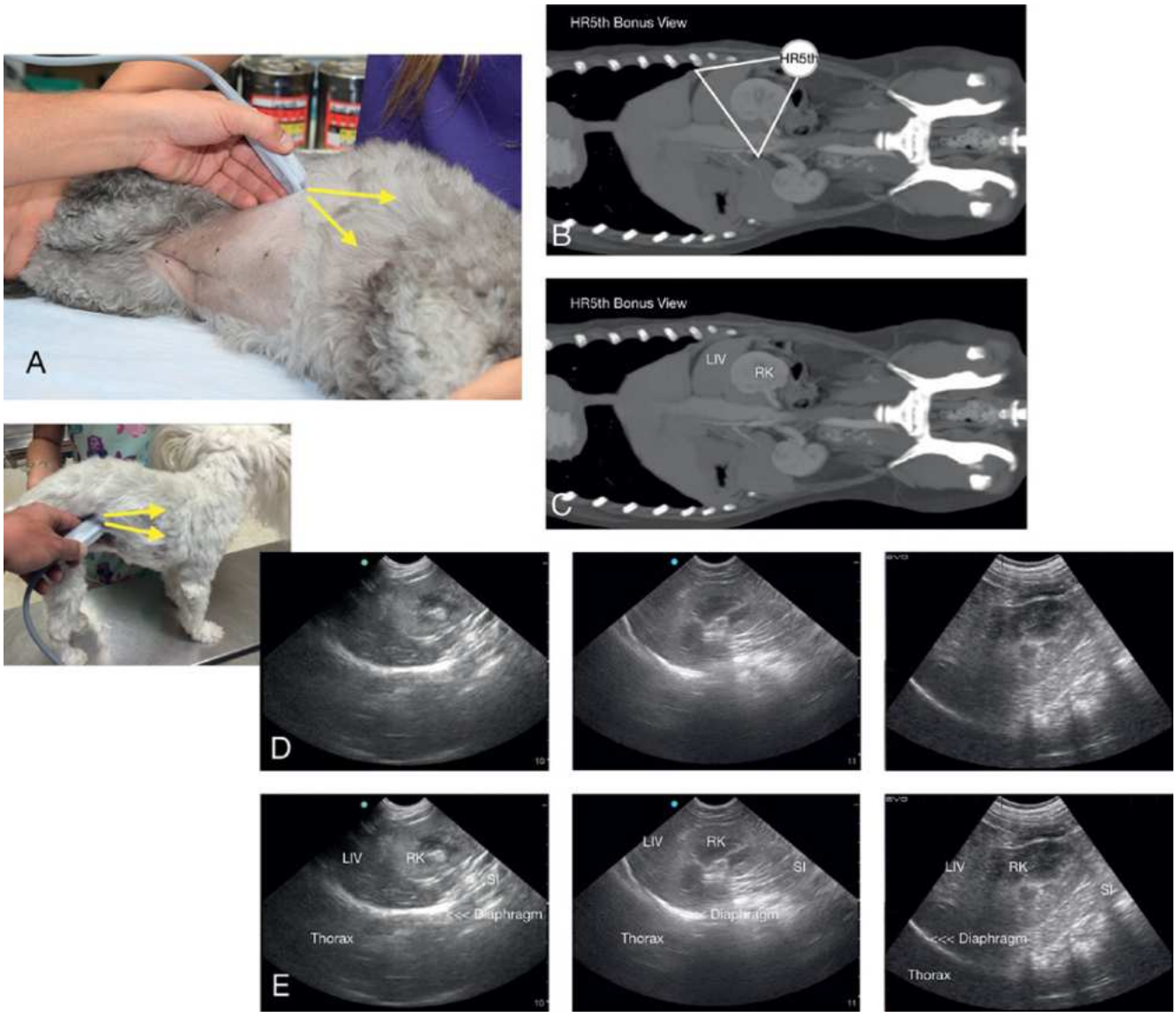


**Figure 6.34.** HR5th view on a dog. In (A) two different approaches are shown imaging the HR5th bonus view in which the right kidney and liver are in fact interrogated. In (A) the lateral recumbent method uses the same landmarks as the SR view where the costal arch meets the hypaxial muscles, but the probe is often directed much more cranially because the right kidney in the dog lies further cranially than its left counterpart (in contrast to cats not so much further cranially). The author prefers performing the HR5th bonus view (or SR5th bonus view in left lateral recumbency) with the patient *standing* after the four views of AFAST, TFAST and Vet BLUE have been completed leaving the HR5th (SR5th) bonus view as the final acoustic window. The same landmarks used in lateral are used in standing. The author avoids imaging between ribs if possible but either approach is acceptable (sonographer preference). In (B) and (C) are unlabeled and labeled CT images to better illustrate the anatomy. In (D) and (E) are typical negative studies of the HR5th bonus view unlabeled and labeled. Use the diaphragm as a landmark to find and follow the liver, which will lead you to the right kidney in dogs. LIV, liver; RK, right kidney. Source: Reproduced with permission of Dr Gregory Lisciandro, Hill Country Veterinary Specialists and FASTVet.com, Spicewood, TX.

- The diaphragm is a good landmark and helps locate the liver since the liver abuts the diaphragm.
- The liver and right kidney are then fanned through, searching for free fluid and screening for soft tissue lesions.

### *Typical HR5th Bonus View Positives*

Free fluid located around the right kidney and between the right kidney and the liver displacing the right kidney from its renal fossa in dogs. The SR5th bonus view is performed just like the SR view.

### *False Positives*

The caudal vena cava and other vasculature, aorta and portal vein, run through this region and can be confounders for free fluid (see Chapter 26). Color flow Doppler and holding the probe stationary in B-mode and watching for pulsation are other options to differentiate free fluid from venous or arterial blood flow. These vessels are generally not problematic at the SR and SR5th bonus views.

### *False Negatives*

Similar to the other AFAST views of missing small volumes, thus always performing at least one more AFAST is recommended as standard of care even in "stable" patients.

**Pearl:** The HR5th (and SR5th) bonus views are not part of the AFS.
**Pearl:** Consider the 5th bonus view as exactly that, a "bonus," not mandated but considered as an add-on skill once image acquisition is perfected at the first four AFAST views.

## AFAST-Focused Spleen

The AFAST-focused spleen should be performed after every AFAST if the spleen is imaged at the HRU (SRU) view (Figure 6.35). The author has routinely adopted this practice since the recognition of medically treated anaphylaxis-induced hemoabdomen in dogs (Lisciandro 2016a,b; Caldwell et al. 2018; Hnatusko et al. 2019; Birkbeck et al. 2019). The approach is that a positive AFAST-focused spleen for a mass is likely highly specific (the mass is real). In contrast, a negative AFAST-focused spleen doesn't rule a mass out (dependent on the operator). The AFAST-focused spleen is a *screening test*. For more detail, see Chapter 9.

- The spleen is identified by the finding of a hyperechoic capsule and the blood supply splitting the capsule.
- The slide and fan technique is repeated through successive sections while overlapping between sections. A more detailed evaluation may be found in Chapter 9.
- Scan cranially and then caudally to each end of the spleen. The author performs this twice and makes sure that the spleen was maximally imaged at the SR view.
- A mass that deforms the capsule of the spleen is always considered a serious finding.

## Recording AFAST Findings on Goal-directed Templates

Recording your findings is imperative for a successful ultrasound program. See Chapter 7 and the Appendices.

## Pearls and Pitfalls, The Final Say

AFAST is a standardized ultrasound examination with exact clarity of its five acoustic windows and how each is performed. AFAST has been shown to be superior to radiography for not only the detection of free intraabdominal fluid but also the volume through its AFAST-applied fluid scoring system (Lisciandro et al. 2009, 2015, 2019). Moreover, the AFAST DH view is an important source of patient information for free fluid, volume status, pericardial and pleural effusion and lung conditions. Chapter 7 covers clinical integration of AFAST-acquired information.

- AFAST has *exact* clarity to its five acoustic windows.
- AFAST and its acoustic windows are *exactly* the same no matter the patient positioning.
- Each view has target organs that are imaged while looking for free fluid (intraabdominal, retroperitoneal, pleural, pericardial) and lung conditions.
- AFAST should be part of any POCUS abdominal examination to make sure that effusions or other obvious target organ pathology are not missed.
- Serial AFAST and an assigned abdominal fluid score should be repeated, called the serial exam, four hours after the initial AFAST in all stable patients and sooner if the patient is unstable or questionable.

## Quick Reference of Normals and Rules of Thumb

- Adult dogs and cats should have no free fluid within their peritoneal cavity or retroperitoneal space (or within the pleural cavity or pericardial sac); however, recent research evaluating anesthetized adult dogs and cats, and puppies and kittens has documented small pockets of free intraabdominal fluid in clinically normal canines and felines.
- The originally published AFAST-applied abdominal fluid scoring system was scored according to number for positive AFAST views (range 0–4)

excluding the bonus 5th view that is not part of the AFS. However, to better categorize small-volume bleed/effusion from large-volume bleed/effusion, AFS at each respective AFAST view now ranges from 0 (negative) to ½ (small pocket <5 mm in cats and <10 mm in dogs) to 1 (>5 mm cats and >10 mm dogs).

- Total AFS remains as originally published, with the categorization of small-volume bleed/effusion defined as AFS <3 (AFS ranges from 0 to 2½, thus including AFS of 1, 1½, 2 and 2½) and large-volume bleed/effusion defined as AFS ≥3 (AFS ranges from 3 to 4, including AFS of 3, 3½ and 4).
- Expect that ~50% of adult dogs will have an AFS of ½ along the diaphragm at the DH view with maximum dimensions of <3 mm that may not be noticeable in unsedated, unanesthetized adults (Lisciandro et al. 2019).
- Expect ~90% of puppies <6 months of age to have an AFS of ½ to 1 along the diaphragm at the DH view and then with fairly equal distribution between the other three AFAST views of ½ to 1 with maximum dimensions of <3 mm (Lisciandro et al. 2019).
- Expect that ~70% of adult cats and kittens <6 months of age will have AFS of ½ along the diaphragm at the DH view and then next most commonly positive in both age groups at the most gravity-dependent umbilical view (SR view in left lateral recumbency) with maximum dimensions at

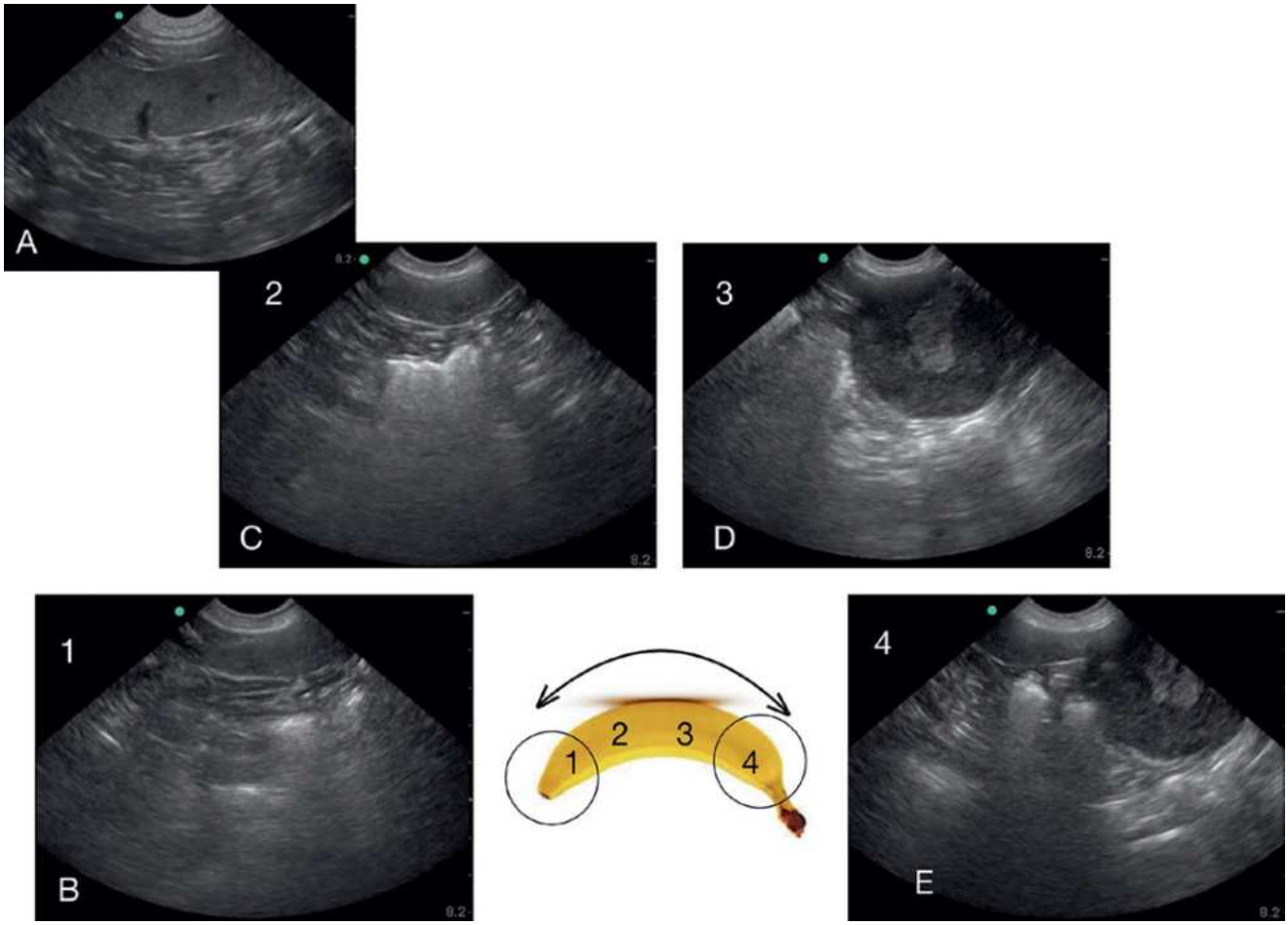


**Figure 6.35.** AFAST-focused spleen. The spleen represented by the banana is interrogated by the "slide and fan" approach, overlapping each section as scanning cranially until there is no more spleen and then scanning caudally until there is no more spleen. The author repeats the technique twice. Its hyperechoic capsule and the blood vessels splitting the capsule as in (A) identify the spleen. (B–E) A scan in a dog that has a splenic mass. In (B) and (C) the spleen is unremarkable until at (D) and (E) a mass that disrupts the contour of the splenic capsule is noted, a serious finding. Source: Reproduced with permission of Dr Gregory Lisciandro, Hill Country Veterinary Specialists and FASTVet.com, Spicewood, TX.

either of these AFAST views of <3 mm that may or may not be noticeable in unsedated, unanesthetized adult cats and kittens (Lisciandro et al. 2015).
- The finding of sonographic striation of the canine gallbladder wall should be considered abnormal in the acute setting (acute collapse and weakness) even when the thickness is in the normal range of 1–3 mm; anaphylaxis, "anaphylactic gallbladder," and right-sided congestive heart failure, "cardiac gallbladder," should be ruled out using the Global FAST approach.
- Although rare in cats, a "cardiac gallbladder" may occur with feline congestive heart failure.
- Characterization of the caudal vena cava may be grouped as a "bounce" and fluid responsive, "FAT" and fluid intolerant, and "flat" and hypovolemic.
- Maximum heights at the FAST DH view may be used to additionally characterize the caudal vena cava (see Tables 7.6 and 36.3).

# References


American College of Emergency Physicians. 2001. ACEP emergency ultrasound guidelines 2001. *Ann Emerg Med* 38:470–481.

Bilello JF, Davis JW, Lemaster D, et al. 2011. Prehospital hypotension in blunt trauma: identifying the "crump factor." *J Trauma* 70(5): 1038–1042.

Birkbeck R, Greensmith T, Humm K, et al. 2019. Haemoabdomen due to suspect anaphylaxis in four dogs. *Vet Rec Case Rep* 7:e000734.

Blackbourne LH, Soofer D, McKenney M, et al. 2004. Secondary ultrasound examination increases the sensitivity of the FAST exam in blunt trauma. *J Trauma* 57(5): 934–938.

Boysen SR, Lisciandro GR. 2013. The use of ultrasound in the emergency room (AFAST and TFAST). *Vet Clin North Am Small Anim Pract* 43(4):773–797.

Boysen SR, Rozanski EA, Tidwell AS, et al. 2004. Evaluation of a focused assessment with sonography for trauma protocol to detect free abdominal fluid in dogs involved in motor vehicle accidents. *J Am Vet Med Assoc* 225(8):1198–1204.

Caldwell DJ, Petras KE, Mattison BL, et al. 2018. Spontaneous hemoperitoneum and anaphylactic shock associated with Hymenoptera envenomation in a dog. *J Vet Emerg Crit Care* 28(5):476–482.

Candotti C, Arntfield R. Pericardial effusion. 2014. In: Point-of-Care Ultrasound, edited by Soni NJ, Arntfield R, Kory P. Philadephia: Elsevier, pp 130–134.

Darnis E, Boysen S, Merveille AC, et al. 2018. Establishment of reference values of the caudal vena cava by fast-ultrasonography through different views in healthy dogs. *J Vet Intern Med* 32(4):1308–1318.

Ferrada P, Vanguri P, Anand RJ, et al. 2012a. Flat inferior vena cava: indicator of poor prognosis in trauma and acute care surgery patients. *Am Surg* 78(12):1396–1398.

Ferrada P, Anand RJ, Whelan J, et al. 2012b. Qualitative assessment of the inferior vena cava: useful tool for the evalutaion of fluid status in criticall ill patients. *Am Surg* 78(4):468–470.

Grimes JA, Fletcher JM, Schmiedt CW. 2018. Outcomes in dogs with uroabdomen: 43 cases (2006–2015). *J Am Vet Med Assoc* 252(1):92–97.

Hnatusko A, Gicking JC, Lisciandro GR. 2019. Anaphylaxis-related hemoperitoneum in 11 dogs. *J Vet Emerg Crit Care*, in press.

Hoffberg JE, Koenigshof AM, Guiot LP. 2016. Retrospective evaluation of concurrent intra-abdominal injuries in dogs with traumatic pelvic fractures: 83 cases (2008–2013). *J Vet Emerg Crit Care* 26:288–294.

Lichtenstein DA. 2010. Gallbladder. In: Whole Body Ultrasound in the Critically Ill, edited by Lichtenstein DA. London: Springer, pp 59–67.

Lisciandro GR. 2011. Abdominal and thoracic focused assessment with sonography for trauma, triage, and monitoring in small animals. *J Vet Emerg Crit Care* 21(2):104–122.

Lisciandro GR. 2012. Evaluation of initial and serial combination focused assessment with sonography for trauma (CFAST) examinations of the thorax (TFAST) and abdomen (AFAST) with the application of an abdominal fluid scoring system in 49 traumatized cats. Abstract. *J Vet Emerg Crit Care* 22(S2):11.

Lisciandro GR. 2014a. The abdominal FAST$^3$ (AFAST$^3$) exam. In: Focused Ultrasound for the Small Animal Practitioner, edited by Lisciandro GR. Ames: Wiley Blackwell, pp 17–43.

Lisciandro GR. 2014b. The thoracic FAST$^3$ (TFAST$^3$) exam. In: Focused Ultrasound for the Small Animal Practitioner, edited by Lisciandro GR. Ames: Wiley Blackwell, pp 140–165.

Lisciandro GR. 2014c. Alanine aminotransferase level (ALT) as a marker for hemoabdomen detected by abdominal FAST (AFAST) in dogs with automobile trauma. *J Vet Emerg Crit Care* 24(S1):S11.

Lisciandro GR. 2016a. The use of the diaphragmatico-hepatic (DH) views of the abdominal and thoracic focused assessment with sonography for triage (AFAST/TFAST) examinations for the detection of pericardial effusion in 24 dogs (2011-2012). *J Vet Emerg Crit Care* 26(1):125–131.

Lisciandro GR. 2016b. Abdominal FAST (AFAST)-detected hemorrhagic abdominal effusion in 11 dogs with acute collapse and gallbladder wall edema (halo sign) with presumed anaphylaxis. Abstract. *J Vet Emerg Crit Care* 26(S1):S8.

Lisciandro GR, Fosgate GT. 2017. Use of AFAST cysto-colic view urinary bladder measurements to estimate urinary bladder volume in dogs and cats. *J Vet Emerg Crit Care* 27(6):713–717.

Lisciandro GR, Lagutchik MS, Mann KA, et al. 2008. Evaluation of a thoracic focused assessment with sonography for trauma (TFAST) protocol to detect pneumothorax and concurrent thoracic injury in 145 traumatized dogs. *J Vet Emerg Crit Care* 18(3):258–269.

Lisciandro GR, Lagutchik MS, Mann KA, et al. 2009. Evaluation of an abdominal fluid scoring system determined using abdominal focused assessment with sonography for trauma in 101 dogs with motor vehicle trauma. *J Vet Emerg Crit Care* 19(5):426–437.

Lisciandro GR, Fosgate GT, Romero LA, Bridgeman CH. 2015. Abdominal FAST (AFAST) and abdominal fluid scores in adult and juvenile cats. Abstract. *J Vet Emerg Crit Care* 25(S1):S8.

Lisciandro GR, Fosgate GT, Romero LA, et al. 2019. The expected frequency and amount of free peritoneal fluid estimated using the abdominal FAST-applied abdominal fluid scores in clinically normal adult and juvenile dogs. *J Vet Emerg Crit Care*, in press.

McMurray J, Boysen S, Chalhoub S. 2016. Focused assessment with sonography in nontruamtized dogs and cats in the emergency and critical care setting. *J Vet Emerg Crit Care* 26(1):64–73.

Narasimhan M, Koenig SJ, Mayo PH. 2016. A whole-body approach to point of care ultrasound. *Chest* 150(4):772–776.

Nelson NC, Drost WT, Lerche P, et al. 2011. Noninvasive estimation of central venous pressure in anesthetized dogs by measurement of hepatic venous blood flow velocity and abdomen al venous diameter. *Vet Radiol Ultrasound* 51(3):313–323.

Ollerton JE, Sugrue M, Balogh Z, et al. 2006. Prospective study to evaluate the influence of FAST on trauma patient management. *J Trauma* 60(4):785–791.

Powell LL, Rozanski EA, Tidwell AS, et al. 1999. A retrospective analysis of pulmonary contusions secondary to motor vehicle accidents in 143 dogs: 1994–1997. *J Vet Emerg Crit Care* 9(3):127–136.

Romero LA, Lisciandro GR, Fosgate GT, Bridgeman CH. 2015. Abdominal FAST (AFAST) and abdominal fluid scores in adult and juvenile dogs. Abstract. *J Vet Emerg Crit Care* 25(S1):S7–S8.

Sigrist NE, Adamik KN, Doherr MG, et al. 2011. Evaluation of respiratory parameters at presentation as clinical indicators of the respiratory localization in dogs and catswith respiratory distress. *J Vet Emerg Crit Care* 21(1):13–23.

Simpson SA, Syring R, Otto CM. 2009. Severe blunt trauma in dogs: 235 cases (1997–2003). *J Vet Emerg Crit Care* 19(6):588–602.

Sobrino J, Shafi S. 2013. Timing and causes of death after injuries. *Proc (Bayl Univ Med Cent)* 26(2):120–123.

Stander N, Wagner WM, Goddard A, et al. 2010. Normal canine pediatric gastrointestinal ultrasonography. *Vet Radiol Ultrasound* 51(1):75–78.

Sutherland-Smith J, Penninck DG, Keating JH, et al. 2007. Ultrasonic intestinal hyperechoic mucosal striations in dogs are associated with lacteal dilation. *Vet Radiol Ultrasound* 48(1):51–57.

Udobi KF, Rodriguez A, Chiu WC, et al. 2001. Role of utrasonography in penetrating abdominal trauma: a prospective study. *J Trauma* 50:475–479.

# Further Reading

Culp WT, Weisse C, Kellogg ME, et al. 2010. Spontaneous hemoperitoneum in cats: 65 cases (1994–2006). *J Am Vet Med Assoc* 236(9):978–982.

Kirkpatrick AW, Sirois M, Ball CG, et al. 2004. The hand-held ultrasound for penetrating abdominal trauma. *Am J Surg* 187:660–665.

Kolata RJ, Dudley EJ. 1075. Motor vehicle accidents in urban dogs: a study of 600 cases. *J Am Vet Med Assoc* 167:938–941.

Mandell DC, Drobatz K. 1995. Feline hemoperitoneum: 16 cases (1986–1993). *J Vet Emerg Crit Care* 5(2):93–97.

Matsushima K, Frankel HL. 2011. Beyond focused assessment with sonongraphy for trauma: ultrasound creep in the trauma resuscitation area and beyond. *Curr Opin Crit Care* 17(6):606–612.

Mohammadi A, Ghasemi-Rad M. 2012. Evaluation of gastrointestinal injury in blunt abdominal trauma "FAST is not reliable": the role of repeated ultrasonography. *World J Emerg Surg* 7(1):2.

Mongil CM, Drobatz KJ, Hendricks JC. 1995. Traumatic hemoperitoneum in 28 cases: a retrospective review. *J Am Anim Hosp Assoc* 31:217–222.

Muir W. 2006. Trauma: physiology, pathophysiology, and clinical implications. *J Vet Emerg Crit Care* 16(4):253–263.

Pintar J, Breitschwerdt EB, Hardie EM, et al. 2003. Acute nontraumatic hemoabdomen in the dog : a retrospective analysis of 39 cases (1987–2001). *J Am Anim Hosp Assoc* 37:518–522.

Quantz JE, Miles MS, Reed AL, et al. 2009. Elevation of alanine transaminase and gallbladder wall abnormalities as biomarkers of anaphylaxis in canine hypersensitivity patients. *J Vet Emerg Crit Care* 19(6):536–544.

Rozycki GS. 1998. Surgeon performed US: its use in clinical practice. *Ann Surg* 228:16–28.

Rozycki GS, Pennington SD, Feliciano DV. 2001. Surgeon-performed ultrasound in the critical care setting: its use as an extension of the physical examination to detect pleural effusion. *J Trauma* 50(4):636–642.

Sgourakis G, Lanitis S, Zacharioudakis C, et al. 2012. Incidental findings in trauma patients during focused assessment with sonography for trauma. *Am Surg* 78(3):366–372.

CHAPTER SEVEN

# POCUS: AFAST – Clinical Integration

Gregory R. Lisciandro

## Introduction

The AFAST, having exact clarity to its five acoustic windows, is a standardized, rapid screening test of the abdominal cavity, retroperitoneal space, and pleural cavity, including the pericardial sac, heart, and lung. Even for the novice sonographer, the AFAST examination likely will take no more than 3½–4 minutes. In the previous AFAST chapter, we covered image acquisition and the AFAST target organ approach, examples of typical negative and positive images, pitfalls, and artifacts.

In this AFAST chapter, we will discuss clinical integration of AFAST findings as well as its limitations. Enjoy this wild AFAST ride of patient information that gives evidence-based information by "seeing" your patient's problem list for a better working diagnosis, a better way to manage bleeding patients, a better way to track effusions, a better diagnostic plan for picking the next best test, and much more.

We will cover the following (Table 7.1).

- The abdominal fluid scoring system in different subsets of bleeding patients including blunt trauma, penetrating trauma, postinterventional, and nontrauma.
- The use of the diaphragmatico-hepatic (DH) view for pericardial and pleural effusion.
- The use of the DH view for lung pathology along the pulmonary-diaphragmatic interface.
- The use of the DH view and the caudal vena cava for volume status.
- The detection and interpretation of gallbladder wall edema, the so-called "gallbladder halo sign," that is a marker for canine anaphylaxis as well as cardiac conditions in the acute collapse, triaged setting.
- Target organ conditions at respective AFAST views that may be easily recognized as "abnormal" to capture cases otherwise missed without ultrasound.

### *What AFAST Clinical Integration Can Do*

- Can detect free fluid within the abdomen, retroperitoneal space, pleural cavity, pericardial sac superior to physical examination and abdominal radiography and comparable to the gold standard of computed tomography (CT).
- Can semiquantitate intraabdominal hemorrhagic and nonhemorrhagic effusions using its AFAST-applied abdominal fluid scoring system.
- Can anticipate degree of anemia in hemorrhaging dogs and cats by using its abdominal fluid scoring system and the small volume versus large volume principle.
- Can help with decision making for blood transfusion and surgical interventions in hemorrhaging dogs and cats including blunt trauma, penetrating trauma, postinterventional (percutaneous biopsy, laparoscopy, and postlaparotomy, i.e., ovariohysterectomy, splenectomy, adrenalectomy, liver lobectomy, nephrectomy, gastrointestinal surgery, bladder surgery, etc.) by applying its abdominal fluid scoring system.
- Can be used serially (repeating AFAST) for surveillance of all patients atrisk for bleeding, peritonitis, and other nonhemorrhagic effusive conditions.

*Point-of-Care Ultrasound Techniques for the Small Animal Practitioner*, Second Edition. Edited by Gregory R. Lisciandro.
© 2021 John Wiley & Sons, Inc. Published 2021 by John Wiley & Sons, Inc.
Companion website: www.wiley.com/go/lisciandro/ultrasound2

**Table 7.1.**
Questions answered during AFAST.

| | |
|---|---|
| Is there any free fluid in the abdominal (peritoneal) cavity? | Yes or no |
| How much free fluid is in the abdominal cavity using the AFAST-applied fluid scoring system? | 0 (negative), 1, 2, 3, and 4 (maximum score) |
| Is there any pericardial effusion? | Yes or no |
| Subjective amount? | Trivial (<0.5 cm), mild (>0.5 and <1.0 cm), moderate (>1.0 and <2 cm), severe (>2 cm) on DH view (Candotti and Arntfield 2015) |
| Is there any pleural effusion? | Yes or no |
| Subjective amount? | Trivial, mild, moderate, severe |
| What does the pulmonary-diaphragmatic surface look like? | Unremarkable or abnormal |
| Are there any lung lesions along the diaphragm? | B-lines, shred sign, tissue sign, nodule sign (Lisciandro 2014c; Lisciandro and Fosgate 2017) |
| What does the gallbladder look like? | Unremarkable, halo sign, abnormalities in its lumen or wall |
| What do the target organs look like at each AFAST view? | Unremarkable or abnormal |
| What do the caudal vena cava and its associated hepatic veins look like? | Unremarkable (bounce) or abnormal (FAT, flat) (see Tables 7.6 and 36.3 and Figures 36.7, 36.10–36.12) and presence of "tree trunk sign" (see Figure 36.8) |
| What is estimated bladder volume? | Length (cm) × width (cm) × height (cm) × 0.625 = estimation in milliliters (mL) |
| What is estimated urine output? | Difference in serial volume measurements/time (Lisciandro and Fosgate 2017) |
| Could I be misinterpreting an artifact or pitfall as pathology? | Know pitfalls and artifacts (see Chapter 6) |

Source: Reproduced with permission of Dr Gregory Lisciandro, Hill Country Veterinary Specialists and FASTVet.com, Spicewood, TX.

- Can serially track bleeding patients as worsening (ongoing) hemorrhage (increasing AFS), static hemorrhage (no change in AFS), and resolution (decreasing AFS).
- Can serially track peritonitis (and other nonhemorrhagic effusions) as worsening (increasing AFS), static (no change in AFS), and resolution (decreasing AFS).
- Can detect retroperitoneal effusion when imaging at the AFAST spleno-renal (SR) and hepato-renal (HR) views.
- Can detect pleural and pericardial effusions by routinely imaging cranial to the diaphragm at the AFAST DH view.
- Can screen for anaphylaxis in dogs through the detection of sonographic striation of the gallbladder wall, referred to as the "halo effect," "double rim effect" or "gallbladder halo sign" at the AFAST DH view; however, the finding is not pathognomonic and cardiac conditions should always be ruled out in the acute triage setting and other more chronic causes.
- Can assess volume status and right-sided cardiac function by evaluating caudal vena caval size and characterization coupled with hepatic venous distension and gallbladder wall edema at the AFAST DH view.
- Can screen for obvious target organ injury or pathology, serving as a soft tissue screening test.
- Can assess urinary bladder integrity (rupture or intact) at the AFAST cysto-colic (CC) view in trauma and urinary obstructed cases.
- Can noninvasively estimate urinary bladder volume and thus urine output through bladder measurements at the AFAST CC view.

## What AFAST Clinical Integration Cannot Do

- Cannot ultrasonographically characterize fluid, so sample acquisition via centesis and fluid analysis and cytology is required when free fluid is safely accessible.
- Lacks sensitivity for injury in penetrating trauma because blood acutely clots, but is likely highly specific for intraabdominal and retroperitoneal injury similar to human studies; serial examinations are imperative in questionable patients.

- Potentially misses peritonitis and small-volume bleeds in dehydrated or hypotensive patients. AFAST examinations should be applied minimally once after resuscitation and rehydration has taken place and as many times as necessary until you are assured that the patient is not surgical
- Cannot replace a detailed complete abdominal ultrasound.
- Cannot replace proper training.

### Indications

In reality, AFAST and the Global FAST approach are everyday imaging modalities for nearly every patient as an extension of the physical examination. However, to better grasp this concept with baby steps to get to "an extension of the physical examination" mentality, we have bulleted the following.

- All blunt and penetrating trauma cases as standard of care for screening for indirect evidence of intraabdominal injury.
- All collapsed (both recovered and unrecovered) cases with unexplained hypotension, tachycardia, or mentation changes.
- All anemic cases.
- All "ain't doing right" (ADR) cases.
- All postinterventional, postsurgical cases, at risk for bleeding, infections, vascular complications.
- All peritonitis suspects, including acute abdomen, for expedient diagnosis through the detection of free fluid (and sampling, fluid analysis testing as deemed appropriate).
- Add-on for *all* POCUS exams (abdomen, thorax, eye, brain) to make sure that forms of peritonitis and pleuritis, presence of bleeding, cardiac and pulmonary complications are not being missed that could have easily been detected with the Global FAST* approach.

*The Global FAST approach includes the combination of AFAST and its fluid scoring system and its target organ approach, the TFAST and Vet BLUE combined as part of the physical examination (see Chapters 36 and 37).

### Objectives

- Perform the five acoustic windows of AFAST and accurately assign and abdominal fluid score.
- Apply the "small-volume bleeder versus large-volume bleeder" principle to hemorrhaging subsets of small animal patients to better direct definitive therapy and decision making, including the need for blood transfusion and exploratory surgery and medical versus surgical management.
- Recognize sonographic striation of the gallbladder wall referred to as the "halo effect," "double rim effect" or "halo sign."
- Know additional rule-outs (cardiac causes) for the collapsed or acutely weak dog with sonographic striation of the gallbladder wall.
- Know additional rule-outs for sonographic striation of the gallbladder wall in dogs and cats without acute collapse and weakness.
- Recognize retroperitoneal free fluid and distinguish it from intraabdominal fluid.
- Recognize pleural and pericardial effusion via the DH view by looking cranial to the diaphragm.
- Know how to assess volume status through characterization of the caudal vena cava and its associated hepatic veins.
- Know common artifacts and pitfalls at each respective AFAST view (see Chapter 6).

### Final Note

The POCUS abdominal, thoracic, ocular, neurological, and musculoskeletal examinations described throughout this textbook, should as a general rule always include an AFAST and an assigned abdominal fluid score, and even better the Global FAST approach. By *only* performing a POCUS examination targeted at a specific organ or system, you risk missing obvious significant conditions to the patient's detriment. Integration of POCUS information is now similarly being advocated in human medicine like the author's Global FAST approach (Lichtenstein 2010; Narasimhan et al. 2016; Ha and Yo 2016).

## Calculating the Abdominal Fluid Score

The AFAST-applied fluid scoring system is a simple and easy to remember 0–4 scoring system developed over a decade ago (Lisciandro et al. 2009). Originally, each AFAST view was scored as 0 being negative or 1 being positive; however, the abdominal fluid scoring system has been further modified, explained subsequently based on more recent studies (Romero et al. 2015; Lisciandro et al. 2019). With this system, an abdominal fluid score (AFS) of 1 was defined as positive at any *single* AFAST view, an AFS of 2 was

positive at any two views, an AFS of 3 was positive at any three views, and the maximum AFS of 4 was positive at all four views (Figure 7.1). The impact of assigning an AFS is that in bleeding patients, an AFS of 1 and 2 is characterized as major injury/pathology, "small-volume bleeder." In contrast, an AFS 3 and 4 are characterized as major injury/pathology, "large-volume bleeder" (Lisciandro et al. 2009; Lisciandro 2011, 2012). "Small-volume" versus "large-volume" effusions may also be semiquantitated regarding fluid loss (third spacing) into the abdominal cavity.

## Modification of the Abdominal Fluid Scoring System – Using Maximum Dimensions

For several years the author has used a modified AFS system to better differentiate between small-volume and large-volume bleeder and effusions. The modified system now includes scores of 0, ½, and 1, which we refer to as the measurement approach (Lisciandro et al. 2015, 2019; Romero et al. 2015). The measurement approach categorizes positives as ½ or 1 dependent on

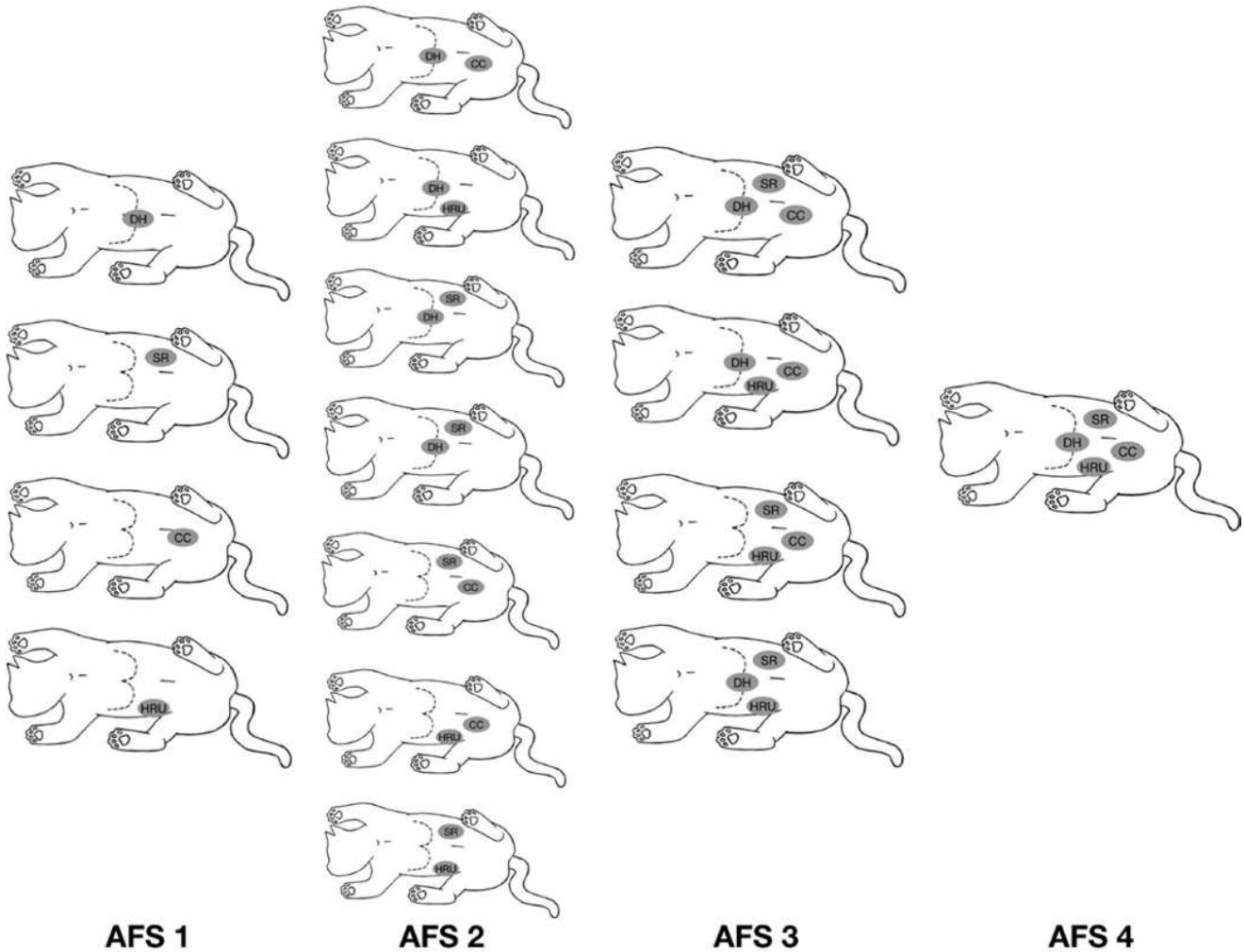


**Figure 7.1.** AFAST-applied abdominal fluid scoring system. Calculating the abdominal fluid score (AFS) using the AFAST-applied fluid scoring system shown on a cat placed in right lateral recumbency as a 0–4 system (the same system applies analogously to left lateral recumbency and to dogs). An AFS of 1 is a positive at any single view, an AFS 2 as any combination of two views, an AFS 3 as any combination of three views, and the maximum AFS of 4 when positive at all four views. Note the author has recently modified the AFS by assigning a score of ½ at views that have smaller pockets with maximum dimensions of ≤1 cm or >1 cm in dogs and ≤0.5 cm or >0.5 cm in cats based on more recent research (see Figure 7.2) (Romero et al. 2015; Lisciandro et al. 2019). Source: Reproduced with permission of Dr Gregory Lisciandro, Hill Country Veterinary Specialists and FASTVet.com, Spicewood, TX. Illustration by Hannah M. Cole, Adkins, TX.

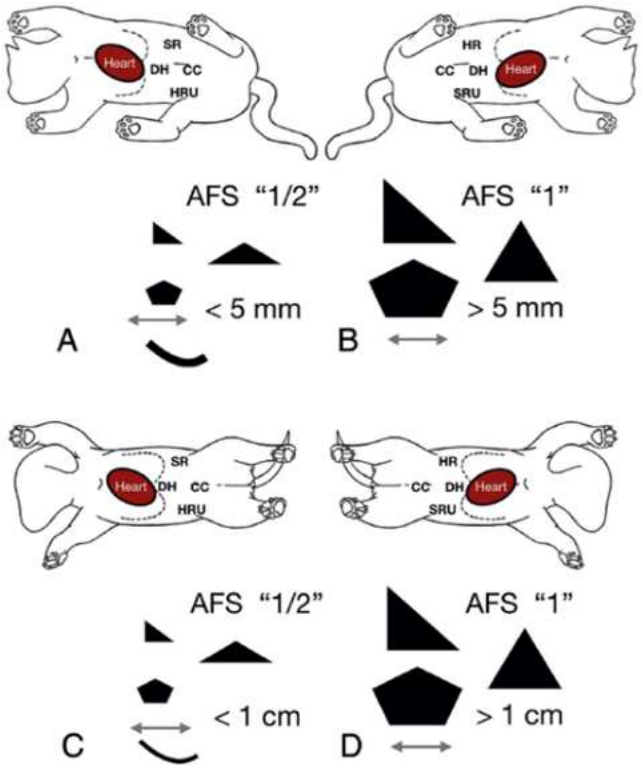


**Figure 7.2.** The "measurement" modification of the AFAST-applied abdominal fluid scoring system. The figure shows the measurement abdominal fluid scoring (AFS) system. (A,B) Cartoons of a cat in right and left lateral recumbency and (C,D) cartoons of a dog in right and left lateral recumbency. The modification of the AFS better distinguishes between "small-volume" and "large-volume" bleeding (and other forms of nonhemorrhagic effusions) by assigning a score of ½ or 1 dependent on the maximum measured dimension at each AFAST view based on recently published studies (Lisciandro et al. 2015, 2019; Romero et al. 2015). The AFS is validated in either right or left lateral recumbency (Lisciandro et al. 2009). See also Figure 7.3. Source: Reproduced with permission of Dr Gregory Lisciandro, Hill Country Veterinary Specialists and FASTVet.com, Spicewood, TX. Illustration by Hannah M. Cole, Adkins, TX.

the maximum dimension at each AFAST view (Figure 7.2). Based on recent research since the first edition, we suggest an "under–over" of 1 cm (10 mm) in dogs and "under–over" of 0.5 cm (5 mm) in cats (Lisciandro et al. 2015, 2019; Romero et al. 2015). Thus, in a dog, when a maximum dimension at an AFAST view is ≤1 cm, it is scored as a ½, and if >1 cm, it is scored as 1; and in a cat ≤0.5 cm is scored as a ½ and >0.5 cm is scored as a 1 (Figure 7.3; see also 7.8).

The "small-volume bleeder versus large-volume bleeder" principle remains the same with a 0–4 system as published (Lisciandro et al. 2009); however, the addition of the ½ helps better semiquantitate and categorize the bleeding dog and cat (Lisciandro et al. 2019). The modified fluid scoring system may also be used with nonhemorrhagic effusions since any effusion potentially contributes to volume loss in your patient. Clinical judgment always should be considered along with the patient's entire clinical picture; however, this AFS modification provides an option to better categorize bleeding patients and those with other nonhemorrhagic effusions. For example, a dog may have small pockets at the DH, CC, and HRU views of <1 cm which would now be deemed a small-volume bleeder (if a bleeding case) with a score of 1½ rather than a 3 (see Figure 7.8).

## *Applying the Abdominal Fluid Scoring System to the Hemoabdomen*

The "abdominal" fluid scoring system was purposely named as such and not the "hemorrhage" scoring system to avoid the system being typecast for only hemorrhage. The name, however, seems to have prevented its routine use in bleeding cases despite its documented ability to semiquantitate volume, rapidly categorize the bleeding patient, and help with decision making regarding blood transfusion(s) and exploratory laparotomy. The AFS system furthermore serves to track patients for worsening hemorrhage (or effusions) by increasing AFS, static hemorrhage (or effusions) by no change in AFS, and resolving hemorrhage (or effusions) by decreasing AFS. Knowing the patient's AFS is incredibly helpful for clinicians performing AFAST to place the degree of hemorrhage into clinical context (Lisciandro et al. 2009). The AFS should be used as standard of care, calculated and recorded for all patients having AFAST.

### Small-Volume Bleeders: AFS 1 and 2 (AFS <3)

- AFS 1 and 2 (AFS <3) are "small-volume bleeders" that reliably will not become significantly anemic from their intraabdominal bleed because, simply put, there is not enough intraabdominal hemorrhage to cause anemia (Figures 7.4 and 7.5). Of course, they must remain an AFS of 1 or 2 (AFS <3) on serial AFAST examinations.
- If an AFS 1 or 2 (AFS <3) dog or cat is or becomes anemic, then there are four major possibilities.
  1. The patient had preexisting anemia.
  2. The patient is bleeding somewhere else, emphasizing the importance of the Global FAST approach and a good physical exam

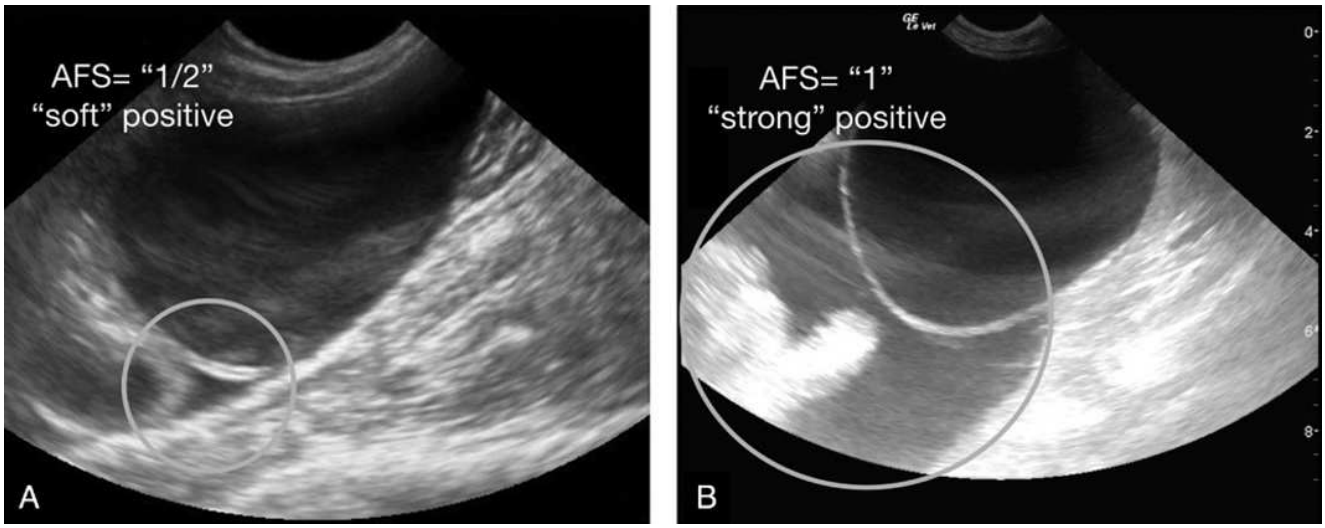


**Figure 7.3.** Modification of the AFAST-applied AFS. The figure shows how size matters, using the AFAST CC view as an example. In (A) the small pocket, anechoic triangulation (circled) would be scored a ½ as a "soft" positive whereas in (B) the larger pocket would be scored a full 1 as a "strong" positive. This visual modification is used at all AFAST views and is an alternative to the measurement modification shown in Figure 7.2. Source: Reproduced with permission of Dr Gregory Lisciandro, Hill Country Veterinary Specialists and FASTVet.com, Spicewood, TX.

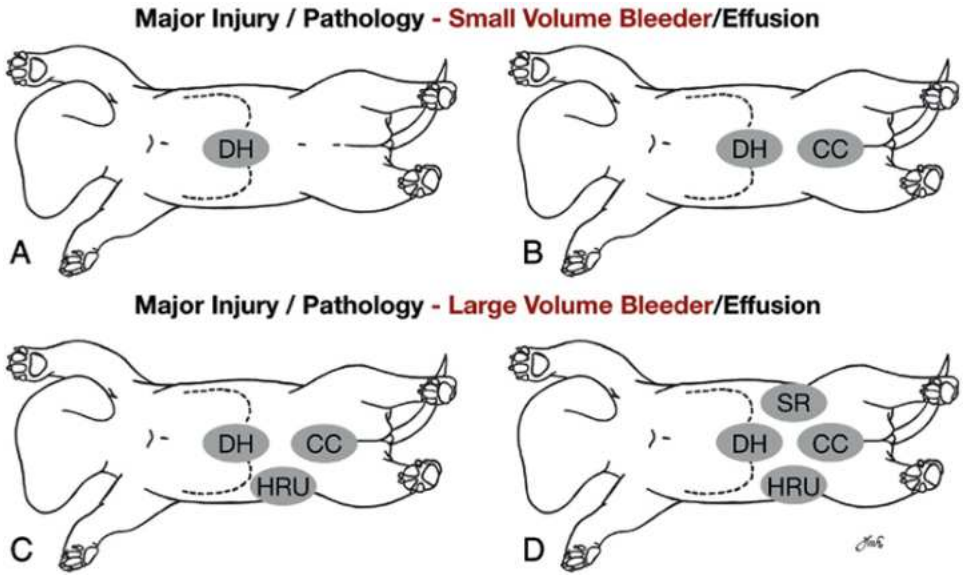


**Figure 7.4.** AFAST-applied AFS and the small-volume versus large-volume bleeder principle. Cartoon of a dog in right lateral recumbency and the "small-volume versus large-volume" bleeder/effusion principle. In (A) and (B) the AFS is 1 and 2, respectively. Anemia is not expected in AFS 1 and 2 (modified AFS system <3) bleeding patients. In (C) and (D) the AFS is 3 and 4 (modified AFS system ≥3), respectively. These bleeding dogs will predictably be or become anemic from the intraabdominal volume of blood. The same principle holds true for cats. The AFS is validated only in lateral recumbency. CC, cysto-colic view; DH, diaphragmatico-hepatic view; HRU, hepato-renal umbilical view; SR, spleno-renal view. Source: Reproduced with permission of Dr Gregory Lisciandro, Hill Country Veterinary Specialists and FASTVet.com, Spicewood, TX. Illustration by Hannah M. Cole, Adkins, TX.

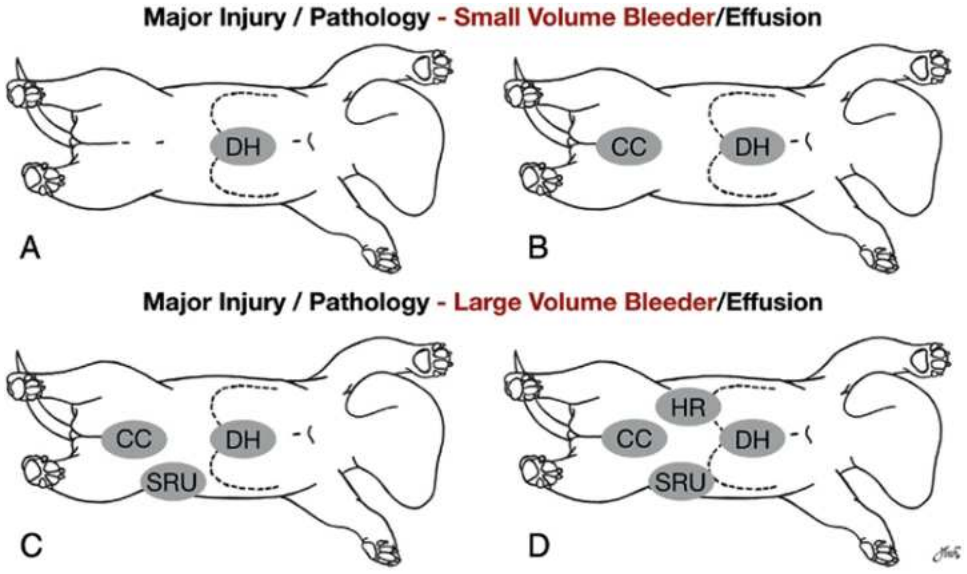


**Figure 7.5.** AFAST-applied AFS system and the small volume versus large volume principle. Cartoon of a dog in left lateral recumbency and the "small-volume versus large-volume" bleeder/effusion principle. In (A) and (B) the AFS is 1 and 2, respectively. Anemia is not expected in AFS 1 and 2 (modified AFS system <3) bleeding patients. In (C) and (D) the AFS is 3 and 4 (modified AFS system ≥3), respectively. These bleeding dogs will predictably be or become anemic from the intraabdominal volume of blood. The same principle holds true for cats. The AFS is validated only in lateral recumbency. CC, cysto-colic view; DH, diaphragmatico-hepatic view; HRU, hepato-renal umbilical view; SR, spleno-renal view. Source: Reproduced with permission of Dr Gregory Lisciandro, Hill Country Veterinary Specialists and FASTVet.com, Spicewood, TX. Illustration by Hannah M. Cole, Adkins, TX.

3. Hemodilution has occurred from fluid therapy, which is much less common than a couple of decades ago because of more recently taught titrated fluid therapy.
4. Lab error.

### Large-Volume Bleeders: AFS 3 and 4 (AFS ≥3)

- AFS 3 and 4 (AFS ≥3) are "large-volume bleeders" that are or will reliably become anemic from their intraabdominal bleed because, simply put, there is enough intraabdominal blood to cause anemia (see Figures 7.4 and 7.5).
- Generally expect a 20–25% decrease from baseline packed cell volume (PCV) for all dogs and cats.
- In the author's experience, ~1 in 4–5 dogs (unknown in cats) will become severely anemic (dogs PCV <25%; cats PCV <20%), requiring a blood transfusion(s).
- Surgical intervention varies with patient subsets (Table 7.2).

A hemoabdomen decision-making algorithm for correlating the AFS to the anticipated degree of anemia and decision making in different patient subsets is provided in Table 7.3.

## *Importance of the Serial Exam*

Serial AFAST with an assigned AFS is key for monitoring changes, and for better detecting the "small-volume bleeder" that is becoming a "large-volume bleeder" often before overt patient decompensation, referred to by some as the "crump factor" (Bilello et al. 2011) (see Figure 7.9). Veterinarians using the AFAST and AFS approach have advantages over human medicine, in which hemorrhage scoring systems are not routinely implemented despite the fact that occult or unrecognized ongoing hemorrhage is the top cause of death next to traumatic brain injury in hospitalized human trauma patients within their first 48 hours of care (Bilello et al. 2011; Sobrino and Shafi 2013). Moreover, the most important intervention that prevented the "crump factor" in people with prehospital hypotension was the "liberal use of FAST" examinations over physical examination, vital signs, and base deficit (Bilello et al. 2011).

In addition, serial exams are important because they allow for the evaluation of the urinary bladder in two major ways: the integrity of the urinary bladder (expected rounded contour versus suspect rupture) and estimation or urinary bladder volume and urine

Vetbooks.ir

**Table 7.2.**
Summary of patient management guidelines for hemoabdomen and positive abdominal fluid scoring (AFS) for different patient subsets.

| Type of trauma | Major injury/pathology, small-volume bleeder (AFS 1, 2; modified AFS system <3) | Major injury/pathology, large-volume bleeder (AFS 3, 4; modified AFS system ≥3) |
|---|---|---|
| **Blunt trauma** | | |
| *Think Medical First* | If stays AFS 1, 2 (AFS <3) no blood transfusion necessary if only bleeding intraabdominally | If an AFS 3, 4 (AFS ≥3) or becomes AFS ≥3 then expect anemia <30% in dogs and <24% in cats |
| Use AFS to help with decision-making regarding transfusions and surgical intervention. | Do NOT expect anemia | Use titrated fluid therapy strategies as 1/3 shock dose and repeat as fluid challenges are needed |
| Blood rapidly defibrinates thus is seen even acutely as anechoic (black) triangulations | Expect PCV to be >30% in dogs and >24% in cats if only bleeding intraabdominally | If patient becomes severely anemic <25% in dogs and <20% in cats then generally treat medically first by blood transfusion(s) |
| | If stays AFS 1, 2 (AFS <3) and becomes anemic <30% in dogs and <24% in cats, rule out another site of bleeding (retroperitoneal, pleural cavity, fracture site, externally) so do Global FAST and a good physical exam | Note most intraabdominal bleeding in this subset will stop with 1 or 2 rounds of blood transfusion +/- replacement of clotting factors |
| | Uncommon but possible for other nonhemorrhagic effusions (uroabdomen, bilioabdomen, other) | Uncommonly need exploratory surgery<br>Uncommon but possible for other nonhemorrhagic effusions (uroabdomen, bilioabdomen, other) |
| **Penetrating trauma** | | |
| *Think Surgical for Any Positive AFS* | Generally best to assume in penetrating trauma that all cases are surgical with ANY positive | Generally best to assume in penetrating trauma that all cases are surgical with ANY positive, especially AFS 3 and 4 |
| Blood often acutely clots from ripping, tearing, crushing of tissue and thus is often missed during AFAST because clotted blood looks like adjacent soft tissue | Combine AFAST (or Global FAST) with other clinical findings and surgical indications (hernia, pneumoperitoneum, septic abdomen, refractory pain, etc.) | Combine AFAST (or Global FAST) with other clinical findings and surgical indications (hernia, pneumoperitoneum, septic abdomen, refractory pain, etc.) |
| In time, blood clots will defibrinate and become free fluid, detected as anechoic (black) triangulations | Sample fluid when safely accessible and characterize the effusion with fluid analysis and cytology | Sample fluid when safely accessible and characterize the effusion with fluid analysis and cytology |
| In time, ruptured, injured viscus organs will also leak or effuse, thus serial AFAST exams are key in cases in which medical vs surgical management is unclear | Serial exams are key – at four, eight, 12 and 24 hours, two, three and five days | CT is the gold standard imaging test |
| Serial AFAST exams are key – at four, eight, 12 and 24 hours, two, three and five days | You will miss a developing septic abdomen, pyothorax, by not using this strategy | |
| You will miss a developing septic abdomen, pyothorax, by not using this strategy | CT is the gold standard imaging test | |

**Table 7.2.**
(*Continued*)

| Type of trauma | Major injury/pathology, small-volume bleeder (AFS 1, 2; modified AFS system <3) | Major injury/pathology, large-volume bleeder (AFS 3, 4; modified AFS system ≥3) |
|---|---|---|
| **Postinterventional trauma** | | |
| *Think Medical for AFS 1, 2 and Surgical for AFS 3, 4* | If stays AFS 1, 2 (AFS <3) on serial exams, then generally NOT surgical | If an AFS 3, 4 and not anemic, then generally it is still best to explore emergently and NOT wait |
| Large-volume bleeding (AFS 3, 4) is generally not going to stop without surgical ligation of the bleeding | Do serial exams to make sure does not change score and become a large-volume bleeder (AFS 3, 4) | If you wait, you will likely have to transfuse your patient with its added cost and more anesthetic risk |
| Correct coagulopathy if present | Sample fluid when safely accessible and characterize the effusion with fluid analysis and cytology | If an AFS 3, 4 and already anemic, transfuse as per patient assessment and explore emergently<br>Sample fluid when safely accessible and characterize the effusion with fluid analysis and cytology |

Source: Reproduced with permission of Dr Gregory Lisciandro, Hill Country Veterinary Specialists and FASTVet.com, Spicewood, TX.

output (Lisciandro and Fosgate 2017) (see Figures 7.9 and 7.15). Soft tissue and luminal conditions (masses, sediment, calculi, thrombus) can also be recognized. Patients change and a minimum of one postresuscitation serial exam should be standard of care, four hours post admission in stable patients and sooner in unstable or questionable patients (Lisciandro et al. 2009; Boysen and Lisciandro 2013).

**Pearl:** If an AFS 1, 2 (modified AFS system <3) "small-volume bleeder" dog or cat without preexisting anemia becomes anemic, the attending clinician should explore other sites as potential sources of hemorrhage, including the retroperitoneal space, pericardial sac, pleural cavity, and lung, using the Global FAST approach along with a good physical exam.

## *Decision Making Using the AFS for the Hemoabdomen*

Tables 7.2 and 7.3 will aid decision making based on the AFAST AFS score in dogs and cats.

In summary, the following general guidelines apply.

### Blunt Trauma (BT)

Bleeding is most commonly medically treated with titrated fluid therapy, blood transfusion(s), and replacement of clotting factors in patients that require more than one transfusion or that are or have become coagulopathic. *Surgery is uncommon so think medical treatment first*.

- Computed tomography (CT) is the gold standard for detecting injury, whereas AFAST provides indirect evidence through the detection of free fluid.
- Radiography is an unreliable test for free fluid not only in terms of its presence or absence but also its inability to semiquantitate volume (Lisciandro et al. 2009).

### Penetrating Trauma (PT)

Any positive is potentially a surgical problem and thus exploratory laparotomy should be considered post resuscitation. There are no veterinary studies evaluating positive AFAST studies and the frequency of medical versus surgical injuries; however, exploratory laparotomy is recommended in people with positive FAST examinations (Udobi et al. 2001).

- Computed tomography is the gold standard for detecting injury, whereas AFAST provides only indirect evidence through the imaging of free fluid.
- Other imaging options include radiography, which is standard of care for PT, for the detection of pneumoperitoneum, herniations, fractures and body wall abnormalities.

**Table 7.3.**
Flowchart providing general guidelines regarding the decision-making process for acutely bleeding dogs and cats when applying the abdominal fluid score (AFS) during AFAST. Note the algorithm assumes the patient is noncoagulopathic or, when coagulopathic, the coagulopathy is corrected.

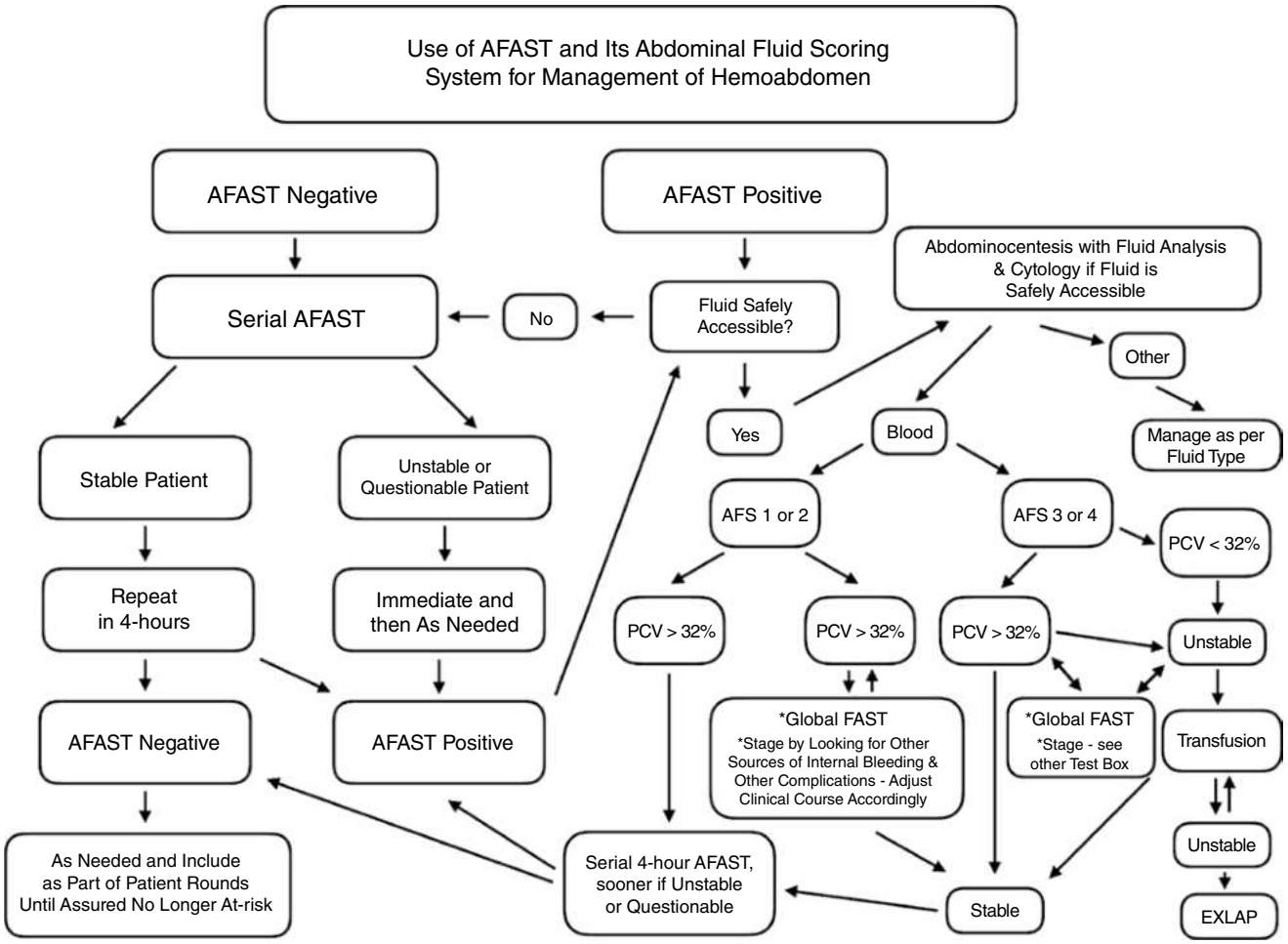


Source: Reproduced with permission of Dr Gregory Lisciandro, Hill Country Veterinary Specialists and FASTVet.com, Spicewood, TX.

## Postinterventional Trauma

Apply the "small-volume bleeder versus large-volume bleeder" principle to determine if the case is medical or surgical. The postinterventional patient includes any invasive procedure in which internal bleeding is a possible complication, such as percutaneous aspirations, needle and Tru-Cut biopsy, laparoscopy, exploratory laparotomy, etc.

### *Small-Volume AFS 1 and 2 Bleeders*

- In general, the "small-volume bleeder" (AFS 1 and 2; modified AFS system <3) is not immediately surgical and serial AFAST with an assigned AFS is an important monitoring tool for detecting increasing AFS often before overt decompensation, referred to as the "crump" (Bilello et al. 2011).
- In stable AFS 1 and 2 (modified AFS system <3) patients, the author routinely repeats AFAST with an assigned AFS ~1 hour post admission and then again four hours post admission, and then as clinical course dictates.
- AFAST with an assigned AFS should continue during patient rounds every 12–24 hours or during recheck examination until ascites resolution, that is, AFS returns to 0, negative.
- In questionable or unstable patients, serial AFAST with an assigned AFS are performed as often as necessary. The Global FAST approach is important to rule in and rule out other internal sites of

bleeding and comorbidities in the thorax, including heart and lung.

### *Large-Volume AFS 3 and 4 Bleeders (AFS ≥3)*

In general, postinterventional bleeding in noncoagulopathic patients will not stop without a surgical intervention, in other words, the ligation of the bleeder(s). Many "large-volume bleeders" are not initially anemic in the acute setting because patients can compensate, especially dogs which have a unique large splenic blood reservoir.

- AFS 3 and 4 (modified AFS system ≥3) initially or on serial examinations are "large-volume bleeders" and in general should be explored or have another appropriate intervention to stop the bleeding as soon as possible, with the caveat that the patient has an acceptable coagulation profile.
- The author follows the axiom "If it's an AFS of 3 or 4, you should explore (surgically intervene)," with the caveat that the patient has an acceptable coagulation profile.

**Pearl:** Waiting on a compensated postinterventional noncoagulopathic "large-volume bleeder" (AFS ≥3) instead of surgically addressing the cause of bleeding often leads to increased morbidity and cost (e.g., transfusion products) and increased patient anesthetic risk, because "large-volume bleeders" predictably become markedly to severely anemic and overtly decompensate in time. Thus, "If it's an AFS of 3 or 4, you should explore (surgically intervene)," with the caveat that the patient has an acceptable coagulation profile.

### Nontrauma

Nontraumatic hemoabdomen requires a more cerebral approach and knowledge base. Coagulopathy should always be ruled out, including minimally performing basic testing of prothrombin time (PT), activated partial thromboplastin time (aPTT), and a buccal mucosal or nail clip bleed time (platelet function test), readily available onsite tests at most practices. In coagulopathic cases, the coagulopathy generally needs to be corrected before invasive procedures. In noncoagulopathic cases, a bleeding mass is most common in dogs and cats and surgical intervention is required for definitive care. However, canine anaphylaxis must also be considered in all dogs with hemorrhagic effusions, some of which may have PT and aPTT times of <25% over the upper reference range, and thus not significantly coagulopathic (Lisciandro 2016b; Hnatusko et al. 2019). Because of this newly described complication in dogs, a focused spleen is now recommended following the AFAST examination in *all* canine hemoabdomens, and in general following any AFAST examinations in both dogs and cats (see Chapter 6 and Figure 6.35. See also canine anaphylaxis and gallbladder wall edema section within this chapter).

The focused spleen is a *rule-in* test, meaning that when a mass is detected, it is probably real (see Figure 6.35). In contrast, if a splenic mass is not seen then it could have been missed, depending on the proficiency of the sonographer and location of the mass. Thus, the focused spleen examination should be considered as it has high specificity as a screening test, but with variable sensitivity. The focused spleen is helpful because when a cavitated midabdominal mass is detected, especially when associated with the spleen and deforming its capsule, such a finding raises the probability of being correct in concluding that the hemoabdomen is due to a bleeding mass (surgical management) rather than canine anaphylaxis (medical management) (Lisciandro 2014a, 2016b). *Any mass that deforms the capsule of the spleen should be considered a serious finding*.

**Pearl:** In contrast to dogs, cats with spontaneous nontraumatic hemoabdomen have a poor prognosis because the cause is likely advanced forms of neoplasia (Mandell and Drobatz 1995; Culp et al. 2010). However, the AFAST-applied AFS is helpful in predicting degree of anticipated anemia, the need for blood transfusion and exploratory laparotomy, or other hemostatic interventions. The Global FAST approach may also be used to stage the feline.

## Major AFAST Difference Between Blunt and Penetrating Trauma

There is a *major* difference that must be understood when applying AFAST to blunt and penetrating trauma. The difference lies in the behavior of blood. In blunt trauma, it generally doesn't matter where the patient bleeds as mesothelial cells lining the abdominal cavity, pleural cavity, and pericardial sac rapidly defibrinate blood, making it readily apparent on AFAST as free fluid (anechoic triangulations). In contrast, victims of penetrating trauma have ripping, tearing and crushing of tissue, especially with bite wounds, and hence blood clots. During AFAST, clotted blood is often difficult to discriminate from adjacent soft tissue and thus is often

initially missed (Figure 7.6). Although there are no large veterinary studies (Lisciandro et al. 2008, 2009; Lisciandro 2012), the importance is likely similar to that in human medicine (Udobi et al. 2001), in that FAST is likely highly specific for surgical trauma but variably sensitive. AFAST (and Global FAST) should still be used as a first-line screening test because of all the clinical questions that may be answered regarding the patient. However, in instances of a negative AFAST, serial examinations should be implemented as standard of care until it is clear whether the patient is surgical versus medical.

In time, clotted blood will defribinate and appear as free fluid, and when viscus organ injury is present, likely the organ will "leak" into the abdominal cavity. Thus, AFAST carries the potential to detect septic peritonitis and other developing complications earlier in their course. In fact, vascular injury, uroabdomen, bilioabdomen, gastrointestinal injury, and others may present over the next several days post injury. Parenchymal injury is also possible and the use of color flow Doppler can be helpful especially for screening for renal injury (Figure 7.7). The author recommends continually performing AFAST serial examinations (or the Global FAST approach) four, eight, 12, and 24 hours post admission, and even two, three, and five days post injury. In other words, repeat the AFAST (Global FAST) as many times as needed until a surgical problem is comfortably ruled out.

Serial FAST examination strategies have proven helpful in human medicine (Blackbourne et al. 2004; Kirkpatrick et al. 2004; Ollerton et al. 2006; Matsushima and Frankel 2011; Mohammadi and Ghasemi-Rad 2012). Although abdominal radiographs are of variable yield for blunt trauma because of their unreliability in detecting free fluid and their inability to semiquantitate volume (Lisciandro et al. 2009), radiography is *always indicated* in penetrating trauma as part of patient evaluation because of its ability to effectively detect hard tissue (fractures, luxations), soft tissue (herniation), and viscus organ injury (free air).

**Pearl:** Although abdominal radiography is typically a low yield diagnostic test in bluntly traumatized patients for abdominal effusion, radiography should *always* be part of the standard work-up in penetrating trauma.

**Pearl:** AFAST often misses clotted blood, which is a common feature of penetrating trauma, because the echogenicity of clots is similar to soft tissue. The use of color flow Doppler can be helpful because clotted blood has no blood flow.

**Pearl:** Serial AFAST exams increase sensitivity for the detection of intraabdominal injury in penetrating trauma suspects and should be routinely performed four hours post admission (sooner if unstable or questionable) and then as often as needed when surgical injury is still possible, including up to five days or more post injury.

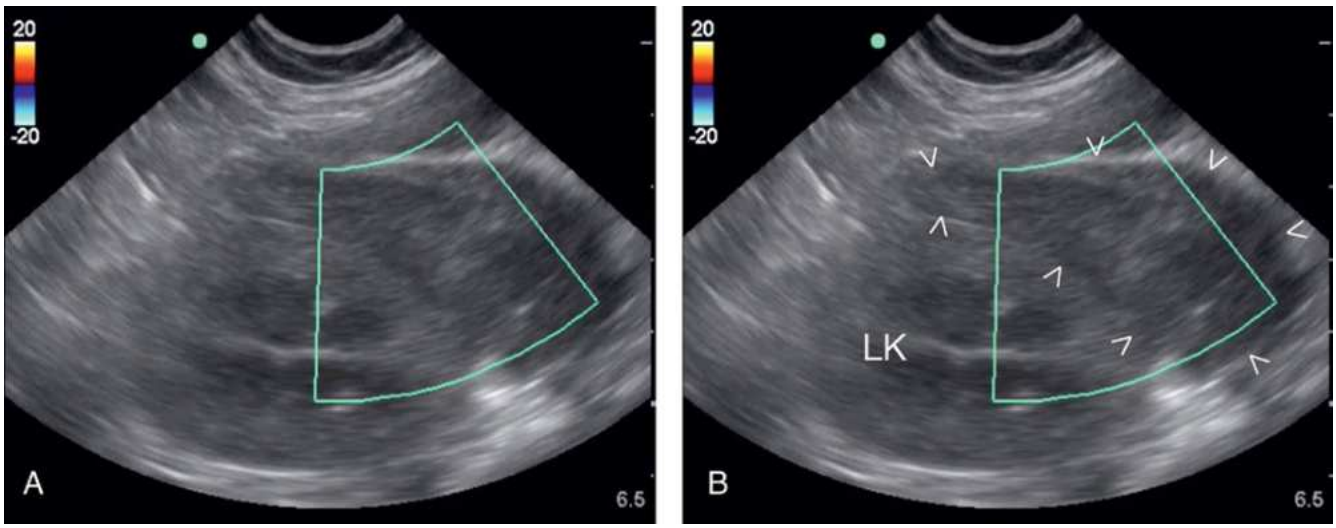


**Figure 7.6.** Clotted blood adjacent to the left kidney at the SR view. In penetrating trauma, blood often clots and clotted blood appears like soft tissue and is easy to miss during AFAST. Where suspected, color flow Doppler may be used. Clotted blood will lack flow. The image at the SR view shows the left kidney and an adjacent large clot with no flow on color Doppler, unlabeled in (A) and labeled in (B). Serial exams are key because if the clot was missed initially, the opportunity to capture the condition remains when repeating AFAST. Clot is outlined with cursors (V). LK, left kidney. Source: Reproduced with permission of Dr Gregory Lisciandro, Hill Country Veterinary Specialists and FASTVet.com, Spicewood, TX.

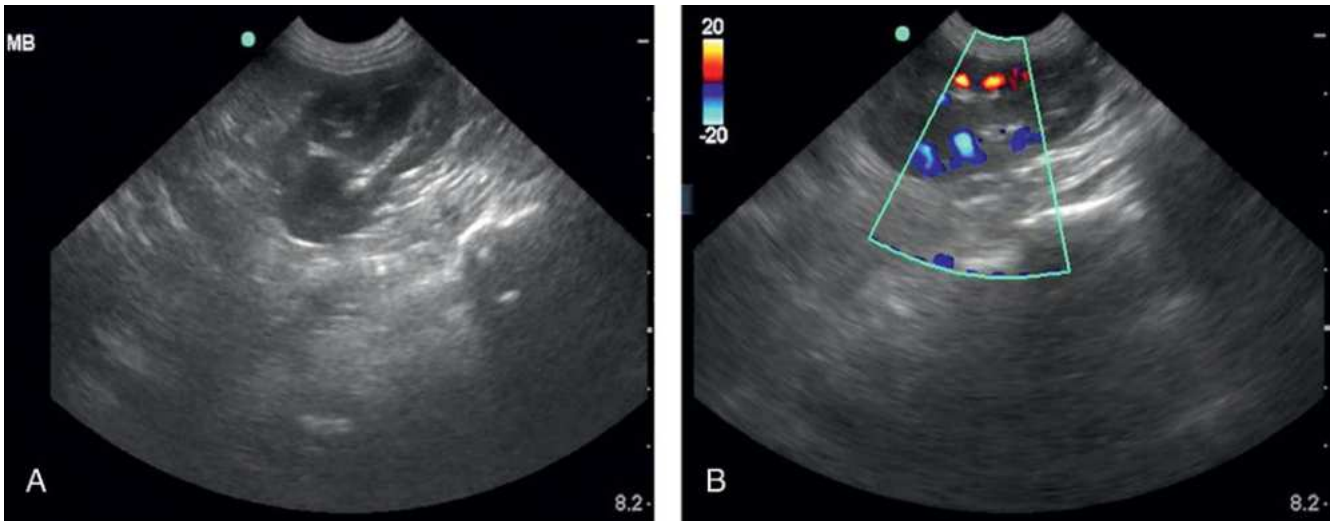


**Figure 7.7.** Evaluating for blood flow of the left kidney at the (SR) view. In (A) is a B-mode image followed by color flow Doppler in (B) showing pulsatile flow. In penetrating injury, especially bite wounds over the lumbar region, or in animals which were shaken by their attacker, renal injury and avulsion are possible. It is a good habit to apply color flow Doppler routinely in these at-risk cases, especially prior to exploratory surgery to help decision making by the surgeon for salvaging or removing the kidney. Source: Reproduced with permission of Dr Gregory Lisciandro, Hill Country Veterinary Specialists and FASTVet.com, Spicewood, TX.

## How Long Does It Take for Cavitary Bleeding to Resolve?

There are no veterinary studies that have established this definitively, but author experience and discussion among colleagues suggest that we should expect cavitary bleeds (peritoneal cavity, pleural cavity, pericardial sac) to resolve (or be very minimal in AFS) within 48 hours *once the bleeding stops* or after coagulopathy has been corrected (and remains corrected). We call this the "AFAST-TFAST 48-hour rule."

### Save All Cavitary Hemorrhage

It is important to harvest all cavitary hemorrhage cleanly into a collection apparatus as basic as clean syringes. The blood in the majority of cases will be naturally defibrinated in both dogs and cats. The collected cavitary hemorrhage may be administered without added anticoagulant through an inline blood filter to prevent administration of blood clots back to the patient (Higgs et al. 2015; Robinson et al. 2016; Cole and Humm 2019).

The question is sometimes posed regarding the older anemic hemoabdomen dog in a situation in which there are no resources for blood transfusion administration and whether leaving the blood in the abdominal cavity is acceptable. The argument is that by leaving the intraabdominal blood, the patient has the benefit of resorbing the cavitary blood postoperatively, and common sense should always prevail in the quest to improve the probability of patient survival. However, when possible, "dry the abdomen" to better interpret the clinical relevance of postoperative effusions.

## How Long Does It Take for Lavage Fluid to be Resorbed?

A fascinating question because, in contrast to cavitary blood that is resorbed quite rapidly within the "AFAST-TFAST 48-hour rule," lavage fluid lasts much longer (several days) in the author's experience. Thus, our recommendation is always "dry the abdomen" before abdominal closure using suction and running lap sponges through the left (mesocolon) and right (mesoduodenum) sided abdominal "gutters." Drying the abdomen gives you a negative AFS (AFS of 0) postoperatively and helps you better interpret the finding of free fluid post-procedure. Moreover, neutrophils work much more effectively in a "dry abdomen" environment than one bathed in lavage fluid.

**Pearl:** Expect abdominal cavitary blood to be resorbed with decreasing AFS and be nearly resolved or at an AFS of 0 within 48 hours – the "AFAST-TFAST 48-hour rule" – once bleeding has stopped.

**Pearl:** Spend an extra few minutes to suction and "dry the abdomen" with lap sponges prior to closure. Neutrophils function better, and your patient has an AFS 0 prior to closure, which helps to interpret positive AFS postoperatively.

### Cats Don't Survive Large-Volume Traumatic Bleeds

AFAST and the AFS system were prospectively studied in 49 traumatized cats. Although 17% of cats had positive fluid scores, feline "large-volume bleeders" were almost nonexistent and those with an AFS of 3 and 4 died during triage or were dead on arrival and not enrolled (Lisciandro 2012). Originally, the conclusion was that AFS was less reliable in cats, but several years of experience suggest that AFS for bleeding works just as well in cats. However, bluntly traumatized cats generally do not survive large-volume bleeds as dogs might (Mandell and Drobatz 1995; Lisciandro 2012). This is likely because the canine spleen serves as a large reservoir of blood whereas the feline spleen does not. Moreover, cats have over the years presented with "soft" positives at multiple AFAST views that would be better scored as a ½ rather than a full 1. The modification of the AFAST-applied AFS system thus recategorizes more accurately these feline cases as "small-volume bleeders" (Figure 7.8).

**Pearl:** Cats with automobile-induced traumatic hemoabdomen are often nonsurvivors before making it to veterinarians because they cannot compensate as dogs do and because of their smaller size, making injury more severe and lacking a splenic blood reservior. Free fluid on AFAST in surviving cats (>12–24 hours) is more likely to be urine than blood.

### Importance of Recording Locations of Where Patients are Positive

It is imperative to not only record the AFS but also locations of where the patient is positive and negative. This is important because the locations of AFAST-positive views in lower-scoring "small-volume bleeders" may be helpful for the localization of the bleeder (Table 7.4). For example, consider a hit-by-car dog or cat with an AFS of 1 at the AFAST DH view that continues to bleed with an increase in AFS to 3 or 4 and that despite blood transfusions becomes a surgical

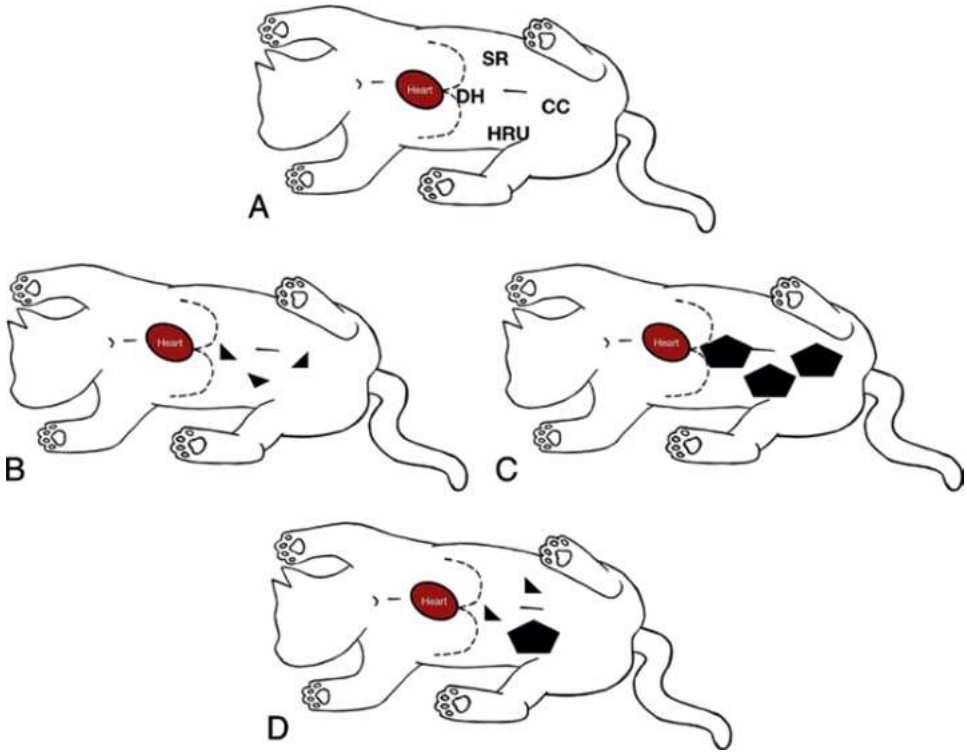


**Figure 7.8.** Example in a cat using the modified AFS system. (A) AFAST in right lateral recumbency and the four AFAST views used for the AFS. In (B) small triangulations (½ + ½ + ½) are found at three of the four views which calculates as an AFS of 1.5, a "small-volume bleeder/effusion." In (C) there are larger pockets of free fluid (1 + 1 + 1) at the same three AFAST views as in (A) and the AFS calculates as 3, a "large-volume bleeder/effusion." In (D) there are small triangulations at the DH and SR views and a larger pocket at the HRU view with a calculated AFS of 2 (½ + ½ + 1), a "small-volume bleeder/effusion." The same concept is applied to dogs. Source: Reproduced with permission of Dr Gregory Lisciandro, Hill Country Veterinary Specialists and FASTVet.com, Spicewood, TX. Illustration by Hannah M. Cole, Adkins, TX.

**Table 7.4.**
Possible sources of abdominal bleeding on AFAST views.

| View | Possible source |
|---|---|
| DH | Liver |
| | Vascular |
| | • Caudal vena cava |
| | • Hepatic vessels |
| | • Portal vessels |
| SR, HR, SR5th, HR5th | Spleen (SR, SR5th) |
| | Liver (HR, HR5th) |
| | Adrenal |
| | Ovary |
| | Vascular |
| | • Caudal vena cava |
| | • Aorta |
| | • Renal vessels |
| | Vertebrae |
| CC | Small intestine |
| | Large intestine |
| | Reproductive tract |
| | • Uterus |
| | • Prostate |
| | Vascular |
| | • Caudal vena cava |
| | • Aorta |
| HRU, SRU | Liver |
| | Spleen |
| | Uterus |
| | Gastrointestinal tract |

Source: Reproduced with permission of Dr Gregory Lisciandro, Hill Country Veterinary Specialists and FASTVet.com, Spicewood, TX.

case. Logic would dictate that the source of intraabdominal bleeding is likely associated with the liver and its vasculature. This information would potentially better prepare the surgeon for the anticipated type of injury, such as liver laceration, hepatic venous or vena caval injury, and for the needed procedure(s) as well as relevant resources. On the other hand, in the same trauma scenario the AFS 1 is positive at an AFAST view further caudally, such as the CC or HR umbilical view, and now logic would dictate that the source of bleeding would be more likely intestinal tract or spleen. Thus, the definitive procedure would likely be less technically challenging than a liver laceration or vascular hepatic injury.

In nontrauma, another example would be a post-ovariohysterectomy bleeding case with an AFS of 1 that is positive at the SR view. Let's say that over time, the patient progresses to an AFS of 3 or 4 that requires surgical exploratory. Logic would dictate the source of bleeding is most likely in the vicinity of the SR view and the left ovarian pedicle would be suspect. This information would again help direct the surgeon to that region as initially AFAST positive for the source of bleeding. In fact, for bleeding postoperative ovariohysterectomy surgeries, the AFAST acoustic windows are in regions of the left ovarian pedicle (SR view), the right ovarian pedicle (HR5th bonus view), and the uterine stump (CC view), which is important to consider in "small-volume bleeders" that progress to "large-volume bleeders" requiring surgical intervention. The upshot is that the sonographer should record both the AFS and specifically what AFAST views are positive and negative to maximize patient information as dictated in AFAST goal-directed templates (see last section of this chapter).

**Pearl:** Use the AFAST and AFS system as a postinterventional exit exam evaluation, e.g., postoperative and postpercutaneous ultrasound-guided procedures, before patients are sent home to ensure no occult bleeding is occurring. The use of this strategy is more sensitive than a physical exam, vital signs, and packed cell volume and total solids.

### Most Common AFAST-Positive Sites in Low-Scoring AFS 1 and 2 Patients

In trauma, the most commonly reported positive sites are the nongravity-dependent DH and CC views, which is against logic, which would dictate that the most gravity-dependent HRU view would be more likely to be positive (SRU view in left lateral recumbency) (Lisciandro et al. 2009, 2019; Romero et al. 2015). In nontrauma, the most gravity-dependent and least gravity-dependent views were most commonly positive and surprisingly in equal distribution (McMurray et al. 2016), also defying logic. Lastly, in clinically normal puppies and kittens, the DH and CC views were most commonly positive (Lisciandro et al. 2015, 2019; Romero et al. 2015). The upshot is that sonographers should be aware of the pitfalls and artifacts for all AFAST views in order to maximize identifying free fluid over confounders since there is variation in the most commonly detected positive AFAST views between patient subsets and ages. These pitfalls and artifacts are well detailed in Chapter 6.

## *AFAST Limitations for Intrapelvic Bleeding*

People with femoral and pelvic fractures can lose 50–75% of their blood volume at the fracture site, respectively (Coccolini et al. 2017). In dogs and cats, this is uncommon but does occur and should be

considered in anemic cases in which the source of the large volume of blood loss is inapparent (Lisciandro 2012). Importantly, FAST has been shown to perform poorly for detecting intrapelvic bleeding and the AFAST sonographer should consider this limitation. Through an understanding of ultrasound and imaging of soft and hard musculoskeletal tissues, however, it seems possible that large blood clots and hemorrhage could potentially be detected at fracture sites through the combined use of B-mode and color flow Doppler (see Chapters 34 and 35).

## Use of the AFAST AFS System as an Exit Exam Postintervention

Physical examination, laboratory testing, and radiography are insensitive and unreliable tests for the presence of free fluid in small animals (Rozycki 1998; Rozycki et al. 1998, 2001; Boysen et al. 2004; Lisciandro et al. 2009; Lisciandro 2012; Boysen and Lisciandro 2013; McMurray 2016), and there is no reason to think that this would be different for postinterventional cases. After any invasive procedure that places your patient at risk for bleeding, the AFAST and its applied fluid scoring system should be used as standard of care. By having an AFAST and AFS documented pre- and postinterventionally (or, even better, the Global FAST approach – see Chapters 36 and 37), during follow-up examinations the continued use of AFAST and AFS (Global FAST) may help to detect complications earlier in their course.

The value of the FAST approach for postinterventional monitoring has clearly been shown in people (Rozycki 1998; Rozycki et al. 1998, 2001). Initial and serial AFAST with an AFS will help survey for ongoing bleeders. In addition, the technique aids in the detection of "large-volume bleeders" and may allow the clinician to have a higher index of suspicion for the possibility of overt clinical decompensation than would be possible by waiting on less sensitive traditional indicators such as packed cell volume and vital signs (Rozycki 1998; Bilello et al. 2010). In humans, it is well known that patients can compensate and fool physicians with unremarkable vital signs, mucous membrane color, heart rate, and pulse quality even with an acute loss of 30% of their blood volume (Muir 2006). Dogs are likely more able to compensate due to the blood reservoir provided through splenic contraction. We recommend performing AFAST and assigning an AFS postoperatively and then again as part of daily rounds and/or as part of the patient's exit exam prior to patient discharge. See information on drying the abdomen in a preceding section.

## Use of the AFAST AFS System in Nonhemorrhagic Effusions

Patients may become hypovolemic from nonhemorrhagic cavitary effusions and effusions within the retroperitoneal space. Analogous to the hypovolemic bleeding patient, nonhemorrhagic effusions are similarly categorized using the AFS system as "small-volume effusion" (AFS 1 and 2 or with the modified AFS system <3) versus "large-volume effusion" (AFS 3 and 4 or with the modified AFS system ≥3). The use of Global FAST helps detect effusions in these three major reservoir cavities and spaces that often are overlooked until effusions are advanced without ultrasound, radiography, and CT. The other two areas surveyed are the smaller reservoirs of the pericardial sac and lung (B-lines). Smaller in that generally a patient cannot tolerate large volumes of pericardial effusion (heart fails) or many B-lines representing alveolar-interstitial edema (lungs fail). Global FAST should be routinely used in all volume-depleted patients, as is advocated in human medicine (RUSH exam) (Perera et al. 2010), and discussed in more detail in Chapters 36 and 37.

### Clinical Examples

An example of the manner in which AFAST with an AFS works in nontrauma monitoring is for the patient with pancreatitis that on day 1 has an AFS of 1 without any AFAST target organ abnormalities. The following day, the Global FAST approach is used, and the AFS has increased to 3. Moreover, Global FAST further evaluates for effusions using TFAST, volume status, and any lung complications using Vet BLUE, and no additional effusions other than the ascites are found. This is significant patient information because likely the disease process is worsening. The finding of an increase from AFS 1 to 3 dictates a more aggressively diagnostic and therapeutic pursuit. Without this approach as an extension of the physical exam, these changes are often missed until the complications advance even more and the patient becomes overtly clinical. In contrast, the following day the AFS has decreased to 0, likely reflecting a positive response to therapy, important information for the clinician as well as the client.

Additional practical Global FAST examples would include cases with right-sided congestive heart (CHF) and making decisions on whether the patient requires therapeutic abdominocentesis as well as tracking ascites using the AFS for response to CHF therapy; and the use of the AFS postoperatively in vomiting septic abdomen cases to screen for abdominal-related complications, including effusions and ileus or dehiscence,

VetBooks.ir

or thoracic-related complications such as aspiration pneumonia or myocardial dysfunction, and so forth. The Global FAST approach screens these systems as part of its standardized protocol.

### *The use of AFAST and AFS in Dehydrated and Hypovolemic Patients*

These subsets of veterinary patients often have no ultrasonographically visible free fluid until after they are resuscitated and rehydrated. In the dehydrated patient with a bowel perforation, the omentum is often adhered to the defect, with the resorption (recruitment) of any available free water from the abdominal cavity. Thus, the serious lesion (same for a "small-volume bleed" from a mass) is not producing substantial free fluid until after rehydration and resuscitation. We use the mantra "Rehydrate, resuscitate, reevaluate with a minimum of at least one additional serial AFAST and AFS" within the next 2–4 hours. In humans with possible bowel injury, serial ultrasound examinations are recommended out to 12-24 hours post-admission (Mohammadi and Ghasemi-Rad 2012) (Figure 7.9).

**Pearl:** Serial AFAST exams increase sensitivity in detecting peritonitis and "small-volume bleed" suspects and should be performed four hours post admission, and again after resuscitation and rehydration. If the patient has not declared itself overtly surgical but remains a candidate, AFAST and AFS should be used serially for at least 12–24 hours and longer if patient status is questionable.

## Use of AFAST for Canine Anaphylaxis

### *Gallbladder Wall Edema – Sonographic Striation*

In 2009, the clinical utility of using point-of-care ultrasound for the rapid diagnosis of canine anaphylaxis (AX) was shown to be clinically helpful. Since the shock organ in dogs is the liver and gastrointestinal tract, hepatic venous congestion occurs rapidly (experimentally within minutes) due to massive histamine release within the portal circulation (Quantz et al. 2009; Caldwell et al. 2018; Hnatusko et al. 2019). As a result of massive histamine release, the intrahepatic venous sphincters tighten, thus causing the marked acute hepatic venous congestion along with degrees of gallbladder wall edema (intramural edema). The gallbladder change is generally easy to recognize during AFAST because the gallbladder is a fluid-filled structure and the intramural edema appears as sonographic striation, alternating hyperechoic and anechoic layering, called the "halo effect" or "double rim effect" and more commonly the "gallbladder halo sign" (Quantz et al. 2009) (Figures 7.10 and 7.11). The sonographic striation is observed as an outer hyperechoic line (outer gallbladder wall) and inner hyperechoic line (inner gallbladder wall) with sonolucency (hypoechoic to anechoic) in between. In other words, a layering of white-black-white or white-gray-white (see Figures 7.10, 7.11, and 18.22).

The gallbladder wall edema is a more rapid (<2–4 minutes) sign of canine AX over traditional markers of liver enzyme elevation such as the alanine transaminase (ALT) level that may peak in as long as 2–4 hours (Quantz et al. 2009). It is important to note that there are additional causes of gallbladder wall edema (Table 7.5). In the acute setting, conditions that cause obstruction to venous and lymphatic return to the heart that also result in hepatic venous congestion are important rule-outs and include pericardial effusion/cardiac tamponade and right-sided congestive heart failure, such as dilated cardiomyopathy, pulmonary hypertension, and tricuspid valvular disease (Lisciandro 2014a,b, 2016a) (see Figure 18.22). In less acute conditions, primary gallbladder diseases (cholecystitis) and diseases that affect the gallbladder such as pancreatitis and cholangiohepatitis can also cause gallbladder wall edema. Other miscellaneous causes include severe hypoalbuminemia and third spacing (d'Anjou and Penninck 2015), immune-mediated hemolytic anemia, post transfusion, and right-sided volume overload from overresuscitation from fluid therapy (Nelson et al. 2010).

Rule-outs are summarized in Table 7.5 with speculative pathogenesis and concurrent expected characterization of the caudal vena cava (see next section). The list is important to know to avoid "satisfaction of search error," the failure to search for additional abnormalities, which is automatically avoided using the Global FAST approach. By failing to rule out these conditions, the patient may be incorrectly resuscitated to its detriment. For example, a canine AX case requires the use of epinephrine and large-volume fluid resuscitation, which would not be the strategy to resuscitate a case of dilated cardiomyopathy, and emergent pericardiocentesis would be the treatment for pericardial effusion/tamponade, with inotropes for dilated cardiomyopathy.

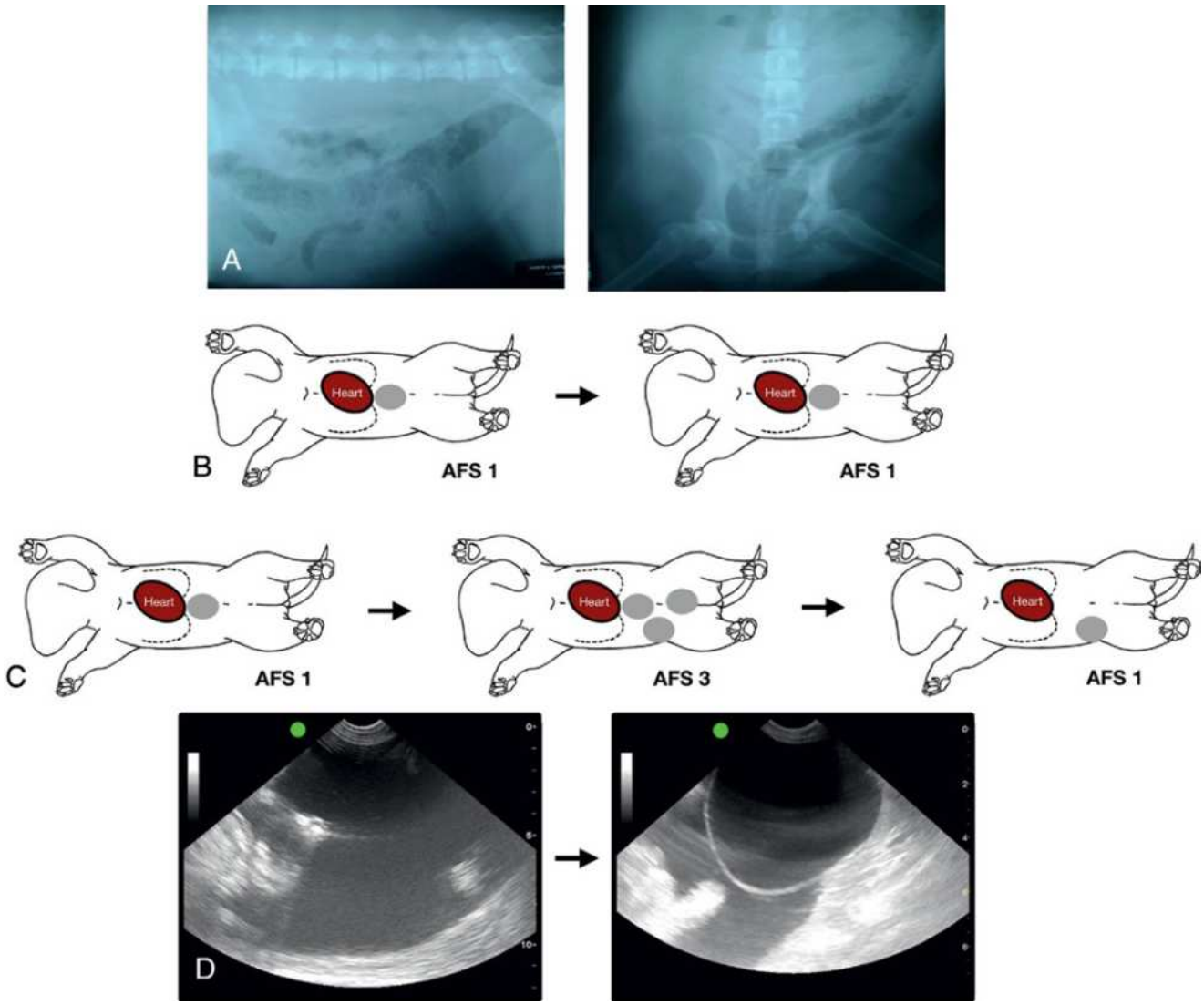


**Figure 7.9.** Composite showing comparison of abdominal radiographic serosal detail to AFS and value of serial examinations. (A) Abdominal radiographs of a dog with automobile trauma with markedly reduced serosal detail. The dog has a minimally displaced left acetabular fracture with an unimaged urinary bladder. (B) The initial AFAST determines that the dog has an AFS of 1 positive only at the DH View (*gray circle*). On the four-hour postadmission AFAST the AFS remains the same. (C) The AFAST on admission is again a 1 which in fact was found with the abdominal radiographs in (A). On serial exam the dog worsened with an AFS of 3. The fluid pocket was large enough to be accessed via abdominocentesis and its fluid analysis documented the large-volume bleeder hemoabdomen. The dog seemed stable based on physical exam, vital signs, and blood pressure with a normal PCV when in fact the dog was exsanguinating. Over time, the AFS was tracked and the dog received a blood transfusion due to developing anemia. Serial exams may be continued every four hours to every 12–24 hours on patient rounds, depending on clinical course. The serial exam thereafter documenting improvement to an AFS of 1 is invaluable patient information. (D) Images of the initial and four-hour postadmission serial AFAST showing absence of a urinary bladder and then its expected rounded contour post fluid resuscitation. The urinary bladder was missed initially likely because it was small and caudally located but in critical patients, the serial AFAST may be better used to decide on urinary bladder integrity post resuscitation. Source: Reproduced with permission of Dr Gregory Lisciandro, Hill Country Veterinary Specialists and FASTVet.com, Spicewood, TX. Illustration by Hannah M. Cole, Adkins, TX.

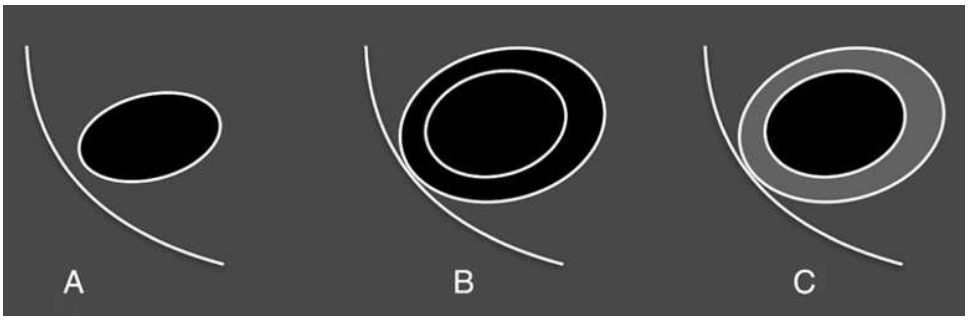


**Figure 7.10.** Normal and edematous gallbladder wall and sonographic striation. The gallbladder is represented by the black oval and the diaphragm is the white curved line mimicking the DH view. In (A) the gallbladder wall is normal and represented as a hyperechoic (white) thin line. In (B) and (C) the gallbladder has sonographic striation that alternates hyperechoic-anechoic-hyperechoic (white-black-white) and hyperechoic-hypoechoic-hyperechoic (white-gray-white). The inner and outer walls are shown as white lines with the intramural edema (black or gray) in between. The gallbladder wall does not have to be of abnormal thickness as dogs with an anaphylactic gallbladder can have sonographic striation with a wall thickness of <3 mm (Lisciandro 2016b) as shown in Figure 7.11B. Source: Reproduced with permission of Dr Gregory Lisciandro, Hill Country Veterinary Specialists and FASTVet.com, Spicewood, TX.

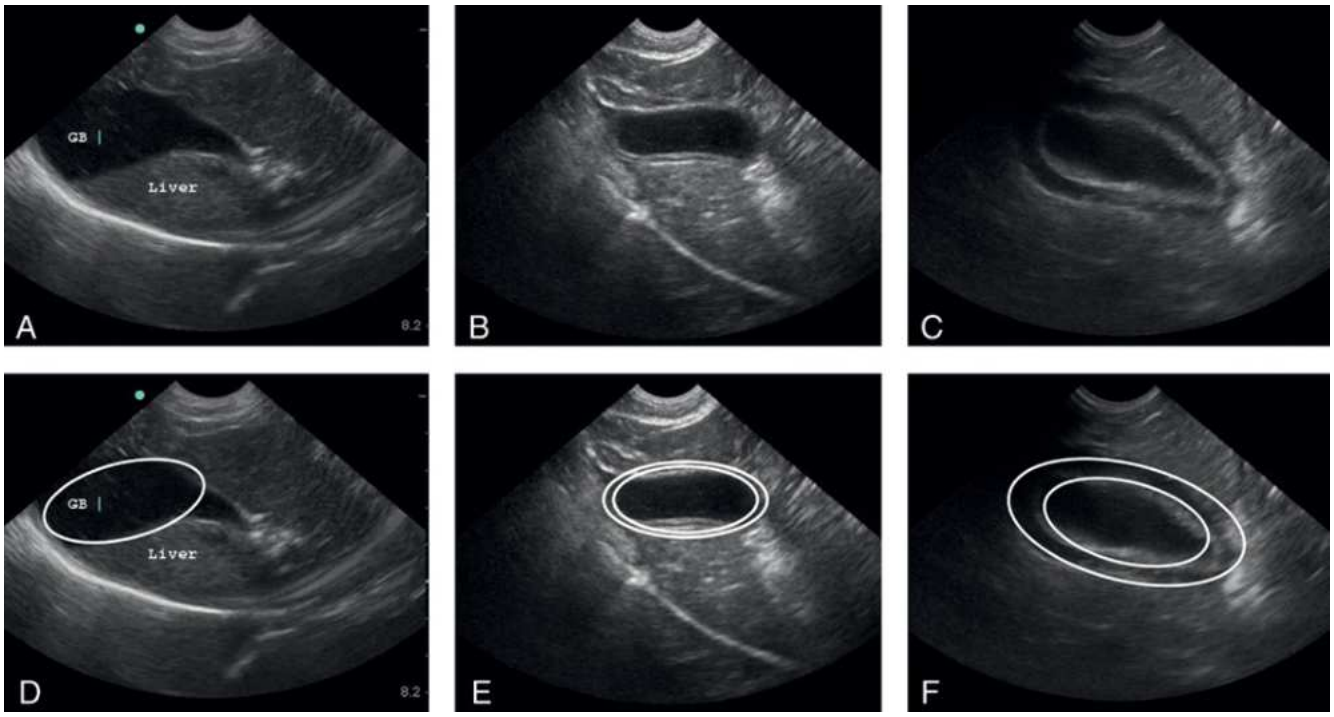


**Figure 7.11.** Gallbladder wall edema in dogs with anaphylaxis. Three different images with two different degrees of gallbladder wall edema in two different dogs at the AFAST DH view. Images in the top row are shown in the bottom row with correlating line drawing overlays. A normal gallbladder wall is for all intents and purposes a thin hyperechoic line as shown in (A) and (D). The gallbladder wall "halo effect" is in fact intramural edema that images as a hyperechoic inner wall, a hypoechoic or anechoic sonographic layer of intramural edema, followed by an outer hyperechoic wall. The sonographic striation, white-black-white or white-gray-white, is also referred to as the "halo sign" or "double rim effect" (Quantz et al. 2009). (B) and (E) is the same image unlabeled and labeled; note the small triangulations of free fluid (outlined with triangles), which would be scored as an AFS of ½. In (C) and (F) is another case with canine anaphylaxis with the same image unlabeled and labeled. The curved white line represents the diaphragm. Degrees of gallbladder wall edema in the author's experience do not correlate with severity of anaphylaxis. Gallbladder wall edema, although a marker for canine anaphylaxis, is not pathognomonic and PCE and right-sided heart failure are major rule-outs in the acutely collapsed or weak-hypotensive dog (see Table 7.5 and Figure 18.22). Source: Reproduced with permission of Dr Gregory Lisciandro, Hill Country Veterinary Specialists and FASTVet.com, Spicewood, TX.

**Table 7.5.**
Rule-outs for the finding of gallbladder wall edema in dogs and cats.

| Condition | Expected characterization of the caudal vena cava (CVC) | Speculated pathophysiology |
|---|---|---|
| Canine anaphylaxis[a] | Flat, hypovolemic CVC, (see Table 7.6) | Massive histamine release resulting in acute marked hepatic venous congestion |
| Pericardial effusion[q] | FAT, distended, hypervolemic CVC, referred to as vena cava plethora in people (see Table 7.6) (Himelman et al. 1988) | Marked hepatic venous congestion from obstruction of blood flow to the right atrium |
| Right-sided congestive heart failure (dilated cardiomyopathy, pulmonary hypertension, tricuspid disease)[a] | FAT, distended, hypervolemic CVC, referred to as vena cava plethora in people (see Table 7.6) (Himelman et al. 1988) | Marked hepatic venous congestion from backflow of blood from the right atrium |
| Cholecystitis | Variable | Direct inflammation |
| Pancreatitis | Variable | Direct inflammation |
| Hypoproteinemia (third spacing) | Variable | Vascular leak |
| Immune-mediated hemolytic anemia | Variable (author experience, unpublished) | Likely immune-mediated and volume overload, does not indicate anaphylaxis in many patients |
| Post transfusion[b] | Variable to FAT, hypervolemia (author experience, unpublished) | Likely immune-mediated and volume overload, does not indicate anaphylaxis in many patients |

[a]Conditions that are most important to consider in the acute triage setting of acute collapse and weakness in a previously healthy patient (dog). FAT, flat, and bounce are defined in the text.
[b]Many posttransfusion cases develop gallbladder wall edema that is not anaphylaxis. Look at your patient and correlate its clinical profile with the finding of gallbladder wall edema.
Source: Reproduced with permission of Dr Gregory Lisciandro, Hill Country Veterinary Specialists and FASTVet.com, Spicewood, TX.

## *Characterizing the Caudal Vena Cava*

### Measurements

Guidelines for caudal vena caval (CVC) *absolute size* in dogs of various weight classes have been created by the author from the data generously provided by Dr Elodie Darnis and colleagues (Darnis et al. 2018). More indepth CVC detail regarding measurements and formulas may be found in her co-authored Chapter 26.

The expected CVC maximum heights for three weight classes of dogs taken in the longitudinal plane at the FAST DH view (subxiphoid) are shown in Table 7.6. The absolute height measurements should be combined with the "eyeball method" of evaluating respirophasic dynamic changes in the CVC. This gestalt "eyeball method" essentially assesses the CVC Collapsibility Index, which is the difference between maximum and minimum diameter divided by the maximum diameter multiplied by 100%.

The author has characterized the CVC as having a "bounce," being "FAT" or "flat" for categorizing its clinical relevance to volume status. A "bounce" is a "fluid-responsive" CVC; a "FAT" CVC is a distended CVC suggesting a "fluid-intolerant" CVC reflective of an abnormally high central venous pressure (hypervolemia); and a "flat" CVC is a "fluid-starved" CVC reflective of a "hypovolemic CVC." The terms "FAT" and "flat" have been descriptively used in the human literature (Ferrada et al. 2012a,b) and many clinicians combine absolute maximum inferior vena cava height measurements with the "eyeball method" (FAT or flat). More and more, these same clinicians are incorporating basic echo views and lung ultrasound findings for more clinical integration to accurately assess volume status and thus guide fluid resuscitation in people (Ferrada et al. 2012a,b). Similar approaches are being investigated in veterinary medicine (Nelson et al. 2010; Lisciandro 2014a, 2016a, Lisciandro and Fosgate 2017; Bucci et al. 2017; Kwak et al. 2017; Tuplin et al. 2017; Darnis et al. 2018; Marshall et al. 2018; Cambournac et al. 2018) (see Chapters 26, 36, and 37 and also Figures 36.8–36.12). The terms "FAT" (fluid intolerant, high central venous pressure, inferior vena cava >2 cm) and "flat" (fluid starved, low central venous pressure, hypovolemia) are routinely used in human medicine in the San Antonio area (Ferrada et al. 2012a,b). The author has added the term "bounce" for a fluid-responsive CVC.

**Table 7.6.**
Reference values for the caudal vena cava (CVC) measured in longitudinal at the subxiphoid[a] view in 126 healthy dogs, grouped into three body weight classes.

| Size | Body weight (kg) | Expected CVC height measurement (cm) | CVC +/-2 standard deviations (cm) | Suggested CVC maximum height (cm) for a "flat" or hypovolemic, fluid-starved CVC | Suggested CVC maximum height (cm) for a "FAT" or fluid-intolerant CVC (high central venous pressure) |
|---|---|---|---|---|---|
| Small/Toy[b] | <9 kg | 0.55 | (0.23–0.86) | <0.25 | >1.0 |
| Medium | >9–15 kg | 0.85 | (0.32–1.38) | <0.35 | >1.5 |
| Large/Giant | >15 kg | 0.96 | (0.51–1.4) | <0.50 | >1.5 |

Data from the study by Darnis et al. (2018) and measurements created with permission by Lisciandro GR and Vientós-Plotts AI. These values are unproven but give some guidelines for veterinary clinicians to combine with the eyeball method – "bounce", "FAT," and "flat."
[a]The subxiphoid view is analogous to the FAST DH view and the CVC imaged in its longitudinal plane.
[b]Suggested starting point for felines while awaiting current research findings.

The suggested CVC measurements shown in Table 7.6 are at least a start and are easy to remember over formulas.

### Integrating Global FAST Information

The characterization of the CVC is key because it helps with clinical integration of information when sonographic striation of the gallbladder is found in acute collapse or weakness in a dog with a previous healthy history (Figure 7.12) (Lisciandro 2014a). In canine AX, the CVC is expected to be "flat" having small maximum diameter with little respirophasic diametrical change because of the severe AX-related hypovolemia (see Figures 7.12, 36.8–36.12). In contrast, patients with pericardial effusion/tamponade and right-sided congestive heart failure have a CVC that is expected to be "FAT" having a large maximum diameter with little respirophasic diametrical change because of the severe cardiac-related hepatic venous congestion (see Figures 7.12, 36.8–36.12). The terms "flat" and "FAT" have been published as terms that similarly characterize the inferior vena cava (IVC) at the subxiphoid view in people (Ferrada et al. 2012a,b). Integration of other POCUS and FAST findings is imperative for accurate interpretation. More information regarding the CVC and its evaluation may be found in Chapters 19, 20, 26, 36, and 37.

## *Canine AX-Related Heparin-Induced Hemoabdomen – Single Witnessed or Unwitnessed Hymenoptera sp. Envenomation*

Although we were the first group to describe the phenomenon in the veterinary literature (Lisciandro 2016b), all the credit goes to Dr Scott Johnson, of Austin, Texas. When Dr Johnson took our Global FAST course in 2010, he remarked that he had observed hemoabdomen in anaphylactic dogs, and that we should start looking during AFAST. We heeded his suggestion and have seen close to 100 canine anaphylactic dogs with positive fluid scores and dozens with confirmed hemoabdomen that responded to medical treatment (Lisciandro 2014a, 2016b; Hnatusko et al. 2019). Importantly, these are witnessed or unwitnessed events likely caused by a presumed single Hymenoptera species envenomation (*not* massive bee envenomation). *The great majority of anaphylactic dogs have no obvious cutaneous signs* (Lisciandro 2016b; Hnatusko et al. 2019).

Heparin, a clinically tangible constituent of mast cells, likely plays a major role, thus the addition of "heparin-induced" by the author to its descriptor (Lisciandro 2016b). The importance of recognizing this AX-related heparin-induced hemoabdomen is that these dogs are medically treated (Lisciandro 2014a, 2016b; Caldwell et al. 2018; Birkbeck et al. 2019; Hnatusko et al. 2019) and inadvertently taking these dogs to surgery will anecdotally result in a fatal outcome (Lisciandro 2014a, 2016b; Hnatusko et al. 2019). Interestingly, in a published case series of 432 dogs with hemoabdomen, 86 were operated, but only 83 were included in the study because the three that were excluded had no histopathological diagnosis (Lux et al. 2013). One has to wonder if these three dogs were AX-related heparin-induced hemoabdomen cases.

## *Small-Volume Bleeders/Effusions*

Anaphylactic dogs commonly have small-volume effusions, AFS 1 and 2 (modified AFS system <3), that are not safely amenable to abdominocentesis (Lisciandro 2014a, 2016b). AFS 1 cases are most commonly positive at the AFAST DH view, with free fluid

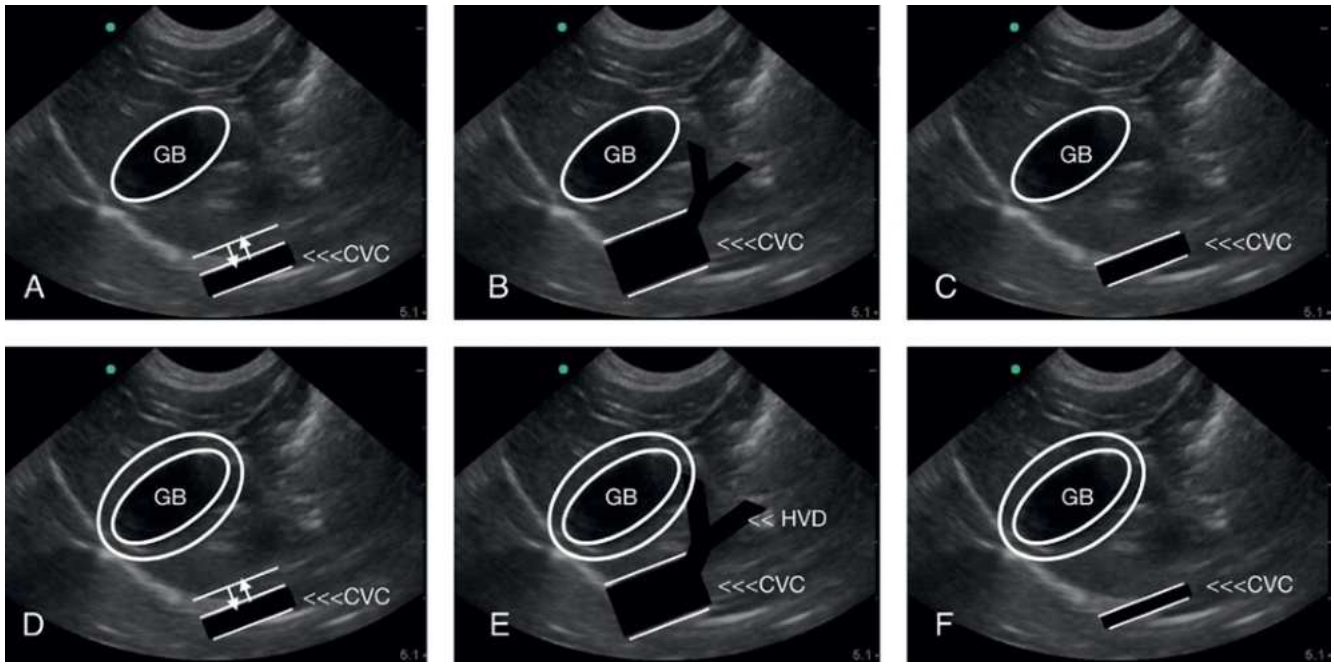


**Figure 7.12.** Integrating gallbladder wall edema with characterization of the caudal vena cava. The top row (A–C) shows a normal gallbladder wall (thin hyperechoic line) with variations of the caudal vena cava (CVC) as being (A) "fluid responsive" with a "bounce" or change to its respirophasic height, (B) "FAT" or distended and "fluid intolerant" with minimal change to its respirophasic height, and (C) "flat" or small sized due to hypovolemia and thus "fluid starved" with minimal change to its respirophasic height. The same images in rows (D–F) show gallbladder wall edema, which can occur with heart failure, as in (B), and referred to as a "cardiac gallbladder," or with canine anaphylaxis as in (F) and referred to as an "anaphylactic gallbladder." In right-sided congestive heart failure the CVC is "FAT," distended with a large maximum height, whereas in canine anaphylaxis with hypovolemic shock the CVC is "flat," small with a small maximum height (see Table 7.6). Note also the distended hepatic veins associated with the "FAT" CVC, referred to as the "tree trunk sign" (Lisciandro 2014a,b) (see also Figure 36.8). There are other causes for gallbladder wall edema (Table 7.5). Source: Reproduced with permission of Dr Gregory Lisciandro, Hill Country Veterinary Specialists and FASTVet.com, Spicewood, TX.

pocketing around the gallbladder, in between adjacent liver lobes, and between the liver and the diaphragm as an anechoic stripe generally with maximum dimensions of <0.5 to 1 cm (Lisciandro 2014a, 2016b). Often this free fluid is not safely accessible via abdominocentesis. AFS 2 cases are most often positive at the AFAST DH and CC views followed by AFS 2 cases being positive at the DH and HRU views (Lisciandro 2014a, 2016b; Hnatusko et al. 2019). It is important not to overreact, but rather acknowledge the complication is likely present in these AFS-positive AX dogs and treat with standard AX therapy to prevent and/or mitigate the "second episode of AX" that likely causes the acquired and persistent coagulopathy prolonged even more without glucocorticoid and antihistamine-2 receptor blockers (Table 7.7) (Simons et al. 2015). Most AFS 1 and 2 (modified AFS system <3) dogs that are appropriately treated do not become markedly coagulopathic and do not require replacement of clotting factors via transfusion products (Lisciandro 2014a, 2016b).

The manner in which the author recommends managing these cases is to get a baseline coagulation profile, when possible, as standard of care. In cases with coagulation profiles >25% of upper reference range, clotting factors should be replaced, that is, fresh frozen plasma (FFP). However, if a coagulation profile is not possible, AFS 1 and 2 (modified AFS system <3) dogs are "small-volume effusions/bleeders" and, having an occult hemoabdomen until proven otherwise, do not have enough blood in their abdominal cavity to be life-threatening. In fact, many AFS 3 and 4 (modified AFS system ≥3) will likewise resolve within 24–48 hours, if not excessively coagulopathic, with appropriate treatment (including initial treatment of glucocorticoids and histamine-2 receptor blockers) to prevent the "second episode of anaphylaxis." These treatment strategies are recommended in people (Simons et al. 2015).

Treat all AFS-positive (AFS 1–4) AX dogs with standard resuscitative care including glucocorticoids and

**Table 7.7.**
The author's treatment and monitoring guidelines for canine anaphylaxis (AX) in all AFAST fluid-positive cases to prevent and treat AX-related heparin-induced hemoabdomen.

| | Intervention | Duration of activity | Comments |
|---|---|---|---|
| **First line** | | | |
| Intravenous (IV) fluids | 30–50 mL/kg IV repeated as needed | Short-acting | |
| Epinephrine (EPI) | Low dose 0.01 mg/kg, intramuscular (IM) or IV repeated as needed every 5–10 minutes; if this fails, injectable EPI then go to constant-rate infusion (CRI) | Ultra short-acting | Can use as a CRI starting at 0.05 µg/kg/min IV then increasing as needed based on blood pressure and taper off as soon as possible due to side effects |
| **Second line** | | | |
| Dexamethasone Sodium phosphate (glucocorticoids)[a] | 0.3 mg/kg IV | Long-acting | Repeat 12 hours post admission at 0.15–mg/kg if not able to take PO prednisone[a] |
| Diphenhydramine (histamine-1 receptor blocker) | 2 mg/kg IM ONCE with maximum dose of 50 mg/dog | Intermediate | Avoid IV due to potential to initiate hypotension |
| Famotidine (histamine-2 receptor blocker) | 0.5 mg/kg IV or IM q12–24h (PO once appropriate) | Intermediate to long-acting | Continue for 5–7 days while patient on steroids |
| Prednisone[a] | 0.25 mg/kg q12h for 3 days then 0.25 mg/kg q24h for 3 days | Long-acting | Tapering steroid regimen to prevent 2nd episode (wave) of inflammation that causes persistent coagulopathy |
| Fresh frozen plasma | Give if PT, aPTT greater than >25% over upper reference range and repeat as needed<br>Delay if PT, aPTT less than <25% over upper reference range and recheck again in 4h and thereafter as needed depending on AFS and clinical course | Intermediate | Follow these cases with frequent PCV q2–4h plus serial AFAST and AFS until you are confident that the coagulopathy and hemoabdomen are resolving |
| **Monitoring** | **AFAST** | **TFAST** | **Vet BLUE** |
| **Global FAST** – combining AFAST and AFS and its target organ Approach, TFAST, and Vet BLUE | **AFAST** and AFS and its target organ approach – on admission and then 4h post admission if stable, sooner if unstable | **TFAST** for pleural and pericardial effusion, volume status and cardiac status | **Vet BLUE** for lung edema and other respiratory complications |
| | **AFAST** and **AFS** as part of daily patient rounds | Left-atrial to aortic (LA:Ao) ratio, fallback nonecho view Vet BLUE for left-sided volume overload | Expect lung to be dry in canine AX unless there are complications |
| | Expect dogs with resolved coagulopathy to have dramatic resolution of their AFS within 24h – AFS 1 or 0 (negative fluid score) | Right ventricular to left ventricular (RV:LV) ratio, fallback nonecho view of the caudal vena cava and hepatic veins for right-sided volume overload | |

[a] Potent arachidonic acid inflammatory pathway blocker (inhibiting phospholipase A2), histamine blocker, and inhibitor of mast cell degranulation.
Source: Reproduced with permission of Dr Gregory Lisciandro, Hill Country Veterinary Specialists and FASTVet.com, Spicewood, TX.

VetBooks.ir

histamine-2 receptor blockers to prevent histamine, heparin, bradykinin and other contributory inflammatory factors, prostacyclins, that contribute to the acquired coagulopathy (see Table 7.7). Monitor by performing serial Global FAST examination(s) that include AFAST and AFS. Expect the AFS to resolve to near 0 within 12–36 hours in dogs that are not continuing to bleed according to the "AFAST-TFAST 48-hour rule" (Lisciandro 2014a, 2016b). Packed cell volume is another inexpensive monitoring tool and is combined with patient AFS regarding blood loss (and the Global FAST approach for other complications and volume status assessment) versus drops in PCV and increases in AFS that become concerning, requiring additional intervention(s), such as coagulation profiles and administration of transfusion products, to maximum a successful patient outcome. For example, an increasing AFS to a 3 or 4 (modified AFS system, AFS ≥3) has become a "large-volume bleeder" and with developing anemia warrants a change in treatment strategy with relevant testing (e.g., confirmatory abdominocentesis with fluid analysis and cytology and coagulation profile). In contrast, a static AFS 1 or 2 "small-volume bleeder" with a stable, nonanemic PCV may be monitored using AFAST and an assigned AFS (or, better, Global FAST). The author always performs one more Global FAST four hours post admission and then on patient rounds every 12–24 hours in stable patients until the effusion has resolved (AFS 0), while also evaluating for any additional complications (TFAST and Vet BLUE). See Table 7.7 for suggested management guidelines.

## Large-Volume Bleeders/Effusions

In lesser numbers of canine AX cases, "large-volume bleeding," AFS 3 and 4 (modified AFS system ≥3), occurs (Lisciandro 2014a, 2016b). When detected, the challenge is again not to overreact because in our experience, dogs with PT and aPTT times that range no more than 25% over upper reference often do not need replacement of clotting factors as long as standard therapy, including glucocorticoids and histamine-2 receptor blockers (second-line medications), is used upfront (without delay) in patient management (see Table 7.7). AFS 3 and 4 (modified AFS system ≥3) cases are often confirmed as AX-related heparin-induced hemoabdomen because the free intraabdominal fluid is safely accessible for abdominocentesis and fluid characterization. These cases require close monitoring and coagulation profile(s). In cases with initial or serial coagulation profiles of >25% of upper reference range, clotting factors should be replaced. However, PCV, vital signs, physical exams, and repeating AFAST with AFS (or Global FAST) can help monitor (track) the patient, whether coagulopathic or not. See Table 7.7 for suggested management guidelines.

## Clinical Examples

Let's look at a couple of case scenarios of large-volume canine AX-related heparin-induced bleeders. For example, if the high normal aPTT is 102 seconds, then an acceptable elevation not requiring FFP would be up to 129 seconds. The author has managed many cases with an AFS of 3 and 4 on admission that responded favorably to resuscitation with epinephrine, intravenous crystalloid fluid therapy, histamine-1 and histamine-2 receptor blockers, and glucocorticoids (see Table 7.7). These cases are continued on a short course of antiinflammatory glucocorticoids and histamine-2 receptor blockers for the next several days with documented hemorrhagic effusion (and others highly suspected that fit the canine AX clinical profile). Often the AFS 3 and 4 is completely resolved (AFS 0) or nearly resolved (AFS 1) the following day on patient rounds. An excellent up-to-date anaphylaxis webinar and additional information regarding this unique and fascinating medically treated canine AX-related complication is available free of charge at www.FASTVet.com

In uncommon to rare instances, packed red blood cells (pRBCs) are additionally needed. In the author's experience, some general guidelines for a clinical course and need for transfusion products would be that 1 in 5–7 AX-hemoabdomen dogs (of any positive AFS) require replacement of clotting factors, 1 in 15 AX-hemoabdomen dogs require a second round of FFP, and 1 in >25 AX-hemoabdomen dogs require pRBCs treating as in Table 7.7, with the caveat that glucocorticoids and histamine-2 receptor blockers are administered initially without delay. A recent case report documented a canine AX-hemoabdomen without gallbladder wall edema, which in our experience is the vast exception rather than the rule (Caldwell et al. 2018; Lisciandro and Lisciandro 2019). Without saving the ultrasound gallbladder image for radiologist review, more subtle sonographic striation could have been missed (Caldwell et al. 2018; Lisciandro and Lisciandro 2019) (see Figure 7.11B).

Lastly, nearly all of our canine AX cases (100+) have had Global FAST performed and we have found a couple more important observations: pericardial and pleural hemorrhage has not been documented as a complication of the acquired AX-related heparin-induced hemoabdomen coagulopathy, and lung has always been "dry" with "absent B-lines All (Vet BLUE)

views (ABAV)" initially and on serial Global FAST examinations (Lisciandro et al. 2016; Hnatusko et al. 2019), in contrast to a single case report in the literature of massive bee envenomation accompanied by marked pulmonary edema (Walker et al. 2005). Importantly, these AX cases are single witnessed or witnessed Hymenoptera sp. envenomation and not massive bee envenomations, a much different subset of dogs. Anecdotally, AX-related hemabdomen has occurred with vaccine-induced AX.

## Speculated Pathogenesis

There is only a single report of which we are aware in the human literature of an AX-related hemoabdomen (Borahay et al. 2011). The case involved a near-term pregnancy in a woman, interestingly from Galveston, Texas, with previous AX to contrast agents. She was anemic and received a blood transfusion prior to a scheduled C-section and tubal ligation. During the procedure, she was given a cephalosporin antibiotic and complained of pruritus and had cutaneous and vital signs supporting a diagnosis of AX. She was started on epinephrine as a constant-rate infusion. Postoperatively she became hypotensive and bedside point-of-care ultrasound was performed and she was positive for free fluid. Coagulation profile supported an acquired coagulopathy and disseminated intravascular coagulopathy (DIC) was diagnosed. She was reoperated after receiving histamine-1 and histamine-2 receptor blockers and glucocorticoids. At surgery, no discrete bleeding was found but only generalized oozing; topical hemostatic agents were placed intraoperatively and FFP was administered. She survived and her coagulopathy corrected within 24 hours (Borahay et al. 2011).

The case is interesting because likely the acquired coagulopathy in these dogs is complex and multifactorial and variable depending on what factor(s) is the major player in each case. However, heparin must play a role because some dogs have obvious discordance in coagulation times with a much higher aPTT than PT time (consistent with heparinization). Mast cell granules contain heparin. Additional factors likely playing a role include histamine, bradykinin, tryptase, platelet-activating factor, and others (Lisciandro 2016b; Caldwell et al. 2018; Hnatusko et al. 2019).

## Therapy for Canine Anaphylaxis

The human case and these AX-related factors are important to recognize for effective therapy. It is equally important to recognize that in people 4–5% (range ~2–20%) experience the "second episode of AX" in which inflammatory by-products create a second wave of inflammation (Simons et al. 2015). The "second episode of AX" is countered therapeutically through the use of histamine-2 receptor blockers (e.g., famotidine) and glucocorticoids, often continued over several days post AX. Histamine-2 receptor blockers are readily available and help mitigate oozing of blood and plasma into the abdominal cavity. Glucocorticoids are important on several fronts, most importantly including: mitigating mast cell degranulation (stopping release of heparin and histamine), and indirectly attenuating the wind-up of bradykinin (BK) through (a) blocking phospholipase A2 and the arachidonic acid pathway and (b) mitigating circulating heparin (Hnatusko et al. 2019) (see Table 7.7). Of note, maropitant and pantoprazole, commonly used drugs for gastrointestinal signs, do not treat AX and are ineffective for mitigating the "second episode of anaphylaxis" and treating the AX-acquired coagulopathy.

In a recent case series of four dogs with AX-hemoabdomen, three of the four dogs had small-volume peritoneal effusion at the DH view and these three had short hospitalization courses (<48 hours). However, the fourth case had progression of the abdominal effusion and became unstable, requiring vasopressors and multiple units of FFP, surviving but hospitalized for five days. None of these four dogs received glucocorticoids or antihistamines to mitigate the "second episode of anaphylaxis." The first three arguably got better on their own and were unlikely to progress no matter the treatment. However, the fourth dog arguably risked a poor outcome (death or euthanasia) and presumably had a large bill for its five days of intensive care with transfusion products and vasopressors (Birkbeck et al. 2019). One has to wonder if treating for the "second episode of AX" would have shortened the patient's course and curbed its complications and still would have been a low-risk, high-benefit, cost-effective preventive therapy for the first three dogs. Moreover, performing a standardized AFAST and assigning an AFS would have provided more clinically relevant patient information rather than performing an unspecified POCUS abdominal exam using subjective descriptive terms for the ascites.

**Pearl:** Anaphylactic dogs commonly have AFAST-positive fluid scores (AFS of 1 and 2, modified AFS system <3) with some developing large-volume medically treated coagulopathic hemoabdomens (AFS 3 and 4, modified AFS system ≥3). Misdiagnosing and taking to surgery likely will be a fatal event.

**Pearl:** All canine AX-hemoabdomen cases need to have as part of their work-up a Global FAST and POCUS spleen evaluation to avoid "satisfaction of search error." The combined evaluation will (1) semiquantitate volume of blood (AFS), (2) screen for gallbladder wall edema (AFAST), (3) screen for pericardial and pleural effusion (TFAST), (4) screen for right-sided heart problems and dilated cardiomyopathy (TFAST), and (5) screen for a splenic mass (focused spleen). This combination of Global FAST and POCUS increases the probability of obtaining an accurate working diagnosis in the acutely collapsed or weak dog.

# AFAST DH View for Pericardial Effusion

## *Anatomy and Advantages over TFAST Transthoracic Views*

The premise is simple – *always, always, always* look cranial to the diaphragm at the FAST DH view (Figure 7.13; see also Figures 6.8 and 6.9) (Lisciandro 2016a, 2019). The use of the DH view for pericardial effusion (PCE) avoids air interference (ultrasound cannot transit through air) from lung at transthoracic views, especially since dogs and cats (and people) often have respiratory distress as their chief complaint. In fact, the subcostal FAST view in human medicine is the number 1 view for PCE that may be used a *single* view because the heart is so well imaged through the acoustic window provided by the liver and gallbladder into the thorax. In dogs and cats, the observation of the "racetrack sign" is essentially pathognomonic for PCE (Lisciandro 2014a, 2016a) (see Figure 7.13).

The best way to comprehend the relevant anatomy at the DH view is to look at an inverted canine (and feline) lateral thoracic radiograph (TXR). The TXR helps in learning the relative locations of the major structures, including the location of the muscular apex of the heart, called the "cardiac bump," the expected positioning of heart chambers relative to the diaphragm, location of the CVC, and the expected location of the canine and feline gallbladder (Figure 7.14; see also Figures 6.11 and 6.12). The "cardiac bump" is the descriptor used for the observation of the beating heart and its muscular apex immediately against and, in dogs, often indenting the surface of the diaphragm where the heart and diaphragm come into contact (see Figures 7.14, 6.11, and 39.5). From our retrospective case series in which the methodology did not establish whether transthoracic TFAST views or the DH view was first performed, ~85% of PCE cases were imaged via the DH view (Lisciandro 2016a). In a prospective case series with subsequent improvements in training since our study, likely the DH view would prove to be nearly 100% sensitive and 100% specific for PCE in standing/sternal positioning in both dogs and cats. In other words, the DH view is a very good screening test.

Interestingly, the cardiac and diaphragmatic interface differs between people and dogs and cats. The human heart has its right ventricle and right atrium closest to the diaphragm whereas it is the left ventricle and left atrium in dogs and cats (see Figure 7.14). This is important when imaging the CVC because in people, the analogous IVC may be imaged as it enters the right atrium whereas in dogs and cats, the closest the CVC may be imaged to the right atrium is where the CVC passes through the diaphragm. Learning the DH view's cardiac orientation is a good add-on skill. The DH cardiac view is helpful in PCE cases that have a left atrial tear/rupture from chronic mitral valve disease because the severely enlarged left atrium is commonly obvious here (conversely finding a small left atrium), and the DH view is generally less stressful and a better acoustic window for respiratory distressed patients.

## *Use for Cardiac Tamponade*

The noncardiologist sonographer will grapple with this clinical question that often causes marked degrees of anxiety – does my patient have cardiac tamponade? And, taking it a step further – does my patient need emergent pericardiocentesis?

The diagnosis of cardiac tamponade is discussed in more detail in Chapters 18 and 21. Most importantly for the AFAST chapter, there exists a nonecho option, the characterization of the patient's CVC (see Figure 7.12)! Think about why and when an emergent pericardiocentesis would be indicated, and the answer – the presence of obstructive shock from PCE. By definition, obstructive shock from PCE results in a "FAT," distended, with little respirophasic diametric CVC change. Thus, if the CVC is not "FAT" or distended and has a diametric respirophasic "bounce" to it, then your patient does not have cardiac tamponade. Moroever, if your patient is weak and collapsed, you need to investigate for other causes (using Global FAST). If your patient

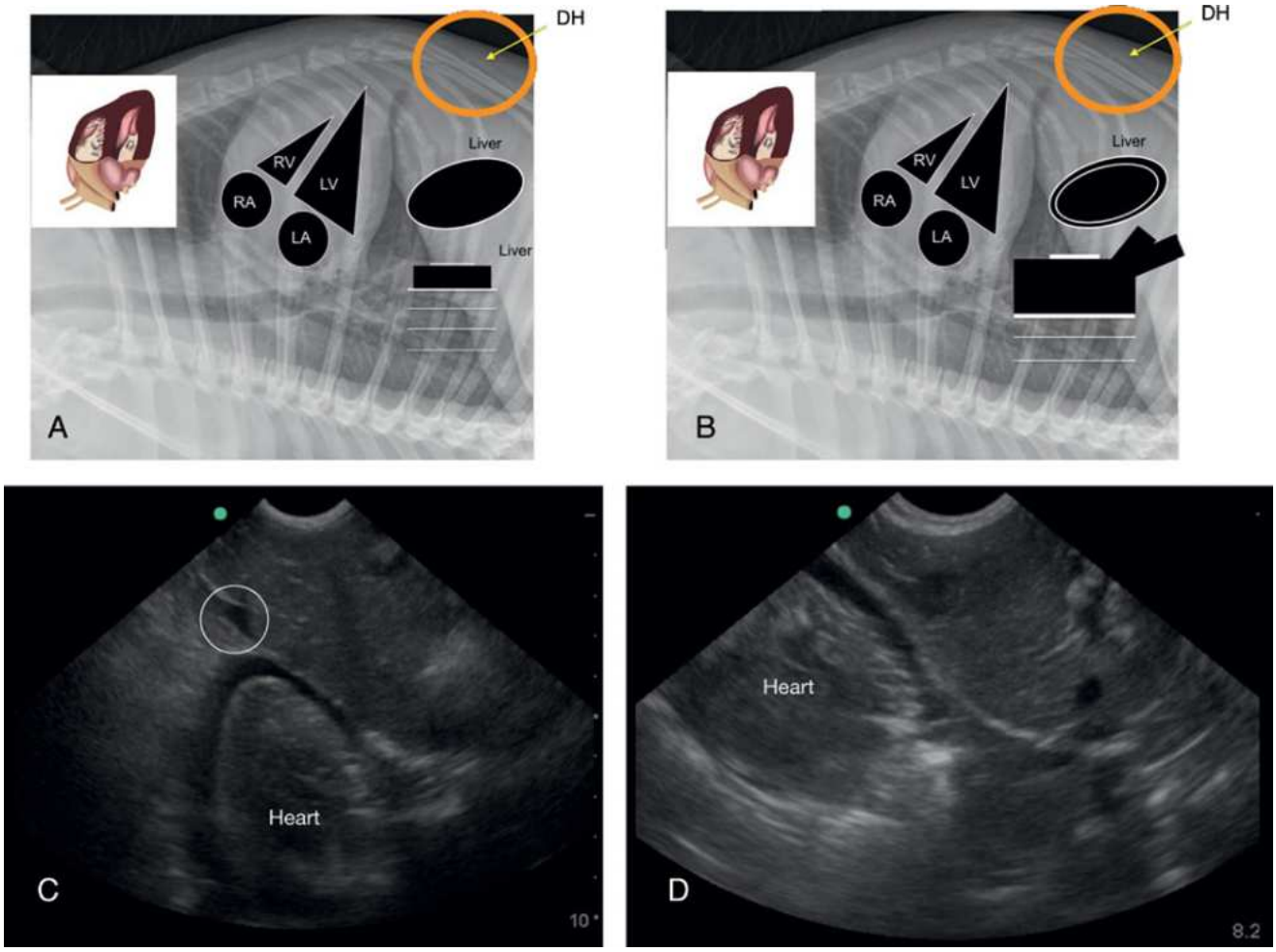


**Figure 7.13.** The racetrack sign of PCE with integration of the CVC characterization. (A,B) Inverted lateral thoracic radiographs to illustrate the anatomy in the ultrasound images in (C) and (D) with PCE evidenced by the rounding of anechoic fluid, referred to as the "racetrack sign" (Lisciandro 2014a,b, 2016a). Characterization of the CVC is helpful for evidence that obstructive shock and tamponade may be present. In (A) the CVC is unremarkable and in (B) the CVC is "FAT" and has associated hepatic venous distension supporting obstruction of blood flow to the right atrium. In (C) there is a small-volume ascites (*circled*) and if a modified transudate, supports a more chronic case of PCE and a better prognosis. In (B) gallbladder wall edema, the "cardiac gallbladder," is shown which is only expected with hepatic venous congestion and more chronicity to the PCE. Source: Reproduced with permission of Dr Gregory Lisciandro, Hill Country Veterinary Specialists and FASTVet.com, Spicewood, TX.

does have CVC characteristics suggestive of cardiac tamponade, look at your patient! If they are alert and in no distress, take a few breaths and relax, you have time on your side, the procedure may be delayed, complete echocardiography may be scheduled, and the procedure, if indicated, performed electively. However, if your patient is weak and unstable, an emergent life-saving pericardiocentesis is indicated.

Interestingly, the use of IVC distension (a "FAT" IVC) in people is only about 40% specific for the presence of cardiac tamponade. Conversely, a nondistended IVC at the subxiphoid view that has its expected normal variation in diameter in spontaneously breathing people effectively rules out cardiac tamponade with a sensitivity of 97% (Candotti and Arntfield 2015; Tchernodrinski and Arntfield 2015). The CVC in small animals likely proves similarly helpful with indirect nonechocardiographic (fallback view) information regarding the presence of obstructive shock from cardiac tamponade. We like the saying "Don't risk your patient's life trying for an echo view" – use the Global FAST fallback views (see Figure 36.7).

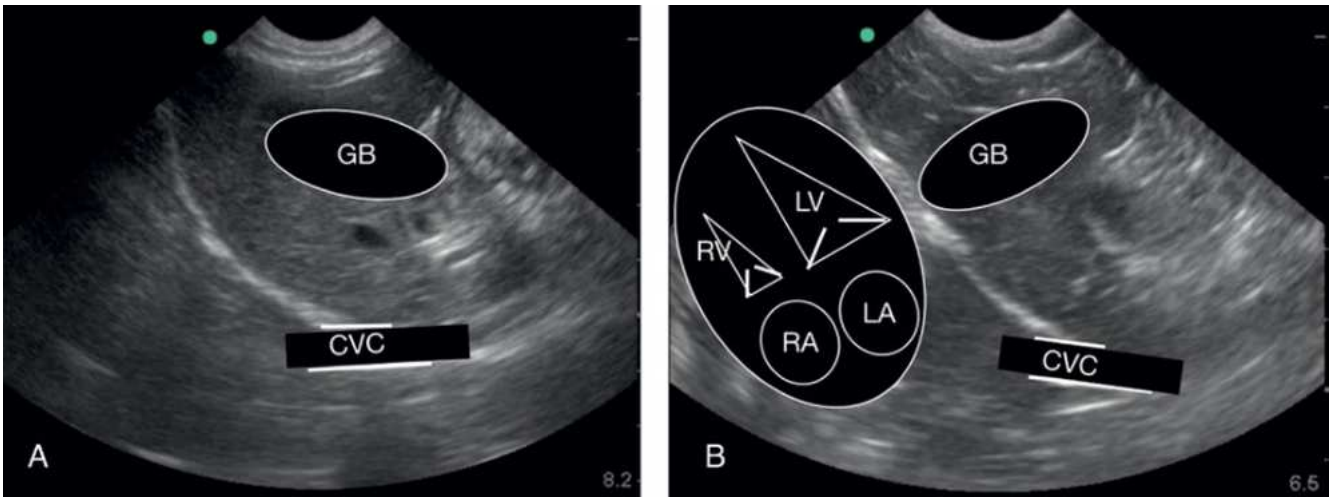


**Figure 7.14.** Relative positioning of gallbladder to diaphragm to caudal vena cava. (A,B) Line drawing overlays of the gallbladder (GB) and caudal vena cava (CVC). In (A) the heart is faintly visible on the still image analogous to the overlay in (B). In real time the beating heart is readily apparent. (B) Orientation of the heart as it lies against the diaphragm in both dogs and cats. LA, left atrium; LV, left ventricle; RA, right atrium; RV, right ventricle. The orientation and proportionality in the longitudinal plane are nearly identical independent of standing/sternal versus right lateral recumbency. Source: Reproduced with permission of Dr Gregory Lisciandro, Hill Country Veterinary Specialists and FASTVet.com, Spicewood, TX.

**Pearl:** Always look cranial to the diaphragm because most cases of clinically relevant pericardial effusion are detected via the DH view, which is part of AFAST, TFAST, and Vet BLUE.

**Pearl:** Ascites (modified transudate) in cases of PCE cases carries a *better* prognosis because the PCE has been a more chronic process in that patient (Johnson et al. 2004). Always stage with Global FAST and encourage pericardiocentesis when indicated in these cases.

**Pearl:** The nonecho option for the presence or absence of cardiac tamponade is characterization of the CVC. A "bounce" to the CVC rules out tamponade versus a "FAT" distended CVC which supports the presence of obstructive shock and cardiac tamponade and the need for emergent pericardiocentesis in weak, collapsed patients, although it's best to look at the patient to make that final decision (stable, can wait; unstable, needs emergent pericardiocentesis).

## Prevalence of Pericardial Effusion

Pericardial effusion brings up a fascinating change in teaching paradigms because a more effective first-line screening test is being used since the FAST movement began in 2004 (Boysen et al. 2004; Lisciandro 2014a,b, 2016a). We were screening with less sensitive imaging, using thoracic radiography, an unreliable test (Guglielmini et al. 2012; Côté et al. 2013; Lisciandro 2016a). Before FAST, the patient was only diagnosed if they were scheduled for echocardiography or CT. As a case in point, the author's practice documented three cases of PCE in 2005 before AFAST-TFAST and 28 cases in 2012 (Lisciandro 2014a,b, 2016a). Why the difference? Simply, we were using the wrong test (Guglielmini et al. 2012; Côté et al. 2013). Ultrasound is arguably the gold standard test for PCE.

## Causes of Pericardial Effusion

So now fast forward through 15 years of AFAST and TFAST. Using ultrasound as a first- line screening test, veterinarians (and physicians) are now capturing PCE cases that would have otherwise been missed (Lisciandro 2014a,b, 2016a). However, what we are finding with the paradigm change is that there are two subsets of PCE, acute and chronic, and they are remarkably different (Table 7.8).

In the past, a feline or canine patient may have had acute PCE and cardiac tamponade but with radiography dominating as first-line imaging, the unremarkable or equivocal cardiac silhouette missed the PCE because many patients were never scheduled for echocardiography. The patient, with or without help from the attending clinician, often declared themselves survivors or nonsurvivors despite care. In those that survived, the patient likely compensated, stretched its

**Table 7.8.**
Most common causes of pericardial effusion in dogs and cats.

| Dogs[a] | Cats[c] |
|---|---|
| Neoplasia[b] (~70%) | Congestive heart failure (≥75%) |
| Idiopathic (~20%) | Idiopathic |
| Right-sided congestive heart failure | Lymphoma |
| Left atrial tear/rupture | Feline infectious peritonitis (FIP) |
| Anticoagulant rodenticides | Hyperthyroidism |
| Foreign body (plant awn, porcupine quill, projectile, other) | Uremia |
| Infectious (bacterial, fungal) | Infectious (fungal, bacterial) |
| Peritoneopericardial diaphragmatic hernia | Peritoneopericardial diaphragmatic hernia |
| Pericardial cyst | Sepsis |
| Uremia | |
| Trauma | |

[a]Ascites is a more favorable diagnosis with median survival reported to be 605 days compared to 45 days in dogs without ascites (Johnson et al. 2004), thus Global FAST should be done first line.
[b]~50–60% have metastatic disease at time of diagnosis (MacDonald et al. 2009), thus Global FAST should be done first line.
[c]Most common cause in cats is congestive heart failure and most common heart disease is hypertrophic cardiomyopathy (Hall et al. 2007).
Data from Hall et al. (2007); Davidson et al. (2008); Shaw and Rush (2007); MacDonald et al. (2009); Ward et al. (2018).
Source: Reproduced with permission of Dr Gregory Lisciandro, Hill Country Veterinary Specialists and FASTVet.com, Spicewood, TX.

pericardium over time before developing the classic globoid heart and ascites, representing as weak with abdominal distension from ascites and generally stable. Pericardiocentesis was more commonly an elective procedure with high success due to PCE chronicity. In this patient subset, the findings of electrical alternans, pulsus paradoxicus, muffled heart sounds, and a globoid heart on thoracic radiography were possible, although with variable reliability (Johnson et al. 2004).

## Nonhemoabdomen Ascites Carries a Better Prognosis

The Global FAST approach is imperative for PCE cases, especially in dogs in which nonhemoabdomen ascites (and echo negative for a mass) has been shown to carry a much more favorable prognosis, with median survival times much different at 605 days versus 45 days (Stafford Johnson et al. 2004). The presence of a mass (echo-positive versus echo-negative) also has great influence on the prognosis, with similar large differences in survival between those without echo-detected masses and those with – 1068 days versus 26 days (Stafford Johnson et al. 2004). Furthermore, in the large study done by MacDonald and colleagues, of those with masses, no matter the type of tumor, metastasis was high (~50–66%) and thoracic radiography only detected ~33% of lung metastasis (MacDonald et al. 2009). Global FAST with its target organ approach has the potential to detect intraabdominal metastasis as well as pulmonary, and Vet BLUE has been shown to perform better than thoracic radiography in a pilot study (Kulhavy and Lisciandro 2015) (see Chapter 36).

## Clinical Signs and Signalment

Historically, the most common presenting signs for dogs with PCE have been weakness, collapse, and labored breathing (Stafford Johnson et al. 2004; MacDonald et al. 2009; Lisciandro 2016a); however, more recently a study documented that approximately 50% of dogs had a history of vomiting within 48 hours of presentation (Fahey et al. 2017). This finding, from the author's experience, argues for performing a Global FAST prior to a complete detailed abdominal ultrasound not only for ordering the indicated ultrasound study but also for the safety of the patient. Placing a patient with PCE into dorsal recumbency risks acute decompensation. Golden retrievers are the most common breed reported and in one study comprised 33% of the case study population, followed by German shepherds and other large breeds (Stafford Johnson et al. 2004; Fahey et al. 2017). In another study, gastrointestinal signs were reported in 16% of canine cases of PCE (Stafford Johnson et al. 2004).

## Changes in the Paradigm – Recognizing Acute Pericardial Effusion

We are recognizing a new patient subset, the acute PCE case, with an unremarkable cardiac silhouette and respiratory distress, and a likely cardiac chamber rupture as the contributing factor. Traditional signs of muffled heart sounds, pulsus paradoxicus, electrical alternans on electrocardiogram, and a globoid heart on thoracic radiography are insensitive even in the chronic PCE case, let alone the acutely collapsed respiratory distressed case (Stafford Johnson et al. 2004; MacDonald et al. 2009; Guglielmini et al. 2012;

Côté et al. 2013). Moreover, treatment strategies differ, as does the success of pericardiocentesis and definitive treatment. For example, if a cardiac chamber has acutely ruptured because of a right atrial mass, then the PCE may return in minutes to hours with repeated cardiac tamponade and obstructive shock. The case of a right atrial mass from hemangiosarcoma is a strong argument for the Global FAST approach, and rapidly staging the patient within minutes of presentation. Metastatic rate is high, 50–66% in one study (MacDonald et al. 2009).

Global FAST screens for hemoabdomen and lung metastasis, because if the patient is staged as isolated disease, then surgical removal of the cardiac tumor may be effective. The insertion of an indwelling pericardial catheter and autotransfusion(s) may be your only effective option (much different from traditional teaching paradigms). Moreover, performing a rough pericardiocentesis and opening the pericardial sac as a temporary pericardial window, used as a cheap, quick option in the past, will backfire with the patient then exsanguinating into an even larger space, the pleural cavity.

### *Pericardiocentesis Becomes a Core Skill*

Veterinarians need to acquire pericardiocentesis as part of their skill set to save these patients (both canine and feline). Pericardiocentesis is not a difficult procedure and is discussed in detail in Chapters 21 and 43. You have nothing to lose and everything to gain if a patient is dying from its PCE and complications are acceptable (Humm et al. 2009).

### *Use of TFAST for Accurate Diagnosis of Pericardial Effusion*

See Chapters 17 and 18.

### *Use of the DH View and TFAST for Accurate Diagnosis of Pleural Effusion*

See Chapters 17 and 18.

### *Use of the DH View and Vet BLUE for Deep Lung Lesions*

See Chapters 22 and 23 for more detail. However, it is important to appreciate that the DH view serves as a deep window into lung pathology along its diaphragmatic interface (see Figures 6.14 and 23.21).

## AFAST Cysto-Colic View Formula for Urinary Bladder Volume Estimation

The use of the CC view formula of length × height × width (cm) × 0.625 = estimation of urinary bladder volume (mL) (Lisciandro and Fosgate 2017) serves as a rapid noninvasive way in which to estimate urinary bladder volume and, with serial measurements over time, provides a noninvasive means to estimate urine production. Moreover, walking dogs and allowing them to void, then confirming an empty urinary bladder with AFAST, is another way to effectively measure urine output in the hospitalized setting.

- Make your best oval in longitudinal orientation of the bladder and acquire length and height in centimeters (cm).
- Rotate the probe into transverse orientation and make your best largest oval and measure width (cm) (Figure 7.15).
- Calculate urinary bladder volume using length × height × width (cm) × 0.625 = estimation of urinary bladder volume (mL) (see Figure 7.15).
- Urine output is estimated using change in urinary bladder volume/time.

## AFAST and Its Target Organ Approach

AFAST was never meant to be a "flash exam" of the abdomen. The "flash" mentality is a quick ultrasound sweep answering a single binary question of whether fluid is present or absent, a positive or negative test. It is often used as a desultory sweep for a midabdominal mass, but without standardization of views and knowledge of anatomy at specific acoustic windows as in AFAST. Without direction, it becomes easy for the sonographer to get lost. Easily detected soft tissue conditions are often missed by abdominal radiography (Table 7.9) and the reader is referred to Chapters 8–12. The objective is through repetition and standardization to be able to tell normal from abnormal (differentiate expected from unexpected) and capture conditions that would otherwise be missed without any imaging or with radiography. As you read through Table 7.9, think about the conditions listed and how often they are missed on plain radiography. Interestingly, incidental findings during FAST exams have been reported in people (Sgourakis et al. 2012).

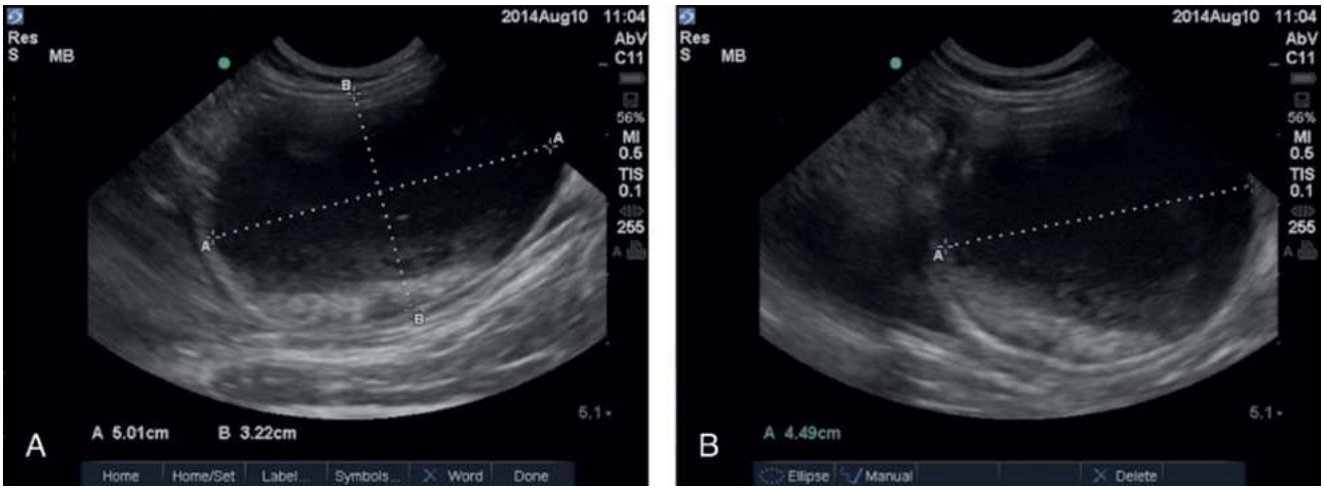


**Figure 7.15.** Measurements at the AFAST CC view for estimating urinary bladder volume. In (A) the best largest oval in the longitudinal plane is used for length (L, cm) and height (H, cm) measured as 5.01 cm and 3.22 cm, respectively. In (B) the best largest oval in the transverse plane is used for width (W, cm) measured as 4.49 cm. With these measurements the equation would be 5.01 × 3.22 × 4.49 cm × 0.625 = 45.3 mL. The volume can be compared to that aspirated when patients are catheterized immediately thereafter to gain confidence in its use (Lisciandro and Fosgate 2017). Source: Reproduced with permission of Dr Gregory Lisciandro, Hill Country Veterinary Specialists and FASTVet.com, Spicewood, TX.

**Table 7.9.**
AFAST and its target organ approach as a soft tissue screening test.

| View | Target organ | Findings |
|---|---|---|
| DH | Gallbladder | Sludge |
| | | Mucocele |
| | | Calculi |
| | | Masses |
| | Liver | Masses |
| | | Obvious mottled echogenicity |
| | Caudal vena cava | Caudal caval size abnormalities |
| | | Caval syndrome |
| | | Hepatic venous congestion |
| | Lung | Alveolar-interstitial edema (B-lines) |
| | | Consolidation |
| | | Masses |
| | Heart | Pericardial effusion |
| | | Left atrial enlargement |
| | Thorax | Pleural effusionMasses |
| SR, HR, SR5th, HR5th | Kidney | Pyelectasia |
| | | Hydronephrosis |
| | | Cortical cyst(s) |
| | | Perinephric cyst(s) |
| | | Polycystic disease |
| | | Masses |
| | Liver | See DH view |
| CC | Urinary bladder | Sediment |
| | | Calculi |
| | | Bladder wall irregularities |
| | | Masses |
| HRU, SRU | Spleen | Masses |
| | | Obvious mottled echogenicity |
| | | Midabdominal masses |

See respective POCUS abdomen-related chapters for examples.
Source: Reproduced with permission of Dr Gregory Lisciandro, Hill Country Veterinary Specialists and FASTVet.com, Spicewood, TX.

VetBooks.ir

# Recording AFAST Findings on Goal-directed Templates

The use of standardized templates is imperative not only for communication of AFAST findings between veterinarians but also for the attending clinician evaluating serial findings (Figure 7.16). Goal-directed templates also clearly define objectives, which is especially important in teaching hospitals and referral hospitals with multiple disciplines of practice including emergency and critical care, cardiology, and radiology. Being goal driven, these standardized templates also accelerate the learning curve and discipline the sonographer by making them look at certain aspects of the target organs (into the thorax for pleural and pericardial effusion [DH view]; looking at the hepatic veins for venous congestion [DH view]). The "Comments" allows for any findings outside the goal-driven standard format to be listed, for example suspect a urinary bladder stone or mass, suspect a splenic mass, etc. Finally, the AFAST protocol and its strengths and weaknesses may be evaluated and improved upon with recorded data. Suggested templates for medical records are shown in Chapter 45 and Appendix I.

# Pearls and Pitfalls, The Final Say

AFAST is superior in detecting hemorrhage to laboratory values (packed cell volume, lactate), physical examination findings, and radiography (Lisciandro et al. 2009; Rozycki 1998; Rozycki et al. 1998, 2001; McMurray et al. 2016). AFAST is an advantageous ultrasonographic format for nonradiologist veterinarians to use for the timely detection of free fluid representing bleeding or forms of peritonitis since ultrasound is superior in sensitivity to physical examination and abdominal radiography.

- Should be a routine add-on for all POCUS abdominal exams (Global FAST is an even better approach).
- Should be standard of care for all bluntly traumatized small animals, as it is in people.
- Should be used in penetrating trauma cases with the understanding that AFAST is generally thought to be very specific for detecting intraabdominal injury (by finding free fluid), but lacks high sensitivity.
- Serial exams should always be performed in bluntly traumatized animals, after rehydration and resuscitation in trauma and nontrauma including suspect peritonitis cases.
- The use of the AFAST-applied abdominal fluid scoring system may be effective in bleeding traumatized and nontraumatized dogs to predict degree of anticipated anemia and may be used also for peritonitis or other effusive conditions as a monitoring tool by scoring (AFS 0–4).
- The diagnosis of anaphylaxis in dogs may be supported with the finding of a sonographic striation of the gallbladder wall (halo effect or double rim effect). However, a Global FAST (including TFAST and Vet BLUE) helps rule out pericardial effusion/cardiac tamponade and right-sided cardiac failure, and placing the constellation of patient information (history, physical examination, laboratory findings, imaging) within the complete clinical picture is important to avoid mistakes and "satisfaction of search error."

# Quick Reference of Normals and Rules of Thumb

- Adult dogs and cats should have no free fluid within their peritoneal cavity or retroperitoneal space (or within the pleural cavity or pericardial sac); however, recent research evaluating anesthetized adult dogs and cats, and puppies and kittens has documented small pockets of free intraabdominal fluid in clinically normal canines and felines.
- The originally published AFAST-applied abdominal fluid scoring system was scored according to number for positive AFAST views (range 0–4) excluding the bonus 5th view that is not part of the AFS. However, to better distinguish small-volume bleeder/effusion from large-volume bleeder/effusion, AFS at each AFAST view now ranges from 0 (negative) to ½ (small pocket <5 mm in cats and <10 mm in dogs) to 1 (>5 mm cats and >10 mm dogs).
- Total AFS remains similar as originally published with the categorization of small-volume bleeder/effusion defined as AFS <3 (AFS ranges from 0 to 2½, thus including AFS of 1, 1½, 2 and 2½) and large-volume bleeder/effusion defined as AFS ≥3 (AFS ranges from 3 to 4, including AFS of 3, 3½, and 4).
- Expect ~50% of adult dogs to have an AFS of ½ along the diaphragm at the DH view with maximum dimensions of <3 mm that may not be noticeable in unsedated, unanesthetized adults (Lisciandro et al. 2019).
- Expect ~90% of puppies <6 months of age to have an AFS of ½ to 1 along the diaphragm at the DH view and then with fairly equal distribution between the other three AFAST views of ½ to 1 with maximum dimensions of <3 mm (Lisciandro et al. 2019).

**Template for AFAST®**

**Patient Positioning:**

Right Lateral ☐ Left Lateral ☐ Modified Sternal ☐ Standing ☐ Sternal ☐

**Gallbladder** unremarkable☐ abnormal ☐ indeterminate ☐ not assessed ☐

**Urinary Bladder** unremarkable☐ abnormal ☐ indeterminate ☐ not assessed ☐

**DH View:**

Pleural Effusion absent ☐ present ☐ indeterminate ☐ not assessed ☐

Pericardial Effusion absent ☐ present ☐ indeterminate ☐ not assessed ☐

Caudal Vena Cava unremarkable (BOUNCE) ☐ small (flat) ☐

distended (FAT) ☐ indeterminate ☐ not assessed ☐

Hepatic Venous Distension unremarkable☐ distended ☐ indeterminate ☐
not assessed ☐

**AFAST Fluid Scoring**

| | | | |
|---|---|---|---|
| DH | 0 ☐ | 1/2 ☐ | 1 ☐ |
| SR/HR | 0 ☐ | 1/2 ☐ | 1 ☐ |
| CC | 0 ☐ | 1/2 ☐ | 1 ☐ |
| HR Umbilical | 0 ☐ | 1/2 ☐ | 1 ☐ |

**Total Abdominal Fluid Score (AFS) 0-4 = _____**

**HR5th View** 0 ☐ 1/2☐ 1☐ *(not part of the AFS)*

**Focused Spleen** unremarkable☐ abnormal ☐ indeterminate ☐ not assessed ☐

**Comments** _____

**Qualifier:** The AFAST exam is an ultrasound examination used to detect the presence of free abdominal fluid (which is generally abnormal) as a screening test in order to better direct resuscitation efforts and diagnostic testing, detect complications, and manage critically ill patients. AFAST allows rapid but indirect assessment for evidence of major internal abdominal organ injury or disease. The AFAST exam is not intended to replace a complete detailed abdominal ultrasound of the abdomen.

**Figure 7.16.** AFAST goal-directed template. Source: Reproduced with permission of Dr Gregory Lisciandro, Hill Country Veterinary Specialists and FASTVet.com, Spicewood, TX.

- Expect that ~70% of adult cats and kittens <6 months of age will have AFS of ½ along the diaphragm at the DH view and then next most commonly positive in both age groups at the most gravity-dependent umbilical view (SR view in left lateral recumbency) with maximum dimensions at either of these AFAST views of <3 mm that may or may not be noticeable in unsedated, unanesthetized adult cats and kittens (Lisciandro et al. 2015).
- Any mass found to deform the splenic capsule on a focused spleen view should always be considered a serious finding.
- The FAST DH view should be considered nearly 100% sensitive and 100% specific for the detection of clinically relevant PCE in both dogs and cats in standing or sternal positioning.
- Serial examinations should always be performed after resuscitation and rehydration of the patient with at least one more AFAST examination (or a Global FAST) and whenever the patient is failing inpatient or outpatient care.
- The finding of sonographic striation of the canine gallbladder wall should be considered abnormal in the acute setting (acute collapse and weakness) even when the thickness is in the normal range of 1–3 mm and anaphylaxis, "anaphylactic gallbladder," and right-sided congestive heart failure, "cardiac gallbladder," should be ruled out using the Global FAST approach.
- Although rare in cats, a "cardiac gallbladder" may occur with feline congestive heart failure.
- Characterization of the CVC may be categorized as a "bounce" and fluid responsive, "FAT" and fluid intolerant, or "flat" and hypovolemic.
- Maximum heights at the FAST DH view may be used to additionally characterize the CVC (see Tables 7.6 and 36.3).

# References


American College of Emergency Physicians. 2001. ACEP emergency ultrasound guidelines – 2001. *Ann Emerg Med* 38:470–481.

Bilello JF, Davis JW, Lemaster D, et al. 2011. Prehospital hypotension in blunt trauma: identifying the "crump factor." *J Trauma* 70(5):1038–1042.

Birkbeck R, Greensmith T, Humm K, et al. 2019. Haemoabdomen due to suspect anaphylaxis in four dogs. *Vet Rec Case Rep* 7:e000734.

Blackbourne LH, Soffer D, McKenney M, et al. 2004. Secondary ultrasound examination increases the sensitivity of the FAST exam in trauma, *J Trauma* 57(5):934–938.

Borahay MA, Harirah HM, Olseon G, et al. 2011. Disseminated intravascular coagulation, hemoperitoneum, and reversible ischemic neurological deficit complicating anaphylaxis to prophylactic antibiotics during cesarean delivery: a case report and review of literature. *Am J Perinatol Reports* 1(1):15–19.

Boysen SR, Lisciandro GR. 2013. The use of ultrasound in the emergency room (AFAST and TFAST). *Vet Clin North Am Small Anim Pract* 43(4):773–797.

Boysen SR, Rozanski EA, Tidwell AS, et al. 2004. Evaluation of a focused assessment with sonography for trauma protocol to detect free abdominal fluid in dogs involved in motor vehicle accidents. *J Am Vet Med Assoc* 225(8): 1198–1204.

Bucci M, Rabozzi R, Guglielmini C, et al. 2017. Respiratory variation in aortic blood peak velocity and caudal vena cava diameter can predict fluid responsiveness in anaesthetised and mechanically ventilated dogs. *Vet J* 227:30–35.

Caldwell DJ, Petras KE, Mattison BL, et al. 2018. Spontaneous hemoperitoneum and anaphylactic shock associated with Hymenoptera envenomation in a dog. *J Vet Emerg Crit Care* 28(5):476–482.

Cambournac M, Goy-Thollot I, Violé A, et al. 2018. Sonographic assessment of volaemia: development and validation of a new method in dogs. *J Small Anim Pract* 59(3):174–182.

Candotti C, Arntfield R. Pericardial effusion. In: *Point-of-Care Ultrasound*, edited by Soni NJ, Arntfield R, and Kory P. Philadephia: Elsevier, pp 130–134.

Coccolini F, Stahel PF, Montori G, et al. 2017. Pelvic trauma: WSES classification and guidelines. *World J Emerg Surg* 12:5.

Cole LP, Humm K. 2019. Twelve autologous blood transfusions in eight cats with hemoperitoenum. *J Feline Med Surg* 21:481–487.

Côté E, Schwarz LA, Sithole F. 2013. Thoracic radiographic findings for dogs with cardiac tamponade attributable to pericardial effusion. *J Am Vet Med Assoc* 243(2):232–235.

Culp WT, Weisse C, Kellogg ME, et al. 2010. Spontaneous hemoperitoneum in cats: 65 cases (1994–2006). *J Am Vet Med Assoc* 236(9):978–982.

d'Anjou M, Penninck D. 2015. Liver. In: *Atlas of Small Animal Ultrasonography*, 2nd edition, edited by d'Anjou M, Penninck D. Ames: Wiley Blackwell, p 220.

Davidson BJ, Paling AC, Lahmers SL, et al. 2008. Disease association and clinical assessment of feline pericardial effusion. *J Am Anim Hosp Assoc* 44(1):5–9.

Darnis E, Boysen S, Merveille AC, et al. 2018. Establishment of references values of the caudal vena cava by fast-ultrasonography through different views in healthy dogs. *J Vet Intern Med* 32(4):1308–1318.

Fahey R, Rozanski E, Paul A, et al. 2017. Prevalence of vomiting in dogs with pericardial effusion. *J Vet Emerg Crit Care* 27(2): 250–252.

Ferrada P, Anand RJ, Whelan J, et al. 2012a. Qualitative assessment of the inferior vena cava: useful tool for the

evaluation of fluid status in critically ill patients. *Am Surg* 78(4):468–470.

Ferrada P, Vanguri P, Anand RJ, et al. 2012b. Flat inferior vena cava: indicator of poor prognosis in trauma and acute care surgery patients. *Am Surg* 78(12):1396–1398.

Gulglielmini C, Diana A, Santarelli G, et al. 2012. Accuracy of radiographic vertebral heart score and sphericity index in the detection of pericardial effusion in dogs. *J Am Vet Med Assoc* 241(8):1048–1055.

Ha YR, Toh HC. 2016. Clinically integrated multi-organ point-of care ultrasound for undifferentiated respiratory difficulty, chest pain, or shock: a critical analytic review. *J Intensive Care* 4:54.

Hall DJ, Schofer F, Meier KC, et al. 2007. Pericardial effusion in cats: a retrospective study of clinical findings and outcome in 146 cats. *J Vet Intern Med* 21:1002–1007.

Higgs VA, Rudloff E, Kirby R, et al. 2015. Autologous blood transfusion in dogs with thoracic or abdominal hemorrhage: 25 cases. *J Vet Emerg Crit Care* 25(6):731–738.

Hnatusko A, Gicking JC, Lisciandro GR. 2019. Anaphylaxis-related hemoperitoneum in 11 dogs. *J Vet Emerg Crit Care*, in press.

Himelman RB, Kircher B, Rockey DC, et al. 1988. Inferior vena cava plethora with blunted respiratory response: a sensitive echocardiographic sign of cardiac tamoponade. *J Am Coll Cardiol* 12(6):1470–1477.

Humm KR, Keenaghan-Clark EA, Boag AK. 2009. Adverse events associated with pericardiocentesis in dogs; 85 cases (1999–2006). *J Vet Emerg Crit Care* 19(4):352–356.

Kirkpatrick AW, Sirois M, Ball CG, et al. 2004. The hand-held ultrasound for penetrating abdominal trauma. *Am J Surg* 187:660–665.

Kulhavy DA, Lisciandro GR. 2015. Use of a lung ultrasound examination called Vet BLUE to screen for metastatic lung nodules in the emergency room. *J Vet Emerg Crit Care* 25(S1):S14.

Kwak J, Yoon H, Kim J, et al. 2018. Ultrasonographic measurement of caudal vena cava to aorta ratios for determination of volume depletion in normal beagle dogs. *Vet Radiol Ultrasound* 59(2):203–211.

Lichtenstein DA. 2010. Gallbladder. In: *Whole Body Ultrasonography in the Critically Ill*, edited by Lichtenstein DA. Heidelberg: Springer, pp 59–68.

Lisciandro GR. 2011. Abdominal and thoracic focused assessment with sonography for trauma, triage, and monitoring in small animals. *J Vet Emerg Crit Care* 21(2):104–122.

Lisciandro GR. 2012. Evaluation of initial and serial combination focused assessment with sonography for trauma (CFAST) examinations of the thorax (TFAST) and abdomen (AFAST) with the application of an abdominal fluid scoring system in 49 traumatized cats. Abstract. *J Vet Emerg Crit Care* 22(S2):S11.

Lisciandro GR. 2014a. The abdominal FAST$^3$ (AFAST$^3$) exam. In: *Focused Ultrasound for the Small Animal Practitioner*, edited by Lisciandro GR. Ames: Wiley Blackwell, pp 17–43.

Lisciandro GR. 2014b. The thoracic FAST$^3$ (TFAST$^3$) exam. In: *Focused Ultrasound for the Small Animal Practitioner*, edited by Lisciandro GR. Ames: Wiley Blackwell, pp 140–165.

Lisciandro GR. 2014c. The Vet BLUE lung scan. In: *Focused Ultrasound for the Small Animal Practitioner*, edited by Lisciandro GR. Ames: Wiley Blackwell, pp. 166–188.

Lisciandro GR. 2016a. The use of the diaphragmatico-hepatic (DH) views of the abdominal and thoracic focused assessment with sonography for triage (AFAST/TFAST) examinations for the detection of pericardial effusion in 24 dogs (2011–2012). *J Vet Emerg Crit Care* 26(1):125–131.

Lisciandro GR. 2016b. Abdominal FAST (AFAST)-detected hemorrhagic abdominal effusion in 11 dogs with acute collapse and gallbladder wall edema (halo sign) with presumed anaphylaxis. Abstract. *J Vet Emerg Crit Care* 26(S1):S8.

Lisciandro GR. 2019. The cardiac gallbladder: case series of 13 dogs and 1 cat with sonographically detected gallbladder wall edema. *J Vet Emerg Crit Care* 29(S1):S24.

Lisciandro GR, Fosgate GT. 2017. Use of AFAST cysto-colic view urinary bladder measurements to estimate urinary bladder volume in dogs and cats. *J Vet Emerg Crit Care* 27(6):713–717.

Lisciandro GR, Lisciandro SC. 2019. Sonographic changes of the gallbladder associated with anaphylaxis in dogs. *J Vet Emerg Crit Care* 29(2):214–215.

Lisciandro GR, Lagutchik MS, Mann KA, et al. 2008. Evaluation of a thoracic focused assessment with sonography for trauma (TFAST) protocol to detect pneumothorax and concurrent thoracic injury in 145 traumatized dogs. *J Vet Emerg Crit Care* 18(3):258–269.

Lisciandro GR, Lagutchik MS, Mann KA, et al. 2009. Evaluation of an abdominal fluid scoring system determined using abdominal focused assessment with sonography for trauma in 101 dogs with motor vehicle trauma. *J Vet Emerg Crit Care* 19(5):426–437.

Lisciandro GR, Fosgate GT, Romero LA, et al. 2015. Abdominal FAST (AFAST) and abdominal fluid scores in adult and juvenile cats. Abstract. *J Vet Emerg Crit Care* 25(S1):S8.

Lisciandro GR, Ward JL, DeFrancesco TC, Mann KA. 2016. Absence of B-lines on lung ultrasound (Vet BLUE protocol) to rule out left-sided congestive heart failure in 368 cats and dogs. *J Vet Emerg Crit Care* 26(S1):S8.

Lisciandro GR, Fosgate GT, Romero LA, et al. 2019. The expected frequency and amount of free peritoneal fluid estimated using the abdominal FAST-applied abdominal fluid scores in clinically normal adult and juvenile dogs. *J Vet Emerg Crit Care*, in press.

Lux CN, Culp WT, Mayhew RD, et al. 2013. Perioperative outcome in dogs with hemoperitoneum: 83 cases (2005–2010). *J Am Vet Med Assoc* 242(10):1385–1391.

MacDonald KA, Cagney O, Magne ML. 2009. Echocardiographic and clinicopathologic characterization of pericardial effusion in dogs: 107 cases (1985–2006). *J Am Vet Med Assoc* 235(12):1456–1461.

Mandell DC, Drobatz K. 1995. Feline hemoperitoneum 16 cases (1986–1993). *J Vet Emerg Crit Care* 5(2):93–97.

Marshall KA, Thomovsky EJ, Brooks AC, et al. 2018. Ultrasound measurements of the caudal vena cava before and after blood donation in 9 greyhound dogs. *Can Vet J* 59(9):973–980.

Matsushima K, Frankel HL. 2011. Beyond focused assessment with sonongraphy for trauma: ultrasound creep in the trauma resuscitation area and beyond. *Curr Opin Crit Care* 17(6):606–612.

McMurray J, Boysen S, Chalhoub S. 2016. Focused assessment with sonography in nontraumatized dogs and cats in the emergency and critical care setting. *J Vet Emerg Crit Care* 26(1):64–73.

Mohammadi A, Ghasemi-Rad M. 2012. Evaluation of gastrointestinal injury in blunt abdominal trauma "FAST is not reliable": the role of repeated ultrasonography. *World J Emerg Surg* 7(1):2.

Muir W. 2006. Trauma: physiology, pathophysiology, and clinical implications. *J Vet Emerg Crit Care* 16(4):253–263.

Narasimhan M, Koenig SJ, Mayo PH. 2016. A whole-body approach to point of care ultrasound. *Chest* 150(4): 772–776.

Nelson NC, Drost WT, Lerche P, et al. 2010. Noninvasive estimation of central venous pressure in anesthetized dogs by measurement of hepatic venous blood flow velocity and abdomen al venous diameter. *Vet Radiol Ultrasound* 51(3):313–323.

Ollerton JE, Sugrue M, Balogh Z, et al. 2006. Prospective study to evaluate the influence of FAST on trauma patient management. *J Trauma* 60:785–791.

Perera P, Mailhot T, Riley D, et al. 2010. The RUSH exam: Rapid Ultrasound in SHock in the evaluation of the critically ill. *Emerg Med Clin North Am* 28(1):29–56.

Pintar J, Breitschwerdt EB, Hardie EM, et al. 2003. Acute nontraumatic hemoabdomen in the dog : a retrospective analysis of 39 cases (1987–2001). *J Am Anim Hosp Assoc* 37:518–522.

Quantz JE, Miles MS, Reed AL, et al. 2009. Elevation of alanine transaminase and gallbladder wall abnormalities as biomarkers of anaphylaxis in canine hypersensitivity patients. *J Vet Emerg Crit Care* 19(6):536–544.

Robinson DA, Kiefer K, Bassett R, et al. 2016. Autotransfusion in dogs using a 2-syringe technique. *J Vet Emerg Crit Care* 26(6):766–774.

Romero LA, Lisciandro GR, Fosgate GT, et al. 2015. Abdominal FAST (AFAST) and abdominal fluid scores in adult and juvenile dogs. Abstract. *J Vet Emerg Crit Care* 25(S1):S7–S8.

Rozycki GS. 1998. Surgeon performed US: its use in clinical practice. *Ann Surg* 228:16–28.

Rozycki GS, Ballard RB, Feliciano DV, et al. 1998. Surgeon-performed ultrasound for the assessment of truncal injuries: lessons learned from 1540 patients. *Ann Surg* 228(4):557–567.

Rozycki GS, Pennington SD, Feliciano DV. 2001. Surgeon-performed ultrasound in the critical care setting: its use as an extension of the physical examination to detect pleural effusion. *J Trauma* 50(4):636–42.

Sgourakis G, Lanitis S, Zacharioudakis C, et al.2012. Incidental findings in trauma patients during focused assessment with sonography for trauma. *Am Surg* 78(3):366–72.

Shaw S, Rush JE. 2007. Canine pericardial effusion: pathophysiology and cause. *Compendium* 29(7):400–404.

Simons FER, Ebisawa M, Sanchez-borges M, et al. 2015. 2015 update of the evidence base: World Allergy Organization anaphylaxis guidelines. *World Allergy Organ J* 8:32.

Sobrino J, Shafi S. 2013. Timing and causes of death after injuries. *Proc (Bayl Univ Med Cent)* 26(2):120–123.

Stafford Johnson M, Martin M, Binns S, et al. 2004. A retrospective study of clinical findings, treatment and outcome in 143 dogs with pericardial effusion. *J Small Anim Pract* 45(11):546–552.

Tchernodrinski S, Arntfield R. 2015. Inferior vena cava. In: *Point-of-care Ultrasound*, edited by Soni NJ, Arntfield R, Kory P. Philadelphia: Elsevier/Saunders, pp 135–144.

Tuplin MC, Romero AE, Boysen SR. 2017. Influence of the respiratory cycle on caudal vena cava diameter measured by sonography in healthy foals: a pilot study. *J Vet Intern Med* 31(5):1556–1562.

Udobi KF, Rodriguez A, Chiu WC et al. 2001. Role of utrasonography in penetrating abdominal trauma: a prospective study. *J Trauma* 50:475–479.

Walker T, Tidwell AS, Rozanski EA, et al. 2005. Imaging diagnosis: acute lung injury following massive bee envenomation in a dog. *Vet Radiol Ultrasound* 46(4):300–303.

Ward JL, Lisciandro GR, Ware WA, et al. 2018. Evaluation of point-of-care thoracic ultrasound and NT-proBNP for the diagnosis of congestive heart failure in cats with respiratory distress. *J Vet Intern Med* 32(5):1530–1540.

# Further Reading

Boston SE, Higginson G, Monteith G. 2011. Concurrent splenic and right atrial mass at presentation in dogs with HSA: a retrospective study. *J Am Anim Hosp Assoc* 47(5): 336–341.

Grimes JA, Fletcher JM, Schmiedt CW. 2018. Outcomes in dogs with uroabdomen: 43 cases (2006–2015). *J Am Vet Med Assoc* 252(1):92–97.

Hoffberg JE, Koenigshof AM, Guiot LP. 2016. Retrospective evaluation of concurrent intra-abdominal injuries in dogs with traumatic pelvic fractures: 83 cases (2008–2013). *J Vet Emerg Crit Care* 26:288–294.

Kim SY, Park KT, Yeon SC, et al. 2014. Accuracy of sonographic diagnosis of pneumoperitoneum using the enhanced peritoneal stripe sign in beagle dogs. *J Vet Sci* 15(2):195–198.

Kolata RJ, Dudley EJ. 1975. Motor vehicle accidents in urban dogs: a study of 600 cases. *J Am Vet Med Assoc* 167: 938–941.

Mongil CM, Drobatz KJ, Hendricks JC. 1995. Traumatic hemoperitoneum in 28 cases: a retrospective review. *J Am Anim Hosp Assoc* 31:217–222.

Sigrist NE, Adamik KN, Doherr MG, et al. 2011. Evaluation of respiratory parameters at presentation as clinical indicators of the respiratory localization in dogs and cats with respiratory distress. *J Vet Emerg Crit Care* 21(1):13–23.

Simpson SA, Syring R, Otto CM. 2009. Severe blunt trauma in dogs: 235 cases (1997–2003). *J Vet Emerg Crit Care* 19(6):588–602.

CHAPTER EIGHT

# POCUS: Liver and Gallbladder

Stephanie C. Lisciandro, Jennifer M. Gambino, and Sarah Young

## Introduction

The goals of using POCUS for evaluation of the liver include recognizing focal and multifocal mass lesions and evaluating diffuse parenchymal echotexture and obvious changes in echogenicity. Evaluation for hepatic venous congestion may also be accomplished. The goals for the POCUS examination of the gallbladder include recognizing gallbladder wall abnormalities, luminal disease processes (e.g., accumulation of echogenic debris and wall nodules or mass lesions), and identification of signs that may support biliary obstruction. The POCUS liver and gallbladder examination can help guide clinical decisions by providing initial information that may not otherwise be evident with radiography.

The POCUS liver and gallbladder examination does not replace a complete detailed abdominal ultrasound study by a veterinarian with advanced training (veterinary radiologist or internist). The use of the POCUS examination may direct the clinician to obtain a complete study since the comprehensive evaluation of the liver and biliary tract is inherently more technically challenging for the novice sonographer than other abdominal organs. It is especially important to note that an unremarkable POCUS liver and gallbladder examination does not rule out the possibility of significant hepatobiliary dysfunction and disease. Liver biopsy may still be indicated when there is evidence of hepatic dysfunction, even with a lack of ultrasound abnormalities.

AFAST and the abdominal fluid scoring system (better the Global FAST approach) should be performed in conjunction with all POCUS abdominal exams, so as not to miss abdominal and retroperitoneal effusion including peritonitis and hemorrhage. Global FAST would be an even better approach to survey for pleural and pericardial effusion, and obvious cardiac and pulmonary abnormalities, and Global FAST is used as a screening test to rapidly discriminate between localized versus disseminated disease and identify complicating comorbidities.

### *What POCUS Liver and Gallbladder Can Do*

- Screen for differences in echogenicity between liver lobes.
- Identify focal or multifocal masses or nodules.
- Evaluate gallbladder wall and luminal contents (mobile vs consolidated, evidence of mucocele).
- Screen for vascular congestion.
- Evaluate for evidence of anaphylaxis if there is an index of suspicion.

### *What POCUS Liver and Gallbladder Cannot Do*

- Cannot differentiate between benign and malignant liver masses.
- Cannot be the sole diagnostic indicator used in the diagnosis of biliary obstruction.
- Cannot diagnose liver conditions based on echogenicity.
- Cannot reliably determine liver size, or hepatomegaly versus microhepatica.
- Cannot rule out severe liver disease such as hepatic neoplasia and cirrhosis or infiltrative processes based on an unremarkable focused liver examination.

*Point-of-Care Ultrasound Techniques for the Small Animal Practitioner*, Second Edition. Edited by Gregory R. Lisciandro.
© 2021 John Wiley & Sons, Inc. Published 2021 by John Wiley & Sons, Inc.
Companion website: www.wiley.com/go/lisciandro/ultrasound2

### Indications

- Increased liver enzymes, total bilirubin, and gamma-glutamyl transferase (GGT).
- Cranial abdominal organomegaly discovered on physical examination/palpation and abdominal radiography (or both).
- Abnormal serum bile acid levels or resting ammonia levels.
- Decreased albumin, cholesterol, blood urea nitrogen (BUN).
- Persistent hypoglycemia.
- Prolonged anorexia (especially cats).
- Vomiting.

### Objectives

- Recognize liver masses (single, multifocal).
- Recognize regional changes in liver echogenicity.
- Recognize venous congestion.
- Recognize gallbladder wall abnormalities.
- Recognize gallbladder luminal conditions such as mucocele, choleliths, biliary sludge, and gallbladder mass lesions.
- Recognize signs supportive of biliary obstruction, abnormal biliary contents (choleliths and inspissated bile), which when found should prompt referral for a complete detailed abdominal ultrasound study by a veterinary radiologist or internist with advanced training.

## Ultrasound Settings and Positioning

When imaging the liver, a 5–10 MHz curvilinear probe may be used depending on the size of the animal. Generally, higher frequency probes (7.5–10 MHz) are used for smaller dogs and cats and lower frequency probes (5 MHz) are used for large dogs to allow for deeper penetration. The depth of field should be adjusted initially (increased) to visualize the interface of the diaphragm and liver in the far-field. Gain should also be adjusted to maximize image quality. Adjustments in depth, gain, and focus position will be made repeatedly during the exam to optimize penetration and image quality.

The patient is most commonly imaged in dorsal recumbency with the transducer placed on the ventral abdomen just caudal to the xiphoid process, and the liver scanned in transverse and sagittal planes. This position generally allows for adequate visualization of the liver in smaller dogs and cats. In deep-chested dogs or larger animals, additional approaches through the right and left intercostal spaces may also be needed. The presence of an overlying gas-distended stomach or colon may also interfere with adequate visualization of the liver in dorsal recumbency. In these instances, positioning the patient in right and/or left lateral recumbency will cause the gas to rise to the upside (least gravity-dependent) of the patient, and scanning planes can be obtained from below the gas-filled structure.

**Pearl:** Best practice is to perform a Global FAST prior to moving and restraining your patient in dorsal recumbency to make sure the patient is stable (ruling out pleural and pericardial effusion, obvious cardiac and pulmonary conditions, poor volume status via caudal vena cava charcterization) and thus not hemodynamically fragile in which dorsal recumbency risks patient decompensation.

## How to Perform the POCUS Liver and Gallbladder Examination

The patient is positioned in dorsal recumbency and the hair is clipped from the ventral abdomen and as needed over intercostal spaces. Acoustic gel is applied to the abdomen, often preceded by 70% isopropyl alcohol that helps strip lipid and remove air from the patient's hair follicles. The transducer is placed caudal to the xiphoid process with the probe marker facing toward the head of the patient using a subcostal approach. Generally, this provides a sagittal view through the midline of the liver. The pleural margin of the diaphragm should be evident as a hyperechoic (bright white line) in the far-field (Figures 8.1A and 8.2B–E). If this is not initially visualized, then depth of field should be adjusted (increased) to bring it into view. Falciform fat may be seen along the ventral margin of the liver in the near-field, especially in overweight animals and should not be mistaken for hepatic parenchyma (see Figures 8.2A–D and 39.2).

The probe should then be fanned to the right side of the patient where the gallbladder should come into view, and can then be rotated to obtain a long-axis image of the gallbladder. The probe is then fanned to the patient's left so that the entirety of the sonographically accessible liver can be evaluated. In larger animals, it may be necessary to move the probe to the right

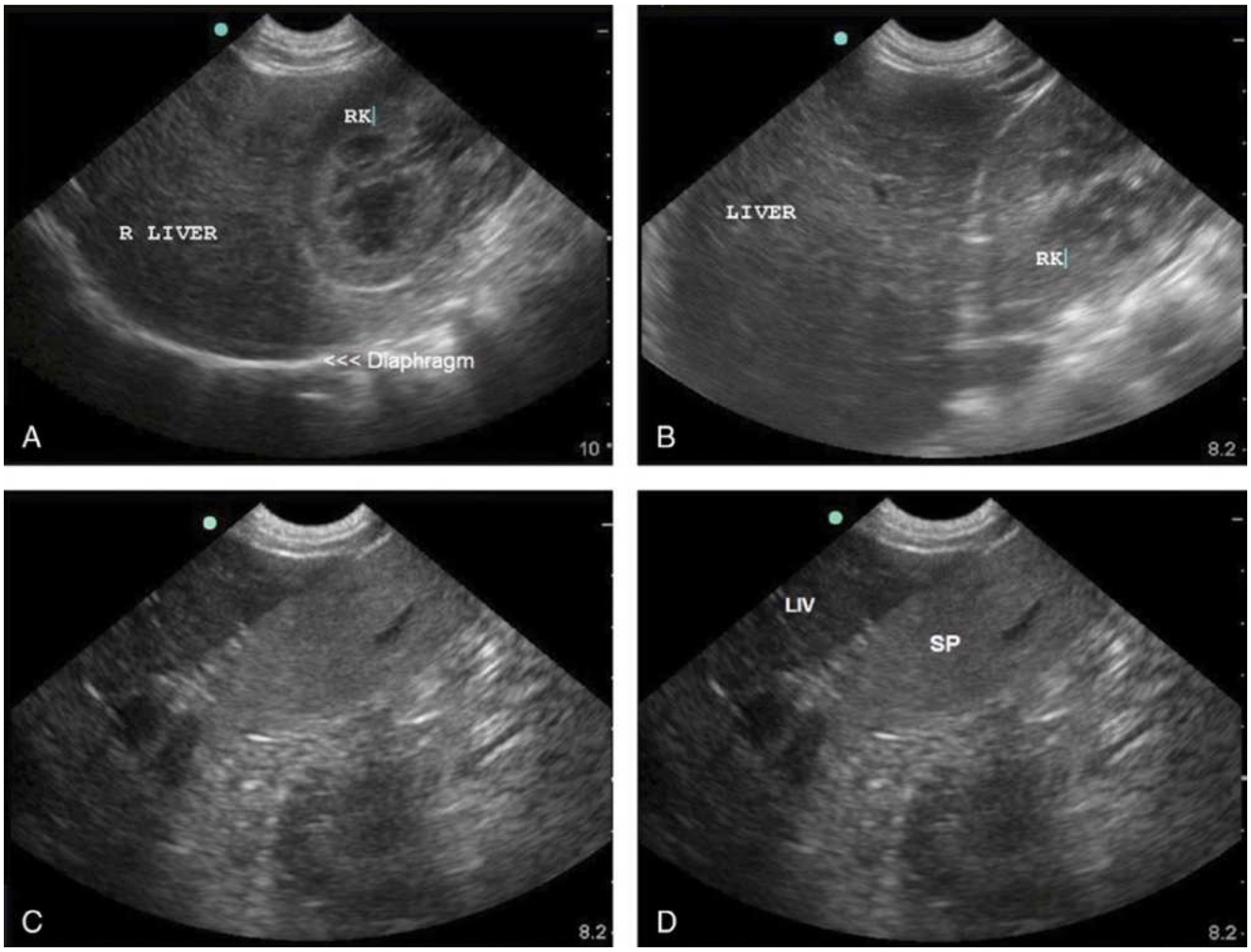


**Figure 8.1.** Comparative echogenicity of the liver to the cortex of the right kidney and spleen. (A) The liver (R LIVER) is normally slightly more echogenic (brighter) or the same echogenicity (isoechoic) as the cortex of the kidney (RK). In (B) another example with the right kidney (RK) compared to the echogenicity of the liver because the RK is located within the renal fossa of the liver's caudate lobe. (C) Normally, the spleen is more echogenic than the liver (unlabeled). (D) Same image as (C) with the liver and spleen labeled. When it is difficult to image the organs being compared in the same image frame, use of the split-screen function of your ultrasound machine facilitates comparative echogenicities of the liver to the spleen and kidney.

and left along the costal arch to visualize the entire liver. As the probe is fanned to the left, the stomach will come into view. After thoroughly scanning in the sagittal view, the probe is then rotated with the marker facing to the right side ("turn left" or counterclockwise) of the patient and the liver is scanned from right to left again in the transverse view. The hepatic and portal veins are imaged within (or immediately adjacent to) the hepatic parenchyma. Portal veins are distinguished by their hyperechoic (brighter) walls.

Large volumes of gas or ingesta can prevent complete visualization of the left side of the liver. A large amount of gas or stool in the descending colon may also interfere with imaging of the left side of the liver. If the stomach or colon interferes with imaging, the patient should be repositioned in right lateral recumbency and a left intercostal approach used. Alternatively, the patient can be reimaged following fasting and/or colonic evacuation if necessary and if the patient is stable. However, in the authors' opinion, some food within the stomach and a full colon can provide natural contrast for evaluation of the gastric and colon walls, and evacuation of the colon is rarely needed.

In deep-chested dogs, the liver may be difficult to image completely using a subcostal approach since the entire liver may lie under the ribcage. In these instances, right and left intercostal approaches are often needed to evaluate portions of the liver. From intercostal

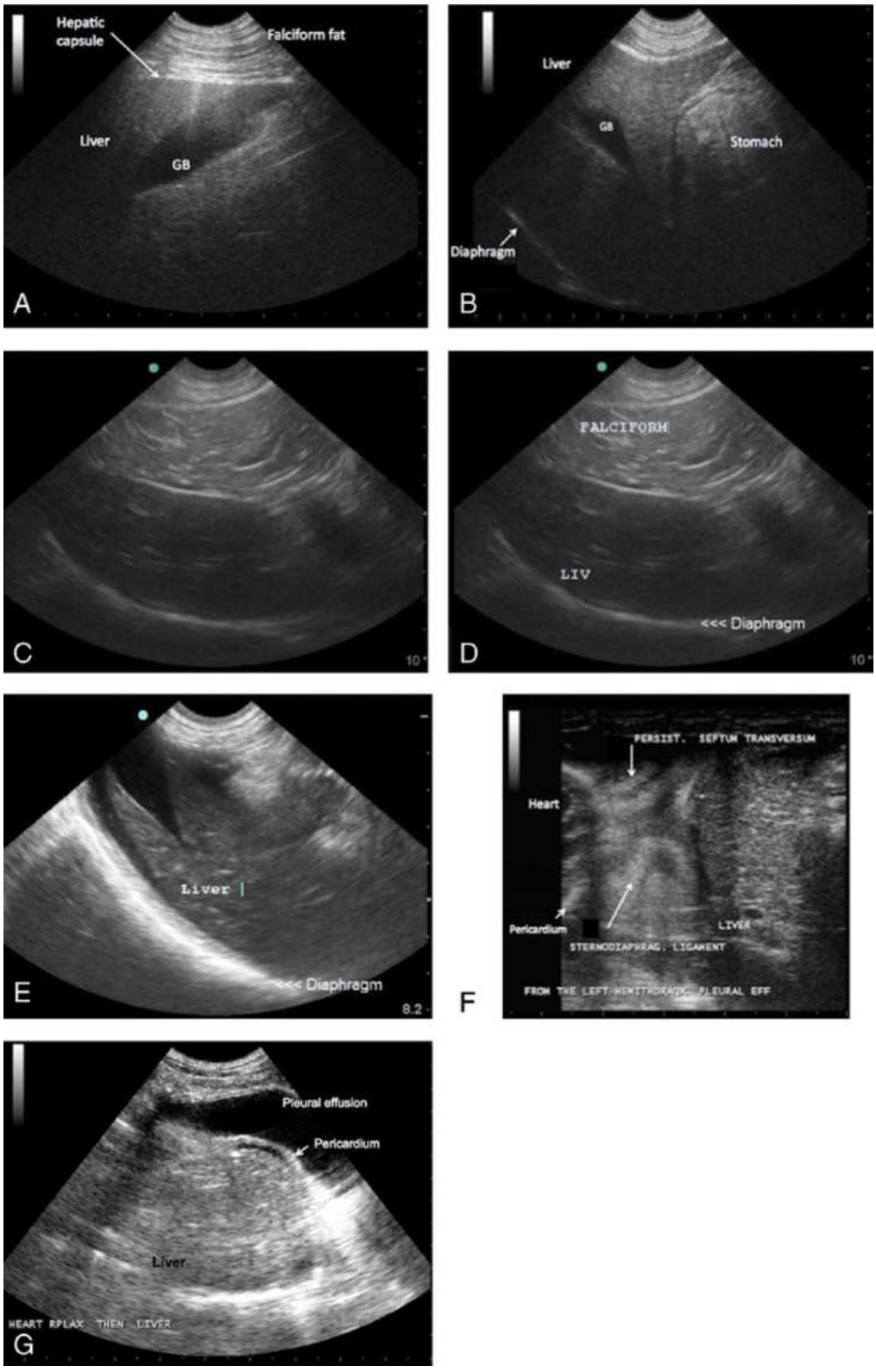


**Figure 8.2.** Liver margination and comparative echogenicity to the falciform fat. (A) Image of the falciform fat. Note the linear subcutaneous facial planes and falciform fat just distal to the point of probe contact. Liver echogenicity can be similar to the falciform fat. This especially depends on sonographic gain settings and hence comparative echogenicity can vary. Notice delineation between the falciform fat and normal liver by the thin echogenic line (*arrow*) representing the liver capsule. (B) Another example of differences in echogenicity between the liver and falciform fat. Note the sharp, normal liver margin. Compare to (A) and (B) and note that the liver capsule can be seen surrounding the hepatic parenchymal and at its contact with

approaches, evaluation may further be hindered by gas shadowing from the caudal lung. The sonographer should be aware that complete ultrasonographic interrogation of the liver may not be possible especially in large-breed dogs, for which computed tomography (CT) may be elected for a more comprehensive evaluation.

# Ultrasonographic Findings: Normal Liver and Gallbladder

The liver is composed of six lobes: left medial and lateral lobes, quadrate lobe, right medial and lateral lobes, and caudate lobe. Sonographically, the distinction between liver lobes is poorly defined. The left liver is largest and may comprise up to half of the liver mass. The gallbladder contacts the quadrate and right medial lobes. The left liver can be seen lateral and to the left of the gallbladder, and medial to the gastric fundus. The caudate process of the caudate lobe contacts the right kidney at the renal fossa (see Figure 8.1A,B). In general, it is difficult to visualize the divisions between liver lobes unless peritoneal fluid is present (see Figure 8.2E). Falciform fat can be imaged in the near-field at the ventral liver margin (see Figures 8.2A–D, 8.10C and 39.2). A hyperechoic (bright white) line is imaged cranial to the liver. While this is commonly referred to as the diaphragm, it is actually the interface of the muscular soft tissue diaphragm and the gas-filled lung (seeFigure 8.2B–E). When this echogenic curvilinear interface is not present or there is interruption of the normal curvilinear continuity of the structure, then congenital or acquired diaphragmatic herniation should be ruled out (see Figure 8.2F,G).

Evaluation of the size of the liver is subjective and is poorly assessed with ultrasound due to variability in patient conformation. Hepatic size estimation is better evaluated on abdominal radiographs. Normal liver margins are sharp and not rounded (see Figure 8.2A,B,E).

Normal hepatic parenchyma is homogeneous and uniform in echogenicity with medium echotexture (coarser echotexture than the spleen) (see Figure 8.1C,D). Echogenicity is generally evaluated in comparison with falciform fat, the right renal cortex and spleen (see Figures 8.1A,B and 8.2A–D). Falciform fat must be distinguished from hepatic parenchyma and is generally isoechoic or hyperechoic to normal hepatic parenchyma (see Figure 8.2A–D and compare to Figure 8.10D), with a coarser echotexture. The liver is hypoechoic (darker) compared to spleen and the left liver can often easily be compared to the head of the spleen whereas the right liver is easily compared to the right kidney, which allows for comparisons at the same image field of view at the same depth, focus and gain (see Figure 8.1C,D). The liver is normally isoechoic to mildly hypoechoic and coarser in echotexture compared to the renal cortex (see Figure 8.1A,B). Subtle changes in echogenicity of the hepatic parenchyma can be difficult to appreciate for the novice sonographer. Using the split-screen B-mode function can be helpful for comparing liver, renal and splenic echogenicity comparisons at the same depth, focus, and gain when these organs cannot be imaged in the same frame on nonsplit-screen B-mode scanning.

**Pearl:** Remember the "SLiCK" pneumonic regarding canine echogenicity: the spleen (S) is hyperechoic (brighter) to liver (Li) which is slightly more hyperechoic (brighter) or isoechoic (same echogenicity) to the cortex of the kidney (CK). In the order of most to least echogenic, this spells "SLiCK." For the feline, hepatic echogenicity is often compared to the adjacent falciform fat and the feline liver should be isoechoic to slightly hypoechoic to the falciform fat.

the diaphragm as a hyperechoic line (<<<). (C) Example of prominent falciform fat in a more obese patient. The falciform in the near-field is juxtaposed to normal liver in the far field. (D) Same image as in (C) but labeled. (E) Delineation of the liver lobes is not sonographically readily apparent unless anechoic free fluid (*) (ascites) is present, as is the case in this image of a peritoneal pericardial hernia in a cat. Normally the caudal margins of the liver lobes are easily identified and sharply demarcated. Imaging of the liver should be deep enough to appreciate the diaphragm. The sharply marginated hyperechoic curvilinear structure is the liver and diaphragm interface (<<<). (F) Although not the gold standard for evaluation of diaphragmatic integrity, evaluation of the diaphragm can be useful in trauma cases and cases in which the integrity of the diaphragm may be compromised (e.g., congenital or acquired types of diaphragmatic hernia). Shown here is a peritoneal pericardial hernia in a cat. Note the embryological persistence of the septum transversum. In this patient, the liver would dynamically slip into the pericardial sac, depending on how the patient was positioned. In many cases, other abdominal organs (such as the spleen, liver or bowel) can be seen within the pericardial sac. These can be an incidental finding or seen in patients with exercise intolerance or respiratory distress. (G) Another example of a peritoneal pericardial diaphragmatic hernia in a cat with concurrent pleural effusion. The apex of the heart is identified to the left of the image. However, the homogeneously echotextured, more solid liver partially occupies a large portion of the pericardial sac. The small bowel is also commonly herniated and easily recognized by the layering of its walls.

Evaluation of hepatic vasculature should generally be reserved for the more experienced sonographer. However, distension of the hepatic veins is fairly easy to identify and can be learned by the novice. Hepatic veins are distinguished from portal veins based on the echogenicity of the walls. Portal veins have bright echogenic walls whereas the walls of the hepatic veins are not visualized (see Figure 8.10A,B). The hepatic veins can be traced through the hepatic parenchyma to the caudal vena cava to confirm their identity. The caudal vena cava traverses the dorsal hepatic parenchyma slightly to the right of midline, and the hepatic veins empty into the cava near the diaphragm (Figure 8.3A,B). See also Chapters 7, 20, 26, and 36.

The gallbladder is surrounded by hepatic parenchyma on the right side of the liver. The size is variable depending on when gallbladder contraction last occurred. In the typical normal state, the gallbladder is an anechoic structure with a uniformly thin echogenic wall. Normal gallbladder wall thickness is

**Figure 8.3.** Hepatic venous congestion. The differentiation between hepatic veins and portal veins can be challenging for the novice. However, imaging the caudal vena cava as it passes through the diaphragm in the longitudinal plane is easy to learn and helps accurately identify distended hepatic veins by their associated branching into the caudal vena cava. Normally, hepatic veins are inconspicuous. Shown in (A) and (B) is the same example of moderate hepatic venous (HV) congestion unlabeled and labeled. Note how the hepatic veins can be seen emptying into the caudal vena cava (CVC) prior to the CVC passing through the diaphragm (Diaphragm →). The image was acquired at the TFAST diaphragmatico-hepatic (DH) view. (C) Another example of HV congestion being traced to the caudal vena cava (CdVC) near the diaphragm (Diaphragm →). Detecting hepatic venous distension is clinically helpful and aids in the detection of right-sided volume overload, right-sided heart failure or an obstructive venous lesion between the liver and right atrium, which would then prompt further investigation and help guide management. (D) A similar correlative figure with overlays to show the anatomy of the area. Source: (B) and (D) courtesy of Dr Gregory Lisciandro, Hill Country Veterinary Specialists and FASTVet.com, Spicewood, TX, and (C) courtesy of Dr Terri DeFrancesco, Raleigh, NC.

less than 1 mm in cats and less than 3 mm in dogs (Hittmair et al. 2001; Spaulding 1993); however, for all intents and purposes, the gallbladder wall should be a thin white line in both species (Figure 8.4A–C; see also Figure 8.11). Gallbladder sludge (echogenic gravity-dependent material within the lumen) is common in dogs and generally a benign finding in the absence of other significant ultrasonographic and clinical findings although the presence of "normal" gallbladder sludge has been more recently questioned (Tsukagoshi et al. 2012) (see Figure 8.12A–D). The finding may be an indication of cholestasis. The intrahepatic bile ducts are not seen unless there is extrahepatic biliary obstruction of at least five days' duration when the fluid dilated ducts will have the appearance of hepatic veins (without the hyperechoic walls of portal veins) (see Figure 8.15A,B). If available, color flow Doppler is useful for differentiating the lack of flow in a dilated biliary duct from the normal blood flow in hepatic and portal vessels; however, tracing structures in real time is often adequate. The common bile duct is small and difficult to see in the normal state in dogs and cats, but is generally easier to identify in the cat.

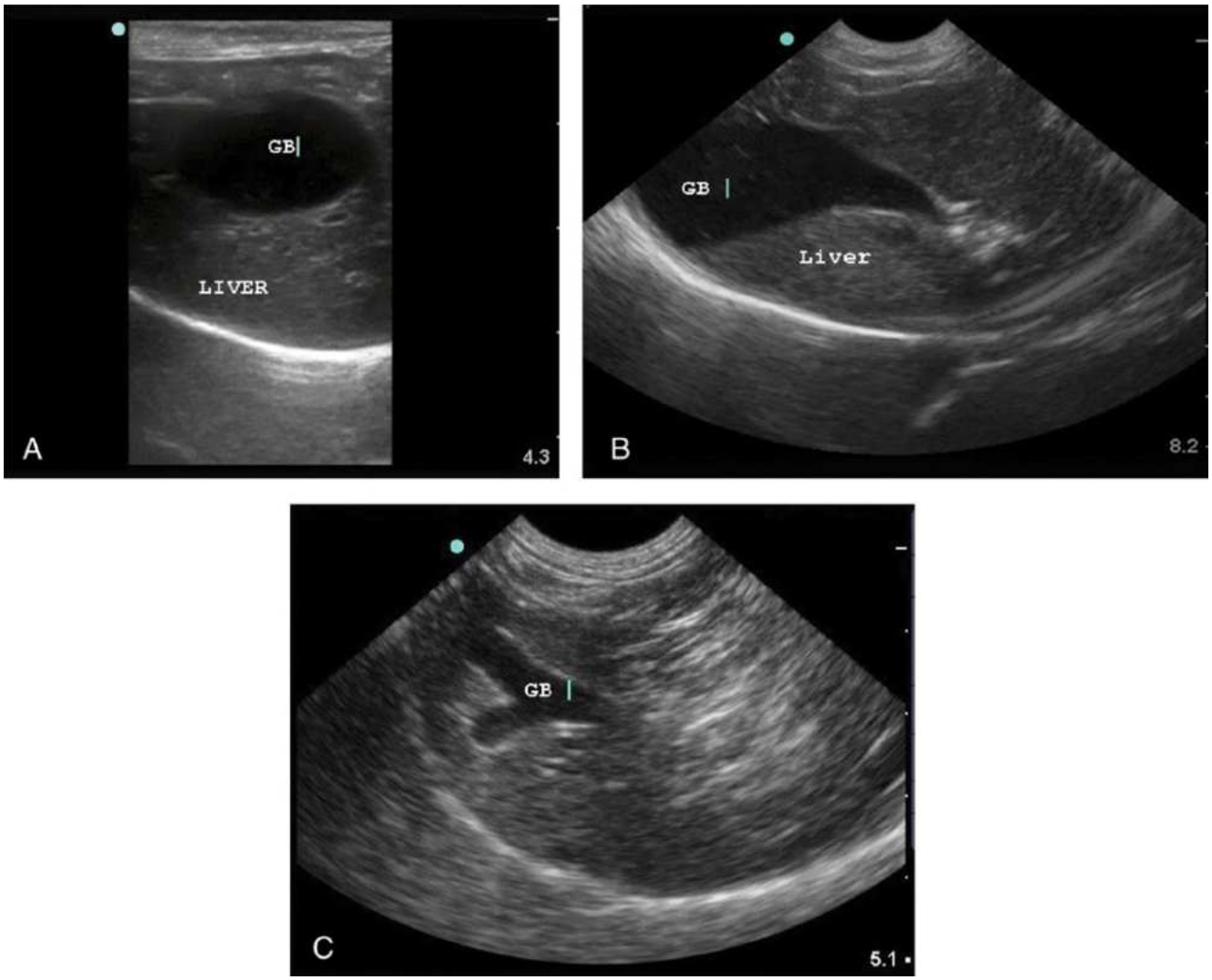


**Figure 8.4.** Normal gallbladder and variations. (A) The normal gallbladder wall (not labeled) is inconspicuous with normal thickness <1 mm in cats and <3 mm in dogs (GB, gallbladder). However, normal wall thickness does not rule out mild, low-grade or chronic inflammation. (B) Similarly labeled image showing a normal canine gallbladder wall. Note the anechoic structure is marginated ultrasonographically by a thin hyperechoic (bright white) line. Evaluation of the margin of the gallbladder in real time provides a global view of the gallbladder wall and can aid in determining gallbladder wall integrity. The curvilinear line in the far-field is created by the interface between the diaphragm and lung (air). (C) Image of a bilobed gallbladder may be seen in both dogs and cats but is more common in cats, as was seen in this normal feline patient (GB, gallbladder).

**Pearl:** It may be difficult to tell the difference between a dilated biliary tract (no flow) and hepatic veins (flow), in which case color flow Doppler may be helpful.

Artifacts are commonly encountered when performing the POCUS liver and gallbladder examination and include mirror image, acoustic enhancement, side-lobe, slice thickness, and edge shadowing. These are discussed in more detail in Chapter 3 and 5.

- **Mirror image**. The most common of these artifacts results in a mirror image of the liver and gallbladder being seen on the far side of the lung–diaphragm interface. This should not be mistaken for a diaphragmatic hernia (see Figure 8.9D).
- **Acoustic enhancement**. Acoustic enhancement is associated with a fluid-filled gallbladder that causes an increase in echogenicity of the hepatic parenchyma on the far side of the gallbladder. *Acoustic enhancement should not be mistaken for increased liver echogenicity*.
- **Side-lobe and slice thickness**. These artifacts involve fluid-filled organs like the gallbladder and give the false impression of the presence of luminal sediment.
- **Edge shadowing**. This artifact also involves fluid-filled organs like the gallbladder and gives the appearance of a defect in the wall that can be mistaken for gallbladder rupture or gallbladder wall mineralization.

**Pearl:** Common artifacts in the liver include mirror image, acoustic enhancement, side-lobe, slice thickness, and edge shadow.

# Clinical Significance and Implications of Abnormal Focused Liver and Gallbladder Findings

Goals of POCUS liver and gallbladder examination include recognition of liver masses (single, multifocal), obvious changes in liver echogenicity, hepatic venous congestion, identification of gallbladder wall abnormalities and gallbladder luminal conditions, and recognition of signs of biliary obstruction. Such findings should prompt referral for a complete detailed abdominal ultrasound as interventions may be indicated.

## *Liver Masses*

Identification of focal liver masses is the easiest task to learn with the POCUS examination. It is important to remember that is not possible to differentiate between benign and malignant processes based on ultrasound alone. Focal lesions may be caused by regenerative nodules or nodular hyperplasia, benign or malignant neoplasia, focal inflammatory disease (e.g., abscesses and granulomas), cysts, and hematomas.

The origin of a large midabdominal mass can sometimes be difficult to determine when the mass contacts multiple origins. In this case, try repositioning the patient from dorsal to lateral recumbency. This will often separate the liver and spleen from one another and help determine the origin of the mass. Generally, the spleen is differentiated from the liver by its hyperechoic capsule (bright white) and its vasculature splitting its capsule unlike the liver.

- *Benign hepatic nodular disease* is common and nodules associated with nodular hyperplasia may be variable in echogenicity when compared to normal hepatic parenchyma (hyperechoic, hypoechoic, isoechoic or mixed echogenicity). Generally, well-defined hyperechoic homogeneous nodules are more likely to be benign but cytology or histopathology is necessary for definitive evaluation. Nodular hyperplasia is common in older dogs (Nyland et al. 2002) (Figure 8.5).
- *Hepatic cysts* consist of round to oval anechoic (fluid-filled) structures with well-defined walls. These are generally benign unless a significant amount of hepatic architecture is disrupted and there is evidence of hepatic dysfunction (polycystic disease). Cysts may be parenchymal or biliary in nature, and may be congenital or acquired. Cysts that have irregular margins or contain echogenic material are less likely to be benign and may represent abscesses, inflammation or neoplastic changes (Figure 8.6A–C).
- Other parenchymal masses may have variable appearances and include abscess, hematoma, nodular hyperplasia and neoplasia.
- *Hepatic abscesses* are uncommon, usually indistinguishable from nodules and mass lesions of other etiology, and may have variable echogenicity, appearance, and margination (Figure 8.7A). Most commonly, abscesses are relatively hypoechoic, thick-walled lesions which may have cystic or cavitary components or mixed echogenicity. A more definitive finding is the presence of gas (due to gas-forming bacteria) within the lesion, which appears as focal areas of hyperechogenicity with distal edge

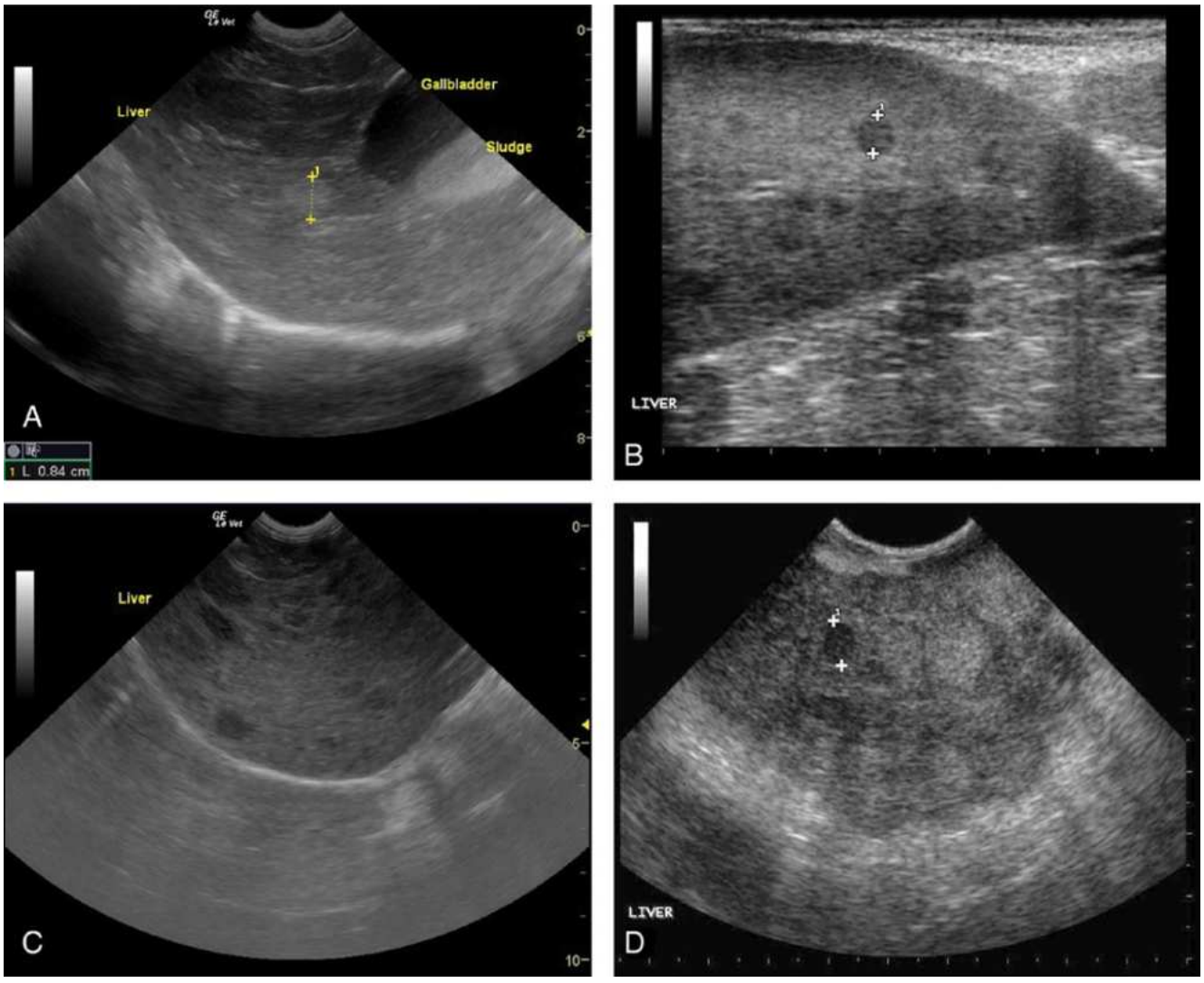


**Figure 8.5.** Nodular hyperplasia. (A) Small hyperplastic nodule as demarcated by the caliper marks made by the sonographer, consistent histopathologically with benign nodular hyperplasia. This is a common finding in older dogs. Generally, nodules are seen as discrete, well-demarcated hyper- or hypoechoic homogeneous nodules and can be singular or multiple and poorly demarcated. Nodules can be any size <3 cm (mass defined as >3 cm). Hence, findings are nonspecific and fine needle aspiration and/or biopsy is needed to differentiate these nodules from malignant processes. (B) Nodular hyperplasia with multiple varying sized, homogeneous, hypoechoic nodules with the largest marked with calipers (+). (C) Example of an older dog with multiple hypoechoic nodules confirmed to be benign nodular hyperplasia. (D) In contrast to (B), an example of a severely nodular liver in a 10-year-old male castrated Chihuahua with poorly controlled diabetes and pancreatitis. The process is diffuse and the liver margins are severely rounded. The calipers (+) demonstrate a hypoechoic cyst. Notice its distal acoustic enhancement and the multiple, hypoechoic (dark) nodules throughout the parenchyma. Fine needle aspiration results were consistent with a vacuolar degeneration and lipidosis. Benign hyperplasia and neoplasia would be considered additional differentials. A biopsy would be more definitive in this case.

shadowing, comet tailing, and reverberation. Fine needle aspiration with cytology and microbial culture and sensitivity is helpful in confirming the diagnosis. However, neoplastic lesions can have necrotic centers that can be mistaken for abscesses and therefore, diagnosis should always be in conjunction with additional clinical findings that support the diagnosis. The Global FAST approach is helpful as a quick screening test for disseminated versus localized disease and the presence or absence of lung nodules (quick pulmonary metastasis check).

- *Hepatic hematomas* may be variable in appearance and initially are generally anechoic or hypoechoic

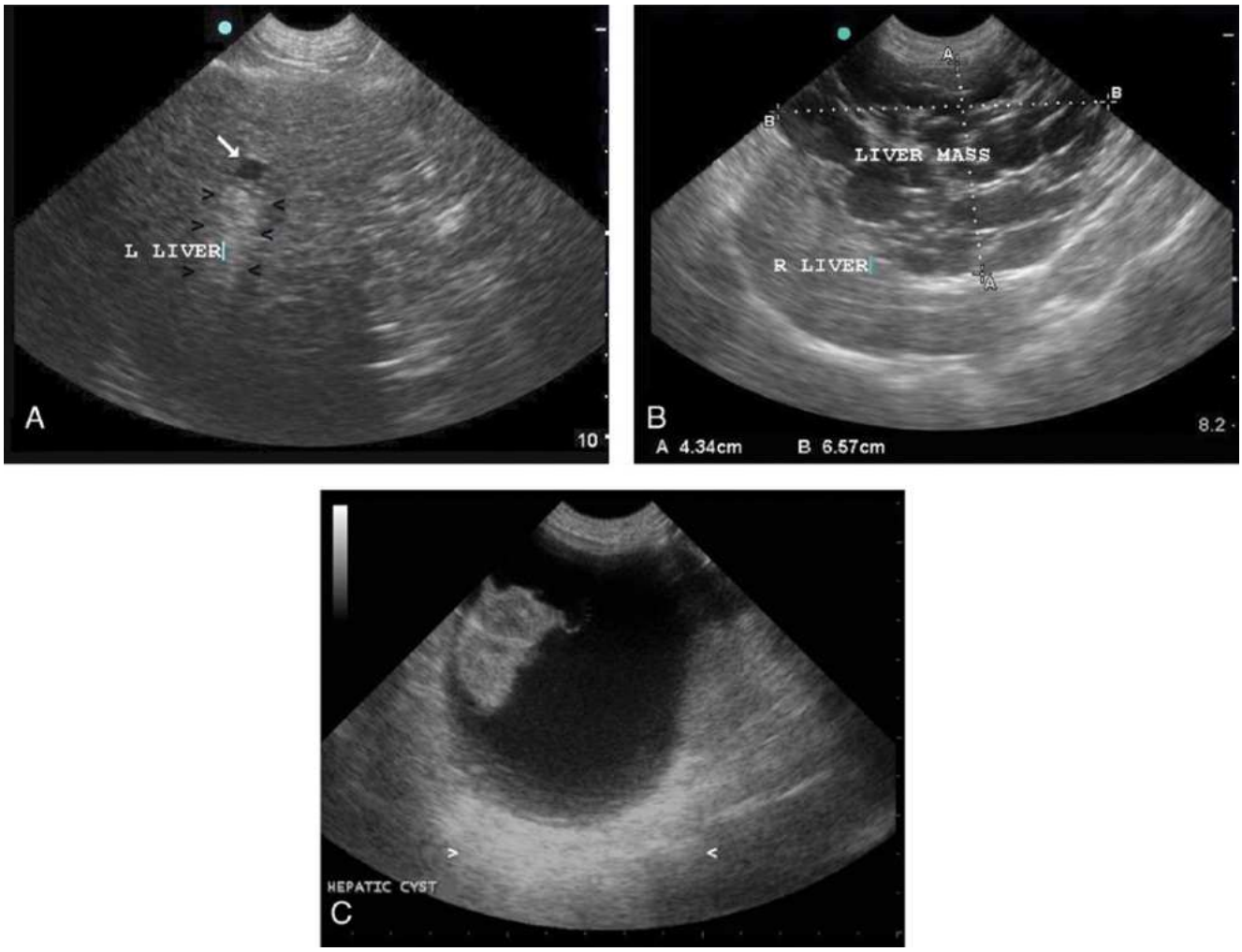


**Figure 8.6.** Hepatic cyst and biliary cysts. **(**A) Hepatic cyst (*arrow*) with distal acoustic enhancement (seen as a hyperechoic, bright enhancement extending from the far margin of the hepatic cyst and marked with subtle black cursors [> <] on both sides of the hyperechoic track). Hepatic cysts are typically thin-walled and filled with anechoic fluid. A fluid-filled structure can be differentiated from a solid nodule by looking in the far-field for *acoustic enhancement* artifact (the bright track extending from the far field of the cyst to the text L LIVER). A solid or mineralized structure will conversely have *acoustic shadowing* artifact in the far-field (a dark track extending from the far-field of the solid or mineralized structure). (B) Multiple benign biliary cystadenomas in a cat (labeled liver masses by the sonographer). This can be mistaken for malignant cystic neoplasia. (C) Large hepatic cyst in a dog. Note the large anechoic structure with distal *acoustic enhancement* artifact extending from the far border of the cyst (labeled > <). Cysts can be complex in architecture and within this cyst is a large, echogenic, ovoid to amorphous structure. Irregularly marginated cysts or those containing echogenic material can be malignant. An additional differential for the structure within the cyst includes fibrinous material or hemorrhage and may represent abscessation, inflammation or neoplastic change. Fine needle aspiration may allude to the diagnosis. Alternatively, excisional biopsy may be needed.

to normal hepatic parenchyma. Hematomas may be difficult to distinguish from other mass lesions, including neoplasia (hemangiosarcoma). Frequently, large hematomas usually form with ruptured hepatic masses and can complicate diagnosis (Figure 8.8A,B; see also Figure 8.7B). Fine needle aspiration of hematomas generally yields nonspecific cytological results and the absence of neoplastic cells on cytology does not rule out neoplasia.

- *Neoplastic lesions* have a wide range of morphological changes. Again, it should be emphasized that it is *not possible to distinguish between benign and malignant lesions* based on ultrasonographic appearance alone. There are a variety of primary liver tumors including hepatocellular adenoma and adenocarcinoma as well

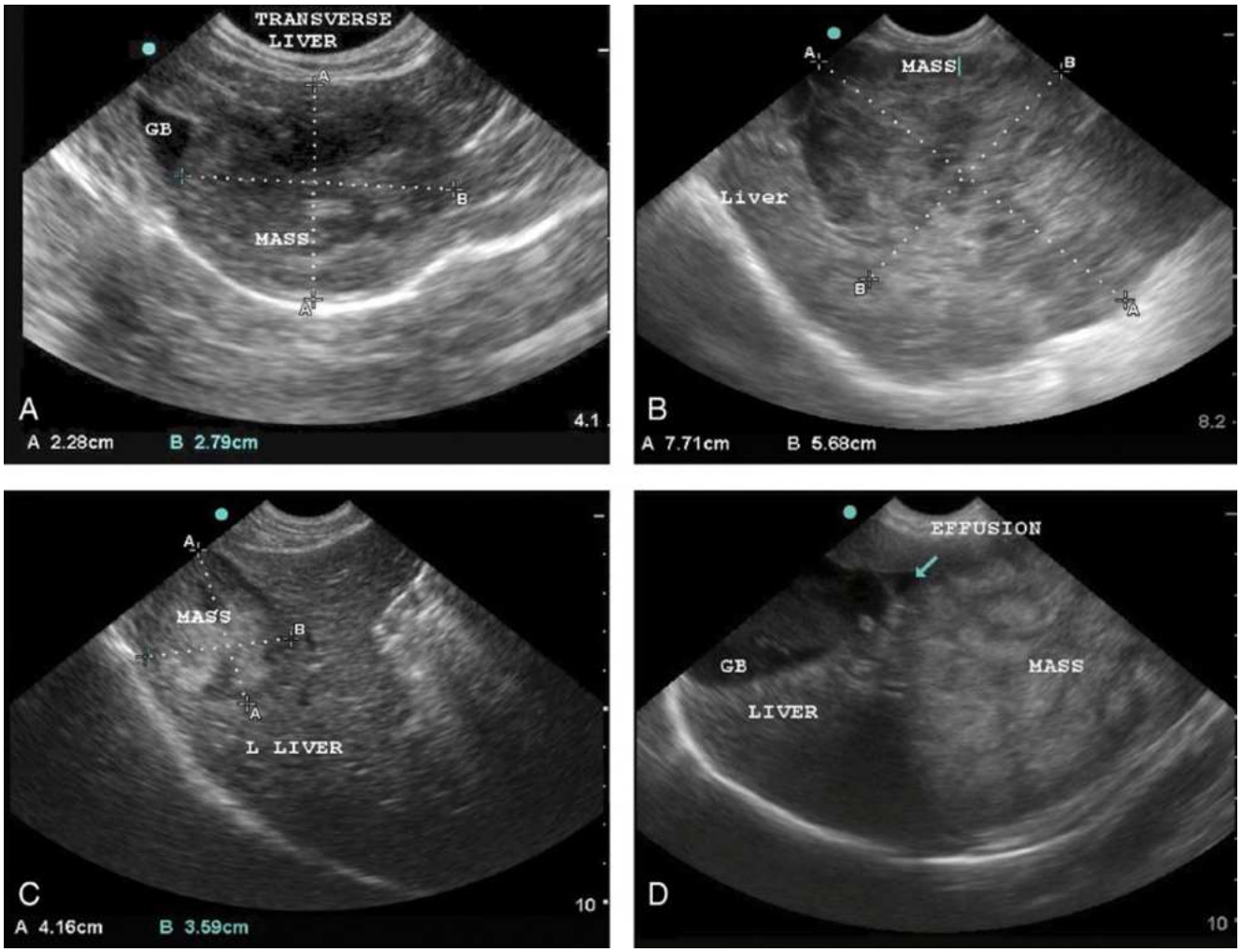


**Figure 8.7.** Various liver masses. Benign and malignant liver masses cannot be differentiated based on ultrasound characteristic alone. (A) Semisolid hepatic mass in a cat confirmed to be a hepatic abscess. The gallbladder (GB) is juxtaposed to the mass and may be confused with free fluid on this still image, highlighting the value of a several-second video when images are submitted to the specialist for interpretation. Although not always present, the hallmark of an abscess regardless of location is the presence of gas within the mass effect as evidenced by comet tails and other air-related artifacts caused by gas-producing bacteria (such artifacts are not evident here). Diagnosis was made by liver biopsy. (B) A large, mixed echogenicity mass (MASS). It can be difficult to determine the origin of large masses. The liver, spleen, kidney or other adjacent structures should be considered if a region of organ confluence cannot be identified. The histopathological diagnosis in this case was hepatic hemangiosarcoma. (C) Another example of mixed echogenicity with a hepatic mass adjacent to the diaphragm. Note the abrupt change of echogenicity between the mass and normal hepatic parenchyma. Percutaneous biopsy result was hepatocellular carcinoma. (D) Large hyperechoic, lobulated mass with mild peritoneal effusion within the gallbladder fossa. The lesion was confirmed to be hepatocellular carcinoma. Note the differences between sonographic appearances of the same tumor type in (C) and (D) demonstrating the poor specificity of ultrasonographic findings with regard to histopathological diagnosis. Additional differentials might have included a hepatoma (benign liver mass) or other types of solid parenchymal neoplasia (GB, gallbladder; RLiver, right liver; RK, right kidney).

as mesenchymal tumors (see Figure 8.7B–D). Lymphosarcoma can appear as either focal or multifocal mass lesions or as diffuse parenchymal disease. Hemangiosarcoma generally appears as complex mass lesions with mixed echogenicity and cavitations (see Figures 8.7B and 8.8A,B). Hematomas can have a similar appearance. Metastatic neoplasia is common in the liver (Figure 8.9A,B). Hepatic mass lesions must be characterized by cytology or histopathology for a definitive diagnosis. Ultrasound-guided fine

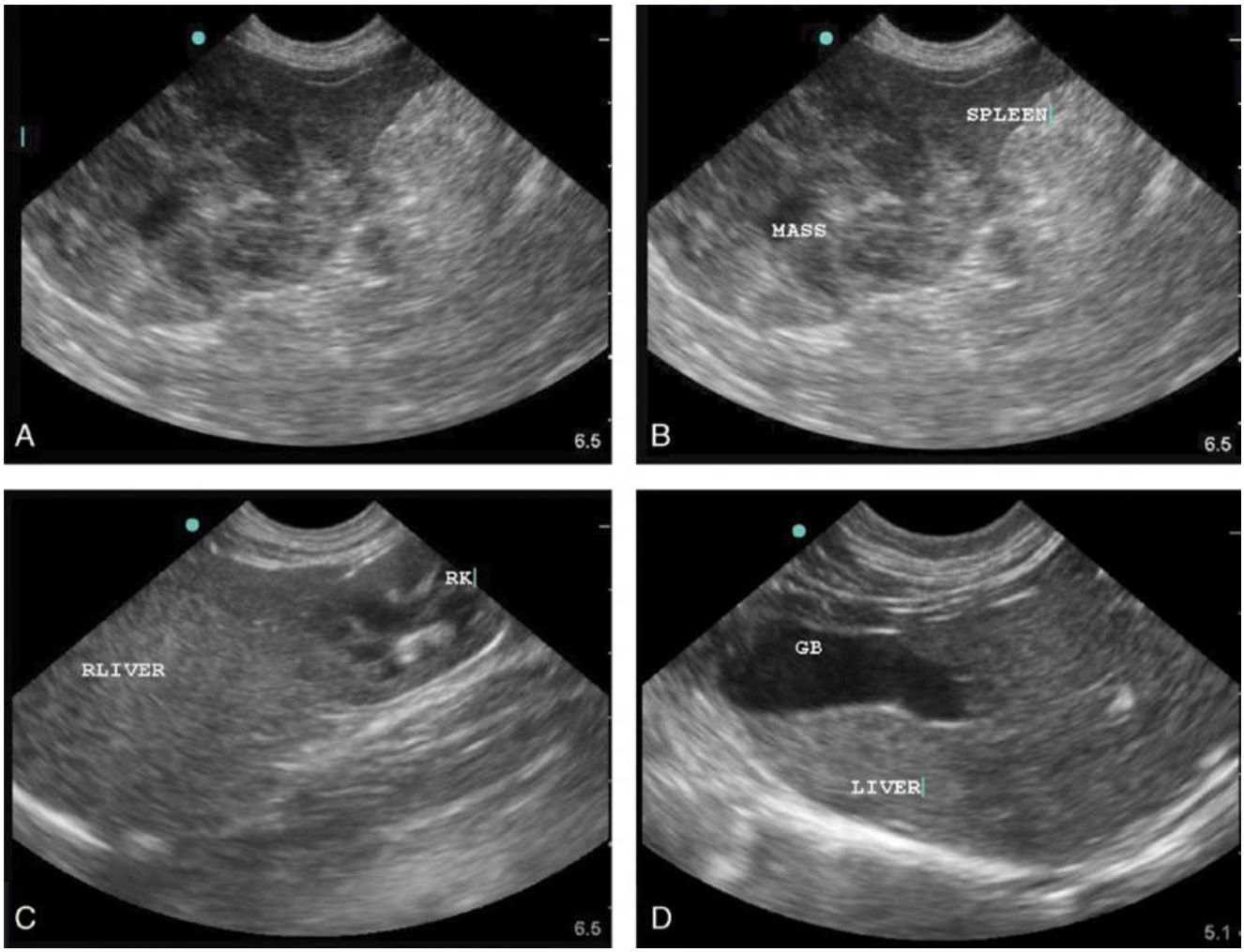


**Figure 8.8.** Liver and splenic masses. The origin of large masses can be challenging to determine ultrasonographically and is sometimes not possible. (A) and (B) show the same large mass in a dog with mixed echogenicity (unlabeled and labeled). Careful evaluation showed confluence of the tumor with the splenic parenchyma. (C,D) Images of a cat (same patient) with hepatic mast cell tumor. Note that a well-defined mass is not seen. Rather, the parenchymal changes are subtle and the liver is coarse in echotexture. This case highlights the importance of fine needle aspirate and/or liver biopsy in obtaining the patient's definitive diagnosis.

needle or Tru-Cut biopsy of mass lesions can usually be accomplished with minimal difficulty and risk, depending on the location of the mass.

- *Target lesions* consist of alternating layers of different echogenicities, giving the appearance of a target or bull's eye. Single target lesions have a high predictive value for malignancy. Multiple target lesions increase the positive predictive value of malignancy up to 74–81% (Cuccovillo and Lamb 2002) (see Figure 8.9A,B). Regardless, target lesions are nonspecific and a biopsy is required for further characterization. If target lesions are detected, then the authors recommend screening for additional evidence of neoplasia with a complete detailed abdominal ultrasound, thoracic radiographs, and lung ultrasound. However, performing a Global FAST immediately following your POCUS examination is helpful for a quick survey of the remaining abdominal structures, the thorax (TFAST), and lung surface, especially for nodules (Vet BLUE).

## Liver Parenchymal Disease

Ultrasonography is not always sensitive for evaluating diffuse parenchymal disease, and diffuse disease may be more challenging to assess than focal disease because sonographic changes are more easily overlooked or

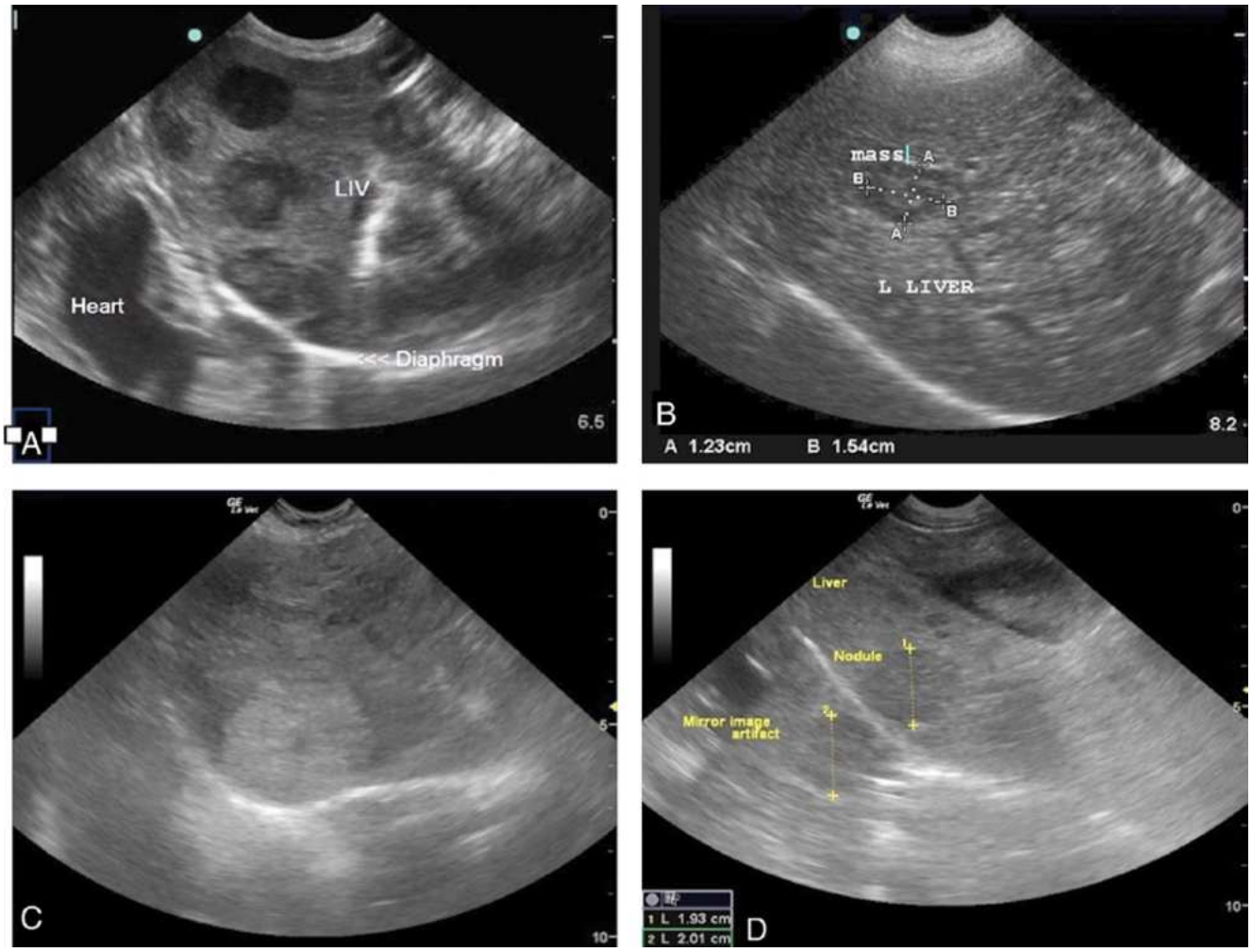


**Figure 8.9.** Liver masses. (A) Image of a dog with target lesions of the hepatic parenchyma. These lesions are generally considered malignant and may be consistent with metastatic disease. Less commonly, this appearance may be seen with primary hepatic neoplasia, granulomatous disease, chronic active hepatitis or even benign hyperplasia. This canine patient also had a large cavitary splenic mass supportive of metastatic disease, pericardial effusion and lung nodules emphasizing the importance of the Global FAST approach for staging. (B) An example of a small hepatic target lesion in a dog with splenic hemangiosarcoma. One must keep in mind that sonographic visualization of a target lesion is nonspecific and a biopsy is required; however, the Global FAST approach can help stage and guide diagnostic testing. (C) A large hyperechoic, well-marginated mass in a dog that was percutaneously biopsied as hepatocellular carcinoma. (D) Another example of hepatocellular carcinoma. Note in both (C) and (D) the commonly encountered mirror image artifact because of the strong, reflective soft tissue–air interface of the liver, diaphragm, and lung. Source: (A) courtesy of Dr Gregory Lisciandro, Hill Country Veterinary Specialists and FASTVet.com, Spicewood, TX.

may not be present. When there is a high index of suspicion for diffuse hepatic disease, fine needle aspiration or biopsy is indicated to confirm a diagnosis, and ultrasound guidance can assist with these procedures. Despite sonographic limitations, some generalizations can be made regarding changes in echogenicity.

- *Diffuse hepatic hypoechogenicity* (parenchyma is darker than normal due to decreased echogenicity) is generally noted when the hepatic parenchyma is significantly hypoechoic to the renal cortex (Figure 8.10A,B). In addition, the portal veins are more conspicuous due to the contrast between their hyperechoic walls and the hypoechoic hepatic parenchyma (see Figure 8.10A,B). The portal veins appear as linear "equal signs" ( = ) when evaluating the liver in real time. As a general rule, if they are prominent and numerous against a hypoechoic

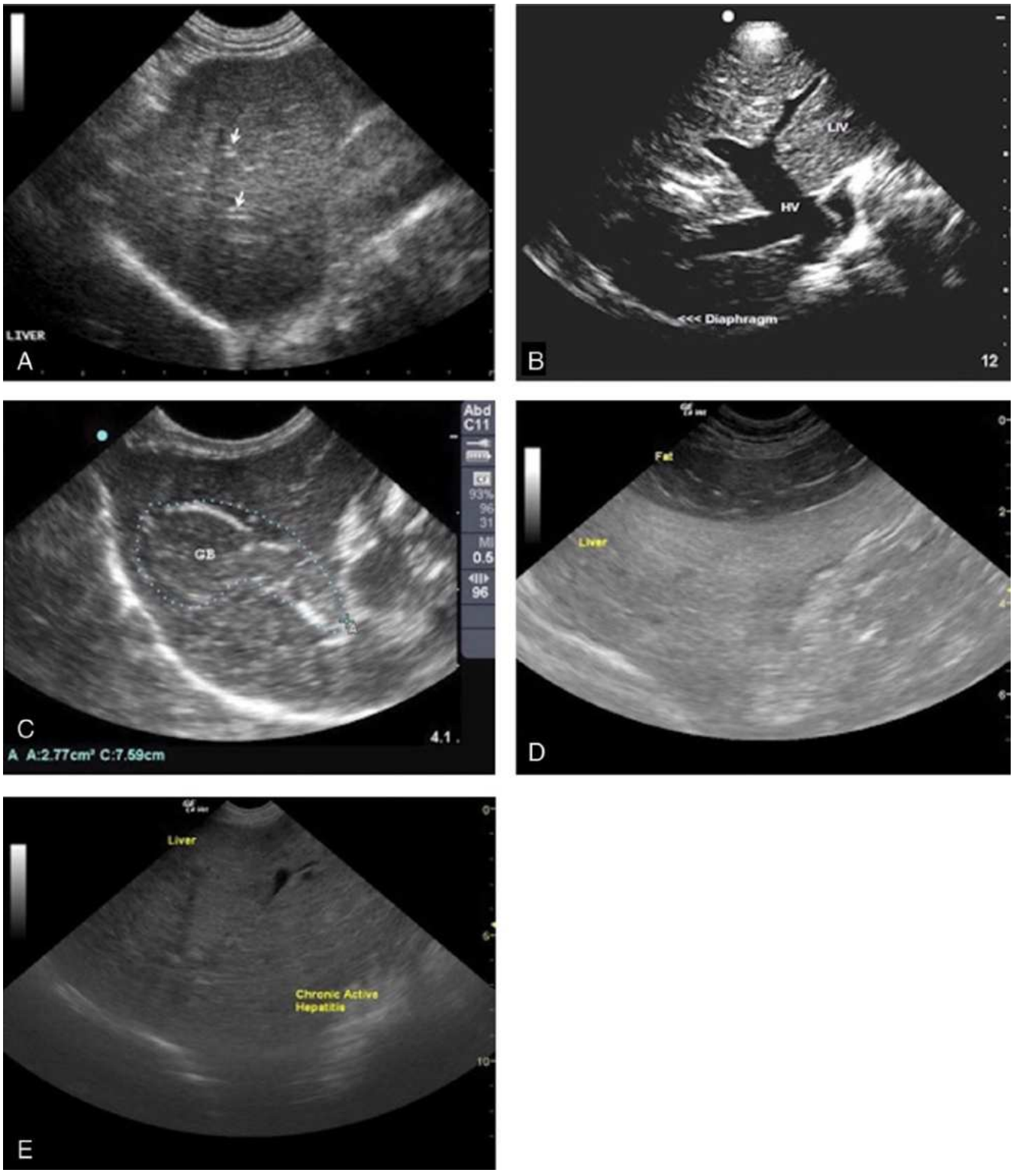


**Figure 8.10.** Diffuse homogeneous hypoechoic and hyperechoic liver. **(**A) Hepatic venous congestion (veins not shown) with a homogeneously hypoechoic (dark) liver. Note the increase in portal markings (arrows and stippled hepatic echogenicity), analogous to a "starry night." The portal vein reflections look like stars against the night sky or hyperechoic (bright white) equal (=) signs, depending on the angle of insonation. (B) Hepatic venous congestion with obvious distended hepatic veins (HV) and a homogeneously hypoechoic liver (LIV). The background hepatic echogenicity is an additional example of the

(dark) background, the liver can be said to be diffusely hypoechoic. Hepatic hypoechogenicity can occur with passive congestion (see Figure 8.10A,B), diffuse inflammatory diseases such as cholangiohepatitis, and diffuse infiltrative diseases such as lymphosarcoma and mast cell disease (see Figures 8.8C,D, 8.10C). Of note, lymphosarcoma can also present with diffuse hyperechoic (brighter) changes or normal echogenicity.

- *Diffuse hepatic hyperechogenicity* (liver is brighter than normal) can be seen with fatty infiltration (hepatic lipidosis in cats), steroid hepatopathy, other metabolic and endocrine hepatopathies (diabetes mellitus), chronic hepatitis and cirrhosis (see Figure 8.10E). In addition to the diffuse hypoechogenicity noted above, infiltrative neoplastic disease such as lymphosarcoma and mast cell tumor can also produce diffuse (homogeneous) hyperechoic changes (see Figure 8.8C,D). Fine needle sampling is a simple and minimally invasive technique for obtaining diagnostic information. If cytology results acquired by fine needle sampling are nonspecific, then a liver biopsy is necessary (percutaneous core biopsy, laparoscopic biopsy or surgical wedge biopsy). Liver biopsies are best in patients in which chronic diffuse hepatic disease is suspected because histopathology is required to evaluate parenchymal architecture. The hepatic parenchyma of cats with hepatic lipidosis is usually hyperechoic to falciform fat. This change can also be an incidental finding in obese cats (Nicoll et al. 1998) (see Figure 8.10D). Liver size is usually increased in cats with hepatic lipidosis, steroid hepatopathy, and infiltrative diseases, and decreased in size in animals with chronic hepatopathies.
- *Mixed hepatic echogenicity* is often associated due to diffuse inflammatory disease (often chronic) or infiltrative disease (neoplasia, fungal infection).
- *Animals with toxic hepatopathies* often have normal hepatic echogenicity (Nyland et al. 2002). Other pathological conditions may also have normal echogenicity and fine needle aspiration and/or biopsy should be considered in the face of a normal ultrasonographic appearance with clinical and biochemical parameters supporting primary liver disease. It is important to remember that animals with severe hepatic dysfunction or diseases may have *normal ultrasound findings* (Nyland et al. 2002). Additional assessment is indicated when clinical findings support hepatic dysfunction and may include fasting ammonia (NH3) levels, pre- and postprandial serum bile acid levels, abdominal CT and, ultimately, liver biopsy.

**Pearl:** *Liver disease cannot be ruled out on the basis of an unremarkable ultrasound examination*. Additional evaluation is indicated if clinical findings support liver disease.

## Hepatic Vasculature

The hepatic veins are best evaluated from the right side of the liver where they join the caudal vena cava (see Figures 8.3A,B and 39.3). Moderate to marked dilation of the hepatic veins is usually secondary to right-sided cardiac insufficiency, including right-sided volume overload in patients receiving intravenous fluid therapy (see Chapters 7, 20, 26, and 36). Obstruction of the caudal vena cava due to thrombosis, stricture (kinking) or neoplasia can also cause marked distention of the hepatic veins (Kolata et al. 1982; Crowe et al. 1984; Lisciandro et al. 1995; Fine et al. 1998). Hepatic venous distension should be evaluated in conjunction with other clinical signs, and congestion with concurrent ascites (modified transudate) further supports the presence of right-sided heart failure or obstruction of the hepatic caudal vena cava (see also Chapters 7, 20, 26, and 36).

"starry night" appearance caused by decreased parenchymal echogenicity and increased conspicuity of the portal markings (<). Notice how the portal vein walls appear as hyperechoic (white) equal (=) signs, and these portal veins are nondistended. Compare to (A). (C) A dog with cholangiohepatitis is an additional example of a disease process that can have homogeneously hypoechoic (dark) liver changes. Note also the inspissated contents of the gallbladder (GB, gallbladder, outlined). (D) Diffusely hyperechoic (bright) liver in a cat diagnosed with hepatic lipidosis. Note that the liver is diffusely hyperechoic (bright) compared to the falciform fat of the near-field; however, this can be a normal variant in some obese cats (Nicoll et al., 1998). The patient's clinical picture, and cytological and histopatholgical sampling must be considered for an accurate diagnosis. (E) Image of a patient with chronic active hepatitis (CAH). Note the homogeneously hyperechoic (bright) liver demonstrating the variability of ultrasonographic findings in livers with changes in echogenicity emphasizing the need for fine needle aspiration and/or liver biopsy for definitive diagnosis.

## Gallbladder

The gallbladder is easily imaged with ultrasound because it is fluid filled. The gallbladder is generally round to oval; however, it may be bilobed, particularly in cats, and this is generally of no clinical consequence (see Figure 8.4C). Several artifacts are common when scanning the gallbladder, due to its fluid-filled nature, and the novice sonographer should become familiar with these artifacts in order to minimize misinterpretations. These include acoustic enhancement, side-lobe artifact, edge shadowing artifact, and mirror image artifact (when the gallbladder contacts the diaphragm–lung interface).

### Gallbladder Wall

Evaluation of the gallbladder wall is generally easily accomplished due to the contact between the anechoic bile and the more echogenic gallbladder wall and surrounding hepatic parenchyma. The normal gallbladder wall appears as an echogenic (white) line surrounding the luminal contents (see Figure 8.4A–C). Diffuse gallbladder wall thickening may occur with a wide range of conditions such as acute or chronic cholecystitis, hepatitis, canine anaphylaxis (Quantz et al. 2009), right-sided heart failure, iatrogenic volume overload (Nelson et al. 2010), and hypoalbuminemia (Nyland et al. 2002) (see Chapters 7, 20, 26, and 36). Therefore, the finding must be interpreted in conjunction with additional ultrasound findings as well as clinical signs and biochemical alterations (Figure 8.11; see also Figures 7.11, 7.12, 18.22, and 39.6).

Generally, gallbladder wall thickening is nonspecific for any of the above conditions and thickening is typically associated with wall edema with similar sonographic features despite the underlying pathologic cause (see Figure 8.11 and Table 7.5). Most commonly, the gallbladder wall appears diffusely hypoechoic with parallel hyperechoic lines on either side, referred to as a "double rim effect" or "halo effect" (Nyland et al. 2002; Quantz et al. 2009) (see Figures 7.11, 7.12, 18.22, and 39.6). This change needs to be distinguished from small-volume fluid external to the gallbladder, where effusion within the gallbladder fossa can mimic the double rim or halo effect. Focal and/or irregular thickening of the gallbladder wall is less common, and may be consistent with chronic cholecystitis or neoplastic change. A flaccid or undulating gallbladder wall may be consistent with wall rupture and warrants correlation to the index of suspicion for biliary peritonitis as well as clinical and biochemical assessment of the patient.

**Pearl:** In patients in which peritonitis is suspected (ruptured gallbladder, perforated bowel, low-grade bleed), especially in dehydration, fluid resuscitation and reevaluation (serial exam within the next 2–4 hours) with AFAST and an abdominal fluid score often prove most helpful because once rehydrated, peritoneal effusion develops or progresses (higher abdominal fluid score) and sampling for fluid characterization becomes possible.

### Gallbladder Lumen

Evaluation of the luminal gallbladder is typically straightforward due to the ease of scanning through a fluid acoustic window.

- *Biliary sediment or sludge* is common in dogs and can be easily recognized (Figure 8.12). In general, the finding of gravity-dependent, mobile material is an incidental finding but could be an indication of cholestasis. Gallbladder wall abnormalities should be correlated to clinical and/or clinicopathological signs of hepatobiliary disease changes (Tsukagoshi et al. 2012). Luminal sediment is usually hyperechoic (bright) and nonshadowing. When mineralized, the debris may cast a distal acoustic shadow (see Figure 8.12D). Biliary sludge is classified as gravity or nongravity dependent and mobile or consolidated. Nongravity-dependent material may further be classified as adherent or nonadherent to the gallbladder wall.
- *Calcified material or choleliths* can occasionally be observed within the biliary tract and may also be an incidental finding. These gallbladder stones will cause *a* distal acoustic shadow similar to a urolith (Figure 8.13; see also 8.12D).

**Pearl:** When suspicion is raised for intraluminal gallbladder contents, the gallbladder can be reexamined at the end of the study to see if the possible intraluminal pathology has settled into gravity-dependent regions.

- *Gallbladder mucoceles* always have significant implications and their presence should be confirmed by an experienced sonographer as surgery is often indicated. Gallbladder mucoceles have a distinct appearance and, in the mature form, have a stellate

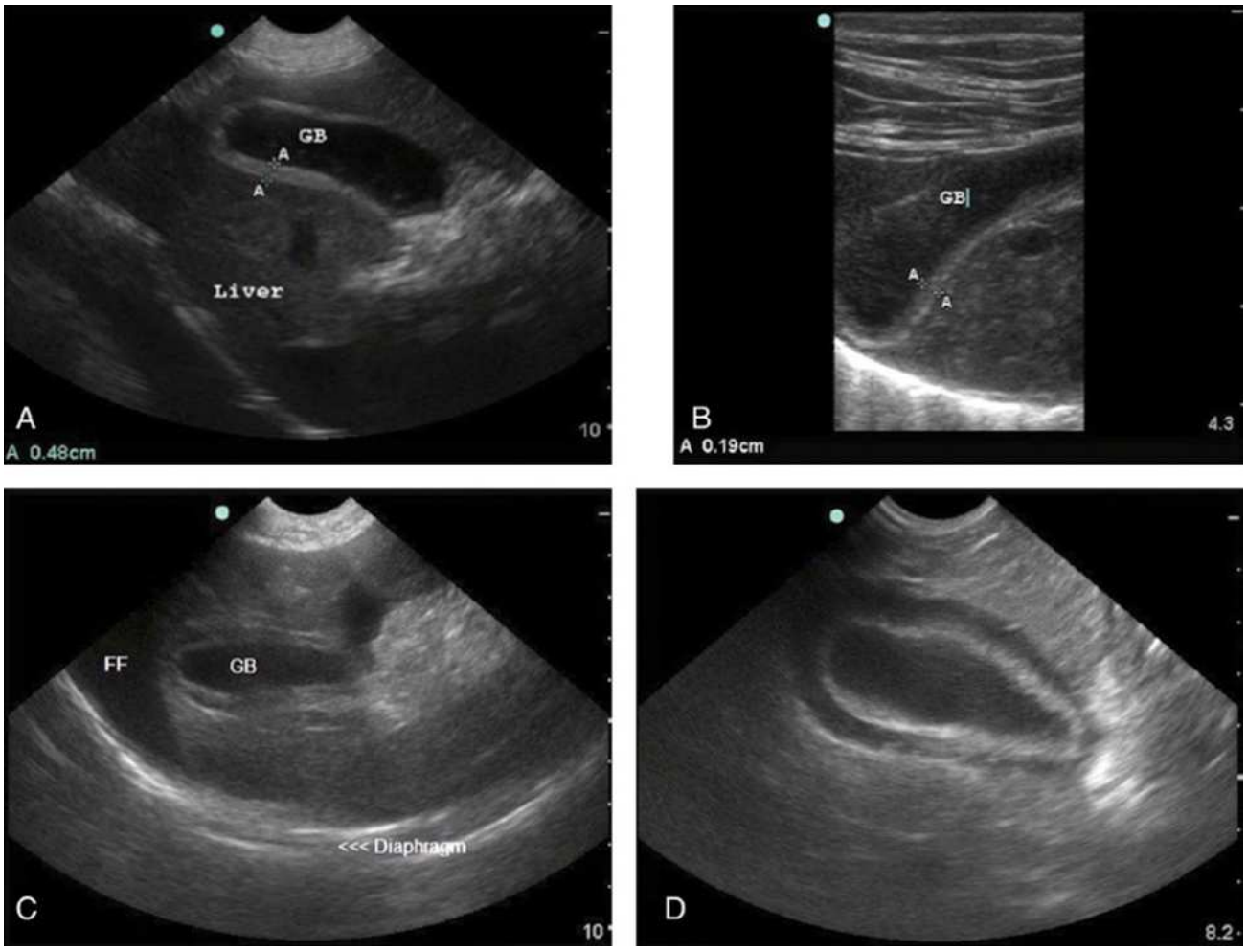


**Figure 8.11.** Gallbladder wall abnormalities. (A) Thickened gallbladder wall seen as a hyperechoic (bright white) rim (marked with calipers) outlining the hypoechoic gallbladder (GB) luminal contents. This has been referred to as a double rim effect, halo effect or halo sign and is caused by several conditions. (B) A mildly thickened gallbladder (GB) wall in a cat similarly outlined with a hyperechoic (bright white) line. The caliper measurement is 1.9 mm in thickness, which is considered thickened in cats (normal <1 mm). C) This image is of a dog seen for acute collapse. Note the halo sign hallmarked by the outer and inner hyperechoic borders of gallbladder wall with central hypoechogenicty (intramural edema), termed sonographic striation (white-black-white sonographic layering). The thickening of the gallbladder wall is consistent with intramural edema. This case illustrates the value of concurrent evaluation of the pleural and pericardial spaces because the cause of collapse (not always known at triage) was obstructive shock secondary to pericardial effusion and cardiac tamponade and not canine anaphylaxis. Emergent pericardiocentesis is indicated as a life-saving procedure. Note the small volume of effusion within the gallbladder fossa and ascites (FF, free fluid). (D) The gallbladder double rim effect or halo effect or halo sign, which can range in its degree of gallbladder wall thickness, has been reported to be supportive of anaphylaxis in dogs. This image depicts an acutely collapsed dog diagnosed with anaphylaxis caused by Hymenoptera (bee) envenomation. The gallbladder double rim or halo effect and wall thickening are severe; however, the sonographic striation (white-black-white) may be similar and more subtle than shown in (C), emphasizing the importance of the Global FAST approach to avoid "satisfaction of search error." In contrast to 8.11C, the emergent treatment for anaphylaxis is rapid intravenous fluid bolus and epinephrine administration, emphasizing the importance of surveying the pleural and pericardial spaces in acutely collapsed dogs for optimizing appropriate therapy (see Chapter 8). Source: (C) and (D) courtesy of Dr Gregory Lisciandro, Hill Country Veterinary Specialists and FASTVet.com, Spicewood, TX.

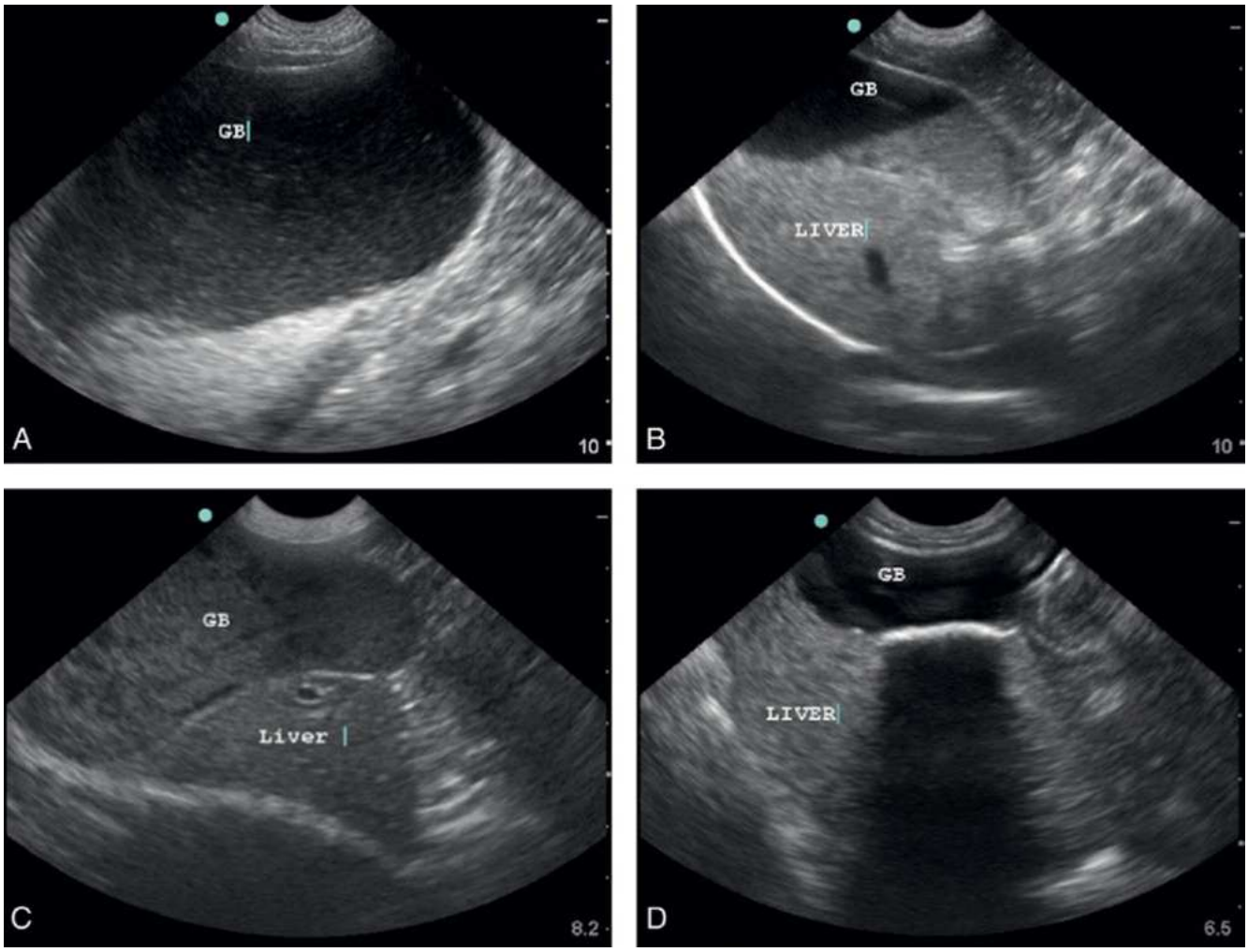


**Figure 8.12.** Degrees of gallbladder sedimentation (sludge). (A) A mild amount of echogenic debris in suspension within the gallbladder lumen with a faint sedimentation line along the gravity-dependent portion in an asymptomatic dog (GB, gallbladder). (B) Moderate echogenic debris settled within the gravity-dependent portion of the gallbladder lumen in an asymptomatic dog. (C) Moderate to severe echogenic debris in suspension, some of which is adherent to the gallbladder wall (this is best appreciated in real time). When differentiating sediment (or a thrombus) from a mass, use color flow Doppler for the presence or absence of blood flow. (D) Shadowing (clean shadowing) debris settled within the gravity-dependent portion of the gallbladder in a dog diagnosed with mineralized biliary sediment, which can be distinguished from a large cholelith by ballottement (agitation) or changes in patient positioning (observing how it moves and resettles into gravity-dependent regions). Images such as these should prompt a complete detailed abdominal ultrasound evaluation of the hepatobiliary tract and liver when there is biochemical or clinical evidence of hepatobiliary disease.

("kiwi fruit-like") appearance caused by fracture lines between mucous collections (Figure 8.14A,B). When immature, there are variable degrees of nonmobile sludge seen between the focal collections of mucus. In addition, the gallbladder wall may be thickened, irregular and hypoechoic or hyperechoic due to wall inflammation, and may lead to wall necrosis and gallbladder rupture (see Figure 8.14C,D). Six ultrasonographic patterns of mucoceles have been described: type 1, immobile echogenic bile; type 2, incomplete stellate pattern; type 3, typical stellate pattern; type 4, kiwi fruit-like pattern and stellate combination; type 5, kiwi fruit-like pattern with residual central echogenic bile; and type 6, kiwi fruit-like pattern. Based on one study, there was no correlation between the ultrasonographic pattern and clinical disease status or gallbladder rupture (Choi et al. 2014).

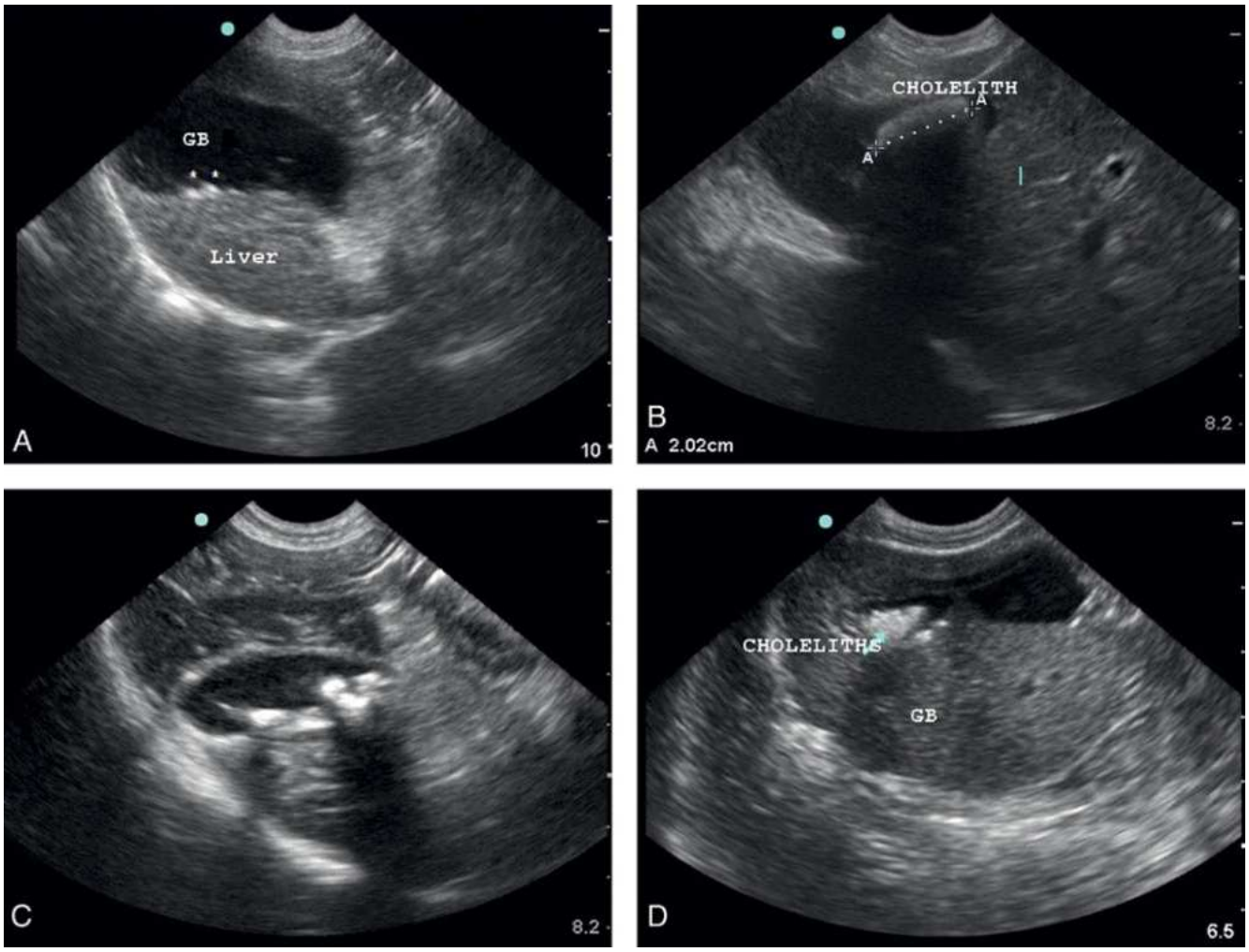


**Figure 8.13.** Gallbladder stones or choleliths. (A) Two small choleliths in a dog (identified by a small asterisk [*] over each cholelith). The finding was incidental. Note the two linear distal "clean" shadows cast by the small solid structures. These hypoechoic (dark) low-amplitude echo regions are caused by the highly attenuating mineralized (cholelith) structures (GB, gallbladder). (B) Large, 2 cm cholelith in a dog with biochemical and clinical evidence of biliary obstruction (marked by calipers). Note the strong (anechoic) distal shadow. A complete detailed abdominal ultrasound evaluation of the biliary tract is indicated by a veterinary radiologist or specialist with advanced ultrasound training to best determine biliary tract obstruction. A good rule of thumb when unable to effectively visualize the gallbladder using ultrasound (likely due to mineralized material or air) is to take an abdominal radiograph. (C) Multiple, clean shadowing choleliths demonstrating the variability of size and number identified by a small asterisk (*) over each cholelith. Such findings can be seen incidentally or in patients with clinical evidence of advanced hepatobiliary obstruction. In cases with signs of severe hepatobiliary disease, the entire biliary tract should be evaluated by an experienced sonographer given the potential need for surgical intervention. (D) Example of a shadowing cholelith in a cat. Note the strong clean acoustic shadowing in the far-field.

## *Biliary System*

Biliary obstruction can be difficult for the novice sonographer to assess. It should be noted that biliary tree distension can mimic other pathology and tortuosity may be a normal variation, especially in cats (Figure 8.15). In cases where biliary obstruction is suspected, it is best to refer for immediate complete detailed abdominal ultrasound to minimize morbidity and the potential for life-threatening biliary peritonitis, especially when gallbladder rupture is suspected (see Figure 8.14C,D). In cats, a bile duct greater than 4 mm is considered to be consistent with extrahepatic biliary obstruction (d'Anjou 2008) (see also Figure 39.4). In cases where peritonitis is clinically suspected or needs to be ruled out, an AFAST with an abdominal fluid score should be performed and used to guide fine needle aspiration of peritoneal effusion for fluid analysis, cytology and culture (see Chapter 43).

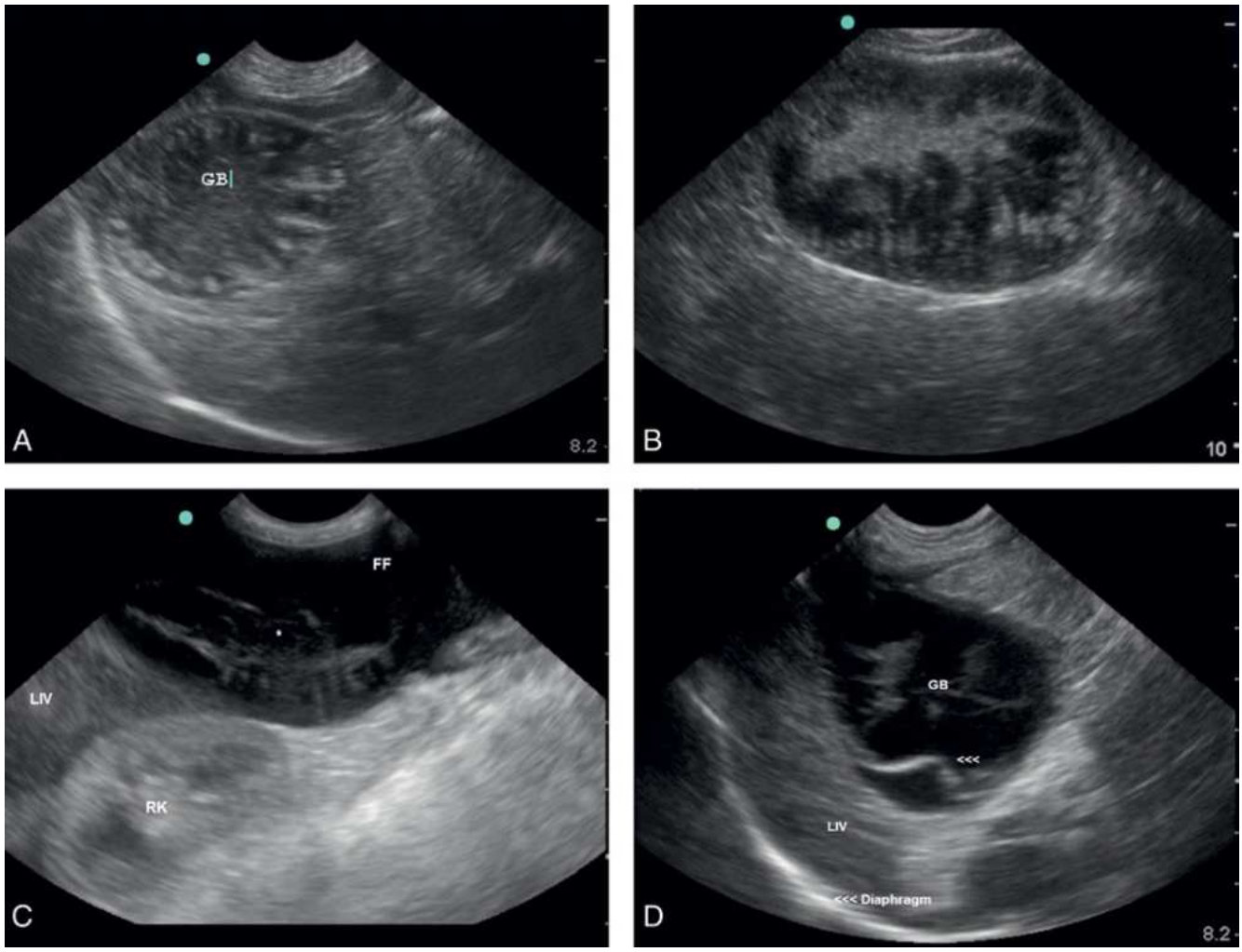


**Figure 8.14.** Gallbladder mucocele. (A) Gallbladder mucocele in a dog. Note the echostructural appearance of the gallbladder lumen (GB, gallbladder). In real time, mucoceles are typically seen as immobile biliary patterns that have a stellate or fine striated character referred to as the "kiwi fruit" appearance. Also note the typical concurrent distension of the gallbladder that is enlarged because of the mucocele. These findings should prompt a complete evaluation of the peritoneal cavity by AFAST and assignment of an abdominal fluid score to search for any evidence of bile peritonitis (free fluid) secondary to gallbladder rupture, and a thorough abdominal ultrasound interrogation of the entire biliary tract by an experienced sonographer. (B) Additional example of a gallbladder mucocele demonstrating the variability of their ultrasonographic appearance. (C) Ruptured gallbladder secondary to mucocele. When a kiwi fruit-like structure (*) is not seen associated with the gallbladder and found in any quadrant of the peritoneal cavity, a mucocele may be eviscerated from the gallbladder and freely floating within the abdomen, as shown in this image. Characterization of the abdominal effusion (anechoic in near-field) as bile peritonitis further supported this clinical suspicion (FF, free fluid; LIV, caudate lobe of liver; RK, right kidney). (D) Ruptured gallbladder secondary to gallbladder mucocele. If the gallbladder is not visualized, or lacks its normal expected curvilinear contour, gallbladder rupture should be suspected. In this image, the dorsal gallbladder wall is deviated from its expected course. Signs of rupture of the gallbladder can also include loculated echogenic fluid within the gallbladder fossa with adjacent hyperechoic reactive mesentery and/or free-floating shadowing cholelith s. Degrees of bile peritonitis (either loculated within the gallbladder fossa or throughout the abdominal cavity) should be present and an AFAST with the assignment of an abdominal fluid score should be performed. Accessible fluid should be aspirated to characterize its nature and direct surgical intervention. Discontinuity of the dorsal aspect of the gallbladder is marked with cursors [<<<]. In cases of gallbladder rupture, emergent exploratory surgery is indicated. Additional, less common rule-outs for lack of visualization of the gallbladder include gallbladder agenesis (which is rare but has been reported) and obstruction of the cystic duct (such as with a mass lesion), that is impairing normal gallbladder and bile duct filling. Moreover, obscured gallbladder visualization may occur with emphysematous cholecystitis or severe cholelithiasis, warranting the use of radiography.

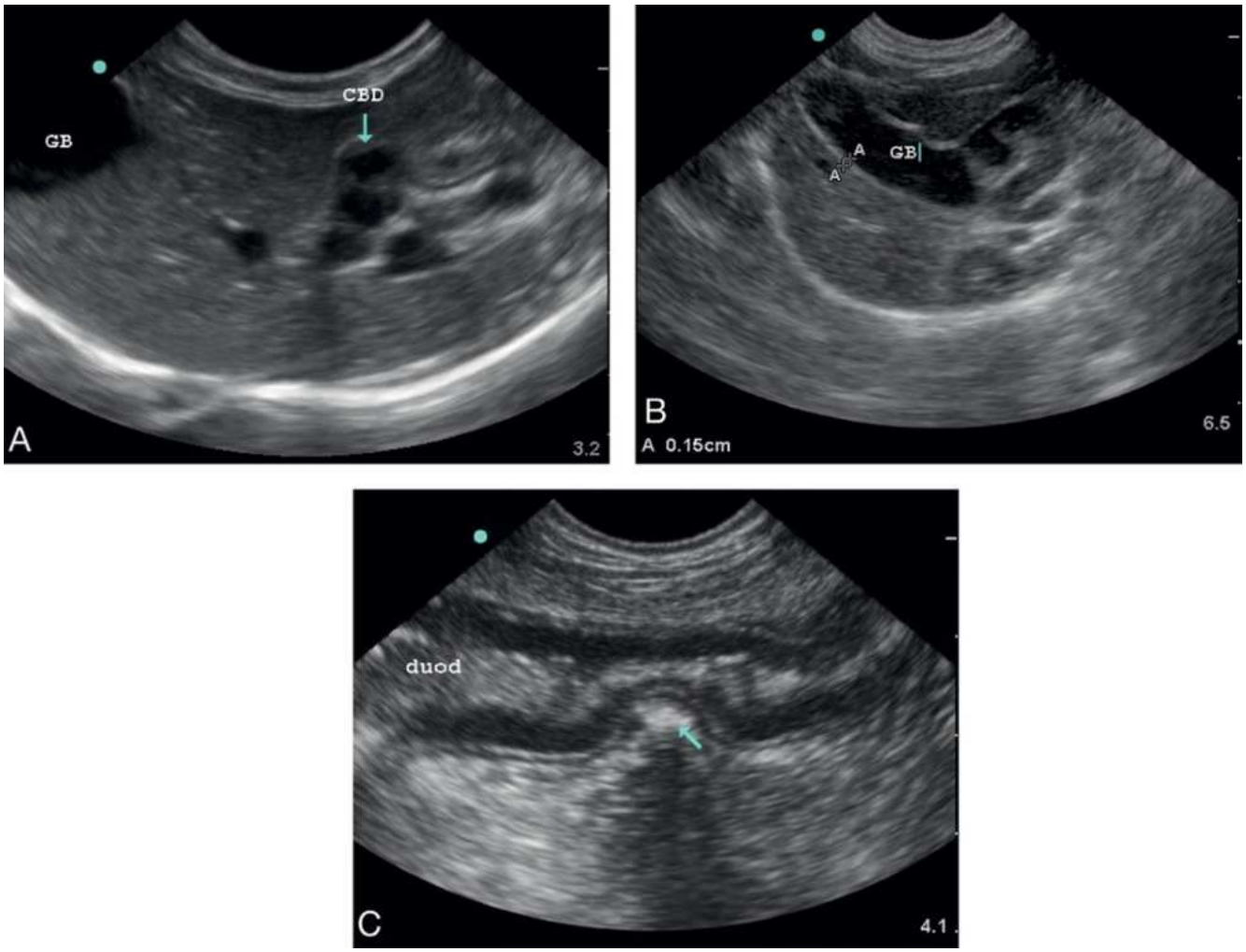


**Figure 8.15.** Biliary tract distension. (A) Cat with bile duct tortuosity which can be a normal variant and common finding. This variant can be easily mistaken for a variety of pathology (nodules, cysts, masses) by the novice or hasty sonographer. Careful correlation with other clinical findings is imperative for an accurate assessment (CBD, common bile duct; GB, gallbladder). (B) A cat with suppurative cholangitis with concurrent pathological tortuosity and dilation of the bile duct. The bile duct is seen ventral to the portal vein and can be distinguished from vessels with color flow Doppler evaluation. In cats, a bile duct greater than 4 mm is considered to be consistent with extrahepatic biliary obstruction. When the biliary duct wall is irregular or unevenly thickened, neoplasia should be a differential. (C) Cholelithiasis can be seen anywhere along the biliary tract and presents challenges for the novice sonographer. This image demonstrates a hyperechoic cholelith at the level of the duodenal papilla in a dog. Note the strong distal acoustic shadow (clean shadow) and lack of normal architecture of the duodenal papilla (duod, duodenum). This example emphasizes the need for a complete detailed abdominal ultrasound evaluation by a veterinary radiologist or specialist with advanced ultrasound training.

# Routine Add-on of AFAST and Abdominal Fluid Scoring System (or Global FAST)

In the authors' experience, it is extremely valuable to perform an AFAST examination with assignment of an abdominal fluid score in either lateral recumbency for the best approach. The positioning of small animals in dorsal recumbency for POCUS abdominal organ exams can obscure small-volume peritoneal effusion and underestimate the volume of effusion present because peritoneal effusion will flow into the less sonographically accessible diaphragmatic recesses. AFAST improves the diagnostic potential of the ultrasound exam by detecting peritoneal effusion. The early detection of abdominal effusion is clinically important and helps direct additional diagnostic recommendations

while avoiding morbidity, complications, and patient mortality in the event the effusion is missed.

The Global FAST approach is used as a screening test to rapidly discriminate between localized and disseminated disease, comorbidities, and complications. Global FAST offers a rapid assessment to survey for pleural and pericardial effusion and cardiac and pulmonary abnormalities, including lung nodules, with minimal restraint upon initial patient triage.

# Pearls and Pitfalls, The Final Say

- *Normal echogenicity rule of thumb*. The spleen (S) is more echogenic (hyperechoic, brighter) than the liver (Li), which is the same or slightly more echogenic (hyperechic, brighter) than the cortex of the kidney (CK). Remember this as S > Li ≥ CK or the mnemonic "SLiCK" for dogs. For the feline, hepatic echogenicity is often compared to the adjacent falciform fat and the feline liver should be isoechoic to slightly hypoechoic to the falciform fat.
- *Benign conditions* may appear ultrasonographically "malignant." Hepatic echogenicity can be difficult to interpret and significant liver disease may still be present even with an unremarkable exam. Ultimately, tissue sampling is necessary for definitive diagnosis of hepatic parenchymal diseases.
- *Be familiar with the possible artifacts* related to the liver and gallbladder. The fluid-filled gallbladder is subject to several artifacts including side-lobe, edge shadowing, and far-field acoustic enhancement. A mirror image artifact of the gallbladder and liver may appear on the thoracic side of the diaphragm due to the air interface between the diaphragm and lung, and can be mistaken for diaphragmatic hernia, pleural and pericardial effusion.
- *The origin of a large midabdominal mass* can sometimes be difficult to determine when the mass contacts multiple origins. In this case, try repositioning the patient from dorsal to lateral recumbency. This will often separate the liver and spleen from one another and help determine the origin of the mass.
- *Always look into the thorax* through the diaphragmatic hepatic interface when evaluating liver to investigate the pleural and pericardial spaces, and the lung surface along the diaphragm.
- *An AFAST and assignment of an abdominal fluid score* should be considered as routine for POCUS liver and gallbladder examinations and the Global FAST approach should be performed so as not to miss comorbidities including intraabdominal bleeding or peritonitis as well as intrathoracic conditions. The AFAST and its fluid scoring system should be used on initial patient evaluation and also to monitor for complications such as hemorrhage or peritonitis after interventional procedures including liver and gallbladder surgeries, percutaneous aspirates and biopsies, and laparoscopic procedures. The Global FAST approach is used for postinterventional intrathoracic complications including aspiration pneumonia (see Chapters 23 and 36).

# Quick Reference of Normals and Rules of Thumb

- Liver assessment is subjective. Edges of the liver lobes should be sharply pointed. Rounded margins of liver lobes and hepatic extension (especially the left lobes) beyond the costal arch suggest enlargement. Abdominal radiography is more reliable for the determination of hepatomegaly.
- *Target lesions*. Single target lesions have a high predictive value for malignancy. When multiple target lesions are seen, the positive predictive value of malignancy increases from 74% to 81% (Cuccovillo and Lamb 2002), and Global FAST is a rapid and quick assessment test for localized versus disseminated disease by surveying the remainder of the abdomen (AFAST), the thorax (TFAST) including heart (TFAST), and lung (Vet BLUE).
- *Normal echogenicity rule of thumb*. The spleen (S) is more echogenic (hyperechoic) than the liver (Li) which is the same or slightly more echogenic (brighter) than the cortex of the kidney (CK), remembered as S > Li ≥ CK or by the mnemonic "SLiCK." For the feline, hepatic echogenicity is often compared to the adjacent falciform fat and the feline liver should be isoechoic to slightly hypoechoic to the falciform fat.
- Gallbladder wall thickness is normally <1 mm in cats and <3 mm in dogs (Hittmair et al. 2001; Spaulding 1993; Quantz et al. 2009).
- Gallbladder luminal content is generally homogeneous anechoic bile although degrees of gallbladder sludge may be considered as clinically irrelevant or may indicate cholestasis based on the patient's clinical profile (Tsukagoshi et al. 2012).
- Being fluid filled, the gallbladder is subject to several artifacts including side-lobe, slice thickness, edge shadowing, and acoustic enhancement in the

far-field; and the liver and gallbladder, being adjacent to the strong soft tissue–air interface between the diaphragm and the aerated lung, are subject to mirror image artifact.

- In cats, tortuosity of the bile duct can be a normal variation; however, a bile duct greater than 4 mm (≥5 mm) is considered to be consistent with extrahepatic biliary obstruction.
- When you are unable to effectively visualize the gallbladder using ultrasound (likely due to mineralized material or air), a good rule of thumb is to add radiography.

# References


Choi J, Kim A, Keh S, et al. 2014. Comparison between ultrasonographic and clinical findings in 43 dogs with gallbladder mucoceles. *Vet Radiol Ultrasound* 55:202–207.

Crowe DT, Lorenz MD, Hardie EM, et al. 1984. Chronic peritoneal effusion due to partial obstruction caudal vena caval obstruction following blunt abdominal trauma: diagnosis and successful surgical management. *J Am Anim Hosp Assoc* 20:231–238.

Cuccovillo A, Lamb CR. 2002. Cellular features of sonographic target lesions of the liver and spleen in 21 dogs and a cat. *Vet Radiol Ultrasound* 43(3):275–278.

d'Anjou MA. 2008. Liver. In: *Atlas of Small Animal Ultrasonography*, edited by Penninck D, D'anjou MA. Ames: Blackwell Publishing, pp 243–247.

Fine DM, Olivier NB, Walshaw R, et al. 1998. Surgical correction of late onset Budd–Chiari-like syndrome in a dog. *J Am Vet Med Assoc* 212(6):835–837.

Hittmair KM, Vielgrader HD, Loupal G. 2001. Ultrasonographic gallbladder wall thickness in cats. *Vet Radiol Ultrasound* 42:149–155.

Kolata RJ, Cornelius LM, Bjorling DE, et al. 1982. Correction of an obstructive lesion of the caudal vena cava in a dog using a temporary intraluminal shunt. *Vet Surg* 11:100–104.

Lisciandro GL, Harvey HJ, Beck KA. 1995. Automobile-induced obstruction of the caudal vena cava in a dog. *J Small Anim Pract* 36(8):368–372.

Nelson NC, Drost WT, Lerche P, et al. 2010. Noninvasive estimation of central venous pressure in anesthetized dogs by measurement of hepatic venous blood flow velocity and abdominal venous diameter. *Vet Radiol Ultrasound* 51(3):313–323.

Nicoll RG, O'Brien RT, Jackson MW. 1998. Qualitative ultrasonography of the liver in obese cats. *Vet Radiol Ultrasound* 39(1):47–50.

Nyland TG, Mattoon JS, Herrgesell EJ, et al. 2002. Liver. In: *Small Animal Diagnostic Ultrasound*, 2nd edition, edited by Nyland TC, Mattoon JS. Philadelphia: WB Saunders, pp 93–127.

Quantz JE, Miles MS, Reed AL, et al. 2009. Elevation of alanine transaminase and gallbladder wall abnormalities as biomarkers of anaphylaxis in canine hypersensitivity patients. *J Vet Emerg Crit Care* 19(6):536–544.

Spaulding KA. 1993. Ultrasound corner: Gallbladder wall thickness. *Vet Radiol Ultrasound* 34:270–272.

Tsukagoshi T, Ohno K, Tsukamoto A, et al. 2012. Decreased gallbladder emptying in dogs with biliary sludge or gallbladder mucocele. *Vet Radiol Ultrasound* 53(1):84–91.


# Further Reading


Harran N, d'Anjou MA, Dunn M, et al. 2011. Gallbladder sludge on ultrasound is predictive of increased liver enzymes and total bilirubin in cats. *Can Vet J* 52(9):999–1003.

Lisciandro GR. 2011. Abdominal and thoracic focused assessment with sonography for trauma, triage and monitoring in small animals. *J Vet Emerg Crit Care* 21(2): 104–122.

Lisciandro GR, Lagutchik MS, Mann KA, et al. 2009. Evaluation of an abdominal fluid scoring system determined using abdominal focused assessment with sonography for trauma in 101 dogs with motor vehicle trauma. *J Vet Emerg Crit Care* 19(5):426–437.

CHAPTER NINE

# POCUS: Spleen

Stephanie C. Lisciandro and Sarah Young

Vetbooks.ir

## Introduction

The POCUS examination of the spleen is a valuable diagnostic tool for guiding clinical care and, with adequate care and awareness, can be effectively performed by a nonradiologist veterinarian. The POCUS spleen examination is not meant to replace a complete detailed abdominal ultrasound study by a veterinarian with advanced training (the veterinary radiologist or internist) but rather serves as a screening test for obvious abnormalities. Ultrasonographic findings involving the spleen may be subjective and nonspecific, including splenic size and generalized changes in echogenicity. Additionally, the frequent close anatomical contact of the spleen and liver can make it difficult to differentiate the origin of a mass, particularly for a less experienced sonographer.

As stated in Chapter 8, a concurrent AFAST examination should be performed with any of the POCUS abdominal organ examinations to rule out intraabdominal, retroperitoneal, pleural and pericardial effusions, and in the case of the POCUS spleen examination, to rule out splenic hemorrhage. The AFAST not only detects free peritoneal fluid but also semiquantitates its volume using its abdominal fluid scoring system and assigning an abdominal fluid score (see Chapter 6). The abdominal fluid score helps predict the degree of anticipated anemia in cases of hemoabdomen (Lisciandro 2011; Lisciandro et al. 2009). Global FAST is an even better approach to survey for pleural and pericardial effusion, cardiac and pulmonary abnormalities, and patient volume status. Moreover, Global FAST is used as a screening test to rapidly discriminate between localized versus disseminated disease, comorbidities, and complications, which may be especially helpful in hemoabdomen cases.

### What the POCUS Spleen Can Do

- Identify focal or multifocal splenic masses or nodules.
- Identify parenchymal changes by screening for changes in echogenicity associated with diffuse splenic diseases.
- Identify splenic infarction and thrombosis.
- Help the clinician to recognize splenic torsion.
- These last three goals are inherently more difficult for the novice sonographer and abnormalities should prompt referral for a complete detailed abdominal ultrasound examination.

### What the POCUS Spleen Cannot Do

- Differentiate benign from malignant splenic masses. The Global FAST approach is a rapid add-on assessment screening test for localized versus disseminated disease through surveying the abdomen (AFAST), the thorax (TFAST) including heart (TFAST), and lung (Vet BLUE) as well as for detecting other comorbidities.
- Definitively diagnose diffuse and localized splenic conditions based on echogenicity.
- Reliably determine splenic size (large or small) in dogs (more reliable for size in cats).

### Indications

- Cranial organomegaly or pendulous abdomen.
- Abdominal pain.
- Abdominal trauma.
- Hematological disorders such as anemia or thrombocytopenia.
- Generalized lymphadenopathy.
- Episodes of collapse, lethargy or vomiting.

*Point-of-Care Ultrasound Techniques for the Small Animal Practitioner*, Second Edition. Edited by Gregory R. Lisciandro.
© 2021 John Wiley & Sons, Inc. Published 2021 by John Wiley & Sons, Inc.
Companion website: www.wiley.com/go/lisciandro/ultrasound2

### Objectives

- Recognize splenic masses (single, multifocal).
- Recognize regional and diffuse changes in splenic echogenicity.
- Recognize splenic venous congestion, thrombosis, and infarction.
- Recognize splenic torsion.

# Patient Positioning and Probe Selection

A curvilinear (microconvex) probe is most frequently used to image the spleen, and the MHz is adjusted for the size of the animal. Smaller dogs and cats are generally imaged using higher frequencies of 7.5–10 MHz (less penetration, better detail) and large dogs are generally imaged using lower frequencies such as 5 MHz (deeper penetration, less detail). In small dogs and cats, a linear probe may also be used in order to maximize image quality (due to the higher resolution) when greater penetration depth is not of concern.

Patients are most commonly imaged in dorsal recumbency. In large dogs, however, the cranial aspect of the spleen is often located under the ribcage on the left side. Repositioning these patients into right lateral recumbency allows visualization of the cranial aspect or head of the spleen using a left intercostal approach (Hecht 2008). The authors recommend performing a Global FAST to screen for any intrathoracic problems including pleural and pericardial effusion, cardiac and pulmonary conditions, and abnormal volume status that may pose patient risk *before* moving the patient into dorsal recumbency.

# How to Perform the POCUS Spleen

The patient is placed in dorsal recumbency, the abdomen is shaved, and acoustic coupling gel is applied for best visualization. Although image quality will be diminished, ample application of 70% isopropyl alcohol to haired skin can be utilized in an emergency situation. The spleen is located caudal to the stomach on the patient's left side and can provide an acoustic window for the left kidney (see also Figures 6.18, 16.3, 16.4, 16.5). The spleen is identified by its hyperechoic (bright white) capsule and blood supply splitting its capsule, unlike the liver. Spleen position and size vary between patients and with the degree of gastric filling. The entire length of the spleen is generally not visualized in one acoustic window and so its entirety must be traced cranially to the head of the spleen and caudally to its tail.

The position of the spleen may vary between patients. The head or cranial aspect of the spleen is generally located on the left side caudal to the last rib. In large dogs, it may be located under the ribcage and therefore, repositioning into right lateral recumbency with a left intercostal approach may be necessary. The spleen is then traced caudally toward its hilus where the splenic vein is imaged and seen branching in a "Y" configuration, referred to by some sonographers as the "whale tail" shaped like the tail fluke (Figure 9.1; see also Figures 39.8 and 39.9). Splenic arteries are usually not visualized (Hecht 2008). Evaluation of the spleen continues as the sonographer follows the spleen distally along the left side of the abdomen to examine the caudal aspect of the spleen to its tail so that the entire organ has been examined. Remember that the spleen is anchored at the head by its short gastric vessels along the greater curvature of the stomach but has a relatively mobile tail. In some patients, the tail of the spleen may be located medial and to the right side of the patient instead of the left. Several sweeps along the length and width of the spleen may be necessary for a thorough interrogation, especially in animals with splenomegaly.

**Pearl:** Identify the spleen by its hyperechoic (bright white) capsule and blood supply splitting its capsule, unlike the liver.

# Ultrasonographic Findings in a Normal Spleen

When assessing the spleen, systematic evaluation should include the following four features: estimation of size (subjective), evaluation of changes in parenchymal echogenicity, interrogation for mass lesions and nodules, and assessment of splenic vasculature.

### Size and Shape

The general contour of the spleen is tongue-shaped and when viewed adjacent to the left kidney, it appears more triangular (than flat) in cross-sectional views. Since the size of the spleen can vary in normal animals, estimation of size is generally subjective in dogs except in cases of marked splenomegaly. In cats, splenomegaly

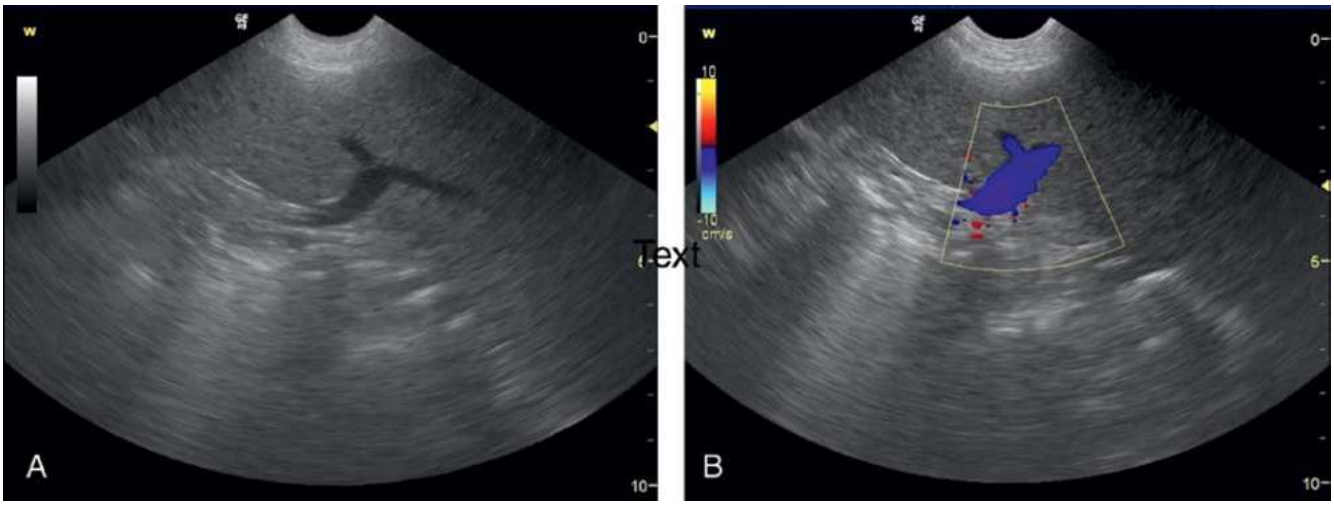


**Figure 9.1.** Normal splenic hilus. (A) The "Y" shape of the splenic vein, also referred to as the whale tail (mimics tail fluke of the whale), as it branches at the hilus is helpful for identifying the spleen and distinguishing it from the liver. (B) Color flow Doppler may be used to assess blood flow and rule out splenic venous thrombosis and splenic torsion when suspected.

**Figure 9.2.** Subjective size evaluation of the spleen. Splenic enlargement as evidenced by its folding. The "Y"-shaped splenic veins departing from its hilus are helpful for identification and distinguishing it from the liver. The spleen here has a homogeneous normal echotexture. Source: Courtesy of Dr Gregory Lisciandro, DVM, Hill Country Veterinary Specialists and FASTVet.com, Spicewood, TX.

is almost always due to pathology and should prompt further evaluation. Spleen thickness greater than 10 mm or a folded spleen invariably indicates splenomegaly in the feline species (Hecht 2008; Reese et al. 2013) (Figure 9.2; see also Figure 39.9). Benign splenomegaly is uncommon in cats and if present, additional evaluation is warranted.

**Pearl:** Moderate splenomegaly occurs in dogs with many forms of sedation or anesthesia (Hecht 2008; Reese et al. 2013); thus, the effects of sedation and anesthesia must be considered.

## *Echogenicity*

The echogenicity of the splenic parenchyma should be evaluated for diffuse and focal changes. Normal splenic parenchyma is homogeneous in appearance with fine echotexture, and its thin hyperechoic (bright white) capsule may be apparent on long-axis (sagittal) views. Spleen parenchyma is generally mildly to moderately hyperechoic (brighter) to normal liver parenchyma (Figure 9.3A,B), and significantly hyperechoic (brighter) to normal renal cortex (Hecht 2008) (see Figure 9.3C,D).

**Pearl**: Remember the mnemonic "SLiCK" regarding relative normal echogenicity of spleen, liver and kidney cortex. Spleen (S) is hyperechoic (brighter) to liver (Li) which is slightly hyperechoic (brighter) or isoechoic (same shades of gray) to the cortex of the kidney (CK). For the feline, hepatic echogenicity is often compared to the adjacent falciform fat and the feline liver should be isoechoic to slightly hypoechoic to the falciform fat.

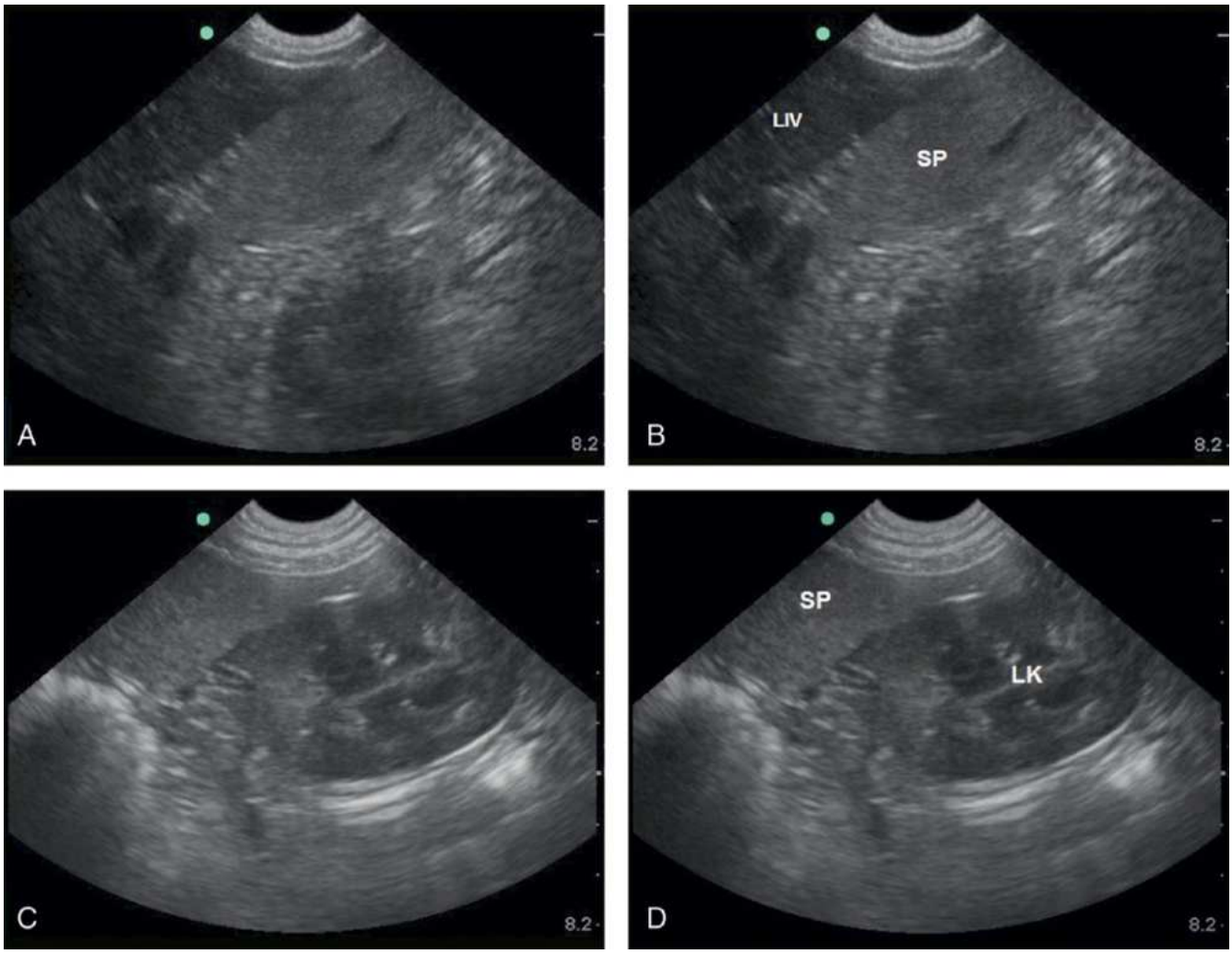


**Figure 9.3.** Echogenicity of spleen relative to liver and cortex of kidney. (A) Comparison of the echogenicity of spleen to the liver, unlabeled. (B) Same as (A) but labeled as liver (LIV) and spleen (SP). (C) Comparison of echogenicity of the spleen to the cortex of the left kidney, unlabeled. (D) Same as (C) but labeled as spleen (SP) and left kidney (LK).

### *Presence of Masses and Nodules*

Normal splenic parenchyma is homogeneous with fine echotexture and free of focal lesions (Figure 9.4).

### *Vasculature*

Splenic veins exit the spleen at the centrally located hilus and merge into the single large splenic vein deep to the spleen, which can be traced transversely across the abdomen to its junction with the portal vein. Color flow Doppler evaluation, if available, allows for additional evaluation of the splenic vein and its branches (see Figures 9.1AB, 9.2 and 39.8).

**Pearl:** The splenic capsule is hyperechoic (bright white) and its vessels cross the splenic capsule. In contrast, the hepatic capsule is not sonographically apparent and its vessels do not cross the hepatic capsule. This anatomical difference can be used to distinguish spleen from liver.

## Clinical Significance and Implications of Abnormal Findings

Abnormal findings that may be appreciated during the POCUS spleen examination include the four features

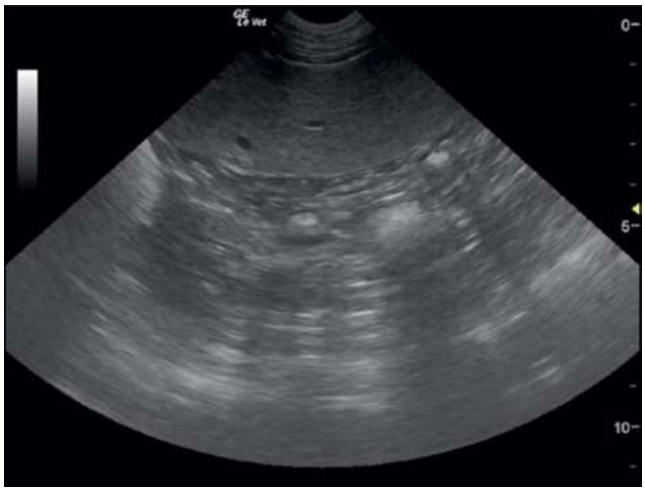

**Figure 9.4.** Normal appearance of spleen. Spleen by itself showing its homogeneous nature with normal echogenicity. The anechoic areas (circular) are normal vasculature and readily appreciated in real time evidenced by their branching. The splenic capsule is recognized as a hyperechoic (bright white) line.

mentioned above: subjective evaluation of size (splenomegaly), changes in echogenicity (evaluation for diffuse parenchyma disorders), presence of mass lesions (solitary and multifocal mass lesions), and assessment of vasculature (thrombosis and torsion).

**Pearl:** The four key features to evaluate with the focused spleen examination are size, echogenicity, presence of nodules or masses and assessment of the vasculature.

## Splenic Size

Splenomegaly is usually a subjective assessment except in cases of severe enlargement. Ultrasonographic clues that help in discriminating between normal size and splenomegaly include the following.

- *Marked enlargement* may result in the distal tip of the spleen folding back on itself (Figure 9.5,B) and therefore the distal tip or tail is visualized medial to the left kidney (see Figure 9.5C,D). In addition, the markedly enlarged spleen may extend caudally and come in contact with a small to medium-sized urinary bladder (Figure 9.6). In cats, a folded spleen supports splenomegaly (Hecht 2008), as does a spleen thicker than 10 mm (Reese et al. 2013) (see Figure 9.9B).

**Pearl:** In cats a folded spleen invariably indicates splenomegaly which is always abnormal in felines; splenic thickness is normally <10 mm in cats.

- *Marked splenomegaly* most commonly occurs with neoplasia (lymphosarcoma), other infiltrative processes (fungal infection), acute inflammation, or in some cases of immune-mediated hemolytic anemia. Extramedullary hematopoiesis can cause marked splenomegaly. Marked splenomegaly may also occur in animals with splenic torsion (see additional description below) (see Figure 9.15).

**Pearl:** With the exception of splenic torsion (often urgent surgical disease), fine needle biopsy with cytological evaluation is indicated in cases of moderate to marked splenomegaly.

When splenomegaly is confidently ascertained, correlation between size and echogencity can be clinically helpful as follows.

- Mild to moderate splenomegaly *with normal echogenicity and architecture* is most commonly associated with sedation, extramedullary hematopoiesis, antigenic stimulation (acute inflammatory and infectious diseases), and passive congestion (Figures 9.7 and 9.8A,B). However, diffuse infiltrative processes including lymphoma and mast cell tumor can also have normal echogenicity.
- Splenomegaly *with mild to moderate hypoechogenicity* may be associated with nodular hyperplasia or extramedullary hematopoiesis, passive congestion, inflammation, infection (fungal, bacterial, rickettsial), immune-mediated diseases, and lymphosarcoma. Comparison with adjacent liver and the renal cortex can help when assessing echogenicity (Figure 9.9; see also Figure 9.8; see normal relative echogenicity in Figure 9.3).

**Pearl:** With the exception of splenic torsion, fine needle biopsy with cytological evaluation is indicated in cases of moderate to marked splenomegaly.

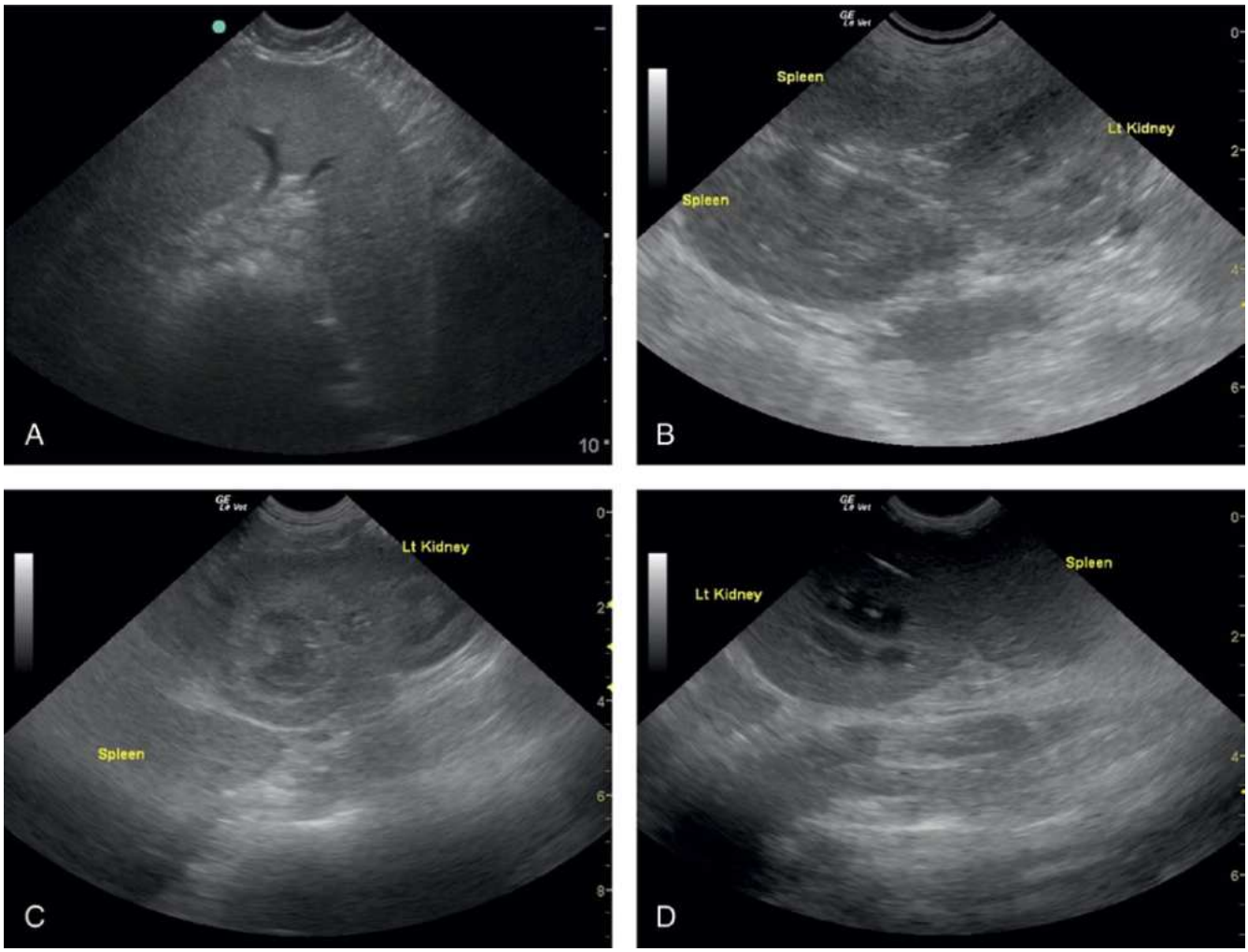


**Figure 9.5.** Splenomegaly. (A) Splenomegaly or splenic enlargement as evidenced by its folding. The "Y"-shaped splenic veins departing from its hilus are helpful for identification and distinguishing it from the liver. The spleen here has a homogeneous normal echotexture. (B) Another example of an enlarged folded spleen enveloping the left kidney (Lt Kidney). (C) Splenic enlargement similar to (B) being folded and medial to the left kidney with comparative normal echogenicity. The spleen is hyperechoic (brighter) when compared to the cortex of the left kidney. (D) Similar to (C), the spleen extends *caudal* to the left kidney.

## *Splenic Mass Lesions*

### Masses and Nodules

The identification of nodules or mass lesions within the splenic parenchyma is the most basic of the four features of the POCUS spleen (size, echogenicity, nodules, vasculature). It is important to recognize, however, that ultrasound does not allow differentiation between benign and malignant processes, unless advanced contrast-enhanced ultrasound studies are performed (limited availability) that still may not prove helpful (Fife et al. 2004; Rossi et al. 2008). The sonographer should keep in mind that according to one study, benign splenic masses are more common than malignant splenic masses in dogs (Fife et al. 2004).

- *Nodular hyperplasia*. Nodules associated with nodular hyperplasia or extramedullary hematopoiesis may be variable in echogenicity (hyperechoic, hypoechoic, isoechoic or mixed echogenicity) when compared to normal splenic parenchyma (Figure 9.10A,B). In addition, nodular hyperplasia may be associated with a mildly irregular splenic capsule without associated nodular lesions. This change is commonly seen in older dogs.

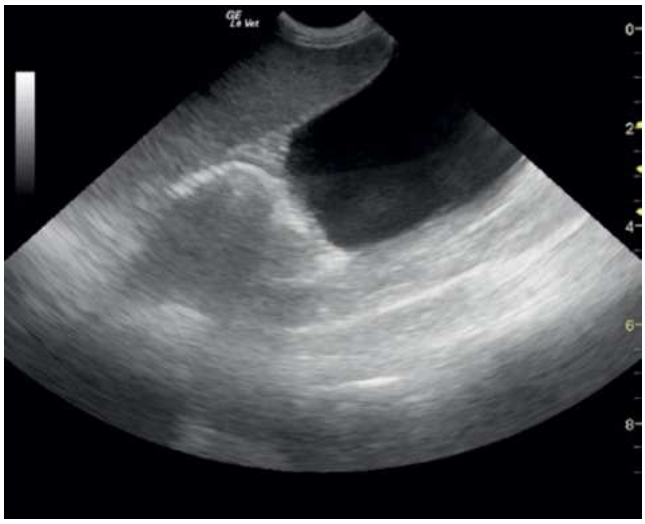

**Figure 9.6.** Splenomegaly with spleen extending to urinary bladder. This severely enlarged spleen extends caudally to the fluid-filled (anechoic) urinary bladder. Although it appears relatively normal regarding its echotexture and echogenicity, this dog had splenic lymphosarcoma diagnosed by percutaneous needle biopsy. Compare to Figure 9.14 showing the ultrasonographic variability of splenic lymphosarcoma (LSA).

**Figure 9.7.** Splenomegaly with normal echogenicity. Infectious diseases can cause splenomegaly with variable changes in echogenicity. Shown here is an image from a dog with ehrlichiosis.

**Pearl:** In cases with nodular lesions, it may be difficult to differentiate changes associated with nodular hyperplasia from other processes without further testing (cytology or histopathology).

- *Myelolipoma*. Myelolipomas are incidental findings in older dogs and are identified as discrete, strongly hyperechoic (bright) and frequently irregularly shaped nodules most often located near the hilus or associated with the parenchymal vessels. Less commonly, they are smooth in shape and buried within the splenic parenchyma. They are generally small in size but are occasionally quite large and can also be seen in cats. Myelolipomas are typically of no clinical consequence (incidental finding) (see Figure 9.10C,D).
- *Hematoma*. Abdominal trauma may be associated with hematomas and splenic parenchymal injury (Figure 9.11). Hematomas (benign masses) may be variable in appearance but initially are generally anechoic to hypoechoic (darker) when compared to normal splenic parenchyma. As the blood within the hematoma forms a clot, the lesion may become more isoechoic or hyperechoic to normal parenchyma. As the clot retracts, the lesion may again become hypoechoic. Anechoic fluid may form around the clot and appear as a cyst-like lesion. These factors may make hematomas difficult to distinguish from other mass lesions, including neoplasia.

**Pearl:** Fine needle biopsy of hematomas generally yields nonspecific cytological results and therefore the absence of neoplastic cells on cytology does not rule out neoplasia. A more definitive diagnosis of hematoma is obtained by splenectomy and histopathological evaluation; however, even this may be complicated by a large hematoma associated with a smaller malignant mass, resulting in a possible misdiagnosis.

- *Abscess*. Splenic abscesses are uncommon and usually cannot be distinguished from other processes that produce nodular or mass lesions. The appearance may be variable with well-defined or indistinct margins and variable echogenicity. Abscesses most commonly appear as hypoechoic lesions, which may have cystic components or mixed echogenicity. A more conclusive finding for an abscess (in contrast to neoplastic processes) is the presence of gas (due to gas-forming bacteria) within the lesion. This appears as focal areas of hyperechogenicity with distal edge shadowing (see Chapter 3).

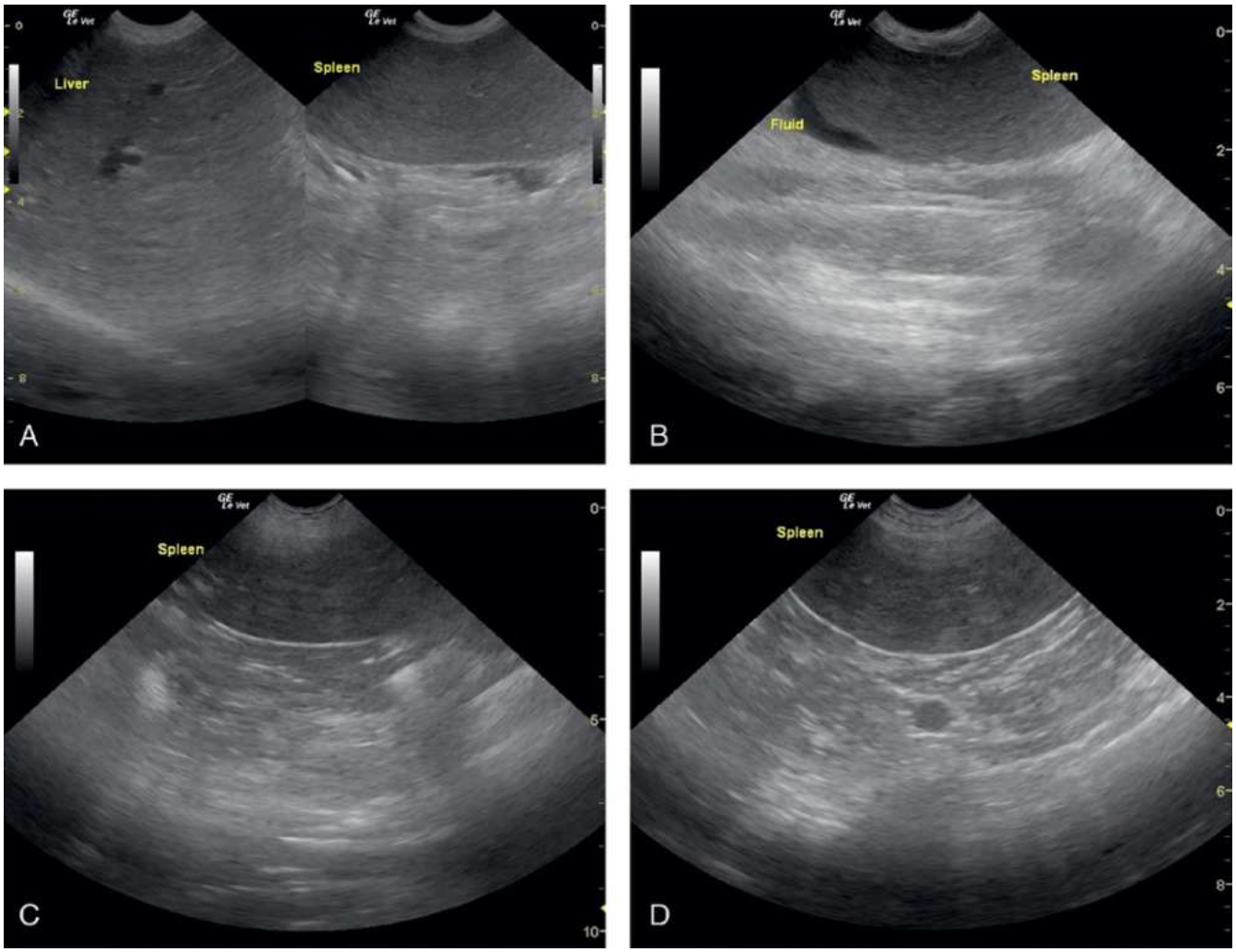


**Figure 9.8.** Splenomegaly with splenic hyperechogenicity (brighter than normal) and hypoechogenicity (darker than normal). (A) Relatively normal homogeneous echotexture in a hyperechoic (brighter than the liver) spleen. The diagnosis by percutaneous needle biopsy was lymphosarcoma (LSA). (B) Another relatively unremarkable hyperechoic spleen in a cat diagnosed with splenic LSA by percutaneous needle biopsy. Note an anechoic triangle of free fluid (Fluid). (C,D) Mottled echotexture with hypoechogenicity (darker) in spleens representing nodular hyperplasia diagnosed by percutaneous needle biopsy.

**Pearl:** Fine needle aspiration/needle biopsy with cytology and bacterial culture and sensitivity is helpful in confirming a splenic abscess diagnosis. Be aware that necrotic centers of neoplastic lesions can be mistaken for abscesses, and so diagnosis should always be in conjunction with clinical findings and in some cases a definitive diagnosis may only be gained with splenectomy and histopathological evaluation.

### Neoplasia

Splenic neoplastic lesions can have a wide range of ultrasonographic changes. As emphasized above, it is not possible to distinguish between benign and malignant lesions based on ultrasonographic appearance alone. The most common types of splenic neoplasia found in dogs are hemangiosarcoma and lymphosarcoma (Hecht 2008) but other primary and metastatic tumors are possible.

- *Hemangiosarcoma* (HSA) generally appears as complex mass lesions with mixed echogenicity and cavitations that distort the splenic capsule (Figure 9.12). HSA of the spleen is often associated with acute or chronic hemorrhage, and animals with ruptured splenic masses causing hemoabdomen have a higher likelihood of malignancy (hemangiosarcoma) (Hammond and Pesillo-Crosby 2008). Definitive preoperative

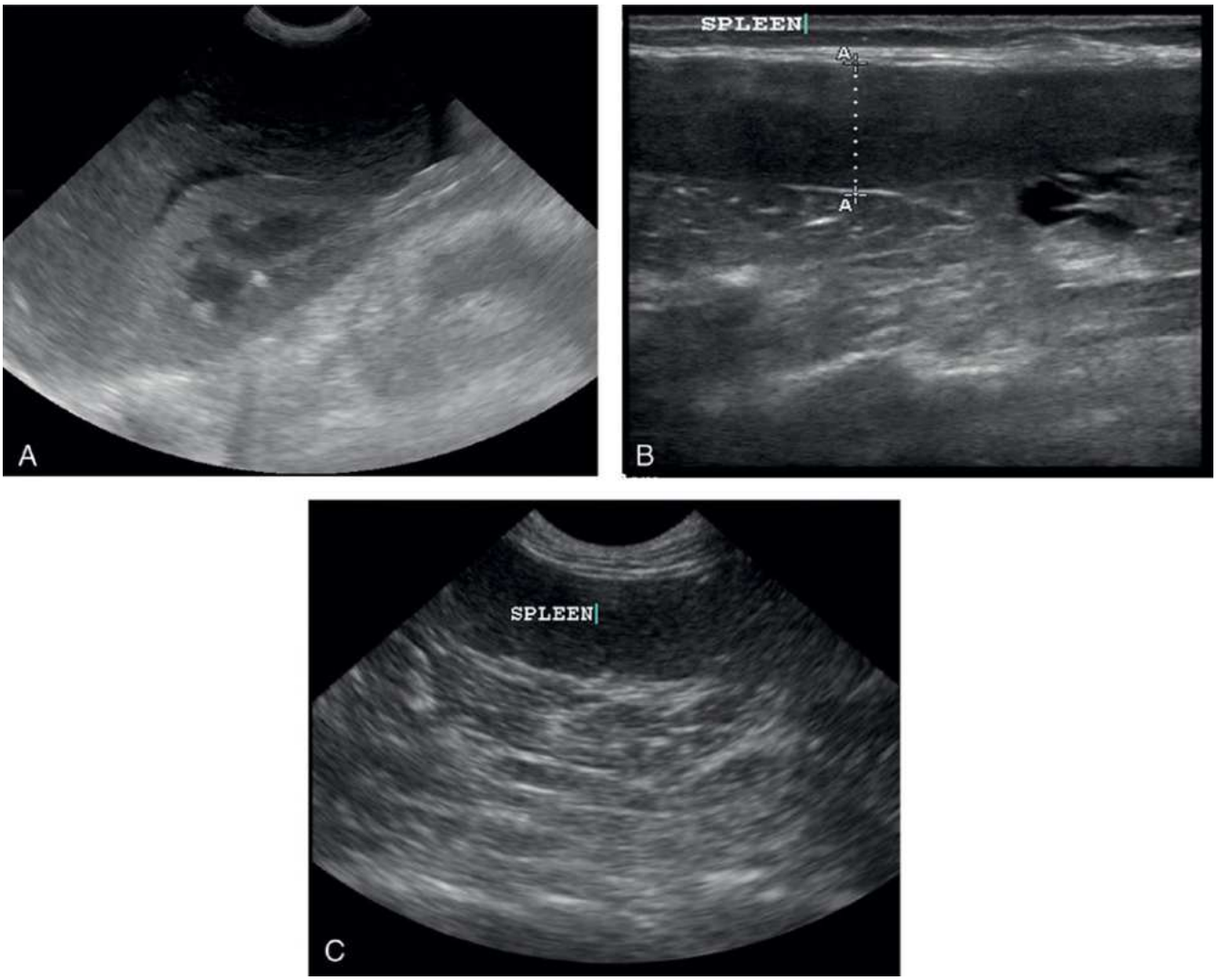


**Figure 9.9.** Splenomegaly with splenic hypoechogenicity (darker than normal). (A) Comparative echogenicity of the spleen to the cortex of the left kidney. Suppurative splenitis was diagnosed by percutaneous needle biopsy. (B) Splenomegaly determined by a splenic thickness that was >10 mm (measured by calipers marked "A") with concurrent hypoechogenicity (darker) in a cat. Histoplasmosis was diagnosed by percutaneous needle biopsy. (C) Diffuse parenchymal changes not much different from (A) and (B) diagnosed by percutaneous needle biopsy as mast cell tumor. These examples illustrate that clinical diagnosis cannot be made based on ultrasonographic appearance alone.

diagnosis of HSA is challenging, however, since rupture of splenic masses with resultant hemoabdomen can occur with both benign and malignant processes, and since benign hematomas and HSA can have similar ultrasonographic appearances. The presence of suspected metastatic nodules elsewhere in the abdomen or thorax increases the index of suspicion for malignancy, but a definitive diagnosis is often not made without splenectomy and histopathology, and even then can be complicated by an associated hematoma.

**Pearl:** Staging of HSA may be assisted by performing a Global FAST to evaluate for hemoabdomen (AFAST), pericardial effusion (and right atrial mass) and Vet BLUE lung ultrasound for pulmonary metastasis.

- *Metastatic lesions* may be hypoechoic or hyperechoic in nature and are more likely to have a "target" appearance consisting of hypoechoic margins with a relatively hyperechoic center (Figure 9.13). Single target lesions have a high

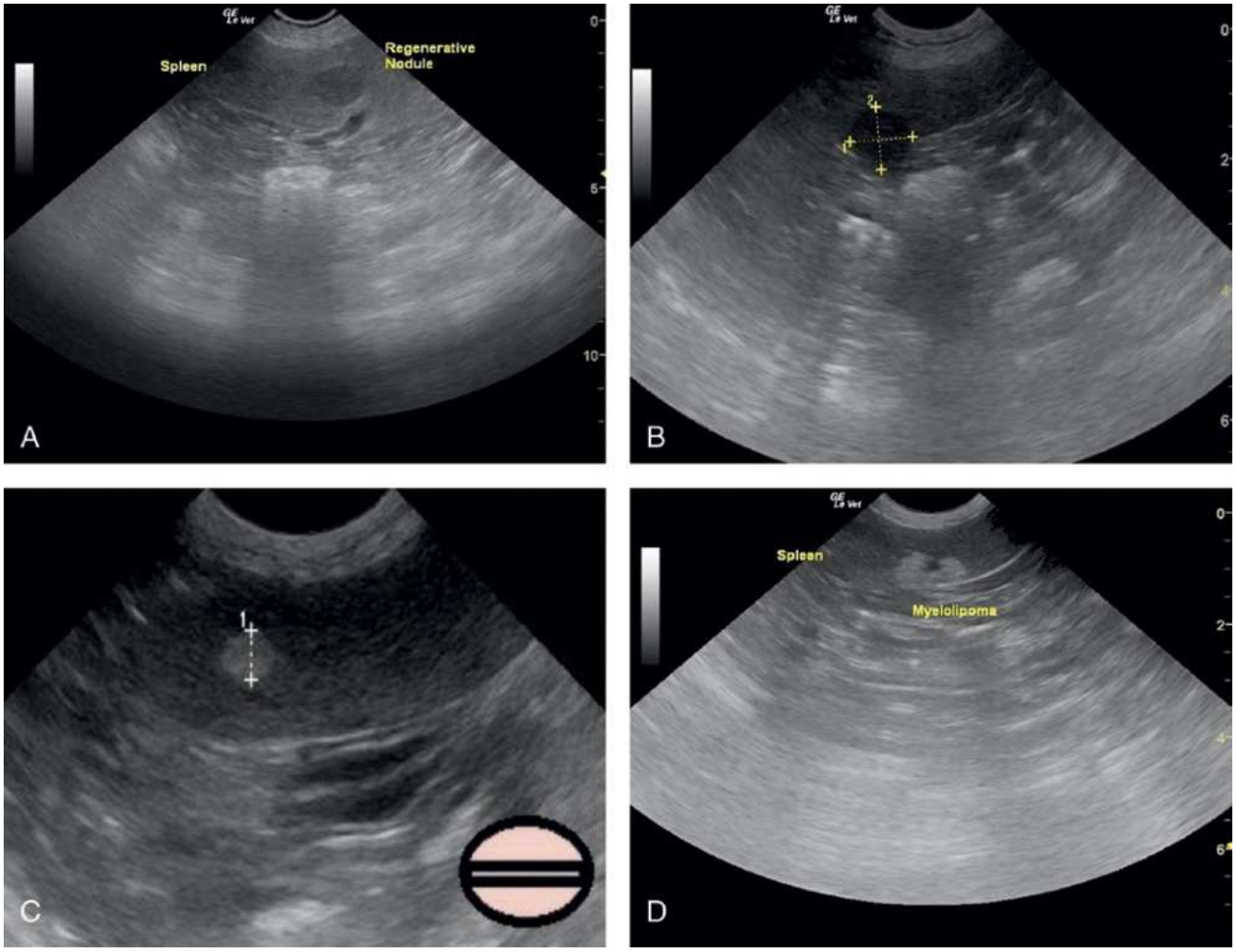


**Figure 9.10.** Splenic nodular hyperplasia and myelolipomas. (A–C) Examples of nodular hyperplasia characterized by homogeneous echogenicity of the mass which may be hyper- or hypoechoic relative to the adjacent splenic parenchyma. Importantly, note that in contrast to fluid-filled structures that have acoustic shadowing artifact extending through their far-field, these solid nodules do not. Also, in the distal field is a transverse image of normal small bowel that appears like a "hamburger" (colored cartoon to the lower right of the small bowel). (D) An example of a myelolipoma, a common incidental finding in older dogs, often hyperechoic (bright) discreet nodules located near the splenic hilus but may also be located parenchymally.

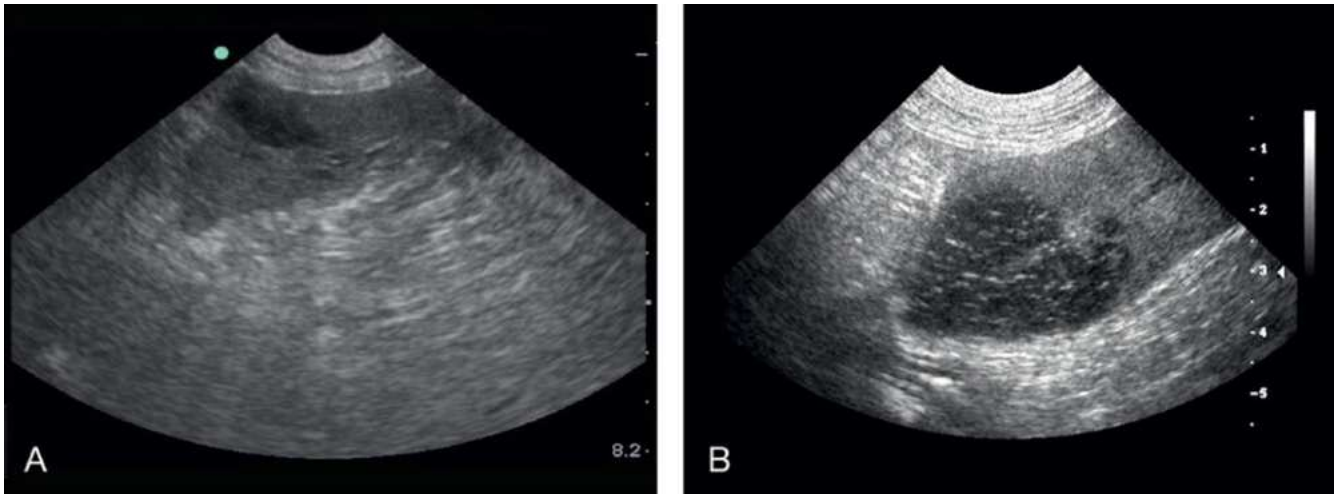


**Figure 9.11.** Splenic hematomas and infarcts. (A) The spleen has a hypoechoic (dark) area within its parenchyma that represents an acute hematoma in a young dog that had just incurred blunt automobile trauma. The splenic finding was observed during an AFAST exam. (B) The spleen has a hypoechoic area within its parenchyma that represents an infarcted region seen in a bluntly traumatized puppy. Source: (B) courtesy of Dr Autumn Davidson and Tomas Baker, University of California, Davis, CA.

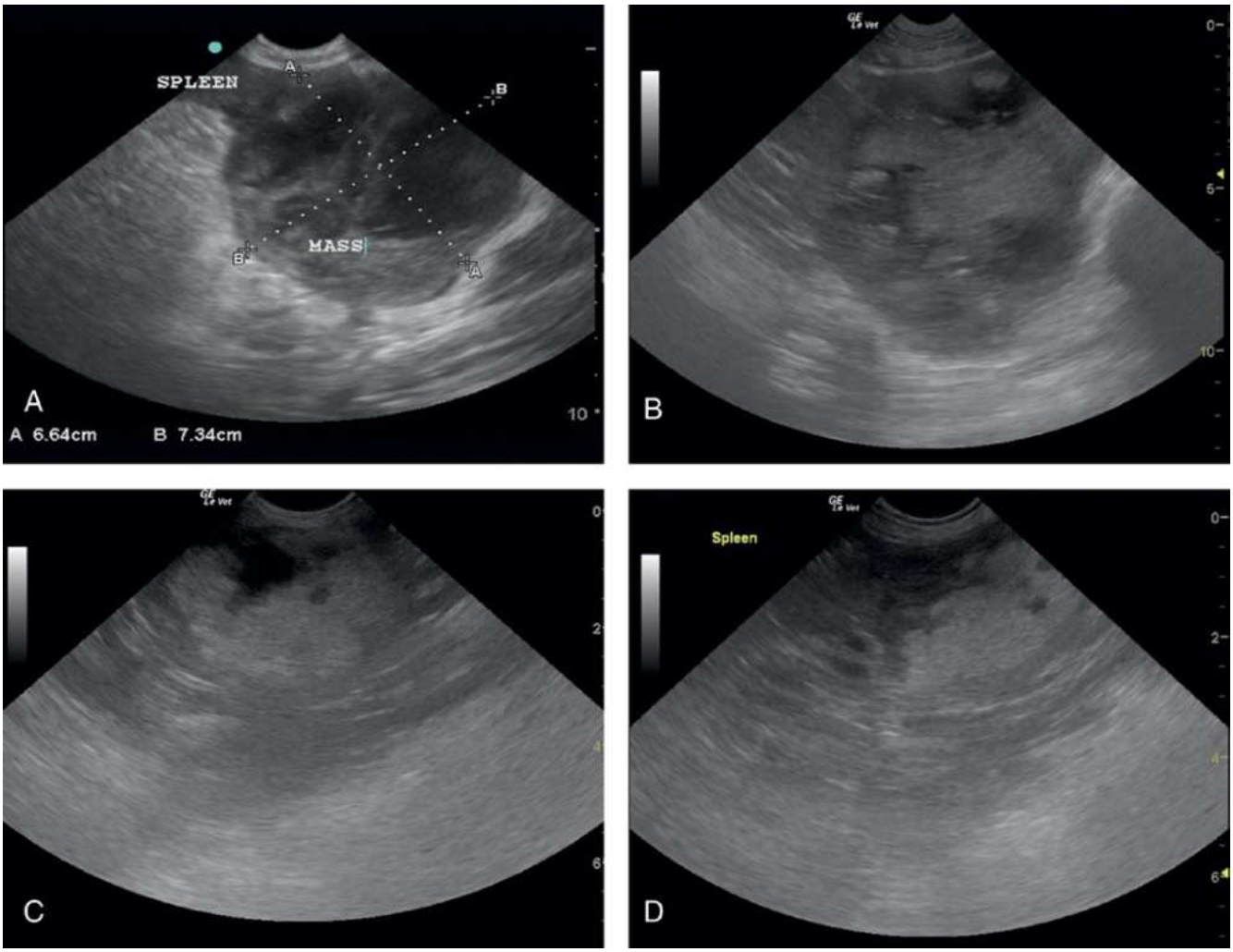


**Figure 9.12.** Splenic hemangiosarcoma (HSA) and its variability. (A) A splenic mass that was diagnosed as HSA by splenectomy and histopathological evaluation. Note normal spleen in the upper left image is confluent with the mass of mixed echogenicity determining its splenic origin. (B,C) Typical mass appearances of splenic HSA. For positive splenic identification, the mass should be traced into obvious splenic parenchyma. Surprisingly, in some cases, HSA and other splenic masses can mimic the less common benign diagnosis of splenic abscess. A large splenic mass of mixed echogenicity or with a necrotic center may also mimic free fluid when depth is inadequate (too zoomed in or the depth set too shallow) or the mass is excessively large (exceeding the depth limits of your ultrasound machine). (D) An example of HSA that is more infiltrative and less mass-like. Note that despite the mixed echogenicity, the spleen has little to no deformation of its normal contour.

predictive value for malignancy and when multiple target lesions are seen, the positive predictive value of malignancy increases from 74% to 81% (Cuccovillo and Lamb 2002). One must keep in mind, though, that a sonographic target lesion is a nonspecific finding and a biopsy is required for diagnosis. When finding a splenic target lesion, look for other intraabdominal or intrathoracic masses using Global FAST, radiography (screening for lung nodules) or both. The identification of additional nodules provides further suspicion for malignancy and may also provide a more accessible scanning plane for percutaneous sampling.

- *Lymphosarcoma* (LSA) has a variable appearance when associated with the spleen. LSA may appear as a focal mass lesion, multifocal mass lesions, or as diffuse parenchymal disease referred to as a "honeycomb," "moth-eaten" or "Swiss cheese" appearance (Figure 9.14) (Nyland et al. 2002). Mass lesions due to LSA are generally hypoechoic with indistinct margins and may be singular or multifocal in nature. However, they can also be isoechoic or slightly hyperechoic to normal splenic parenchyma, and may or may not distort the splenic contour (see Figures 9.6 and 9.8A,B).

**Figure 9.13.** Target lesion. Target lesions suggest metastatic neoplasia and should trigger a search for a primary tumor as well as other sites of metastasis, and the Global FAST approach serves as a rapid screening staging test.

**Figure 9.14.** Lymphosarcoma (LSA). The "Swiss cheese" or "moth-eaten" appearance of the spleen is often caused by LSA. However, LSA has variable presentations including a diffuse homogeneous echogenicity change that is hyper- or hypoechoic. Moreover, splenic LSA may appear ultrasonographically unremarkable. Compare to Figure 9.6 showing the variability of splenic LSA and Figure 9.16 showing the lacy appearance of splenic torsion.

**Pearl:** Diagnosis of all presentations of lymphosarcoma may be made via percutaneous needle biopsy (Crabtree et al. 2010).

- *Other tumors* may have similar variability in size, echogenicity, and the ability to distort the splenic contour. Therefore, it is always important to base a diagnosis on other clinical findings as well as cytological and histopathological evaluation.

## Echogenicity and Parenchymal Conditions

Evaluation of diffuse parenchymal disease is subjective and can be difficult for the novice sonographer. Echogenicity of the spleen is assessed by comparing splenic parenchyma to the adjacent liver and left renal (kidney) cortex as described above. Changes in echogenicity can be seen with extramedullary hematopoiesis, passive congestion, nodular hyperplasia, inflammation, infection, neoplasia, and splenic torsion.

- *Extramedullary hematopoiesis*. Generally associated with mildly reduced echogenicity (hypoechoic).
- *Passive splenic congestion*. Generally associated with hypoechoic changes in acute phases but may be associated with hyperechoic changes in more chronic processes. Architecture is rarely disrupted.
- *Nodular hyperplasia*. May be associated with either hypoechoic or hyperechoic changes which are relatively mild. The splenic capsule may be mildly irregular as described above. Nodular hyperplasia is a benign condition commonly seen in older dogs (see Figure 9.8C,D).
- *Inflammatory or infectious diseases* (fungal, bacterial, rickettsial). Generally these conditions cause mild to moderate splenomegaly with diffuse hypoechogenicity. With acute inflammation or infection, the changes are more pronounced with more prominent hypoechogenicity and a finely mottled appearance (see Figures 9.7 and 9.9A,B).
- *Neoplastic conditions*. Lymphosarcoma, mast cell tumor, and other myeloproliferative diseases generally produce an appearance of generalized coarse mottling referred to as a "honeycomb", "moth-eaten" or "Swiss cheese" appearance (Nyland et al. 2002) (compare Figure 9.14 to Figures 9.6 and 9.8A,B). It is important to remember that both lymphosarcoma and mast cell tumor can also be present with very mild diffuse changes and the spleen may even have a normal appearance. As a result, fine needle biopsies of the spleen may be indicated even in the absence of sonographic abnormalities.
- *Splenic torsion*. Marked splenomegaly with a diffusely hypoechoic to anechoic lacy appearance (compared to the hyperechoic [brighter] lacy appearance seen with LSA of the parenchyma) is typical of

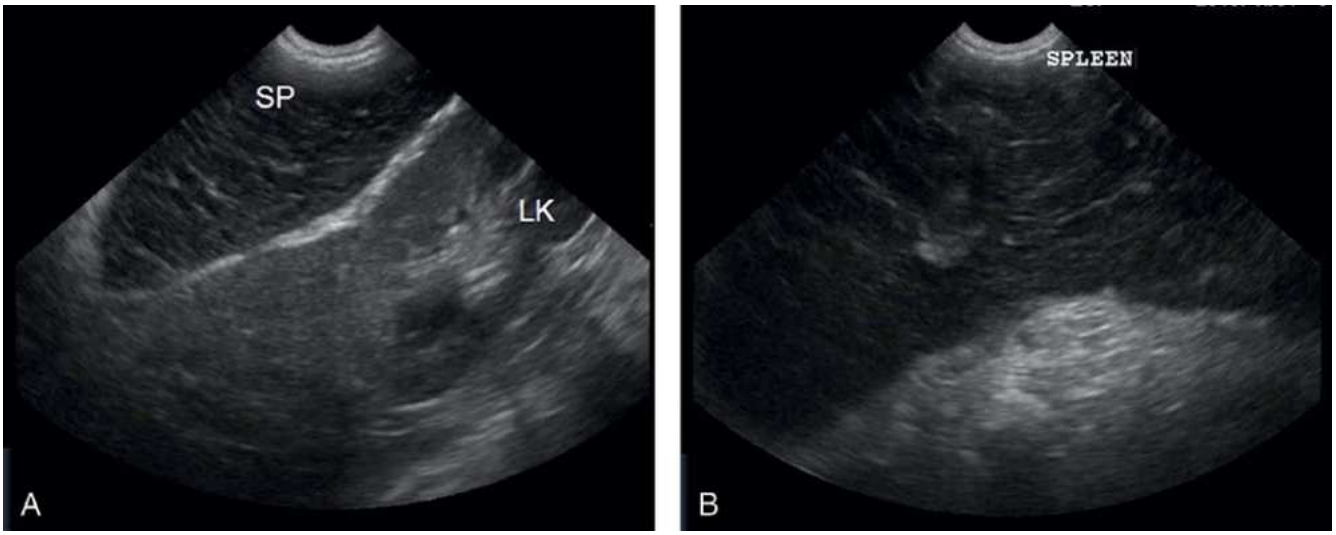


**Figure 9.15.** Splenic torsion parenchymal lesion. (A) Note the hypoechoic (dark) lacy appearance to the spleen (SP) shown adjacent to the left kidney (LK). (B) Another view of the same spleen in (A) showing its thickness and its hypoechoic (dark) lacy parenchymal appearance. Compare to the hyperechoic (bright) lacy appearance of splenic lymphosarcoma in Figure 9.14. The perihilar region is hyperechoic (bright) without clear imaging of the hyperechoic triangle shown in Figure 9.16. Color flow Doppler was helpful in this case (not shown) documenting the lack of perihilar blood flow.

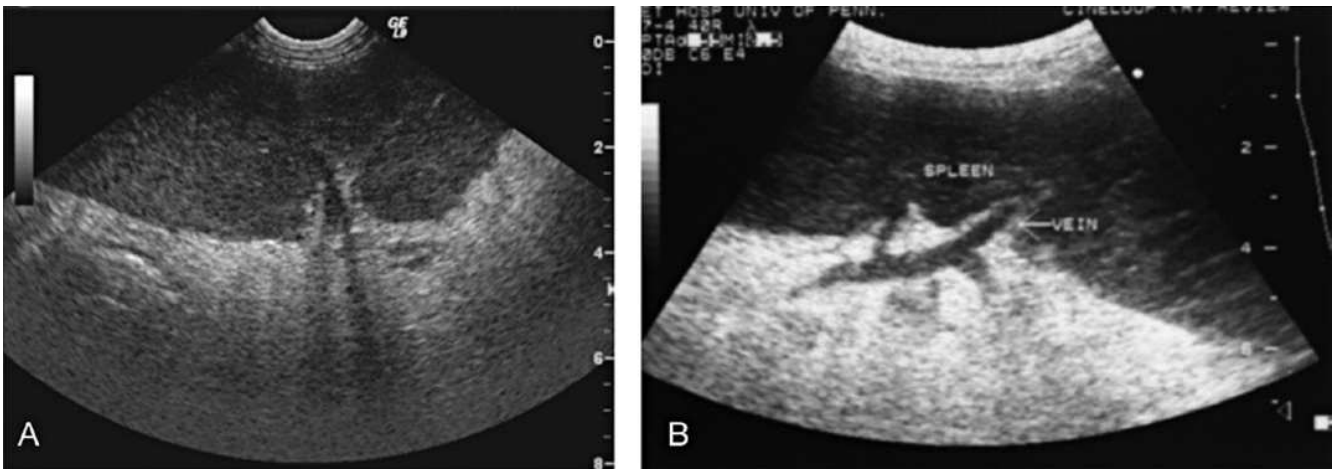


**Figure 9.16.** Splenic torsion vascular lesion. (A) Image of the splenic hilus in a dog with splenic torsion. Note the hyperechoic triangular region around the vessel, continuous with the hyperechoic and hyperattenuating mesenteric fat. (B) Image of the splenic hilus in another dog with splenic torsion. There is a hyperechoic triangular region around the splenic veins, continuous with the mesenteric fat, which is markedly hyperechoic and hyperattenuating. There are also intraluminal echoes in the splenic veins consistent with thrombosis. Both (A) and (B) show the perivenous hyperechoic triangle supportive of splenic torsion. Source: (A) and (B) reproduced with permission from Mai (2006).

splenic torsion (Figure 9.15). If color flow Doppler is available, then absence of blood flow in the splenic vein is consistent with torsion. Thrombus formation may also be identified within the splenic vein in some cases of splenic torsion. Additionally, a perivenous hyperechoic triangle at the level of the splenic hilus has been described as a common feature in dogs with splenic torsions (Mai 2006; Hecht 2008).

### *Vasculature*

Finally, evaluation of the splenic vasculature may help identify splenic torsion (Figure 9.16) (see above), thrombus formation, and splenic infarction.

- *Thrombi* are visualized as echogenic structures within the splenic vein or parenchymal splenic

vessels, and may or may not have clinical consequences depending on the degree of occlusion of the vessel (Figure 9.17; compare to Figure 9.1). Their presence, however, does raise clinical suspicion for lymphosarcoma (Laurenson et al. 2010). See also Chapter 25.

**Pearl:** Splenic thrombi are most commonly associated with lymphosarcoma (Laurenson et al. 2010). They can also be seen with splenic torsion.

- *Splenic infarction* is a possible sequela to splenic thrombi and occurs when blood flow is occluded to an area of splenic parenchyma due to torsion or trauma. Infarcted areas tend to be hypoechoic due to edema in the acute phase, while having borders that are variable in appearance ranging from poorly defined to sharply delineated margins. The lesions generally become smaller and hyperechoic with time (see Figures 9.11 and 16.10B).

# Routine Add-on of AFAST and Its Abdominal Fluid Scoring System (or Global FAST)

In the authors' experience, it is extremely valuable to perform an AFAST examination with assignment of an abdominal fluid score in either lateral recumbency for the best approach. The positioning of small animals in dorsal recumbency for POCUS abdominal organ examinations can obscure small-volume peritoneal effusion and underestimate the volume of effusion present because peritoneal effusion will flow into the less sonographically accessible diaphragmatic recesses. AFAST improves the diagnostic potential of ultrasound by detecting peritoneal effusion. The early detection of abdominal effusion is clinically important and helps direct additional diagnostic recommendations while avoiding morbidity, complications, and patient mortality in the event the effusion is missed.

The Global FAST approach is used as a screening test to rapidly discriminate between localized and

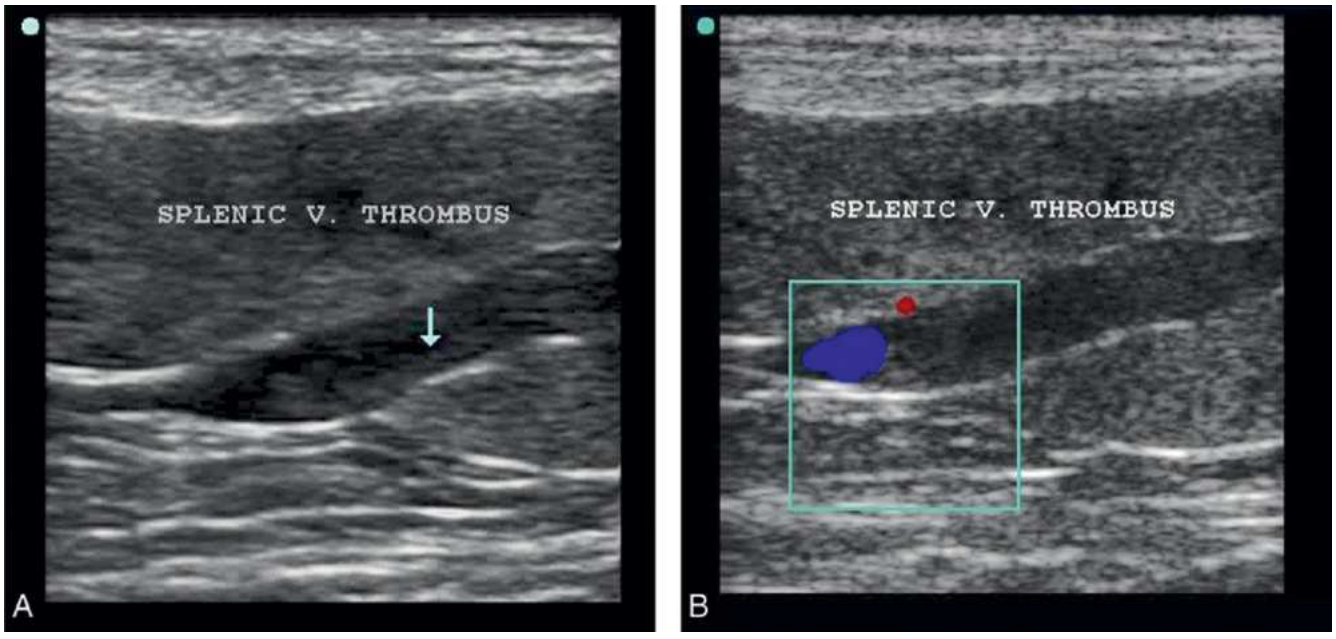


**Figure 9.17.** Splenic thrombus. (A) The splenic vein near the hilus appearing distended by its relative size to the body of the spleen. Within the lumen there appear to be isoechoic material/intraluminal echoes. (B) Same image as (A) confirming the presence of the suspected splenic thrombus using color flow Doppler. Splenic thrombi are most commonly associated with lymphosarcoma but are also associated with other prothrombotic conditions.

VetBooks.ir

disseminated disease, comorbidities, and complications. Global FAST offers a rapid assessment of the abdomen (AFAST) and to survey for pleural and pericardial effusion (TFAST),and cardiac and pulmonary abnormalities (TFAST and Vet BLUE), including lung nodules, with minimal restraint upon initial patient triage.

# Pearls and Pitfalls, The Final Say

It is important for the nonradiologist veterinarian to respect the limitations of the POCUS spleen examination because of the sonographic variability of many diffuse and nodular conditions. Fortunately, the spleen is amenable to minimally invasive cytological evaluation by percutaneous needle biopsy or aspirates when sonographic abnormalities are identified.

Although hemorrhage is an uncommon complication of percutaneous fine needle biopsy, the AFAST format with fluid scoring system (see Chapters 6 and 7) is an excellent tool for postsampling monitoring (four hours post procedure and as needed thereafter), and is more sensitive than traditional means such as packed cell volume (hematocrit) for occult hemorrhage. Finally, a splenectomy with appropriate culture and histopathological testing may be required for definitive diagnosis and treatment plan, and the spleen may be surgically removed with little long-term consequence in both dogs and cats. Global FAST is an especially helpful approach to rapidly survey for pleural and pericardial effusion, and cardiac and pulmonary abnormalities, and is used as a screening test to rapidly discriminate between localized and disseminated disease, comorbidities, and complications (see Chapters XX and XX).

- Evaluation of splenomegaly is a subjective assessment in dogs unless splenic enlargement is severe.
- Splenomegaly in cats is almost always due to pathology and warrants additional evaluation.
- Nodular and mass lesions within the splenic parenchyma are common and usually easy to identify. It is not possible to distinguish benign and malignant processes without cytology or histopathology.
- Splenic hematoma and hemangiosarcoma cannot be differentiated on the basis of ultrasound alone, and may be concurrent. However, use of the Global FAST approach is helpful to rapidly screen for localized versus disseminated disease.
- If the origin of an abdominal mass is difficult to determine, move the patient from dorsal to lateral recumbency. By doing so, the liver and spleen will often separate from one another, helping to better determine the origin of the mass.
- Needle visualization by ultrasound facilitates fine needle percutaneous biopsy of the spleen. Nonspecific cytology results with fine needle biopsy do not rule out the possibility of a malignant lesion, and further diagnostics are required. However, the use of the Global FAST approach is helpful to rapidly screen for localized versus disseminated disease.
- Mild diffuse changes in echogenicity are subjective and can be challenging for the novice sonographer.
- Remember the mnemonic "SLiCK" regarding the echogenicity between the spleen (S), liver (Li), and cortex of the kidney (CK). The echogenicity of the spleen is greater (brighter) than the liver, which is slightly greater (brighter) or isoechoic (same as) than the cortex of the kidney. For the feline, hepatic echogenicity is often compared to the adjacent falciform fat and the feline liver should be isoechoic to slightly hypoechoic to the falciform fat.
- Several benign processes cause mild to moderate diffuse changes in echogenicity including extramedullary hematopoiesis, passive congestion, and antigenic stimulation.
- Diffuse changes associated with lymphosarcoma or other myeloproliferative disorders can be variable in appearance and occasionally can be associated with a normal or unremarkable splenic appearance.
- Fine needle percutaneous biopsies are indicated in cases of moderate to severe splenomegaly or in animals with diffuse changes in echogenicity.

# Quick Reference of Normals and Rules of Thumb

- Spleen size is subjective. A spleen that extends to a small or medium-sized urinary bladder is considered enlarged.
- A folded spleen in a cat is always as a general rule considered abnormal and indicates splenomegaly (Hecht 2008).

- Normal cat spleen thickness is <10 mm (Reese et al. 2013).
- Benign nodular hyperplasia usually consists of nodules that are of homogeneous echotexture being either hypoechoic or hyperechoic.
- Single target lesions have a high predictive value for malignancy. When multiple target lesions are seen, the positive predictive value of malignancy increases from 74% to 81% (Cuccovillo and Lamb 2002).
- Normal echogenicity rule of thumb: the spleen (S) is more echogenic (hyperechoic) than the liver (Li) which is the same or slightly more echogenic (brighter) than the cortex of the kidney (CK), remembered as S > Li ≥ CK or by the mnemonic "SLiCK." For the feline, hepatic echogenicity is often compared to the adjacent falciform fat and the feline liver should be isoechoic to slightly hypoechoic to the falciform fat.

# References


Crabtree AC, Spangler E, Beard D, et al. 2010. Diagnostic accuracy of gray-scale ultrasonography for the detection of hepatic and splenic lymphoma in dogs. *Vet Radiol Ultrasound* 51(6):661–614.

Cuccovillo A, Lamb CR. 2002. Cellular features of sonographic target lesions of the liver and spleen in 21 dogs and a cat. *Vet Radiol Ultrasound* 43(3):275–278.

Fife WD, Samii VF, Drost JS, et al. 2004. Comparison between malignant and nonmalignant splenic masses in dogs using contrast enhanced computed tomography. *Vet Radiol Ultrasound* 45:289–297.

Hammond TN, Pesillo-Crosby SA. 2008. Prevalence of hemangiosarcoma in anemic dogs with a splenic mass and hemoperitoneum requiring a transfusion: 71 cases (2003–2005). *J Am Vet Med Assoc* 232(4):553–558.

Hecht S. 2008. Spleen. In: *Atlas of Small Animal Ultrasonography*, edited by Penninck D, d'Anjou M. Ames: Blackwell Publishing, pp 263–280.

Laurenson MP, Hopper K, Herrera MA, et al. 2010. Concurrent diseases and conditions in dogs with splenic vein thrombosis. *J Vet Intern Med* 24:1298–1304.

Lisciandro GR. 2011. Abdominal and thoracic focused assessment with sonography for trauma, triage, and monitoring in small animals. *J Vet Emerg Crit Care* 21(2):104–122.

Lisciandro GR, Lagutchik MS, Mann KA, et al. 2009. Evaluation of an abdominal fluid scoring system determined using abdominal focused assessment with sonography for trauma in 101 dogs with motor vehicle trauma. *J Vet Emerg Crit Care* 19(5):426–437.

Mai W. 2006. The hilar perivenous hyperechoic triangle as a sign of acute splenic torsion in dogs. *Vet Radiol Ultrasound* 47(5):487–491.

Nyland TG, Mattoon JS, Herrgesell EJ, Wisner ER. 2002. Spleen. In: *Small Animal Diagnostic Ultrasound*, 2nd edition, edited by Nyland TG, Mattoon JS. Philadelphia: WB Saunders, pp 132–133.

Reese SH, Zekas LJ, Iazbik MC, et al. 2013. Effect of sevoflurane anesthesia and blood donation on the sonographic appearance of the spleen in 60 healthy cats. *Vet Radiol Ultrasound* 54(2):168–175.

Rossi F, Leone VF, Vignoli M, et al. 2008. Use of contrast-enhanced ultrasound for characterization of focal splenic lesions. *Vet Radiol Ultrasound* 49(2):154–164.

CHAPTER TEN

# POCUS: Kidney

Stephanie C. Lisciandro and Sarah Young

Vetbooks.ir

## Introduction

POCUS to evaluate the kidneys can provide valuable clinical information to the nonradiologist veterinarian to expedite diagnosis and treatment. The POCUS kidney examination may be especially beneficial in patients with an index of suspicion for acute kidney injury, kidney failure of undetermined cause and postrenal obstruction by screening for several easily recognizable ultrasonographic findings. The POCUS kidney cannot predict kidney function and, in most instances, does not provide information regarding response to therapy. Animals may have a normal ultrasonographic examination with severe kidney dysfunction. Conversely, some animals may have an abnormal ultrasonographic examination with normal kidney function. The POCUS kidney does not replace a complete detailed abdominal ultrasound study performed by a veterinarian with advanced training (a veterinary radiologist or internist).

As with all imaging modalities, ultrasound has inherent weaknesses and should be used in conjunction with, and not to the exclusion of, other diagnostic tests such as abdominal radiography and other renal imaging procedures (e.g., intravenous radiographic, enhanced computed tomography, or retrograde positive contrast pyelography), tissue and fluid sampling, microbial urine culture, sampling of peritoneal effusions, renal cortical fine needle aspiration or biopsy, or other renal function screening and confirmatory tests.

Finally, as with all POCUS abdomen-related organ examinations, the concurrent use of an AFAST is recommended for further patient assessment. The AFAST increases the likelihood of identifying effusive conditions (e.g., hemorrhage, ascites, uroperitoneum and uroretroperitoneum, or other forms of peritonitis), which plays an important role in guiding clinical care and decision making. Global FAST provides further assessment for pleural and pericardial effusion (TFAST), and cardiac (TFAST) and pulmonary abnormalities (Vet BLUE), and can help differentiate between localized and obvious disseminated disease, while aiding in the diagnosis of comorbidities and complications (see Chapter 36).

### What POCUS Kidney Can Do

- Recognize renal parenchymal abnormalities such as cysts, nodules, and masses.
- Identify kidney stones (nephroliths).
- Evaluate for pyelectasia and dilation of the proximal ureter.
- Identify hydronephrosis.
- Determine the presence of retroperitoneal fluid.
- Help determine the presence of renal infarcts (especially cats).
- Measure kidney size and margination and evaluate for asymmetry. In addition, serial assessment may be beneficial in acute kidney injury.

### What POCUS Kidney Cannot Do

- Differentiate benign versus malignant kidney masses.
- Diagnose pyelonephritis.
- Define the character of retroperitoneal fluid.
- Provide reliable information regarding renal function and glomerular filtration; ultrasound also cannot determine potential response to therapy.
- Definitively diagnose ethylene glycol toxicity or other causes of acute kidney failure.

*Point-of-Care Ultrasound Techniques for the Small Animal Practitioner*, Second Edition. Edited by Gregory R. Lisciandro.
© 2021 John Wiley & Sons, Inc. Published 2021 by John Wiley & Sons, Inc.
Companion website: www.wiley.com/go/lisciandro/ultrasound2

### Indications

- Hematuria.
- Polyuria and polydipsia of undetermined cause.
- Acute kidney failure of undetermined cause.
- Discrepancies in comparative palpable or radiographic kidney size.
- Uncharacterized, perceived back pain, peritoneal or retroperitoneal abnormalities of uncertain etiology.
- Abdominal pain.

### Objectives

- Recognize changes in echogenicity consistent with diffuse parenchymal disease.
- Recognize focal parenchymal changes such as kidney cysts and masses.
- Recognize kidney stones (nephroliths).
- Recognize acute and chronic renal infarcts.
- Recognize pyelectasia.
- Recognize hydronephrosis/hydroureter.
- Recognize retroperitoneal and perirenal (subcapsular) fluid.
- Determine the presence of renal agenesis.

## Patient Positioning and Probe Selection

Imaging the kidneys is most frequently performed using a curvilinear (microconvex) probe of the highest possible frequency that allows adequate penetration. Higher frequency linear probes (7.5–10 MHz) provide less penetration but better detail and may be used in smaller dogs and cats. Conversely, a lower frequency probe (5 MHz) provides more penetration but less image detail, and is usually required in larger dogs. Depth should be adjusted to visualize the entire kidney in both the long-axis and short-axis views.

Dogs and cats may be scanned in dorsal or right and left lateral recumbency. In most small animals, both kidneys can be adequately imaged in dorsal recumbency. However, in large or deep-chested dogs, it is often necessary to also image kidneys in lateral recumbencies (right decubitus for the left kidney and left decubitus for visualization of the right kidney) due to their dorsal position within the retroperitoneal space. Left lateral recumbency and an intercostal or subcostal scanning acoustic window are particularly helpful for the right kidney because of its more cranial and sometimes subcostal orientation. The left kidney, located caudal to the last rib and caudomedial to the spleen, is generally easy to image in dorsal recumbency in both dogs and cats regardless of patient size. A gas-filled gastrointestinal tract (particularly the transverse or descending colon) can obscure complete renal visualization because ultrasound does not transmit through air. Minor adjustments in patient positioning to redistribute intestinal gas can address this issue.

**Pearl:** The intestinal tract falls away from the nongravity-dependent kidney when the patient is in lateral recumbency.

## Patient Preparation

Image quality is improved by shaving the ventral abdomen for evaluation of the kidneys. If an intercostal approach is used, additional clipping may be required, but clipping may be avoided for cosmetic reasons by parting the hair and applying alcohol to the skin in addition to acoustic coupling gel.

## How to Perform the POCUS Kidney

When the patient is in dorsal recumbency, the left kidney is visualized caudal to the stomach and spleen within the left dorsolateral abdomen. The spleen is visualized in the near-field and provides an acoustic window for visualization of the left kidney, which is deep to the spleen (Figure 10.1A,B; see also Figures 6.17, 6.18, and 39.13). The entire kidney can be seen on the ultrasound screen by adjusting the depth of field as needed. In some very large patients, the full sagittal length of the kidney may not be visualized regardless of depth. In these cases, fanning while scanning with rocking and sliding motions of the probe should help to fully evaluate all aspects of the organ.

The kidney should be completely scanned from just beyond the serosal margins in both the long (longitudinal/sagittal) and short (transverse) axes (or image scanning planes). Scanning and fanning can be facilitated by obtaining the long-axis (longitudinal/sagittal/dorsal) view and then gently fanning the probe medially and laterally followed by reorientation of the probe 90° counterclockwise to the long axis. This motion leads to the short-axis (transverse) view upon which continued slow fanning and scanning with the probe from the cranial to caudal pole can be performed.

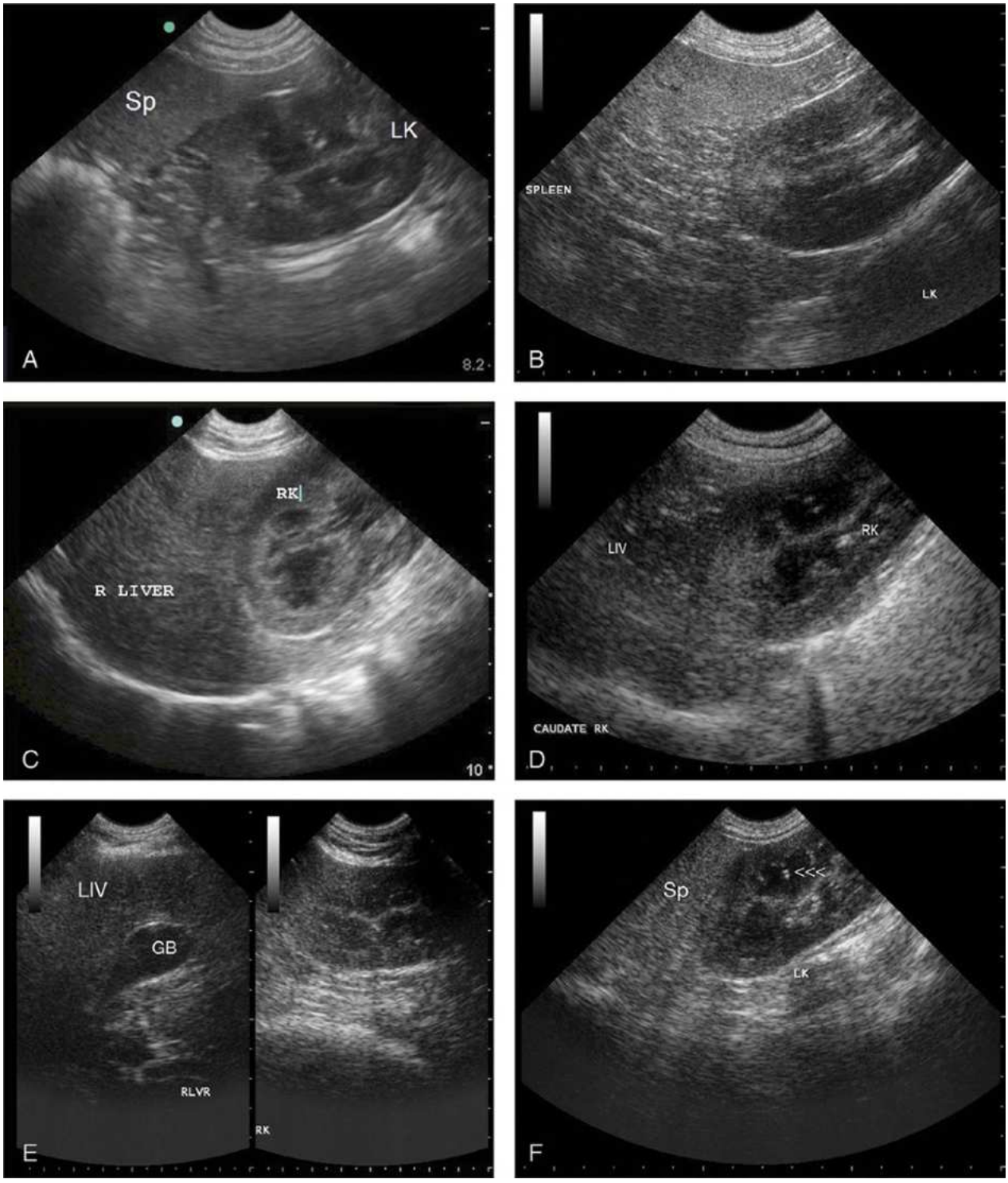


**Figure 10.1.** Left and right kidneys and comparative echogenicity. (A,B) Images from different ultrasound machines showing normal renal echogenicity in relation to spleen and liver. When normal, the spleen (Sp) is hyperechoic (brighter) when compared to the renal cortex. The left kidney (LK) is easier to image than the right because it is more caudally located beyond the costal arch and is thus more ultrasonographically accessible. Following the spleen caudolaterally can aid in locating the left kidney. The spleen can also serve as an acoustic window enhancing renal imaging when in the near-field to the kidney. (C,D) Images from different ultrasound machines as in (A) and (B), respectively. These images show the more cranially located right kidney (RK), which is often found within the costal arch and tucked into the renal fossa of the caudate liver lobe (LIV). Intercostal and subcostal imaging and moving the patient into left lateral recumbency may be necessary for adequate imaging of the right kidney, especially in large and deep-chested dogs. The liver is slightly hyperechoic (brighter) to isoechoic (the same as) when compared to the echogenicity of the cortex of the kidney. (E) The split-screen function may be used to compare relative echogenicity between right liver (RLVR, LIV) and right kidney (RK) when they are not easily imaged side by side on a single screen. Note the gallbladder (GB) is also in the image of the right liver. (F) The highly echogenic interlobar/arcuate vessels appear as bright white dots or equal signs marked (<<<) along the corticomedullary junction of the left kidney (LK) next to the spleen (Sp). Compare to Figure 10.3B and C. The mnemonic "SLiCK" (see text) is a good way to remember the order of normal echogenicity.

**Pearl:** Follow the spleen caudolaterally to find the left kidney.

The right kidney is generally more difficult to find due to its location, especially in large or deep-chested dogs. The right kidney is located more cranially than the left kidney and in dorsal recumbency is typically found tucked under the right costal arch, caudal to the liver, and sits in the renal fossa of the caudate liver lobe (see Figures 10.1C,D and 6.34) so that the cranial right renal cortex contacts hepatic parenchyma. The right kidney is also anatomically caudal to the pyloric outflow tract and adjacent to the duodenum. Remember that the kidneys are located *dorsally* and it may be necessary to sweep to the right and caudally, following the caudal border of the costal arch to find the right kidney. In large and deep-chested dogs, it may be necessary to angle the probe (its beam) cranial under the last rib, or to reposition the patient in left lateral recumbency for an intercostal approach. Left lateral recumbency generally allows for better long-axis (longitudinal/sagittal) views of the kidney through an intercostal space, rather than the angled appearance of the kidney when imaged from caudal to the costal margin in dorsal recumbency.

Once the desired long-axis (longitudinal/sagittal) image is obtained, the probe is gently fanned from medial to lateral to obtain images through all planes of the kidney. The probe is then rotated 90° counterclockwise (turn to the left) for the short-axis (transverse) view and moved from the cranial to caudal pole to allow for evaluation of the entire kidney.

# Ultrasonographic Findings in a Normal Kidney

Four main organ features (anatomy, size, margination, and symmetry) should be assessed when determining whether or not the kidneys are normal or have changes consistent with pathology. Furthermore, in normalcy, fluid is absent. No perirenal (subcapsular) or retroperitoneal fluid should be evident in clinically normal patients. Basic normal renal ultrasonographical anatomy is shown in Figures 10.2 and 10.3.

**Pearl:** The four main features of a POCUS Kidney are anatomy, size, margination and symmetry.

## *Kidney Anatomy*

The kidney is divided into three distinct regions that need to be assessed: the cortex, medulla, and renal pelvis.

### Cortex

The cortex is the outermost region of the kidney and is hyperechoic (or brighter than) the inner medullary tissue. A distinct demarcation is noted between these two areas and is generally referred to as corticomedullary distinction. Corticomedullary distinction may be classified as normal or decreased by variable degrees (mild, moderate, severe). The margin of the cortex

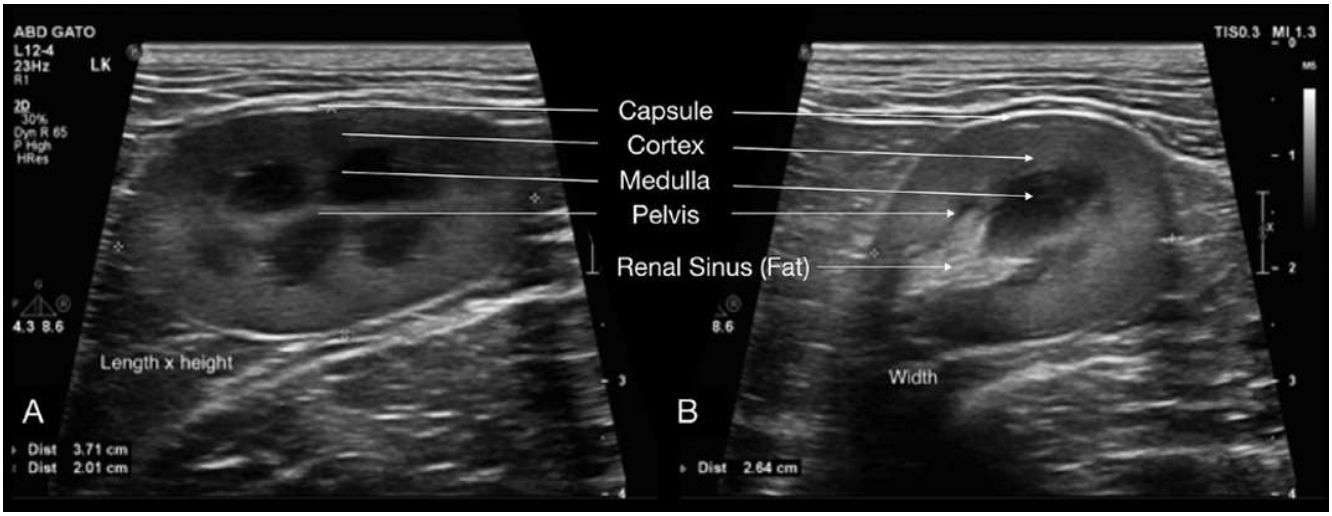


**Figure 10.2.** Basic normal renal ultrasonographic anatomy. The kidney is shown in (A) in the sagittal or longitudinal orientation (long axis) and in (B) in transverse orientation (short axis). Basic renal anatomy is labeled.

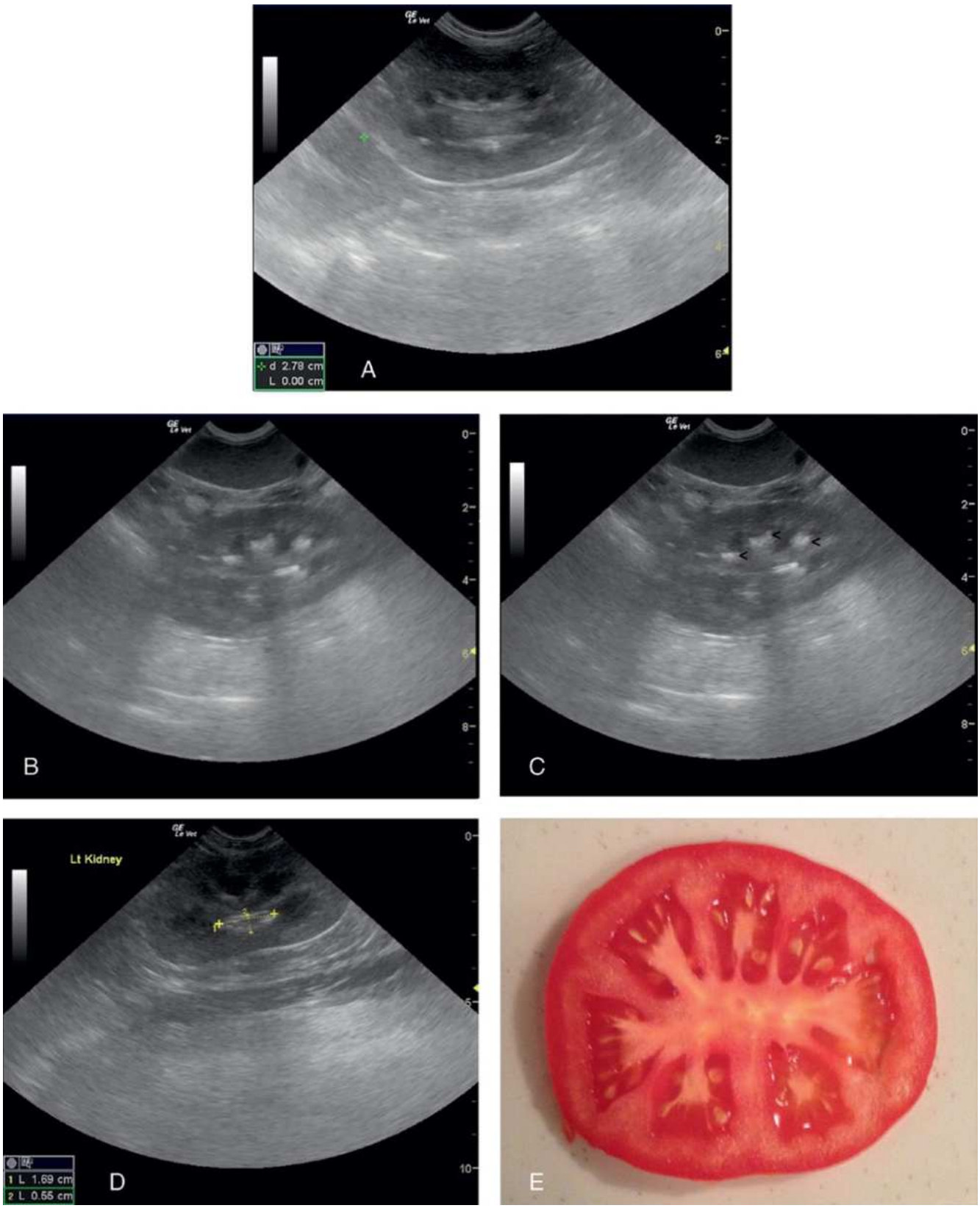


**Figure 10.3.** Normal kidney architecture. (A) Sagittal image of the left kidney demonstrating normal corticomedullary architecture. The appearance of a kidney in longitudinal section is likened to a tomato in cross-section. (B) and (C) are the same image unlabeled and labeled. The interlobar/arcuate vessels are hyperechoic (bright white) and should not be mistaken for mineralization. In (C) the hyperechoic (bright white) interlobar/arcuate vessels (<) are labeled. Note there is no distal acoustic shadowing which makes mineralization less likely. Note here how the comparative splenic echogenicity is abnormal. The spleen is hypoechoic or darker than the cortex of the left kidney. Compare this image to the normal comparative echogenicity of spleen and renal cortex in Figure 10.1A and B. (D) The renal pelvic fat (identified by the sonographer by the caliper lines showing its borders) can be prominent and very hyperechoic (bright white). As with the interlobar/arcuate vessels (<<<), this should not be mistaken for mineralization. Other good examples are Figures 10.4B, 10.8B and 10.10A. (E) A tomato cut in cross-section mimics the sagittal or longitudinal (long-axis) orientation of the kidney.

(also called the renal contour) is also assessed and should be smooth with a thin echogenic renal capsule. Normal cortical tissue is isoechoic or slightly hypoechoic to normal liver tissue, although it may also be slightly hyperechoic to the liver in cats in the normal state due to increased renal tubular fatty deposition (see Figures 39.10 and 39.11) (Yeager and Anderson 1989) and in some dogs as a normal variation (see Figure 10.1C,D,E). Renal cortical tissue is hypoechoic to the echogenicity of normal splenic tissue (see Figure 10.1A,B).

Apparent alteration in the normal echogenicity between adjacent organs generally indicates pathology in one or more of the organs being compared. However, echogenicity is affected by the type of probe, frequency, depth of evaluation, and gain settings. Therefore, the ability to perceive subtle differences in comparative echogenicity may require more operator experience or may sometimes not be possible (see Figure 10.3E). The astute sonographer must consider the concurrent conditions of organs (liver, spleen) to which the renal cortex is being compared in order to determine which, if any, are normal or abnormal.

**Pearl:** Remember the "SLiCK" mnemonic regarding canine echogenicity: the spleen (S) is hyperechoic (brighter) to liver (Li) which is slightly more hyperechoic (brighter) or isoechoic (same echogenicity) to the cortex of the kidney (CK). In the order of most echogenic to least echogenic, this spells "SLiCK." For the feline, hepatic echogenicity is often compared to the adjacent falciform fat and the feline liver should be isoechoic to slightly hypoechoic to the falciform fat.

### Medulla

The medulla is hypoechoic or darker than normal renal cortical tissue and there is a clear demarcation between normal cortical and medullary tissue. The normal medullary margin has a circumferentially symmetrical appearance with radiating linear echogenicities due to the presence of interlobar vessels (see Figures 10.1F and 10.3B,C) and pelvic diverticula (see Figure 10.3D) which are uniformly arranged (like the appearance of a tomato in cross-section) (see Figures 10.3A, 39.10, and 39.11). In addition, some animals may have a linear hyperechoic (bright) medullary rim sign (incidental rim sign) that can be of normal variation and clinically irrelevant (d'Anjou 2008).

**Pearl:** The normal renal medulla appears like a tomato in cross-section. Medullary rim signs, while once thought to be clinically relevant, are found in both normal and abnormal kidneys and in many cases are clinically irrelevant.

### Renal Pelvis

The renal pelvis is more difficult to evaluate, especially in normal animals where it may not be readily visualized (see Figure 10.3A–D). The renal pelvis may be distended and thus more apparent in animals receiving intravenous fluids or diuretic therapy. In these cases, the degree of distension is usually bilaterally symmetrical and mild (but can be unilateral) (Pugh et al. 1994; Felkai and Voros Fenyes 1995) (see section on Pyelectasia later in this chapter, and Figure 10.11). The pelvis is frequently surrounded by fat, especially in felines, which is hyperechoic (bright) and is distinguished from mineralized material by the absence of an acoustic shadow (see Figure 10.2D). The renal pelvis appears linear or "T"-shaped in sagittal views and "V-shaped" in transverse views.

There is variability of normal pelvic measurements in both cats and dogs. Normal renal diameter in cats is typically 1.5–2 mm, with a maximum diameter of 2.8 mm, and in dogs is 2–3 mm, with a maximum diameter of 3.8 mm (d'Anjou et al. 2011) (see Figures 10.13A–D, 39.10, and 39.11). The normal ureter should not contain fluid and is difficult to image due to the small luminal diameter (typically 1–1.8 mm) (Neuwirth et al. 1993). Any degree of ureteral dilation typically indicates pathology (see Figure 10.13C).

**Pearl:** The renal pelvis should be considered dilated (referred to as pyelectasia) if it measures ≥3 mm in cats and ≥4 mm in dogs.

**Pearl:** Renal anatomy, including the cortex, medulla and pelvis, is one of the basic characteristics to assess when evaluating the kidney.

## *Kidney Size*

Kidney size should be evaluated through measurement of long-axis views. Symmetry of size and architecture between the right and left kidney is equally important (Figure 10.4; see also Figures 39.10 and 39.11).

- *Cats*. Normal kidney size in cats is generally considered to be 3.0–4.4 cm in length depending on the reference (Nickel et al. 1973; Walter et al. 1987).

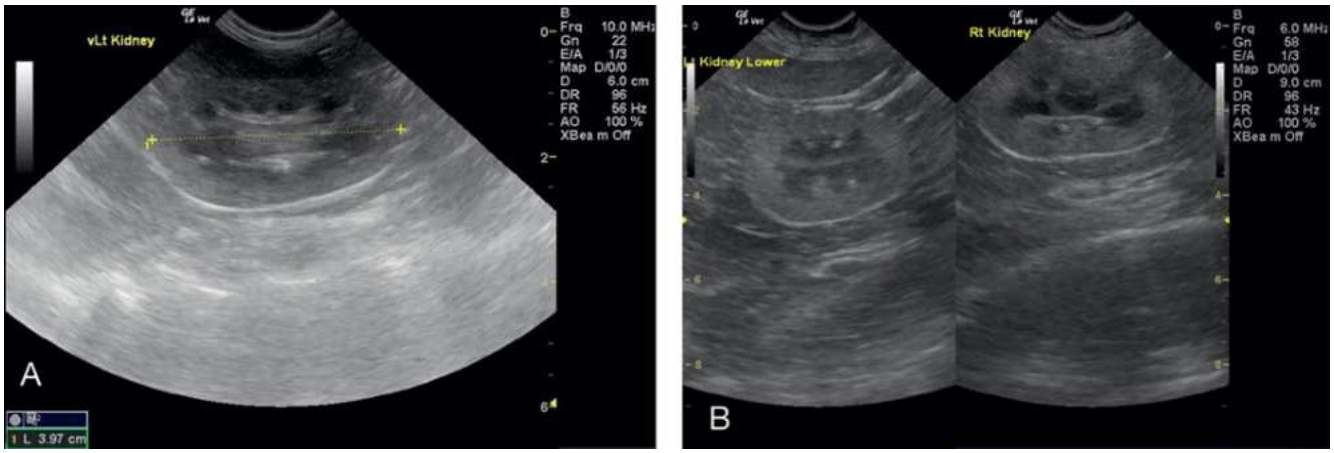


**Figure 10.4.** Assessing kidney size and symmetry. Normal size is established for cats and the kidneys should be symmetrical when normal. There are no established normal reference ranges for renal size in dogs; thus, comparison of symmetry is most important in dogs. (A) The proper placement of calipers for renal measurement. This kidney measures 3.97 cm (bottom left corner of image [not shown]). (B) Split-screen B-mode images showing side-by-side comparisons of the left (Lt) and right (Rt) kidney. This is a common feature of many ultrasound machines. Note the asymmetry of the kidneys in this example.

- *Dogs*. Normal kidney size in dogs varies significantly with body weight, and normal size values for dog kidneys have not been established. Thus, renal size in dogs is a subjective assessment, and assessment of symmetry is more important. Asymmetry of size or architecture supports kidney pathology.

**Pearl:** Evaluation of renal symmetry is important in both dogs and cats, but is especially important in dogs where there are no established normals for renal size.

## *Clinical Significance and Implications of Abnormal Kidney Findings*

The goal of the POCUS kidney is to identify abnormalities such as parenchymal disorders, kidney stones (nephroliths), renal infarcts, subcapsular renal fluid, margin irregularity, renal pelvic abnormalities such as pyelectasia and hydronephrosis, and perinephric or retroperitoneal fluid.

## *Kidney Parenchymal Disorders*

Evaluation for kidney parenchymal disease should include the ability to detect the presence of diffuse abnormalities as well as focal abnormalities such as masses and cysts.

### Diffuse Parenchymal Disease

Diffuse parenchymal disease may be more difficult to detect for a less experienced sonographer. Changes are evaluated by comparing renal cortical echogenicity to normal liver and splenic tissue. Recall the "SLiCK" mnemonic discussed previously for normal echogenicity: splenic parenchyma is brighter than liver parenchyma which is slightly brighter or the same echogenicity as the cortex of the kidney (see Figure 10.1A–E).

In general, disorders that result in increased echogenicity (cortical tissue that is hyperechoic or brighter than spleen and liver) include ethylene glycol toxicosis, pyelonephritis, other acute toxicities, glomerular disease, interstitial nephritis, end-stage kidney disease, infiltrative neoplasia (lymphosarcoma), amyloidosis, and hypercalcemic nephropathy (see Figure 10.4). The presence of a hyperechoic medullary rim sign in animals with hyperechoic cortical tissue (medullary rim sign) is nonspecific, but may increase the suspicion for hypercalcemic nephropathy, ethylene glycol toxicosis, pyogranulomatous inflammation due to feline infectious peritonitis, leptospirosis, and chronic interstitial nephritis (Adams et al. 1991; d'Anjou 2008) (Figure 10.5C). It must also be noted, however, that these changes (both hyperechoic cortices and hyperechoic medullary rim signs) can be seen in normal cats and occasionally in normal dogs (see Figure 10.5C). Therefore, evaluation of a patient's full clinical picture, further assessment by an experienced sonographer, and interventional diagnostics such as cortical aspirates or renal biopsy are often necessary to determine the significance of these changes.

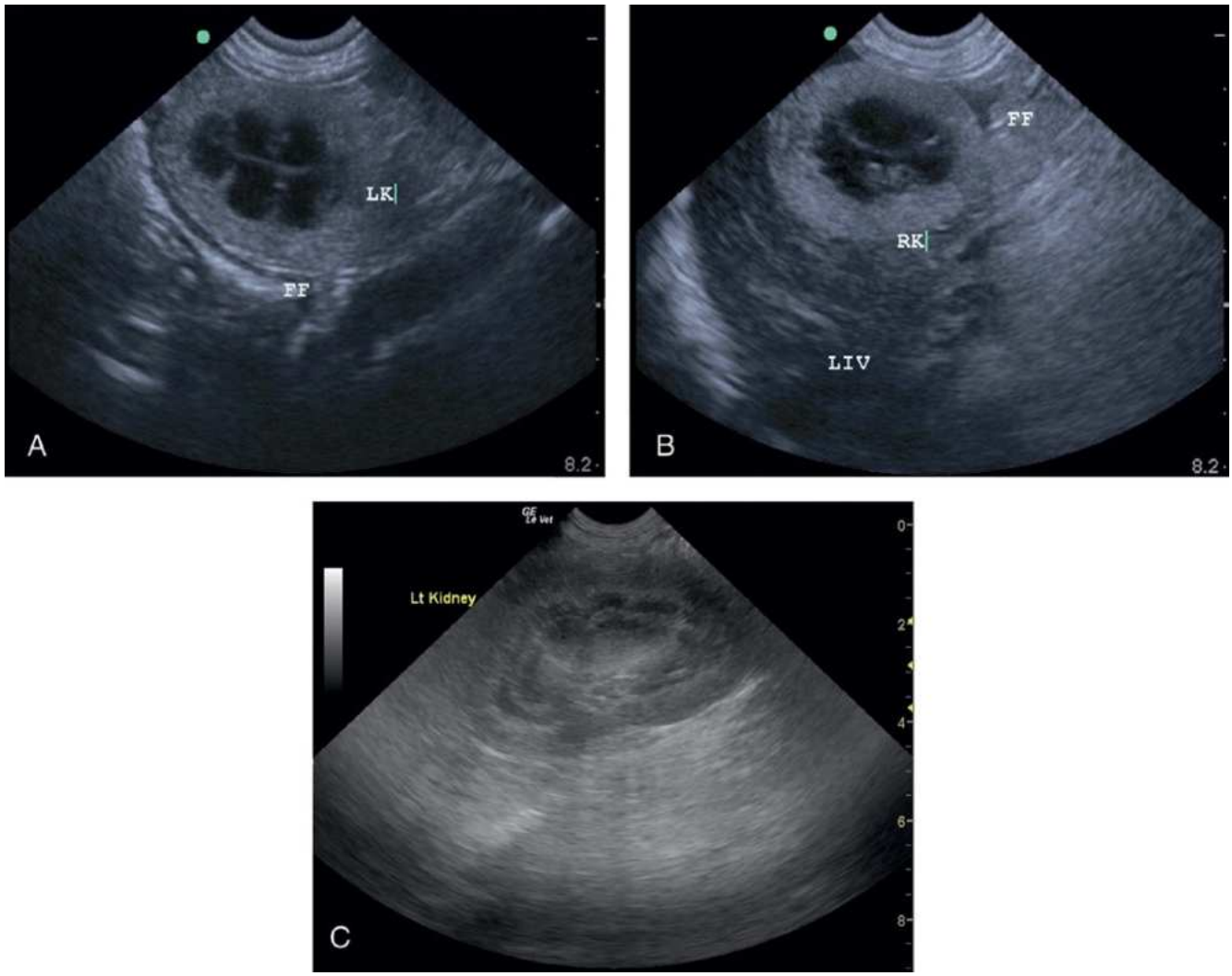


**Figure 10.5.** Hyperechoic kidneys and medullary rim sign. (A,B) Images from a middle-aged dog with unexplained acute kidney injury that was minimally responsive to intravenous fluid diuresis and antibiotic therapy. The kidneys were asymmetrical. Note the severely hyperechoic renal cortices. Differentials for these ultrasonographic changes include hypercalcemic nephropathy, pyogranulomatous inflammation due to feline infectious peritonitis (FIP), leptospirosis, amyloidosis, and chronic interstitial nephritis. It should be noted that in fact hyperechoic cortices may be a normal finding more commonly seen in cats (because of a higher renal tubular fat content) than dogs (FF, free fluid; LIV, liver; LK, left kidney; RK, right kidney). (C) The medullary rim sign may or may not represent true renal pathology and has been referred to as the halo sign through its observation in dogs and cats with ethylene glycol (EG) toxicosis. However, its observation should be cautiously interpreted because there are other causes than EG and the sign may be seen in canine kidneys with normal renal function.

**Pearl:** The halo sign and medullary rim sign are two different renal ultrasonographic findings. The halo sign is a hypoechic (dark) rim in between hyperechoic (bright) medullary and cortical regions and is best known as occurring with ethylene glycol toxicosis (Adams et al. 1989, 1991). The medullary rim sign is a hyperechoic line within the medulla parallel to the corticomedullary junction and is nonspecific (Biller et al. 1992).

## Focal Parenchymal Disorders

Focal parenchymal conditions such as cysts and masses are easier to detect than diffuse abnormalities and are subdivided into mass lesions, renal cysts, and other fluid-filled pathology (e.g., abscess, granuloma, hematoma).

### *Mass Lesions*

Mass lesions may occur in the renal cortex or medulla and frequently result in distortion of the renal contour.

Mass lesions have many possible appearances and should be described by size (measuring the lesion), echogenicity (hyperechoic, isoechoic or hypoechoic) as compared to normal cortical tissue, margination, and character (complex, mixed echogenicity, homogeneous, lobulated) (Figure 10.6). It is not possible to differentiate benign from malignant processes based on sonographic appearance alone. For example, benign processes such as retroperitoneal hemorrhage and subsequent large blood clot, or fungal disease causing a granuloma, can mimic a mass lesion and be misinterpreted as a malignant process (Figure 10.7).

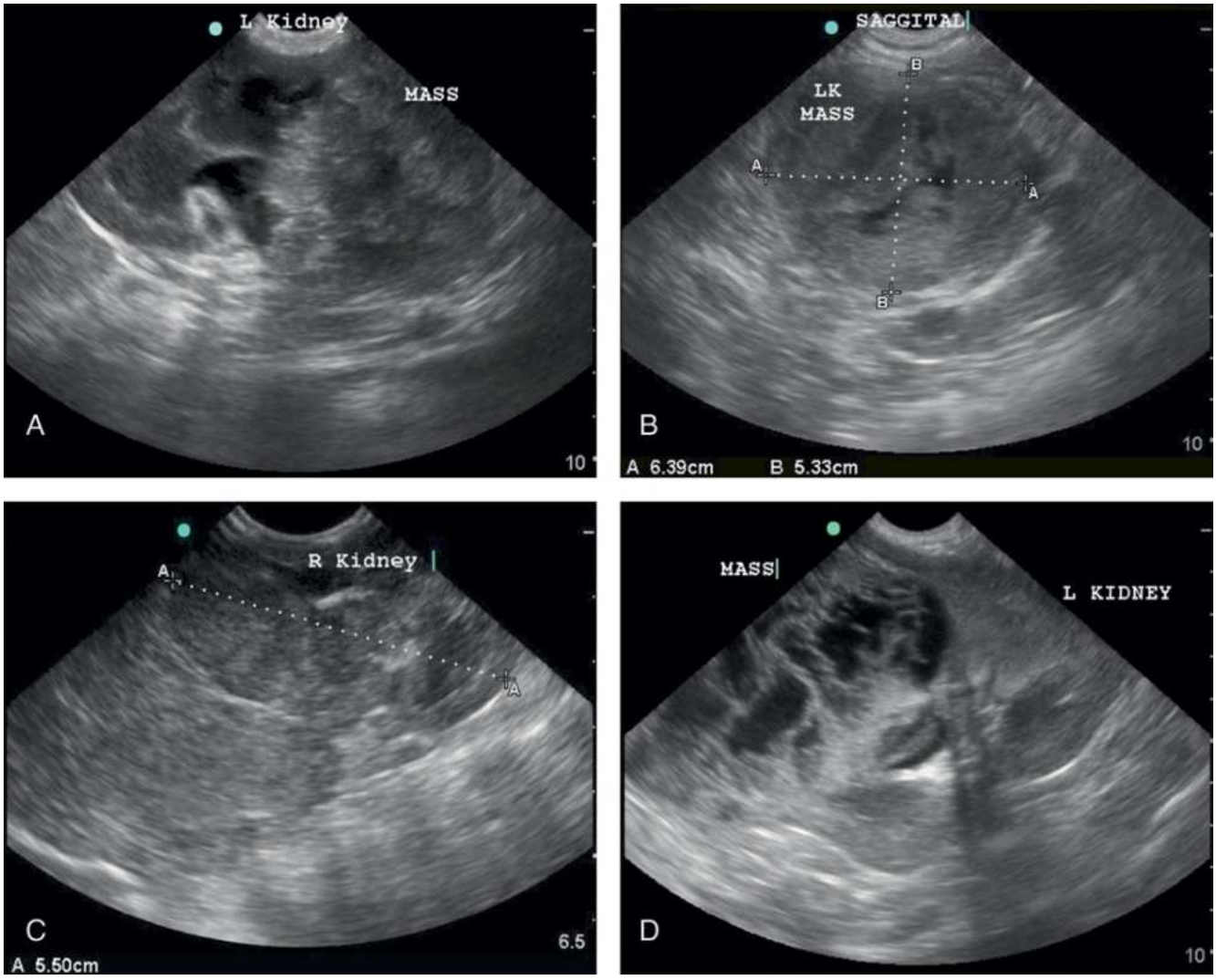


**Figure 10.6.** Various renal tumors. (A) Mass off the caudal pole of the kidney. Biopsy of the mass demonstrated renal adenocarcinoma. It is not uncommon for these tumors and other kidney-related masses to rupture and result in significant retroperitoneal hemorrhage. (B) Same mass as in (A) shown in transverse orientation (short-axis). Note the lack of normal renal anatomy. The renal origin of the mass was obvious in real time during longitudinal and transverse interrogation. (C) Invasive mass involving the cranial pole of the kidney. The diagnosis in this young adult dog was nephroblastoma. It can be difficult differentiating the true origin of large masses. Careful tracing and identification of other nearby structures are imperative to improve accuracy. (D) Cavitary mass of the cranial renal pole. The diagnosis in this case was hemangiosarcoma. Again, the origin of large masses can be difficult to definitively ascertain as finding an area of organ to mass confluence can only sometimes be achieved with ultrasonography.

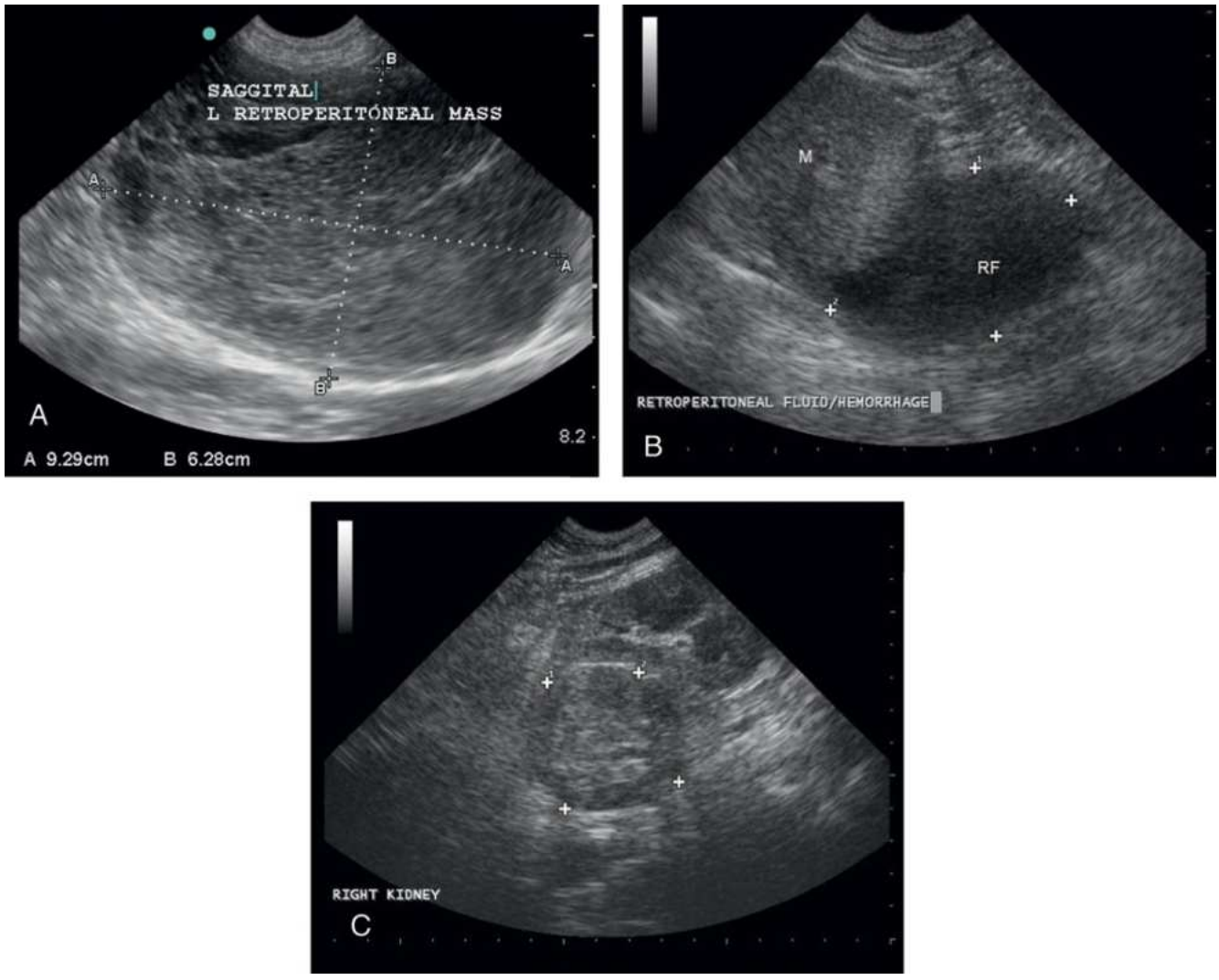


**Figure 10.7.** Hematoma in a coagulopathic dog and a dog with a ruptured adrenal mass. (A) Large mass in the retroperitoneal space in a dog with anticoagulant (warfarin) rodenticide toxicosis. The diagnosis was retroperitoneal hematoma. Color flow Doppler is helpful to document the presence or absence of blood flow. (B) A similar-appearing anechoic tubular mass effect (M) off the pole of the kidney with adjacent retroperitoneal anechoic fluid (RF and marked with calipers [+]) that cannot be characterized without fluid sampling. (C) Same dog as in (B) showing that further interrogation suggests a renal mass of the cranial pole, and antemortem fine needle aspiration for cytological evaluation was considered. Postmortem diagnosis was retroperitoneal hematoma secondary to a bleeding pheochromocytoma of the right adrenal gland eroding the caudal vena cava. Fine needle aspiration potentially could have led to significant complications, including uncontrolled hemorrhage. The case stresses the point that a more thorough ultrasonographic interrogation may provide important information in the decision-making process regarding FNA versus exploratory laparotomy. It can be difficult to differentiate benign, as in (A), from malignant conditions as in (B) and (C) based on ultrasonographic appearance alone. The use of Global FAST to stage the patient should be considered as an adjunct evaluation.

**Pearl:** Masses should be described by the following features: size (measuring the lesion), echogenicity (hyperechoic, isoechoic or hypoechoic) as compared to normal cortical tissue, margination, and character (complex, mixed echogenicity, homogeneous, lobulated).

When renal masses are identified, perform Global FAST to differentiate between localized and obvious disseminated and comorbidities. Referral for additional imaging and possible percutaneous aspirates or biopsies by an experienced sonographer should be considered.

### *Renal Cysts*

Renal cysts are easy to identify and may either be due to benign processes or associated with functional disease. Characteristics of true cysts include the presence of thin walls with central anechoic fluid and distal acoustic enhancement artifact. Cysts may be solitary or multiple and involve one or both kidneys. Benign cysts are generally cortical although they may extend into the medulla, and may result in distortion of the renal contour but rarely disturb the corticomedullary architecture. They may be relatively large and the significance of cysts is determined not by size but by number (Figure 10.8A,B; see also Figure 16.18). In animals with congenital polycystic kidney disease (as can occur in long-haired cats and cairn terriers), the cysts are generally numerous and result in distortion of both the renal contour and the corticomedullary architecture (d'Anjou 2008) (see Figure 10.8C,D).

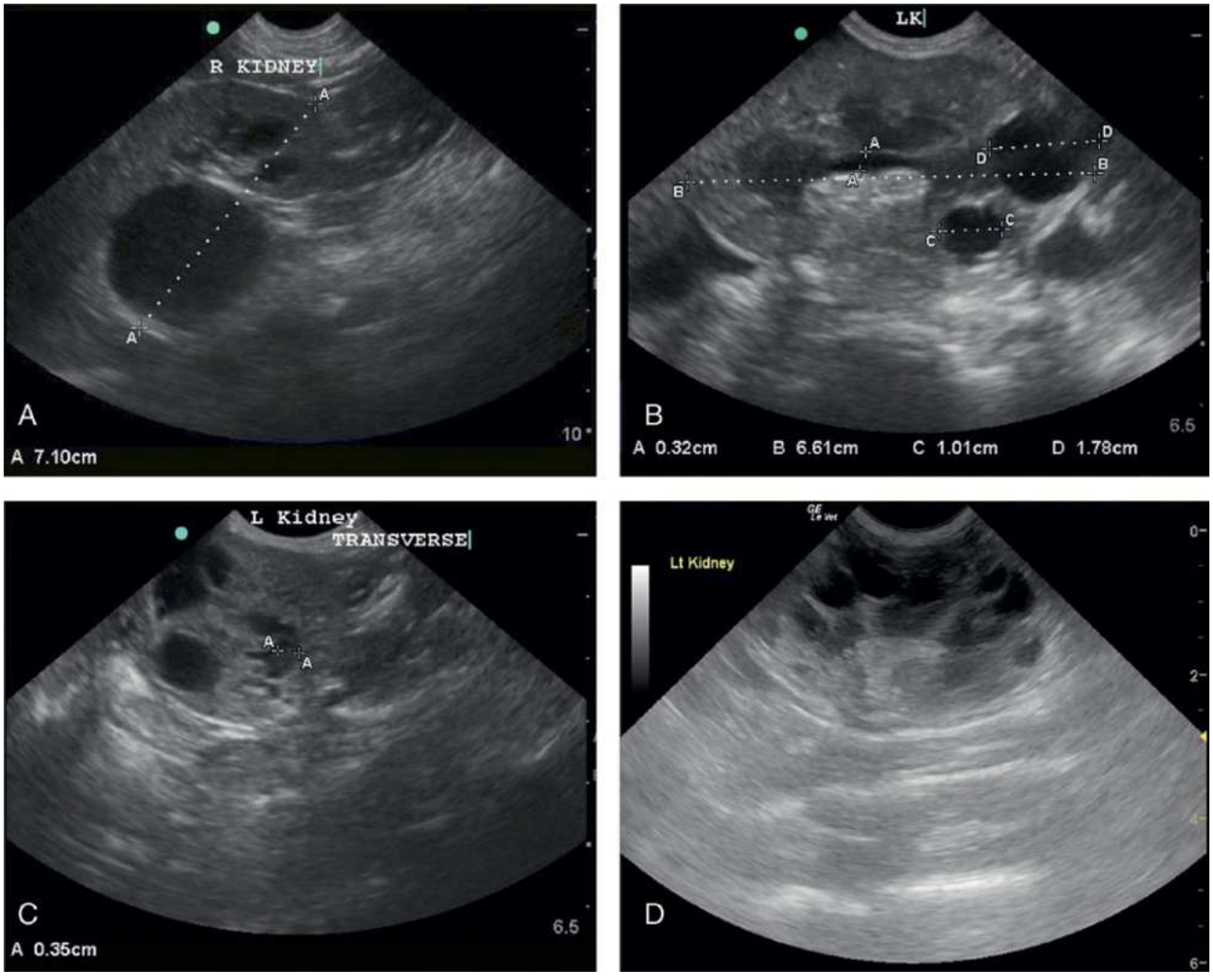


**Figure 10.8.** Renal cysts and polycystic kidney disease. (A) Large renal cortical cyst. Note the thinly encapsulated, large anechoic structure. In real time, one would note distal acoustic enhancement typical of fluid-filled (versus solid masses) structures. The kidney's length is measured by calipers (A-A) at 7.10 cm. (B) Other examples of renal cortical cysts. Note here the mild renal pelvic dilation (caliper marks A-A, as identified by the sonographer). Note also how the typical cortical cyst(s) (identified by the sonographer and marked C-C and D-D) do not cause distortion of the inner anatomy (medulla) of the kidney. Renal length is shown by caliper marks B-B. The measurements in centimeters are located along the bottom of the image. (C) Polycystic renal disease. When compared to previously shown renal cortical cysts, these cysts are greater in number, distort the renal capsule and typically distort the normal kidney architecture in a destructive manner. (D) Feline polycystic kidney disease (PKD). Again, note the "destructive" distortion of the normal renal architecture.

**Pearl:** Polycystic kidney disease is most common in domestic long-haired cats and cairn terriers.

VetBooks.ir

#### *Perinephric Pseudocysts*

Pseudocysts are accumulations of fluid under the renal capsule creating the appearance of a cyst (a pseudocyst). A kidney can be identified within the large volume of pseudocyst fluid, which is typically anechoic. As they are frequently associated with chronic renal disease, the kidney is often small and may have chronic degenerative changes (such as irregular margination or cortical hyperechogenicity).

#### *Other Fluid-filled Structures*

True cysts must also be differentiated from other pathological processes such as abscess, hematoma or tumor. These disorders are more likely to be present if the cystic structure has a thick wall, echogenic contents, or the presence of internal septations (Figure 10.9). Aspiration of fluid may help to identify and characterize these disorders and should generally be performed by an experienced sonographer.

#### Infiltrative Processes

Infiltrative conditions such as renal lymphosarcoma or diffuse renal carcinoma result in changes in echogenicity as well as distortion of the normal corticomedullary architecture (enlarged irregular kidneys and loss of symmetry) (Figure 10.10A,B). Lymphosarcoma in cats is typically diffusely infiltrative and associated with increased cortical echogenicity. In dogs, lymphosarcoma may be infiltrative but more commonly causes mass lesions (typically hypoechoic). These disorders are often accompanied by the presence of a rim of subcapsular perinephric fluid as well as distortion of normal corticomedullary architecture (see Figure 10.10C,D).

## *Kidney Stones*

Kidney stones (nephroliths) may be detected by POCUS kidney. Kidney stones or renal calculi have bright reflective surfaces and typically cause strong acoustic shadowing distal to the mineralized area (Figure 10.11A–D). Very small calculi may cast negligible acoustic shadows. The calculi may be nonobstructive or obstructive and assessment of the renal pelvis for dilation will help to determine significance. Renal calcification, also referred to as dystrophic mineralization, may involve the parenchymal tissue usually at the corticomedullary junction or the renal pelvis (see Figure 10.11E,F). Calcification of the corticomedullary tissue must be differentiated from the normal hyperechoic tissue seen at the corticomedullary junction due to the presence of interlobar/arcuate vessels (see Figures 10.1F and 10.3B,C). These normal structures do not result in acoustic shadows. Calcification at the renal pelvis must be differentiated from the presence of renal pelvic fat (see Figure 10.2).

More recently, a new artifact described using color Doppler, called the "twinkle artifact," has been used to detect uroliths (renal, ureteral, and bladder) that are <5 mm in people (Gliga et al. 2017). See Chapter 11 for greater detail.

**Pearl:** Kidney stones (renal calculi, nephroliths) are usually identified in B-mode by the presence of strong acoustic shadowing distal to the mineralized area. This helps differentiate mineralization from normal hyperechoic findings due to interlobar/arcuate vessels at the corticomedullary junction or fat in the renal pelvis. In other words, interlobar/arcuate vessels and renal pelvic fat may be hyperechoic (bright white) but generally do not cast a distal shadow.

**Pearl:** Small nephroliths and renal mineralization may be more readily visible by abdominal radiography.

## *Pyelectasia*

Pyelectasia is defined as renal pelvic dilation without other dilation of the collecting system. It should be characterized as unilateral or bilateral and its symmetry as symmetrical or asymmetrical in determining the significance of this finding (Figure 10.12; see also Figure 16.18). The normal renal pelvis is collapsed, typically measuring less than 2 mm. Normal renal pelvic dilation ranges in cats from 1.5 to 2 mm, with maximum height of 2.8 mm, and in dogs from 2 to 3 mm with a maximum height of 3.8 mm (d'Anjou et al. 2011). A general rule of thumb is to consider the renal pelvis abnormal if it measures ≥3 mm cats and ≥4 mm dogs.

Causes of pyelectasia include pyelonephritis, total or partial obstruction of urine flow, intravenous fluid therapy, diuretic therapy, a distended urinary bladder, acute kidney injury, and some congenital disorders (Pugh et al. 1994; Felkai and Voros Fenyes 1995; Cole et al. 2019) (Table 10.1).

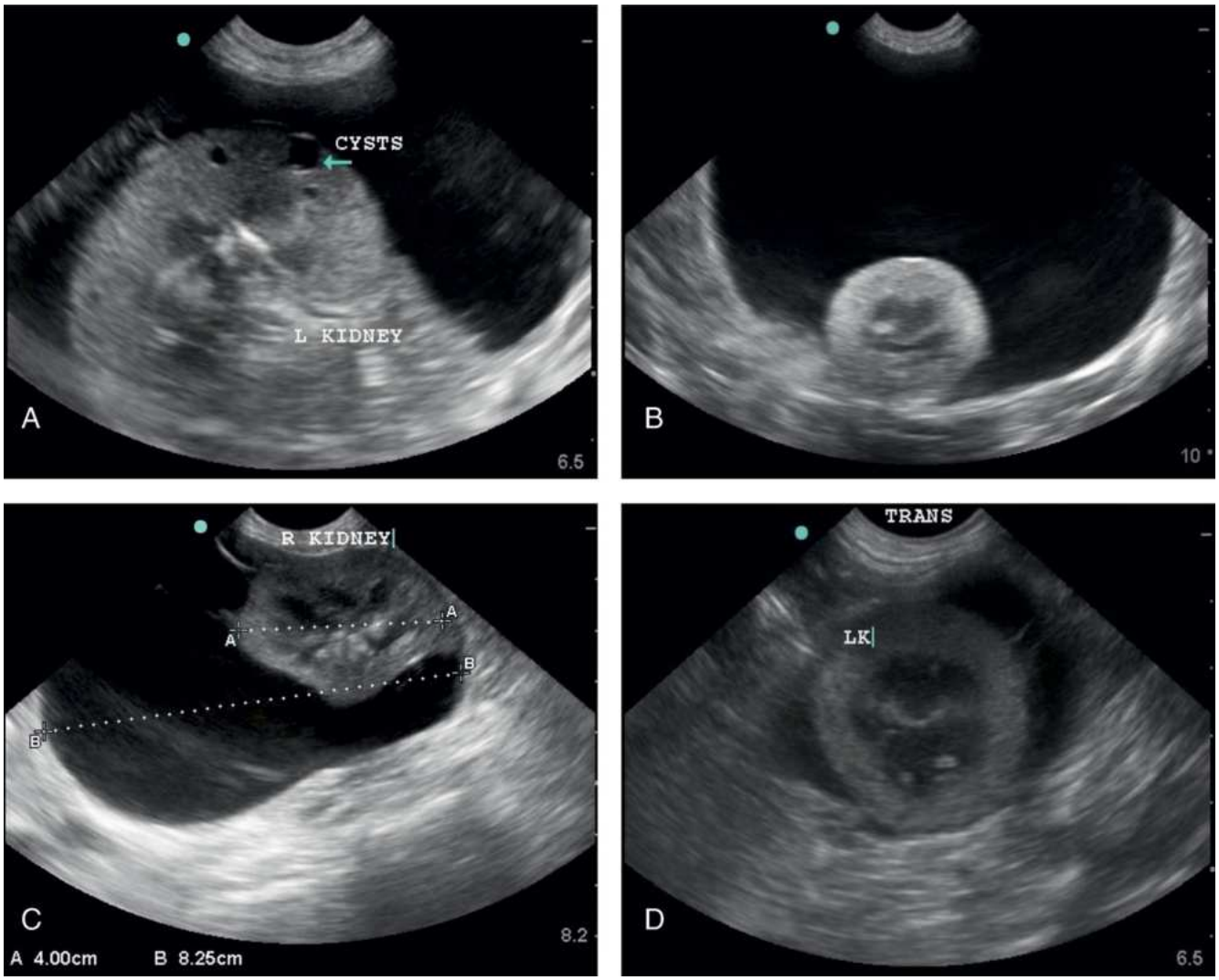


**Figure 10.9.** Renal cortical cysts and polycystic renal disease. (A) Renal cortical cysts with concurrent perinephric pseudocyst. Renal cortical cysts are intraparenchymal, anechoic, and typically do not distort the renal capsule or its normal architecture. The large amount of perirenal fluid contained within the kidney's capsule is more commonly related to perinephric pseudocysts. (B) Another example of a perinephric pseudocyst. Note the lack of renal parenchymal involvement. (C) Example of a perinephric pseudocyst that distorts the renal shape and causes secondary changes in its renal architecture from pressure necrosis. (D) Perinephric pseudocyst in transverse orientation. These types of cysts that may or may not completely surround the kidney have been reported in dogs and cats. Histopathologically, perinephric cysts do not have a true epithelial lining, hence the term *pseudocyst*. The cause of these cysts is commonly unknown and treatment generally involves intermittent drainage, surgically placed portal systems or nephrectomy in cases of impaired renal function.

Pyelonephritis cannot be determined on the basis of ultrasound alone but is more likely when associated with clinical signs (polyuria/polydipsia, active urine sediment). Generally, pyelonephritis causes mild to moderate dilation of the renal pelvis, which is usually unilateral but may be bilateral with chronic infection. The dilation is usually asymmetrical and concurrent dilation of the proximal ureter (>1.8–2 mm) may also be seen (Neuwirth et al. 1993). The absence of pyelectasia does not rule out the presence of pyelonephritis, especially in acute disease, and the presence of pyelectasia does not confirm pyelonephritis.

In contrast, diuresis (from either intravenous fluid therapy or diuretic therapy) often results in mild symmetrical dilation of the renal pelvis and therefore the symmetrical form of pyelectasia seen in these patients is usually of lesser clinical concern.

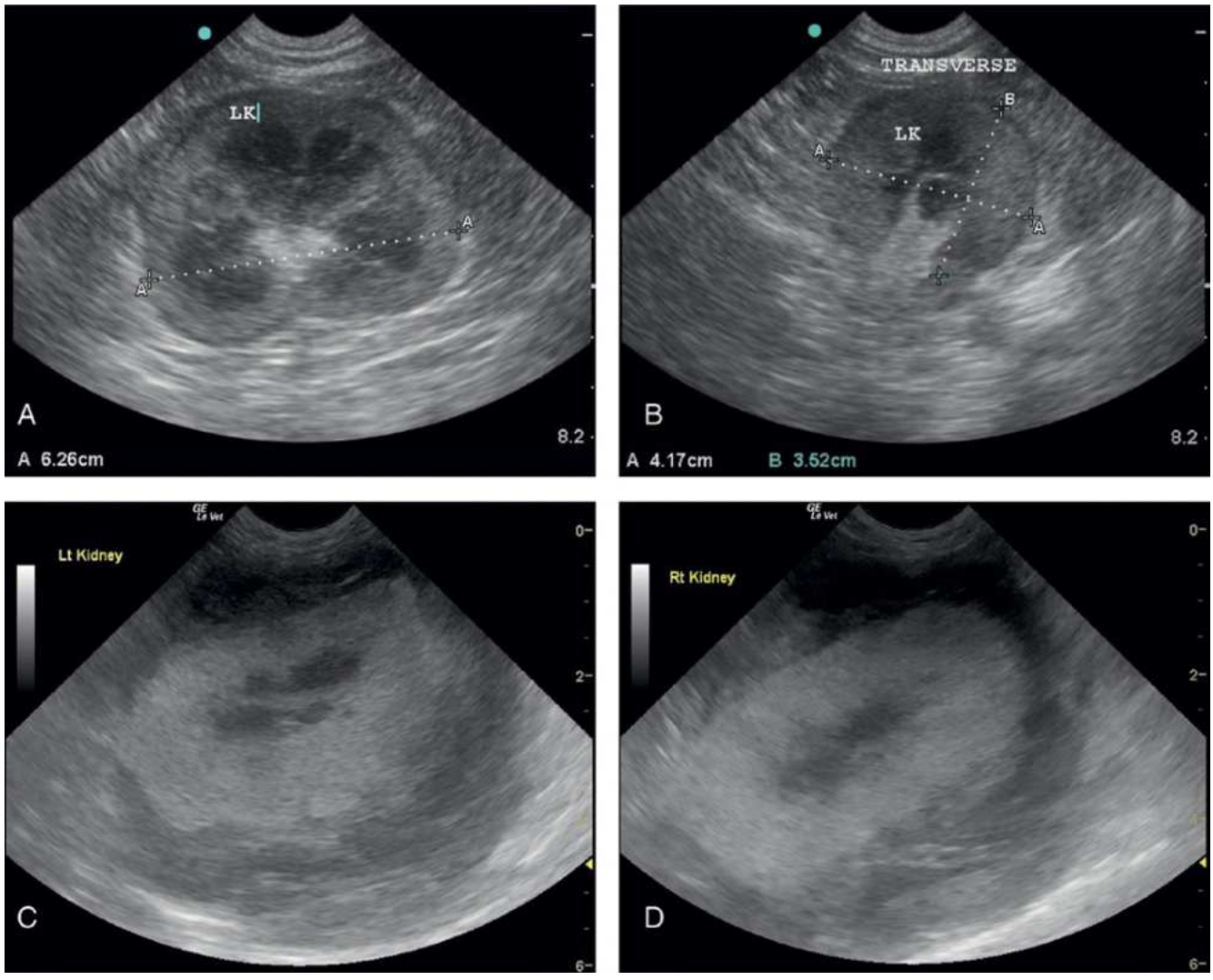


**Figure 10.10.** Renal lymphosarcoma (LSA) and its variations. (A) and (B) illustrate homogeneously hyperechoic renal cortices. This is due to the infiltrative nature of feline LSA. Images show the disease state in longitudinal and transverse planes. Both kidneys were similarly affected in this cat. (C,D) The left and right kidney of another cat with LSA. Note the variation in degrees of hyperechogenicity of renal LSA. Note also the homogeneous hyperechoic infiltration of the cortices, loss of normal renal architecture, indistinct corticomedullary definition, and the various degrees of subcapsular/perirenal fluid of images A–D.

**Pearl:** Mild to moderate symmetrical pyelectasia may be seen in animals on intravenous fluid therapy or receiving diuretics and should not be overinterpreted.

**Pearl:** Pyelonephritis cannot be diagnosed on the basis of ultrasound alone and ultrasound findings must be interpreted in light of concurrent clinical signs.

## *Hydronephrosis*

Hydronephrosis is defined as dilation of the renal pelvis and renal collecting system. It is most commonly seen with obstruction of the ureters or lower urinary tract (d'Anjou 2008) (Figure 10.13; see also Figure 16.18), and is classified by degrees varying with severity (d'Anjou 2008). Hydronephrosis is also occasionally seen as a congenital malformation.

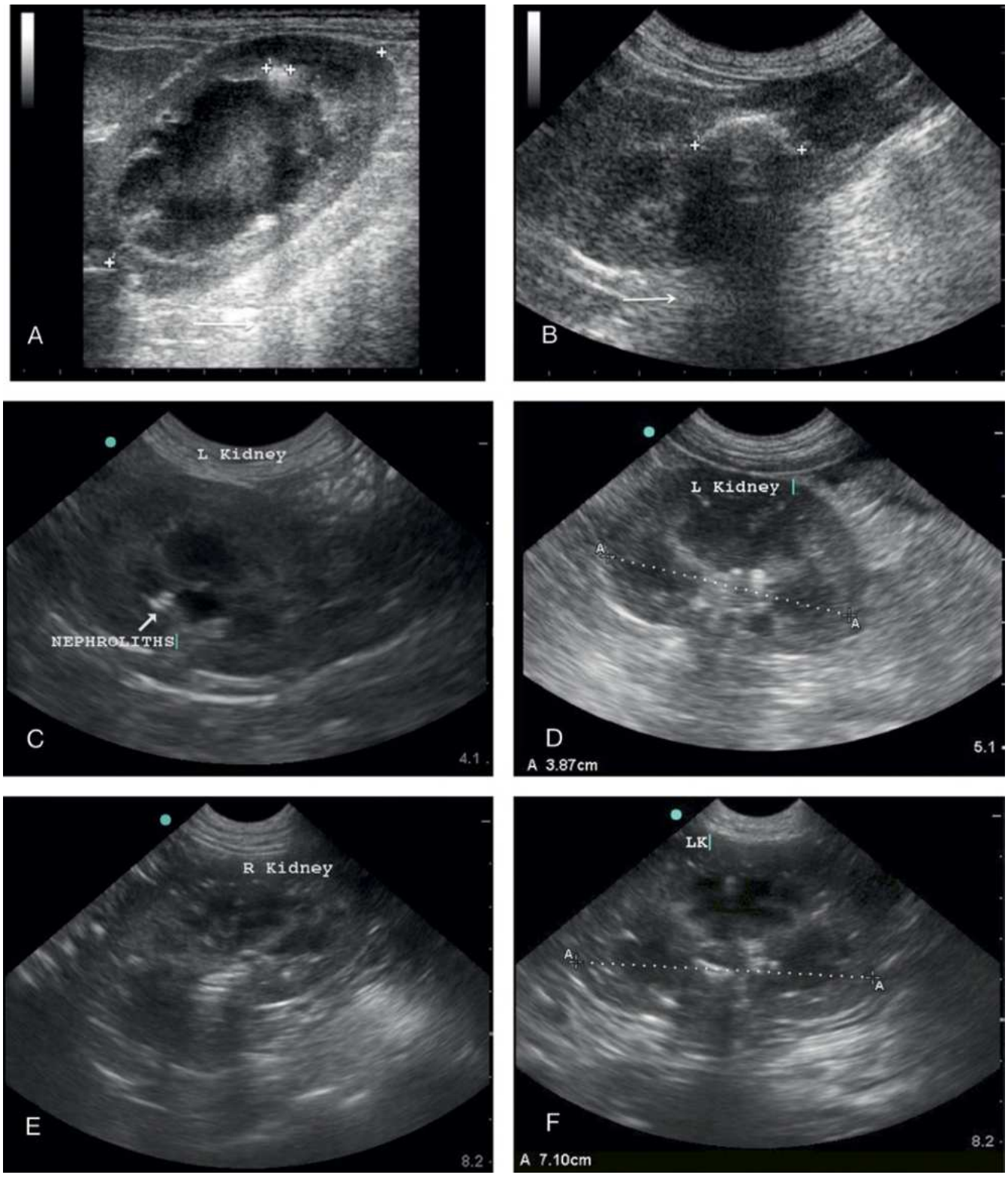


**Figure 10.11.** Nephroliths and dystrophic mineralization. (A) Patient with obstructive hydronephrosis secondary to ureterolithiasis (not shown) using a linear probe. Note the small nephrolith at the level of the renal diverticula (as denoted by the sonographer with the calipers) with subtle distal acoustic shadowing (*arrow*). Scanning and fanning in real-time imaging make these hyperechogenicities and their shadowing more readily apparent. (B) Same patient as in (A). Large nephrolith located at the level of the renal pelvis with distal acoustic shadowing (*arrow*). (C,D) Additional examples of nephroliths with more subtle acoustic shadowing. Small nephroliths may be more readily visible by abdominal radiography and some do not readily produce acoustic shadowing. Recently, the use of color flow Doppler has been documented to help diagnose people with presence of the "twinkle artifact" (see Chapter 11). (E) and (F) show dystrophic mineralization (linear hyperechoic lines) within the renal cortex that does not fit the expected pattern for interlobar/arcuate vessels or the location of renal pelvic fat. Compare to Figures 10.1F and 10.3B–D.

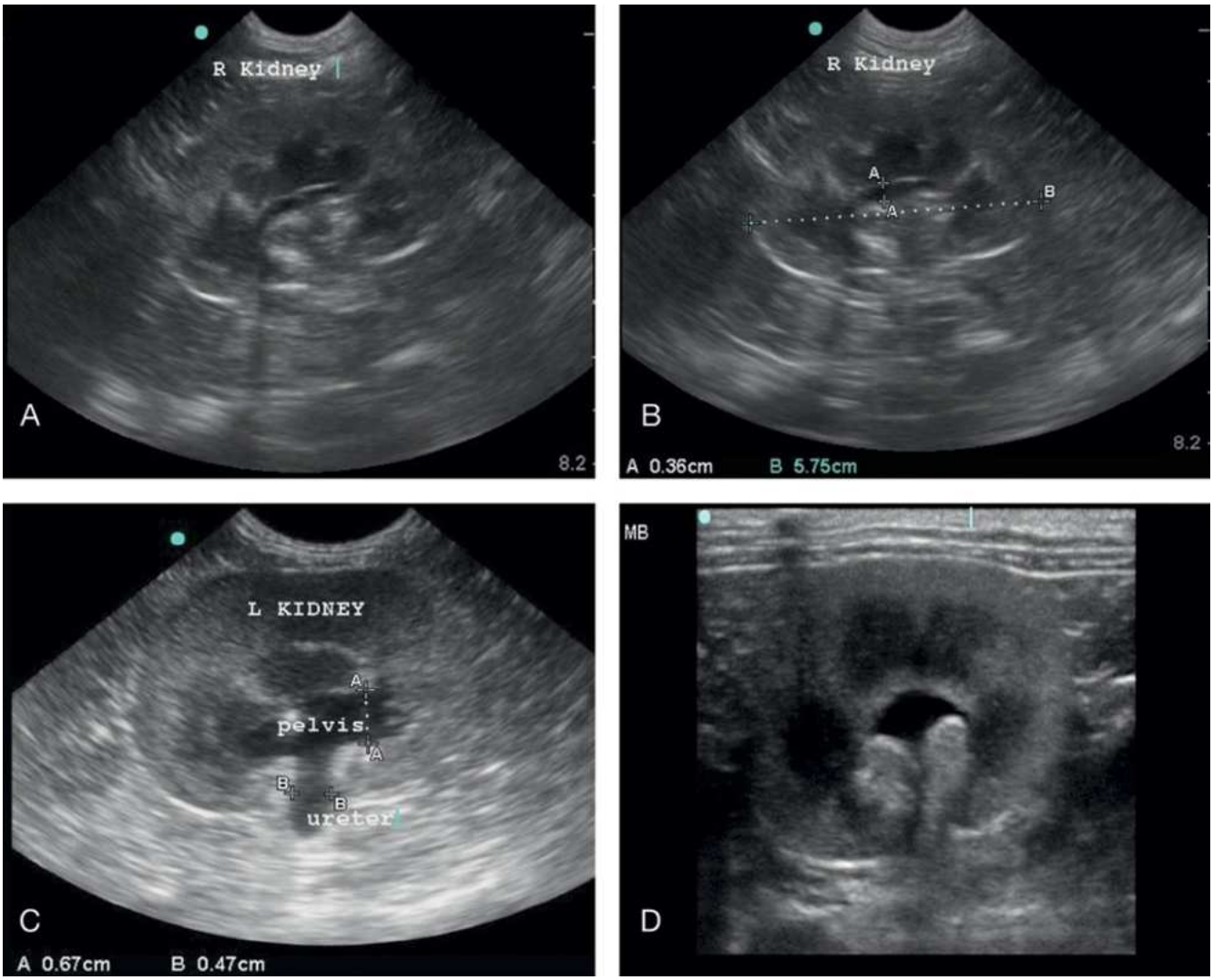


**Figure 10.12.** Various degrees of pyelectasia. (A) Mild pyelectasia in a right kidney (R Kidney). (B) Same image demonstrating caliper measurement of 0.36 cm of the renal pelvis (labeled A-A, by the sonographer) and measurement of renal length length, 5.75 cm (labeled B). (C) Severe pyelectasia, 0.67 cm (or mild hydronephrosis) (labeled A-A) with proximal ureteral distension (hydroureter). (D) Moderate to severe pyelectasia with an image from a linear probe (note the rectangular-shaped ultrasound image). Typical rule-outs for mild pyelectasia include normal variant, fluid diuresis, moderate to severely distended (full) normal urinary bladder, pyelonephritis, acute kidney injury or diuretic therapy. Partial ureteral obstruction should also be considered, especially in cases of more moderate distension. Total ureteral obstruction is highly suspected in cases of severe renal pelvic dilation or hydronephrosis, and should be ruled out with complete abdominal ultrasonography or other forms of imaging.

**Table 10.1.**
Causes of pyelectasia.

| |
|---|
| Pyelonephritis |
| Total or partial obstruction of urine flow |
| Intravenous fluid therapy |
| Diuretic therapy |
| Distended urinary bladder |
| Acute kidney injury |
| Some congenital disorders |

It is important to recognize whether or not the change is unilateral or bilateral as this will greatly affect prognosis.

Obstructive processes of the lower urinary tract (calculi, stricture, tumor) result in progressive dilation of the renal pelvis and ureter (hydroureter) with alteration of the renal architecture. Initial changes include loss of corticomedullary distinction and progressive dilation of the renal diverticuli. This

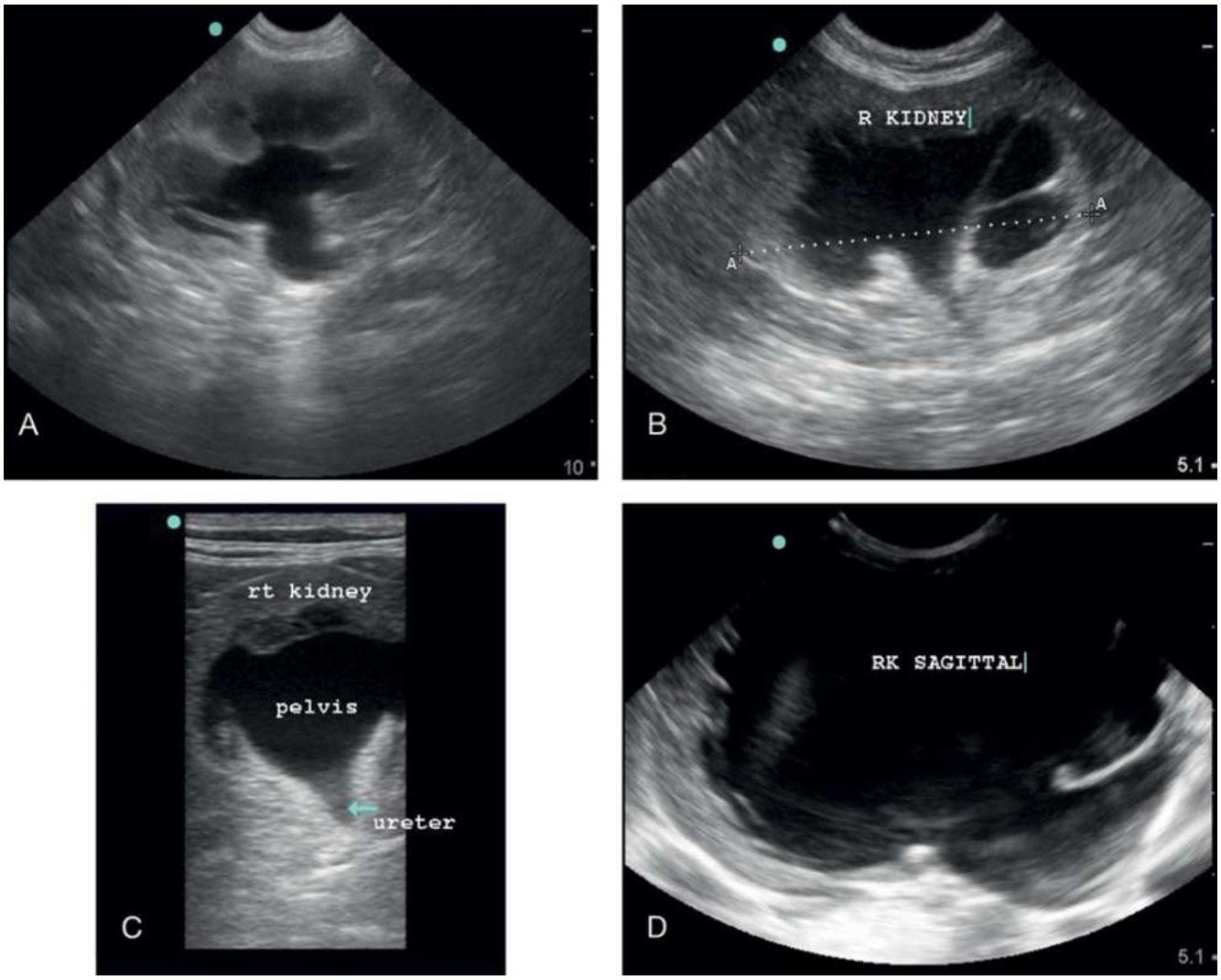


**Figure 10.13. Various degrees of hydronephrosis.** Images (A–C) depict mild to moderate hydronephrosis. A loss of normal renal architecture occurs secondary to pressure necrosis. (B) and (C) are the same kidney in longitudinal and sagittal views using curvilinear (microconvex) and linear probes, respectively. (D) Severe hydronephrosis with pressure necrosis and severe loss of renal parenchyma. The difference between pyelectasia and hydronephrosis is the absence (pyelectasia) or presence (hydronephrosis) of a total obstruction to urine flow distal to the renal pelvis. Typical causes of hydronephrosis include ureteral stones, obstructive masses in the retroperitoneal space between the kidney and the ureteral stoma, or tumors within the bladder wall and trigone that obstruct ureteral urine flow.

proceeds to enlargement of the affected kidney with a gradual decrease in the volume of normal parenchymal tissue. As the renal diverticula continue to distend, they become rounded in appearance and may be mistaken for cysts by the inexperienced sonographer, particularly in the sagittal scanning plane. The ureter may also become progressively dilated and an attempt should be made to identify the cause of obstruction (calculi, tumor, external compression by suture, etc.) by following it toward the urinary bladder (d'Anjou 2008).

**Pearl:** Findings consistent with hydronephrosis should prompt additional assessment with a complete detailed abdominal ultrasound by an experienced sonographer to evaluate for potential causes of obstruction.

## *Kidney Infarcts*

Renal infarction generally results when the blood supply to part of the kidney is impaired. The appearance of renal infarcts can be variable and is based on

the age of the insulting occlusive event. Renal infarcts may be hypoechoic (dark) initially and gradually become more echogenic (brighter) over the course of 7–17 days when they generally appear as focal-shaped, triangular hyperechoic (bright) regions within the cortex, followed by depression and shrinkage of the parenchyma due to fibrosis (Figure 10.14). Other causes of focal hyperechoic renal cortical lesions include calcification, papillary necrosis, and neoplasia.

Infarcts typically have a wedge-shaped appearance with the broad base of the wedge near the surface of the kidney and the point of the wedge extending toward the medulla. When chronic, the infarcted tissue may cause a flattening, distortion or indentation of the cortex along the surface of the kidney due to fibrosis. Infarcts do not produce a distal acoustic shadow as is expected with calcified lesions. An absence of perfusion may also be noted upon color flow Doppler interrogation of acute renal infarcts.

### *Perirenal and Retroperitoneal Fluid*

Perirenal fluid and retroperitoneal fluid are generally easy to recognize but may be challenging to differentiate. Perirenal fluid is subcapsular between the renal

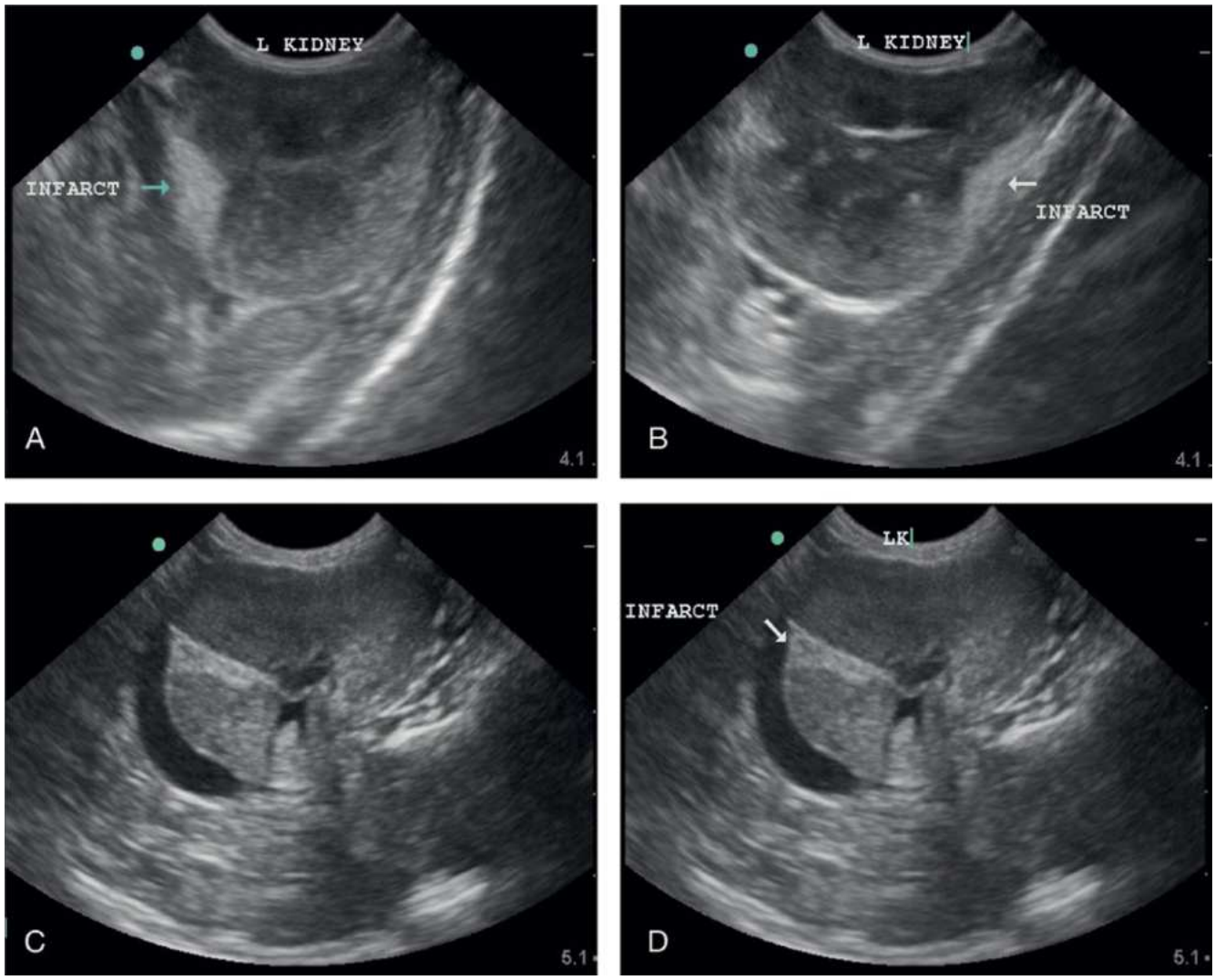


**Figure 10.14.** Renal infarcts. (A,B) Small renal infarcts. Infarcts are classically triangular or wedge-shaped and hyperechoic (bright) with their widest margin at the periphery of the renal cortex. There is no acoustic shadowing associated with such hyperechogenicity, thus differentiating infarcts from mineralization. Larger infarcts are shown in (C) and (D). These are the same images without and with labeling (LK, left kidney). Note there is a region of anechoic subcapsular fluid located immediately outside the infarction.

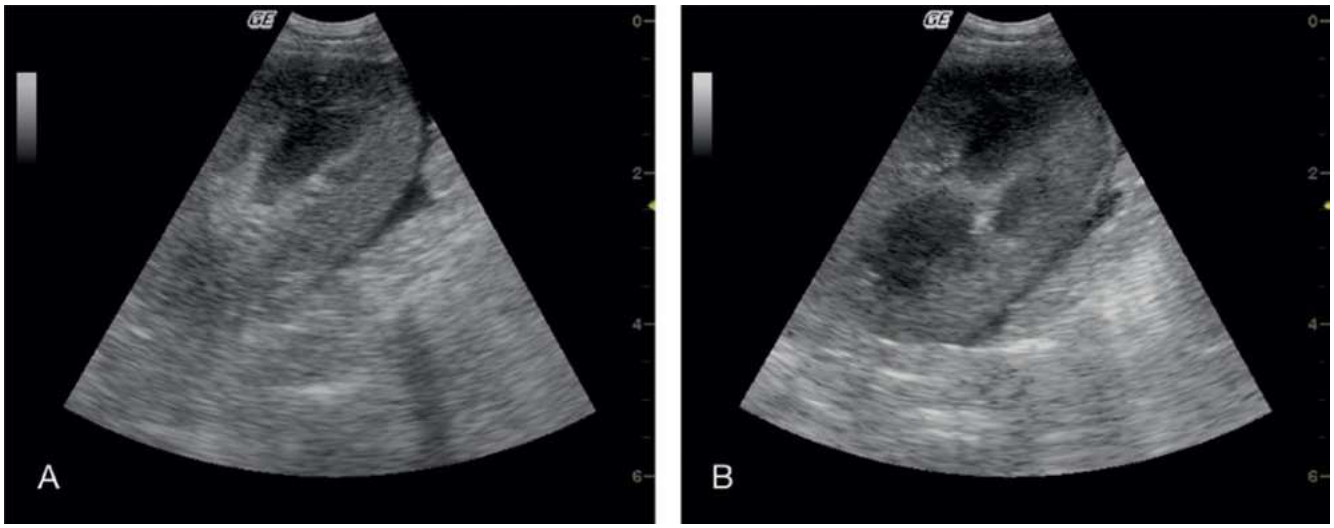


**Figure 10.15.** Acute kidney injury. Dog with a diagnosis of heat stroke 48 hours earlier. (A) and (B) show the hyperechoic cortices with a rim of perirenal fluid around each. After 24 hours of intravenous fluid diuresis, the kidney values improved and the perirenal fluid completely resolved on serial examination. The thin rim of fluid would not be safely amenable to aspiration noting that the greatest width is less than 0.5 cm using the "eyeball method" and the centimeter scale to the right of the image. Serial renal imaging can provide great value in monitoring the progression or regression of lesions, as was the case in this patient.

cortex and the renal capsule. Small amounts of perirenal fluid may be seen with infection including feline infectious peritonitis (FIP) and leptospirosis, inflammation, toxicities, coagulopathy and other causes of acute kidney injury (AKI) (Figure 10.15). Neoplasia such as renal lymphosarcoma may cause variable degrees of perirenal fluid, especially in the cat (see Figure 10.10C,D). Correlating the presence of perirenal fluid with the overall renal appearance may help determine the cause of the change. Fluid within the retroperitoneal space is external to the kidney capsule and separate from the peritoneal space. Retroperitoneal fluid may be secondary to urine leakage from a compromised or injured urinary tract, hemorrhage from a coagulopathy or traumatic injury, and abscessation (such as with migrating grass awns) (Nevins et al. 2015). In cases with accessible volumes of fluid, fine needle aspiration for fluid analysis, cytology, and culture may be accomplished with ultrasound guidance.

# Routine Add-on of AFAST and Its Abdominal Fluid Scoring System

In the authors' experience, it is invaluable to include an AFAST examination with an abdominal fluid score (AFS) to improve the diagnostic potential of the POCUS kidney. In the authors' experience, the positioning of small animal patients in dorsal recumbency for complete detailed abdominal ultrasound exams can preclude the discovery of small-volume peritoneal effusions and at the same time underestimate volume. As a result, moving the patient into lateral recumbency (right or left, with right lateral generally preferred), waiting a few minutes for any free intraabdominal fluid to redistribute, and then performing AFAST with an AFS is now the authors' standard protocol. The addition of AFAST and AFS adds little extra time, while improving diagnostic evaluation.

Although no veterinary studies have compared the detection and volume estimation of abdominal effusions in dorsal versus lateral recumbency, AFAST performed in right lateral recumbency through experience has proven to better detect small-volume intraabdominal effusions and the AFS allows for objective assessment of volume over the terms trivial, mild, moderate, and severe. The early detection of abdominal effusion is clinically important as it helps direct additional diagnostics and decision making, while reducing morbidity and mortality when such effusions are missed.

Lastly, the use of Global FAST helps rapidly differentiate localized from obvious disseminated disease, as well as screening for comorbidities and complications, by imaging the thorax for pleural and pericardial effusions (TFAST) and echo views (TFAST), and lung (Vet BLUE).

VetBooks.ir

# Pearls and Pitfalls, The Final Say

- Most patients can be imaged in dorsal recumbency for the POCUS kidney examination. However, in large and deep-chested dogs, repositioning to lateral recumbency may be needed and is particularly beneficial when imaging the right kidney which may require an intercostal approach.
- Changes in kidney parenchymal echogenicity may be identified by comparison to the adjacent organs. The renal cortex is normally isoechoic or slightly hypoechoic to normal liver and significantly hypoechoic to normal spleen. As a normal variation, however, the renal cortex may be hyperechoic to liver in cats and some dogs. Remember the "SLiCK" mnemonic regarding canine echogenicity. For the feline, hepatic echogenicity is often compared to the adjacent falciform fat and the feline liver should be isoechoic to slightly hypoechoic to the falciform fat.
- Subtle changes in echogenicity of the renal parenchyma are subjective. Changes may indicate pathology in either the kidney or the comparative organ (liver, spleen) and the patient's clinical picture must be considered to avoid interpretation errors.
- In addition, the presence of normal anatomy, and the size and symmetry between the right and left kidneys should be used to evaluate for pathology.
- A hyperechoic medullary rim sign may be seen with multiple pathological conditions including hypercalcemia, acute toxicities such as ethylene glycol, and infectious diseases such as feline infectious peritonitis (FIP) or leptospirosis. It is, however, a nonspecific finding that may also be seen in animals with normal renal function, and must be interpreted in association with additional clinical findings.
- Mineralization within the kidney can occur due to calculi or dystrophic mineralization. Both will create a strongly echogenic near-field margin and an acoustic shadow. This can be confused with hyperechoic vascular walls at the corticomedullary junction caused by interlobar/arcuate vessels, and with fat around the renal pelvis. Neither of these confounders causes a distal acoustic shadow.
- Mild symmetrical pyelectasia may occur with intravenous fluid administration or diuretic therapy and should not be misinterpreted as pyelonephritis.
- The presence of pyelectasia or hydronephrosis should prompt further evaluation for a cause of partial (pyelectasia) or total (hydronephrosis) ureteral obstruction. Additional evaluation by an experienced sonographer and perhaps additional imaging techniques (such as intravenous pyelography or computed tomography) are warranted.

# Quick Reference of Normals and Rules of Thumb

- Normal kidney size for cats is generally considered to be 3.0–4.4 cm in length depending on the reference (Nickel et al.1973; Walter et al. 1987).
- Normal kidney size in dogs is variable and depends on the size of the dog so assessment is generally subjective. Therefore, assessment of symmetry and size between the two kidneys is particularly important in dogs.
- Normal renal pelvis size (height in mm). Variability in both species. Cat 1.5–2 mm with maximum of 2.8 mm; dogs 2–3 mm with a maximum of 3.8 mm. As a general rule of thumb, consider abnormal if ≥3 mm cats and ≥4 mm dogs) (d'Anjou et al. 2011).

# References

Adams WH, Toal RL, Walker MA, et al. 1989. Early renal ultrasonographic findings in dogs with experimentally-induced ethylene glycol nephrosis. *Am J Vet Res* 50(8):137–1376.

Adams WH, Toal RL, Breider MA. 1991. Ultrasonographic findings in dogs and cats with ethylene glycol intoxication: 15 cases (1984–1988). *J Am Vet Med Assoc* 199(4):492–496.

Biller DS, Bradley GA, Partington BP. 1992. Renal medullary rim sign: ultrasonographic evidence of renal disease. *Vet Radiol Ultrasound* 33(5):286–290.

Cole LP, Mantis P, Humm K. 2019. Ultrasonographic findings in cats with acute kidney injury: a prospective study. *J Feline Med Surg* 21:475–480.

D'Anjou MA. 2008. Kidneys and ureters. In: *Atlas of Small Animal Ultrasonography*, edited by Penninck D, d'Anjou MA. Ames: Blackwell, pp 351–357.

d'Anjou MA, Bédard A, Dunn ME. 2011. Clinical significance of renal pelvic dilatation on ultrasound in dogs and cats. *Vet Radiol Ultrasound* 52(1):88–94.

Felkai C, Voros Fenyes B. 1995. Lesions of the renal pelvis and proximal ureter in various nephro-urological conditions: an ultrasonographic study. *Vet Radiol Ultrasound* 39:397–401.

Gliga ML, Chirila CN, Podeanu DM, et al. 2017. Twinkle, twinkle, little stone: an artifact improves the ultrasound performance! *Med Ultrasound* 19(3):272–275.

Neuwirth L, Mahaffey M, Crowell W, et al. 1993. Comparison of excretory urography and ultrasonography for the detection of experimentally induced pyelonephritis in dogs. *Am J Vet Res* 54:660–669.

Nevins JR, Mai W, Thomas E. 2015. Association between ultrasound and clinical findings in 87 cats with urethral obstruction. *Vet Radiol Ultrasound* 56(4):439–447.

Nickel R, Schummer A, Seiferle E, et al. 1973. Urogenital system. In: *The Viscera of Domestic Mammals*, edited by Schummer A, Nickel R, Sack WO. Berlin: Paul Parcy, pp 291–293.

Pugh CR, Schelling CG, Moreau RE, et al. 1994. Iatrogenic renal pyelectasia in the dog. *Vet Radiol Ultrasound* 35:50–51.

Walter PA, Feeney DA, Johnston GR, Fletcher TF. 1987. Feline renal ultrasonography: quantitative analyses of imaged anatomy. *Am J Vet Res* 48:596–599.

Yeager AE, Anderson WI. 1989. Study of association between histologic features and echogenicity of architecturally normal cat kidneys. *Am J Vet Res* 50:860–863.

# Further Reading

Barella G, Lodi M, Sabbadin LA, et al. 2012. A new method for ultrasonographic measurement of kidney size in healthy dogs. *J Ultrasound* 15(3):186–191.

Spies JB, Hricak H, Slemmer TM, et al. 1984. Sonographic evaluation of experimental acute renal arterial occlusion in dogs. *Am J Roentgenol* 142(2):341–346.

CHAPTER ELEVEN

# POCUS: Urinary Bladder

Stephanie C. Lisciandro and Sarah Young

## Introduction

POCUS assessment of the urinary bladder is relatively easy to learn because, as with the gallbladder, fluid-filled structures are easily imaged with ultrasound. As a result, ultrasound examination is more sensitive than abdominal radiography for detecting abnormalities of the urinary bladder wall and evaluating for nonmineral dense luminal contents such as sediment, proteinaceous and cellular debris, and radiolucent calculi. The use of the POCUS urinary bladder examination optimizes patient care and clinical course with improved diagnosis and recognition of abnormalities otherwise undetected by traditional radiographic means. POCUS urinary bladder examination does not replace a complete abdominal and urinary tract ultrasound study by a veterinarian with advanced training (radiologist or internist) and provides only a limited evaluation of the proximal urethra. A combination of ultrasonography and special contrast-assisted radiographic studies may still be needed for a comprehensive evaluation of the urinary tract and adjacent structures.

### What the POCUS Urinary Bladder Can Do

- Recognize abnormalities of the bladder wall such as cystitis, polyps, and tumors.
- Recognize abnormalities of the urinary bladder lumen such as stones (calculi), sediment, and blood clots.
- Take advantage of a newly described technique for the detection of small uroliths (<5 mm) using color flow Doppler and the "twinkle artifact."

### What the POCUS Urinary Bladder Cannot Do

- Cannot differentiate benign from malignant urinary bladder wall infiltration or mass lesions.
- Cannot confirm urinary bladder infection (bacterial cystitis).
- Cannot accurately diagnose bladder wall abnormalities in a poorly filled urinary bladder.

**Pearl:** Be aware of ultrasound artifacts that may lead to a misdiagnosis. Gas in the colon and small intestine may be mistaken for a calculus or mineralized sediment, edge shadowing artifact may be mistaken for a wall defect, and slice thickness and side-lobe artifact may be misinterpreted as luminal sediment or a mass.

### Indications

- Hematuria, dysuria, stranguria, and signs of urinary tract infection.
- History of previously confirmed urolithiasis.
- Undifferentiated caudal abdominal pain or spinal pain.
- Unexplained urinary retention and urinary bladder distension.

### Objectives

- Identify urinary bladder wall (mural and extramural) abnormalities such as cystitis, polyps, and tumors.

*Point-of-Care Ultrasound Techniques for the Small Animal Practitioner*, Second Edition. Edited by Gregory R. Lisciandro.
© 2021 John Wiley & Sons, Inc. Published 2021 by John Wiley & Sons, Inc.
Companion website: www.wiley.com/go/lisciandro/ultrasound2

- Recognize urinary bladder luminal abnormalities such as urinary bladder stones (calculi), sediment, and blood clots.

VetBooks.ir

# Patient Positioning and Probe Selection

A 7.5–10 MHz curvilinear (microconvex) probe is adequate for evaluation of the urinary bladder in most patients. A 7.5–10 MHz linear probe provides increased image resolution (but less penetration) and can be useful for smaller dogs and cats, or when subtle changes of the urinary bladder wall are noted. A linear probe can be of particular benefit when evaluating the urinary bladder neck and proximal urethra for mural and luminal abnormalities. Moderate distension of the urinary bladder is ideal for complete evaluation of the bladder wall and lumen, and reduces the incidence of misdiagnoses due to artifact. If reevaluation within 5–8 hours does not lead to sufficient urinary bladder distension, then a low dose of injectable furosemide or infusion of sterile saline into the bladder via catheterization are strategies to consider in order to obtain optimal bladder distention.

**Pearl:** A urine-filled bladder optimizes sonographic imaging of the bladder wall and lumen. When possible, refrain from walking dogs and remove the litter box from cats several hours prior to their POCUS urinary bladder examination.

The patient is typically positioned in dorsal recumbency but in reluctant patients, lateral recumbency may be used. Clipping the caudoventral abdominal hair and applying acoustic coupling gel will maximize image quality. If calculi or other intraluminal abnormalities are suspected, then changing patient body position throughout the scan, for example from lateral to standing, can discriminate moveable from nonmoveable abnormalities. Unless they are adherent to the urinary bladder wall, sediment, blood clots, and calculi will fall to the gravity-dependent luminal surface, whereas artifacts and mural abnormalities will persist.

The authors recommend performing a Global FAST to screen for any intrathoracic problems including pleural and pericardial effusion, cardiac and pulmonary conditions, and abnormal volume status that may pose patient risk *before* moving the patient into dorsal recumbency.

# How to do POCUS Urinary Bladder

With the patient in dorsal recumbency, the caudal abdomen is scanned using a transabdominal approach. The entire urinary bladder should be visualized in both longitudinal and transverse planes. This can be achieved by fanning from just beyond the apex to the shadowing brim of the bony pelvis in the transverse plane, and from just beyond either side of the serosal margins of the urinary bladder in the sagittal plane. This is especially important when assessing for wall thickening or mass lesions since reverberation artifacts may alter the appearance of the bladder wall and may mimic abnormalities (Figure 11.1A). These artifacts can be minimized by examining from multiple scanning angles. If review of the POCUS urinary bladder is submitted for specialty evaluation, submission of cine clips in both the transverse and sagittal planes is imperative for an accurate assessment.

In addition, the proximal urethra should be assessed for dilation, normal wall thickness, and intraluminal abnormalities. The prostate should be subjectively assessed for size (expected to be approximately 1 cm in the neutered male dog), symmetry, pain upon interrogation and parenchymal abnormalities such as abnormalities of echogenicity and mural lesions (e.g., masses, polyps, and cysts), and intraluminal and intramural mineralization (see Chapter 13).

The primary purposes of the POCUS urinary bladder examination are to evaluate for obvious abnormalities of the urinary bladder wall (diffuse thickening versus focal abnormalities) and for intraluminal abnormalities such as calculi, sediment, and blood clots.

# Ultrasonographic Findings in a Normal Urinary Bladder

The normal urinary bladder wall consists of four layers: an outer serosal layer (hyperechoic), muscularis layer (hypoechoic), submucosa (hyperechoic), and inner mucosal layer (hypoechoic). These layers are not well delineated and the inner mucosal layer is rarely distinguishable from the urine unless inflamed and irregular. As a result, when the layers are visible, the wall typically has a three-layered appearance, having two thin mildly hyperechoic (bright white) layers with a thin hypoechoic (dark) central layer (see Figure 11.1B).

The thickness of the urinary bladder wall varies with bladder distension. In cats, reported normal wall

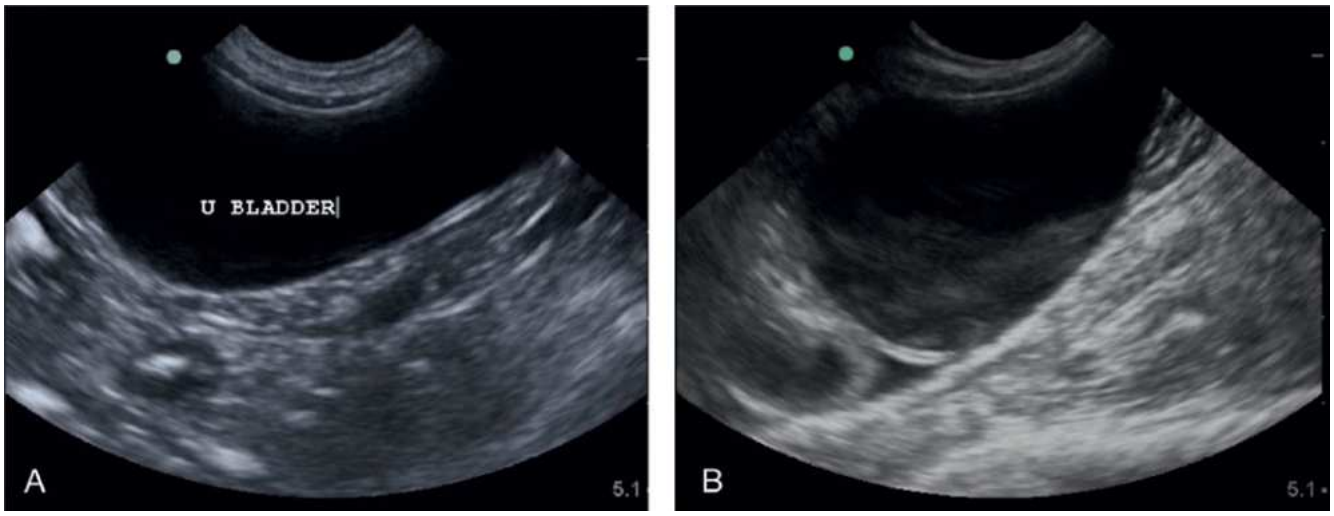


**Figure 11.1.** Normal urinary bladder and its wall. (A) A normal urine-filled (pure anechoic [black] urine) urinary bladder with subtle artifact in the far-field. Notice how thin the normal urinary bladder wall is when the organ is distended. The normal wall has outer and inner hyperechoic lines with an inner hypoechoic sonolucent line (double line effect) that is most visible on the right third of the wall in the far-field. (B) A normal urinary bladder with mild side-lobe and slice thickness artifact mimicking sediment. Note the urinary bladder wall is against ("kissing") the abdominal wall (bright white line) in the far-field. A small triangle of free fluid is present between its apex and the body wall in the gravity-dependent far-field. In general, the urinary bladder apex, with the patient placed in lateral recumbency, is a good location to search for small-volume peritoneal effusion. The normal urinary bladder wall (double line) is seen only near the bladder's apex in this image.

thickness ranges from 1.3 to 1.7 mm (Finn-Bodner 1995). In dogs, the reported normal range is from 1.4 mm in moderately distended bladders to 2.3 mm in minimally distended bladders (Geisse et al. 1997), with normal generally being less than 3 mm. Additionally, wall thickness increases with body size by up to 1 mm in heavier dogs (Geisse et al. 1997).

**Pearl:** Urinary bladder wall thickness in dogs should not exceed 3 mm in moderately distended bladders.

## Urine

Normal urine is uniformly anechoic (black) in dogs; however, cats have more concentrated urine and may have lipid droplets which affect echogenicity (see Chapter 39). The presence of echogenic, amorphous material within the urinary bladder lumen may be consistent with crystalline, proteinaceous, lipid or cellular debris. Side-lobe, slice thickness, and edge shadowing artifacts should not be misinterpreted as luminal debris or mural lesions, and care should be taken to distinguish these artifacts from true lesions (see Figure 11.1; see also Chapter 3).

## Ureters

Normal ureters are difficult to identify as they enter at the trigone. With experience, they may be identified as two small echogenic structures approximately 1–2 mm shaped as "equalsigns" on either side of the trigone, best seen in the transverse plane. The ureters should not be fluid filled; however, the ureteral papillae (ureterovesicular junctions) are occasionally seen as paired small, isoechoic to slightly hyperechoic (white) bumps protruding into the lumen from the caudodorsal bladder wall, which is in the far-field in dorsal recumbency and should not be mistaken for a bladder wall mass (Figure 11.2). Urine may at times be seen jetting into the urinary bladder from either ureter. This vesiculoureteral reflex typically appears as a faint jet of echogenic moving or swirling fluid, and is visible due to the slight difference in specific gravity between the urine from the kidney and the urine within the bladder. Color flow Doppler or power Doppler can also be used to visualize the urine jet and thus distinguish a ureteral papilla from other causes of focal wall thickening (see Figure 11.2B).

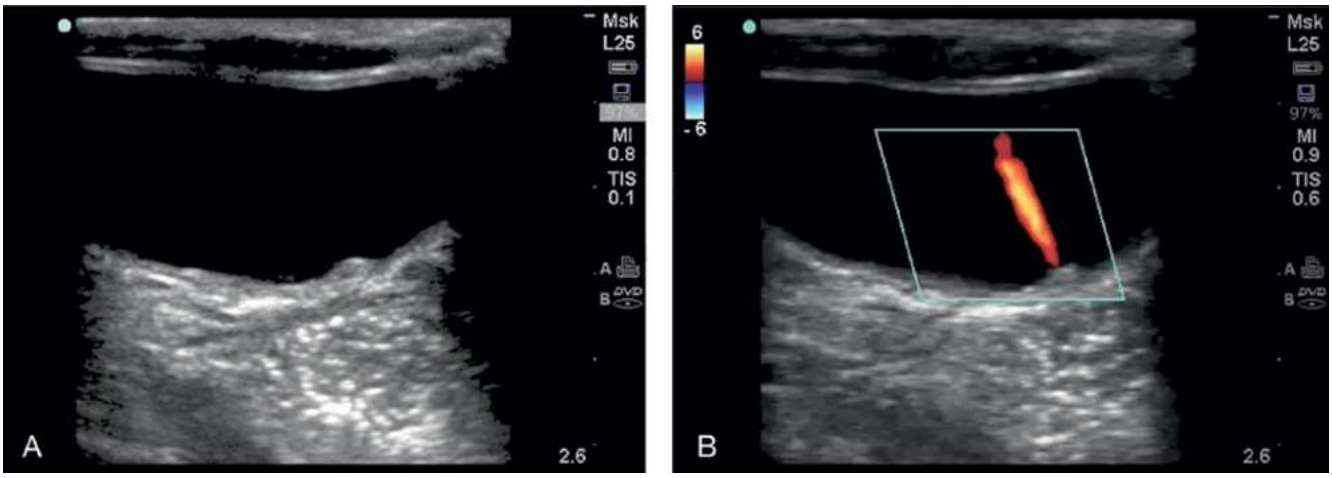


**Figure 11.2.** Normal ureteral papilla. (A) A linear probe ultrasound image showing the ureteral papilla. In real-time two-dimensional B-mode, the urine can be seen swirling or jetting. (B) Swirling or jetting of urine entering the urinary bladder lumen from the same ureteral papilla as in (A) is obvious using color flow Doppler. Note the red flow toward the transducer, and the normal urinary bladder wall (double line) in the near-field along the ventrum of the patient positioned in dorsal recumbency.

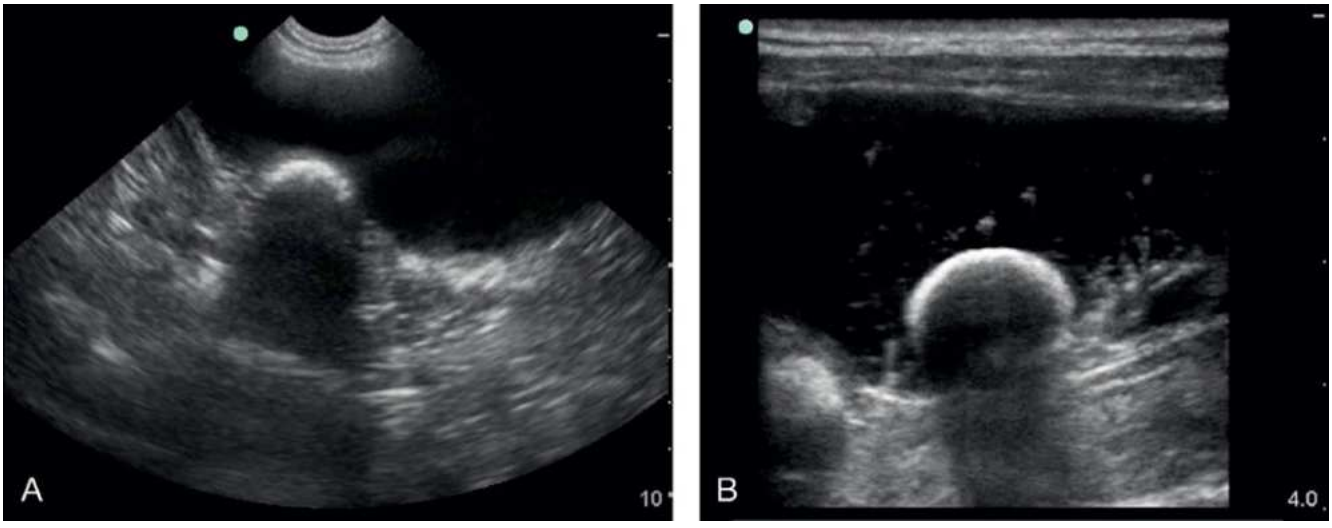


**Figure 11.3.** Colon shadowing compared to a bladder stone. (A) The air- and fecal-filled colon can mimic cystic calculi by causing strong or "clean" distal acoustic shadowing through the distal or far-field. Removing some of your probe pressure, reevaluating in different planes, and/or placing the animal in a standing position can aid in mitigating the artifact. (B) Compare to (A); this is shadowing created by a similarly shaped bladder stone rounded in the near-field. Multiple views that are gravity dependent help discriminate colon artifact from true bladder stones.

# Artifacts Associated with POCUS Urinary Bladder

It is very important to be familiar with artifacts associated with the fluid-filled urinary bladder and the closely associated and potentially air- or fecal-filled colon. Fluid-related artifacts include side-lobe, slice thickness, edge shadowing (refraction), and acoustic shadowing and enhancement (see Chapter 3). Air-related artifacts or reverberation artifacts can cause false abnormalities of the bladder wall and lumen. Both fluid- and air-related artifacts can mimic pathology and combinations of the aforementioned may confound ultrasound interpretation of the urinary bladder (Figure 11.3; see also Figures 11.1B, 11.9, 11.10B, and Chapter 3). A recently described and practical artifact, referred to as the

"twinkle artifact," may allow detection of small uroliths (renal, ureteral, and bladder) that are <5 mm in people, a traditionally difficult size range to diagnose accurately with B-mode (Gliga et al. 2017) (see section on Calculi below). In this study, the artifact was over 90% sensitive and specific and over 90% for positive and negative predictive values. The twinkle artifact (also referred to as the color comet tail artifact) employs color flow Doppler evaluation of the region of interest to evaluate for a focus of alternating colors behind a reflective object (such as a calculus) (Gliga et al. 2017).

# Clinical Significance and Implications of Abnormal POCUS Urinary Bladder Findings

The primary purpose of the POCUS urinary bladder is to detect obvious abnormalities of the wall and lumen. Abnormalities of the proximal urethra and prostate may also be identified and may be clinically relevant.

## *Abnormalities of the Bladder Wall*

The urinary bladder wall should be assessed for diffuse and focal changes.

### Diffuse Changes

Diffuse changes in the urinary bladder wall are most consistent with cystitis or other infiltrative or systemic disease processes, such as mural hemorrhage due to coagulopathy or rodenticide toxicity.

#### *Cystitis*

Cystitis is the most common cause of diffuse change and may result in diffuse changes in echogenicity, such as hypoechoic urinary bladder thickening, but can especially occur along the cranioventral and apical aspects of the bladder. Cystitis may also result in irregularity of the luminal surface (Figure 11.4A,C). Polypoid cystitis is a chronic form of cystitis occasionally seen in dogs that results in multiple pedunculated masses projecting into the lumen (see Figure 11.6B–D).

#### *Emphysematous Cystitis*

This uncommon form of cystitis is most often seen in diabetic animals secondary to chronic bacterial infection with mural extension and gas-producing bacteria within the urinary bladder wall. It results in hyperechoic foci of gas within the wall and subsequent mural reverberation (comet tail and ringdown) artifacts (Figure 11.5). In some cases, the changes may be severe and can be confused with neoplasia. The appearance may be very confusing for the unsuspecting sonographer as the gas-associated artifacts from within the wall can be so severe that they obscure visualization of a normal urinary bladder altogether. The general rule of thumb during ultrasound when you cannot acquire an acceptable image is to perform radiography. In the case of emphysematous cystitis, radiography should reveal a gas bubble within the lumen of the bladder consistent with air within the lumen.

**Pearl:** When diffuse wall thickening is noted, a urinalysis and microbial urine culture should be performed to rule out bacterial cystitis. If clinical signs and diffuse sonographic changes persist following appropriate therapy, then traumatic catheterization, ultrasound-guided fine needle aspiration or biopsies are indicated for definitive diagnosis.

### Focal Irregularities

Focal irregularities in the urinary bladder wall are generally easy to detect when the bladder is urine filled and appropriately distended. These focal changes most commonly are due to either benign polyps or neoplasia. Remember that the presence of the ureteral papillae protruding from the dorsal wall of the bladder at the trigone is normal and should not be confused with a mass lesion (see Figure 11.2).

#### *Benign Polyps*

Usually have a pedunculated appearance and are attached to the mucosa by a narrow stalk (Figure 11.6 B–D). However, it *is not possible to* distinguish between benign and malignant bladder tumors based on ultrasonographic appearance alone.

#### *Neoplasia*

The most common neoplasia of the urinary bladder is transitional cell carcinoma (TCC). The appearance is variable but generally the tumor presents as an irregular, hyperechoic, broad-based mural lesion (Figure 11.7). Other possible tumors of the urinary bladder wall include squamous cell carcinoma, leiomyosarcoma, lymphoma, and a variety of

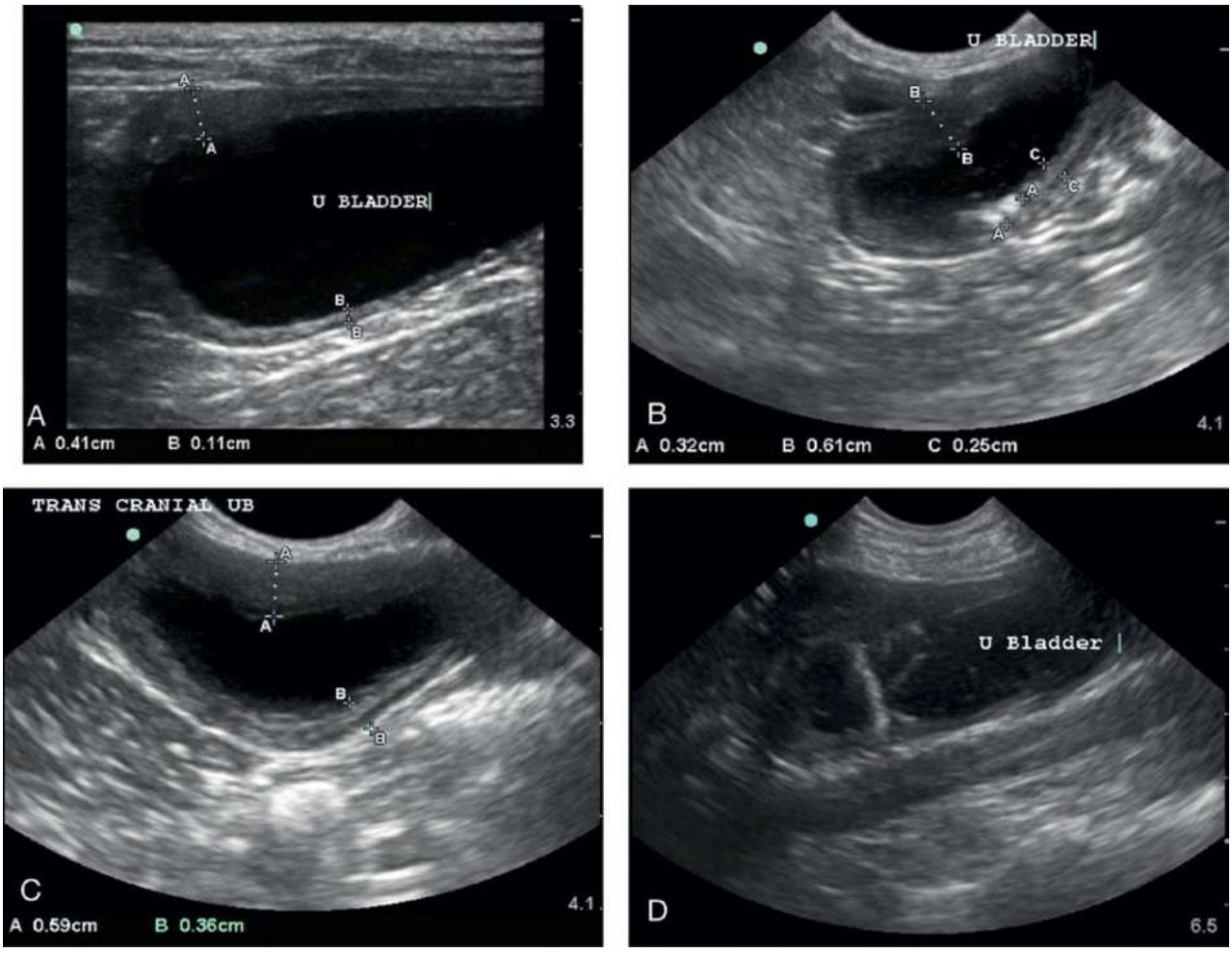


**Figure 11.4.** Examples of the variability of cystitis. (A) Irregular bladder wall thickening extending out to the apex is typical of bacterial cystitis, Note the echogenicity is hypoechoic to the adjacent normal wall. (B) Bacterial cystitis with multiple lesions including circumferential mural thickening (B and C cursors) and settled urinary bladder debris noted by a few small echogenic stones (A cursor). (C) Another example similar to (A) of generalized irregular wall thickening. (D) A good example of how a nondistended urinary bladder (labeled "U Bladder") wall may be difficult to interpret ultrasonographically. The image is further complicated by echogenic debris, which in this case is luminal hemorrhage and blood clot (thrombus).

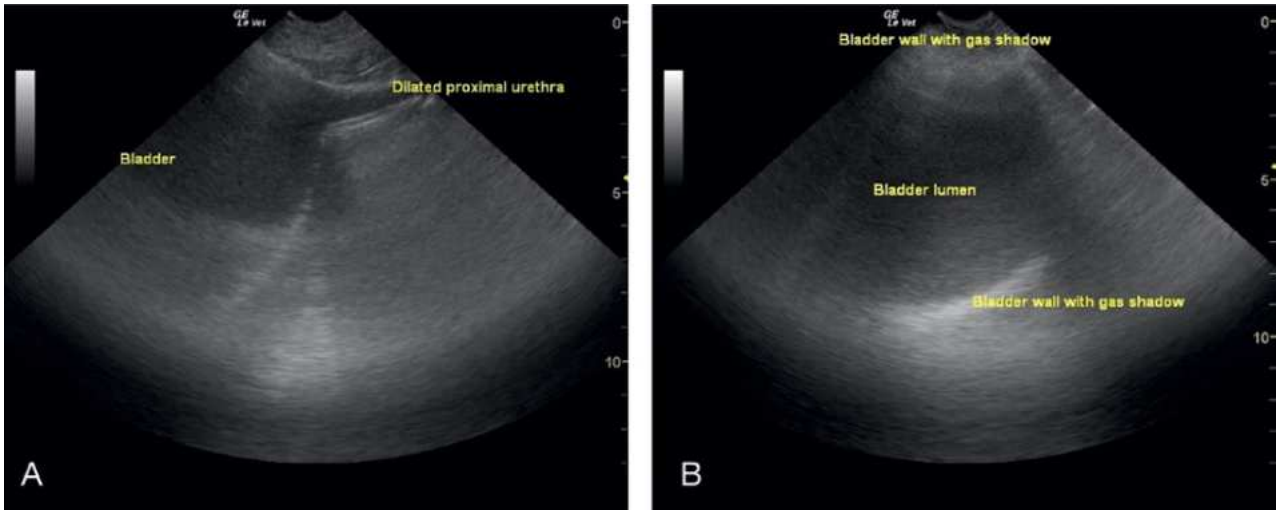


**Figure 11.5.** Emphysematous cystitis. An uncommon form of bacterial cystitis with severe gas-associated artifacts (shadowing, reverberation, and ringdown) due to an emphysematous urinary bladder wall in a dog with pituitary-dependent hyperadrenocorticism and diabetes mellitus. (A) Sagittal labeled view of the urinary bladder lumen with reverberation artifact obscuring the trigone region. (B) A transverse view (labeled) of the same urinary bladder. In both views, the lumen is difficult to view clearly because of the air interference of gas shadowing. A good general rule of thumb is add-on radiography when ultrasound imaging fails to be acceptable no matter what adjustments you make with your machine.

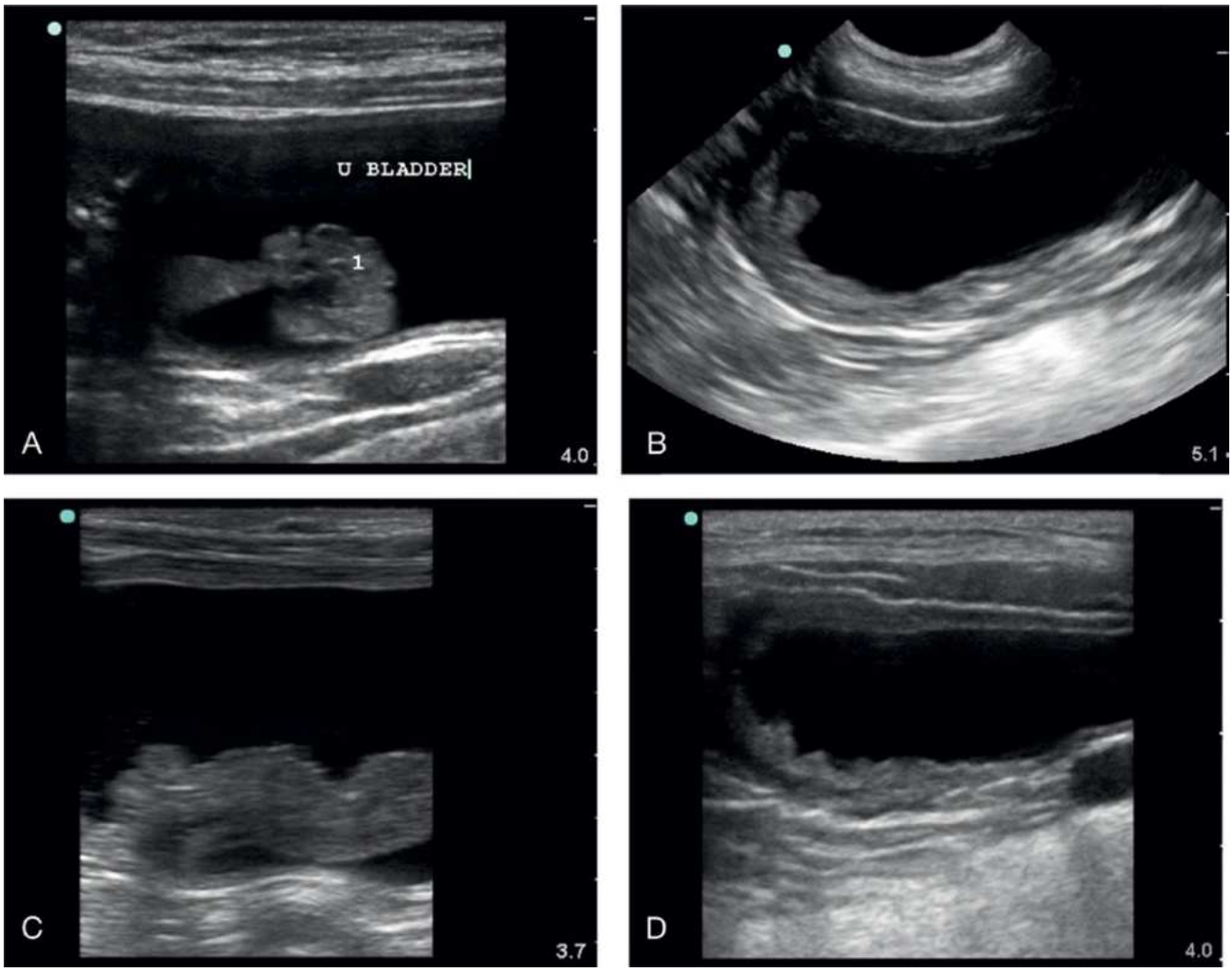


**Figure 11.6.** Benign polyps. (A) An image using a linear probe of a classic benign polyp appearing with its pedunculated stalk. (B) A small polyp extending into the bladder lumen near its apex. (C) Another example of a large mass-like polyp as in (A). (D) Diffuse benign polypoid cystitis located along the dorsal urinary bladder (patient in dorsal recumbency).

mesenchymal tumors. Thrombi (blood clots), which have varying degrees of echogenicity, can be mistaken for neoplasia. Thrombi are typically mobile within the bladder and will organize and contract with time. Changing patient body position to assess for movement within the lumen and serial monitoring for changes in appearance may be helpful. Use of color flow Doppler can generally differentiate between neoplasia and thrombi based on the presence or absence of blood flow within the structure. Neoplasia will have blood flow and thrombi will not (neither will artifact). Thrombi may be iatrogenic and associated with a recent history of cystocentesis. Regardless of etiology, these should shrink and resolve with time, whereas neoplasia will typically progress over time (see Figure 11.11).

In the dog, the most common location of TCC is near the trigone (Leveille et al. 1992) but they can occur in any region of the bladder wall or urethra, and can occasionally be seen extending into the urethra from the bladder lumen or into the bladder lumen from the urethra. TCC is more common in females. Obstruction of the ureters with secondary hydronephrosis may occur due to obstruction of the ureteral papillae by tumor. Therefore, assessment of the ureters and kidneys is indicated, and easily performed for further evaluation of the urinary tract in patients with suspected TCC. In fact, the Global FAST approach allows for rapid same-day staging for obvious hydronephrosis, liver, and pulmonary metastasis as well as any cardiac complications (see Chapters 10 and XX).

In cats, TCC is less common than in dogs and more often seen in older males. In cats, TCC is more commonly located near the apex of the bladder and thus may be more amenable to surgical resection; median

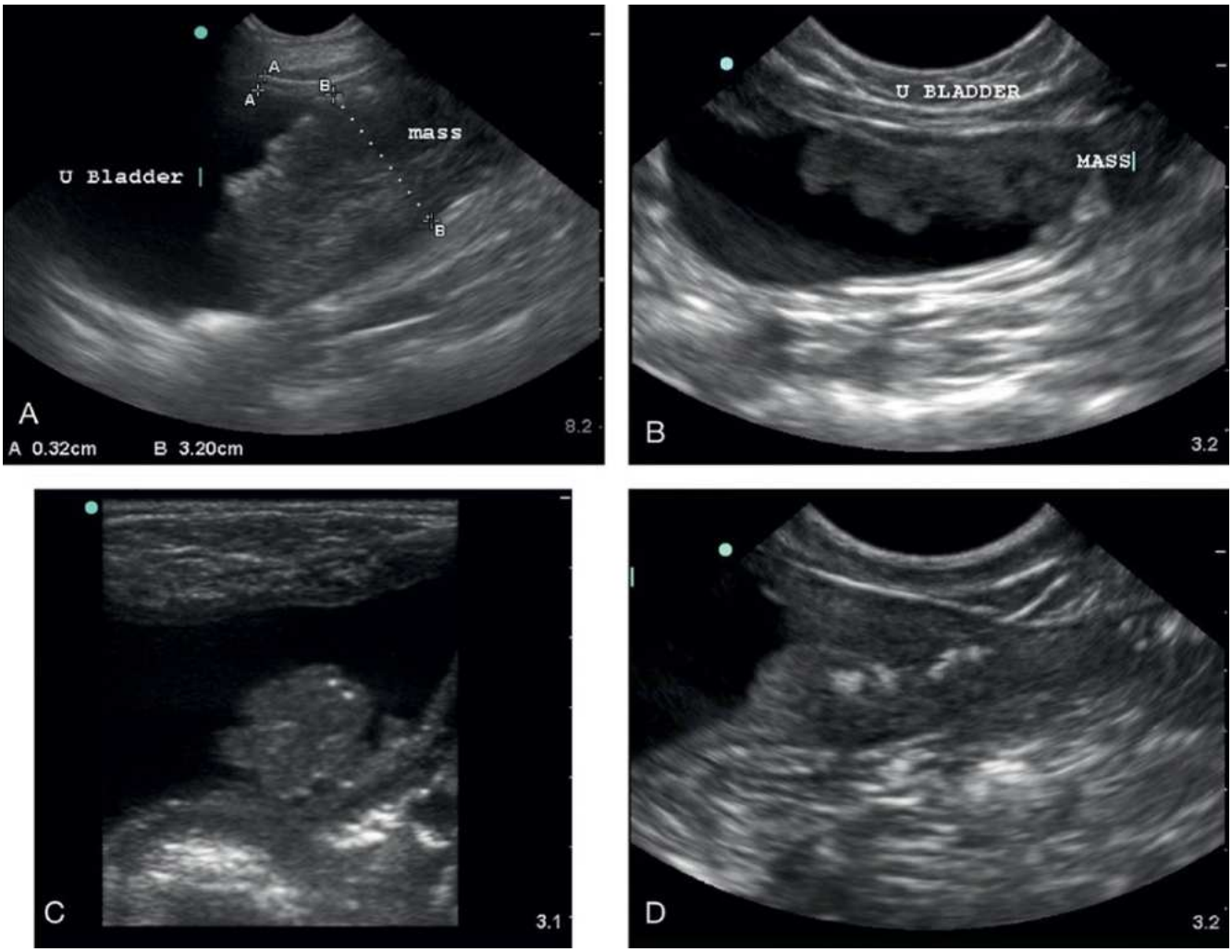


**Figure 11.7.** Mural urinary bladder neoplasia. (A) Transitional cell carcinoma (TCC) in a dog. In contrast to cystitis, the lesions more typically afflict the trigone region (versus apex), but can occur anywhere along the urinary bladder wall. (B) Similar to (A), the mass lesion is away from the apex and is another example of TCC. (C) An example of how TCC may have a polypoid appearance. (D) Trigone-related urinary bladder neoplasia (away from the apex). The visible proximal urethral lumen is obstructed by the mass, the full extent of which would require a special positive contrast radiographic study to completely evaluate, for example vaginocystourethrography in the female patient or retrograde positive contrast urethrography in the male patient. Notice the hyperechoic stippling throughout the mass consistent with either malignant mural mineraliztion or concurrent urolithiasis.

survival times are similar to dogs. Feline TCC, however, originates from any region of the bladder wall and the entire bladder should be thoroughly evaluated (Wilson et al. 2007).

Sonographic characteristics of TCC bladder tumors include a broad base and an irregular luminal surface and they may contain foci of mineralization. Concurrent bladder sediment, calculi, and/or cystitis are common. More recently, TCC of the urinary bladder has been referred to as a urothelial carcinoma (Sommer et al. 2018; Lin et al. 2018).

**Pearl:** Diagnosis of bladder neoplasia requires cytological or histopathological confirmation. Cytology may be acquired via urinalysis, traumatic catheterization or fine needle aspiration (risk of seeding tumor). Alternately, Cadet® BRAF Mutation Detection Assay (Sentinel Biomedical, Raleigh, NC) may be helpful to assess for bladder neoplasia (TCC/urothelial carcinoma). A urinary bladder wall biopsy may be necessary to definitively determine the tumor type in order to guide therapy and assess prognosis.

Percutaneous fine needle aspiration of bladder tumors should be pursued with caution. Although extremely rare, TCC has the potential to seed along the needle track, resulting in regional spread of the tumor (Nyland et al. 2002; Vignoli et al. 2007; Liffman and Courtman 2017). Ultrasound-guided suction biopsy of the mass by urinary catheter may provide ample cells or tissue for diagnosis. Referral for a complete detailed abdominal ultrasound by an experienced sonographer is recommended if fine needle aspirates are to be pursued.

## *Intraluminal Abnormalities*

Intraluminal abnormalities of the urinary bladder include calculi, blood clots (thrombi), and sediment.

### Calculi (Bladder Stones)

Calculi (bladder stones) are discrete mobile objects with curvilinear hyperechoic (bright) surfaces within the lumen of the bladder. They are generally round in appearance but may be variable in shape and size, and may be clustered together. Calculi usually have a distal acoustic shadow but very small calculi (<1–2 mm) may not produce an appreciable shadow (Figure 11.8).

However, in people, a new artifact, referred to as the "twinkle artifact," has been used to detect uroliths (renal, ureteral, and bladder) that are <5 mm, a traditionally difficult size range to accurately diagnose with B-mode (Gliga et al. 2017). This twinkle artifact, created by intrinsic ultrasound machine noise seen with color flow Doppler, has been shown to be more sensitive for the detection of small stones (<5 mm) than acoustic shadowing. The twinkle artifact is most apparent when the reflecting surface of the urolith (renal, ureteral, or cystic) is irregular and the focal zone is placed below the reflecting surface of the suspect object. In summary, the twinkle artifact occurs when color flow Doppler is applied to the region (suspect stone) in question and red/blue turbulent or pulse-like "twinkling" is seen behind the mineralization (Gliga et al. 2017). Interestingly, the twinkle artifact may be applied to other organs with suspected mineralization (Gliga et al. 2017).

Size of the calculi is important to note and record as it may have clinical implications regarding therapy, particularly for evaluating the likelihood of a calculus safely passing through the urethra either spontaneously or by voiding hydropropulsion. The following guidelines for voiding urohydropulsion (VUH) have been published (Defarges et al. 2013).

- Female dogs (>2 kg) can typically void stones <3–4 mm.
- Female cats may be able to void stones <3 mm.
- Male dogs weighing 5–10 kg may be able to void stones <2–3 mm; male dogs >10 kg may be able to void stones <3 mm.
- Male cats: voiding urohydropulsion is not recommended.

**Pearl:** The ease of passing a 9 French urinary catheter correlates with the successful voiding of 3 mm stones.

The number of calculi is also important to assess, although cannot often be accurately established, particularly when calculi are clustered together. Note also that calculi may be located within the urethra, and the proximal and prostatic urethra should be visualized for intraluminal calculi.

**Pearl:** The presence of echogenic urine is not specific for urinary tract infection or other pathology and a urinalysis (and urine culture) should be obtained to determine the significance of the ultrasonographic finding(s).

**Pitfall and Pearl:** Gas, formed fecal matter in the colon, and associated artifacts (i.e., acoustic shadow) can mimic a urinary calculus when the bladder rests against the colon, and the bladder wall indents and curves to the contour of the fecal-filled colon. While centering on the possible calculus, slide the transducer cranially. If the hyperechoic mass with the acoustic shadow can be followed cranial to the bladder, then it is not a calculus. Alternately, turn the transducer 90° and if the suspected item elongates into a tubular structure, then it is not a calculus (see Figure 11.3).

**Pearl:** The "twinkle artifact" is a recently described effective technique (>90% sensitivity, specificity, positive and negative predictive values) to detect small calculi and mineralization of <5 mm in the urinary tract from the kidney to the urinary bladder through the use of color flow Doppler. The technique may in fact be applied to any organ with suspect mineralization (Gliga et al. 2017).

**Pearl:** Calculi can be assessed for mobility within the lumen by agitating the bladder (ballottement) with the transducer or by changing patient body position. Repositioning into a standing position is

very helpful as mobile calculi will fall to the gravity-dependent area of the urinary bladder, and thus should be adjacent to the far-field (dorsal) bladder wall when in dorsal recumbency, and adjacent to the near-field (ventral) bladder wall when standing. In these views, the probe is placed on the ventral abdomen and directed dorsally.

### Thrombi

Thrombi, also referred to as blood clots, may result from infection, inflammation, bleeding disorders, neoplasia or trauma (see Figure 11.11). They may be isoechoic, hyperechoic or hypoechoic to the urinary bladder wall, do not display distal acoustic shadowing and can often have mixed echogenicity with an indistinct layered appearance. Blood clots consist of irregular focal echogenic structures within the urinary bladder lumen and are generally mobile but may occasionally be adhered to the urinary bladder mucosa. When mobile, the luminal location of the clot will vary with changes in patient body position. When adherent, they can sometimes be difficult to differentiate from a mural mass. Color flow or power Doppler interrogation can be useful in this case, as there is no blood flow within a clot, but flow should be visualized within a bladder tumor.

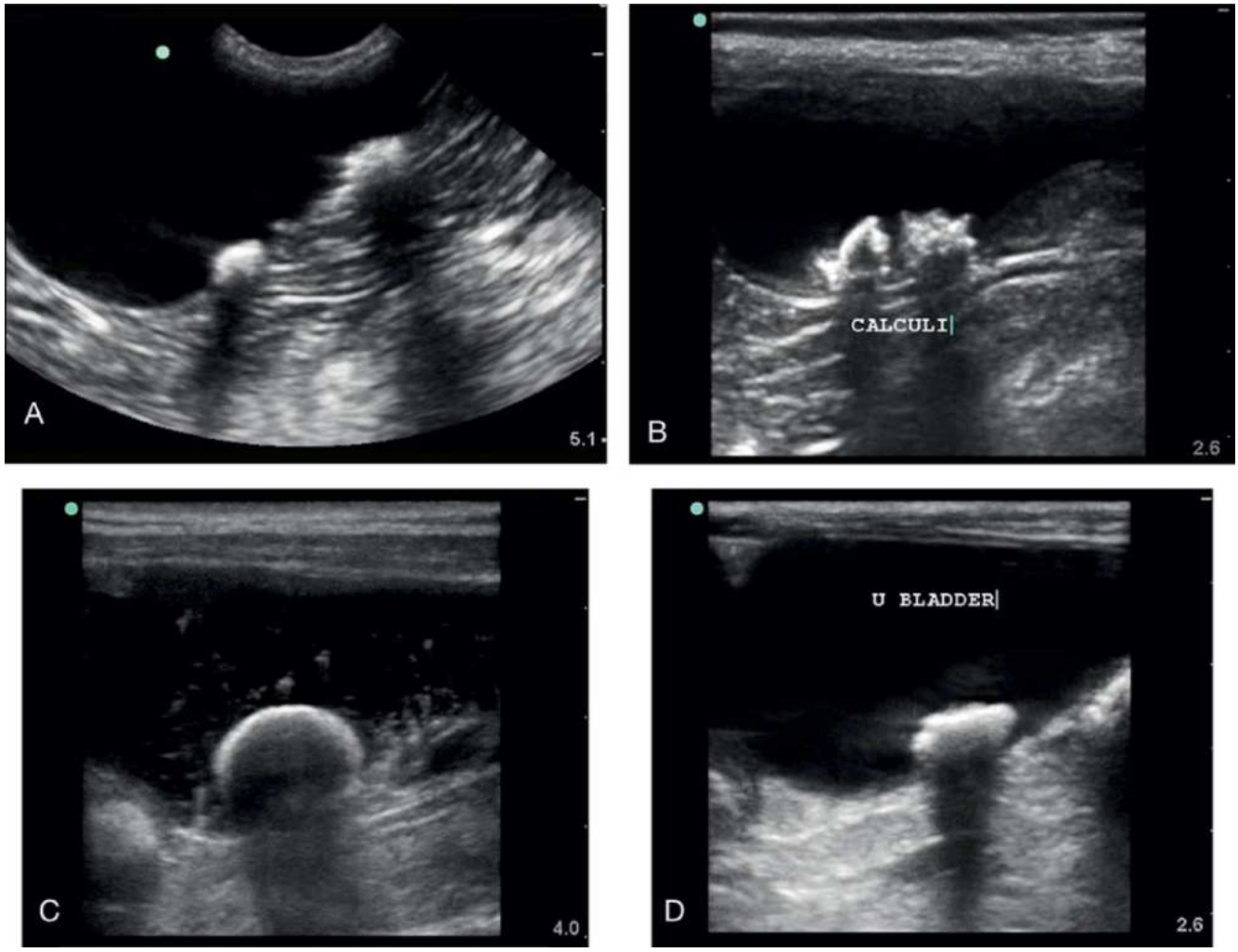


**Figure 11.8.** Bladder stones. (A) Multiple urinary bladder stones with a strong surface hyperechoic interphase (bright white) acoustic line followed by a strong distal acoustic shadow through the far-field. (B) Similar to (A) but with the hyperechoic echogenic interphase suggesting at least two, stellate-shaped urinary bladder stone(s). (C) Similar to (B) but with the hyperechoic echogenic interphase suggesting a round bladder stone. (D) Similar to (C) but with the echogenic interphase being consistent with a more ovoid-shaped, flat urinary bladder stone.

**Pearl:** The patient history, clinical pathology data, and ultrasound findings should all be correlated to determine the significance of blood clots (thrombi) within the bladder lumen.

### Sediment

Sediment typically appears as gravity-dependent hyperechoic particulate material within the bladder. It will produce an acoustic shadow when mineralized (i.e., crystals, sand, tiny calculi). Agitation of the bladder (ballottement) is recommended in all urinary bladder interrogations and may result in suspension and swirling of the sediment or the so-called "snow globe" appearance. Repositioning the patient can also result in movement of the sediment to the gravity-dependent surface (see repositioning for cystic calculi above). A urinalysis should be performed to evaluate the significance and composition of sediment seen on ultrasound examination (Figures 11.9 and 11.10; see also Figure 11.8B).

**Pearl:** Ultrasound-guided cystocentesis allows collection of urine from the area of greatest sediment, thus improving diagnostic accuracy.

**Pearl:** Remember that wall abnormalities and intraluminal abnormalities often occur concurrently. For example, animals with cystic calculi often have cystitis or sediment, and animals with urinary bladder wall tumors may have blood clots (Figure 11.11), sediment, mural mineralization or calculi.

## Routine Add-on of AFAST and Its Abdominal Fluid Scoring System (or Global FAST)

In the authors' experience, it is invaluable to perform an AFAST examination with assignment of an abdominal fluid score in either lateral recumbency for the best approach. The positioning of small animals in dorsal recumbency for POCUS abdominal organ examinations can obscure small-volume peritoneal effusion and underestimate the volume of effusion present because peritoneal effusion will flow into the less sonographically accessible diaphragmatic recesses. AFAST improves the diagnostic potential of the ultrasound examination by detecting peritoneal effusion. The early detection of abdominal effusion is clinically important and helps direct additional diagnostic recommendations while avoiding

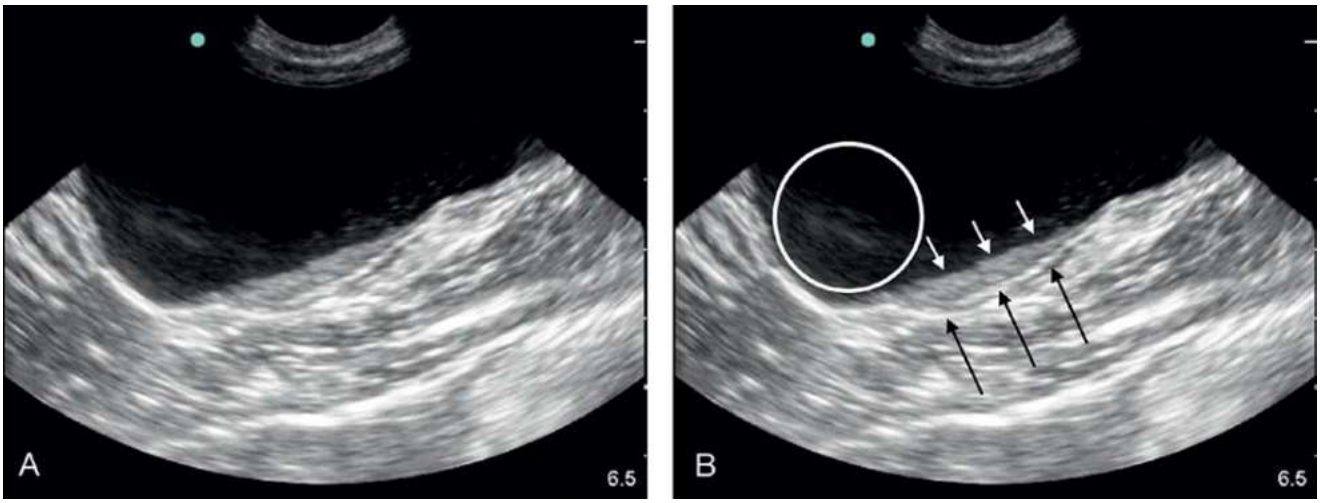


**Figure 11.9.** Urinary bladder sediment and artifact. Shown is the same image unlabeled in (A) and labeled in (B). Toward the apex the intraluminal echogenicity is due to side-lobe and slice thickness artifact (*circled*) in contrast to the area in the middle third and trigone regions consistent with actual sediment (*arrows*). The best ways to differentiate artifact from sediment is by changing patient position to see if sediment drops to gravity-dependent areas or through ballottement for a "snow globe" effect, as sediment will swirl in suspension within the luminal urine (artifact will not behave this way). Color flow Doppler is another way in which to evaluate for blood flow through the suspect mass as a mass has flow while a thrombus or artifact does not.

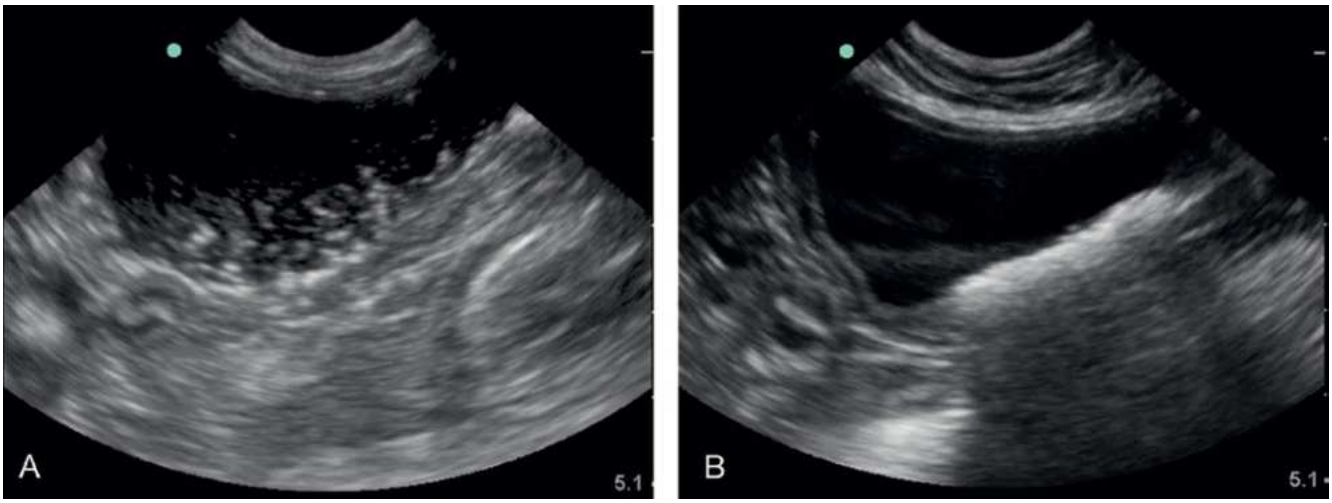


**Figure 11.10.** Urinary bladder sediment and artifact. (A) Sediment is best appreciated in real time and can be made up of echogenic partially mineralized material that falls to the gravity-dependent aspect of the urinary bladder with changes in patient positioning or appears as a "snow globe" effect with gentler agitation or ballottement (artifact does not). (B) An example of intraluminal side-lobe and slice thickness artifact near the apex, distal acoustic shadowing distal to the middle third of the urinary bladder where the sediment is located and flattening of the apical contour of the urinary bladder wall, in this case caused by the adjacent, cranial intestinal tract (small bowel).

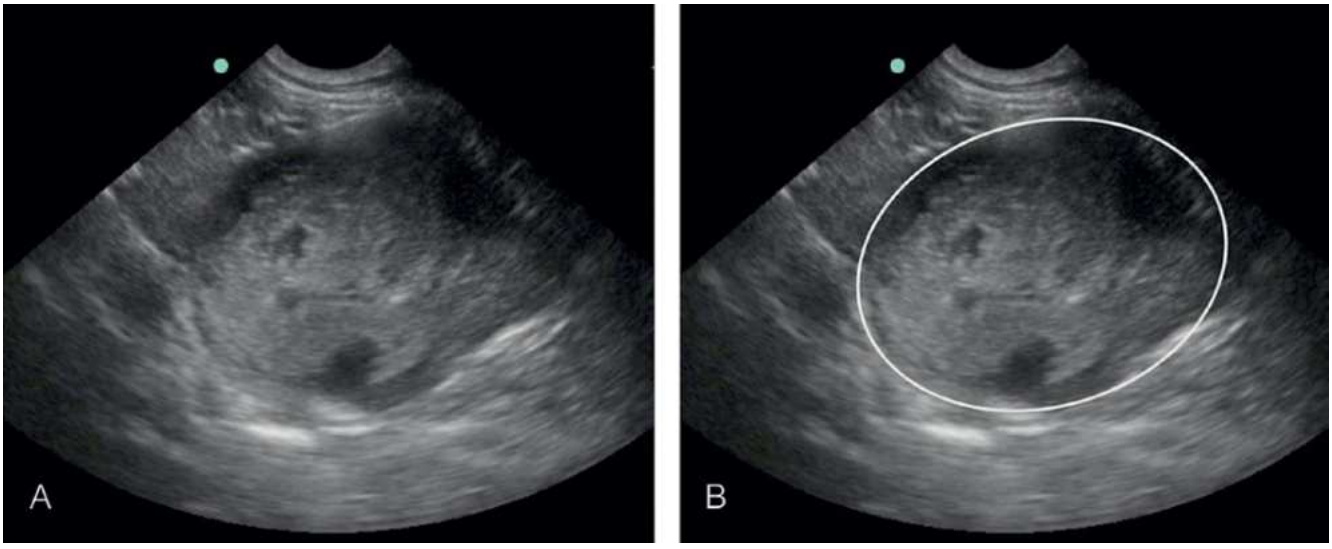


**Figure 11.11.** Intraluminal blood clot (thrombus). (A) Large echogenic to heterogeneous structure filling the lumen of the urinary bladder in a dog that sustained urinary bladder hemorrhage due to recent vehicular trauma. Notice the blood clot filling nearly the entirety of the urinary bladder lumen. The echogenicity is similar to that of bladder wall masses. The structure lacked evident blood flow on color flow and power Doppler interrogation (not shown). In (B) the urinary bladder with its intraluminal thrombus is outlined. Source: Courtesy of Dr Gregory Lisciandro, Hill Country Veterinary Specialists and FASTVet.com, Spicewood, TX.

morbidity, complications, and patient mortality in the event the effusion is missed.

The Global FAST approach is used as a screening test to rapidly discriminate between localized and disseminated disease, comorbidities, and complications. Global FAST offers a rapid assessment to survey for additional abdominal abnormalities (AFAST and fluid scoring), pleural and pericardial effusion (TFAST), and cardiac (TFAST) and pulmonary (Vet BLUE) abnormalities including lung nodules with minimal restraint upon initial patient triage.

# Pearls and Pitfalls, The Final Say

- The urinary bladder is generally easy to evaluate for obvious intraluminal (e.g., calculi or blood clots) and mural (e.g., mass lesions) abnormalities.
- Moderate distension of the urinary bladder is necessary for optimal assessment for urinary bladder wall thickness and the presence of focal wall abnormalities. An empty urinary bladder can often be misinterpreted as having a thickened urinary bladder wall.
- When evaluating for diffuse changes, cystitis generally results in hypoechoic thickening, most often along the cranioventral or apical aspect of the urinary bladder.
- Severe or polypoid cystitis is not distinguishable from diffuse mural urinary bladder neoplasia. If ultrasonographic changes persist or worsen during/following medical therapy for cystitis, tissue sampling should be pursued. However, the add-on of a Global FAST rapidly screens for localized versus disseminated disease and should be used the *same* day for staging the patient.
- Ureteral papillae occasionally may be seen on the dorsal surface of the bladder wall near the trigone and should not be confused with a urinary bladder wall abnormality.
- The contents of the colon can cause shadowing artifacts that may be mistaken for calculi or sediment and moving the patient to a standing position will help discriminate artifact from true abnormalities. Unless adhered, uroliths and sediment will fall to the gravity-dependent location (artifact will not) and pressure impingement from the colon along the ventral urinary bladder surface will be relieved.
- The ultrasonographic interrogation of the urinary bladder is susceptible to many artifacts, which may lead to misinterpretation. Therefore, it is imperative to be familiar with these artifacts and how to mitigate them as with interrogating the urinary bladder from multiple vantage points or changing patient position in order to provide an accurate assessment of the findings and paying attention to gravity-dependent regions where sediment, calculi, and blood clots would settle.
- Blood clots (thrombi) may be variable in echogenicity and may be difficult to distinguish from bladder wall masses, especially if they are adhered to the wall. Use color flow Doppler to help differentiate them as neoplasia generally has positive (blood) flow and blood clots and artifacts do not.
- Additional diagnostic techniques may be needed following the POCUS urinary bladder examination to further define disorders of the lower urinary tract. This may include referral for a complete detailed abdominal ultrasound by an experienced sonographer and/or additional perineal radiography in the male patient for urethral evaluation, special radiographic studies or computed tomographic imaging of the entire urinary tract, which are especially helpful in further assessing the kidneys, ureters, urethra, and pelvic inlet.

# Quick Reference of Normals and Rules of Thumb

- The thickness of the urinary bladder wall varies depending on the degree of distension.
- Normal range for urinary bladder wall thickness is cats 1.3–1.7 mm (Finn-Bodner 1995).
- Normal ranges for urinary bladder wall thickness in dogs are from 1.4 mm in moderately distended bladders to 2.3 mm in minimally distended bladders (Geisse et al. 1997). However, wall thickness in dogs has been reported to increase with body size, with heavier dogs having increased thickness by up to 1 mm or a maximum normal thickness of ≤3 mm (Geisse et al. 1997).
- The urinary bladder, being fluid filled, is subject to several artifacts including side-lobe, edge shadowing, and acoustic enhancement in the far-field.
- Voiding urohydropulsion guidelines are as follows.
    - Female dogs (>2 kg) can typically void stones <3–4 mm.
    - Female cats may be able to void stones <3 mm.
    - Male dogs weighing 5–10 kg may be able to void stones <2–3 mm; male dogs >10 kg may be able to void stones <3 mm.
    - Male cats: VUH is not recommended.

# References

Defarges A, Dunn M, Berent AC. 2013. New alternatives for minimally invasive management of uroliths: lower urinary tract uroliths. *Compend Contin Educ Vet* 35(1):E1.

Finn-Bodner ST. 1995. The urinary bladder. In: *Practical Veterinary Ultrasound*, edited by Cartee RE. Baltimore: Williams and Wilkins, pp 200–235.

Geisse AL, Lowry JE, Schaefer DJ, Smith CW. 1997. Sonographic evaluation of the urinary bladder wall thickness in normal dogs. *Vet Radiol Ultrasound* 38:132–137.

Gliga ML, Chirila CN, Podeanu DM, et al. 2017. Twinkle, twinkle, little stone: an artifact improves the ultrasound performance! *Med Ultrasound* 19(3):272–275.

Leveille R, Biller DS, Partington BP, et al. 1992. Sonographic investigation of transitional cell carcinoma of the urinary bladder in small animals. *Vet Radiol Ultrasound* 33:103–107.

Liffman, R, Courtman N. 2017. Fine needle aspiration of abdominal organs: a review of current recommendations for achieving a diagnostic sample. *J Small Anim Pract* 58(11):599–609.

Lin SJ, Kao CF, Wang FI, et al. 2018. Urothelial carcinomas of the urinary bladder with plasmacytic or rhabdoid features and tendency of epithelial-mesenchymal transition in 3 dogs. *Vet Pathol* 55(5):673–677.

Nyland TG, Wallack ST, Wisner ER. 2002. Needle-tract implantation following US-guided fine-needle aspiration biopsy of transitional cell carcinoma of the bladder, urethra, and prostate. *Vet Radiol Ultrasound* 43(1):50–53.

Sommer BC, Dhawan D, Ratliff TL, et al. 2018. Naturally-occurring canine invasive urothelial carcinoma: a model for emerging therapies. *Bladder Cancer* 4(2):149–159.

Vignoli M, Rosi F, Chierici C, et al. 2007. Needle tract implantation after fine needle aspiration biopsy (FNAB) of transitional cell carcinoma of the urinary bladder and adenocarcinoma of the lung. *Schweiz Arch Tierheilkd* 149(7):314–318.

Wilson HM, Chun R, Larson VS, et al. 2007. Clinical signs, treatments, and outcome in cats with transitional cell carcinoma of the urinary bladder: 20 cases (1990–2004). *J Am Vet Med Assoc* 231(1):101–106.

CHAPTER TWELVE

# POCUS: Gastrointestinal Tract and Pancreas

Søren R. Boysen and Jennifer M. Gambino

## Introduction

Typically, a point-of-care ultrasound (POCUS) examination is not extensive, thorough or complete. Rather, it provides a limited examination designed to answer brief and important clinical questions in an organ system or for a symptom involving multiple organ systems (Mateer et al. 1994). In the emergency setting, it can provide early diagnostic information that can guide treatment of the critical patient. This is especially true in situations where delaying ultrasonographic evaluation until a specialist is available, or positioning the patient for complete ultrasonographic evaluation or radiography, might lead to further patient compromise.

Some gastrointestinal (GI)-related conditions that have been evaluated with emergency ultrasound in people include intussusception, small bowel obstruction, pyloric stenosis, appendicitis, gastric ulcers, perforated hollow viscus, gallbladder rupture, septic peritonitis, acute mesenteric ischemia, and acute pancreatitis (Rozycki 2001; Dean et al. 2002; Unluer et al. 2010; Testa et al. 2010; Jang et al. 2011).

Using the AFAST examination technique to evaluate for the presence of peritoneal fluid has been validated in dogs (Boysen et al. 2004; Lisciandro et al. 2009) and whether or not peritonitis exists is an important clinical question to answer. However, a more detailed approach to scanning of the gastrointestinal tract (GIT) and pancreatic pathologies requires considerably more expertise and training, which may limit the use of POCUS GIT and pancreas by some emergency clinicians. It must be stressed that POCUS GIT and pancreas should not replace abdominal radiographs, complete detailed abdominal ultrasound or computed tomography (CT) examination for a more comprehensive peritoneal cavity evaluation. Furthermore, in people the correlation obtained between emergency physician POCUS and a gold standard pathology confirmation varies by operator experience and the extent and type of training received for the abovementioned GI conditions (Raymond-Dufresne and Ghanayem 2012; Hasani et al. 2015). This emphasizes the potential advantages and limitations of POCUS GIT and pancreas emergency examination in the acute GI setting.

However, abnormal ultrasonographic findings (a positive result) can be extremely valuable in providing a diagnosis and guiding initial case management. A negative emergency POCUS GIT and pancreas examination is not uncommon and does not necessarily rule out disease (false negative) indicating the need for further diagnostic testing, serial POCUS GIT and pancreas plus AFAST, or follow-up with an imaging specialist. In other words, POCUS GIT and pancreas should be considered a rule-in test for organ pathology. On the other hand, AFAST for intraabdominal fluid detection, evidence for peritonitis, is both a rule-in (highly specific) and rule-out (highly sensitive) test for the nonradiologist sonographer (Boysen et al. 2004). For the sonographer who is not confident in assigning the GIT or pancreas with a pathological sonographic diagnosis in acute abdomen cases, AFAST remains a very good screening test for peritonitis, a POCUS GIT and pancreas-related consideration that warrants a prompt diagnosis.

No studies exist evaluating the efficiency, accuracy, sensitivity or specificity of equivalent POCUS emergency GI ultrasound when performed by

*Point-of-Care Ultrasound Techniques for the Small Animal Practitioner*, Second Edition. Edited by Gregory R. Lisciandro.
© 2021 John Wiley & Sons, Inc. Published 2021 by John Wiley & Sons, Inc.
Companion website: www.wiley.com/go/lisciandro/ultrasound2

VetBooks.ir

veterinary emergency clinicians compared to a boarded radiologist or internal medicine specialist. However, evidence suggests that the diagnostic accuracy of detecting small intestinal mechanical obstruction in dogs using ultrasound is lower when performed by a novice sonographer compared to a boarded radiologist and that the learning curve is steeper for ultrasonographic GI assessment than for many other emergency POCUS techniques (Sharma et al. 2011). Currently, there are no standardized guidelines or recommendations in the veterinary literature for performing POCUS emergency GI examinations. The accuracy, sensitivity, and specificity of our POCUS GIT and pancreas examination have not been evaluated. We propose that POCUS GIT and pancreas be adapted and/or tailored to the critical patient and that, in many cases, it will provide valuable diagnostic information to better direct resuscitation, screen post resuscitation, and better keep patients alive for gold standard testing and treatment.

The specific application of POCUS emergency examinations of the GIT depends on patient status, history, physical examination findings, clinical suspicion, and operator experience. Whether or not POCUS emergency examination for suspected GIT and pancreatic disease is warranted should be dictated by the availability of an experienced sonographer or radiologist and the assessment of preliminary diagnostic tests and dependent on the clinical questions to be answered by the attending veterinarian.

In summary, when negative, POCUS GIT and pancreas should not be considered a definitive test in the assessment of patients with suspected acute GI conditions. Instead, the application should be used as an initial screening, ancillary test to supplement the history, physical examination findings, and other preliminary diagnostic screening tests given its potential ability to direct initial therapy and guide appropriate diagnostic testing, especially when other imaging modalities might be detrimental to the patient's critical status, such as in those patients with profound anemia or complicating respiratory distress. When combined with AFAST, life-threatening peritonitis can be ruled in or out, and a Global FAST approach can screen for thoracic (TFAST), cardiac (TFAST), and pulmonary comorbidities (Vet BLUE) (see Chapters 7, 18, 23, and 36).

## What POCUS Gastrointestinal Tract and Pancreas Can Do

- Provide a preliminary evaluation of patients with GI signs or evidence of acute abdomen in an effort to answer a specific question when complete abdominal ultrasonography is not available.
- Rapidly assess the unstable patient with GI signs in an effort to rule in (or out) significant diffuse peritoneal effusion.
- Complement radiographic findings in cases with GI signs.
- Support the clinical suspicion of moderate GI and pancreatic pathology for further testing to obtain a definitive diagnosis (i.e., ultrasound-guided fine needle tissue sampling).
- Detect the presence of peritonitis through the add-on of AFAST in initial and serial evaluations, and be complemented by Global FAST for further assessment of the thorax, heart, lung, and volume status.

## What POCUS Gastrointestinal Tract and Pancreas Cannot Do

- Cannot replace a complete abdominal ultrasound examination or abdominal radiographs.
- Cannot rule out focal or specific causes of GI pathology (particularly pancreatitis) when results are negative.

## Indications

Two key factors to consider for POCUS GIT and pancreas examinations are what the emergency clinician suspects is the underlying cause for presentation, and the urgency of finding an answer to the question asked. The stable patient may benefit more from a complete abdominal ultrasound exam whereas the unstable patient presenting "after hours" with signs of acute abdomen/GI signs is considered the ideal candidate for the POCUS GIT and pancreas examination.

The indications and type of POCUS GIT and pancreas examination vary and depend on the operator's level of experience and training, presenting complaint, preliminary minimum database bloodwork results, physical examination findings, and suspected underlying condition of the patient.

The indications for POCUS GIT and pancreas (plus AFAST) examination in the veterinary patient with acute GI signs include the clinical suspicion of pancreatitis, screening for peritoneal effusion that might suggest perforated intestines, septic or biliary peritonitis, right-sided cardiac failure, hemo- or uroabdomen or an underlying neoplastic process. The peritoneal space, stomach, and small and large bowel are readily evaluated for supportive evidence of GI perforation such as effusion shadowing GI foreign bodies, bowel intussusception, intestinal obstruction, and evidence of ileus.

VetBooks.ir

Although not the ideal screening test for pneumoperitoneum, peritoneal gas may also be detected.

Examples of scenarios where an emergency clinician has a specific question that could potentially be answered by POCUS GIT and pancreas examination include the following.

- In a patients with an acute abdomen, vomiting and unexplained hypotension, it is reasonable to ask if the patient has peritoneal effusion, which could be indicative of GI perforation and septic peritonitis. In these patients, an emergent AFAST examination may be performed to evaluate for effusion and aid in ultrasound-guided abdominocentesis to screen for cytological evidence of sepsis.
- In patients with acute abdominal pain and vomiting that are negative for peritoneal effusion, the emergency clinician may ask if the patient has localized or indirect evidence supportive of GI perforation or if a shadowing intestinal foreign body is present. POCUS GIT and pancreas examination of the intestines may then be perfomed and may lead to the discovery of an ultrasonographically detectable foreign body or raise the index of suspicion of intestinal obstruction. Indirect evidence of obstruction, such as a severely dilated jejunum with luminal dilation measuring greater than 1.5 cm, may highlight the need for a more extensive and complete ultrasonographic evaluation, abdominal radiographs, upper GI series or exploratory surgery (Sharma et al. 2011). The history, physical examination, and other ancillary tests should be correlated with, and supportive of, the findings.
- If the emergency clinician is experienced with ultrasonographic evaluation of the pancreas and the patient is hypotensive with a history suggestive of pancreatitis (such as exposure to a high-fat meal followed by vomiting, diarrhea, and abdominal pain), then a POCUS GIT and pancreas examination may be performed to evaluate for ultrasonographic evidence of pancreatitis. If criteria for acute pancreatitis are present (e.g., hyperechoic or hyperattenuating mesentery with parenchymal pancreatic hypoechogenicity and elicitable pain in response to probe pressure during pancreatic evaluation), the emergency clinician can then institute preliminary supportive measures while considering further diagnostic and therapeutic options.
- In patients that have undergone GI surgery and are deteriorating, the clinician may ask if dehiscence, septic peritonitis or postoperative ileus is present and may elect to perform an AFAST examination which would aid in ultrasound-guided abdominocentesis if peritoneal effusion is present.
- In the postoperative patient that is vomiting, anorexic or painful, it is reasonable to ask if the patient has functional ileus and perform a POCUS emergency GIT examination to assess GI motility. Although perioperative gas may obscure ultrasonographic peritoneal evaluation, if postoperative functional ileus is present, the clinician should search for and try to correct the underlying cause while considering specific therapies directed at addressing ileus.

These are only a few examples of specific POCUS GIT and pancreas examination applications designed to answer a specific question. Although many factors dictate the clinical value of an AFAST study (the experience of the operator, patient's presenting complaint, and physical examination findings), there are many other clinical situations in which a patient can benefit from POCUS GIT and pancreas examination.

### *Objectives*

- To identify the location, size, and shape of normal and abnormal peritoneal structures.
- To identify pathology warranting specific or emergent treatment, optimizing early diagnosis and outcome of intraperitoneal disease, particularly in the unstable patient.

## Patient Positioning and Probe Selection

### *Peritoneal Effusion*

See Chapters 6 and 7 for information on patient positioning to look for the presence of peritoneal effusion.

### *Gastrointestinal Evaluation*

Depending on the comfort level of the patient and preference of the sonographer, the POCUS emergency examination of the intestines may be performed in dorsal, left or right lateral recumbency.

The overall status of the patient, with a particular focus on the cardiovascular and respiratory systems, should be determined to ensure patients are stable before placing them in dorsal recumbency. If there is any doubt regarding clinical status, the patient should have thoracic POCUS, such as TFAST and Vet BLUE,

performed to screen for intrathoracic problems including pleural and pericardial effusion, cardiac and pulmonary conditions, and abnormal volume status that may pose patient risk *before* moving the patient into dorsal recumbency (see Chapters 18, 23, and 36).

- Left lateral recumbency helps with visualization of the pylorus and duodenum while right lateral recumbency allows for evaluation of the fundus (Penninck 2008a).
- Repositioning the patient may redistribute intestinal gas and fluid allowing for specific regional evaluation.
- Ultrasound probes with a frequency of at least 7.5 MHz are recommended for bowel evaluation (Penninck 2008a; Garcia et al. 2011).

### Pancreas

Pancreatic scanning is frequently performed in dorsal recumbency although left and right lateral recumbency may also be used (Nyland et al. 2002; Penninck 2008b).

- For pancreatic evaluation, a 5–7.5 MHz or higher transducer is preferred as higher frequencies improve visualization of the pancreas (Nyland et al. 2002).
- Avoid examining the pancreas under high output or gain settings as the increased reflectivity of the pancreatic region prevents visualization of abnormalities and leads to both false-negative and false-positive results (Nyland et al. 2002; Hecht and Henry 2007).

## Scanning Technique

### Intestinal Tract

The detection of GI lesions may be challenging given the difficulty of consistently evaluating the entire intestinal tract. Many factors, including normal or abnormal gas accumulation in the GI tract and operator skill, influence the success of identifying GI lesions. A consistent and systematic technique will minimize false-negative results.

We propose the following POCUS GIT with the probe in the longitudinal plane.

- One common technique involves starting in the region of the pylorus/stomach on the right side of the patient just caudal to the ribs and fanning the probe from the right to the left of the patient, paying specific attention to the stomach (located caudal to the xiphoid and liver) on the first pass.
- Slide the probe 1–2 cm caudally and fan toward the far left side of the patient. Then fan back across the abdomen from left to right while paying specific attention to the bowel loops.
- Repeated fanning of the probe across the abdomen in this fashion with a zig-zag (or grid-like) pattern while moving caudally will aid evaluation. If stable enough, the patient may be repositioned in various recumbencies for redistribution of fluid and gas, while repeating the evaluation (Figure 12.1).
- The intestines are orientated in many directions. The above described approach results in the evaluation of many sections of small intestine in multiple planes (sagittal, transverse, and various oblique planes), which depends on the probe-to-intestinal tract orientation.
- Once completed, if no irregularities are seen, the pylorus and descending duodenum can be evaluated in greater detail by returning the probe to the right side of the patient, just caudal to the ribcage (or, depending on patient conformation, sometimes between the last ribs). The body of the stomach may first be located and traced to the pylorus, and then the descending duodenum.
- This is a good time to get a general and subjective impression of overall gastric and small bowel motility (see section on Ileus below).
- If a specific area of pain, mass or foreign object is palpated on initial physical examination, specific attention should be paid to the area in longitudinal and transverse planes.
- Abnormal findings in close proximity to the area of suspicion might include intestinal wall structure layering abnormalities, abnormal intestinal peristalsis, focal loculations of peritoneal fluid, segmental focal dilations of small bowel, plicated bowel, target-like lesions or hyperattenuating/hyperechoic fat or mesentery.
- Suspicious areas of intestine should be followed both orad and aborad to allow a more detailed assessment of these areas.
- If structures within the GI lumen are visible, they should be carefully examined for a hyperechoic reflective interface and the presence of acoustic shadowing.

### Pancreas

There are several scanning techniques that may be used to identify the pancreas, but a preferred technique for POCUS emergency evaluation has not been

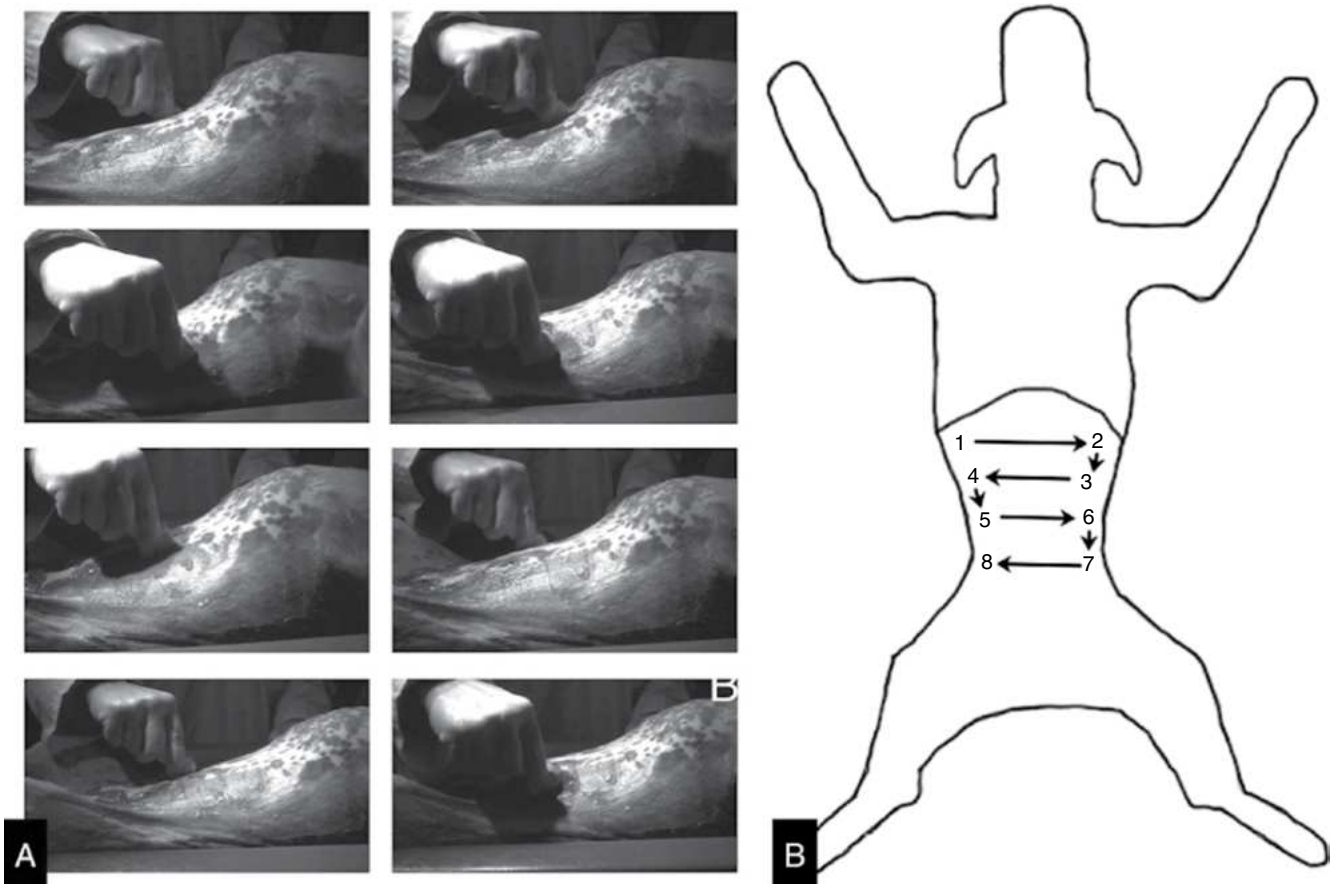


**Figure 12.1.** Scanning the gastrointestinal tract. The zig-zag scanning method of the abdomen shown (A) externally on a dog in dorsal recumbency and (B) on a simple line drawing labeled 1–8 for the sequence from start to finish.

formally described for veterinarians. One of the more commonly used techniques in dogs involves an initial search for the right lobe of the pancreas as the right lobe is more easily imaged than the body and left lobe. Furthermore, the right lobe is more frequently affected by acute pancreatitis in the dog (Nyland et al. 2002; Hecht and Henry 2007; Penninck 2008b) whereas a higher prevelance is seen within the left pancreatic limb in cats with combined chronic pancreatic and gastrointestinal disease (De Cock et al. 2007).

We propose the following POCUS pancreas.

- The ultrasound probe is placed over the right kidney in transverse orientation.
- After identifying the right kidney, the probe is slowly fanned laterally and medially until the descending duodenum is identified in transverse orientation.
- The probe is then oriented in the sagittal plane, demonstrating that the duodenum may be evaluated along its length medial to the right abdominal body wall.
- The pancreas is triangular shaped, and iso- to slightly hypoechoic (darker than) to surrounding mesenteric fat. It has an echogenic capsule and is found dorsomedial to the duodenum, directly ventral to the right kidney (Hecht and Henry 2007).
- The pancreaticoduodenal vessels and pancreatic duct may be seen as round anechoic structures within the pancreas (compare Figures 12.2 and 12.3). Color flow Doppler evaluation, if available, provides differentiation between the structures (see Figure 12.3A,B).
- The portal vein may be seen and can be a useful landmark. It lies left and dorsal-left to the pancreas and is best evaluated from a right dorsal intercostal approach (Brinkman-Furguson and Biller 2009).
- In very large or deep-chested dogs, it may be easier to evaluated the right limb of the pancreas

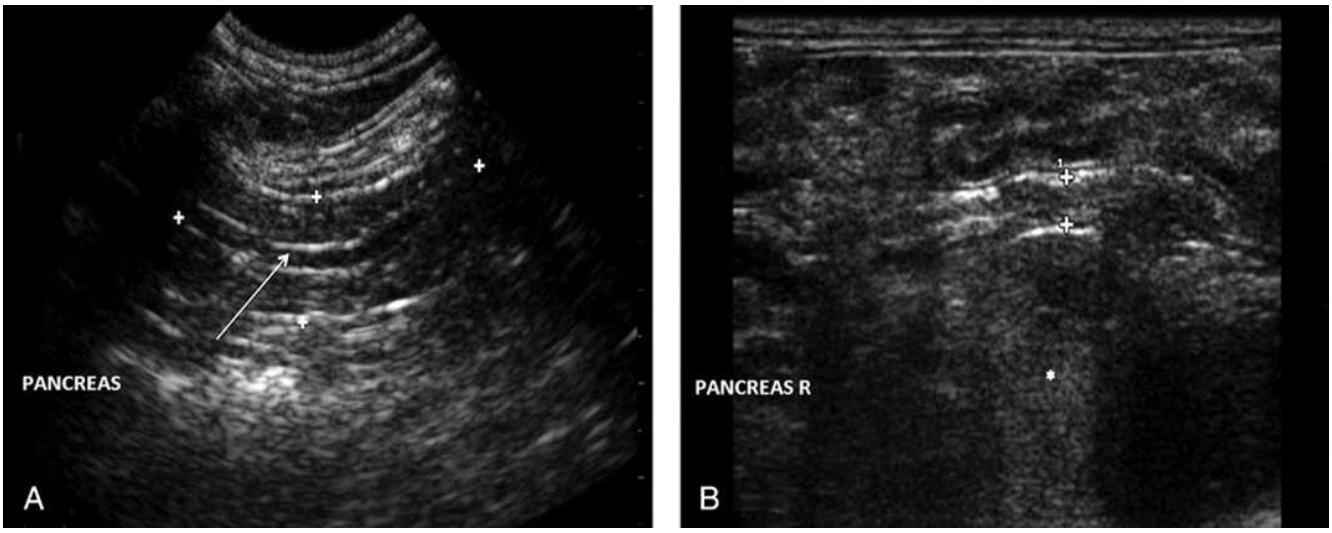


**Figure 12.2.** Normal pancreas. (A) Normal right pancreatic limb in the sagittal plane in a dog (boundaries identified by the crosses, +). Note the tubular hypoechoic structure within the midpancreatic parenchyma (*arrow*). Color flow Doppler can aid in differentiating whether this structure is vessel (pancreaticoduodenal artery or vein) or pancreatic duct. (B) Right pancreatic limb in the sagittal plane in a cat. The pancreas is typically isoechoic to the surrounding mesentery (*asterisk*). In the authors' experience, the echogenicity of the pancreatic parenchyma can vary in normal animals without clinical signs or laboratory evidence of pancreatitis. The pancreas can range in echogenicity from mildly hypoechoic to mildly hyperechoic to the surrounding mesentery, but is typically isoechoic to the surrounding mesentery in the normal state. Pancreatic echogenicity is especially dependent on *gain and acoustic output settings*. Decreasing the gain settings can aid in pancreatic identification. Serosal margins of the pancreas are typically hyperreflective and can be used to identify the organ's boundaries. Identification of the descending duodenum along the right dorsolateral aspect of the patient while fanning and scanning medially and laterally along the length of the descending duodenum will aid in identification of the right limb. The sonographer can then follow the right limb to the body of the pancreas. To identify the left limb of the pancreas, the sonographer can begin scanning and fanning in the sagittal plane along the left lateral cranial abdominal wall at the level of the last rib. Here, the gastric fundus and spleen can be easily identified and the sonographer can move caudally along the medial and lateral aspects of the spleen to the cranial pole of the left kidney in search of the organ.

through the 10th–12th right intercostal spaces with the dog in left lateral recumbency (Hecht and Henry 2007).

- If the right lobe of the pancreas can be located, it may then be traced to the body. The pancreatic body is located between the right and left lobes of the pancreas in close proximity to the portal vein, dorsocaudal to the pylorus.
- The left lobe of the pancreas is located between the stomach and transverse colon and medial to the splenic head. It may be seen cranial to the gastric fundus and caudal to the left liver from the left of the patient caudal to the ribs. It is often difficult to identify these parts of the pancreas, especially in normal dogs (Hecht and Henry 2007).
- It should be noted that gas within the GI tract may hamper evaluation of the pancreas.
- The pancratic body and left limb should not exceed 1 cm in width (8.5 mm and 9.5 mm, respectively) in the cat, regardless of age, whereas the left pancreatic duct should not exceed 2.5 mm (Larson et al. 2005).

Excessive probe pressure may displace the duodenum, affecting its normal anatomical orientation to the right kidney. Remember that the *normal pancreas may not be visible* because it is often isoechoic (similar) to the surrounding mesenteric fat.

**Pearl:** Remember that the normal pancreas may not be visible because it is often isoechoic to the surrounding mesenteric fat and it is a small structure (i.e., well under 1 cm in width). However, the findings of moderately hyperechoic (bright white) peripancreatic fat and peritoneal fluid adjacent to an enlarged hypoechoic pancreas should prompt a suspicion of pancreatitis.

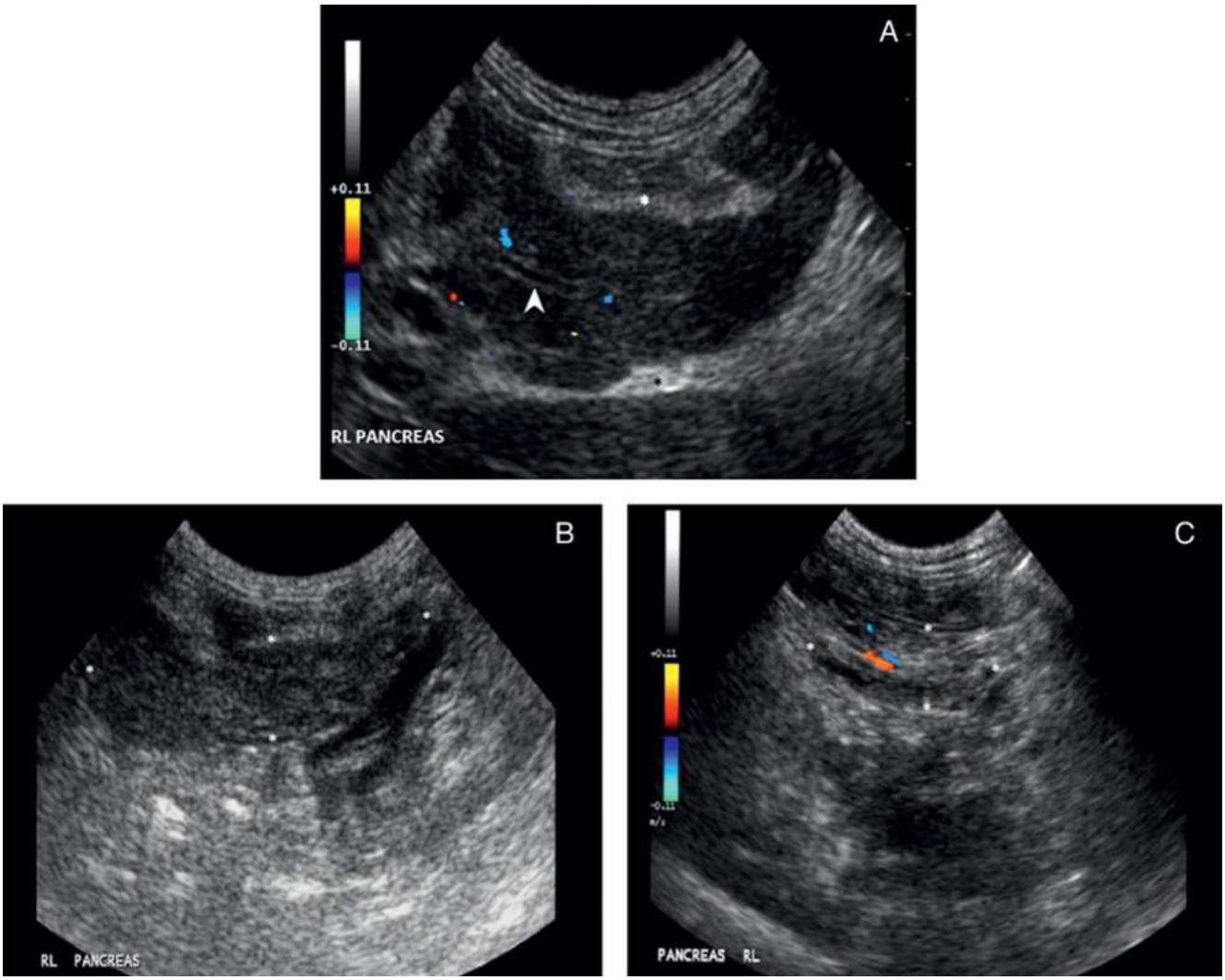


**Figure 12.3.** Pancreatitis. (A) Sagittal image of the right pancreatic limb in an 11-year-old female spayed Shetland sheepdog with pancreatitis. The pancreas is severely hypoechoic and subjectively enlarged. The surrounding mesentery is severely hyperechoic (*asterisk*). Note the lack of color flow Doppler within the anechoic tubular structure, the pancreatic duct (*arrowhead*), coursing along the midaspect of the right pancreatic limb. (B) Sagittal image of the right limb of the pancreas in a 7-year-old female spayed Siamese cat with pancreatitis. The patient had a history of weight loss, vomiting, and lethargy. Pancreatitis is typically found more often in the left limb of the pancreas in cats. This patient's entire pancreas was severely hypoechoic and enlarged. (C) Color flow Doppler evaluation of the right limb of the pancreas in a cat with mild pancreatitis and renal disease. In this case, the blue vessel represents the pancreaticoduodenal artery and the red vessel represents the flow within the pancreaticoduodenal vein. Recall that blood flowing away from the transducer is blue and blood flowing toward the transducer is red.

It must be stressed that a *significant number of dogs with pancreatitis will not have ultrasonographic evidence of pancreatitis*, and the success of diagnosing acute pancreatitis will vary with sonographer experience (Hess et al. 1989). Failure to detect evidence of pancreatitis during the POCUS GIT and pancreas examination does not rule out acute pancreatitis, and further testing should be pursued if the history and other clinical findings support a diagnosis of acute pancreatitis.

# POCUS GIT and Pancreas Findings and Their Significance

## *Small Bowel*

To be able to identify intestinal lesions, it is important to gain familiarity with the normal ultrasonographic appearance of the bowel.

- In adults, the normal small intestine typically has five ultrasonographicaly identifiable layers, which tend to resemble a "hamburger" on cross-section (Figures 12.4, 12.5; see also Figure 16.9).
- The five layers from the lumen to the serosal surface include the hyperechoic luminal–mucosal gas interface, hypoechoic mucosa, hyperechoic submucosa, hypoechoic muscular layer, and hyperechoic subserosa and serosa.
- When thinking of the ultrasonographic layers of the GI tract, the mnemonic "the sun is bright and it's dark at midnight" may be helpful in remembering that layers starting with an "s," like the sun, are bright (submucosa and serosa are hyperechoic), while layers starting with an "m," like midnight, are dark (mucosa and muscular layer are hypoechoic) on the ultrasound image.

**Pearl:** Normal small bowel looks like a "hamburger" in transverse orientation.

**Pearl:** Use the mnemonic "the sun is bright and it's dark at midnight" to remember that layers starting with an "s" like the sun are bright (submucosa and serosa are hyperechoic [bright]) while layers starting with an "m" like midnight are dark (mucosa and muscular layer are hypoechoic [dark]) on the ultrasound image.

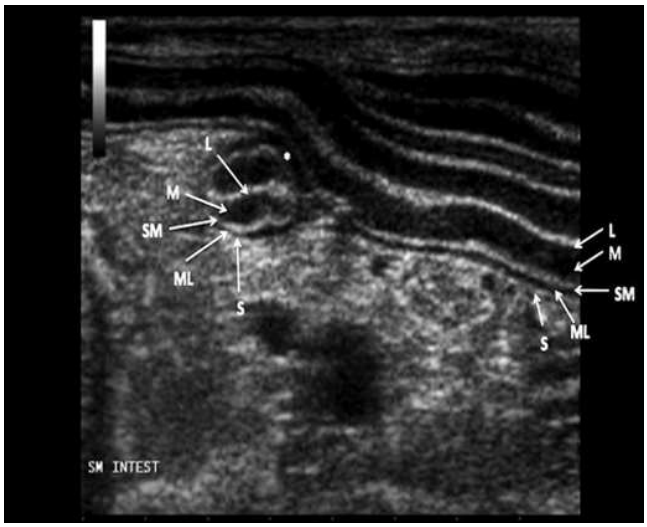


**Figure 12.4.** Normal layering of small bowel. Normal image of adjacent loops of small bowel in both sagittal and transverse planes in a 9-year-old diabetic, female spayed miniature pinscher who presented for acute vomiting due to foreign body ingestion. Luminal GI contents can vary in echogenicity. In this example, the small bowel is predominantly empty with mild admixed gas and chyme causing the hyperechoic lumen. There are five layers of the normal small intestine that are most sonographically evident and easily identified. From lumen to serosal surface, the layers are as follows: the luminal-mucosal layer (L) is hyperechoic and represents the gas–mucosal interface, the hypoechoic mucosa (M), the hyperechoic submucosa (SM), the hypoechoic muscular layer (ML), and the hyperechoic subserosa/serosa (S). A small amount of anechoic peritoneal effusion (*asterisk*) was noted due to pancreatitis. Care should be taken not to confuse this finding with an increase in thickness of the muscularis layer.

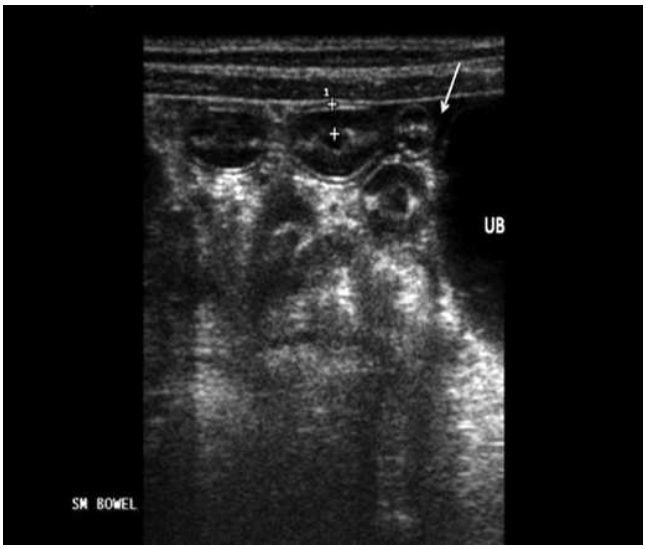


**Figure 12.5.** Normal small bowel. Normal image of small bowel in the transverse plane, in a 5-year-old Jack Russell terrier with a two-month duration of vomiting and radiographically evident pyloric outflow obstruction. Note the anechoic luminal small bowel fluid in some of the small bowel adjacent to the urinary bladder (UB). A small amount of anechoic peritoneal fluid was also noted (*arrow*), consistent with modified transudate. Surgical and histopathological diagnosis was giant hypertrophic gastropathy (not shown). The small bowel was normal and the patient had a successful outcome with partial gastrectomy.

## Foreign Bodies

The acoustic appearance of GI foreign bodies detected ultrasonographically varies depending on their physical properties. The margins of foreign objects that allow sound to pass through them can be visualized within the GI lumen whereas objects that reflect or attenuate sound often have a hyperechoic interface and produce shadowing beyond their superficial surface (Figures 12.6 and 12.7) (Tidwell and Penninck 1992; Sharma et al. 2011).

- The majority of ultrasonographically detectable GI foreign bodies typically involve a well-defined hyperechoic, hyperreflective acoustic interface with strong distal acoustic shadowing (Tidwell and Penninck 1992; Garcia et al. 2011).
- This is in contrast to intraluminal gas, which tends to result in reverberation artifact (Figures 12.8 and 12.9; see also Figures 16.9–16.13) (Tidwell and Penninck 1992; Tyrrell and Beck 2006; Sharma et al. 2011). However, there is some overlap in the shadowing seen with foreign bodies and intraluminal gas that may render the identification of a foreign body difficult (Tidwell and Penninck 1992).
- The acoustic shadowing of foreign bodies may be masked by air, but manipulation of bowel with the probe and changes in patient position can aid evaluation.
- Dilation of the intestine orad to a distally shadowing structure that has a hyperechoic interface between the mucosa and lumen lends support to the presence of intestinal obstruction and suggests the need for surgical exploration (Garcia et al. 2011).
- GI foreign bodies should be considered and ruled out when ultrasonographic findings suggest mechanical obstruction or GI irritation.
- In the face of appropriate history and physical examination findings, the ultrasonographic detection of peritoneal effusion, gas distension, and abnormal motility (particularly hyperperistalsis with failure to advance intraluminal contents) warrants a careful search of the GIT for foreign bodies (Tidwell and Penninck 1992; Sharma et al. 2011).

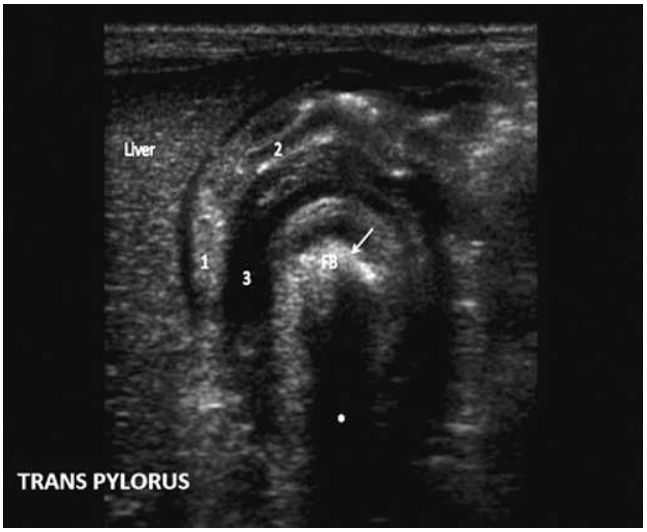


**Figure 12.6.** Pyloric foreign body. Same patient as in Figure 12.4. Transverse image of the pylorus. A smoothly contoured hyperattenuating foreign body (FB) is present within the pylorus. Note the hyperreflective acoustic interface (*arrow*) associated with a well-defined band of hypoechoic distal acoustic shadowing (*asterisk*). The pylorus can be found by identifying the gastric fundus in the left cranial abdominal quadrant and following the gastric wall medially and toward the right aspect of the patient. The stomach can be imaged with the patient in multiple positions (dorsal, right lateral, left lateral and standing) for a global view. In deep-chested dogs, it may be necessary to place the animal in left lateral recumbency and image from a right intercostal vantage for pyloric evaluation. Isoechoic fat (1), small bowel (2), pyloric muscularis layer (3). Note that the muscularis layer of the pyloric region is quite thick, representing the pyloric sphincter. In cases with suspected pyloric outflow obstruction or gastric foreign body, attempts should be made to evaluate the entire stomach and gastroduodenal junction in both transverse and sagittal planes. This patient recovered well with gastrotomy, diabetic management, and supportive care for pancreatitis.

## Linear Foreign Bodies

Linear foreign bodies often appear as persistent echogenic or hyperechoic linear structures within the center of plicated small intestinal loops that do not move with peristalsis and remain static throughout the examination (Figures 12.10 and 12.11; see also Figures 16.9–16.13).

- The finding of bowel plication is strongly suggestive of a linear foreign body and should prompt careful evaluation of the intestine (longitudinal and transverse images) at sites where plication is seen (Tidwell and Penninck 1992; Garcia et al. 2011).
- Intestinal corrugation has also been associated with linear foreign bodies (Tidwell and Penninck 1992) but is less specific than plication. Care should be taken to avoid mistaking bowel plication for corrugation (a sign of spasticity and inflammation/enteritis which may be seen with toxins, primary enteropathy or underlying infectious causes) (Figure 12.12) (see later).

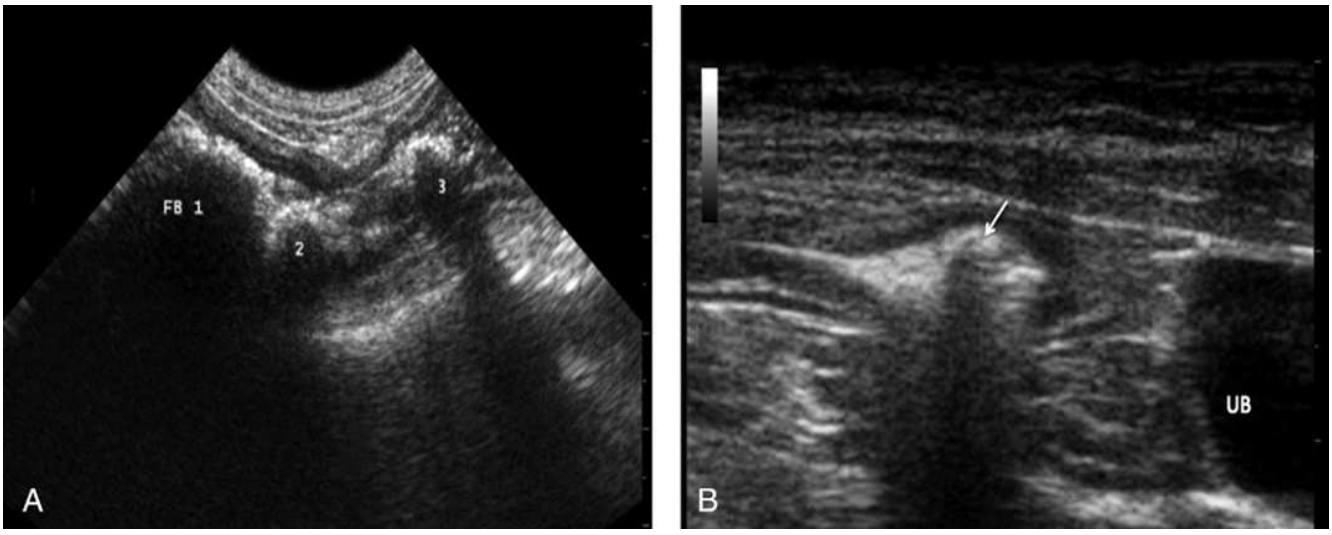


**Figure 12.7.** Additional examples of small bowel intestinal foreign bodies. (A) Multiple duodenal foreign objects (FB 1, 2, 3) in a dog, demonstrating various degrees of distal acoustic shadowing. Foreign body 1 demonstrates the strongest and "cleanest" degree of shadowing. (B) Distal small bowel adjacent to the urinary bladder (UB), with an intraluminal, shadowing, incidental small intestinal foreign body (*arrow*) in a 7-year-old cat. The patient did well without surgical intervention.

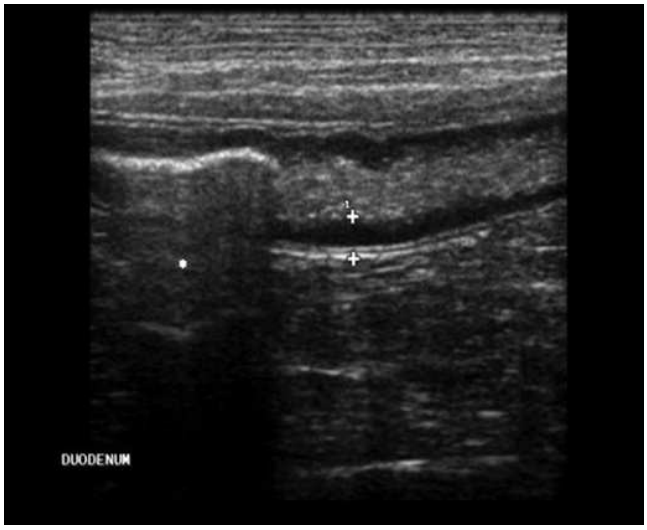


**Figure 12.8.** Normal small bowel. Image of a normal duodenum with normal luminal gas. Note the dirty distal shadow (*asterisk*) cast by the movement of gas within the small bowel lumen which could be mistaken for a luminal foreign body.

## Intestinal Obstruction

The ultrasonographic diagnosis of intestinal obstruction may be indirect based on the presence of a combined segmental luminal (fluid) distension, hypermotility in the absence of luminal content progression (Ogata et al. 1996; Manczur et al. 1998), nonuniform intestinal peristalsis and the presence of hyper- and hypomotility in the same animal (Schmutz et al. 1997; Manczur et al. 1998).

- Patients with these ultrasonographic findings should be carefully evaluated for luminal foreign bodies, intussusception, or even obstructive neoplasia as their presence further supports a diagnosis of intestinal obstruction (Tidwell and Penninck 1992; Penninck 2008a; Garcia et al. 2011).
- The ultrasonographic presence of any two of the above findings has a reported sensitivity of 100% and specificity 98.5% for the diagnosis of intestinal obstruction in cats and dogs (Garcia et al. 2011). However, the presence of only intestinal hyper- or hypomotility and concurrent segmental intestinal dilation without progression of luminal content may result in a false-positive diagnosis of intestinal obstruction (Garcia et al. 2011). Thus, it is imperative to continue to search for the presence of foreign bodies, intussusception or mass lesions that would further support mechanical obstruction and surgical decision making.

## Intussusception

Intestinal intussusception is readily diagnosed with ultrasonography due to a characteristic and easily recognized pattern.

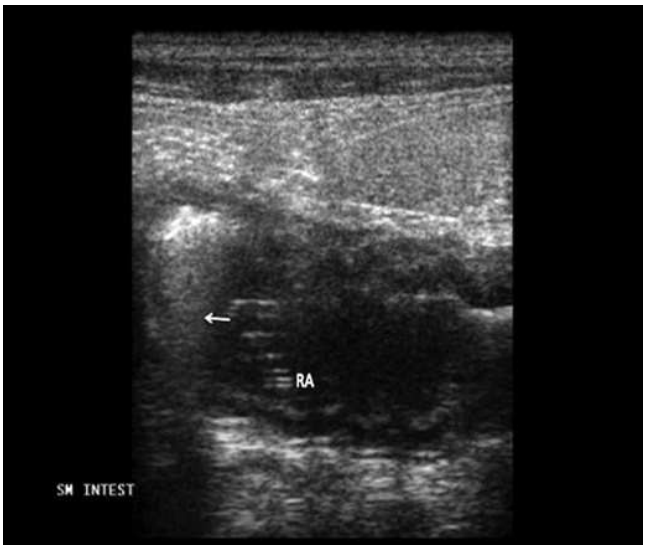


**Figure 12.9.** Corrugated small bowel. Sagittal image of a loop of small bowel in a 5-month-old male Labrador retriever with a two-day history of vomiting and diarrhea following dietary indiscretion and a diagnosis of severe enteritis. The small bowel is abnormally corrugated and fluid distended. There is a small amount of intraluminal gas (*arrow*) and reverberation artifact (RA). Corrugation and plication can be difficult to differentiate. Notice the lack of deep invagination of the serosal margin. It is important to evaluate the bowel from different angles in both the sagittal and transverse planes to aid in differentiation of corrugation from plication and reverberation artifact from a linear foreign body. This can be achieved in real time with investigative fanning and scanning of the bowel loop in question. The authors recommend video documentation of such investigations for the medical record. A foreign body was not identified, the patient was not obstructed and recovered with supportive care. See also Figures 12.10–12.12.

- In the transverse plane, the lesion has a series of multilayered concentric rings (bull's eye or target lesion). In the longitudinal plane, the multilayered lesion has linear streaks of hyperechoic and hypoechoic tissue (Figures 12.13 and 12.14; see also Figure 16.13) (Penninck et al. 1990; Larson and Biller 2009; Garcia et al. 2011).
- The outer layer of affected intestine may be thickened and signs of bowel obstruction are often present.
- Fluid distension oral to the site of invagination, increased peristalsis without signs of content progression, and signs of hypo- or normal motility distant from the intussusception may also be noted (Larson and Biller 2009; Garcia et al. 2011).

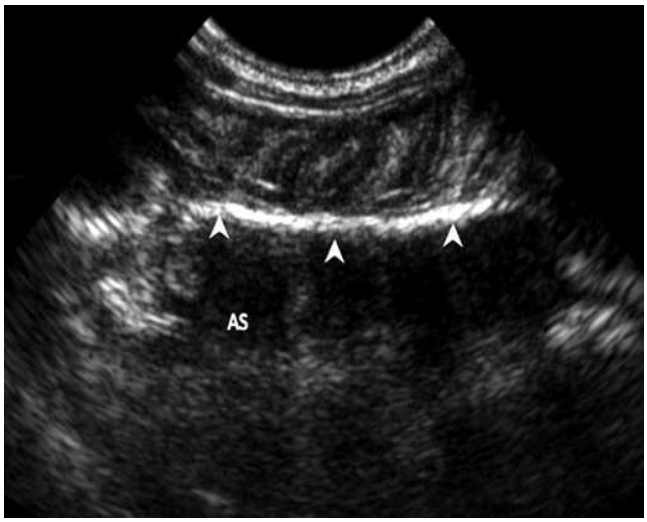


**Figure 12.10.** Plicated small bowel. Small bowel plication in a 3-month-old French bulldog with a two-day history of vomiting. An intraluminal linear foreign body (*arrowheads*) can sometimes be easily identified within the lumen of plicated small intestine. Note the clean acoustic shadowing (AS) distal to the linear foreign body. A toy mouse on a long string was removed surgically via multiple enterotomies.

## *Septic Peritonitis and Pneumoperitoneum*

Septic peritonitis (often secondary to GI perforation) is a life-threatening emergency that may be challenging to diagnose presurgically.

- The AFAST examination (see Chapters 6 and 7) is particularly helpful in identifying peritoneal effusion (a common finding in patients with septic peritonitis).
- Moderate amounts of fluid are easily detectable via ultrasound. Ultrasound-guided fine needle aspiration may subsequently provide the definitive diagnosis of sepsis (see Chapter 43).
- In addition to the presence of fluid, which may be anechoic, anechoic with hyperechoic particles suspended throughout or echogenic and swirling, ultrasound may also detect the presence of intraperitoneal gas in cases of GI or other hollow organ perforation (Boysen et al. 2003).
- Although radiographs are indicated for the detection of pneumoperitoneum, survey radiographs may fail to detect the presence of small-volume intraperitoneal gas. Ultrasound has been used successfully to diagnose pneumoperitoneum in both people and veterinary patients (Boysen et al. 2003).
- In dogs and cats, the ultrasonographic detection of intraperitoneal gas is characterized by

**Figure 12.11.** Plicated small bowel. Same patient as in Figure 12.10. Sagittal image of severely plicated small bowel secondary to linear foreign body (not shown). If this characteristic zig-zag pattern of small bowel is seen it should prompt the sonographer to look carefully for the presence of a linear foreign body (not seen in this image). The small bowel is plicated and bunched with deep invaginations of the serosa/subserosa. The presence of such a pattern should also prompt *strong* recommendations for surgical intervention.

reverberation and comet-tailing artifacts interposed between the nondependent abdominal wall and organs such as the liver and stomach, stomach and body wall or kidney and body wall (Figure 12.15) (Boysen et al. 2003). However, it should be noted that air-filled bowel can be difficult to differentiate from intraperitoneal air. Careful identification of the peritoneal lining and the enhanced peritoneal strip sign (EPSS) will help differentiate intraperitoneal air from air-filled bowel (see later) (Kim et al. 2014). In cases where there is a high index of suspicion for small-volume intraperitoneal gas or if the etiology of the suspected gas is unclear, ancillary diagnostics such as abdominal radiography or computed tomography should be considered.

- Detection of the EPSS aids in the diagnosis of pneumoperitoneum. The EPSS is the linear enhancement and thickening of the peritoneal lining with either dirty shadowing or multiple reflection artifacts. It occurs where the peritoneum comes in contact with free abdominal gas. The associated shadowing or reflection artifact is transmitted through the peritoneal cavity and underlying soft tissue structures (Figure 12.16) (Grechenig et al. 1999; Kim et al. 2014).

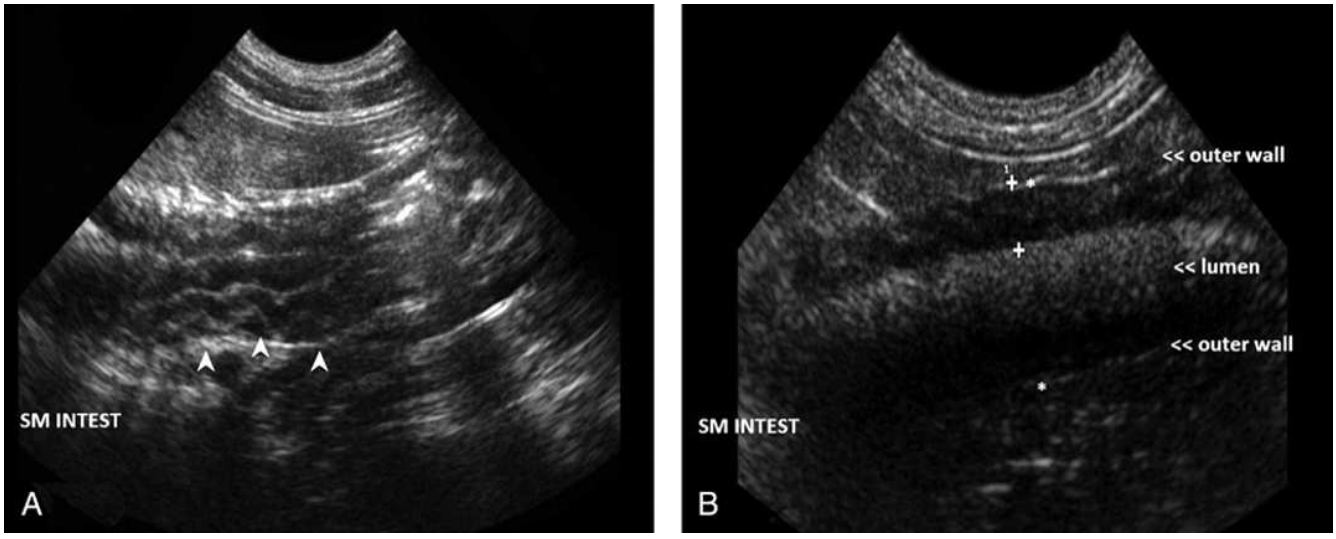


**Figure 12.12.** Examples of small bowel corrugation. (A) Image of the small bowel corrugation in the same patient as in Figure 12.9. Note the various degrees of corrugation and fluid distension of the small bowel in this patient. It may be difficult to distinguish between corrugation and plication. (B) Intestinal corrugation in a 15-year-old male rat terrier with severe pancreatitis and pancreatic abscessation. Compare Figures 12.7–12.11. Note that corrugated bowel appears as a wavy pattern of the intestinal wall; however, the intestine tends to follow a straight line.

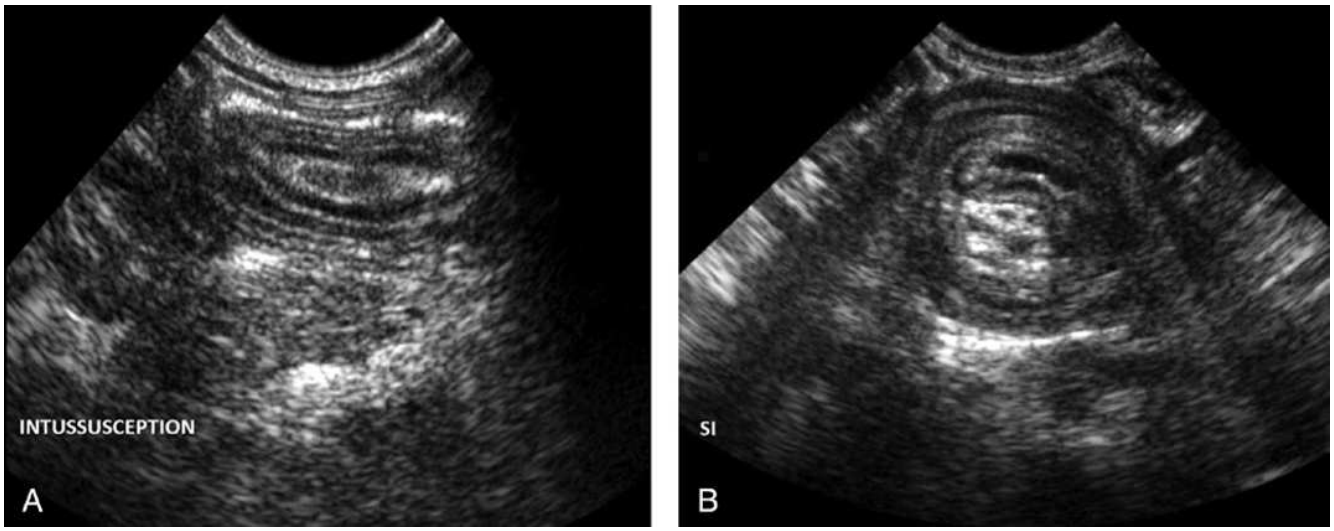


**Figure 12.13.** Intussusception. Intussusception of the small bowel (jejuno-jejunal) in the same patient as in Figure 12.10. (A) Sagittal plane image. Note the multilayered lesion with linear streaks of hyperechoic and hypoechoic tissue. Six jejuno-jejunal intussusceptions were noted during surgery and manually reduced. The patient recovered without complication. (B) A cross-sectional image of a small intestinal intussusception (labeled SI by the sonographer) in a 9-year-old greyhound with vomiting and hematochezia. Note the series of multilayered concentric rings (bull's eye or ring sign).

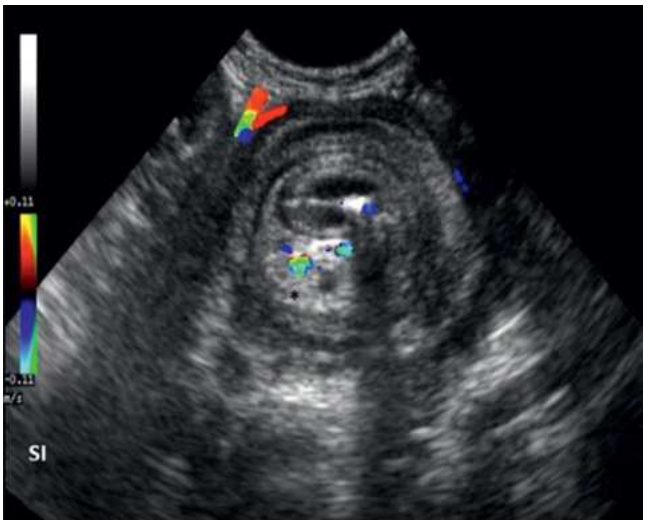


**Figure 12.14.** Intussusception. Transverse image of a small intestinal intussusception in the same patient as in Figure 12.13B. The final diagnosis was linear foreign body with secondary ascending duodenal intussusception. The patient recovered well following resection and anastomosis. Note the series of multilayered concentric rings (bull's eye or ring sign) and hyperechoic invaginated mesenteric fat (*asterisk*). Color flow or power Doppler evaluation can aid in providing information about the viability and perfusion of the intussuscepted bowel.

- As little as 0.2 mL of abdominal free gas can be detected ultrasonographically in dogs (Kim et al. 2014). However, depending on patient positioning and the area of abdomen evaluated, detection of a false-positive EPSS may occur in proximity to the linea alba of dogs positioned in dorsal recumbency, particularly if the linea alba is focally thickened (Kim et al. 2014).
- In people and animals, pneumoperitoneum may be ultrasonographically apparent by the detection of reverberation or comet-tailing artifacts between the anterior abdominal wall and the liver in the right upper quadrant with an 85% sensitivity and 100% specificity (Pattison et al. 1997; Muradali et al. 1999; Ferrell and Graham 2003; Chao et al. 2015). The authors have seen similar sonographic findings within the left dorsal aspect of the dog between the fundus and left liver. To increase the chances of detecting air between the fundus and left liver, the animal should remain in right lateral recumbency for a minimum of 10–15 minutes to allow intraperitoneal gas to rise to the nongravity-dependent sites.
- Scanning cranially along an imaginary line of the diaphragmatic crura and at the approximate level of the costophrenic angle, between the ribs

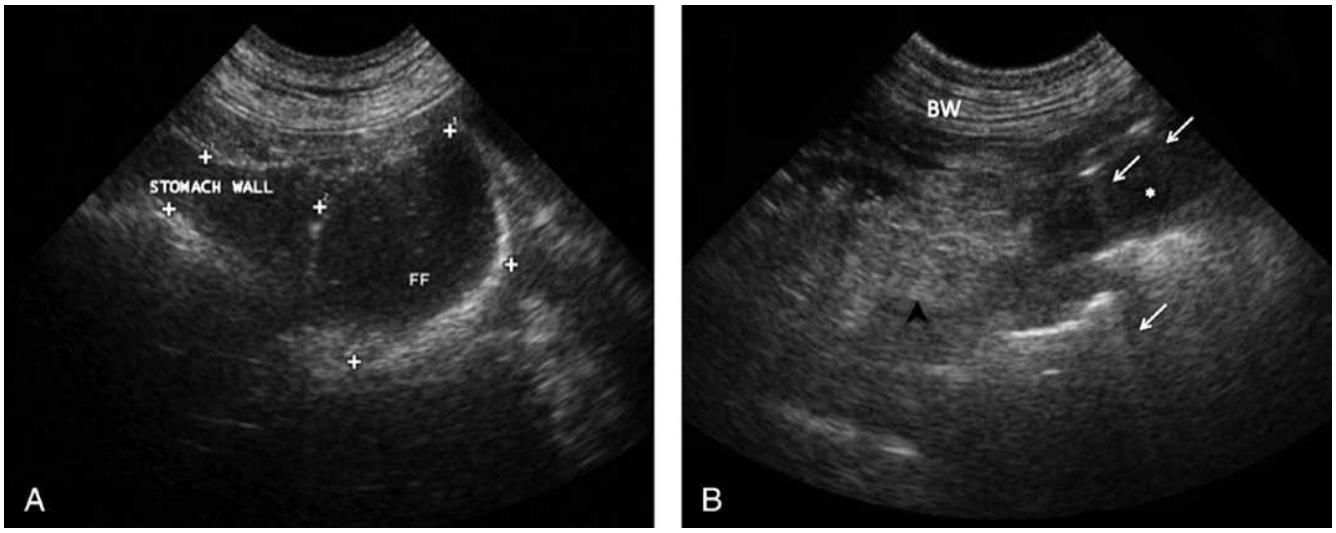


**Figure 12.15.** Ruptured gastric ulcer and peritonitis. Images of the left cranial abdominal quadrant of a 9-year-old English bulldog that presented with lethargy and hematemesis. The patient had been on chronic nonsteroidal antiinflammatory therapy for arthritis. (A) Note the severely thickened gastric wall measuring approximately 0.9 cm, which displays a loss of normal wall layering and is hypoechoic. Immediately adjacent to the stomach is a loculation of anechoic fluid with echogenic particles noted in suspension (labeled FF and identified by the cross marks, +). (B) Intraperitoneal gas in the same patient. Fanning and scanning of this region in real time revealed faint echogenic streaking (reverberation artifact) and comet-tails interposed between the nondependent body wall and stomach (*arrows*), liver and body wall (not shown) and within the loculated fluid and mesentery (*arrows*). Gastric wall (*asterisk*) with adjacent hyperechoic mesentery (*black arrowhead*). Multiple comet-tails present (*white arrows*) consistent with intraperitoneal gas. The patient was diagnosed surgically with a perforated gastric ulcer and had a full recovery following surgical resection and supportive care.

while fanning, may aid in the detection of small amounts of intraperitoneal gas trapped between the liver and diaphragm. Furthermore, in the authors' experience, evaluating the mid-highest point of the abdomen, regardless of recumbency, may aid in the detection of a small volume of intraperitoneal gas.

- Regardless of patient positioning, particular attention should be paid to the nongravity-dependent areas of the abdomen when looking for intraperitoneal gas (as gas rises) (Asrani 2007).
- If the history and physical examination are supportive of acute GI disease and an AFAST examination is performed to look for septic peritonitis, it is also reasonable to look for the presence of intraperitoneal gas (particularly along the nongravity-dependent body wall as gas rises) while simultaneously searching for fluid, which might alternatively be seen along the gravity-dependent aspects of the patient as fluid falls or settles.
- Failure to detect gas does not rule out GI perforation. Its presence in patients with supporting history and clinical findings expedites the decision for exploratory surgery.

**Pearl:** Serial AFAST (and POCUS GIT and pancreas) examinations *after resuscitation and rehydration* are helpful (four hours post admission out to 12 and 24 hours) to detect initially occult peritonitis or bowel perforation because peritoneal fluid and gas will often develop over time and as the patient becomes hydrated.

**Pearl:** AFAST and POCUS GIT and pancreas examinations are helpful initial screening tests for penumoperitoneum (Shanaman et al. 2013; Chao et al. 2015). Although CT is generally considered the gold standard for detection of pneumoperitoneum, abdominal radiography (including horizonal beam techniques) are good ancillary tests when pneumoperitoneum is suspected (Chao et al. 2015).

## Functional Ileus

Ultrasonographically, GI motility can be recorded as the number of gastrointestinal contractions observed over a one-minute time period.

- To determine the number of contractions per minute, the number of contractions are recorded

**Figure 12.16.** Intraperitoneal gas and the enhanced peritoneal stripe sign. Image of the right cranial abdominal quadrant of a young adult dog with intraperitoneal gas secondary to traumatic ballistic trauma (gunshot wound) with subsequent multiple intestinal perforations. The enhanced peritoneal stripe sign (EPSS) (*arrowhead*) is visible where free gas within the abdomen contacts the peritoneum, making the peritoneum appear more hyperechoic. Reverberation artifact is also noted arising from the EPSS or peritoneal–gas interface (*short white arrows*) extending deep into the far-field of the image, which obscures structures located in its path. Note the loss of image detail as the reverberation artifact passes though the duodenum.

twice over a three-minute time period, averaged, and then divided by 3 to get the number of contractions per minute (Penninck et al. 1989; Sanderson et al. 2017).

- Fasting or anorexia of 12–24 hours duration decreases GI motility in dogs. Thus, knowing when the animal last ate is important when interpreting GI motility. If possible, GI motility should be assessed within six hours of ingesting a meal (Sanderson et al. 2017).
- Caution should be exercised when diagnosing hypomotility based on the presence of food within the GI tract, as food can be ultrasonographically detected in the GI lumen of healthy dogs following 24 hours of fasting. However, the absence of GI contraction in the presence of food supports a diagnosis of ileus (Sanderson et al. 2017).
- Normal contractility varies depending on the section of GIT evaluated. The mean number of peristaltic contractions of the stomach and proximal duodenum is 4–5 contractions per minute. The number of contractions of the small intestine in the midabdomen is more variable and ranges from one to six contractions per minute (Penninck et al. 1989; Sanderson et al. 2017).
- Certain GI disorders are associated with changes in intestinal motility, including mechanical bowel obstruction, gastric ulcers, severe pancreatitis, inflammatory bowel disease, and neoplastic processes (Garcia et al. 2011). Functional ileus, during which the lumen of the bowel remains patent, may also be caused by pain, metabolic disterbances, poor perfusion, and sedative agents (Sanderson et al. 2017).

**Pearl:** The mean number of gastric and proximal duodenal peristaltic contractions is 4–5 per minute, which tend to be easy areas to consistently assess ultrasongraphically. The sonographic finding of food within the GI lumen and absence of GI contractions should prompt consideration of ileus.

- A generalized decrease in GI motility is reported in small animals with functional and chronic mechanical ileus, whereas a generalized increase in motility is most commonly reported in cases of acute mechanical obstruction (Penninck 2008a).
- There is considerable overlap in motility changes between dogs that do and do not have small intestinal obstruction. Changes in motility alone do not indicate the need for surgery (Sharma et al. 2011; Garcia et al. 2011).
- If the emergency clinician notes increased or decreased GI motility in a patient with clinical signs of GI disease, further diagnostics (abdominal radiographs or complete abdominal ultrasound examination) should be considered as several surgical conditions (foreign bodies, intussusception, and neoplasia) are frequently associated with altered GI motility (Penninck 2008a; Garcia et al. 2011). A thorough evaluation of the GI tract to rule out these conditions is warranted.

Decreased intestinal motility due to functional ileus is commonly seen in postoperative patients.

- This condition results in a transient cessation of coordinated propulsive motility, most commonly following abdominal surgery (Koscienly and Kalff 2011).
- In people, it is associated with abdominal distension, nausea, vomiting, and the inability to pass stools or tolerate a solid diet.

- In addition to the discomfort reported in people, postoperative ileus may predispose patients to wound dehiscence, intussusception, and pulmonary and thromboembolic complications (van Bree et al. 2012).
- Several predispositions are associated with acute ileus following postoperative abdominal surgery in people, including intestinal handling during surgery, anesthetic agents, and opioid analgesics (Kehlet 2008; van Bree et al. 2012).
- Many small animals are routinely fasted pre- and postoperatively, which can also contribute to ileus (Sanderson et al. 2017). Unless otherwise contraindicated, food should be reintroduced to patients as soon as possible following surgical procedures.
- If the impression of ileus is due to fasting, reintroducing solid food within 24 hours of fasting should promote GI motility (Sanderson et al. 2017). However, if reintroduction of solid food fails to stimulate motility in the patient that has been fasted for less than 24 hours, other causes of functional ileus should be considered. It is currently unknown if liquid diets have the same effect on GI motility as solid diets following a period of fasting.
- Long-term ileus following abdominal surgery is believed to result from inflammation of the intestinal muscularis externa (Kalff et al. 1999).
- Postoperative ileus involving the entire gastrointestinal tract can occur even if only part of the intestine had been handled or is inflamed (van Bree et al. 2012).
- If postoperative ileus is noted, measures should be taken to ascertain the underlying cause (opioids, postoperative surgery, abdominal pain, electrolyte imbalances, and peritonitis).
- Therapeutic interventions should be implemented and include feeding soon after surgery, early ambulation, epidural analgesia (decreases the need for systemic opioid analgesia which is often associated with ileus), nonsteroidal antiinflammatory agents, and minimally invasive surgery (Behm and Stollman 2003; van Bree et al. 2012).

## Corrugated Intestine

Although not always easy to do, it is *important to differentiate corrugated bowel from plicated bowel* as the two pathologies have different etiologies.

- *Plicated bowel*. Plicated bowel is usually associated with intestinal linear foreign bodies that cause the small intestine to bunch around a linear object, resulting in an asymmetrical intestinal pattern (see Figures 12.10, 12.11, 16.9–16.13). The loop of small intestine may weave as it cinches together and contracts around the linear foreign body. The finding of plicated bowel may indicate the need for surgery, even if the linear foreign body is not ultrasonographically detected (Tidwell and Penninck 1992) (see Figures 12.9, 12.11, 16.9–16.13).
- *Corrugated bowel*. In contrast, corrugated bowel is a very nonspecific ultrasonographic finding that suggests intestinal dysfunction or inflammation, which could result from several different causes (peritonitis, enteritis, pancreatitis and pancreatic neoplasia, diffuse abdominal neoplasia, enteritis, thrombosis/infarction, protein-losing enteropathy, and acute renal failure) (Moon et al. 2003) (see Figure 12.9).
- *Corrugated intestine*. Corrugated intestine occurs secondary to abnormal spastic peristalsis of the bowel resulting in an abnormal wavy (corrugated) pattern to the wall (Moon et al. 2003). The overall direction of the intestine (and serosal margin) tends to appear straight, in contrast to bunched or weaved with plicated bowel (see Figures 12.9, 12.12, 16.9–16.13).
- Both conditions are most apparent in the sagittal (longitudinal) plane of the small intestine and may be evident in a single loop or sporadically throughout the scan in several loops.
- If corrugated bowel is noted in the unstable patient, a POCUS examination of the pancreas and a search for peritoneal fluid using AFAST is warranted as the condition is commonly associated with pancreatitis and peritonitis. Pancreatitis is particularly common when corrugation of the duodenum is noted (Moon et al. 2003).
- If POCUS of the pancreas and/or AFAST examination are unremarkable, or if the patient is stable, a complete abdominal ultrasound exam (or other diagnostic tests) may be indicated to search for other pathologies associated with corrugated bowel, including enteritis (parvovirus, inflammatory bowel disease, lymphocytic plasmacytic enteritis), pancreatic neoplasia, diffuse abdominal neoplasia, thrombosis/infarction, protein-losing enteropathy, and acute renal failure (Moon et al. 2003).

**Pearl:** In differentiating corrugated from plicated bowel, overall direction of the intestine tends to appear straight with corrugated bowel (as with enteritis or pancreatitis). In contrast, the serosal margin follows the contour of the bunching with plicated bowel (as with surgically indicated linear foreign body) (see Figures 12.10, 12.11, 12.12, 16.9–16.13).

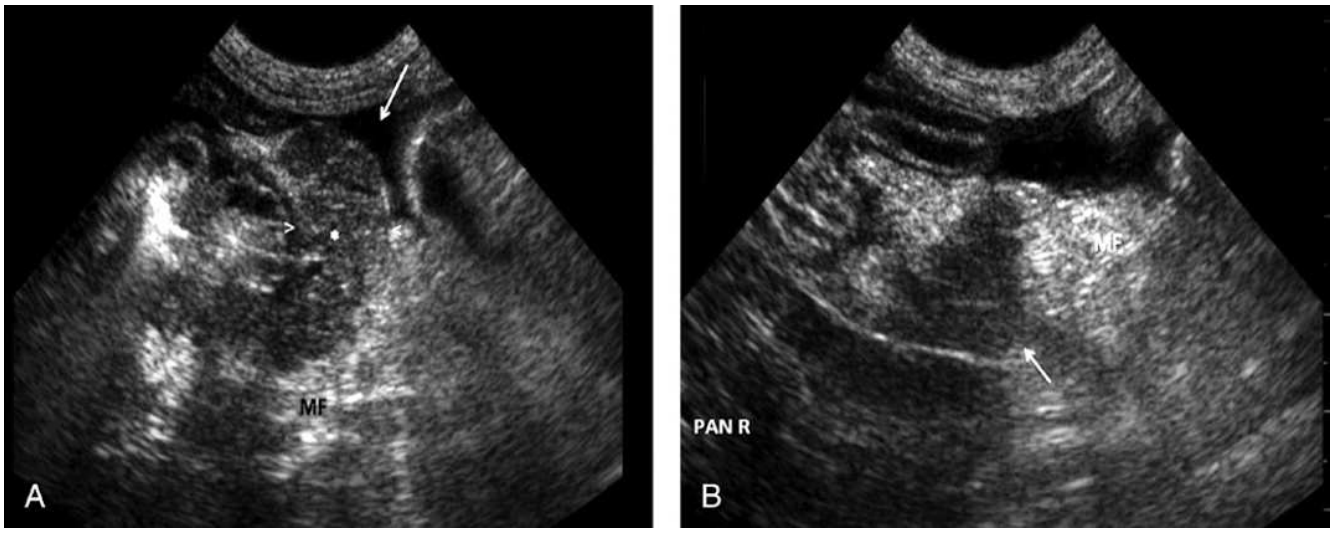


**Figure 12.17.** Pancreatitis. (A) Image of an 8-year-old male neutered Yorkshire terrier with acute pancreatitis. Note the enlarged and diffusely hypoechoic pancreatic body (*asterisk*). Variable amounts of peritoneal effusion may accompany pancreatitis (fluid echogenicity can vary from anechoic to echogenic and cellular) and can be seen in proximity to the pancreas (*arrow*). The surrounding mesenteric fat (MF) often appears moderately hyperechoic. (B) Same patient, right limb of the pancreas. The right pancreatic limb (*arrow*) is surrounded by hyperechoic and hyperattenuating mesenteric fat.

### *Pancreatitis*

Acute pancreatitis is generally a clinical diagnosis supported by history and physical examination findings. If suspected, a POCUS pancreas examination may further support the diagnosis of pancreatitis. However, ultrasonographic findings may be inconsistent and may not reliably produce sufficient pancreatic parenchymal change.

- A normal ultrasonographic finding does not rule out pancreatitis.
- Ultrasound has limited sensitivity (68%) for the detection of pancreatitis, even in severe acute cases (Hess et al. 1998).
- Evidence of acute pancreatitis includes an enlarged and diffusely hypoechoic pancreas (Figure 12.17) (Lamb and Simpson 1995; Hecht and Henry 2007).
- Variable amounts of peritoneal effusion may be present, and may be amenable to sampling for cytological evaluation.
- Surrounding mesenteric fat often appears hyperchoic (bright) due to inflammation, necrosis, and saponification (see Figure 12.17) (Hecht and Henry 2007; Penninck 2008b).
- Corrugation of the duodenum or jejunum, and focal pain at the scan site may be present (Hecht and Henry 2007).
- Extrahepatic biliary obstruction may accompany pancreatits with bile duct and gallbladder distension. These findings in patients with appropriate history and clinical findings warrant the initiation of therapy for acute pancreatitis. One disadvantage to a POCUS pancreas examination is that the entire biliary and pancreatic ductal system requires a greater time commitment and skill level that is typically beyond that of the nonradiologist veterinarian.
- If the preliminary POCUS pancreas examination is negative, a complete abdominal ultrasound may be warranted.
- When suspected or diagnosed, recheck of the pancreas in 1–3 days should be considered as ultrasonographic signs may become evident with time. Further, follow-up evaluation will aid in monitoring response to treatment and progression or resolution of changes.

### *Peritoneal Effusion*

See Chapters 6 and 7.

## Pearls, Pitfalls, The Final Say

- Fasting the patient 12 hours prior to ultrasound evaluation is historically desired to avoid having to scan around a distended stomach, but is not

usually feasible in the emergent POCUS GIT and pancreas examinations; fasting can also affect GI motility.
- Gastrointestinal gas may cause reverberation, comet-tail, and acoustic shadowing artifacts, which may obscure bowel evaluation. Gas artifacts may be difficult to distinguish from the shadowing associated with some GI foreign bodies.
- The stomach is easy to identify due to the presence of rugal folds, but can be difficult to completely image due to luminal ingesta and gas. Luminal contents, or lack thereof, can also affect wall measurements. For example, an empty stomach may give the impression of having a thickened wall.
- In dogs, the descending duodenal wall is thicker than other small intestinal segments and can normally measure up to 6 mm in large-breed dogs. For the remainder of the small bowel, greater than 5 mm (4 mm for the ileum) in dogs and 2.5 mm in cats would generally be considered as thickened (Penninck et al. 1989; Newell et al. 1999).
- In cats, the ileum is identified by its bright submucosal layer.
- The colon can often be differentiated from the small intestinal wall by its thinner wall and lack of motility in normal instances.
- Using an acoustic window such as the spleen can enhance imaging of the intestine.

# Quick Reference of Normals and Rules of Thumb

## Gastrointestinal Tract

- *Normal stomach wall thickness*. Dogs 3–5 mm (higher in some giant breeds); cats 2 mm interrugal (up to 4.4 mm if rugal fold is measured) (Nyland et al. 2002). Measure from the hyperechoic outer serosal margin to the inner hyperechoic mucosoluminal surface.
- *Duodenal wall thickness*. In dogs, the descending duodenal wall is *thicker* than other small intestinal segments and can normally measure up to 5 mm in large-breed dogs (Newell et al. 1999). Measure from the hyperechoic outer serosal margin to the inner hyperechoic mucosoluminal surface.
- *Small intestinal measurements*. Small bowel wall measurements, *other than the duodenum*, of greater than 4 mm in dogs and 2.5 mm in cats would generally be considered as abnormally thickened (Newell et al. 1999). Measure from the hyperechoic outer serosal margin to the inner hyperechoic mucosoluminal surface.
- *Remembering the five layers of the small intestine*. Use the mnemonic "the sun is bright and it's dark at midnight" to remember that on the US image, layers starting with an "s" like the sun are bright (submucosa and serosa are hyperechoic [bright]), while layers starting with an "m" like midnight are dark (mucosa and muscular layer are hypoechoic [dark]).
- *Direct evidence of GIT foreign bodies*. The majority of ultrasonographically detectable GIT foreign bodies typically involve a well-defined hyperechoic, hyperreflective acoustic interface with strong distal acoustic shadowing (Tidwell and Penninck 1992; Garcia et al. 2011).
- *Linear GIT foreign bodies: plication versus corrugation*. The finding of bowel plication is strongly suggestive of a linear foreign body and should prompt careful evaluation of the intestine (longitudinal and transverse images) at sites where plication is seen (Tidwell and Penninck 1992; Garcia et al. 2011). Intestinal corrugation has also been associated with linear foreign bodies (Tidwell and Penninck 1992) but is less specific than plication.
- *Corrguated versus plicated*. In differentiating corrugated from plicated bowel, overall direction of the intestine tends to appear straight with corrugated bowel (medical causes – enteritis/pancreatitis) in contrast to bunched or weaved with plicated bowel (surgical causes – linear foreign body) (Tidwell and Penninck 1992; Moon et al. 2003).
- *Indirect evidence of obstruction*. Suspect obstruction with the finding of a severely dilated jejunum with luminal dilation measuring greater than 1.5 cm, which may highlight the need for a more extensive and complete abdominal ultrasonographic evaluation, abdominal radiographs or exploratory surgery. Measure from serosal to serosal surface.
- *Normal peristalsis – counting contractions*. Determine the number of contractions per minute by recording the number of contractions over a three-minute time period and average to get the number of contractions per minute (Penninck et al. 1989).
  - The mean number of peristaltic contractions of the stomach and proximal duodenum is 4–5 contractions per minute.
  - The mean number of peristaltic contractions of the jejunum averages 1–3 contractions per minute.
  - The mean number of peristaltic contractions in other areas of small intestine is variable and ranges from one to six contractions per minute (Penninck et al. 1989; Sanderson et al. 2017).
  - The large bowel (colon) normally has no peristalsis.

- *Ileus*. A generalized decrease in GI motility is reported in small animals with functional and chronic mechanical ileus, whereas a generalized increase in motility is most commonly reported in cases of *acute* mechanical obstruction (Penninck 2008a). However, because of considerable overlap in motility findings, motility alone does not indicate the need for surgery (Sharma et al. 2011; Garcia et al. 2011).

### Pancreas

- The right pancreatic limb is generally easiest to image in dogs and is the lobe more commonly affected by pancreatitis (Nyland et al. 2002; Hecht and Henry 2007; Penninck 2008b).
- The left pancreatic limb is generally easiest to image in cats.
- The reference range for pancreatitic thickness in dogs is 3.5–16 mm (Respess et al. 2012).
- Identification of the pancreas can be challenging for the novice sonographer because it is isoechoic to adjacent tissues. As a result, its identification commonly relies on the observance of its duct and vasculature.
- Historically, it has been thought that a normal pancreas is generally not seen; however, the normal pancreas is in fact frequently imaged with high-frequency transducers and newer machines.
- Pancreatitis is particularly common when corrugation of the duodenum is noted (Moon et al. 2003).
- Even in cases of severe acute pancreatitis, the sensitivity of ultrasound may only be 68% (Hess et al. 1998).

# References


Asrani A. 2007. Sonographic diagnosis of pneumoperitoneum using the 'enhancement of the peritoneal stripe sign.' A prospective study. *Emerg Radiol* 14:29–39.

Behm B, Stollman N. 2003. Postoperative ileus: etiologies and interventions. *Clin Gastroenterol Hepatol* 1:71–80.

Boysen SR, Tidwell AS, Penninck DG. 2003. Ultrasonographic findings in dogs and cats with gastrointestinal perforation. *Vet Radiol Ultrasound* 44(5):556–564.

Boysen SR, Rozanski EA, Tidwell AS, et al. 2004. Evaluation of a focused assessment with sonography for trauma protocol to detect free abdominal fluid in dogs involved in motor vehicle accidents. *J Am Vet Med Assoc* 225(8):1198–1204.

Brinkman-Furguson EL, Biller DS. 2009. Ultrasound of the right lateral intercostal space. *Vet Clin North Am Small Anim Pract* 39(4):761–781.

Chao A, Gharahbaghian L, Perera P. 2015. Diagnosis of pneumoperitoneum with bedside ultrasound. *West J Emerg Med* 16(2):302.

Dean A, Lafferty K, Villaneuva T. 2003. Emergency medicine bedside ultrasound diagnosis of intussusception in a patient with chronic abdominal pain and unrecognized Peutz–Jeghers syndrome. *J Emerg Med* 24(2):203–210.

De Cock HE, Forman FA, Farver TB, et al. 2007. Prevalence and histopathologic characteristics of pancreatitis in cats. *Vet Pathol* 44(1):39–49.

Ferrell EA, Graham JP. 2003. Ultrasound corner – diagnosis of pneumoperitoneum. *Vet Radiol Ultrasound* 44(3):307–308.

Garcia DA, Froes TR, Vilani OC, et al. 2011. Ultrasonography of small intestinal obstructions: a contemporary approach. *J Small Anim Pract* 52:484–490.

Grechenig W, Peicha G, Clement HG, Grechenig M. 1999. Detection of pneumoperitoneum by ultrasound examination: an experimental and clinical study. *Int J Care Injured* 30:173–178.

Hasani SA, Fathi M, Daadpey M, et al. 2015. Accuracy of bedside emergency physician performed ultrasound in diagnosing different causes of acute abdominal pain: a prospective study. *Clin Imaging* 39(3):476–479.

Hecht S, Henry G. 2007. Sonographic evaluation of the normal and abnormal pancreas. *Clin Tech Small Anim Pract* 22:115–121.

Hess RS, Saunders HM, van Winkle TJ, et al. 1998. Clinical, clinicopathological, radiographic and ultrasonographic abnormalities in dogs with fatal acute pancreatitis: 70 cases (1986–1985). *J Am Vet Med Assoc* 213:665–670.

Jang T, Schindler D, Kaji D. 2011. Bedside ultrasonography for the detection of small bowel obstruction in the emergency department. *Emerg Med J* 28:676–678.

Kalff JC, Carlos TM, Schraut WH, et al. 1999. Surgically induced leukocytic infiltrates within the rat intestinal muscularis mediate postoperative ileus. *Gastroenterology* 117:378–387.

Kehlet H. 2008. Postoperative ileus – an update on preventive techiques. *Nat Clin Pract Gastroenterol Hepatol* 5:552–558.

Kim SY, Park KT, Yeon SC, et al. 2014. Accuracy of sonographic diagnosis of pneumoperitoneum using the enhanced peritoneal stripe sign in Beagle dogs. *J Vet Sci* 15(2):195–198.

Koscielny A, Kalff JC. 2011. T-helper cell type 1 memory cells and postoperative ileus in the entire gut. *Curr Opin Gastroenterol* 27:509–514.

Lamb CR, Simpson KW. 1995. Ultrasonographic findings in cholecystokinin-induced pancreatitis in dogs. *Vet Radiol Ultrasound* 36:139–145.

Larson MM, Biller DS. 2009. Ultrasound of the gastrointestinal tract. *Vet Clin North Am Small Anim Pract* 39:747–759.

Larson MM, Panciera DL, Ward, DL, et al. 2005. Age-related changes in the ultrasound appearance of the feline pancreas. *Vet Radiol Ultrasound* 46(3):238–242.

Lisciandro GR, Lagutchik MS, Mann KA, et al. 2009. Evaluation of an abdominal fluid scoring system determined using abdominal focused assessment with sonography for trauma in 101 dogs with motor vehicle trauma. *J Vet Emerg Crit Care* 19(5):426–437.

Manczur F, Voros F, Vrabely T, et al. 1998. Sonographic diagnosis of intestinal obstruction in the dog. *Acta Vet Hung* 46:35–45.

Mateer J, Plummer D, Heller M, et al. 1994. Model curriculum for physician training in emergency ultrasonography. *Ann Emerg Med* 23:95–102.

Moon M, Biller D, Armburst L. 2003. Ultrasonographic appearance and etiology of corrugated small intestine. *Vet Radiol Ultrasound* 44(2):199–203.

Muradali D, Wilson S, Burns PN, et al. 1999. A specific sign of pneumoperitoneum onsonography: enhancement of the peritoneal stripe. *Am J Roentgenol* 173:1257–1262.

Newell SM, Graham JP, Roberts GD, et al. 1999. Sonography of the normal feline gastrointestinal tract. *Vet Radiol Ultrasound* 40(1):40–43.

Nyland TG, Mattoon JS, Herrgesell EJ, et al. 2002. Pancreas. In: *Small Animal Diagnostic Ultrasound*, 2nd edition, edited by Nyland TG, Mattoon JS. Philadelphia: WB Saunders, pp 144–157.

Ogata M, Mateer JR, Condon RE. 1996. Prospective evaluation of abdominal sonography for the diagnosis of bowel obstruction. *Ann Surg* 223:237–241.

Pattison P, Jeffrey RB, Mindelzum RE, et al. 1997. Sonography of intraabdominal gas collections. *Am J Roentgenol* 169:1559–1564.

Penninck D. 2008a. Gastrointestinal tract. In: *Ultrasound of Small Animal Ultrasonography*, edited by Penninck D, d'Anjou MA. Ames: Blackwell Publishing, pp 281–318.

Penninck D. 2008b. Pancreas. In: *Ultrasound of Small Animal Ultrasonography*, edited by Penninck D, d'Anjou MA. Ames: Blackwell Publishing, pp 319–338.

Penninck D, Nyland T, Fisher P, et al. 1989. Ultrasonography of the normal canine gastrointestinal tract. *Vet Radiol* 30(6):272–276.

Penninck D, Nyland T, Kerr L, et al. 1990. Ultrasonographic evaluation of gastrointestinal diseases in small animals. *Vet Radiol* 31(3):134–141.

Raymond-Dufresne É, Ghanayem H. 2012. Towards evidence-based emergency medicine: best BETs from the Manchester Royal Infirmary. BET 2: Can emergency physicians safely rule in or rule out paediatric intussusception in the emergency department using bedside ultrasound? *Emerg Med J* 29(10):854–855.

Respess M, O'Toole TE, Taeymens O, et al. 2012. Portal vein thrombosis in 33 dogs: 1998–2011. *J Vet Intern Med* 26:230–237.

Rozycki GS, Pennington SD, Feliciano DV, et al. 2001. Surgeon-performed ultrasound in the critical care setting: its use as an extension of the physical examination to detect pleural effusion. *J Trauma* 50:636–642.

Sanderson JJ, Boysen SR, McMurray JM, et al. 2017. The effect of fasting on gastrointestinal motility in healthy dogs as assessed by sonography. *J Vet Emerg Crit Care* 27(6):645–650.

Schmutz GR, Benko A, Fournier L, et al. 1997. Small bowel obstruction: role and contribution of sonography. *Eur Radiol* 7:1054–1058.

Shanaman MM, Schwarz T, Gal A. 2013. Comparison between survey radiography, B-mode ultrasonography, contrast-enhanced ultrasonography and contrast-enhanced multidetector computed tomography findings in dogs with acute abdominal signs. *Vet Radiol Ultrasound* 54(6):591–604.

Sharma A, Thompson M, Scrivani P, et al. 2011. Comparison of radiography and ultrasonography for diagnosing small-intestinal mechanical obstruction in vomiting dogs. *Vet Radiol Ultrasound* 52(3):248–255.

Testa A, Lauritano C, Giannuzzi R, et al. 2010. The role of emergency ultrasound in the diagnosis of acute non-traumatic epigastric pain. *Intern Emerg Med* 5:401–409.

Tidwell AS, Penninck DG. 1992. Ultrasonography of gastrointestinal foreign bodies. *Vet Radiol Ultrasound* 2(33) 160–169.

Tyrrell D, Beck C. 2006. Survey of the use of radiography vs. ultrasonography in the investigation of gastrointestinal forein bodies in small animals. *Vet Radiol Ultrasound* 47:404–408.

Unluer E, Yavasi O, Eroglu O, et al. 2010. Ultrasonography by emergency medicine and radiology residents for the diagnosis of small bowel obstruction. *Emerg Med* 17:260–264.

van Bree SH, Nemethova CC, Gomez-Pinilla PJ, et al. 2012. New therapeutic strategies for postoperative ileus. *Nat Rev Gastroenterol Hepatol* 9:675–683.

# Further Reading

American College of Emergency Physicians. 2001. Use of ultrasound imaging by emergency physicians. *Ann Emerg Med* 38:469–470.

Capak D, Simpraga M, Maticic D et al. 2001. Incidence of foreign-body-induced ileus in dogs. *Berl Munch Tierarzl Wochenschr* 114:290–296.

Heller M, Jehle D. 1995. Primary applications of ultrasound. In: *Ultrasound in Emergency Medicine*, edited by Heller M, Jehle D. Philadelphia: WB Saunders, pp 131–134.

Jones R. 2007. Recognition of pneumoperitoneum using bedside ultrasound in critically ill patients presenting with acute abdominal pain. *Am J Emerg Med* 25:838–841.

Lisciandro GR. 2011. Abdominal and thoracic focused assessment with sonography for trauma, triage, and monitoring in small animals. *J Vet Emerg Crit Care* 21(2):104–122.

Mohammadi A, Ghasemi-Rad M. 2012. Evaluation of gastrointestinal injury in blunt abdominal trauma "FAST is not reliable": the role of repeated ultrasonography. *World J Emerg Surg* 7(1):2.

SECTION III

# Reproductive and Pediatric

CHAPTER THIRTEEN

# POCUS: Reproductive – Male

Robert M. Fulton

Vetbooks.ir

## Introduction

In the grand scheme of things, reproductive ultrasonography probably gets the short end of the stick since most of our patients in the United States lack their reproductive organs (testicles, ovaries, and uterus) through surgical sterilization. However, one should not assume that reproductive sterilization has taken place simply because the altered pet is more common. It is very important to confirm your patient's reproductive status since many adopted dogs and cats have unknown medical histories. The sexual status of the male is typically easy to ascertain from the physical examination; however, do not overlook cryptorchidism.

Ultrasonographically, the majority of the reproductive tract may be imaged. In females, POCUS reproductive includes the ovaries, uterus, cervix, and mammary glands (see Chapters 14 and 15) and for males, the prostate, scrotum, and testes (Figure 13.1). Of these structures, the uterus makes up the vast majority of POCUS reproductive examinations. This chapter, however, will focus on the male reproductive tract.

**Pearl:** In many areas of the United States, dogs and cats sterilized in shelters are tattooed either within or adjacent to their surgical site. A ¼–½ inch lime green linear tattoo is commonplace. Cats may also have a partial amputation of their left ear tip identifying them as sterilized (Figure 13.2).

**Pearl:** Cryptorchid testosterone-producing male cats have penile spines readily recognized on physical examination (Figure 13.3).

### *What the POCUS Reproductive – Male Can Do*

- Help determine causes of scrotal swelling. Screen for:
  - testicular torsion
  - orchitis
  - epididymitis
  - cryptorchidism
  - prostatic pathology.

### *What the POCUS Reproductive – Male Cannot Do*

- Cannot differentiate between different types of testicular tumors.
- Cannot differentiate benign versus malignant prostatic conditions.
- Cannot fully screen for intraabdominal free fluid.

**Note:** An AFAST and the assignment of an abdominal fluid score should be minimally performed to screen for any effusions or other obvious AFAST target organ pathology; the Global FAST approach provides even more information regarding the thorax (TFAST), including heart (TFAST) and lung (Vet BLUE), as a quick assessment imaging test for localized versus disseminated disease, comorbidities, and complications.

*Point-of-Care Ultrasound Techniques for the Small Animal Practitioner*, Second Edition. Edited by Gregory R. Lisciandro.
© 2021 John Wiley & Sons, Inc. Published 2021 by John Wiley & Sons, Inc.
Companion website: www.wiley.com/go/lisciandro/ultrasound2

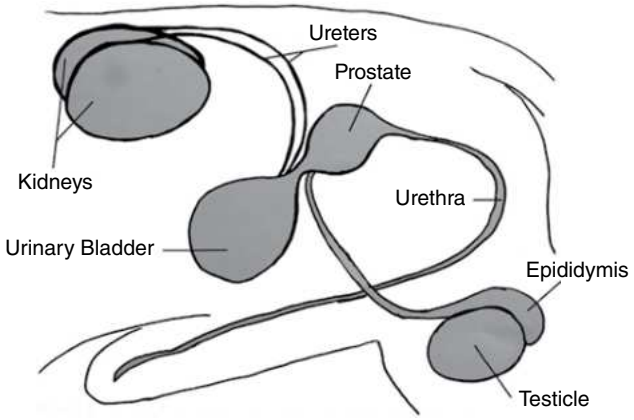


**Figure 13.1.** General male dog urogenital anatomy. Source: Courtesy of Robert M. Fulton, DVM, Richmond, VA.

**Figure 13.2.** Marking surgically sterilized animals. (A,B) Green-colored tattoos indicating the animal has been neutered (spayed or castrated). Source: Courtesy of Dr Courtney Bridgeman, Dragonfly Veterinary Services, Boerne, TX.

**Figure 13.3.** Penile spines of the tom cat. Presence of the spines serves as a physical bioassay of circulating testosterone. The penile spines start to appear around 12 weeks of age and are fully developed by the end of puberty. They are absent in the castrated male cat, disappearing about six weeks following castration. Source: Courtesy of Dr Courtney Bridgeman, Dragonfly Veterinary Services, Boerne, TX.

### *Indications*

- Acute abdomen especially in intact males with caudal abdominal pain.
- Scrotal swellings.
- Testicular swellings.
- Cryptorchidism.

### *Objectives*

- Be able to image the basic features of the male reproductive tract (scrotum, testicles, prostate).
- Identify common ultrasonographic reproductive pathology of the male or minimally be able to assess that the structure is abnormal.

## Reproductive Conditions of the Male

The male less commonly than the female has indications for the POCUS reproductive examination; however, it is useful for canine prostatic, scrotal, and testicular

problems including cryptorchidism. Interestingly, most male scans will be performed on dogs since the feline male seems immune to most reproductive conditions.

# The Prostate

All male dogs have a prostate, neutered or not (Figure 13.4). It is the dog's only accessory sex gland and it increases in size and weight with age due to glandular hyperplasia (Johnston et al. 2001a). Interestingly, the neutered male is more prone to prostatic neoplasia (prostatic adenocarcinoma) than the intact male (Root-Kustritz 2010). Finding an enlarged prostate in a neutered male of any age should be considered neoplastic until proven otherwise. Ultrasound may be helpful as an adjunctive test for aspirates and biopsies, but a digital rectal examination is invaluable for determining the presence of often painful prostatic enlargement in neutered males. Intact male dogs, on the other hand, have several possible conditions such as benign prostatic hypertrophy, bacterial prostatitis, prostatic abscesses, prostatic cysts, and paraprostatic cysts. Thus, the POCUS reproductive – male examination can be helpful in sorting through these conditions.

The feline prostate is a rather small structure of rare clinical importance and is rarely, if ever, imaged. Still, imaging the bladder and surrounding structures may be useful.

**Figure 13.4.** The normal prostate gland in a castrated dog in the longitudinal plane. The prostate (denoted by the caliper marks) is of medium echogenicity similar to that of the normal canine uterus. Source: Courtesy of Robert M. Fulton, DVM, Richmond, VA.

## *Imaging the Prostate - Dorsal and Standing Positioning*

- *Dorsal*. Place the dog in dorsal recumbency. Find the prostate by locating the urinary bladder. Move your probe to longitudinal orientation and then follow the bladder caudally until it narrows into the trigone region. Now, focus on the urethra (an anechoic linear stripe in longitudinal, anechoic circle in transverse). Once you have the urethra in the long axis, follow it caudally a short distance to the prostate.
- Standing. The standing or lateral positions may also be used for prostatic imaging and standing is actually preferred by many sonographers.

**Pearl:** Do not walk the patient (dogs) or give a litter box (cats) before the POCUS reproductive – male examination. The urine-filled bladder improves imaging by providing an acoustic window and serves as a landmark in identifying caudal abdominal structures.

- A healthy prostate is bilobed and symmetrical. The symmetry is readily appreciated in transverse orientation. Except for ductal tissue, the prostatic parenchyma is homogeneous in appearance. The echogenicity is similar to the surrounding fat but has a finer echotexture (Lattimer and Essman 2007).

**Pearl:** A hyperechoic "butterfly" pattern is typically apparent in the transverse view. The "butterfly" corresponds with distribution of relatively more hyperechoic (brighter) ductal tissue than the hypoechoic glandular connective tissue (Mattoon and Nyland 2002; Davidson and Baker 2009).

- Stay transverse and assess symmetry (normal) and for homogeneous echogenicity other than the "butterfly."
- Some veterinary radiologists more easily image the prostate with the dog in a standing position.

## *Prostate of the Castrated Male*

The normal dog prostate ultrasound appearance after involution, shrinking in size as a response to castration, has not been strictly defined or classified; however,

studies are currently ongoing to define this. In general, the prostate in the castrated dog appears as a smooth, homogeneous swelling around the proximal urethra with total width being approximately 3–4 times the width of the urethra. The overall echogenicity is similar to that of the uterine body in the female (see Figure 13.4).

## Benign Prostatic Hypertrophy (BPH)

*Ultrasonographic appearance*: enlarged, uniformly hyperechoic with a smooth margin. The enlargement may be different between dorsal and ventral areas, but is symmetrical when viewed in the transverse plane (Figure 13.5A). In time, the expected symmetry and uniform echogenicity of BPH may be lost as the condition progresses into the cystic stage (Lattimer and Essman 2007).

## Prostatitis

*Ultrasonographic appearance*: a wide variety depending on severity of disease. The shape is generally normal but the echogenicity may increase or decrease and some degree of mottling (mixed echogenicity) is appreciated. A hypoechoic rim may be evident in some dogs. If prostatitis is severe enough, surrounding fat may become hyperechoic (bright) (Lattimer and Essman 2007).

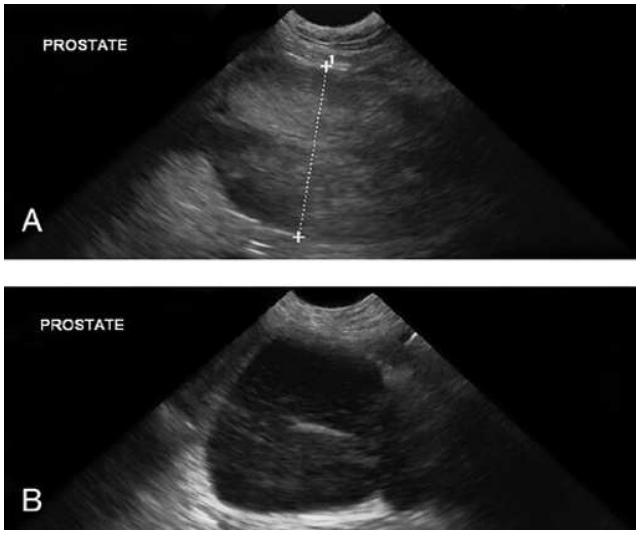


**Figure 13.5.** Benign prostatic hypertrophy in the transverse plane. In (A) the prostate is enlarged and relatively hyperechoic (brighter) consistent with benign prostatic hypertrophy. In (B) the prostate gland is diffusely hypoechoic (darker) and was diagnosed on cytological evaluation with prostatic lymphoma. Initially, the sonographer's objective is to identify the prostate and be able to differentiate normal from abnormal. Source: Courtesy of Robert M. Fulton, DVM, Richmond, VA.

## Prostatic Abscesses and Cysts

*Ultrasonographic appearance*: abscesses and cysts may be found within or attached to the prostatic parenchyma. They are typically thin-walled structures with either anechoic or hypoechoic centers. The presence or absence of acoustic enhancement in the far-field helps differentiate fluid from soft tissue. Septation and echogenic fluid are more suggestive of prostatic abscess than cyst(s) (Lattimer and Essman 2007). Gas formation by bacteria may be present with some abscesses. Air will typically be represented by multiple hyperechoic foci within the prostatic parenchyma and may be confused with tissue mineralization as may be found with some malignancies. Acoustic shadowing with gas is typically weaker than that seen with mineral.

## Paraprostatic Cysts

*Ultrasonographic appearance*: in contrast to prostatic cysts, which are found within the prostatic parenchyma, paraprostatic cysts are found adjacent to the gland and may appear confluent with it. They are thin-walled structures of varying size often appearing similar to the urinary bladder. The fluid contained within the paraprostatic cyst may be anechoic to echoic with or without intraluminal debris (Lisciandro 1995; Davidson and Baker 2009). Paraprostatic cysts are thought to be remnants or associated with remnants of the Müllerian duct (Lisciandro 1995; Smith 2008; Davidson and Baker 2009).

**Pearl:** When a paraprostatic cyst is suspected, it is often immediately helpful to catheterize the patient and radiographically perform a positive contrast study to define the location of the urinary bladder compared to the suspect paraprostatic cyst.

## Prostatic Neoplasia

*Ultrasonographic appearance*: prostatic neoplasia may show similarities to prostatitis, abscesses, or cysts (see Figure 13.5B). Calcification and severe loss of symmetry are suggestive of malignancy. Calcification will result in bright echoes with strong acoustic shadowing. This finding should prompt the pursuit of an aspirate or needle biopsy. Additionally, there is often severe

loss of architecture with advanced neoplastic disease (Lattimer and Essman 2007).

The ultrasonographic appearance of the prostate should not be the sole determinant in making a specific diagnosis. Digital rectal examination will provide clues in firmness, symmetry, and pain, and tissue sampling, either by aspirate or biopsy, is typically required to make the definitive diagnosis while culture is recommended for suspect cases of bacterial infection. Fine needle aspiration has been shown to diagnose prostatic carcinoma in about 50% of cases and biopsy has been reported to improve diagnosis to as high as 89% (Johnston et al. 2001a).

# Scrotum and Testicles

The descended scrotal testicles are easy to image using ultrasound. Keeping with previous probe positioning recommendations, begin with longitudinal orientation. A thin, hyperechoic line, the mediastinum testis, is easily identified in the center of the organ (Figure 13.6). By placing both testicles side by side, transverse imaging allows for assessing differences between them regarding echogenicity and texture. The epididymis begins dorsocaudally and is hypoechoic to the testicular parenchyma (Davidson and Baker 2009).

**Pearl:** The testicular parenchyma is a medium gray and homogeneous pattern, similar to the spleen (Davidson and Baker 2009). The testes should be the same size. The tunica albuginea, the dense white fibrous capsule that immediately covers the testicle, is hyperechoic (brighter) compared to the parenchyma (Johnston et al. 2001b).

## *Cryptorchidism*

Descent of testicles normally occurs by 10 days after birth; however, in the young puppy and kitten, the testicles can move between the scrotum and inguinal canal (Hoskins and Taboada 1992). Most clinicians will allow up to 6 months of age, by which time the inguinal canal has closed and any movement is precluded, to confirm cryptorchidism (Johnston et al. 2001b).

Cryptorchidism ("hidden testis") is a heritable, developmental defect in which descent of one or both testes does not occur by 6 months of age. Unilateral cryptorchidism is more common than bilateral. Retained testes are smaller than scrotal testes with size directly correlated with the degree of retention. Testes retained within the abdomen are smaller than those

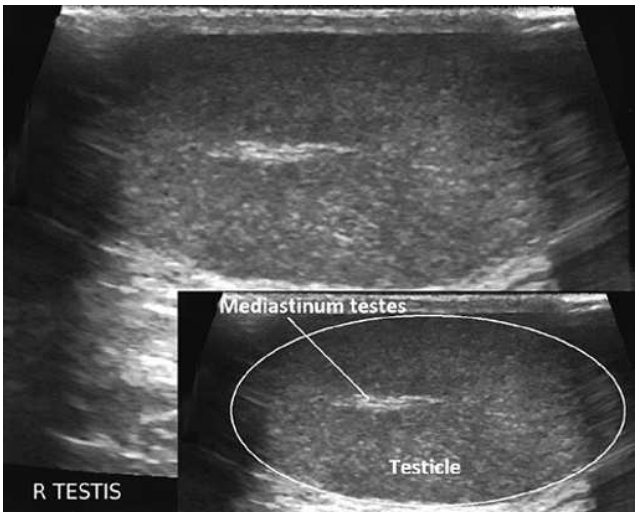


**Figure 13.6.** Normal canine testicle. The parenchyma is homogeneous and of medium echogenicity similar to the spleen. The hyperechoic line in the center represents the mediastinum testes, or the testicular landmark. (*Inset*) Outline of testicle (longitudinal plane). Source: Courtesy of Robert M. Fulton, DVM, Richmond, VA.

retained within the inguinal canal (Johnston et al. 2001b) (Figure 13.7).

- *Ultrasonographic scan and appearance*: the cryptorchid testes, while smaller than the scrotal testes, often will retain its normal anatomical structure, including the mediastinum testes with normal expected echogenicity (see Figure 13.7). The retained testicle may be located anywhere from the inguinal canal to the ipsilateral kidney (Davidson and Baker 2009); however, the inguinal location is more common. The cryptorchid testes can be difficult to find (Johnston et al. 2001b).
- The POCUS examination is often performed in lateral recumbency with the contralateral side down. The ipsilateral leg is raised to allow access to the inguinal region. With the probe in longitudinal orientation, a systematic scan is advanced from the inguinal canal to the caudal pole of the ipsilateral kidney. The lateral positioning allows for gravity to pull viscera away from the inguinal and retroperitoneal areas of interest, improving ultrasonographic imaging. The POCUS examination may also be performed in dorsal recumbency.

## *Orchitis and Epididymitis*

Orchitis (inflammation of the testicle) and epididymitis may occur singly or in combination and are typically painful conditions. Acute orchitis is usually

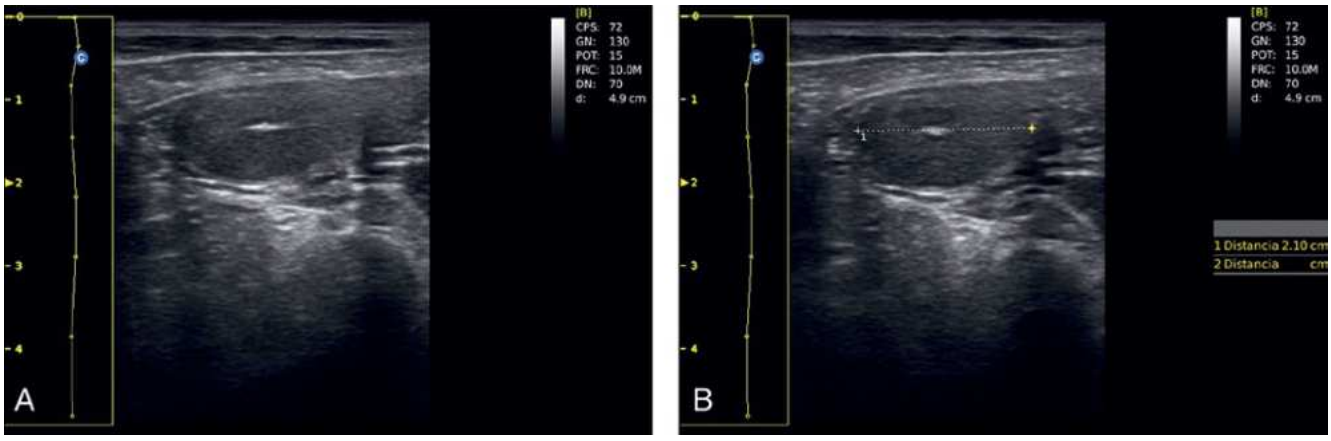


**Figure 13.7.** Cryptorchidism. Shown in (A) and (B) is the same image unlabeled and labeled (calipers) of the left intraabdominal retained testicle of a 1-year-old Doberman with cryptorchidism. The dog was placed in right lateral recumbency and the high-frequency linear probe positioned in the longitudinal plane. Note the testicle has its characteristic identifying landmark feature of the mediastinum testes. Compare to Figure 13.6. Source: Courtesy of Karin Vomend, MVZ, Clínica Veterinaria Río Mayo, Cuernavaca, Morelos, Mexico.

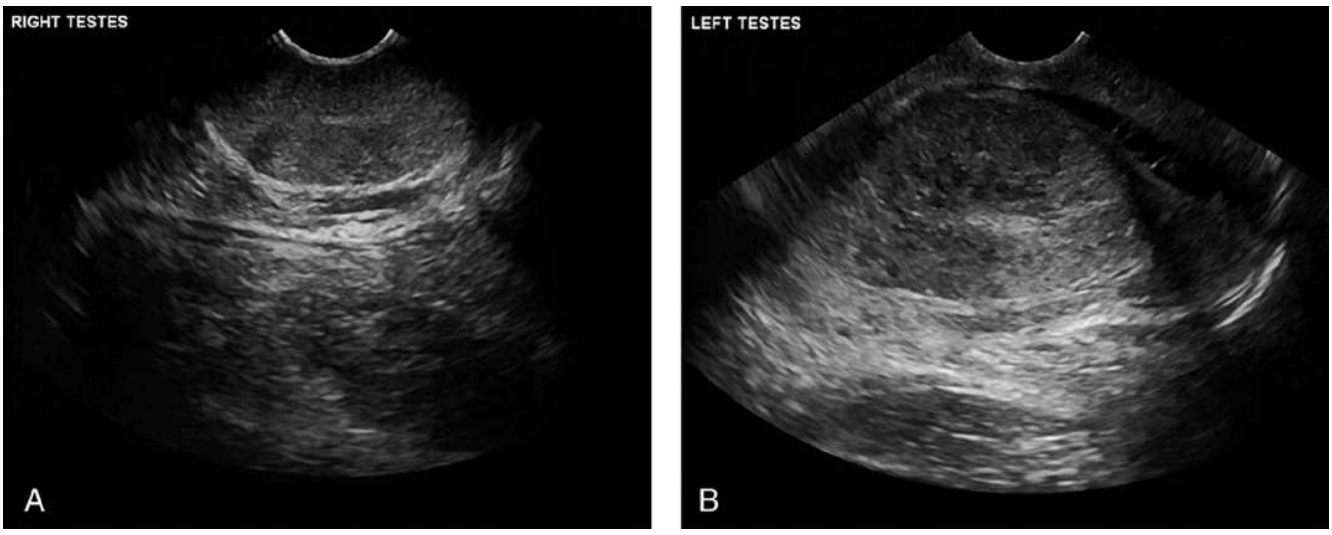


**Figure 13.8.** Orchitis in the dog. Orchitis may be unilateral as seen in this dog. The image in (A) is of the normal sized right testicle and the image in (B) is of the affected left testicle. Note the irregular texture of the affected testicle as well as the degree of enlargement. Both images were obtained with the same ultrasound settings. Initially, the sonographer's objective is to identify the testicle and be able to differentiate normal from abnormal. Compare to Figure 13.6. Note in (B) the edge shadowing artifact off the curved surface of the testicle, especially off its caudal pole. Source: Courtesy of Robert M. Fulton, DVM, Richmond, VA.

characterized by enlargement of the testicle with the parenchyma taking on a patchy, hypoechoic texture (Figure 13.8). Epididymitis is characterized by testicular enlargement with focal parenchymal changes. Fluid may be evident around the testicle or epididymis with either condition (Feeney and Johnston 2007; Davidson and Baker 2009) (Figure 13.9).

**Pearl:** Acute orchitis and epididymitis can be caused by zoonotic diseases, including brucellosis, which should be considered in all sexually active males.

The immunocompetent human tends to be more resistant to *Brucella canis* infection than other species;

**Figure 13.9.** Epididymitis in the dog. The head of the inflamed epididymis is seen as an ovoid hypoechoic structure to the lower right of the testicle. Also note the hypoechoic rim around the testicle. Source: Courtesy of Robert M. Fulton, DVM, Richmond, VA.

however, the immunocompromised individual, children, and pregnant women are considered to be at higher risk and should avoid exposure (Johnston et al. 2001a,b). Care must be taken to protect oneself and other members of the healthcare team by following standard procedures such as wearing exam gloves and avoiding contact with or aerosolization of body fluids. Proper disinfection of surfaces and equipment is mandatory. Rapid slide agglutination tests (RSAT) are available for quick screening tests and agar gel immunodiffusion (AGID) can be used to confirm suspected cases. Serological tests have their limitations as *B. canis* evokes little humoral response. Recent advances in molecular biology have yielded PCR tests but are not yet widely available. A positive identification of the causative organism from blood culture is the definitive proof for brucellosis (Hollett 2010).

## Testicular Torsion

Testicular torsion is more appropriately termed torsion of the spermatic cord. Dogs will typically present with signs of an acute abdomen including abdominal pain, vomiting, dysuria, hematuria, pyrexia, anorexia, lethargy, or stiff gait. Other physical examination findings may be related to concurrent testicular neoplasia such as truncal, symmetrical alopecia or a pendulous prepuce seen with Sertoli cell tumors.

*Ultrasonographic appearance*: the testicle of the affected cord is typically enlarged and has a uniform hypoechogenicity. There may or may not be fluid associated with the epididymis. Absence of blood flow when interrogated with color flow or power Doppler imaging is the most supportive sign ultrasonographically; definitive diagnosis is made at the time of surgery which is the treatment of choice (Johnston et al. 2001b).

**Pearl:** The intraabdominal cryptorchid spermatic cord is more often affected in torsions than the scrotal cord (Johnston et al. 2001b).

## Testicular Tumors

Testicular neoplasia is the most common tumor type in male dogs, second only to skin tumors. Tumors may be unilateral or bilateral and different tumors may be present within the same testicle. The three most common types of tumor are Sertoli cell tumor, seminoma, and interstitial (Leydig) cell tumors. Dogs with testicular neoplasia commonly present with testicular enlargement as the only sign; however, dogs with Sertoli cell tumor may present with bone marrow toxicity (anemia), symmetrical truncal hair loss, and male feminization due to excessive estrogen production (Johnston et al. 2001b). Testicular tumors may appear as focal masses of varying degrees of distinction from surrounding parenchyma with varying degrees of echogenicity (Davidson and Baker 2009). Ultrasonographic appearance is not specific for tumor cell type and cannot differentiate between benign and malignant conditions (Feeney and Johnston 2007). The Global FAST approach may be used for staging (see Chapter 36).

**Pearl:** The enlarged testicle in the older dog in the absence of testicular pain prioritizes neoplasia over orchitis (Johnston et al. 2001b).

## Miscellaneous Scrotal Swellings

- *Hernias*: herniation of small bowel into the scrotum may be detected by finding the normal bowel layers adjacent to the testes; intestinal peristalsis may also be present, helping with the ultrasonographic diagnosis (see additionally Chapter 34) (Mattoon and Nyland 2002).
- *Hematomas, abscesses, and sperm granulomas*: may all appear similar to other extratesticular pathology. These causes of scrotal swellings often have poorly

demarcated margins with variable echogenicity and texture (Foster 2010).
- *Hydrocele or noninflammatory fluid within the scrotum*: may occur in cases of ascites (Foster 2010).

# Pearls and Pitfalls, The Final Say

Given the external location and relatively simple anatomy, the testicles are easy to image. Still, make sure to systematically evaluate the three main areas.

- *Scrotal space* – evaluate for fluid, intestines (as in the case of inguinal hernia) or other extratesticular structures, and position of the testicle based upon the epididymis (head caudal, body dorsal, tail dorsocranial).
- *Testicular parenchyma* – evaluate for symmetry in size and shape, tumors, overall echogenicity.
- *Epididymis* – evaluate for focal or diffuse swelling, position (see above), surrounding fluid.

Remember, a scrotum that does not contain testicles is not always synonymous with castration; do not forget about cryptorchidism.

The prostate is slightly more challenging to image than the testicles, but use the proximal urethra as a guide to lead you directly to it. Evaluate for changes in symmetry and echogenicity in transverse planes. Thoroughly image all edges as paraprostatic pathology can extend well beyond the expected prostatic location.

# Quick Reference of Normals and Rules of Thumb

Given the large variation in size of dogs between breeds, there are no objective measurements to apply across our patients. Symmetry, rather, is the best rule of thumb. The testicles should be ultrasonographically symmetrical to each other, and the prostate should be ultrasonographically symmetrical about its median plane.

In general, the prostate in the castrated dog appears as a smooth, homogeneous swelling around the proximal urethra, with total width being approximately 3–4 times the width of the urethra. The overall echogenicity is similar to that of the uterine body in the female.

# References

Davidson A, Baker T. 2009. Reproductive ultrasound of the dog and tom. *Top Compan Anim Med* 24(2):64–70.

Feeney D, Johnston G. 2007. The uterus, ovaries, and testes. In: *Textbook of Veterinary Diagnostic Radiology*, 5th edition, edited by Thrall DE. St Louis: Saunders/Elsevier, pp 735–749.

Foster R. 2010. Pathology of male reproductive organs. *Clin Theriogenol* 2(4):531–544.

Hollett B. 2010. Update on canine brucellosis. *Clin Theriogenol* 1(2):257–295.

Hoskins JD, Taboada J. 1992. Congenital defects of the dog. *Comp Contin Educ Pract Vet* 14:873–897.

Johnston S, Root-Kustriz M, Olson P. 2001a. Disorders of the canine prostate. In: *Canine and Feline Theriogenology*, edited by Johnston S, Root-Kustriz M, Olson P. Philadelphia: WB Saunders, pp 337–355.

Johnston S, Root-Kustriz M, Olson P. 2001b. Disorders of the canine testes and epididymes. In: *Canine and Feline Theriogenology*, edited by Johnston S, Root-Kustriz M, Olson P. Philadelphia: WB Saunders, pp 312–332.

Lattimer J, Essman S. 2007. The prostate gland. In: *Textbook of Veterinary Diagnostic Radiology*, 5th edition, edited by Thrall DE. St Louis: Saunders/Elsevier, pp 729–737.

Lisciandro GR. 1995. What is your diagnosis? Large, round mass with intramural mineralization in the mid-to-caudal portion of the abdominal cavity – prostatomegaly. *J Am Vet Med Assoc* 206(2):171–172.

Mattoon J, Nyland T. 2002. Ovaries and uterus. In: *Small Animal Diagnostic Ultrasound*, 2nd edition, edited by Nyland T, Mattoon J. Philadelphia: WB Saunders, pp 231–249.

Root-Kustritz M. 2010. Pathogenesis of prostatic neoplasia in castrated dogs: why the increased risk? *Clin Theriogenol* 2(3):152–154.

Smith J. 2008. Canine prostatic disease: a review of anatomy, pathology, diagnosis, and treatment. *Theriogenology* 70:375–353.

CHAPTER FOURTEEN

# POCUS: Reproductive – Female

Robert M. Fulton

## Introduction

In the grand scheme of things, reproductive ultrasonography probably gets the short end of the stick since most of our patients lack their reproductive organs (testicles, ovaries, and uterus) through surgical sterilization. However, one should *not assume* that reproductive sterilization has taken place simply because the altered pet is more common. It is very important to confirm reproductive status since many adopted dogs and cats have unknown medical histories. For instance, a pet owner may assume their female is spayed when in reality she may have never been observed to go into heat. When sexual status is questionable, the shaving of hair and evaluation for surgical spay and neutering scars is helpful, as are other physical examination findings such as the lack of mammary development in an older female dog or cat.

With ultrasound, most of the reproductive tract may be imaged. In females, this includes the ovaries, uterus, cervix, and mammary glands, and for males, the prostate, scrotum, and testes (see Chapter 13). Of these structures, the uterus makes up the vast majority of POCUS reproductive – female examinations. However, other important conditions of the female and male reproductive tracts are discussed in this chapter and Chapter 13.

**Pearl:** In many areas throughout the United States, dogs and cats sterilized in shelters are tattooed either within or adjacent to their surgical site. A ¼–½ inch lime green linear tattoo is commonplace (Figure 14.1). Cats may also have a partial amputation of their left ear tip identifying them as sterilized.

### *What the POCUS Reproductive – Female Can Do*

- Diagnose pregnancy.
- Aid in the diagnosis of pyometra, mucometra, and hydrometra.
- Aid in the diagnosis of pseudopregnancy.
- Aid in the medical management of pyometra.

### *What the POCUS Reproductive – Female Cannot Do*

- Cannot definitively differentiate pyometra from mucometra and hydrometra.
- Cannot provide an accurate fetal count.
- Cannot fully screen for intraabdominal free fluid.

**Note:** An AFAST and the assignment of an abdominal fluid score should be minimally performed to screen for any effusions or other obvious AFAST target organ pathology. The Global FAST approach provides even more information regarding the thorax (TFAST), including heart (TFAST) and lung (Vet BLUE), as a quick assessment test for localized versus disseminated disease and comorbidities and complications.

### *Indications*

- Any ill intact female cat or dog to rule out pyometra.
- Acute abdomen, especially in intact females with abdominal pain.

*Point-of-Care Ultrasound Techniques for the Small Animal Practitioner*, Second Edition. Edited by Gregory R. Lisciandro.
© 2021 John Wiley & Sons, Inc. Published 2021 by John Wiley & Sons, Inc.
Companion website: www.wiley.com/go/lisciandro/ultrasound2

**Figure 14.1.** Spay tattoo. Lime green tattoo scar indicating this female dog has been spayed. Source: Courtesy of Robert M. Fulton, DVM, Richmond, VA.

- Dystocia.
- Vaginal discharge.
- Uncertainty of pregnancy.
- Mammary gland abnormalities.

### *Objectives*

- Be able to image the basic features of the female reproductive tract.
- Identify common ultrasonographic reproductive pathology of the female.
- Diagnose pregnancy.

# Reproductive Conditions of the Female

Female reproductive anatomy is shown in Figure 14.2. The major structure involved in most concerning conditions of the bitch or queen is the uterus, and two of its major problems are pyometra and dystocia. Fortunately, the enlarged uterus is very accessible with ultrasound and recognizable by the novice sonographer with minimal training. These conditions and other less common uterine and mammary conditions will be discussed but dystocia is covered in a separate chapter (see Chapter 15).

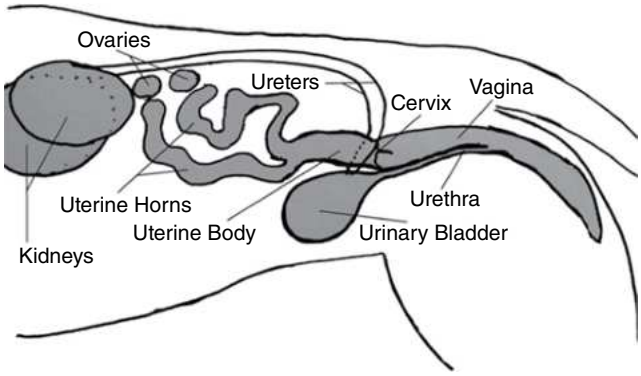


**Figure 14.2.** General female reproductive anatomy of the dog or cat. Source: Courtesy of Robert Fulton, Richmond, VA.

# Patient Positioning and Probe Selection

Patients are best evaluated in dorsal recumbency with a curvilinear probe and a urine-filled bladder; however, lateral recumbency and standing position may also be used. Depending on the ultrasound machine, use a medium or comparable abdominal preset. Primarily focusing on longitudinal orientation rather than transverse orientation is usually easier when beginning because the female anatomy is more recognizable. However, performing the POCUS Reproductive – Female examination in standing may be less stressful for some patients.

**Pearl:** Do not walk the patient (dogs) or give a litter box (cats) before the examination. The urine-filled bladder improves imaging by providing an acoustic window and also serves as a landmark for identifying caudal abdominal structures.

# Imaging the Normal Ovary

The ovaries lie just caudal to the kidneys. To image the kidneys, start in longitudinal orientation and visualize the ipsilateral kidney. Slide the probe caudally and then fan through this area immediately behind the kidney (Figure 14.3). The normal ovary is often difficult to visualize as it is nearly isoechoic to surrounding tissues but will usually have a subtle cystic appearance (Figure 14.4). For this reason, a linear probe providing greater detail may be useful, especially in small dogs and cats. In large dogs, linear probes may not be able to image deep enough. Overlying gas from small intestine and large bowel can interfere with imaging in this area.

Ovarian disease is uncommon in the dog and cat and the reader is referred to additional texts regarding ovarian pathology. Most ovarian disease is associated with changes in size (larger) and echogenicity (often hyperechoic), or cystic change (single or multiple anechoic structures) and is at least screened for using the POCUS reproductive – female examination.

**Figure 14.3.** Scanning position to image the ovary. The probe is in longitudinal orientation and placed just caudally to the ipsilateral kidney. In this image, the left ovary is being imaged. Source: Courtesy of Robert Fulton, Richmond, VA.

# Imaging the Normal Uterus

Begin the examination with the animal in dorsal recumbency. Keep in mind the normal caudal abdominal anatomy. The female reproductive tract lies in between the urinary bladder and colon (Figure 14.5) (Feeney and Johnston 2007). However, performing the POCUS reproductive – female examination in standing (or lateral recumbency) may be less stressful for some patients.

- Place the ultrasound probe in longitudinal orientation just cranial to the pubis where you would expect to find the urinary bladder.
- Direct by rocking and sliding the probe caudally to the trigone of the bladder, fanning longitudinally and following urine (normally anechoic [black]) until it triangulates and narrows into the urethra.

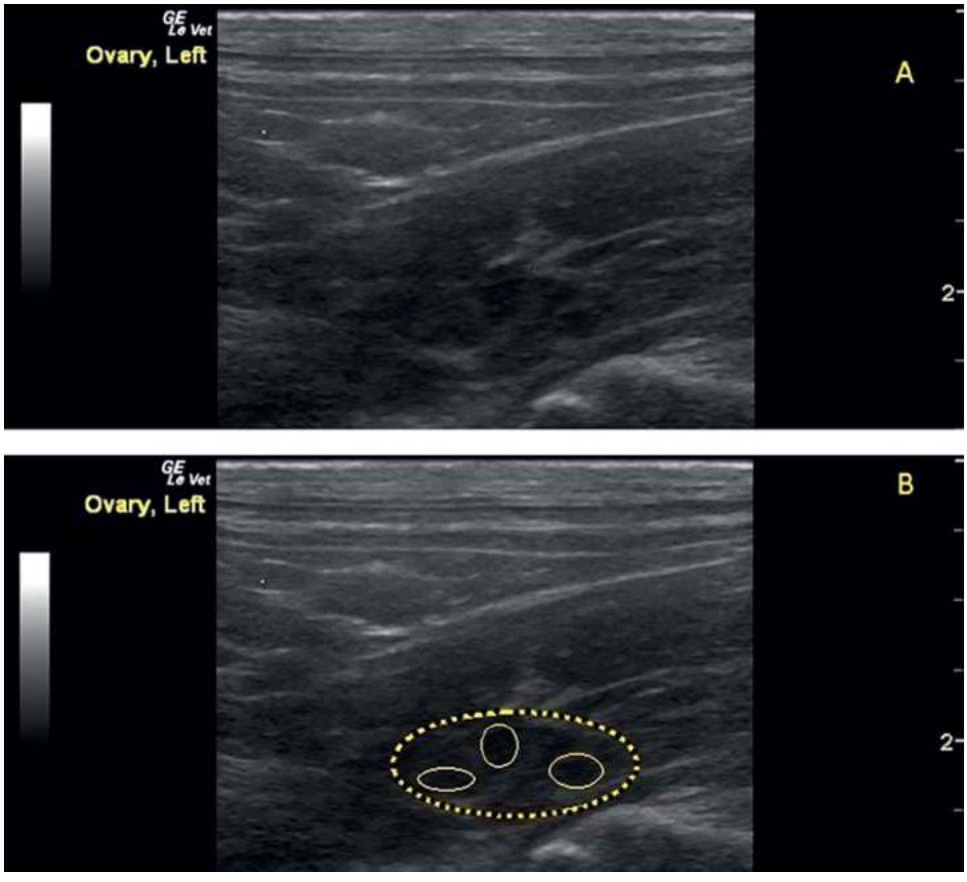


**Figure 14.4.** Normal canine ovary. (A) The normal ovary is isoechoic to surrounding tissues but has a subtle cystic appearance. (B) The ovary is outlined by a dashed line; follicles are outlined by small circles. Source: Courtesy of Robert M. Fulton, DVM, Richmond, VA.

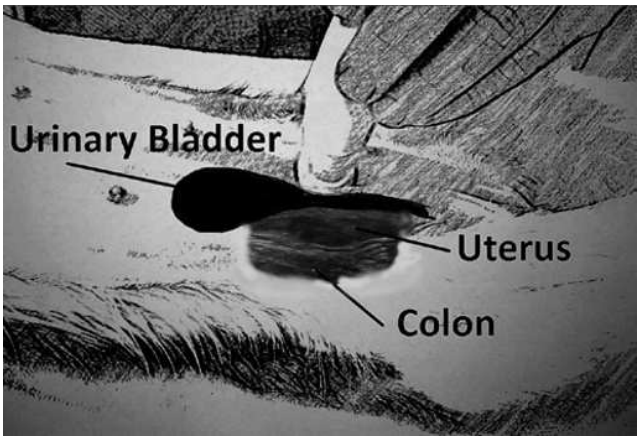


**Figure 14.5.** General scanning position with patient in dorsal recumbency and positioning of the probe in longitudinal orientation. The uterine body will be dorsal to the bladder and ventral to the colon. Source: Courtesy of Robert Fulton, Richmond, VA.

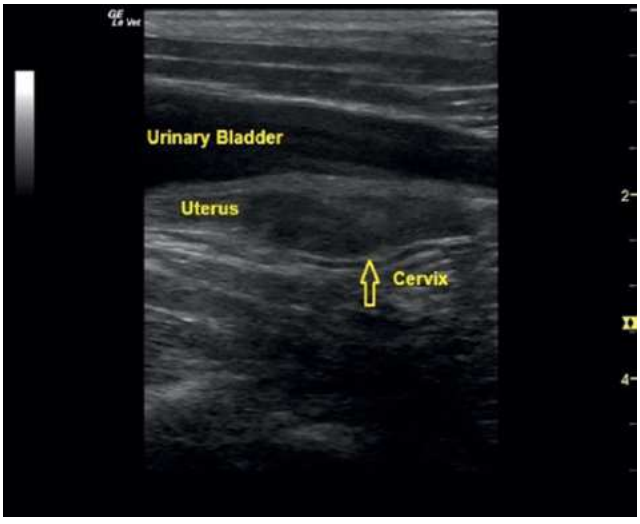


**Figure 14.6.** Cervix, long axis. The uterus flares slightly at the junction with the cervix (*small arrow*). The normal cervix is often difficult to distinguish from surrounding structures. Source: Courtesy of Robert M. Fulton, DVM, Richmond, VA.

- At the trigone, search for the cervix or the uterine body just cranial and dorsal to the trigone. The cervix is slightly larger than the uterine diameter with the two structures blending into one another (Figure 14.6).The uterine body is of medium, homogeneous echogenicity (shades of gray) and is easier to identify than the cervix. The uterus appears as a tubular structure similar in size to small intestine. The uterine lumen lacks a central echogenic stripe in the normal anestrous bitch (Figures 14.7 and 14.8). However, in estrus, a thin, echogenic (bright) stripe within the uterine lumen may be seen (Figure 14.9) (Feeney and Johnston 2007).

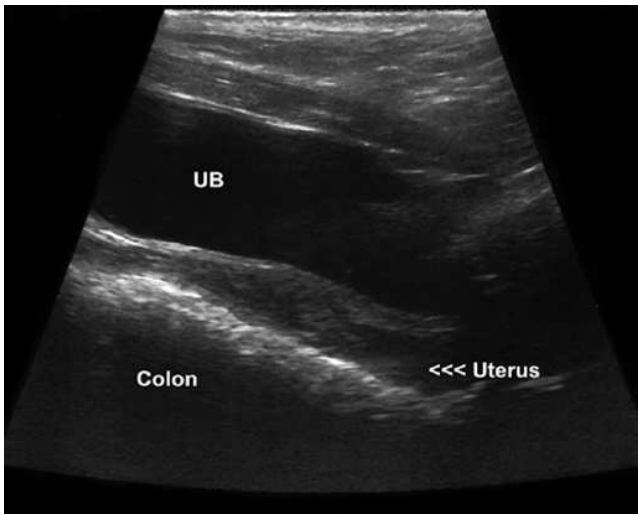


**Figure 14.7.** Uterus, long axis. The canine uterus is the medium gray structure between the urinary bladder and the colon shown in longitudinal orientation. Source: Courtesy of Robert M. Fulton, DVM, Richmond, VA.

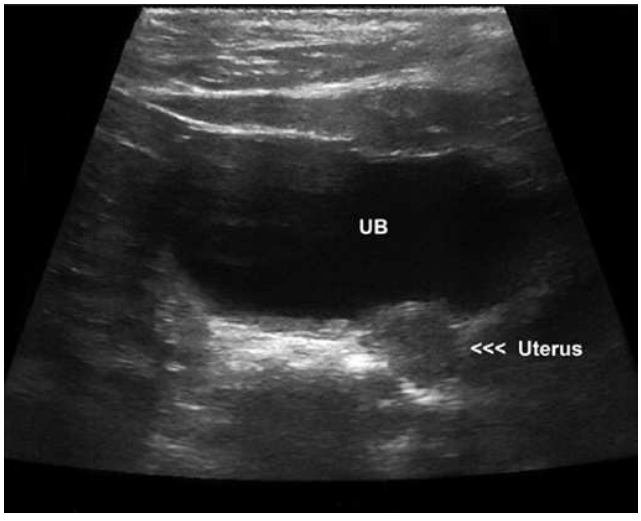


**Figure 14.8.** Uterus, short axis. In this image, the uterus is seen in short axis as the circular medium gray structure to the right between the urinary bladder ventrally and the colon dorsally. Source: Courtesy of Robert M. Fulton, DVM, Richmond, VA.

**Pearl:** The cervix may be difficult to differentiate from the uterine body so do not spend too much time attempting to precisely localize the structure.

**Pearl:** Any free fluid within the uterus greater than the expected thin echogenic stripe of estrus is considered abnormal.

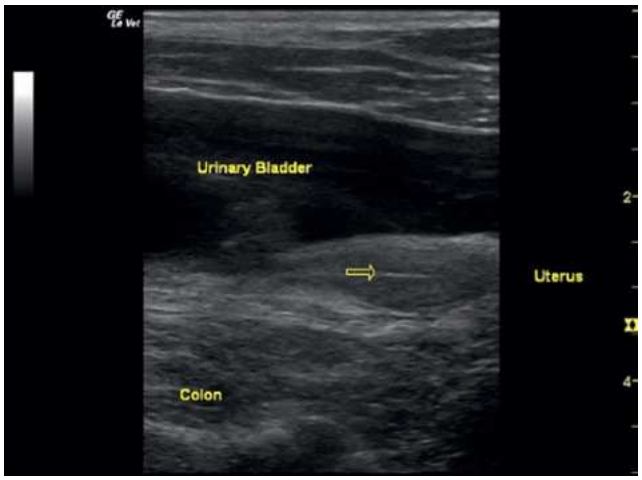


**Figure 14.9.** Canine estrus uterus Note the thin, hyperechoic (white) line within the lumen of the uterus (*small arrow*). This line may be seen during estrus. Source: Courtesy of Robert M. Fulton, DVM, Richmond, VA.

- Approximately one-third of the way along the urinary bladder, depending on bladder size, the uterine body will bifurcate into its two horns.
- Follow the uterine horns cranially as they make their way caudal to the kidneys, using combinations of longitudinal and transverse views. This can be challenging given the many twists and turns the uterine horns can make. If you are having problems tracing nongravid, nonfluid-filled uterine horns, then they are probably not clinically relevant. Although rare, some females may have abnormalities of the tubular reproductive tract such as uterine atresia (not formed), more common in cats. Atresia may involve both or only one uterine horn (Johnston et al. 2001b).

**Pearl:** In the nongravid or fluid-filled uterus, it may not be possible to image the uterine horns for their full length.

# Cystic Endometrial Hyperplasia-Pyometra

Cystic endometrial hyperplasia (CEH)-pyometra complex is the most common and important uterine disorder in bitches. CEH-pyometra occurs during the luteal phase of diestrus although there are some reports of it occurring during anestrus (Verstegen et al. 2008). General classifications of the complex have been suggested according to criteria outlined by Dow and DeBosschere. Dow's classification scheme uses gross pathology findings and histological lesions while DeBosschere's scheme also uses the degree of inflammatory reaction, fibroblast proliferation, and endometrium to myometrium ratio. Ultrasonography has been shown to be valuable in the diagnosis of CEH-pyometra and an efficient tool in the identification of more severe disease as described in both Dow's and DeBosschere's schemes (Bigliardi et al. 2004).

As pyometra should be included in the differential diagnosis for any intact bitch, regardless of the presenting signs, the focused female reproductive examination for pyometra is indicated for any ill intact female dog or cat and should be considered in combination with AFAST (the Global FAST approach is better). Ultrasound has a higher sensitivity than radiography for determining the presence of uterine enlargement and fluid accumulation (Feeney and Johnston 2007). The ultrasound scan is similar to that for dystocia with a primary difference of searching for a *fluid*-filled uterus rather than a gravid (*fetus*-filled) uterus.

## *Pyometra*

The initial physical examination finding of purulent vaginal discharge should be an immediate trigger for performing an ultrasound examination to determine the presence of pyometra. Conversely, the finding of a fluid-filled uterus should trigger a more thorough search for purulent vaginal discharge that may be subtle or initially overlooked on physical examination.

- Begin the scan in dorsal recumbency. Start over the urinary bladder in longitudinal orientation, moving along the ventral midline from the caudal abdominal region to the xiphoid as described with the dystocia evaluation. However, performing the POCUS reproductive – female in standing (or lateral recumbency) may be less stressful for some patients.
- Follow the midline evaluation with the lateral to the mammary gland scan on both the left and right sides to help differentiate the fluid-filled uterus from the urinary bladder and fluid-distended small bowel.
- Careful scanning should be performed along each horn as thoroughly as possible to avoid a false-negative evaluation for pyometra.

The amount and echogenicity of fluid can vary greatly independent of the pyometra being "open" (cervix open, vaginal discharge) or "closed" (cervix closed, no vaginal discharge), although a "closed" pyometra generally leads to a greater degree of fluid distension. Echogenicity of intraluminal fluid in pyometra ranges from anechoic (pure black) to viscous and echogenic (Figure 14.10). In cases with echogenic fluid, its movement may be characterized by slow, swirling patterns (Mattoon and Nyland 2002).

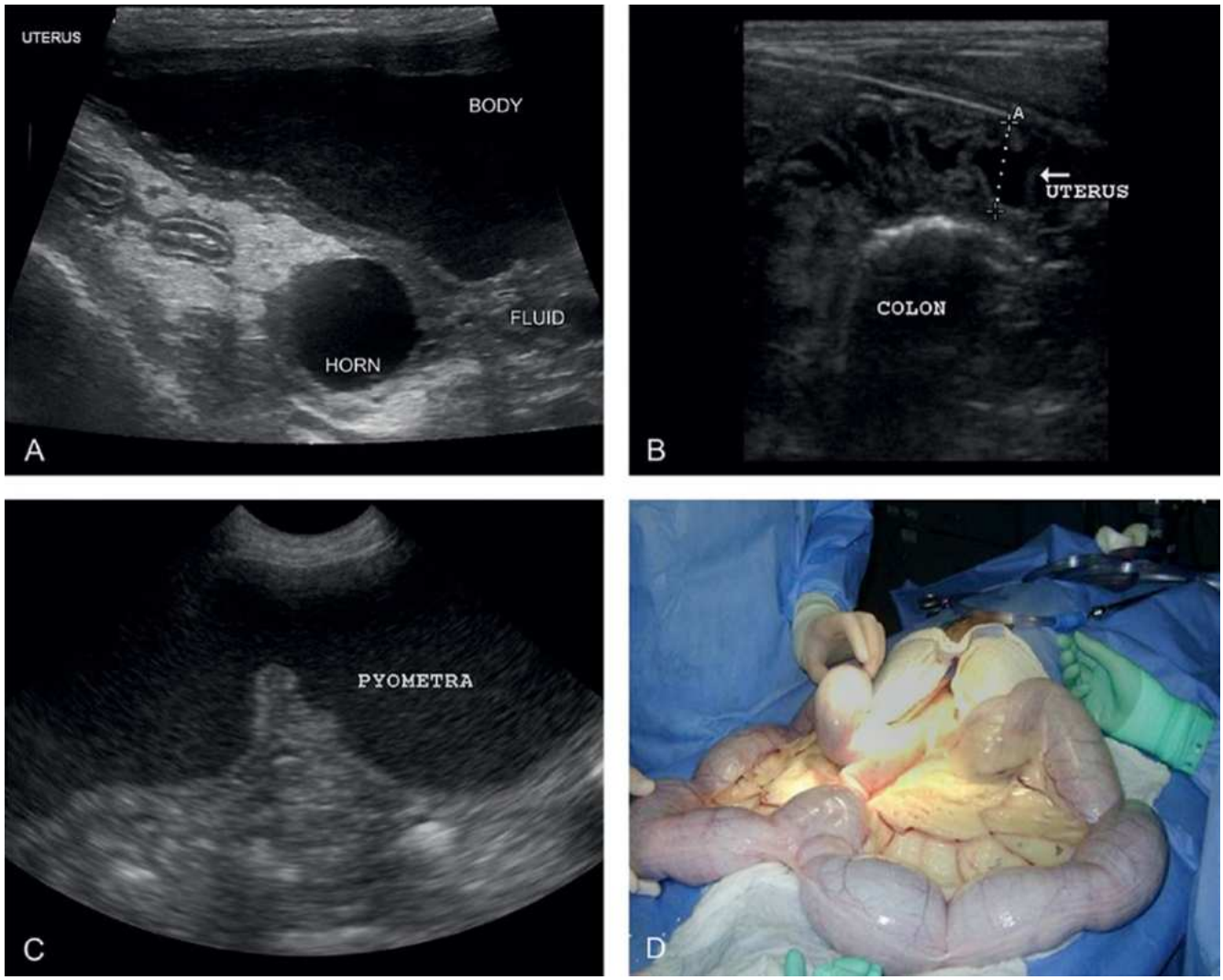


**Figure 14.10.** Pyometra. (A) There is severe fluid distension of the uterine body and uterine horn of this feline with pyometra. The severely hyperechoic (bright) appearance of the mesentery is consistent with peritonitis. The free fluid noted in the lower right-hand corner warrants an AFAST exam and assigned abdominal fluid score, abdominoocentesis, and cytology for fluid characterization. This patient was determined to have a septic abdomen caused by a ruptured pyometra confirmed at surgery. (B) The compartmentalized fluid-filled uterus often typical of pyometra is in the near-field to the air-filled colon, helping with its identification. (C) In a severely enlarged, distended pyometra, uterine compartmentalization can be less obvious; however, the uterine wall is quite different in appearance from the multilayered small bowel. (D) A gross correlation of the severe uterine distension found at surgery compared to the ultrasound findings shown in (C). Source: Courtesy of Robert M. Fulton, DVM, Richmond, VA.

**Pearl:** Remember, there typically is no luminal fluid during anestrus, but the estrus uterus may normally have a thin echogenic stripe (Mattoon and Nyland 2002; Verstegen et al. 2008) (see Figure 14.9).

**Pearl:** *Pus can appear anechoic ultrasonographically*. Don't misdiagnose benign hydrometra or mucometra for more serious pyometra. Use the rest of your diagnostic information and physical examination clues, including presence of vaginal discharge, in the decision-making process.

**Pearl:** Pyometra is often diffuse throughout both uterine horns but may appear compartmentalized as the horns fold on themselves; however, segmental pyometra is also possible in dogs and cats (Johnston et al. 2001a,b; Verstegen et al. 2008).

VetBooks.ir

One form of segmental uterine pathology that is likely misdiagnosed as CEH-pyometra has been termed pseudoplacentational endometrial hyperplasia (PEH). First reported in 1914, PEH also occurs during the luteal phase, with the endometrium remodeling in a way that is very similar to the normal histology of the endometrium at normal placentation sites in pregnancy (Schlafer and Gifford 2008). While histologically different, clinical presentation and management are the same as for CEH-pyometra. PEH is likely to form approximately two months post estrus compared to the typical two weeks postestrus occurrence more common with CEH-pyometra.

#### Surgical versus Medical Management

The old adage holds true: "Don't let the sun set on a pyometra." Often spoken by a surgeon, this does not mean that all cases of pyometra should be immediately addressed with the scalpel. The unstable, compromised, septic patient should be resuscitated before operation. By optimizing patient status for anesthesia through the initiation of appropriate antibiotics, correction of hypovolemia, hypoglycemia, and acid–base and electrolyte abnormalities, a favorable outcome is more likely. Detailed preoperative management is beyond the scope of this chapter but may be found in other reference materials (Johnston et al. 2001a,b; Traas 2008).

While surgery remains the best option for the vast majority of cases, medical management has been shown to be a viable therapeutic option for the valuable breeding bitch (Verstegen et al. 2008). Because of the potent drugs and unfamiliarity with protocols by most general practitioners and emergency and critical care veterinarians, medical management is best referred to a small animal specialist in theriogenology or other veterinarian experienced in reproductive work.

**Pearl:** Always use ultrasound for guided cystocentesis for obtaining urine with a suspect pyometra case. Failure to do so may result in inadvertent aspiration of the pus-filled uterus and contamination of the abdomen.

### *Stump Pyometra*

A stump pyometra should always be on the differential of any acute abdomen in a female spayed dog whatever matter their age and its location would be anatomically between the urinary bladder and the colon. Stump pyometra may occur following ovariohysterectomy if a portion of the uterine horns or uterine body is not removed and the animal has increased progesterone concentrations. Progestins may come from endogenous sources such as residual ovarian tissue, sex hormone-secreting adrenal tumors, or exogenous sources such as progestational compounds used to treat dermatitis, or may be potentially absorbed from creams used for treatment of menopausal symptoms in women (Howe 2006). Stump pyometra will not occur in a patient that has undergone ovariectomy as there is no "stump." The entire uterus is left intact. Common in European nations, the procedure is beginning to gain popularity in the United States. The same concerns for the development of pyometra (endogenous or exogenous progestin exposure) exist for stump pyometra but at least one study of 72 bitches that underwent ovariectomy did not show any incidence of pyometra over a 6–8-year follow-up (Howe 2006).

The POCUS reproductive –female examination for stump pyometra is identical to that for pyometra but the primary area of interest is the caudal abdomen, specifically the region between the trigone of the bladder and colon. At this location, search for an area of mixed echogenicity indicative of complex mass effect (England et al. 2003; Davidson and Baker 2009). Other local diseases mimicking or causing a stump pyometra include stump granuloma caused by excess residual devitalized uterine body tissue, use of inappropriate suture material, or poor surgical asepsis. Additionally, hematoma formation caused by poor surgical technique or a coagulopathy can serve as a nidus for infection. The finding of free fluid suggestive of acute hemorrhage or peritonitis is another indication for the AFAST scan and assigning an abdominal fluid score (see Chapters 6 and 7) and the Global FAST is a more thorough examination for staging (see Chapter 36). Free fluid may only be characterized by abdominocentesis and subsequent fluid analysis. If the case is not urgent, that is, does not have a septic abdomen or large bleed, then a complete detailed abdominal ultrasound may be warranted.

## Uterine Torsion

Uterine torsion in the dog and cat is uncommonly reported. However, the ultrasonographic appearance is as expected for pyometra. The diagnosis of uterine torsion is typically made at surgery (Misumi et al. 2000; Chambers et al. 2011). An AFAST and an assigned fluid score help screen for effusions including secondary hemoabdomen, and a Global FAST can assess for

thorax-related complications, including aspiration pneumonia, lung edema, and volume depletion (see Chapter 36), and help direct fluid resuscitation.

**Pearl:** Uterine torsion is an emergent surgical condition that cannot be definitively diagnosed by ultrasound.

# Mounting of Postoperative Recently In-heat Spayed Females

In-heat (estrus) spayed females should be kept away from male dogs for two weeks postoperatively because they remain receptive to interested males. Mounting postoperatively can lead to trauma and rupture of the surgical site and insemination of the peritoneal cavity, leading to potentially life-threatening sterile or septic peritonitis (Morley 2006). AFAST and fluid scoring would be the scan best suited to determining whether obvious peritonitis exists (evidence of free fluid), with subsequent characterization of ascites by abdominocentesis.

# Pseudopregnancy

All bitches experience the same progesterone profile whether they become pregnant or not. As the progesterone falls at the end of diestrus, some bitches will experience overt signs of imminent whelping with fully developed mammary glands and milk letdown, nesting behavior, and even abdominal contractions (Johnston et al. 2001c). Although rare, the queen may also show signs of pseudopregnancy. The owners may be convinced their female dog has not been bred but we are all aware of unsupervised receptive females left in the backyard becoming pregnant. A POCUS reproductive – female examination will reliably confirm or refute the presence or absence of fetuses during midgestation and later.

# Pregnancy Diagnosis

Pregnancy is ultrasonographically characterized by segmental fluid distension of the uterine horns. The hallmark is the fetal structures with the segments of fluid (Figure 14.11). These segments are the fetal vesicles. Fetal heart rate can typically be detected ultrasonographically after day 21 post luteinizing hormone (LH) surge. A more thorough discussion of fetal development can be found in Chapter 15.

**Figure 14.11.** Gestational vesicles. The vesicles are visualized as spherical to oval structures filled with anechoic fluid. The fetal structures are easily seen as hyperechoic objects with the lumen. The urinary bladder is seen to the far right of the image. Source: Courtesy of Robert M. Fulton, DVM, Richmond, VA.

**Pitfall:** Ultrasound is a *relatively inaccurate* method for determining litter size. Litter size is best done radiographically 45 days post LH surge, counting fetal skull-vertebral column units.

# Mammary Glands

Due to its superficial location and small thickness, the mammary gland is best imaged with a high-frequency linear probe. However, if using a curvilinear probe, use the highest frequency available. The normal developed mammary gland at parturition is of a homogeneous appearance. The larger blood vessels may be noted entering the gland. With disease such as mastitis and neoplasia, there is loss of the homogeneous appearance (Mattoon and Nyland 2002).

The ultrasonographic appearance of mammary gland neoplasia can be quite variable depending on its severity. Small mammary tumors may appear as poorly defined hypoechoic structures with acoustic enhancement artifact, and larger tumors may appear hyperechoic, sometimes with the presence of cysts (Figure 14.12). The spread of tumor tissue among the mammary glands can be successfully detected by ultrasound, and it is very sensitive for detecting such lesions of the mammary gland. The involvement of the regional lymph nodes (axillary and superficial inguinal)

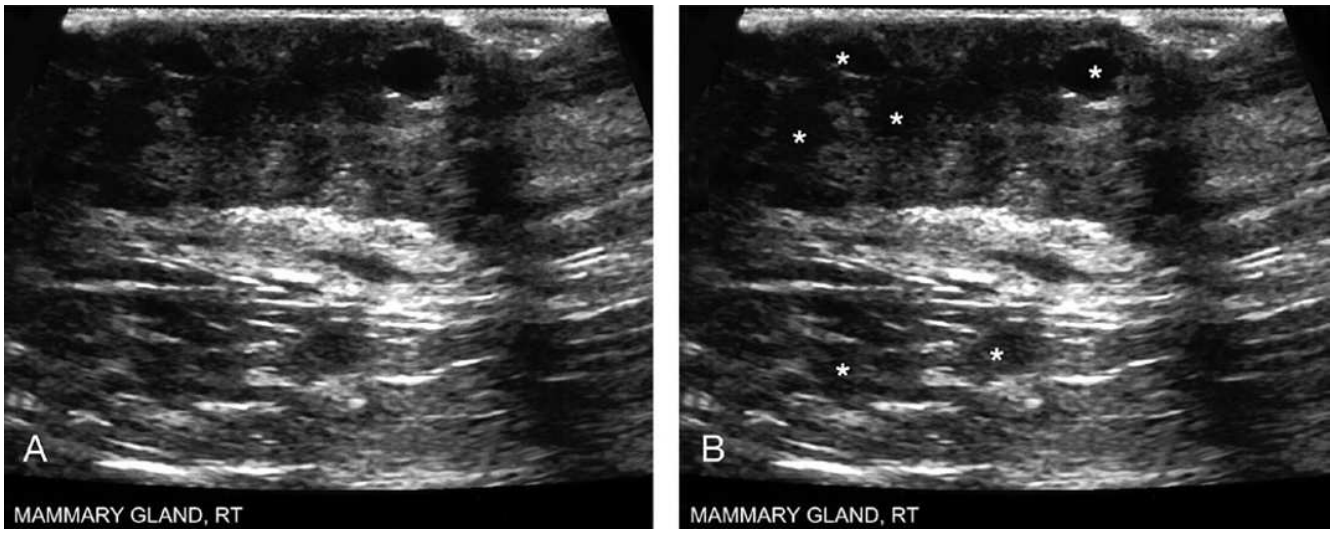


**Figure 14.12.** Canine mammary neoplasia. The ultrasonographic appearance of mammary gland neoplasia can be quite variable. Small mammary tumors may appear as poorly defined hypoechoic structures with acoustic enhancement artifact in the far-field, and larger tumors may appear hyperechoic, sometimes with the presence of cysts. (A) Mammary gland adenocarcinoma from a cat with typical mixed echogenicity and (B) overlays (*asterisks*) on the several cysts and overall mammary gland. The add-on Global FAST provides rapid same-day screening for localized versus disseminated disease by surveying the AFAST target organs and the thorax, including heart and lung, by TFAST and Vet BLUE. Source: Courtesy of Robert M. Fulton, DVM, Richmond, VA.

can also be successfully scrutinized for abnormal changes. Ultrasound, however, cannot determine whether lymphadenopathy is due to metastatic spread of tumor tissue or inflammatory reaction (Zuki and Boyd 2004).

# Pearls, Pitfalls, The Final Say

The POCUS reproductive – female examination can lend insight to many disorders such as pyometra, hydrometra, and mucometra. Because these diseases are characterized by fluid, ultrasound is a sensitive imaging modality for these conditions. Be careful not to confuse the urinary bladder or fluid-filled gastrointestinal tract (as with small bowel obstruction or severe diarrhea distending the colon) with a diseased uterus. Similar evaluation of the uterus can help diagnose pregnancy and ultrasound is a fast, noninvasive method to do so.

# Quick Reference of Normals and Rules of Thumb

- In anestrus, there is no uterine luminal fluid in normalcy; however, in estrus there may be a thin echogenic stripe also considered as a normal finding (Mattoon and Nyland 2002; Verstegen et al. 2008).
- The nongravid uterus is tubular, homogeneous in echotexture, with a lumen that is not readily seen and is differentiated from small intestine by lack of peristalsis and intraluminal gas, and absence of the layered appearance characteristics (Mattoon and Nyland 2015). Uterine width varies from 3 to 5 mm in cats and 5 to 10 mm in dogs.
- A sonographic hallmark of pyometra is diffuse or segmental fluid dilation of the uterus.
- Abdominal radiography is the most accurate way of determining the number of puppies or kittens in the litter (Davidson and Baker 2009). When talking to clients, avoid confirming numbers in the litter using ultrasound because of its inaccuracy.
- Normal ultrasonographic layering of the small bowel in the fetus may be used as a guideline for full-term maturation of puppies and kittens (Mattoon and Nyland 2002) – see Chapter 15.

# References

Bigliardi E, Parmigiani E, Cavirani S et al. 2004. Ultrasonography and cystic hyperplasia-pyometra complex in the bitch. *Reprod Domest Anim* 39;136–140.

Chambers B, Laksito M, Long F, et al. 2011. Unilateral uterine torsion secondary to an inflammatory endometrial polyp in the bitch. *Aust Vet J* 59(8):350–354.

England G, Yeager A, Concannon P. 2003. Ultrasound imaging of the reproductive tract of the bitch. In: *Recent Advances in Small Animal Reproduction*, edited by Concannon PW, England G, Verstegen J, Linde-Forsberg C. New York: International Veterinary Information Service.

Davidson A, Baker T. 2009. Reproductive ultrasound in the bitch and queen. *Top Compan Anim Med* 24(2):55–63.

Feeney D, Johnston G. 2007. The uterus, ovaries, and testes. In: *Textbook of Veterinary Diagnostic Radiology*, 5th edition, edited by Thrall EJ. St Louis: Saunders/Elsevier, pp 735–749.

Foster R. 2010. Pathology of male reproductive organs. *Clin Theriogenol* 2(4):531–544.

Howe L. 2006. Surgical methods of contraception and sterilization. *Theriogenology* 66:500–509.

Johnston S, Root-Kustriz M, Olson P. 2001a. Canine parturition – eustocia and dystocia. In: *Canine and Feline Theriogenology*, edited by Johnston S, Root-Kustriz M, Olson P. Philadelphia: WB Saunders, pp 105–128.

Johnston S, Root-Kustriz M, Olson P. 2001b. Disorders of the feline uterus and uterine tubes (oviducts). In: *Canine and Feline Theriogenology*, edited by Johnston S, Root-Kustriz M, Olson P. Philadelphia: WB Saunders, pp 463–471.

Johnston S, Root-Kustriz M, Olson P. 2001c. Disorders of the mammary glands of the bitch. In: *Canine and Feline Theriogenology*, edited by Johnston S, Root-Kustriz M, Olson P. Philadelphia: WB Saunders, pp 243–256.

Mattoon J, Nyland T. 2002. Ovaries and uterus. In: *Small Animal Diagnostic Ultrasound*, 2nd edition, edited by Nyland TG, Mattoon JS. Philadelphia: WB Saunders, pp 231–249.

Mattoon JS, Nyland TG. 2015. Ovaries and Uterus. In: *Small Animal Diagnostic Ultrasound*, 3rd edition, edited by Nyland TG, Mattoon JS. St. Louis: Elsevier Saunders, pp 634–654.

Misumi K, Fujiki M, Miura N, et al. 2000. Uterine horn torsion in two non-gravid bitches. *J Small Anim Pract* 41(8):465–471.

Morley DL. 2006. Acute peritonitis secondary to traumatic breeding in the bitch. *J Vet Emerg Crit Care* 16(2);128–130.

Schlafer DH, Gifford AT. 2008. Cystic endometrial hyperplasia, pseudo-placentational endometrial hyperplasia, and other cystic conditions of the canine and feline uterus. *Theriogenology* 70:349–358.

Traas AM. 2008. Surgical management of canine and feline dystocia. *Theriogenology* 40:337–342.

Verstegen J, Dhaliwal G, Verstegen-Onclin K. 2008. Mucometra, cystic endometrial hyperplasia, and pyometra in the bitch: advances in treatment and assessment of future reproductive success. *Theriogenology* 70:364–374.

Zuki ABZ, Boyd JS. 2004. Ultrasonographic imaging of neoplasia of the canine mammary glands and their regional lymph nodes. *J Anim Vet Adv* 3:604–612.

# Further Reading

Serrano S, McMillian M. 2009. Dystocia. *Standards Care Emerg Crit Care Med* 11(1):1–11.

Smith F. 2008. Canine pyometra. *Theriogenology* 66: 610–612.

Yeager AE, Mohammed HO, Meyers-Wallen V, et al. 1992. Ultrasonographic appearance of the uterus, placenta, fetus, and fetal membranes throughout accurately timed pregnancy in beagles. *Am J Vet Res* 53:342–351.

CHAPTER FIFTEEN

# POCUS: Dystocia

Robert M. Fulton

Vetbooks.ir

## Introduction

Canine and feline dystocia cases are challenging with the clinician having to juggle maternal, fetal, client, and breeder factors. While POCUS dystocia examination cannot help in managing all these elements, it is a valuable tool to gain insight into the fetal side of things and, when combined with the Global FAST approach, the maternal side of things. Assessing fetal development, viability, and fetal stress helps the clinician to make critical decisions in the management of dystocia.

### What the POCUS Dystocia Can Do

- Help assess fetal maturity.
- Screen for the presence of fetal stress.
- Help manage dystocia by using serial examinations for the screening of fetal distress.

### What the POCUS Dystocia Cannot Do

- Cannot provide an accurate fetal count.
- Cannot consistently allow the scrutiny of every individual fetus for fetal stress.
- Cannot fully screen for intraabdominal free fluid.

**Note:** It is a good idea to routinely perform an AFAST with an assigned abdominal fluid score to screen for obvious peritonitis and any evidence of intraabdominal and retroperitoneal hemorrhage as well as AFAST target organ abnormalities. By implementing the Global FAST approach, important complications regarding the thorax (TFAST), heart (TFAST), and lung (Vet BLUE), such as aspiration pneumonia (Vet BLUE), volume contraction (TFAST), and comorbidities (target organ approach), are also surveyed.

### Indications

- Parturition in any dog or cat.
- Diagnosed dystocia.
- Vaginal discharge during pregnancy.
- Green vaginal discharge not followed by passage of a puppy or kitten.

### Objectives

- Discuss final fetal organogenesis.
- Discuss fetal heart rate in relation to fetal stress.

## Dystocia

Dystocia: from the Greek *dys*, meaning difficult, and *tokos*, meaning birth, or, more simply put, a difficult birthing. More specifically, dystocia is defined as the inability to expel fetuses through the birth canal during parturition and may result from maternal or fetal factors that prevent delivery from taking place (Jutkowitz 2005).

Dogs and cats, like many mammals, tend to undergo parturition during the relative safety of night time. Therefore, dystocia often occurs outside normal business hours for the small animal clinician and becomes the responsibility of the overnight emergency veterinarian. A synergistic relationship between melatonin and oxytocin may, in part, explain this phenomenon (Sharkey et al. 2009). If the clinician presented with a dystocia has been managing the pregnancy from conception, they have a huge body of clinical information that can greatly aid important decision making, particularly in relation to determining if pregnancy is term and parturition is imminent. Many times, however, the managing clinician is novel to the pregnancy and must rely on often

*Point-of-Care Ultrasound Techniques for the Small Animal Practitioner*, Second Edition. Edited by Gregory R. Lisciandro.
© 2021 John Wiley & Sons, Inc. Published 2021 by John Wiley & Sons, Inc.
Companion website: www.wiley.com/go/lisciandro/ultrasound2

inaccurate or incomplete historical information. For either party, ultrasound is an invaluable tool to manage parturition, including dystocia. Two primary pieces of vital information that POCUS can help determine during parturition and dystocia management are fetal maturation and fetal stress.

**Pearl:** Fetal heart rate is a key indicator of fetal stress. The lower the heart rate, the higher the fetal stress.

# Fetal Maturation: Imaging Puppies and Kittens *In Utero*

The pregnant bitch is often scanned in dorsal recumbency. However, during term gestation when the gravid uterus may place undue pressure on the bitch's diaphragm, scan in lateral recumbency (or standing position) (Figure 15.1) Dorsal recumbency has the advantage of allowing the uterine horns to fall away from each other and allows for a more systematic approach of scanning the entire uterus. Lateral recumbency results in less pressure on the diaphragm but the uterine horns stack on top of each other.

From either position, start with the probe in longitudinal orientation along the ventral midline near the pelvic brim. Fan the probe laterally to both sides. Return to the starting position, slide the probe cranially and repeat the lateral scanning movements. Repeat this process until most of the abdomen has been scanned and you have the general layout of the uterine horns and fetuses. Upon finding a fetus, align the probe along its long axis parallel to its spine to examine fetal abdominal and thoracic structures.

**Pearl:** Term fetuses are easy to identify. With their anatomy formed in miniature, internal fetal structures are recognizable in normalcy and may be used for fetal aging.

- Start with the fetal abdomen and find the liver, which is generally the easiest to image because of its size and location adjacent to the thorax.
- After identifying the liver, look caudally for the kidneys (Figure 15.2) and small intestine (Figure 15.3).

These are some of the last organs to form and serve as a guide for fetal maturation. As they develop, the kidneys begin to appear similar to adults with distinct cortical and medullary regions (see Chapters 10 and 16). The intestines are the final organ to develop their ultrasonographic identity and typically mark the end of fetal organogenesis (Mattoon and Nyland 2002; Gil et al. 2015) (see also Figures 12.4 and 16.9, and Chapters 12 and 16).

There are four sonographic phases of fetal intestinal maturation beginning between days 39 and 44 of gestation as measured from the luteinizing hormone (LH) surge, with the final phase of fetal intestinal

**Figure 15.1.** Lateral scanning of the bitch. Scanning the term bitch or queen can be performed in either dorsal or lateral recumbency (also standing position). The dorsal position may lead to respiratory and cardiovascular compromise due to compression of the gravid uterus on the great vessels and diaphragm so the lateral position is preferred for these patients. Source: Courtesy of Robert M. Fulton, DVM, Richmond, VA.

**Figure 15.2.** Fetal kidney. The fetal kidney develops recognizable corticomedullary distinction around days 39–47 post luteinizing hormone (LH) peak. The kidney is marked with calipers in this image (see also Chapters 10 and 16). Note that neonates commonly have a variable degree of free anechoic intraabdominal fluid (ascites) present in normalcy. Source: Courtesy of Robert M. Fulton, DVM, Richmond, VA.

maturation beginning between days 57 and 62 of gestation (Tables 15.1 and 15.2). This final phase is characterized not only by intestinal layering (see Figures 12.4 and 16.9), but also by consistent and frequent peristalsis. The three visible bowel wall layers are the hyperechoic mucosal surface (intestinal lumen), the hypoechoic combined mucosa, submucosa, and muscularis, and the hyperechoic serosa. As ultrasound technologies continue to improve, it may be possible in the future to differentiate the middle layer into its component parts, thus giving a more accurate determination of final, functional fetal maturity. In phase three of sonographic intestinal maturation, the intestines develop peristalsis but this is only intermittent and it may take over one minute of visualizing the intestines to see peristalsis. In the fourth final phase, intestinal motility is constant and visible immediately with ultrasound (Gil et al. 2015).

**Figure 15.3.** Fetal intestine. The fetal intestine is the last organ to develop recognizable features, normally between days 57 and 63 post LH peak. The normal intestinal layers can be seen in this fetal abdomen. The small intestine in cross-section has distinct layering and has been referred to as looking like "hamburgers" (see Chapters 12 and 16 and Figures 12.4 and 16.9). Source: Courtesy of Robert M. Fulton, DVM, Richmond, VA.

**Table 15.1.**
Fetal ultrasonographic maturation – canine.

| Fetal structure | Days post luteinizing hormone surge |
|---|---|
| Gestational sac | 20 |
| Embryo | 23–25 |
| Cardiac activity | 23–25 |
| Yolk sac, U-shaped | 25–28 |
| Yolk sac, tubular | 27–31 |
| Fetal orientation (head and body) | 28 |
| Limb buds, fetal movement | 35 |
| Fetal skeleton | 33–39 |
| Stomach, urinary bladder | 35–39 |
| Lungs – hyperechoic to liver | 38–42 |
| Kidneys, eyes | 39–47 |
| Cardiac chambers | 40 |
| Intestines – layered appearance | 57–63 |

Source: Adapted from Mattoon and Nyland (2015).

**Table 15.2.**
Fetal ultrasonographic maturation – feline.

| Fetal structure | Days post luteinizing hormone surge |
|---|---|
| Gestational sac – spherical shape | 10–11 |
| Gestational sac – lemon shape | 19–21 |
| Embryo | 23–25 |
| Cardiac activity | 16–18 |
| Yolk sac, tubular | 25–27 |
| Fetal orientation (head and body) | 24–27 |
| Limb buds, fetal movement | 30–34 |
| Fetal skeleton | 30–33 |
| Stomach, urinary bladder | 29–32 |
| Kidneys, eyes | 38–41 |
| Cardiac chambers | 48–50 |
| Intestines – layered appearance | 52–56 |

Source: Adapted from Zambelli et al. (2002).

**Pitfall:** As the onset of consistent intestinal peristalsis may be as much as four days from natural delivery, visualization of intestinal motility should not be the sole determinant for C-section.

**Pearl:** Ultrasound may be used to accurately age fetuses but must be done between 19 and 37 days post LH peak (Lopate 2008); this is not addressed in this text.

After scanning the fetal abdomen, follow the fetal trunk cranially into the thorax, which is readily identified by the ribcage. There the beating heart is readily identifiable in the live, unstressed fetus.

The ribs will minimally and variably shadow the intrathoracic structures although less than the adult because of their decreased mineralization (mostly cartilage) and small size. Here the fetal heart should be easily recognized by its fluttering chambers. The fetal heartbeat is the hallmark characteristic of fetal vitality.

**Pearl:** The fetal heart can be difficult to image in fetal death because of both lack of heart movement and varying degrees of fetal decomposition. Intrauterine gas typically representing fetal death and decomposition may also be evident during ultrasound by dirty shadowing and air reverberation artifacts, which further interfere with fetal cardiac imaging.

# Fetal Stress

## *Determining Fetal Heart Rate*

One of the most sensitive indicators of fetal stress is heart rate.

**Pearl:** Normal canine or feline fetal heart rates should be greater than 200 beats/min and often well above 220 beats/min. Fetal cat heart rates are often around 265 beats/min (Jutkowitz 2005).

**Pearl**: Normal fetal heart rate is approximately double the dam's heart rate (Mattoon and Nyland 2015).

There are two ways to determine fetal heart rate. The first, the "eyeball method," is simple but lacks accuracy. Visualize the fetal heart and count how many beats per minute. The second method is to use M-mode imaging. This is preferred as it is more accurate and allows for better documentation. The M-mode image may be digitally saved or printed for the medical record. Using M-mode is more time-consuming and technically more challenging when first learning the technique but in time it becomes much more expedient. In comparison, the eyeball method is generally an estimate while the M-mode method is an accurate measurement of fetal heart rate (Figure 15.4).

**Pitfall:** Know how your ultrasound machine is set in M-mode to determine heart rate. Some measure a single cycle while others measure two cycles and take the average.

## *Fetal Heart Rates and Fetal Stress*

With increasing fetal stress come decreasing fetal heart rates. Specific values for heart rate in relation to fetal stress can vary among clinicians. From a clinical viewpoint, Traas (2008) uses the following guidelines.

- Fetal heart rates of *160–180 beats/min* indicate mild distress and clinical intervention should be considered.
- Fetal heart rates between *140 and 160 beats/min* indicate moderate distress and high risk of fetal death if not delivered within the next 2–3 hours.
- Fetal heart rates less than *140 beats/min* indicate severe distress and that immediate intervention (C-section) is required because fetal death is imminent.

A study by Zone and Wanke (2001) suggests more conservative values.

- Fetal heart rates between *180 and 220 beats/min* indicate mild distress.
- Fetal heart rates less than *180 beats/min* indicate severe fetal distress.

**Pitfall:** As they pass over a fetus, segmental uterine contractions may result in transient reduction of fetal heart rate (Lopate 2008).

An additional marker of fetal stress is fetal bowel movements. All fetuses under severe stress exhibit bowel movements (Zone and Wanke 2001), which may be seen ultrasonographically as an echogenic character to the amniotic fluid. Similar echogenicity of the amniotic fluid may also be seen with premature placental separation and hemorrhage (Lopate 2008).

**Pearl:** When evaluating for fetal stress, bear in mind that stress may be variable within the litter and that a single individual may not reflect the general status of others. There may be fetal death in one or two fetuses, yet the others are healthy.

- Avoid telling a client the number of puppies or kittens in a litter based on a fetal count using ultrasound because of its unreliability. The most accurate way of determining the number of puppies or kittens in a litter is by radiography (Davidson and Baker 2009).

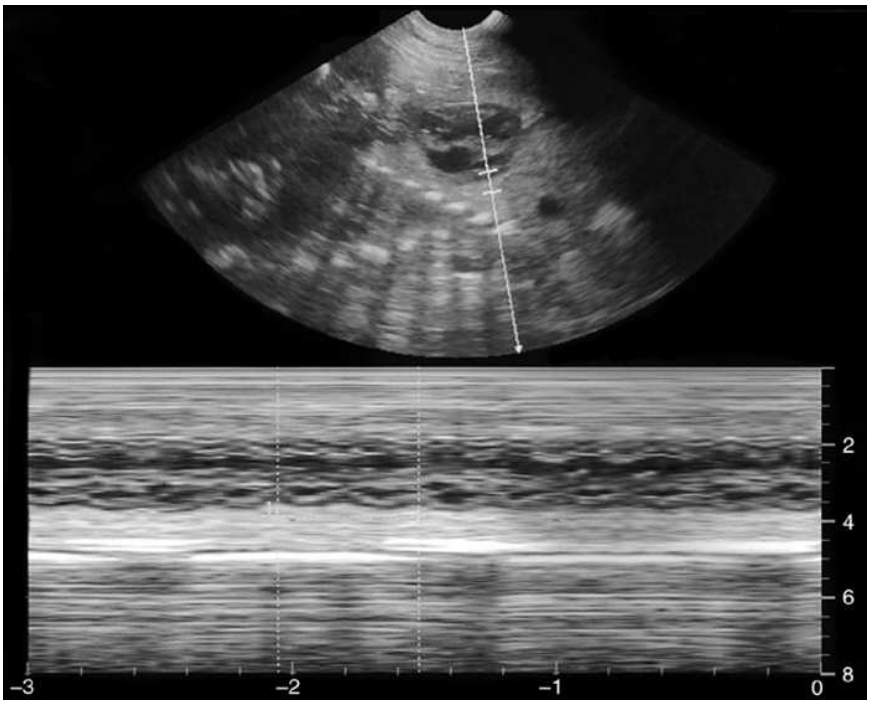


**Figure 15.4.** M-mode of fetal heart rate. By using M-mode, the sonographer can accurately determine fetal heart rate and eliminate error of estimation that occurs with the "eyeball method." This ultrasound machine was set to measure two cycles and take the average. Source: Courtesy of Robert M. Fulton, DVM, Richmond, VA.

- If uterine rupture or hemorrhage is a possibility, then an AFAST and assigned fluid score should be performed (see Chapters 6 and 7).

Clinical intervention, whether surgical or medical, should not be solely premised on ultrasonographic findings since ultrasound cannot evaluate all forms of dystocia. Abdominal radiography should also be used to assess fetal size relative to the mother's pelvic diameter to rule out forms of mechanical dystocia. Bloodwork should be used to rule out metabolic causes of dystocia. History (duration of time between births, duration of hard pushing), physical examination findings, and the owner's observations and expectations must all be included the decision-making process.

## Serial POCUS Dystocia during Medical Management

The use of ultrasound for monitoring signs of fetal stress during medical management is superior to traditional means. Moreover, its use carries the potential to positively influence the decision-making process regarding medical versus surgical management, thus optimizing the chance for a favorable outcome for the fetuses, bitch, client, and veterinarian.

**Pearl:** During medical management of dystocia, assess for fetal stress by measuring heart rates prior to each oxytocin injection, or minimally every 30 minutes (Traas 2008). See the correlation between fetal stress and heart rates mentioned above.

## Pearls, Pitfalls, The Final Say

Ultrasonography is a very useful clinical tool for managing dystocia. The most important relevant skill is also perhaps the easiest to learn and that is determining the fetal heart rate. A steady hand is required to visualize the small fetal heart but once this skill is developed, measuring fetal heart rate becomes quick and easy. Imaging the remainder of the fetal structures takes a little more time to develop the fine motor and visual interpretation skills, and is machine dependent, requiring greater ultrasound detail, but sonographer proficiency will come with time and practice. Using POCUS to assess fetal maturity can aid in the timing of C-sections and other clinical interventions.

# Quick Reference of Normals and Rules of Thumb

- *Fetal heart rates and distress*: HR >180 – normal; 180 > HR > 160 – early fetal stress, prompt intervention required; 160 > HR > 140 – moderate fetal stress, C-section warranted next 2–3 hours; HR <140 – severe fetal stress, reduced fetal viability, immediate surgical intervention required (Traas 2008). Note that variability exists in litters where one fetus may be severely distressed and another normal.
- *Normal ultrasonographic layering* of the small bowel coupled with peristalsis in the fetus may be used as a guideline for full-term maturation of puppies and kittens (Mattoon and Nyland 2002).
- *In anestrus* there is no uterine luminal fluid in normalcy; however, in estrus there may be a thin echogenic stripe also considered as a normal finding (Mattoon and Nyland 2002).
- *Abdominal radiography* is the most accurate way of determining the number of puppies or kittens in the litter (Davidson and Baker 2009). Avoid advising clients about numbers in the litter using ultrasound because of its inaccuracy.

# References


Davidson A, Baker T. 2009. Neonatal and pediatric ultrasonography – part II. *Clin Theriogenol* 1(1):156–150.

Gil E, Garcia D, Froes T. 2015. In utero development of the fetal intestine: sonographic evaluation and correlation with gestational age and fetal maturity in dogs. *Theriogenology* 84:681–686.

Jutkowitz L. 2005. Reproductive emergencies. *Vet Clin North Am Small Anim Pract* 35:397–420.

Lopate C. 2008. Estimation of gestational age and assessment of canine fetal maturation using radiology and ultrasonography: a review. *Theriogenology* 70:397–402.

Mattoon J, Nyland T. 2002. Ovaries and uterus. In: *Small Animal Diagnostic Ultrasound*, 2nd edition, edited by Nyland TG, Mattoon JS. Philadelphia: WB Saunders, pp 231–249.

Mattoon J, Nyland T. 2015. Ovaries and uterus. In: *Small Animal Diagnostic Ultrasound*, 3rd edition, edited by Mattoon JS, Nyland TG. St Louis: Elsevier/Saunders, pp 634–654.

Sharkey JT, Puttaramu R, Word RA, Olcese J. 2009; Melatonin synergizes with oxytocin to enhance contractility of human myometrial smooth muscle cells. *J Clin Endocrinol Metab* 94:421–427.

Traas AM. 2008. Surgical management of canine and feline dystocia. *Theriogenology* 40:337–342.

Zambelli D, Caneppele B, Bassi S, et al. 2002. Ultrasound aspects of fetal and extrafetal structures in pregnant cats. *J Feline Med Surg* 4:95–106.

Zone MA, Wanke M. 2001. Diagnosis of canine fetal health by ultrasonography. *J Reprod Fertil* 57(suppl):215–219.


# Further Reading


Feeny D, Johnston G. 2007. The uterus, ovaries, and testes. In: *Textbook of Veterinary Diagnostic Radiology*, 5th edition, edited by Thrall EJ. St Louis: Saunders/Elsevier, pp 735–749.

Johnston S, Root-Kustriz M, Olson P. 2001. Canine parturition – eustocia and dystocia. In: *Canine and Feline Theriogenology*, edited by Johnston S, Root-Kustriz M, Olson P. Philadelphia: WB Saunders, pp 105–128.

Johnston S, Root-Kustriz M, Olson P. 2001. Disorders of the feline uterus and uterine tubes (oviducts). In: *Canine and Feline Theriogenology*, edited by Johnston S, Root-Kustriz M, Olson P. Philadelphia: WB Saunders, pp 463–471.

Serrano S, McMillan M. 2009. Dystocia. *Standards Care Emerg Crit Care Med* 11(1):1–11.

Yeager AE, Mohammed HO, Meyers-Wallen V, et al. 1992. Ultrasonographic appearance of the uterus, placenta, fetus, and fetal membranes throughout accurately timed pregnancy in beagles. *Am J Vet Res* 53:342–351.

CHAPTER SIXTEEN

# POCUS: Pediatrics

Autumn P. Davidson and Tomas W. Baker

Vetbooks.ir

## Introduction

Pediatric patients are commonly presented to the veterinarian due to signs referable to the abdominal cavity. Abdominal disorders can rapidly progress to serious conditions in pediatric dogs and cats; anorexia or fasting can result in hypoglycemia, vomiting can result in aspiration pneumonia, diarrhea can result in intussusception, and perforation from a foreign body can cause peritonitis. Congenital anomalies can first become clinically apparent in the pediatric patient. Dietary indiscretions are common. Parasitic infestation and viral infectious disease have the greatest incidence in pediatric patients. Contagious diseases result in confinement in an isolation ward where continuous monitoring can be difficult. Rapid, accurate diagnostic evaluation permits timely effective intervention.

Physical examination findings, fecal examination for cytology, parasites and viral antigens, fecal culture for pathogenic bacteria, and abdominal radiography can all contribute useful diagnostic information. Cageside POCUS pediatrics and its abdominal ultrasound provide valuable clinical information about the peritoneal cavity, great vessels, abdominal viscera, and lymph nodes and can usually be obtained without sedation or anesthesia unless the patient is markedly painful. Ultrasound thus greatly facilitates prompt and ongoing diagnostic evaluation of the pediatric patient with abdominal disorders.

### What POCUS Pediatrics Can Do

- Support or negate clinical suspicions based on less sensitive evaluations of physical examination, laboratory testing, and abdominal radiography.
- Confirm/support the presence of an absolute indication for surgery (e.g., intussusception, obstructive foreign body, perforated bowel).
- Provide support for further diagnostics (suspected vascular anomaly, upper or lower urinary tract disorders).

### What POCUS Pediatrics Cannot Do

- Cannot replace a complete detailed abdominal ultrasound scan performed by a veterinary radiologist or trained specialist.

### Indications

- Acute abdomen.
- Abdominal free fluid (urine, blood, transudate, exudate).
- Protracted vomiting or diarrhea not responsive to supportive care.
- Unexplained clinical deterioration.

### Objectives

- Perform a basic ultrasound exam in a structured format.
- Answer important clinical questions especially in confirming or refuting clinical suspicions based on physical examination, laboratory findings, and abdominal radiography to better direct pediatric care.
- Answer important clinical questions when delays exist in being able to schedule a complete abdominal ultrasound by a veterinary radiologist or trained specialist.

## Equipment

Pediatric patients are best evaluated using an ultrasound machine equipped with a curvilinear (microconvex) variable frequency scanhead (6.0–8.0 MHz)

*Point-of-Care Ultrasound Techniques for the Small Animal Practitioner*, Second Edition. Edited by Gregory R. Lisciandro.
© 2021 John Wiley & Sons, Inc. Published 2021 by John Wiley & Sons, Inc.
Companion website: www.wiley.com/go/lisciandro/ultrasound2

(Nyland et al. 2002a). Many portable machines now have a high-frequency linear scanhead (8.0–13.0 MHz) which will improve image quality and also allow evaluation of even smaller superficial anatomy, but these are not essential. Portability permits cageside POCUS pediatrics evaluation.

# Patient Preparation

The pediatric patient should be gently placed in dorsal recumbency, ideally in a small padded V-trough, and restrained by assistant(s) holding the fore- and hindlimbs (Figure 16.1A). Permit the pediatric patient to become accustomed to this restraint before initiating clipping or scanning; this usually minimizes struggling and resultant aerophagia. If sedation or analgesia is required, the use of a reversible narcotic agent such as hydromorphone or butorphanol is preferable. However, lateral recumbency or standing positioning is now being used for AFAST, TFAST, and Vet BLUE and provides another option, especially in stressed or critical pediatric patients.

**Pearl:** Panting as commonly seen in adult dogs under narcotic sedation is less prevalent in pediatric dogs and cats.

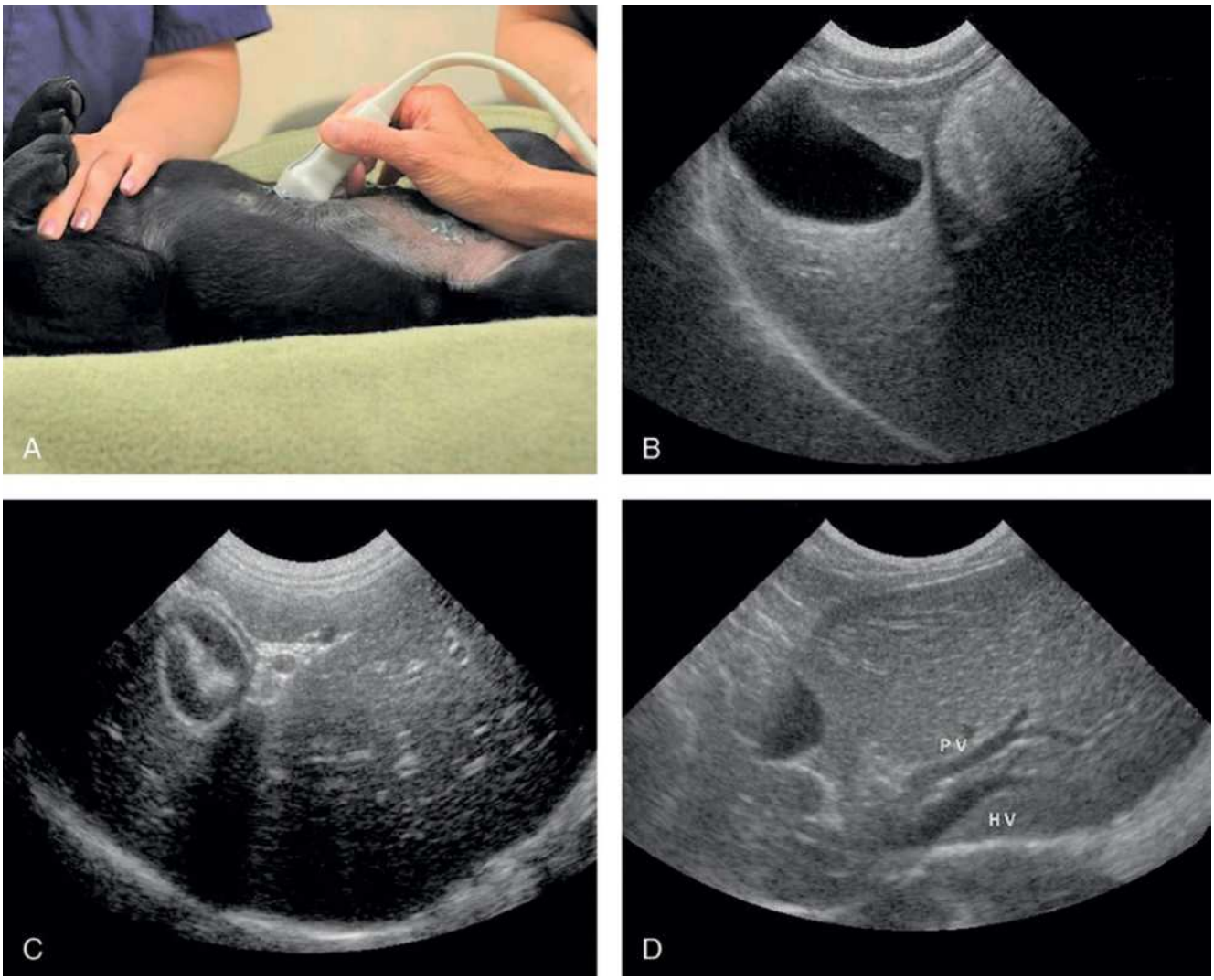


**Figure 16.1.** Abdominal scanning. (A) Scanning the pediatric canine in a comfortable, warm trough. (B) Sagittal image of normal gallbladder, liver, and stomach. (C) Transverse image of the liver and duodenum. (D) Walls of the hepatic veins (HV) are less echogenic than portal veins (PV).

Clipping hair is usually minimally necessary in the pediatric patient. Clipping the cranioventral abdominal hair, using a quiet set of electric clippers with a #40 blade in the direction of hair growth, rather than against it, minimizes cutaneous trauma. Wetting the clipped skin with tepid water, tincture of zephran or 70% isopropyl alcohol, followed by a liberal amount of ultrasound gel, permits the best acoustic coupling of the scanhead to the patient, improving the image obtained. Care should be taken to avoid excessive chilling of pediatric patients secondary to the application of cool, room-temperature liquids and gels followed by evaporation. Alcohol-based hand sanitizer is another coupling medium option that is less noxious.

**Pearl:** Electronic warming devices (warm water blankets, 3M™ Bair Hugger™) may cause electronic interference with the ultrasound equipment (a wavy screen); warm water blankets or fluid bags are superior for preventing hypothermia (Penninck 2002a; Baker and Davidson 2006).

Fasting as much as is safely possible in the pediatric patient minimizes gastric ingesta obscuring imaging of the liver and gastrointestinal gas accumulation interfering with visualization of other abdominal viscera. Preventing urination immediately prior to the examination permits better evaluation of the urinary bladder and dorsal sublumbar structures. Nauseated patients should be closely monitored for vomiting or regurgitation and immediately repositioned to ventral recumbency with the head lowered should it occur to help prevent aspiration pneumonia.

Serial evaluations can provide useful information when the clinical status of the pediatric patient has changed. clinicopathological deterioration, progressive lethargy or obtundation, acute or progressive pain, changes in abdominal palpation findings, or refractory vomiting or diarrhea warrant repeat evaluation for ultrasonographic findings indicating that gastrointestinal obstruction, intussusception, visceral perforation, and/or peritonitis have occurred.

**Pearl:** Serial examinations are very helpful and should be used in patients with worsening signs when ultrasound findings are initially equivocal or indeterminate.

# Ultrasound of the Normal Pediatric Abdomen

Regardless of the clinical history, the abdomen should always be evaluated completely and methodically, in a clockwise direction starting with the liver. Performing a complete abdominal scan in an organized fashion saves time and often identifies disorders that might otherwise be missed if only a focused study (i.e., bladder scan) is done. The complete scan should only take 10–15 minutes (Baker 2009).

**Pearl:** Always do the POCUS pediatrics examination in the same manner each time, going in a clockwise direction.

To begin, place the scanhead under the xiphoid with the beam in the sagittal plane. Visualization of the liver is achieved by fanning the beam from the patient's right to left. The gallbladder is seen on the right; the left liver lobes are seen ventral and sometimes caudal to the stomach (see Figure 16.1B). Turning the scanhead to transverse allows for visualization of the liver between the stomach and gallbladder. This view is good for evaluation of the hepatic border, echogenicity of hepatic parenchyma, and the portal architecture (see Figure 16.1C). The portal vessels have more echogenic walls than the hepatic veins (see Figure 16.1D).

**Pearl:** Portal veins have more echogenic walls than hepatic veins.

Evaluation of the body and left limb of the pancreas is actually possible at this point, by looking caudal to the stomach. In sagittal, point the scanhead directly into the dog (Figure 16.2). This visualizes the pancreatic trapezoid where the body and the left limb of the pancreas are located. The spleen appears in the near-field; the splenic vein divides the pancreatic body from the left limb. Realize that if the pancreas is normal, it is isoechoic to the surrounding mesentery and not visualized readily (Figure 16.3A). The normal pancreas can be visualized in the pediatric patient at times, due to the paucity of fat within the abdomen; lack of gastric gas is also helpful (see Figure 16.3B).

Continuing in the sagittal plane, scan to the left past the stomach to the spleen. The spleen will be visualized ventrally in the near-field, confirmed by the

**Figure 16.2.** Liver and pancreas. (A) Scanhead in sagittal for evaluation of the liver. (B) Scanhead in sagittal for evaluation of the body and left limb of the pancreas.

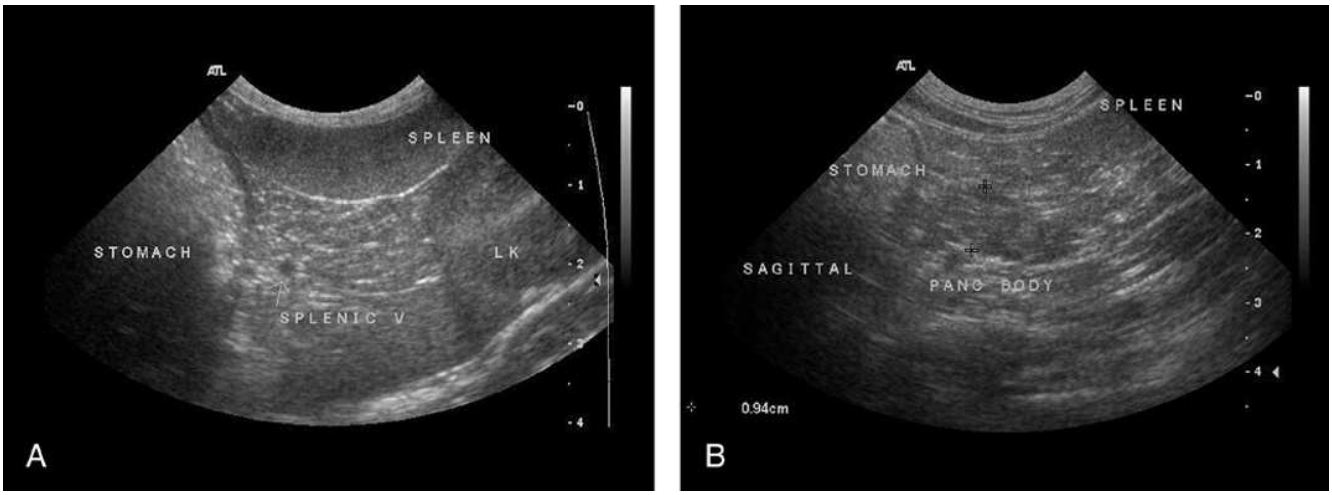


**Figure 16.3.** Additional pancreas. (A) Pancreatic trapezoid created by the caudal gastric wall, spleen, and cranial pole of the left kidney. (B) Normal pancreas (cursors).

splenic vein (Figure 16.4). Splenic border, parenchyma, and shape should be evaluated. Following the spleen transversely down the left body wall, you will see the left kidney.

**Pearl:** The tail of the spleen often rests near the left kidney – "follow the spleen caudolaterally to the left kidney."

**Pearl:** Remember "SLiCK" for the order of echogenicity between spleen, liver, and kidney. In other words, the spleen (S) is normally more echogenic (brighter) than the liver (Li), which is normally equal or slightly more echogenic (brighter) than the cortex of the kidney (CK).

Once visualization of the left kidney is achieved, turn to the sagittal plane and evaluate the renal border, cortical echogenicity, and pelvic architecture (see Figure 16.4B). Dilation of the renal pelvis is best seen in the transverse plane. Bear in mind that mild renal pelvic dilation can be associated with fluid loading and diuresis (Figure 16.5).

The adrenal is located medial to the cranial pole of the kidney. In sagittal, scan medially from the kidney in order to visualize the linear aorta and the renal artery. The left adrenal is located cranial to the left renal artery and caudal to the left cranial mesenteric artery. The left adrenal is visualized as a bilobed structure with the phrenicoabdominal vein at its waist (Figure 16.6A).

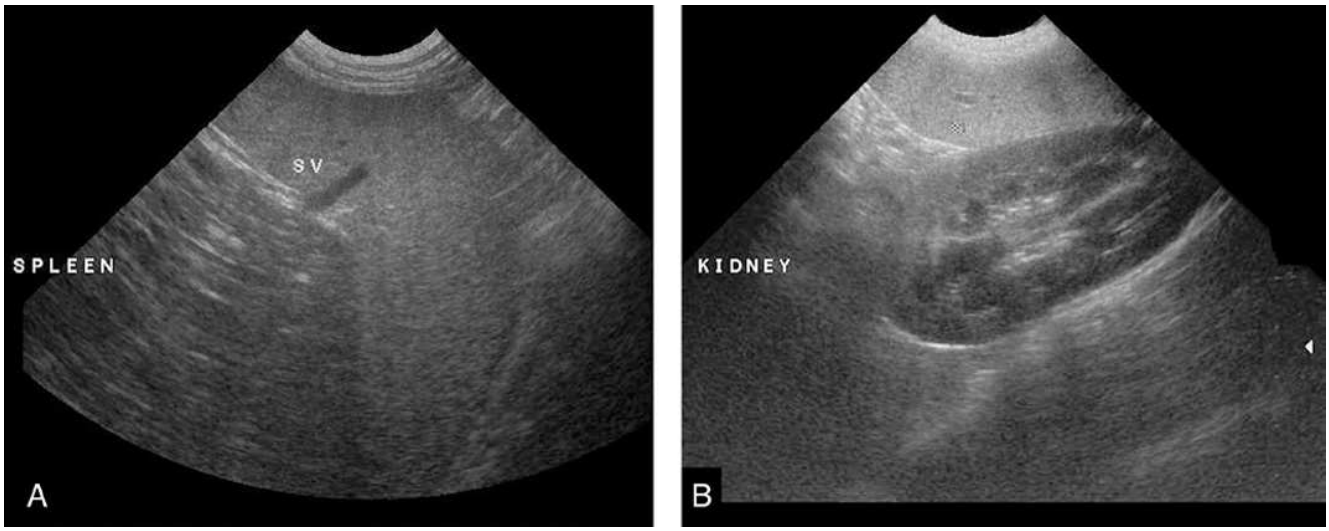


**Figure 16.4.** Spleen and left kidney. (A) Normal spleen, splenic vein (SV). (B) Normal left kidney in sagittal plane.

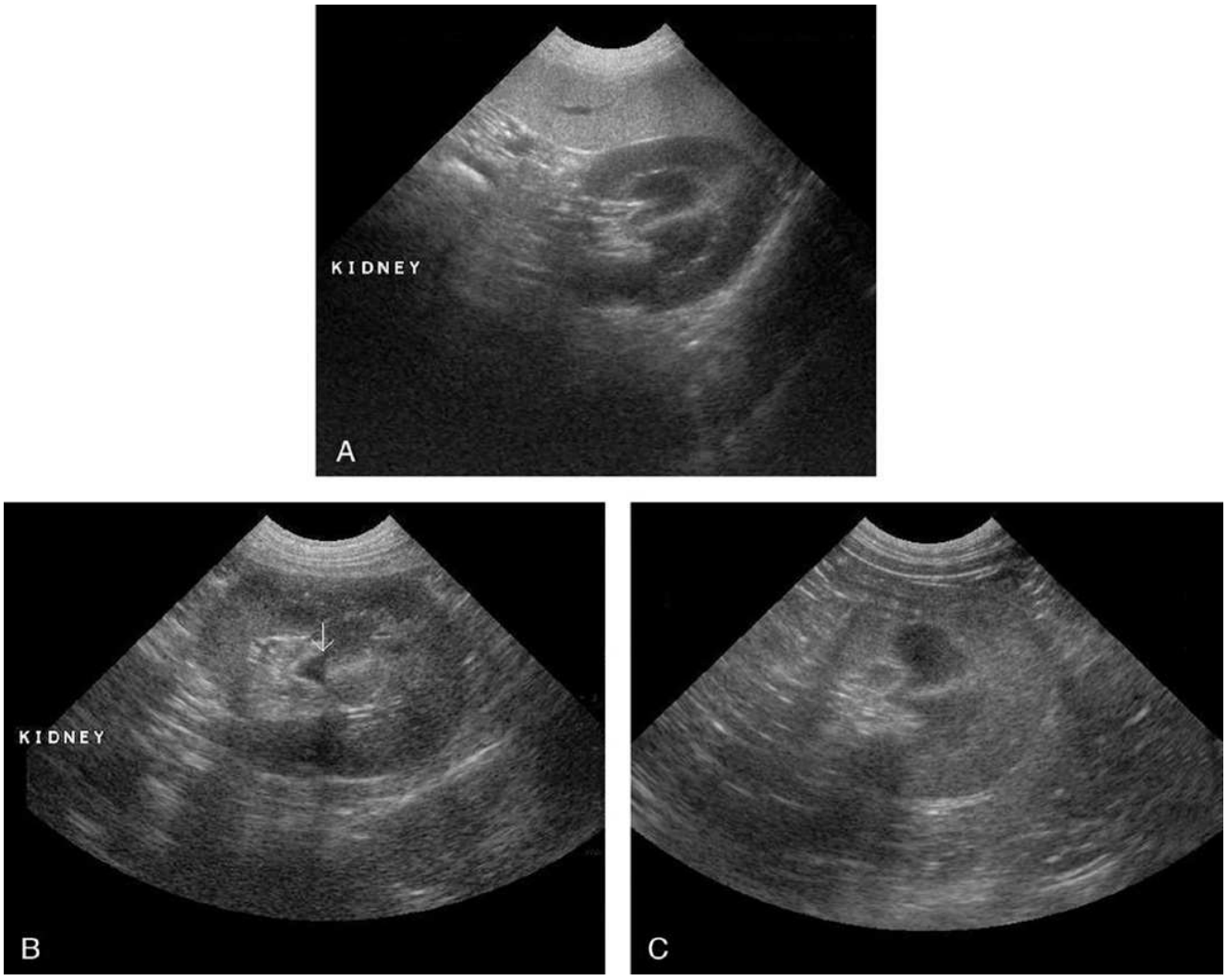


**Figure 16.5.** Left kidney. (A) Normal left kidney in transverse plane with normal renal pelvis. (B) Dilated renal pelvis (*arrow*). (C) Diuresis-induced renal pelvic dilation.

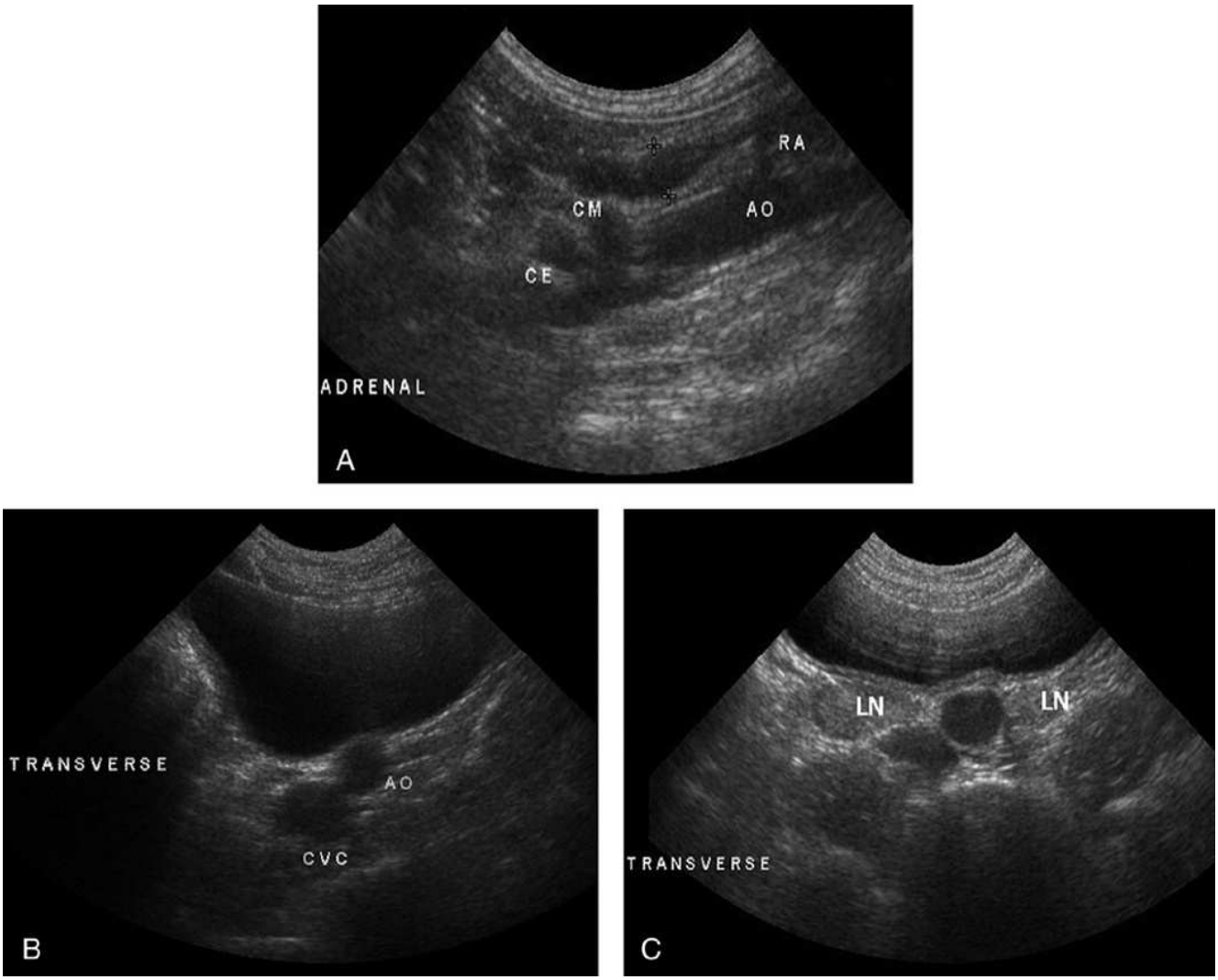


**Figure 16.6.** Left adrenal gland and retroperitoneal structures. (A) Left adrenal (cursors) surrounded by celiac artery (CE), cranial mesenteric artery (CM), aorta (AO), and renal artery (RA). (B) Urinary bladder in transverse; aorta (AO) and caudal vena cava (CVC) dorsally. (C) Normal pediatric sublumbar lymph nodes (LN).

With a transverse beam back in the middle of the abdomen, scan caudally to a large hypoechoic structure, the urinary bladder. Evaluate bladder wall and lumen contents and, dorsal to the bladder, the major vessels (caudal vena cava and aorta) (see Figure 16.6B). Sublumbar lymph nodes will be seen at the aortic bifurcation into the iliac arteries, adjacent to the bladder wall. The abdominal lymph nodes are readily visible in pediatric patients due to nonspecific immune stimulation at that period of development; this is usually considered normal if their appearance is homogenous (see Figure 16.6C). The bladder should be scanned in both the transverse and sagittal planes. Sagittal scanning of the urinary bladder caudally will allow visualization of the proximal urethra (and pediatric prostate in the male) (Figure 16.7A). The pediatric uterus is best seen in transverse, dorsal to the bladder and adjacent to the colon (see Figure 16.7B). The testes should be found in the scrotum after 6 weeks of age (see Figure 16.7C).

At the edge of the right ribcage, within the renal fossa of the liver, the right kidney will be found. The right kidney should be evaluated as was the left (renal border, cortical echogenicity, and pelvic architecture). By scanning sagittally between the right kidney and the caudal vena cava using a fanning technique, the right adrenal is visualized just lateral to the caudal vena cava (Figure 16.8A).

In transverse, return to the right kidney and, lateral to the kidney, find the duodenum. At the cranial end of

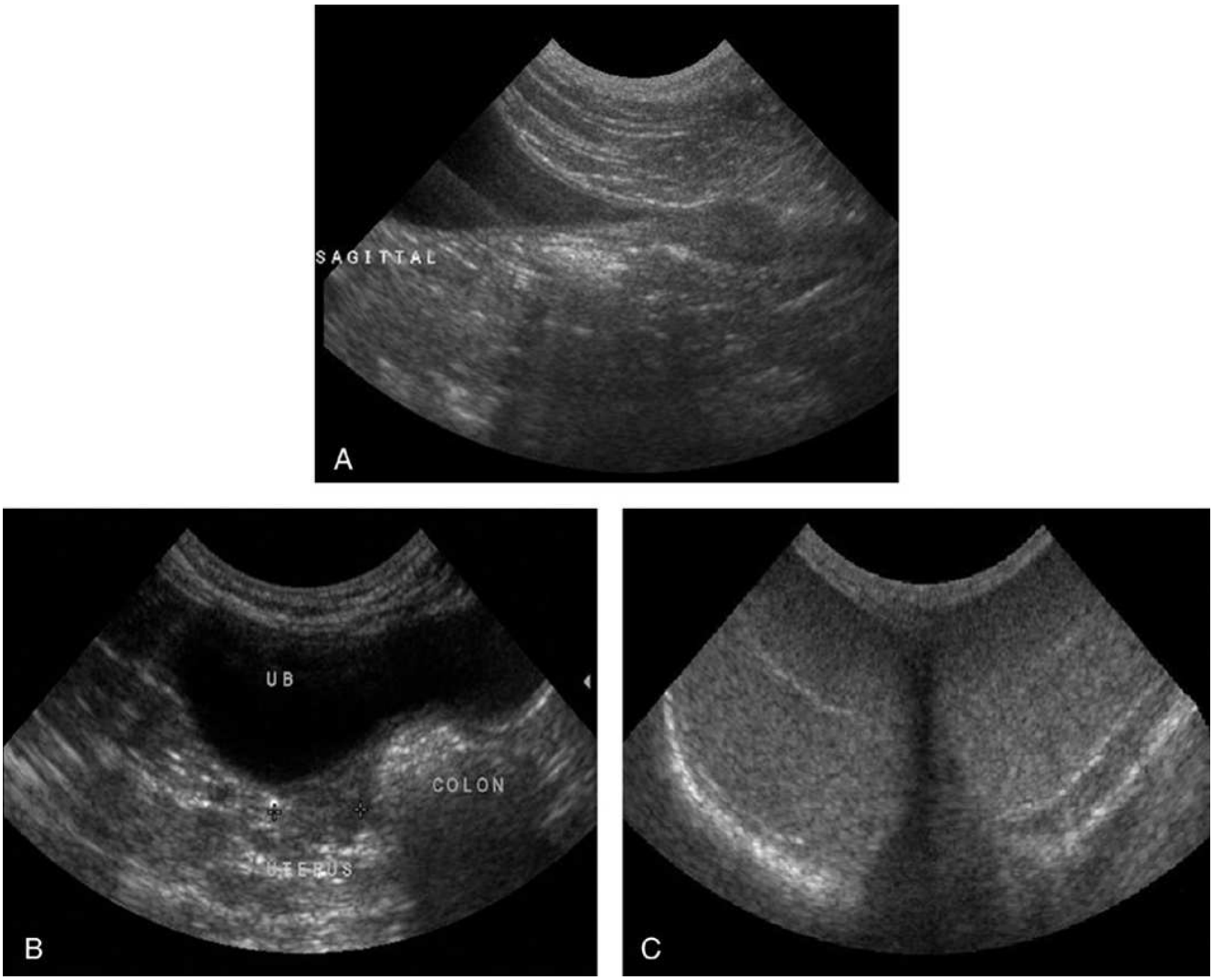


**Figure 16.7.** Prostate, testes, and uterus. (A) Pediatric prostate gland in sagittal. (B) Pediatric uterine body in transverse (cursors). (C) Pediatric testes; note hyperechoic mediastinum testis in each.

the kidney adjacent to the duodenum will be the right limb of the pancreas. The right pancreatic limb is identified by visualizing the caudal pancreaticoduodenal vein (see Figure 16.8B). The right limb of the pancreas is best seen in sagittal in the kitten, caudal to the gallbladder and the duodenum (see Figure 16.8C). The pancreatic body is seen caudal to the stomach, cranial to the splenic vein. The left limb is found caudal to the splenic vein and midline to the cranial pole of the left kidney (see Figure 16.8D).

Returning to the transverse plane in the cranial midabdomen at the mesenteric root, scan for mesenteric lymph nodes and small bowel wall architecture. It may take 2–3 craniocaudal passes to evaluate the entire bowel in a thorough fashion. Canine and feline small bowel has distinct layering and motile ingesta in the lumen. Normally, the small bowel appears sonographically as four distinct layers. The bowel lumen appears hyperechoic, as the mucosal interface is echogenic. The compression of gas and ingesta also visually strengthens this hyperechoic line. The layer just outside the lumen is the mucosa; it is hypoechoic and normally the thickest appearing section. Outside the mucosa is the submucosa, which is hyperechoic to the mucosa and about one-third the thickness. The muscularis, the bowel muscle layer, is outside the submucosa and appears as a very thin hypoechoic black line. The outermost layer, the serosa, is not seen as linearly as the other wall layers, but is very hyperechoic and about the same thickness as normal muscularis (Figure 16.9).

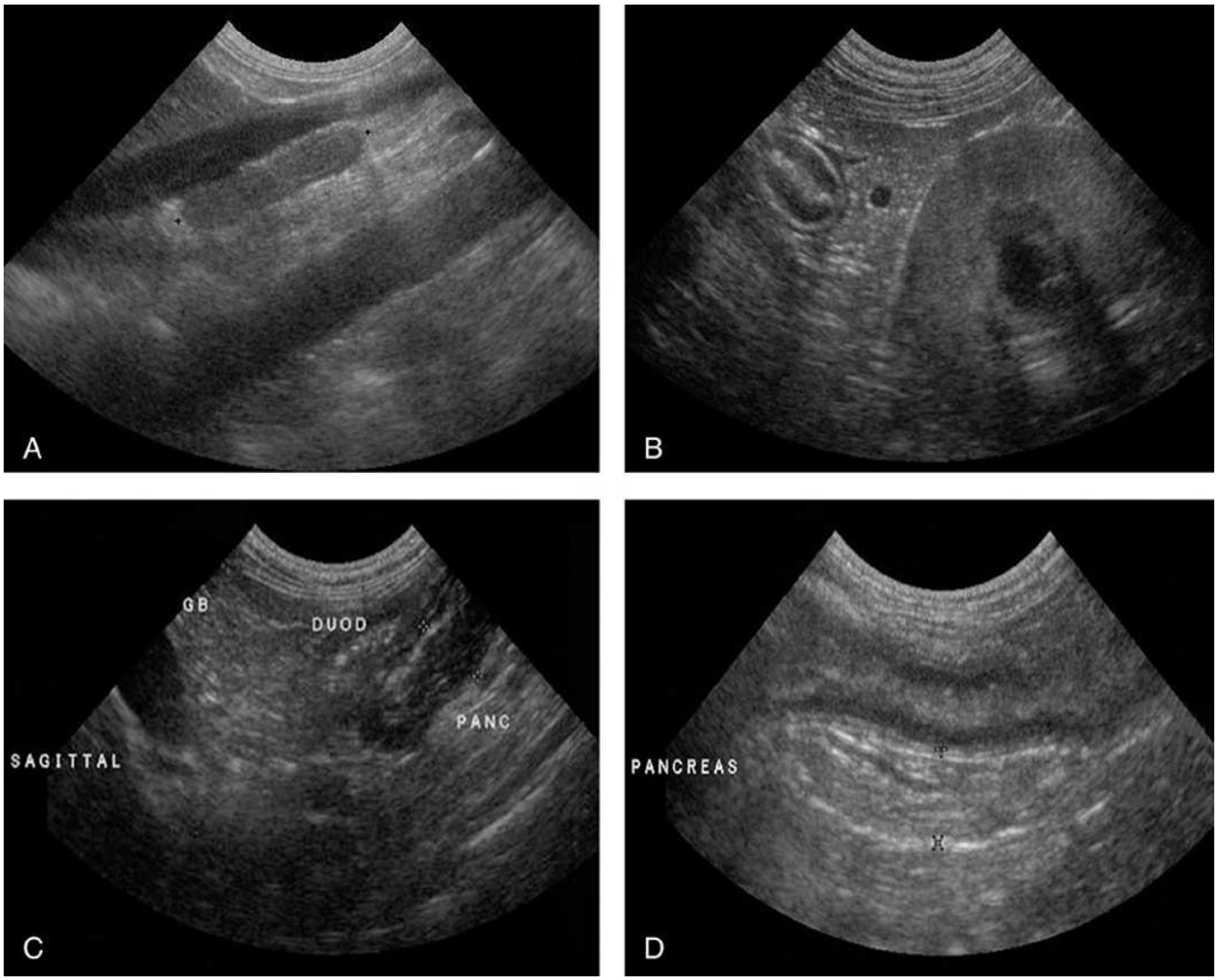


**Figure 16.8.** Right adrenal and pancreas. (A) Sagittal image of right adrenal between the aorta (dorsal) and vena cava. (B) The pancreaticoduodenal vein identifying the right limb of the pancreas. (C) Feline right limb of the pancreas caudal to the duodenum. (D) The pancreatic body in sagittal (cursors).

**Pearl:** Use the mnemonic "The sun is bright and it's dark at midnight" to remember that layers starting with an "s" like the sun are bright (submucosa and serosa are hyperechoic [bright]), while layers starting with an "m" like midnight are dark (mucosa and muscularis layer are hypoechoic [dark]).

Mesenteric lymph nodes will be readily visible in pediatric patients, but are likely normal when other enteric abnormalities are lacking. Look for mesenteric lymph nodes at the confluence of the renal vessels and the major vessels (aorta and caudal vena cava). Transverse scanning midline to the kidneys in a focused routine pattern will help with the visualization of normal mesenteric nodes (see Figure 16.9C).

Document your findings by storing images. Labeling images is ideal but time-consuming; if the abdominal scan is always performed in the same clockwise order, labeling is not essential (i.e., the left kidney is always scanned before the right).

**Pearl:** If the abdominal scan is always performed in the same clockwise order, labeling is not essential since organs will be viewed in the same order on every POCUS pediatrics examination.

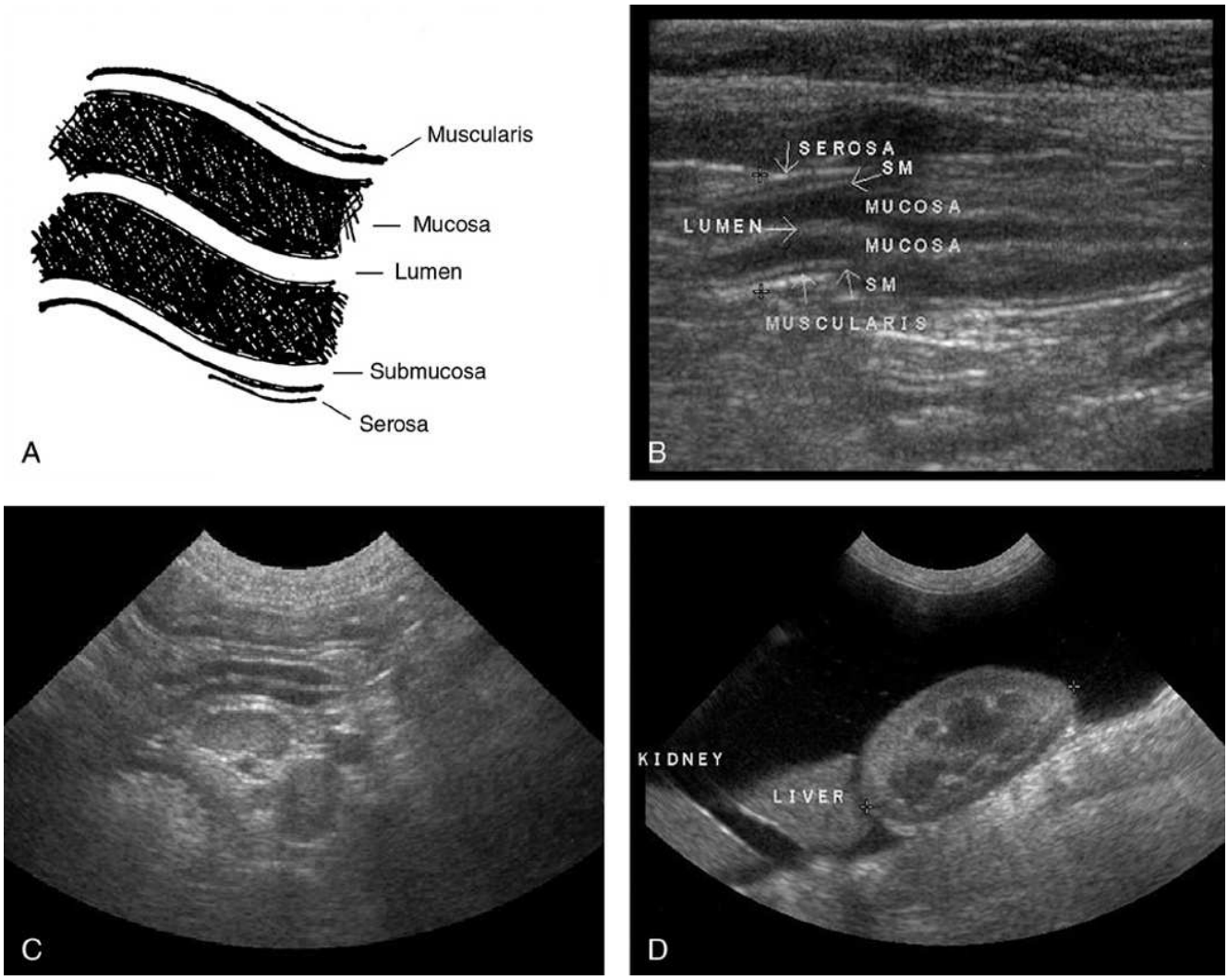


**Figure 16.9.** Small intestine, mesenteric lymph nodes, and ascites. (A) Schematic of normal small bowel wall layering. (B) Named normal small bowel wall layering. (C) Normal pediatric mesenteric lymph nodes. (D) Ascites, anechoic fluid likely representing a pure or modified transudate seen in the region of the right kidney.

# Common Pediatric Abdominal Disorders

## *Gastrointestinal Disease*

Abdominal ultrasonography provides additional and complementary information about the presence or absence of fluid in the peritoneal cavity (hemorrhage, effusion), intraabdominal gas suggesting bowel perforation (or postoperative), the appearance of gastrointestinal contents (appropriate vs foreign), gastrointestinal tract motility (ileus vs hyperkinetic), gastrointestinal wall morphology (infiltrative, disrupted or edematous), and mesenteric lymph node appearance (anticipated pediatric reactivity vs pathological).

## *Peritonitis/Peritoneal Effusion*

Pediatric patients have a small amount of free, scant, anechoic peritoneal fluid that appears in an abdominal ultrasound (best visualized lateral to the spleen when in dorsal recumbency) and represents normalcy. Increased fluid volume or echogenicity can indicate hemorrhage, septic peritonitis (exudative), transudative ascites, or rupture of the gallbladder or urinary tract (see Figure 16.9D). Septic peritonitis and biliary

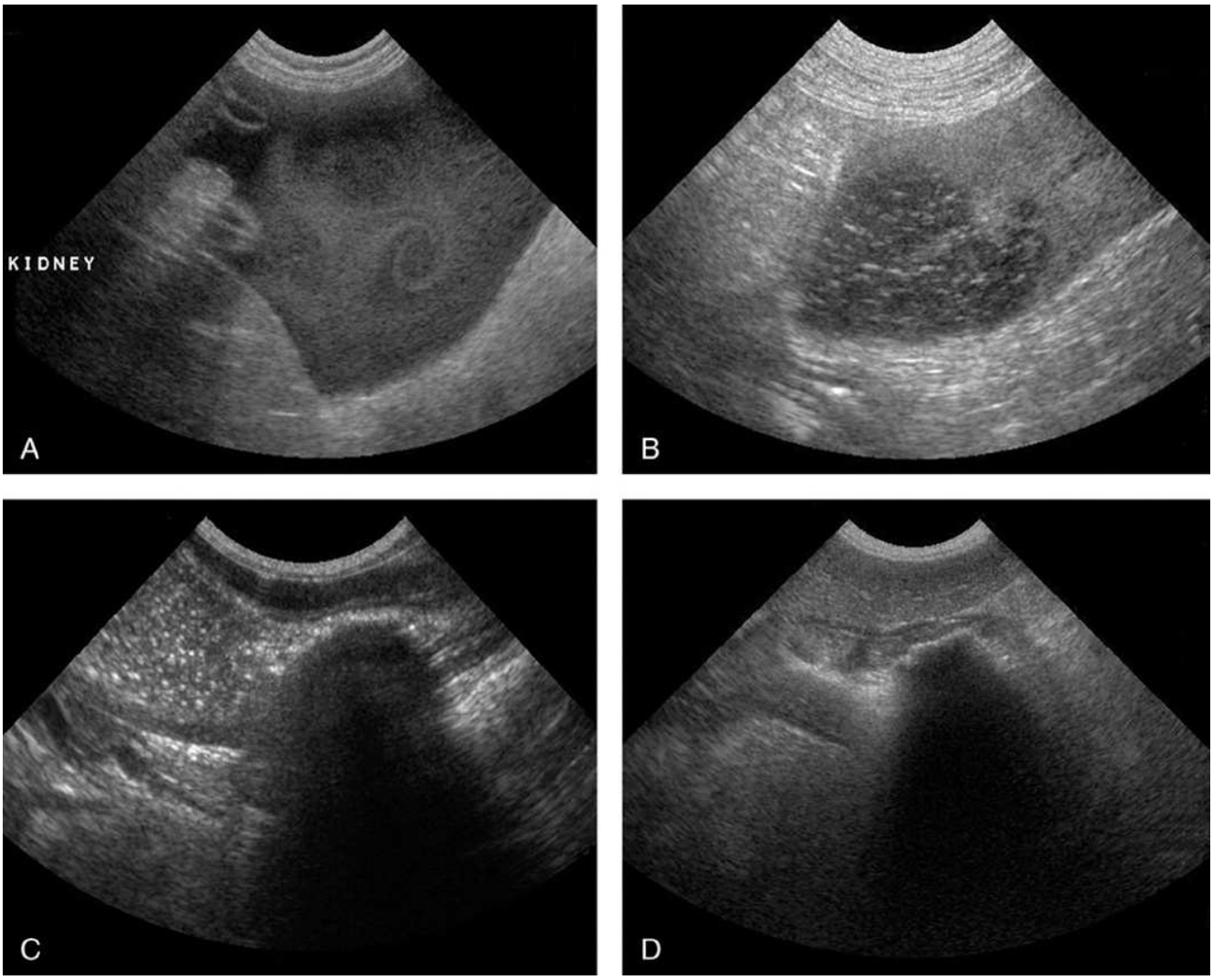


**Figure 16.10.** (A) Echogenic ascites, likely representing an exudate, seen adjacent to the right kidney. (B) Splenic infarction; typical hypoechoic parenchyma with echogenic slashes. (C) Colonic foreign body (oval ball) showing hard shadowing and fluid distension of the proximal bowel. (D) Hard shadowing associated with an irregularly shaped foreign body causing partial obstruction of the pylorus.

or urinary tract rupture are usually accompanied by evidence of inflammation causing progressively increased echogenicity (brightness) of the serosal surfaces over time (Figure 16.10A).

Blunt trauma resulting in hemoabdomen is best evaluated with FAST ultrasound (see also Chapters 6 and 7). Rupture or crushing trauma to the liver or infarction of the spleen is readily differentiated from normal homogenous parenchyma (see Figure 16.10B). The localization and normal appearance of fluid-filled viscera (bladder, gallbladder) can be reassuring but does not eliminate the possibility of an occult rupture; serial evaluation is advised along with the accumulation of clinical data (e.g., ultrasound-guided centesis for peritoneal fluid evaluation) (Penninck 2002b; Baker 2012).

## *Gastrointestinal Foreign Body: Nonobstructive versus Obstructive*

A common clinical dilemma results from the ingestion of foreign objects by pediatric patients. Foreign bodies can cause gastrointestinal inflammation and perforation even if they are not obstructive. Obstruction and/or perforation are absolute indications for laparotomy, albeit an invasive and expensive procedure. On the other hand, an unnecessary (negative) laparotomy in the pediatric patient can increase morbidity and mortality from anesthetic events, hypotension, hypovolemia, and surgical trauma, and is less likely to be tempered by the acquisition of meaningful biopsies as would occur in the adult pet.

Unless radiopaque, gastrointestinal foreign bodies are often difficult to confirm radiographically; they are usually suspected clinically based on intraluminal gas and fluid accumulation proximal to the mechanical obstruction caused by their presence. Serial radiography can support progression of a nonobstructive foreign body but requires time. Contrast radiography can complicate subsequent endoscopy or laparotomy, and can be difficult to accomplish in the vomiting patient. Ultrasonography can provide supportive information and sometimes confirm the diagnosis if the foreign body has a characteristic appearance (such as a ball, a trichobezoar or a linear foreign body).

**Pearl:** Ultrasound is now considered the best clinical tool for noninvasive diagnosis of intestinal obstruction.

Typically, a bright interface associated with strong shadowing suggests a foreign body. Fluid distension and peristalsis proximal to the object can confirm the suspicion. Balls have a rounded interface with uniform acoustic shadowing (see Figure 16.10C) whereas other foreign bodies may have more irregular hyperechoic borders with distal shadowing (see Figure 16.10D). Trichobezoars have irregular bright interfaces and strong shadowing. Linear foreign bodies produce bowel plication recognized as undulation (Figure 16.11A) and must be differentiated from undulation of the bowel wall which more commonly represents milder forms of enteritis. Complete obstruction results in pronounced dilation of the bowel cranial to the object. Pyloric obstruction can result in gastric atony and distension (Penninck 2002b; Baker and Davidson 2006). Do not mistake gastric ingesta for a foreign body (see Figure 16.11B), or an empty stomach with prominent rugal folds as abnormal (see Figure 16.11C).

**Pearl:** Do not mistake gastric ingesta for a foreign body or an empty stomach with prominent rugal folds as abnormal.

## Anatomical Obstruction

Enteric duplication or agenesis can be confirmed ultrasonographically in pediatric patients. Duplication is rare and can occur anywhere in the intestinal tract; the clinical signs may be nonspecific (abdominal distension, discomfort). A fluid-filled juxtaintestinal formation with variable peristalsis and contents can be seen. Enteric agenesis usually results in severe, life-threatening clinical signs in the neonatal period. Ultrasonographic findings usually include marked fluid and gas distension of bowel proximal to the defect (see Figure 16.11E).

Pyloric stenosis secondary to hypertrophic gastritis has been reported in the pediatric dog. Focal circumferential thickening of the pylorus primarily involving the muscularis is typical (Penninck 2002b; Baker and Davidson 2006).

## Bowel Perforation

Intestinal perforation can result in focal changes in bowel wall layer ratios, with thickening of the muscularis and submucosal layer due to inflammation and edema. A focal hypoechoic mass can be visualized where total effacement has occurred (Figure 16.12A). Hyperechoic slashes within the hypoechoic wall can represent gas trapping. Free abdominal air denotes bowel perforation unless the patient has recently undergone a laparotomy or laparoscopy or has a penetrating abdominal wall wound. Free abdominal air is best visualized ventral to the spleen when the patient is in dorsal recumbency (see Figure 16.12B) and in nongravity lateral sites when in lateral recumbency; radiography can confirm the suspicion (Penninck 2002b; Baker 2009).

**Pearl:** Abdominal radiography should be used to definitively document free abdominal air suspected in an ultrasound examination (see Chapter 12).

## Gastroenterocolitis

Mild to moderate thickening of the gastrointestinal wall with preservation of wall layering and moderate mesenteric lymphadenomegaly are the most common ultrasonographic findings with nonspecific pediatric gastroenterocolitis, such as that resulting from dietary indiscretion or bacterial overgrowth. More severe pathology, such as extensive bowel edema or hemorrhage accompanying severe infectious gastroenterocolitis, can be associated with changes in fluid volume within the bowel lumen, wall thickening, corrugation, and loss of normal wall layering (Figure 16.13A; see also Figure 16.12C,D). These changes can be regional or diffuse. Fluid distension of the bowel with generalized decreased motility can be seen with functional ileus accompanying gastroenterocolitis.

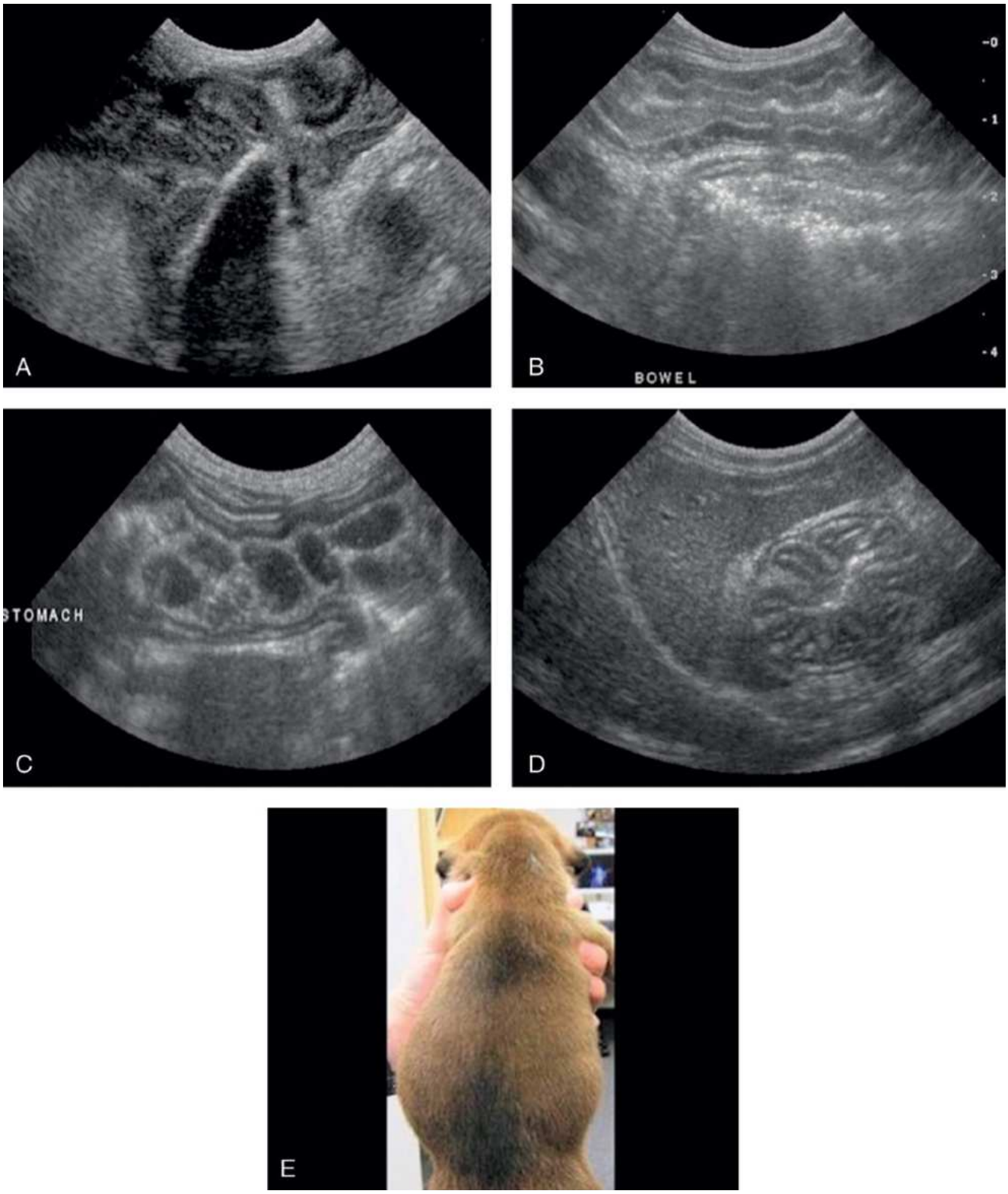


**Figure 16.11.** (A) Linear foreign body producing plication of the small bowel. (B) Undulating appearance of small bowel wall in enteritis. (C) Kibble within the gastric lumen. (D) Normal gastric rugae in the pyloric antrum. (E) Marked abdominal distension in a 3-week-old boxer puppy with an imperforate anus secondary to rectal agenesis.

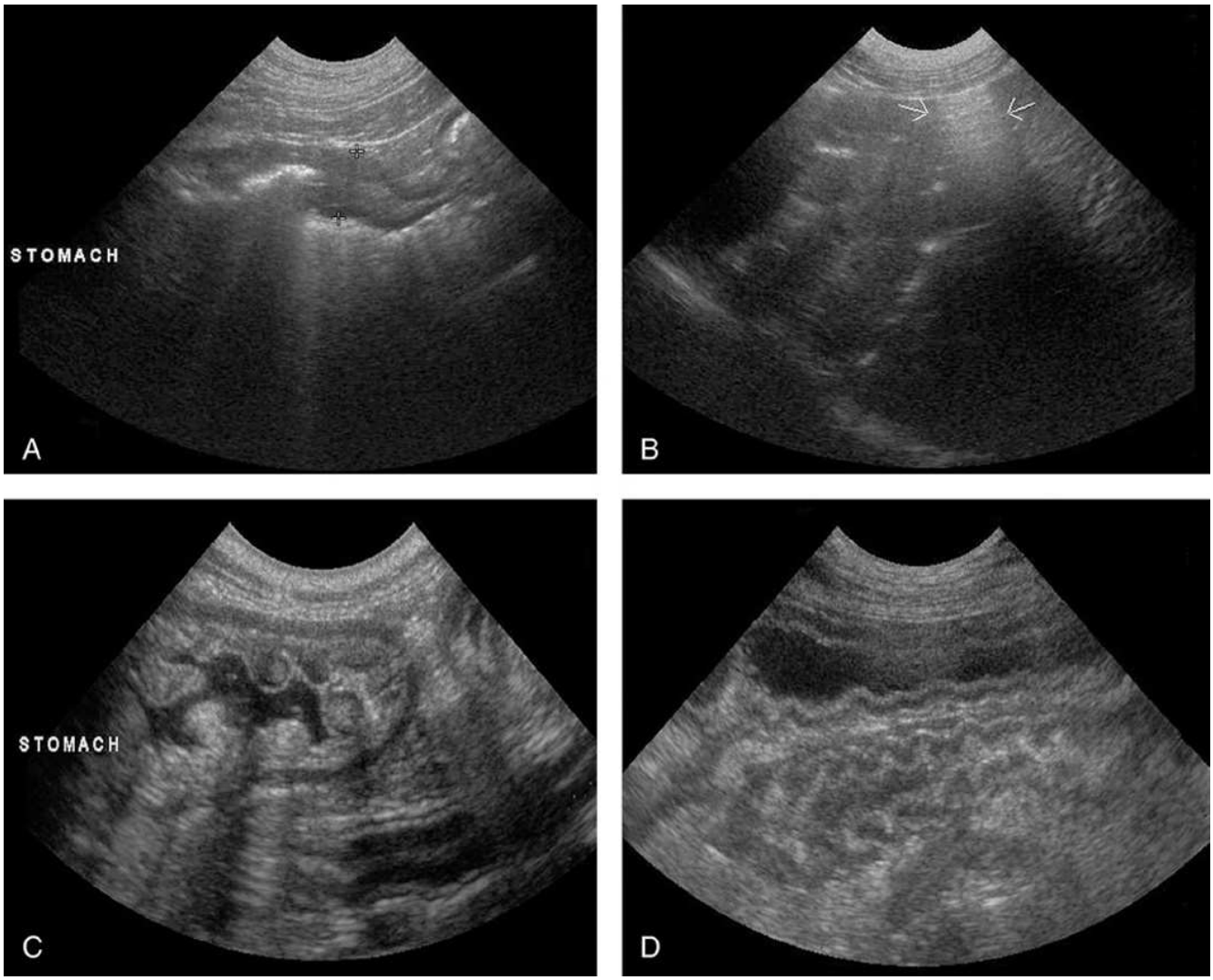


**Figure 16.12.** (A) Disrupted bowel wall (cursors) secondary to perforation. (B) Free air (*arrows*) within the peritoneal space. (C) Edema of the gastric wall associated with viral gastroenterocolitis in a puppy. (D) Increased fluid in the small bowel lumen, corrugated appearance of the bowel wall seen with hemorrhagic viral enteritis.

Several breeds of dogs have a reported genetic predilection for small intestinal disease. An immunoproliferative enteropathy is seen in the Basenji, which is characterized by lymphangiectasia, intermittent diarrhea, weight loss, hypoalbuminemia and hyperglobulinemia, and lymphoplasmacytic mucosal infiltrates throughout the gastrointestinal tract. Histopathology is diagnostic, but abdominal ultrasonography can identify bowel in which disruption of the normal layering has occurred. Chinese sharpei dogs have been identified with a lymphoplasmacytic-eosinophilic infiltrative enteropathy that is characterized by poor weight gain, weight loss, or intermittent diarrhea episodes, with onset of signs typically between 2 and 6 months of age. Infiltrative enteropathies can be characterized ultrasonographically as having changes in the normal bowel wall echogenicity and layering (Penninck 2002b; Baker and Davidson 2006).

## *Intussusception*

Intussusception is not uncommon in young dogs and cats, occurring most frequently at the ileocecocolic junction in dogs and in the jejunum in cats. Pediatric patients are prone to intussusception because they lack the intrinsic enteric neural mechanisms for aboral motility present in adult animals; instead,

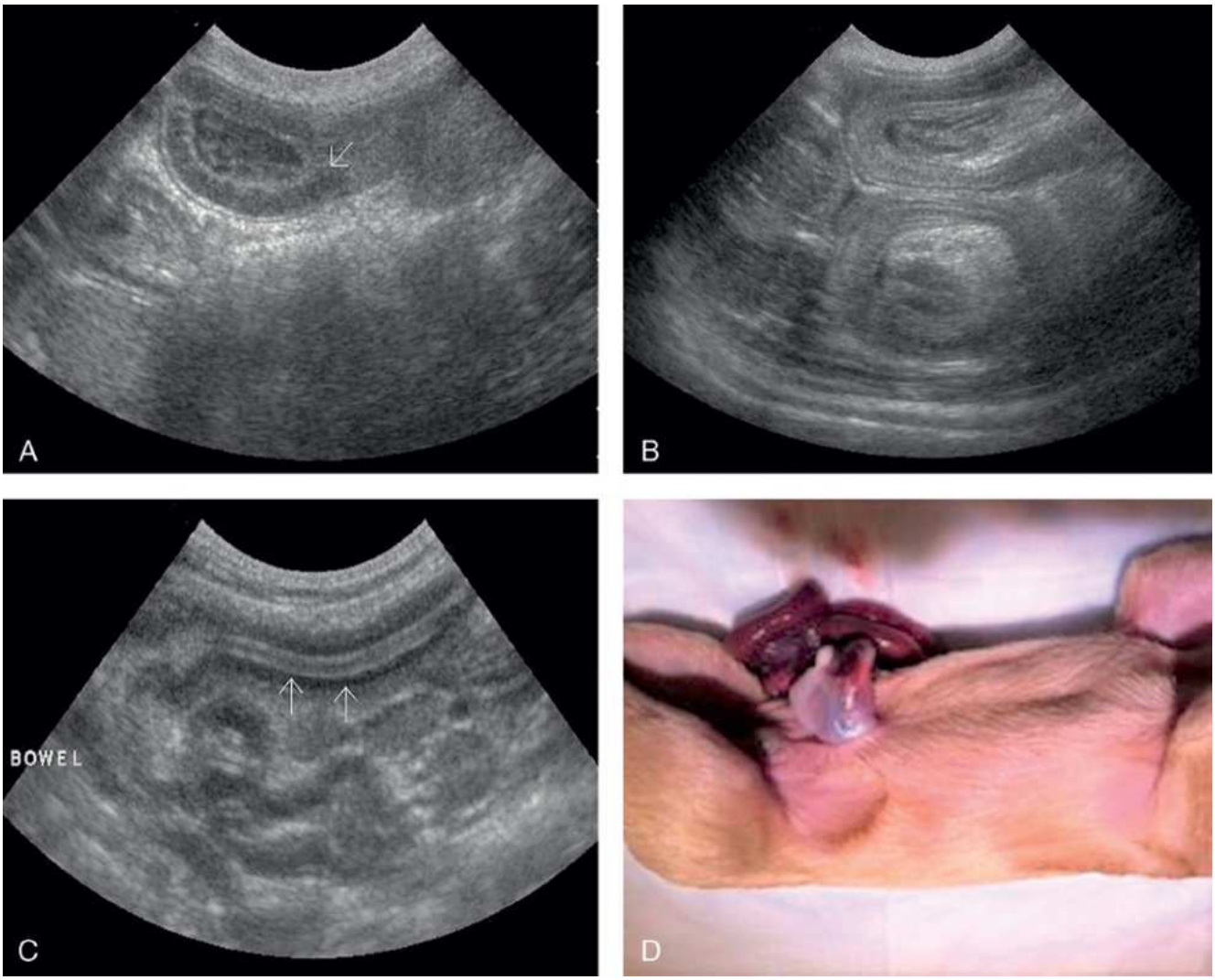


**Figure 16.13.** (A) Small bowel wall thickening and loss of normal layering (*arrow*). (B) Intussusception in two bowel segments; typical bowel within the bowel appearance. (C) Ascarid (*arrows*) in small bowel. (D) Omphalocele in a neonatal dog.

gastrointestinal motility is pressure dependent and based on the sequential ingestion of food. Fasting or vomiting results in ileus and increases the risk of intussusception.

The classic transverse ultrasonographic appearance of intussusception is a multilayered series of concentric rings representing the invaginated bowel wall layers; the outer layer can be edematous (hypoechoic) and the inner layers more normal in appearance (see Figure 16.13B). Discomfort is typically displayed when scanhead pressure is placed over the affected area of bowel. Doppler evaluation of the bowel and associated mesenteric vessels can provide information about bowel viability. Serial examinations are important when evaluating the pediatric patient with a palpable abdominal mass, unanticipated clinical deterioration or increased abdominal pain (Penninck 2002b; Baker and Davidson 2006).

**Pearl:** If an intussusception is diagnosed in the pediatric veterinary patient in a timely fashion, reduction rather than resection might be possible.

### *Enteric Parasites*

Enterocolitis from intestinal parasites can be severe in pediatric patients with high worm burdens. Small bowel helminths can be visualized ultrasonographically as double-walled structures within the fluid-filled lumen (see Figure 16.13C). Movement of helminths can be appreciated with real-time ultrasonography (Penninck 2002b).

### Enteric Thrombosis

A serious consequence of hypercoagulopathic enterocolitis is mesenteric thrombosis resulting in bowel ischemia. Doppler imaging is necessary to identify the thrombus; the resultant hypoechoic bowel wall appearance is visible with real-time ultrasonography (Baker 2009) (see also Section V).

### Congenital Herniation

A developmental anomaly resulting in extrusion of a portion of the gastrointestinal tract outside the body wall, occurring within the umbilical canal (omphalocele) or lateral to the umbilical canal (gastroschisis), has been reported in humans and occurs in both dogs and cats (see Figure 16.13D). The condition is usually hopeless in small pediatric patients presented to the veterinarian hours after birth; however, a 30–70% survival rate is reported in humans with immediate postpartum surgical intervention. Diagnosis is made prepartum with abdominal ultrasound, based on the recognition of fetal gastric wall (rugal) structures or intestinal contents in an abnormal location. Earlier surgical intervention before inevitable septic contamination occurs may improve the prognosis in veterinary patients.

Congenital peritoneopericardial diaphragmatic hernias occur in both the dog and cat; ultrasonography provides an additional modality for their diagnosis. As with other diaphragmatic hernias, careful evaluation for continuity of the echogenic diaphragm differentiates a true hernia from mirror image artifacts (see Figure 16.14F). Evaluation of the pericardial contents can be made from the subcostal (across the liver) or intercostal (using the heart as an acoustic window) approach (Figure 16.14A). Abnormal pericardial contents can include falciform fat, liver, gallbladder, and/or intestines (see Figure 16.14B).

Umbilical hernias can be significant if large enough to permit bowel evisceration and strangulation (see Figure 16.14B). Omentum can become trapped in an open umbilical hernia in immature dogs and cats; closure of the hernia then results in a benign mass effect often alarming to clients. Evaluation of a painful or enlarging umbilical mass usually permits

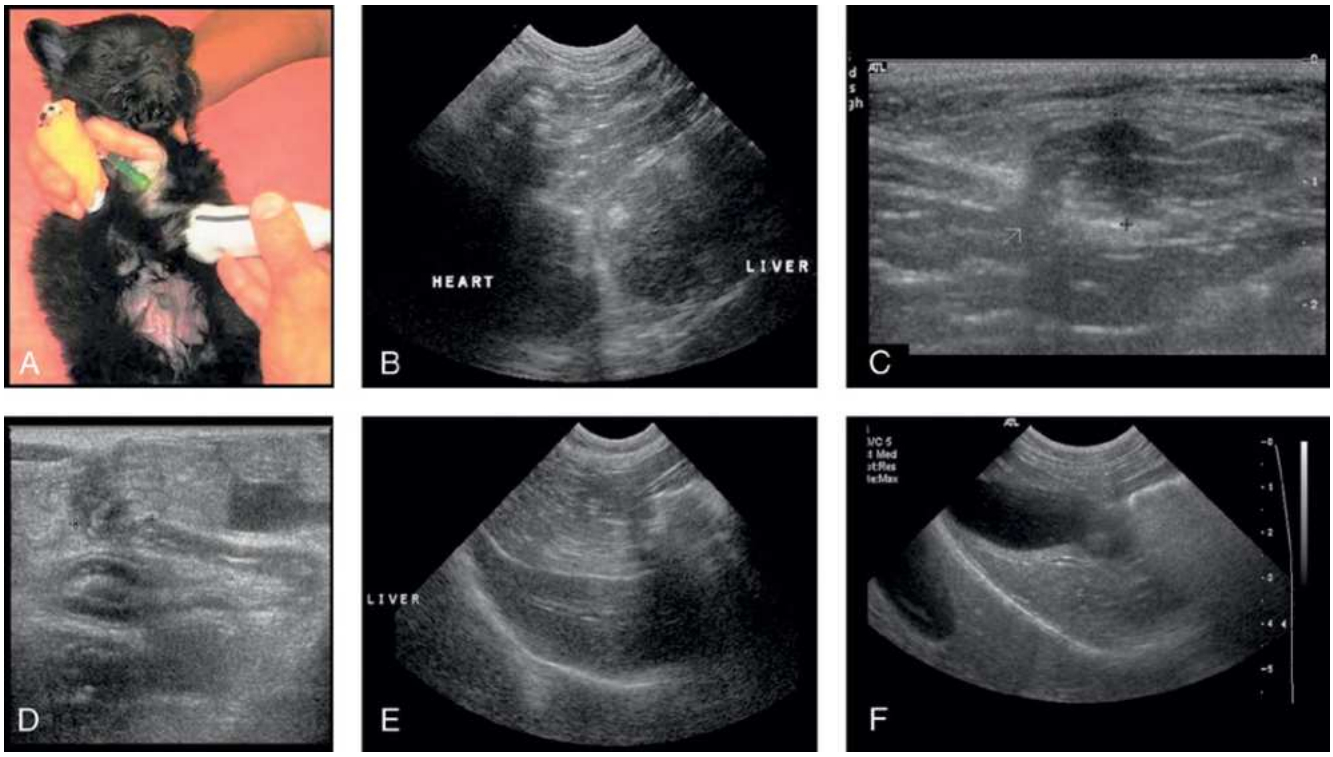


**Figure 16.14.** (A) Intercostal imaging in the pediatric canine. (B) Peritoneopericardial diaphragmatic hernia. (C) Omentum (cursors) trapped in an open umbilical hernia (*arrow*). (D) Inguinal hernia showing entrapment of omentum; small bowel remains within the peritoneal cavity. (E) Microhepatica; falciform fat is seen ventral to the hepatic border. (F) Artifactual mirror image of the gallbladder seen across the diaphragm.

differentiation of omentum from entrapped bowel, which has a typical enteric appearance.

Congenital inguinal hernias can similarly be confirmed by ultrasonographic identification of intestinal structures within the subcutaneous space of the affected groin. This can be a dynamic finding. Mesenteric fat may alternatively be entrapped through the hernia and sometimes becomes strangulated (see Figure 16.14C).

Congenital hiatal hernias are more difficult to confirm with ultrasound because of the inherent difficulty in imaging the gas-filled stomach and the intermittent (sliding) nature of the disorder. Stomach wall with characteristic rugal folds can be imaged crossing the diaphragm into the thoracic cavity (Suter 1984; Baker and Davidson 2006).

**Pearl:** Fluoroscopic evaluation can be more informative in dynamic hiatal hernia cases.

### Acquired Herniation

Traumatic diaphragmatic herniation can result in the presence of stomach, liver, spleen, intestines, and falciform fat in the thorax, usually accompanied by effusion of fluid enhancing imaging (see Figure 16.14D). Failure to identify a contiguous diaphragmatic image supports the diagnosis.

**Pearl:** Thoracic radiography or positive contrast peritoneography can be used to confirm the diagnosis if ultrasound findings are not conclusive (Suter 1984).

## Metabolic Conditions of the Pediatric Patient

### Congenital Portosystemic Shunts

Portosystemic shunts are congenital malformations of the hepatic portal venous drainage system and can have either a familial, that is, genetic, or random occurrence. Congenital portosystemic shunts can be either intrahepatic or extrahepatic; breed predilections for extrahepatic shunts include Yorkshire terrier, Maltese, poodle, miniature schnauzer, dachshund, Lhasa Apso, Pekingese, pug, and shih tzu, whereas intrahepatic shunts are more commonly identified in large-breed dogs such as golden retrievers, German shepherds, Irish wolfhounds, Irish setters, and samoyeds. Portosystemic shunts are uncommon in cats.

Ultrasonography provides a rapid and noninvasive method for screening patients suspected to have congenital portosystemic shunts. Although scintigraphy is considered the most reliable noninvasive method of documenting a portosystemic shunt, its availability is limited to specialty and university practices, and its use requires special handling of the radioactive patient for at least 12 hours. The liver may be small and difficult to image in patients with congenital portosystemic shunts (see Figure 16.14E). Imaging the liver from the standard ventral approach can be improved in some cases by using the left ventral intercostal or right dorsal intercostal approaches (Figure 16.15A). The presence of ascites can facilitate the study, as can adding fluid to the stomach, and positioning the patient to shift gas away from the scanhead and shift abdominal organs caudally (see Figure 16.15B). Ultrasound evaluation of portosystemic anomalies can be facilitated by positive pressure ventilation under anesthesia for the same reason.

Extrahepatic shunts most commonly arise from the portal vein, splenic vein or left gastric vein in the dog, and from the left gastric vein in the cat. Identification of a shunting vessel emptying into the caudal vena cava is difficult but confirmatory. These shunts are often tortuous; Doppler helps identify altered blood flow (see Figure 16.15C,D). Intrahepatic shunts can be more difficult to identify because of patient size, bowel gas, and liver size. Clipping the hair coat intercostally on the right can allow for transverse vessel stacking (of the aorta, vena cava, and portal vein) and visualization of ductal shunts (Figure 16.16). There can be right and left shunting of the ductus (Nyland and Hager 1985; Nyland et al. 2002a; Baker and Davidson 2006; Baker 2009).

### Seizure Disorders

Pediatric patients with focal, partial or grand mal seizures for which no metabolic or toxic etiology can be identified can benefit from intracranial ultrasound. Scanning the brain through the fontanelle, usually partially open in pediatric patients, permits noninvasive evaluation of the ventricles (Baker, personal communication). Evaluation of a normal littermate facilitates recognition of excessive cerebral spinal fluid accumulation by serving as a control (Figure 16.17).

**Pearl:** Evaluation of a normal littermate facilitates recognition of excessive cerebral spinal fluid accumulation by serving as a control.

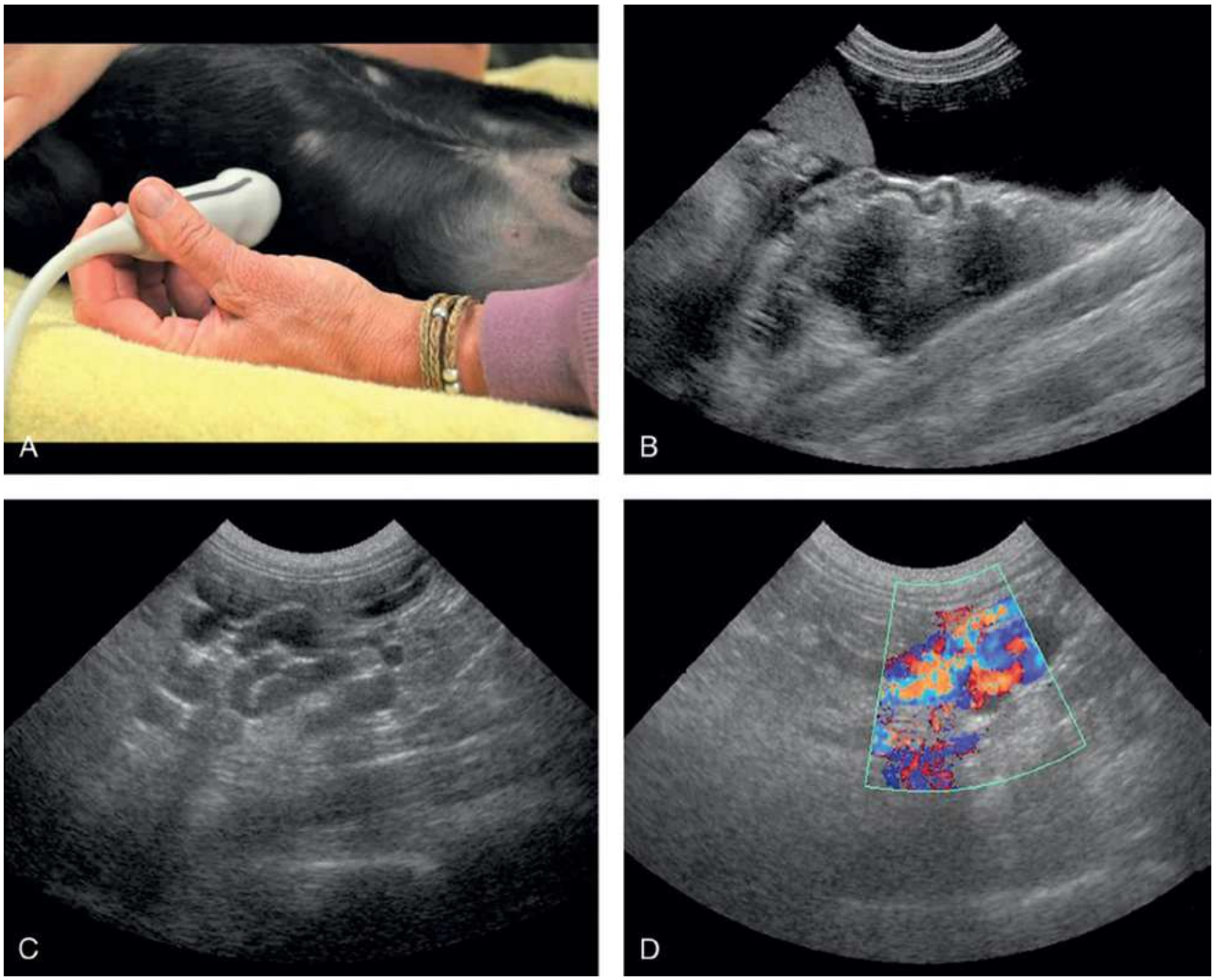


**Figure 16.15.** (A) Intercostal approach for imaging patients with a very small liver. (B) Tortuous extrahepatic shunt vessel seen caudal to the spleen; note ascites. (C) Hairpin extrahepatic shunt vessel. (D) Doppler imaging of extrahepatic shunt showing turbulence.

## *Genitourinary Disorders*

Young dogs and cats are commonly presented to the veterinarian for perceived genitourinary system disorders. While gastrointestinal disorders account for most acute presentations, perceived urogenital disorders account for many others. Clinical differentiation between the characteristics of normal pediatric housebreaking and immature renal function and true urogenital disease can be challenging and is facilitated with ultrasound

### Renal Agenesis

Congenital renal agenesis resulting in the absence of a kidney can be confirmed with ultrasound, but is usually an incidental finding. The contralateral kidney typically has normal internal anatomy, but is enlarged as a consequence of obligatory hypertrophy (Baker and Davidson 2006).

### Renal Dysplasia

Until reliable genetic markers are available for all of the various breed-specific congenital renal dysplasias, ultrasound provides the best method of screening young dogs and cats for these likely heritable disorders. Early ultrasonographic screening is possible in breeds in which morphological changes are grossly evident (i.e., cairn terriers, German shepherd dogs, Persian cats). The kidneys lack normal corticomedullary interface and the renal border can be irregular (Figure 16.18A). The condition is usually bilateral (Baker 2009).

**Pearl:** Severe pyelonephritis can mimic the ultrasonographic appearance of renal dysplasia; clinical differentiation with urinalysis and urine culture helps with discriminating between these conditions (see Figure 16.18A). Feline polycystic disease, also congenital and heritable, can be effectively screened for with ultrasound (see Figure 16.18A).

**Pearl:** Renal function of the pediatric patient does not equal that of the adult until 4–6 months of age; azotemia secondary to renal dysplasia may not occur until adulthood.

### Urogenital Ectopia

Congenital ectopic placement of the distal ureter into the urethra, vestibule or vagina is usually associated with ureteral dilation with or without renal pelvic dilation. Dilation of the ureter improves the sensitivity of the ultrasound study but the diagnosis can still be elusive. Visualization of a nonvascular fluid-filled structure with a hyperechoic wall passing dorsal to the urinary bladder, or obvious insertion of the structure into the proximal urethra suggests the diagnosis. Ectopic ureters display peristalsis if monitored for a few moments. Visualization of a ureteral jet in the bladder suggests normalcy (see Figure 16.18A), but

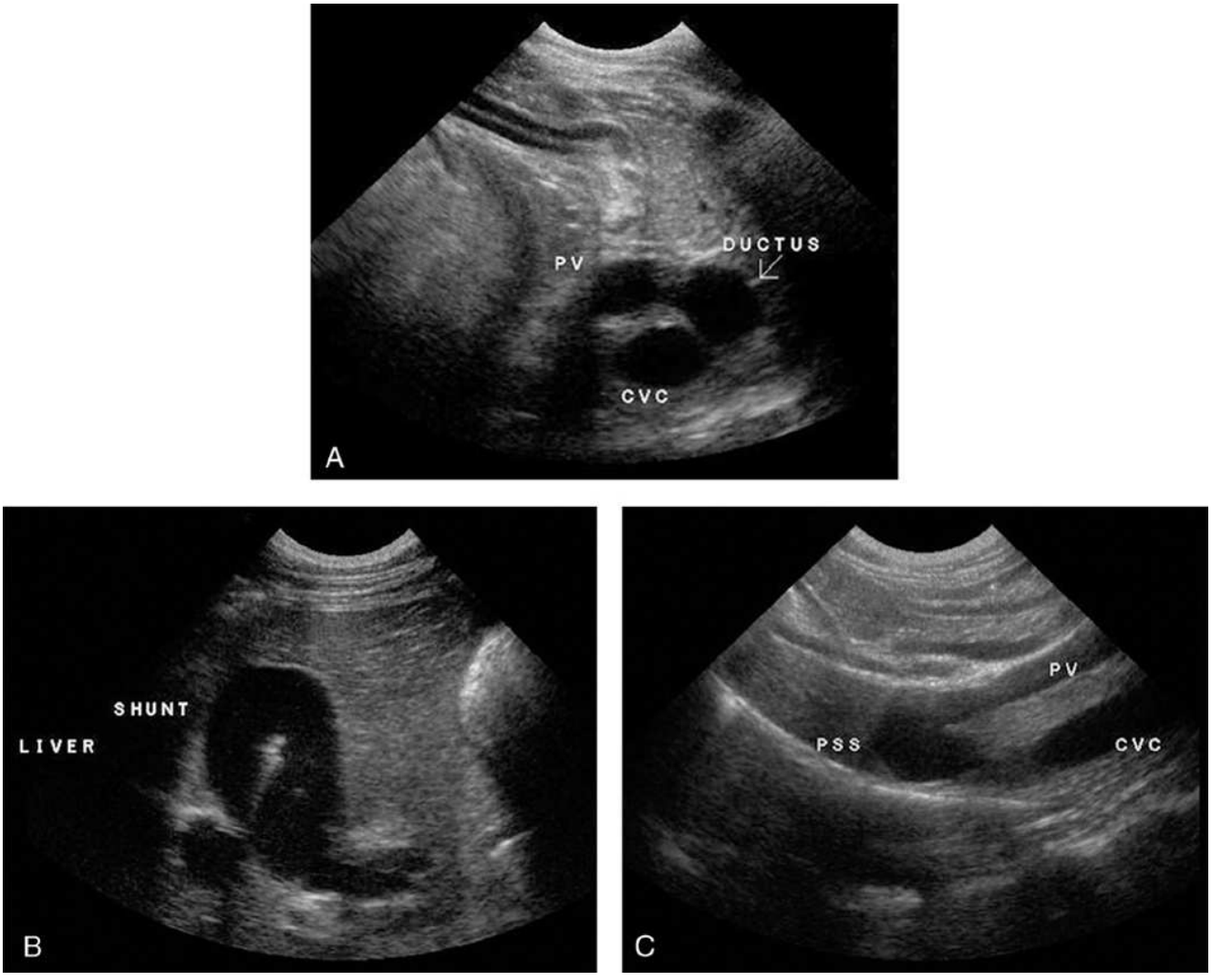


**Figure 16.16.** Examples of intrahepatic shunts. (A) Intrahepatic ductal portocaval shunt (*arrow*). Note the stacking of the vena cava and portal vein. (B) Hairpin intrahepatic shunt vessel; transverse view. (C) Sagittal image of intrahepatic portocaval shunt.

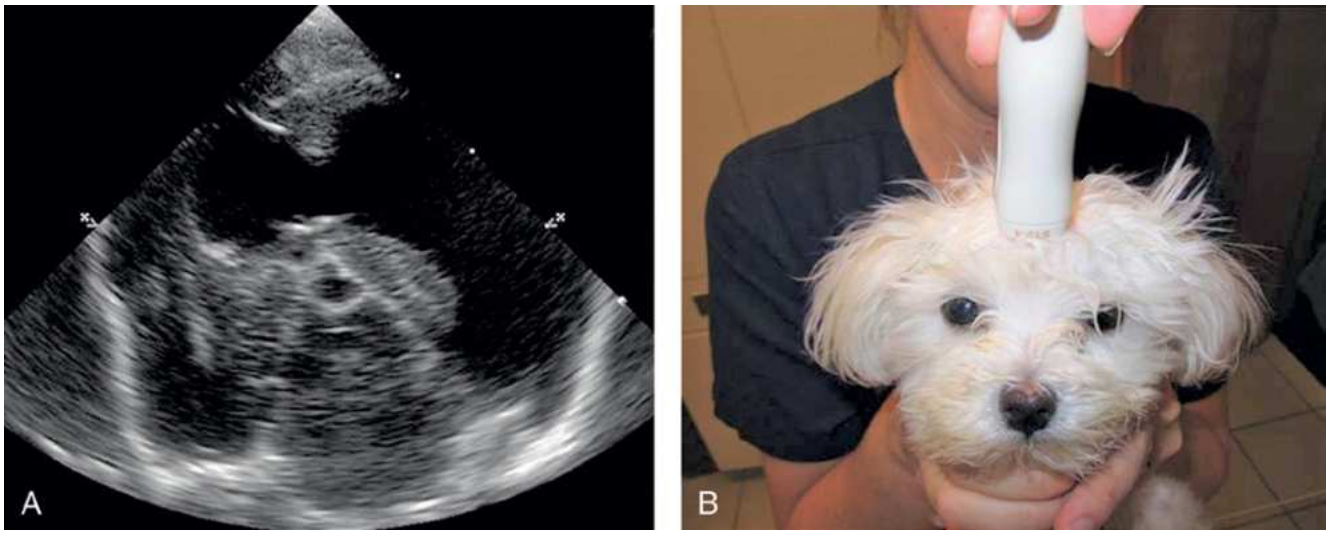


**Figure 16.17.** Hydrocephalus, imaging through open fontanelle. (A) Increased fluid within the ventricles of a hydrocephalic puppy, scanned through the fontanelle. (B) Scanhead placement for imaging through the open fontanelle.

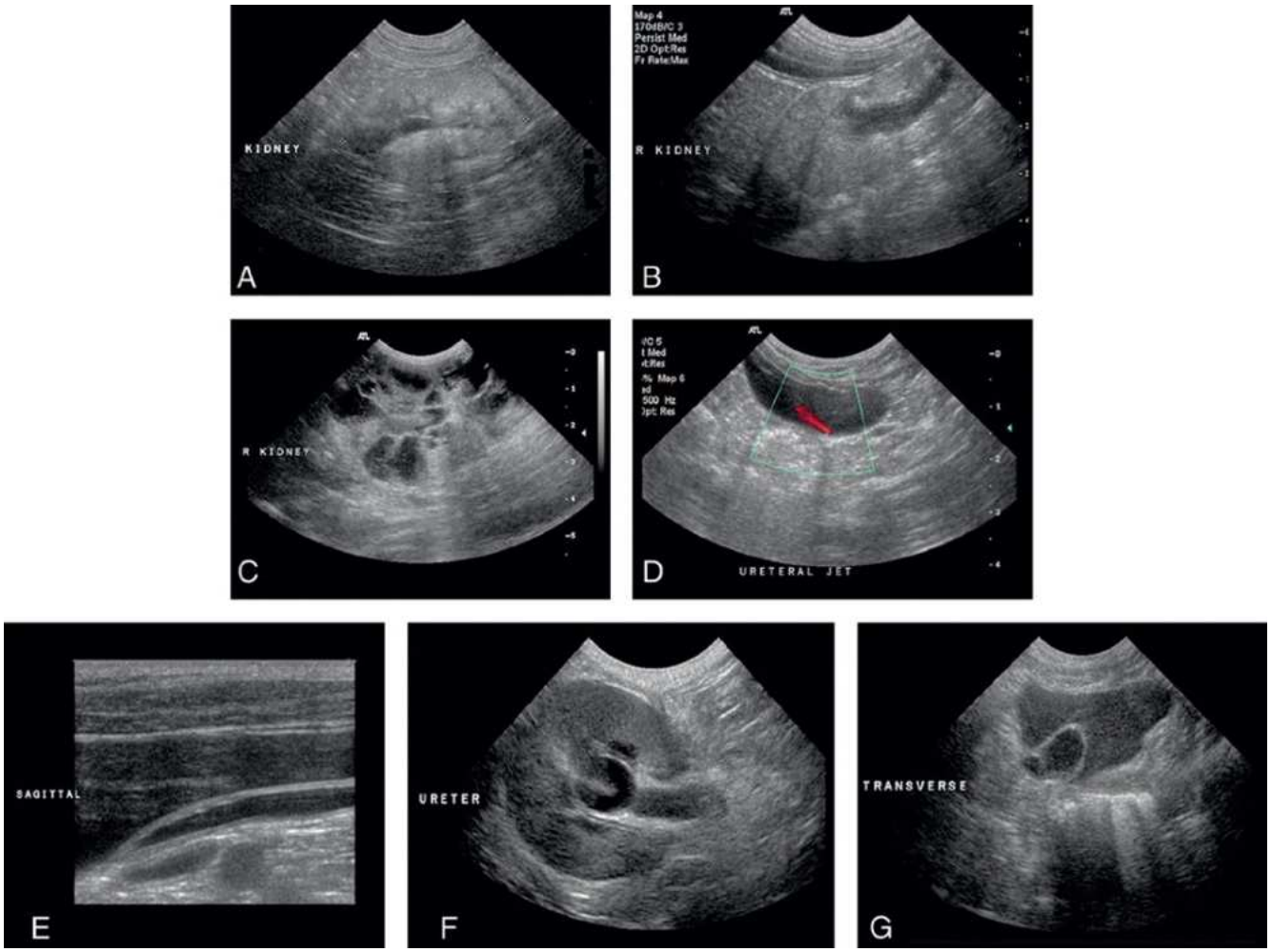


**Figure 16.18.** (A) Renal dysplasia; abnormal kidney structure; note loss of normal corticomedullary interface (thickened cortex). (B) Pyelonephritis; similar appearance to renal dysplasia with chronic dilation of the renal pelvis. (C) Feline polycystic kidney disease; note loss of normal parenchymal anatomy. (D) Visualization of normal ureteral jet in the bladder. (E) Ectopic ureter dorsal to urinary bladder; note hyperechoic walls. (F) Hydronephrosis, with proximal hydroureter. (G) Transverse image of a ureterocele seen in the dorsal right urinary bladder.

some ectopic ureters insert initially into the bladder and additionally tunnel distally to terminate in an abnormal site. Visualization of the dilated ureter usually occurs near the urinary bladder (see Figure 16.18B). Visualization of the bladder neck and proximal urethra may be obscured by the pubic bone, making identification of such termination difficult.

Hydronephrosis can eventually result from an uncorrected ectopic ureter due to flow impedance at the abnormal site of insertion (see Figure 16.18C). Urinary tract infection is commonly associated with ectopia, due to accompanying urethral sphincter mechanism anomalies, and if not detected and treated, can progress to pyelonephritis and ureteritis. Infection and its associated inflammation in the tract can further alter the ultrasonographic appearance of the kidneys, bladder, ureters, and urethra.

Contrast-enhanced computed tomography is the most sensitive and specific modality for the diagnosis of ectopia but, like double-contrast radiography, requires anesthesia, making initial evaluation with ultrasound desirable when ectopia is suspected clinically. Endoscopic evaluation of the vestibule, vagina, bladder, and ureters can also confirm the diagnosis; laser correction of intramural ectopia is possible. The condition is thought to be heritable, and is more common in females (Lamb 1988; Nyland et al. 2002b; Baker and Davidson 2006; Baker 2009).

### Ureterocele

A ureterocele is an uncommon congenital dilation of the ureter near the bladder, appearing as a cystic structure within the bladder lumen or wall. The ureterocele occurs most commonly in association with an ectopic ureter. Diagnosis can be made by scanning the urinary bladder in the transverse plane and watching for strong peristalsis of the tunneling ureter (Lamb 1988; Nyland et al. 2015; Baker and Davidson 2006; Baker 2009) (see Figure 16.18D).

### Urinary Tract Infection

Puppies are frequently presented to the veterinarian because of owner concerns about difficulty achieving housebreaking and the perception that urination is excessively frequent (pollakiuria). Historical differentiation between a history of true pollakiuria and dysuria associated with cystourethritis and the normal frequency of urination in pediatric dogs with immature renal concentrating abilities can be difficult. A urinalysis/urine culture with urine obtained by ultrasound-guided cystocentesis can be diagnostic. The bladder can appear normal in acute urinary tract infection. Chronic urinary tract infection can induce bladder wall thickening (greater than 1–2 mm in a fully distended bladder), especially in the cranioventral portion of the bladder (Figure 16.19A). Similarly, early pyelonephritis can have a normal ultrasonographic appearance; chronic pyelonephritis can produce a dilated renal pelvis, sometimes accompanied by poor corticomedullary definition, increased echogenicity, reduction in renal size, and irregular renal contour (Nyland et al. 2002b; Baker and Davidson 2006) (see Figure 16.19B).

### Urolithiasis

Cystic calculi (radiopaque or radiolucent), visualized as discrete hyperechoic focal echogenicities in the dependent portion of the bladder, occur most commonly in pediatric patients with urinary tract infection (struvite or triple phosphate uroliths) and portosystemic shunts (ammonium biurate uroliths); the presence of a cystic calculus without urinary tract infection in the pediatric patient should actually prompt evaluation for developmental hepatic vascular anomalies. Both urinary tract infection and cystic calculi are more common in female pediatric patients (Nyland et al. 2002b; Baker and Davidson 2006) (see Figure 16.19C,D).

**Pearl:** Both urinary tract infection and cystic calculi are more common in female pediatric patients.

### Patent Urachus

The urachus permits the flow of urine from the bladder into the allantoic sac of the fetus, and normally atrophies at birth. A patent urachus in the neonate is characterized clinically by urine dribbling from the umbilicus. The fluid-filled urachus can be identified ultrasonographically, extending cranially from the cranioventral bladder wall (Figure 16.20A). If an incompletely patent urachus is present in the neonate, a urachal diverticulum may result, seen as a divot in the apex of the bladder (see Figure 16.20B). Urachal diverticula can predispose the bladder to recurrent infection because of abnormal bladder flow in the region, and surgical excision can be indicated (Nyland et al. 2002b; Baker and Davidson 2006).

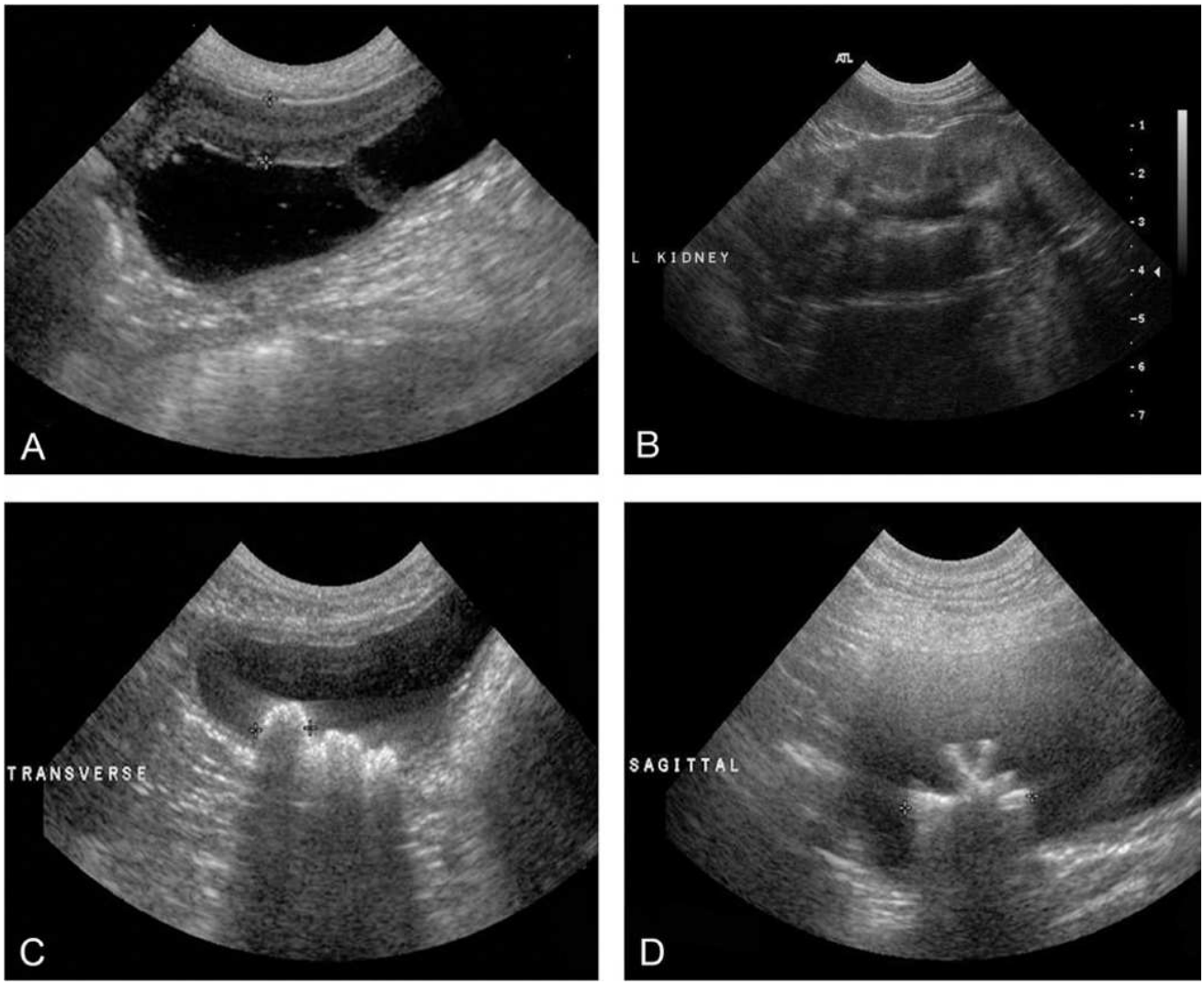


**Figure 16.19.** (A) Thickened urinary bladder wall (cursors) associated with cystitis. (B) Pyelonephritis left kidney; note poor corticomedullary interface, thickened, echogenic cortex and abnormal renal pelvis. (C) Multiple cystic calculi (cursors) identified by strong distal shadowing. (D) Jackstone cystic calculi (cursors).

### Cryptorchidism

Ultrasound localization of cryptorchidism can confirm the condition in pediatric patients with bilateral involvement whose neutering status is unknown, and assist the surgeon in planning the approach (i.e., inguinal vs cranial abdominal). Retained testes can torse and present as an acute abdomen. The retained testis can be positioned anywhere between the ipsilateral kidney and the scrotum. A systematic evaluation of the region from the caudal renal pole to the inguinal canal can identify an oval, homogeneously echogenic structure with a mildly hyperechoic border representing the parietal and visceral tunics (see Figure 16.20C). The epididymis is usually distinctly less echoic than the testicular parenchyma, as in the scrotal testis. The cryptorchid testis will maintain the anatomical structure, the mediastinum testis (a hyperechoic slash), and normal testicular echogenicity despite being reduced in size compared to a scrotal testis, unless malignant transformation has occurred (Eilts et al. 1988; Baker and Davidson 2006) (see Figure 16.20D).

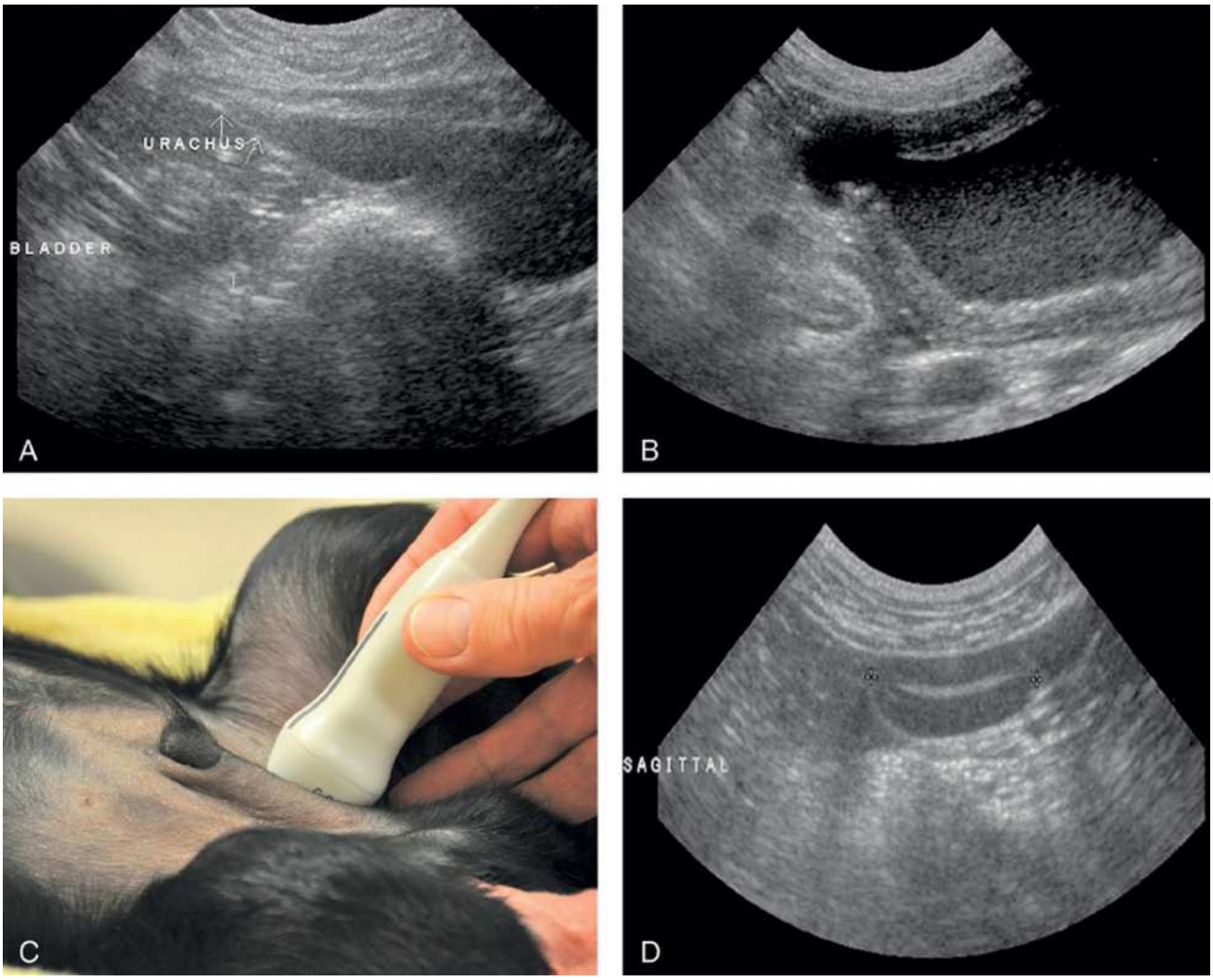


**Figure 16.20.** (A) Patent urachus imaged sagittally at the apex of the bladder (arrows). (B) Urinary bladder wall persistent diverticulum resulting from incomplete regression of the urachus. (C) Sagittal scanning lateral to the prepuce to localize a cryptorchid testis. (D) Cryptorchid testis (cursors); note hyperechoic mediastinum testis.

# Pearls and Pitfalls, The Final Say

POCUS pediatrics performed in a structured manner following basic ultrasonographic principles has the potential to expediently answer important clinical questions when radiographic and laboratory testing are inconclusive or indicate more definitive confirmation; or, conversely, ultrasound findings trigger additional laboratory testing or ancillary imaging; or when delays exist in being able to schedule a complete detailed abdominal ultrasound exam by a veterinary radiologist or ultrasonographically trained specialist to improve pediatric care. The use of the POCUS pediatrics evaluation importantly has the potential to improve pediatric patient care.

# References

Baker TW. 2009. *What's That? A Guide to Basic Veterinary Abdominal Ultrasound*. Lakewood: AAHA Press.

Baker TW. 2012. *What's Next? A Guide to Veterinary Ultrasound of the Eye, Neck and Shoulder and Guided Sampling Techniques*. Lakewood: AAHA Press.

Baker TW, Davidson AP. 2006. Pediatric abdominal ultrasonography. *Vet Clin North Am Small Anim Pract* 36:641–655.

Eilts BE, Pechman RD, Hedlund CS. 1988. Use of ultrasonography to diagnose Sertoli cell neoplasia and cryptorchidism in a dog. *J Am Vet Med Assoc* 192:533–534.

Lamb CR. 1988. Ultrasonography of the ureters. *Vet Clin North Am Small Anim Pract* 28:823–848.

Nyland TG, Hager DA. 1985. Sonography of the liver, gallbladder, and spleen. *Vet Clin North Am Small Anim Pract* 15:1123–1148.

Nyland TG, Mattoon JS, Herrgesell EJ, Wisner ER. 2002a. Physical principles, instrumentation, and safety of diagnostic ultrasound. In: *Small Animal Diagnostic Ultrasound*, 2nd edition, edited by Nyland TG, Mattoon JS. Philadelphia: WB Saunders, pp 1–18.

Nyland TG, Mattoon JS, Herrgesell EJ, Wisner ER. 2002b. Urinary tract. In: *Small Animal Diagnostic Ultrasound*, 2nd edition, edited by Nyland TG, Mattoon JS. Philadelphia: WB Saunders, pp 158–195.

Penninck DG. 2002. Artifacts. In: *Small Animal Diagnostic Ultrasound*, 2nd edition, edited by Nyland TG, Mattoon JS. Philadelphia: WB Saunders, pp 19–29.

Penninck DG. 2002. Gastrointestinal tract. In: *Small Animal Diagnostic Ultrasound*, 2nd edition, edited by Nyland TG, Mattoon JS. Philadelphia: WB Saunders, pp 207–230.

Suter PF. 1984. Abnormalities of the diaphragm. In: *Thoracic Radiography: A Text Atlas of Thoracic Disease in the Dog and Cat*, edited by Suter PF, Lord PF. Wettswil, Switzerland: Peter F. Suter, pp 180–204.

SECTION IV

# Thorax

CHAPTER SEVENTEEN

# POCUS: TFAST – Introduction and Image Acquisition

Gregory R. Lisciandro

## Introduction

The thoracic FAST (TFAST) examination was first published in 2008, focusing on the diagnosis of pneumothorax in a large prospective study of 145 dogs with blunt and penetrating trauma (Lisciandro et al. 2008). The study also documented other intrathoracic injuries by detecting free fluid (pleural and pericardial effusion) and lung injury. TFAST was the first standardized, nonecho ultrasound examination of the thorax for veterinarians. The original study did not publish the diaphragmatico-hepatic (DH) view but this view is advantageous on a number of fronts including serving as an acoustic window via the liver and gallbladder into the thorax for pleural and pericardial effusion and lung pathology along the pulmonary-diaphragmatic surface (Boysen et al. 2004; Lisciandro et al. 2009; Lisciandro 2011, 2012, 2014a,b, 2016; Boysen and Lisciandro 2013; McMurray et al. 2016). Moreover, the caudal vena cava is imaged for volume status during fluid resuscitation, which is helpful for detecting right-sided cardiac strain/failure/overload, the abdominal cavity is surveyed for free fluid, and the liver and gallbladder for any soft tissue abnormalities (Quantz et al. 2009; Nelson et al. 2010; Lisciandro 2011, 2016, 2019; Lisciandro and Armenise 2014; Darnis et al. 2018).

Since day 1 in 2005 when the author developed AFAST and TFAST, the two examinations have been combined and referred to as combination (Combo) FAST, learning quickly by experience that by doing only one or the other FAST examination, serious conditions are easily missed (Lisciandro 2012). Moreover, the author has advocated that AFAST and TFAST be used *first line* as an extension of the physical exam. With the more recent addition of a more comprehensive lung examination, called Vet BLUE (Lisciandro et al. 2014, 2017), the author has since changed the term from Combo FAST to Global FAST, which is AFAST, TFAST, and Vet BLUE combined into a single ultrasound format (Lisciandro 2012, 2019; Lisciandro and Armenise 2014). The use of AFAST, TFAST, and Vet BLUE extends beyond trauma to triage (nontrauma) and tracking (monitoring).

In 2016, a prospective nontrauma case series applied AFAST and TFAST in combination to 100 cases (82 dogs, 18 cats). The authors found that 75% of cardiovascularly unstable or respiratory-compromised patients were positive for free fluid. They also documented a positive rate of approximately 10% for those considered to be stable. Interestingly, this nontrauma study had a median time post presentation to the AFAST-TFAST studies of 1.75 and 2.5 hours for unstable and stable patients, respectively, with an overall median time of two hours (range 0–12 hours) (McMurray et al. 2016). In other words, AFAST-TFAST generally were not used first line as part of initial patient assessment. One has to wonder during the interval of ~2 hours between presentation and AFAST-TFAST examination: How accurate and appropriate were the types of resuscitation? The ordered therapy? The diagnostic testing? Despite the much lower positive rate of ~10% in the stable patients, it is important to realize that missing a serious condition in one out of 10 dogs and cats, *your* patients, would be considered *significant* to many

*Point-of-Care Ultrasound Techniques for the Small Animal Practitioner*, Second Edition. Edited by Gregory R. Lisciandro.
© 2021 John Wiley & Sons, Inc. Published 2021 by John Wiley & Sons, Inc.
Companion website: www.wiley.com/go/lisciandro/ultrasound2

clinicians and pet owners. Moreover, Vet BLUE was not included and could have potentially added more positive studies by surveying more lung. Lastly, the study was important in (1) documenting the clinical relevance of applying AFAST and TFAST in combination (Lisciandro 2012), (2) the high frequency of positive examinations in unstable patients, and (3) that AFAST-TFAST proficiency could be attained with proper training and proctored examinations although there was only a single sonographer involved in the scanning (McMurray et al. 2016).

Before we begin this chapter, it is important to acknowledge that TFAST is far more than a "flash exam" of the thorax (Lisciandro and Mann 2019). It is also important to acknowledge that relative to AFAST and Vet BLUE, TFAST is the most challenging to learn. TFAST is more complex because of the probe handling and machine manipulation to acquire images that involves the dynamics of a beating heart and phases of respiration as well as interpretation of air-related artifacts. TFAST, like AFAST, is a cerebral approach, assessing the thorax and its components of thoracic wall, pleural cavity, pericardial sac, lung and volume status in a standardized goal-directed manner with clearly defined acoustic windows. Moreover, TFAST is generally completed in a matter of minutes (Lisciandro et al. 2008, 2009; Lisciandro 2011, 2014a; Boysen and Lisciandro 2013; McMurray et al. 2016). The standardized approach helps rule in and rule out easily identified serious conditions that would otherwise be missed or delayed in their detection based on less sensitive means of physical examination, blood and urine testing, and radiography (see Table 18.1). TFAST (and Global FAST) gives diagnostic power (evidence-based) to the attending veterinarian by actually "seeing" the problem list by "seeing" the conditions. Lastly, since his internship, the author has abided by the axiom to "never send a patient out the door with something you could have easily diagnosed." The Global FAST approach is the new "quick assessment test" that modernizes this statement.

## What TFAST Can Do

- Can rapidly detect with high accuracy, sensitivity, and specificity pneumothorax in traumatized dogs and cats.
- Can determine the degree of pneumothorax (in other words, its severity) as "partial" versus "massive" by finding the "lung point."
- Can detect and monitor pleural effusion, initially and serially.
- Can detect and monitor pericardial effusion, initially and serially.
- Can determine the presence or absence of cardiac tamponade.
- Can be used as a soft tissue examination of the heart.
- Can detect and monitor lung contusions initially and serially; however, lung contusions are better detected, tracked and scored using the Vet BLUE lung contusion scoring system (see Chapters 22 and 23).
- Can detect thoracic wall, pleural space, and lung pathology through the presence of the "step sign."
- Can assess volume status and contractility (fractional shortening, FS%) by using the TFAST right pericardial site (PCS) view to evaluate the left ventricular short-axis "mushroom" view.
- Can assess left cardiac strain/failure/overload by using the TFAST right PCS view to evaluate the left atrial to aortic ratio (LA:Ao) on short-axis.
- Can assess right cardiac strain/failure/overload by using the TFAST right PCS view to evaluate the right ventricular to left ventricular ratio (RV:LV) on long-axis.
- Can screen for right atrial and auricular masses at the TFAST left PCS view.
- Can screen for intracardiac and extracardiac masses at any of the TFAST echo views.
- When combined with Vet BLUE, can assist in respiratory distress evaluation, rapidly determining pulmonary versus cardiac causes.
- When combined with Vet BLUE, can assist in respiratory distress cases by rapidly supporting different types of lung disease including forms of pulmonary edema (cardiogenic, noncardiogenic), pneumonia, pulmonary thromboembolism, and neoplastic conditions.
- Can be used to serially monitor intrathoracic conditions including pleural, pericardial, heart and lung conditions at point of care in place of serial radiography or computed tomography (CT).

## What TFAST Cannot Do

- Cannot reliably characterize pleural fluid; sample acquisition (thoracocentesis) and fluid analysis is necessary.
- Cannot reliably characterize pericardial fluid; sample acquisition (pericardiocentesis) and fluid analysis is necessary.
- Cannot fully replace thoracic radiography (TXR).
- Cannot fully replace complete echocardiography.

- Cannot fully replace computed tomography (CT).
- Cannot diagnose nonthoracic causes of respiratory distress, the so-called nonrespiratory lookalikes within the peritoneal cavity – hemoabdomen, canine anaphylaxis, and causes of acute abdomen; and retroperitoneal space conditions – bleeding from adrenal, vena cava, and aortic sources and other renal-related or spinal-related sources of free retroperitoneal fluid, without AFAST.
- TFAST is limited in its pulmonary evaluation because it has only two acoustic windows for lung compared to the nine acoustic windows of Vet BLUE.

### Indications

- Blunt and penetrating trauma.
- Nontrauma triaged cases (weakness, collapsed, "ain't doing right" (ADR), changes in breathing patterns).
- All respiratory distress.
- Trauma cases for lung contusions.
- Nontrauma cases for evidence of various forms of alveolar-interstitial edema and pulmonary hemorrhage.
- Pneumothorax (PTX) for detecting and assessing severity using the "lung point" in standing or sternal, tracking pneumothorax using the "lung point," and deciding whether thoracocentesis is indicated by the "TFAST PTX 1/3s Rule" for the "lung point" as the upper third, middle third, and lower third of the thorax (see Chapter 18).
- Pleural effusion for detecting, tracking, and estimating its severity using the PCS view measurements at the level of the costochondral junction (see Chapter 18).
- Pericardial effusion for detecting, tracking, and estimating its severity using widest measurements at the DH view and PCS view measurements at the level of the costochondral junction (see Chapter 18).
- Surveying at-risk small animals for pneumothorax, pleural effusion, and pericardial effusion, including any and all postinterventional/procedural cases (thoracic surgery, thoracoscopy, lung lobe aspirates, other at-risk procedures, mechanical ventilation, and post anesthesia).

### Objectives

- Understand TFAST and its five acoustic windows.
- Be able to perform TFAST image acquisition.

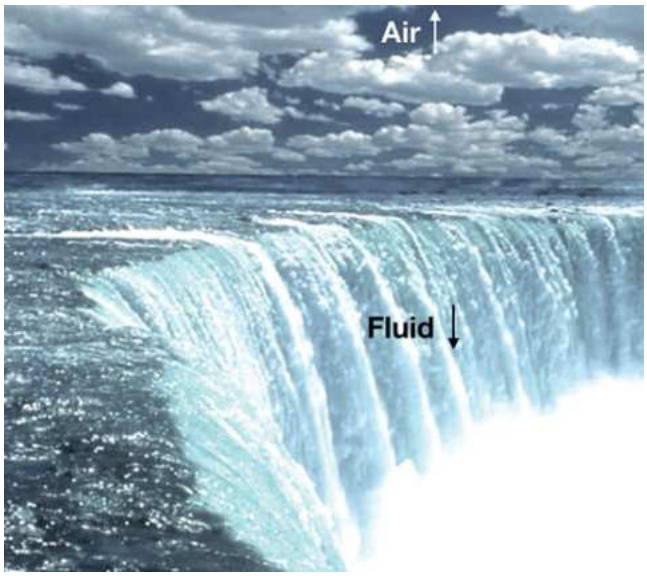


**Figure 17.1.** Air rises and fluid falls. Air rises (nongravity dependent) and fluid falls (gravity dependent) within cavities and spaces (*arrows*). Thus the chest tube site (CTS) view is used for pneumothorax and the pericardial site (PCS) and DH views for pleural and pericardial effusion.

- Understand the principle that air rises (nongravity dependent) and fluid falls (gravity dependent) (Figure 17.1).
- Understand the pitfalls and artifacts of each of the TFAST views.

## What Clinical Questions are Answered using TFAST

### Binary Answers – Yes or No, Unremarkable or Abnormal

- Does the patient have pleural effusion (PE) – free fluid in the pleural space?
- Does the patient have pericardial effusion (PCE) – fluid in the pericardial sac?
- Does the patient have cardiac tamponade?
- Does the patient have pneumothorax – free air in the pleural space?
- Does the patient have evidence of systolic dysfunction?
- Does the patient have evidence of right-sided heart dysfunction/strain/failure/overload?
- Does the patient have evidence of left-sided heart dysfunction/strain/failure/overload?
- Does the patient have any intracardiac abnormalities?
- What is the patient's volume status?
- Does the patient have any obvious lung pathology?

### *Cerebral Approach – Integrating Information*

- What is the degree of PE (measure)?
- What is the degree of PCE (measure)?
- What is the degree of pneumothorax using the "lung point" and the TFAST PTX 1/3s Rule?
- What is the patient's volume status (Global FAST)?
- Where is the volume loss (Global FAST)?
- Does the patient have left-sided congestive heart failure (Global FAST)?
- Does the patient have right-sided congestive heart failure (Global FAST)?

## TFAST and Its Five Acoustic Windows

TFAST consists of five acoustic windows (views) having exact clarity as follows: bilaterally the chest tube site (CTS) and PCS views, plus the single DH view (Figure 17.2) (Lisciandro 2014b, 2016; McMurray et al. 2016). The DH view is part of the TFAST, AFAST, and Vet BLUE formats, providing a large amount of clinical information including screening for pleural and pericardial effusion, lung conditions, cardiac problems, and patient volume status, and within the abdomen for soft tissue screening of the gallbladder and liver and for ascites (Lisciandro 2011, 2014a,b, 2016; Boysen and Lisciandro 2013; McMurray et al. 2016).

The strengths of the respective views are as follows.

- The CTS views are for pneumothorax, free air in the pleural cavity, because air rises (see Figures 17.1 and 17.2), and it is best practice to have your patient in standing or sternal for the "lung point" (see Chapter 18).
- The PCS views are for detecting pleural and pericardial effusion, free fluid in the pleural cavity and pericardial sac, because fluid falls because it is gravity dependent (see Figures 17.1 and 17.2), and for the TFAST echo views.
- The DH view is for pleural cavity, pericardial sac, heart and lung imaging with less air interference than the transthoracic TFAST views, taking advantage of the acoustic window of the liver and gallbladder; for ascites and soft tissue abnormalities of the liver and gallbladder; and volume status via the caudal vena cava and hepatic veins.

## Peforming TFAST – General Set-Up

### *Ultrasound Settings and Probe Preferences*

- Curvilinear (microconvex) probe with a range of 5–10 MHz. A linear probe may also be used for lung ultrasonography (see Chapters 22 and 23) and a phased-array probe for cardiac imaging, although the curvilinear probe is sufficient and faster without probe changes during TFAST.
- Presets of either the abdominal or cardiac settings may be used depending on how your ultrasound machine performs. Most ultrasound machines perform well on the abdominal preset for the entire Global FAST, which is favored by the author and much faster than switching presets.
- The focus cursor, on most machines, should be placed at the level of the region of interest, generally midscreen or across from the "lung line" when evaluating lung (see Chapter 5).

### *Ultrasound Screen Orientation*

The abdominal preset and all others on your machine likely are consistent with cranial (the head) to the left of the screen and caudal (the tail) to the right of the screen. When using cardiac presets, the orientation is switched, which is very confusing for the noncardiologist sonographer. The cardiac preset may be maintained but the orientation changed back using the reverse button on the machine or rotating the probe 180° to maintain the consistency of orientation with the head always to the left (cranial) of the screen and the tail to the right (caudal). In human medicine, institutions have decided on implementing this uniform orientation in people even with cardiac imaging.

**Figure 17.2.** (*Continued*) the patient's left, which will at the same time accelerate DH view image acquisition proficiency. In (B) the CTS view is performed the same as on the left. The TFAST right PCS view cartoons of the echo views must be learned and compared to (A) as they are uniquely different. The DH view, although shown on the right side, is better performed from the patient's *left* side because of the anatomical features of the gallbladder and CVC lying more right-sided in both dogs and cats. Although shown on a dog, the TFAST examination is analogous for cats. Source: Reproduced with permission from Dr Gregory Lisciandro, Hill Country Veterinary Specialists and FASTVet.com, Spicewood, TX.

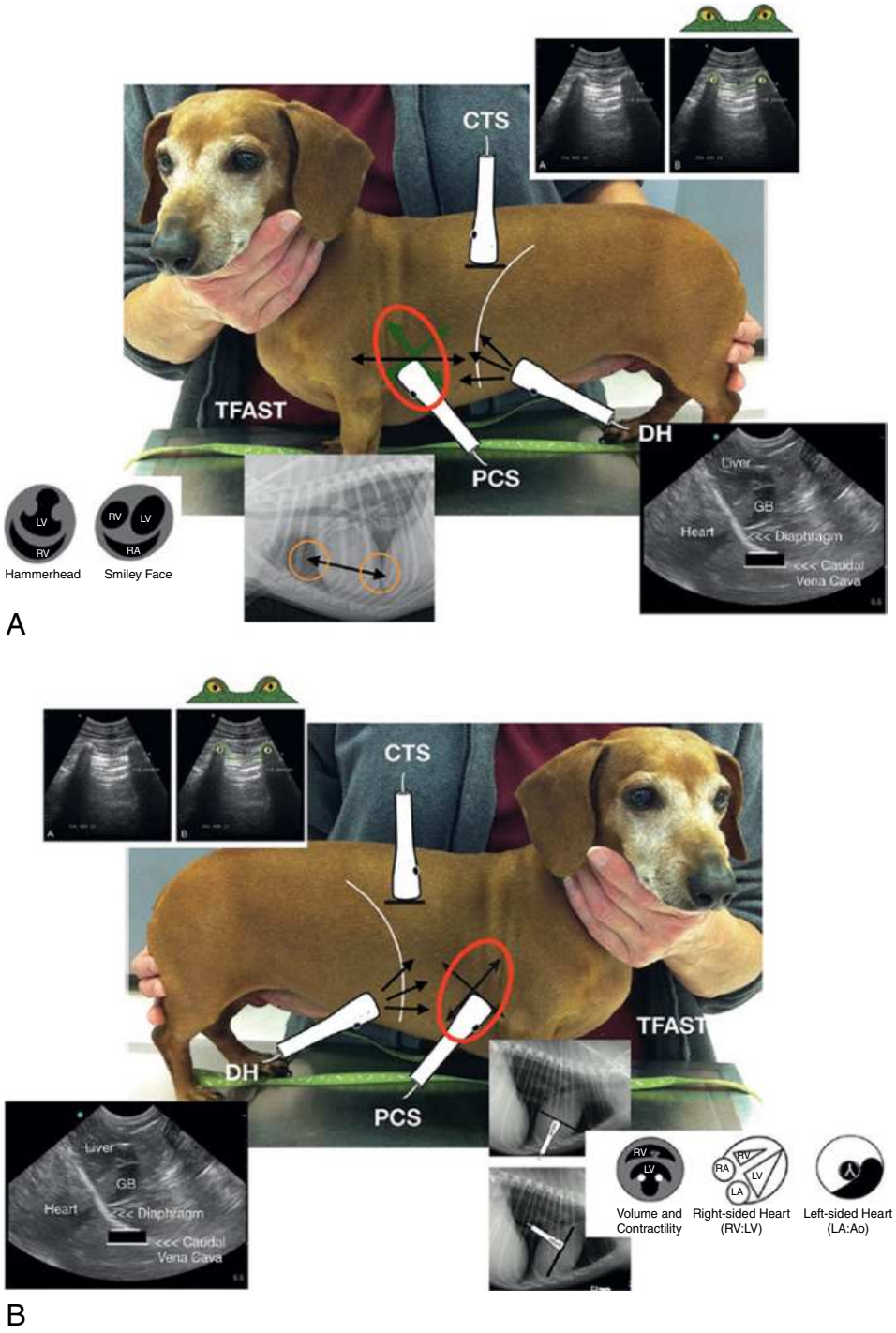


**Figure 17.2.** The five acoustic windows of TFAST in a standing dog. There is a lot of information in these figures showing TFAST on the patient's left and right sides. In (A) the *left* TFAST is shown. The CTS view is the same on both hemithoraces and its "gator sign" orientation for identifying the view's intercostal space(s). The heart's relative position is indicated by the red outlined oval. The left PCS view is quite different from the right PCS view. The probe is held *horizontally* for imaging the left apical view and then slid cranial and caudal to the heart (*arrow*), called the "TFAST slide," for pleural effusion and other pleural cavity abnormalities. The cartoons of the left PCS view heart orientation should be learned and compared to the very different echo views at the right PCS view in (B). The DH view also is dependent on side. The caudal vena cava (CVC) and the gallbladder are more right-sided, so performing the DH view from the patient's left is generally more comfortable and works far better for right-handed sonographers. Muscle memory occurs through performing the DH view the same way every time from

The important point here is to note that commonly, the head is no longer to the left of the screen when changing to a cardiac preset (unless you reverse the marker or modify your probe orientation), and the change in orientation must be acknowledged by the sonographer for proper spatial awareness and interpretation (see Figures 1.6 and 5.3).

## Machine Positioning

Where the machine is located is hugely important for imaging the patient accurately and for the safety of the sonographer, assisting staff, and patient. The machine and the head of the patient should always be in the *same* sightline (see Figure 5.3). When this rule of thumb is violated, spatial orientation for the sonographer may be affected as well as the performance of ultrasound-assisted and ultrasound-guided procedures. Moreover, the sonographer and assisting staff are generally looking at the ultrasound screen and not the head of the patient so if the patient is becoming cyanotic or decompensating, it may not be recognized when their head is facing the other way. Moreover, if the patient turns to bite or scratch the sonographer and assistant(s), it is more difficult to move quickly out of the way. Pain is a powerful teacher, and insisting on the patient's head and machine in the same sightline was a lesson learned the painful way (dog bite) by the author when developing TFAST in 2005.

## Patient Positioning

In patients that present standing or in sternal, it is generally a good idea to perform TFAST prior to any patient restraint in case the patient is hemodynamically fragile. By beginning with TFAST (and Vet BLUE), intrathoracic life-threatening conditions that can potentially become catastrophic with patient restraint or transport are initially detected and promptly addressed, such as need for centesis for PTX, PE or PCE. When critical patients present in lateral recumbency, TFAST and AFAST are generally performed without moving the patient, and before moving the patient to sternal or standing to evaluate the contralateral hemithorax for the opposing CTS and PCS views.

Right lateral recumbency (versus left lateral recumbency) is generally preferred because it is the standard positioning for electrocardiographic and echocardiographic evaluations and may be arguably more reliable for gallbladder, caudal vena cava, and hepatic venous imaging, although sonographers skilled at performing TFAST and AFAST in left lateral may disagree. In either lateral, the four AFAST views and the ipsilateral TFAST PCS view can be performed at nearly the same depth setting (7–15 cm) on the abdominal preset prior to going to a more shallow depth (4–8 cm) for the CTS view. Thus, six of the eight TFAST-AFAST views are rapidly completed (Figure 17.3). If PTX is suspected, move to sternal or standing to search for the lung point to more accurately assess the degree of PTX (see lung point section) and perform thoracocentesis immediately if unstable as per clinical judgment.

A modified lateral-sternal recumbency position is another option to allow the patient to ventilate more efficiently when in respiratory distress. The modified lateral-sternal position is acquired by allowing the thorax to be in sternal while having the forelegs positioned laterally toward the sonographer (Figure 17.4). The position gives an estimate of the abdominal fluid score without the patient having to be in purely a lateral recumbent position (see Figure 6.4).

Dorsal recumbency should *never* be used for several important reasons, including the increased stress in dorsal recumbency for respiratory and hemodynamically fragile patients, and the invalidation of the AFAST-applied fluid scoring system (validated only in lateral recumbency; see Chapters 6 and 7). When moving a patient into dorsal recumbency, their ventilation is changed by the weight of the abdominal organs against the diaphragm and reversing the least gravity-dependent, most aerated lung to become the most gravity-dependent position within the thorax. The combination negatively affects ventilation. In addition, dorsal recumbency causes the weight of the abdominal organs to compress the cauda vena cava and aorta, affecting circulation and, most importantly, venous return to the heart (see Figure 6.5). Thus, if your patient had a known or unknown preload problem prior to being moved to dorsal recumbency, their status could catastrophically change if placed and restrained in dorsal recumbency. In human medicine, it has been said, "Death begins in radiology. Never send a human patient to radiology without a good physical exam and an EFAST (essentially a Global FAST)." The same could be said in veterinary medicine when deciding on the safety of dorsal recumbency positioning for your patient.

**Pearl:** A tip for gaining a TFAST PCS view is to place a rolled towel under the forelegs of a sternally recumbent patient (see Chapters 19 and 39). By doing so, the sternum is elevated off the tabletop, optimizing maneuverability of the ultrasound probe (see Figures 19.2 and 39.28).

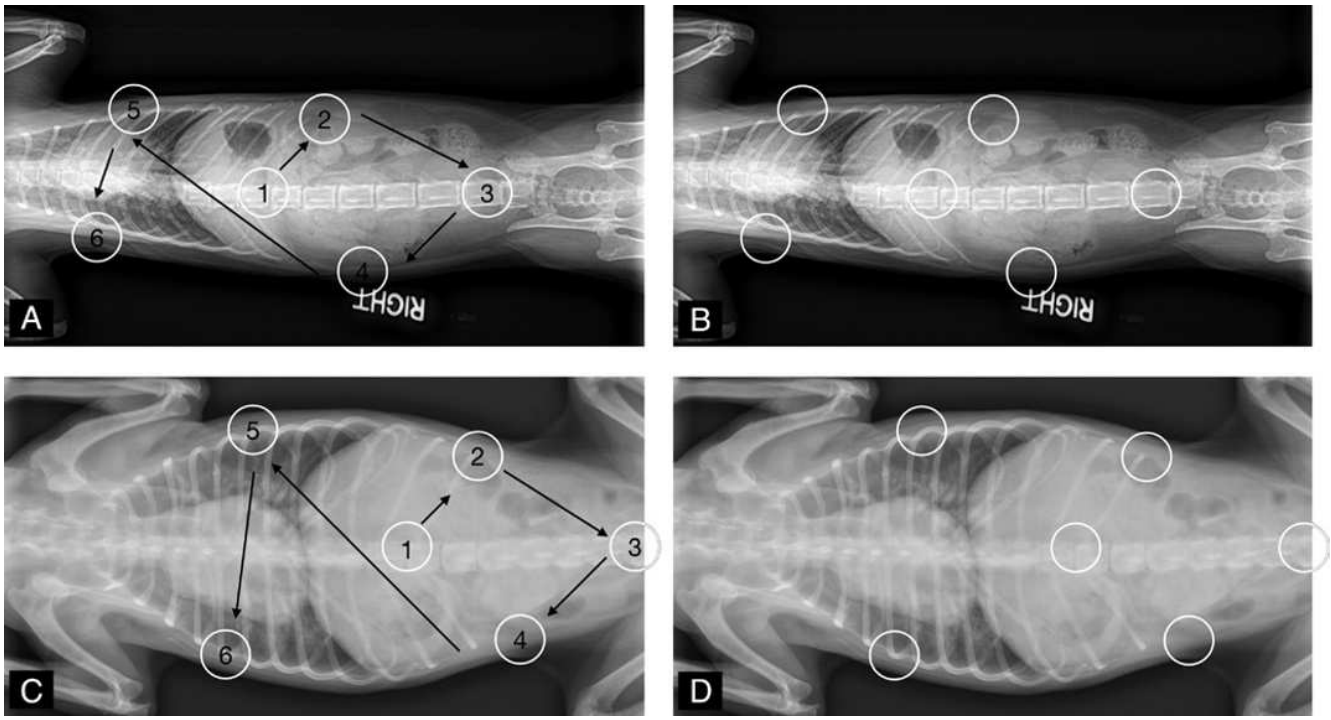


**Figure 17.3.** Most efficient way to perform the AFAST-TFAST echo view blend in right lateral recumbency. If your patient presents in either lateral recumbency you may quickly and efficiently blend AFAST and TFAST echo views as shown with a cat (A,B) and dog (C,D) in right lateral recumbency, correlating a radiograph to better show the acoustic windows of each respective view (*circles*). In (A) and (B), the views in a cat are labeled as ordered 1–6 and unlabeled. In (C) and (D) the views in a dog are likewise labeled and unlabeled. Right lateral is advantageous over left lateral mainly for the right pericardial TFAST echo views because the heart will fall against the thoracic wall, displacing lung within the cardiac notch. As a result, right lateral provides a superior acoustic window than other positioning. Source: Reproduced with permission from Dr Gregory Lisciandro, Hill Country Veterinary Specialists and FASTVet.com, Spicewood, TX.

**Pearl:** The abdominal (preset) setting works well for TFAST and the entire Global FAST approach in the vast majority of cases. Note that the screen marker and image are automatically reversed by most machines when using the cardiac preset.

**Pearl:** Dorsal recumbency risks clinical decompensation in compromised, hemodynamically fragile patients and *should never be used* for TFAST (or in fact any part of Global FAST) exams (see Figure 6.5).

## Patient Preparation

Similar to AFAST and Vet BLUE, hair is generally left unshaved but it is imperative to wet and part the hair and place the probe as directly on skin as possible to prevent air trapping, which negatively affects your image quality (see Figures 5.1 and 5.2). The author prefers smaller amounts of 70% isopropyl alcohol and larger amounts of alcohol-based hand sanitizer, a Mississippi State Radiology Department trick. Acoustic coupling gel may also be used, but it is gooey and does not wipe off or evaporate like hand sanitizer (and with hand sanitizer your hands may be a little dry but always clean!). As for alcohol, it is much more noxious to the patient's skin and to the patient's lungs when enclosed in oxygen cages. Furthermore, alcohol should not be used if electrical defibrillation is anticipated since it presents a burn/fire hazard and thus is even more dangerous in oxygen-enriched environments. Of note, some manufacturers do not recommend isopropyl alcohol placed directly on the probe head because it can damage (desiccate) the rubber footprint (see Figure 4.13). Thus, placing a small amount of acoustic coupling gel on the probe head may be an easy protective solution (check manufacturer recommendations).

## To Shave or Not Shave

By not shaving, the cosmetic appearance of the patient is preserved, the patient and staff are generally less stressed, and exam time is lessened. Imaging quality is sufficient with most newer ultrasound machines,

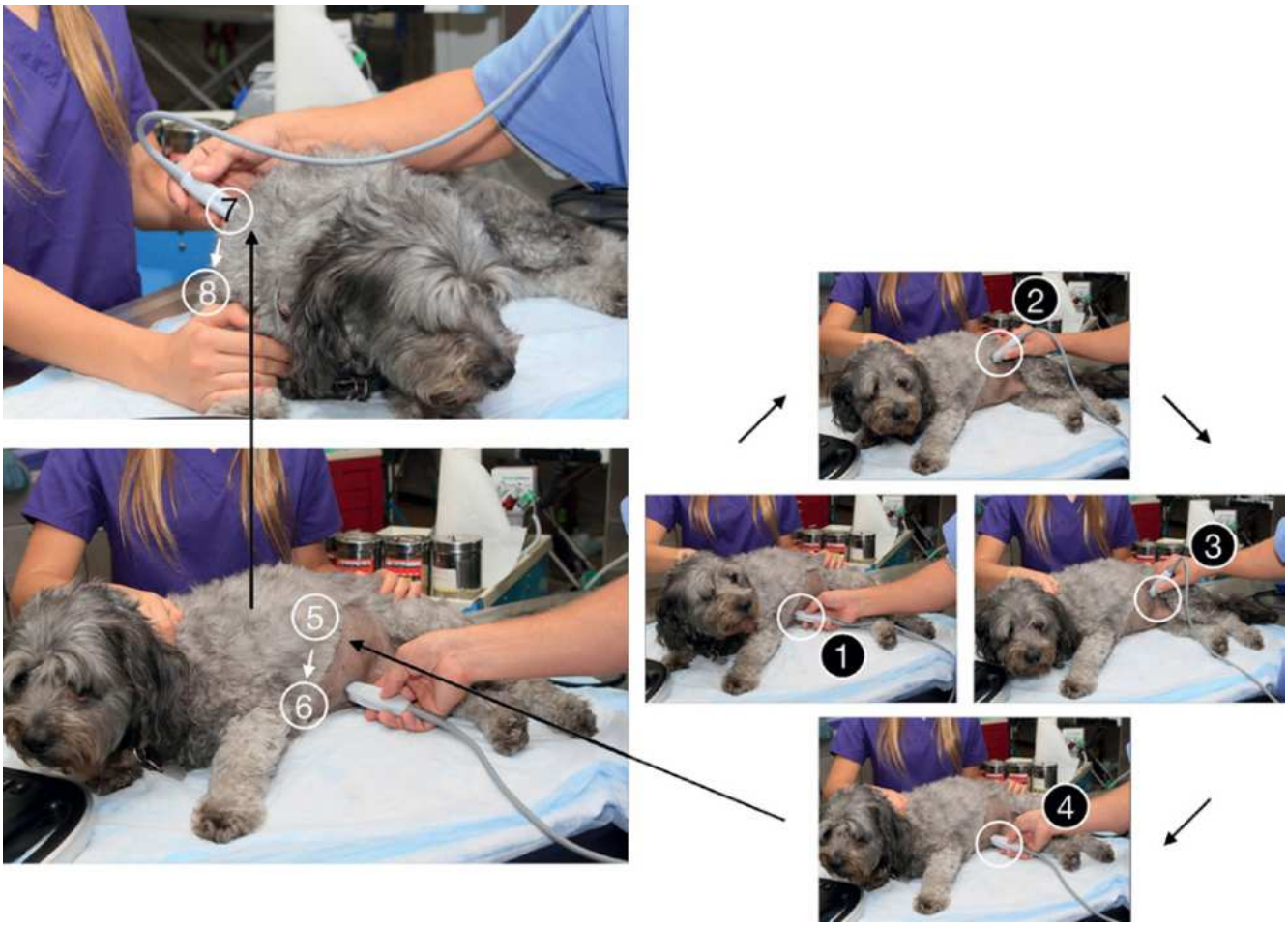


**Figure 17.4.** AFAST-TFAST blend with a dog in right modified lateral-sternal recumbency. Starting at the DH view (1), then to the SR view (2), then to the CC view (3), the HRU view (4), the ipsilateral CTS view (5), ipsilateral PCS view (6), ending on the opposing CTS view (7) and opposing PCS view (8). The analogous approach can be performed in a left modified lateral-sternal recumbency. *Note*: In contrast to what is shown, it is best to swap sides with your holder and be present on the right side of the patient looking directly at the views rather than reaching over the patient. CC, cysto-colic; CTS, chest tube site; DH, diaphragmatico-hepatic; HRU, hepato-renal umbilical; SR, spleno-renal; PCS, pericardial site. Although shown on a dog, the TFAST concept is analogous for cats. Source: Reproduced with permission from Dr Gregory Lisciandro, Hill Country Veterinary Specialists and FASTVet.com, Spicewood, TX.

especially if the probe head is placed directly on skin and not a wet matted area of hair, which has lots of air trapping and produces a poor image (see Figures 5.1 and 5.2). In the original TFAST and AFAST studies, and all Vet BLUE studies, no animals were shaved and the published images are from unshaved patients (Lisciandro 2014a,b, 2016a: Lisciandro et al. 2008, 2009, 2014, 2017; Boysen and Lisciandro 2013; McMurray et al. 2016; Ward et al. 2017, 2019). In cases when it is necessary to improve image quality, limited shaving of small viewing windows by using small-width clippers is a good idea. You can make the shaving of hair more cosmetic and pleasing to the owner by the small clipped areas and leaving hair feathered above to cover the clipped area.

**Pearl:** When you have a good probe-to-skin acoustic window, do not lift the probe to move through the view(s) but rather, if the skin is moveable, take the nonprobe hand and slide the skin and probe together to the adjacent intercostal spaces. Every time you lift the probe off a nice acoustic window, you have to start over for image acquisition, losing valuable time (see Figure 5.4).

### To Dim or Not Dim the Lights

The author rarely dims lights. This is also a risk/benefit decision because when lights are dimmed in critical patients requiring life-saving interventions, it can be difficult to locate equipment. Poor lighting also may affect how rapidly staff can move around when vision is decreased. Image quality in human studies has been shown to be acceptable in ambient light with most ultrasound machines (Breitkreutz et al. 2010).

## Performing the TFAST Chest Tube Site View

The chest tube site (CTS) views are applied bilaterally for the diagnosis of pneumothorax (PTX) because they are the highest point, least gravity-dependent site (air rises), on the thoracic wall over the pleural cavity, where air would accumulate in PTX (collapsed lung away from the intercostal space that is occupied with free air) (Figure 17.5). The TFAST CTS view is analogous to human PTX protocols (Kirkpatrick et al. 2004; Reissig et al. 2011) in which the most anterior, least gravity-dependent chest region over the pleural cavity is imaged first. The premise is that if lung is observed in opposition to the intercostal space, then PTX is not present in spontaneously breathing patients, especially when in standing and sternal (versus lateral in which pockets can bubble, causing the "double lung point" effect) (Copetti and Cattarossi 2007; Volpicelli et al. 2013). The orientation for all lung ultrasound is the "gator sign" (Figures 17.6 and 17.7) (Lisciandro et al. 2014, 2017) explained in more detail in the "gator sign orientation" section.

The CTS view has historically been defined as directly dorsal to the xiphoid process between the eighth and ninth intercostal spaces (ICS); however, experience has taught us that most often this location is likely to be the "transition zone" of the pleural (thorax) and peritoneal (abdominal) cavities (Figures 17.8 and 17.9). We refer to this as the "caudodorsal transition zone" (CdTZ). This is important because the CdTZ can be a confusing region to evaluate for PTX because of the motion of the lung, the pleural cavity, and air shadowing coupled with abdominal structures moving simultaneously. We now teach that the sonographer first locates the CdTZ by finding the "curtain sign" where the linear caudal border of dirty shadowing of lung moves to and fro obscuring abdominal contents (Figure 17.9) (Neelis et al. 2015). From the CdTZ, the probe is then moved (slid) cranially 2–3 intercostal spaces to move away from the CdTZ and more clearly evaluate for "lung sliding" without the diaphragmatic reflection and its adjacent abdominal structures (see Figure 17.12). When PTX is suspected, the probe is moved through Vet BLUE views – "TFAST PTX 1/3s Rule," middle third and lower third of the thorax – searching for the "lung point," defined as where lung recontacts the thoracic wall (Lisciandro 2011; Lisciandro et al. 2008) (see Figure 18.5). Any evidence of lung recontacting the thoracic wall supports the presence of the "lung point," most commonly by observing the resumption of "lung sliding" or B-lines (see Chapter 18 for more detail).

Being confused in the CdTZ can lead to many errors, including mistaking movement of the diaphragmatic reflection and its adjacent abdominal structures as "lung sliding" or a "step sign" (see Step Sign section) and also mistaking abdominal structures for some of the Vet BLUE lung ultrasound signs, such as the rugal folds of the stomach as a shred sign (pseudo shred sign) or the liver as a tissue sign (pseudo tissue sign), or air and fluid in the stomach lumen for B-lines (pseudo gastric B-lines), or the gallbladder for free fluid (see Pitfalls TFAST, Chapter 18, and Pitfalls Vet BLUE, Chapter 23) (see Figures 23.20, 17.9, 3.2, and 3.6).

### Optimizing the Image at the CTS View and the Gator Sign

#### Pitfalls – Machine Settings

##### *Depth Setting*

At the CTS view, depth is generally set between 4 and 8 cm. For smaller patients start with 4–5 cm and for large canine patients increase to 7–8 cm (and sometimes up to 9–10 cm in giant-breed dogs) (Figure 17.10; see also Figures 17.6 and 17.7). As a general rule, have a little more depth for an overview and to see your landmarks and then decrease depth accordingly (magnify).

##### *Gain*

Turning down the gain in the near-field is important, as the contrast is better for recognizing "lung sliding." A common mistake is making the screen along the pulmonary-pleural interface (lung line) too bright (too white) (see Figure 17.10B) or undergained (too dark) through the far-field (see Figure 17.10C). The ideal image at the CTS view is to have some gain to be able to see whether artifacts and suspected pathology extend through the far-field (Figure 17.10A).

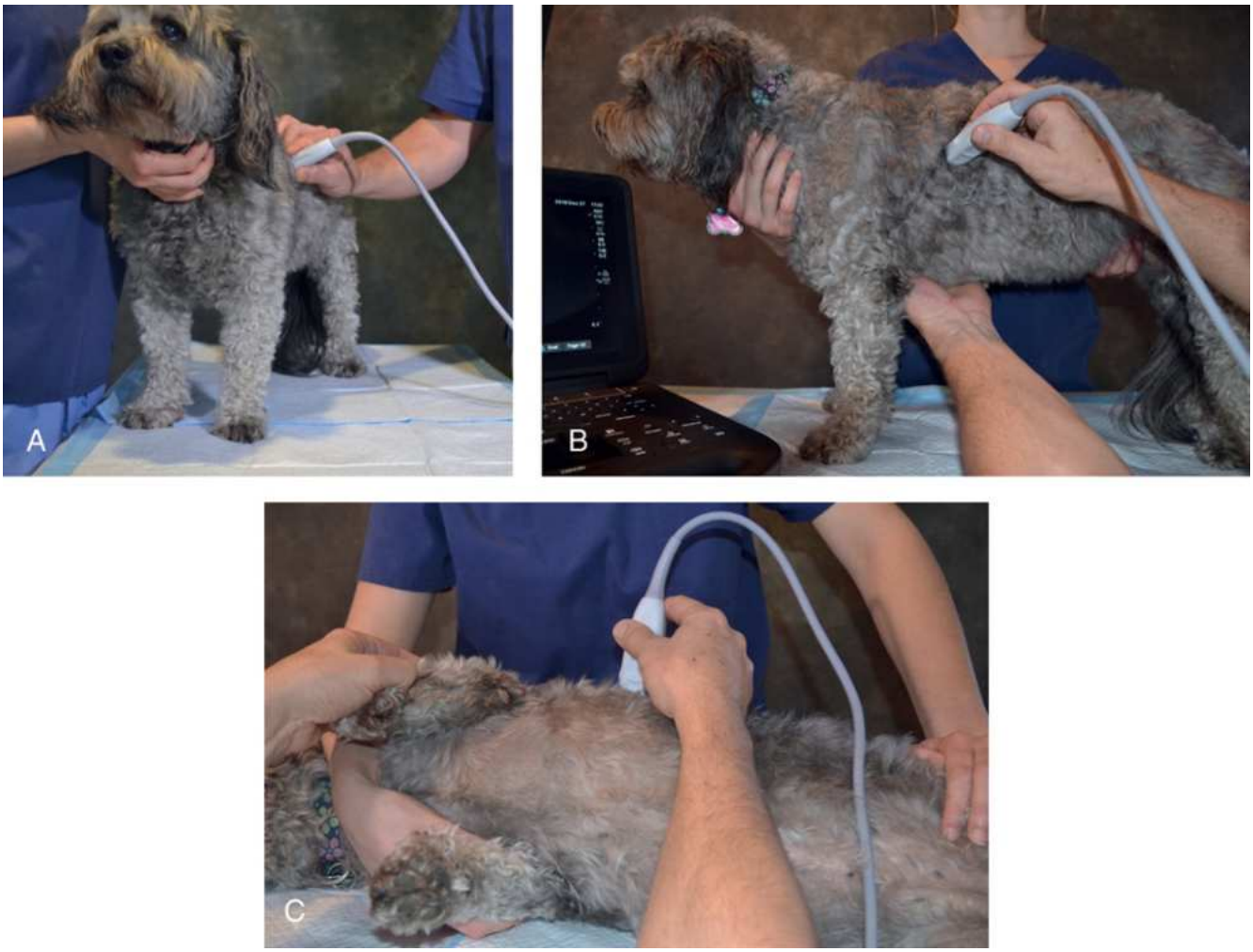


**Figure 17.5.** The chest tube site view in standing and lateral recumbency in a dog. The pictures show probe placement for the CTS view, which is the highest location over the pleural cavity. In standing/sternal positioning, too dorsal places the sonographer over rib heads as they attach to the vertebral column and too far caudal will be over the liver, stomach, and kidneys. The following three concepts will best assure accurate pneumothorax evaluation. First, pay attention to where the probe is placed externally on your patient. Second, lung cannot be accurately imaged without establishing the "gator sign" orientation (see Figures 17.6 and 17.7). Third, the probe should be placed over the highest point over the pleural cavity, in which the "gator sign" is established, understanding that the free cap of air in the pleural space in PTX rises to this location. In (A) and (B) the probe placement is shown in standing and in (C) the highest point in lateral. Although shown on a dog, the TFAST concept is analogous for cats. Source: Reproduced with permission from Dr Gregory Lisciandro, Hill Country Veterinary Specialists and FASTVet.com, Spicewood, TX.

**Figure 17.6.** *(Continued)* deep enough to the pulmonary-pleural interface (PPI), referred to as the "lung line" by the author, in between the ribs (R). Because ultrasound does not transit through bone (it's reflected), the ribs cleanly shadow distally as anechoic (black) rays through the far field. In (F) the beam strikes aerated lung and reflects off the lung surface and thus dirty shadows through the far-field along with air reverberation artifact(s) called A-lines. A-lines are equidistant approximating the distance from the probe head to the first reflective aerated surface that then extend through the far-field *ad infinitum*. In between these A-lines are A', A", and A" lines, again repetitive horizontal bars parallel to the PPI and "lung line." Air artifact(s) are always *horizontal* lines, a very important concept when discussing other lung artifacts and lung ultrasound signs. Note the depth is circled in the bottom right of the images in (B), (D) and (F). Source: Reproduced with permission from Dr Gregory Lisciandro, Hill Country Veterinary Specialists and FASTVet.com, Spicewood, TX.

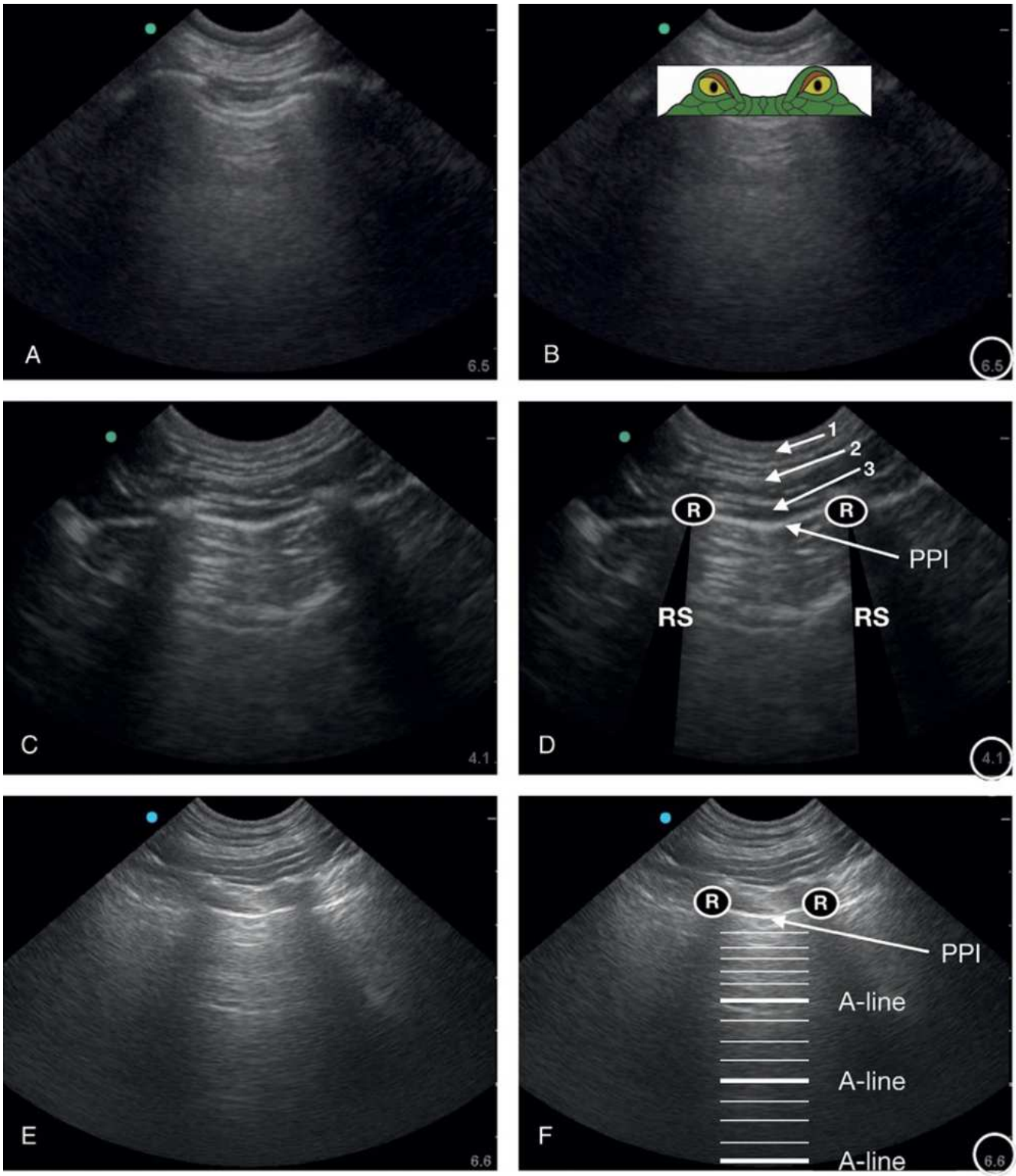


**Figure 17.6.** The "gator sign" and anatomy of the intercostal space. In (A), (C) and (E) the images of the intercostal space over the pleural cavity and lung are unlabeled with the same image labeled to each one's right side. The "gator sign" represents the lung orientation mandated to accurately image the lung. It is composed of two ribs with the interposing intercostal space in between. The rounded ribs are the alligator's (gator) eyes and the intercostal space in between is the bridge of its nose (Lisciandro 2014b,c, Lisciandro et al. 2014, 2017; Ward et al. 2017). It is important to understand the anatomy to accelerate learning. Relative structures are in image (D) as follows: (1) skin, (2) subcutaneous tissue, (3) intercostal space before getting

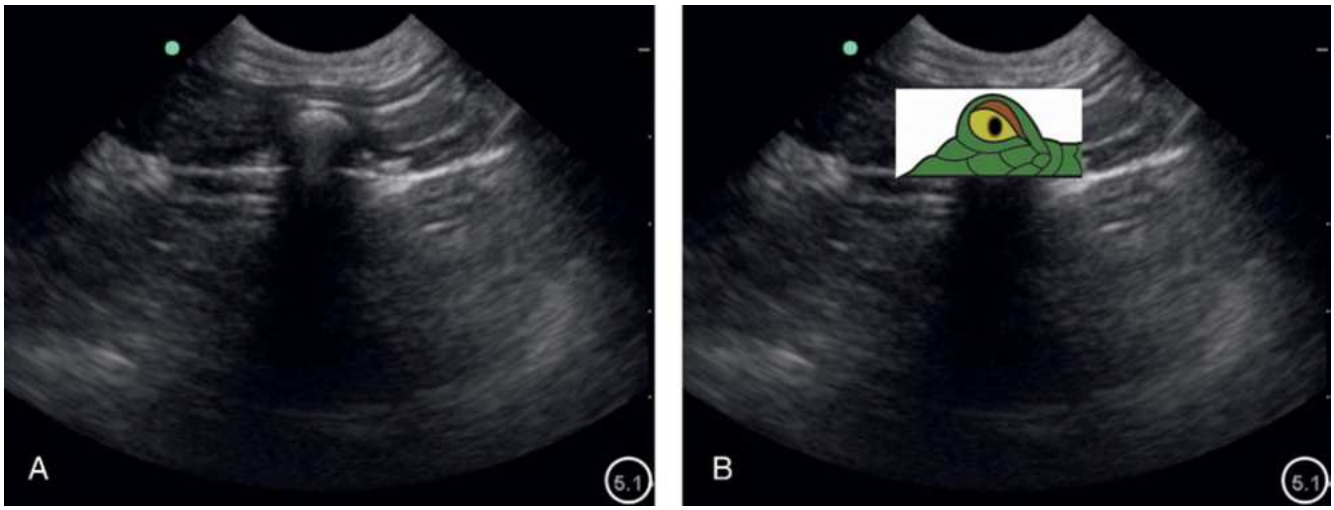


**Figure 17.7.** The "one-eyed gator." Unlabeled in (A) with an illustrative overlay in (B). Placing the rib in the center of the image is a "Trick of the Trade" developed by the author that scatters the echoes off the reflective bone (rib) and brings out the to-and-fro "lung sliding" of the lung along the intercostal space during inspiration and expiration likened to an Etch-a-Sketch® cursor. The pulmonary–pleural interface, referred to as the "lung line" by the author, is evident as a hyperechoic line on either side of the rib. Source: Reproduced with permission from Dr Gregory Lisciandro, Hill Country Veterinary Specialists and FASTVet.com, Spicewood, TX.

### *Angle of Insonation*

The angle of insonation is very useful for imaging lung. A 90° angle of the ultrasound beam to the aerated pulmonary-pleural interface (PPI) produces a sharp, crisp hyperechoic (bright white) "lung line" with distinct A-lines ("A" for "air") (Figure 17.11) (Lisciandro 2014b,c). An angle that deviates from 90° makes the PPI and its "lung line" appear less distinct with softer grays, but despite losing the crisp detail of the "lung line" (as in Figure 17.11E), this imaging strategy is helpful for imaging "lung sliding" (see Tricks of the Trade section below) (Lisciandro 2014b,c).

## Pitfall – Probe Positioning and Orientation

### *Longitudinal or Perpendicular to Ribs*

The "gator sign" orientation must be acquired with the probe held stationary perpendicular to the long axis of the ribs, or what some sonographers would describe as a longitudinal orientation (parallel to the long axis (spine) of the patient's body) (Figure 17.12) (Lisciandro et al. 2014, 2017). Without clearly establishing the "gator sign" orientation, the PPI and "lung line" cannot be accurately located. There are two ways to describe the PPI. The first is where lung is directly opposed to the intercostal space, preferred by the author and referred to as the "lung line," which also serves accurately our terminology when pleural space disease is present. The second description is where parietal and visceral pleura are directly opposed; however, in disease states, such as pleural effusion, there is separation of the two pleura so again the "lung line" seems to be a better descriptor (see Figures 17.9, 17.10, and 17.12).

### *Transverse or Parallel to Ribs*

Some lung sonographers will advocate rotating the probe so that it is parallel to the long axis of the ribs, or in transverse orientation to the patient's long axis. However, this can be a dangerous proposition because it is easy to lose sight of where the PPI and "lung line" are located (see Figures 22.5 and 41.21). The spine of the scapula, subcutaneous emphysema, and even air in the stomach can be easily mistaken for the lung surface (see Figures 18.12, 18.13, and 41.21). When moving to the transverse orientation of lung, the lung sonographer must always continually double-check by returning to the "gator sign" orientation and reconfirming that the "lung line" is being accurately tracked.

## Pitfall – Subcutaneous Emphysema and Fat

In people, subcutaneous emphysema (SQE) and fat seem to be a much bigger problem than in small animals. The presence of SQE is low in trauma cases (Lisciandro et al. 2008) but presents an imaging problem by causing shadowing by air proximal to the "gator sign" so the "gator sign" cannot be imaged. However, in most cases of SQE, gently applying probe pressure

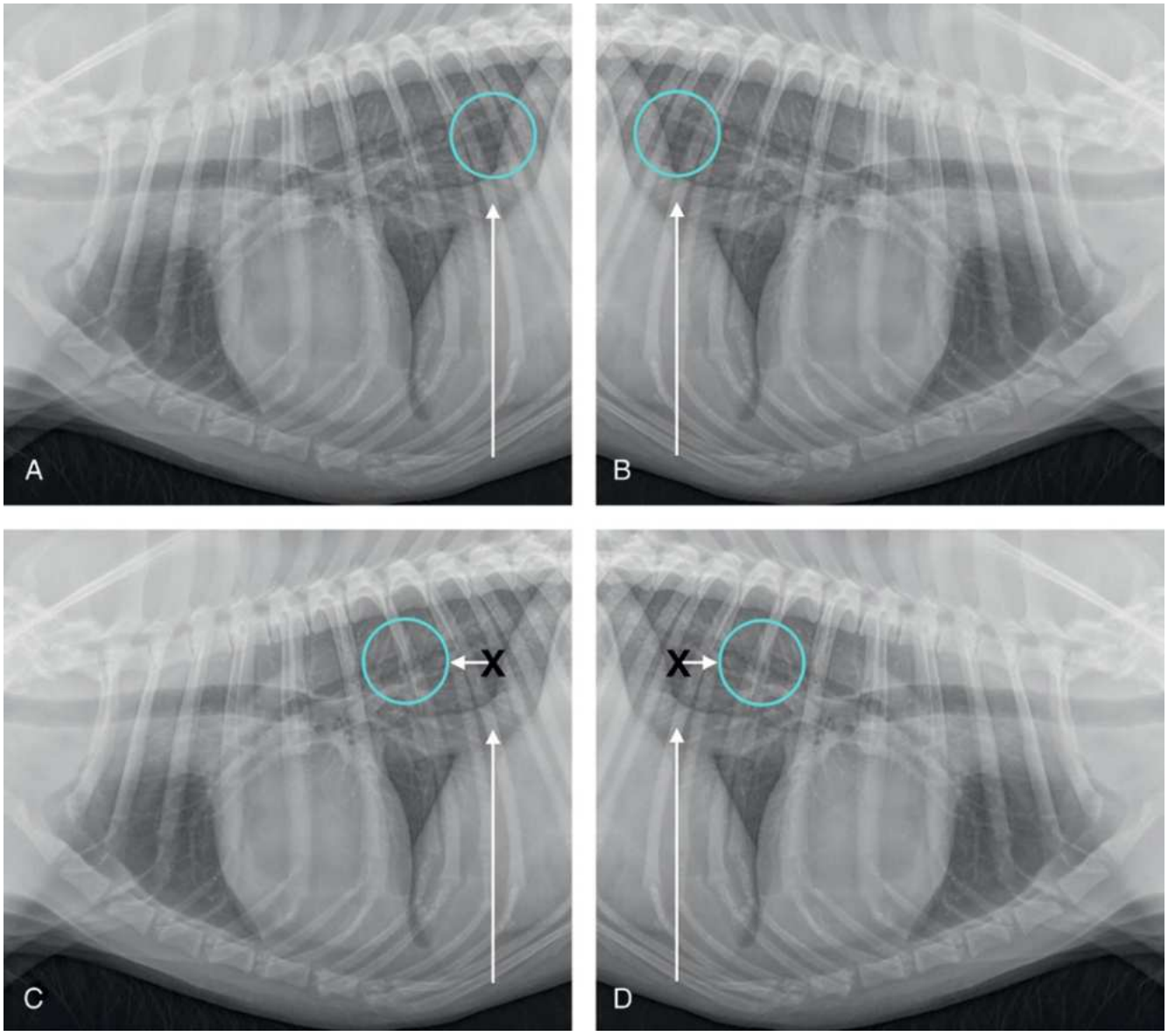


**Figure 17.8.** Chest tube site and the caudodorsal transition zone (CdTZ). The original CTS view was defined as directly above the xiphoid in the uppermost dorsal third of the thorax. The thoracic radiograph helps show the CTS view in (A) and (B) and its pitfall of commonly being in the CdTZ where there are both the pleural and peritoneal cavities in the same view (*circle*). This CdTZ confounds the observation of "lung sliding" and can lead the sonographer to mistake abdominal structures for lung pathology. The circle where the original CTS view was defined in (A) and (B) is in fact over lung, diaphragm, and cranial abdomen marked with an "X" in (C) and (D). The long arrow indicates the original landmark of being directly dorsal to the xiphoid. In (C) and (D) the "X" marks the original CTS view and the circle 2–3 spaces cranial from the CdTZ, which is now the preferred starting point for the CTS view, taking the sonographer reliably over lung without the confounding movement and structures of the diaphragmatic reflection and its adjacent abdominal structures. Although shown on a canine thoracic radiograph, the TFAST concept is analogous for cats. Source: Reproduced with permission from Dr Gregory Lisciandro, Hill Country Veterinary Specialists and FASTVet.com, Spicewood, TX.

often adequately displaces the SQE so the "gator sign" orientation may be established (see Figures 18.12 and 18.13) (Lisciandro et al. 2008). Obese patients are also problematic because fat attenuates the ultrasound beam, making the image less clear. See Chapter 18 for greater detail. The bottom line is that if you cannot acquire the "gator sign" orientation, you cannot accurately image the lung (see Figures 17.6 and 17.7).

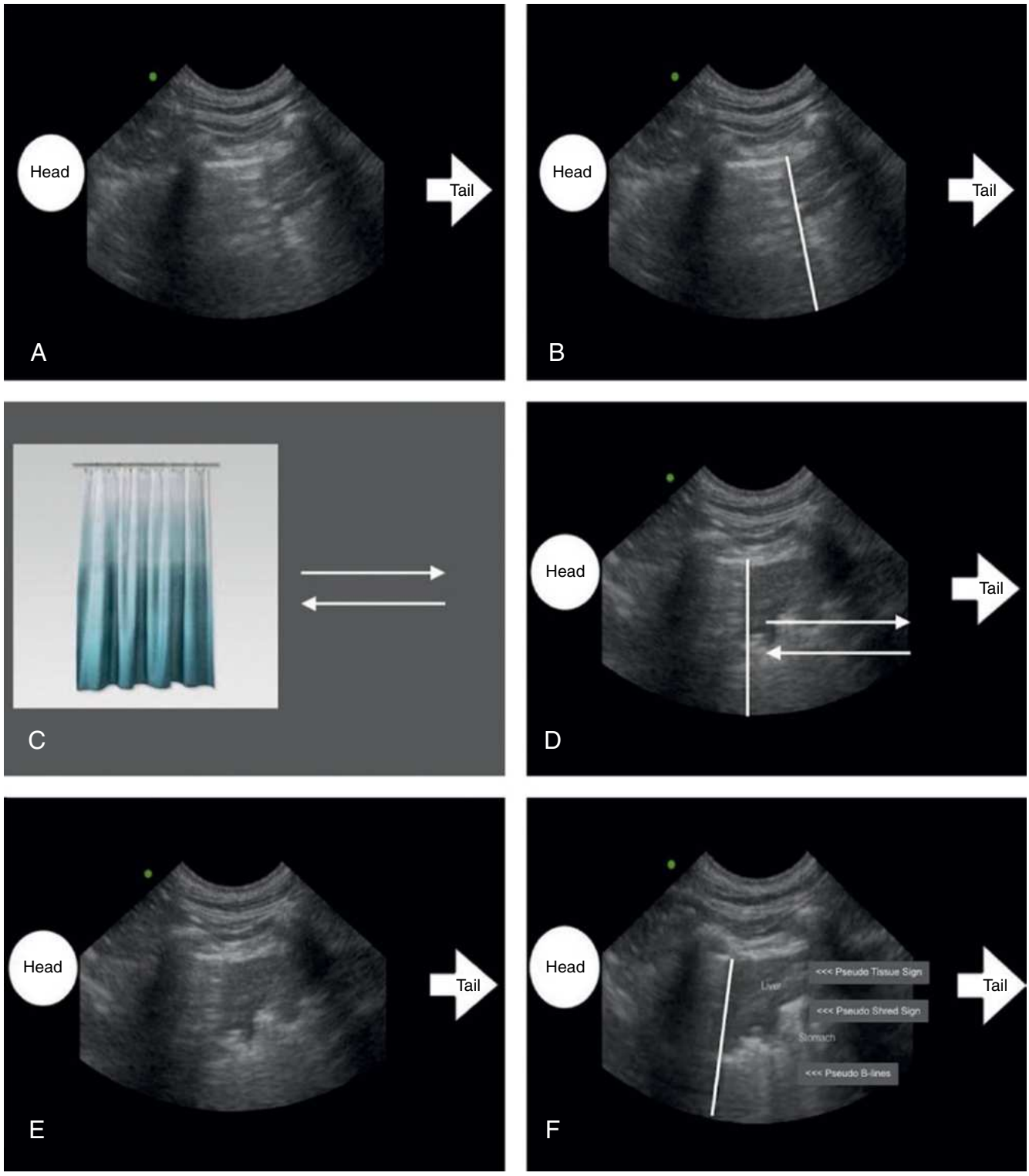


**Figure 17.9.** The "curtain sign" identifies the caudodorsal transition zone. In (A) and (B) the "gator sign" is evident, defining the intercostal space. The head is always maintained to the left of the screen and the tail to the right to keep track of the screen direction from which the abdominal cavity is expected (abdomen thus always comes into view from the right). The vertical line highlights the linear caudal border of the aerated lung that creates the "curtain sign" illustrated in (C) and (D). In real time the linear shadowing slides back and forth as if a curtain is being opened and closed. In (E) and (F), from the same patient as in (A–C), the same CTS view with *expiration* shows how the liver and rugal folds of the stomach now come into view. (E) is unlabeled and (F) is labeled, showing how abdominal structures mimic Vet BLUE lung ultrasound signs (text on image (F), "pseudo tissue," "pseudo shred," "pseudo gastric B-lines"). The CdTZ also shows what is called a "pseudo step sign" where the expected linear continuity along the PPI is lost. In locations away from the transition zone, pathology should be suspected. See the "step sign" section in Chapter 18 and Chapters 22 and 23 for more detail. Source: Reproduced with permission from Dr Gregory Lisciandro, Hill Country Veterinary Specialists and FASTVet.com, Spicewood, TX.

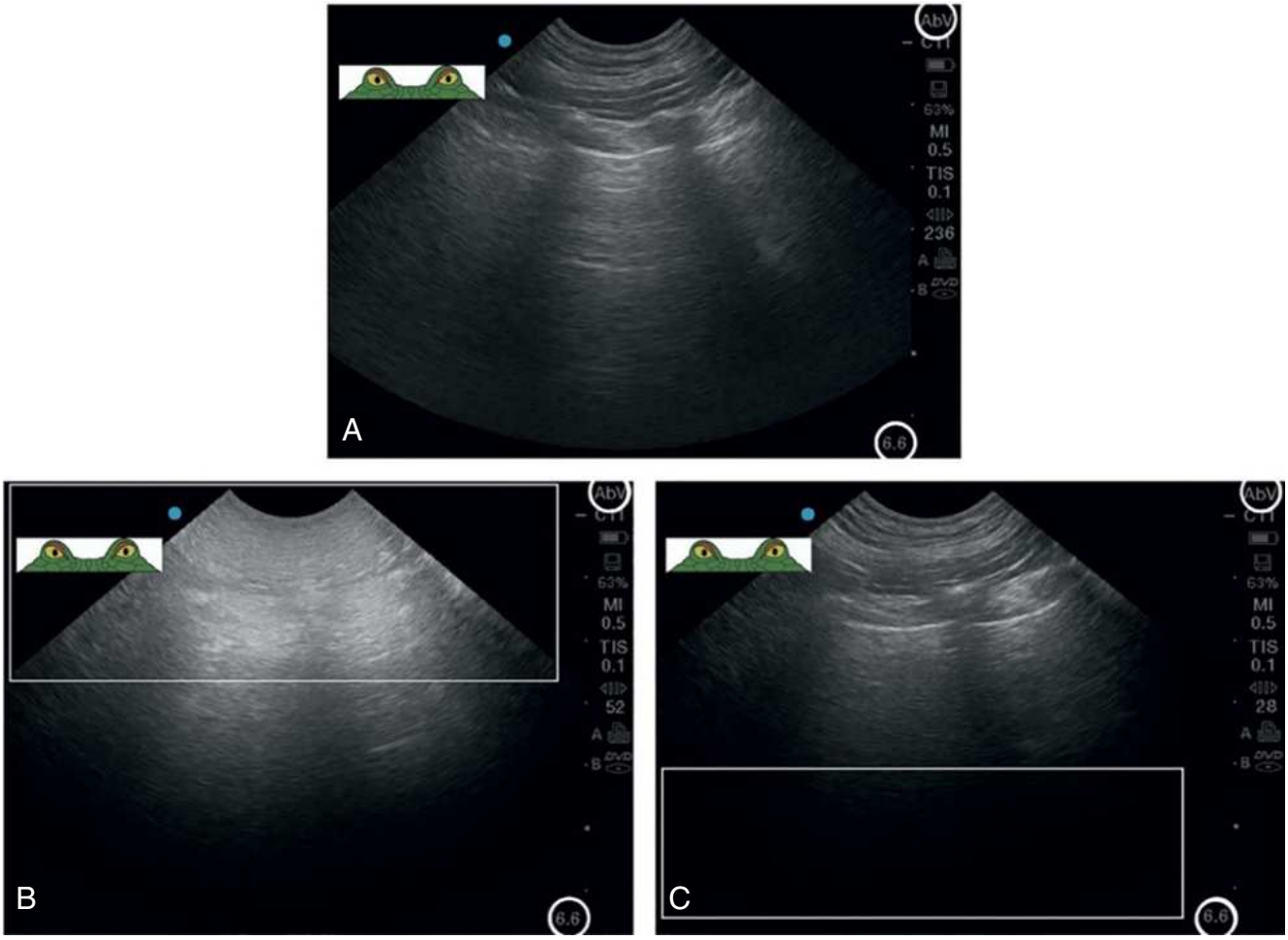


**Figure 17.10.** Effect of gain on the chest tube site view. (A–C) Images of the same dog, at the same view, at the same time, on the *abdominal* preset with the same machine and curvilinear (microconvex) probe and the same settings other than variations in the gain. The "gator sign" cartoon is shown in the left upper corner of each image to help see the actual "gator sign" orientation on each image. The circles are highlighting the abdominal preset (AbV) and the depth (6.6 [cm]) in each image. Pay attention to the information on your screen when imaging. In (A) is a nice image with gain setting showing a clear PPI and "lung line." In (B) the near-field (*rectangle outline*) is overgained so you cannot see the PPI and its "lung line" clearly and the "gator sign" cannot be confidently identified. In (C) the PPI and its "lung line" and accompanying "gator sign" are clearly seen, but the far-field (*rectangle outline*) is too undergained (dark) and artifacts and lung ultrasound signs are not clearly assessed and possibly missed. Source: Reproduced with permission from Dr Gregory Lisciandro, Hill Country Veterinary Specialists and FASTVet.com, Spicewood, TX.

### Pitfall – Lateral Recumbent Positioning

#### *Being Over the Top*

The probe should be placed at the highest point where air would rise along the thoracic wall (see Figure 17.5); however, when your patient is in lateral recumbency, this will not likely be the uppermost dorsal third of the thorax because of the barrel-shaped nature of the canine and feline thorax. By not appreciating this concept, the probe is mistakenly placed on the other side of the highest point or lower than it should be (Figure 17.13). The easiest way to prevent this is to look at your patient's thorax. At eye level, double-check as to whether you are at the highest point where air would rise or incorrectly over the backside of the thorax (see Figure 17.13). Furthermore, in lateral recumbency, the CdTZ is found similarly as when standing or sternal and evaluation for "lung sliding" is identically performed 2–3 intercostal spaces cranial to the CdTZ (see Figures 17.8 and 17.9).

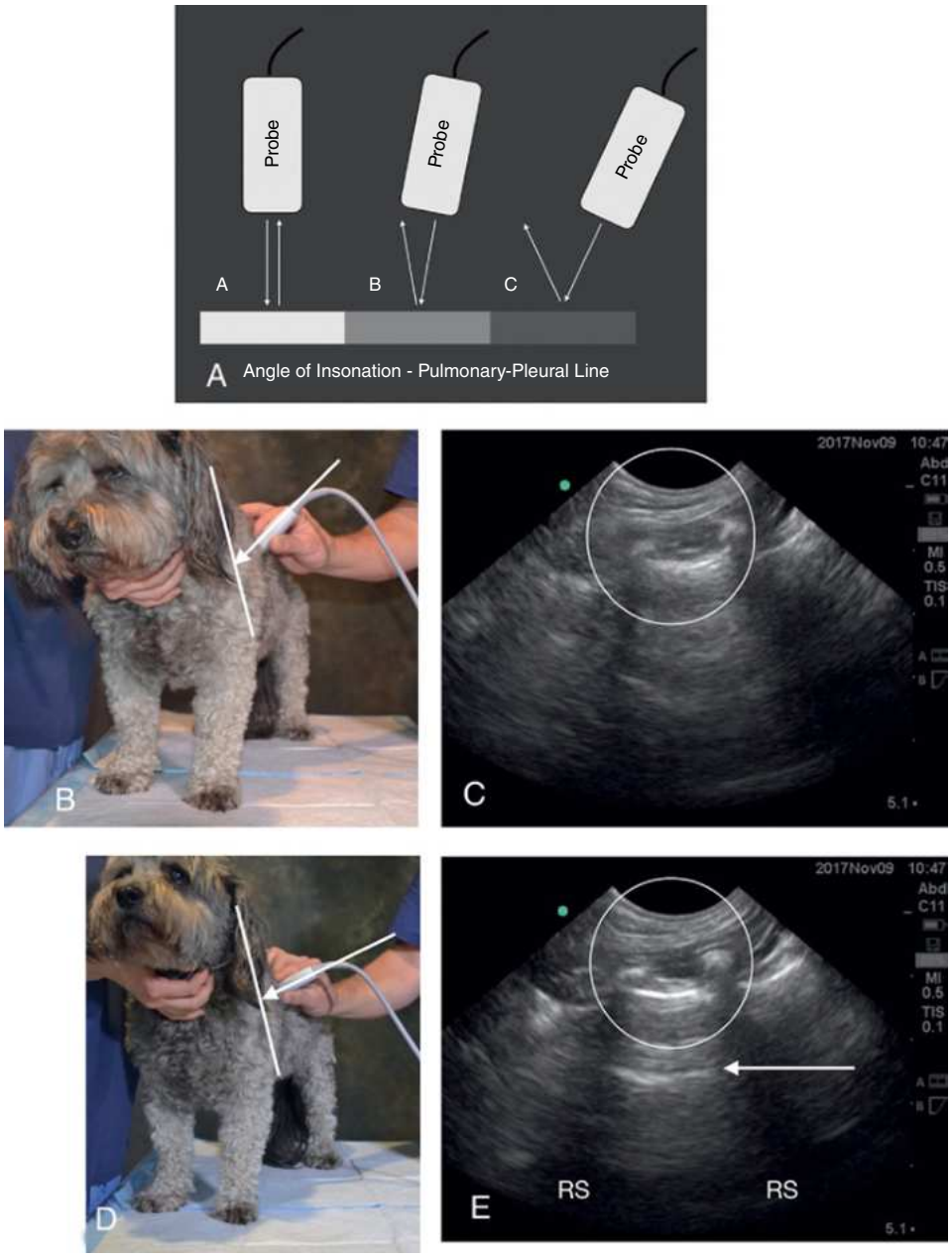


**Figure 17.11.** Angle of insonation for "lung sliding." In (A) is a cartoon showing the angle of insonation and the hyperechoic to hypoechoic degrees of the PPI or "lung line." The 90° angle produces the crisp hyperechoic "lung line" that is a crisp white line as in (D) and (E) that is so important for Vet BLUE, and angled to 75° makes a hypoechoic "lung line" that is a softer, less crisp gray as in (B) and (C) that helps image "lung sliding" by obliquing or ricocheting the echoes (Lisciandro 2011, 2014b,c; Boysen and Lisciandro 2013). These images were taken at the same time, from the same dog, with the same settings, which are included to the right of each partially cropped ultrasound image. We call it the angle of insonation "Trick of the Trade," "obliquing or ricocheting the echoes" and often combine it with the "one-eyed gator" to rapidly detect the presence or absence of "lung sliding" (see Figure 17.7). Although shown on a dog, the TFAST concept is analogous for cats. Source: Reproduced with permission from Dr Gregory Lisciandro, Hill Country Veterinary Specialists and FASTVet.com, Spicewood, TX.

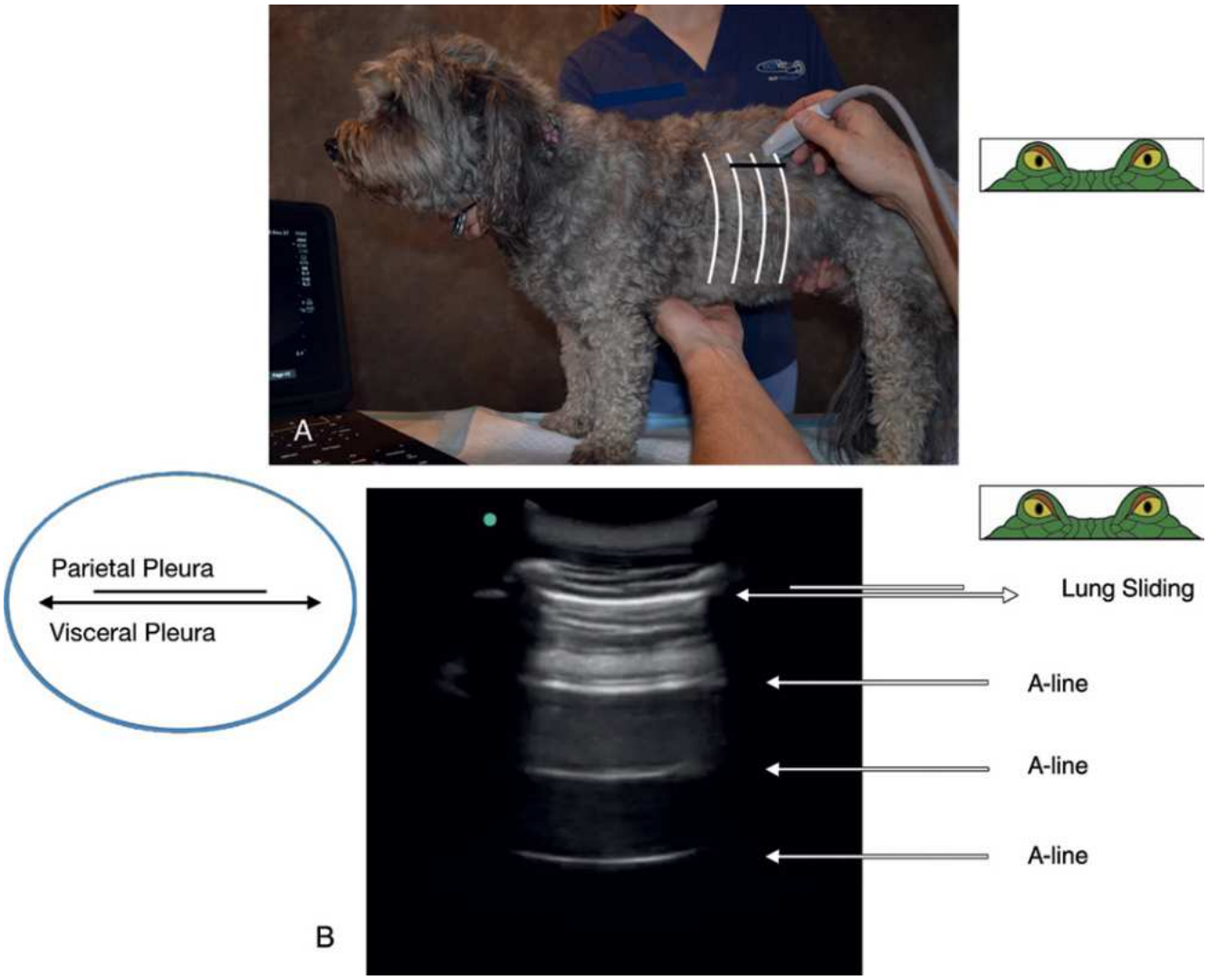


**Figure 17.12.** Anatomy at the CTS view and the "gator sign" orientation. In (A) the probe is held perpendicular and stationary to the long axis of the ribs (*white curved lines*) as shown by the black line. By doing so the "gator sign" orientation is achieved. (B) Correlating still image with a distinct PPI and "lung line" where "lung sliding" is observed, indicated by an outer white line being the parietal pleura and the inner white line with arrows (←) the visceral pleura. These overlying arrows represent the lung surface sliding to and fro with phases of respiration immediately against the stationary parietal pleura along the thoracic wall in the absence of pleural space disease. The air reverberation artifact called A-lines, remembered by the "A" standing for air, are evident on the still image as equidistant horizontal bars parallel to the "lung line" and extending through the far-field. Although shown on a dog, the TFAST concept is analogous for cats. Source: Reproduced with permission from Dr Gregory Lisciandro, Hill Country Veterinary Specialists and FASTVet.com, Spicewood, TX.

### *Double Lung Point*

The "double lung point" has been described in people with smaller volume pneumothorax and occurs when the free air does not completely pocket at the highest point within the pleural cavity (Volpicelli et al. 2013). The smaller volume of free air in the pleural space gets pushed into different locations or, as the author likes to put it, bubbles unevenly. The effect is having "lung sliding" interposed with an absent "lung sliding" (the pneumothorax) in the same field of view. This effect is seen in people in supine positioning. It may be immediately eliminated in small animals by moving them to sternal or standing, when possible, when pneumothorax is suspected (see Figure 18.8). The effect is also more problematic with positive pressure ventilation.

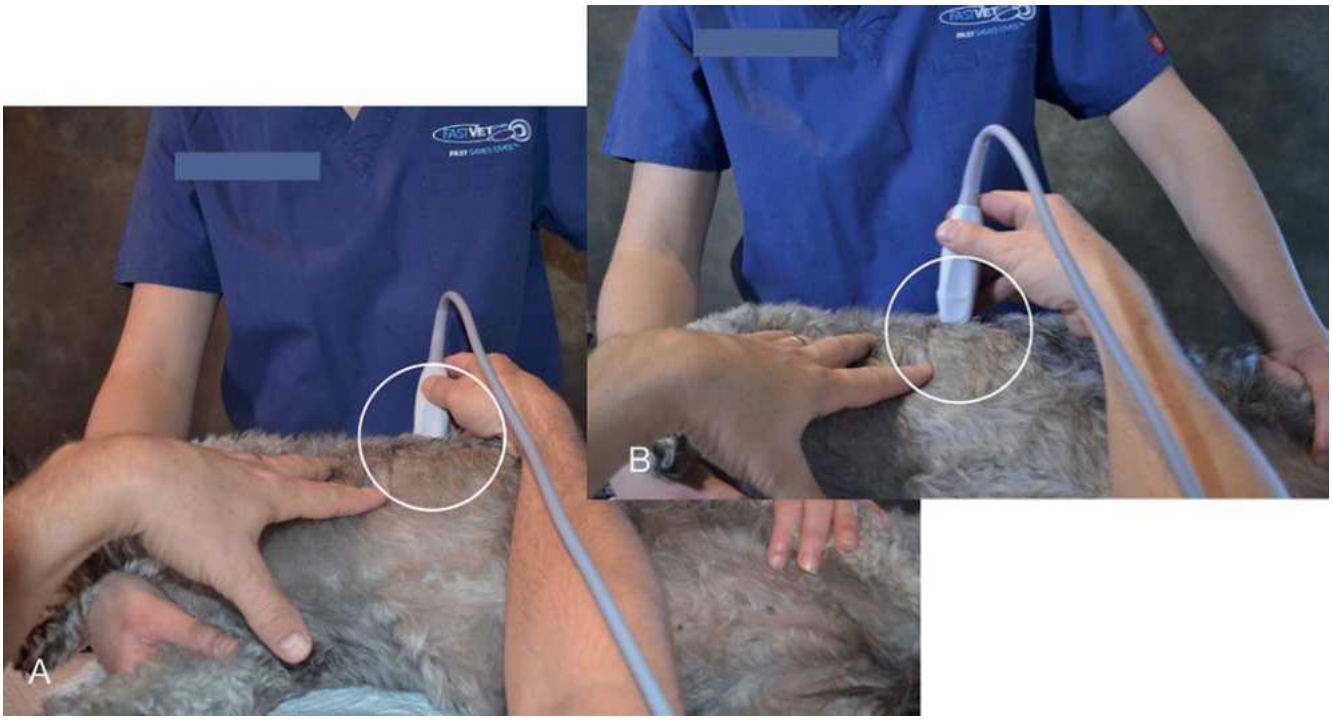


**Figure 17.13.** Pitfall of lateral recumbency and being over the top of the thorax. The CTS view needs to be at the highest point where the free air in the pleural cavity would rise. In (A) the probe is "over the top" and down the other side, which is a common mistake. In (B) the probe is at the highest point where free air would rise. If pneumothorax is suspected, it's best to avoid searching for the "lung point" in lateral because of phenomena like the "double lung point" and move the patient to standing or sternal position. See Chapter 18 for the "lung point" and the "parking garage versus skyscraper effect" (see Figure 18.8). Although shown on a dog, the TFAST concept is analogous for cats. Source: Reproduced with permission from Dr Gregory Lisciandro, Hill Country Veterinary Specialists and FASTVet.com, Spicewood, TX.

## *Tricks of the Trade for Imaging "Lung Sliding"*

These are a few strategies that we have learned over the past several years.

- *Obliquing or ricocheting the echoes*. Change the angle of insonation from 90° to ~75° or in other words, fan the probe slowly, making the PPI and "lung line" less hyperechoic, or rather more gray than white, and then hold the probe stationary and observe for "lung sliding" (see Figures 17.11 and 22.8). This is called "obliquing the echoes" or you may think of as "ricocheting the echoes (ultrasound beam)" off the highly reflective surface of air whether in aerated lung or in the presence of pneumothorax (see Figures 17.11 and 22.8) (Lisciandro 2014b; Lisciandro et al. 2014, 2017).
- *One-eyed gator*. Move the rib to the center of the screen. Observe for lung sliding on either side of the rib. This is called "scattering the echoes" because essentially you are having echoes reflect off the rib (bone) and scatter to its sides and before then striking the reflective surface of air at different angles (see Figures 17.7 and 22.8) (Lisciandro 2011, 2014b,c: Boysen and Lisciandro 2013).
- *Combine obliquing and ricocheting the echoes with the one-eyed gator*. Do both – change the angle of insonation and place the rib centered in the screen simultaneously (see Figures 17.7, 17.11, and 22.8). The author typically does both maneuvers to start TFAST and not waste any time for efficiently observing for the presence or absence of "lung sliding."
- *Butorphanol*. It is also helpful to give light sedation that calms the patient and is safe, low risk and short-acting, and generally does not induce panting. We can accept the limited risk and benefits of subcutaneous butorphanol that generally reduces patient anxiety and slows their breathing pattern without causing panting.

### *Troubleshooting Inconsistent Imaging of the Pulmonary-Pleural Interface and "Lung Line"*

- Manipulating the machine is another option.
  - Make sure the focus cursor is directly across from the PPI and "lung line" (see Figure 5.12).
  - Turn down the overall gain to make the near-field darker, providing more contrast along the PPI (see Figure 17.10).
  - Change from the abdominal preset to the cardiac preset, which is rarely done by the author but a consideration. The cardiac preset, however, will change the screen orientation by reversing and making the head to the right and tail to the left of the screen unless you use the reverse button present on many machines, or turn the probe 180° to revert back to having the head to the left and tail to the right on the screen, as is done with all other ultrasound imaging.
- Watch the patient's breathing pattern while observing for "lung sliding"; during breath holding or apnea, "lung sliding" will not be seen. Thus, "lung sliding" is best appreciated if the sonographer is paying attention to when the patient inspires and expires during each spontaneous breath (or when administered positive pressure ventilation).
- If "lung sliding" is not observed then the "lung point" is sought by moving through the Vet BLUE views in the middle third (perihilar lung region) and lower third (middle lung region) of the thorax (see Chapter 18, PTX section) and best practice is to move your patient into sternal or standing position when possible (see Figure 18.8).
- Use the opposing hemithorax as a control, meaning if you can clearly see "lung sliding" on the opposing hemithorax with the same settings, then likely PTX is present on the suspected side, especially if a "lung point" is determined.

**Pearl:** "Lung sliding" is now the accepted term in human medicine (Volpicelli et al.2012), replacing the term "glide sign" previously used in veterinary medicine (Nyland and Mattoon 2002; Lisciandro et al. 2008; Lisciandro 2011) (see Figure 17.12).

**Pearl:** Make sure your patient and ultrasound machine are in the same sight line for sonographer, staff, and patient safety (see Figure 5.3).

### *Summary – How to Image the Chest Tube Site View Step by Step in Standing or Sternal Recumbency*

- Find the CTS view by going directly dorsal to the xiphoid and into the uppermost dorsal third of the thorax over aerated lung (see Figures 17.8 and 17.9).
- Adjust depth to 4–5 cm to 7–8 cm (and even 9 cm in giant breeds) (see Figure 17.10).
- Acquire the "gator sign" orientation (see Figure 17.12).
- Adjust gain for a good-looking image (see Figure 17.10).
- Find the CdTZ, defined as having the pleural cavity (thorax) to the *left* of the screen and the peritoneal cavity (abdomen) to the *right* of the screen. The "curtain sign" is your landmark (see Figures 17.8 and 17.9).
- After finding the "curtain sign", find the proximal generally most hyperechoic line representing the PPI or, in other words, the aerated lung surface referred to as the "lung line" to the left of the screen away from the abdominal structures (see Figure 17.12).
- Follow the "lung line," sliding the probe cranial away from the CdTZ 2–3 intercostal spaces in order to eliminate the abdominal cavity from view, which may not be possible in small canine patients and cats (see Figure 17.8).
- At this location, 2–3 intercostal spaces cranial from the CdTZ, observe for "lung sliding," the to-and-fro movement with inspiration and expiration along the intercostal space, or the sliding of parietal and visceral pleura over one another (see Figure 17.12). "Lung sliding" has been likened to an Etch-a-Sketch® cursor being moved back and forth over the same line (Lisciandro 2011; Lisciandro et al. 2008, 2014, 2017; Boysen and Lisciandro 2013).
- The angle of insonation is important (see Figure 17.11). Oblique or ricochet the echoes off the "lung line" to help bring out "lung sliding" if not observed with 90° angle of insonation.
- If "lung sliding" is still not obvious, add on the "one-eyed gator sign" by placing the rib in the center of the screen, called scattering the echoes (see Figure 17.6) (see Tricks of the Trade above).

## Performing the TFAST Pericardial Views

The PCS views are bilaterally applied in the region of the third to fifth intercostal spaces, generally at the level of the costochondral junctions, with the objective

of interrogating the most gravity-dependent regions of the thorax for pleural and pericardial effusion (fluid falls) and imaging the TFAST echo views (see Figures 17.1, 17.2, and 17.3). The left and right PCS views are similar to the parasternal views of echocardiography (Lisciandro et al. 2008; Lisciandro 2011, 2016; Boysen and Lisciandro 2013; Lisciandro and Armenise 2014); however, the appearance of the heart is markedly different (Figure 17.14). In contrast to the CTS view, in which lung is imaged as a stationary view, the PCS views are dynamically interrogated (see Figure 17.2).

The heart is both used as a landmark for the diagnosis of pleural and pericardial effusion and imaged directly for cardiac assessment, including the left short-axis view (left PCS view) and right PCS views of short- and long-axis views. With the patient in right lateral recumbency, the heart is most rapidly located by palpating the thorax with your nonprobe hand (helper hand) and then placing the probe on the patient's thoracic wall, where the apical beat is strongest (see Figure 17.16). In the absence of a palpable apical beat, the probe may be placed just below the level of the costochondral junctions of the third and

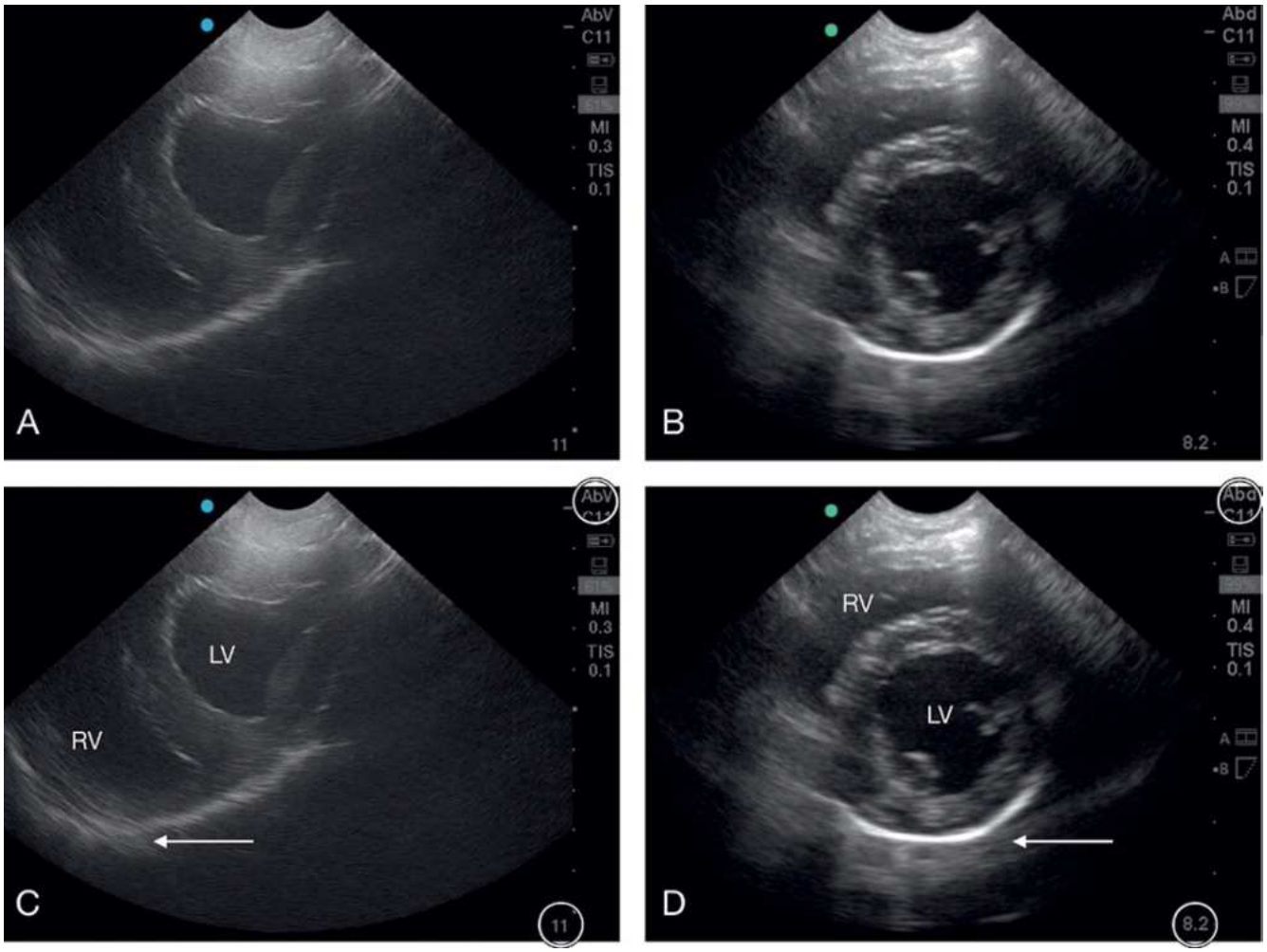


**Figure 17.14.** Differences of the heart between left and right pericardial views. In (A) and (B) are unlabeled left and right PCS views with the heart shown in short-axis. The general impression and cardiac shape are quite different. In (C) and (D) the ventricles are labeled and note the difference in the left ventricle in the near-field at the left PCS view and in the far-field from the right PCS view. It is important to always have enough depth to see the bright pericardium landmark (*arrow*) in the far-field. Without having the pericardium in view, it's easy to get confused on cardiac anatomy and mistake heart chambers for pleural or pericardial effusion. The preset is abdomen (circled at top [Abd]) and the depth is circled in the bottom right corner in (C) as 11 cm and in (D) 8.2 cm. Source: Reproduced with permission from Dr Gregory Lisciandro, Hill Country Veterinary Specialists and FASTVet.com, Spicewood, TX.

fourth intercostal spaces. The importance of clearly locating the heart and having enough depth to see the bright pericardium in the far-field is to avoid mistaking it for pleural or pericardial effusion since it is the only structure in the thorax that may be mistaken for either (Figures 17.14 and 17.15).

## *Left Pericardial Site View*

### Finding the Heart at the Left Pericardial Site View

The heart is located as previously described (Figure 17.16). Place the probe on your patient however is most comfortable for you (holding like a pencil often works well). The heart is recognized by its motion (beating). From the left TFAST PCS view, the heart's left ventricle (LV) is viewed in short-axis in the near-field and the crescent-shaped right ventricle (RV) in the far-field, both uniquely different from the heart's short-axis appearance on the right TFAST PCS view (see Figure 17.14). The author calls the most ventral appearance of the heart the "hammerhead view" because the inverted LV "mushroom" on short axis looks like the head of a hammerhead shark. If the probe is fanned or swept immediately dorsal to the "hammerhead view," the "smiley face" appearance is appreciated in

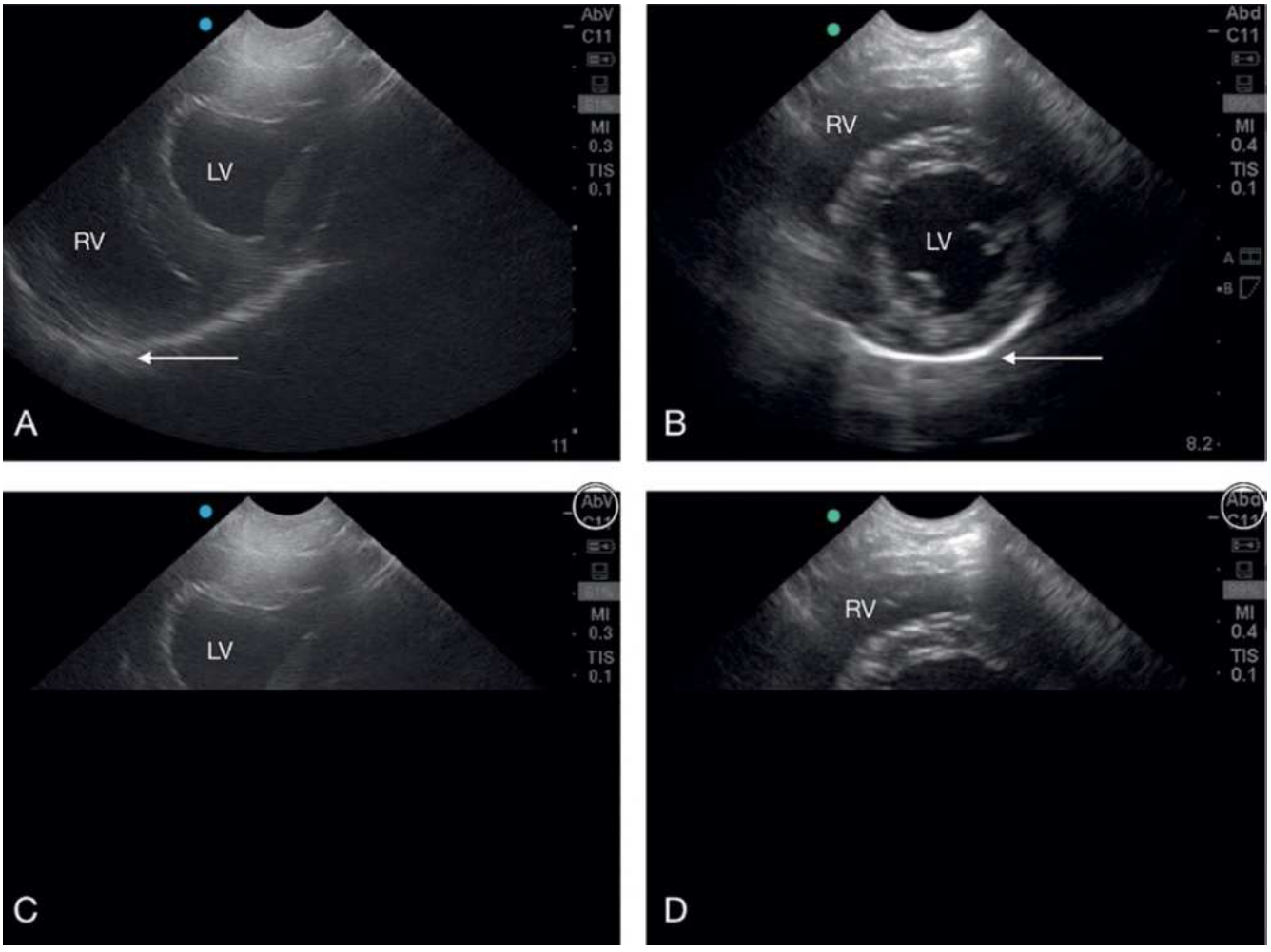


**Figure 17.15.** TFAST echo views – too shallow a depth is dangerous. This shows how easy it is for the sonographer to get confused when the heart is not viewed in its entirety. Use cardiac motion and the hyperechoic (brightest line in the far-field) pericardium as landmarks to make sure the entire heart is in the field of view. In (A) and (B) short-axis images of the heart from the left and right side (PCS views), respectively, are shown adhering to the practice of having enough depth to see the bright pericardium in the far-field. Notice the shape of the heart is radically different between left and right views. In (C) and (D) too shallow a depth is being used and the cardiac chambers are confusing and may be easily mistaken for pleural or pericardial effusion. Source: Reproduced with permission from Dr Gregory Lisciandro, Hill Country Veterinary Specialists and FASTVet.com, Spicewood, TX.

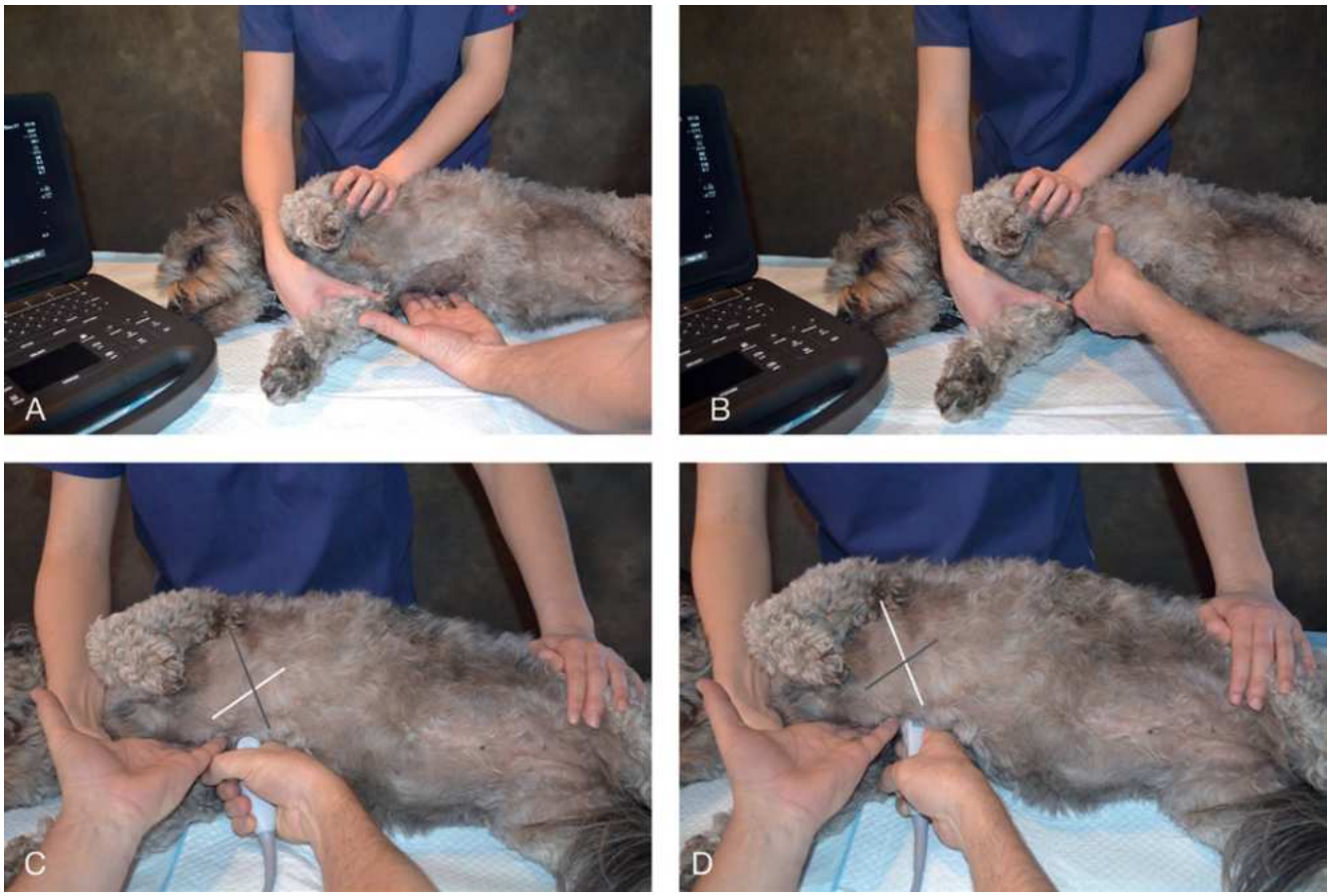


**Figure 17.16.** Finding the heart and short- and long-axis lines. Start as in (A) with an open left nonprobe (helper) hand with the fingers on one side of the thorax and the thumb on the other; with the probe held in your right hand, palpate for the apical beat. Once the apical beat is palpated at its maximum, place your thumb on the left thorax as in (B). Your thumb marks where to begin your left PCS view. "X" on the thorax in (C) and (D) shows the short- and long-axis imaging lines. In (C) the probe is run under the patient and directed on the short-axis line (*white line*) and in (D) the long-axis line (*white line*). Although shown on a dog, the TFAST concept is analogous for cats. Source: Reproduced with permission from Dr Gregory Lisciandro, Hill Country Veterinary Specialists and FASTVet.com, Spicewood, TX.

which there are three fluid-filled chambers including the left ventricle (LV), right ventricle (RV) and the right atrium and auricle (RA) (see Figures 17.25 and 17.26). This is one of the views used to screen for right auricular masses (see Chapters 19–21). With the heart identified and depth increased to always see the hyperechoic pericardium in the far-field (see Figure 17.14), the TFAST caudal and then cranial "slide" are performed to screen for smaller volume pleural effusions within the "cardiac-diaphragmatic pouch," the area between the caudal heart and diaphragm, and the cranial heart and thoracic inlet within the "cardiac-cervical pouch" (Figure 17.17; see also Figure 17.2). We refer to this probe maneuver as the "TFAST slide" and it is identically performed at the left and right TFAST PCS views.

Think anatomy as you perform the "TFAST slide." Sliding caudally brings you over the diaphragm and the liver, which are readily recognized because of their similarity to the FAST DH view. By identifying the liver and diaphragm, small-volume effusions may be appreciated in the "cardiac-diaphragmatic pouch" caudally. Being too ventral along the heart, pericardial and mediastinal fat are often imaged with a triangular fat pad between the apex of the heart and the diaphragm and a linear appearance along the heart between its caudal and cranial boundaries along the intercostal spaces, especially at the level of the "hammerhead view" (see Figures 17.17, 18.25, and 18.26) (Lamb 2000). To avoid mistaking pericardial and peristernal fat for pleural effusion (PE), sweep immediately dorsal and the lung will dirty shadow when there is

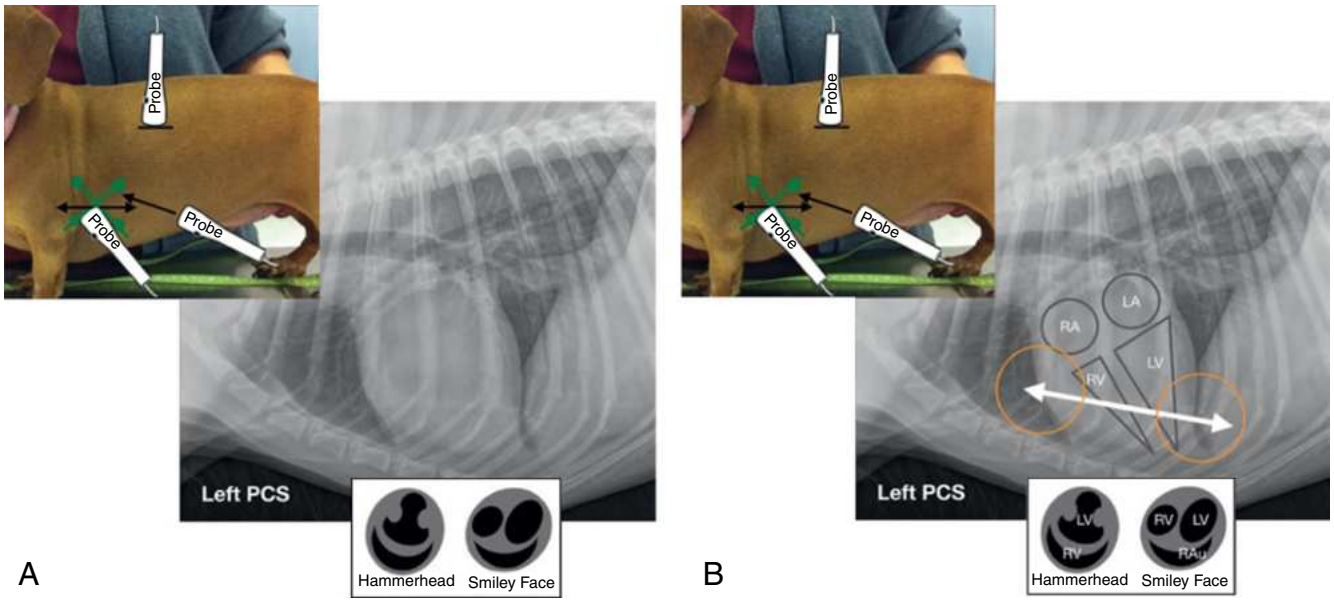


**Figure 17.17.** "TFAST slide" for pleural effusion from the left pericardial site view. The "TFAST slide" principle is best remembered by imaging caudal and then cranial to the heart in the "cardiac-diaphragmatic pouch" and the "cardiac-cervical pouch" respectively, shown unlabeled in (A) and labeled in (B) by the circles. Cartoons of the TFAST echo views from the left PCS view are shown. Although shown on a dog, the TFAST concept is analogous for cats. Source: Reproduced with permission from Dr Gregory Lisciandro, Hill Country Veterinary Specialists and FASTVet.com, Spicewood, TX.

absent PE. In the presence of PE, the PE will separate lung from thoracic wall, creating fluid stripes and triangulations and a "curtain sign" of pleural effusion (Neelis et al. 2015) (see Figure 18.25). PE is described in more detail in Chapter 18.

## *Right TFAST Pericardial Site View*

### Locating the Heart

The apical beat is palpated with an opened left non-probe (helper) hand and the probe is held in the right hand with the patient in right lateral recumbency as described at the left TFAST PCS view (see Figure 17.16). The probe is placed on the underside of the patient over the strongest palpable apical beat (see Figure 17.16). The "TFAST slide" is performed similarly to the left TFAST PCS view for PE, however, TFAST short-axis and long-axis views are acquired there too (Figure 17.18).

### Optimizing the TFAST Cardiac Image – Depth, Gain, Presets, and Focus Cursor

#### *Depth*

Depth should be set so that the heart is always imaged in its entirety using the hyperechoic line in the far-field, the pericardium, as a mandated landmark (see Figures 17.14 and 17.15). By not imaging the heart in its entirety, identifying heart chambers becomes confusing and lends itself to mistaking fluid-filled heart chambers for pleural and pericardial effusion or other pathology. Enough depth to clearly see the heart in its entirety is the most important fundamental imaging concept for TFAST.

#### *Gain*

Moving from lung (Vet BLUE) to TFAST, your image likely will be undergained (too dark) and generally the gain will need to be increased. In contrast, when moving from AFAST to TFAST, the gain for similar soft tissue densities of abdominal organs to heart requires minimal if any change (see Figure 17.10).

#### *Presets*

Often TFAST echo views (as with AFAST and Vet BLUE) are acceptable on the abdominal presets, but for small abdomen, medium abdomen, and large abdomen (or pediatric and adult) the frequencies for each preset will be different, depending on your machine. Smaller or pediatric abdominal presets have higher frequencies (7.5–10 MHz) with more detail but less penetration; large or adult abdominal presets have lower frequencies

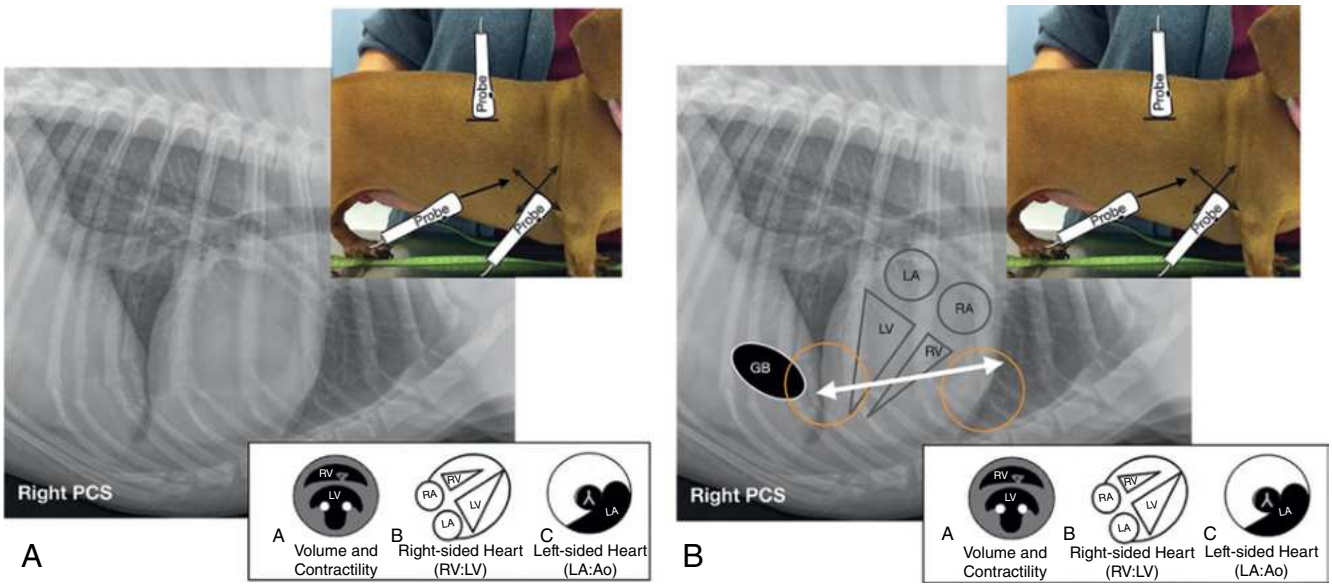


**Figure 17.18.** "TFAST slide" for pleural effusion from the right pericardial site view. The "TFAST slide" principle is best remembered by imaging caudal and then cranial to the heart in the "cardiac-diaphragmatic pouch" and the "cardiac-cervical pouch" respectively, shown unlabeled in (A) and labeled in (B) by the circles. The gallbladder is often seen when the diaphragm and liver are in view from the right side, unlike the left side. Cartoons of the TFAST echo views from the right PCS view are shown. Although shown on a dog, the TFAST concept is analogous for cats. Source: Reproduced with permission from Dr Gregory Lisciandro, Hill Country Veterinary Specialists and FASTVet.com, Spicewood, TX.

(~5 MHz) with more penetration but less detail. So the small abdomen preset may not image the large dog heart well. In general, during TFAST we are not that concerned with detail but rather want a general overview of contractility, chamber sizes and ratios so err toward lower frequencies for most patients.

Cardiac presets may be used with the curvilinear (microconvex) probe but the sonographer must recall that cranial and caudal are automatically reversed by the preset (see Chapters 19–21). The sonographer may note the change in orientation and image as dictated by the cardiac preset, or maintain cranial to the left and caudal to the right (head to the left and tail to the right) as with all other ultrasound imaging by either pressing the reverse button of some machines that will change the orientation for you, or rotating the probe 180°.

The bottom line for presets is that you have to learn what you like on your machine, stay consistent with cardiac orientation so as to know where to expect cardiac structures, and ultimately recognize which direction on the screen is cranial and caudal (see Figures 1.6, 17.25, and 17.26).

### *Focus Cursor*

The image may not look as good as you would like, then you realize the focus cursor was left in the near-field because you were looking at lung and forgot to move the cursor to the center of the cardiac image. Get into the habit of checking the position of the focus cursor (see Figure 5.12).

### *Freezing and Rolling the Cine Ball*

This skill is mandatory for optimizing image interpretation, especially for cats that have much higher heart rates than dogs; higher feline heart rates make eyeballing their TFAST echo views more prone to error. The "freeze" button captures images and, depending on how your machine is set up, saves several frames retrospectively, for frame-by-frame review. The "cine ball" is usually a roller ball on the machine's keyboard but may be buttons. In either case, they permit frame-by-frame capture that allows for *post hoc* review without the stresses of real time, especially in unstable or fractious patients.

## Optimizing the TFAST Cardiac Image – Handling the Probe

To gain an advantage for imaging a right laterally recumbent dog or cat on a triage table, the probe must be placed between the thorax and the table, a disadvantage when compared to a cardiac table with a cut-out window (Figure 17.19). Thus, the sonographer must handle the probe differently; we call it "knuckling the

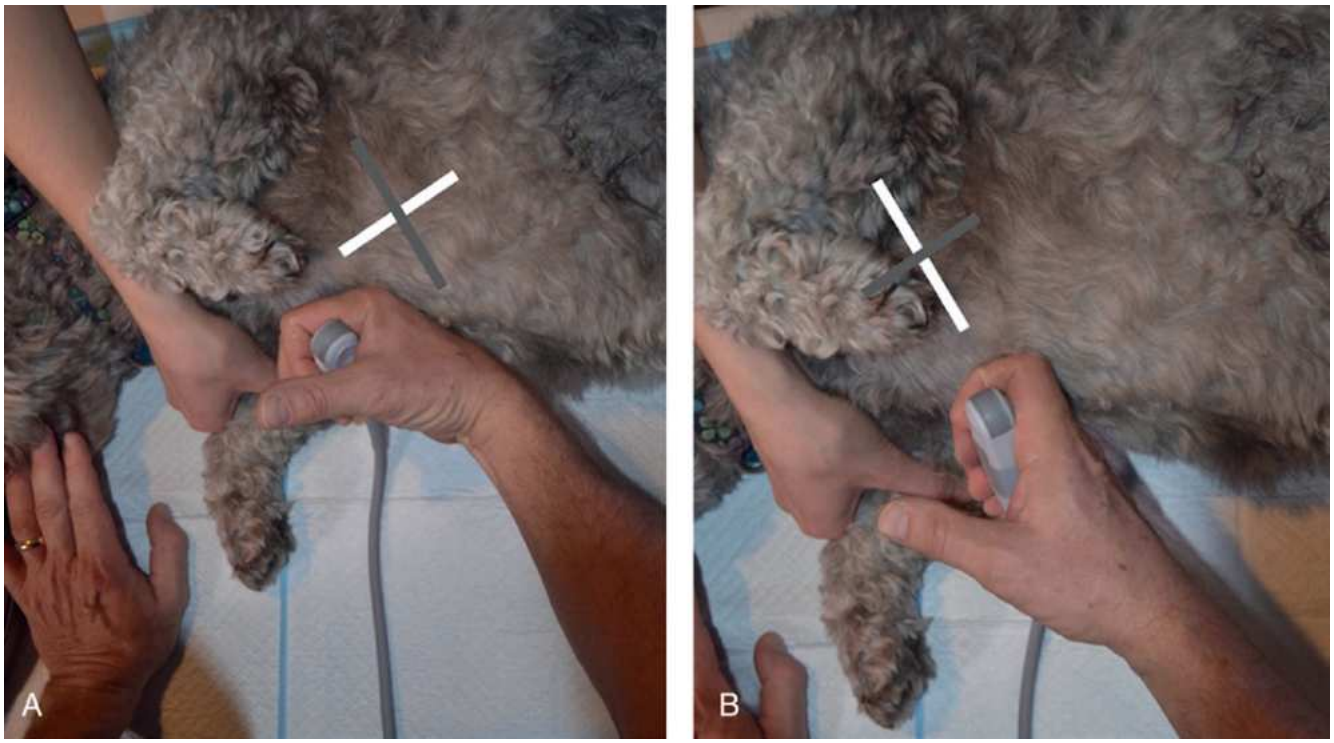


**Figure 17.19.** Knuckling the probe for short- and long-axis right TFAST pericardial site views. This technique is only for right lateral recumbency for right TFAST echo views (not left) and not for standing-sternal positioning. Place your index finger like a trigger finger on a gun and then comfortably wrap your hand around the rest of the probe as shown (A). It should be comfortable. Then as in (B), "open" your hand so that your knuckles are straight and practice this until it is reflexive. In (A) the probe is oriented for short-axis views (*white line*) and in (B) for long-axis views (*white line*). If you master this probe handling technique and it works for you, TFAST echo views will quickly become consistently good. The short-axis and long-axis lines are automatic. Although shown on a dog, the probe maneuvering is identical for cats. Source: Reproduced with permission from Dr Gregory Lisciandro, Hill Country Veterinary Specialists and FASTVet.com, Spicewood, TX.

probe" and it works really well for many sonographers although it takes some practice (Figure 17.20). *This technique is only for right lateral recumbency and not standing-sternal positioning*. By placing your index (trigger) finger on the probe marker and comfortably wrapping your hand around the probe head, you can buttress the pressure between the probe head and the patient's thoracic wall. Without this type of handling, you have two major problems: the probe head is jammed into the intercostal spaces of your patient, which is uncomfortable/painful (you will see the patient's pain-induced tachycardia on the screen), and the weight of your patient upon the probe head makes it difficult to fan and move the probe in small increments for your short-axis and long-axis views. For some, this probe-handling trick works very well and others just won't grasp it (no pun here). Practicing with the probe and repeating the motions away from the patient as in Figure 17.19 helps you learn the maneuver.

## *Right TFAST Pericardial Site Echo Views and Clinical Relevance*

There are three TFAST echo views imaged at this location which include both short-axis and long-axis views (Figure 17.21).

- The left ventricular short-axis (LVSA) view for volume and contractility (fractional shortening, FS%).
- The left atrial to aortic ratio (LA:Ao) on short-axis view for left heart strain/overload/failure.
- The right ventricular to left ventricular ratio (RV:LV) on long-axis four-chamber view (LA4CV) for right heart strain/overload/failure.

A bonus fourth TFAST echo view is slightly offset from the LA4CV in which the left ventricular (aortic) outflow tract (LVOT) may be imaged (see Chapters 19–21).

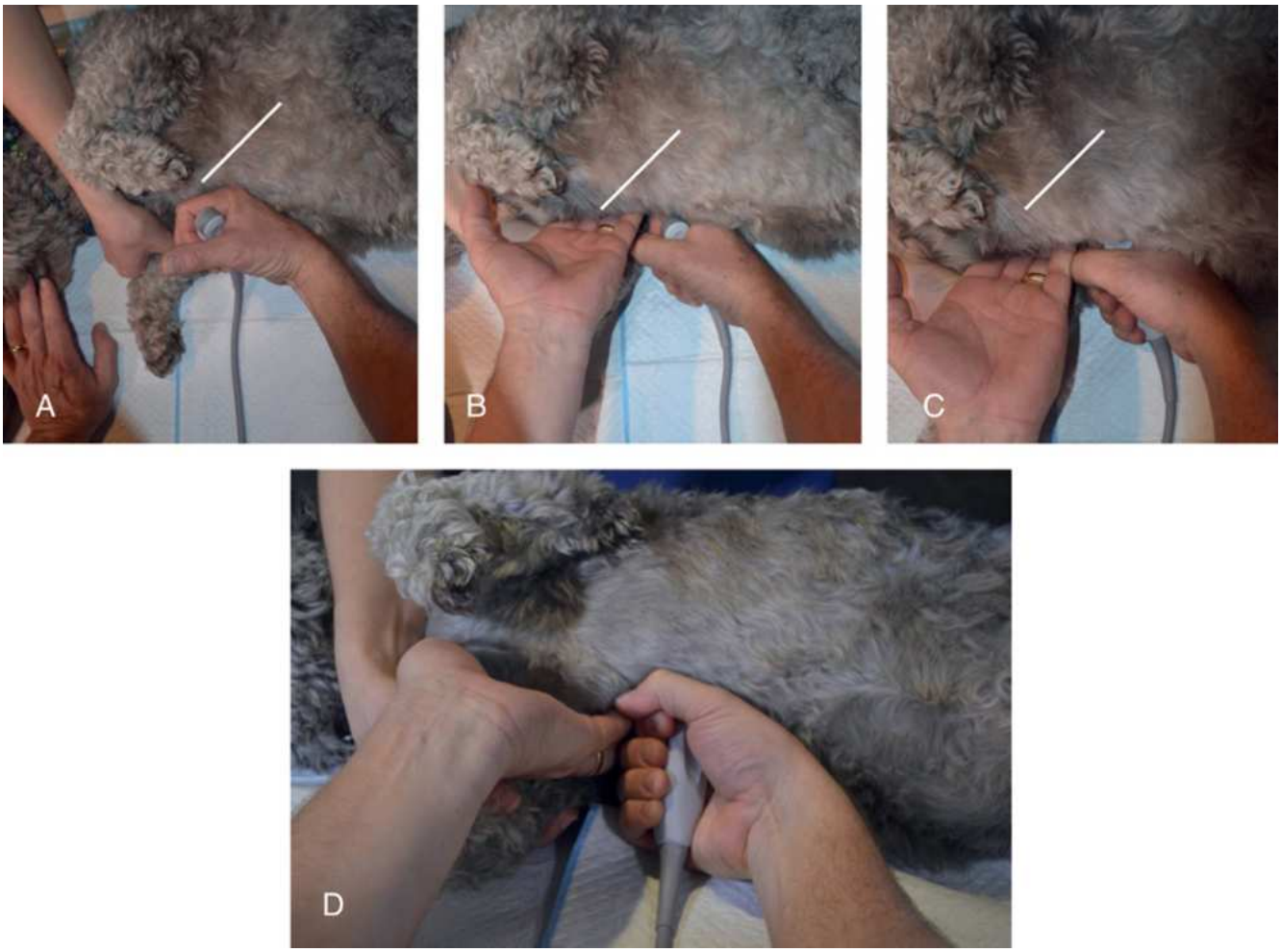


**Figure 17.20.** Working the short-axis TFAST echo lines. In (A) the probe is "knuckled" as in Figure 17.19. The probe head is held parallel to the short-axis line (white line on all the images) and placed under the patient where the apical beat is palpated shown in Figure 17.16. If you stay parallel to the short-axis line (4 o'clock to 10 o'clock) when placing the probe under your patient, as shown in (A–C) you will be very close to the correct short-axis view. In (D) the helper hand lifts the sternum and thorax to take pressure off the probe head to facilitate the small fanning increments that take you through the short-axis TFAST echo views (see also Figures 17.25 and 17.26). Source: Reproduced with permission from Dr Gregory Lisciandro, Hill Country Veterinary Specialists and FASTVet.com, Spicewood, TX.

Image acquisition for these three right PCS TFAST echo views follows the mantra "marker toward the elbow" for the short-axis line (4 o'clock to 10 o'clock) and "marker toward the spine" for the long-axis line (1 o'clock to 7 o'clock); no matter if the patient is in lateral recumbency or standing or sternal, the lines remain the same (Figure 17.22; see also Figures 17.20, 17.25, and 17.26). Learning to image on these short-axis and long-axis lines accelerates the learning process. The probe on the short-axis line of marker toward the elbow is a fanning maneuver "playing" on this line.

The probe is fanned on the long-axis line (1 o'clock to 7 o'clock) by having the probe marker toward the spine (1 o'clock) but angled slightly cranial since the heart is angled slightly cranially within the thorax (see Figures 17.19, 17.22, 17.25, and 17.26). On the long-axis line, fanning takes place for long-axis image acquisition. The appreciation of the position of the heart within the thorax and understanding the importance of the short- and long-axis lines accelerates the learning curve for imaging the heart (see Figures 17.19 and 17.22). Once the probe is rotated off these short-axis and long-axis lines, the echo images appear confusing and the sonographer becomes lost. Keep the probe head parallel to these lines while fanning in very small increments.

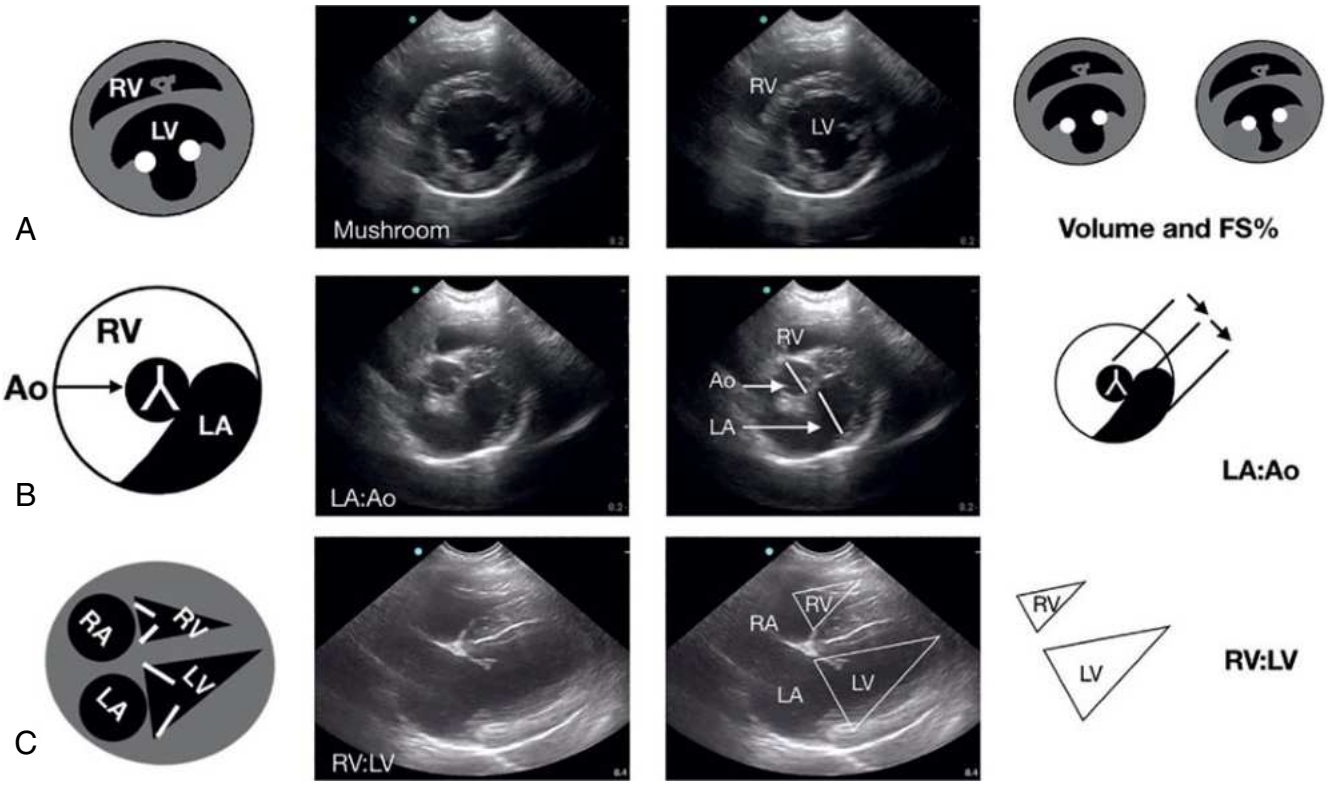


**Figure 17.21.** TFAST pericardial site echo views: rogue orientation, eyeballing volume and contractility and evidence for left- and right-sided enlargement. This figure shows the three major TFAST echo views: (1) the left ventricular short-axis view (LVSA) for volume and contractility (fractional shortening, FS%), (2) the short-axis left atrial (LA) to aortic (Ao) ratio (LA:Ao), and (3) the long axis four-chamber view for the right ventricular (RV) to left ventricular (LV) ratio (RV:LV). The long-axis LVOT image is a small movement off the long-axis four-chamber view and easily learned (see Chapters 19–21). In (A) the top row represents the LVSA, showing line drawing and images that correlate with expected volume and contractility (FS%). In (B) the middle row, the short-axis LA:Ao is showing line drawings and images for an unremarkable LA:Ao ratio. In (C) the lower row is the long-axis four-chamber view with line drawings and images for an unremarkable RV:LV ratio. The major focus for the long-axis four-chamber view is the "small triangle (RV) to large triangle (LV)" impression. In long-axis views, the atria and LVOT are *bonus* information but routinely imaged by the author. Abnormals are shown in Chapter 18. Source: Reproduced with permission from Dr Gregory Lisciandro, Hill Country Veterinary Specialists and FASTVet.com, Spicewood, TX.

In summary, the short-axis line and long-axis TFAST echo lines are the same whether in lateral recumbency or standing or sternal.

## *Defining the Levels of the TFAST Echo Views and the Cardiac Ladder*

Shown in Figures 17.22, 17.23, and 17.24 are line drawings and B-mode images on the abdominal preset of a dog, which would be analogous in the cat. In Figures 17.25 and 17.26 are the author's TFAST echo charts that must be understood in order to achieve success with TFAST echo view image acquisition. There are two versions. The rogue version has the standard imaging for all other ultrasound studies with the head to the left of the screen and the tail to the right. The classic version is the reverse screen orientation with the head to the right and the tail to the left. For some reason, echo orientation was reversed by radiologists/cardiologists. This echo view reversal from all other ultrasound imaging is confusing for the nonradiologist and noncardiologist because probe movements mirror what is done during all other ultrasound studies. In human medicine, the rogue version orientation is permitted at many institutions for this same reason, to remain consistent with all other imaging.

Learn the general shapes and impressions of heart chambers at all levels on our TFAST echo chart. Print and laminate the TFAST echo chart for your ultrasound stand. The heart is "eyeballed" for its assessment and used as a screening test in people *without* measurements

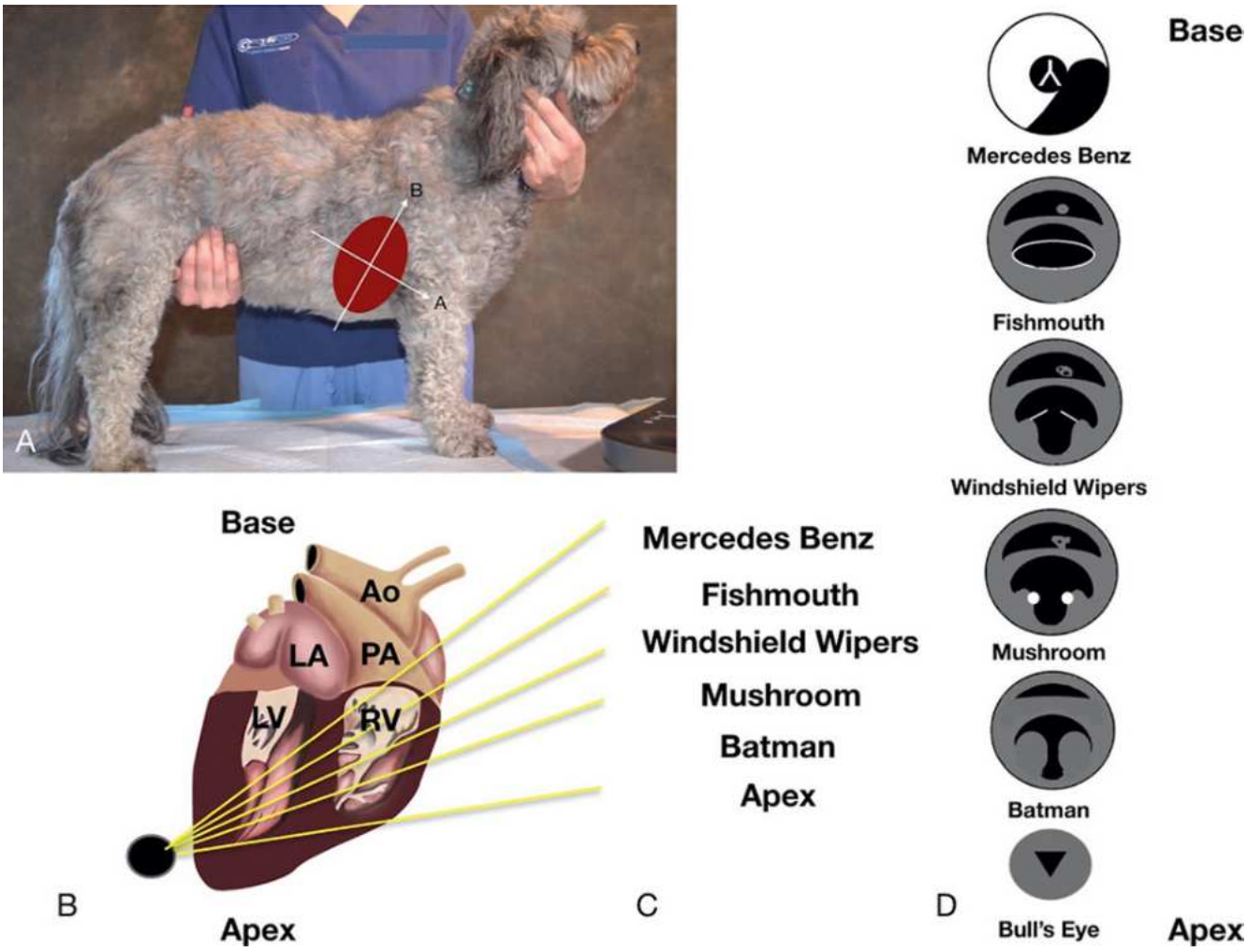


**Figure 17.22.** Right TFAST pericardial site short-axis echo views: rogue orientation in a standing dog. In (A) the dog is standing and the heart cartoon has overlays with the short-axis line "A" (4 o'clock to 10 o'clock) and long-axis line "B" (1 o'clock to 7 o'clock). In (B) the heart figure is labeled to give an idea of how the short-axis views image through the heart at different levels and it's worth spending time correlating (B) with (C) and (D). We have given unique names that help reflect the image to each of the levels. Note the levels go from the heart's apex to its base and knowing which is above and below each level helps you know which way to direct the probe for the level you want. Although shown on a dog, the TFAST concept is analogous for cats. See Figures 17.25 and 17.26. Ao, aorta; LA, left atrium; LV, left ventricle; RV, right ventricle. Source: Reproduced with permission from Dr Gregory Lisciandro, Hill Country Veterinary Specialists and FASTVet.com, Spicewood, TX.

(Ferrada et al. 2011; Atkinson et al. 2017). The objective of "eyeballing" echo views is to capture cases for gold standard testing and treatment while using a superior test, TFAST, over radiography. In most echocardiography courses, the sonographer is taught to start with long-axis views. For TFAST, we start sonographers on the more recognizable cardiac ladder of the short-axis views in the rogue version (see Figure 17.25).

### TFAST Right Pericardial Site Short-axis Views

Many of us focus on the shape of the left ventricle, but it is imperative to recognize the variability in the crescent-shaped right ventricle so it is not mistaken for pleural or pericardial effusion and centesis is catastrophically performed on the heart (Lisciandro 2016). So as you go through the figures, force yourself to pay attention to the crescent-shaped right ventricle and its variability in normalcy. See more detail regarding pitfalls in Chapter 18.

The short-axis levels are named as follows, beginning at the heart's apex and moving toward its base (see Figure 17.23).

- *Bull's eye*: the region of the muscular apex of the heart where there are no heart chambers to be confused when diagnosing pericardial effusion on TFAST. The soft tissue of the muscular apex of the

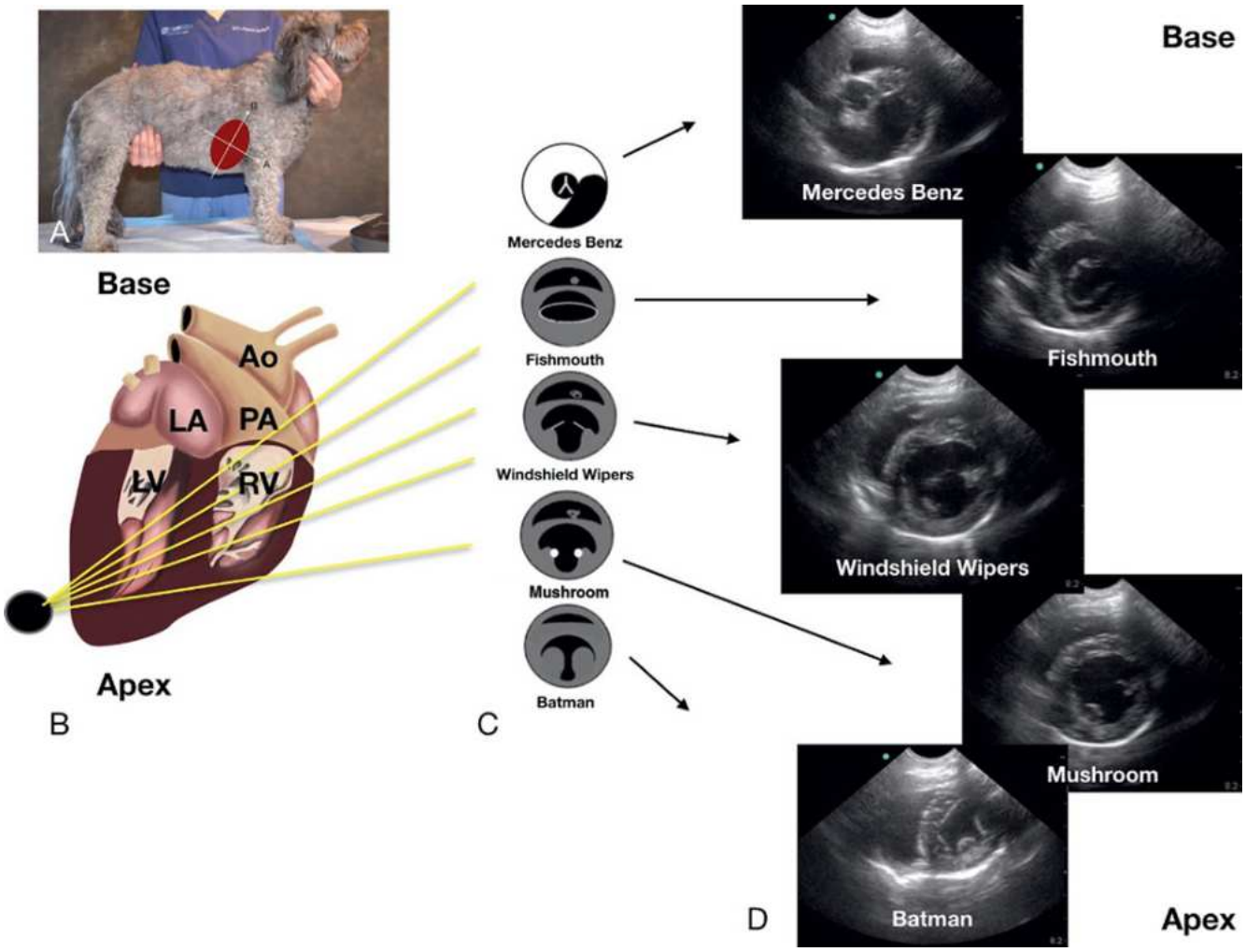


**Figure 17.23.** Right TFAST pericardial site short-axis echo views: rogue orientation in a standing dog with B-mode. In (A) the dog is standing and the heart cartoon has overlays with the short-axis line "A" (4 o'clock to 10 o'clock) and long-axis line "B" (1 o'clock to 7 o'clock). In (B) the heart figure is labeled to give an idea of how the short-axis views image through the heart at different levels and it's worth spending time correlating (b) with (C) and (D). We have given unique names that help reflect the image to each of the levels. Note the levels go from the heart's apex to its base and knowing which is above and below helps you know which way to direct the probe. Although shown on a dog, the TFAST concept is analogous for cats. See Figures 17.25 and 17.26. Ao, aorta; LA, left atrium; LV, left ventricle; RV, right ventricle. Source: Reproduced with permission from Dr Gregory Lisciandro, Hill Country Veterinary Specialists and FASTVet.com, Spicewood, TX.

heart appears as a gray circle in normalcy; however, when pericardial effusion is present, the gray circle is surrounded typically by anechoic fluid that gives the image of a "bull's eye."

- *Batman*: the next level toward the base of the heart involves the left ventricular papillary muscles with a variable crescent-shaped right ventricle. The effect looks like the superhero "Batman sign" projected in the sky when Batman is called for help. The importance of recognizing this view is that hypovolemia is often described as the papillary muscles contacting or "kissing" one another. This effect can be seen in normal patients by being too low on the heart in the Batman region.
- *Mushroom*: this level is clinically significant for the "eyeball method" of determining volume (filling of the left ventricle), contractility (fractional shortening, FS%), and chamber size (LA:Ao). The two white (hyperechoic) dots off the papillary muscles are landmarks created by the chordae tendinae coming off the papillary muscles to the semilunar mitral valves. The left ventricle appears like a "mushroom" and thus the name has been applied to this level that is where M-mode measurements are taken during complete detailed echocardiography.
- *Windshield wipers*: this level is where the mitral valves are first in view. They appear synchronously, mimicking car windshield wipers. When

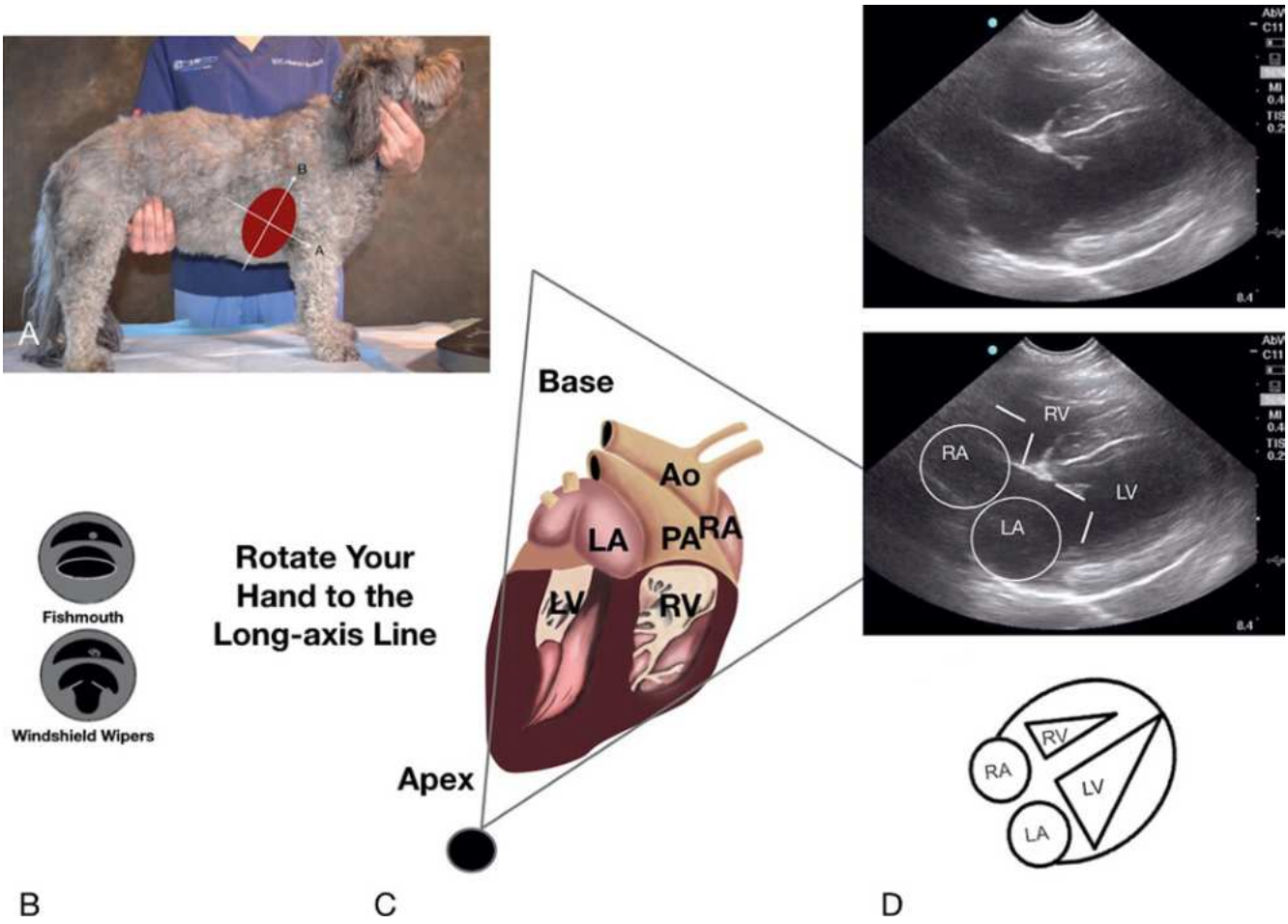


**Figure 17.24.** Long-axis right TFAST pericardial site echo view in a standing dog with still B-mode images. In (A) the dog is standing and the heart cartoon has overlays with the short-axis line "A" (4 o'clock to 10 o'clock) and long-axis line "B" (1 o'clock to 7 o'clock). In (B) the short-axis levels named "windshield wipers" and "fishmouth" are shown because on either of these levels, rotate 90° (when in lateral, you "open your hand" as in Figure 17.20). In (C) the cutaway of the heart is actually showing long axis so a triangle is used to represent the slice of the ultrasound beam. The image in (D) correlates with an unlabeled and labeled still image of the long-axis four-chamber view along with a didactic cartoon in the same orientation. Although shown on a dog, the TFAST concept is analogous for cats. See Figures 17.25 and 17.26. Ao, aorta; LA, left atrium; LV, left ventricle; RV, right ventricle. Source: Reproduced with permission from Dr Gregory Lisciandro, Hill Country Veterinary Specialists and FASTVet.com, Spicewood, TX.

dyssynchronous, conditions such as valvular disease and ruptured chordae tendinae should be suspected.

- *Fishmouth*: this level is in between the windshield wipers and the Mercedes-Benz view. The mitral valves touch and form an annulus that has been likened to a fishmouth. This level can be very confusing without considering where you are along short-axis views because the effect can mimic pleural and pericardial effusion without double-checking by fanning below and above this view.
- *Mercedes-Benz*: this level is called "Mercedes-Benz" by cardiologists because of the three aortic valves that look like the well-known logo. Often with curvilinear (microconvex) probes, the Mercedes-Benz sign is not that clear but the circle in the middle of the short-axis image is the giveaway because it can only be in the region of the heart base (most dorsal). Double-checking is always important and fanning the probe toward the heart's apex will bring you back into the mitral valves. This is a relevant view for evaluating volume status, cardiac function

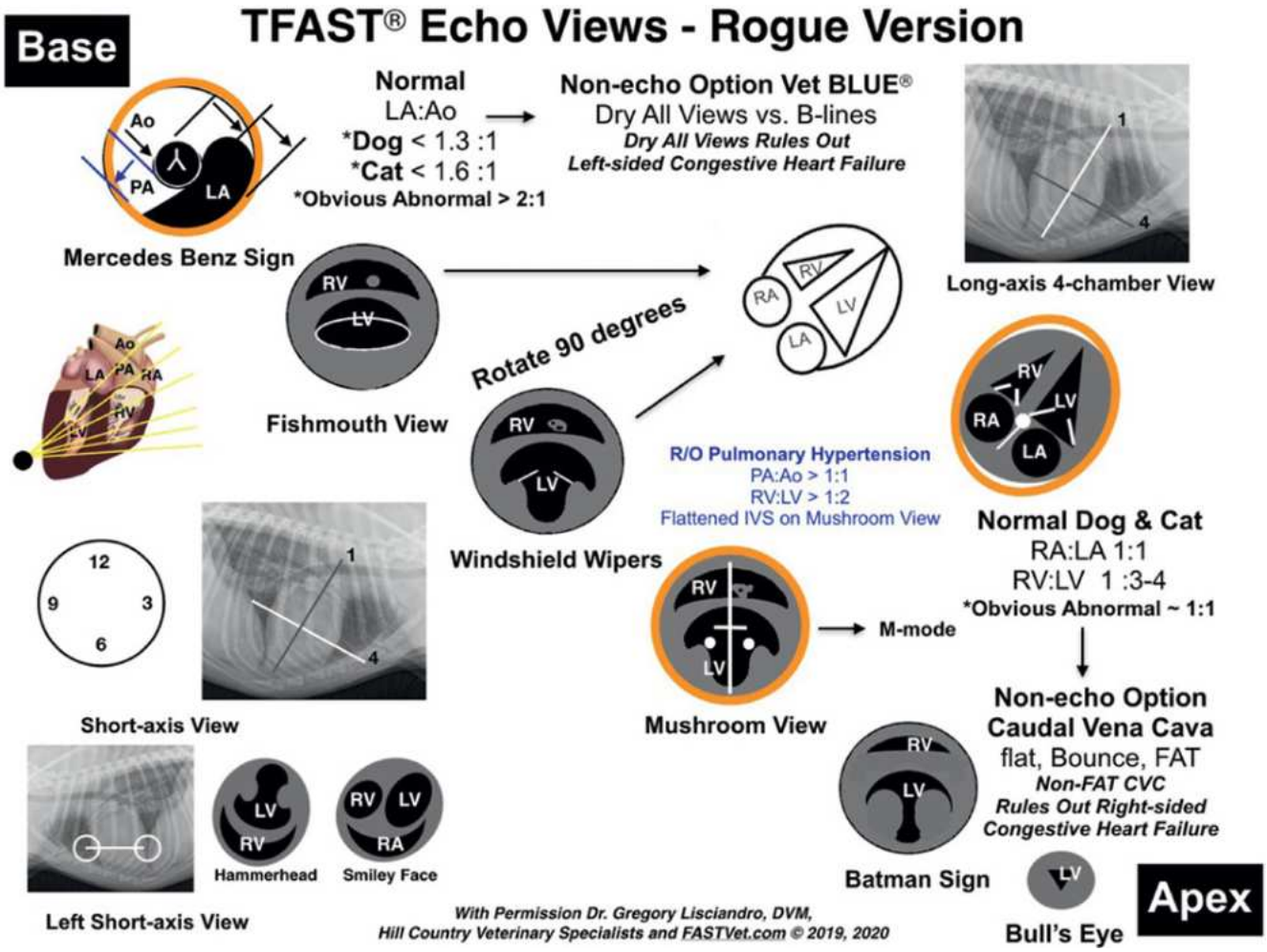


**Figure 17.25.** Rogue version of the TFAST pericardial site echo chart and its cardiac ladder. The rogue version with the head to the left of the screen as all other ultrasound imaging is performed. See the text for detailed explanation of the TFAST echo chart. The circled views (orange) are the three major TFAST echo views. The author images TFAST echo views according to the rogue version. Note the overlays on the radiograph with the short-axis line along 4 o'clock to 10 o'clock and the long-axis line along 1 o'clock to 7 o'clock. In order to be successful, the probe's scanning plane must stay along these lines (footprint parallel to these lines) as the sonographer fans in very small increments. For the rogue TFAST echo version images, the probe marker is toward 4 o'clock for short axis and 1 o'clock for long axis. Although shown with a canine thoracic radiograph, the TFAST concept is analogous for cats. Source: Reproduced with permission from Dr Gregory Lisciandro, Hill Country Veterinary Specialists and FASTVet.com, Spicewood, TX.

(FS%), and chamber size (LA:Ao). Normal LA:Ao is shown on the TFAST echo chart as 1.3:1 in dogs and 1.6:1 in cats. A good rule of thumb in either species is that the LA:Ao should never be more than 2:1.

### Right TFAST Pericardial Site Long-axis Views

The long-axis view is begun by moving to the mitral valve levels of either "windshield wiper" or "fishmouth" and rotating the probe 90°. If the patient is in lateral and you like "knuckling" the probe, then "open your hand" as shown in Figure 17.19, which automatically brings you 90°. The long-axis four-chamber view is the major view here although the LVOT view is just a small fan away from the long-axis four-chamber view and is useful to screen for aortic outflow and aortic valve abnormalities. See Chapters 19–21 regarding this additional view not shown on our chart. In human medicine, the major evaluation here is the right ventricular to left ventricular (RV:LV) ratio over atrial size and ratios. When the right ventricle approximates the size of the left ventricle then right-sided

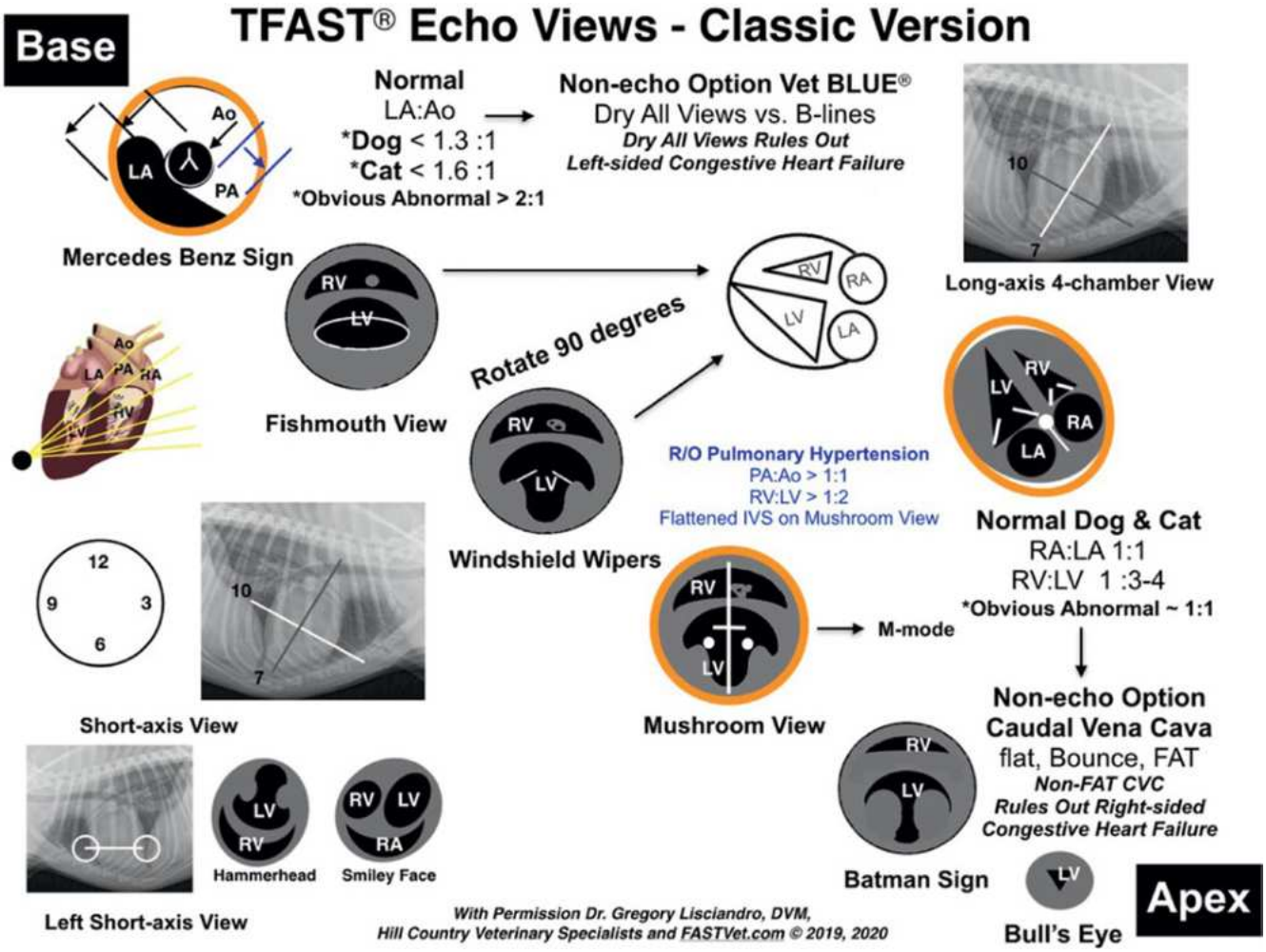


**Figure 17.26.** Classic version of the TFAST pericardial site echo chart and its cardiac ladder. The classic version with the head to the right of the screen is the opposite of the orientation of all other ultrasound imaging. The circled views (orange) are the three major TFAST echo views. Note the overlays on the radiograph with the short-axis line along 4 o'clock to 10 o'clock and the long-axis line along 1 o'clock to 7 o'clock. In order to be successful, the probe's scanning plane must stay along these lines (footprint parallel to these lines) as the sonographer fans in very small increments. For the classic TFAST echo version images, the probe marker is toward 10 o'clock for short axis and 7 o'clock for long axis. See the text for more detailed explanation of the TFAST echo chart. Although shown with a canine thoracic radiograph, the TFAST concept is analogous for cats. Source: Reproduced with permission from Dr Gregory Lisciandro, Hill Country Veterinary Specialists and FASTVet.com, Spicewood, TX.

cardiac problems should be suspected and a complete echocardiogram strongly considered.

Normal RV:LV is on the TFAST echo chart and the same for both dogs and cats as 1:3–4; in other words, the right ventricle is a "small triangle" and the left ventricle a "large triangle." Whenever the RV:LV approximates 1:1, right-sided strain/failure/overload should be suspected with integration of characterization of the caudal vena cava and hepatic veins (right-sided fallback view). See Chapters 7, 18, 19, 20, 26, and 36 for more detail.

### Left TFAST Pericardial Site Short-axis Views

The left short-axis views of the heart from the left TFAST PCS view are quite different from the right TFAST PCS views. The levels shown are ventral along the thoracic wall in the region of the costochondral junction with the probe held more or less parallel to the sternum, as shown in the lower left corner of the TFAST echo chart (see Figures 17.2, 17.25, and 17.26).

- *Hammerhead*: this is the lowest level (most ventral) at the left PCS view and named because the

upside-down mushroom looks like the head of a hammerhead shark. Along this level, it is common to see pericardial fat, which should be borne in mind to prevent mistaking for free fluid or pathology (Lamb 2000) (see Figures 18.25 and 18.26).

- *Smiley face*: this level is slightly dorsal from the "hammerhead view" where the right atrium and right auricle make up the lower "smile" part of the cardiac image. At the right commissure of the "smile" is where right auricular masses may be sought. See Chapters 19–21 for greater detail as an add-on TFAST skill.

## How to Image the Right TFAST Pericardial Site View Step by Step

### Right TFAST PCS Short-axis Views

- Locate the heart by palpating for the apical beat and placing the probe on the thoracic wall where the strongest palpated apical beat is found. This holds true for both lateral and standing or sternal recumbency (see Figure 17.16).
- Place the probe under the laterally recumbent (right side down) patient on the short-axis line with the marker toward the elbow. We start on short-axis views because it is easier to understand on what level you are by memorizing our TFAST echo chart (see Figures 17.16, 17.19, 17.20, and 17.25). You may also do the TFAST echo views in a standing patient, which the author prefers and does >95% of the time in stable dogs and cats. Echo measurements are validated in standing dogs (Chetboul et al. 2005).
- Wait through a couple of breaths if the heart is not immediately in view because your acoustic window may be intermittent (especially in sternal or standing patients) between inspiration and expiration from lung (air) interference.
- Make sure you have adequate coupling medium on the thorax with the hair parted before starting your approach. Without this strategy, you may get a nice acoustic window but without ample coupling medium you have to remove the probe from the patient to apply more medium, and you may not get a great acoustic window a second time.
- If the heart is not located after a couple of breaths, while remaining on the short-axis line, move the probe ventrally to get closer to the sternum and away from aerated lung (air rises).
- If the heart is not in view, likely it is an intercostal space cranial to where you are so slide one space cranially, looking for the beating heart.
- Once the heart is located, identify where you are on the left ventricular short-axis views (see Figures 17.19, 17.22, 17.23, and 17.25) and then fan along the short-axis line. These are generally very small hand movements of just a few millimeters while fanning that take you through the full range of short-axis views.

You must memorize the short-axis views on the echo chart so you know what direction to direct the probe, toward the heart base (more dorsal) or toward the heart apex (more ventral or toward the sternum), to get your images. The author images right TFAST PCS echo views according to the rogue version. These short-axis levels are named from the apex to the heart base from the "bull's eye" to the "batman sign" to the "mushroom" to the "windshield wipers" to the "fishmouth" to the "Mercedes-Benz sign" (circle in the middle of the screen) that represents the aorta. The "Mercedes-Benz," created by the three aortic semilunar valves, is often difficult to appreciate with the curvilinear (microconvex) probe in most patients. Thus, the "circle in the middle" on the next level toward the heart base (dorsal) from the "fishmouth" is the key to identifying the aorta. The "circle in the middle" is unique to the heart base region and is therefore an important landmark.

### Right TFAST Pericardial Site Long-axis Views

- After working through all the short-axis cardiac levels (short-axis cardiac ladder), move to where the mitral valves are located at either the "windshield wipers" or the "fishmouth."
- While on the mitral valves, rotate the marker toward the patient's spine but angled a little cranially to get on the long-axis line (see Figures 17.16, 17.19, and 17.24). Once on the long-axis line, fan one way and then the other while maintaining the footprint parallel to the long-axis line to get the long-axis four-chamber views.
- While the fan is occurring cranially and then caudally, watch the left ventricle to see it "open up" with its mitral valves appearing as "windshield wipers" (and if the left ventricle is closing down then fan the other direction). These movements are generally just a few millimeters, a very tight window, while fanning through this view.
- The long-axis four-chamber view has a hyperechoic focal point at the interventricular septum and then a thin white line extending from it representing the intraatrial septum (see Figure 17.24).
- A very small fanning from the long-axis four-chamber view will get you to the LVOT, an anechoic

circle representing the aorta (and possibly the Mercedes-Benz sign) and/or a hypoechoic (black) linear tract through the circle representing the LVOT (see Chapters 19–21).
- The Mercedes-Benz sign is often difficult to appreciate with the curvilinear (microconvex) probe in most patients, so the "circle" is the key to identifying the aorta, dependent on the view (short axis versus long axis).

## *Pitfalls at the TFAST Pericardial Views*

### Machine Settings

#### *Screen Orientation*

Make sure that you are aware of the screen orientation and which side of the screen is cranial. In abdominal presets and all other imaging, cranial is to the left of the screen. When changing to the cardiac preset, the screen orientation marker will be reversed. Either push the reverse button on your screen or rotate the probe 180° to maintain screen left as cranial if you prefer.

#### *Depth*

Always have enough depth to see the landmark of the bright pericardium in the far-field.

### Artifacts

There are three major artifacts that are the most relevant at the PCS views.

#### *Edge Shadowing*

Can produce hypoechoic and anechoic regions on either side of the heart, being a rounded structure. Scan by the axiom that "One view is no view" and combine multiple views (PCS and DH) to improve your interpretation.

#### *Mirror Image*

With dry lung against the far side of the heart, mirror image artifact is not uncommon in which the heart is partially or completely mirrored in the far-field.

#### *Slice-thickness and Side-lobe*

With rounded borders to cardiac chambers, slice-thickness and side-lobe artifacts can mimic soft tissue abnormalities.

### Anatomy – Left TFAST Pericardial Site View

The left TFAST PCS view is unique in that commonly an anechoic stripe is present between the heart and the thoracic wall representing pericardial fat (Lamb 2000) (see Figures 18.25 and 18.26). The best way to interpret this is to combine views and observe for the complete dirty shadowing from aerated lung in the absence of pleural effusion during the "TFAST slide" maneuver. If the stripe does not continue into the "cardiac-diaphragmatic pouch" caudally or the "cardiac-cervical pouch" cranially during the "TFAST slide" or is not supported by findings at combined views (DH view), then the suspect finding is likely not pleural effusion but rather pericardial fat as seen radiographically (Lamb 2000). A fat pad also exists in many patients in between the apex of the heart that is triangular but variably echogenic (shades of gray) (see Figures 18.25 and 18.26). To differentiate the pericardial fat pad from pleural effusion, the probe is swept dorsally to see if dirty shadowing from the thoracic wall obscures imaging or when free fluid is present the effect is absent along with a "curtain sign" of pleural effusion (Neelis et al. 2015) (see Figure 18.25). Furthermore, combine multiple views, especially the DH view, because this will interrogate the "cardiac-diaphragmatic pouch" from a different scanning plane.

# Performing the TFAST Diaphragmatico-Hepatic View

The TFAST DH view is performed identical to the AFAST DH view and the DH view should look nearly identical whether the patient is in lateral, right lateral or left lateral recumbency (Figure 17.27; see also Figures 6.8–6.12). Typically, three structures (the "Big 3") are rapidly located to get a feel for the depth and proportions of the view: gallbladder, "cardiac bump," and caudal vena cava. The best way in which to start the view is to begin at 10–15 cm depth, depending on the size of the patient (10 cm smaller to 15 cm larger patients), so that time is not wasted trying to find the Big 3 structures while being at too shallow a depth.

Once structures are identified, the depth may be reduced so the caudal vena cava is at the limit of the far-field. In severe respiratory compromised sternally (or standing) positioned small animals, the subxiphoid location is modified to accommodate the patient and may be used subcostally off midline and not immediately caudal to the xiphoid if safer. Importantly, the

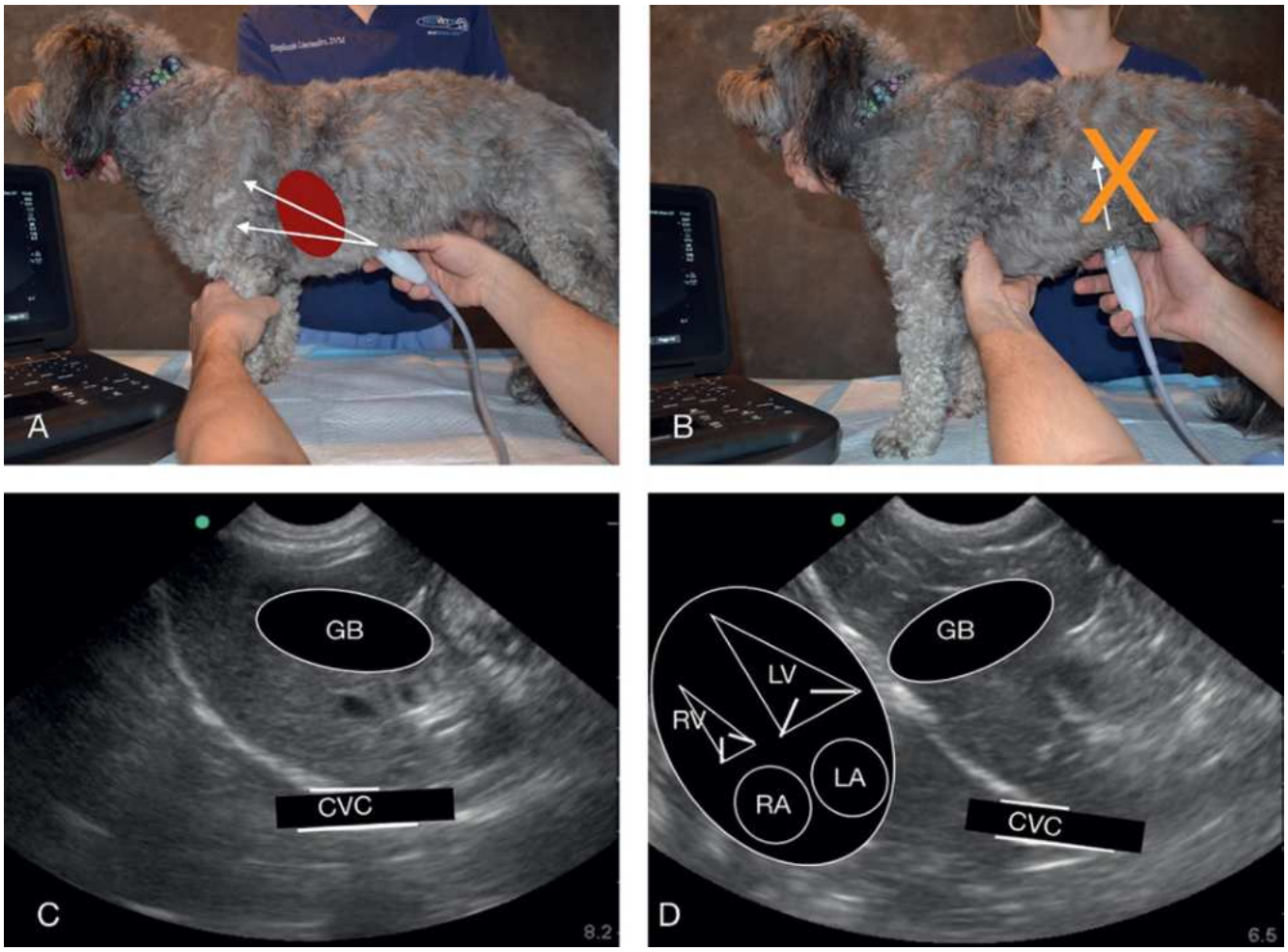


**Figure 17.27.** Diaphragmatico-hepatic view in a standing dog. In (A) the probe is directed toward the head in the longitudinal scanning plane of the patient which brings in the Big 3 when having lots of depth to start (8–15 cm) shown in (C) and (D). The arrows show how the ultrasound beam should be directed and the probe orientation is longitudinal, nearly parallel to the sternum. Note how the curved white (hyperechoic) line representing the diaphragmatic–pulmonary interface is nearly to the probe head in the near-field – a helpful tip for how far to rock the probe cranially. When done correctly, the DH view whether in right lateral, standing or sternal looks identical. In (B) the probe is directed toward the spine and this will not give you your target organs and is not recommended (X). The author always does the DH view from the patient's left side as shown because it is easier to image the gallbladder in both dogs and cats since the gallbladder lies to the right of midline and your right hand works naturally fanning right. In (C) and (D) are overlays showing the anatomy of the DH view that looks virtually the same whatever the patient positioning. CVC, caudal vena cava; GB, gallbladder; LA, left atrium; LV, left ventricle; RA, right atrium; RV, right ventricle, See the many detailed DH view figures in the AFAST chapters. Although shown on a dog, the TFAST concept is analogous for cats. Source: Reproduced with permission from Dr Gregory Lisciandro, Hill Country Veterinary Specialists and FASTVet.com, Spicewood, TX.

caudal vena cava will be more difficult to image and the heart will look different because of the oblique angle. However, the basic interrogation for free intraabdominal, pleural, and pericardial fluid may be completed, with some interrogation of the liver depending on what side the patient is imaged (the gallbladder is on the patient's right side). The gallbladder lies to the right of midline so it may be difficult to view from a modified left subcostal view, especially in cats.

The TFAST DH view is part of AFAST, TFAST, and Vet BLUE (see Chapters 6 and 22). The reader is referred to Chapter 6 in which the DH view is outlined in great detail.

Briefly, the DH view is performed as follows.

- The DH view begins with longitudinal placement of the probe with the probe marker towards the patient's head immediately caudal to the xiphoid

process. Stay longitudinal because transverse planes are confusing (see Figure 4.3).

- The probe is then directed far more cranially than most sonographers expect, being almost parallel to the sternum (see Figure 17.27). Attempting to bring the curved white (hyperechoic) line, representing the diaphragm-pulmonary interface as close (to the probe head) as possible in the near-field is another helpful tip. Don't direct toward the spine as you will get too much gastrointestinal tract and often there is lots of gas shadowing.
- Depth should be adjusted so that the diaphragm courses through the distal two-thirds of the image on the screen so that the near-field is two-thirds abdomen and the far-field one-third thorax (see Figures 6.8–6.12 and 17.27). This allows for adequately screening both the abdomen and thorax.
- The gallbladder, if not in view, is sought by fanning toward the tabletop (when in right lateral recumbency) or when the patient is standing and the sonographer is on the patient's left, fans toward the patient's right side (or the assistant if standing on the other side of the patient) because the gallbladder is located to the right of midline in both dogs and cats.
- In this same plane or close by, and making sure that the probe is immediately against the xiphoid, look for the caudal vena cava (CVC) as it traverses the diaphragm in both canines and felines (see Figures 6.8–6.12 and 17.27).
- The CVC is recognized by the two hyperechoic (bright white) lines that make up the near wall (short line) and far wall (long line) with reverberation artifact (A-lines) parallel hyperechoic lines to the far wall extending through the far-field, dependent on depth setting and the presence or absence of dry lung against the CVC's far wall (see Figures 6.9, 6.11, and 6.12).
- The mantra at the DH view is to see the Big 3 (gallbladder, "cardiac bump", CVC) as a general overview and for proper depth setting before starting the fanning and rocking (see Figure 17.27).
- Once the Big 3 have been identified and the image looks good, then in a sequential way specifically interrogate in the same order every time as follows.
  - Check the abdominal cavity for free fluid by fanning through the gallbladder (and its adjacent liver) in both directions, then followed by…
  - Rocking the probe toward the sternum to best image the cardiac bump, where the muscular apex of the heart is very near or immediately against the diaphragm for pericardial effusion, then followed by…
  - Imaging along the diaphragm for pleural effusion, and lung pathology along the pulmonary-diaphragmatic interface.

### Soft Tissue Findings at the DH View

If the canine and feline gallbladder is not visualized, its rupture, displacement (diaphragmatic herniation), or the presence of gallbladder stones, mineralization, sludge, mucoceles, and emphysematous cholecystitis should all be considered within the clinical context of the patient's history, presenting complaint, and other diagnostic findings (see Chapters 6 and 8).

### Pitfalls of the Diaphragmatico-Hepatic View

See Chapter 6.

## Summary of TFAST Views and Their Clinical Utility

TFAST now consists of five acoustic windows that include the bilaterally applied CTS and PCS views and a single midline DH view. The premise here is that fluid falls (gravity dependent) and air rises (nongravity dependent) (see Figure 17.1). Thus, it is easy to remember the clinical utility of the TFAST views.

The right and left CTS views are best used to rule out PTX and serve as a single-point survey for lung conditions. Vet BLUE should always be performed to search for the "lung point" when applicable (see Chapter 18) and for more comprehensive lung screening assessment.

The right and left PCS views are used to screen for the presence of pleural and pericardial effusions, and assess volume status and contractility (FS%), and left- and right-sided strain/failure/overload through the four TFAST echo views (see Chapter 18).

The single DH view is a first-line view for pericardial and pleural effusions because of less lung interference using the acoustic window of the liver and gallbladder (Lisciandro 2016a). The view is also used to assess CVC characterization and size, hepatic venous distension, and gallbladder wall edema (cardiac gallbladder) for volume status and right-sided heart strain/failure/overload (Nelson et al. 2010; Lisciandro 2011, 2014a,b, 2016; Lisciandro and Armenise 2014; Darnis et al. 2018). See also Chapters 6, 18, 26, and 36.

# Recording TFAST Findings on Goal-directed Templates

Recording your findings is imperative for a successful ultrasound program. See Chapter 18 and Appendix I.

# Pearls and Pitfalls, The Final Say

TFAST is more than a "flash exam" of the thorax (Lisciandro and Mann 2019). The TFAST examination rapidly answers many important clinical questions to help with decision making not only for patient resuscitation but also directing diagnostic efforts and patient management. TFAST is a superior imaging modality for pneumothorax, pericardial effusion, and soft tissue conditions of the heart which are suspected or completely missed radiographically. TFAST can help determine patient volume status and be used as a tracking tool for pleural and pericardial effusions and pneumothorax.

### *For the TFAST Chest Tube Site*

- You can't reliably image lung if you can't obtain the "gator sign" orientation.
- Use the "Tricks of the Trade" for manipulating the echoes either by the "one-eyed gator sign" and scattering the echoes or by the angle of insonation and ricocheting the echoes, or do both to enhance the observation of "lung sliding."
- Understand that gain, focus cursor, angle of insonation, and depth play a large role in image quality.
- Observe the CdTZ on every patient when defining the CTS view so that you become used to the pitfalls of lung ultrasound and avoid mistaking abdominal structures for lung pathology.

### *For the TFAST Pericardial Sites*

- Always image the heart in its entirety with enough depth to be able to identify the hyperechoic pericardium as your landmark in the far-field to avoid mistaking heart chambers for pleural and pericardial effusion and other pathology.
- Always start with the TFAST short-axis views for right PCS views.
- Learn to fan along the short-axis and long-axis TFAST echo lines. If you understand this concept you will quickly excel in TFAST echo image acquisition.
- Memorize the TFAST echo chart because it will help you know where you are and what direction you should go for image acquisition.
- The DH view should always be used because of its advantageous acoustic window via the liver and gallbladder into the pleural and pericardial spaces.

### *Eyeballing TFAST Echo Views*

- Especially in cats, the "freeze and roll the cine ball" maneuver must be mastered because the faster feline heart rate makes "eyeballing" more error prone.

# Quick Reference of Normals and Rules of Thumb

- If any evidence of lung, most commonly lung sliding and B-lines, observed against the intercostal space at the TFAST CTS view rules out PTX, especially in the preferred standing or sternal position.
- B-lines in trauma are lung contusions until proven otherwise.
- Always image the heart in its entirety using the hyperechoic (bright white) pericardium as a landmark in the far-field.
- Adhere to the axiom that "One view is no view" for the accurate diagnosis of pleural effusion and pericardial effusion.
- The FAST DH view is likely nearly 100% sensitive and 100% specific for detecting clinically relevant pericardial effusion in dogs and cats.
- Dogs and cats have no pleural or pericardial effusion that is evident in normalcy; however, pericardial fat mimics pleural effusion especially (1) along the heart at the left TFAST PCS view as an anechoic stripe (linear) between the heart and intercostal spaces, and (2) as an echogenic triangulation (fat pad) within the cardiacdiaphragmatic pouch.
- The "eyeball method" is accepted in people as a screening test for obvious cardiac abnormalities.
- A left atrial to aortic ratio (LA:Ao) that is >2:1 would be obviously abnormal in both dogs and cats.
- A right ventricular to left ventricular ratio (RV:LV) on the four-chamber long-axis view approximating a ratio of 1:1 would be obviously abnormal in both dogs and cats.
- An abnormal fractional shortening (FS%) for dogs and cats would be <20%.

- Sonographic striation of the gallbladder wall in dogs and cats can be due to right-sided congestive heart failure (most commonly pericardial effusion), referred to as a "cardiac gallbladder."
- TFAST right-sided cardiac markers that screen for obvious right-sided cardiac problems include the RV:LV, characterization of the CVC and hepatic veins, and gallbladder wall edema, that is, sonographic striation and the "cardiac gallbladder."

# References


American College of Emergency Physicians (ACEP). 2001. ACEP emergency ultrasound guidelines – 2001. *Ann Emerg Med* 38:470–481.

Atkinson P, Bowra J, Milne J, et al. 2017. International Federation for Emergency Medicine Consensus Statement: sonography in hypotension and cardiac arrest (SHoC): an international consensus on the use of point of care ultrasound for undifferentiated hypotension and during cardiac arrest. *Can J Emerg Med* 19(6): 459–470.

Ball CG, Ranson KM, Rodriguez-Galvez M, et al. 2009. Sonographic depiction of posttraumatic alveolar-interstitial disease: the handheld diagnosis of a pulmonary contusion. *J Trauma* 66(3):962.

Bilello JF, Davis JW, Lemaster D, et al. 2011. Prehospital hypotension in blunt trauma: identifying the "crump factor". *J Trauma* 70(5):1038–1042.

Blackbourne LH, Soffer D, McKenney M, et al. 2004. Secondary ultrasound examination increases the sensitivity of the FAST exam in blunt trauma. *J Trauma* 57: 934–938.

Boysen SR, Lisciandro GR. 2013. The use of ultrasound in the emergency room (AFAST and TFAST). *Vet Clin North Am Small Anim Pract* 43(4):773–797.

Boysen SR, Rozanski EA, Tidwell AS, et al. 2004. Evaluation of a focused assessment with sonography for trauma protocol to detect free abdominal fluid in dogs involved in motor vehicle accidents. *J Am Vet Med Assoc* 225(8): 1198–1204.

Breitkreutz R, Price S, Steiger HV, et al. 2010. Focused echocardiographic evaluation in life support and peri-resuscitation of emergency patients: a prospective trial. *Resuscitation* 81:1527–1533.

Brockman DJ, Puerto DA. 2004. Pneumomediastinum and pneumothorax. In: *Textbook of Respiratory Diseases in Dogs and Cats*, edited by King LG. Philadelphia: WB Saunders, pp 617–621.

Candotti C, Arntfield R. Pericardial effusion. In: *Point-of-Care Ultrasound*, edited by Soni NJ, Arntfield R, Kory P. Philadelphia: Elsevier, pp 130–134.

Chetboul V, Tidholm A, Nicolle A, et al. 2005. Effects of animal position and number of repeated measurements on selected two-dimensional and M-mode echocardiographic variables in healthy dogs. *J Am Vet Med Assoc* 227(5): 743–747.

Copetti R, Cattarossi L. 2007. The "double lung point": an unusual ultrasound sign diagnostic of transient tachypnea in the newborn. *Neonatology* 91:203–209.

Côté E, Schwarz LA, Sithole F. 2013. Thoracic radiographic findings for dogs with cardiac tamponade attributable to pericardial effusion. *J Am Vet Med Assoc* 243(2):232–235.

Cunningham J, Kirkpatrick AW, Nicolaou S, et al. 2002. Enhanced recognition of "lung sliding" with power color Doppler in the diagnosis of pneumothorax. *J Trauma* 52:769–772.

Darnis E, Boysen S, Merveille AC, et al. 2018. Establishment of references values of the caudal vena cava by fast-ultrasonography through different views in healthy dogs. *J Vet Intern Med* 32(4):1308–1318.

Ferrada P, Anand RJ, Whelan J, et al. 2011. Limited transthoracic echocardiogram: so easy any trauma attending can do it. *J Trauma* 71(5):1327–1331.

Ferrada P, Evans D, Wolfe L, et al. 2014. Findings of a randomized controlled trial using limited transthoracic echocardiogram (LTTE) as a hemodynamic monitoring tool in the trauma bay. *J Trauma Acute Care Surg* 76(1): 31–37.

Gargani L, Lionetti V, di Cristofano C, et al. 2007. Early detection of acute lung injury uncoupled to hypoxemia in pigs using ultrasound lung comets. *Crit Care Med* 35(12):2769–2774.

Guglielmini C, Diana A, Santarelli G, et al. 2012. Accuracy of radiographic vertebral heart score and sphericity index in the detection of pericardial effusion in dogs. *J Am Vet Med Assoc* 241(8):1048–1055.

Hwang TS, Yoon YM, Jung DI, et al. 2018. Usefulness of transthoracic lung ultrasound for the diagnosis of mild pneumothorax. *J Vet Sci* 19(5):660–666.

Hyacinthe AC, Broux C, Francony G, et al. 2012. Diagnostic accuracy of ultrasonography in the acute assessment of common thoracic lesions after trauma. *Chest* 141(5): 1177–1183.

Kirkpatrick AW, Sirois M, Laupland KB, et al. 2004. Handheld thoracic sonography for detecting post-traumatic pneumothoraces: the extended focused assessment with sonography for trauma (EFAST). *J Trauma* 57:288–295.

Koegelenberg CF, von Groote-Bidlingmaier F, Bolliger CT. 2012. Transthoracic ultrasonography for the respiratory physician. *Respiration* 84(4):312–318.

Kolata RJ, Dudley EJ. 1975. Motor vehicle accidents in urban dogs: a study of 600 cases. *J Am Vet Med Assoc* 167: 938–941.

Lamb CR. 2000. Radiology Corner: Ability to visualize the cardiac silhouette in animals with pleural fluid: the pericardial fat stripe. *Vet Radiol Ultrasound* 41(6):519–520.

Lichtenstein DA. 2007. Ultrasound in the management of thoracic disease. *Crit Care Med* 35(S5):S250–S261.

Lichtenstein DA. 2010. Should lung ultrasonography be more widely used in the assessment of acute respiratory disease? *Expert Rev Respir Med* 4(5):533–538.

Lichtenstein D. 2012. Fluid administration limited by lung sonography: the place of lung ultrasound in assessment of acute circulatory failure (the FALLS-protocol). *Expert Rev Respir Med* 6(2):155–162.

Lichtenstein D, Karakitsos D. 2012. Integrating lung ultrasound in the hemodynamic evaluation of acute circulatory failure (the fluid administration limited by lung sonography protocol). *J Crit Care* 27(5):533.

Lichtenstein DA, Meziere GA. 2008. Relevance of lung ultrasound in the diagnosis of acute respiratory failure: the BLUE protocol. *Chest* 134(1):117–125.

Lichtenstein D, Meziere G, Biderman P, et al. 2000. The "lung point": an ultrasound sign specific to pneumothorax. *Intens Care Med* 26:1434–1440.

Lichtenstein DA, Lascos N, Meziere GA, et al. 2004. Ultrasound diagnosis of alveolar consolidation in the critically ill. *Intens Care Med* 30:276–281.

Lichtenstein D, Meziere G, Lagoueyte JF et al. 2009. A-lines and B-lines: lung ultrasonography as a bedside tool for predicting pulmonary artery occlusion pressure in the critically ill. *Chest* 136:1014–1020.

Lisciandro GR. 2011. Abdominal and thoracic focused assessment with sonography for trauma, triage, and monitoring in small animals. *J Vet Emerg Crit Care* 21(2): 104–122.

Lisciandro GR. 2012. Evaluation of initial and serial combination focused assessment with sonography for trauma (CFAST) examinations of the thorax (TFAST) and abdomen (AFAST) with the application of an abdominal fluid scoring system in 49 traumatized cats. Abstract. *J Vet Emerg Crit Care* 22(S2):11.

Lisciandro GR. 2014a. The Abdominal FAST$^3$ (AFAST$^3$) Exam. In: *Focused Ultrasound for the Small Animal Practitioner*, edited by Lisciandro GR. Ames: Wiley Blackwell, pp 17–43.

Lisciandro GR. 2014b. The Thoracic FAST$^3$ (TFAST$^3$) Exam. In: *Focused Ultrasound for the Small Animal Practitioner*, edited by Lisciandro GR. Ames: Wiley Blackwell, pp 140–165.

Lisciandro GR. 2014c. The Vet BLUE lung scan. In: *Focused Ultrasound for the Small Animal Practitioner*, edited by Lisciandro GR. Ames: Wiley Blackwell, pp 166–188.

Lisciandro GR. 2016. The use of the diaphragmatico-hepatic (DH) views of the abdominal and thoracic focused assessment with sonography for triage (AFAST/TFAST) examinations for the detection of pericardial effusion in 24 dogs (2011–2012). *J Vet Emerg Crit Care* 26(1):125–131.

Lisciandro GR. 2019. The cardiac gallbladder: case series of 13 dogs and 1 cat with sonographically - detected gallbladder wall edema. *J Vet Emerg Crit Care* 29(S1): S24.

Lisciandro GR, Armenise A. 2014. Focused or COAST$^3$ – Cardiopulmonary Resuscitation (CPR), Global FAST (GFAST$^3$) & the FAST-ABCDE Exam. In: *Focused Ultrasound for the Small Animal Practitioner*, edited by Lisciandro GR. Ames: Wiley Blackwell, pp 269–285.

Lisciandro GR, Mann KA. 2019. Methodological questions regarding focused assessment sonography for trauma comparison with computed tomography in dogs. *J Vet Emerg Crit Care* 29(2): 211–213.

Lisciandro GR, Lagutchik MS, Mann KA, et al. 2008. Evaluation of a thoracic focused assessment with sonography for trauma (TFAST) protocol to detect pneumothorax and concurrent thoracic injury in 145 traumatized dogs. *J Vet Emerg Crit Care* 18(3):258–269.

Lisciandro GR, Lagutchik MS, Mann KA, et al. 2009. Evaluation of an abdominal fluid scoring system determined using abdominal focused assessment with sonography for trauma in 101 dogs with motor vehicle trauma. *J Vet Emerg Crit Care* 19(5):426–437.

Lisciandro GR, Fosgate GT, Fulton RM. 2014. Frequency of ultrasound lung rockets using a regionally-based lung ultrasound examination named veterinary bedside lung ultrasound exam (Vet BLUE) in 98 dogs with normal thoracic radiographic lung findings. *Vet Radiol Ultrasound* 55(3):315–322.

Lisciandro GR, Fulton RM, Fosgate GT, Mann KA. 2017. Frequency of B-lines using a regionally-based lung ultrasound examination (the Vet BLUE protocol) in 49 cats with normal thoracic radiographical lung findings. *J Vet Emerg Crit Care* 27(3):267–277.

Lisciandro GR, Romero L, Fosgate GT. 2018. The frequency of B-Lines and other lung ultrasound artifacts during Vet BLUE in 91 healthy puppies and kittens. Abstrac*t*. *J Vet Emerg Crit Care* 28(S1):S16.

McMurray J, Boysen S, Chalhoub S. 2016. Focused assessment with sonography in nontruamtized dogs and cats in the emegrency and critivcal care setting. *J Vet Emerg Crit Care* 26(1):64–73.

Narasimhan M, Koenig SJ, Mayo PH. 2016. A whole-body approach to point of care ultrasound. *Chest* 150(4): 772–776.

Neelis DA, Mattoon JS, Nyland TG. 2015. Thorax. In: *Small Animal Diagnstic Ultrasound*, 3rd edition, edited by Mattoon JS, Nyland TG. St Louis: Elsevier, pp 188–217.

Nelson NC, Drost WT, Lerche P, et al. 2010. Noninvasive estimation of central venous pressure in anesthetized dogs by measurement of hepatic venous blood flow velocity and abdominal venous diameter. *Vet Radiol Ultrasound* 51(3):313–323.

Nyland TC, Mattoon JS. 2002. Thorax. In: *Small Animal Diagnostic Ultrasound*, 2nd edition, edited by Nyland TC, Matton JS. Philadelphia: WB Saunders, p 335.

Ollerton JE, Sugrue M, Balogh Z, et al. 2006. Prospective study to evaluate the influence of FAST on trauma patient management. *J Trauma* 60:785–791.

Peris A, Zagli G, Barbani F, et al. 2010. The value of lung ultrasound monitoring in H1N1 acute respiratory distress syndrome. *Anaesthesia* 65(3):294–297.

Powell LL, Rozanski EA, Tidwell AS, et al. 1999. A retrospective analysis of pulmonary contusions secondary to motor vehicle accidents in 143 dogs: 1994–1997. *J Vet Emerg Crit Care* 9(3):127–136.

Quantz JE, Miles MS, Reed AL, et al. 2009. Elevation of alanine transaminase and gallbladder wall abnormalities as biomarkers of anaphylaxis in canine hypersensitivity patients. *J Vet Emerg Crit Care* 19(6):536–544.

Rademacher N, Pariaut R, Pate J, et al. 2010. Comet-tail artifacts in normal dogs and dogs with cardiogenic pulmonary edema. *J Vet Intern Med* 24(3):729.

Reissig A, Copetti R, Kroegel C. 2011. Current role of emergency ultrasound of the chest. *Crit Care Med* 39(5):1–8.

Sargsyan AE, Hamilton DR, Nicolau S, et al. 2001. Ultrasound evaluation of the magnitude of pneumothorax: a new concept. *Am Surg* 67:232–235.

Scansen BA. 2001. Interventional cardiology for the criticalist. *J Vet Emerg Crit Care* 21(2):123–136.

Sigrist NE, Doherr MG, Spreng DE. 2004. Clinical findings and diagnostic value of post-traumatic thoracic radiographs in dogs and cats with blunt trauma. *J Vet Emerg Crit Care* 14:259–268.

Simpson SA, Syring R, Otto CM. 2009. Severe blunt trauma in dogs: 235 cases (1997–2003). *J Vet Emerg Crit Care* 19(6):588–602.

Soldati G, Testa A, Silva FR, et al. 2006. Chest ultrasonography in lung contusion. *Chest* 130(2):533–538.

Soldati G, Sher S, Testa A. 2011. Lung and ultrasound: time to "reflect." *Eur Rev Med Pharmacol Sci* 15:223–227.

Volpicelli G, Boero E, Stefano V, et al. 2013. Unusual new signs of pneumothorax at lung ultrasound. *Crit Ultrasound J* 5(1):10.

Ward JL, Lisciandro GR, Keene BW, et al. 2017. Accuracy of point-of-care lung ultrasonography for the diagnosis of cardiogenic pulmonary edema in dogs and cats with acute dyspnea. *J Am Vet Med Assoc* 250:666–675.

Ward JL, Lisciandro GR, Ware WA, et al. 2019. Lung ultrasound findings in 100 dogs with various etiologies of cough. *J Am Vet Med Assoc* 255(5):574–583.

CHAPTER EIGHTEEN

# POCUS: TFAST – Clinical Integration

Gregory R. Lisciandro

## Introduction

TFAST is an examination of the thorax that extends beyond the "flash mentality" because with its cerebral approach, a tremendous amount of clinical information may be gained in a matter of minutes, similar to the AFAST examination. Chapter 17 reviews image acquisition principles, to which the reader is referred. This chapter will discuss the clinical integration of TFAST and its five acoustic windows as they relate to pleural and pericardial effusion, pneumothorax, the TFAST echo views for cardiac conditions, and the caudal vena cava for volume status combined with other TFAST findings.

Before beginning this chapter, it is important to acknowledge the uniqueness of the thorax, with its two major organs, compared to the abdomen, with more than six major organs, regarding effusions and free air. First, there is only one major fluid-filled structure within the thorax that the sonographer can mistake for free fluid and that is your patient's heart. The heart, unlike the abdominal organs, is not as forgiving regarding misguided centesis (sticking a needle in your patient's heart versus the liver or spleen or urinary bladder). Second, the other major thoracic organ, lung, is air-filled and occupies most of the thorax, posing problems not only with its direct imaging but also interfering with the imaging of the heart and pleural cavity because ultrasound does not transmit through air but rather reflects. Thus, transthoracic acoustic windows are much more challenging and intimidating to many sonographers who are comfortable imaging the abdominal cavity, but lack confidence in tackling the thorax.

Free fluid in the thorax also differs from the abdominal cavity and retroperitoneal space, in which free fluid commonly images as anechoic (black) triangulations. Whereas pleural effusion often behaves similarly, pericardial effusion is contained within the pericardial sac and is rounded (not triangulated) in appearance. Then finally, we can have pathological free air in the pleural cavity, called pneumothorax, which involves an array of intimidating air-related artifacts that must be differentiated from aerated lung.

Get ready for a wild but achievable TFAST ride through the small animal thorax!

### *What TFAST Can Do*

- Can rapidly detect pneumothorax in traumatized dogs and cats with high accuracy, sensitivity, and specificity.
- Can determine the degree of pneumothorax (in other words, its severity) as "partial" versus "massive" by finding the "lung point."
- Can detect and monitor pleural effusion, initially and serially.
- Can detect and monitor pericardial effusion, initially and serially.
- Can determine the presence or absence of cardiac tamponade.
- Can be used as a soft tissue examination of the heart.
- Can crudely detect and monitor lung contusions initially and serially. However, lung contusions are better detected, tracked, and scored with Vet BLUE, using the Vet BLUE lung contusion scoring system.

*Point-of-Care Ultrasound Techniques for the Small Animal Practitioner*, Second Edition. Edited by Gregory R. Lisciandro.
© 2021 John Wiley & Sons, Inc. Published 2021 by John Wiley & Sons, Inc.
Companion website: www.wiley.com/go/lisciandro/ultrasound2

- Can detect thoracic wall, pleural space, and lung pathology through the presence of the "step sign" which is, however, better characterized by Vet BLUE (more extensive lung examination than TFAST).
- Can assess volume status and contractility by using the TFAST right pericardial site (PCS) view to evaluate the left ventricular short-axis "mushroom view."
- Can assess left cardiac strain/failure/overload by using the TFAST right PCS view to evaluate the short-axis left atrial to aortic ratio (LA:Ao).
- Can assess right cardiac strain/failure/overload by using the TFAST right PCS view to evaluate the long-axis right ventricular to left ventricular ratio (RV:LV).
- Can screen for right atrial and right auricular masses at the TFAST left PCS view using its short-axis "smiley face" echo view.
- Can screen for intracardiac and extracardiac masses at any of the TFAST echo views.
- When combined with Vet BLUE, can assist in respiratory distress evaluation by rapidly determining pulmonary versus cardiac causes based on Vet BLUE's regional pattern-based approach.
- When combined with Vet BLUE, can assist in respiratory distress cases by rapidly supporting types of lung disease including forms of pulmonary edema (cardiogenic, noncardiogenic), pneumonia, and neoplastic conditions based on regional pattern-based lung distribution of the Vet BLUE six lung ultrasound signs.
- Can be used to serially monitor intrathoracic conditions including pleural, pericardial, heart, and lung conditions at cageside in place of serial radiography and computed tomography (CT) in many patients. See Table 18.1 for summary.

## What TFAST Cannot Do

- Cannot characterize pleural fluid; sample acquisition (thoracocentesis) and fluid analysis are necessary.
- Cannot characterize pericardial fluid; sample acquisition (pericardiocentesis) and fluid analysis are necessary.
- Cannot fully replace thoracic radiography (TXR).
- Cannot fully replace computed tomography (CT).
- Cannot fully replace complete echocardiography.
- Cannot diagnose nonthoracic causes of respiratory distress, the so-called nonrespiratory lookalikes such as, within the peritoneal cavity, hemoabdomen, canine anaphylaxis, and causes of acute abdomen, and in the retroperitoneal space, bleeding from adrenal, vena cava, and aortic sources, other renal-related or spinal-related sources of free fluid. Therefore, the Global FAST approach should be incorporated with TFAST.
- TFAST is limited in its pulmonary evaluation without the additional six acoustic windows of Vet BLUE. See Table 18.1 for summary.

**Important:** Vet BLUE should be considered as an extension from the TFAST chest tube site (CTS) and used routinely for better lung evaluation.

## Indications

- Blunt and penetrating trauma.
- Nontrauma triaged cases, for example, weakness, collapsed, "ain't doing right" (ADR), and with changes in breathing patterns.
- All respiratory distress.
- Trauma cases for lung contusions.
- Nontrauma cases for evidence of various forms of alveolar-interstitial edema and pulmonary hemorrhage.
- Pneumothorax (PTX) for detecting and assessing PTX severity using the "lung point."
- Tracking and decision making for PTX using the "TFAST PTX 1/3s Rule."
- Pleural effusion (PE) for detecting, tracking, and estimating severity using the TFAST PCS view measurement at the 4th–5th intercostal space at the level of the costochondral junction.
- Pericardial effusion (PCE) for detecting, tracking, and estimating severity using widest measurements at the diaphragmatico-hepatic (DH) view in standing or sternal, or at the 4th–5th intercostal space at the level of the costochondral junction.
- Surveying at-risk small animals for PTX, PE, and PCE, including any and all postinterventional/procedural cases (thoracic surgery, thoracoscopy, lung lobe aspirates, other at-risk procedures, mechanical ventilation, and post anesthesia).

## Objectives

- Be able to rapidly diagnose PTX, estimate the degree of PTX, and track it using the "Lung point" and the "TFAST PTX 1/3s Rule."
- Be able to identify a lung condition at the CTS view including the six Vet BLUE lung ultrasound signs.

- Be able to rapidly diagnose PE, estimate the degree of PE, and track PE using TFAST measurements.
- Be able to rapidly diagnose PCE, estimate the degree of PCE, and track PCE using TFAST measurements.
- Be able to detect left- and right-sided strain/failure/overload through the use of TFAST echo views of the left ventricular short-axis view, the LA:Ao on short-axis, and the RV:LV on long-axis.
- Be able to assess patient volume status by using the TFAST right-sided cardiac markers of the RV:LV ratio on long-axis, caudal vena cava characterization and measurement, hepatic venous distension, and gallbladder wall edema ("halo effect").
- Be able to suspect pleural space conditions other than PTX and PE, such as diaphragmatic herniation, by recognizing changes from the expected contour of the diaphragm at the DH view and the presence of abdominal structures at the PCS views.
- Understand that the Global FAST approach should be used to better assess the patient for other concurrent conditions by integrating information.

# Findings at the Chest Tube Site View

## *Concept of Wet versus Dry Lung*

### Lung Sliding and A-lines Indicate Dry Lung and Rule Out Pneumothorax

"Lung sliding" is defined as the to-and-fro motion of the lung along the intercostal space represented by the bright white, hyperechoic, (proximal) line or the pulmonary–pleural interface (PPI) or where the parietal and visceral pleura slide across one another (micro description) or where the "lung line" and intercostal space slide across one another (macro description) (see Figure 17.6). All these descriptions are synonymous and are descriptive in normalcy. However, when pleural space disease exists, the PPI is most commonly disrupted by fluid, air, abdominal organs, or soft tissue and we refer to the lung surface as the "lung line." "Lung sliding" has replaced the veterinary term of "glide sign" (Volpicelli et al. 2012).

In normalcy, "lung sliding" of aerated lung is accompanied by strong air reverberation artifacts called A-lines (remember "A" is for "air"). The observation of A-lines is dependent on your angle of insonation (make it as close to 90° to the lung surface as possible) and your machine settings (frequency, depth, focus cursor), explained in more detail in Chapter 17. Primary A-lines are identified by their equidistance from one another as parallel lines (or bars) through the far-field (see Figure 17.6). Their spacing is approximately the distance from the probe head to the first soft tissue–air interface (in normalcy aerated lung against the thoracic wall or pneumothorax when air is in the pleural space). A-lines are also present, dependent on settings and your machine's software, as secondary and tertiary A-lines or, in other words, as A-double prime and A-triple prime (A'-, A"-, A"-) lines (see Figure 17.6). The key is the presence of repeated horizontal parallel lines (or bars) from the "lung line" through the far-field. The presence of "lung sliding" with A-lines defines the term "dry lung" and, with its absence, pneumothorax (PTX) (Lichtenstein et al. 2000; Kirkpatrick et al. 2004; Volpicelli et al. 2006; Lisciandro 2011, 2014a,b, Lisciandro et al. 2014, 2017).

Importantly, "lung sliding" is a real-time finding. It requires correlating with phases of respiration, the to-and-fro movement in concert with inspiration and expiration. The presence of "lung sliding" differentiates "dry lung" from PTX since both conditions have strong A-lines because both have air immediately adjacent to the thoracic wall and its intercostal space. In PTX there are strong A-lines but no "lung sliding" (Volpicelli et al. 2012; Lisciandro 2011; Lichtenstein et al. 2000; Kirkpatrick et al. 2004) (Figure 18.1). Moreover, the finding of the "lung point" (described later) increases the sensitivity and specificity of a PTX diagnosis (Lichtenstein et al. 2000; Lisciandro et al. 2008, Lisciandro 2011, 2014a) (see Figures 18.5 and 18.6).

### B-Lines and Wet Lung Rule Out Pneumothorax

B-lines have also been referred to as "ultrasound lung rockets" and represent forms of alveolar-interstitial edema; however, in trauma, B-lines are lung contusions until proven otherwise (Ball et al. 2009; Lisciandro 2011, 2014a,b; Lisciandro et al. 2014; Dicker et al. 2019). You cannot see the B-line artifact when PTX is present because free air in the pleural space images as A-lines, a uniquely different artifact (Lichtenstein et al. 1999; Ball et al.2009; Lisciandro 2011). B-lines are now the preferred nonvisual term for artifacts historically referred to as comet-tail artifact, ultrasound lung rockets, and ring-down artifact (Lichtenstein et al. 1997, 1999, 2009; Volpicelli et al. 2012; Louvet and Bourgeois 2008).

It is important to note that B-lines are created differently from true comet-tails. Comet-tails were first used to describe the ultrasound artifact created by strong reflectors (metal) of the ultrasound beam, whereas B-lines are created by the large difference in acoustic

Vetbooks.ir

**Table 18.1.**
What clinical questions can be answered using TFAST? Binary? Qualitative-quantitive?.

| Clinical questions answered using TFAST | Binary | Qualitative-quantitive | Examples | Sensitivity (Se)[a]<br>Specificity (Sp)[a] |
|---|---|---|---|---|
| • Does the patient have free fluid in the pleural cavity –pleural effusion? | √<br>Yes or no | √<br>No standardized established easy objective measurement techniques<br>Trivial, mild, moderate, severe | Transudate<br>Modified transudate<br>Hemothorax<br>Pyothorax<br>Chylothorax<br>Pseudochylothorax<br>Other exudates | Se – high<br>Sp – high |
| • Does the patient have free fluid in the pericardial sac – pericardial effusion? | √<br>Yes or no | √<br>No standardized established easy objective measurement techniques<br>Trivial, mild, moderate, severe | | Se – high<br>Sp – high |
| • Does the patient have any obvious TFAST target organ abnormalities of the heart? | √<br>Yes or no | √ | Pericardial effusion<br>Chamber enlargement<br>• Pulmonary hypertension (increased RV:LV)<br>• Dilated cardiomyopathy (poor FS%)<br>• Mitral valve disease (increased LA:Ao)<br>Intracardiac masses<br>Heartworms (*Dirofilaria immitis*) | Se – variable, operator dependent<br>Sp – high |
| • Does the patient have any obvious TFAST target organ abnormalities of or related to the pleural space? | √<br>Yes or no | √ | Diaphragmatic hernia<br>Pericardioperitoneal hernia<br>Masses (thoracic wall, intrathoracic, pericardial, cardiac, intracardiac, pulmonary) | Se – unknown, operator dependent<br>Sp – likely high |
| • Does the patient have any obvious TFAST target organ abnormalities of or related to the lung surface? | √<br>Yes or no | √<br>Vet BLUE 6 lung ultrasound signs<br>Vet BLUE B-line scoring | | Se – variable, only a single lung-specific transthoracic acoustic window bilaterally<br>Sp – high |
| • Does the patient have lung pathology along the pulmonary–diaphragmatic interface? | √<br>Yes or no | √<br>Vet BLUE 6 lung ultrasound signs<br>Vet BLUE B-line scoring | | Se – unknown, operator dependent<br>Sp – likely high |
| • What is the patient's volume status? | √<br>Unremarkable or abnormal | √<br>Characterizing the caudal vena cava | | Hypervolemia[b]<br>Se – likely high<br>Sp – likely high<br>Hypovolemia[b]<br>Se – likely variable<br>Sp – likely high<br>Euvolemia[b]<br>Se – variable<br>Sp – variable |

[a]Clinical experience, limited veterinary and human studies.
[b]Integrating TFAST echo and Vet BLUE pulmonary information likely improves both Se and Sp.
Source: Reproduced with permission from Dr Gregory Lisciandro, Hill Country Veterinary Specialists and FASTVet.com, Spicewood, TX.

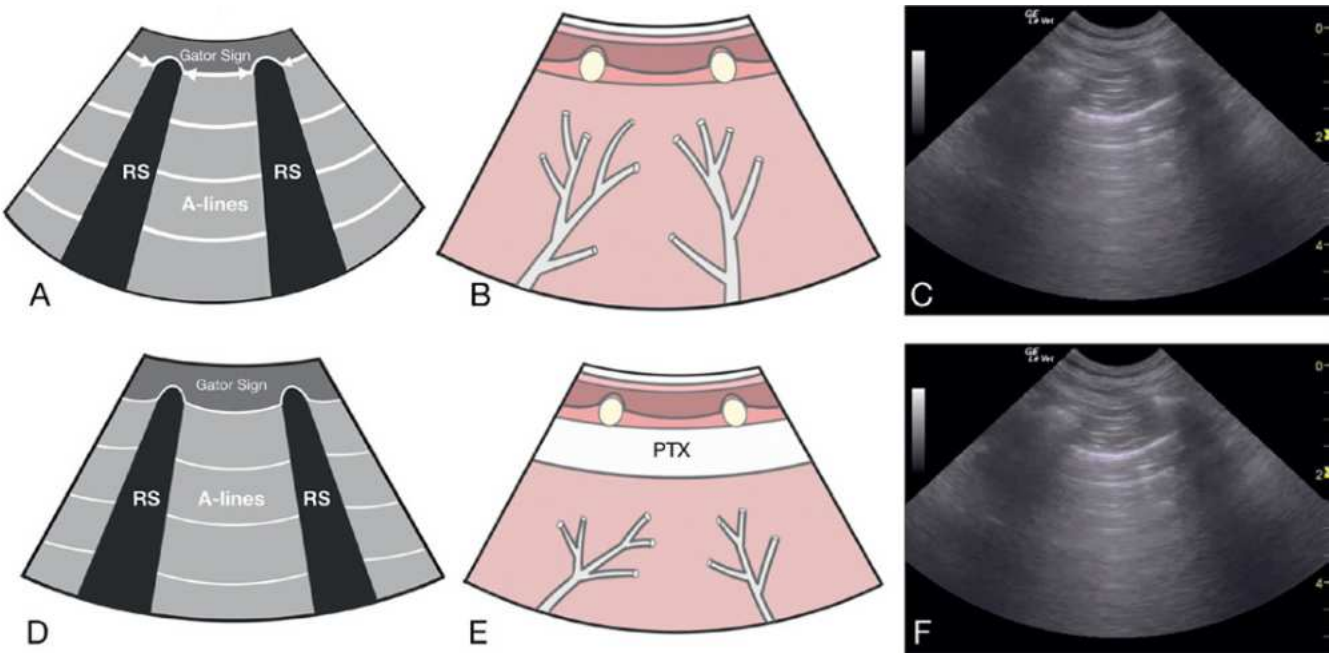


**Figure 18.1.** Dry aerated normal lung and pneumothorax. Shown in the top row are the (A) line drawing, followed by (B) a pictorial of the anatomy, followed by (C) the B-mode ultrasound image of normal aerated lung at its periphery. Shown in the bottom row are the (D) line drawing, followed by (E) a pictorial of the anatomy, followed by)F) the B-mode ultrasound image of pneumothorax. Note how the line drawings and B-mode ultrasound images look identical. To differentiate normal aerated lung at the periphery from pneumothorax in B-mode, "lung sliding" must be observed in real time. Source: Reproduced with permission from Dr Gregory Lisciandro, Hill Country Veterinary Specialists and FASTVet.com, Spicewood, TX. Illustration by Dr Judy Brown, Toronto, Canada.

impedance between a fluid–air interface (Volpicelli et al. 2006). B-lines are defined as laser-like hyperechoic (bright white) vertical streaks that oscillate in synchrony with phases of respiration while obliterating A-lines and extend through the far-field of the ultrasound screen without fading (Figure 18.2). Their laser-like appearance is why they have also been referred to as "ultrasound lung rockets" (Lichtenstein 2007, 2010b; Lisciandro 2011, 2014a,b). B-lines, despite extending through the far-field, represent a superficial fluid–air juxtaposition along the very outer 1–3 mm of lung surface in people (Volpicelli et al. 2006; Soldati et al. 2011), which likely holds true for all mammalian lung. B-lines are referred to as "wet lung" since they most commonly represent forms of alveolar-interstitial edema (Volpicelli et al. 2006; Lisciandro 2011, 2014a,b, Lisciandro et al. 2014, 2017).

Importantly, B-lines are nonspecific and thus their presence is referred to as alveolar-interstitial syndrome (AIS) because their distribution with a regional pattern-based approach must be used for their causative interpretation, that is, Vet BLUE (see Figure 18.2). In people, older lung (>65 years of age) and fibrosis along the lung surface from chronic respiratory diseases can also cause B-lines that are not truly representative of AIS (Shyamsundar et al. 2013). In trauma, B-lines are lung contusions until proven otherwise and a Vet BLUE B-line scoring system and lung contusion severity score have been developed (Ball et al. 2009; Lisciandro 2011; Dicker et al. 2019). See Chapters 22 and 23 for more detail and Figure 23.29.

The clinical advantages of the observation of B-lines are several (Lichtenstein et al. 1997, 1999; Lichtenstein and Karakitsos 2012; Lisciandro 2011, 2014a,b; Lichtenstein 2012; Lisciandro et al. 2014, 2017; Ward et al. 2017).

- B-lines are easily and rapidly recognizable with minimal training and immediately rule out PTX at that specific point along the thoracic wall because they cannot be seen in the presence of PTX.
- B-line distribution helps diagnose lung conditions using the Vet BLUE regional pattern-based approach along with being placed into clinical context.
- Numbers of B-lines, the Vet BLUE B-line scoring system, and their distribution during Vet BLUE are used to reach a Vet BLUE lung contusion severity score in trauma patients and for semiquantitating

**Figure 18.2.** Correlation of line drawings and B-mode still image for B-lines. (A) Line drawing, followed by (B) a pictorial of the anatomy, followed by (C) the B-mode ultrasound image of alveolar-interstitial edema. B-lines immediately rule out pneumothorax at that location along the thoracic wall. In trauma, B-lines represent pulmonary contusions until proven otherwise. Numbers of B-lines and numbers of positive Vet BLUE regional views provide a Vet BLUE Lung Contusion Severity Score (Lisciandro 2011, 2014; Dicker 2019) (see Chapters 22 and 23 and Figures 23.6 and 23.9). Source: Reproduced with permission from Dr Gregory Lisciandro, Hill Country Veterinary Specialists and FASTVet.com, Spicewood, TX. Illustration by Dr Judy Brown, Toronto, Canada.

degree of alveolar-interstitial edema in nontrauma (Lisciandro 2011, 2014a,b; Dicker et al. 2019) (see Figures 23.26 and 23.29). See Chapters 22 and 23 for more detail on lung ultrasound.

## Pseudo B-lines

### *The "Shimmy Line" or Z-line*

The "shimmy line," a term coined by the author, is a tight band of horizontal A-lines extending through the far-field that may appear at first glance as a B-line(s) (Figure 18.3). However, the "shimmy line" does not swing like a pendulum with inspiration and expiration and lacks the discrete laser-like hyperechoic character of a B-line, and "shimmy lines" do not extend through the far-field (Lichtenstein 2010b; Neto et al. 2016; Lee 2016). In the author's experience, these lines are generally observed with really "dry lung" and are most often seen at angles of insonation of 90° to strongly aerated lung surface. Since they are in fact created off the thoracic wall and its reflective fascial planes, they do not swing to and fro with inspiration and expiration, they fade, unlike true B-lines, they do not obliterate A-lines, unlike true B-lines, and are in essence short comet-tails (Soldati, personal communication). These "shimmy lines" have also been referred to as "Z-lines" and clinically mean nothing, having no relevant lung pathology implications, and thus were given the last letter in the alphabet for that reason (Lichtenstein 2010b; Lee 2016). It is important to note that the use of the "Z-line" nomenclature is controversial and for many lung sonographers the line nomenclature adds further confusion over merely stating that "shimmy lines" lack the characteristics of B-lines and are inconsequential. Moreover, in our experience, they are overlooked when using the definition of B-lines. With fairly minimal experience with your machine and its settings, you will be able to readily differentiate the B-line(s) from a "shimmy line."

### *Gastric "Pseudo B-lines"*

The presence of fluid immediately adjacent to air at the outer surface of lung creates the B-line artifact. The same artifact can be similarly created within the gastric lumen when liquid (fluid) ingesta and air are juxtaposed (see Figures 3.6 and 18.3). Typically, these "pseudo gastric B-lines" are seen at the TFAST CTS view since air rises within the gastric lumen to its least gravity-dependent region as air similarly rises within the pleural cavity (see Figure 18.3). The "pseudo gastric B-lines" are a major reason why we now teach to find and move away from the caudodorsal transition zone (CdTZ) at the TFAST CTS view (and during Vet BLUE) to avoid mistaking these lines for lung pathology. Moreover, abdominal structures such as the rugal folds of the stomach and liver may be mistaken for "pseudo shred sign" and "pseudo tissue sign," respectively (see Figures 23.13, 23.16, and 23.20 and Chapters 22 and 23).

### *Nodule "Pseudo B-lines"*

Nodules along the surface of the lung, due to their difference in acoustic impedance of soft tissue and aerated lung, cast "pseudo B-lines" through the far-field (see Figures 3.6 and 18.3). Usually, it is obvious that there is a nodule(s) in the near-field from which the "pseudo B-line" is cast. However, nodule "pseudo B-lines" may be associated with nodules that are very

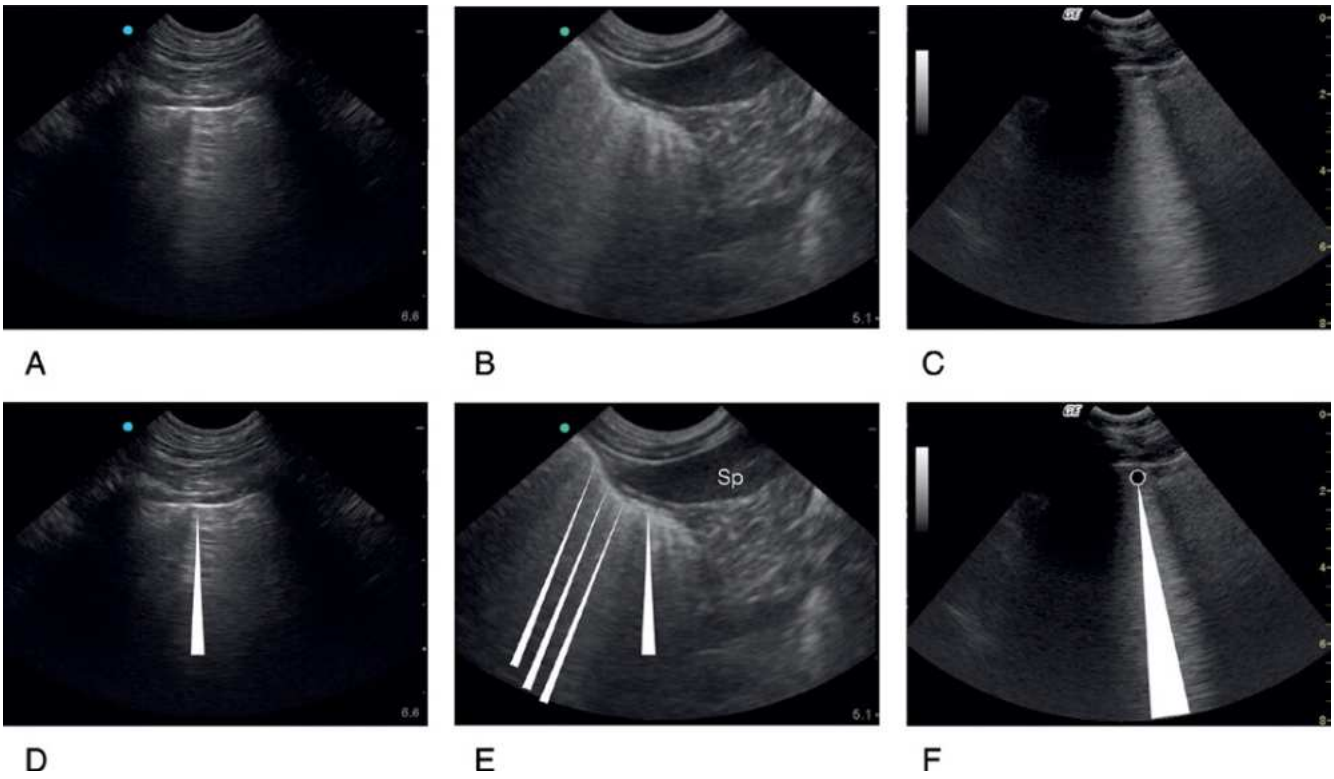


**Figure 18.3.** Correlating images with pseudo B-lines and overlays. In the top row are shown "pseudo B-lines" in images (A) through (C) that are unlabeled and then labeled in (D) through (F). In (A) and (D) is a centrally located "shimmy line" or "Z-line" that does not extend through the far-filed nor does it oscillate with inspiration and expiration. Note how the linear streak fails to extend though the far-field, lacking the characteristics of true B-lines. In (B) and (E) are "pseudo gastric B-lines" originating off the gastric wall and caused by fluid–ingesta–air interfaces within the gastric lumen. Locating the caudodorsal transition zone (transition of the pleural-peritoneal [abdominal] cavities) helps avoid mistaking abdominal structures for lung pathology (see Figure 17.9 and Chapters 22 and 23). In (C) and (F) a small nodule creates a "pseudo nodule B-line" coming off the "lung line" that behaves identically to a true B-line with the difference being the recognition of the nodule in the near-field. Source: Reproduced with permission from Dr Gregory Lisciandro, Hill Country Veterinary Specialists and FASTVet.com, Spicewood, TX.

small (<1–3 mm), and unless the depth is adequate and the sonographer follows the B-line to the lung surface, these small nodules could be mistakenly misinterpreted as true B-lines. The nodule "pseudo B-line" is similarly created, but with air encompassing soft tissue rather than fluid. Each of these conditions has a strong enough difference in acoustic impedance that a B-line is cast through the far-field. Since alveolar-interstitial edema is different from a nodule, we refer to the former as a B-line and the latter as a "pseudo B-line."

### Pseudo Lung Sliding

The movement at the CdTZ along the interface of pleural and peritoneal (abdominal) cavities can easily be mistaken for "lung sliding." As a result, we now train lung sonographers to find the CdTZ and then slide cranial 2–3 intercostal spaces away from it. By doing so, the sonographer may more accurately observe for "lung sliding" without being confounded by movement of the diaphragm and abdominal structures in the same view as lung. The upshot is that the sonographer can ideally observe for "lung sliding" with the abdomen out of view at the TFAST CTS view (see Figures 17.6, 17.8, and 17.9). "Lung sliding" is also difficult to see when the patient is panting because of short, rapid, "lung sliding" movements (in contrast to deep breaths) (Lisciandro et al. 2008). Use the "Tricks of the Trade" explained in Chapter 17.

### Pseudo Pleural Effusion

This is an important concept to understand. The gastric wall has an anechoic (black) layering and thus can mimic a sonographic fluid stripe at the CdTZ (Figure 18.4). Pleural effusion would unlikely be severe

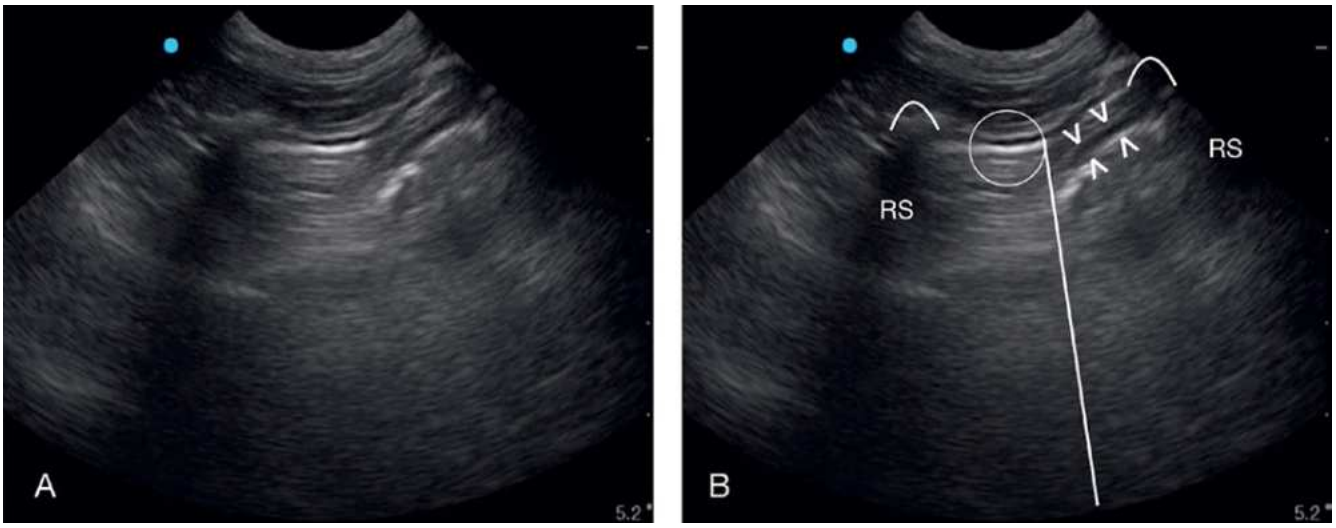


**Figure 18.4.** Pseudo pleural effusion from the gastric wall. Shown in (A) and (B) are unlabeled and labeled images taken at the CdTZ where the pleural–peritoneal (abdominal) interface exists. The gastric wall is anechoic (black) and may be mistaken for pleural effusion; however, lung floats on top of pleural effusion and it would be rare to ever see a pleural effusion fluid stripe at the least gravity-dependent CTS view. In (B) the rib shadows (RS) are apparent by the ribs (*curved lines*) and clean acoustic rib shadowing through the far-field. The "curtain sign," the transition zone of pleural and peritoneal (abdominal cavities), is labeled with a vertical line. See also Figure 17.9. The gastric wall is outlined (<). Source: Reproduced with permission from Dr Gregory Lisciandro, Hill Country Veterinary Specialists and FASTVet.com, Spicewood, TX.

enough to be observed at the highest point of the patient's thorax. Moreover, lung floats on the pleural effusion. In cases in which PE is suspected at the CTS view, the sonographer can move to the more ventral gravity-dependent TFAST PCS views to confirm or refute clinical suspicion. The finding of an anechoic stripe at the CTS view is always the stomach wall until proven otherwise (see Figure 18.4).

## *TFAST Pneumothorax: A-lines with Absent "Lung Sliding"*

"Dry lung," A-lines with "lung sliding," and PTX look identical on B-mode still images. The difference must be made in real time or on cine clips. The difference between "dry lung" and PTX is the presence and absence of "lung sliding," respectively (Lichtenstein et al. 2000, Lichtenstein 2007; Kirkpatrick et al. 2004; Lisciandro et al. 2008; Volpicelli et al. 2012). The CTS view was selected because if "lung sliding" is observed at the CTS view, the highest reasonable point over the pleural cavity, then PTX is immediately ruled out (Lisciandro 2008). The same strategy of the least gravity-dependent or highest reasonable point over the anterior chest is used in human medicine (Lichtenstein et al. 1999, 2000; Lichtenstein 2007; Kirkpatrick et al. 2004).

## *Lung Point: Improves the Diagnosis, Semiquantifies the Degree, and Helps Monitor PTX (Figures 18.5 and 18.6)*

### Effect of Positioning

When PTX is suspected, move your patient to standing or sternal if possible for several important reasons. First, standing or sternal is generally safer because your patient as a rule can ventilate more easily and efficiently. Second, the "lung point" is better categorized by using greater differences in height between the most and least gravity-dependent sternum and upper limits of the pleural cavity, referred to by the author as the "parking garage-skyscraper concept" (Figures 18.7 and 18.8) (Lisciandro 2011). Third, air rises to the least gravity-dependent regions of the thorax and the cap of air within the pleural cavity is more evenly distributed (not "bubbled") than in a patient in lateral recumbency, eliminating confounding findings such as the "double lung point" and the "reverse sliding sign" (Volpicelli et al. 2013; Hwang et al. 2018) (see Figure 18.6). Recently, a newer concept that shows promise has been described, referred to as the "double curtain sign" and the "reverse curtain sign" observed at the CdTZ in standing or sternal (Boysen et al. 2019). It is important to understand these confounding PTX

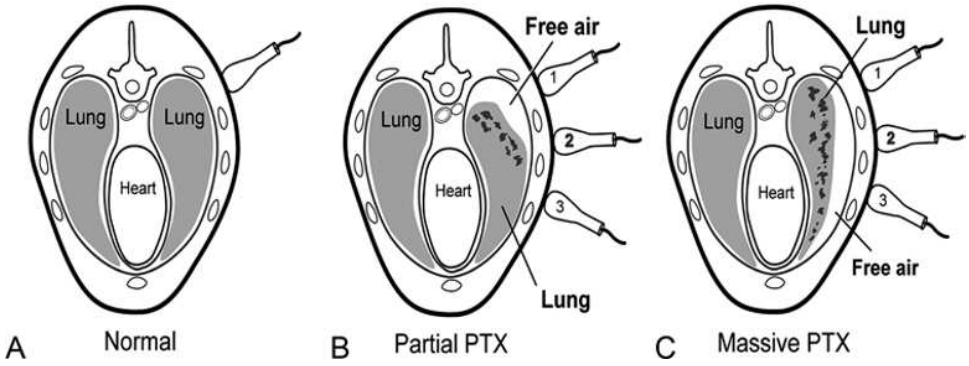


**Figure 18.5.** The "lung point" on a cross-section of the thorax. For best evaluation of the "lung point," place your patient into standing or sternal positioning when possible. Shown in (A) is a cross-section of the thorax in standing or sternal positioning with no PTX. The probe placed at the most dorsal region over the thorax will lead to the observation of "lung sliding" and A-lines, ruling out PTX. In (B) the patient has a pneumothorax and the transition zone of PTX and lung recontacting the thoracic wall, referred to as the "lung point," is found at probe position 2 and the PTX is semiquantitated as being "partial." In (C) no "lung point" is found along the thoracic wall and the PTX is semiquantitated as "massive." See Table 18.2 for a diagnostic algorithm. Source: Reproduced with permission from Dr Gregory Lisciandro, Hill Country Veterinary Specialists and FASTVet.com, Spicewood, TX and Lisciandro et al. *J Vet Emerg Crit Care* 2008;18(3):258–269 and Lisciandro. *J Vet Emerg Crit Care* 2011;21(2):104–122.

features; and how standing or sternal positioning in spontaneously ventilating patients (and likely mechanically ventilated patients) and imaging away from the CdTZ avoids them.

First, these confounding PTX findings are commonly described in human patients in supine positioning, thus the thorax is like a "parking garage" with minimal differences in height from the sternum to the highest reasonable, least gravity-dependent point on the chest wall, where free air would rise (PTX) within the pleural cavity. Lateral recumbency in small animals would correlate with supine positioning in people. Thus this "parking garage effect" places minimal differences between levels for locating the "lung point" (see Figures 18.7 and 18.8). Second, respiration is important because in either spontaneously breathing patients or those being supported with positive pressure ventilation (PPV), the type of ventilation changes how free air in the pleural space (PTX) behaves. During PPV, the free air in the pleural cavity is pushed or "bubbled" unnaturally into different regions with each breath, whatever the positioning. This PPV effect does not occur in spontaneously breathing small animals in which the free air within the pleural cavity more naturally rises to the least gravity-dependent region, and collapsed lung falls into gravity-dependent regions, especially when the patient is in standing or sternal positioning (see Figure 18.7).

### Searching for the Lung Point Improves Sensitivity

The "lung point" is defined as the point along the thoracic wall where there is evidence of lung recontacting intercostal spaces (see Figures 18.5–18.8), in other words, the transition zone of free air within the pleural space and lung reopposed to the thoracic wall. Most commonly, the "lung point" is found through the observation of "lung sliding" or B-lines; however, any ultrasonographic evidence of lung recontacting the thoracic wall determines the "lung point," including the "shred sign," "tissue sign," "nodule sign," "wedge sign" (see Chapters 22 and 23 and Figures 23.2, 23.5, 23.7–11), and the "lung pulse," explained in greater detail in the next section (Lichtenstein et al. 2000, 2003; Lichtenstein 2007). The sonographer must consider this lung information because "lung sliding" with "dry lung" differs from the condition of B-lines or "wet lung" in which the lung likely has forms of alveolar-interstitial edema. Moreover, the findings of consolidation (shred sign, tissue sign, wedge sign, nodule sign) indicate that lung function, ventilation, is even more severely compromised.

In the presence of significant pleural effusion, such as hemothorax in trauma, the "lung point" will be affected because the PE displaces air and lung floats on the PE, making positioning again important for expected findings. Sternal or standing will be least confounding (Lisciandro et al. 2008; Lisciandro 2011,

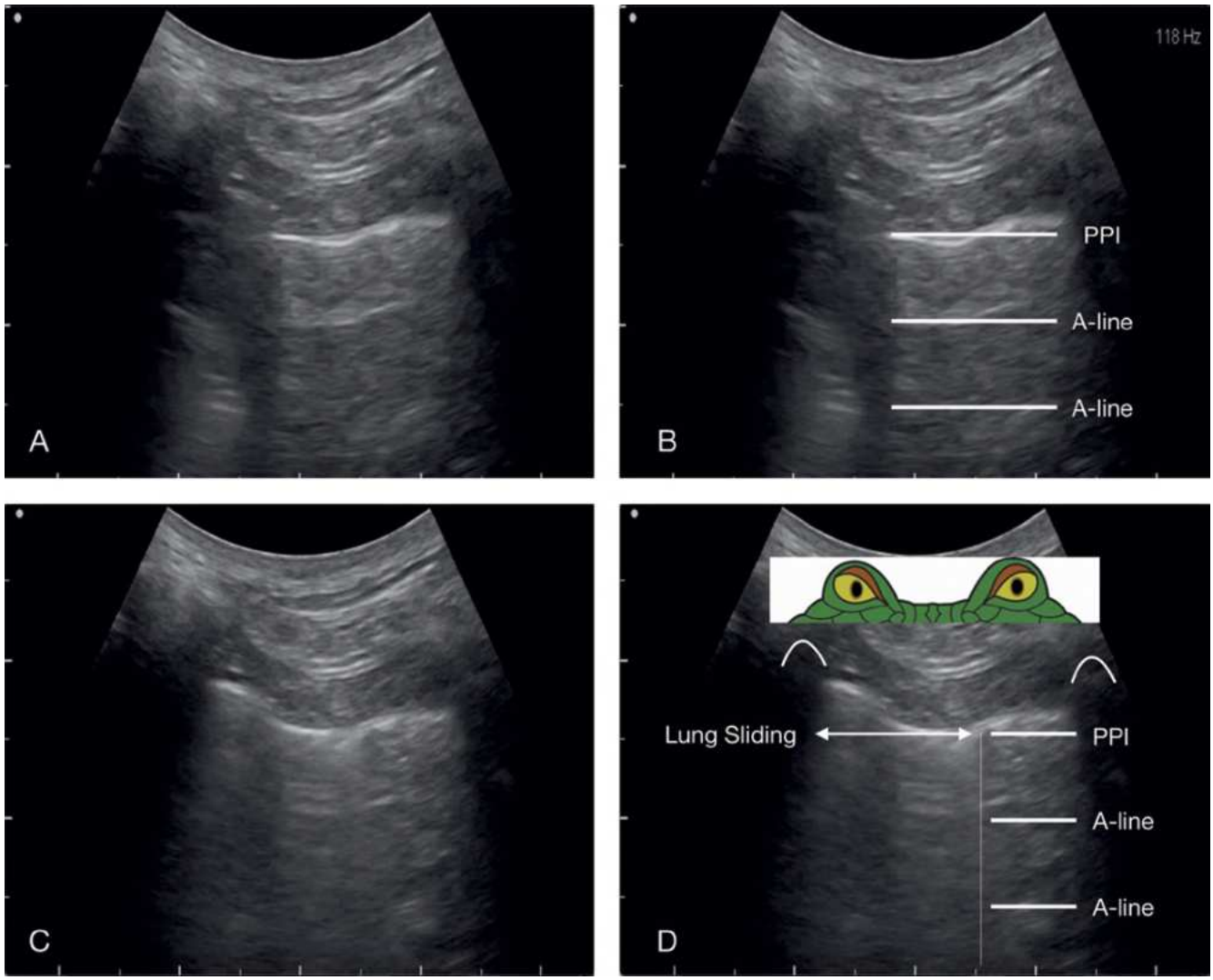


**Figure 18.6.** The "lung point" with the finding of "lung sliding." The "lung point" is shown unlabeled in (A) and (C) and labeled in (B) and (D). In (A) and (C) "lung sliding" is entering the screen from cranial or screen left. The PTX is clearly seen by the A-lines to the right of the screen labeled in (B). In (C) and (D) the "lung point" is shown taken a split second later with the "lung sliding" nearly across the entire intercostal space. A-lines are eliminated with the "lung sliding" as shown in (D). The overlay of the "gator sign" emphasizes the importance of proper orientation and being able to identify where the "to and fro" motion of "lung sliding" is accurately observed (←→). For best evaluation of the "lung point," have your patient in standing or sternal positioning when possible. Source: Reproduced with permission from Dr Gregory Lisciandro, Hill Country Veterinary Specialists and FASTVet.com, Spicewood, TX. Illustration by Suji Park, Englewood Cliffs, NJ.

2014a; Boysen and Lisciandro 2013; Neelis et al. 2015). The "curtain sign" will likely be seen with the free air of PTX and PE (Neelis et al. 2015; Boysen et al. 2019).

**Pearl:** It is best practice to observe for PTX at the CTS view after the initial five breaths since air needs to redistribute when moving your patient from lateral to sternal or standing recumbency, or vice versa (Lisciandro et al. 2008). See Table 18.2.

### Lung Pulse

The "lung pulse" is a term coined for the observation of "lung sliding" often accompanied by the shred sign or tissue sign of severely collapsed lung that moves with each heartbeat rather than with expected phases of respiration (Lichtenstein et al. 2003). In other words, the "lung pulse" occurs when nonaerated, severely collapsed (consolidated) lung is in direct opposition to the thoracic wall while at the same time against the heart to cause the movement of "lung sliding" with

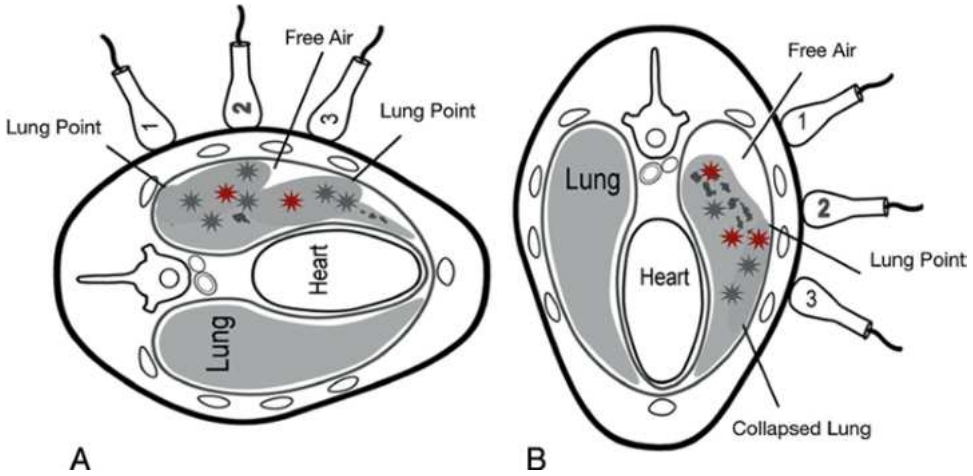


**Figure 18.7.** Differences in positioning and the effect on the location of the "lung point." In (A) the patient with PTX is in lateral recumbency and because of the "parking garage effect" the free air bubbles into different regions, creating a "double lung point" phenomenon (see Figure 18.8). Moreover, if the patient in (A) is receiving positive pressure ventilation the free air is pushed into multiple locations unnaturally between collapsed lung. In (B) the effect is eliminated or reduced by moving the patient to standing or sternal positioning, thus creating a "skyscraper effect" in which the difference between the sternum and least gravity-dependent CTS view is greatest. Thus, it is unlikely a "double lung point" will be observed. Source: Reproduced with permission from Dr Gregory Lisciandro, Hill Country Veterinary Specialists and FASTVet.com, Spicewood, TX.

each heart beat rather than with inspiration and expiration (Lichtenstein et al. 2000, 2003; Volpicelli et al. 2012). The upshot again is for the sonographer to consider any evidence of lung, the observation of any of the six Vet BLUE lung ultrasound signs, recontacting the thoracic wall for detecting the "lung point" then placed into clinical context (see Chapters 22 and 23).

**Pearl:** Keep it simple. Any observation of the six Vet BLUE lung ultrasound signs, in other words, any evidence of lung recontacting the thoracic wall, defines the "lung point."

### The Lung Point Semiquantitates Degree of PTX

The location of the "lung point" with your patient in sternal or standing semiquantitates and thus categorizes the degree of PTX (Lichtenstein et al. 2000; Sargsyan et al. 2001; Lisciandro 2011). Although not yet published at the time of writing this chapter, degree of PTX likely correlates with the location of the "lung point," most effectively in standing or sternal positioning over lateral recumbency. We have used a systematic approach, referred to as the "TFAST PTX 1/3s Rule," of an upper third, middle third, and lower third for location of the "lung point" with the patient in standing or sternal position and designating each third as trivial, moderate, or severe (Lisciandro 2011, 2014a) (Figure 18.9, Table 18.3). The use of this TFAST systematic approach is important for several clinically relevant reasons.

- It allows for decision making on whether thoracocentesis should be performed.
- It provides a tracking or monitoring tool (static, resolving or worsening).
- It minimizes iatrogenic lung trauma via empirical thoracocentesis.

We use the rule of thumb that a "lung point" in the upper third is "trivial PTX" and thus PTX can be monitored by tracking the location of the "lung point" over time; a middle third is "moderate PTX" and treatment (minimally thoracocentesis) should be seriously considered; and a lower third is "severe PTX" (serious) that mandates treatment (thoracocentesis) (see Figure 18.9).

### Use of the TFAST PTX 1/3s Rule for Pneumothorax Monitoring

The location of the "lung point" serves as a monitoring tool, using its distance from the CTS view (Lichtenstein et al. 2000; Sargsyan et al. 2001; Lisciandro 2011). Examples of its clinical relevance are given here.

- *Example 1* – a case that has a thoracostomy tube removed. Prior to thoracostomy tube removal, "lung sliding" was evident at the CTS view documenting absent PTX prior to thoracostomy tube removal. The "lung sliding" with A-lines supports

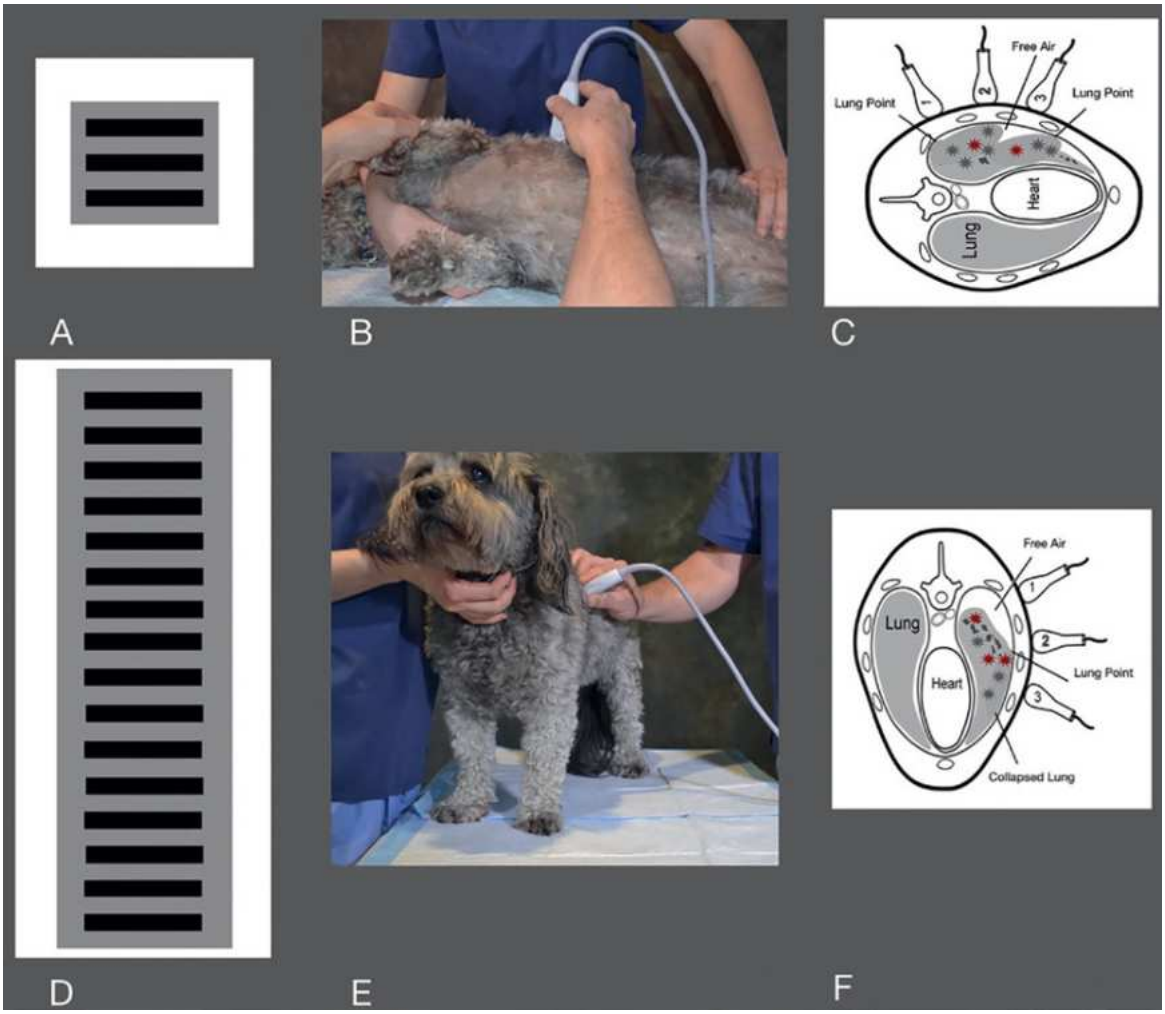


**Figure 18.8.** The "parking garage - skyscraper effect" for the "lung point." In (A) through (C) the patient with PTX is in lateral recumbency and note that probe 1 and probe 3 are gravity-equal, and thus free air creates the "double lung point" phenomenon on either side of collapsed lung. Moreover, the "parking garage effect" in (A) through (C) occurs because of only 3 levels (black rectangles) available for assessing the degree of PTX. In contrast, the standing or sternal positioning makes collapsed lung fall toward the sternum, minimizing the possibility of the "double lung point" phenomenon as illustrated in (D) through (F). Note that probe 1 and probe 3 are now gravity-unequal, making the "lung point" more true than in lateral recumbency. Furthermore, the "skyscraper effect" creates more levels to locate the "lung point" and thus better assess the degree or semi-quantification of PTX. Source: Reproduced with permission from Dr Gregory Lisciandro, Hill Country Veterinary Specialists and FASTVet.com, Spicewood, TX.

normal aerated "dry lung" at the periphery. Post removal, the attending determines PTX with a "lung point" in the upper third of the thorax, determined as "trivial PTX," and thus close TFAST monitoring suffices to track the location of the "lung point" over time on serial TFAST examinations. On the next shift and thereafter, PTX is not found, remaining absent, providing reassurance that the patient's PTX is not only stable but also resolved, and accompanying lung is normal and aerated at the periphery (see Figure 18.9).

- *Example 2* – a PTX case in which the "lung point" is in the middle third of the thorax that qualifies as "moderate PTX" and the increased respiratory effort supports a more serious form of PTX. This patient has thoracocentesis performed and using serial TFAST the PTX is confirmed to be resolved – absent "lung point" post thoracocentesis with "lung sliding." Later on the same shift, the PTX has recurred with the finding of a "lung point" in the upper third of the thorax, thus qualifying as "trivial PTX." During the next shift, the new attending veterinarian is aware of

**Table 18.2.**
Pneumothorax diagnostic algorithm using TFAST. Refer to the text for more detail.

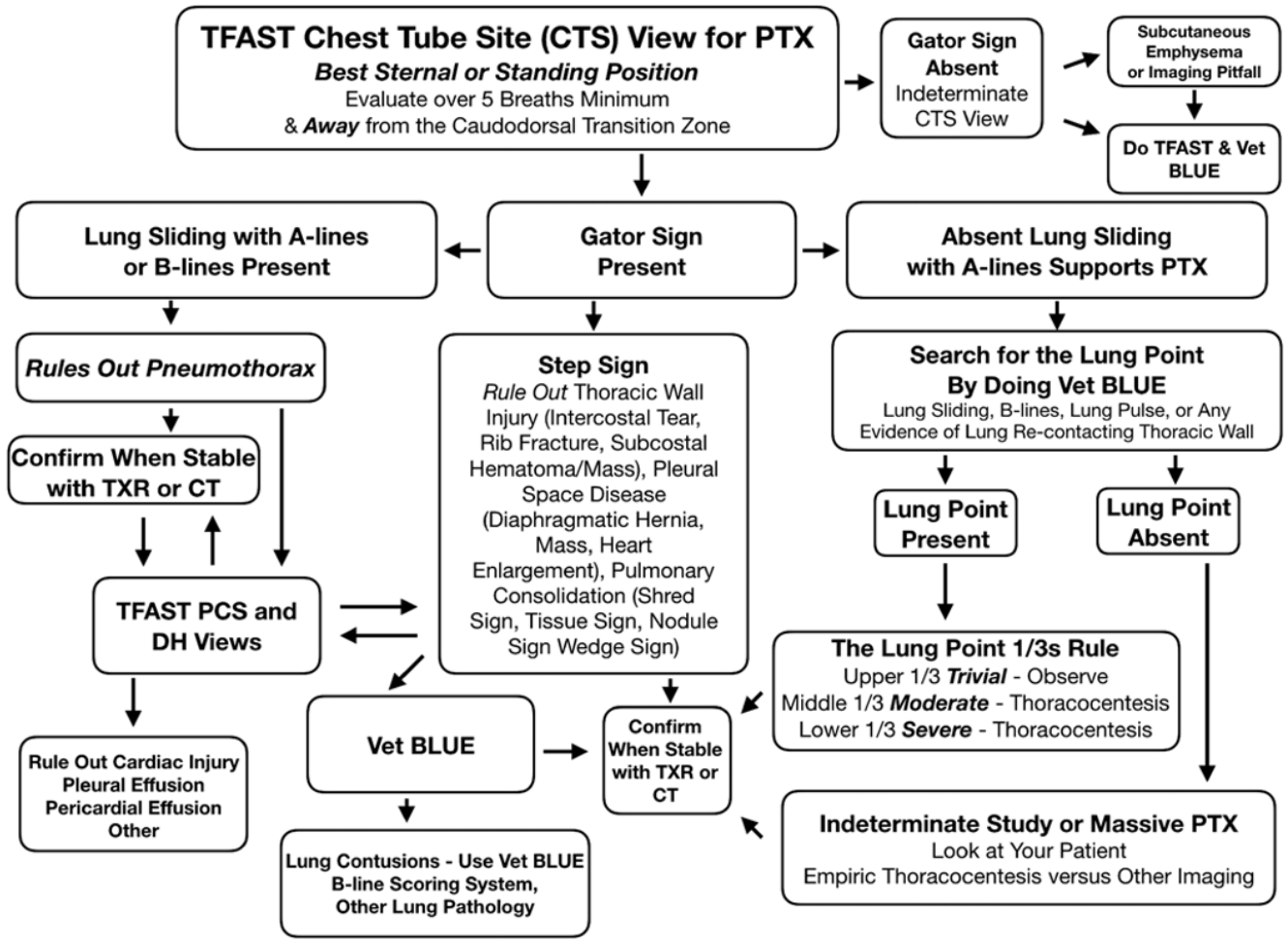


Source: Reproduced with permission from Dr Gregory Lisciandro, Hill Country Veterinary Specialists and FASTVet.com, Spicewood, TX.
CT, computed tomography; CTS, chest tube site view; DH, diaphragmatico-hepatic view; PTX, pneumothorax; TXR, thoracic radiography.

the "lung point" being in the upper third of the thorax, discussed on patient rounds and also recorded in medical record. During this next shift, the PTX is found to be worsening with the finding of the "lung point" located in the middle (or lower) third of the thorax, qualifying it as "moderate (or severe) PTX" and triggering intervention rather than waiting for the patient to overtly decompensate.

If the patient is stable and low risk, thoracic radiography may be performed to document the PTX and help gain confidence in our TFAST PTX 1/3s Rule. The "lung point" may be compared to the radiographic severity, followed by thoracocentesis. Post thoracocentesis, the patient is again monitored using TFAST and determining the location of the "lung point" when PTX is present (see Figure 18.9).

The observation of the location of the PTX using the TFAST PTX 1/3s Rule and characterization of the lung surface using the Vet BLUE six lung ultrasound signs help to better anticipate respiratory and ventilatory complications. For example, a resolved PTX with aerated lung in a patient is very different from resolved PTX, with forms of consolidation noted within the lung, such as the shred sign and tissue sign. Forms of consolidation support atelectatic lung that is abnormally ventilated having varying consequences on clinical course, and Vet BLUE signs of consolidation could also represent aspiration pneumonia and other important respiratory complications that would otherwise be missed (see Chapters 22 and 23).

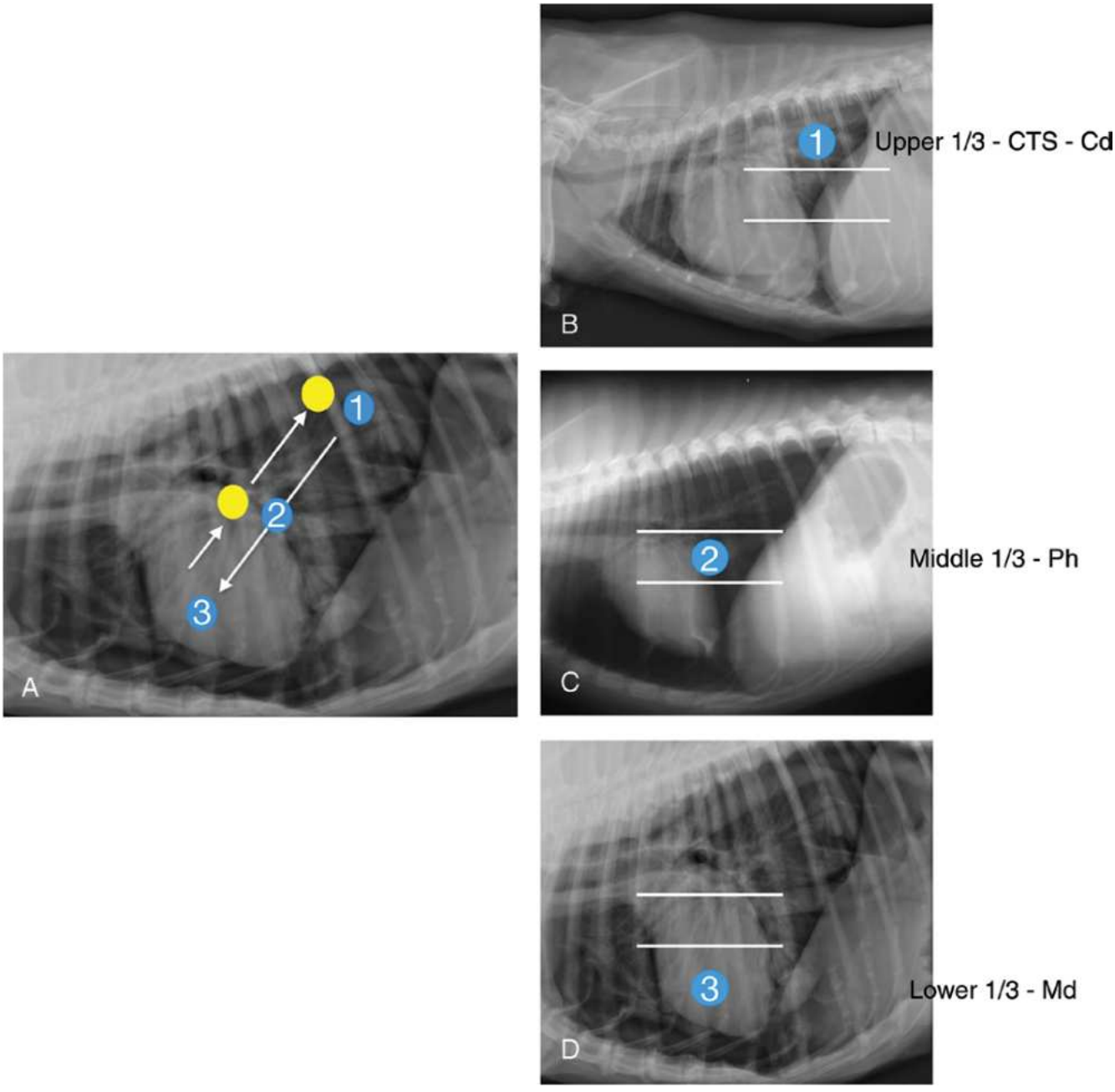


**Figure 18.9.** Pneumothorax and the TFAST PTX 1/3s Rule. (A) Performing Vet BLUE and moving through the upper, middle, and lower thirds of the thorax, most reliably performed in standing or sternal positioning, referred to as the TFAST PTX 1/3s Rule. Points 1–3 are moving through Vet BLUE Caudodorsal (same as CTS view), Perihilar, and Middle lung regions. Where lung recontacts the thoracic wall determines where there is no PTX at that level, from which smaller increments are made moving dorsally in search of the "lung point", the transition zone of lung recontacting the thoracic wall and PTX. The Vet BLUE strategy is more rapid than moving in small increments ventrally from the TFAST CTS view to more gravity-dependent regions trying to find the "lung point." In (B), (C) and (D) each has the "lung point" marked as point 1, point 2, and point 3 superimposed on the correlating thoracic radiographs showing the correlative differences between trivial, moderate, and severe comparing Vet BLUE to thoracic radiographs. Clinically, each dog was remarkably different. In (B) the patient was asymptomatic, in (C) stable but with increased effort, and in (D) the dog was in overt respiratory distress from its tension PTX. Source: Reproduced with permission from Dr Gregory Lisciandro, Hill Country Veterinary Specialists and FASTVet.com, Spicewood, TX.

**Table 18.3.**
Using the author's TFAST PTX 1/3s Rule for location of the "lung point" to categorize the degree of pneumothorax (PTX).

| | Degree of PTX |
|---|---|
| Upper third of thorax | Trivial PTX – expect mild if any clinical signs |
| Middle third of thorax | Moderate PTX – expect increased respiratory effort |
| Lower third of thorax | Severe PTX – expect overt respiratory distress |
| Not found along thorax | Indeterminate study or most severe form of PTX – look at your patient's respiratory effort! |

Source: Reproduced with permission from Dr Gregory Lisciandro, Hill Country Veterinary Specialists and FASTVet.com, Spicewood, TX.

## *Missing PTX on TFAST*

### Tricks of the Trade

The original TFAST study evaluated 145 dogs and showed that with experience and in slower breathing patients, PTX could be diagnosed with ~95% sensitivity and specificity (Lisciandro et al. 2008).

The major reasons for missing PTX during TFAST include the following.

- Panting patients – administer butorphanol routinely for respiratory patients because it is safe and serves as an anxiolytic without causing hemodynamic compromise and panting, while also being short-acting.
- Not incorporating the author's Tricks of the Trade by manipulating the echoes during image optimization either by using the "one-eyed gator sign" – rib in the middle of the screen – or obliquing or ricocheting the echoes by changing the angle of insonation (see Figures 17.7 and 17.11)
- Not having proper machine settings, especially regarding depth and gain (see Figure 17.10),
- Not searching for the "lung point."
- Improper training.

Through our continued understanding of these factors, we have been able to markedly improve training, including accelerating the learning curve and gaining proficiency in the accurate diagnosis of PTX (Lisciandro 2011, 2014a,b; Dicker et al. 2019).

### False Negatives

It is possible to mistake "lung sliding" for abdominal structure movement at the CdTZ, when in fact the patient has PTX. Sliding cranial 2–3 intercostal spaces away from the CdTZ and searching for the "lung point" eliminates this error (see Figures 17.8 and 17.9). A helpful intervention is the use of subcutaneous injectable butorphanol (or other cardiovascular and respiratory forgiving form of sedation) that is low risk, fairly rapid onset, short-acting, and does not cause panting, while serving as an anxiolytic and slowing breathing patterns.

### False Positives

It is also possible to mistake "lung sliding" in PTX for panting or rapid shallow breathing in dogs and cats (Lisciandro et al. 2008). Sliding cranial away from the CdTZ and searching for the "lung point" helps eliminate this confounder (see Figures 17.8 and 17.9). A helpful intervention is the use of subcutaneous injectable butorphanol (or other cardiovascular and respiratory forgiving form of sedation) that is low risk, fairly rapid onset, short-acting, and does not cause panting, while serving as an anxiolytic and slowing breathing patterns.

## *Use of M-mode and Power Doppler for Detecting PTX*

The demand for still image documentation of PTX in people has resulted in the use of M-mode and power Doppler ultrasonography (Cunningham et al. 2002; Lichtenstein 2007, 2010b). The reason for these alternate modalities is that still images are easier to archive and consume less data than storing cine clips for PTX documentation. M-mode has not only proven helpful as an adjunct to B-mode but is also now used as a primary diagnostic modality in people (Lichtenstein 2007, 2010b).

### Use of M-mode: Seashore Sign, Stratosphere Sign, and Rain Sign

When using M-mode, "dry lung" is represented by the "seashore sign," likened to the graininess of sand along the shoreline (Figure 18.10) (Lichtenstein 2007, 2010b). The "seashore sign" is created by the movement of "lung sliding" and rules out PTX and supports "dry lung." In contrast, when no "lung sliding" exists along the "lung line," as in PTX, a "stratosphere sign" (also called the "bar code sign") is observed (Lichtenstein 2007, 2010b). The "stratosphere sign" ("bar code sign") is observed in PTX as linear horizontal bars that fill the entire screen from near- to far-field because there is no

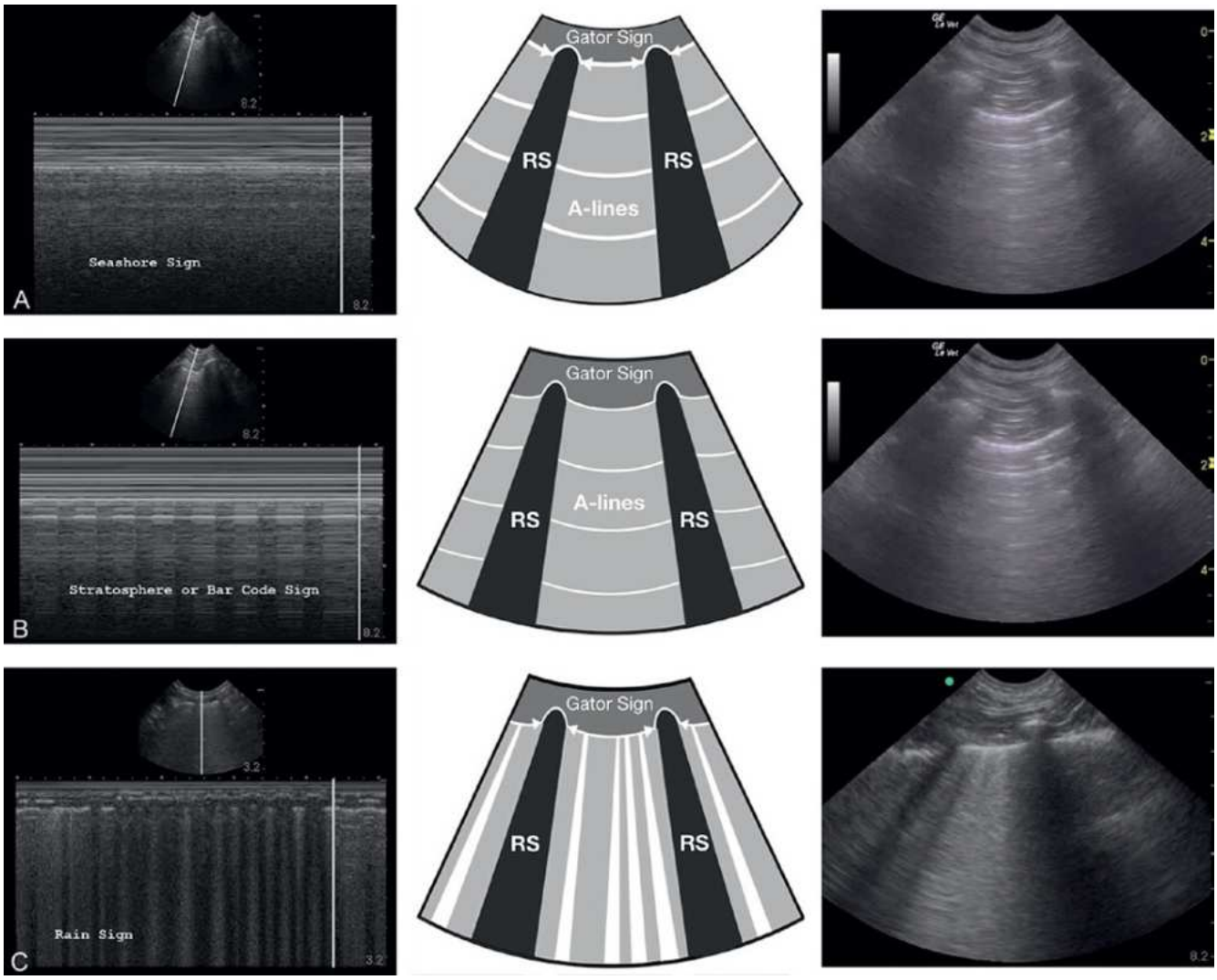


**Figure 18.10.** M-mode findings correlated to line drawings and B-mode images. In the top row (A) shows normal expected aerated lung at the periphery with "lung sliding." The M-mode is typified by the "seashore sign" and B-mode in real-time with A-lines and "lung sliding." In (B) M-mode documents the presence of PTX with observation of the "stratosphere sign" or "bar code sign" typified in B-mode by the observation of A-lines with absent "lung sliding." In (C) the M-mode shows the "rain sign" with vertical bands originating off the "lung line" extending through the far-field without fading and typified in B-mode as B-lines (also called ultrasound lung rockets). The line drawings correlate with the respective M-mode and B-mode images. Source: Reproduced with permission from Dr Gregory Lisciandro, Hill Country Veterinary Specialists and FASTVet.com, Spicewood, TX. Illustration by Dr Judy Brown, Toronto, Canada.

movement from "lung sliding" along the PPI because lung is collapsed.

Lastly, when B-lines are present, M-mode shows linear vertical streaks extending from the "lung line" through the far-field, referred to by the author as the "rain sign" (Lisciandro 2014a). The "lung point" will most commonly appear with a combination of either "seashore sign" or "rain sign" with the "stratosphere sign" ("bar code sign") (Lichtenstein 2010b).

### Tweaking M-mode

The author has not had good success using M-mode even in patients with slow thoracic excursions. In the author's experience, there is too much thoracic wall movement in spontaneously breathing patients to be able to reliably use M-mode. However, in patients with controlled ventilation, M-mode may prove more helpful. Recently, in a study involving horses with experientially induced small–volume PTX (without thoracic

wall movements typical in small animal respiratory distress), B-mode performed better than M-mode; however, M-mode was found to be an effective imaging modality in most study horses (Partlow et al. 2017).

A couple of considerations when using M-mode for lung are to reduce the frame speed to "slow" or as low as possible to minimize confounding thoracic wall movement, and use different transducers such as linear or phased array rather than a curvilinear (microconvex) probe. Another variable is the actual ultrasound machine and its software; some ultrasound machines may perform better using M-mode for lung than others. Despite these modifications, the author remains more confident with using B-mode for observing the presence or absence of "lung sliding" and when PTX is suspected, in searching for the "lung point" in B-mode.

## *Use of Power Doppler and the "Power Slide"*

The use of power Doppler seems to have never made the mainstream in human medicine. In short, the presence of the colored pixels of power Doppler along the "lung line" supports the movement of "lung sliding" and the absence of colored pixels suggests the diagnosis of PTX (Cunningham et al. 2002). Thus, power Doppler in theory could be used for medical records as a still image (Figure 18.11). In the author's experience, as with M-mode, there is generally too much thoracic wall movement in spontaneously breathing small animals for power Doppler to be as reliable as B-mode (Lisciandro 2014a), and M-mode is superior as an adjunct technique, making power Doppler the lesser of the three modalities (Table 18.4).

## *Other Confounders*

### Subcutaneous Emphysema and Its Effects on TFAST

The presence of subcutaneous emphysema (SQE) is problematic because ultrasound does not transit (image) through air and, depending on where the SQE is present, any or all of the acoustic windows of TFAST may be affected (Lisciandro et al. 2008; Lisciandro 2011). In the only study to the author's knowledge reporting SQE, only 7/145 (~5%) cases were affected (Lisciandro et al. 2008). If the sonographer is unable to displace the SQE with probe pressure and is thus unable to observe the "gator sign" orientation, then TFAST evaluation of lung (and pleural cavity) will be indeterminate. In other words, if the "gator sign" cannot be imaged then the TFAST sonographer cannot confidently interrogate lung (or image the pleural cavity) (see Table 18.2). Displacing SQE with gentle probe pressure is successful for acquiring the "gator sign" orientation and PCS views in most small animals, thus allowing for TFAST lung, cardiac, and pleural cavity examination (Lisciandro et al. 2008). In human medicine, some sonographers have referred to SQE as having E-lines, with "E" standing for emphysema (Lichtenstein 2010b; Lee 2016; Neto et al. 2016). However, the "line language" becomes confusing since often there are no "lines" at all in SQE; and air performs as air – A-lines or dirty shadowing dependent on the angle of insonation. The use of "E-lines" is not preferred by the author (Figures 18.12 and 18.13).

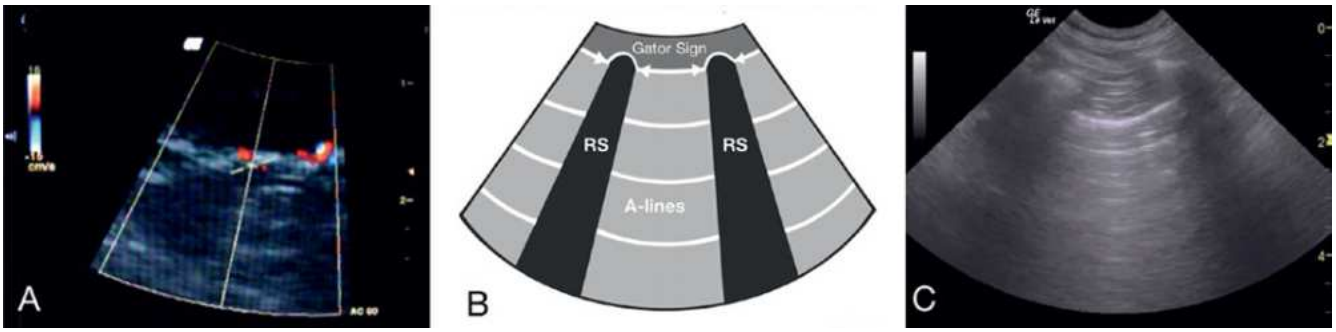


**Figure 18.11.** Power Doppler for "lung sliding." Shown in (A) is the use of power Doppler for the "power slide" indicating that "lung sliding" is present along the PPI. In (B) is a correlative line drawing and (C) a B-mode image in which the difference between "lung sliding" from pneumothorax is only evident in real-time imaging. In PTX there would be no colored pixels along the PPI. Although first described over a decade ago, the use of power Doppler has not become mainstream in lung ultrasound imaging. Source: Reproduced with permission from Dr Gregory Lisciandro, Hill Country Veterinary Specialists and FASTVet.com, Spicewood, TX. Illustration by Dr Judy Brown, Toronto, Canada.

Table 18.4.
Findings at the CTS view using different ultrasound modalities.

| Condition | B-mode | M-mode | Power Doppler |
|---|---|---|---|
| Normal aerated lung | Lung sliding with A-lines | Seashore sign | Pixels where expect "lung sliding" |
| Pneumothorax | Absent "lung sliding" with A-lines | Stratosphere sign (bar code sign) | Absent pixels |
| Alveolar-interstitial edema (lung contusions in trauma) | B-lines | Rain sign | N/A |

Source: Reproduced with permission from Dr Gregory Lisciandro, Hill Country Veterinary Specialists and FASTVet.com, Spicewood, TX.

### Obesity

Fat attenuates the ultrasound beam and thus negatively affects the image quality by decreasing image's sharpness and contrast. Obesity is not as problematic in small animals as with people.

## *The "Step Sign" of TFAST and the CTS View*

The term "step sign" was coined in the original TFAST study to describe the ultrasound finding of a disruption to the expected linear continuity of the PPI (Lisciandro et al. 2008: Lisciandro 2014a; Dicker et al. 2019) (Figure 18.14). The "step sign" often correlated with abnormal findings on thoracic radiography (TXR) that included pleural space abnormalities such as pleural effusion and diaphragmatic hernia, thoracic wall abnormalities such as intercostal tear(s), rib fracture(s), and subcostal hematomas, and other intrathoracic abnormalities including comorbidities such as an anterior mediastinal mass, severe left atrial enlargement, and others (Lisciandro et al. 2008). The "step sign" also can be seen as a normal finding at the CdTZ and is described in Chapter 17 (see Figure 17.9). "Step sign" rule-outs are summarized in Table 18.5. The upshot is that when a "step sign" is observed at the CTS view away from the transition zone of pleural and abdominal cavities, a potentially serious abnormality should be suspected. Vet BLUE for more comprehensive lung evaluation and radiography should be pursued and the "step sign" placed into clinical context with other findings.

The term "step sign" has also been used to describe disruption of the expected linear continuity of long bones as a sonographic feature of bone fractures and an accurate screening test for rib fractures in foals and skull and long bone fractures in children (Picandet et al. 2007; Barata et al. 2012; et al. Parri 2013) (see Figures 35.7 and 35.9).

## *Summary for the CTS View*

### Three Major Lung-related Findings

There are three major findings at the CTS view: (1) "lung sliding" and A-lines, referred to as "dry lung" representing normal aerated lung at the periphery and immediately ruling out PTX; (2) B-lines, referred to as "wet lung" most commonly representing forms of alveolar-interstitial edema at the periphery, immediately ruling out PTX; and (3) pneumothorax, A-lines with absent "lung sliding" and a "lung point."

- "Lung sliding" and A-lines also referred to as "dry lung."
  - Expect for adult dogs and cats, and puppies and kittens >6 weeks of age to have a "dry lung" profile with absent B-lines (Lisciandro et al. 2014, 2017, 2018; Lisciandro and Fosgate 2018).
- B-lines, also referred to as ultrasound lung rockets and "wet lung."
  - Immediately rules out PTX at that specific point on the thoracic wall because the artifact cannot be observed when air is in the pleural space (PTX) (Lichtenstein et al. 2000; Kirkpatrick et al. 2004; Lisciandro et al. 2008; Lisciandro 2011).
  - Represent various forms of alveolar-interstitial edema; however, in trauma cases B-lines represent lung contusions until proven otherwise (Lisciandro et al. 2008; Lisciandro 2011; Ball et al. 2009; Dicker et al. 2019).
  - The Vet BLUE B-line scoring system provides a way in which to score the degree of lung contusions in trauma patients. See the Vet BLUE Lung Contusion Severity Score in Chapters 22 and 23 (Lisciandro 2011, 2014b; Dicker et al. 2019).
- Pneumothorax as A-lines with absent "lung sliding."
  - Search for the "lung point" (Lisciandro et al. 2008; Lisciandro 2011).

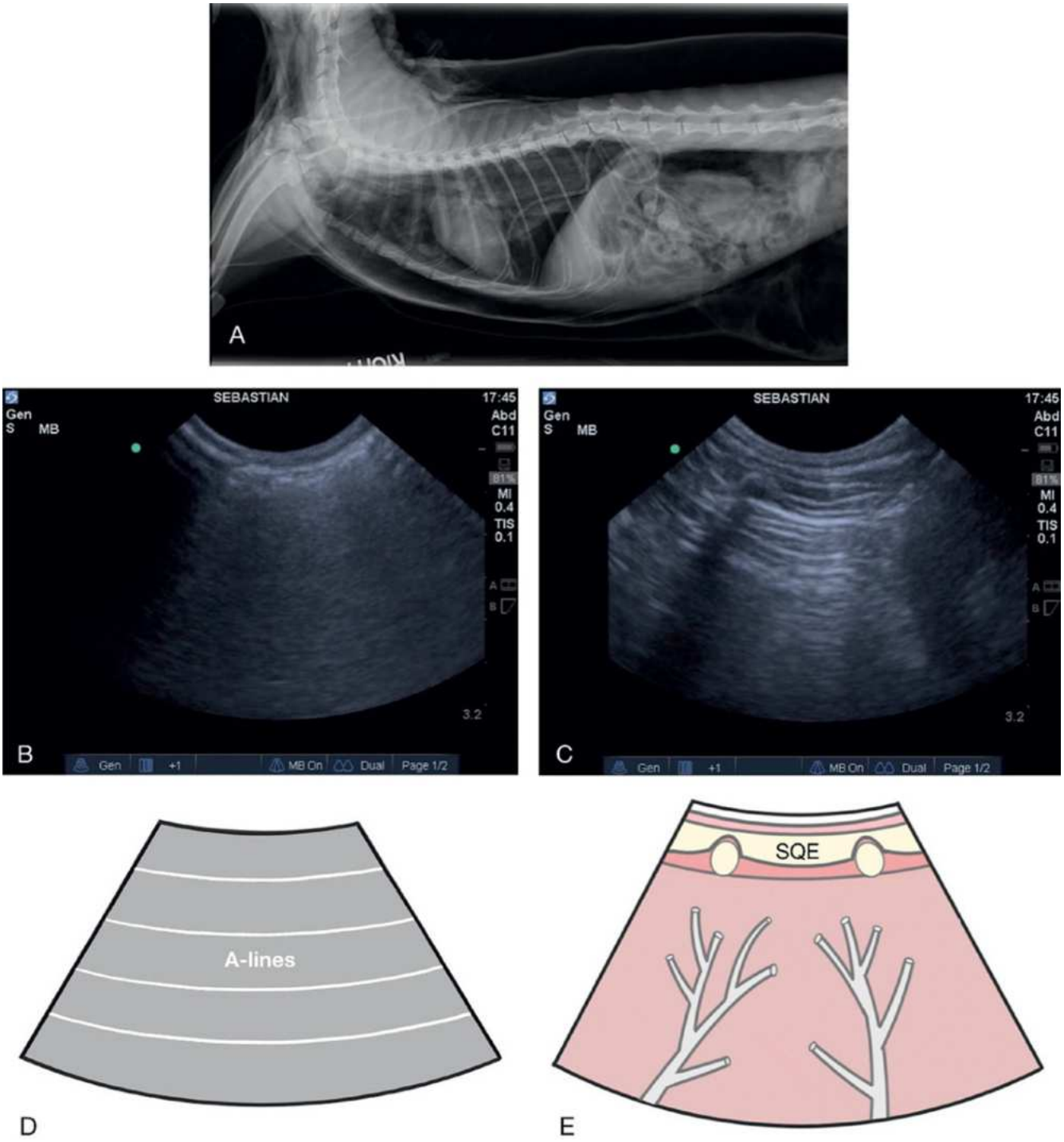


**Figure 18.12.** Subcutaneous emphysema and probe pressure technique. In (A) is shown a cat with severe subcutaneous emphysema on thoracic radiography. In (B) the B-mode still image lacks a "gator sign" orientation. If a "gator sign" orientation in unachievable then lung ultrasound will be indeterminate. (C) In the same patient as (A) and (B), through gentle probe pressure, subcutaneous emphysema (SQE) is adequately displaced so that the "gator sign" orientation may be acquired, and the TFAST CTS examination may be accurately performed. In (D) is a line drawing of SQE to be compared with other Vet BLUE signs in Chapter 23. In (E) is the anatomical line drawing showing the SQE in the near-field. Normal aerated lung parenchyma is shown in (E), but the lung cannot be accurately assessed without a "gator sign" orientation and any number of conditions may be obscured through the far-field in the presence of SQE. Compare to other line drawings in Chapter 23. Uncommonly, SQE invalidates the TFAST examination in small animal patients (Lisciandro et al. 2008). Source: Reproduced with permission from Dr Gregory Lisciandro, Hill Country Veterinary Specialists and FASTVet.com, Spicewood, TX. Illustration by Dr Judy Brown, Toronto, Canada.

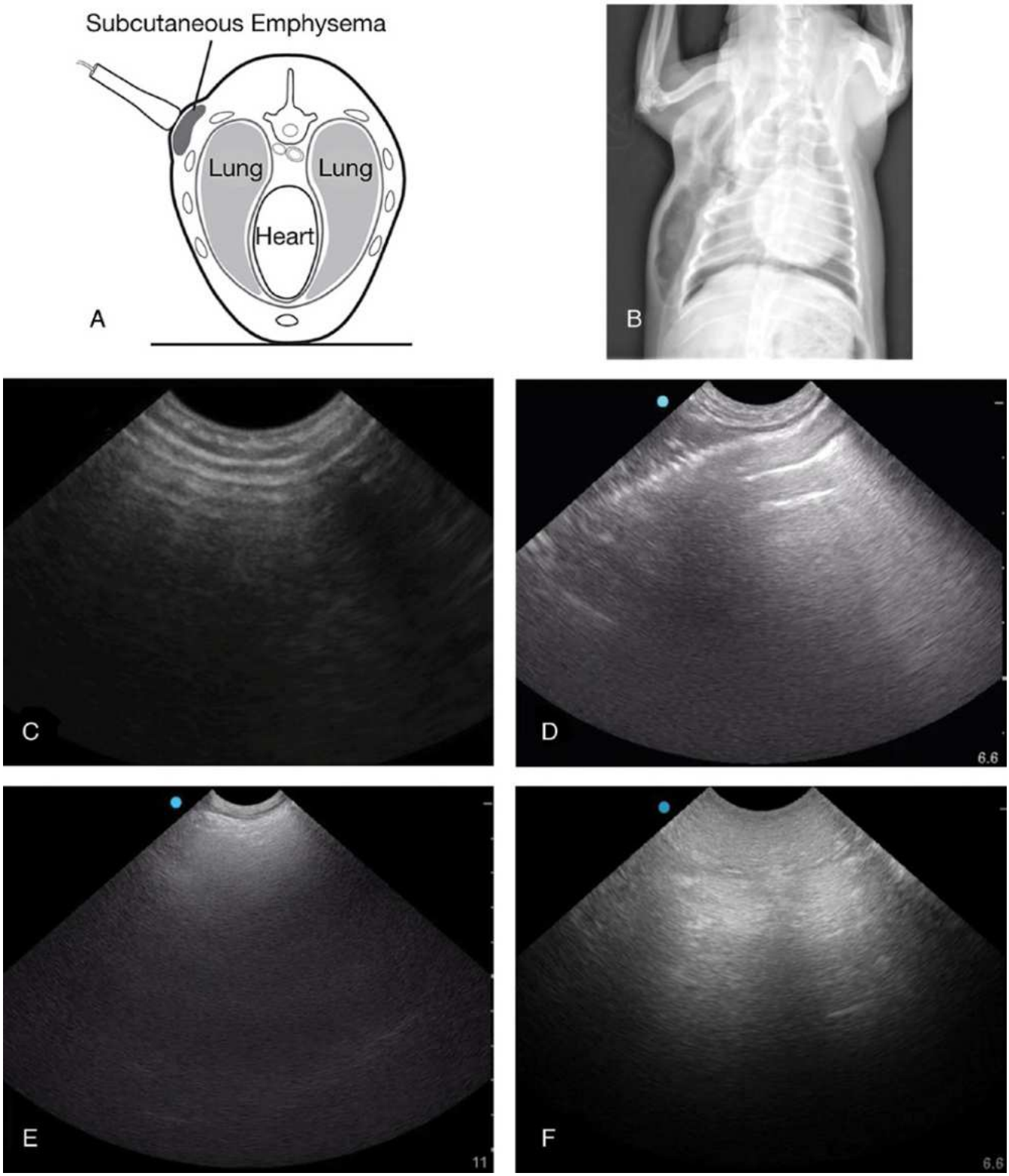


**Figure 18.13.** Subcutaneous emphysema and its B-mode appearance. (A) Cartoon of SQE along a cross-section of the thorax at the CTS view. In (B) is the correlative thoracic radiograph. B-mode images (C) through (F) show how SQE images, with its most striking feature being expected A-lines or dirty shadowing. In (D) there are actually multiple A-lines from both the SQE and aerated lung. However, without the "gator sign" orientation, the "lung line" cannot be accurately identified (see Table 18.2). The bottom line is that if you cannot establish the "gator sign" orientation, then you cannot accurately image lung because you cannot tell what hyperechoic line represents the "lung line." Gentle probe pressure to displace the SQE and acquire the "gator sign" orientation is possible in most cases (Lisciandro 2008). Source: Reproduced with permission from Dr Gregory Lisciandro, Hill Country Veterinary Specialists and FASTVet.com, Spicewood, TX.

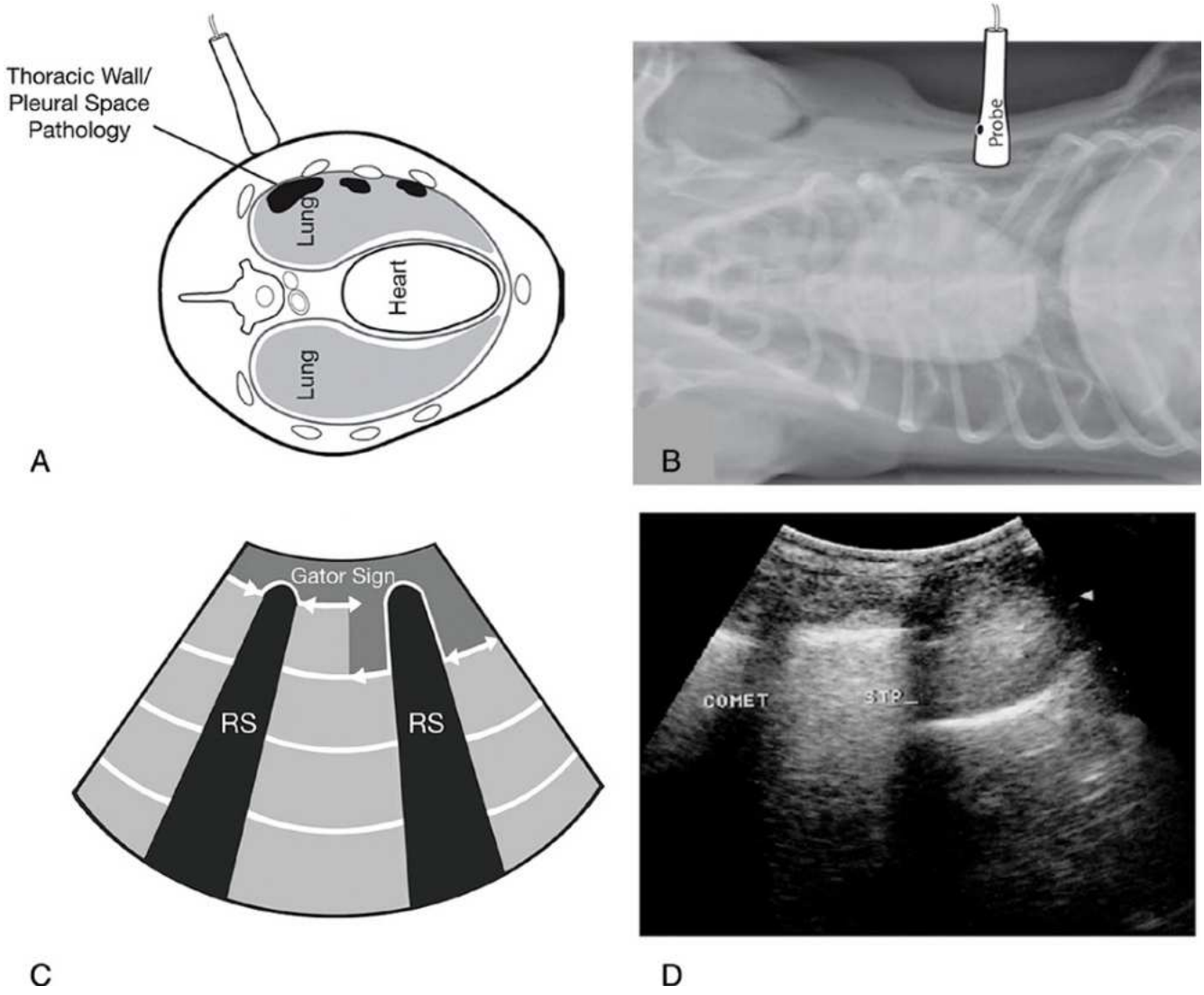


**Figure 18.14.** The "step sign." The "step sign" is the loss of the expected normal linear continuity along the PPI that when found away from transition zones between the pleural and peritoneal (abdominal) cavity often represents forms of pathology (Lisciandro et al. 2008). In (A) is a cartoon of a cross-section of thorax that correlates with the radiograph (B) of an intercostal tear and rib fractures, with a illustrative line drawing in (C) and the B-mode still image in (D). Source: Reproduced with permission from Dr Gregory Lisciandro, Hill Country Veterinary Specialists and FASTVet.com, Spicewood, TX. Illustration in (C) by Dr Judy Brown, Toronto, Canada.

- Categorize the degree of PTX by the TFAST PTX 1/3s Rule as upper third, middle third and lower third (see Figure 18.9 and Table 18.3) (Lisciandro et al. 2008; Lisciandro 2011).

### Pitfalls and Pleural Effusion

Pleural effusion is nonexistent at the CTS view because when free fluid is within the pleural cavity, lung floats. Thus, anechoic stripes at the least gravity-dependent TFAST CTS view should be questioned by the following process.

- An anechoic stripe at this view is most likely stomach wall and artifacts associated with stomach wall include confounders, pseudo gastric B-lines, pseudo shred sign, and pseudo tissue sign (see Figure 18.4).
- Confirm PE through the combination of TFAST views including the gravity-dependent PCS views where fluid falls.

## *Final Comments Regarding the TFAST Lung and Pneumothorax Evaluation*

Pneumothorax has been dubbed the most preventable cause of death in traumatized people (Kirkpatrick

**Table 18.5.**
Rule-outs for the "step sign" of lung.

| | Rule out |
|---|---|
| Pleural space abnormalities | Diaphragmatic hernia |
| | Peritoneopericardial hernia |
| | Pleural effusion |
| Thoracic wall abnormalities | Intercostal tear |
| | Rib fractures |
| | Subcostal hematomas |
| | Thoracic wall masses |
| Pulmonary abnormalities | Consolidation – shred sign, tissue sign, wedge sign |
| | Nodules and masses – nodule sign (granulomas, neoplastic, abscess, other) |
| Other conditions | Anterior mediastinal mass |
| | Other mass effect including lymph nodes, thymus (juveniles) |
| | Enlarged left atrium |
| Pitfall – pseudo step sign | Transition zone of pleural and peritoneal cavities |

Source: Reproduced with permission from Dr Gregory Lisciandro, Hill Country Veterinary Specialists and FASTVet.com, Spicewood, TX.

et al. 2004), and the use of lung ultrasound is an effective, sensitive, specific and accurate, point-of-care imaging modality that may be brought directly to the patient even in austere environments for diagnosing PTX, categorizing the degree of PTX, and monitoring (tracking) PTX that exceeds lung auscultation and radiography and compares favorably with CT (Sargsyan et al. 2001; Kirkpatrick et al. 2004; Lisciandro et al. 2008; Lisciandro 2011; Partlow et al. 2017). Greater detail on lung ultrasound is found in Chapters 22 and 23.

# Pericardial Effusion

## *General TFAST Considerations Regarding Pericardial Effusion*

Several years ago, we posed the question "How would you teach me to accurately diagnose pericardial effusion (PCE) using ultrasound?" Colleagues would reply, "It just looks like pericardial effusion" and textbooks would read, "Imaging features of pericardial effusion are the presence of a sonolucent space between the epicardium and pericardial/mediastinal interface, an influence of gravity on the localization of fluid" (Bonagura and Fuentes 2015), a virtually meaningless answer from a teaching standpoint, especially for the nonradiologist, noncardiologist sonographer. From such answers, the author realized that TFAST tenets for the accurate diagnosis of PCE needed to be created and that knowledge of cardiac anatomy on both short- and long-axis views was imperative to prevent mistakes (Lisciandro 2016).

The left ventricular short-axis view is a most confusing and dangerous proposition as a primary view because of the crescent-shaped right ventricle that mimics the rounding of PCE within the pericardial sac (Figure 18.15). Moreover, the FAST DH view needed to become a primary view in small animals. The FAST DH view is advantageous because it avoids air interference from transthoracic views and directly images for PCE without the confusion of cardiac chambers and for these reasons is the number 1 view in human medicine (see Figure 18.18) (Lisciandro 2014a, 2016, 2019).

### Pericardial Effusion and Pleural Effusion are Quite Different

The differences between PCE and PE ultrasonographically are significant and must be acknowledged by the sonographer on a number of fronts. First, the sonographer must understand the intrathoracic anatomy to accurately differentiate PCE from PE and recognize when both are concurrently present. Second, thoracic radiography is generally a good test for pleural effusion but unreliable for pericardial effusion (Guglielmini 2012; Côté 2013). Lastly, the prevalence of PCE is likely much higher than previously reported because historically unless the patient underwent advanced imaging, either complete echocardiography or CT, the diagnosis of PCE was missed because thoracic radiography is unreliable (Guglielmini et al. 2012; Côté et al. 2013).

Now that TFAST and AFAST have become first-line imaging tests for many clinicians, and ultrasound is arguably the gold standard test for PCE, cases of PCE are captured as part of initial patient assessment rather than being missed or delayed. In 2005, pre-FAST, the author's practice had three documented cases of PCE in comparison to when TFAST became a first-line test, after which 28 documented cases were detected (Lisciandro 2014a, 2016). The true prevalence of PCE is likely higher than reported pre-FAST, as are likely many other cardiac-related conditions, such as intracardiac masses, pulmonary hypertension, dilated cardiomyopathy, left atrial tear in chronic mitral valve disease, caval syndrome, and others, because unless a complete echocardiogram or CT was performed, the condition was missed. The bottom line is that we were using the wrong imaging modality as our screening test.

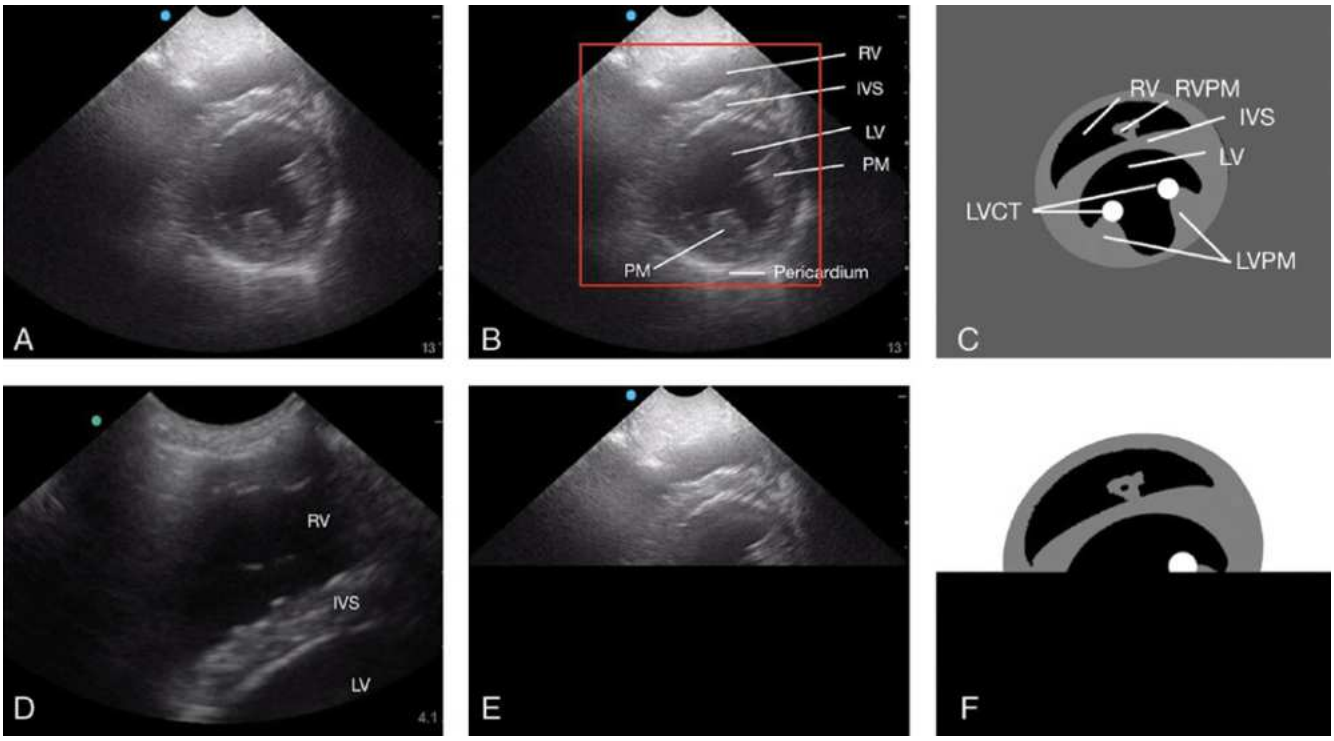


**Figure 18.15.** Anatomy of the heart and its right TFAST pericardial short-axis views. (A) and (B) are identical images unlabeled and labeled followed by a correlative line drawing in (C). The heart should always be imaged in its entirety using the bright hyperechoic line in the far-field representing the pericardium as your landmark. In (D) and (E) are examples of being too shallow in depth (magnified) in which heart chambers in the near-field become very confusing, followed by a correlative line drawing in (F). By being in too close to the heart, its chambers may be easily mistaken for free fluid, which may lead to performing the most catastrophic of mistakes – centesis on your patient's heart. The image in (E) is actually the same image as in (A) and (B) but showing how shallow depth is confusing for the sonographer. In real time, air interference from lung makes the acoustic window to the heart very intermittent, especially in patients in respiratory distress. IVS, interventricular septum; LV, left ventricle; LVCT, left ventricular chordae tendinae; LVPM, left ventricular papillary muscle; RV, right ventricle; RVPM, right ventricular papillary muscle. Source: Reproduced with permission from Dr Gregory Lisciandro, Hill Country Veterinary Specialists and FASTVet.com, Spicewood, TX.

## *Accurate TFAST Diagnosis of Pericardial Effusion*

The sonographer should have a set of rules to follow for the accurate sonographic diagnosis of PCE. The only major fluid-filled structure in the thorax that can be mistaken for PCE (or PE) is your patient's heart. And it's not generally a good thing for your patient to perform centesis on their heart chamber.

These are the TFAST tenets that will be subsequently explained in greater detail.

- *Always, always, always* image the heart in its entirety with enough depth to see the bright hyperechoic pericardium, your habitual landmark, in the far-field. By adhering to this tenet, the probability of mistaking the heart for PCE (or PE) is greatly reduced (Figure 18.16; see also Figure 18.15). We call this the "DeFrancesco Rule."
- Image toward the muscular apex of the heart where there are no confusing heart chambers. Pericardial effusion rounds the muscular apex of the heart, referred to as the "racetrack sign" and "bull's eye sign" (Lisciandro 2014a, 2016). We call this the "Lisciandro Rule I."
- The sole echo view from the right TFAST PCS view would be the long-axis four-chamber view when all four chambers are clearly identified and the free fluid is observed outside the heart and between the heart and hyperechoic pericardium (Lisciandro 2014a, 2016) (Figures 18.17, 18.18, and 18.19). We call this the the "Lisciandro Rule II."
- The sole echo view from the left TFAST PCS view would be the left short-axis view at the level

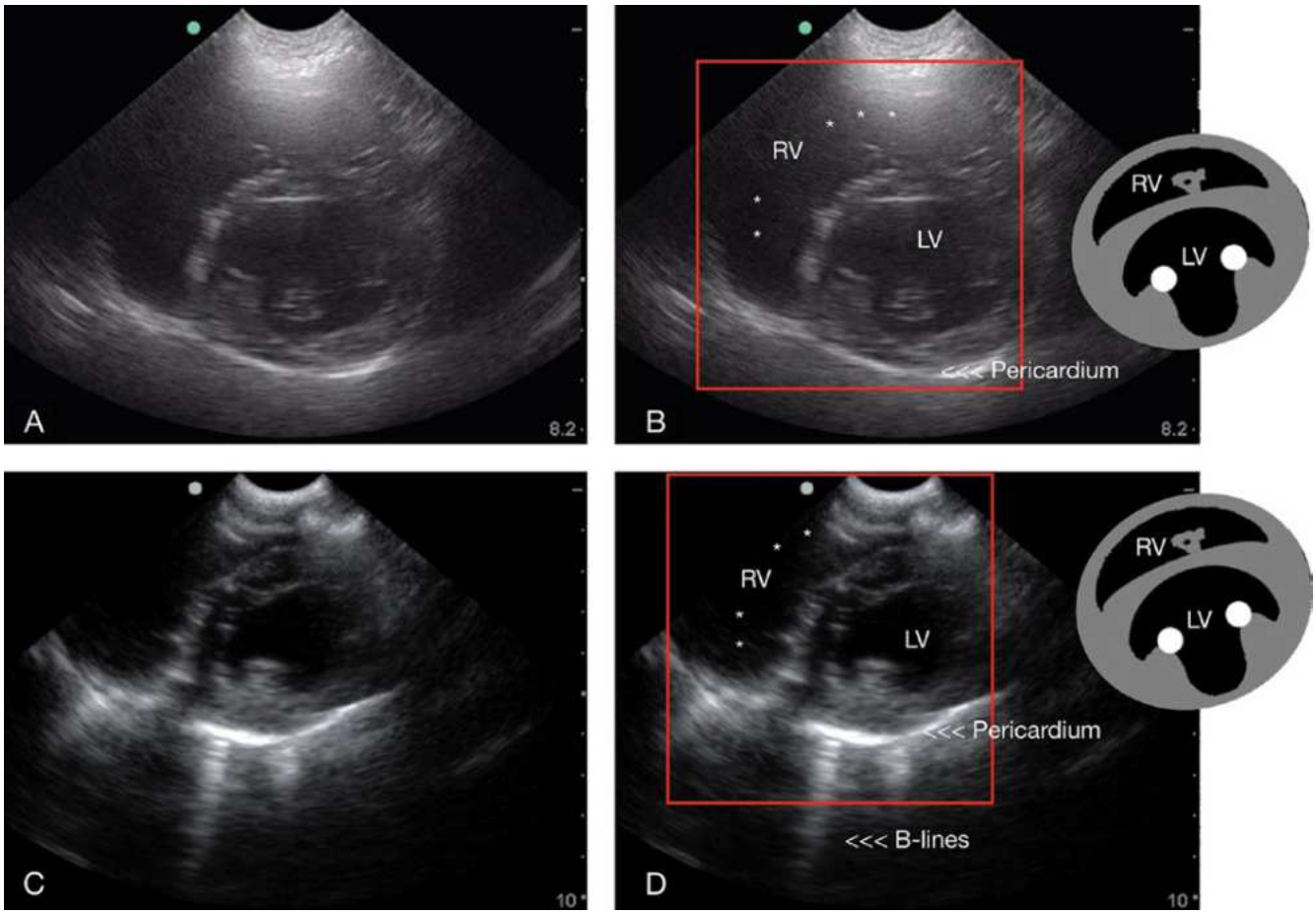


**Figure 18.16.** Right pericardial short-axis views and their danger zone. Corresponding images are unlabeled (A,B) and labeled (C,D) followed by a correlative line drawing of the left ventricular short-axis view for orientation. The landmark of the bright hyperechoic pericardium is obvious in all images, ensuring that the heart is viewed in its entirety. The red box indicates what the author calls the "danger zone" because the right ventricle can look so variable, ranging from a crescent-shaped sliver to being pooched out without clear borders as in both (B) and (D) outlined with (*). The size of the right ventricle (RV and *) is so variable on right TFAST PCS short-axis views that it is much more reliably assessed in its long-axis four-chamber view. The images are from dogs with normal hearts. Note a couple of B-lines off the pericardial-pulmonary interface in images (C) and (D). LV, left ventricle; RV, right ventricle. Source: Reproduced with permission from Dr Gregory Lisciandro, Hill Country Veterinary Specialists and FASTVet.com, Spicewood, TX.

referred to as the "hammerhead view" in which both ventricles are clearly identified and pericardial effusion is outside both ventricles and contained within the hyperechoic pericardial sac (see Figures 18.17 and 18.19). We call this the "Lisciandro Rule III."

- One view is no view! Combine views. This is an axiom from human medicine.
- Never use the right PCS short-axis views of the heart as a single view for PCE (and PE) because it is too confusing with the crescent-shaped right ventricle and risks the most catastrophic of mistakes – centesis on your patient's heart (Lisciandro 2016). We refer to the TFAST PCS short-axis views of the heart from the right side as the "danger zone" and stay away from them as sole views when attempting to determine if PCE (or PE) is present (see Figure 18.16).

## *Causes of Pericardial Effusion*

See Table 7.8 in Chapter 7.

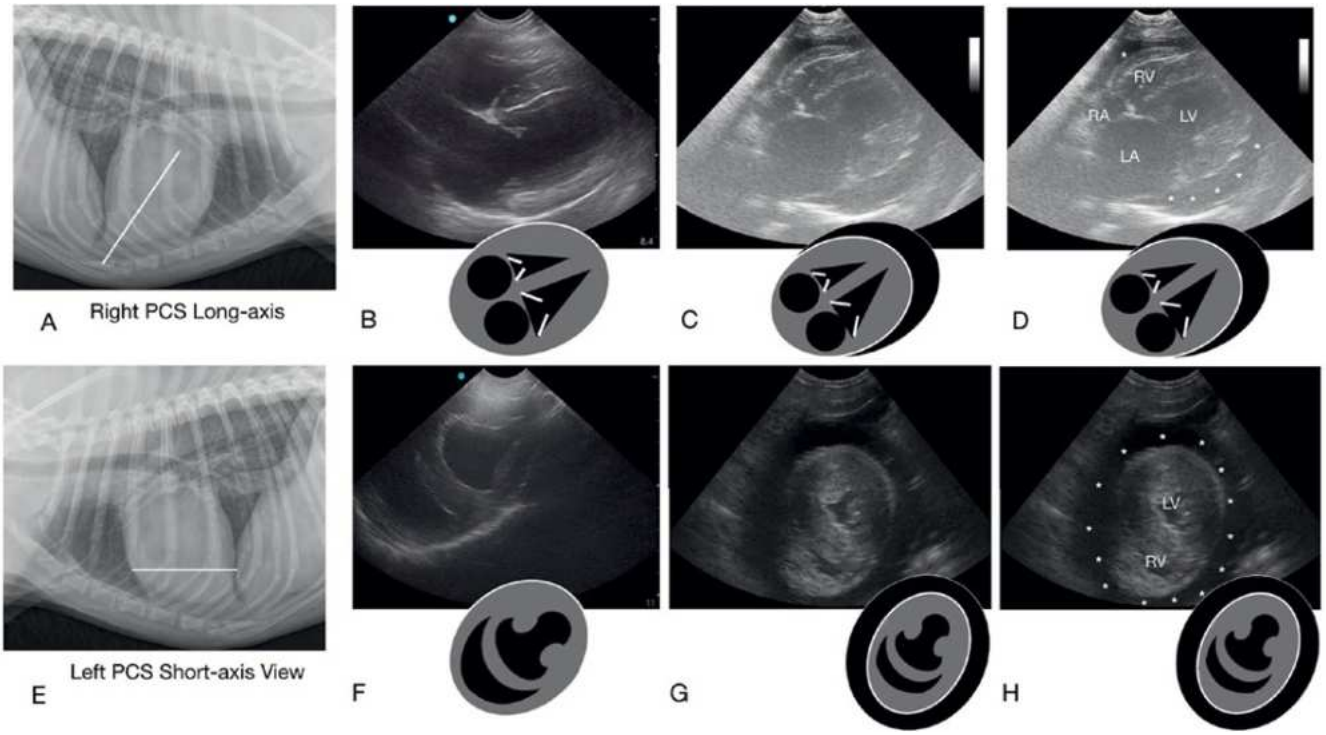


**Figure 18.17.** Most reliable echo views for pericardial effusion. (A–D) show the right TFAST PCS long-axis four-chamber view. The line on the thoracic radiograph shows the long-axis line along which the probe's footprint should be parallel. In (B) is shown a normal long-axis four-chamber view, and in (C) and (D) are unlabeled and labeled long-axis four-chamber views with pericardial effusion (*), respectively. (E–H) Left TFAST PCS short-axis views of the heart. The probe is positioned nearly parallel to the sternum as shown in (E) with corresponding B-mode images of a normal "hammerhead view" followed by one with pericardial effusion that is unlabeled and labeled in (G) and (H), respectively. In both of these TFAST echo views, all heart chambers are clearly identified and PCE is clearly identified outside the heart (*). See also the TFAST echo charts in Figures 17.25 and 17.26. LA, left atrium; LV, left ventricle; RA, right atrium; RV, right ventricle. Source: Reproduced with permission from Dr Gregory Lisciandro, Hill Country Veterinary Specialists and FASTVet.com, Spicewood, TX.

## *Does My Patient have Cardiac Tamponade?*

### Defining Cardiac Tamponade

The question increases the anxiety of the sonographer when finding PCE. Cardiac tamponade occurs when intrapericardial pressure exceeds right atrial and right ventricular pressures, causing their collapse seen on either short-axis or long-axis views (Figure 18.20). In real time, the right atrium and right ventricle often dynamically collapse with a rippling effect. As a result of cardiac tamponade, obstructive shock occurs in which blood cannot be pumped from the right heart to the lung and right-sided congestive heart failure ensues. Different degrees of cardiac tamponade can be present (see Chapters 19–21) with more severe forms being life-threatening and warranting emergent pericardiocentesis (see Chapters 21 and 43).

### Using the Characterization of the Caudal Vena Cava and Hepatic Veins

By definition, obstructive shock secondary to cardiac tamponade will result in a distended caudal vena cava (CVC), referred to as FAT or fluid-intolerant CVC, along with hepatic venous distension because the hepatic veins drain into the CVC, referred to as the "tree trunk sign" (Lisciandro 2014a, 2016) (see Figures 18.20D and 36.8). If the patient survives, in time hepatic venous congestion becomes chronic and right-sided congestive heart failure develops with ascites (modified transudate) (see Figures 6.8, 6.9,

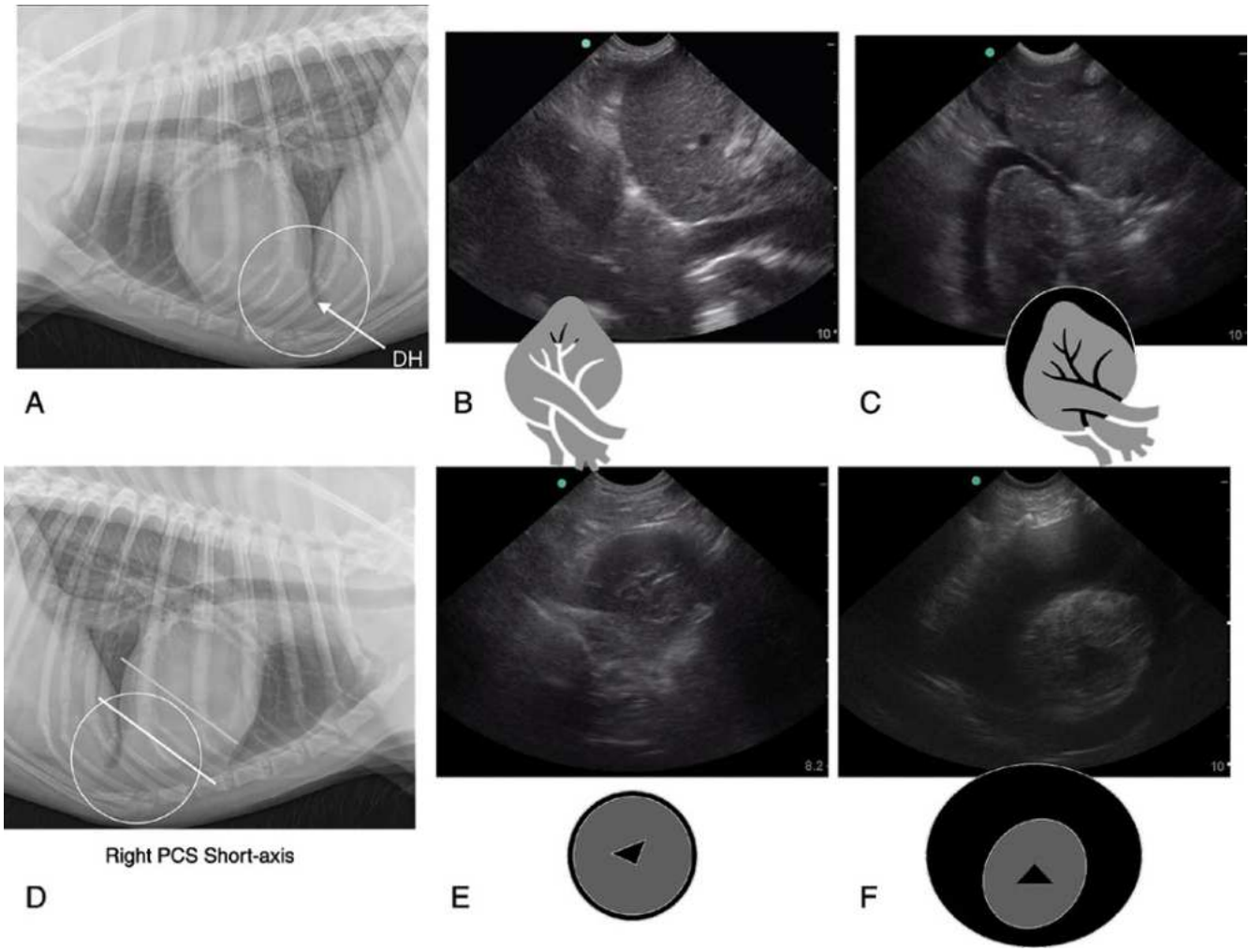


**Figure 18.18.** Imaging strategy for PCE is toward the muscular apex of the heart where there are no confounding heart chambers. In (A) through (D), the FAST DH view is shown in which imaging the muscular apex of the heart is automatic. This view is the number 1 view in human medicine for the same reason, that it is very difficult to mistake a heart chamber for PCE. In (B) is the normal heart against the diaphragm referred to in real time as the "cardiac bump" by the author (see also Figure 17.27). In (C) and (D) are the same images unlabeled and labeled from a patient that clearly has PCE (*) evidenced by the "racetrack sign" of PCE rounding the muscular apex of the heart (Lisciandro 2014a, 2016, 2019). In (E) through (H) are images from the right TFAST PCS views showing how the short-axis plane is taken from the most ventral of the short-axis lines (bars) of the TFAST cardiac ladder referred to as the "bull's eye" sign (*circled*) because the muscular apex of the heart is imaged (see Figures 17.25 and 17.26). Source: Reproduced with permission from Dr Gregory Lisciandro, Hill Country Veterinary Specialists and FASTVet.com, Spicewood, TX.

6.10, 6.11, and 18.20). Thus, characterizing the CVC and its associated hepatic veins provides a nonecho alternative to echo views as well as invaluable supplemental information regarding the significance of the PCE in your canine patient. Be smart – a nondistended CVC with a bounce rules out cardiac tamponade without an echo view. A distended CVC with hepatic venous distension supports cardiac tamponade but always consider the status of your patient as being stable or unstable. An unstable patient with this clear supportive evidence for cardiac tamponade and obstructive shock, that is FAT CVC and hepatic venous congestion, mandates emergent pericardiocentesis. In contrast, a stable alert patient with PCE may have a FAT CVC but a lesser degree of cardiac tamponade in which pericardiocentesis is not immediately emergent.

See more detailed information on the CVC in Chapters 7 (Figure 7.12 and Table 7.6), 26, and 36 and cardiac tamponade in Chapters 19–21.

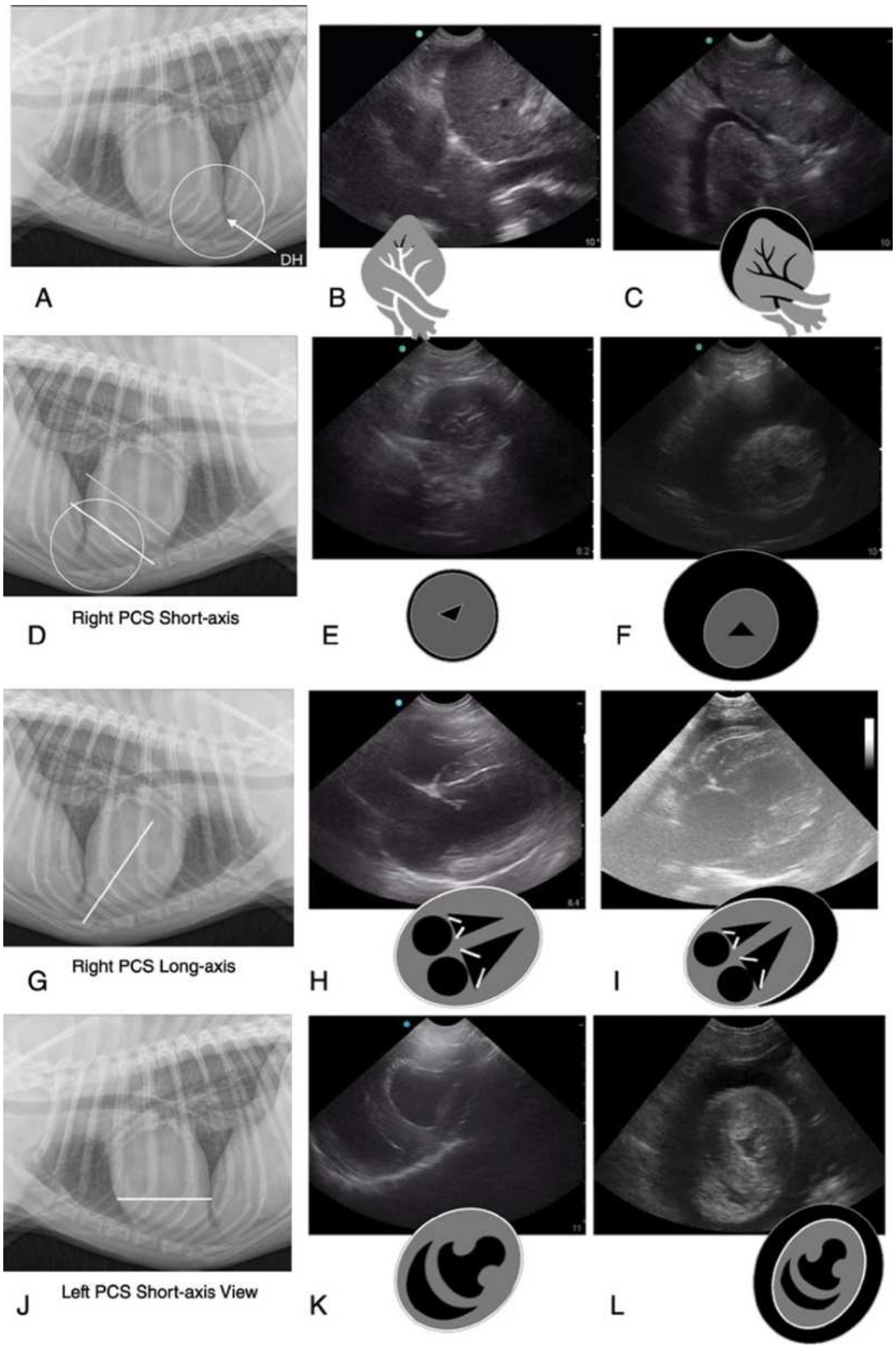


**Figure 18.19.** "One view is no view" – composite of multiple views for the accurate TFAST diagnosis of pericardial effusion. In (A) through (C) is the sequence of images for detecting PCE at the FAST DH view and its "racetrack sign." In (D) through (F) is the sequence of imaging the right TFAST PCS views and imaging toward the muscular apex of the heart for the "bull's eye" sign. In (G) through (I) is the sequence of long-axis four-chamber views, arguably the only reliable echo view in which all four chambers of the heart may be identified and the PCE identified outside the heart and within the pericardial sac. In (J) through (L) the left TFAST PCS short-axis view is another view in which the left ventricle and right ventricle are clearly visible at this level and PCE is outside the heart within the pericardial sac. In (B), (E), (H), and (K) negative images are contrasted with the positive PCE images of (C), (F), (I), and (L). Source: Reproduced with permission from Dr Gregory Lisciandro, Hill Country Veterinary Specialists and FASTVet.com, Spicewood, TX.

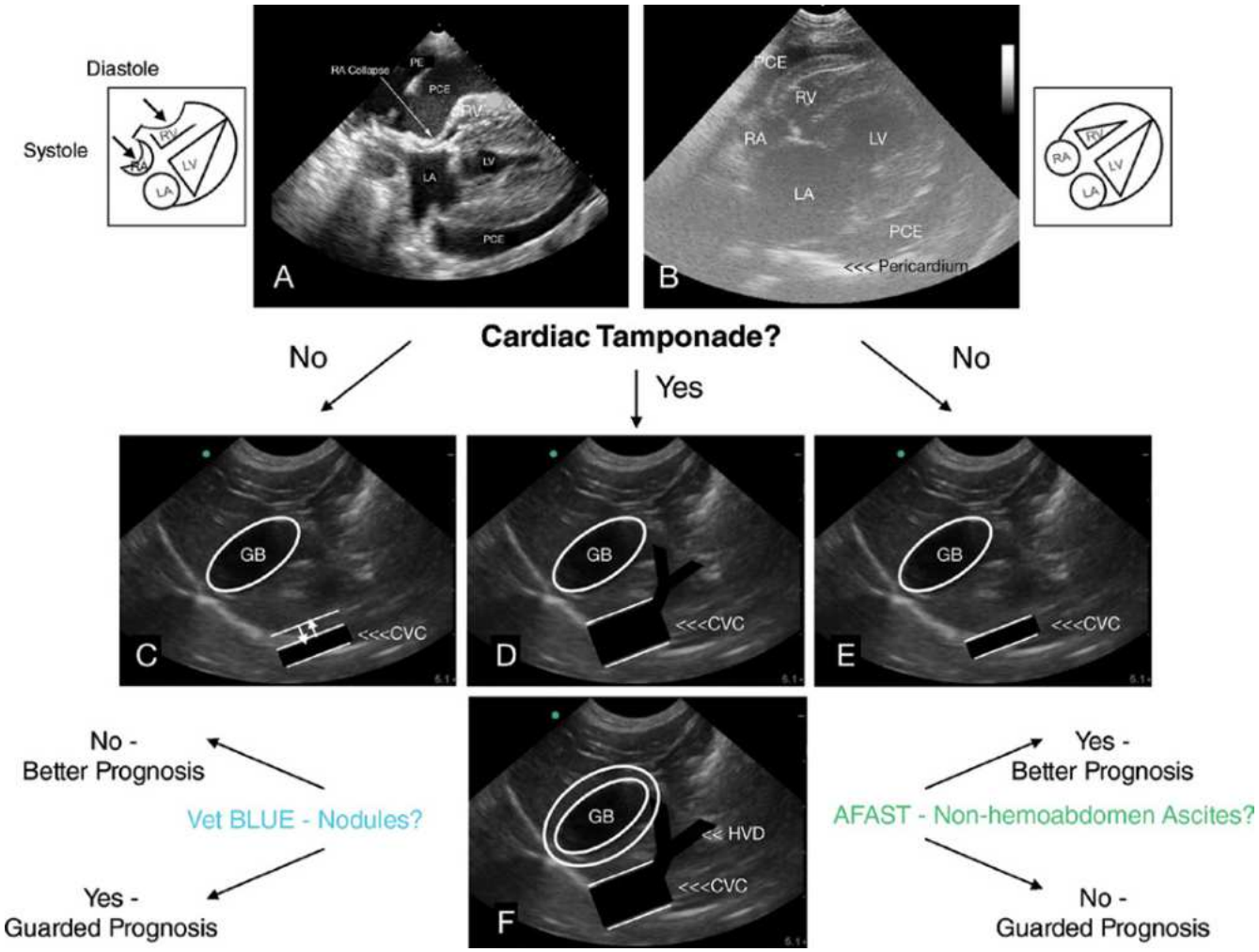


**Figure 18.20.** Integration of information in PCE and the presence and absence of cardiac tamponade. In (A) cardiac tamponade is present with collapse of the right atrium (RA) during systole with a correlative cartoon of right atrial and right ventricular collapse during systole and diastole, respectively. With cardiac tamponade, by definition the intrapericardial pressure within the pericardial sac exceeds filling pressures of the right heart and thus venous return to the right heart is compromised. In (B) the patient has pericardial effusion and an enlarged left atrium (LA), likely due to a left atrial tear. No signs of cardiac tamponade are seen. In (C) through (E) illustrated with overlays is caudal vena cava (CVC) and hepatic venous characterization because, by definition, cardiac tamponade results in hepatic venous congestion due to obstruction of blood flow to the right heart. The use of the CVC and hepatic venous characterization serves as a "right-sided Global FAST nonecho fallback view." In (C) and (E) there are no signs of right-sided obstruction of flow whereas in (D) there is, supporting a degree of cardiac tamponade with a FAT CVC and hepatic venous distension referred to as the "tree trunk sign." In (F) is the same image as (D) but showing gallbladder wall edema as a result of a "cardiac gallbladder." When PCE is found, Global FAST is helpful to search quickly for signs of pulmonary metastasis using Vet BLUE and for the presence of ascites, which have significant implications for patient care, nonhemoabdomen ascites carrying a better prognosis (Stafford Johnson et al. 2004). Source: Reproduced with permission from Dr Gregory Lisciandro, Hill Country Veterinary Specialists and FASTVet.com, Spicewood, TX.

### The Presence of Ascites - Better or Worse?

The presence of a nonhemoabdomen ascites, which should be a modified transudate due to posthepatic portal hypertension, generally carries a much better prognosis. The presence of a nonhemoabdomen ascites supports a long-standing presence of PCE because the ascites occurred over time, supporting a more chronic process (see Figures 6.8, 6.9, 6.10, 6.11, 18.18C,D, and 18.20 and see Chapter 7) (Stafford Johnson et al. 2004). One canine pericardial effusion study (143 dogs) documented a median survival of 605 days with ascites (and echo negative for a mass) versus 45 days without

ascites (Stafford Johnson et al. 2004). This is another example of how targeted POCUS exams can miss important clinical information that could have a profound effect on patient management. With the Global FAST approach, ascites may be rapidly ruled in or out and the CVC and its associated hepatic veins characterized using AFAST (see Chapter 36). Moreover, AFAST and its target organ approach rapidly screens for obvious soft tissue abnormalities, such as obvious liver masses or other abdomen-related pathology.

In another canine pericardial effusion study of 107 dogs, 50–66% had evidence of pulmonary metastasis based on surgical and necropsy findings as the gold standard, of which only 33% were detected via thoracic radiography (TXR) (MacDonald et al. 2009); Vet BLUE screens for any obvious lung abnormalities including pulmonary metastasis and may prove better than three-view TXR (Kulhavy and Lisciandro 2015). These studies make a strong case for initially staging all canine PCE cases using the Global FAST approach over targeted POCUS exams, in which important information is often missed (satisfaction of search error) or delayed in its detection (see Figure 18.20). See Patient Staging in Chapter 36 and Figure 36.23.

In summary, there are different degrees of cardiac tamponade and the best approach is as follows.

- Look at your patient. Are they hemodynamically stable? If the answer is yes, then take a few breaths and relax. If the patient is unstable, then emergent pericardiocentesis is indicated as a life-saving intervention (see Chapters 19–21and 43 and Section IX).
- Look at the CVC (see Figure 18.20). It is a nonecho option that is often less stressful for the patient because it can be performed rapidly without the air interference and restraint needed for echocardiography, including TFAST echo views and POCUS heart.
  - If the CVC has a bounce, then the patient *does not have obstructive shock*, in other words, does not have cardiac tamponade (see Figures 7.12 and 18.20 and Table 7.6). And if a CVC bounce is present, do Global FAST (and an electrocardiogram) to look for another reason for weakness and shock because it's unlikely to be primarily due to the PCE!
  - If the CVC is FAT, then there is evidence of obstructive shock or cardiac tamponade. Look at your patient. Are they stable or unstable? An unstable patient requires emergent pericardiocentesis versus a stable patient that favors pericardiocentesis as an elective procedure (see Figures 7.12 and 18.20 and Table 7.6).

In human medicine, it has been shown that an unremarkable inferior vena cava (IVC) rules out cardiac tamponade and a FAT or distended IVC is only 40% specific, meaning that even if the IVC is FAT or distended, the patient still may not have cardiac tamponade requiring emergent pericardiocentesis (Himelman et al. 1988; Candotti and Arntfield 2014; Tchernodrinski and Arntfield 2015). Moreover, in weak hypotensive people with PCE and a non-distended IVC, it is possible that the PCE is not the cause because there is no cardiac tamponade (Himelman et al. 1988; Candotti and Arntfield 2014; Tchernodrinski and Arntfield 2015). So again, look at your patient and do Global FAST to look for other causes!

## When Should Emergent Pericardiocentesis Be Performed?

### *Chronic versus Acute PCE*

Emergent pericardiocentesis should be performed in hemodynamically unstable cases with obstructive shock. The procedure is straightforward and complications are most commonly related to arrhythmias over cardiac puncture or bleeding (Humm et al. 2009). With that being said, we now capture acute PCE that was historically missed, and some of these dogs have acute cardiac chamber rupture, in which the pericardial sac is protective by keeping the hemorrhage in a closed system. Clinically, this is important because pericardiocentesis may be indicated, but the PCE and cardiac tamponade may recur quickly, ranging from minutes to the next several hours. Tearing the pericardium, the so-called "rough pericardiocentesis" to create an inexpensive temporary pericardial window, would be contraindicated in these cases as they may exsanguinate into their pleural space. Management also is different and likely requires a pericardial catheter for intermittent as needed pericardiocentesis of which the blood, often *without* anticoagulant, could be repeatedly autotransfused with an inline blood filter, and the patient potentially kept alive for definitive surgical intervention (Morges et al. 2011; Higgs et al. 2015; Ployart et al. 2013; Robinson et al. 2016).

**Pearl:** When performing pericardiocentesis, *leave a small volume of fluid in the pericardial sac* if complete echocardiography will be subsequently performed because the pericardial fluid provides an acoustic window for the detection of a pericardial or heart-based mass (Scansen 2011).

**Pearl:** Some cardiac and systemic conditions result in a small rim of hemodynamically benign pericardial fluid (often <5 mm) that is clinically silent. TFAST provides a monitoring tool by measuring the widest dimension at the DH view in standing or sternal positioning (so gravity dependent) with "trivial" <5 mm, "mild" 5 mm–1 cm, "moderate" >1 cm–<2 cm, and "severe" >2 cm, similar to human medicine (Candotti and Arntfield 2014; Tchernodrinski and Arntfield 2015).

### *Other Pericardial Effusion Subsets*

#### Left Atrial Rupture/Tear

The author captures the complication of left atrial tear/rupture (LAT) several times a year because TFAST is an extension of the physical exam (actually the Global FAST approach is used as an extension of the physical exam). TFAST-Global FAST is performed on all cardiac patients and suspects (Figure 18.21). The complication is fascinating because it has been traditionally overlooked. LAT is also covered in Chapter 21 from the veterinary cardiologist perspective. The classic presentation in the author's experience is acute respiratory signs, usually with respiratory distress but sometimes just persistent relentless coughing. The PCE most often has a clot (Reineke et al. 2008; Nakamura et al. 2014) and the key to an accurate diagnosis is PCE in a mitral valve heart disease dog with a severely enlarged left atrium. Look for the severely enlarged left atrium (LA:Ao >2:1) not only via the right TFAST PCS short-axis echo views, but also advantageously (generally less patient stress) via the DH view (see Figures 17.27, 18.17C, and 18.32B).

The LAT aspects which are important from the non-cardiologist perspective are as follows.

- LAT is routinely missed by radiography.
- Most patients are small dogs with chronic mitral valve disease.
  - Dachshunds and Shetland sheepdogs are most common (DeFranceso, personal communication).
- Pericardial effusion in a dog with the appropriate clinical profile and a severely enlarged left atrium.
- A clot present within the PCE is a hallmark for LAT but variably present (Reineke et al. 2008; Nakamura et al. 2014).
- LAT dogs often have only mild pulmonary edema (use Vet BLUE).
  - The Vet BLUE B-line scoring system guides loop diuretic usage.
  - Vet BLUE prevents overtreating with loop diuretics.
- Emergent pericardiocentesis is generally avoided, but in the unstable patient it may be needed and care should be taken not to tear open the pericardium (author experience, <5% of cases).
- Treatment includes lowering left atrial pressure by including pimobendan and afterload reducers such as amlodipine (Suzuki et al. 2011).
- Most LAT cases survive hospitalized care, but the long-term prognosis is guarded because of their unpredictable clinical course. In a small case series, 10/11 were discharged with a median survival of 203 days, found to be better for those with first-event congestive heart failure. The left atrium can heal and these dogs survive several months or more (Nakamura et al. 2014).

#### Cardiac Chamber Rupture and Pericardial Effusion: Traumatic and Nontraumatic

Cardiac chamber rupture can be caused by trauma (blunt and penetrating) and nontrauma (usually a ruptured tumor). Trauma-induced PCE has been reported and successfully treated surgically in both penetrating (projectiles and foreign bodies) and blunt trauma (Witt and Mayhew 2011; Elliott and Mayhew 2011), and neoplastic causes have had successful outcomes (Ployart et al. 2013; Treggiari et al. 2017). Keys for success include early detection, patient stabilization and management, and a willing surgeon. Catheterization of the pericardial sac and initial and repeated autotransfusion will likely be required for patient stabilization.

## *Gallbladder Wall Edema: the "Cardiac Gallbladder"*

Gallbladder wall edema (GWE) has gained a lot of press regarding its use in the triage setting, especially with anaphylactic dogs (see Chapters 6 and 7). However, GWE may also be a result of right-sided cardiac conditions and right-sided congestive heart failure (Nelson et al. 2010; Lisciandro 2014a, 2019) (Figures 18.22 and 18.23). The terms "anaphylactic gallbladder" and "cardiac gallbladder" have been created by the author for these patient subsets (Figure 18.22; see also Figure 7.12) and the author has a case series of dogs and cats with PCE, dilated cardiomyopathy, right-sided congestive heart failure (congenital, pulmonary hypertension, tricuspid disease) and volume overload from fluid therapy (Nelson et al. 2010; Lisciandro 2014a, 2019). Thus, in the acute setting

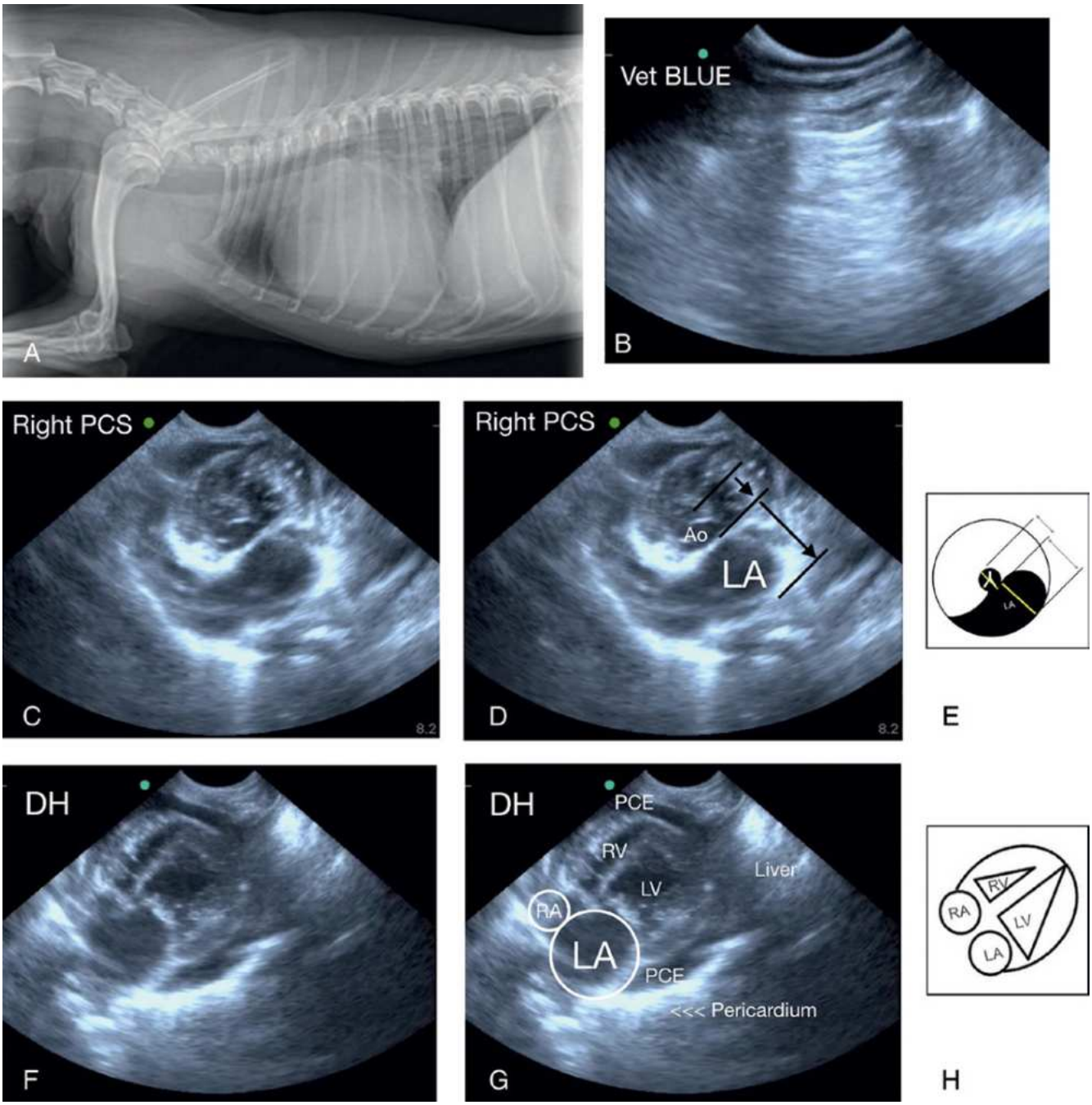


**Figure 18.21.** Composite of images in a dog with a left atrial tear secondary to mitral valve disease. In (A) the thoracic radiograph misses the complication of a left atrial tear (LAT) from mitral valve disease in this older dachshund. In (B) the Vet BLUE confirms radiographically that the dog has no significant pulmonary edema. (C) and (D) are the same image unlabeled and labeled showing the severely enlarged left atrium as noted by the arrows (LA:Ao >2:1), with a cartoon of normal left ventricular short-axis view and cardiac chamber ratios in (E). In (F) and (G) the same image is unlabeled and labeled as imaged from the right TFAST PCS view. A cartoon of the expected normal long-axis four-chamber view is shown in (H). Note the severely enlarged left atrium (>1:1 relative to the right atrium). The pericardial effusion of a LAT often has a clot (see Figure 18.32B). LA, left atrium; LV, left ventricle; PCE, pericardial effusion; PCS, pericardial site view; RA, right atrium; RV, right ventricle. Source: Reproduced with permission from Dr Gregory Lisciandro, Hill Country Veterinary Specialists and FASTVet.com, Spicewood, TX.

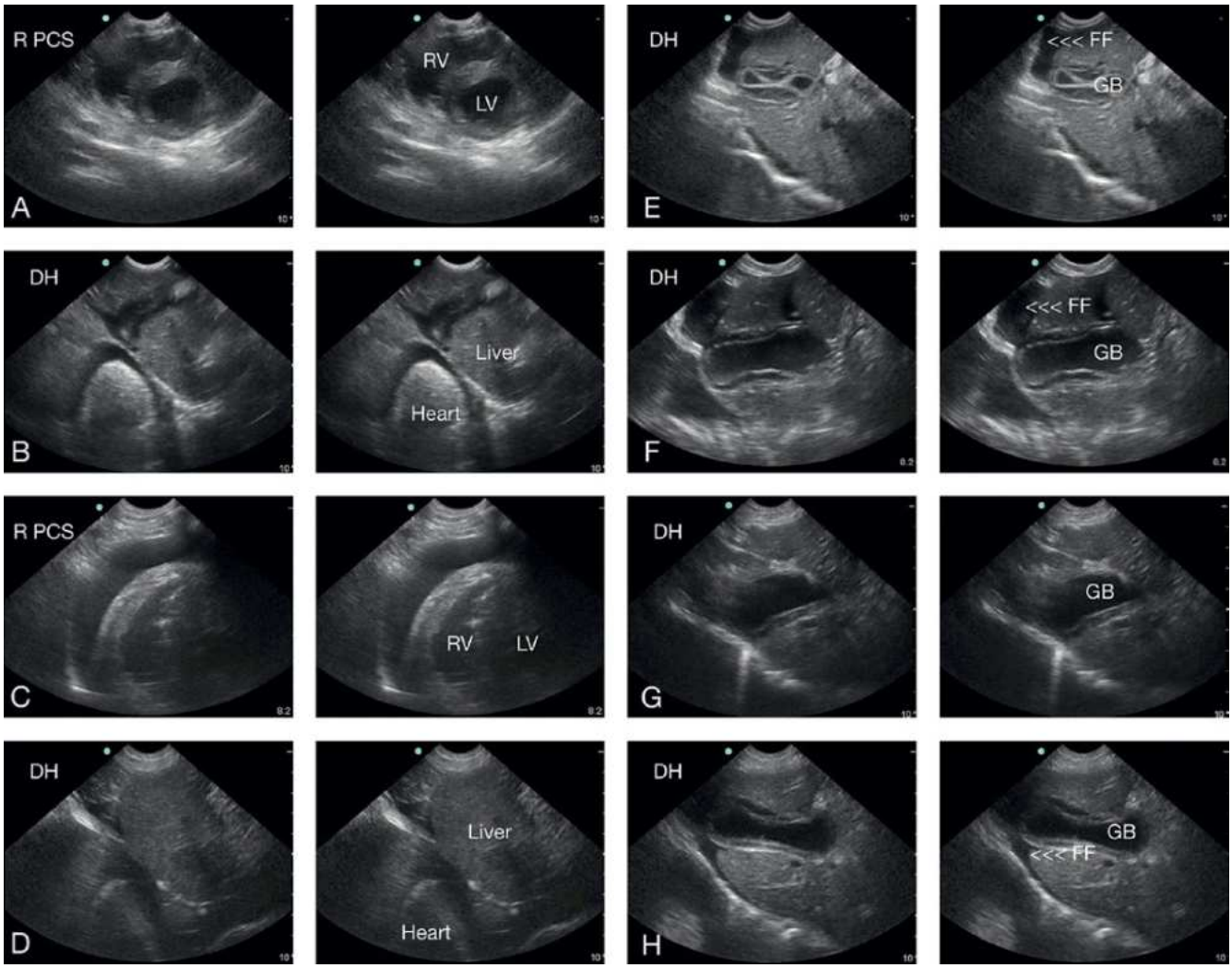


**Figure 18.22.** The "cardiac gallbladder" in a case series of dogs. In (A) and (E) are unlabeled and labeled images from the same dog. The right TFAST PCS view shows the left ventricular short-axis view and the right ventricle in real time is distended and has poor systolic function. In (E) is the patient's FAST DH view showing the ascites (<<< FF) in between the liver and diaphragm and the obvious gallbladder wall edema (sonographic striation). In (B) and (F) another dog is shown with unlabeled and labeled images at the FAST DH view of the "racetrack sign" of pericardial effusion and the obvious ascites (<<< FF) and gallbladder wall edema (sonographic striation). In (C) and (G) is a third dog with pericardial effusion viewed from the right PCS view; caution should be exercised if this is used as a sole view because of the crescent-shaped right ventricle. In (G) the gallbladder wall edema is obvious, as in the preceding cases. In (D) and (H) is shown a final example in another dog with pericardial effusion via the FAST DH view and obvious ascites (<<< FF) and gallbladder wall edema (sonographic striation). FF, free fluid; GB, gallbladder; LA, left atrium; LV, left ventricle; RA, right atrium; R PCS, right pericardial site view; RV, right ventricle. Source: Reproduced with permission from Dr Gregory Lisciandro, Hill Country Veterinary Specialists and FASTVet.com, Spicewood, TX.

the rule-out list should be known to sonographers performing and interpreting images; the Global FAST approach prevents satisfaction of search error since it mandates imaging acoustic windows in the abdomen (AFAST) and thorax (TFAST), including heart and lung (Vet BLUE). Always look past the diaphragm for PCE, the most common cause of a "cardiac gallbladder" (Lisciandro 2016, 2019) (see Figures 18.22 and 18.23). See Table 7.5 for GWE rule-outs and Table 7.6 for characterization of the CVC.

## *Use of Radiography for the Diagnosis of Pericardial Effusion and Tamponade*

Thoracic radiography and vertebral heart scores are unreliable tests for detecting PCE and tamponade (Guglielmini et al. 2012; Côté et al. 2013) (see Figures 18.21 and 18.32A,B). The view that PCE should be considered in "globoid hearts" is an unreliable test and many unremarkable cardiac silhouettes have significant PCE that is missed (Stafford Johnson et al. 2004; MacDonald et al. 2009).

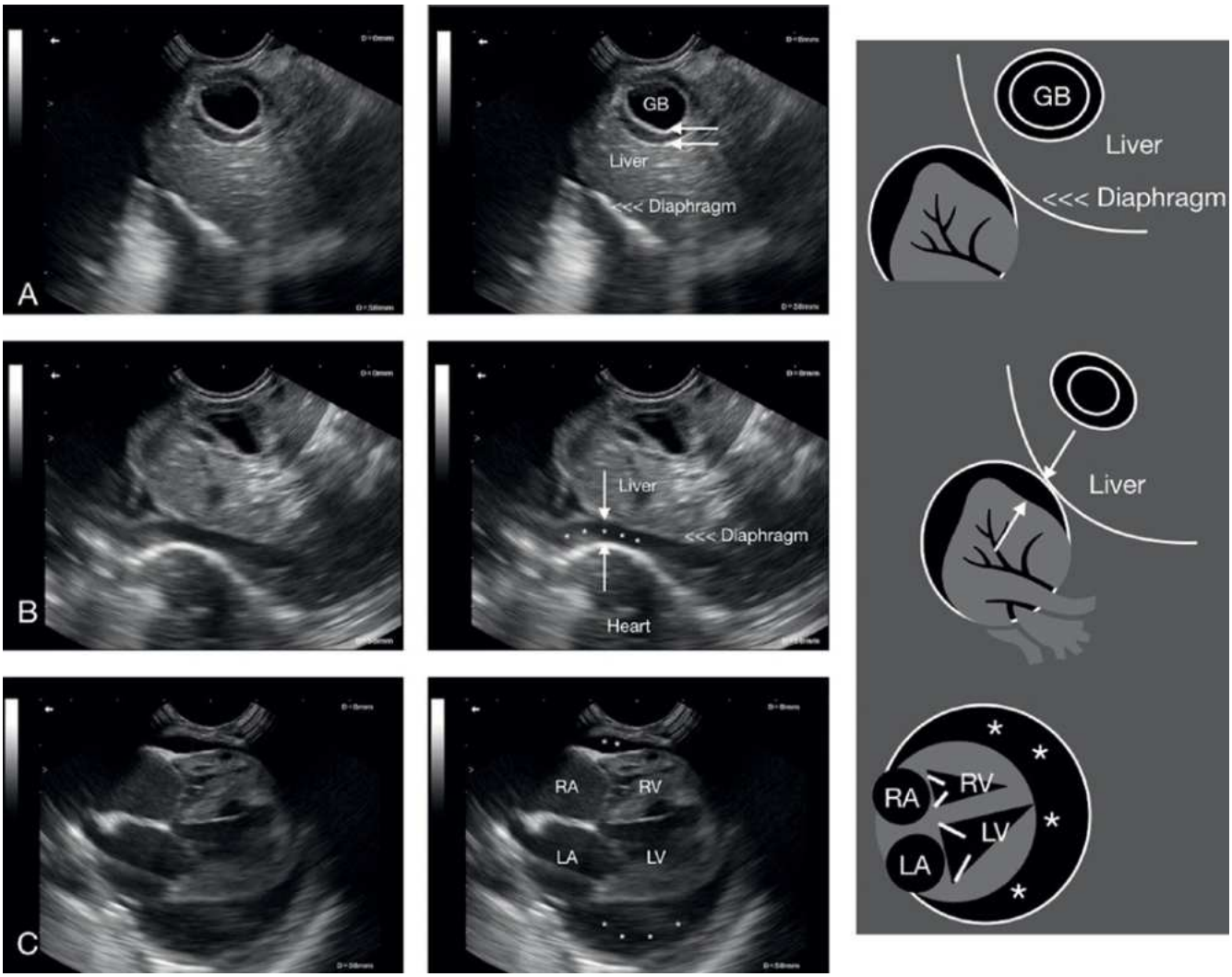


**Figure 18.23.** The "cardiac gallbladder" in a cat. In rows (A) through (C) are labeled and unlabeled images and correlative line drawings from a juvenile cat with a ventricular septal defect and left to right shunting. In (A) the FAST DH view is shown with the obvious gallbladder wall edema, with the arrows pointing out the inner and outer gallbladder wall and the sonographic striation representing intramural edema in between. There is some ascites noted, which is unusual for the feline with right-sided congestive heart failure. In (B) the obvious "racetrack sign" of pericardial effusion (*, ←) is seen through a slightly different longitudinal scanning plane through the FAST DH view. In (C) from the TFAST right PCS view is the long-axis four-chamber view clearly showing the four chambers and pericardial effusion (*) outside the heart and within the pericardial sac. GB, gallbladder; LA, left atrium; LV, left ventricle; RA, right atrium; RV, right ventricle. Source: Courtesy of Dr Chris Johnson, DVM, Tulsa, OK.

So why the increased prevalence of PCE? We have historically been using the wrong test as our first line-screening. Ultrasound is arguably the gold standard test for PCE and with widespread use of TFAST, these cases are now being captured.

**Pearl:** If PCE remains an uncertainty and the patient is hemodynamically stable, then arrange for complete echocardiography for confirmation (or perform serial TFAST examinations or both).

# Pleural Effusion

## *General TFAST Considerations Regarding Pleural Effusion*

Pleural effusion (PE) has major important differences from pericardial effusion. First, PE is generally uncontained and unrestrained within the pleural cavity and thus, it often appears triangulated ultrasonographically, similar to free intraabdominal fluid. In contrast, PCE is contained and restrained within a much smaller

pericardial sac and thus PCE is not triangulated but rounded (Figure 18.24).

Second, PE can be more tricky to diagnose ultrasonographically because it may be unilateral versus bilateral or in one quadrant and no others, or compartmentalized with and without adhesions, or be associated with soft tissue solid or cavitated masses, along with having various degrees of echogenicity, such as anechoic in heart failure to being very echogenic (high cellularity) and viscous in pyothorax. Furthermore, PE may be complicated by lung pathology that mimics soft tissue masses. The upshot is you have to think about and integrate your TFAST findings.

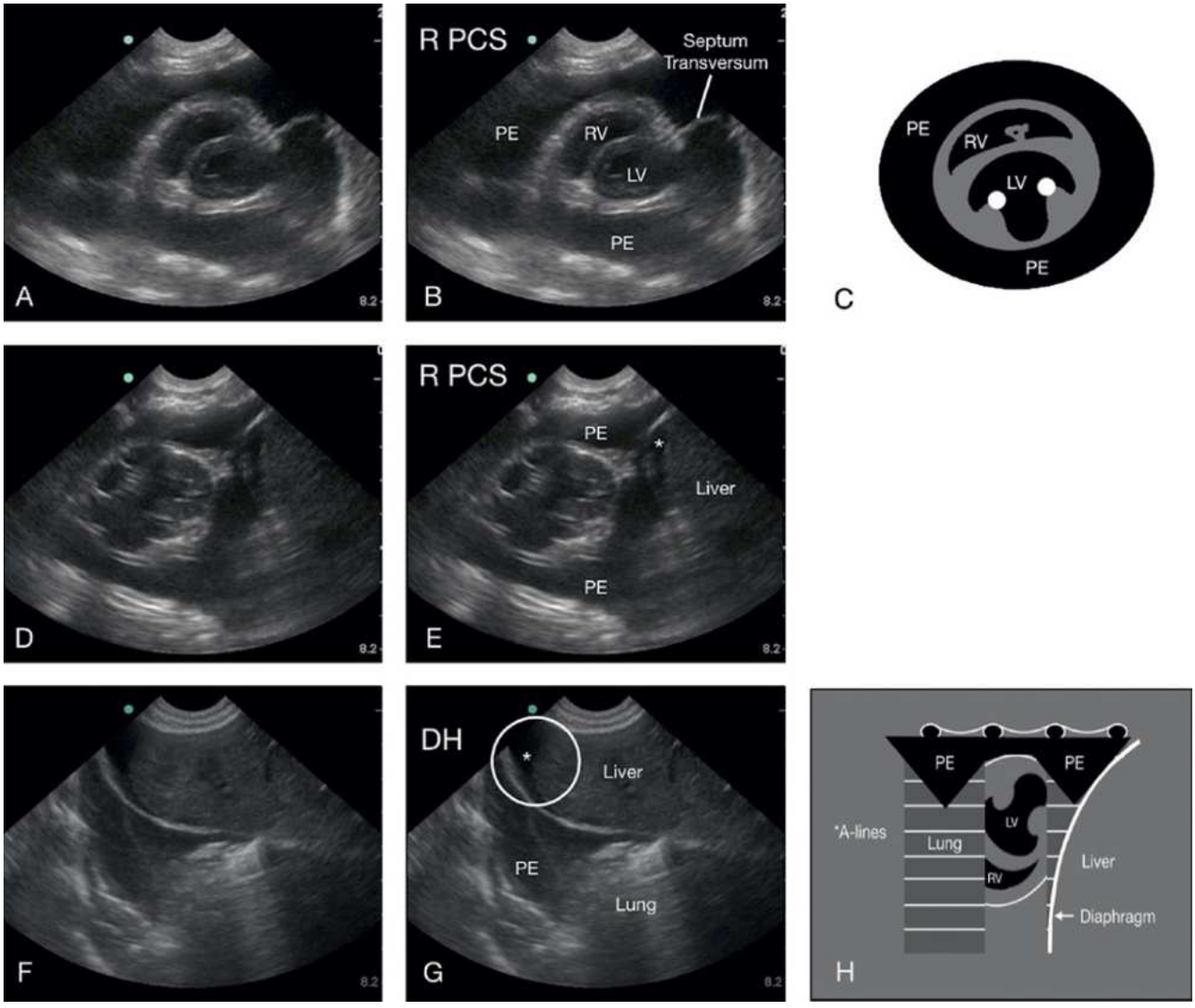


**Figure 18.24.** Composite of pleural effusion in a cat. Same images are shown unlabeled and labeled. In (A) and (B) the pleural effusion is seen via the right TFAST PCS view with a correlative line drawing in (C). Note that depth is set to see the heart in its entirety so that the heart is clearly identified and the pleural effusion is clearly outside the heart, preventing heart chambers for being mistaken as free fluid (pleural or pericardial). In (D) and (E) the image is from a TFAST PCS view using the "TFAST slide" and imaging the "cardiac-diaphragmatic pouch" or the gravity-dependent region between the heart. Note that the diaphragm and liver are clearly seen. In (F) and (G) is the DH view with the triangulation of pleural effusion clearly seen and no "racetrack sign" or rounding typical of pericardial effusion. In (H) is an approximate correlative line drawing. LV, left ventricle; PE, pleural effusion; R PCS, right pericardial site view; RV, right ventricle. Source: Reproduced with permission from Dr Gregory Lisciandro, Hill Country Veterinary Specialists and FASTVet.com, Spicewood, TX.

For example, feline congestive heart failure and its associated modified transudate is most commonly anechoic and bilateral in contrast to feline pyothorax that can almost appear as echogenic as soft tissue and have very little fluid movement, being purulent, of high viscosity, and compartmentalized with adhesions. Furthermore, pressure atelectatic lung can mimic masses so care must be taken not to overinterpret PE-related soft tissue abnormalities but rather wait until after thoracocentesis and reevaluate along with more advanced imaging, such as detailed nonthoracic ultrasound study, thoracic radiography, or CT. In general, blood and transudates tend to be anechoic while exudates, including chylous/pseudochylous/purulent effusions, tend to more echogenic.

Third, TXR is complementary to ultrasonography for detecting PE (unlike PCE in which TXR is unreliable) (Guglielmini et al. 2012; Côté et al. 2013). Following a set of TFAST sonographic rules or tenets helps maximize the probability of an accurate PE diagnosis.

## Accurate TFAST Diagnosis of Pleural Effusion

The sonographer should have a set of rules to follow for the accurate TFAST diagnosis of PE (as with PCE). The only major fluid-filled structure in the thorax to be mistaken for PE is your patient's heart. And it is not generally a good thing for your patient to perform centesis on their heart chamber.

These are the TFAST tenets that will be subsequently explained in greater detail.

- *Always, always, always* image the heart in its entirety with enough depth to see the bright pericardium, your habitual landmark, in the far-field. By adhering to this tenet, the probability of mistaking the heart for PE (or PCE) is greatly lessened (see Figures 18.15 and 18.16).
- One view is no view! Combine views. This is an axiom from human medicine.
- Use the "TFAST slide" maneuver, sliding caudal from the heart toward the diaphragm and then cranial from the heart toward the cervical region, to evaluate the "cardiac-diaphragmatic pouch" and "cardiac-cervical pouch," respectively (see Figures 17.2, 17.17, and 17.18).
- Rotate from a position of perpendicular to the ribs to parallel to the ribs for a "one view is no view" approach during the "TFAST slide" – the "Boysen maneuver."
- Use the DH view where heart chambers are avoided as confounders and with the advantage of much less air (lung) interference over transthoracic views (Lisciandro 2014a, 2016).

## TFAST "Slide" for Pleural Effusion

### Left PCS View

After identifying the location of the heart from the left PCS view, the "TFAST slide" is performed (see Figures 17.2, 17.17, and 17.18). The "TFAST slide" is composed of a caudal slide and then a cranial slide from the heart toward the diaphragm and from the heart toward the neck, respectively. The caudal "TFAST slide" interrogates the "cardiac-diaphragmatic pouch," the most gravity-dependent region in the standing or sternal patient. With minimal training, the sonographer can easily recognize the liver and diaphragm to the right of the screen and then image between it and the heart for PE. The probe is next slid cranially across the heart past the cranial thoracic border of the heart to the "cardiac-cervical pouch," the most gravity-dependent region in the standing or sternal patient cranial to the heart.

Pleural effusion is characterized by the separation of the parietal and visceral pleural, in other words disruption of the PPI or the "lung line" displaced away from the thoracic wall and often accompanied by the "curtain sign" (Neelis et al. 2015). If PE is questionable in either pouch, then the "Boysen Maneuver" can next be performed by rotating the probe parallel to the long axis of the ribs at either of the TFAST cardiac pouches, especially helpful for detecting small amounts of pleural effusion (Boysen, personal communication).

#### *Pitfalls at the Left PCS View*

##### Anechoic/Hypoechoic Stripes

If small anechoic/hypoechoic stripes (1–5 mm) are seen in between the heart at its most ventral left short-axis view (referred to as the hammerhead view) and the thoracic wall in the near-field, the linear anechoic/hypoechoic stripe is unlikely to be pleural effusion (Figure 18.25) but rather pericardial fat (Lamb 2000). Pleural effusion will be best identified away from this pitfall by performing the "TFAST slide" into the "cardiac-diaphragmatic" and "cardiac-cervical pouches" and finding anechoic-hypoechoic triangulations away from the heart (Figures 18.26). Another way to rule out PE is if the stripe is lost because of dirty shadowing from air in lung during the "TFAST slide" into these pouches, by moving slightly dorsal so that you are not imaging the lowest extreme of the pleural cavity (Neelis et al. 2015), or by adding the "Boysen maneuver."

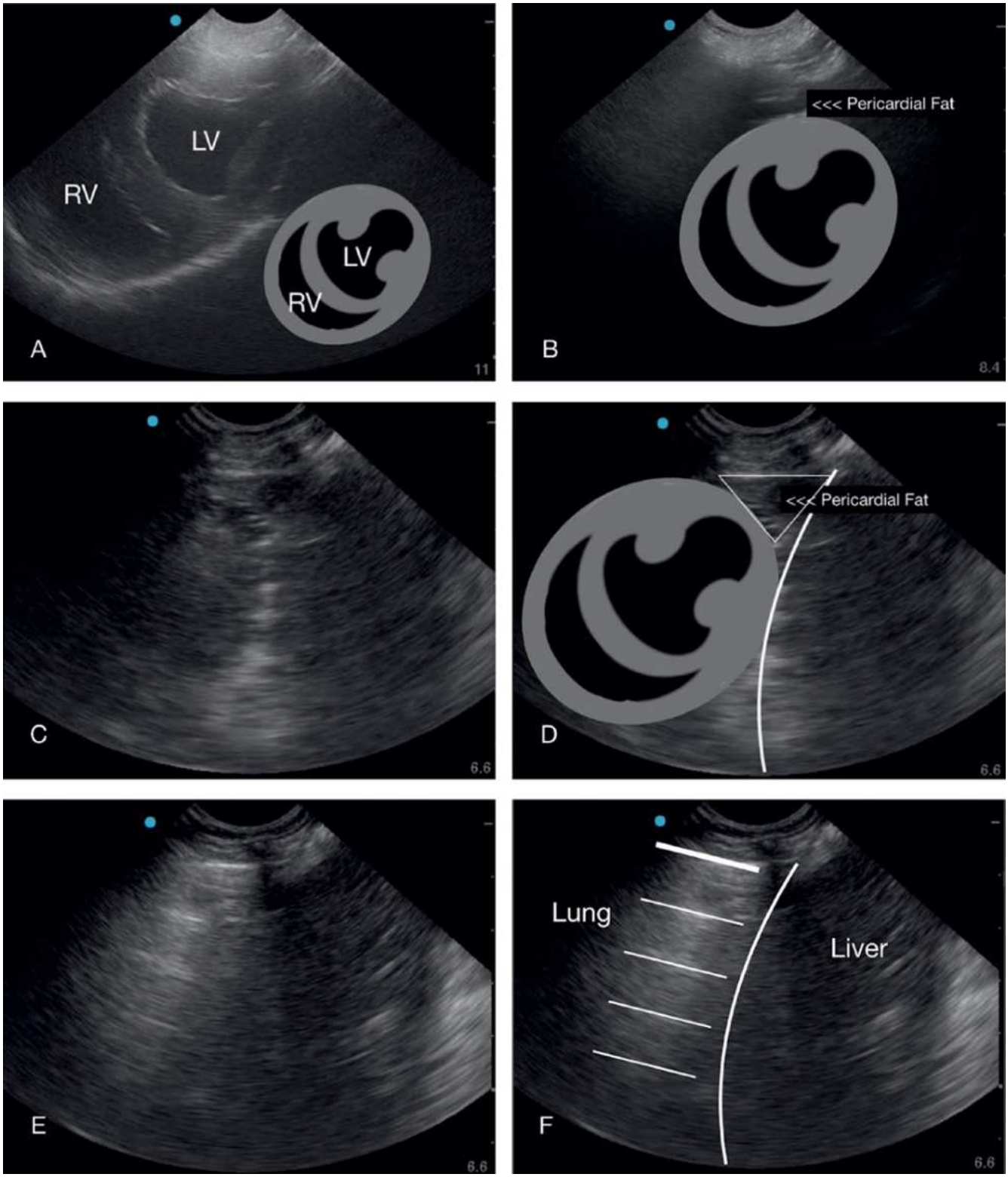


**Figure 18.25.** Pitfall of pericardial FAST at the TFAST PCS views. In (A) and (B) are images showing the left TFAST PCS short-axis view of the heart referred to as the "hammerhead view" (see TFAST echo charts in Figures 17.25 and 17.26). Along the heart and the thoracic wall at the "hammerhead view," it is common to see a hypoechoic "pseudo fluid stripe" that is pericardial fat. In (C) and (D) the images show where the triangular pericardial fat pad (triangle overlay) is located in between the apex of the heart and the diaphragm in the "cardiac-diaphragmatic pouch" that should not be mistaken for free fluid or a mass. (E) and (F) show the maneuver of sweeping the probe dorsal to the region for dirty shadowing of lung obscuring the area with a hyperechoic near-field from the "lung line" and A-lines (parallel line overlay) through the far-field which rules out pleural effusion. In doubt, use multiple views including the FAST DH view that images the same "cardiac-diaphragmatic pouch" but from a different angle and scanning plane. See Figure 18.26 for line drawings of this pitfall. Source: Reproduced with permission from Dr Gregory Lisciandro, Hill Country Veterinary Specialists and FASTVet.com, Spicewood, TX.

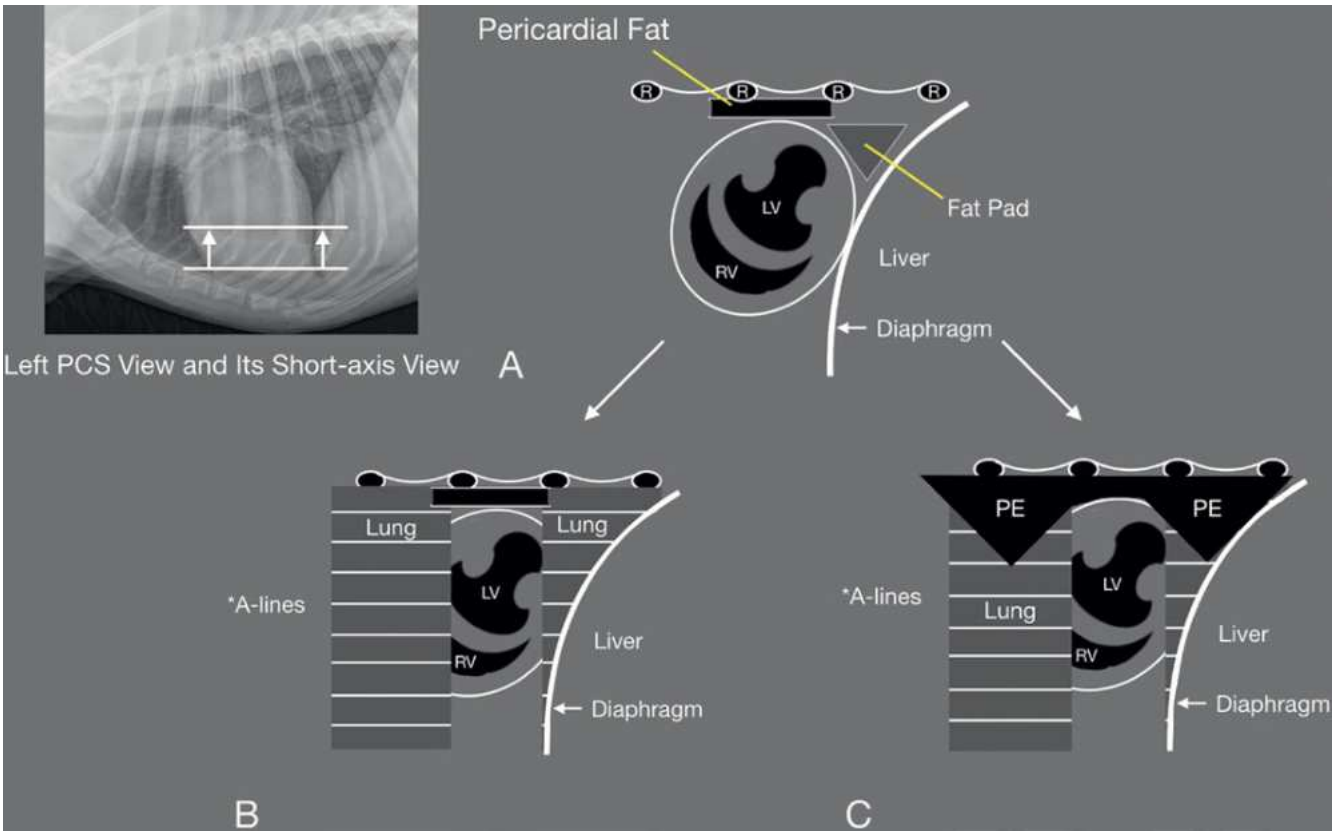


**Figure 18.26.** Pitfall of pericardial fat. Shown is from the left TFAST PCS the short-axis view of the heart called the "hammerhead view" where this pitfall is most commonly seen. The thoracic radiograph shows the caudal and cranial "TFAST slide" by the white bars and how sweeping the probe dorsal helps differentiate pericardial fat from pleural effusion. In (A) the thoracic wall is shown with intercostal spaces and the "hammerhead view" with the heart in close proximity to the diaphragm. The black rectangle depicts the pericardial fat that is a pseudo (anechoic to hypoechoic) pleural effusion stripe that is common between the heart and the thoracic wall. The pericardial fat is linear and can have substantial thickness (~1–1.5 cm in some dogs). In (B) the dorsal sweep creates dirty shadowing obscuring the pericardial fat. In (C) when pleural effusion is present, the pleural effusion stripe triangulates out on either side of the heart in its "cardiac-diaphragmatic pouch" caudally and "cardiac-cervical pouch" cranially. The axiom "one view is no view" should be adhered to by adding the FAST DH view that images the "cardiac-diaphragmatic pouch" from a different scanning plane. LV, left ventricle; PE, pleural effusion; R, rib; RV, right ventricle. Source: Reproduced with permission from Dr Gregory Lisciandro, Hill Country Veterinary Specialists and FASTVet.com, Spicewood, TX.

The anechoic-hypoechoic stripe represents pericardial-mediastinal fat (Lamb 2000).

### Apical Hypoechoic Triangle

When sliding caudal from the heart into the "cardiac-diaphragmatic pouch," especially when most ventral at the left TFAST PCS short-axis hammerhead view, it is common to see a triangle of soft tissue echogenicity between the apex of the heart and the diaphragm, which is fat around the pericardial ligament until proven otherwise (see Figures 18.25 and 18.26). A "curtain sign" for PE will be lacking. The probe again may be swept immediately dorsal to this area because in the absence of PE, the lung should dirty shadow (obliterate) any hint of pleural effusion in normalcy. The "Boysen maneuver" may also be used.

One key here is that "one view is no view" and combining sonographic information from the DH view and the right PCS view helps more accurately diagnose PE. Another key is to have plenty of depth so that the heart is always viewed in its entirety, thus eliminating cardiac chambers as confounders. The brightest line through the far-field is generally the pericardium which serves as a landmark that the heart is entirely in the field of view (see Chapters 19–21).

## Right PCS View

After locating the heart from the right TFAST PCS view, the "TFAST slide" is performed identically as at the left TFAST PCS view, following the same principles.

### Combining Views

*DH View*

The key to performing the DH view is to rock the probe toward the head of the patient in the longitudinal orientation (see Chapter 6). The pocketing of fluid will occur in the "cardiac-diaphragmatic pouch" imaged through a different plane and direction from the TFAST PCS views. The "lung line" will separate from the diaphragmatic surface and PE is triangulated with no rounding as seen with the "racetrack sign" of PCE (Figure 18.27; see also Figure 18.24). The DH view is very useful for the diagnosis of PE in that air interference is minimized through the acoustic window through the liver and gallbladder into your patient's thorax. The appearance of PE is quite different from PCE because there will be triangulations with PE in contrast to the rounding and "racetrack sign" with PCE. The DH view will look different from normalcy because the hyperechoic line created by aerated lung immediately against the soft tissue diaphragm is lost with fluid (PE) against the diaphragm. Moreover, aerated and atelectatic lung will be wafting in the triangulations of PE, which is not a feature of PCE.

The dog in Figure 18.27 has a serious, likely vascular intrathoracic injury that is missed on thoracic radiography. By documenting the injury, trauma sequelae may be better detected if complications occur over time like intrathoracic CVC obstruction and ascites, and the complication, kinked CVC syndrome, is treatable with surgery (Cornelius and Mahaffey 1985; Lisciandro et al. 1995; Fine et al. 1998).

## *Pleural Effusion: TFAST is a Better Option than the POCUS Thoracic or Flash Approach*

In using the combined TFAST-Vet BLUE approach, a much greater amount of information may be gained in about the same time as those performing thoracic "flash exams" in which only a simple binary question is being addressed – the presence or absence of PE. The author has always advocated moving beyond the "flash mentality" by observing for lung findings along the "lung line" (see Chapters 22 and 23 and the six Vet BLUE lung ultrasound signs) and for the presence or absence of PCE, especially in cats (Figure 18.28) (Ward et al. 2018). So much more clinically relevant information can be

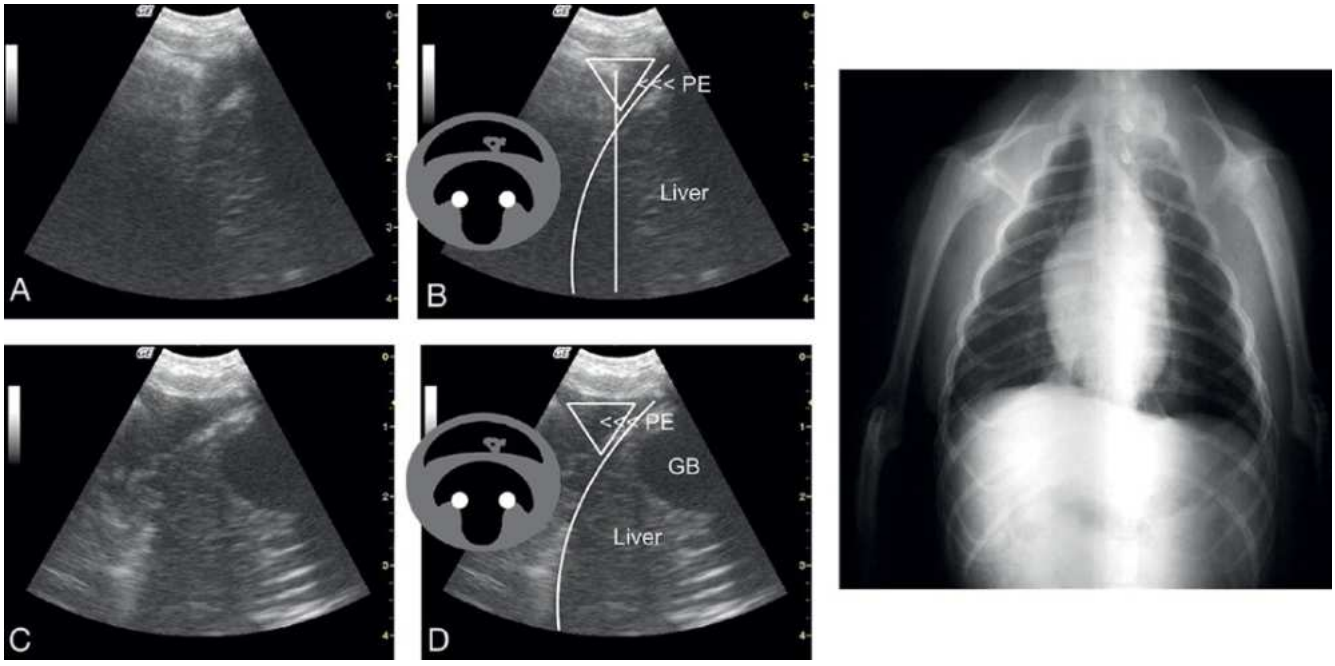


**Figure 18.27.** Hemothorax in a bluntly traumatized dog occult on thoracic radiography. Shown in (A) and (B) is the same image within the "cardiac-diaphragmatic pouch" unlabeled and labeled with overlays of the left ventricular short-axis view from the right TFAST PCS view with the diaphragm as the curved line, the pleural effusion as a triangle. The vertical straight line designates the "curtain sign." In (C) and (D) is the same patient a split second later with the shadowing of lung now out of view due to phases of respiration. The same overlays are present without the "curtain sign," which is now absent. The triangulation of pleural effusion is obvious. The radiograph shows how the injury is occult and missed without TFAST. The dog has a hemothorax and an important, likely vascular injury within its thorax. Source: Reproduced with permission from Dr Gregory Lisciandro, Hill Country Veterinary Specialists and FASTVet.com, Spicewood, TX.

gained with a standardized TFAST approach over the thoracic "flash" in similar time frames.

### Concurrent Pleural and Pericardial Effusion in Dogs

The prevalence of having both PCE and PE concurrently has been reported in a few retrospective canine pericardial effusion studies as ranging from 21% to 34% (Stafford Johnson et al. 2004; MacDonald et al. 2009; Lisciandro 2016).

### Concurrent Pleural and Pericardial Effusion in Cats

The most common cause of PCE in cats is hypertrophic cardiomyopathy and congestive heart failure, reported to be 75% of feline cases in one study (Hall et al. 2007;

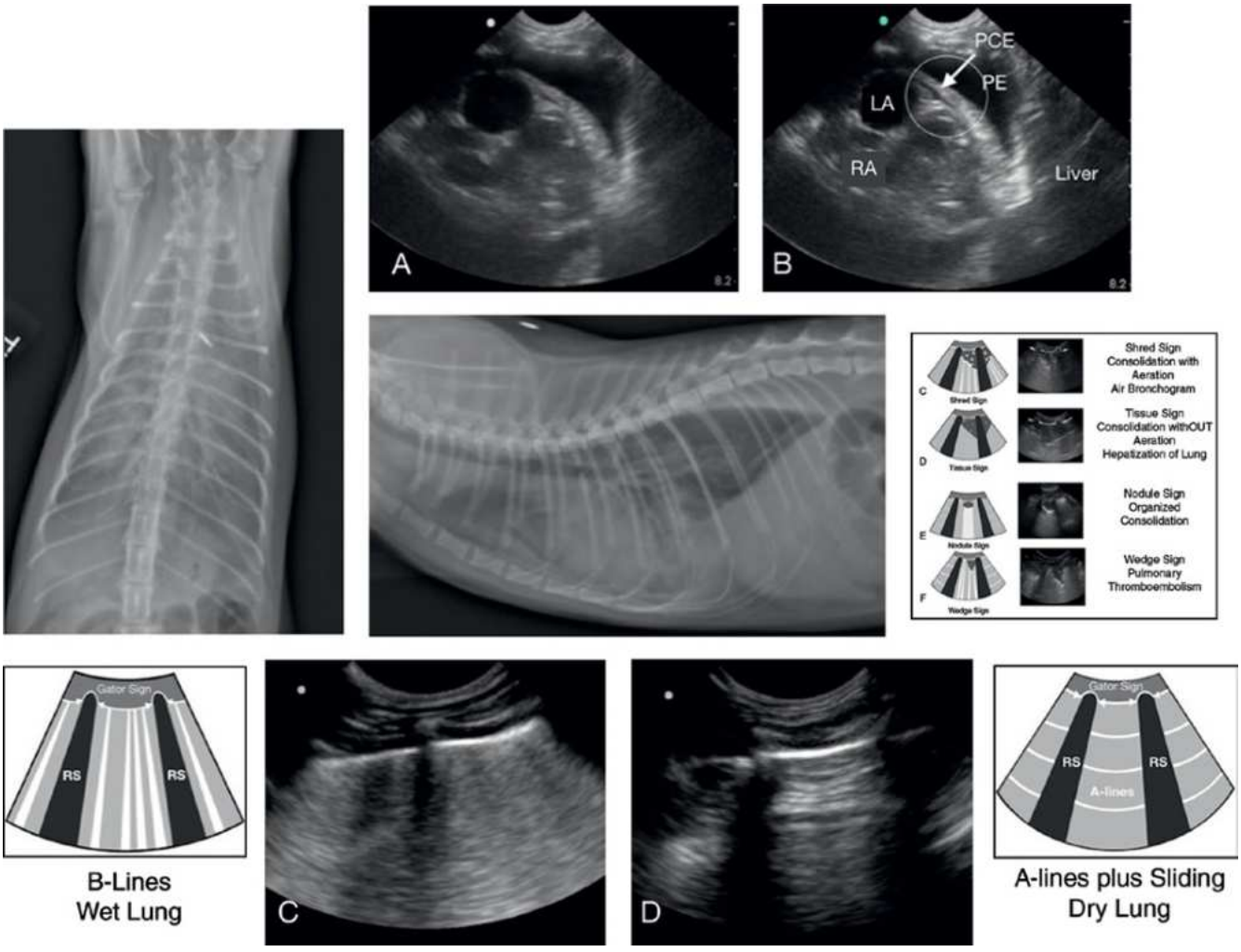


**Figure 18.28.** TFAST is better for patient care than the "flash" approach. (A) and (B) are the same images unlabeled and labeled. The sonographer has ample depth to see the feline heart in its entirety and can clearly document fluid outside the four chambers of the heart, and the triangulations of pleural effusion (PE). With the "flash exam" the sonographer is satisfied with the finding of pleural effusion. With TFAST and, better, Global FAST more information is rapidly gained. In this cat pericardial effusion (PCE) is a significant finding (circled in B). The small volume of pericardial effusion supports a diagnosis of congestive heart failure in cats (Hall et al. 2007; Ward et al. 2018). In (C) and (D) lung is shown, wet with B-lines in (C) and dry with A-lines and "lung sliding" in (D), helping guide diuretic usage. The TFAST-Vet BLUE approach (and, better, Global FAST) better directs care and places congestive heart failure at the top of the differential list prior to discussing patient status with the client. Note the left atrium (LA) is much larger than the right atrium (RA) as they should be ~1:1 in normalcy on the long-axis four-chamber view. The Vet BLUE visual lung language composite with shred sign, tissue sign, nodule sign, and wedge sign are also shown to remind the sonographer of the possibility of other lung surface pathology while also considering that pressure atelectasis can cause false positives. Serial Vet BLUE exams post thoracocentesis are key as atelectatic lung typically resolves in stable spontaneously breathing dogs (unknown in cats) within three hours (Lisciandro and Fosgate 2018). Source: Reproduced with permission from Dr Gregory Lisciandro, Hill Country Veterinary Specialists and FASTVet.com, Spicewood, TX. Illustration by Dr Judy Brown, Toronto, Canada.

Davidson et al. 2008). Recently, it was shown that PCE detected in any degree with or without PE using ultrasound was 100% specific for congestive heart failure in cats presenting to veterinary hospitals at North Carolina State and Iowa State (Ward et al. 2018) (see Figure 18.28). Using TFAST echo views and CVC and hepatic venous characterization (and, better, Global FAST), other important feline patient information may be obtained, and generally in the same amount of time as a targeted POCUS exam or thoracic "flash" that only addresses the binary question of the presence or absence of PE. Other findings during TFAST may include the suspicion for intrathoracic masses (see Chapters 19–21).

## Use of Radiography for the Diagnosis of Pleural Effusion

If the TFAST sonographer cannot confidently diagnose PE, the use of TXR should be incorporated into the work-up, or nonthoracic ultrasound or complete echocardiography by someone more skilled, or combinations thereof. However, TXR has limitations in that it is unreliable for PCE, especially with the presence of PE that obscures the cardiac silhouette, and is unreliable and generally ineffective for pulmonary evaluation (see Figure 18.28). Conversely, PE actually enhances imaging of the heart and its chambers and the presence of PCE; it also enhances imaging of the "lung line" for the six Vet BLUE lung ultrasound signs, and the presence or absence of PCE, which is especially helpful in the diagnosis of congestive heart failure in cats (see Chapters 19–21).

## Overall Pitfalls of Imaging the Heart

- Using the left ventricular short-axis views between the "mushroom" view and the heart base and its "Mercedes-Benz" sign can be very confusing and lead to mistaking the crescent-shaped right ventricle for PCE.
- The difficulty in getting a good acoustic window to visualize the heart transthoracically in cases of severe respiratory distress.
- Mirror artifact off the far side of the heart when "dry lung" is immediately against the pericardium in the far-field.

**Pearl:** Use the DH view to determine the presence and absence of PCE as likely it is a sole view for both dogs and cats (Lisciandro 2016).

**Pearl:** Use the DH view as a nonecho alternative for cardiac tamponade because in a patient with a CVC that has a "bounce", cardiac tamponade is ruled out by definition. If a FAT distended CVC is present, then look at your patient. In people, a FAT IVC, analogous to the CVC, is 92–97% sensitive but not specific (40%) (Himelman et al. 1998; Candotti and Arntfield 2014; Tchernodrinski and Arntfield 2015). Thus, when a collapsible "bounce" to the IVC is found in people with PCE, cardiac tamponade is unlikely. The IVC (and CVC) provides a nonecho view option that is often easier to acquire (and generally safer and faster) than echo views in distressed, unstable, and hemodynamically fragile patients.

## Definitive Characterization of Pleural and Pericardial Effusions Requires Sampling

Ultrasound's strength is imaging fluid and fluid-filled structures, but it cannot reliably characterize or diagnose the etiology of the fluid. Fluid acquisition via thoracocentesis or pericardiocentesis with fluid analysis and cytology is necessary because there are many different types of effusion (transudate, modified transudate, exudates [pyothorax, chylous, and pseudochylous], and neoplastic). Before pursuing sample acquisition, the risks and benefits must be weighed by the attending veterinarian (Table 18.6). Ultrasound-guided or assisted thoracocentesis and pericardiocentesis are described in Chapters 43 and 21.

## Measuring and Monitoring Pleural Effusion

Attempts have been made in cadaver models to measure PE from the sternum through cardiac cut-out tables to the lateral thorax. However, atelectatic lung in cadaver dog and cat models lacks the respirophasic dynamics and the floating of aerated lung in live breathing patients (Newitt et al. 2009; Shimali et al. 2010). The author suggests measuring patients in sternal or standing at the 4th–5th intercostal space at the level of the costochondral junction with the maximum respirophasic distance from the thoracic wall to the heart. A method will need to be developed from live patients using consistent methodology and comparison to actual volumes aspirated in live dogs and cats with PE.

**Table 18.6.**
Accurate TFAST diagnosis of pericardial and pleural effusion.

| Imaging strategies | FAST DH view | TFAST PCS view | Thoracic radiography | Gold standard |
|---|---|---|---|---|
| Pericardial effusion (PCE)<br>(1) Image toward the muscular apex of the heart where no heart chambers that can be mistaken for free fluid | Racetrack sign | Bull's eye sign | Unreliable test for PCE and for cardiac tamponade | Ultrasound and computed tomography (CT) |
| (2) Long-axis four-chamber view where all four chambers are identified is the only echo view for diagnosis<br>(3) Image the heart in its entirety using the hyperechoic pericardium in the far-field as a landmark | Enlarged left atrium supports left atrial tear in the mitral valve disease dog | TFAST right PCS view Long-axis four-chamber view | | |
| Pleural effusion<br>(1) Image the heart in its entirety using the hyperechoic pericardium in the far-field as a landmark<br>(2) Image toward the muscular apex of the heart where no heart chambers that can be mistaken for free fluid | Anechoic triangulations | TFAST right and left PCS Anechoic triangulations | Good test | Debatable between ultrasound, CT, and thoracoscopy |

Source: Reproduced with permission from Dr Gregory Lisciandro, Hill Country Veterinary Specialists and FASTVet.com, Spicewood, TX.

### *Other Pleural Cavity Findings During TFAST*

#### Diaphragmatic Herniation

Through repetition in performing the DH view, the loss of the expected curvilinear continuity of the diaphragm will often be appreciated in the presence of both traumatic and congenital types of diaphragmatic herniation (Figures 18.29 and 18.30). Additionally, the lack of finding the gallbladder at its expected location can be helpful in triggering suspicion that the diaphragm is herniated (or ruptured). The axiom of "one view is no view" is also helpful because visualization of the heart may be obscured by solid organs or viscous structures (air-filled/fluid-filled) including liver, gallbladder, spleen, loops of small intestine and stomach, which become readily apparent with minimal training to the nonradiologist sonographer experienced with AFAST and its target organ approach. Furthermore, this observation will help guide therapy and avoid blindly performing thoracocentesis into abdominal structures before a confirmatory thoracic radiograph with or without contrast is acquired (see Figures 18.29 and 18.30).

#### Masses

Diagnosis of masses within the thorax during TFAST can be problematic and may require advanced training. Lung may develop pressure atelectasis in PE cases, and atelectatic lung may appear as a tissue sign mimicking a mass lesion. Moreover, the lung may in fact have forms of pathological consolidation and nodules. The best strategy is to reimage after thoracocentesis, allowing time for spontaneous breathing and/or positive pressure ventilation to reexpand normal atelectatic lung to better differentiate if the suspect lesions persist or resolve.

## Additional Clinical Relevance of the DH View

The DH view also serves as a soft tissue evaluation of the gallbladder and liver, screens for ascites, characterizes the CVC and its associated hepatic veins, and determines lung surface pathology along the pulmonary-diaphragmatic interface (see Chapters 7, 22, 23, and 36 for more detail). Moreover, the DH view

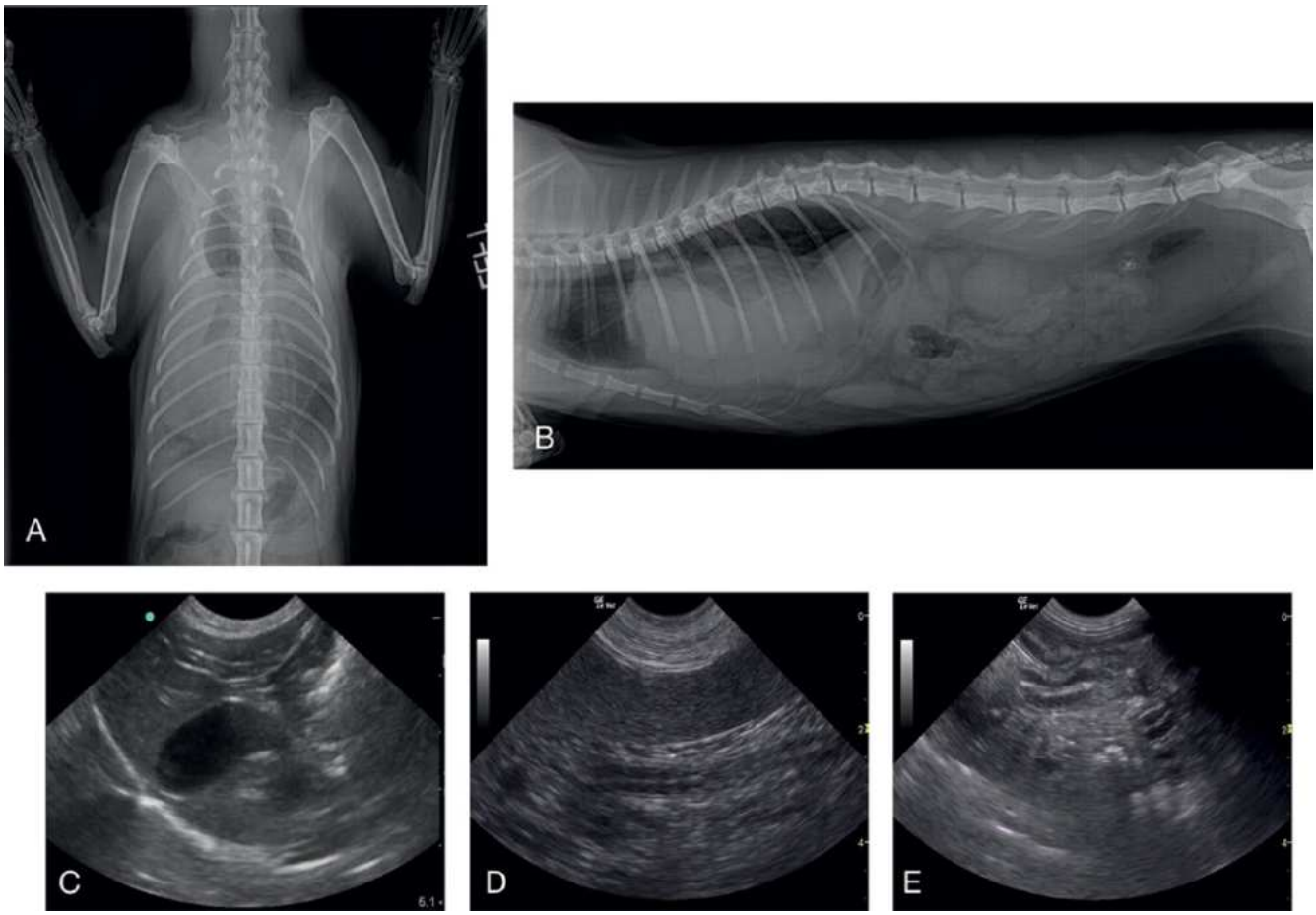


**Figure 18.29.** Peritoneopericardial hernia detected during TFAST. The cat presents with (or without) respiratory signs. The Global FAST approach provides first-line low-impact imaging (AFAST, TFAST, and Vet BLUE) and is used as an extension of the physical exam. The approach will rapidly pick up the abnormality with minimum training because the expected "normal" anatomy at the TFAST DH and PCS views deviate from what is expected as shown in C) from a normal patient, with the expected curved line to the diaphragm and liver and gallbladder compared to the abnormal in Figures 18.30A through C; and spleen (or liver) as in (D) and small intestine (E) at the PCS views as in 18.30D rather than the expected heart. Source: Reproduced with permission from Dr Gregory Lisciandro, Hill Country Veterinary Specialists and FASTVet.com, Spicewood, TX.

is an important acoustic window for lung pathology along the pulmonary-diaphragmatic interface that is otherwise inaccessible sonographically via transthoracic views (see Chapters 22 and 23, and Figure 23.21).

# TFAST Echo Views

## *TFAST Cardiac Evaluation*

The TFAST screening for soft tissue cardiac abnormalities (and Vet BLUE for lung surface conditions) is analogous to the AFAST target organ approach, meaning that TFAST cardiac evaluation is a rule-in test (Figure 18.31). In other words, if the condition is seen, then it likely exists and gold standard confirmation would be indicated next with a higher probability of having a positive test. However, if the condition is not seen, then it is possible that it was missed since detection is user dependent and the patient may require more expert or sophisticated interrogation or the gold standard test for diagnosis.

These conditions include dilated cardiomyopathy (DCM), hypertrophic cardiomyopathy (HCM), pulmonary hypertension (PHT), left-sided cardiac conditions/volume overload/failure, right-sided cardiac conditions/volume overload/failure, intracardiac masses, heartworms, and LAT in chronic mitral valve disease. In other words conditions that are traditionally missed may now be screened for with a more effective test, TFAST. By capturing these cardiac-related

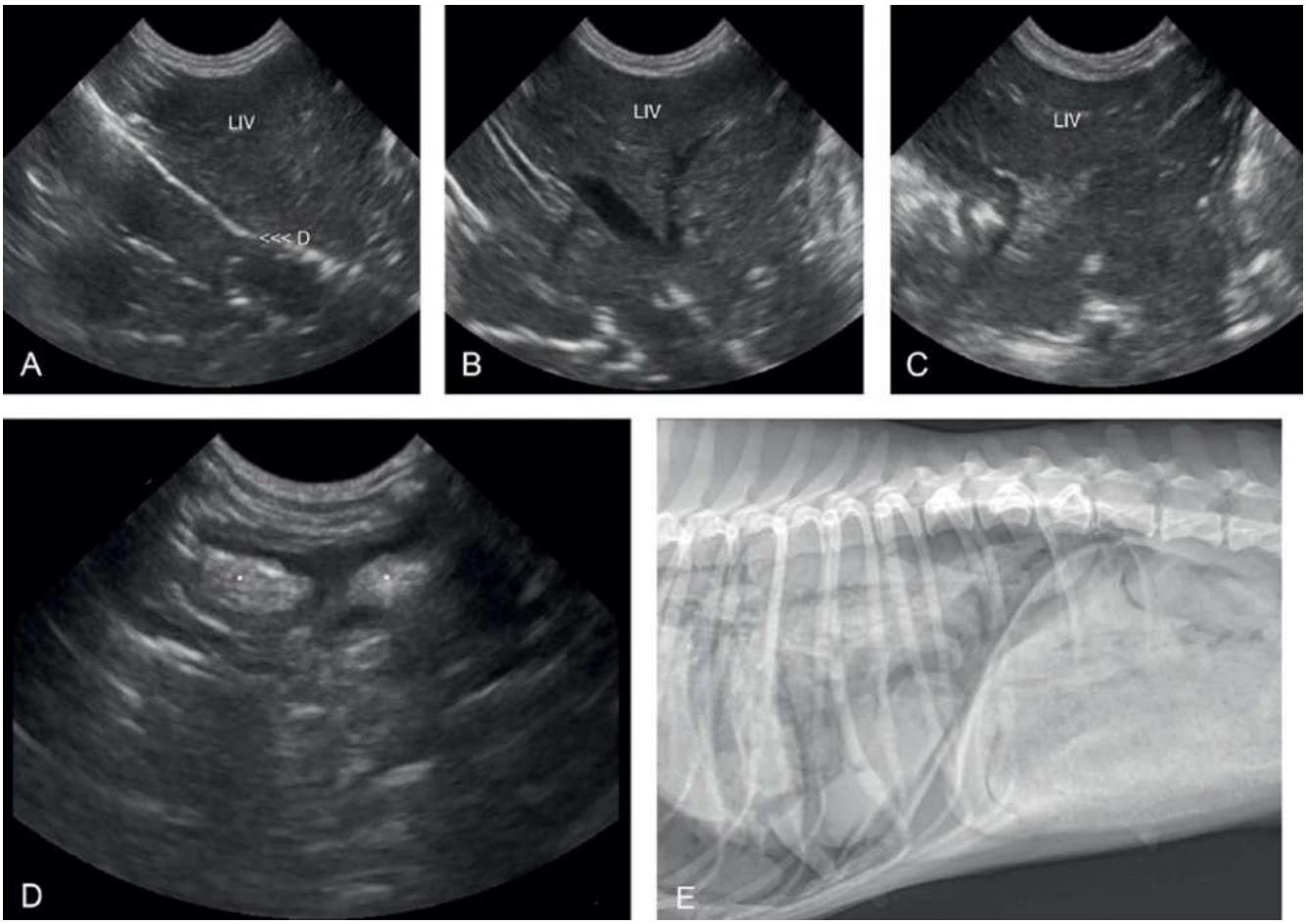


**Figure 18.30.** Diaphragmatic hernia in a dog. The same concept in the cat in Figure 18.29 is shown in a dog with a diaphragmatic hernia (E). The expected normal contour of the diaphragm and the gallbladder in close proximity is lost in (A–C) and (D) shows loops of small intestine at the TFAST PCS views (*). Source: Reproduced with permission from Dr Gregory Lisciandro, Hill Country Veterinary Specialists and FASTVet.com, Spicewood, TX.

conditions, patients are potentially more accurately and better treated and better kept alive for gold standard testing, such as complete echocardiography and CT.

The TFAST echo views are eyeballed, meaning they are subjectively assessed in most instances (Ferrada et al. 2012a, 2014; Atkinson et al. 2017). There is evidence on the human side that eyeballing works well in screening for obvious disease and a recent international point-of-care echocardiography consensus statement advocated for the eyeball method (Ferrada et al. 2012a, 2014; Atkinson et al. 2017).

The sonographer looks to see if basic echo views appear to be unremarkable or not, a simple binary question as a screening test. Will more subtle conditions be missed? Possibly, but consider how much you are missing every day on traditional training of physical examination and radiography. You have nothing to lose so look and see if the heart has PCE, chamber abnormalities, soft tissue problems, intracardiac (within its chambers), extracardiac, and intramural masses, or parasitic organisms (heartworms), as well as valvular conditions such as asynchrony from ruptured chordae tendinae or vegetations. Moreover, the TFAST echo views may be evaluated in standing in dogs and cats (Chetboul et al. 2005; Loughran et al. 2019).

The three major TFAST echo views plus a fourth bonus view are as follows (see Figure 18.31).

- The left ventricular short-axis view (LVSA) at the level of the chordae tendinae, same as for M-mode measurements, to assess volume and contractility.
- The left atrial to aortic ratio on short-axis view (LA:Ao) for left-sided cardiac conditions, the so-called "quick peek" view for left-sided cardiac conditions (heart strain/failure/overload).

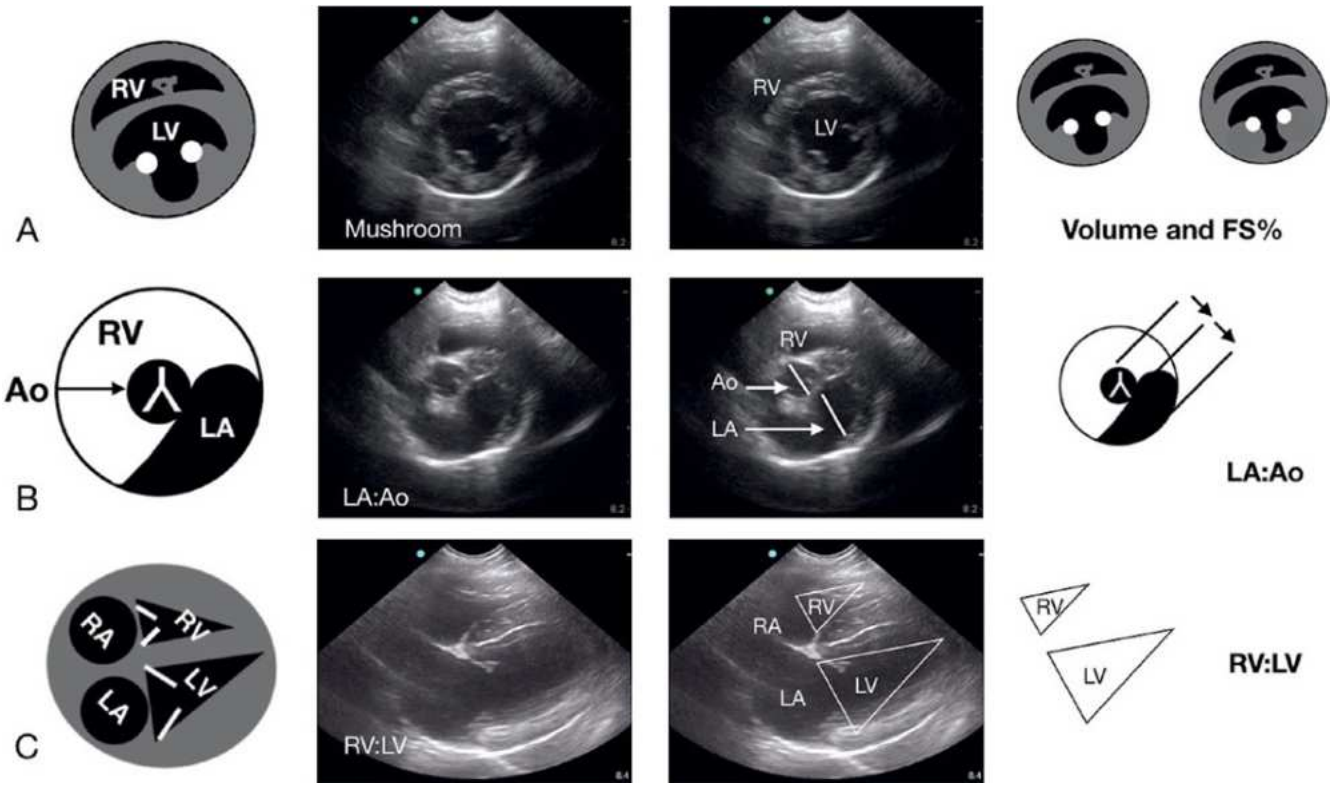


**Figure 18.31.** Composite of echo views from the right TFAST PCS view. The top row (A) shows the expected left ventricular short-axis views in which volume and fractional shortening (FS%) are evaluated by the "eyeball method" for unremarkable versus abnormal. In the middle row (B), the left ventricular short-axis left atrial to aortic ratio (LA:Ao) is shown with the expected normal ratios. A general guideline is that the LA:Ao ratio should not be >2:1 in dogs and cats. In the bottom row (C) is shown the expected normal right ventricular to left ventricular ration on long-axis four-chamber view (RV:LV). Source: Reproduced with permission from Dr Gregory Lisciandro, Hill Country Veterinary Specialists and FASTVet.com, Spicewood, TX.

- The long-axis four-chamber view (LA4CV) for the right ventricular to left ventricular ratio (RV:LV) for right-sided cardiac conditions (heart strain/failure/overload).
- Bonus – the long-axis five-chamber view (LA5CV) with the left ventricular (aortic) outflow tract for masses.

The use of these three major TFAST echo views, as the patient allows, serves as a soft tissue scan of the heart, with the potential for capturing traditionally difficult conditions such as pulmonary hypertension and right-sided cardiac strain/failure, DCM, HCM (dogs and cats), left-sided cardiac strain/failure, PCE, left atrial tear/rupture, intracardiac massses, myocardial masses, vegetative valve lesions, and caval syndrome (*Dirofilaria immitis*).

The TFAST sonographer must understand that they are using TFAST as a screening test that is more effective than physical examination and radiography because TFAST is in fact a soft tissue (and free fluid) exam of the heart (Figure 18.32). You have nothing to lose by looking for cardiac-related problems. In addition to noting that TFAST is a screening test, the TFAST sonographer only has to answer the minimal question of whether the heart looks normal or not. These conditions are easy to recognize and can develop a better working diagnosis to keep the patient alive for gold standard testing and treatment. Over time, the TFAST sonographer will build more

**Figure 18.32.** (*Continued*) complaint of urinating on himself. A urinary tract infection would likely be pursued, but it is the intracardiac mass leading to mild episodes of weakness and syncope that is causing the inappropriate urinations. The dog is at risk for sudden death as the mass is occluding the left ventricular outflow tract and moves into the aortic valves with heartbeats. These are all examples of conditions missed with ultrasound (or CT) that are missed on TXR and easily screened for using TFAST (and the Global FAST approach for staging). The prevalence of each of these conditions is likely much higher than previously reported because unless a complete echocardiogram was performed, these conditions were missed. Source: Reproduced with permission from Dr Gregory Lisciandro, Hill Country Veterinary Specialists and FASTVet.com, Spicewood, TX.

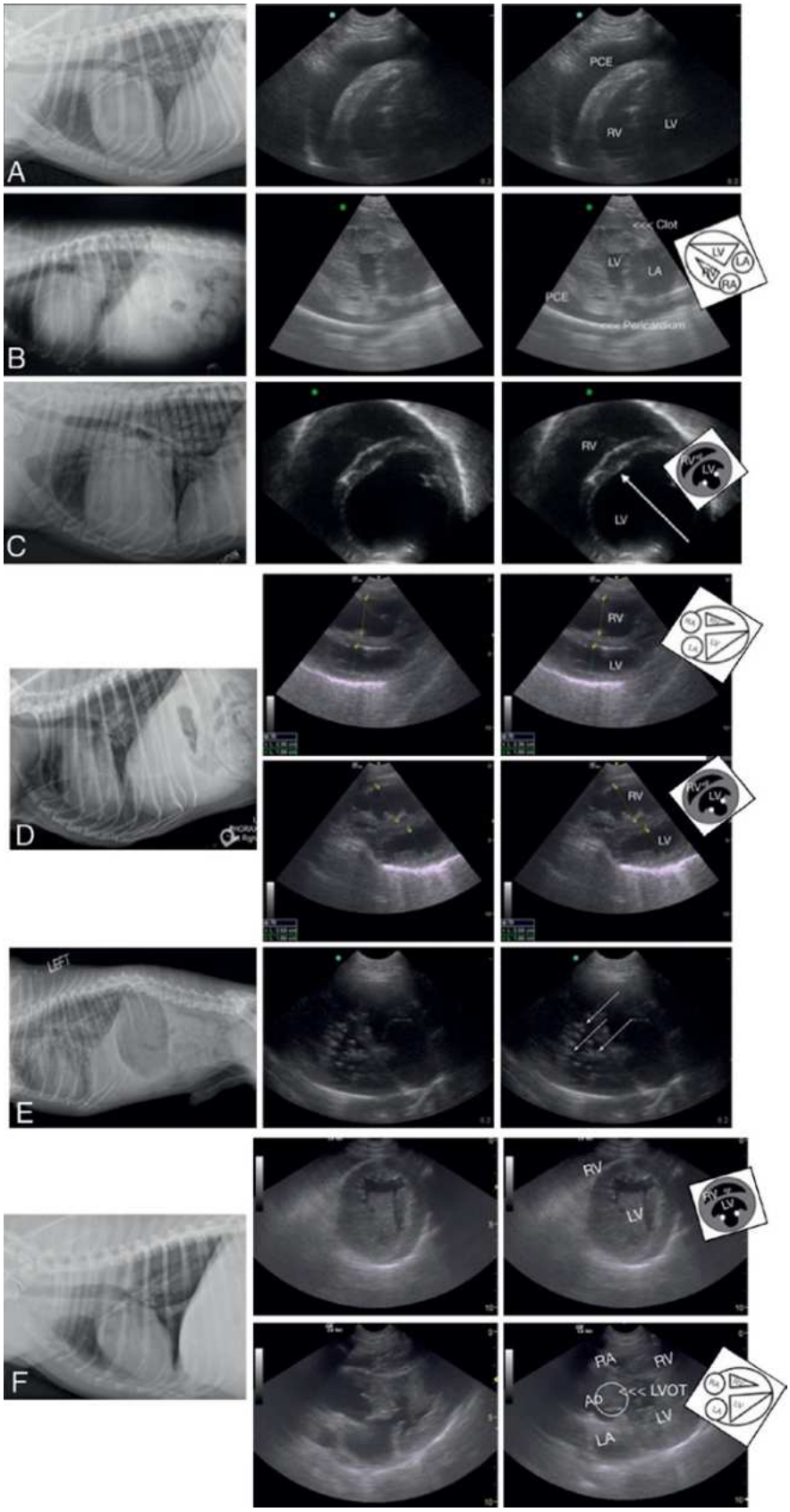


**Figure 18.32.** Composite for how TFAST echo views are a screening test for various cardiac conditions likely missed on radiography. In (A) pericardial effusion is missed on TXR. In (B) the left atrial tear is missed on TXR and the left atrial enlargement based on the cardiac silhouette leads to "satisfaction of search error" without TFAST. In (C) the dilated cardiomyopathy may be suspected or pericardial effusion or right-sided heart diseases based on TXR; however, the TFAST approach rapidly detects the likely diagnosis of dilated cardiomyopathy. In (D) the dog has severe pulmonary hypertension that again is missed on TXR (and actually has aspiration pneumonia detected on Vet BLUE). Note the severely enlarged right ventricle that is larger than the left ventricle. In (E) the dog has abnormal lungs from heartworm disease (*Dirofilaria immitis*), but without the use of TFAST the diagnosis is delayed or possibly missed. Heartworms are clearly evident in the right heart. In (F) the dog has an obvious intracardiac mass with a chief

advanced echo skills including left apical views and subcostal views of the heart.

- Pulmonary hypertension – enlarged right ventricle (RV:LV ~1).
- Dilated cardiomyopathy – enlarged heart with poor contractility (FS%).
- Left atrial tear/rupture – PCE +/- an intrapericardial clot and a severely enlarged left atrium (LA) with a severe increase in the LA:Ao of >2:1
- Intracardiac masses – echogenic material within heart chambers.
- Valvular abnormalities – vegetative lesions (echogenic material off the valves) and ruptured chordae tendinae (asynchronous valvular movement).
- Caval syndrome (*Dirofilaria immitis*) – heartworms within the right heart and pulmonary arteries.

### Integrating TFAST Echo Views with Nonecho Fallback Views for Volume Status and Congestive Heart Failure

Integrating TFAST echo views with the characterization of the CVC at the DH view and evaluating lung using Vet BLUE help to confirm or refute clinical impressions of right- and left-sided congestive heart failure (Figure 18.33). For example, if TFAST suggests left-sided heart disease, left-sided congestive failure may be rapidly screened for using Vet BLUE and determining if lung is wet or dry. If TFAST suggests right-sided heart disease, then right-sided congestive failure may be screened for by characterizing the CVC and its associated hepatic veins (see Figure 18.33). By definition, right-sided CHF should have CVC and hepatic venous distension. These integration concepts of TFAST, Vet BLUE, and AFAST are detailed in

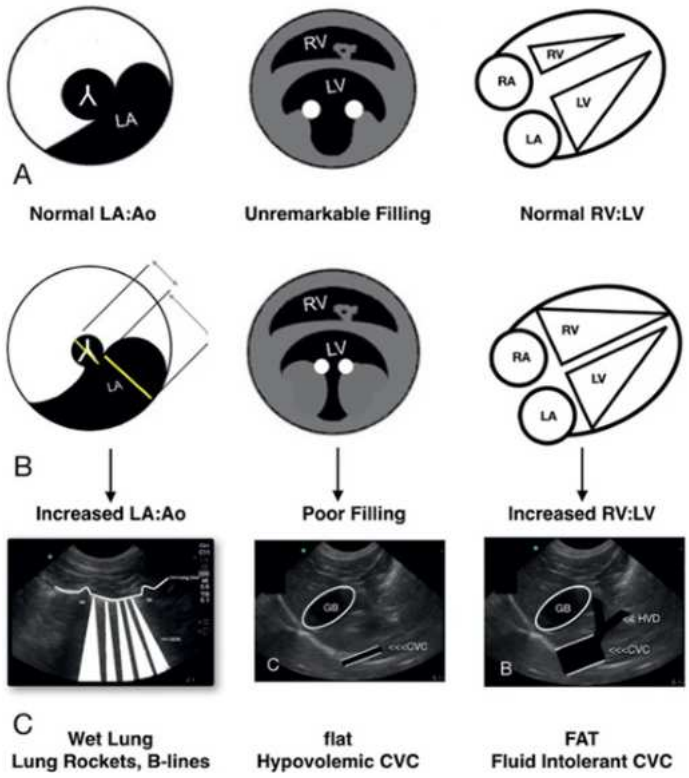


**Figure 18.33.** Composite of the TFAST echo views and expected normals and abnormals and nonecho fallback views of Global FAST. In row (A) the TFAST right PCS short-axis views are shown with cartoons of expected normalcy. In row (B) are shown abnormals, including an increased left atrial to aortic ratio (LA:Ao >2:1), poor filling at the left ventricular short-axis "mushroom view" and an enlarged right ventricular to left ventricular ratio (RV:LV) on long-axis four-chamber view. In row (C) are the "Global FAST nonecho fallback views" of Vet BLUE and "wet lung" (left-sided congestive heart failure) versus "dry lung" (absent left-sided congestive heart failure) and characterization of the caudal vena cava and hepatic veins at the FAST DH View as flat, reinforcing the clinical impression of poor volume versus a FAT CVC with hepatic venous distension. Source: Reproduced with permission from Dr Gregory Lisciandro, Hill Country Veterinary Specialists and FASTVet.com, Spicewood, TX.

VetBooks.ir

Chapters 36 and 37 (see Figure 36.7). The Global FAST non-echo fallback views work in the opposite direction too. For example, "dry lung" or absent B-lines in all Vet BLUE views rule out left-sided CHF (Lisciandro 2016: Ward et al. 2017; Vezzosi et al. 2017) and a "bounce" or fluid-responsive CVC rules out right-sided CHF (Himelman et al. 1988; Candotti and Arntfield 2014; Tchernodrinski and Arntfield 2015). Thus, if there is no evidence for congestive heart failure on Global FAST nonecho fallback views, then echo views can wait in critical patients until they are more stable.

## The Global FAST Approach is Key to Averting Satisfaction of Search Error

The use of Global FAST automatically helps avoid satisfaction of search error by applying AFAST, TFAST, and Vet BLUE as a single examination. In respiratory compromised or distressed patients or those that may be hemodynamically fragile, Global FAST may be performed entirely in standing and then, only if indicated, performed in part in lateral recumbency when the patient is more stable if needed.

## Recording TFAST Findings on Goal-directed Templates

To achieve success with TFAST you must record your patient data, save images for review and learning and teaching purposes, and review final outcomes, especially comparing to subsequent imaging. Entries should be marked "indeterminate" and "not assessed" as they are important for learning and training purposes (Figure 18.34). "Indeterminate" means that the DH view was imaged but the findings were inconclusive. "Not assessed" means that the DH view was never evaluated for whatever reason (patient too stressed, fractious, or because of triaging other cases). For example, if the DH view was marked as an "indeterminate" entry and then subsequently you found out there was a pneumothorax, a pneumoabdomen, a diaphragmatic hernia, or an emphysematous gallbladder, then lessons are learned regarding the limitations of TFAST in addition to modifying teaching paradigms. On the other hand, if you don't record your data, then you can't measure performance. If you can't measure performance, then you can't evaluate and improve.

See Chapter 45 and the Appendices for additional examples of goal-directed templates.

## Quick Reference of Normals and Rules of Thumb

- Any evidence of lung, most commonly "lung sliding" or the presence of B-lines, that is observed at the TFAST CTS view rules out clinically relevant PTX, especially in the positioning of standing or sternal.
- B-lines in trauma are lung contusions until proven otherwise.
- Always image the heart in its entirety using the hyperechoic (bright white) pericardium as a landmark in the far-field.
- Adhere to the axiom that "one view is no view" for the accurate diagnosis of PE and PCE.
- The FAST DH view is likely nearly 100% sensitive and 100% specific for detecting clinically relevant PCE in dogs and cats.
- Dogs and cats have no pleural or pericardial effusion that is evident in normalcy; however, pericardial fat mimics pleural effusion especially (1) along the heart at the left TFAST PCS view as an anechoic stripe (linear) between the heart and intercostal spaces, and (2) as an echogenic triangulation (fat pad) within the cardiac-diaphragmatic pouch.
- The "eyeball method" is accepted in people as a screening test for obvious cardiac abnormalities.
- A left atrial to aortic ratio (LA:Ao) that is >2:1 would be obviously abnormal in both dogs and cats.
- A right ventricular to left ventricular ratio (RV:LV) on the four-chamber long-axis view of >1:2 or ~1:1 would be obviously abnormal in both dogs and cats.
- An abnormal fractional shortening (FS%) for dogs and cats would be <20%.
- Sonographic striation of the gallbladder wall in dogs and cats can be due to right-sided congestive heart failure (most commonly pericardial effusion), referred to as a "cardiac gallbladder" (Lisciandro 2019).
- TFAST right-sided cardiac markers that screen for obvious right-sided cardiac problems include the RV:LV, characterization of the CVC and hepatic veins, and gallbladder wall edema, that is, sonographic striation and the "cardiac gallbladder" (Lisciandro 2016, 2019).

**Template for TFAST®**

**Pneumothorax?**
Left CTS: absent ☐ present ☐ indeterminate ☐ not assessed ☐
Lung Point : upper 1/3 ☐ middle 1/3 ☐ lower 1/3 ☐

Right CTS: absent ☐ present ☐ indeterminate ☐ not assessed ☐
Lung Point : upper 1/3 ☐ middle 1/3 ☐ lower 1/3 ☐

**Pleural Effusion?**
Left PCS: absent ☐ present ☐ indeterminate ☐ not assessed ☐
mild ☐ moderate ☐ severe ☐
Right PCS: absent ☐ present ☐ indeterminate ☐ not assessed ☐
mild ☐ moderate ☐ severe ☐

**Pericardial Effusion?**
absent ☐ present ☐ indeterminate ☐ not assessed ☐
trivial < 5 mm ☐ mild < 1 cm ☐
moderate > 1 cm< 2 cm ☐ severe >2 cm ☐

**TFAST Echo Views**

**Right PCS**
LVSA Volume - unremarkable ☐ abnormal ☐
indeterminate ☐ not assessed ☐
LVSA Contractility (FS%) - unremarkable ☐ abnormal ☐
indeterminate ☐ not assessed ☐
LA:Ao Ratio - unremarkable ☐ abnormal ☐
indeterminate ☐ not assessed ☐
RV:LV Ratio - unremarkable ☐ abnormal ☐
indeterminate ☐ not assessed ☐

Caudal Vena Cava
unremarkable (BOUNCE) ☐ small (flat) ☐ distended (FAT) ☐
indeterminate ☐ not assessed ☐

Hepatic Venous Distension
unremarkable ☐ distended ☐
indeterminate ☐ not assessed ☐

**Comments** _____

**KEY: CTS** = chest tube site; **PCS** = pericardial sac; **LV** = left ventricle, **PTX** = pneumothorax, **LVSA**: left ventricular short-axis view, **LA:AO** aortic to left atrial ratio on short-axis view, **RVLV**: right ventricular to left ventricular ratio on long-axis view.

**Qualifier:** The TFAST exam is an ultrasound examination used to detect pleural and pericardial effusion, major thoracic wall, lung, and heart abnormalities as a screening test in order to better direct resuscitation efforts or manage hospitalized critically ill patients. TFAST exam is not intended to replace thoracic radiographs, or complete detailed echocardiography.

*Created by Gregory Lisciandro, DVM, DABVP, DACVECC, CEO of FASTVet.com and President, International Veterinary Point-of-care Ultrasound Society, IVPOCUS.org*

**Figure 18.34.** TFAST goal-directed template. Source: Reproduced with permission from Dr Gregory Lisciandro, Hill Country Veterinary Specialists and FASTVet.com, Spicewood, TX.

# Pearls and Pitfalls, The Final Say

- TFAST should be used as a first-line imaging test, as a quick assessment test as an extension of the physical exam, to "see" your problem list, and to rule in and out important potentially life-threatening conditions.
- TFAST has clear advantages over thoracic radiography for pericardial effusion, pleural effusion, cardiac conditions including abnormal chamber ratios, soft tissue abnormalities, and includes one of the AFAST views, the DH view, that provides information regarding ascites, soft tissue abnormalities of the liver and gallbladder, and volume status via the CVC.
- TFAST can not only diagnose but also monitor pneumothorax using the "lung point" concept.
- TFAST is not a "flash exam" of the thorax.

# References


Atkinson P, Bowra J, Milne J, et al. 2017. International Federation for Emergency Medicine Consensus Statement: Sonography in hypotension and cardiac arrest (SHoC): an international consensus on the use of point of care ultrasound for undifferentiated hypotension and during cardiac arrest. *Can J Emerg Med* 19(6):459–470.

Ball CG, Ranson KM, Rodriguez-Galvez M, et al. 2009. Sonographic depiction of posttraumatic alveolar-interstitial disease: the handheld diagnosis of a pulmonary contusion. *J Trauma* 66(3):962.

Barata I, Spencer R, Suppiah A, et al. 2012. Emergency ultrasound in the detection of pediatric long bone fractures. *Pediatr Emerg Care* 28(11):1154–1157.

Blackbourne LH, Soffer D, McKenney M, et al. 2004. Secondary ultrasound examination increases the sensitivity of the FAST exam in blunt trauma. *J Trauma* 57:934–938.

Bonagura JD, Fuentes VL. 2015. Echocardiography. In: *Small Animal Diagnostic Ultrasound*, 3rd edition, edited by Mattoon JS, Nyland TC. St Louis: Elsevier, p 312.

Breitkreutz R, Price S, Steiger HV, et al. 2010. Focused echocardiographic evaluation in life support and peri-resuscitation of emergency patients: a prospective trial. *Resuscitation* 81: 1527–1533.

Brockman DJ, Puerto DA. 2004. Pneumomediastinum and pneumothorax, In: *Textbook of Respiratory Diseases in Dogs and Cats*, edited by King LG. Philadelphia: WB Saunders, pp 617–621.

Candotti C, Arntfield R. 2014. Pericardial effusion. In: *Point-of-Care Ultrasound*, edited by Soni NJ, Arntfield R, Kory P. Philadelphia: Elsevier, pp 130–134.

Chetboul V, Tidholm A, Nicolle A, et al. 2005. Effects of animal position and number of repeated measurements on selected two-dimensional and M-mode echocardiographic variables in healthy dogs. *J Am Vet Med Assoc* 227(5):743–747.

Cornelius L, Mahaffey M. 1985. Kinking of the intra-thoracic caudal vena cava in 5 dogs. *J Small Anim Pract* 26:67–80.

Côté E, Schwarz LA, Sithole F. 2013. Thoracic radiographic findings for dogs with cardiac tamponade attributable to pericardial effusion. *J Am Vet Med Assoc* 243(2):232–235.

Cunningham J, Kirkpatrick AW, Nicolaou S, et al. 2002. Enhanced recognition of "lung sliding" with power color Doppler in the diagnosis of pneumothorax. *J Trauma* 52:769–772.

Darnis E, Boysen S, Merveille AC et al. 2018. Establishment of references values of the caudal vena cava by fast-ultrasonography through different views in healthy dogs. *J Vet Intern Med* 32:1308–1318.

Davidson BJ, Paling AC, Lahmers SL, et al. 2008. Disease association and clinical assessment of pericardial effusion. *J Am Anim Hosp* 44(1):5–9.

Dicker SA, Lisciandro GR, Newell SM, et al. 2019. Diagnosis of pulmonary contusions with point-of-care lung ultrasonography and thoracic radiography compared to thoracic computed tomography in dogs with motor vehicle trauma: 29 cases (2017–2018). *J Vet Emerg Crit Care*, in press.

Elliot JM, Mayhew PD. 2011. Diagnostic challenges and treatment options of a suspected pericardial metallic projectile foreign body in a dog. *J Vet Emerg Crit Care* 21(6): 684–691.

Ferrada P, Anand RJ, Whelan J, et al. 2012a. Limited transthoracic echocardiogram: so easy any trauma attending can do it. *J Trauma* 71(5):1327–1331.

Ferrada P, Vanguri P, Anand RJ, et al. 2012b. Flat inferior vena cava: indicator of poor prognosis in trauma and acute care surgery patients. *Am Surg* 78(12):1396–1398.

Ferrada P, Anand RJ, Whelan J, et al. 2012. Qualitative assessment of the inferior vena cava: useful tool for the evalutaion of fluid status in criticall ill patients. *Am Surg* 78(4):468–470.

Ferrada P, Evans D, Wolfe L, et al. 2014. Findings of a randomized controlled trial using limited transthoracic echocardiogram (LTTE) as a hemodynamic monitoring tool in the trauma bay. *J Trauma Acute Care Surg* 76(1):31–37.

Fine DM, Olivier NB, Walshaw R, et al. 1998. Surgical correction of late-onset Budd–Chairi-like syndrome in a dog. *J Am Vet Med Assoc* 212(6):835–837.

Gargani L, Lionetti V, di Cristofano C, et al. 2007. Early detection of acute lung injury uncoupled to hypoxemia in pigs using ultrasound lung comets. *Crit Care Med* 35(12): 2769–2774.

Guglielmini C, Diana A, Santarelli G, et al. 2012. Accuracy of radiographic vertebral heart score and sphericity index in the detection of pericardial effusion in dogs. *J Am Vet Med Assoc* 241(8):1048–1055.

Hall DJ, Shofer F, Meier CK, Sleeper MM. 2007. Pericardial effusion in cats: a retrospective study of clinical findings and outcome in 146 cats. *J Vet Intern Med* 21(5):1002–1007.

Higgs VA, Rudloff E, Kirby R, Linklater AK. 2015. Autologous blood transfusion in dogs with thoracic or abdominal hemorrhage: 25 cases (2007–2012). *J Vet Emerg Crit Care* 25(6):731–738.

Himelman RB, Kircher B, Rockey DC, et al. 1988. Inferior vena cava plethora with blunted respiratory response: a sensitive echocardiographic sign of cardiac tamoponade. *J Am Coll Cardiol* 12(6):1470–1477.

Humm KR, Keenaghan-Clark EA, Boag AK. 2009. Adverse events associated with pericardiocentesis in dogs: 85 cases (1999–2006). *J Vet Emerg Crit Care* 19(4):352–356.

Hwang TS, Yoon YM, Jung DI, et al. 2018. Usefulness of transthoracic lung ultrasound for the diagnosis of mild pneumothorax. *J Vet Sci* 19(5):660–666.

Hyacinthe AC, Broux C, Francony G, et al. 2012. Diagnostic accuracy of ultrasonography in the acute assessment of common thoracic lesions after trauma. *Chest* 141(5): 1177–1183.

Jambrik Z, Monti S, Coppola V, et al. 2004. Usefulness of ultrasound lung comets as a nonradiologist sign of extravascular lung water. *Am J Cardiol* 93:1265–1270.

Kirkpatrick AW, Sirois M, Laupland KB, et al. 2004. Hand-held thoracic sonography for detecting post-traumatic pnuemothoraces: the extended focused assessment with sonography for trauma (EFAST). *J Trauma* 57:288–295.

Koegelenberg CF, von Groote-Bidlingmaier F, Bolliger CT. 2012. Transthoracic ultrasonography for the respiratory physician. *Respiration* 84(4):312–318.

Kolata RJ, Dudley EJ. 1975. Motor vehicle accidents in urban dogs: a study of 600 cases. *J Am Vet Med Assoc* 167:938–941.

Kulhavy DA, Lisciandro GR. 2015. Use of a lung ultrasound examination called Vet BLUE to screen for metastatic lung nodules in the emergency room. *J Vet Emerg Crit Care* 25(S1):S14.

Lamb CR. 2000. Radiology Corner: Ability to visualize the cardiac silhouette in animals with pleural fluid: the pericardial fat stripe. *Vet Radiol Ultrasound* 41(6):519–520.

Lee FCY. 2016. Lung ultrasound – a primary survey of acutely dyspneic patient. *J Intens Care* 4:57.

Lichtenstein DA. 2007. Ultrasound in the management of thoracic disease. *Crit Care Med* 35(S5):S250–S261.

Lichtenstein DA. 2010a. Gallbladder. In: *Whole Body Ultrasonography in the Critically Ill*, edited by Lichtenstein DA. Heidelberg: Springer, pp 59–68.

Lichtenstein DA. 2010b. Should lung ultrasonography be more widely used in the assessment of acute respiratory disease? *Expert Rev Respir Med* 4(5):533–538.

Lichtenstein D. 2012. Fluid administration limited by lung sonography: the place of lung ultrasound in assessment of acute circulatory failure (the FALLS protocol). *Expert Rev Respir Med* 6(2):155–162.

Lichtenstein D, Karakitsos D. 2012. Integrating lung ultrasound in the hemodynamic evaluation of acute circulatory failure (the fluid administration limited by lung sonography protocol). *J Crit Care* 27(5):533.

Lichtenstein DA, Meziere GA. 2008. Relevance of lung ultrasound in the diagnosis of acute respiratory failure: the BLUE protocol. *Chest* 134(1):117–125.

Lichtenstein DA, Meziere G, Biderman P, et al. 1997. The comet-tail artifact. An ultrasound sign of alveolar-interstitial syndrome. *Am J Respir Crit Care Med* 156(5):1640–1646.

Lichtenstein DA, Meziere G, Biderman P, et al. 1999. Comet-tail artifact: an ultrasound sign of ruling out pneumothorax. *Intens Care Med* 25(4):383–388.

Lichtenstein D, Meziere G, Biderman P, et al. 2000. The "lung point": an ultrasound sign specific to pneumothorax. *Intens Care Med* 26:1434–1440.

Lichtenstein DA, Lascos N, Meziere GA, et al. 2004. Ultrasound diagnosis of alveolar consolidation in the critically ill. *Intens Care Med* 30:276–281.

Lichtenstein D, Meziere G, Lagoueyte JF, et al. 2009. A-lines and B-lines: lung ultrasonography as a bedside tool for predicting pulmonary artery occlusion pressure in the critically ill. *Chest* 136:1014–1020.

Lisciandro GR. 2011. Abdominal and thoracic focused assessment with sonography for trauma, triage and monitoring in small animals. *J Vet Emerg Crit Care* 21(2): 104–122.

Lisciandro GR. 2012. Evaluation of initial and serial combination focused assessment with sonography for trauma (CFAST) examinations of the thorax (TFAST) and abdomen (AFAST) with the application of an abdominal fluid scoring system in 49 traumatized cats. *J Vet Emerg Crit Care* 22(S2):11.

Lisciandro GR. 2014a. The Thoracic FAST$^3$ (TFAST$^3$) Exam. In: *Focused Ultrasound for the Small Animal Practitioner*, edited by Lisciandro GR. Ames: Wiley Blackwell, pp 140–165.

Lisciandro GR. 2014b. The The Vet BLUE lung Scan. In: *Focused Ultrasound for the Small Animal Practitioner*, edited by Lisciandro GR. Ames: Wiley Blackwell, pp 166–188.

Lisciandro GR. 2016. The use of the diaphragmatico-hepatic (DH) views of the abdominal and thoracic focused assessment with sonography for triage (AFAST/TFAST) examinations for the detection of pericardial effusion in 24 dogs (2011–2012). *J Vet Emerg Crit Care* 26(1):125–131.

Lisciandro GR. 2019. The cardiac gallbladder: case series of 13 dogs and 1 cat with sonographically detected gallbladder wall edema. *J Vet Emerg Crit Care* 29(S1):S24.

Lisciandro GR, Armenise A. 2014. Focused or COAST$^3$ – Cardiopulmonary Resuscitation (CPR), Global FAST (GFAST$^3$) and the FAST-ABCDE Exam. In: *Focused Ultrasound for the Small Animal Practitioner*, edited by Lisciandro GR. Ames: Wiley Blackwell, pp 269–287.

Lisciandro GR, Fosgate GT. 2018. Use of Vet BLUE protocol for the detection of lung atelectasis and sonographic gallbladder wall evaluation for anaphylaxis and volume overload in 63 dogs undergoing general anesthesia. *J Vet Emerg Crit Care* 28(S1):S15–S16.

Lisciandro GR, Harvey HJ, Beck KA. 1995. Automobile-induced obstruction of the intrathracic caudal vena cava in a dog. *J Small Anim Pract* 36(8):368–372.

Lisciandro GR, Lagutchik MS, Mann KA, et al. 2008. Accuracy of Focused Assessment with Sonography for Trauma (TFAST) to detect pneumothorax in 145 dogs with blunt and penetrating trauma. *J Vet Emerg Crit Care* 18(3): 258–269.

Lisciandro GR, Lagutchik MS, Mann KA, et al. 2009. Evaluation of an abdominal fluid scoring system determined using abdominal focused assessment with sonography for trauma in 101 dogs with motor vehicle trauma. *J Vet Emerg Crit Care* 19(5):426–437.

Lisciandro GR, Fosgate GT, Fulton RM. 2014. Frequency of ultrasound lung rockets using a regionally-based lung ultrasound examination named veterinary bedside lung ultrasound exam (Vet BLUE) in 98 dogs with normal thoracic radiographic lung findings. *Vet Radiol Ultrasound* 55(3):315–322.

Lisciandro GR, Fulton RM, Fosgate GT, Mann KA. 2017. Frequency of B-lines using a regionally-based lung ultrasound examination (the Vet BLUE protocol) in 49 cats with

normal thoracic radiographical lung findings. *J Vet Emerg Crit Care* 27(3):267–277.

Lisciandro GR, Romero L, Fosgate GT. 2018. The frequency of B-Lines and other lung ultrasound artifacts during Vet BLUE in 91 healthy puppies and kittens. *J Vet Emerg Crit Care* 28(S1):S16.

Lisciandro GR, Johnson CB, Gambino JM, et al. 2019. The prevalence of sonographically-detected gallbladder wall edema in dogs with acute hemorrhagic diarrhea syndrome. In review.

Little AA, Steffey M, Kraus MS. 2007. Marked pleural effusion causing right atrial collapse simulating cardiac tamponade in a dog. *J Am Anim Hosp Assoc* 43(3):157–162.

Loughran KA, Rush JE, Rozanski EA, et al. 2019. The use of focused cardiac ultrasound to screen for occult heart disease in asymptomatic cats. *J Vet Intern Med* 33(5):1892–1901.

Louvet A, Bourgeois JM. 2008. Lung ring-down artifact as a sign of pulmonary alveolar-interstitial disease. *Vet Radiol Ultrasound* 49(4): 374–377.

MacDonald KA, Cagney O, Magne ML. 2009. Echocardiographic and clinicopathologic characterization of pericardial effusion in dogs: 107 cases (1985–2006). *J Am Vet Med Assoc* 235(12):1456–1461.

Mellanby RJ, Herrtage ME. 2005. Long-term survival of 23 dogs with pericardial effusions. *Vet Rec* 156(18):568–571.

Morges M, Worley DR, Withrow SJ, et al. 2011. Pericardial free patch grafting as a rescue technique in surgical management of right atrial HSA. *J Am Anim Hosp Assoc* 47(3):224–228.

Nakamura RK, Tompkins E, Russell NJ, Zimmerman SA. 2014. Left atrial rupture secondary to myxomatous mitral valve disease in 11 dogs. *J Am Anim Hosp Assoc* 50(6): 405–408.

Neelis DA, Mattoon JS, Nyland TG. 2015. Thorax. In: *Small Animal Diagnstic Ultrasound*, 3rd edition, edited by Mattoon JS, Nyland TG. St Louis: Elsevier, pp 188–217.

Nelson NC, Drost WT, Lerche P, et al. 2010. Noninvasive estimation of central venous pressure in anesthetized dogs by measurement of hepatic venous blood flow velocity and abdominal venous diameter. *Vet Radiol Ultrasound* 51(3):313–323.

Neto MJ, Junior AR, Vieira FA, et al. 2016. Advances in lung ultrasound. *Einstein* 14(3):443–448.

Newitt AL, Cripps PJ, Shimali J. 2009. Sonographic estimation of pleural fluid in dogs. *Vet Radiol Ultrasound* 50(1):86–90.

Nielsen C, Todd JM, Cronk DE, et al. 2005. What is your diagnosis? A wood fragment was detected within the mediastinum, penetrating the cranial aspect of the pericardial sac and in contact with the right auricle. *J Am Vet Med Assoc* 226(7):1055–1056.

Nyland TC, Mattoon JS. 2002. Thorax. *In: Small Animal Diagnostic Ultrasound*, 2nd edition, edited by Nyland TC, Matton JS. Philadelphia: WB Saunders, p 335.

Ollerton JE, Sugrue M, Balogh Z, et al. 2006. Prospective study to evaluate the influence of FAST on trauma patient management. *J Trauma* 60:785–791.

Parri N, Crosby BJ, Glass C, et al. 2013. Ability of emergency ultrasonography to detect pediatric skull fractures. *J Emerg Med* 44(1):135–141.

Partlow J, David F, Hunt LM, et al. 2017. Comparison on thoracic ultrasonography and radiography for the detection of induced small volume pneumothorax in the horse. *Vet Radiol Ultrasound* 58(3):354–360.

Pate J, Rademacher N, Pariaut R, et al. 2010. Comet-tail artifacts in normal dogs and dogs with cardiogenic pulmonary edema. *J Vet Intern Med* 24(3):729.

Peris A, Zagli G, Barbani F, et al. 2010. The value of lung ultrasound monitoring in H1N1 acute respiratory distress syndrome. *Anaesthesia* 65(3):294–297.

Picandet JD, Macieira S, Beauregard G, et al. 2007. Detection of rib trauma in newborn foals in equine critical care unit: a comparison of ultrasonography, radiography, and physical examination. *Equine Vet J* 39(2):158–163.

Ployart S, Libermann S, Doran I, et al. 2013. Thoracoscopic resection of right auricular masses in dogs: 9 cases (2003–2011). *J Am Vet Med Assoc* 242(2):237–241.

Powell LL, Rozanski EA, Tidwell AS, et al. 1999. A retrospective analysis of pulmonary contusions secondary to motor vehicle accidents in 143 dogs: 1994–1997. *J Vet Emerg Crit Care* 9(3):127–136.

Reineke EL, Burkett DE, Drobatz KJ. 2008. Left atrial rupture in dogs: 14 cases (1990–2005). *J Vet Emerg Crit Care* 18(2): 158–164.

Reissig A, Copetti R, Kroegel C. 2011. Current role of emergency ultrasound of the chest. *Crit Care Med* 39(5):1–8.

Robinson DA, Kiefer K, Bassett R, Quandt J. 2016. Autotransfusion in dogs using a 2-syringe technique. *J Vet Emerg Crit Care* 26(6):766–774.

Sandanaga KK, MacDonald MJ, Buchanan JW. 1990. Echocardiography and surgery in a dog with left atrial rupture and hemopericardium. *J Vet Intern Med* 4:216–221.

Sargsyan AE, Hamilton DR, Nicolau S, et al. 2001. Ultrasound evaluation of the magnitude of pneumothorax: a new concept. *Am Surg* 67:232–235.

Scansen BA. 2011. Interventional cardiology for the criticalist. *J Vet Emerg Crit Care* 21(2):123–136.

Shaw SP, Rush JE. 2007. Canine pericardial effusion: pathophysiology and cause. *Compend Contin Educ Vet* 29(7): 400–403.

Shimali J, Cripps PJ, Newitt AL. 2010. Sonographic pleural fluid volume estimation in cats. *J Fel Med Surg* 12:113–116.

Shyamsundar M, Attwood B, Keating L, et al. 2013. Clinical review: the role of ultrasound in estimating extra-vascular lung water. *Crit Care* 17(5):237–244.

Sigrist NE, Doherr MG, Spreng DE. 2004. Clinical findings and diagnostic value of post-traumatic thoracic radiographs in dogs and cats with blunt trauma. *J Vet Emerg Crit Care* 14:259–268.

Simpson SA, Syring R, Otto CM. 2009. Severe blunt trauma in dogs: 235 cases (1997–2003). *J Vet Emerg Crit Care* 19(6): 588–602.

Soldati G, Testa A, Silva FR, et al.2006. Chest ultrasonography in lung contusion. *Chest* 130(2):533–538.

Soldati G, Sher S, Testa A. 2011. Lung and ultrasound: time to "reflect." *Eur Rev Med Pharmacol Sci* 15:223–227.

Stafford Johnson M, Martin M, Binns S, Day MJ. 2004. A retrospective study of clinical findings, treatment and outcome in 143 dogs with pericardial effusion. *J Small Anim Pract* 45(11):546–552.

Suzuki S, Fukushima R, Ishikawa T, et al. 2011. The effect of pimobendan on left atrial pressure in dogs with mitral valve regurgitation. *J Vet Intern Med* 25(6):1328–1333.

Tchernodrinski S, Arntfield R. 2015. Inferior vena cava. In: *Point-of-Care Ultrasound*, edited by Soni NJ, Arntfield R, Kory P. Philadelphia: Elsevier, pp 135–141.

Treggiari E, Pedro B, Dukes-McEwan J, et al. 2017. A descriptive review of cardiac tumors in dogs and cats. *Vet Comp Oncol* 15(2):273–288.

Vezzosi T, Mannucci A, Pistoresi F, et al. 2017. Assessment of lung ultrasound B-Lines in dogs with different stages of chronic valvular heart disease. *J Vet Intern Med* 31(3): 700–704.

Volpicelli G, Mussa A, Garofalo G, et al. 2006. Bedside lung ultrasound in the assessment of alveolar-interstitial syndrome. *Am J Emerg Med* 24:689–696.

Volpicelli G, Elbarbary M, Blaivas M, et al. 2012. International evidence-based recommendations for point-of-care lung ultrasound. *Intens Care Med* 38:577–591.

Volpicelli G, Boero E, Stefano V, et al. 2013. Unusual new signs of pneumothorax at lung ultrasound. *Crit Ultrasound J* 5(1):10.

Ward JL, Lisciandro GR, Keene BW, et al. 2017. Accuracy of point-of-care lung ultrasonography for the diagnosis of cardiogenic pulmonary edema in dogs and cats with acute dyspnea. *J Am Vet Med Assoc* 250:666–675.

Ward JL, Lisciandro GR, DeFrancesco TD, et al. 2018. Evaluation of point-of-care thoracic ultrasound and NT-proBNP for the diagnosis of congestive heart failure in cats with respiratory distress. *J Vet Intern Med* 32(5):1530–1540.

Witt JM, Mayhew PD. 2011. Diagnostic challenges and treatment options of a suspected pericardial metallic projectile foreign body in a dog. *J Vet Emerg Crit Care* 21(6): 684–691.

CHAPTER NINETEEN

# POCUS: Heart – Introduction and Image Acquisition

Teresa DeFrancesco

## Introduction

Focused cardiac ultrasound (FCU) or focused echocardiography are terms used to describe a limited ultrasound examination of the cardiovascular system, typically performed by a noncardiology specialist and as an adjunct to the physical examination, to recognize specific sonographic signs that represent a narrow list of potential diagnoses in specific clinical settings (Spencer et al. 2013). Most commonly, FCU is performed in symptomatic or at-risk small animal patients in the acute or primary care setting. Unlike complete echocardiography, FCU is usually a time-sensitive exam investigating the cause of a patient's clinical signs in order to make immediate treatment decisions by rapidly diagnosing potentially life-threatening conditions and improving the management of a critically ill patient (Beaulieu 2007; Labovitz et al. 2010; Arntfield and Millington 2012). Frequently, FCU is part of a more comprehensive and integrated thoracic ultrasound including interrogation of the pleural space, anterior mediastinum, and lungs (see also Chapters 17, 18, 22, and 23).

Recently, FCU has shown clinical utility in veterinary medicine as an aid in the diagnosis of heart failure (Ward et al. 2018) and other nontraumatic conditions causing cardiovascular instability and respiratory distress (McMurray et al. 2016). Recent studies also support the assessment of the caudal vena cava as an aid in diagnosis of fluid responsiveness and volume status and as a noninvasive estimate of right atrial pressure (Nelson et al. 2010; Cambournac et al. 2018; Kwak et al. 2018; Marshall et al. 2018). See also Chapters 6, 7, 17, 18, 26, 36, and 37.

With limited didactic and hands-on training, noncardiologist or nonradiologist veterinarians can achieve an acceptable proficiency in identifying pleural and pericardial effusions, and detecting the presence of right and left atrial enlargement (Tse et al. 2012). Achievable goals discussed in the next three chapters include not only the detection of pleural and pericardial effusion, left and right atrial enlargement but also the assessment of significant abnormalities in contractility, valvular anatomy, volume status, identification of obvious masses and right sided-heart disease.

Similar to other focused ultrasound exams, the FCU provides a rapid, point-of-care, safe (radiation sparing), noninvasive, and portable assessment of patients. FCU is indicated in dogs and cats presenting with respiratory signs or distress, significant arrhythmias and persistent or episodic hemodynamic collapse, especially to rapidly rule out pericardial effusion with cardiac tamponade and pleural effusion, and to help diagnosis heart failure or other causes of hemodynamic compromise.

The author finds FCU particularly useful for cats in respiratory distress to differentiate heart failure from other causes of respiratory distress (see also Chapters 17, 18, 22, 23, 36, and 37) because physical examination and radiographic findings are notoriously nonspecific in felines. In fact, up to 30% of cats in heart failure have no murmur or gallop sound on initial cardiac auscultation (Rush et al. 2002). Furthermore, distribution of radiographic lesions is variable in cats with cardiogenic pulmonary edema caused by left-sided heart

*Point-of-Care Ultrasound Techniques for the Small Animal Practitioner*, Second Edition. Edited by Gregory R. Lisciandro.
© 2021 John Wiley & Sons, Inc. Published 2021 by John Wiley & Sons, Inc.
Companion website: www.wiley.com/go/lisciandro/ultrasound2

failure (versus the predictable perihilar distribution in dogs), and pleural effusion, a common manifestation of feline heart failure, obscures the cardiac silhouette, making radiographic assessment of heart size difficult. On the other hand, ultrasound is superior in detecting pleural and pericardial effusion (arguably the gold standard) (Reissig et al. 2011), and cardiac imaging is enhanced when effusions are present rather than diminished compared to thoracic radiography. Thus, a cat with pleural effusion may be clearly imaged with ultrasound with minimal stress, allowing more accurate assessment of heart chamber dimensions and specifically left atrial size (Schober et al. 2014).

In conclusion, the added diagnostic value of FCU was highlighted by a study in which the diagnostic accuracy of minimally trained first-year medical students performing bedside echocardiography was superior to that of board-certified cardiologists performing cardiac physical examinations for the detection and evaluation of selected valvular and nonvalvular cardiac abnormalities (Kobal et al. 2005). The improved diagnostic accuracy of FCU in certain conditions over the cardiac physical examination alone is the reason why point-of-care thoracic ultrasound has been termed the "visual stethoscope of the 21st century" (Moore and Copel 2011).

## What Focused Cardiac Ultrasound Can Do

- Identify severely enlarged cardiac chambers, even in the presence of pleural effusion, thus providing useful and timely corroborative evidence for either left- or right-sided heart failure.
- Assess left ventricular contractility by either the "eyeball method" or by measurement of its fractional shortening, thus helping with detection of left ventricular systolic failure and diagnosis of dilated cardiomyopathy in dogs.
- Detect obvious thickened mitral or tricuspid valves and possibly ruptured chordae tendineae.
- Assess severe left ventricular concentric hypertrophy (thickening), thus helping with the diagnosis of hypertrophic cardiomyopathy in cats.
- Detect severe left atrial enlargement and screen for left atrial thrombus or echogenic "smoke" in cats with aortic thromboembolism (ATE).
- Detect heartworms in the right heart in cats with respiratory distress or in dogs with caval syndrome.
- Detect pleural effusion and characterize its distribution.
- Estimate the amount of pleural fluid, its location(s), identify a suitable site for thoracocentesis, and track (monitor) for recurrence of effusion.
- Detect pericardial effusion, determine the presence of cardiac tamponade and possibly the etiology of the effusion.
- Estimate the amount of pericardial fluid, identify a suitable site for pericardiocentesis, and track (monitor) for recurrence of effusion.
- Assess the size and degree of respiratory variation of the caudal vena cava to determine if a patient is fluid tolerant or intolerant.

## What Focused Cardiac Ultrasound Cannot Do

- Cannot be used as a stand-alone diagnostic test for the definitive diagnosis of heart failure (echocardiography by itself can only diagnose heart disease, not failure).
- Cannot replace complete echocardiography by a veterinary cardiologist or radiologist, and sonographers should know their limitations.
- Cannot provide proficient use of color flow, pulsed, continuous wave or tissue Doppler echocardiography (not covered).

## Indications

- Respiratory distress, respiratory compromise, or uncharacterized tachypnea or dyspnea.
- Congestive heart failure (left- and right-sided) suspects.
- Pericardial effusion with or without cardiac tamponade suspects.
- Uncharacterized persistent or intermittent hemodynamic instability or collapse.
- Uncharacterized syncope, collapse or generalized weakness.
- Uncharacterized tachycardia (rapid heart rate) or significant cardiac arrhythmia.
- Feline aortic thromboembolism.
- Cardiovascular assessment of volume status and heart contractility.
- Tracking (monitoring) using serial exams for recurrence of pericardial or pleural effusions post centesis or during course of therapy.

## Objectives

- Be able to perform basic echocardiographic views of the short and long axis at the right and left parasternal and subxiphoid sites.
- Be able to recognize normal heart anatomy including the atria, ventricles, and associated valves and walls.
- Identify a severely enlarged left atrium (LA) in small animals with suspected left-sided heart failure.

VetBooks.ir

- Identify severe right heart enlargement, caudal vena cava, and hepatic venous distension suggestive of right heart failure or possibly secondary to chronic pulmonary hypertension/cor pulmonale in a dog with respiratory distress.
- Be able to qualitatively assess left ventricular (LV) systolic function as normal, hypo- or hyperdynamic. Additionally, be able to measure left ventricular fractional shortening (FS%), a commonly used quantitative parameter of LV function.
- Be able to measure the LV wall thickness in diastole, LV lumen in systole and diastole, and left atrial (LA) and aortic (Ao) dimensions, and know cut-off values for normal and abnormal.
- Identify pericardial effusion and cardiac tamponade. Additionally, identify the cause of the pericardial effusion.
- Identify pleural effusion.
- Identify masses within the heart, in heart walls or heart base, and pleural space, prompting confirmation by complete echocardiography or other advanced imaging technique or procedures.
- Be able to assess extreme abnormalities in volume status as fluid tolerant or fluid intolerant. Additionally, be able to serially assess cardiac measurements in response to intravenous fluid resuscitation and therapy.

# Ultrasound Settings and Probe Preferences

The use of the cardiac setting (presets) on your ultrasound unit generally provides more contrast in echogenicity, making identification of cardiac chambers and assessing their motion (valves and walls) easier (than abdominal presets). Images in this chapter (cardiac preset) may be compared to cardiac images in Chapters 17 and 18 (abdominal preset). Most built-in cardiac presets will also flip the left to right orientation of the image, which is different from other built-in presets. Cardiologists prefer viewing so that the cranial aspects of the heart and the marker indicator are on the right side of the screen, which is in the opposite orientation from all other ultrasound imaging. If you do not use a cardiac preset to image the heart, then the image on the screen will be a mirror image of what is typically seen in cardiology and echocardiographic textbooks (see Figures 19.3 and 19.6). Image quality of the heart is best with ultrasound machines (or settings) with high frame or sampling rates. Inadequate (too slow) frame or sampling rates are recognized by a real-time image that is choppy.

- Use of curvilinear (microconvex) or phased-array sector probes (3–10 MHz) is ideal for imaging the heart between ribs (creating an acoustic window). Use the highest megahertz (MHz) possible to obtain the highest resolution images. If given a choice, the phased-array probe is preferred for cardiac imaging because of better temporal resolution and typically a small footprint, resulting in less rib (shadowing) interference. The curvilinear (microconvex) probe is a multipurpose probe that can be used for cardiac imaging and enhanced by using a cardiac preset. Linear probes generally do not image the heart well because of their long footprint and rib interference (ultrasound does not transmit through bone).
- Adjust the depth setting so that the entire heart is visualized and the heart makes up the majority of the image of the screen. In large or giant breeds, this may require a depth of up to 30 cm, which is often not available in some of the compact ultrasound machines. The focus setting is placed in the area of interest or near distal edge of the cardiac image.
- Adjusting the depth and optimizing the size of the heart on the image are important to avoid artifacts and misinterpretations. If the depth setting is too high relative to the heart size (small heart at top of image with a large void in the far field), a mirror (double image) artifact may result (and be confusing to the sonographer).

**Pitfall:** If you are unable to image the entire heart, cardiac chambers, especially if enlarged, may be easily misinterpreted for pleural and pericardial effusions, leading to the potentially catastrophic mistake of performing centesis on a heart chamber (see also Chapters 17, 18, 43, and 44) and cardiac chamber dimensions may not be accurately measured.

**Pearl:** Adhere to the axiom "One view is no view" to avoid misinterpreting normal heart anatomy for pleural or pericardial effusions, especially when the necessary depth for imaging the heart in its entirety is not possible on your ultrasound machine.

# How to Perform a Focused Cardiac Ultrasound

## *Patient Positioning and Preparation*

- Depending on patient stability and comfort, the FCU can be performed with the patient in either lateral or sternal recumbency (or standing). If the

**Figure 19.1.** Dog on an echo table in right lateral recumbency with the sonographer acquiring images in the right parasternal transducer position from below. Source: Image by Nathan Latil, courtesy of North Carolina State College of Veterinary Medicine.

patient is in respiratory distress, the exam is performed in sternal recumbency (or standing) while the patient receives flow-by oxygen.

- In a dog or cat with respiratory distress, the exam performed in sternal or standing recumbency will be more challenging because of lung interference and chest wall motion. Commonly, one may see "quick peeks" of the heart in between respiration cycles.
- The heart is best visualized when closest to the thoracic wall because of less lung (air) interference (ultrasound does not transmit through air). Thus, lateral recumbency with the probe positioned on the thorax of the patient's recumbent side is ideal (Figure 19.1; see also Figures 19.3, 19.6, and 19.7).

**Pearl:** Place rolled-up towels or a blanket under the cranial thorax to tilt the patient upward in either sternal or lateral recumbency to allow more probe maneuverability and permit better visualization of the heart, particularly the heart base (Figure 19.2). Bringing the patient as close to the edge of the table as possible will also improve your success in imaging the heart if scanning in lateral recumbency without an "echo table."

**Figure 19.2.** A cat in sternal recumbency with a rolled-up towel under the forelegs to elevate the thorax and facilitate FCU views.

- The heart also can be visualized from the nonrecumbent side of the thorax, especially if the animal has a narrow thoracic confirmation (see Figure 19.7).
- Focused cardiac ultrasound can be performed on a special table designed for echocardiography ("echo table") that elevates the patient off the tabletop and has a cut-out hole where the heart is, facilitating probe maneuverability and enabling a more comfortable and complete focused evaluation (see Figure 19.1).
- Typically, generous amounts of alcohol and acoustic coupling gel are applied while parting the hair to allow the coupling agents to reach the skin.
- Shaving is usually unnecessary but may be warranted if the patient has extremely thick hair. Shaving minimizes the amount of alcohol and acoustic coupling gel needed to obtain acceptable ultrasound images and because of the cooling effects of alcohol, may be best for hypothermic patients.
- The use of alcohol is contraindicated when electrical defibrillation is anticipated (ventricular fibrillation, cardiopulmonary arrest) because the alcohol presents a serious fire hazard.

## *Performing the Focused Cardiac Ultrasound Exam and the Three Main Acoustic Windows*

- The *right parasternal window* and its long- and short-axis cardiac views (Figures 19.3, 19.4, 19.5, and 19.6).

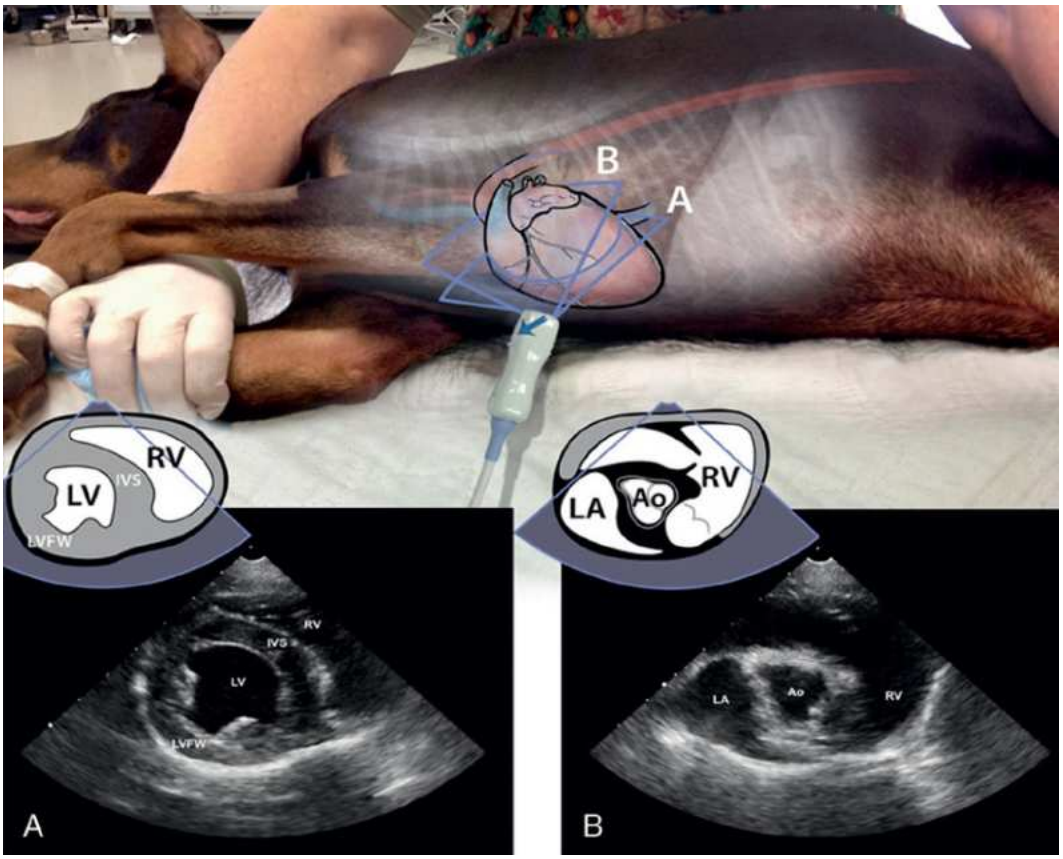


**Figure 19.3.** Dog with transducer probe positioned on the right recumbent side with the patient's thorax near the edge of the table for short-axis views. Probe showing "marker toward the elbow" for short-axis views with slice(s) of the heart labeled as "A" and "B" on the dog. (A) Corresponding schematic drawing for the echocardiogram labeled "A" of a normal right parasternal short-axis view of the left ventricle or "mushroom" view used for the assessment of patient volume status and heart contractility. (B) Corresponding schematic drawing for the echocardiogram labeled "B" of a normal short-axis view of the heart base also called the "quick peek" view used for supporting evidence of left atrial dilation and left-sided heart disease (LA:Ao ratio). The view is acquired by tipping the probe from "A" to "B" as shown on the dog. Ao, aorta; IVS, interventricular septum; LA, left atrium; LV, left ventricle; LVFW, left ventricular free wall; RV, right ventricle. Source: Courtesy of Alice MacGregor Harvey, Medical Illustrator, North Carolina State College of Veterinary Medicine.

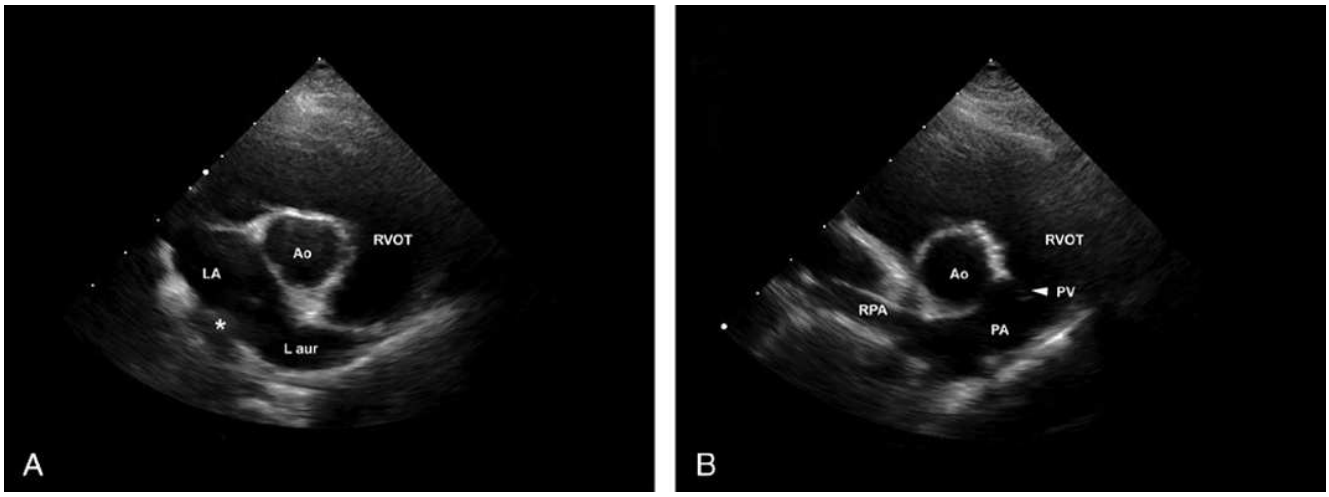


**Figure 19.4.** Normal right parasternal short-axis views at heart base optimized for left atrial appendage versus pulmonary artery. (A) Image optimized for the LA appendage ("whale tail view") used to estimate left atrial size. Echolucency depicted by (*) is a pulmonary vein entering the left atrium. (B) Image optimized for the pulmonary artery to estimate relative PA size compared to aorta. The pulmonary artery and aortic diameters should be the same. Ao, aorta; LA, left atrium; L auricle; PA, pulmonary artery; PV, pulmonary vein; RPA, right pulmonary artery; RVOT, right ventricular outflow tract.

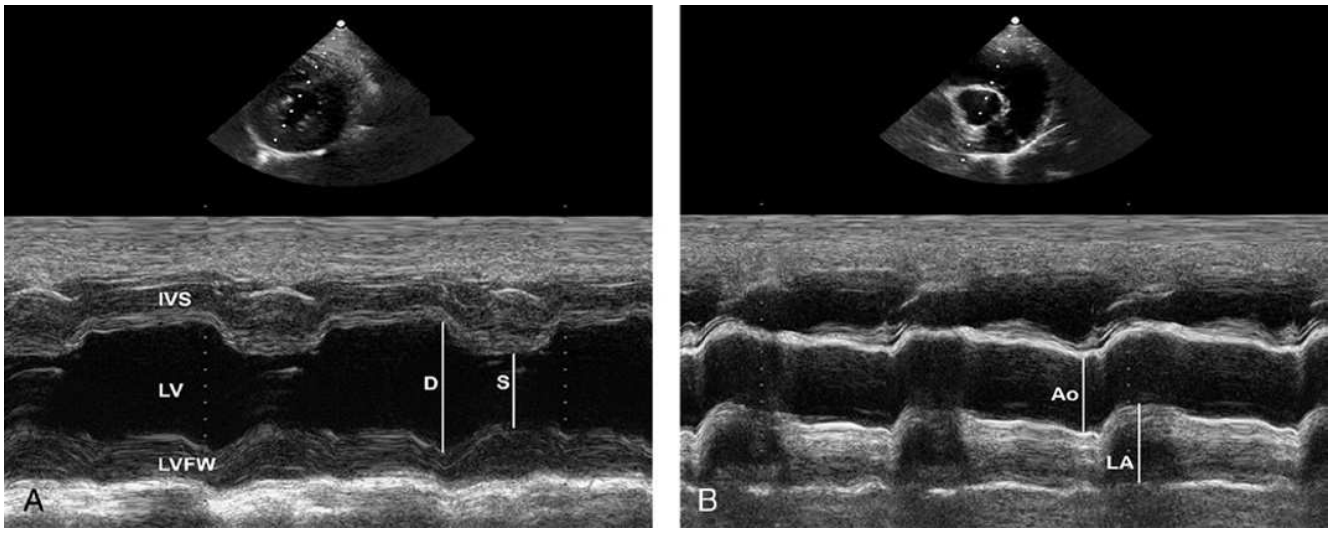


**Figure 19.5.** Normal M-mode views of the left heart. (A) Normal M-mode of the left ventricle. (B) Normal M-mode of the left atrium (LA) and aorta (Ao) with a normal LA:Ao ratio. Ao, aorta; D, diastole; IVS, interventricular septum; LA, left atrium; LV, left ventricle; LVFW, left ventricular free wall; S, systole.

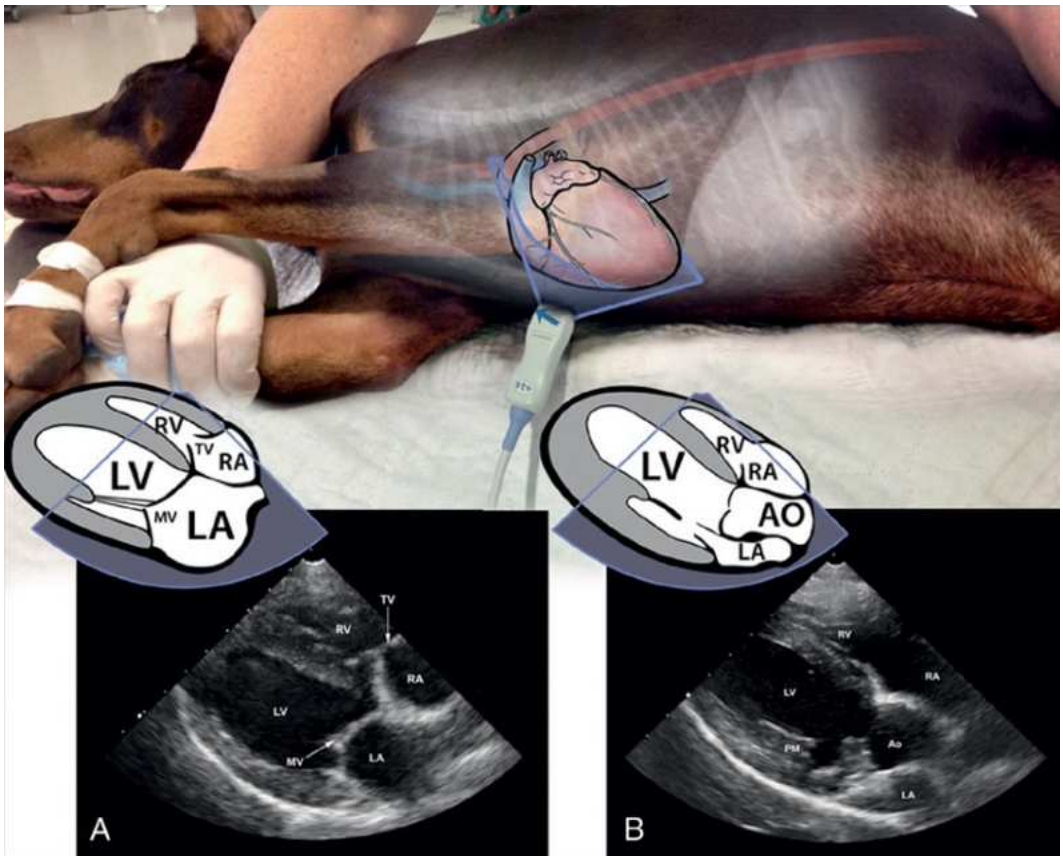


**Figure 19.6.** Dog with transducer probe positioned on the recumbent right side with the patient's thorax near the edge of the table for long-axis views. Probe showing "marker toward the head" for long-axis views with slice(s) of the heart. (A) Corresponding schematic drawing for the echocardiogram of a normal right parasternal long-axis view showing the four-chamber view. (B) Corresponding schematic drawing for the echocardiogram of a normal five-chamber view with the addition of the left ventricular outflow tract into the aorta (Ao) acquired by fanning the probe slightly dorsally from the four-chamber view. Ao, aorta; LA, left atrium; LV, left ventricle; MV, mitral valve; PM, papillary muscle; RA, right atrium; RV, right ventricle; TV, tricuspid valve. Source: Courtesy of Alice MacGregor Harvey, Medical Illustrator, North Carolina State College of Veterinary Medicine.

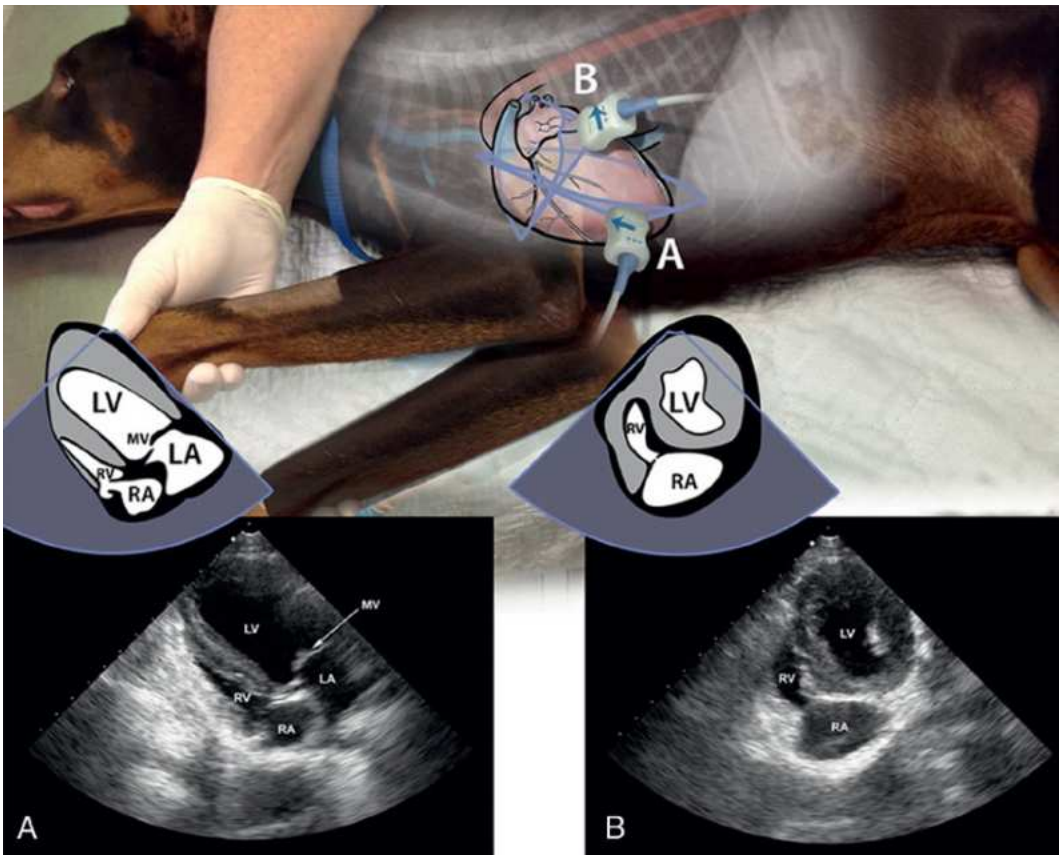


**Figure 19.7.** Dog with the probe positioned on the left hemithorax (nonrecumbent side) to obtain left-sided POCUS heart views while in right lateral recumbency for left apical views. (A) Corresponding schematic drawing labeled "A" with "marker toward the head" for the echocardiogram showing a normal left apical four-chamber view. (B) Corresponding schematic drawing labeled "B" with probe marker towards the spine and the probe rotated clockwise for the echocardiogram showing a normal left cranial view for optimal imaging of the right atrium and ventricle looking for right heart pathology including masses. LA, left atrium; LV, left ventricle; MV, mitral valve; RA, right atrium; RV, right ventricle. Source: Courtesy of Alice MacGregor Harvey, Medical Illustrator, North Carolina State College of Veterinary Medicine.

- The *left parasternal window* and its apical and cranial cardiac views (Figures 19.7 and 19.8).
- The *subcostal or subxiphoid window* and its four- and five-chamber cardiac views and imaging the caudal vena cava (Figure 19.9).

### Right Parasternal Short-axis Views

- Place the probe at the right 4th–5th intercostal space near the costochondral junction or at the site where there is a palpable heart beat (place your hand on the patient's thorax) preempting probe placement.
- To obtain the LV short-axis views, position the probe so that the marker on the probe is pointing towards the elbow (marker toward the elbow) (see Figure 19.3). Take a little time to find the best acoustic window by slightly sliding, sweeping or rocking the probe to get the best view of the heart.
- Because of rib and lung interference, and unlike abdominal ultrasound, the probe position during echocardiography remains relatively static on the chest after finding the best acoustic window.

**Pearl:** Once you have found the best image or "acoustic window" of the heart between the ribs, the probe generally is not moved much other than to rotate and fan to visualize the various cardiac chambers. Image quality may be improved in obese animals by applying firm pressure on the probe.

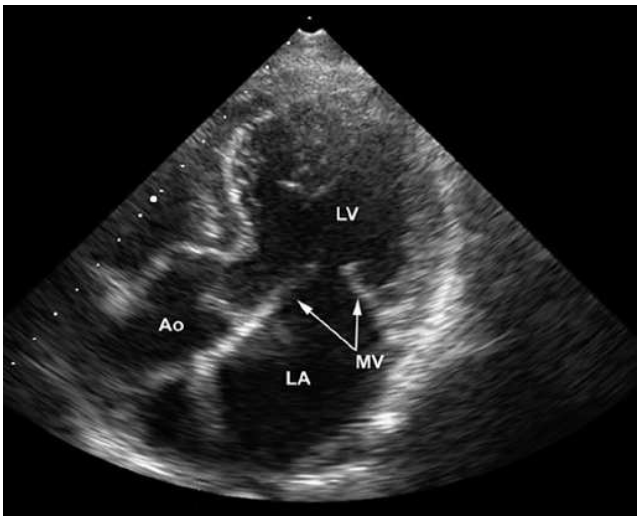


**Figure 19.8.** Normal two-dimensional image of the left ventricular outflow tract from a left apical view. Ao, aorta; LA, left atrium; LV, left ventricle; MV, mitral valve.

- An important first view to obtain will be the LV short-axis view just below the mitral valve, also called the LV "mushroom" view, as it is most helpful for the assessment of contractility and left ventricular chamber dimensions (see Figure 19.3A).
- Rotate and fan the probe until the LV short-axis "mushroom" view of the LV is as round and symmetrical as possible.

**Pearl:** Within this acoustic window, angulate or fan the probe just below and then through and above the mitral valve to get the various views.

- The LV in the "mushroom" view should normally have a circular appearance and the RV should be crescent shaped (see Figure 19.3A). Flattening of the interventricular septum (IVS) suggests right ventricular volume or pressure overload (see Figure 20.9A).
- Now fan upward above the mitral valve to visualize the heart base in short-axis view. In other words, from the LV "mushroom" view, angulate or fan the probe upward towards the cervical spine until the aorta and aortic valves are in view in cross-section.
- Rotate and angulate the probe so that the cross-section of the aorta is round and all three cusps of the aortic valves are visible (see Figure 19.3B), recognized as the "Mercedes-Benz" sign (or the "peace sign" or "Y"). At the heart base, the probe can be angulated to optimize for either the left atrial appendage (looks like a "whale tail") or the pulmonary artery (PA) (see Figure 19.4). The diameter of the PA should normally be the same as the diameter of the aorta in this view.
- When comparing the diameters of the left atrium (LA) and aorta (Ao), the image should be optimized for the left atrial appendage. Normally, the diameters of LA and Ao in this view, whether in 2D B-mode or M-mode, are similar in size (LA:Ao is 1:1) (see Figures 19.3B, 19.4, and 19.5). If the left atrium is greater than 1.3 times the aorta in dogs, then the left atrium is enlarged (see Figure 20.2); and greater than 1.6 in cats (LA:Ao >1.3:1 dogs, >1.6:1 cats) (Rishniw and Erb 2000; Abbott and Maclean 2006).

**Pearl:** In the short-axis view, a left atrial diameter that is twice the aortic diameter is very suggestive of left-sided heart failure in an animal with consistent clinical signs (see abnormal examples in Chapter 20).

In summary, the right parasternal short-axis views at the heart base are helpful in assessing left atrial, pulmonary artery size, and the presence of a heart base mass (e.g., chemodectoma) (see abnormal examples in Chapter 20).

**Pitfalls:** Be cautious not to overinterpret normal fat at the heart base as a mass lesion. Adipose or fat tissue is quite hyperechoic with irregular borders. A heart base mass usually has a smooth border and is *less* echogenic (see Chapter 20).

### Right Parasternal Long-axis Views

- To obtain the LV long-axis views, start with the short-axis (marker to the elbow) view and simply rotate the probe about 90° in a *clockwise* direction so that the marker on the probe is pointing towards the neck and head (see Figure 19.6). Note that the rotation of the probe is similar to the methodology of the TFAST echo views, but the screen orientation is opposite (see Figures 17.25 and 17.26).
- The marker on the probe is pointed towards the neck and head to obtain the sagittal or long-axis views with the probe angulated slightly caudally (see Figure 19.6).
- The right (and left) parasternal long-axis views are most helpful to estimate the size and relative proportions of the right and left heart.

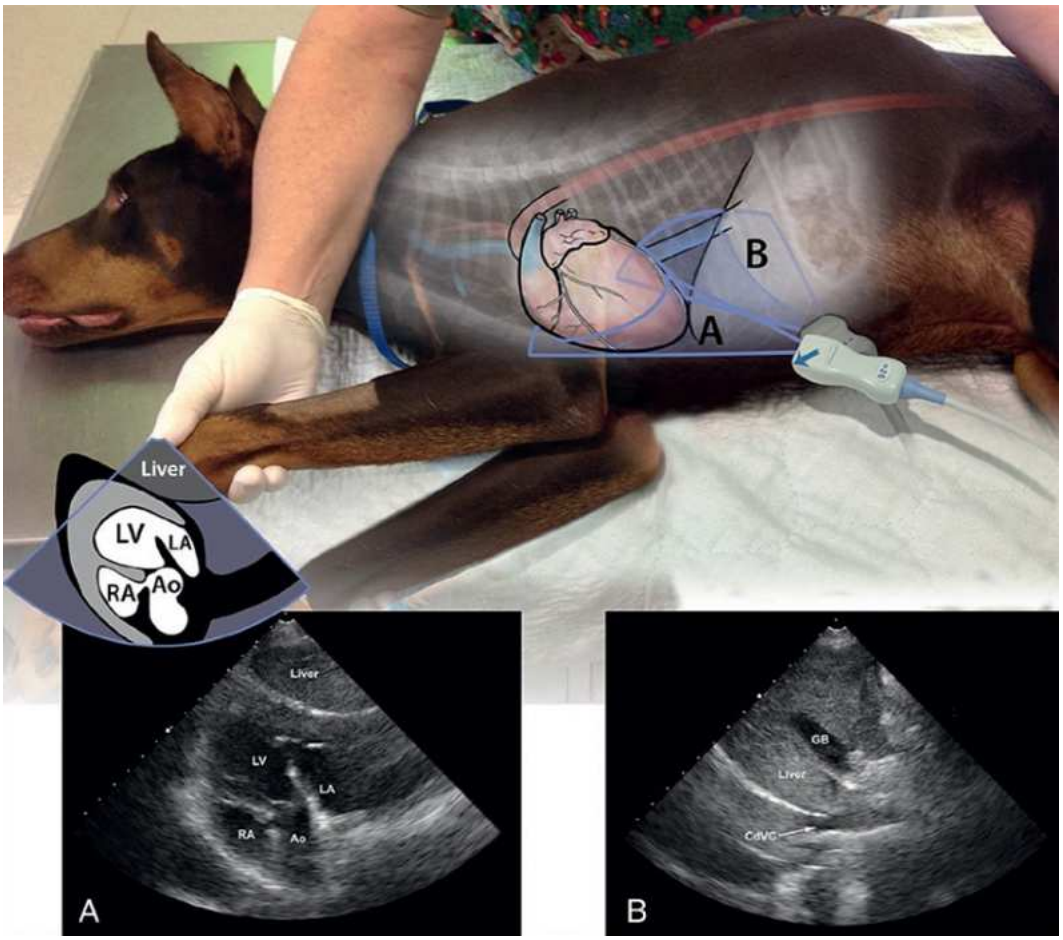


**Figure 19.9.** Dog positioned for subcostal views with the probe positioned just below the xiphoid at midline. Probe marker is towards the elbow and the probe's scanning plane (beam) is directed towards the dog's head. (A) Corresponding schematic drawing for the echocardiogram labeled "A" of a normal subcostal LV outflow tract view. (B) Rotation of the probe towards liver and diaphragm on the dog shown as "B" will result in an ultrasound labeled "B" image of the caudal vena cava and liver in its longitudinal plane as described and taught at the FAST DH view (see also Figures 7.12, 7.13, and 7.14). Note that these images are in the standard orientation of all other imaging, with the head to the left and tail to the right of the screen. Ao, aorta; CdCV, caudal vena cava; GB, gallbladder; LA, left atrium; LV, left ventricle; RA, right atrium. Source: Courtesy of Alice MacGregor Harvey, Medical Illustrator, North Carolina State College of Veterinary Medicine.

### *The Ventricles*

In normalcy, the LV should be 3–4 times bigger than the right ventricle (RV) in the right parasternal four-chamber view. The LV lumen is normally shaped like a bullet. The interventricular septum is generally straight (see Figure 19.6A). The LV should contract uniformly and its papillary muscles appear symmetrical.

- If the RV is the same size as the LV, severe right ventricular enlargement can be diagnosed (see abnormal examples in Chapter 20).

**Pearl:** Remember in the long-axis view the ratio of right to left ventricle is 1:3 (the right ventricle is much smaller since it pumps blood to the lower pressure lung circulation).

**Pitfall:** Be cautious about overinterpreting irregular echogenicities within the right ventricle. These may be normal trabeculae and papillary muscles, either of which can look abnormal when they are of no clinical significance (and are normal).

### *The Atria*

In normalcy, the left and right atria are approximately the same size (1:1) with a neutral (nondeviated) interatrial septum.

### *The Valves*

In normalcy, all cardiac valves should be thin with no evidence of prolapsing or areas of focal thickening. The semilunar valves (mitral and tricuspid) are generally easy and less challenging to evaluate (than the aortic and pulmonary valves) by the inexperienced sonographer.

### *Overall Long-axis Assessment*

A semiquantitative assessment of LV contractility, mitral valvular anatomy, pericardial and pleural effusion can also be obtained in this view and is achievable for the noncardiologist or nonradiologist sonographer.

- With slight angulation towards the animal's head and slight counterclockwise rotation of the probe, one can also image the ascending aorta, aortic valves, left atrium, and left ventricular outflow tract (see Figure 19.6B).
- The LA and Ao in this view should be the same size (LA:Ao should be 1:1).

### *Normal Canine Cardiac Chamber Dimensions*

These vary based on body weight and breed (Table 19.1). In contrast to dogs, normal feline cardiac chamber dimensions do not vary based on body weight (Table 19.2).

- *To obtain cardiac chamber dimensions*, freeze a loop (cine function) and scroll between systole (when the LV lumen is the smallest) and diastole (when the lumen is the biggest) to obtain a fractional shortening (FS%) using 2D B-mode and to measure LV wall thicknesses.
- *Alternatively, M-mode echocardiography can be used*. The M-mode view is an "ice pick" view with the cursor placed in the center of the LV short-axis "mushroom" view or at the level of the mitral valve. Use of M-mode enhances assessment of both LV contractility and its wall thickness (see Figure 19.5A).
- *For LV wall thickness*, both the IVS and LV free wall (LVFW) are measured in diastole with either 2D B-mode or M-mode echocardiography.

**Table 19.1.**
Normal mean echocardiographic values (cm) in dogs.

| BW(kg) | LVEDD | LVESD | IVSD | LVFWD | Ao | LA |
|---|---|---|---|---|---|---|
| 3 | 2.0 | 1.1 | 0.5 | 0.6 | 1.1 | 1.3 |
| 5 | 2.4 | 1.3 | 0.6 | 0.7 | 1.3 | 1.5 |
| 10 | 3.0 | 1.8 | 0.7 | 0.8 | 1.6 | 1.8 |
| 15 | 3.4 | 2.1 | 0.8 | 0.8 | 1.9 | 2.0 |
| 20 | 3.8 | 2.4 | 0.9 | 0.9 | 2.1 | 2.2 |
| 25 | 4.0 | 2.6 | 0.9 | 0.9 | 2.1 | 2.4 |
| 30 | 4.3 | 2.8 | 1.0 | 1.0 | 2.4 | 2.5 |
| 35 | 4.5 | 3.0 | 1.0 | 1.0 | 2.5 | 2.6 |
| 40 | 4.7 | 3.1 | 1.0 | 1.0 | 2.6 | 2.7 |
| 45 | 4.9 | 3.3 | 1.1 | 1.1 | 2.7 | 2.8 |
| 50 | 5.0 | 3.4 | 1.1 | 1.1 | 2.8 | 2.9 |

Ao aortic diameter; BW, body weight; IVSD, interventricular septal thickness in diastole; LA, left atrial diameter; LVEDD, left ventricular end-diastolic diameter; LVESD, left ventricular end-systolic diameter; LVFWD, left ventricular free wall thickness in diastole.
Source: Reproduced with permission from Kittleson MD, Kienle RD. 1998. Small Animal Cardiovascular Medicine. St Louis: Mosby, Table 6-2, p 104.

**Table 19.2.**
Normal ranges of echocardiographic values (cm) in cats.

| Cardiac parameter | Normal range |
|---|---|
| LVEDD | 11.0–17.5 |
| LVESD | 0.40–1.0 |
| IVSD | 0.35–0.55 |
| LVFWD | 0.35–0.55 |
| Ao | 0.7–1.3 |
| LA | 0.9–1.4 |
| LA/Ao (sax 2D) | 0.9–1.4 |
| FS% | 33–66% |

Ao, aortic diameter; FS%, fractional shortening %; IVSD, interventricular septal thickness in diastole; LA, left atrial diameter; LA/Ao (sax 2D), ratio of left atrial and aortic diameter measured in short-axis view in 2D echo; LVEDD, left ventricular end-diastolic diameter; LVESD, left ventricular end-systolic diameter; LVFWD, left ventricular free wall thickness in diastole.

- Normally, the *RV free wall thickness* (RVFW) is about half the thickness of the LVFW.
- *Normal values* are stratified by body weight in dogs (see Table 19.1). In contrast to dogs, size is independent of weight in cats and thus feline IVS and LVFW thickness in diastole should be approximately 3–4 mm. LV wall thickness in diastole ≥6 mm is diagnostic for LV hypertrophy (see Table 19.2 and Figures 20.5 and 20.6).

**Pearl:** Cardiac chamber dimensions and LV systolic function can be influenced by the breed of dog, the patient's volume and hydration status, the presence of a tachy- or bradyarrhythmia, and systemic inflammation.

**Pitfall:** Interpretation of LV systolic function and cardiac size thus should be interpreted in the context of the patient's complete clinical picture, with attention given to these confounding factors (breed, volume and hydration status, arrhythmias, and systemic inflammation).

### *Fractional Shortening Values (FS%)*

Keep in mind that normal FS% can vary by breed and loading (~ volume status) conditions. In general, normal FS% is 28–45% in the dog and 30–50% in the cat. A FS% below 20% is suggestive of severe myocardial systolic failure and a FS% above 55% would be considered hyperdynamic LV function (see Tables 19.1 and 19.2).

$$FS\% = \frac{\left[\text{LV internal dimension (diastole)} - \text{LVID (systole)}\right]}{\text{LVID (diastole)}} \times 100$$

## Left Parasternal Apical and Cranial Views

The left cranial or basilar views allow additional and excellent views of the aorta, pulmonary artery, left atrium, right atrium and ventricle. These views are obtained with the probe positioned at the 3rd–4th intercostal spaces on the left side with analogous positioning to the right parasternal view (see Figure 19.7). Image quality is best when moving the patient to left lateral recumbency so the heart falls against the thoracic wall (moving lung [air] out of the way since ultrasound does not transmit through air). However, depending on the dog's thoracic conformation, left-sided views could be obtained with the dog remaining in right lateral recumbency immediately after obtaining right parasternal views or imaging in sternal recumbency. Not having to reposition the animal saves time.

The main reasons to image from the left side are to further assess the right heart, further assess valvular anatomy and motion, discriminate pleural from pericardial effusions when present, and search for possible masses when indicated.

### *Left Parasternal Apical View*

The left four- and five-chamber apical views are obtained with the probe marker pointing towards the spine and the probe angulated up towards the neck about the fifth intercostal space near the costochondral junction (see Figure 19.7).

- The left four-chamber apical view allows simultaneous visualization of both right and left ventricles and their atria.
- The RV tricuspid and LV mitral valves should be thin with no evidence of prolapsing (see Figure 19.7A).
- The left five-chamber apical view is obtained with a slight angulation toward the head and a slight rotation of the marker towards the head until the aorta comes into view (see Figure 19.8).

### *Left Parasternal Cranial View*

From the left apical view, the probe is moved one or two intercostal spaces cranially with the probe marker towards the spine angulated slightly to optimize the visualization of the right atrium and ventricle (see Figure 19.7B).

- The left cranial view allows for optimal visualization of the right heart, including the right auricle and tricuspid valve.
- This is the best view to visualize a small right auricular mass in a dog with pericardial effusion and cardiac tamponade (see examples in Chapter 21).

## Subxiphoid or Subcostal View

- The transducer (probe) is positioned just caudal to the xiphoid, typically with the patient in right lateral recumbency, similar to the TFAST and AFAST diaphragmatico-hepatic (DH) view (see Figure 19.9).
- The marker is pointed towards the elbow and the probe angulated towards the head almost parallel with the body wall. Adjust the depth and rotate the probe until a four- or five-chamber view is seen (see Figure 19.9A). Note: The view may not be possible in some very large dogs depending on the depth limits of your ultrasound machine.
- From the subcostal cardiac views, angulate the probe and decrease the depth to visualize the liver, caudal vena cava, and hepatic veins (see Figure 19.9B). The liver is assessed primarily for passive congestion (signs of right-sided failure) as evidenced by caudal vena caval and hepatic venous

distension with ascites between the liver lobes (see also Chapters 6–8, 17, and 18) (Nelson et al. 2010).
- Hepatic venous distension is judged subjectively. The ability to see large anechoic vessels, larger branches and then smaller branches, extending peripherally into hepatic tissue is compatible with enlarged hepatic veins. The concurrent findings of ascites and an enlarged and hypoechoic liver add confidence to the diagnosis of right-sided heart failure (see abnormal examples in Chapter 20 and also see also Chapters 6–8, 17, and 18).
- Hepatic veins can be differentiated from portal veins in the liver because they have much less echogenic vessel walls and portal veins have hyperechoic (much brighter) walls (see also Chapters 6–8, 17, and 18). When measured at the same depth, portal veins and hepatic veins should be about the same size.
- Now obtain an image of the caudal vena cava near the diaphragm from this subxiphoid view. The probe is angulated almost perpendicularly towards the spine with slight upward tilting of the tail of the probe as the caudal vena cava is slightly to the right of midline just below the spine (see Figure 19.9B).
- Alternatively, the caudal vena cava can be imaged from the left sublumbar region with the patient in right lateral recumbency. The caudal vena cava is ventral (more right-sided) than the pulsating aorta (see Chapter 26).
- The caudal vena cava can be assessed for respiratory fluctuation in size as an indicator of volume status. Optimize the image by fanning through the caudal vena cava to obtain a sagittal view with the largest diameter. M-mode can be useful to visualize respiratory fluctuations of the caudal vena cava (Figure 19.10). Be careful with translational motion of the probe with respirations.
- Respiratory fluctuations are greater in animals that may be fluid responsive (generally >50–60% fluctuation). No respiratory fluctuations, only static distension, of the caudal vena cava are seen in animals that have high right atrial pressure (Feissel et al. 2004; Beigel et al. 2013).

# Pearls and Pitfalls, The Final Say

- Focused cardiac ultrasound can expedite diagnosis and treatments, especially in patients that are hemodynamically unstable or in respiratory distress.

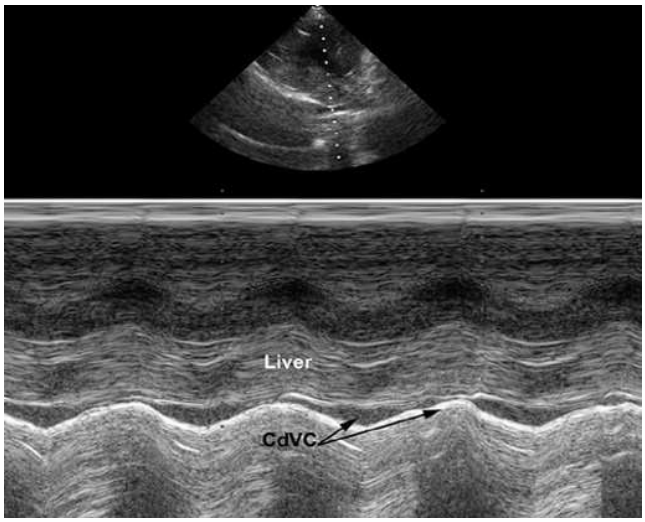


**Figure 19.10.** Subcostal view of fluctuations of caudal vena cava diameter during respiration using M-mode. More caudal vena cava assessment is provided in Chapters 7, 26, and 36. CdVC, caudal vena cava; LV, left ventricle.

- The specific cardiac views and images differ depending on clinical need. The right parasternal and subxiphoid views are easier than the left-sided views to acquire proficiency.
- While canine normal values for cardiac chambers are listed based on body weight, these values can vary based on dog breed, body conformation, volume status, arrhythmias, and systemic diseases.
- With training, one should be able to identify severe left atrial enlargement, decreased systolic function, right ventricular enlargement, pericardial effusion, and a dilated plethoric caudal vena cava.

# Quick Reference of Normals and Rules of Thumb

- In normalcy, the LV should be 3–4 times larger than the RV in the right parasternal four-chamber view (3:1).
- If the RV is the same size as the LV, then severe right ventricular enlargement can be diagnosed (and its various rule-outs considered).
- In normalcy, the left and right atria are approximately the same size or 1:1 with a neutral (nondeviated) interatrial septum.
- In normalcy, the LA and Ao in the short-axis right parasternal view should be nearly the same size.
- If the LA is greater than 1.3 times the aorta in dogs, then the LA is enlarged; greater than 1.6 times in cats (LA:Ao >1.3:1 dogs, >1.6:1 cats).

# References


Abbott JA, MacLean HN. 2006. Two-dimensional echocardiographic assessment of the feline left atrium. *J Vet Intern Med* 20:111–119.

Arntfield RT, Millington SJ. 2012. Point of care cardiac ultrasound applications in the emergency department and intensive care unit – a review. *Curr Cardiol Rev* 8:98–108.

Beigel R, Cercek B, Luo H, et al. 2013. Noninvasive evaluation of right atrial pressure. *J Am Soc Echocardiograph* 26:1033–1042.

Beaulieu Y. 2007. Bedside echocardiography in the assessment of the critically ill. *Crit Care Med* 35(5S):S235–249.

Cambournac M, Goy-Thollot I, Violé A, et al. 2018. Sonographic assessment of volaemia: development and validation of a new method in dogs. *J Small Anim Pract* 59:174–182.

Feissel M, Michard F, Faller JP, et al. 2004. The respiratory variation in inferior vena cava diameter as a guide to fluid therapy. *Intens Care Med* 30:1834–1837.

Kobal SL, Trento L, Baharami S, et al. 2005. Comparison of effectiveness of hand-carried ultrasound to bedside cardiovascular physical examination. *Am J Cardiol* 96:1002–1006.

Kwak J, Yoon H, Kim J et al. 2018. Ultrasonographic measurement of caudal vena cava to aortic ratios for determination of volume depletion in normal beagle dogs. *Vet Radiol Ultrasound* 59:203–211.

Labovitz AJ, Noble V, Beirig M, et al. 2010. Focused cardiac ultrasound in the emergent setting: a consensus statement of the American Society of Echocardiography and American College of Emergency Physicians. *J Am Soc Echocardiograph* 23:1225–1230.

Marshall KA, Thomovsky EJ, Brooks AC, et al. 2018. Ultrasound measurements of the caudal vena cava before and after blood donation in 9 greyhound dogs. *Can Vet J* 59:973–980.

McMurray J, Boysen S, Chalhoub S. 2016. Focused assessment with sonography in nontraumatized dogs and cats in the emergency and critical care setting. *J Vet Emerg Crit Care* 26:64–73.

Moore CL, Copel JA. 2011. Point of care ultrasonography. *N Engl J Med* 364:749–757.

Nelson NC, Drost WT, Lerche P, et al. 2010. Noninvasive estimation of central venous pressure in anesthetized dogs by measurement of hepatic venous blood flow velocity and abdominal venous diameter. *Vet Radiol Ultrasound* 51:313–323.

Reissig A, Copetti R, Kroegel C. 2011. Current role of emergency ultrasound of the chest. *Crit Care Med* 39(5):1–8.

Rishniw M, Erb HN. 2000. Evaluation of four 2-dimensional echocardiographic methods of assessing left atrial size in dogs. *J Vet Intern Med* 14:429–435.

Rush JE, Freeman LM, Fenollasa NK, et al. 2002. Population and survival characteristics of cats with hypertrophic cardiomyopathy: 260 cases (1990–1999). *J Am Vet Med Assoc* 220:202–207.

Schober KE, Wetli E, Drost WT. 2014. Radiographic and echocardiographic assessment of left atrial size in 100 cats with acute left-sided congestive heart failure. *Vet Radiol Ultrasound* 55:359–367.

Spencer KT, Kimura BJ, Korcarz CE, et al. 2013. Focused cardiac ultrasound: recommendations from the American Society of Echocardiography. *J Am Soc Echocardiograph* 26:567–581.

Tse Y, Bulmer B, Cunningham S, et al. 2012. Evaluation of a training course in focused echocardiography for the non cardiology house officer. *J Vet Emerg Crit Care* 22:S2–10.

Ward JL, Lisciandro GR, Ware WA, et al. 2018. Evaluation of point-of-care thoracic ultrasound and NT-proBNP for the diagnosis of congestive heart failure in cats with respiratory distress. *J Vet Intern Med* 32:1530–1540.

CHAPTER TWENTY

# POCUS: Heart - Abnormalities of Valves, Myocardium, and Great Vessels

Teresa DeFrancesco

## Introduction

Focused cardiac ultrasound (FCU) can provide vital and noninvasive detailed information about cardiac structure and function, beyond the capabilities of the physical examination and thoracic radiographs. This valuable information can aid in the rapid diagnosis and improved management of suspected heart failure, pericardial and pleural effusion or other hemodynamically unstable patients. Even with limited experience, significant cardiac abnormalities such as marked chamber enlargements, pericardial effusion, and myocardial failure can be determined. The integration of other point-of-care information of the lung, pleural and peritoneal space will provide valuable corroborative evidence of left-sided or right-sided congestive heart failure and justify loop diuretic usage (see Chapters 22, 23, and 36).

### *What Focused Cardiac Ultrasound Abnormalities Can Do*

- Identify severely enlarged left atrium, providing useful and timely corroborative evidence for left-sided heart failure in a dog or cat with respiratory signs.
- Identify severely enlarged right atrium and ventricle, providing useful evidence for right heart failure in a dog with ascites or severe pulmonary hypertension in a dog with respiratory distress.
- Provide a qualitative or quantitive assessment of left ventricular chamber size, systolic function, and wall thickness to aid in the diagnosis of cardiomyopathies.
- Detect obviously thickened or abnormal cardiac valvular anatomy, providing supportive evidence for degenerative valvular heart disease or infectious endocarditis.
- Detect heartworms in the right heart in dogs with caval syndrome or in cats with respiratory distress.
- Detect an obvious cardiac mass such as a heart base mass or right atrial hemangiosarcoma in a dog with respiratory or hemodynamic compromise. Assess the size and degree of respiratory variation of the caudal vena cava to determine if a patient is fluid tolerant or intolerant.

### *What Focused Cardiac Ultrasound Abnormalities Cannot Do*

- Cannot be used as a stand-alone diagnostic test for the definitive diagnosis of heart failure. Heart failure is a clinical diagnosis incorporating the FCU with the history, physical exam, and other imaging and diagnostic tests.

*Point-of-Care Ultrasound Techniques for the Small Animal Practitioner*, Second Edition. Edited by Gregory R. Lisciandro.
© 2021 John Wiley & Sons, Inc. Published 2021 by John Wiley & Sons, Inc.
Companion website: www.wiley.com/go/lisciandro/ultrasound2

- Cannot replace a complete and diagnostic echocardiography by a veterinary cardiologist or other specialist. Ultrasound is a user-dependent modality and sonographers should know the limitations of their ultrasound unit and skill level.
- Cannot teach how to utilize more advanced echocardiographic features of heart assessment.

Follow-up echocardiography by a boarded specialist after initial diagnosis by FCU will provide corroborative evidence of the initial diagnosis or feedback of an initial incorrect diagnosis.

### Indications

- Respiratory distress, uncharacterized tachypnea or other respiratory signs.
- Body cavity effusions (pleural, pericardial or peritoneal effusion) suspected or confirmed based on physical exam or other imaging.
- Suspect right-sided or left-side heart failure based on physical exam or imaging.
- Uncharacterized syncope, collapse, generalized weakness or hemodynamic instability.
- Uncharacterized tachycardia (rapid heart rate) or significant cardiac arrhythmia.
- Feline aortic thromboembolism (ATE).
- Suspect heartworm caval syndrome in a dog.

### Objectives

- Identify a severely enlarged left atrium (LA) in dogs and cats with suspected left-sided heart failure and integrate the FCU findings with the lung and thoracic ultrasound exams (see Chapters 17, 18, 22, 23, 26, 36, and 37).
- Identify severe right heart enlargement, caudal vena cava, and hepatic venous distension suggestive of right heart failure or possibly secondary to chronic pulmonary hypertension/cor pulmonale in a dog with respiratory distress.
- Identify severely diminished left ventricular (LV) systolic dysfunction.
- Know the FCU abnormalities of the common acquired heart diseases in dogs and cats – specifically, degenerative valvular heart disease and dilated cardiomyopathy in dogs and hypertrophic cardiomyopathy in cats.
- Know the common locations and FCU appearances of the common etiologies of cardiac neoplasia.

# Valvular Heart Diseases

## Degenerative Mitral Valve Disease

Mitral valve disease (MVD) is the most common cause of heart disease in dogs. It is estimated that MVD accounts for 75–85% of all heart disease in dogs, so it is the most common cause of canine heart failure (Fox 2012). MVD is most prevalent in older, small-breed dogs but can also affect large-breed dogs to a lesser degree. Commonly affected breeds include the cavalier king charles spaniel, dachshund, chihuahua, toy poodle, beagle, cocker spaniel, maltese, pomeranian, shetland sheepdog, miniature schnauzer, whippet, and many small mixed breeds (Borgarelli and Buchanan 2012). Cats rarely get degenerative valvular heart disease. MVD causes progressive degeneration and thickening of the mitral valve, leading to backwards blood flow from the LV to the LA due to mitral valve insufficiency. Over time, chronic mitral valvular insufficiency may lead to left-sided congestive heart failure. Not uncommonly, MVD can manifest with acute fulminant heart failure as a result of a chordae tendineae rupture or, less commonly, as a result of a LA tear with pericardial effusion (see Figures 18.21, 18.32B, and 21.5). Dogs with a ruptured LA typically present in severe respiratory distress and have a history of heart murmur and recent collapse episode (Reineke et al. 2008; Nakamura et al. 2014).

#### Common FCU findings in MVD

- Thickened mitral valve (MV) leaflets with possible prolapsing of an MV leaflet, usually the anterior mitral valve leaflet (Figure 20.1).

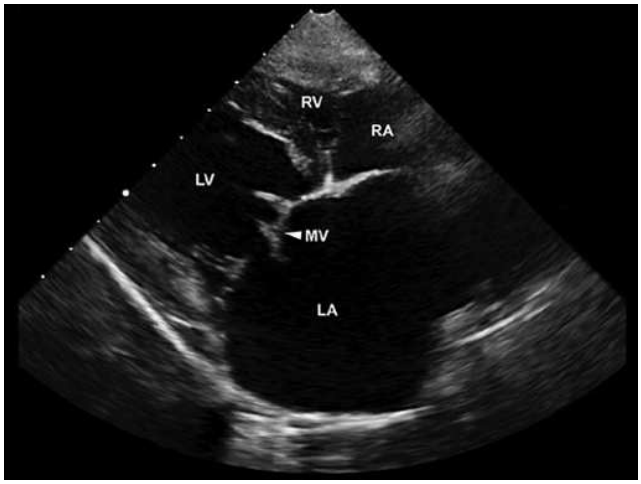


**Figure 20.1.** Right parasternal long-axis view of severe left atrial enlargement in a dog with mitral valvular disease. Arrowhead highlights prolapsing of the anterior mitral valve leaflet.

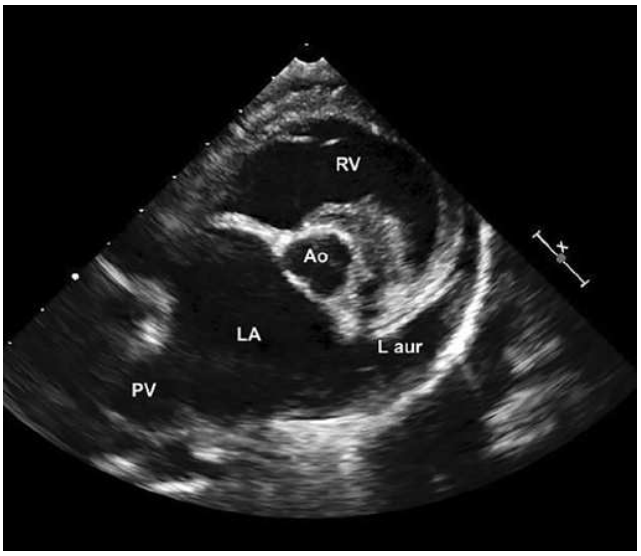


**Figure 20.2.** Right parasternal short-axis view of severe left atrial enlargement in a dog with mitral valvular disease. The left atrial (LA) diameter is more than twice the diameter of the aorta (Ao), LA:Ao ratio is >2:1. Ao, aorta; LA, left atrium; PV, pulmonary vein; RV, right ventricle.

- In left-sided congestive heart failure, severe LA enlargement is present typically with a LA:Ao ratio of >2:1. Left ventricular enlargement is also present (Figure 20.2).
- In early left-sided volume overload, the LV maintains its systolic function and may appear to be *hyperdynamic* (higher than normal FS%). In later, end-stage MV disease, LV systolic myocardial function becomes diminished.
- Concurrent degeneration and thickening of the tricuspid valve is common.

**Pitfall:** Many older small-breed dogs with respiratory disease have concurrent MV disease. The size of the LA may be used to determine if respiratory clinical signs are due to heart disease or respiratory disease as well as the presence of cardiogenic pulmonary edema or pneumonia represented by regional and pattern-based distribution and numbers of B-lines on lung ultrasound (see Chapters 22 and 23).

**Pearl:** The LA size in a dog with acute chordae tendineae rupture may not be severely enlarged. However, these dogs typically have severe cardiogenic pulmonary edema and clinical signs. Use of the Vet BLUE B-line scoring system can help estimate extravascular lung water and guide loop diuretic usage (Lisciandro et al. 2014, 2016, 2017; Gargani et al. 2015; Ward et al. 2017; Vezzosi et al. 2017; Ward et al. 2018) (see Chapters 22 and 23).

**Pearl:** In a dog with severe cardiogenic pulmonary edema due to MVD, B-lines are usually present in all lung fields (Lisciandro et al. 2014; Ward et al. 2017).

**Pearl:** Pericardial effusion seen in a dog with congestive heart failure and cardiogenic shock may be a result of LA rupture as a complication of severe MV disease and LA dilation (see Figures 18.21, 18.32B, and 21.5) (Reineke et al. 2008; Nakamura et al. 2014).

## *Infectious Endocarditis*

Infectious endocarditis (IE) is an uncommon disease in dogs and is rarely seen in cats. Despite its low prevalence, IE is a disease in which FCU can be extremely helpful in expediting a diagnosis. The diagnosis is difficult without the use of FCU or an echocardiogram because of its vague clinical signs and nonspecific clinical presentations. Animals usually succumb to acute congestive heart failure because of extensive valvular damage and insufficiency. They can also present with clinical signs related to other disease complications such as polyarthritis, glomerulonephritis, thromboembolism, and lethal arrhythmias (MacDonald et al. 2010).

Focused cardiac ultrasound is extremely helpful in diagnosing IE through detection of vegetative lesions on the valvular surfaces. The most commonly affected valves in the dog and cat are the aortic and mitral valves (MacDonald et al. 2010). In fact, the finding of an irregular echogenic thickening or mobile mass on the aortic valve is highly suggestive of IE in a clinically ill dog or cat. Unfortunately, clearly distinguishing DMV disease (endocardiosis) from MV endocarditis can be difficult based solely on the ultrasound images. However, the finding of an independently oscillating focal lesion on the MV can be very suggestive of IE, especially in a sick dog. It is important to emphasize that the FCU findings need to be interpreted in light of the clinical presentation and progression of clinical signs.

### Common FCE findings in IE

- Vegetative lesion (irregular thickened and often mobile mass) on the "blood flow" side of the aortic and/or mitral valve (Figure 20.3).
- Left atrial and ventricular volume overload are common due to valvular insufficiencies.

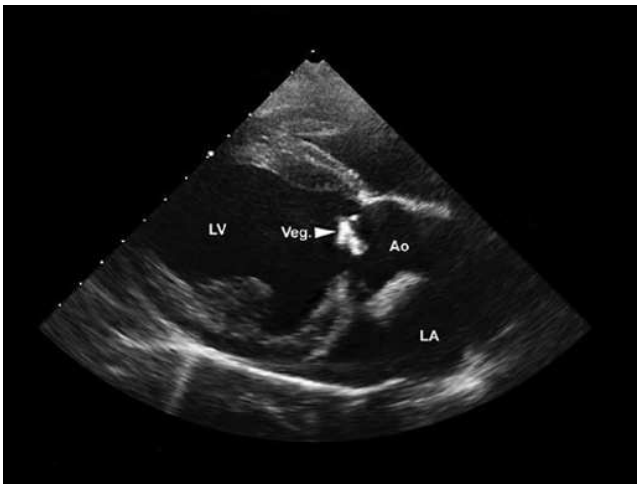


**Figure 20.3.** Right parasternal long-axis view of the left ventricular outflow tract and aorta in a dog with infectious endocarditis. The vegetative lesion is seen on the aortic valve (arrowhead). Ao, aorta; LA, left atrium; LV, left ventricle; Veg, vegetative lesion.

**Pearl:** Predisposing factors such as chronic infections or bacteremia, congenital heart disease, and immunosuppressive therapy are common in dogs with IE.

**Pitfall:** Infectious endocarditis is a clinical diagnosis usually in an extremely ill dog or cat. If IE is suspected based on FCU, a complete detailed echocardiogram and systemic evaluation is advised (see Chapter 36).

# Myocardial Diseases

## *Dilated Cardiomyopathy and Other Causes of Left Ventricular Myocardial Failure*

Left ventricular performance by FCU should be assessed in any hemodynamically unstable patient. Global assessment of LV contractility can be a qualitative "eyeball" assessment and/or a quantitative assessment by fractional shortening (FS%) or ejection fraction. The value of the "eyeball" assessment of LV function should not be underestimated. An experienced and trained clinician can make real-time assessments of LV wall kinetics and chamber dimensions to make an immediate diagnosis. The simplest quantitative approach is to measure the LV end-diastolic dimension and the LV end-systolic dimension for determination of the fractional shortening. This can be done in 2-D or via M-mode echo (see Figures 19.5, 36.6, and 37.5). Normal FS% is 28–45% in the dog and 30–50% in the cat. A FS% below 20% is suggestive of severe myocardial systolic failure and a FS% above 55% would be considered hyperdynamic LV function.

Left ventricular systolic myocardial failure can be caused by a primary myocardial disease or could be the end-result of various different insults or diseases. The most common cause of LV myocardial failure in veterinary medicine is breed-associated dilated cardiomyopathy (DCM) in Doberman pinschers, Great Danes, and boxers with arrhythmogenic cardiomyopathy with DCM phenotype (Stern and Ueda 2019). However, many other causes of LV myocardial failure are possible such as nutritional cardiomyopathies (carnitine, taurine, grain-free diet), doxorubicin cardiomyopathy, tachycardia-induced cardiomyopathy, sepsis-induced myocardial dysfunction, cardiomyopathy of volume overload in dogs with end-stage MV disease, and end-stage hypertrophic cardiomyopathy (HCM), referred to as "burn-out" HCM of cats (Meurs 2010).

## *Dilated Cardiomyopathy*

Dilated cardiomyopathy (DCM) is a common cause of heart disease and heart failure in certain large- and giant-breed dogs (Figure 20.4; see also Figures 18.32B and 37.5). DCM is uncommonly diagnosed in cats. It causes myocardial failure and cardiac dilation. DCM is often breed associated and is usually identified when a dog is symptomatic with congestive heart failure. Commonly affected breeds include Doberman pinschers, Great Danes, boxers, Irish wolfhounds, Labradors, and golden retrievers. Dogs with DCM may be young, middle-aged or older and males are more commonly affected than females. Cardiac arrhythmias are often associated with DCM (Martin et al. 2009).

### Common FCU Findings in DCM

- Dilated LV with spherical appearance in the long-axis views with a markedly hypodynamic LV systolic function (poor contractility) (see Figure 20.4A). The internal dimension of the normal canine LV in diastole should not exceed 5 cm in dogs less than 120 lb.
- Fractional shortening is typically <20% (normal FS% is 28–45% in dogs, 30–50% in cats) (see Figure 20.4B).
- Dilated LA and increased LA:Ao ratio but not increased as much as in MVD.

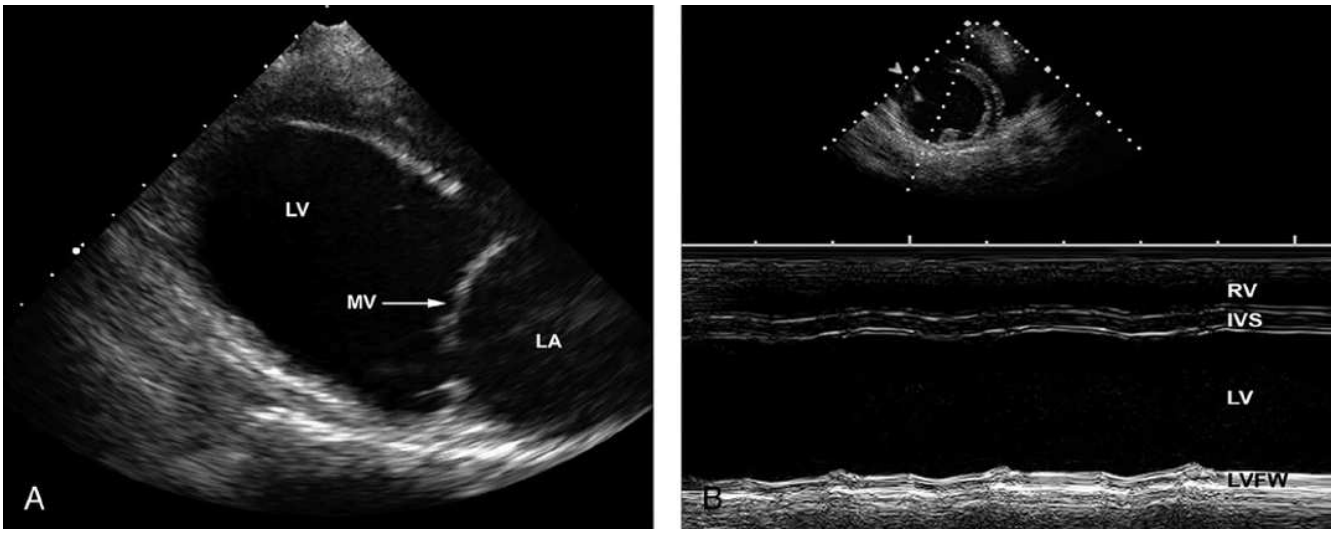


**Figure 20.4.** Canine dilated cardiomyopathy. (A) Right parasternal long-axis view of left atrial and left ventricular dilation in a dog with DCM. (B) Severely hypodynamic left ventricular wall motion (low fractional shortening [FS%]) is seen in an M-mode view of the left ventricle in a dog with DCM. LA, left atrium; LV, left ventricle; MV, mitral valve; RA, right atrium; RV, right ventricle.

- Not uncommonly, all four cardiac chambers may be dilated, especially if biventricular heart failure is present.
- Normal MV anatomy with reduced MV motion.

**Pearl:** Tachyarrhythmias and sepsis syndrome may also markedly diminish myocardial function, causing misinterpretation of echocardiographic findings. Reevaluation of myocardial function once arrhythmias and sepsis have resolved is advised for best patient assessment.

**Pitfall:** Be careful not to overinterpret what may appear by the "eyeball method" to be subnormal LV systolic function in a large- or giant-breed dog. These dogs have LV systolic function parameters that are lower than a small-breed dog.

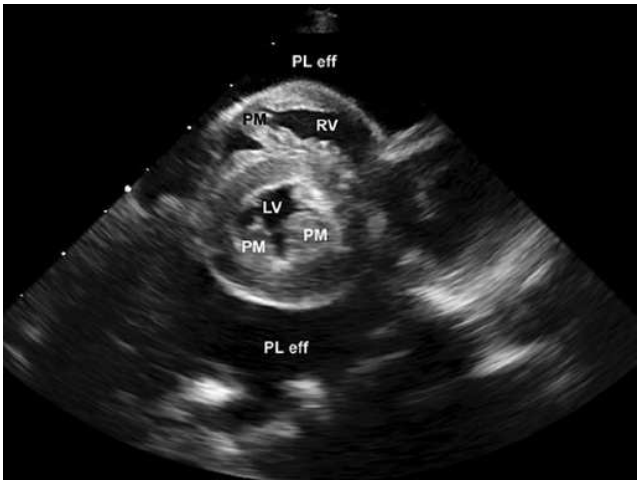


**Figure 20.5.** Feline hypertrophic cardiomyopathy. Right parasternal short-axis view of left ventricular hypertrophy and pleural effusion in a cat with HCM and congestive heart failure. LV, left ventricle; PL eff, pleural effusion; PM, papillary muscles; RV, right ventricle.

## *Hypertrophic Cardiomyopathy*

Hypertrophic cardiomyopathy is the most common cause of heart disease and heart failure in cats (Rush et al. 2002; Hall et al. 2007; Payne et al. 2015) but is extremely rare in the dog. Congestive heart failure is a common cause of respiratory distress in the cat. HCM is defined as LV hypertrophy in the absence of diseases that can lead to hypertrophy. A wall thickness of either the interventricular septum (IVS) or LV free wall of >6 mm in a cat is suggestive of HCM (Payne et al. 2013) (Figure 20.5). Other causes of LV hypertrophy that mimic HCM include systemic hypertension, hyperthyroidism, congenital aortic stenosis, acromegaly, infiltrative disease and, importantly, "pseudohypertrophy" associated with volume contraction and dehydration (Luis-Fuentes and Wilkie 2017). The "eyeball method" of FCU is more challenging in the feline species because they have higher heart rates than dogs. Thus, freezing and rolling the cine ball to move through captured frames improves FCU assessment and should become habitual for the feline FCU sonographer.

Hypertrophic cardiomyopathy generally affects young, middle-aged, and older cats and more commonly affects males than females. Although the most commonly affected cat is the mixed-breed cat, certain breeds, such as the Maine coon, ragdoll, Bengal, British shorthair, Sphinx, and Persian breeds, have a high prevalence of HCM (Luis-Fuentes and Wilkie 2017).

Hypertrophic cardiomyopathy typically causes heart failure due to LV diastolic dysfunction causing elevated filling pressures with normal, subnormal or even supranormal LV systolic function parameters. Cats in congestive heart failure secondary to HCM will usually have an enlarged left atrium (Schober et al. 2014; Ward et al. 2018).

In cats with respiratory distress, lung ultrasound (Vet BLUE) provides an option to rapidly rule out left-sided congestive heart failure in the absence of B-lines even if there is evidence of some cardiac abnormalities. Other differentials such as feline asthma, neoplasia or upper airway obstructions are other common conditions causing respiratory distress (Lisciandro et al. 2016; Ward et al. 2017, 2018). Loop diuretics are not indicated in the absence of B-lines and the FCU or complete echocardiogram may wait until the patient is more stable.

### Common FCU Findings in HCM

- Concentric LV hypertrophy, including the LV papillary muscles. The LV hypertrophy can be either symmetrical or segmental (Figure 20.6A).
- A LV wall in diastole measuring greater than 6 mm (>6 mm) is generally considered hypertrophic. In some cats with chronic HCM, LV walls may be high normal thickness because of a phenomenon called LV remodeling (Luis-Fuentes and Wilkie 2017).
- In a cat with suspect heart failure, the LA is severely dilated with typically a LA:Ao ratio >2:1 (see Figure 20.6B).
- Variable amounts of pleural effusion are often a unique manifestation of congestive heart failure (HF) in cats (see Figure 20.5).
- Small amount of pericardial effusion (typically <5 mm) without evidence of cardiac tamponade may be seen in cats with congestive HF as a consequence of their HF and is commonly not due to pericardial disease. In fact, the most common cause of pericardial effusion in cats is heart failure (see Figure 20.6A) (Hall et al. 2007; Ward et al. 2018).
- Typically, HCM cats have normal to hyperdynamic (high FS%) LV function. However, in end-stage or remodeled HCM, LV function can be diminished (lower FS%) (normal FS% in cats is 30–50%) (Payne et al. 2015).
- Possible LA thrombus, most commonly within the left auricle, may be present. The thrombus can be adhered to the atrial wall or freely mobile (see Figure 20.6C). "Smoke" or a swirling appearance of blood in the LA can be seen in cats with severe LA enlargement and stagnant blood flow. This finding, known as spontaneous echo contrast, may be seen in cats that have suffered an aortic thromboembolism (ATE) or are at high risk for thromboembolism (Schober and Maerz 2006).

**Pearl:** Hypertrophic cardiomyopathy is diagnosed when LV hypertrophy is present in the absence of hyperthyroidism, hypertension, severe hypovolemia, including from dehydration, and aortic stenosis.

**Pitfall:** Left atrial thrombus has clear edges and should be confirmed in multiple views. The edges of a thrombus should not be hazy. Be careful not to overinterpret a side-lobe artifact in the LA for a thrombus (see Chapters 3 and 5, and Figures 3.7 and 15.17).

**Pitfall:** Extreme hypovolemia causing "pseudohypertrophy of the left ventricle" can be confused with HCM in the cat. The LA size should be enlarged in a symptomatic HCM cat, while LA size will be normal to small in hypovolemia and LV pseudohypertrophy. Moreover, the evaluation of lung using Vet BLUE is another strategy to rule out left-sided congestive heart failure in the critical unstable cat (Lisciandro et al. 2016, 2017; Ward et al. 2017, 2018).

## Cardiac Neoplasia

Primary and metastatic tumors of the heart are relatively uncommon. Despite the lower prevalence, FCU can be quite helpful in expediting a diagnosis. Cardiac tumors are more common in dogs than cats. Dogs usually present for clinical signs related to obstruction of blood flow in or out of the heart, compression of the airways or cardiac tamponade and pericardial effusion. Common owner complaints include respiratory signs such as coughing, retching, tachypnea, or dyspnea. They also present for collapse, weakness or abdominal distension. Occasionally, a dog with a cardiac neoplasia, usually a heart base tumor, will be asymptomatic. The clinically silent cardiac tumor usually is identified when an echocardiography or thoracic radiography is performed for another problem, such as a heart murmur (Guglielmini et al. 2016).

When a mass lesion is identified in the heart or at the heart base, the etiology of the mass is typically deduced

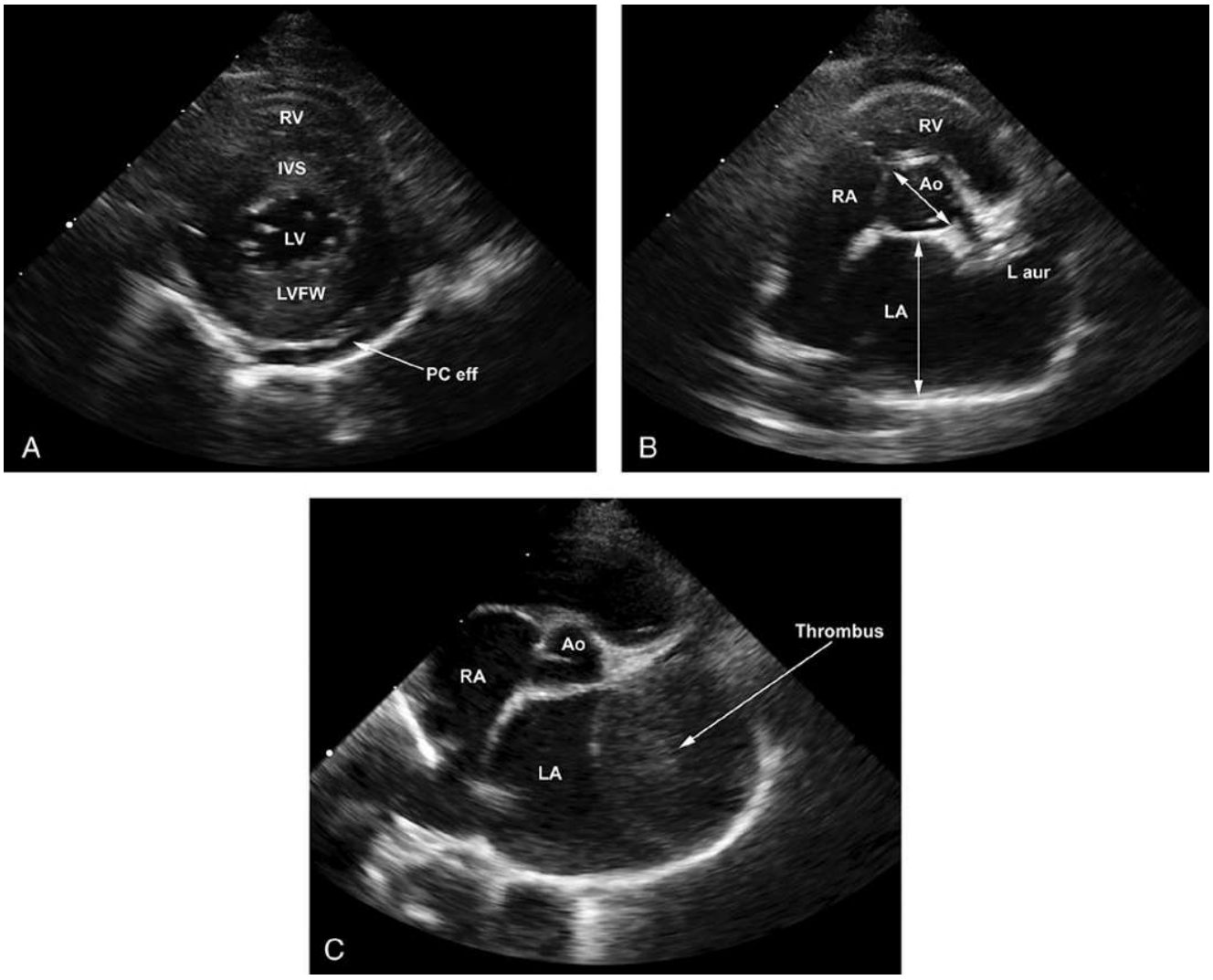


**Figure 20.6.** Feline hypertrophic cardiomyopathy and its complications. Right parasternal short-axis views of (A) left ventricular hypertrophy in a cat with HCM and heart failure. A small amount of pericardial effusion is present. (B) Severe left atrial enlargement in a cat with HCM and congestive heart failure. (C) Large left atrial thrombus in a cat with aortic thromboembolism and congestive heart failure due to HCM. Using the freeze function and rolling the cine ball through captured frames overcomes the higher heart rate and difficulties in accurately "eyeballing" echocardiography views of cats. Ao, aorta; IVS, interventricular septum; LA, left atrium; L aur, left auricle; LV, left ventricle; LVFW, left ventricular free wall; PC eff, pericardial effusion; RA, right atrium; RV, right ventricle.

by its location, shape, and echogenicity, and the clinical context (Rajagopalan et al. 2013). The most common cause of a cardiac neoplasia is hemangiosarcoma, typically located in the right atrium or right atrial appendage (Waters et al. 1988; Boston et al. 2011). Dogs with a right atrial hemangiosarcoma typically present for signs associated with cardiac tamponade and pericardial effusion (MacDonald et al. 2009). The second most common cardiac tumor is an aortic body tumor (also called chemodectoma) at the heart base. Dogs with chemodectomas can also present with pericardial effusion and cardiac tamponade. Alternatively, these tumors can get quite large and cause airway compression or obstruction to blood flow. Cardiac tumors can also be located in the pericardium, left or right ventricle and on cardiac valves. Other less common types of cardiac neoplasia include lymphoma, mesothelioma, leiomysarcoma, fibrosarcoma, chondrosarcoma, myxosarcoma, hamartoma, thyroid adenoma, and melanoma (Treggiari et al. 2017). Other less likely nonneoplastic causes of a cardiac mass in the dog are a fungal granuloma or an intracardiac thrombus (MacDonald et al. 2009; Treggiari et al. 2017).

German shepherd dogs, golden and Labrador retrievers are at increased risk for cardiac hemangiosarcoma while brachycephalic dog breeds (boxers, bulldogs, and Boston terriers) are at increased risk for aortic body tumors (MacDonald et al. 2009; Treggiari et al. 2017). With a high metastatic rate for some cardiac tumors, performing thoracic radiography and the use of Global FAST including Vet BLUE to stage the patient should be considered (MacDonald et al. 2009) (see Chapter 36).

## Common FCU Findings of Cardiac Neoplasia

- Cardiac hemangiosarcoma is often an irregular mass of varying size and mixed echogenicity located in the wall of the right atrium or right atrial appendage. Concurrent pericardial effusion and cardiac tamponade is common and less commonly a splenic mass (Figure 20.7) (Waters et al. 1988; Boston et al. 2011).
- Clinically significant heart base chemodectomas are usually large masses of homogeneous echogenicity with smooth borders located adjacent to the ascending aorta. Concurrent pericardial effusion is also common (Figure 20.8) (Rajagopalan et al. 2013).
- Mesothelioma usually does not cause a discrete mass and is often associated with a thickened pericardium and pericardial effusion (MacDonald et al. 2009).

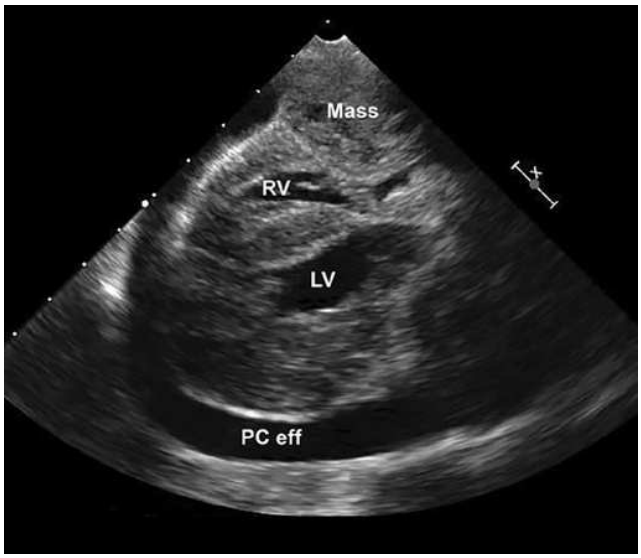


**Figure 20.7.** Large right atrial tumor and pericardial effusion in a dog. Right parasternal long-axis view of large mixed echogenic mass in the wall of the right atrium. Based on location and echogenicity, the mass is most likely a hemangiosarcoma. Staging with the Global FAST approach is warranted (see Chapter 36 and Figure 36.23). LA, left atrium; LV, left ventricle; PC eff, pericardial effusion; RA, right atrium; RV, right ventricle.

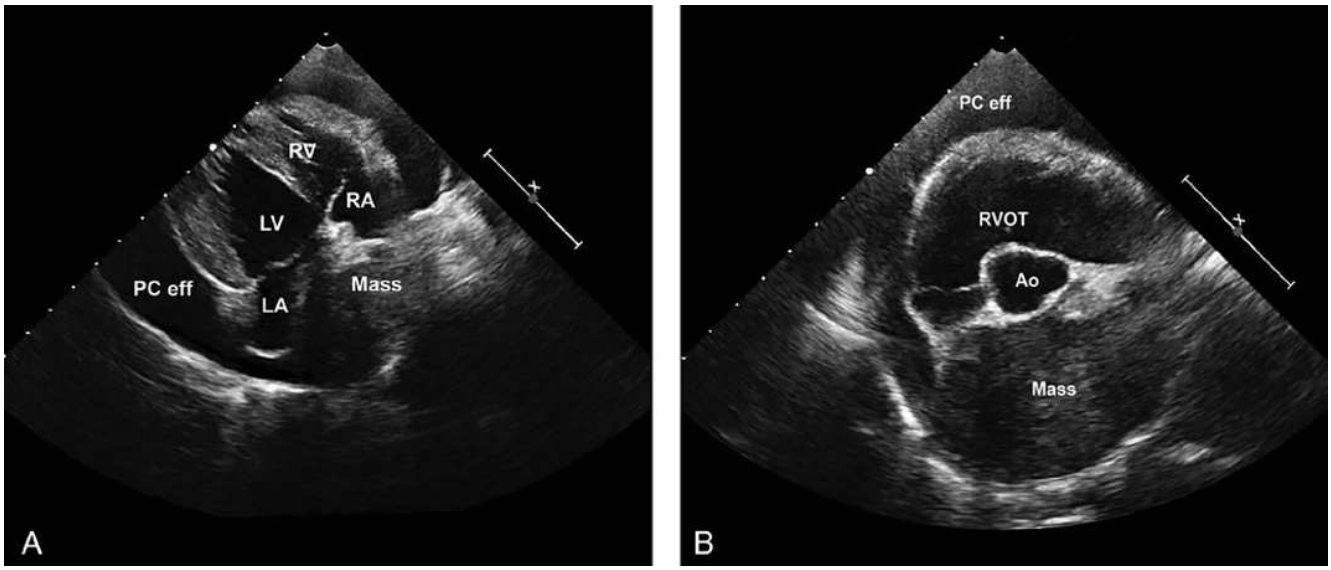


**Figure 20.8.** Large heart base tumor, likely a chemodectoma, in a dog with pericardial effusion. (A) Right parasternal long-axis view of a large oval mass with homogeneous echogenicity seen deforming the atria. (B) Right parasternal short-axis view of the mass adjacent to the aorta and dorsal to the left atrium. Staging with the Global FAST approach is warranted (see Chapter 36 and Figure 36.20). Ao, aorta; LA, left atrium; LV, left ventricle; PC eff, pericardial effusion; RA, right atrium; RV, right ventricle; RVOT, right ventricular outflow tract.

- Cardiac lymphoma typically causes an infiltrative hypertrophy of the left or right ventricular myocardium and when associated with pericardial effusion can be diagnosed on fluid analysis and cytology (MacGregor et al. 2005).

**Pearl:** Most masses at the heart base are chemodectomas, tumors of the chemoreceptors in the aorta. Other possible causes of a heart base mass include ectopic thyroid gland tissue, hemangiosarcomas, and mesothelioma (Treggiari et al. 2017).

**Pearl:** A right atrial hemangiosarcoma is typically best seen from the left parasternal view optimized for the right atrium and auricle. Make sure to fan through the entire mass to estimate the mass size and extent of involvement. If a mass is very large, it can be seen in any view and may compress the atria or great vessels, impinging the inflow and/or outflow of blood (see Figure 18.32F).

**Pitfall:** In an extremely overweight dog or cat, be careful not to overinterpret adipose tissue at the heart base as a cardiac mass.

# Abnormalities of Great Vessels

## *Pulmonary Hypertension*

Pulmonary hypertension (PHT) is defined as a systolic pressure in the pulmonary artery of greater than 30 mmHg or greater than ¼ of systemic blood pressure (Kellihan and Stepien 2010). PHT is a complex syndrome that can be caused by many diseases and is often idiopathic. PHT can be categorized into precapillary or postcapillary based on the disease causing the elevated pulmonary arterial pressure (PAP). Causes of precapillary PHT include heartworm disease, pulmonary embolus, chronic lung disease, primary or idiopathic PHT. PHT can also be due to postcapillary etiologies relating to increased left heart filling pressures, or pulmonary venoocclusive disease (Kellihan and Stepien 2010).

Common presenting complaints for PHT are syncope and dyspnea. Other clinical signs include worsening cough, increased respiratory rate, "can't sleep or get comfortable," lethargy, and decreased appetite (Johnson et al. 1999). Severe PHT can also result in right-sided congestive heart failure and ascites. PHT can be difficult to diagnose without the aid of FCU or a complete detailed echocardiogram because radiographs and physical examination findings can be difficult to interpret and are nonspecific (Kellihan and Stepien 2010).

In dogs with severe PHT due to heartworm disease, heartworms may be seen as double-lined structures within the pulmonary artery. With caval syndrome, a severe form of heartworm disease, the heartworms will be seen in the right atrium and ventricle and caudal vena cava (Figure 20.9C; see also Figure 18.32E). Careful interrogation of the main pulmonary artery (PA) for a possible pulmonary embolism is advised.

### Common FCU Findings in Severe Pulmonary Hypertension

- Severe RV hypertrophy (RV > LV) on the right parasternal long-axis four-chamber view. Its short-axis view is too variable for the noncardiologist sonographer as a sole view.
- Flattening of the IVS in the LV short-axis "mushroom" view (see Figures 20.9A and 37.6).
- Small internal LV lumen suggests poor filling of the LV and low cardiac output due to the PHT.
- Right atrial dilation, caudal vena caval, and hepatic venous distension may be seen in severe PHT and right-sided congestive heart failure (Figure 20.10; see also Figure 37.6).
- Main PA enlargement (larger than the aorta) (see Figure 20.9B) (Sutherland-Smith et al. 2018).

**Pearl:** FCU findings of right-sided congestive heart failure typically include right ventricular and right atrial enlargement, caudal vena cava and hepatic venous distension, and ascites.

**Pearl:** With acute PHT such as in an acute pulmonary thromboembolism (PTE), the right ventricle will be enlarged. Other FCU findings of more chronic PHT include a RV that is eccentrically hypertrophied, PA enlargement, and diminished RV function. RV hypertrophy results from chronic severe PHT.

**Pitfall:** With severe chronic PHT, the RV papillary muscles will also be severely hypertrophied. In the right parasternal short-axis views, these RV papillary muscles can mistaken for a mass or thrombus (see Figures 20.9A and 37.6).

## *Assessment of the Caudal Vena Cava*

Caudal vena cava (CVC) diameter and its respiratory variations can be used to estimate right atrial filling pressures and guide volume responsiveness (Feissel

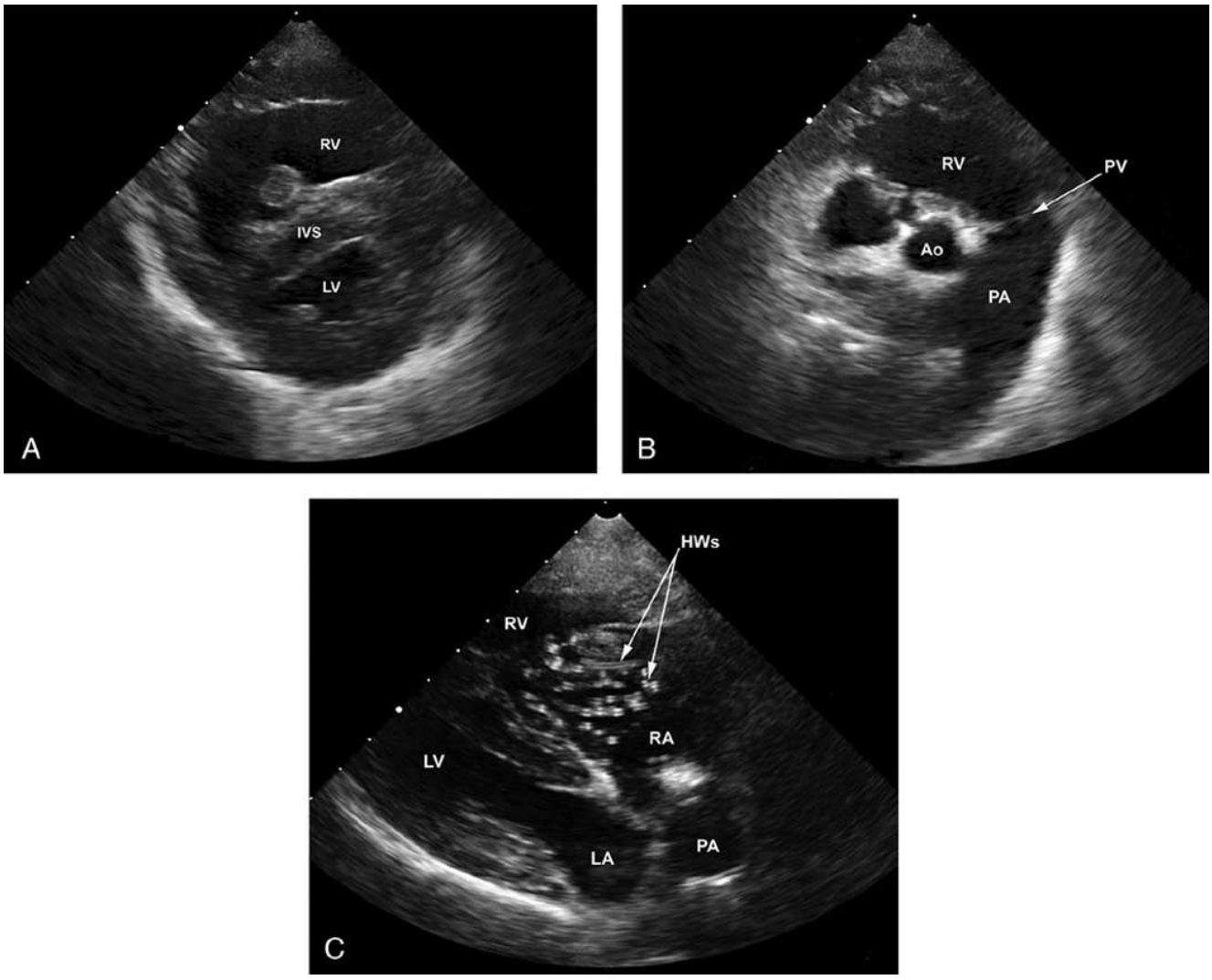


**Figure 20.9.** Canine pulmonary hypertension. (A) Right parasternal short axis-view of severe RV hypertrophy in a dog with pulmonary hypertension (PHT). Note the flattening of the IVS. (B) Right parasternal short-axis view of severe pulmonary arterial dilation in a dog with severe PHT. (C) Right parasternal long-axis view of severe right atrial and ventricular enlargement with heartworms visualized in a dog with caval syndrome and right-sided heart failure due to severe end-stage heartworm disease. HWs, heartworms; IVS, interventricular septum; LA, left atrium; LV, left ventricle; PA, pulmonary artery; PV, pulmonic valve; RA, right atrium; RV, right ventricle.

et al. 2004; Beigel et al. 2013). This section will primarily focus on the assessment of the CVC as it relates to elevated right heart filling pressure.

Elevated right atrial pressures can result from right-sided congestive heart failure due to structural acquired or congenital heart diseases, severe PHT, and pericardial effusion with cardiac tamponade. Elevated right atrial pressure can also result from excessive volume expansion in a critically ill patient (Nelson et al. 2010). In spontaneously breathing animals, the CVC normally collapses during inspiration. In patients with severely elevated right atrial pressure (>15 mmHg), the CVC diameter will be increased with no respiratory fluctuations noted (see Figures 20.10 and 37.6). Hepatic veins will also be distended and ascites may be seen between the liver lobes. The visualization of a dilated nonfluctuating CVC can be quite helpful to expedite the diagnosis of right-sided congestive heart failure in a dog with ascites or cat with large-volume pleural effusion.

It is important to know that the degree of respiratory fluctuation can be affected by the depth and volume of the breath in a spontaneously breathing patient. In a patient who is panting or taking short shallow breaths, the fluctuations may not accurately correlate with right atrial filling pressure. However, the respiratory

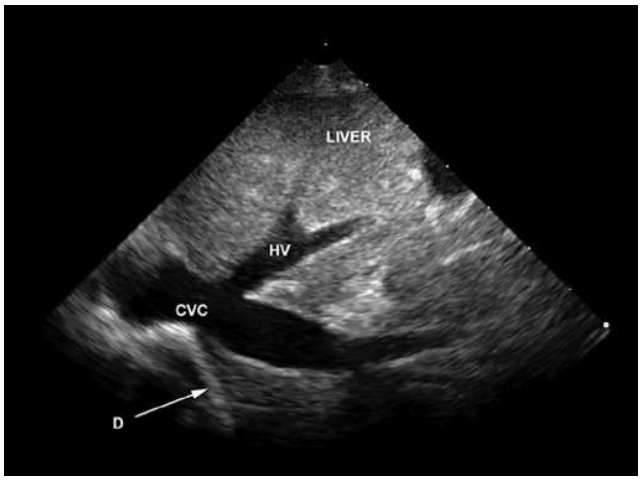


**Figure 20.10.** Subcostal view of severe caudal vena caval and hepatic venous distension in a dog with right-sided congestive heart failure. AFAST and abdominal fluid scoring can semiquantitate the ascites, depending on patient status, and Vet BLUE is used for signs of left-sided congestive heart failure (see Chapters 22, 23, 26, and 36). CVC, caudal vena cava; D, diaphragm; HV, hepatic vein.

fluctuations of extreme situations can be helpful; that is, a flat and highly collapsible vena cava (>50% collapse) would suggest volume responsiveness. Conversely, a distended and plethoric (blood-filled) CVC would suggest fluid intolerance and elevated right atrial pressure (see also Figures 7.12, 7.13, 26.1, 26.4, 36.7, and 36.11).

A long-axis view of the CVC as it crosses the diaphragm is the author's recommended view from a subxiphoid transducer position (the same as the FAST diaphragmatico-hepatic [DH] view). The view allows easy qualitative assessment of the CVC, hepatic veins and presence of ascites in the abdomen and thorax, and screens for both pleural and pericardial effusion. M-mode assessment of the CVC can be helpful in visualizing the respiratory fluctuations. There are a few other views that can be used to visualize the CVC at the porta hepatis and cranial and caudal to the right kidney (Darnis et al. 2018; Marshall et al. 2018) (see Chapter 26). The advantage of the subxiphoid view (FAST DH view) is that the respiratory fluctuations can be better assessed at the level of the diaphragm and the CVC can be easily imaged in most dogs and cats (Figure 20.11). However, this view can be challenging in extremely deep-chested dogs.

**Pearl:** The author finds CVC distension easier to observe by FCU than the detection of distended jugular veins on physical exam, especially in a long-haired patient.

**Pitfall:** To accurately assess the diameter of the CVC in a longitudinal orientation, the scanning plane needs to be centered in the middle of the vessel. An offcentered or oblique view will result in a falsely smaller diameter (see Figures 36.11 and 36.12).

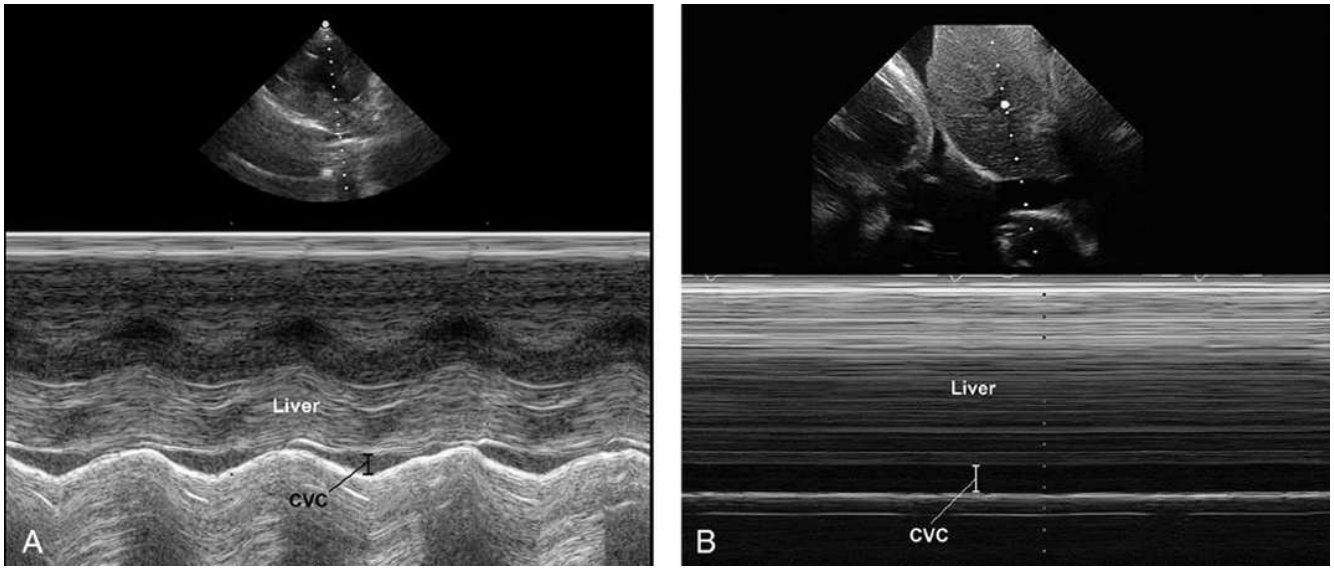


**Figure 20.11.** Subcostal view of fluctuations of the caudal vena caval diameter in two dogs during respiration using M-mode. (A) Note the >50% collapse of the CVC with inspiration, suggesting the dog is "fluid responsive." (B) Note the dilated and nonfluctating CVC motion with respirations, suggesting that this dog is "fluid intolerant" and has an elevated right atrial pressure. CVC, caudal vena cava.

VetBooks.ir

# Cardiopulmonary Arrest

Both the American Heart Association and the European Resuscitation Council recommend the use of ultrasound in cardiac arrest situations (Link et al. 2015; Soar et al. 2015). Point-of-care ultrasound (POCUS) is helpful in the diagnosis of any possible correctable causes of cardiac arrest while resuscitation is ongoing (see Table 37.1). Possible reversible causes of cardiac arrest in which ultrasound can aid in the diagnosis include hypovolemia, tension pneumothorax, cardiac tamponade, and pulmonary thromboembolism. Additionally, ultrasound can be used to assess myocardial motion and prognosis. The use of ultrasound should not delay the onset or the intervals between cardiac compressions. Typical protocols propose use brief 10-second ultrasound exams of the heart and lungs after each continuous two-minute round of chest compressions and basic life support. Cardiac standstill visualized by the FCU suggests no return to spontaneous circulation despite electrical activity. If cardiac standstill is documented, it would be reasonable to terminate resuscitation efforts. Conversely, if coordinated cardiac motion is observed, continue CPR while searching for its cause.

# Pearls and Pitfalls, The Final Say

The images obtained from the FCU can expedite the diagnosis of structural heart disease in patients presenting with clinical signs suggesting left-sided and right-sided heart failure. These patients are typically in respiratory distress or can be hemodynamically unstable. The FCU is a low-stress, low-impact, noninvasive tool that will lead to expedited treatment and improved patient care. Even without the use of advanced echocardiographic techniques, such as 2D and M-mode, FCU images of significant cardiac abnormalities such as marked chamber enlargements and myocardial failure can be determined.

# Quick Reference of Normals and Rules of Thumb

- Fractional shortening (FS%) is typically <20 % in DCM with normal FS% being 28–45% in dogs and 30–50% in cats.
- Hypertrophic cardiomyopathy in cats is supported by a LV wall measured in diastole to be >6 mm. In some cats with chronic disease, LV walls may be high normal thickness because of a phenomenon referred to as LV remodeling.
- In a cat with suspected heart failure, the LA is severely dilated with typically a LA:Ao ratio >2:1.
- Variable amounts of pleural effusion are often a unique manifestation of congestive heart failure in cats.
- Small amounts of pericardial effusion (typically <5 mm) without evidence of cardiac tamponade may be seen in cats with congestive heart failure. In fact, the most common cause of pericardial effusion in cats is heart failure (~75%).
- Extreme hypovolemia can be mistaken for HCM in cats, a phenomenon referred to as "pseudohypertrophy of the left ventricle."
- Features of severe pulmonary hypertension include: (1) severe RV hypertrophy (RV > LV) on the right parasternal long-axis four-chamber view, (2) flattening of the IVS in the LV short-axis "mushroom" view", (3) small internal LV lumen suggests poor filling of the LV and low cardiac output due to the PHT, 4) right atrial dilation, CVC, and hepatic venous distension in severe PHT and right-sided congestive heart failure, and 5) main pulmonary artery enlargement (larger than the aorta).
- The most common cause of a cardiac neoplasia in dogs is hemangiosarcoma, typically located in the right atrium or right atrial appendage.
- Most masses at the heart base are chemodectomas, tumors of the chemoreceptors in the aorta. Other possible causes of a heart base mass include ectopic thyroid gland tissue, hemangiosarcomas, and mesothelioma.
- Left atrial to aortic ratio (LA:Ao) >2:1 is extremely suggestive of left-sided heart failure in a dog or cat with respiratory distress, especially with the presence of B-lines providing further supportive evidence using the Vet BLUE regional, pattern-based approach (see Chapters 22 and 23). B-lines are nonspecific and must be placed into a regional, pattern-based approach, i.e. Vet BLUE.
- Normally the LV is 3–4 times the size of the RV. An RV that is larger than the LV with a distended and nonfluctuating CVC is extremely suggestive of right-sided heart failure, especially in a dog with ascites.
- Normal LV chamber size, wall dimensions and systolic function can vary based on body weight, breed of dog, heart rate/rhythm, volume status and systemic disease. Careful clinical integration of all influences on chamber dimensions is advised before making assessments of LV size and function.

# References


Beigel R, Cercek B, Luo H, et al. 2013. Noninvasive evaluation of right atrial pressure. *J Am Soc Echocardiogr* 26:1033–1042.

Borgarelli M, Buchanan JW. 2012. Historical review, epidemiology and natural history of degenerative mitral valve disease. *J Vet Cardiol* 14:93–101.

Boston SE, Higginson G, Montleith G. 2011. Concurrent splenic and right atrial mass at presentation in dogs with HSA: a retrospective study. *J Am Anim Hosp Assoc* 47(5):336–341.

Darnis E, Boysen S, Merveille AC, et al. 2018. Establishment of reference values of the caudal vena cava by fast-ultrasonography through different views in healthy dogs. *J Vet Intern Med* 32:1308–1318.

Feissel M, Michard F, Faller JP, et al. 2004. The respiratory variation in inferior vena cava diameter as a guide to fluid therapy. *Intens Care Med* 30:1834–1837.

Fox PR. 2012. Pathology of myxomatous mitral valve disease in the dog. *J Vet Cardiol* 14:103–126.

Gargani L, Pang PS, Frassi F, et al. 2015. Persistent pulmonary congestion before discharge predicts rehospitalization in heart failure: a lung ultrasound study. *Cardiovasc Ultrasound* 13:40.

Guglielmini C, Baron Toaldo M, Quinci M, et al. 2016. Sensitivity, specificity, and interobserver variability of survey thoracic radiography for the detection of heart base masses in dogs. *J Am Vet Med Assoc* 248(12):1391–1398.

Hall DJ, Shofer F, Meier CK, Sleeper MM. 2007. Pericardial effusion in cats: a retrospective study of clinical findings and outcome in 146 cats. *J Vet Intern Med* 21(5):1002–1007.

Johnson L, Boon J, Orton EC. 1999. Clinical characteristics of 53 dogs with Doppler-derived evidence of pulmonary hypertension: 1992–1996. *J Vet Intern Med* 13:440–447.

Kellihan HB, Stepien RL. 2010. Pulmonary hypertension in dogs: diagnosis and therapy. *Vet Clin Small Anim* 40:623–641.

Link MS, Berkow LC, Kudenchuk PJ, et al. 2015. Part 7: Adult Advanced Cardiovascular Life Support: 2015 American Heart Association Guidelines Update for Cardiopulmonary Resuscitation and Emergency Cardiovascular Care. *Circulation* 132(18 Suppl 2):S444–464.

Lisciandro GR, Fosgate GT, Fulton RM. 2014. Frequency of ultrasound lung rockets using a regionally-based lung ultrasound examination named veterinary bedside lung ultrasound exam (Vet BLUE) in 98 dogs with normal thoracic radiographic lung findings. *Vet Radiol Ultrasound* 55(3):315–322.

Lisciandro GR, Ward JL, DeFrancesco TC, et al. 2016. Absence of B-lines on lung ultrasound (Vet BLUE protocol) to rule out left-sided congestive heart failure in 368 cats and dogs. *J Vet Emerg Crit Care* 26(S1):S8.

Lisciandro GR, Fulton RM, Fosgate GT, Mann KA. 2017. Frequency of B-lines using a regionally-based lung ultrasound examination (the Vet BLUE protocol) in 49 cats with normal thoracic radiographical lung findings. *J Vet Emerg Crit Care* 27(3):267–277.

Luis Fuentes V, Wilkie LJ. Asymptomatic hypertrophic cardiomyopathy: diagnosis and therapy. *Vet Clin North Am Small Anim Pract* 47:1041–1054.

MacDonald K. Infective endocarditis in dogs: diagnosis and therapy. *Vet Clin North Am Small Anim Pract* 40:665–684.

MacDonald KA, Cagney O, Magne ML. 2009. Echocardiographic and clinicopathologic characterization of pericardial effusion in dogs: 107 cases (1985–2006). *J Am Vet Med Assoc* 235:1456–1461.

MacGregor JM, Faria ML, Moore AS, et al. 2005. Cardiac lymphoma and pericardial effusion in dogs: 12 cases (1994–2004). *J Am Vet Med Assoc* 227(9):1449–1453.

Marshall KA, Thomovsky EJ, Brooks AC, et al. 2018. Ultrasound measurements of the caudal vena cava before and after blood transfusion in 9 greyhound dogs. *Can Vet J* 59(9):973–980.

Martin MW, Stafford Johnson MJ, Celona B. 2009. Canine dilated cardiomyopathy: a retrospective study of signalment, presentation and clinical findings in 369 cases. *J Small Anim Pract* 50:23–29.

Meurs KM. 2010. Myocardial diseases: canine. In: Textbook of Veterinary Internal Medicine, 7th edition, edited by Ettinger SJ, Feldman EC. St Louis: Saunders Elsevier, pp 1320–1328.

Nakamura RK, Tompkins E, Russell NJ, Zimmerman SA. 2014. Left atrial rupture secondary to myxomatous mitral valve disease in 11 dogs. *J Am Anim Hosp Assoc* 50(6):405–408.

Nelson NC, Drost WT, Lerche P, et al. 2010. Noninvasive estimation of central venous pressure in anesthetized dogs by measurement of hepatic venous blood flow velocity and abdominal venous diameter. *Vet Radiol Ultrasound* 51(3):313–323.

Payne JR, Borgeat K, Connolly DJ, et al. 2013. Prognostic indicators in cats with hypertrophic cardiomyopathy. *J Vet Intern Med* 27:1427–1436.

Payne JR, Borgeat K, Brodbelt DC et al. 2015. Risk factors associated with sudden death vs. congestive heart failure or arterial thromboembolism in cats with hypertrophic cardiomyopathy. *J Vet Cardiol* 17:S318–S328.

Rajagopalan V, Jesty SA, Craig LE, et al. 2013. Comparison of presumptive echocardiographic and definitive diagnoses of cardiac tumors in dogs. *J Vet Intern Med* 27:1092–1096.

Reineke EL, Burkett DE, Drobatz KJ. 2008. Left atrial rupture in dogs: 14 cases (1990–2005). *J Vet Emerg Crit Care* 18(2):158–164.

Rush JE, Freeman LM, Fenollasa NK, et al. 2002. Population and survival characteristics of cats with hypertrophic cardiomyopathy: 260 cases (1990–1999). *J Am Vet Med Assoc* 220:202–207.

Schober KE, Maerz I. 2006. Assessment of left atrial appendage flow velocity and its relation to spontaneous echocardiographic contrast in 89 cats with myocardial disease. *J Vet Intern Med* 20:120–130.

Schober KE, Wetli E, Drost WT. 2014. Radiographic and echocardiographic assessment of left atrial size in 100 cats with acute left-sided congestive heart failure. *Vet Radiol Ultrasound* 55:359–367.

Soar J, Nolan JP, Böttiger BW, et al. 2015. European Resuscitation Council Guidelines for Resuscitation 2015: Section 3. *Adult advanced life support. Resuscitation* 95:100–147.

Stern JA, Ueda Y. 2019. Inherited cardiomyopathies in veterinary medicine. *Pflugers Arch* 471:745–753.

Sutherland-Smith J, Hankin EJ, Cunningham SM, et al. 2018. Comparison of a computed tomographic pulmonary trunk to aorta diameter ratio with echocardiographic indices of pulmonary hypertension in dogs. *Vet Radiol Ultrasound* 59(1):18–26.

Treggiari E, Pedro B, Dukes-McEwan J, et al. 2017. A descriptive review of cardiac tumours in dogs and cats. *Vet Comp Oncol* 15:273–288.

Vezzosi T, Mannucci A, Pistoresi F, et al. 2017. Assessment of lung ultrasound B-Lines in dogs with different stages of chronic valvular heart disease. *J Vet Intern Med* 31(3):700–704.

Ward JL, Lisciandro GR, Keene BW, et al. 2017. Accuracy of point-of-care lung ultrasonography for the diagnosis of cardiogenic pulmonary edema in dogs and cats with acute dyspnea. *J Am Vet Med Assoc* 250:666–675.

Ward JL, Lisciandro GR, Ware WA, et al. 2018. Evaluation of point-of-care thoracic ultrasound and NT-proBNP for the diagnosis of congestive heart failure in cats with respiratory distress. *J Vet Intern Med* 32:1530–1540.

Waters DJ, Caywood DD, Hayden DW, et al. 1988. Metastatic pattern in dogs with splenic hemangiosarcoma: clinical implications. *J Small Animal Pract* 29:805.

CHAPTER TWENTY-ONE

# POCUS: Heart – Pericardial Effusion and Pericardiocentesis

Teresa DeFrancesco

## Introduction

Pericardial effusion (PCE) is an excess of fluid in the pericardial sac. The normal pericardial sac has a small amount of clear serous fluid that is usually not detectable with ultrasound. Abnormal accumulations of pericardial fluid develop as a result of many disease processes. Neoplastic and idiopathic PCE disorders are the most common in the dog, particularly large-breed and brachycephalic dogs (MacGregor et al. 2005; MacDonald et al. 2009; Boston et al. 2011). Less commonly, PCE may be caused by a left atrial tear (mitral valve disease dogs), coagulopathies, uremia, systemic inflammation, infectious pericarditis (e.g., coccidioidomycosis), trauma or foreign bodies (Reineke et al. 2008; Nakamura et al. 2014; Covey and Connolly 2018). In cats, PCE is most commonly a manifestation of congestive heart failure (Hall et al. 2007). Much less commonly, lymphoma and feline infectious peritonitis (FIP) can result in pericardial effusion in cats.

Cardiac tamponade is a frequent consequence of PCE in the dog and a life-threatening condition. Cardiac tamponade results when the intrapericardial pressure is higher than the right ventricular filling pressure. This high intrapericardial pressure causes poor right ventricular filling, low cardiac output, and right heart failure. Both the amount of the effusion and its rate of formation determine the degree of hemodynamic compromise. A dog can have cardiac tamponade and poor cardiac output with a small amount of pericardial effusion if the rate of accumulation of the effusion is fast. Common clinical signs include collapse, lethargy, cough, vomiting, inappetence, abdominal distension and possible difficulty breathing. Dogs with chronic mitral valve disease that have suffered a left atrial tear will be acutely dyspneic and extremely weak (Reineke et al. 2008; Nakamura et al. 2014).

While there are some classic physical examination findings such as muffled heart sounds, weak pulses, jugular venous distension and abdominal distension, these can be nonspecific. Focused cardiac ultrasound (FCU) can provide a rapid and accurate diagnosis, especially in a dog with cardiac tamponade and small-volume pericardial effusion. Despite some suggestive findings such as globoid cardiomegaly, thoracic radiography is often not a valuable imaging modality for the diagnosis of PCE (Côté et al. 2013). FCU is a sensitive diagnostic test for pericardial effusion; pericardial effusion can be reliably recognized with a 95% degree of accuracy by noncardiologists with POCUS training (Tse et al. 2013; Ceriani and Cogliati 2016).

### *What Focused Cardiac Ultrasound Pericardial Effusion Can Do*

- Detect the presence of PCE and cardiac tamponade.
- Based on the absence or presence of a mass (its location, size, shape, echogenicity, and behavior), suggest the suspected etiology of the PCE.
- Estimate the amount and echogenicity of PCE (small, moderate, large) and identify an optimal site for POCUS-assisted or POCUS-guided pericardiocentesis.

*Point-of-Care Ultrasound Techniques for the Small Animal Practitioner*, Second Edition. Edited by Gregory R. Lisciandro.
© 2021 John Wiley & Sons, Inc. Published 2021 by John Wiley & Sons, Inc.
Companion website: www.wiley.com/go/lisciandro/ultrasound2

- Monitor for recurrence of the PCE, which is not uncommon with a right atrial mass and highly probable with hemangiosarcoma.

### What Focused Cardiac Ultrasound Pericardial Effusion Cannot Do

- Care should be taken to not overzealously definitively diagnose the etiology of the pericardial effusion without corroborative or confirmatory evidence.

### Indications

- Collapse, weakness, and hemodynamic compromise.
- Vague clinical signs with muffled heart sounds and weak pulses.
- Sudden-onset collapse and dyspnea in a dog with advanced mitral valve disease.
- Abdominal distension and jugular venous distension.
- Globoid radiographic appearance to the cardiac silhouette.

### Objectives

- To accurately identify pericardial effusion and distinguish it from pleural effusion.
- To identify right atrial collapse, the sonographic finding of cardiac tamponade, in a dog with pericardial effusion.
- To be familiar with the two most common neoplastic causes of pericardial effusion in the dog, specifically a right atrial mass (likely a hemangiosarcoma) or heart base mass (likely a chemodectoma) (Treggiari et al. 2017).
- To be familiar with the FCU findings of a left atrial tear in a dog with advanced mitral valve disease.
- To know that PCE in the cat is often associated with congestive heart failure and is managed medically.
- To know the indications for and be familiar with how to perform an emergency pericardiocentesis in a dog with cardiac tamponade and PCE (see also Chapter 43).

# Pericardial Effusion

The pericardium consists of a tough fibrous parietal layer and a membranous visceral layer adhered to the epicardium. In normality, the parietal and visceral layers are seen as one hyperechoic (bright white) line adjacent to the epicardium. When there is PCE, the two layers separate. PCE is typically seen as an anechoic (black) space encircling the heart between the myocardium and the highly echogenic parietal layer of the pericardium (Figure 21.1).

Occasionally, the PCE could have a more echogenic appearance, suggesting increased cellularity to the fluid, such as in a left atrial tear or infectious pericarditis. Multiple views of the heart as well as visualizing the entire heart are necessary to avoid mistaking a dilated atrium or ventricle for pericardial (or pleural) effusions, resulting in a catastrophic error and performing centesis of a cardiac chamber (see also Chapters 17 and 18). In the smaller compact ultrasound units, the maximum depth of 13 or 15 cm may not allow viewing of the entire heart in a large-breed dog. In these cases, viewing the fluid and heart from multiple views is of the utmost importance. The axiom "One view is no view" is sage advice when diagnosing pericardial effusion (see also Chapters 17 and 18 and Figures 18.18, and 18.19). PCE is seen from all standard views including the subxiphoid (Lisciandro 2016), right parasternal, and left-sided views (Figure 21.2). Neoplasia, most commonly right auricular hemangiosarcoma and heart base chemodectoma, is the most common cause of pericardial effusion in an older dog. The presence of a possible cardiac mass is generally better evaluated prior to pericardiocentesis depending on patient stability.

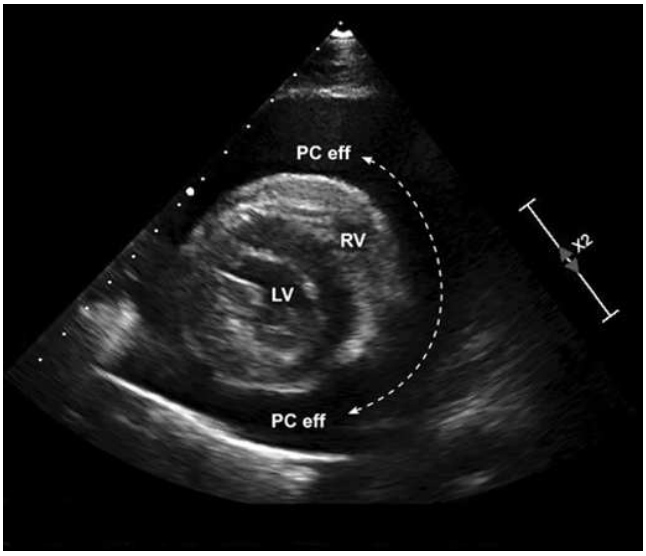


**Figure 21.1.** Right parasternal short-axis view of pericardial effusion in a dog. The pericardial effusion is the anechoic space encircling the heart depicted by the curved double-sided arrow. LV, left ventricle; PC eff, pericardial effusion; RV, right ventricle.

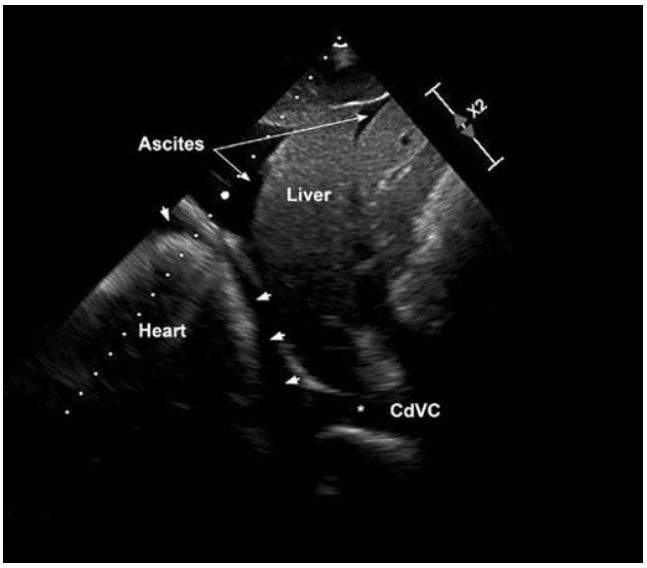


**Figure 21.2.** Subxiphoid (or diaphragmatic hepatic) view of pericardial effusion and ascites in a dog. The pericardial effusion is depicted by the arrowheads. The caudal vena cava (*) is distended and nonfluctuating, suggestive of cardiac tamponade. CdVC, caudal vena cava.

Pleural effusion is often present concurrently with PCE. The distinction between pleural and pericardial effusion can be challenging. Moderate- to large-volume PCE is seen as circumferential anechoic space encircling the ventricles in short-axis view, while pleural effusion will be seen as angular anechoic spaces near the heart and between the lung lobes. PCE should taper as it nears the top of the left atrium in the long-axis views as the pericardium attaches to the top of the atrium (Figure 21.3A). The parietal pericardium is usually the most hyperechoic (brightest) structure within the thorax. You can turn down the gain of the ultrasound machine and generally the last linear echo structure is the pericardium. If no PCE is present then the pericardium (the last white line) should be adjacent to the epicardial surface of the heart. Lastly, pleural effusion is gravity dependent and will shift to the recumbent side down. As previously mentioned, multiple views are key for interrogation of the pleural and pericardial spaces (see also Chapters 17 and 18 and Figures 18.18 and 18.19).

### *Common FCU findings in Pericardial Effusion*

- Anechoic fluid around the heart that is delineated by the pericardium, which appears as a bright white (hyperechoic) linear echo in the far-field (mostly because of acoustic enhancement) (see Figures 18.19, 21.1, 21.3A,B).
- Echocardiographic criteria for cardiac tamponade are right atrial and possibly right ventricular diastolic collapse (see Figures 18.19, 18.20, and 21.3A).
- Cardiac tamponade and obstruction of right heart filling are further corroborated by a distended and nonfluctuating caudal vena cava (see Figures 18.20 and 21.2).
- A heart base mass is usually best visualized in the right-sided parasternal views (see Figures 20.8 and 21.3A) while a right atrial or auricular hemangiosarcoma is typically best seen from a left-sided parasternal view optimized for the right atrium and auricle (Figure 21.4). If a mass is very large, it can be seen in any view and may compress the atria or great vessels, impinging the inflow or outflow of blood (see Figure 18.32F).
- Nonstandard views may be best to fully determine the extent of the mass.
- PCE caused by a left atrial tear in a dog with mitral valve disease will have an increased echogenicity representing a tubular-shaped blood clot. The left atrium is typically enlarged and the mitral valve will be thick and abnormal (Figure 21.5; see also Figures 18.21 and 18.32B).

**Pearl:** If patient stability allows, search for a mass when PCE is present (prior to pericardiocentesis). Masses are seen more easily with pericardial fluid around them.

**Pitfall:** Furosemide and vasodilators are contraindicated in the setting of cardiac tamponade. Typically, fluid expansion with intravenous crystalloids is used to transiently improve cardiac output while awaiting pericardiocentesis. Medical treatment with diuretics and other conventional medications, however, is indicated for the management of PCE in cats with congestive heart failure.

**Pitfall:** Some very obese cats will have a large fat deposit on their pericardium that can be misdiagnosed as pericardial effusion or a mass. Fat has a more echogenic (brighter) appearance than fluid.

## Pericardiocentesis

The main indication for pericardiocentesis is the urgent and life-saving removal of PCE from a dog with cardiac tamponade and hemodynamic compromise. If time and patient conditions allow, an attempt

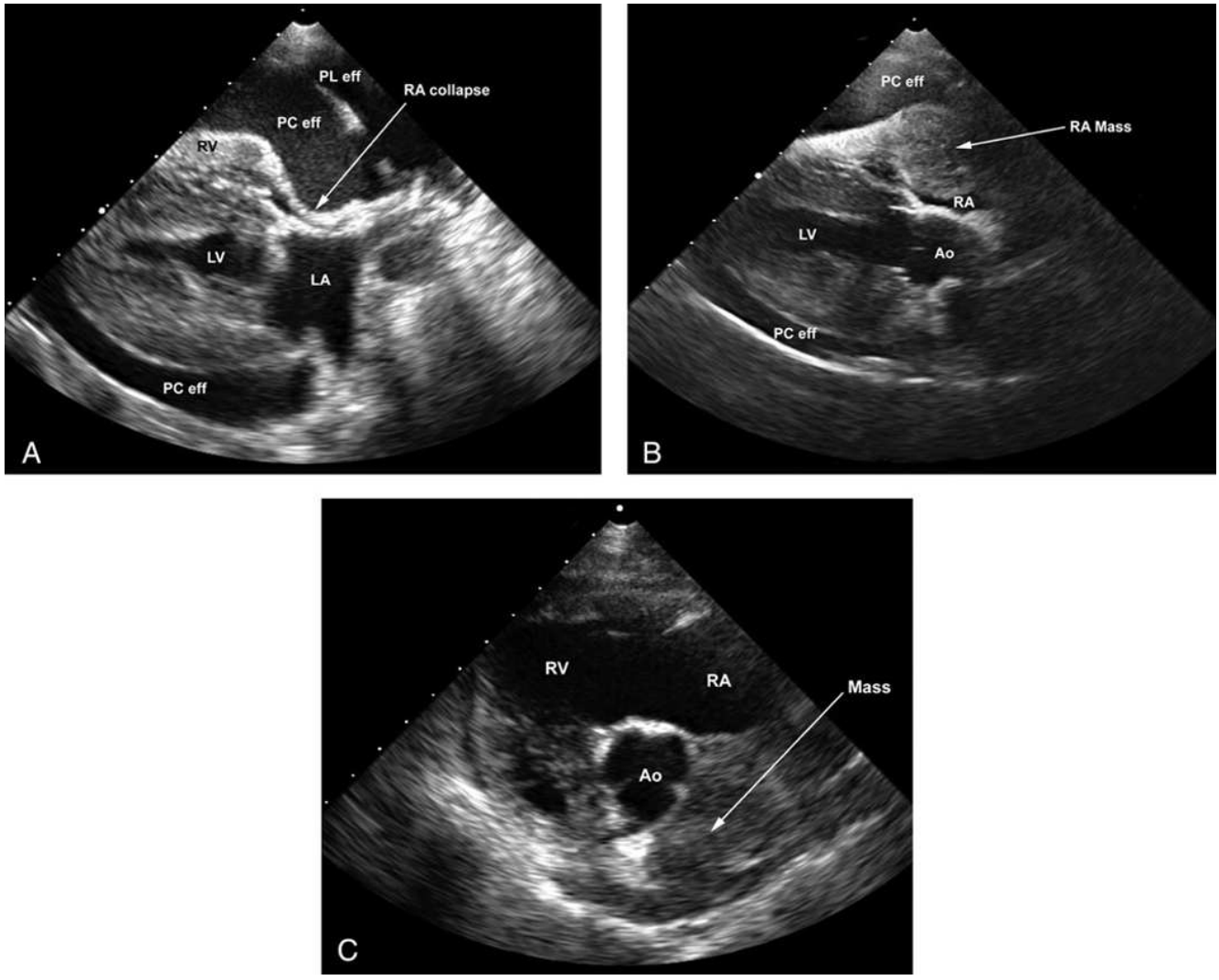


**Figure 21.3.** Cardiac tamponade, right atrial tumor, and heart base tumor. (A) Right long-axis view of pericardial effusion and cardiac tamponade showing clear right atrial collapse. (B) Right long-axis view of a right atrial tumor, most likely hemangiosarcoma, in a dog with pericardial effusion. (C) Right short-axis view of a heart base tumor most likely chemodectoma. Ao, aorta; LA, left atrium; LV, left ventricle; PC eff, pericardial effusion; PL eff, pleural effusion; RA, right atrium; RA Mass, right atrial mass; RV, right ventricle.

to identify a possible mass prior to pericardiocentesis is warranted as the mass may be missed after centesis. While there is some risk associated with this procedure, the risks are typically outweighed by the benefits. The removal of the pericardial fluid is the only therapeutic maneuver that will allow the heart to fill normally and significantly improve cardiac output. Medical management of cardiac tamponade with diuretics and vasodilators is harmful. In addition, the fluid analysis of the PCE may have some limited diagnostic utility (MacDonald et al. 2009; Cagle et al. 2014). PCE without evidence of cardiac tamponade does not need to be urgently removed. Small-volume PCE is commonly a manifestation of heart failure in the cat and occasionally the dog (Ward et al. 2018). When PCE without cardiac tamponade is thought to be a manifestation of heart failure, then conventional heart failure medical management is advised.

The complications associated with pericardiocentesis are uncommon but significant (Humm et al. 2009). Cardiac puncture, pneumothorax, arrhythmias, and potential death should be discussed as potential complications. If a specialty center is close by and the dog's condition is reasonably stable, these cases are often referred to a center that commonly performs pericardiocentesis. However, if there is concern that the

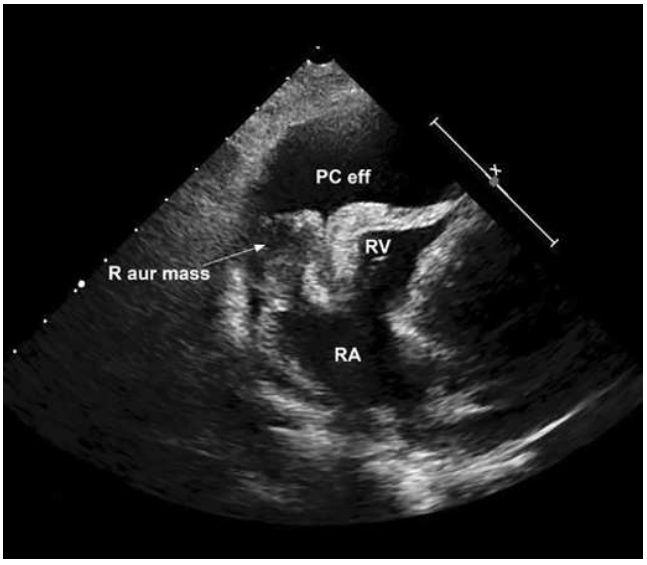


**Figure 21.4.** Right atrial mass (probable hemangiosarcoma) in a dog with pericardial effusion. In this left cranial view, the right auricular mass is visualized well enhanced with the pericardial effusion. PC eff, pericardial effusion; RA, right atrium; R aur mass, right auricular mass; RV, right ventricle.

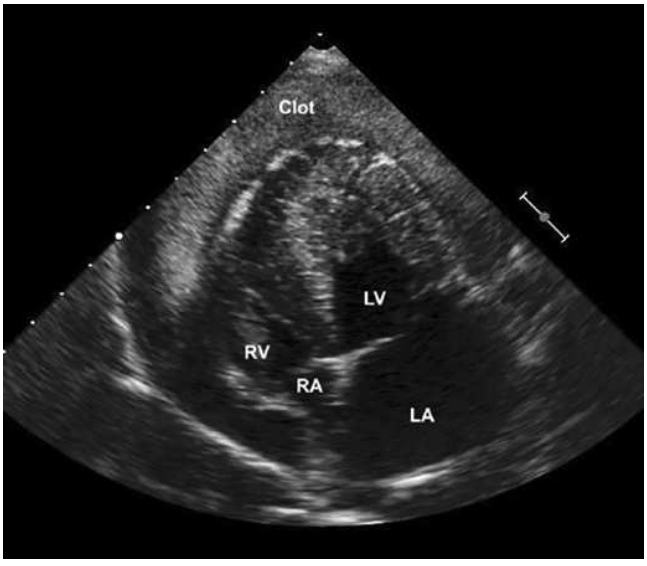


**Figure 21.5.** Left atrial tear in a dog with advanced degenerative mitral valve disease. In this left apical view, the hyperechoic blood clot, labeled "Clot," can be seen encircling the heart from the left atrium to the right ventricle. The left atrium is enlarged and right atrium is collapsed, suggesting increased intrapericardial pressure. LA, left atrium; LV, left ventricle; PC eff, pericardial effusion; RA, right atrium; RV, right ventricle.

patient may not survive transport to a specialty center, then emergency pericardiocentesis is warranted.

Pericardiocentesis is typically performed on the right hemithorax because it is considered safer due to the cardiac notch, the space between the right cranial and middle lung lobes, and reduced chance of lacerating a coronary artery. It is of the utmost importance that the patient does not move during the procedure. Sedation is sometimes needed but some patients are so hemodynamically compromised that sedation is not necessary. The larger the volume of PCE, the safer the procedure because there is more distance between the needle and the heart.

In human medicine, ultrasound guidance has decreased the complication rate of pericardiocentesis (Tsang et al. 1998; Lindenberger et al. 2003). In veterinary medicine, ultrasound is most commonly used either to assist or to guide pericardiocentesis. Ultrasound-guided pericardiocentesis is real-time visualization of the needle draining the pericardial sac while ultrasound-assisted pericardiocentesis helps to find the optimal location for catheter insertion into the pericardium with intermittent ultrasound monitoring the fluid drainage. The author prefers the ultrasound-*assisted* method because moderate- to large-volume PCE is most common and the preference is to introduce and maintain a soft catheter in the pericardial sac for the duration of draining the fluid rather than a sharp needle that is often used for ultrasound-*guided* centesis (Degirmencioglu et al. 2013). The author performs ultrasound-guided pericardiocentesis for small-volume pericardial effusion usually for diagnostic purposes under heavy sedation.

## *Ultrasound-assisted Pericardiocentesis with an Over-the-Needle Catheter*

- A short peripheral intravenous (IV) catheter is placed for administration of drugs (sedation, antiarrhythmic drugs, or IV fluids).
- The sedated patient is placed in sternal or left lateral recumbency, depending on the preference of the veterinarian performing the procedure.
- A large area on the right hemithorax (3rd to 8th intercostal space from just below the costochondral junction [CCJ] to midthorax) over the heart is clipped.
- Prior to surgically prepping the skin, the optimal location is chosen for the introduction of the catheter with the aid of the ultrasound (Figure 21.6A). The optimal site should be at or above the CCJ to avoid the internal thoracic artery, and where there is a clear and central view of the PCE with minimal lung interference. Once the optimal puncture site is

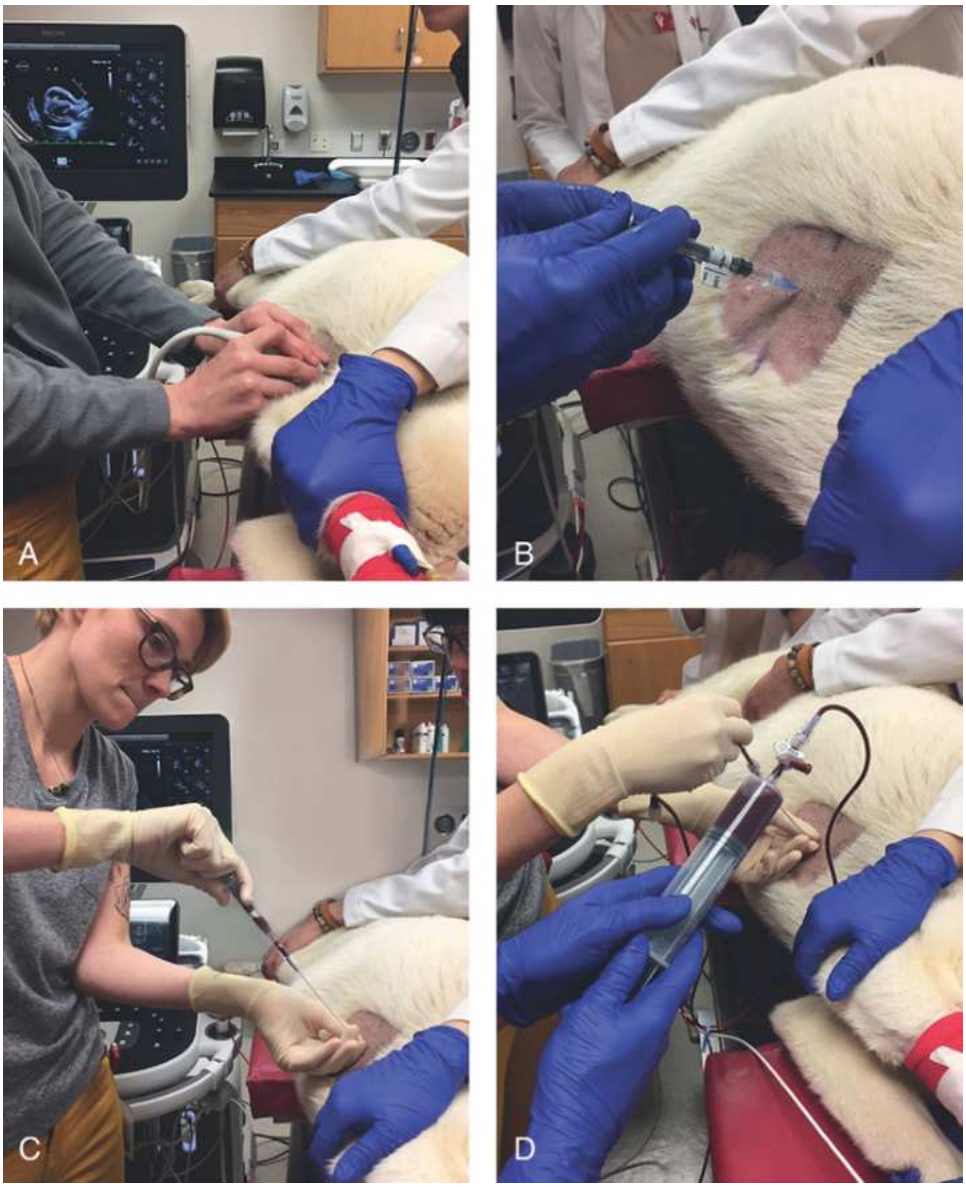


**Figure 21.6.** Ultrasound-assisted pericardiocentesis in a dog. (A) After clipping hair and prior to surgical preparation of the skin, the optimal location is chosen in the right hemithorax for the introduction of the catheter with the aid of ultrasound with the dog in left lateral recumbency. (B) Local anesthesia is administered in the skin, subcutaneous tissues, and intercostal muscles. (C) The over-the-needle catheter is advanced into the pericardial sac with negative suction applied by a small syringe until hemorrhagic pericardial fluid fills the syringe. (D) Once in the pericardial sac, the catheter is advanced and the needle stylet removed. The catheter is connected to tubing and syringe to allow drainage of the fluid.

chosen, every effort should be made to keep the patient in the same position.

- Local anesthesia with lidocaine is infiltrated in the subcutaneous tissues and intercostal muscles and pleura at the desired puncture site (see Figure 21.6B).
- Continuous electrocardiogram (ECG) is monitored for any possible arrhythmias that may represent myocardial contact with the pericardiocentesis catheter.
- The size and length of the needle or catheter depend on the size of the patient and the volume and nature of the fluid. In large dogs, a 16 G or 14 G × 3.25 to 5 inch over-the-needle catheter with optional side-hole fenestrations works well.
- The over-the-needle catheter is inserted through a releasing incision in the skin to minimize the drag or burring of the catheter through the skin.

A Luer-Slip 3 cc syringe is connected to the catheter. Once the catheter tip is through the skin, at least 1 cc of negative suction is applied to the syringe. The catheter is inserted perpendicular to the chest wall and advanced through the subcutaneous tissues and intercostal muscles until dark red hemorrhagic fluid fills the syringe, signaling that you have entered the pericardial space (see Figure 21.6C).

- Pleural effusion is often present together with PCE. Pleural fluid is typically serosanginous or pink in color. One should continue to advance the catheter until the dark red fluid fills the syringe. If there is any doubt about the location of the catheter (pleural or pericardial space), you can inject a small amount of agitated saline and ensure that the catheter is located in the correct space and not in the pleural space or right heart (Schussler and Grayburn 2010).
- Once in the pericardial sac, the catheter is advanced over the needle stylet. The needle stylet is then removed. Extension tubing, a three-way stopcock, and a large syringe are quickly attached to the hub of the catheter and drainage of the fluid begins. The fluid should come easily with minimal negative suction (see Figure 21.6D).
- You should try to completely drain the PCE. Complete emptying of the fluid will be noted by the absence of more fluid with gentle negative suction. Arrhythmias will often be noted as the catheter tip will be touching the epicardium when little fluid is in the pericardial sac.
- Careful monitoring of the ECG during insertion of the needle and during the centesis is advised. If arrhythmias are noted, slight retraction of the needle/catheter should result in resolution of the arrhythmia.
- After the pericardiocentesis, the dog should be monitored with FCU for possible reeffusion, especially if a right atrial mass is identified. Reeffusion within a few hours is not uncommon with hemorrhaging right atrial hemangiosarcomas.

**Pearl:** Most PCEs are hemorrhagic and can be similar in appearance to blood. If you are concerned about an accidental right ventricular puncture and frank blood, wait to see if the hemorrhagic fluid clots. PCE should not clot while blood from a cardiac puncture will clot after a couple of minutes. You may also feel the rhythmic pulsation of the heart on the catheter.

**Pearl:** Even if you are unsuccessful in advancing the catheter into the pericardial sac, just the puncture of the pericardium will likely relieve the cardiac tamponade. The PCE will often drain into the pleural space. Reevaluating the amount of PCE and the presence of right atrial collapse after an attempted pericardiocentesis is advised.

Ultrasound-guided pericardiocentesis is very similar to ultrasound-assisted with a few differences. With ultrasound-guided centesis, the sonographer will hold the probe with their nondominant hand and a reasonably long centesis needle with the dominant hand. The needle hub is connected to extension tubing, three-way stopcock, and syringe. An assistant will apply negative suction with the syringe as the needle is advanced into the skin and subcutaneous tissues. The sonographer will watch the insertion of the needle into the pericardial space that should coincide with fluid filling the collection system and syringe. The sonographer will continuously watch while the needle is in the pericardial sac while the fluid is drained, exercising caution to keep the needle tip from touching the heart.

## Pearls and Pitfalls, The Final Say

Focused cardiac ultrasound is the most sensitive and specific diagnostic modality that is readily available to veterinarians to diagnose PCE and cardiac tamponade. Physical examination, chest radiographs, and electrocardiography will suggest the diagnosis of PCE but POCUS will:

- provide a definitive diagnosis of PCE
- provide a diagnosis of cardiac tamponade (right atrial collapse in diastole, distended caudal vena cava [CVC])
- possibly determine the cause of the PCE (often a cardiac neoplasia)
- aid in pericardiocentesis.

A significant challenge is in accurately distinguishing PCE from pleural effusion, a severely dilated cardiac chamber or excessive pericardial fat. Always try to view the entire heart with fluid *encircling* it from multiple views and transducer positions. Also try to identify a mass if possibly prior to pericardiocentesis. Scan the right atrium (including the auricle) and heart base carefully for possible hemangiosarcoma or chemodectoma, respectively. Pericardiocentesis, either by

ultrasound assistance or ultrasound guidance, is the only therapeutic maneuver that will relieve the life-threatening cardiac tamponade.

# Quick Reference of Normals and Rules of Thumb

- Always increase your depth to be able to see the heart in its entirety using the hyperechoic (bright white) pericardium in the far-field as your landmark.
- Mirror image of the heart is possible with excessive depth that can be confounding to the sonographer.
- Pericardial effusion is most commonly caused by neoplasia in dogs and congestive heart failure in cats.
- Pericardial effusion is most commonly hemorrhagic and differentiated between true cardiac puncture and pericardial effusion by the presence and absence of a clot, respectively.
- Pericardial effusion is most accurately diagnosed sonographically through the use of multiple views, being careful not to mistake a cardiac chamber for pericardial (or pleural) effusion.
- The safest echocardiogram views for the diagnosis of pericardial effusion are those in which the chambers are clearly identified with pericardial effusion clearly outside the heart and in between it and the pericardial sac.
- Cardiac tamponade is a life-threatening condition requiring emergent pericardiocentesis.

# References


Boston SE, Higginson G, Montleith G. 2011. Concurrent splenic and right atrial mass at presentation in dogs with HSA: a retrospective study. *J Am Anim Hosp Assoc* 47(5):336–341.

Cagle LA, Epstein SE, Owens SD, et al. 2014. Diagnostic yield of cytologic analysis of pericardial effusion in dogs. *J Vet Intern Med* 28:66–71.

Ceriani E, Cogliati C. 2016. Update on bedside ultrasound diagnosis of pericardial effusion. *Intern Emerg Med* 11:477–480.

Côté E, Schwarz LA, Sithole F. 2013. Thoracic radiographic findings for dogs with cardiac tamponade attributable to pericardial effusion. *J Am Vet Med Assoc* 243:232–235.

Covey HL, Connolly DJ. 2018. Pericardial effusion associated with systemic inflammatory disease in seven dogs (January 2006 – January 2012). *J Vet Cardiol* 20:123–128.

Degirmencioglu A, Karakus G, Güvenc TS, et al. 2013. Echocardiography-guided or "sided" pericardiocentesis. *Echocardiography* 30(9):997–1000.

Hall DJ, Shofer F, Meier CK, Sleeper MM. 2007. Pericardial effusion in cats: a retrospective study of clinical findings and outcome in 146 cats. *J Vet Intern Med* 21(5):1002–1007.

Humm KR, Keenaghan-Clark EA, Boag AK. Adverse events associated with pericardiocentesis in dogs: 85 cases (1999–2006). *J Vet Emerg Crit Care* 19(4):352–356.

Lindenberger M, Kjellberg M, Karlsson E, et al. 2003. Pericardiocentesis guided by 2-D echocardiography: the method of choice for treatment of pericardial effusion. *J Intern Med* 253:411–417.

Lisciandro GR. 2016. The use of the diaphragmatico-hepatic (DH) views of the abdominal and thoracic focused assessment with sonography for triage (AFAST/TFAST) examinations for the detection of pericardial effusion in 24 dogs (2011–2012). *J Vet Emerg Crit Care* 26:125–131.

MacDonald KA, Cagney O, Magne ML. 2009. Echocardiographic and clinicopathologic characterization of pericardial effusion in dogs: 107 cases (1985–2006). *J Am Vet Med Assoc* 235:1456–1461.

MacGregor JM, Faria ML, Moore AS, et al. 2005. Cardiac lymphoma and pericardial effusion in dogs: 12 cases (1994–2004). *J Am Vet Med Assoc* 227(9):1449–1453.

Nakamura RK, Tompkins E, Russell NJ, Zimmerman SA. 2014. Left atrial rupture secondary to myxomatous mitral valve disease in 11 dogs. *J Am Anim Hosp Assoc* 50(6):405–408.

Reineke EL, Burkett DE, Drobatz KJ. 2008. Left atrial rupture in dogs: 14 cases (1990–2005). *J Vet Emerg Crit Care* 18(2):158–164.

Schussler JM, Grayburn PA. 2010. Contrast guided two-dimensional echocardiography for needle localization during pericardiocentesis: a case report. *J Am Soc Echocardiogr* 23:683.

Treggiari E, Pedro B, Dukes-McEwan J, et al. 2017. A descriptive review of cardiac tumours in dogs and cats. *Vet Comp Oncol* 15:273–288.

Tsang TSM, Freeman WK, Sinak LJ, et al. 1998. Echocardiographically guided pericardiocentesis: evolution and state of the art technique. *Mayo Clin Proc* 73:647–652.

Tse Y, Bulmer B, Cunningham S, et al. 2013. Evaluation of a training course in focused echocardiography for the non cardiology house officer. *J Vet Emerg Crit Care* 22:S2–10.

Ward JL, Lisciandro GR, Ware WA, et al. 2018. Evaluation of point-of-care thoracic ultrasound and NT-proBNP for the diagnosis of congestive heart failure in cats with respiratory distress. *J Vet Intern Med* 32:1530–1540.

CHAPTER TWENTY-TWO

# POCUS: Vet BLUE – Introduction and Image Acquisition

Gregory R. Lisciandro and Stephanie C. Lisciandro

## Introduction

The Vet BLUE protocol was developed in 2010 after finding pulmonary pathology at the TFAST chest tube site view and was first described in our first edition (Lisciandro 2014a,b). Vet BLUE added seven more acoustic windows (views) beyond TFAST for lung evaluation and is the veterinary modification of the BLUE Protocol (Bedside Lung Ultrasound Examination) in humans (Lichtenstein and Meziere 2008). Vet BLUE (Veterinary Brief Lung Ultrasound Exam) is designed so that its regional pattern-based approach may be applied rapidly and at the point of care in any respiratory small animal (Lisciandro 2014a,b; Lisciandro et al. 2014, 2017, 2018; Ward et al. 2017). Without the delay of radiography and computed tomography, Vet BLUE helps guide therapy to stabilize the patient for continued work-up (Ward et al. 2017, 2019; Dicker et al. 2019). Vet BLUE findings may be correlated to thoracic radiography (TXR) and computed tomography (CT). Moreover, Vet BLUE is consistent with how most veterinarians interpret thoracic radiography with its regional pattern-based approach of Caudodorsal, Perihilar, Middle, and Cranial lung region views (Lisciandro 2014b; Lisciandro et al. 2014, 2017; Ward et al. 2017, 2018b, 2019).

So why the delay in the uptake of lung ultrasound (LUS) use in small animal veterinary medicine? It is true that ultrasound waves do not transmit through air but rather are reflected, and therefore ultrasonography does not allow visualization of aerated lung parenchyma in the way that is allows visualization of nonviscous soft tissue and fluid-filled structures. However, the surface of the lung is visible on ultrasound, and the epiphany is that LUS is extremely sensitive for lung surface pathology (Volpicelli et al. 2006, 2012; Lichtenstein and Meziere 2008; Rademacher et al. 2014; Kulhavy and Lisciandro 2015; Ward et al. 2017, 2018b; Dicker et al. 2019). Furthermore, many types of lung pathology, including alveolar-interstitial edema, consolidation, and nodules, cause easily recognizable LUS artifacts that can be detected with high sensitivity and specificity (Kulhavy and Lisciandro 2015; Ward et al. 2017, 2018b; Dicker et al. 2019).

In fact, Vet BLUE may actually be more sensitive than TXR for detecting alveolar-interstitial edema, metastatic nodules, and lung contusions (Kulhavy and Lisciandro 2015; Lisciandro et al. 2016; Ward et al. 2018b; Vezzosi et al. 2017; Dicker et al. 2019); and performs well when compared to CT for many respiratory conditions in people and lung contusions in dogs (Volpicelli et al. 2006; Dicker et al. 2019). For example, CT is sensitive enough to reliably detect metastatic lung nodules as small as 1–2 mm in contrast to radiography, which has a threshold of 7–9 mm (Nemanic et al. 2006). In this same study, TXR compared to CT only detected metastatic nodules in 9% of cases. Vet BLUE gives you another option for cost-effective pulmonary metastasis screening as a same-day, same-patient visit, rapid, point-of-care imaging modality. In a comparative study with TXR, Vet BLUE outperformed TXR and was shown to detect nodules

*Point-of-Care Ultrasound Techniques for the Small Animal Practitioner*, Second Edition. Edited by Gregory R. Lisciandro.
© 2021 John Wiley & Sons, Inc. Published 2021 by John Wiley & Sons, Inc.
Companion website: www.wiley.com/go/lisciandro/ultrasound2

at the lung surface that were smaller than 1 mm (Kulhavy and Lisciandro 2015).

In people, it has been shown that most acute lung pathology extends to the lung surface and is thus detected by LUS (Lichtenstein and Meziere 2008; Volpicelli et al. 2006, 2012). Through our published and unpublished Vet BLUE research, we have found similar findings: acute conditions make it to the lung surface in dogs and cats (Lisciandro 2012, unpublished data). There is no reason to suspect that this differs from any other mammalian lung (Smith et al. 2012; Yarto and Lisciandro 2017, unpublished data). The limitation of any LUS examination is that in order to be visualized, pathology must extend very near to the peripheral, lung referred to as the "lung line" by the authors, which in people represents the outer 1–3 mm of lung (Volpicelli et al. 2006). Thus, if the pulmonary pathology occurs centrally within the lung and/or does not extend to the "lung line" at the acoustic window being used, then the pulmonary lesion will not be imaged regardless of protocol used. Thus, a major limitation of LUS is that it can only detect peripheral lesions present in an acoustic window being imaged; however, you will quickly find out how much Vet BLUE improves your current respiratory diagnostic and monitoring practice – the limitation approximates triviality.

In this chapter, we will cover how to perform the Vet BLUE lung ultrasound examination including relative anatomy, basic artifacts, the Vet BLUE B-line scoring system, and briefly its regional pattern-based approach. We will also cover its comparison to the other veterinary LUS protocols and differences in B-line scoring. Chapter 23 integrates the six Vet BLUE lung ultrasound signs with practical clinically relevant Vet BLUE applications.

Enjoy the ride into this new imaging frontier! We have made proactive lung ultrasound relevant and no small animal veterinarian has done as much proactive lung ultrasound as we have … 1000+ exams over 16 years.

## What Vet BLUE Can Do

- Provide a standardized regional pattern-based approach for lung ultrasound examination.
- Provide a systematic manner in which to record findings.
- Can rapidly rule out clinically relevant alveolar-interstitial edema including left-sided congestive heart failure by the finding of absent B-lines at all Vet BLUE views.
- Can rapidly detect signs of alveolar-interstitial syndrome (cardiogenic or noncardiogenic pulmonary edema, pneumonia, or other causes of increased extravascular lung water) with the finding of B-lines at Vet BLUE views.
- Can "score" the degree of alveolar-interstitial edema by using the Vet BLUE B-line scoring system.
- Can justify the use of loop diuretics in patients with left-sided congestive heart failure using the Vet BLUE B-line scoring system.
- Can guide loop diuretic therapy for patients with left-sided congestive heart failure using the Vet BLUE B-line scoring system.
- Can "score" the degree of lung contusions using the Vet BLUE B-line lung contusion scoring system.

## What Vet BLUE Cannot Do

- Provide a definitive diagnosis for underlying cause of lung pathology.
- Detect centrally (deeper) located lung pathology or conditions that are not in contact with the lung surface at a Vet BLUE acoustic window.
- Replace a complete physical examination, thoracic radiography, or CT imaging when indicated.

## Indications

- Point-of-care screening for patients with respiratory-related clinical signs (tachypnea, respiratory distress, cough) and for patients at risk for respiratory complications.
- Rapid assessment of patients with respiratory-related clinical signs deemed too unstable for TXR or CT, or when additional imaging is delayed because of lack of resources.
- Serial monitoring of respiratory patients using a rapid, noninvasive, radiation-sparing, point-of-care imaging modality.
- Use as a guide for diuretic therapy by monitoring persistence or resolution of B-lines and the Vet BLUE B-line scoring system.
- Use as a guide for fluid resuscitation or for detection of volume overload (cardiogenic pulmonary edema) in at-risk hospitalized and critically ill patients.
- Use in hospitalized patients for the presence and absence of volume overload, aspiration pneumonia, atelectatic lung, pulmonary thromboembolism, and others.

## Objectives (Table 22.1)

- Be able to perform Vet BLUE and understand the principles of image acquisition and its pitfalls.

**Table 22.1.**
Clinical questions answered using Vet BLUE lung examination.

| | |
|---|---|
| Does lung pathology exist on the lung surface? | Binary (Yes or no, present or absent) plus integrative with other findings using Global FAST, i.e., Vet BLUE visual lung ultrasound signs |
| Does the patient have alveolar-interstitial syndrome (fluid in the interstitial space or alveoli)? | Binary (yes or no, present or absent) plus integrative with other findings using Global FAST, i.e., TFAST Echo views |
| Does the patient have lung consolidation? | Binary (yes or no, present or absent) plus integrative with other findings using Global FAST |
| Does the patient have lung nodules? | Binary (yes or no, present or absent) plus integrative with other findings using Global FAST, i.e., other masses |
| Does the patient have pneumonia? | Binary (yes or no, present or absent) plus integrative with other findings using Global FAST, i.e., TFAST echo views |
| Does the patient have pulmonary thromboembolism (PTE)? | Binary (yes or no, present or absent) plus integrative with other findings using Global FAST, i.e., TFAST echo views |
| Does the patient have lung contusions? | Binary (yes or no, present or absent) plus integrative with other findings using Global FAST, i.e., Vet BLUE B-line lung contusion scoring |
| Does the patient have left-sided congestive heart failure? If so, what is the severity of pulmonary edema? Might the patient need diuretics? | Binary (yes or no, present or absent) plus integrative with other findings using Global FAST, i.e., TFAST echo views, Vet BLUE B-line scoring system |
| Is the patient developing lung pathology secondary to an intervention (blood transfusion, fluid therapy, etc.)? | Binary (yes or no, present or absent) plus integrative with other findings using Global FAST, i.e., TFAST echo views, caudal vena cava assessment, wedge sign |
| Is the coagulopathic patient bleeding into lung? | Binary (yes or no, present or absent) plus integrative with other findings using Global FAST, i.e., searching other internal spaces and cavities for other sites of bleeding |
| Does the patient have atelectatic lung? | Binary (yes or no, present or absent) plus integrative with other findings using Global FAST, Vet BLUE visual lung ultrasound signs, directly recruit lung using real-time imaging and positive pressure ventilation |

Source: Reproduced with permission from Dr Gregory Lisciandro, Hill Country Veterinary Specialists and FASTVet.com, Spicewood, TX.

- Be able to recognize normal appearance of aerated lung by A-lines with lung sliding at the pulmonary–pleural interface, also referred to as the "lung line."
- Be able to recognize LUS artifacts associated with alveolar-interstitial syndrome by the presence of B-lines (previously called ultrasound lung rockets).
- Be able to recognize the shred sign, tissue sign, nodule sign, and wedge sign.
- Be able to integrate the Vet BLUE regional pattern-based approach with the patient's clinical profile for an evidence-based working diagnosis by "seeing" the condition.

# Patient Preparation

## *To Clip or Not?*

Hair is generally not shaved but rather parted, with acoustic coupling medium applied as directly to the skin as possible, minimizing air trapping (see Figure 5.2). Isopropyl alcohol is often used alone or as a component of the coupling medium. Isopropyl alcohol should not be used when electrical defibrillation is anticipated (fire/burn hazard) or if prohibited by the transducer manufacturer due to risk of probe head damage. Commercially available acoustic coupling gel may be used on the probe head while the isopropyl alcohol is used to wet and part the hair, maximizing transducer–skin contact. Alcohol-based hand sanitizer, which has the advantage of being an excellent coupling medium, is much less noxious (not as chilling) to the skin and lungs (irritating fumes) than isopropyl alcohol, and wipes off much more easily than commercially available acoustic coupling gel. If the sonographer prefers clipping, clip in patients with longer hair using the smallest clipping width possible from ventral to dorsal so that the hair may be feathered to cover the clipped area, making clients much happier.

### Lights On or Off?

Imaging quality is generally sufficient without dimming lights in most indoor environments. Dimming lights potentially detracts from finding important equipment and avoiding hazards during resuscitation when time is critical. In all of the published AFAST, TFAST and Vet BLUE studies, lights were rarely dimmed for the ultrasound examinations (Lisciandro et al. 2008, 2009, 2014, 2017, 2018). In a human prospective study evaluating the efficacy of ultrasound during cardiopulmonary resuscitation (CPR), similar favorable conclusions regarding ambient light were reached (Breitkreutz et al. 2010a,b; McEntee et al. 2011). However, depending on the machine and sonographer's preference and the clinical situation, lighting may be appropriately dimmed for image optimization.

## Patient Positioning

### Standing and Sternal are Safest

Vet BLUE is most often performed in standing position because its nine acoustic windows are readily accessible in this position (Figure 22.1). Moreover, standing is generally safer and more comfortable for the patient. Sternal recumbency is also used in fragile respiratory or compromised patients. A roll of towels may be placed under the forelegs to access more ventral Vet BLUE (and TFAST) acoustic windows, especially helpful in felines (see Figures 19.2 and 39.28). When patients present recumbent, Vet BLUE may be performed on the exposed hemithorax along with the FAST diaphragmatico-hepatic (DH) view, with the opposing hemithorax performed by moving the patient to sternal/standing or to their opposing side. Most importantly, sternal or standing is preferred for patients with confirmed or suspected respiratory disease, those that are respiratory compromised or respiratory distressed, and those that are questionably stable and hemodynamically fragile.

Dorsal recumbency should never be used in unstable or questionably stable patients (Sigrist et al. 2004, 2011; Lisciandro et al. 2008, 2011; Boysen and Lisciandro 2013). A Vet BLUE/TFAST approach should be performed first before any significant restraint to rule out obvious pulmonary conditions, pleural effusion, and other pleural space-occupying conditions, pericardial effusion, cardiac abnormalities, and ascites (see Chapters 17 and 18). Excessive restraint or placing a hemodynamically fragile patient in dorsal recumbency is risky because the additional restraint and stress/anxiety can lead to increased oxygen demand, which is then compounded by the reduction of tidal volume and venous return through the weight of abdominal organs on the diaphragm and the caudal vena cava, respectively (see Figure 6.5). In human medicine, it is suggested to "never send a patient to radiology without a good physical exam and an extended FAST (EFAST)"; in other words, first perform a good physical exam and a Global FAST.

### Machine Positioning

The ultrasound machine and head of the patient should be in the same sightline for better spatial orientation and overall safety (see Figure 5.3). For example, if the patient is decompensating (cyanotic, open-mouth breathing) or turns to bite the sonographer or the animal holder, adjustments can be more easily made if the patient's head is in the sightline of the ultrasound screen. If the patient's head is facing in the opposite direction and away from the machine, the holder and sonographer are at risk for injury and the patient for unwitnessed decompensation – for example, if the patient is open-mouth breathing or becoming cyanotic, the sonographer and the assistant cannot see the patient's head directly.

## Ultrasound Settings and Probe Preferences

### Curvilinear Probe on Abdominal Preset versus Other

- A curvilinear (microconvex) probe with a frequency of 5–10 MHz is generally preferred for Vet BLUE, and this same probe may be used for the entire Global FAST examination. Linear probes will provide the best detail along the lung surface; however, most clinically relevant lung pathology is easily appreciated with the curvilinear probe, and curvilinear probes fit best within the contours of rib spaces. Phased-array probes have a "pinpoint" focal point and excellent temporal resolution, and are thus preferred for cardiac ultrasound. However, preliminary studies in which the author is involved suggest that phased-array probes are inferior to curvilinear probes for visualization and enumeration of B-lines.
- Depth is set at 4–8 (up to 9–10) cm for most patients. For cats and small dogs, start with 4–5 cm and for

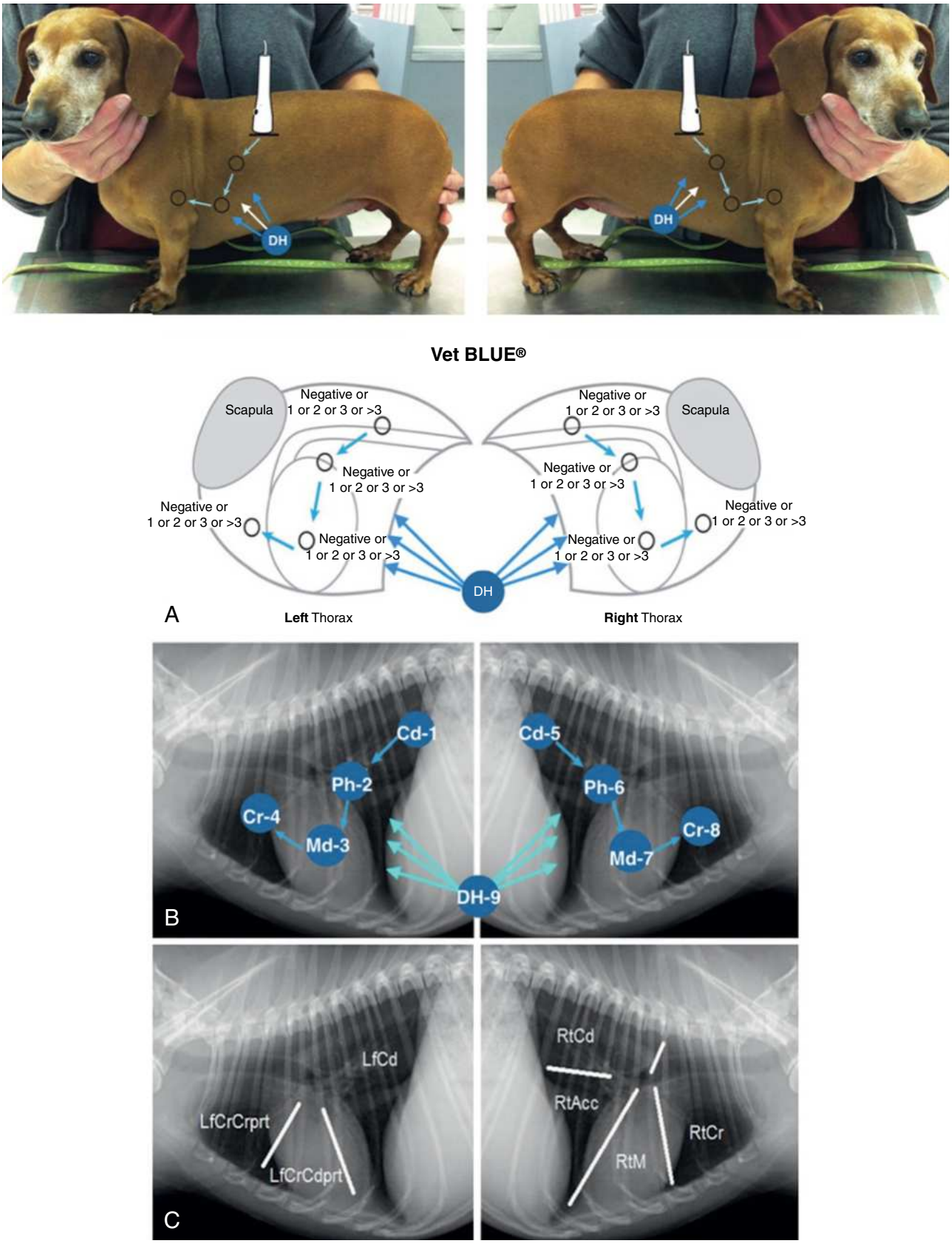


**Figure 22.1.** Vet BLUE performed in standing showing correlation with lung regions. In the unlabeled top row, the nine Vet BLUE acoustic windows are shown on a dachshund including four transthoracic views and the DH view. (A) A cartoon of the Vet BLUE with the cardiac silhouette, aorta, diaphragm, and scapula depicted. In (B) the Vet BLUE views overlay a lateral thoracic radiograph and in (C) the divisions of lung lobes is depicted showing that Vet BLUE is not exactly anatomical and thus it is possible that two different lung lobes or two different parts of lung may be viewed via the same Vet BLUE acoustic window. Source: Reproduced with permission from Dr Gregory Lisciandro, Hill Country Veterinary Specialists and FASTVet.com, Spicewood, TX.

larger dogs set initial depth up to 8 cm; and in some giant-breed dogs a depth up to 9–10 cm may provide the best imaging. Depth settings that are too low ("too close" to the lung) make it possible to miss lung lesions that fill the screen, and depth settings that are too high ("too far away" from the lung) make it possible to miss smaller lung surface pathology (see Chapter 23). Depth may be *decreased* (magnify) to investigate smaller lung pathology and to view details of the pulmonary–pleural interface (PPI), also referred to as the "lung line," but then should be again *increased* to the general guidelines of 4–8 cm (and 9–10 cm for giant breeds) (Figure 22.4).

- The focal zone cursor, featured on most ultrasound machines, should be placed at the level of the PPI represented by the hyperechoic line where the visceral and parietal pleura meet in normalcy in the absence of pleural space disease or where the "lung line" is located in pleural space conditions (see Figures 22.2 and 22.3).
- Appropriate gain settings are very important. "Overgaining," making the image too bright (too white), makes it difficult to see the PPI (see Figure 17.10) and artifacts along the lung surface. In general, the gain setting for Vet BLUE should be less than that for soft tissue during TFAST and AFAST, such that the screen is darker with more contrast. However, gain must also be high enough so that imaging is possible through the far-field of the screen to accurately identify B-lines and deeper lesions (see Figure 17.10).
- Because the abdominal preset is generally used for the rest of the Global FAST examination, this preset is also often used for Vet BLUE. However, the cardiac preset may provide more contrast and be preferred by some sonographers. The author, however, does the entire Global FAST on the abdominal preset and with a single probe type (curvilinear).
- The "gator sign" is the same intercostal orientation as for the TFAST CTS view and used for *all* lung ultrasound orientation (see Figures 22.2 and 22.3). See the Probe Orientation section below.

**Pearl:** Consider Vet BLUE as an "extension" from the TFAST CTS view, applied to three additional transthoracic lung regions per hemithorax plus the FAST DH view providing a more comprehensive lung ultrasound examination.

# How to Do a Vet BLUE Exam

## *Lung Orientation and the Gator Sign*

The "gator sign" is an orientation where the probe head is positioned perpendicular to the long axis of the ribs, or in the longitudinal plane for lung. The standard orientation for all lung ultrasound (LUS) begins with the observation of the "gator (alligator) sign" (Figures 22.2 and 22.3). The "gator sign" is created by the rounded rib (alligator's eyes) with a proximal hyperechoic line in between (alligator's bridge of nose) creating the image of a partially submerged alligator peering over the water at the sonographer. The space between the rib (alligator's eyes) is the intercostal region with the hyperechoic line (alligator's bridge of nose) created by the strong air–soft tissue interface representing the PPI and the "lung line (surface)" (see Figures 22.2 and 22.3). The author prefers the term "lung line" because when pleural space conditions are present, the integrity of the PPI is lost, and the term "lung line" is more accurate for what is being located and evaluated.

The "gator sign" orientation is the starting point for all lung ultrasound (Lisciandro 2011; Lisciandro et al. 2014, 2017; Ward et al. 2017). This orientation is the same as described for the TFAST CTS view (Lisciandro et al. 2008; Lisciandro 2011; Boysen and Lisciandro 2013) (see Figure 17.12). The "gator sign" orientation also allows observation of the to-and-fro motion of "lung sliding" (Volpicelli et al. 2012), previously referred to as the "glide sign" in the veterinary literature (see Figure 22.2) (Nyland and Mattoon 2002). "Lung sliding" represents the to-and-fro sliding of visceral and parietal pleura during inspiration and expiration, or "lung sliding" along the intercostal space. Its appearance resembles the back-and-forth movement of an Etch-a-Sketch® cursor (see Figures 22.2 and 22.3) (Lisciandro et al. 2008, 2014a,b; Lisciandro 2011).

## *Probe Orientation: Rotate or Not*

Some sonographers advocate rotating the probe parallel to the ribs to get another plane of lung during LUS (Figure 22.4). Caution should be exercised unless the sonographer has an extensive knowledge of LUS imaging and its anatomical borders and pitfalls. Rotating the probe and losing sight of the "lung line" can lead to misinterpretations of abdominal structures, dorsal and ventral borders of the pleural cavity

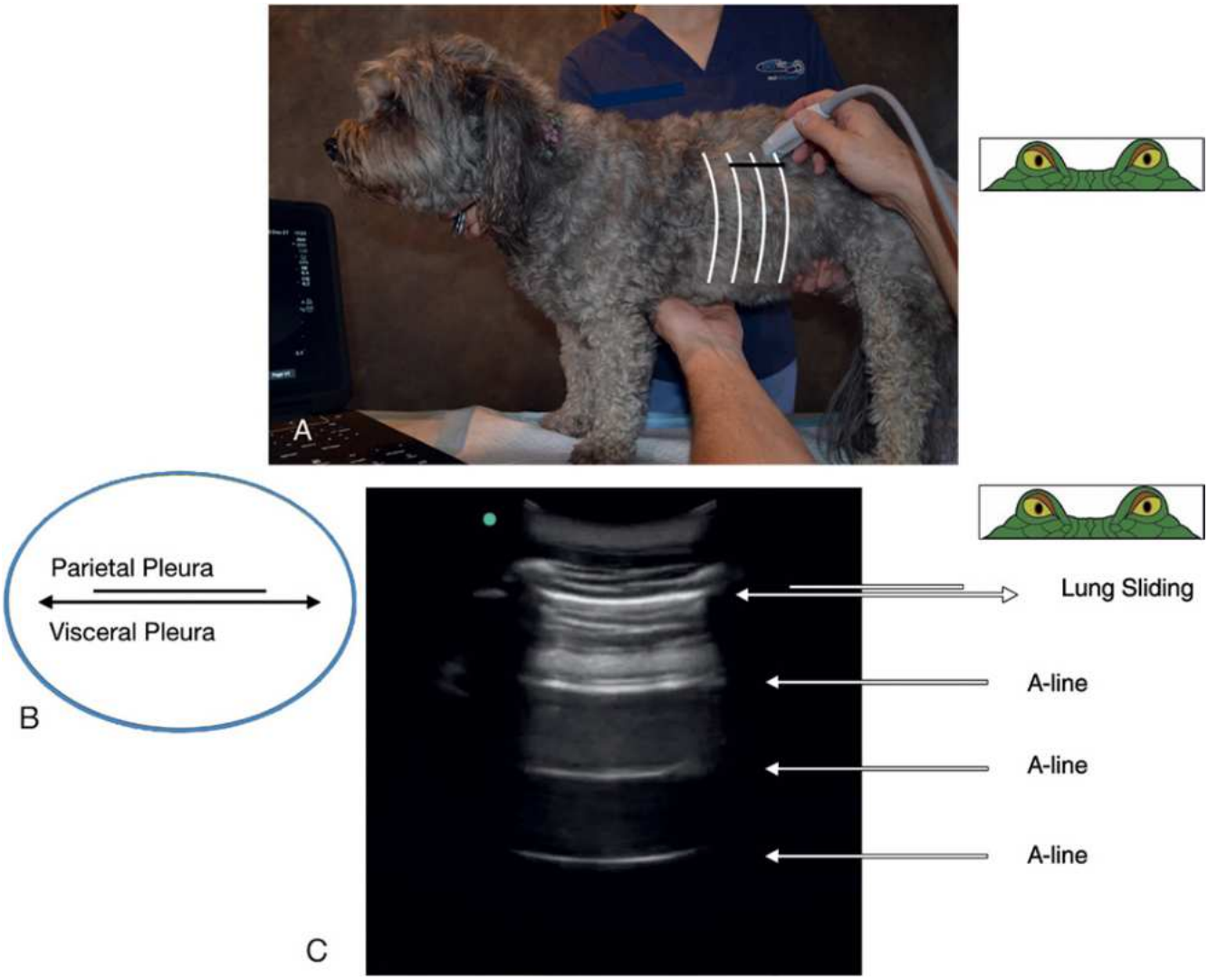


**Figure 22.2.** Gator sign orientation externally on a dog. Shown in (A) is the orientation externally on a dog with white curved lines as an overlay depicting the intercostal spaces and acquisition of the "gator sign" by orientating the probe perpendicular to the long axis of the ribs. In the absence of pleural space disease (free fluid, free air, diaphragmatic hernias, masses) the sonographer observes for the "lung sliding" sign of visceral and parietal pleura sliding along the intercostal space (B) likened to an Etch-a-Sketch® cursor. In (C) "lung sliding" is accompanied by air reverberation artifact and these horizontal equidistant lines extending from the aerated lung surface are referred to as A-lines. Source: Reproduced with permission from Dr Gregory Lisciandro, Hill Country Veterinary Specialists and FASTVet.com, Spicewood, TX. Illustration by Suji Park, Englewood Cliffs, NJ.

(muscle), and cranial borders (thoracic inlet and periscapular muscles and scapula) for lung pathology (Figure 22.5; see also Figures 22.17 and 41.21). If transverse orientation is attempted, the lung sonographer must always double-check by appreciating the "gator sign" while rotating the probe from longitudinal to transverse and then returning to longitudinal, the author's recommended methodology (see Chapter 41). See Confounders of the "Gator Sign" Orientation section later in this chapter.

## *Image Optimization of the "Lung Line"*

During Vet BLUE, the angle of insonation should be close to 90° (scanning plane perpendicular to the "lung line") to maximize sonographic clarity of the lung

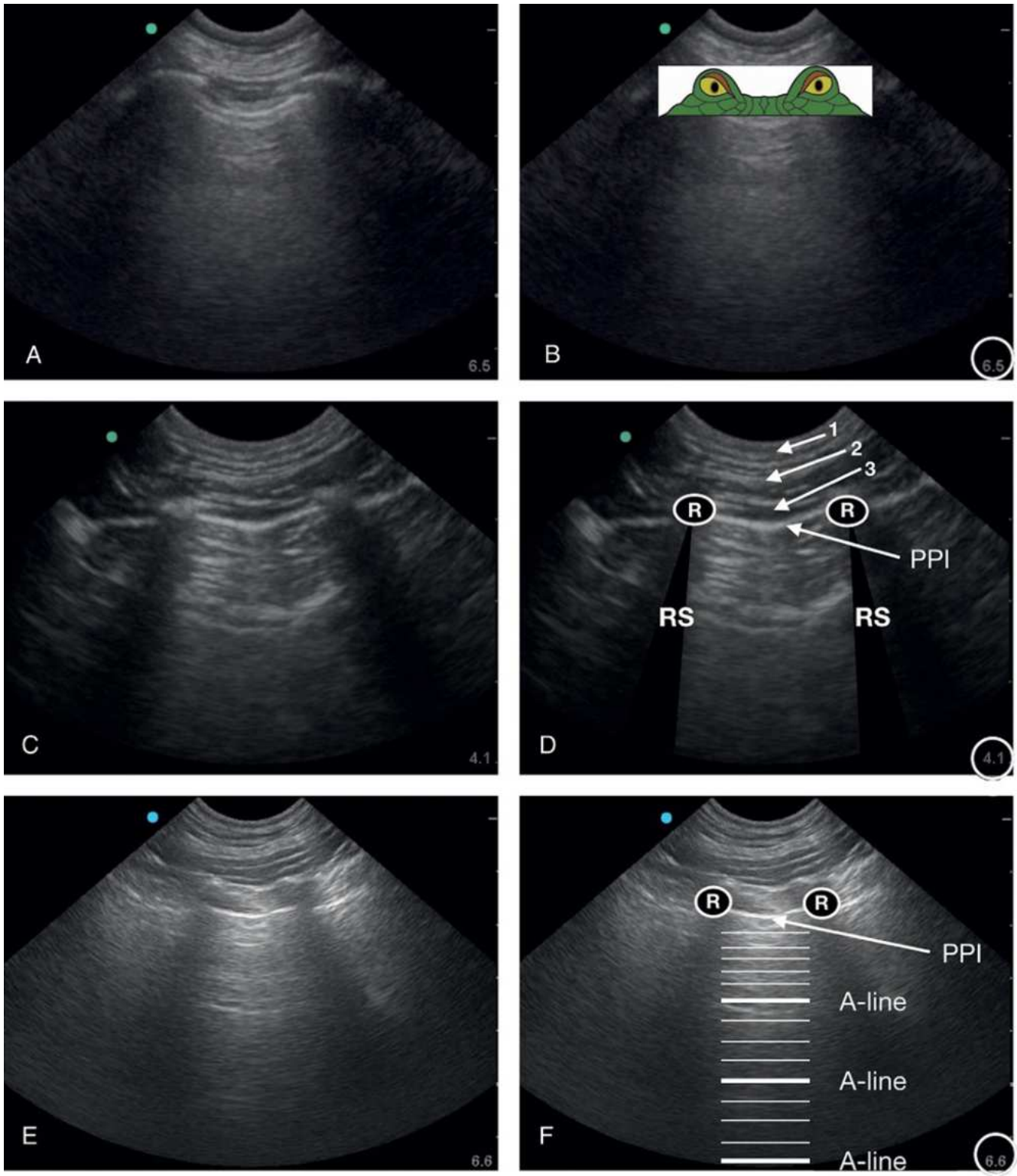


**Figure 22.3.** Gator sign orientation on B-mode. The "gator sign" orientation is imperative to understand for successful Vet BLUE imaging because it locates the lung surface, at the pulmonary–pleural line (PPI), that the author calls the "lung line." The term "lung line" would be more accurate in patients with pleural space disease since the PPI is no longer representative of where lung is expected. Without being able to confidently determine where the intercostal space is located and where the lung surface is expected by establishing the "gator sign" orientation, lung cannot be accurately imaged. In (A) an unlabeled "gator sign" image is shown. In (B) an overlay showing the "gator sign" is placed over the same image. In (C) another example shows the proper "gator sign" orientation in a cat. Shown in (D) is the same image but labeled pointing out the soft tissue between the probe head and the "lung line." In (E) and (F) are again unlabeled and labeled images. In (D) the arrows labeled 1, 2 and 3 point out the skin, subcutaneous tissue and intercostal muscle, respectively. A-lines are depicted by horizontal line overlays, which are always parallel to the "lung line" and proceed through the far-field of the screen. To optimize visualization of the A-line artifact, the angle of insonation must be at 90° to the "lung line." Circled R, rib; RS, rib shadow. Source: Reproduced with permission from Dr Gregory Lisciandro, Hill Country Veterinary Specialists and FASTVet.com, Spicewood, TX. Illustration by Suji Park, Englewood Cliffs, NJ.

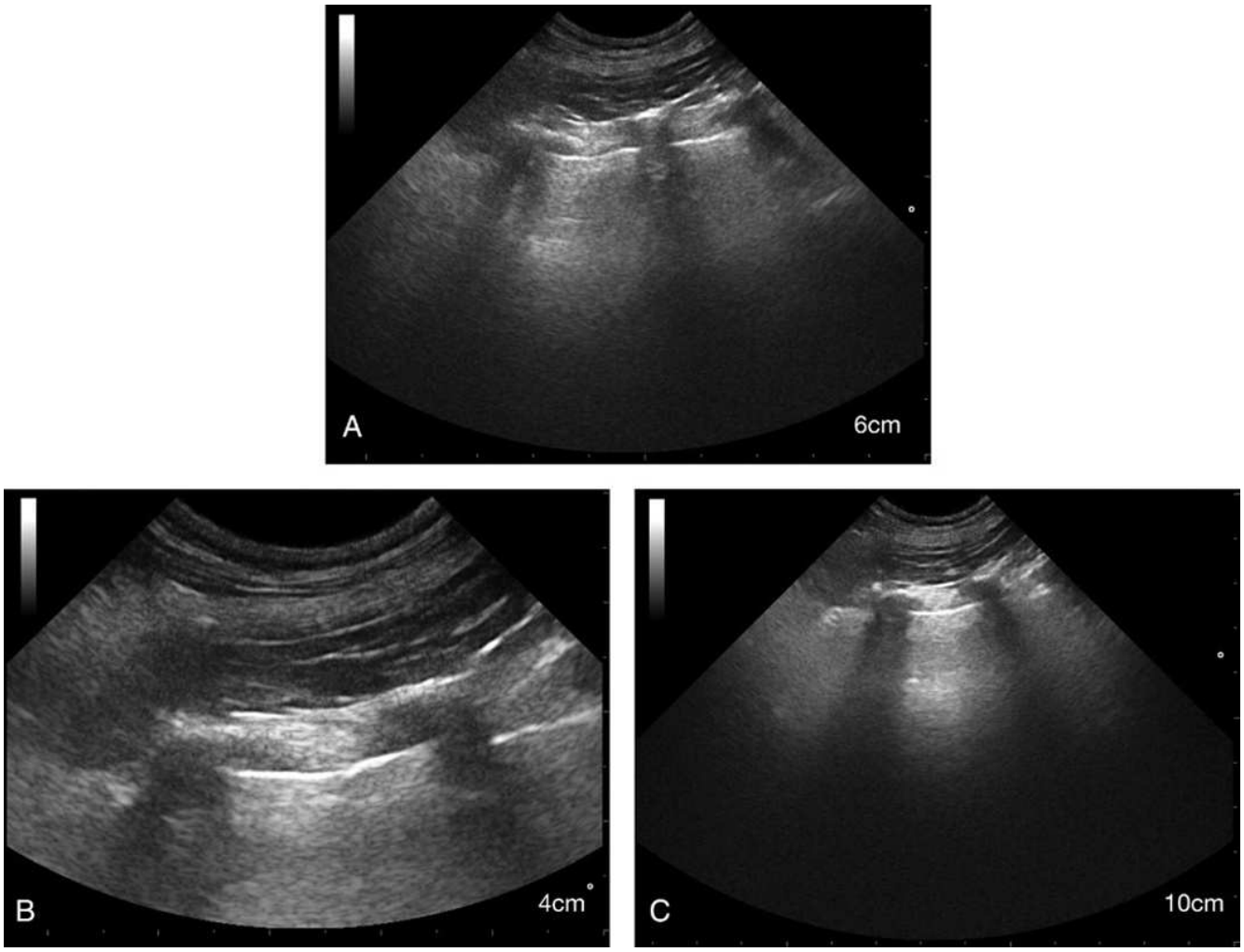


**Figure 22.4.** Depth and proportionality. Depth is generally set at 4–8 cm (up to 9–10 cm in giant-breed dogs). In (A) the depth setting is closest to ideal at 6 cm. In (B) the depth is too shallow or magnified (4 cm) as lung pathology may be missed when extending beyond the far-field of the screen. In (C) the depth is too deep (10 cm) and the intercostal space very small, making it difficult to appreciate lung surface pathology. Source: Reproduced with permission from Dr Gregory Lisciandro, Hill Country Veterinary Specialists and FASTVet.com, Spicewood, TX.

surface (Figure 22.6; see also Figure 22.7). This Vet BLUE angle of insonation differs from the TFAST approach for pneumothorax (PTX), in which the presence (normal aerated lung) or absence (PTX) of "lung sliding" is often best observed by fanning the probe to a 60–75° angle of insonation and then holding the probe still (Figure 22.7). This TFAST strategy is referred to by the author as "obliquing" or "ricocheting" the echoes (Lisciandro 2014a: Boysen and Lisciandro 2013; Lisciandro et al. 2014) (see Chapter 17 Tricks of the Trade Section). In Vet BLUE, the probe is held stationary at 90° to optimize imaging of LUS artifacts other than "lung sliding" and thus allowing best visualization of the six Vet BLUE lung ultrasound signs (see Chapter 23) (Figure 22.8).

## Vet BLUE and Its Nine Acoustic Windows

It is very important for the sonographer to understand that Vet BLUE views *do not correspond exactly* to anatomical locations of lung lobes, and that when surveying intercostal spaces (ICS), different parts of lung lobes or different lung lobes may be present over the

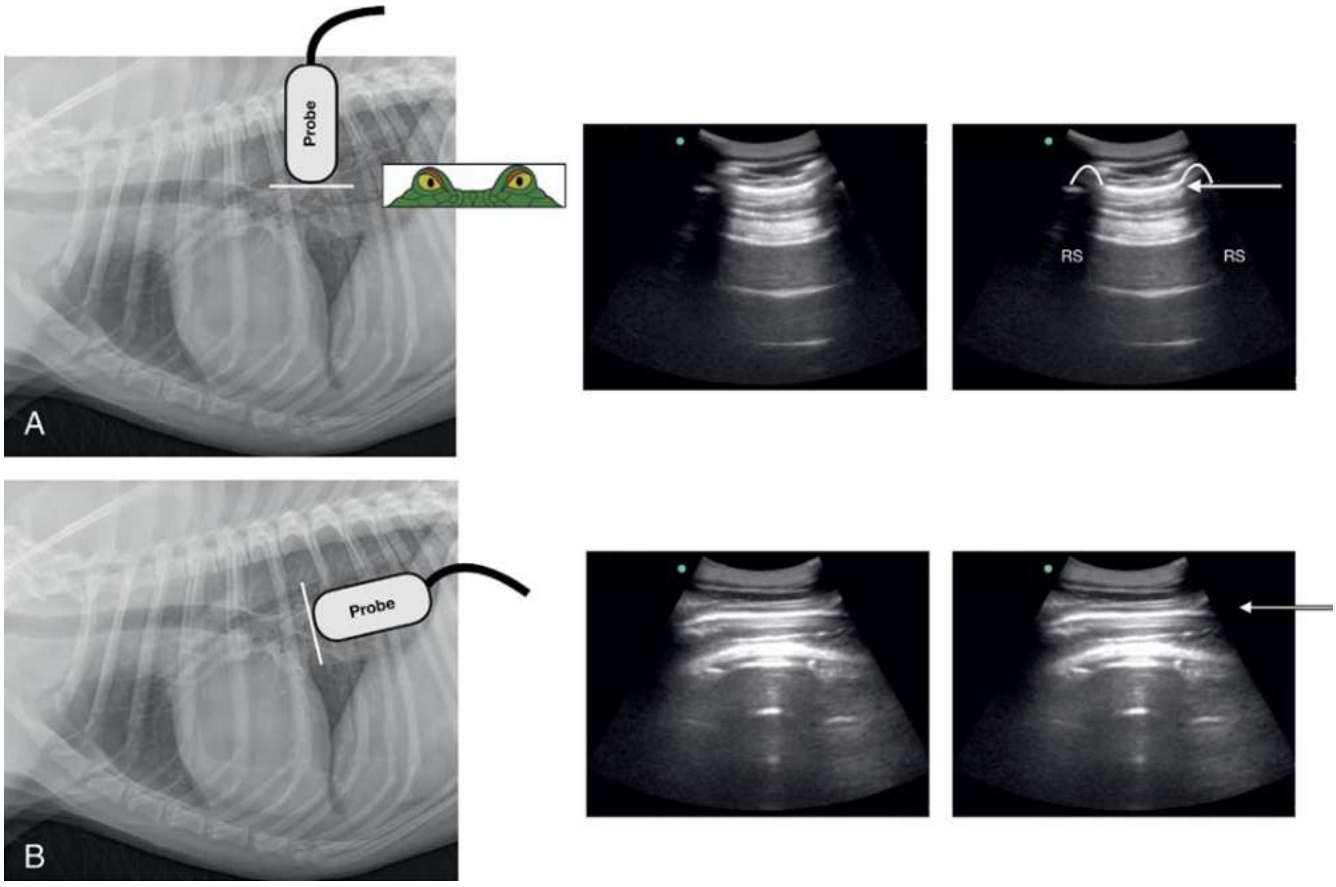


**Figure 22.5.** Difference in appearance of longitudinal versus transverse orientation of lung and losing the "gator sign." Shown in (A) is the "gator sign" orientation with the direction of the probe head superimposed on a lateral thoracic radiograph and perpendicular to the long axis of the ribs, followed by unlabeled and labeled B-mode images. The curved overlays help point out the ribs, the arrows point out the PPI and "lung line", and RS is rib shadow. Note the strikingly obvious A-lines. Contrast row (A) with row (B) in which the probe is rotated parallel to the ribs resulting in the "gator sign" orientation being lost. Now the location of the PPI and "lung line" becomes confusing if the PPI and "lung line" are not first established and recognized via the "gator sign." The arrow points out the actual PPI and "lung line." Source: Reproduced with permission from Dr Gregory Lisciandro, Hill Country Veterinary Specialists and FASTVet.com, Spicewood, TX.

three intercostal spaces of each Vet BLUE acoustic window (see Figure 22.1). Thus, the Vet BLUE acoustic windows are referred to as "lung regions."

## Naming of the Nine Acoustic Windows

There are eight bilaterally applied *transthoracic* acoustic windows plus the ninth acoustic window as the DH view.

- Caudodorsal (Cd) lung region, right and left
- Perihilar (Ph) lung region, right and left
- Middle (Md) lung region, right and left
- Cranial (Cr) lung region, right and left
- Diaphragmatico-hepatic view, single acoustic window

## Defining the Locations of the Nine Acoustic Windows (Views)

### Transthoracic Views

#### *Caudodorsal Lung Region (Cd, point 1)*

This is defined as directly dorsal to the xiphoid in the upper third of the thorax in its 9th–10th intercostal space near the highest point over the pleural cavity with lung. The Cd view starting point is the same acoustic window used for the TFAST CTS. At this region, the sonographer looks for the caudodorsal transition zone (CdTZ) where pleural and abdominal cavities meet because you will move cranial, away from this region to start Vet BLUE. There are two ways

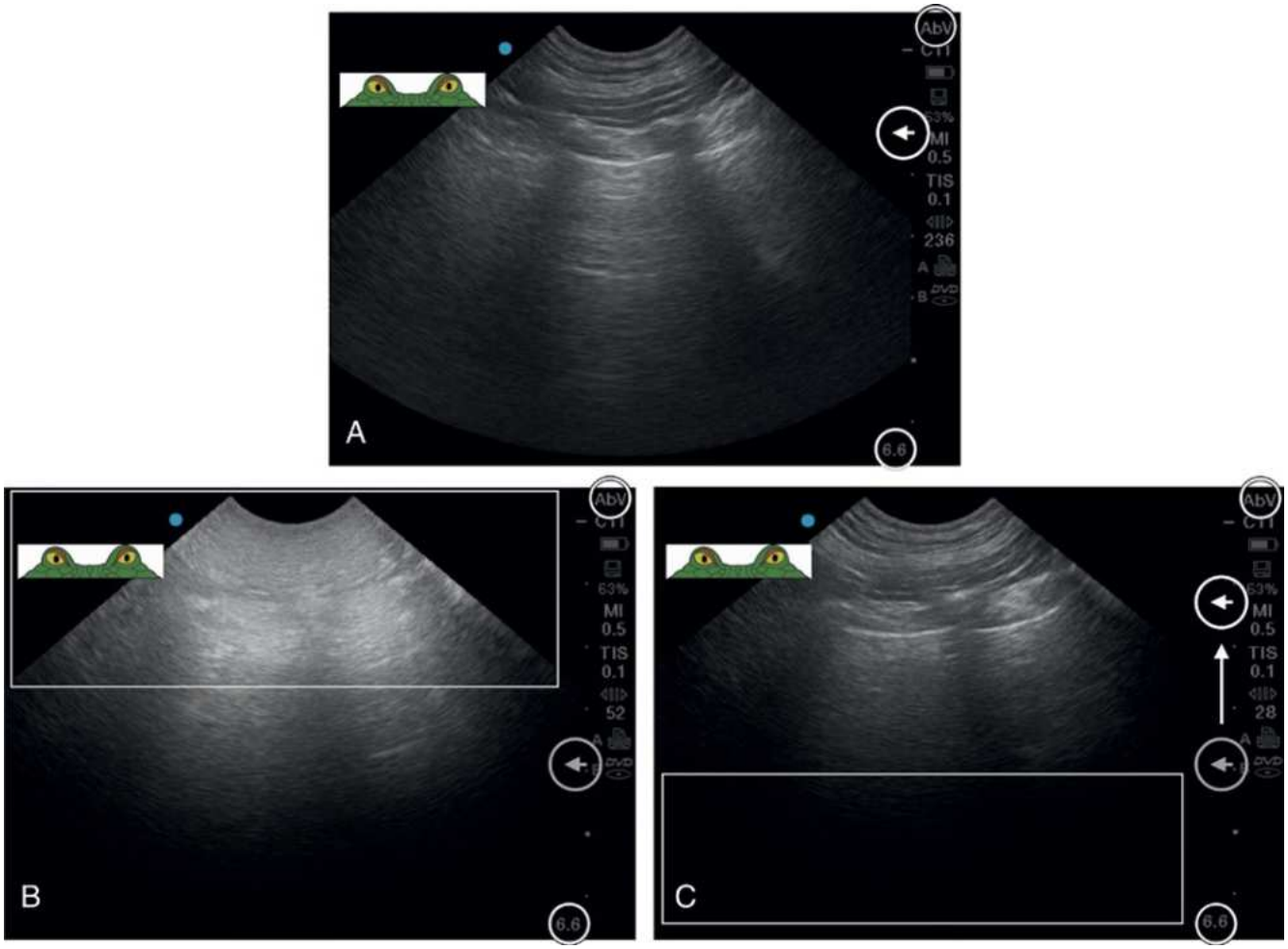


**Figure 22.6.** Optimizing the image – gain, depth, and focus cursor. Major ultrasound machine adjustments to optimize the image. A "gator sign" overlay is also present to show the appropriate orientation and proportionality for good lung ultrasound image acquisition. All are on the same abdominal preset noted by the circle in the upper right corner of all images. Depth is shown by the circle in the bottom right corner and is in centimeters (cm). All ultrasound machines have a depth and ruler (hash marks in cm) on their screen and the sonographer should be familiar with this feature. The focus cursor is denoted by an arrow overlay. In (A) the focus cursor is directly across from the "lung line" which is at the pulmonary–pleural interface (PPI). In (B) the focus cursor is in the middle of the screen, appropriate for soft tissue imaging with AFAST and TFAST. In (C) a vertical area is a prompt that if the "lung line" and PPI are not acceptable to the lung sonographer, moving the focus cursor to directly across from either often proves helpful. Lastly, the boxed area shows how the near-field is overgained in (B), making it difficult to observe the "lung line" and PPI. Turn down the gain. The gain is likely set higher for soft tissue of AFAST and TFAST (and depth likely deeper too) so get used to making these adjustments going from AFAST and TFAST to Vet BLUE and the opposite adjustment when starting with Vet BLUE and moving to AFAST and TFAST. In (C) the far-field is undergained (boxed overlay), making it difficult to see artifacts and lung pathology through the far-field which can lead to inaccurate interpretation. Source: Reproduced with permission from Dr Gregory Lisciandro, Hill Country Veterinary Specialists and FASTVet.com, Spicewood, TX.

to find this transition zone: (1) find the "curtain sign" where a linear border from the dirty shadowing of air-filled lung comes across the screen from left to right, and (2) identify abdominal structures and then slide cranial away from the abdominal cavity (Figures 22.9 and 22.10). Once the CdTZ is located, slide 2–3 intercostal spaces cranially away from it. This maneuver is important for two major reasons: so the sonographer's eyes are not tricked into thinking abdominal structures are lung pathology, and the sonographer's eyes are not tricked into thinking that diaphragmatic-abdominal movement is "lung sliding." While sliding cranially and away from the CdTZ, pay attention to the lung surface.

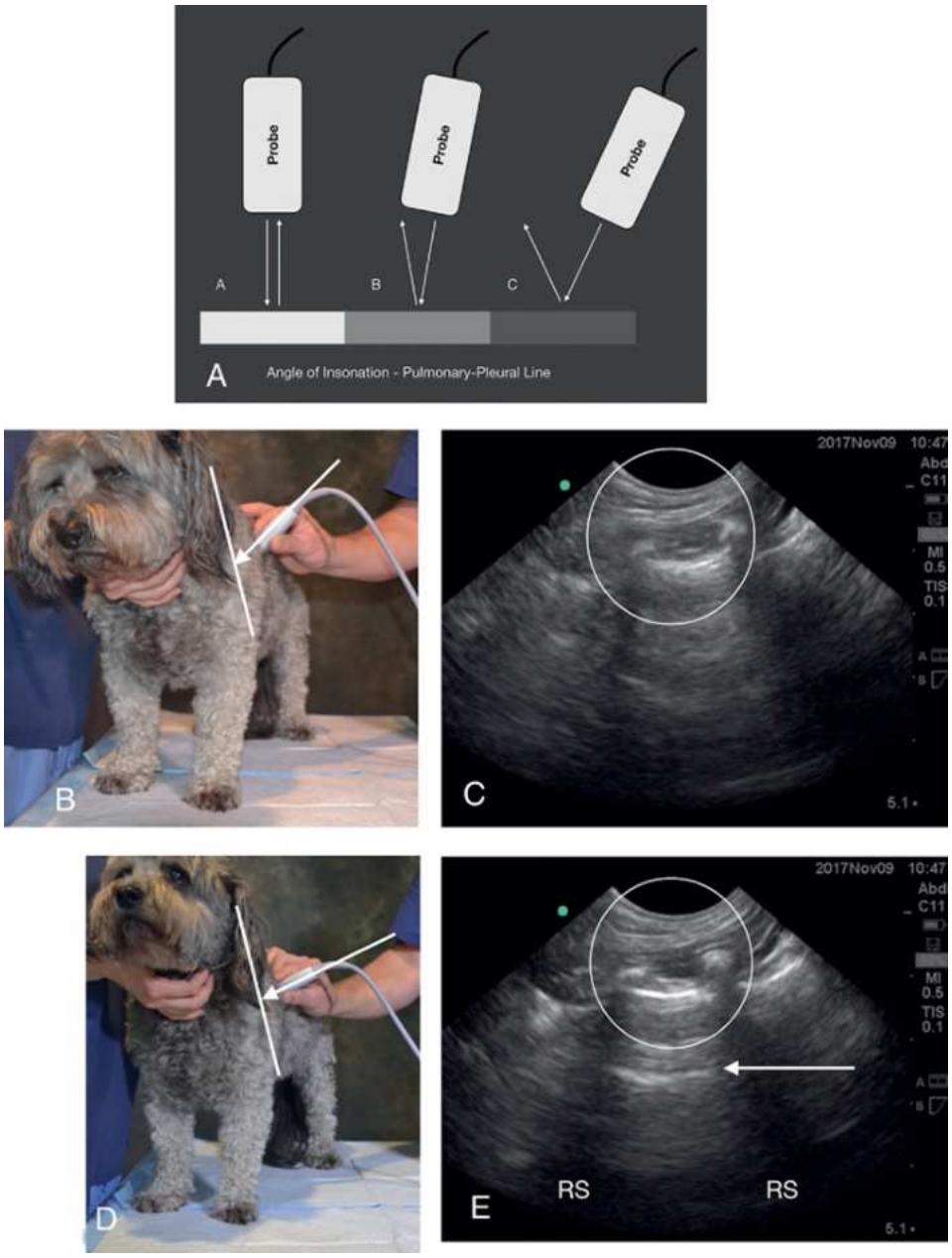


**Figure 22.7.** The effect of angle of insonation and lung ultrasound artifacts. The cartoon in (A) shows different angles of insonation along the PPI and "lung line." The best for appreciating LUS artifacts other than "lung sliding" is 90°. However, fanning the probe to an angle of ~75° (in other words, making the hyperechoic "lung line" less white and more gray) and then holding the probe stationary "ricochets" or "obliques" the echoes, helping to recognize "lung sliding." In (B) and (C) the angle is shown externally on a dog's thoracic wall with a corresponding B-mode image with an angle more ideal for "lung sliding" in contrast to (D) and (E) where the angle of insonation approximates 90° that better shows artifacts, A-lines, and a sharper "lung line" for evaluation of lung surface pathology. Circled is the intercostal space, RS, rib shadow. Source: Reproduced with permission from Dr Gregory Lisciandro, Hill Country Veterinary Specialists and FASTVet.com, Spicewood, TX.

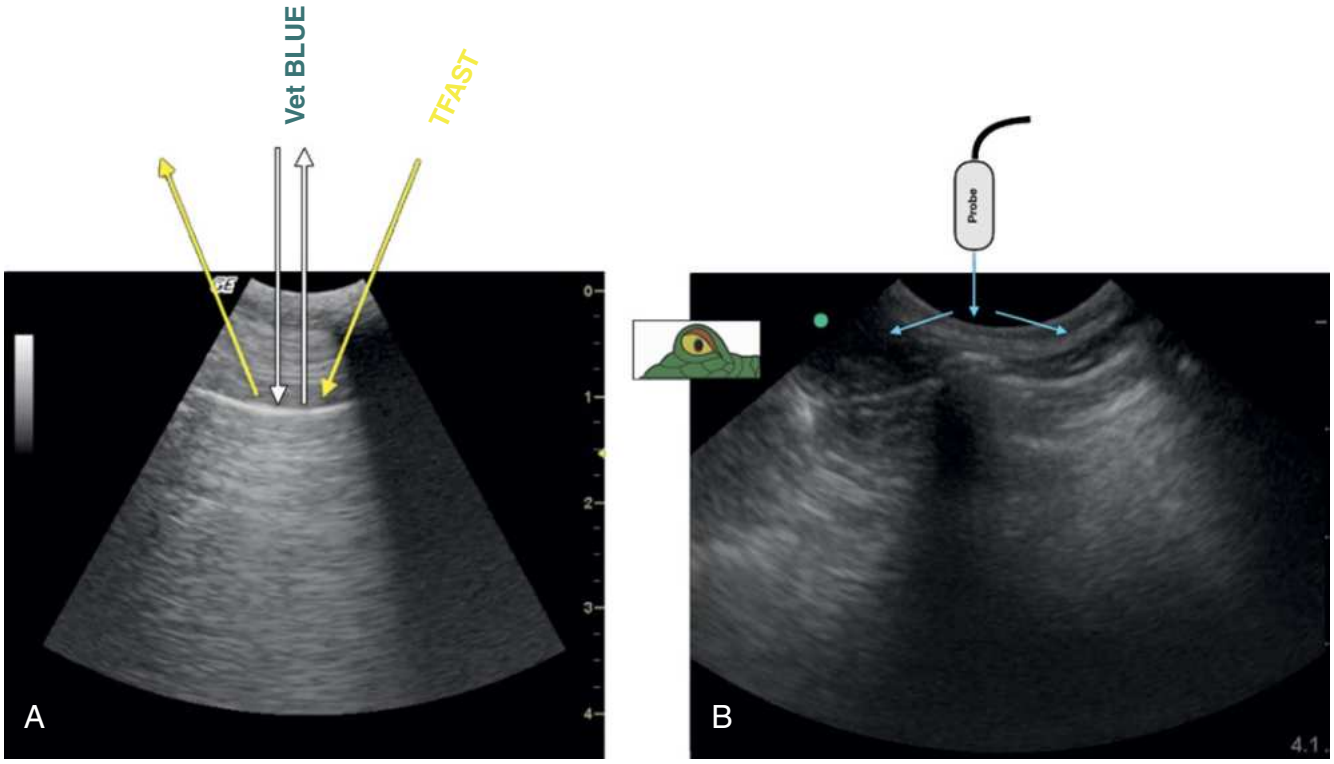


**Figure 22.8.** Imaging the "lung line" and angle of insonation. (A) Changing the angle of insonation for the "lung line" and for "lung sliding" by 90° (Vet BLUE) and ~75° (TFAST). Shown in (B) is the "one-eyed gator sign" and an approach discovered by the author placing the rib centered in the middle of the screen to scatter echoes off the lung surface, which enhances the observation of "lung sliding" (see also Figures 17.7 and 17.11). Source: Reproduced with permission from Dr Gregory Lisciandro, Hill Country Veterinary Specialists and FASTVet.com, Spicewood, TX. Illustration by Suji Park, Englewood Cliffs, NJ.

### *Perihilar Lung Region (Ph, point 2)*

This is defined as the point in the middle third of the thorax between the 6th and 7th intercostal spaces approximating the perihilar region on a thoracic radiograph. The Ph (point 2) is found by "drawing" a line from the Cd (point 1) to the elbow. This is done with your acoustic coupling medium and your hand by roughing the hair along this "Vet BLUE line." Halfway from the Cd (point 1) is the Ph (point 2) (Figure 22.11).

### *Middle Lung Region (Md, point 3)*

This region is defined as the lower half of the thorax over the heart approximating the 4th–5th intercostal spaces. If the heart is in view and obscuring lung, then sweep immediately dorsal in that same intercostal space(s), finding the "lung line" and then performing the Vet BLUE examination (Figure 22.12).

### *Cranial Lung Region (Cr, point 4)*

This is defined as the 1st, 2nd, and 3rd intercostal spaces – in other words, in the region caudal to the thoracic inlet and cranial to the heart. The foreleg often needs to be gently extended cranially to get this view (see Figure 22.11). The soft tissue and vessels of the thoracic inlet help define the Cr (point 4). Identify the thoracic inlet's soft tissue structures, the cranial transition zone (CrTZ) (Figure 22.13), and then slide caudally over the first three intercostal spaces. The author recommends always extending the foreleg from the elbow region rather than the paw because some dogs (and cats) do not like their paws touched and become stressed or bite when their paws are handled.

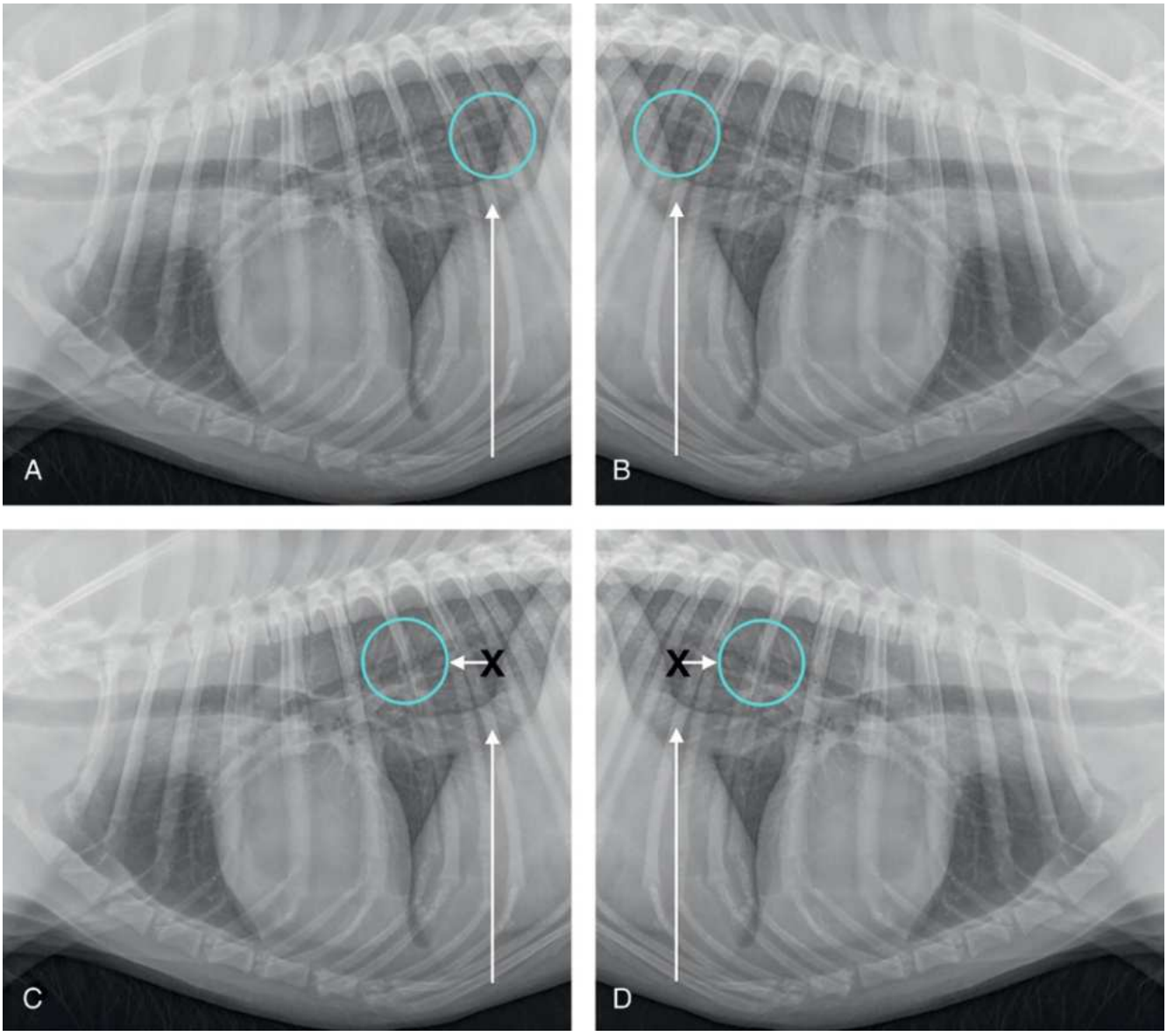


**Figure 22.9.** Caudodorsal transition zone depicted radiographically. All images are the same lateral thoracic radiograph used for illustrative purposes for the spatial relationship of the pleural and peritoneal cavity and identifying the CdTZ. Directly dorsal to the xiphoid was originally defined at our TFAST CTS view (A) and (B), but commonly the location places you at the CdTZ (circle) and through experience we have learned that the region can become confusing with the movement of the pleural cavity, lung, diaphragm and abdominal structures and their respirophasic sliding. This makes "lung sliding" difficult to observe as well as confusing the lung sonographer who may be unable to accurately differentiate lung from abdominal structures. The CdTZ is now identified (X) and then the probe is slid cranially 2–3 intercostal spaces (horizontal arrow) to move away from and when possible eliminate the CdTZ (circle) from view for evaluating lung shown in (C) and (D). Source: Reproduced with permission from Dr Gregory Lisciandro, Hill Country Veterinary Specialists and FASTVet.com, Spicewood, TX.

### The Ninth Acoustic Window

The ninth acoustic window (view) is the DH view, serving as a deep window where lung contacts the diaphragmatic surface, referred to by the author as the pulmonary–diaphragmatic interface.

This view is defined as immediately caudal to the xiphoid on midline with the probe directed far cranially toward the patient's head with the same DH view methodology used for AFAST and TFAST. Along the diaphragm, the Vet BLUE six lung

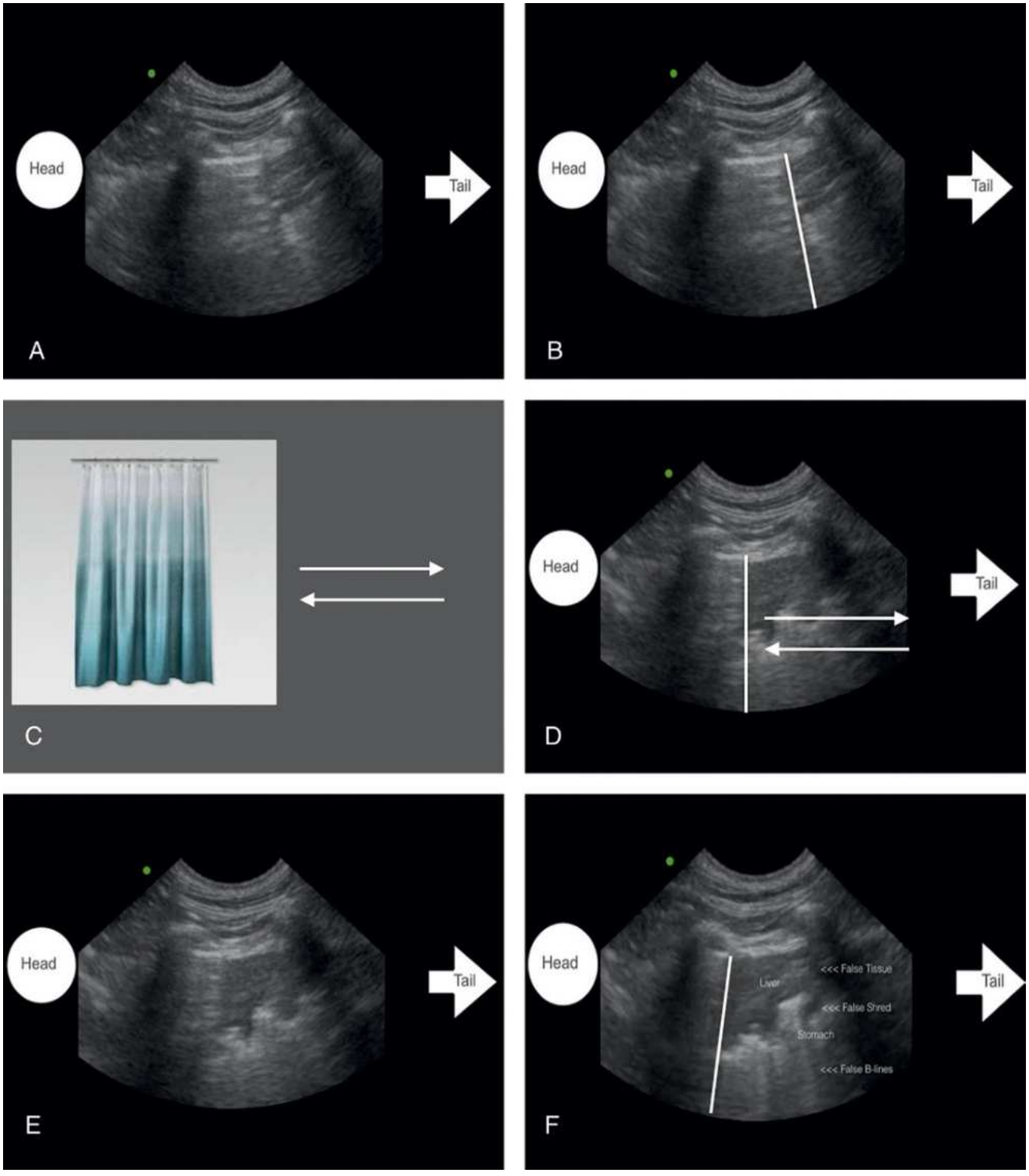


**Figure 22.10.** Caudodorsal transition zone on B-mode and "curtain sign." All B-mode images are the same image but with different overlays to point out the various features of the CdTZ. The head should always be to the left of the screen because it helps keep track of the abdominal structure pitfalls that are then always expected from the right of the screen. In (A) unlabeled and (B) labeled the line shows the linear "curtain sign" that is the caudal aspect of the dirty shadowing from air within the thorax (either aerated lung or pneumothorax). In (C) is a "shower curtain" that helps convey the effect of the pleural cavity and peritoneal cavity transition zone like a curtain sliding over a region with a linear border as in (D). In (E) is an unlabeled B-mode image showing the CdTZ compared to the labeled version in (F) showing how abdominal structures may be mistaken for lung pathology – pseudo B-lines from fluid and air within the lumen of the stomach, pseudo shred sign, pseudo tissue sign. The shred sign and tissue sign are explained in Chapter 23 and the B-lines explained subsequently in this chapter. Source: Reproduced with permission from Dr Gregory Lisciandro, Hill Country Veterinary Specialists and FASTVet.com, Spicewood, TX.

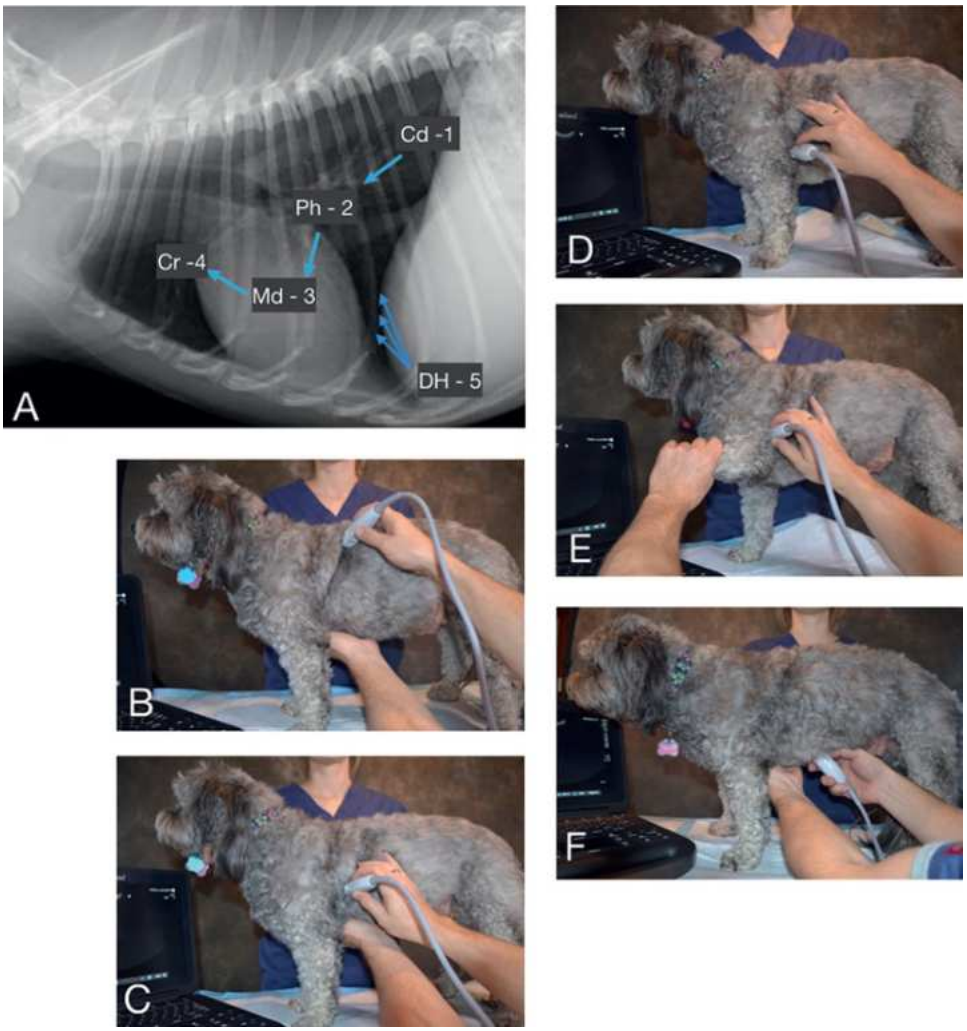


**Figure 22.11.** Left-sided Vet BLUE views. The lateral thoracic radiograph in (A) is helps correlate the external Vet BLUE views on a standing dog. Shown in (B) is the Caudodorsal lung region (Cd, point 1), in (C) the Perihilar lung region (Ph, point 2), in (D) the Middle lung region (Md, point 3) and in (E) the Cranial lung region (Cr, point 4). The Cranial lung region (point 4) requires extending the foreleg to place the probe over the first three intercostal spaces in the axillary area. The DH view shown in (F) is also part of Vet BLUE providing a deep window into lung along the pulmonary–diaphragmatic interface (see Figure 22.14). Source: Reproduced with permission from Dr Gregory Lisciandro, Hill Country Veterinary Specialists and FASTVet.com, Spicewood, TX.

ultrasound signs, described subsequently, are sought along the pulmonary-diaphragmatic interface. In fact, "lung sliding" may be observed here, although in standing or sternal patients, the region is generally least gravity dependent. Primarily the left and right caudal lung lobes that are inaccessible along the Vet BLUE transthoracic views are visualized (see Chapter 23).

Although inconsistently published (Boysen and Lisciandro 2013; Lisciandro 2014a,b; Lisciandro et al. 2014, 2017; Kulhavy and Lisciandro 2015; Ward et al. 2017, 2018b; Dicker et al. 2019), this view has been used by the author since the original development of Vet BLUE in 2010 (Figure 22.14). The FAST DH view allows imaging of the lung along its pulmonary–diaphragmatic interface where lung is inaccessible

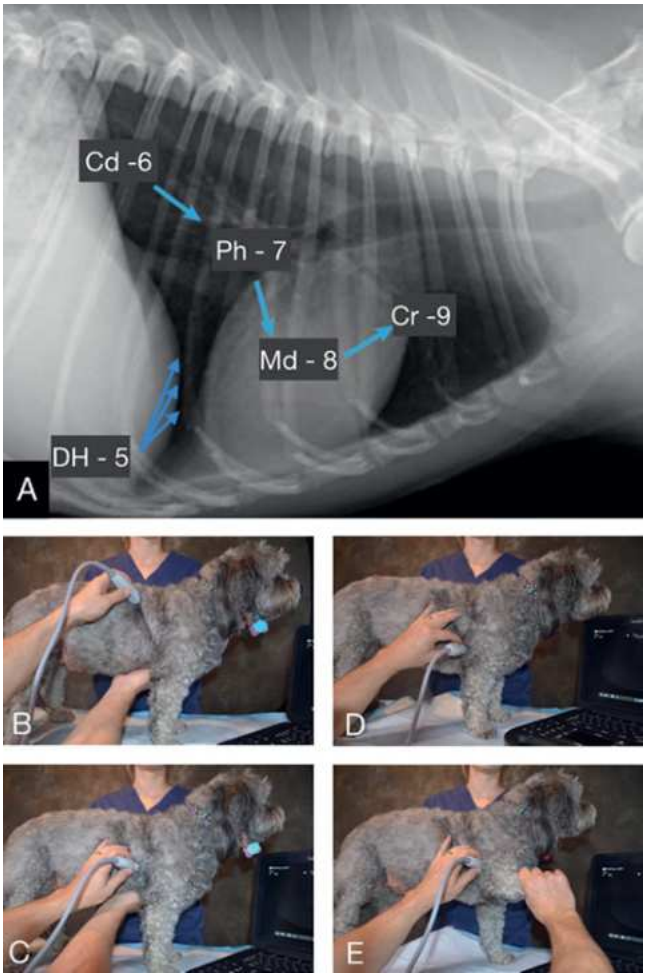


**Figure 22.12.** Right-sided Vet BLUE views. The lateral thoracic radiograph in (A) is used to help correlate the external Vet BLUE views on a standing dog. Shown in (B) is the Caudodorsal lung region (Cd, point 1), in (C) the Perihilar lung region (Ph, point 2), in (D) the Middle lung region (Md, point 3) and in (E) the Cranial lung region (Cr, point 4). The Cranial lung region (point 4) requires lifting and flexing the foreleg to place the probe over the first three intercostal spaces in the axillary area. The DH view is also part of Vet BLUE providing a deep window into lung along the pulmonary–diaphragmatic interface but is done from the left side by the author who is right-handed because it is easier for the right-handed to image the gallbladder and caudal vena cava (right-sided structures) from the left side of the patient. Source: Reproduced with permission from Dr Gregory Lisciandro, Hill Country Veterinary Specialists and FASTVet.com, Spicewood, TX.

via the transthoracic Vet BLUE acoustic windows. Thus, the FAST DH view is very important for detecting lung pathology associated with the accessory and the right and left caudal lung lobes and the mediastinal area that would otherwise be missed (see Chapter 23 and Figure 23.21).

# Performing the Vet BLUE

## *Order of Vet BLUE*

The Vet BLUE acoustic windows are generally performed in the following order moving from dorsal to ventral and cranial: left Cd → Ph → Md → Cr view, then DH, followed by right Cd → Ph → Md → Cr views. The reason for beginning dorsal is to rule in or rule out pneumothorax (PTX); and when suspected the "lung point" is automatically sought by moving ventrally along the subsequent Ph and Md lung regions. However, in most patients in which PTX is unlikely, the repetition of performing Vet BLUE after Vet BLUE after Vet BLUE on a daily basis will help the sonographer become confident with observing "lung sliding" while also learning how to optimize image acquisition with the Tricks of the Trade (see Chapter 17) and adjustments in the focus cursor, gain, depth, etc.

The protocol detailed below includes numerous updates and methodological improvements from the original Vet BLUE examination described in 2014 (Lisciandro 2014b; Lisciandro et al. 2014, 2017; Ward et al. 2017, 2019). For example, previously the Md lung region was defined as the lower third of the thorax in between the 4th and 5th intercostal spaces, and if heart was in view, we previously recommended sliding the

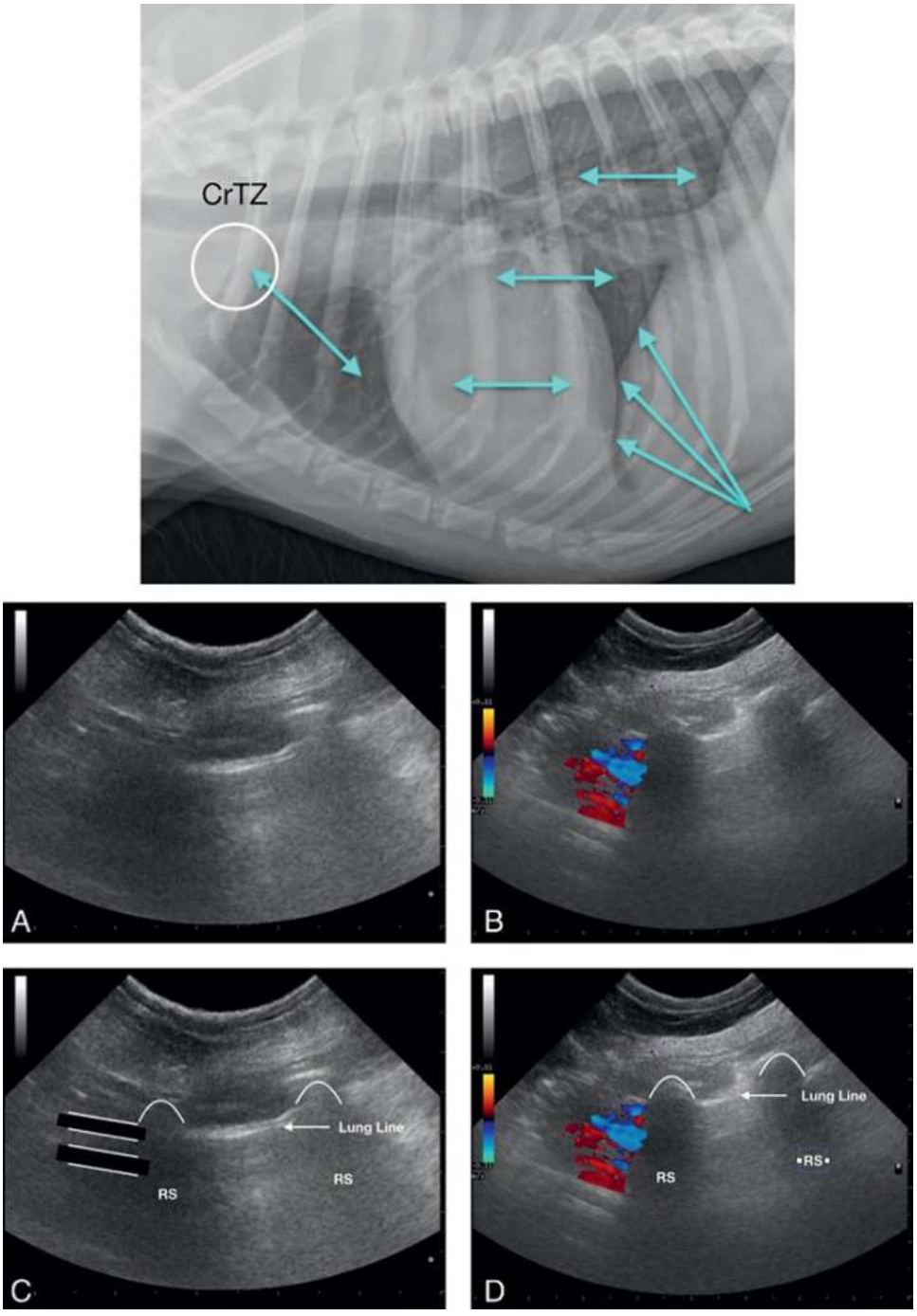


**Figure 22.13.** The cranial transition zone. The top image shows Vet BLUE on a lateral radiograph for the spatial relationships of its acoustic windows. In (A) and (B) are B-mode and the same patient and same acoustic window with color flow Doppler to show the CrTZ. The methodology has changed to improve consistency of the Cranial lung region view by finding the CrTZ and then sliding caudally over the first three intercostal spaces. The author likes to find the CrTZ and then slide over first rib – first intercostal space – second rib – second space – third rib – third space and that is a repeatable and defined Cranial lung region. Note the Cranial lung region view is found by moving craniodorsally from the previous Middle lung region. In (C) and (D) are the same images as (A) and (B) with overlays. The horizontal bars represent vessels (jugular vein and carotid) that in real time are appreciated by pulsation. The rib shadow clearly obscures the vessels at the transition of thorax and vertical soft tissue at the thoracic inlet. Curved lines, ribs; RS, rib shadow. Source: Reproduced with permission from Dr Gregory Lisciandro, Hill Country Veterinary Specialists and FASTVet.com, Spicewood, TX.

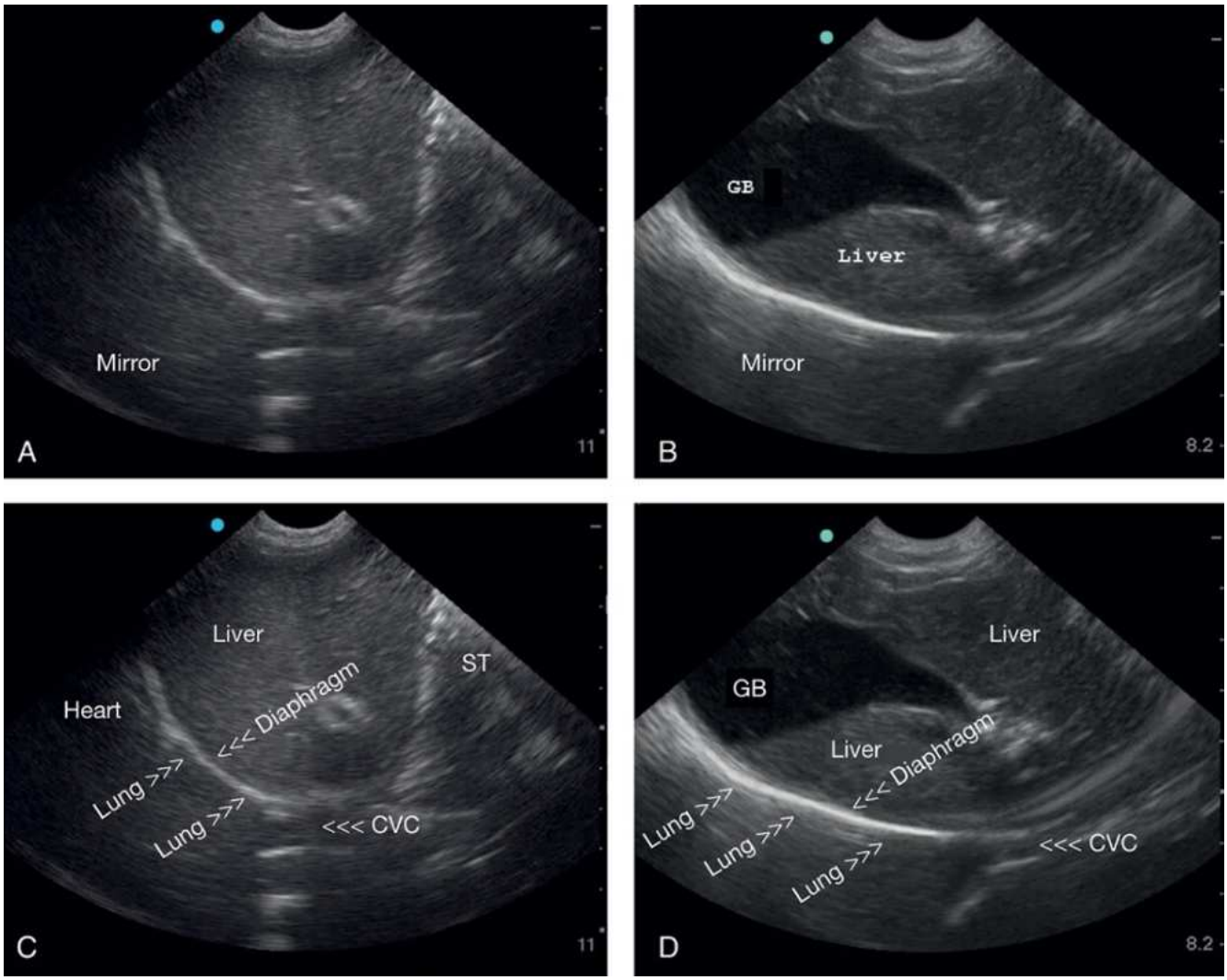


**Figure 22.14.** Vet BLUE DH view. The view is shown without (A) and with (B) the gallbladder in view with the proper depth and proportionality of pleural and peritoneal cavity with the expected curved hyperechoic (white) line indicating the whereabouts and integrity of the diaphragm. (C) and (D) are the same images as (A) and (B) but more extensively labeled. The pulmonary–diaphragmatic interface is interrogated for any obvious signs of lung pathology, often inaccessible via Vet BLUE transthoracic views, making the DH view invaluable. Note in (A) and (B) the mirror image artifact marked "mirror" on the cranial side of the diaphragm. The mirror image artifact immediately rules out pleural effusion at the scanning plane. The pulmonary–diaphragmatic interface is shown by the labeling of the diaphragm (<<<) and the lung (>>>) in (C) and (D). The other structures in the longitudinal scanning plane along the diaphragmatic surface include the heart proximally in the near-field and the caudal vena cava distally in the far-field. CVC, caudal vena cava; GB, gallbladder; ST, stomach. Source: Reproduced with permission from Dr Gregory Lisciandro, Hill Country Veterinary Specialists and FASTVet.com, Spicewood, TX.

probe caudally. This is no longer recommended because in most standing patients, sliding caudally places you over the abdominal cavity and sonographers easily mistake abdominal structures for lung pathology. Thus, the Middle lung region is better performed by moving immediately dorsal to the heart, until the sonographer is comfortable identifying abdominal structures along the Vet BLUE Line of the Cd, point 1, Ph, point 2, and Md, point 3 acoustic windows, each of which has the potential to image the pleural cavity-peritoneal cavity (abdomen) transition zone (Figure 22.15).

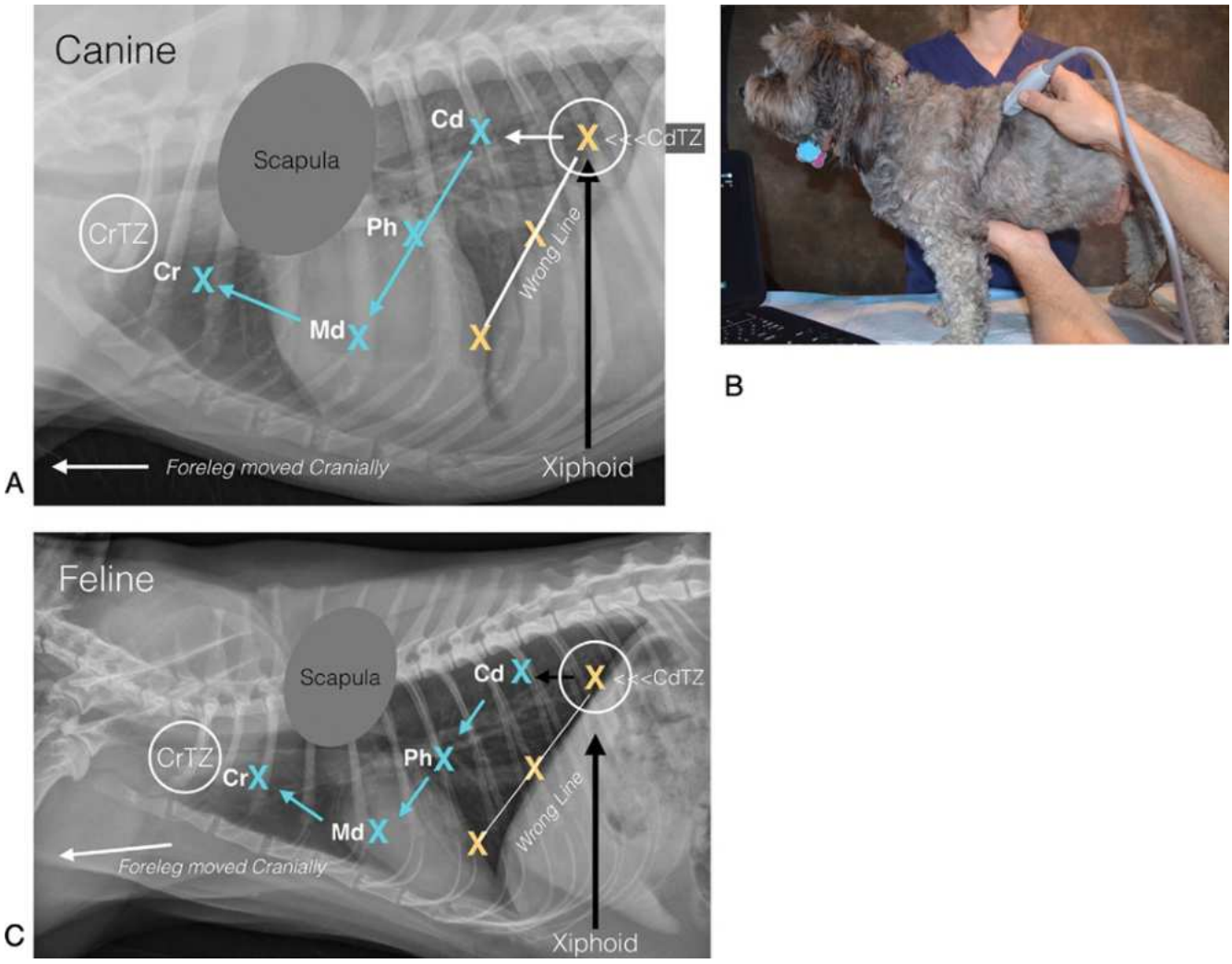


**Figure 22.15.** Determining and following the Vet BLUE line. In (A) and (C) the Vet BLUE protocol is an overlay on a lateral radiograph dog and cat, respectively. The methodology is the same for both species. Find the CdTZ, locating the "curtain sign" that indicates where the pleural and peritoneal cavity meet (transition). The "curtain sign" is the linear dirty shadowing from the pleural cavity that slides to and fro over abdominal structures (see Figure 22.10). From the CdTZ, slide the probe cranially 2–3 intercostal spaces away from the CdTZ to exclude abdominal structures from view when possible. This is the Caudodorsal lung region (Cd, point 1) where lung is then surveyed by moving one intercostal space caudally and then one intercostal space cranially from point 1. A line is often drawn with the acoustic coupling medium from point 1 to the elbow that is shown in (B). This is the Vet BLUE line and following it keeps the sonographer away from the transition zone of pleural and peritoneal cavities, limiting mistaking abdominal structures along the Vet BLUE line for lung pathology. The methodology is the same for Perihilar (Ph, point 2) and Middle lung regions (Md, point 3). Always slide one intercostal space caudally first, checking how close the acoustic window is to the abdominal cavity and being aware of this confounder. Then slide one intercostal space cranially so that three intercostal spaces are surveyed along the Vet BLUE line (points 1–3). For the final Cranial lung region view (Cr, point 4), the probe is slid along the "lung line" cranially and dorsally to lose the "lung line" and gain the soft tissue neck and its vessels. This is the cranial transition zone (CrTZ) and is located to the left of the screen. The probe is then slid caudally over the first rib, first intercostal space (ICS), second rib, second ICS, third rib, third ICS making the methodology standardized and repeatable between sonographers for imaging Cr (point 4). Source: Reproduced with permission from Dr Gregory Lisciandro, Hill Country Veterinary Specialists and FASTVet.com, Spicewood, TX.

### *Performing Vet BLUE Step by Step (Figure 22.16)*

- Locate the Cd, Point 1 lung region, which is the same methodology as for the TFAST CTS view by palpating the xiphoid and then moving dorsally to the upper third of the thorax. To recognize the pitfall, slide more dorsally to see the difference between being over the PPI and the "lung line" and being over the hypaxial and epaxial muscles along the vertebral column and proximal rib heads.
- Place the probe perpendicular to the long axis of the ribs and appreciate the hyperechoic PPI and "lung line" (air).
- Identify the "gator sign" orientation with two ribs and an interposing intercostal space starting with depth of 4–8 cm for smaller and larger patients (and giant breeds up to 9–10 cm), respectively.
- With the probe stationary and the angle of insonation 90° to the PPI, make the "lung line" sharp and hyperechoic as a crisp, bright white line. The gain may need to be turned down more than was used on soft tissues, but have some gain through the far-field so that artifacts may be seen through the entire screen. Too much gain results in poor detail along the "lung line" (see Figure 22.6).
- Find the CdTZ where pleural and abdominal cavities meet by identifying the "curtain sign" and then slide 2–3 intercostal spaces cranially away from abdominal structures and the diaphragm (see Figures 22.9 and 22.10). This is the starting Caudodorsal lung region (Cd, point 1).
- From here, slide an intercostal space caudally first, being aware of how close you are to the abdominal cavity, then return to your starting point, and then slide an intercostal space cranially before returning to your Cd (point 1) starting point. You have surveyed three intercostal spaces at the Vet BLUE Cd view.
- From the Vet BLUE Cd starting point, draw your Vet BLUE line to the patient's elbow using your acoustic coupling medium and a finger to roughen the hair coat along this line so it is obvious (see Figure 22.11B).
- Along your Vet BLUE line, halfway to the elbow is Ph (point 2). Survey three intercostal spaces as done at Cd. Slide caudally first, being aware of possible abdominal structures coming into view, and then slide cranially. You again surveyed three intercostal spaces.
- Along your Vet BLUE line, move to the elbow region for the Md (point 3). If heart is observed and obscuring lung, the probe is swept immediately dorsal until the heart is just out of view and a "gator sign" and "lung line" are identified as performed for the previous two views. The methodology is repeated – slide caudally first, being aware of abdominal structures possibly coming into view, and then slide cranially. You have again surveyed three intercostal spaces.
- Now begin the final Cr (point 4) by gently extending the foreleg cranially to allow room to slide the probe into the axillary region (see Figures 22.10 and 22.11). The probe is held similar to all other views perpendicular to the ribs directly over the space with minimal rocking.
- Slide cranial dorsal through the axillary region and identify the thoracic inlet of cervical soft tissue and vessels, keeping in mind the "check mark" track of the Vet BLUE line. Vessels, jugular vein, and carotid arteries are identified on B-mode by pulsation and their linear and circular anechoic appearance being blood-filled (fluid). Generally, color flow Doppler is not necessary but may be used. This is the cranial transition zone (CrTZ) and is located to the left of the screen.
- By sliding too ventral, the "gator sign" will be lost in pectoral muscles that have a pennate appearance sonographically. To recognize the pitfall, slide ventrally and image the pectoral muscles to become familiar with their pennate appearance (see Figures 22.17D, 34.1, 35.1, and 35.14).
- Slide caudally from the CrTZ and see in the following order: rib 1, intercostal space 1, rib 2, intercostal space 2, rib 3, intercostal space 3. You have now surveyed the first three intercostal spaces of Cr (point 4).
- The transthoracic Vet BLUE acoustic windows have been completed on the left hemithorax and the same methodology is performed on the right hemithorax (see Figure 22.12).
- The DH view is the nontransthoracic acoustic window that provides a deep window into lung along the pulmonary–diaphragmatic interface and is invaluable in identifying lung pathology not evident at the three transthoracic acoustic windows (see Figure 22.14).

In summary, three intercostal spaces have been surveyed at each of the respective Vet BLUE views. Always slide caudally first so that the question may

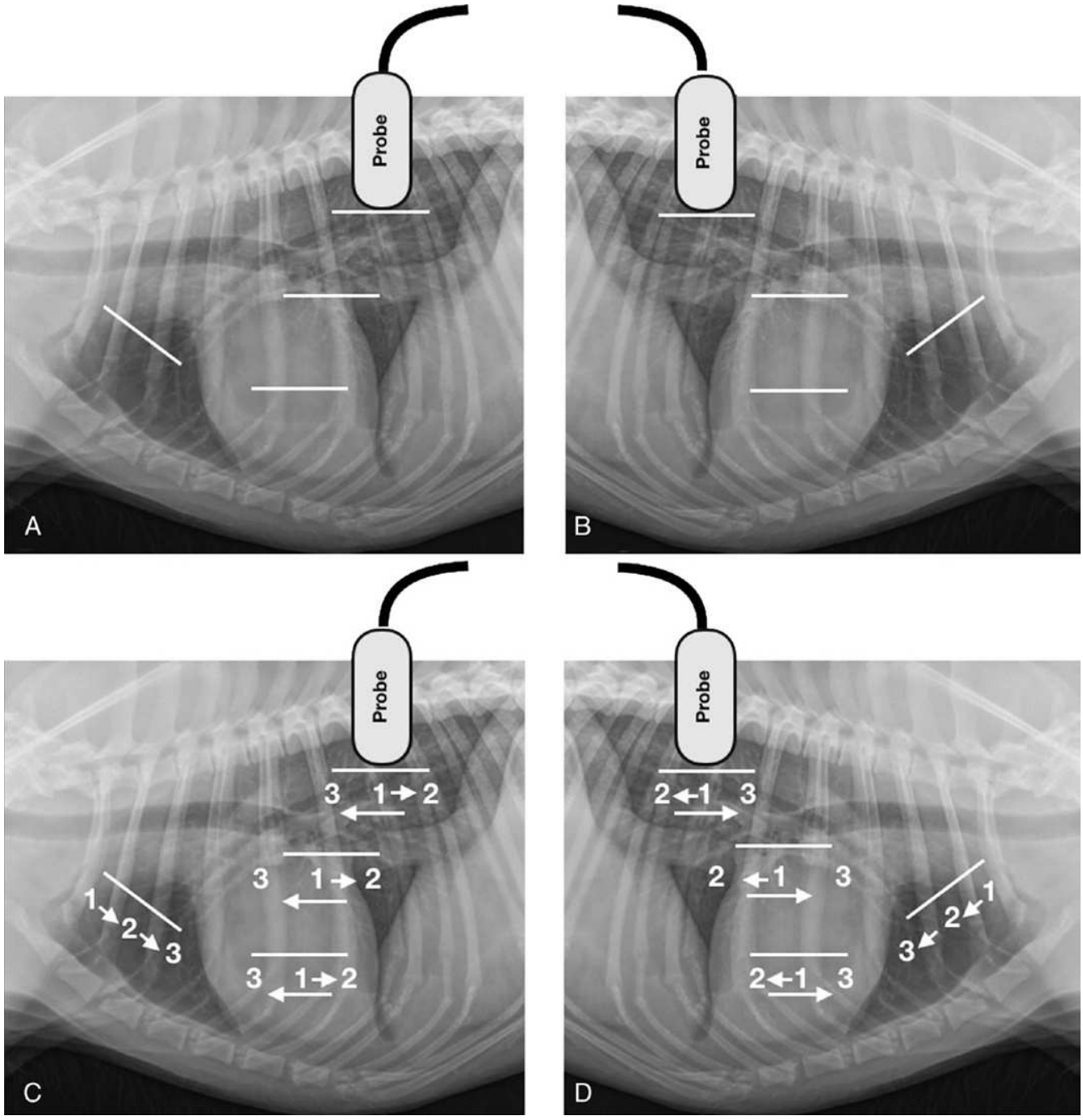


**Figure 22.16.** Vet BLUE protocol and its three intercostal spaces. In (A) and (B) are the left and right hemithoraces with the white lines showing the four transthoracic Vet BLUE acoustic windows. In (C) and (D) the three intercostal spaces are shown over each acoustic window or view. The sonographer should check where the probe is placed externally on the patient to approximate these regions radiographically. Moreover, in very large dogs (and other species), Vet BLUE may be modified as shown in Chapter 41 on dolphins. By having discrete, defined acoustic windows, Vet BLUE regionality and its pattern-based approach is better appreciated and findings are readily recorded, creating a tracking (monitoring) tool. Source: Reproduced with permission from Dr Gregory Lisciandro, Hill Country Veterinary Specialists and FASTVet.com, Spicewood, TX.

VetBooks.ir

be asked "how close am I to the transition zone of pleural and peritoneal cavities (to prevent mistaking abdominal structures for lung pathology)?" The lung sonographer also quickly becomes attuned to the variability in amount of liver, stomach wall and lumen, and gallbladder that is viewed along the pleural-peritoneal transition zone of points Cd-1, Ph-2, and Md-3 and how easily these structures can be mistaken for pathology. The methodology described here is improved from our original publication by better recognizing pitfalls and being a more repeatable LUS examination and will soon be published.

Vet BLUE is a proactive screening test that is regional and pattern based. The findings within each region may be recorded and followed over time. In contrast, the scanning of every intercostal space loses regionality and a pattern-based approach and lacks specific Vet BLUE data points for monitoring (see Vet BLUE B-line Scoring and Comparison to Other Lung Ultrasound Formats below).

# Trouble Shooting

## *Avoiding the Phenomenon of Drifting*

Drifting occurs by the weight of your hand moving the probe into a different location than where you think you are imaging by watching the screen and ignoring the external position of the probe on your patient. Make a habit of placing fingers (or part of your hand) of your probe hand on the patient's thoracic wall, so-called "kickstanding" of the probe, so that you can comfortably maintain contact with your patient and thus prevent drifting away from where you think you are imaging (see Figure 5.9). Moreover, V-troughing the patient with your helper hand (nonprobe hand) prevents your patient from swaying and losing probe-to-skin contact and thus your nice acoustic window, which delays the study and often leads to sonographer frustration (see Figure 5.7).

## *Confounders of Lung Ultrasound*

Adhering to the following axiom serves the lung sonographer well: If you cannot appreciate the "gator sign" orientation and accurately identify the "lung line" then you cannot be certain that you are in fact looking at lung.

Confounders include the following.

### Imaging Outside the Boundaries of the Pleural Cavity

#### *Caudally*

Abdominal structures including the liver, stomach and its rugal folds, and the gallbladder.

- The liver can be mistaken for lung consolidation, a "pseudo tissue sign," defined in Chapter 23.
- The stomach wall can be seen as an anechoic stripe mimicking and thus potentially being mistaken for pleural effusion, although pleural effusion generally occurs ventrally with aerated lungs rising (floating) dorsally and would never be noted at the least gravity-dependent region.
- The stomach and its rugal folds can be mistaken for a "pseudo shred sign," defined in Chapter 23.
- The stomach and its gastric luminal contents (ingesta having fluid and air) can create "pseudo gastric B-lines," defined in Chapter 23 (see Figures 18.3 and 22.10).
- The gallbladder, depending on its luminal contents, can be mistaken for lung pathology or pleural/pericardial effusion.

#### *Dorsally*

The hypaxial muscles along the rib heads and spine (Figures 22.17 and 22.18).

#### *Ventrally*

The pectoral muscles and soft tissue along the sternum including vessels. Muscle has an ultrasonographically pennate appearance (see Figures 22.17, 34.1, 35.1, and 35.14).

#### *Cranially*

The thoracic inlet and its soft tissue including vessels (see Figure 22.17).

#### *Craniodorsal*

The periscapular muscles and the scapula. The bony scapula is a smooth surface and can mimic the "lung line" (see Figures 22.17 and 41.21C).

### Subcutaneous Emphysema

- Air between the skin and intercostal space, subcutaneous emphysema (SQE), will obscure the "lung line" by dirty shadowing, often with A-lines as expected at any strong air–soft tissue interface

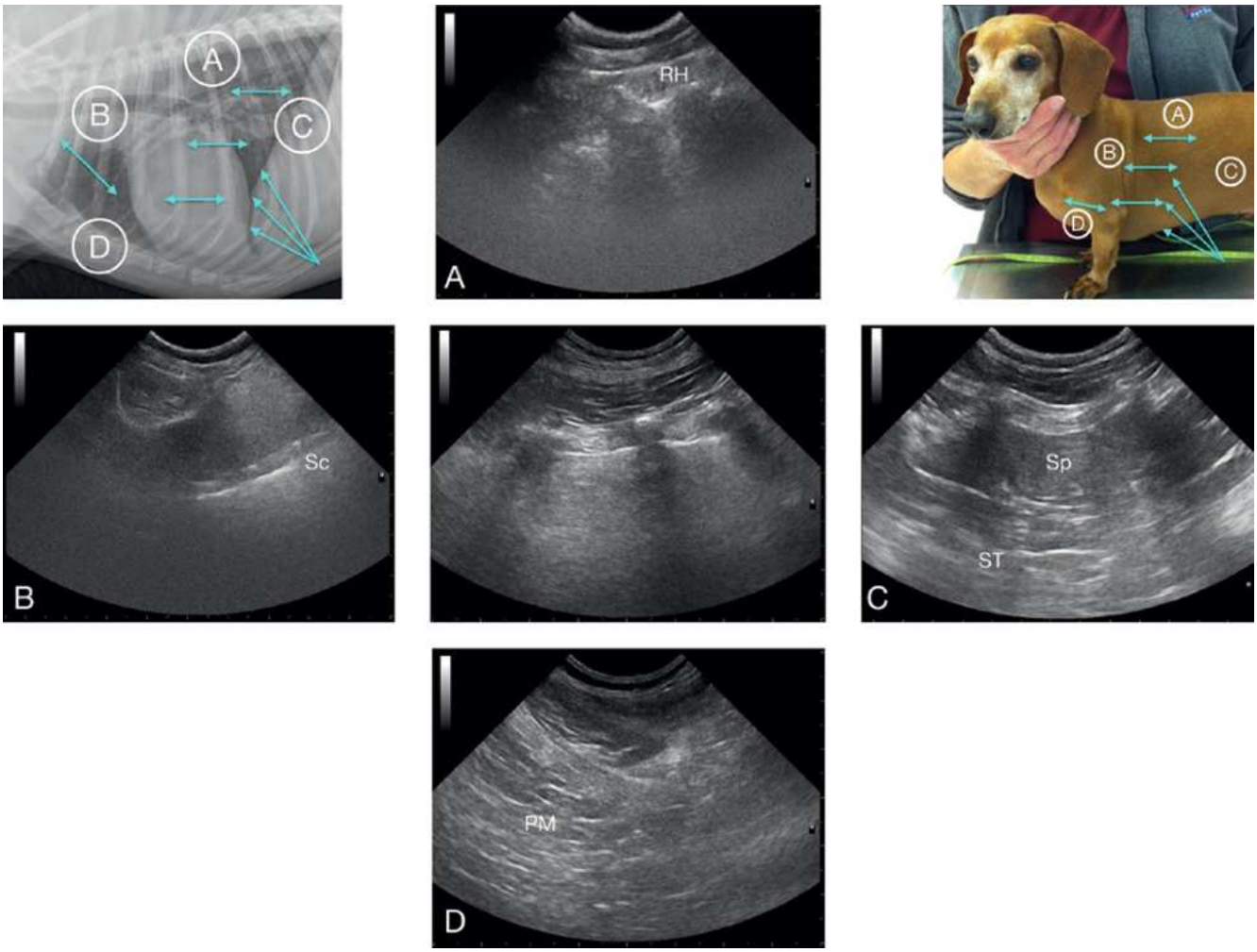


**Figure 22.17.** Boundaries of lung. The boundaries of lung are correlated to the thoracic radiograph as well as externally on a dog as (C) caudally – abdomen (Sp, spleen; ST, stomach), (A) dorsally – hypaxial and epaxial muscles, rib heads (RH) and vertebral column, (B) cranially – the scapula (Sc) and associated muscles, and (D) ventrally – the sternum and pectoral muscles. Note the pennate appearance of the pectoral muscles. The hyperechoic line in (B) is in fact the spine of the scapula and mimics the "lung line." Without recognizing these boundaries, the sonographer may mistake them for lung pathology. Adhering to the following axiom serves the lung sonographer well: If you cannot appreciate the "gator sign" orientation and accurately identify the "lung line" then you cannot be certain that you are in fact looking at lung. Source: Reproduced with permission from Dr Gregory Lisciandro, Hill Country Veterinary Specialists and FASTVet.com, Spicewood, TX.

(Figure 22.19). This rule is universal for all lung ultrasound: if you cannot image the "gator sign" orientation, than you cannot be sure that you are imaging lung.

- Subcutaneous emphysema is more problematic in people than in small animal patients. In most instances, gentle probe pressure displaces SQE so that the "gator sign" orientation may be obtained (see Figure 22.19). With "gator sign" orientation, LUS may proceed with an acceptable Vet BLUE (and TFAST) study (Lisciandro et al. 2008; Lisciandro 2011, 2014a,b; Boysen and Lisciandro 2013).

### Fat and Excessive Soft Tissue

Fat and excessive soft tissue in between the transducer and the thoracic wall will also obscure imaging because of the attenuation of the ultrasound beam (travelling through more soft tissue than with a thinner patient). This is far more problematic in people, who are

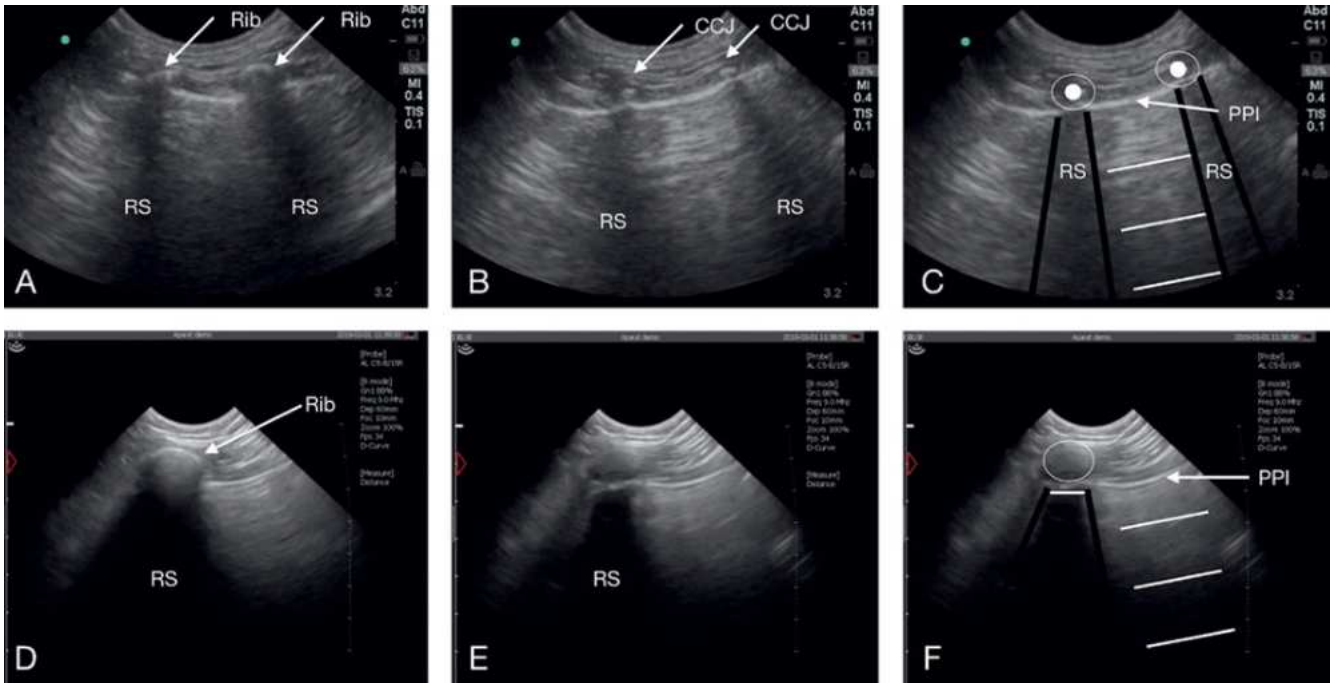


**Figure 22.18.** Ribs versus costochondral junction. (A–C) Images from the same juvenile cat along different levels of the thoracic cage. In (A) the ossified rib creates a shadow through the far-field as expected. In (B) minimally labeled and (C) more extensively labeled are the same image but more ventral at the level of the costochondral junction (CCJ) to show how different ribs may appear. In (C) the outline shows a bull's eye or target-like effect. Note these images are on the abdominal preset, upper right hand corner "Abd", and the depth setting is 3.2 cm, noted in the lower right hand corner, magnified more than normal for adults because of the small size of the feline. The proportionality of the image is very good, as is the gain, allowing for artifact to appear through the far-field (see also Figure 22.4). (D–F) Analogous images from a human illustrating how osseous rib clean shadows and CCJ shows the circle and ring effect because of the cartilage. The CCJ is a pitfall in that the sonographer may think that the effect is a lesion such as a nodule or mass. The black bars in (C) and (F) help distinguish the borders of the rib shadowing. The horizontal bars in (C) and (F) indicate A-lines associated with aerated lung in the absence of pneumothorax. CCJ, costochondral junction; PPI, pulmonary–pleural interface; RS, rib shadow. Source: Reproduced with permission from Dr Gregory Lisciandro, Hill Country Veterinary Specialists and FASTVet.com, Spicewood, TX.

generally more obese than our small animal patients. Interestingly, Vet BLUE performed in bottlenose dolphins yields excellent quality lung images as the "gator sign" orientation is easily observed with little beam attenuation through the blubber (see Chapter 41) (Yarto and Lisciandro, unpublished data 2017).

**Pearl:** The presence of SQE prevents orientation of the "gator sign," thus negating the use of TFAST and Vet BLUE. However, SQE almost always can be displaced with gentle probe pressure allowing for visualization of the "gator sign," accurate identification of the "lung line" and thus for TFAST and Vet BLUE to be satisfactorily performed (Lisciandro et al. 2008; Lisciandro 2011, 2014a,b) (see Figure 22.19).

# Vet BLUE Six Lung Ultrasound Signs

## *Dry Lung versus Wet Lung, A-lines, "Lung Sliding," and B-lines*

A-lines with "lung sliding" represent "dry lung" at its surface (Figure 22.20). A-lines with absent "lung sliding" represent pneumothorax (PTX).

B-lines (previosuly referred to as ultrasound lung rockets) represent "wet lung" or forms of alveolar-interstitial edema (Figures 22.21; see also Figure 22.20) (Lisciandro et al. 2014). B-lines are nonspecific in that they cannot tell you what type of alveolar-interstitial edema is present, thus referred to as alveolar-interstitial syndrome, making a regional pattern-based Vet BLUE approach more clinically relevant

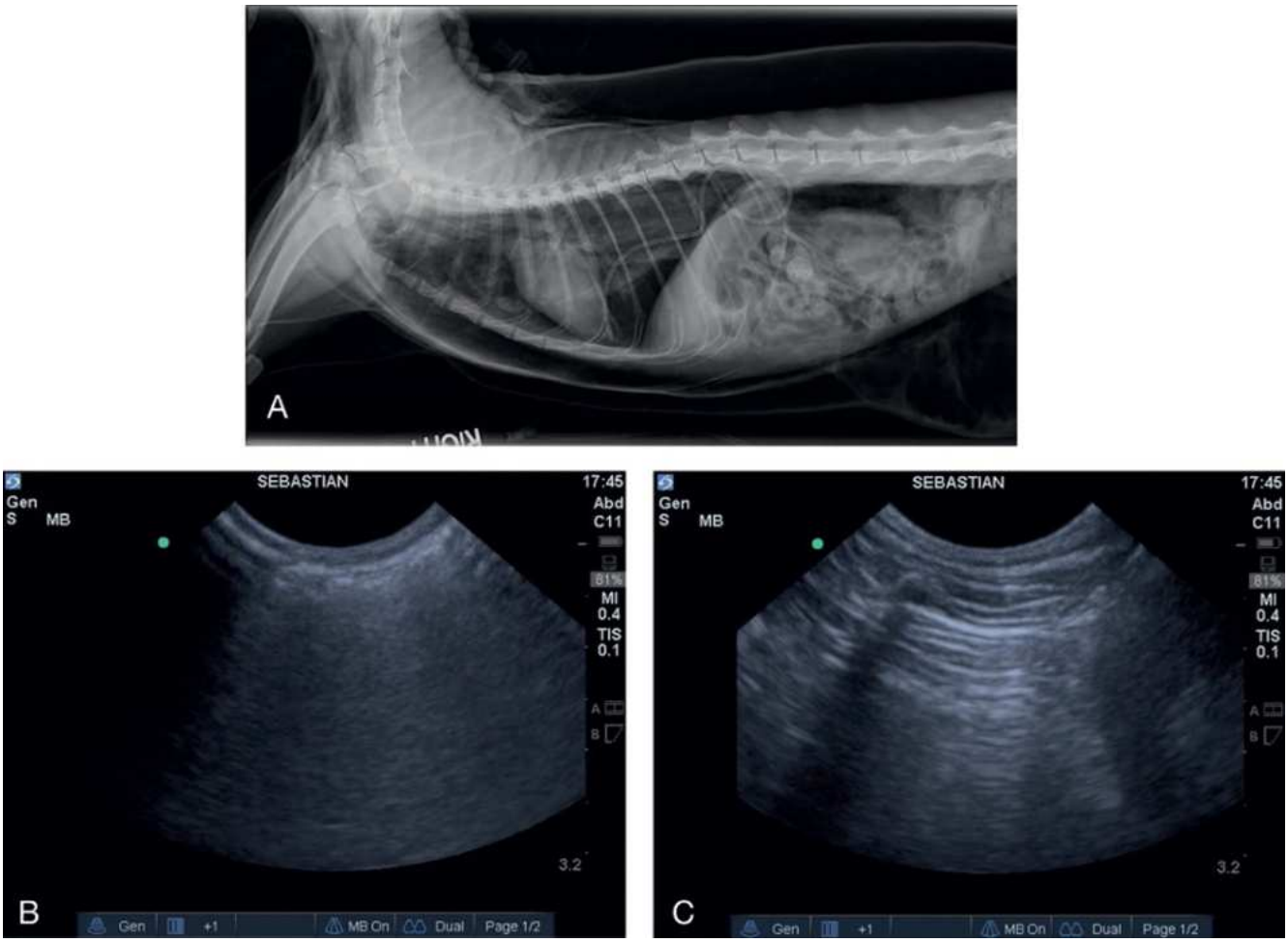


**Figure 22.19.** Subcutaneous emphysema. Shown in (A) is radiographically evident subcutaneous emphysema (SQE) in a cat caused by a tracheal tear during extubation postoperatively (note also the pneumoretroperitoneum). The initial Vet BLUE Caudodorsal lung region view (same as the TFAST CTS view) does not show a "gator sign" orientation, thus lung cannot be assessed as shown in (B). In (C), with gentle probe pressure, the SQE is displaced and the Vet BLUE (TFAST) study may be performed. Note that SQE dirty shadows from the near-field through the far-field. The sonographer can also anticipate how the AFAST spleno-renal (SR) view will appear with the air within the retroperitoneal space as widespread dirty shadowing and the inability to image its target organs. Source: Reproduced with permission from Dr Gregory Lisciandro, Hill Country Veterinary Specialists and FASTVet.com, Spicewood, TX.

for a working diagnosis. B-lines less commonly are caused by senescent lung and fibrosis, more relevant to people who live longer than our small animal patients (Lichtenstein et al. 1997; Shyamsundar et al. 2013). However, B-line scoring has been found to correlate with degree of alveolar-interstitial edema in human lung when compared to the gold standard test of computed tomography (CT) (Volpicelli et al. 2006). A Vet BLUE B-line scoring system has been published (Figure 22.22) (Lisciandro et al. 2014, 2017; Ward et al. 2017).

## Comparison of Vet BLUE to Other Lung Ultrasound Protocols

Other researchers have published lung ultrasound protocols that differ from Vet BLUE in various ways. It is important to understand how these other LUS protocols are performed as well as how their scoring systems are defined. We will briefly review these ultrasound protocols as follows: the four-quadrant

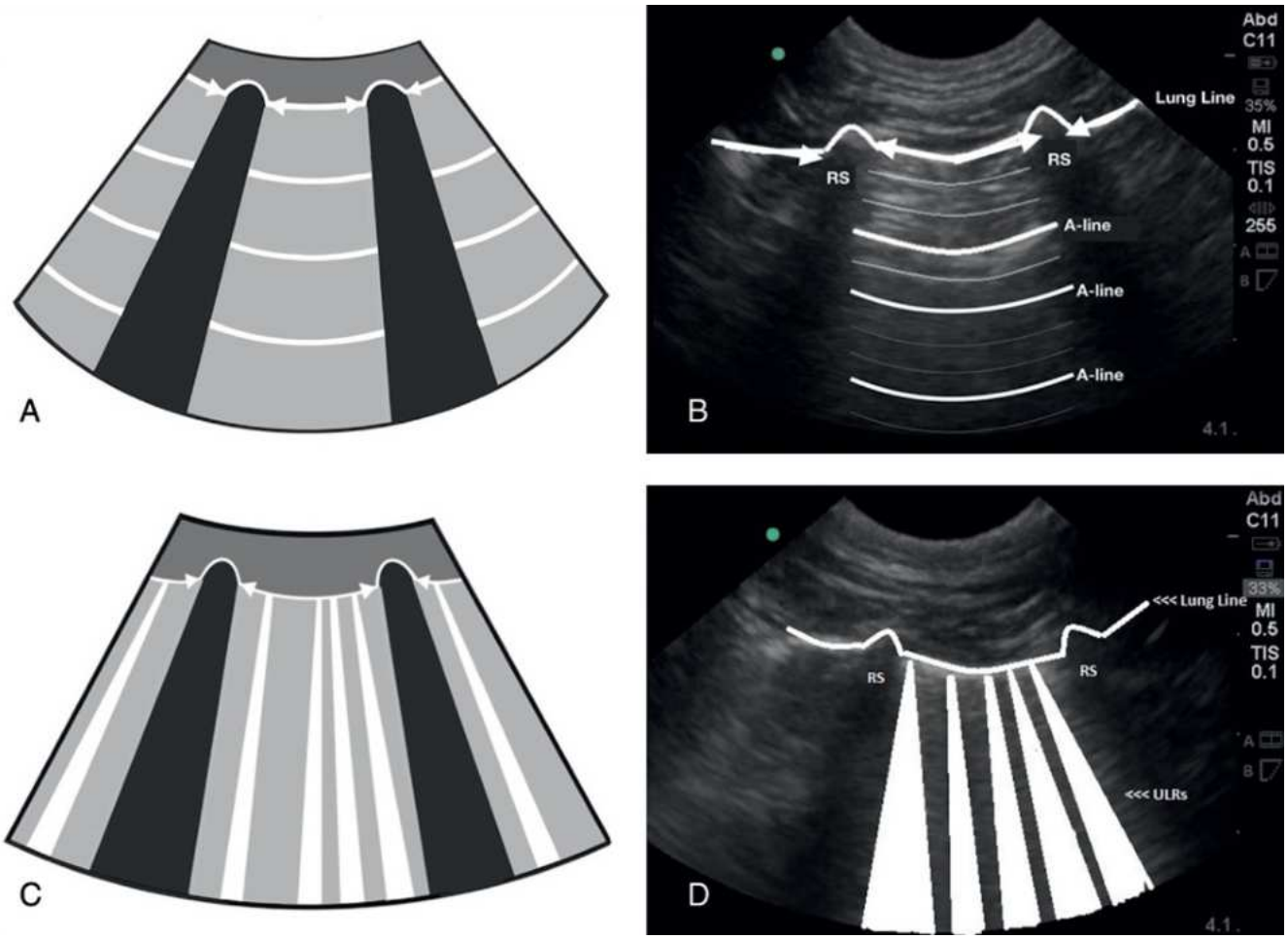


**Figure 22.20.** Wet Versus dry lung. Shown in (A) and (B) are a line drawing of dry lung, "lung sliding" with A-lines, with a correlative B-mode image with overlays. A-lines are horizontal equidistant lines that are evident through the far-field and maximized by having a 90° angle of insonation to the PPI and "lung line." "Dry lung" is "lung sliding" with A-lines and indicated by the arrows along the "lung line." Shown in (C) and (D) are a line drawing of "wet lung," B-lines with a correlative B-mode image with overlays. B-lines are laser-like, hyperechoic vertical lines that extend through the far-field without fading while obliterating A-lines. B-lines swing like a pendulum in synchrony with phases of respiration. The lung sonographer adhering to this definition will avoid being confounded by other vertical artifacts. Source: Reproduced with permission from Dr Gregory Lisciandro, Hill Country Veterinary Specialists and FASTVet.com, Spicewood, TX. Illustration by Dr Judy Brown, Toronto, Canada.

approach (Rademacher et al. 2014; Hwang et al. 2018), and the ZigZag Intercostal Continuum Approach (author's term) (Vezzosi et al. 2017).

## *Four-Quadrant Approach*

The four-quadrant approach has been published with two slightly different methodologies for two different purposes by two different institutions (Figure 22.23). One study evaluated dogs with and without left-sided congestive heart failure (CHF) and the other study evaluated PTX (Rademacher et al. 2014; Hwang et al. 2018).

The left-sided CHF study evaluated a four-quadrant LUS examination in 31 clinically normal, spontaneously breathing dogs along with a comparative cohort of nine spontaneously breathing dogs with left-sided CHF (Rademacher et al. 2014). The PTX study evaluated a slightly different four-quadrant approach (essentially the same) in dogs with experimentally

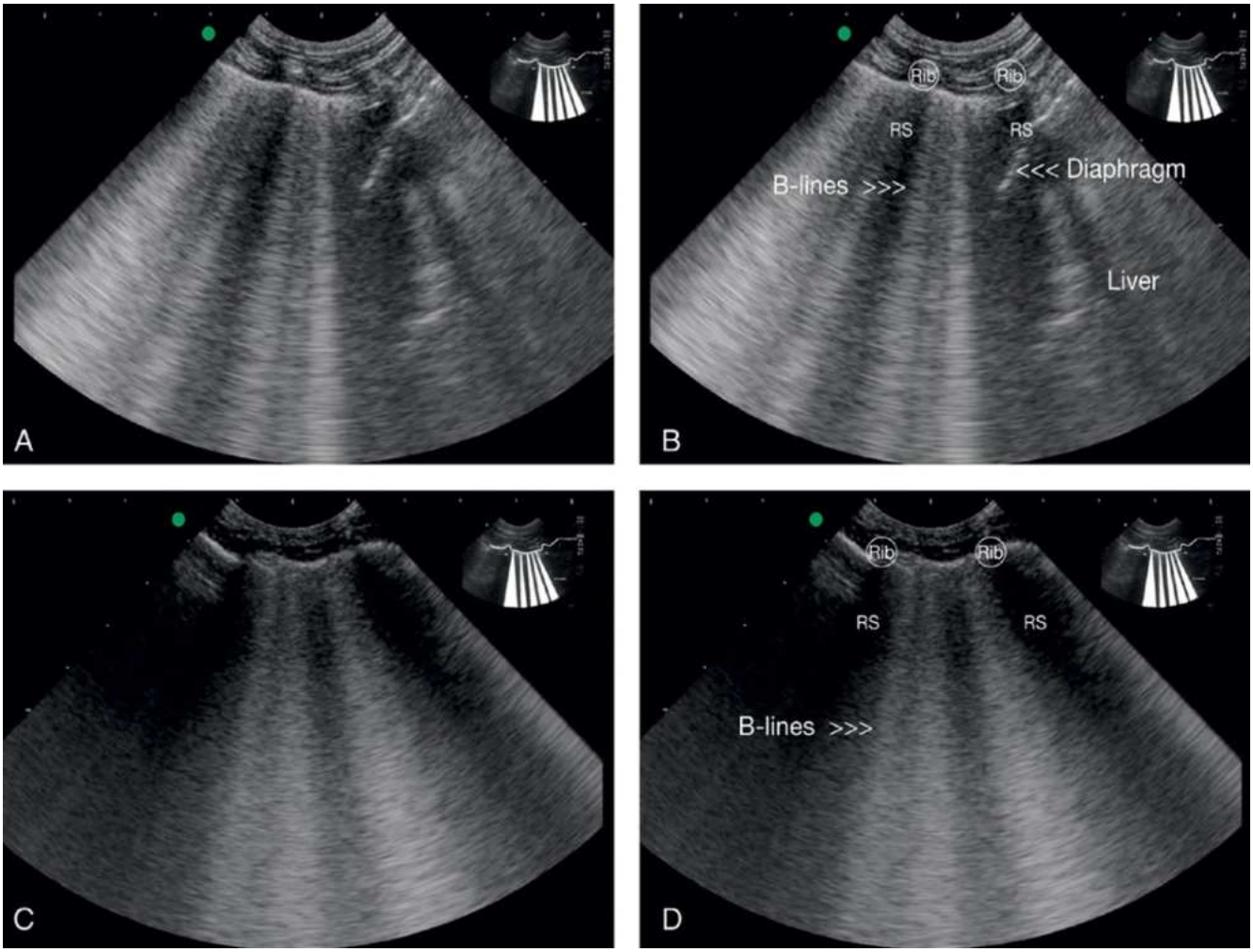


**Figure 22.21.** B-lines previously referred to as ultrasound lung rockets. Examples of B-lines in (A) and (C) with the same images labeled in (B) and (D). Note the laser-like hyperechoic vertical lines (rocket like) that extend from the "lung line" through the far-field that in real time swing synchronously with inspiration and expiration while obliterating A-lines. An illustrative cartoon of B-lines is present in the upper right hand corner of each image. Note the features on these images and then compare with Figures 22.4 and 22.20. The recognition of B-lines is "all or none" – they are either present or not present. In (A) and (B) the image shows the CdTZ labeled with diaphragm and liver. The images have too much depth (7 cm) and should be magnified in this cat to 4–5 cm. Ribs are labeled and circled. RS, rib shadow. Source: Reproduced with permission from Dr Gregory Lisciandro, Hill Country Veterinary Specialists and FASTVet.com, Spicewood, TX. Illustration by Dr Judy Brown, Toronto, Canada.

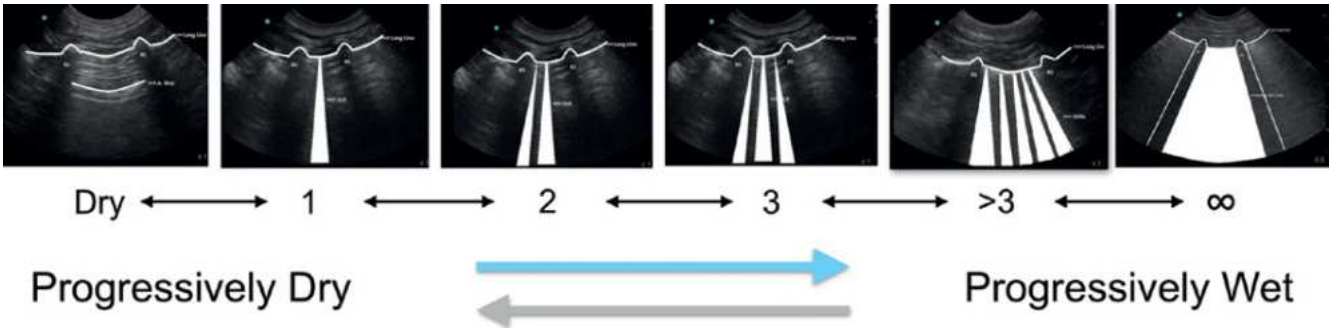


**Figure 22.22.** Vet BLUE B-line scoring system. Numbers of B-lines have been shown to correlate with degree of alveolar-interstitial edema on computed tomography (CT) in human lung. The scoring is 0 (no B-lines) or when B-lines are present, the maximum number over a single representative intercostal space as 1, 2, 3, >3, and infinity (∞). Source: Reproduced with permission from Dr Gregory Lisciandro, Hill Country Veterinary Specialists and FASTVet.com, Spicewood, TX.

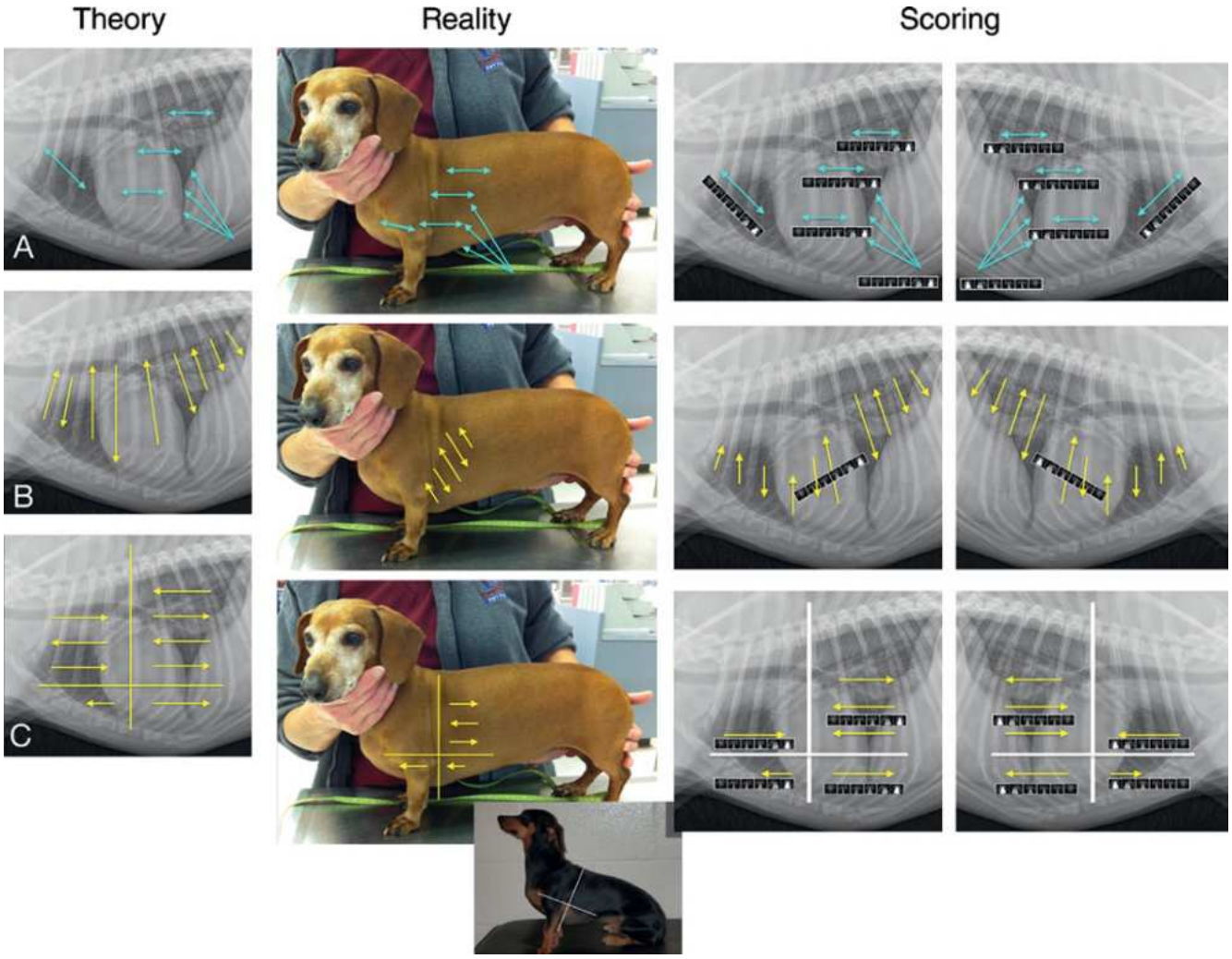


**Figure 22.23.** Composite of three different published lung ultrasound formats. The composite emphasizes how important critical thinking is when determining what lung ultrasound format works best for the patient. In each row is a different LUS format illustrated with "theory" and "reality" to show what the actual acoustic windows survey. In row (A), the Vet BLUE theory and reality has acoustic windows that are the same. The Vet BLUE B-line scoring system (0, 1, 2, 3, >3, and infinity [∞]), explained in detail in Chapter 23, is applied to each of its nine views, thus there are nine scores. In row (B), the ZigZag Intercostal Continuum (ZZIC) method is applied to every intercostal space; however, this is impossible because of the scapula and its associated musculature especially in a standing (sternal) patient so "theory" and "reality" are quite different. The scoring system is per hemithorax, thus two scores, making it difficult to assess the degree of alveolar-interstitial edema (B-lines). For example, once >3 B-lines are observed, focally or diffusely over an individual hemithorax, the ZZIC score is the same, ">3," when degrees of edema are radically different (focal score of >3 is much less edema than diffusely >3). Moreover, with a Vet BLUE pattern-based approach, the patient with the score of >3 B-lines focally over a middle lung region likely has aspiration pneumonia, and the patient with >3 B-lines diffusely likely has left-sided congestive heart failure. These differences are lost with a per hemithorax scoring system. In row (C) is the four-quadrant approach, and the amount of lung is markedly different between "theory" and "reality." The black and tan dachshund is in fact the published four-quadrant format (Rademacher et al. 2014). The methodology is sliding cranially and caudally as shown with arrows and each quadrant is scored. The asymmetry of amount of lung coupled with sliding over the same lung may contribute to a higher score than the patient really has (likewise, it is possible Vet BLUE underestimates and the ZZIC loses semiquantitation inherently through a per hemithorax approach). It is worth taking the time to think out these three formats. Source: Reproduced with permission from Dr Gregory Lisciandro, Hill Country Veterinary Specialists and FASTVet.com, Spicewood, TX. The image of the black and tan dachshund with overlays is reproduced with permission from Rademacher et al. (2014).

induced PTX, presumably intubated and mechanically ventilated although this is unclear from the publication (Hwang et al. 2018). However, the use of positive pressure ventilation has important implications on LUS findings because free air in the pleural space is unnaturally pushed into different regions (see Figures 18.7 and 18.8). In both LUS formats, the canine thorax was divided into four quadrants: caudal dorsal, caudal ventral, cranial dorsal, and cranial ventral. The level of the elbow was defined as the border between dorsal and ventral in the left-sided CHF study (Rademacher et al. 2014) and the shoulder in the PTX study (Hwang et al. 2018). Using these landmarks as LUS boundaries, the reality is an asymmetrical division of lung (see Figure 22.23). In both LUS four-quadrant formats, the dorsal regions encompass more potential lung than the ventral regions, and the caudal dorsal and caudal ventral regions are in reality over very little lung (see Figure 22.23).

The four-quadrant left-sided CHF study used a linear probe (versus microconvex with Vet BLUE) and the average time per examination was 10 minutes (Rademacher et al. 2014), much longer than a Vet BLUE (<2 minutes) (Lisciandro et al. 2014, 2017; Ward et al. 2017). Each quadrant was evaluated using a "sliding" methodology, moving the probe caudal to cranial and then cranial to caudal within each of the four quadrants (see Figure 22.23). Numbers of B-lines were totaled per quadrant. The authors found that 31% of unaffected dogs had at least one B-line, with a mean number of 0.9 +/- 0.3 B-lines per normal dog. In contrast and as expected, in left-sided CHF there was a much higher mean number of B-lines per patient (6.2 +/- 3.8). A major difference between the four-quadrant CHF approach and Vet BLUE is that by "sliding" over each quadrant, the overlapping of previously imaged lung is possible, which may account for the higher numbers of B-lines seen in normal dogs in that study (Rademacher et al. 2014) than in Vet BLUE studies (Lisciandro et al. 2014, 2017; Ward et al. 2017, 2018a, 2019), or conversely Vet BLUE may underestimate. Importantly, locations of LUS-detected cardiogenic pulmonary edema correlated with locations found on thoracic radiography (Rademacher et al. 2014) similar to Vet BLUE studies (Lisciandro et al. 2014, 2017; Ward et al. 2017, 2018b). However, the four-quadrant approach does not inherently correlate LUS regions and their respective findings to thoracic radiography as Vet BLUE does. Moreover, with the disproportionality of lung in the four-quadrant approach, degrees of alveolar-interstitial edema likely seem more difficult to appreciate.

The other four-quadrant approach study evaluated experimentally induced PTX and compared three imaging modalities – LUS, thoracic radiography (TXR), and computed tomography (CT) – within 30 minutes (Hwang et al. 2018). This study presents an interesting approach, but unless the reader is experienced in LUS, they may overlook its nuances. Briefly, thoracostomy tubes were placed under general anesthesia and it is unclear whether ventilation was controlled via positive pressure ventilation (PPV) or these dogs were spontaneously breathing. This is important because PPV manipulates how free air within the pleural cavity is distributed because PPV presumably pushes (redistributes) the free air (PTX) unnaturally into pockets (see Figures 18.7 and 18.8). Moreover, their four quadrants are unequal and asymmetrical regarding amount of lung surveyed and lack the ability to find a "lung point" (see Figure 18.9). In fact, their caudal dorsal and caudal ventral quadrants are over very little if any lung. Their methodology, however, provides an interesting approach for diagnosing PTX. Historically, the CdTZ has been avoided because the respirophasic dynamics for observing "lung sliding" are confounded by the complexity of movement by the lung, its "curtain sign," and the adjacent abdominal structures. However, Hwang and colleagues suggest that the CdTZ region is an effective site for detecting small-volume PTX, supported by comparative imaging of TXR and CT, and more recent research has shown similar more understandable findings (and technique) using the CdTZ with PTX diagnosed using the "reverse curtain sign" and "double curtain sign" (Boysen et al. 2019).

### *Zigzag Intercostal Continuum Approach*

The Zigzag Intercostal Continuum (ZZIC) Approach (author's term) was published by investigators who evaluated dogs with different stages of degenerative mitral valve disease based on the ACVIM classification system (Vezzosi et al. 2017). The study was well done, but without critically reviewing the methodology, its nuances and weaknesses may not be appreciated by the reader. Dogs were not shaved but rather the hair was parted and isopropyl alcohol and acoustic coupling gel were used for imaging the entire hemithorax. Every intercostal space was evaluated using a linear probe (see Figure 22.23). The study found that significant numbers of B-lines were only detected in dogs with stage C degenerative mitral valve disease with active left-sided congestive heart failure, a well-founded and clinically relevant

finding. Dogs with preclinical degenerative mitral valve disease (B1, B2) and dogs with treated/compensated stage C disease had none to rare B-lines, again a well-founded and clinically relevant finding. LUS correlated with findings of cardiogenic pulmonary edema on TXR similar to findings on the other studies (Rademacher et al. 2014; Lisciandro et al. 2014, 2016, 2017; Ward et al. 2017, 2018b). In fact, it was suggested that LUS may have been more sensitive than TXR for detecting cardiogenic pulmonary edema by finding B-lines in some dogs that had unremarkable TXR lung, similar to other studies (Rademacher et al. 2014; Lisciandro et al. 2016; Ward et al. 2017, 2018b).

The LUS examination methodology, though, has important features that should be critically considered. The ZZIC scoring system was an estimation of total number of B-lines per hemithorax (numerous/confluent vs absent/rare), and inherently lacked the ability to assess the presence and number of B-lines at any discrete views other than per hemithorax. Thus, the ZZIC not only is deficient in being able to semiquantitate degree of cardiogenic pulmonary edema (numbers of B-lines), but it also lacks a regional pattern-based approach and is unable to differentiate causes of alveolar-interstitial edema (distribution of B-lines) (see Figure 22.23). Secondly, similar to the four-quadrant approach, the ZZIC in theory appears to be an extensive lung evaluation, but the scapula and its associated musculature prevent much of the cranial dorsal thoracic lung being evaluated (see Figure 22.23). Thirdly, and very importantly and similar to the four-quadrant approach, knowledge of the pitfalls of LUS along its caudal, cranial, dorsal, and ventral boundaries is essential to avoid mistaking each of these regions for lung pathology, important for lung sonography training (see Figure 22.17). Moreover, extreme margins of highly reflective aerated lung inherently lend themselves to creating artifact by the ultrasound striking reflective margins and thin portions of lung (author's experience).

Some final questions not specifically covered in the ZZIC methodology should be considered. How does the lung sonographer image every intercostal space dorsal to ventral in a thickly coated breed with no shaving and isopropyl alcohol and coupling gel? How cold does a smaller patient get with the amount of isopropyl alcohol over each hemithorax? Moreover, are there any patient problems with the resultant noxious fumes if the patient is placed in a closed environment like an oxygen cage? Where do you accurately restart your ZZIC study when the patient moves? How were ZZIC sonographers trained to recognize the caudal, cranial, ventral, and dorsal borders of the lung along the thorax? These features of the ZZIC methodology were recognized in part by the author when evaluating both LUS methods, ZZIC and Vet BLUE, in dolphins (see Chapter 41).

# Recording Vet BLUE Findings on Goal-directed Templates

Recording your findings is imperative for a successful ultrasound program. See Chapter 23.

# Pearls and Pitfalls, The Final Say

- Vet BLUE is a regional pattern-based approach that is standardized with exact clarity to its acoustic windows.
- Vet BLUE is correlative to the manner in which most veterinarians view thoracic radiography.
- The caudodorsal transition zone is important to be able to identify because the lung sonographer may easily mistake abdominal structures without recognizing this pitfall.
- The first three Vet BLUE acoustic windows of Caudodorsal, Perihilar, and Middle are along the Vet BLUE line to the elbow and importantly the sonographer always slides caudally first to ask "How close am I to the transition zone of the pleural and peritoneal cavity abdominal cavity?"
- All Vet BLUE acoustic windows survey three intercostal spaces.
- The cranial transition zone is identified by soft tissue structures of the neck and the probe then slides caudally over the first three intercostal spaces for a repeatable and accurate Cranial lung region.
- Boundaries to lung should generally be avoided, but the sonographic appearance of these structures should be known to the lung sonographer to avoid mistaking them for lung pathology.
- The pulmonary–pleural interface and "lung line" are optimized by adjusting depth, gain, and focus cursor with a depth of 4–8 cm for small to large patients (up to 9–10 cm in giant breeds), respectively.
- There are major differences in lung imaged and scoring systems between Vet BLUE, the four-quadrant approach, and the ZigZag Intercostal Continuum that must be understood.

# Quick Reference of Normals and Rules of Thumb

- Expect adult dogs and cats and puppies and kittens >6 weeks of age to have "dry lung" artifacts predominate (absent B-lines). In other words, no more than a single B-line at only one of the eight transthoracic Vet BLUE views.
- Numbers of B-lines correlate to the degree of alveolar-interstitial edema in human lung and likely similar in other mammalian lung including small animals.
- "Absent B-lines All (Vet BLUE) Views (ABAV)" rules out clinically relevant left-sided congestive heart failure in both dogs and cats (and likely for all mammalian lung) (see Chapter 23).
- The Volpicelli Strong Positive Model is an effective screening test to rule in left-sided congestive heart failure in cats (see Chapter 23).
- Shred sign in gravity-dependent Vet BLUE views supports aspiration and bacterial bronchopneumonia (see Chapter 23).
- Wedge sign in the dorsal nongravity-dependent Vet BLUE views supports pulmonary thromboembolism (see Chapter 23).
- Nodule sign supports neoplastic, granulomatous processes including fungal, parasitic and bacterial, and abscessation (see Chapter 23).

# References


Boysen SR, Lisciandro GR. 2013. The use of ultrasound in the emergency room (AFAST and TFAST). *Vet Clin North Am Small Anim Pract* 43(4):773–797.

Boysen S, McMurray J, Gommeren K. 2019. Abnormal curtain signs identified with a novel lung ultrasound protocol in six dogs with pneumothorax. *Front Vet Sci* 6:291.

Breitkreutz R, Walcher F, Seeger FH, et al. 2007. Focused echocardiographic evaluation in resuscitation management (FEER): concept of an advanced life support-conformed algorithm. *Crit Care Med* 35(S5):S150–161.

Breitkreutz R, Price S, Steiger HV, et al. 2010. Focused echocardiographic evaluation in life support and peri-resuscitation of emergency patients: a prospective trial. *Resuscitation* 81:1527–1533.

Dicker SA, Lisciandro GR, Newell SM, et al. 2019. Diagnosis of pulmonary contusions with point-of-care lung ultrasonography and thoracic radiography compared to thoracic computed tomography in dogs with motor vehicle trauma: 29 cases (2017–2018). *J Vet Emerg Crit Care*, in press.

Hwang TS, Yoon YM, Jung DI, et al. 2018. Usefulness of transthoracic lung ultrasound for the diagnosis of mild pneumothorax. *J Vet Sci* 19(5): 660–666.

Kulhavy DA, Lisciandro GR. 2015. Use of a lung ultrasound examination called Vet BLUE to screen for metastatic lung nodules in the emergency room. *J Vet Emerg Crit Care* 25(S1):S14.

Lee FCY. 2016. Lung ultrasound – a primary survey of acutely dyspneic patients. *J Intens Care* 4:57.

Lichtenstein DA. 2010. Should lung ultrasonography be more widely used in the assessment of acute respiratory disease? *Expert Rev Respir Med* 4(5):533–538.

Lichtenstein DA, Meziere GA. 2008. Relevance of lung ultrasound in the diagnosis of acute respiratory failure: the BLUE protocol. *Chest* 134(1):117–125.

Lichtenstein DA, Meziere G, Biderman P, et al. 1997. The comet-tail artifact. An ultrasound sign of alveolar-interstitial syndrome. *Am J Respir Crit Care Med* 156(5):1640–1646.

Lisciandro GR. 2011. Abdominal and thoracic focused assessment with sonography for trauma, triage, and monitoring in small animals. *J Vet Emerg Crit Care* 21(2):104–122.

Lisciandro GR. 2014a. The Thoracic FAST$^3$ (TFAST$^3$) Exam. In: *Focused Ultrasound for the Small Animal Practitioner*, edited by Lisciandro GR. Ames: Wiley Blackwell, pp 140–165.

Lisciandro GR. 2014b. The Vet BLUE Lung Scan. In: *Focused Ultrasound for the Small Animal Practitioner*, edited by Lisciandro GR. Ames: Wiley Blackwell, pp 166–188.

Lisciandro GR, Armenise A. 2014. Focused or COAST$^3$ – Cardiopulmonary Resuscitation (CPR), Global FAST (GFAST$^3$) & the FAST-ABCDE Exam. In: *Focused Ultrasound for the Small Animal Practitioner*, edited by Lisciandro GR. Ames: Wiley Blackwell, pp 269–285.

Lisciandro GR, Lagutchik MS, Mann KA, et al. 2008. Evaluation of a thoracic focused assessment with sonography for trauma (TFAST) protocol to detect pneumothorax and concurrent thoracic injury in 145 traumatized dogs. *J Vet Emerg Crit Care* 18(3):258–269.

Lisciandro GR, Lagutchik MS, Mann KA, et al. 2008. Accuracy of Focused Assessment with Sonography for Trauma (TFAST) to detect pneumothorax in 145 dogs with blunt and penetrating trauma. *J Vet Emerg Crit Care* 18(3):258–269.

Lisciandro GR, Fosgate GT, Fulton RM. 2014. Frequency of ultrasound lung rockets using a regionally-based lung ultrasound examination named veterinary bedside lung ultrasound exam (Vet BLUE) in 98 dogs with normal thoracic radiographic lung findings. *Vet Radiol Ultrasound* 55(3):315–322.

Lisciandro GR, Ward JL, DeFrancesco TC, Mann KA. 2016. Absence of B-lines on lung ultrasound (Vet BLUE protocol) to rule out left-sided congestive heart failure in 368 cats and dogs. *J Vet Emerg Crit Care* 26(S1):S8.

Lisciandro GR, Fulton RM, Fosgate GT, Mann KA. 2017. Frequency of B-lines using a regionally-based lung

ultrasound examination (the Vet BLUE protocol) in 49 cats with normal thoracic radiographical lung findings. *J Vet Emerg Crit Care* 27(3):267–277.

Lisciandro GR, Romero L, Fosgate GT. 2018. The frequency of B-Lines and other lung ultrasound artifacts during Vet BLUE in 91 healthy puppies and kittens. *J Vet Emerg Crit Care* 28(S1):S16.

McEntee MF, Donohoe C, Stanton M, et al. 2011. The effects of varying ambient lighting of the detection of liver lesions in soft-copy reporting of ultrasound. Poster, European Society of Radiology. https://pdfs.semanticscholar.org/48ed/3c78acf9c0e3e04240cedf0c7b9dc07efb66.pdf

Nemanic S, London CA, Winser ER. 2006. Comparison of thoracic radiographs and single breath-hold helical CT for detection of pulmonary nodules in dogs with metastatic neoplasia. *J Vet Intern Med* 20(3):508–515.

Nyland TC, Mattoon JS. 2002. Thorax. In: *Small Animal Diagnostic Ultrasound*, 2nd edition, edited by Nyland TC and Mattoon JS. Philadelphia: WB Saunders, p 335.

Rademacher N, Pariaut R, Pate J, et al. 2014. Transthoracic lung ultrasound in normal dogs and dogs with cardiogenic pulmonary edema: a pilot study. *Vet Radiol Ultrasound* 55(4):447–452.

Reef VB. 1998. Thoracic ultrasonography: non-cardiac imaging. In: *Equine Diagnostic Ultrasound*, edited by Reef VB. Philadelphia: WB Saunders, pp 187–214.

Shyamsundar M, Attwood, B, Keating L, et al. 2013. Clinical review: The role of ultrasound in estimating extravascular lung water. *Cri Care* 17(5):237.

Sigrist NE, Doherr MG, Spreng DE. 2004. Clinical findings and diagnostic value of post-traumatic thoracic radiographs in dogs and cats with blunt trauma. *J Vet Emerg Crit Care* 14:259–268.

Sigrist NE, Adamik KN, Doherr MG, et al. 2011. Evaluation of respiratory parameters at presentation as clinical indicators of the respiratory localization in dogs and cats with respiratory distress. *J Vet Emerg Crit Care* 21(1):13–23.

Smith CR, Solano M, Lutmerding BA, et al. 2012. Pulmonary ultrasound findings in bottlenose dolphin Tursiops truncatus population. *Dis Aquat Organ* 101(3):243–255.

Vezzosi T, Mannucci A, Pistoresi F, et al. 2017. Assessment of lung ultrasound B-lines in dogs with different stages of chronic valvular heart disease. *J Vet Intern Med* 31(3):700–704.

Volpicelli G, Mussa A, Garofalo G, et al. 2006. Bedside lung ultrasound in the assessment of alveolar-interstitial syndrome. *Am J Emerg Med* 24:689–696.

Volpicelli G, Elbarbary M, Blaivas M, et al. 2012. International evidence-based recommendations for point-of-care lung ultrasound. *Intens Care Med* 38:577–591.

Ward JL, Lisciandro GR, Keene BW, et al. 2017. Accuracy of point-of-care lung ultrasonography for the diagnosis of cardiogenic pulmonary edema in dogs and cats with acute dyspnea. *J Am Vet Med Assoc* 250:666–675.

Ward JL, Lisciandro GR, DeFrancesco TD, et al. 2018a. Evaluation of point-of-care thoracic ultrasound and NT-proBNP for the diagnosis of congestive heart failure in cats with respiratory distress. *J Vet Intern Med* 32(5):1530–1540.

Ward JL, Lisciandro GR, DeFrancesco TC. 2018b. Distribution of alveolar-interstitial syndrome in dyspneic veterinary patients assessed by lung ultrasound versus thoracic radiography. *J Vet Emerg Crit Care* 28(5):415–428.

Ward JL, Lisciandro GR, Ware WA, et al. 2019. Lung ultrasound findings in 100 dogs with various etiologies of cough. *J Am Vet Med Assoc* 255(5):574–583.

# Further Reading

Ball CG, Ranson MK, Adamicza A, et al. 2009. Sonographic depiction of posttraumatic alveolar-interstitial disease: the hand-held diagnosis of a pulmonary contusion. *J Trauma* 66(3):962.

Cunningham J, Kirkpatrick AW, Nicolaou S, et al. 2002. Enhanced recognition of "lung sliding" with power color Doppler in the diagnosis of pneumothorax. *J Trauma* 52:769–772.

Filly RA. 1988. Ultrasound: the stethoscope of the future, alas. *Radiology* 167:400.

Gargani L, Lionetti V, di Cristofano C, et al. 2007. Early detection of acute lung injury uncoupled to hypoxemia in pigs using ultrasound lung comets. *Crit Care Med* 35(12): 2769–2774.

Hecht S. 2008. Thorax. In: *Atlas of Small Animal Ultrasonography*, edited by Penninck D, d'Anjou MA. Ames: Blackwell Publishing, pp 119–150.

Jambrik Z, Monti S, Coppola V, et al. 2004. Usefulness of ultrasound lung comets as a nonradiologic sign of extravascular lung water. *Am J Cardiol* 93(10):1265–1270.

Jambrik Z, Gargani L, Adamicza A, et al.2010. B-lines quantify the lung water content: a lung ultrasound versus lung gravimetry study in acute lung injury. *Ultrasound Med Biol* 36(12):2004–2010.

Kulhavy DA, Lisciandro GR. 2018. The use of VetBLUE to evaluate lung pathology in dogs with severe pulmonary hypertension without left-sided heart disease. *J Vet Emerg Crit Care* 28(S1):S15.

Lichtenstein DA. 2007. Ultrasound in the management of thoracic disease. *Crit Care Med* 35(S5):S250–S261.

Lichtenstein D. 2010. Should lung ultrasonography be more widely used in the assessment of acute respiratory disease? *Expert Rev Respir Med* 4(5):533–538.

Lichtenstein D. 2012. Fluid administration limited by lung sonography: the place of lung ultrasound in assessment of acute circulatory failure (the FALLS-protocol). *Expert Rev Respir Med* 6(2):155–162.

Lichtenstein D, Karakitsos D. 2012. Integrating lung ultrasound in the hemodynamic evaluation of acute circulatory failure (the fluid administration limited by lung sonography protocol). *J Crit Care* 27(5):533.

Lichtenstein D, Meziere G, Bideman P, et al. 1997. The comet-tail artifact. An ultrasound sign of alveolar-interstitial syndrome. *Am J Respir Crit Care Med* 156(5):1640–1646.

Lichtenstein D, Meziere G, Lagoueyte JF, et al. 2009. A-lines and B-lines: lung ultrasonography as a bedside tool for predicting pulmonary artery occlusion pressure in the critically ill. *Chest* 136:1014–1020.

Lisciandro GR. 2012. Evaluation of initial and serial combination focused assessment with sonography for trauma (CFAST) examinations of the thorax (TFAST) and abdomen (AFAST) with the application of an abdominal fluid scoring system in 49 traumatized cats. *J Vet Emerg Crit Care* 22(S2):11.

Lisciandro GR. 2014. Ultrasound in animals. In: *Critical Care Ultrasound*, edited by Lumb P, Karakitsos D. St Louis: Elsevier, pp 290–293.

Lisciandro GR. 2019. Point-of-care ultrasound. In: *Small Animal Diagnostic Ultrasound*, edited by Mattoon JS, Sellon R, Berry CR. St Louis: Elsevier, in press.

Peris A, Zagli G, Barbani F, et al. 2010. The value of lung ultrasound monitoring in H1N1 acute respiratory distress syndrome. *Anaesthesia* 65(3):294–297.

Rozycki GS, Pennington SD, Feliciano DV. 2001. Surgeon-performed ultrasound in the critical care setting: its use as an extension of the physical examination to detect pleural effusion. *J Trauma* 50:636–642.

Simpson S, Syring R, Otto CM. 2009. Severe blunt trauma in dogs: 235 cases (1997–2003). *J Vet Emerg Crit Care* 19(6):588–602.

Soldati G, Testa A, Silva FR, et al. 2006. Chest ultrasonography in lung contusion. *Chest* 130(2):533–538.

Soldati G, Sher S, Testa A. 2011. Lung and ultrasound: a time to "reflect." *Eur Rev Med Pharmacol Sci* 15(2):223–227.

Ward JL, Lisciandro GR, Ware WA, et al. 2019. Lung ultrasound findings in 100 dogs with various etiologies of cough. *J Am Vet Med Assoc* 255(5):574–583.

CHAPTER TWENTY-THREE

# POCUS: Vet BLUE – Clinical Integration

Gregory R. Lisciandro and Stephanie C. Lisciandro

## Introduction

Over thirty 30 years ago, a physician, Roy Filly, MD, dubbed the ultrasound probe "the modern stethoscope." Although lung ultrasound (LUS) has been utilized by large animal veterinarians for decades, especially on the equine side, there has been no easily understandable *lung language* until the first edition of this book (Lisciandro 2014b). The lung language that we propose, including the terms "dry lung," "wet lung," shred sign, tissue sign, nodule sign, and wedge sign to describe specific findings, allows clear communication of findings between colleagues. The use of lung ultrasound in veterinary practice is proving to be an invaluable tool to assess patients for pulmonary disease.

Lung ultrasound artifacts and their integration into a regional pattern-based approach have provided a new tool that in human medicine replaces the subjectivity of lung auscultation as well as the unreliability of supine chest radiography and breathing patterns (Volpicelli et al. 2012). The ultrasound probe is the "visual stethoscope" and allows the sonographer to "see" versus hearing (and guessing) as to the type of lung pathology (Filly 1988, Lichtenstein and Mezière 2008; Volpicelli et al. 2006; Lisciandro 2011, 2012, 2013, unpublished data; Moore and Copel 2011; Lisciandro et al. 2014; Gillman and Kirkpatrick 2012). Vet BLUE (Brief Lung Ultrasound Exam) is a protocol for lung ultrasound that provides an additional imaging modality which serves as both a practical pulmonary screening test and an adjunct for the often problematic interpretation of radiographic lung.

The use of the ultrasound probe as a visual stethoscope allows point-of-care imaging of lung ultrasound artifacts and signs along the lung surface, providing evidence-based clinical information. Vet BLUE lung ultrasound when used in clinical practice may function as a screening test or a primary and ancillary imaging modality as well as a point-of-care monitoring tool without the restraint and risk of radiographic studies (see Table 23.1).

In this chapter, we describe our lung language, including the six Vet BLUE lung ultrasound signs and their clinical applications. We use the term "B-lines" in place of "ultrasound lung rockets" (Volpicelli et al. 2012; Lisciandro et al. 2014). We expand on the information from the first edition of this textbook adding years of additional information we have learned about lung ultrasound since its publication. Enjoy the ride into this new frontier!

## What Vet BLUE Can Do

- Can rapidly rule out clinically relevant alveolar-interstitial edema by the finding of "dry lung."
- Can rapidly rule out left-sided congestive heart failure in patients with respiratory distress by the finding of "dry lung all (Vet BLUE) views" abbreviated as ABAV (Absent B-lines All Views).
- Can rapidly detect signs of alveolar-interstitial syndrome (cardiogenic and noncardiogenic pulmonary edema) using the "wet lung" (B-lines) principle.
- Can rapidly and preemptively detect the development of alveolar-interstitial syndrome using the "wet lung" principle in patients at risk for volume overload (fluid resuscitation, transfusion administration, mechanical ventilation, kidney failure, hypoalbuminemia, heart disease,

*Point-of-Care Ultrasound Techniques for the Small Animal Practitioner*, Second Edition. Edited by Gregory R. Lisciandro.
© 2021 John Wiley & Sons, Inc. Published 2021 by John Wiley & Sons, Inc.
Companion website: www.wiley.com/go/lisciandro/ultrasound2

**Table 23.1.**
Vet BLUE lung examination and the clinical questions it answers.

| | Questions answered |
|---|---|
| Does lung pathology exist on the lung surface? | Binary plus Integrative, Global FAST |
| Does the patient have alveolar-interstitial syndrome (fluid in the interstitial space or alveoli)? | Binary plus Integrative, Global FAST |
| Does the patient have lung consolidation? | Binary plus Integrative, Global FAST |
| Does the patient have lung nodules? | Binary plus Integrative, Global FAST |
| Does the patient have pneumonia? | Binary plus Integrative, Global FAST |
| Does the patient have pulmonary thromboembolism (PTE)? | Binary plus Integrative, Global FAST |
| Does the patient have lung contusions? | Binary plus Integrative, Global FAST |
| Does the patient have left-sided congestive heart failure? If so, what is the severity of pulmonary edema? Might the patient need diuretics? | Binary plus Integrative, Global FAST |
| Is the patient developing lung pathology secondary to an intervention (blood transfusion, fluid therapy, etc.)? | Binary plus Integrative, Global FAST |
| Is the coagulopathic patient bleeding into lung? | Binary plus Integrative, Global FAST |
| Does the patient have atelectatic lung? | Binary plus Integrative, Global FAST |

Source: Courtesy of Dr Gregory Lisciandro, Hill Country Veterinary Specialists and FASTVet.com, Spicewood, TX.

etc.) and those at risk for pulmonary hemorrhage (coagulopathic).
- Can guide loop diuretic therapy using the Vet BLUE B-line scoring system by counting B-lines at each respective Vet BLUE view and combining with numbers of positive Vet BLUE regions.
- Can rapidly and often preemptively detect the development of acute lung injury/acute respiratory distress syndrome (ARDS) and its related subsets.
- Can rapidly and often preemptively detect aspiration pneumonia in at risk patients.
- Can screen for pulmonary thromboembolism (PTE) and be used as a tool to trigger thromboprophylaxis and thrombolytics.
- Serves as a rapid point-of-care pulmonary metastasis check.
- Can detect lung surface pathology not evident on thoracic radiography.
- Can help when combining with Global FAST and its TFAST echo views to differentiate true respiratory conditions from nonrespiratory look-alikes.
- Can provide evidence-based information to help determine your next best diagnostic test in work-ups.
- Can detect lung patterns in trauma patients that support pulmonary contusions.
- Can provide a Vet BLUE lung contusion severity score by numbers of B-lines at each respective Vet BLUE view combined with the number of positive Vet BLUE regions.
- Can provide an evidence-based working diagnosis for respiratory and nonrespiratory conditions that helps keep patients alive for subsequent imaging and gold standard testing and treatment.
- Can be used for monitoring response to therapy (serial exams) in many lung conditions, including cardiogenic and non-cardiogenic pulmonary edema, pulmonary contusions, pulmonary hemorrhage, pneumonias, neoplasia, and granulomatous disease.

## What Vet BLUE Cannot Do

- Cannot give a definitive diagnosis. Vet BLUE provides regional pattern-based evidence for certain lung conditions similar to interpretative conclusions using thoracic radiography (TXR) and computed tomography (CT) although likely with higher sensitivity for lung surface pathology.
- Cannot detect lung pathology that is deep to the peripheral margin of lung or pathology that is not present at one of its views. Vet BLUE is limited to lung disease that makes it to the lung periphery and must also be present at the view being used.
- Cannot fully replace TXR or CT but may be used as an adjunctive diagnostic aid, a screening test, and a monitoring tool for many diagnosed conditions.

## Indications

- A screening test for patients with respiratory signs, respiratory compromise or distress, and for patients at risk for respiratory complications.
- Point-of-care rapid assessment for patients too unstable for TXR or CT, or when additional imaging is delayed because of lack of resources.

- Monitoring response to therapy in many respiratory patients as a rapid, noninvasive, radiation-sparing, and point-of-care imaging modality.
- As a guide for loop diuretic usage by using the Vet BLUE B-line scoring system.
- Use as a guide for fluid resuscitation or for early detection of volume overload (cardiogenic pulmonary edema) in at-risk hospitalized and critically ill patients, especially when combined with the Global FAST approach including its TFAST echo views.

### *Objectives*

- Apply the simple "wet lung" and "dry lung" lung ultrasound concepts in a regional pattern-based approach following the Vet BLUE protocol; thus, be able to categorize respiratory distressed patients into probable causes including upper airway versus lower airway, lung disease versus congestive heart failure, and nonrespiratory (so-called respiratory look-alikes) versus respiratory causes.
- Recognize additional lung conditions through recognition of the Vet BLUE visual lung language of shred sign, tissue sign, nodule sign, and wedge sign.
- Preemptively anticipate thoracic radiographic findings by using the Vet BLUE visual lung language in a regional pattern-based approach.
- Make evidence-based decisions regarding therapeutic course (initial assessment as well as monitoring) in patients with respiratory disease or affected animals.

The Global FAST exam includes Vet BLUE combined with AFAST and TFAST. We recommend always performing the complete Global FAST approach because a problem list is "seen," and thus, the interpretation and clinical integration of Vet BLUE findings are optimized. For example, a nodule sign found during AFAST in a younger outdoor cat in central Texas with an enlarged spleen (>10 mm in thickness) and no other apparent masses may dictate fungal serology as the next best test because of the high suspicion of histoplasmosis. Multiple nodule signs on Vet BLUE in a dog with a hemoabdomen and cavitated splenic mass may support metastatic disease. A dog with dilated cardiomyopathy (DCM) will present with a dry cough and unremarkable TXR but on TFAST has obvious poor contractility (DCM) that would otherwise be missed. By only performing Vet BLUE, satisfaction of search error often occurs, and essential information is missed, as in the cases mentioned above. See Chapters 36 and 37 for staging the patient on day 1 (Table 23.1).

# Important Considerations and Limitations of Vet BLUE and Lung Ultrasound

Before beginning this chapter, there are several points that must be appreciated by the lung sonographer and those using the Vet BLUE protocol.

- Significant, acute, common, clinically relevant pulmonary disease most likely extends to the lung periphery in dogs and cats and other mammalian lung, similar to what has been found in people (Lichtenstein and Mezière 2008; Lichtenstein 2010a; Soldati et al. 2011; Volpicelli et al. 2012; Lisciandro 2012, unpublished data; Lisciandro et al. 2014, 2016, 2017; Ward et al. 2017, 2018b). However, if lung pathology doesn't extend in close proximity to the "lung line" (outer ~1–3 mm of human lung), the lung's peripheral surface at an acoustic window being used during lung ultrasound, then it will be missed (Volpicelli et al. 2006) (Figure 23.1).
- Centrally located lung disease will be missed (occult lesion) by lung ultrasound because ultrasound cannot image through aerated lung (Soldati et al. 2011; Volpicelli et al. 2006, 2012; Kulhavy and Lisciandro 2015; Dicker et al. 2019) (see Figure 23.1).

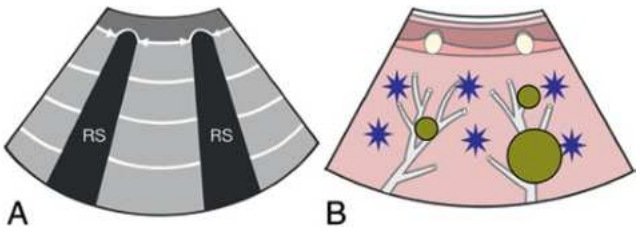


**Figure 23.1.** Lung pathology *must* touch the lung line to be detected. Simple line drawings of lung and its standard orientation of the "gator sign." In (A) the arrows along the pulmonary–pleural interface (PPI) and "lung line" represent "lung sliding" and the A-lines "dry lung" at the lung periphery at that specific LUS acoustic window. In (B) is the lung anatomy and what is being missed in (A) because the pathology does not touch the "lung line." The stars represent lung pathology such as alveolar-interstitial syndrome that does not extend to the lung surface and thus will go undetected during LUS. The circle represents a nodule that also doesn't make it to the lung surface and thus will likewise go undetected. Even though the lung is considered "dry lung" and normal at its surface, the line drawing shows how deeper lesions may be missed, a limitation of LUS. Source: Reproduced with permission of Dr Gregory Lisciandro, Hill Country Veterinary Specialists and FASTVet.com, Spicewood, TX. Illustration by Dr Judy Brown, Toronto, Canada.

- B-lines in most instances represent forms of alveolar-interstitial edema, referred to as alveolar-interstitial syndrome (AIS), but B-lines are nonspecific for the cause of alveolar-interstitial edema (Lichtenstein et al. 1997; Lichtenstein and Mezière 2008; Volpicelli et al. 2006, 2012).
- Alveolar-interstitial syndrome is referred to as a "syndrome" because B-lines are nonspecific and thus may represent forms of cardiogenic and noncardiogenic pulmonary edema, pneumonia, hemorrhage and other inflammatory conditions (Soldati et al. 2006; Lisciandro 2011, 2014a,b; Volpicelli et al. 2012; Rademacher et al. 2014; Lisciandro et al. 2014, 2017; Ward et al. 2017, 2019). In trauma patients, the finding of AIS supports lung contusions until proven otherwise (Ball et al. 2009; Lisciandro et al. 2008; Lisciandro 2011, 2014a,b; Dicker et al. 2019). Think of AIS most commonly as "wet lung" with the presence of B-lines.
- Vet BLUE can effectively detect AIS that correlates with radiographic lung (Rademacher et al. 2014; Lisciandro et al. 2014, 2016, 2017; Ward et al. 2017, 2018b; Vezzosi et al. 2017; Szymczak et al. 2018), and with higher frequency than TXR and comparable to CT in human, canine, and feline lung (Volpicelli et al. 2006, 2012; Lichtenstein 2010b; Ward et al. 2018b; Dicker et al. 2019).
- Vet BLUE can effectively detect pulmonary contusions with higher sensitivity and specificity than TXR and fares well compared to the gold standard of CT (Dicker et al. 2019).
- Alveolar-interstitial edema (B-lines) represents extravascular lung water, and precedes alveolar flooding, a more serious and more difficult lung condition to treat; thus B-lines serve as an early warning sign to alter therapeutic course (Lichtenstein et al. 2009a; Lichtenstein 2010a; Lichtenstein and Karakitosos 2012; Jambrik et al. 201; Soldati et al. 2011; Shyamsundar et al. 2013; Lisciandro et al. 2016; Ward et al. 2017, 2018b; Vezzosi et al. 2017).
- Infiltrative lung conditions such as lung consolidation and nodular disease are sonographically detected through observation of the shred sign, tissue sign, nodule sign, and wedge sign (Lichtenstein et al. 2004, 2009b; Lichtenstein 2010a,b; Volpicelli et al. 2012; Lee et al. 2015; Kulhavy and Lisciandro 2015; Ward et al. 2017, 2019).

# Vet BLUE Visual Lung Language

## Most Normal to Least Normal

A composite of the Vet BLUE visual lung language is illustrated in Figure 23.2 (Lichtenstein 2010b; Lisciandro 2014b; Lee et al. 2015).

- Dry lung – normal aerated lung surface, A-lines with "lung sliding" (Figure 23.5). Dry lung only to be confounded with pneumothorax, which is A-lines without "lung sliding" (Figure 23.6).
- Wet lung – alveolar-interstitial syndrome, B-lines (Figures 23.3, 23.4, 23.7). There are other causes of "wet lung" that are far less common, one of which is pleural thickening from pulmonary fibrosis and senescent lung, which is more common in people than small animals (Tardella et al. 2012; Shyamsundar et al. 2013; Wang et al. 2017) as well as types of "pseudo- B-lines" (see Nodular Disease).
- Shred sign – air bronchogram (Figure 23.8).
- Tissue sign – hepatization (Figure 23.9).
- Nodule sign (mass sign) – nodule (mass if >3 cm) (Figure 23.10).
- Wedge sign – infarct, PTE (Figure 23.11).

## Dry Lung versus Wet Lung: A-lines, Lung Sliding, and B-lines

*A-lines* with "lung sliding" represents "dry lung" at its surface (see Figure 23.5; see also Figures 17.6 and 22.3). A-lines with no "lung sliding" represent pneumothorax (PTX) (Figure 23.6).

*B-lines* represent "wet lung" and most commonly forms of alveolar-interstitial edema (Figure 23.7). B-lines are nonspecific in that they cannot tell you what type of alveolar-interstitial edema is present. Thus, the presence of B-lines is commonly referred to as alveolar-interstitial *syndrome* (AIS) and a regional pattern-based approach, Vet BLUE, is used to place their presence into clinical relevance (see Figure 23.13). B-lines less commonly are caused by senescent lung and fibrosis, more relevant to people who live longer than our small animal patients (Shyamsundar et al. 2013); and must be differentiated from "pseudo B-lines" (see Figure 23.10).

## Shred Sign, Tissue Sign, Nodule Sign, and Wedge Sign

*Shred sign* is lung consolidation seen as a fractal (irregular) line from the expected linear continuity of the "lung line" with hyperechoic foci (air) within the consolidation. The shred sign represents an air bronchogram (see Figure 23.8) (Lichtenstein et al. 2004, 2009b; Lisciandro 2014b; Lichtenstein 2010a; Lee et al. 2015; Neelis et al. 2015).

*Tissue sign* is lung consolidation similar to the shred sign, but more severe. The tissue sign is complete consolidation without any aeration and thus appears as liver (or spleen), referred to as hepatization of lung. In other words, the tissue sign is when lung lacking

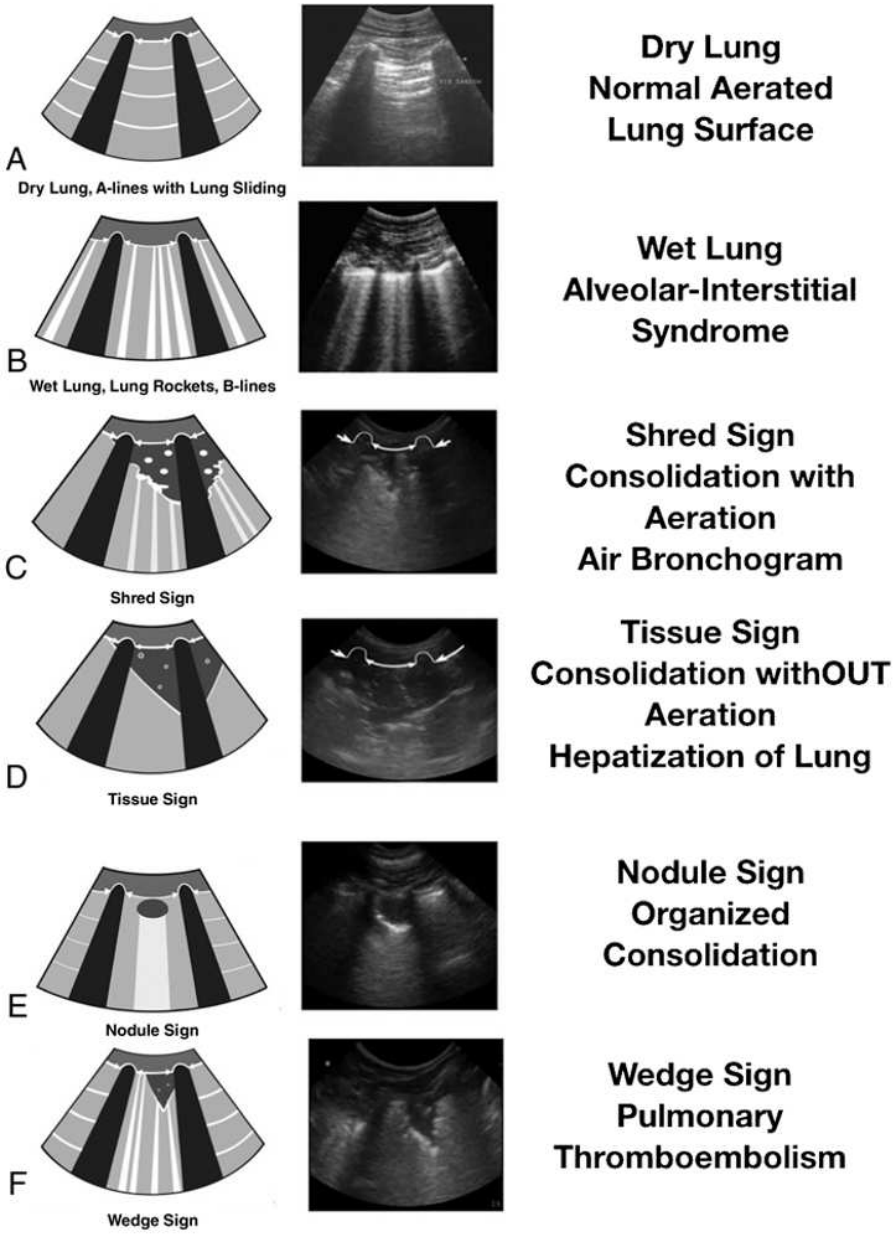


**Figure 23.2.** Vet BLUE six lung ultrasound signs. The Vet BLUE visual lung language allows easy communication of findings over the alphabetical line nomenclature system. From top to bottom are escalating degrees from normal to abnormal of LUS findings beginning with normal aerated lung that progresses to alveolar-interstitial syndrome to forms of more severe consolidation. The six Vet BLUE lung ultrasound signs are (A) "dry lung" defined as A-lines with "lung sliding," representing aerated lung at its periphery, (B) "wet lung" defined as B-lines, representing forms of alveolar-interstitial syndrome and less commonly fibrosis and senescent lung and others, (C) shred sign, consolidated lung with aeration, representing an air bronchogram, (D) tissue sign, complete consolidation with no aeration, representing hepatization of lung, (E) nodule sign, organized consolidation into a nodule or mass, and lastly (F) wedge sign, a triangulation of tissue necrosis from lung infarction, supporting PTE when observed in the least gravity-dependent Caudodorsal and Perihilar Vet BLUE views. Line with rounding and an interposing straight line represents the intercostal space and the "gator sign" orientation. Source: Reproduced with permission of Dr Gregory Lisciandro, Hill Country Veterinary Specialists and FASTVet.com, Spicewood, TX. Illustration by Dr Judy Brown, Toronto, Canada.

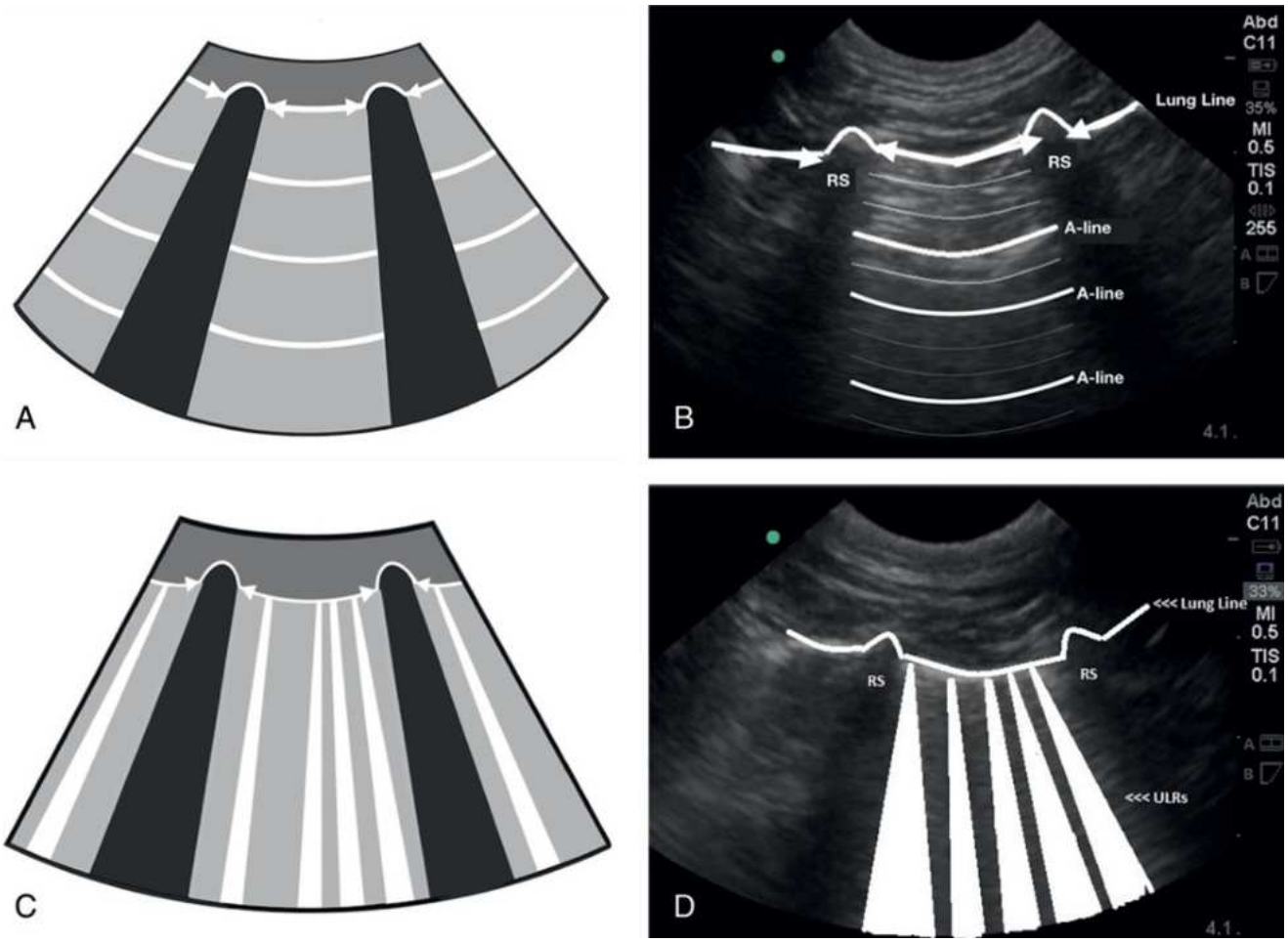


**Figure 23.3.** "Wet" versus "dry lung." (A,B) Line drawings of "dry lung," "lung sliding" with A-lines, and "wet lung," B-lines, with a correlative B-mode image with overlays, respectively. A-lines are horizontal parallel (to the "lung line") equidistant lines that are evident through the far-field and enhanced by having a 90° angle of insonation to the pulmonary–pleural interface (PPI) and "lung line." "Dry Lung" is "lung sliding" with A-lines and indicated by the arrows along the "lung line." (CD) Line drawing of "wet lung" with a correlative B-mode image with overlays. B-lines are laser-like, hyperechoic vertical lines that extend through the far-field *without* fading while obliterating A-lines. B-lines swing in real time like a pendulum in respirophasic synchrony. The lung sonographer adhering to this definition will avoid being confounded by other vertical-like artifacts. Line with rounding and an interposing straight line represents the intercostal space and the "gator sign" orientation. Source: Reproduced with permission of Dr Gregory Lisciandro, Hill Country Veterinary Specialists and FASTVet.com, Spicewood, TX. Illustration by Dr Judy Brown, Toronto, Canada.

aeration appears like a parenchymal organ (liver) (see Figure 23.9) (Lichtenstein 2010a; Lisciandro 2014b; Neelis et al. 2015).

*Nodule sign* is lung consolidation organized into the shape of an oval or circle and usually represents neoplastic, granulomatous, and infectious processes (abscess). The nodule is often anechoic to hypoechoic with a far border that is hyperechoic with a pseudo B-line extending from it through the far-field (Lisciandro 2014b; Neelis et al. 2015; Ward et al. 2019) (see Figure 23.10). Radiographically, a nodule is generally defined as <3 cm and a mass as >3 cm and a mass sign could be added to the nodule sign (Alpert et al. 2015).

*Wedge sign* is a subset of the shred sign and less commonly the tissue sign that has a triangular wedge shape representing lung surface infarction and vascular necrosis of peripheral lung. When the wedge sign is observed in dorsal Vet BLUE lung regions (Caudodorsal and Perihilar lung regions) the presence of PTE should be suspected (see Figure 23.11) (Lisciandro 2013, unpublished data). In gravity-dependent views a wedge sign would be difficult to distinguish from pneumonia and other forms of gravity-dependent consolidation, emphasizing the importance of using the regional pattern-based approach for the most probable working diagnosis (Mathis et al. 2005; Mastruzzo et al. 2008; Nazerian et al. 2014).

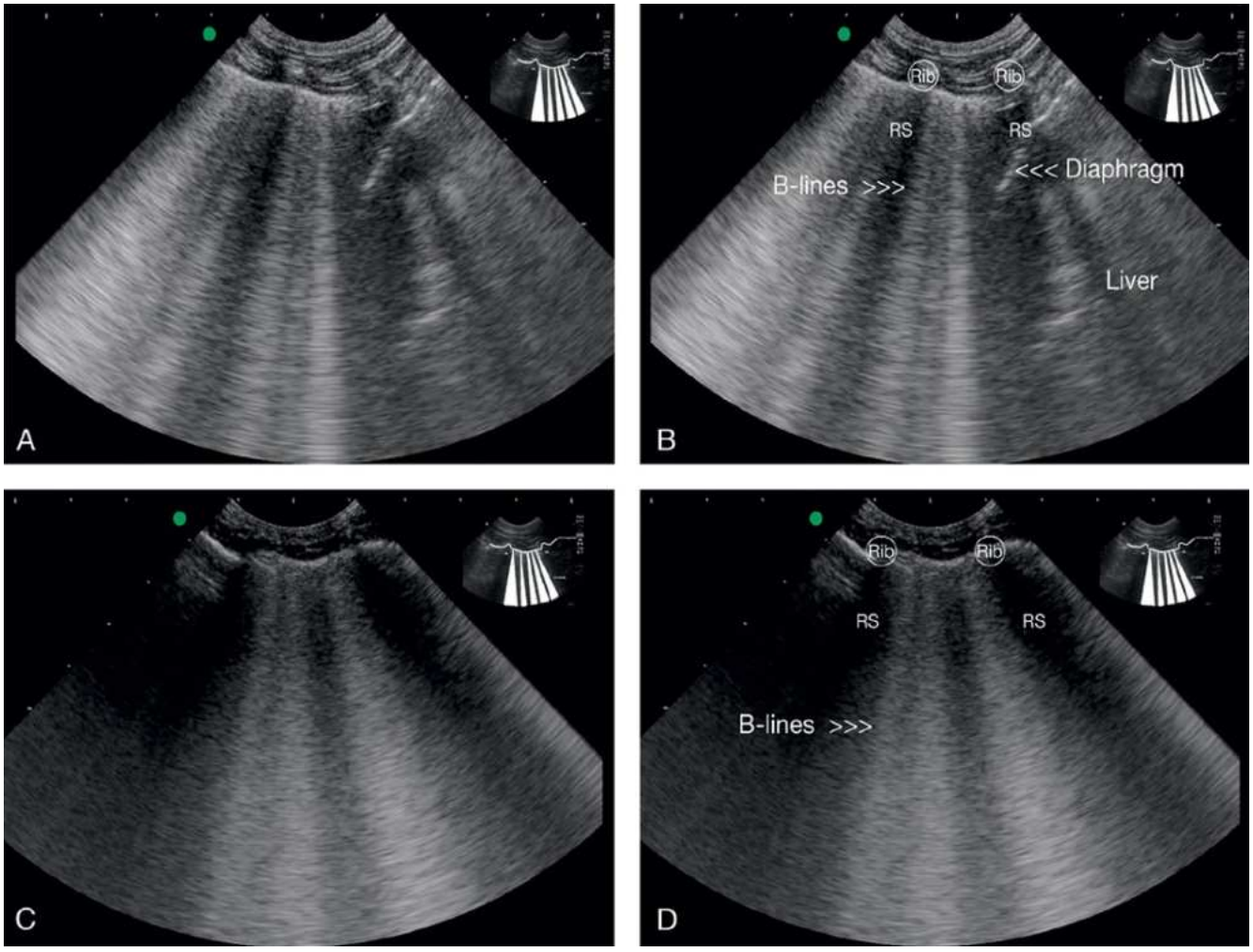


**Figure 23.4.** B-lines also referred to as ultrasound lung rockets. Examples of B-lines in (A) and (C) with the same images labeled in (B) and (D). Note the laser-like hyperechoic vertical lines (rocket like) that extend from the "lung line" through the far-field that in real time swing synchronously with inspiration and expiration while obliterating A-lines. An illustrative icon of B-lines (>3) is present in the upper right hand corner of each image. Note the features on these images and then compare with Figure 23.3 and the confounders in Figures 22.17, 23.20, and 23.22. The recognition of B-lines is "all or none"— they are either present or not present. In (A) and (B) the image shows the caudodorsal transition zone (CdTZ) labeled with diaphragm and liver. The images are acceptable for overall LUS orientation but for Vet BLUE have too much depth (7 cm) and should be magnified in this cat to 4–5 cm. Ribs are labeled and circled. RS, rib shadow. Source: Reproduced with permission of Dr Gregory Lisciandro, Hill Country Veterinary Specialists and FASTVet.com, Spicewood, TX.

**Figure 23.5.** "Dry lung" – A-lines with "lung sliding." Correlative images of (A) line drawing of "dry lung" with strong A-lines and "lung sliding," (B) the relevant lung anatomy with lung immediately against the intercostal space, and (C) the B-mode image. Note the B-mode image for "dry lung" and "PTX" are the same because the difference is "lung sliding" that must be observed in real time. Source: Reproduced with permission of Dr Gregory Lisciandro, Hill Country Veterinary Specialists and FASTVet.com, Spicewood, TX. Illustration by Dr Judy Brown, Toronto, Canada.

**Figure 23.6.** Pneumothorax – A-lines with absent "lung sliding." Correlative images of (A) line drawing of PTX with strong A-lines and absent "lung sliding," (B) the relevant lung anatomy with air shown within the pleural cavity, and (C) the B-mode image. Source: Reproduced with permission of Dr Gregory Lisciandro, Hill Country Veterinary Specialists and FASTVet.com, Spicewood, TX. Illustration by Dr Judy Brown, Toronto, Canada.

**Figure 23.7.** "Wet lung" – B-lines. Correlative images of (A) line drawing of B-lines extending from the "lung line" without fading while obliterating A-lines and swinging like a pendulum in respirophasic synchrony, (B) the relevant lung anatomy with alveolar-interstitial edema (*blue splotches*) that touch the "lung line" and can thus be detected during LUS, and (C) the B-mode image. The presence and absence of B-lines is an "all or none" phenomenon and their presence, referred to as alveolar-interstitial syndrome (AIS), is nonspecific. AIS and its edema component may commonly be water next to air (cardiogenic and noncardiogenic edema), blood next to air (lung hemorrhage or contusions in trauma) or pus next to air (pneumonia) (see Figure 23.13). Source: Reproduced with permission of Dr Gregory Lisciandro, Hill Country Veterinary Specialists and FASTVet.com, Spicewood, TX. Illustration by Dr Judy Brown, Toronto, Canada.

**Figure 23.8.** Shred sign – air bronchogram, consolidation with aeration. Correlative images of (A) line drawing of the shred sign where the expected normal linear continuity along the pulmonary–pleural interface (PPI) is fractal or irregular and the "lung line" is absent, (B) the relevant lung anatomy as an air bronchogram in which lung is consolidated but the airways are open for ventilation, and (C) the B-mode image. Source: Reproduced with permission of Dr Gregory Lisciandro, Hill Country Veterinary Specialists and FASTVet.com, Spicewood, TX. Illustration by Dr Judy Brown, Toronto, Canada.

**Figure 23.9.** Tissue sign – hepatization, consolidation without aeration. Correlative images of (A) line drawing of the tissue sign where the expected normal linear continuity along the pulmonary–pleural interface (PPI) may be linear or fractal or irregular and the hyperechoic "lung line" in the near-field may be absent, (B) the relevant lung anatomy is complete consolidation without aeration (see illustrative plugged airways) and lung appears like liver, referred to as "hepatization" of lung, and (C) the B-mode image. Source: Reproduced with permission of Dr Gregory Lisciandro, Hill Country Veterinary Specialists and FASTVet.com, Spicewood, TX. Illustration by Dr Judy Brown, Toronto, Canada.

**Figure 23.10.** Nodule sign. Correlative images of (A) line drawing of the nodule sign where along the pulmonary–pleural interface (PPI) are rounded or oval hypoechoic consolidations, (B) the relevant lung anatomy with nodules along the "lung line" and deeper, and (C) the B-mode image. Only nodules reaching the "lung line" will be detected. The nodule sign has an accompanied "pseudo B-line" similarly created in alveolar-interstitial syndrome (fluid–air) by strong differences in acoustic impedance, but instead regarding nodules between soft tissue–air and thus termed "pseudo B-lines" to reflect this distinction. See the single nodule sign in Figure 23.19E. Source: Reproduced with permission of Dr Gregory Lisciandro, Hill Country Veterinary Specialists and FASTVet.com, Spicewood, TX. Illustration by Dr Judy Brown, Toronto, Canada.

**Figure 23.11.** Wedge sign. Correlative images of (A) line drawing of the wedge sign where along the PPI is a triangulated shred sign or tissue sign, (B) the relevant lung anatomy with lung surface infarction, and (C) the B-mode image. The wedge sign in the Caudodorsal and Perihilar lung regions are highly suggestive of PTE. Often, the wedge sign has accompanying B-lines (alveolar-interstitial syndrome) associated with it. Source: Reproduced with permission of Dr Gregory Lisciandro, Hill Country Veterinary Specialists and FASTVet.com, Spicewood, TX. Illustration by Dr Judy Brown, Toronto, Canada.

## Lung Ultrasound Artifacts Further Defined: "Lung Sliding," A-lines, and B-lines

"*Lung sliding*" is the "to and fro" respirophasic movement of the visceral and parietal pleura over one another. The macrodescription preferred by the author is the "to and fro" respirophasic movement of the "lung line" (surface) along the intercostal space. In other words, as the patient inspires and expires, the expanded (inspiration) and contracted (expiration) lung surface will slide along the intercostal space and is imaged as "sliding" using ultrasound (see Figure 23.5). The absence of "lung sliding" diagnoses PTX (see Figure 23.6). Panting, shallow breathing, and apnea will all confound "lung sliding" which along with PTX is explained in more detail in Chapters 17 and 18 (Lichtenstein et al. 2000; Kirkpatrick et al. 2004; Lisciandro et al. 2008).

*A-lines* are air reverberation artifact and "A" stands for air, a good way to remember A-lines. These are equidistant horizontal lines parallel to the intercostal space and extending from the first reflective hyperechoic surface, generally the "lung line" of aerated lung in normalcy, that then repeat themselves and their equidistant spacing through the far-field of the ultrasound screen (Figure 23.12; see also Figures 17.6, 17.12, 18.6, 22.2, 22.3, 23.3, 23.5, 23.6) (Volpicelli et al. 2006, 2012; Lichtenstein 2009a). A-lines indicate a strong aerated presence and are observed in either "dry lung" or pneumothorax (air in the pleural space) with the differentiating feature being the presence or absence of "lung sliding." The A-lines of PTX are also parallel to the pulmonary-pleural interface and where the "lung line" is expected, but lung is collapsed and displaced from the thoracic wall (see Figure 23.6). A-lines may also be present in "dry lung" in patients with pleural effusion, thus the term "lung line" is used by the author when lung is not directly opposed to the thoracic wall. A-lines, air reverberation, are also possible when air is present in other regions, such as free air in the peritoneal cavity, pleural cavity, pericardial sac, retroperitoneal space, stomach, etc.

*B-lines* usually represent forms of alveolar-interstitial edema and are most commonly the ultrasonographic result of a small amount of fluid next to a small amount of air at the outermost periphery of lung. Simplistically, the strong difference in acoustic impedance creates the vertical lines that synchronously swing in real time with respirophasic movement, although it's a bit more complex than this, These laser-like strongly hyperechoic lines do not fade while obliterating A-lines and must extend through the far-field of the ultrasound screen (Lichtenstein et al. 1997; Volpicelli et al. 2006, 2012; Lisciandro et al. 2008, 2014, 2017; Lisciandro 2011, 2014a,b). Despite the artifact extending through the far-field of the screen, they are caused by the very outermost surface of lung (Volpicelli et al. 2006; Lichtenstein et al. 2009a).

The term "B" for B-lines has an unknown basis other than the letter "B" follows "A" in the alphabet; however, the author likes to remember B-lines as approximating Kerley B lines that represent pulmonary interstitial edema on radiographs (Volipicelli et al. 2006, 2012; Louvet and Bourgeois 2008; Lichtenstein et al. 2009a,b; Lisciandro 2011). Importantly, B-lines are nonspecific for the type of alveolar-interstitial edema, thus referred to as alveolar-interstitial

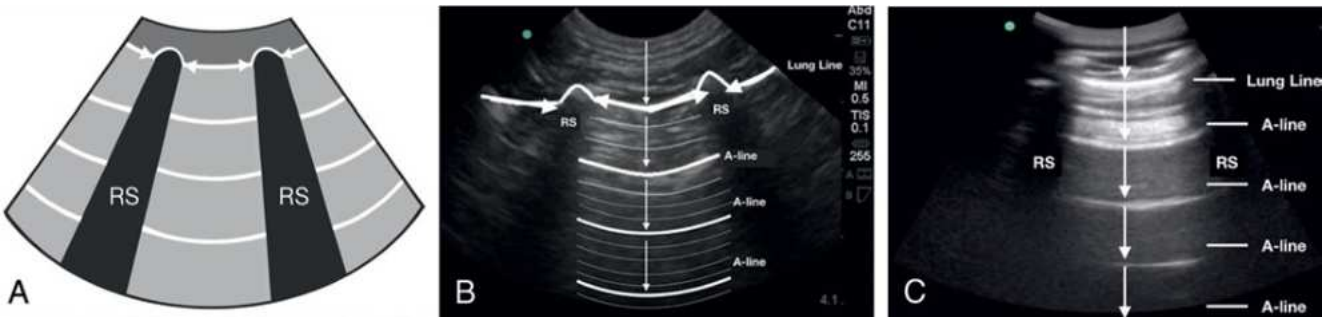


**Figure 23.12.** "Dry lung" – A-lines and "lung sliding." Correlative line drawing with labeled B-mode images. In (A) the "gator sign" orientation is established and an angle of insonation of 90° will best bring out A-line artifacts as noted by horizontal equidistant lines extending through the far-field from the "lung line." The arrows indicate the "lung sliding" that may only be observed in real time. In (B) and (C) are B-mode images labeled with (B) from a feline and (C) from a bottlenose dolphin. The "lung line" and A-lines are labeled. RS, rib shadow. The importance of the "gator sign" orientation is to not mistake an A-line for the "lung line" or another reflective surface, i.e., spine of the scapula. Line with rounding and an interposing straight line represents the intercostal space and the "gator sign" orientation. Source: Reproduced with permission of Dr Gregory Lisciandro, Hill Country Veterinary Specialists and FASTVet.com, Spicewood, TX. Illustration by Dr Judy Brown, Toronto, Canada.

syndrome (AIS) in people (Lichtenstein et al. 1997; Volpicelli et al. 2006). Since Vet BLUE uses a pattern-based assessment, this provides a strategy for placing B-lines into clinical context. For example, B-lines created by water next to air would be caused by cardiogenic and noncardiogenic causes; blood next to air, lung contusions in trauma, or lung hemorrhage in coagulopathic cases; and pus next to air, pneumonia (Figure 23.13). B-lines immediately rule out pneumothorax at that point along the thoracic wall (Lichtenstein et al. 1997, 1999; Lisciandro et al. 2008; Lisciandro 2011). Integrating other patient information with a Global FAST approach helps determine the more likely working diagnosis in many patients (see

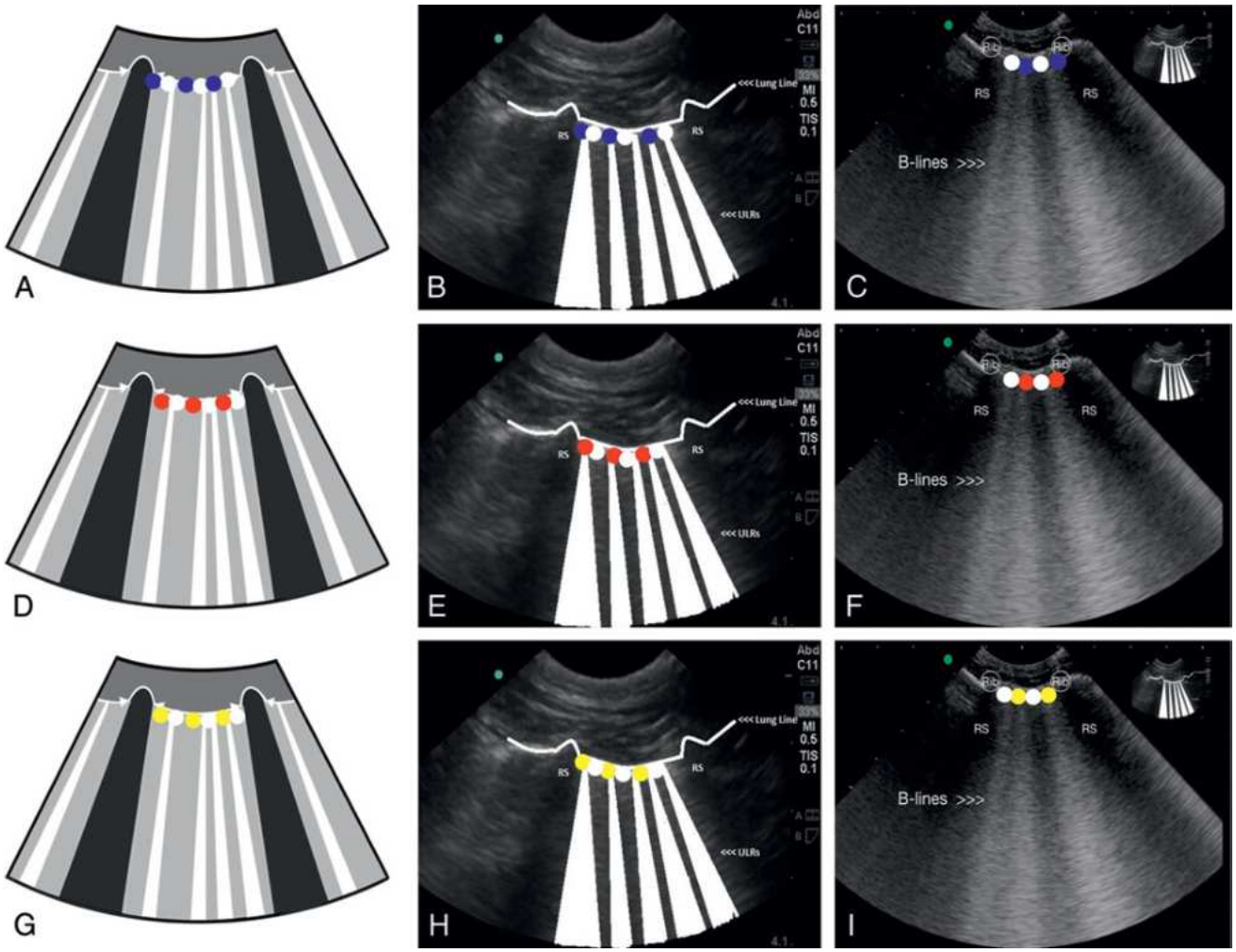


**Figure 23.13.** "Wet lung" – B-lines most commonly a result of fluid next to air at the lung line. Correlative line drawings and B-mode with overlays and without overlays in each row. Fluid next to air is illustrated with colored circles of blue and white, red and white, yellow and white in (A), (D) and (G). B-lines are a result of fluid next to air (fluid encompassed by air) along the lung surface. B-lines are nonspecific and must be placed into clinical context through the clinical profile of the patient and the regional pattern-based Vet BLUE approach to formulate the most probable working diagnosis. In rows (A), (B), and (C) are illustrated B-lines for cardiogenic and noncardiogenic edema with water (blue) next to air (white). In (D), (E) and (F) are illustrated lung contusions in trauma or pulmonary hemorrhage in a coagulopathic patient with blood (red) next to air (white). In (G), (H), and (I) is illustrated pneumonia that would predominate with "wet lung" artifacts in gravity-dependent regions represented by pus (yellow) next to air (white). The other Vet BLUE lung signs when present are also used to help formulate the working diagnosis. For example, shred sign in nontrauma in gravity-dependent Vet BLUE views supports bacterial pneumonia. Line with rounding and an interposing straight line represents the intercostal space and the "gator sign" orientation. Source: Reproduced with permission of Dr Gregory Lisciandro, Hill Country Veterinary Specialists and FASTVet.com, Spicewood, TX. Illustration by Dr Judy Brown, Toronto, Canada.

Chapters 36 and 37 and Table 23.4) (Lisciandro 2012; Lisciandro and Armenise 2014; Nazerian et al. 2014; Narasimhan et al. 2016). Conversely, absent B-lines rule out left-sided congestive heart failure in dogs and cats in a rapid, highly sensitive manner (Lisciandro 2014b; Lisciandro et al. 2014, 2016, 2017; Rademacher et al. 2014; Ward et al. 2017; Vezzosi et al. 2017) and likely for *all* mammalian lung (Yarto and Lisciandro 2017, unpublished data).

Counting numbers of B-lines has been shown to correlate with degree of pulmonary edema on the gold standard test of CT in human lung (Volipcelli et al. 2006). In one comparative study in dogs and cats, Vet BLUE fared better than three-view TXR for detecting AIS (Ward et al. 2018b) and in another, Vet BLUE exceeded TXR and compared favorably with CT (Dicker et al. 2019). Thus, the Vet BLUE B-line scoring system, described below, is clinically relevant (Figures 23.14 and 23.15). Lastly, in humans, in whom pulmonary fibrosis is much more common, thickened pleural surfaces can also cause B-lines, as does senescent lung (Tardella et al. 2012; Shyamsundar et al. 2013).

### *Expectations for Frequency of Wet Lung Artifacts in Normalcy*

Adult canine and feline lung and puppies and kittens >6 weeks of age carry the expectation of having infrequent numbers of B-lines during Vet BLUE (Lisciandro et al. 2014, 2016, 2017, 2018; Ward et al. 2017, 2018b). Expect adult dog, adult cat, and puppies and kittens >6 weeks of age to have predominantly "dry lung" artifacts at all nine acoustic windows of Vet BLUE, meaning the absence of B-lines (Lisciandro 2014b; Lisciandro et al. 2014, 2016, 2017, 2018; Ward et al. 2017). The low frequency of B-lines is nearly the same between adult dogs, adult cats, and puppies and kittens >6 weeks of age with no more than a single B-line at a single Vet BLUE view about ~10–12% of the time (Lisciandro et al. 2014, 2017, 2018). The upshot is that every B-line is potentially significant in feline and canine lung >6 weeks of age and should be recorded on the patient's Vet BLUE template for comparison to later studies.

## Vet BLUE B-line Scoring System

### *Counting B-lines During Vet BLUE*

First and foremost, the author's clinical research has shown that during Vet BLUE dogs, cats, and puppies and kittens (and dolphins) have predominantly "dry lung" artifacts, A-lines, at all Vet BLUE views (Figure 23.16) (Lisciandro et al. 2014, 2017, 2018; Ward et al. 2017; Yarto and Lisciandro 2017, unpublished data). Thus, B-lines are unexpected and when observed expected to be only sporadically present in low numbers (Lisciandro et al. 2014, 2016, 2017; Ward et al. 2017, 2018; Yarto and Lisciandro 2017, unpublished data). Exceptions are in regions where lung is very thin (lung

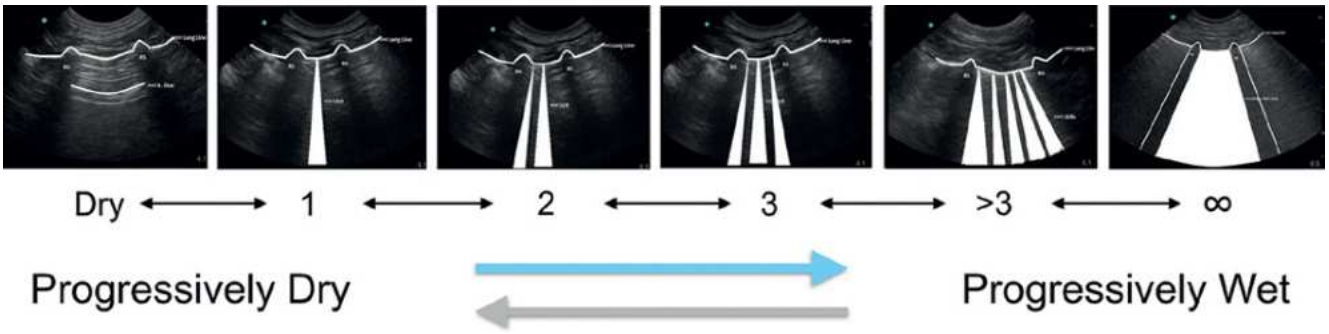


**Figure 23.14.** Vet BLUE B-line scoring system. Numbers of B-lines correlate with the degree of alveolar-interstitial edema in human lung and likely the same holds true for all mammalian lung. Thus, counting B-lines is clinically relevant. Expect "dry lung" artifacts, A-lines, and "lung sliding" to predominate (Lisciandro et al. 2014, 2016, 2017, 2018). Single B-lines are uncommon. When single B-lines are present in multiple views, they are abnormal and should be recorded on goal-directed templates and placed into clinical context. The lung sonographer knows, however, that lower numbers mean lesser degrees of alveolar-interstitial edema, and conversely more B-lines mean greater degrees (severity) of alveolar-interstitial edema. The Vet BLUE B-line scoring system counts the maximum number over a single intercostal space at each of the Vet BLUE acoustic windows (views) (see Figure 23.15). The scoring is 1, 2, 3, as weak positives, and >3 and infinity (∞), as strong positives. Line with rounding and an interposing straight line represents the intercostal space and the "gator sign" orientation. Source: Reproduced with permission of Dr Gregory Lisciandro, Hill Country Veterinary Specialists and FASTVet.com, Spicewood, TX.

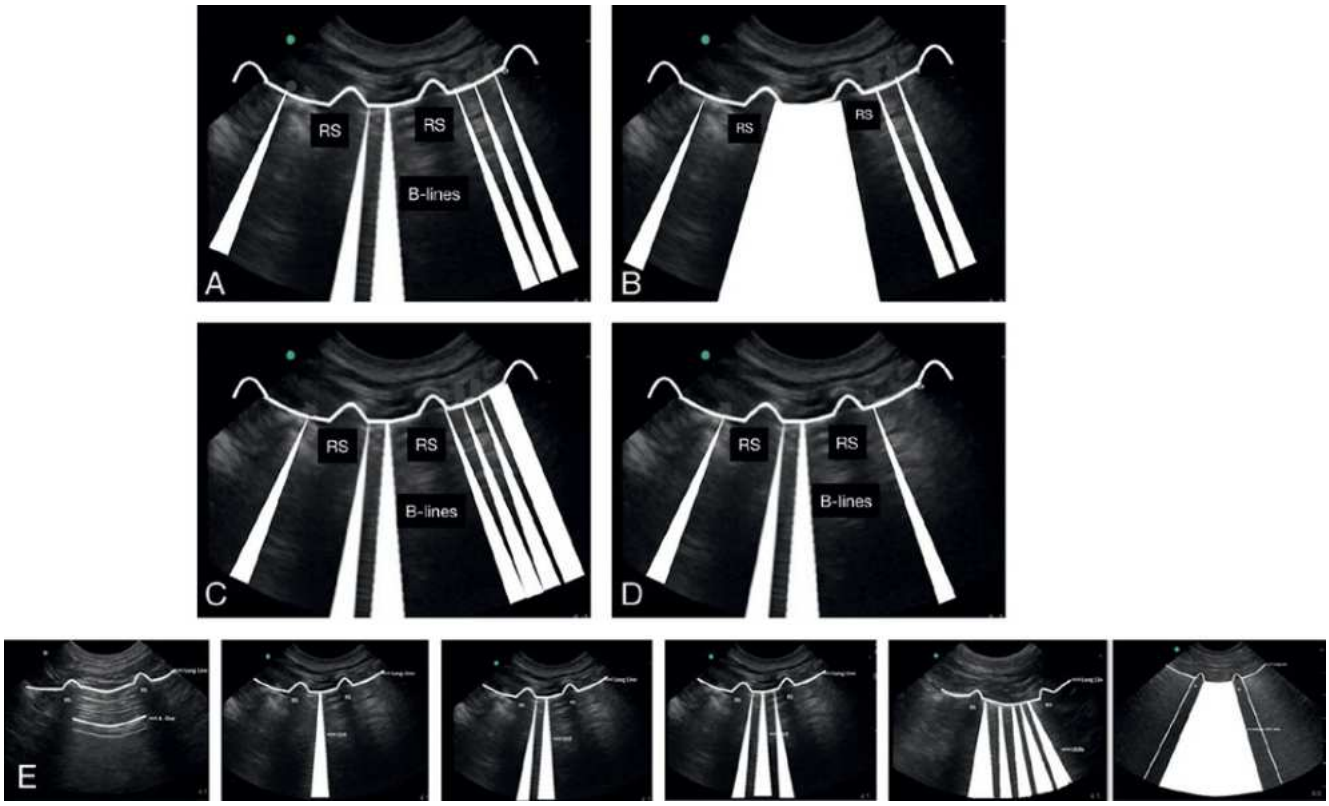


**Figure 22.15.** Examples of how to score each regional Vet BLUE view by maximum number over a single intercostal space. Although unknown in canine and feline lung, numbers of B-lines correlate with the amount of alveolar-interstitial edema on CT in human lung (Volipcelli et al. 2006) and are directly proportional to amount of extravascular lung water. Numbers are scored as 1, 2, 3, as weak positives, and >3 and infinity (∞), as strong positives The Vet Blue B-line scoring system helps with placing numbers into clinical perspective and aids in monitoring response to therapy, and in left-sided congestive heart failure, helps guide diuretic usage. The B-lines that reflect pulmonary fibrosis, much less common in small animals, may be similarly scored (Wang et al. 2017). In (A) the score is 3 because 3 is the highest number over those three intercostal spaces at the Vet BLUE regional view. The same principle scores (B) as infinity, (C) as >3, and (D) as 2. The echelon of Vet BLUE B-line scoring (0 through infinity) is shown in (E). RS, rib shadow. Line with rounding and an interposing straight line represents the intercostal space and the "gator sign" orientation. Source: Reproduced with permission of Dr Gregory Lisciandro, Hill Country Veterinary Specialists and FASTVet.com, Spicewood, TX.

adjacent to heart at the Middle lung region or at most caudal extent along the Caudodorsal, Perihilar, and Middle lung regions) or where lung bends away from the scanning plane (the cupula of lung at the thoracic inlet). Vet BLUE acoustic windows generally avoid these peripheral lung margins and extremities at all but the cranial transition zone (see Chapter 22 and Different LUS Formats).

During LUS it is necessary to (1) avoid extreme boundaries of lung (Figure 23.17), (2) place any B-line during Vet BLUE into clinical context (Figure 23.18), (3) incorporate serial examinations to detect changes in Vet BLUE profiles (increasing, decreasing or static numbers of B-lines combined with numbers of positive Vet BLUE views), and (4) 1–3 B-lines represent mild degrees of AIS (weak positive) versus >3 and infinity (see numbers of B-lines subsequently defined) that represent moderate to more severe degrees (strong positive) of alveolar-interstitial syndrome (see Figures 23.14, 23.17, and 23.18). Thus, when a few B-lines are observed, weak positive, the lung sonographer knows it is milder AIS versus when many B-lines, strong positive, are observed (Volpicelli et al. 2006; Jambrik et al. 2010; Shyamsundar et al. 2013). In order for your data to be valuable, findings must be recorded on goal-directed templates (see Table 23.5).

In 2006, Volpicelli and colleagues published a landmark study regarding the clinical utility of lung ultrasound and the quantification of alveolar-interstitial edema by numbers of B-lines compared to CT

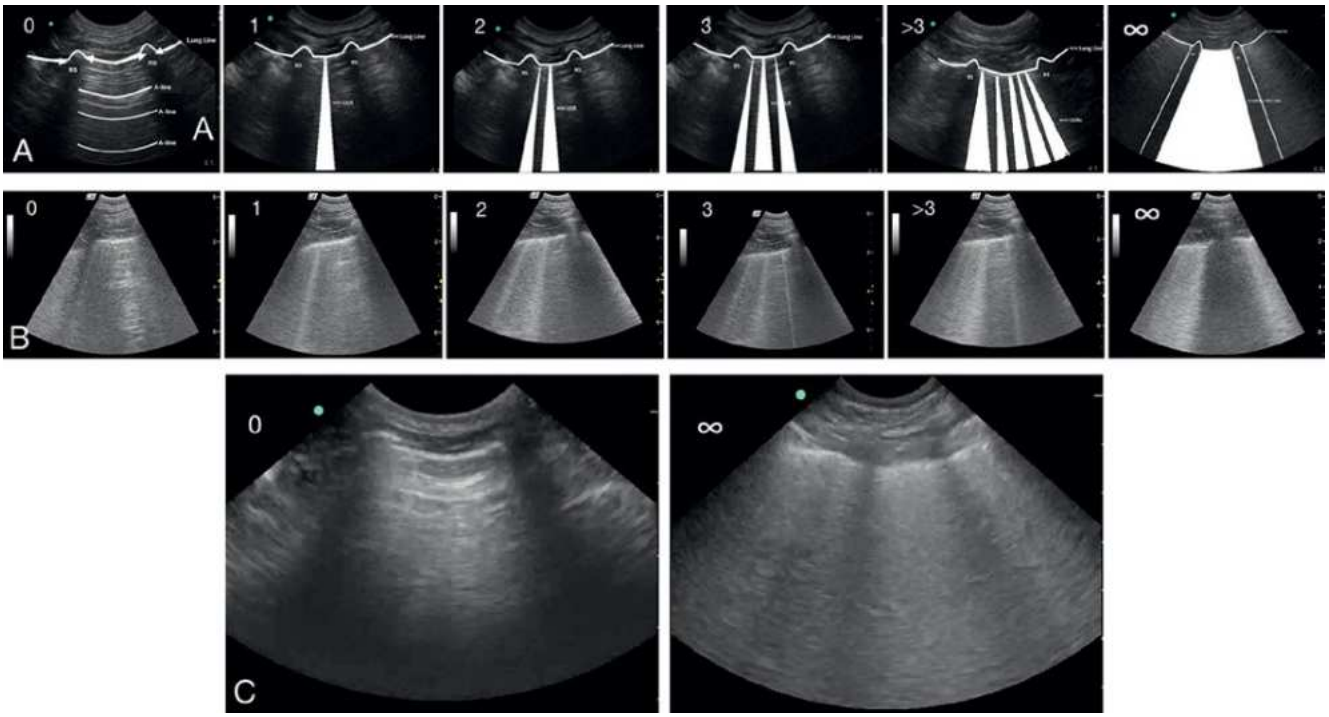


**Figure 23.16.** Vet BLUE B-line scoring system. Line drawings in row (A) correlate with B-mode images in row (B) to illustrate the Vet BLUE B-line scoring system. The images in row (B) are all from the same machine. The B-mode images do not necessarily show the entire intercostal space, but the scoring system is assessed over an entire single intercostal space. In row (C) are comparisons of completely "dry lung," A-lines and "lung sliding" to completely "wet lung," infinity (∞) B-lines, that initially can be difficult to distinguish until the sonographer learns how their ultrasound machine images infinity (confluent) B-lines. Line with rounding and an interposing straight line represents the intercostal space and the "gator sign" orientation. Source: Reproduced with permission of Dr Gregory Lisciandro, Hill Country Veterinary Specialists and FASTVet.com, Spicewood, TX.

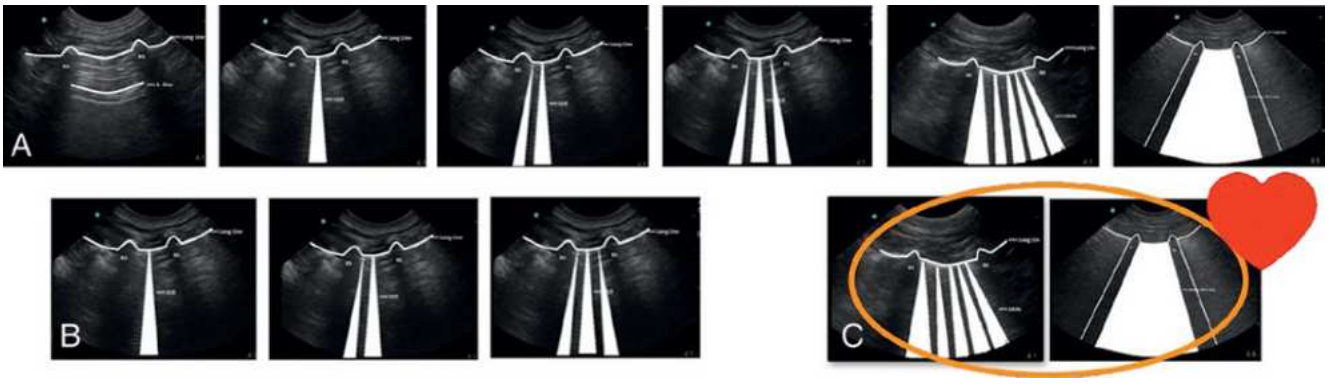


**Figure 23.17.** Vet BLUE B-line scoring system compared to the Volpicelli Strong Positive Model. In (A) the upper row shows the Vet BLUE B-line scoring system that includes the total number of B-lines over a single intercostal space at that Vet BLUE regional view. Scoring is as follows: 1, 2, 3, as weak positives, and >3 and infinity (∞), as strong positives. In (B) scores of 1, 2, and 3 are divided from scores of >3 and infinity (∞) shown in (C) to better illustrate the so-called Volpicelli Strong Positive model (VSP). The VSP counts only strongly positive >3 and infinity (∞) views while discrediting scores of 1, 2, and 3. The use of the VSP has a bias for more severe degrees of AIS, working well for feline congestive heart failure but missing less affected abnormal lung, the so-called weak positives. From several clinical studies, it has been shown that "dry lung" artifacts predominate on a Vet BLUE examination. Thus, *any number* of B-lines is potentially significant and should be recorded on goal-directed templates and placed into clinical context. Line with rounding and an interposing straight line represents the intercostal space and the "gator sign" orientation. Source: Reproduced with permission of Dr Gregory Lisciandro, Hill Country Veterinary Specialists and FASTVet.com, Spicewood, TX.

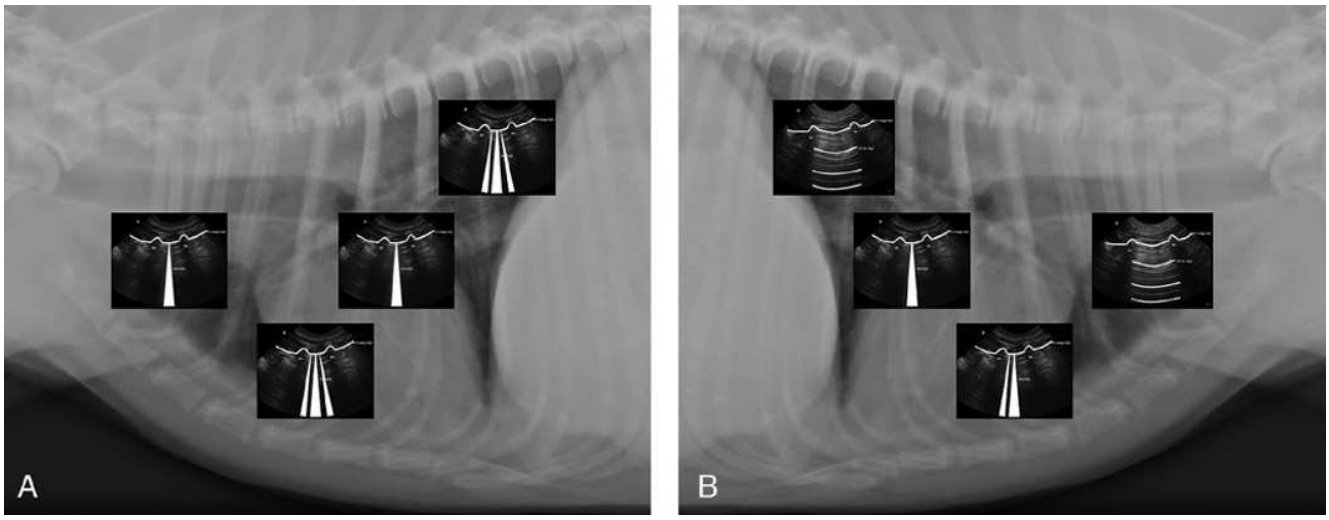


**Figure 23.18.** Example of an abnormal Vet BLUE considered negative by the Volpicelli Strong Positive Model. During Vet BLUE, it is found that the patient is positive for B-lines at most left and right Vet BLUE views as shown in (A) and (B); however, all positive views are <3 B-lines and thus would be considered a negative LUS examination using the VSP model. Through clinical research it is known that adult dogs and cats and puppies and kittens >6 weeks of age are expected to have absent B-lines all views (rare single B-lines). Thus, *any number* of B-lines is potentially relevant and should be placed into clinical context. The example, although having mild degrees of alveolar-interstitial syndrome, has very abnormal lung. Serial Vet BLUE or additional imaging is warranted. Source: Reproduced with permission of Dr Gregory Lisciandro, Hill Country Veterinary Specialists and FASTVet.com, Spicewood, TX.

(Volpicelli et al. 2006). They found that numbers of B-lines correlated with the degree of alveolar-interstitial edema when compared to the gold standard test of CT in human lung. Thus, the author developed a simple, easy to remember Vet BLUE B-line scoring system (Lisciandro 2014b; Lisciandro et al. 2014, 2016, 2017; Ward et al. 2017, 2018b): the highest number of B-lines over a single intercostal space at each Vet BLUE view is recorded as 0 (negative), 1 (a single B-line), 2 (two B-lines), 3 (three B-lines), >3 (more than three B-lines but not confluent over the entire intercostal space), and infinity, when confluent over an entire intercostal space, referred to by some sonographers as "white lung" (see Figures 23.14, 23.15, and 23.16) (Gargani and Volpicelli 2014). Consider B-line scores of 1–3 as weak positive and scores of >3 and infinity as strong positives (Volpicelli Strong Positive Model).

The use of this scoring system helps gauge how much AIS is present at that regional view (acoustic widow). B-lines have not only shown good clinical correlation for detection of AIS (cardiogenic pulmonary edema and lung contusions) in both dogs and cats (Lisciandro et al. 2014, 2016, 2017; Ward et al. 2017, 2018b; Dicker et al. 2019), but also interobserver agreement is high (kappa values >0.85) in two different studies (Ward et al. 2017; Dicker et al. 2019). Vet BLUE findings should be recorded on goal-directed templates (see below and Table 23.5).

# Other B-line Scoring Systems

## *Volpicelli Strong Positive Model - Cardiac Bias*

The Volpicelli Strong Positive (VSP) model differs from the Vet BLUE B-line scoring system in that only >3 and infinity B-lines are scored as "positive" (see Figure 23.17). In other words, B-line numbers of 1, 2, and 3 are discredited, when in fact the expectation during Vet BLUE is to have rare B-lines (see Figure 23.18) (Ward et al. 2017). The VSP model has strengths in evaluating human patients especially in left-sided congestive heart failure because only the most strongly positive acoustic windows are counted; however, this is not universally accepted for the evaluation of B-lines (Volpicelli et al. 2006; Lichtenstein 2009a; Gargani and Volpicelli 2014; Lee et al. 2015). The VSP model does have a place as it proved useful in diagnosing felines with left-sided congestive heart failure using the VSP criteria and with ≥2 Vet BLUE views being positive bilaterally (Ward et al. 2017). Using this VSP scoring modification with a left-sided congestive heart failure bias in felines, Vet BLUE had the same sensitivity (89%) and specificity (87%) as TXR (Ward et al. 2017). The advantage of using VSP scoring modification during Vet BLUE is that pulmonary imaging is rapid without restraint, which effectively rules in left-sided CHF

without the risk of radiography until the patient is more stable. The upshot is that by understanding the scoring strategy and placing regional findings into a pattern-based approach, the lung sonographer has different ways to integrate LUS findings during Vet BLUE (Jambrik et al. 2004; Volpicelli et al. 2006; Gargani and Volpicelli 2014; Wang et al. 2017).

**Pearl:** To best integrate Vet BLUE, the lung sonographer must place findings into clinical context, perform serial examinations, and record Vet BLUE data on goal-directed templates (see Table 23.5).

### Why are They Called B-lines?

There are two answers to this: (1) "B" follows "A" in the alphabet, and (2) "B-lines" are named for radiographic Kerley B-lines that represent interlobar edema (pulmonary edema) (Louvet and Bourgeois 2008; Lisciandro 2011, 2014b; Lisciandro et al. 2014).

### Why are They Not Comet-tails?

The "wet lung" artifact has been published as comet-tail artifacts (Lichtenstein et al. 1997). However, comet-tail artifact (CTA) is a poor descriptor because the CTA was first described by the reflective artifacts extending beyond metallic buckshot in a human liver, which does not represent the ultrasonographic phenomenon of alveolar-interstitial syndrome having fluid next to air with the artifact not reflective but rather due to strong differences in acoustic impedance (between air and fluid) (Lichtenstein et al. 1997; Volpicelli et al. 2006; Lichtenstein 2010b). CTAs observed during LUS have no defined clinical relevance and in the author's experience are often created by small (<1 mm) lung surface irregularities and also found along extreme thin margins of aerated lung.

### Comet-tail Artifact

The comet-tail artifact is an extension of LUS artifact that comes off the thoracic wall (parietal pleura) or lung surface (visceral pleura) but does not extend through the far-field in laser-like fashion as defined for B-lines (Lichtenstein 2007, 2010b; Lichtenstein and Mezière 2008). It is imperative to have enough gain through the far-field to be able to differentiate between comet-tails and B-lines (Lichtenstein et al. 2009a; Lichtenstein 2010a; Lisciandro 2014b; Gargani and Volpicelli 2014) (see Figures 17.10 and 22.6). Comet-tail artifacts observed during LUS have no defined clinical relevance and in the author's experience are created by small (<1 mm) lung surface irregularities and also along extreme thin margins of aerated lung, and are rarely observed during Vet BLUE.

## Six Signs-Further Information

### Shred Sign – Air Bronchogram

The shred sign is the irregularity (fractal, shredding) and lack of the expected linear continuity of the pulmonary–pleural interface and its "lung line" that represents lung consolidation along the intercostal space (Figure 23.19; see also Figure 23.8) (Lisciandro 2014b; Lisciandro et al. 2014, 2017; Ward et al. 2017). Importantly, the lung consolidation has air within the consolidation and thus shred sign represents an air bronchogram (Lichtenstein et al. 2004; Lichtenstein and Mezière 2008; Lisciandro 2014b; Neelis et al. 2015). These air bronchograms appear as hyperechoic (bright white) flecks or foci throughout the consolidation and can be dynamic or static (Lisciandro 2014b; Lichtenstein et al. 2004, 2009b; Neelis et al. 2015). Remember, air on ultrasound is white (hyperechoic) which is the opposite of radiography! The air bronchogram may still have air exchange occurring with air movement during phases of respiration, referred to as a "dynamic" air bronchogram, or have stagnant air, referred to as a "static" air bronchogram (Lichtenstein et al. 2004; Lichtenstein 2009a,b; Gillman and Kirkpatrick 2012; Mongodi et al. 2016). The movement of air through these airways can be difficult to appreciate in spontaneously breathing dogs and cats; however, with controlled positive pressure ventilation (under anesthesia, mechanical ventilation), the differentiation of "dynamic" from "static" may be made by observing whether the air "slides" or wisps through the hyperechoic foci (air bronchograms).

Thus, a shred sign is consolidation with aeration and must be placed into clinical context for developing an accurate working diagnosis since the sign is nonspecific in and of itself. Generally, shred signs in gravity-dependent Vet BLUE regions in nontrauma patients represent bacterial bronchopneumonia or aspiration pneumonia until proven otherwise (Lisciandro 2014b; Ward et al. 2017, 2019).

### Tissue Sign – Hepatization of Lung

In contrast to the shred sign, the tissue sign is a gradation of more severe consolidation because lung in the tissue sign lacks aeration and thus the consolidation appears like liver (see Figures 23.9 and 23.19) (Lichtenstein

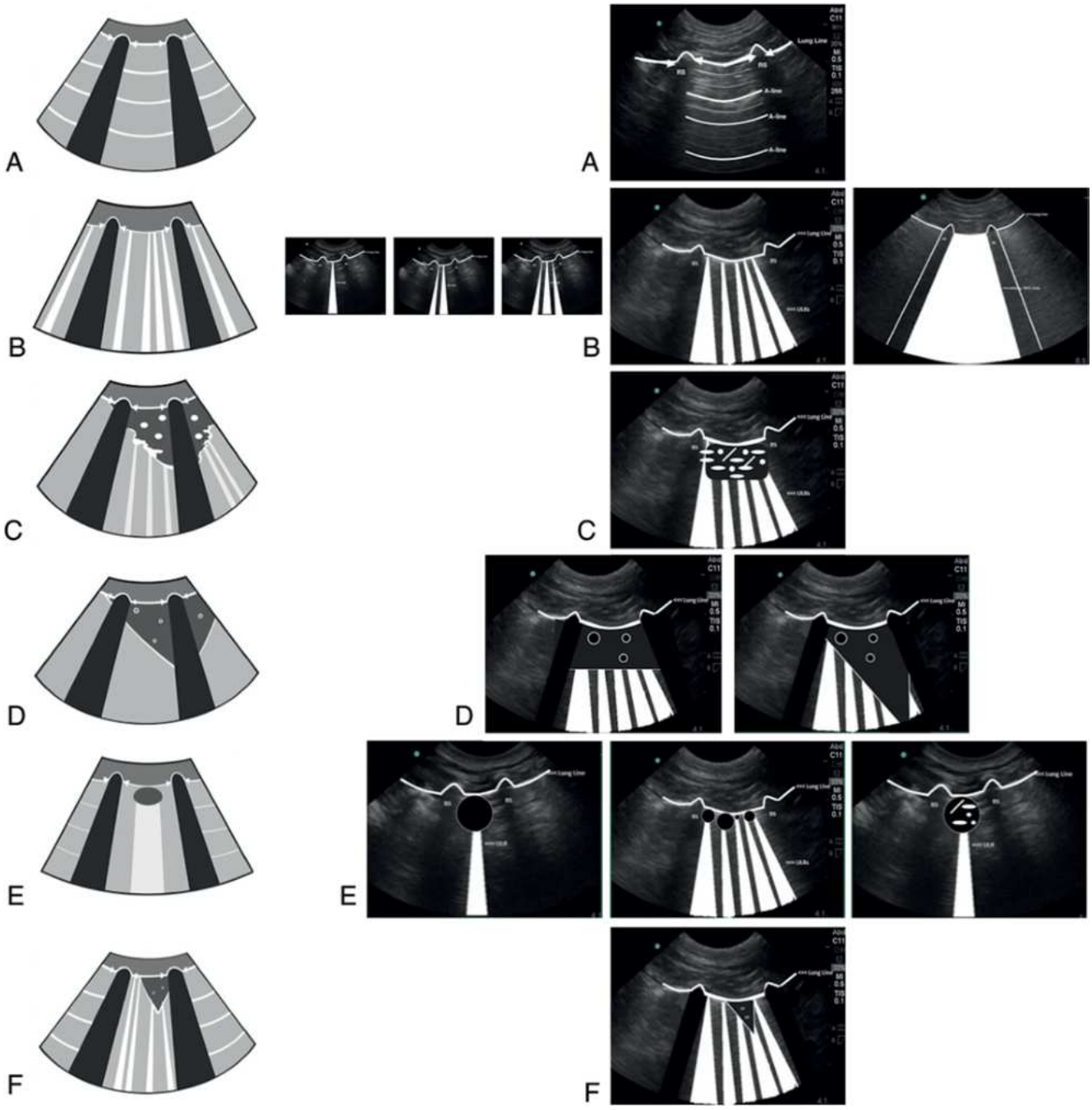


**Figure 23.19.** Line Drawings and overlays of the six Vet BLUE lung ultrasound signs. (A) "Dry lung" with A-lines (horizontal lines) and "lung sliding" represented by arrows (only seen in real time). (B) B-lines and the scoring system of 1, 2, 3, as weak positives, and >3 and infinity (∞), as strong positives. (C) The shred sign where the normal expected continuity is lost along the "lung line" and fractal due to lung consolidation, but air remains in the bronchi (hyperechoic foci within the consolidation; air is white on ultrasound). Thus, the shred sign represents an air bronchogram. (D) Tissue sign with two examples. The consolidation has bronchi that are no longer air filled, making the lung appear liver-like (hepatization of lung). (E) Nodule sign. Note the hypoechoic to anechoic ovals and circles that represent organized consolidation. These nodules have "pseudo B-lines" extending through the far-field. Note the nodule sign with intralesional air supporting a bacterial abscess. (F) Wedge sign. Note the accompanying B-lines as often there is adjacent inflammation (alveolar-interstitial edema). RS, rib shadow. Line with rounding and an interposing straight line represents the intercostal space ("gator sign"). Source: Reproduced with permission of Dr Gregory Lisciandro, Hill Country Veterinary Specialists and FASTVet.com, Spicewood, TX. Illustration by Dr Judy Brown, Toronto, Canada.

2009a,b; Lichtenstein et al. 2010b; Lisciandro 2014b; Neelis et al. 2015). The airways are fluid-filled or infiltrated or obstructed "upstream" to cause the tissue sign. The term "hepatization" has historically been applied to this lung ultrasound finding (Neelis et al. 2015). Color flow Doppler is a good option to document whether pulsatile blood flow is present through the lung with a tissue sign to differentiate a lung lobe torsion (no flow with fluid bronchograms) from a mass (pulsatile blood flow) (Hecht and Penninck 2015).

## *Nodule Sign*

The nodule sign is an organized infiltrating mass. It is a step up in severity from the shred sign and tissue sign because now the abnormal consolidation is in fact organized consolidation along the lung surface within its parenchyma. The nodule sign is generally characterized by a hypoechoic or anechoic circle or oval along the "lung line" with pseudo B-lines extending through the far-field with respirophasic synchrony (see Figures 23.10, 23.19, 23.35, and 23.26) (Lisciandro 2014b; Neelis et al. 2015). A nodule sign that does not oscillate to and fro with respirophasic movement is more likely originating from the thoracic wall (Neelis et al. 2015). The effect is similarly created as for alveolar-interstitial edema, with strong differences in acoustic impedance but rather than fluid next to air is soft tissue cuffed by air. Thus, B-lines associated with the nodule sign are referred to as pseudo B-lines since they do not represent AIS. Thus, when vertical streaks are seen on lung ultrasound, the sonographer should follow them to the "lung line" to look for the nodule sign. By definition, nodules are generally considered ≤3 cm and a mass >3 cm. The author has not created a "mass sign" as an additional descriptor but certainly the term could be applied for nodule signs that are >3 cm (Alpert et al. 2015).

In some instances, the nodule sign may be associated with adjacent inflammation (edema, hemorrhage) and pathology and thus with other Vet BLUE lung ultrasound signs including B-lines, shred sign, tissue sign, and wedge sign. The nodule sign is only ultrasonographically apparent if these nodules (and masses) are located at the periphery of lung within the examined acoustic window (see Figure 23.1). Centrally located (deeper) nodules (and masses) that do not touch the "lung line" at the LUS acoustic windows will be missed. However, in a pilot study, Vet BLUE performed better than TXR for pulmonary metastasis (Kulhavy and Lisciandro 2015) and three-view TXR has been shown to perform poorly when compared to the gold standard of CT (Nemanic et al. 2006; Armbrust et al. 2012; Alexander et al. 2012). In another study evaluating pulmonary contusions, Vet BLUE outperformed TXR and fared well compared to CT (Dicker et al. 2019). The million dollar question is how well does Vet BLUE fare when compared to CT? Certainly we can answer that it performs likely better than TXR for many respiratory conditions (Kulhavy and Lisciandro 2015; Ward et al. 2018b; Dicker et al. 2019).

### Use of Vet BLUE for Detecting Pulmonary Nodules

A pilot comparing Vet BLUE to three-view TXR showed that all three-view TXR studies that had nodules determined by a blinded, board-certified radiologist had nodules on Vet BLUE; however, several cases that had the nodule sign on Vet BLUE were not apparent on TXR (Kulhavy and Lisciandro 2015). The gold standard test of CT has been shown in small animals to be able to detect nodules as small as 1–2 mm (Nemanic et al. 2006; Armbrust et al. 2012) and clearly is a better test than three-view TXR (Nemanic et al. 2006; Eberle et al. 2010; Armbrust et al. 2012; Alexander et al. 2012). In fact, in one study evaluating dogs with osteosarcoma (OSA), of the 11 dogs with metastatic disease seen on CT, only two had metastasis detected by TXR (Eberle et al. 2010). Interestingly, another study found no difference in detecting nodules between traditional film screen and computed radiography (Alexander et al. 2012). Comparative studies have shown that the threshold for radiography to detect nodules is somewhere between 3 and 7 mm, a wide range (Armbrust et al. 2005; Nemanic et al. 2006; Alexander et al. 2012), and clearly TXR greatly underestimates the numbers of nodules compared to CT (Nemanic et al. 2006; Eberle et al. 2010; Armbrust et al. 2012; Alexander et al. 2012). One study determined that in the case population, the right middle and left and right caudal lung regions most commonly had nodules compared to other lung lobes (Alexander et al. 2012).

In our experience, Vet BLUE and lung ultrasound can readily detect lung surface nodules <1 mm. The author is a collaborator in ongoing research comparing these three imaging modalities to help answer the clinical question: How good is Vet BLUE as a pulmonary metastasis check? The author would answer, from experience and preliminary clinical research, "very good" and better than three-view TXR. Another important factor that must be considered is how often lung metastases reach the lung surface, because if nodules are not along the "lung line" at one of the nine Vet BLUE acoustic windows, then the pulmonary metastasis will be missed (see Figure 23.1).

VetBooks.ir

The answer is to perform Global FAST on all cancer-aged patients to "stage" their disease on day 1 (see Chapters 36 and 37). By doing so, you provide more clinical information to your client regarding their pet. Moreover, the client may better decide on cost/benefit for the recommended work-up. The Global FAST approach serves as a same-day screening test to let the owner know whether the disease has obviously spread (or is disseminated) versus appearing localized. The same approach may be used for staging any disease (infectious) as being localized or disseminated as well as screening for comorbidities and complications.

### Wedge Sign

The wedge sign represents lung infarction (PTE) (Lisciandro 2013, unpublished data). This is arguably the most abnormal or severe Vet BLUE sign by representing a pie-shaped region of vascular necrosis (see Figures 23.11 and 23.19; see also for case examples Figures 37.9 and 37.10) (Mathis et al. 2005; Mastruzzo et al. 2008). The wedge sign may also be considered a subset of the shred sign and tissue sign. In gravity-dependent Vet BLUE acoustic windows, the wedge sign would be difficult to distinguish from bacterial and aspiration pneumonias and other ventral pathology; however, in the least gravity-dependent left and right Caudodorsal and Perihilar Vet BLUE views, the wedge sign is very convincing for PTE, giving clinicians a means to justify and trigger thromboprophylaxis and thrombolytics, and a way to monitor and track PTE (resolving, worsening with more wedge signs, or static) (Mastruzzo et al. 2008). See Chapter 25 and Chapter 37 for CPR.

**Pearl:** Abdominal structures are situated farther cranially in standing dogs and cats than you would think; thus, finding caudal Vet BLUE transition zones and sliding cranially away from them helps to avoid mistaking abdominal structures for lung pathology (Figure 23.20).

### Summary

In summary, the Vet BLUE six lung ultrasound signs are arranged by degree of lung infiltration/consolidation, beginning with unremarkable "dry lung" followed by "wet lung" (B-lines representing AIS), followed by degrees of lung consolidation with shred sign (consolidation *with* aeration), tissue sign (consolidation *without* aeration), nodule(s) sign (organized infiltrate), and lastly the wedge sign, representing lung surface infarction (pie-shaped vascular wedge of necrosis) (see Figures 23.5, 23.6–11, and 23.19). The diaphragmatico-hepatic (DH) view should not be underestimated as an integral part of Vet BLUE as it can detect lung pathology that was missed or questionable at the eight transthoracic Vet BLUE views (Figure 23.21).

Combinations of any and all of the signs may be present in severely diseased dogs and cats, especially in dogs with heartworm disease (*Dirofilaria immitis*). Lastly, the visual system provides veterinarians with a Vet BLUE visual lung language to freely communicate findings during conversation and within medical records.

## Other Lines: Are They Really Lines?

The use of a pulmonary line nomenclature is not necessarily the best way proceed with teaching lung ultrasound to veterinarians and is not fully accepted in human medicine. The author has earmarked C-lines, E-lines, I-lines, and Z-lines for discussion, but there are many more types of LUS lines (Lichtenstein and Mezière 2008; Lichtenstein 2007, 2009a, 2010a,b; Lee et al. 2015; Lee 2016). The author prefers the Vet BLUE visual lung language over creating esoteric "lines" for all possible LUS findings (Figure 23.22). A similar visual lung language is also used in human point-of-care ultrasound textbooks and published reviews (Lee et al. 2015; Lichtenstein 2010a). The visual lung language system eliminates the need for so many different lines, many of which are not really lines at all, e.g., C-lines, E-lines, I-lines, Z-lines (Lisciandro 2014b).

### C-lines

C-lines are not lines because consolidation is most often a fractal irregular effect that deviates from the expected normal linear continuity of the "lung line" (see Figure 23.22) (Lichtenstein and Mezière 2008; Lichtenstein 2007, 2010a,b). The author prefers the terms shred sign, tissue sign, nodule sign, and wedge sign because they are visual, each has clinically relevant implications and are more descriptive than lumping them all into a general category of C-lines. "C-lines" are nonspecific and too generalized.

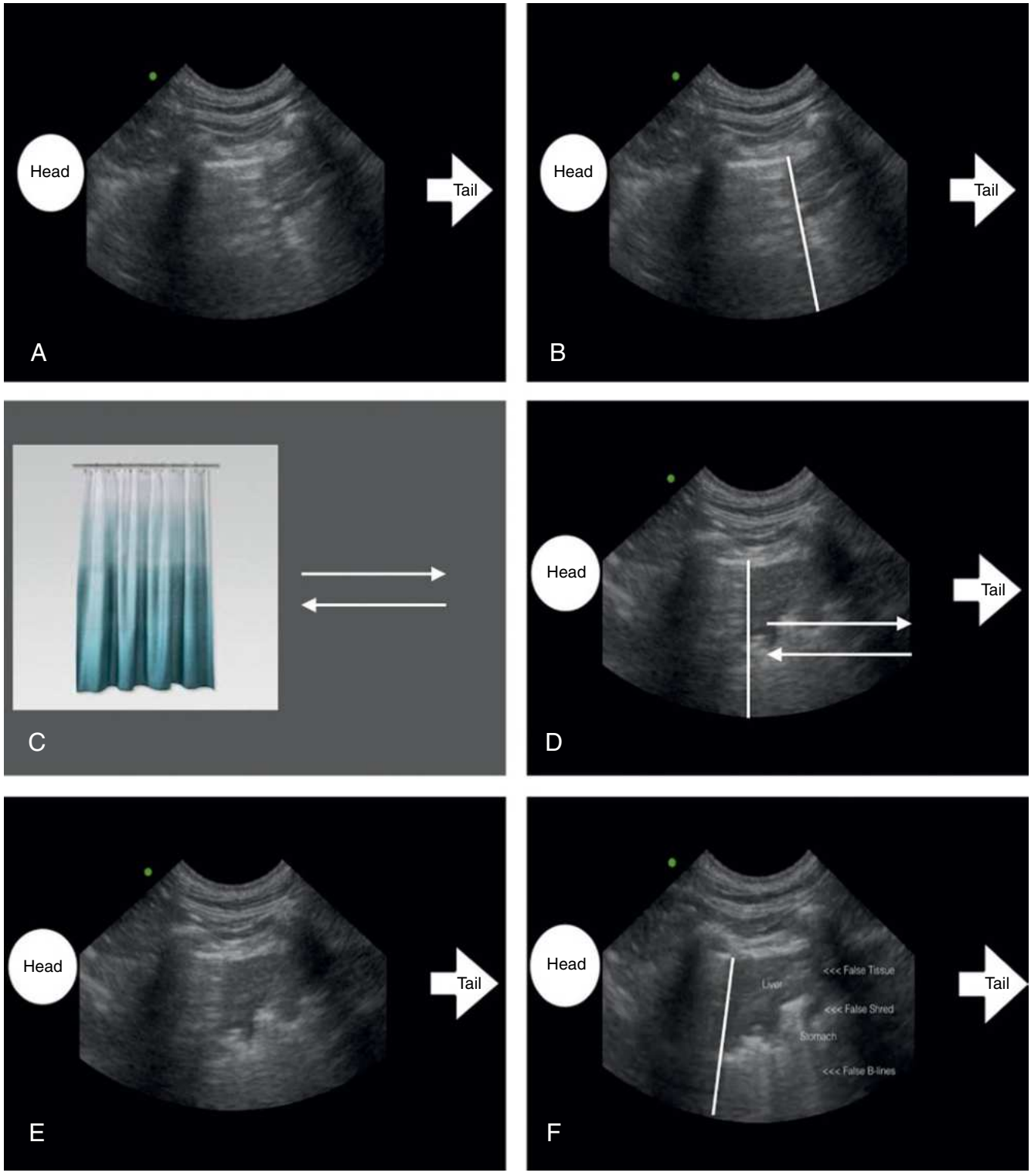


**Figure 23.20.** Caudodorsal transition zone (CdTZ). The curtain sign is the term used to illustrate the dirty shadowing of air in the pleural cavity with respirophasic movement (caudal-cranial) over the abdominal cavity. This is likened to a curtain being opened and closed across a window. In (A) and (B) the same image is unlabeled and labeled with the vertical line in (B) showing the linear dirty shadowing of lung over the peritoneal cavity. In (C) a shower curtain is used to illustrate in real time the effect of air within the pleural cavity moving "to and fro" with phases of respiration across the peritoneal cavity (*arrows*) in (D). The CdTZ is important to locate because abdominal structures may easily be mistaken for lung pathology, unlabeled and labeled as shown in (E) and (F) with the liver as a "pseudo tissue sign," rugal folds of the stomach as a "pseudo shred sign" and gastric luminal contents as "pseudo gastric B-lines." The other important point regards orientation and that the head should always be to the right of the screen so the sonographer knows to expect confounding abdominal structures to be to the right of the screen at the CdTZ. Source: Reproduced with permission of Dr Gregory Lisciandro, Hill Country Veterinary Specialists and FASTVet.com, Spicewood, TX.

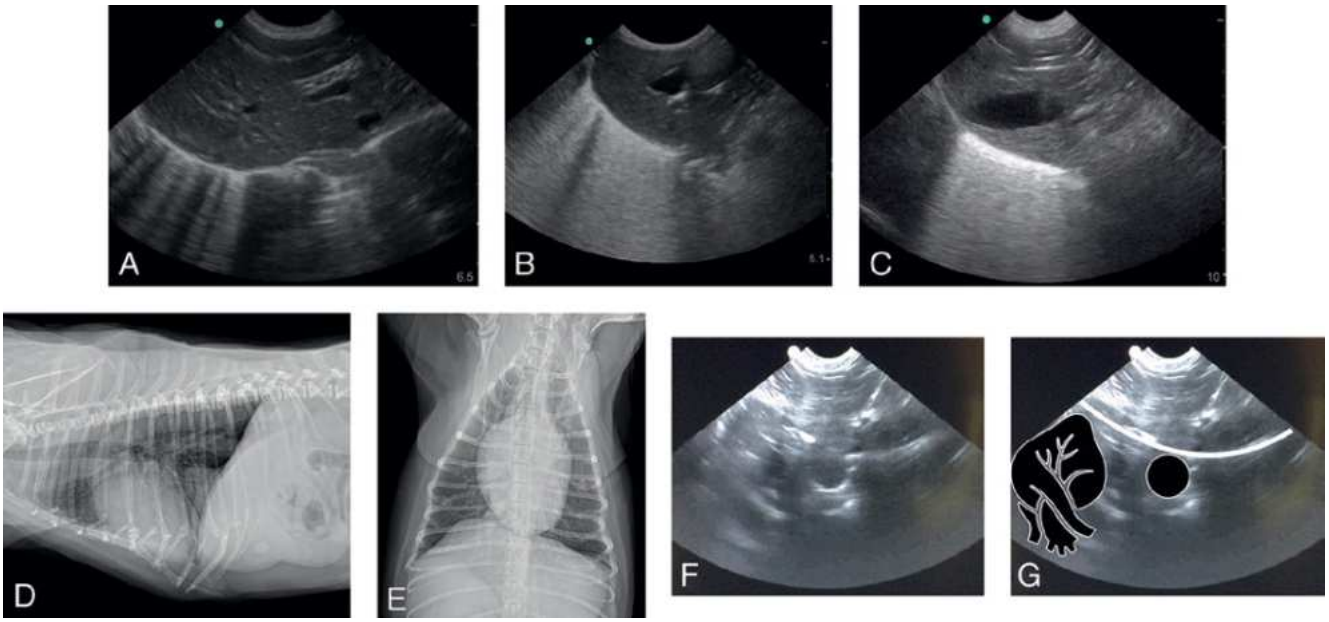


**Figure 23.21.** Lung pathology during Vet BLUE at the DH view. (A–C) Various degrees of B-lines. In (A) and (B) there are >3 and infinity B-lines, respectively. In (D) is an acoustic enhancement effect through the fluid-filled gallbladder; however, their presence is likely real because lung still should be dry (A-lines and "lung sliding") in all adult dogs and cats, and puppies and kittens > 6 weeks of age. (D–G) A case with a questionable lung mass on thoracic radiography but clearly detected via Vet BLUE along the pulmonary–diaphragmatic interface. (F,G) Images unlabeled and labeled with overlays of the heart and a circle representing the mass in (F). Source: Figures (D–G) courtesy of Dr Kara LaRue, Portland, OR.

### *E-lines*

E-lines are a moot point if the lung sonographer focuses on the basic premise for all LUS – if you cannot image the "gator sign" orientation, then you can't accurately image lung. E-lines make the simple far more complicated and in most instances of subcutaneous emphysema (SQE), there are no lines at all but rather the expected air-related principle of the dirty shadowing effect and/or A-lines (see Figures 18.12, 18.13, and 23.22). Moreover, most SQE is readily recognized during physical exam.

### *I-lines*

I-lines are comet-tail artifacts that most often originate from the lung surface but fade, unlike B-lines. Comet-tail artifacts observed during LUS generally have no defined clinical relevance and in the author's experience are created by small (<1 mm) lung surface irregularities and also observed along extreme thin margins of aerated lung (Figure 23.23).

### *Z-lines*

Z-lines are yet another example where simply abiding by the definition of B-lines avoids the addition of the "Z-line." Z-lines are potentially mistaken for B-lines because they are vertical streaks, but they fade and do not oscillate with respirophasic movement and do not obliterate A-lines (see Figure 23.22). They are most commonly created by the reflective fascial planes in the near-field (intercostal muscles and those more superficial) away from the pulmonary–pleural interface (PPI). Thus, "Z-lines" do not oscillate in synchrony with phases of respiration. In the author's experience, these Z-lines, called "shimmy lines" by the author, go unnoticed by most sonographers once B-lines are learned on your machine. The letter "Z" was given to these "lines" by Lichtenstein because they have no clinical relevance other than being a confounder (Lichtenstein 2010b; Lee 2016). See also Chapter 17.

## Clinical Use of Regional Pattern-based Vet BLUE Approach

The Vet BLUE regional pattern-based pattern approach may be used for ruling in (specificity) and ruling out (sensitivity) respiratory and nonrespiratory look-alike causes (Table 23.2). True Vet BLUE accuracy and its strength compared to other imaging modalities will

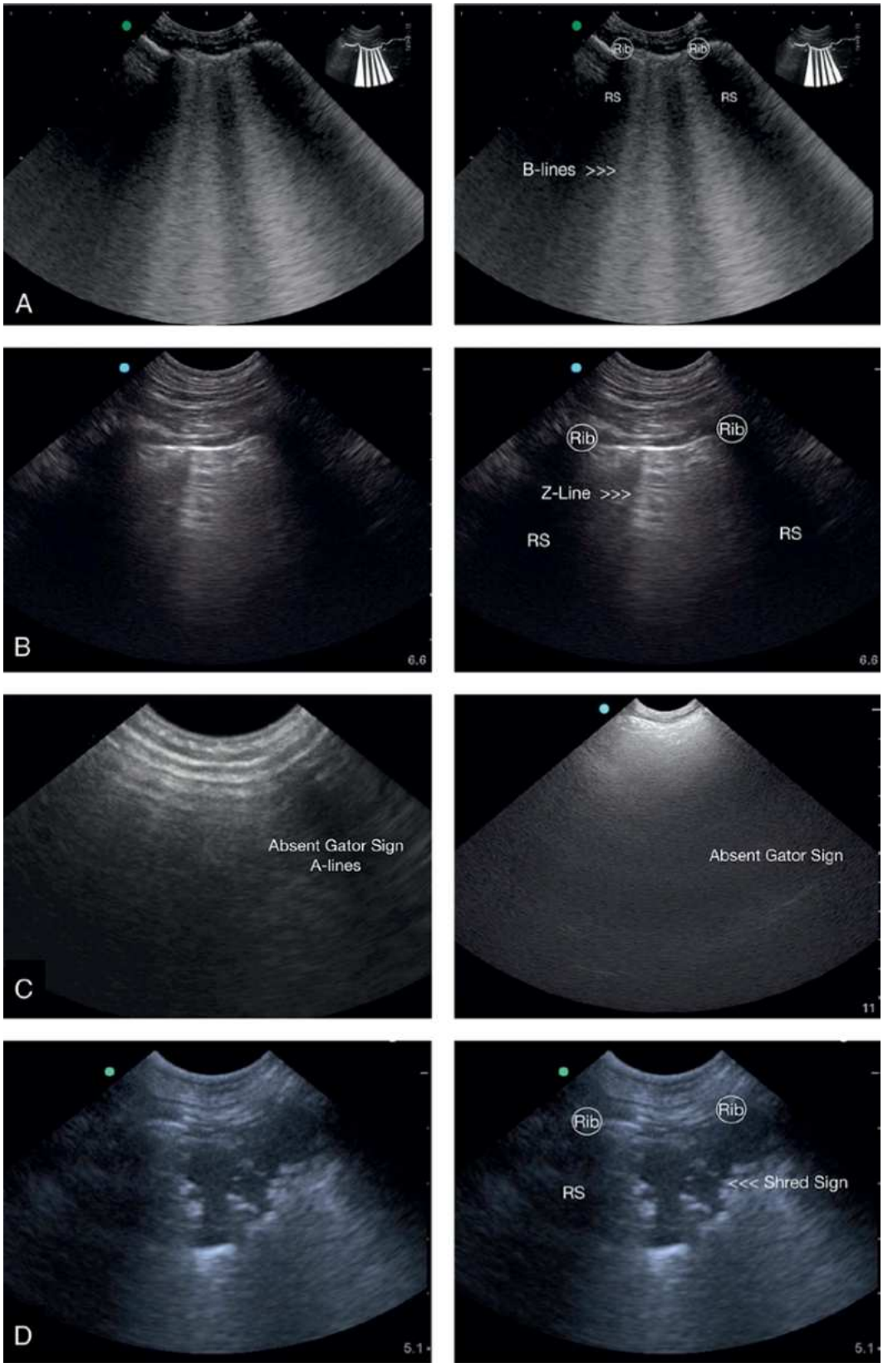
A
Rib
Rib
RS
RS
B-lines >>>
B
6.6
Rib
Rib
Z-Line >>>
RS
RS
6.6
Absent Gator Sign
A-lines
C
Absent Gator Sign
11
D
5.1
Rib
Rib
RS
<<< Shred Sign
5.1

become known in time as more comparative imaging studies are published.

To illustrate the Vet BLUE regional pattern-based pattern approach, examples of nonrespiratory look-alikes, left-sided congestive heart failure, noncardiogenic pulmonary edema, pneumonia, nodular disease, and pleural effusion are shown on several figures using lateral thoracic radiographs with Vet BLUE illustrative overlays (Figure 23.24; see also Figures 23.25, 23.26, 23.28, and 23.29).

## "Dry Lung" Conditions

The finding of "dry lung all (Vet BLUE) views" or "absent B-lines all (Vet BLUE) views (ABAV)" is important in patients with respiratory distress (Lisciandro et al. 2016) (Figure 23.25). The finding effectively rules out any clinically relevant left-sided congestive heart failure in dogs and cats with 88–96% sensitivity and likely holds true for all mammalian lung (Lichtenstein 2009a; Lisciandro et al. 2016; Ward et al. 2017). The finding of absent B-lines also rules against the use of loop diuretics because no clinically relevant alveolar-interstitial edema exists (Rademacher et al. 2014; Lisciandro 2014b; Lisciandro et al. 2016, 2017; Ward et al. 2017, 2019; Vezzosi et al. 2017). The patient may have heart disease, but no clinically relevant left-sided congestive heart failure is present.

Rule-outs for "dry lung all (Vet BLUE) views" or ABAV are summarized in Table 23.3. Importantly, ABAV respiratory conditions will most commonly include upper airway disease, feline asthma, tracheobronchitis/bronchitis, severe pneumothorax, and PTE and lung pathology that does not make it to the "lung line" (lung surface) or pathology that is not present at any of the Vet BLUE acoustic windows or other LUS formats being used. For nonrespiratory look-alikes, in other words conditions that present with respiratory signs that are not truly respiratory, the categories include: (1) cardiac such as arrhythmias, dilated cardiomyopathy, pulmonary hypertension, right-sided congestive heart failure, and pericardial effusion, (2) uncharacterized hypotension such as internal hemorrhage (hemoabdomen, hemothorax, hemoretroperitoneum), gastric dilation-volvulus (GDV), sepsis, canine anaphylaxis, and (3) miscellaneous causes such as high fever, pyrexia, heat stroke, severe metabolic acidosis, and anemia (Lisciandro 2012, 2013, unpublished data; Hnatusko et al. 2019).

## "Wet Lung" Conditions

### Left-sided Congestive Heart Failure

Most cases of canine left-sided congestive heart failure have a dorsal perihilar distribution (think the classic perihilar edema on the thoracic radiograph) or generalized distribution of B-lines (alveolar-interstitial edema), unless the dog is a Doberman, which often have a random patchy alveolar-interstitial pattern like felines (Fox 1988; Benigni et al. 2009). Early cardiogenic pulmonary edema has been reported to be asymmetrical and more right-sided (caudodorsal lung fields) than left (Guglielmini et al. 2009). The Volipcelli strong positive (VSP) model was used to better categorize pulmonary edema as cardiogenic or noncardiogenic with manipulation of the Vet BLUE B-line scoring system (Figure 23.26; see also Figures 23.14–17). The VSP model is more conservative, making only B-lines scores of >3 and infinity "positive," thus discrediting scores of 1, 2, and 3 (see Figures 23.16 and 23.18). However, if the Vet BLUE sonographer understands the VSP model cardiac bias, then the VSP model helps to rule in left-sided congestive heart failure (L-CHF) from other causes of respiratory distress, especially for cats (Ward et al. 2017). In cats, two or more VSP positive

**Figure 23.22.** How the lung ultrasound line system lacks illustrative purposes. In (A–D) are examples that are unlabeled to the left and labeled to the right. (A) B-lines, defined within the text. (B) So-called Z-lines that may confound the lung sonographer, however, in comparing to (A) and adhering to the definition of B-lines, these Z-lines are only academic and esoteric. Note they originate from fascial planes of the intercostal muscles and those more superficial, they are partial in their extent toward the far-field, they fade, and they do not obliterate A-lines, appearing nothing like a B-line. Moreover, because their origin is proximal to the "lung line," they do not move in respirophasic synchrony but rather have "shimmy" motion. In (C) there are two examples of subcutaneous emphysema (SQE). To the left, the SQE behaves as expected, showing A-lines *without* a "gator sign" and to the right is dirty shadowing again as expected with SQE and again *without* a "gator sign." Air is air is air anywhere. The need for E-lines is only academic and esoteric. If you cannot identify the "gator sign" then you cannot confidently evaluate lung. Finally, in (D) are C-lines for consolidation. It may be difficult for the sonographer to find where these C-lines exist as there are no discrete lines *per se*, and the use of the shred sign and tissue sign is much more tangible, descriptive, and better conveys the type of consolidation. The author supports the use of the Vet BLUE visual lung language over the esoteric line nomenclature. RS, rib shadow. Rib with circle, ribs in cross-section. Icon of >3 B-lines. Source: Reproduced with permission of Dr Gregory Lisciandro, Hill Country Veterinary Specialists and FASTVet.com, Spicewood, TX.

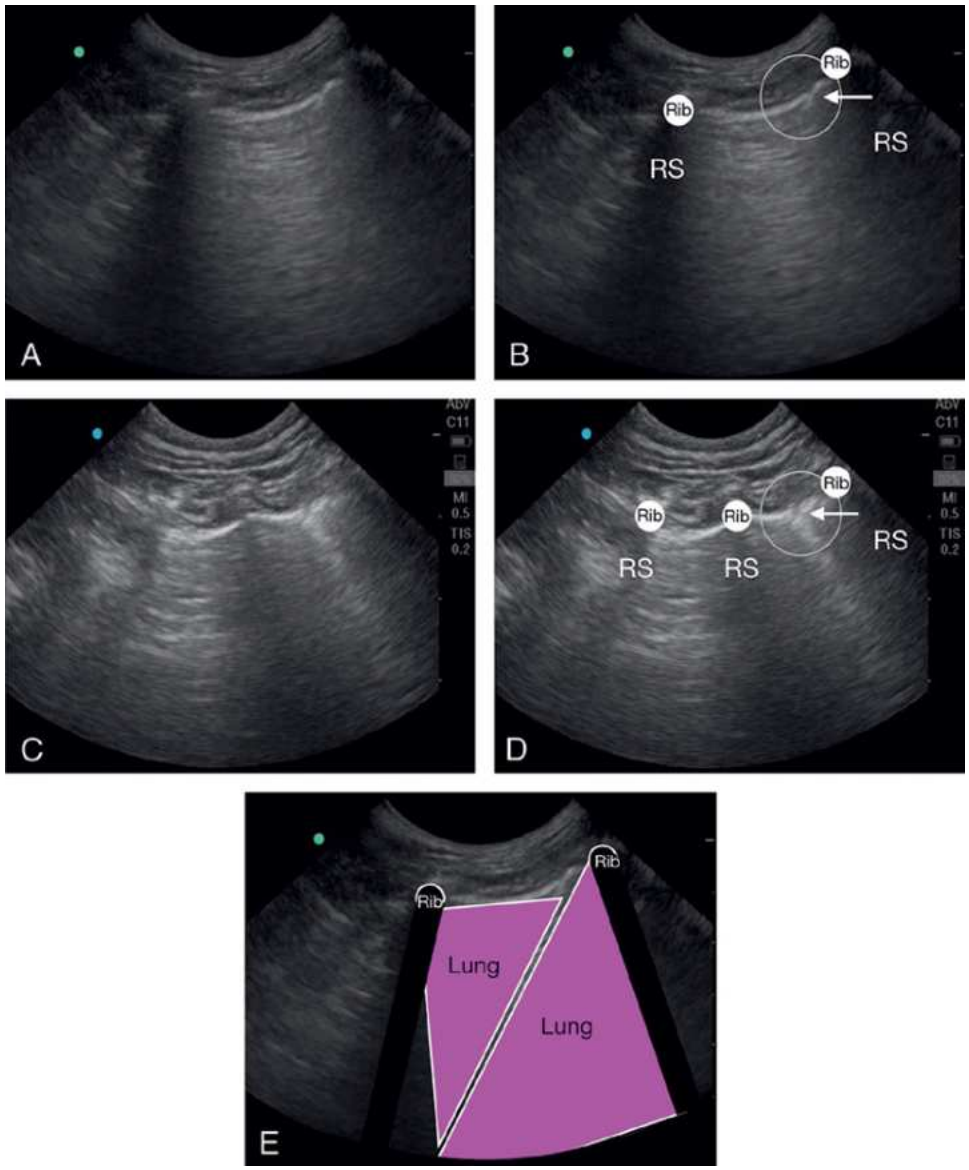


**Figure 23.23.** Hitches and blips. Lung ultrasound is extremely sensitive for lung surface pathology and during Vet BLUE it is important for the sonographer to acknowledge that regional views involve different lung lobes that have respirophasic movement through the same intercostal spaces being interrogated. Thus, hitches and blips along the lung surface may be noted and may represent different anatomical lung overriding one another. Two examples are shown. In (A) and (B) are unlabeled and labeled images showing a clear deviation off the "lung line" that gives the effect of overriding lung. In (C) and (D) is another similar image, with the overriding lung resulting in a "comet-tail" artifact. (E) Two different lung parts or lobes are illustratively shown as overriding one another ("shaking hands") that commonly results in these LUS findings. Source: Reproduced with permission of Dr Gregory Lisciandro, Hill Country Veterinary Specialists and FASTVet.com, Spicewood, TX.

views bilaterally during Vet BLUE have the same sensitivity and specificity (87% and 89%) as TXR (Ward et al. 2017). For the feline, this VSP approach is important because radiology is so risky for the cat. The VSP scoring model was less helpful in diagnosing L-CHF in dogs because of other canine "wet lung" conditions, such as ARDS, pneumonias, hemorrhage, pulmonary hypertension, PTE, and others that have moderate to severe generalized pulmonary edema (Ward et al. 2017). For this reason, the regional pattern-based approach along with findings on Global FAST and the patient's clinical profile provides a more probable working diagnosis (Lisciandro 2012, unpublished data; Ward et al. 2019).

**Table 23.2.**
Vet BLUE algorithm for acute respiratory distress in dogs and cats.

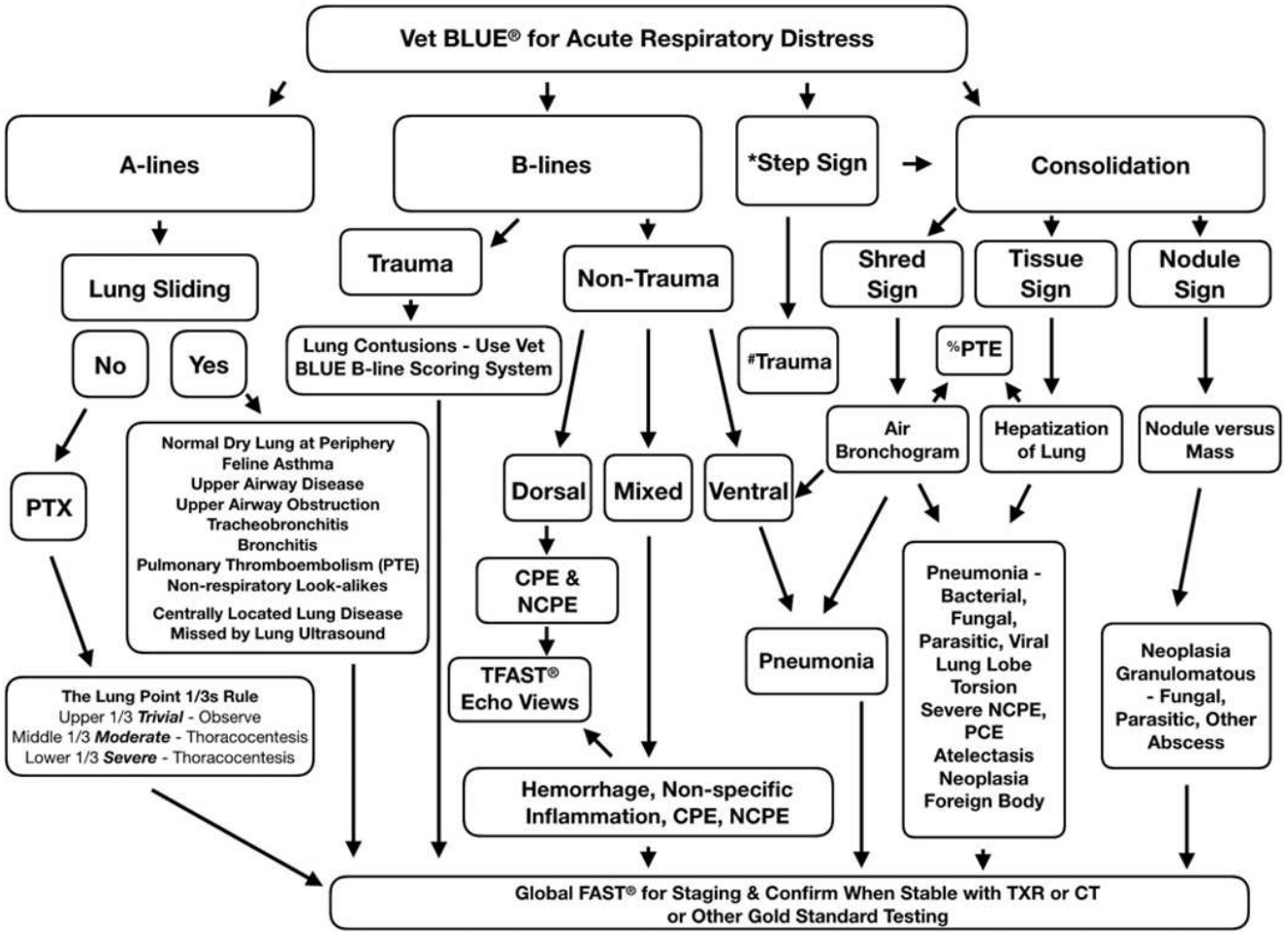


*Step sign is a deviation from the linear expectation of the PPI and the "lung line."
#In trauma the step sign's rule-out list includes thoracic wall injury (intercostal tear, rib fracture(s), subcostal hematoma/mass), pleural space disease (diaphragmatic hernia, mass, heart enlargement), and pulmonary consolidation (shred sign, tissue sign, nodule sign, wedge sign).
%Pulmonary thromboembolism (PTE) is supported by triangulated shred sign or tissue sign-like findings in the Perihilar and Caudodorsal lung regions (Lisciandro 2013, unpublished data).
PTE, pulmonary thromboembolism; PTX, pneumothorax; CPE, cardiogenic pulmonary edema; NCPE, noncardiogenic pulmonary edema; TXR, thoracic radiography; CT, computed tomography. Source: Courtesy of Dr Gregory Lisciandro, Hill Country Veterinary Specialists and FASTVet.com, Spicewood, TX.

### Numbers of B-lines Guide Loop Diuretic Usage

Numbers of B-lines and the Vet BLUE B-line scoring system help direct loop diuretic usage (Jambrik et al. 2004; Volpicelli et al. 2006; Lisciandro 2011; Lisciandro et al. 2014, 2016, 2017; Shyamsundar et al. 2013; Gargani et al. 2015; Gargani 2019) (Figure 23.27). Studies in dogs have shown that LUS-detected cardiogenic lung edema correlates with findings on TXR (Rademacher et al. 2014; Vezzosi et al. 2017; Ward et al. 2017, 2018b) and has been suggested as a point-of-care, low-impact imaging modality for patient monitoring (Rademacher et al. 2014; Ward et al. 2017, 2018b; Vezzosi et al. 2017). Conversely, when low B-line numbers exist, much less aggressive (and delaying) loop diuretic therapy appears to be supported by several studies (Rademacher et al. 2014; Lisciandro et al. 2014, 2016, 2017; Ward et al. 2017, 2018b; Vezzosi et al. 2017). The scoring of B-lines and categorizing as weak and strong positives provides a new tool for small animal clinicians

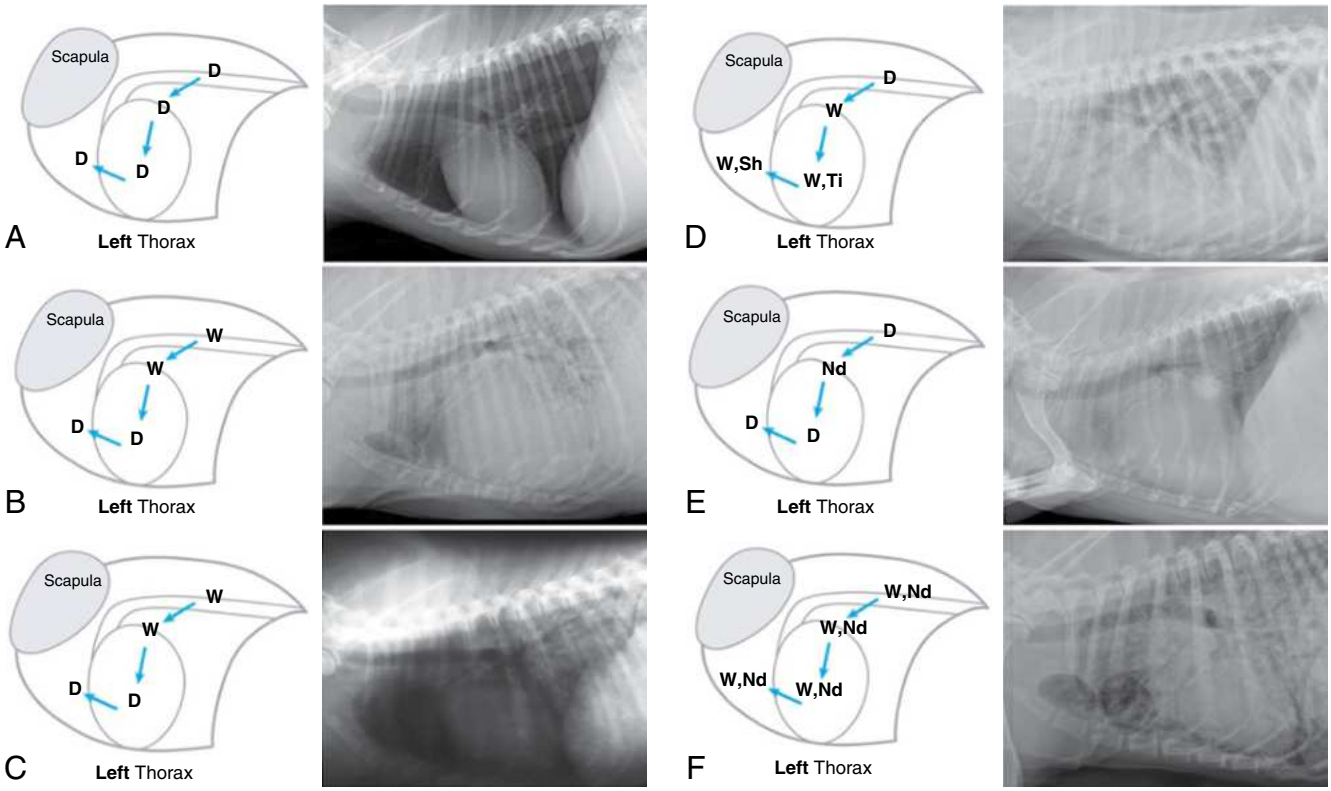


**Figure 23.24.** Vet BLUE profiles using its regional pattern-based approach. In (A) a Vet BLUE dry profile all views rules out left-sided *congestive* heart failure and develops a working problem list (see Tables 23.2 and 23.3). In (B) the finding of a wet profile in the Caudodorsal and Perihilar lung regions supports left-sided CHF and forms of noncardiogenic pulmonary edema. TFAST echo views are key to differentiate between these two causes (see Table 23.4). In this case the dog has left-sided CHF (increased LA:Ao ratio). In (C) the finding of a wet profile in the Caudodorsal and Perihilar lung regions supports left-sided CHF and forms of noncardiogenic pulmonary edema (NCPE). In this case the dog has NCPE (unremarkable echo views). In (D) the Vet BLUE profile supports bacterial bronchopneumonia with a wet profile and signs of consolidation (shred sign, tissue sign) ventrally. In (E) the Vet BLUE profile detects a solitary lung nodule (nodule sign) at the left Perihilar lung region. In (F) the Vet BLUE profile is a combination of a wet profile and multiple nodules (nodule sign) supporting metastatic or diffuse granulomatous disease. Source: Reproduced with permission of Dr Gregory Lisciandro, Hill Country Veterinary Specialists and FASTVet.com, Spicewood, TX.

to help prevent unwanted loop diuretic side-effects such as hemoconcentration from loss of free water, metabolic alkalosis, and azotemia. Moreover, for patients receiving aggressive loop diuretic therapy, including by constant-rate infusion, Vet BLUE may be performed as often as hourly as a more reliable test than lung auscultation and radiography (Rademacher et al. 2014; Gargani et al. 2015; Lisciandro et al. 2016; Vezzosi et al. 2017; Ward et al. 2018b).

### Noncardiogenic Pulmonary Edema

Noncardiogenic pulmonary edema (NCPE) has historically been described as symmetrical caudodorsal distribution of alveolar-interstitial infiltrate on TXR (Bouyssou et al. 2017), for example neurogenic (post seizure), asphyxiation/choked, electrocution, drowning, smoke inhalation, ARDS, and transfusion-related lung injury (TRALI) (Figure 23.28). A recent retrospective study came to contradictory TXR pattern conclusions, but the study evaluated small animals with presumed NCPE in very low, diluted numbers by several subsets of patients (49 dogs, 11 cats). The conclusions drawn were that NCPE may be more randomly distributed and asymmetrical, being more right- than left-sided (Bouyssou et al. 2017). In the author's experience, NCPE remains a top differential in small animals with a predominantly caudodorsal "wet lung" distribution; and integrating Global FAST findings helps increase the probability of a correct working diagnosis, especially incorporating TFAST echo views and characterization of the caudal vena cava and hepatic veins.

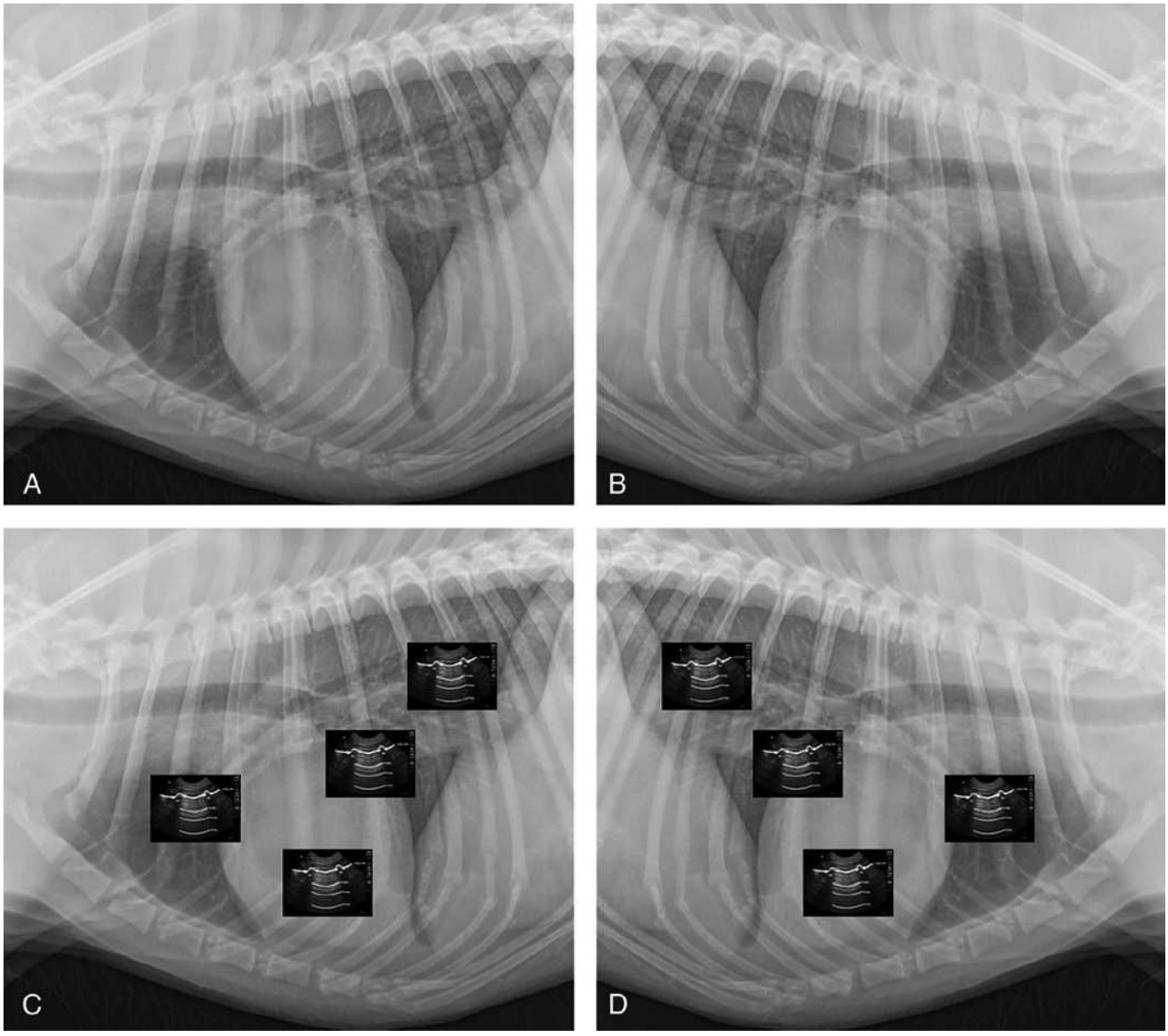


**Figure 23.25.** "Dry lung" All Vet BLUE Views also called Absent B-lines All (Vet BLUE) Views (ABAV). (A) through (D) are the same lateral radiographs with the Vet BLUE findings of dry lung overlays in (C) and (D). An effective means to rapidly (<60 seconds) and safely rule out left-sided CHF with minimal to no restraint in both dogs and cats (likely all mammalian lung) and argues against the empiric use of loop diuretic therapy that can have deleterious side-effects for the patient. See Table 23.3 for common rule-outs. Source: Reproduced with permission of Dr Gregory Lisciandro, Hill Country Veterinary Specialists and FASTVet.com, Spicewood, TX.

### Aspiration Pneumonia and Bacterial Pneumonias

Aspiration pneumonia and bacterial pneumonias are generally gravity dependent and are recognized during Vet BLUE as a predominantly ventral distribution with B-lines with and without signs of consolidation such as shred sign and tissue sign (Lisciandro 2012, unpublished data; Ward et al. 2019) (Figure 23.29; see also Figure 23.34).

### Nodular Disease

The nodule sign creates "pseudo B-lines", B-lines not created by types of fluid next to air, so the lung sonographer must evaluate the origin of the B-line off the "lung line" for the presence of nodules. The presence of nodules is not always neoplastic in origin. Fungal granulomas, parasitic granulomas, and bacterial granulomas along with bacterial abscesses (hallmark is air

**Table 23.3.**
Rule-outs for Dry Lung All Views.

| |
|---|
| **Respiratory** |
| Pulmonary thromboembolism (PTE) |
| Severe pneumothorax |
| Dynamic upper airway conditions (e.g., collapsing trachea, laryngeal paralysis) |
| Upper airway obstruction (e.g., mass, foreign body, oropharyngeal swelling, severe upper airway inflammation, nasopharyngeal polyp [cats], granulomatous laryngitis [cats]) |
| Chronic obstructive pulmonary disease (COPD), bronchitis |
| Feline asthma |
| Tracheobronchitis (e.g., infectious, inflammatory, irritant) |
| Centrally located lung pathology away from the "lung line" (missed by Vet BLUE) |
| Lung surface pathology that is Absent at All Vet BLUE Views (missed by Vet BLUE) |
| **Nonrespiratory look-alikes** |
| **Cardiac** |
| Pericardial effusion/cardiac tamponade |
| Cardiac arrhythmia |
| Dilated cardiomyopathy (DCM) |
| Right-sided congestive heart failure |
| Pulmonary hypertension |
| **Undifferentiated hypotension** |
| Canine anaphylaxis |
| Hemoabdomen |
| Hemothorax |
| Hemoretroperitoneum |
| Other cavitary or space hemorrhage |
| Gastric dilation-volvulus/bloat |
| Sepsis |
| **Other nonrespiratory** |
| Pyrexia/heat stroke |
| High fever |
| Severe metabolic acidosis |
| Severe anemia |

Source: Reproduced with permission of Dr Gregory Lisciandro, Hill Country Veterinary Specialists and FASTVet.com, Spicewood, TX.

within the mass) including from foreign bodies are other common considerations. The nodule sign may be accompanied by inflammation so true B-lines may be present along the adjacent "lung line" in contrast to "pseudo B-lines" that are directly associated with the nodule sign (see Figure 23.10) (Lisciandro 2014b; Neelis et al. 2015). Nodular diseases may also have concurrent shred and tissue signs, thus the overall Vet BLUE profile coupled with clinical findings best dictate the working diagnosis.

### Pulmonary Thromboembolism

The wedge sign is in some ways a subset of the shred and tissue signs although the pulmonary parenchyma has been affected differently by vascular necrosis from infarction. The wedge sign would be difficult to differentiate from pneumonia in gravity-dependent Vet BLUE views, but when in Caudodorsal and Perihilar views, PTE should be strongly suspected and placed into clinical context with other supportive information. Subpleural lesions similar to the wedge sign have supported the diagnosis of PTE in people (Mathis et al. 2005; Mastruzzo et al. 2008; Nazerian et al. 2014); however, in the author's experience PTE in dogs is much more wedge-shaped (triangular) than that described in people (Lisciandro 2013, unpublished data). See Figures 37.9 and 37.10 for illustrative case examples.

### Other Diffusely Wet Conditions

Lung contusions, pulmonary hemorrhage in coagulopathic patients, feline anaphylaxis, canine pulmonary hypertension, allergic and irritant pneumonitis, dirofilariasis (canine heartworm disease), feline histoplasmosis, and feline *Alurostrongylus* and *Paragominus* infections are additional conditions which the author has encountered that may mimic left-sided CHF, being diffusely "wet lung" using the VSP model. Metastatic neoplasia, although appearing to have diffuse "wet lung"-like artifacts, has in fact "pseudo B-lines" created by strong differences in acoustic impedance between soft tissue cuffed by aerated lung (Soldati, personal communication). These "pseudo B-lines" likewise oscillate in synchrony with phases of respiration so careful evaluation of the "lung line" to evaluate for surface nodules and other Vet BLUE LUS signs is important. Moreover, several nodules of various sizes should be detected during Vet BLUE to draw the final conclusions for nodular lung. Care should be taken to avoid overinterpreting small blips along the "lung line," where divisions of lung lobes and parts of lung contact one another, that may mimic small nodules (see Figure 23.23). Repeating the Vet BLUE in 10–14 days is a viable option as well.

Close observation of the "lung line" from which the B-line originates is important to rule in and out the presence of the nodule sign for neoplastic disease, abscesses and granulomatous disease. For example, a cat with left-sided CHF will have diffuse "wet lung" but so will a cat with pulmonary histoplasmosis. Thus, the finding of the nodule sign in this feline example

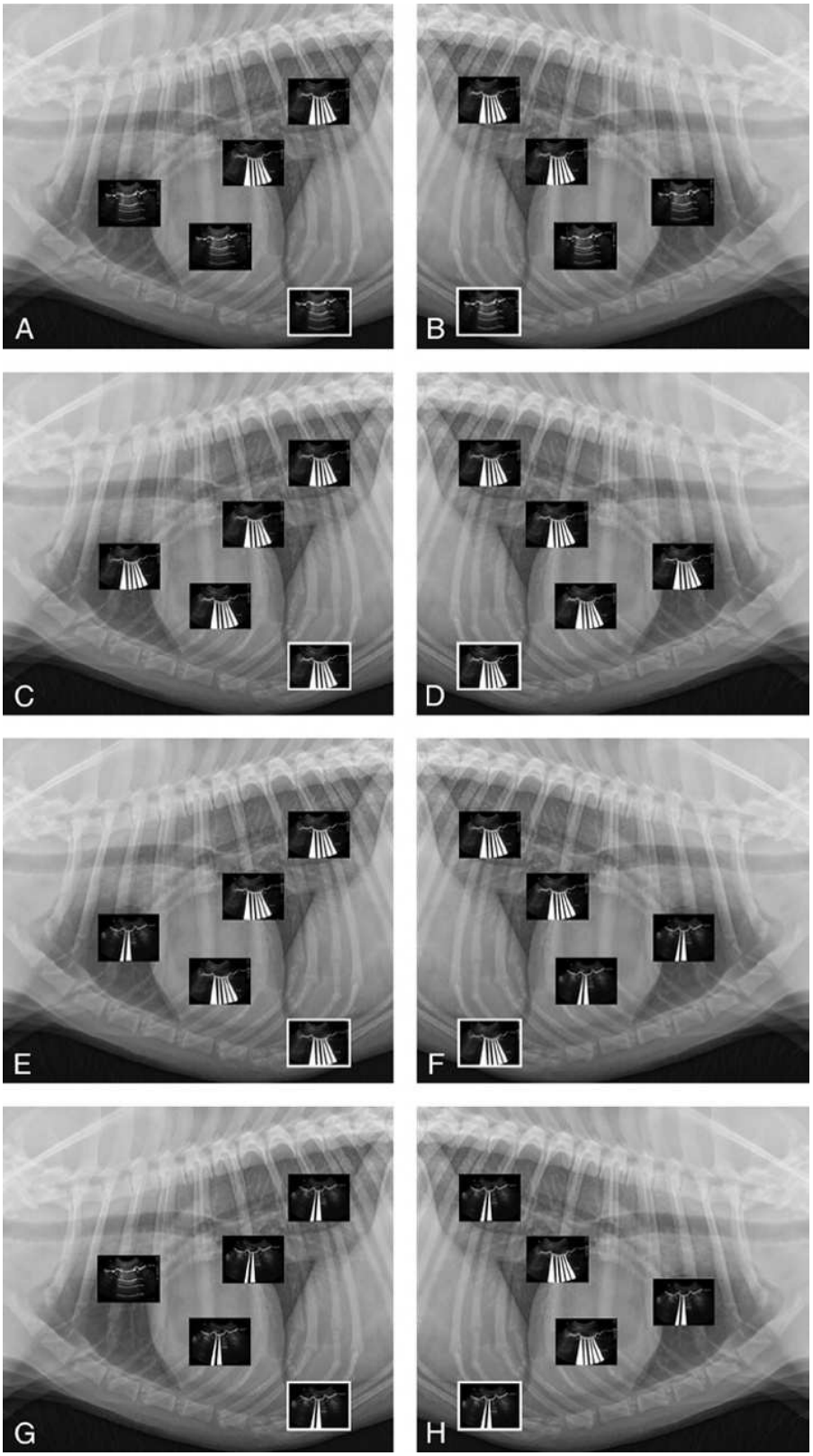


**Figure 23.26.** Examples of Vet BLUE left-sided congestive heart failure profile. Lateral thoracic radiographs are used with overlays of "dry lung" and "wet lung" (>3 B-lines) icons. In left-sided CHF "wet lung" predominates in dorsal and perihilar regions as in (A) and (B), or may be more right- than left-sided dorsal and perihilar as in (G) and (H), or generalized in most Vet BLUE regions as in (C) and (D). In (E) and (F) note that edema predominates in Caudodorsal and Perihilar lung regions. See Table 23.4 for integrating additional Global FAST information to better interpret the cause(s) for the "wet lung." Source: Reproduced with permission of Dr Gregory Lisciandro, Hill Country Veterinary Specialists and FASTVet.com, Spicewood, TX.

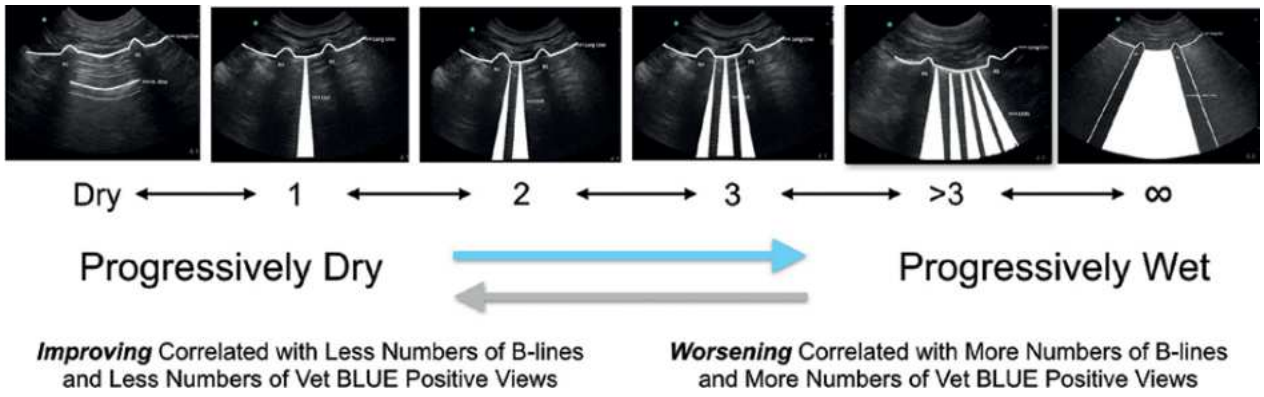


**Figure 23.27.** Use of the Vet BLUE B-line scoring system for guiding loop diuretic therapy. Numbers of B-lines help guide diuretic therapy, with low to no numbers ruling against aggressive loop diuretic therapy versus high numbers over many Vet BLUE views ruling for more aggressive therapy. As a monitoring tool, Vet BLUE replaces the stethoscope and may be used hourly in patients receiving heavy loop diuretics, including while receiving constant rate infusions to help prevent the many side-effects of these drugs. Line with rounding and an interposing straight line represents the intercostal space and the "gator sign" orientation. Source: Reproduced with permission of Dr Gregory Lisciandro, Hill Country Veterinary Specialists and FASTVet.com, Spicewood, TX.

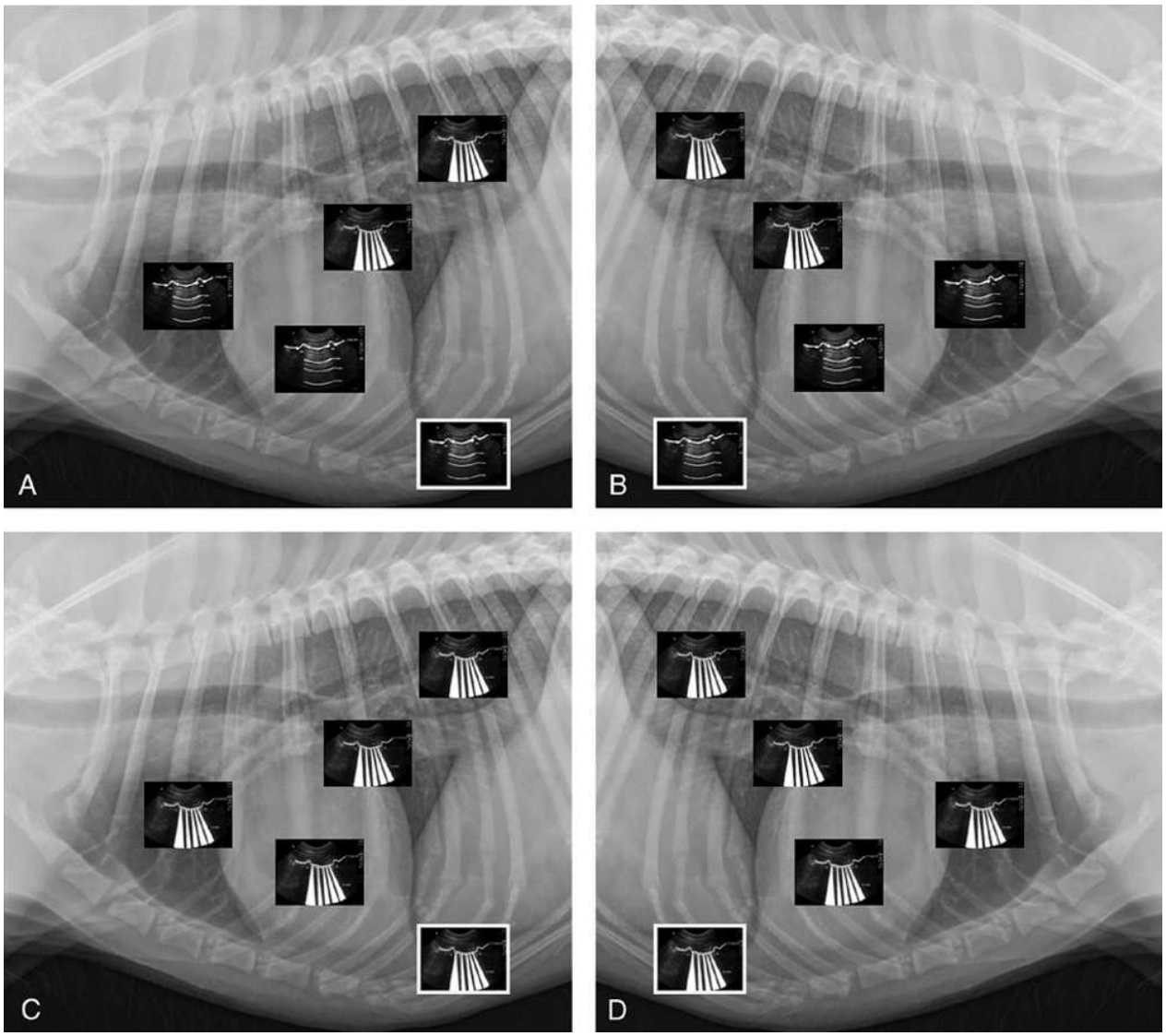


**Figure 23.28.** Examples of Vet BLUE noncardiogenic lung edema profile. Lateral thoracic radiographs are used with overlays of "dry lung" and "wet lung" (>3 B-lines) icons. In NCPE "wet lung" predominates in Caudodorsal and Perihilar regions as in (A) and (B) or is generalized in most Vet BLUE regions as in (C) and (D) and generally is symmetrical. See Table 23.4 for integrating additional Global FAST information to better interpret the cause(s) for the "wet lung." Source: Reproduced with permission of Dr Gregory Lisciandro, Hill Country Veterinary Specialists and FASTVet.com, Spicewood, TX.

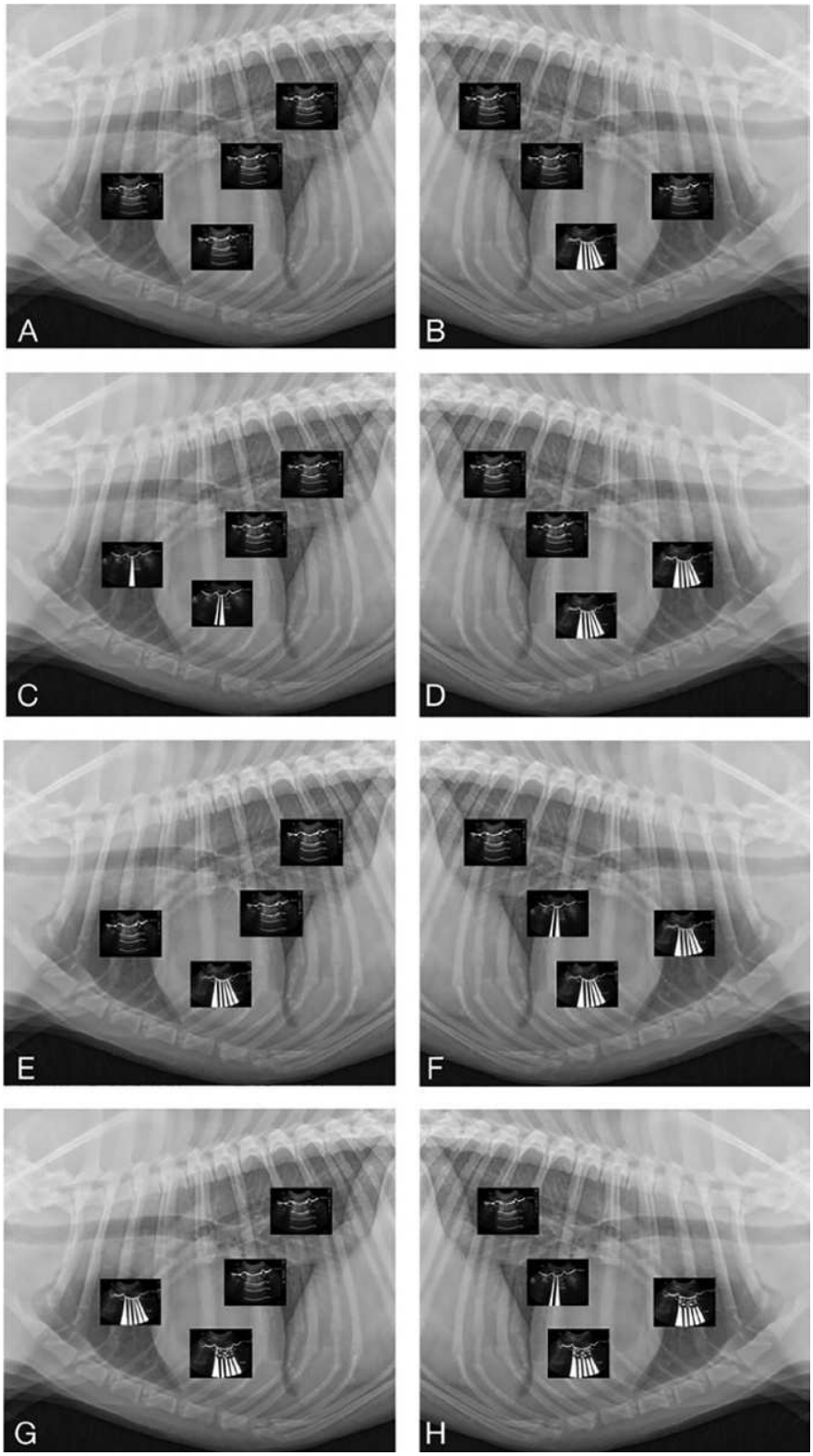


**Figure 23.29.** Examples of Vet BLUE pneumonia profile. Lateral thoracic radiographs are used with "dry lung", "wet lung", and "shred sign" in paired left and right Vet BLUE examples of different degrees of pneumonia characterized by gravity-dependent predominance in Middle and Cranial lung regions along with asymmetrical patterns. In (A) and (B) the Vet BLUE pattern supports canine aspiration pneumonia into the most common right middle lung lobe by the presence of >3 B-lines. More severe right middle lung lobe aspiration would be the presence of the shred sign and then tissue sign. In (C) and (D), (E) and (F), and (G) and (H), the Vet BLUE patterns again support bacterial bronchopneumonia, however, in more progressive severity with (C) and (D) having lesser numbers of B-lines than (E) and (F); and (G) and (H) more severe with B-lines plus shred signs of consolidation. See Table 23.4 for integrating additional Global FAST information to better interpret the cause(s) for the "wet lung." Source: Reproduced with permission of Dr Gregory Lisciandro, Hill Country Veterinary Specialists and FASTVet.com, Spicewood, TX.

Table 23.4.

**Algorithm for diffuse B-lines.** Algorithm for diffuse B-lines and sorting out cardiogenic pulmonary edema (PCE), various forms of noncardiogenic pulmonary edema (NPCE), pulmonary hypertension (PHT) plus other major considerations. Integration of other information including the TFAST echo views is key for an accurate assessment.

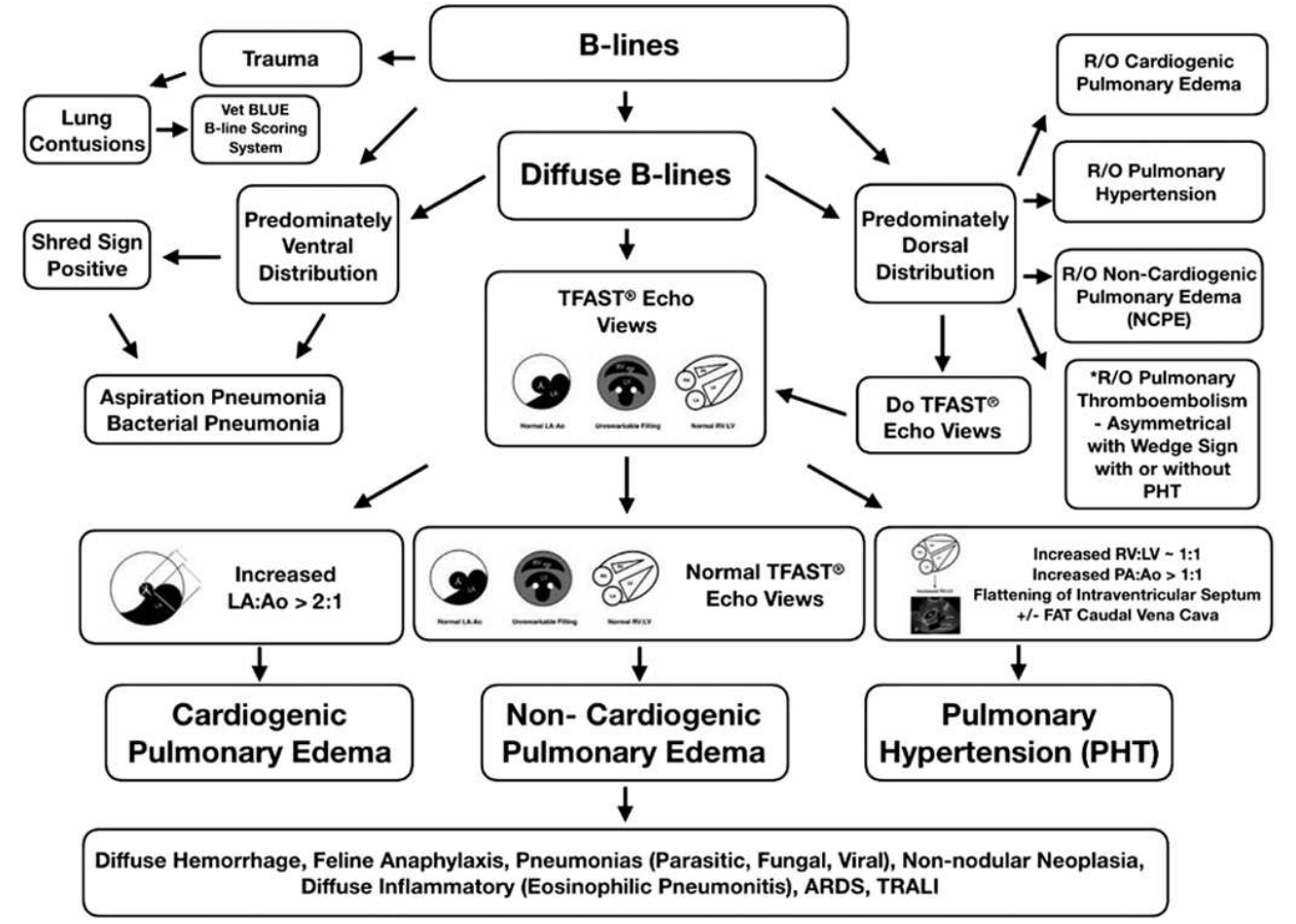


Source: Reproduced with permission of Dr Gregory Lisciandro, Hill Country Veterinary Specialists and FASTVet.com, Spicewood, TX.

weights the working diagnosis more toward fungal pneumonia over left-sided CHF since the nodule sign is not expected in left-sided CHF. Thus, Vet BLUE findings help direct treatment and choice of the next best test, and a Global FAST approach incorporates TFAST echo views to better differentiate cardiogenic from noncardiogenic causes of "wet lung" as well as other abnormalities (Table 23.4).

### Differentiating Causes of "Wet Lung" Requires Clinical Integration

When diffusely marked "wet lung" is present, TFAST echo views and POCUS heart evaluation are very helpful. Global FAST nonecho fallback views are also useful, especially in equivocal echo assessment and unstable patients that may not tolerate the restraint and risk of prolonged cardiac imaging (see Chapters 36 and 37) (Gargani and Volpicelli 2014; Lisciandro and Armenise 2014; Ha and Toh 2016). Clinical integration of Vet BLUE findings with TFAST echo views and Global FAST nonecho fallback views and their expected findings are listed.

- Cardiogenic pulmonary edema – increased LA:Ao ratio.
- Noncardiogenic pulmonary edema – unremarkable TFAST echo views.
  - Choking/asphyxiation.
  - Neurogenic.
  - Electrocution.

VetBooks.ir

- Smoke (other irritant) inhalation.
- Drowning.
- Acute respiratory distress syndrome.
- Transfusion-related lung injury.

- Miscellaneous that also have unremarkable TFAST echo views.
  - Diffuse hemorrhage – coagulopathic.
  - Lung contusions – history of trauma.
  - Pneumonitis.
  - Fungal pneumonias.
  - Viral pneumonias.
  - Parasitic pneumonias.
- Canine pulmonary hypertension – increased RV:LV ratio, flattening of the interventricular septum, increased pulmonary artery to aorta ratio, distended or "FAT" caudal vena cava and hepatic venous distension, and possibly gallbladder wall edema (the "cardiac gallbladder") (Lisciandro 2019) – see Chapters 6, 7, 16, and 17).

# Using the Vet BLUE "Wet Lung" versus "Dry Lung" Concept for Monitoring During Fluid Therapy

Combining numbers of B-lines using the Vet BLUE B-line scoring system with numbers of positive views, B-lines are "sentinels" for developing lung edema and serve as a rapid point-of-care, low-impact monitoring tool for detecting increased extravascular lung water (EVLW) (Jambrik et al. 2004; Lichtenstein et al. 2009a; Lichtenstein and Karakitsos 2012; Shyamsundar et al. 2013; Gargani et al. 2015; Gargani 2019). The gold standard test for EVLW of transpulmonary thermodilution cardiac output (PICCO) is invasive and of limited availability (Anile et al. 2017). Thus, Vet BLUE and its simple B-line scoring system coupled with numbers of positive regional views carries tremendous potential for estimation of EVLW in our small animal patients (Anile et al. 2017). Moreover, the finding of increased EVLW (B-line, alveolar-interstitial edema) anticipates the possible development of alveolar flooding (shred sign, tissue sign, air bronchograms, and lung consolidation), which is far more difficult to treat. Moreover, unrecognized EVLW risks overt patient decompensation (labored breathing, respiratory distress) before being detected by more traditional means of lung auscultation and vital signs. By recognizing the development of B-lines in patients receiving intravenous fluid therapy, the attending clinician can modify the clinical course, especially regarding fluid therapy and loop diuretics, and further investigate causes.

# Lung Contusions and Vet BLUE

## *Using Vet BLUE for Scoring Severity of Lung Contusions in Trauma*

Numbers of B-lines combined with number of positive Vet BLUE views semiquantitates overall lung contusion severity, providing a Vet BLUE lung contusion severity score (Lisciandro 2011, 2014b; Lisciandro 2012, unpublished data; Dicker et al. 2019). In other words, the more B-lines at higher numbers of positive Vet BLUE regional views, the more severe the lung contusions are in that patient. Focally, numbers of B-lines in a Vet BLUE view also semiquantitate the degree of lung contusions within that region of lung, and the distribution of lung contusions is also appreciated by combining positive views with numbers of B-lines. In severe lung contusions, shred sign and tissue sign are present (Dicker et al. 2019).

For example, a puppy that has a crush injury from being stepped on by a large adult presents in overt and severe respiratory distress. The puppy is found to have >3 B-lines at all Vet BLUE views, including the DH view, indicating severe pulmonary contusions. This patient information is gained immediately following the physical exam with minimal to no restraint and little patient risk (no restraint and no transport to radiology). In contrast, a dog that has been bluntly traumatized by an automobile or was kicked by a horse has only >3 B-lines at only two of nine Vet BLUE views – the left Caudodorsal and Perihilar lung region views (absent at the other seven Vet BLUE views). The Vet BLUE sonographer can readily appreciate the difference in severity of the lung contusions between the puppy being stepped on and the hit-by-car or kicked by a horse examples. Serial Vet BLUE and scoring may then be used as a monitoring tool for assessing worsening, resolving, and static lung contusions (Figure 23.30).

## *Comparative Imaging: Vet BLUE, Radiography, and Computed Tomography*

The use of Vet BLUE does not negate the need for radiographical studies. Radiography is generally a better imaging test for fractures, bone lesions, projectile foreign bodies, thoracic wall injuries, and herniations; and CT is generally considered the gold

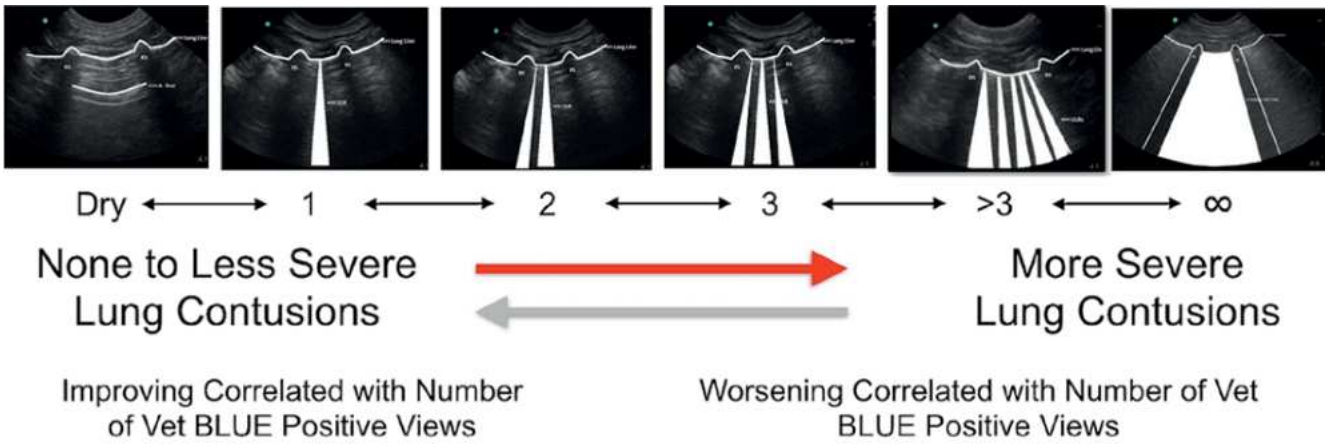


**Figure 23.30.** Vet BLUE severity scoring of lung contusions. As with assessing degree of pulmonary edema by combining numbers of B-lines with numbers of positive Vet BLUE views, a Vet BLUE lung contusion severity score may be used for decision making (Lisciandro 2011, 2014b; Dicker et al. 2019). Line with rounding and an interposing straight line represents the intercostal space and the "gator sign" orientation. Source: Reproduced with permission of Dr Gregory Lisciandro, Hill Country Veterinary Specialists and FASTVet.com, Spicewood, TX.

standard imaging test for most patients. However, Vet BLUE provides a lower risk, lower impact, point-of-care first-line imaging test for the critical and unstable patient that exceeds radiography for lung surface pathology and may be used diagnostically for many common respiratory conditions while comparing favorably with CT for many conditions. Moreover, Vet BLUE may be subsequently used as a cost-effective monitoring tool. In traumatized canine lung, Vet BLUE is more sensitive than TXR and fares well when compared to CT (Figure 23.31) (Dicker et al. 2019). The limitations of Vet BLUE when compared to CT were found to be the missing of deeper (away from the lung surface) lung contusions and those associated with the mediastinum (Dicker et al. 2019).

# Pitfalls, False Negatives, False Positives, and Limitations

## *False Negatives, Limitations*

- Centrally located (deep to the lung's surface) lung disease is ultrasonographically inaccessible (missed or occult) (see Figure 23.1).
- Peripheral lung lesions are missed when they are not present at a Vet BLUE (or other LUS) acoustic window (see Figure 23.1).
- Peripheral lung lesions are missed because they are not accessible because of the patient's foreleg (scapula and its associated musculature).
- Pneumothorax and SQE (see Figures 18.12, 18.13, 23.6, and 23.21) negate LUS beyond the strong air interface each presents because ultrasound cannot image past air. Thus …
- LUS may be performed when PTX has resolved or at any regions where lung is in direct contact with the thoracic wall ventral to the "lung point" (see Figures 18.6–9).
- SQE can often be eliminated by applying enough probe pressure to displace the interfering subcutaneous air so that the "gator sign" orientation becomes visible (see Figure 18.12).
- Obese patients or those with a large amount of soft tissue interposed between skin and intercostal space and "lung line" may be difficult to image because of the attenuation of the ultrasound beam.

**Pearl:** If you cannot acquire the "gator sign" orientation then you cannot be certain you are looking at the "lung line."

## *False Positives, Limitations*

- Pleural space and pericardial conditions such as diaphragmatic hernia, peritoneopericardial hernia and thoracic wall disease may be confounders creating a step sign, which is a deviation from the expected linear continuity of "lung sliding" along the intercostal space (Lisciandro et al. 2008; Lisciandro 2014b).
- Abdominal structures may be falsely considered as a shred sign (rugal folds of the stomach) and tissue

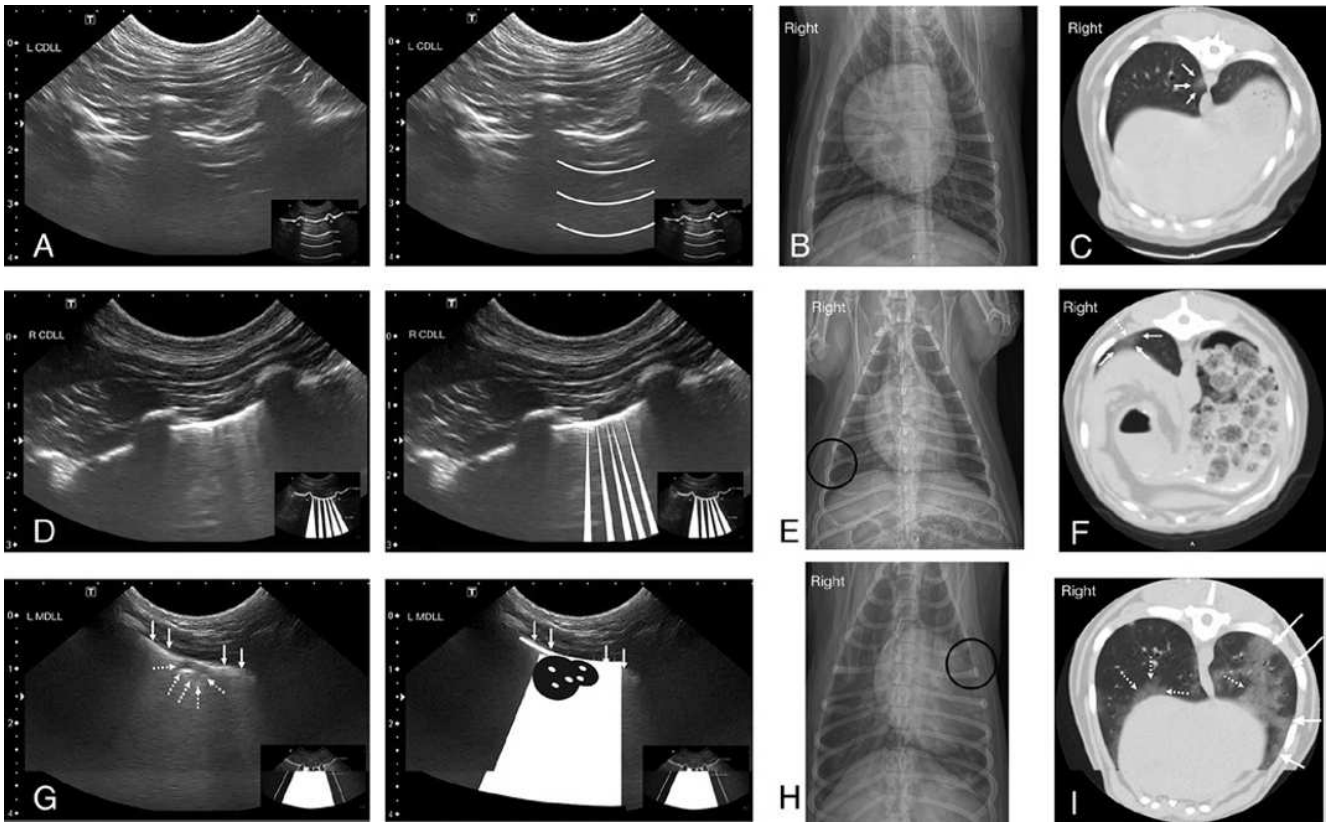


**Figure 23.31.** Comparative imaging of Vet BLUE, TXR, and CT. Shown in the top row of (A), (B) and (C) are mild lung contusions inapparent on Vet BLUE and TXR but detected on CT (*arrows*). In the middle row of (D), (E), and (F) the patient has moderate lung contusions evidence by >3 B-lines in (D) missed on TXR in (E) and detected in the same region on CT in (F). In the bottom row of (G), (H) and (I) severe contusions are evidenced by infinity B-lines and shred sign on Vet BLUE in (G) that are difficult to detect on TXR in (H) that correlate to the severity on CT in (I). The case in the top row was a 1-year-old female Australian shepherd that was positive for pulmonary contusions only on CT. In (A) the Vet BLUE examination at the right Caudodorsal lung region showed "dry lung" with no B-lines or other Vet BLUE LUS signs along with the correlative ventrodorsal thoracic radiograph in (B) that likewise showed no evidence of pulmonary contusions. In (C) the CT image detected pulmonary contusions in the right caudal lung lobe (*solid arrows*). This image series (A–C) serves as an example of pulmonary contusions not visible with Vet BLUE due to the central location of lung pathology. The case in the middle row is a 1-year-old male Chihuahua mix that was positive for pulmonary contusions on Vet BLUE and CT, but went undetected on TXR. In (D) is the image from the right Caudodorsal lung region with >3 B-lines with an overlay of artifacts to its right. The white arrows indicate the pulmonary-parietal pleural interface and "lung line" from which the B-lines originate and in (E) is the ventrodorsal TXR with no evidence of pulmonary contusions. In (F) is the CT image of pulmonary contusions (*solid arrows*) in the right caudal lung lobe that touch the pulmonary-pleural surface (*dashed arrow*) and correlate with the Vet BLUE finding. This case serves as an example of Vet BLUE outperforming TXR and correlating with CT. The final case in the bottom row is a 2-year-old male neutered Chihuahua mix that was positive for pulmonary contusions on all three imaging modalities. In (G) the Vet BLUE image from the right Middle (Md) lung region shows a small shred sign and infinity B-lines originating from the pulmonary-parietal pleural interface (*solid arrows*) and "lung line" with an overlay of artifacts to its right. In (H) the ventrodorsal TXR has a correlative interstitial pattern in its left Cd and right Md lung regions as well as an alveolar pattern in the left Md lung region (lateral radiographs not shown). In (I) the CT image shows pulmonary contusions in both the left and right lungs. Some of the pulmonary contusions (*solid arrows*) reach the pulmonary-parietal pleural surface, "lung line," and other pulmonary contusions are more central (*dashed arrows*), which would not be visible on Vet BLUE. Note the depth shown is too shallow for a complete Vet BLUE assessment and should be increased (4–8 cm) to make sure the lung is adequately surveyed. Source: Courtesy of Dr Sam Dicker, West Hills Animal Hospital Emergency and Critical Care Center, Huntington, New York and Dr Gregory Lisciandro, Hill Country Veterinary Specialists and FASTVet.com, Spicewood, TX.

VetBooks.ir

sign (liver) and B-lines (ingesta in the stomach lumen) and thus our current training practice is to ensure Vet BLUE sonographers acknowledge transition zones of (1) the peritoneal and pleural cavities (caudodorsal transition zone, CdTZ), and (2) the thoracic inlet and pleural cavity (cranial transition zone, CrTZ) (see Chapter 22, Figures 22.13 and 23.20).

- Ventral and dorsal, caudal and cranial borders involve muscle, soft tissue and abdominal structures that must be learned to avoid mistaking these structures for lung and lung pathology (see Chapter 22 and Figure 22.17).

# Vet BLUE Examples

## *Dogs*

### Heart Disease Patient Before and After Anesthesia

Preanesthetic evaluation with the Global FAST approach helps detect morbidities while at the same time establishing a baseline of data imaging points to which future studies post anesthesia may be compared. A practical common example is the mitral valve disease dog coming in for an anesthetic procedure that has "dry lung" before the procedure and is coughing post procedure (Figure 23.32). By having a preprocedure baseline, the cause of coughing is better determined with serial Vet BLUE plus the Global FAST approach.

### Choked on Rawhide

The first example is a patient with Dry Lungs (D) all views and used for comparison for the subsequent examples of different respiratory conditions.

Let's work through the following example of a dog that has choked on a rawhide that presents stable but with an increased respiratory rate. There are three common scenarios causing the increased respiratory rate: (1) stress, anxiety, oropharyngeal and tracheal irritation, (2) noncardiogenic pulmonary edema, and (3) aspiration pneumonia. Think about the Vet BLUE profiles for each. In (1) the dog will have "dry lung" (D) (see Figure 23.25), or in other words be dry all Vet BLUE views with ABAV. In (2) the dog will likely have a predominantly dorsal or generalized distribution of "wet lung" (W) (see Figure 23.26). In (3) the dog will likely have a predominantly ventral gravity-dependent distribution of "wet lung" (W) (see Figures 23.29 and 23.34). Vet BLUE profiles may be established within 90 seconds in most patients and an evidence-based approach is used point of care, leading to more accurate assessment and treatment. Additional imaging and testing is then triggered as indicated, but importantly can be delayed until the patient is more stable.

## *Cats*

### Abdominal Breathing and Nostril Flaring

The respiratory distressed feline presents with similar breathing patterns of abdominal breathing and nostril flaring (Figure 23.33). A physical exam and watching the patient spontaneously breathe without restraint is good practice. However, if you can place a stethoscope on the patient, you can place an ultrasound probe. In these felines, the Vet BLUE-TFAST approach (always better to use Global FAST with AFAST performed with the cat in standing or sternal) is very helpful and can cut to the chase diagnostically by "seeing" the condition.

There are four common conditions in cats to be considered: (1) feline asthma, (2) left-sided CHF, (3) pleural effusion, and (4) metastatic disease. Each of these has radically different Vet BLUE profiles that, in fact, would have already been sorted out in about the time it took me to type this paragraph.

In (1) the cat has feline asthma and will have "dry lung" all views, absent B-lines all (Vet BLUE) views (ABAV), ruling out left-sided CHF (Lisciandro et al. 2016; Ward et al. 2017). In (2) the cat has left-sided CHF and will have "wet lung" in most if not all Vet BLUE views (Lisciandro et al. 2017; Ward et al. 2017). In fact, the VSP model works as well in cats with left-sided CHF as three-view TXR (Ward et al. 2017). In (3) the cat has pleural effusion and will have free fluid identified during Vet BLUE-TFAST (Ward et al. 2018a). In (4) the cat with metastatic disease has nodules of various sizes in multiple views during Vet BLUE coupled with mammary gland tumors (Kulhavy and Lisciandro 2015). A good physical exam and an AFAST help search for additional supportive information to formulate a working diagnosis. Each of these four felines has radically different Vet BLUE profiles despite very similar breathing patterns and lung auscultation.

### Feline Pleural Effusion – Get Over the Flash Mentality

A "flash exam" is taught to many veterinary students and veterinarians as an unstructured approach of sweeping over the abdomen and thorax with the ultrasound probe to answer a simple binary question of

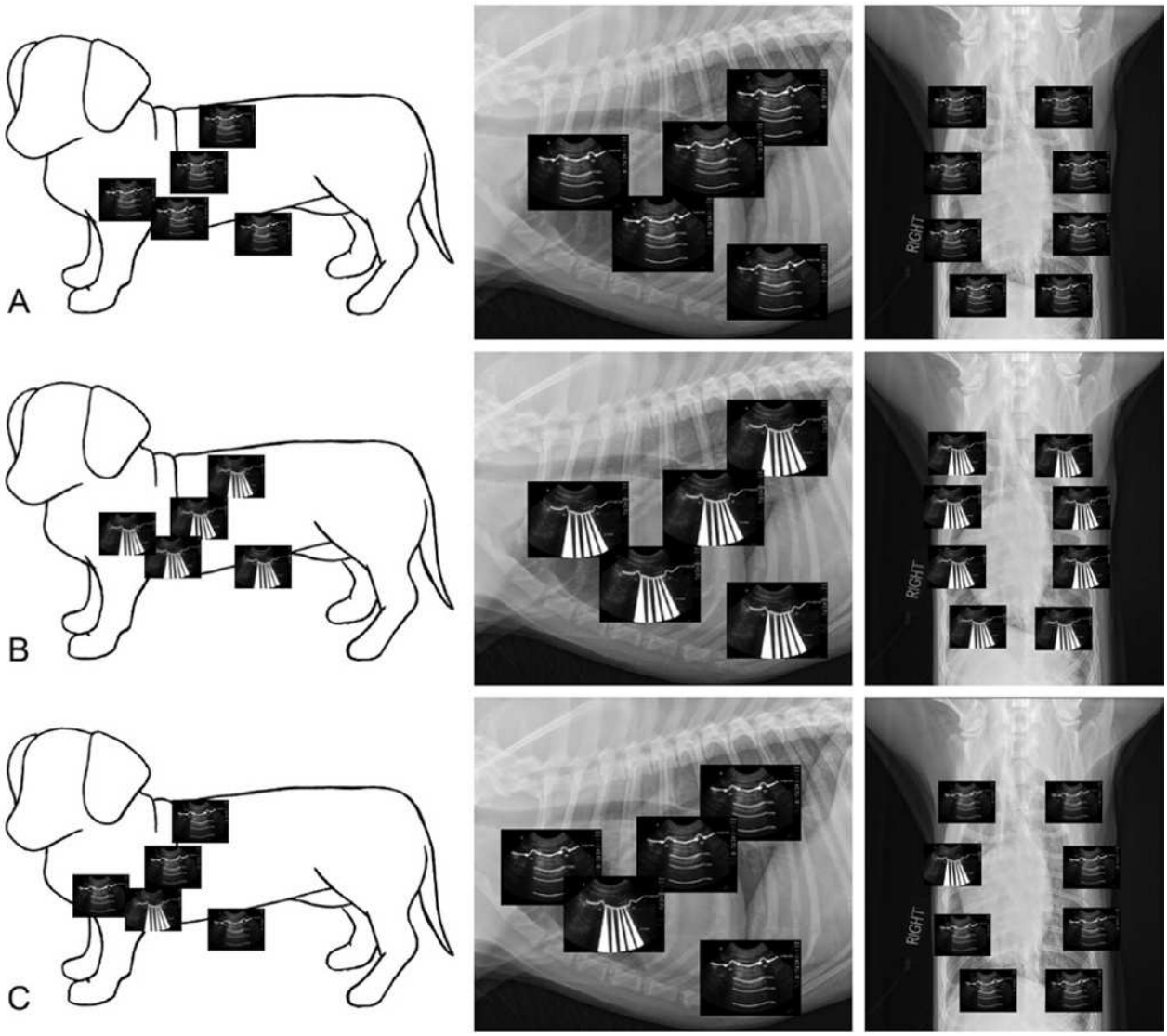


**Figure 23.32.** Coughing dog post anesthesia event. This heart disease (class B2) patient had a "dry lung" Vet BLUE profile before anesthesia (dental procedure). The following day the dog was coughing. (A) Vet BLUE supports upper airway inflammation such as endotracheal irritation or mainstem bronchial compression *without* clinically relevant cardiogenic lung edema. (B) The Vet BLUE profile supports cardiogenic pulmonary edema. (C) The Vet BLUE profile supports aspiration pneumonia. Vet BLUE provides a rapid screening test for a point-of-care working diagnosis to help direct diagnostics and therapy and may be used in a serial manner for monitoring. Line with rounding and an interposing straight line represents the intercostal space and the "gator sign" orientation. Source: Reproduced with permission of Dr Gregory Lisciandro, Hill Country Veterinary Specialists and FASTVet.com, Spicewood, TX.

"fluid positive" or "fluid negative." There is so much more to gain during similar amounts of time through standardized, structured views of the TFAST-Vet BLUE approach, and the Global FAST approach, by also surveying the abdomen using AFAST (done in standing in respiratory compromised patients).

The following are important factors that will reduce satisfaction of search error and provide more patient information for a better working diagnosis, therapeutic and diagnostic working plan.

### *Look for Pericardial Effusion*

The most common cause of pericardial effusion in cats is congestive heart failure. Other causes are possible but less common. In one study, pericardial effusion

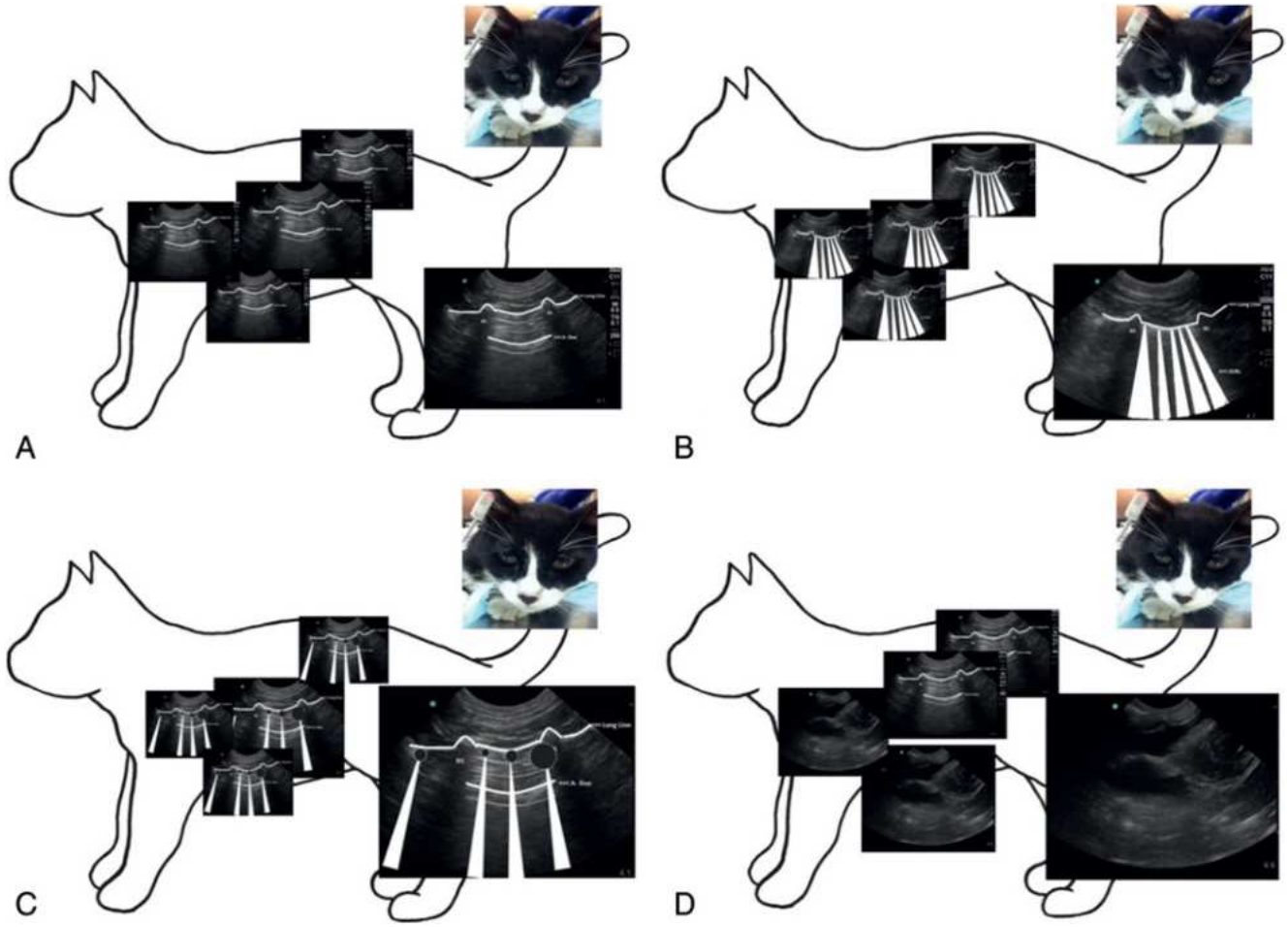


**Figure 23.33.** Respiratory distress feline. (A) The Vet BLUE profile is "Dry Lung All (Vet BLUE) Views" or "Absent B-lines All Views (ABAV)" that rapidly rules out left-sided CHF, which argues against the use of loop diuretics, and supports feline asthma as the most common working diagnosis (see Table 23.3). (B) The Vet BLUE profile is "wet" supporting the working diagnosis of left-sided CHF. Other generalized wet Vet BLUE profiles are listed (see Tables 23.2 and 23.4). (C) The Vet BLUE profile shows multiple nodules of various sizes at multiple views, supporting the working diagnosis of a granulomatous or neoplastic process. In (D) the lung is "dry" in the dorsal Vet BLUE views and pleural effusion is present ventrally. By looking past the "lung line," important information in the pleural effusion cat is gained using the "wet lung" versus "dry lung" concept as well as observing for the other Vet BLUE lung ultrasound signs. Serial Vet BLUE exams are important in cases of pleural effusion to distinguish between pressure atelectatic lung and true pathology. Line with rounding and an interposing straight line represents the intercostal space and the "gator sign" orientation. Source: Reproduced with permission of Dr Gregory Lisciandro, Hill Country Veterinary Specialists and FASTVet.com, Spicewood, TX.

was caused by CHF in 75% of the study population of cats (Hall et al. 2007). However, more recently a study showed that feline pericardial effusion, in any degree from scant to more severe, was 100% specific for CHF in cats presenting to North Carolina State and Iowa State veterinary colleges including those with concurrent pleural effusion (Ward et al. 2018a). However, the attending clinician must consider other endemic diseases in their area, for example prevalence of feline infectious peritonitis (FIP), retroviral positive cats and lymphoma, and other infectious diseases. Still, the presence of pericardial effusion with or without pleural effusion puts CHF highest on the differential list, and looking for PCE is generally an easy task with increased depth and minimal patient restraint. Moreover, looking at lung using Vet BLUE provides additional important information over a "flash exam."

### *Look at the "Lung Line"*

In pleural effusion cats, not only look for pericardial effusion but also look at the lung surface using Vet BLUE and its six lung ultrasound signs. For example,

VetBooks.ir

"dry lung," lung sliding and A-lines rule against aggressive loop diuretic therapy and for delaying or administering lower doses. "Wet lung" gives evidence-based information that loop diuretics are potentially indicated because left-sided CHF may be present. Additional findings of the shred sign and tissue sign suggest marked to severe lung consolidation that must be placed into clinical context. The nodule sign generally suggests neoplastic or granulomatous disease (fungal, parasitic) and the wedge sign in Caudodorsal and Perihilar lung regions suggests PTE. Atelectatic lung can cause "wet lung" artifacts as well as forms of consolidation due to pressure atelectasis, making repeat or serial examinations after thoracocentesis necessary to see if the Vet BLUE lung findings resolve or persist.

#### *Considering Pressure Atelectatic Lung*

This is a very good clinical question. Are the Vet BLUE lung signs of "wet lung," shred sign, and tissue sign in fact a result of pressure atelectasis? Each could very well be, so the best strategy is to treat and reassess. As a general rule, atelectatic lung resolves post thoracocentesis in spontaneously breathing patients within three hours (three-hour rule), as shown in a recent pilot study of 63 dogs (Lisciandro and Fosgate 2018). Clinical studies in feline cases are warranted, but at least the "three-hour rule" derived from dogs gives the attending clinician a general guideline and stresses the importance of serial (repeat) Vet BLUE exams. Persistence of abnormal Vet BLUE findings of >3 hours suggests that the lung lesions are more than pressure atelectasis, placed into clinical context and used to develop a more streamlined diagnostic plan (lung lobe aspirate, different types of fluid analysis testing, direct airway evaluation and sampling, CT, etc.).

The use of this TFAST-Vet BLUE approach in cats (and dogs) provides clear advantages over TXR because TXR is a less reliable evaluation of the lung surface and intrathoracic abnormalities in the presence of pleural effusion, and ineffective for diagnosing pericardial effusion (ultrasound is arguably the gold standard test) (Guglielmini et al. 2012; Côté et al. 2013).

# Monitoring Applications for Vet BLUE

## *Vet BLUE for Left-sided Congestive Heart Failure and Volume Overload*

Effective uses of Vet BLUE include determination of whether clinically relevant left-sided heart failure is present (Lichtenstein and Mezière 2008; Lichtenstein and Karakitsos 2012; Lisciandro et al. 2014, 2016, 2017; Lee et al. 2015; Ward et al. 2017) and evaluating the current status of the patient's lung relative to degrees of alveolar-interstitial edema (left-sided congestion, extravascular lung water) (Gargani et al. 2007; Peris et al. 2010; Jambrik et al. 2010). In probably any and all mammalian lung, the finding of "dry lung all (Vet BLUE) views" (or ABAV) rules out with high sensitivity (>96%) any clinically relevant left-sided CHF (Lichtenstein and Mezière 2008; Lichtenstein et al. 2009a; Volpicelli et al. 2012; Lisciandro et al. 2014, 2016, 2017; Ward et al. 2017). Conversely, the presence of B-lines supports the diagnosis of left-sided CHF, especially when using the VSP model, and in dogs when distributed in the upper (dorsal) lung views of the Caudodorsal and Perihilar areas (pneumonia being predominantly ventrally distributed, being gravity dependent) (Ward et al. 2017, 2019). Assessment of the LA:Ao ratio is by far the most important additional piece of information, the so-called "quick peek" echo view. Interestingly, in people discharged after having left-sided CHF, those with persistent B-lines are more likely to return sooner with recurrence of left-sided CHF than those having "dry lung" on their exit exams (Gargani et al. 2015).

It is so important to realize that a dog or cat with "dry lung all (Vet BLUE) views" (ABAV) can have other intrathoracic pathology that is missed without always combining Vet BLUE and TFAST (see Table 23.4). A good example is PCE that often results in respiratory distress in both dogs and cats. Being predominantly a right-sided phenomenon in dogs, the Vet BLUE profile is expected to be "dry lung" all views (ABAV) whereas in cats lung likely would be wet because their most common cause for PCE is congestive heart failure (Hall et al. 2007; Ward et al. 2018a), so by only performing Vet BLUE as a standalone format, the PCE is missed. In canine PCE, Global FAST should be performed as the patient may have a midabdominal mass that is missed and AFAST with an abdominal fluid score allows you to rule in and rule out effusion, whether a modified transudate or a hemoabdomen, and semiquantitate the volume when present. Another example that is very common is the coughing dashchund or Shetland sheepdog that has respiratory signs and some with persistent cough. The Vet BLUE is dry all views (ABAV), but the dog has a left atrial tear/rupture, a serious complication of chronic mitral valve disease, that would be missed and treatment potentially erroneously pursued as increased cardiogenic edema without Vet BLUE. Moreover, think about this hemodynamically fragile patient being restrained in radiology risking the patient coding (cardiopulmonary arrest, CPA), or having an

unremarkable thoracic radiograph that missed the PCE caused by the left atrial rupture/tear (Guglielmini et al. 2012; Côté et al. 2013).

For efficiency, we recommend doing a Vet BLUE-TFAST blend by, for example, doing a left Vet BLUE from Caudodorsal (Cd) to Perihilar (Ph) to Middle (Md) to Cranial (Cr) lung regions then sliding caudally over the left TFAST PCS and imaging the heart and interrogating for pleural effusion followed by the DH view from the patient's left side. After the DH, move to the patient's right side and make the depth shallow (4–8 cm) for Vet BLUE performing the right Cd to Ph to Md to Cr before ending at the right TFAST PCS, and its most time-consuming echo views. However, prior to the TFAST right PCS, the sonographer already knows if the lungs are predominantly wet or dry, and where the lung pathology exists, if any, if any pleural effusion (PE) or PCE is present, and how the caudal vena cava and hepatic veins are characterized. Thus, by our recommended Vet BLUE-TFAST order, the sonographer gains a good idea of how important the TFAST echo views at the right PCS view are by ending at them.

## Vet BLUE for Pulmonary Hypertension

Dogs with pulmonary hypertension (PHT) not uncommonly have alveolar-interstitial edema (Kellihan et al. 2015; Kulhavy and Lisciandro 2018). This is very important to recognize because the PHT-pulmonary edema is refractory to loop diuretics and the "quick peek approach" will miss the problem, a danger in POCUS heart examination without a Global FAST approach. These TFAST right-sided cardiac markers (R-SCMs) are defined as (1) an enlarged right ventricular to left ventricular ratio on long axis (RV:LV), (2) a FAT caudal vena cava with hepatic venous distension, (3) gallbladder wall edema, and (4) ascites at the FAST DH view. The findings of an increased RV:LV and a FAT caudal vena cava with hepatic venous distension (tree trunk sign) should *always* warrant a complete detailed echocardiogram. The true sensitivity and specificity of TFAST R-SCMs are under study for detecting different subsets of right-sided heart disease, but a recent study suggested that the nonecho TFAST R-SCMs, i.e., excluding the RV:LV, were not effective as a screening test for canine PHT, concluding that a complete echocardiogram is necessary to rule in or out this subset of right-sided canine heart disease (Vientós-Plotts et al. 2019). However, it should be kept in mind that the addition of TFAST echo views (and POCUS heart – focused cardiac ultrasound), including an increased right ventricular to left ventricular ratio (RV:LV), interventricular flattening at the short-axis left ventricular mushroom view, and an increased pulmonary artery to aortic ratio on short-axis (PA:Ao), may increase the effectiveness of this type of first-line screening test for PHT in dogs (see Figures 37.6, 17.25 and 17.26).

## Vet BLUE for Pneumonias

Vet BLUE may be used for tracking (monitoring) pneumonias by recording findings at the regional views and expecting in resolving pneumonias to see the most consolidated/abnormal lung signs resolving to B-lines followed by "dry lung" (A-lines and "lung sliding"). On the other hand, worsening pneumonia will progress from alveolar-interstitial edema ("wet lung") of B-lines to shred sign to tissue sign and possibly, depending on the type of pneumonia, nodule sign. Findings must be recorded and of course a definitive diagnosis sought through gold standard testing to make sure that the diagnosis is correct (bronchoalveolar lavage [BAL], blind BAL, endotracheal wash, fungal testing, lung lobe aspirates, lung biopsy, additional imaging studies). The Vet BLUE examination provides a monitoring tool to trigger additional intervention, testing, and imaging along the patient's clinical course that is low cost, effective, and gives clinicians more confidence using this ancillary imaging modality. Vet BLUE should be combined with Global FAST because other comorbidities may be developing that will be otherwise missed. For example, a feline patient had respiratory signs and maybe a more conservative approach was pursued and on recheck, the spleen is now enlarged (>1 cm) and a splenic aspirate, a safer procedure than a lung lobe aspirate or less costly than a thoracic CT, is performed, yielding the diagnosis of feline histoplasmosis. Without this Global FAST approach, tunnel vision takes the feline down a different path possibly with delays and more risk (and more cost).

## Vet BLUE for Nodular Disease

Vet BLUE may also be used to monitor response to therapy by measuring changes in the size and numbers of nodule(s) (neoplastic, fungal, bacterial or other types of granulomas). The use of Vet BLUE and lung ultrasound in this manner can help determine whether the chemotherapy or antifungal or anthelminthic or antibiotic therapy is working more effectively and with less cost than serial thoracic radiography or CT, carrying the potential that medication strategies may be changed sooner than later. The advantage of Vet BLUE over other published formats is that Vet BLUE has discrete defined regions that may be evaluated, scored and findings recorded that can then be compared and followed.

# The Future of Proactive Vet BLUE and Lung Ultrasound in Small Animals

The use of proactive Vet BLUE lung ultrasound is novel. Historically, lung ultrasound in small animals has primarily been utilized as a secondary imaging pulmonary modality based on thoracic radiography, ironically a less sensitive modality. We are not reinventing the wheel, and large animal practitioners, especially on the equine side, have been using LUS for a couple of decades, but their approach generally lacks a visual easily understandable lung language and discrete regions like Vet BLUE in which locations may be scored and patient data recorded for future comparison. Vet BLUE through its standardization serves as a platform for clinical research regarding the sensitivity, specificity, and accuracy of the regional pattern-based LUS examination for acute and chronic respiratory conditions, and continues to accelerate the long overdue general use of LUS in small animals. Finally, Vet BLUE may be the greatest advancement for respiratory medicine and possibly veterinary medicine this decade, regarding its impact on care. It is worth learning and implementing Vet BLUE on a daily basis.

# Recording Vet BLUE Findings on Goal-Directed Templates

# Case Examples of Vet BLUE Advantage over Thoracic Radiography

Vet BLUE has advantages over TXR on several fronts, including being low impact, point-of-care imaging and extremely sensitive for lung surface pathology.

**Table 23.5.**
Template for Vet BLUE.

**Ask yourself:** Wet vs Dry? Number of B-lines? Anything off the "lung line"? Are you mistaking abdominal contents for lung pathology?

**Left Cd** 0 ☐ 1–3 ☐ >3 ☐ ∞ ☐
Sh ☐ __cm Ti ☐__cm Nd ☐__cm Wedge ☐__cm OR indeterminate ☐ not assessed ☐
**Ph** 0 ☐ 1–3 ☐ >3 ☐ ∞ ☐
Sh ☐ __cm Ti ☐__cm Nd ☐__cm Wedge ☐__cm OR indeterminate ☐ not assessed ☐
**Md** 0 ☐ 1–3 ☐ >3 ☐ ∞ ☐
Sh ☐ __cm Ti ☐__cm Nd ☐__cm Wedge ☐__cm OR indeterminate ☐ not assessed ☐
**Cr** 0 ☐ 1–3 ☐ >3 ☐ ∞ ☐
Sh ☐ __cm Ti ☐__cm Nd ☐__cm Wedge ☐__cm OR indeterminate ☐ not assessed ☐
Comments_____

**Right Cd** 0 ☐ 1–3 ☐ >3 ☐ ∞ ☐
Sh ☐ __cm Ti ☐__cm Nd ☐__cm Wedge ☐__cm OR indeterminate ☐ not assessed ☐
**Ph** 0 ☐ 1–3 ☐ >3 ☐ ∞ ☐
Sh ☐ __cm Ti ☐__cm Nd ☐__cm Wedge ☐__cm OR indeterminate ☐ not assessed ☐
**Md** 0 ☐ 1–3 ☐ >3 ☐ ∞ ☐
Sh ☐ __cm Ti ☐__cm Nd ☐__cm Wedge ☐__cm OR indeterminate ☐ not assessed ☐
**Cr** 0 ☐ 1–3 ☐ >3 ☐ ∞ ☐
Sh ☐ __cm Ti ☐__cm Nd ☐__cm Wedge ☐__cm OR indeterminate ☐ not assessed ☐
Comments_____

**DH**0 ☐ 1–3 ☐ >3 ☐ ∞ ☐
Sh ☐Ti ☐ Nd ☐Wedge ☐ OR indeterminate ☐ not assessed ☐
Comments _____
Conclusion _____

Sh, shred sign;Ti, tissue sign; Nd, nodule. Cd, Caudodorsal lung region; Cr, Cranial lung region; Md, Middle lung region; Ph, Perihilar lung region.
**Qualifier:** The Vet BLUE lung ultrasound exam is a screening test for many conditions that affect the lung surface such as heart failure, pneumonia, nodular disease and others. Vet BLUE helps characterize respiratory conditions as a screening test. Vet BLUE is not meant to replace thoracic radiography or computed tomography.
Created by Gregory Lisciandro, DVM, DABVP, DACVECC, CEO of FASTVet.com and President, International Veterinary Point-of-care Ultrasound Society, IVPOCUS.org.

VetBooks.ir

Common diseases make it to the lung surface, and thus Vet BLUE is an effective means to rapidly categorize veterinary patients using its regional, pattern-based approach, ranging from left-sided CHF to pneumonia to pulmonary thromboembolism to nonrespiratory look-alikes to different types of nodular disease. Moreover, through the recording of results, lung conditions may be tracked or monitored using Vet BLUE. Some everyday examples are presented below.

## *Aspiration Pneumonia and Other Bacterial Pneumonias*

The finding of the shred sign in gravity-dependent Vet BLUE views, Cranial and Middle lung regions, strongly supports the presence of aspiration pneumonia and bacterial pneumonias (Figure 23.34; see also Figures 23.29 and 23.32). Nebulous TXR findings may be better clarified through the use of Vet BLUE. The bulldog cross has an expiratory TXR and coupled with its conformation is problematic in interpretation. However, a Vet BLUE clearly shows "dry lung" at all Vet BLUE views except the right and left Middle (Md) and Cranial (Cr) lung regions that rule in aspiration pneumonia until proven otherwise. The case could have been a hospitalized vomiting parvoviral puppy or pancreatitic dog, any postoperative case, a dog with laryngeal paralysis, a dog with CHF with worsening respiratory signs, a brachiocephalic breed, etc. The list goes on and on. The use of Vet BLUE as a screening test is obvious and detection of the shred sign is readily learned with proper training.

### Vet BLUE Template (Caudodorsal [Cd], Perihilar [Ph], Middle [Md], Cranial [Cr])

Left: 0, 0, Shred 3 cm, Shred 3 cm
Right: 0, 0, Shred 2.5 cm, 0
Diaphragmatico-Hepatic View: 0

## *Old Dog Lungs*

The case is an older mixed-breed dog who has gastrointestinal signs and has just had a complete detailed abdominal ultrasound by a specialist with a mobile consulting service, confirming the working diagnosis of pancreatitis. The dog had an intermittent cough so the primary care veterinarian performed a three-view TXR that also included the abdomen. The thoracic radiograph was read out as "old dog lungs" by the board-certified radiologist (Figure 23.35). The primary care veterinarian was not confident with the TXR diagnosis and having been trained in Global FAST, performed Vet BLUE, finding various sized nodules. The working diagnosis was then changed to a neoplastic process with complicating pancreatitis and the dog approached much differently with palliative care. The nodules were followed using Vet BLUE in recheck examinations, increased in size and the respiratory signs worsened over the following three weeks. The Vet BLUE alternatively may have detected shred signs in gravity-dependent lung region views and the pancreatitis dog could very well have had the complication of aspiration pneumonia missed or nebulous (occult) on TXR (see Figure 23.34).

### Vet BLUE Template (Caudodorsal [Cd], Perihilar [Ph], Middle [Md], Cranial [Cr])

Left: Nodules (1–4 mm) × 4, nodules (1–4 mm) × 2, nodules (2–3 mm) × 3, nodule (3 mm) × 1
Right: Nodule (3–4 mm) × 1, nodules (1–4 mm) × 3, nodules (2–3 mm) × 2, 0
Diaphragmatico-Hepatic View: Nodules (1–3 mm)

## *Lung Nodules – Fungal Granulomas*

A 5-year-old spayed female, English springer spaniel is scheduled for a complete detailed abdominal ultrasound to search for a cause for two weeks of weight loss, fever and rare dry cough. Basic lab work including blood testing is unremarkable, as is the physical examination. The complete detailed abdominal ultrasound is unremarkable. The cough is so intermittent that the decision to treat conservatively is made, a historically typical approach in the author's experience. In this scenario, the dog is sent home with antibiotics and fails therapy. A few days later the client phones the veterinarian who changes the antibiotic and again the dog fails therapy. Now 5–7 days later, failing two different antibiotics, the dog returns for imaging. The patient is scheduled for an endotracheal wash or referred for BAL with airway sampling and testing. The diagnosis may be made (or not, further delayed) and results from the BAL (or other airway sampling), including culture, further delay definitive care. The upshot is that the diagnosis has been delayed for several days and possibly up to two weeks. Let's consider another scenario – the client determines that the cough is no big deal and watches the dog's respiratory signs worsen for the next three weeks until ultimately rechecking at the point of respiratory distress. Thoracic radiographs now have severe changes in the lungs. The respiratory disease has become advanced and the opportunity to treat and cure, diminished.

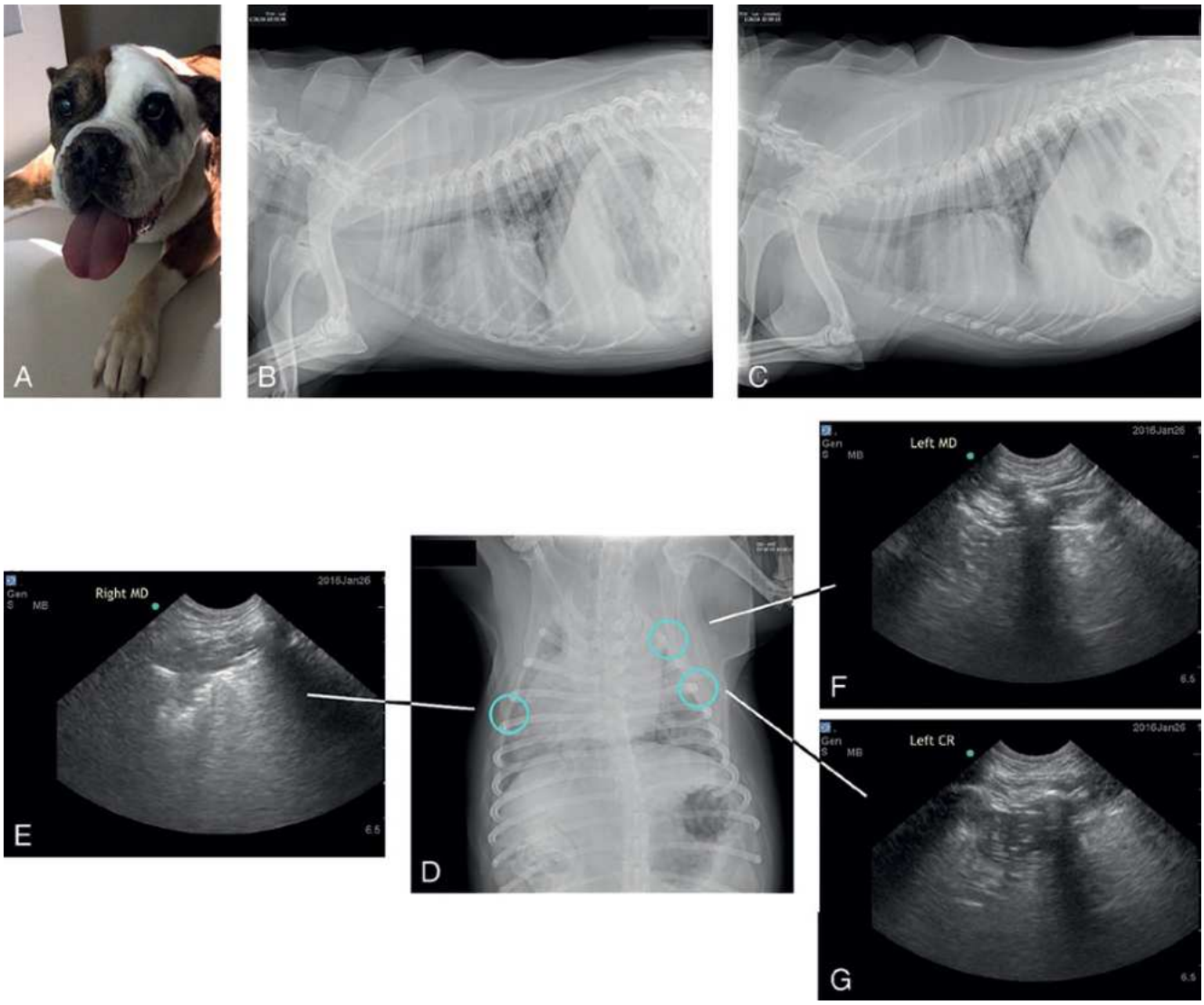


**Figure 23.34.** Aspiration pneumonia detected on Vet BLUE over thoracic radiography. (A) This dog presents with respiratory signs and harsh lung sounds all fields on auscultation, an insensitive test. The TXR is difficult to interpret because of it being expiratory and the conformation of the bulldog cross with right lateral in (B), left lateral in (C) and ventrodorsal in (D). The Vet BLUE clearly shows shred sign in right Middle (E), left Middle (G) and Cranial (F) lung regions, an imaging test that is performed without restraint, in standing or sternal, and rapidly in <90 seconds. Recording your findings on goal-directed templates establishes credibility for your ultrasound examination (see Table 23.5). Source: Reproduced with permission of Dr Gregory Lisciandro, Hill Country Veterinary Specialists and FASTVet.com, Spicewood, TX and Dr Kyle Crowley, Acres North Animal Hospital, San Antonio, TX.

The new paradigm involves the Global FAST approach because Vet BLUE by itself misses other comorbidities in the thorax and abdomen that may have significant relevant consequences for patient care. In the new approach, Vet BLUE clearly shows multiple nodules, some as large as 5.2 mm and 7.2 mm in diameter, that are missed on the TXR (Figure 23.36). This important clinical information is garnered on day 1 of care, immediately following the complete detailed abdominal ultrasound. Digital radiography has been purported to detect nodules as small as 3 mm, but TXR misses these larger 5.2 and 7.2 mm nodules. These Vet BLUE findings trigger fungal testing on day 1 (or a lung lobe aspirate), and the diagnosis of coccidioidomycosis is expediently made, giving the opportunity to treat (and monitor) when the disease is early in its course. This is great patient care with the opportunity to cure!

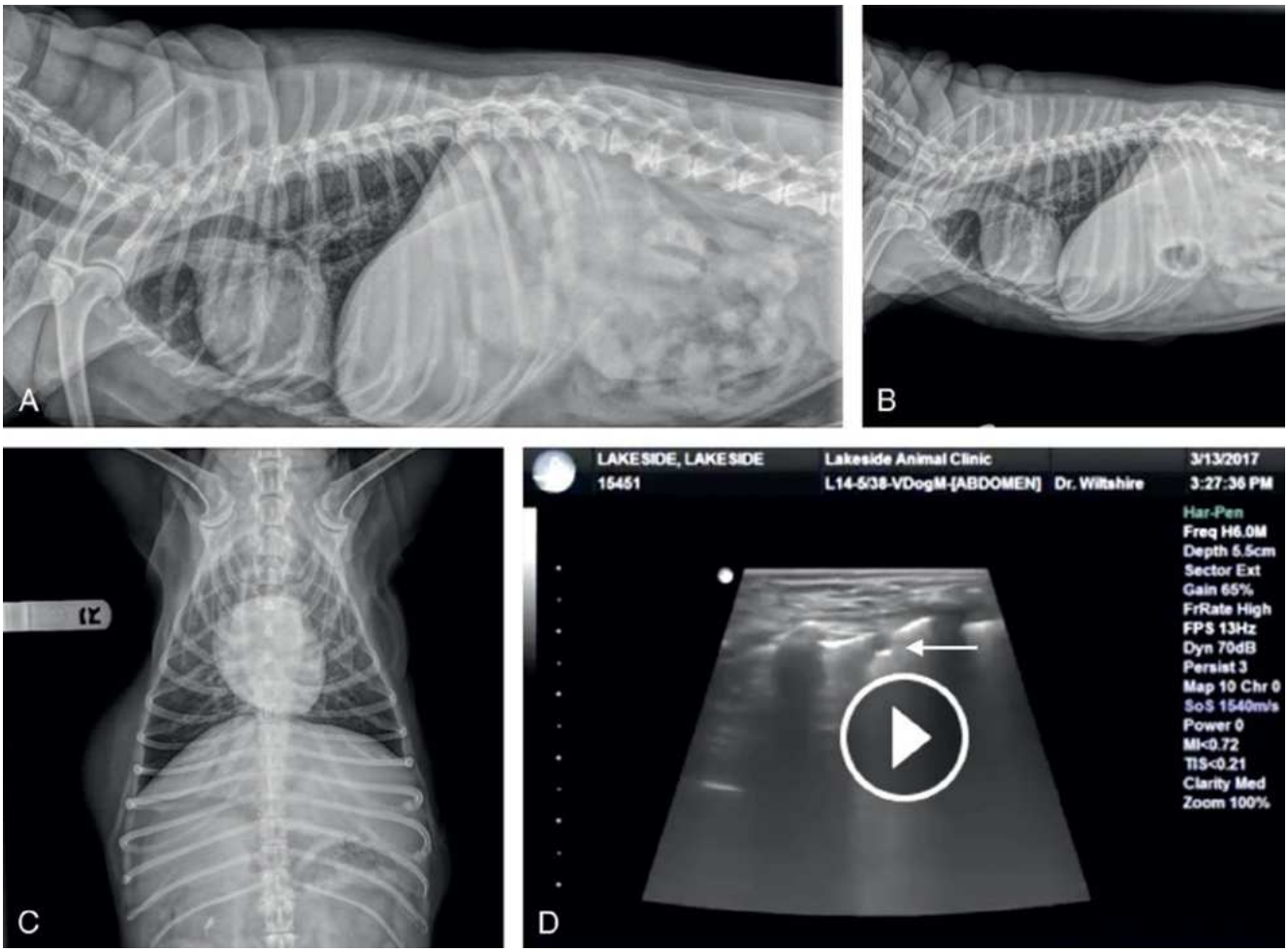


**Figure 23.35.** Old dog lungs. The "old dog lungs" on three-view radiography (XR) (A–C) that were in fact many nodules of various sizes 1–4 mm seen during Vet BLUE but occult (missed) on thoracic radiography (TXR) shown in (D). The arrow points to the nodule sign and its size can be estimated from the centimeter scale on the screen or measured with calipers as in Figure 23.35. The nodule sign as a rule should be accompanied by a "pseudo B-line." These "pseudo B-lines" are created similar to true B-lines by a strong difference in acoustic impedance; however, the difference is between fluid–air in AIS and between soft tissue–air with the nodule sign. Source: Reproduced with permission of Dr Gregory Lisciandro, Hill Country Veterinary Specialists and FASTVet.com, Spicewood, TX, and Dr Randy Wiltshire, Lakeshore Animal Clinic, Houston, TX.

### Vet BLUE Template (Caudodorsal [Cd], Perihilar [Ph], Middle [Md], Cranial [Cr])

Left: Nodule (5.2 mm) × 1, nodule (7.2 mm) × 1, 0, nodule (3 mm) × 1

Right: 0, nodules (3.7 mm) × 1, 0, 0

Diaphragmatico-Hepatic View: 0

## *Determining Whether a Lung Lobe Aspirate Would Be a Productive Test*

Historically, TXR has been used to determine if lung disease is present along the lung periphery. Vet BLUE provides an extremely sensitive modality to evaluate the lung surface for the presence of significant lung surface disease amenable to percutaneous lung sampling. In Figure 23.37 the older cat has a centrally located, away from the thoracic wall, mass in the left caudal lung lobe appearing too far away for percutaneous sampling. Moreover, it is unclear if the mass represents localized or disseminated disease. Using a Global FAST approach, the patient may be surveyed for obvious additional comorbidities as well as for any evidence of lung pathology along the lung surface. The Vet BLUE shows many small 1–3 mm nodules along the lung surface at multiple views. A lung lobe aspirate now becomes a viable diagnostic intervention and

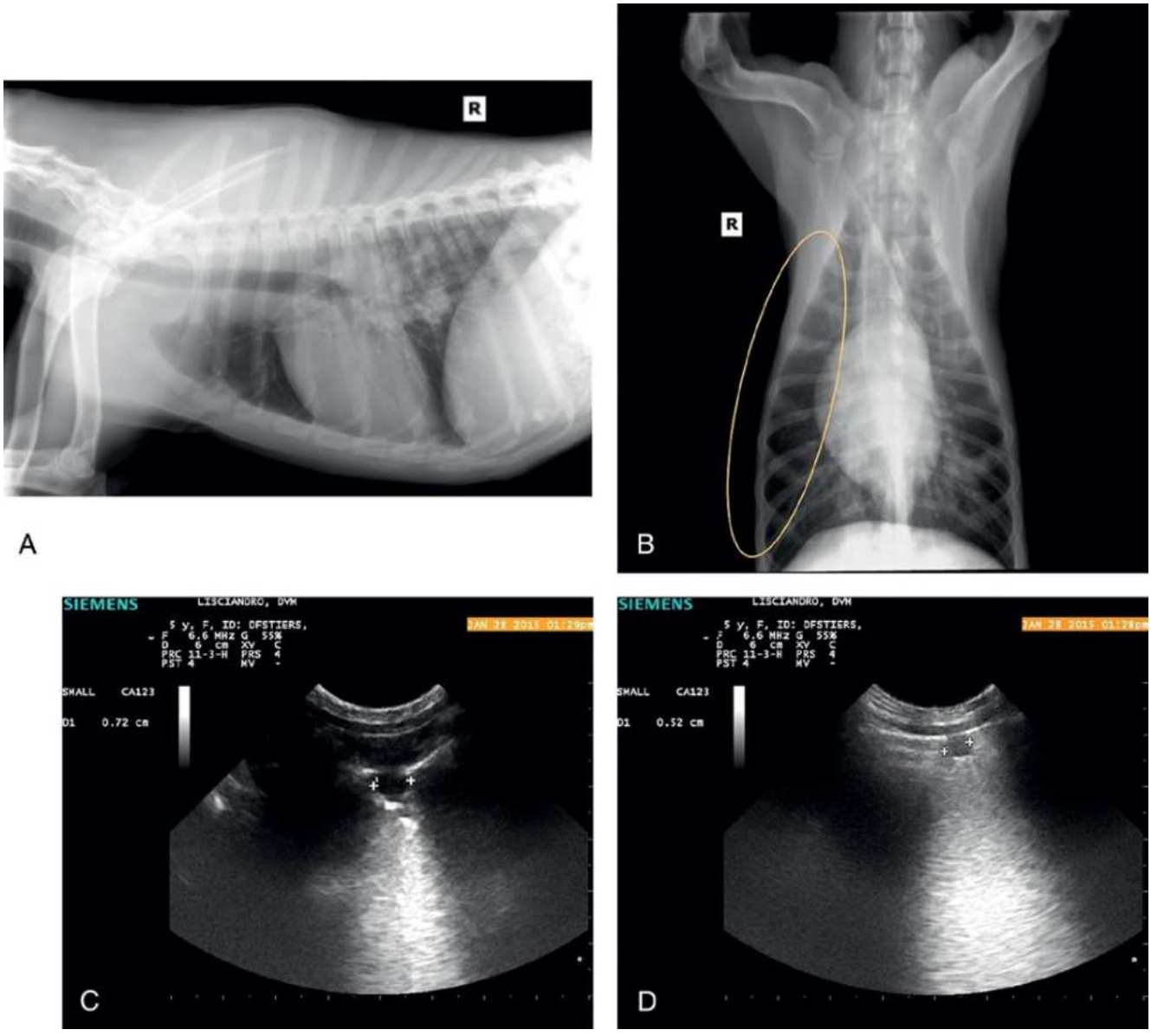


**Figure 23.36.** Fungal granulomas easily detected on Vet BLUE missed on thoracic radiography. (A,B) Digital radiographs of a dog with perihilar lymphadenopathy and a two-week history of intermittent fever and weight loss with a sporadic dry cough. The TXR was performed because of the Vet BLUE findings of the nodule sign. (C,D) Vet BLUE images that correlate with the TXR show the obvious nodule sign. These nodules are measured with calipers as 5.2 and 7.2 mm. Each nodule sign has a "pseudo B-line" associated with it. The circled area emphasizes that these nodules are undetected on TXR along all visible radiographic lung surfaces. The finding of the nodule sign triggered fungal testing and captured the case on day 1 with a diagnosis of coccidioidomycosis. This case exemplifies how a Vet BLUE–Global FAST approach on initial presentation provides game-changing care in a case that likely would have been delayed or missed without this approach. Source: Reproduced with permission of Dr Gregory Lisciandro, Hill Country Veterinary Specialists and FASTVet.com, Spicewood, TX, and Dr Stephanie Lisciandro, Hill Country Veterinary Specialists and Oncura Partners, Austin, TX.

these findings better direct the next best test(s) by placing the evidence of disseminated disease into clinical context (neoplasia versus fungal versus parasitic versus other).

### Vet BLUE Template (Caudodorsal [Cd], Perihilar [Ph], Middle [Md], Cranial [Cr])

Left: Nodules (1–3 mm) >4, nodules (1–3 mm) >4, nodules (1–3 mm) >4, nodules (1–3 mm) >4

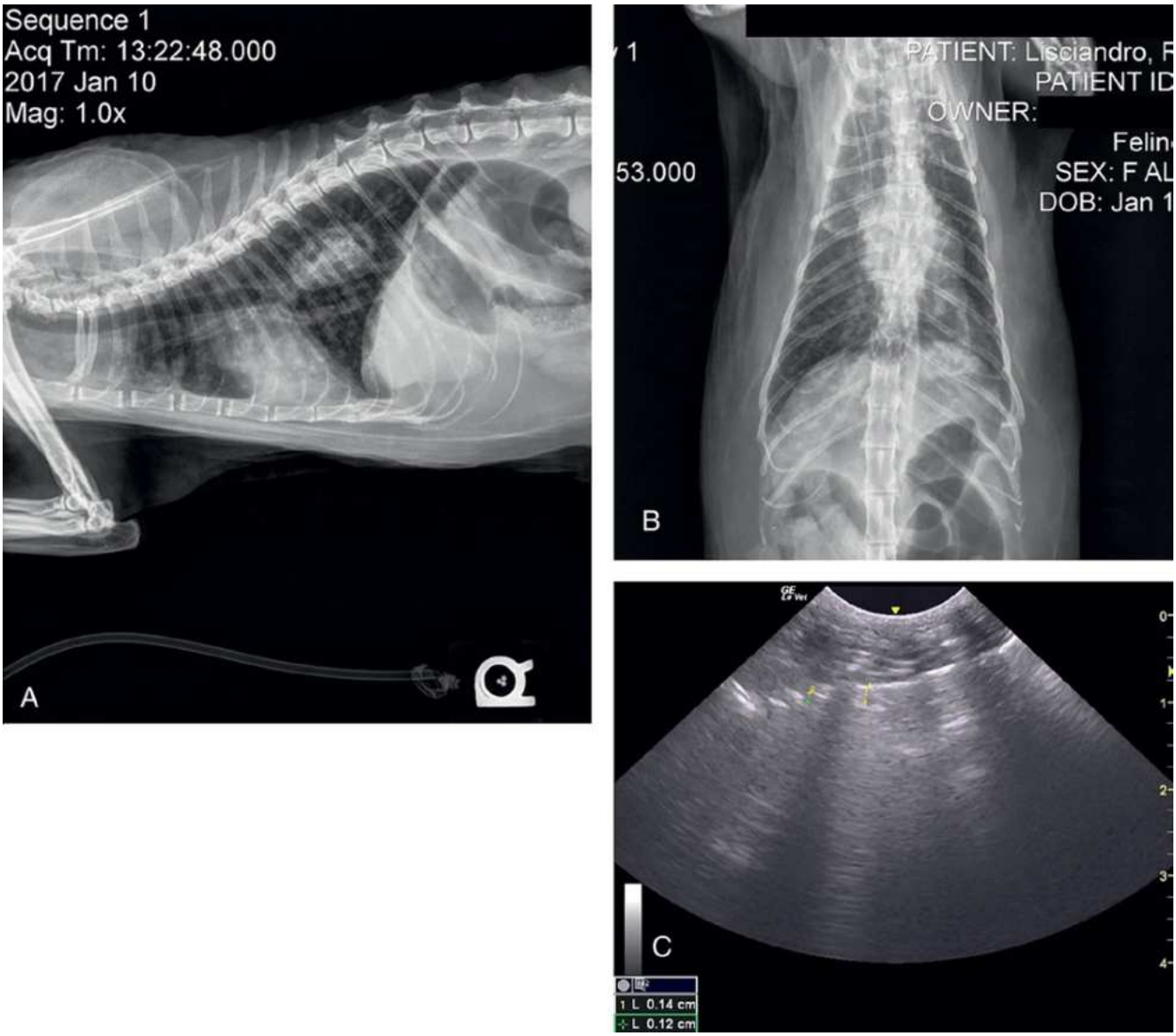


**Figure 23.37.** Primary lung lobe mass versus disseminated lung disease. The three-view thoracic radiograph (TXR) in (A) and (B) is questionable and potentially misses the presence of lung surface disease in this older cat with respiratory signs and an obvious caudodorsal lung lobe mass. Historically, the decision has been made based on TXR on whether percutaneous lung lobe sampling is a diagnostic option. In this cat, Vet BLUE clearly showed many obvious 1–3 mm nodules at multiple views, shown in (C) and measured with the calipers. The presence of these small nodules indicates two things: (1) that disease is disseminated (versus localized) and that a lung lobe aspirate is a diagnostic option with high probability for a diagnosis. This case exemplifies how disseminated disease may be missed without the Vet BLUE–Global FAST approach. Source: Reproduced with permission of Dr Gregory Lisciandro, Hill Country Veterinary Specialists and FASTVet.com, Spicewood, TX.

Right: Nodules (1–3 mm) >4, nodules (1–3 mm) >4, nodules (1–3 mm) >4, nodules (1–3 mm) >4

Diaphragmatico-Hepatic View: >B-lines, possible small nodules.

# Pearls and Pitfalls, The Final Say

- Vet BLUE is the most studied lung ultrasound examination in veterinary medicine.
- Vet BLUE provides a regional pattern-based approach that surveys three intercostal spaces at each transthoracic view.
- The identification of the transition zones helps to avoid mistaking abdominal structures for lung pathology and makes the examination more repeatable between colleagues and with recheck examinations.
- Vet BLUE is the fastest and safest way in which to rule out left-sided CHF in both dogs and cats.

- Vet BLUE has a "visual lung language" that helps with communication of findings.
- Vet BLUE has a B-line scoring system to better estimate the degree of alveolar-interstitial edema.
- Vet BLUE and its B-line scoring system help to direct diuretic usage in left-sided CHF patients.
- Vet BLUE has a lung contusion scoring system.

# Quick Reference of Normals and Rules of Thumb

- Expect adult dogs and cats and puppies and kittens >6 weeks of age to have "dry lung" artifacts predominate (absent B-lines). In other words, no more than a single B-line at only one of the eight transthoracic Vet BLUE views.
- Numbers of B-lines correlate to the degree of alveolar-interstitial edema in human lung and likely in other mammalian lung, including small animals.
- "Absent B-lines all (Vet BLUE) views (ABAV)" rules out clinically relevant left-sided CHF in both dogs and cats (and likely for all mammalian lung).
- The Volpicelli Strong Positive model is an effective screening test to rule in left-sided CHF in cats.
- Shred sign in gravity-dependent Vet BLUE views supports aspiration and bacterial bronchopneumonia.
- Wedge sign in the dorsal nongravity-dependent Vet BLUE views supports pulmonary thromboembolism.
- Nodule sign supports neoplastic, granulomatous processes including fungal, parasitic and bacterial, and abscessation.

# References


Alexander K, Joly H, Blond L, et al. 2012. A comparison of computed tomography, computed radiography, and film-screen radiography for the detection of canine pulmonary nodules. *Vet Radiol Ultrasound* 53(3):258–265.

Alpert JB, Lowry CM, Ko JP. 2015. Imaging the solitary pulmonary nodule. *Clin Chest Med* 36(2):161–178.

Anile A, Russo J, Castiglione G, et al. 2017. A simplified lung ultrasound approach to detect increased extravscular lung water in critically ill patients. *Crit Ultrasound J* 9:13

Armbrust LJ, Hoskinson JJ, Biller DS, et al. 2005. Comparison of digitized and direct viewed (analog) radiographic images for detection of pulmonary nodules. *Vet Radiol Ultrasound* 46(5):361–367.

Armbrust LJ, Biller DS, Bamford A, et al. 2012. Comparison of three-view thoracic radiography and computed tomography for detection of pulmonary nodules in dogs with neoplasia. *J Am Vet Med Assoc* 240(9):1088–1094.

Ball CG, Ranson MK, Rodriguez-Galvez M, et al. Sonographic depiction of posttraumatic alveolar-interstitial disease: the hand-held diagnosis of a pulmonary contusion. *J Trauma* 66(3):962.

Benigni L, Morgan N, Lamb CR. 2009. Radiographic appearance of cardiogenic pulmonary oedema in 23 cats. *Small Anim Pract* 50(1):9–14.

Bouyssou S, Specchi S, Desquilbet L, et al. 2017. Radiographic appearance of presumed noncardiogenic pulmonary edema and correlation with the underlying cause in dogs and cats. *Vet Radiol Ultrasound* 58(3):259–265.

Diana A, Guglielmini C, Pivetta M, et al. 2009. Radiographic features of cardiogenic pulmonary edema in dogs with mitral regurgitation: 61 cases (1998–2007). *J Am Vet Am Assoc* 235(9):1058–1063.

Dicker SA, Lisciandro GR, Newell SM, et al. 2019. Diagnosis of pulmonary contusions with point-of-care lung ultrasonography and thoracic radiography compared to thoracic computed tomography in dogs with motor vehicle trauma: 29 cases (2017–2018). *J Vet Emerg Crit Care*, in press.

Eberle N, Fork M, von Babo I, et al. 2010. Comparison of examination of thoracic radiographs and thoracic computed tomography in dogs with appendicular osteosarcoma. *Vet Comp Oncol* 9(2):131–140.

Filly RA. 1988. Ultrasound: the stethoscope of the future, alas. *Radiology* 167:400.

Fox PR. 1988. Canine myocardial disease. In: *Canine and Feline Cardiology*, edited by Fox PR. New York: Churchill Livingstone, pp 467–494.

Gargani L. 2019. Ultrasound of the lungs: more than a room with a view. *Heart Fail Clin* 15(2):297–303.

Gargani L, Volpicelli G. 2014. How I do it: Lung ultrasound. *Cardiovasc Ultrasound* 12:25.

Gargani L, Pang PS, Frassi F, et al. 2015. Persistent pulmonary congestion before discharge predicts rehospitalization in heart failure: a lung ultrasound study. *Cardiovasc Ultrasound* 13:40.

Gillman LM, Kirkpatrick AW. 2012. Portable bedside ultrasound: the visual stethoscope of the 21st century. *Scand J Trauma Emerg Med* 20:18.

Goggs R, Chan DL, Benigni L, et al. 2014. Comparison on computed tomography pulmonary angiography and point-of-care tests for pulmonary thromboembolism diagnosis in dogs. *J Small Anim Pract* 55:190–197.

Guglielmini C, Diana A, Santarelli G, et al. 2012. Accuracy of radiographic vertebral heart score and sphericity index in the detection of pericardial effusion in dogs. *J Am Vet Med Assoc* 241(8):1048–1055.

Ha YR, Toh HC. 2016. Clinically integrated multi-organ point-of-care ultrasound for undifferentiated respiratory difficulty, chest pain, or shock: a critical analytic review. *J Intensive Care* 4:54.

Hall DJ, Shofer F, Meier CK, Sleeper MM. 2007. Pericardial effusion in cats: a retrospective study of clinical findings and outcome in 146 cats. *J Vet Intern Med* 21(5):1002–1007.

Hecht S, Penninck D. 2015. Thorax. In: *Atlas of Small Animal Ultrasonography*, 2nd edition, edited by Penninck D, d'Anjou M. Ames: Wiley Blackwell, pp 81–110.

Jambrik Z, Monti S, Coppola V, et al. 2004. Usefulness of ultrasound lung comets as a nonradiologic sign of extravascular lung water. *Am J Cardiol* 93(10):1265–1270.

Jambrik Z, Gargani L, Adamicza A, et al. 2010. B-lines quantify the lung water content: a lung ultrasound versus lung gravimetry study in acute lung injury. *Ultrasound Med Biol* 36(12):2004–2010.

Johnson LR, Lappin MR, Baker DC. 1999. Pulmonary thromboembolism in 29 dogs: 1985–1995. *J Vet Intern Med* 13(4):338–345.

Kellihan HB, Waller KR, Pinkos A, et al. 2015. Acute resolution of pulmonary alveolar infiltrates in 10 dogs with pulmonary hypertension treated with sildenafil citrate: 2005–2014. *J Vet Cardiol* 17:182–191.

Kirkpatrick AW, Sirois M, Laupland KB, et al. 2004. Hand-held thoracic sonography for detecting post-traumatic pneumothoraces: the Extended Focused Assessment with Sonography for Trauma (EFAST). *J Trauma* 57(2):288–295.

Kulhavy DA, Lisciandro GR. 2015. Use of a lung ultrasound examination called Vet BLUE to screen for metastatic lung nodules in the emergency room. *J Vet Emerg Crit Care* 25(S1):S14.

Kulhavy DA, Lisciandro GR. 2018. The use of lung ultrasound (Vet BLUE Protocol) to evaluate for pulmonary hypertension-associated pulmonary edema in dogs without left atrial enlargement. *J Vet Emerg Crit Care* 28(S1):S15.

Lamb CR, Tyler M, Boswood A, Skelly BJ, Cain M. 2000. Assessment of the value of the vertebral heart scale in the radiographic diagnosis of cardiac disease in dogs. *Vet Rec* 146:687–690.

Lamb CR, Wikeley H, Boswood A, et al. 2001. Use of breed-specific ranges for vertebral heart scale in dogs as an aid to radiographic diagnosis of cardiac disease. *Vet Rec*148:707–711.

Lee FC. 2016. Lung ultrasound – a primary survey of acutely dyspneic patient. *J Intens Care* 4:57.

Lee P, Tofts R, Kory P. 2015. Lung ultrasound interpretation. In: *Point-of-Care Ultrasound*, edited by Soni N, Arntfield R, Kory P. Philadelphia: Elsevier Saunders, pp 59–69.

Lichtenstein DA. 2007. Ultrasound in the management of thoracic disease. *Crit Care Med* 35(S5):S250–261.

Lichtenstein DA. 2010a. Should lung ultrasonography be more widely used in the assessment of acute respiratory disease? *Expert Rev Respir Med* 4(5):533–538.

Lichtenstein DA. 2010b. Basic applications of lung ultrasound in the critically ill – a bedside alternative to CT and other irradiating techniques. In: *Whole Body Ultrasonography in the Critically Ill*, edited by Lichtenstein DA. Berlin: Springer, pp 181–188.

Lichtenstein D, Karakitsos D. 2012. Integrating lung ultrasound in the hemodynamic evaluation of acute circulatory failure (the fluid administration limited by lung sonography protocol). *J Crit Care* 27(5):533.

Lichtenstein DA, Mezière GA. 2008. Relevance of lung ultrasound in the diagnosis of acute respiratory failure: the BLUE protocol. *Chest* 134(1):117–125.

Lichtenstein D, Mezière G, Bideman P, et al. 1997. The comet-tail artifact. An ultrasound sign of alveolar-interstitial syndrome. *Am J Respir Crit Care Med* 156(5):1640–1646.

Lichtenstein D, Mezière G, Biderman P, et al. 1999. The comet-tail artifact: an ultrasound sign ruling out pneumothorax. *Intensive Care Med* 25(4):383–388.

Lichtenstein D, Mezière G, Biderman P, et al. 2000. The "lung point": an ultrasound sign specific to pneumothorax. *Intensive Care Med* 26(10):1434–1440.

Lichtenstein DA, Lascos N, Mezière GA, et al. 2004. Ultrasound diagnosis of alveolar consolidation in the critically ill. *Intens Care Med* 30:276–281.

Lichtenstein D, Mezière G, Lagoueyte JF et al. 2009a. A-lines and B-lines: lung ultrasonography as a bedside tool for predicting pulmonary artery occlusion pressure in the critically ill. *Chest* 136:1014–1020.

Lichtenstein D, Mezière G, Seitz J. 2009b. The dynamic air bronchogram. A lung ultrasound sign of alveolar consolidation ruling out atelectasis. *Chest* 135(6):1421–1425.

Lisciandro GR. 2011. Abdominal and thoracic focused assessment with sonography for trauma, triage and monitoring in small animals. *J Vet Emerg Crit Care* 21(2):104–122.

Lisciandro GR. 2012a. Evaluation of initial and serial combination focused assessment with sonography for trauma (CFAST) examinations of the thorax (TFAST) and abdomen (AFAST) with the application of an abdominal fluid scoring system in 49 traumatized cats. Abstract. *J Vet Emerg Crit Care* 22(S2):11.

Lisciandro GR. 2012b. Comparison of Vet BLUE to thoracic radiography – 432 cases (2010–2012). Unpublished data.

Lisciandro GR. 2013. The Vet BLUE wedge sign for detecting pulmonary thromboembolism: case series of 6 dogs. Unpublished data.

Lisciandro GR. 2014a. The thoracic FAST$^3$ (TFAST$^3$) exam. In: *Focused Ultrasound for the Small Animal Practitioner*, edited by Lisciandro GR. Ames: Wiley Blackwell, pp 140–165.

Lisciandro GR. 2014b. The Vet BLUE lung Scan. In: *Focused Ultrasound for the Small Animal Practitioner*, edited by Lisciandro GR. Ames: Wiley Blackwell, pp 166–188.

Lisciandro GR. 2019. The cardiac gallbladder: case series of 13 dogs and 1 cat with sonographically-detected gallbladder wall edema. *J Vet Emerg Crit Care* 29(S1):S24.

Lisciandro GR, Armenise A. 2014. Focused or COAST$^3$ – cardiopulmonary resuscitation (CPR), Global FAST (GFAST$^3$) and the FAST-ABCDE exam. In: *Focused Ultrasound for the Small Animal Practitioner*, edited by Lisciandro GR. Ames: Wiley Blackwell, pp 269–287.

Lisciandro GR, Fosgate GT. 2018. Use of Vet BLUE protocol for the detection of lung atelectasis and sonographic gallbladder wall evaluation for anaphylaxis and volume overload in 63 dogs undergoing general anesthesia. *J Vet Emerg Crit Care* 28(S1):S15–S16.

Lisciandro GR, Lagutchik MS, Mann KA, et al. 2008. Accuracy of Focused Assessment with Sonography for Trauma (TFAST) to detect pneumothorax in 145 dogs with blunt and penetrating trauma. *J Vet Emerg Crit Care* 18(3):258–269.

Lisciandro GR, Fosgate GT, Fulton RM. 2014. Frequency of ultrasound lung rockets using a regionally-based lung ultrasound examination named veterinary bedside lung ultrasound exam (Vet BLUE) in 98 dogs with normal thoracic radiographic lung findings. *Vet Radiol Ultrasound* 55(3):315–322.

Lisciandro GR, Ward JL, DeFrancesco TC, Mann KA. 2016. Absence of B-lines on lung ultrasound (Vet BLUE protocol) to rule out left-sided congestive heart failure in 368 cats and dogs. *J Vet Emerg Crit Care* 26(S1):S8.

Lisciandro GR, Fulton RM, Fosgate GT, Mann KA. 2017. Frequency of B-lines using a regionally-based lung ultrasound examination (the Vet BLUE protocol) in 49 cats with normal thoracic radiographical lung findings. *J Vet Emerg Crit Care* 27(3):267–277.

Lisciandro GR, Romero L, Fosgate GT. 2018. The frequency of B-Lines and other lung ultrasound artifacts during Vet BLUE in 91 healthy puppies and kittens. *J Vet Emerg Crit Care* 28(S1):S16.

Louvet A, Bourgeois JM. 2008. Lung ring-down artifact as a sign of pulmonary alveolar-interstitial disease. *Vet Radiol Ultrasound* 49(4):374–377.

MacDonald KA, Cagney O, Magne ML. 2009. Echocardiographic and clinicopathologic characterization of pericardial effusion in dogs: 107 cases (1985–2006). *J Am Vet Med Assoc* 235(12):1456–1461.

Mastruzzo C, Perrachio G, Poidomani G, et al. 2008. Subsegmental pulmonary embolism: value of the thoracic ultrasound for the diagnosis and follow-up. *Intern Med* 47:1415–1417.

Mathis G, Blank W, Reibig A, et al. 2005. Thoracic ultrasound for diagnosing pulmonary embolism. *Chest* 128(3):1531–1538.

Mongodi S, Via G, Girard M, et al. 2016. Lung ultrasound for early diagnosis of ventilator-associated pneumonia. *Chest* 149(4):969–980.

Moore CL, Copel JA. 2011. Point of care ultrasonography. *N Engl J Med* 364:749–757.

Narasimhan M, Koenig SJ, Mayo PH. 2016. A whole body approach to point of care ultrasound. *Chest* 150(4):772–776.

Nazerian P, Vanni S, Volpicelli G, et al. 2014. Accuracy of point-of-care multiorgan ultrasonography for the diagnosis of pulmonary embolism. *Chest* 145(5):950–957.

Neelis DA, Mattoon JS, Nyland TG. 2015. Thorax. In: *Small Animal Diagnostic Ultrasound*, edited by Mattoon JS, Nyland TG. Philadelphia: Elsevier Saunders, pp 188–216.

Nemanic S, London CA, Wisner ER. 2006. Comparison of thoracic radiographs and single breath-hold helical CT for detection of pulmonary nodules in dogs with metastatic neoplasia. *J Vet Intern Med* 20:508–515.

Rademacher N, Pariaut R, Pate J, et al. 2014. Transthoracic lung ultrasound in normal dogs and dogs with cardiogenic pulmonary edema: a pilot study. *Vet Radiol Ultrasound* 55(4):447–452.

Schober KE, Hart TM, Stern JA, et al. 2010. Detection of congestive heart failure in dogs by Doppler echocardiography. *J Vet Intern Med* 24(6):1358–1368.

Shyamsundar M, Attwood, B, Keating L, et al. 2013. Clinical review: The role of ultrasound in estimating extravascular lung water. *Crit Care* 17(5):237.

Soldati G, Testa A, Silva FR, et al. 2006. Chest ultrasonography in lung contusions. *Chest* 130(2):533–538.

Soldati G, Giunta V, Sher S, et al. 2011. "Synthetic" comets" a new look at lung sonography. *Ultrasound Med Biol* 37(11):1762–1770.

Stafford Johnson M, Martin M, Binns S, et al. 2004. A retrospective study of clinical findings, treatment and outcome in 143 dogs with pericardial effusion. *J Small Anim Pract* 45(11):546–552.

Szymczak J, Kielbowicz Z, Kinda W, et al. 2018. Transthoracic lung and pleura ultrasonography as a diagnsotic tool of pulmonary edema in dogs and cats. *Pol J Vet Sci* 21(3):475–481.

Tardella M, Guttierez M, Salaffi F, et al. 2012. Ultrasound in the assessment of pulmonary fibrosis in connective tissue disorders: correlation with high-resolution computed tomography. *J Rheumatol* 39(8):1641–1647.

Vezzosi T, Mannucci A, Pistoresi F, et al. 2017. Assessment of lung ultrasound B-Lines in dogs with different stages of chronic valvular heart disease. *J Vet Intern Med* 31(3):700–704.

Vientós-Plotts AI, Wiggen KE, Lisciandro GR, et al. 2019. The utility of point-of-care ultrasound non-echo right-sided cardiac markers as a screening test for moderate to severe pulmonary hypertension in dogs. *Vet J* 250:6–13.

Volpicelli G, Mussa A, Garofalo G, et al. 2006. Bedside lung ultrasound in the assessment of alveolar-interstitial syndrome. *Am J Emerg Med* 24:689–696.

Volpicelli G, Elbarbary M, Blaivas M, et al. 2012. International evidence-based recommendations for point-of-care lung ultrasound. *Intens Care Med* 38:577–591.

Wang Y, Gargani L, Barskova T, et al. 2017. Usefulness of lung ultrasound B-lines in connective tissue disease-associated interstitial lung disease: a literature review. *Arthritis Res Ther* 19(1):206.

Ward JL, Lisciandro GR, Keene BW, et al. 2017. Accuracy of point-of-care lung ultrasonography for the diagnosis of cardiogenic pulmonary edema in dogs and cats with acute dyspnea. *J Am Vet Med Assoc* 250:666–675.

Ward JL, Lisciandro GR, DeFrancesco TD, et al. 2018a. Evaluation of point-of-care thoracic ultrasound and NT-proBNP for the diagnosis of congestive heart failure in cats with respiratory distress. *J Vet Intern Med* 32(5):1530–1540.

Ward JL, Lisciandro GR, DeFrancesco TC. 2018b. Distribution of alveolar-interstitial syndrome in dyspneic veterinary patients assessed by lung ultrasound versus thoracic radiography. *J Vet Emerg Crit Care* 28(5):415–428.

Ward JL, Lisciandro GR, Ware WA, et al. 2019. Lung ultrasound findings in 100 dogs with various etiologies of cough. *J Am Vet Med Assoc* 255(5):574–583.

Yarto E, Lisciandro GR. 2017. Evaluation of a Global FAST protocol in bottlenose dolphins (Tursiops truncatus). Unpublished data.

SECTION V

# Vascular

CHAPTER TWENTY-FOUR

# POCUS: Central Venous and Arterial Catheterization

Scott Chamberlin

## Introduction

Vascular access is a requirement for nearly every emergent and/or critical case, and the more emergent or critical the patient, the more difficult obtaining vascular access seems to be. Moreover, many elective procedures require vascular access for administration of sedatives, analgesics, anesthetics, medications, and emergency drugs. Factors like anatomical conformation and local hematoma formation from failed intravascular catheter attempts can potentially jeopardize patients' safety and add to their discomfort. Ultrasound guidance for vascular access is point-of-care and noninvasive, increases reliability, and is generally unaffected by common complications like patient size, obesity, local hematoma formation, and peripheral edema that can frustrate blind catheterization procedures (also referred to as the landmark technique). As a result, ultrasound-guided central venous catheter placement has become standard of care in human medicine for both adult and pediatric patients across multiple disciplines and is similarly recommended for arterial catheterization (Miller et al. 2002; Milling et al. 2005; Wigmore et al. 2007; Ringold and Kelmer 2008; Froelich et al. 2009; AIUM 2013; Mustapha et al. 2016). Although sparsely described in the veterinary literature, ultrasound guidance during these procedures delivers the same advantages as in human medicine (Ringold and Kelmer 2008; Chamberlin et al. 2013; Izer et al. 2017; Pavlisko et al. 2018).

Through comparison with traditional blind catheterization, ultrasound-guided techniques have documented greater success rates with fewer complications in the emergency, critical care, and anesthesia settings. Furthermore, ultrasound guidance is less invasive than surgical cut-down techniques, which often sacrifice the vessel and risk neuropraxia (Miller et al. 2002; Karakitsos et al. 2006; Pirotte and Veyckmans 2007; Ringold and Kelmer 2008; Theodoro et al. 2010). Perhaps most importantly, ultrasound-guided vascular access techniques have been shown to be achievable by minimally trained, nonradiologist clinicians (Miller et al. 2002; Froehlich et al. 2009) and veterinarians (Ringold and Kelmer 2008; Chamberlin et al. 2013).

### *Veterinary Central Venous Catheterization*

The author's veterinary study describing ultrasound guidance for central venous catheter placement demonstrated that the procedure was technically easy and rapid, with a median time of 1.9 minutes without hematoma formation and 4.3 minutes with hematoma formation. Ultrasound guidance additionally had a relatively shallow learning curve among nonradiologist residents and faculty involved in learning and then performing the procedure. Despite complicating factors such as iatrogenic perivascular hematoma formation and cardiovascular collapse post cardiac arrest, ultrasound-guided central venous catheter placement was achievable with a 100% success rate across all participants in the study (Chamberlin et al. 2013). And, now with a realistic training model also described within this chapter, learning this ultrasound-related skill is even more practical.

*Point-of-Care Ultrasound Techniques for the Small Animal Practitioner*, Second Edition. Edited by Gregory R. Lisciandro.
© 2021 John Wiley & Sons, Inc. Published 2021 by John Wiley & Sons, Inc.
Companion website: www.wiley.com/go/lisciandro/ultrasound2

VetBooks.ir

### Veterinary Arterial Catheterization

The most common site in veterinary medicine for arterial catheter placement is the dorsal pedal artery, which is a challenging target in small or unstable patients. The larger femoral artery is an excellent alternative and thus also may be used for obtaining direct blood pressure as well as respiratory and acid–base laboratory values; this larger artery is also the preferred access site for cardiac catheterizations and other interventional radiology procedures (Ringold and Kelmer 2008; Kweon et al. 2012; Izer et al. 2017; Pavlisko et al. 2018). Ultrasound guidance may be used to visually place femoral arterial catheters in veterinary patients. The target vessel and the insertion of the stylet, guidewire, and catheter are not only imaged during real-time ultrasound for greater accuracy during catheter insertion, but the procedure helps identify and avoid nearby anatomical structures, thus minimizing complications over the traditional blind landmark techniques (Ringold and Kelmer 2008; Chamberlin et al. 2013). In fact, higher intravascular pressures make perivascular hematomas larger and more common; repeated attempts are virtually impossible using the landmark technique at the same site. Perivascular fluid (like a hematoma) does not hinder but in fact often enhances target vessel imaging in the far-field through acoustic enhancement artifact. Ultrasound thus delivers a huge advantage in these situations.

### Applications for Peripheral Vessels

While distal and peripheral vessels are commonly used by veterinarians for short-term simple vascular access, ultrasound-guided catheterization of vessels like the cephalic vein or dorsal pedal artery in cats and dogs is generally of minimal benefit due to their small limb radius and the shallow depth of tissue between skin surface, vessel of interest, and underlying bone. Ultrasound machines are also generally unable to image that closely in the near-field. Although acoustically permeable "stand-off" blocks are used for denser superficial musculoskeletal structures such as tendons, ligaments, and bones, they are generally cumbersome and thus ineffective for catheterizing superficial and distal limb vessels in dogs and cats (see Chapters 34 and 35).

### Recent Training Advancements

A novel, simple, affordable, realistic training model has recently been described for teaching and practicing ultrasound-guided vascular access (Rippey et al. 2015). A recipe for creating these useful chicken breast phantoms is provided later in this chapter.

In summary, ultrasound guidance for central venous and arterial catheterization delivers the potential to provide significant benefits in patient care by facilitating vessel cannulation success rates, especially when patient factors like hypotension, conformation, or hematomas make vascular access particularly challenging. Recent training advances, experience, and knowledge should help accelerate providers' proficiency and comfort with ultrasound guidance as a core skill for veterinarians.

### What POCUS Central Venous and Arterial Catheterization Can Do

- Rapidly identify the jugular vein or femoral artery for catheterization independent of vascular collapse, peripheral edema, obesity, patient size, and local hematoma formation.
- Guide central venous or femoral arterial catheter placement, preventing damage to adjacent structures otherwise unrecognized via the traditional blind landmark method.
- Provide a less invasive option over surgical cutdown procedures.
- Facilitate the use of central venous catheters, which allow more rapid fluid and drug delivery to central circulation and simplify repeated blood sampling.
- Enable administration of hyperosmolar or other fluids that cause peripheral phlebitis, and allow for otherwise incompatible fluid administration via multilumen central venous catheters.
- Enable early goal-directed therapy including central venous pressure (CVP) measurement and central venous oxygen saturation.
- Facilitate arterial catheterization which allows arterial blood sampling, direct arterial blood pressure measurements, and interventional radiology techniques.
- Enable and then confirm a reliable "clean stick" for safe and successful cannulation of a desired vein or artery, particularly useful for interventional or high-flow procedures such as hemodialysis.

### What POCUS Central Venous and Arterial Catheterization Cannot Do

- Cannot guide cannulation of superficially located small veins and arteries.
- Cannot replace adequate ultrasound training because vascular ultrasound techniques are operator dependent.

VetBooks.ir

### Indications

- Failure or anticipated failure in obtaining any vascular access by traditional blind landmark techniques due to cardiovascular collapse, hypotension, or hematoma formation.
- Inability to identify the target vessel (central vein or femoral artery) due to cardiovascular collapse, hypotension, or hematoma formation.
- Requirement for central venous access for administration of caustic or high osmolarity drugs poorly suited for peripheral administration, and/or administration of parenteral nutrition and multiple incompatible drugs or transfusion products by use of multilumen central venous catheters.
- Requirement for frequent blood sampling for critically ill and fractious animals.
- Requirement for arterial sampling and access for direct arterial blood pressure readings and/or respiratory and acid–base monitoring when traditional distal arterial sampling sites are compromised or unavailable.
- Requirement for cannulation of large vessels with minimal trauma for interventional radiology, hemodialysis, and other special procedures.

### Objectives

- Ultrasonographically recognize the regional vasculature and anatomy of the neck.
- Use ultrasound guidance for central venous placement using the jugular vein.
- Ultrasonographically recognize regional vasculature and nerves of the hindlimbs.
- Use ultrasound guidance for femoral arterial catheterization and direct arterial sampling.
- Be aware that a simple model (phantom) can be made locally using inexpensive, readily available supplies that provides hands-on training with realistic images including normal tissue planes and echogenicity.

# Placement of an Ultrasound-guided Central Venous Jugular Catheter

### Equipment and Materials

#### Probe

Most of the probes commonly used in small animal medicine can be used to gain vascular access. Linear array probes with a minimum frequency of 7.5 MHz are preferred because of their superior detail at shallow depths. Curvilinear (microconvex) 5–8 MHz probes are the most widespread probe type in veterinary medicine, having the ability to magnify to a depth of <4 cm.

**Pearl:** Utilizing "Small Parts" or "Vascular" presets on your machine can improve imaging detail.

- Some ultrasound machines have a "needle enhancement" feature; these can be helpful and are most commonly featured with linear probes.
- Probes should be cleaned and disinfected according to manufacturer guidelines before and after use in ultrasound-guided vascular access.
- Although not required, color flow Doppler ultrasound is helpful to gain confidence in differentiating vein from artery. However, most sonographers become proficient with ultrasound-guided procedures using only B-mode. In fact, several large studies recommend *against* using color flow Doppler because the pulse in the artery can also make the vein move, which can lead to operator confusion (Bowra 2006).

**Pearl:** For aseptic ultrasound imaging, the probe may be placed in a sterile surgical glove or sterile obstetric sleeve as a protective barrier that is filled with acoustic coupling gel (Figure 24.1).

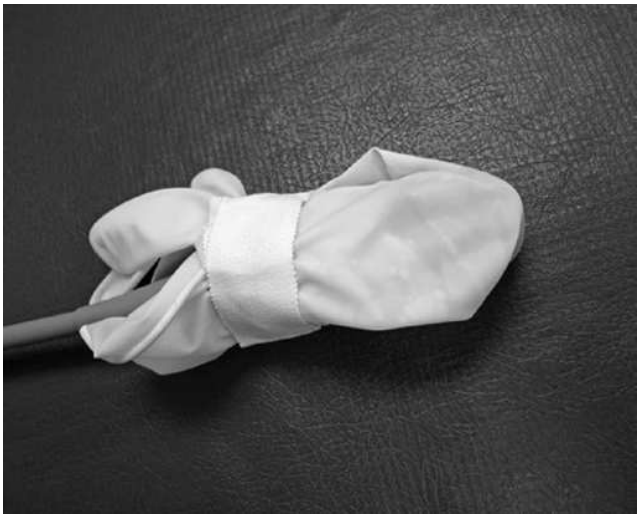

**Figure 24.1.** Sterile probe preparation. Sterile probe preparation using a sterile glove barrier. Acoustic coupling gel is on the probe inside the glove. Alcohol with or without sterile acoustic coupling gel is applied to the patient's skin for optimal imaging at the probe-glove-skin interface.

### Central Venous Catheter Selection

There are different styles of central venous catheters available, including the through-the-needle Venocath® (Hospira, Inc., Lake Forest, IL) and Seldinger-type designs (Mila International, Erlanger, KY; Cook, Inc., Bloomington, IL) which come in variable lengths with variable numbers of lumens (single, double, triple).

**Pearl:** In general, it is best to use a 16 gauge central venous catheter for larger dogs (>7.5 kg) and an 18 gauge central venous catheter for smaller dogs and cats (<7.5 kg).

### Central Venous Catheter Line Length

Premeasuring from the insertion site to the patient's 4th–5th rib is imperative to prevent catheter-associated complications because advancing the central line too far risks placing the catheter into the right heart and/or pulmonary artery. Excessive advancement of the catheter can cause direct injury to the heart or coiling and knotting of the central line, rendering it irretrievable (Mitchell and Clark 1979; Kusminsky 2007).

**Pearl:** Premeasure the catheter to the fourth or fifth rib on the patient and note the length on the catheter (most central venous catheters have length demarcations printed on them). Confirm central venous catheter location with postprocedure radiographs.

The central venous catheters placed using the Seldinger technique are preferred; however, both central venous catheter designs can be unquestionably foreign and intimidating to the novice. Sacrifice a Venocath or single-lumen Seldinger-technique central venous catheter for familiarity with the device; the latter includes several components including a needle or stylet, a guidewire, a dilator, and the actual central venous catheter (used sequentially). Some excellent supplementary step-by-step descriptions are available including Silverstein and Hopper's *Small Animal Critical Care Medicine*, Hackett and Mazzaferro's *Veterinary Emergency and Critical Care Procedures* (2012 edition includes online videos), as well as other video demonstrations available on YouTube.

**Pearl:** Sacrifice a Venocath or Seldinger-technique catheter for familiarity and practice with the device.

# How to Place an Ultrasound-guided Central Venous Jugular Catheter

## *Static versus Dynamic and One- versus Two-person Techniques*

As with any medical procedure, there are multiple ultrasound-guided vascular access techniques available to the veterinarian. Each technique has inherent advantages and disadvantages with regard to comfort, efficacy, and safety. The points for ultrasound-guided central venous catheter placement reviewed below relate to how much the probe is used during actual catheter placement (static vs dynamic or real-time placement vs combinations thereof) and probe orientation (transverse [out of plane] vs longitudinal [in plane] vs combinations thereof). Because needle guides (devices that attach to the probe) are too cumbersome for vascular access techniques, only free-hand descriptions are used in this text (Ringold and Kelmer 2008; Chamberlin et al. 2013).

### Static Technique

The static technique uses ultrasound as a screening tool to localize structures (vessels, nerves, etc.) prior to blindly placing the catheter in the traditional landmark manner. This technique has been described in the human literature as acceptable, though it is less successful than the dynamic technique. The static technique may be an option for the novice who has difficulty coordinating both the probe and the stylet as guided by the ultrasound image during catheter introduction.

### Dynamic Technique

In the dynamic technique, ultrasound is used to actually guide the catheter into the vessel using ultrasound in real time. Because this method tracks the target vessel and the surrounding structures in relation to the sharp stylet, it is safer and typically more successful than the static technique, especially when a single operator manipulates both the catheter and the ultrasound probe. Note that an assistant is generally still needed to place digital pressure in the jugular furrow to "hold off the vein," just like during the traditional blind technique. The novice sonographer performing the dynamic technique may be tempted to have an assistant maneuver the probe; however, communication and coordination between

the person placing the catheter and the person holding the probe is often a source for error. With minimal training to develop comfort with ultrasound imaging and coordinating both the probe and stylet, the one-person technique will quickly prove more successful and lead to fewer errors than the static or two-person options (Milling et al. 2005; Chamberlin et al. 2013).

Traditionally, jugular vein catheterization is abandoned when hematomas obscure palpable and visual landmarks. However, ultrasound becomes more effective when imaging through fluid in such circumstances (acoustic enhancement artifact) and permits continued attempts for central venous catheter placement at the discretion of the attending veterinarian. Moreover, stylets, needles, and catheter components may be ultrasonographically visualized in real time, providing distinct advantages over both the static and blind landmark methods. Coated needles have been specifically developed for increased ultrasonographic visualization (Havel's, Mila).

### Honing Your Skills

Simple and affordable homemade models using Jello® or commercially available phantoms are great practice options (Wells and Goldstein 2010; Rippey et al. 2015), and a description for a recently published realistic phantom model using chicken breast filets and balloons is included in this chapter. We have found the chicken breast phantom model hugely helpful in accelerating the perfection of ultrasound-guided catheterization skills.

The dynamic real-time technique is subsequently described. Keep in mind the aforementioned options because it is not uncommon for any veterinary procedure to become modified based on the particular circumstances at that time, such as bailing on the dynamic technique because the static technique lends itself better to the situation at hand.

## Anatomy

The external jugular veins are the preferred central venous catheter sites in veterinary patients. Each jugular vein runs ventrolaterally on the left and right sides of the neck superficially under the skin, traversing from the angle of the mandible to the thoracic inlet. Each jugular vein is bounded throughout its slightly angulated course ventrally by the sternocephalicus muscle and laterally by the cleidocervicalis muscle.

## Patient Preparation

Place the patient in lateral recumbency consistent with typical positioning for jugular catheterization, then clip hair and aseptically prep the skin as fully as possible, depending on patient stability.

- All attempts should be made to adequately shave over the jugular furrow (ventrolateral cervical region) to give ample room to aseptically prep the skin over the central venous catheter insertion site and comfortably protect the site post insertion (neck wrap).
- Liberal local use of 70% isopropyl alcohol, either by itself (which is often sufficient) or in combination with acoustic coupling gels mentioned below, improves probe contact or greatly enhances image quality while maintaining a clean catheter insertion site.

However, the attending veterinarian should keep in mind the following precautions.

- Alcohol-induced hypothermia (external cooling) may occur in any patient, especially smaller animals.
- The inherent flammability of alcohol also poses burn risks to the patient in the event of electrical defibrillation.

Sterile acoustic coupling gels are commercially available and ideal (Aquasonics, Parker Laboratories, Fairfield, NJ). Although it lacks viscosity and tends to fall off the site, sterile K-Y® Jelly (Johnson and Johnson, New Brunswick, NJ) serves as a replacement option to sterile commercially available acoustic coupling gel.

**Pearl:** Excess alcohol and gel should be wiped off the hair and skin as soon as it is no longer needed.

## Orientation

- Verify the ultrasound probe-to-screen marker orientation so that direction is accurate during the procedure.
- The ultrasound monitor must be located in a comfortable line of sight and generally the head of the patient and the ultrasound screen should be in the *same* sightline.

**Pitfall:** It is unsafe for the patient, not to mention difficult, fatiguing and uncomfortable for the sonographer, to insert a central venous catheter (or arterial catheter) when craning to look over your shoulder at the ultrasound screen (Bowra 2006).

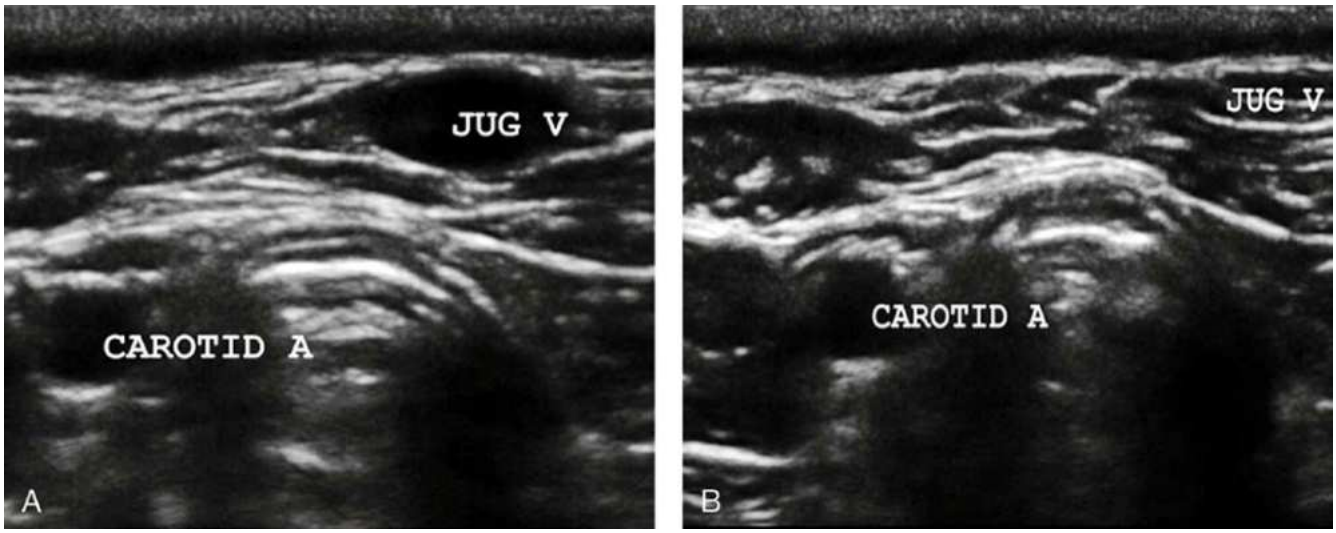


**Figure 24.2.** Compression technique to discriminate jugular vein from carotid artery. (A) Transverse image depicting normal probe pressure (no significant compression) with both the jugular vein and carotid artery visible. (B) Transverse image depicting the disappearance of the jugular vein with gentle probe pressure (compression) while the lumen of the carotid artery remains visible (circular). The compression technique is effective and reliable in discriminating between arteries and veins.

- With the nondominant hand of the person placing the central venous catheter, the ultrasound probe is placed in the jugular groove in transverse orientation just caudal to the desired catheter entry point on the skin, searching for the anechoic (black) circles of the vessels (Figure 24.2A).
- Structures (particularly artery versus vein) are most easily identified by their anatomical location and by intermittent gentle probe pressure (compression technique) since veins will collapse (flatten) while arteries will not flatten but remain relatively circular (see Figure 24.2).

**Pearl:** As with traditional landmark techniques, having an assistant "hold off" the jugular vein by applying digital pressure at the thoracic inlet can prove helpful in visualizing as well as cannulating the jugular vein.

- Color flow Doppler, when available, may be helpful in the learning phases to gain confidence in differentiating vein from artery. However, color flow Doppler is not required as proficiency may be obtained without it, and in fact it is not recommended in several larger published human studies and protocols (Bowra 2006).
- Color flow Doppler *does not identify artery and vein by color* but rather is generally coded as "red" flowing towards the probe and "blue" flowing away.

**Pearl:** Color flow Doppler imaging for pulsatile arterial flow is not 100% reliable as the artery's "jump" can transmit motion to the nearby vein, causing misidentification.

The sonographer can either remain in transverse orientation (needle out of plane) throughout the catheter placement (often easier for the novice and advantageous in short-necked animals) (Blaivas et al. 2003), rotate the probe 90° to a longitudinal alignment (needle in plane), obtaining an anechoic (black) linear tract representative of the jugular vein (Figure 24.3), or use combinations of transverse and longitudinal views.

In either transverse or longitudinal views, the probe is placed just caudal (closer to the heart) to the desired catheter entry point on the skin. For safety and by convention when using longitudinal orientation (very important), the ultrasound probe marker should point rostrally, thus positioning the probe marker on the same side as the catheter insertion site.

## *Transverse Orientation*

With the jugular vein identified, move the ultrasound probe and alter image depth and focus so that the vessel appears in the center of the ultrasound screen as an anechoic circle (transverse orientation), thus "landmarking" the jugular vein's position (Figures 24.2 and 24.4). With the dominant hand, insert the stylet (or

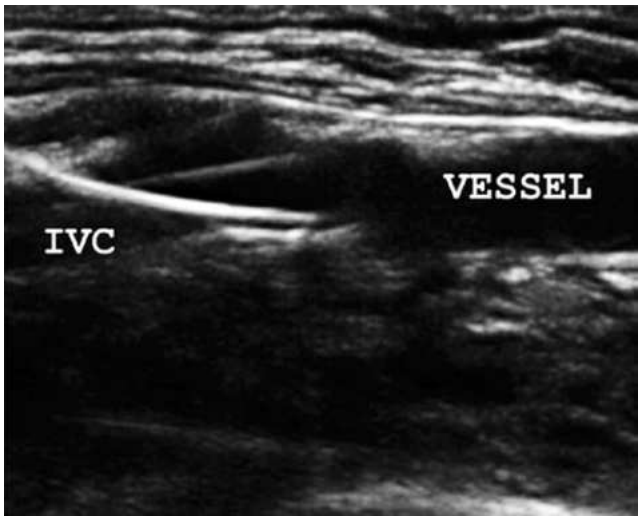


**Figure 24.3.** Ultrasound-guided central line placement. Longitudinal view showing the horizontally aligned anechoic (black) lumen of jugular vein. The central venous catheter is seen within the vessel. The anechoic (black) perivascular fluid immediately superficial to the jugular vein is due to hematoma formation. Ultrasound actually images better through fluid, making it advantageous when hematoma formation occurs allowing for the procedure to continue whereas the blind landmark technique would need to be aborted.

needle in some Seldinger kits; the terms will be used interchangeably hereafter for simplicity) through the skin directly over the jugular vein at approximately 1–2 cm rostral to the ultrasound probe. Placing the stylet 1–2 cm rostral to the ultrasound probe keeps the sharp point of the stylet from damaging the rubber probe head (Figure 24.5).

**Pearl:** In transverse probe orientation, inserting the stylet 1–2 cm rostral to the ultrasound probe and at a 45° angle (steeper than when using the blind landmark technique) makes it easier to keep track of the sharp tip of the stylet, as well as avoiding damage to the rubber probe head.

- Using a #11 scalpel blade or an 18 gauge needle to nick the skin 3–5 mm lateral to the jugular vessel facilitates getting the stylet through otherwise tough skin. This nick can then be moved directly over the jugular vein for the subsequent introduction of the stylet into the vessel (Crowe 2009).
- Once the stylet is through the skin (not yet puncturing the jugular vein), slide the probe rostrally to visualize the tip of the hyperechoic (bright) stylet

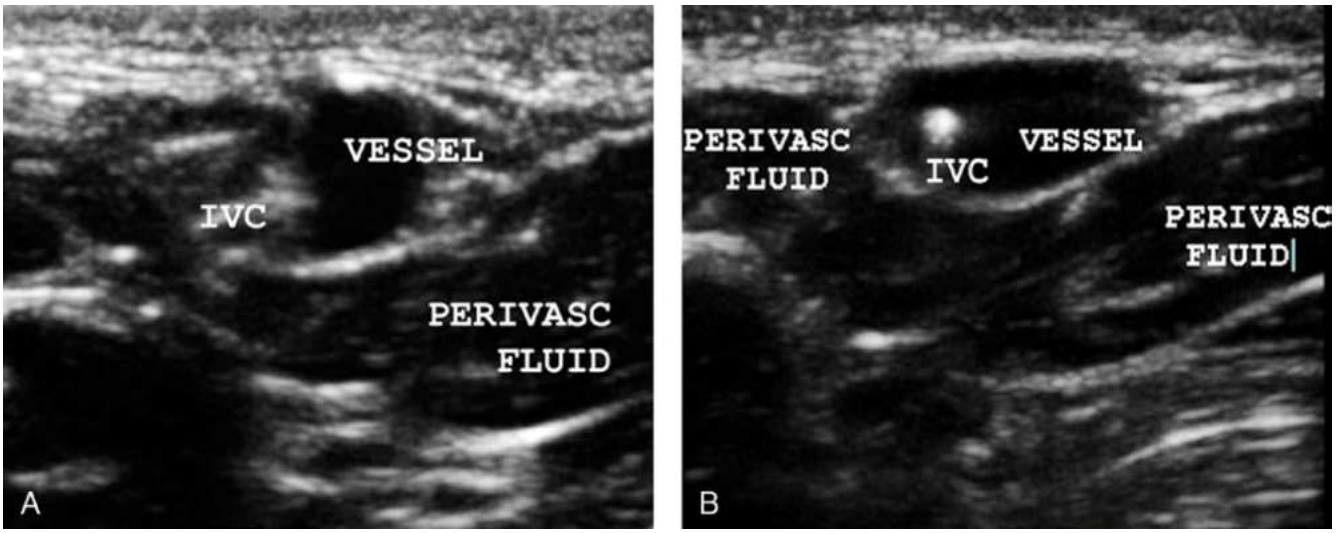


**Figure 24.4.** Ultrasound-guided central line placement. (A) Transverse view of stylet (labeled IVC) beside the jugular vein, indenting but not penetrating the vessel lumen. The direction of approach of the stylet is directly down from the top of the figure while the vessel has "rolled" and "tented" laterally. (B) Transverse view showing successful vascular access with the stylet (labeled IVC) in the vessel. The presence of perivascular fluid (labeled) is due to hematoma formation. Ultrasound actually images better through fluid, making it advantageous when hematoma formation occurs and allowing for the procedure to continue, whereas the blind landmark technique would need to be aborted.

**Figure 24.5.** Probe head damage. Probe head damaged by chronic needling during ultrasound-guided aspirates and biopsies. Source: Reproduced with permission of Dr Stephanie Lisciandro, Hill Country Veterinary Specialists, Spicewood, TX.

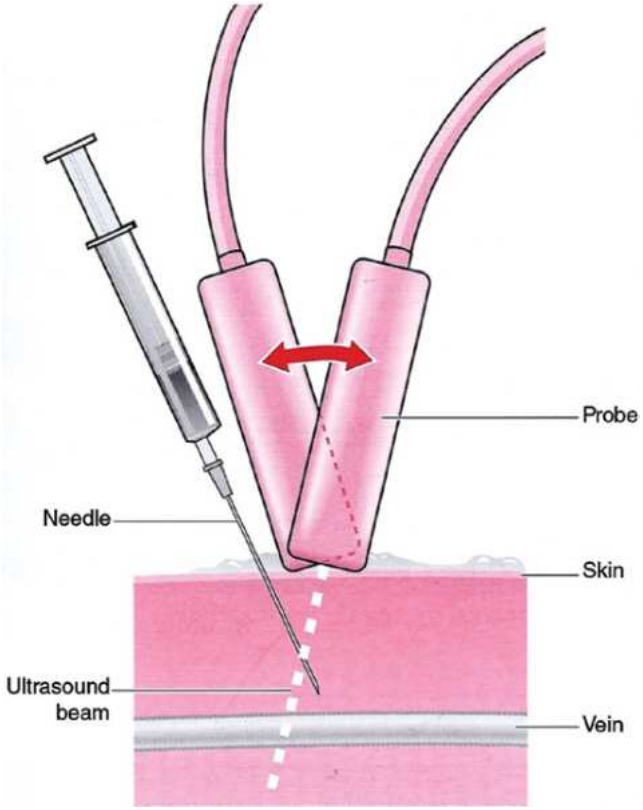


**Figure 24.6.** Changing probe angle. Changing the probe angle until the target vessel and needle are visualized. Source: Reproduced from Bowra (2006) with permission from Churchill Livingstone Elsevier.

and the anechoic (dark) vessel simultaneously in the middle of the screen. Use the image to direct the stylet and penetrate the proximal wall of the jugular vein and cannulate the vessel (see Figure 24.4). Inserting the stylet at a slightly steeper angle to the skin (than typically angled for traditional blind landmark central venous catheter placement) and sliding the ultrasound probe back and forth slightly as the stylet is moved helps ensure that the needle tip intersects the jugular vein in the field of view of the transverse ultrasound image. This steeper angle prevents overshooting the vein and is recommended in human central venous catheter placement guidelines to increase patient safety by facilitating the accurate tracking of the stylet tip (Bowra 2006; AIUM 2013) (Figure 24.6).

- Rotating the probe slightly or partially between transverse and longitudinal orientations so the target vessel appears oval versus circular may also help maintain both the jugular vessel and the stylet tip in the ultrasound field of view.
- Watch for tenting of the vessel's superficial wall inward as the stylet encounters the jugular vein while maintaining positioning of the stylet dorsal to the vein. The vessel may tent even if it rolls away. When this occurs, slightly withdraw the stylet to reposition more advantageously directly above the vein (see Figure 24.4).
- When the jugular vein's lumen is penetrated, tenting should diminish even if you don't see the stylet in the vessel, and you should get a flash of venous blood.

**Note:** You will likely need to slide the probe along the vessel to visualize the stylet tip within the vessel's lumen on the ultrasound screen because the ultrasound beam is quite narrow and moving the probe this way can bring the tip back into the field of view.

**Pearl:** As with the traditional blind landmark technique, a sharp yet smooth and deliberate motion may be needed to get the stylet through the dorsal superficial wall of the vessel and into its lumen.

**Figure 24.7.** Transverse orientation. Transverse placement of the ultrasound probe for identifying and then gaining jugular central venous access. Jugular venous blood is aspirated to confirm successful vascular access.

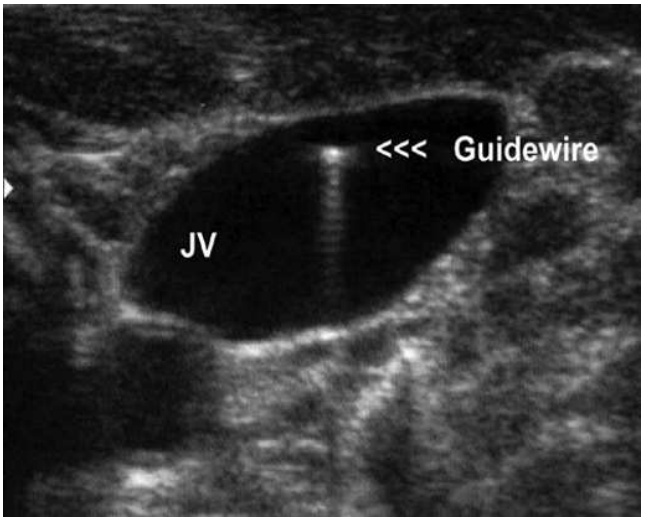


**Figure 24.8.** Ultrasound-guided needle location. Transverse view showing successful vascular access with ring-down artifact depicting the guidewire in the jugular vein (JV). Any metallic strong reflector of ultrasound will create the same artifact, including needles, stylets, implants, and foreign bodies (Bowra 2006).

- Further advance the stylet a few millimeters after getting the flash of venous blood, and confirm jugular luminal placement by observing continuous blood exiting the stylet and/or by blood aspiration into a syringe attached to the stylet (or catheter) (Figure 24.7).
- Now lessen the angle to the jugular vein for feeding the next component (guidewire followed by the venous dilator for Seldinger technique or the central venous catheter for the Venocath technique) depending on the central venous catheter style used (as with the blind landmark technique).
- Once the central venous catheter is completely placed, secure it to the skin (usually sutured) via the manufacturer's provided butterfly adapters or similar devices, and cover the entry site with a sterile Telfa pad with triple antibiotic ointment followed by a few gauze sponges and a light protective cervical wrap.

**Pearl:** Correct placement may also be confirmed (if needed) by visualizing a ring-down artifact of streaking hyperechoic (bright white) lines emanating from the metal stylet or guidewire from their surface through the far-field (Figure 24.8).

### *Longitudinal Orientation*

With the jugular vein identified in transverse orientation, move the probe and alter the image depth and focus so that the jugular vein appears in the center of the screen as an anechoic (black) circle. Now, slowly rotate the probe 90° into longitudinal orientation, ending with the jugular vein as an anechoic (black) linear tract in the middle of the screen and the probe marker pointing rostrally, closest to the point of desired catheter insertion (see Figure 24.3).

- By keeping the target vessel (jugular vein) centered on the ultrasound screen, the sonographer is less likely to lose the visualization and misidentify the jugular vein for another structure (see Figure 24.3).
- Watch for tenting of the vessel's superficial wall inward as the stylet encounters the jugular vein while maintaining positioning of the stylet dorsal to the vein. The vessel may tent even if it rolls away.
- When this occurs, slightly withdraw the stylet to reposition more advantageously directly above the vein (see Figure 24.4).
- When the jugular vein's lumen is penetrated, tenting should diminish even if you don't see the stylet in the vessel, and you should get a flash of venous blood.
- Further advance the stylet a few millimeters after getting the flash of venous blood, and confirm

jugular luminal placement by observing continuous blood exiting the stylet and/or by blood aspiration into a syringe attached to the stylet (or catheter) (see Figure 24.7).

- Now lessen the angle to the jugular vein to feed the next component (guidewire followed by the venous dilator for Seldinger technique or the central venous catheter for the Venocath technique) depending on the central venous catheter style used (as with the blind landmark technique).
- Once the central venous catheter is completely placed, secure it to the skin (usually sutured) via the manufacturer's provided butterfly adapters or similar devices, and cover the entry site with a sterile Telfa pad with triple antibiotic ointment followed by a few gauze sponges and a light protective cervical wrap.

### Sensible Use of a Short Temporary Jugular Catheter

In emergency resuscitation situations, in which time is critical for rapid venous access and a full-length central venous catheter may be too cumbersome, an excellent intermediate option is to use ultrasound guidance to percutaneously place a short large-bore (18 gauge or larger) 1.5 inch catheter in the jugular vein. The temporary short catheter permits rapid administration of resuscitative fluids through a large central vein (jugular). This short jugular catheter may be temporarily secured with any combination of tape, adhesive catheter covers, or one or two looped sutures incorporating both the catheter's hub and the patient's skin.

Be careful because the skin over the vessel is highly mobile in this area and the short catheter can come out of the jugular vein into the subcutaneous space during patient movement. If you have resuscitated the patient and you don't have a long central venous catheter in stock, place another short peripheral catheter for fluid/drug administration, but consider leaving the short jugular catheter secured with a saline lock.

Be smart! The short, large-bore catheter in the jugular vein may be used after initial stabilization as a conduit using the central venous catheter kit's guidewire for a long central line, taking advantage of this temporary catheter to complete a modified Seldinger technique with a single or multilumen central venous catheter or the Venocath. Of course, time and patient stability permitting, a true central venous catheter may be placed at the outset (see above). The responsible use of a central venous catheter is a welcome addition to patient care in any emergency and critical care center or 24-hour general practice. Please note, however, that significant hemorrhage or other complications can occur if the catheter is dislodged or severed, so 24-hour veterinary surveillance and monitoring is warranted.

**Pearl:** In general, it is best to use a 16 gauge central venous catheter for larger dogs (>7.5 kg) and 18 gauge central venous catheter for smaller dogs and cats (<7.5 kg). See the equipment section above.

## Placement of Ultrasound-guided Femoral Arterial Catheters and Sampling

### Ultrasound Settings and Probe Preferences

See Placement of an Ultrasound-guided Central Venous Jugular Catheter above.

### Equipment

For special procedures such as cardiac catheterization, use equipment (stylets, catheters) designed for that procedure. For general blood pressure monitoring and sampling (including via the femoral artery), arterial access can be maintained with standard short catheters (18–24 gauge, 1–1.5 inches) commonly used for peripheral (cephalic, saphenous) venous access.

**Pearl:** It is extremely important to secure any arterial catheter via tape and/or padding around the limb to prevent dislodgment and life-threatening hemorrhage while moving anesthetized or even awake patients.

### Procedure

The dynamic real-time technique with combinations of longitudinal and transverse orientation is described here, as briefly outlined under the central venous catheter section.

### Anatomy

The femoral artery is a continuation of the external iliac artery and courses along the medial aspect of the femur. Proximally, the femoral artery lies cranial to the femoral vein and caudal or medial to the saphenous nerve within the femoral triangle (formed by the sartorius muscle cranially, pectineus muscle caudally, and iliopsoas and vastus lateralis muscle

laterally); the femoral artery is covered only by the deep medial femoral fascia and a thin layer of skin, thus providing a convenient place for vascular access. Distal to the femoral triangle, these vessels are covered by the caudal belly of the semimembranosus muscle and course caudodistally in relation to the femur, crossing the mid to distal third of the femoral diaphysis at an angle of approximately 35° (Ringold and Kelmer 2008).

## Patient Preparation

Place the patient in lateral recumbency with the nondependent hindlimb abducted, extended, and immobilized by tethering it to the table by appropriate physical and/or chemical restraint techniques to allow access to the dependent limb's inguinal region (proximal medial thigh). Shave the medial thigh, giving ample room to aseptically prep the skin over the femoral artery insertion site.

**Pearl:** For aseptic ultrasound imaging, the probe may be placed in a sterile surgical glove or sterile obstetric sleeve as a protective barrier that is filled with acoustic coupling gel (see Figure 24.1).

Liberal local use of 70% isopropyl alcohol either by itself (which is often sufficient) or in combination with the gels mentioned below improves probe contact and greatly enhances image quality while maintaining a clean central venous catheter insertion site.

The attending veterinarian should keep in mind the following precautions.

- Alcohol-induced hypothermia (external cooling) may occur in any patient, especially smaller animals.
- The inherent flammability of alcohol is environmentally dangerous (fire, explosion) and poses burn risks to the patient in the event of electrical defibrillation.

Sterile acoustic coupling gels are commercially available and ideal (Aquasonics, Parker Laboratories, Fairfield, NJ). Although it lacks viscosity and tends to fall off the site, sterile K-Y Jelly can be used instead of sterile commercially available acoustic coupling gel.

**Pearl:** Excess alcohol and gel should be wiped off the fur and skin as soon as it is no longer needed.

## Orientation

Verify the ultrasound probe-to-screen marker orientation so that direction is accurate during the procedure. The ultrasound monitor must be located in a comfortable line of sight.

**Pearl:** It is difficult and potentially hazardous to insert a central venous catheter or arterial catheter when craning to look over your shoulder at the screen (Bowra 2006).

- Using the nondominant hand, place the ultrasound probe over the femoral triangle in transverse orientation relative to the axis of the proximal limb, proximal to the desired entry point on the skin, searching for the anechoic (black) circles of the vessel lumens (Figure 24.9).
- Structures (particularly artery vs vein) are most easily identified by anatomical location (the femoral artery is cranial to the femoral vein) and by intermittent gentle probe pressure because veins flatten (collapse) and arteries remain relatively circular (maintain their lumen and do not collapse) (Figure 24.10). Generally, the pulsatile motion of the artery is often observable in B-mode without the use of color flow Doppler. Color flow Doppler, when available, may be helpful in the learning phases to gain confidence in differentiating femoral artery from vein.

**Pearl:** Remember that the colors do not identify the vessel but rather are generally coded as red with flow toward the probe and blue with flow away from the probe.

**Pearl:** Color flow Doppler ultrasound imaging for pulsatile arterial flow is not 100% reliable because the artery's "jump" can transmit misinterpreted motion to the nearby vein, causing misidentification (Bowra 2006).

- Once the artery is identified, move distally along the femoral triangle to approximately middiaphysis of the femur in case multiple attempts are needed. By starting distally, the proximal femoral artery is spared and may be used for repeated attempts if necessary.
- Using a #11 scalpel blade or an extra 18 gauge to nick the skin 3–5 mm lateral to the vessel may facilitate getting the stylet through tough skin.

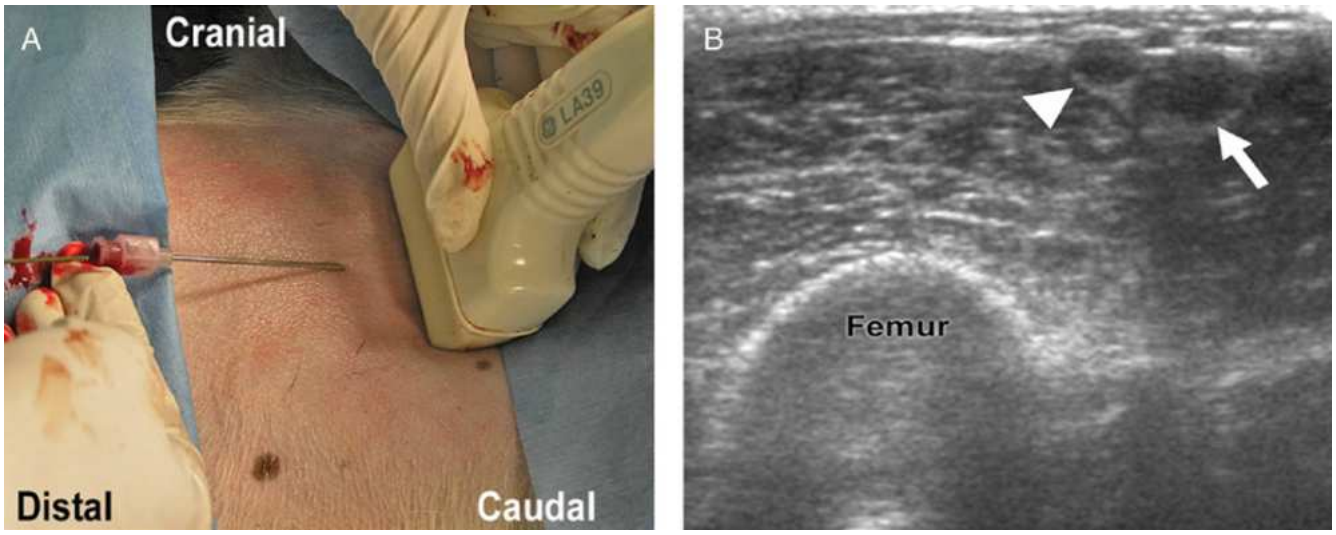


**Figure 24.9.** Femoral artery catheterization. (A) Orientation of the ultrasound transducer and introducer needle during catheterization of the femoral artery in a dog. (B) Transverse image of the femoral artery (*arrowhead*) and vein (*arrow*) with 12 MHz transducer at the level of the midfemoral diaphysis. The medial surface of the femur is seen as a curvilinear, hyperechoic (bright white) line (Ringold and Kelmer 2008).

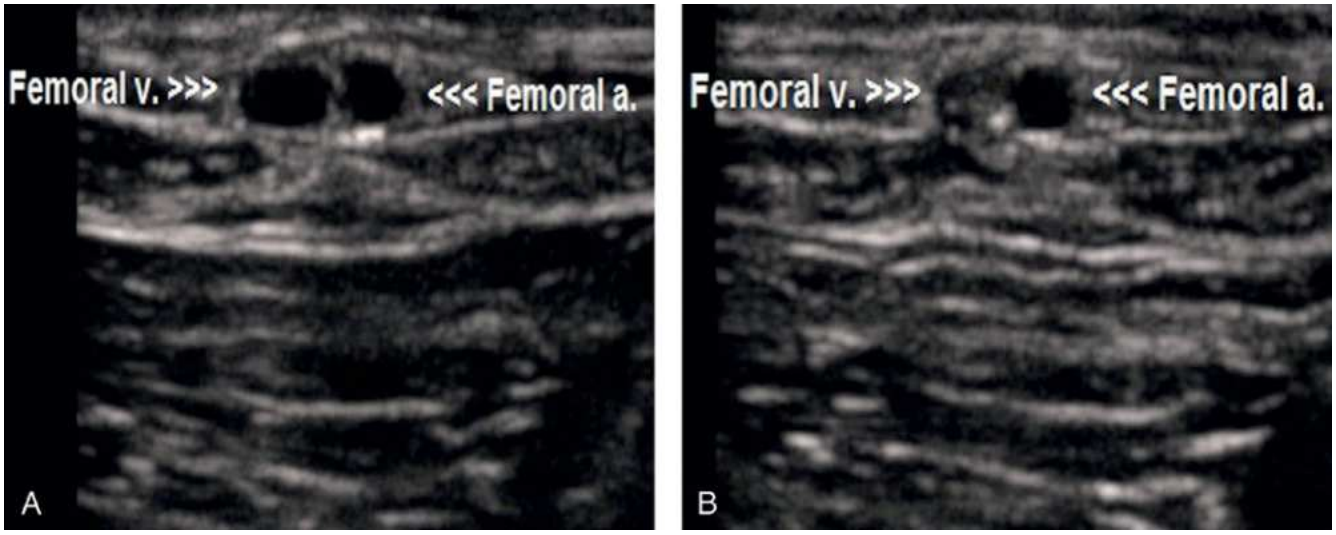


**Figure 24.10.** Compression technique for differentiating femoral vein from femoral artery. (A) Transverse image depicting normal probe pressure (no compression) with both femoral vein and artery visible. (B) Transverse image depicting disappearance of femoral vein with gentle probe pressure (compression) while femoral artery lumen remains an anechoic (dark) circle. The patient is in left lateral recumbency, so cranial is to the right. The compression technique is effective and reliable in discriminating between arteries and veins. Source: Reproduced with permission of Dr Gregory Lisciandro, Hill Country Veterinary Specialists and FASTVet.com, Spicewood, TX.

The skin can then be moved over to set up the subsequent introduction of the stylet into the vessel (Crowe 2009).

- With the probe in transverse orientation on the proximal (inguinal) side of the puncture site, the stylet (or needle) is then passed through the tented skin 1–2 cm away from the probe head at an approximate angle of 10–30° between the stylet and the plane of the skin, avoiding prematurely puncturing the femoral artery (stay superficial and off to its side).

**Pearl:** By keeping the stylet's tip 1–2 cm away from the probe, the maneuver also keeps the sharp point from damaging the rubber probe head.

- With the femoral artery reidentified, move the probe and alter the image depth and focus so the vessel appears in the center of the screen as an anechoic circle (transverse orientation), landmarking the femoral artery's position similar to the central venous catheter procedure previously described.
- The sonographer can either remain in transverse orientation, maintaining the anechoic (black) circle of the femoral artery throughout catheter placement (which is often easier for the novice), rotate the probe 90° to a longitudinal alignment, obtaining an anechoic (black) linear tract (representing the femoral artery), or use combinations of transverse and longitudinal orientation while keeping the femoral artery centered in the field of view.
- In either transverse or longitudinal orientation, the probe is placed just proximal (inguinal side) to the desired catheter entry point on the skin; however, in longitudinal orientation (very important), by convention for safety, the probe marker should be on the same side as the stylet or needle insertion.
- With the needle tip and artery visualized, maneuver the stylet and advance the tip into the femoral artery with a smooth and deliberate motion (to prevent it rolling away). If rolling occurs, withdraw the tip minimally to reposition the tip over the artery and reperform the advancement steps noted immediately above.
- For arterial catheterization, further advance the needle tip a few millimeters after getting the flash of bright red pulsatile blood from penetrating the artery's lumen.
- The tip of the stylet or the catheter may or may not be visible in the vessel's lumen, depending upon the relationship of the stylet and the beam and resultant echo interpretation by the ultrasound machine.
- Arteries do not tent as much as veins (see central venous catheter placement, above) due to their stiffer, more muscular walls.
- Backflow of pulsatile red blood is the best confirmation of successful arterial catheterization along with visualization of the stylet in the vessel lumen.

**Pearl:** As with the traditional blind technique, a sharp yet smooth and deliberate motion may be needed to get the stylet through the superficial wall of the vessel and into the lumen.

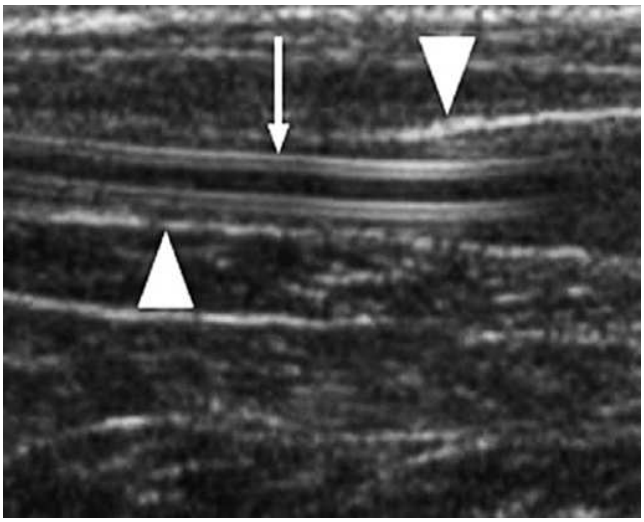

**Figure 24.11.** Longitudinal orientation. Longitudinal ultrasound image for the arterial catheter (*arrow*) inside the femoral artery (its wall is delineated by the solid triangle) (Ringold and Kelmer 2008).

- Now lessen the angle of the stylet to the artery and feed the catheter off into the vessel (for standard monitoring and sampling with a short catheter) or proceed with the Seldinger technique or other steps as required for special procedure equipment.
- Correct stylet placement in the femoral artery is confirmed via pulsatile red blood flow.
- Correct placement can also often be confirmed by visualizing a ring-down artifact of streaking hyperechoic (bright white) lines emanating from the metal stylet or guidewire if performing the Seldinger technique (see Figure 24.8) or, if a short catheter has been placed, visualization of the arterial catheter is possible (Figure 24.11).

**Pearl:** It can be harder to advance an arterial catheter off the stylet than the same (familiar) procedure in a peripheral vein. A moderately steady push will generally overcome the arteriospasm and allow the catheter to slide off the stylet. If the catheter remains in the lumen, pulsatile red blood will flow when the stylet is removed.

**Pearl:** It is extremely important to secure any arterial catheter with tape and/or padding around the limb to prevent dislodgment and life-threatening hemorrhage while moving anesthetized or even awake patients.

# General Comments regarding Transverse versus Longitudinal Orientation

As with any intravenous catheter placement, regardless of ultrasound guidance, the most challenging aspect of the procedure after finding the vein or artery is penetrating the superficial vessel wall without the vessel sliding or rolling away.

The longitudinal approach provides direct visualization of the stylet entering the skin while directing the stylet toward the jugular vein and during penetration of the lumen. It is easier to maintain visualization of the sharp tip of the stylet and relevant structures using the longitudinal orientation, avoiding complications such as inadvertent puncturing of the vessel's far wall and damage to other structures. The longitudinal approach is thus considered the safest orientation because it allows visualization of the stylet tip through the entire central venous catheter placement process.

On the other hand, some users find the longitudinal approach to be more difficult when redirecting the catheter if the vessel rolls away because of the difficulty discerning in real time which direction the stylet goes relative to the target vessel (medial vs lateral). Once this occurs, the sonographer may need to partially or fully rotate back to transverse orientation to determine how to redirect the stylet into the target vessel.

**Pearl:** Using a combination of transverse and longitudinal orientation may help keep the stylet and target visible in the ultrasound field of view at all times.

The transverse approach provides better visualization of the vessel of interest relative to other structures and more efficiently helps visualize redirection of the stylet when the vein or artery rolls. Moreover, transverse orientation is better suited where space is limited (i.e., for smaller or short-necked patients). However, there is a greater risk of losing track of the stylet's sharp tip and thus inadvertently damaging surrounding structures.

On the other hand, if the probe is placed too far rostrally over the stylet's midpoint or even as high as the hub (which can definitely occur while the clinician's attention is divided between the probe, the stylet, and the ultrasound image), then visualization of the sharp tip of the stylet within the narrow fan of the ultrasound beam will be lost. It is easier to lose track of the tip of the stylet in transverse than longitudinal orientation as mentioned above, thus risking damage to other structures.

**Pearl:** Use a slightly steeper approach angle to the skin with the stylet (than the traditional blind or landmark technique), and consider using combinations of transverse orientation and longitudinal orientation to keep the stylet and jugular vein visible in the field of view at all times (see Figure 24.6).

# How to Make a Realistic Practice Phantom

Ultrasound-guided vascular access has a shallow learning curve but the opportunity to gain proficiency before attempting the technique in an emergent or unstable patient supports patient safety and operator success. A simple model (phantom) using inexpensive, readily available supplies was recently developed that provides hands-on training with realistic high-fidelity images including normal tissue planes and echogenicity. The author has used this easily constructed model in international settings to successfully teach ultrasound-guided vascular access to veterinary care providers of varying levels of experience. The materials and techniques are highlighted here, and more details including videos are available at www.vascular-access.info (Rippey et al. 2015).

## *Supplies*

A photograph of the supplies needed to construct the chicken breast phantom model is shown in Figure 24.12.

- Modeling balloons (the long thin ones used to make balloon animals work best to simulate veins, available at party or hobby shop retailers) and/or Pezzer tubes (arteries).
- Colored fluid (simulated "blood").
- 60 cc catheter-tipped syringe, to load the blood into the balloon simulated vessels.
- Plastic cling wrap, i.e., Saran Wrap®.
- Acoustic coupling gel.
- IV catheters (short and/or long).
- Boneless skinless chicken breasts (not too thick, or the catheter is too short to feed effectively).
- Exam gloves (both for the user and to put the ultrasound gel and probe into – the image quality remains good while your probe is further protected from contact with the chicken).

- Shallow aluminum or plastic tray/pan (to hold the model during practice).
- Table drape and/or chuck towels.
- Sanitizing spray and wipes.

### *Assembling the Chicken Breast Phantoms*

- Fill the balloons with the colored fluid using the catheter-tipped syringe. Try to remove all air before tying off or clamping the balloon to avoid this artifact in your simulated vessel.

**Figure 24.12.** Chicken breast phantom supplies. Layout of most key items for creating the chicken breast phantom to practice ultrasound-guided vascular access.

- Filling until you have a small (1–2 cm) "bleb" seems to provide a good pressure and facilitates a "flash" of fluid when the catheter stylet punctures the balloon simulating the vessel. The balloon can generally be reused a few times in the phantom before being replaced and with smaller volumes simulates patient hypotension.
- Next place the chicken breast flat on a single layer of Saran Wrap. Lay your new "vessels" down on the exposed surface of the chicken breast, then place another breast on top and wrap the phantom "sandwich" in Saran Wrap (Figures 24.13 and 24.14). You can also roll the vessels up within the same (large) breast and the Saran Wrap.
- Remove all the air to avoid artifact; adding some gel next to the vessels before wrapping the phantom can also help.
- To hygienically protect your ultrasound probe, place some acoustic coupling gel into an exam glove, then insert the probe (the same technique used for sterile ultrasound-guided procedures – see Figure 24.1).
- For hygiene and safety, discard the models and use the sanitizing spray/wipes to clean the area after training.

You are now ready to practice the vascular access procedures described in this chapter. Try the different strategies and orientations to see what works best for you. It's wise to develop some level of proficiency with each of the techniques; longitudinal may be your

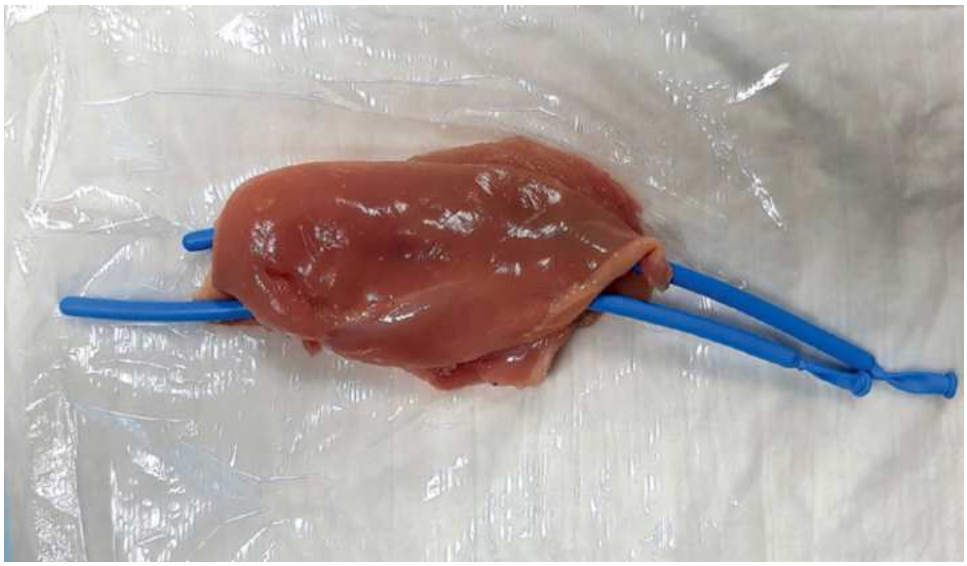

**Figure 24.13.** Chicken breast model assembly part I. Fluid-filled modeling balloons placed as simulated vessels between two chicken breast fillets before being wrapped in plastic wrap.

**Figure 24.14.** Chicken breast model assembly part II. Chicken breasts and balloon "vessels" wrapped in 2–3 layers of Saran Wrap. Note that alcohol provides great contact and image quality on actual patients, but gel is required for this Saran Wrap-wrapped phantom chicken breast model.

favorite method but transverse may be the only option in some small patients. Note that alcohol provides great contact and image quality on actual patients, but gel is required for this Saran Wrap-wrapped phantom chicken breast model.

# Pearls and Pitfalls, The Final Say

Real-time ultrasound-guided vascular access can be technically challenging at first but has a relatively shallow learning curve. It has been shown that proficiency may be readily mastered by the nonradiologist veterinary sonographer with minimal training (enabled by simple and affordable models), the procedure is fast and has the potential to become an invaluable asset to your practice.

A few key points.

- Place the ultrasound screen in a line of vision that is comfortable for you. This is safest for your patient as well.
- Liberal use of 70% isopropyl alcohol is generally sufficient for good image quality; however, some probe heads will incur damage (check manufacturer's guidelines), and alcohol may excessively cool the patient and increase risk of burns if electrical defibrillation is required.
- For initial emergency resuscitation, a short, large-bore (18 gauge, 1.5 inch) catheter can be placed in the jugular vein for rapid easy vascular access and high fluid rates. Just be careful because the skin over the vessel is highly mobile in this area, and the short catheter can come out of the jugular vein into the subcutaneous space during patient movement.
- The short catheter also provides an excellent conduit after initial stabilization for a guidewire and replacement with a true central venous catheter using a modified Seldinger technique.
- Color flow Doppler can sometimes be helpful but is not required for vasculature structure identification, and it has some inherent artifactual problems if a patient is uncooperative because movement compromises its diagnostic utility.
- The compression technique during B-mode is often adequate to discriminate veins (which collapse with compression) from arteries (which do not collapse).
- Focus on keeping the sharp tip of the stylet and the target vessel visible in the field of view at all times for success and safety. Using combinations of transverse and longitudinal orientation is sometimes helpful.

**Pearl:** Remember, the width of the ultrasound beam emitted by the probe is actually quite narrow.

- Move the stylet (or needle in some kits, see above) slowly, and look for tenting as the tip lands on the superficial proximal wall of the vessel.
- Models or phantoms can be made with Jello (incorporating embedded objects like grapes or tomatoes as targets), polony, or chicken breasts and modeling balloons (Wells and Goldstein 2010; Rippey et al. 2015; www.vascular-access.info).
- Phantoms also can be purchased for practicing stylet orientation and tracking. Starting with a large dog with more easily recognized and larger anatomy instead of a pug or a cat may also be helpful.

- Obesity, hematomas, hypotension, and so on do not appear to affect success rates or perceived difficulty for ultrasound-guided vascular access techniques, and the learning curve is shallow (Ringold and Kelmer 2008; Chamberlin et al. 2013).
- The axiom "See one, do one, teach one" works well in training multiple members of the staff to become confidently proficient.

# References


AIUM. 2013. AIUM practice guideline for the use of ultrasound to guide vascular access procedures. *J Ultrasound Med* 32:191–215.

Blaivas M, Brannam L, Fernandez E. 2003. Short-axis versus long-axis approaches for teaching ultrasound-guided vascular access on a new inanimate model. *Acad Emerg Med* 10(12):1307–1311.

Bowra J. 2006. Central venous access. In: *Emergency Ultrasound Made Easy*, edited by Bowra J, McLaughlin RE. Edinburgh: Churchill Livingstone Elsevier, pp 59–72.

Chamberlin S, Sullivan L, Boscan P. 2013. Evaluation of ultrasound-guided vascular access in dogs. *J Vet Emerg Crit Care* 23(5):498–503.

Crowe DT. 2009. Patient triage. In: *Small Animal Critical Care Medicine*, edited by Silverstein D, Hopper K. St Louis: Saunders, pp 5–9.

Froehlich CD, Rigby MR, Rosenberg ES, et al. 2009. Ultrasound-guided central venous catheter placement decreases complications and decreases placement attempts compared with the landmark technique in patients in a pediatric intensive care unit. *Crit Care Med* 37(3):1090–1096.

Izer J, Wilson R, Hernon K, Undar A. 2017. Ultrasound-guided vessel catheterization in adult Yorkshire cross-bred pigs. *Vet Anaesth Analg* 44(1):133–137.

Karakitsos D, Labropoulos N, de Groot E, et al. 2006. Real-time ultrasound-guided catheterization of the internal jugular vein: a prospective comparison with the landmark technique in critical care patients. *Crit Care Med* 10(6):162.

Kusminsky RE. 2007. Complications of central venous catheterization. *J Am Coll Surg* 204(4):681–696.

Kweon MV, Bhamidipaty A, Holden A. 2012. Antegrade superficial femoral artery versus common femoral artery punctures for infrainguinal occlusive disease. *J Vasc Interv Radiol* 23(9):1160–1164.

Miller AH, Roth BA, Mills TJ, et al. 2002. Ultrasound guidance versus the landmark technique for the placement of central venous catheters in the emergency department. *Acad Emerg Med* 9(8):800–805.

Milling TJ, Rose J, Briggs WM, et al. 2005. Randomized, controlled clinical trial of point-of-care limited ultrasonography assistance of central venous cannulation: the Third Sonography Outcomes Assessment Program (SOAP-3) Trial. *Crit Care Med* 33(8):1764.

Mitchell SE, Clark RA. 1979. Complications of central venous catheterization. *Am J Roentgenol* 133(3):467–476.

Mustapha JA, Sandoval-Diaz LJ, Jaff MR, et al. 2016. Ultrasound-guided arterial access: outcomes among patients with peripheral artery disease and critical limb ischemia undergoing peripheral interventions. *J Invasive Cardiol* 28:259–264.

Pavlisko, N, Soares J, Henao-Guerrero N, et al. 2018. Ultrasound-guided catheterization of the femoral artery in a canine model of acute hemorrhagic shock. *J Vet Emerg Crit Care* 236(6):579–584.

Pirotte T, Veyckemans F. 2007. Ultrasound-guided subclavian vein cannulation in infants and children: a novel approach. *Br J Anaesth* 98(4):509–514.

Ringold SA, Kelmer E. 2008. Freehand ultrasound-guided femoral arterial catheterization in dogs. *J Vet Emerg Crit Care* 18(3):306–311.

Rippey JC, Blanco P, Carr PJ. 2015. An affordable and easily constructed model for training in ultrasound-guided vascular access. *J Vasc Access* 16:422–427.

Theodoro D, Bausano B, Lewis L, et al. 2010. A descriptive comparison of ultrasound-guided central venous cannulation of the internal jugular vein to landmark-based subclavian vein cannulation. *Acad Emerg Med* 17(4):416–422.

Wells M, Goldstein L. 2010. The polony phantom: a cost-effective aid for teaching emergency ultrasound procedures. *Int J Emerg Med* 3(2):115–118.

Wigmore TJ, Smythe JF, Hacking MB, et al. 2007. Effect of the implementation of NICE guidelines for ultrasound guidance on the complication rates associated with central venous catheter placement in patients presenting for routine surgery in a tertiary referral centre. *Br J Anaesth* 99(5):662–665.


# Further Reading


Emerman CL, Pinchak AC, Hancock D, et al. 1988. Effect of injection site on circulation times during cardiac arrest. *Crit Care Med* 16(11):1138–1141.

Prittie J. 2006. Optimal endpoints of resuscitation and early goal-directed therapy. *J Vet Emerg Crit Care* 16(4):329–339.

Rivers E, Nguyen B, Havstad S, et al. 2001. Early goal-directed therapy in the treatment of severe sepsis and septic shock. *N Engl J Med* 345(19):1368–1377.

Szatmári V, Sótonyi P, Voros K. 2001. Normal duplex Doppler waveforms of major abdominal vessels in dogs: a review. *Vet Radiol Ultrasound* 42(2):93–107.

Zwingenberger A, Wisner ER. 2008. Neck. In: *Atlas of Small Animal Ultrasonography*, edited by Penninck D, d'Anjou MA. Ames: Blackwell Publishing, pp 102–105.

CHAPTER TWENTY-FIVE

# POCUS: Vascular – Veins and Arteries

Gregory R. Lisciandro

## Introduction

Throughout this textbook, you are learning image acquisition and the ultrasonographic appearance of fluid (cavitary effusions to fluid-filled organs to viscus organs), various soft tissues (muscle to solid organs to nerves), bone and air (lung to viscus organs). Imaging fluid-filled vessels is another skill to add to your armamentarium with the potential to improve patient care and outcome.

POCUS vascular is not meant to be a standalone examination without the Global FAST approach. Applying Global FAST should be an extension of your physical examination and POCUS vascular an add-on so that major easily detected conditions within the abdomen, retroperitoneal space, and thorax are not missed. Moreover, most thromboembolic disease is a result of another disease process, which may be treatable. And, by using Global FAST as a more effective surveillance system and a first-line evaluation, the triggering of thromboprophylaxis and thrombolytics becomes more evidence based by "seeing" the problem(s) for decision making.

This chapter will briefly review the major sites and principles for the detection (or suspicion) of venous and aortic thrombosis and thromboembolism in small animals, of which very little is known. The use of POCUS and FAST ultrasound has the ability to change another traditionally difficult paradigm.

### *What POCUS Vascular Can Do*

- Identify fluid-filled vessels and distinguish veins from arteries using the compression technique.
- Screen for sonographic evidence of venous thrombosis, arterial thrombosis, and pulmonary thromboembolism.
- Screen for abnormalities in veins and arteries supported by their distension, collapse and soft tissue thrombi within using the general principles of obstruction to flow within a conduit.
- Provide a means to dictate thrombolytics and thromboprophylaxis and monitor response to therapy.
- Develop your use of color Doppler.

### *What POCUS Vascular Cannot Do*

- Cannot identify superficially located small veins and arteries without a stand-off device.
- Cannot replace adequate training because vascular imaging often requires more knowledge of your ultrasound machine, imaging techniques, probe changes, and ultrasonographic anatomy.

### *Indications*

- Add-on to all at-risk patients for venous and arterial thrombosis and pulmonary thromboembolism.
- Edematous limbs.

*Point-of-Care Ultrasound Techniques for the Small Animal Practitioner*, Second Edition. Edited by Gregory R. Lisciandro.
© 2021 John Wiley & Sons, Inc. Published 2021 by John Wiley & Sons, Inc.
Companion website: www.wiley.com/go/lisciandro/ultrasound2

- Acute respiratory signs.
- Post heartworm treatment.
- Patients undergoing chemotherapy.
- Total hip replacement surgery, and other postsurgical invasive bone procedures.

### Objectives

- Distinguish between veins and arteries using the compression technique with and without the use of color Doppler.
- Understand how to use color flow Doppler.
- Survey major vessels for evidence of venous and arterial thrombosis and thromboembolism.

## Equipment, Materials, and General Preparation

### Probe

Most curvilinear (microconvex) probes with frequency ranges of 5–10 MHz on abdominal presets that are commonly used in small animal practice may be used for vascular imaging of the larger vessels within the abdominal cavity. However, for more superficial vessels, especially with limbs, linear transducers with a minimum frequency of 7.5 MHz are preferred because of their superior detail at shallow depths. Additionally, the "Small Parts" or "Vascular" presets on your machine will optimize the imaging detail with either probe type, and a stand-off device further optimizes image quality and may be mandatory for superficial vessels (see Chapters 30–35).

### Patient Preparation

In general, shaving of hair is not required for POCUS, but in thickly coated patients or those in which imaging is not satisfactory for the detail required for interrogation of the area of interest, shaving will likely improve your image. Parting the hair is often helped by wetting the hair first with 70% isopropyl alcohol, which is then reapplied to the skin as needed with the addition of either alcohol-based hand sanitizer or commercially available acoustic coupling gel, dependent on sonographer preference. Maximize probe head to skin contact with ample coupling medium using combinations of 70% isopropyl alcohol, commercially available gel, and alcohol-based hand sanitizer.

### General Principles and Compression Technique

By combining principles you will have a better probability of being correct in your assessment of venous and arterial thrombosis, thromboembolism and the degree of their obstruction. As with any obstructive process to unidirectional flow within a conduit, the proximal side will have dilation and the distal side attenuation. Importantly and generally counter to logic, the acute nascent thrombus (clot) is poorly echogenic and often anechoic (like blood), being difficult to directly image. Thus, color Doppler is important to apply to the vessel(s) of interest to enhance imaging of the thrombus as well as the deviations of expected blood flow within an unobstructed vessel. Physically, pressure compression is important for a couple of reasons: (1) veins, being a lower pressure system and thinner-walled, collapse before arteries in normalcy, and (2) veins, when obstructed, become less compressible. The use of the compression technique is often adequate for differentiating vein from artery (Figure 25.1). This principle is used as a diagnostic strategy for detecting deep venous thrombosis (DVT) in the lower limbs of people using B-mode, often without color flow Doppler (Crisp et al. 2010; Kory et al. 2011). However, importantly, venous blood can be sluggish and echogenic, especially in larger veins, mimicking soft tissue, advocating for the use of color Doppler in veterinary patients (Nyland and Mattoon 2015; Nyland et al. 2015).

### Color Doppler

There are a few different types of color Doppler but most commonly color flow Doppler, which gives an overview of flow, will be used by the nonradiologist. Color flow Doppler is necessary for two major reasons: acute thrombi often are poorly echogenic and not obvious with gray-scale B-mode imaging, and to differentiate sluggish venous flow from a thrombus (Nyland and Mattoon 2015; Nyland et al. 2015). However, color flow Doppler has some limitations including patient movement (panting, trembling, or struggling), which leads to motion artifacts causing the Doppler colors to "jump" to other areas. Similarly, the color flow Doppler gain setting has a profound effect (aliasing) on image quality and overgaining leads to a similar problem with colors "jumping" to other areas (Figure 25.2). Color flow is also affected by other basics such as the angle of insonation and the focus cursor. Learn how to adjust the gain, place the focus cursor across from the area of interest, and manipulate the

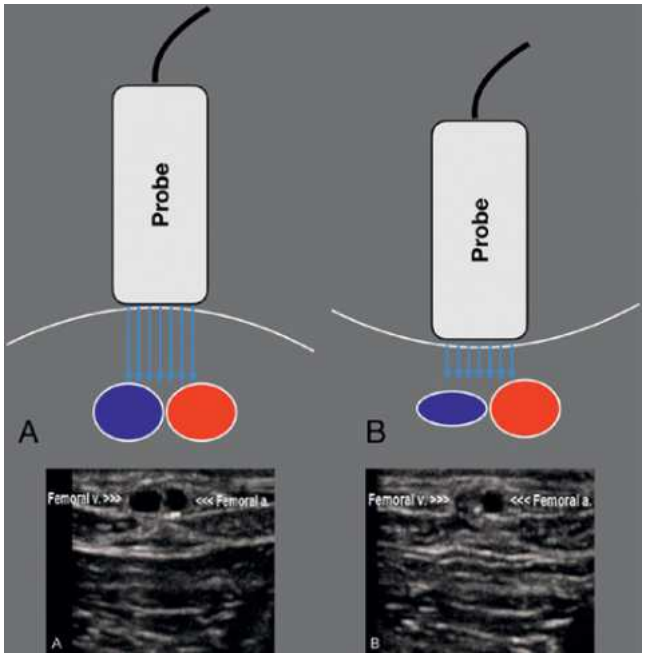


**Figure 25.1.** Compression technique. The use of compression with the probe head will as a general rule collapse veins before collapsing arteries. In (A) both the femoral vein and artery are shown on a B-mode image using a linear probe. In (B) probe pressure is applied and the femoral vein collapses while the integrity of the femoral artery is maintained. The compression technique allows for identification of vessels without color Doppler (Crisp et al. 2010). Moreover, noncompressible veins support deep venous thrombosis. Source: Reproduced with permission of Dr Gregory Lisciandro, Hill Country Veterinary Specialists and FASTVet.com, Spicewood, TX.

angle of insonation for best imaging using color flow Doppler. In most machines, the color flow Doppler gain is the same wheel or button as the overall B-mode gray-scale gain.

### *Vessel Orientation and Slice-thickness Artifact*

Vessels are imaged in their longitudinal (also referred to as long-axis) and transverse (also referred to as short-axis) planes. Longitudinal elongates the vessel as a tube and transverse brings the vessel into the shape of a circle or oval (Figure 25.3). Slice-thickness artifact can occur in larger veins that are within solid organs (primarily hepatic veins and the caudal vena cava passing through the liver) and mimic a thrombus when imaged in longitudinal planes. To help differentiate slice-thickness artifact from a true thrombus, rotate the probe to the transverse plane, which will as a rule eliminate the artifact (Figure 25.4) (Nyland and Mattoon 2015; Nyland et al. 2015).

### *Porta Hepatis Anatomy*

It is important to learn the anatomy of the closely associated aorta, caudal vena cava (CVC), and portal vein imaged via the 10–12th intercostal spaces in a transverse plane with the probe oriented parallel to the ribs. At this porta hepatis view, the aorta, CVC, and portal vein may be imaged side by side from cranial to caudal within the same view (see Chapter 26) (see also Figures 16.15, 16.16, 26.2, 26.5, and 39.3).

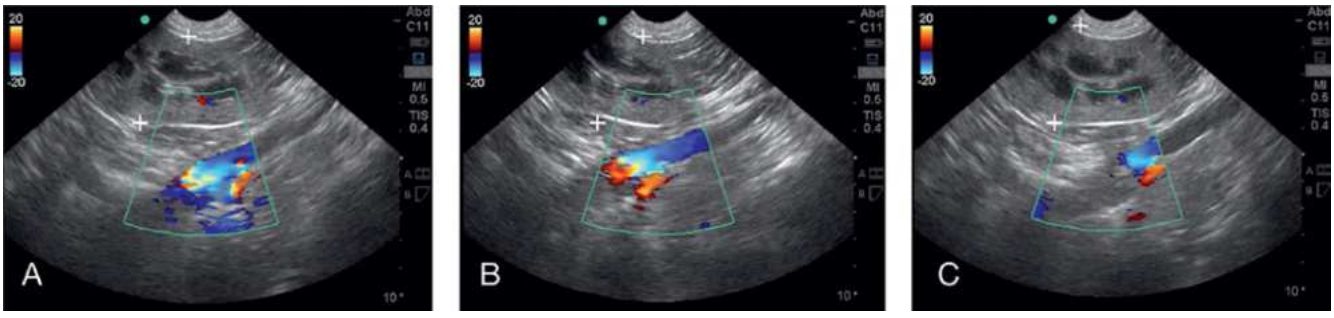


**Figure 25.2.** Optimizing color flow Doppler. Changes achieved by lowering the gain on the great vessels (caudal vena cava and aorta) along the left kidney at the AFAST spleno-renal (SR) view of the same dog. In (A) the color flow Doppler (CFD) is overgained followed by successive lowering of gain adjustments. Note how the CFD is more limited to flow within the vessels and not "jumping" to other areas in (B) followed by (C). The image and use of CFD are optimized in (C). Patient movement will also cause "jumping" of the color to adjacent areas. Crosses (+) outline the borders of the left kidney. Source: Reproduced with permission of Dr Gregory Lisciandro, Hill Country Veterinary Specialists and FASTVet.com, Spicewood, TX.

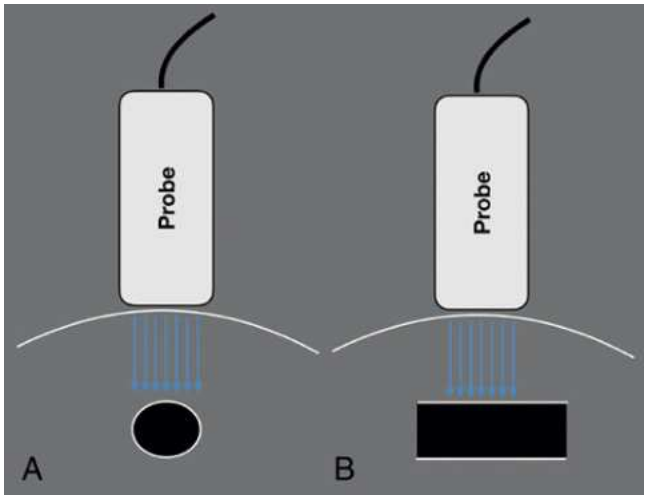


**Figure 25.3.** Transverse (short-axis) and longitudinal (long-axis) orientation planes of the vessel. (A) The short-axis or transverse plane of the vessel and (B) the long-axis or longitudinal plane. In general, measuring vessels in short-axis/transverse planes is more accurate than in long-axis/longitudinal planes (Darnis et al. 2018). Moreover, artifact (slice-thickness) is less problematic in vessels in short-axis/transverse planes (Nyland and Mattoon 2015; Nyland et al. 2015). It is best practice to do both planes habitually. Source: Reproduced with permission of Dr Gregory Lisciandro, Hill Country Veterinary Specialists and FASTVet.com, Spicewood, TX.

# Venous and Arterial Thromboembolism

## *Central and Deep Venous Thrombosis*

Central venous thrombosis is seen in small animals, often in the CVC (see Figure 25.6) and splenic veins. Other venous thrombosis sites detected ultrasonographically in small animals include hepatic, portal, renal, jugular cranial vena cava and pulmonary veins (Nyland and Mattoon 2015). Venous thrombosis is relatively unstudied in small animals in terms of prevalence and causes. However, neoplastic, inflammatory (immune-mediated disease, pancreatitis, sepsis), cardiac, and infectious diseases, including parasitic, and glucocorticoids are common risk factors as they relate to Virchow's triad (hypercoagulability, endothelial injury, and stasis or turbulence of flow) (Goggs et al. 2009; Laurenson et al. 2010; Nyland and Mattoon 2015; Nyland et al. 2015).

## *Hepatic Venous and Caudal Vena Cava Thrombosis*

The hepatic veins empty into the CVC and are routinely visualized at the FAST diaphragmatico-hepatic (DH) view and during POCUS liver and gallbladder.

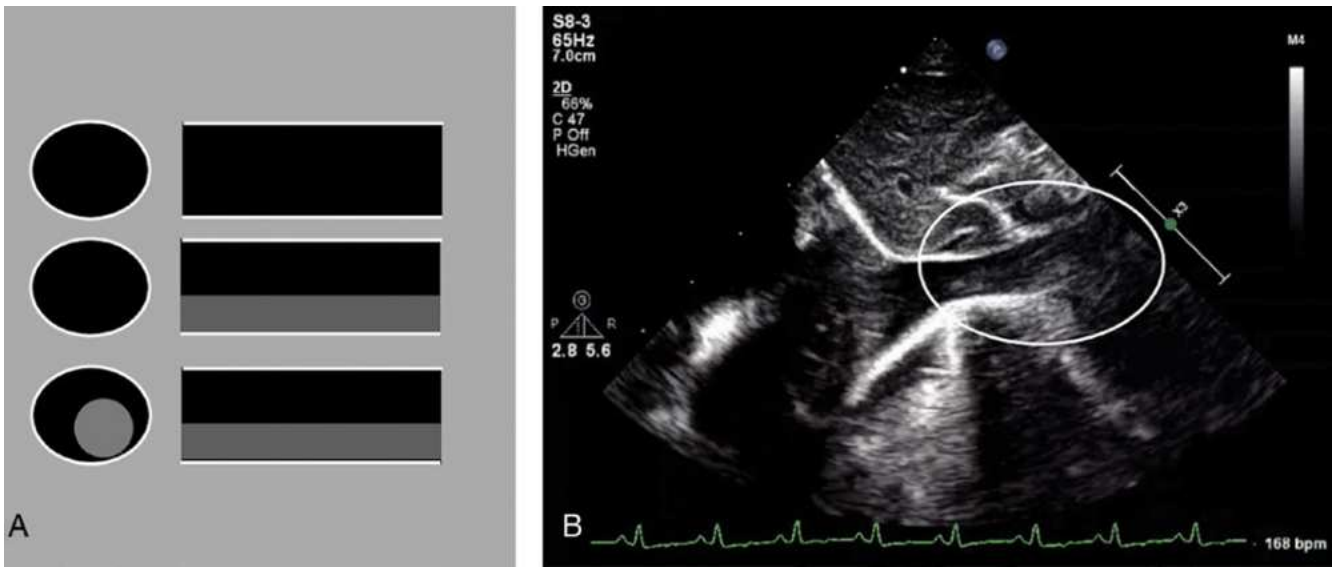


**Figure 25.4.** Slice-thickness artifact and correlation between short-axis/transverse and long-axis/longitudinal orientation planes. (A) The contrast between short-axis/transverse planes and long-axis/longitudinal planes with echogenicity that correlates between each plane (*top*), and then echogenic material in long-axis/longitudinal planes without (*middle*) and with (*bottom*) correlation between the two planes. When the echogenic material is seen in both planes, a thrombus is more likely versus when only seen in long-axis/longitudinal and lacking in short-axis/transverse planes, slice-thickness artifact is more likely (Nyland and Mattoon 2015; Nyland et al. 2015). In (B) the caudal vena cava (CVC) is shown as it traverses the diaphragm at the FAST DH view. Its near wall and far wall are hyperechoic lines. The oval outlines the portion of the CVC that has slice-thickness artifact, which could be mistaken for a thrombus without careful interrogation. Source: Reproduced with permission of Dr Gregory Lisciandro, Hill Country Veterinary Specialists and FASTVet.com, Spicewood, TX, and ultrasound image in (B) courtesy of Dr Jessica Ward, Ames, Iowa.

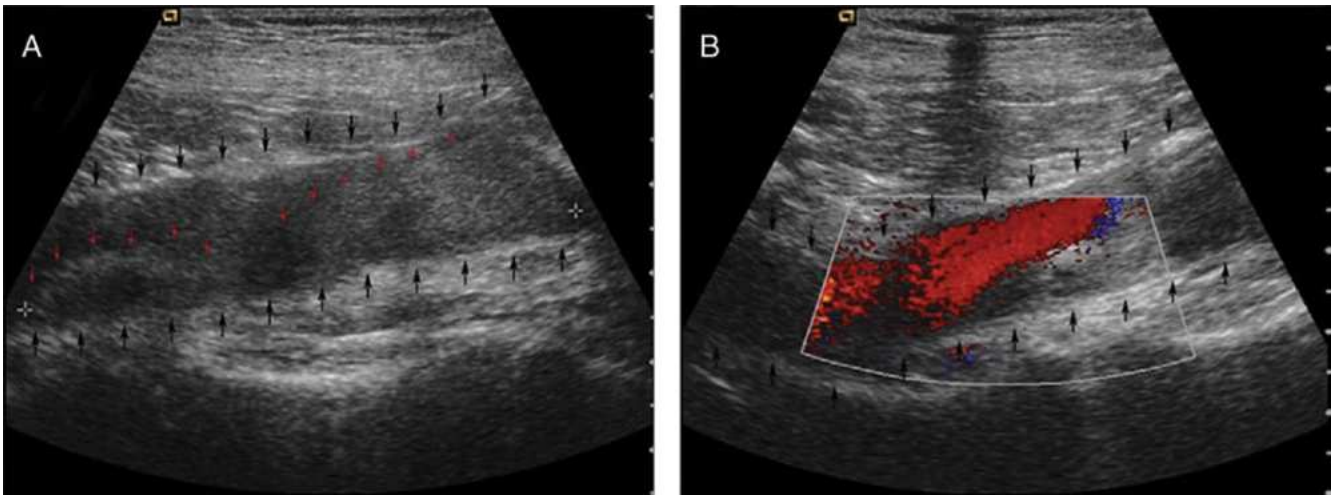


**Figure 25.5.** Arterial thromboembolism comparing B-mode to color flow Doppler. Two-dimensional ultrasonography image in (A) of the distal aorta of a dog with aortic thrombosis (AT). Black arrows outline the aorta. Blood flow (*red*) within the aorta is diminished at the location of the thrombus. Blood flow at the distal aorta would be cranial to caudal (left to right). (B) The B-mode image shows how a clot and slice-thickness artifact (or in veins sluggish flow) could look similar. The image emphasizes the use of color flow Doppler and the thought process to use to increase the probability of a correct interpretation. Source: Reproduced from Gonçalves et al. (2008) with permission from John Wiley and Sons.

Hepatic veins as a general rule are inapparent in lateral and standing and sternal recumbency during FAST examinations. Anecdotally, hepatic venous distension occurs to some extent in dogs and cats placed into dorsal recumbency (Lisciandro 2014, unpublished). Principles of upstream venous distension due to downstream obstruction to flow and echogenic material within the venous lumen are characteristic. However, acute nascent clots may appear as anechoic as the blood in the venous lumen, and thus not apparent with B-mode gray-scale imaging (Nyland and Mattoon 2015). Furthermore, hepatic veins can have slice-thickness artifact mimicking a thrombus, and thus rotating the probe to the transverse plane will help eliminate the artifact (see Figure 25.4) (Nyland and Mattoon 2015). When hepatic venous distension is thought to be a thrombus, color flow Doppler should be added to differentiate sluggish flow from obstruction (Nyland and Mattoon 2015). In another example, the use of color flow Doppler is also shown contrasting B-mode and color flow Doppler in a case of aortic arterial thromboembolism in a dog. Also, direction of flow is important to consider depending on whether imaging veins or arteries (Figures 25.5 and 25.6) (see also Figures 16.6, 26.2, 26.3, 26.6, 26.7, and 39.3).

Obstruction of the hepatic venous system, when severe enough, leads to hepatic venous congestion and ascites (see Chapters 6, 7, 19–21, and 26). The Global FAST approach surveys for other causes of hepatic venous congestion, such as right-sided congestive heart failure including pericardial effusion, dilated cardiomyopathy, and pulmonary hypertension, while incorporating lung (Vet BLUE) and the CVC and hepatic veins. More directed POCUS examinations might then follow, such as POCUS heart, POCUS caudal vena cava, and POCUS kidney.

## *Splenic Venous Thrombosis*

Anatomically, the splenic vein is part of the portal system and joins with the cranial and caudal mesenteric veins and the gastroduodenal vein to form the portal vein. Concurrent diseases have been documented in 80 dogs with splenic venous thrombosis (SVT) detected by ultrasound (Laurenson et al. 2010). In this case series, 33% of the dogs had concurrent splenic infarction (see Chapter 9), and 18 % had concurrent portal venous thrombosis, of which 64% had ascites (Laurenson et al. 2010). SVT was found to be most prevalent in dogs with concurrent neoplasia (54%) with 25% having round cell neoplasia (lymphosarcoma > leukemia > mast cell > histiocytic > melanoma). Concurrent nonneoplastic conditions included systemic inflammatory response syndrome (26%), disseminated intravascular coagulation (20%), pancreatitis (18%), immune-mediated anemia (16%), and renal failure without proteinuria (14%), with many dogs having more than one concurrent condition. Interestingly, dogs with protein-losing nephropathy and hyperadrenocorticism made up <10% of cases. Exogenous steroid administration was also common among SVT dogs (43%) (Laurenson et al. 2010).

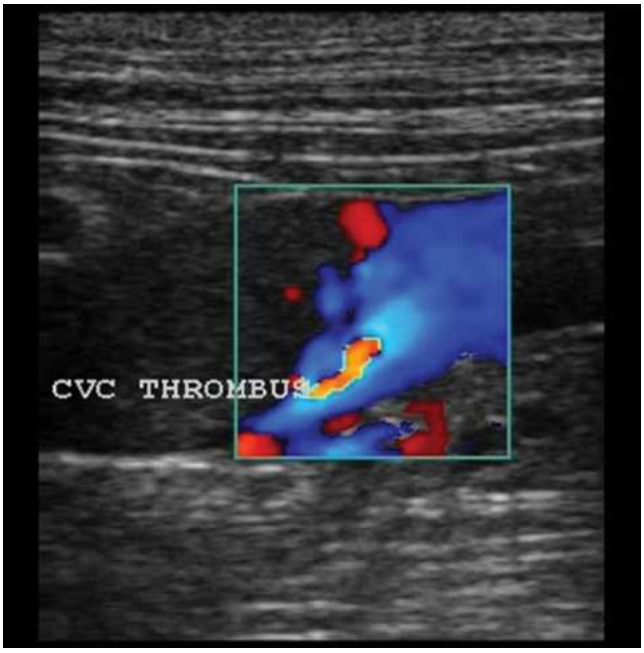


**Figure 25.6.** Thrombus associated with an adrenal tumor in a dog. The thrombus is nearly occluding all of the caudal vena cava (CVC) lumen as evidenced by the echogenic material and attenuation of the color flow Doppler due to obstruction of flow to the heart (cranial to the left and caudal to the right). The adrenal tumor is not shown. With the head to the left of the screen, blood flows caudal to cranial (obstructed going cranially) and is different from the flow in the aortic thrombosis/thromboembolism images in which the direction is opposite (obstructed flowing caudally) (see also Figure 16.6). Source: Image courtesy of Dr Sarah Young, Echo Service for Pets, Ojai, CA.

The SVT was commonly detected in the region of the splenic hilus (Figure 25.7) (see also Figures 9.11, 16.10B, and 39.8). The splenic hilus is easily recognizable during a POCUS spleen because of the obvious splenic venous branching forming a "Y" shape or "whale tail" effect in both dogs and cats (see Chapters 9 and 39, Figure 39.8). The splenic artery runs along the splenic vein, but splenic arterial branches are difficult to image and the splenic artery is less conspicuous than its vein. Color flow Doppler is needed to differentiate sluggish splenic flow from a true thrombus (Nyland and Mattoon 2015). With repetition, the nonradiologist performing Global FAST and POCUS will be able to recognize the splenic vein and the splenic hilus as abnormal (and its parenchyma as abnormal from splenic infarction), thus capturing the case for a complete detailed abdominal ultrasound, other indicated testing, and triggering adjustment in clinical course including treatment. Global FAST is important to stage the patient including detecting concurrent effusions and obvious soft tissue abnormalities of the abdominal organs, heart, and lung surface (see Chapters 36 and 37).

## *Portal Venous Thrombosis*

The portal vein is closely related to the splenic vein and CVC. Principles are similar to other centrally located venous thrombosis and if portal vein thrombosis is severe enough, ascites and shunting of the collateral venous system will occur. The most definitive region to recognize the portal vein for the nonradiologist

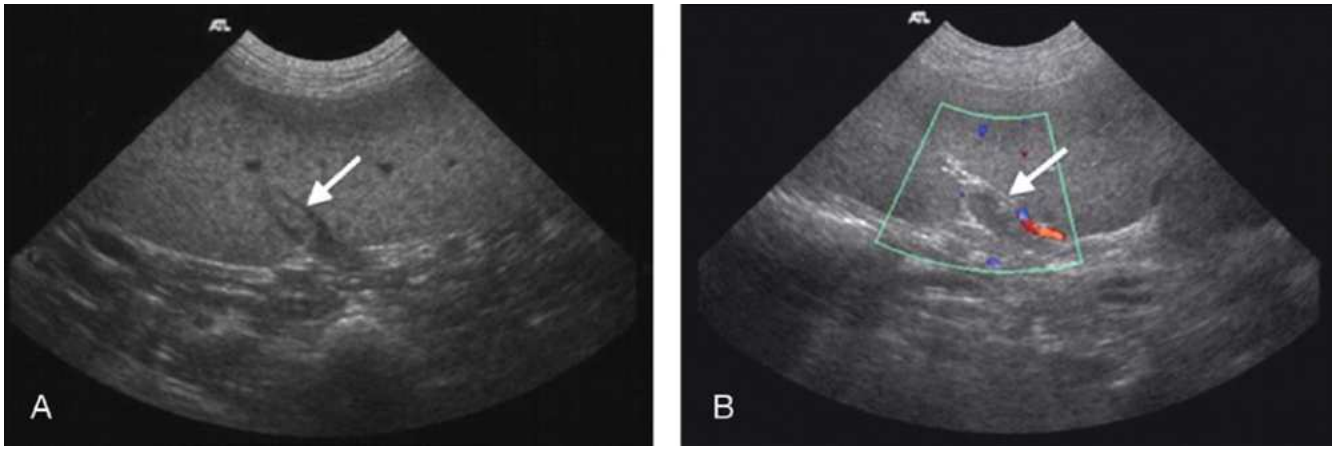


**Figure 25.7.** Splenic venous thrombosis in a dog. (A) Abdominal ultrasound image demonstrating an echogenic thrombus in one of the splenic veins. (B) Abdominal ultrasound with color Doppler demonstrating lack of blood flow within one of the splenic veins. Source: Reproduced from Laurenson et al. (2010) with permission from John Wiley & Sons.

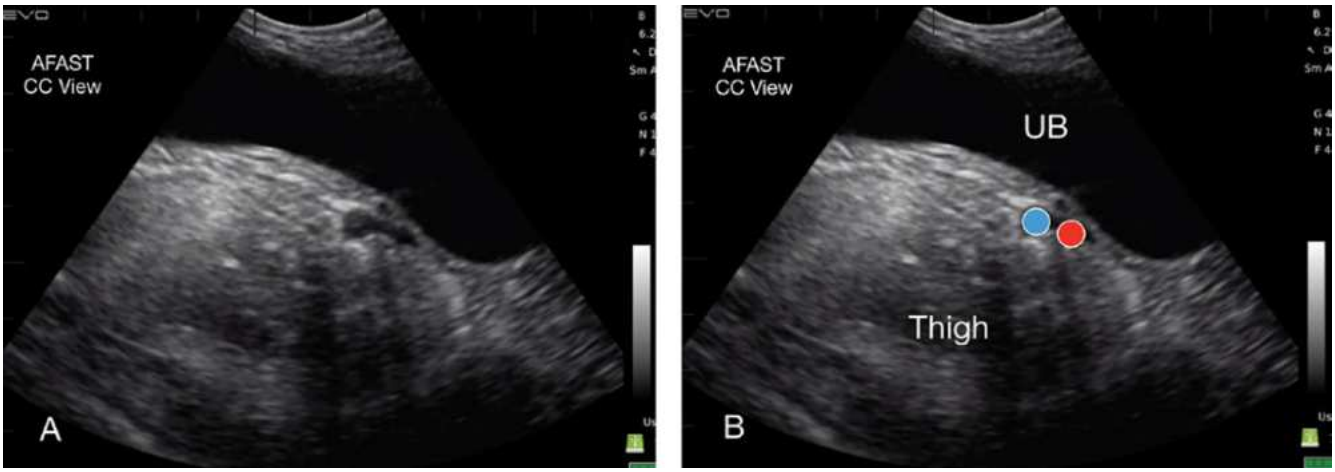


**Figure 25.8.** Femoral vein and artery at the AFAST cysto-colic view in a dog. (A) AFAST CC view with the urinary bladder in longitudinal orientation with cranial to screen left and caudal to screen right. The femoral artery and vein are clearly seen in the center of the B-mode image as adjacent anechoic (dark) circles. In (B) the same image is labeled and a blue circle represents the femoral vein and a red circle the femoral artery. The thigh is labeled. UB, urinary bladder. Source: Reproduced with permission of Dr Gregory Lisciandro, Hill Country Veterinary Specialists and FASTVet.com, Spicewood, TX.

sonographer is at the porta hepatis (see also Figures 16.15, 16.16, and 38.9) (see Chapter 26).

### Renal Vein Thrombosis

The renal vein courses a short distance from the CVC to its respective kidney in close proximity with the renal artery (see also Figures 16.6, 26.8–10). This retroperitoneal region of interest will also have the abdominal aorta (and adrenal glands) typically in view. Invasive adrenal tumors are a common cause for thrombi in the adjacent CVC and occasionally in the renal artery. Secondary changes in the kidney are also expected, including hypoechoic cortical regions from the infarction that over time will lead to hyperechoic renal parenchymal triangulation, loss of corticomedullary detail, and contracture of the renal parenchyma. In acute renal vein thrombosis, renal enlargement and perinephric fluid may also be present (Nyland et al. 2015). The principal objective for the nonradiologist novice and intermediate sonographer is to be able to recognize the region as abnormal (and everything else is bonus information), capturing the case for additional imaging. In patients with suspect adrenal tumors, staging with Global FAST is indicated *before* letting the patient leave your care (see Chapters 36 and 37).

### Deep Venous Thrombosis

Deep venous thrombosis is a fascinating translational topic from people, being bipeds, to veterinary medicine, in which the vast majority of our patients are quadrupeds. The prevalence of DVT in veterinary medicine is completely unknown. Moreover, no standardized systematic ultrasonographic surveillance approach has been developed for dogs and cats, unlike people in which DVT is prevalent and leads to potentially catastrophic pulmonary thromboembolism (PTE). However, the opposing femoral artery and vein may be easily imaged during AFAST at its cysto-colic (CC) view with a curvilinear (microconvex) probe. In the CC view, the urinary urine-filled bladder serves as a stand-off and acoustic window for the femoral artery and vein (Figure 25.8). The CC view may be helpful to screen for abnormalities in high-risk dogs and cats.

So what is the required proficiency of the nonradiologist performing ultrasound scans for DVT? One study demonstrated that emergency physicians who had undergone a 10-minute training session on the technique of two-point compression ultrasonography could detect DVT in people with a sensitivity and specificity of 100% and 99% (Crisp et al. 2010). In another prospective study, intensivists performed bedside compression ultrasonography and findings were compared to a formal vascular study (the gold standard) with high sensitivity and specificity of 86% and 96%, and an accuracy of 95%. The prevalence of DVT in these patients was 20% (Kory et al. 2011). Importantly, bedside-intensivist ultrasonographic compression scans could be performed promptly while formal vascular studies took a median time of 13.8 hours from ordering to their execution by the radiology department (Kory et al. 2011). In addition, contrast venography, historically considered the gold standard

test, involves radiation, is invasive, and carries some risk for complications (Crisp et al. 2010; Kory et al. 2011). The use of ultrasound has become the standard at most institutions.

Deep vein thrombosis is a common and severe problem in human medicine, annually affecting 1–5 patients out of every 1000 in the United States (White 2012). Moreover, 2 million people are affected annually, resulting in 600 000 hospitalizations. Of these, 200 000 deaths result from the most dreaded complication of PTE (Crisp et al. 2010). To our knowledge, no studies have reported the clinical relevance, if any, of DVT in peripheral limbs in veterinary medicine. It seems plausible that DVT probably exists but is unrecognized in small animals, and may explain sudden death or rapid deterioration in critically ill small animal patients (see Chapters 36 and 37). However, we now have some tools to survey for PTE and DVT. Future veterinary studies with standardized protocols are required to determine whether POCUS vascular and lung ultrasound studies will be helpful in diagnosing these conditions in small animals (Szatmári et al. 2001; Dean and Ku 2008).

## *Pulmonary Thromboembolism*

Preexisting PTE factors are similar to those for other sites of venous thromboembolism (Goggs et al. 2009; Crisp et al. 2010; Kory et al. 2011; White 2012) (Table 25.1). Pulmonary thromboembolism is a frequent life-threatening problem in people and early detection is key for patient survival, triggering treatment including thrombolytics and prophylaxis. Computed tomography contrast angiography (CTPA) is considered the gold standard test, but many PTE patients are too unstable for CTPA. Moreover, small PTE at the lung periphery may not be detected by CTPA. Dependent on where the PTE is located, ultrasound carries some advantages, being low impact for the patient, rapid and cageside. POCUS evaluations including cardiac (POCUS heart, TFAST) and pulmonary (Vet BLUE) assessment can be helpful (see Figures 23.11, 37.6, 37.9, and 37.10). Supportive evidence for PTE includes acute right ventricular dilation in an acutely respiratory-distressed or hypoxemic patient (POCUS Heart, TFAST). Thrombi or "echogenic smoke" or heartworms (dirofilariasis) may be seen within the right heart and

**Table 25.1.**
Predisposing factors for aortic and venous thrombosis and thromboembolism in dogs and cats (Goggs et al. 2009; Williams et al. 2017).

| Predisposing factors for aortic thrombosis and thromboembolism | | Predisposing factors for deep venous and pulmonary venous thrombosis and thromboembolism | |
|---|---|---|---|
| Dog | Cat | Dog | Cat |
| Idiopathic | Cardiac | Corticosteroids | Cardiac |
| Hyperadrenocorticism | Hyperthyroidism | Dirofilariasis | Feline infectious peritonitis |
| Corticosteroids | Other | Diabetes mellitus | Dirofilariasis |
| Neoplasia | | Disseminated intervascular coagulation (DIC) secondary to other diseases | Other |
| Protein-losing nephropathy | | Endocarditis | |
| Protein-losing enteropathy | | Hypothyroidism | |
| Diabetes mellitus | | Hyperadrenocorticism | |
| Hypothyroidism | | Hypoadrenocorticism | |
| Immune-mediated anemia | | Immune-mediated anemia | |
| Endocarditis | | Cardiac | |
| Liver disease | | Neoplasia | |
| Radiation | | Pancreatitis | |
| Spirocercosis | | Amyloidosis | |
| Ehrlichiosis | | Protein-losing nephropathy | |
| | | Protein-losing enteropathy | |
| | | Sepsis | |
| | | Surgery | |
| | | Trauma | |
| | | Intravenous catheters | |

Source: Reproduced with permission of Dr Gregory Lisciandro, Hill Country Veterinary Specialists and FASTVet.com, Spicewood, TX.

heartworms and thrombi in the CVC as a predisposing factors (see Chapters 19–21). The wedge sign may be seen along the lung periphery during Vet BLUE in upper lung regions (see Chapters 22 and 23) (see Figures 23.11, 37.6, 37.9, and 37.10). These different locations for PTE argue for the use of Global FAST with POCUS add-on imaging and for having a baseline Global FAST recorded on goal-directed templates for every patient admitted for care (and even at-risk outpatients). Furthermore, Global FAST should become part of the work-up for dogs and cats with heartworm.

Having this baseline information recorded is invaluable for comparison to future studies (see Chapters 36 and 37). For example, knowing on admission that an at-risk patient with pancreatitis has an unremarkable long-axis right ventricular to left ventricular ratio, and that their lung surface is smooth without any Vet BLUE lung ultrasound signs, is key for those developing respiratory signs, some subtle (Liska and Poteet 2003; Tidwell et al. 2007). Finding cardiac and pulmonary PTE evidence, changes from the patient's initial Global FAST profile that you recorded, gives evidence-based information that PTE treatment is likely indicated.

### *Arterial Thromboembolism and Thrombosis*

Arterial thromboembolism (ATE) and aortic thrombosis (AT) are most commonly located in the distal aorta at or in close proximity to its bifurcation to the hindlimbs in both dogs and cats (Fuentes 2012; Williams et al. 2017). However, causes are different between the two species. In dogs, ATE appears to be less frequently documented than AT in a recent review article (Williams et al. 2017). Most canine cases of AT (~50%) are idiopathic (Winters et al. 2012; Williams et al. 2017); however, a number of diseases have been reported as causing ATE/AT in dogs including cardiac, hyperadrenocorticsim, protein-losing nephropathy, infectious diseases, including ehrlichiosis and spirocercosis, immune-mediated diseases, glucocorticoid administration, and others. In cats, cardiac disease is most common and results in ATE rather than AT. In felines, the bifurcation of the distal aorta is the classic location (with a saddle thrombus), with the right subclavian artery as the second most common feline arterial thromboembolic site. Other more common feline causes are hyperthyroidism and pulmonary neoplasia (Fuentes 2012). The bottom line is that ATE and AT are typically a result of fulfillment of Virchow's triad.

The diagnosis often requires the use of color flow Doppler to enhance imaging of the poorly echogenic nascent clot similar to venous thrombosis/thromboembolism in which early stage thrombi often have poor contrast to the normal blood-filled vessel lumen (Szatmári et al. 2001; Zwingenberger and Wisner 2008). Furthermore, familiarity with the anatomy of the region is important as well as correlating the anatomy to patient positioning. An air-filled or stool-filled colon can interfere with imaging and patient positioning and restraint can carry risk, especially with patients moved to dorsal recumbency. These factors must be considered during POCUS vascular assessment.

Principles of venous blood flow obstruction likewise apply to arterial obstruction, including vessel dilation upstream and vessel attenuation downstream although vasoconstriction is more intense than with venous events. Ultrasonographic strategies used by physicians for ATE include looking for "smoke" representing proximal turbulent blood flow as well as proximal dilation of the vessel. Importantly, color flow Doppler has its limitations including patient movement and adjusting the color flow Doppler gain to prevent motion artifact and overgaining, which both lead to the same problem of Doppler colors "jumping" to other areas, thwarting accurate interpretation. With that being said, the identification of ATE in dogs and cats may be made with caution by nonradiologists, keeping in mind that mistakes may impact unfavorably on patient prognosis and therapy (Lake-Bakaar et al. 2012). A readily identifiable aortic thrombus in a dog is shown without the use of color flow Doppler (Figure 25.9) (see also Figure 25.5) and a saddle thrombus in a cat (Figure 25.10).

If ATE is suspected but not confirmed, a complete detailed abdominal ultrasound evaluation by a veterinary radiologist or specialist skilled in ultrasound or other advanced imaging (CT, MRI) may be indicated. However, a Global FAST approach can be helpful in surveying for additional information and comorbidities. A similar approach is used in people for gaining additional supportive evidence as well as rapidly detecting complications and comorbidities (Nazerian et al. 2014; Squizzato et al. 2015). Future study is needed regarding the sensitivity, specificity, and accuracy of ultrasonographic diagnosis of ATE/AT in dogs by nonradiologists.

## Pearls and Pitfalls, The Final Say

The use of ultrasound to survey for vascular abnormalities is exciting for a traditionally difficult problem in veterinary medicine – the detection of venous and arterial thrombosis and thromboembolism. With the strategies listed in this chapter, we have a starting

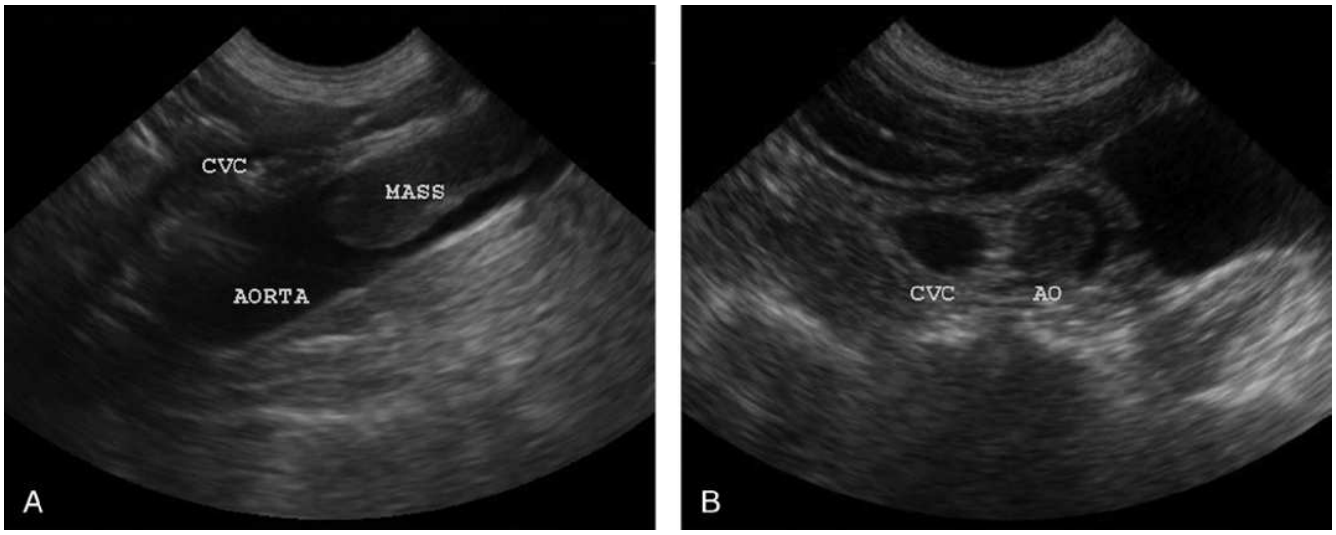


**Figure 25.9.** Aortic thrombosis in a dog. Shown is the aortic thrombus in both the long-axis/longitudinal (A) and short-axis/transverse (B) planes which adheres to the axiom "one view is no view." By imaging the suspect area of interest in multiple views, the probability of a correct conclusion is higher and limits mistaking an artifact such as slice-thickness for a thrombus. Source: Image courtesy of Dr Sarah Young, Echo Service for Pets, Ojai, CA.

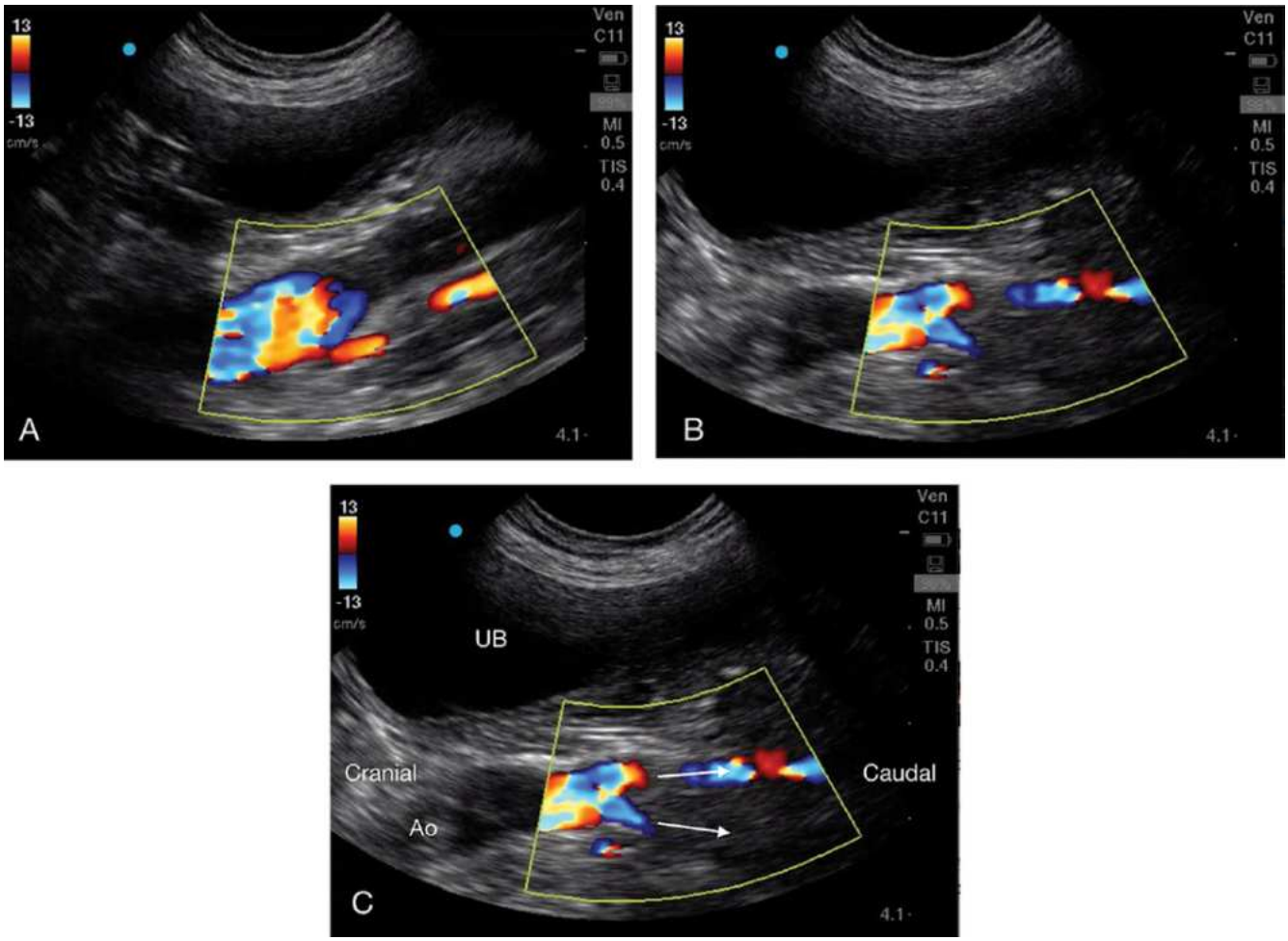


**Figure 25.10.** Aortic thromboembolism in a cat. The application of color flow Doppler at the caudal abdominal aorta documenting aortic thromboembolism and a saddle thrombus where the distal caudal aorta bifurcates into the left and right iliac arteries. The CFD shows some flow past the ATE and outlines the clot itself in (A) through (C). The arrows in (C) show the direction of the iliac arteries and "cranial" and caudal" are labeled for orientation in (C). The images are all the same orientation from the same cat. Ao, aorta; UB, urinary bladder. Source: Reproduced with permission of Dr Gregory Lisciandro, Hill Country Veterinary Specialists and FASTVet.com, Spicewood, TX.

point for evaluating for what the author likes to call "the drop dead patient." Earlier detection, evidence-based information, and using POCUS and FAST as a monitoring tool during therapy may prove helpful.

# References


Crisp JG, Lovato LM, Jang TB. 2010. Compression ultrasonography of the lower extremity with portable vascular ultrasonography can accurately detect deep venous thrombosis in the emergency department. *Ann Emerg Med* 56(6):601–610.

Darnis E, Boysen S, Merveille AC, et al. 2018. Establishment of references values of the caudal vena cava by fast-ultrasonography through different views in healthy dogs. *J Vet Intern Med* 32(4):1308–1318.

Dean A, Ku B. 2008. Deep venous thrombosis. In: *Ultrasound Guide for Emergency Physicians*, edited by Hoffmann B. www.acep.org/sonoguide/dvt.html

Fuentes L. 2012. Arterial thromboembolism: risks, realities and a rational first-line approach. *J Feline Med Surg* 14(7):459–470.

Goggs R, Benigni L, Fuentes VL, et al. 2009. Pulmonary thromboembolism. *Vet Emerg Crit Care* 19(1):30–52.

Gonçalves R, Penderis J, Chang YP, et al. 2008. Clinical and neurological characteristics of aortic thromboembolism in dogs. *J Small Anim Pract* 49(4):178–184.

Kory PD, Pellecchia CM, Shiloh AL, et al. 2011. Accuracy of ultrasonography performed by critical care physicians for the diagnosis of DVT. *Chest* 139(3):538–542.

Lake-Bakaar GA, Johnson EG, Griffiths LG. 2012. Aortic thrombosis in dogs: 31 cases (2000–2010). *J Am Vet Assoc* 241(7):910–915.

Laurenson MP, Hopper K, Herrera MA, et al. 2010. Concurrent diseases and conditions in dogs with splenic vein thrombosis. *J Vet Intern Med* 24:1298–1304.

Liska WD, Poteet BA. 2003. Pulmonary embolism associated with canine total hip replacement. *Vet Surg* 32(2):178–186.

Nazerian P, Vanni S, Volpicelli G, et al. 2014. Accuracy of point-of-care multiorgan ultrasonography for the diagnosis of pulmonary embolism. *Chest* 145(5):950–957.

Nyland TG, Mattoon JS. 2015. Spleen. In: *Small Animal Diagnostic Ultrasound*, 3rd edition, edited by Nyland TG, Mattoon JS. Philadelphia: WB Saunders, pp 400–437.

Nyland TG, Wydmer WR, Mattoon JS. 2015. Urinary tract. In: *Small Animal Diagnostic Ultrasound*, 3rd edition, edited by Nyland TG, Mattoon JS. Philadelphia: WB Saunders, pp 557–607.

Squizzato A, Galli L, Gerdes V. 2015. Point-of-care ultrasound in the diagnosis of pulmonary thromboembolism. *Crit Ultrasound J* 7:7.

Szatmári V, Sótonyi P, Voros K. 2001. Normal duplex Doppler waveforms of major abdominal vessels in dogs: a review. *Vet Radiol Ultrasound* 42(2):93–107.

Tidwell SA, Graham JP, Peck JN, et al. 2007. Incidence of pulmonary embolism after non-cemented total hip arthroplasty in eleven dogs: computed tomographic pulmonary angiography and pulmonary perfusion scintigraphy. *Vet Surg* 36(1):37–42.

White RH. 2012. Identifying risk factors for venous thromboembolism. *Circulation* 125(17):2051–2053.

Williams TP, Shaw S, Porter A, et al. 2017. Aortic thrombosis. *J Vet Emerg Crit Care* 27(1):9–22.

Winters RL, Sedacca CD, Adams A, et al. 2012. Aortic thrombosis in dogs: presentation, therapy, and outcome in 26 cases. *J Vet Cardiol* 14(2):333–342.

Zwingenberger A, Wisner ER. 2008. Neck. In: *Atlas of Small Animal Ultrasonography*, edited by Penninck D, d'Anjou MA. Ames: Blackwell Publishing, pp 91–118.


# Further Reading


Boswood A, Lamb CR, White RN. 2000. Aortic and iliac thrombosis in six dogs. *J Small Anim Pract* 41(3):109–114.

Bressler C, Himes LC, Moreau RE. 2003. Portal vein and aortic thromboses in a Siberian husky with ehrlichiosis and hypothyroidism. *J Small Anim Pract* 44(9):408–410.

Johnson LR, Lappin MR, Baker DC. 1999. Pulmonary thromboembolism in 29 dogs: 1985–1995. *J Vet Intern Med* 13(4):338–345.

CHAPTER TWENTY-SIX

# POCUS: Caudal Vena Cava

Kris Gommeren, Elodie Darnis, and
Anne-Christine Merveille

## Introduction

In the last decade a lot of attention has been given to the evaluation of volume status using ultrasonography of the inferior and/or superior vena cava and the effect of passive leg raising on the caval size and its collapsibility in people. Besides the evaluation of the larger vessels, adding evaluation of certain basic cardiac images and of the lungs, pleural space and abdomen allows for a more complete assessment of the cardiovascular system in an emergency and critical care setting. In this chapter, the focus will be on ultrasonography of the caudal vena cava (CVC) in small animals and three published methodologies. The reader is referred to the chapters on cardiac, pulmonary and thoracic ultrasonography for integrating additional POCUS information for complete patient volume assessment (see Chapters 17, 18–23, 36 and 37).

POCUS caudal vena cava (POCUS CVC) by no means replaces a complete physical examination and other traditional volume assessment measures, but rather serves as an adjunct for confirming or refuting clinical suspicion. By using POCUS CVC, the clinician has another tool for assessing patient volume status that is noninvasive, rapid, repeatable, permits comparison of findings (serial examinations), and requires minimal patient restraint and stress in contrast to the traditional use of central lines for central venous pressure, which is no longer advocated in human medicine (Marik and Cavallazzi 2013). Moreover, POCUS CVC is easily taught to students and veterinarians and does not require any additional equipment besides your ultrasound machine.

Over the past 10 years, we've been developing the use of POCUS in our emergency and critical care (ECC) service and have lead research regarding the assessment of the CVC in dogs (Darnis et al. 2018, 2019). Indeed, POCUS CVC and cardiovascular-pulmonary POCUS integration have allowed us to objectivate clinical findings that better dictate therapeutic decisions, reassuring the attending veterinarian. Most importantly, POCUS examinations in our experience seem to positively affect the prognosis of small animals presented to our service.

### *What POCUS Caudal Vena Cava Can Do*

- Provide various methodologies for assessing the CVC including three studied methods: subxiphoid CVC view, intercostal CVC view, paralumbar CVC view.
- Identify hypovolemic patients by demonstrating flat CV, a decreased CVC to aorta ratio, and high variability in CVC dimensions across the respiratory cycle.
- Identify hypervolemic patients by demonstrating a fat CVC, an increased CVC to aorta ratio, a low variability in CVC dimensions across the respiratory cycle, and prominent hepatic vessels.

*Point-of-Care Ultrasound Techniques for the Small Animal Practitioner*, Second Edition. Edited by Gregory R. Lisciandro.
© 2021 John Wiley & Sons, Inc. Published 2021 by John Wiley & Sons, Inc.
Companion website: www.wiley.com/go/lisciandro/ultrasound2

- Help guide fluid resuscitation and track and monitor volume status throughout initial stabilization as well as during hospitalized care.

### What POCUS Caudal Vena Cava Cannot Do

- Replace complete echocardiography.
- Replace the physical examination.
- Replace clinical integration of the complete patient profile including POCUS cardiovascular and pulmonary findings.
- Serve as a single POCUS assessment for volume status.

### Indications

- Assessment of volume status.
- Patients with a suspicion of cardiovascular compromise: shock, collapse, respiratory compromise or distress.
- Patients with conditions associated with large shifts in intravascular volume: severe gastrointestinal losses, anaphylaxis, internal hemorrhage, acute renal injury, post removal of large quantities of cavitary fluid.
- During fluid resuscitation to evaluate the efficacy of treatment.
- During transfusion or hemodialysis.
- Whenever an acute circulatory change is noted: development of tachycardia, decrease in arterial blood pressure.

### Objectives

- Evaluate the CVC through one or more of the following methods.
  - Subxiphoid CVC view, visualizing at the level where the CVC crosses the diaphragm in a longitudinal orientation in a cineloop allowing evaluation of size and size change throughout the respiratory cycle.
  - Intercostal CVC view, visualizing a cross-section of both the CVC and the aorta in a single frame, recording a cineloop allowing evaluation of size and size-change throughout the respiratory cycle and comparison with the size of the aorta.
  - Paralumbar CVC view, visualizing the CVC and the aorta in a single frame in either a longitudinal or a transverse orientation. At this location the effect of respiratory movement on the venous system will often be negligible.
- Be able to integrate POCUS CVC with basic echocardiographic views.
  - Right parasternal view – long axis.
  - Right parasternal view – short axis.
    - Transverse or short-axis ventricular view for fractional shortening (FS%).
    - Transverse or short-axis left atrium (LA) and aortic (Ao) view for the LA/Ao ratio.
- Evaluate chamber sizes and systolic function including heterogeneous and homogeneous motion.
- Evaluate wall thickness of the ventricles – pseudohypertrophy versus true hypertrophy.
- Identify pericardial effusion and evaluate the presence of pericardial tamponade.
- Identify pleural effusion.
- Identify intraabdominal and retroperitoneal effusions.

## How to Do a POCUS Caudal Vena Cava

### Ultrasound Settings and Probe Preferences

The entire POCUS CVC procedure can be performed using a curvilinear (microconvex) 5–7 MHz probe. Most views can be obtained at 7 MHz, except for the subxiphoid CVC and intercostal CVC views in larger breed dogs, in which a 5 MHz probe will improve the depth penetration and generally allow better CVC visualization. Most interpretations are made cageside, based on the subjective "eyeball approach" of real-time ultrasonography, but still images and captured cineclips that encompass an entire respiratory cycle are advised for CVC and aortic measurements, review, and interpretation.

### Patient Positioning and Preparation

As for most of the POCUS techniques, clipping hair is generally not required for imaging. Rather, hair is parted and isopropyl alcohol and additional acoustic coupling medium are applied to the exposed skin. In rare cases insufficient image quality occurs in dogs with unclipped hair. These tend to be outdoor dogs with longer, thick haircoats, especially during wintertime.

## The Three Methods for POCUS Caudal Vena Cava

Three different methods have been described and studied in the veterinary literature: the subxiphoid

CVC view (Darnis et al. 2018, 2019; Finnerty et al. 2017); the intercostal CVC view (Meneghini et al. 2016; Darnis et al. 2018); and the paralumbar CVC view (Cambournac et al. 2018; Darnis et al. 2018). Placing the patient in left lateral recumbency is preferred, especially for the intercostal CVC view, in contrast to right lateral recumbency for basic echocardiography. These three methods may also be acquired in a standing patient; however, in our experience, especially when obtaining the subxiphoid CVC view, dogs will tend to move when pressure is exerted behind their xiphoid process.

As the CVC is a low-pressure vessel, it can easily be compressed through excessive probe pressure, leading to erroneous measurements. A simple technique is to exert ample pressure while locating the CVC followed by minimal pressure without compromising the quality of the image for best characterizing the CVC and taking measurements.

The benefits and downsides of each of our three described POCUS CVC methods are determined by the ease of acquisition of the image, the motion artifacts observed at each respective region, and the degree of size change generated by intrathoracic pressure changes during the patient's respiratory cycle. We typically assess all three POCUS CVC methods since their acquisition only demands a couple of minutes; and by comparing these methods, the probablity of misinterpreting volume status is lessened in our opinion.

## Subxiphoid Caudal Vena Cava View

The CVC is assessed in a longitudinal orientation as it crosses the diaphragm (Figure 26.1) (Darnis et al. 2018). The CVC is easily located slightly right from midline, just next to the gallbladder. The hepatic veins dorsally drain into the CVC (see Figures 20.10, 36.7, and 36.8). In the case of right-sided congestive heart disease, these vessels also become more apparent (see Figure 36.9). In deep-chested dogs, a lower frequency probe might be required (5 MHz) due to the deeper location of the CVC. At the subxiphoid CVC view, pressure changes during the respiratory cycle are maximal because of its proximity to the thorax, and therefore this location is ideal to evaluate dynamic changes in the CVC. However in our experience, B-mode evaluation of the CVC is more reliable than M-mode because of movement of the diaphragm and CVC during phases of respiration (see also Figures 20.11, 36.11, and 36.12). Moreover, the subxiphoid CVC view does not allow comparison of the size of the CVC to the aorta. The CVC:Ao ratio is helpful to negate the effect of body size on CVC evaluations in dogs (Cambournac et al. 2018; Darnis et al. 2018).

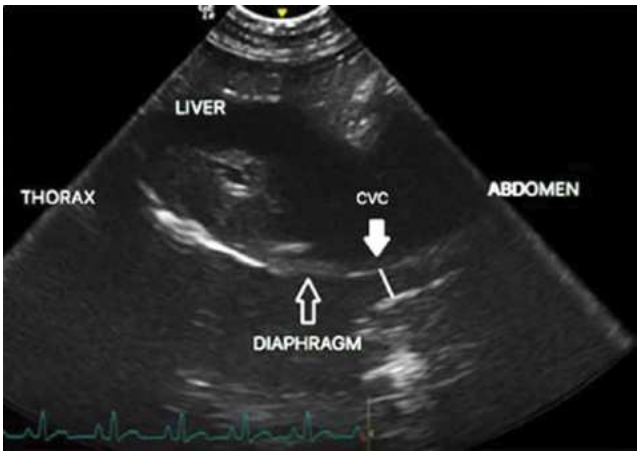


**Figure 26.1.** Subxiphoid CVC view in a healthy dog. The probe is placed longitudinally immediately caudal to the subxiphoid process and angled cranially to visualize the diaphragm as at the FAST DH view (see Chapters 6 and 7). The probe is then fanned to the right of midline until the CVC is identified where it crosses the diaphragm. The probe is then slowly fanned off either side of the CVC and returned to the position where the CVC is subjectively felt to be at its widest diameter with an image similar to that shown. Diaph, diaphragm.

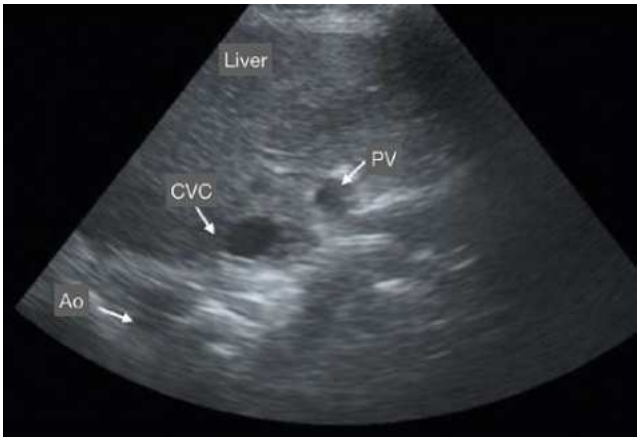


**Figure 26.2.** Hepatic CVC view at the porta hepatis of a healthy dog. To locate the porta hepatis, the probe is placed parallel to the ribs for transverse orientation of the CVC and aorta at the 10th to 12th right intercostal space immediately ventral to the epaxial muscles in the upper third of the thorax. Ao, aorta; CVC, caudal vena cava; PV, portal vein.

## Intercostal Caudal Vena Cava View

This CVC approach starts from a view of the porta hepatis at which a transverse orientation of the CVC, portal vein, and aorta can all be imaged on a single view (Figure 26.2; see also Figure 16.15) (Meneghini et al. 2016; Darnis et al. 2018). At the intercostal CVC

view, size changes of the CVC can be observed throughout the respiratory cycle, while at the same time motion artifacts are rather small in comparison to the subxiphoid CVC view. Therefore, the intercostal CVC view theoretically would be better for both the "eyeball method" and actual measurements of CVC size while additionally providing CVC:aortic ratios since the aorta is imaged. However, due to the proximity of the caudal lung field as well as the stomach, the intercostal CVC view can be complicated by aerated lung or gas in the stomach. This problem is most often encountered in dogs presented with respiratory compromise and distress (caudal lung field tends to expand along with aerophagia) and deep-chested dogs. Whenever air interference occurs with visualization of the porta hepatis, a "modified view" is used by sliding the probe further caudally until the left kidney is located. At this level, a transverse orientation of both the CVC and aorta is visible within the same acoustic window, but at a cost of losing the portal vein that is often not visible within this "modified window." At the modified view, the "eyeball method" and actual measurements may be similarly made (Darnis et al. 2018).

### *Paralumbar Caudal Vena Cava View*

This approach is the most caudal position for the evaluation of the canine CVC (Figure 26.3; see also Figure 26.6) (Cambournac et al. 2018; Darnis et al. 2018). At this location, the CVC and aorta are located rather superficially and can be evaluated in a transverse or longitudinal plane. The major advantage of the paralumbar CVC view is the lack of both motion artifacts and interference by aerated lung or gas-filled stomach or intestines. This makes it easy to acquire both B- and M-mode cineloops for measurements of the CVC and aorta. However, its superficial location makes the paralumbar CVC view sensitive to pressure artifacts, so the probe should be gently manipulated with as little pressure as possible. Moreover, due to its distance from the thorax, size changes of the CVC are much less dynamic, unless the patient is severely respiratory distressed. For this reason, fluid responsiveness should not be primarily evaluated at the paralumbar CVC view (Darnis et al. 2018).

## Image Acquisition and Measurements for POCUS Caudal Vena Cava

### *Subxiphoid Caudal Vena Cava View*

In order to visualize the CVC at the level of the diaphragm, the probe is placed under the subxiphoid process, angled cranially in a longitudinal orientation (Figure 26.4; see also Figure 26.1). The diaphragm and the liver are identified on the screen. Typically, the

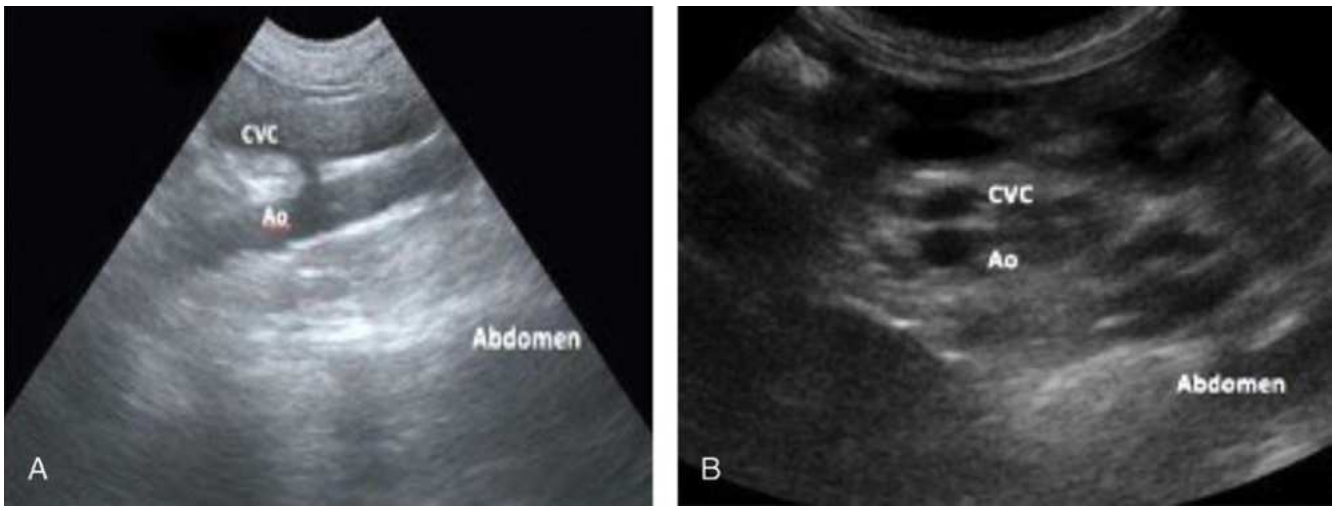


**Figure 26.3.** Paralumbar CVC view with both longitudinal (A) and transverse (B) orientations in a healthy dog. To obtain the paralumbar CVC view the probe is moved caudally under the last rib pointing in a cranial direction from behind the last rib, allowing visualization of the right kidney. The probe is slowly moved or fanned medially off the right kidney until the CVC and aorta are identified. The probe is slowly rotated and fanned to obtain a longitudinal orientation in (A) where the CVC and Ao are parallel to each other within the same acoustic window, and (B) transverse orientation where the CVC and Ao become oval. Ao, aorta; CVC, caudal vena cava.

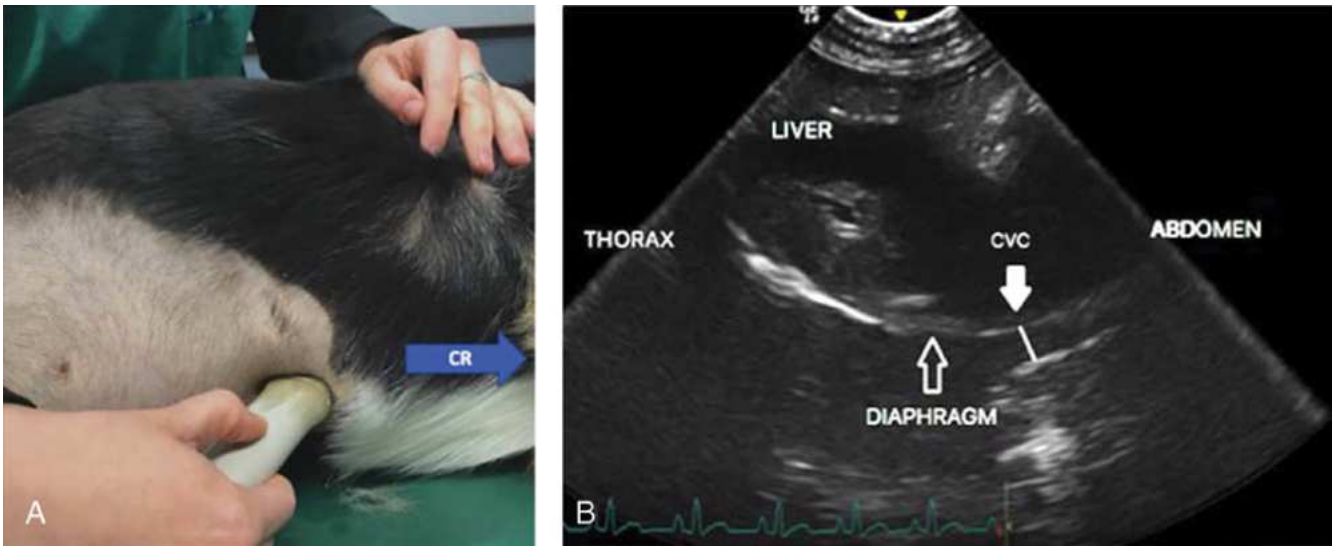


**Figure 26.4.** Probe placement and measurement for evaluation of the subxiphoid CVC view. In (A) the probe is oriented in a longitudinal plane caudal to the subxiphoid process and angled cranially to visualize the diaphragm identical to the FAST DH view. In (B) the cineloop is assessed for the widest and narrowest diameter of the CVC on the abdominal side of the diaphragm during expiration and inspiration, respectively. Measurements are taken perpendicular to the walls of the CVC (*vertical white bar*). CR, cranial; CVC, caudal vena cava (see also Figures 6.9B,D and 6.11).

probe must then be fanned slightly to the right of midline, without excessive pressure, to bring the gallbladder and CVC into view. Here the CVC is then identified at the point where it crosses the diaphragm. As soon as the CVC is visualized, the probe can be slowly fanned and/or slightly rotated to obtain the optimal view, in essence where the CVC has a maximal diameter, and where the vessel wall can be followed over a longer distance (Darnis et al. 2018).

In spontaneously breathing patients, The maximal diameter of the CVC is seen during expiration, as the positive intrathoracic pressure will prevent blood moving towards the heart across the diaphragm, thus causing blood to pool within the abdominal CVC. Conversely, the CVC has its minimal diameter at the end of inspiration, as the negative intrathoracic pressure draws the blood from the abdominal CVC into the thoracic CVC and the right atrium. Measurements are performed where the ventral wall of the CVC crosses the diaphragam perpendicular to its dorsal wall (Figure 26.4) (Darnis et al. 2018).

## *Intercostal Caudal Vena Cava View*

In order to obtain this view, the probe is placed just below the right epaxial muscles in the upper third of the thorax (see Figures 26.2 and 26.5) (Meneghini et al. 2016; Darnis et al. 2018). The probe should be somewhere between the 10th and 12th right intercostal spaces, parallel with the ribs. If aerated lung obscures the image, then the sonographer has two options: the probe is angled caudally and/or moved an intercostal space caudally, or the probe is placed more dorsally over the epaxial muscles and then slowly slid ventrally into the respective intercostal space until the porta hepatis is visualized (Meneghini et al. 2016; Darnis et al. 2018). Alternately, after the right kidney is identified, the probe can be angled cranially or moved an intercostal space cranially.

When the porta hepatis is visualized, a transverse image of the aorta, CVC, and portal vein can be identified as three hypoechoic round (aorta and possibly the CVC and portal vein) to oval (CVC and portal vein) structures within the same view (see Figure 26.5B). The vessels are ordered from left to right as aorta, CVC, and portal vein. Note the CVC at this location often is ovoid rather than circular, thus the size of the vessel rather than its diameter should be evaluated (Darnis et al. 2018).

The size of the CVC is calculated via measurement of its short and long axis using B-mode (see Figure 26.5B) (Darnis et al. 2018). The maximal CVC area ($CVC_a$) on expiration ($CVC_{max}$) and the minimal $CVC_a$ on inspiration ($CVC_{min}$) are then estimated using the following mathematical formula for ellipsoid structures:

$$\pi \times \frac{CVC\,short-axis}{2} \times \frac{CVC\,long-axis}{2}$$

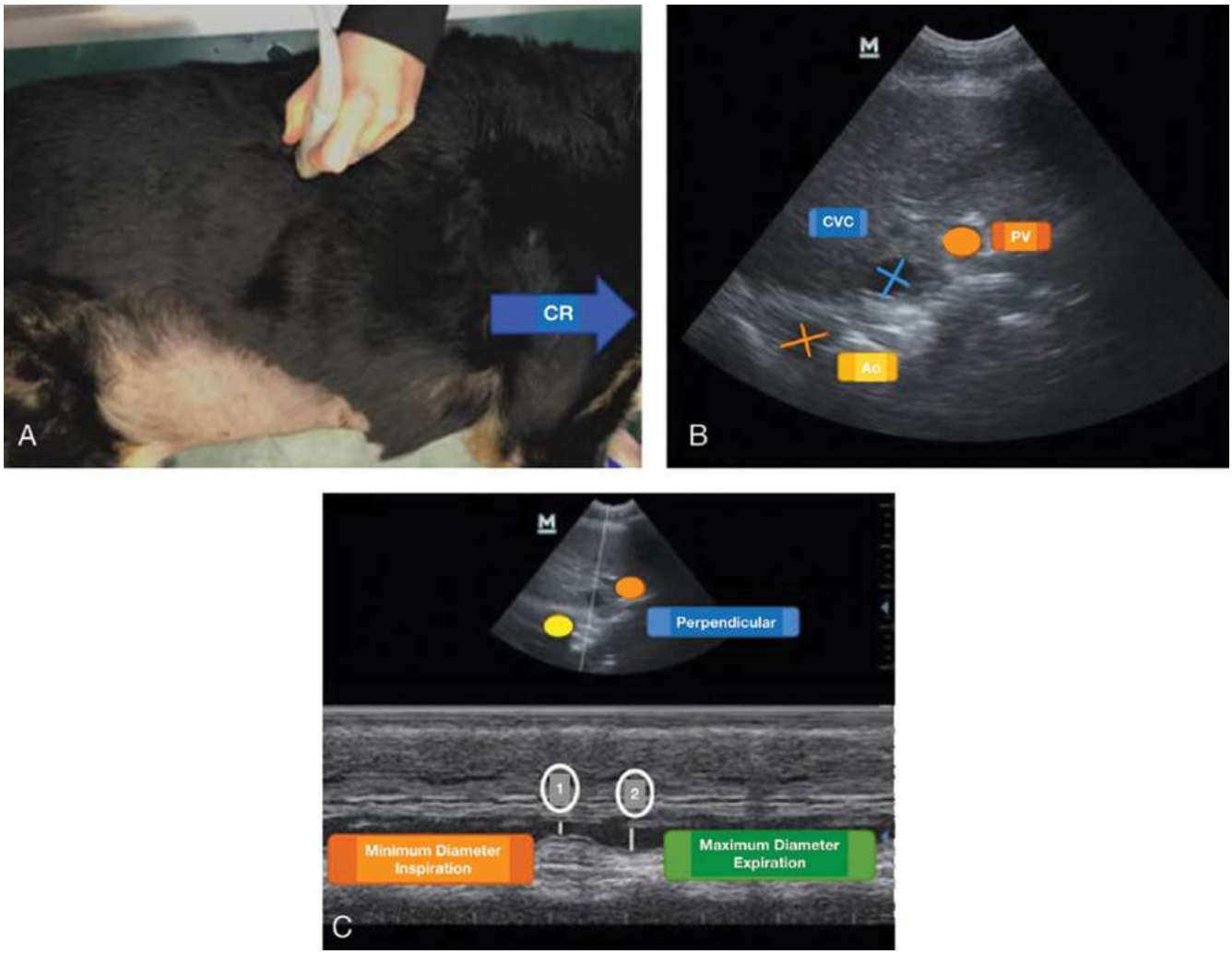


**Figure 26.5.** Probe placement and measurements for evaluation of the intercostal CVC view. (A) To locate the porta hepatis, the probe is placed parallel to the ribs in transverse plane for the CVC and aorta at the 10th to 12th right intercostal space immediately ventral to the epaxial muscles in the upper third of the thorax. The short axis and long axis of the CVC and aorta are measured at the narrowest diameter on inspiration and maximum diameter on expiration within a single cineloop of five cardiac cycles. (B,C) Short-axis in B-mode and M-mode, respectively, illustrating dynamic changes in diameter during inspiration and expiration in (C). Cranial is to the left and caudal to the right of the screen. Ao, aorta (orange X); Cr, cranial; CVC, caudal vena cava (blue X); PV, portal vein (orange circle).

The maximal size of the CVC is measured during the expiratory phase and the minimal size is measured during the inspiratory phase the same as for the subxiphoid CVC view (see Figure 26.5C). The diameter of the aorta is typically measured at the same moment as the CVC because the dimensions of the aorta do not change with respiration, and change only minimally between systole and diastole. If a simultaneous electrocardiogram (ECG) tracing is available, we tend to measure the aorta at the beginning of systole, when its size is maximal (Darnis et al. 2018). Alternatively, rather than assessing size, the diameter of the CVC can be assessed using an M-mode view after positioning the cursor in the middle of the CVC, and maximal and minimal CVC size can be measured and then evaluated including their difference for a CVC distensibility index (Darnis et al. 2018) (see Figure 26.5, 36.11 and 36.12).

## *Paralumbar Caudal Vena Cava View*

In order to obtain this view, the probe is placed behind and pushed *under* the last rib, directed cranially, allowing visualization of the right kidney (Figure 26.6).

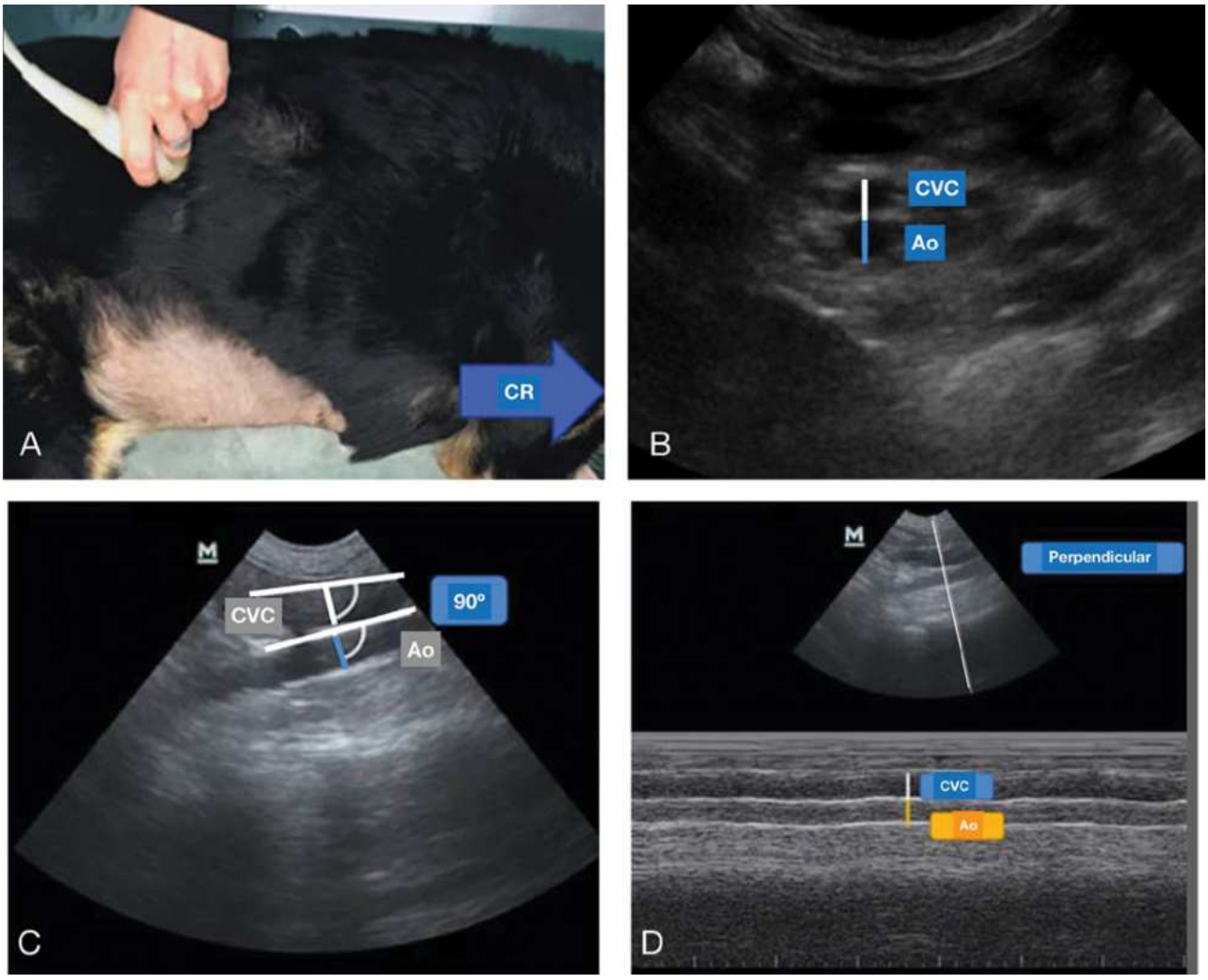


**Figure 26.6.** Probe placement and measurements for evaluation of the paralumbar CVC view in longitudinal and transverse orientation. In (A) the probe is moved or fanned medially off the right kidney until the CVC and aorta are identified as in (B). In (B) the $CVC_D$ and $Ao_D$ are estimated in the middle of both vessels (*vertical bars*). The probe is then rotated and fanned to obtain a longitudinal plane in which the CVC and Ao are parallel to each other within the same acoustic window as in (C) using B-mode and (D) using M-mode. As the diameters of the CVC and aorta do not tend to change with the respiratory cycle at this location, only a single measurement of the CVC and aorta is made. The measurement is made perpendicular to the wall of the CVC, shown in (C) with B-mode and in (D) with M-mode for the $CVC_D$ and $Ao_D$ measurements. Ao, aorta; Cr, cranial; CVC, caudal vena cava.

The probe is moved or fanned dorsomedially from the right kidney. Ideally, an acoustic window is obtained that visualizes part of the right kidney, as well as the CVC and the aorta, which are located parallel to each other. The aorta can be easily identified in B-mode as the pulsatile vessel, while the CVC can be identified by applying some extra pressure on the probe, which will demonstrate its collapsibility (the high-pressure aorta does not collapse as easily). Both the CVC and aorta are circular structures at this location, and therefore a single measurement of their diameter can be obtained (Cambournac et al. 2018; Darnis et al. 2018).

For evaluation of the CVC and aortic size, the probe is rotated to ensure that a optimal transverse (Figure 26.6B) or longitudinal (Figure 26.6C,D) orientation of both vessels is obtained. The transverse orientation is usually preferred, as it assesses minimal and maximal diameter of both vessels more reliably. When the longitudinal orientation is chosen, care must be taken to properly evaluate both vessels at their

maximal diameter by cross-sectioning each vessel within their middle because erroneous measurements are possible (see Figure 36.12). Measurements may be made in B- or M-mode. The vessel distance from the diaphragm is greatest at this CVC view, thus the CVC and aorta are least affected by intrathoracic pressure changes throughout the respiratory cycle. However, in brachycephalic dogs, often having exaggerated negative intrathoracic pressure due to their unique airway conformation, respiratory variations might be observed (Darnis et al. 2018).

# Use of Allometric Scaling Formulas for CVC Assessment

CVC evaluation in small animals still requires further scientific validation in actual clinical settings. However, the authors have established reference values that may be used for the CVC using the three described POCUS CVC methods in healthy dogs (Darnis et al. 2018). Reference values for the hepatic and paralumbar CVC views, expressed via allometric scaling, are presented in Table 26.1. The subxiphoid CVC view had poorer repeatability, and therefore no references values have been calculated, although absolute CVC height values have been recently suggested (see Tables 7.6 and 36.2).

The poorer subxiphoid CVC view measurement repeatability is likely due to several factors: movement of the diaphragm causing difficulties in performing both B- and M-mode measurements, a more pronounced effect of the force of respiratory movement on CVC imaging, and variability in the observed angle at the diaphragm of the CVC during measurement (see also Figures 36.11 and 36.12). Although at first glance it seems to indicate that the subxiphoid CVC view is of less clinical utility than the other two views, changes observed in a clinical setting seem to be more pronounced at the subxiphoid view (see cineloops on the Companion Website). Therefore, the subxiphoid CVC view merits further investigation, as it may be the best view to make "eyeball method" evaluations (Darnis et al. 2018, 2019).

**Table 26.1.**
Reference values using allometric scaling with body weight (BW) for the caudal vena cava (CVC) and aorta (Ao) in healthy dogs using different views (Darnis et al. 2018).

| View | Variable) | Dimension | Formula |
|---|---|---|---|
| Hepatic view | $CVC_{min}$ | Area ($mm^2$) | $6.16 \times BW^{0.762}$ |
| *B-mode* | $CVC_{max}$ | Area ($mm^2$) | $7.24 \times BW^{0.787}$ |
| | $Ao_{max}$ | Diameter (mm) | $3.85 \times BW^{0.323}$ |
| Paralumbar view | $CVC_D$ | Diameter (mm) | $2.79 \times BW^{0.390}$ |
| *B-mode* | $Ao_D$ | Diameter (mm) | $3.49 \times BW^{0.328}$ |
| Paralumbar view | $CVC_D$ | Diameter (mm) | $2.53 \times BW^{0.419}$ |
| *M-mode* | $Ao_D$ | Diameter (mm) | $3.49 \times BW^{0.332}$ |

$CVC_{min}$ – minimal caudal vena cava area at the hepatic view.
$CVC_{max}$ – maximal caudal vena cava area at the hepatic view.
$Ao_{max}$ – maximal aortic diameter at the hepatic view.
$CVC_D$ – caudal vena cava diameter at the paralumbar view.
$Ao_D$ – aortic diameter at the paralumbar view.

# Integration of POCUS CVC Findings

The main purpose of a POCUS CVC is the evaluation of volume status and indirectly cardiovascular function of the patient (see Chapter 36 for integration of information). Both the CVC and right heart are closely related (referred to as fallback view in the Global FAST approach), as right-sided cardiac disease often leads to hepatic venous congestion, which shares several characterisitics with hypervolemia, such as distended CVC and hepatic veins. Additionally, hypervolemia also causes right atrial dilation, and right ventricular dilation in more chronic and severe situations, and the left heart may also be involved (see also Figures 36.7 and 36.8 and Chapter 36). Therefore, evaluation of volume status should always include a cardiac and lung evaluation and a survey for effusions (see Chapters 17–21 and 36). Lastly, abnormalities suspected during POCUS CVC at the authors' critical care department trigger a complete detailed echocardiogram by the cardiology department.

# Inherent Differences Between Volume Status in People and Small Animals

POCUS CVC research in companion animals remains ongoing, and much scientific data and evidence have yet to be determined. However, the inferior vena cava and volume status in human medicine has been well studied (Dipti et al. 2012; Ferrada et al. 2012a,b; Monnet et al. 2016a,b), and many parallels with companion animals appear to exist. For example, in human medicine evaluation of volume status is typically assessed by the "eyeball method" using both sonographic size

and dynamic changes of the inferior vena cava as fat (distended without collapsability) or flat (attenuated without collapsability) (Perera et al. 2010; Ferrada et al. 2012a,b; Lee et al. 2016). Of note, IVC sonographic assessment is usually performed in people at the subxiphoid view.

When the flat versus fat inferior vena cava distinction is not clearcut in people, several approaches exist to avoid fluid overload. The first technique is the comparison of inferior vena cava (IVC) parameters while administering a true or "virtual" fluid bolus by passive leg raising, or by actively changing intrathoracic pressures in ventilated patients (Vieillard-Baron et al. 2004; Monnet et al. 2016a). Passive leg raising carries the benefit that only a "virtual" bolus is administered, and consequently the risk of active and true volume overload is minimized because no fluids are actually administered.

Although effective in people, this technique is unlikely to become commonplace in companion animals because of differences between anatomy and blood volume in the hindlegs of bipeds and quadrapeds for the following reasons. First, the amount of blood pooled in the venous system of hindlegs of companion animals is unlikely to be similar to humans. Second, veterinary exam and triage tables are not designed to comfortably raise our patient's hindlimbs. Moreover, such patient positional changes and lack of patient understanding of the procedure would more likely induce a stress response affecting POCUS CVC findings. Third, although thoracic pressures can be manipulated in ventilated small animals, this represents a minority of our emergency and critical care case population, most of which are spontaneously breathing. Consequently, we are left to evaluate the effect of the administration of intravenous fluid boluses on CVC assessment. Furthermore, to scientifically detect CVC differences, actual measurements will need to be correlated to the "eyeball method." In people, a minimal change of ~15% in IVC diameter is generally accepted as a positive reaction to fluid loading conditions. Whether the same threshhold exists in small animals remains to be determined.

# Pearls and Pitfalls, The Final Say

We have evaluated three different POCUS CVC methodologies for assessing the CVC in dogs. Each has its own limitations including distance from the thorax, effect of respiratory patterns and patient status, and reliability and repeatability of measuring the CVC and aorta dependent on location of each view. Until further studies correlate the utility of these three POCUS CVC methodologies to clinical cases, we do not know which is best. However, to make an accurate volume status assessment, POCUS cardiovascular and pulmonary findings must be combined with POCUS CVC findings.

# References


Cambournac M, Goy-Thollot I, Violé A, et al. 2018. Sonographic assessment of volaemia: development and validation of a new method in dogs. *J Small Anim Pract* 59(3):174–182.

Darnis E, Boysen S, Merveille AC, et al. 2018. Establishment of references values of the caudal vena cava by fast-ultrasonography through different views in healthy dogs. *J Vet Intern Med* 32(4):1308–1318.

Darnis E, Merveille AC, Desquilbet L, et al. 2019. Interobserver agreement between non-cardiologist veterinarians and a cardiologist after a 6-hour training course for echographic evaluation of basic echocardiographic parameters and caudal vena cava diameter in fifteen healthy Beagles. *J Vet Emerg Crit Care* 29:495–504.

Dipti A, Soucy Z, Surana A, et al. 2012. Role of inferior vena cava diameter in assessment of volume status: a meta-analysis. *Am J Emerg Med* 30(8):1414–1419.

Ferrada P, Vanguri P, Anand RJ, et al. 2012a. Flat inferior vena cava: indicator of poor prognosis in trauma and acute care surgery patients. *Am Surg* 78(12):1396–1398.

Ferrada P, Attand RJ, Whelan J, et al. 2012b. Qualitative assessment of the inferior vena cava: useful tool for the evaluation of volume status in criticall ill patients. *Am Surg* 78(4):468–470.

Finnerty NM, Panchal AR, Boulger C, et al. 2017. Inferior vena cava measurement with ultrasound: what is the best view and best mode? *West J Emerg Med* 18(3):496–501.

Lee CW, Kory PD, Arntfield RT. 2016. Development of a fluid resuscitation protocol using inferior vena cava and lung ultrasound. *J Crit Care* 31(1):96–100.

Marik P, Cavallazzi R. 2013. Does the central venous pressure predict fluid responsiveness? An updated meta-analysis and a plea for some common sense. *Crit Care Med* 41(7):1774–1781.

Meneghini C, Rabozzi R, Franci P. 2016. Correlation of the ratio of caudal vena cava diameter and aorta diameter with systolic pressure variation in anesthetized dogs. *Am J Vet Res* 77(2):137–143.

Monnet X, Marik P, Teboul JL. 2016a. Passive leg raising for predicting fluid responsiveness: a systematic review and meta-analysis. *Intensive Care Med* 42(12):1935–1947.

Monnet X, Marik PE, Teboul JL. 2016b. Prediction of fluid responsiveness: an update. *Ann Intensive Care* 6(1):111.

Perera P, Mailhot T, Riley D, et al. 2010. The RUSH exam: Rapid Ultrasound in SHock in the evaluation of the critically lll. *Emerg Med Clin North Am* 28(1):29–56.

Vieillard-Baron A, Chergui K, Rabiller A, et al. 2004. Superior vena caval collapsibility as a gauge of volume status in ventilated septic patients. *Intensive Care Med* 30(9):1734–1739.

# Further Reading

DeFrancesco T. 2014. Focused or COAST-ECHO (Heart). In: *Focused Ultrasound Techniques for the Small Animal Practitioner*, edited by Lisciandro GR. Ames: Wiley-Blackwell, pp 189–205.

Di Segni E, Preisman S, Ohad DG, et al. 1997. Echocardiographic left ventricular remodeling and pseudohypertrophy as markers of hypovolemia. An experimental study on bleeding and volume repletion. *J Am Soc Echocardiogr* 10(9):926–936.

Hollerbach S, Schultze K, Muscholi M, et al. 2001. Ultrasonography of the inferior vena cava (IVC) in the diagnosis and monitoring of therapy in patients with chronic congestive heart failure. *Dtsch Med Wochenschr* 126(6):129–133.

Kwak HS, Im HG, Shim EB. 2016. A model for allometric scaling of mammalian metabolism with ambient heat loss. *Integr Med Res* 5(1):30–36.

Lichtenstein D. 2015. FALLS-protocol: lung ultrasound in hemodynamic assessment of shock. *Heart Lung Vessel* 5(3):142–147.

Lisciandro G, Ward J, DeFrancesco T, et al. 2016. Absence of B-lines on lung ultrasound (Vet BLUE Protocol) to rule out left-sided congestive heart failure in 368 cats and dogs. *J Vet Emerg Crit Care* 26(S1):S8–9.

Lisciandro GR, Fulton RM, Fosgate GT, Mann KA. 2017. Frequency of B-lines using a regionally-based lung ultrasound examination (the Vet BLUE protocol) in 49 cats with normal thoracic radiographical lung findings. *J Vet Emerg Crit Care* 27(3):267–277.

Marik PE. 2009. Techniques for assessment of intravascular volume in critically ill patients. *J Intensive Care Med* 24(5):329–337.

Merveille AC, Darnis E, Gommeren K. 2017. Caudal vena cava assessment in dogs with right-sided congestive heart failure: a pilot study. Abstract, 27th ECVIM Congress, Malta.

Nelson NC, Drost WT, Lerche P. 2010. Noninvasive estimation of central venous pressure in anesthetized dogs by measurement of hepatic venous blood flow velocity and abdominal venous diameter. *Vet Radiol Ultrasound* 51(3):313–323.

Poelaert J. 2015. Assessment of loading conditions with cardiac ultrasound. A comprehensive review. *Anaesth Intensive Ther* 47(5):464–470.

Smith S, Dukes-McEwan J. 2012. Clinical signs and left atrial size in cats with cardiovascular disease in general practice. *J Small Anim Pract* 53(1):27–33.

Vermeiren GL, Malbrain ML, Walpot JM. 2015. Cardiac ultrasonography in the critical care setting: a practical approach to asses cardiac function and preload for the "non-cardiologist." *Anaesthesiol Intensive Ther* 47S:s89–104.

Vezzosi T, Mannucci T, Pistoresi A, et al. 2017. Assessment of lung ultrasound B-Lines in dogs with different stages of chronic valvular heart disease. *J Vet Intern Med* 31(3):700–704.

Ward JL, Lisciandro GR, Keene BW, et al. 2017. Accuracy of point-of-care lung ultrasonography for the diagnosis of cardiogenic pulmonary edema in dogs and cats with acute dyspnea. *J Am Vet Med Assoc* 250(6):666–675.

SECTION VI

# Ocular, Neurological, and Musculoskeletal

CHAPTER TWENTY-SEVEN

# POCUS: Eye

Jane Cho

Vetbooks.ir

## Introduction

The nonophthalmologist veterinarian is often faced with the challenges of having to assess eye conditions that require urgent attention, such as those that might need emergent referral and/or specific medications or surgery to save vision or the globe. Using ocular ultrasonography to obtain evidence-based information and increase the probability of an accurate diagnosis over solely traditional clinical diagnostic means is an underutilized option for the nonophthalmologist veterinarian in busy general or emergency and critical care practices. While a complete ocular ultrasound exam by a veterinary ophthalmologist or radiologist may be indicated when there is ocular opacity and/or extraocular inflammation or injury, a POCUS eye examination can help alleviate the practitioner's frustration of not being able to visualize intraocular and periorbital structures. The use of ocular ultrasonography by nonophthalmologist veterinarians can help answer important clinical questions quickly when a complete clinical eye examination alone does not reveal a diagnosis.

### What POCUS Eye Can Do

- Provide a diagnostic window into an eye not amenable to direct examination by traditional means.
- Provide anatomical information about an opaque or inaccessible eye without resorting to more costly imaging methods.
- Diagnose or support a clinical diagnosis of anterior or posterior lens luxation, intraocular masses, retinal detachments, and scleral rupture.
- Expedite referral for salvage of vision or the globe by detecting otherwise occult conditions.
- Assist in providing an initial prognosis for vision and the globe.

### What POCUS Eye Cannot Do

- Cannot substitute for a full clinical ocular examination.
- Cannot provide a diagnosis in the absence of a basic level of clinician skill and knowledge of ocular anatomy and disease.
- Cannot overcome any inherent mechanical limitations of your ultrasound machine and probe.

**Note:** While ocular ultrasound can significantly assist in diagnosis, it cannot always allow for a specific etiological diagnosis due to variations in ultrasound appearances and a wide variety of possible pathology.

**Note:** Use Global FAST to help determine if the ocular problem is localized or part of disseminated disease. Global FAST surveys the abdomen (AFAST), thorax (TFAST) including heart (TFAST) and lung (Vet BLUE) and also helps assess patient volume status (see Chapters 6, 7, 17, 18, 22, 23, 36, and 37).

### Indications

- Opaque eye: cannot visualize through the cornea or anterior chamber because of corneal, anterior chamber, or other structural opacity (Figures 27.1, 27.2, 27.3) (see also Table 27.3).
- Bulging eye: to differentiate exophthalmos (protruding normal-sized globe) from buphthalmos (enlarged globe), and determine the presence and sonographic characterization of a retrobulbar mass (Figure 27.4)
- Cloudy eye: cannot visualize the fundus because of opacities in the normally clear ocular media

*Point-of-Care Ultrasound Techniques for the Small Animal Practitioner*, Second Edition. Edited by Gregory R. Lisciandro.
© 2021 John Wiley & Sons, Inc. Published 2021 by John Wiley & Sons, Inc.
Companion website: www.wiley.com/go/lisciandro/ultrasound2

**Figure 27.1.** Corneal opacity. Various types of corneal opacity can make directly viewing the intraocular structures difficult or impossible, including (A) corneal edema, (B) corneal pigmentation, and (C) other types of corneal scarring.

(cornea, anterior chamber, lens, and vitreous) (see Figures 27.1–3).
- Traumatized eye: especially with swollen periocular structures preventing examination of the eye, to evaluate for injury to the globe or its structures (with great caution) (see Figures 27.25 and 27.26A).

### *Objectives*

- To identify the location, size, and shape of normal and abnormal ocular and periocular structures, allowing for a more correct ophthalmic diagnosis.
- To better define the existence of pathology warranting specific treatment, especially emergent treatment, thus optimizing preservation of vision and the globe.

## Ultrasound Settings

For imaging the globe, the ultrasound probe with the highest frequency available should be used. A 7.5–10 MHz probe is preferable.

- A 7.5 MHz probe is adequate for imaging deeper structures (orbit). A 5 MHz probe may be acceptable for detecting deeper large lesions at the expense of losing detail. Higher MHz (7.5–12 MHz) provides better detail in the nearer fields. However, a newer modality called high-resolution ultrasound (HRUS), also called ultrasound biomicroscopy, uses very high-frequency probes of 35–50 MHz to image the very near parts of the eye (<1 cm) in great detail, but is only rarely available and requires sedation or anesthesia.

**Figure 27.2.** Opacities in the anterior chamber. Various types of pathology can render the anterior chamber cloudy or opaque, obscuring the rest of the intraocular structures, including (A) hyphema, (B) hypopyon, and (C) fibrin and other structures.

- A probe with a small scan head diameter (linear or sector) is preferred.
- If the machine allows, a "Small Parts" or "Eye" or similar setting optimizing focus in the very near field (1–5 cm) is preferred.
- Reduced depth of the image (using a "depth" dial if present on your machine) also helps to magnify small structures.
- If the machine has a foot pedal, install prior to the eye exam, to allow hands-free freezing of images.

**Pearl:** Gain can be turned up or down during the exam to highlight certain structures. This can be used to better define differences in echogenicity, but care should be taken to not "create" or "remove" lesions while adjusting gain.

# Patient Eye Preparation

- Ideally, a sterile, viscous, aqueous-based ultrasound gel that is nontoxic to the eye and ocular surfaces should be used. The author routinely uses Aquasonic 100 (Parker Laboratories, Fairfield, NJ) ultrasound gel, a very commonly used and readily available gel, on the intact ocular surface, with no ill effects (Dziezyc and Hager 1988). Aquasonic is also available in sterile form. Gel such as K-Y® (which is less viscous and thus tends to fall off the eye, making its use more difficult) or ophthalmic 2.5% methylcellulose gel can be used. Clean the probe well and dry it according to manufacturer's instructions before placing it on the eye. In cases of possible globe rupture, a sterile gel such as individual packets of K-Y should be used and the

**Figure 27.3.** Ocular opacities. Structural opacities in the eye can prevent direct viewing of the anatomy of the eye behind the opacity, such as (A) iris adhesions that close the pupil, (B) cataract, and (C) other abnormal structures or masses in the anterior chamber (in this case, a formed blood clot with fibrin).

probe should be placed on intact eyelid or periocular skin and not the eye (see later in this chapter).

- If a stand-off is needed for imaging the anterior, most superficial parts of the eye, either a thicker layer of gel or a water-filled glove may be used, though the latter can be unwieldy to handle.
- All gel should be gently and completely flushed off the ocular surfaces with sterile saline eyewash immediately after the exam. Fluorescein staining of the cornea after the exam is also recommended to ensure that no corneal damage has occurred during the examination.

# How to do the POCUS Eye

First, topically anesthetize the cornea with several drops of ophthalmic proparacaine, tetracaine, or another appropriate topical ophthalmic anesthetic. Note that this is likely stored in the refrigerator. If adequate topical anesthetic effect is not achieved with 10–15 drops over two minutes, additional chemical restraint may be needed. This should be tailored to the patient, and titrated to the lightest sedative/anesthetic plane needed. No specific sedation or anesthetic protocols are required, although a reversible one may be preferable.

**Figure 27.4.** The bulging eye. Exophthalmos and buphthalmos can clinically look very similar on initial inspection. Both dogs have one eye that is bulging, but further examination would be needed to differentiate a globe that is merely large versus one that is being pushed out of the orbit. Ocular ultrasound can help determine the nature of the problem, and thus the correct course of action. The eye in (A) is exophthalmic, and (B) is buphthalmic.

Unless the patient is excessively mobile or very painful, sedation and/or general anesthesia are typically unnecessary, and may make examination more difficult due to resulting changes in globe position.

Second, regarding restraint, the animal should be able to sit, lie sternal, or stand normally in a comfortable position. If sitting or standing, make sure the animal is not allowed to scoot or slide backwards. At least one assistant is needed to hold the animal's head still. Either that assistant or the sonographer can hold the eyelids open (Figure 27.5). An additional assistant may be needed to work the freeze button.

Third, regarding probe pressure and positioning, avoid pressing the probe directly onto the cornea. Maintain a layer of ultrasound gel 3–10 mm thick between the probe and the cornea (Figure 27.6).

**Pearl:** Maintain a layer of ultrasound gel 3–10 mm thick between the probe and the cornea. This technique will allow better imaging of the near fields (cornea, anterior chamber, iris) and be more comfortable for the patient.

Be mindful of the direction of the patient's gaze. By keeping the probe correctly oriented, you will be more likely to properly localize ocular and periocular structures.

**Figure 27.5.** Ocular ultrasound setup. An assistant should hold the patient in a comfortable position in which the patient cannot slide backwards. This person can also hold the patient's eye open for the exam. Another assistant should be available to freeze the image if needed.

**Figure 27.6.** Probe with aqueous-based gel. *Do not use alcohol-based gel, which may be harmful to the cornea*. Apply a large amount of coupling gel that is safe for eyes (see text for specifics) to the ultrasound probe before applying to the eye. The probe *should not be pressed* onto the eye, but held with a 3–10 mm "stand-off layer" of gel between the probe and the cornea if possible, to allow for better imaging of the most superficial structures.

**Pearl:** Look at the position *of the other eye* and the facial muscles for help in orienting the images of the eye being evaluated.

Fourth, regarding probe positioning, several views can be used, including vertical, horizontal, and lateral, and behind the orbital ligament (viewing posterior to anterior). Begin by placing the probe vertically (bisecting the globe into medial and lateral halves) on the central cornea (Figure 27.7) to image the globe from the anterior to the posterior pole. Sweep the probe, moving the point of contact from one side of the cornea to the other, imaging the entire globe. Alternately, pivot the angle of the probe while keeping the probe contact point stationary.

A second viewing angle to consider is horizontal, with the probe placed parallel to the floor (bisecting the globe into top and bottom halves). The probe is then swept/angled from top to bottom (Figure 27.8).

A third (and less commonly used) view places the probe parallel to the iris from the lateral aspect of the globe (bisecting the globe into anterior and posterior halves), sweeping/angling the probe from front to back (Figure 27.9).

**Figure 27.7.** Vertical probe position. The initial view should be with the probe held vertically, dividing the globe into lateral and medial halves, and either tilting the probe from side to side or moving it from side to side (changing the contact point on the eye) to image the whole structure. Note the thick layer of gel that is maintained between the probe and the eye.

**Figure 27.8.** Horizontal probe position. This view divides the globe into upper and lower halves, providing additional directional information on intraocular structures.

A fourth possible angle is a retrobulbar one from behind the orbital ligament, producing a lower quality image directed from the back to the front of the eye (Figure 27.10). This view may be worth considering if the cornea might be ruptured, or the lids are extremely thickened or swollen, but you need to proceed with caution to prevent causing additional damage.

**Figure 27.9.** Lateral probe position. This view places the probe so that it divides the globe into anterior and posterior sections. It is easiest to access from the lateral sclera where the limbus is most exposed. This view is not commonly used but may allow for further orientation of intraocular structures.

**Figure 27.10.** Probe position from behind orbital ligament. If possible, palpate the orbital ligament and feel for the slight depression behind it. You may need to palpate the other side to locate the ligament, as orbital injury is often what necessitates this view. Shaving or completely wetting down the skin in this area before applying gel will improve the image. Orient the probe forward. Note that the probe will be in contact with the skin and a thick gel layer is not necessary with this view. Images obtained using this view will not be of as good quality as those obtained with corneal contact.

**Pearl:** If imaging through skin, shaving or thoroughly wetting down the skin hairs improves the image quality.

**Important:** In cases where globe rupture is suspected (gross hyphema, hypotony [low intraocular pressure], or visible globe deformation/deflation), if imaging is required, *it is preferred to image through closed lids or intact skin, rather than through the cornea,* to prevent contamination of the intraocular space. *Do not press* on the globe or lids, as this will easily further damage the eye.

In summary, these additional views can provide further information as to the location and orientation of lesions if needed, although generally not all views are necessary to make most urgent clinical decisions. Performing the scan first at higher gain, then at lower gain, will allow for differentiation of smaller, more subtle, and lower-intensity lesions.

## Ultrasonographic Findings in a Normal Eye

When imaging using the vertical or horizontal probe position, under your layer of gel, the most superficial structure seen will be the cornea, represented by a single bright 1 mm thick curved line or (depending on your probe frequency) two very thin bright parallel curved lines (the anterior and posterior corneal surfaces) about 1 mm apart (Figure 27.11). If there is not enough stand-off space between the probe and eye, it may not be visible at all.

Just posterior to this is the anechoic anterior chamber. This should always be anechoic as it is filled with the aqueous humor, an acellular solution, and is normally about 3–5 mm deep in the central axis (Cottrill et al. 1989). It is bordered posteriorly by the iris and axial anterior lens capsule, and peripherally by the iridocorneal angle (which is not typically seen in any detail with standard ultrasound).

**Pearl:** The normal anterior chamber is always anechoic (uniformly black).

The iris might be visible as a thin linear area of increased echogenicity at the peripheral anterior lens but is often not distinguishable from the adjacent structures (Figure 27.12). It should be thin with an approximately flat anterior surface, with no asymmetrical thickness (medial vs lateral), though it may be slightly thicker when the pupil is dilated and thinner when the pupil is constricted.

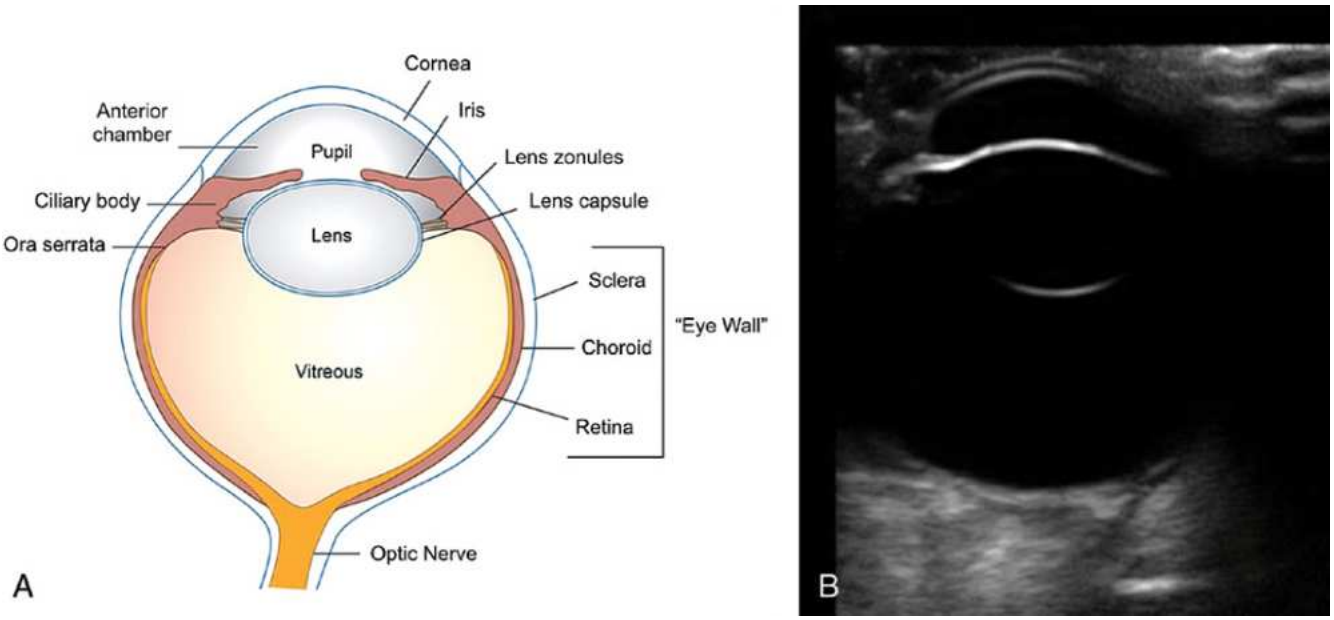


**Figure 27.11.** Normal ocular anatomy and ultrasound. (A) Illustration of normal ocular anatomy. (B) Ultrasound image of a normal eye. Note the bright concave curved cornea with two thin bright parallel lines (which may seen as a single echogenic band, or not at all) anteriorly (at the top of the image), the anechoic anterior chamber behind it, the bright iris (seen here peripherally on the left) and bright thin curved anterior and posterior lens capsules (axially), the anechoic vitreous, and the bright convex posterior eye wall. A band of hypoechoic retrobulbar muscle is visible behind the globe to the right of the visual axis. This still image does not show the ciliary body or peripheral eye wall well, as not all parts of the eye may be visualized at any one time. Source: Reproduced with permission of Dr Gregory Lisciandro, Hill Country Veterinary Specialists and FASTVet.com, Spicewood, TX.

The lens is directly behind the iris, and the anterior lens capsule may not be distinguishable from the iris where they are in contact. The lens capsule is a thin bright line surrounding the lens in an oval shape. It should be smooth and curvilinear, though it appears brightest along the central axis of the image (at the central anterior and posterior lens capsules, when the vertical and horizontal views are used) and often "disappears" towards the periphery (see Figure 27.11). The ability to see even a part of the lens capsule with its characteristic appearance allows the user to reliably locate the lens, especially when the lens is not in a normal position. The lens material inside the capsule is generally fairly echolucent, but it can be more echogenic than the aqueous in front of it and the vitreous behind it, and may not be uniform. Nuclear sclerosis and cataracts may appear as variable echogenic structures within the normally hypoechoic lens. The lens should always be centered in the visual axis.

The lens zonules, small structures that attach the lens equator to the ciliary body, are generally not visible on ultrasound. The ciliary body, which is the posterior continuation of the iris, may be seen as a small mound of echogenic tissue peripheral to the lens equator, but is also often not easily distinguishable from the iris, or even visible. The posterior chamber is defined as the space between the iris and the lens (not the retina), and as such is actually a very small and thin space in front of and to the sides of the lens that is not easily discernible on ultrasound.

Posterior to the lens is the large, gel-like, uniformly echolucent vitreous body, composed mainly of water and collagen fibers. No echogenic structures should be present in the vitreous (see Figure 27.11). However, various vitreal abnormalities (asteroid hyalosis, vitreal strands) may be ultrasonographically present without being a clinically significant cause for disease (Labruyère et al. 2008).

Posterior to the vitreous is the posterior eye wall, a smooth and echogenic curved line representing the back of the globe. The posterior eye wall is made up of three thin layers (the retina, choroid, and sclera) that are normally so closely opposed to each other as not to be ultrasonographically distinguishable from each other.

**Pearl:** In the vertical and horizontal views, all ocular structures should be symmetrical within the globe; *asymmetry is abnormal*.

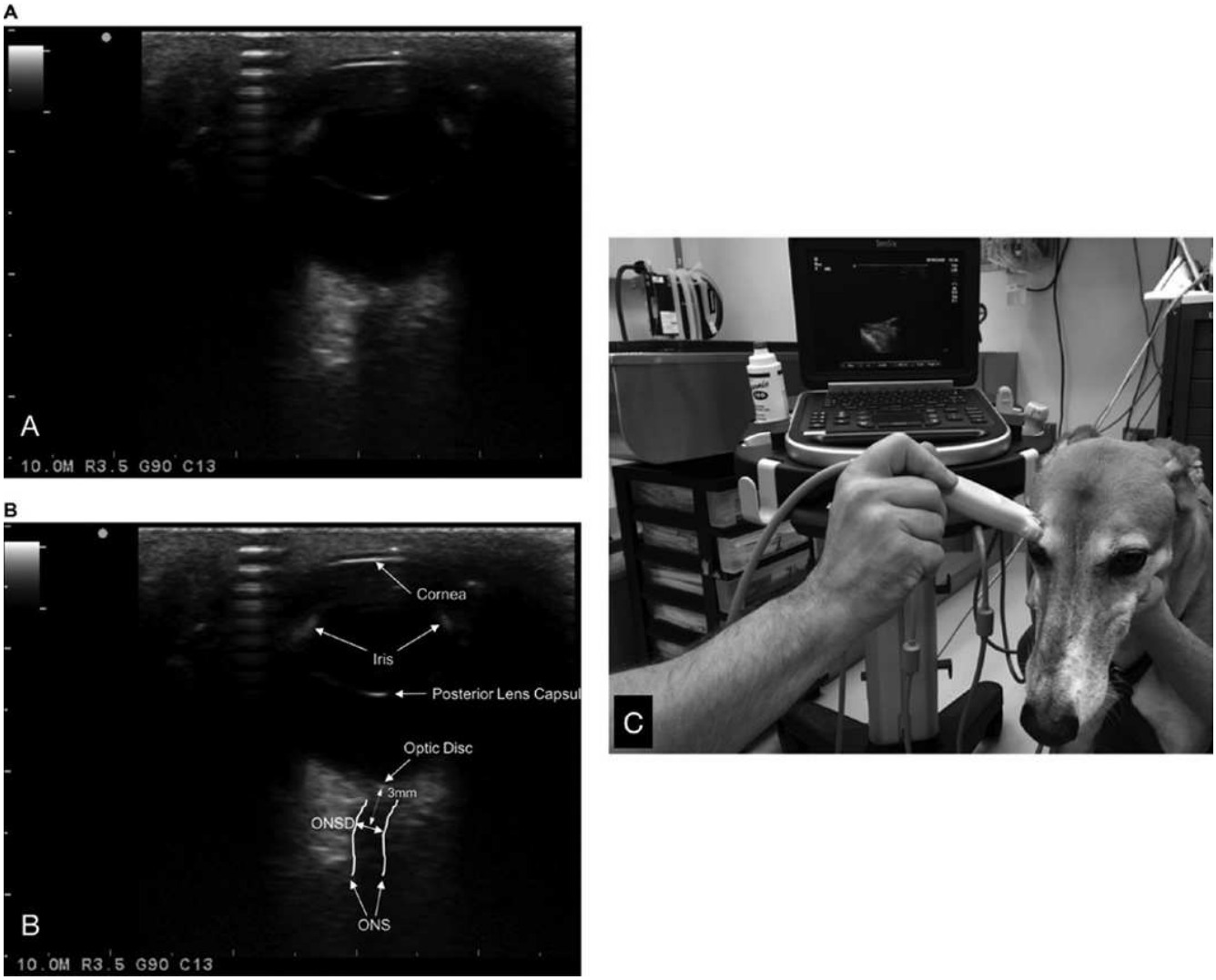


**Figure 27.12.** Optic nerve and optic nerve sheath diameter. Transpalpebral ultrasonography is performed on a standing awake dog. The transducer (probe) is placed on the upper eyelid and fanned dorsoventrally until the optic nerve is detected in the longitudinal plane. Transpalpebral ocular ultrasonographic image from a 7 kg, 3-year-old dog. An image of the entire globe is obtained and fills the screen as in (A). Depth is optimized to allow adequate retrobulbar space for visualization of the optic nerve. The same image in (B) with structures labeled: cornea, posterior lens capsule, hyperechoic optic disc, hypoechoic optic nerve within the hyperechoic optic nerve sheath (ONS), delineated by the white lines. The optic nerve sheath diameter (ONSD) is measured 3 mm posterior to the optic disc. In (C) the external placement of the probe is shown. Source: Reproduced with permission from Smith et al. 2018. *J Vet Emerg Crit Care* 28(1):33–34.

Behind the globe, it may be possible to identify the hypoechoic optic nerve, originating just ventral to the back of the globe and sometimes appearing as two thin parallel and occasionally curved lines extending towards the posterior orbit (see Figure 27.12). Note that it is normally off center from the axis of the anterior segment, more so in dogs than in cats. It may also appear as a hypoechoic linear (or possibly curvilinear) structure without the brighter borders. It is often surrounded by a thin layer of bright fat and the hypoechoic extraocular muscle bellies, all oriented as a cone towards the posterior orbit. The diameter of the optic nerve sheath may be measured in the retrobulbar tissues. The optic nerve is surrounded by cerebrospinal fluid (CSF) within its outer layer of dura (the outer layer of the optic nerve sheath), making the optic nerve sheath potentially distensible by CSF in this area and thus a potential transient indicator for increased

intracranial pressure (Ilie et al. 2015). In general, these structures are not nearly as easy to discern as the intraocular structures.

Finally, a very bright line representing the ventromedial bony wall of the orbit may be seen behind these retrobulbar soft tissue structures. This is a smooth and bright line that curves away from the globe ventrally.

Normal ocular findings are listed in Table 27.1 and abnormal findings in Table 27.2.

**Pearl:** Imaging the other eye for comparison is often very helpful for distinguishing lesions and better identifying what is normal for that animal.

# Clinical Significance and Implications of Abnormal Findings

## *Anterior Lens Luxation*

### Clinical Findings

- History: acute change in the eye (trauma is not required).
- Signalment: terrier breeds most commonly affected; also poodles, but can occur in any dog breed; cats may also be affected.
- Eye exam: corneal edema – usually most pronounced in the center or wherever the lens is touching the cornea; may not be able to visualize iris or anterior chamber well; directing focal light from the side may highlight a relucent (brightly reflective) "rim" of the luxated lens in the peripheral anterior chamber (Figure 27.14); pupil dilated with a poor pupillary light response (PLR); cannot see fundus well; high intraocular pressure (IOP) – often over 30–40 mmHg; menace response and vision is variable.

### Ultrasonographic Findings

- Lens in anterior chamber – usually can only see the thin bright line of the axial anterior lens capsule just behind the cornea, or the posterior lens capsule just in front of pupil; sometimes can see an echolucent lens-shaped structure with a thin bright border in anterior chamber right behind the cornea and anterior to the normal lens location (Figure 27.15).

**Table 27.1.**
Normal findings (see Figures 27.11 and 27.12).

| | Structure | Echo appearance |
|---|---|---|
| Should always see: | Anterior chamber | Should be anechoic |
| | Axial anterior and posterior lens capsule (axial = along the central visual axis) | Thin bright line of specular reflection curving backwards and forwards (though often cannot see where they meet peripherally) |
| | Vitreous | Should be anechoic |
| | Axial posterior eye wall | Smooth curved bright white line with no hyperechoic adjoining structures |
| Will often see: | Cornea | Linear, uniform, moderately echogenic structure forming anterior eye wall – usually not visible unless using a thick layer of gel or some other standoff is used |
| | Retrobulbar extraocular muscle cone | Hypoechoic muscle bellies originating in a ring around the optic nerve and converging at the back of the orbit, forming a cone |
| | Frontal bone | A bright hyperechoic angled line behind and ventromedial to globe |
| Might see: | Iris | A very thin hyperechoic linear structure peripheral and anterior to, but not often distinguishable from, the anterior lens surface |
| | Optic nerve | A straight or curved hypoechoic linear structure from just below the globe's posterior pole with parallel linear borders, surrounded by echogenic fat and the retrobulbar extraocular muscle cone |
| | Fat around optic nerve | Hyperechoic material around the hypoechoic optic nerve |
| Should not see: | | Any bright structures in the anterior chamber or vitreous, especially in the center of your image |
| | | Any anechoic structures in the orbit (behind the globe) |

**Table 27.2.**
Types of abnormal ultrasonographic findings and possible causes.

| Finding | Possible cause |
|---|---|
| Deep anterior chamber | • true deep anterior chamber due to chronic glaucoma and buphthalmos<br>• posterior lens luxation<br>• prior lens removal surgery (aphakia) |
| Shallow anterior chamber | • mass in anterior chamber (Figures 27.19, 27.20, 27.23)<br>• anterior synechiae<br>• intumescent (swollen) cataract (Figure 27.13A)<br>• iatrogenic (compressing cornea with probe)<br>• ruptured cornea with loss of aqueous humor<br>• aqueous misdirection syndrome (rare and only in cats) |
| Echogenic material in anterior chamber | • anterior lens luxation (Figure 27.15)<br>• blood, fibrin, and/or cells in anterior chamber (Figures 27.2, 27.3, 27.26)<br>• cysts in anterior chamber<br>• anterior synechiae<br>• iris (or other) mass (Figures 27.19, 27.20, 27.23)<br>• anteriorly displaced vitreous (would be very weakly echogenic)<br>• foreign body (rare) |
| Echogenic lens (other than axial lens capsules) | • cataract (varying degrees and distribution of echogenicity possible)<br>• nuclear sclerosis<br>• gain turned too high<br>• artificial intraocular lens implant due to prior cataract surgery (lens implant would be thinner than a normal lens, and highly echogenic) |
| Abnormal lens shape or size | • hypermature cataract (lens smaller than normal)<br>• intumescent cataract (lens larger than normal) (Figure 27.13A)<br>• lens capsule rupture (can occur with diabetic cataracts)<br>• cells or other material adherent to lens surface (for example, as occurs with lens capsule rupture or persistent hyaloid remnant)<br>• lenticonus (rare) |
| Abnormal lens location | • lens subluxation or luxation (Figures 27.14, 27.15, 27.16, 27.17) |
| Echogenic structure(s) in posterior segment | • vitreal degeneration (forming strands, membranes, clumps, and/or dots in vitreous)<br>• asteroid hyalosis (usually poorly defined and in central vitreous) (Figure 27.22)<br>• vitreal hemorrhage and fibrin<br>• posterior lens luxation (lens-shaped mass in vitreous, may be mobile and in a dependent position) (Figure 27.17)<br>• retinal detachment (Figure 27.18)<br>• retinal/vitreal hemorrhage (Figure 27.26)<br>• mass or other abnormal accumulation of cells in posterior segment (Figure 27.21)<br>• foreign body (rare)<br>• hyaloid vessel remnant (hyperechoic linear structure oriented along a line from posterior pole of lens to posterior pole of globe, possibly patent with blood flow - rare)<br>• marked optic nerve head swelling (slightly raised echogenic structure at optic nerve head protruding into vitreous) |
| Abnormal globe shape | • scleral or corneal rupture<br>• phthisis bulbi<br>• large intraocular or scleral mass deforming globe<br>• retrobulbar mass (indenting globe focally) (Figure 27.24)<br>• staphyloma or coloboma (a focal bulge in eye wall – rare)<br>• scleral thickening (e.g., inflammation, foreign body, etc.) |
| Abnormal globe size | • buphthalmos due to chronic glaucoma (larger globe) (Figure 27.23B)<br>• phthisis bulbi or microphthalmos (smaller globe) |

(*Continued*)

**Table 27.2.**
(*Continued*)

| Finding | Possible cause |
|---|---|
| Mass-like structure in or around eye | • neoplasia (Figures 27.19, 27.20, 27.21, 27.23, 27.24)<br>• inflammation/granuloma<br>• blood clots and hemorrhage<br>• foreign body (rare)<br>• displaced, enlarged or swollen normal tissue<br>• cystic structure |
| Poor image quality | • inappropriate probe position or angle<br>• air under lids or in gel<br>• eye or patient motion<br>• inadequate amount of gel<br>• settings on machine (gain, probe type, zoom, etc.) require adjustment<br>• technical probe or machine issues |

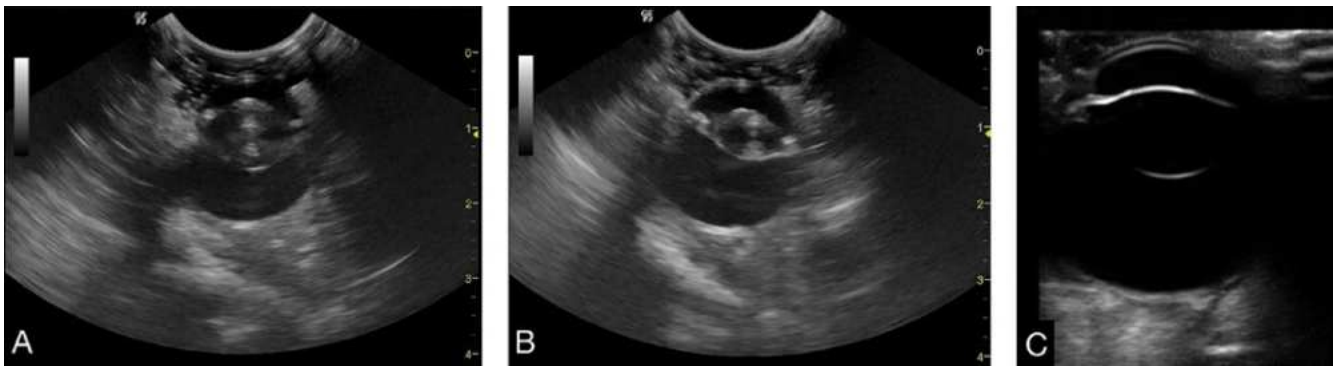


**Figure 27.13.** Shallow anterior chamber. (A) Shows an eye with a shallow anterior chamber; compare with (B), which is the fellow eye of the same dog. The difference in anterior chamber depth is due to the size of the lens. The lens in (A) is an intumescent (swollen) cataract, and the lens in (B) is a normal-sized cataract. In (C) is the normal B-mode image of the eye for comparison.

- No lens in normal location (posterior lens capsule is *not* just anterior to center of globe) – reliable finding.
- Mobile, thin, somewhat amorphous strands in vitreous (in posterior segment) might be present.
- Possible retinal detachment (see Retinal Detachments below).

### Actions

- Measure IOP (preferably with an applanation or rebound tonometer, not with a Schiotz tonometer). Avoid using the center of the cornea where the lens is likely to be touching the cornea inside. If acute glaucoma (IOP >25 mmHg) is present (onset of ocular pain and high IOP <24 hours), immediately refer to ophthalmologist for evaluation and possible surgery. Vision might be able to be saved if the lens can be surgically removed or possibly repositioned before the retina has been permanently damaged by high IOP.
- If available, start the antiglaucoma medications 0.5% timolol every 12 hours and/or 2% dorzolamide q8h (or the combination drop timolol/dorzolamide q8h), +/- oral methazolamide 1 mg/lb up to q8–12h. The latter may be difficult to find and can be considered optional.
- Short-term glaucoma treatment like a dose of IV mannitol might be worth considering especially if IOP increase is very high and recent, if vision may still be present, and/or referral to an ophthalmologist for lensectomy surgery is imminent.
- Do *not* give mydriatics (tropicamide, atropine) as this may exacerbate glaucoma. *Do not* give miotics (latanoprost, pilocarpine, etc.) as these will block the normal flow of aqueous humor, trapping the lens in the anterior chamber and exacerbating glaucoma.

**Figure 27.14.** Anterior lens luxation. This 3-year-old Jack Russell terrier presented with acute ocular pain and cloudiness. Note the dilated pupil, very mild focal corneal edema, and a relucent (brightly reflective) "rim" indicating the equator of the lens in the anterior chamber. This rim can be highlighted by shining a light from the side of the anterior chamber. The IOP is 64 mmHg. In this case the cornea is still clear so that the lens is visible, but in some cases the corneal opacity can be pronounced enough that the lens may not be directly visible and ultrasound may be necessary. Figure 27.15 shows the ultrasound image of an anterior lens luxation.

**Pearl:** All the above ophthalmic medications are human drugs, and drops are generally available at human pharmacies.

Additionally consider the following on an individual basis.

- Topical antiinflammatories if cornea is fluorescein negative.
- Analgesia, systemic pain medications.
- Make patient nil per os (NPO) for referral as applicable for possible surgery.
- Place E-collar to prevent self-trauma.

**Pearl:** If the IOP is not reduced quickly (approximately 24–48 hours depending on IOP level), the eye will not only remain painful but will also become irreversibly blind.

**Pearl:** If the globe is already enlarged (buphthalmos) and blind, then the glaucoma has been chronic and is *not* an emergency.

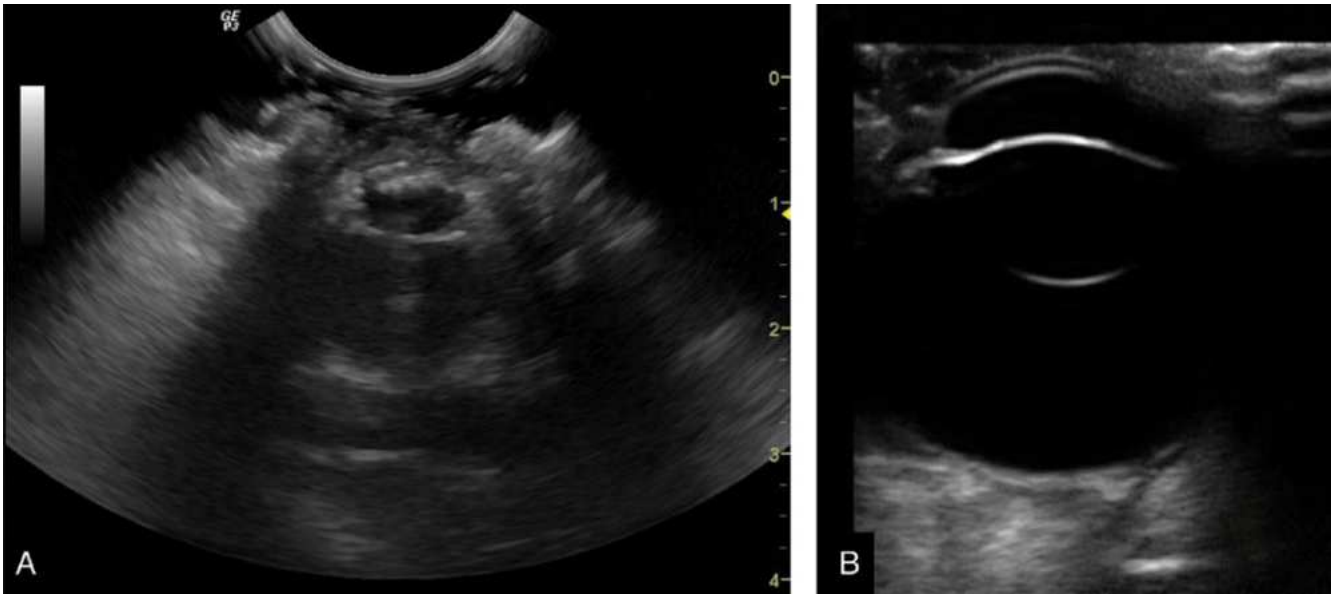


**Figure 27.15.** Anterior lens luxation. The lens, highlighted by its relatively bright lens capsule, is in the anterior chamber just behind the cornea, and is more anterior than it should be. Note that the posterior lens capsule is not visible in its normal location in the center of the globe. In (B) is the normal B-mode image of the eye for comparison. Source: Image (A) courtesy of Dr Andra Voges, College Station, TX.

## *Posterior Lens Luxation*

### Clinical Findings

- History: variable; typically the chief complaint will not implicate lens disease; chronic or acute.
- Signalment: variable.
- Eye exam: variable, as it depends on the cause of the posterior lens luxation. An aphakic crescent may be visible (Figure 27.16), and the lens may luxate anywhere posteriorly, though most commonly it will luxate ventrally and posteriorly. If due to trauma, there may be hyphema, posterior segment bleeding, retinal detachment, globe rupture, etc. If due to chronic glaucoma, there may be blindness, buphthalmos, mydriasis, a deep anterior chamber, retinal degeneration, optic nerve cupping, etc. If due to previous primary anterior lens luxation, there may be focal axial corneal edema, a deep anterior chamber, and possibly other signs of previous glaucoma. If due to chronic anterior uveitis (seen more in cats), other signs of uveitis may be present (aqueous flare, fibrin in anterior chamber, iris hyperemia, etc.).

### Ultrasonographic findings (Figure 27.17)

- No lens in normal position just behind iris and in anterior half of globe.
- Thin curvilinear lens capsule in posterior segment, in characteristic lens shape.
- Lens position is variable and may be gravity dependent.
- Mobile, thin, somewhat amorphous strands in vitreous may be present (vitreal degeneration).
- If present, ultrasonographic signs of vitreal hemorrhage, retinal detachment, scleral rupture, buphthalmos, etc.

**Figure 27.16.** Aphakic crescent. This illustrates the clinical appearance of an aphakic crescent when visible. A posteriorly and ventrally luxated lens (which happens to be a cataract) is in the lower pupil, allowing for the appearance of an aphakic ("without lens") area in the upper part of the pupil (in this case) where the lens is absent. A corresponding ultrasonographic appearance would be seen depending on the lens location.

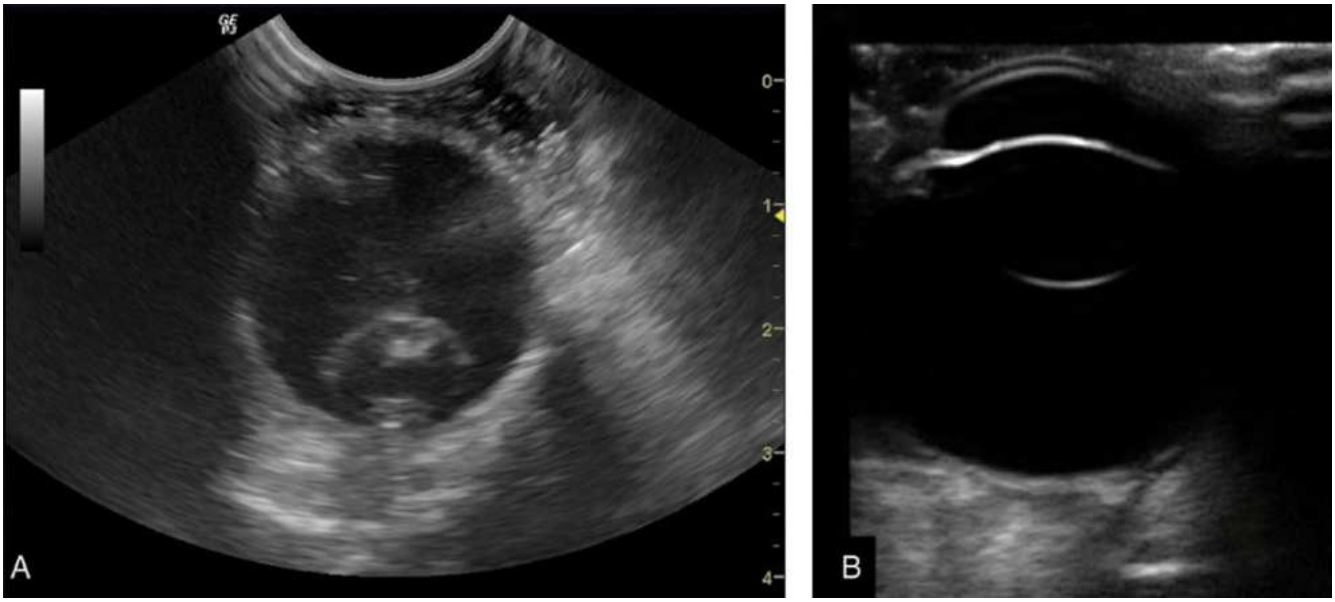


**Figure 27.17.** Posterior lens luxation. In this eye with chronic glaucoma and buphthalmos, the lens zonules have broken down, allowing the lens to become mobile and rest in the dependent part of the globe along the posterior eye wall as shown in (A). Note that there is no lens visible in its normal location. In (B) is the normal B-mode image of the eye for comparison.

### Actions

- Measure IOP, and treat glaucoma if needed. Do *not* give mydriatics (atropine, tropicamide) if the IOP is high, as this may exacerbate glaucoma. Miotics (latanoprost, pilocarpine) are not specifically contraindicated and may help to keep the lens trapped in the posterior segment.
- Topical antiinflammatories may be needed if there are clinical signs of anterior uveitis.
- Based on clinical signs and history, need to determine primary cause as discussed above. The posterior location of the lens, alone, does not necessarily require specific treatment but is more an indicator of possibly more significant ocular pathology that must be identified and addressed. Consider referral to a veterinary ophthalmologist.

## *Retinal Detachment*

### Clinical Findings

- History: possible acute or subacute vision loss (may not be noticeable to owner if unilateral).
- Signalment: variable.
- Eye exam: reduced or absent PLR, menace and dazzle; hyphema (blood in anterior chamber); resting mydriasis (in affected eye), especially with anisocoria; possible retinal hemorrhages or generalized red color from behind pupils; visible retinal detachment seen on fundic exam (best seen using indirect ophthalmoscopy, rather than direct ophthalmoscopy (for examination techniques see Cho 2019).

### Ultrasonographic Findings

- If intraocular bleeding is present, this may be visible as echogenic structures (see Intraocular Hemorrhage section below).
- The retinal detachment itself is seen as a thin bright continuous curvilinear structure in the posterior segment that can be followed back to the optic nerve head, often making a V- or Y-shape or "gull wing" appearance (Figure 27.18A).
- This linear structure is almost always attached at the ora serrata (junction between retina and ciliary body) (Figure 27.18B).
- Often accompanied by other echogenic structures (vitreal strands, hemorrhage, asteroid hyalosis) in the posterior segment.
- Retinal detachments may be bullous (retina separated from the posterior eye wall) or "flat" (retina close to the posterior eye wall) (Figure 27.18C).
- Retinal detachments may be completely detached (only attached at the optic nerve head and ora serrata) or partial (still attached to the choroid in some areas).
- It is possible to see discontinuities (tears or holes) in the detached retina, but not common.
- The subretinal space is more often echolucent (indicating a serous retinal detachment) than echogenic (indicating subretinal blood, cells or a mass), and is very often more echolucent than either the retina or the posterior eye wall.
- The presence of vitreal blood and vitreal membranes/degeneration can make identification of a retinal detachment, especially a partial detachment, much more difficult (see Figure 27.26). These findings can significantly reduce image contrast, causing a missed diagnosis of detachment, or a false positive if vitreal membranes are oriented to masquerade as a detachment (Gallhoefer et al. 2013).
- If available, the use of contrast enhancement may improve the ability to differentiate a detached retina from vitreal membranes by identifying vascularization within the suspect structure(s), and may be more useful than using Doppler (Labruyère et al. 2011).
- Seeing attachment points of a suspected retinal detachment (especially at the optic nerve and ora serrata) greatly increases the chance that a suspected detachment is truly a retinal detachment. Sweeping the probe across a suspect area in different directions will improve your ability to see this.

### Actions

- Measure blood pressure especially if retinal detachment is nontraumatic and bilateral; treat systemic hypertension (systolic blood pressure >180 mmHg) if present and consistent with clinical signs.
- Look for signs of anterior or posterior uveitis (miosis, aqueous flare, hypotony, iris hyperemia, etc.). If present, and cornea is fluorescein negative, and if patient will *not* be seen by a veterinary ophthalmologist within 48–72 hours, begin topical treatment, such as NeoPolyDex drops or ointment, or 1% pred acetate suspension q6–12h, and systemic nonsteroidal antiinflammatories. If patient will be seen immediately, therapy may be delayed until examination.
- If hyphema is present, measure IOP, and treat with antiglaucoma medications if IOP >25 mmHg (0.5% timolol q12h and/or 2% dorzolamide q8h, or the combination drop timolol/dorzolamide q8h), +/- oral methazolamide 1 mg/lb up to q8–12h). The latter may be difficult to find and can be considered optional.

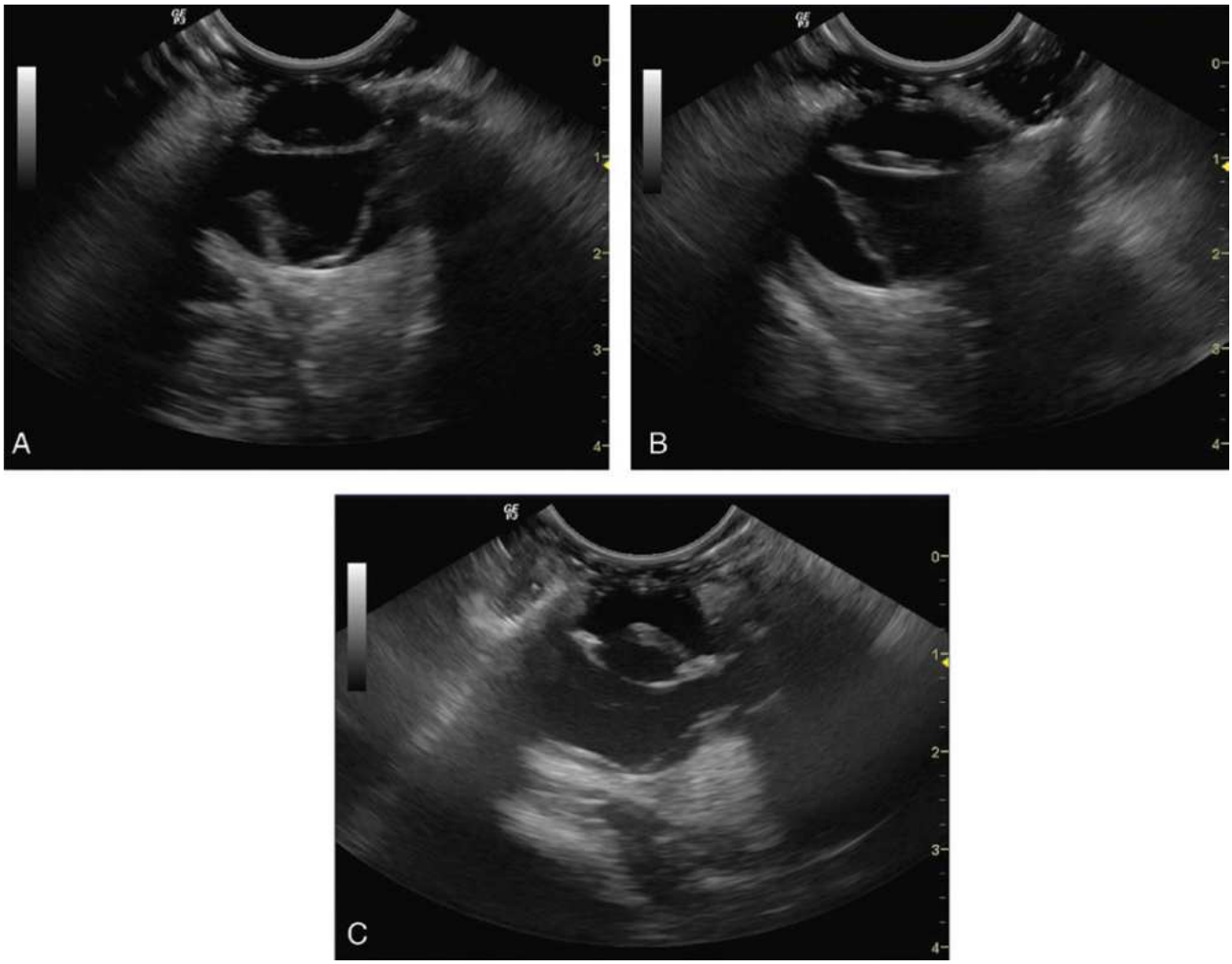


**Figure 27.18.** Retinal detachments. (A) Note the curvilinear bright line in a "gull wing" shape that connects to the optic nerve head at the back of the globe. The space between the retina and the choroid/sclera is echolucent here, as is often the case in serous retinal detachments. The posterior lens capsule is also seen in this image, but the anterior lens capsule is not. (B) Retinal detachment. In this different view of the same eye, on the left of the image, the retina is seen as a thin bright membrane attached posteriorly at the optic nerve head at the back of the globe, and anteriorly extending towards the ora serrata (the junction between the ciliary body and retina), both natural anatomical attachment points. The full lens is not seen at this angle. (C) Retinal detachment. This retinal detachment (a different patient from Figure 27.18A and B) is less pronounced than in the previous figures, as the retina is much closer to the posterior eye wall (a so-called "flat detachment"). Note the thin separation of the retina on the left side of the image. The presence of an echogenic space between the retina and the eye wall confirms this to be a retinal detachment.

**Pearl:** All the above ophthalmic medications are human drugs, and drops are generally available at human pharmacies.

- Note that other differentials for retinal detachment include primary retinal detachment, systemic disease (systemic infection, neoplasia) as well as idiopathic/immune-mediated pathologies, so a complete physical exam and/or additional laboratory testing and imaging (thoracic radiographs, +/- abdominal radiographs or ultrasound) for systemic disease may be indicated if other clinical signs are abnormal.
- Consider referral to a veterinary ophthalmologist for further evaluation and possible advanced additional treatment.

**Pearl:** Retinal reattachment surgery, while not as commonly performed in animals as it is in humans, is increasingly available for animals with primary retinal detachment.

**Pearl:** The prognosis for vision is better if the subretinal space is echolucent (transudate) and worse if echogenic (blood, cells, mass). The prognosis also worsens with increasing duration of the detachment.

**Pearl:** If retinal detachment is present and associated with trauma, the prognosis for vision is guarded to poor (Book et al. 2008).

## *Intraocular Masses*

### Clinical Findings

- History: variable; many owners are unaware of the eye looking abnormal and the eye is often not painful until either uveitis, glaucoma or hyphema develops; signs referable to these secondary problems are often the presenting complaint.
- Signalment: variable, but generally middle-aged to older animals.
- Eye exam: variable but any of the following: deformed globe in advanced cases (outward focal bulging of eye wall); hyphema; focal peripheral corneal edema if mass is touching inside of cornea (Figure 27.19A), dyscoria, iris thickening, presence of a visible mass in either anterior or posterior segment (pigmented or nonpigmented, and especially near eye wall) (Figures 27.20 and 27.21); lens subluxation; focal retinal detachment associated with a solid-looking structure; any of the above with glaucoma.

### Ultrasonographic Findings

- A bulge in the normally spherical eye wall might be seen in advanced cases, with a mass as described below just under the area of the bulging eye wall.
- Hyphema might be seen as indistinct, echogenic material in the anterior chamber.
- Dyscoria would be difficult to appreciate on ultrasound, but an area of iris thickening might be seen if thickening is marked (see Figures 27.19B and 27.20C).
- The most common type in dogs (uveal melanoma) usually appears as an attached, rounded, uniformly echogenic structure in the area of the iris or ciliary body (less commonly the choroid) with a sharp border, possibly slightly pushing the lens off-center (see Figure 27.19B,C).
- Differentiate masses from uveal cysts, which would be very thin-walled, echolucent within, and either free-floating or attached to the posterior iris, pupil margin or ora serrata.
- Masses are often broad-based (on the eye wall) and not pedunculated (see Figure 27.21).

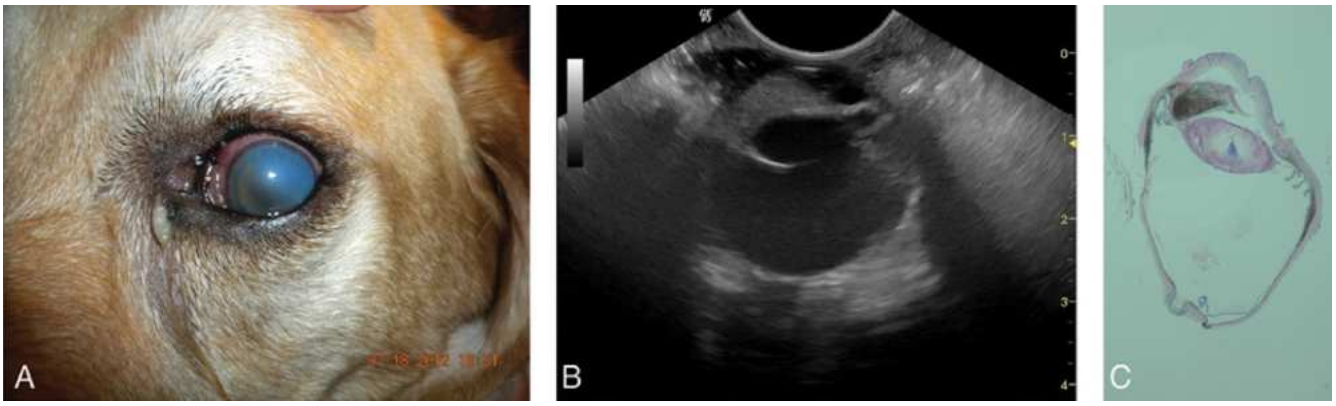


**Figure 27.19.** Anterior chamber mass in a dog. (A) The left eye of this 9-year-old dog has focal corneal edema, obscuring a large dark mass of the iris. The corneal edema has resulted from the mass growing large enough to contact and damage the corneal endothelium. The eye is buphthalmic and blind, and the IOP is 43 mmHg. (B) A large, uniformly echogenic mass is present in the anterior chamber of the same eye, originating from the iris and slightly pushing the lens to the right side of the image. Note the rounded, relatively distinct border between the mass and the anterior chamber and lens. The lens itself, as well as the vitreous, is otherwise normal and echolucent. Left is lateral in this image. (C) Subgross photo of the globe in (A) and (B). The eye was enucleated and a large, solid, pigmented mass is visible in the lateral anterior chamber. Some distortion of the globe shape is present but this is a common processing artifact. The mass was diagnosed histopathologically as a uveal melanocytoma.

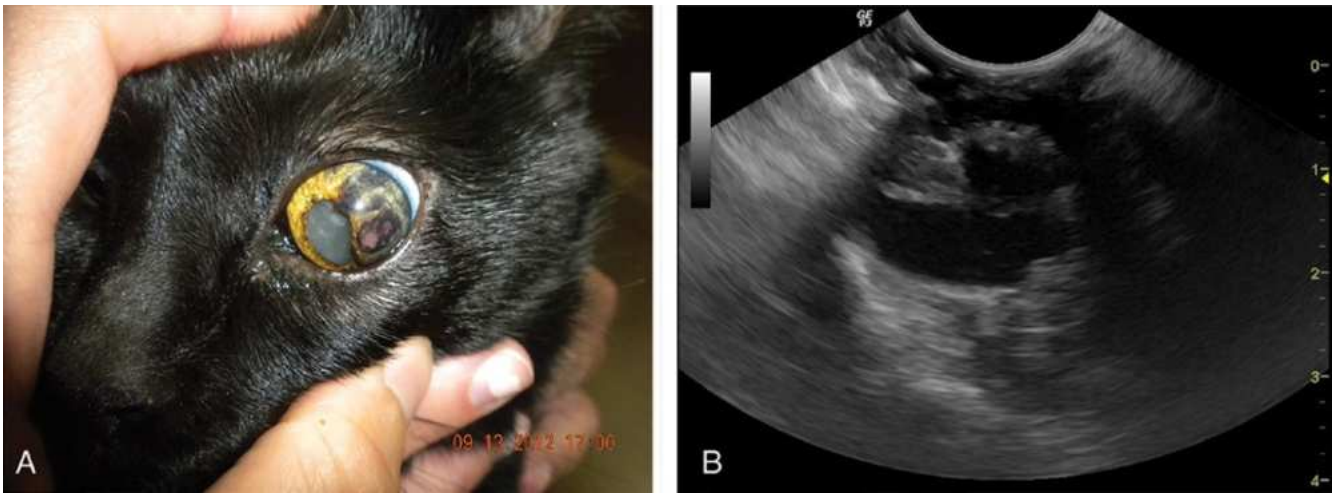


**Figure 27.20.** Anterior chamber mass in a cat. (A) In this adult cat, the lateral iris is clearly distorted. The lateral iris face is raised, discolored and causing dyscoria (abnormal pupil shape). There is also a cataract, blocking direct viewing of the inside of the eye. (B) An ocular ultrasound was done to better identify the extent of the iris mass effect. The ultrasound shows gross thickening of the area of the iris and ciliary body (left is lateral in this image). The iris mass appears to be uniformly echogenic, suggesting a mass and not a cystic structure, and in this case does not extend posteriorly.

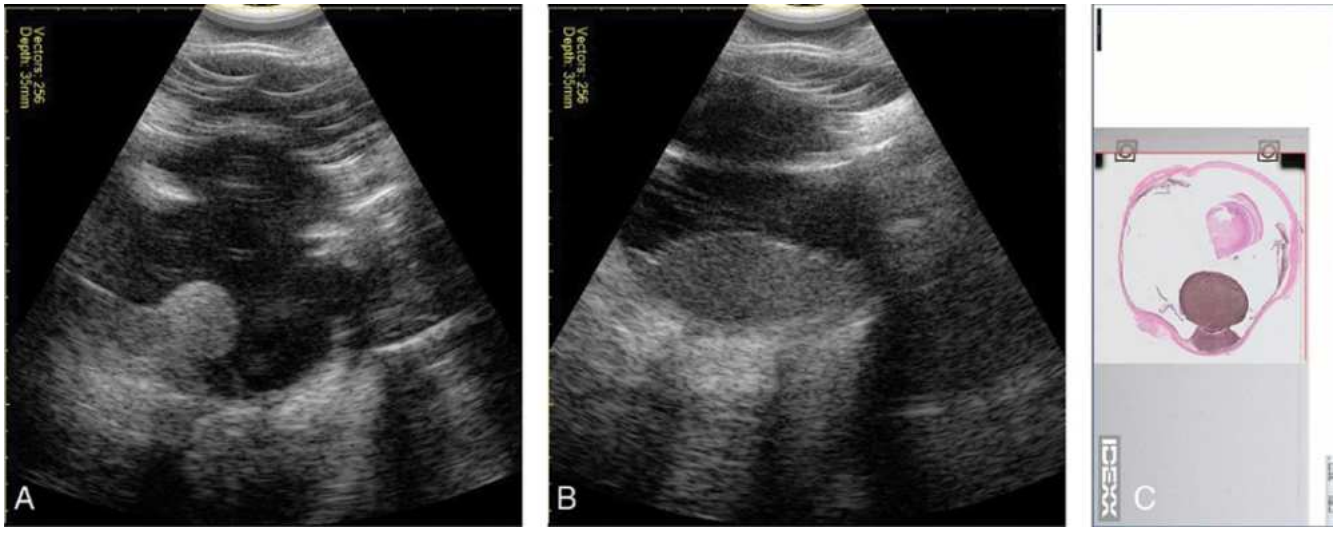


**Figure 27.21.** Posterior segment mass in a dog. In this 7-year-old mixed-breed dog, an abnormal appearance to the fundus was seen incidentally by the referring veterinarian. A dark structure was seen at the posterior eye wall, difficult to discern directly. Ocular ultrasound confirms a solid, lobulated, uniformly echogenic, broad-based mass, and different shapes are seen with the probe held at different angles (A,B). Ultimately, the eye was enucleated, and histopathology confirmed the presence of a lobulated choroidal melanocytoma (C). The complete lens is not visible in this subgross histo section due to processing artifact.

- Doppler might show blood flow within a mass but absence of Doppler-confirmed blood flow does not rule out neoplasia.
- Masses may also be seen with vitreal hemorrhage, vitreal strands, and possibly retinal detachment.
- Intraocular masses would be rarely associated with a foreign body (Welihozkiy et al. 2011).

### Actions

- Look for signs of uveitis and hyphema; if anterior uveitis or hyphema is present and cornea is fluorescein negative, begin topical antiinflammatories, such as NeoPolyDex drops or ointment, or 1% pred acetate suspension q6–12h. If patient will be seen

by a veterinary ophthalmologist immediately, topical therapy can be delayed until examination.
- Measure IOP; if glaucoma present (IOP >25 mmHg), begin antiglaucoma medications, such as 0.5% timolol q12h, 2% dorzolamide q8h, or dorzolamide/timolol q8h, if not being seen by an ophthalmologist within 24 hours. Do *not* give mydriatics (tropicamide, atropine) as this may exacerbate glaucoma.

**Pearl:** All the above ophthalmic medications are human drugs, and drops are generally available at human pharmacies.

- Most intraocular neoplasms (such as melanoma, adenoma) are primary and late to metastasize; however, a minimal systemic work-up with baseline bloodwork, urinalysis, and thoracic radiographs, with or without abdominal imaging (ultrasonography, radiography), is indicated if systemic illness is present since intraocular neoplasia (such as lymphosarcoma, hemangiosarcoma, etc.) may represent metastatic disease.
- Enucleation may ultimately be needed for both diagnostic and therapeutic purposes.
- Consider timely referral to a veterinary ophthalmologist as necessary for confirmation and definitive therapy.

## *Intraocular Hemorrhage*

### Clinical Findings

- History: variable; possible vision loss, possible trauma, change in appearance, possible history of coagulopathy.
- Signalment: variable.
- Eye exam: hyphema (see Figure 27.2A), red or red-black haze visible inside eye from behind iris and lens, inability to visualize any fundic details; pupil may be any size and may still be responsive to light. Since the possible causes of intraocular hemorrhage include retinal detachment, posterior segment mass or injury, trauma, systemic hypertension, coagulopathy and possibly vascular disease, accompanying history and clinical signs vary with the underlying cause. IOP may be low, normal or high.

**Pearl:** In the absence of trauma, two of the most common causes for spontaneous intraocular bleeding in older dogs are retinal detachment and intraocular neoplasia. In cats, neoplasia and hypertensive retinopathy with retinal detachment are the most common in the author's experience.

### Ultrasonographic Findings

- If hyphema is present, diffuse echogenic material will be present in the anterior chamber.
- Variably sized and shaped structure(s) within the vitreous with poorly defined borders that are semi-mobile (try jiggling the eye) but not completely gravity dependent; can be multifocal; may be densely and uniformly echogenic, anechoic, hypoechoic or heterogeneous; may be composed of multiple point-like echoes; are often near the eye wall (where the original bleeding occurred) (see Figure 27.26).
- Differentiate on ultrasound from asteroid hyalosis, which tends to have a lucent peripheral vitreal border and is generally uniform (Figure 27.22) but both have partial mobility and may also have concurrent vitreal strands.
- May be associated with retinal detachment, intraocular masses and scleral rupture (see corresponding sections in this chapter). The presence of echogenic blood in any location could greatly obscure the ultrasonographic visibility of both normal structures and actual lesions.
- Need to differentiate from a solid intraocular mass, which will not be mobile at all, will always be attached to the eye wall, and will typically have a more distinct interior border than a hemorrhage.

**Figure 27.22.** Optic nerve and asteroid hyalosis. Asteroid hyalosis, a common finding in older dogs, is typically seen as an amorphous, fairly uniform, semimobile echogenic material in the normally echolucent vitreous. It is often denser in the center of the vitreous, leaving the more peripheral vitreous echogenic.

### Actions (Table 27.3)

- Look for signs of hyphema and uveitis (aqueous flare, miosis, hypotony); if uveitis is present and cornea is fluorescein negative, start topical steroids, such as NeoPolyDex drops or ointment or 1% prednisone acetate q6–12h, and consider systemic antiinflammatories. If IOP is low-normal and uveitis is present, consider topical mydriatic cycloplegics (atropine q12–48h); IOP should be monitored.
- If not associated with trauma, and especially if seen with hyphema, pursue a timely work-up for coagulopathy including clotting times, platelet count, etc.
- If not associated with trauma, and seen with retinal detachment, especially if bilateral, measure blood pressure; if hypertensive (systolic blood pressure >180 mmHg), then start systemic antihypertensive therapy.
- Measure IOP, and treat with antiglaucoma medications if IOP >25 mmHg (0.5% timolol q12h and/or 2% dorzolamide q8h, or timolol/dorzolamide q8h), +/- oral methazolamide 1 mg/lb up to q8–12h). The latter may be difficult to find and can be considered optional.

**Table 27.3.**
Intraocular bleeding.

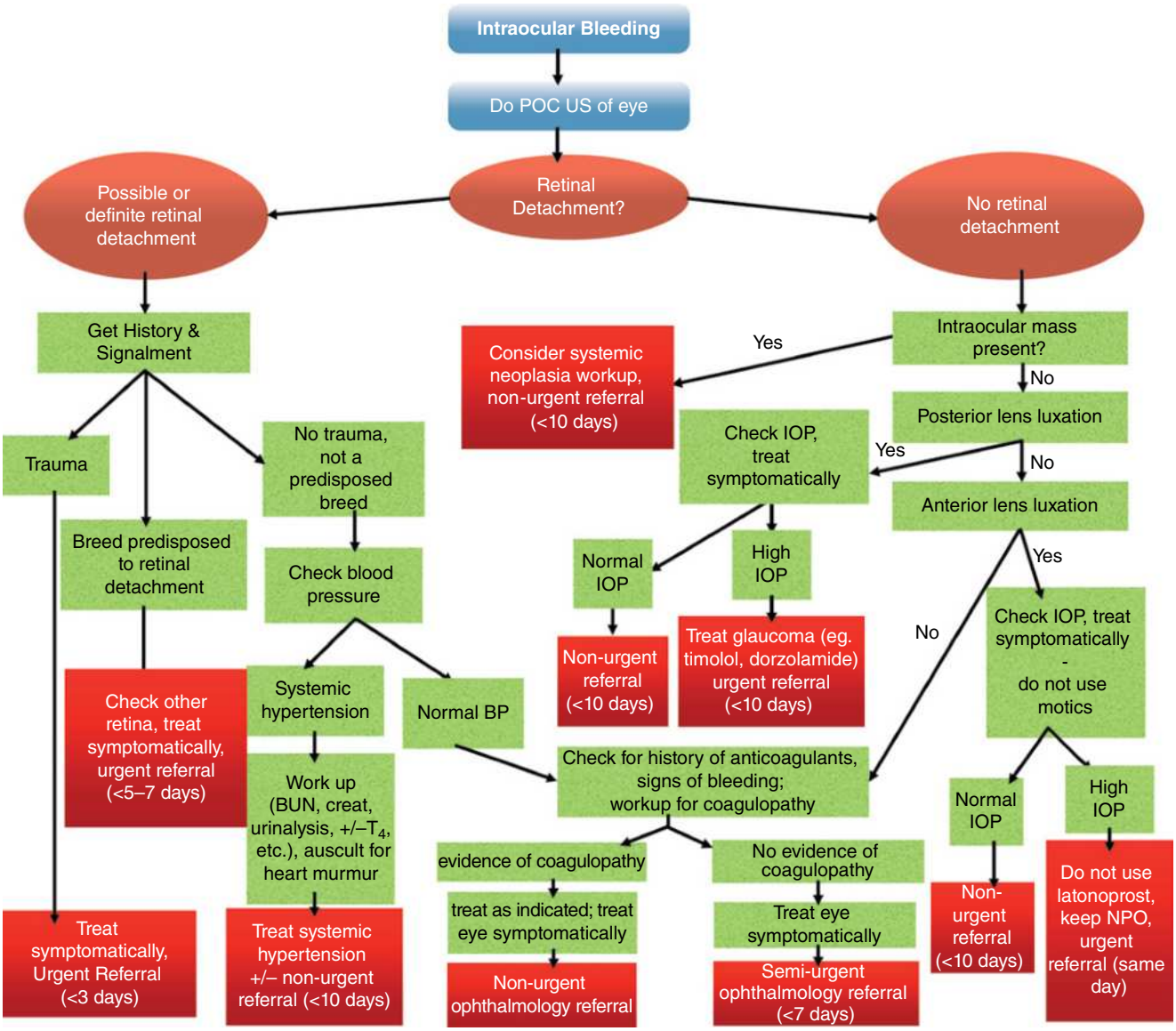


**Note: symptomatic treatment includes treatment for IOP elevation, inflammation, and ulceration as indicated. See Text**

**Pearl:** Intraocular bleeding is a nonspecific finding. Differentials include systemic disease (systemic hypertension, coagulopathy, vasculitis, etc.), ocular disease (uveitis, retinal detachment, neoplasia, possibly lens luxation, etc)., trauma, etc. Referral is indicated unless the cause is definitively identified, treated, and managed.

## *Suspected Retrobulbar Masses/ Exophthalmos*

Distinguishing between exophthalmos and buphthalmos is key to choosing the right treatment plan when the eye is "bulging" (see Figure 27.4).

### Clinical Findings of Exophthalmos (Pushed-Out Eye)

- History: variable, may be acute or gradual onset.
- Signalment: variable due to the varying etiologies.
- Eye exam: globe protrudes and has reduced retropulsion (compare to the other side by palpating gently with an index finger on each closed eye) but is *not* enlarged in size (see below); globe deviation, not necessarily with strabismus; elevated nictitans; secondary lagophthalmos and central corneal exposure; indentation of sclera may be seen on fundic exam but fundus is otherwise normal; variable changes in vision and in IOP – most cases still have intact vision and normal IOP.
- Physical exam: also look for possible ipsilateral dental disease or evidence of inflammation in soft palate; pain on opening mouth (variable); local lymphadenopathy; ipsilateral nasal disease; sneezing and nasal discharge; palpable periocular/orbital bony abnormalities.

### Clinical Findings Supportive of Buphthalmos (Large Eye)

- History: gradual or chronic onset.
- Signalment: for dogs, a breed predisposed to primary glaucoma, for example any terrier breed, bassett hound, cocker, beagle, sharpei, Siberian husky, shih tzu, Dalmatian, Great Dane, etc. For cats, clinical signs and history of chronic or recurrent uveitis. Secondary glaucoma can occur with any age or breed having prior intraocular disease.
- Eye exam: enlarged (and not just pushed out) globe; signs of chronic glaucoma including blindness, episcleral injection, diffuse corneal edema, corneal striae, negative PLR, mydriasis, high IOP, hyperreflective tapetum, thin retinal vessels, dark and/or cupped optic nerve head.

**Note:** Differentiate exophthalmos from buphthalmos using ultrasound by measuring globe at widest front-to-back diameter and compare to normal eye (normal typically around 19–21 mm) (Figure 27.23). Buphthalmos is only caused by glaucoma, and is thus distinctly different in pathology from exophthalmos.

**Pearl:** Cases of buphthalmos still warrant timely referral to a veterinary ophthalmologist for glaucoma treatment for the affected blind eye and glaucoma prophylaxis for the remaining sighted eye.

### Ultrasonographic Findings of Retrobulbar Mass/ Exophthalmos

- Affected globe is normal size.
- Globe indentation by the mass may be seen (Figure 27.24B,C).

**Pearl:** Indentation is more consistent with a mass or cyst rather than cellulitis.

- Mass effect of variable echotexture behind the globe (Figure 27.24B,C).

**Pearl:** Echogenicity versus echolucency is often *not predictive* of the etiology of a retrobulbar mass (Mason et al. 2001).

- Variably discrete mass borders.

**Pearl:** Cellulitis/abscesses usually have very indistinct borders and variable echogenicity, and obliterate/obscure normal structures; cystic structures typically are more sharply marginated with anecholucent/anechoic interior; neoplastic masses tend to be more discrete (than cellulitis/abscess) and more uniform, but may have cavitation, indistinct borders, and variable echogenicity and even be occult via ultrasonography (Mason et al. 2001).

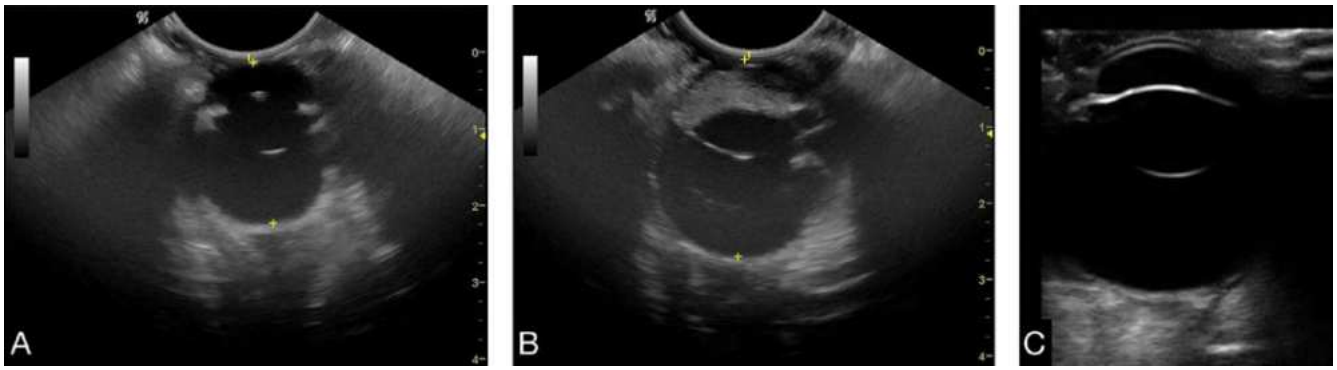


**Figure 27.23.** Measuring globe size. The probe has been placed so that the maximal length of the globe from anterior to posterior (the A-P diameter) can be measured, and the image frozen for measurement. In (A), the normal eye, the normal A-P diameter measured is 2.10 cm. In (B), an image of the fellow eye which is glaucomatous and blind, this same measurement is 2.57 cm. Note: These are additional images from the dog in Figure 27.19. In (C) is the normal B-mode image of the eye for comparison.

- The mass may be attached to or separate from the globe.

**Pearl:** Check ultrasonographically or on fundic exam, if visible, for any motion of the mass relative to the globe; if the mass stays separate from the globe when the gaze is redirected, it is more likely to be noninflammatory (neoplasia or a cystic structure).

- Most common differentials include abscesses (generally acute onset and very painful on opening mouth), soft tissue or bony neoplasia (generally gradual onset and of varying degrees of pain – may not be painful at all).
- Other less likely differentials include cysts (including sialoceles), foreign bodies, cellulitis or inflammation of retrobulbar tissues (sialoadenitis, extraocular muscle myositis), bony orbital masses, hamartomas, vascular anomalies, parasitic disease. These may be very difficult to distinguish (Welihozkiy et al. 2011).

**Pearl:** A lateral orbital location may be more suggestive of abscess than neoplasm.

- Bony destruction is more indicative of neoplasia, and is more easily detected using radiography.

### Actions

- If neoplasia is suspected, initiate a work-up to screen for metastatic disease including baseline bloodwork, urinalysis, skull and thoracic radiography with or without abdominal imaging (ultrasonography, radiography); referral to a veterinary ophthalmologist or surgeon may be necessary.
- If an orbital abscess is suspected supported by findings of pain, ipsilateral soft palate swelling, gross dental disease, leukocytosis, lethargy, +/- fever, perform an oral exam and appropriate imaging, such as dental and skull radiographs, with applicable dental treatment; if found, oral abscess exploration, drainage, cytology, biopsy, and culture as indicated; systemic antibiotics and analgesics; advanced imaging and referral to a veterinary ophthalmologist, surgeon, or dentist, as per clinical impression may be necessary (Hartley et al. 2007).

Fine needle aspiration of suspected retrobulbar masses carries the risk of hemorrhage, possible iatrogenic globe puncture or nerve damage, but is often diagnostic for neoplasia and infection when the needle is appropriately placed. Aspiration aided by simultaneous ultrasound can reduce these risks. Vascular anomalies, although extremely rare, may develop significant bleeding when aspirated or biopsied, and may not be amenable to typical hemorrhage control maneuvers.

Most cases of primary orbital/periorbital neoplasia are malignant, for example nasal or third eyelid adenocarcinoma, soft tissue sarcomas, osteosarcoma, squamous cell carcinoma, meningioma, glioma, lymphoma (Kern 1985; Attali-Soussay et al. 2001).

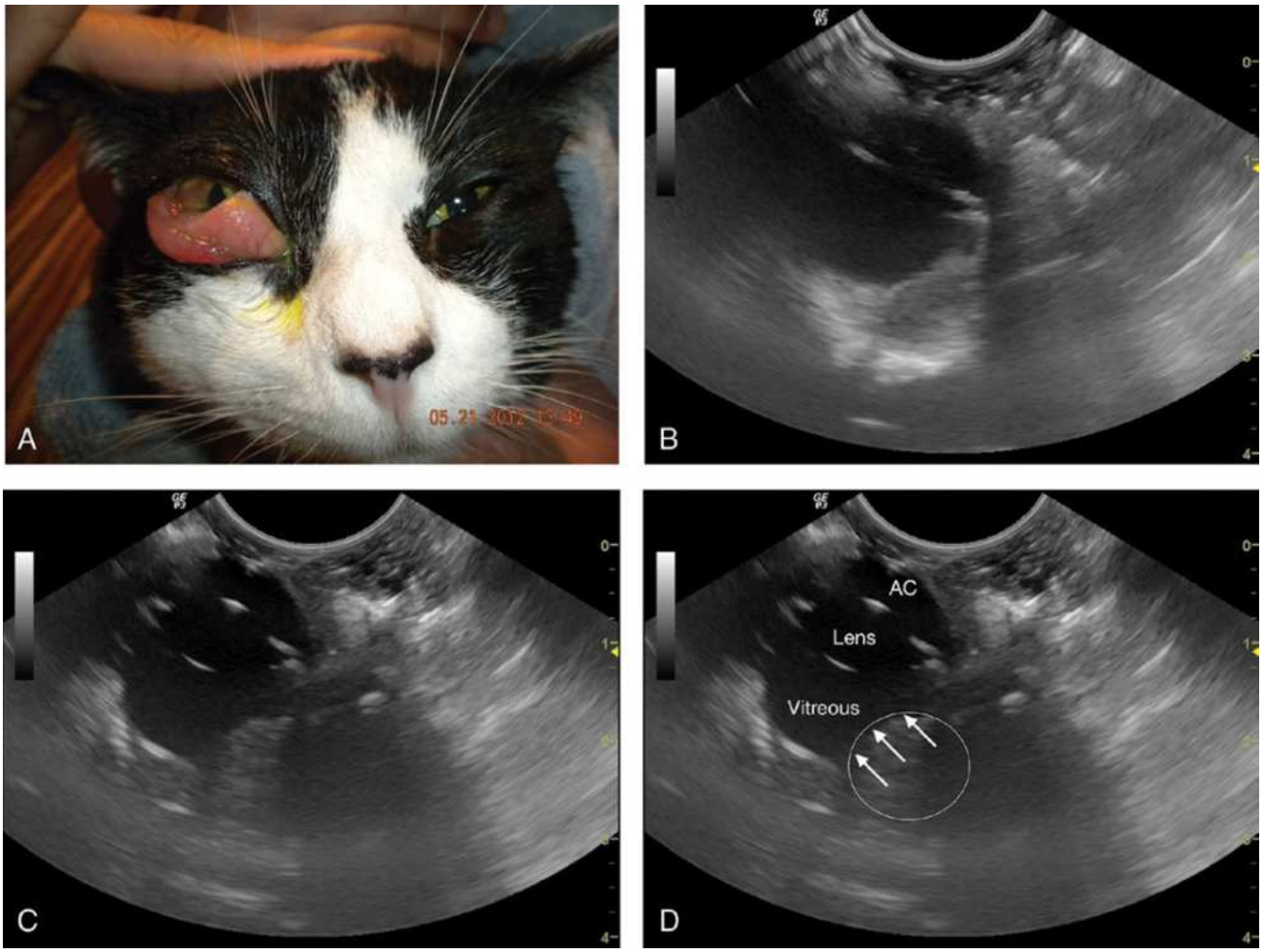


**Figure 27.24.** Retrobulbar mass/exophthalmos. (A) This 10-year-old cat has had progressive exophthalmos for 3–4 weeks. Note the exophthalmos, elevated nictitans, chemosis, and globe deviation dorsally without strabismus. The globe is so exophthalmic that the lids cannot close (lagophthalmos), causing a small corneal exposure ulcer and secondary uveitis with mild miosis. The marked chemosis and hyperemia of the bulbar conjunctiva and nictitans are due to the protruding globe causing tight compression of the lower lid against the globe. (B) Ocular ultrasound shows a distinct rounded echogenic mass behind the globe. Note that the mass is slightly indenting the globe, which is causing a visible indentation that can be seen when viewing the fundus. The full lens is not imaged well at this angle but is normal. In (C) and (D) are unlabeled and labeled second views of the same mass in (B), respectively. A larger more echolucent area is seen to extend from the mass, causing even more distortion to the normal globe contour (*arrows*). This mass was most likely neoplastic, but further diagnostics were declined by the owner. AC, anterior chamber.

### Suspected Globe Rupture

#### Clinical Findings

- History: suspected or known trauma (vehicular trauma, being struck by objects like doors, furniture or toys, fights with other animals including clawed cats and larger dogs, etc.); outdoor animals.
- Signalment: variable.
- Eye exam: acute ocular pain; globe deformation, gross hypotony, chemosis, subconjunctival hemorrhage; other periocular injuries, lid swelling and bruising; hyphema and/or anterior uveitis (Figures 27.25 and 27.26; see also Figure 27.2); blood, fibrin and dark brown-black uveal tissue may be mounded externally at site of rupture

**Figure 27.25.** Traumatic globe rupture in a dog. This unfortunate dog had been kicked by a moose, causing major ocular injury. Note that the corneal contour of this left eye is not spherical but rather appears squashed into a flatter shape by the eyelids. This is because the globe has lost its tension and shape due to a large rent at the limbus. Hyphema obscures all the intraocular structures, but a carefully performed ocular ultrasound (not shown) from behind the orbital ligament might reveal a posterior rent and the presence of a retinal detachment, lens luxation or lens extrusion. ***Important:*** In cases of suspected globe rupture, extreme caution should be exercised when considering ocular ultrasonography. Avoid any direct contact with the suspected ruptured area and if ultrasound imaging is necessary (to confirm or clarify clinical suspicion) use only sterile gel after adequate topical anesthesia, or the retrobulbar view, if at all. Any pressure at all to the globe or resistance by the patient may be painful and will cause further eye damage. The patient may be better served by avoiding ultrasound altogether and simply referring to an ophthalmologist for definitive care.

(which might be located somewhere behind the front exposed part of the eye and thus not visible externally) (Rampazzo et al. 2006); orbital or skull fractures.

**Pearl:** Stabilize animal systemically first before working up the eye!

### Ultrasonographic Findings

Extreme care should be used in approaching ocular ultrasonography in these cases, if at all. Avoid any direct contact with the suspected ruptured area; use sterile gel and adequate topical and anesthesia (see above) or the retrobulbar angle for probe placement; *avoid any pressure at all to the globe and excessive restraint*.

**Pearl:** If the eye is too painful to be imaged with topical anesthesia and other clinical signs are suggestive of globe rupture, the patient may be better served by avoiding ultrasound altogether due to the potential for causing further damage.

- Globe not spherical like normal.
- Globe may be smaller than the other eye (compare diameter of each eye).
- Eye wall may not be clearly visible in all views – intraocular structures may seem to blend in with adjacent extraocular structures consistently in one location (see Figure 27.26B,C).
- Will often be accompanied by sonographic evidence of retinal detachment, vitreal hemorrhage, and/or lens luxation or loss (see above corresponding sections).
- The interior of the whole globe may appear heterogeneously echogenic (due to the presence of blood and fibrin) with no discernible normal structures except for the lens, which will remain echolucent against this echogenic background if present.

### Actions

- Evaluate first for life-threatening trauma such as skull fractures, traumatic brain injury, cavitary hemorrhage, lung contusions, pneumothorax, etc. with a basic trauma work-up.

**Pearl:** Stabilize the critical patient before addressing the ocular component.

- Do *not* aggressively clean off adherent mucus-like material from the eye surface. This may be fibrin that is actually sealing the defect, and removing it may cause a releak of intraocular contents as well as acute pain.
- Administer systemic pain medications, systemic antiinflammatories and analgesics, systemic antibiotics, and topical ophthalmics (antibiotics, atropine; drops preferred, avoid ointments) as dictated by patient.

**Pearl:** The owner's ability to give topical medications may be limited due to patient pain. Due to the possibility of further injury in the act of topical drug administration, topical medications may not be worth the trouble.

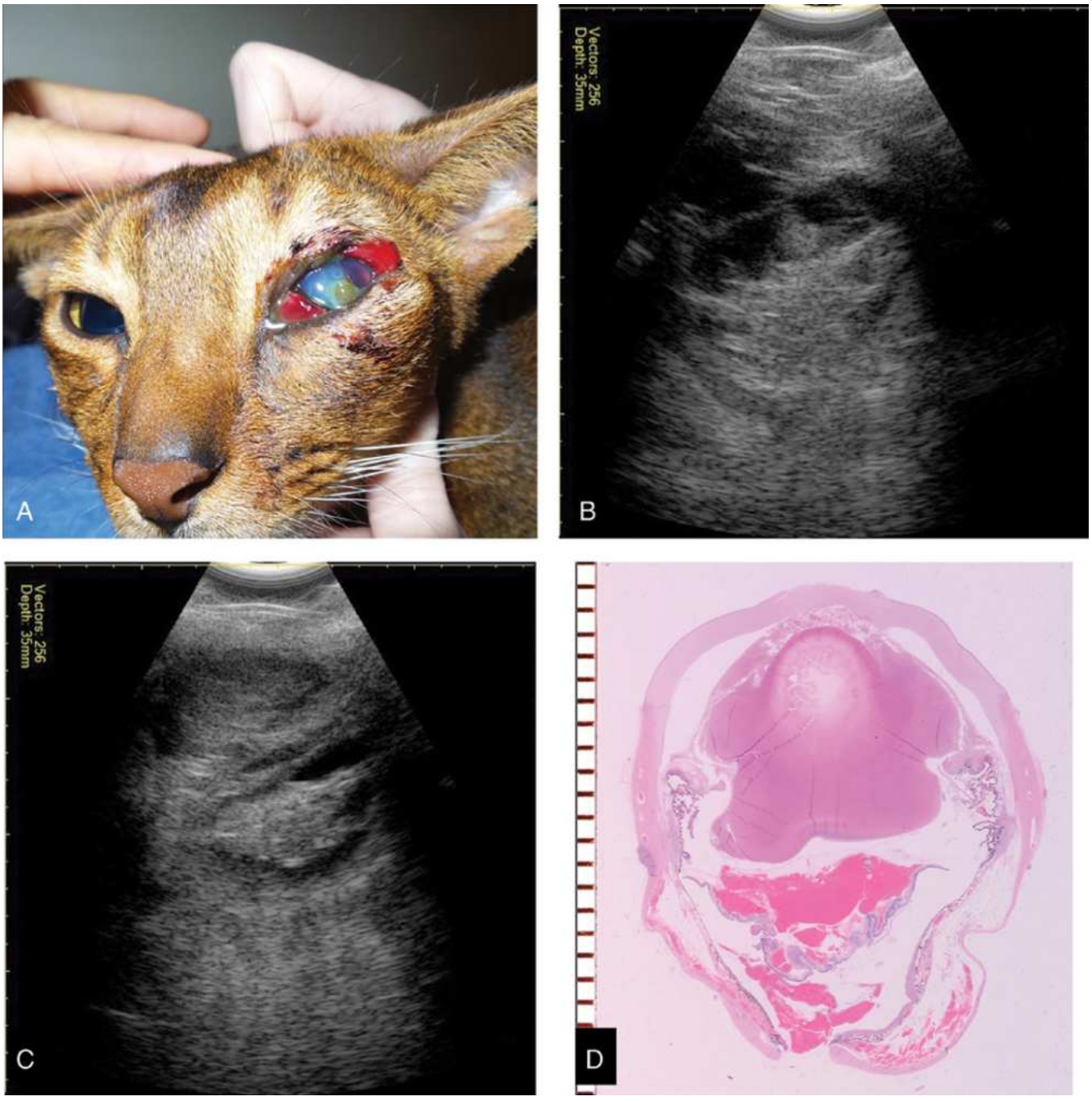


**Figure 27.26.** Globe trauma in an outdoor cat. This 3-year-old male Abyssinian sustained unknown trauma while outdoors. Significant subconjunctival hemorrhage and a central corneal rupture were seen, and the entire anterior chamber was full of fibrin, obscuring visibility of iris and posterior structures (A). Ocular ultrasound shows extensive echogenic material with unorganized linear structures mixed with smaller echolucent areas. The anterior chamber cannot be distinguished and the lens is not clearly seen, and while a retinal detachment may be present, it cannot be distinguished ultrasonographically due to the diffuse presence of surrounding echogenic structures (probably blood). In addition, the posterior eye wall is not clearly visible and cannot be followed continuously through its normal extent (B,C). Ultimately the eye was removed, and histopathological evaluation confirmed the presence of retinal detachment with expulsive vitreal and subretinal hemorrhage, posterior scleral rupture, as well as cataract and lens capsule rupture as shown in (D), and (not seen in this section) corneal rupture. A ballistic foreign body was suspected based on histopathological findings.

VetBooks.ir

- Very carefully place an E-collar to prevent self-trauma.
- If a penetrating foreign body is seen, leave it in place if immediate, timely referral is possible; if a foreign body is clearly visible, very mobile and loose enough to fall out on its own before referral to an ophthalmologist is possible, it may be *very carefully* removed in the clinic under clean conditions with at least topical anesthesia; however, there is risk of damaging the eye and causing leakage of intraocular contents, allowing for intraocular infection, bleeding, and increased risk of loss of the eye.
- Many cases will require enucleation, but referral to a veterinary ophthalmologist may provide options for salvaging the globe and possibly vision.

# Pearls and Pitfalls, The Final Say

- Important to correlate ultrasound findings with clinical ophthalmic signs! Always do a complete ocular examination first when presented with an ocular complaint.
- Very helpful to compare the abnormal eye to the other eye as a control, especially when the other eye is unaffected.
- Adjust magnification (depth) to a level adequate to distinguish lesions.
- Adjust gain both by increasing and decreasing to help distinguish real findings from artifacts.
- Unless you are very comfortable with your diagnosis and treatment plan, it is wise to adhere to the following statement: if an eye is diseased enough to require ultrasound, it should most likely be referred to an ophthalmologist for follow-up.
- Use Global FAST to help determine if the ocular problem is localized or part of disseminated disease. Global FAST surveys the abdomen (AFAST), thorax (TFAST) including heart (TFAST) and lung (Vet BLUE) and also helps assess patient volume status (see Chapters 6, 7, 17, 18, 22, 23, 36, and 37).

# References


Attali-Soussay K, Jegou J, Clerc B. 2001. Retrobulbar tumors in dogs and cats: 25 cases. *Vet Ophthalmol* 4(1):19–27.

Book BP, van der Woerdt A, Wilkie DA. 2008. Ultrasonographic abnormalities in eyes with traumatic hyphema obscuring intraocular structures: 33 cases (1991–2002). *J Vet Emerg Crit Care* 18(4):383–387.

Cho J. 2019. Ophthalmic examination. In: *Veterinary Clinical Advisor*, 4th edition, edited by Cohn L, Cote E. St Louis: Elsevier Mosby, pp 1137–1139.

Cottrill NB, Banks WJ, Pechman RD. 1989. Ultrasonographic and biometric evaluation of the eye and orbit of dogs. *Am J Vet Res* 50(6):898–903.

Dziezyc J, Hager DA. 1988. Ocular ultrasonography in veterinary medicine. *Semin Vet Med Surg (Small Anim)* 3(1):1–9.

Gallhoefer NS, Bentley E, Ruetten M, et al. 2013. Comparison of ultrasongraphy and histologic examination for identification of ocular diseases in animals: 113 cases. *J Am Vet Med Assoc* 243(3):365–388.

Hartley C, McConnell JF, Doust R. 2007. Wooden orbital foreign body in a Weimaraner. *Vet Ophthalmol* 10(6):390–393.

Ilie LA, Thormovsky EJ, Johnson PA, et al. 2015. Relationship between intracranial pressure as measured by an epidural intracranial pressure monitoring system and optic nerve sheath diameter in healthy dogs. *Am J Vet Res* 76: 724–731.

Kern TJ. 1985. Orbital neoplasia in 23 dogs. *J Am Vet Med Assoc* 186:489–491.

Labruyère JJ, Hartley C, Roders K, et al. 2008. Ultrasonographic evaluation of vitreous degeneration in normal dogs. *Vet Radiol Ultrasound* 49(2):165–171.

Labruyère JJ, Hartley C, Holloway A. 2011. Contrast-enhanced ultrasonography in the differentiation of retinal detachment and vitreous membrane in dogs and cats. *J Small Anim Pract* 52(10):522–530.

Mason DR, Lamb CR, McLellan GJ. 2001. Ultrasonographic findings in 50 dogs with retrobulbar disease. *J Am Anim Hosp Assoc* 37:757–762.

Rampazzo A, Eule C, Speier S, et al. 2006. Scleral rupture in dogs, cats and horses. *Vet Ophthalmol* 9(3):149–155.

Welihozkiy A, Pirie CG, Pizzirani S. 2011. Scleral and suprachoroidal foreign body in a dog – a case report. *Vet Ophthalmol* 14 (5):345–351.


# Further Reading


Bayón A, Tovar MC, Fernández del Palacio MJ, et al. 2001. Ocular complications of persistent hyperplastic primary vitreous in three dogs. *Vet Ophthalmol* 4(1):35–40.

Dietrich UM. 2007. Ophthalmic examination and diagnostics part 3: diagnostic ultrasonography. In: *Veterinary Ophthalmology*, 4th edition, edited by Gelatt KN. Ames: Blackwell Publishing, pp 507–519.

Gonzalez EM, Rodriguez A, Garcia I. 2001. Review of ocular ultrasonography. *Vet Radiol Ultrasound* 42(6):485–495.

Jinks MR, Olea-Popelka F, Freeman KS. 2017. Causes and outcomes of dogs presenting with hyphema to a referral hospital in Colorado: a retrospective analysis of 99 cases. *Vet Ophthalmol* 21(2):160–166.

Spaulding K. 2008. Eye and orbit. In: *Atlas of Small Animal Ultrasonography*, edited by Penninck D,d'Anjou MA. Ames: Blackwell Publishing, pp 49–90.

Williams J, Wilkie DA. 1996. Ultrasonography of the eye. *Compend Contin Educ Pract Vet* 18:667–678.

CHAPTER TWENTY-EIGHT

# POCUS: Brain – Image Acquisition

Cibele F. Carvalho

## Introduction

Magnetic resonance imaging (MRI) is the gold standard for brain imaging. However, this technique involves high costs such as equipment acquisition and maintenance, making it difficult to perform as a routine anywhere, especially in veterinary medicine. Moreover, MRI requires some form of chemical restraint, which is commonly inhaled general anesthesia via endotracheal intubation, which carries patient risk. On the other hand, transcranial ultrasonography (TCUS) has the advantage of being noninvasive and low cost, which has great value in the diagnosis of brain disorders such as hydrocephalus, tumors, congenital malformations, and traumatic processes, and can be performed without the need to anesthetize the patient.

Transcranial ultrasonography is considered a screening method for neuroimaging examination in many situations. It may be applied to cases of trauma, patients with anesthesia limitations and owners' economical restrictions, before patients are imaged by computed tomography (CT) or MRI.

In human medicine, TCUS has been compared to CT and MRI in children in order to detect the cause of headache. While CT and MRI were able to detect tumors as the primary disease in 3.8% of these cases, TCUS was less effective, detecting tumors as primary disease in 2.2% of cases. However, the low cost, lower patient risk, and convenience through point-of-care imaging applications make TCUS an option in clinical practice not only as a screening test but also when measurements and monitoring are needed (Abrão et al. 1998; Wang et al. 2002). In children, the temporal, parietal, and suborbital acoustic windows are commonly utilized when performing TCUS (Wang et al. 2002). These acoustic windows may be used for animals but the bregmatic fontanelle and temporal bone have been most studied as acoustic windows for TCUS in veterinary medicine (Gallagher et al. 1995; Lorigados and Pinto 2013; Cintra et al. 2014). Both human and veterinary protocols additionally use the foramen magnum as an acoustic window to assess the caudal fossa.

Despite many published veterinary studies (Hudson et al. 1998; Carvalho et al. 2007; Duque et al. 2009) some neurologists still remain uncomfortable with the potential use of TCUS. However, many small animal patients have suitable transcranial acoustic windows that allow screening for structural lesions with the advantages of being a rapid, safe (no anesthesia requirement and minimal restraint), point-of-care, imaging application. One of the main indications for TCUS is ventricular system evaluation. Ventricular measurements may be used clinically and compared to normal published reference values (Table 28.1).

### *What POCUS Brain Can Do*

- Screen for anatomical abnormalities of the brain.
- Screen for structural abnormalities of the brain.
- Provide monitoring measurements (ventricular system, focal lesions).

### *What POCUS Brain Cannot Do*

- Account for variables of skull bone thickness.
- Account for anatomical variations between patients and species.
- Differentiate between malignant and benign lesions.

*Point-of-Care Ultrasound Techniques for the Small Animal Practitioner*, Second Edition. Edited by Gregory R. Lisciandro.
© 2021 John Wiley & Sons, Inc. Published 2021 by John Wiley & Sons, Inc.
Companion website: www.wiley.com/go/lisciandro/ultrasound2

**Table 28.1.**
Guidelines for measurements of the ventricular system as currently available in the literature.

| Parameter | How measured | Normal | Ventriculomegaly |
|---|---|---|---|
| Lateral ventricular height: transverse[a] | Measure the dorsoventral dimension of the lateral ventricle with the probe perpendicular at or caudal to the interthalamic adhesion | 0.04–0.35 cm (mean: 0.15 cm) | >0.35 cm |
| Cerebral mantle thickness: transverse[a] | Measure the thickness of brain tissue dorsal to each lateral ventricle | 1.63–1.91 cm | Often decreased; may be very thin |
| Ventricle- hemisphere ratio (measured on transverse images)[a] | Ratio of the lateral ventricular height to the width of the ipsilateral hemisphere | Mean 0.19 | >0.19 |
| Ventricle- mantle ratio (measured on transverse images)[a] | Ratio of the lateral ventricular height to the thickness of the mantle | Mean 0.25 | >0.25 |
| Lateral ventricular height: sagittal[a] | Measure the dorsoventral dimension of the lateral ventricle with the probe perpendicular at the thalamocaudate sulcus | Mean 0.14 cm | |
| Dorsoventral dimension of the lateral ventricle[b] | Measure the dorsoventral dimensions of the lateral ventricle at the level of the pituitary fossa | NA | NA |
| Dorsoventral percentage[b] | Ratio of the dorsoventral dimension of the lateral ventricle to the dorsoventral dimension of the brain | 0–14% | 15–25% moderate ventriculomegaly<br>>25% severe ventriculomegaly |

[a]Hudson et al. 1991
[b]Spaulding et al. 1990
Source: Reproduced with permission from Penninck D, d'Anjou M (eds). 2008. *Atlas of Small Animal Ultrasonography*. Ames: Blackwell Publishing.

## Indications

- Any small-breed dog or cat with neurological signs and accessible transcranial acoustic windows.

## Objectives

- Understand how to image the three transcranial acoustic windows.
- Appreciate basic ultrasonographic brain anatomy.
- Understand the value and limitations of transcranial Doppler ultrasound (TCUS).

## How to do POCUS Brain

## Probe Type

Real-time B-mode TCUS probe requirements are as follows.

- Linear probes of 5–10 MHz with depth range of 1.0–4.0 cm for neonates with or without an open rostral fontanelle.
- Curvilinear (microconvex) probes of 2–6 MHz with high resolution and depth range of 1.0–6.0 cm for mature small-breed dogs without an open bregmatic fontanelle.

## Acoustic Windows for POCUS Brain

Three transcranial acoustic windows may be used for POCUS brain: rostral, temporal, and suboccipital.

### Rostral Acoustic Window

The rostral window is used in patients with an open bregmatic fontanelle, including puppies <1–3 months old, kittens <5 months old, and many toy breeds. However, even in a closed bregmatic fontanelle having a thin frontal bone, an acoustic window may be present because ultrasound can image through thin bone.

### Temporal and Suboccipital Acoustic Windows

The temporal window is located above zygomatic arch, and the suboccipital window should be used in all cases (Figures 28.1, 28.2, 28.3, and 28.4).

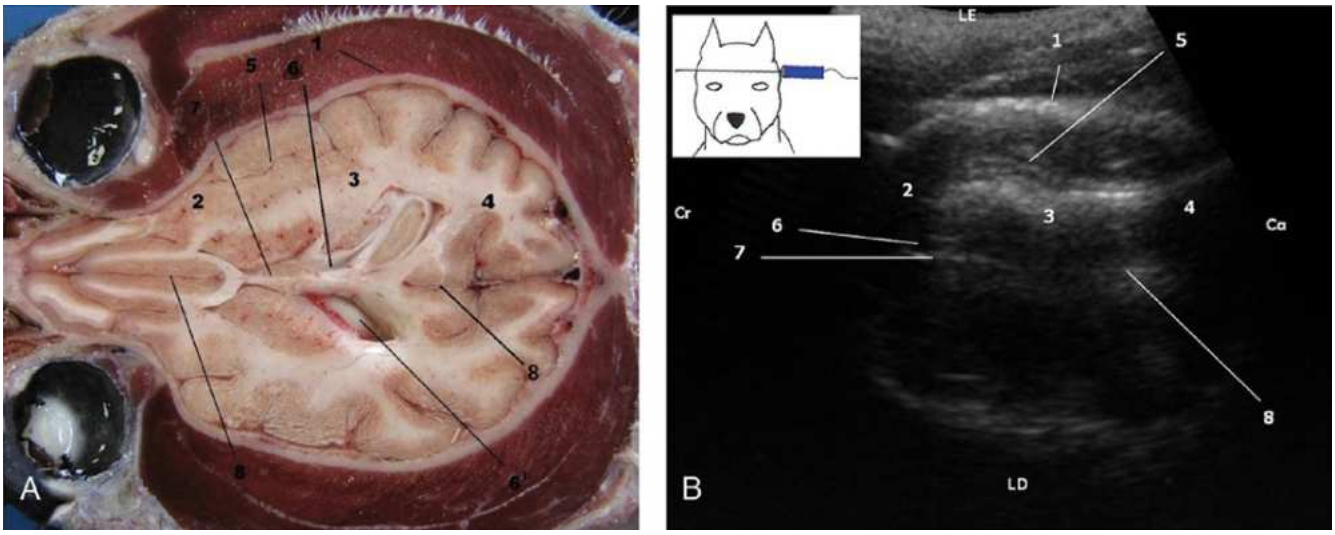


**Figure 28.1.** Temporal acoustic window – for dorsal planes. Middle dorsal plane, probe located above zygomatic arch, with comparative gross, B-mode, and line drawing images in (A) and (B). Line drawing in (B) shows the plane of image. 1, temporal bone; 2, frontal bone; 3, temporal lobe; 4, occipital lobe; 5, suprasylvian sulcus; 6 and 6′, (left and right) lateral ventricles; 7, septum pellucidum; 8, longitudinal fissure. LE, left; LD, right; Cr, cranial; Ca, caudal. Source: Courtesy of Dr Thassila C.F. Cintra, São Paulo, Brasil.

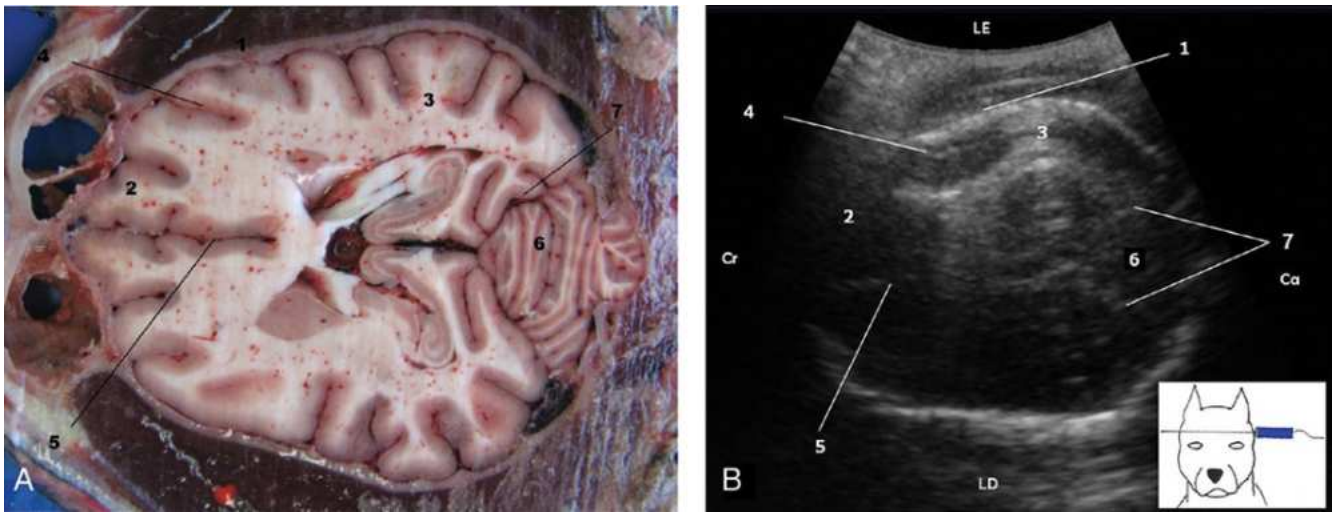


**Figure 28.2.** Temporal acoustic window – fanning lateral for oblique dorsal planes. Oblique dorsal caudal plane (temporal window), probe 45° rotated, with comparative gross, B-mode, and line drawing images in (A) and (B). Line drawing at right inferior shows the plane of image. 1, temporal bone; 2, frontal lobe; 3, reverberation on temporal lobe; 4, ectosylvian sulcus; 5, longitudinal fissure; 6, cerebellum; 7, tentorium of cerebellum. LE, left; LD, right; Cr, cranial; Ca, caudal. Source: Courtesy of Dr Thassila C.F. Cintra, São Paulo, Brasil.

## *Technique for POCUS Brain*

Each acoustic window should be scanned in all planes if possible, including rostral to caudal, laterally through the sagittal plane, and fanning dorsal to ventral.

At the temporal acoustic window located above the zygomatic arch, and fanning the probe from dorsal to ventral, the sonographer obtains the dorsal planes (Figures 28.5, 28.6, 28.7, 28.8, 28.9, 28.10, 28.11, 28.12, and 28.13; see also Figures 28.1–4).

At the rostral acoustic window, sliding the probe in the rostral to caudal direction, the sonographer obtains the transverse planes (Figures 28.21, 28.22, 28.23, 28.24, and 28.25).

At the rostral acoustic window, fanning the probe in lateral direction, the sonographer obtains its sagittal planes (Figure 28.17, 28.18, 28.19 and 28.20).

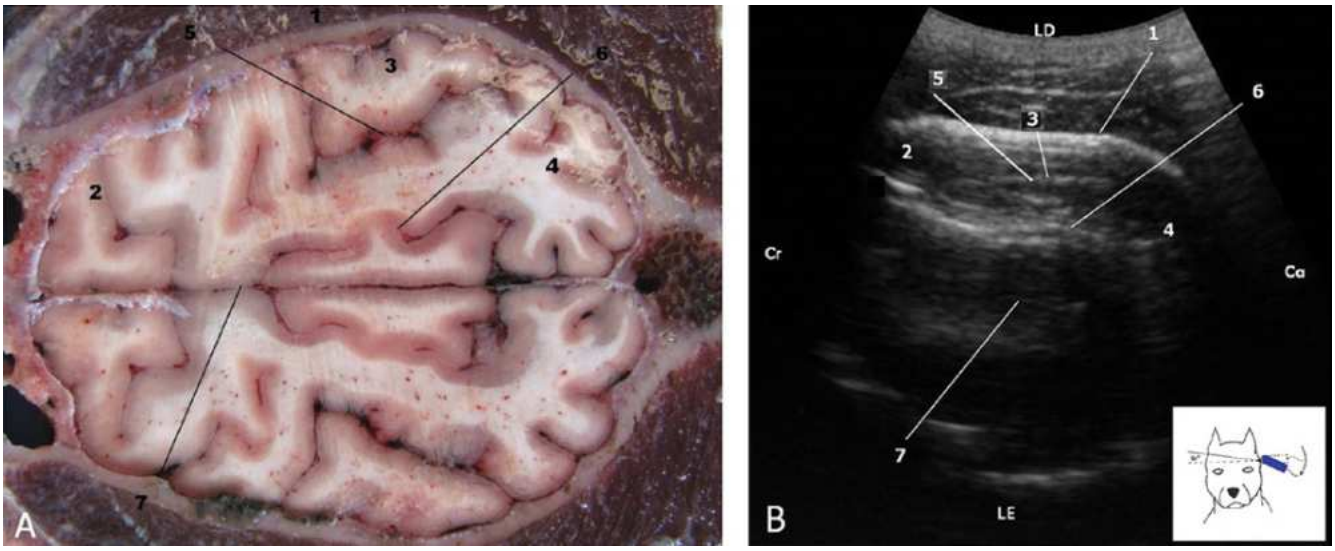


**Figure 28.3.** Temporal acoustic window – fanning dorsal to ventral. Oblique dorsal caudal plane (temporal window), probe 10° dorsally, with comparative gross, B-mode, and line drawing images in (A) and (B). Line drawing at right inferior shows the plane of image. 1, temporal bone; 2, frontal lobe; 3, temporal lobe; 4, occipital lobe; 5, suprasylvian sulcus; 6, splenial sulcus; 7, longitudinal fissure. LE, left; LD, right; Cr, cranial; Ca, caudal. Source: Courtesy of Dr Thassila C.F. Cintra, São Paulo, Brasil.

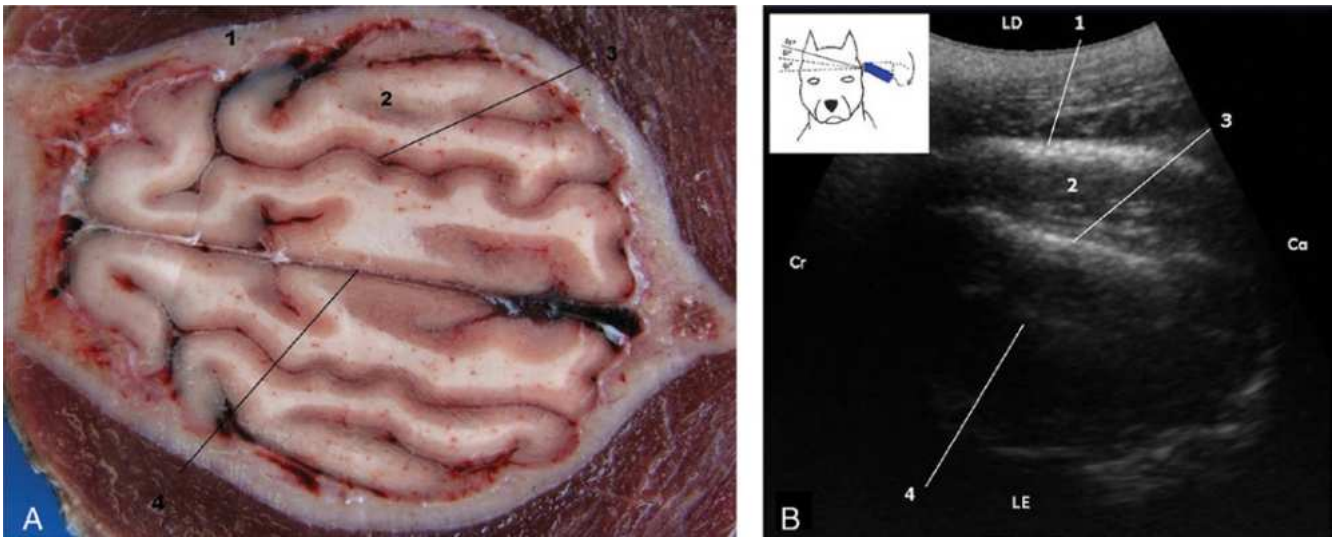


**Figure 28.4.** Temporal acoustic window – oblique dorsal planes. Oblique dorsal caudal plane (temporal window), probe 45° rotated, elevated 20° dorsally, with comparative gross, B-mode, and line drawing images in (A) and (B). Line drawing at right inferior shows the plane of image. 1, parietal bone; 2, parietal lobe; 3, marginal sulcus; 4, longitudinal fissure. LE, left; LD, right; Cr, cranial; Ca, caudal. Source: Courtesy of Dr Thassila C.F. Cintra, São Paulo, Brasil.

Finally, at the suboccipital acoustic window, the sonographer obtains transverse and sagittal planes (Figures 28.14, 28.15, and 28.16).

# Ultrasonographic Anatomy

The brain is surrounded by the bones of the skull and during fetal development, fibrous sutures appear between them. These sutures extend to intersections called the fontanelles. Compared to humans, at birth most dogs and cats have either a very small fontanelle (approximately 0.5–3 mm) or one that is completely ossified. The toys and chondrodystrophic breeds are exceptions, in which the fontanelle between the frontal and parietal bones is relatively greater in size and can remain open for up to three months or in some cases remain persistently open throughout life.

Sonographically, the encephalic structures seen in dogs present aspects similar to those described for

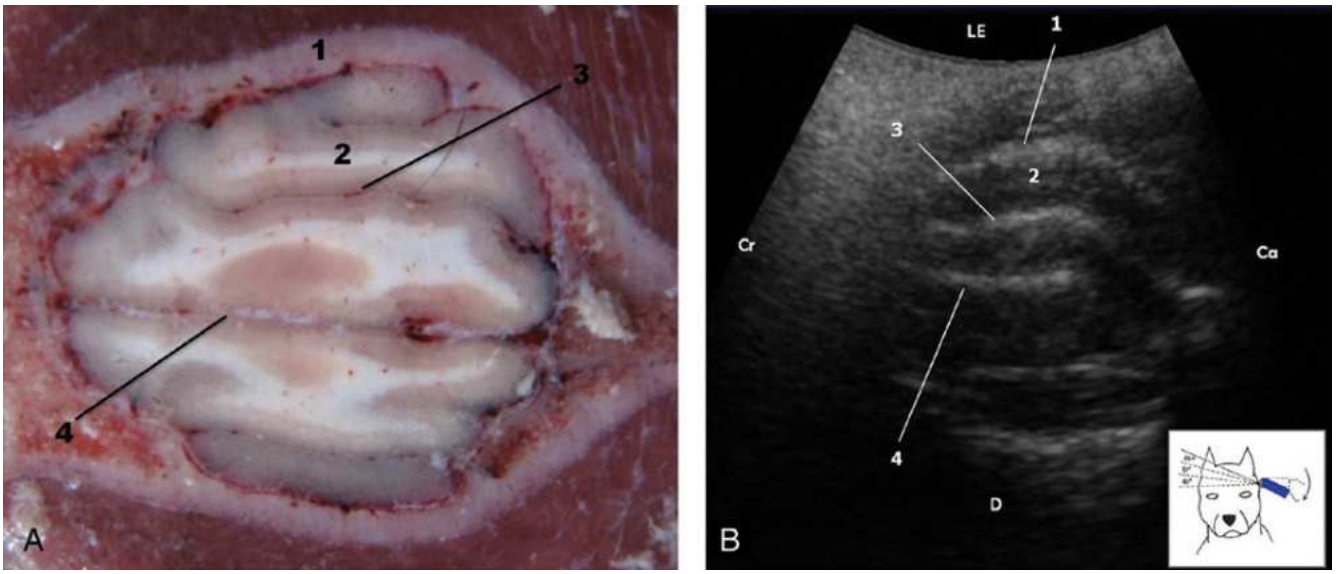


**Figure 28.5.** Temporal acoustic window. Oblique dorsal caudal plane (temporal window), probe 45° rotated, elevated 30° dorsally, with comparative gross, B-mode, and line drawing images in (A) and (B). Line drawing at right inferior shows the plane of image. 1, parietal bone; 2, parietal lobe; 3, marginal sulcus; 4, longitudinal fissure. LE, left; D, dorsal; Cr, cranial; Ca, caudal. Source: Courtesy of Dr Thassila C.F. Cintra, São Paulo, Brasil.

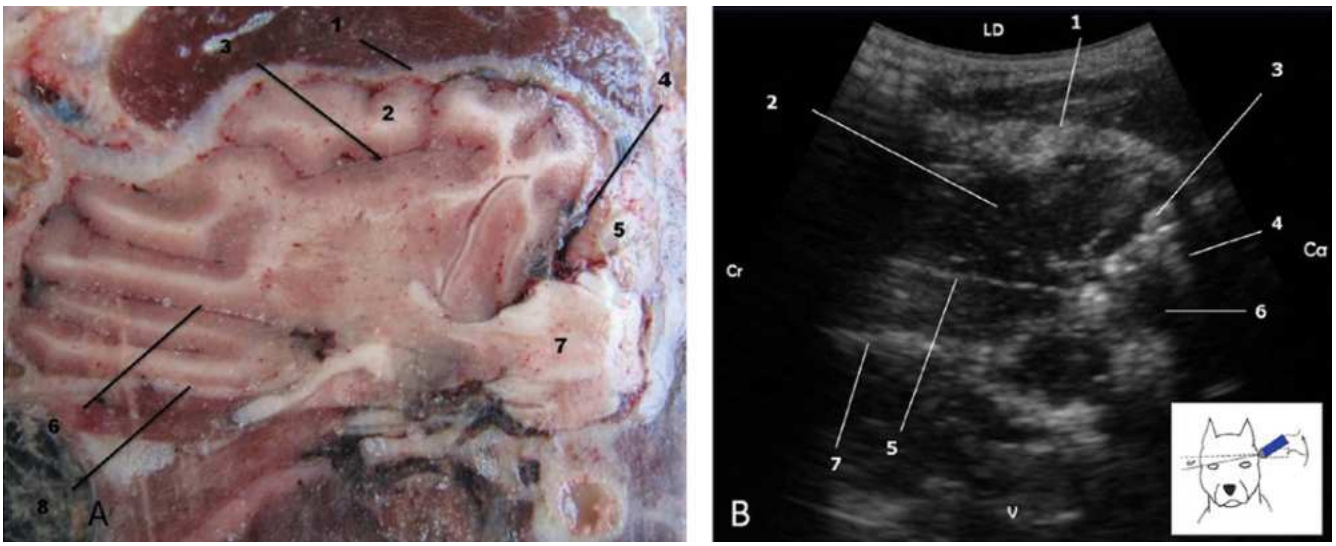


**Figure 28.6.** Temporal acoustic window. Oblique dorsal caudal plane (temporal window), probe 45° rotated, elevated 10° to ventral direction, with comparative gross, B-mode, and line drawing images in (A) and (B). Line drawing at right inferior shows the plane of image. 1, temporal bone; 2, temporal lobe; 3, presylvian sulcus; 4, tentorium of cerebellum; 5, cerebellum; 6, longitudinal fissure; 7, mesencephalon; 8, ethmoid bone. LD, right; V, ventral; Cr, cranial; Ca, caudal. Source: Courtesy of Dr Thassila C.F. Cintra, São Paulo, Brasil.

humans. The contours of the bone can be identified as a hyperechogenic (bright white) arcuate line in the near-field of the image, with brain parenchyma (gray and white brain matter) appearing with moderate degrees of echogenicity.

The encephalon is contained in a cavity inside the skull, whose rostral border is limited by a bony plate, called the ethmoid, and caudally limited by the occipital bone. Laterally, the cavity is limited by the temporal, parietal, and frontal bones. The dome of the cavity (calvaria) is formed by the frontal and parietal bones, and the base is formed by the ethmoid, prephenoid, and basisphenoid bones. Its most prominent internal anatomical feature is the cerebellar tentorium, which is a large projection at the junction of the dorsal and caudal walls, forming the middle portion of the cerebellum in the transverse fissure of the brain (Hudson et al. 1989; Cartee et al. 1993; Homco 1996).

The meninges that surround the brain are called the dura, arachnoid, and pia mater. Within the dura mater

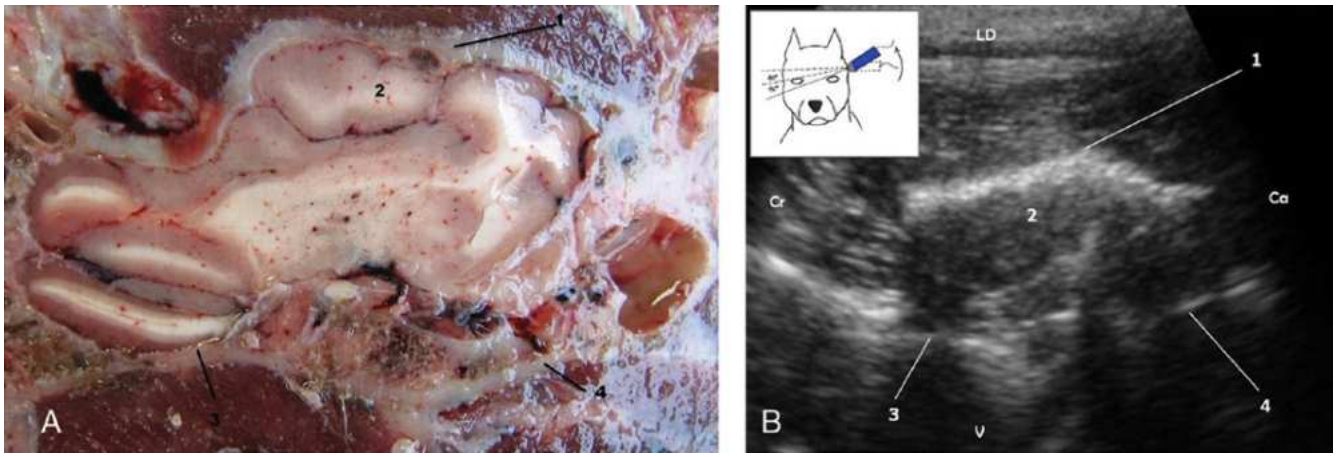


**Figure 28.7.** Temporal acoustic window. Oblique dorsal caudal plane (temporal window), probe 45° rotated, elevated 20° to ventral direction, with comparative gross, B-mode, and line drawing images in (A) and (B). Line drawing at right inferior shows the plane of image. 1, temporal bone; 2, temporal lobe; 3, ethmoid bone; 4, sphenoid bone. LD, right; V, ventral; Cr, cranial; Ca, caudal. Source: Courtesy of Dr Thassila C.F. Cintra, São Paulo, Brasil.

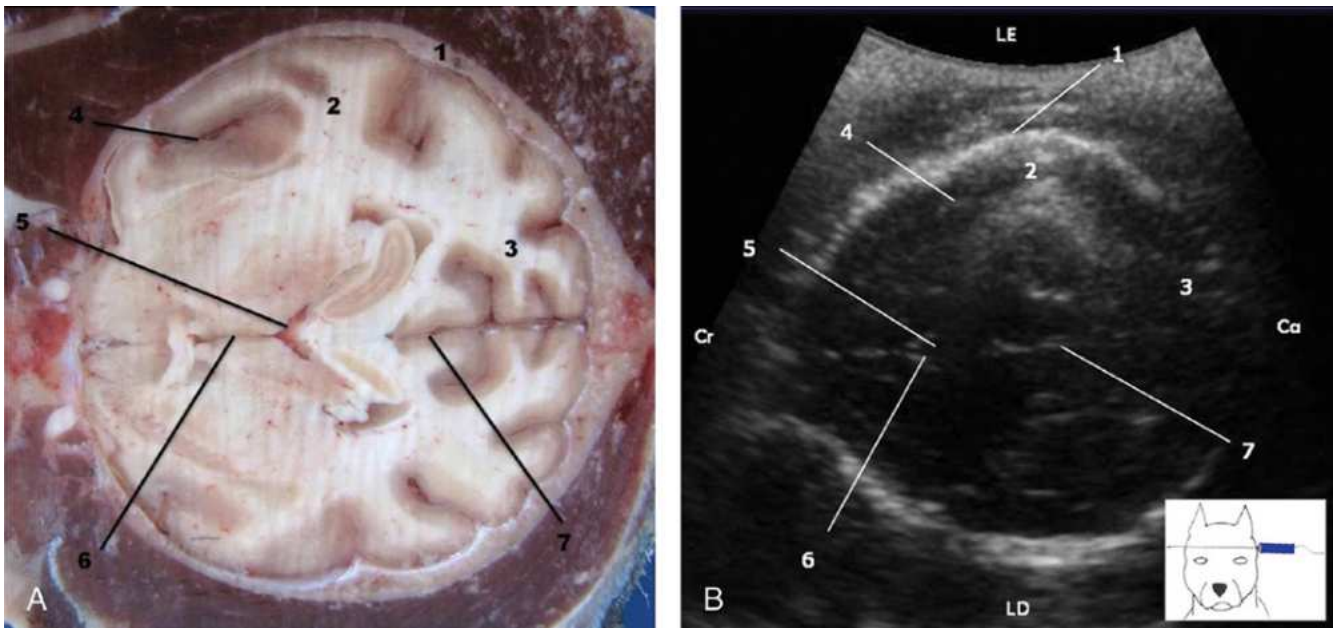


**Figure 28.8.** Temporal acoustic window. Oblique dorsal cranial plane (temporal window), probe rotated 45°, with comparative gross, B-mode, and line drawing images in (A) and (B). Line drawing at right inferior shows the plane of image. 1, temporal bone; 2, temporal lobe; 3, occipital lobe; 4, presylvian sulcus; 5, lateral ventricle; 6, septum pellucidum; 7, longitudinal fissure. LD, right; LE, left; Cr, cranial; Ca, caudal. Source: Courtesy of Dr Thassila C.F. Cintra, São Paulo, Brasil.

are blood vessels that are identified as linear hyperechoic (bright white) areas ultrasonographically.

The cerebral hemispheres are divided from each other by a deep longitudinal fissure; the cerebellum is divided by a transverse fissure. Each hemisphere is divided into lobes denominated by the corresponding bone portion that covers them. The frontal lobe is the most rostral portion, limited caudally by the crossed groove. The parietal lobe is caudal to the folded and dorsal groove of the Sylvian gyrus and extends caudally to the caudal third of the cerebral hemisphere. The occipital lobe includes the caudal third of the cerebral hemisphere. The temporal lobe consists of the spins and grooves of the ventrolateral portion of the cerebral hemispheres, and part of the Sylvian spins are located in that region (Hudson et al. 1989;

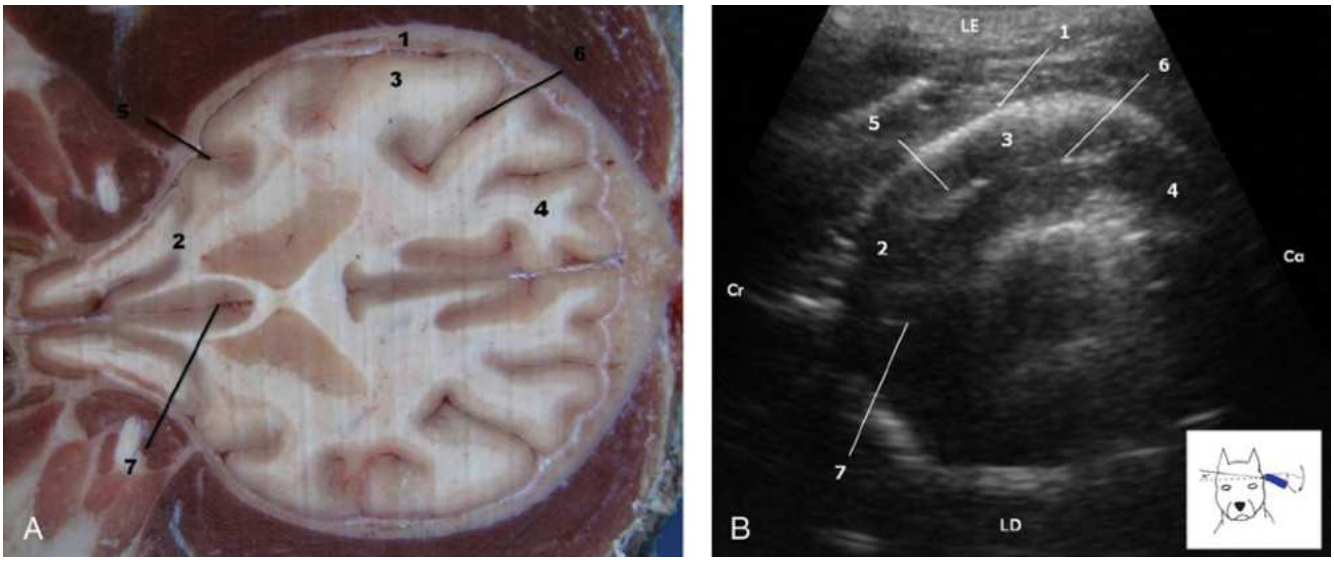


**Figure 28.9.** Temporal acoustic window. Oblique dorsal cranial plane (temporal window), probe in 45° rotated, elevated 10° dorsally, with comparative gross, B-mode, and line drawing images in (A) and (B). Line drawing at right inferior shows the plane of image. 1, temporal bone; 2, frontal lobe; 3, temporal lobe; 4, occipital lobe; 5, presylvian sulcus; 6, suprasylvian sulcus; 7, longitudinal fissure. LD, right; LE, left; Cr, cranial; Ca, caudal. Source: Courtesy of Dr Thassila C.F. Cintra, São Paulo, Brasil.

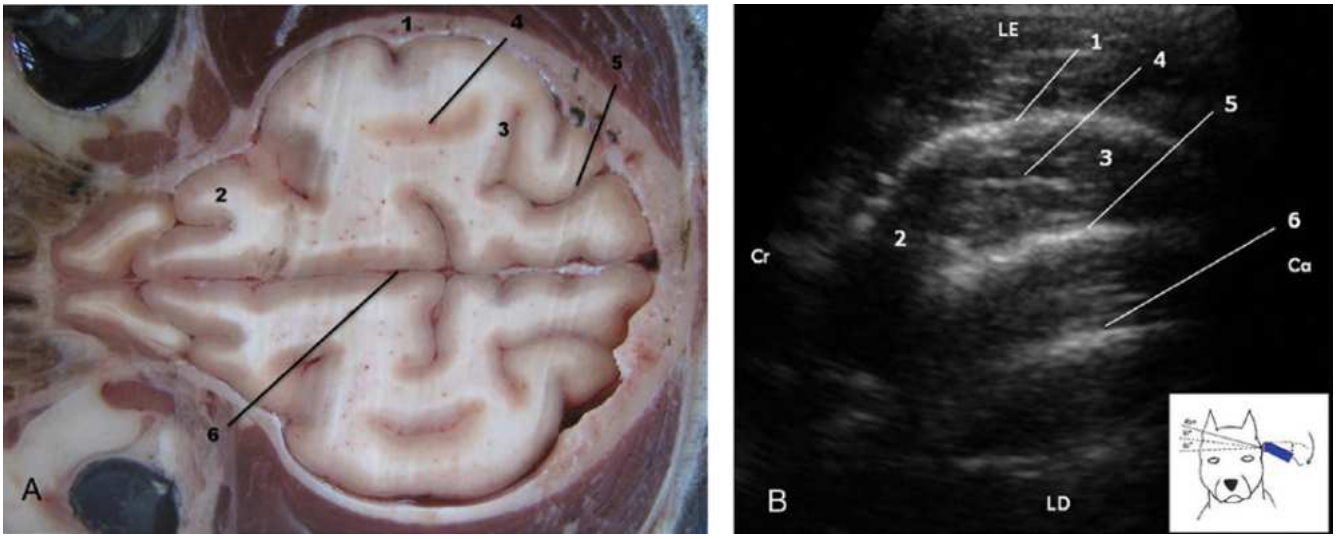


**Figure 28.10.** Temporal acoustic window. Oblique dorsal cranial plane (temporal window), probe in 45° rotated, elevated 20° dorsally, with comparative gross, B-mode, and line drawing images in (A) and (B). Line drawing at right inferior shows the plane of image. 1, temporal bone; 2, frontal lobe; 3, parietal lobe; 4, ectomarginal sulcus; 5, marginal sulcus; 6, longitudinal fissure. LD, right; LE, left; Cr, cranial; Ca, caudal. Source: Courtesy of Dr Thassila C.F. Cintra, São Paulo, Brasil.

Cartee et al. 1993; Homco 1996). The brain lobes cannot be seen as distinct areas, but can be identified according to their topography (Homco 1996).

In the dorsal plane, performed through the temporal acoustic window, the suprasylvian groove is represented by a hyperechoic linear structure. The lateral ventricles appear as two anechogenic areas separated by a thin hyperechogenic rostral line representing the septum pellucidum. The longitudinal fissure of the brain can be seen as a hyperechogenic (bright white) line in the center of this image (see Figure 28.1) (Spaulding et al. 1990; Cintra et al. 2014).

In dorsal planes through the temporal window, it is possible to observe images of some brain grooves as

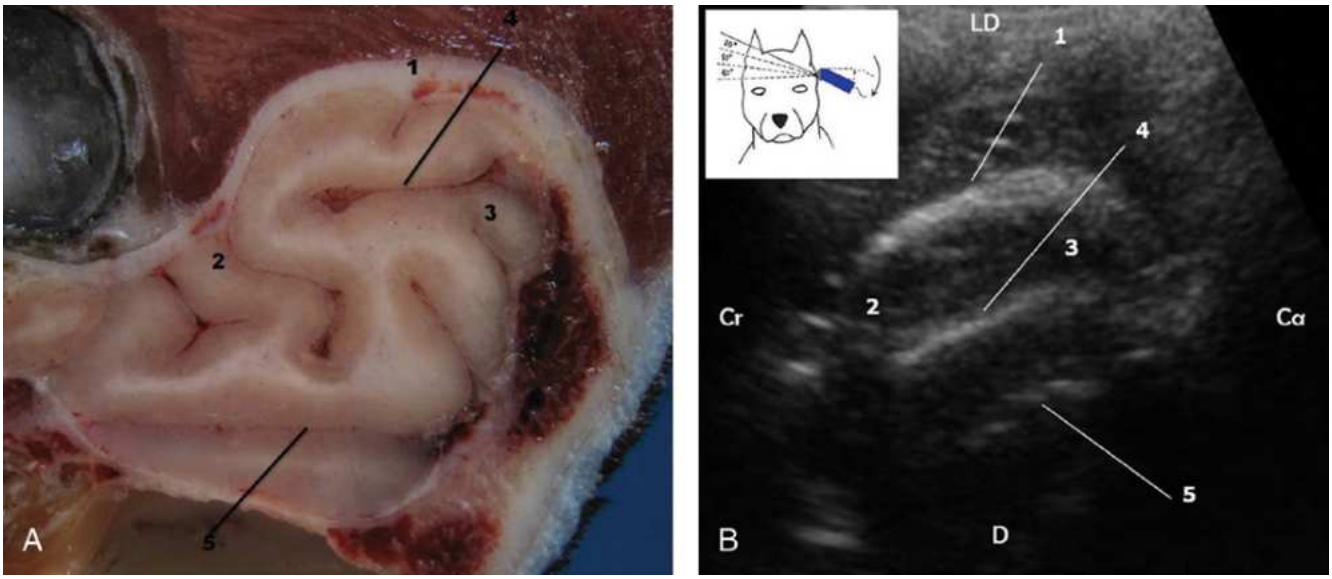


**Figure 28.11.** Temporal acoustic window. Oblique dorsal cranial plane (temporal window), probe in 45° rotated, elevated 30° dorsally, with comparative gross, B-mode, and line drawing images in (A) and (B). Line drawing at right inferior shows the plane of image. 1, parietal bone; 2, frontal lobe; 3, parietal lobe; 4, coronal sulcus; 5, longitudinal fissure. LD, right; D, dorsal; Cr, cranial; Ca, caudal. Source: Courtesy of Dr Thassila C.F. Cintra, São Paulo, Brasil.

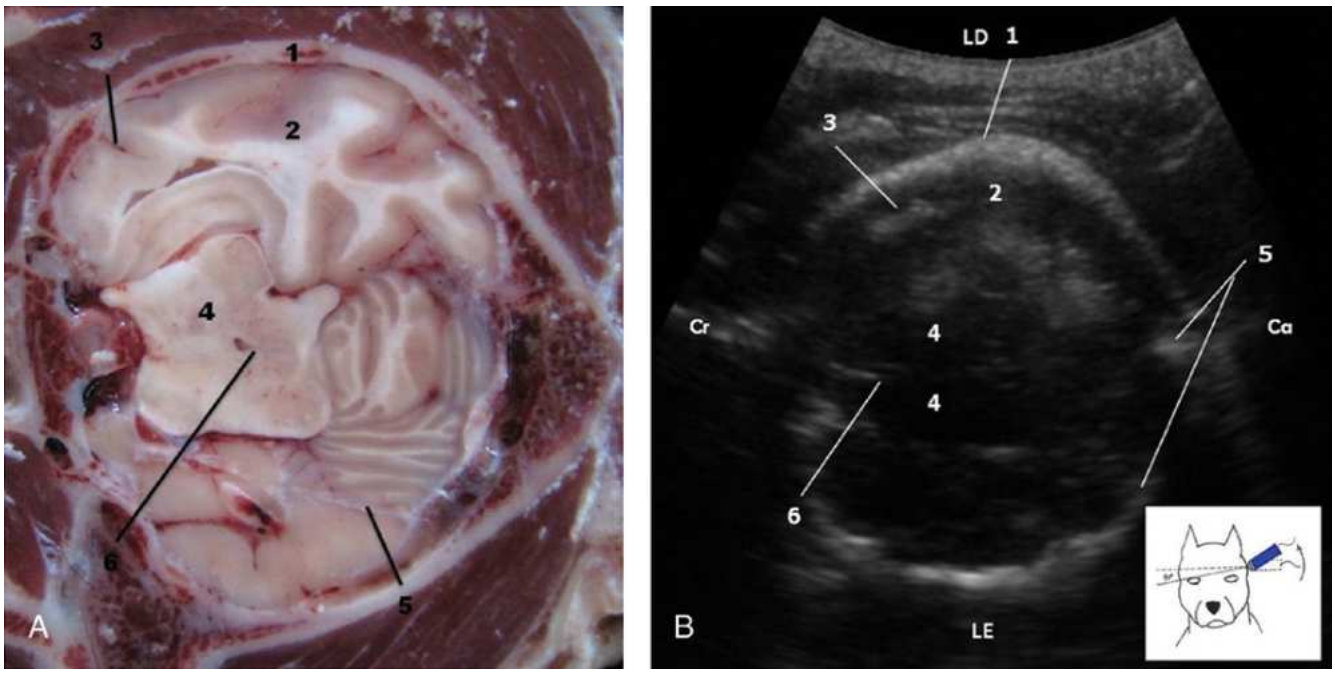


**Figure 28.12.** Temporal acoustic window. Oblique dorsal cranial plane (temporal window), probe 45° rotated, elevated 10° to ventral direction, with comparative gross, B-mode, and line drawing images in (A) and (B). Line drawing at right inferior shows the plane of image. 1, temporal bone; 2, temporal lobe; 3, pseudosylvian fissure; 4, diencephalon; 5, tentorium of cerebellum; 6, longitudinal fissure. LD, right; LE, left; Cr, cranial; Ca, caudal. Source: Courtesy of Dr Thassila C.F. Cintra, São Paulo, Brasil.

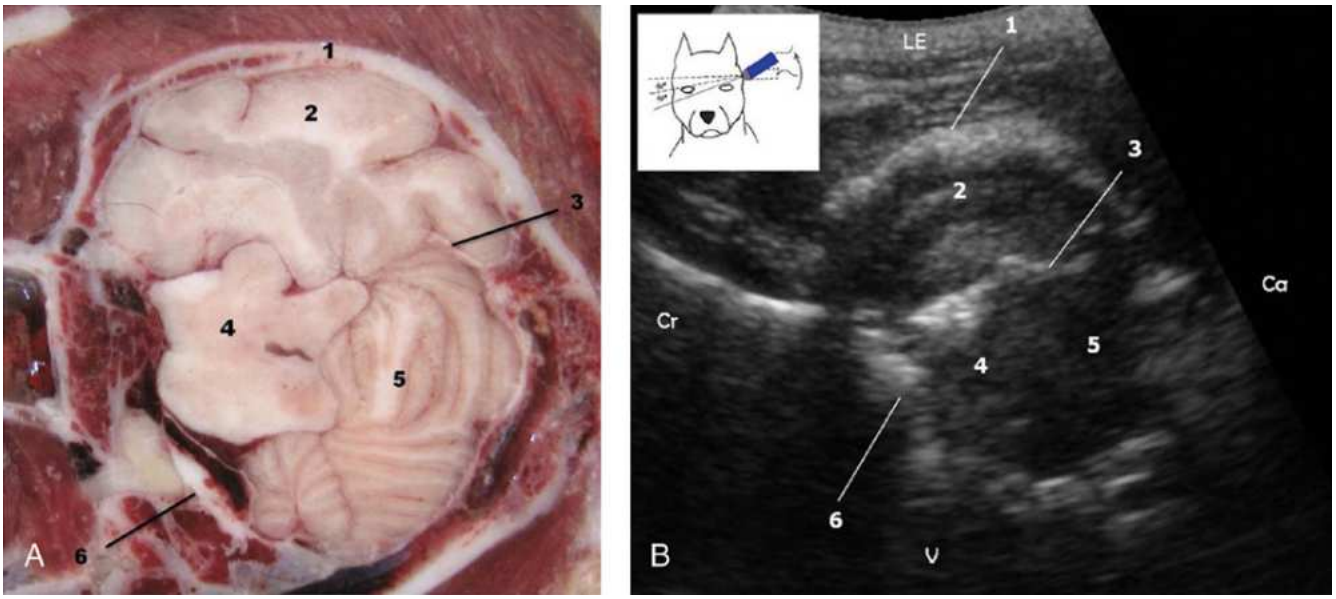


**Figure 28.13.** Temporal acoustic window. Oblique dorsal cranial plane (temporal window), probe 45° rotated, elevated 20° to ventral direction, with comparative gross, B-mode, and line drawing images in (A) and (B). Line drawing at right inferior shows the plane of image. 1, temporal bone; 2, temporal lobe; 3, tentorium of cerebellum; 4, thalamus and mesencephalon; 5, cerebellum; 6, basisphenoid bone. V, ventral; LE, left; Cr, cranial; Ca, caudal. Source: Courtesy of Dr Thassila C.F. Cintra, São Paulo, Brasil.

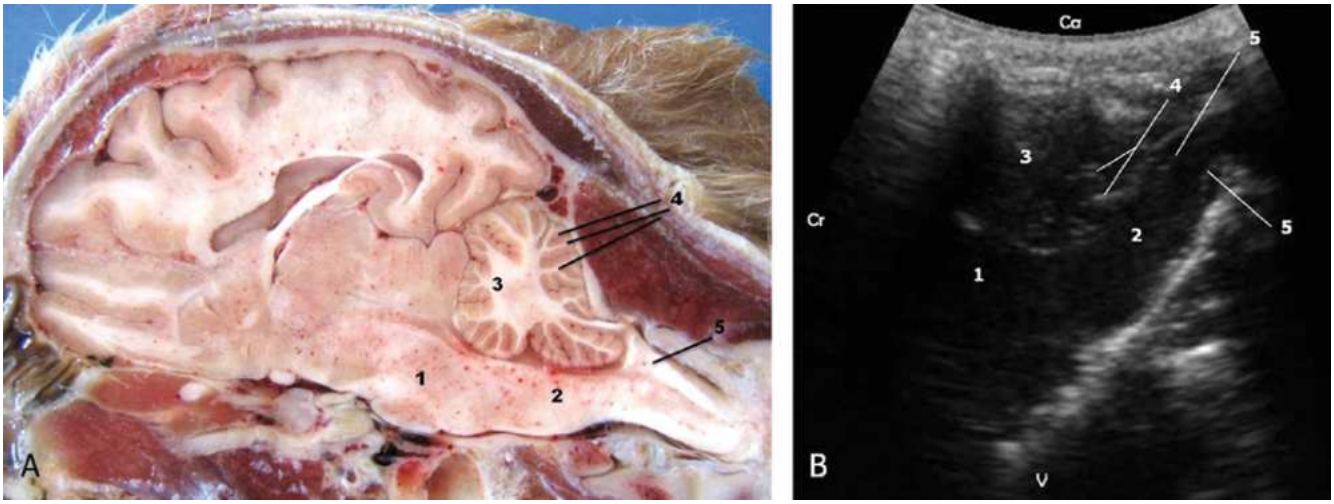


**Figure 28.14.** Suboccipital acoustic window. Sagittal plane of image (occipital window); probe perpendicular to foramen magnum, with comparative gross, B-mode, and line drawing images in (A) and (B). 1, pons; 2, medulla oblongata; 3, cerebellum; 4, vermis of cerebellum; 5, white and gray matter interface. V, ventral; Cr, cranial; Ca, caudal. Source: Courtesy of Dr Thassila C.F. Cintra, São Paulo, Brasil.

hyperechogenic (bright white) linear structures emphasizing the echogenic parenchyma and the cerebellar bone tentorium represented by a strong hyperechogenic (bright white) line in the caudal fossa region (see Figures 28.2–7). In oblique cranial dorsal planes, the mesencephalon, telencephalon, and diencephalon appear as hypoechogenic (darker) areas compared to the rest of the parenchyma (see Figures 28.8–13) (Spaulding et al. 1990; Homco 1996).

Dorsal planes through the occipital window allow visualization of the caudal portion of the encephalon, composed of the medulla oblongata, pons, and cerebellum (Dyce and Sack 2004). The cerebellum is seen as a rounded echogenic structure with large lateral

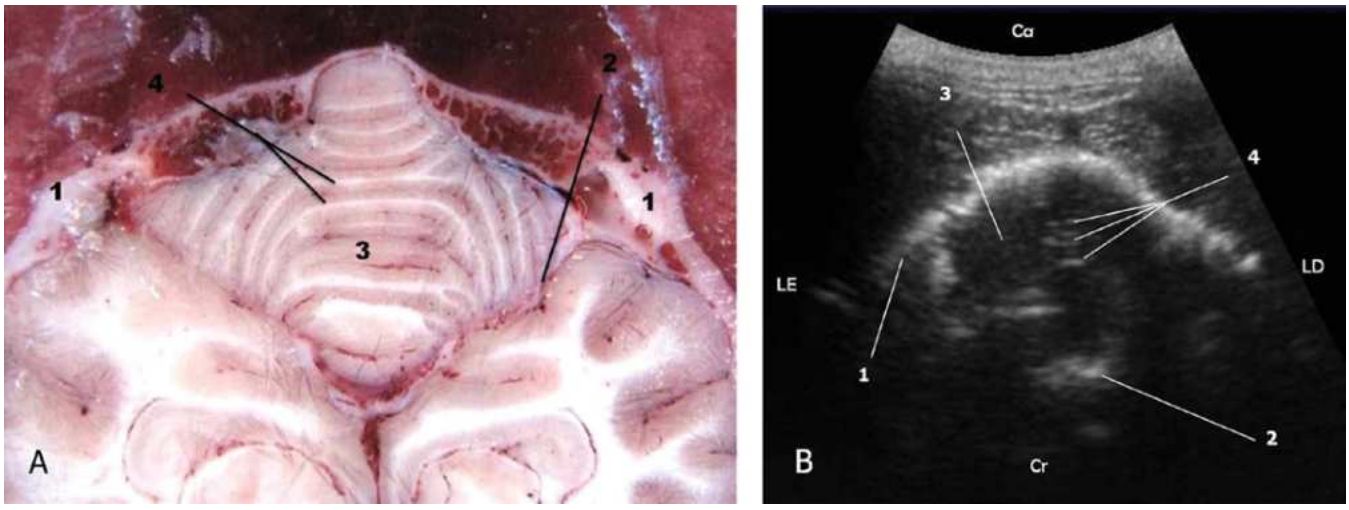


**Figure 28.15.** Subocciptal acoustic window. Dorsal plane of image (occipital window), and rotated 90°, with comparative gross, B-mode, and line drawing images in (A) and (B). 1, occipital bone; 2, tentorium of cerebellum; 3, cerebellum; 4, vermis of cerebellum. LE, left lateral; LD, right lateral; Cr, cranial; Ca, caudal. Source: Courtesy of Dr Thassila C.F. Cintra, São Paulo, Brasil.

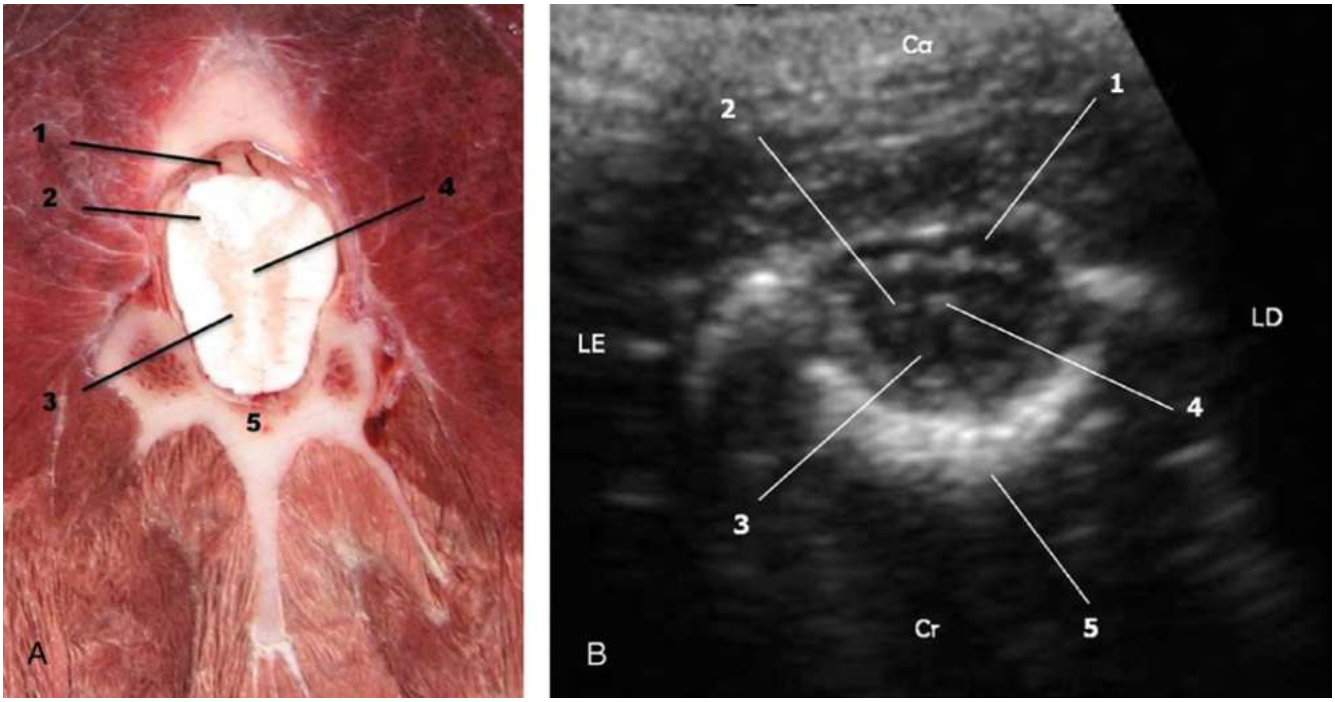


**Figure 28.16.** Subocciptal acoustic window. Oblique dorsal plane of image (occipital window), rotated 90° and 10° caudally, with comparative gross, B-mode, and line drawing images in (A) and (B). 1, subarachnoid space; 2, dorsal horn; 3, ventral horn; 4, central canal; 5, atlas body. LE, left lateral; LD, right lateral; Cr, cranial; Ca, caudal. Source: Courtesy of Dr Thassila C.F. Cintra, São Paulo, Brasil.

hemispheres and a narrow medial protrusion called the vermis; cerebellar worms are seen as parallel hyperechogenic (bright white) lines (Spaulding et al. 1990; Homco 1996). The medulla oblongata is an elongated, echogenic structure, located ventrally in the image of the cerebellum. The two hyperechogenic (bright white) lines in the medullar region represent the interfaces between the white and gray matter in this region. The pons may be observed as an echogenic area with poorly defined contours in the region adjacent to the medulla

**Figure 28.17.** Rostral acoustic window. Sagittal plane from rostral window showing measurements. CM, cerebral mantle; LV, lateral ventricle; green arrow, choroid plexus. Source: Courtesy of Dr Thassila C.F. Cintra, São Paulo, Brasil.

oblongata and identified according to its topography (see Figures 28.14 and 28.15) (Cintra et al. 2014).

The spinal cord is an elongated, more or less cylindrical structure, which can be seen in oblique dorsal planes performed through the suboccipital acoustic window as a hypoechoic (dark) circular structure in the center of the image (Gallagher et al. 1995; Lorigados and Pinto 2013; Cintra et al. 2014). When imaged, the dura mater and pia mater are hyperechogenic (bright white). The subarachnoid space, replete with cerebrospinal fluid, appears as an anechogenic (black) area surrounding the medulla. The central canal of the medulla is represented by a hyperechogenic (bright white) point in the center of the image. The gray matter, which looks like a butterfly, is commonly described as having dorsal and ventral horns appearing as an echogenic tissue in a region adjacent to the central canal (see Figure 28.16) (Lorigados and Pinto 2013; Cintra et al. 2014). The cerebral ventricles

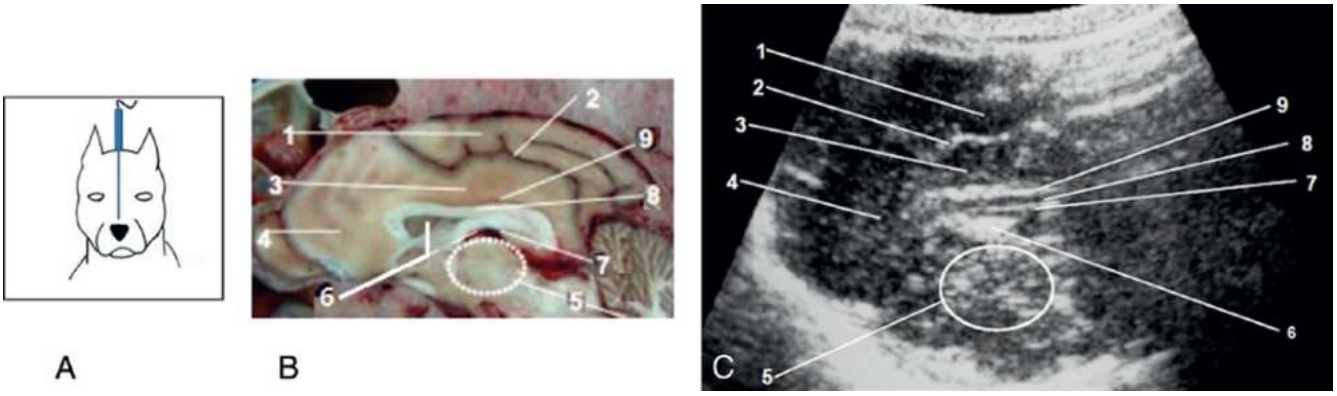


**Figure 28.18.** Rostral acoustic window. Sagittal plane rostral window, with comparative line drawing, gross, and B-mode images in (A), (B) and (C), respectively. 1, splenial gyrus; 2, splenial sulci; 3, cingulate gyrus; 4, frontal lobe; 5, diencephalon; 6, choroid plexus; 7, lateral ventricle; 8, corpus callosum; 9, callosum sulci. Source: Courtesy of Dr Thassila C.F. Cintra, São Paulo, Brasil.

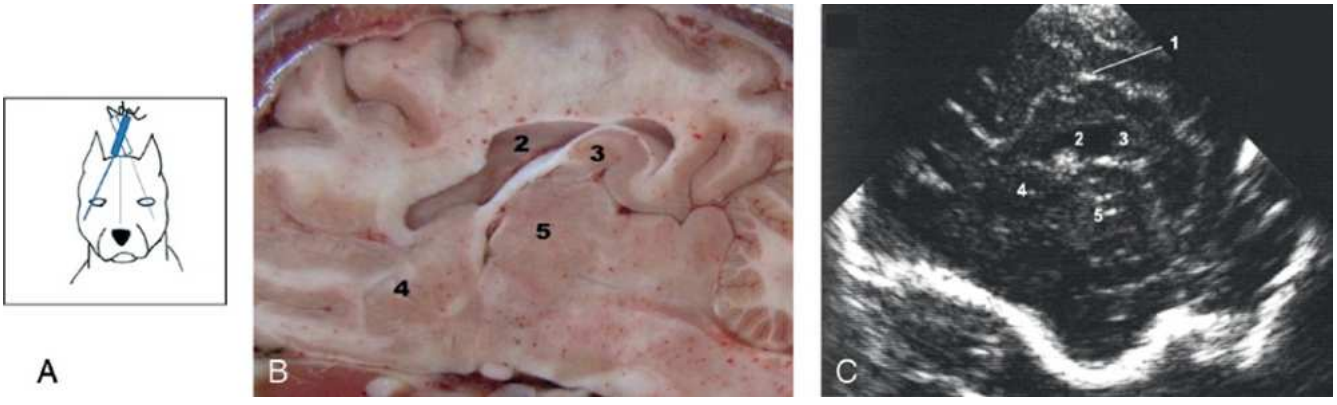


**Figure 28.19.** Rostral acoustic window. Sagittal oblique lateral plane from rostral window, with comparative line drawing, gross, and B-mode images in (A), (B) and (C), respectively. 1, splenial sulci; 2, lateral ventricle; 3, hippocampus; 4, nucleus caudatum; 5, diencephalon. Source: Courtesy of Dr Thassila C.F. Cintra, São Paulo, Brasil.

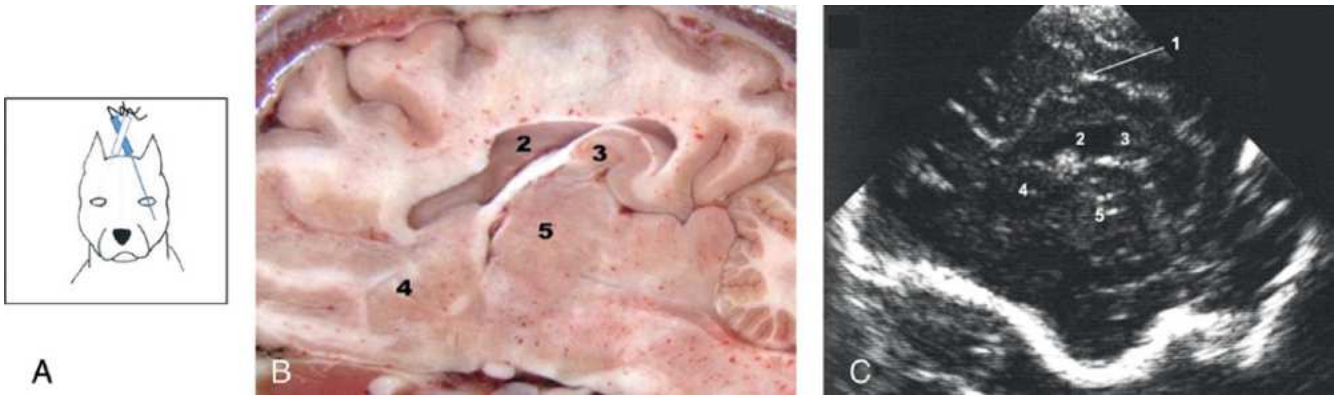


**Figure 28.20.** Rostral acoustic window. Sagittal (more) oblique lateral plane from rostral window, with comparative line drawing, gross, and B-mode images in (A), (B) and (C), respectively. 1, splenial sulci; 2, lateral ventricle; 3, hippocampus; 4, caudatum nucleus; 5, diencephalon. Source: Courtesy of Dr Thassila C.F. Cintra, São Paulo, Brasil.

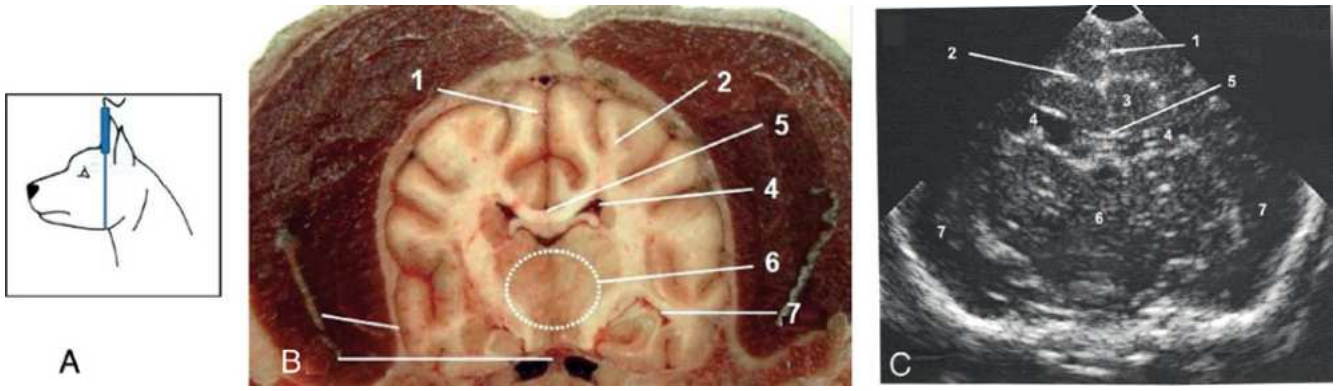


**Figure 28.21.** Rostral acoustic window. Transverse plane, with comparative line drawing, gross, and B-mode images in (A), (B) and (C), respectively. 1, longitudinal fissure; 2, splenial sulci; 3, cingulate gyrus; 4, lateral ventricle; 5, corpus callosum; 6, diencephalon; 7, piriform lobe. Source: Courtesy of Dr Thassila C.F. Cintra, São Paulo, Brasil.

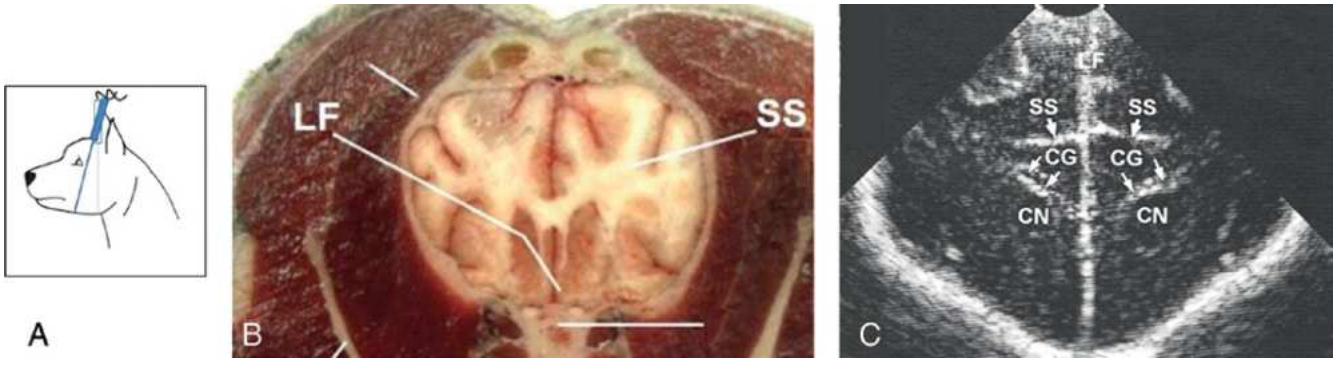


**Figure 28.22.** Rostral acoustic window. Transverse plane fanning rostral, with comparative line drawing, gross, and B-mode images in (A), (B) and (C), respectively. LF, longitudinal fissure; SS, splenial sulci; CG, cingulate gyrus; CN, caudatum nucleus. Source: Courtesy of Dr Thassila C.F. Cintra, São Paulo, Brasil.

are important anatomical references for sonographic diagnosis and contain cerebrospinal fluid. This fluid is produced by the choroid plexus in the ventricles (see Figure 28.17) and circulates within the central canal of the spinal cord and through three openings in the fourth ventricle into the subarachnoid space.

The spaces of the lateral ventricles and the third ventricle are filled by a small amount of cerebral spinal fluid under normal conditions. The lateral ventricles present hyperechogenic (bright white) contours because of the vascular plexuses, delineating the region of their floor, where the most prominent hyperechoic

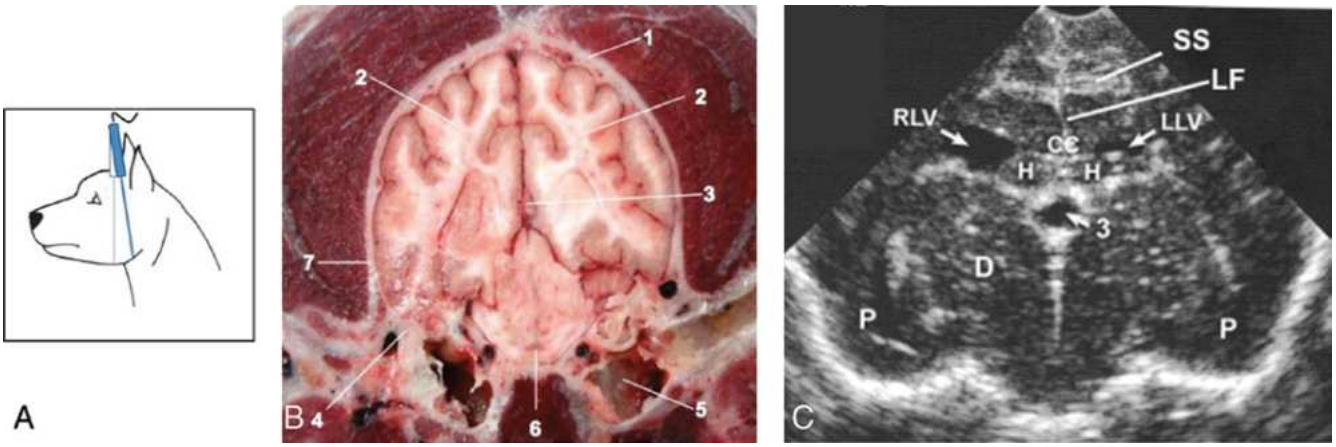


**Figure 28.23.** Rostral acoustic window. Transverse plane fanning caudal, with comparative line drawing, gross, and B-mode images in (A), (B) and (C), respectively. 1, bone; 2, splenial sulci (SS); 3, third ventricle; 4, sphenoid bone; 6, subarachnoid space. RLV, right lateral ventricle; LLV, left lateral ventricle; CC, corpus callosum; D, diencephalon; P, piriform lobe. Source: Courtesy of Dr Thassila C.F. Cintra, São Paulo, Brasil.

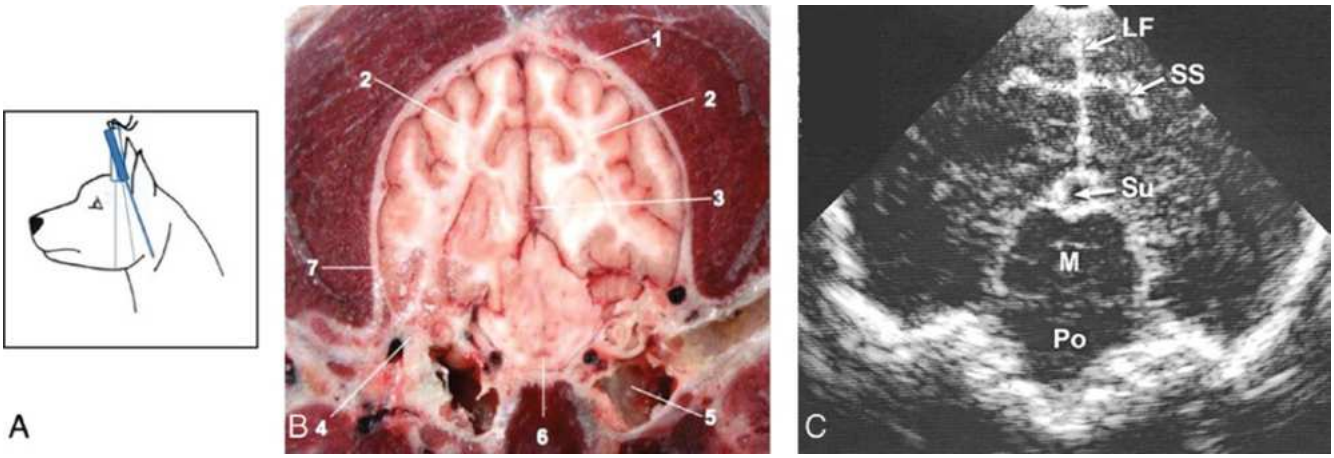


**Figure 28.24.** Rostral acoustic window. Transverse plane fanning more caudally, with comparative line drawing, gross, and B-mode images in (A), (B) and (C), respectively. LF, longitudinal fissure; SS, splenial sulci; Su, subarachnoid space; M, mesencephalon; Po, pons. Source: Courtesy of Dr Thassila C.F. Cintra, São Paulo, Brasil.

(bright white) area corresponds to the choroid plexus (see Figure 28.17). Rostral to this structure is the caudate nucleus. The hippocampus can be seen caudomedial to the lateral ventricle with greater echogenicity (brighter) when compared to the thalamus (darker). The third ventricle appears as a hypo- to anechoic (dark to black) area around the interthalamic adhesion (Homco 1996). These structures can be more easily seen in longitudinal and transversal planes using the rostral acoustic window. Transverse planes of this acoustic window with a rostral direction (see Figure 28.18) image the dorsal portions of the caudate nucleus close to the telencephalic region (Carvalho and Andrade neto 2005).

The lateral ventricles are located in a paramedian region in the cerebral hemispheres. The third ventricle lies within the diencephalon and hints toward the mesencephalic aqueduct. The fourth ventricle lies within the rhombencephalon and communicates with the outer spaces of the cerebral fluid. The third and fourth ventricles in the dog and cat under normal conditions are too small to be measured sonographically. The corpus callosum and callus groove sometimes are not seen, but are represented by a dorsal hyperechoic (bright white) line with less intense echoes. All these anatomical landmarks are best viewed at the rostral window on sagittal and transverse planes (see Figures 28.18–25).

When the ventricles are distended, they appear as anechoic cavities and may or may communicate with one another, particularly in their rostral portion. The dorsoventral measurement of the ventricles, obtained

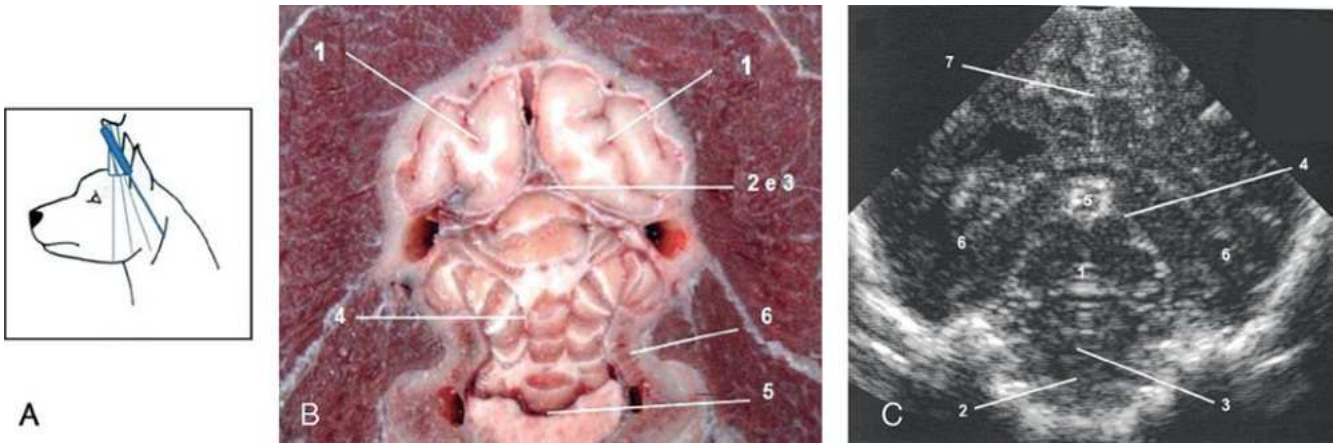


**Figure 28.25.** Rostral acoustic window. Transverse plane fanning more caudally than Figure 28.24 as shown in the line drawing (A). (B) 1, cerebellum; 2, medulla oblongata; 3, fourth ventricle; 5, subarachnoid space; 6, occipital lobe; 7, longitudinal fissure. (C) 1, occipital lobes; 2, 3, subarachnoid space; 4, cerebellum; 5, medulla oblongata; 6, bone. Source: Courtesy of Dr Thassila C.F. Cintra, São Paulo, Brasil.

through the rostral fontanelle in the transverse plane, should not exceed 0.15 cm in neonatal dogs and similar in normal adults. This ventricular diameter should be measured in a transverse plane at the level of the interthalamic adhesion. Ventriculomegaly is considered when the dorsoventral measurement of the lateral ventricles is greater than or equal to 0.35 cm at this point. The use of corresponding longitudinal planes help better interrogate this three-dimensional structure of the ventricles. Another applied measurement is the distance between the dorsoventral point of the ventricle to the surface of the brain which ranges from 1.63 to 2.06 cm in young dogs (Hudson 1998). At the interthalamic adhesion level in longitudinal plane obtained through the rostral acoustic window, the thickness of the cerebral mantle is measured as the distance from the ceiling of the ventricle to the surface of the brain (see Figure 28.17).

In a dorsal plane obtained at the temporal acoustic window, it is also possible to measure the width of lateral ventricles. The measurement should be made between the septum pellucidum and the lateral wall of the ventricle (see Figure 28.8). In a study of 37 normal adult dogs (mesaticephalics), the mean lateral ventricle width obtained in the anterior parietotemporal region was 0.27 ± 0.03 cm (Spaulding et al. 1990).

There are some noteworthy differences between the neonatal brain and the adult brain of animals. The tentorium of the cerebellum is cartilaginous, allowing its visibility through access through the dorsal midline in puppies. The grooves and spines, however, are less developed in puppies than in adult dogs. The hippocampus is a prominent structure in the encephalon of adult animals, but is not clearly visible in the neonate brain for similar reasons (Carvalho et al. 2007). However, no references exist in the literature establishing the anatomical differences expected in elderly adult animals.

# Pearls and Pitfalls, The Final Say

POCUS brain is an alternative imaging modality to be considered in neurological patients, especially in cats and small- and toy-breed dogs that have viable transcranial acoustic windows. POCUS brain may be used for both initial assessment and serial monitoring, being economical, fast, safe, and radiation sparing, and carries less patient risk and cost when compared with CT and MRI.

# References

Abrão N, Junior EA, Cerri GG. 1998. *Ultrassonografia Intracraniana – Anatomia Ultrassonográfica Afecções Hemorrágicas e Hipóxico-Isquêmicas*, edited by Abrão N, Junior EA, Cerri GG. São Paulo: Savier.

Carvalho CF, Chammas MC, Andrade neto JP, et al. 2007. Ultra-Sonografia transcraniana em cães com distúrbios neurológicos de origem central (Transcranial ultrasonography in dogs with central neurologycal disorders). *Arq Bras Med Vet Zootec* 59:1412–1416.

Carvalho CF, Andrade neto JP. 2005. Ecoencefalografia. In: *Ultrassonografia em Pequenos Animais*, edited by Carvalho CF. São Paulo: Roca, pp 265–277.

Cartee RE, Hudson JA, Finn-Bodner, ST. 1993. Ultrasonography. *Vet Clin North Am Small Anim Pract* 23(2):345–377.

Cintra TCF, Carvalho CF, Canola JC, et al. 2014. Transcranial ultrasonography in healthy dogs: technique standardization and anatomic description. *Braz J Vet Res Anim Sci* 66(1):61–68.

Duque FL, Dominguez JM, Ruiz P, et al. 2009. Assessing circle of Willis blood circulation in dogs with transcranial color-coded duplex sonography. *Vet Radiol Ultrasound* 50(5):530–535.

Dyce KM, Sack WO. 2004. O sistema nervoso. In: *Tratado de Anatomia Veterinária*, edited by Dyce KM, Sack WO. Rio de Janeiro: Elsevier, pp 256–317.

Gallagher JG, Penninck D, Boudrieau RJ, et al. 1995. Ultrasonography of the brain and vertebral canal in dogs and cats: 15 cases (1988–1993). *J Am Vet Med Assoc* 207:1320–1324.

Homco LD. 1996. Ultrasound scanning techniques. In: *Small Animal Ultrasound*, edited by Green RW. Philadelphia: Lippincott-Raven, p 52.

Hudson JA, Cartee RE, Simpson ST, et al. 1989. Ultrasonographic anatomy of the canine brain. *Vet Radiol* 30:13–21.

Hudson JA, Simpson ST, Cox NR, et al. 1991. Ultrasonographic examination of the normal canine neonatal brain. *Vet Radiol* 32(2):50–59.

Hudson JA, Finn-Bodner ST, Steiss J E. 1998. Neurosonography. *Vet Clin North Am Small Anim Pract* 28:943–972.

Lorigados CAB, Pinto ACBF. 2013. Comparison between ultrasound images of the dog brain with and without the calvaria and its correlation with real anatomy. *Braz J Vet Res Anim Sci* 50(2):105–113.

Spaulding KA, Nicholas JH, Sharp B. 1990. Ultrasonographic imaging of the lateral cerebral ventricles in the dog. *Vet Radiol* 3:59–64.

Wang HS, Kuo MF, Huang SC, et al. 2002. Transcranial ultrasound diagnosis of intracranial lesions in children with headaches. *Pediatr Neurol* 26:43–46.

# Further Reading

Babcock DS, Han BK. 1981. The accuracy of high-resolution real-time ultrasonography of the head in infancy. *Radiology* 139:665–676.

Berg D, Godau J, Walter U. 2008. Transcranial sonography in movement disorders. *Lancet Neurol* 7:1044–1055.

Evans HE. 1993. The skeleton. In: *Anatomy of the Dog*, edited by Evans HE. Philadelphia: Saunders, pp 122–218.

Konig HE, Liebich HG, Cerveny C. 2004. Sistema nervoso. In: *Anatomia Dos Animais Domésticos*, edited by Konig HE, Liebich HG, Cerveny C. Porto Alegre: Artmed, pp 203–275.

Molenaar GJ. 1997. O sistema nervoso. In: *Tratado de Anatomia Veterinária*, 2nd edition, edited by Dyce KM. Rio de Janeiro: Guanabara Koogan, pp 206–257.

Saito M, Olby JN, Spaulding K. 2001. Identification of arachnoid cysts in the quadrigeminal cistern using ultrasonography. *Vet Radiol Ultrasound* 42:435–439.

Schaller O. 1999. *Nomenclatura Anatômica Veterinária Ilustrada*, edited by Schaller O. São Paulo: Manole.

CHAPTER TWENTY-NINE

# POCUS: Brain – Clinical Integration

Cibele F. Carvalho

## Introduction

Traumatic brain injury (TBI) is a common occurrence in veterinary medicine and is associated with a high rate of morbidity and mortality in both humans (Ghajar 2000) and small animals (Dewey 2000). TBI is most frequently caused by road traffic accidents, but can also be due to falls, kicks, gunshot wounds, and animal bites; nontrauma causes include metabolic, toxic, hypoxic, infectious, vascular, and space-occupying lesions (Vianna and Arias 2013). Successful outcome depends upon the severity and location of injury, appropriate management, and timely identification of complications. Advanced imaging has been the gold standard evaluation of TBI but is limited by availability, patient risk, and expense. Moreover, many veterinarians are unfamiliar with the potential use of ultrasound for central neurological evaluation despite published veterinary studies (Hudson et al. 1989; Carvalho et al. 2007; Duque et al. 2013). The fact that ultrasound cannot pass through bone has contributed to this reluctance. However, many small animal patients have suitable transcranial acoustic windows that allow for both screening for structural lesions and assessing vascular perfusion along with the advantages of being a rapid, safe, point-of-care, imaging application.

With the brain being bathed in cerebral spinal fluid which is circulated through a system of ventricles and the subarachnoid space, the organ is structurally amenable to sonographic assessment since ultrasound's strength is imaging fluid. As a result, dilation of its ventricular system is easily appreciated, and standardized measurements may be performed and used clinically with normal reference values (Table 29.1).

A more challenging ultrasound skill, transcranial Doppler ultrasonography (TCDUS), used for vascular mapping and flow measurements, is also discussed in this chapter, involving the vasculature itself and some vascular-derived factors, using Doppler for the assessment of brain perfusion and the degree of intracranial pressure. Traditional methods used most frequently for such monitoring cerebral perfusion and intracranial pressure are technically challenging, invasive, and can cause complications (Werner et al. 1995). On the other hand, TCDUS of cerebral arteries has distinct advantages of being not only noninvasive with less patient risk, but also a low-cost, readily available imaging method when compared to computed tomography (CT) and magnetic resonance imaging (MRI).

Transcranial Doppler ultrasonography was introduced to human medicine in the early 1980s (Berg et al. 2008; Carvalho Andrade Neto 2014), and is a method which may be used repeatedly, allowing real-time measurement of blood flow velocity in the major cerebral arteries without the need for contrast agents (CT and MRI). More recently, TCDUS has been used to confirm changes in cerebral hemodynamics in several neurological disorders of people and small animals, and can provide the Doppler velocimetry parameters of velocity, resistive and pulsatility index (PI) in the various cerebral arteries (Carvalho et al. 2007). Normal RI reference ranges have been determined in dogs as 0.55 ± 0.04 for cerebral arteries (Seo et al. 2005) and 0.5–0.78 for the basilar artery (Saito et al. 2003). The clinical significance of the RI is that it has been shown to correlate with the degree of intracranial pressure (ICP) (Fukushima et al. 2000a,b) with RI measurements (ICP = –37.35 + 109.85 × RI) investigated in

*Point-of-Care Ultrasound Techniques for the Small Animal Practitioner*, Second Edition. Edited by Gregory R. Lisciandro.
© 2021 John Wiley & Sons, Inc. Published 2021 by John Wiley & Sons, Inc.
Companion website: www.wiley.com/go/lisciandro/ultrasound2

**Table 29.1.**
Guidelines for measurements of the ventricular system as currently available in the literature.

| Parameter | How measured | Normal | Ventriculomegaly |
|---|---|---|---|
| Lateral ventricular height: transverse[a] | Measure the dorsoventral dimension of the lateral ventricle with the probe perpendicular at or caudal to the interthalamic adhesion | 0.04–0.35 cm (mean 0.15 cm) | >0.35 cm |
| Cerebral mantle thickness: transverse[a] | Measure the thickness of brain tissue dorsal to each lateral ventricle | 1.63–1.91 cm | Often decreased; may be very thin |
| Ventricle- hemisphere ratio (measured on transverse images)[a] | Ratio of the lateral ventricular height to the width of the ipsilateral hemisphere | Mean 0.19 | >0.19 |
| Ventricle- mantle ratio (measured on transverse images)[a] | Ratio of the lateral ventricular height to the thickness of the mantle | Mean 0.25 | >0.25 |
| Lateral ventricular height: sagittal[a] | Measure the dorsoventral dimension of the lateral ventricle with the probe perpendicular at the thalamocaudate sulcus | Mean 0.14 cm | |
| Dorsoventral dimension of the lateral ventricle[b] | Measure the dorsoventral dimensions of the lateral ventricle at the level of the pituitary fossa | NA | NA |
| Dorsoventral percentage[b] | Ratio of the dorsoventral dimension of the lateral ventricle to the dorsoventral dimension of the brain | 0–14% | 15–25% moderate ventriculomegaly<br>>25% severe ventriculomegaly |

[a]Hudson et al. 1991.
[b]Spaulding et al. 1990.
Source: Reproduced with permission from Penninck D, d'Anjou MA (eds). 2008. *Atlas of Small Animal Ultrasonography*. Ames: Blackwell Publishing.

veterinary and human medicine literature (Fukushima et al. 1999). Thus, TCDUS has the potential to be a useful tool for monitoring TBI cases for the presence of ICP and its changes during treatment (McCormick et al. 2017).

## What POCUS Brain Can Do

- Screen for structural abnormalities of the brain.
- Evaluate brain perfusion via TCDUS.
- Serve as a monitoring tool for intracranial pressure (ICP).

## What POCUS Brain Cannot Do

- Account for variability of skull bone thickness.
- Account for variables that affect TCDUS including hematocrit, blood glucose, ventilatory status (oxygenation, carbon dioxide levels), and cardiac output.
- Account for anatomical variations between patients and species.

## Indications

- Any small animals with neurological signs and accessible transcranial acoustic windows.
- Patients with suspect or confirmed TBI, increased ICP, or central neurological disease.

## Objectives

- Be aware of the 3 transcranial acoustic windows.
- Be able to appreciate basic ultrasonographic brain anatomy.
- Be familiar with the required transcranial color Doppler ultrasound (TCDUS) images.
- Be familiar with Doppler velocimetry indices.
- Understand the value and limitations of transcranial color Doppler ultrasound (TCDUS).

# How to do POCUS Brain

## *Probe Type*

Both real-time B-mode and TCDUS probe requirements are as follows.

- Linear probes of 5–10 MHz in neonates with or without an open rostral fontanelle with depth range of 1.0–4.0 cm.
- Microconvex probes of 2–6 MHz with high resolution for more mature small-breed dogs with bregmatic fontanelle with depth range of 2.0–6.0 cm.
- Color flow and pulsed Doppler for TCDUS.

## *Acoustic Windows for POCUS Brain*

Three transcranial acoustic windows may be used for POCUS brain.

- Rostral acoustic window.
- Temporal acoustic window.
- Suboccipital acoustic window.

### Rostral Acoustic Window

The rostral window is used in patients with an open bregmatic fontanelle: puppies <1–3 months of age and kittens <5 months of age, and many toy breeds. The window is accessible when a closed bregmatic fontanelle has a thin frontal bone.

### Temporal and Subocciptal Acoustic Windows

The temporal window is located above the zygomatic arch, and the suboccipital window should be used in all cases.

## *Technique for POCUS Brain*

Each acoustic window should be scanned in all planes if possible.

At the rostral window, sliding the probe in the rostral to caudal direction, the sonographer obtains transverse planes (Figure 29.1).

At the rostral window, fanning the probe in lateral direction, the sonographer obtains sagittal planes (Figure 29.2).

**Figure 29.1.** Image acquisition at the rostral acoustic window – transverse planes. Picture and schematic drawings showing how to obtain the transverse planes at the rostral acoustic window and fanning the probe through the rostral to caudal directions.

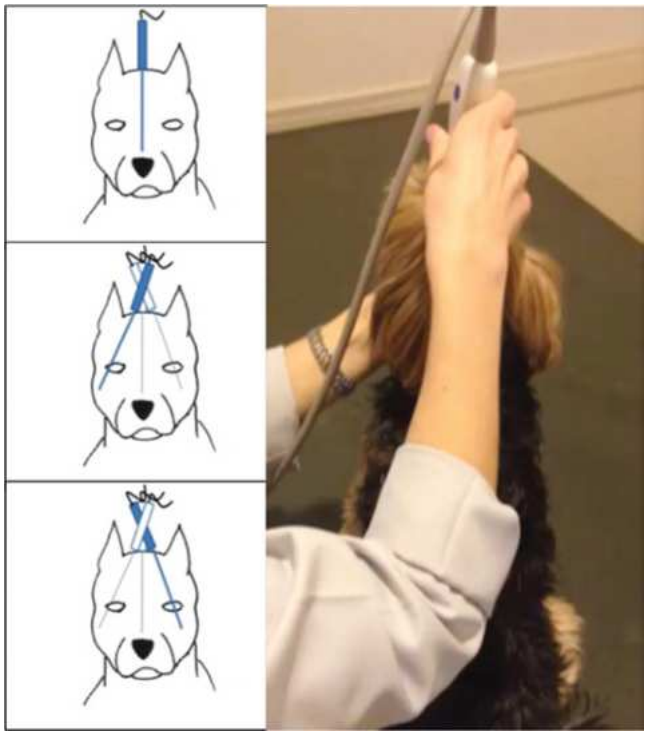

**Figure 29.2.** Image acquisition at the rostral acoustic window – sagittal planes. Picture and schematic drawings showing how to obtain the sagittal planes at the rostral acoustic window and fanning the probe from through the lateral directions. Source: Courtesy of Dr Thassila C.F. Cintra, São Paulo, Brasil.

At the temporal window located above the zygomatic arch, and fanning the probe from dorsal to ventral, the sonographer obtains dorsal planes (Figure 29.3).

Finally, at the suboccipital window, the sonographer obtains transverse and sagittal planes (Figure 29.4).

### Transcranial Ultrasonography without Color Flow Doppler – Imaging the Parenchyma

Publications exist documenting normal ultrasonographic findings using transcranial ultrasonography in healthy dogs (Hudson et al. 1989, 1991) and correlating transcranial ultrasound images with encephalic anatomy (Carvalho et al. 2009; Cintra et al. 2014). In smaller dogs and cats with thin skull bones and those with an open bregmatic fontanelle, it is possible to see several anatomical landmarks sonographically (Figure 29.5) including various sulci, the interhemispheric fissure, ventricular system (lateral ventricle, third and fourth ventricles and the mesencephalic aqueduct that connects the third and fourth ventricles), cerebellum, caudal brainstem, and medulla.

### Transcranial Ultrasonography with Color Flow Doppler – Imaging the Vasculature

The brain's main arterial anatomy is composed of the vertebrobasilar system and the cerebral arterial circle (Figure 29.6A). Vascular anatomy can be further assessed by TCDUS (Figure 25.6B). The temporal window is the best acoustic window to assess the cerebral arterial circle. The additional arteries within the cerebral arterial circle are best assessed by TCDUS via the rostral window. The suboccipital window is the best to assess the vertebrobasilar system, in both the transverse and sagittal planes.

A few reports have described vascular anatomy and its reference values (Spaulding et al. 1990; Saito et al. 2003; Duque et al. 2010; Carvalho and Andrade Neto 2014). TCDUS can be used to confirm changes in cerebral hemodynamics (Werner et al. 1992, 1993, 1995; Carvalho et al. 2012a). In a temporal approach, directing the probecaudally, we obtain dorsal planes. Color Doppler is performed (as a kind of guide) to identify the cerebral arterial circle (Figure 29.7). Once the vessels are identified, pulsed Doppler is initiated, paying attention to the optimal angle of insonation (>60°) to maximize signal. Freeze the image when you get three similar sequential waveforms (Figure 29.8), and then measure a representative spectral waveform to determine the patient's peak systolic velocity, end-diastolic velocity, and resistive index (Figure 29.9, Table 29.2).

## Sonographic Features of Traumatic Brain Injury from Trauma

Head trauma is the most common cause of bleeding in the subarachnoid space of small animals (Braund 2003; Vianna and Arias 2013; De LaHunta et al. 2014), with the possible complications of epidural and subdural hematomas, and intracerebral and intraventricular hemorrhage. Clinical consequences of focal lesions vary with location, regional extent and collateral damage, i.e. coup contrecoup phenomenon (Braund 2003).

Epidural and subdural hematomas generally are seen as hypoechoic lesions (Figure 29.10); however, brain edema and demyelinization appear similar sonographically and may be concurrently present. Intraventricular hemorrhage is identified by the presence of echogenic debris within the lateral ventricle cavities (Figure 29.11). Intraparenchymal hemorrhage

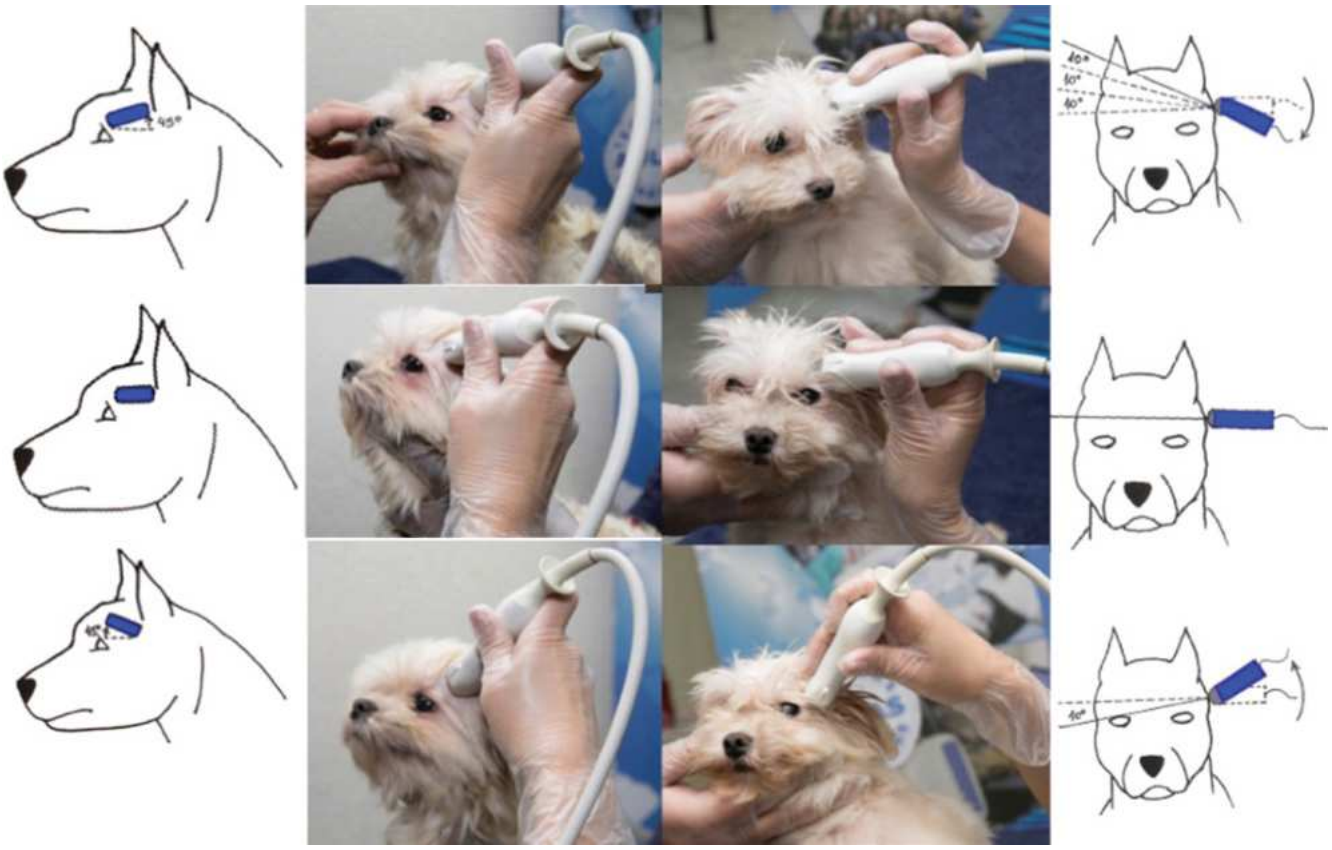

**Figure 29.3.** Image acquisition at the temporal acoustic window. Pictures and schematic drawings showing how to obtain the dorsal planes at the temporal acoustic window, which is dorsal to the zygomatic arch, and fanning the probe through dorsal to ventral directions.

usually appears as focal hyperechoic lesions (Figure 29.12). Over time, hemorrhage organization can sonographically appear as a mass effect and perilesional edema may be seen as a hypo- or anechoic halo around the lesion (Figure 29.13). Any intracavitary lesion can cause a space-occupying "mass effect" that may result in disruption of cerebral spinal fluid circulation or both effects may lead to increased intracranial pressure (ICP) (Figure 29.14) because of the Monro–Kellie Doctrine.

Real-time imaging in B-mode and TCDUS may be used for assessing injury and its potential ramifications, including via estimating ICP TCDUS (Carvalho et al. 2012a). Furthermore, vasospasm secondary to TBI (Werner et al. 1995) may be assessed through mapping with color flow Doppler, and calculations of Doppler velocimetry using TCDUS. POCUS brain findings may also be clinically integrated with the patient's modified Glasgow Coma Score (Platt et al. 2001) for decision making.

# Sonographic Features of Brain Pathology from Nontrauma

## *Hydrocephaly*

Prevalence studies of central neurological disease in dogs indicate that congenital anomalies constitute approximately 6% of total diagnoses, with hydrocephalus accounting for ~50% of these cases, making hydrocephalus one of the more common canine congenital defects (Spaulding et al. 1990). Small-breed and brachycephalic dogs are most commonly affected by hydrocephalus (Spaulding et al. 1990), with many patients presenting with nonspecific signs. Moreover, the significance of the degree of ventriculomegaly can be difficult to determine. Although POCUS brain imaging may demonstrate ventriculomegaly (Figure 29.15), B-mode parameters may not be sensitive and specific enough for accurate monitoring during treatment and clinical course of these patients (Spaulding et al. 1990).

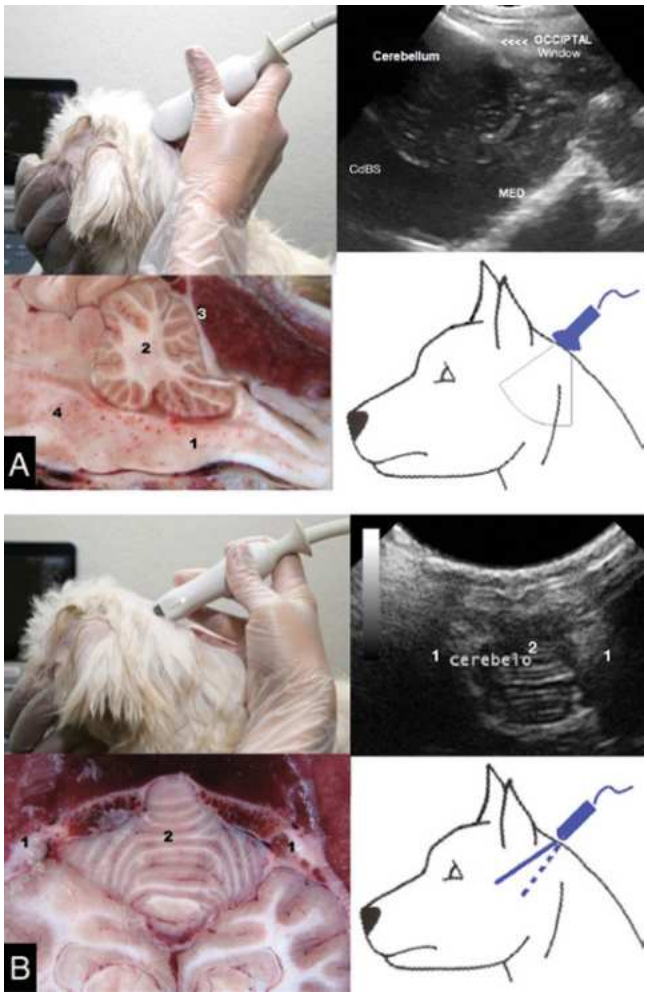


**Figure 29.4.** Image acquisition at the suboccipital acoustic window. (A) Picture of sagittal plane position, drawing and sonographic image at suboccipital window with corresponding anatomy labeled as (1) medulla (MED), (2) cerebellum (Cerebellum), (3) occipital bone (OCCIPTAL), and (4) caudal brainstem (CdBS). (B) Picture of the transverse plane position, drawing and sonographic image at suboccipital window with corresponding anatomy labeled as (1) cerebellar tentorium and (2) cerebellum vermis.

Reports in the veterinary literature better correlate TCDUS resistive index (RI) of the basilar artery to clinical signs in hydrocephalic dogs than B-mode (Fukushima et al. 1999, 2000a,b). One clinical study showed that with experimentally induced acute hydrocephalus in cats, a 22% reduction in the blood flow of the brain, cerebellum, and encephalic trunk occurred, and differed in variable ways in each part of the encephalon (Hochwald et al. 1975). Thus, TCDUS is a more accurate method of cerebral hemodynamic assessment than B-mode with the potential to monitor treatment of hydrocephalus by measuring the RI of the cerebral arteries (Figure 29.16), combined with other clinical information.

In summary, TCDUS measurement of the RI is likely more useful than B-mode measurements of the lateral ventricles (Carvalho et al. 2009).

## Strokes

Cerebrovascular diseases in dogs are defined as brain abnormalities caused by blood supply impairment (Garosi 2010), which often affect the cognitive and neurological status of the dog. Previously considered uncommon in animals, cerebrovascular disease is being recognized with greater frequency in veterinary medicine since brain imaging techniques such as ultrasonography, CT and MRI have become more readily available. Stroke is currently one of the leading causes of human death (Lillehei et al. 1984; Garosi 2010) but its overall occurrence in dogs is not well known.

Stroke, also referred to as a cerebrovascular accident (CVA), is the most common clinical manifestation of cerebrovascular disease, and can be broadly divided into ischemic stroke and hemorrhagic stroke (Braund 2003). Once the diagnosis of ischemic or hemorrhagic stroke is confirmed, potential underlying causes should be sought and treated. In one study of 42 small-breed dogs showing acute onset of clinical signs with no progressive focal cerebral dysfunction with the diagnosis of cerebrovascular disease confirmed at necropsy, coexisting diseases included cerebral amyloid microangiopathy, endocrinopathy, coagulopathy, neoplasias, and hyperlipemia with published antemortem sonographic features (Figure 29.17) (Carvalho et al. 2012b). However, further studies are needed to fully investigate the potential of TCDUS to monitor the treatment and clinical course of this patient subset.

## Encephalitis

As a representative example of inflammatory disease of the canine central nervous system (CNS), granulomatous meningoencephalitis (GME) is the second most common inflammatory CNS disease in dogs, following canine distemper. GME is an acute, nonsuppurative, and progressive disease that mainly affects small- and toy-breed dogs, especially young and middle-aged terriers and poodles (mean age 5 years; range 6 months to 12 years); thus POCUS brain has the potential to evaluate and monitor this disease. Lesions are often restricted to the CNS and most commonly occur within the white matter of the cerebrum, cerebellum, caudal brainstem, and cervical spinal cord.

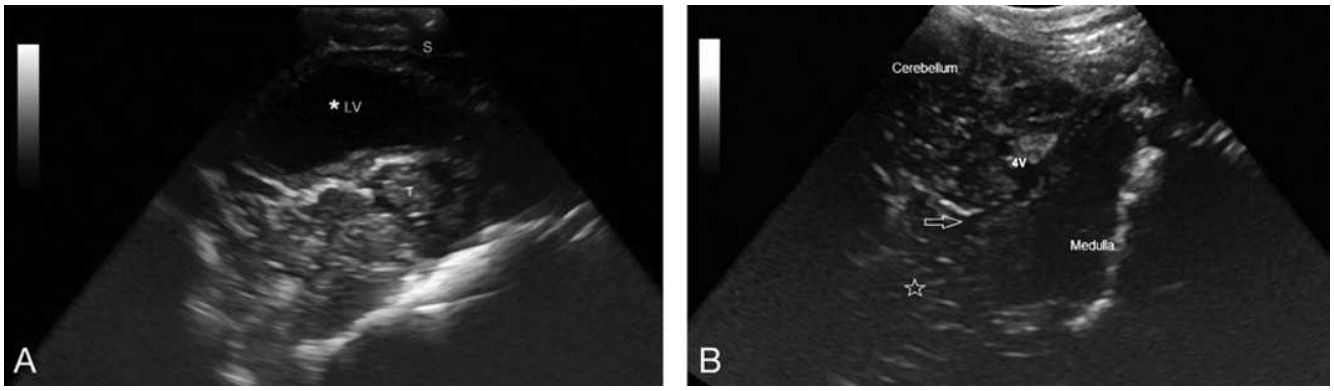


**Figure 29.5.** Landmarks at the bregmatic fontanelle and suboccipital acoustic window in sagittal planes. (A) Sonographic image of the anatomical landmarks in a sagittal plane obtained via a bregmatic fontanelle labeled as (S) sulci, dilated lateral ventricle (LV) and thalamus (T). (B) Sonographic image of the anatomical landmarks in a sagittal plane at the suboccipital window labeled as fourth ventricle (4V), mesencephalic aqueduct (⇒), cerebellum (Cerebellum), caudal brainstem (★), and medulla (Medulla).

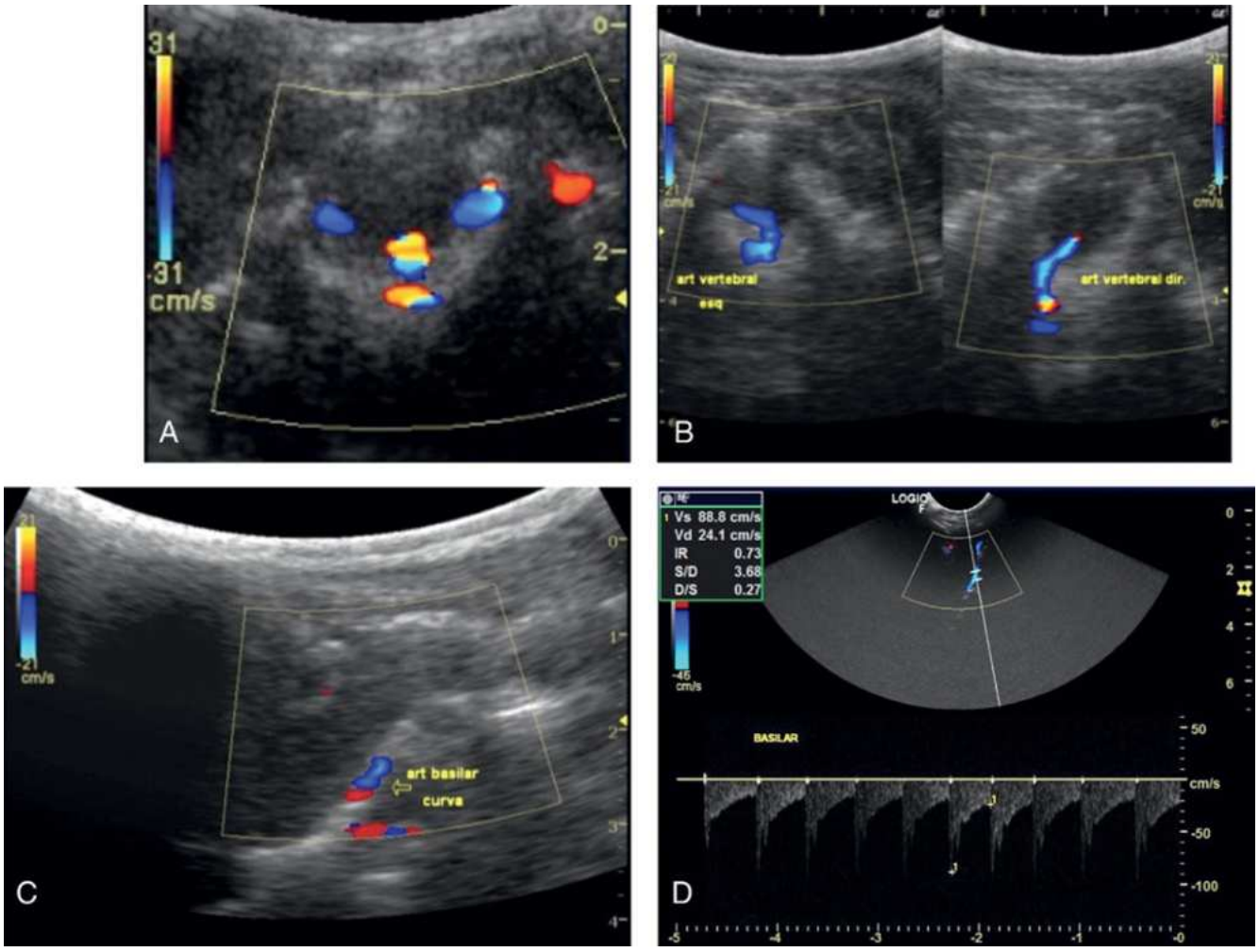


**Figure 29.6.** Color flow Doppler mapping of vertebrobasilar system obtained at the suboccipital acoustic window. (A,B) Transverse planes showing vertebral arteries. (C) Sagittal plane showing the basilar artery. (D) Application of triplex Doppler showing stenosis of the basilar artery in a dog after partial cerebellar herniation. Note the high systolic velocity (Vs).

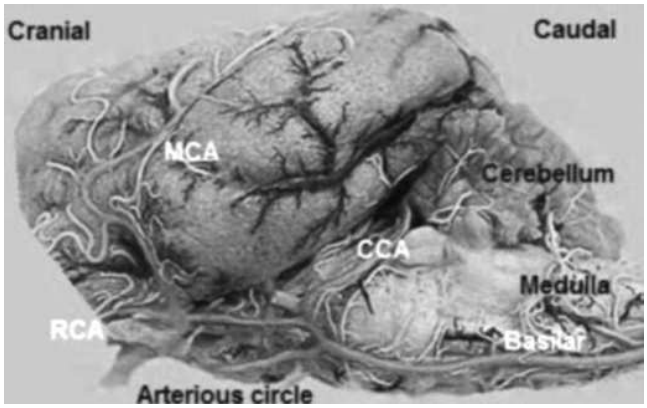


**Figure 29.7.** Cerebral arterial circle on canine brain. Showing the cerebral arterial circle on a drawing of the canine brain with the arteries labeled as the rostral cerebral artery (RCA), middle cerebral artery (MCA), caudal cerebral artery (CCA), and basilar artery (Basilar).

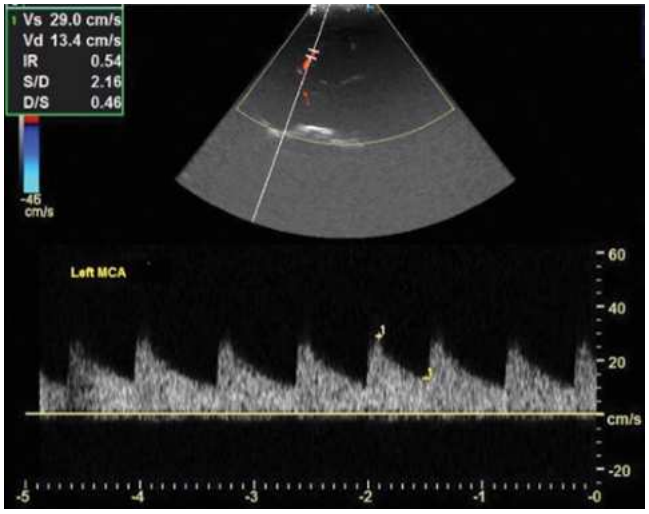


**Figure 29.8.** Triplex Doppler with a spectral image. Triplex Doppler with a spectral image showing similar sequential waveforms of a normal left middle cerebral artery (MCA) in a dog and peak systolic velocity (Vs), end-diastolic velocity (Vd), and resistive index (IR).

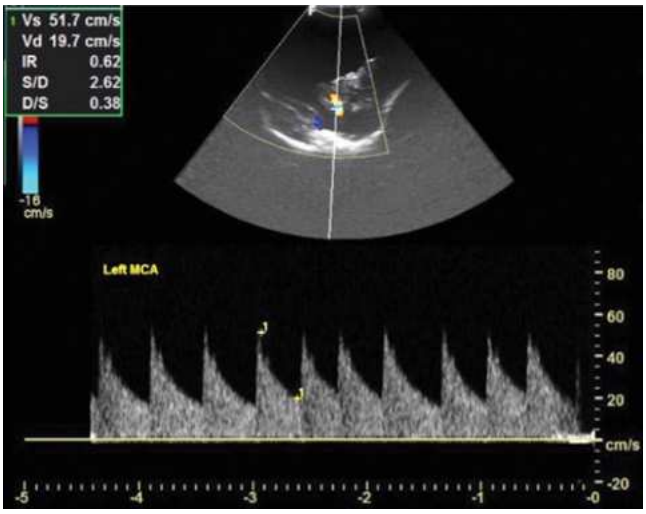


**Figure 29.9.** Triplex Doppler with a spectral image. Triplex Doppler with a spectral image showing measurements made on a representative spectral waveform to determine the peak systolic velocity (Vs), end-diastolic velocity (Vd) and resistive index (IR) of the left middle cerebral artery (MCA) in a dog with ventriculomegaly post TBI.

**Table 29.2.**
Guidelines for measurements of the resistive index as currently available in the literature.

| Window | Plane of image | Structure assessed | Resistive index value |
|---|---|---|---|
| Temporal | Oblique dorsal | Middle cerebral artery | 0.55 ± 0.04[a] |
| Rostral | Sagittal | Cerebral arteries | 0.55 ± 0.04[a] |
| Occipital | Sagittal | Basilar artery | 0.5–0.78[b] |

[a]Reference ranges of cerebral arteries in dogs (Seo et al. 2005).
[b]Reference ranges of canine basilar artery (Saito et al. 2003).

Three types of GME have been described based on the site of the lesions: focal, disseminated, and ocular (Fisher 2002). Historically, the presumptive diagnosis of GME has been based on nonspecific findings of history, laboratory testing, advanced imaging (CT and MRI), and cerebrospinal fluid (CSF) analysis. Disseminated GME may be confounded with infection and inflammation, and focal GME with neoplasia and nonneoplastic space-occupying lesions such as inflammatory/infectious/parasitic-related granulomas, cysts, and infarcts. Ocular GME may be confounded by other causes of optic neuritis. In general, CT scan and MRI, although useful diagnostic imaging tools for detecting brain injuries, cannot differentiate benign space-occupying masses from neoplastic lesions and their expense and need for chemical restraint make serial examination often impractical.

Recently, ultrasound has been applied to a small series of GME cases, showing some promise (Carvalho et al. 2012a). The study showed a supportive constellation of

sonographic findings for GME combining B-mode and TCDUS, including:

- diffuse decreased brain parenchyma echogenicity during early stages
- ventriculomegaly
- brain atrophy assessed via temporal or rostral windows
- hyperechoic focal lesions.

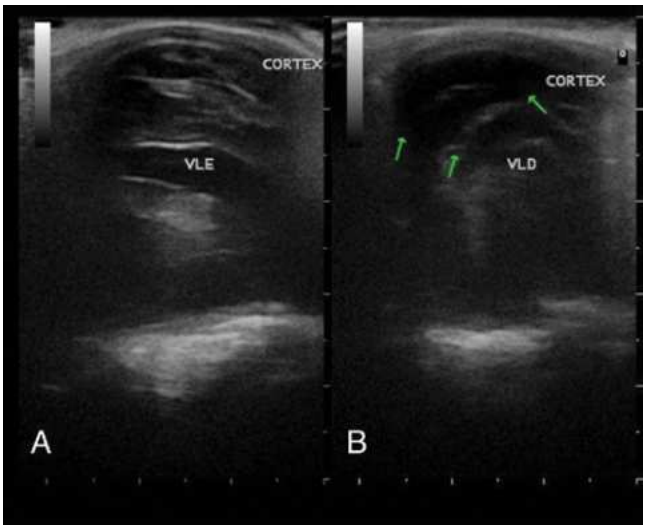


**Figure 29.10.** Epidural and subdural hematomas. Sagittal plane obtained at the rostral acoustic window showing epidural and subdural hematomas seen as hypoechoic focal lesion (*green arrows*) in the near-field above right lateral ventricle (VLD) post TBI in a dog. There is an additional sequela of unilateral ventriculomegaly at the left lateral ventricle (VLE).

Color flow Doppler ultrasound showed more obvious vessels of the arterial circle (with color mapping showing arterial trajectory to the periphery) and pulsed Doppler showed variation of RI values in the outlined arteries (Figure 29.18). Although not definitive, further B-mode and TCDUS veterinary studies may show that tracking RI of cerebral arteries, and B-mode and color flow Doppler changes may be helpful for diagnosis and monitoring response to therapy as well as evaluating effectiveness of different therapeutic regimens as an alternative to CT and MRI (Carvalho et al. 2012a).

## Pearls and Pitfalls, The Final Say

POCUS brain is an imaging modality to be considered in neurological patients, especially small- and toy-breed dogs and cats, that have transcranial acoustic windows, for many different types of TBI. POCUS brain may be used for initial assessment and serial monitoring, and TCDUS can be used for the assessment and monitoring of intracranial pressure. POCUS brain is fast, economical, safe, and radiation-sparing, and carries less risk compared with CT and MRI.

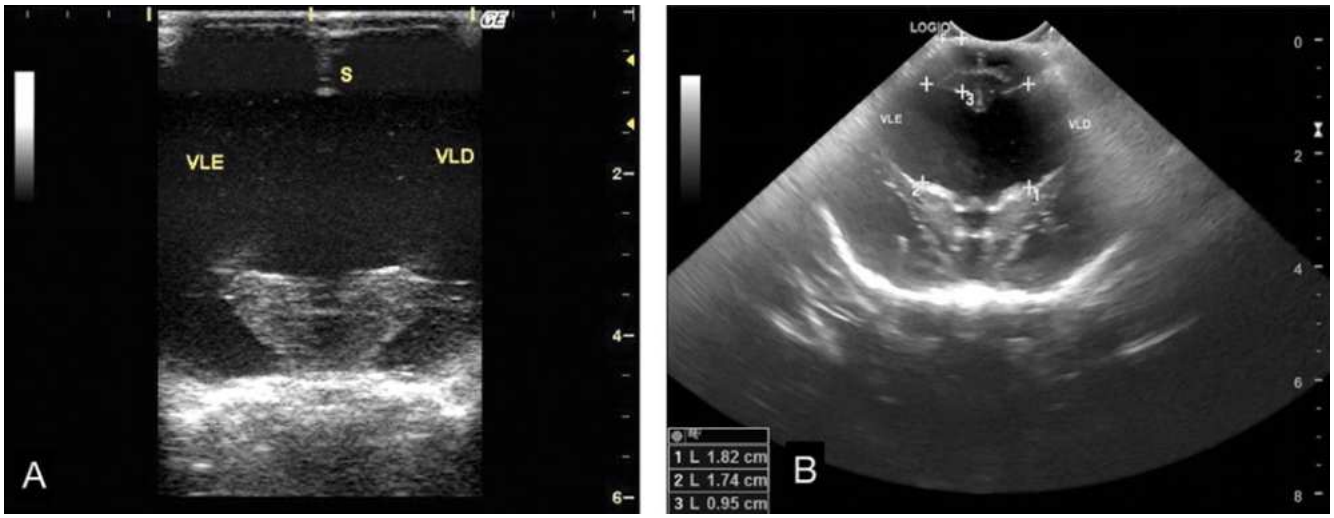


**Figure 29.11.** Intraventricular hemorrhage. Comparative gross, B-mode, and line drawing images in (A) and (B). Line drawing in (B) shows the transverse plane at the rostral acoustic window. Intraventricular hemorrhage identified by the presence of echoic debris inside dilated lateral ventricular cavities labeled as left lateral ventricle (VLE), right lateral ventricle (VLD), and telencephalic septum (S).

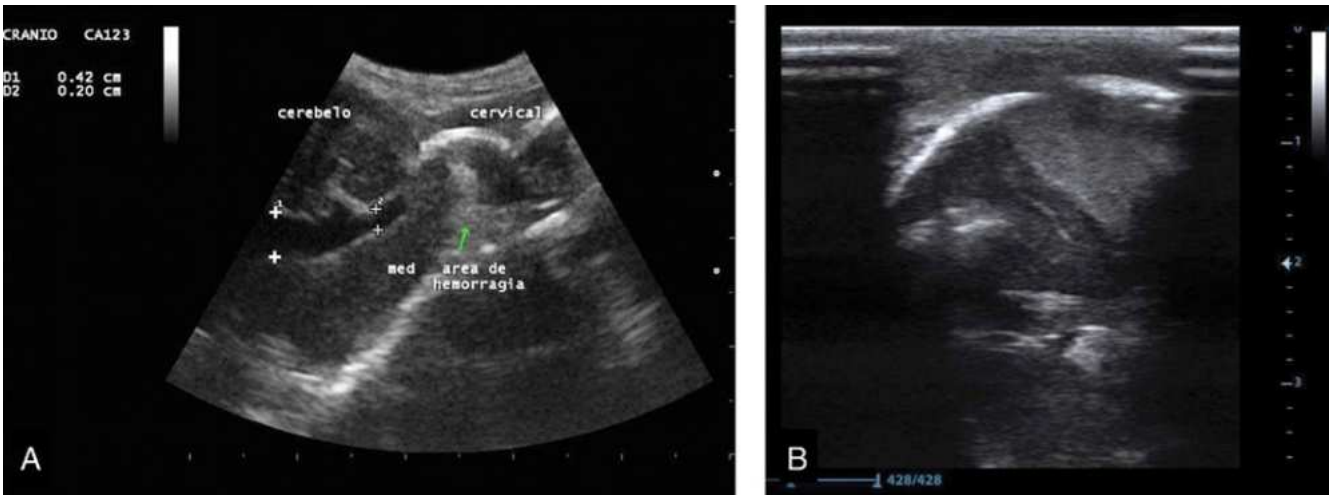


**Figure 29.12.** Intraparenchymal hemorrhage cases. (A) Sagittal plane at the occipital acoustic window showing focal hyperechoic lesion (*green arrow*) with hypoechoic halo (edema) with concurrent obstruction of the mesencephalic aqueduct caused by local edema and medullar deformity in a dog with compression trauma (skull fracture). (B) Sagittal plane at the rostral acoustic window with skull bone fracture and focal hyperechoic lesion in the near-field in a dog with blunt force TBI.

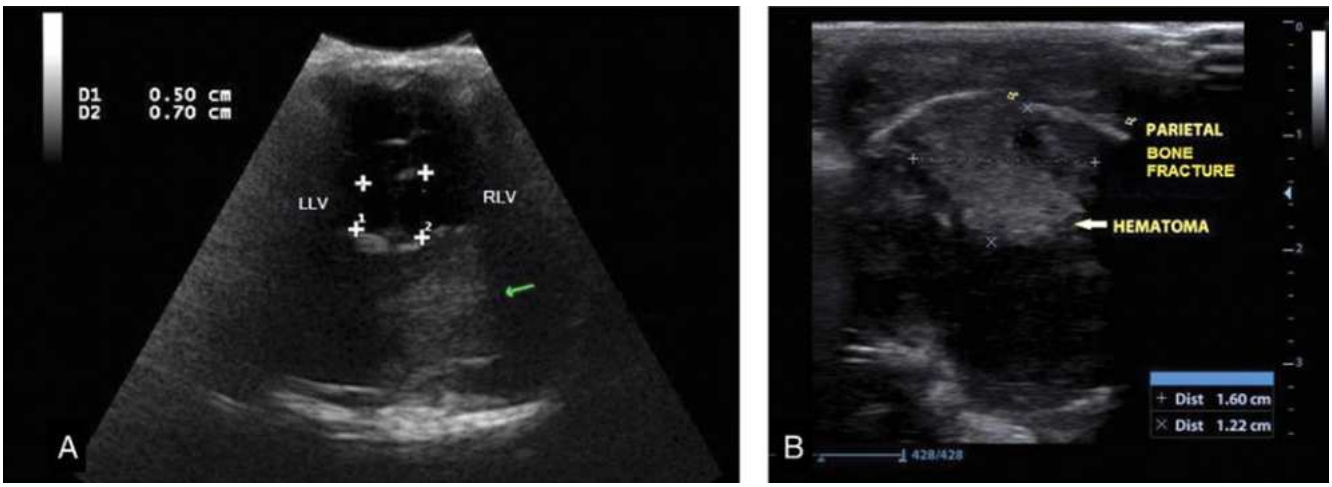


**Figure 29.13.** Skull fracture. (A) Transverse plane at the rostral acoustic window showing the mass effect caused by a hematoma and its associated perilesional edema seen sonographically as a hypo- to anechoic halo around the lesion (*green arrow*) and labeled as left lateral ventricle (LLV), right lateral ventricle (RLV). (B) Dorsal plane at the temporal acoustic window showing the mass effect caused by hematoma and its associated perilesional edema from a skull bone fracture in a dog with blunt force trauma.

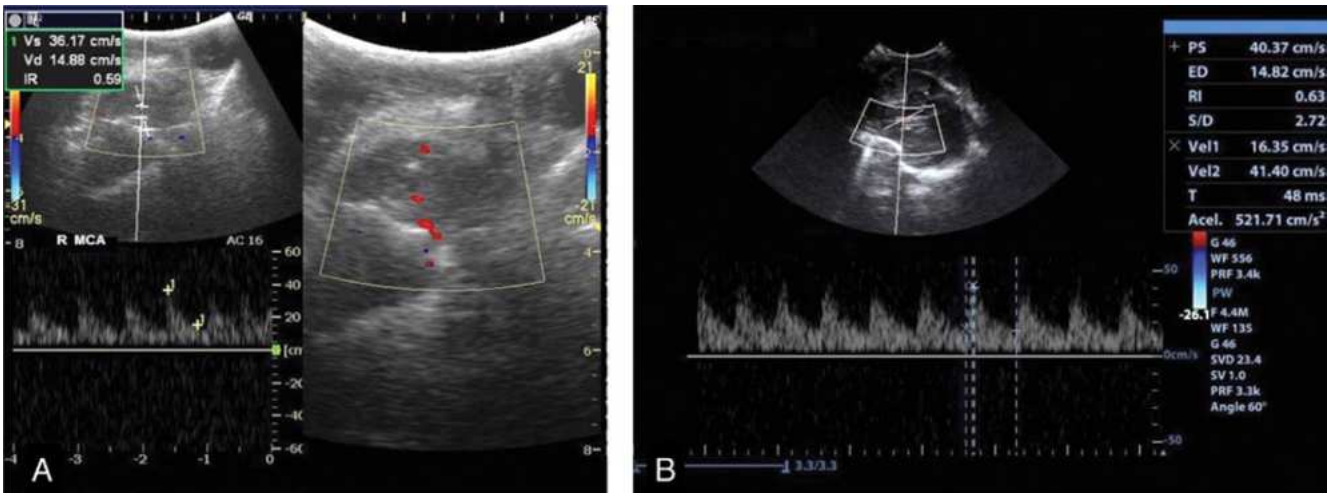


**Figure 29.14.** Intracranial mass lesion. (A) Focal lesion causing a mass effect resulting in increased ICP. Note the pulsed color flow Doppler of the middle cerebral artery (R MCA) shows an increased resistive index (IR) near the focal lesion. (B) Pulsed Doppler of the cerebral artery in a dog three hours post TBI showing an increased resistive index (RI) representative of elevated ICP.

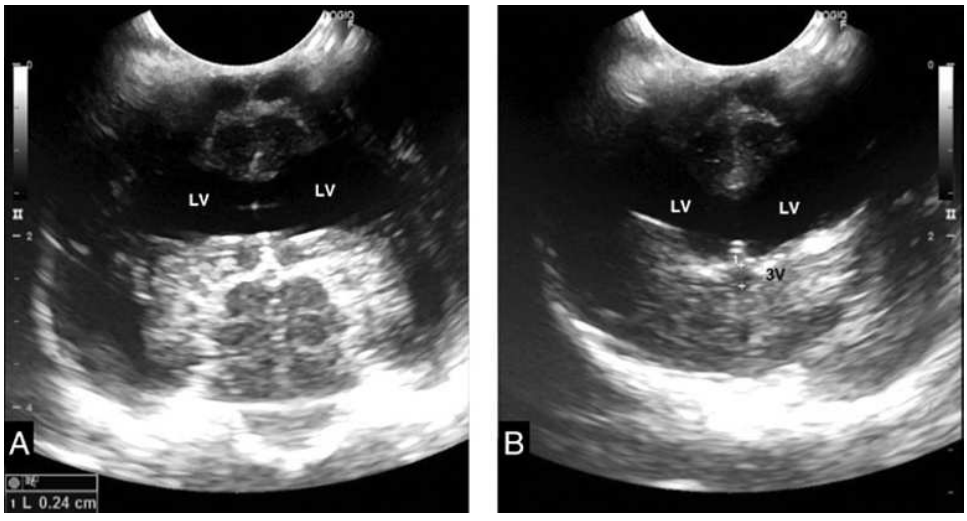


**Figure 29.15.** Ventriculomegaly. Transverse plane at the rostral window in (A) and (B). Lateral ventricles (LV) and third ventricle (3V) are increased – ventriculomegaly. The third ventricle is between the crosses (+).

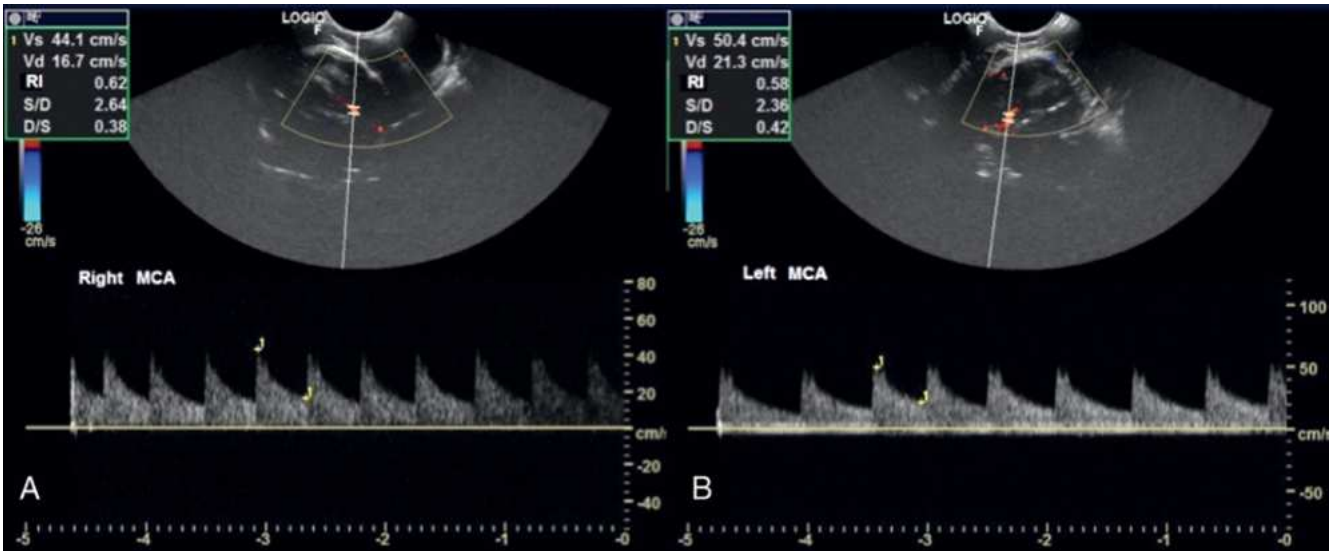


**Figure 29.16.** Hydrocephaly. Pulsed Doppler of right (A) and left (B) middle cerebral arteries (MCA) in a dog with hydrocephaly. Note the resistive index (RI) of both arteries is increased. The normal RI would be 0.55 ± 0.04.

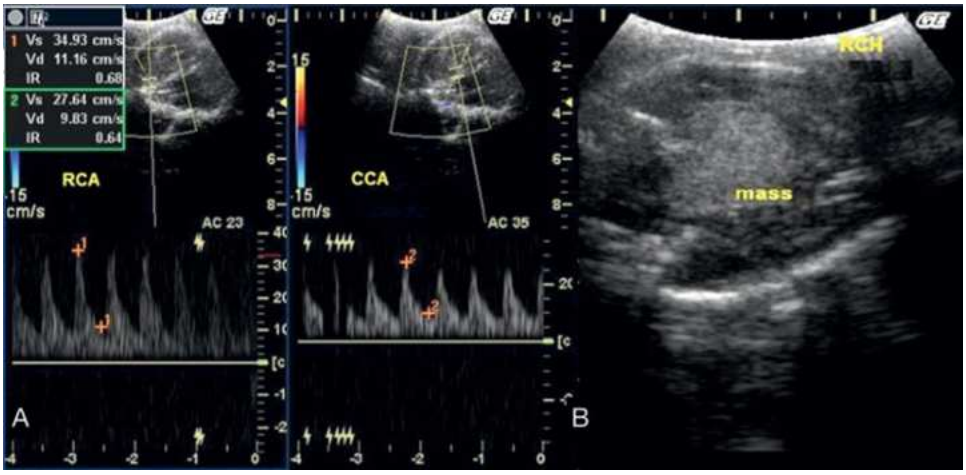


**Figure 29.17.** Intracranial space-occupying lesion. Dorsal plane at transtemporal window. Sonographic image of focal hyperechoic space-occupying lesion (mass) in (B). Note the increased RI in (A) of the rostral (RCA) and caudal (CCA) cerebral arteries. The normal RI would be 0.55 ± 0.04.

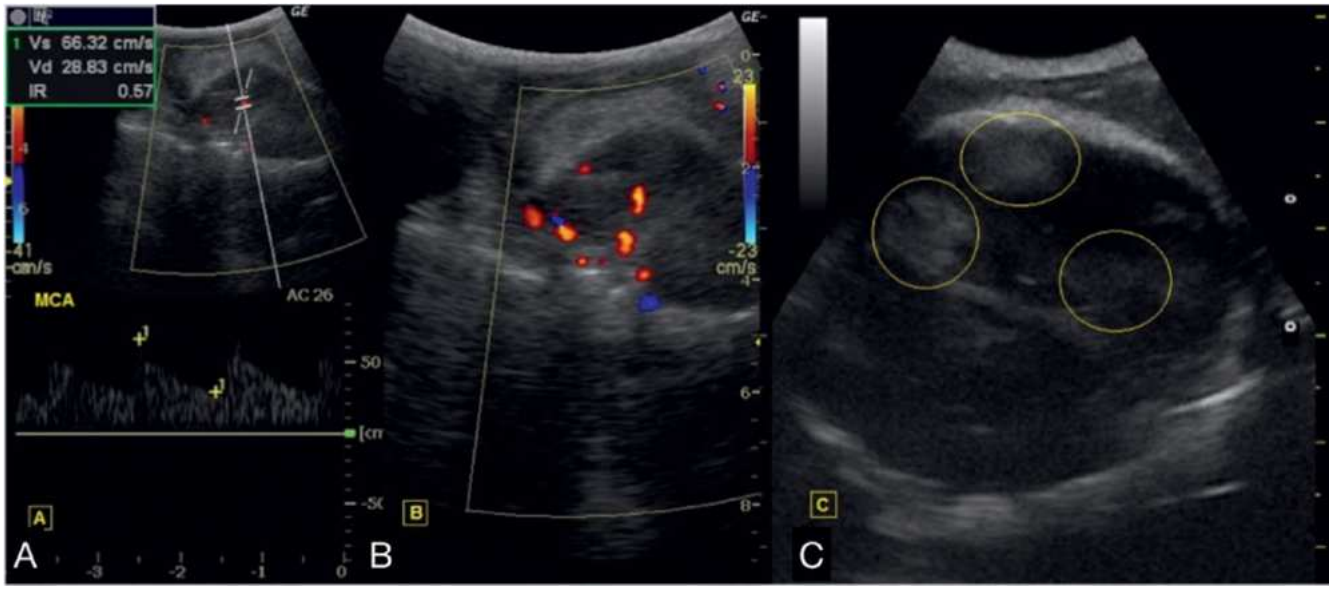


**Figure 29.18.** Granulomatous meningoencephalitis (GME). Dorsal oblique planes at transtemporal window. (A) Pulsed Doppler of middle cerebral artery (MCA) in a dog with GME, demonstrating a high RI. (B) Color flow Doppler showing more obvious arteries and veins. (C) B-mode showing focal nodular hyperechoic lesions in the same patient with GME.

# References


Berg D, Godau J, Walter U. 2008. Transcranial sonography in movement disorders. *Lancet Neurology* 7:1044–1055.

Braund KG. Neurological syndromes. In: *Clinical Neurology in Small Animals: Localization, Diagnosis and Treatment*. New York: International Veterinary Information Service, 2003.

Carvalho CF, Andrade Neto JP, Jimenez CD, et al. 2007. Ultrassonografia transcraniana em cães com distúrbios de origem central. *Arq Bras Med Vet Zootec* 59(6):1412–1416.

Carvalho CF, Cintra TC, Andrade Neto JP. 2009. Ultrassonografia Doppler transcraniana. In: *Ultrassonografia Doppler em Pequenos Animais*, edited by Carvalho CF. São Paulo: Roca.

Carvalho CF, Perez RB, Chammas MC, et al. 2012a. Transcranial Doppler sonographic findings in granulomatous meningoencephalitis in small breed dogs. *Can Vet J* 53:855–859.

Carvalho CF, Andrade Neto JP, Diniz SA. 2012b. Small breed dogs with confirmed stroke: concurrent diseases and sonographic findings. *Arq Bras Med Vet Zootec* 64(5):1177–1183.

Carvalho CF, Andrade Neto JP. 2014. Encéfalo. In: *Ultrassonografia em Pequenos Animais*, 2nd edition, edited by Grupo Editora Nacional. São Paulo: Roca.

Cintra TCF, Carvalho CF, Canola JC, et al. 2014. Ultrassonografia transcraniana em cães hígidos: padronização da técnica e descrição anatômica. *Arq Bras Med Vet Zootec* 66(1):61–68.

De LaHunta A, Glass E, Kentt M. *Veterinary Neuroanatomy and Clinical Neurology*, 4th edition, edited by DeLaHunta A. Philadelphia: WB Saunders, p 600.

Dewey CW. 2000. Emergency management of the head trauma patient. *Vet Clin North Am Small Anim Pract* 30:207–225.

Duque FJ, Barrera-Chacon R, Ruiz P, et al. 2010. Effect of transient carotid artery compression during transcranial Doppler ultrasonography in dogs. *Vet Rec* 167(13):481–484.

Duque FJ, Dominguez-Roldan JM, Martinez-Taboada F, et al. 2013. Effects of medetomidine and medetomidine-butorphanol on transcranial color-coded duplex ultrasonography in healthy dogs. *Res Vet Sci* 95(2):648–53.

Fisher M. 2002. Disseminated granulomatous meningoencephalomyelitis in a dog. *Can Vet J* 43:49–51.

Fukushima U, Sasaki S, Okano S, et al. 1999. The comparison between the cerebral blood flow directly measures and cerebral blood flow velocity in the middle and basilar cerebral arteries measured by transcranial Doppler ultrasonography. *J Vet Med Sci* 61(12):1293–1297.

Fukushima U, Miyashita K, Okano S, et al. 2000a. Evaluation of intracranial pressure by transcranial Doppler ultrasonography in dogs with intracranial hypertension. *J Vet Med Sci* 62(3):353–355.

Fukushima U, Sasaki S, Okano S, et al. 2000b. Non-invasive diagnosis of ischemic brain damage after cardiopulmonary resuscitation in dogs by using transcranial Doppler ultrasonography. *Vet Radiol Ultrasound* 41(2):172–177.

Garosi LS. 2010. Cerebrovascular disease in dogs and cats. *Vet Clin North Am Small Anim Pract* 40(1):65–79.

Ghajar J. 2000. Traumatic brain injury. *Lancet* 356:923–929.

Hochwald GM, Boal RD, Marlin AE, et al. 1975. Changes in regional blood-flow and water content of brain and spinal cord in acute and chronic experimental hydrocephalus. *Dev Med Child Neurol* 17(Suppl. 35):42–50.

Hudson JA, Cartee RE, Simpson ST, et al. 1989. Ultrasonographic anatomy of the canine brain. *Vet Radiol* 30(1):13–21.

Hudson JA, Simpson ST, Cox NR. 1991. Ultrasonographic examination of the normal canine neonatal brain. *Vet Radiol* 32(2):50–59.

Lillehei KO, Chandler WF, Knake JE. 1984. Real time ultrasound characteristics of the acute intracerebral hemorrhage as studied in the canine model. *Neurosurgery* 14(1):48–51.

McCormick T, Chilstrom M, Childs J, et al. 2017. Point of care ultrasound for the detection of traumatic intracranial hemorrhage in infants: a pilot study. *Pediatr Emerg Care* 33(1):18–20.

Platt SR, Radaelli ST, McDonnell JJ. 2001. The prognostic of the modified coma scale in head trauma in dogs. *J Vet Intern Med* 15:581–584.

Saito M, Olby NJ, Spaulding K, et al. 2003. Relationship among basilar artery resistance index, degree of ventriculomegaly and clinical signs in hydrocephalic dogs. *Vet Radiol Ultrasound* 44(6):687–694.

Seo M, CHoi H, Lee K, et al. 2005. Transcranial Doppler ultrasound analysis of resistive index in rostral and caudal cerebral arteries in dogs. *J Vet Sci* 6(1):61–66.

Spaulding KA, Nicholas JH, Sharp B. 1990. Ultrasonographic imaging of the lateral cerebral ventricles in the dog. *Vet Radiol* 31(2):59–64.

Vianna CG, Arias MVB. 2013. Prospective study of 32 dogs with traumatic brain injury. *Rev Bras Med Vet* 35(1):93–99.

Werner C, Hoffman WE, Kochs E, et al. 1992. The effects of propofol on cerebral blood flow in correlation to cerebral blood flow velocity in dogs. *J Neurosurg Anesth* 4(1):41–46.

Werner C, Hoffman WE, Kochs E, et al. 1993. Cerebral blood flow and cerebral blood flow velocity during angiotensin-induced arterial hypertension in dogs. *Can J Anaesth* 40(8):755–760.

Werner C, Hoffman WE, Kochs E, et al. 1995. Transcranial Doppler sonography indicates critical brain perfusion during hemorrhagic hypotension in dogs. *Anesth Analg* 81(6):1203–1207.

CHAPTER THIRTY

# POCUS: Nerve Blocks – Forelimb

Pablo E. Otero and Diego A. Portela

## Introduction

Peripheral nerve blocks of the forelimb are used to provide analgesia in both medical and surgical situations. Peripheral nerve blocks are indicated for the alleviation of perioperative pain, chronic pain, and traumatic pain of the shoulder, brachium, antebrachium, carpus, metacarpus, and phalanges. Peripheral nerve blocks may be used as a primary analgesic procedure or more commonly as part of a multimodal analgesic approach to small animals with acute and chronic pain as inpatients and outpatients. Moreover, the use of POCUS nerve blocks allows the clinician to more accurately locate target nerves, thus better insuring success and avoiding nearby structures such as blood vessels and body cavities, thus minimizing complications. The use of POCUS nerve blocks provides clear advantages over blind techniques. In fact, ultrasound-guided nerve blocks are becoming standard of care in human medicine.

### What POCUS Nerve Blocks – Forelimb Can Do

- Can assist with accurately performing nerve blocks over blind techniques.
- Can help avoid complications by imaging nearby structures such as vessels and body cavities, and other structures to be avoided.

### What POCUS Nerve Blocks – Forelimb Cannot Do

- Cannot replace the need for familiarity with the anatomy at each nerve block location.
- Cannot replace ultrasound-guided skills and the hand–eye and spatial coordination necessary for needle placement and advancement.

### Indications

- Regional anesthesia of the forelimb during procedural anesthetic events, and nonprocedural options for acute and chronic pain.
- Part of multimodal anesthesia of the forelimb.
- The paravertebral approach is indicated to provide analgesia/anesthesia to the shoulder and proximal brachium.
- The subscalene approach is indicated to provide analgesia/anesthesia to the shoulder, brachium, and elbow.
- The axillary approach is indicated to provide analgesia/anesthesia to the distal brachium and elbow.
- The radial, ulnar, median, and musculocutaneous nerve block (RUMM) is indicated to provide analgesia/anesthesia to the antebrachium, carpus, metacarpus, and digits.

### Objectives

- Be able to identify relevant anatomy of the forelimb.
- Be able to perform the regional blocks of the forelimb.
- Know the clinical utility of each of the three approaches, and what part of the forelimb is anesthetized in each.

*Point-of-Care Ultrasound Techniques for the Small Animal Practitioner*, Second Edition. Edited by Gregory R. Lisciandro.
© 2021 John Wiley & Sons, Inc. Published 2021 by John Wiley & Sons, Inc.
Companion website: www.wiley.com/go/lisciandro/ultrasound2

# How to Perform POCUS Nerve Blocks – Forelimb

## Approaches and Locations

The nerves of the forelimb via the brachial plexus may be blocked at different locations by different approaches – the paravertebral, subscalene and axillary (Table 30.1).

## Relevant Anatomy of the Brachial Plexus

- The brachial plexus is formed by the ventral roots of the spinal nerves C6, C7, C8, and T1 (Evans and de Lahunta 2013). Occasionally the brachial plexus receives contributions from C5 and T2.
- The ventral branches of C6 and C7 emerge through the intervertebral foramen of C5–6 and C6–7, respectively, and course through the muscles in the intertransverse space towards the medial aspect of the scalenus muscle.
- The ventral roots of C8 and T1 emerge through the intervertebral foramen of C7–T1 and T1–T2, respectively. The branches of C8 course ventrally parallel to the cranial aspect of the first rib, and the branches of T1 course lateral to the axillary artery.
- The nerve branches then descend into the cervical area bordered laterally by the deep fascia of the neck and medially by the prevertebral fascia.

**Pearl:** For the most effective and long-lasting nerve block, the anesthetic solution must be injected between the deep fascia of the neck and the prevertebral fascia (Otero and Portela 2019).

## Probe Type Used to Perform Forelimb Blocks

- Ultrasound machine with a linear transducer (probe) of ≥10 MHz.
- 2–4 cm depth depending on animal size.

## Materials Needed to Perform Forelimb Blocks

- Clippers and skin preparation solutions.
- Sterile gloves.
- Sterile drapes.
- Local anesthetic (in sufficient quantity).
- 50 mm 21 gauge isolated unipolar needles (for cats and dogs weighing less than 15 kg).
- 100 mm 21 gauge isolated unipolar needles (for dogs weighing more than 15 kg).
- Sterile transducer (probe) drapes and gel.
- Multiparametric monitor (electrocardiogram [ECG], noninvasive blood pressure [NIBP], pulse oximetry [$SpO_2$], temperature).
- Emergency drugs.

# Ultrasound-guided Brachial Plexus: Paravertebral Approach

The brachial plexus paravertebral approach consists of the deposit of an anesthetic solution at the ventral roots of spinal nerves C6, C7, C8, and T1 (Bagshaw et al. 2009). The paravertebral approach provides analgesia/anesthesia to the entire forelimb, but it is indicated for procedures involving the shoulder and proximal brachium.

**Table 30.1.**
Approaches to the forelimb, where on the forelimb analgesia/anesthesia is provided, and important nearby structures.

| Approach | Where analgesia/ anesthesia provided | Important nearby structures | Comments |
|---|---|---|---|
| Paravertebral | Shoulder and entire forelimb | Shoulder, brachium, elbow | Epidural spread could affect the cervical portion of the spinal cord |
| Subscalene | Shoulder and entire forelimb | Shoulder, brachium, elbow | Phrenic nerve is blocked, *therefore bilateral block should be avoided* |
| Axillary | Distal to midbrachium | Distal brachium, elbow, antebrachium, carpus | Pleural puncture and pneumothorax could be a complication of this technique.<br>Phrenic nerve is blocked, *therefore bilateral block should be avoided* |
| Radial, ulnar, median, and musculocutaneous (RUMM) | Distal to the elbow | Antebrachium, carpus, metacarpus, digits | Pressure exerted on the transducer can easily collapse the brachial vein, increasing the risk of vascular puncture |

### Ultrasound Probe Placement and Block Technique

- *C6 and C7 block*. Place the probe parallel to the longitudinal axis of the cervical spine, immediately below the lateral border of the transverse process of C6.
- *C8 through T1 block*. Place the probe parallel to the longitudinal axis of the cervical spine, cranial to the first rib and above the costochondral joint.
- The block is performed using an in-plane needle advancement (Figure 30.1).
- Check through gentle aspiration for extravascular needle placement *and abort if blood is aspirated or if resistance to the injection occurs*.
- During anesthetic injection, the needle should be repositioned if necessary to obtain a homogeneous distribution of anesthetic around the target nerve.

### Drugs and Volume Administered

- Drug and concentration: bupivacaine 0.5%, ropivacaine 0.5%, levobupivacaine 0.5%.
- Suggested volume: 0.05 mL/kg per branch.

**Note:** The protocol generally provides analgesia/anesthesia for up to eight hours. Epidural spread of local anesthetics could result in phrenic nerve paralysis and sympathetic blockade of the cardioaccelerator nerves. *Careful cardiorespiratory monitoring is mandatory after a paravertebral brachial plexus block.*

**Pearl:** The paravertebral approach to block the brachial plexus promotes block of the ipsilateral phrenic nerve. This block does not significantly impair ventilation in animals without respiratory compromise unless performed bilaterally.

**Figure 30.1.** Paravertebral approach. Insertion of the needle to perform a block of the ventral branch of C6 through a paravertebral approach, using an in-plane technique. Source: Reproduced with permission from Otero and Portela (2019).

### Scan of Brachial Plexus at the Paravertebral Space

#### Scanning of the Paravertebral Spaces C5–6 and C6–7

The transverse process of C6 is the most prominent landmark. The ventral branches of C6 and C7, cranial or caudal to the transverse process of C6 respectively, are visualized as bilobular ovoid structures of anechoic appearance (Figures 30.2 and 30.3).

#### Scanning of the C8–T1 Complex

The most relevant landmark is the first rib, which is seen as a hyperechoic semicircular line, and a sharp acoustic shadow, which extends medially. The acoustic window allows visualization of the C8–T1 nerve complex, medial to the belly of the scalenus muscle (Figures 30.4 and 30.5).

## Ultrasound-guided Brachial Plexus Block through a Subscalene Approach

The Subscalene approach for the brachial plexus block consists of the deposit of local anesthetic on the ventral branches of spinal nerves C6, C7, C8, and T1,

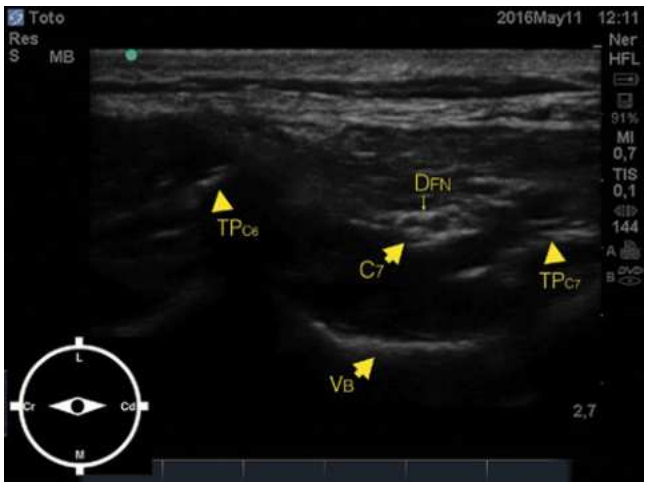


**Figure 30.2.** Paravertebral approach. The acoustic window shows the C6–7 paravertebral space, performed with a linear probe, oriented parallel to the longitudinal axis of the spine. L, lateral; M, medial; Cr, cranial; Cd, caudal. DFN, deep fascia of the neck; TPC6, transverse process of C6; TPC7, transverse process of C7; C7, ventral branches of C7; VB, vertebral body. Source: Modified and used with permission from Otero and Portela (2019).

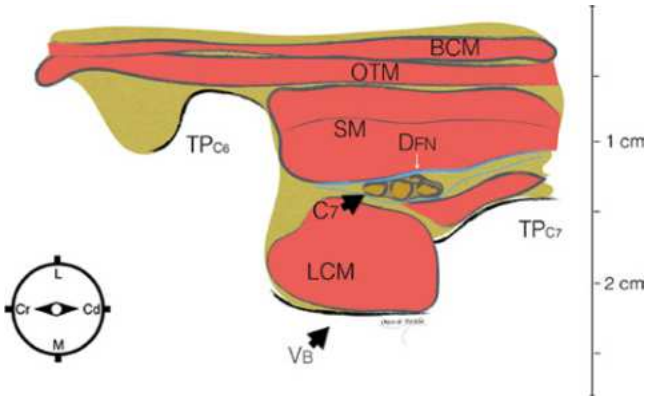


**Figure 30.3.** Paravertebral approach. Schematic illustration of the structures shown in Figure 30.2. BCM, brachiocephalicus muscle; OTM, omotransversarius muscle; SM, scalenus muscle; DFN, deep fascia of the neck; LCM, longus colli muscle; TPC6, transverse process of C6; TPC7, transverse process of C7; C7, ventral branches of C7; VB, vertebral body. Source: Modified and used with permission from Otero and Portela (2019).

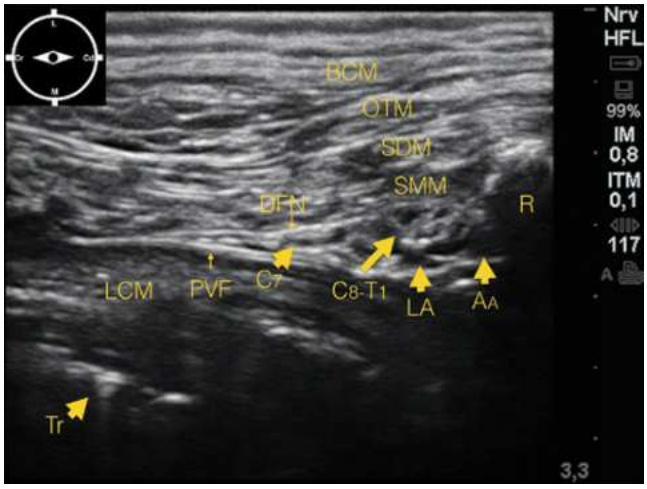


**Figure 30.4.** Paravertebral approach. The acoustic window shows the C8–T1 nerve complex, performed with a linear probe, oriented parallel to the longitudinal axis of the spine, and placed cranial to the cranial border of the first rib. L, lateral; M, medial; Cr, cranial; Cd, caudal. BCM, brachiocephalicus muscle; OTM, omotransversarius muscle; SM, scalenus muscle; DFN, deep fascia of the neck; PVF, prevertebral fascia; C7, ventral branches of C7; AA, axillary artery; R, first rib; LA, local anesthetic; LCM, longus colli muscle; E, esophagus; Tr, trachea. Source: Modified and used with permission from Otero and Portela (2019).

when they pass between the belly of the scalenus muscle and the longus colli muscle (Otero et al. 2017) (Figures 30.7 and 30.8). The subscalene approach provides analgesia/anesthesia to the *entire forelimb*, but is indicated for procedures involving the shoulder, brachium, and elbow.

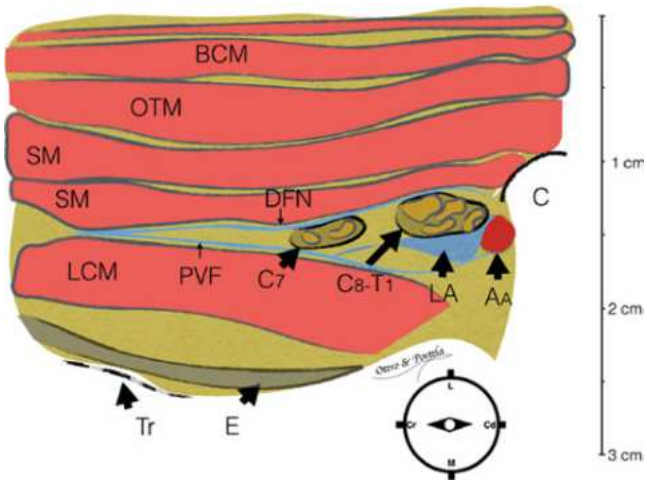


**Figure 30.5.** Paravertebral approach. Schematic illustration of the structures shown in Figure 30.4. BCM, brachiocephalicus muscle; OTM, omotransversarius muscle; SM, scalenus muscle; DFN, deep fascia of the neck; PVF, prevertebral fascia; C7, ventral branches of C7; AA, axillary artery; R, first rib; LA, local anesthetic; LCM, longus colli muscle; E, esophagus; Tr, trachea. Source: Modified and used with permission from Otero and Portela (2019).

**Figure 30.6.** Subscalenus approach. Dog positioned for subscalene block of the brachial plexus. The probe is placed parallel to the longitudinal axis of the scalenus muscle, cranial to the first rib, and above the costochondral joint. The needle is introduced with an in-plane approach, in a craniocaudal direction. Source: Used with permission from Otero and Portela (2019).

## *Ultrasound Probe Placement and Block Technique*

- Place the probe parallel to the longitudinal axis of the cervical spine, cranial to the first rib and above the costochondral joint (Figure 30.6).
- The block is performed using an in-plane needle advancement. The needle is advanced through the belly of the scalenus muscle, and the deep fascia of

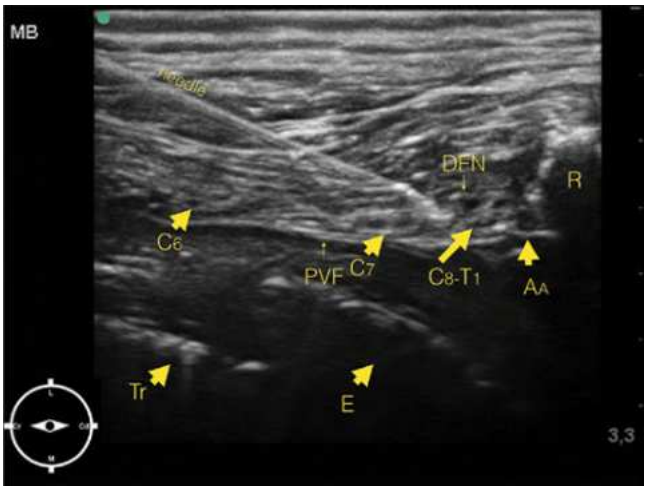


**Figure 30.7.** Subscalenus approach. The acoustic window shows the ventral branches of the brachial plexus aligned below the belly of the scalenus muscle.Note the position of the tip of the needle between C8 and C7 for the injection of the first aliquot of the local aesthetic. L, lateral; M, medial; Cr, cranial; Cd, caudal. DFN, deep fascia of the neck; PVF, prevertebral fascia; C7, ventral branches of C7; C6, ventral branches of C6; AA, axillary artery; R, first rib; E, esophagus; Tr, trachea. Source: Modified and used with permission from Otero and Portela (2019).

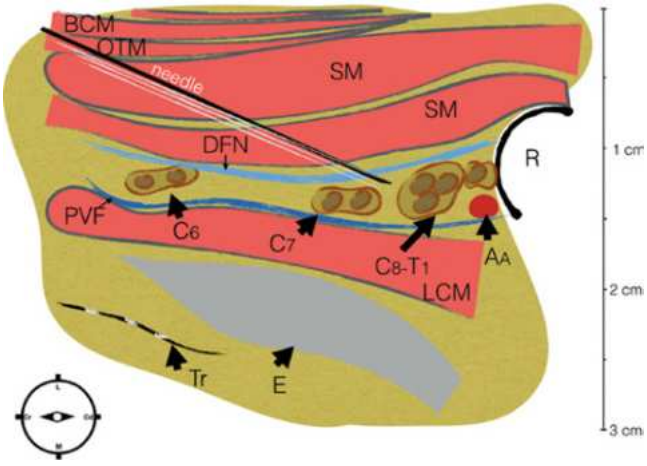


**Figure 30.8.** Subscalenus approach. Schematic illustration of the structures present in Figure 30.7. SM, scalenus muscle; C8–T1, C8–T1 complex; C7, ventral branches of C7; R, first rib; LCM, longus colli muscle. Source: Modified and used with permission from Otero and Portela (2019).

the neck is punctured (see Figure 30.6). The total volume is divided into two aliquots and injected caudal and cranial to the C7 nerve roots.

- Check for extravascular needle placement and *avoid injection if resistance is perceived*. If necessary, the needle should be repositioned to obtain a homogeneous distribution around the target nerve.

**Pearl:** The needle should not be advanced further than the cranial border of the first rib in order to avoid pleural puncture. Puncturing of the prevertebral fascia should also be avoided.

### *Drugs and Volume Administered*

- Drug and concentration: bupivacaine 0.5%, ropivacaine 0.5%, levobupivacaine 0.5%.
- Suggested volume: 0.4 mL/kg, divided into the nerve branches of the plexus.

**Note:** The protocol generally provides analgesia/anesthesia for up to eight hours. This technique produces block of the phrenic nerve, *therefore bilateral blocks should be avoided because they can adversely affect ventilation*.

**Pearl:** The subscalene approach to block the brachial plexus promotes block of the ipsilateral phrenic nerve (Fuensalida et al. 2017). This block does not significantly impair ventilation in animals without respiratory compromise unless performed bilaterally.

### *Scan of the Ventral Branches of the Brachial Plexus at the Subscalene Level*

See Figures 30.7 and 30.8.

## Ultrasound-guided Brachial Plexus Block through an Axillary Approach

The brachial plexus block through an axillary approach consists of instillation of local anesthetic solution around the nerves responsible for innervation of the forelimb in the axillary space (Figure 30.9). The target nerves are the musculocutaneous nerve, axillary nerve, radial nerve, and median-ulnar nerve trunk (Campoy et al. 2010; Ansón et al. 2015). The axillary approach provides analgesia/anesthesia to structures located distal to the midbrachial region, and it is indicated for procedures involving the distal humerus, elbow, antebrachium, and carpus.

### *Ultrasound Probe Placement and Block Technique*

- Place the probe on the axillary space, between the manubrium of the sternum and the supraglenoid tubercle of the scapula, with a ventrodorsal orientation in a parasagittal approach (see Figure 30.9).

**Figure 30.9.** Axillary approach. Ultrasound-guided axillary plexus block being performed in a dog. A linear probe is positioned in the axillary space, between the manubrium of the sternum and the supraglenoid tubercle of the scapula, with a ventrodorsal orientation in a parasagittal approach. The needle is introduced in-plane, in a craniocaudal direction. Source: Used with permission from Otero and Portela (2019).

- Once positioned, gently direct the ultrasound beam until a transverse view of the axillary vessels and nerves is obtained.
- Identify the axillary fascia surrounding these structures.
- The brachial plexus block in the axillary space is performed with an in-plane technique.
- The needle is introduced through the belly of the superficial pectoral muscle and lateral to the jugular vein, in a caudodorsal direction.
- Check for extravascular needle placement *and avoid injection if resistance is perceived*. If necessary, the needle should be repositioned to obtain a homogeneous distribution around the target nerve.

**Pearl:** In order to achieve a deep and long-lasting block, the local anesthetic must be injected after puncturing the axillary fascia.

### Drugs and Volume Administered

- Drug and concentration: bupivacaine 0.5%, ropivacaine 0.5%, levobupivacaine 0.5%.
- Suggested total volume: 0.15–0.2 mL/kg.

**Note:** The protocol generally provides analgesia for up to eight hours. Since the phrenic nerve could be blocked with this technique, *bilateral blocks should be avoided*. There is a potential risk of producing an iatrogenic pneumothorax if the needle pierces the parietal pleura at the thoracic inlet, therefore *it is important to avoid introducing the needle caudal to the brachial artery*.

**Pearl:** The axillary approach to block the brachial plexus promotes block of the ipsilateral phrenic nerve. This block does not significantly impair ventilation in animals without respiratory compromise *unless performed bilaterally*.

### Scan of the Axillary Space

The axillary artery, represented as a pulsatile and anechoic circle structure, is the main reference of the image. The axillary vein, situated caudal to the artery, is an ovoid and anechoic structure, easily collapsible when gentle pressure is applied with the transducer. The acoustic window permits identification of the nerves of the brachial plexus, located cranial and slightly dorsal to the axillary vessels (Figures 30.10 and 30.11).

**Pearl:** Under probe compression, veins initially collapse while arteries do not.

**Pearl:** The nerves that supply the thoracic limb run through the axillary space from medial to lateral and should be memorized. For this reason, when the ultrasound probe is placed parasagittal to this area in a ventrodorsal orientation, a transverse view of the nerves and vessels is obtained.

## Ultrasound-guided Radial, Ulnar, Median, and Musculocutaneous (RUMM) Nerve Block

The RUMM block desensitizes the antebrachium, carpal joint, and forepaw. It consists of the instillation of anesthetic solution over the radial, musculocutaneous, median, and ulnar nerves at the middle third of the brachium (Portela et al. 2013; Castiñeiras et al. 2015).

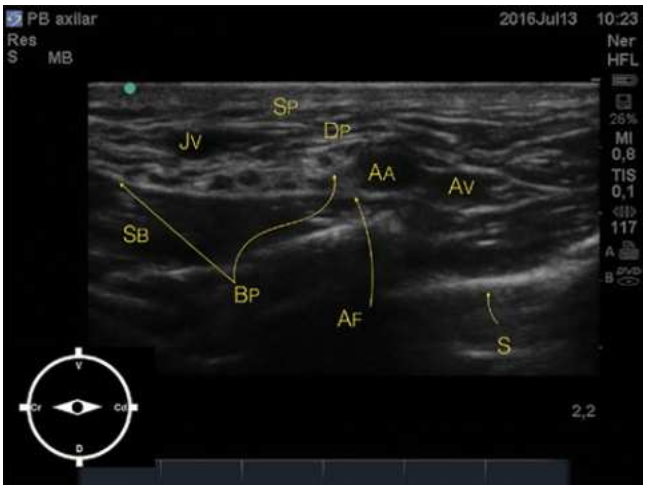


**Figure 30.10.** Axillary approach. Ultrasound image of the axillary space, performed with a linear probe, positioned between the manubrium of the sternum and the supraglenoid tubercle of the scapula, with a ventrodorsal orientation in a parasagittal approach. Cr, cranial; Cd, caudal; V, ventral; D, dorsal. SP, superficial pectoral muscle; DP, deep pectoral muscle; AA, axillary artery; AV, axillary vein; JV, jugular vein; BP, brachial plexus; AF, axillary fascia; SB, subscapular muscle; S, scapula. Source: Modified and used with permission from Otero and Portela (2019).

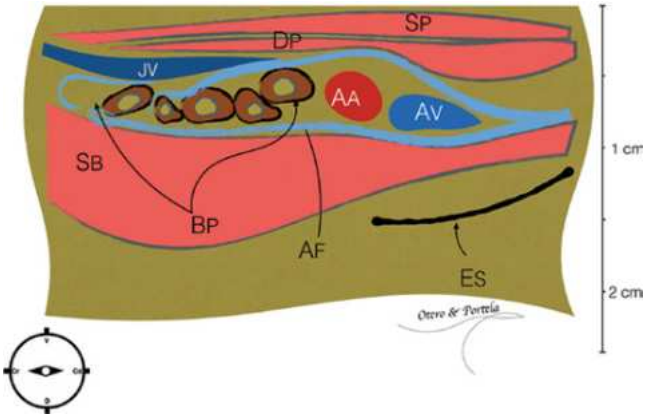


**Figure 30.11.** Axillary approach. Schematic view of the structures present in Figure 30.10. SP, superficial pectoral muscle; DP, deep pectoral muscle; AA, axillary artery; AV, axillary vein; JV, jugular vein; BP, brachial plexus; AF, axillary fascia; SB, subscapular muscle; S, scapula. Source: Modified and used with permission from Otero and Portela (2019).

## *Relevant Anatomy of the Radial, Ulnar, Median, and Musculocutaneous Nerves*

- At the level of the middle third of the humerus, the nerves of the brachial plexus start to separate (Figures 30.12 and 30.13).

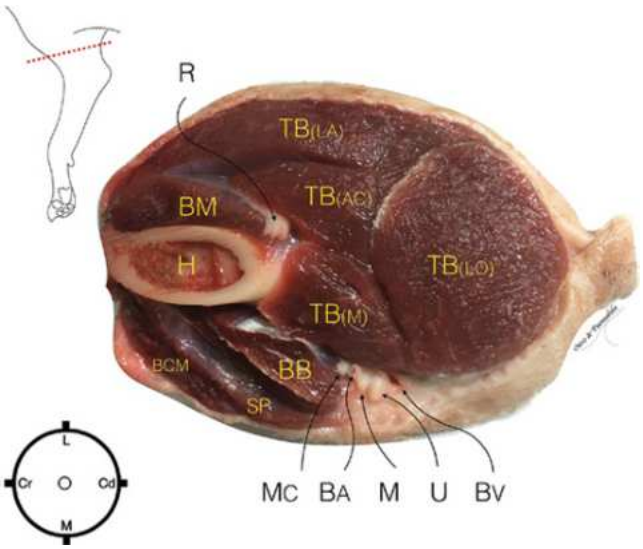


**Figure 30.12.** Brachial anatomy. Transverse view of the forelimb at the middle third of the brachium. SP, superficial pectoral muscle; BB, biceps brachii muscle; B, brachial muscle; BC, brachiocephalicus muscle; TB(LO), triceps brachii muscle (long head); TB(L), triceps brachii muscle (lateral head); TB(A), triceps brachii muscle (accessory head); TB(M), triceps brachii muscle (medial head); H, humerus; BA, brachial artery; BV, brachial vein; MC, musculocutaneous nerve; R, radial nerve; M, median nerve; U, ulnar nerve. Source: Modified and used with permission from Otero and Portela (2019).

- The radial nerve runs spirally around the humerus, from medial to lateral, to lie between the lateral and accessory heads of the triceps brachii muscle and the brachial muscle.
- On the medial aspect of the arm, the musculocutaneous nerve runs distally in contact with the caudal border of the belly of the biceps brachii muscle, cranial to the brachial artery.
- The median and ulnar nerves run distally flanked by the brachial vessels (artery in cranial and vein in caudal).

## *Ultrasound-guided Radial Nerve Block*

### Ultrasound Probe Placement and Block Technique

- Place the probe on the lateral aspect of the brachium, at the level of the middle third, transversal to the longitudinal axis of the humerus (Figure 30.14).
- The humerus, brachialis, and triceps brachii muscles can be easily identified at this level (see Figure 30.15).

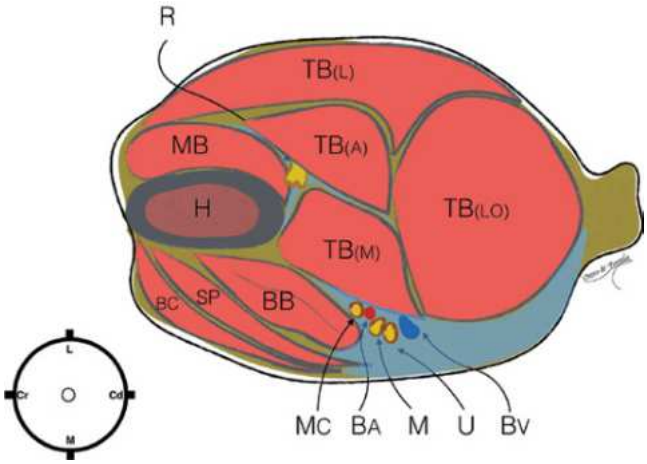


**Figure 30.13.** Brachial anatomy. Schematic illustration of Figure 30.12. SP, superficial pectoral muscle; BB, biceps brachii muscle; B, brachial muscle; BC, brachiocephalicus muscle; TB(LO), triceps brachii muscle (long head); TB(L), triceps brachii muscle (lateral head); TB(A), triceps brachii muscle (accessory head); TB(M), triceps brachii muscle (medial head); H, humerus; BA, brachial artery; BV, brachial vein; MC, musculocutaneous nerve; R, radial nerve; M, median nerve; U, ulnar nerve. Source: Modified and used with permission from Otero and Portela (2019).

**Figure 30.14.** RUMM block. Linear probe placement for radial nerve visualization, on the lateral aspect of the brachium. The needle is advanced in-plane, in a caudomedial direction. Source: Used with permission from Otero and Portela (2019).

- Then, slide the probe distally until the radial nerve appears between the muscle bellies.
- The needle is introduced at the cranial border of the ultrasound probe through the belly of the brachialis muscle, in a caudomedial direction, and tilted enough to allow a lateral approach to the target nerve.
- Check for extravascular needle placement and *avoid injection if resistance is perceived*. If necessary, the needle should be repositioned to obtain a homogeneous distribution around the target nerve.

### Drugs and Volume Administered

- Drug and concentration: bupivacaine 0.5%, ropivacaine 0.5%, levobupivacaine 0.5%.
- Suggested volume: 0.1 mL/kg.

### Scanning of the Radial Nerve

See Figures 30.15 and 30.16.

**Note:** The protocol generally provides analgesia for up to eight hours. Use gentle pressure on the transducer to avoid collapsing the brachial vein, which can make visualization of the target nerves more difficult and increase the risk of vascular puncture.

## *Ultrasound-guided Musculocutaneous, Median, and Ulnar Nerves Block*

### Ultrasound Probe Placement and Block Technique

- Place the probe on the medial aspect of the brachium, at the level of the middle third, transversal to the longitudinal axis of the humerus (Figure 30.17).
- The brachial artery and vein, the humerus, the brachialis and the accessory head of the triceps brachii muscle can be easily identified at this level (see Figure 30.18).
- Applying color flow Doppler mode can be useful to differentiate vessels from nerves.
- Once the target is identified, the depth and angle of insertion of the needle should be measured.
- The needle is introduced in-plane at the caudal border of the ultrasound.
- Check for extravascular needle placement and *avoid injection if resistance is perceived*. If necessary, the needle should be repositioned to obtain a homogeneous distribution around the target nerve.

### Drugs and Volume Administered

- Drug and concentration: bupivacaine 0.5%, ropivacaine 0.5%, levobupivacaine 0.5%.
- Suggested volume: 0.05 mL/kg, for musculocutaneous nerve and 0.1 mL/kg for median and ulnar nerves.

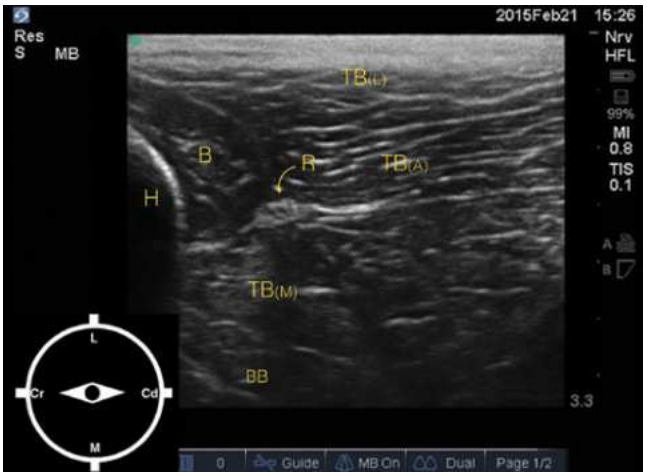


**Figure 30.15.** RUMM block. The acoustic window shows the lateral aspect of the brachium, obtained with a linear probe, placed transversal to the longitudinal axis of the humerus, at the level of its middle third. L, lateral; M, medial; Cr, cranial; Cd, caudal. BM, brachialis muscle; TB(L), triceps brachii muscle (lateral head); TB(A), triceps brachii muscle (accessory head); TB(M), triceps brachii muscle (medial head); BB, biceps brachialis muscle; H, humerus; R, radial nerve. Source: Modified and used with permission from Otero and Portela (2019).

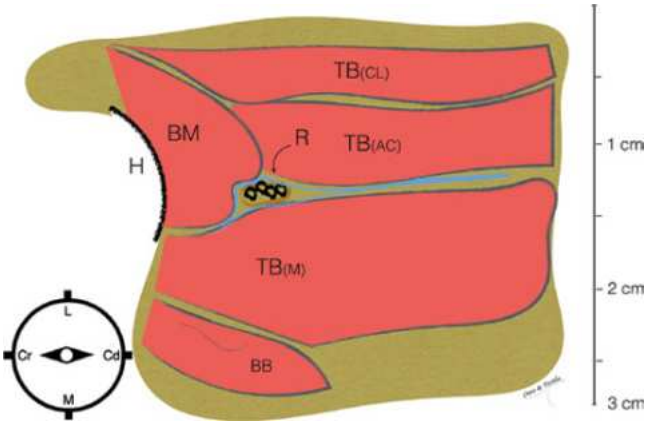


**Figure 30.16.** RUMM block. Schematic illustration of structures present in Figure 30.15. BM, brachialis muscle; TB(L), triceps brachii muscle (lateral head); TB(A), triceps brachii muscle (accessory head); TB(M), triceps brachii muscle (medial head); BB, biceps brachialis muscle; H, humerus; R, radial nerve. Source: Modified and used with permission from Otero and Portela (2019).

**Note:** The protocol generally provides analgesia/anesthesia for up to eight hours.

**Figure 30.17.** RUMM block. Ultrasound probe placement to allow visualization of the musculocutaneous, median, and ulnar nerves in the medial aspect of the brachium. The needle is advanced in-plane, in a caudocranial direction. Source: Reproduced with permission from Otero and Portela (2019).

### Scanning of the Musculocutaneous, Median, and Ulnar Nerves

See Figures 30.18 and 30.19.

## Pearls and Pitfalls, The Final Say

- When performing the subscalene approach, place a cushion under the scapula in contact with the table to facilitate the procedure. This should allow better caudal movement of the limb to be blocked.
- In the axillary space, the axillary fascia is disposed between the nerves, allocating them in different compartments. This might explain an incomplete block when the local anesthetic is administered in a single injection.
- At the level of the axillary space, when the animal is positioned in dorsal recumbency, the axillary artery is located ventral and caudal to the brachial plexus
- Always confirm extravascular positioning of the needle through gentle aspiration and the absence of resistance during injection.
- To perform surgical procedures such as shoulder joint arthroscopy or thoracic limb amputation, the entire brachial plexus should be blocked so the subscalene or paravertebral approach are approach is the indicated technique.

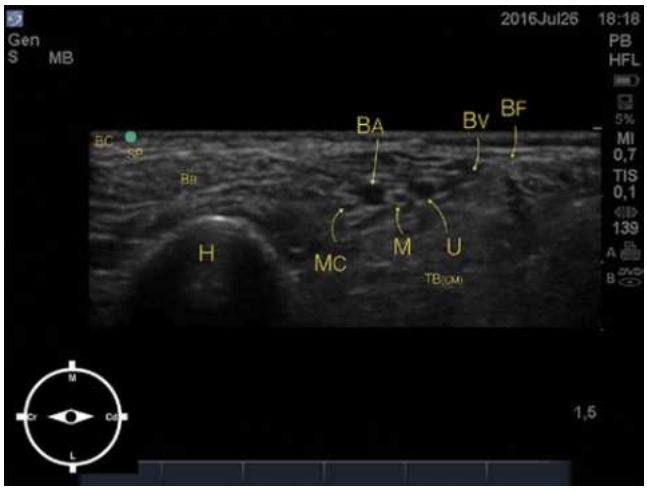


**Figure 30.18.** RUMM block. The acoustic window shows the medial aspect of the brachium obtained with a linear probe, placed transversal to the longitudinal axis of the humerus, at the level of its middle third. L, lateral; M, medial; Cr, cranial; Cd, caudal. BC brachiocephalicus muscle; SP, superficial pectoral muscle; BB, biceps brachii muscle; TB(M), triceps brachii muscle (medial head); H, humerus; BF, brachial fascia; BA, brachial artery; BV, brachial vein; MC, musculocutaneous nerve; M, median nerve; U, ulnar nerve. Modified and used with permission from Otero and Portela 2019.

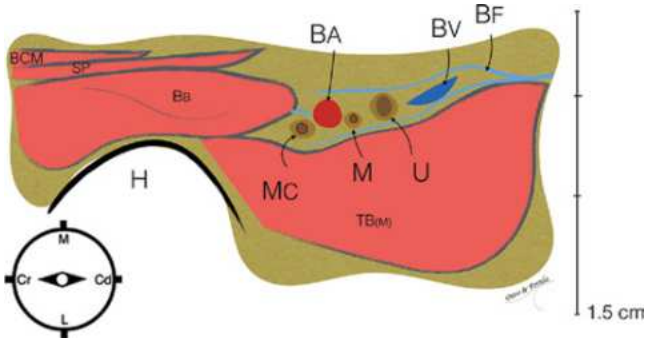


**Figure 30.19.** RUMM block. Schematic representation of structures present in Figure 30.18. BC brachiocephalicus muscle; SP, superficial pectoral muscle; BB, biceps brachii muscle; TB(M), triceps brachii muscle (medial head); H, humerus; BF, brachial fascia; BA, brachial artery; BV, brachial vein; MC, musculocutaneous nerve; M, median nerve; U, ulnar nerve. Source: Modified and used with permission from Otero and Portela (2019).

- To perform surgical procedures involving the brachium such as a humeral fracture or soft tissue intervention, a subscalene approach is the indicated technique.
- To perform surgical procedures involving the elbow and antebrachium, an axillary approach is the indicated technique.
- The RUMM block can be used to provide analgesia in surgeries involving the antebrachium, carpus, and digits.

# References

Ansón A, Laredo FG, Gil F, et al. 2015. Comparison of two techniques for ultrasound-guided axillary brachial plexus blockade in cats. *J Feline Med Surg* 17(6):476–485.

Bagshaw HS, Larenza MP, Seiler GS. 2009. A technique for ultrasound-guided paravertebral brachial plexus injections in dogs. *Vet Radiol Ultrasound* 50:649–654.

Campoy L, Bezuidenhout AJ, Gleed RD, et al. 2010. Ultrasound-guided approach for axillary brachial plexus, femoral nerve, and sciatic nerve blocks in dogs. *Vet Anaesth Analg* 37:144–153.

Castiñeiras D, Viscasillas J, Seymour C. 2015. A modified approach for performing ultrasound-guided radial, ulnar, median and musculocutaneous nerve block in a dog. *Vet Anaesth Analg* 42:659–661.

Evans HE, de Lahunta A. 2013. Spinal nerves. In: *Miller's Anatomy of the Dog*, 4th edition, edited by Evans HE, de Lahunta A. St Louis: Saunders Elsevier, pp 611–657.

Fuensalida SE, Ceballos M, Verdier N, et al. 2017. Sonographic evaluation of diaphragm function during a subscalene brachial plexus block in dogs: technique and clinical applications. Proceedings of the Spring Meeting of the Association of Veterinary Anaesthetists, Manchester, UK. *Vet Anaesth Analg* 44:983–988.

Otero PE, Portela DA. 2019. *Manual of Small Animal Regional Anesthesia: Illustrated Anatomy for Nerve Stimulation and Ultrasound-Guided Nerve Blocks*, 2nd edition, edited by Otero PE, Portella DA. Buenos Aires: Inter-Médica S.A.I.C.I.

Otero PE, Fuensalida SE, Briganti A. 2017. Ultrasound-guided subscalene brachial plexus block in dogs: a cadaveric study. Proceedings of the Spring Meeting of the Association of Veterinary Anaesthetists, Manchester, UK. *Vet Anaesth Analg* 44:983–988.

Portela DA, Raschi A, Otero PE. 2013. Ultrasound guided mid-humeral block of the radial, ulnar, median and musculocutaneous (RUMM block) nerves in a dog with traumatic exposed metacarpal luxation. *Vet Anaesth Analg* 40:552–554.

# Further Reading

Ansón A, Gil F, Laredo FG, et al. 2013. Correlative ultrasound anatomy of the feline brachial plexus and major nerves of the thoracic limb. *Vet Radiol Ultrasound* 54:185–193.

Ansón A, Laredo FG, Gil F, et al. 2017. Evaluation of an ultrasound-guided technique for axillary brachial plexus blockade in cats. *J Feline Med Surg* 19(2):146–152.

CHAPTER THIRTY-ONE

# POCUS: Nerve Blocks – Pelvic Limb

Pablo E. Otero and Diego A. Portela

## Introduction

Peripheral nerve blocks of the hindlimb are indicated for numerous clinical and surgical procedures, and they can in some cases replace neuraxial anesthesia techniques. The nerves that innervate the hindlimb, mainly the femoral and sciatic nerves, can be blocked from their emergence from the intervertebral foramen to their distal branches in the thigh region. The specific nerve to be blocked should be chosen according to the area to be desensitized. The use of POCUS nerve blocks and the use of ultrasound for visualizing structures may reduce both failure and complication rates associated with many of the blind techniques.

### What POCUS Nerve Blocks – Pelvic Limb Can Do

- Can assist with accurately performing nerve blocks over blind techniques.
- Can help reduce complications by imaging nearby structures such as vessels and body cavities, and other structures to be avoided.

### What POCUS Nerve Blocks – Pelvic Limb Cannot Do

- Cannot replace the need for familiarity with the involved anatomy at each nerve block location.
- Cannot replace ultrasound-guided skills and the hand–eye and spatial coordination necessary for needle placement and advancement.

### Indications

- Regional anesthesia of the pelvic limb during procedural anesthetic events, and nonprocedural options for acute and chronic pain (Table 31.1).
- Part of multimodal anesthesia of the pelvic limb.
- Combination of psoas compartment with lumbosacral trunk block is indicated to provide analgesia/anesthesia to the hip, thigh, and knee.
- The combination of femoral and sciatic nerve block is indicated to provide analgesia/anesthesia to the femur area and knee.
- The combination of saphenous and sciatic nerve block is indicated to provide analgesia/anesthesia to the to the knee, tibia and tarsus.

### Objectives

- Be able to identify regional anatomy of the pelvic limb and caudal vertebral column.
- Be able to perform regional blocks of the pelvic limb.
- Know the clinical utility of each of the lumbar plexus nerve blocks, including the psoas compartment nerve block, the femoral nerve block, and the saphenous nerve block.
- Know the clinical utility of each of the sacral plexus nerve blocks, including, the lumbosacral trunk block and the sciatic nerve block
- Be able to choose the correct approach relating to the area to be blocked (Table 31.1).

*Point-of-Care Ultrasound Techniques for the Small Animal Practitioner*, Second Edition. Edited by Gregory R. Lisciandro.
© 2021 John Wiley & Sons, Inc. Published 2021 by John Wiley & Sons, Inc.
Companion website: www.wiley.com/go/lisciandro/ultrasound2

Table 31.1.
Approach to the pelvic limb, where on the pelvic limb analgesia/anesthesia is provided, and important nearby structures.

| Approach | Where analgesia/anesthesia is provided | Important nearby structures | Comments |
|---|---|---|---|
| Psoas compartment block | Hemipelvis and thigh region innervated by the lumbar plexus | Proximal thigh, knee joint | Combined with a parasacral approach to the lumbosacral trunk, produces blockade of the entire pelvic limb, including the hip |
| Femoral/saphenous nerve block | Medial and cranial aspect of the distal thigh, knee joint and medial aspect of the leg | Distal femur and knee joint | The superficial circumflex iliac artery helps to identify the femoral nerve at the femoral triangle |
| Saphenous nerve block distal thigh | Medial and cranial aspect of the distal thigh, knee joint and medial aspect of the leg | Distal femur and knee joint | This block preserves the function of the quadriceps muscle |
| Sciatic nerve lateral thigh | Caudal aspect of the thigh, lateral, cranial and caudal aspect of leg and foot | Caudal knee joint, tarsus, digits (except first) | This block is usually combined with a femoral or saphenous nerve block |

# How to Perform POCUS Nerve Blocks – Pelvic Limb

## *Approaches and Locations*

The femoral nerve can be blocked as it passes through the psoas compartment or when it exits the muscle at the level of the femoral triangle on the medial aspect of the thigh. Additionally, the saphenous nerve, the main sensory component of the femoral nerve, can be blocked during its passage through the medial aspect of the thigh.

## *Relevant Anatomy of the Lumbar Plexus*

- After exiting the intervertebral foramen, the ventral branches of the fourth, fifth, and sixth lumbar spinal nerves penetrate the iliopsoas muscle and interconnect to form the lumbar plexus (Evans and de Lahunta 2013).
- The most important nerves of the lumbar plexus are the femoral and obturator nerves.
- The femoral nerve and its ramification, the saphenous nerve, penetrate the belly of the iliopsoas muscle and course between the sartorius and pectineus muscles, lateral to the iliac fascia in the proximal third of the femoral triangle.
- At the level of the thigh, the saphenous nerve, already separated from the femoral nerve, is located cranial to the femoral artery, sharing the same interfascial space.

## *Materials Needed to Perform Pelvic Limb Blocks*

- Clippers and skin preparation solutions.
- Sterile gloves.
- Sterile drapes.
- Local anesthetic (in sufficient quantity).
- 50 mm 21 gauge isolated unipolar needles (for cats and dogs weighing less than 15 kg).
- 100 mm 21 gauge isolated unipolar needles (for dogs weighing more than 15 kg).
- Sterile transducer (probe) drapes and gel.
- Multiparametric monitor (electrocardiogram [ECG], noninvasive blood pressure [NIBP], pulse oximetry [$SpO_2$], temperature).
- Emergency drugs.

# Ultrasound-guided Femoral Nerve Block in the Psoas Compartment

The ultrasound-guided femoral nerve block in the psoas compartment consists of the injection of local anesthetic between the major and minor psoas muscles, at the level of the seventh lumbar vertebra (L7). Due to its proximity to the femoral nerve, the obturator nerve is blocked when local anesthetic is injected in the psoas compartment (Echeverry et al. 2012a,b; Mahler 2012; Tayari et al. 2017).

**Pearl:** The block of the femoral nerve in the psoas compartment should be combined with the lumbosacral trunk block for most of the procedures of the pelvic limb to guarantee adequate analgesia.

Vetbooks.ir

### Probe Type

- Ultrasound machine with a linear transducer (probe) of ≥10 MHz.
- 1–5cm depth depending on the animal size and nerve to be blocked.

### Ultrasound Probe Placement and Block Technique for the Psoas Compartment

- Place the probe perpendicular to the long axis of the spine in line with the ventral side of the sublumbar muscles at the level of L7 (Figure 31.1).
- Once the probe is in place, the lumbar vertebrae are visualized and, ventral to them, the iliopsoas muscle.
- The iliac artery is an important reference and can be identified medially and ventrally to the psoas compartment (Figures 31.2 and 31.3).
- Once the target is identified, measure the insertion depth using calipers and the centimeter scale on your screen, and calculate the angle of entrance of the needle.
- An in-plane approach is suggested to perform the femoral nerve block in the psoas compartment.
- Check for extravascular needle placement and *avoid injection if resistance is perceived or blood is aspirated*. If necessary, the needle should be repositioned to obtain a homogeneous distribution around the target nerve.

**Pearl:** In order to scan the psoas compartment, the probe should be placed over the abdominal wall, which should be pushed against the sublumbar muscles. Then, the probe should be slid or swept caudally until the body of the lumbar vertebra and the external iliac artery are visualized.

**Pearl:** Ultrasound visualization of the femoral nerve inside the psoas compartment varies according to the probe position. If the scanning is in the cranial aspect of the compartment, the nerve will be seen more dorsal (close to the intervertebral foramina). As the probe is moved caudally, the nerve is identified in the caudoventral quadrant of the iliopsoas muscle.

### Drugs and Volume Administered

- Drug and concentration: bupivacaine 0.5%, ropivacaine 0.5%, levobupivacaine 0.5%.
- Suggested volume: 0.15 mL/kg.

**Note:** This block usually provides analgesia/anesthesia for up to eight hours. *Epidural spread of local anesthetics could result in bilateral pelvic limb blockade.*

**Figure 31.1.** Dog positioned in lateral recumbency with the limb to be blocked uppermost and extended caudally for the ultrasound-guided femoral nerve block through a psoas compartment block. Source: Reproduced with permission from Otero and Portela (2019).

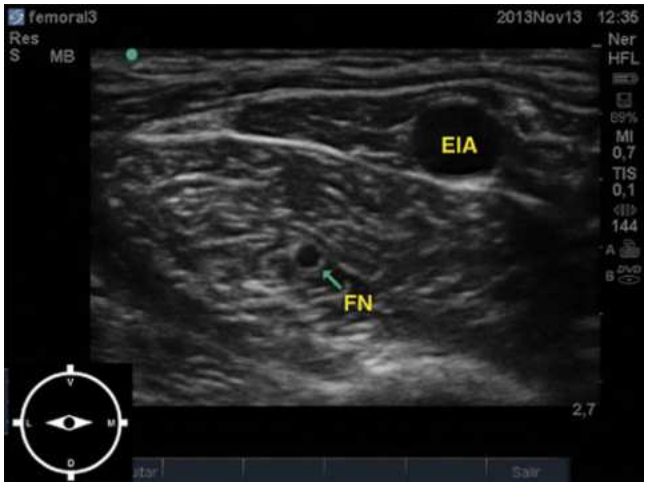


**Figure 31.2.** Ultrasound image of the sublumbar region at the level of L7 obtained with a linear transducer placed over the abdominal wall, orientated perpendicular to the long axis of the spine. L, lateral; M, medial; Cr, cranial; Cd, caudal. FN, femoral nerve; EIA, Source: Modified and used with permission from Otero and Portela (2019).

### Scan of Lumbar Plexus at the Psoas Compartment

The external iliac artery is an important reference easily identified as an anechoic (black) circle and pulsatile structure located in the ventromedial quadrant of the screen. The vertebral body is seen as a hyperechoic (bright white) line and acoustic shadow below. The femoral nerve can be seen inside the belly of the psoas muscle, as a circular hyperechoic

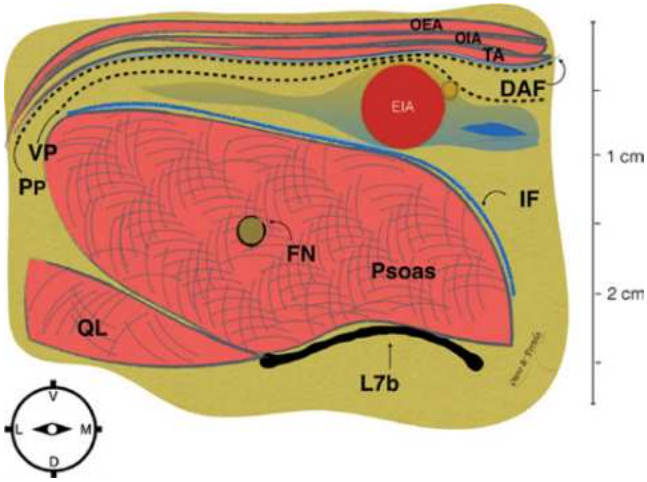


**Figure 31.3.** Schematic illustration of the structures present in Figure 31.2. TA, transversus abdominis muscle; EIA, external iliac artery; OEA, obliquus externus abdominis muscle; OIA, obliquus internus abdominis muscle; DAF, deep abdominal fascia; PP, parietal peritoneum; VP, visceral peritoneum; IF, iliac fossa; QL, quadratus lumborum muscle; FN, femoral nerve; L7b, 7th lumbar vertebra, transverse process. Source: Modified and used with permission from Otero and Portela (2019).

(bright) structure with a hypoechoic (dark) center (see Figures 31.2 and 31.3).

# Ultrasound-guided Femoral Nerve Block in the Inguinal Region

The block of the femoral nerve consists of the injection of local anesthetic on the femoral nerve after exits the psoas compartment and enters the femoral triangle (Campoy et al. 2010; Echeverry et al, 2010).

**Pearl:** Injections performed distally to the bifurcation of the saphenous nerve can produce blockade of the main muscular component of the femoral nerve without affecting the saphenous nerve (Evangelista et al. 2017).

**Pearl:** Block of the femoral nerve in the femoral triangle should be combined with block of the sciatic nerve for most procedures of the hindlimb to guarantee adequate analgesia.

## *Probe Type*

- Linear transducer (probe) of ≥10 MHz.
- 1–2 cm depth depending on the animal size.

## *Ultrasound Probe Placement and Block Technique*

- Place the probe on the medial aspect of the thigh and center the femoral artery in the middle of the screen (Figure 31.4).
- Identify the iliac fascia below the femoral vessels.
- Once the nerve complex is identified in a craniolateral position in relation to the femoral artery, perform the block as close as possible to the belly of the psoas muscle.
- Introduce the needle from the cranial border of the probe, and advance it through the belly of the sartorius muscle in a craniocaudal direction.
- Once the tip of the needle is on the target nerve and after negative aspiration has been obtained, inject an aliquot of the calculated volume. This should be observed as an anechoic (black) image that distributes around the nerve seen in real time.

**Pearl:** When this block is performed through an inguinal approach, it is necessary to inject the anesthetic after puncturing the iliac fascia. *Injection above the fascia will result in a perivascular distribution and block failure.*

**Figure 31.4.** Position of the linear transducer to visualize the femoral nerve in the inguinal region. The probe is placed perpendicular to the long axis of the limb, on the proximal area of the femoral triangle. The needle is introduced in an in-plane approach and advanced in a craniocaudal direction through the belly of the sartorius muscle. Source: Reproduced with permission from Otero and Portela (2019).

### Drugs and Volume Administered

- Drug and concentration: bupivacaine 0.5%, ropivacaine 0.5%, levobupivacaine 0.5%.
- Suggested volume: 0.1 mL/kg.

**Note:** This block usually provides analgesia/anesthesia for up to eight hours. Motor weakness of the quadriceps muscle is generally observed after this block. The superficial circumflex iliac artery is located medially (superficially) to the femoral nerve and can be used as a landmark to identify the femoral nerve at the femoral triangle (Garcia-Pereira et al. 2018).

### Scan of the Femoral Triangle

The femoral artery is identified as a pulsatile anechoic (black) round structure in between the medial femoral fascia and the iliac fascia. The femoral nerve is located below (lateral to) the caudal portion of the sartorius muscle, *always* cranial and lateral to the femoral artery, and in its own interfascial space. It is always slightly more echogenic than the surrounding structures (Figures 31.5 and 31.6).

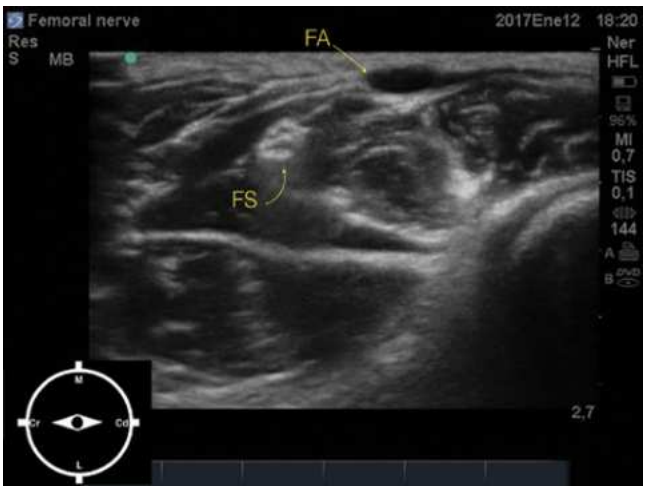


**Figure 31.5.** Ultrasound view of the inguinal region, obtained with a linear probe placed on the proximal area of the femoral triangle, orientated perpendicular to the long axis of the limb. L, lateral; M, medial; Cr, cranial; Cd, caudal. FS, femoral-saphenous nerve complex; FA, femoral artery. Source: Modified and used with permission from Otero and Portela (2019).

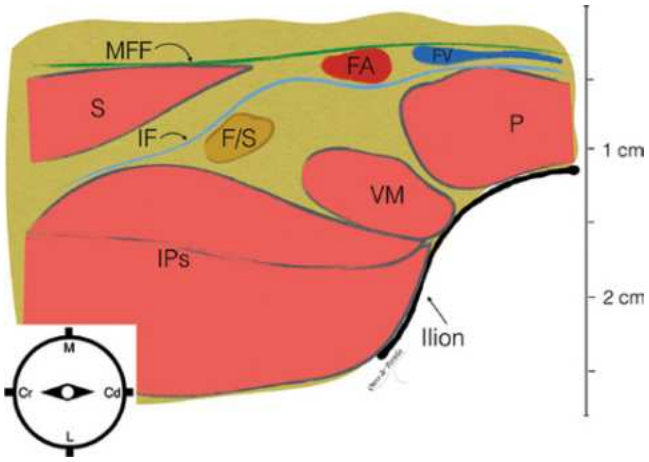


**Figure 31.6.** Schematic illustration of the structures present in Figure 31.5. MFF, medial femoral fascia; S, sartorius muscle (caudal portion); FA, femoral artery; FV, femoral vein; IF, iliac fascia; FS, femoral-saphenous nerve complex; P, pectineus muscle; VM, vastus medialis muscle; IPs, iliopsoas muscle. Source: Modified and used with permission from Otero and Portela (2019).

## Ultrasound-guided Saphenous Nerve Block in the Distal Thigh Region

The saphenous nerve, the main sensory branch of the femoral nerve, can be blocked in the middle third of the thigh region, where it shares the same interfascial space with the femoral artery, to provide analgesia of the stifle without affecting the motor function of the quadriceps muscle (Shilo et al. 2010; Costa-Farré et al. 2011).

### Probe Type

- Linear transducer (probe) of ≥10 MHz
- Depth set at 1.5–2 cm.

### Ultrasound Probe Placement and Block Technique

- Place the probe perpendicular to the long axis of the limb, on the medial aspect of the thigh, at the junction between the proximal and middle thirds (Figure 31.7).
- Identify the femoral artery and move the probe to place it in the center of the image (Figure 31.8).
- The saphenous nerve runs cranial to the femoral artery, until it branches at the level of midthigh.

**Figure 31.7.** Dog positioned in lateral recumbency for the ultrasound-guided saphenous nerve block. The limb to be blocked is placed uppermost, abducted 90° and extended caudally. The probe is placed perpendicular to the long axis of the limb, at the level of the middle third of the femur. The needle is introduced in-plane and advanced in a craniocaudal direction. Source: Reproduced with permission from Otero and Portela (2019).

**Figure 31.8.** Acoustic window of the inguinal region obtained with a linear probe, placed perpendicular to the long axis of the limb, at the level of the distal third of the femoral triangle. Note the femoral artery and vein and the saphenous nerve cranially. L, lateral; M, medial; Cr, cranial; Cd, caudal. Source: Modified and used with permission from Otero and Portela (2019).

Therefore, it can be blocked at any point from its emergence from the femoral nerve, at the middle third of the femoral triangle, to the articular branch emerging from it.

- Introduce the needle through the quadriceps and advance it in a caudomedial direction through an in-plane approach.
- Once the tip of the needle is on the target nerve and after negative aspiration has been obtained, inject an aliquot of the calculated volume. This should be observed as an anechoic (black) image that distributes around the nerve seen in real time.

**Pearl**: Block of the saphenous nerve is the one most commonly used to provide analgesia of the stifle due to the easy recognition of the reference structures and the angle of entrance of the needle.

### *Drugs and Volume Administered*

- Drug and concentration: bupivacaine 0.5%, ropivacaine 0.5%, levobupivacaine 0.5%.
- Suggested volume: 0.05–0.1 mL/kg.

**Note:** This block could potentially provide analgesia/anesthesia for 12–18 hours. Motor weakness of the quadriceps muscle is not commonly observed with this block because the femoral nerve is not affected by the local anesthetic injection.

**Pearl:** Although ultrasound visualization of the saphenous nerve is not always possible, perivascular injection produces a predictable blockade (Costa-Farré et al. 2011).

### *Scan of the Saphenous Nerve*

The femoral artery is identified as a pulsatile anechoic (black) round structure superficially near the skin. The saphenous nerve can be identified as a small hyperechoic (bright), oval structure, situated immediately cranial to the femoral artery and sharing the same fascial plane (Figures 31.8. and 31.9).

## Ultrasound-guided Sciatic Nerve Block

The sciatic nerve can be blocked as it passes through the medial aspect of the ilium where it is part of the lumbosacral trunk or when it is located on the lateral aspect of the thigh, between the biceps femoris and abductor muscles.

### *Relevant Anatomy of the Sacral Plexus*

The lumbosacral trunk originates from the ventral branches of the sixth and seventh lumbar and first sacral nerves, with a variable contribution of the

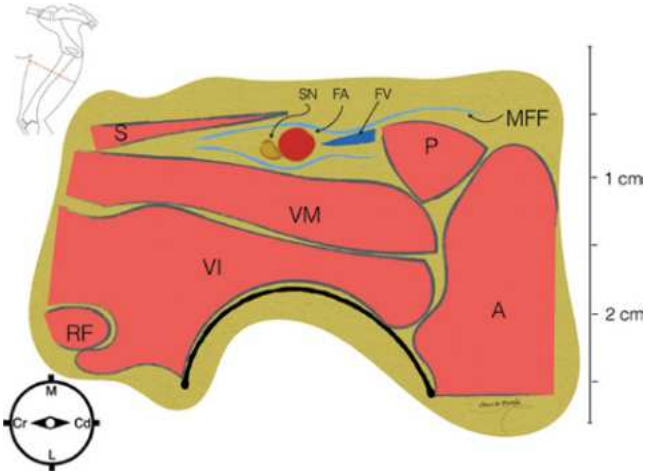


**Figure 31.9.** Schematic representation of the structures presented in Figure 31.8. SN, saphenous nerve; FA, femoral artery; MFF, medial femoral fascia; S, sartorius muscle; P, pectineus muscle; VM, vastus medialis; VI, vastus intermedius; RF, rectus femoris muscle; A, adductor muscle; Source: Modified and used with permission from Otero and Portela (2019).

second sacral nerve (Evans and de Lahunta 2013). Through its intrapelvic path, the lumbosacral trunk is located on the medial aspect of the ilium in relationship with the gluteal vessels under the superficial and medium gluteal muscles. The main nerves arising from the lumbosacral trunk are the sciatic nerve, formed by the tibial and peroneus nerves, the cranial and caudal gluteal nerves, and the caudal cutaneous femoral nerve.

**Pearl:** Blockade of the lumbosacral trunk covers a large area of desensitization, including an important region of the hip and knee joints and the dermatomes, myotomes, and osteotomes of the lateral and posterior aspects of the pelvic limb.

## Ultrasound-guided Lumbosacral Trunk Block

Block of the lumbosacral trunk consists of the injection of local anesthetic on the origin of sciatic nerve involving at the same time the cranial and caudal gluteal nerves and the caudal cutaneous femoral nerve (Shilo et al. 2010).

**Pearl:** To reach the lumbosacral trunk, the block should be performed at the medial aspect of the ilium, at the level of its greater ischiatic notch.

**Pearl:** Block of the lumbosacral trunk should be combined with block of the femoral nerve in the psoas compartment for most procedures of the hip and hindlimb to guarantee adequate analgesia.

### Probe Type

- Linear transducer (probe) of ≥10 MHz for (for cats and dogs weighing less than 15 kg): 2–4 cm depth.
- Microconvex transducer (probe) 5–8 MHz (for dogs weighing more than 15 kg): 3–6 cm depth.

### Ultrasound Probe Placement and Block Technique

- Place the probe perpendicular to the long axis of the ilium over its greater ischiatic notch (Figure 31.10).
- Identify the caudal gluteal vessels and pelvic fascia (Figure 31.11).
- The lumbosacral trunk will be visualized over the medial aspect of the ilium, lateral to the caudal gluteal artery.
- Introduce the needle in-plane through the gluteal muscles from medial to lateral, and advance in a ventrolateral direction.

**Figure 31.10.** Dog positioned in lateral recumbency for a lumbosacral trunk blockade with the limb to be blocked uppermost. The probe is placed perpendicular to the long axis of the ilium, over its greater ischiatic notch. The needle is introduced in an in-plane approach and advanced in a ventrolateral direction through the bellies of the gluteal muscles. Source: Modified and used with permission from Otero and Portela (2019).

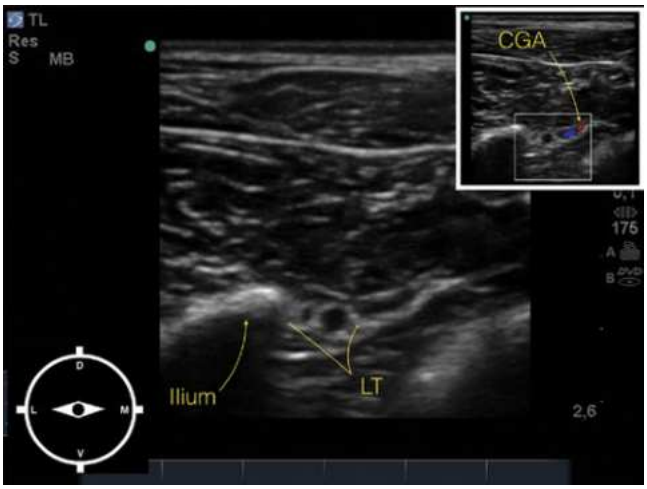


**Figure 31.11.** Acoustic window obtained with a linear probe positioned over the gluteal region, at the level of the greater ischiatic notch, with an orientation transverse to the ilium. In the box, the same view with color Doppler mode, D, dorsal; V, ventral; L, lateral; M, medial; Cr, cranial; Cd, caudal; LT, lumbosacral trunk; CGA, caudal gluteal artery. Source: Modified and used with permission from Otero and Portela (2019).

- Once the tip of the needle is on the target nerve and after negative aspiration has been obtained, inject an aliquot of the calculated volume. This should be observed as an anechoic (black) image that distributes around the nerve seen in real time.

### *Drugs and Volume Administered*

- Drug and concentration: bupivacaine 0.5%, ropivacaine 0.5%, levobupivacaine 0.5%.
- Suggested volume: 0.15 mL/kg.

**Note:** The protocol generally provides analgesia/anesthesia for up to eight hours.

### *Scan of the Lumbosacral Trunk at the Parasacral Space*

The body of the ilium is an important reference easily identified as a hyperechoic line and acoustic shadow located in the lateral quadrant of the screen. The lumbosacral trunk can be seen as a couple of circular hyperechoic (bright) structures with hypoechoic (dark) centers, between the ilium and the gluteal vessels, and surrounded by the pelvic fascia (Figures 31.11 and 31.12).

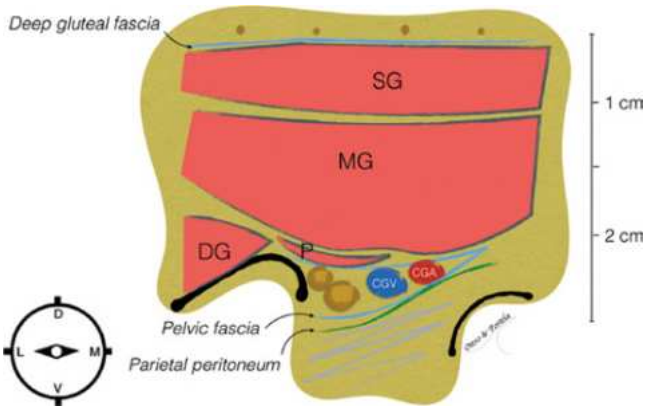


**Figure 31.12.** Schematic representation of the structures presented in Figure 31.11. LT, lumbosacral trunk; SG, superficial gluteal muscle; MG, middle gluteal muscle; DG, deep gluteal muscle; P, piriformis muscle; CGA, caudal gluteal artery; CGV, caudal gluteal vein. Source: Modified and used with permission from Otero and Portela (2019).

## Ultrasound-guided Sciatic Nerve Block in the Lateral Thigh Region

The block of the sciatic nerve is performed immediately distal to the greater trochanter, between the biceps femoris and the abductor muscles in the lateral aspect of the thigh (Campoy et al. 2010; Echeverry et al. 2010).

### *Probe Type*

- Linear transducer (probe) of ≥10 MHz for (for cats and dogs weighing less than 15 kg).
- 2–4 cm depth depending on the size of the animal.

### *Ultrasound Probe Placement and Block Technique*

- Place the probe perpendicular to the long axis of the femur immediately distal to the greater trochanter (Figure 31.13).
- Identify the bellies of the biceps femoris and abductor muscles.
- The sciatic nerve will be visualized in the intermuscular space, caudal to the femur (Figures 31.14).
- Introduce the needle in-plane through the semitendinosus muscle and advance in a caudocranial direction.
- Once the tip of the needle is on the target nerve and after negative aspiration has been obtained, inject an aliquot of the calculated volume. This should be observed as an anechoic (black) image that distributes around the nerve seen in real time (Figure 31.16).

**Figure 31.13.** Dog positioned in lateral recumbency for an ultrasound-guided sciatic nerve block with the limb to be blocked uppermost. The probe is placed perpendicular to the longaxis of the femur, distal to the greater trochanter. The needle is introduced in plane, and advanced in a cranial direction through the semitendinosus muscle, until its tip is positioned close to the perineural tissues. Source: Reproduced with permission from Otero and Portela (2019).

**Figure 31.14.** Acoustic window obtained with a linear probe positioned distal to the greater trochanter of the femur, with a transverse orientation to the long-axis of the limb. L, lateral; M, medial; Cr, cranial; Cd, caudal. BF, biceps femoris muscle A, abductor muscle; SM, semimembranosus muscle; ACC, caudal crural abductor muscle; T, tibial nerve; P, common peroneal nerve. Source: Modified and used with permission from Otero and Portela (2019).

## Drugs and Volume Administered

- Drug and concentration: bupivacaine 0.5%, ropivacaine 0.5%, levobupivacaine 0.5%.
- Suggested volume: 0.05–0.1 mL/kg.

**Note**: The protocol generally provides analgesia/anesthesia for up to eight hours.

## Scan of the Sciatic Nerve at the Lateral Thigh Region

See Figures 31.14 and 31.15.

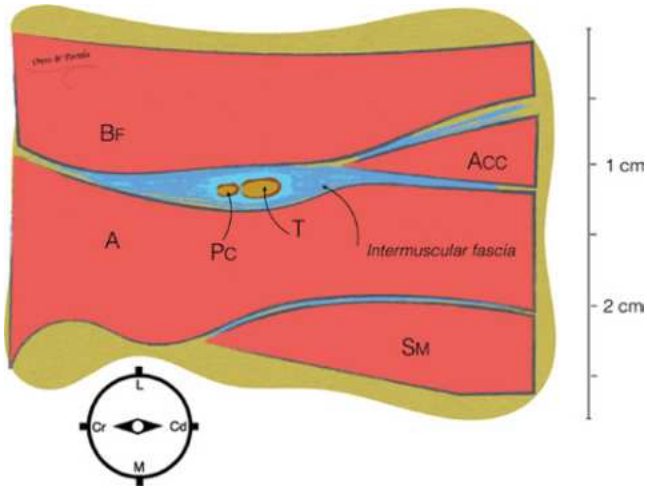


**Figure 31.15.** Schematic representation of the structures presented in Figure 31.14. BF, biceps femoris muscle A, abductor muscle; SM, semimembranosus muscle; ACC, caudal crural abductor muscle; T, tibial nerve; Pc, common peroneal nerve. Source: Modified and used with permission from Otero and Portela (2019).

**Figure 31.16.** Acoustic window obtained with a linear transducer positioned distal to the greater trochanter of the femur, with a transverse orientation to the long axis of the limb. Note the needle in an in-plane approach and deposit of local anesthetic (LA) around the sciatic nerve (ScN). L, lateral; M, medial; Cr, cranial; Cd, caudal. Source: Modified and used with permission from Otero and Portela (2019).

VetBooks.ir

# Pearls and Pitfalls, The Final Say

- Lumbar plexus block combined with a parasacral plexus block can be successfully used for hindlimb amputation.
- These blocks are being used in small animals in lieu of epidural anesthesia with fewer side-effects.
- Invasive surgeries of the pelvic limb can be performed without giving opioids to the animal and still maintain an excellent analgesic plane.
- Lumbar plexus block (i.e., psoas compartment block) produces deep muscular relaxation of the entire limb, so animals should be carefully evaluated during recovery until they can accommodate the limb.
- With practice, the pelvic limb can be blocked in less than five minutes.

# References


Campoy L, Bezeuidenhout AJ, Gleed RD, et al. 2010. Ultrasound-guided approach for axillary brachial plexus, femoral nerve, and sciatic nerve blocks in dogs. *Vet Anaesth Analg* 37(2):144–153.

Costa-Farré C, Blanch XS, Cruz JI, et al. 2011. Ultrasound guidance for the performance of sciatic and saphenous nerve blocks in dogs. *Vet J* 187:221–224.

Echeverry DF, Gil F, Laredo F, et al. 2010. Ultrasound-guided block of the sciatic and femoral nerves in dogs: a descriptive study. *Vet J* 186(2):210–215

Echeverry DF, Laredo FG, Gil F, et al. 2012a. Ventral ultrasound-guided suprainguinal approach to block the femoral nerve in the dog. *Vet J* 192:333–337.

Echeverry DF, Laredo FG, Gil F, et al. 2012b. Ultrasound-guided "two-in-one" femoral and obturator nerve block in the dog: an anatomical study. *Vet Anaesth Analg* 39:611–617.

Evans HE, de Lahunta A. 2013. Spinal nerves. In: *Miller's Anatomy of the Dog*, 4th edition, edited by Evans HE, de Lahunta A. St Louis: Saunders Elsevier, pp 611–657.

Evangelista MC, de Lassalle J, Chevrier C, et al. 2017. Distribution of bupivacaine hydrochloride after sciatic and femoral nerve blocks in cats: a magnetic resonance imaging study. *Res Vet Sci* 115:61–65.

Garcia-Pereira FL, Boruta D, Tenenbaum S, et al. 2018. Ultrasonographical identification of the superficial circumflex iliac artery as a landmark for location of the femoral nerve in the dog. *Vet Anaesth Analg* 45(5):703–706.

Mahler SP. 2012. Ultrasound guidance to approach the femoral nerve in the iliopsoas muscle: a preliminary study in the dog. *Vet Anaesth Analg* 39:550–554.

Otero PE, Portela DA. 2019. *Manual of Small Animal Regional Anesthesia: Illustrated Anatomy for Nerve Stimulation and Ultrasound-Guided Nerve Blocks*, 2nd edition, edited by Otero PE and Portela DA. Buenos Aires: Inter-Médica S.A.I.C.I.

Shilo Y, Pascoe PJ, Cissell D, et al. 2010. Ultrasound-guided nerve blocks of the pelvic limb in dogs. *Vet Anaesth Analg* 37:460–470.

Tayari H, Tazioli G, Breghi G, et al. 2017. Ultrasound-guided femoral and obturator nerves block in the psoas compartment in dogs: anatomical and randomized clinical study. *Vet Anaesth Analg* 44(5):1216–1226.


# Further Reading


Benigni L, Corr SA, Lamb CR. 2007. Ultrasonographic assessment of the canine sciatic nerve. *Vet Radiol Ultrasound* 48:428–433.

Graff SM, Wilson DV, Guiot LP, et al. 2015. Comparison of three ultrasound-guided approaches to the lumbar plexus in dogs: a cadaveric study. *Vet Anaesth Analg* 42:394–404.

Haro P, Laredo F, Gil F, et al. 2013. Ultrasound-guided dorsal approach for femoral nerve blockade in cats: an imaging study. *J Feline Med Surg* 15:91–98.

Haro P, Laredo F, Gil F, et al. 2016. Validation of the dorsal approach for the blockade of the femoral nerve using ultrasound and nerve electrolocation in cats. *J Feline Med Surg* 18:620–625.

Mogicato G, Layssol-Lamour C, Mahler S, et al. 2015. Anatomical and ultrasonographic study of the femoral nerve within the iliopsoas muscle in beagle dogs and cats. *Vet Anaesth Analg* 42:425–432.

CHAPTER THIRTY-TWO

# POCUS: Nerve Blocks – Trunk

Pablo E. Otero and Diego A. Portela

## Introduction

Peripheral nerve blocks of the trunk are indicated to provide perioperative analgesia in animals having intrathoracic, thoracic wall, abdominal or mammary surgery. The nerves involved in the sensory innervation of the abdominal and thoracic wall can be blocked to alleviate pain related to intraabdominal and intrathoracic surgeries, and lesions associated with the abdominal and thoracic wall. Ultrasound guidance is a useful tool for identifying location of these nerves, to monitor needle placement, and visualize local anesthetic spread. The use of POCUS nerve blocks improves success while reducing complications over blind techniques.

### What POCUS Nerve Blocks – Trunk Can Do

- Can assist in accurately performing nerve blocks, reducing the subjectivity of blind technique blocks.
- Can help to reduce complications by visually identifying nearby structures such as blood vessels and body cavities, or other important anatomical structures to be avoided.

### What POCUS Nerve Blocks – Trunk Cannot Do

- Cannot replace the need for familiarity of the anatomy at each nerve block location.
- Cannot replace ultrasound-guided skills and the hand–eye and spatial coordination necessary for needle placement and advancement.

### Indications

- To treat acute or chronic pain originating in the abdominal and thoracic wall, and the peritoneal and pleural cavities.
- Important part of a multimodal anesthetic/analgesic strategy for the trunk.
- The thoracic paravertebral block is indicated to provide analgesia/anesthesia to the thorax (wall and cavity).
- The ultrasound-guided intercostal blocks are indicated to provide analgesia/anesthesia to the thoracic wall and ribs.
- The transversus abdominis plane (TAP) block is indicated to provide analgesia/anesthesia to the abdominal wall and parietal peritoneum.

### Objectives

- Be able to identify regional anatomy of the thoracic and abdominal walls and the associated paravertebral regions of the thoracic and lumbar spine.
- Be able to perform regional blocks of the trunk.
- Know the clinical utility of each of the approaches to block the trunk, including the thoracic paravertebral, intercostal, and transverse abdominal plane blocks (Table 32.1).

*Point-of-Care Ultrasound Techniques for the Small Animal Practitioner*, Second Edition. Edited by Gregory R. Lisciandro.
© 2021 John Wiley & Sons, Inc. Published 2021 by John Wiley & Sons, Inc.
Companion website: www.wiley.com/go/lisciandro/ultrasound2

Table 32.1.
Approach to the trunk, where on the trunk analgesia/anesthesia is provided, and important nearby structures.

| Approach | Where analgesia/ anesthesia is provided | Important nearby structures | Comments |
|---|---|---|---|
| Thoracic Paravertebral Block | Dermatome in concordance with the injected thoracic level | Spinal nerve (dorsal, ventral and sympathetic rami communicans) at the site of injection | This block provides excellent quality of analgesia in animals undergoing thoracotomies |
| Intercostal block | Dermatome in concordance with the intercostal nerve blocked | Intercostal nerve | This block does not provide visceral analgesia. Useful block to alleviate pain from rib fractures |
| Transversus abdomins plane (TAP) block | Dermatomes from T9 to L3 | Abdominal wall and parietal peritoneum | This block provides good-quality postoperative analgesia in patients undergoing laparotomies and mastectomies. It can also be used to provide analgesia in cases with pancreatitis |

# Ultrasound-guided Thoracic and Abdominal Wall Blocks

## *Relevant Anatomy of the Truncal Nerves*

- The thoracic spinal nerves (13 pairs) exit the spinal canal through their respective intervertebral foramina (Evans and de Lahunta 2013).
- When located in the paravertebral space, they have a dorsal branch, a ventral branch, and the ramus communicans of the sympathetic chain (Figure 32.1).
- The ventral branch crosses the paravertebral space to reach the intercostal space as the intercostal nerve.
- Along its route to the ventral midline, the intercostal nerve gives several cutaneous motor and sensory ramifications, the latter responsible for the innervation of the middle and ventral regions of the thoracic wall.
- The communicating branch carries autonomic fibers and connects the spinal nerve with the thoracic sympathetic chain.
- The limits of the thoracic paravertebral space are as follows.
  - Dorsal: internal intercostal membrane.
  - Ventral: parietal pleura.
  - Medial: intervertebral foramen, intervertebral discs, and vertebral bodies.
  - Lateral: there is no clear lateral limit.
- The abdominal wall is innervated by the ventral branches of the caudal intercostal (T9 to T12), costoabdominal, cranial iliohypogastric, caudal iliohypogastric, and ilioinguinal nerves (Evans and de Lahunta).
- The nerves of the abdominal wall run embedded in a fascial plane located between the obliquus internus abdominis and transversus abdominis muscles, known as the transversus abdominis plane (Castañeda-Herrera et al. 2017).

# Ultrasound-guided Thoracic Paravertebral Block

This technique produces an ipsilateral somatic and sympathetic nerve blockade and it is used to provide perioperative analgesia of the thoracic wall and cavity (Monticelli et al. 2017; Portela et al. 2017).

## *Probe Type*

- Linear transducer (probe) of ≥10 MHz for (for cats and dogs weighing less than 30 kg): 2–4 cm depth.
- Microconvex transducer (probe) 5–8 MHz (for dogs weighing more than 30 kg): 4–7 cm depth.

## *Materials Needed*

- Clippers and skin preparation solutions.
- Sterile gloves.
- Local anesthetic (in sufficient quantity).
- 20 gauge 75 mm Tuohy needle attached to an extension line.
- Sterile transducer (probe) drapes and gel.
- Permanent marker.

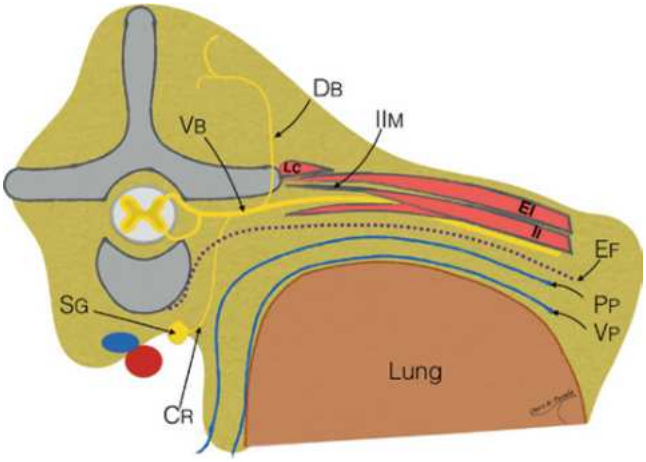


**Figure 32.1.** Truncal anatomy. Schematic of the components of the paravertebral space and the relationship between its anatomical structures. VB, ventral branch of the spinal nerve; DB, dorsal branch of the spinal nerve; IIM, internal intercostal membrane; EF, endothoracic fascia; PP, parietal pleura; VP, visceral pleura; RC, ramus communicans of the sympathetic chain; SG, sympathetic ganglion; LC, levator costae muscle; EI, external intercostal muscle; II, internal intercostal muscle.

- Multiparametric monitor (electrocardiogram [ECG], noninvasive blood pressure [NIBP], pulse oximetry [$SpO_2$], temperature)
- Emergency drugs.

## Ultrasound Probe Placement and Thoracic Paravertebral Block Technique

- Place the probe parallel to the long axis of the spine, close to the dorsal midline, and gradually slide laterally until the two consecutive transverse processes of the respective thoracic paravertebral spaces are included on the screen.
- To allow a better angle for the needle entrance, the probe should be rotated to an oblique orientation to show the transverse process cranially and the neck of the immediately caudal rib (Figure 32.2).
- Once the probe is in place, the following echographic features should be recognized: transverse process, parietal pleura, internal intercostal membrane, and paravertebral space.
- Once the target is identified, measure the insertion depth using calipers and the screen's centimeter scale and calculate the angle of entrance of the needle.
- An in-plane approach is suggested to perform the block.

**Figure 32.2.** Thoracic paravertebral block. Dog positioned in sternal recumbency. The needle is introduced in-plane from the caudal aspect of the transducer (probe) and advanced in a medial-ventral-cranial direction until its tip is positioned between the internal intercostal membrane and the parietal pleura. Source: Modified and used with permission from Otero and Portela (2019).

- The needle is advanced in a medial-ventral-cranial direction until its tip is positioned between the internal intercostal membrane and the parietal pleura.
- Check for extravascular needle placement *and avoid injection if resistance is perceived or blood is aspirated*.

**Pearl:** During local anesthetic injection at the thoracic paravertebral space, a ventral displacement of the pleura during injection is associated with a successful block.

## Drugs and Volume Administered

- Drug and concentration: bupivacaine 0.5%, ropivacaine 0.5%, levobupivacaine 0.5%.
- Suggested volume: 0.05 mL/kg per site.

**Note:** The protocol generally provides analgesia/anesthesia for up to eight hours. An oblique orientation of the transducer (probe) helps to introduce the needle to the desired endpoint.

**Pearl:** The authors currently suggest blocking at *least 3–5 thoracic paravertebral segments* associated with the location of the incision(s) when ultrasound guidance is used in animals undergoing lateral thoracotomies.

### Scan of the Thoracic Paravertebral Space

See Figures 32.3 and 32.4.

# Ultrasound-guided Intercostal Block

The intercostal block consists of injection of a local anesthetic solution alongside the caudal border of the rib, between the internal intercostal muscle and the parietal pleura.

### Probe Type

- Linear transducer (probe) of ≥10 MHz.
- 2–4 cm depth depending on the size of the animal.

### Materials Needed

- Clippers and skin preparation solutions.
- Sterile gloves.
- Local anesthetic (in sufficient quantity).
- 22 gauge 50–75 mm spinal needles.
- Prefilled extension line.
- Sterile transducer (probe) drapes and gel.

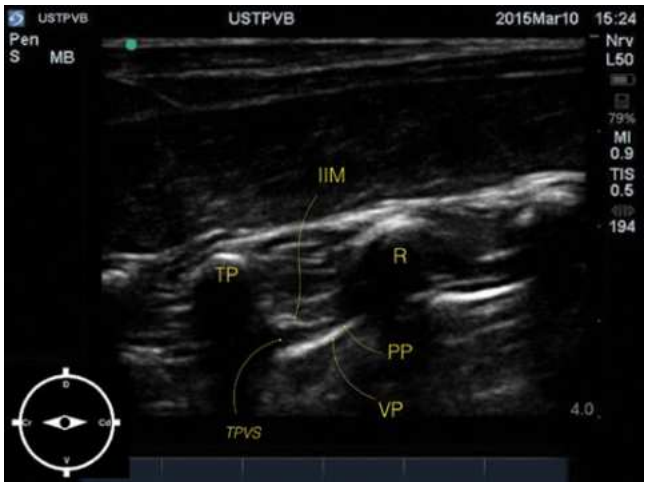


**Figure 32.3.** Thoracic paravertebral block. Acoustic window of the thoracic paravertebral space obtained with a linear probe positioned in a parasagittal, slightly oblique orientation. Note that the oblique orientation will show the transverse process cranially and the neck of the immediately caudal rib. D, dorsal; V, ventral; Cr, cranial; Cd, caudal. TPVS, thoracic paravertebral space; TP, transverse process; R, rib; IIM, internal intercostal membrane; PP, parietal pleura; VP, visceral pleura. Source: Modified and used with permission from Otero and Portela (2019).

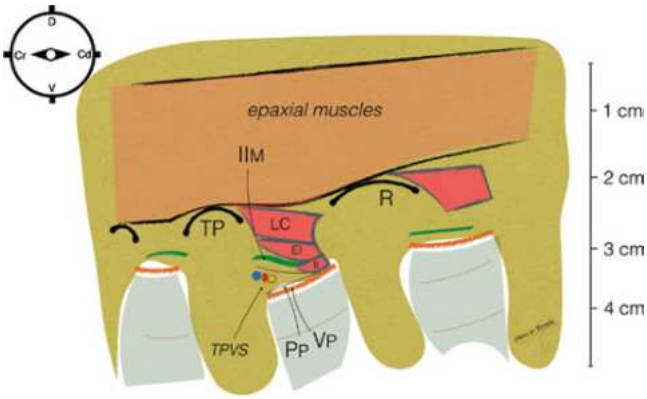


**Figure 32.4.** Thoracic paravertebral block. Schematic illustration of the structures present in Figure 32.3. TPVS, thoracic paravertebral space; TP, transverse process; R, rib; IIM, internal intercostal membrane; PP, parietal pleura; VP, visceral pleura; LC, levatores costarum muscle; EI, external intercostal muscle; II, internal intercostal muscle. Source: Modified and used with permission from Otero and Portela (2019).

- Multiparametric monitor (electrocardiogram [ECG], noninvasive blood pressure [NIBP], pulse oximetry [$SpO_2$], temperature).
- Emergency drugs.

### Ultrasound Probe Placement and Intercostal Block Technique

- Place the probe perpendicularly to the long axis of the rib, at the level of the angle of the rib (Figure 32.5).
- Once the probe is in place, the following echographic features should be recognized: ribs, parietal pleura, internal intercostal muscle.
- The needle is advanced in-plane in a caudocranial direction until its tip is positioned between the internal intercostal muscle and the parietal pleura.
- Check for extravascular needle placement and *avoid injection if resistance is perceived or blood is aspirated*.

### Drugs and Volume Administered

- Drug and concentration: bupivacaine 0.5%, ropivacaine 0.5%, levobupivacaine 0.5%.
- Suggested volume: 0.05 mL/kg per site.

**Note:** The protocol generally provides analgesia/anesthesia for up to six hours.

**Figure 32.5.** Intercostal block. Dog positioned in lateral recumbency for an intercostal block. The needle is introduced in-plane from the caudal aspect of the probe and advanced in a caudocranial direction until its tip is positioned between the internal intercostal muscle and the parietal pleura. Source: Modified and used with permission from Otero and Portela (2019).

**Figure 32.6.** Intercostal block. Acoustic window of the intercostal space obtained with a linear probe positioned perpendicular to the long axis of the rib. In the box, the needle is shown between the internal intercostal muscle and the pleura. L, lateral; Cr, cranial; Cd, caudal; M, medial. EI, external intercostal muscle; II, internal intercostal muscle; IN, intercostal nerve; PP, parietal pleura. Source: Modified and used with permission from Otero and Portela (2019).

**Pearl:** The number of intercostal spaces to be blocked will be determined according to the procedure. The authors currently suggest blocking *at least 3–5 thoracic intercostal segments* when ultrasound guidance is used in animals undergoing lateral thoracotomies.

### *Scan of the Intercostal Space*

See Figures 32.6 and 32.7.

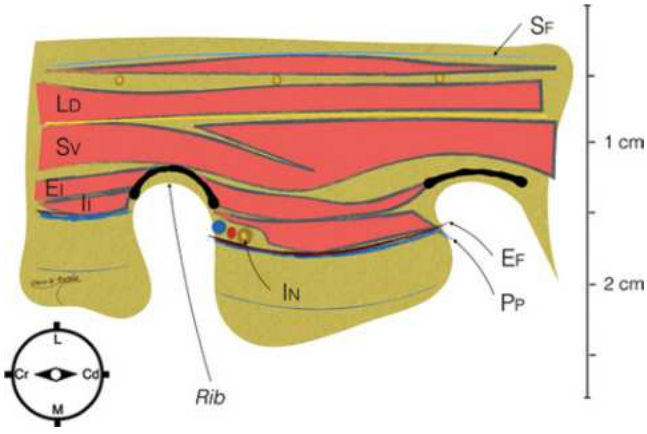


**Figure 32.7.** Intercostal block. Schematic illustration of the structures present in Figure 32.6. EI, external intercostal muscle; II, internal intercostal muscle; IN, intercostal nerve; PP, parietal pleura; LD, longissimus dorsi muscle; SV, serratus ventralis muscle; SF, superficial fascia; EF, endothoracic fascia. Source: Modified and used with permission from Otero and Portela (2019).

# Ultrasound-guided Transversus Abdominis Plane Block

The Transversus abdominis plane (TAP) block consists of guiding the needle with ultrasound to the plane between the transversus abdominis and internal oblique muscles, to block the ventral branches of the thoracic and lumbar nerves involved in the innervation of the abdominal wall (Schroeder et al. 2011; Portela et al. 2014; Drożdżyńska et al. 2017).

### *Probe Type*

- Linear transducer (probe) of ≥10 MHz.
- 2–4 cm depth depending on the size of the animal.

### *Materials Needed*

- Clippers and skin preparation solutions.
- Sterile gloves.
- Local anesthetic (in sufficient quantity).
- 22 gauge 75 mm spinal needles for dogs weighing less than 15 kg and 90 mm for dogs weighing more than 15 kg.

- Prefilled extension line.
- Sterile transducer (probe) drapes and gel.
- Multiparametric monitor (electrocardiogram [ECG], noninvasive blood pressure [NIBP], pulse oximetry [$SpO_2$], temperature).
- Emergency drug.

### Ultrasound Probe Placement and Transversus Abdominis Plane Block Technique

- Place the probe parallel to the caudal edge of the last rib (subcostal approach) and in cranial to the ilium crest (umbilical approach) (Figure 32.8).
- Identify the muscular planes and the parietal peritoneum. Individualize the Transversus abdominis plane.
- The needle enters in-plane until its tip is between the obliquus internus and transversus abdominis muscles.
- Inject a small aliquot to check the instillation site of the anesthetic. In case of an intramuscular injection, withdraw or insert the needle a few millimeters to the targeted place. Repeat this maneuver until the objective is achieved.
- Check the extravascular and extraabdominal position of the needle.
- Inject the calculated volume of local anesthetic in the intermuscular plane. To increase the distribution surface of the anesthetic, the needle can be moved in a caudodorsal direction as the injection is made.

**Pearl:** Among the muscles of the abdominal wall, the internal abdominal oblique is the thickest.

**Pearl:** To desensitize the abdominal wall bilaterally, the transverse abdominal plane procedure should be performed on both hemiabdomens.

### Drugs and Volume Administered

- Drug and concentration: bupivacaine 0.25%, ropivacaine 0.25%, levobupivacaine 0.25%.
- Suggested volume: 0.25–0.3 mL/kg per point accounting for a total volume per animal of 1 to 1.2 mL/kg corresponding.

**Note:** The protocol generally provides analgesia/anesthesia for up to six hours. This block has been also used to provide analgesia in animals suffering from pancreatitis.

**Figure 32.8.** Transverse abdominal plane (TAP) block. Dog positioned in dorsal recumbency for a transversus abdominis plane block. The linear transducer (probe) is positioned caudal and parallel to the last rib for the subcostal approach and then slid caudally to the midabdomen for the midabdominal injection. The needle is introduced in-plane from the cranial edge of the transducer (probe). Source: Reproduced with permission from Otero and Portela (2019).

**Pearl:** Due to the high volume required for bilateral blockade of the abdominal wall (1.0–1.2 mL/kg), it is always recommended to *calculate the maximum dose* allowed for the chosen anesthetic and then complete the volume with a sufficient amount of saline solution. The final concentration will vary but the final dose of local anesthetics will be the same in all animals.

### Scan of the Abdominal Wall

See Figures 32.9 and 32.10.

## Pearls and Pitfalls, The Final Say

- Thoracic paravertebral blocks might require more time to be performed, compared to other blocks, until good skills are developed.
- Thoracic paravertebral blocks usually provide complete analgesia for lateral thoracotomies, significantly reducing the need for opioids in the perioperative period.
- Transversus abdominis plane (TAP) block is a very useful and simple procedure, indicated to control pain after any abdominal surgical procedures, that

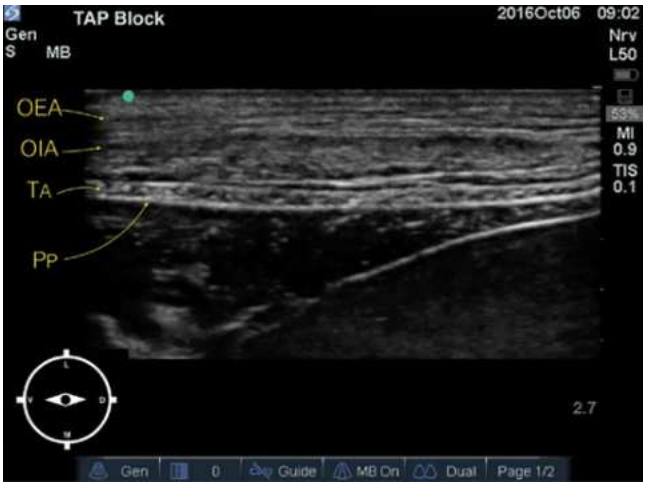


**Figure 32.9.** Transversus abdomins plane (TAP) block. Acoustic window of the abdominal wall obtained with a linear transducer positioned caudal and parallel to the last rib D, dorsal; V, ventral; L, lateral; M, medial. OEA, obliquus externus abdominis muscle; OIA, obliquus internus abdominis muscle; TA, transversus abdominis muscle; RA, rectus abdominis muscle; PP, parietal peritoneum. Source: Modified and used with permission from Otero and Portela (2019).

**Figure 32.10.** Transversus abdomins plane (TAP) block. Acoustic window of the abdominal wall obtained with a linear transducer positioned caudal and parallel to the last rib. Note the needle and the pocket seen after the injection of local anesthetic and watched in real-time. D, dorsal; V, ventral; L, lateral; M, medial. OIA, obliquus internus abdominis muscle; TA, transversus abdominis muscle. Source: Modified and used with permission from Otero and Portela (2019).

should be applied bilaterally and is best performed preoperatively.

- In order to obtain a complete spread to the entire abdomen, two injections per hemiabdomen are recommended: one cranial, caudal and perpendicular to the last rib (subcostal) and the other at the midabdominal region.
- In small dogs and cats, the abdominal wall is very thin, so it is mandatory to introduce the needle very superficially (close to the probe) in order to avoid intraabdominal punctures.
- Transversus abdomins plane block performed after surgery could be more complicated because the pneumoperitoneum could make it difficult to visualize the normal landmarks.

# References

Castañeda-Herrera FE, Buriticá-Gaviria EF, Echeverry-Bonilla DF. 2017. Anatomical evaluation of the thoracolumbar nerves related to the transversus abdominis plane block technique in the dog. *Anat Histol Embryol* 46:373–377.

Drożdżyńska M, Monticelli P, Neilson D, Viscasillas J. 2017. Ultrasound-guided subcostal oblique transversus abdominis plane block in canine cadavers. *VetAnaesth Analg* 44(1):183–186.

Evans HE, de Lahunta A. 2013. Spinal nerves. In: *Miller's Anatomy of the Dog*, 4th edition, edited by Evans HE, de Lahunta A. St Louis: Saunders Elsevier, pp 611–657.

Monticelli P, Jones I, Viscasillas J. 2017. Ultrasound-guided thoracic paravertebral block: cadaveric study in foxes (Vulpes vulpes). *Vet Anaesth Analg* 44(4):968–972.

Otero PE, Portela DA. 2019. *Manual of Small Animal Regional Anesthesia: Illustrated Anatomy for Nerve Stimulation and Ultrasound-Guided Nerve Blocks*, 2nd edition, edited by Otero PE, Portela DA. Buenos Aires: Inter-Médica S.A.I.C.I.

Portela DA, Romano M, Briganti A. 2014. Retrospective clinical evaluation of ultrasound guided Transversus abdomins plane block in dogs undergoing mastectomy. *Vet Anaesth Analg* 41(3):319–324.

Portela DA, Campoy L, Otero PE, et al. 2017. Ultrasound-guided thoracic paravertebral injection in dogs: a cadaveric study. *Vet Anaesth Analg* 44(3):636–645.

Schroeder CA, Snyder LB, Tearney CC, et al. 2011. Ultrasound-guided transversus abdominis plane block in the dog: an anatomical evaluation. *Vet Anaesth Analg* 38(3):267–271.

# Further Reading

Read MR, Schroeder CA. 2013. The trunk. In: *Small Animal Regional Anesthesia and Analgesia*, edited by Campoy L, Read MR. Ames: Wiley-Blackwell, pp 167–198.

CHAPTER THIRTY-THREE

# POCUS: Nerve Blocks – Neuroaxial

Pablo E. Otero and Diego A. Portela

## Introduction

Ultrasound examination of the spine is a valuable tool when performing different regional anesthetic approaches. Ultrasound allows differentiation of the bony structures and the contents of the spinal canal, such as ligaments, meninges, spinal cord, and nerve roots. Additionally, it is useful to determine the path and depth of needle introduction. Neuraxial blocks can be achieved by an intrathecal or an epidural approach. The epidural space can be accessed at different levels such as in the sacrococcygeal, lumbosacral (LS), lumbar or thoracic intervertebral spaces. These approaches are summarized in Table 33.1.

### What POCUS Nerve Blocks – Neuroaxial Can Do

- Can assist in the identification of intervertebral space to perform epidural anesthesia/analgesia through a sacrococcygeal, lumbosacral or thoracolumbar approach.
- Can assist in intrathecal needle placement, avoiding bone contact.
- Can assist epidural/intrathecal injection in patients with abnormal spinal anatomy.
- Provides the only available method for confirmation of epidural/intrathecal drug administration in real time before drug injection.

### What POCUS Nerve Blocks – Neuroaxial Cannot Do

- Cannot replace the need for familiarity with the involved anatomical landmarks.
- Cannot avoid laceration of dura mater during needle handling.
- Cannot replace ultrasound-guided skills and hand–eye and spatial coordination necessary for needle placement and advancement.

### Indications

- Surgeries involving perineal region, tail, pelvic limbs, abdominal wall/cavity, and thoracic wall/cavity.
- Treatment of postoperative pain.
- Treatment of pain associated with traumatic events.
- Treatment of chronic pain.

### Objectives

- Be able to identify regional anatomy of the vertebral column.
- Be able to identify the contents of the spinal canal.
- Be able to guide the needle using an in-plane technique.
- Know the clinical utility of each of the neuroaxial approaches – sacrococcygeal, lumbosacral and thoracolumbar.
- Know the difference between epidural and intrathecal anesthesia/analgesia.
- Understand the "ultrasound-signs" of epidural/intrathecal drug administration; color flow Doppler test, dural sac collapse and enlargement of epidural space.

## Sonoanatomy of the Spine

In order to obtain an adequate ultrasound image of the vertebral canal, the ultrasound beam needs to reach the vertebral canal from dorsal to ventral, regardless

*Point-of-Care Ultrasound Techniques for the Small Animal Practitioner*, Second Edition. Edited by Gregory R. Lisciandro.
© 2021 John Wiley & Sons, Inc. Published 2021 by John Wiley & Sons, Inc.
Companion website: www.wiley.com/go/lisciandro/ultrasound2

Table 33.1.
Approach to the neuroaxial nerve blocks, where analgesia/anesthesia is provided, and important nearby structures.

| Approach | Where analgesia/anesthesia is provided | Important nearby structures | Comments |
|---|---|---|---|
| Sacrococcygeal (SC) | Caudal to the 3rd lumbar vertebra | Perineal region, tail, and pelvic limbs | Due to the lack of dural sac at SC space, dural puncture is not possible |
| Lumbosacral | Caudal to the 3rd lumbar vertebra | Perineal region, tai,l and pelvic limbs | Accidental intrathecal injection is a potential complication |
| Thoracolumbar | From the 5th thoracic to the 3rd lumbar vertebrae | Thoracic and abdominal cavities. The sympathetic innervation is also blocked | Allows segmental anesthesia/ analgesia, without affecting the ability to walk |
| Intrathecal (hyperbaric solutions) | From the 5th thoracic to the 3rd lumbar vertebrae | Thoracic and abdominal cavities. The sympathetic innervation is also blocked | To supplement general anesthesia/ analgesia for thoracoabdominal surgery |
| Intrathecal (isobaric solution) | From the 3rd lumbar vertebra to caudal | Perineal region, tail, and pelvic limbs | To supplement general anesthesia/ analgesia for pelvic and pelvic limb surgery |
| Intrathecal (hypobaric solution) | Nondependent side, from the 3rd lumbar vertebra to caudal | Pelvic limb | To supplement general anesthesia/ analgesia for pelvic limb surgery |

of the probe position. This approach allows the identification of two parallel hyperechoic (bright white) lines flanked by an acoustic shadow produced by the high impedance of the surrounding bones (see Figure 33.3). The hyperechoic line that is observed in the roof of the vertebral canal is the representation of the interarcuate ligament, in close contact with the dura mater, and is called "the dorsal complex (see Figure 33.3)." Occasionally, a hypoechoic (dark) line can be visualized between these structures, which is fatty tissue lodged in the dorsal aspect of the vertebral canal. The line on the floor of the vertebral canal represents the dura mater and the longitudinal dorsal ligament, and is called "the ventral complex" (see Figure 33.3). Due to the scarce adipose tissue in the ventral aspect of the vertebral canal and the weight exerted by the dural sac, these structures are visualized as a single hyperechoic (bright white) line. Depending on the level of the spine scanned, between the dorsal and ventral complexes the subarachnoid space and the spinal cord or cauda equina can be distinguished (Otero et al. 2016; Viscasillas et al. 2016).

**Pearl:** In dogs and cats, ultrasound visualization of the structures within the vertebral canal is only possible through the space between adjacent vertebrae.

**Pearl:** It is important to consider that, due to their impedance, bones are visualized as hyperechoic (bright white) linear structures with compact or clean acoustic shadowing. The ligaments are also hyperechoic (bright white) although less dense than bone images. Fat and cerebrospinal fluid are represented as hypoechoic (dark) due to their very low acoustic impedance.

# Longitudinal Ultrasound Scan of the Lumbosacral Area

A longitudinal ultrasound scan of the vertebral column allows identification of the intervertebral level and direction of the needle when an in-plane neuraxial blockade is performed.

## *Probe Type*

- Linear transducer (probe) of ≥10 MHz for (for cats and dogs weighing less than 20 kg): 2–4 cm depth.
- Microconvex transducer (probe) 5–8 MHz (for dogs weighing more than 20 kg): 4–6 cm depth.

## Materials Needed

- Clippers and skin preparation solutions.
- Sterile gloves.
- Local anesthetic and adjuvants (in sufficient quantity).
- 18 or 20 gauge, 50 or 75 mm Tuohy needle and an extension line.
- Sterile transducer drapes and gel.
- Low-resistance syringe.
- Multiparametric monitor (electrocardiogram [ECG], noninvasive blood pressure [NIBP], pulse oximetry [$SpO_2$], temperature).
- Emergency drugs.

## Ultrasound Probe Placement

- Place the probe over the spinous processes, at the level of the lumbosacral space, with a longitudinal orientation.
- Slide the probe to a parasagittal plane, until the articular processes are visualized.
- Tilt the probe obliquely towards the sagittal plane, in order to obtain an oblique parasagittal view of the vertebral canal (Figure 33.1).
- The typical image of the fusion of the sacral vertebrae and the respective acoustic shadow will be visualized, caudal to the lumbosacral (LS) space (Figure 33.2).

**Figure 33.1.** Dog positioned in sternal recumbency for a longitudinal ultrasound scanning of the LS area. The probe is placed in a sagittal plane, near to midline, and is tilted to obtain an oblique parasagittal view of the vertebral canal. Source: Reproduced with permission from Otero and Portela (2019).

- Once the LS space is identified, if necessary, move the probe cranially or caudally, until the desired intervertebral space is reached.
- The acoustic window should allow visualization of the dorsal and ventral complexes parallel to each other at the same time. This confirms the correct alignment of the probe (Figure 33.3).

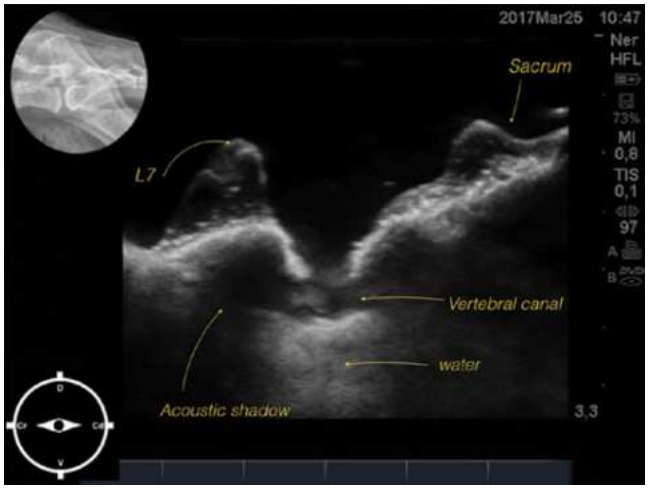


**Figure 33.2.** Water-based phantom and sonograms of the L7 and sacrum spinous processes, articular processes and the lumbosacral space. Cr, cranial; Cd, caudal; V, ventral; D, dorsal. In the box, an X-ray (radiograph) of the area. Source: Modified and used with permission from Otero and Portela (2019).

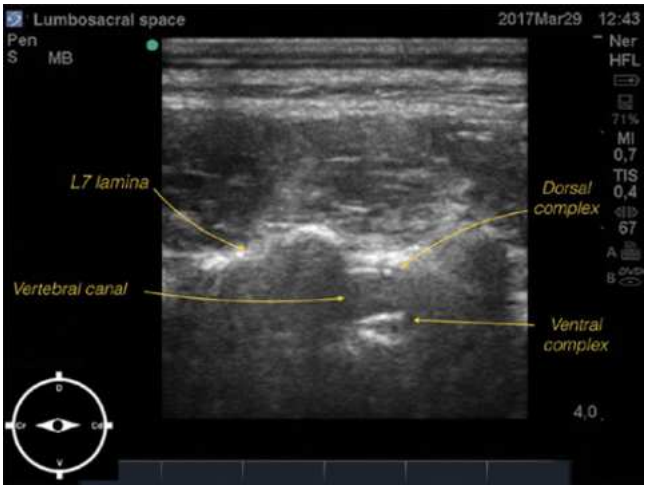


**Figure 33.3.** Acoustic window of an oblique parasagittal view, at the level of the lumbosacral space, performed with a linear probe. Cr, cranial; Cd, caudal; V, ventral; D, dorsal. Source: Modified and used with permission from Otero and Portela (2019).

**Pearl:** To identify an intervertebral space, begin scanning the spine from the LS space and move the probe cranially or caudally to the target position.

# Transverse Ultrasound Scan of the Lumbosacral Area

A transverse ultrasound scan of the vertebral column allows identification of bony structures, the dorsal and ventral borders of the vertebral canal and direction of the tip of the needle when an out-of-plane neuraxial blockade is performed.

**Pearl:** A transverse view of the spinal canal can be used to confirm epidural or intrathecal injections in real time. When a solution is injected into the epidural space, ultrasound allows determination of (1) collapse of the dural sac, (2) enlargement of the epidural space and (3), if color flow Doppler mode is being used, a positive signal. The absence of the aforementioned signs indicates an intrathecal injection or a wrong position of the tip of the needle.

## *Ultrasound Probe Placement*

- Place the probe over the LS intervertebral space, orienting it perpendicularly to the vertebral column and centering it on the midline.
- When the beam is aligned with the interlaminae space, the probe should be tilted cephalad to a 70° angle relative to the spine to improve visualization of the structures inside the vertebral canal (Figure 33.4).
- The acoustic window should allow visualization of the dorsal and ventral complexes. This confirms correct alignment of the probe (Figures 33.5 and 33.6).

**Figure 33.4.** Dog positioned in sternal recumbency for a transverse ultrasound scanning of the LS area. The probe is placed over LS intervertebral space and tilted cephalad to improve visualization of the structures inside the vertebral canal. Source: Reproduced with permission from Otero and Portela (2019).

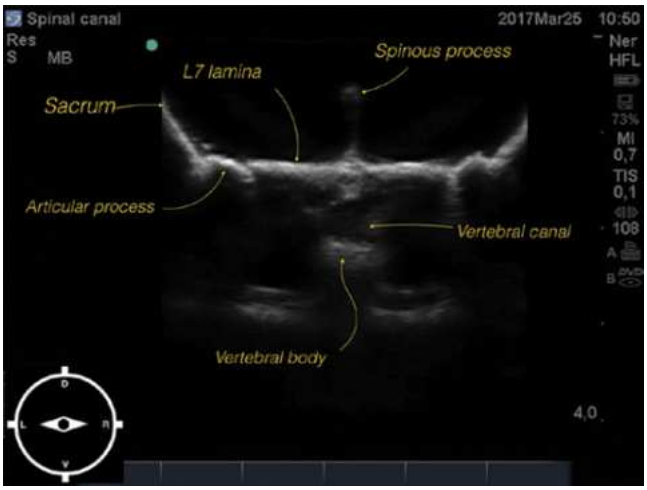


**Figure 33.5.** Water-based phantom and simplified sonogram of the LS intervertebral space and its structures. L, left; R, right; V, ventral; D, dorsal. Compare with an analogous sonogram with anatomy in Figure 33.6. Source: Modified and used with permission from Otero and Portela (2019).

# Longitudinal Scan of the Thoracolumbar Area

A longitudinal scan of the vertebral column at the thoracolumbar area allows visualization of the desired intervertebral level and also allows real-time visualization of the needle when a thoracic epidural in-plane approach is performed (Etienne et al. 2010; Gregori et al. 2014; Liotta et al. 2015).

## *Ultrasound Probe Placement*

- Place the probe over the spinous processes, at the level of T13–L1 or L1–L2 intervertebral spaces, with a longitudinal orientation (Figure 33.7).
- Move the probe to a parasagittal plane, until the articular processes are visualized.

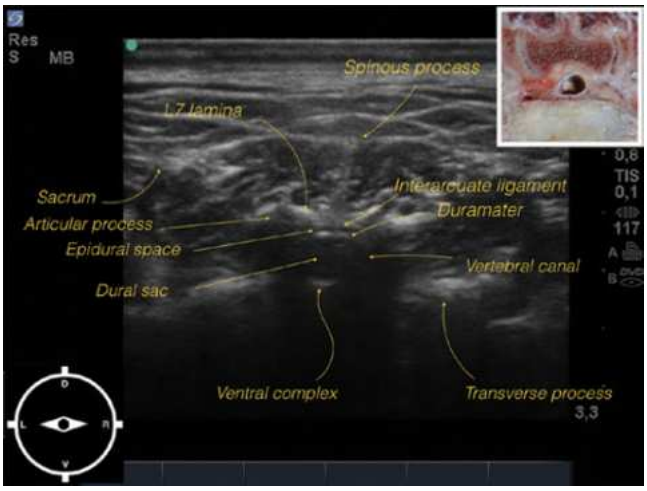


**Figure 33.6.** Acoustic window of a transverse section at the level of the LS space, obtained with a linear probe. L, left; R, right; V, ventral; D, dorsal. In the box is a cross-section of the spine at the LS intervertebral space. Compare to Figure 33.5. Source: Modified and used with permission from Otero and Portela (2019).

**Figure 33.7.** Dog positioned in sternal recumbency for a longitudinal ultrasound scanning of the thoracolumbar area. Source: Reproduced with permission from Otero and Portela (2019).

- Tilt the ultrasound beam towards the sagittal plane to obtain an oblique parasagittal view of the vertebral canal (Figure 33.8).
- At this point, the articular process of the vertebrae and the dorsal and ventral complexes should be identified (Figure 33.9).

## *Ultrasound-guided Epidural Approach*

- Perform a longitudinal scan of the spinal canal at the target intervertebral space and align the probe in order to identify the dorsal and the ventral complexes as two parallel hyperechoic (bright white) lines.
- Introduce a Tuohy needle gently through the epaxial musculature until its tip is located above the interarcuate ligament.
- The site of insertion of the needle as well as its inclination angle will depend on the target site and the technique used (Figures 33.10, 33.11, and 33.12).

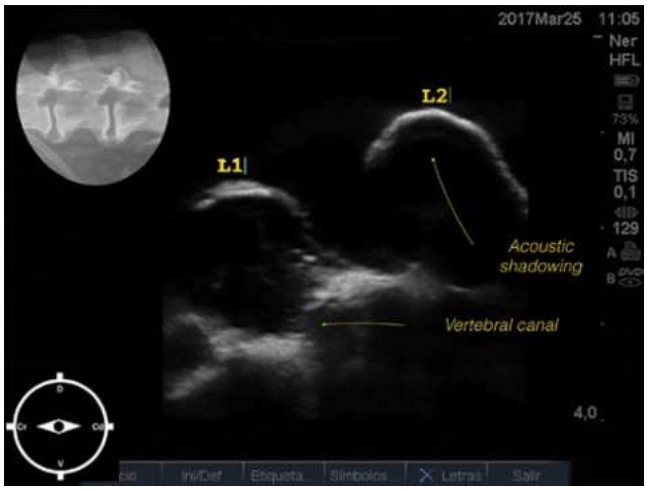


**Figure 33.8.** Water-based phantom and sonograms of the L1–2 intervertebral space. Cr, cranial; Cd, caudal; V, ventral; D, dorsal. Source: Modified and used with permission from Otero and Portela (2019).

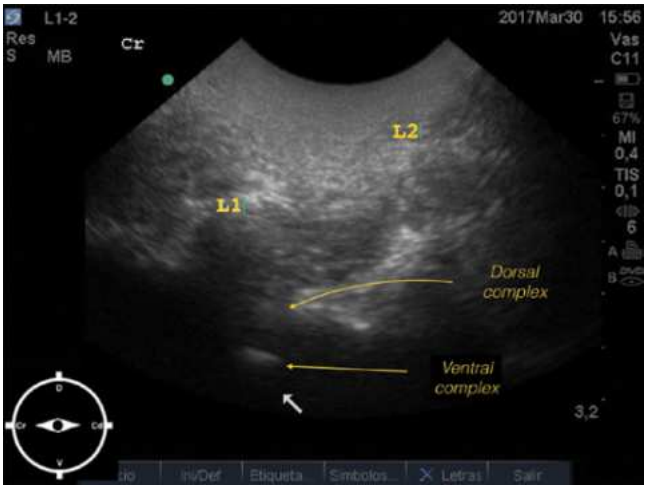


**Figure 33.9.** Acoustic window of an oblique parasagittal section, at the level of the L1–2 intervertebral space, obtained with a convex probe. Cr, cranial; Cd, caudal; V, ventral; D, dorsal. Source: Modified and used with permission from Otero and Portela (2019).

**Figure 33.10.** Ultrasound-guided LS epidural approach. The needle is advanced in-plane. Source: Reproduced with permission from Otero and Portela (2019).

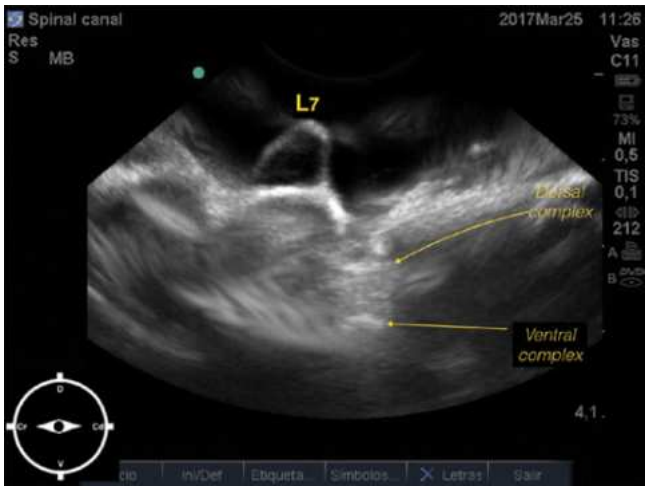


**Figure 33.11.** Acoustic window of an oblique parasagittal section, at the L1–2 intervertebral space, obtained with a microconvex probe. Cr, cranial; Cd, caudal; V, ventral; D, dorsal. Source: Modified and used with permission from Otero and Portela (2019).

- Check for resistance to injection by pushing the plunger of the low-resistance syringe. To perform this technique, an assistant should hold the probe or check for loss of resistance.
- Advance the needle in order to penetrate the interarcuate ligament by exerting a continuous pressure (40–60 cm$H_2O$) on the plunger of the syringe.
- After piercing the interarcuate ligament, needle advancement should be stopped. perforation of the interarcuate ligament produces a sudden loss of resistance. The jet of fluid that enters the epidural space collapses the dural sac and enlarges the epidural space considerably.
- After confirming absence of blood or cerebral spinal fluid (CSF) flow through the hub of the needle, inject the solution at a rate of 0.15 mL/sec.

**Figure 33.12.** Ultrasound-guided thoracolumbar approach. The needle is introduced in a parasagittal approach between the first and second lumbar vertebrae and advanced in a craniomedial direction, with an inclination of 45° to the skin and 15° to the dorsal midline (*upper box*). In the lower box is the ultrasound image (the yellow line indicates the path of the needle).

**Pearl:** During ultrasound scanning of the lumbar and thoracic spine, animals should be placed in the position in which the block will be performed, which is most commonly sternal recumbency.

**Pearl:** For ultrasound-guided neuraxial blocks, the authors recommend using a microconvex probe (5–8 MHz) to guide the needle, because this will facilitate recognition of reference structures and the handling of the needle.

## *Ultrasound-guided Lumbosacral Epidural Approach*

In order to perform a LS epidural injection, a Tuohy needle should be introduced and advanced in a caudocranial direction with an angle of 60° in relation to the skin. During needle advancement, the tip of the needle as well as the interarcuate ligament should be continuously visualized. Due to the relatively large space

between L7 and S1 vertebrae, the landmarks are easy to recognize. See Figures 33.10 and 33.11 for details.

### Ultrasound-guided Thoracolumbar Epidural Approach

In order to access the epidural space through the L1–2 intervertebral space, the operator should use a Tuohy needle and advance it in a caudocranial direction with an angle of 45° in relation to the skin and 15° to the dorsal midline. During needle advancement, the tip of the needle as well as the interarcuate ligament should be continuously visualized. Due to the relatively small space between the lumbar vertebrae and the inclination of the spinous processes, the landmarks are difficult to recognize (see Figure 33.12).

## Ultrasound-guided Intrathecal Approach

The intrathecal approach is performed through the L5–6 or L6–7 intervertebral spaces. In order to increase the pressure and size of the dural sac, the authors recommend placing the animal in anti-Trendelenburg position of 10° (Figure 33.13).

**Figure 33.13.** L5–6 ultrasound-guided approach using a in-plane technique. The probe is placed on the spinous processes of L5 and L6 with the mark of the probe facing cranially. Once the target space is centered on the screen, the needle is inserted and advanced in a cranial direction with an inclination of 60–80° in relation to the skin, towards the subarachnoid space.

### Probe Type

- Linear transducer (probe) of ≥10 MHz for (for cats and dogs weighing less than 20 kg): 2–4 cm depth.
- Microconvex transducer (probe) 5–8 MHz (for dogs weighing more than 20 kg): 4–6 cm depth.

### Materials Needed

- Clippers and skin preparation solutions.
- Sterile gloves.
- Local anesthetic/analgesic (in sufficient quantity). The density of the final solution should be checked using a portable refractometer.
- 25 gauge × 2″, 22 gauge × 1.5″, 22 gauge × 2.5″ Quincke spinal needles.
- Refractometer.
- Multiparametric monitor (electrocardiogram [ECG], noninvasive blood pressure [NIBP], pulse oximetry [$SpO_2$], temperature).
- Emergency drugs.

### In-plane Approach

- Place the probe over the spinous processes, at the level of the LS space, with a longitudinal orientation.
- Move the probe to a parasagittal plane, until the articular processes are identified
- Tilt the ultrasound probe towards the sagittal plane to obtain an oblique parasagittal view of the vertebral canal.
- The fusion of the sacral vertebrae and the respective acoustic shadow can be visualized caudal to the LS space.
- Once the LS space is identified, move the probe cranially until the desired space is reached (L5–6, L6–7).
- The acoustic window should allow visualization of the dorsal and ventral complexes as they parallel one another at the same time. This indicates correct alignment of the probe (Figure 33.14).
- Introduce the spinal needle gently through the epaxial musculature until its tip enters the vertebral canal and perforates the dura mater.
- Due to the angle of entrance, after perforating the yellow ligament the tip of the needle will be located below the acoustic shadow of the vertebral lamina of L5 and it will not be visualized (Figure 33.15).
- Then, remove the stylet from the spinal needle and check for absence of cerebral spinal fluid (CSF) free flow.

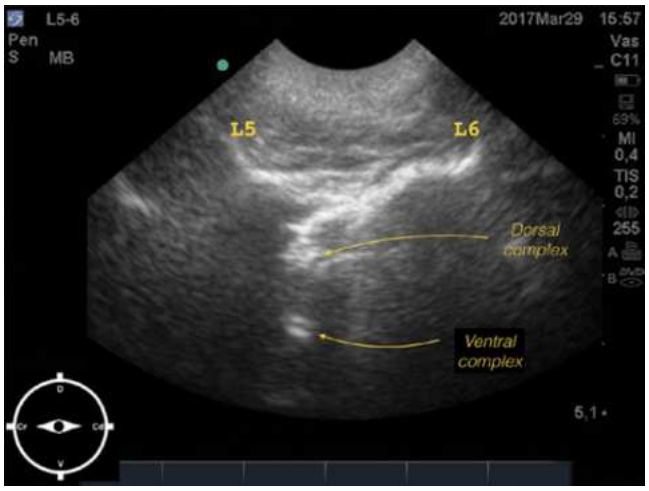


**Figure 33.14.** Acoustic window of an oblique parasagittal section, at the level of the L5–6 intervertebral space, obtained with a convex transducer. Cr, cranial; Cd, caudal; V, ventral; D, dorsal. Source: Modified and used with permission from Otero and Portela (2019).

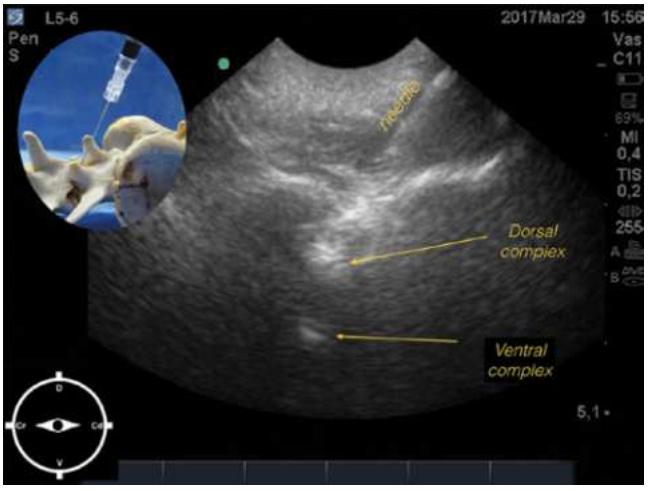


**Figure 33.15.** Ultrasound-guided intrathecal injection at the L5–6 intervertebral space. Note the hyperechoic (bright white) contour of the spinal needle. Cr, cranial; Cd, caudal; V, ventral; D, dorsal. In the box are the bony landmarks. Source: Modified and used with permission from Otero and Portela (2019).

- Depending on the solution to inject, position the animal:
  - in Trendelenburg position (5–10°) if hyperbaric solutions are used
  - with the limb of interest uppermost if hypobaric solutions are used
  - in neutral position if isobaric solutions are used.
- Attach the syringe and inject the anesthetic/analgesic solution.

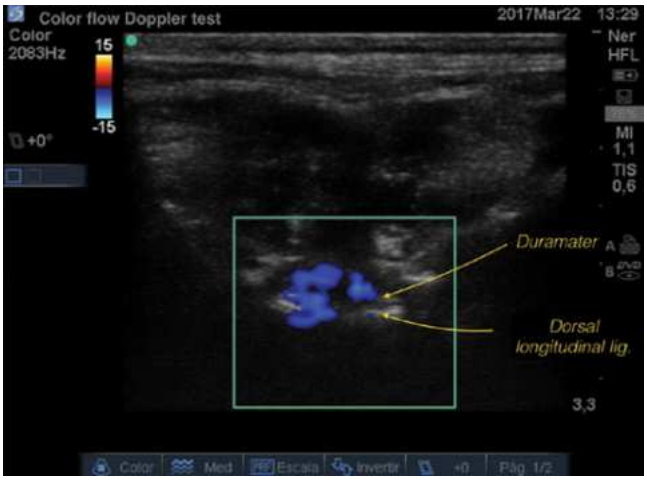


**Figure 33.16.** Acoustic window obtained with a linear probe positioned over the spine, at the level of the LS space with the color Doppler mode on during an epidural injection at the sacrococcygeal space. Source: Modified and used with permission from Otero and Portela (2019).

# Ultrasound Signs of Epidural/Intrathecal Injection

In addition to simplifying access to neuraxial blockade by providing preprocedure scanning of the spinal canal (Karmakar et al. 2009; Chin and Perlas 2011; Chin et al. 2011), real-time assessment of needle placement and spread of injection (Liotta et al. 2015; Vicasillas et al. 2016), ultrasound is a reliable method for unambiguous identification of epidural or intrathecal injection with the presence or absence of a color flow Doppler signal (Tsui et al. 2013; Otero et al. 2016), dural sac collapse, and enlargement of the epidural space.

## *Color Flow Doppler Test*

When ultrasound is performed in color Doppler mode, the epidural injection coincides with the occurrence of a positive Doppler signal that colors the vertebral canal mainly (Figure 33.16). This is due to the turbulent flow experienced by the solution injected at this level. It is important to pay attention to the dorsal and ventral complexes and to confirm passage of the fluid (positive flow color Doppler test) through the epidural space (Tsui et al. 2013; Otero et al. 2016). On the other hand, the injection of fluid into an already fluid-filled area like the subarachnoidal space does not produce coloring of the epidural space. However,

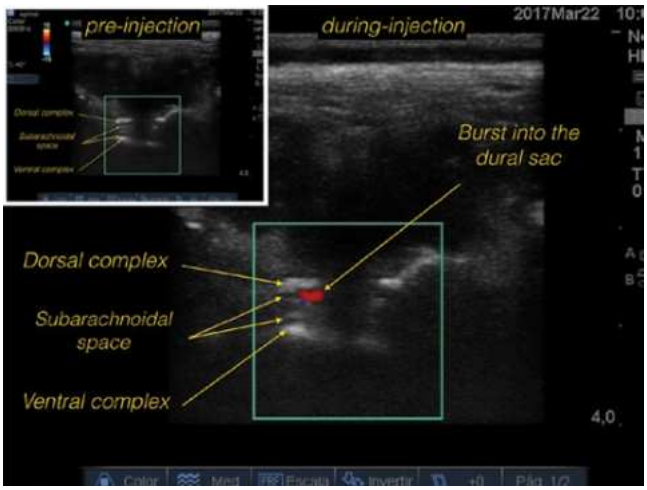


**Figure 33.17.** Acoustic window obtained with a linear probe positioned over the spine, at the level of the L4–5 intervertebral space with the color Doppler mode on during an intrathecal injection performed at the L5–6 intervertebral space. In the box is the same image before the injection. Source: Modified and used with permission from Otero and Portela (2019).

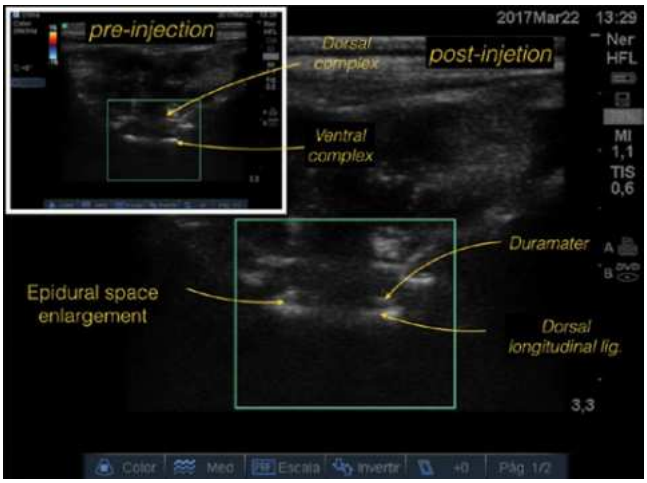


**Figure 33.18.** Acoustic window obtained with a linear probe positioned over the spine, at the level of the LS space after an epidural injection. Note the enlargement of the epidural space, now hypoechoic (dark) due to the presence of liquid. In the box is the same image before the injection. Source: Modified and used with permission from Otero and Portela (2019).

sometimes a weak signal can be seen inside the dural sac that does not compromise the epidural space (Figure 33.17).

### *Collapse of the Dural Sac*

During injection of a solution into the epidural space, the fluid distends the space between the interarcuate ligament and the dura mater. Thus, collapse of the dural sac during injection is a real-time confirmation sign of epidural injection (Otero et al. 2016).

### *Epidural Space Enlargement*

After injection, the fluid remaining in the epidural space can be identified as a typical anechoic (black) pool between the interarcuate ligament and the superficial longitudinal ligaments and the dura mater, and this can be used as confirmation of epidural injection (Otero et al. 2016) (Figure 33.18).

## Pearls and Pitfalls, The Final Say

- Ultrasound offers several advantages when used to guide needle placement for neuraxial anesthesia/analgesia.
- Ultrasound provides real-time images.
- It is noninvasive, safe, and avoids exposure to radiation.
- Ultrasound real-time approaches may be beneficial in animals with abnormal spinal anatomy.
- It has been shown in human medicine that in expert hands, the use of ultrasound for epidural needle insertion reduces the number of puncture attempts, improves the success rate of epidural access on the first attempt, and reduces the need to puncture multiple levels.

## References

Chin KJ, Perlas A. 2011. Ultrasonography of the lumbar spine for neuraxial and lumbar plexus blocks. *Curr Opin Anaesthesiol* 24(5):567–572.

Chin KJ, Karmakar MK, PengP. 2011. Ultrasonography of the adult thoracic and lumbar spine for central neuraxial blockade. *Anesthesiology* 114:1459–1485.

Etienne AL, Peeters D, Busoni V. 2010. Ultrasonographic percutaneous anatomy of the caudal lumbar region and ultrasound-guided lumbar puncture in the dog. *Vet Radiol Ultrasound* 51(5):527–532.

Gregori T, Viscasillas J, Benigni L. 2014. Ultrasonographic anatomy of the sacrococcygeal region and ultrasound-guided epidural injection at the sacrococcygeal space in dogs. *Vet Record* 175(3):68.

Karmakar MK, Li X, Ho AM, et al. 2009. Real-time ultrasound-guided paramedian epidural access: evaluation of a novel in-plane technique. *Br J Anaesth* 102(6):845–854.

Liotta A, Busoni V, Carrozzo MV, et al. 2015. Feasibility of ultrasound-guided epidural access at the lumbo-sacral space in dogs. *Vet Radiol Ultrasound* 56(2):220–228.

Otero PE, Portela DA. 2019. *Manual 0f Small Animal Regional Anesthesia: Illustrated Anatomy for Nerve Stimulation and Ultrasound-Guided Nerve Blocks*, 2nd edition, edited by Otero PE, Portela DA. Buenos Aires: Inter-Médica S.A.I.C.I.

Otero PE, Verdier N, Zaccagnini AS, et al. 2016. Sonographic evaluation of epidural and intrathecal injections in cats. *Vet Anaesth Analg* 43(6):652–661.

Tsui B, Leipoldt C, Desai S. 2013. Color flow Doppler ultrasonography can distinguish caudal epidural injection from intrathecal injection. *Vet Anaesth Analg* 116(6):1376–1379.

Viscasillas J, Gregori T, Castiñeiras D, et al. 2016. Description and evaluation of four ultrasound-guided approaches to aid spinal canal puncture in dogs. *Vet Anaesth Analg* 43(4):444–452.

CHAPTER THIRTY-FOUR

# POCUS: Musculoskeletal – Soft Tissue

Susanne M. Stieger-Vanegas

## Introduction

The skin, soft tissue, and large parts of the musculoskeletal (MSK) system are relatively superficially located compared to visceral organs and are therefore easily accessible using ultrasound. In recent years, ultrasound has gained popularity in evaluation of soft tissues for the presence of lesions, especially tumors. However, soft tissue ultrasound can be used for a wide range of other etiologies, including further evaluation of areas of palpable soft tissue thickening or decrease in soft tissue, areas of abnormal soft tissue function or anatomy, and when the patient has experienced physical trauma (vehicular, ballistic, foreign body, animal abuse, etc.).

The advantages of ultrasound include its wide availability, relatively low cost, the benefit of performing real-time imaging, the ability to perform dynamic evaluations of structures, and the lack of ionizing radiation. Ultrasound can not only differentiate between fluid-filled structures and masses in the soft tissue but can also detect mineralization of or within the soft tissue before it can be detected with radiography or computed tomography. Many lesions have a nonspecific appearance on ultrasound but ultrasound allows better characterization of the soft tissue lesion and, if indicated, provides the ability for ultrasound-guided sampling.

This chapter will cover basic ultrasound imaging of the normal soft tissue including normal expected anatomy of the skin, subcutaneous tissue and fat, muscle, fascia, bone, and salivary glands. Additionally, ultrasound characteristics of abnormalities of soft tissues are described and illustrated.

### *What POCUS Musculoskeletal – Soft Tissue Can Do*

- Provide diagnostic access to a soft tissue structure which is not accessible to direct evaluation.
- Provide anatomical information about soft tissue structures to better formulate a treatment plan and provide prognostic information.
- Help in differentiating between various soft tissue injuries.
- Help in decision making if an immediate intervention is necessary, such as surgical correction of abdominal wall rupture with vascular impaired intestine.
- Allow for ultrasound-guided aspiration of abnormal content such as fluid within or adjacent to soft tissue structures.
- Evaluate soft tissue structures to assess if they move normally. including movement together or independent of each other.

### *What POCUS Musculoskeletal – Soft Tissue Cannot Do*

- Cot substitute for a thorough physical and clinical evaluation as these will guide where the ultrasound examination is to be performed.
- Cannot substitute for lack of anatomical knowledge for the area examined.

*Point-of-Care Ultrasound Techniques for the Small Animal Practitioner*, Second Edition. Edited by Gregory R. Lisciandro.
© 2021 John Wiley & Sons, Inc. Published 2021 by John Wiley & Sons, Inc.
Companion website: www.wiley.com/go/lisciandro/ultrasound2

- Cannot overcome depth limitations of the ultrasound transducer (probe), which may limit access to soft tissue structures deep within the body.
- Cannot overcome physical limitations of ultrasound such as penetration through gas-containing structures, bone, and structures which limit the travel of ultrasound waves and cause strong distal shadowing, such as surgical implants, stones, etc.
- Cannot always differentiate between different etiologies because many pathologies have a similar ultrasound appearance.
- Cannot always replace a musculoskeletal ultrasound study performed by a radiologist or veterinarian specifically trained in musculoskeletal ultrasound. Often a close working relationship with other specialists and a multidisciplinary approach are crucial for successful management and outcome for the patient with soft tissue injuries.

### Indications

Soft tissue injuries can be caused by a wide variety of disease, some of which may occur acutely and some chronically; however, despite being chronic, the patient might present acutely due to pain, swelling, asymmetry or decreased appetite and lethargy similar to an acute injury. Common soft tissue injuries in veterinary patients involve the musculoskeletal system, the thoracic or abdominal wall or superficial soft tissues and can be caused by a wide range of reasons such as traumatic injuries including vehicular, ballistic, foreign body trauma or due to animal abuse. These causes can result in visible superficial injuries or injuries which may not be as easily noted on a physical examination. Performing an ultrasound of an area where pain or swelling is noted on clinical examination or a site of known trauma can provide valuable information complementing the clinical examination. Commonly noted soft tissue injuries include edema, cellulitis, fistulous tracts without or with visible foreign bodies, tendon injuries, and fractures. One of the most common reasons to use ultrasound to evaluate an area of soft tissue injury is to attempt to differentiate between the various types of soft tissue lesions.

### Objectives

The reasons for performing a soft tissue ultrasound include the screening and diagnosis of soft tissue injuries, therefore providing more information about the location, shape, margination, internal characteristics, and vascularity of the lesion. Furthermore, regional lymph nodes may be included in the assessment and this can be helpful in the decision-making process. Thus, ultrasound can provide clinicians with a higher certainty of the extent and type of soft tissue lesion, thus providing a prompt diagnosis, which may alter and improve the management and treatment of a patient.

## Equipment and Settings for POCUS Musculoskeletal – Soft Tissue

Usually minimal preparation of the patient is necessary when performing a soft tissue ultrasound. Preferentially, the ultrasound transducer (probe) with the highest frequency available, providing adequate depth for the anatomy in the area of interest, should be used. In some cases, lower frequency transducers with a smaller contact surface might be used in small patients or in areas with limited physical space to gain good images of the area of soft tissue injury.

It can be useful having a stand-off pad available to increase image depth if very superficial structures are imaged or to compensate and enhance contact in an area of a very uneven surface (see Chapter 35, Figure 35.1). Stand-off pads are made of an acoustically transparent medium. If no stand-off pad is available, ultrasound gel can be placed into a glove and used instead. When using a glove filled with ultrasound gel as a stand-off pad, ensure that only minimal air is mixed into the gel while filling an area of the glove, as the presence of air bubbles results in image degradation.

### Transducer

- Linear array transducer (probe) with a wide range of frequencies.
- A small or large curvilinear transducer with a wide range of frequencies to evaluate deeper soft tissue structures or to access areas where only limited surface contact is available and the larger footprint of the linear transducer limits contact.
- A "hockey stick" transducer often works well where access to an area of interest for ultrasound examination is very small.

### Settings

- Adjustments of gain, frequency, and focal zone are crucial and the focal zone(s) may have to be adjusted frequently during an imaging examination.

- It can be helpful to have a dual image function available so that contralateral structures can be compared at the same time.
- Doppler function, whether conventional, power or microvascular, is helpful to evaluate for vascular flow in a lesion.
- Video capabilities to allow storage of images of areas that were evaluated dynamically or where the lesion extends over a greater length than can be captured in one image.

# Patient Preparation

- Frequently, minimal preparation is necessary.
- Often ultrasound examination does not require anesthesia; some patients require sedation while other patients tolerate the examination well without sedation. However, sedation or anesthesia may be recommended in cases of extensive soft tissue injury for pain management and should be considered before the ultrasound examination is started.
- Depending on the location of the soft tissue, the patient can be placed in dorsal or lateral recumbency. If a lesion of the abdominal wall or inguinal area is suspected, it can be helpful to perform the examination with the patient spatial standing while considering where gravity-dependent regions are located. Standing (or sternal) position may increase abdominal pressure therefore further displacing abdominal organs, which may help in outlining abdominal organs, which move into abnormal locations and help to identify their potential incarceration within a hernia.
- Clipping of the hair in an area of interest to improve transducer (probe) contact, thereby reducing the presence of artifacts and optimizing the image. However, soft tissue ultrasound may be performed without clipping, especially in longer-haired patients, where the hair can be parted to gain direct access to the skin.
- To achieve a good contact between the transducer and skin, 70% isopropyl alcohol should be applied, the hair parted, and ultrasound coupling gel should be used. In patients with skin injuries, sterile water or sterile ultrasound gel or alternatives such as K-Y® jelly, should be used instead of 70% isopropyl alcohol or commercially available ultrasound gel for patient comfort and to prevent wound contamination.
- In patients where fine needle aspirates or biopsies are planned, sterile ultrasound gel can be used or the examination can alternatively be performed using sterile water or 70% isopropyl alcohol.
- When fine needle aspirates or biopsies are performed, clean the patient's skin appropriately with the necessary level of hygiene. Importantly, ultrasound coupling gel during fine needle aspiration or biopsy can cause significant artifacts on cytological specimens (Molyneux and Coghill 1994; Lalzad et al. 2012) and should therefore be removed prior to the fine needle aspiration or biopsy. Sterile saline solution or alcohol can be used to achieve transducer contact.

# How To Do the POCUS Musculoskeletal – Soft Tissue

Once the area of interest is prepared, it is easiest to start the soft tissue ultrasound a short distance away from the area of interest within normal anatomy. As a standard when performing a soft tissue ultrasound, both sagittal and transverse plane images should be acquired. In a sagittal image, the probe is usually oriented towards the patient's head or proximal in the limb. In transverse images, the patient's left side of the image is oriented towards the right side of their body and the opposite for the patient's right side. However, some veterinarians change this based on their preference or dominant hand. Make it a habit to first perform the scan with a higher depth to gain a general overview of the soft tissue lesion and then to zoom in (decrease depth) on the area of interest to best evaluate anatomical detail. Furthermore, the highest frequency possible that provides the necessary depth penetration should be used for optimal detail. Remember that increasing the frequency improves spatial resolution while reducing penetration, whereas lower frequency has better depth penetration with less spatial resolution.

It is important to scan the entire area or lesion until normal anatomy is again noted. When scanning superficial injuries, use only light pressure so that the area of interest is not compressed, which distorts the structure. It is also helpful to hold the transducer (probe) so that part of your hand such as a finger or ulnar aspect of your arm rests on the patient's body, which will help to stabilize the probe during scanning and prevent "drifting" while focusing on the screen (see Chapters 4 and 5) or placing too much pressure on the lesion while scanning.

Additionally, it can be helpful to gently move the area of interest, so that the lesion can be evaluated dynamically. This is especially important in areas where the normal function of structures is disrupted, such as body wall, muscle and tendon injuries.

# Ultrasonographic Findings of Common Soft Tissue Structures

## Dermis and Epidermis

The dermis and epidermis may only be differentiated ultrasonographically if a high-frequency transducer is used. The first layer adjacent to the head of the transducer (probe) is hyperechoic (bright white) and is more correctly termed the "epidermal echo" (Figure 34.1). Deep to the epidermis layer, the dermis is noted, which is heterogeneously hypoechoic (dark) with small hyperechoic reflectors (white) caused by the collagen fibers. Deep to the dermis is the subcutaneous tissue, which is also heterogeneous in echogenicity and hypoechoic relative to the dermis and epidermis.

## Fascia

The fascia is the next deeper layer to the subcutaneous tissue and is usually relatively linear, thin and hyperechoic (see Figure 34.1).

## Muscle

The ultrasonographic appearance of muscle is relatively distinct. Normal muscle is diffusely hypoechoic. In the transverse plane, perpendicular to the long axis of the muscle, the muscle has a speckled appearance (see Figure 34.1).

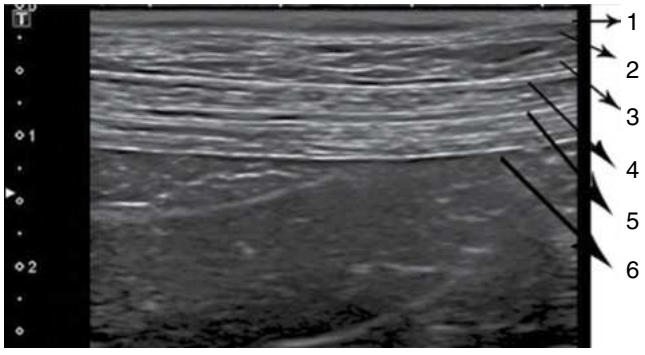


**Figure 34.1.** Normal superficial ultrasound anatomy of the ventral abdominal wall. Longitudinal ultrasound image of the ventral abdominal wall with the individual wall layers and soft tissue structures labeled. 1, ultrasound gel, 2, epidermis/dermis, 3, subcutaneous tissue, 4, muscle fascia, 5, abdominal muscles, 6, fascia/peritoneum.

## Bone

The cortical surface of bone is usually smooth except in areas of attachments of tendons and ligaments. The surface of bone is hyperechoic, causing complete distal acoustic shadowing because ultrasound cannot transmit through bone (see several examples in Chapter 35).

## Salivary Gland

On ultrasound, the normal salivary gland is usually homogeneous and tends to be hyperechoic in comparison to adjacent muscle tissue. Dependent on the fat content of the salivary gland, it might appear more hyperechoic relative to other adjacent structures. The salivary glands are usually well defined from surrounding adjacent soft tissue structures.

### Parotid Salivary Gland

The parotid salivary gland is located cranioventral to the ear and at the cranioventrolateral aspect of the sternomastoideus muscle and has an irregular triangular shape. The excretory duct of the parotid salivary gland runs rostrally and ends opposite the second maxillary molar tooth.

### Mandibular Salivary Gland

The mandibular salivary gland is round to ovoid and is located at the caudoventral angle of the mandible, ventral and often mildly caudal to the parotid salivary gland. The mandibular salivary gland parenchyma is uniformly hypoechoic (Figure 34.2). At the rostroventral aspect of the mandibular salivary gland, the mandibular lymph nodes can be found, which are normally smaller than the adjacent mandibular salivary gland but can be similar in echogenicity. The excretory duct of the mandibular salivary gland exits the hilus of the gland running along the ventrolateral aspect of the mylohyoid muscle and rostrally to the sublingual caruncle, which is a small papilla at the base of the frenulum of the tongue seen on visual and physical examination of this area.

### Sublingual Salivary Gland

The sublingual salivary gland is located at the rostral aspect of the mandibular salivary gland and is smaller and less distinct than the mandibular salivary gland.

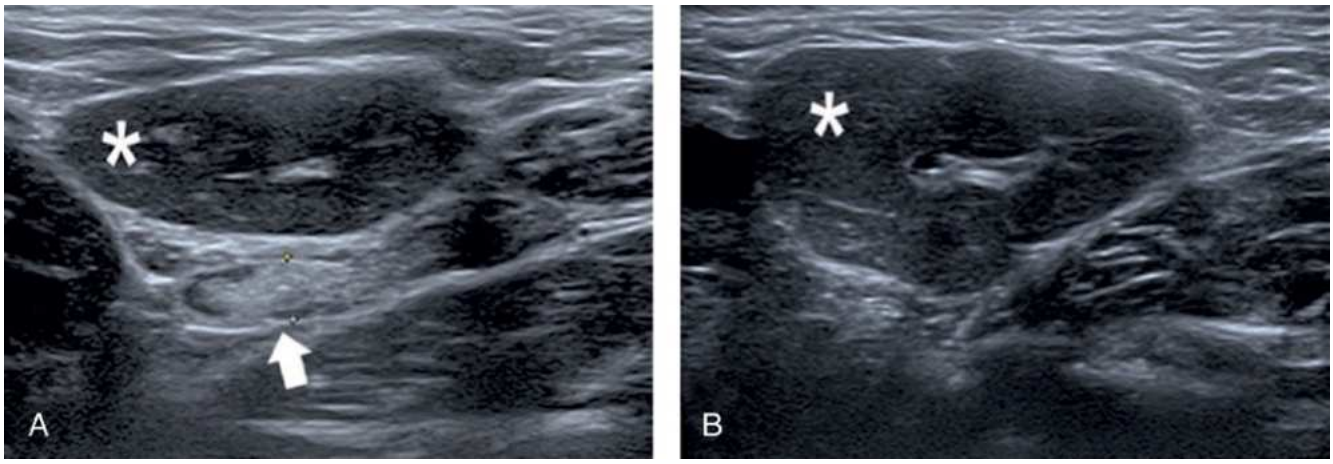


**Figure 34.2.** Normal mandibular salivary gland and medial retropharyngeal lymph node. (A) Longitudinal ultrasound images of the mandibular salivary gland (*asterisk*) with the adjacent normal medial retropharyngeal lymph node (*white arrow*). The mandibular salivary gland has a mildly lobulated border and the parenchyma has uniform echogenicity. The medial retropharyngeal lymph node is mildly heterogeneous in echogenicity and normal in size. (B) Centrally within the salivary gland, the mandibular salivary duct is noted as a small round anechoic structure with mild distal acoustic enhancement.

The dorsal aspect of the sublingual salivary gland is in part covered by the parotid salivary gland. The sublingual salivary gland in the dog has a monostomatic and polystomatic part. The monostomatic aspect of the sublingual and the mandibular gland are in part connected by a common tissue capsule. The monostomatic aspect of the sublingual gland empties into the sublingual duct, which runs together with the mandibular duct rostrally to the sublingual caruncle lateral to the base of the frenulum. The mandibular and sublingual salivary glands may open together or separately at the sublingual caruncle. When separate, the mandibular gland opening tends to be located rostral to the sublingual gland opening.

The rostral, polystomatic aspect of the sublingual salivary gland is strongly lobulated and extends diffusely along the sublingual duct on the medial aspect of the mandible rostrally. The polystomatic aspect of the sublingual gland has multiple small ducts, which empty directly into the oral cavity at the medial aspect of the mandible.

### Zygomatic Salivary Gland

The zygomatic salivary gland is ultrasonographically more challenging to scan because it is located ventromedial to the eye and caudal or adjacent to the zygomatic arch. The salivary duct of the zygomatic gland ends at an opening at the dorsolateral aspect of the maxillary first to second molar teeth adjacent to the opening of the parotid salivary gland.

## Common Soft Tissue Lesions

### *Cellulitis and Edema*

Cellulitis is a frequent pathological condition of the subcutaneous tissues caused by an infection. Cellulitis is usually a clinical diagnosis and patients may present with a focal area of increased temperature (heat), hyperemia, swelling, and leukocytosis. Edema may palpate similarly compared to cellulitis but patients usually do not have a fever, hyperemia, or leukocytosis. Edema is frequently caused by congestive heart failure but can also be secondary to lymphatic disease. The ultrasonographic appearance may vary dependent on the severity and chronicity of the cellulitis or edema but most commonly cellulitis has a heterogeneous echogenicity created by a mixture of hyperechoic and hypo- to anechoic tissue (Figure 34.3) referred to as striated or having a cobblestone appearance in people. Additional features of cellulitis include skin thickening and increased vascularity that may be better detected using color Doppler ultrasound (Figure 34.4). Larger focal fluid accumulations are not typical for either cellulitis or peripheral edema and other conditions such as seroma, abscess, or cystic structures should then be considered.

In summary, cellulitis and edema have similar ultrasonographic findings and the difference between the two is usually based on combining clinical findings and clinical impression.

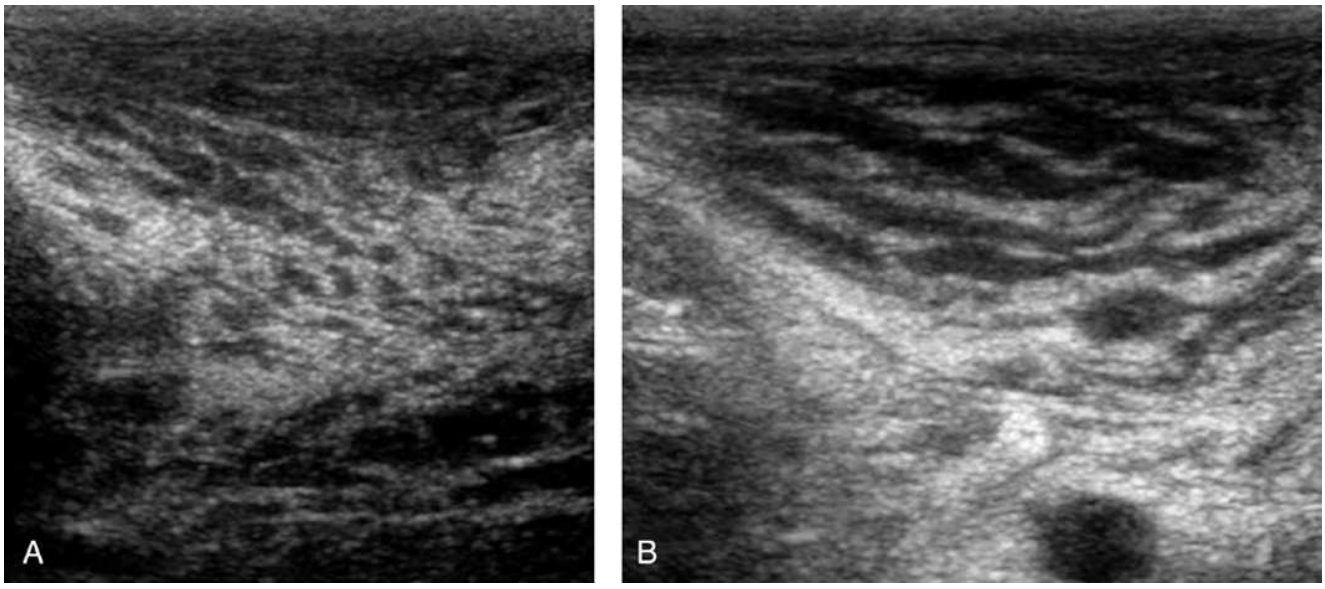


**Figure 34.3.** Cellulitis. (A,B) Classic ultrasound features of cellulitis as noted by the hypoechoic stranding and thickening of the subcutaneous tissue with no cavitary fluid accumulations.

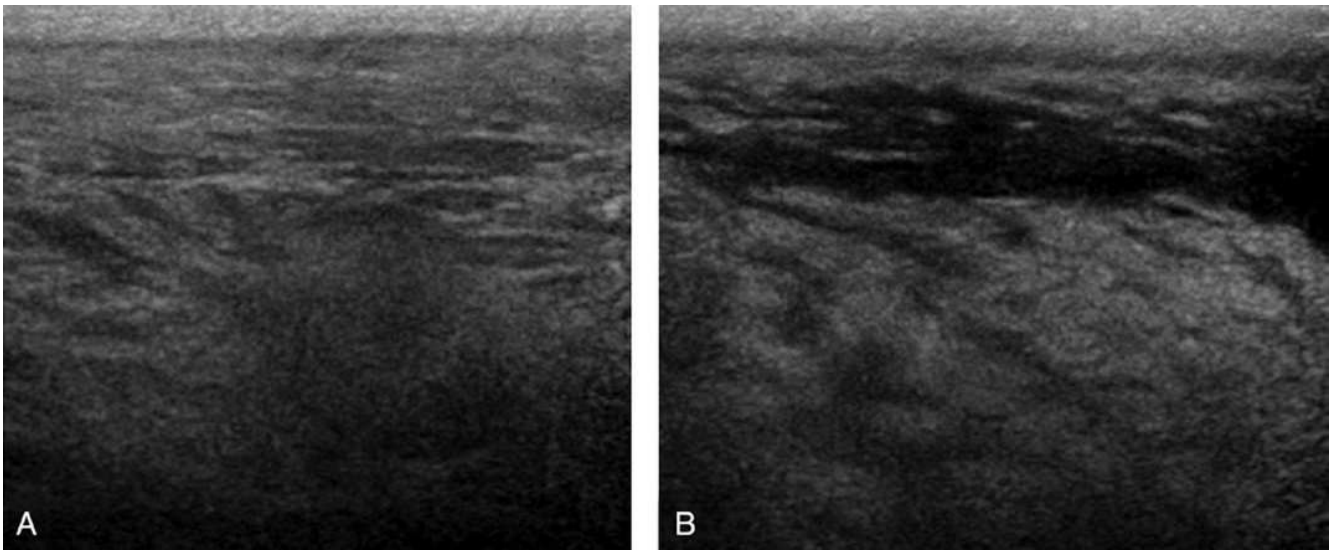


**Figure 34.4.** Cellulitis with suspected abscessation. (A) Longitudinal images of the dermis and subcutaneous tissue reveal a marked thickening of the subcutaneous tissue. Hypoechoic strands are noted throughout the subcutaneous tissue. (B) An indistinct fluid accumulation with ill-defined hypoechoic strands of tissue is noted and local abscessation was suspected. The pattern has been described as a cobblestone appearance in human medicine. Ultrasound-guided fluid sampling was performed with fluid analysis, cytology, and culture confirming the suspicion of abscessation.

## *Seroma*

Seroma is thought to be a local fluid accumulation secondary to a trauma or surgery. Seroma is usually identified by its simple fluid appearance, meaning the fluid is anechoic (black), with either no wall or a thin, hyperechoic circumferential wall surrounding the seroma (Figure 34.5). Remember that distal to a fluid-filled structure such as a seroma, distal acoustic enhancement will be noted. Postsurgical seroma formation occurs frequently and it is important to evaluate if suture dehiscence occurred or if there is any infection at the surgical site. Infected seromas may

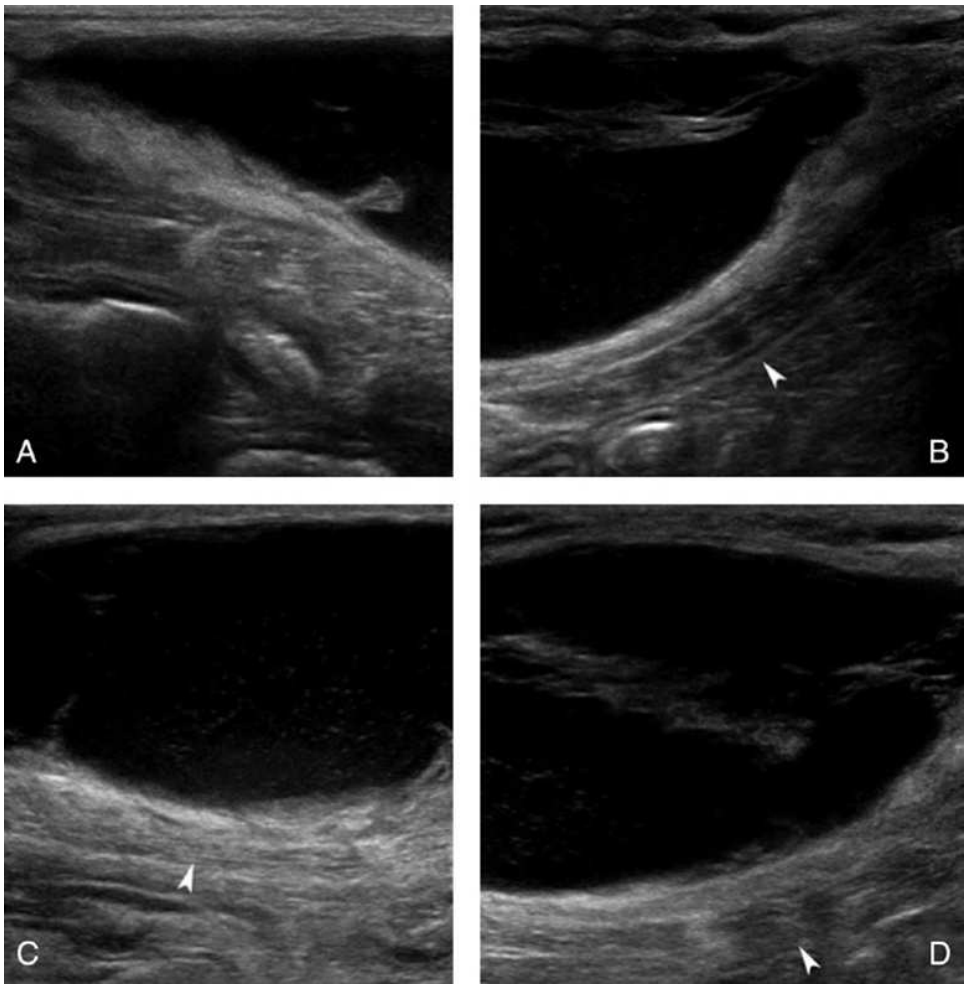


**Figure 34.5.** Features of a body wall seroma. (A–D) Longitudinal images of the ventral caudal abdominal wall. A localized, well-defined, anechoic cavitary lesion is noted in the subcutaneous tissue with mild displacement of the ventral abdominal wall musculature (*white arrowhead*) in images B–D. (C) A minimal amount of echogenic particles within the seroma are present. (D) A few hyperechoic strands crossing through the seroma are noted.

have a similar ultrasonographic appearance to an uninfected seroma, but generally infected seromas have an increase in particle content (hyperechoic specular reflectors), and rarely intralesional gas (gas-producing bacteria) within the fluid. Ultrasound-guided fluid sampling and fluid analysis with cytology and culture may be needed to differentiate between the sterile and infected seromas.

## Hematoma

Hematomas can occur nearly anywhere for a wide range of reasons. A hematoma is an accumulation of blood outside the vascular system secondary to hemorrhage.

In the early stage, a hematoma may appear similar in echogenicity to a seroma, but frequently echogenic particles are noted within the hematoma's anechoic fluid. Sedimentation of these particles within the hematoma may be noted in addition to hyperechoic septations dividing the hematoma into smaller areas. Additionally, hematomas may have components consisting of anechoic fluid and other parts with heterogeneous hypoechogenicity suggesting organization of the hematoma. In later stages, the hematoma may be heterogeneously hypoechoic and well defined from adjacent soft tissue. In these stages of organization, it can be difficult to diffeentiate the hematoma from a soft tissue mass (e.g. granuloma or neoplasia).

## Abscess

Abscesses often can be diagnosed clinically without the need for ultrasonographic imaging. However, in cases where an extension into deeper tissues is suspected, where large vessels are in close proximity to the abscess, or where there is concern for adjacent osteomyelitis, ultrasound imaging can be helpful.

An abscess has a mixed central echogenicity surrounded by thickened, hypo- to hyperechoic tissue (Figure 34.6). Additionally, within or adjacent to an abscess gas may be noted by the presence of gas reverberation artifacts. As a reminder, gas appears on ultrasound as a bright reflective surface with shadowing, which obscures the underlying anatomy; when the amount of gas is small, a short acoustic shadow or reverberation (ring-down) artifact may be noted, whereas when the amount of gas is large, a long reverberation artifact can be seen. Adjacent to an abscess, fat may be hyperechoic, suggesting focal or localized

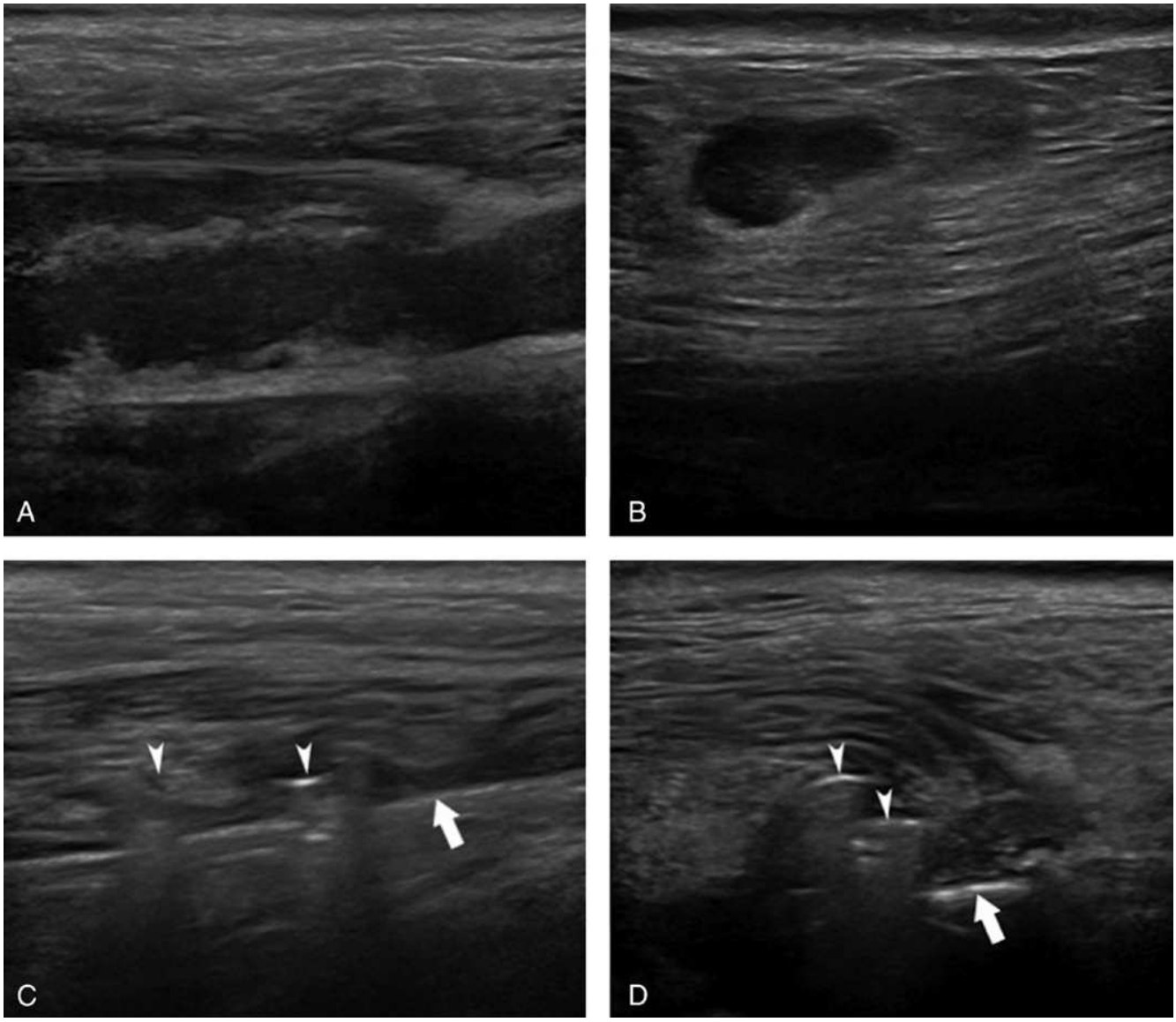


**Figure 34.6.** Abscess next to femur and its femoral surgical repair site. (A–D) Longitudinal and transverse images of the soft tissues on the lateral aspect of the femur having had an orthopedic repair with a bone plate and screws. (A) A large cavitary structure with irregular borders, thick wall and fluid containing echogenic particles is noted in the soft tissues on the lateral aspect of the femur. This cavitary structure extends into the adjacent musculature in (B) and in (C) and (D) towards the screw heads (*white arrowheads*) adjacent to the lateral aspect of the femoral cortex (*white arrow*).

inflammation (e.g., steatitis). Movement or gentle pressure on the abscess can result in movement of the particles within the abscess, helping to differentiate an abscess from a soft tissue mass. Color Doppler allows further soft tissue evaluation for the presence or absence of vascular flow, allowing differentiation between abscess (no vascular flow) and soft tissue mass (vascularity) (Figure 34.7).

Ultimately, sampling will often be necessary and ultrasound guidance allows for planning a safe route for aspiration and/or drainage of the abscess by avoiding associated structures including major blood vessels, nerves, and body cavities, thus reducing the risk of complications. Using ultrasound guidance for aspiration and drainage is becoming standard of care in human medicine for these reasons.

## Foreign Body

Foreign bodies are frequently not visualized on initial clinical examination. Radiopaque foreign bodies can be well visualized using radiography but many foreign bodies are not radiopaque and are therefore missed on radiographic examination. Ultrasound is an excellent imaging modality for identifying foreign bodies. The echogenicity and pattern visualized secondary to a foreign body are very dependent on foreign body composition, size, and time post injury. Fluid surrounding the foreign body, when present, can be a helpful visual clue for foreign body localization (Figure 34.8). However, highly echogenic fluid with intralesional echogenic tissue strands from an abscess may obscure visualization of the foreign body. In general, foreign bodies are always hyperechoic with or without distal acoustic shadowing (Mohammadi et al. 2011).

Distal acoustic shadowing may be seen in approximately 60–75% of patients with wooden, thorn and grass awn foreign bodies and in over 90% of cases with broken glass or metallic foreign bodies. Moreover, broken glass or metallic foreign bodies often also cause comet-tail artifacts, which are characterized by a thin band of reverberation artifacts. Grass awns may be directly identified by their spindle shape and hyperechogenicity within the soft tissue (Figure 34.9) (Gnudi et al. 2005).

Lastly, minimally invasive ultrasound-guided techniques have been described for foreign body removal (Stades et al. 2003; Staudte et al. 2004; Della Santa et al. 2008). When using ultrasound guidance, it is best to use small-sized surgical instruments because distal acoustic shadowing caused by the surgical tools often reduces the ability to visualize the foreign body during the ultrasound-guided procedure.

## Sialadenitis and Sialocele

Sialadenitis is the inflammation of a salivary gland, including the parotid, sublingual, mandibular, and

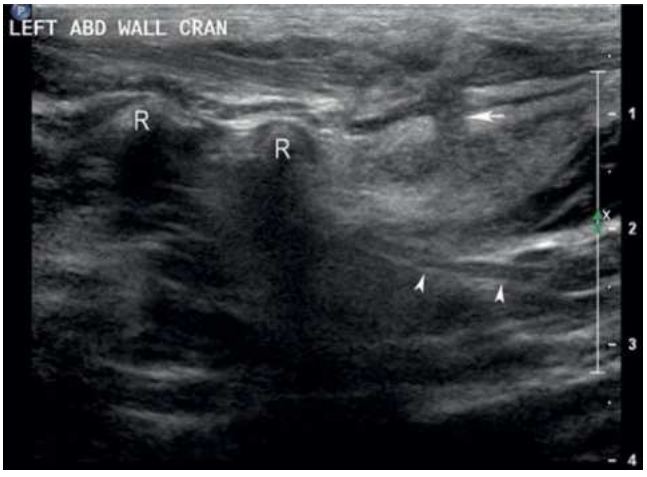


**Figure 34.7.** Abdominal wall abscess with fistula tract. Longitudinal image of the left craniolateral abdominal wall. In the subcutaneous tissue of the left cranial abdominal wall, a mixed echogenic subcutaneous lesion is noted with a tubular, hypoechoic tract (*white arrow*) extending from the subcutaneous tissue into and in part through the craniolateral abdominal wall, displacing the peritoneum (*white arrowheads*) medially. No perforation into the peritoneal cavity was identified. The ribs (R) cause incomplete distal acoustic shadowing.

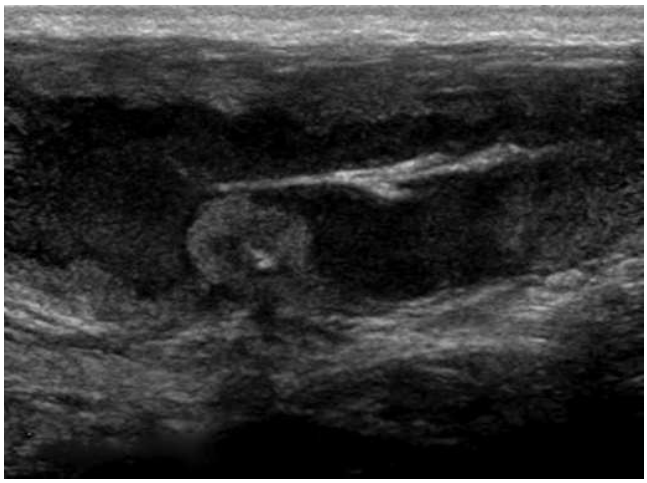

**Figure 34.8.** Grass awn foreign body with local abscess. In the subcutaneous tissue, a thick-walled, cavitary structure with internal fluid and a linear to mildly irregular hyperechoic structure is noted. The structure shows minimal distal acoustic shadowing. The fluid within the cavity is hypoechoic with mobile particle content consistent with an abscess.

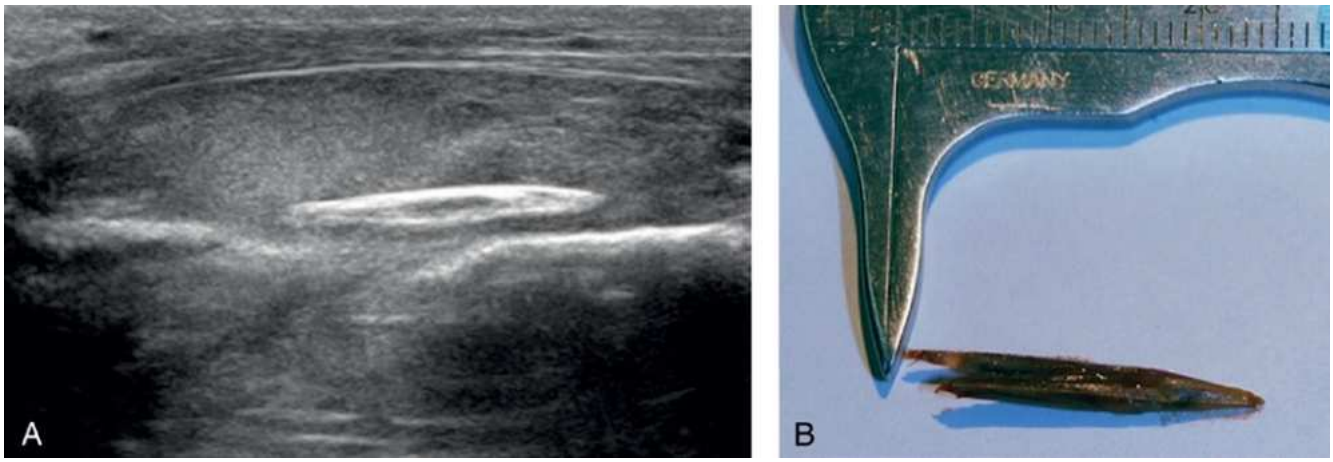


**Figure 34.9.** Grass awn foreign body. (A) Longitudinal image of the soft tissues on the dorsal aspect of the metacarpus. A spindle-shaped hyperechoic (bright white) structure is noted in the soft tissues dorsal to the metacarpal bones. (B) The small grass awn which was surgically removed. The caliper outlined is in millimeters and each small checkmark represents 1 mm.

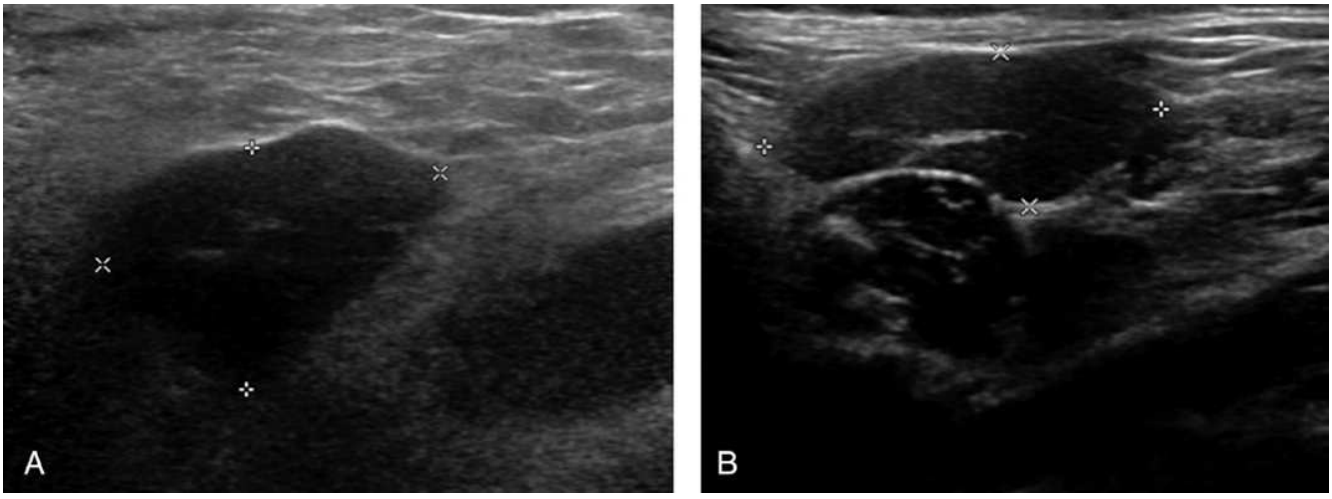


**Figure 34.10.** Mandibular sialadenitis. Longitudinal images of the right (A) and left (B) mandibular salivary gland demonstrate an enlargement of the right salivary gland with marked increased echogenicity of the adjacent fat and subcutaneous tissue. The calipers outline the borders of the mandibular salivary glands. No initiating cause was identified.

zygomatic salivary glands. The most commonly involved glands are the zygomatic, parotid, and mandibular involved salivary glands. Despite a variety of implicated causes including ascending infection from the oral cavity and trauma to the head and neck, frequently no inciting cause is apparent.

Generally, swelling in the area of the gland is noted on physical examination. On ultrasound, the affected salivary gland may be enlarged and is often heterogeneously hypoechoic (Figure 34.10). If the salivary ducts are dilated, they can be visualized on ultrasound. If visualized, the dilated ducts can be followed along their expected anatomical path and, if present, sialoliths are visualized as hyperechoic, distally acoustic shadowing structures. In rare cases, a foreign body may be identified as the cause for the obstruction and inflammation of the salivary duct or gland (sialadenitis).

A sialocele, also referred to as a salivary mucocele, is the accumulation of saliva in the submucosal or subcutaneous tissues that most commonly occurs in the head and neck due to damage to the duct or capsule of a salivary gland. The most commonly involved salivary ducts are the ducts of the mandibular and sublingual salivary glands (Figures 34.11 and 34.12). In rare cases,

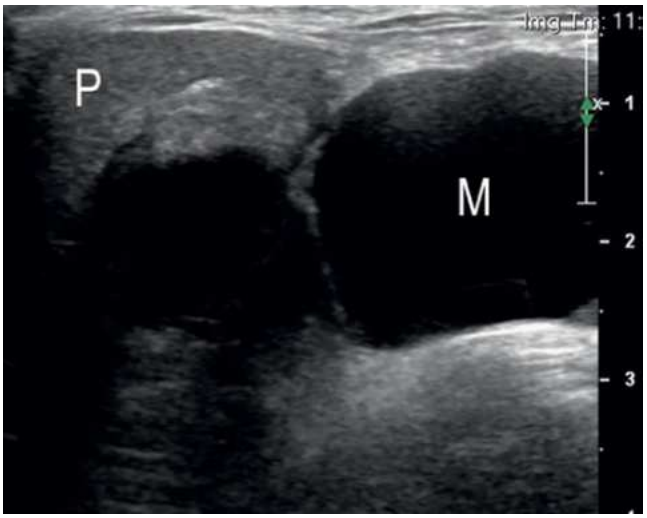


**Figure 34.11.** Mandibular sialocele. Longitudinal image of the left mandibular salivary gland. The right mandibular salivary gland (M) is a well-defined, relatively round structure, and anechoic with distal acoustic enhancement. The parotid salivary gland (P) is uniformly hypoechoic.

the salivary gland or duct can rupture, leading to the development of fascial swelling with or without signs of pain (Figure 34.13). In any event, aspiration of thick mucinous saliva raises a strong clinical suspicion for sialocele. The most common causes for sialocele include trauma (iatrogenic and noniatrogenic), sialolithiasis, rarely neoplasia. Similar to sialadenitis, it is not uncommon that no inciting cause is identified. Malignant neoplasia of the salivary glands is rare in dogs and most commonly involves the parotid and mandibular salivary glands and requires tissue sampling for diagnosis.

# Abdominal Wall Injury or Hernia

Abdominal wall injuries occur frequently secondary to nonpenetrating and penetrating trauma. Additionally, congenital abdominal wall defects can be present. A wide range of injuries of the abdominal wall are

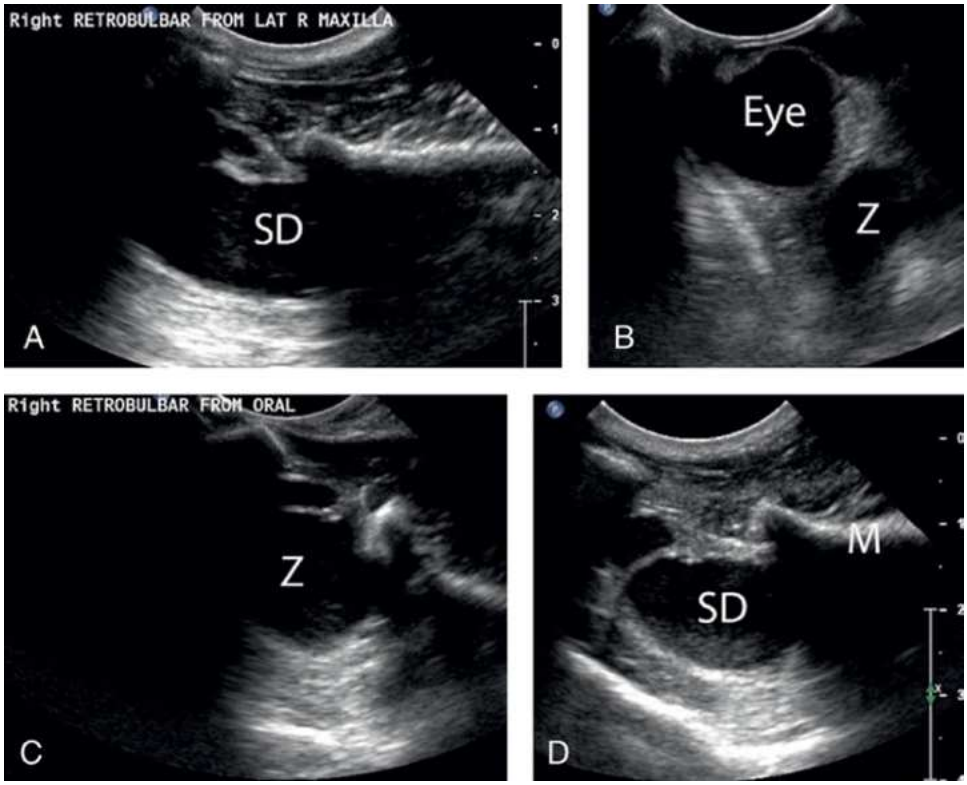


**Figure 34.12.** Zygomatic sialocele with severe dilation of the salivary duct. An ultrasound of the right retrobulbar space revealed a severely enlarged and anechoic zygomatic salivary gland (Z) lateral to the right maxilla at the ventral aspect of the eye. The eye is compressed and abnormal in shape. The salivary duct (SD) of the zygomatic salivary gland was severely dilated and could be followed to the lateral aspect of the maxilla (M) at the level of the first to second maxillary molar teeth. (A,B) The transducer was placed on the lateral aspect of the maxilla and in (C,D) was placed from orally caudal to the last maxillary molar teeth angled dorsally towards the retrobulbar space.

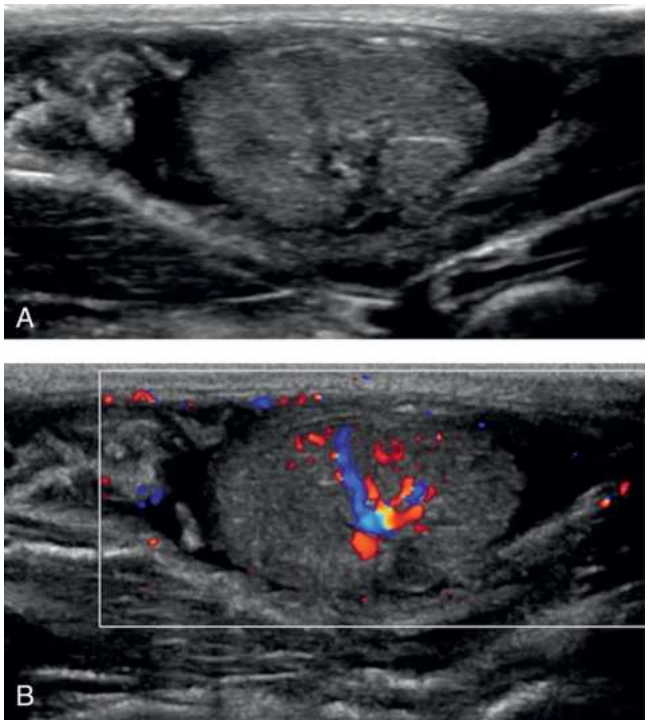


**Figure 34.13.** Suspected mandibular salivary gland rupture secondary to blunt trauma. (A) Longitudinal image of the mandibular salivary gland, which is surrounded by a rim of anechoic fluid. At the cranial aspect, the tissue adjacent to the mandibular salivary gland is heterogeneous. (B) Vascularity of the mandibular salivary gland is evident via color Doppler ultrasound. No vascularity within the fluid adjacent to the mandibular salivary gland is detected.

possible, from a local hematoma to severe abdominal wall rupture with displacement of abdominal contents. Not uncommonly, these injuries are overlooked or not considered to be serious as they truly are, because other more serious injuries are present. However, diagnosis of the abdominal wall injury can be critical as it can lead to visceral and, less commonly, vascular compromise. Abdominal wall ruptures can lead to inguinal herniation, which is best diagnosed early as herniation can lead to strangulation of the intestines, and displacement of the urinary bladder into the hernia can lead to urinary bladder wall compromise and inability to urinate and compress the urinary bladder.

The abdominal wall consists of superficial to deep layers; the outer layer is the skin, followed by the subcutaneous tissue, fat, muscles, and fascia, with the innermost layer being the peritoneum. Ventral on either side of midline and separated by the linea alba is the rectus abdominis muscle. On the inner surface of the abdominal wall, the thin, hyperechoic peritoneum is located. In the near-field, the dermis and subcutaneous fat are recognized as explained previously.

Abdominal wall rupture or herniation is commonly very noticeable on ultrasound as separation of the abdominal wall layers can be seen (Figures 34.14 and 34.15; see also Figure 16.14). Furthermore, Doppler ultrasound can be used to evaluate the extent of vascular perfusion in displaced abdominal organs. If a transient or dynamic herniation is present along the abdominal wall such as at the umbilical or inguinal region, eliciting a cough by tracheal palpation may adequately increase the intraabdominal pressure to better diagnose the condition.

# Neoplasia of Superficial Structures

## *Benign Neoplastic Masses*

Lipomas are benign fat-containing masses, which occur frequently in subcutaneous and intramuscular locations, and are considered the most common soft tissue neoplasm. They are heterogeneously hyperechoic to isoechoic to surrounding subcutaneous fat and tissue (Figure 34.16). Lipomas are often ovoid in shape, well defined from surrounding tissue, and tend to have low vascularity and therefore only minimal blood flow is seen using color Doppler. Lipomas tend not to have distal acoustic shadowing or acoustic enhancement as fluid-filled structures would (Nyman et al. 2006). Although lipomas are common, it is important to remember that ultrasonographically they can appear similar to the less commonly occurring low-grade liposarcoma.

## *Malignant Neoplastic Masses*

Malignant superficial masses can be primary or metastatic neoplasias. A wide range of superficial masses are reported including mast cell tumors, melanoma, squamous cell carcinoma, soft tissue sarcoma, tumors of the skin glands or follicles, and epitheliotropic lymphoma. Frequently, these masses are hypoechoic on ultrasound and the vascularity is variable. Masses with heterogeneous echogenicity and irregular borders (Figure 34.17; see also Figure 14.12) are more likely to be malignant than benign tumors (Nyman et al. 2006). Fine needle aspirates or biopsies are needed to differentiate between the various superficial neoplasias. Moreover, the Global FAST approach can rapidly screen for other abnormalities (see Chapters 36 and 37).

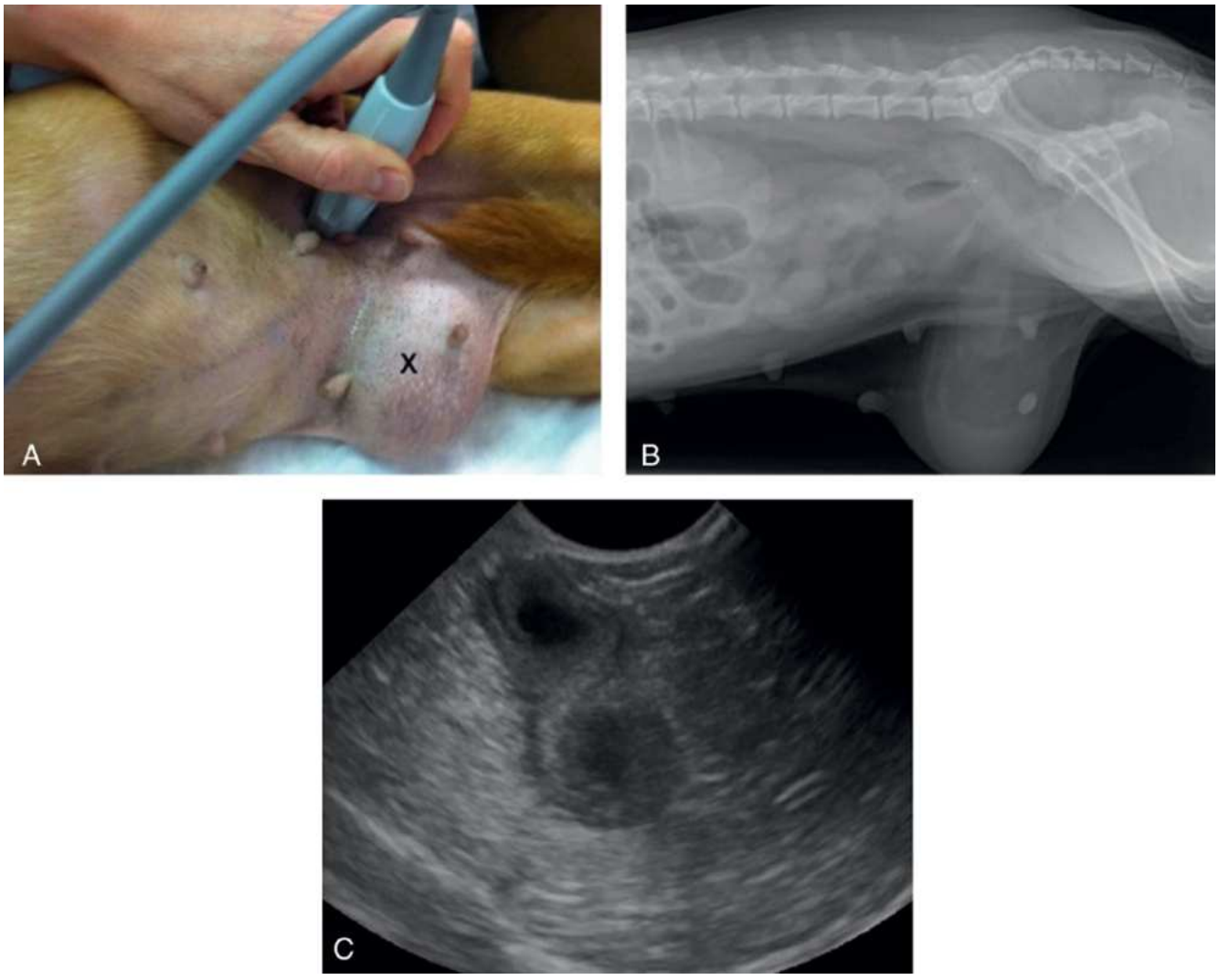


**Figure 34.14.** Inguinal hernia. (A) External view of the inguinal region of a dog with anorexia and vomiting for 48 hours. (B) Lateral abdominal radiograph (ventrodorsal view not shown) with no urinary bladder identified in the caudal abdomen and with gas within the swelling. (C) Using point-of-care ultrasound, the urinary bladder was seen within the abdominal cavity with the probe as shown. Loops of bowel with little peristalsis were found in the swelling by placing the probe at the location marked "X." Adding on an AFAST helps screen for free fluid (peritonitis, hemorrhage, or sterile effusions) and adding color Doppler assesses blood flow (see Figure 34.15). Source: Reproduced with permission of Dr Greg Lisciandro, Spicewood, TX.

# Pearls and Pitfalls, The Final Say

- Point-of-care ultrasound is increasingly used to evaluate palpable soft tissue masses.
- Point-of-care ultrasound of the soft tissues allows clinicians to evaluate structures underneath the skin, which are otherwise not accessible to clinical evaluation.
- Superficial masses can easily be identified using point-of-care ultrasound; however, fine needle aspiration or biopsies are often necessary to differentiate between the various benign and malignant mass etiologies.
- Hematomas cannot reliably be differentiated from soft tissue masses.
- Lipomas tend to be ovoid, similar in echogenicity to adjacent fat, and can often be differentiated

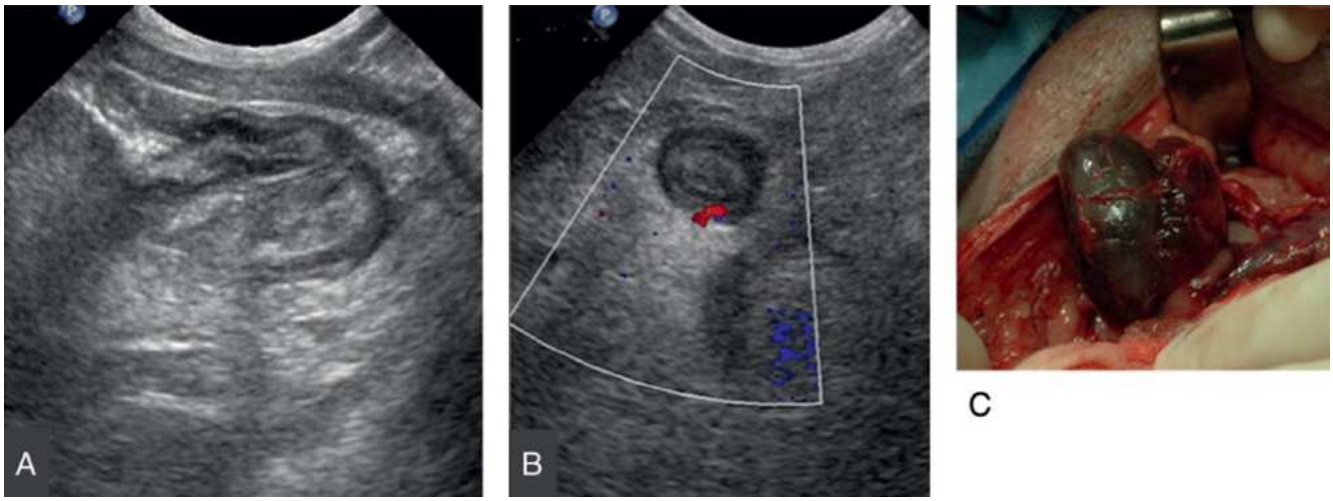


**Figure 34.15.** Inguinal hernia with displacement and vascular impairment of a segment of small intestine. (A) The inguinal canal is increased in width and a loop of small intestine is extending through the inguinal canal into the subcutaneous tissue. This segment of small intestine shows mildly reduced definition of wall layers. (B) Minimal vascular flow of the intestinal wall is noted on color Doppler and moderately reduced definition of the wall layers of the displaced small intestine is also noted. (C) In surgery, a severely hyperemic segment of small intestine was found in the subcutaneous tissue.

**Figure 34.16.** Subcutaneous lipoma. In the subcutaneous tissue at the caudal aspect of the stifle joint, a well-defined, heterogeneous, hyperechoic small mass consistent with lipoma is outlined by calipers (x and x). Ultrasound-guided fine needle aspirates confirmed lipoma.

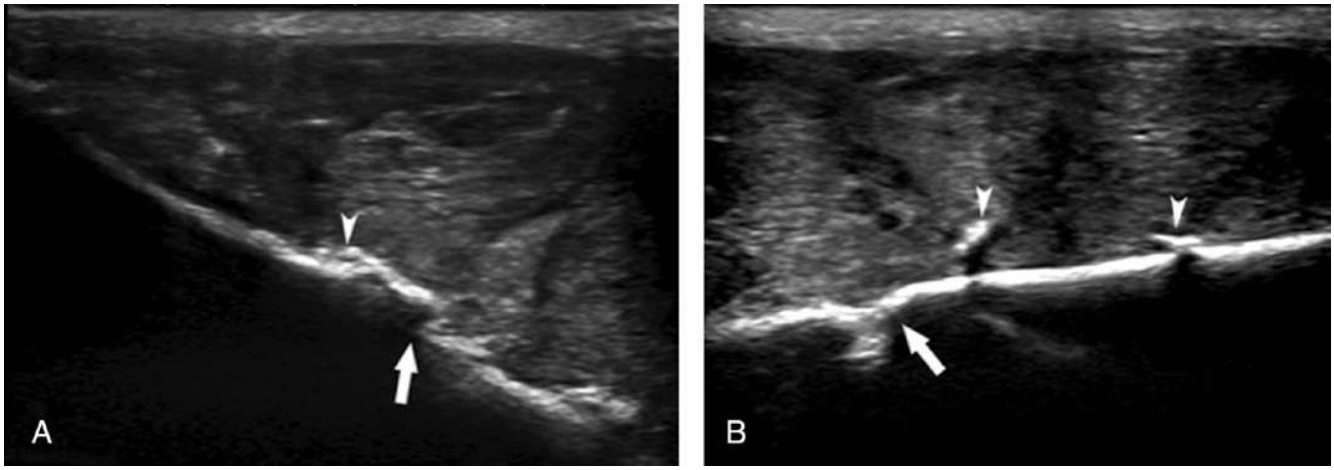


**Figure 34.17.** Subcutaneous hemangiosarcoma left tibia. (A,B) Longitudinal images of the medial aspect of the left tibia are shown. A heterogeneous, indistinctively defined soft tissue mass with adjacent periosteal remodeling (*white arrowheads*) and permeative cortical lysis (*white arrow*) of the tibia is noted. Ultrasound-guided fine needle aspirates revealed a sarcoma and full-thickness biopsies confirmed hemangiosarcoma.

from most other soft tissue masses by use of ultrasound.

- Traumatic abdominal wall lesions are frequently caused by a substantial impact and therefore associated with significant visceral trauma. A Global FAST approach and potentially a complete detailed abdominal ultrasound or computed tomography examination may be needed for thorough patient assessment.

# References & Further Reading

Della Santa DF, Rossi F, Carlucci M, et al. 2008. Ultrasound-guided retrieval of plant awns. *Vet Radiol Ultrasound* 49(5):484–486.

Gnudi G, Volta A, Bonazzi M, et al. 2005. Ultrasonographic features of grass awn migration in the dog. *Vet Radiol Ultrasound* 46(5):423–426.

Lalzad AD, Ristitsch W, Downey AF, et al. 2012. Effect of ultrasound transmission gel on ultrasound-guided fine needle aspiration cytological specimens of thyroid. *Cytopathology* 23(5):330–333.

Mohammadi A, Ghasemi-Rad M, Khodabakhsh M. 2011. Non-opaque soft tissue foreign body: sonographic findings. *BMC Med Imaging* 11:9.

Molyneux AJ, Coghill SB. 1994. Cell lysis due to ultrasound gel in fine needle aspirates: an important new artefact in cytology. *Cytopathology* 5(1):41–45.

Nyman HT, Kristensen AT, Lee MH, et al. 2006. Characterization of canine superficial tumors using gray-scale B mode, color flow mapping, and spectral doppler ultrasonography – a multivariate study. *Vet Radiol Ultrasound* 47(2):192–198.

Stades FC, Djajadiningrat-Laanen SC, Boroffka SA, et al. 2003. Suprascleral removal of a foreign body from the retrobulbar muscle cone in two dogs. *J Small Anim Pract* 44(1):17–20.

Staudte KL, Hopper BJ, Gibson NR, et al. 2004. Use of ultrasonography to facilitate surgical removal of non-enteric foreign bodies in 17 dogs. *J Small Anim Pract* 45(8):395–400.

CHAPTER THIRTY-FIVE

# POCUS: Musculoskeletal – Bones and Joints

Susanne M. Stieger-Vanegas

## Introduction

In the last 20 years, ultrasound has emerged as an alternative imaging modailty for the musculoskeletal (MSK) system. The soft tissues and MSK structures are often located relatively superficially and therefore are ultrasonographically accessible.

Musculoskeletal emergencies are often a result of trauma such as a vehicular accident, high-rise or foreign body injury. These patients frequently have serious internal injuries, which require more immediate attention, so that the MSK trauma is often assigned a lower priority in the initial triage and treatment. However, MSK injuries often require surgical intervention and long-term treatment, and affect the prognosis for the patient. Moreover, these MSK-related factors can be costly and affect the owner's decision regarding further treatment. Therefore, early evaluation of MSK injuries is critical for a timely diagnosis, assessing prognosis, and developing a treatment plan and POCUS MSK carries the potential to provide such information.

Emergency veterinarians are generally less familiar with imaging MSK and soft tissue compared to other ultrasound applications like FAST examinations, which are used to rapidly survey for internal injuries. However, many principles learned from FAST examinations, such as recognizing free fluid, soft tissue and bony structures and their associated artifacts, can translate to POCUS MSK.

In this chapter, we will describe basic POCUS MSK applications in the immediate care and emergency setting as an adjunct to patient evaluation as well as including some nonemergent and monitoring applications.

### *What POCUS Musculoskeletal – Bones and Joints Can Do*

- Provide imaging of bone, muscle, and tendons.
- Provide imaging of bone, muscles, tendons and joints that would be otherwise delayed by patient status and risk of transport to radiology.
- Provide structural information regarding the integrity of cortical bone (detect cortical disruption).
- Provide ultrasound-guided access to the bone, including its medullary area, for sampling.
- Provide structural information about muscles and tendons for the presence of partial or complete muscle or tendon tears.
- Provide an imaging modality for monitoring soft tissue injury site(s) for healing and scarring.
- Provide structural information about joints, including their associated bone surface and surrounding soft tissue.
- Evaluate for the presence of cartilage defects and the thickness of the joint capsule and qualitatively and quantitatively evaluate synovial fluid in regard to its echogenicity and volume.
- Evaluate MSK structures dynamically for normal and abnormal movement and for the presence of partial or complete tendinous, ligamentous and

*Point-of-Care Ultrasound Techniques for the Small Animal Practitioner*, Second Edition. Edited by Gregory R. Lisciandro.
© 2021 John Wiley & Sons, Inc. Published 2021 by John Wiley & Sons, Inc.
Companion website: www.wiley.com/go/lisciandro/ultrasound2

muscle tears, and whether muscles and tendons move independently or if adhesions are developing during convalescence.
- Localize injury sites to plan interventional procedures, especially when areas have accompanying adjacent body cavities, vessels, and nerves that need to be avoided.
- Help in decision making on whether an immediate intervention is necessary, for example when a bone is fractured or shows signs of osteomyelitis, or when a muscle or tendon is ruptured.
- Perform ultrasound-guided injections for regenerative medicine therapies, such as stem cell or platelet-rich plasma injections, more accurately than blind techniques.
- Provide MSK information in patients with pacemakers, metallic implants or fragments in the body, when other MSK imaging modalities such as magnetic resonance imaging (MRI) are contraindicated.
- Provide MSK information in cooperative patients requiring little if any chemical restraint with a higher anesthetic risk due to the presence of other comorbidities.

### What POCUS Musculoskeletal – Bones and Joints Cannot Do

- Cannot substitute for a thorough clinical evaluation which preemptively guides the location and objectives for the applicable POCUS MSK examination.
- Cannot overcome depth limitations of the available ultrasound transducer (probe).
- Cannot overcome physical limitations of ultrasound, including the penetration of air, ballistic materials, and intact bone, or associated implants that reflect ultrasound, such as metallic implants (plates, screws, wires, rods, etc.).
- Cannot replace a detailed MSK study by a skilled sonographer with specialized training.

### Indications

- For cooperative higher risk patients due to comorbidities and critical patients that need imaging but are intolerant of chemical restraint.
- For guiding determining MSK problematic sites and thus helping plan and guide therapeutic intervention(s).
- For patients with surgical metallic implants when the MSK region of interest is superficial to the reflective metallic implant.
- For differentiating soft tissue hypoechoic fluid-filled structures from soft tissue masses using color Doppler.
- For more safely performing diagnostic and therapeutic interventions using ultrasound guidance to more accurately direct needles and devices while avoiding larger blood vessels, nerves, and cavities, for example avoiding the axillary nerve and associated vessels and the pleural cavity when targeting an axillary mass.
- For draining or obtaining a sample(s) from fluid-filled structure (s) including a cyst or abscess in soft tissue.
- For obtaining or draining fluid from a joint or bursa.
- As an adjunct to MRI because ultrasound provides better axial resolution and thus better images smaller lesions and smaller sized veterinary patients when limited by currently available MRI scanners.
- For real-time dynamic evaluation of MSK structures and their functionality, especially injuries missed in resting muscle or tendon that are only detected if dynamic stress and limb motion is applied, such as collateral ligamentous injuries and dynamic widening of the joint space.

### Objectives

POCUS MSK provides some basic ultrasound scanning principles for identifying and localizing MSK injuries. Moreover, POCUS MSK can help characterize the type of injury and what structures are involved and be complementary to radiography and MRI. The information acquired using POCUS MSK also assists in specific treatment(s) and interventional procedure(s), and serves as a low-impact, cost-effective, point-of-care dynamic and static imaging modality for many MSK conditions.

## Equipment and Settings

### Clipping Hair and Coupling Medium

If possible, the area of interest should be clipped of hair. A mixture of 70% isopropyl alcohol and water should be applied to the scanning area followed by acoustic coupling gel to optimize the image quality while limiting artifacts. In patients with dermal injuries, sterile water, sterile saline solution, and K-Y® jelly may be used individually or in combination instead of irritating isopropyl alcohol and commercially available coupling gel. Remember that ultrasound waves do not

travel through air and therefore optimal acoustic coupling of the transducer (probe) to the skin is crucial for achieving high image quality.

## Transducer (Probe) Types

The transducer with the highest frequency available while providing adequate imaging depth should be used. It is advantageous to have a variety of probes with various contact surfaces (footprints) available during POCUS MSK, as smaller probes allow access to small or very curved areas, whereas larger probes provide a better general overview, allowing the imaging of a larger area of tendon or muscle and associated structures. Interchanging probes during scanning may be needed for gaining the most POCUS MSK information.

- Linear array transducer (probe) with a wide range of frequencies (8–20 MHz). The footprint of most linear array transducers is larger and straighter when compared to curvilinear (microconvex) probes.
- A small curvilinear (microconvex) transducer (probe) with a wide range of frequencies to evaluate deeper MSK structures or to access areas where only limited surface contact is available.
- A "hockey stick" transducer (probe) for accessing very small acoustic windows, and this probe can also be used for intraoral applications.

## Stand-off Pads

A stand-off pad can be helpful to artificially increase depth if very superficial structures are to be imaged while at the same time improving contact (acoustic coupling) when uneven surfaces are being imaged (Figure 35.1). Stand-off pads are commercially available and made of an acoustically transparent medium; however, makeshift stand-offs may be assembled by placing ultrasound gel into a glove. When using a

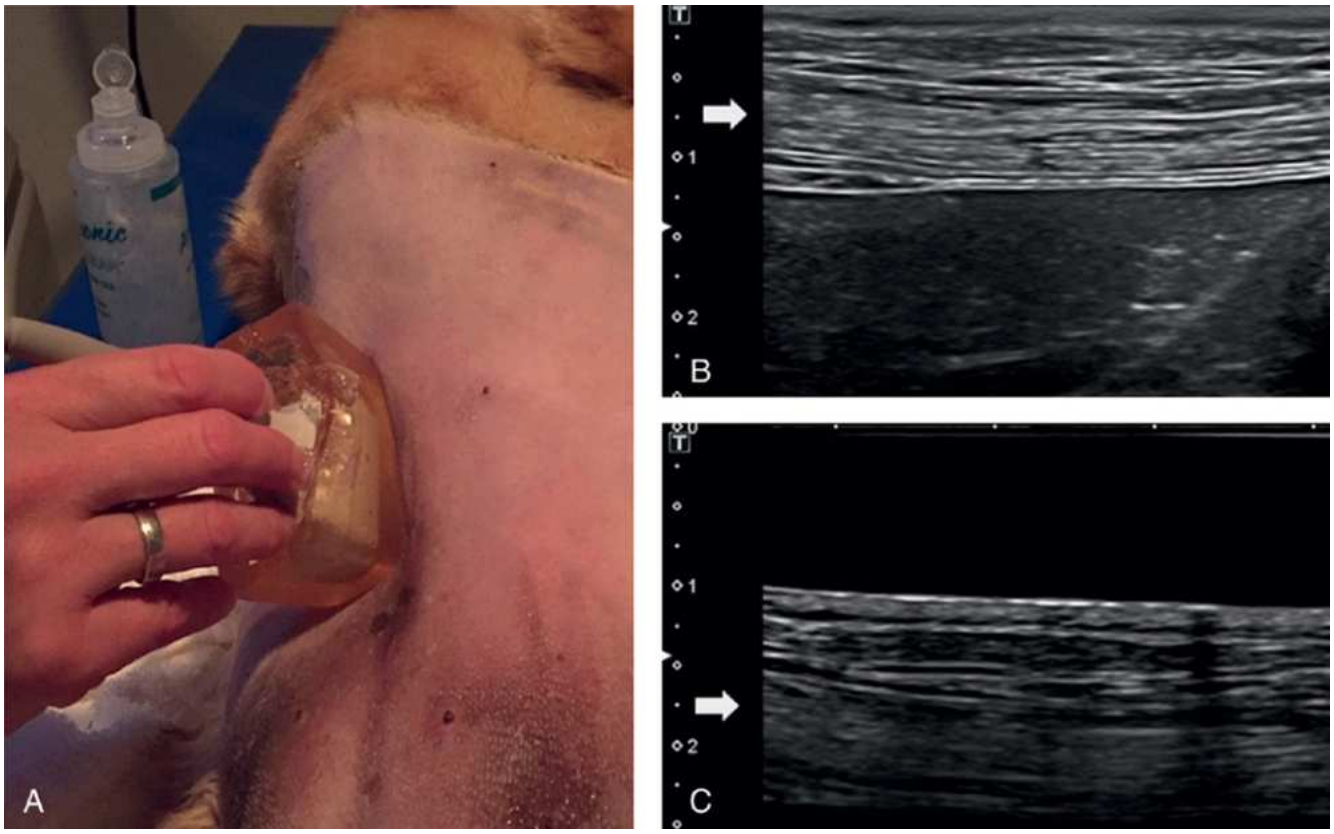


**Figure 35.1.** Stand-off pad. (A) A slip-on stand-off pad is used to evaluate the abdominal wall. A stand-off pad is an acoustically inert structure which is placed between the probe and the area of interest. Images of the ventral abdominal wall without (B)and with (C) stand-off pad. The stand-off pad moves superficial structures from the near-field more distally into the field of view, therefore allowing better evaluation of superficial structures.

makeshift stand-off, minimize the amount of air that is mixed into the gel because reflective air bubbles (air trapping) result in image degradation.

### Settings

- Adjustments of gain, frequency, and focal zone are crucial and the focal zone(s) may have to be adjusted frequently during an imaging examination.
- A dual image function can be helpful so that contralateral structures can be compared at the same time.
- Doppler function, either conventional color flow, power or microvascular, is advantageous to evaluate for the presence of vascular flow in a MSK structure
- Video storage of POCUS MSK areas evaluated dynamically can be useful when a lesion is monitored over time, as still images may lack the complete information of a lesion.

## Minimizing MSK-related Artifacts

### Anisotropy and Off-axis Side-lobe Artifacts

Importantly, muscles and especially tendons should always be imaged perpendicular to their fiber structures otherwise the tendons and their myotendinous junctions will be artifactually reduced in echogenicity (hypoechoic). When the perpendicular angle to the fiber is not ultrasonographically maintained, anisotropy and off-axis artifact result (Cook 2016) (Figure 35.2).

Structures such as tendons, including their myotendinous junction, are strongly reflective surfaces and therefore more affected by anisotropy artifact than muscles, nerves, and other tissues. Anisotropy artifact must be recognized and minimized by the sonographer for accurate MSK image interpretation. For example, tendinous structures imaged at oblique angles may falsely appear hypo- to anechoic due to the anisotropy artifact, resulting in misinterpretation, including falsely identifying a tendon injury or fluid accumulation in areas where the structures are in fact normal. Off-axis artifacts include the secondary lobe artifacts commonly referred to as side-lobe artifact in which a nearby out-of-view structure reflects enough beam to create a "ghost image" within the primary field of view (Mattoon and Nyland 2015).

**Pearl:** Anisotropy artifact is an angle-generated artifact produced in tissue that contains multiple, parallel linear sound interfaces, most commonly in tendons and ligaments, that leads to preferential reflection of the beam in one direction. Clinically, the area of interest is more (falsely) hypoechoic.

**Pearl:** Off-axis artifacts include the side-lobe artifact generated by lateral beams from the primary beam striking an "out of sight structure" creating a "ghost image" that is falsely placed within the primary beam that can confound interpretation (see Chapter 3). Alter or eliminate this artifact by changing probes, dropping the focal point, or lowering the gain. The artifact will disappear whereas true pathology will persist (Mattoon and Nyland 2015).

### Acoustic Shadowing, Acoustic Enhancement, and Reverberation Artifacts

Similar to other body areas, acoustic shadowing (dirty/incomplete and clean/complete), acoustic enhancement, and reverberation artifacts can occur (see Chapter 3).

Acoustic shadowing occurs when a sound wave is attenuated by a very dense object, such as bone, that reflects nearly all the sound waves. However, acoustic shadowing also occurs secondary to dense foreign bodies or calcifications.

Acoustic enhancement is caused by the sound wave traveling through an anechoic fluid that results in an area of increased echogenicity (hyperechoic) distal to the fluid-filled structure when compared to adjacent tissues.

Reverberation artifacts result when sound waves are reflected back and forth between a highly echogenic structure's surface and the probe surface, resulting in an image with evenly spaced parallel horizontal lines off the structure through the far-field, referred to as A-lines and ring-down artifact. These lines are usually less echogenic than the previous line moving from near- to far-field. This common artifact is associated with reflectors of ultrasound, such as air, glass and metallic objects like projectiles and needles in soft tissue (see Chapters 22, 23, 30–33).

Furthermore, similar to other body areas, MSK structure(s) should be habitually evaluated in both transverse and longitudinal planes to reduce the probability of misinterpreting an artifact for a true lesion.

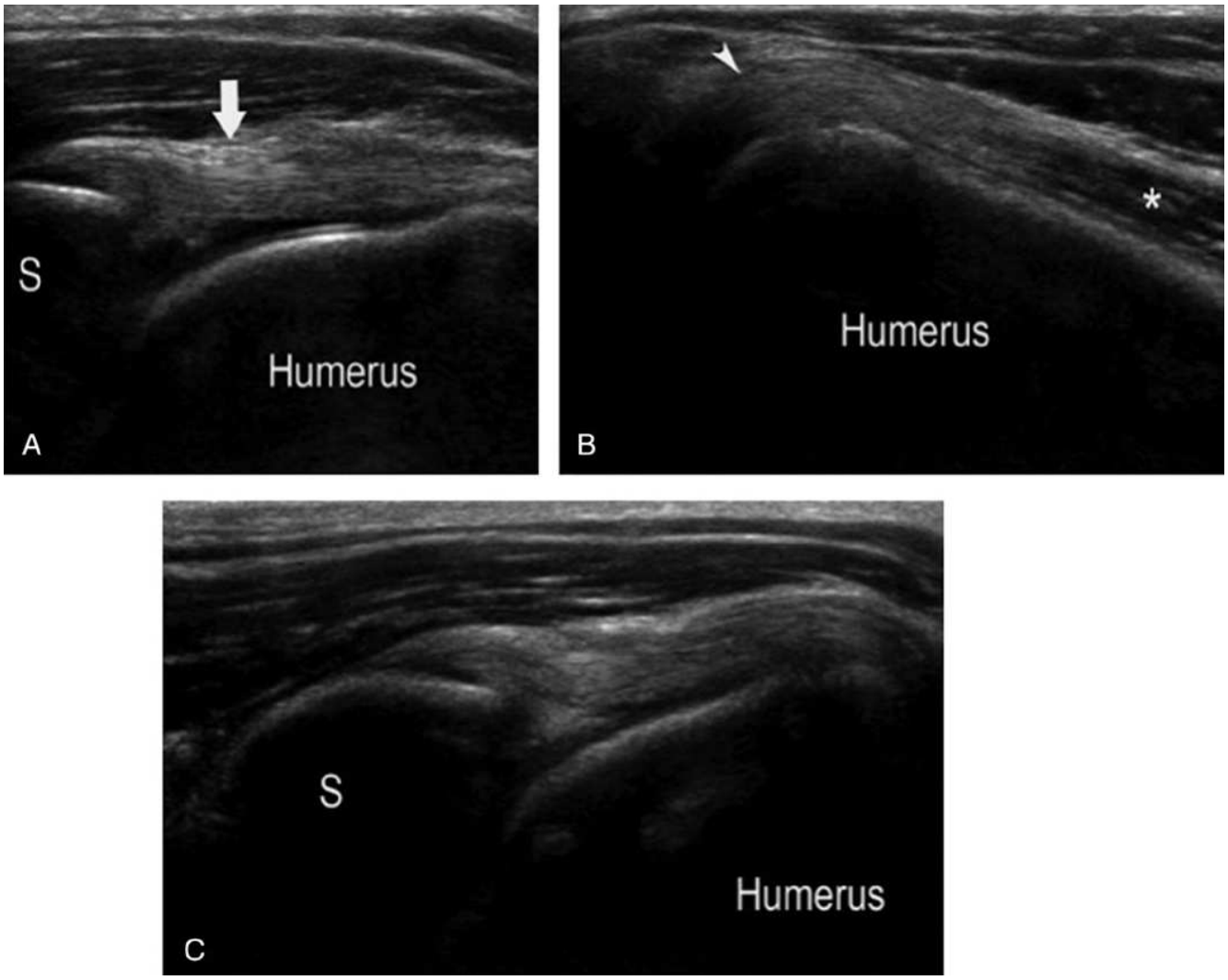


**Figure 35.2.** Normal biceps tendon. Longitudinal images of the biceps tendon of a dog. (A) The supraglenoid tubercle of the scapula (S) is smooth in outline and hyperechoic with acoustic distal shadowing, consistent with normal bone. The origin of the biceps tendon (*arrow*) shows a normal hyperechoic echogenicity and fiber structure. (B) The proximal to mid aspect of the biceps tendon proximal to the bicipital groove is reduced in echogenicity and hypoechoic (*arrowhead*). This is caused by anisotropy and is artifactual due to scanning of the biceps tendon at an oblique angle. This should not be misinterpreted as a tendon lesion. Distally the tendon diverges into the muscular aspect (*) of the biceps and the mildly heterogeneous hypoechogenicity is normal for muscle tissue. (C) The proximal aspect of the biceps tendon shows a mild loss of normal linear fiber architecture secondary to scanning of the tendon in incomplete extension. The limb should always be positioned in a way that the tendon structure is imaged in maximal extension. It is important to remember that this position has to be adjusted between the various tendinous and ligamentous structures.

# Ultrasonographic Findings in the Normal Bone, Muscle, and Tendon

## *Transducer Orientation*

As a standard when performing an ultrasound in a sagittal or dorsal plane, the probe is usually oriented towards the head or proximal in the limb. In transverse images, often the left side of the image is oriented towards the right side of the animal's body and the other way around for the right side. However, some veterinarians change this based on preference or hand dominance.

When performing an ultrasound of a MSK structure, it is helpful to note the distance to an easily palpable or prominent structure (using the centimeter scale on the

VetBooks.ir

screen or measuring with calipers), as this will allow an easier recheck of the area of interest and it is best practice to note this distance in the acquired images and the medical record. Furthermore, and unique to MSK imaging, recording position of the limb or area that was scanned as either in full or partial extension or flexion is important. Imaging of incompletely stretched muscles and tendons will have an effect on the echogenicity of the targeted structure.

Each body area should be carefully evaluated from proximal to distal or dorsal to ventral in both transverse and longitudinal planes.

## Normal Bone

Normal bone has a highly reflective, hyperechoic (bright white), smooth surface with complete distal acoustic shadowing due to the reflection of the ultrasound wave back to the probe from the cortical margin of the bone. Normal bone has a smooth, hyperechoic cortex along the diaphysis to epiphysis, which changes along the joint margins to a thin hypoechoic curvilinear area representing the joint cartilage. The transition between the osseous and cartilaginous surfaces is smooth. In the area of the attachments of tendons and ligaments, the normal bone surface is more irregular. If the sonographer is not familiar with the ultrasonographic anatomy of the area evaluated, comparison with the contralateral limb can easily be performed.

## Normal Joint

The normal joint is most easily evaluated in longitudinal (sagittal) planes with a high-frequency probe; however, as previously noted, all structures should also be evaluated in transverse planes. It is important to hold the probe very lightly to reduce pressure on the normal joint structures. Increased pressure during ultrasound examination of the joint can cause compression of the synovia and joint fluid, resulting in lack of visualization of the synovial fluid. The joint fluid (synovial fluid) is anechoic and often only present in small quantities. When performing a joint ultrasound, it is important to also evaluate the extraarticular and intraarticular structures of the joint. The joint capsule is overall thin, often mildly hypoechoic with an articular thin, hyperechoic lining, which is usually well defined from the synovial fluid. Normally, only minimal vascular flow is noted in the synovia when using Doppler ultrasound. Mild synovial folding might be normally present in various joints. The articular cartilage is a thin, well-defined, hypoechoic line along the articular, hyperechoic surfaces of the bones. The thickness of the articular cartilages varies minimally between the various joints.

## Normal Skeletal Muscle

Normal skeletal muscle has a very characteristic ultrasound appearance and can easily be differentiated from subcutaneous fat bone and vascular structures. In some cases, the nerves within or adjacent to the muscle tissue can also be differentiated using ultrasound (see Chapters 30–33). Normal muscle has a relatively heterogeneous echogenicity with hypoechoic muscle bundles surrounded by hyperechoic epimysium and perimysium. In transverse imaging planes, normal muscle has a more speckled ("starry night") appearance and in a longitudinal view relative to the length axis of the muscle, the muscle has a more pennate appearance similar to barbs on a feather (see Figure 35.14A) (Stevenson 2013). Within the muscle, a strong hyperechoic linear area consistent with the myotendinous junction may be noted into which the adjacent muscle bundles converge. From the myotendinous junction, the fibers can be followed into the tendon of the muscle. It is important to remember to evaluate ultrasonographically whether the movement of the muscle is normal or abnormal.

## Normal Tendon

Normal tendon fibrils have a hyperechoic (bright white) echogenicity interposed with hypoechoic signals resulting from the surrounding connective tissue. In a longitudinal image, a strong linear, hyperechoic fiber pattern is noted. On a transverse image, well-defined hyperechoic tendon fibrils interspersed with hypoechoic connective tissue are seen.

## Normal Ligament

Similar to tendons, normal ligaments have a linear, hyperechoic (bright white) fiber pattern (Figure 35.3). In small animals, the ligaments are often evaluated most easily in a longitudinal view. As ligaments are often oriented in a curved pattern, alignment of the probe is crucial to reduce the occurrence of anisotropy artifacts.

## Normal Nerve

In veterinary patients, small nerves may not be discernible and differentiated from surrounding tissue. Larger nerves may be identified as a round to oval structure consistent with hypoechoic nerve fascicles

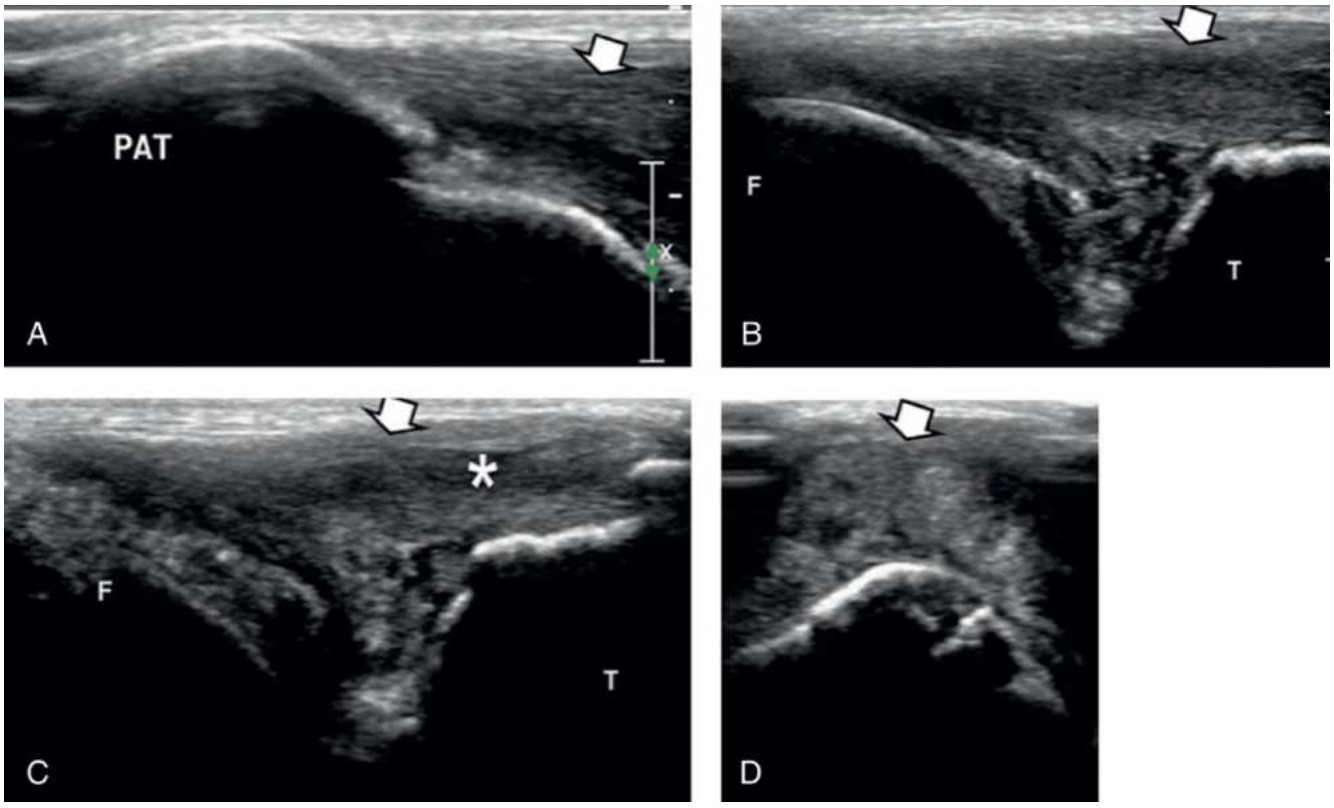


**Figure 35.3.** Normal and partially ruptured patellar ligament. (A) The normal patellar ligament has a linear hyperechoic fiber structure (*white arrow*) extending from the distal aspect of the patella (PAT). (B) The infrapatellar fat pad is noted at the caudal aspect of the patellar ligament (*white arrow*) proximal of the tibia (T) and distal of the femur (F). Longitudinal (C) and transverse (D) images of the distal aspect of the patellar ligament. The patellar ligament is increased in thickness and a loss of normal fiber alignment with a heterogeneous echogenicity and diffuse hypoechoic areas (white asterisk) of the patellar ligament is noted.

surrounded by hyperechoic epineurium. In a transverse image, the nerve may appear as a round, small structure with an "onion ring" or "honeycomb" pattern (Figure 35.4) (see also Chapters 30–33). In a longitudinal image, the nerves have a linear fiber structure and can be noted as small, mildly mixed echogenic tubes.

### Normal Cartilage

Normal hyaline cartilage will be seen as a homogeneously anechoic layer covering an articular bone surface (Figure 35.5). The hyaline cartilage has a very thin, superficial and deep hyperechoic layer, which allows differentiation of the cartilage from adjacent bone and joint fluid.

### Normal Subcutaneous Tissue

Superficially a bright echogenic line caused by the dermis and epidermis is followed deep by a hypoechoic area created by fat that often has a more recognizable heterogeneous and granular appearance (see Figure 34.1).

## Ultrasonographic Findings in Diseased Bone, Muscle, and Tendon

### Fracture

The most commonly used technique to evaluate fractures is radiography. However, fractures of superficially located bones, such as the skull (Figures 35.6 and 35.7; see also Figures 29.12 and 29.13), ribs, long bones (Figures 35.8 and 35.9; see also Figures 35.11–13), can be easily identified using ultrasound by finding disruption of the expected smooth linear cortical margin as a step formation ("step sign") or by obvious cortical

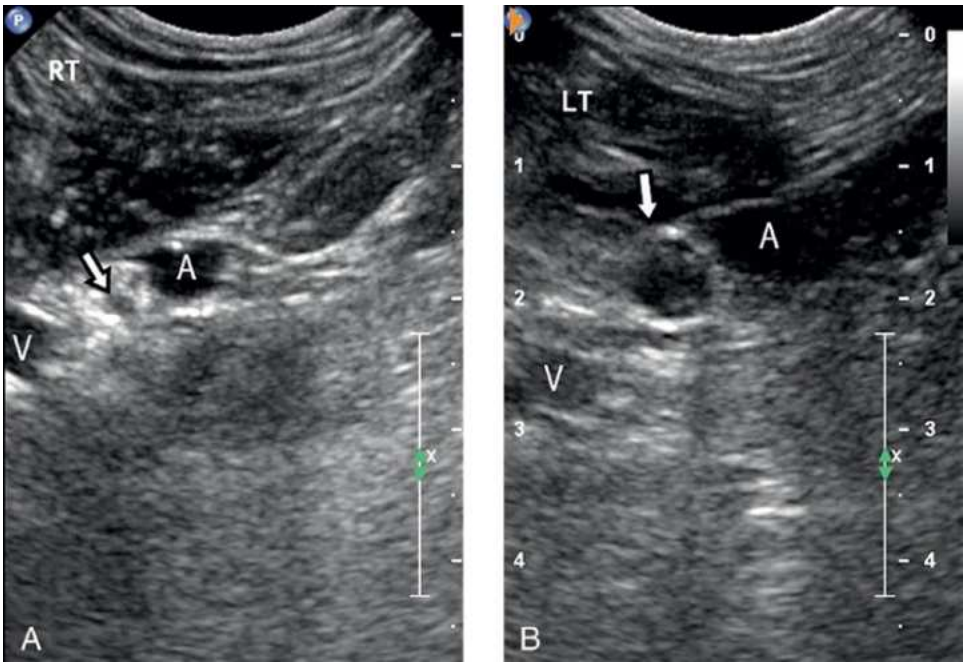


**Figure 35.4.** Normal and peripheral nerve sheath tumor of axillary nerve. Comparison images of the right (A) and left axilla (B). The normal right axillary nerve shown in (A) is noted as a small round, hypoechoic structure between the right axillary vein (V) and artery (A). On the left side, the axillary nerve shown in (B) is enlarged and mildly heterogeneous in echogenicity and similarly located between the right axillary vein (V) and artery (A). Ultrasound-guided fine needle aspirates confirmed a peripheral nerve sheath tumor.

displacement. Hematoma formation is recognized by a hypoechoic or mixed echogenic area and adjacent soft tissue swelling can be used to guide the ultrasound examination. It is important to remember that very irregular shaped and deeper located bones, such as tarsal, carpal, vertebra, are not well evaluated using ultrasound, necessitating additional imaging techniques for their proper evaluation.

## *Osteomyelitis and Bone Tumors*

Osteomyelitis and bone neoplasia can vary in ultrasonographic appearance. Often, on ultrasound, the cortical margin of the bone may be more irregular and contain small defects compared to adjacent normal areas of bone and additionally, a fine hyperechoic (bright white) band of tissue might be noted next to the cortex, indicating a periosteal response (Figure 35.10). The adjacent soft tissue might be increased in thickness, more heterogeneous in echogenicity and texture (Figures 35.11 and 35.12). In osteomyelitis, the adjacent inflamed tissues may be reduced in echogenicity (Figure 35.13).

Importantly, osteomyelitis and bone neoplasia can have similar ultrasonographic features and therefore ultrasound-guided fine needle aspirates or bone biopsies are generally recommended for further evaluation of the lesion. Ultrasound can be useful for identifying the cortical defect through which a needle can be guided for optimal sampling.

In osteomyelitis, the degree of cortical lysis is generally less severe than in some forms of bone neoplasia. In advanced primary bone neoplasia, often large, heterogeneous and irregular defects are present in the cortex of the diaphyseal to the metaphyseal aspect of the bone in addition to irregular, hyperechoic periosteal new bone formation (Codman's triangle). As a reminder, the Codman triangle is not pathognomonic for neoplasia and this triangular periosteal response can also be seen in inflammatory processes. The adjacent soft tissues are often very heterogeneous and can be highly vascularized.

**Pearl:** In cases in which neoplasia is on the differential, a Global FAST has tremendous value in rapidly surveying the patient for any obvious signs of metastasis including lung, any comorbidities, and for staging the patient; it is also used as preanesthetic evaluation for scheduled sampling procedures.

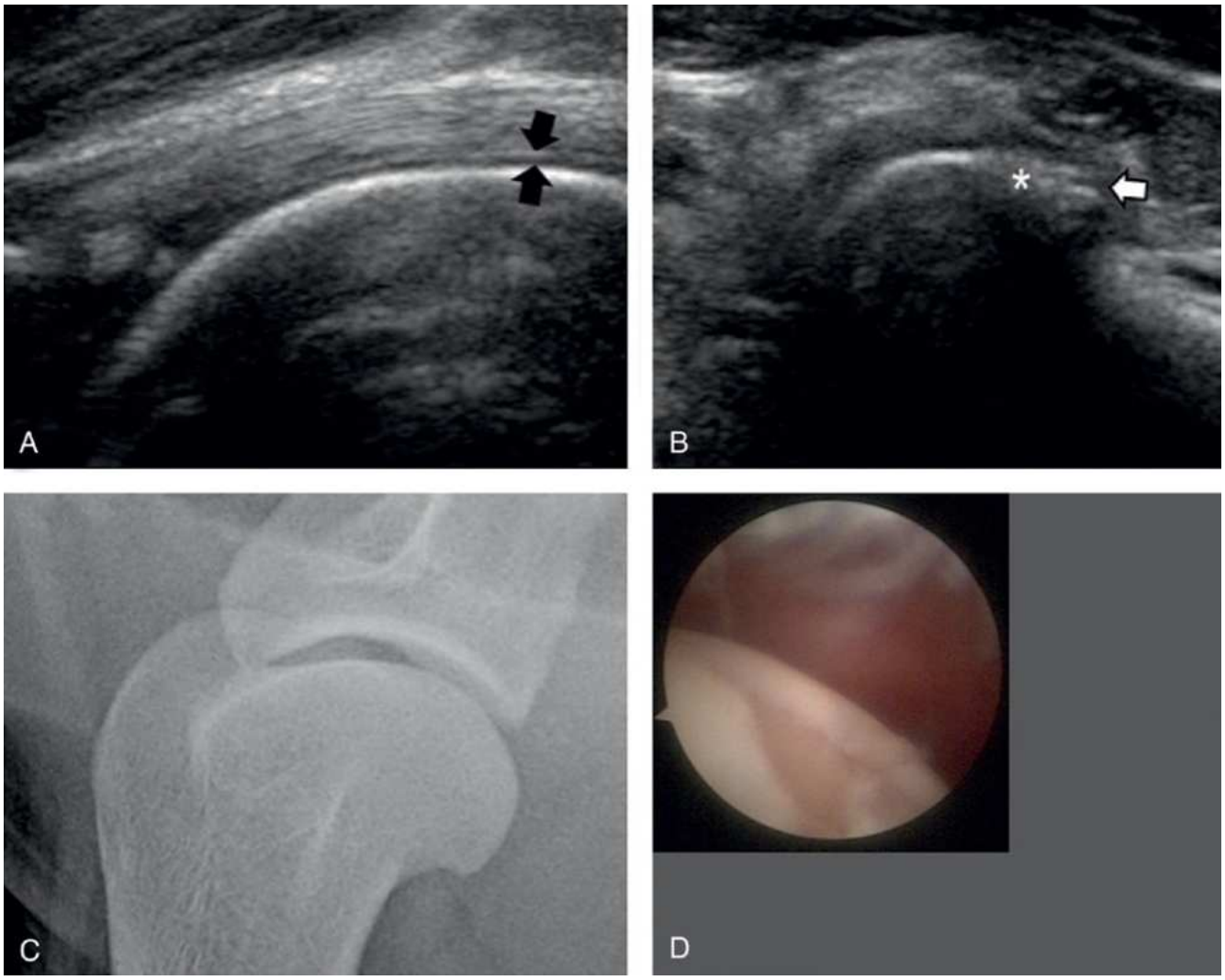


**Figure 35.5.** Normal cartilage and osteochondrosis of the caudal aspect of the humeral head. (A) Longitudinal ultrasound image of the cranioproximal aspect of the humeral head shows a smoothly outlined, hypoechoic line in parallel (*black arrows*) with the hyperechoic subchondral bone of the humeral head, which is consistent with normal cartilage. (B) At the caudodistal aspect, the cartilage is focally mildly increased in thickness and irregularly outlined. Additionally, an area of decreased, heterogeneous echogenicity of the subchondral bone (*) of the caudal aspect of the humeral head with adjacent periarticular bone formation (*white arrow*) is noted. (C) Lateromedial radiograph of the shoulder joint. No distinct lesion of the humeral head is noted. A faint linear mineral opacity is noted at the caudal aspect of the humeral head. Questionable, minimal flattening of the humeral head is present. (D) On arthroscopy, a defect is noted in the cartilaginous aspect of the humeral head consistent with osteochondrosis.

## *Assessment of Fracture Healing Using Ultrasound*

Evaluation of bone using ultrasound is still viewed controversially, but especially in the early stages of healing, callus formation might be better evaluated using ultrasound than radiography (Maffulli and Thornton 1995). Studies in human patients have shown that periosteal new bone formation evaluation using ultrasound correlated well with radiography and is likely similar in veterinary patients (see Figures 35.8 and 35.9). Furthermore, color flow Doppler can be used to evaluate for the presence of blood flow at the fracture site and within the callus (see Figure 35.9).

## *Muscle Injuries*

Muscle and tendon injuries can be noted as a disruption of the normal fiber structure. In extrinsic muscle injuries caused by blunt trauma or laceration, tearing

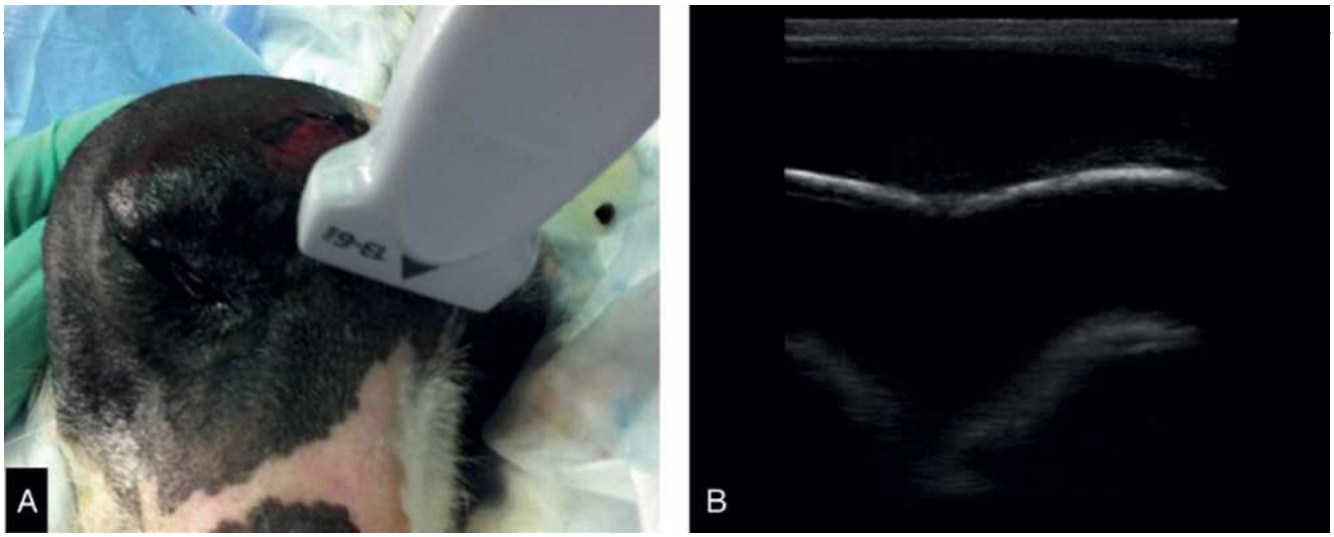


**Figure 35.6.** Skull imaging. Shown are probe placement in (A) and the corresponding B-mode image in (B) of the linear continuity of the proximal hyperechoic line of the normal contour of the frontal bone. Source: Reproduced with permission from Dr Gregory Lisciandro, Hill Country Veterinary Specialists and FASTVet.com, Spicewood, TX.

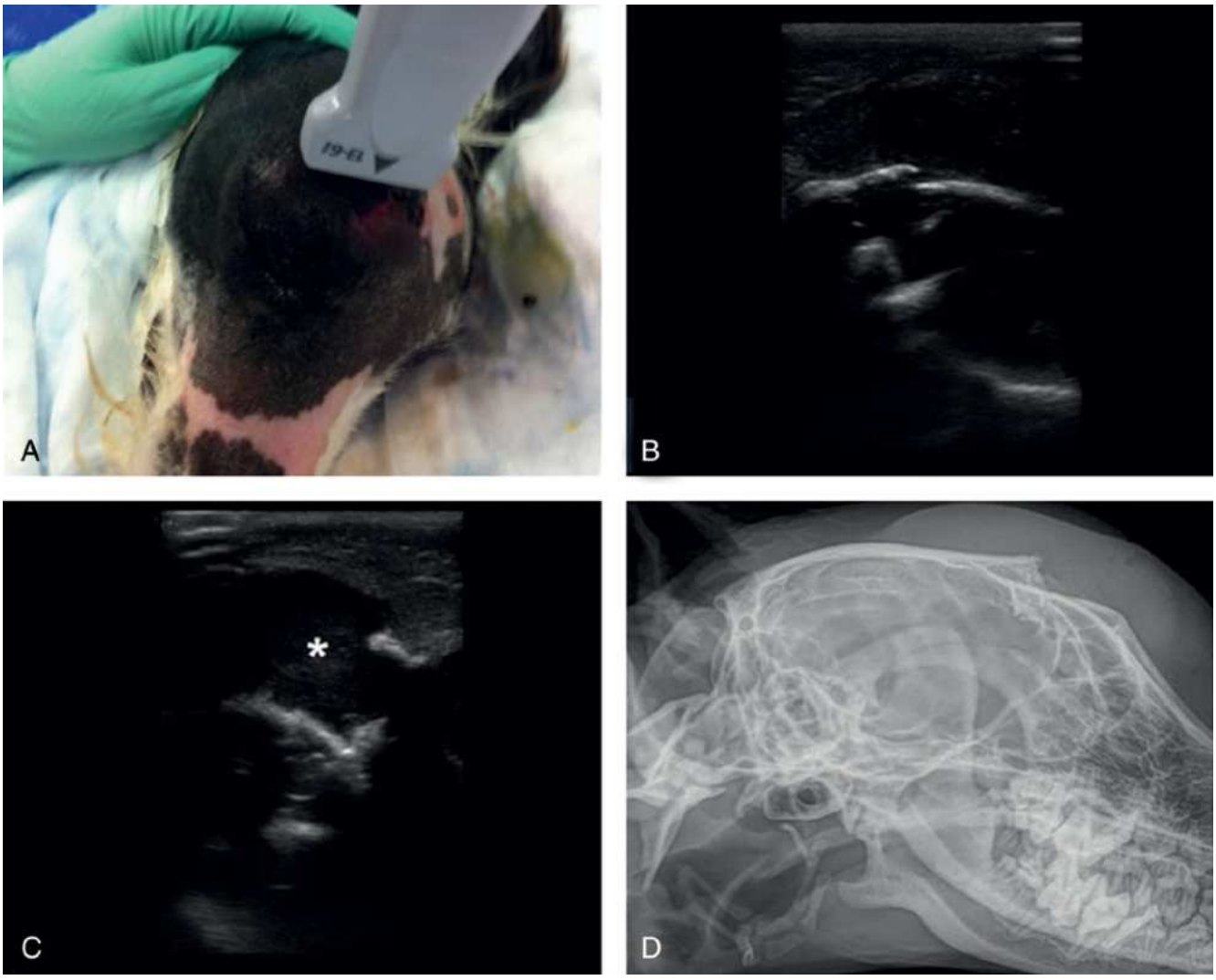


**Figure 35.7.** Skull fractures with confirmatory skull radiograph. Same dog as Figure 35.6. Shown here are probe placement in (A) and the corresponding B-mode images in (B) and (C) where there is clear disruption of the expected linear continuity of the proximal hyperechoic line, a "step sign," indicating that a skull fracture is present. The asterisk (*) marks the hematoma (anechoic area). (D) The confirmatory skull radiograph. Source: Reproduced with permission from Dr Gregory Lisciandro, Hill Country Veterinary Specialists and FASTVet.com, Spicewood, TX.

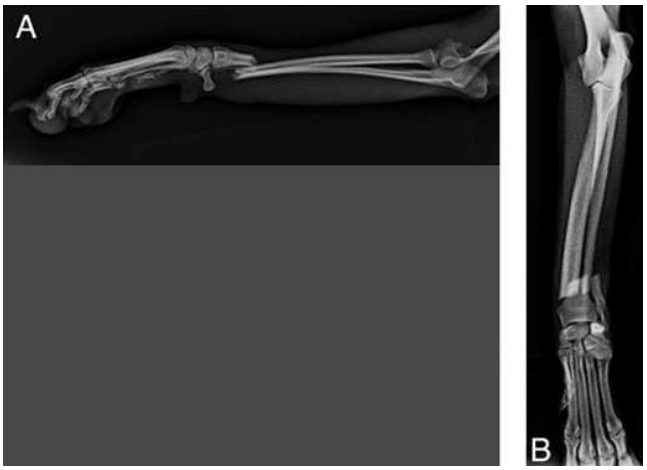


**Figure 35.8.** Long bone fracture. Acute, short oblique fracture of the distal diaphysis of the left radius and ulna in a 9-month-old Chihuahua mixed-breed dog. (A) Mediolateral and (B) craniocaudal radiographs of the left antebrachium. A short, oblique fracture of the distal diaphysis of the radius and ulna with proximodorsal displacement is noted.

of the muscle fibers is recognized ultrasonographically as areas of anechogenicity and/or hypoechogenicity with concomitant loss of the normal muscular fiber pattern (Figure 35.14). In mild injuries, only an increase in size (swelling) of the muscle may be present that may only involve a portion of the muscle body. In more severe injuries, areas of reduced echogenicity consistent with hematoma and/or seroma formation may also be noted. In earlier acute phases, a hematoma may appear relatively anechoic whereas in later chronic phases, hematomas become heterogeneous and hyperechoic secondary to coagulation.

Intrinsic injuries can be caused by a wide range of traumas affecting the myotendinous junction of the muscle (see Figure 35.14). These injuries can range from mild to severe, involving only a small area or resulting in complete rupture of the muscle at its myotendinous junction (Draghi et al. 2013).

## *Tendon Injuries*

The injured tendon is often mixed or reduced in echogenicity with loss of normal fiber structure. Frequently, an increase in the size of the tendon (focal or diffuse) can be noted. Additionally, tenosynovitis may be present, recognized as an increased amount of fluid causing distension of the tendon sheath (Figure 35.15). The fluid can be variable in echogenicity, ranging from anechoic to mixed echogenic secondary to inflammation, hemorrhage or infection. The synovial layer of the tendon sheath might be increased in thickness and have an irregular border. If concern about an infectious tenosynovitis exists, sampling and analysis of the fluid should be performed as hemorrhage and an infectious process can have a similar ultrasonographic appearance (see Figure 35.15).

## *Common Sites of Muscle and Tendon Injuries in Small Animal Patients*

### Supraspinatus Muscle (Supraspinatus Tendinopathy)

The most common site of supraspinatus injuries, especially in the dog, is the tendon of insertion at the greater tubercle of the humerus. In an acute injury, an area of decreased echogenicity and loss of normal fiber structure may be noted in this area (Figure 35.16). Importantly, the aspect of the tendon immediately proximal to the greater tubercle normally has an area of decreased echogenicity, in part due to its different fiber anatomy at this location. In chronic lesions, areas of increased echogenicity without and with distal shadowing can be noted. When areas of hyperechogenicity with distal shadowing are present, areas of mineralization secondary to chronic fiber disruption should be suspected.

### Biceps and Achilles Tendon Rupture

Injuries to tendons can be partial or complete (Figures 35.17 and 35.18). When a partial tendon rupture is identified, it is important to evaluate the extent of it, as partial rupture can develop into complete rupture of a tendinous structure. Often a "core" lesion may be noted, which is an area of hypoechogenicity and fiber loss within the tendon (see Figure 35.17). Adjacent soft tissue should always be evaluated, including tendon sheaths and adjacent joints. It is important to remember that tendinous structures are not well vascularized and healing is often slow, requiring a long duration of stabilizing support and/or exercise restriction.

### Iliopsoas Muscles

This type of injury can be challenging to diagnose; however, it is not uncommon in active (sporting) dogs and can be associated with a significant level of patient pain and discomfort. Injuries in dogs can occur in both parts of the iliopsoas muscle (psoas major and iliacus). It is important to note that the

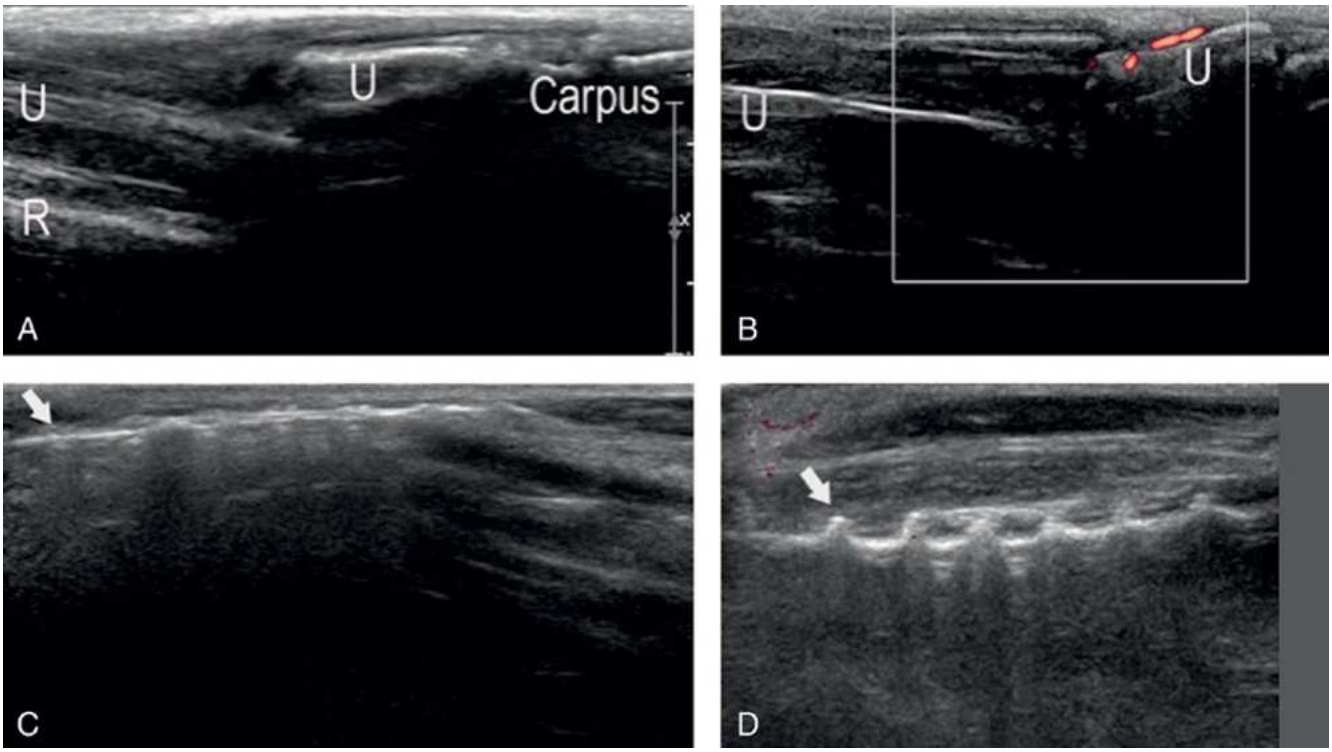


**Figure 35.9.** Fracture and healing. Acute short oblique fracture of the distal diaphysis to metaphyseal area of the left radius and ulna in the same Chihuahua mixed-breed dog as in Figure 35.8. Initial imaging in (A) and (B) and five months post surgical repair in (C) and (D) with longitudinal ultrasound images of the distal aspect of the left radius and ulna. (A) A fracture of the distal diaphysis to metaphyseal area of the radius (R) and ulna (U) with moderate dorsal and mild proximal displacement of the distal ulnar fragment is noted. On ultrasound, the diaphyseal fracture is evident by a "step sign" in which there is a break in the hyperechoic bright white line representing the expected linear continuity of the bone surface. The scale in the image represents a length of 2.5 cm. The distal radial fragment is not well visualized due to being off plane in the image provided. (B) Mild vascular flow is noted along the distal ulna fragment using power Doppler imaging. (C) The plate positioned along the dorsal cortex of the radius and the screws are well defined. The heads of several screws are noted as round, hyperechoic structures with a central area of hypoechogenicity (*arrow*) five months post surgical repair of the fracture. (D) On the caudodistal aspect of the radius, the tips of the screws can be noted (*arrow*). In the five months postsurgery ultrasound scan, the fracture line is not identified.

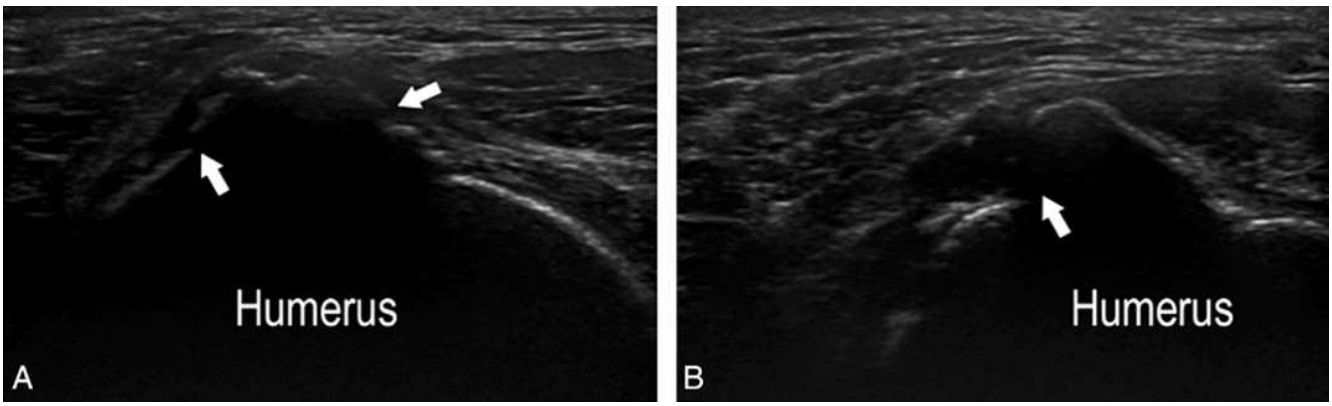


**Figure 35.10.** Osteosarcoma of the humerus. Osteosarcoma of the humerus in a 6-year-old pitbull mixed-breed dog with a history of progressive lameness. (A,B) Longitudinal ultrasound images of the proximal humerus. A point-of-care ultrasound of the left proximal humerus diaphysis to metaphysis revealed a severe irregular cortical margin with areas of cortical defects (*arrows*). Irregular, hyperechoic areas are noted adjacent to the cortical defects in the proximal humerus consistent with periosteal new bone formation. Additionally, adjacent to the cortical defects, a small, broad-based, hypoechoic to mixed echogenic mass lesion is noted. The cranial aspect of the humeral head is smoothly outlined and hyperechoic.

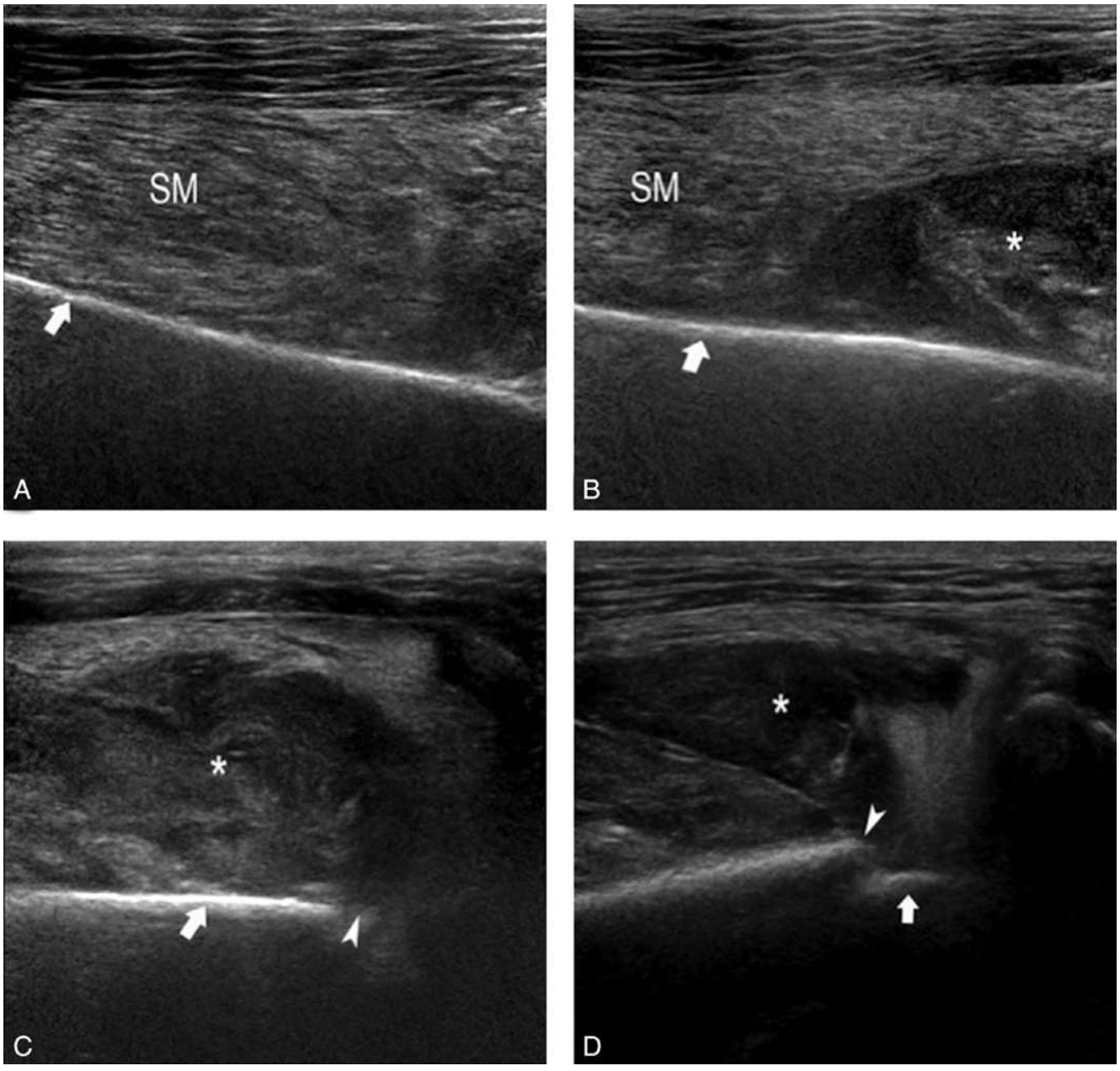


**Figure 35.11.** Osteosarcoma of the scapula. Pathological fracture of the neck of the scapula in a 7-year-old Labrador retriever mixed-breed dog. The dog showed pain in the shoulder area and hyperextension of the toes. (A–D) Longitudinal images of the supraspinatus muscle and left scapula (*arrow*). (A) The cortical margin of the scapula is hyperechoic, smooth outlined and well defined with strong acoustic distal shadowing. The supraspinatus muscle (SM) has a mildly heterogeneous echogenicity with abnormal fiber alignment. (B) In the distal aspect of the supraspinatus muscle a well-defined, mixed echogenic mass is noted (*). The spine of the scapula is persistently smooth outlined. (C) The mass (*) within the supraspinatus muscle extends distally towards the neck of the scapula and a defect is noted in the cortical margin of the neck of the scapula (*arrowhead*). At this level, the osseous margins of the scapula are less distinct and irregular. (D) A fracture of the neck of the scapula (*arrows*) is noted. The fracture ends (*arrowhead*) are irregular outlined and rounded, suggesting a chronic or pathological fracture. The mass lesion (*) within the supraspinatus muscle is persistently noted. Ultrasound-guided fine needle aspirates of the mass within the supraspinatus muscle revealed a sarcoma.

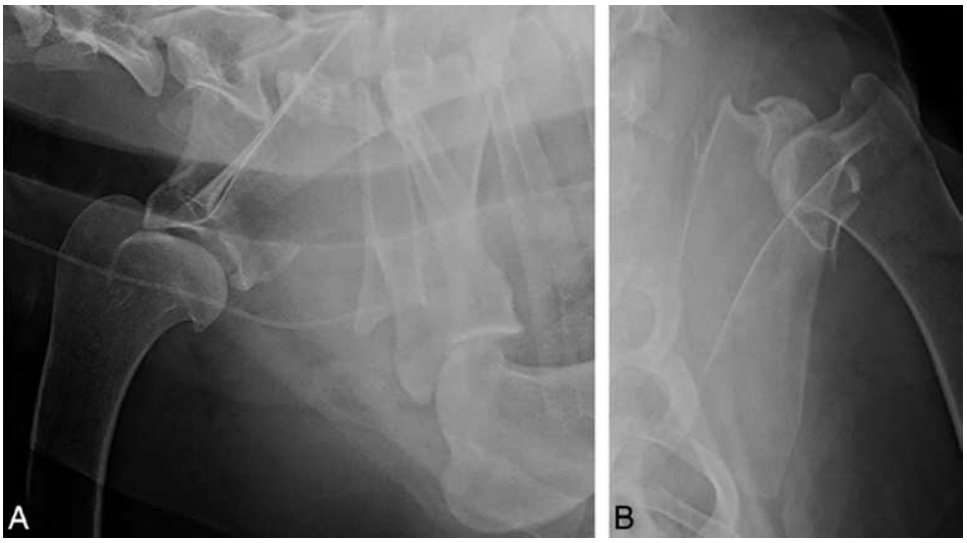


**Figure 35.12.** Pathological fracture of scapula. Pathological fracture of the neck of the scapula of the 7-year-old Labrador retriever mixed-breed dog in Figure 35.11. Mediolateral (A) and craniocaudal (B) radiographs of the left scapula and shoulder revealed an articular T-shaped fracture of the scapula neck and spine. The distal aspect of the scapula has a heterogeneous bone opacity with reduced definition of the cortical margins consistent with a pathological fracture. Mild degenerative shoulder joint disease is noted.

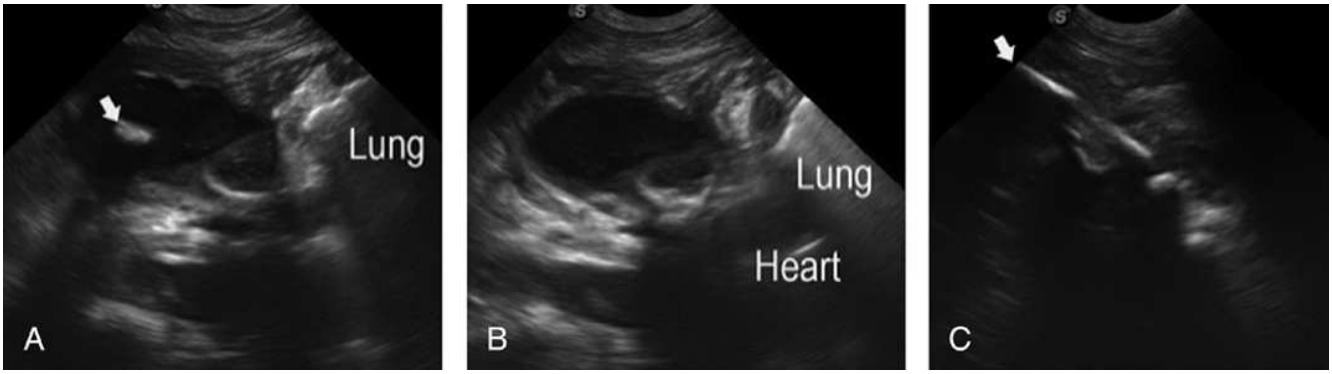


**Figure 35.13.** Rib fracture and abscess. Rib fracture and abscess in a 3-month-old, male German shepherd dog with a history of lethargy, pain, and pyrexia (40.4 °C). The dog got acutely more painful and was unwilling to walk. Ultrasound images of the axillary area (A,B) revealed a thick-walled fluid-filled cavity circumferentially surrounding the fractured left first rib (*arrow*). The cavity caused mild medial displacement of the left cranial lung. No pleural fluid is noted. No distinct foreign body is identified. The adjacent lung parenchyma shows normal acoustic reverberation artifacts. Ultrasound-guided fluid aspiration and emptying of the cavity revealed a thick, gray to yellow fluid consistent with an abscess. (C) After ultrasound-guided emptying of the abscess, areas of loss of normal cortical margins of the left first rib with adjacent areas of hyperechogenicity with distal shadowing consistent with fractures are noted. Additionally, the small hypoechoic defects in the cortical margin of the left first rib and the lack of blood flow (not shown in the images provided) were concerning for bone necrosis and/or osteomyelitis causing the abscess or being caused by the abscess. No external injury was identified in the patient but the dog lives on a property with horses.

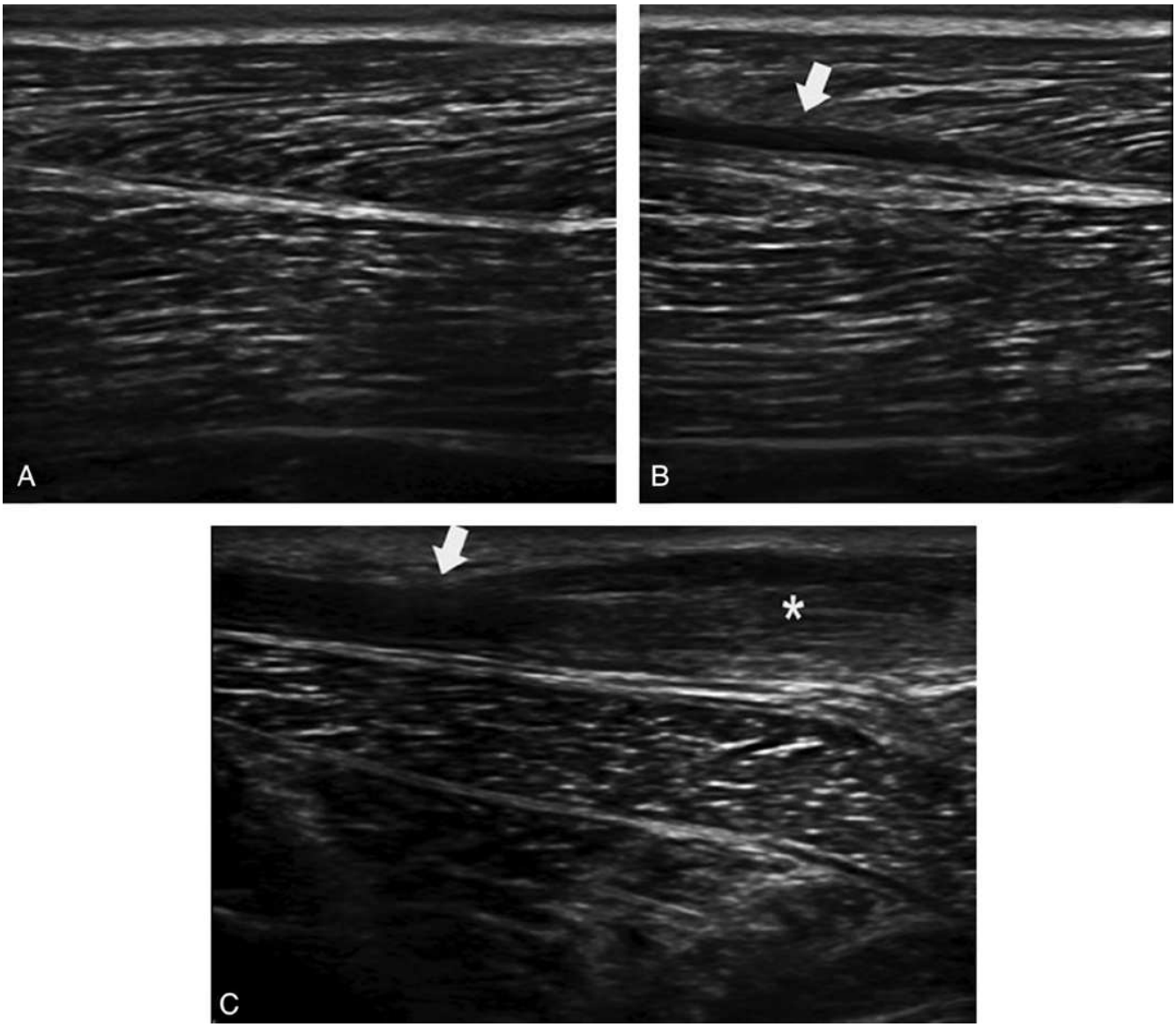


**Figure 35.14.** Semimembranosus muscle. Partial rupture of the semimembranosus muscle and tendon of insertion in a 8-year-old male intact Border collie with an acute nonweight-bearing lameness and a palpable nodular lesion in the right thigh musculature. Longitudinal ultrasound images of the (A) normal and injured (B,C) semimembranosus muscle. In (A) the pennate appearance of the normal semimembranosus muscle is noted. Centrally in the semimembranosus muscle, the hyperechoic myotendinous junction is present. (B) Adjacent to the myotendinous junction of the semimembranosus muscle a hypo- to anechoic linear area is noted (*arrow*), with loss of the normal adjacent muscle fiber alignment. (C) This partial fiber disruption continues distally (*asterisk*) and extends along the tendon of insertion of the semimembranosus muscle (*arrow*) distally to the tibia (not included in the image). The distal aspect of the semimembranosus muscle to tendon is increased in size, which is most noticeable at the level of the asterisk (*).

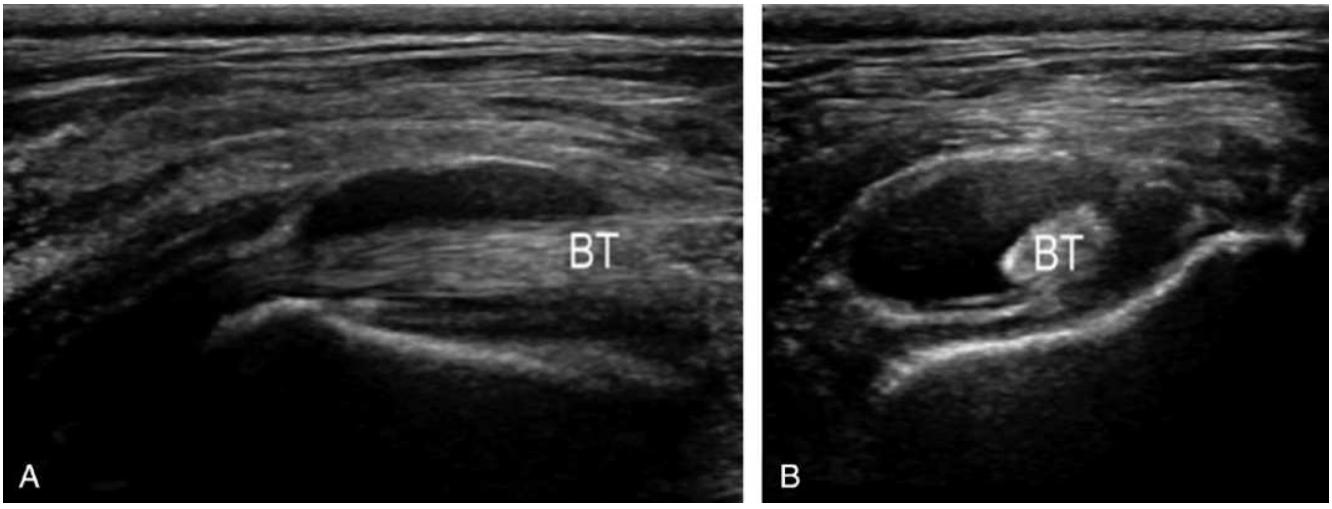


**Figure 35.15.** Biceps tenosynovitis. In both longitudinal (A) and transverse (B) ultrasound images of the biceps tendon (BT), an increased amount of anechoic fluid is noted in the biceps brachii tendon sheath. The tendon sheath is severely distended and the wall is mildly thickened. The biceps tendon has a mildly heterogeneous echogenicity.

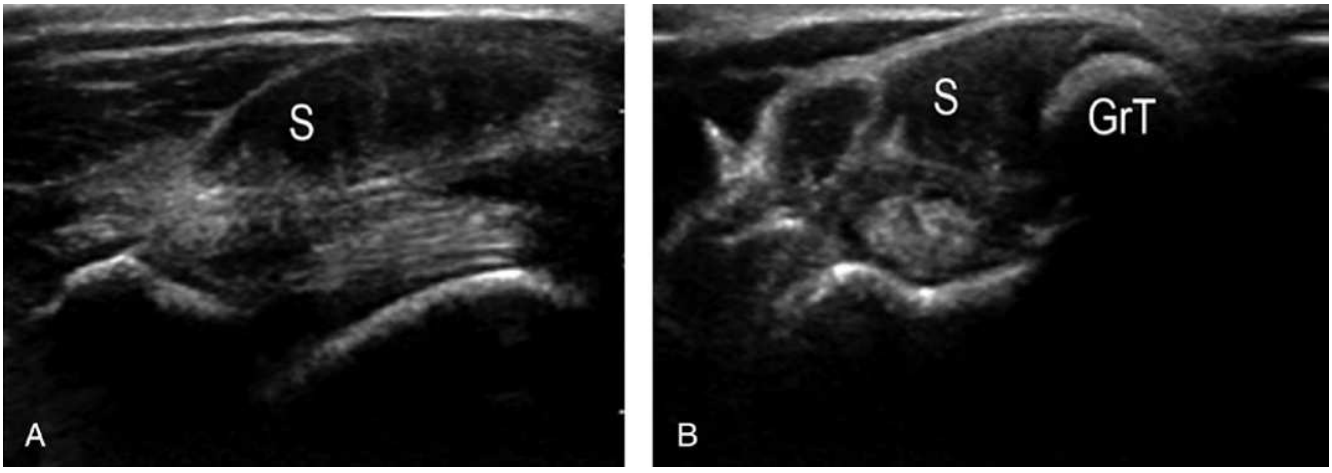


**Figure 35.16.** Supraspinatus tendinopathy. (A) Longitudinal and (B) transverse image of the supraspinatus tendon (S) at the insertion at the greater tubercle (GrT) of the humerus. The supraspinatus tendon of insertion shows diffusely reduced echogenicity and a loss of normal fiber architecture. The biceps tendon shows a mildly heterogeneous echogenicity in its origin in the longitudinal and transverse plane ultrasound images.

psoas muscle originates from the ventrolateral aspect of the lumbar spine and the iliacus muscle from the ilium, and both insert together at the lesser tubercle of the femur. If a lesion is suspected, the entire length of these muscles from the lumbar spine and the pelvis to the lesser tubercle of the femur needs to be evaluated, as lesions can occur anywhere along this path. Moreover, lesions frequently occur bilaterally and thus a comparison with the contralateral side might look similar if both are equally injured.

### *Muscle Atrophy*

Atrophied muscle is smaller when compared to the contralateral limb or body area. Often a heterogeneous, patchy and striped echogenicity with hypoechoic areas in between may be noted (Figure 35.19). In human patients, it has been demonstrated that when a muscle atrophies, such as in neuromuscular disorders, the muscle tissue gets replaced by fat and fibrous tissue, resulting in increased echogenicity of the muscle.

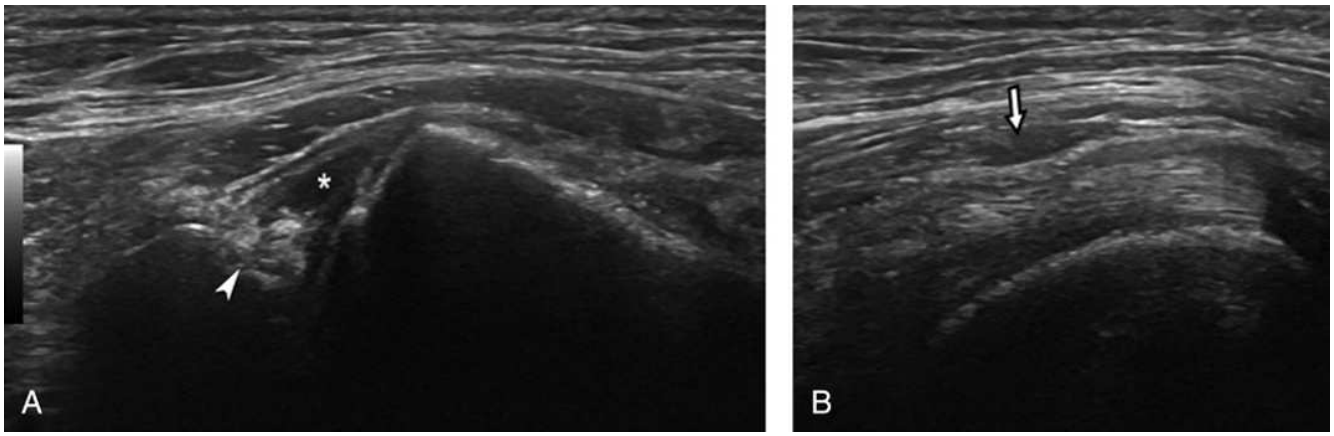


**Figure 35.17.** Avulsion fracture of the supraglenoid tubercle of the scapula and rupture of the biceps tendon at the level of the supraglenoid tubercle. (A) Longitudinal image of origin of the biceps tendon. The distal aspect of the supraglenoid tubercle (*arrowhead*) is markedly irregular with a small round to irregularly shaped, hyperechoic structure distal to it. A large hypoechoic defect (*) is noted in the proximal aspect of the biceps tendon distal to the supraglenoid tubercle of the humerus. (B) Longitudinal image of the biceps tendon at the level of the bicipital groove. A small amount of anechoic to hypoechoic fluid is noted in the biceps tendon sheath circumferentially surrounding the biceps tendon (*white arrow*) and minimally distending the biceps tendon sheath.

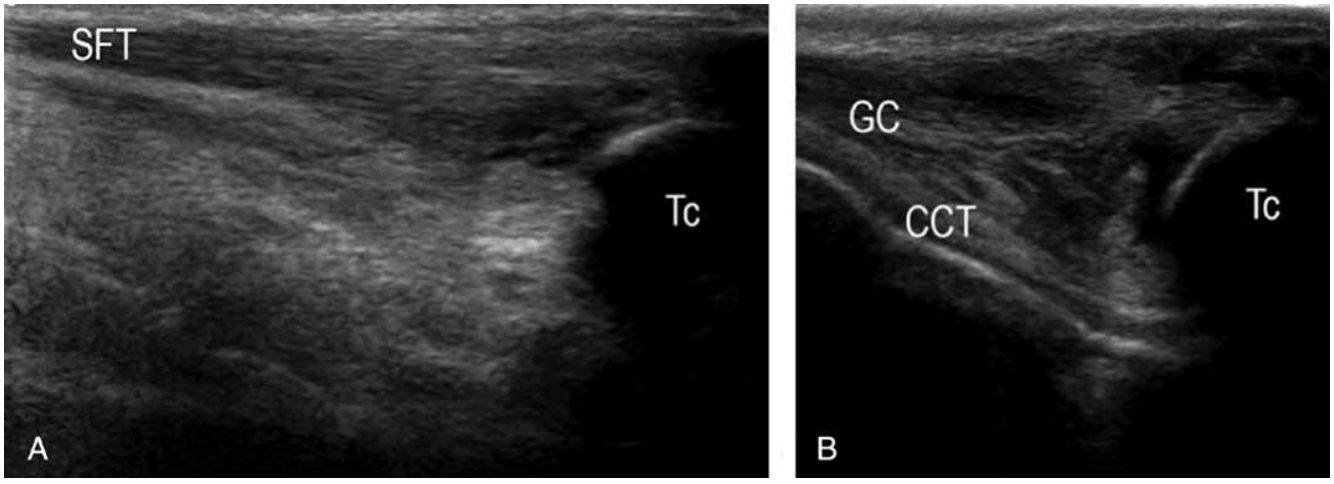


**Figure 35.18.** Partial Achilles tendon rupture. Longitudinal ultrasound images of the distal aspect of the Achilles tendon proximal to the calcaneal tubercle (TC). (A) The superficial flexor tendon shows at the level of the calcaneal tubercle an increased thickness and reduced echogenicity with loss of normal fiber structure. (B) The distal aspect of the gastrocnemius muscle and tendon is severely heterogeneous in echogenicity with loss of fiber attachment at the calcaneal tubercle. The common calcaneal tendon is mildly dorsally displaced and shows distally a reduced echogenicity and loss of normal fiber structure.

Furthermore, this increase in muscle echogenicity can be quantified, used to stage disease, and subsequently compared for assessing response to treatment (Pillen and van Alfen 2011).

## Muscle Masses

POCUS MSK can provide valuable information evaluating the extent of a mass and its relationship to surrounding structures, including lymph nodes. Color Doppler may provide additional information regarding vascularity and blood flow within the mass (Figure 35.20). Muscle mass lesions can appear widely variable ultrasonographically, and ultrasound has shown poor correlation with final histopathological diagnosis. Therefore, tissue sampling is necessary and ultrasound-guided sampling techniques may be used to more accurately sample affected tissue and avoid important associated structures (lowering complications).

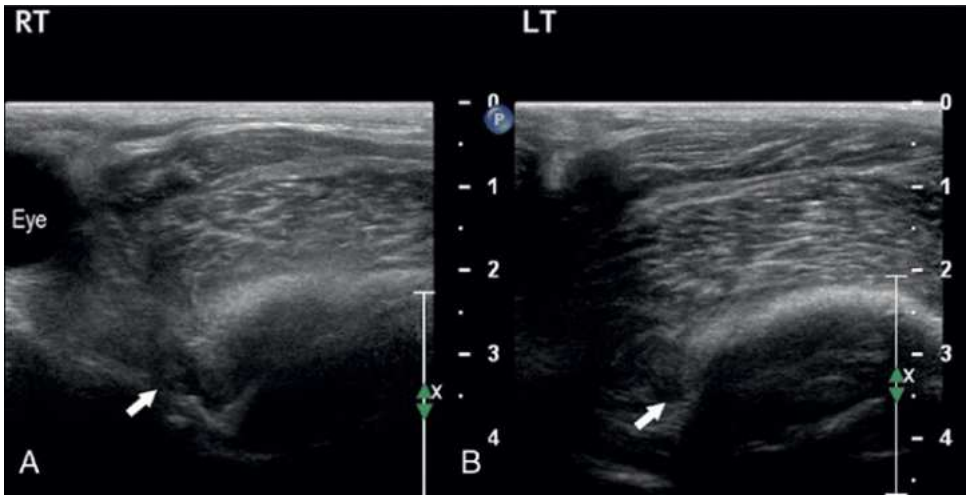


**Figure 35.19.** Neuritis and regional muscle atrophy. A 9-year-old Portuguese water dog was presented with a recent history of lethargy, inappetence, squinting, and difficulty opening the mouth. On computed tomography, a focal area of contrast enhancement was noted in the area of the maxillary branch of the trigeminal to oculomotor nerve. A focused ultrasound of this area was performed to obtain fine needle aspirates. Comparative ultrasound images ventral to the eye and medial to the zygomatic arch revealed that the maxillary branch of the trigeminal or oculomotor nerve on the right (RT) (shown in A) and left (LT) (shown in B) sides of the head are similar in size and echogenicity (*white arrow*). The adjacent masseter and to a lesser extent zygomaticus muscles on the right side (B) are mildly reduced in size and heterogeneous in echogenicity with a mildly patchy and striped pattern. No mass lesion was identified. Cytology revealed a septic suppurative inflammation and a focal neuritis was suspected.

# Pearls and Pitfalls, The Final Say

- Correlate POCUS MSK findings with clinical findings because some diseases, such as osteomyelitis and bone neoplasia, appear ultrasonographically similar and additional tissue sampling is necessary for a definitive diagnosis.
- Compare the suspected lesion with the contralateral side or adjacent normal tissue, especially when the contralateral side or adjacent area is not affected.
- Routinely evaluate MSK lesions both statically and dynamically to evaluate for conditions more recognizable with changes in flexion and extension, the presence of adhesions, and to ensure normal movement (function) of the tissue.
- POCUS MSK can provide additional information regarding bone healing, specifically when the degree of vascularization is of concern, and when there is concern whether infection exists. Ultrasound-guided sampling of regions of concern containing fluid may then be pursued using color flow Doppler to avoid vascular structures.
- Image POCUS MSK in two steps. First, evaluate the area of interest as an overview, and then second, magnify (decrease depth) so that smaller lesions may be detected and not overlooked.
- Acute muscle injuries often present with subtle findings of focal swelling and minor fiber inhomogeneity that will change over time, emphasizing the importance of serial POCUS MSK examination and comparison(s) and the need for saving and archiving these images.
- When imaging tendons, anisotropy artifact is common and avoided by continuous adjustment of the imaging plane and ensuring that the tendon is scanned at its maximum echogenicity. By not scanning in this manner, artifactual anisotropy resulting in areas of decreased echogenicity within a tendon might be misinterpreted as a lesion.
- POCUS MSK may be used as an ancillary technique to other imaging modalities to more completely evaluate the extent of a lesion, such as skull fracture and traumatic brain injury. Head injuries with suspected brain involvement can initially be quickly evaluated with a POCUS MSK and POCUS brain, followed by computed tomography and/or MRI after patient stabilization.
- POCUS MSK is effective for detecting injuries such as rib fractures, but assessment for related intrathoracic injury should not be overlooked, including the Global FAST approach, followed by additional imaging as indicated such as thoracic radiography and computed tomography when the patient is stabilized for complete trauma evaluation.

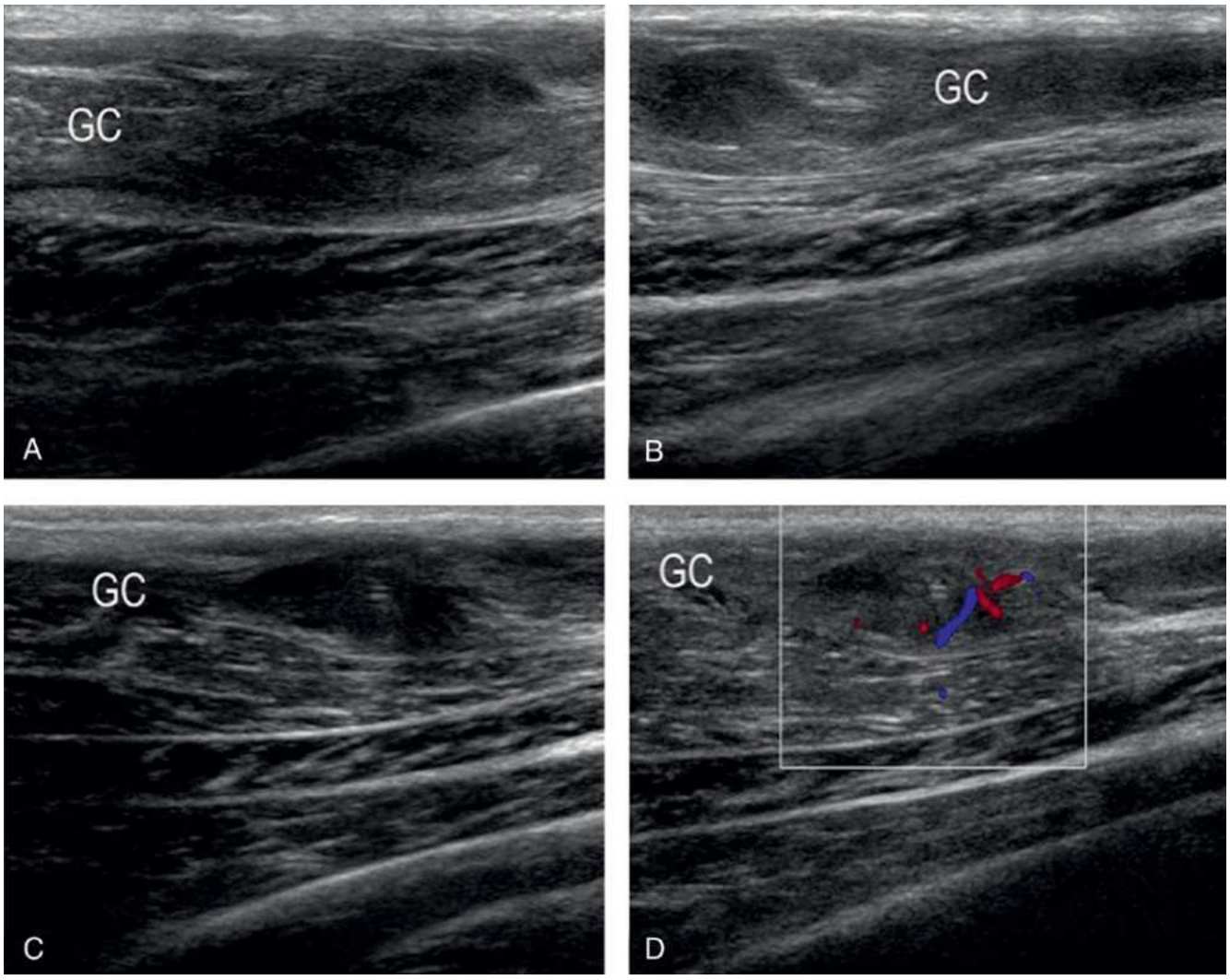


**Figure 35.20.** Benign, chronic, degenerative muscle mass. Four longitudinal ultrasound images of the distal aspect of the gastrocnemius muscle (GC). (A) Proximal to the myotendinous junction of the gastrocnemius muscle, a heterogeneous, hypoechoic area causing increased size of the gastrocnemius muscle and loss of normal fiber structure is noted. (B) This lesion extends distally into the proximal aspect of the gastrocnemius tendon, which is decreased in echogenicity. (C) The lesion is proximally well defined and does not show invasion into adjacent musculature or extension into the subcutaneous tissue. (D) This lesion is distally well vascularized as noted on color Doppler imaging. Ultrasound-guided fine needle aspiration and cytology of the lesion revealed no signs of neoplasia or inflammation. Follow-up biopsies were performed and no signs of neoplasia or infection were noted. The lesion was described as a collagenous proliferation with myxomatous change.

# References

Cook CR. 2016. Ultrasound imaging of the musculoskeletal system. *Vet Clin North Am Small Anim Pract* 46:355–371.

Draghi F, Zacchino M, Canepari M, et al. 2013. Muscle injuries: ultrasound evaluation in the acute phase. *J Ultrasound* 16:209–214.

Maffulli N, Thornton A. 1995. Ultrasonographic appearance of external callus in long-bone fractures. *Injury* 26:5–12.

Mattoon JS, Nyland TG. 2015. Fundamentals in diagnostic ultrasound. In: *Small Animal Diagnostic Ultrasound*, 3rd edition, edited by Nyland TG, Mattoon JS. Philadelphia: WB Saunders, pp 1–49.

Pillen S, van Alfen N. 2011. Skeletal muscle ultrasound. *Neurol Res* 33:1016–1024.

Stevenson JH. 2013. Tissue scanning. In: *Basics of Musculoskeletal Ultrasound: A Workbook*, edited by Daniels JM, Dexter WW. New York: Springer, pp 15–27.

# Further Reading

Adeyemo WL, Akadiri OA. 2011. A systematic review of the diagnostic role of ultrasonography in maxillofacial fractures. *In J Oral Maxillofac Surg* 40(7):655–661.

Barata I, Spencer R, Suppiah A, et al. 2012. Emergency ultrasound in the detection of pediatric long-bone fractures. *Pediatr Emerg Care* 28(11):1154–1157.

Bradley M. 2012. Image-guided soft-tissue foreign body extraction – success and pitfalls. *Clin Radiol* 67(6):531–534.

Hosomi S, Rinka H, Watanabe Y, et al. 2012. Cervical impalement injury to a child by a chopstick diagnosed with computed tomography and ultrasonography. *J Anesth* 26(4):598–600.

Ogunmuyiwa SA, Fatusi OA, Ugboko VI, et al. 2012. The validity of ultrasonography in the diagnsosi of sygomaticomexiallry complex fractures. *Int J Oral Maxillofac Surg* 41(4):500–505.

Parri N, Crosby BJ, Glass C, et al. 2013. Ability of emergency ultrasonography to detect pediatric skull fractures: a prospective, observational study. *J Emerg Med* 44(1):135–141.

Picandet JD, Macieira S, Beauregard G, et al. 2007. Detection of rib trauma in newborn foals in equine critical care unit: a comparison of ultrasonography, radiography and physical examination. *Equine Vet J* 39(2):158–163.

Ramirez-Schrempp D, Vinci RJ, Liteplo AS. 2011. Bedside ultrasound in the diagnosis of skull fractures in the pediatric emergency department. *Pediatr Emerg Care* 27(4):312–314.

Teng M, Doniger SJ. 2012. Subungual wooden splinter visualized with bedside sonography. *Pediatr Emerg Care* 28(4):392–394.

SECTION VII

# Monitoring and Surveillance

CHAPTER THIRTY-SIX

# POCUS: Global FAST – Patient Monitoring and Staging

Gregory R. Lisciandro

## Introduction

This chapter covers two major principles: the use of Global FAST for patient monitoring, and the use of Global FAST for staging disease. The Global FAST approach is the combination of AFAST and its abdominal fluid scoring system, its target organ approach; TFAST for pleural and pericardial effusion, its TFAST echo views, and its target organ approach to the heart; and lastly Vet BLUE for detection of alveolar-interstitial edema and other lung surface pathology.

The Global FAST approach consists of exact clarity to its 15 acoustic windows with clear objectives on its goal-directed templates (Boysen and Lisciandro 2013; Lisciandro and Armenise 2014; Lisciandro 2014a,b,d, 2019b) (see Figures 36.3, 36.4, 37.1, and 37.2). Furthermore, Global FAST provides a set of unbiased imaging data points that avoid satisfaction of search error and picking and choosing POCUS examinations based on the preconceived bias of the clinician. For example, the finding of sonographic gallbladder wall edema in a collapsed dog may erroneously lead to the diagnosis of canine anaphylaxis when the patient in fact has pericardial effusion as its cause for the sonographic gallbladder wall edema and its collapse (see Figure 7.12, 7.13, 18.22, 18.23, 36.8, and 36.9) (Lisciandro 2014a,d, 2019a). A Vet BLUE with "dry lung" all views (absent B-lines) rules out left-sided congestive heart failure with high sensitivity in both cats (96%) and dogs (89–96%) (see Table 23.3) (Lisciandro et al. 2016) but without TFAST, the dilated cardiomyopathy or the intracardiac mass is missed (see Figure 18.32) while without AFAST, the low-grade hemoabdomen with a midabdominal mass is missed (Figure 36.1).

Expanding further on the case of pericardial effusion with gallbladder wall edema, referred to as a "cardiac gallbladder" (Lisciandro 2019a), the Global FAST approach provides even more clinically relevant information, allowing assessment of volume status via the caudal vena cava (CVC) at the FAST diaphragmatico-hepatic (DH) view and its characterization. In this case, the CVC is determined to be FAT, or distended CVC (fluid intolerant, high central venous pressure) along with hepatic venous distension (tree trunk sign), which is indirect evidence for cardiac tamponade and obstructive shock (Himelman et al. 1988: Candotti and Arntfield 2015; Lisciandro 2014a,d, 2016). Moreover, the TFAST echo views provide direct evidence for cardiac tamponade and obstructive shock through the observation of right atrial and ventricular collapse. The AFAST screens for the presence of a non-hemoabdomen ascites (better prognosis) and Vet BLUE for the presence of pulmonary metastasis (poor prognosis) (see Figures 18.20 and 36.21) (Stafford Johnson et al. 2004; MacDonald et al. 2009).

The Global FAST approach is clearly more informative than a "flash exam," which consists of no defined acoustic windows other than a sweep of the abdomen and thorax to answer a single binary question of fluid positive or fluid negative. Furthermore, it is important to critically consider whether the terms "AFAST", "TFAST" and "Vet BLUE" are being misused for "flashing" (Lisciandro and Mann 2019). The targeted POCUS exam, focusing on a single area of interest, also is

*Point-of-Care Ultrasound Techniques for the Small Animal Practitioner*, Second Edition. Edited by Gregory R. Lisciandro.
© 2021 John Wiley & Sons, Inc. Published 2021 by John Wiley & Sons, Inc.
Companion website: www.wiley.com/go/lisciandro/ultrasound2

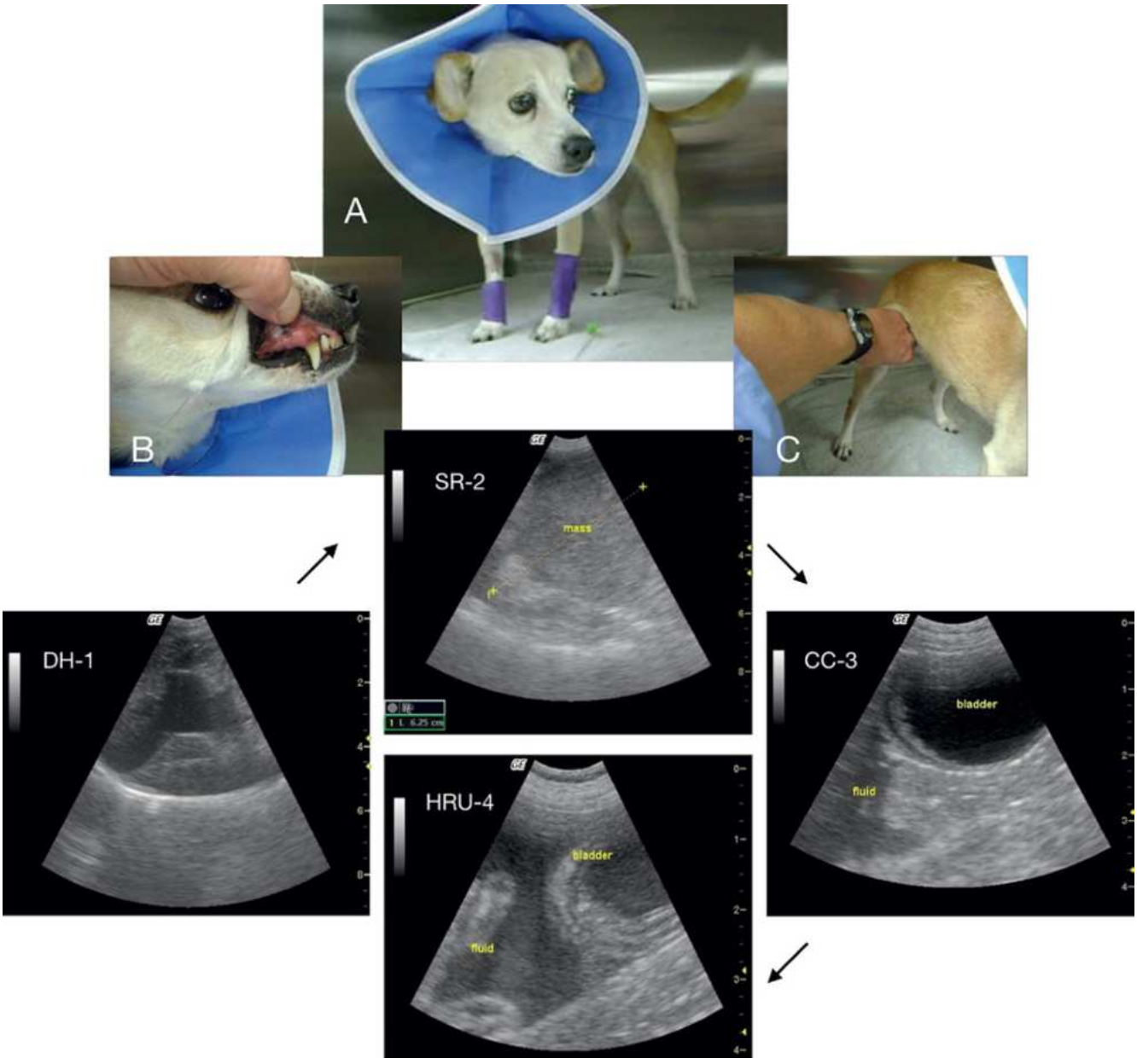


**Figure 36.1.** Occult low-grade hemoabdomen in a dog. A 12-year-old, female spayed Chihuahua that presented for lethargy and poor appetite for 48 hours. Physical examination was unremarkable other than a low-grade fever, mild dehydration, and melena. Laboratory testing yielded a mild nonregenerative anemia and mild azotemia. The dog was treated through the day with intravenous fluids, antibiotics, and gastrointestinal protectorants. (A–C) The dog post treatment is now bright and alert with pink mucous membrane color and good peripheral pulses. However, the Global FAST shows soft tissue mass at the SR view and free intraabdominal fluid at the CC and HRU views, thus assigning an AFS of 2. The presence of safely accessible intraabdominal fluid led to abdominocentesis. Fluid analysis and cytology confirmed a hemoabdomen from the likely bleeding splenic mass. The AFS of 2 made the dog a small-volume bleeder and with an AFS of 2 there would be no anticipated anemia pretreatment unless the dog had preexisting anemia. The mass was determined to be splenic in origin during a focused spleen exam (or a complete detailed abdominal ultrasound dependent on operator proficiency). Global FAST staged the dog with localized disease. The dog is assessed as a surgical candidate and the presurgical work-up continues with hope for definitive surgical care. Source: Reproduced with permission from Dr Gregory Lisciandro, Hill Country Veterinary Specialists and FASTVet.com, Spicewood, TX.

VetBooks.ir

potentially detrimental to patient care by missing the big clinical picture (Narasimhan et al. 2016). The POCUS targeted examination, focused organ or system exam clearly has its place, but should be performed *after* a Global FAST. The cases at the end of this chapter further emphasize this point (see Figures 36.18–24).

The use of Global FAST for patient monitoring continues to evolve from its original concept with the publication of subsequent clinical studies (Lisciandro 2012, 2016; Boysen and Lisciandro 2013; Lisciandro and Armenise 2014; Lisciandro et al. 2014, 2016, 2017, 2019; McMurray et al. 2016; Ward et al. 2017, 2018a,b, 2019: Dicker et al. 2019; Hnatusko et al. 2019; Lisciandro and Lisciandro 2019; Vientós-Plotts et al. 2019). Global FAST is advantageous over the individual use of POCUS Heart, POCUS Caudal Vena Cava, Vet BLUE, and AFAST by integrating important global patient information (see Figures 36.5, 36.18–24). Integration of other relevant findings increases the probability of being correct. Conversely, when selecting individual POCUS exams, important patient information is potentially overlooked to the detriment of the patient through selective imaging and satisfaction of search error.

A good example would be performing a POCUS Heart along with a POCUS Caudal Vena Cava for volume status during fluid resuscitation. The patient is assessed as volume contracted based on poor left ventricular filling and a flat caudal vena cava warranting more aggressive fluid therapy; however, the question always raised is where is the volume loss? In other words, where is the "leak in the tank"? By applying Global FAST, the AFAST component detects free intraabdominal fluid with an abdominal fluid score (AFS) of 4. The fluid is sampled and evaluated, documenting a hemoabdomen. The postinterventional life-threatening bleed is detected before overt patient decompensation but likely missed with POCUS Heart and POCUS Caudal Vena Cava. To the detriment of the bleeding patient, they will likely worsen with a more aggressive fluid resuscitation approach based on only a POCUS Heart and POCUS Caudal Vena Cava. The AFAST findings rapidly provide a complete global evaluation and trigger blood transfusion and interventions to stop the otherwise occult ongoing hemorrhage missed by targeted POCUS Heart and POCUS Caudal Vena Cava.

Moreover, the clinical question of "Where is the volume loss ("leak in the tank")?" is automatically evaluated by Global FAST that includes searching for effusion within the peritoneal and pleural cavities, retroperitoneal space, pericardial sac, and lung (Tables 36.1 and 36.2). The patient can often "leak" large volumes of effusion in the peritoneal and pleural cavities and retroperitoneal spaces, forgiving areas, before the "leak in the tank" is recognized, and in bleeding patients, large volumes that are potentially catastrophic before being recognized without ultrasound based on less sensitive means of physical exam, vital signs, laboratory testing, and radiography (Lisciandro et al. 2009; Perera et al. 2010; Bilello et al. 2011). The pericardial sac and lung differ in that they are *unforgiving* areas for "leaks" because much smaller volumes lead to obvious negative changes in patient status, including poor cardiac output and obstructive shock (pericardial effusion) and deterioration in ventilation ("wet lung") from increased extravascular lung water, respectively.

The use of the Global FAST approach for staging patients for localized versus disseminated disease is helpful for conveying prognostic information to clients and also for following response to treatment. For example, fungal granulomas may be tracked during antifungal therapy using Vet BLUE. Moreover, the Global FAST approach helps dictate the next best diagnostic test for the general practitioner as well as the specialist. For example, a cat may have lung nodules on Vet BLUE and an enlarged spleen on AFAST with the suspicion of disseminated fungal disease diverting the lung lobe aspirate to a potentially less risky splenic aspirate, or the combination of Global FAST findings triggers fungal testing or a lung lobe aspirate (see Figures 23.35–23.37).

In patients suspected of having neoplastic processes, use Global FAST to rapidly stage the patient for localized versus disseminated disease (see Figures 36.19–36.21). For example, a splenic mass deforming the splenic capsule, a serious finding, is detected using POCUS abdomen with a "flash approach," the general ultrasound sweep of the abdominal cavity without any standardization. The client is given the news of a cancerous process, which likely triggers much anxiety compounded by the prospect of an overwhelming and costly diagnostic "staging" work-up. As a result, many of these cases are euthanized (Lux et al. 2013).

A new approach is Global FAST the same day before the patient departs, looking for obvious disseminated disease. For the splenic mass, peritoneal hemorrhage is screened for by AFAST and its fluid scoring system, and when hemoabdomen is present, the free fluid is categorized as a small-volume bleeder versus large-volume bleeder, thus helping with decision making on the need for a blood transfusion (Lisciandro et al. 2009; Boysen and Lisciandro 2013). Moreover, liver masses and pericardial effusion are rapidly screened for via the DH view, pleural and

**Table 36.1.**
Comparison of Global FAST and the RUSH (Rapid Ultrasound in Shock) exam.

| Echo views | RUSH | Global FAST | Comments |
|---|---|---|---|
| Volume and contractility (FS%) | Right parasternal short-axis and long-axis views | Right PCS TFAST short-axis and long-axis views | Similar –echocardiography views and the "eyeball method" *without* measurements (Ferrada et al. 2011) |
| Left-sided strain/ overload | Unclear | Short-axis view from right pericardial site for LA:Ao | Similar – "eyeball method" *without* measurements (Ferrada et al. 2011) |
| Right-sided strain/ overload | Long-axis view for RV:LV | Long-axis view from right pericardial site for RV:LV | Similar – "eyeball method" *without* measurements (Ferrada et al. 2011) |
| Thoracic effusions | | | |
| Pleural effusion | E-FAST (extended FAST) | TFAST | Similar – E-FAST developed in 2004 (Kirkpatrick 2004), TFAST developed in 2005 (Lisciandro et al. 2008) |
| Pericardial effusion | E-FAST | TFAST | Similar – E-FAST developed in 2004 (Kirkpatrick et al. 2004), TFAST developed in 2005 (Lisciandro et al. 2008) |
| Pneumothorax | E-FAST | TFAST | Similar – E-FAST developed in 2004 (Kirkpatrick et al. 2004), TFAST developed in 2005 (Lisciandro et al. 2008); E-FAST has no "lung point" for degree of PTX (see Figure 36.16) |
| "Lung Point" | Similar but *without* a semiquantitative approach | TFAST PTX 1/3s Rule – upper, middle, lower in standing or sternal (see Figure 36.16) | Different – evaluating in sternal or standing better categorizes degree of PTX (see Figure 36.16); lacking in E-FAST and RUSH (Lisciandro et al. 2008; Lisciandro 2011) |
| Lung ultrasound | Minimal approach without a B-line scoring system; lacking regional and pattern-based approach | Vet BLUE B-line scoring system; regional pattern-based approach; Vet BLUE 6 lung ultrasound signs (Figure 36.17 and see also Figures 23.2, 22.1, 22.11, 22.12, 22.15) | Different – Global FAST does more; Vet BLUE B-line scoring system and Vet BLUE lung contusion severity score and Vet BLUE 6 lung ultrasound signs with a regional pattern-based approach (Figure 36.17 and see also Figures 23.2, 22.1, 22.11, 22.12, 22.15) (Lisciandro 2014b; Lisciandro et al. 2014, 2017) |
| Vena cava | Inferior vena cava (IVC) - FAT, flat or fluid responsive – 2 cm rule and sniff test (Ferrada et al. 2012a,b; Erhardt 1996) | Caudal vena cava – FAT, flat or bounce (Ferrada et al. 2012a,b) | Similar – longitudinal plane at the subxiphoid view is analogous to the FAST DH view (Ferrada et al. 2012a,b; Tchernodrinski and Arntfield 2015); maximum CVC height guidelines established for dogs and suggested for cats (see Tables 36.3 and 36.4) (Darnis et al. 2018) |
| FAST | Fluid only, no scoring system | AFAST – target organ approach, AFAST – abdominal fluid scoring system – "small-volume bleeder/effusion" versus "large-volume bleeder/ effusion" (Lisciandro et al. 2009, 2019a; Lisciandro 2011; Boysen and Lisciandro 2013) | Different – Global FAST does more; RUSH has no fluid scoring system for bleeding patients regarding decision making for blood transfusion and expected anemia from the intraabdominal bleed (Perera et al. 2010); no soft tissue scan (Perera et al. 2010) |

**Table 36.1.**
(*Continued*)

| Echo views | RUSH | Global FAST | Comments |
|---|---|---|---|
| Search for a "leak in the tank" | Pleural and pericardial effusions, retroperitoneal space, peritoneal cavity | Pleural and pericardial effusions, retroperitoneal space, peritoneal cavity plus lung using the Vet BLUE B-line scoring system for estimating extravascular lung water (Jambrik et al. 2004, 2010; Volpicelli et al. 2006; Lichtenstein et al. 2009; Lisciandro et al. 2008, 2009; Lisciandro 2014, 2016, 2017; Ward et al. 2017, 2018; Dicker et al. 2019) | Different – Global FAST does more through more lung examination (pulmonary hemorrhage and increased extravascular water) (Jambrik et al. 2004, 2010; Volpicelli et al. 2006; Lichtenstein et al. 2009, 2012; Lichtenstein and Karakitsos 2012; Lisciandro 2011; Lisciandro et al. 2014, 2016, 2017; Ward et al. 2017; Dicker et al. 2019) |
| Urinary bladder volume estimation and urine output | N/A | Length × height × width (W) in centimeters × 0.625 = estimation urinary bladder volume in milliliters (Lisciandro and Fosgate 2017) | Global FAST does more; RUSH has no urinary bladder estimation formula although a formula is described in people (Hassani 2015) |
| Aortic evaluation | RUSH screens for aortic aneurysm and dissection | N/A | Unlikely relevance for dogs and cats; may be relevant for other species, especially birds and reptiles with vitamin D toxicosis |
| Deep venous thrombosis (DVT) | RUSH screens for DVT through a leg survey | N/A | Unknown relevance for dogs and cats; however, the femoral artery and vein may be imaged via the AFAST CC view using the urinary bladder as an acoustic window and stand-off |
| Inferior jugular vein | | N/A | Unknown relevance for dogs and cats, although anecdotally imaging the caudal vena cava at the FAST DH view is more reliable (see Chapter 19) |

Source: Reproduced with permission of Dr Gregory Lisciandro, Hill Country Veterinary Specialists and FASTVet.com, Spicewood, TX.

pericardial effusion using TFAST (indirect evidence for metastasis), and obvious lung metastasis via Vet BLUE (MacDonald et al. 2009; Stafford Johnson et al. 2004; Boston et al. 2011; Kulhavy and Lisciandro 2015; Lisciandro 2016a; Lisciandro 2019b). If the patient is negative on the Global FAST staging, a very different presentation may be made to the owner of encouragement and the possibility of cure with the diagnostic steps of X, Y, and Z. The conclusion is that "Your pet is a surgical candidate!"

Conversely, departing clients left to "think about it" often despair about the potentially catastrophic disease process that is suspected along with being guilt ridden and torn between pursuing treatment or not. When patients stage with obvious disseminated disease using the Global FAST approach, the patient–client–veterinarian bond is strengthened through the helping of patient and client in the pet's final stages of life, rather than the client feeling abandoned (see Figures 36.22, 36.23). The author has been on both ends of this spectrum, being a general practitioner the first half of his 28-year career and an emergency veterinarian and specialist the second half. Case examples are presented at the end of this chapter and the reader is referred to specific AFAST, TFAST, Vet BLUE, and POCUS chapters for more detail.

The Global FAST approach is a game-changer for patient evaluation and one of the most impactful paradigm changes for better patient care this decade. A similar ultrasound approach will likely do the same in human medicine (Skubas 2015; Narasimhan et al. 2016; Tavares et al. 2019).

Vetbooks.ir

**Table 36.2.**
Global FAST for patient volume assessment and detecting treatable forms of shock, modified from the RUSH Exam (Perera et al. 2010).

| Global FAST evaluation | Hypovolemic shock | Cardiogenic shock | Obstructive shock | Distributive shock |
|---|---|---|---|---|
| **Pump – How Contracting?** | **Works** | **Deficient** | **Works –Overloaded** | **Works – Deficient** |
| **Inotropy** | Hypercontractile heart | Hypocontractile heart | Hypercontractile heart | Hypercontractile heart (early sepsis) |
| | Small chamber size | Dilated heart | PCE/tamponade | |
| | | | RV strain (increased RV:LV) when PTE, cardiac thrombus | Hypocontractile heart (late sepsis) |
| | Dry Lung | Wet Lung | Dry >> Wet Lung | Dry > Wet Lung |
| **Tank – How Full?** | **Empty** | **Overfilled** | **Overfilled** | **Empty or Overfilled** |
| **Volume** | Flat CVC | Distended CVC | Distended CVC | Normal or small CVC (early sepsis) |
| | Flat jugular veins | Distended jugular vein | Distended jugular | Peritoneal fluid (exudate/sepsis source) |
| | | B-lines (lung edema) | PTX (A-lines and no glide sign) | PE (exudate/ sepsis source) |
| | Dry Lung | Wet Lung | Dry or Wet Lung | Dry or Wet Lung |
| **Pipes – Leaky?** | **Leaky** | **Normal** | **Obstructed** | **Leaky or Distended** |
| | Peritoneal fluid (loss) | Peritoneal fluid (ascites) | Thromboembolism | Acute respiratory distress syndrome (ARDS) |
| | PE (loss) | PE | | Third spacing |
| | Splenic or other intraabdominal bleeding tumor | | | |
| **Comments** | Use Vet BLUE and AFS | Use Vet BLUE and AFS | Vet BLUE can detect PTE | Vet BLUE and TFAST can detect noncardiogenic edema |

Source: Reproduced with permission from Dr Gregory Lisciandro, Hill Country Veterinary Specialists and FASTVet.com, Spicewood, TX.
PTE, pulmonary thromboembolism; PTX, pneumothorax; AFS, abdominal fluid score; ARDS, acute respiratory distress syndrome; PE, pleural effusion; PCE, pericardial effusion; RV, right ventricle; LV, left ventricle.

## What Global FAST – Patient Monitoring and Staging Can Do

- Can rapidly assess patient volume status by integrating the TFAST echocardiography views with the "Global FAST nonecho fallback" strategies of the FAST DH view for caudal vena cava and hepatic venous distension characterization and Vet BLUE for "wet lung" versus "dry lung."
- Can rapidly screen for effusions causing hypovolemia, by surveying the peritoneal and pleural cavities, retroperitoneal space, pericardial sac, and lung.
- Can trigger ultrasound-guided procedures with the finding of free fluid and soft tissue abnormalities.
- Can rapidly semiquantitate and categorize intraabdominal hemorrhage as small-volume bleeder versus large-volume bleeder by assigning a numerical fluid score (0–4) and decision making for the need for transfusion therapy and surgical interventions.
- Can rapidly semiquantitate and categorize nonhemorrhagic effusions as small-volume effusion versus large-volume effusion by assigning a numerical fluid score.
- Can rapidly estimate urinary bladder volume using the AFAST cysto-colic formula and with serial measurements estimate urine output noninvasively.
- Can rapidly screen for obvious soft tissue abnormalities using the AFAST target organ approach.
- Can semiquantitate pleural effusion.
- Can semiquantitate pericardial effusion.
- Can rapidly screen for left- and right-sided cardiac strain/failure/overload using the TFAST echocardiography views.
- Can rapidly screen for cardiac soft tissue abnormalities.
- Can rapidly screen for lung conditions and categorize them by the distribution of the six Vet BLUE lung ultrasound signs.
- Can semiquantitate degree of pneumothorax (PTX) and track its severity using the TFAST "lung point" concept and TFAST PTX 1/3s Rule.
- Can help determine need for and guide use of vasopressors using the Global FAST volume status approach.
- Can help determine need for and guide use of thromboprophylaxis and thrombolytics using the Global FAST approach for pulmonary thromboembolism.

## What Global FAST – Patient Monitoring and Staging Cannot Do

- Cannot replace the physical examination but rather serves as an extension of the physical exam.
- Cannot replace blood pressure and electrocardiographic monitoring.
- Cannot replace arterial and venous blood gas evaluation and other respiratory function assessment.
- Cannot definitively characterize effusions and mass lesions based on echogenicity because sampling and fluid analysis with cytology and tissue sampling and testing are required, respectively.
- Cannot replace advanced imaging, including complete detailed ultrasound studies of the abdomen and thorax, computed tomography (CT) and magnetic resonance imaging (MRI).

## Indications

- All hospitalized patients on fluid therapy.
- All perioperative patients using Global FAST as their preanesthetic screening test.
- All postinterventional cases for the presence of complications.
- All patients with serious conditions (neoplasia, sepsis, infectious diseases, i.e., fungal) for staging as localized versus disseminated disease.
- Any patient with suspect stability, uncharacterized forms of shock, and uncharacterized hypotension.
- All patients with cardiopulmonary arrest (CPA) or those needing cardiopulmonary resuscitation (CPR).
- All patients with return of spontaneous circulation (ROSC) as part of advanced life support and post-CPR resuscitation.

## Objectives

- Understand the clinical utility of combining AFAST, TFAST, and Vet BLUE as a single examination called Global FAST as an extension of the physical examination for any abnormal or preinterventional patient.
- Understand how staging using Global FAST helps "see" your problem list and better determine your next best test(s).
- Understand how Global FAST may be used perioperatively and postinterventionally for detecting comorbidities and complications otherwise missed without ultrasound.
- Understand how Global FAST can detect left- and right-sided strain/failure/volume overload so that adjustments may be made during resuscitation efforts.
- Understand how Global FAST can trigger thrombolytics and thromboprophylactics.
- Understand how Global FAST may be used for patient monitoring.

# Ultrasound Settings, Probe Preferences, Patient Positioning, and Preparation

## Ultrasound Settings and Probe Preference

A curvilinear (microconvex) probe with a frequency range of 5–10 MHz. The appropriate abdominal preset with a depth range of 3–15 cm is generally acceptable for the entire Global FAST examination in most dogs and cats. Changing probes is unnecessary and often prolongs the completion of the Global FAST examination.

## Optimizing Image Quality and Probe–Skin Contact

Hair is generally not shaved but rather parted for probe-to-skin contact (minimizing air trapping) (Figure 36.2) with the use of isopropyl alcohol and/or alcohol-based hand sanitizer, and/or acoustic coupling gel (see Figures 5.2 and 39.29). The author uses minimal amounts of isopropyl alcohol primarily to wet and part the hair (also strips out air and lipid in hair follicles) followed by alcohol-based hand sanitizer or acoustic coupling gel. Smaller amounts of isopropyl alcohol are less noxious to your patient by minimizing the coolness and wetness of alcohol along with its fumes, especially when the patient is then placed in an oxygen cage. Alcohol-based hand sanitizer has the added benefit of being easily wiped off while also evaporating quickly. Isopropyl alcohol *should not be used if electrical defibrillation is anticipated* because it poses a burn/fire hazard. The clinician should be aware that isopropyl alcohol may cause probe head damage (see Figure 4.13).

**Pearl:** The author generally does not shave patients and does not dim the lighting when performing any part of Global FAST, which is supported by similar findings regarding environmental lighting and that ultrasound imaging is generally not compromised (Breitkreutz et al. 2007, 2010).

## Patient Positioning and Most Efficient Ways to Perform Global FAST

There are a couple of highly efficient ways to perform the 15 acoustic windows (views) of Global FAST in standing/sternal and lateral recumbency that minimize depth changes and moving to different sides of the patient (Figure 36.3).

**Figure 36.2.** Global FAST with low patient impact imaging with minimal restraint. The photo shows the low impact of Global FAST imaging on a patient that is unshaved and unrestrained. The sonographer is starting with the Vet BLUE part of Global FAST. See also Figure 37.23. Source: Reproduced with permission from Dr Gregory Lisciandro, Hill Country Veterinary Specialists and FASTVet.com, Spicewood, TX.

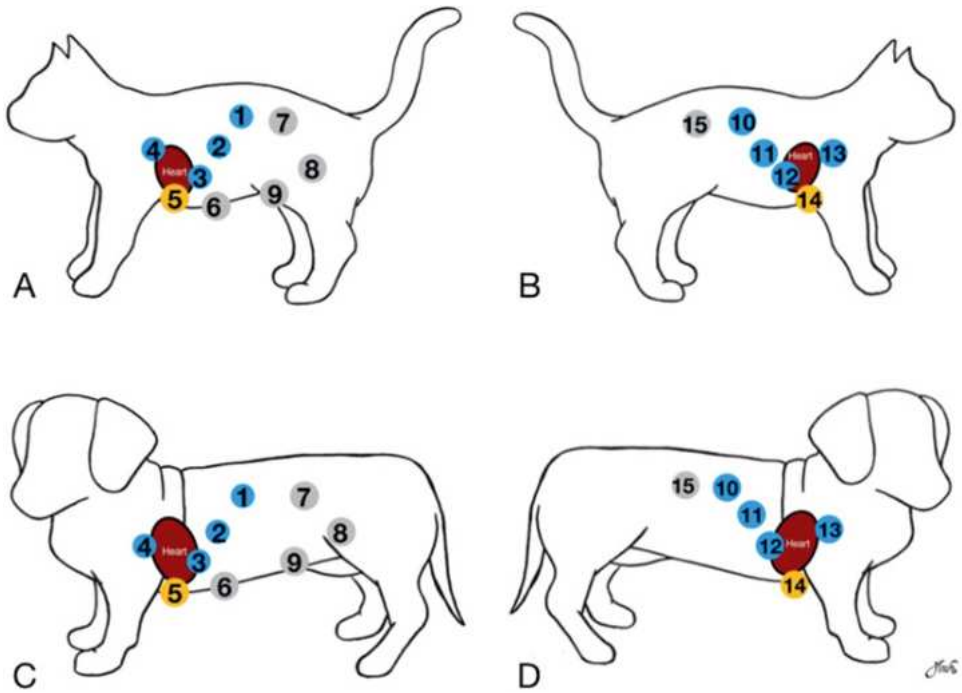


**Figure 36.3.** Global FAST standing position. Shown is an efficient manner in which to perform Global FAST in a standing patient. The sonographer starts from the left side and performs Vet BLUE first (1–4) and then performs the TFAST left PCS view (5) followed by the FAST DH view (6). By performing the DH View from the *left* side, the gallbladder is imaged by fanning toward the patient's *right* side which gives much easier hand motion for the right-handed sonographer. After the DH View, the AFAST is completed by performing the SR view (7) followed by the CC view (8) and the HRU view (9) and a focused spleen (not shown) as illustrated in (A) and (C) for cats and dogs, respectively. The sonographer then moves to the patient's right side as shown in (B) and (D) and performs the right Vet BLUE (10–13) and then the TFAST right PCS view (14) with its most time-consuming TFAST echo views. Finally, the HR5th bonus view is performed (15). Another advantage is that by performing in this order, the sonographer has a good idea of how important the TFAST echo views are because lung has been surveyed (Vet BLUE) including pneumothorax and alveolar-interstitial edema, the thorax has been surveyed for pleural and pericardial effusion, and the CVC and its associated hepatic veins have been characterized. If there is no free fluid detected on AFAST then lateral recumbency is not necessary for fluid scoring. The AFAST views look identical independent of positioning and are performed with the same probe maneuvers as if the patient were in lateral recumbency. Source: Reproduced with permission from Dr Gregory Lisciandro, Hill Country Veterinary Specialists and FASTVet.com, Spicewood, TX. Illustration by Hannah M. Cole, Adkins, TX.

In fact, Global FAST may be reduced to six achievable probe maneuvers as follows.

### *AFAST*

A single maneuver for all five AFAST views: fan, rock cranially, and return to the starting position.

### *TFAST*

Three maneuvers.

- "TFAST slide" caudal and cranial into the "cardiac-diaphragmatic pouch" and "cardiac-cervical pouch" respectively.
- Right TFAST pericardial site (PCS) short-axis views.
- Right TFAST PCS long-axis views.

### *Vet BLUE*

Two maneuvers.

- Three intercostal spaces (ICS) – one caudal and one cranial from the primary for the Caudodorsal, Perihilar, and Middle lung region views.
- Sliding from the cervical region, the cranial transition zone, across the first rib, first ICS, second rib, second ICS, and third rib, third ICS for the Cranial lung region view.

## Lateral Recumbency

When a patient presents in lateral recumbency and is best left in that position for initial Global FAST examination, AFAST is generally performed followed by

TFAST and its PCS views with depth and gain settings that are similar, thus rapidly completing six of eight views (Figure 36.4). The use of the DH view first is the author's choice in lateral recumbency because it rapidly surveys the thorax for pleural and pericardial effusion and pulmonary conditions, the caudal vena cava for volume status, the liver and gallbladder for obvious soft tissue changes including gallbladder wall edema, and the abdomen for the presence of ascites. As a single view, the DH view provides a huge amount of clinically relevant patient information including surveying the thorax without the air interference of lung at transthoracic TFAST views.

Findings at the DH view can dictate whether the TFAST is performed next followed by Vet BLUE or AFAST is completed before moving to TFAST and Vet BLUE.

- The AFAST DH view is performed with lots of depth (10–15 cm) depending on the size of the patient. The higher depth setting allows for a quick overview to see your expected big three landmarks of diaphragm, heart ("cardiac bump"), and caudal vena cava. Depth may then be magnified (decreased) to place the caudal vena cava nearer to the bottom (far-field) of the screen.
- Depth and gain setting are generally similar between AFAST and the TFAST PCS views and both the left TFAST PCS and right TFAST PCS views are evaluated in this order (see Figure 36.4).
- After completing the TFAST PCS views, depth is decreased and the gain turned down for more contrast for lung for the ipsilateral TFAST CTS view for pneumothorax (PTX) and continuing through the ipsilateral Vet BLUE. Right lateral (over left lateral) is advantageous because of the cardiac notch and the heart falling against the thoracic wall for the most valuable of the TFAST echocardiography views, the right PCS view for the left ventricular short axis (LVSA), the short-axis left atrial to aortic ratio (LA:Ao), and the long-axis four-chamber (LA4C) view for the right ventricular (RV) to left ventricular (LV) ratio (RV:LV).
- Left lateral recumbency is used when the patient presents in this position and is most comfortable in left lateral. The AFAST applied abdominal fluid scoring system is validated in either lateral recumbency; however, the TFAST echocardiography

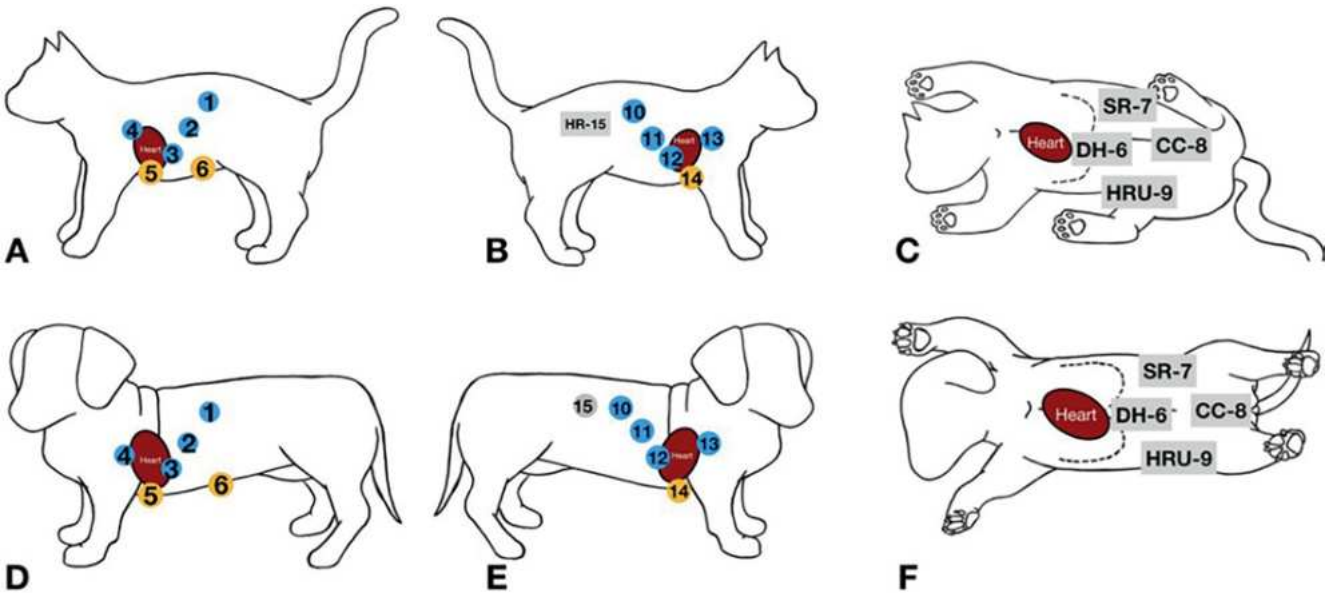


**Figure 36.4.** Global FAST standing position with movement to lateral for fluid scoring. Shown is another manner in which to perform Global FAST efficiently. Compare to Figure 36.3. Vet BLUE and TFAST are blended together as shown in (A) and (B) in the cat, and (D) and (E) in the dog, to get information about the thorax including heart and lung and the FAST DH view for characterization of the CVC and its associated hepatic veins numbered 0–6 from the left and then 10–15 from the right as shown in (A) and (B) in the cat and (D) and (E) in the dog. Now the sonographer has a better idea of patient stability by assessing for pleural and pericardial effusion, lung disease, cardiac conditions, and volume status before moving the patient to right lateral recumbency as shown in (C) and (F). Note the order differs from Figure 36.3, but both versions start with Vet BLUE-TFAST to screen for any compromising conditions that put the patient at risk for restraint as well as determining the need for emergent thoracocentesis and pericardiocentesis. Source: Reproduced with permission from Dr Gregory Lisciandro, Hill Country Veterinary Specialists and FASTVet.com, Spicewood, TX. Illustration by Hannah M. Cole, Adkins, TX.

views are generally more reliable in *right* lateral recumbency but may be attempted from left lateral.

- An imaging trick is to slide the probe closer to the sternum and then direct the scanning plane to the expected location of the heart, attempting to avoid air interference from lung.

### Standing or Sternal

Most patients are less stressed and Global FAST is low impact in standing (or sternal) position and the entire Global FAST format may be performed in < 6 minutes (360 seconds for 15 views is ~25 seconds per view), keeping in mind that eight of the 15 views are transthoracic Vet BLUE views, which are typically faster (~15 seconds) than AFAST and TFAST views. Again, Global FAST is performed without shaving hair and with minimal patient restraint (see Figures 36.2 and 36.3).

Beginning on the left side (author preference) of the patient, the left Vet BLUE transthoracic views are performed first, starting at the Caudodorsal lung region and then moving ventrally and cranially through the subsequent Vet BLUE views. Vet BLUE requires less depth, more magnification, and lower gain (darker screen with more contrast) than soft tissue imaging of AFAST and TFAST. Following the left Vet BLUE, depth is increased to see the landmark of the pericardium in the far-field, gain is generally increased, and the left TFAST PCS view is performed with its "TFAST slide" caudally and then cranially, within the respective cardiac pouches (see Chapter 17). The FAST DH view with nearly same settings as the PCS view is performed next and double checks the "cardiac-diaphragmatic pouch." While standing, the AFAST spleno-renal view, cysto-colic view, hepato-renal umbilical view, and focused spleen are then performed with identical image acquisition as in lateral recumbency and as shown in Chapter 6. In other words, there is no difference in the look of the AFAST views between positioning as target organs are fanned through in nearly identical imaging planes. AFAST, Vet BLUE, and TFAST have now been completed on the left side.

The right Vet BLUE is then performed, requiring a depth change (less depth, magnified) and a gain change (less gain, darker for more contrast along the "lung line"). As on the left side, Vet BLUE begins with the Caudodorsal lung region view followed by the Perihilar, Middle, and Cranial lung regions before blending with the right TFAST PCS echocardiography views (LVSA, LA:Ao, LA4CV) (Figures 36.5 and 36.6). The HR5th bonus view is performed last with fanning, rocking, and returning to the starting point as with the other AFAST views; however, this view is not part of the AFAST-applied abdominal fluid scoring system.

Now the entire Global FAST has been completed and standing-sternal is the positioning of choice for the detection of pleural and pericardial effusion because it is safer and gravity dependency is ventral bilaterally at the TFAST PCS views and FAST DH view. As for ascites, if the standing-sternal patient is negative for free intraabdominal fluid, then lateral recumbency is only necessary to repeat the FAST DH View and TFAST echocardiography views in patients with ambiguity in standing-sternal. If the patient is positive for ascites, then when safe to do so, the patient is placed into either lateral recumbency and then three minutes are allowed to pass so that fluid may distribute, prior to assigning an AFS (Lisciandro et al. 2009).

### Why Start Left and then Move Right for the Global FAST Blend?

The author prefers beginning with the left side of the patient as described. By moving from left to right with the Vet BLUE-TFAST blend, the sonographer already has ruled pneumothorax in or out, knows not only whether lung is wet (B-lines) or dry (A-lines) but also to what degree by using the Vet BLUE B-line scoring system (plus the presence of any other Vet BLUE lung ultrasound signs). Furthermore, the sonographer knows whether pleural and/or pericardial effusion are present, what the liver and gallbladder look like, if there is obvious ascites, and the characterization of the caudal vena cava *before* arriving at the most time-consuming right TFAST PCS view where the TFAST echocardiography views are performed (see Figure 36.6). Thus, the sonographer knows how important these TFAST echocardiography views are because if lung is dry (absent B-lines all views) and the caudal vena cava has a fluid-responsive appearance, then the TFAST echo views for left- and right-sided heart failure are less important on the *initial* survey. TFAST echocardiography views *may wait* until the patient is more stable or less stressed, and if the patient has no pleural effusion (PE), pericardial effusion (PCE), or PTX and has "dry lung" then the restraint for TFAST echocardiography views is less risky.

### Never Dorsal Recumbency

Dorsal recumbency should not be used for several reasons but most importantly because of increasing patient risk. A hemodynamically fragile patient that is unknowingly placed in dorsal recumbency undergoes significant negative changes in ventilation and

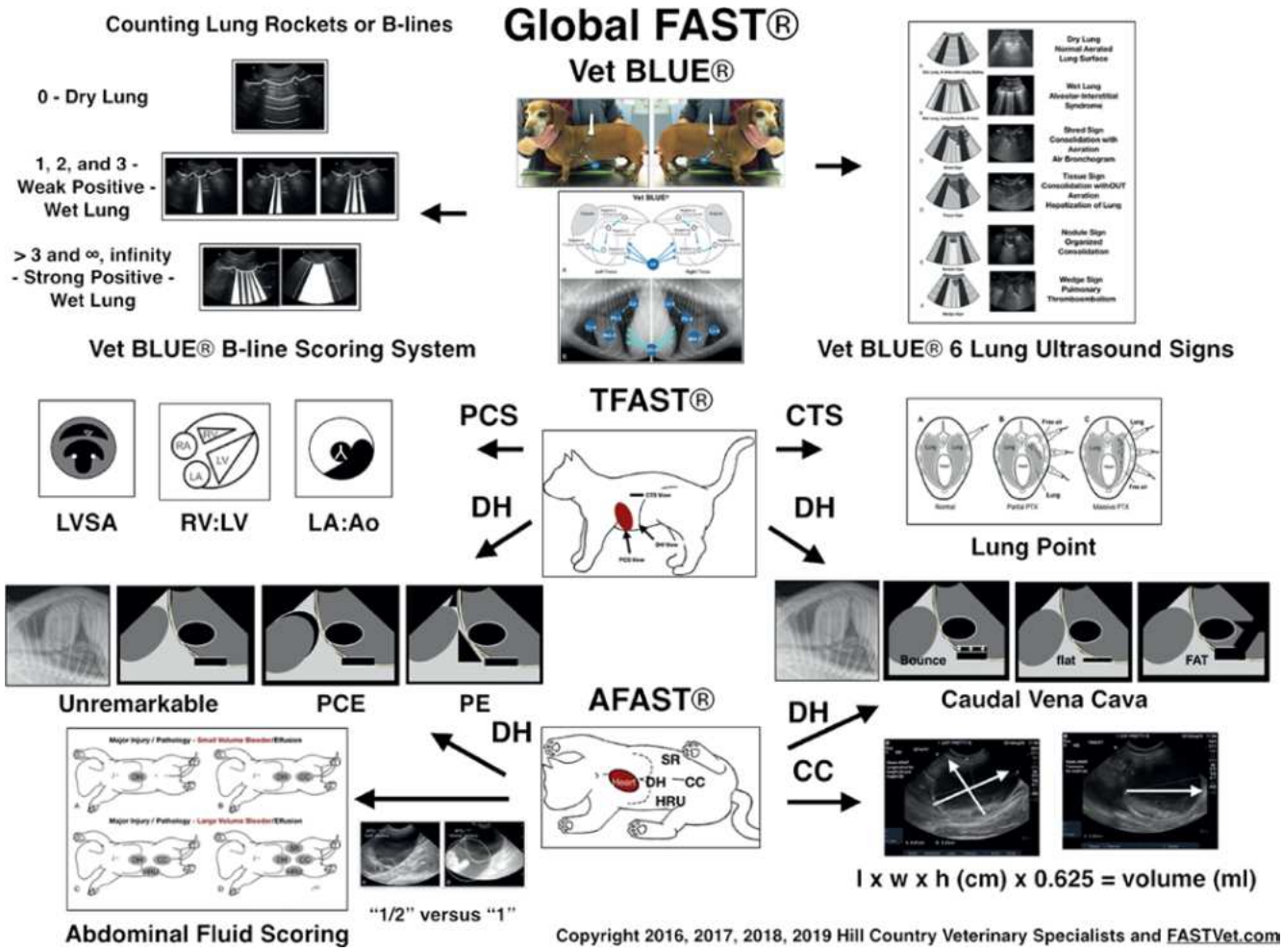


**Figure 36.5.** Global FAST for patient monitoring and integration of its components. A great deal of amount of information may be integrated by the sonographer. The reader is encouraged to spend some time looking through this chart after studying the chapters on AFAST, TFAST and Vet BLUE and this Global FAST chapter. Source: Reproduced with permission from Dr Gregory Lisciandro, Hill Country Veterinary Specialists and FASTVet.com, Spicewood, TX. Cat and dog illustrations by Hannah M. Cole, Adkins, TX.

circulation, specifically venous return (see Figure 6.5). Add to these respiratory and cardiovascular stresses the increased oxygen demand in a struggling, anxious patient, and the patient risks acute and potentially catastrophic decompensation. When considering trauma, many dogs and cats have concurrent lung contusions and other thoracic-related injuries (Powell et al. 1999; Sigrist et al. 2004; Lisciandro et al. 2008; Armenise et al. 2019); hemoabdomen (Boysen et al. 2004; Lisciandro et al. 2009; Lisciandro 2012); and in non-trauma, many hypotensive triaged patients have pleural and/or pericardial effusion and intracavitary bleeds often accompanied by anemia (McMurray et al. 2016; Lisciandro 2016a,b). Moreover, the abdominal fluid scoring system is not validated in dorsal recumbency and only subjective terms of mild, moderate, and severe have been used (Sutherland-Smith et al. 2007; Stander et al. 2010).

# Global FAST for Patient Monitoring

The use of Global FAST for volume status includes the following.

- TFAST echocardiography (echo) views for left- and right-sided strain/failure/overload.
- TFAST PCS views and the FAST DH view for pleural and pericardial effusion.

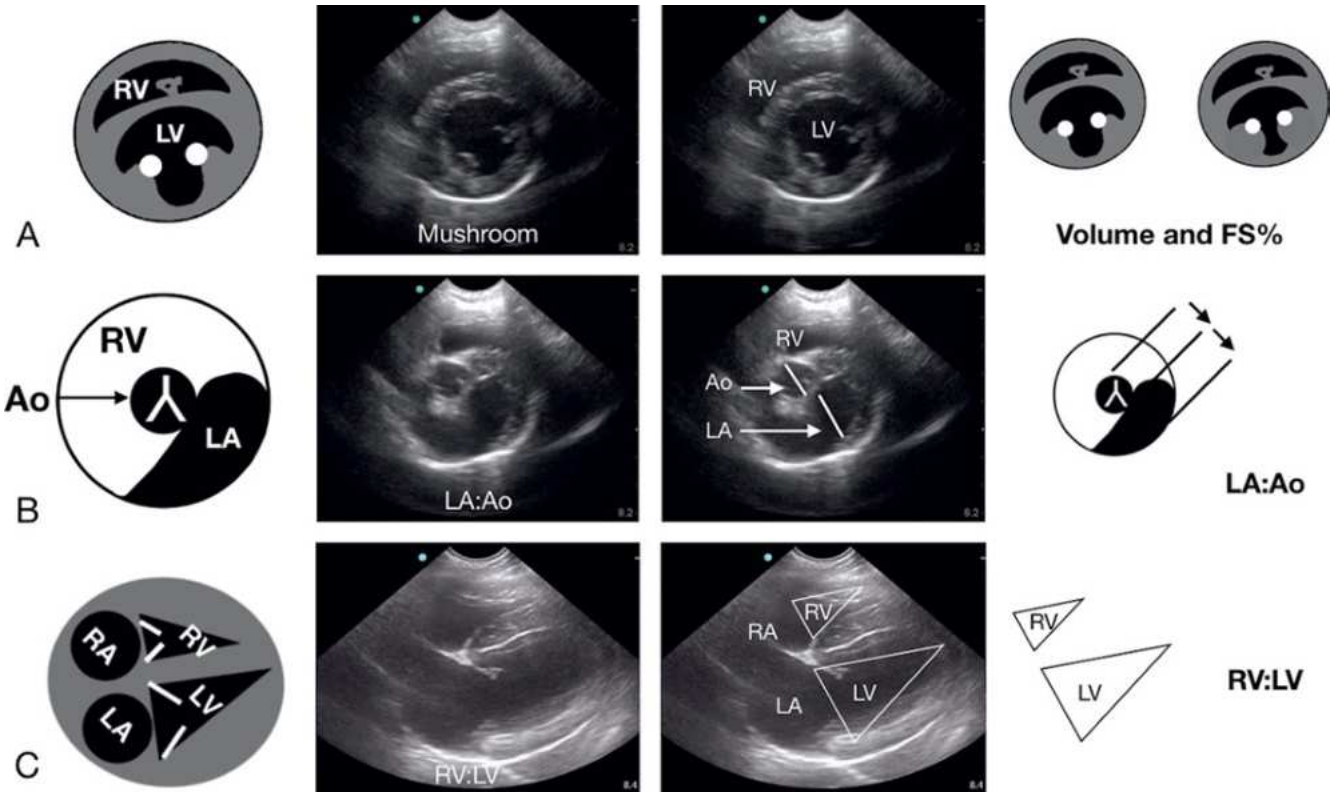


**Figure 36.6.** Integrating TFAST echocardiography views with fallback views. In row (A) is shown the left ventricular short-axis (LVSA) "mushroom view" from the right TFAST PCS view. The view is used for subjective assessment of volume and contractility by looking at its maximum (diastole) left ventricular filling and the change in its filling between diastole (maximum) and systole (minimum) for an estimation of fractional shortening (FS%). In row (B) the short-axis view from the right TFAST PCS view is used to assess the LA:Ao, screening for left-sided cardiac strain/failure/overload. Shown with the arrows is the approximation of the comparative measurements (LA:Ao) with the expected normal ratio of ~1:1 in dogs and ~1.5:1 in cats. Obvious abnormal for either species would be >2:1. In row (C) the LA4CV from the right TFAST PCS view is shown to assess the RV:LV, screening for right-sided cardiac strain/failure/overload. Shown with the triangles is the expected ratio of the RV to LV as ~1:3–4 as the RV should be much smaller than the LV. Global FAST nonecho fallback views are important to further reinforce clinical impression regarding these TFAST echo views (see Figures 36.7 and 36.8). Source: Reproduced with permission from Dr Gregory Lisciandro, Hill Country Veterinary Specialists and FASTVet.com, Spicewood, TX.

- TFAST for pneumothorax.
- TFAST for soft tissue lesions of the heart.
- FAST DH view for caudal vena cava and hepatic venous characterization.
- Vet BLUE for lung.
- AFAST and its fluid scoring system.
- AFAST for interrogation of the retroperitoneal space.
- AFAST for soft tissue obvious abnormalities using the target organ approach.
- AFAST cysto-colic view for estimating urinary bladder volume over time with serial measurements used for noninvasive estimation of urine output.

There is no need for a veterinary RUSH (Rapid Ultrasound in Shock) protocol or other similar protocols (Neri et al. 2007; Perera et al. 2010; Lichtenstein and Malbrain 2015) because Global FAST does everything RUSH does and more (Perera et al. 2010; Boysen and Lisciandro 2013; Lisciandro and Armenise 2014Lisciandro 2019b). The RUSH exam lacks an abdominal fluid scoring system, a "lung point" assessment for degree of pneumothorax (while also serving as a monitoring tool), and a urinary bladder estimation formula, and has much less lung evaluation (Lisciandro et al. 2008, 2014, 2017; Lisciandro 2011; Lisciandro and Armenise 2014; Lisciandro and Fosgate 2017).

## *Global FAST for Volume Status*

### Clarity, Rapidity, Standardization

The use of Global FAST for volume status includes TFAST echocardiography (echo) views and pleural and pericardial effusion (Lisciandro et al. 2008; Lisciandro 2011, 2014a, 2016a; Boysen and Lisciandro 2013; McMurray et al. 2016) and pneumothorax (Lisciandro et al. 2008; Lisciandro 2011, 2014b; Boysen and Lisciandro 2013), the FAST DH views for caudal vena cava and hepatic venous characterization (Nelson et al. 2010; Boysen and Lisciandro 2013; Lisciandro and Armenise 2014; Darnis et al. 2018), Vet BLUE for lung (Lisciandro et al. 2014, 2017; Ward et al. 2017, 2018a; Dicker et al. 2019), and AFAST and its fluid scoring system and interrogation of the retroperitoneal space (Lisciandro et al. 2009; Boysen and Lisciandro 2013; Lisciandro 2011, 2014a, 2019b; Lisciandro et al. 2019a; McMurray et al. 2016; Armenise et al. 2019), and its cysto-colic view for estimating urinary bladder volume, that over time may be used for noninvasive estimation of urine output (Lisciandro and Fosgate 2017). Integrating information is key for increasing the probability of an accurate assessment. Time is also important and Global FAST is 15 defined acoustic windows (views) with *exact clarity* that with its standardized methodology requires only six different probe maneuvers. Moreover, the Global FAST components of AFAST, TFAST, and Vet BLUE are the most studied in veterinary medicine with over 16 relevant publications at the time of writing (Lisciandro et al. 2008, 2009, 2014, 2017, 2019; Lisciandro 2016a; Lisciandro and Fosgate 2017; Ward et al. 2017, 2018a,b, 2019; Dicker et al. 2019; Hnatusko et al. 2019; Vientós-Plotts et al. 2019).

### Integrating Echocardiography and the "Global FAST Nonecho Fallback Views"

The use of Global FAST for volume status includes TFAST echocardiography (echo) views and the "Global FAST nonecho fallback views," a term created by the author. The strategy of using "Global FAST nonecho fallback views" spares your patient the risk of echocardiography and radiography, when your patient is critical. For example, left- and right-sided congestive heart failure is rapidly ruled out by the finding of "dry lung" all views during Vet BLUE (or absent B-lines) (Lisciandro et al. 2014, 2016, 2017; Ward et al. 2017) and a nondistended CVC (bounce) and hepatic veins at the FAST DH view, respectively (Ferrada et al. 2012a,b; Boysen and Lisciandro 2013; Lisciandro and Armenise 2014; Tchernodrinski and Arntfield 2015). These "Global FAST nonecho fallback views" are generally easier (and faster) and require minimal patient restraint when compared to TFAST echocardiography views and radiography. In other words, don't risk patient decompensation and the potential for cardiopulmonary arrest (CPA) in a patient that has unremarkable "Global FAST nonecho fallback views." Heart disease may exist, but left- and right-sided congestive heart failure are as a general rule ruled out. In other words, echocardiography and radiology can wait until your patient is more stable.

### TFAST Cardiac Imaging

The four TFAST echocardiography views and their clinical utility are explained below.

#### *Short-axis Views*

The TFAST echocardiography views consist of two short-axis views.

Volume and Contractility

Left ventricular short-axis (LVSA) "mushroom" view.

- Volume – *subjective* size of left ventricle in diastole (maximum size).
- Fractional shortening percentage (FS%) – subjective changes in size from systole to diastole (change in size through the cardiac cycle).
- Normal dog FS 25–45%; cat FS 30–50%.
- Obvious abnormal.
  - Heart that is both enlarged and fluttering, lacking robust contractions.
  - LVSA internal maximum diameter >5 cm in dogs (DeFrancesco, personal communication 2019).

Left-sided Strain/Failure/Overload

Left ventricular short-axis "Mercedes-Benz" view.

- Left ventricular short-axis left atrial (LA) to aortic (Ao) ratio (LA:Ao).
- Normal generally is a ratio of <1.3:1 in dogs and <1.6:1 in cats.
- Obvious abnormal enlargement is LA:Ao >2:1 in both dogs and cats.

#### *Long-axis Views*

The TFAST echocardiography views consist of two long-axis views.

Right-sided Strain/Failure/Overload

Long-axis four-chamber view (LA4CV).

- RV:LV.
- Normal generally is a ratio of approximately 1:3–4 in dogs and cats or, in other words, the RV should be 1/3 to 1/4 of the size of the LV.
- Obvious abnormal enlargement is an RV:LV of approximately 1:1 in both dogs and cats.

Abnormalities within the Ascending Aorta

Left ventricular outflow tract (LVOT) on long axis.

- Any obvious soft tissue abnormalities in the LVOT including masses, dilation (aneurysm), and vegetation(s) on the aortic valves.

Freeze the image and roll the cine ball through multiple frames to get a more accurate assessment of the heart when it cannot be done in real time with the "eyeball method." This is especially helpful in cats that have much higher heart rates than dogs, and in dogs with tachycardia, in which the "eyeball method" is problematic and more error prone.

## Nonecho Fallback Strategies for Right-sided Heart Problems

### *FAST DH View and Its Right-sided Cardiac Markers*

The FAST DH view is the "Global FAST nonecho fallback view," often safer than TFAST echocardiography views for critical patients. By definition, right-sided congestive heart failure results in a distended or FAT caudal vena cava along with concomitant hepatic venous congestion.

The features of right-sided congestive heart failure may be "seen" sonographically by observing what the author terms the four "TFAST right-sided cardiac markers" (RSCM).

Caudal Vena Cava

Characterization of its dynamic changes over several respiratory cycles combined with its maximum height where it crosses the diaphragm (Figure 36.7 and Tables 36.3 and 36.4) (Nelson et al. 2010; Lisciandro 2011, 2014a,d, 2016a; Boysen and Lisciandro 2013; Lisciandro and Armenise 2014; Darnis et al. 2018; Vientós-Plotts et al. 2019).

- "FAT" (fluid intolerant) – distended with <10% change in height.
- "Flat" (fluid starved or hypovolemic) – small with <10% change in height.
- "Bounce" (fluid responsive) – normal sized with 35–50% change in height.

Hepatic Veins

Hepatic veins are normally unremarkable and inconspicuous at the FAST DH view in patients positioned in lateral or standing-sternal. Thus, hepatic venous distension serves as a marker for increased central venous pressure, especially when combined with a "FAT" or distended CVC (Nelson et al. 2010; Ferrada 2012a,b; Lisciandro 2014a,d, 2016a, 2019a; Tchernodrinski and Arntfield 2015; Vientós-Plotts et al. 2019).

- "Tree trunk sign" (Figure 36.8) (Lisciandro 2014a,d, 2016a, 2019a; Vientós-Plotts et al. 2019).

Gallbladder Wall Edema (Lisciandro et al. 2019b)

- "Cardiac gallbladder" (Figure 36.9) (Lisciandro 2014a,d, 2016a, 2019a; Vientós-Plotts et al. 2019).
- The finding of sonographic striation similar to the "gallbladder halo effect" in canine anaphylaxis, and when caused by anaphylaxis referred to as the "anaphylactic gallbladder"(Quantz et al. 2009).

**Ascites** (Nelson et al. 2010; Lisciandro and Armenise 2014; Vientós-Plotts et al. 2019)

- Modified transudate confirmed when free fluid is safely accessible typically caudal or near the hepato-renal umbilical (HRU) view for sampling with subsequent fluid analysis and cytology (see Figures 6.10, 6.19, 6.25, and 6.32).
- In cats, unlike dogs, ascites is generally not present in right-sided congestive heart failure but felines rather have pleural effusion that is often accompanied by degrees of pericardial effusion (Ward et al. 2018a).

### *Ruling Out Right-sided Congestive Heart Failure*

A dog or cat (or rabbit, gerbil, or ferret) with a fluid-responsive CVC (bounce) without hepatic venous distension has as a rule no evidence of right-sided *congestive* heart failure which serves as a helpful approach when the TFAST echocardiography view(s) are equivocal or are not possible due to patient status.

## Nonecho Fallback Strategies for Left-sided Heart Problems

### *Vet BLUE for Lung and Wet Lung Versus Dry Lung Findings*

By definition, left-sided *congestive* heart failure results in pulmonary edema. Thus, if a dog or cat has absent B-lines at all Vet BLUE views (ABAV), then the patient

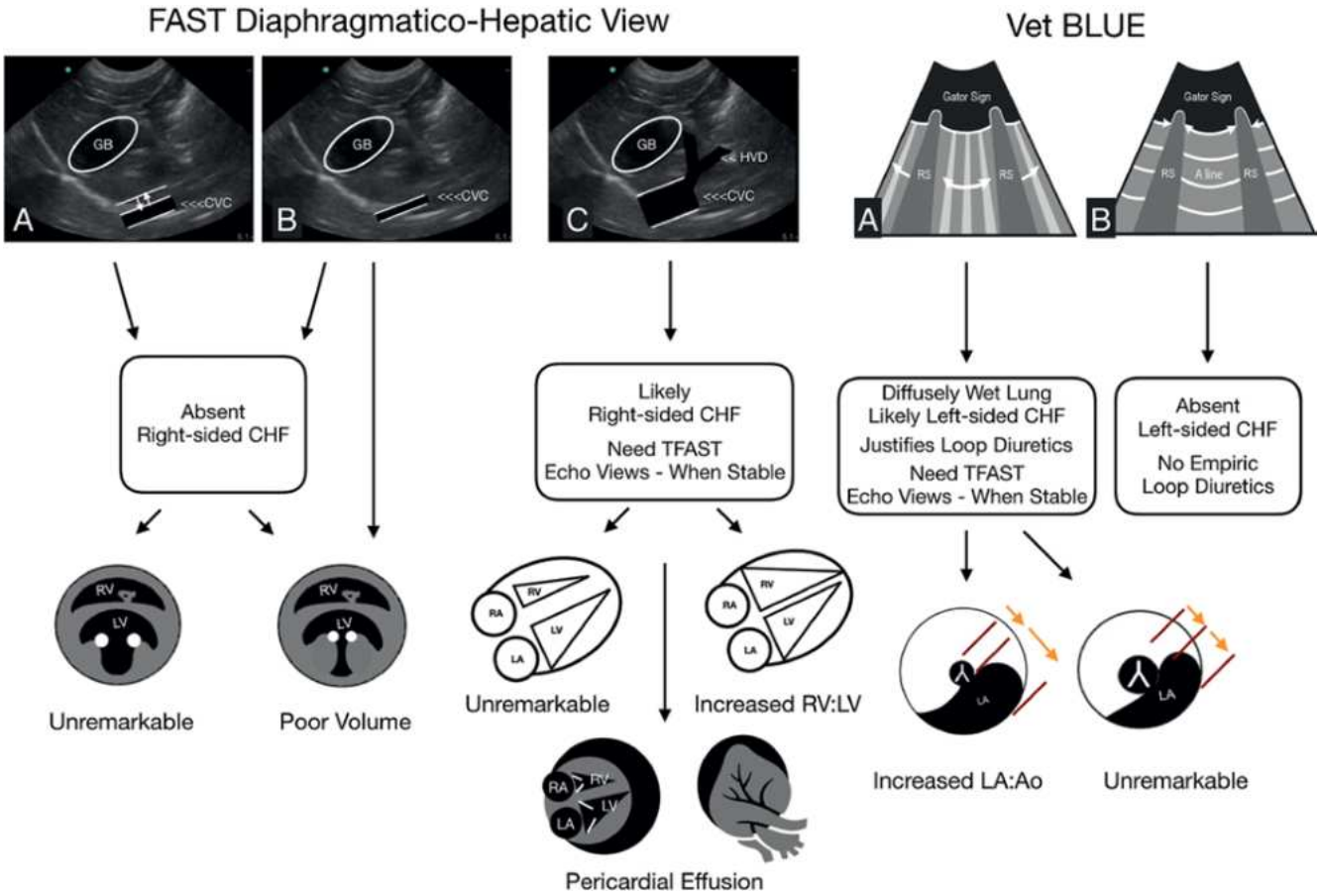


**Figure 36.7.** Taking advantage of the Global FAST nonecho fallback views. When assessing cardiovascular status, integrating cardiac findings with lung (Vet BLUE) and the CVC and its hepatic venous characterization (FAST DH view) is important to maximize the probability of correct assessment. (A,B) Images of the CVC and hepatic veins at the FAST DH view with an algorithm for deciding if cardiac images support the findings of the CVC and its hepatic veins. The "wet lung" versus "dry lung" concept helps better interpret findings of the LA:Ao. Conversely, in unstable patients, these Global FAST nonecho fallback views lend themselves to ruling out and ruling in the presence of left- and right-sided congestive heart failure. They provide strategies for the sonographer who is newer to TFAST echo views as well as the more experienced sonographer in which an unstable patient is too risky for the restraint for TFAST echo views. Source: Reproduced with permission from Dr Gregory Lisciandro, Hill Country Veterinary Specialists and FASTVet.com, Spicewood, TX.

**Table 36.3.**
Absolute measurement suggested guidelines for maximum CVC height in dogs at the FAST DH view relative to body weight.

| Dogs | Body weight | Suggested CVC maximum height (cm) for a "flat" or hypovolemic CVC (low CVP)[a] | Suggested CVC maximum height (cm) for a "FAT" or fluid-intolerant CVC (high CVP)[a] |
|---|---|---|---|
| Small/Toy[b] | <9 kg | 0.25 | >1.0 |
| Medium | >9 kg but <15 kg | 0.35 | >1.5 |
| Large | >15 kg | 0.50 | >1.5 |

[a] The CVC measurements were extrapolated with permission by Lisciandro GR and Vientós-Plotts AI from data provided by Darnis et al. (2018).
[b] Use the Small/Toy values for felines until further guidelines are available.
CVC, caudal vena cava; CVP, central venous pressure; cm, centimeters; kg, kilograms.

**Table 36.4.**
Characterization of the CVC and hepatic veins for canines at the FAST DH view.

| | | | Clinical implications |
|---|---|---|---|
| Bounce – range of normovolemia | Fluid-responsive CVC | Change in CVC height ~35–50% with respiration; maximum height should be between 0.55 and 0.96 cm; combine the dynamic characterization (bounce, FAT, or flat) with maximum CVC DH view height (see Table 7.6); and TFAST echo views and Vet BLUE lung for best integrative volume assessment | Safe to fluid challenge if the attending clinician feels the patient needs volume and lungs are dry on Vet BLUE |
| FAT – hypervolemia | Fluid-intolerant CVC | Minimal change in CVC height of < 10% and the CVC is enlarged often with distended hepatic veins (tree trunk sign); [a]CVC maximum height when > 1.0 cm for dogs < 9 kg is considered FAT; and dogs > 9 kg when maximum height is > 1.5 cm (see Table 36.3); combine the dynamic characterization (bounce, FAT, or flat) with maximum DH view height and TFAST echo views and Vet BLUE lung for best integrative volume assessment | The central venous pressure (CVP) is severely elevated and the right heart is volume overloaded; fluids discontinued and consider vasopressors if hypotensive; if normotensive reduce or stop intravenous fluid therapy; investigate the heart for pericardial effusion, enlarged right ventricle, and evidence of right-sided congestive failure, including ascites |
| Flat – hypovolemia | Hypovolemic CVC | Minimal change in CVC height of < 10% and the CVC is small; [a]CVC maximum DH view height when < 0.25 cm is considered flat in dogs < 9 kg; and < 0.35 cm in dogs > 9 kg and < 15 kg; and < 0.5 cm in dogs > 15 kg (see Table 7.6); combine the dynamic characterization (bounce, FAT, or flat) with maximum DH view height and TFAST echo views and Vet BLUE lung for best integrative volume assessment | The patient is severely volume depleted until proven otherwise; consider where the fluid loss is and evaluate with [b]Global FAST for effusions in the peritoneal cavity, retroperitoneal space, pleural cavity, and pericardial sac (plus lung edema using Vet BLUE) |

[a]The CVC measurements were extrapolated with permission by Lisciandro GR and Vientós-Plotts AI from data provided by Darnis et al. (2018) (see Table 7.6).
[b]Use Global FAST to search for possible internal volume loss, and combine CVC information with TFAST echo views and the patient's Vet BLUE lung findings for best integrative patient assessment.
Source: Reproduced with permission from Dr Gregory Lisciandro, Hill Country Veterinary Specialists and FASTVet.com, Spicewood, TX.

by definition has no evidence of left-sided *congestive* heart failure. Moreover, there is generally no indication for immediate loop diuretic therapy (Lisciandro et al. 2014, 2016, 2017; Rademacher et al. 2014; Ward et al. 2017; Vezzosi et al. 2017). In fact, Vet BLUE has been shown to detect alveolar-interstitial syndrome more frequently than three-view thoracic radiography, especially in the cranial lung regions (Ward et al. 2018b).

Conversely, when "wet lung" is present the use of the Vet BLUE B-line scoring system is predictive for the presence of cardiogenic pulmonary edema based on B-line scoring and numbers of positive views in dogs and cats (Lisciandro et al. 2014, 2016, 2017; Ward et al. 2017, 2018b). In a comparative study of Vet BLUE and three-view thoracic radiography and final diagnosis, Vet BLUE performed with the same sensitivity and specificity as TXR in cats with the advantage of being rapid, simple, and without the transport to and restraint for radiography (Ward et al. 2017). Moreover, Vet BLUE is helpful is estimating degree of alveolar-interstitial edema and sorting out other causes using its regional, pattern-based approach (see Figures 22.1, 23.2, and 23.4). Greater numbers of B-lines and numbers of positive lung ultrasound views directly correlate with amount of alveolar-interstitial edema and extravascular lung water in human lung on computed

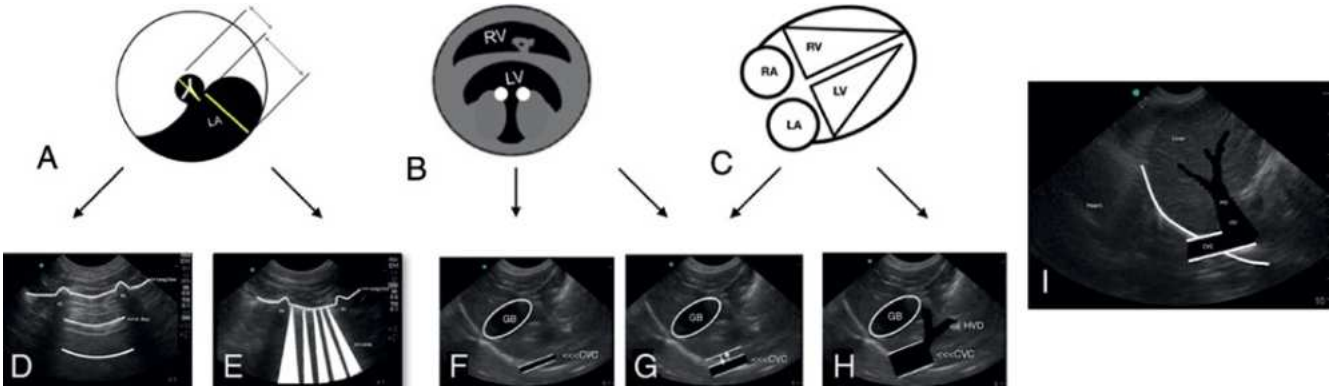


**Figure 36.8.** Double-checking TFAST echocardiography views with Global FAST nonecho fallback views. (A–C) Three TFAST echo views and how clinical suspicions for either of their abnormalities may be double-checked by comparing findings at the respective nonecho fallback views shown in a different light than Figures 36.5, 36.6, and 36.7. When left-sided cardiac problems are suspected by an increased LA:Ao view, then lung is examined during Vet BLUE for the presence (E) and absence (D) of B-lines because the absence of "wet lung" rules out left-sided congestive heart failure (Lisciandro et al. 2014, 2016, 2017; Ward et al. 2017; Vezzosi et al. 2017). In (B) based on the left ventricular short-axis view at the proper level of the chordae tendinae, poor volume status is suspected that may be double-checked by characterizing the CVC and hepatic veins as in (F–H). A CVC and hepatic veins that are not distended (not FAT) as in (F) and (G) rules out right-sided congestive heart failure (Nelson et al. 2010; Tchernodrinski and Arntfield 2015). In (C) an increased RV:LV may be double-checked by characterizing the CVC. A CVC and hepatic veins that are not distended (not FAT) rules out right-sided congestive heart failure as shown in (F) and (G). In (H) and (I) distension of the hepatic veins, referred to as the "tree trunk sign," is shown, indicative of right-sided volume overload and congestive heart failure (Lisciandro 2014a,d, 2016a). Source: Reproduced with permission from Dr Gregory Lisciandro, Hill Country Veterinary Specialists and FASTVet.com, Spicewood, TX.

tomography (Jambrik et al. 2004; Volpicelli et al. 2006; Lichtenstein et al. 2009; Gargani et al. 2015). See Figure 36.17 and Chapters 22 and 23 for greater detail.

## Assessing and Measuring the Caudal Vena Cava and Assessing Hepatic Venous Distension

### *Where to Evaluate the Caudal Vena Cava?*

Multiple regions have been used to assess and measure the CVC in dogs (Nelson et al. 2010; Lisciandro 2014a,d, 2016a; Meneghini et al. 2016; Tuplin et al. 2017; Bucci et al. 2017; Kwak et al. 2018; Cambournac et al. 2018; Darnis et al. 2018; Vientós-Plotts et al. 2019) (Figure 36.10) (see Chapter 26).

- Where the CVC traverses the diaphragm (subxiphoid or FAST DH view) having the advantage of combining hepatic venous characterization and being closest to the right heart and pleural cavity, making it most predictive of central venous pressure (Nelson et al. 2010; Lisciandro 2014a,d; 2016; 2019a; Tchernodrinski and Arntfield 2015; Tuplin et al. 2017). This is the view detailed by the author in this chapter.
- At the porta hepatis at the 11–13th intercostal spaces of the right hemithorax where hepatic veins are not assessed but rather the CVC is compared to the adjacent abdominal aorta. See more detail in Chapter 26 (Bucci et al. 2017; Darnis et al. 2018; Armenise et al. 2019).
- Cranial to the right kidney (or left kidney).
- Caudal to the right kidney where hepatic veins are not assessed but rather the CVC is compared to the adjacent abdominal aorta (Meneghini et al. 2016; Kwak et al. 2018; Marshall et al. 2018; Cambournac et al. 2018). See more detail in Chapter 26.

### *Characterizing the Caudal Vena Cava and Hepatic Veins – "Eyeball Method"*

Assessing the CVC and its dynamic change in height over several respiratory cycles as "FAT," "flat," or having a "bounce" (Figure 36.11; see also Figure 36.9).

### *Measuring the Caudal Vena Cava*

At the FAST DH view, two options are available in its longitudinal plane, M-mode and B-mode, each having limitations (Figure 36.12). Either is acceptable in the opinion of the author, who prefers the simplicity of the B-mode measurement (see Figures 36.11 and 36.12). Table 36.3 is created from data from Darnis et al. (2018) and adapted by the author for CVC char-

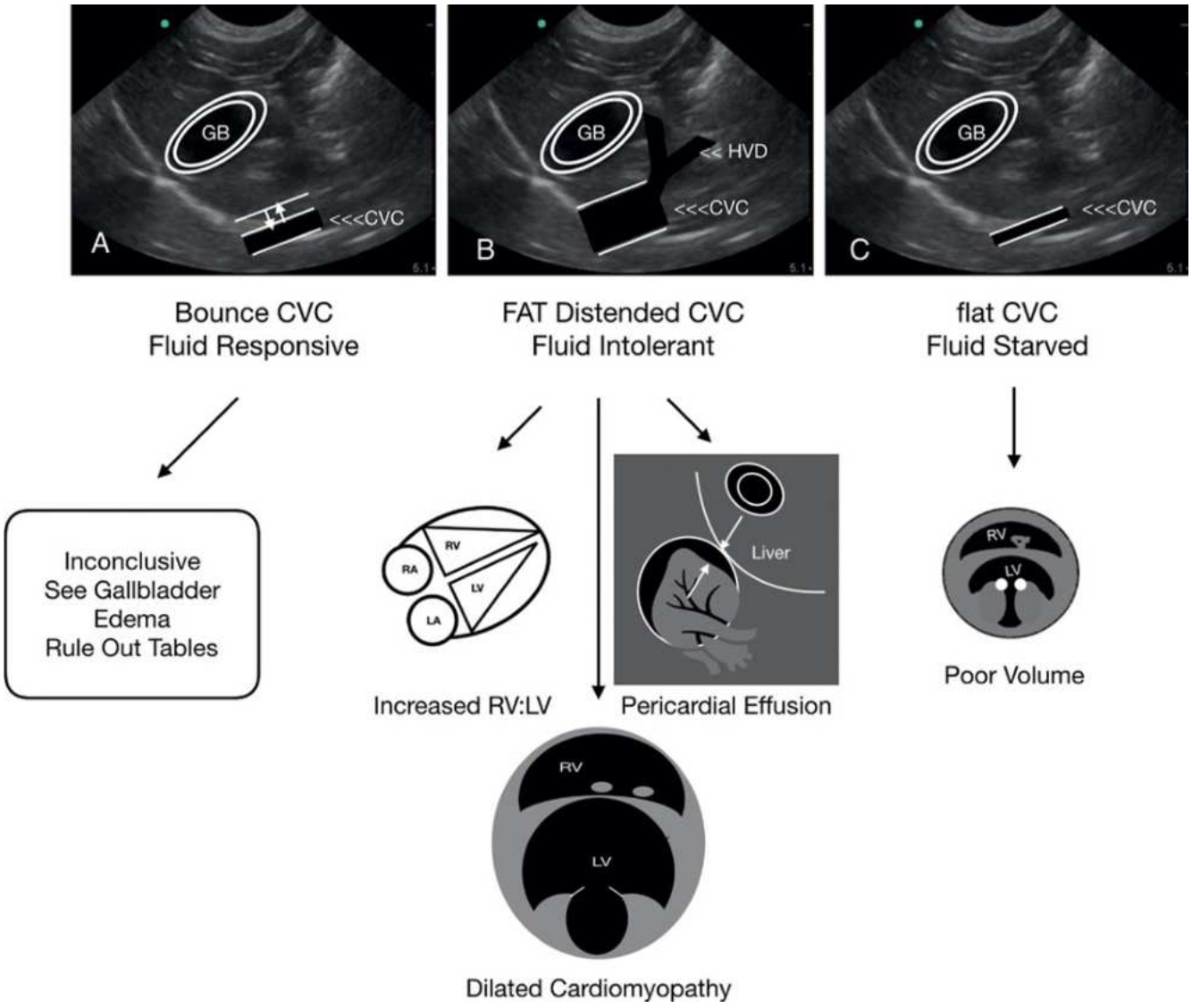


**Figure 36.9.** Gallbladder wall edema and integrating information to increase the probability for an accurate assessment. (A–C) Patients with clear sonographic striation of the gallbladder wall representing intramural gallbladder edema. When the patient is acutely collapsed or weak, looking at the CVC and heart is imperative to determine if the gallbladder wall edema is an "anaphylactic gallbladder" (dogs only) (Quantz et al. 2009) or a "cardiac gallbladder" (dogs, cats, people) (Lichtenstein 2010; Lisciandro 2014a,d, 2016, 2019a). Note that a FAT CVC and distended hepatic veins support the presence of pericardial effusion and right-sided heart failure including dilated cardiomyopathy and pulmonary hypertension (Lisciandro 2014a,d, 2016a). Note that a flat CVC suggests severe hypovolemia and the presence of canine anaphylaxis. Lastly, when gallbladder wall edema is present and the CVC has a "bounce" (fluid-responsive CVC), then the assessment is inconclusive, as there are several other causes for gallbladder wall edema (see Table 37.2) (Lisciandro et al. 2019b). Maximum height measurements of the CVC as it traverses the diaphragm may also be combined with the "eyeball method" of the CVC and its dynamic changes (see Table 36.3). See also Figures 37.4 and 37.13. RV, right ventricle; LV, left ventricle; RA, right atrium; LA, left atrium; CVC, caudal vena cava; HVD, hepatic venous distension; GB, gallbladder. Source: Reproduced with permission from Dr Gregory Lisciandro, Hill Country Veterinary Specialists and FASTVet.com, Spicewood, TX.

acterization as "flat" or "FAT" using maximum CVC heights in the longitudinal plane at the FAST DH view. Other CVC measurements in experimentally induced right-sided volume overload from excessive crystalloid administration are also available (Nelson et al. 2010). The associated hepatic veins when distended provide even more evidence that hepatic congestion from right-sided strain/failure/overload is occurring,

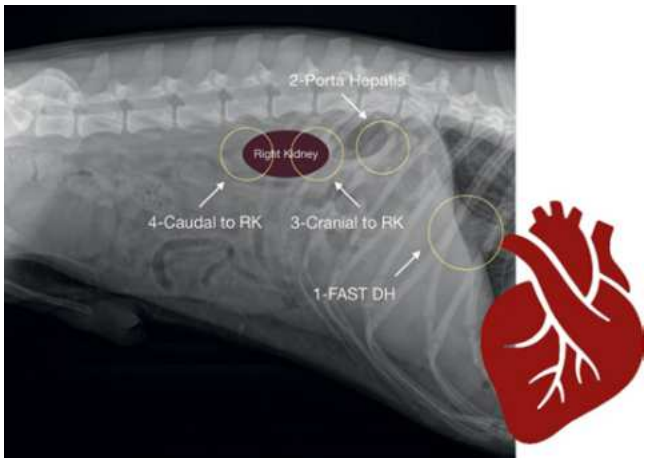


**Figure 36.10.** Different locations for characterization of the CVC in dogs. Several locations have been studied in dogs for hypovolemia based on the characterization and measurements of the CVC. These are numbered as 1 FAST DH, 2 porta hepatis, 3 cranial to the right kidney (RK) and left kidney (not shown), and 4 caudal to the RK. It is important to understand a few concepts, the first being that volume status is likely best assessed as close as possible to the right atrium. Second, CVC characterization is correlated to the adjacent hepatic veins at site 1; however, for sites 2–4, the CVC is being compared to the aorta and although reproducibly measured between different observers, the question must be raised as to how relevant volume status is with increasing distances from the patient's right atrium. The author favors site 1 where the CVC traverses the diaphragm and also provides information regarding hepatic venous distension. Clinical studies have shown that site 2 is measured well (CVC and aorta for their comparison) and has correlated with hypovolemia although the view is not part of Global FAST (see Chapter 26 for greater detail). Source: Reproduced with permission from Dr Gregory Lisciandro, Hill Country Veterinary Specialists and FASTVet.com, Spicewood, TX.

although only via subjective assessment, the finding of the "tree trunk sign" is currently used (Nelson et al. 2010; Lisciandro 2014a,d, 2016a, 2019a; Lisciandro and Armenise 2014; Vientós-Plotts et al. 2019) (see Figures 36.7 and 36.9). Combining both the "eyeball method" and actual measurements at the FAST DH view would likely give the best overall assessment, but this is speculative and likely dependent on types of heart conditions.

As a final note, the FAST DH view provides characterizations of both the CVC and hepatic veins at the same view, whereas other published CVC locations do not give hepatic venous characterization but rather compare size of the CVC to the adjacent abdominal aorta (see Figure 36.10 and also Figures 38.8 and 38.9 and Chapter 26 for greater detail). CVC methods further away from the diaphragm are at increasing distance from the pleural cavity and right heart and are thus in theory less sensitive predictors of patient volume status.

## *Global FAST for Volume Loss*

### The Leak in the Tank

Whenever a patient presents as volume contracted, the important question is always asked "Where is the fluid loss?" referred to as a "leak in the tank" by the RUSH examination (Perera et al. 2010). By finding the "leak in the tank," the volume loss has a better chance of being corrected. For example, a postoperative dog may be mildly tachycardic, hypothermic, quiet and alert with a normal blood pressure. The focused cardiac ultrasound (FCU) or a POCUS caudal vena cava (CVC) exam may reveal volume contraction. An intravenous fluid bolus may be administered along with serial FCU or POCUS CVC. However, Global FAST not only rapidly detects the ascites but also triggers an abdominocentesis and a hemoabdomen is diagnosed along with categorization of a small-volume bleeder versus large-volume bleeder (see Chapter 7). Another example would be a dog with acute hemorrhagic diarrhea syndrome (previously referred to as hemorrhagic gastroenteritis syndrome, HGE) (Busch et al. 2015; Mortier et al. 2015). The dog is stable, unremarkable on physical examination, with normal vital signs and blood pressure assessment, and is being treated for mild tachycardia with analgesia. However, Global FAST shows that the patient is volume contracted with poor left ventricular filling on the right TFAST PCS view and the CVC is flat at the FAST DH view. Fluid resuscitation is better approached with the checks and balances using the Global FAST approach.

### Global FAST Automatically Surveys for the Leak in the Tank

#### *Four Spaces Plus Lung and Maybe More*

Global FAST automatically surveys for internal volume loss by interrogating four spaces plus lung (see Maybe More section below) including:

- the peritoneal cavity
- the retroperitoneal space
- the pleural cavity
- the pericardial sac
- the lung (extravascular lung water).

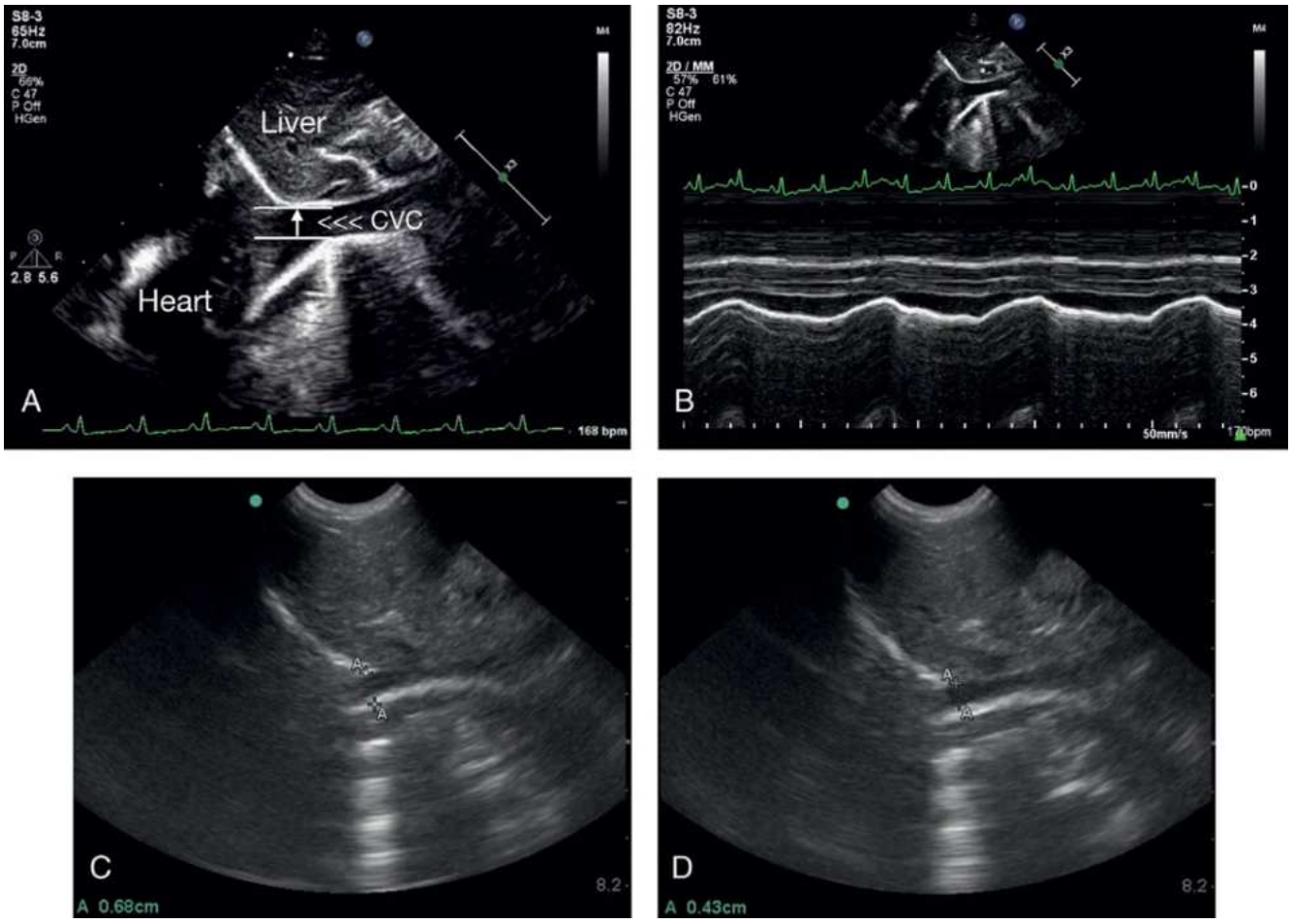


**Figure 36.11.** Different methods for measuring the CVC at the FAST DH view. (A,B) B-mode image of the CVC at the FAST DH view using M-mode. (C,D) The CVC is measured using B-mode with freezing and rolling the cine ball through several frames to find the maximum and minimum diameters for an appreciation of their change to assess the CVC. Either method may be used. Source: (A,B) Images courtesy of Dr Jessica Ward, DVM, Iowa State University, Ames IA, and (C,D) courtesy of Dr Gregory Lisciandro, Hill Country Veterinary Specialists and FASTVet.com, Spicewood, TX.

The patient may lose marked volume in the three "forgiving areas" of the peritoneal cavity, retroperitoneal space, and pleural cavity before it is obvious to the attending veterinarian that the patient has developed serious complication(s). The "unforgiving areas" of the pericardial sac and lung are also surveyed; however, large "leaks" in these two regions lead to obvious changes in patient status because much smaller relative volumes of pericardial effusion will affect cardiac output and increases in extravascular lung water (B-lines and Vet BLUE B-line scoring system) in lung will quickly affect ventilation.

The Vet BLUE examination has been shown to detect alveolar-interstitial syndrome with higher frequency than thoracic radiography, providing clear advantages by being point-of-care, rapid and a regional pattern-based approach (Lisciandro et al. 2016; Ward et al. 2017, 2018b; Dicker et al. 2019), and is comparable to computed tomography (CT) for lung contusions (Dicker et al. 2019). The detection of "leaks" in these areas can trigger interventions to better treat the patient by directing care with evidence-based information by "seeing" the problem and assessing its degree through AFAST (abdominal fluid scoring system), TFAST ("lung point" for degree of pneumothorax) and Vet BLUE (B-line and pulmonary contusion scoring systems).

### *Maybe More – Other Leaks and Plugs*

Through Global FAST, soft tissue information is garnered. For example, during TFAST and AFAST and

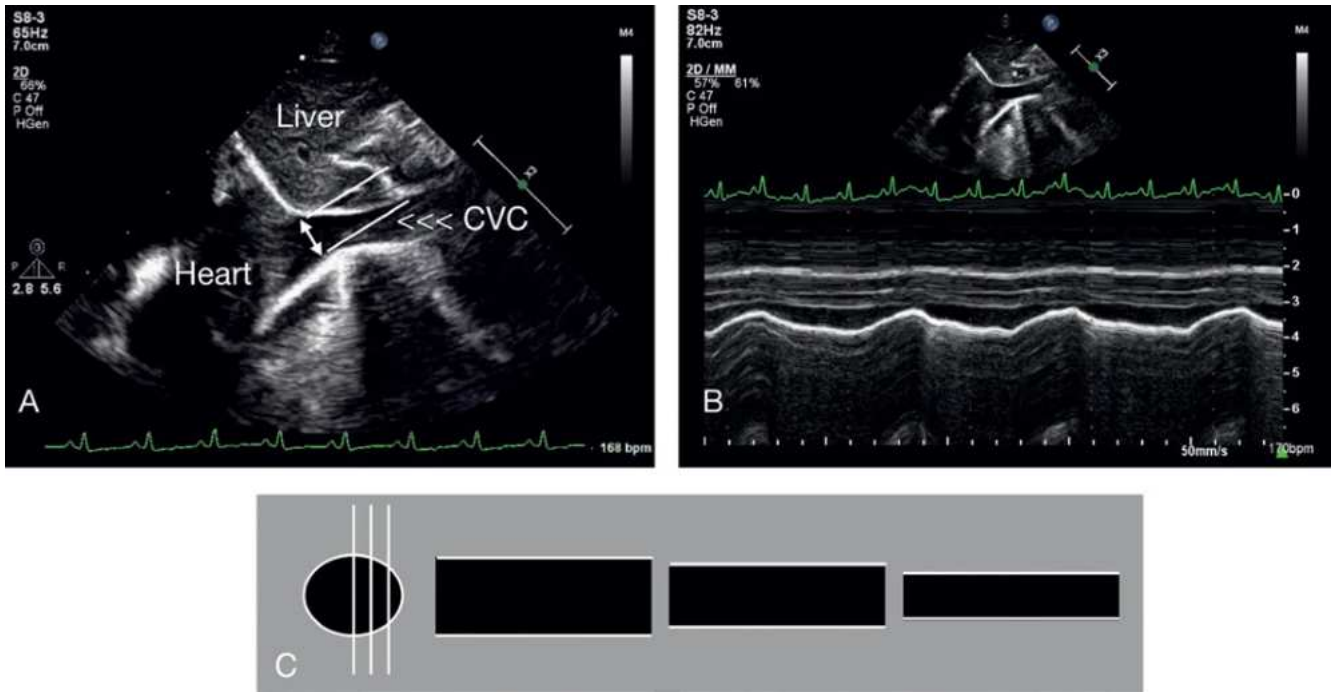


**Figure 36.12** Limitations and errors in measuring the CVC in longitudinal planes. The measurement of the CVC poses some inherent problems as shown in these figures. In (A) the M-mode cursor is placed through the CVC and in (B) measurements may be taken by looking at the changes in CVC height over several respiratory cycles. However, shown in (C) is how the M-mode cursor may not truly represent the actual CVC height measurement because of where the scanning plane exists. For illustrative purposes, three CVC different locations are shown on the black oval (transverse plane) that correlate to the black rectangles (longitudinal plane) showing an accurate CVC height measurement along with two inaccurate measurements, dependent on where the scanning plane is positioned. Measurements should be combined with the eyeball method for best CVC interpretation. Source: (A,B) Images courtesy of Dr Jessica Ward, DVM, Iowa State University, Ames IA, and (C) courtesy of Dr Gregory Lisciandro, Hill Country Veterinary Specialists and FASTVet.com, Spicewood, TX.

their target organ approach, each automatically screens for plugs (obstruction of flow), thrombi (blood clots) in the urinary bladder and cardiac chambers, and various vessels including renal, splenic, hepatic, and the CVC, and other leaks such as a fluid-distended gastrointestinal and urogenital tract that may be easily appreciated through the observation of distended fluid-filled loops and thrombus in the urinary bladder. These findings can trigger investigative interventions ranging from the simple during physical examination (digital rectal examination for gastrointestinal bleeding and free catch urine samples) to more advanced imaging and diagnostic testing (D-dimers, coagulation testing, advanced imaging).

Through Global FAST, infarction potentially may be recognized within the spleen, lung, and renal cortex. Other obstructions to flow would be poor vascular tone such as in sepsis, and poor venous tone likely would be better recognized through CVC and splanchnic pooling during AFAST by a distended (or "FAT") CVC with hepatic venous distension ("tree trunk sign") and edematous small intestine, respectively (Lisciandro 2014a,d, 2016a, 2019a).

## Summary

The objective of the Global FAST approach is to recognize deviations from what is expected at each of its 15 acoustic windows to allow further assessment with the potential to positively affect outcome (Blackbourne et al. 2004; Ollerton et al. 2006; Neri et al. 2007; Lisciandro et al. 2008, 2009, 2014, 2017; Lisciandro 2011, 2012; Boysen and Lisciandro 2013; Perera et al. 2010; Ferrada et al. 2011, 2012a,b; Lisciandro and Armenise 2014; Lichtenstein and Malbrain 2015; Tavares et al. 2019). There will always be exceptions, but this approach provides a solid foundation from which skills may be further developed. For example, the septic patient may have poor vascular tone resulting in poor ventricular filling on the left ventricular "mushroom" view, triggering intravenous volume expansion when in fact the patient requires vasopressors.

## Global FAST Monitoring Tools

### Use of the AFAST-applied Abdominal Fluid Scoring System for Ascites

The use of the abdominal fluid score is important for semiquantitating intraabdominal small-volume bleeder/effusion (AFS 1–2, <3 with modification of AFS) versus large-volume bleeder/effusion (AFS 3–4, ≥3 with modification of AFS) and estimating both hemorrhagic and nonhemorrhagic volume loss within the abdominal cavity. With hemoabdomen, the decisions for blood transfusion(s) may be made using AFS (see Chapters 6 and 7, and Table 7.3). This facet of Global FAST is not part of the RUSH exam.

### Use of TFAST for Estimating Pleural and Pericardial Effusion

#### *Pleural Effusion*

Studies have been performed in cadaver cats and dogs positioned in sternal using an off-the-sternum imaging methodology for measuring distance between the heart and the thoracic wall; however, the estimation formulas were unreliable (Newitt et al. 2009; Shimali et al. 2010). A suggestion by the author is to measure the distance of pleural effusion from the thoracic wall at the fourth or fifth intercostal spaces at the level of the costochondral junction and/or via the FAST DH view in a standing or sternal patient, although this methodology has never been studied (Figure 36.13). Ideally, such a method would need to be developed from spontaneously breathing subjects with lung naturally aerated rather than in cadaver studies because the dynamics of aerated lung floating in pleural effusion would presumably differ between antemortem and postmortem (Newitt et al. 2009; Shimali et al. 2010).

#### *Pericardial Effusion*

No studies to the author's knowledge have been formulated to measure the volume of pericardial effusion in dogs and cats. Descriptors for amount of pericardial effusion have been published in people and include trivial <0.5 cm, mild 0.5–1.0 cm, moderate >1.0 and <2.0 cm, and severe >2.0 cm (Candotti and Arntfield 2015). The question remains: where to measure? A suggestion by the author is to measure the distance of pericardial effusion from the pericardial sac to the heart (visceral pericardium) at the fourth or fifth intercostal spaces at the level of the costochondral junction with the patient in sternal-standing, although this methodology has never been studied (Figure 36.14).

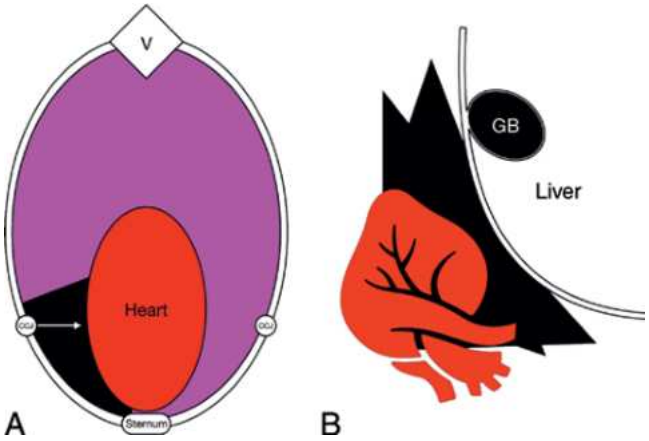


**Figure 36.13.** Measuring pleural effusion with illustrative line drawings of the cross-section of the thorax and the FAST DH view. Transthoracic PCS view of TFAST (A) and the FAST DH view (B). There is no established methodology for measuring PE and estimating PCE volume in live patients, but logic would dictate that standing or sternal position would be ideal because the PE would accumulate in gravity-dependent regions. The author suggests measuring the greatest width at the FAST DH view as shown in (B) with the patient in standing or sternal (*arrow*). A second option is measuring the greatest width at the level of the costochondral junction bilaterally between the 4th–5th intercostal space approximating the positioning of the probe for the right and left TFAST PCS views as shown in (A) in standing or sternal (*arrow*) positioning. GB, gallbladder; CCJ, costochondral junction; V, vertebra. Source: Reproduced with permission from Dr Gregory Lisciandro, Hill Country Veterinary Specialists and FASTVet.com, Spicewood, TX.

Another methodology that would seem logical would be to measure the maximum distance in a standing or sternal patient between the pericardial sac and the heart (visceral pericardium) from the FAST DH view (see Figure 36.14).

### Use of Global FAST for Estimating Urine Output

Formulas exist for estimating urinary bladder volume (Atalan et al. 2007; Lisciandro and Fosgate 2017) and the ellipsoid formula of length (cm) × height (cm) × width (cm) × 0.625 estimates the urinary bladder volume in milliliters (mL) (Figure 36.15). To the author's knowledge, only a single study has been performed in cats (Lisciandro and Fosgate 2017). Thus, with serial measurements, urine output may be estimated noninvasively by change in volume over change in time (Δ urine volume/Δ time). Although not known for cats, residual urine volume in dogs has been reported to be <0.2 mg/kg (Atalan et al. 1999). Dogs

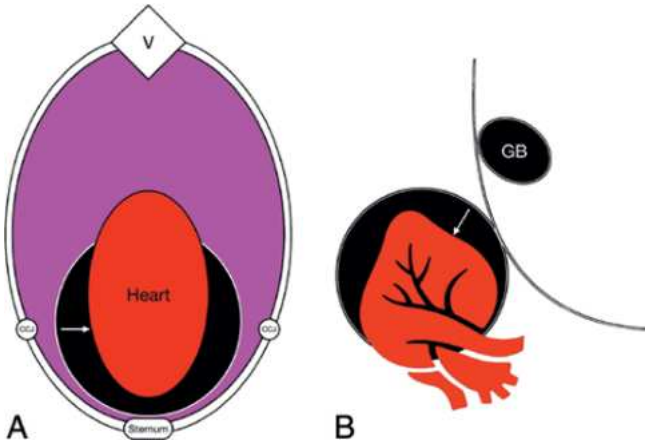


**Figure 36.14.** Measuring pericardial effusion with illustrative line drawings of the cross-section of the thorax and the FAST DH view. Transthoracic PCS view of TFAST (A) and the FAST DH view (B). There is no established methodology for measuring PCE and estimating PCE volume in live patients, but logic would dictate that standing or sternal position would be ideal because the PCE would accumulate in gravity-dependent regions. The author suggests measuring the greatest width at the FAST DH view as shown in (B) with the patient in standing or sternal (*arrow*). A second option is measuring the greatest width at the level of the costochondral junction bilaterally between the 4th–5th intercostal space approximating the positioning of the probe for the right and left TFAST PCS views as shown in (A) in standing or sternal (*arrow*) positioning. GB, gallbladder; CCJ, costochondral junction; V, vertebra. Source: Reproduced with permission from Dr Gregory Lisciandro, Hill Country Veterinary Specialists and FASTVet.com, Spicewood, TX.

have the advantage of being walked and voiding so that measurements begin with minimal urine at time 0. This facet of Global FAST is not part of the RUSH exam.

### Use of Global FAST for Estimating Pneumothorax Using The "Lung Point"

The use of the "lung point" serves as a means not only to assess the degree of PTX but also to monitor PTX (Lisciandro et al. 2008; Lisciandro 2011, 2014a; Lisciandro and Armenise 2014) (Figure 36.16). When PTX is suspected, the patient is best moved to sternal or standing position (if in lateral) and the sonographer continues with a Vet BLUE, searching for any evidence of lung recontacting the thoracic wall, most commonly "lung sliding" or B-lines, but any Vet BLUE lung ultrasound signs can determine the location of the "lung point" (Lisciandro et al. 2008; Lisciandro 2011, 2014b; Lisciandro and Armenise 2014). In other words, when PTX is suspected at the Caudodorsal lung region, then the sonographer continues to the Perihilar (Ph) lung region (middle third) followed by the Middle (Md) lung region (lower third), referred to as the TFAST PTX 1/3s Rule.

If a "lung point" is not found at either, then the sonographer may slide even lower along the thoracic wall ventral to the Md lung region. If evidence of lung contacting the thoracic wall is found, then the sonographer moves dorsal from that view until lung contacting the thoracic wall is lost (because of PTX). The transition zone of PTX and lung contacting the thoracic wall is the "lung point." The TFAST PTX 1/3s Rule

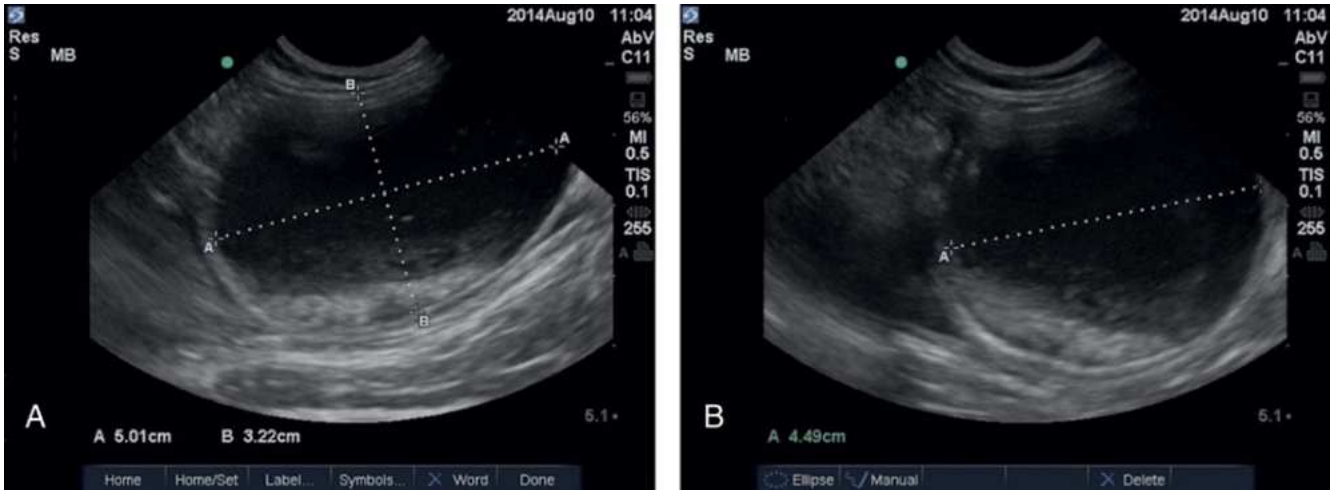


**Figure 36.15.** Estimating urinary bladder volume. Measurements of the urinary bladder may be made to help estimate urinary bladder volume. In (A) is shown how to acquire the length and height measurements at the AFAST CC view in the longitudinal (sagittal) plane, and in B) by rotating the probe 90°, the width measurement can be obtained in the transverse plane. Using the formula L × H × W (cm) × 0.625 estimates urinary bladder volume (mL) and thus over time provides a non-invasive means to estimate urine output in both dogs and cats (Lisciandro and Fosgate 2017). Source: Reproduced with permission from Dr Gregory Lisciandro, Hill Country Veterinary Specialists and FASTVet.com, Spicewood, TX.

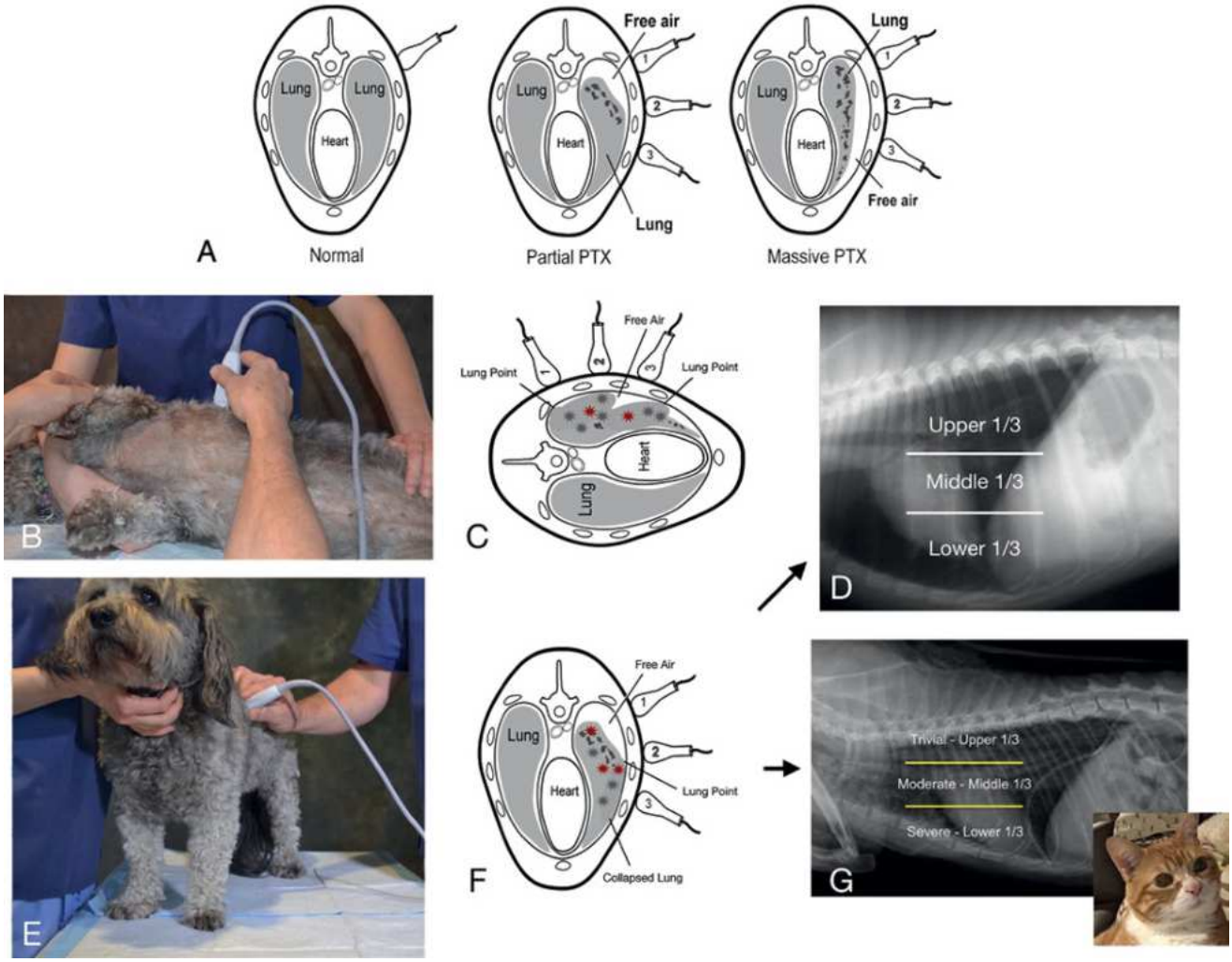


**Figure 36.16.** Estimating degree of pneumothorax and the TFAST PTX 1/3s Rule. (A–C) The patient with PTX is in lateral recumbency and because of the "parking garage effect" the free air bubbles into different regions, creating a "double lung point" phenomenon in which a "lung point" is potentially seen on either side of the collapsed lung. Moreover, if the patient is receiving positive pressure ventilation, the free air (PTX) is pushed into multiple locations unnaturally between the collapsed lung. In (D–F) the effect is eliminated or greatly reduced by moving the patient to standing or sternal position, thus creating a "sky scraper effect" in which the difference between the sternum and least gravity-dependent chest tube site (CTS) view is greatest. Thus, it is unlikely a "double lung point" will be observed. In (F) the probe is moved along the lateral thoracic wall searching for the "lung point." The TFAST 1/3s Rule is used to assess as trivial, moderate, and severe PTX, dependent on the location of the "lung point," the upper 1/3, middle 1/3, and lower 1/3, respectively. In (G) the degree of PTX may be characterized as trivial, moderate, and severe depending on where the lung point is located. Source: Reproduced with permission from Dr Gregory Lisciandro, Hill Country Veterinary Specialists and FASTVet.com, Spicewood, TX.

serves as a qualifier of the degree of PTX as upper third being trivial, middle third moderate, and lower third severe. This facet of Global FAST is not part of the RUSH exam. See Chapter 18 for greater detail.

### Use of the Vet BLUE B-line Scoring System

Numbers of B-lines are counted as the largest number at each Vet BLUE view and scored as 0, 1, 2, 3, >3, and infinity (∞). Consider scoring of 1, 2, and 3 as weak positives and >3 and infinity (∞) as strong positives (Ward et al. 2017). The scoring system is detailed in Chapter 23 and may be applied to patients with alveolar-interstitial syndrome (AIS) and lung contusions. In people, scoring numbers of B-lines is also used in pulmonary fibrotic conditions. This facet of Global FAST is not part of the RUSH exam.

### *B-line Scoring for Estimating Degrees of Alveolar-Interstitial Edema and Extravascular Lung Water*

Numbers of B-lines have been shown to correlate with degree of alveolar-interstitial edema on computed tomography and directly correlate with extravascular lung water (Jambrik et al. 2004, 2010; Volpicelli et al. 2006; Gargani et al. 2015). In other words, greater numbers of B-lines in most patients means greater degree of alveolar-interstitial edema and extravascular lung water (EVLW) (Figure 36.17). This is important because the degree of EVLW correlates with survival in people, so by detecting increases in B-lines, interventions may potentially take place *prior to* overt patient decompensation (Jambrik et al. 2004, 2010; Volpicelli et al. 2006; Lichtenstein and Karakitsos 2012; Shyamsundar et al. 2013). This facet of Global FAST is not part of the RUSH exam. See Chapters 22 and 23 for greater detail.

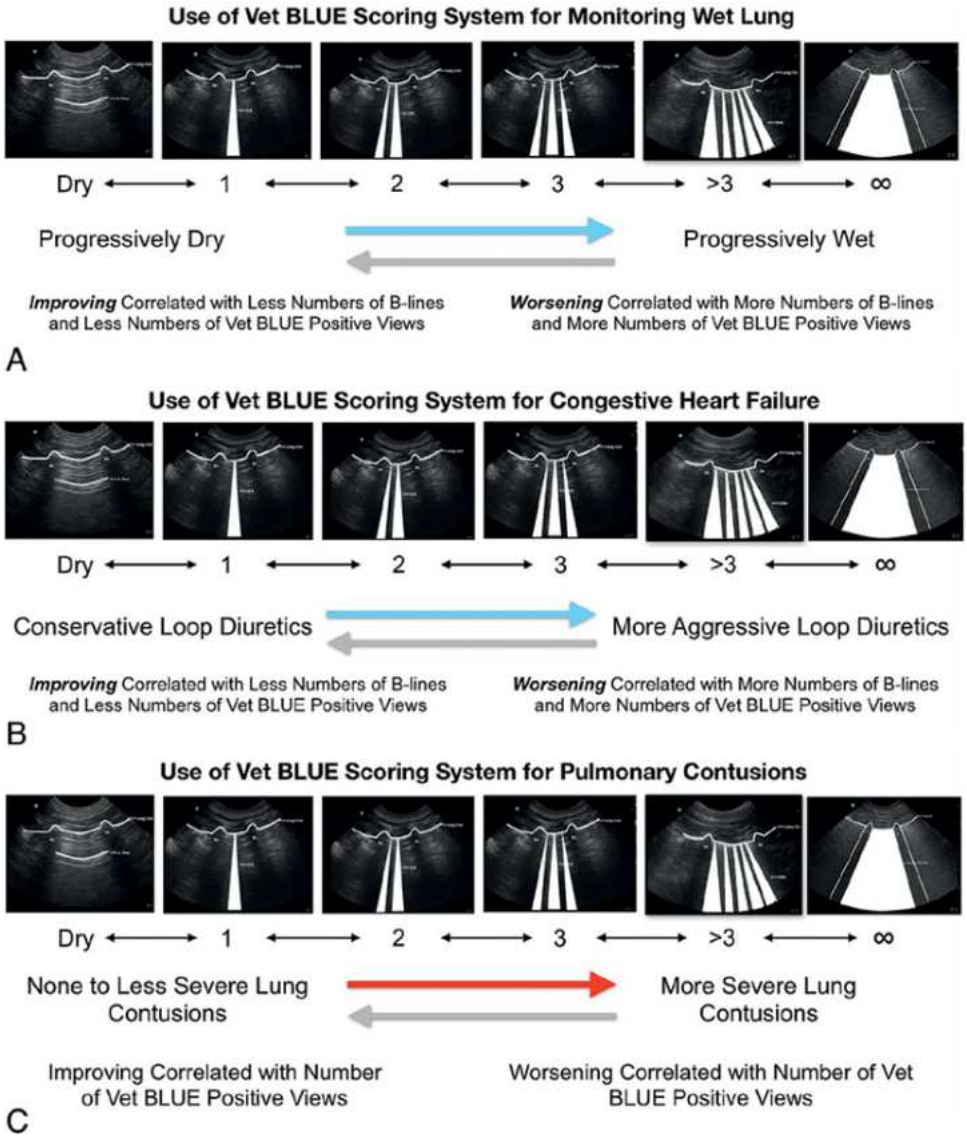


**Figure 36.17.** The Vet BLUE B-line scoring system. The amount of extravascular lung water may be estimated by its direct correlation with numbers of B-lines. In (A) a patient developing B-lines may be determined as having left-sided volume overload or pneumonia (as well as other causes) based on the Vet BLUE regional pattern-based approach and integrating TFAST echocardiography views and the Global FAST nonecho fallback views (see Tables 23.2, 23.3, and 23.4). In (B), a patient with left-sided congestive heart failure, loop diuretic usage may be guided by the Vet BLUE B-line scoring system. Lots of B-lines (>3 and infinity) at most Vet BLUE views dictates more aggressive loop diuretics than one or two positive Vet BLUE views with smaller numbers of B-lines (0–3). In (C) lung contusions may be similarly semiquantitated by numbers of B-lines combined with distribution of positive Vet BLUE views. Source: Reproduced with permission from Dr Gregory Lisciandro, Hill Country Veterinary Specialists and FASTVet.com, Spicewood, TX.

VetBooks.ir

### *B-line Scoring System for Guiding Diuretic Usage*

Numbers of B-lines can help justify the need for loop diuretics (see Figure 36.17). In dogs and cats with absent B-lines during Vet BLUE (likely holds true for all mammalian lung), loop diuretics should not be given empirically (Lisciandro et al. 2014, 2016, 2017; Rademacher et al. 2014; Ward et al. 2017, 2018b; Vezzosi et al. 2017). When B-lines are present, their numbers and distribution help guide loop diuretic usage. In patients with small numbers of B-lines, loop diuretics likely may be administered more conservatively versus patients with high numbers of B-lines (>3 and infinity) at many Vet BLUE views. Numbers of B-lines most commonly represent alveolar-interstitial syndrome, meaning B-lines are nonspecific and must be placed in clinical context. For example, a predominance of B-lines dorsally or generalized is more likely cardiogenic and noncardiogenic forms of lung edema, especially when combined with TFAST echo views and other supportive evidence including physical exam findings, patient history, signalment, and other imaging. This facet of Global FAST is not part of the RUSH exam. See Figure 36.17, Table 23.4, and Chapters 22 and 23 for greater detail.

### *B-line Scoring System for Lung Contusions*

In trauma cases, numbers of B-lines may be combined with numbers of positive Vet BLUE views and their distribution to assign a Vet BLUE lung contusion severity score to the patient (Lisciandro 2011, 2014b; Boysen and Lisciandro 2013; Dicker et al. 2019) (see Figures 23.30, 36.17). For example, a trauma patient with >3 B-lines at its left Ph and Md lung regions has focal contusions compared to another trauma patient that has >3 B-lines at all transthoracic Vet BLUE views as well as at the DH view. This facet of Global FAST is not part of the RUSH exam. See Chapters 22 and 23 for greater detail.

# Global FAST for Staging Disease – Localized Versus Disseminated Disease

Having practiced veterinary medicine as a general practitioner and a clinical specialist for over 28 years and having trained 1000+ veterinarians throughout the United States, the following scenarios are not uncommon and drive home an important and necessary paradigm change. The "flash approach" of ultrasound for imaging patients is a huge detriment for patient care in the author's opinion, likened to performing an incomplete physical examination. Moreover, the "flash approach" not only lends itself to desultory methodology but also obviates the mandatory requirement for recording patient data other than "fluid positive" or "fluid negative" and other freehanded data entries. Finally, the "flash approach" and targeted "POCUS" examination, without a standardized set of data imaging points provided by Global FAST, lends itself to the dangerous problem of satisfaction of search error. A case in point is canine anaphylaxis and its marker of sonographic striation of the gallbladder wall, discovered in a brilliant study by Quantz (2009); however, its flaw was doing just a targeted or focused gallbladder examination and not a Global FAST. By performing Global FAST, the added rule-outs of pericardial effusion and right-sided congestive heart failure, including dilated cardiomyopathy, and the unique canine complication of hemoabdomen would likely have been detected sooner than post-study by other investigators (Lisciandro 2014a,d, 2016b; Lisciandro et al. 2019b; Hnatusko et al. 2019).

Let's look at several scenarios and the positive effect that the Global FAST approach has on patient care (Figure 36.18).

## *Staging the Hemoabdomen*

### Canine Hemoabdomen

A retrospective study described numbers of canine hemoabdomen cases and those that proceeded to definitive surgical care. Of the 432 cases, only 86 were operated, or 20% (Lux et al. 2013). Many factors enter into the decision to pursue a diagnostic work-up and the decision for definitive care; however, the author will describe a typical scenario that many veterinarians would recognize. The acute collapsed nontraumatic hemoabdomen patient is triaged and because a physical exam is ambiguous, the ultrasound probe is used to "flash" the abdomen, answering a simple binary question of "fluid positive" or "fluid negative" with or without an additional sweep of the abdomen for a "mass." The subsequent discussion with the client goes as follows: "Your dog has a bleed within its abdominal cavity. The bleeding likely has a splenic tumor as its cause (Lux et al. 2013). The most likely diagnosis is a malignant tumor with a probability of benign ranging from ~25% to 33% to malignant ranging from ~67% to 75% (Hammond and Pesillo-Crosby 2008; Aronsohn et al. 2009; Levinson et al. 2009; Eberle et al. 2012; Lux et al. 2013; Lynch et al. 2015). We need to do X, Y, and Z for a cost of X." This work-up of X, Y, and Z is likely expensive, including blood work +/- coagulation profile, three-view thoracic radiograph as a pulmonary metastasis

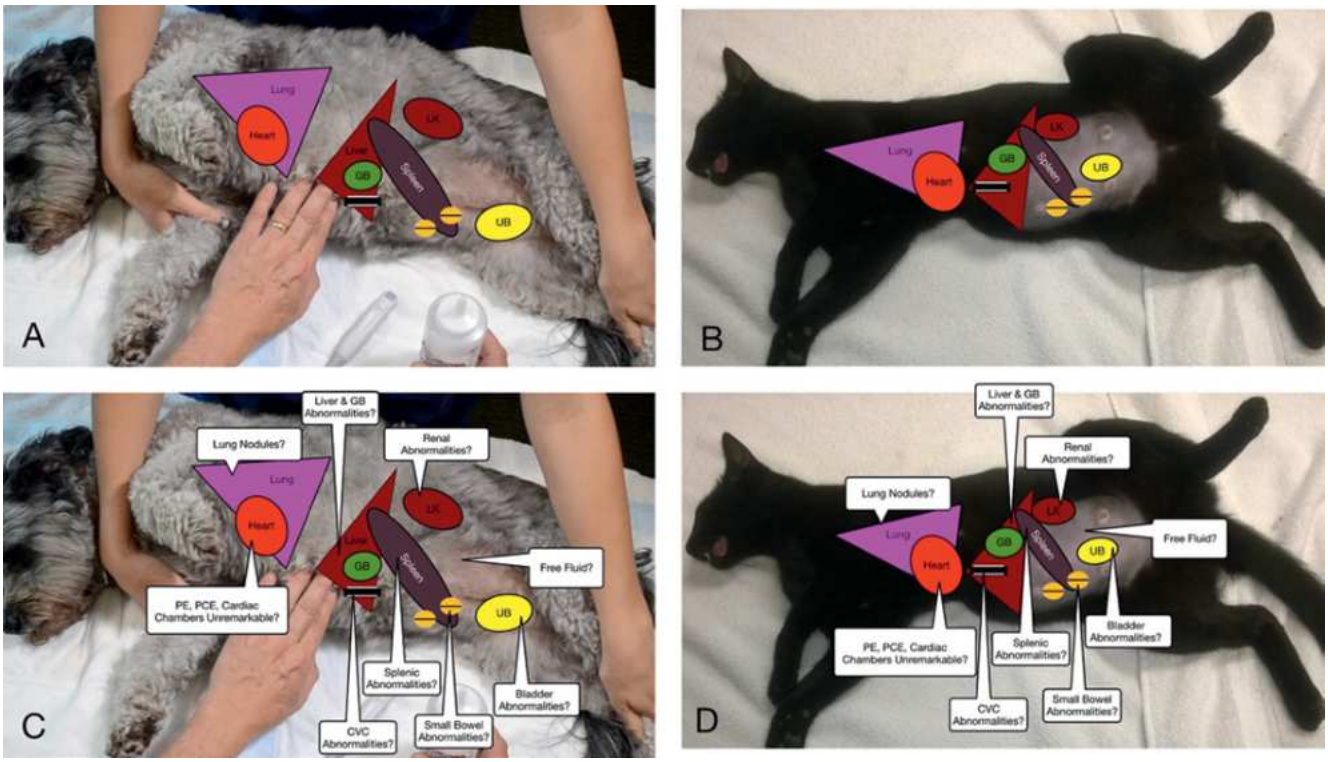


**Figure 36.18.** Questions asked during staging with Global FAST. (A,B) Overlays of target structures evaluated during the Global FAST approach including within the abdomen and thorax, including heart and lung. In (C,D) clinically relevant questions are shown on overlays for the staging of disease and conditions as being localized or disseminated. The Global FAST approach provides a means to not only quickly screen for local versus disseminated disease but also to determine the diagnostic path, including the next best test(s). Moreover, by "seeing" the problem list with evidence-based information, treatment is potentially better directed. See the text for greater detail. Source: Reproduced with permission from Dr Gregory Lisciandro, Hill Country Veterinary Specialists and FASTVet.com, Spicewood, TX.

check, and a complete detailed abdominal ultrasound to confirm the bleeding mass, its origin, and whether intraabdominal metastasis is apparent. The end-result is that the patient is euthanized, given palliative care or not treated (Lux et al. 2013).

So let's think about this work-up and the study's data a bit more (Lux et al. 2013). If the ratio of benign to malignant is as poor as 25–33%% to 67–75% then likely there are many dogs with benign tumors being euthanized. If we think about the effectiveness of staging with a three-view thoracic radiograph (TXR) study for pulmonary metastasis and pericardial effusion, common sites for hemangiosarcoma to metastasize, the literature has shown that there are real limitations to this approach. Three-view TXR misses lung nodules, for which computed tomography is the gold standard (Eberle et al. 2010; Alexander et al. 2012; Armbrust et al. 2012), and misses pericardial effusion, for which ultrasound is arguably the gold standard (Guglielmini et al. 2012; Côté et al. 2013).

The questions must be asked: "If the patient is staged negative on Global FAST for any obvious metastasis, would the benign to malignant tumor frequency be improved?" and "Would we be able to better determine surgical candidacy and thus treat with the potential to cure benign splenic neoplastic disease?"

The advantages of the Global FAST approach for staging this subset of patients with the most clinically relevant questions are as follows (Figure 36.19).

### *AFAST*

- DH view – are there obvious liver metastases (target lesions)?
- SR and HRU views – is there an obvious splenic or midabdominal mass?
- What is the AFS? Determine small-volume bleeder versus large-volume bleeder to help with the decision regarding blood transfusion(s).

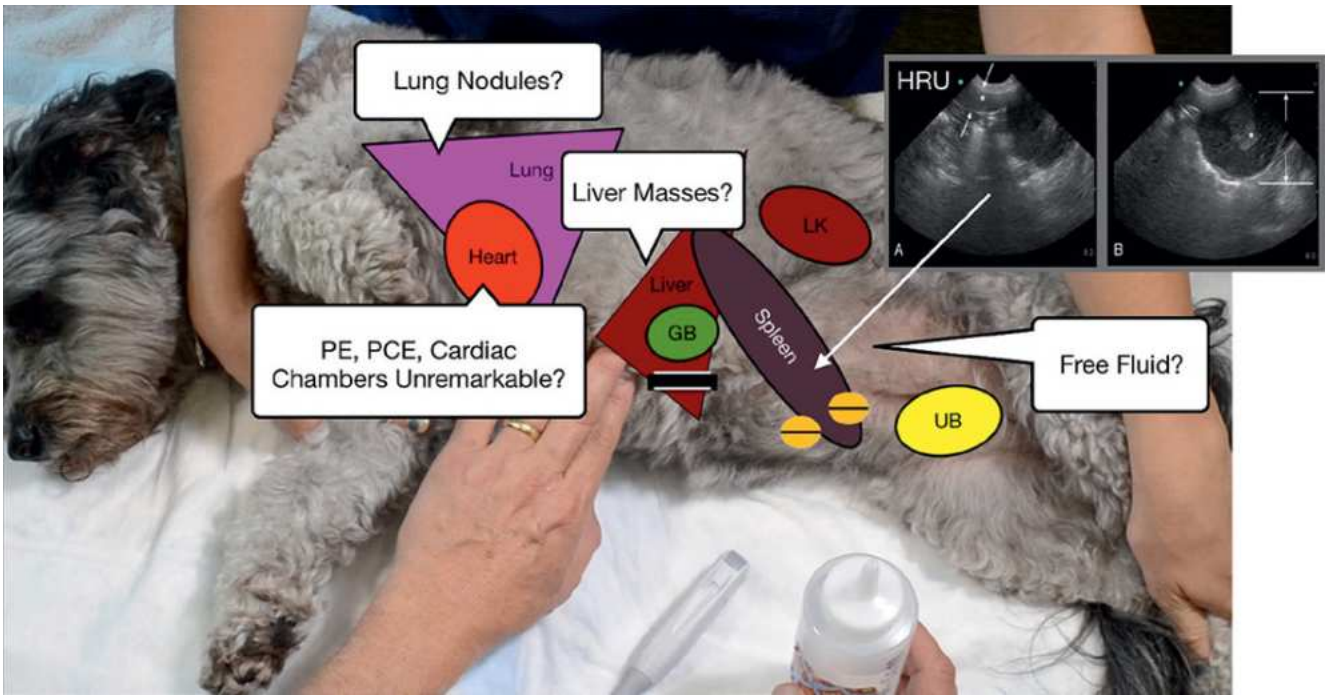


**Figure 36.19.** Global FAST approach for hemoabdomen and splenic mass. Shown on a dog with overlays are important target structures during Global FAST that help stage the hemoabdomen case caused by a bleeding splenic mass by answering clinically relevant questions to determine if the patient is a good surgical candidate. The Global FAST approach for staging shows clear advantages over radiography for the detection of pleural and pericardial effusion, liver masses, and pulmonary metastatic disease. See the text for greater detail. The approach would be analogous for the cat and other species. Source: Reproduced with permission from Dr Gregory Lisciandro, Hill Country Veterinary Specialists and FASTVet.com, Spicewood, TX.

*TFAST*

- Is there pleural effusion?
- Is there pericardial effusion?
- Is there any obvious intracardiac mass?

*Vet BLUE*

- Are there any obvious lung nodules?
- Any lung surface abnormalities?

The attending clinician is searching for any obvious signs of metastasis and thus is helped in their presentation of the condition to the client with the potential of hope for definitive surgical care in those staging negative for obvious metastasis. Further work-up, including possible additional imaging, then takes place with more confidence that the patient has localized disease and is more likely to be a surgical candidate.

### Feline Hemoabdomen

As with dogs, cats have neoplasia as the top differential with nontraumatic hemoabdomen (Culp et al. 2010). The staging of the cat would be identical and from experience without using first-line Global FAST ultrasound, blood transfusions were administered to cats with obvious widespread disseminated disease. On the other hand, staging may determine localized disease, affording the opportunity to stabilize, work up, and treat. The clinically relevant questions are the same as for dogs.

## Staging for Urinary Bladder Mass

### Canine Bladder Masses

Many clinicians are performing ultrasound-guided cystocentesis and are using ultrasound on a daily basis and appreciating obvious urinary bladder pathology such as sediment, cystic calculi, thrombi, and masses. A common scenario is the finding of a soft tissue bladder wall mass. The cystocentesis procedure is stopped because of the finding of a suspicious mass. The client is told of the concerning finding, and that a diagnostic work-up of X, Y, and Z is indicated that includes blood and urine testing (free-catch, voided

sample urinalysis), confirmation of the mass via a complete detailed abdominal ultrasound (AUS), staging the disease for any complications or metastasis with the abdomen (AUS), and complications or pulmonary metastasis within the thorax with three-view TXR. Not uncommonly, the AUS is delayed either by scheduling in-house evaluation by a third party or the client and patient are sent to a referral practice with or without a three-view TXR the same day. With a stable patient, the client may elect to think about it and get back to the veterinarian, with or without returning, and likely overwhelmed by the finding on emotional and financial fronts. The same client may have not been told that the most common tumor of the urinary bladder is treatable with oral chemotherapy with good long-term results.

A better approach would be to perform Global FAST on day 1, not letting the client depart before staging the patient to determine the following information (Figure 36.20).

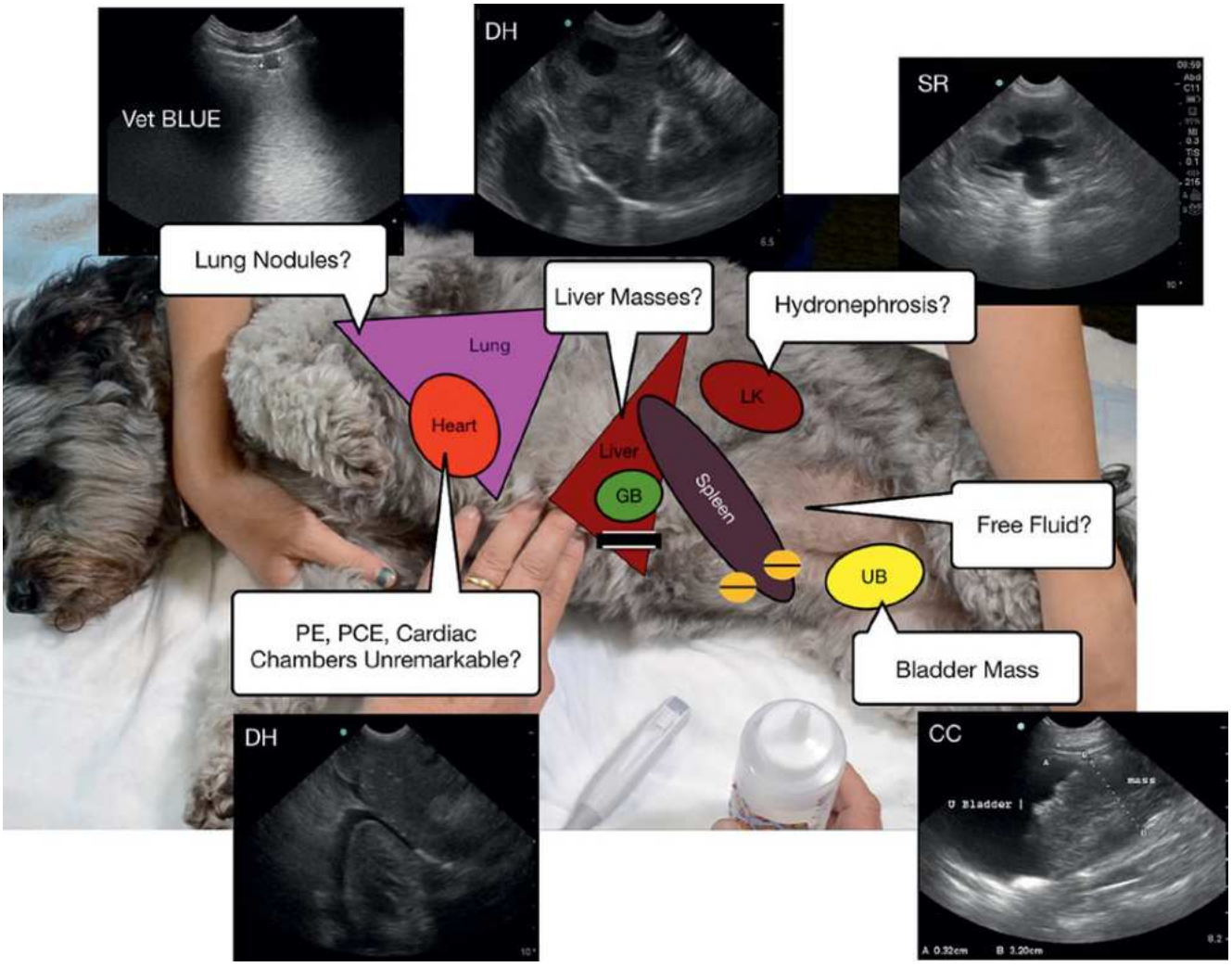


**Figure 36.20.** Global FAST approach for urinary bladder mass. Shown are overlays of clinically relevant target structures evaluated during the Global FAST approach for staging the patient as localized or disseminated disease. These questions are readily answered with minimal training including the presence of an actual bladder mass (versus a thrombus or artifact), the presence of hydronephrosis in the kidneys (obstruction of ureters), liver masses, pulmonary metastatic disease, and pleural effusion, providing clear advantages over radiography and the "flash approach." Moreover, cardiac and bladder masses can be related and the TFAST echo view allows a search for any obvious soft tissue cardiac abnormalities. B-mode images are near the respective overlay as examples of easily detected abnormalities. Staging provides hope for the client on day 1 in those patients staging without obvious complications. See the text for greater detail and the respective POCUS chapters. The approach would be analogous for the cat and other species. Source: Reproduced with permission from Dr Gregory Lisciandro, Hill Country Veterinary Specialists and FASTVet.com, Spicewood, TX.

*AFAST*

- DH view – any obvious liver metastasis?
- SR view – any obvious renal masses or renal pelvic dilation – hydronephrosis?
- HRU view – any obvious midabdominal masses?
- HR5th bonus view – any obvious renal masses or renal pelvic dilation – hydronephrosis?

*TFAST*

- Is there pleural effusion?
- Is there pericardial effusion?
- Is there any obvious intracardiac mass?

*Vet BLUE*

- Are there any obvious lung nodules?
- Any lung surface abnormalities?

The attending clinician is searching for any obvious complications and signs of metastasis and thus is helped in their presentation of the condition to the client with the potential for hope and definitive care. The traditional work-up will take place with more confidence for the possibility for definitive gold standard treatment for the patient.

### Feline Bladder Masses

As with dogs, cats have neoplasia as the top differential but the signalment, sex, and location generally differ, with bladder tumors more common in older males (versus middle-aged female dogs) and nearer the apex (cats) than the trigone (dogs). Moreover, the prognosis may be guarded to good as well as in dogs (Wilson et al. 2007; Griffin et al. 2018). The staging of the cat would be identical and determining localized disease before the patient departs on day 1 affords the opportunity to work up and treat. The clinically relevant questions are the same as for dogs.

## *Staging Pericardial Effusion*

### Canine Pericardial Effusion

Pericardial effusion is far more prevalent than previously recorded because we were using the wrong first-line screening test, namely thoracic radiography, which is unreliable (Stafford Johnson et al. 2004; MacDonald et al. 2009; Guglielmini et al. 2012; Côté et al. 2013). With first-line use of AFAST and TFAST and the emphasis to look past the diaphragm for PCE and following specific tenets for its accurate diagnosis (Lisciandro 2014a,d, 2016a, 2019a), the sonographer is less intimidated by the thorax and is becoming more confident in accurately diagnosing PCE. With increased detection comes the need to better understand the causes and prognoses for pericardial effusion in both the dog and cat.

In the dog, it has been reported that a nonhemoabdomen ascites along with echocardiography negative for a heart mass carries a significantly better prognosis (605 days versus 45 days), thus emphasizing the importance of a Global FAST approach over the "flashing of the thorax" in which the presentation to the client likely will involve neoplasia as a top differential (Stafford Johnson et al. 2004). The advantage with "flashing the thorax" or selectively imaging the heart lies more in the PCE diagnosis and that the finding carries a poor prognosis rather than staging the patient with the Global FAST approach in an attempt to pursue treatment. Moreover, pulmonary metastasis is commonly missed by thoracic radiography, detecting only 33% of cases with thoracoscopy with necropsy as the gold standard comparison test (MacDonald et al. 2009). By staging with Global FAST, ascites may be easily screened for with high sensitivity and specificity, as well as lung nodules during Vet BLUE (Kulhavy and Lisciandro 2015).

Staging with a more favorable prognosis helps direct the client to performing life-saving pericardiocentesis (so more and more veterinarians will need to acquire this skill) and understanding that pericardiocentesis buys time for the client to make decisions, including gold standard testing of a complete detailed echocardiogram and possibly surgery. Even slow-growing, mildly inflammatory heart base tumors may be treated for months with pericardiocentesis and other minimal interventions. Moreover, dogs echo negative for cardiac masses may have foreign bodies, infectious and inflammatory causes, or acquired coagulopathies that have the potential to be cured. See Chapters 18, 20, and 21 for greater detail.

The advantages of the Global FAST approach for staging this subset of patients with the most clinically relevant questions are as follows (Figure 36.21).

*AFAST*

- DH view – are there obvious liver metastases (target lesions)?
- SR and HRU views – is there an obvious splenic or midabdominal mass?
- What is the AFS? What is the fluid type? If nonhemorrhagic, a modified transudate carries a much better prognosis (Stafford Johnson et al. 2004). If

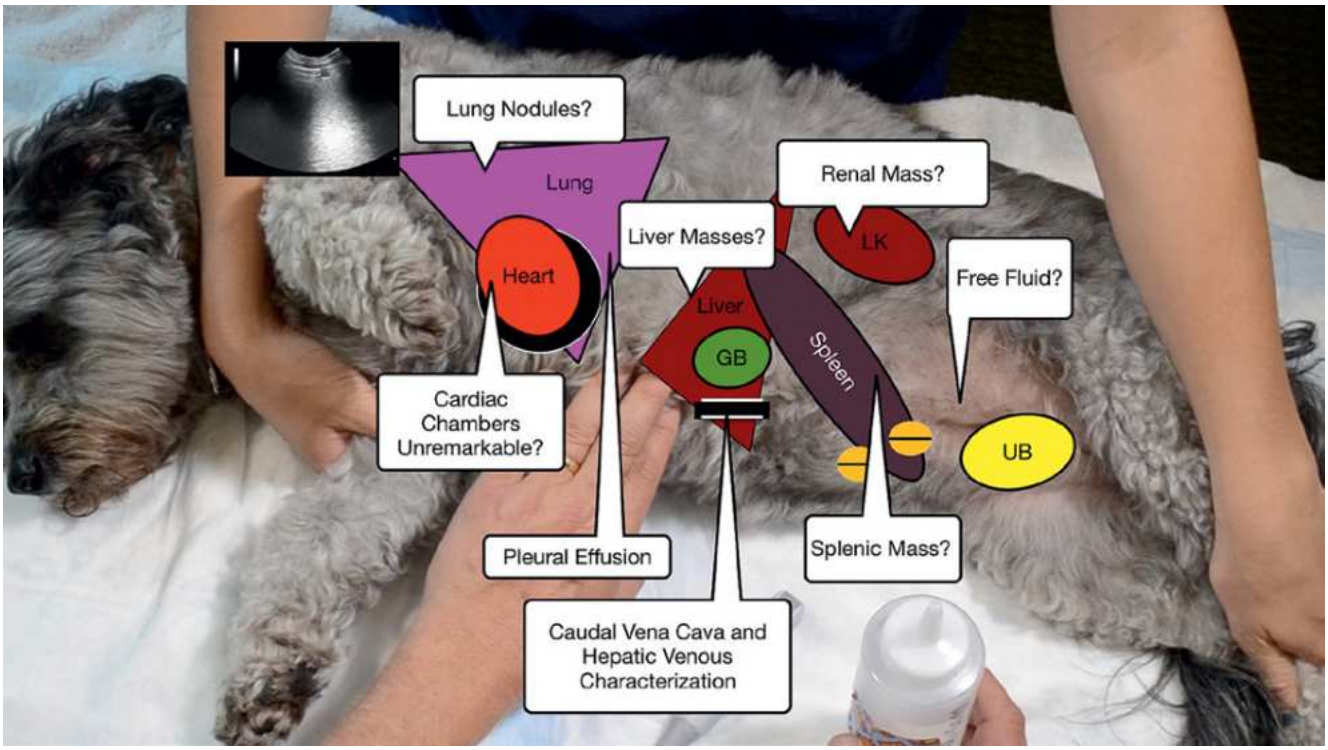


**Figure 36.21.** Global FAST approach for pericardial effusion. Shown are overlays of clinically relevant target structures evaluated during the Global FAST approach for staging the patient as localized or disseminated disease. This is especially important in dogs because pericardial effusion can be associated with primary pericardial disease from infectious causes, foreign bodies, and pericardial and cardiac neoplasia, as well as secondary to primary cardiac masses and metastatic disease, i.e., hemangiosarcoma. Source: Reproduced with permission from Dr Gregory Lisciandro, Hill Country Veterinary Specialists and FASTVet.com, Spicewood, TX.

hemorrhagic, then categorize as a small-volume bleeder versus large-volume bleeder to help with decisions regarding blood transfusion(s).
- Focused spleen for an obvious splenic mass (Boston et al. 2011; Fleming et al. 2018) (see Figure 6.35).

### *TFAST*

- Is there concurrent pleural effusion?
- Is there any obvious intracardiac mass?

### *Vet BLUE*

- Are there any obvious lung nodules?
- Any lung surface abnormalities?

The attending clinician is searching for any obvious signs of metastasis and thus is helped in their presentation of the condition to the client with the potential of hope for definitive care if pericardial effusion screens as isolated or nondisseminated disease.

### Feline Pericardial Effusion

Unlike dogs, cats have congestive heart failure (hypertrophic cardiomyopathy, HCM) as the top differential when PCE is detected (Hall et al. 2007; Ward et al. 2018a). In the largest published study, 75% of cats with PCE were ultimately diagnosed with heart failure most commonly from HCM (Hall et al. 2007). In another more recent study, the finding of PCE was 100% specific, meaning every cat with any degree of PCE was ultimately diagnosed with heart failure (Ward et al. 2018a). Thus, the clinically relevant questions differ with cats. Staging is important but in terms of cats with pleural effusion, "flashing the thorax" may be detrimental with a long list of differentials, when the observation of PCE places heart failure as the top differential and changes the presentation to the client as well as directing care along the lines of this treatable disease. Moreover, the use of Vet BLUE helps guide diuretic usage by using the B-line Scoring system. The Global FAST approach helps guide treatment of the congestive heart failure patient,

looks for comorbidities, and also screens for other causes of PCE and disseminated disease. For example, if lung nodules were found with PCE, then heart failure would be a much less probable diagnosis but rather granulomatous disease (fungal, parasitic, bacterial) and neoplasia.

# Global FAST Approach Case Examples

The use of Global FAST would have made me a better veterinarian if I had known then what I know now, having been on both sides of the equation as a primary care veterinarian and as a emergency veterinarian at referral practices. On the primary care side, the client felt guilty about not pursuing a work-up for a presumed cancerous condition, often leaving to "think about it (the plan and its cost without much hope)," never to return. On the flip side, as an emergency veterinarian, that same client saw me for the euthanasia because they felt too guilty to return to the primary care veterinarian. Either way, care is less than optimal, to the detriment of the patient.

Now let's look at three cases to illustrate the point.

## *Case 1*

The patient is a 13-year-old male (neutered at 6 months of age) Jack Russell terrier that presents with stranguria and hematuria (Figure 36.22). On physical examination, the most significant finding by digital rectal examination is an asymmetrical enlarged and painful prostate. The top differential is straight forward as a prostatic adenocarcinoma. The diagnostic work-up includes confirmation of the mass as well as staging the abdominal cavity by a complete detailed diagnostic abdominal ultrasound, a three-view TXR as a pulmonary metastatic check, and blood and urine testing. The client departs to discuss with her family the patient assessment and proposed diagnostic work-up with a top differential of prostatic neoplasia with a fairly guarded to poor prognosis.

Let's look at the client's perspective. She got the dog before she was married and now it's part of her family with three young children. She won't return to the primary veterinarian due to the guilt of not pursuing the work-up with little hope. However, several days later, she told her story to a recent acquaintance, who happened to be not only a veterinarian but a specialist in small animal internal medicine and skilled in advanced ultrasound, who offered to perform a Global FAST. Vet

**Figure 36.22.** Jack Russell terrier with prostatic adenocarcinoma. Global FAST begins with the Vet BLUE as shown. The sonographer, a specialist in small animal internal medicine, readily detects multiple various sized nodules throughout the Vet BLUE examination. The patient has disseminated disease, which is important to tell the client on day 1, and set up a plan that includes palliative end-of-life hospice care. Source: Reproduced with permission from Dr Gregory Lisciandro, Hill Country Veterinary Specialists and FASTVet.com, Spicewood, TX.

BLUE was performed initially as a rapid screening test for pulmonary metastasis, low impact, without shaving and restraint, and on the living room coffee table. At the first two Vet BLUE views, variable sized nodules were observed along the lung surface and were subsequently detected throughout the Vet BLUE. The remainder of the Global FAST along with a focused prostate and the clinical profile of the patient supported metastatic disease to the lungs and sublumbar lymph nodes.

The information provided by Global FAST was important on a number of fronts: the client is informed of the disseminated disease (and not left to feel guilty and not know), and palliative therapy is offered (instead of no therapy) and the dog made as comfortable as possible, providing end-of-life time for the dog with its family. In this scenario, the client will return to the primary practitioner for end-of-life decisions rather than go elsewhere. A solid bond of trust has been formed between the client and her primary care veterinarian and case management and care greatly improved. Global FAST may be continued for monitoring progression as well as response to treatment, if attempted.

Another possible scenario is that this same case is sent by the primary care veterinarian to a referral practice and the pulmonary metastasis may or may not be detected initially. When detected initially, the client wonders why you, as the primary care veterinarian, didn't spare them the trip and cost by detecting these nodules *before* referral. The Global FAST should have been performed on day 1 before the client departed. The other possibility is that the detection of the pulmonary metastases is delayed or missed by less sensitive imaging such as three-view TXR (Armbrust et al. 2012; Alexander et al. 2012; Kulhavy and Lisciandro 2015).

## Case 2

The patient is Tootsie, a 15-year-old female spayed dachshund that had a gingival mass removed and biopsied at the time of her recent dental (Figure 36.23). The histopathology came back with the diagnosis of malignant melanoma and a three-view TXR was recommended to screen for metastatic disease to her lungs. The imaging was declined due to cost compounded by the information that the tumor was highly malignant (so why bother?). The client was instructed for home monitoring, including "watching" for coughing and changes in breathing that likely would occur with pulmonary metastasis. The "watching at home" creates client anxiety – every time Tootsie, the dog she loves dearly, coughs or breathes a little differently the owner wonders if her dog is succumbing to the highly malignant tumor.

**Figure 36.23.** Dachshund named Tootsie with malignant melanoma removed during dental. The dog has a tumor removed off the gingiva during a dental procedure and the histopathology returns with the diagnosis of malignant melanoma. The dog is doing fine at home and returns for a recheck and discussion of the plan with the concerning diagnosis. The client decides not to pursue imaging and is instructed to monitor at home as their other option, thinking that good money is poorly spent for the recommended three-view TXR. Every time Tootsie coughs or looks different to the owner, the client thinks her dog is going to succumb to metastasis. Option 2 is imaging with Global FAST on day 1. The dog is imaged at its home on a coffee table in the living room and the "lung line" has no pathology, including no nodules. The rest of Global FAST is unremarkable. The imaging plan of repeating every three weeks out to 16-weeks is followed and Tootsie never develops any signs of pulmonary or other metastasis and is still alive nine months after the procedure, doing very well. Global FAST as in the previous example (Figure 36.22) would have served the patient well by performing the imaging on day 1 and sparing the client of the anxiety of "not knowing." Source: Reproduced with permission from Dr Gregory Lisciandro, Hill Country Veterinary Specialists and FASTVet.com, Spicewood, TX.

Global FAST imaging is offered to screen for not only pulmonary metastasis but any other obvious abnormalities in the abdomen and thorax, including the heart. The low-impact study, requiring little to no

VetBooks.ir

restraint and no shaving of hair, is performed at the client's home on a coffee table, and is unremarkable. The good news is given to the client and Global FAST examinations are carried out every three weeks to 16 weeks post dental. No evidence of disseminated metastatic is found and Tootsie is alive and doing well 12 months later. Another client–patient–veterinary bond has been solidified. Do Global FAST on day 1! On the other hand, if lung surface abnormalities were detected during Vet BLUE then three-view thoracic radiograph would be indicated and likely agreed to by the owner.

### *Case 3*

The ultrasound probe is naive to the patient and a Global FAST approach is easily applied to this rat (Figure 36.24). The AFAST portion easily can detect ascites and soft tissue lesions of the target organs including caudal vena cava and hepatic venous distension, TFAST screens for pleural and pericardial effusion with unlikely TFAST echo views because of the depth limits of the probe, and Vet BLUE easily screens for "wet lung" versus "dry lung" as well as lung surface pathology. The Global FAST was an unremarkable scan and the neurological rat was treated supportively and symptomatically. Global FAST may be used for monitoring.

**Figure 36.24.** Global FAST on a rat. The application of Global FAST may be translated to any mammalian species. Here, the microconvex probe is placed on the abdomen of a rat and AFAST is readily performed using the same target organ approach as for TFAST and Vet BLUE. The sonographer can easily see that there is no free intraabdominal fluid, retroperitoneal fluid, obvious soft tissue abnormalities including the caudal vena cava and hepatic veins, pleural or pericardial effusion and that the lungs are dry with absent B-lines. The TFAST echo views are indeterminate because of the small size of the heart, requiring a smaller, higher frequency probe. Source: Reproduced with permission from Dr Gregory Lisciandro, Hill Country Veterinary Specialists and FASTVet.com, Spicewood, TX.

## Global FAST for Urinary Obstruction and Renal Failure

Global FAST is invaluable for the renal failure patient, including postrenal, renal, and pre-renal causes. It is not uncommon for urinary obstructed dogs and cats to have free intraabdominal fluid and retroperitoneal and perirenal effusion (Nevins et al. 2015; Gerken et al. 2019. The prognosis in the vast majority is good with standard treatment as these typically are medically treated complications even with the confirmation of a uroabdomen. Serial Global FAST examinations are key to track the effusion, which is expected to resolve within 24–48 hours.

See more detail in Chapters 10 and 37.

## Global FAST for Pulmonary Thromboembolism

Global FAST carries the potential to detect pulmonary thromboembolism (PTE) in dogs and cats (and other mammalian species) through screening for acute right ventricle dilation and the wedge sign during Vet BLUE (Lisciandro 2013, unpublished data). More skilled sonographers may also survey the pulmonary arteries for saddle thrombi as well. The sensitivity and specificity for this approach are unknown in veterinary medicine but it has proven effective in people in both detection and monitoring response to treatment applications (Mathis et al. 2005; Mastruzzo et al. 2008). The Global FAST approach also has clear advantages over contrast pulmonary angiography using computed tomography that poses risk and requires specialized equipment (Goggs et al. 2014). Serial Global FAST examinations are key to track the progression and resolution of PTE. See more detail in Chapters 25 and 37.

## Global FAST and Anesthesia

### *Global FAST as a Preanesthetic Test*

The Global FAST approach serves as a soft tissue scan of the abdomen and thorax, including heart and lung, and is becoming best practice for evaluating patients

prior to any anesthetic procedures (Nomura and Watanabe 2017). Recording Global FAST findings provides a baseline to which postanesthetic profiles may be compared and complications detected (Lisciandro et al. 2015; Lisciandro and Fosgate 2018). For example, the dental prophylaxis case that has concurrent but otherwise occult bladder stones is best detected *before* the dental, or the same case with a splenic mass, or with poor systolic function (dilated cardiomyopathy), or with small-volume pleural or pericardial effusion. The use of Global FAST also includes patients ranging from a skin mass removal to an elective procedure to an emergency procedure.

### *Global FAST Perioperatively*

The Global FAST approach may be used for monitoring for volume status and complications, including those resulting in free fluid such as hemorrhage, infection, inflammation, and vascular in the four spaces (peritoneal and pleural cavity, retroperitoneal space, pericardial sac) and lung (Lisciandro and Fosgate 2018). Moreover, Global FAST surveys for soft tissue abnormalities and cardiovascular and pulmonary complications, as outlined in Chapter 37, including the Hs and Ts of CPR and treatable forms of hypotension and shock.

#### Lung Atelectasis and Gallbladder Wall Edema

Lung atelectasis is common in anesthetized people, including for minor sedation events. It has been shown in a pilot study that dogs undergoing short anesthetic procedures maintained "dry lung" Vet BLUE profiles post procedure without obvious signs of atelectasis, such as B-lines, shred sign, tissue sign (Lisciandro et al. 2015). However, dogs receiving tiletamine-zolazepam trended toward more atelectatic lung, making a case for periodic positive pressure breath sighing during anesthesia (Lisciandro and Fosgate 2018). In a more recent study of 63 anesthetized dogs, the following were important findings (Lisciandro and Fosgate 2018):

- dogs with spontaneous breathing were more likely to develop signs of lung atelectasis than those on anesthetic ventilators
- dogs undergoing anesthesia did not develop gallbladder wall edema from splanchnic venous pooling
- dogs receiving morphine as a premedication and during their procedure (even those that vomited) did not develop gallbladder wall edema
- dogs receiving contrast agents did not develop gallbladder wall edema
- a dog that received a blood transfusion did develop gallbladder wall edema (Lisciandro and Fosgate 2018).

The Global FAST baseline is important for detecting preanesthetic complications and for comparison to perioperative findings for complications and for optimizing resuscitation and volume status.

## Use of Global FAST as Geriatric Health Screening

The reader likely has a good idea of the potential for Global FAST to capture disease earlier in its course in older patients presenting once or twice a year for preventive medicine.

## Global FAST and Saving Images

The Global FAST approach takes ~7 minutes for the experienced and properly trained sonographer to acquire its 15 acoustic windows (see Figures 36.3, 36.4, 37.1, and 37.2), which is ~20–25 seconds per view. The author recommends setting your machine for a minimum of 6-second cine clips prospectively and performing each of the 15 views initially as a "pilot" and then repeating and recording the same view so every view is interrogated twice.

Unless unrecognizable, the AFAST and TFAST views require no labeling as each are distinct when target organs are included and the heart is unique from the right and left TFAST PCS views. Vet BLUE poses the greatest challenge, which is easily surmountable by making each of its transthoracic views unique. The Caudodorsal lung regions are marked with the caudodorsal transition zone by including it at the beginning of the clip. The Perihilar lung regions are marked by only having intercostal spaces. The Middle lung region is marked (or identified) by including the heart at the beginning of its clip. Lastly, the Cranial lung region is marked by including the cranial transition zone of the thoracic inlet at the beginning of its clip. Moreover, performing the AFAST, TFAST, and Vet BLUE examinations in the same order every time maintains consistency, although the author performs the Global FAST order dependent on patient positioning (see Figures 36.3, 36.4, 37.1, and 37.2). Findings are *always* recorded on standardized goal-directed templates (Figure 36.25).

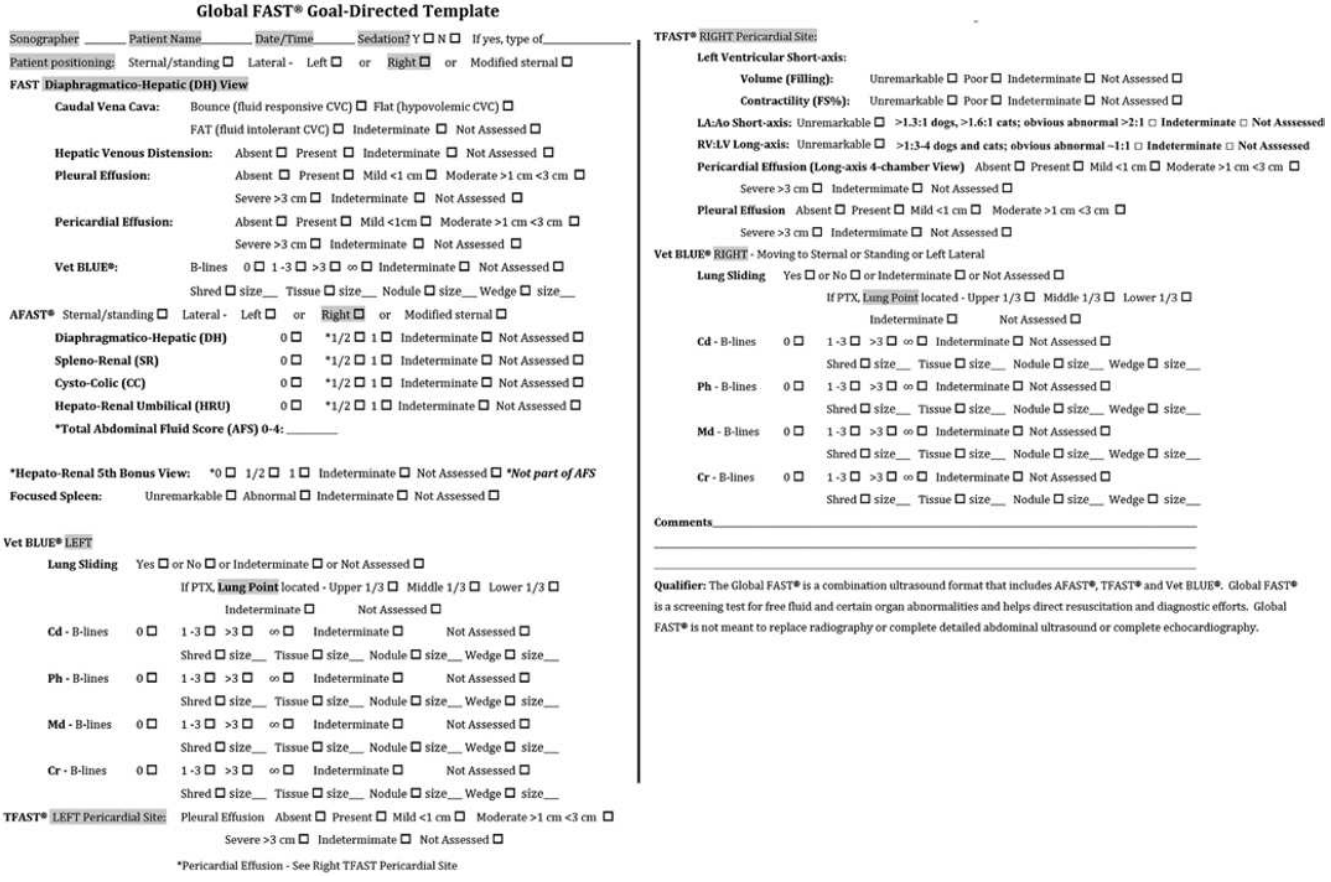

**Global FAST® Goal-Directed Template**

Sonographer _____ Patient Name_____ Date/Time_____ Sedation? Y ☐ N ☐ If yes, type of_____

Patient positioning: Sternal/standing ☐ Lateral - Left ☐ or Right ☐ or Modified sternal ☐

**FAST Diaphragmatico-Hepatic (DH) View**

**Caudal Vena Cava:** Bounce (fluid responsive CVC) ☐ Flat (hypovolemic CVC) ☐
FAT (fluid intolerant CVC) ☐ Indeterminate ☐ Not Assessed ☐

**Hepatic Venous Distension:** Absent ☐ Present ☐ Indeterminate ☐ Not Assessed ☐

**Pleural Effusion:** Absent ☐ Present ☐ Mild <1 cm ☐ Moderate >1 cm <3 cm ☐
Severe >3 cm ☐ Indeterminate ☐ Not Assessed ☐

**Pericardial Effusion:** Absent ☐ Present ☐ Mild <1cm ☐ Moderate >1 cm <3 cm ☐
Severe >3 cm ☐ Indeterminate ☐ Not Assessed ☐

**Vet BLUE®:** B-lines 0 ☐ 1 -3 ☐ >3 ☐ ∞ ☐ Indeterminate ☐ Not Assessed ☐
Shred ☐ size__ Tissue ☐ size__ Nodule ☐ size__ Wedge ☐ size__

**AFAST®** Sternal/standing ☐ Lateral - Left ☐ or Right ☐ or Modified sternal ☐

**Diaphragmatico-Hepatic (DH)** 0 ☐ *1/2 ☐ 1 ☐ Indeterminate ☐ Not Assessed ☐

**Spleno-Renal (SR)** 0 ☐ *1/2 ☐ 1 ☐ Indeterminate ☐ Not Assessed ☐

**Cysto-Colic (CC)** 0 ☐ *1/2 ☐ 1 ☐ Indeterminate ☐ Not Assessed ☐

**Hepato-Renal Umbilical (HRU)** 0 ☐ *1/2 ☐ 1 ☐ Indeterminate ☐ Not Assessed ☐

***Total Abdominal Fluid Score (AFS) 0-4:** _____

***Hepato-Renal 5th Bonus View:** *0 ☐ 1/2 ☐ 1 ☐ Indeterminate ☐ Not Assessed ☐ ***Not part of AFS***

**Focused Spleen:** Unremarkable ☐ Abnormal ☐ Indeterminate ☐ Not Assessed ☐

**Vet BLUE® LEFT**

**Lung Sliding** Yes ☐ or No ☐ or Indeterminate ☐ or Not Assessed ☐
If PTX, Lung Point located - Upper 1/3 ☐ Middle 1/3 ☐ Lower 1/3 ☐
Indeterminate ☐ Not Assessed ☐

**Cd - B-lines** 0 ☐ 1 -3 ☐ >3 ☐ ∞ ☐ Indeterminate ☐ Not Assessed ☐
Shred ☐ size__ Tissue ☐ size__ Nodule ☐ size__ Wedge ☐ size__

**Ph - B-lines** 0 ☐ 1 -3 ☐ >3 ☐ ∞ ☐ Indeterminate ☐ Not Assessed ☐
Shred ☐ size__ Tissue ☐ size__ Nodule ☐ size__ Wedge ☐ size__

**Md - B-lines** 0 ☐ 1 -3 ☐ >3 ☐ ∞ ☐ Indeterminate ☐ Not Assessed ☐
Shred ☐ size__ Tissue ☐ size__ Nodule ☐ size__ Wedge ☐ size__

**Cr - B-lines** 0 ☐ 1 -3 ☐ >3 ☐ ∞ ☐ Indeterminate ☐ Not Assessed ☐
Shred ☐ size__ Tissue ☐ size__ Nodule ☐ size__ Wedge ☐ size__

**TFAST® LEFT Pericardial Site:** Pleural Effusion Absent ☐ Present ☐ Mild <1 cm ☐ Moderate >1 cm <3 cm ☐
Severe >3 cm ☐ Indeterminate ☐ Not Assessed ☐

*Pericardial Effusion - See Right TFAST Pericardial Site

**TFAST® RIGHT Pericardial Site:**

**Left Ventricular Short-axis:**

**Volume (Filling):** Unremarkable ☐ Poor ☐ Indeterminate ☐ Not Assessed ☐

**Contractility (FS%):** Unremarkable ☐ Poor ☐ Indeterminate ☐ Not Assessed ☐

**LA:Ao Short-axis:** Unremarkable ☐ **>1.3:1 dogs, >1.6:1 cats; obvious abnormal >2:1 ☐ Indeterminate ☐ Not Asssessed**

**RV:LV Long-axis:** Unremarkable ☐ **>1:3-4 dogs and cats; obvious abnormal ~1:1 ☐ Indeterminate ☐ Not Asssessed**

**Pericardial Effusion (Long-axis 4-chamber View)** Absent ☐ Present ☐ Mild <1 cm ☐ Moderate >1 cm <3 cm ☐
Severe >3 cm ☐ Indeterminate ☐ Not Assessed ☐

**Pleural Effusion** Absent ☐ Present ☐ Mild <1 cm ☐ Moderate >1 cm <3 cm ☐
Severe >3 cm ☐ Indeterminate ☐ Not Assessed ☐

**Vet BLUE® RIGHT - Moving to Sternal or Standing or Left Lateral**

**Lung Sliding** Yes ☐ or No ☐ or Indeterminate ☐ or Not Assessed ☐
If PTX, Lung Point located - Upper 1/3 ☐ Middle 1/3 ☐ Lower 1/3 ☐
Indeterminate ☐ Not Assessed ☐

**Cd - B-lines** 0 ☐ 1 -3 ☐ >3 ☐ ∞ ☐ Indeterminate ☐ Not Assessed ☐
Shred ☐ size__ Tissue ☐ size__ Nodule ☐ size__ Wedge ☐ size__

**Ph - B-lines** 0 ☐ 1 -3 ☐ >3 ☐ ∞ ☐ Indeterminate ☐ Not Assessed ☐
Shred ☐ size__ Tissue ☐ size__ Nodule ☐ size__ Wedge ☐ size__

**Md - B-lines** 0 ☐ 1 -3 ☐ >3 ☐ ∞ ☐ Indeterminate ☐ Not Assessed ☐
Shred ☐ size__ Tissue ☐ size__ Nodule ☐ size__ Wedge ☐ size__

**Cr - B-lines** 0 ☐ 1 -3 ☐ >3 ☐ ∞ ☐ Indeterminate ☐ Not Assessed ☐
Shred ☐ size__ Tissue ☐ size__ Nodule ☐ size__ Wedge ☐ size__

**Comments**_____

**Qualifier:** The Global FAST® is a combination ultrasound format that includes AFAST®, TFAST® and Vet BLUE®. Global FAST® is a screening test for free fluid and certain organ abnormalities and helps direct resuscitation and diagnostic efforts. Global FAST® is not meant to replace radiography or complete detailed abdominal ultrasound or complete echocardiography.

**Figure 36.25.** Global FAST goal-directed templates. Examples of Global FAST goal-directed templates and order for imaging views in positioning of (A) right lateral and (B) standing-sternal. Source: Reproduced with permission from Dr Gregory Lisciandro, Hill Country Veterinary Specialists and FASTVet.com, Spicewood, TX.

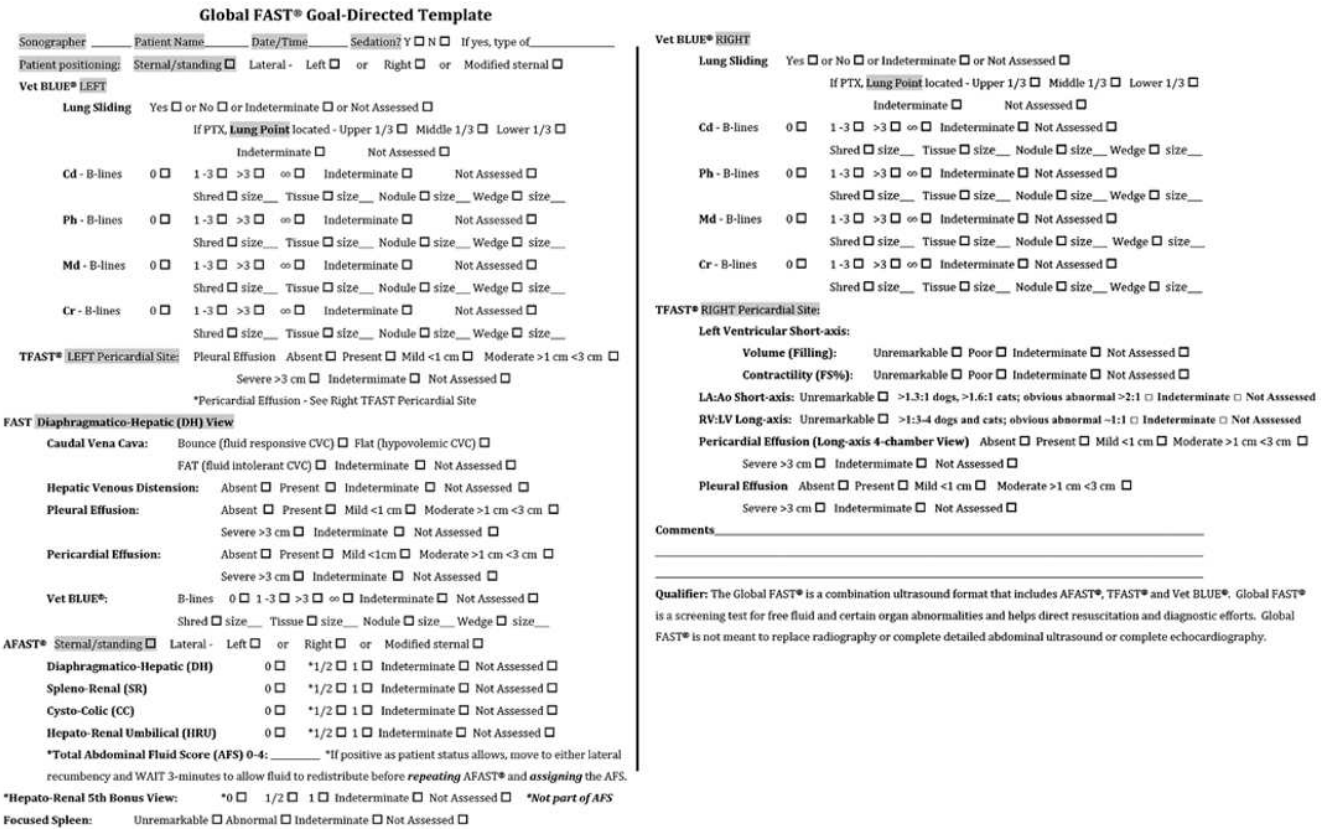

**Global FAST® Goal-Directed Template**

Sonographer _____ Patient Name_____ Date/Time_____ Sedation? Y ☐ N ☐ If yes, type of_____

Patient positioning: Sternal/standing ☐ Lateral - Left ☐ or Right ☐ or Modified sternal ☐

**Vet BLUE® LEFT**

**Lung Sliding** Yes ☐ or No ☐ or Indeterminate ☐ or Not Assessed ☐

If PTX, **Lung Point** located - Upper 1/3 ☐ Middle 1/3 ☐ Lower 1/3 ☐

Indeterminate ☐ Not Assessed ☐

**Cd** - B-lines 0 ☐ 1 -3 ☐ >3 ☐ ∞ ☐ Indeterminate ☐ Not Assessed ☐

Shred ☐ size___ Tissue ☐ size___ Nodule ☐ size___ Wedge ☐ size___

**Ph** - B-lines 0 ☐ 1 -3 ☐ >3 ☐ ∞ ☐ Indeterminate ☐ Not Assessed ☐

Shred ☐ size___ Tissue ☐ size___ Nodule ☐ size___ Wedge ☐ size___

**Md** - B-lines 0 ☐ 1 -3 ☐ >3 ☐ ∞ ☐ Indeterminate ☐ Not Assessed ☐

Shred ☐ size___ Tissue ☐ size___ Nodule ☐ size___ Wedge ☐ size___

**Cr** - B-lines 0 ☐ 1 -3 ☐ >3 ☐ ∞ ☐ Indeterminate ☐ Not Assessed ☐

Shred ☐ size___ Tissue ☐ size___ Nodule ☐ size___ Wedge ☐ size___

**TFAST® LEFT Pericardial Site:** Pleural Effusion Absent ☐ Present ☐ Mild <1 cm ☐ Moderate >1 cm <3 cm ☐

Severe >3 cm ☐ Indeterminate ☐ Not Assessed ☐

*Pericardial Effusion - See Right TFAST Pericardial Site

**FAST Diaphragmatico-Hepatic (DH) View**

**Caudal Vena Cava:** Bounce (fluid responsive CVC) ☐ Flat (hypovolemic CVC) ☐

FAT (fluid intolerant CVC) ☐ Indeterminate ☐ Not Assessed ☐

**Hepatic Venous Distension:** Absent ☐ Present ☐ Indeterminate ☐ Not Assessed ☐

**Pleural Effusion:** Absent ☐ Present ☐ Mild <1 cm ☐ Moderate >1 cm <3 cm ☐

Severe >3 cm ☐ Indeterminate ☐ Not Assessed ☐

**Pericardial Effusion:** Absent ☐ Present ☐ Mild <1cm ☐ Moderate >1 cm <3 cm ☐

Severe >3 cm ☐ Indeterminate ☐ Not Assessed ☐

**Vet BLUE®:** B-lines 0 ☐ 1 -3 ☐ >3 ☐ ∞ ☐ Indeterminate ☐ Not Assessed ☐

Shred ☐ size___ Tissue ☐ size___ Nodule ☐ size___ Wedge ☐ size___

**AFAST®** Sternal/standing ☐ Lateral - Left ☐ or Right ☐ or Modified sternal ☐

**Diaphragmatico-Hepatic (DH)** 0 ☐ *1/2 ☐ 1 ☐ Indeterminate ☐ Not Assessed ☐

**Spleno-Renal (SR)** 0 ☐ *1/2 ☐ 1 ☐ Indeterminate ☐ Not Assessed ☐

**Cysto-Colic (CC)** 0 ☐ *1/2 ☐ 1 ☐ Indeterminate ☐ Not Assessed ☐

**Hepato-Renal Umbilical (HRU)** 0 ☐ *1/2 ☐ 1 ☐ Indeterminate ☐ Not Assessed ☐

***Total Abdominal Fluid Score (AFS) 0-4:** _____ *If positive as patient status allows, move to either lateral recumbency and WAIT 3-minutes to allow fluid to redistribute before ***repeating*** AFAST® and ***assigning*** the AFS.

***Hepato-Renal 5th Bonus View:** *0 ☐ 1/2 ☐ 1 ☐ Indeterminate ☐ Not Assessed ☐ ***Not part of AFS***

**Focused Spleen:** Unremarkable ☐ Abnormal ☐ Indeterminate ☐ Not Assessed ☐

**Vet BLUE® RIGHT**

**Lung Sliding** Yes ☐ or No ☐ or Indeterminate ☐ or Not Assessed ☐

If PTX, **Lung Point** located - Upper 1/3 ☐ Middle 1/3 ☐ Lower 1/3 ☐

Indeterminate ☐ Not Assessed ☐

**Cd** - B-lines 0 ☐ 1 -3 ☐ >3 ☐ ∞ ☐ Indeterminate ☐ Not Assessed ☐

Shred ☐ size___ Tissue ☐ size___ Nodule ☐ size___ Wedge ☐ size___

**Ph** - B-lines 0 ☐ 1 -3 ☐ >3 ☐ ∞ ☐ Indeterminate ☐ Not Assessed ☐

Shred ☐ size___ Tissue ☐ size___ Nodule ☐ size___ Wedge ☐ size___

**Md** - B-lines 0 ☐ 1 -3 ☐ >3 ☐ ∞ ☐ Indeterminate ☐ Not Assessed ☐

Shred ☐ size___ Tissue ☐ size___ Nodule ☐ size___ Wedge ☐ size___

**Cr** - B-lines 0 ☐ 1 -3 ☐ >3 ☐ ∞ ☐ Indeterminate ☐ Not Assessed ☐

Shred ☐ size___ Tissue ☐ size___ Nodule ☐ size___ Wedge ☐ size___

**TFAST® RIGHT Pericardial Site:**

**Left Ventricular Short-axis:**

**Volume (Filling):** Unremarkable ☐ Poor ☐ Indeterminate ☐ Not Assessed ☐

**Contractility (FS%):** Unremarkable ☐ Poor ☐ Indeterminate ☐ Not Assessed ☐

**LA:Ao Short-axis:** Unremarkable ☐ **>1.3:1 dogs, >1.6:1 cats; obvious abnormal >2:1 ☐ Indeterminate ☐ Not Asssessed**

**RV:LV Long-axis:** Unremarkable ☐ **>1:3-4 dogs and cats; obvious abnormal ~1:1 ☐ Indeterminate ☐ Not Asssessed**

**Pericardial Effusion (Long-axis 4-chamber View)** Absent ☐ Present ☐ Mild <1 cm ☐ Moderate >1 cm <3 cm ☐

Severe >3 cm ☐ Indeterminate ☐ Not Assessed ☐

**Pleural Effusion** Absent ☐ Present ☐ Mild <1 cm ☐ Moderate >1 cm <3 cm ☐

Severe >3 cm ☐ Indeterminate ☐ Not Assessed ☐

**Comments**_____

_____

_____

**Qualifier:** The Global FAST® is a combination ultrasound format that includes AFAST®, TFAST® and Vet BLUE®. Global FAST® is a screening test for free fluid and certain organ abnormalities and helps direct resuscitation and diagnostic efforts. Global FAST® is not meant to replace radiography or complete detailed abdominal ultrasound or complete echocardiography.

**Figure 36.25.** (*Continued*)

# Pearls and Pitfalls, The Final Say

The use of the Global FAST approach has clear advantages for patient care through its application as an extension of the physical exam in nearly all patients for all clinical specialists, with the following everyday applications.

- Seeing your problem list to help pick the next best test and dictate a more streamlined diagnostic plan in abnormal patients as well as health screening.
- Monitoring tool for patients with effusions in the abdomen and thorax.
- Monitoring tool for pneumothorax.
- Staging patients for localized versus disseminated disease.
- Use as a preanesthetic screening test.
- Use perioperatively.

# References


Alexander K, Joly H, Blond L, et al. 2012. A comparison of computed tomography, computed radiography, and film-screen radiography for the detection of canine pulmonary nodules. *Vet Radiol Ultrasound* 53(3):258–265.

Andrus P. 2015. Cardiac arrest. In: *Point-of-Ultrasound*, edited by Soni N, Arntfield R, Kory P. Philadelphia: Elsevier Saunders, pp 359–365.

Armbrust LJ, Biller DS, Bamford A, et al. 2012. Comparison of three-view thoracic radiography and computed tomography for detection of pulmonary nodules in dogs with neoplasia. *J Am Vet Med Assoc* 240(9):1088–1094.

Armenise A, Neri L, Storti E, et al. 2012a. Evaluation of a FAST-ABCDE protocol (Focused Assessment with Sonography for Trauma-Airway, Breathing, Circulation, Disability, and Exposure) to detect multiple injuries in canine trauma patients: preliminary data. *J Vet Emerg Crit Care* 22(S2):S20.

Armenise A, Ricciardi M, Giannuzzi AP, et al. 2012b. Ultrasonographic measure of the optic nerve sheath in canine patients with signs of raised intracranial pressure. A preliminary study. *J Vet Emerg Crit Care* 22(S2):S20.

Armenise A, Boysen RS, Rudloff E, et al. 2019. Veterinary-focused assessment with sonography for trauma-airway, breathing, circulation, disability and exposure: a prospective observational study in 64 canine trauma patients. *J Small Anim Pract* 60(3):173–182.

Aronsohn MG, Dubiel B, Roberts B, et al. 2009. Prognosis for acute nontraumatic hemoperitoneum in the dog: a retrospective analysis of 60 cases (2003–2006). *J Am Anim Hosp Assoc* 45(2):72–77.

Atalan G, Barr FJ, Holt PE. 1999. Frequency of urination and ultrasonographic estimation of residual urine in normal and dysuric dogs. *Res Vet Sci* 67(3):295–299.

Atalan G, Barr FJ, Holt PE. 2007. Estimation of the volume of the gall bladder of 32 dogs from linear ultrasonographic measurements. *Vet Rec* 160(4):118–122.

Atkinson P, Bowra J, Milne J, et al. 2017. International Federation for Emergency Medicine Consensus Statement: Sonography in hypotension and cardiac arrest (SHoC): An international consensus on the use of point of care ultrasound for undifferentiated hypotension and during cardiac arrest. *Can J Emerg Med* 19(6):459–470.

Bilello JF, Davis JW, Lemaster D, et al. 2011. Prehospital hypotension in blunt trauma: identifying the "crump factor." *J Trauma* 70(5):1038–1042.

Birkbeck R, Greensmith T, Humm K, et al. 2019. Haemoabdomen due to suspected anaphylaxis in four dogs. *Vet Rec Case Rep* 2019;7:e000734. doi:10.1136/vetreccr-2018-000734.

Blackbourne LH, Soofer D, McKenney M, et al. 2004. Secondary ultrasound examination increases the sensitivity of the FAST exam in blunt trauma. *J Trauma* 57(5): 934–938.

Boller M, Fletcher DJ. 2012. RECOVER evidence and knowledge gap analysis on veterinary CPR. Part 1: Evidence analysis and consensus process: collaborative path toward small animal CPR guidelines. *J Vet Emerg Crit Care* 22(S1):S4–S12.

Boston SE, Higginson G, Monteith G. 2011. Concurrent splenic and right atrial mass at presentation in dogs with HSA: a retrospective study. *J Am Anim Hosp Assoc* 47(5): 336–341.

Boysen SR, Lisciandro GR. 2013. The use of ultrasound in the emergency room (AFAST and TFAST). *Vet Clin North Am Small Anim Pract* 43(4):773–797.

Boysen SR, Rozanski EA, Tidwell AS, et al. 2004. Evaluation of a focused assessment with sonography for trauma protocol to detect free abdominal fluid in dogs involved in motor vehicle accidents. *J Am Vet Med Assoc* 225(8): 1198–1204.

Breitkreutz R, Walcher F, Seeger FH, et al. 2007. Focused echocardiographic evaluation in resuscitation management (FEER): concept of an advanced life support–conformed algorithm. *Crit Care Med* 35(S5):1527–1533.

Breitkreutz R, Price S, Steiger HV, et al. 2010. Focused echocardiographic evaluation in life support and peri-resuscitation of emergency patients: a prospective trial. *Resuscitation* 81:1527–1533.

Bucci M, Rabozzi R, Gugliemini C, et al. 2017. Respiratory variation in aortic blood peak velocity and caudal vena cava dimater can predict fluid responsiveness in anesthetized and mechanically ventilated dogs. *Vet J* 227:30–35.

Busch K, Suchodolski JS, Kuhner KA, et al. 2015. Clostridium perfringens enterotoxin and Clostridium difficile toxin A/B do not play a role in acute haemorrhagic diarrhea syndrome in dogs. *Vet Record* 176:253.

Caldwell DJ, Petras KE, Mattison BL, et al. 2018. Spontaneous hemoperitoneum and anaphylactic shock asscoiated with Hymenoptera envenomation in a dog. *J Vet Emerg Crit Care* 28(5):476–482.

Cambournac M, Goy-Thollot I, Violé A, et al. 2018. Sonographic assessment of volaemia: development and validation of a new method in dogs. *J Small Anim Pract* 59(3):174–182.

Candotti C, Arntfield R. 2015. Pericardial effusion. In: *Point-of-Care Ultrasound*, edited by Soni NJ, Arntfield R, Kory P. Philadelphia: Elsevier Saunders, pp 130–134.

Côté E, Schwarz LA, Sithole F. 2013. Thoracic radiographic findings for dogs with cardiac tamponade attributable to pericardial effusion. *J Am Vet Med Assoc* 243(2):232–235.

Culp WT, Weisse C, Kellog ME, et al. 2010. Spontaneous hemopertoneum in cats: 65 cases (1994–2006). *J Am Vet Med Assoc* 236(9):978–982.

Darnis E, Boysen S, Merveille AC, et al. 2018. Establishment of references values of the caudal vena cava by fast-ultrasonography through different views in healthy dogs. *J Vet Intern Med* 32(4):1308–1318.

Dicker SA, Lisciandro GR, Newell SM, et al. 2019. Diagnosis of pulmonary contusions with point-of-care lung ultrasonography and thoracic radiography compared to thoracic computed tomography in dogs with motor vehicle trauma: 29 cases (2017–2018). *J Vet Emerg Crit Care*, in press.

Eberle N, Fork M, von Babo I, et al. 2010. Comparison of examination of thoracic radiographs and thoracic computed tomography in dogs with appendicular osteosarcoma. *Vet Comp Oncol* 9(2):131–140.

Eberle N, von Babo V, Nolte I, et al. 2012. Splenic masses in dogs. Part I: Epidemiologic, clinical characteristics as well as histopathologic diagnosis in 249 cases (2000–2011). *Tierarztl Prax Ausg K Kleintiere Heimtiere* 40(4):250–260.

Eom K, Moon K, Seong Y, et al. 2008. Ultrasonographic evaluation of tracheal collapse in dogs. *J Vet Sci* 9(4):401–405.

Erhardt C. 1996. Inferior vena caval syndrome and the sniff test for elevated central venous pressure and its contributing factors. *J Diag Med Sonography* 12:27–33.

Ferrada P, Anand RJ, Whelan J, et al. 2011. Limited transthoracic echocardiogram: so easy any trauma attending can do it. *J Trauma* 71(5):1327–1331.

Ferrada P, Vanguri P, Anand RJ, et al. 2012a. Flat inferior vena cava: indicator of poor prognosis in trauma and acute care surgery patients. *Am Surg* 78(12):1396–1398.

Ferrada P, Attand RJ, Whelan J, et al. 2012b. Qualitative assessment of the inferior vena cava: useful tool for the evaluation of volume status in criticall ill patients. *Am Surg* 78(4):468–470.

Fleming J, Giuffrida A, Runge JJ, et al. 2018. Anatomical site and etiology of hemorrhage in small versus large dogs with spontaneous hemopertoneum. *Vet Surg* 47(8):1031–1038.

Gargani L, Pang PS, Frassi F, et al. 2015. Persistent pulmonary congestion before discharge predicts rehospitalization in heart failure: a lung ultrasound study. *Cardiovasc Ultrasound* 13:40.

Geeraerts T, Launey Y, Martin L, et al. 2007. Ultrasonography of the optic nerve sheath may be useful for detecting raised intracranial pressure after severe brain injury. *Intensive Care Med* 33:1704–1711.

Gerken KK, Cooper ES, Butler AS, et al. 2019. Association of abdominal effusion with a single decompression cystocentesis prior to catheterization in male cats with urethral obstruction. *J Vet Emerg Crit Care* [Epub ahead of print].

Goggs R, Chan DL, Benigni L, et al. 2014. Comparison on computed tomography pulmonary angiography and point-of-care tests for pulmonary thromboembolism diagnosis in dogs. *J Small Anim Pract* 55:190–197.

Griffin MA, Culp W, Rebuhn RB. 2018. Lower urinary tract neoplasia. *Vet Sci* 5(4):96.

Guglielmini C, Diana A, Santarelli G, et al. 2012. Accuracy of radiographic vertebral heart score and sphericity index in the detection of pericardial effusion in dogs. *J Am Vet Med Assoc* 241(8):1048–1055.

Hall DJ, Shofer F, Meier CK, Sleeper MM. 2007. Pericardial effusion in cats: a retrospective study of clinical findings and outcome in 146 cats. *J Vet Intern Med* 21(5):1002–1007.

Hammond TN, Pesillo-Crosby SA. 2008. Prevalence of hemangiosarcoma in anemic dogs with a splenic mass and hemoperitoneum requiring a transfusion: 71 cases: 2003–2005. *J Am Vet Med Assoc* 232(4):553–558.

Hassani B. 2015. Bladder. In: *Point-of-Care Ultrasound*, edited by Soni NJ, Arntfield R, Kory P. Philadelphia: Elsevier Saunders, pp 162–165.

Himelman RB, Kircher B, Rockey DC, et al. 1988. Inferior vena cava plethora with blunted respiratory response: a sensitive echocardiographic sign of cardiac tamoponade. *J Am Coll Cardiol* 12(6):1470–1477.

Hnatusko AL, Gicking JC, Lisciandro GR. 2019. Anaphylaxis-related hemoperitoneum in 11 dogs. *J Vet Emerg Crit Care*, in press.

Jambrik Z, Monti S, Coppola V, et al. 2004. Usefulness of ultrasound lung comets as a nonradiologic sign of extravascular lung water. *Am J Cardiol* 93(10):1265–1270.

Jambrik Z, Gargani L, Adamicza A, et al. 2010. B-lines quantify the lung water content: a lung ultrasound versus lung gravimetry study in acute lung injury. *Ultrasound Med Biol* 36(12):2004–2010.

Johnson LR, Lappin MR, Baker DC. 1999. Pulmonary thromboembolism in 29 dogs: 1985–1995. *J Vet Intern Med* 13(4):338–345.

Kirkpatrick AW, Sirois M, Laupland KB, et al. 2004. Hand-held thoracic sonography for detecting post-traumatic pneumothoraces: the extended focused assessment with sonography for trauma (EFAST). *J Trauma* 57:288–295.

Kulhavy DA, Lisciandro GR. 2015. Use of a lung ultrasound examination called Vet BLUE to screen for metastatic lung nodules in the emergency room. *J Vet Emerg Crit Care* 25(S1):S14.

Kulhavy DA, Lisciandro, GR. 2018. The use of VetBLUE to evaluate lung pathology in dogs with severe pulmonary hypertension without left-sided heart disease. *J Vet Emerg Crit Care* 28(S1):S15.

Kwak HS, Im HG, Shim EB. 2016. A model for allometric scaling of mammalian metabolism with ambient heat loss. *Integr Med Res* 5(1):30–36.

Kwak J, Yoon H, Kim J, Kim M, Eom K. Ultrasonographic measurement of caudal vena cava to aorta ratios for determination of volume depletion in normal beagle dogs. *Vet Radiol Ultrasound* 2018;59(2):203–211.

Levinson JG, Bouma JL, Althouse GC, et al. 2009. Prevalence of malignancy when solitary versus multiple lesions are detected during abdominal ultrasonographic examination of dogs with spontaneous hemopertoneum: 31 cases (2003–2008). *J Vet Emerg Crit Care* 19(5):496–500.

Lichtenstein DA. 2010. Gallbladder. In: *Whole Body Ultrasonography in the Critically Ill*, edited by Lichtenstein DA. Heidelberg: Springer, pp 59–68.

Lichtenstein D. 2012. Fluid administration limited by lung sonography: the place of lung ultrasound in assessment of acute circulatory failure (the FALLS-protocol). *Expert Rev Respir Med* 6(2):155–162.

Lichtenstein D, Karakitsos D. 2012. Integrating lung ultrasound in the hemodynamic evaluation of acute circulatory failure (the fluid administration limited by lung sonography protocol). *J Crit Care* 27(5):533.

Lichtenstein D, Malbrain ML. 2015. Critical care ultrasound in cardiac arrest. Technological requirements for performing the SESAME-protocol – a holistic approach. *Anaesthesiol Intensive Ther* 47(5):471–481.

Lichtenstein D, Mezière G, Lagoueyte JF, et al. 2009. A-lines and B-lines: lung ultrasonography as a bedside tool for predicting pulmonary artery occlusion pressure in the critically ill. *Chest* 136:1014–1020.

Lisciandro GR. 2011. Abdominal and thoracic focused assessment with sonography for trauma, triage and monitoring in small animals. *J Vet Emerg Crit Care* 21(2): 104–122.

Lisciandro G. 2012. Evaluation of initial and serial combination focused assessment with sonography for trauma (CFAST) examinations of the thorax (TFAST) and abdomen (AFAST) with the application of an abdominal fluid scoring system in 49 cats. Abstract. *J Vet Emerg Crit Care* 22(S2):S11.

Lisciandro GR. 2014a. The Thoracic FAST$^3$ (TFAST$^3$) Exam. In: *Focused Ultrasound for the Small Animal Practitioner*, edited by Lisciandro GR. Ames: Wiley Blackwell, pp 140–165.

Lisciandro GR. 2014b. The Vet BLUE Lung Scan. In: *Focused Ultrasound for the Small Animal Practitioner*, edited by Lisciandro GR. Ames: Wiley Blackwell, pp 166–188.

Lisciandro GR. 2014c. Alanine aminotransferase level (ALT) as a marker for hemoabdomen detected by abdominal FAST (AFAST) in dogs with automobile trauma. Abstract. *J Vet Emerg Crit Care* 24(S1):S11.

Lisciandro GR. 2014d. The abdominal FAST$^3$ (AFAST$^3$) exam. In: *Focused Ultrasound for the Small Animal Practitioner*, edited by Lisciandro GR. Ames: Wiley Blackwell, pp 17–43.

Lisciandro GR. 2016a. The use of the diaphragmatico-hepatic (DH) views of the abdominal and thoracic focused assessment with sonography for triage (AFAST/TFAST) examinations for the detection of pericardial effusion in 24 dogs (2011–2012). *J Vet Emerg Crit Care* 26(1):125–131.

Lisciandro GR. 2016b. Abdominal FAST (AFAST)-detected hemorrhagic abdominal effusion in 11 dogs with acute collapse and gallbladder wall edema (halo sign) with presumed anaphylaxis. Abstract. *J Vet Emerg Crit Care* 26(S1):S8.

Lisciandro GR. 2019a. The cardiac gallbladder: case series of 13 dogs and 1 cat with sonographically-detected gallbladder wall edema. Abstract. *J Vet Emerg Crit Care* 29(S1): S24.

Lisciandro GR. 2019b. Point-of-care ultrasound. In: *Small Animal Diagnostic Ultrasound*, edited by Mattoon JS, Sellon R, Berry CR. St Louis: Elsevier, in press.

Lisciandro GR, Armenise AA. 2014. Focused or COAST$^3$ - Cardiopulmonary Resuscitation (CPR), Global FAST (GFAST$^3$), and the FAST-ABCDE Exam. In: *Focused Ultrasound for the Small Animal Practitioner*, edited by Lisciandro GR. Ames: Wiley Blackwell, pp 269–285.

Lisciandro GR, Fosgate GT. 2017. Use of AFAST cysto-colic view urinary bladder measurements to estimate urinary bladder volume in dogs and cats. *J Vet Emerg Crit Care* 27(6):713–717.

Lisciandro GR, Fosgate GT. 2018. Use of Vet BLUE Protocol for the detection of lung atelectasis and sonographic gallbladder wall evaluation for anaphylaxis and volume overload in 63 dogs undergoing general anesthesia. *J Vet Emerg Crit Care* 28(S1):S15–S16.

Lisciandro GR, Lisciandro SC. 2019. Sonographic changes of the gallbladder associated with anaphylaxis in dogs. *J Vet Emerg Crit Care* 29(2): 214–215.

Lisciandro GR, Mann KA. 2019. Methodological questions regarding focused assessment sonography for trauma comparison with computed tomography in dogs. *J Vet Emerg Crit Care* 29(2): 211–213.

Lisciandro GR, Lagutchik MS, Mann KA, et al. 2008. Accuracy of Focused Assessment with Sonography for Trauma (TFAST) to detect pneumothorax in 145 dogs with blunt and penetrating trauma. *J Vet Emerg Crit Care* 18(3): 258–269.

Lisciandro GR, Lagutchik MS, Mann KA, et al. 2009. Evaluation of an abdominal fluid scoring (AFS) system determined using abdominal focused assessment with sonography for trauma (AFAST) in 101 dogs with motor vehicle trauma. *J Vet Emerg Crit Care* 19(5):426–437.

Lisciandro GR, Fosgate GT, Fulton RM. 2014. Frequency of ultrasound lung rockets using a regionally-based lung ultrasound examination named veterinary bedside lung ultrasound exam (Vet BLUE) in 98 dogs with normal thoracic radiographic lung findings. *Vet Rad Ultrasound* 55(3):315–322.

Lisciandro GR, Romero LA, Bridgeman CH. 2015. Pilot Study: Vet BLUE profiles pre- and post-anesthesia in

31 dogs undergoing surgical sterilization. *J Vet Emerg Crit Care* 25 (S1):S8–S9.

Lisciandro GR, Ward JL, DeFrancesco TC, Mann KA. 2016. Absence of B-lines on lung ultrasound (Vet BLUE protocol) to rule out left-sided congestive heart failure in 368 cats and dogs. *J Vet Emerg Crit Care* (S1):S8.

Lisciandro GR, Fulton RM, Fosgate GT, Mann KA. 2017. Frequency and number of B-lines using a regionally-based lung ultrasound examination in cats with radiographically normal lung compared to cats with left-sided congestive heart failure. *J Vet Emerg Crit Care* 27(3):267–277.

Lisciandro GR, Romero L, Fosgate GT. 2018. The frequency of B-Lines and other lung ultrasound artifacts during Vet BLUE in 91 healthy puppies and kittens. *J Vet Emerg Crit Care* 28(S1):S16.

Lisciandro GR, Fosgate GT, Romero LA, et al. 2019a. The frequency and amount of free peritoneal fluid estimated using abdominal FAST- applied abdominal fluid scores in clinically normal adult and juvenile dogs. *J Vet Emerg Crit Care*, in press.

Lisciandro GR, Johnson CB, Gambino JM, et al. 2019b. The prevalence of sonographically-detected gallbladder wall edema in dogs with acute hemorrhagic diarrhea syndrome. In review.

Lynch AM, O'Toole TE, Hamilton J. 2015. Transfusion practices for treatment of dogs undergoing splenectomy for splenic masses: 542 cases (2001–2012). *J Am Vet Med Assoc* 247(6):636–642.

Lux CN, Culp, WT, Mayhew RD, et al. 2013. Perioperative outcome in dogs with hemoperitoneum: 83 cases (2005–2010). *J Am Vet Med Assoc* 242(10):1385–1391.

MacDonald KA, Cagney O, Magne ML. 2009. Echocardiographic and clinicopathologic characterization of pericardial effusion in dogs: 107 cases (1985–2006). *J Am Vet Med Assoc* 235(12):1456–1461.

Machare-Delgado E, Decaro M, Marik PE. 2011. Inferior vena cava variation compared to pulse contour analysis as predictors of fluid responsiveness: a prospective cohort study. *J Intensive Care Med* 26(2):116–124.

Marshall KA, Thomovsky EJ, Brooks AC, et al. 2018. Ultrasound measurements of the caudal vena cava before and after blood donation in 9 greyhound dogs. *Can Vet J* 59(9):973–980.

Mastruzzo C, Perrachio G, Poidomani G, et al. 2008. Subsegmental pulmonary embolism: value of the thoracic ultrasound for the diagnosis and follow-up. *Intern Med* 47:1415–1417.

Mathis G, Blank W, Reibig A, et al. 2005. Thoracic ultrasound for diagnosing pulmonary embolism. *Chest* 128(3):1531–1538.

McMurray J, Boysen S, Chalhoub S. Focused assessment with sonography in nontraumatized dogs and cats in the emergency and critical care setting. *J Vet Emerg Crit Care* 2016; 26(1): 64–73.

Meneghini C, Rabozzi R, Franci P. 2016. Correlation of the ratio of caudal vena cava diameter and aorta diameter with systolic pressure variation in anesthetized dogs. *Am J Vet Res* 77(2):137–143.

Moretti R, Pizzi B. 2010. Inferior vena cava distensibility as a predictor of fluid responsiveness in patients with subarachnoid hemorrhage. *Neurocrit Care* 13(1):3–9.

Mortier F, Strohmeyer K, Hartmann K, et al. 2015. Acute haemorrhagic diarrhea syndrome on dogs: 108 cases. *Vet Rec* 176:627.

Narasimhan M, Koenig SJ, Mayo PH. 2016. A whole body approach to point of care ultrasound. *Chest* 150(4):772–776.

Nelson NC, Drost WT, Lerche P, et al. 2010. Noninvasive estimation of central venous pressure in anesthetized dogs by measurement of hepatic venous blood flow velocity and abdominal venous diameter. *Vet Radiol Ultrasound* 51(3):313–323.

Neri L, Storti E, Lichtenstein D. 2007. Toward an ultrasound curriculum for critical care medicine. *Crit Care Med* 35(5 Suppl):S290–304.

Neumar RW, Otto CW, Link MS, et al. 2010. Part 8: Adult advanced cardiovascular life support: 2010 American Heart Association guidelines for cardiopulmonary resuscitation and emergency cardiovascular care. *Circulation* 122:S729–S767.

Nevins JR, Mai W, Thomas E. 2015. Associations between ultrasound and clinical findings in 87 cats with urethral obstruction. *Vet Radiol Ultrasound* 56(4):439–447.

Newitt AL, Cripps PJ, Shimali J. 2009. Sonographic estimation of pleural fluid in dogs. *Vet Radiol Ultrasound* 50(1):86–90.

Nomura T, Watanabe I. 2017. Pre-anesthetic whole body point-of-care ultrasonography. *Masui* 66(5):522–529.

Ollerton JE, Sugrue M, Balogh Z, et al. 2006. Prospective study to evaluate the influence of FAST on trauma patient management. *J Trauma* 60(4):785–791.

Perera P, Mailhot T, Riley D, et al. 2010. The RUSH exam: Rapid Ultrasound in SHock in the evaluation of the critically ill. *Emerg Med Clin North Am* 28(1):29–56.

Pfeiffer P, Bache S, Isbye L, et al. 2012. Verification of endotracheal intubation in obese patients – temporal comparison of ultrasound vs. auscultation and capnography. *Acta Anaesthesiol Scand* 56:571–576.

Powell LL, Rozanski EA, Tidwell AS, et al. 1999. A retrospective analysis of pulmonary contusions secondary to motor vehicle accidents in 143 dogs: 1994–1997. *J Vet Emerg Crit Care* 9(3):127–136.

Quantz JE, Miles MS, Reed AL, et al. 2009. Elevation of alanine transaminase and gallbladder wall abnormalities as biomarkers of anaphylaxis in canine hypersensitivity patients. *J Vet Emerg Crit Care* 19(6):536–544.

Rademacher N, Pariaut R, Pate J, et al. 2014. Transthoracic lung ultrasound in normal dogs and dogs with cardiogenic pulmonary edema: a pilot study. *Vet Radiol Ultrasound* 55(4):447–452.

Ritchie JV, Horne ST, Perry J, et al. 2012. Ultrasound triage of ocular blast injury in the military emergency department. *Mil Med* 177(2):174–178.

Rudorf H, Barr FJ, Lane JG. 2001. The role of ultrasound in the assessment of laryngeal paralysis in the dog. *Vet Radiol Ultrasound* 42(4):338–343.

Shimali J, Cripps PJ, Newitt AL. 2010. Sonographic pleural fluid volume estimation in cats. *J Feline Med Surg* 12:113–116.

Sigrist NE, Doherr MG, Spreng DE. 2004. Clinical findings and diagnostic value of post-traumatic thoracic radiographs in dogs and cats with blunt trauma. *J Vet Emerg Crit Care* 14:259–268.

Skubas NJ. 2015. Teaching whole body point-of-care ultrasound: advancing the skills of tomorrow's anesthesiologists. *Anesthesiology* 123(3):499–500.

Spaulding K. Eye and orbit. In: *Atlas of Small Animal Ultrasonography*, edited by Penninck D, d'Anjou MA. Ames: Blackwell Publishing, p 61.

Stafford Johnson M, Martin M, Binns S, Day MJ. 2004. A retrospective study of clinical findings, treatment and outcome in 143 dogs with pericardial effusion. *J Small Anim Pract* 45(11):546–552.

Stander N, Wagner WM, Goddard A, et al. 2010. Normal canine pediatric gastrointestinal ultrasonography. *Vet Radiol Ultrasound* 51(1):75–78.

Sutherland-Smith J, Penninck DG, Keating JH, et al. 2007. Ultrasonic intestinal hyperechoic mucosal striations in dogs are associated with lacteal dilation. *Vet Radiol Ultrasound* 48(1):51–57.

Shyamsundar M, Attwood, B, Keating L, et al. 2013. Clinical review: The role of ultrasound in estimating extravascular lung water. *Crit Care* 17(5):237.

Tavares J, Ivo R, Gonzalez F, et al. 2019. Global ultrasound check for the critically ill (GUCCI) – a systematized protocol unifying point-of-care ultrasound in critically ill patients based on clinical presentation. *Emerg Med* 11:133–145.

Tchernodrinski S, Arntfield R. 2015. Inferior vena cava. In: *Point-of-Care Ultrasound*, edited by Soni NJ, Arntfield R, Kory P. Philadelphia: Elsevier, pp 135–141.

Tuplin MC, Romero AE, Boysen SR. 2017. Influence of the respiratory cycle on the caudal vena cava diameter measured by sonography in healthy foals: a pilot study. *J Vet Intern Med* 31(5):1556–1562.

Vezzosi T, Mannucci A, Pistoresi F, et al. 2017. Assessment of lung ultrasound B-Lines in dogs with different stages of chronic valvular heart disease. *J Vet Intern Med* 31(3): 700–704.

Vientós-Plotts AI, Wiggen KE, Lisciandro GR, et al. 2019. The utility of point-of-care ultrasound non-echo right-sided cardiac markers as a screening test for moderate to severe pulmonary hypertension in dogs. *Vet J* 250:6–13.

Volpicelli G, Mussa A, Garofalo G, et al. 2006. Bedside lung ultrasound in the assessment of alveolar-interstitial syndrome. *Am J Emerg Med* 24:689–696.

Volpicelli G, Elbarbary M, Blaivas M, et al. 2012. International evidence-based recommendations for point-of-care lung ultrasound. *Intens Care Med* 38(4):577–591.

Ward JL, Lisciandro GR, Tou SP, Keene BW, DeFrancesco TC. 2017. Accuracy of point-of-care lung ultrasound (Vet BLUE protocol) for the diagnosis of cardiogenic pulmonary edema in dogs and cats with acute dyspnea. *J Am Vet Assoc* 250(6):666–675.

Ward JL, Lisciandro GR, DeFrancesco TD, et al. 2018a. Evaluation of point-of-care thoracic ultrasound and NT-proBNP for the diagnosis of congestive heart failure in cats with respiratory distress. *J Vet Intern Med* 32(5):1530–1540.

Ward JL, Lisciandro GR, DeFrancesco TD. 2018b. Distribution of alveolar-interstitial syndrome in dogs and cats with respiratory distress assessed with lung ultrasound versus thoracic radiographs. *J Vet Emerg Crit Care* 28(5):415–428.

Ward JL, Lisciandro GR, Ware WA, Miles KG, DeFrancesco TC. 2019. Lung ultrasonography findings in dogs with various underlying causes of cough. *J Am Vet Med Assoc* 255(5):574–583.

Weaver B, Lyon M, Blaivas M. 2006. Confirmation of endotracheal tube placement after intubation using the ultrasound sliding lung sign. *Acad Emerg Med* 13:239–244.

Wilson HM, Chun R, Larson VS, et al. 2007. Clinical signs, treatments and outcome in cats with transitional cell carcinoma of the urinary bladder: 20 cases (1990–2004). *J Am Vet Med Assoc* 231(1):101–106.

Zechner PM, Breitkreutz R. 2011. Ultrasound instead of capnography for confirming endotracheal tube placement in emergency? *Resuscitation* 82(10):1259–1261.

CHAPTER THIRTY-SEVEN

# POCUS: Global FAST – Rapidly Detecting Treatable Forms of Shock, Advanced Life Support, and Cardiopulmonary Resuscitation

Gregory R. Lisciandro

## Introduction

The use of point-of-care ultrasound (POCUS) for uncharacterized shock, cardiopulmonary arrest (CPA), advanced life support (ALS), and cardiopulmonary resuscitation (CPR) has become an important intervention for rapidly addressing treatable causes of impending and actual CPA (Breitkreutz et al. 2007, 2010; Link et al. 2015; Soar et al. 2015; Henry et al. 2018). The American Heart Association's (AHA) CPR guidelines have an important section entitled *Knowing your Hs and Ts* that lists these potentially treatable conditions (Neumar et al. 2010; Lisciandro and Armenise 2014; Andrus 2015; Link et al. 2015; Soar et al. 2015). The "Ruling Out the Hs and Ts Chart" (Table 37.1) is provided with the author's modifications for small animals and provides the basis for this chapter. Using Global FAST can be lifesaving and helps delegate resources more accurately for those patients that can be saved if their treatable problem is detected soon enough.

For example, according to the AHA CPR guidelines and clinical studies, pulseless electrical activity (PEA) in people is often due to a treatable underlying condition (Breitkreutz et al. 2007, 2010; Neumar et al. 2010; Link et al. 2015; Soar et al. 2015). In the author's experience, these are conditions that are typically causing a preload problem or, in other words, poor venous return to the heart. Such conditions include pneumothorax, pericardial effusion, internal bleeding, pulmonary thromboembolism, anaphylaxis, hypoglycemia in a septic patient, and hyperkalemia in urinary obstruction, all treatable with potentially good outcomes for the patient. Thus, if these treatable conditions are detected quickly before the patient incurs significant complications or dies, there is a chance for a favorable patient outcome. The Global FAST approach rapidly screens for many of these treatable conditions and forms of shock (see Tables 37.1, 37.3, and 37.4).

What is the most effective screening method for cardiac assessment? A most telling prospective CPR study from several years ago documented that ~75% of people diagnosed with PEA (~51% of the total CPR study population) and ~35% of those with asystole had in fact on echocardiogram demonstrable *coordinated* cardiac contractions (Breitkreutz et al. 2007, 2010). As a

*Point-of-Care Ultrasound Techniques for the Small Animal Practitioner*, Second Edition. Edited by Gregory R. Lisciandro.
© 2021 John Wiley & Sons, Inc. Published 2021 by John Wiley & Sons, Inc.
Companion website: www.wiley.com/go/lisciandro/ultrasound2

**Table 37.1.**
Ruling out your Hs and Ts. Use of the Global FAST approach for rapidly ruling out and ruling in the Hs and Ts in patients nearing cardiopulmonary arrest (CPA) and during cardiopulmonary resuscitation (CPR). Hs and Ts are rapidly evaluated for by physical exam, vital signs, venous (or arterial) blood gas, and the Global FAST approach.

| The Hs | The Ts |
|---|---|
| Hypothermia | Tension pneumothorax (PTX) (TFAST and "lung point") |
| Hypotension/hypovolemia[a] | Trauma, hemorrhage (AFAST and abdominal fluid scoring system, TFAST, Vet BLUE, cavitary bleeds) |
| Hyperkalemia, hypokalemia[b] | Thromboembolism (pulmonary thromboembolism) (TFAST, Vet BLUE) |
| Hypoglycemia | Tamponade, (pericardial effusion) (TFAST, FAST DH view) |
| Hydrogen ion (acidosis) | Toxin, canine anaphylaxis (FAST DH view) |
| Hypocontractility (dilated cardiomyopathy) (TFAST) | |
| Hypertension (pulmonary hypertension, heartworm disease/caval syndrome) (TFAST) | |

Source: Reproduced with permission from Dr Gregory Lisciandro, Hill Country Veterinary Specialists and FASTVet.com, Spicewood, TX. Modified by the author for veterinary medicine from AHA CPR Guidelines (Neumar et al. 2010; Andrus 2015).
[a] AFAST, TFAST, Vet BLUE, to search for cavitary bleeds and effusions and alveolar-interstitial syndrome.
[b] AFAST, target organ approach for urinary obstruction including findings of large urinary bladder, distended urethra, dilated ureters, and renal pelvic dilation.

result, the terms "true PEA" and "true asystole" have been applied to people without coordinated cardiac contractions and "pseudo-PEA" and "pseudo-asystole" for those having coordinated cardiac contractions. The relevance of this is that people with coordinated cardiac contractions seen using ultrasound had increased survival (Breitkreutz et al. 2007, 2010).

Tying this altogether, the Global FAST approach not only surveys for treatable causes of CPA but also assesses for coordinated cardiac contractions, thus helping to direct resources for those patients with treatable conditions, while also serving as a missing link in the veterinary CPR efforts for improvement (Lisciandro and Armenise 2014; Boller and Fletcher 2012). Even more convincing when considering the AHA guidelines, ultrasound is either the gold standard test or has higher sensitivity, specificity, and accuracy for most of these Hs and Ts of CPR over traditional approaches without ultrasound. For this reason, Global FAST should be standard of care for CPR and ALS protocols for our veterinary patients (currently lacking), carrying the potential to improve outcome by more accurately directing lifesaving interventions as in human guidelines (Breitkreutz et al. 2010; Boller and Fletcher 2012; Lisciandro and Armenise 2014; Callaway et al. 2015; Soar et al. 2015; Link et al. 2015; Henry et al. 2018).

The RUSH and FAST-ABCDE ultrasound examinations have likewise been developed in people for these same reasons (Neri et al. 2007; Perera et al. 2010; Armenise et al. 2019); however, the Global FAST approach is *fast* and does more than the RUSH examination (see Table 36.1) and has distinct advantages over both RUSH and VetFAST-ABCDE. Although VetFAST-ABCDE is a more comprehensive head-to-toe approach, it has additional aspects that are more challenging for nonradiologist sonographers and other related time-consuming issues such as patient preparation and probe changes. Furthermore, the VetFAST-ABCDE exam has many objectives that are generally lower yield, not primary causes for shock, CPA and CPR, and are often known based on physical examination, such as ocular injury, neurological status, laryngeal function, collapsing trachea, and tracheal cervical injury. Moreover, VetFAST-ABCDE likely underestimates its time for completion.

The Global FAST approach is a standardized protocol and has exact clarity to all its 15 acoustic windows that take <7 minutes to complete. POCUS eye, POCUS heart, POCUS MSK, POCUS brain, etc. are more often appropriate *after* resuscitation as add-on examinations as clinical course dictates. More detailed information on Global FAST is provided in Chapters 6, 7, 17, 18, 22, 23, and 36, and clinically relevant POCUS chapters for the add-on examinations.

## *What Global FAST for Treatable Shock, ALS, and CPR Can Do*

- Can detect many of the AHA Hs and Ts of CPR within minutes when minutes count.
- Can help dictate resources during CPA and CPR as well as post CPR.
- Can rapidly trigger lifesaving ultrasound-guided procedures.

- Can rapidly trigger life-saving therapeutic interventions by providing a more accurate diagnosis when Hs and Ts are detected.
- Can determine return of spontaneous circulation (ROSC) by direct visualization of synchronized heart contractions.
- Can differentiate between ROSC and PEA.
- Can differentiate between true asystole and pseudo-asystole by "seeing" whether coordinated cardiac contractions are present.
- Can assist in tracking (monitoring) resuscitation by detecting the presence or loss of ROSC and surveying for developing complications.
- Can assist in tracking (monitoring) resuscitation by assessing volume status through the use of TFAST echo views, FAST DH characterization of the caudal vena cava (CVC) and hepatic veins, and lung through Vet BLUE.
- Can guide use of vasopressors using the Global FAST (volume status) approach (see Chapter 36).
- Can semiquantitate intraabdominal hemorrhage and need for blood transfusion using the AFAST-applied fluid scoring system (see Chapter 7).
- Can assess urinary output using the AFAST cystocolic view formula for urinary bladder volume estimation (see Chapters 7 and 36).
- Can semiquantitate degree of pneumothorax and track its severity by finding the "lung point" and utilizing the TFAST PTX 1/3s Rule (see Chapters 17 and 36).

### What Global FAST for Treatable Shock, ALS and CPR Cannot Do

- Cannot assess several of the AHA Hs and Ts of CPR, including electrolyte disturbances, blood glucose abnormalities (hyperglycemia and hypoglycemia), body (or core) temperature disturbances (hyperthermia, hypothermia), intracranial hypertension and vascular accidents, and hypoxemia.
- Cannot replace the physical exam.
- Cannot replace blood pressure and electrocardiographic monitoring.
- Cannot replace arterial and venous blood gas evaluation and other respiratory function assessment.
- Cannot characterize effusions based on echogenicity, so, sampling and fluid analysis and cytology are required.

### Indications

- Any patient with questionable cardiovascular stability.
- Any patient with uncharacterized forms of shock.
- Any patient with uncharacterized hypotension.
- All patients with CPA.
- All patients with ROSC as part of ALS and post-CPR resuscitation.

### Objectives

- Understand the clinical utility of combining AFAST, TFAST, and Vet BLUE as a single examination called the Global FAST approach for critical patients.
- Understand how the Global FAST approach may be used to rule out the Hs and Ts of the AHA CPR guidelines.
- Understand how the Global FAST approach may be used for monitoring patients for complications and during resuscitation as a part of ALS.
- Understand how the Global FAST approach does more than the RUSH (ultrasound) exam used in people.

## Ultrasound Settings, Probe Preferences, and Patient Positioning and Preparation

### Ultrasound Settings and Probe Preference

A curvilinear (microconvex) probe with a frequency range of 5–10 MHz and abdominal preset(s) with a depth range of 3–15 cm is generally acceptable for the entire Global FAST examination in most dogs and cats.

### Optimizing Image Quality and Probe–Skin Contact

Hair is generally not shaved but rather parted for as direct as possible probe-to-skin contact with the use of isopropyl alcohol, and/or alcohol-based hand sanitizer, and/or acoustic coupling gel. The author prefers the use of minimal amounts of isopropyl alcohol to effectively part the hair followed by alcohol-based hand sanitizer. The strategy is much less noxious to your patient by minimizing the cold wetness of isopropyl alcohol and its fumes, especially when moved to an oxygen cage. Alcohol-based hand sanitizer is an excellent coupling medium and has the added benefit of being easily wiped off and evaporates quickly. Isopropyl alcohol should not be used if electrical defibrillation is anticipated because it poses a burn/fire hazard. The clinician should also be aware that isopropyl alcohol may cause probe head damage and contributes to hypothermia (see Figure 4.13).

**Pearl:** The author does not shave patients and does not dim the lighting when performing any part of Global FAST, which is supported by similar findings regarding environmental lighting in the FEEL protocol – that ultrasound imaging is generally not compromised (Breitkreutz et al. 2007, 2010). Moreover, dark environments are potentially hazardous when staff are moving around and not time efficient when attempting to locate equipment during CPR and ALS.

## *Patient Positioning and Most Efficient Ways to Perform*

There are a couple of highly efficient ways to perform Global FAST in standing and lateral recumbency that minimize depth changes and moving to different sides of the patient.

### Lateral Recumbency

AFAST, beginning with its diaphragmatico-hepatic (DH) view, is performed first followed by TFAST and its left and right pericardial site (PCS) views with depth and gain settings that are similar, thus rapidly completing six of the 15 Global FAST views (Figure 37.1). After completing the TFAST PCS views, depth is decreased (magnify) for the ipsilateral TFAST chest tube site (CTS) view for performing Vet BLUE. Right lateral is advantageous because of the cardiac notch and the heart falling against the thoracic wall for the three major TFAST echo views (see Figures 37.1, and also 17.16, 17.20, 17.21, and 19.3).

Left lateral recumbency is used when the patient presents in this position and is most comfortable in left lateral. The AFAST-applied abdominal fluid scoring system is validated in either lateral recumbency but TFAST echo views are generally much easier in right lateral recumbency because of the heart falling against the thoracic wall along with the cardiac notch (see Chapters 17–21).

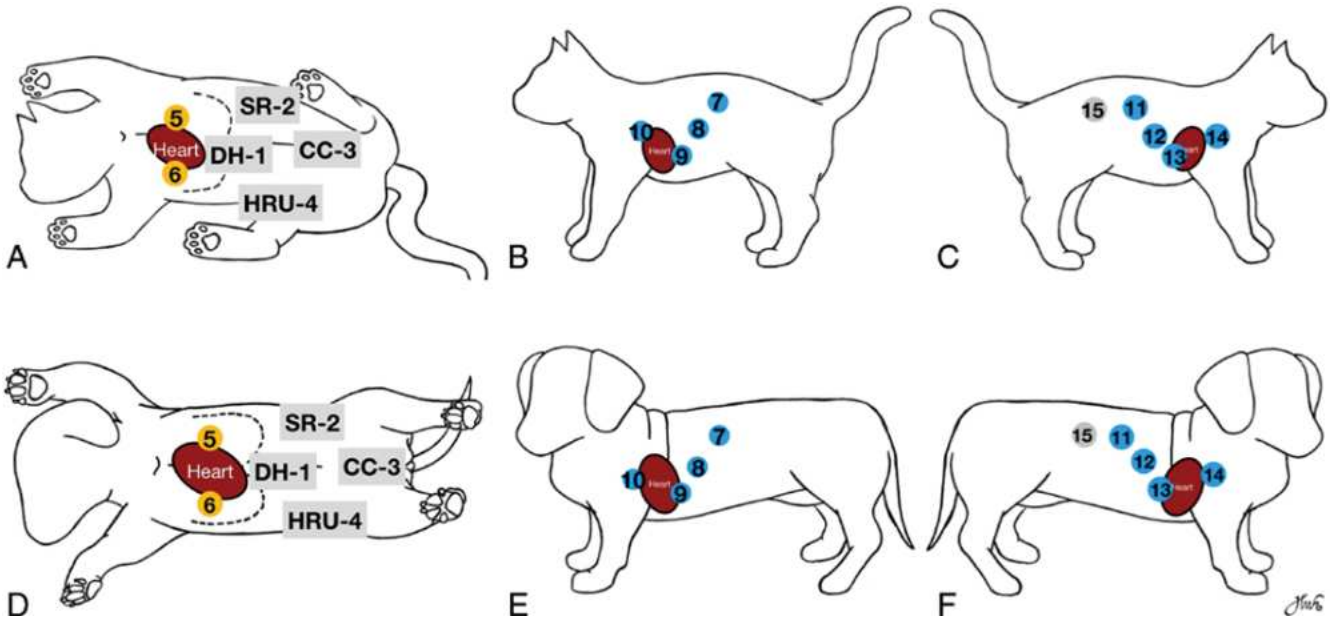


**Figure 37.1.** Global FAST in lateral recumbency. When the patient presents in lateral recumbency, the FAST DH view is performed first because it is a window into the thorax without the air interference of the transthoracic views and quickly assesses for obvious pericardial and pleural effusion, cardiac motion, and the CVC as well as providing a deep window into lung along the pulmonary–diaphragmatic interface and information within the abdominal cavity. (A–C) AFAST in a cat is performed first since it is rapid, followed by similar gain and depth setting for the TFAST pericardial site views, and then either in lateral the ipsilateral hemithorax may be evaluated using Vet BLUE and then moving the patient to the opposing lateral for the final Vet BLUE views (both shown) or the patient moved to sternal or standing (shown) to complete the Vet BLUE and HR5th bonus view (right kidney and associated liver). The analogous standardized order is shown in the dog in (D–F). There are 15 acoustic windows for Global FAST performed with the same microconvex probe and abdominal preset with only changes in depth, gain, and the focus cursor needed during most studies. Source: Reproduced with permission from Dr Gregory Lisciandro, Hill Country Veterinary Specialists and FASTVet.com, Spicewood, TX. Illustration by Hannah M. Cole, Adkins, TX.

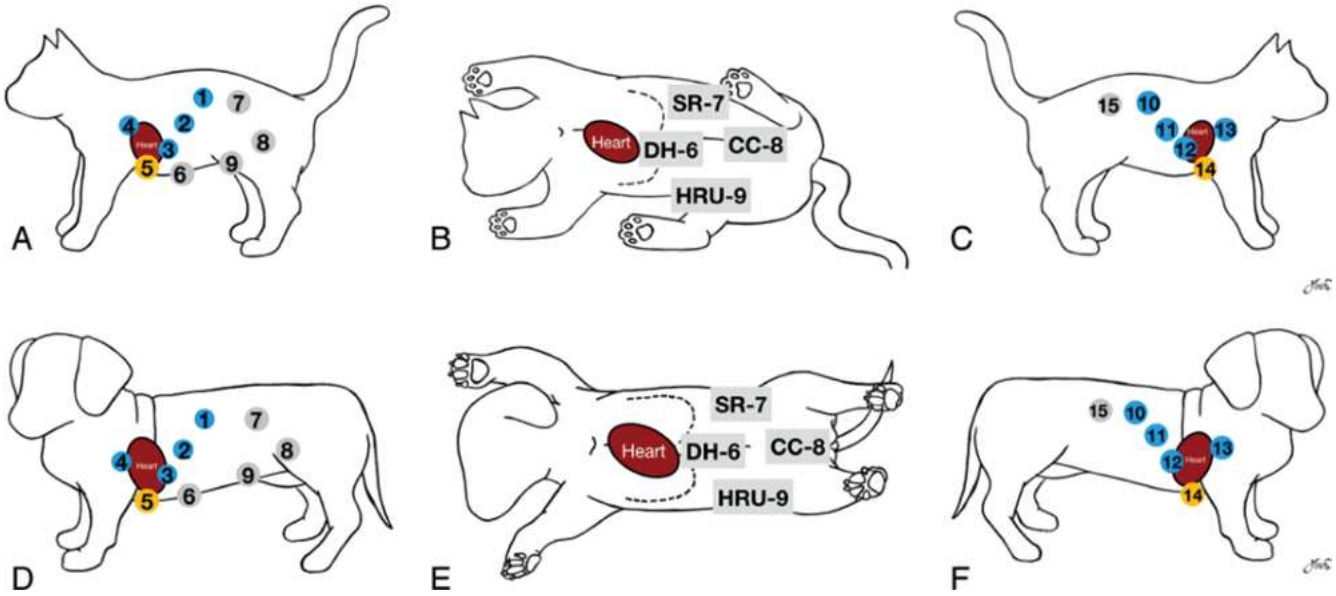


**Figure 37.2.** Global FAST in standing (or sternal) positioning. When the patient is standing or sternal, Global FAST may be performed rapidly starting with the Vet BLUE-TFAST blend of left Vet BLUE, numbered 1–4, and then the left TFAST pericardial site view, numbered 5, and DH view, numbered 6, as shown in (A) and (D) in a cat and dog, respectively. AFAST may be continued in standing or sternal using the same external landmarks and probe maneuvering as in right lateral recumbency, or the patient moved to right lateral recumbency as shown in (B) and (E). The patient is then turned and the machine moved or the sonographer moves to the opposing side of the patient so the patient, its holder, and sonographer are all facing the ultrasound screen to perform the right Vet BLUE, numbered 10–13, and right TFAST echocardiography views, numbered 14, followed by the final AFAST view, numbered 15 as shown in (C) and (F). If the AFAST is negative in standing or sternal, then lateral recumbency is generally unnecessary for AFAST fluid scoring. If AFAST is positive in standing or sternal, then when acceptably stable, move the patient to either lateral recumbency, right lateral shown here in (B) and (E), wait 3-minutes to allow fluid to re-distribute, and then abdominal fluid score, repeating the AFAST, numbered 6–9. Source: Reproduced with permission from Dr Gregory Lisciandro, Hill Country Veterinary Specialists and FASTVet.com, Spicewood, TX. Illustration by Hannah M. Cole, Adkins, TX.

### Standing or Sternal Recumbency

Beginning on the left side of the patient, the left Vet BLUE transthoracic views are performed first followed by the left TFAST PCS view, the DH view, spleno-renal (SR) view, cysto-colic (CC) view, and the hepato-renal umbilical (HRU) view and then the AFAST focused spleen (see Chapters 6–9). The sonographer then moves to the right side of the patient and performs the right Vet BLUE followed by the right TFAST PCS views, ending with the HR5th bonus view (Figure 37.2).

Beginning on the left side is advantageous because by the time the sonographer gets to the most time-consuming TFAST echo views at the TFAST right PCS views, lung, pleural effusion (PE) and pericardial effusion (PCE), caudal vena cava (CVC) assessment, and volume status have already been assessed before ending at the most time-consuming TFAST echo views. Furthermore, the sonographer already has a good idea of how important these TFAST echo views are and can delay them in unstable patients, having already performed the "Global FAST nonecho fallback views" for left- and right-sided congestive heart failure and volume status, being Vet BLUE and the CVC at the DH view, respectively (see Chapter 36).

Dorsal recumbency should always be avoided for several reasons, most importantly because of increased patient risk (Boysen and Lisciandro 2013; Lisciandro 2014a,b,c; Lisciandro and Armenise 2014). A hemodynamically fragile patient that is unknowingly placed in dorsal recumbency undergoes significant negative changes in ventilation and circulation, specifically venous return. Add to these respiratory and cardiovascular stresses the increased oxygen demand in a struggling, anxious patient, and the patient risks acute and potentially catastrophic decompensation. Considering trauma, most dogs and cats have concurrent lung contusions and other thoracic-related injuries (Powell et al. 1999; Sigrist et al. 2004; Lisciandro et al. 2008, 2009; Boysen et al. 2014; Lisciandro 2011) and considering nontrauma, many hypotensive triaged patients have pleural and/or PCE and intracavitary bleeds often accompanied by anemia (McMurray et al. 2016; Lisciandro 2016a). Moreover, the abdominal fluid scoring system is not

validated in dorsal recumbency and only subjective terms of mild, moderate, and severe have been used (Sutherland-Smith et al. 2007; Stander et al. 2010; Cooper et al. 2010; Gerken et al. 2019).

# How to Do Global FAST

See Chapters 6, 7, 17, 18, 22, and 23.

# The Hs Covered by Global FAST

### *Hypotension/Hypovolemia*

Hypotension may be rapidly detected directly during TFAST at its echo views and indirectly by characterization of the CVC and its associated hepatic veins (Figures 37.3, 37.4; see also Table 37.1). The integration

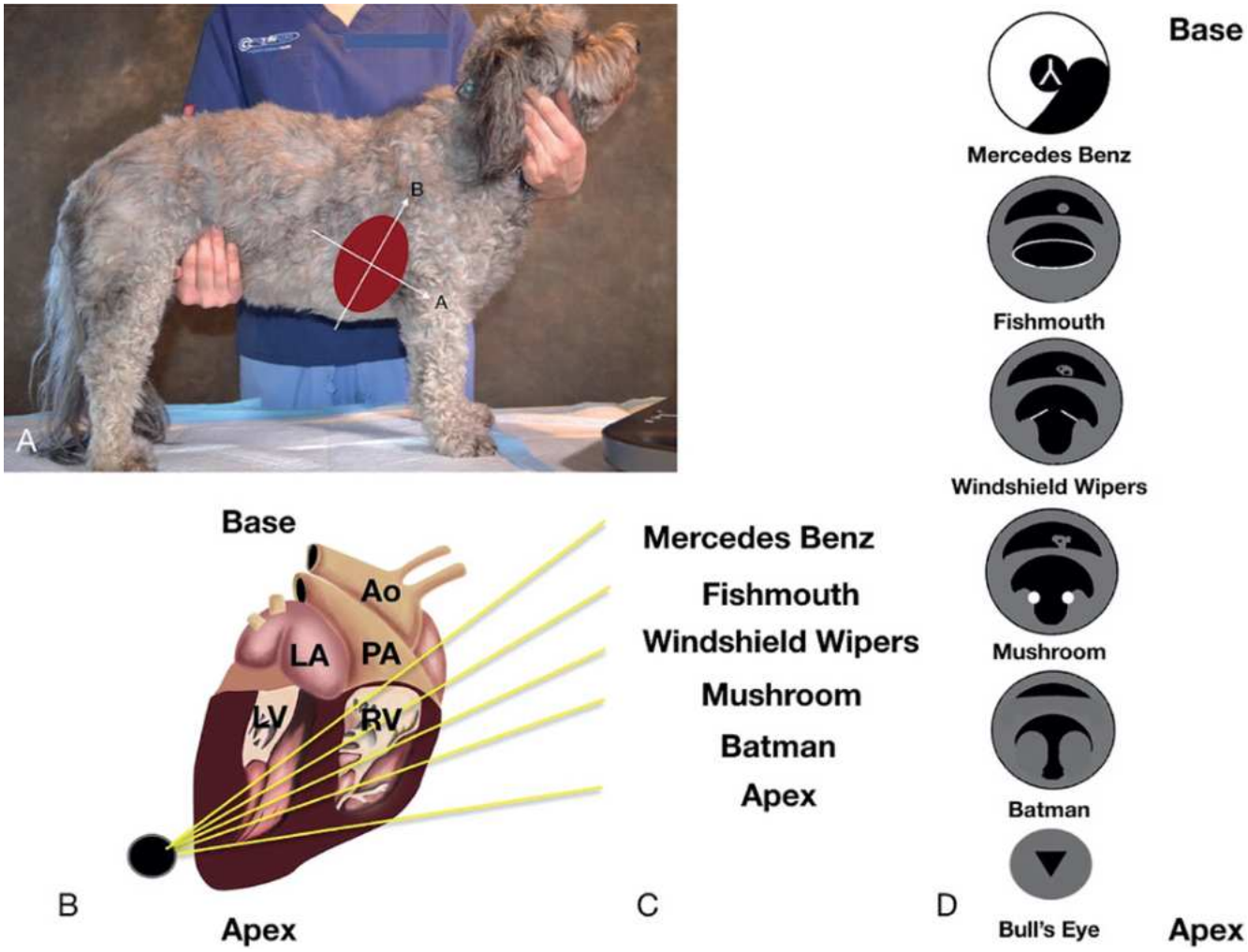


**Figure 37.3.** Proper right TFAST pericardial site view for short-axis view. The short-axis and long-axis lines are shown on a standing dog in (A). The short-axis line is fanned in very small increments to acquire the various short-axis levels that as shown as overlays in (B) and (C). These short-axis levels are named for didactic reasons and need to be recognized for proper cardiac assessment as labeled in (D). For example, the site for volume and contractility (fractional shortening, FS%) is the "mushroom" level, with the two white dots off the left ventricular (LV) papillary muscles representing the hyperechoic chordae tendinae that attach to the mitral valves seen at the next level. Knowing these levels helps to double-check for accuracy. Not understanding these differences leads to false interpretations. For example, "kissing left ventricular papillary muscles" suggestive of hypovolemia may be created in nearly any patient by being at the incorrect level, i.e., Batman. For more detail, see Chapters 17 and 18, and Figures 17.25 and 17.26 for didactic echo charts. Source: Reproduced with permission from Dr Gregory Lisciandro, Hill Country Veterinary Specialists and FASTVet.com, Spicewood, TX.

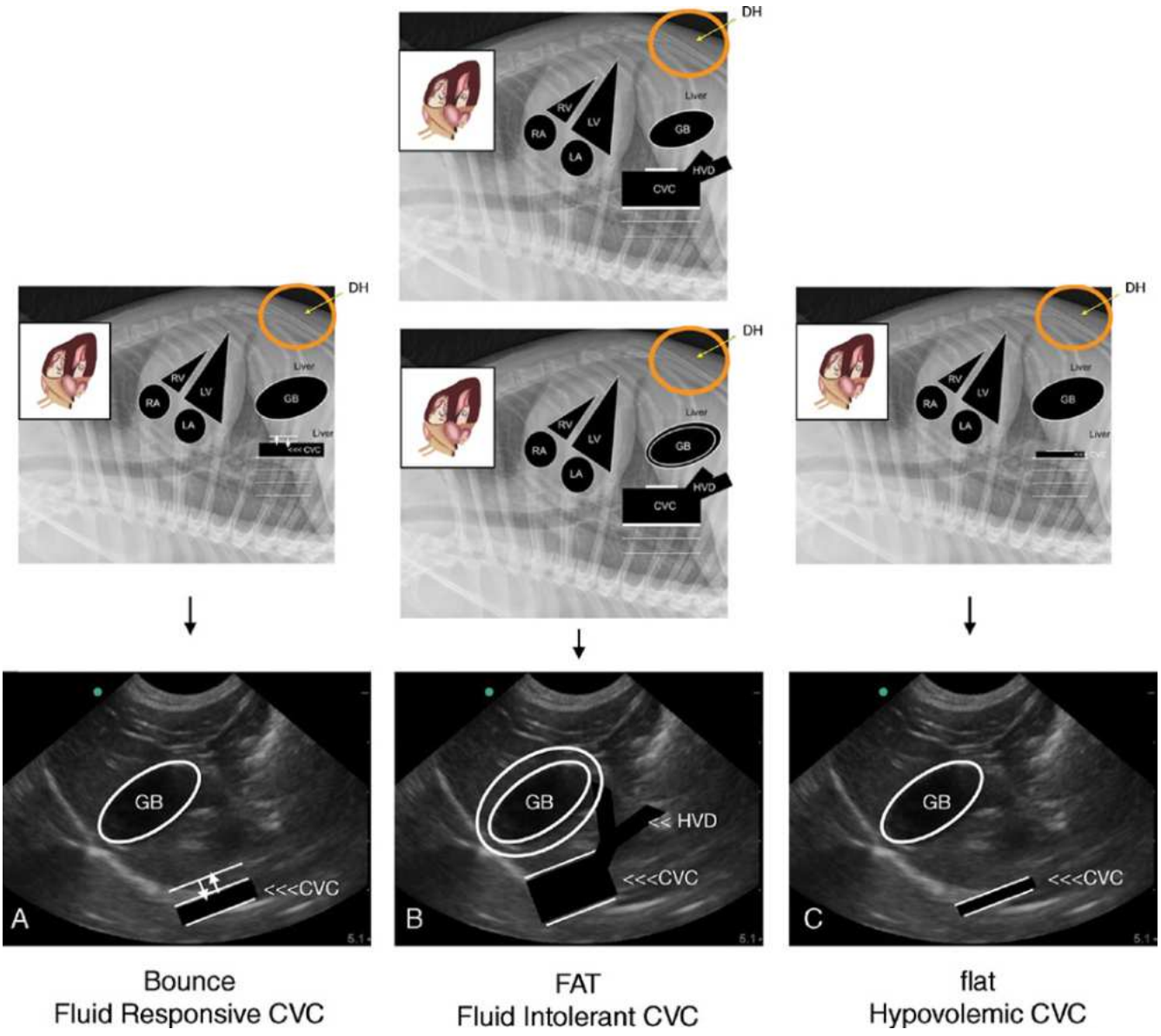


**Figure 37.4.** Characterization of the caudal vena cava. The use of the CVC and its associated hepatic veins (HV) has become a favored approach for volume status in people. The columns correlate with inverted lateral thoracic radiographs of the same dog used for overlays of the expected anatomy and the changes in the CVC and HV and gallbladder (GB). The terms in people have been "FAT" in (B) and "flat" in (C) with the "bounce" in (A) being the author's term. The optional CVC descriptive terms are "fluid responsive" in (A), "fluid intolerant" in (B), and "hypovolemic" in (C). Note in (B) the distended "fluid intolerant" CVC (FAT) with little change in height and with hepatic venous distension referred to as the "tree trunk sign" with and without gallbladder wall edema (the "cardiac gallbladder"). In contrast, note in (C) the small "hypovolemic" CVC (flat) with little change in the CVC height without hepatic venous distension; and in (A) the "fluid-responsive" CVC having recognizable changes in height (35–50%) characterized as a "bounce." The findings of the CVC, HV and GB are correlated with the TFAST echo views (see also Figure 36.9 for "cardiac gallbladder" and Figure 7.12 for "anaphylactic gallbladder") and the Vet BLUE and other Global FAST findings for best patient assessment. Further detailed integrative information is found in Chapter 36. Source: Reproduced with permission from Dr Gregory Lisciandro, Hill Country Veterinary Specialists and FASTVet.com, Spicewood, TX.

of a right TFAST PCS view with an attenuated left ventricular short-axis "mushroom view" combined with a flat or fluid-starved CVC helps quickly determine that the patient has hypovolemia (see Figures 17.25, 17.26, 36.7, 36.8, 36.9, and 37.4). Whenever hypovolemia is determined, then the search for a "leak in the tank" is pursued, and the Global FAST approach automatically does this by imaging the peritoneal and pleural cavities, retroperitoneal space, pericardial sac, and lung (Lisciandro 2011, 2012, 2016a; Lisciandro and Armenise 2014; McMurray et al. 2016). Moreover, the AFAST-applied fluid scoring system is invaluable in semiquantitating volume of blood (and any other effusions) and the patient as a small-volume versus large-volume intraabdominal bleeder (Lisciandro et al. 2009, 2015, 2019a; Lisciandro 2011, 2012, 2016b; Boysen and Lisciandro 2013).

Although no definitive formula exists for estimating pleural and pericardial effusion in clinical situations (Newitt et al. 2009; Shimali et al. 2010), distances can still be measured for each and estimations as trivial (>0.5 cm), mild (0.5–1 cm), moderate (1–3 cm), and severe (>3 cm) may be made at the suggested level of the costochondral junction at the TFAST PCS views from the intercostal space to the heart in standing and sternal small animals (see Figures 36.13, 36.14). Combining the Global FAST approach findings with the complete clinical profile of the patient helps place cavitary and spatial bleeding (and effusions) into clinical relevance as to the degree of their contribution to the "leak in the tank" or patient volume loss.

## Hyperkalemia

In part, the Global FAST approach helps trigger hyperkalemia as a major rule-out or rule-in for shock, CPA and need for CPR by the finding of an enlarged urinary bladder, dilated ureters, and even prepubic abdominal urethral dilation using the AFAST target organ approach. During AFAST, the kidneys are interrogated routinely at the SR, HR, and 5th bonus views. Fluid-associated urinary tract conditions such as retroperitoneal effusion and kidney-related soft tissue abnormalities resulting from urinary tract obstruction (distended urinary bladder, dilated ureters, renal pelvic dilation, hydronephrosis) and acute renal failure can thus readily be detected with minimal training and have been documented in the veterinary literature (Hall et al. 2015; Nevins et al. 2015; Reineke et al. 2017) (see Chapter 11). Often this information is acquired prior to any blood testing when Global FAST is applied as an extension of the physical examination, as advocated by the author (Lisciandro and Armenise 2014). Furthermore, ascites and retroperitoneal effusion are rapidly detected. Ascites, when present, should be assigned an abdominal fluid score (AFS) with positive and negative AFAST views also recorded (see Chapter 7 and Appendices). The free fluid should be sampled when safely accessible for fluid analysis and cytology. This Global FAST approach provides evidence-based information and expedites diagnosis when minutes count (Table 37.2). See Chapters 6, 7, 10, 11, and 39 and also Figure 39.15.

As an aside, urinary obstructed dogs and cats develop ascites that is consistent with a uroabdomen. However, the uroabdomen is medically treated. In a recent feline study, ~60% of obstructed cats were positive for pericystic fluid (analogous to the AFAST CC view) and ~35% were positive for retroperitoneal effusion (Nevins et al. 2015). Importantly, the clinical course for the great majority of these cats (and assume the same for dogs) is unaltered from standard care of unblocking with placement of an indwelling urinary collection system along with resuscitation followed by supportive and symptomatic care. The ascites and retroperitoneal effusion will commonly resolve in time as the patient recovers (Nevins et al. 2015). The author proposes that the cause for the effusions lies in inflammation and backpressure of urine against the urinary bladder wall and renal capsule over alternative speculation (Cooper et al. 2010; Gerken et al. 2019). The AFAST-applied fluid scoring system not only provides an objective semiquantification of the volume but also specifies positive and negative AFAST views, and, as logic would dictate, the origin of the effusion (Lisciandro et al. 2009, 2019a; Lisciandro 2011, 2014a, 2016b; Hnatusko et al. 2019; Gerken et al. 2019). The abdominal fluid scoring system (score and locations) provides distinct advantages over the subjective terms trivial, mild, moderate, and severe (Cooper et al. 2010; Gerken et al. 2019). Assigning an AFS provides a means to monitor these cats including on daily patient rounds and recheck evaluations. From author experience, expect the free fluid (medically treated uroabdomen) to nearly or completely resolve within 48 hours post unblocking in cases in which the patient is successfully resuscitated and its azotemia is resolving.

## Hypocontractility – Dilated Cardiomyopathy

The TFAST echo views are screening tests for left-sided and right-sided strain/failure/overload and generalized systolic cardiac dysfunction. Thus, TFAST rapidly screens for dilated cardiomyopathy (DCM),

**Table 37.2.**
Causes of gallbladder wall edema in the acutely collapsed dog that was previously healthy.

| Condition | Expected characterization of the caudal vena cava (CVC) | Speculative pathophysiology |
|---|---|---|
| Canine anaphylaxis[a] | Flat, hypovolemic CVC, (see Tables 7.6 and 36.3 and 36.4) | Massive histamine release resulting in acute marked hepatic venous congestion. A recent pilot study suggests that hemorrhagic gastroenteritis syndrome (HGE) dogs with elevated alanine transaminase also have gallbladder wall edema (Lisciandro et al. 2019b), thus HGE dogs may be another category for gallbladder wall edema or are anaphylactic and mistaken for HGE |
| Pericardial effusion[a] | FAT, distended, hypervolemic CVC, referred to as vena cava plethora in people (see Tables 7.6 and 36.3 and 36.4) | Marked hepatic venous congestion from obstruction of blood flow to the right atrium |
| Right-sided congestive heart failure (dilated cardiomyopathy, pulmonary hypertension, tricuspid disease)[a] | FAT, distended, hypervolemic CVC, referred to as vena cava plethora in people (see Tables 7.6 and 36.3 and 36.4) | Marked hepatic venous congestion from backflow of blood from the right atrium |
| Post transfusion | Variable to FAT, hypervolemia, author experience, unpublished | Likely immune mediated and volume overload, does not indicate anaphylaxis in many patients |

[a] Conditions that are most important to consider in the acute triage setting of acute collapse and weakness in a previously absolutely healthy patient (dog). FAT, flat, and bounce are defined in the Characterizing the Caudal Vena Cava section. There are other causes listed in Table 7.5 not listed here. Transfusion is listed because many dogs post blood transfusion develop gallbladder wall edema that does not necessarily indicate anaphylaxis.
Source: Reproduced with permission from Dr Gregory Lisciandro, Hill Country Veterinary Specialists and FASTVet.com, Spicewood, TX. Modified from Chapter 7 and Table 7.5.

low fractional shortening (FS%). From the right TFAST PCS view and its left ventricular short-axis "mushroom view," poor contractility is often readily apparent to even the most novice, properly trained sonographer (Figure 37.5; see also Figure 37.3). Of course, there are exceptions to the rule and an asystolic heart or a patient with PEA or marked arrhythmias may have an indeterminate TFAST cardiac assessment. However, the Global FAST approach incorporating TFAST echo views carries diagnostic potential to detect DCM over physical exam, blood and urine testing, vital signs and radiography, and by suspecting DCM, appropriate therapy and a much different resuscitation strategy takes place. In other words, the capturing of a DCM case helps better keep alive (manage using inotropes and arterial afterload reducers) for the gold standard test of a complete detailed echocardiogram that is generally not immediately available when minutes count during triage (see Table 37.2). Normal FS% ranges from 25–45% in dogs and 30–50% in cats (see Chapter 20). Chapters 17, 18, and 21 provide greater detail.

## *Hypertension – Pulmonary Hypertension*

The TFAST echo views are screening tests for left-sided and right-sided strain/failure/overload and generalized systolic cardiac dysfunction (FS%). Thus, TFAST rapidly screens for pulmonary hypertension (PHT), which is generally easy to appreciate with minimal training and missed by thoracic radiography because of its nonspecific radiographic features (Kellihan and Stepien 2010; Kellihan et al. 2015). From the right TFAST pericardial view, the right ventricular (RV) to left ventricular (LV) ratio is used to assess for right ventricular dilation. An enlarged RV:LV, in which the RV is almost the same size as the LV, supports types of right-sided failure including PHT.

Integrating information is a key part of the Global FAST approach. Thus, the additional finding at the left ventricular short-axis "mushroom view" of flattening of the interventricular septum and observing a distended or FAT CVC with hepatic venous distension, referred to as the "tree trunk sign" (Lisciandro 2014a,b,

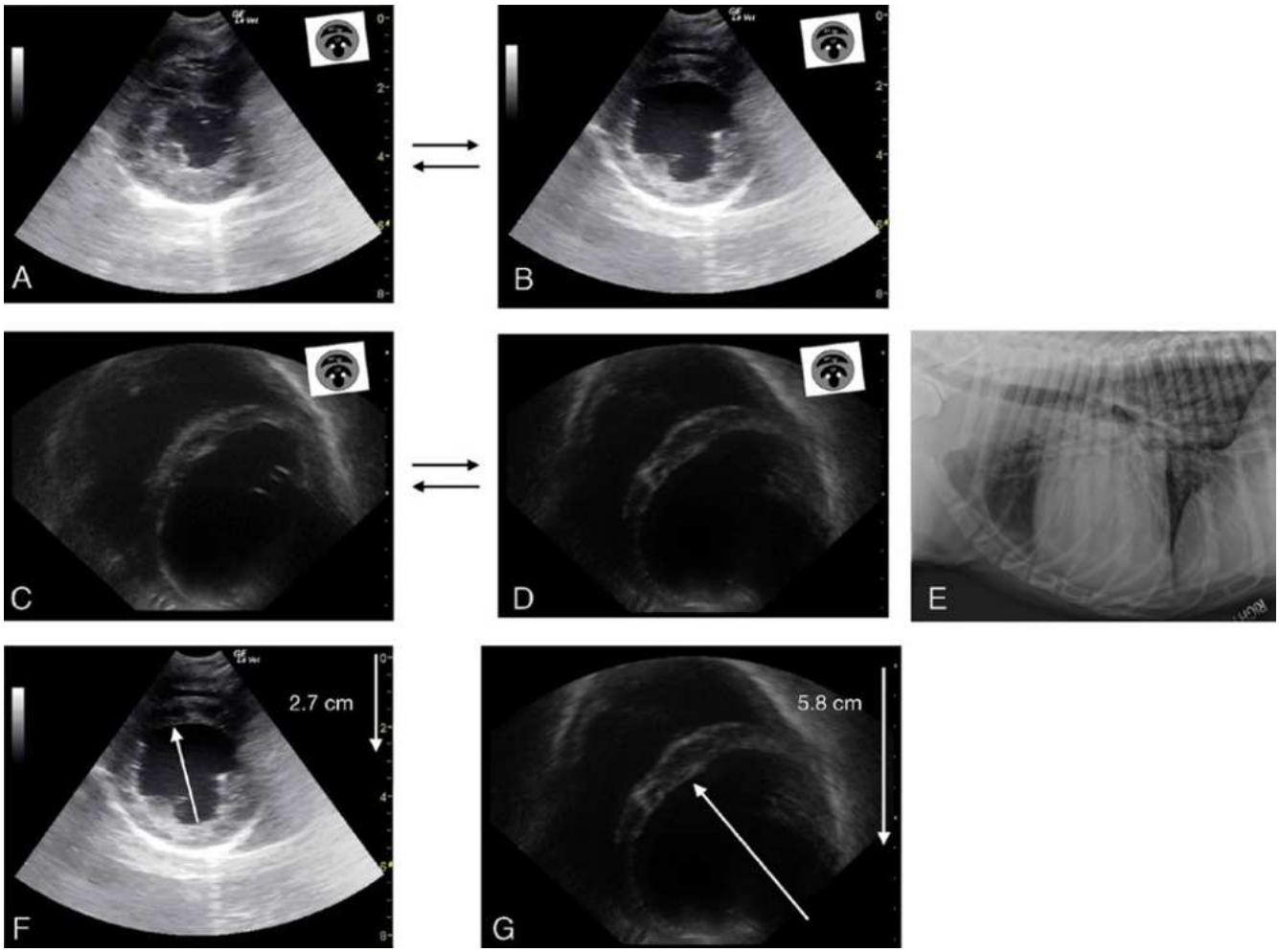


**Figure 37.5.** Dilated cardiomyopathy. In (A) and (B) shown in still B-mode images is the left ventricular "mushroom" view from the right TFAST pericardial site view in systole (A) and diastole (B). The change in internal dimensions is "eyeballed" for an assessment of FS%. In (C) and (D) is a canine patient with obvious poor FS% that is captured as a case of DCM that would likely be missed or delayed in diagnosis based on the thoracic radiograph (E). The heart in real time flutters with very little change between systole and diastole as well as having overall enlarged size with often obvious thinner ventricular walls. Internal dimensions may also be measured in questionable cases as the dog in (F) is unremarkable in contrast to the dog with DCM in (G) that exceeds 5 cm. An unpublished rule of thumb is that this dimension should never be greater than 5 cm in any dog (DeFrancesco, personal communication). The centimeter (cm) scale to the right of the screen is used for measurements listed on the images in (F) as 2.7 cm and (G) as 5.8 cm. Source: Reproduced with permission from Dr Gregory Lisciandro, Hill Country Veterinary Specialists and FASTVet.com, Spicewood, TX.

2016a, 2019a) (Figure 37.6), is further evidence for right-sided cardiac failure and PHT. The pulmonary artery to aortic ratio (PA:Ao) on short-axis (TFAST Mercedes-Benz sign) view, easily learned but not detailed here, is further evidence for PHT. In a recent study, nonecho right-sided cardiac markers failed to identify PHT in a case series of dogs (Vientós-Plotts et al. 2019), emphasizing the need to use TFAST echo views including the PA:Ao as screening tests (see Figures 20.9 and 37.6).

In summary, characterization of the CVC and hepatic veins, gallbladder wall edema, ascites, and TFAST echo views that include the long-axis RV:LV, short-axis "mushroom view" for displacement of the interventricular septum into the LV and the Mercedes-Benz sign view for increased PA:Ao should be combined as a screening test for PHT (see Figure 20.9B).

Naturally, there are exceptions to the rule and an asystolic heart or a patient with PEA or marked arrhythmias will have an indeterminate TFAST cardiac

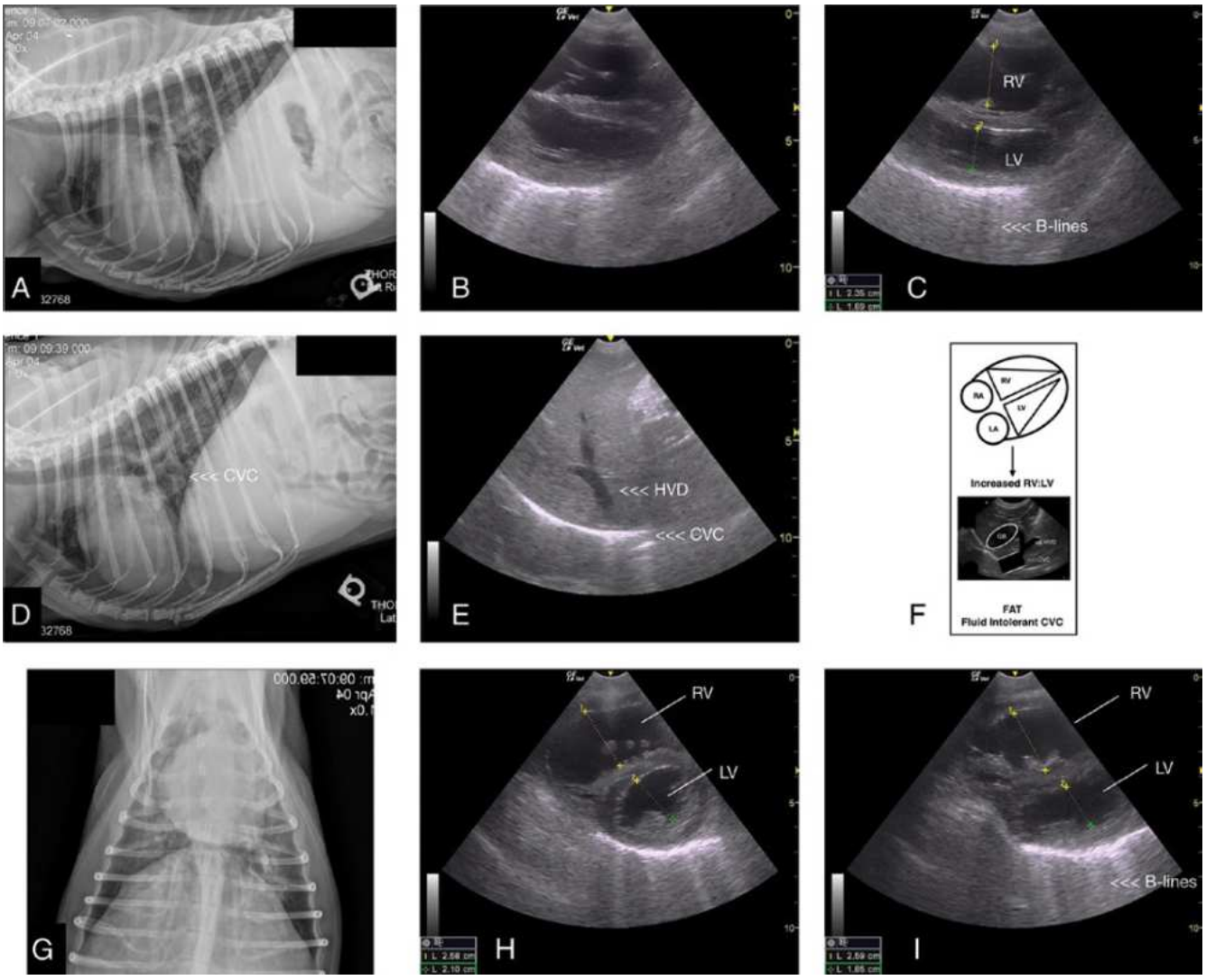


**Figure 37.6.** Pulmonary hypertension. In (A), (D), and (G) thoracic radiographs are shown from the same patient with B-mode still images of the long-axis four-chamber view unlabeled (B) and labeled (C) showing the severe right ventricular (RV) enlargement with the RV larger than the left ventricle (LV). In (E) and (F) is the B-mode still image of the hepatic venous distension (note the "tree trunk sign") and in (F) is a cartoon illustrating the integration of information, taking into account the enlarged RV and then looking at the CVC and hepatic veins for signs of distension (right-sided congestive heart failure) and ascites, present but not shown in the image. In (H) and (I) is shown the classic flattening of the intraventricular septum (unlabeled) due to the severe elevated right pulmonary arterial pressure. Note the collapse of the expected left ventricular "mushroom's" top as shown in (I), the B-lines indicative of alveolar-interstitial edema in (C) and (I), and the papillary muscles that appear within the RV in (H) that should not be mistaken for a mass. See also Figure 20.9B. RV, right ventricle; LV, left ventricle; HVD, hepatic venous distension. Source: Reproduced with permission from Dr Gregory Lisciandro, Hill Country Veterinary Specialists and FASTVet.com, Spicewood, TX.

assessment. However, the Global FAST approach incorporating these TFAST echo views along with information regarding the CVC and hepatic veins carries diagnostic potential over physical exam, blood and urine testing, vital signs and radiography to detect PHT and trigger appropriate therapy and a much different resuscitation strategy over the presumed hypovolemic patient. The capturing of a PHT case helps better keep alive (manage using arterial vasodilators) for gold standard testing of a complete detailed echocardiogram that is generally not immediately available when minutes count. Many of these canine cases are misdiagnosed with pneumonia or left-sided congestive heart failure and the combined use of TFAST, Vet BLUE and AFAST helps build the case for PHT (see Table 37.2) (Kulhavy and Lisciandro 2018).

# The Ts Covered by Global FAST

## *Tension Pneumothorax*

The rapid detection of pneumothorax (PTX) is possible using the Global FAST approach in both spontaneously and mechanically ventilated patients. Imaging strategies have improved for "lung sliding" through the incorporation of the TFAST and Vet BLUE "tricks of the trade." These include the "one-eyed gator sign" by placing rib in the middle of the screen to scatter echoes, changing the angle of insonation to ricochet the echoes off the reflective aerated lung surface, or performing both sonographic maneuvers simultaneously. These sonographic manipulations are explained and illustrated in more detail in Chapters 17, 18, 22, and 23. In intubated patients, controlled positive pressure ventilation helps easily rule PTX in and out because the respirophasic timing for observing "lung sliding" is controlled. Lastly, use of the "lung point" concept not only further supports the accurate diagnosis of PTX but also semiquantitates the degree of PTX as well as serving as a tracking tool, the TFAST PTX 1/3s Rule (Lisciandro et al. 2008;

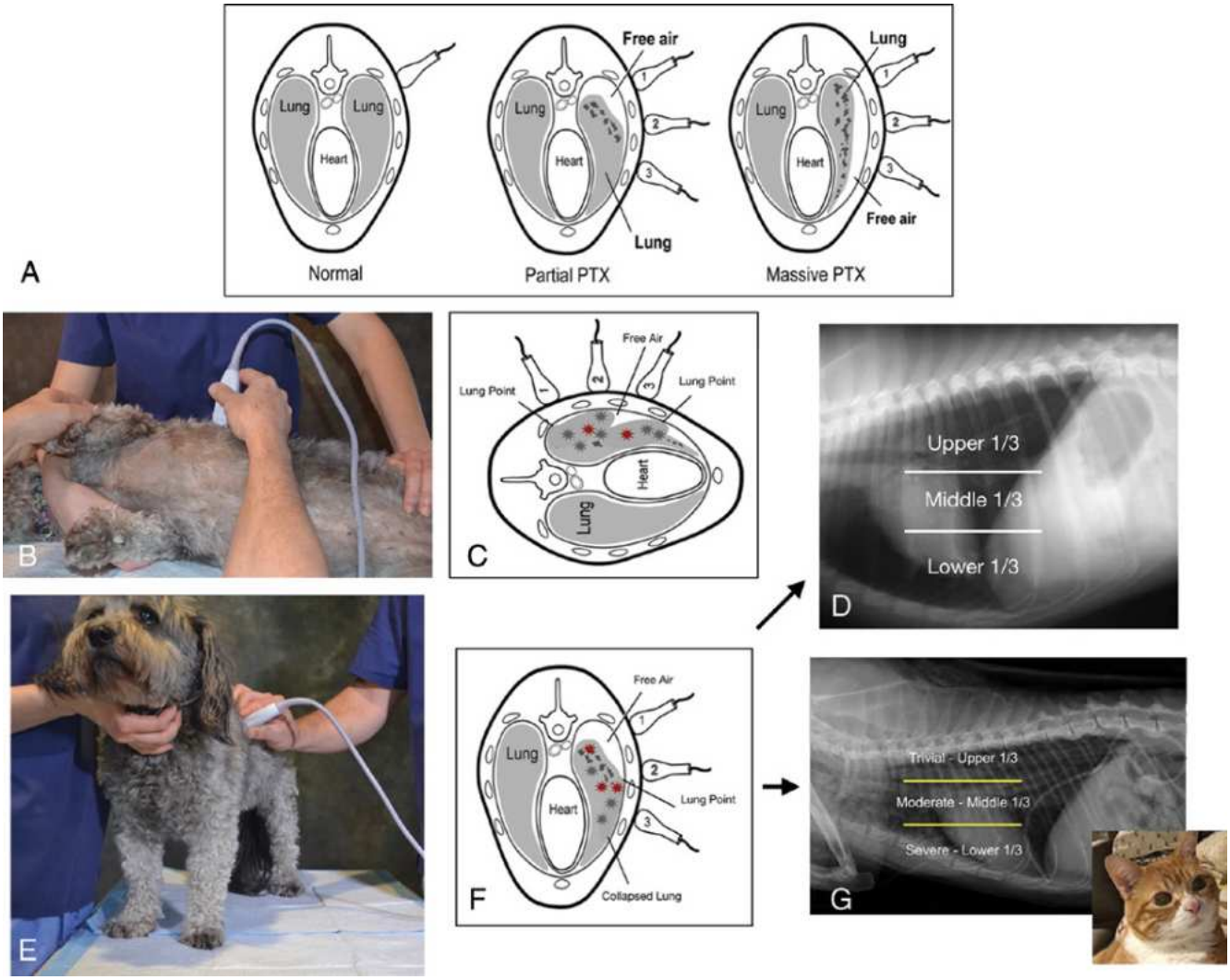


**Figure 37.7.** Tension pneumothorax and using the "lung point" and TFAST PTX 1/3s Rule for semiquantitating degree of pneumothorax. The use of the "lung point" and the TFAST PTX 1/3s Rule with the patient in sternal or standing helps differentiate trivial from moderate and severe PTX. The author calls the difference in positioning of lateral to sternal-standing the "parking garage – skyscraper effect" that is obvious in being able to categorize PTX with more levels. Moreover, in lateral recumbency, especially with positive pressure ventilation, the free air gets pushed into unnatural regions and has been referred to as a "double lung point." Be aware of the phenomenon if your patient must be in lateral recumbency and avoid the confounder by moving your patient into sternal-standing when possible. See Chapter 18 for more detail on pneumothorax. Source: Reproduced with permission from Dr Gregory Lisciandro, Hill Country Veterinary Specialists and FASTVet.com, Spicewood, TX.

Lisciandro 2011, 2014b,c) (Figure 37.7). See Chapter 18 for more detail.

## Trauma – Hemorrhage

Hemorrhage (and other effusions) may be rapidly screened for using the Global FAST approach with four cavities or spaces plus lung (Lisciandro et al. 2009; Lisciandro 2011, 2012, 2014a,b,c; Lisciandro and Armenise 2014; Lisciandro 2016a; McMurray et al. 2016). These four areas are the peritoneal cavity, retroperitoneal space, pleural cavity, pericardial sac plus lung. Importantly, the volume of hemorrhage that can be maximally present varies with each of these locations, as large blood volumes are possible within the peritoneal and pleural cavities and retroperitoneal space but only much smaller blood volumes are generally possible in the less forgiving pericardial sac (affects cardiac output) and lung (affects ventilation). The accumulation within these two locations leads to cardiac and ventilatory failure detected much sooner as secondary events in contrast to the other three locations in which much larger volumes are generally necessary for overt clinical signs. However, the Vet BLUE B-line scoring system provides a severity score (numbers of B-lines and their distribution) and serves as a monitoring tool. Furthermore, the AFAST-applied fluid scoring system can semiquantitate the volume and expected degree of anticipated anemia through the small-volume versus large-volume bleeder concept (see Chapter 7) (Figure 37.8; see also Figures 7.2, 7.3, 7.4, 7.5, and 7.8 and for cats Figures 39.24, 39.25, and 39.26). The use of the AFAST-applied fluid scoring system helps with decision making regarding need for blood transfusion and exploratory surgery dependent on the clinical profile of the patient (Table 37.3). See Chapters 6, 7, 22, and 23 for more detailed information.

## Thromboembolism – Pulmonary Thromboembolism

The detection of thromboembolism in small animals (quadrupeds) is different than in people (bipeds) for two major reasons. The first, deep venous thrombosis (DVT) readily detectable using POCUS in people, has not been described to our knowledge in the canine and feline hindleg(s), and it is unknown if there is indeed any clinical relevance in small animals (see Chapter 25). Thus, within this category, pulmonary thromboembolism (PTE) appears to be the major player in veterinary medicine, although other major veins have been reported to have thrombi (see Chapter 25). The second reason is the ability to detect PTE, which is dependent on whether it may be imaged directly, such as in the pulmonary arteries in the vicinity of their bifurcation, or its effects seen indirectly during Global FAST, such as right ventricular enlargement from acute pulmonary hypertension or the periphery of lung and the "wedge sign" of Vet BLUE (Figures 37.9 and 37.10) (Lisciandro 2013).

The gold standard test for PTE is contrast pulmonary angiography using computed tomography (CTPA) along with specialized equipment for contrast injection (Goggs et al. 2014). However, this modality carries risks, including patient movement to radiology, intravenous contrast agents, chemical restraint and often endotracheal intubation for full breath studies (Goggs et al. 2014). Furthermore, CTPA is limited to larger PTE and may miss smaller PTE in the lung periphery that would be potentially detected using lung ultrasound. Alternatively, the Global FAST approach may be used for both direct and indirect evidence of PTE directly by visualization of the PTE within the pulmonary artery(ies) or indirectly by acute cor pulmonale and an enlarged right ventricle during TFAST (see Chapters 17–21) and the "wedge sign" in upper lung fields, Caudodorsal and Perihilar regions during Vet BLUE (Mathis et al. 2005; Mastruzzo et al. 2008; Lisciandro 2013; Lee et al. 2015) (see Chapters 22 and 23, Figures 23.2 and 23.19).

## Tamponade – Pericardial Effusion

The TFAST sonographic diagnosis for PCE is generally easier for most sonographers than determining the presence of cardiac tamponade. The accurate TFAST diagnosis of PCE is described in Chapter 17 (Figure 37.11) (Lisciandro 2014b, 2016a). The determination of cardiac tamponade can be an intimidating proposition for the noncardiologist sonographer. Most specifically, the diagnosis of cardiac tamponade is the imaging of diastolic collapse of the right atrium and ventricle. However, supportive evidence for tamponade often includes larger volume pericardial effusions (>0.5–1.0 cm), a distended CVC and hepatic veins (FAT CVC and tree trunk sign), along with a patient history of acute collapse and weakness (Figure 37.12). In people, a fluid-responsive CVC rules out cardiac tamponade because by definition, cardiac tamponade is obstructive shock and thus the CVC would be a FAT with little change in height during phases of respiration. In people with a fluid-responsive CVC with PCE, the attending clinician is to look elsewhere (do a Global FAST-like approach, i.e., FAST and RUSH) for the cause of acute weakness and collapse because the CVC does not support cardiac tamponade (Himelman et al. 1988; Candotti and Arntfield 2015; Tchernodrinski and Arntfield 2015). In people with PCE, a FAT inferior vena cava (IVC),

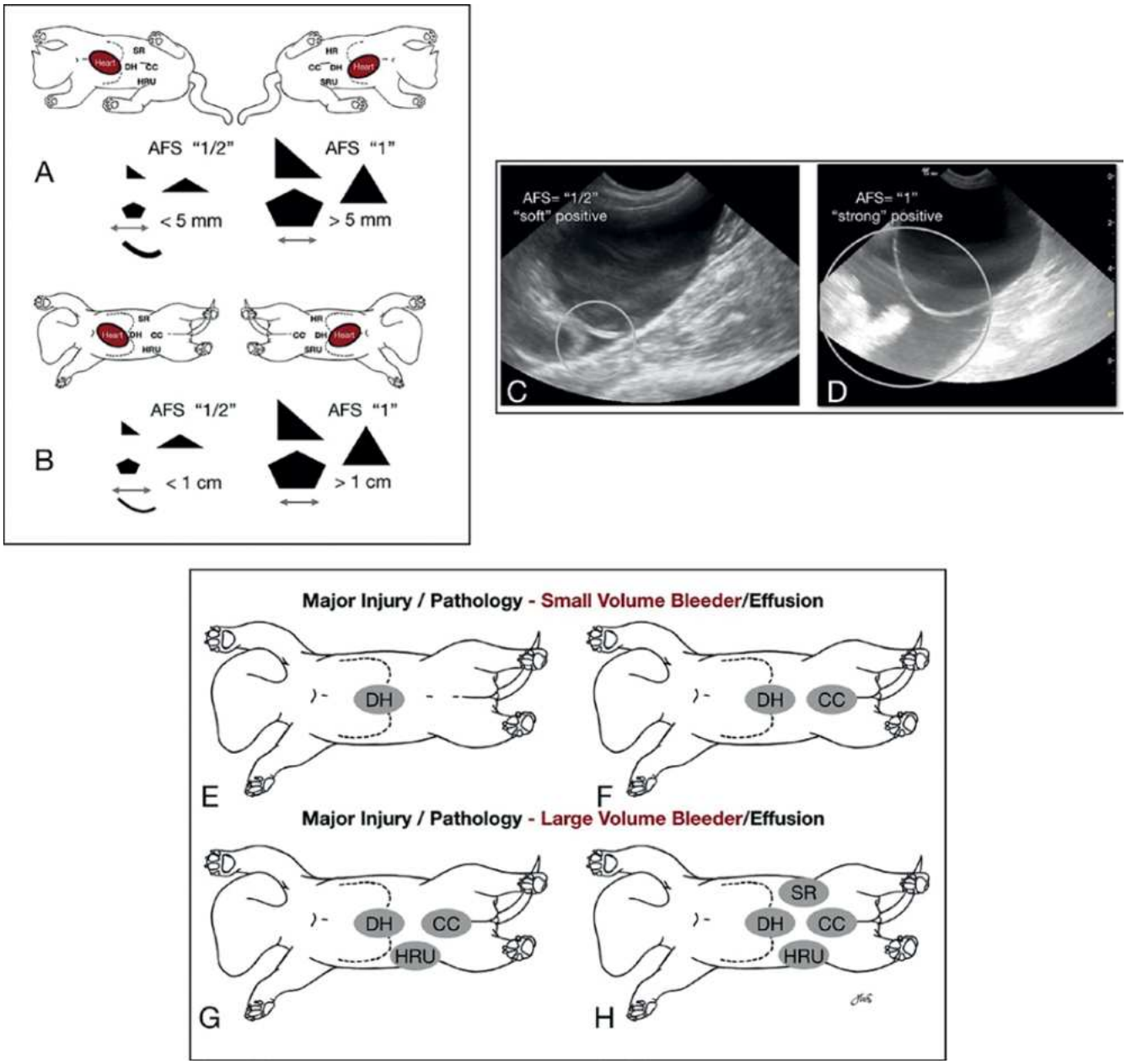


**Figure 37.8.** AFAST-applied abdominal fluid scoring for the bleeding patient. The AFAST-applied abdominal fluid scoring system for the bleeding patient is very useful. The scoring has been modified by further differentiating positive AFAST views by scoring as 0, 1/2 and 1 based on research performed in healthy adult and juvenile dogs and cats (Lisciandro et al. 2015, 2019a). In (A) and (B) maximum dimensions of <5 mm and <1 cm in cats and dogs, respectively, may be used to score as an AFS of 1/2 at that AFAST view; conversely, pockets of fluid with maximum dimensions >5 mm and >1 cm are scored as a full 1. (C) and (D) show the modification of the AFS system as 1/2 and 1. In (E–H), the small-volume bleeder versus large-volume bleeder concept is pictured. Importantly, the use of the modified scoring system that now includes 1/2 still uses the total score for small-volume bleeder (AFS 1 and 2, modified <3) and large-volume bleeder (AFS 3 and 4, modified ≥3). Source: Reproduced with permission from Dr Gregory Lisciandro, Hill Country Veterinary Specialists and FASTVet.com, Spicewood, TX. Illustration by Hannah M. Cole, Adkins, TX.

Vetbooks.ir

**Table 37.3.**
Detecting treatable forms of shock – using Global FAST to rule out Hs and Ts of cardiopulmonary resuscitation (CPR) with the best practice to survey prior to cardiopulmonary arrest (CPA).

| H and T | Component of Global FAST | Comments |
|---|---|---|
| Hypotension/ hypovolemia (AFAST, TFAST, Vet BLUE, cavitary bleeds and effusions) | Short-axis right pericardial TFAST echo views | Make sure at proper short-axis level of the heart, double-check by moving through all short-axis levels of the heart from the bull's eye to the Mercedes-Benz and know that at Batman the heart in normal patients will appear volume contracted being at the incorrect level; double-check TFAST echo interpretation by correlating with caudal vena caval characterization and its maximum height at FAST DH view (see Figures 17.25, 17.26 and Chapter 36) |
| Hyperkalemia, hypokalemia (AFAST, urinary obstruction[a]) | AFAST SR and HR views for renal pelvic dilation, hydronephrosis, perirenal fluid (Nevins et al. 2015); AFAST cysto-colic view for enlarged urinary bladder and for dilation of the intraabdominal urethra, especially cats | The cat has a significant viewable intraabdominal urethra possible at the CC view and urethral obstruction will result in its dilation (as well as the renal pelvis); abdominal effusion is not uncommon in urinary obstructed dogs and cats |
| Hypocontractility (dilated cardiomyopathy) (TFAST) | Right pericardial site TFAST view and the short-axis left ventricular "mushroom view" using the "eyeball method" for poor FS%; a left ventricular "mushroom view" measurement of ≥5 cm (DeFrancesco, personal communication 2019); and on long-axis four-chamber view increase of end-point septal separation (EPSS); return of spontaneous circulation (ROSC) by directly observing for otherwise occult coordinated cardiac movements | Performed in B-mode as a screening test generally without measurements |
| Hypertension (pulmonary hypertension) (TFAST) | Right pericardial site TFAST view and its long-axis four-chamber view with increased right ventricular to left ventricular (RV:LV) ratio; left ventricular short-axis "mushroom view" for intraventricular septal flattening; and short-axis "Mercedes-Benz view" for increased pulmonary artery to aortic ratio (PA:Ao) (see Figures 37.6, 20.9B and Table 23.4) | Eyeballing right ventricular size at the short-axis left ventricular short-axis "mushroom view" from the right TFAST pericardial site view is too variable for judging size; use the long-axis view for "eyeballing" RV enlargement |
| Tension pneumothorax (TFAST and "lung point") | Best practice when possible is moving the patient sternal or standing and then determining the location of the "lung point" and semiquantitating the PTX using the TFAST PTX 1/3s Rule[a] | Lateral recumbency is prone to confounders because of the "parking garage – skyscraper effect" (see Chapter 18) and air is pushed into unnatural locations during positive pressure ventilation; standing and sternal avoids these confounders |
| Trauma, hemorrhage (AFAST and abdominal fluid scoring system, TFAST, Vet BLUE, cavitary bleeds) | AFAST abdominal fluid scoring system and its small-volume bleeder versus large-volume bleeder concept (see Chapter 7); and additionally TFAST surveys the pleural cavity and pericardial sac, and Vet BLUE lung (B-lines) along with the Vet BLUE B-line scoring system for degree of hemorrhage (see Chapter 23) | Ultrasound cannot characterize the type of fluid, only sampling with fluid analysis and cytology; ultrasound may be used to guide sampling |
| Thromboembolism (pulmonary thromboembolism) (TFAST, Vet BLUE) | Vet BLUE and the finding of a wedge sign in upper nongravity-dependent regions is supportive of PTE (Lisciandro 2013, unpublished data); TFAST with right ventricular dilation (increased RV:LV ratio) for acute cor pulmonale and pulmonary hypertension | Using the urinary bladder as an acoustic window to the upper femoral artery and vein is a consideration in small animals; the compression technique in people has not been applied to small animals to the author's knowledge, see Chapter 25 |
| Tamponade (pericardial effusion) (TFAST, FAST DH View) | Following the TFAST tenets for an accurate diagnosis of PCE is paramount (see also Chapter 18); during CPR the FAST DH view permits evaluation of the thorax without interrupting compressions | Gallbladder wall edema occurs in acutely collapsed or weak dogs and cats with right-sided congestive heart failure including DCM and PCE that will have a concurrent distended or "FAT" CVC (large maximum height, see Table 7.6) and hepatic venous distension ("tree trunk sign") |
| Toxin, canine anaphylaxis (FAST DH view) | | Gallbladder wall edema occurs in acutely collapsed or weak dogs with anaphylaxis that will have a concurrent attenuated or "flat" CVC (small maximum height) (see Tables 7.6 and Figures 7.12, 36.7, and 36.8) |

Source: Reproduced with permission from Dr Gregory Lisciandro, Hill Country Veterinary Specialists and FASTVet.com, Spicewood, TX.
[a] Upper 1/3 (trivial), Middle 1/3 (moderate), Lower 1/3 (severe); and Middle 1/3 and Lower 1/3 warrant strong consideration for thoracocentesis.

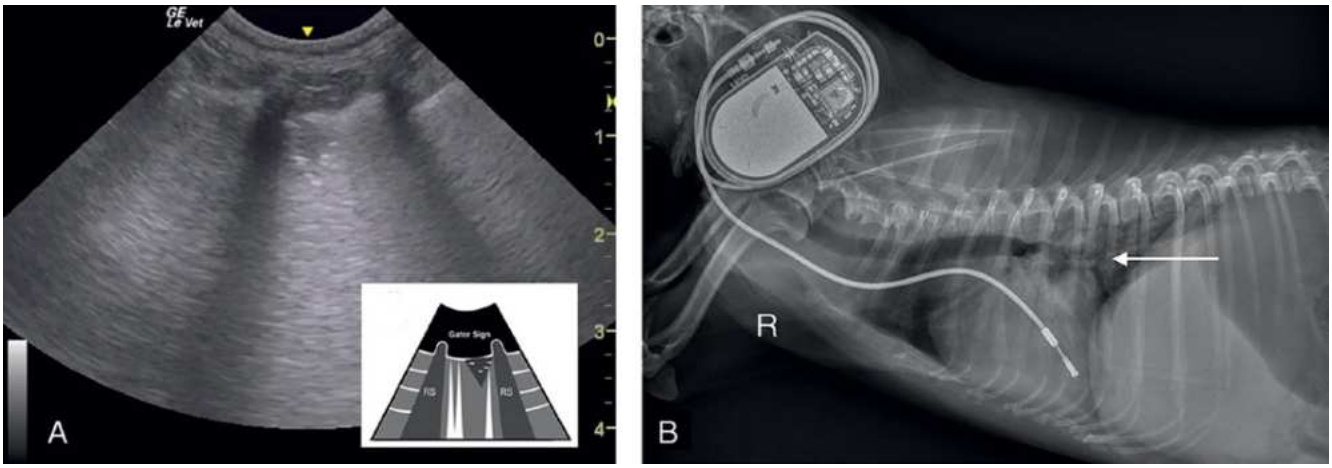


Vet BLUE® (Cd, Ph, Md, Cr)

| | | | | |
|---|---|---|---|---|
| Left: | >3 Wdge | 0, | 0, | 0 |
| Right: | 0, | 0, | 0, | 0 |

DH: 0

C

Key: Shred (Sh), Tissue (Ti), Nodule (Nd), Wedge (Wdge)

**Figure 37.9.** Pulmonary thromboembolism. (A) B-mode image of infinity (labeled as >3) B-lines with a triangulation along the periphery of lung at the left Caudodorsal region of Vet BLUE. The dog has predisposing factors for PTE including a pacemaker lead and a severe protein-losing nephropathy (urine protein:creatinine ratio of >15). The patient was admitted for acute respiratory distress, was extremely critical and questionably stable, and thus was being treated for left-sided congestive heart failure based on history and physical examination findings. However, the Vet BLUE study is listed in (C) and does not fit left-sided congestive heart failure. The thoracic radiograph does not reveal the diagnosis of PTE either. The dog subsequently had D-dimers that were out of range, acute pulmonary hypertension with right ventricular dilation, and thoracic radiography read out as a focal interstitial pattern at the same location of the "wedge sign" and associated B-lines on Vet BLUE. This is a convincing case for PTE diagnosed by Vet BLUE. The dog was too unstable to have the gold standard imaging test of computed tomography contrast angiography but was treated for PTE with a Factor Xa inhibitor plus supportive care and survived. The overlay in (A) shows the "wedge sign," described in more detail in Chapter 23 (Lisciandro 2013, unpublished data). Source: Reproduced with permission from Dr Gregory Lisciandro, Hill Country Veterinary Specialists and FASTVet.com, Spicewood, TX.

referred to as "plethora" (blood-filled), is suggestive, being 40% specific but not pathognomonic for cardiac tamponade (Himelman et al. 1988; Candotti and Arntfield 2015; Tchernodrinski and Arntfield 2015). Importantly, radiography is an unreliable test (Guglielmini et al. 2012; Côté et al. 2013).

The DH view is a rapid way to rule PCE in *and* out, and make a case for cardiac tamponade (see Figures 17.13, 18.18, and 37.11). The DH view advantageously images through the acoustic window of the liver and gallbladder, avoiding interference from lung that is often problematic via transthoracic TFAST and POCUS heart views (Lisciandro 2014a,b, 2016a, 2019a). Furthermore, if CPR is being performed, the DH view may be performed without interrupting thoracic compressions.

The DH view utilizes the strategy of imaging toward the muscular apex of the heart. The "racetrack sign" represents the rounding of PCE around the muscular apex of the heart where there are no heart chambers to confound the sonographer and less interference of lung (air) using the acoustic window provided by the liver and gallbladder (see Figures 7.13, 18.17, 18.18, and Chapter 18) (Lisciandro 2014a,b, 2016a, 2019a).

The other tenets for rapidly and accurately diagnosing PCE are explained in more detail in Chapters 17 and 18.

- Always, always, always image the heart in its entirety, making sure there is ample depth to see the landmark of the hyperechoic (bright white) pericardium in the far-field (see Figure 18.16).

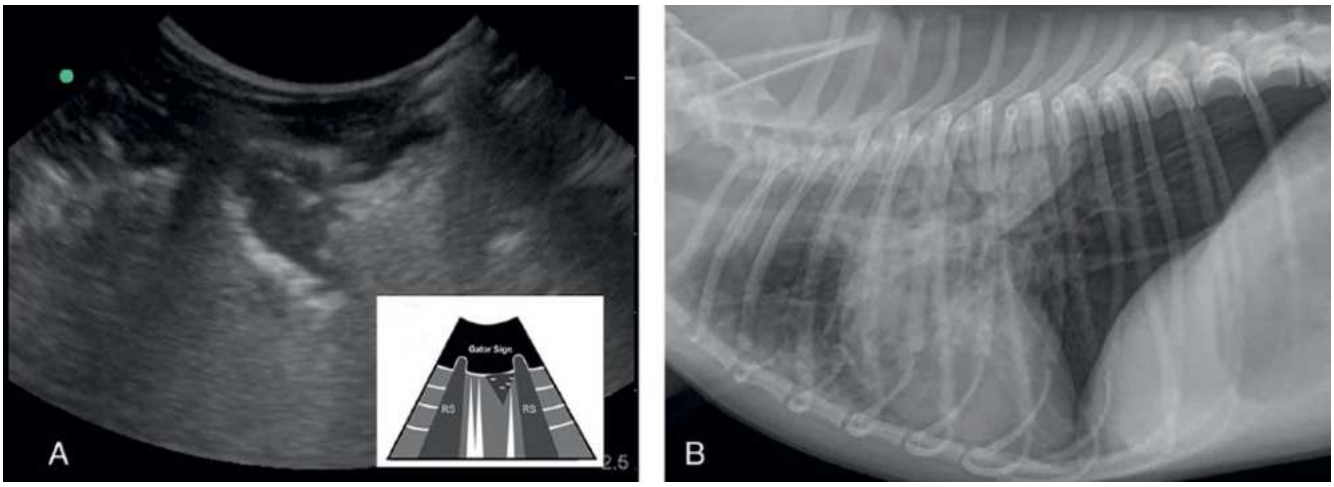


Vet BLUE® (Cd, Ph, Md, Cr)

| | | | | |
|---|---|---|---|---|
| Left: | 0, | 0, | 0, | 0 |
| Right: | ∞ Wdge, | >3, | 0, | 0 |

DH: 0

C Key: Shred (Sh), Tissue (Ti), Nodule (Nd), Wedge (Wdge)

**Figure 37.10.** Pulmonary thromboembolism in a dog with caval syndrome. This dog presented with acute weakness and collapse with heartworms evident in the right ventricular outflow tract and pulmonary arteries during TFAST. The Vet BLUE profile supports PTE in (C). The "wedge sign" and associated B-lines were detected in the right Caudodorsal and Perihilar Vet BLUE lung regions and correlate with the wedge-shaped infarction noted on the lateral thoracic radiograph taken when the dog was more stable. The overlay in (A) shows the "wedge sign" described in more detail in Chapters 20 and 23, Figures 23.2, 23.11, 23.19 (Lisciandro 2013, unpublished data). Source: Reproduced with permission from Dr Gregory Lisciandro, Hill Country Veterinary Specialists and FASTVet.com, Spicewood, TX.

- One view is no view – combine views to increase the probability of being correct.
- Image toward the muscular apex of the heart where there are no heart chambers to mistake for PCE (or PE) referred to as the "racetrack sign" (DH view) and "bull's eye sign" (right TFAST PCS view) (see Figures 18.18 and 37.11).
- The sole right TFAST PCS echo view that may be accurately used is the long-axis four-chamber view in which all four heart chambers are clearly identified and PCE can be clearly observed outside the heart chambers and in between the myocardium and pericardium (or visceral and parietal pericardium) (see Figure 37.11).
- The sole left TFAST PCS view would be its short-axis "hammerhead view" in which the left and right ventricles are clearly identified and PCE can be clearly seen in between the myocardium and pericardium (or visceral and parietal pericardium) (see Figures 37.11 and 43.1). At this level there are no atria.

The finding of PCE causing obstructive shock that has lead to CPA and the need for CPR is an immediate indication for lifesaving emergent pericardiocentesis (Boller and Fletcher 2012; Callaway et al. 2012; Link et al. 2015; Soar et al. 2015). Moreover, open-chest CPR and pericardotomy may be indicated depending on the patient subset (Neumar et al. 2010; Callaway et al. 2012; Link et al. 2015; Soar et al. 2015; Henry et al. 2018). If open-chest CPR takes place, the attending veterinarian must be prepared to surgically address a ruptured cardiac chamber (Sandanaga et al. 1990; Witt et al. 2000; Witt and Mayhew 2011; Neilsen et al. 2005; Morges et al. 2011; Ployart et al. 2013).

## *Toxin – Canine Anaphylaxis*

Canine anaphylaxis (AX) is likely overlooked in many acutely collapsed animals that often have accompanying gastrointestinal signs in an otherwise previously healthy dog. In 2009, Quantz et al. published a brilliant study showing how the finding of sonographic

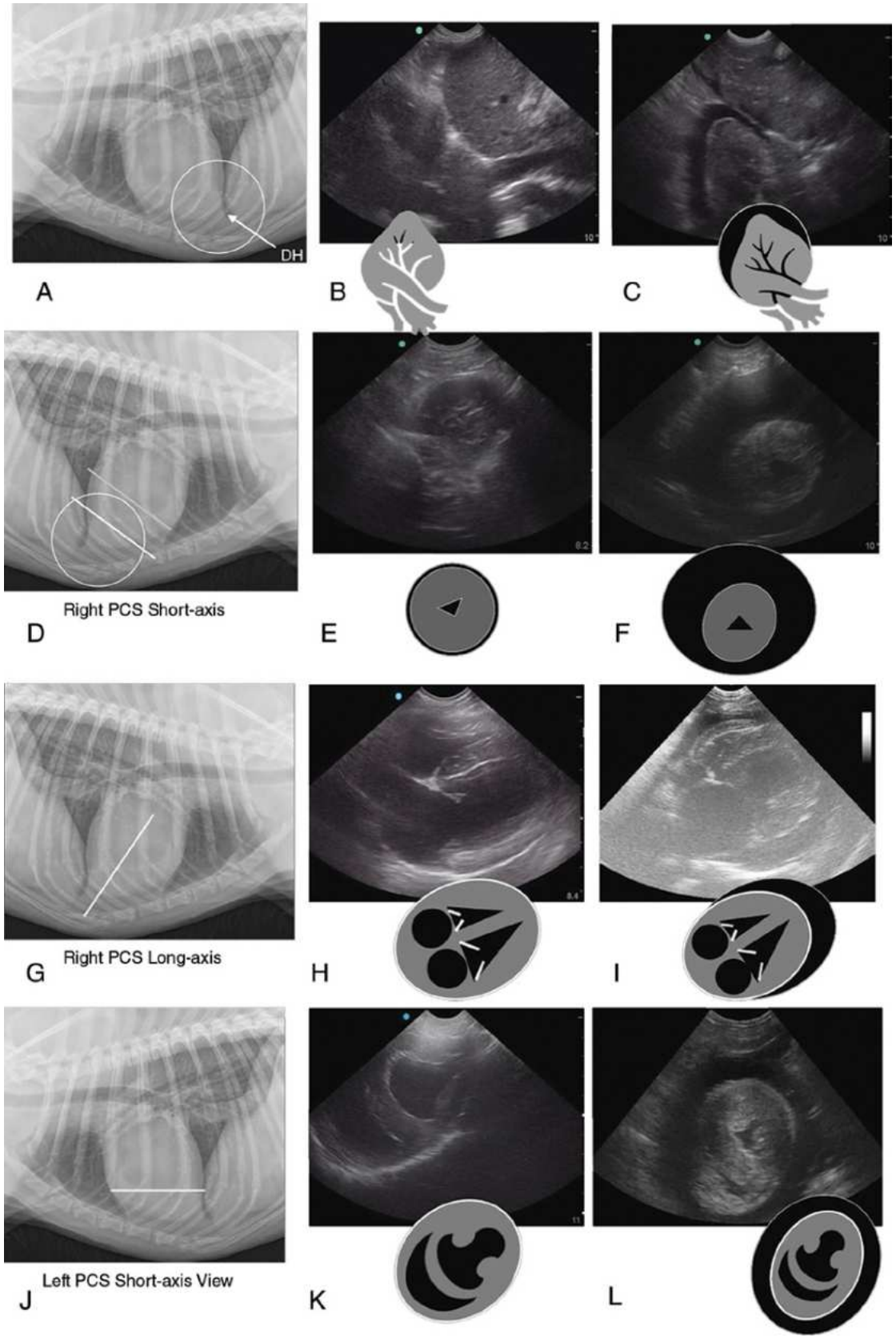
DH
A
B
C
D
Right PCS Short-axis
E
F
G
Right PCS Long-axis
H
I
J
Left PCS Short-axis View
K
L

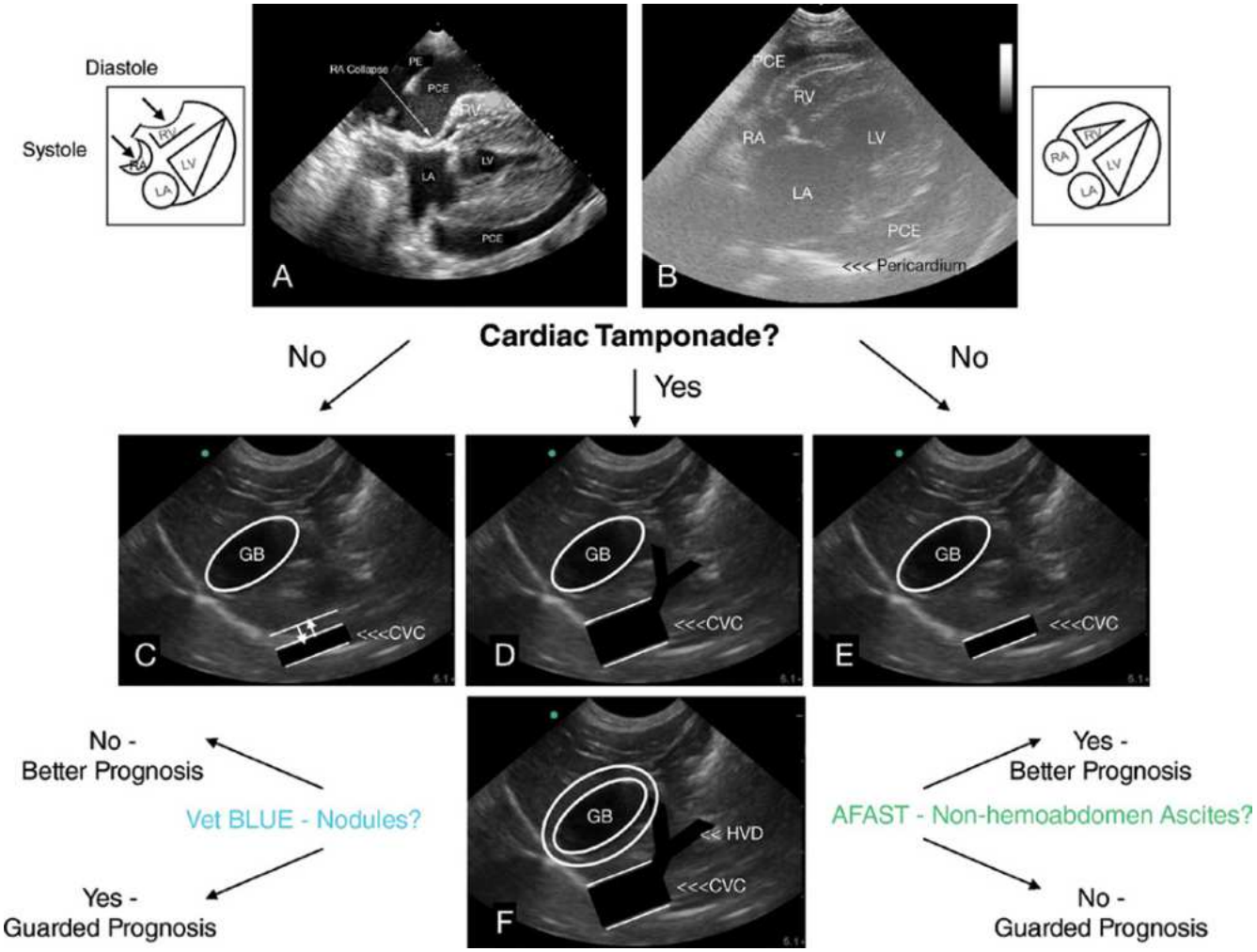


**Figure 37.12.** Pericardial effusion and cardiac tamponade. (A) Pericardial effusion (PCE) with right atrial collapse indicative of cardiac tamponade with a correlative line drawing. Shown in (B) for comparison is PCE without cardiac tamponade. Note it is diagnosed in the right TFAST pericardial site view on the long axis four-chamber view. The CVC and hepatic venous characterization is the "Global FAST nonecho fallback view" as well as an integrative view in questionable cases. In obstructive shock as a result of cardiac tamponade, the CVC by definition should be distended or "FAT" without or with gallbladder wall edema (D) and (F), respectively, and thus a CVC with a "bounce" as in (C), or that is "flat" as in (E), rules out clinically relevant cardiac tamponade. Dogs with PCE often have lung metastasis at the time of diagnosis that is occult on thoracic radiography, which argues for the use of Vet BLUE for rapid staging of the patient, and performing AFAST because median survival times are much higher in dogs with ascites consistent with right-sided congestive heart failure (modified transudate) (Stafford Johnson et al. 2004; MacDonald et al. 2009). In other words, stage these cases with Global FAST (see Chapter 36). Source: Reproduced with permission from Dr Gregory Lisciandro, Hill Country Veterinary Specialists and FASTVet.com, Spicewood, TX.

**Figure 37.11.** Pericardial effusion and its accurate diagnosis during TFAST. The tenets for accurate TFAST diagnosis of pericardial effusion are the following: (1) have enough depth to see the heart in its entirety on TFAST pericardial site views using the bright pericardium as the landmark in the far-field, (2) use the FAST DH view where the muscular apex of the heart is against the diaphragm in the vast majority of clinically relevant PCE (Lisciandro 2014a,b, 2016a, 2019a) and observe for the "racetrack sign" as shown in (A–C), (3) use the right TFAST pericardial site view and image toward the muscular apex of the heart (toward the sternum) and observe for the "bull's eye sign" as shown in (D–F), (4) use the right TFAST long axis four-chamber view where all four chambers are clearly identified and fluid is outside the heart and in between the myocardium and pericardial sac (parietal pericardium) as shown in (G–I), and (5) the left TFAST pericardial site view at the "hammerhead view" in which the two ventricles are clearly identified and PCE encircles the heart in the pericardial sac as shown in (J– L). Avoid the right TFAST left ventricle "mushroom view" because the crescent-shaped right ventricle is too confusing and easily mistaken for PCE (or PE) by the non-cardiologist sonographer (see Figure 18.15). See the didactic TFAST echo chart in Figures 17.25 and 17.26. Source: Reproduced with permission from Dr Gregory Lisciandro, Hill Country Veterinary Specialists and FASTVet.com, Spicewood, TX.

gallbladder wall striation, the "halo sign," "halo effect" or "double rim effect," representing intramural gallbladder wall edema, by performing a focused gallbladder examination at triage has high sensitivity and specificity for the diagnosis of canine anaphylaxis (Figure 37.13) (Quantz et al. 2009). The most common cause for canine AX is witnessed or unwitnessed single Hymenoptera sp. (bee) envenomation that is without cutaneous signs (Quantz et al. 2009; Lisciandro 2016b; Hnatusko et al. 2019). With the Global FAST approach, gallbladder wall edema and its sonographic gallbladder wall striation is easily recognized (see Chapter 7). However, the attending veterinarian must be aware of other important rule-outs, which in the acutely collapsed or hypotensive canine include cardiac causes, such as PCE, DCM, and right-sided

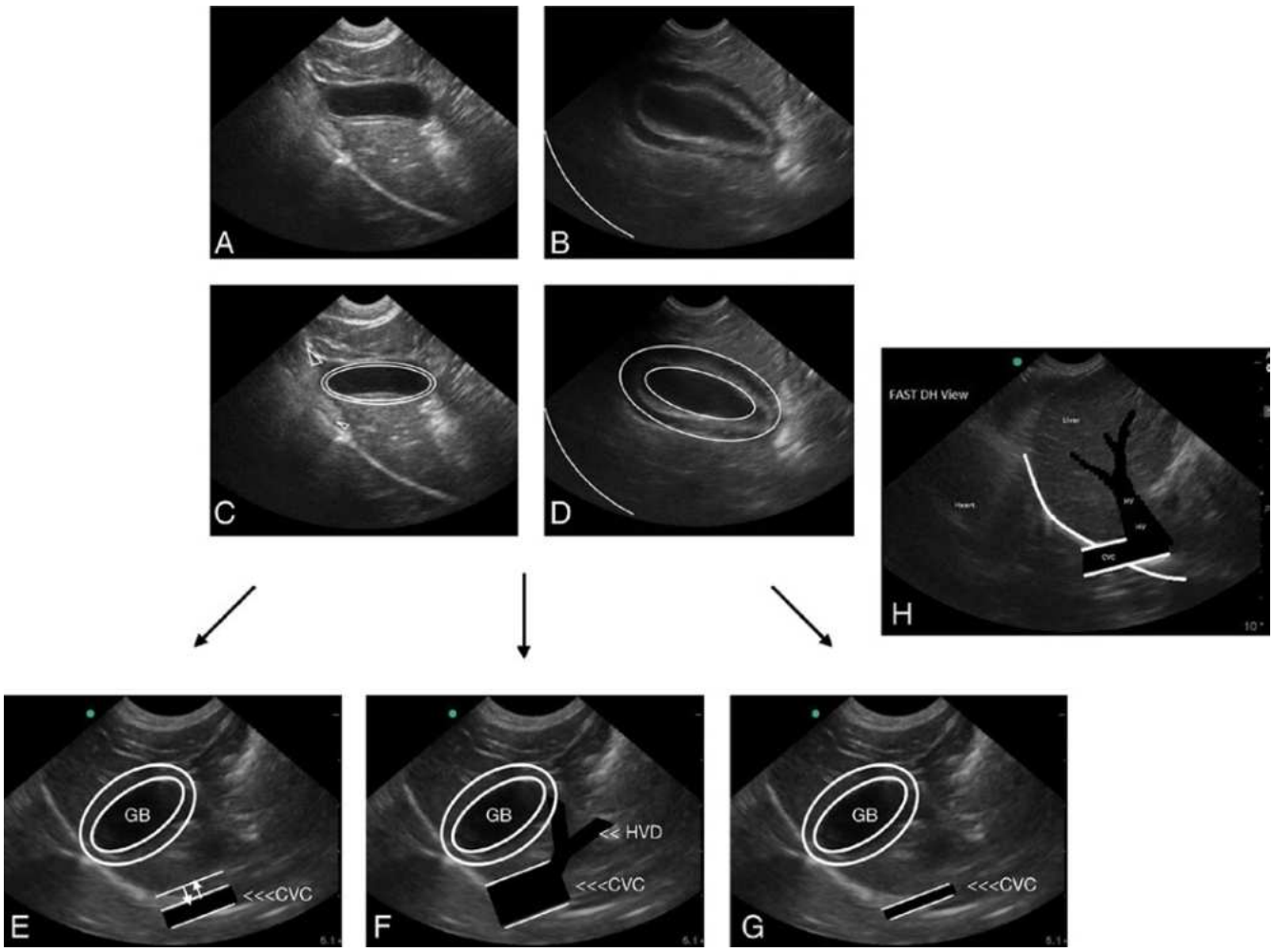


**Figure 37.13.** Gallbladder wall edema and integrating information from the caudal vena cava. (A,C) Correlative images of a more subtle sonographic striation, "gallbladder halo effect," and intramural gallbladder wall edema without (A) and with (C) overlays in a dog that fit the profile of acute canine anaphylaxis from a presumed Hymenoptera sp. envenomation. In (B) and (D) are correlative images of marked sonographic striation and intramural gallbladder wall edema without (B) and with (D) overlays in a dog that fit the profile of acute canine anaphylaxis from a presumed Hymenoptera sp. envenomation. The curved line overlay indicates the diaphragm and (A–G) are representative of the DH view. (E–G) Overlays to show how the finding of sonographic striation and intramural gallbladder wall edema is integrated with the CVC and hepatic venous characterization. The "cardiac gallbladder" would be represented by the finding of a "FAT" CVC with the distension of hepatic veins, "tree trunk sign," as in (F) and (H) plus a supportive clinical profile; the "anaphylactic gallbladder" by a finding of a "flat" CVC *without* hepatic venous distension plus a supportive clinical profile; and inconclusive in (E) when sonographic striation is detected with a CVC that has a "bounce" due to respirophasic height changes that make the integration inconclusive. Source: Reproduced with permission from Dr Gregory Lisciandro, Hill Country Veterinary Specialists and FASTVet.com, Spicewood, TX.

VetBooks.ir

congestive heart failure, including pulmonary hypertension, and dogs that fit the profile of hemorrhagic gastroenteritis syndrome (HGE) (see Tables 37.2 and 7.5) (Lisciandro 2014a,b, 2016a, 2019a; Vientós-Plotts et al. 2019). The use of the Global FAST approach in these cases prevents satisfaction of search error because the gallbladder halo sign is not pathognomonic, and differentiating the "anaphylactic gallbladder" from the "cardiac gallbladder" is imperative in the triage setting.

The differentiation between "anaphylactic gallbladder and "cardiac gallbladder" can be accomplished at the DH view by characterizing the CVC and its associated hepatic veins. In canine anaphylaxis, the CVC is flat with a small maximum height and little dynamic change in its height over several respiratory cycles, versus right-sided heart failure, including PCE and DCM, in which the CVC is FAT with increased maximum height and little dynamic change in height over several respiratory cycles (see Tables 7.6 and 36.11). The Global FAST approach is very important for avoiding satisfaction of search error by including imaging of the abdomen, AFAST, and thorax, TFAST and Vet BLUE, including the pleural cavity, pericardial sac, heart, and lung. Thus, the Global FAST approach should be considered standard of care by providing an unbiased standardized set of imaging data points.

# Comparison of Global FAST and the RUSH Examination

Global FAST provides more information in small animals than the RUSH (Rapid Ultrasound in Shock) protocol by having a fluid scoring system that predicts the degree of anemia and semiquantitates volume, a "lung point" and the TFAST PTX 1/3s Rule for degree of PTX (sternal or standing position), a urinary bladder estimation formula that over time can estimate urine output, and more lung via Vet BLUE with its six lung ultrasound signs, its B-line scoring system, and its lung contusion severity score (Perera et al. 2010; Lisciandro 2011, 2014c; Lisciandro et al. 2014, 2016, 2017; Ward et al. 2017; Lisciandro and Fosgate 2017; Dicker et al. 2019) (see Table 36.1). Global FAST and RUSH have a similar general premise to use clinically relevant lifesaving ultrasound information that is readily available in the abdomen, retroperitoneal space and thorax, and in RUSH for cardiac conditions including the aorta and indirect signs of PTE by searching for DVT (compression technique on legs), conditions unique to people, in addition to both formats' use for patient volume assessment (Perera et al. 2010). The RUSH protocol may be used as a primary or secondary survey and helps guide resuscitative efforts and similarly address the Hs and Ts of CPR, ideally before CPA occurs and CPR is needed.

In the San Antonio area, trauma surgeons and emergency physicians are trained to combine FAST and RUSH, which better approximates the Global FAST approach. In other words, the mindset is one of integrating information. And the sonographer during FAST is right there imaging heart, lung, vena cava, and hepatic veins (with the addition of aorta and deep venous thrombosis in people). So why not pay more attention with a standardized cerebral integrative Global FAST approach rather than just "flashing"?

Global FAST has the following features lacking in FAST-RUSH approach:

- an AFAST-applied abdominal fluid scoring system that predicts the degree of anticipated anemia
- an AFAST target organ approach for obvious soft tissue abnormalities
- an AFAST cysto-colic view urinary bladder volume estimation formula for noninvasive urine output estimation
- the "lung point" and TFAST PTX 1/3s Rule for assessing the severity of pneumothorax and tracking its course
- Vet BLUE for a more comprehensive lung evaluation (see Table 36.1).

The major difference between RUSH and Global FAST is the evaluation of the aorta (and for DVT) because people have a higher prevalence of aortic aneurysm and dissection that would be missed during FAST without this add-on ultrasound assessment.

# Global FAST for Rapidly Detecting Treatable Forms of Shock

By dividing the cardiovascular-respiratory systems into the RUSH exam categories of the "pump" (TFAST echocardiography), the "tank" (the CVC and hepatic veins, and TFAST and AFAST for effusions), and the "pipes" (TFAST and AFAST for effusions and Vet BLUE for PTE and other lung pathology), types of shock may be distinguished. The different types of shock and their features regarding the "pump," "tank," and "pipes" are summarized in Table 37.4.

**Table 37.4.**
Use of the Global FAST approach for the rapid assessment and monitoring of the critical dog and cat.

| Global FAST evaluation | Hypovolemic shock | Cardiogenic shock | Obstructive shock | Distributive shock |
|---|---|---|---|---|
| **Pump – How Contracting?** | **Works** | **Deficient** | **Works –Overloaded** | **Works – Deficient** |
| **Inotropy** | Hypercontractile heart<br>Small chamber size | Hypocontractile heart<br>Dilated heart | Hypercontractile heart<br>PCE/tamponade<br>RV strain (increased RV:LV) when PTE, cardiac thrombus | Hypercontractile heart (early sepsis)<br>Hypocontractile heart (late sepsis) |
| | Dry Lung | Wet Lung (B-lines) | Dry >> Wet Lung (B-lines) | Dry > Wet Lung (B-lines) |
| **Tank – How Full?** | **Empty** | **Overfilled** | **Overfilled** | **Empty or Overfilled** |
| **Volume** | Small flat CVC<br>Flat jugular veins<br>Dry Lung | Distended FAT CVC plus hepatic venous distension<br>Distended jugular vein<br>B-lines (alveolar-interstitial edema)<br>Wet Lung (B-lines) | Distended FAT CVC plus hepatic venous distension<br>Distended jugular<br>PTX (A-lines and no glide sign)<br>Dry or Wet Lung (B-lines) | Normal or small CVC (early sepsis)<br>Peritoneal effusion (exudate/sepsis source)<br>Pleural effusion (exudate/sepsis source)<br>Dry or Wet Lung (B-lines) |
| **Pipes – Leaky?** | **Leaky**<br>Peritoneal fluid (loss)<br>Pleural effusion (loss)<br>Do Focused spleen for most common source of intraabdominal bleeding tumor | **Normal**<br>Peritoneal fluid (ascites)<br>Pleural effusion | **Obstructed**<br>Thromboembolism | **Leaky or Distended**<br>Acute respiratory distress syndrome<br>Third spacing |
| **Comments** | Use Vet BLUE and AFS | Use Vet BLUE and AFS | Vet BLUE can detect PTE via "wedge sign" in upper caudodorsal and perihilar views | Vet BLUE and TFAST can detect noncardiogenic edema using its regional pattern-based approach |

Source: Reproduced with permission from Dr Gregory Lisciandro, Hill Country Veterinary Specialists and FASTVet.com, Spicewood, TX. Modified from the RUSH Examination (Perera et al. 2010).

# Final Comments on the Global FAST Approach

The Global FAST approach provides a baseline of an unbiased set of 15 data imaging points of the abdomen and thorax. Its 15 acoustic windows (views) have *exact* clarity in relation to their image acquisition and their objectives through the use of goal-directed templates. Importantly, the Global FAST approach avoids selective imaging and satisfaction error. Thus, Global FAST should be performed in all patients followed by targeted POCUS exams to avoid such error. Lastly, the components of Global FAST have been studied more than any other FAST or POCUS exams in veterinary medicine, with over 16 clinical studies (Lisciandro et al. 2008, 2009, 2014, 2015, 2017, 2018, 2019a,b; Lisciandro and Fosgate 2017, 2018; Kulhavy and Lisciandro 2015, 2018; Lisciandro 2012, 2013, 2016a,b, 2019a; McMurray et al. 2016; Ward et al. 2017, 2018a,b, 2019; Yarto and Lisciandro 2017; Dicker et al. 2019; Hnatusko et al. 2019).

# Global FAST and Saving Images

The Global FAST approach takes ~6–7 minutes for the experienced and properly trained sonographer with efficient ways to acquire its 15 acoustic windows

VetBooks.ir

(see Figures 37.1 and 37.2), which averages ~20–25 seconds per view. Think about the Global FAST examination and its acoustic windows. The five AFAST views have a standardized probe maneuver of fan, rock cranially, and return to the starting point of that view. Vet BLUE is the repetition of the same methodology for six and arguably eight of its transthoracic windows. The Global FAST examination may be in reality reduced to 4–5 different probe maneuvers. The author's point is the true simplicity of performing the Global FAST approach with our current improved and evolving methodology.

The author recommends setting your machine for a minimum of 6-second cine clips prospectively and performing each of the 15 views initially as a "pilot," followed by repeating and recording the same view so it is interrogated twice. Global FAST images, unless unrecognizable, generally require no labeling as each of its acoustic windows is distinct. When the AFAST order and its target organ approach are performed according to protocol (see Chapters 6 and 7), labeling is not required unless the view is unrecognizable. TFAST and its echo views are undeniable from the left pericardial to the right pericardial site views because the orientation of the heart is so inherently different dependent on left versus right side. Lastly, Vet BLUE poses the most identification problems which are easily overcome by performing the protocol moving from Caudodorsal to Perihilar to Middle and then finishing at the Cranial lung region view and marking each as follows: the Caudodorsal lung region view by its caudodorsal transition zone, which will be from the *right* of the screen, while including abdominal structures; the Perihilar lung region with no defining features; the Middle lung region by briefly including the heart in the image; and the Cranial lung region with its cranial transition zone, which will from the *left* of the screen, while including soft tissue neck. Furthermore, performing the AFAST, TFAST and Vet BLUE examinations in the same order (following protocol) every time maintains consistency.

## Global FAST and Goal-Directed Templates

The sonographer must record their findings for an effective Global FAST ultrasound program (see Figure 36.25A,B). The Global FAST template should be blended with the AFAST, TFAST, and Vet BLUE in the order that you typically perform the examination. Two Global FAST goal-directed template versions are probably best, one with the patient standing and one for when the patient presents in lateral recumbency. The methodology and order are explained in the beginning sections of this chapter and Chapter 36. The entire examination may be performed in standing-sternal, making lateral unnecessary unless the patient is AFAST positive for free fluid, or right lateral positioning would provide better TFAST echo views, imaging of the caudal vena cava, or other suspect abnormalities requiring additional scanning planes.

## Global FAST for Advanced Life Support and Patient Management

Global FAST is used as a tool to direct resuscitation and screen for complications. See Chapter 36 for life-saving surveillance to maximize a favorable outcome in the patient in shock, that has experienced CPA, and those that have ROSC.

## Pearls and Pitfalls, The Final Say

- Global FAST and its 15 defined acoustic windows have exact clarity and thus provide a standardized unbiased set of imaging data points of the abdomen and thorax, including heart and lung.
- Global FAST is the most published, clinically validated approach in the peer-reviewed veterinary literature for each of its components – AFAST, TFAST, and Vet BLUE.
- Global FAST takes approximately 6–7 minutes (~25 seconds per acoustic window) for the experienced properly trained sonographer and may be performed in standing/sternal or lateral recumbency or combinations thereof.
- Global FAST is an effective means to evaluate for the AHA Hs and Ts of CPR for rapid detection of treatable forms of shock, impending CPA, ALS and during CPR.
- As dictated by clinical course, POCUS examinations may be added as adjunctive POCUS evaluations, such as ocular, musculoskeletal, abdominal organs, heart and vascular.

# References


Andrus P. 2015. Cardiac arrest. In: *Point-of-Care Ultrasound*. edited by Soni N, Arntfield R, Kory P. Philadelphia: Elsevier Saunders, pp 359–365.

Armenise A, Neri L, Storti E, et al. 2012a. Evaluation of a FAST-ABCDE protocol (Focused Assessment with Sonography for Trauma-Airway, Breathing, Circulation, Disability, and Exposure) to detect multiple injuries in canine trauma patients: preliminary data. *J Vet Emerg Crit Care* 22(S2):S20.

Armenise A, Ricciardi M, Giannuzzi AP, et al. 2012b. Ultrasonographic measure of the optic nerve sheath in canine patients with signs of raised intracranial pressure. A preliminary study. *J Vet Emerg Crit Care* 22(S2):S20.

Armenise A, Boysen RS, Rudloff E, et al. 2019. Veterinary-focused assessment with sonography for trauma-airway, breathing, circulation, disability and exposure: a prospective observational study in 64 canine trauma patients. *J Small Anim Pract* 60(3):173–182.

Atkinson P, Bowra J, Milne J, et al. 2017. International Federation for Emergency Medicine Consensus Statement: Sonography in hypotension and cardiac arrest (SHoC): An international consensus on the use of point of care ultrasound for undifferentiated hypotension and during cardiac arrest. *Can J Emerg Med* 19(6):459–470.

Boller M, Fletcher DJ. 2012. RECOVER evidence and knowledge gap analysis on veterinary CPR. Part 1: Evidence analysis and consensus process: collaborative path toward small animal CPR guidelines. *J Vet Emerg Crit Care* 22(S1):S4–S12.

Boysen SR, Lisciandro GR. 2013. The use of ultrasound in the emergency room (AFAST and TFAST). *Vet Clin North Am Small Anim Pract* 43(4):773–797.

Boysen SR, Rozanski EA, Tidwell AS, et al. 2004. Evaluation of a focused assessment with sonography for trauma protocol to detect free abdominal fluid in dogs involved in motor vehicle accidents. *J Am Vet Med Assoc* 225(8):1198–1204.

Breitkreutz R, Walcher F, Seeger FH, et al. 2007. Focused echocardiographic evaluation in resuscitation management (FEER): concept of an advanced life support-conformed algorithm. *Crit Care Med* 35(S5):1527–1533.

Breitkreutz R, Price S, Steiger HV, et al. 2010. Focused echocardiographic evaluation in life support and peri-resuscitation of emergency patients: a prospective trial. *Resuscitation* 81:1527–1533.

Callaway CW, Soar J, Aibiki M, et al. 2015. Part 4: Advanced Life Support. 2015 International Consensus on Cardiopulmonary Resuscitation and Emergency Cardiovascular Care Science with Treatment Recommendations. *Circulation* 132(Suppl):S84–S145.

Candotti C, Arntfield R. 2015. Pericardial effusion. In: *Point-of-Care Ultrasound*. edited by Soni N, Arntfield R, Kory P. Philadelphia: Elsevier Saunders, pp 130–134.

Cooper ES, Owens TJ, Chew DJ, et al. 2010. A protocol for manging urethral obstruction in male cats without uerthral catheterization. *J Am Vet Med Assoc* 237(11):1261–2166.

Côté E, Schwarz LA, Sithole F. 2013. Thoracic radiographic findings for dogs with cardiac tamponade attributable to pericardial effusion. *J Am Vet Med Assoc* 243(2):232–235.

Darnis E, Boysen S, Merveille AC, et al. 2018. Establishment of references values of the caudal vena cava by fast-ultrasonography through different views in healthy dogs. *J Vet Intern Med* 32(4):1308–1318.

DeFrancesco TD. 2018. Use of the "5cm interventricular dimension rule" for screening for canine dilated cardiomyopathy. Personal communictaion.

Dicker SA, Lisciandro GR, Newell SM, et al. 2019. Diagnosis of pulmonary contusions with point-of-care lung ultrasonography and thoracic radiography compared to thoracic computed tomography in dogs with motor vehicle trauma: 29 cases (2017–2018). *J Vet Emerg Crit Care*, in press.

Eom K, Moon K, Seong Y, et al. 2008. Ultrasonographic evaluation of tracheal collapse in dogs. *J Vet Sci* 9(4): 401–405.

Ferrada P, Anand RJ, Whelan J, et al. 2011. Limited transthoracic echocardiogram: so easy any trauma attending can do it. *J Trauma* 71(5):1327–1331.

Ferrada P, Vanguri P, Anand RJ, et al. 2012a. Flat inferior vena cava: indicator of poor prognosis in trauma and acute care surgery patients. *Am Surg* 78(12):1396–1398.

Ferrada P, Attand RJ, Whelan J, et al. 2012b. Qualitative assessment of the inferior vena cava: useful tool for the evaluation of volume status in criticall ill patients. *Am Surg* 78(4):468–470.

Geeraerts T, Launey Y, Martin L, et al. 2007. Ultrasonography of the optic nerve sheath may be useful for detecting raised intracranial pressure after severe brain injury. *Intensive Care Med* 33:1704–1711.

Gerken KK, Cooper ES, Butler AS, et al. 2019. Association of abdominal effusion with a single decompression cystocentesis prior to catheterization in male cats with urethral obstruction. *J Vet Emerg Crit Care*, Epub ahead of print.

Goggs R, Chan DL, Benigni L, et al. 2014. Comparison on computed tomography pulmonary angiography and point-of-care tests for pulmonary thromboembolism diagnosis in dogs. *J Small Anim Pract* 55:190–197.

Guglielmini C, Diana A, Santarelli G, et al. 2012. Accuracy of radiographic vertebral heart score and sphericity index in the detection of pericardial effusion in dogs. *J Am Vet Med Assoc* 241(8):1048–1055.

Hall J, Hall K, Powell LL, et al. 2015. Outcome of male cats managed for urethral obstruction with decompressive cystocentesis and urinary catheterization: 47 cats (2009–2012). *J Vet Emerg Crit Care* 25(2):256–262.

Henry S, Brasel K, Stewart RM. 2018. *ATLS® Advanced Trauma Life Support*, 10th edition. Chicago: American College of Surgeons.

Himelman RB, Kircher B, Rockey DC, et al. 1988. Inferior vena cava plethora with blunted respiratory response: a

sensitive echocardiographic sign of cardiac tamoponade. *J Am Coll Cardiol* 12(6):1470–1477.

Hnatusko AL, Gicking JC, Lisciandro GR. 2019. Anaphylaxis-related hemoperitoneum in 11 dogs. *J Vet Emerg Crit Care*, in press.

Jambrik Z, Monti S, Coppola V, et al. 2004. Usefulness of ultrasound lung comets as a nonradiologic sign of extravascular lung water. *Am J Cardiol* 93(10):1265–1270.

Jambrik Z, Gargani L, Adamicza A, et al. 2010. B-lines quantify the lung water content: a lung ultrasound versus lung gravimetry study in acute lung injury. *Ultrasound Med Biol* 36(12):2004–2010.

Johnson LR, Lappin MR, Baker DC. 1999. Pulmonary thromboembolism in 29 dogs: 1985–1995. *J Vet Intern Med* 13(4):338–345.

Kellihan HB, Stepien RL. 2010. Pulmonary hypertension in dogs: diagnosis and therapy. *Vet Clin Small Anim* 40:623–641.

Kellihan HB, Waller KR, Pinkos A, et al. 2015. Acute resolution of pulmonary alveolar infiltrates in 10 dogs with pulmonary hypertension treated with sildenafil citrate: 2005–2014. *J Vet Cardiol* 17:182–191.

Kulhavy DA, Lisciandro GR. 2015. Use of a lung ultrasound examination called Vet BLUE to screen for metastatic lung nodules in the emergency room. *J Vet Emerg Crit Care* 25(S1):S14.

Kulhavy DA, Lisciandro, GR. 2018. The use of VetBLUE to evaluate lung pathology in dogs with severe pulmonary hypertension without left-sided heart disease. *J Vet Emerg Crit Care* 28(S1):S15.

Lee P, Tofts R, Kory P. 2015. Lung ultrasound interpretation. In: *Point-of-Care Ultrasound*. edited by Soni N, Arntfield R, Kory P. Philadelphia: Elsevier Saunders, pp 59–69.

Lichtenstein DA. 2010. Gallbladder. In: *Whole Body Ultrasonography in the Critically Ill*, edited by Lichtenstein DA. Heidelberg: Springer, pp 59–68.

Lichtenstein D. 2012. Fluid administration limited by lung sonography: the place of lung ultrasound in assessment of acute circulatory failure (the FALLS protocol). *Expert Rev Respir Med* 6(2):155–162.

Lichtenstein D, Karakitsos D. 2012. Integrating lung ultrasound in the hemodynamic evaluation of acute circulatory failure (the fluid administration limited by lung sonography protocol). *J Crit Care* 27(5):533.

Lichtenstein D, Mezière G, Lagoueyte JF et al. 2009. A-lines and B-lines: lung ultrasonography as a bedside tool for predicting pulmonary artery occlusion pressure in the critically ill. *Chest* 136:1014–1020.

Link MS, Berkow LC, Kudenchuk PJ, et al. 2015. Part 7: Adult Advanced Cardiovascular Life Support: 2015 American Heart Association Guidelines Update for Cardiopulmonary Resuscitation and Emergency Cardiovascular Care. *Circulation* 132(18 Suppl 2):S444–464.

Lisciandro GR. 2011. Abdominal and thoracic focused assessment with sonography for trauma, triage, and monitoring in small animals. *J Vet Emerg Crit Care* 21(2):104–122.

Lisciandro G. 2012. Evaluation of initial and serial combination focused assessment with sonography for trauma (CFAST) examinations of the thorax (TFAST) and abdomen (AFAST) with the application of an abdominal fluid scoring system in 49 cats. *J Vet Emerg Crit Care* 22(S2):S11.

Lisciandro GR. 2013. The Vet BLUE wedge sign for detecting pulmonary thromboembolism: case series of 6 dogs. Unpublished data.

Lisciandro GR. 2014a. The Abdominal FAST$^3$ (AFAST$^3$) Exam. In: *Focused Ultrasound for the Small Animal Practitioner*, edited by Lisciandro GR. Ames: Wiley Blackwell, pp 17–43.

Lisciandro GR. 2014b. The Thoracic FAST$^3$ (TFAST$^3$) Exam. In: *Focused Ultrasound for the Small Animal Practitioner*, edited by Lisciandro GR. Ames: Wiley Blackwell, pp 140–165.

Lisciandro GR. 2014c. The Vet BLUE lung Scan. In: *Focused Ultrasound for the Small Animal Practitioner*, edited by Lisciandro GR. Ames: Wiley Blackwell, pp 166–188.

Lisciandro GR. 2016a. The use of the diaphragmatico-hepatic (DH) views of the abdominal and thoracic focused assessment with sonography for triage (AFAST/TFAST) examinations for the detection of pericardial effusion in 24 dogs (2011–2012). *J Vet Emerg Crit Care*26(1):125–131.

Lisciandro GR. 2016b. Abdominal FAST (AFAST)-detected hemorrhagic abdominal effusion in 11 dogs with acute collapse and gallbladder wall edema (halo sign) with presumed anaphylaxis. Abstract. *J Vet Emerg Crit Care* 26(S1):S8.

Lisciandro GR. 2019a. The cardiac gallbladder: case series of 13 dogs and 1 cat with sonographically-detected gallbladder wall edema. *J Vet Emerg Crit Care* 26(S1):S8.

Lisciandro GR. 2019b. Point-of-care ultrasound. In: *Small Animal Diagnostic Ultrasound*, 4th edition, edited by Mattoon JS, Sellon R, Berry CR. St Louis: Elsevier, in press.

Lisciandro GR, Armenise AA. 2014. Focused or COAST$^3$ – Cardiopulmonary Resuscitation (CPR), Global FAST (GFAST$^3$), and the FAST-ABCDE Exam. In: *Focused Ultrasound for the Small Animal Practitioner*, edited by Lisciandro GR. Ames: Wiley Blackwell, pp 269–285.

Lisciandro GR, Fosgate GT. 2017. Use of AFAST cysto-colic view urinary bladder measurements to estimate urinary bladder volume in dogs and cats. *J Vet Emerg Crit Care* 27(6):713–717.

Lisciandro GR, Lagutchik MS, Mann KA, et al. 2008. Evaluation of a thoracic focused assessment with sonography for trauma (TFAST) protocol to detect pneumothorax and concurrent thoracic injury in 145 traumatized dogs. *J Vet Emerg Crit Care* 18(3):258–269.

Lisciandro GR, Lagutchik MS, Mann KA, et al. 2009. Evaluation of an abdominal fluid scoring system determined using abdominal focused assessment with sonography for trauma in 101 dogs with motor vehicle trauma. *J Vet Emerg Crit Care* 19(5):426–437.

Lisciandro GR, Fosgate GT, Romero LA, et al. 2015. Abdominal FAST (AFAST) and abdominal fluid scores in adult and juvenile cats. *J Vet Emerg Crit Care* 25(S1):S8.

Lisciandro GR, Ward JL, DeFrancesco TC, Mann KA. 2016. Absence of B-lines on lung ultrasound (Vet BLUE protocol) to rule out left-sided congestive heart failure in 368 cats and dogs. *J Vet Emerg Crit Care* 26(S1):S8.

Lisciandro GR, Fosgate GT, Romero LA, et al. 2019a. The expected frequency and amount of free peritoneal fluid estimated using the abdominal FAST-applied abdominal fluid scores in clinically normal adult and juvenile dogs. *J Vet Emerg Crit Care*, in press.

Lisciandro GR, Johnson CB, Gambino JM, et al. 2019b. The prevalence of sonographically-detected gallbladder wall edema in dogs with acute hemorrhagic diarrhea syndrome. *J Vet Emerg Crit Care*, in press.

MacDonald KA, Cagney O, Magne ML. 2009. Echocardiographic and clinicopathologic characterization of pericardial effusion in dogs: 107 cases (1985–2006). *J Am Vet Med Assoc* 235(12):1456–1461.

Machare-Delgado E, Decaro M, Marik PE. 2011. Inferior vena cava variation compared to pulse contour analysis as predictors of fluid responsiveness: a prospective cohort study. *J Intensive Care Med* 26(2):116–124.

Mastruzzo C, Perrachio G, Poidomani G, et al. 2008. Subsegmental pulmonary embolism: value of the thoracic ultrasound for the diagnosis and follow-up. *Intern Med* 47:1415–1417.

Mathis G, Blank W, Reibig A, et al. 2005. Thoracic ultrasound for diagnosing pulmonary embolism. *Chest* 128(3): 1531–1538.

McMurray J, Boysen S, Chalhoub S. 2016. Focused assessment with sonography in nontraumatized dogs and cats in the emergency and critical care setting. *J Vet Emerg Crit Care* 26(1):64–73.

Moretti R, Pizzi B. 2010. Inferior vena cava distensibility as a predictor of fluid responsiveness in patients with subarachnoid hemorrhage. *Neurocrit Care* 13(1):3–9.

Morges M, Worley DR, Withrow SJ, et al. 2011. Pericardial free patch grafting as a rescue technique in surgical management of right atrial HSA. *J Am Anim Hosp Assoc* 47(3):224–228.

Narasimhan M, Koenig SJ, Mayo PH. 2016. A whole body approach to point of care ultrasound. *Chest* 150(4):772–776.

Nelson NC, Drost WT, Lerche P, et al. 2010. Noninvasive estimation of central venous pressure in anesthetized dogs by measurement of hepatic venous blood flow velocity and abdominal venous diameter. *Vet Radiol Ultrasound* 51(3):313–323.

Neri L, Storti E, Lichtenstein D. 2007. Toward an ultrasound curriculum for critical care medicine. *Crit Care Med* 35(5 Suppl):S290–304.

Neumar RW, Otto CW, Link MS, et al. 2010. Part 8: Adult advanced cardiovascular life support: 2010 American Heart Association guidelines for cardiopulmonary resuscitation and emergency cardiovascular care. *Circulation* 122:S729–S767.

Nevins JR, Mai W, Thomas E. 2015. Associations between ultrasound and clinical findings in 87 cats with urethral obstruction. *Vet Radiol Ultrasound* 56(4):439-447.

Newitt AL, Cripps PJ, Shimali J. 2009. Sonographic estimation of pleural fluid in dogs. *Vet Radiol Ultrasound* 50(1):86–90.

Nielsen C, Todd JM, Cronk DE, et al. 2005. What is your diagnosis? A wood fragment was detected within the mediastinum, penetrating the cranial aspect of the pericardial sac and in contact with the right auricle. *J Am Vet Med Assoc* 226(7):1055–1056.

Perera P, Mailhot T, Riley D, et al. 2010. The RUSH exam: Rapid Ultrasound in SHock in the evaluation of the critically ill. *Emerg Med Clin North Am* 28(1):29–56.

Pfeiffer P, Bache S, Isbye L, et al. 2012. Verification of endotracheal intubation in obese patients – temporal comparison of ultrasound vs. auscultation and capnography. *Acta Anaesthesiol Scand* 56:571–576.

Ployart S, Libermann S, Doran I, et al. 2013. Thoracoscopic resection of right auricular masses in dogs: 9 cases (2003–2011). *J Am Vet Med Assoc* 242(2):237–241.

Powell LL, Rozanski EA, Tidwell AS, et al. 1999. A retrospective analysis of pulmonary contusions secondary to motor vehicle accidents in 143 dogs: 1994–1997. *J Vet Emerg Crit Care* 9(3):127–136.

Quantz JE, Miles MS, Reed AL, et al. 2009. Elevation of alanine transaminase and gallbladder wall abnormalities as biomarkers of anaphylaxis in canine hypersensitivity patients. *J Vet Emerg Crit Care* 19(6):536–544.

Rademacher N, Pariaut R, Pate J, et al. 2014. Transthoracic lung ultrasound in normal dogs and dogs with cardiogenic pulmonary edema: a pilot study. *Vet Radiol Ultrasound* 55(4):447–452.

Reineke EL, Thomas EK, Syring RS, et al. 2017. The effect of prazosin on outcome in feline urethral obstruction. *J Vet Emerg Crit Care* 27(4):387–396.

Ritchie JV, Horne ST, Perry J, et al. 2012. Ultrasound triage of ocular blast injury in the military emergency department. *Mil Med* 177(2):174–178.

Rudorf H, Barr FJ, Lane JG. 2001. The role of ultrasound in the assessment of laryngeal paralysis in the dog. *Vet Radiol Ultrasound* 42(4):338–343.

Sandanaga KK, MacDonald MJ, Buchanan JW. 1990. Echocardiography and surgery in a dog with left atrial rupture and hemopericardium. *J Vet Intern Med* 4:216–221.

Shimali J, Cripps PJ, Newitt AL. 2010. Sonographic pleural fluid volume estimation in cats. *J Fel Med Surg* 12:113–116.

Sigrist NE, Doherr MG, Spreng DE. 2004. Clinical findings and diagnostic value of post-traumatic thoracic radiographs in dogs and cats with blunt trauma. *J Vet Emerg Crit Care* 14:259–268.

Soar J, Nolan JP, Böttiger BW, et al. 2015. Adult Advanced Life Support Section Collaborators. European Resuscitation Council Guidelines for Resuscitation 2015: Section 3. Adult advanced life support. *Resuscitation* 95:100–147.

Spaulding K. 2008. Eye and orbit. In: *Atlas of Small Animal Ultrasonography*, edited by Penninck D, d'Anjou MA. Ames: Blackwell Publishing, p 61.

Stafford Johnson M, Martin M, Binns S, Day MJ. 2004. A retrospective study of clinical findings, treatment and outcome in 143 dogs with pericardial effusion. *J Small Anim Pract* 45(11):546–552.

Stander N, Wagner WM, Goddard A, et al. 2010. Normal canine pediatric gastrointestinal ultrasonography. *Vet Radiol Ultrasound* 51(1):75–78.

Sutherland-Smith J, Penninck DG, Keating JH, et al. 2007. Ultrasonic intestinal hyperechoic mucosal striations in dogs are associated with lacteal dilation. *Vet Radiol Ultrasound* 48(1):51–57.

Tchernodrinski S, Arntfield R. 2015. Inferior vena cava. In: *Point-of-Care Ultrasound*, edited by Soni NJ, Arntfield R, Kory P. Philadelphia: Elsevier, pp 135–141.

Vientós-Plotts AI, Wiggen KE, Lisciandro GR, et al. 2019. The utility of point-of-care ultrasound non-echo right-sided cardiac markers as a screening test for moderate to severe pulmonary hypertension in dogs. *Vet J* 250:6–13.

Volpicelli G, Mussa A, Garofalo G, et al. 2006. Bedside lung ultrasound in the assessment of alveolar-interstitial syndrome. *Am J Emerg Med* 24:689–696.

Volpicelli G, Elbarbary M, Blaivas M, et al. 2012. International evidence-based recommendations for point-of-care lung ultrasound. *Intens Care Med* 38(4):577–591.

Ward JL, Lisciandro GR, DeFrancesco TD, et al. 2018a. Evaluation of point-of-care thoracic ultrasound and NT-proBNP for the diagnosis of congestive heart failure in cats with respiratory distress. *J Vet Intern Med* 32(5):1530–1540.

Ward JL, Lisciandro GR, DeFrancesco TD. 2018b. Distribution of alveolar-interstitial syndrome in dogs and cats with respiratory distress assessed with lung ultrasound versus thoracic radiographs. *J Vet Emerg Crit Care* 28(5):415–428.

Ward JL, Lisciandro GR, Ware WA, Miles KG, DeFrancesco TC. 2019. Lung ultrasonography findings in dogs with various underlying causes of cough. *J Am Vet Med Assoc* 255(5):574–583.

Weaver B, Lyon M, Blaivas M. 2006. Confirmation of endotracheal tube placement after intubation using the ultrasound sliding lung sign. *Acad Emerg Med* 13:239–244.

Witt AL, Mathews KA, Holmberg DL. 2000. Management of traumatic right atrial rupture. *J Vet Emerg Crit Care* 10(2):85–89.

Witt JM, Mayhew PD. 2011. Diagnostic challenges and treatment options of a suspected pericardial metallic projectile foreign body in a dog. *J Vet Emerg Crit Care* 21(6):684–691.

Yarto E, Lisciandro GR. 2017. Evaluation of a Global FAST protocol in bottlenose dolphin (Tursiops truncatus). Unpublished data.

Zechner PM, Breitkreutz R. 2011. Ultrasound instead of capnography for confirming endotracheal tube placement in emergency? *Resuscitation* 82(10):1259–1261.

CHAPTER THIRTY-EIGHT

# POCUS: VetFAST-ABCDE

Andrea Armenise

Vetbooks.ir

## Introduction

The FAST-ABCDE protocol was first developed in human medicine to identify, manage, and treat the most common injuries in traumatized patients (Neri et al. 2007) and has been recently adapted to veterinary patients (Armenise et al. 2019). The intent of the human protocol was to provide credentials through specific training programs after the achievement of accepted standards of knowledge in diagnostic ultrasonography (Neri et al. 2007). FAST-ABCDE consists of a transversal approach to problems and solutions with three different levels of ultrasonography practice, general, comprehensive and expert, consistent with the multiple goal-directed, multisystem, time-dependent vision of critical care professionals (Neri et al. 2007).

Ultrasound skills expected for the general level are known alphabetically as:

- A – airway (airway – patency and ventilation; trachea – displacement, lesion, hematomas, tumors; esophagus – endotracheal tube displacement, prandial status)
- B – breathing (lung – absence of ventilation, pneumothorax [PTX], subcutaneous emphysema, pleural effusion, alveolar-interstitial syndrome, lung consolidation, diaphragmatic lesions)
- C – circulation (cardiac/hemodynamic assessment – asystole, pulseless electrical activity [PEA] vs pseudo-PEA, cardiac tamponade, severe left ventricular [LV] dysfunction, acute cor pulmonale, biventricular dysfunction, cardiac tumors, evaluation of inferior vena cava [IVC]; pericardial effusion; abdominal effusion; retroperitoneal space abnormalities; placenta abnormalities; central deep vein thrombosis; aorta abdominal and proximal arch aneurysm)
- D – disability (optic nerve sheath diameter [ONSD] enlargement, neonatal/infant hemorrhage, pupil evaluations, cerebral midline shift, cervical spine displacement)
- E – exposure (full access to all areas, preventing the misdiagnosis of life-threatening ABCDE lesions and emerging conditions) (Neri et al. 2007).

Additionally, some ultrasound-guided procedures are included, such as evaluation of endotracheal intubation, tracheostomy, thoracentesis, pericardiocentesis, peripheral and central vascular puncture, venous cutdown, nasogastric tube insertion, and urinary catheterization (Neri et al. 2007). The entire curriculum described may be adapted to the canine and feline critically ill patient, to provide a full ultrasonographic evaluation in time-dependent scenarios with the final objective of more accurately and expediently diagnosing life-threatening injuries, thus potentially improving critical diagnosis and treatment processes.

The veterinary FAST-ABCDE (VetFAST-ABCDE) shows a higher accuracy compared to conventional radiology for the diagnosis of trauma lesions (Armenise et al. 2019), similar to prospective AFAST and TFAST studies (Lisciandro et al. 2008, 2009). VetFAST-ABCDE consists of serial exams often completed in <10 minutes, similar to findings in human applications (Neri et al. 2007). After mastering the skills needed for the lungs, heart and abdominal views, add-on evaluations of the eye and upper airway should be learned.

VetFAST-ABCDE, although more technically challenging, incorporates the evaluation of the upper airways, a variant of lung and heart scans, and the evaluation of the ONSD as a marker for intracranial hypertension.

*Point-of-Care Ultrasound Techniques for the Small Animal Practitioner*, Second Edition. Edited by Gregory R. Lisciandro.
© 2021 John Wiley & Sons, Inc. Published 2021 by John Wiley & Sons, Inc.
Companion website: www.wiley.com/go/lisciandro/ultrasound2

## What POCUS: VetFAST-ABCDE Can Do

- Rapidly detect several of the Ts of cardiopulmonary arrest (CPA) including Tension PTX, Tamponade (pericardial effusion), Trauma (bleeding in large spaces such as pleural, peritoneal, retroperitoneal), and possibly Thromboembolism (lung) and Thrombosis (heart [myocardial infarction and its sequelae of ventricular fibrillation]).
- Rapidly assist in differentiating shock syndromes (hypovolemic, cardiogenic, distributive, obstructive and hypoxic).
- Rapidly assist in diagnosis through the triggering of interventional guided-ultrasound procedures (see Chapters 43 and 44).
- Determine the return of spontaneous circulation (ROSC) by direct visualization of synchronized heart contractions.
- Differentiate between ROSC and PEA.
- Confirm whether "pseudo" or "true" asystole is present as shown in humans with flat line ECG tracings who have coordinated heart movements with POCUS heart scans.
- Assist in resuscitation by detecting the presence or loss of ROSC, the patient's volume status and contractility (left ventricular short-axis "mushroom" view and long-axis views), left-sided heart status (presence of B-lines), and right-sided volume status (FAST diaphragmatico-hepatic [DH] view, CVC responsiveness and size, and degree of hepatic venous distension).
- Potentially assist in resuscitation by detecting the presence of intracranial hypertension through a measurement of the ONSD.
- Monitor for complications of cardiopulmonary resuscitation (CPR) such as PTX, pulmonary edema or lung contusions, bleeding into any major spaces, hypovolemia, the development of intracranial hypertension, and others.
- May be able to indirectly characterize interstitial edema (B-lines) as blood (lung contusions) versus forms of pulmonary edema by correlating lung ultrasound findings with the patient's clinical profile.

## What POCUS: VetFAST-ABCDE Cannot Do

- Cannot detect several of the Hs of CPA including electrolyte, blood glucose, body (or core) temperature disturbances, and hypoxemia.
- Cannot replace blood pressure, electrocardiographic and central venous pressure monitoring.
- Cannot replace arterial venous blood gas and other respiratory monitoring.
- Cannot characterize effusions based on echogenicity.
- Cannot replace appropriate ultrasound training for some of the advanced imaging tasks in the VetFAST-ABCDE platform.

## Indications

In the emergency and critical care scenarios, using a problem-based, multidisciplinary approach during resuscitation efforts (shock, advanced life support [ALS], and CPR). Expected abnormal findings are summarized in Table 38.1.

**Table 38.1.**
VetFAST-ABCDE abnormal findings.

| Airway | Breathing | Circulation | Disability | Exposure |
|---|---|---|---|---|
| Laryngeal paralysis | Absent lung sliding sign | Left ventricular (LV) "empty" with kissing walls | ↑ Optic nerve sheath diameter | Monitoring for any new appearance of abnormal ultrasound findings |
| Laryngeal masses | Irregular pleural line | ↑ LA:Ao ratio | | Ultrasound-guided procedures |
| Tracheal abnormalities | Pleural effusion | Systolic dysfunction | | |
| Tracheal dislocation | More than three B-lines per hemithorax | ↑ Heart chambers volume | | |
| Tracheal collapse | Focal or diffuse B-lines | Diastolic dysfunction | | |
| Incorrect tracheal intubation (double trachea sign) | Coalescent/fused B-lines (white lung) | Pericardial effusion with or without cardiac tamponade | | |
| | Focal or diffuse lung consolidation with or without air bronchogram | Abdominal effusion | | |
| | | Flattened caudal vena cava | | |
| | | Distended caudal vena cava | | |

### Objectives

VetFAST-ABCDE is used in critical scenarios including shock states, during, before and after CPR and ALS.

- Assess upper airway for injury.
- Assess laryngeal function.
- Assess for pneumothorax.
- Assess for pleural and pericardial effusion.
- Assess cardiac function.
- Assess for abdominal effusion.
- Assess eye injury.
- Assess for intracranial hypertension via ONSD.
- Monitor for developing injuries and complications during and post resuscitation.

## Ultrasound Settings, Probe Preferences, and Patient Positioning

A multifrequency curvilinear (microconvex) probe (5–8 MHz) is used for the entire VetFAST-ABCDE exam, allowing adequate evaluation of both superficial and deep structures over a wide range of patient sizes in dogs and cats. However, a phased-array (sector) probe is preferred to better evaluate cardiac performance and a linear probe is preferred over a curvilinear probe for superficial structures such as ONSD evaluation, airway, and thoracic views.

Patient positioning is adapted to how the patient presents, thus minimizing the stress of respiratory compromised patients by allowing sternal recumbency, which is preferred by the author. Lateral recumbency is acceptable, and after evaluation of the presented side, the patient is repositioned onto the opposite side to complete the exam. The author prefers to clip the hair to reduce artifacts. Solutions of 70% isopropyl alcohol should not be used if skin wounds are present or electrical defibrillation is anticipated, since alcohol poses a burn hazard to the patient and fire/explosion hazard to the hospital environment. Alternatively, the author uses acoustic coupling gel or saline solution.

## How to do the POCUS: VetFAST-ABCDE Exam

### Airway (A)

Ultrasound airway assessment begins with a rapid transverse scan of the larynx and the trachea, then proceeding distally to the thoracic inlet. The larynx normally appears sonographically as a hypoechoic structure behind the thyroid cartilages (Figure 38.1A,B). In contrast, the trachea appears as a hypoechoic curve surrounding a hyperechoic space followed by air reverberation artifact noted by several A-lines due to the presence of free air (Figure 38.1C,D). Endotracheal placement may also be confirmed using ultrasound as follows: directly by looking for the presence of a hyperechoic linear artifact below the normal tracheal appearance (Chou et al. 2013) or by visualizing an improperly esophageally placed endotracheal tube next to the trachea, referred to as the "double tract sign" (Figure 38.2); or indirectly looking for the presence of "lung sliding" (Weaver et al. 2006; Zechner and Breitkreutz 2011). The latter has been shown to be faster and equally or more reliable than chest auscultation and capnography for confirming endotracheal intubation in people (Pfeiffer et al. 2012).

The complete upper airway evaluation in the author's experience is performed in <1.5 minutes, providing important information regarding the presence or absence of normal regional anatomy (muscles, veins and arteries, thyroid) and the integrity of upper airway structures. The upper airway evaluation also helps in the diagnosis of laryngeal paralysis by observing for laryngeal motion during respiration and the diagnosis of tracheal collapse by direct visual estimates and comparison between the diameter of the first and most distally accessible cervical tracheal rings during the phases of respiration (Rudorf et al. 2001; Eom et al. 2008) (Figure 38.3).

### Breathing (B)

Thoracic evaluation consists of a scan of both hemithoraces by surveying the thorax in the upper, middle, and lower thirds between the fourth and ninth intercostal spaces (Figure 38.4). The "B" exam is performed as a continuum along intercostal spaces cranially to caudally and dorsally to ventrally. The "B" lung ultrasound carries the potential to characterize different types of lung injury, including pneumothorax (A-lines with no lung sliding), pulmonary contusions (B-lines), forms of pulmonary edema, although B-lines are nonspecific and must be placed into clinical context; and lung consolidation, also placed into clinical context to discriminate between severe lung contusions and bronchopneumonia or other forms of lung consolidation (see Chapters 22 and 23).

The "B" scan evaluates the thorax in upper, middle, and lower thirds so when PTX is present, it may determine the location of the "lung point" and thus assess the degree of PTX as partial based on where the "lung

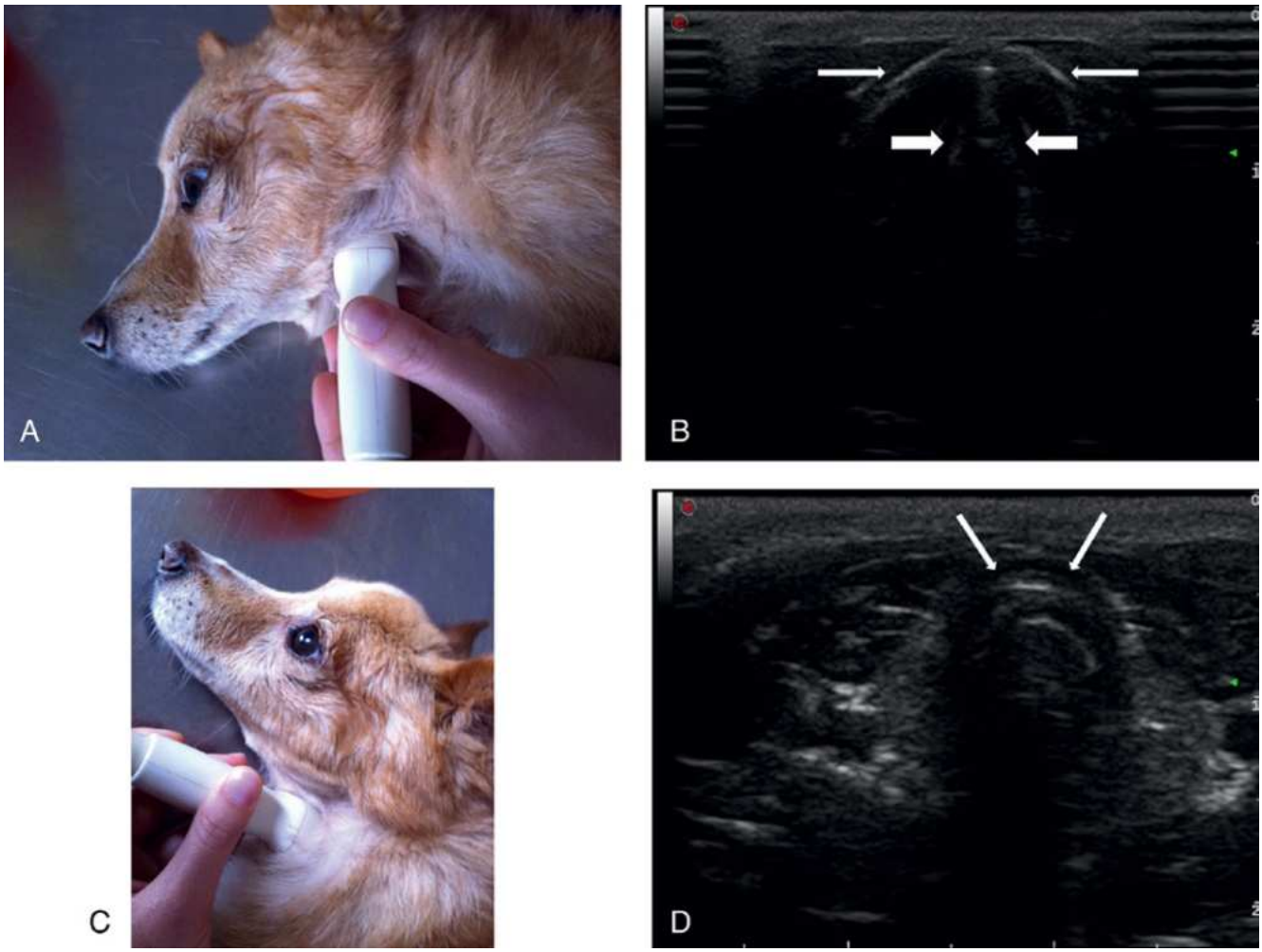


**Figure 38.1.** Upper airway evaluation using VetFAST-ABCDE. (A) External probe position on the neck of a dog for laryngeal evaluation. (B) Transverse image of a normal canine larynx (with a linear probe). The thyroid cartilages appear as hypoechoic structure surrounded by two hyperechoic lines (*thin arrows*). The arytenoid cartilages appear as hypoechoic structure surrounded by two echoic lines (*thick arrows*). (C) External probe position on the neck of a dog for tracheal evaluation which continues from the caudal laryngeal region to the thoracic inlet. (D) Transverse image of a normal canine trachea (with a linear probe). The trachea appears as a hypoechoic curvilinear structure (*arrows*) surrounded by two hyperechoic lines. Only the ventral aspect of the trachea can be visualized when it is air filled (ultrasound does not transmit through air) characterized by a near-field hyperechoic (bright white line) followed by air reverberation and strong distal shadowing.

point" is found on the thoracic wall, or deemed massive when not found (Figure 38.5) (Lisciandro 2011; Volpicelli et al. 2012). The "lung point" is the physical location along the thorax where aerated lung reopposes the thoracic wall, most commonly determined by finding the resumption of "lung sliding" (Figure 38.6A–C) or ultrasound lung rockets also called B-lines (Figure 38.6D). The lung pulse, however, is a third lung ultrasound finding, defined as collapsed lung directly against the thoracic wall gliding rhythmically with each heart beat (Volpicelli et al. 2012). The VetFAST-ABCDE breathing evaluation in the author's experience usually requires <3–4 minutes (Armenise et al. 2019).

## *Circulation (C)*

### Thoracic

Right thoracic circulation views are identical to the TFAST right pericardial site (PCS) views and right parasternal echocardiographic views, located along

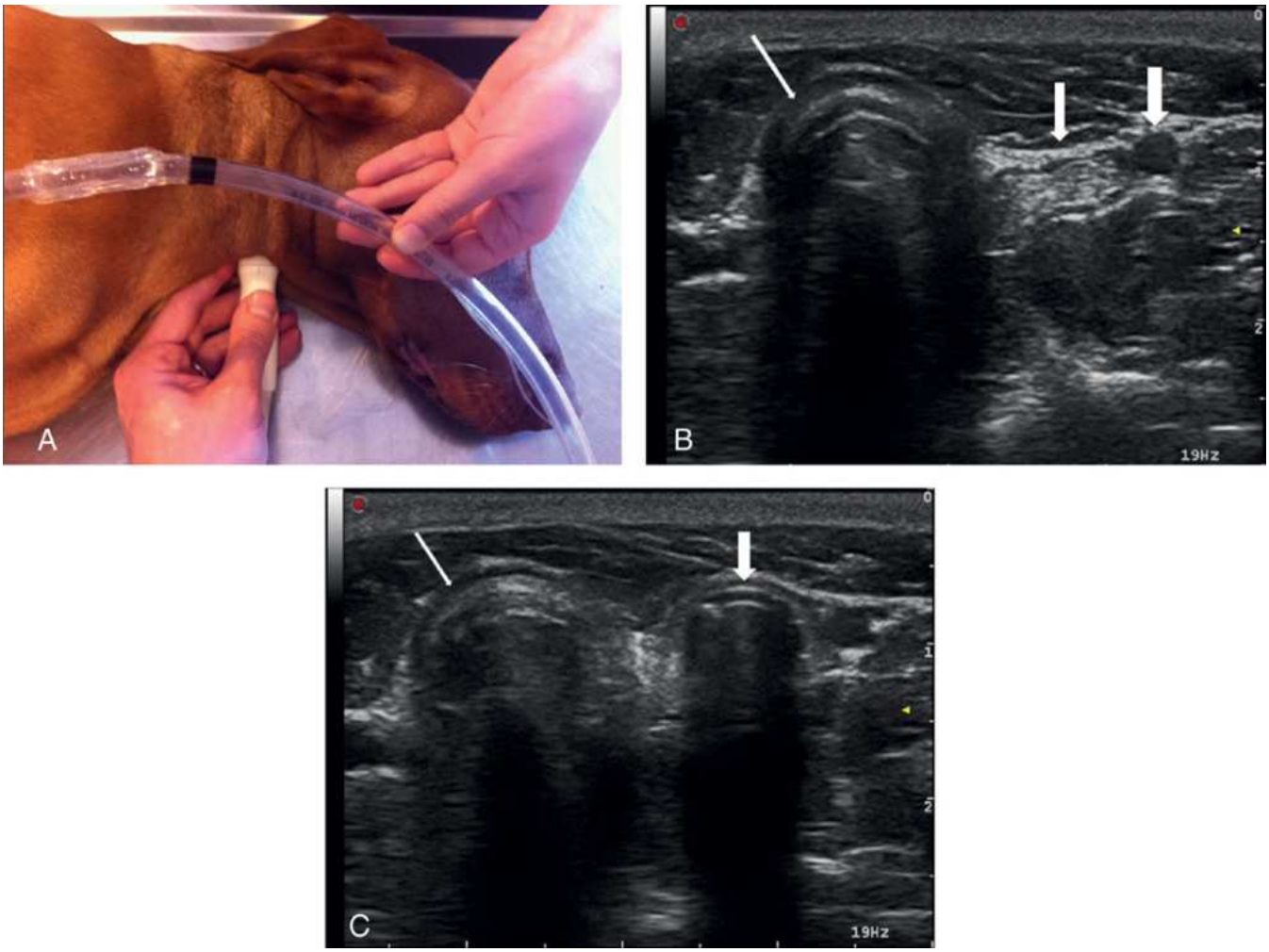


**Figure 38.2.** Endotracheal placement confirmation using ultrasound. (A) Dog in lateral recumbency with an endotracheal tube (ET) mimicking its course when placed in the animal. When first learning the technique of ultrasound confirmation of proper ET placement, place gel (or sterile KY® jelly if you are going to place the ET in the patient) on the ET to get an idea of what its ultrasonographic appearance will look like (near-field hyperechoic [bright white] rounded border with distal shadowing). (B) In normal conditions, the esophagus (*medium arrow*) is located on the left of the trachea (*thin arrow*), and the left carotid artery is seen (*thick arrow*). (C). Double trachea sign. The trachea appears on the left of the screen (*thin arrow*), and the "second trachea" (esophagus with incorrect intubation) is located on the right (*thick arrow*).

the right fourth to sixth intercostal space on the ventrolateral thoracic wall between the sternum and costochondral junctions. The right parasternal view is used for both the long-axis four-chamber (LA4C) and short-axis left ventricular "mushroom" view (LVSA) and the short-axis left atrium-aorta (LA:Ao) view of the heart, described in more detail in Chapters 17–21 (Figure 38.7A–D). A left parasternal view is performed similarly to the right parasternal view, but with the probe placed close to the sternum and directed to obtain the left apical four-chamber view (Figure 38.7E,F). These echocardiographic views rapidly provide important information regarding the presence of pericardial and pleural effusion, heart contractility, valve integrity, and subjective chamber dimensions for volume status and left atrial size assessment (see also Chapters 17–21).

### Abdominal

Abdominal circulation includes AFAST for the detection of hemoabdomen, hemoretroperitoneum and other effusions (see Chapters 6 and 7) and the VetFAST-ABCDE evaluation of the CVC for volume assessment obtained with a right lateral longitudinal and transverse scan at tenth to 12th intercostal

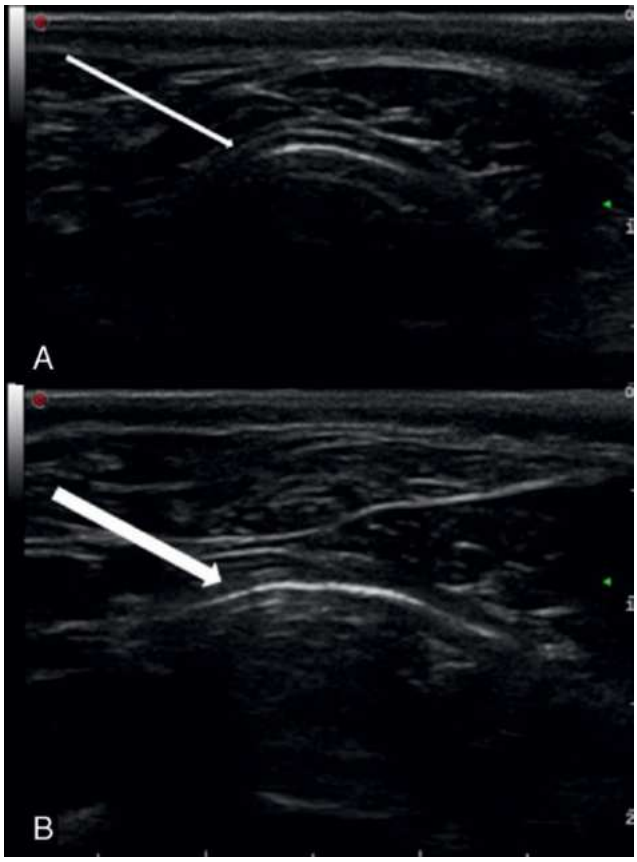


**Figure 38.3.** Tracheal collapse. Ultrasonographic evaluation of tracheal collapse of a 14-year-old male Yorkshire terrier dog. (A) First tracheal ring, close to larynx. (B) The last tracheal ring before the thoracic inlet, with a more concave appearance, compared to (A).

spaces at the dorsal/middle part of the thorax (Cambournac et al. 2018).

The general rule in human resuscitation is that fluid resuscitation continues as long as the IVC diameter shows responsiveness during fluid challenges by distending (larger diameter) and contracting (smaller diameter) with pre- and postfluid boluses, respectively, or until resuscitation endpoints have been met. However, when the IVC becomes distended, losing this dynamic change, patient preload has been maximized (Moretti and Pizzi 2010; Machare-Delgado et al. 2011). More detailed information may be found in Chapters 26, 36, and 37.

A veterinary study similarly evaluated the responsiveness of CVC diameter during fluid challenges, finding that the CVC at the level of the diaphragm, a different location than VetFAST-ABCDE but the same used for Global FAST, became distended with volume overload. The CVC and associated hepatic veins

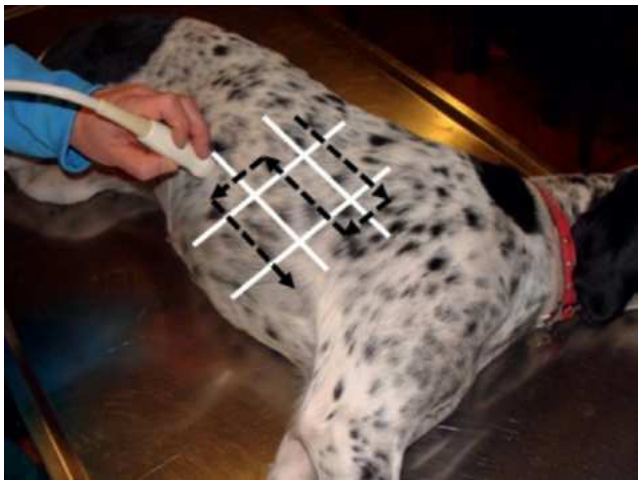

**Figure 38.4.** Lung ultrasound technique. Following the direction of the arrows, looking at each intercostal space starting from the upper dorsal caudal ninth intercostal spaces, then moving cranially to the fourth then in the middle third moving caudally to the ninth and finally in the ventral third moving cranially to the fourth. A longitudinal scan with the marker of the probe cranially was performed during the exam.

reflected a high central venous pressure in their experimentally resuscitated dogs (Nelson et al. 2010). Furthermore, the same study sonographically detected gallbladder wall edema ("halo sign") and pancreatic edema with volume overload (Nelson et al. 2010) (Figure 38.8). In dogs, the CVC diameter ($CVC_d$) and aortic (Ao) ratio ($CVC_d$:Ao) independent of patient size have been shown to be a third way in which to guide fluid resuscitation (Cambournac et al. 2018) (Figure 38.9) (see Chapter 26).

## *Disability (D)*

Disability consists of measuring the ONSD for intracranial hypertension assessment. Safe eye preparation is mandated with the use of an aqueous-based ultrasound gel labeled for eye use to prevent serious corneal injury (see Chapter 27). The ONSD is measured 3 mm behind the globe, using an electronic caliper and an axis perpendicular to the optic nerve (Figure 38.10). For consistent results, the ONSD technique should be standardized by scanning in the same manner. The author evaluates the left eye with a transverse view through the ventral eyelid with the marker of the probe on the right side, thus visualizing the optic nerve on the right of the screen with the probe marker on the left of the screen (see Figure 38.10). The optic nerve has a curved course

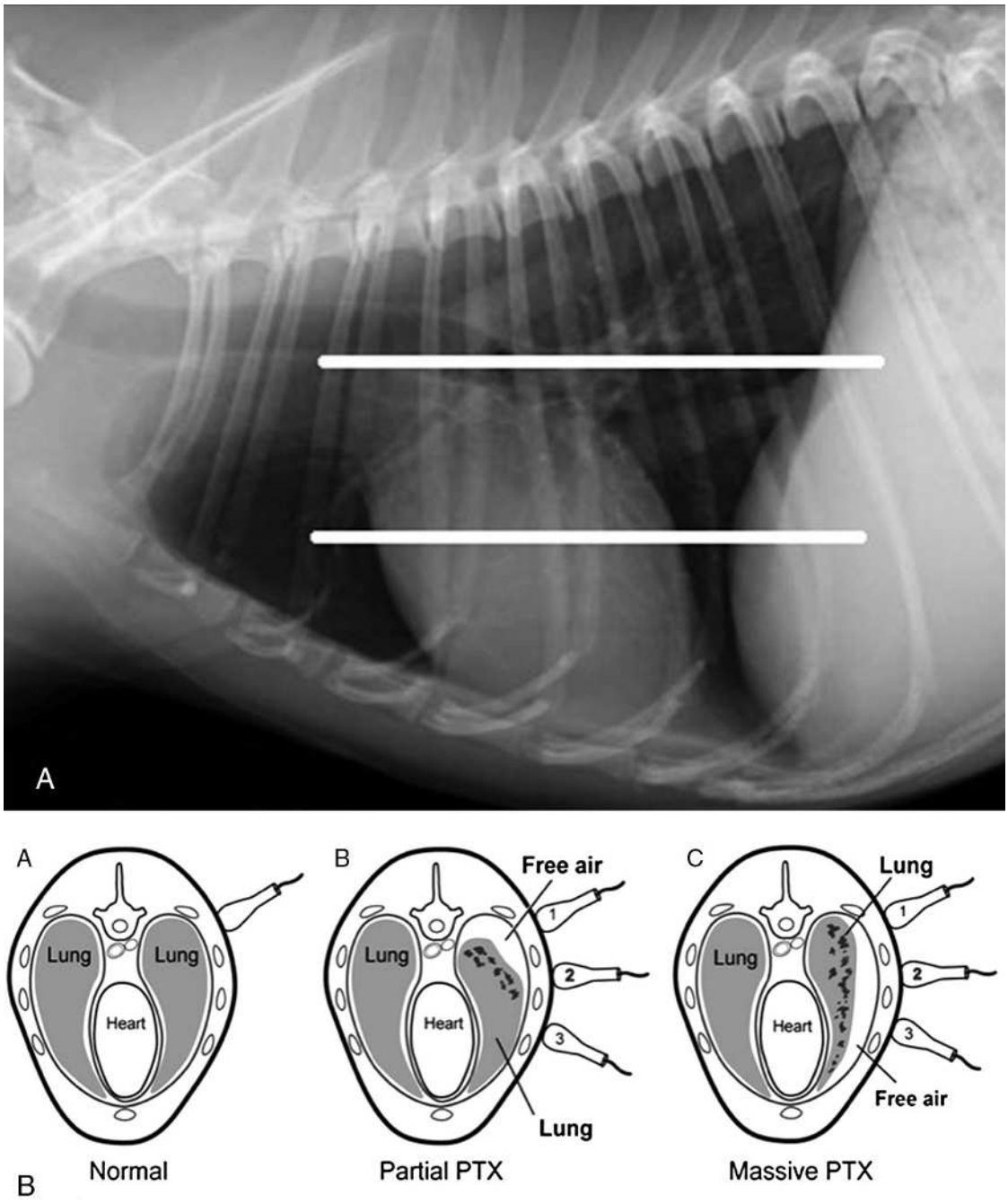


**Figure 38.5.** Finding the "lung point" for degree of pneumothorax, partial versus massive. (A) A normal lateral thoracic radiograph of a dog divided into upper, middle, and lower thirds to didactically help with understanding the search for and clinical relevance of the "lung point" in cases of PTX. If the "lung point" is found in the upper thorax, relatively close to the TFAST chest tube site (CTS), it would be considered as partial and smaller volume than a point in the lower third of the thorax (larger volume PTX). The absence of a "lung point" in true PTX (and not a false positive) would be considered massive. (B) Pictorial representation of the search for the "lung point" by moving the probe along the thoracic wall from the TFAST CTS (highest point where air would accumulate in PTX) to the sternum to determine degree of PTX as partial versus massive with the patient in standing or sternal position (see Chapters 18 and 36 and TFAST PTX 1/3s Rule). Source: Reproduced with permission from Lisciandro (2011).

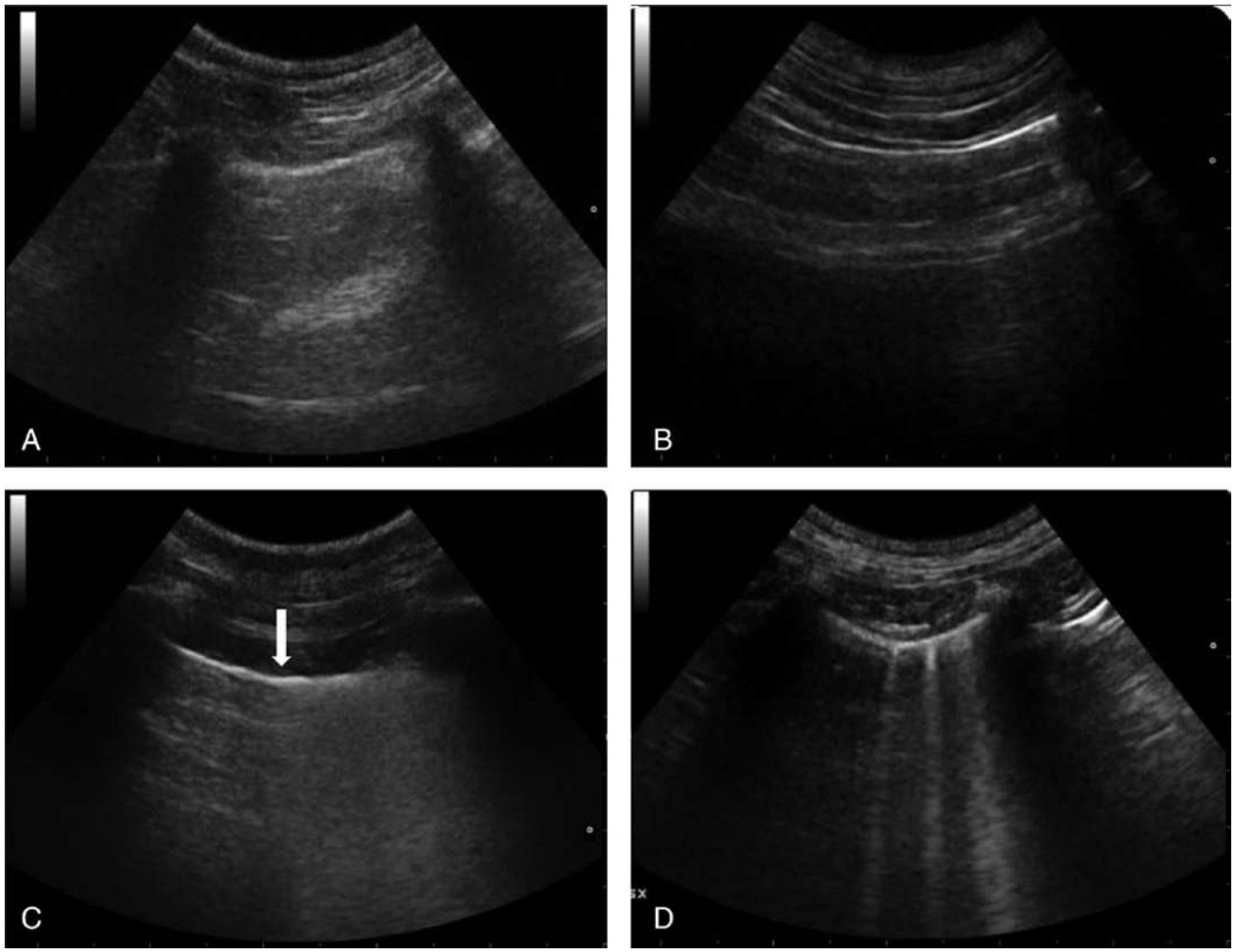


**Figures 38.6.** Normal and abnormal appearances of pleura. (A) "Lung sliding" in real time with A-lines representing dry lungs. The pleura appear regular and thick. (B) Pneumothorax. The pleura appear very thin and linear, and "lung sliding" in real time is not seen. (C) "Lung point." The image is divided into two sections: on the left of the arrow, the pleura is thin and linear without "lung sliding"; on the right, the pleura is thickened and several fused B-lines do not permit the A-lines to be seen, which correspond to the second position of the probe in Figure 38.5B – partial PTX. (D) Three B-lines starting from the pleural line. The B-line on the right is a fusion of two B-lines, which indicates a serious injury.

as it leaves the posterior eye and appears as an isoechoic line bordered by a hypoechoic line, both laterally and medially (Figure 38.10B). Alternately, the ONSD scan may be performed by placing the probe directly on the cornea with the use of acoustic coupling gel or other medium approved as safe for ophthalmic use.

The optic nerve is an extension of the central nervous system (CNS) because of the intraorbital subarachnoid space that surrounds it. Thus, it is subjected to the same pressure changes as the intracranial compartment (Geeraerts et al. 2007). The ONSD may be used as an ultrasonographically visible marker for the detection of increased intracranial pressure (ICP) by measurements of its diameter and increases in its width. Conversely, decreases in the measurements would support a decreasing ICP. In patients with pathologically elevated ICP (intracranial hypertension), perineural cerebrospinal fluid (CSF) is displaced into the intraorbital sheath, enlarging the animal's ONSD. In dogs, a correlation between increased ICP and increased ONSD has been demonstrated in experimentally induced increased ICP (Ilie et al. 2015).

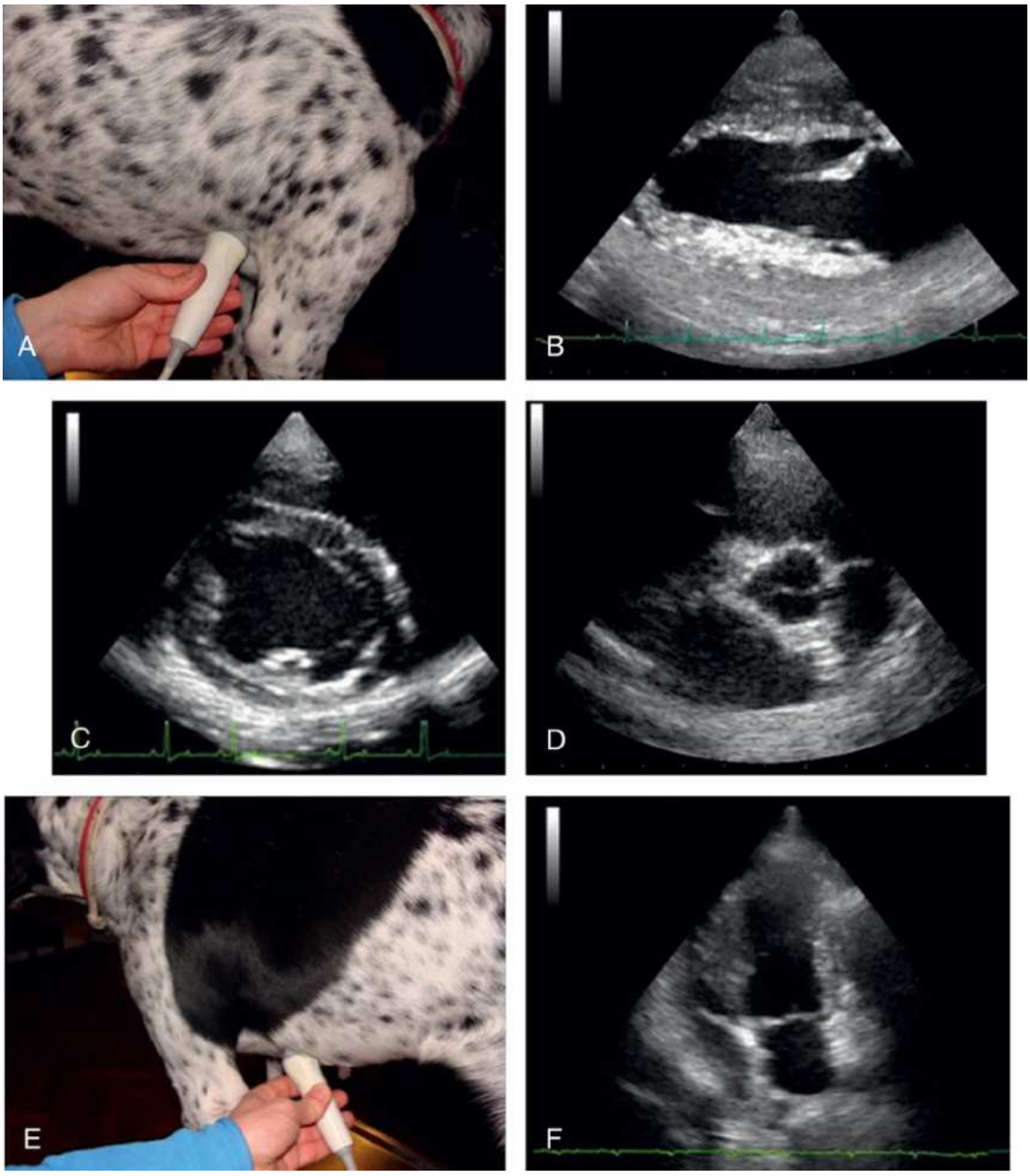


**Figure 38.7.** Probe orientation for heart views with the patient in standing position. (A) Probe positioning for right long-axis and short-axis views. The probe marker toward the elbow for the short-axis view; for the long-axis view, we need to make a 90° probe rotation on the left. (B) Left ventricle long-axis view. (C) Left ventricle short-axis view. (D) Left atrium – aorta view. (E) Probe positioning for left apical view. (F) Left apical four-chamber view.

In dogs, normal ONSD measured 3 mm from the eye's posterior wall is ≤2.7 mm, and ≥3.0 mm is considered abnormal (Armenise et al. 2012) (Figure 38.10C). In patients with abnormally measured ONSD and clinical signs related to intracranial hypertension, management to decrease ICP is urgently warranted and importantly, response to therapy should be monitored by serial ONSD measurements. The use of the ONSD is especially helpful in heavily sedated or anesthetized veterinary patients unable to have accurate mentation assessment.

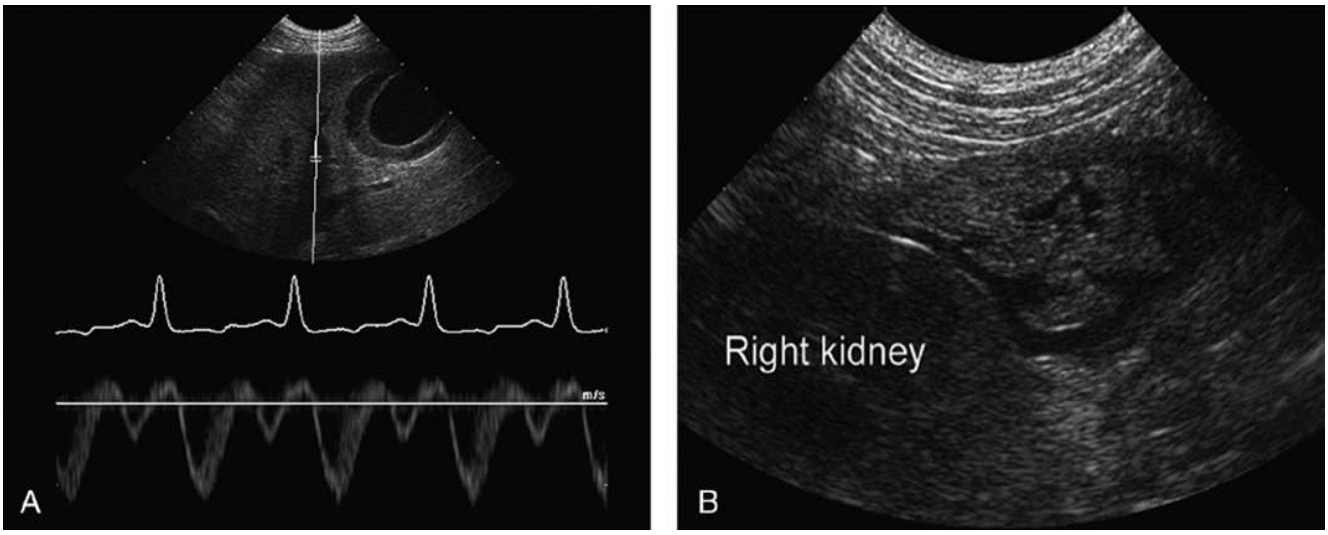


**Figure 38.8.** Caudal vena cava and hepatic venous distension from volume overload during fluid resuscitation in a dog. (A) Duplex Doppler image. Note the relationship of the right medial hepatic vein, quadrate hepatic vein, and gallbladder. The 2 mm Doppler gate is placed within the right medial hepatic vein, approximately 1 cm from the bifurcation from the quadrate vein. This is also the site of hepatic vein diameter measurement, perpendicular to the long axis of the vessel. The gallbladder wall (in the upper right of the B-mode image) is thickened. The pulsed wave Doppler display is below the B-mode image. A simultaneous electrocardiogram tracing is also recorded. (B) Transverse B-mode image of the right lobe of the pancreas. The pancreas is enlarged, triangular in shape, and has internal and peripheral hypoechoic striations. A transverse section of the right kidney is visible at the bottom left of the image. When volume overload occurs as a result of intravenous fluid therapy, the gallbladder and pancreas become edematous. The gallbladder develops a "halo effect" (thickened wall characterized by hyperechoic [bright white] inner and outer borders with a sonolucent [dark] middle) and the right lobe of the pancreas becomes readily obvious ultrasonographically (while in normalcy it is difficult to image). See also Chapters 6 and 8. Source: Reproduced with permission from Nelson et al. (2010).

Recently, a similar method was proposed for scanning from the upper eyelid, fanning the probe dorsally and ventrally to optimize the ONSD evaluation (Smith et al. 2018). Although a comparison between ultrasound and MRI was not performed, there seems to exist a correlation between age, breed, body weight, and ONSD measurements in normal patients so further studies are necessary to better use ultrasound as a non-invasive method to monitor ICP in dogs and cats (Smith et al. 2018). In summary, ocular ultrasound has been shown to be superior in some trauma-related conditions when compared to computed tomography (Ritchie et al. 2012).

### *Exposure (E)*

Serial VetFAST-ABCDE evaluations are clinically helpful because serial FAST exams have been shown to increase sensitivity by detecting occult or missed potentially life-threatening injuries and conditions on initial scans (Blackbourne et al. 2004; Ollerton et al. 2006). Moreover, serial exams may be used to detect complications and for monitoring response to therapy. Serial VetFAST-ABCDE examinations should be performed in all stable patients four hours post admission, as recommended by the American College of Emergency Physicians (www.acep.org) and as frequently as every 15–30 minutes in unstable patients.

## Clinical Significance and Implications of Abnormal VetFAST-ABCDE Exam Findings

The VetFAST-ABCDE format represents an important clinical tool for the nonradiologist emergency physician, trauma surgeon, intensivist, anesthesiologist, and other pertinent specialties. The protocol is used to assess the "3 Ts" ($T^3$), standing for trauma, triage and tracking, to expediently diagnose and better manage life-threatening injuries otherwise occult or speculated based on traditional means without ultrasound and advanced imaging. It is also used for ultrasound-guided interventions (see Chapters 43 and 44) as well

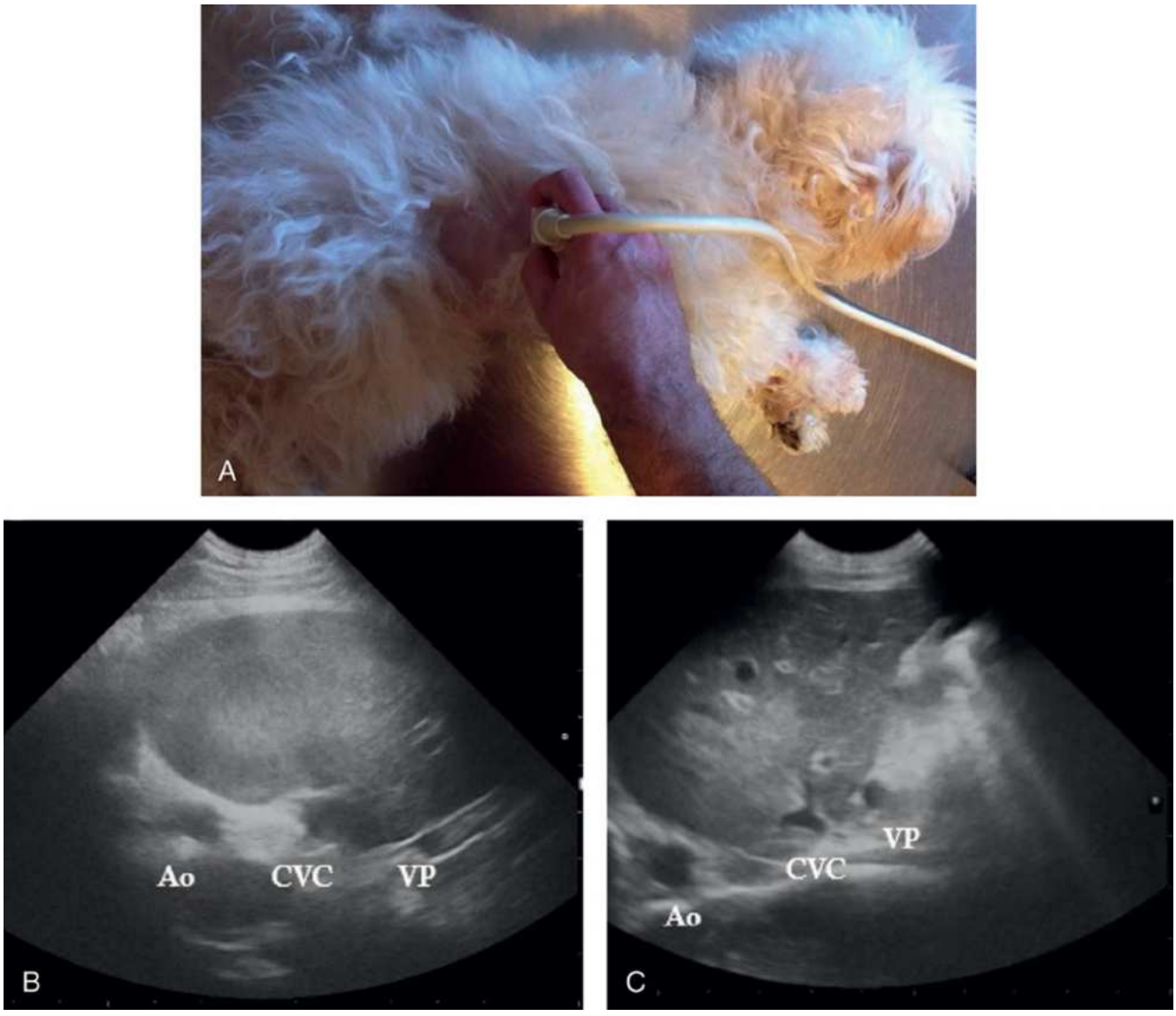


**Figure 38.9.** Caudal vena cava assessment. **(**A) Probe orientation, with the patient in right lateral recumbency, with the probe transverse for CVC:Ao ratio, and sagittal for longitudinal CVC evaluation with the marker placed dorsally, at the 10th–11th intercostal spaces. (B) The CVC is located at the center of the image, between the aorta (Ao) and the portal vein (PV). In normal volume status, the CVC appears rounded with a minimum inspiratory collapse. (C) In hypovolemic patients, the CVC appears elliptical with an increased collapsibility. CVC, caudal vena cava; Ao, aorta; PV, portal vein.

as their applications during and after CPR. Potential VetFAST-ABCDE detected abnormal findings are summarized in Table 38.1.

## *Differences Between VetFAST-ABCDE and Global FAST*

In dogs, the VetFAST-ABCDE exam has been helpful to diagnose and manage similar conditions such as Global FAST, the combination of AFAST and its fluid scoring system, TFAST, and Vet BLUE, but additionally with the following.

## *Airway (A)*

Confirmation of endotracheal tube (ET) placement may be made in two ways: *directly* by the "double trachea sign" or *indirectly* by looking for bilateral "lung sliding" with positive pressure ventilation (see Chapters 17 and 18). Regarding the direct method,

**Figure 38.10.** Probe positioning and orientation for optic nerve imaging for optic nerve sheath diameter measurements. Horizontally oriented image of a normal canine left eye as shown in (A). The transducer was placed on the ventral eyelid with the probe marker to the right. The optic nerve (located on the right of the image) is visualized as an isoechoic linear structure surrounded by two hyperechoic lines which represent the intraorbital subarachnoid space unlabeled and labeled in (B) and (C), respectively. Discrimination between extraocular muscles (located on the left of the image) and the optic nerve, which can look similar, may be made using color flow Doppler, since the optic nerve has blood vessels on either side. While mastering identification of the optic nerve, it is recommended that the exam be performed in the same manner for each evaluation.

improperly placed ET tubes may be recognized by observing the "double trachea sign" in which two hyperechoic (bright white) curved structures (the trachea and the misplaced esophageally located ET tube) are side by side (see Figure 38.2C). Otherwise, the indirect method should be performed after all ET intubation, to rule out improper esophageal intubation and unwanted single bronchi intubation.

Upper airway obstruction is suspected from the loss of normal A-lines extending beyond the tracheal rings, because of echogenic material displacing air in the near-field. Soft tissue may echogenically reflect more benign signs such as significant intratracheal secretions or the more concerning mass. In either case, secretions versus masses are indistinguishable without a more formal ultrasound study, additional imaging, or direct visual examination (by sight or fiberoptically).

Laryngeal paralysis may be diagnosed through monolateral or bilateral absence or asymmetry of movement with the respiratory cycle of the arytenoid cartilages, although no studies exist, to the author's knowledge, regarding the learning and accuracy of this skill.

**Figure 38.11.** Tracheal injury. Tracheal rupture, laceration or other injury is recognized by observing disruption of the normal continuity of the trachea's near-field (bright white line) border, a step sign. Here in transverse with a microconvex probe, the trachea's normal linear continuity is not visualized because of tracheal rupture and its associated deviations and shadowing from maligned cartilaginous tracheal rings.

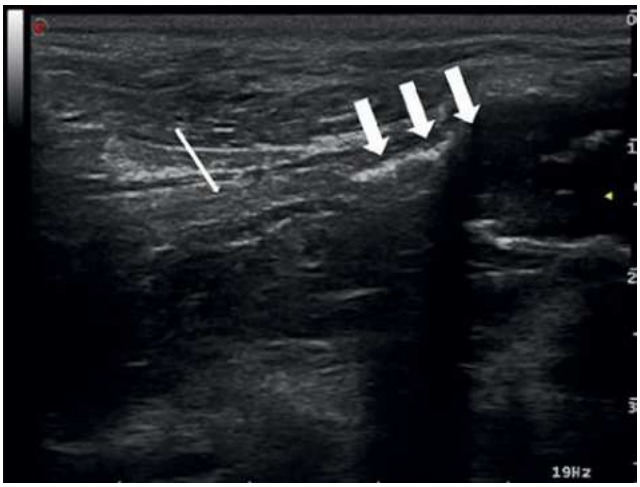


**Figure 38.12.** Longitudinal scan of the esophagus. In the caudal part of the espohagus, an irregular hyperechoic structure (*thin arrow*) is seen with an associated hypoechoic structure (bone foreign body) (*thick arrows*).

Tracheal rupture can be detected through recognized deviations, step signs, from the expected curved or linear continuity of the trachea throughout its cervical course (Figure 38.11).

Regional hematomas/masses may be detected by the presence of echogenic irregularities to adjacent soft tissues and their displacement of the larynx, trachea, veins or arteries.

Foreign bodies within the cervical esophageal lumen can be responsible for airway obstruction and respiratory distress (Figure 38.12).

Jugular veins and carotid artery abnormalities may be detected by the presence of thrombi or aneurisms.

## Breathing (B)

VetFast-ABCDE consists in ~18 intercostal spaces per each hemithorax (~6 in each – the upper, middle and lower thirds), compared to TFAST (two pulmonary acoustic windows per hemithorax) and Vet BLUE (12 pulmonary acoustic per hemithorax plus the FAST diaphragmatico-hepatic [DH] view), dividing the thoracic scan field differently. The formats use the same "wet lung" versus "dry lung" concept and the use of the "lung point."

## Circulation (C)

Valvular function may be evaluated for obvious mitral and tricuspid abnormalities, looking for any degenerative proliferation and insufficiency. Right-sided and left-sided conditions and volume status problems are similarly screened for as with Global FAST (see Chapters 36 and 37).

**Pearl:** Small-volume effusions may be missed on initial scanning or may not be present despite significant injury, and thus serial exams are imperative to increase the sensitivity of VetFAST-ABCDE, the "E" aspect of VetFAST-ABCDE being similar to the premise of Global FAST.

## Disability (D)

Ocular sonography is used to screen for any obvious ocular trauma or pathology (retinal detachment, lens luxation, intraocular abnormalities within the eye and periocular) and to measure ONSD (Figure 38.13). Canine ONSD >3 mm according to one study suggests intracranial hypertension (ICH) and the finding placed within clinical context potentially triggers (ICH) therapy (Armenise et al. 2019). Moreover, ONSD may also be used serially to monitor response to therapy. ONSD has not been evaluated in cats and the full clinical utility of ONSD in dogs for ICH requires continued study. The reader is referred to Chapter 27 for greater detail on safely performing ocular ultrasound and examples of eye pathology.

Fractures and herniation may also be sonographically detected at triage, when either radiography is not readily available or the patient cannot be transported.

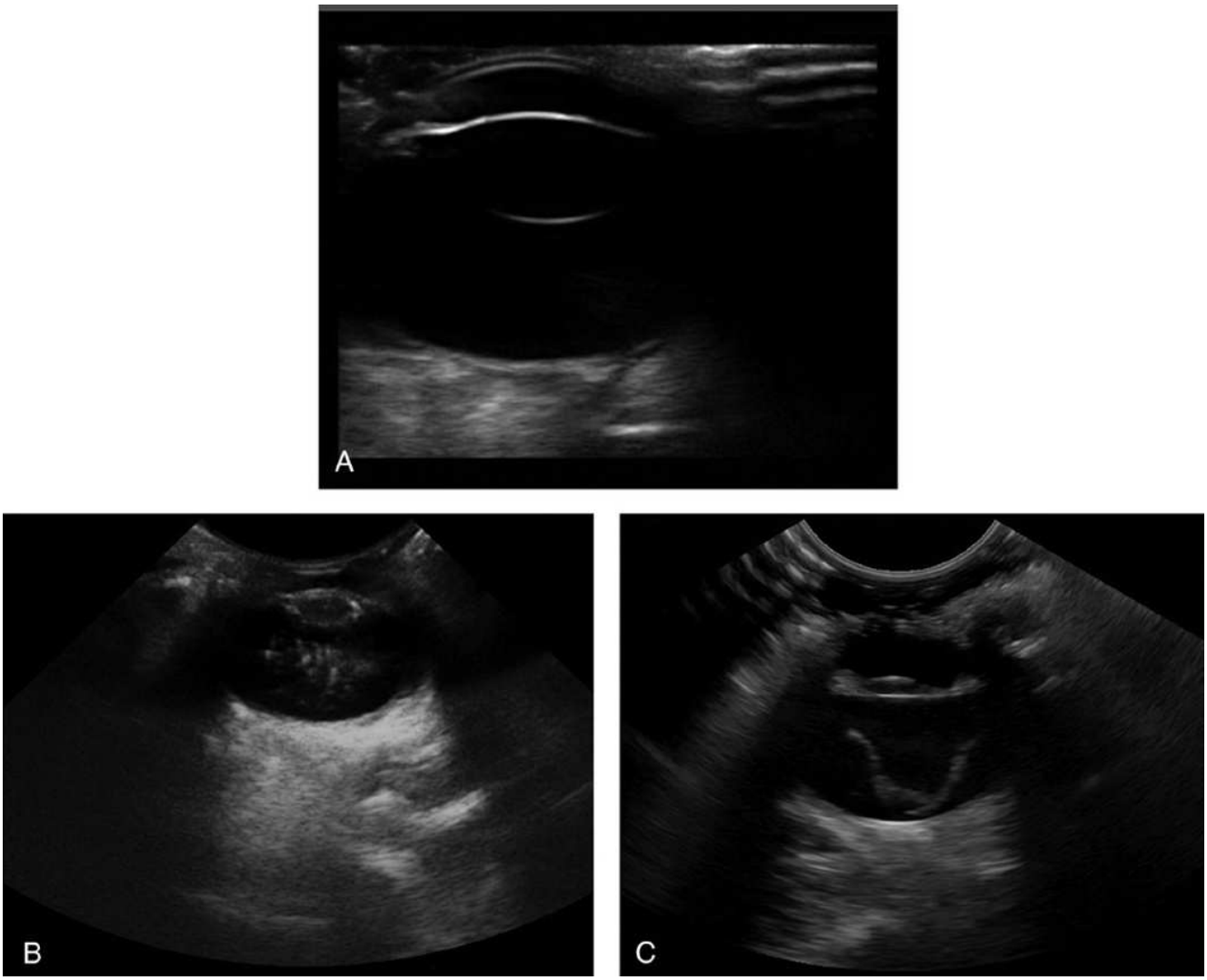


**Figure 38.13.** Normal eye and some lesions associated with ocular trauma. (A) Ultrasound image of the normal canine eye in horizontal probe orientation (see also Chapter 27). Note the hyperechoic (bright white curve) cornea in the near-field followed by the anechoic (pure black) anterior chamber, followed by hyperechoic (bright white lines) curved lines representing the anterior and posterior aspects of the lens followed by an anechoic (pure black) vitreous to the posterior wall. The eye requires nontoxic safe and approved ocular acoustic gels and the reader is referred to Chapter 27. (B) Vitreal hemorrhage recognized by the echogenic material within the posterior chamber, noting that artifacts and some benign conditions may appear similarly. (C) Retinal detachment as evidenced by a hyperechoic irregular line extending and reconnecting to and from the posterior eye wall (see also Chapter 27). Source: Image (A) reproduced with permission from Dr Gregory Lisciandro, Hill Country Veterinary Specialists and FASTVet.com, Spicewood, TX; images (B) and (C) courtesy of Dr Jane Cho, Veterinary Eye Specialists, Ardsley, New York.

Ultrasound has been shown to have good sensitivity and specificity for certain fracture types including skull, ribs, and long bones (see Chapter 35).

## *Exposure (E)*

Serial VetFAST-ABCDE exams increase the probability of initially detecting significant injury and pathology and over time provide a means to detect potentially life-threatening conditions and complications beyond traditional laboratory testing, radiographic imaging and physical examination. In stable veterinary patients, a serial exam should be performed four hours post admission as recommended with Global FAST, and as often as every 15–30 minutes in unstable and critical patients.

# Ultrasound-Guided and -Assisted Procedures

The reader is referred to Chapter 43 for abdominocentesis, thoracocentesis, and pericardiocentesis; Chapter 35 for arthrocentesis; Chapter 24 for placement of intravenous and intraarterial catheters; and Chapter 44 for other ultrasound-guided and ultrasound-assisted procedures.

# POCUS: VetFAST-ABCDE in Shock Syndrome, CPR, and ALS

The use of POCUS for detecting forms of shock (Table 38.2) and causes of CPR is becoming standard of care (Breitkreutz et al. 2007, 2010). The American Heart Association's (AHA) CPR guidelines include "Knowing your Hs and Ts," listing treatable causes of

**Table 38.2.**
Abnormal findings for categories of the VetFAST-ABCDE exam in different forms of shock.

| | Hypovolemic | Cardiogenic | Distributive | Obstructive | Hypoxic |
|---|---|---|---|---|---|
| Airway | Normal<br>Laryngeal or tracheal injuries (trauma) | Normal<br>Tracheal collapse | Normal | Normal | Normal<br>Laryngeal paralysis<br>Laryngeal masses<br>Tracheal masses |
| Breathing | Normal pleural line<br>Normal glide sign<br>Pleural effusion (trauma) | Normal pleural line<br>Normal glide sign<br>Pleural effusion (right-sided CHF)<br>↑ B-lines (left-sided CHF)<br>Infinite B-lines lung (left-sided CHF) | Normal pleural line<br>Irregular/thickened pleural line<br>Pleural effusion (sepsis)<br>↑ B-lines<br>Normal glide sign surrounded by areas with multiple B-lines (spared areas) (sepsis)<br>Small or large areas of lung consolidation with or without air bronchogram (sepsis) | Normal pleural line<br>Normal glide sign<br>Pleural effusion (caval syndrome) | Normal pleural line<br>Irregular/thickened pleural line<br>Pleural effusion (ARDS)<br>↑ B-lines<br>Normal glide sign surrounded by areas with multiple ULRs (spared areas) (ARDS)<br>Small or large areas of lung consolidation with or without air bronchogram (ARDS) |
| Circulation (thoracic) | ↓ LV volume | Normal LV volume<br>↓LV volume<br>↑ LA:Ao ratio (left-sided CHF or HCM – especially cats)<br>Systolic dysfunction<br>↑ All chambers volume (DCM)<br>↑ LV thickness (HCM – especially cats) | Normal LV volume<br>↓ LV volume<br>Systolic dysfunction | ↑ Right side heart chambers (caval syndrome)<br>↓LV volume<br>Pericardial effusion with cardiac tamponade | Normal LV volume<br>↓ LV volume<br>Normal LA:Ao ratio |
| Circulation (abdominal) | Flattened CVC<br>Abdominal effusion (trauma or hypoalbuminemia) | Normal CVC<br>Distended CVC (right-sided CHF)<br>Abdominal effusion (right-sided CHF) | Halo sign (canine anaphylaxis)<br>Flattened CVC<br>Abdominal effusion (sepsis) | Abdominal effusion (caval syndrome)<br>Distended CVC | Normal CVC<br>Flattened CVC |
| Disability (ONSD) | Normal<br>Increased (TBI) | Normal | Normal<br>Increased (sepsis) | Normal | Normal |

Ao, aorta; LV, left ventricle; CVC, caudal vena cava; CHF, congestive heart failure; HCM, hypertrophic cardiomyopathy; LA, left atrium; LA:Ao, left atrial to aortic ratio; ULRs, ultrasound lung rockets; ARDS, acute respiratory distress syndrome; ONSD, optic nerve sheath diameter; TBI, traumatic brain injury.

VetBooks.ir

CPA (Neumar et al. 2010). VetFAST-ABCDE addresses this rule-out list rapidly, including the Ts – Tension pneumothorax, Tamponade (cardiac), Thromboembolism and the veterinary additions of Toxin and Trauma, and the Hs of Hypotension, Hypocontractility, and Hypertension (see Chapter 36 and Table 38.2). These Hs and Ts are screened for using both VetFAST-ABCDE and Global FAST (see Chapter 36). Interestingly, these rapidly identifiable Hs and Ts as causes of CPA are not addressed in current veterinary CPR guidelines (Boller and Fletcher2012), and neither is the use of POCUS, Global FAST, and VetFAST-ABCDE, for not only for rapid diagnosis but likewise for patient monitoring. The use of POCUS exams such as VetFAST-ABCDE and Global FAST has tremendous potential to improve survival by detecting treatable conditions and better directing resources when minutes count. The POCUS strategy is becoming part of advanced trauma life support (ATLS) in human medicine in North America and Europe (Callaway et al. 2015; Soar et al. 2015). Although the utility of POCUS has not been standardized, it may be used as an adjunct to standard patient evaluation (Callaway et al. 2015; Soar et al. 2015). Additional detail is given in Chapters 36 and 37.

VetFAST-ABCDE has the added facets of evaluating ET placement, upper airway evaluation, and ocular evaluation including eye injury and increased ONSD. Abnormal findings in each part of the exam in different shock presentations are summarized in Table 38.2.

# Pearls and Pitfalls, The Final Say

The VetFAST-ABCDE is a more recent format that is similar to Global FAST with the most notable exceptions of upper airway, cardiac, ocular, and musculoskeletal evaluations. The VetFAST-ABCDE format may be used in trauma and nontrauma conditions to manage, diagnose, treat, and serially monitor to optimize veterinary critical care.

# References


Armenise A, Ricciardi M, Giannuzzi AP, et al. 2012. Ultrasonographic measure of the optic nerve sheath in canine patients with signs of raised intracranial pressure. A preliminary study. Abstract. *J Vet Emerg Crit Care* 22(S2):S20.

Armenise A, Boysen RS, Rudloff E, et al. 2019. Veterinary-focused assessment with sonography for trauma-airway, breathing, circulation, disability and exposure: a prospective observational study in 64 canine trauma patients. *J Small Anim Pract* 60(3):173–182.

Blackbourne LH, Soffer D, McKenney M, et al. 2004. Secondary ultrasound examination increases the sensitivity of the FAST exam in trauma, *J Trauma* 57(5):934–938.

Boller M, Fletcher DJ. 2012. RECOVER evidence and knowledge gap analysis on veterinary CPR. Part 1: Evidence analysis and consensus process: collaborative path toward small animal CPR guidelines. *J Vet Emerg Crit Care* 22(S1):S4–S12.

Breitkreutz R, Walcher F, Seeger FH, et al. 2007. Focused echocardiographic evaluation in resuscitation management (FEER): concept of an advanced life support-conformed algorithm. *Crit Care Med* 35(S5):1527–1533.

Breitkreutz R, Price S, Steiger HV, et al. 2010. Focused echocardiographic evaluation in life support and peri-resuscitation of emergency patients: a prospective trial. *Resuscitation* 81:1527–1533.

Callaway CW, Soar J, Aibiki M, et al. 2015. Part 4: Advanced Life Support. 2015 International Consensus on Cardiopulmonary Resuscitation and Emergency Cardiovascular Care Science with Treatment Recommendations. *Circulation* 132 (Suppl):S84–S145.

Chou HC, Chong KM, Sim SS, et al. 2013. Real-time tracheal ultrasonography for confirmation of endotracheal tube placement during cardiopulmonary resuscitation. *Resuscitation* 84:1708–1712.

Eom K, Moon K, Seong Y, et al. 2008. Ultrasonographic evaluation of tracheal collapse in dogs. *J Vet Sci* 9(4):401–405.

Geeraerts T, Launey Y, Martin L, et al. 2007. Ultrasonography of the optic nerve sheath may be useful for detecting raised intracranial pressure after severe brain injury. *Intensive Care Med* 33:1704–1711.

Ilie LA, Thomovsky EJ, Johnson PA, et al. 2015. Relationship between intracranial pressure as measured by an epidural intracranial pressure monitoring system and optic nerve sheath diameter in healthy dogs. *Am J Vet Res* 76:724–731.

Lisciandro GR. 2011. Abdominal and thoracic focused assessment with sonography for trauma, triage, and monitoring in small animals. *J Vet Emerg Crit Care* 21(2):104–122.

Lisciandro GR. 2012. Evaluation of initial and serial combination focused assessment with sonography for trauma (CFAST) examinations of the thorax (TFAST) and abdomen (AFAST) with the application of an abdominal fluid scoring system in 49 traumatized cats. *J Vet Emerg Crit Care* (S2): S11.

Lisciandro GR. 2016. The use of the diaphragmatico-hepatic (DH) views of the abdominal and thoracic focused assessment with sonography for triage (AFAST/TFAST) examinations for the detection of pericardial effusion in 24 dogs (2011–2012). *J Vet Emerg Crit Care* 26(1):125–131.

Lisciandro GR, Armenise AA. 2014. Focused or COAST[3] – Cardiopulmonary Resuscitation (CPR), Global

FAST (GFAST[3]), and the FAST-ABCDE Exam. In: *Focused Ultrasound for the Small Animal Practitioner*, edited by Lisciandro GR. Ames: Wiley Blackwell, pp 269–285.

Lisciandro GR, Lagutchik MS, Mann KA, et al. 2008. Evaluation of a thoracic focused assessment with sonography for trauma (TFAST) protocol to detect pneumothorax and concurrent thoracic injury in 145 traumatized dogs. *J Vet Emerg Crit Care* 18(3):258–269.

Lisciandro GR, Lagutchik MS, Mann KA, et al. 2009. Evaluation of an abdominal fluid scoring system determined using abdominal focused assessment with sonography for trauma in 101 dogs with motor vehicle trauma. *J Vet Emerg Crit Care* 19(5):426–437.

Machare-Delgado E, Decaro M, Marik PE. 2011. Inferior vena cava variation compared to pulse contour analysis as predictors of fluid responsiveness: a prospective cohort study. *J Intensive Care Med* 26(2):116–124.

Moretti R, Pizzi B. 2010. Inferior vena cava distensibility as a predictor of fluid responsiveness in patients with subarachnoid hemorrhage. *Neurocrit Care* 13(1):3–9.

Nelson NC, Drost WT, Lerche P, et al. 2010. Noninvasive estimation of central venous pressure in anesthetized dogs by measurement of hepatic venous blood flow velocity and abdominal venous diameter. *Vet Radiol Ultrasound* 51(3):313–323.

Neri L, Storti E, Lichtenstein D. 2007. Toward an ultrasound curriculum for critical care medicine. *Crit Care Med* 35(5 Suppl):S290–304.

Neumar RW, Otto CW, Link MS, et al. 2010. Part 8: Adult advanced cardiovascular life support: 2010 American Heart Association guidelines for cardiopulmonary resuscitation and emergency cardiovascular care. *Circulation* 122:S729–S767.

Ollerton JE, Sugrue M, Balogh Z, et al. 2006. Prospective study to evaluate the influence of FAST on trauma patient management. *J Trauma* 60:785–791.

Pfeiffer P, Bache S, Isbye L, et al. 2012. Verification of endotracheal intubation in obese patients – temporal comparison of ultrasound vs. auscultation and capnography. *Acta Anaesthesiol Scand* 56:571–576.

Ritchie JV, Horne ST, Perry J, et al. 2012. Ultrasound triage of ocular blast injury in the military emergency department. *Mil Med* 177(2):174–178.

Rudorf H, Barr FJ, Lane JG. 2001. The role of ultrasound in the assessment of laryngeal paralysis in the dog. *Vet Radiol Ultrasound* 42(4):338–343.

Smith JJ, Fletcher DJ, Cooley SD, et al. 2018. Transpalpebral ultrasonographic measurement of the optic nerve sheath diameter in healthy dogs. *J Vet Emerg Crit Care* 28(1):31–38.

Soar J, Nolan JP, Böttiger BW, et al. 2015. European Resuscitation Council Guidelines for Resuscitation 2015: Adult advanced life support. *Resuscitation* 95:100–147.

Volpicelli G, Elbarbary M, Blaivas M, et al. 2012. International evidence-based recommendations for point-of-care lung ultrasound. *Intens Care Med* 38(4):577–591.

Weaver B, Lyon M, Blaivas M. 2006. Confirmation of endotracheal tube placement after intubation using the ultrasound sliding lung sign. *Acad Emerg Med* 13:239–244.

Zechner PM, Breitkreutz R. 2011. Ultrasound instead of capnography for confirming endotracheal tube placement in emergency? *Resuscitation* 82(10):1259–1261.

SECTION VIII

# Felines and Exotic Species

CHAPTER THIRTY-NINE

# POCUS: Feline Differences – Abdomen and Thorax

Daniel Rodriguez and Gregory R. Lisciandro

## Introduction

The anatomy of the dog and cat has important differences, requiring a thorough understanding for accurate sonographic image interpretation and clinical integration. With the widespread use of point-of-care ultrasound (POCUS) by nonradiologists and noncardiologists brought on through the development of standardized FAST ultrasound exams, screening evaluations of the abdomen (AFAST), thorax (TFAST), heart (TFAST), and lung (Vet BLUE) have become commonplace – the Global FAST approach (Lisciandro et al. 2008, 2009, 2015, 2017; Lisciandro 2011, 2012, 2014a–d, 2016; Boysen and Lisciandro 2013; Ward et al. 2017, 2018a,b). This chapter will describe the pertinent sonographic abdominal, thoracic, pulmonary, and cardiac differences between felines and canines.

### *What POCUS: Feline Differences – Abdomen and Thorax Can Do*

- Clarify major abdominal differences between felines and canines.
- Clarify major thoracic differences between felines and canines.
- Clarify Global FAST differences – AFAST and its fluid scoring system, TFAST, and Vet BLUE.

### *What POCUS: Feline Differences – Abdomen and Thorax Cannot Do*

- Account for individual variations in the abdomen.
- Account for individual variations in the thorax.
- Replace a complete detailed diagnostic abdominal ultrasound.
- Replace complete detailed diagnostic echocardiography.
- Replace consultation with a radiologist.
- Replace clinical judgment.

### *Indications*

Sonographers should know these important feline differences if they are performing POCUS examinations and Global FAST in cats.

### *Objectives*

Know the major abdominal and thoracic sonographic differences between felines and canines.

The feline abdomen and feline thorax sections will contrast differences between cats and dogs that are most clinically relevant for POCUS, AFAST, TFAST, and Vet BLUE examinations. This chapter is meant to supplement the respective POCUS and FAST ultrasound chapters.

*Point-of-Care Ultrasound Techniques for the Small Animal Practitioner*, Second Edition. Edited by Gregory R. Lisciandro.
© 2021 John Wiley & Sons, Inc. Published 2021 by John Wiley & Sons, Inc.
Companion website: www.wiley.com/go/lisciandro/ultrasound2

# Feline Abdomen

Complete detailed abdominal ultrasound and many of the POCUS abdominal examinations are performed in dorsal recumbency. In contrast, the AFAST is performed in either lateral recumbency or in standing or sternal, and *not* in dorsal recumbency. The sonographer should always consider differences in positioning and the associated scanning planes for best interpreting what is imaged within each respective acoustic window. For example, the thigh is rarely ever in view when imaging the urinary bladder with a patient in dorsal recumbency; however, during AFAST at its cysto-colic (CC) view, the thigh is almost always in view through the far-field in either lateral recumbency when imaging the urinary bladder.

## *AFAST in Cats*

Briefly, image acquisition of the five acoustic windows of AFAST is the same regardless of patient positioning. The AFAST order and its image acquisition using its target organ approach are independent of positioning and performed in the same order at every examination to avoid satisfaction of search error and incomplete examinations (Figure 39.1). The target organs are fanned through in both directions in longitudinal planes and then the probe is rocked cranially before being returned to your starting point for one final look. Sites are mostly named by the target organs you will image at each AFAST view rather than external sites, with the exception of the hepato-renal (HR) and spleno-renal (SR) umbilical views (Lisciandro et al. 2009, 2015; Lisciandro 2011, 2012, 2014a; Boysen and Lisciandro 2013; McMurray et al. 2016). The AFAST probe maneuver mantra of "fan, rock cranially, and return to your starting point" is applied to all five AFAST acoustic windows (see Chapters 6 and 7 for more detail) (Lisciandro 2011, 2012, 2014a; Lisciandro et al. 2015). Transverse orientation may be used but can be initially confusing to many nonradiologist veterinarians and should be considered an "add-on" skill to be developed once the initial AFAST format is mastered.

### Liver and Gallbladder

#### *Hepatic Echogenicity*

The normal canine and feline liver echotexture is described as coarse. The structures that can be recognized

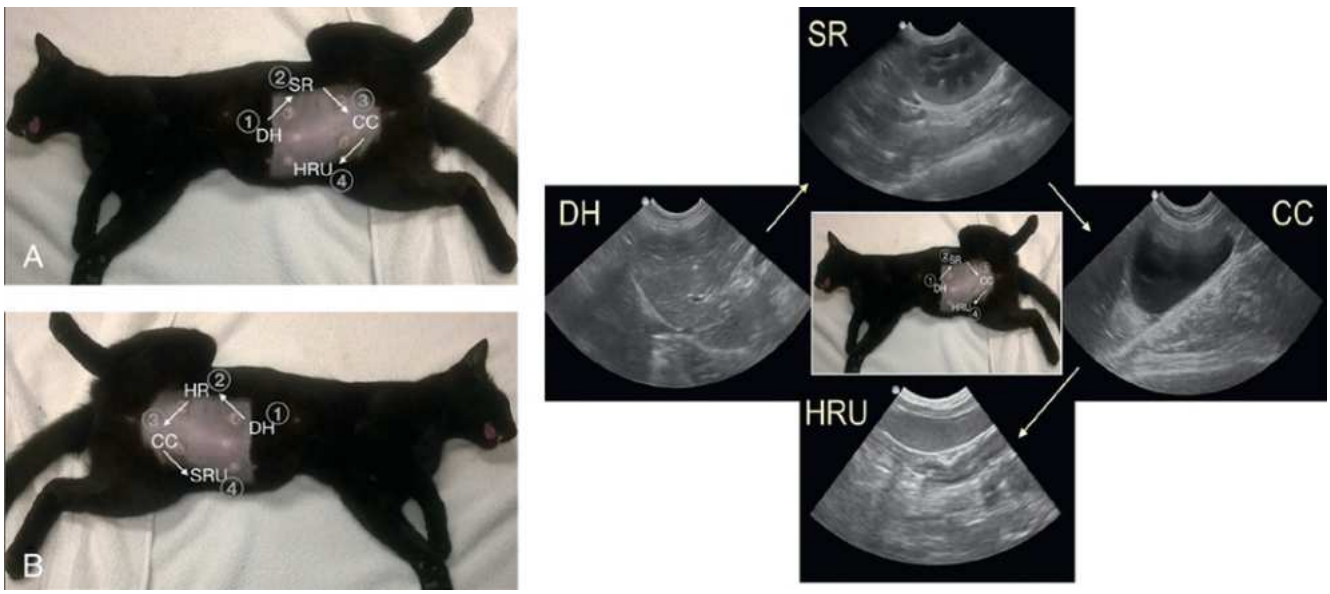


**Figure 39.1.** AFAST views and order in right and left lateral recumbency. The AFAST shown in (A) is a cat in right recumbency. The order is always the same – DH view to SR view to CC view to HRU view completing the examination at the most gravity-dependent region where abdominocentesis is likely performed. (B) AFAST is performed analogously on a cat in left lateral recumbency. The order is always the same – DH to HR to CC to the respective umbilical view completing the examination at the most gravity-dependent region where abdominocentesis is likely performed. To the right is a composite of the AFAST and its classic starting point images at each of the AFAST views. These starting points are independent of positioning and look nearly identical between lateral recumbency and standing and sternal (not shown). The cat was sedated for intubation for an ovariohysterectomy procedure. Source: Reproduced with permission from Dr Gregory Lisciandro, Hill Country Veterinary Specialists and FASTVet.com, Spicewood, TX. Illustration by Hannah M. Cole, Adkins, TX.

within the liver parenchyma in both dogs and cats are the hepatic veins and the intrahepatic portal vasculature, the gallbladder and its associated biliary system, and the porta hilus. The nearby falciform fat in cats may be robust and a confounder during hepatic imaging. The falciform fat is described in more detail below.

The determination of normal versus abnormal liver echogenicity differs between dogs and cats. In dogs, hepatic echogenicity is determined by comparing the echogenicity of liver next to spleen; however, in cats comparisons are made between the liver and adjacent falciform fat. The canine liver is hypoechoic to the spleen (darker) and the feline liver is hyperechoic (brighter) to isoechoic (same) to the falciform fat (d'Anjou 2008b; Nyland et al. 2015c). In order to accurately compare echogenicity in different windows (dual comparison), the parameters of gain, depth, and transducer frequency must be equal so that the comparison of echogenicity is objective. Using echogenicity alone to determine if pathology is present is unreliable since the echogenicity of an organ is dependent on factors intrinsic and extrinsic to its composition, such as angle of insonation, and hence anisotropy, acoustic impedance, position of the focal point, and transducer technology, such as compound or harmonic imaging. The echogenicity of images without harmonics tends to be slightly more echogenic and with a coarser echotexture (Figure 39.2).

### *Differences in Falciform Fat*

The differentiation of falciform fat from liver parenchyma can be difficult if the appropriate depth is not adjusted. The heterogeneous appearance of fat with multiple small hyperechoic (white) lines can be similar to that of the portal veins seen in the normal liver parenchyma. This seems to be a major concern in cats where the falciform fat pad can be robust even in thin body conditions. The echogenicity of falciform fat is usually hypoechoic (darker) to the liver and is some instances isoechoic (same as) to liver (see Figure 39.2).

### *Differences in Hepatic Venous System*

The hepatic veins in both dogs and cats are anechoic (black) tubular structures that drain into the caudal vena cava (CVC) near the middorsal portion of the diaphragm. The hepatic veins have anechoic inconspicuous walls unless the ultrasound beam is perpendicular to the vein (angle of insonation being 90°) where faint hyperechoic (white), thin walls are noted due to its particular specular properties. The portal veins, on the other hand, will depict hyperechoic (white) walls regardless of the angle of insonation and may look like equal signs (=) (see also Figure 8.10A). This appearance is due to the fatty content of the portal triad and also to the echogenicity generated by the bile duct and the hepatic artery (d'Anjou 2008b; Nyland et al. 2015c).

If there is a question over whether or not the vessel of interest is a portal or hepatic vein, the use of color flow Doppler will make this difference clear. The hepatic veins will be depicted in blue with flow away from the transducer (probe) and towards the CVC, and the portal veins depicted in red with flow towards the transducer (probe), away from the porta hepatis, and towards the periphery of the liver parenchyma (Figure 39.3).

### *Differences in Gallbladder Shape and Lumen*

The shape of the feline gallbladder is more variable than in canines. A bilobed gallbladder is a common normal variant found in cats that is possible but uncommon in dogs (see also Figure 8.4). The orientation of the long axis of the gallbladder also varies in the cat where it is uniquely parallel to the ribs and perpendicular to the sternum or obliquely angled with respect to the sternum (Carlisle 1977).

In cats, there are two common and one uncommon presentations of a bilobed gallbladder. The most common feline variant has a longitudinal septum dividing the fundus of the gallbladder into two fundices internally, each fusing to form a single cystic duct. This variant often is not appreciated grossly during laparotomy and generally only detected sonographically. The second common feline bilobed variant occurs when there are actually two different lumens, each forming a fundus, but fused at the neck of the gallbladder. The third variant and the rarest is the presence of a duplex gallbladder with two independent cystic ducts (Moentk and Biller 1993).

### *Differences in Gallbladder Common Bile Duct*

In cats with a full gallbladder, the bile duct may be looped or tortuous as it approaches the porta hepatis, which may be falsely interpreted as extrabiliary obstruction or a cystic mass. The rule of thumb when interpreting the degree of distension of a tortuous common bile duct is that a bile duct diameter of >5 mm supports extrabiliary tract obstruction and a diameter of <4 mm would be considered within normal limits (Figure 39.4) (d'Anjou 2008b).

### *Differences in Gallbladder Sludge*

Historically, the presence of a small amount of echogenic sludge has been considered a normal finding in

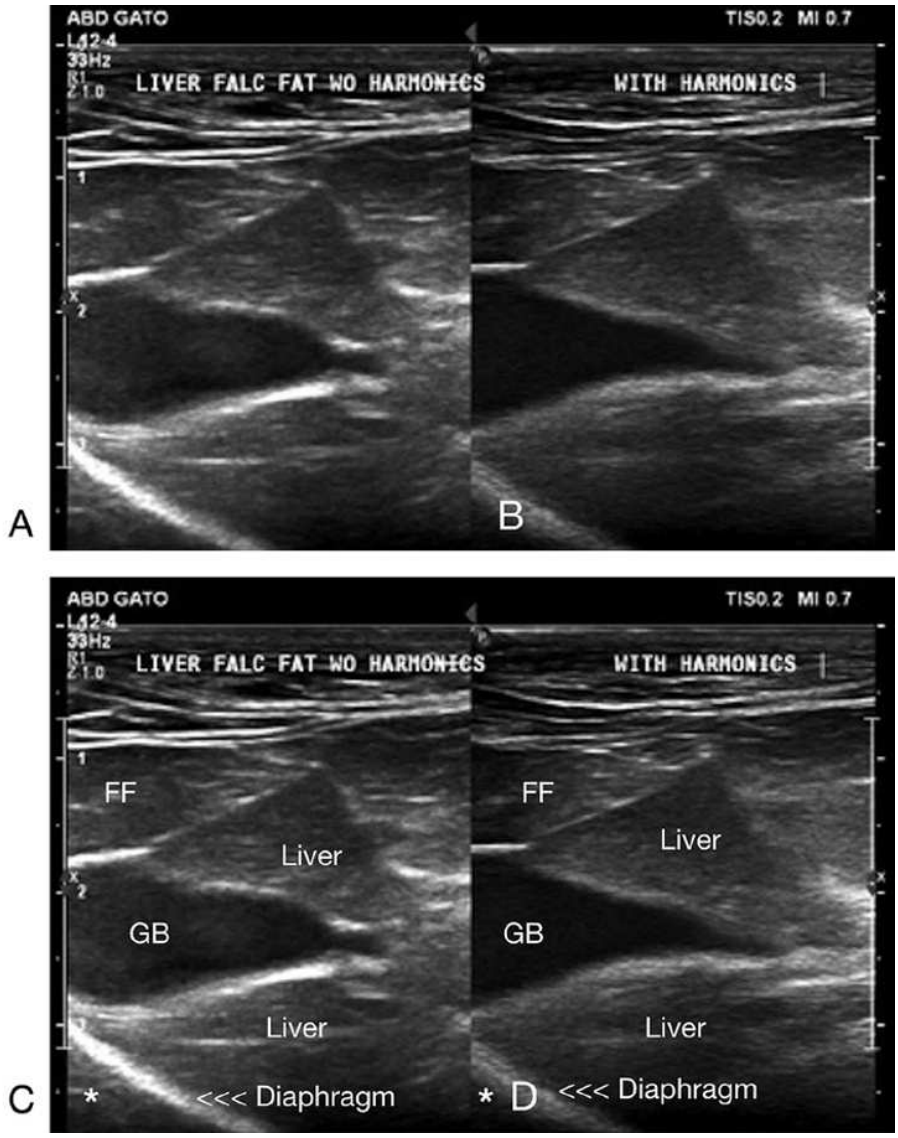


**Figure 39.2.** Comparison of feline liver to adjacent falciform fat. The images show in a longitudinal plane the liver and gallbladder with (A) and without (B) tissue harmonic imaging (THI). When comparing the echogenicity of the superficial falciform fat to that of the liver, note the differences sonographically. There is a mild difference in echogenicity in the B-mode still images between (A) with THI, having a slightly more echogenic liver parenchyma, and (B) without THI. (C,D) The same images are duplicated but labeled. GB, gallbladder; FF, falciform fat; (*), pleural cavity. Source: Reproduced with permission from Dr Daniel Rodriguez, DVM, DACVR, Mexico City, Mexico.

dogs. Recently, the "normal" amount of canine gallbladder sludge has been suggested to be at least partly false based on the difference in ejection fraction between dogs with anechoic bile and those having sludge, and those having sludge with a hyperechoic appearance along with distal acoustic shadowing and those with a mucocele. This recent finding suggests that the presence of sludge in the canine gallbladder may cause a certain degree of biliary stasis and possibly be indicative of early biliary disease. Rather than qualifying the finding as "normal," the presence of biliary sludge likely warrants close monitoring and assessment of hepatobiliary function, such as repeating the ultrasound exam in 3–4 weeks and then periodically thereafter (Tsukagoshi et al. 2012).

Feline bile should be homogeneously anechoic (black). The presence of even a small amount of echogenic sludge is always considered abnormal in cats. Recently, a clinical study suggested a relationship between elevated liver enzymes and the presence of

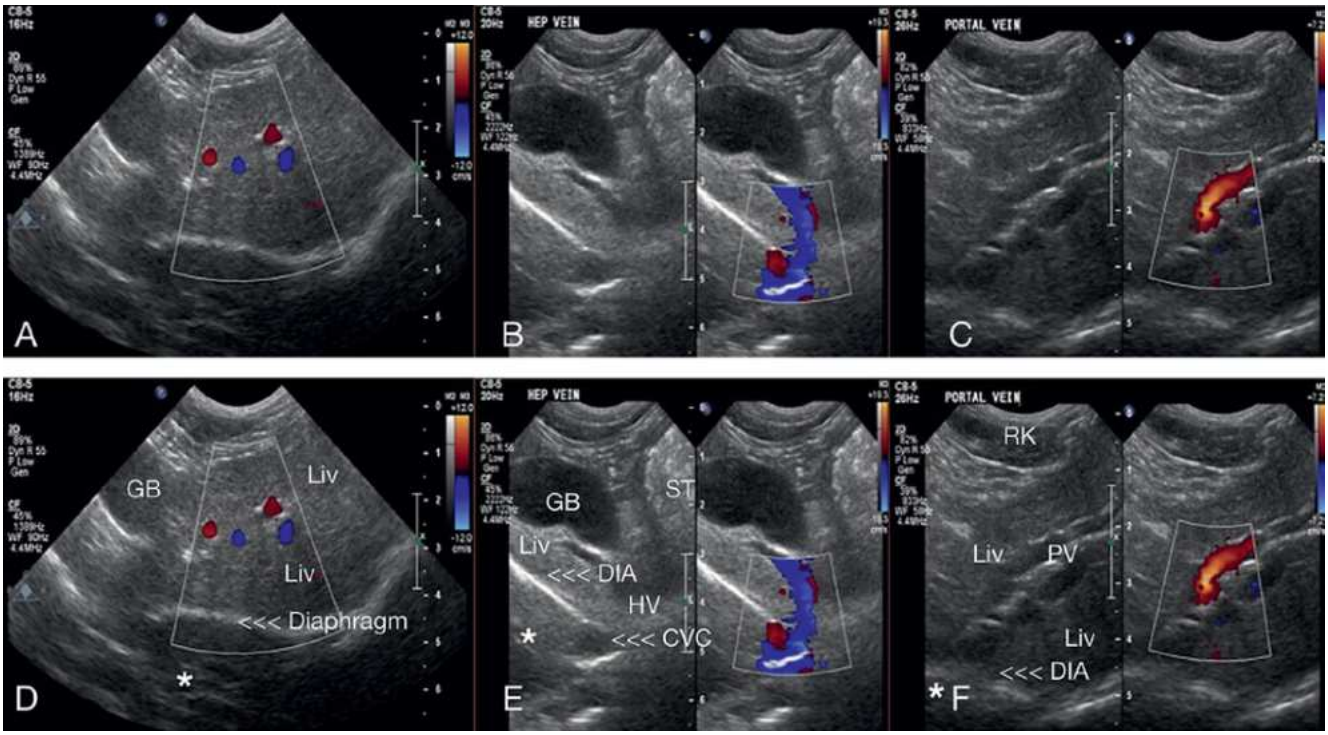


**Figure 39.3.** Differentiating hepatic from portal veins using color flow Doppler. In image (A) shown in the transverse plane of the liver near its hilus are the portal veins in red (blood traveling towards the liver and toward the probe) and the hepatic veins in blue (blood flow away from the probe, towards the CVC near the diaphragm). In (B) the image is labeled "HEP VEIN" and shows comparative images with and without color flow Doppler identifying the hepatic venous system draining into the CVC as the CVC traverses the diaphragm in a longitudinal plane as at the AFAST DH view. In (C) the image is labeled "PORTAL VEIN" and shows comparative images with and without color flow Doppler indicating the portal venous system with flow in red from the right side at the porta hepatis. Note the right kidney in the near-field. (D–F) The same images as (A–) but labeled. Liv, liver; DIA, diaphragm; HV, hepatic veins; PV, portal veins; CVC, caudal vena cava; (*), pleural cavity; GB, gallbladder; RK, right kidney; ST, stomach. Source: Reproduced with permission from Dr Daniel Rodriguez, DVM, DACVR, Mexico City, Mexico.

biliary sludge in cats when compared to feline cohorts with anechoic bile.

In summary, the presence of biliary sludge in both dogs and cats should be correlated with laboratory results and clinical signs and should be monitored through recheck ultrasound evaluation(s) (Harran et al. 2011).

## FAST Diaphragmatico-Hepatic (DH) View

### *Differences in Heart and Gallbladder next to the Diaphragm*

In dogs, the canine heart will routinely image in the long axis along the diaphragmatic interface, the gallbladder along the diaphragm's caudal surface, and the beating heart along the cranial diaphragmatic surface, referred to as the "cardiac bump" (see Chapters 6, 7, 17, 18, and Figures 6.11 and 17.27). The cardiac orientation consistently has the left ventricle (LV) and the left atrium (LA) immediately against or in close proximity to the diaphragm that is sonographically viewable in many dogs (see Figure 6.11).

In cats, however, cardiac imaging along the diaphragm is much less reliable because of more interposing aerated lung. Thus, a very faint ultrasonographic impression of the feline beating heart may or may not be present. One of the reasons for this inconsistency may be appreciated radiographically with the increased space of aerated lung in between the normal heart and the diaphragm that is more dramatic in cats than dogs (Figure 39.5). In contrast to dogs, the feline gallbladder variably lies against the caudal aspect of the diaphragm because anatomically the feline gallbladder lies further caudally and further to the right of midline.

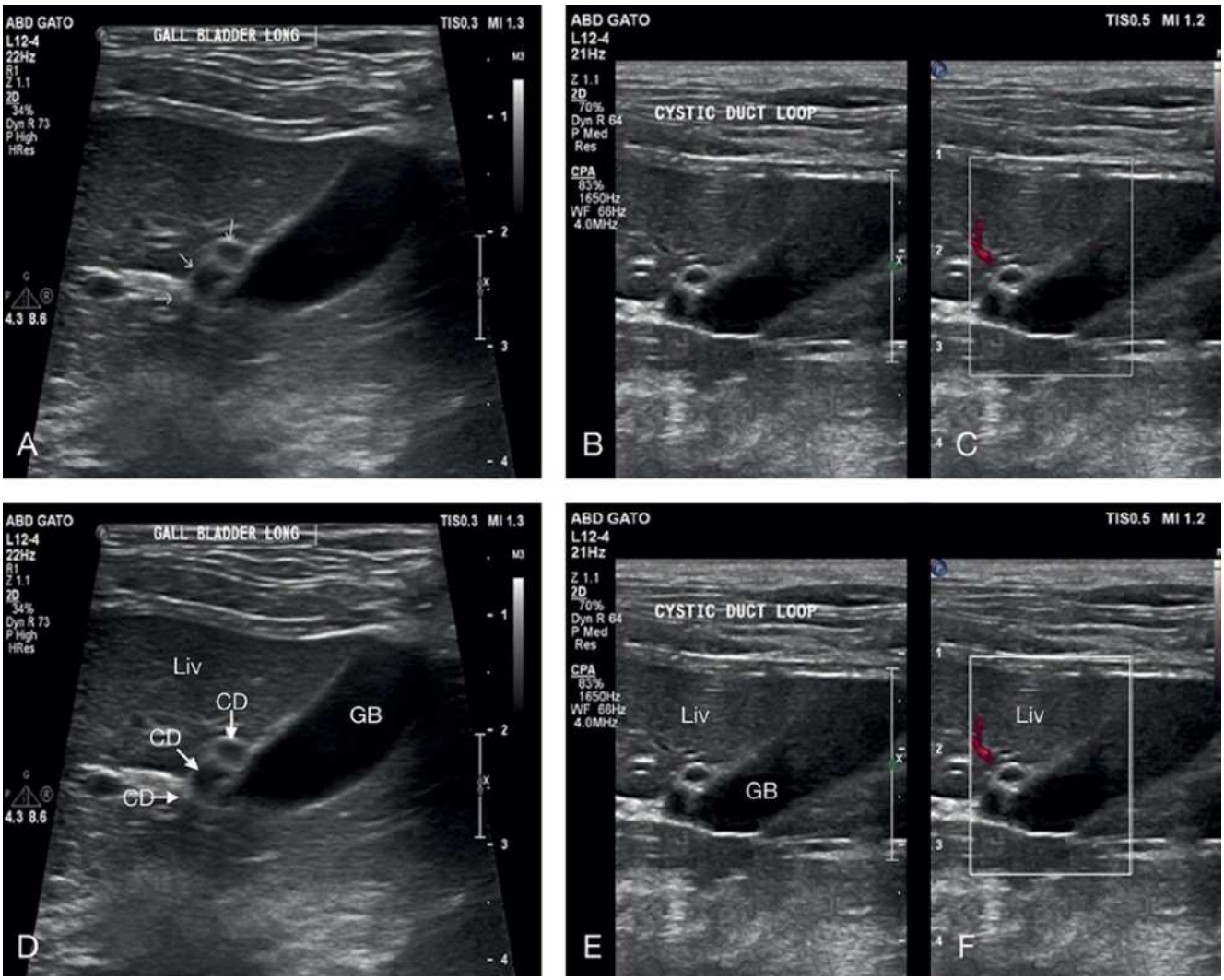


**Figure 39.4.** The tortuous or looped bile duct of cats. The bile duct in the cat may have a tortuosity in normalcy as shown in (A) with an undulating appearance (arrows) creating loops near the porta hepatis in a transverse plane. These bile duct (cystic duct, CD) loops may mimic the presence of multiple small, dilated, intrahepatic ducts, and be mistaken for pathology. The small fluid-filled looped structures adjacent to the gallbladder near the porta hepatis represent a normal bile duct as it curves (tortuosity) in this region (*arrows*). In the paired images to the right (B,C) using the split screen feature, color flow Doppler is used to differentiate fluid-filled cystic ducts *without* pulsatile flow from the regional vasculature, which would show pulsatile flow. The boxed area is the color Doppler gate. In (D–F) the same images are labeled. Liv, liver; GB, gallbladder, CD, cystic ducts. Source: Reproduced with permission from Dr Daniel Rodriguez, DVM, DACVR, Mexico City, Mexico.

### *Differences in the Caudal Vena Cava*

Although limited information is available regarding caudal vena cava (CVC) size and hepatic venous distension at the level of the diaphragm, author experience over 10 years of assessing for CVC and hepatic venous distension has proven the CVC to be reliable for right-sided congestive heart failure (CHF) and right-sided volume overload during hospitalized care, as supported in the human literature (Ferrada 2012a,b). In felines receiving fluid therapy, the finding of developing CVC and hepatic venous distension warrants discontinuing fluid therapy (or if hypotensive, changing the strategy to vasopressors). The terms fluid-responsive CVC (bounce), fluid-intolerant CVC (FAT), and hypovolemic CVC (flat) are used by the authors (Table 39.1) (Ferrada 2012a,b). See also Table 7.6 for CVC measurements.

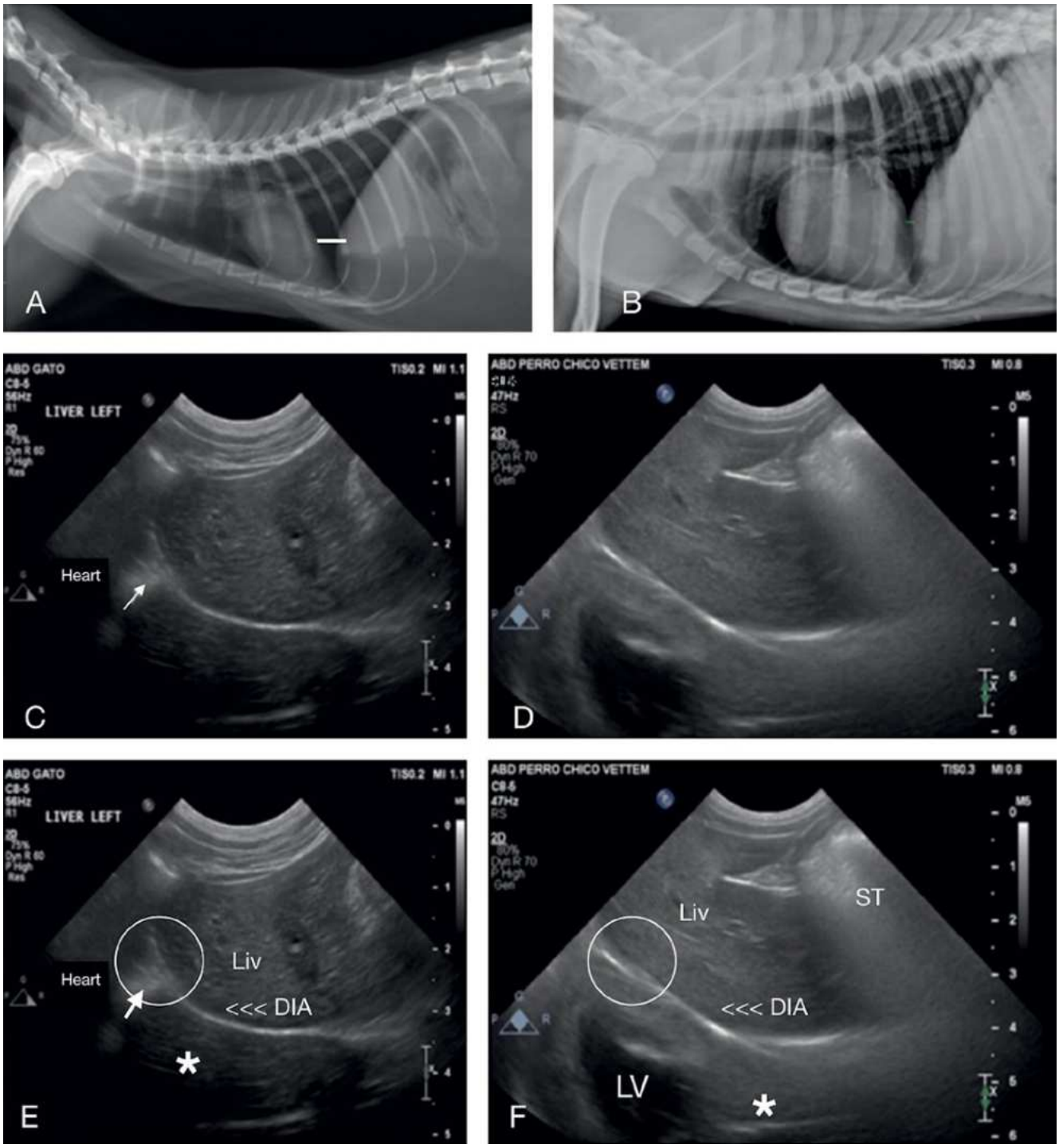


**Figure 39.5.** Differences in relative location of heart to diaphragm at the FAST DH view. (A) A right lateral radiograph of a cat's thorax showing the aerated space between the heart and diaphragm (see the bar overlay between heart and diaphragmatic surface). In contrast, (B) is a right lateral view of a dog's thorax showing the left ventricle against the diaphragm. Beneath each radiograph is the corresponding B-mode image at the feline and canine FAST DH views in longitudinal orientation. (C) Longitudinal B-mode image of the liver and the faintly seen beating heart in a healthy cat. (D) Longitudinal B-mode image that clearly shows the canine heart and its left ventricle against the diaphragmatic surface. (E,F) The same images labeled. The circle and arrow overlay show where to expect the heart beating against the diaphragm, referred to as the "cardiac bump" (see also Figure 6.11). Liv, liver; LV, left ventricle; DIA, diaphragm; (*), pleural cavity with mirror image artifact. Source: Reproduced with permission from Dr Daniel Rodriguez, DVM, DACVR, Mexico City, Mexico.

**Table 39.1.**
Characterization of the caudal vena cava and hepatic veins.

| Caudal vena cava (CVC) characterization at the FAST DH view | | | Clinical implications |
|---|---|---|---|
| Bounce – range of normovolemia | Fluid-responsive CVC | Change in CVC height ~35–50% with respiration; maximum height should be between 0.45 and 0.70 cm; combine the dynamic characterization (bounce, FAT, or flat) with maximum CVC DH view height (see Table 7.6), TFAST echo views and Vet BLUE lung for best integrative volume assessment | Safe to fluid challenge if the attending clinician feels the patient needs volume and lungs are dry on Vet BLUE |
| FAT – hypervolemia | Fluid-intolerant CVC | Minimal change in CVC height of <10% and the CVC is enlarged often with distended hepatic veins (tree trunk sign); [a]CVC maximum height when >1.0 cm is considered FAT (see Table 7.6); combine the dynamic characterization (bounce, FAT, or flat) with maximum DH view height and TFAST echo views and Vet BLUE lung for best integrative volume assessment | The central venous pressure (CVP) is severely elevated and the right heart is volume overloaded; discontinue fluids and consider vasopressors if hypotensive; if normotensive reduce or stop intravenous fluid therapy; investigate the heart for pericardial effusion, enlarged right ventricle, and evidence of right-sided congestive failure including ascites and pleural effusion |
| Flat – hypovolemia | [b]Hypovolemic CVC | Minimal change in CVC height of <10% and the CVC is small; [a]CVC maximum DH view height when <0.25 cm is considered flat (see Table 7.6); combine the dynamic characterization (bounce, FAT, or flat) with maximum DH view height and TFAST echo views and Vet BLUE lung for best integrative volume assessment | The patient is severely volume depleted until proven otherwise; consider where the fluid loss is and evaluate with Global FAST for effusions in the peritoneal cavity, retroperitoneal space, pleural cavity and pericardial sac (plus lung edema using Vet BLUE) |

[a]The CVC measurements were extrapolated from small dog measurements by the author (GL) giving a starting point for feline CVC assessment (see Table 7.6) (Darnis et al. 2018).
[b]Use Global FAST for searching for possible internal volume loss and combine CVC information with TFAST echo views and the patient's Vet BLUE lung findings for best integrative patient assessment.
Source: Reproduced with permission from Dr Gregory Lisciandro, Hill Country Veterinary Specialists and FASTVet.com, Spicewood, TX.

### *Differences in Gallbladder Wall Edema – Halo Sign*

Gallbladder wall edema in cats is not a marker for anaphylaxis, as in dogs, because shock organs are different (Quantz et al. 2009; Lisciandro 2014a, 2016b). In canines, the shock organ, where the highest concentration of mast cells reside, is the liver and gastrointestinal tract whereas in cats (and humans) the shock organ is the lung. However, gallbladder wall edema in cats does serve as a marker for right-sided CHF, right-sided volume overload, and the presence of pericardial effusion, similar to that of dogs, although sensitivity and specificity are unknown (Lisciandro 2014a,b, 2019) (Figure 39.6). Thus, when gallbladder wall edema is detected in cats, pericardial effusion and right-sided CHF (primary or secondary to volume overload) should be ruled out using TFAST and then other causes considered (see Table 7.5).

Combining gallbladder wall edema with CVC and hepatic venous characterization integrates clinical information to more accurately interpret the cause for the finding of gallbladder wall edema. In other words, a cat with gallbladder wall edema and a FAT CVC along with hepatic venous distension has convincing evidence without an echo view that pericardial effusion or right-sided failure likely is occurring. By knowing this information, adjustments may be made to better treat and stabilize for gold standard testing (complete echocardiography) when the cat is more stable or when a more detailed ultrasound study is

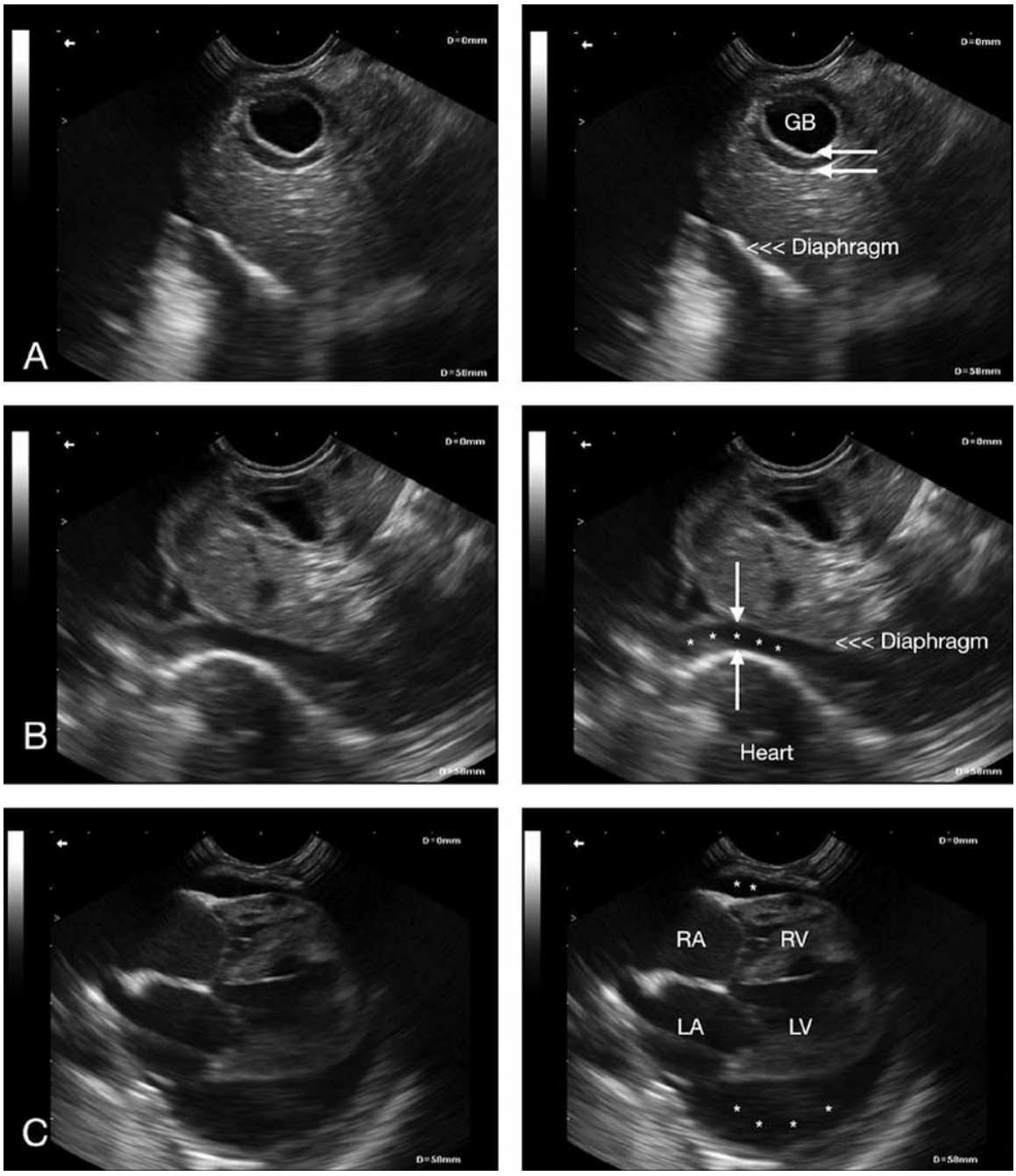


**Figure 39.6.** Gallbladder wall edema due to congestive heart failure – "cardiac gallbladder." (A) Gallbladder wall edema or "cardiac gallbladder" in a cat at the FAST DH view. To the right is the same image labeled. The gallbladder is labeled "GB" and the inner lumen and outer lumen marked with arrows. The anechoic striation in between is the intramural edema. (B) Looking cranial to the diaphragm at the FAST DH view is pericardial effusion recognized by the "racetrack sign." To the right is the same image labeled. The arrows mark the parietal and visceral pericardium and the pericardial effusion is outlined with asterisks (*) along the classic "racetrack sign." (C) Pericardial effusion is evident on the long-axis four-chamber view at the right TFAST PCS view. Note there is also biatrial enlargement. To the right is the same image labeled. RV, right ventricle, LV, left ventricle, RA, right atrium, LA, left atrium. Source: Image courtesy of Dr Chris Johnson, Tulsa, OK.

indicated. On the other hand, in cats with cardiac disease, it is important to consider that the sonographically detected gallbladder wall edema is likely related to right-sided heart failure, and may not be a comorbidity of cholecystitis or other causes (see Table 7.5).

## Spleen

### *Differences in Splenic Vessels, Echogenicity, Size, and Location*

The canine spleen is divided into two main regions: the dorsal extremity (head) and the ventral extremity (body and tail). The dorsal extremity is most often located along the 11th to 12th dorsal intercostal spaces and will move to some extent according to the size of the stomach. The body of the canine spleen will generally be close enough to the left kidney that it is often readily seen at the AFAST SR view using its dorsolateral acoustic window caudal to the last rib where the costal arch meets the hypaxial muscles. The ventral extremity is seen along the left to midventral abdominal wall and in the presence of splenomegaly, seen cranial to a full urinary bladder. The canine spleen is more echogenic (brighter) than the liver parenchyma, but this is not true in cats, where the splenic and hepatic echogenicity are equal (isoechoic) (Figure 39.7). Finally, the splenic veins may be surrounded by fat in the dog whereas this occurs uncommonly in the cat (Nyland and Mattoon 2015c).

In the cat, the spleen is consistently much smaller than the dog and its maximal width should be less than 1 cm (<10 mm) (Reese et al. 2013). The major reason for its smaller size and thickness is that the

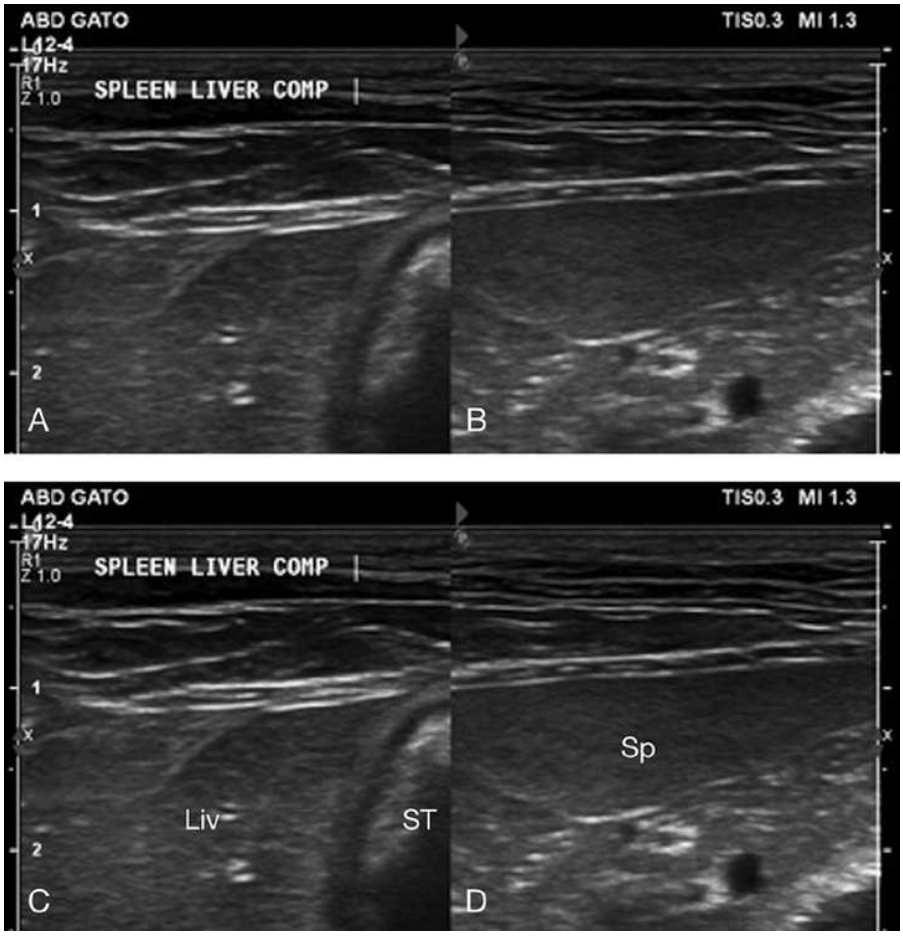


**Figure 39.7.** Echogenicity of the feline spleen compared to the liver. In the cat, the spleen is as echogenic (isoechoic) as the liver. The image in (A) shows the liver parenchyma in a dual comparison with the spleen shown in (B). Note echogenicity is nearly the same (isoechoic). (C,D) The the same images but labeled. Liv, liver; ST, stomach; Sp, spleen. Source: Reproduced with permission from Dr Daniel Rodriguez, DVM, DACVR, Mexico City, Mexico.

feline spleen is not an important reservoir of blood as in the dog. The position of the spleen in very large and obese cats is more dorsal and commonly missed by novice sonographers at the AFAST SR view. The normal feline spleen has an echogenic and homogeneous appearance nearly equal to that of the liver, markedly different from the canine spleen which is hyperechoic (brighter) to the canine liver. Also, the spleen does not commonly abut the left kidney as in the dog. The splenic veins are not as conspicuous in cats, especially when using curvilinear (microconvex) transducers at medium frequencies. The conspicuity of splenic vessels at the splenic hilus has improved with the linear transducer using newer technology such as cross-beam B-mode images, where multiple scan lines are sent from multiple directions instead of the traditional B-mode where the scan lines follow a consecutive and sequential order (Figure 39.8).

Even though splenomegaly can be nonspecific for both dogs and cats in differentiating malignant from benign disease, anecdotally and based on the authors' experience, feline splenomegaly is more commonly associated with malignancies and infectious causes rather than extramedullary hematopoiesis (EMH) or hyperplasia. EMH causes none to mild enlargement, although statistically based studies are needed to confirm this information.

It is important to mention that with new transducer technology, splenic echotexture becomes slightly more heterogeneous in both dogs and cats since newer high-frequency transducers are more likely to depict small centers of hyperplasia (Figure 39.9). As a result, there is a learning curve for proper splenic interpretation. Lastly, although splenic abnormalities in both dogs and cats have been described, it is important to know that serious splenic disease may be present in sonographically

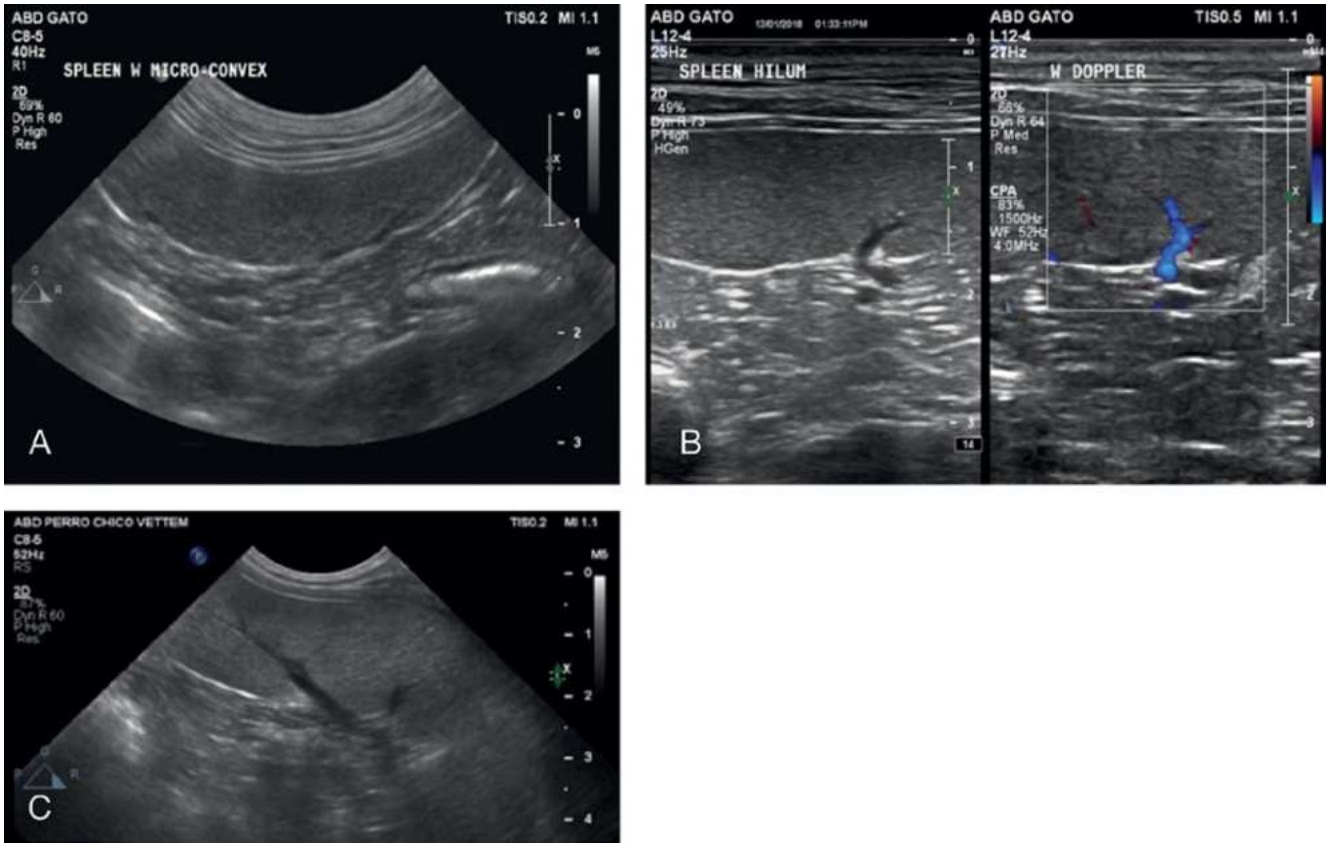


**Figure 39.8.** Differences in the splenic hilum. (A) The splenic hilum of the cat (image labeled "ABD GATO"). Note that the feline splenic hilum is not as distinct as the splenic hilum of the dog (image labeled "ABD PERRO") shown in (C). Both (A) and (C) were imaged with a curvilinear (microconvex) probe. The splenic vessels can be followed much deeper into the parenchyma of the dog than the cat as shown in comparing (A) to (C). (B) Comparative images using a linear probe with and without color flow Doppler to show the feline splenic hilum and its vessels more readily than with B-mode alone. Note the improved quality of detail with the linear transducer. Source: Reproduced with permission from Dr Daniel Rodriguez, DVM, DACVR, Mexico City, Mexico.

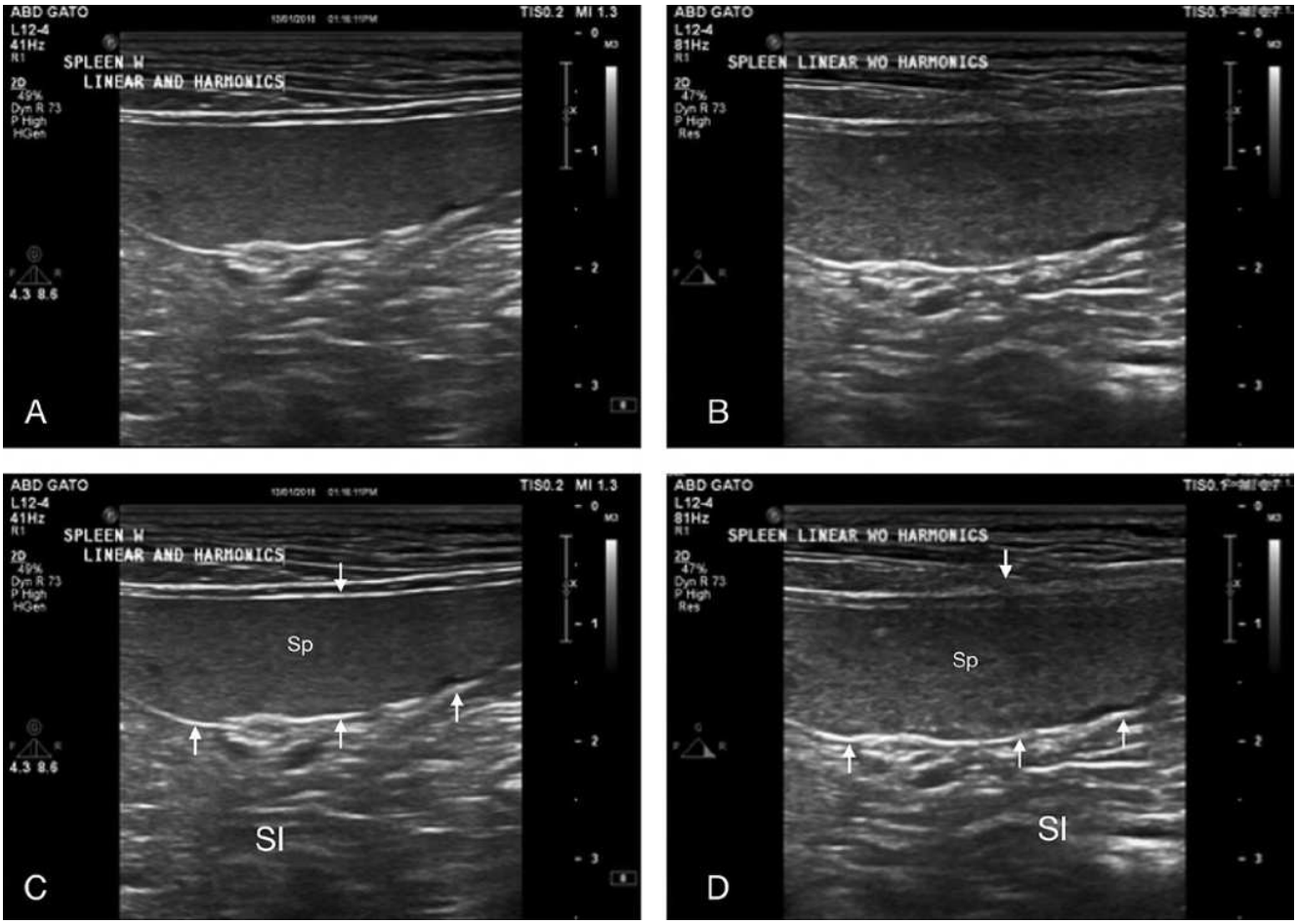


**Figure 39.9.** Differences in echogenicity with and without tissue harmonics. The effect of tissue harmonic imaging (THI) on the echotexture of the spleen can be seen by comparing B-mode images in (A) and (B). Note in image (A) with THI, the splenic (Sp) parenchyma has a more homogeneous and smooth echotexture in contrast to the image in (B) without THI, which shows a more heterogeneous echotexture mimicking pathology. The sonographer should become familiar with the THI feature and use it to their advantage when available on their machine. In (C) and (D) the same images are labeled and illustrate the hyperechoic splenic capsule, one of its identifying sonographic features (*arrows*). Normal splenic thickness should be <10Imm. Small intestine (SI) is throughout the far-field. Source: Reproduced with permission from Dr Daniel Rodriguez, DVM, DACVR, Mexico City, Mexico.

normal spleens of both dogs and cats so correlation with history and laboratory findings is always warranted and splenic sampling may be necessary.

## Kidney

### *Differences in Renal Size, Echogenicity, and Location*

#### Renal Size

There is no standardized method to determine normal renal size in dogs because of the great range of canine size, so renal size is subjectively assessed. A canine kidney length to aorta ratio is described, but the range is rather broad and thus unreliable. The measurement of canine kidneys is best done radiographically using the dorsal ventral view. Basic renal anatomy and the methodology for measuring its dimension of length, height, and width are easily learned (Figure 39.10).

The normal range of feline kidney dimensions includes length from 3 to 4.5 cm, width from 2.2 to 2.8 cm, and height from 1.9 to 2.5 cm (see Figure 39.10) (Nickel et al. 1973; Walter et al. 1987; d'Anjou 2008a). The more homogeneous body size in cats makes determination of volume or area measurements more clinically useful. Normal renal volume in cats has been

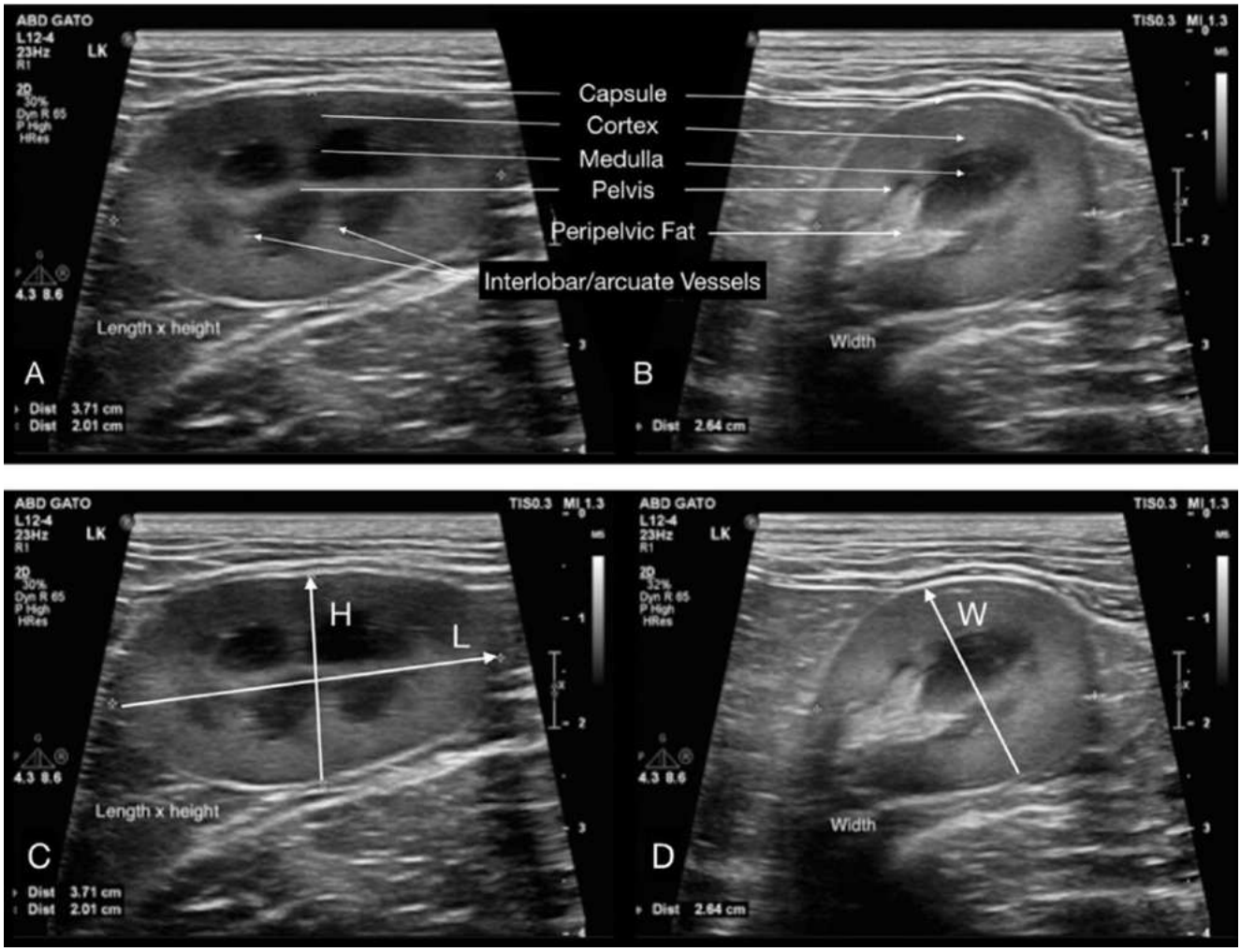


**Figure 39.10.** Renal anatomy and measuring its dimensions. (A,B) The basic anatomical features of the feline kidney. (C,D) Measurements of length (L) and height (H) in the longitudinal (sagittal) plane and width (W) in the transverse plane. Quick reference values are listed in Table 39.3. Source: Reproduced with permission from Dr Daniel Rodriguez, DVM, DACVR, Mexico City, Mexico.

reported to range from 11.9 to 17.7 $cm^3$ using the prolate ellipsoid method of measurement (volume [mL] = length [cm] × width [cm] × height [cm] × 0.523). However, it should be noted that the volume formula range was derived from a group of only five normal female cats, and for this reason many radiologists prefer using renal length (Nyland et al. 2015a) (Figure 39.11).

### Echogenicity

The cortex of the feline kidney contains more fat vacuoles than the canine renal cortex so feline renal cortical echogenicity is higher (brighter) than that expected in dogs. The comparison of echogenicity between the spleen and the cortex of the left kidney is similar (isoechoic) and a normal finding in cats (Figure 39.12). In the dog, the spleen is more echogenic (brighter) than the cortex of the kidney (d'Anjou 2008a; Nyland et al. 2015a).

**Pearl:** The cortex of the canine kidney is less echogenic to the spleen and less or equal (isoechoic) to the liver. The order is remembered by the mnemonic "SLiCK" with S for spleen, Li for liver, and CK for cortex of the kidney. For the feline, hepatic echogenicity is often compared to the adjacent falciform fat and the feline liver should be isoechoic to slightly hyperechoic (brighter) to the falciform fat. The feline liver, spleen, and cortex of the kidney are isoechoic to one another.

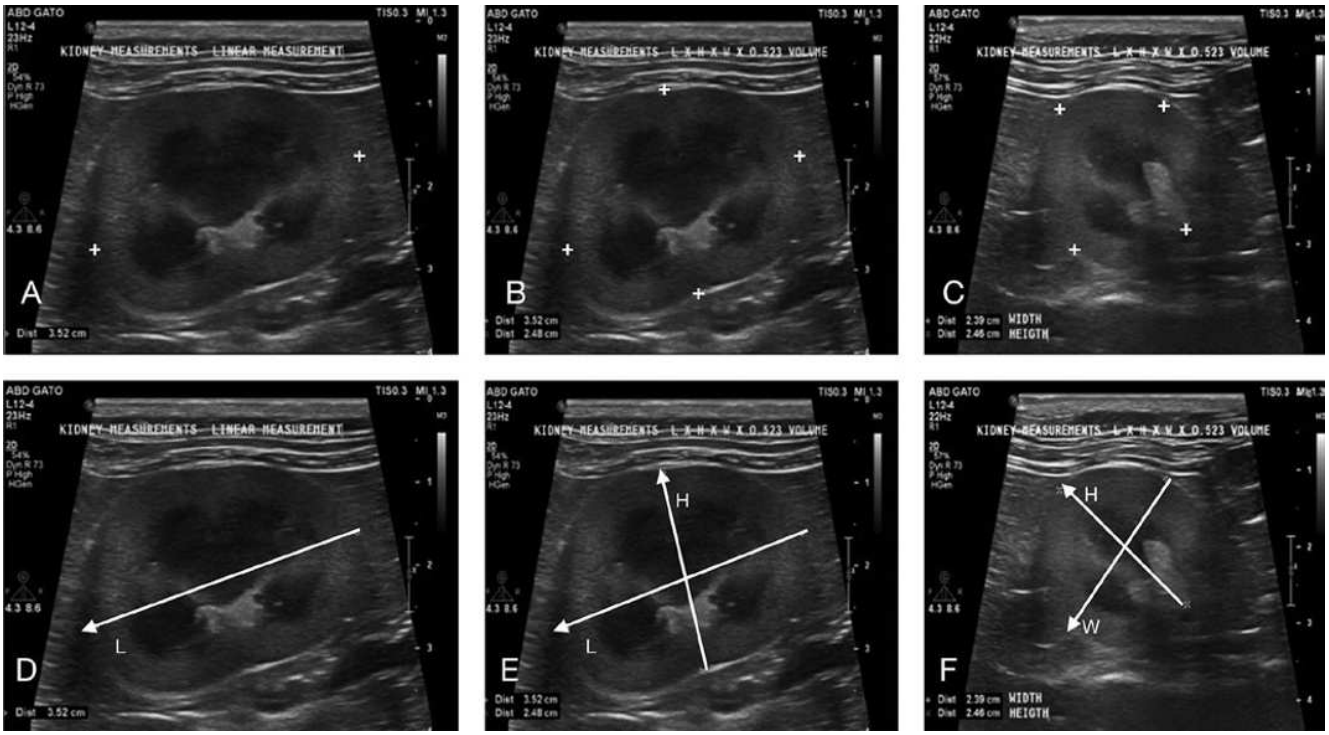


**Figure 39.11.** Measuring the feline kidney length versus volumetric measurements. Different methods of measuring kidney size in the cat. (A) Linear measurement only in the long axis. (B,C) Volumetric measurement option (Nyland et al. 2015a). In contrast, the renal size of kidneys in dogs is variable and judged subjectively, often comparing the canine left kidney to its right counterpart due to lack of standardization in the canine species. The image in (C) shows the feline kidney imaged in transverse orientation for measurements of width and height. In (D–F) there are arrow overlays showing the measurements. L, length; H, height, W, width. Source: Reproduced with permission from Dr Daniel Rodriguez, DVM, DACVR, Mexico City, Mexico.

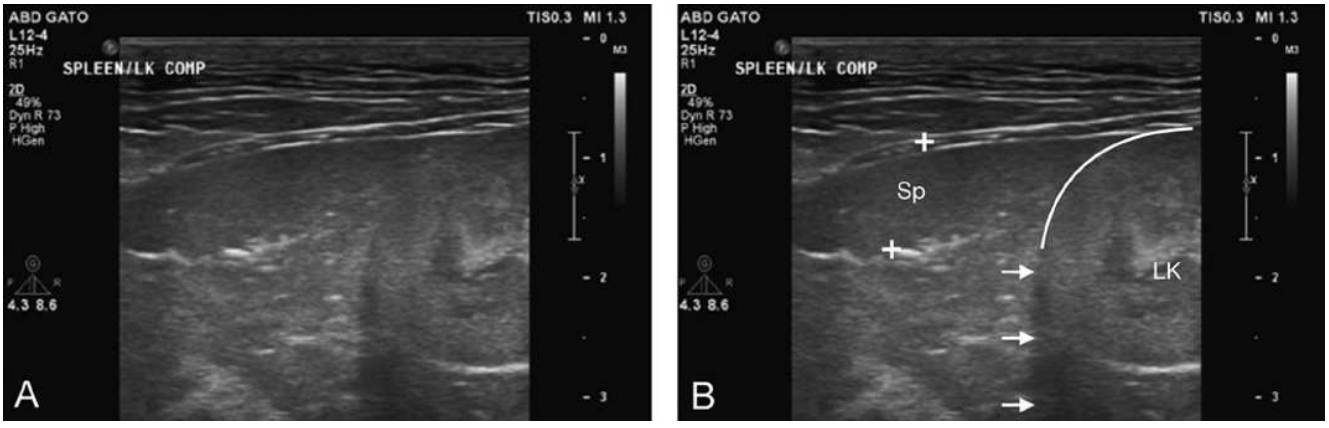


**Figure 39.12.** Echogenicity comparison of the feline kidney to the spleen. The comparison of echogenicity between the spleen and the cortex of the left kidney is similar (isoechoic) and a normal finding in cats. In the dog, the spleen is more echogenic (brighter) than the cortex of the kidney. In (A) the spleen and left kidney are adjacent to one another. In (B) the same image is labeled as SP, spleen, and outlined with (+); LK, left kidney and outlined (curved line); and arrows pointing out the edge shadowing artifact as the anechoic line extending off the rounded edge of the kidney through the far-field that should not be mistaken for free fluid. Source: Reproduced with permission from Dr Daniel Rodriguez, DVM, DACVR, Mexico City, Mexico.

Location

As a rule of thumb, the appropriate depth should be to have approximately 75% of the field of view filled with the organ of interest unless performing AFAST. Regarding renal imaging of cats and small thinner dogs placed in lateral recumbency, both the left and right kidneys are often viewed together with greater depth settings. Care should be taken to ensure that the correct kidney is identified and labeled accurately, and know that rarely would this be a result of a mirror image artifact. The right kidney may be discriminated from the left by its position within the renal fossa of the liver in dogs. In other words, the canine right kidney is cupped by the liver, and the canine left kidney is not. However, in cats, both kidneys are located away from the liver and sometimes more difficult to identify as one being the left or right kidney.

## AFAST Spleno-Renal and Hepato-Renal Views

### *Differences in Spleen next to the Left Kidney*

Both the canine and feline spleen are attached to the greater curvature of the stomach by their short gastric vessels, making the head of the canine and feline spleen reliably in close proximity to its left kidney. The spleen is thus imaged consistently in both species at the AFAST SR view by rocking the probe cranially under the rib cage unless gas-filled bowel is interposed (ultrasound does not transmit through air). Thus, both the feline and canine spleen are expected to be seen at the SR view and the feline right kidney is often imaged through the same SR view acoustic window (Figure 39.13). Conversely, the right kidney is viewed analogously from the HR view.

### *Differences in Imaging the Left and Right Kidneys*

Both kidneys are commonly imaged in cats via the SR view in right lateral or standing or sternal (or analogously the HR view in left lateral) rendering the AFAST HR5th bonus view (when in right lateral recumbency) unnecessary in most feline cases (see Figures 6.21, 6.34, and 39.1). Thus, the cat's left and right retroperitoneal spaces and kidneys are confidently interrogated through the SR view when in right lateral recumbency, and the HR view when in left lateral recumbency. The feline kidney will often sonographically appear different in echogenicity and detail than in dogs and the feline right kidney is not as intimately associated within a fossa of the right liver because of interposing fat (described in the preceding paragraphs).

### *Imaging Feline Ureters*

The feline as a species is more prone to ureteral calculi that will partially or completely obstruct urine flow from the renal pelvis to the trigone of the urinary bladder. During AFAST and its target organ approach, renal pelvic dilation and degrees of hydronephrosis are usually obvious because the conditions are fluid-associated changes and for some sonographers

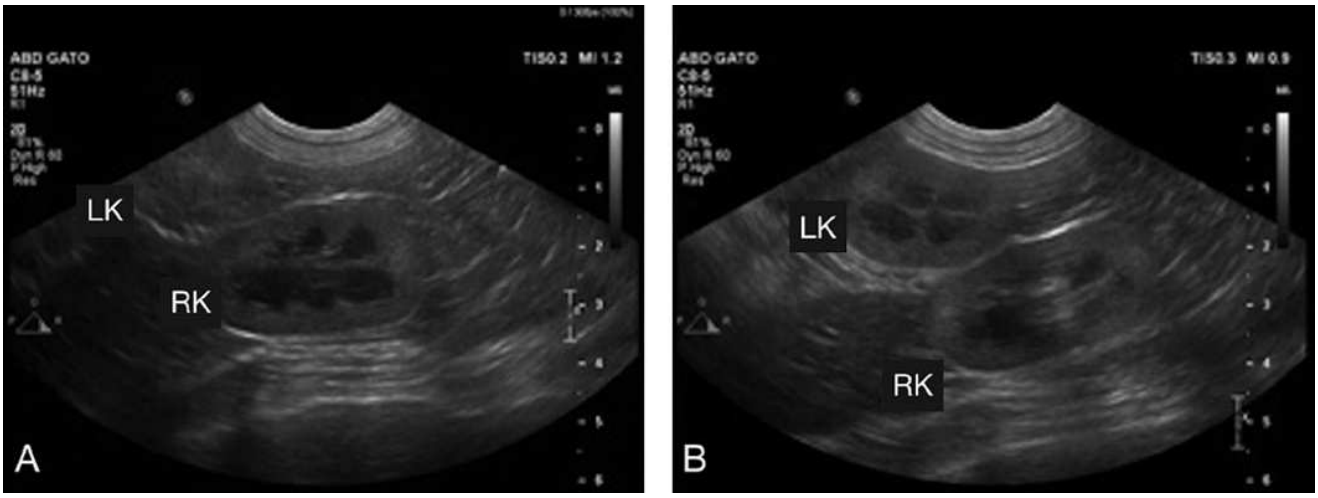


**Figure 39.13.** Differentiating feline left from right kidney. In (A) the right kidney (RK) is seen in the center of the image, and the left kidney (LK) was missed superficially. However, when the depth was increased and the probe was fanned, the LK appeared in the near-field and the RK in the far-field in the same cat as shown in (B). The RK could have easily been misidentified as the LK. Source: Reproduced with permission from Dr Daniel Rodriguez, DVM, DACVR, Mexico City, Mexico.

ureteral dilation may also be recognized as an AFAST abnormality (Figure 39.14). Importantly, these ultrasound-detected changes are missed by physical examination, blood and urine testing, and radiography. Color flow Doppler may be used to determine if the fluid-filled structure is a vessel (obvious pulsatile flow) versus ureteral distension (absent pulsatile flow). The use of AFAST is a good screening test for soft tissue conditions of the kidneys and associated structures, since most are fluid associated, and carries the potential to trigger more advanced imaging.

## Urinary Bladder, Urine, Urethra, and Reproductive Structures

### *Differences in Urinary Bladder, Urethra, and Reproductive Structures*

#### Artifacts

There are several artifacts that may mimic pathology when evaluating the urinary bladder, including sidelobe that can mimic wall thickening, nearby small cystic structures, or pseudo sludge, and slice-thickness artifact that creates images of false sediment. These artifacts can be reduced by adjusting gain (generally decreasing) and focal zone, and using tissue harmonic imaging (THI).

#### Urethra

The cat's urethra is more abdominal in location and much longer than dogs and is thus often readily imaged in cats with a full urinary bladder (Figure 39.15) (d'Anjou 2008a; Nyland et al. 2015a).

#### Prostate

The prostatic urethra can be seen in most dogs, but especially in small-breed dogs, the prostate seems to be directly abutting the neck of the urinary bladder. Having a patient with a full urinary bladder is always helpful for prostatic evaluation, especially in neutered dogs, since the plethoric bladder will pull the prostate cranially from the pelvic inlet.

Usually, determination of canine prostatic size using ultrasound is subjective. A more reliable determination is via the use of a lateral radiograph. On a lateral radiograph, the height of the normal prostate should not exceed 70% of the height measured from the sacral promontory to the pubis. An objective determination of prostatic size by length (L), depth (height) (D), and width (W) measurements is straightforward with the use of electronic cursors. The basic equation used to determine prostate volume (V) is an ellipsoid model ($V = 0.524 \times L \times W \times H$) (Nyland and Mattoon 2015b).

The male cat's prostate is rarely seen sonographically due to the rarity of prostatic disease in the feline and the fact that most cats in general practice are neutered. The normal prostate of intact male cats has been described as being small and oval with hyperechoic prostatic parenchyma. Feline prostatic disease is rare, with the most common neoplasia being prostatic

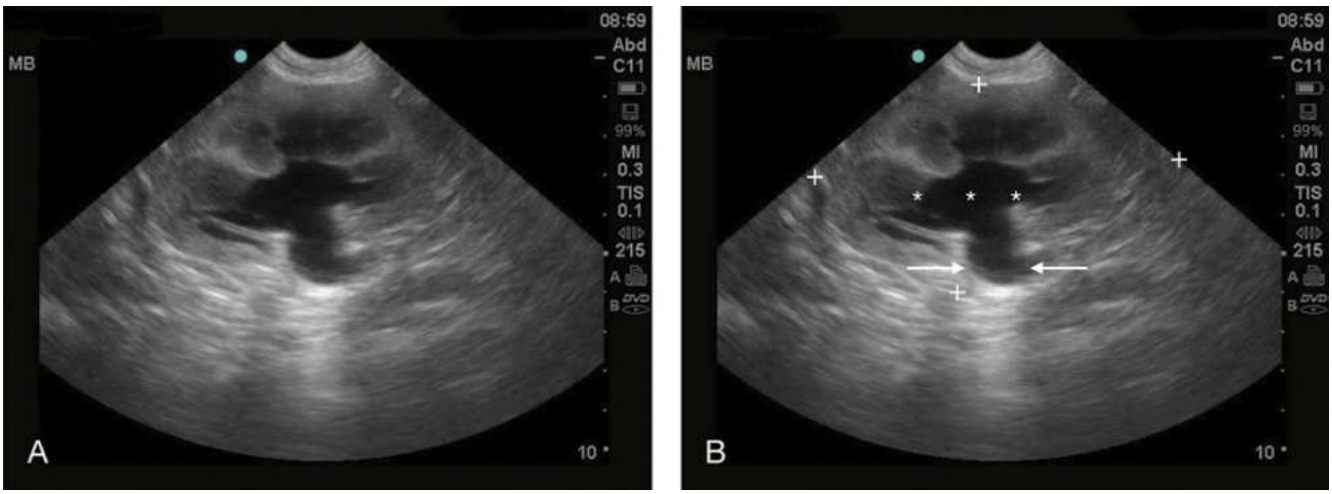


**Figure 39.14.** Hydronephrosis. Shown in (A) unlabeled and in (B) labeled is dilation of the renal pelvis, more specifically hydronephrosis, an easily detected abnormality when fanning through the kidney in the longitudinal (long-axis) plane. The borders of the kidney are outlined in (B) with (+). The finding should prompt a search for dilated ureters in a cat with suspect ureteral obstruction secondary to ureteral calculi or another obstructive process along the course of the ureter to the urinary bladder and its ureteral papilla. Note the tubular structure coursing caudally extending from the renal pelvis (*asterisks*) marked with arrows. Tracing in B-mode as well as color flow Doppler are ways in which to increase the probability of achieving a correct interpretation. The use of color flow Doppler is not shown. Source: Image courtesy of Dr Sarah Young, Ojai, CA.

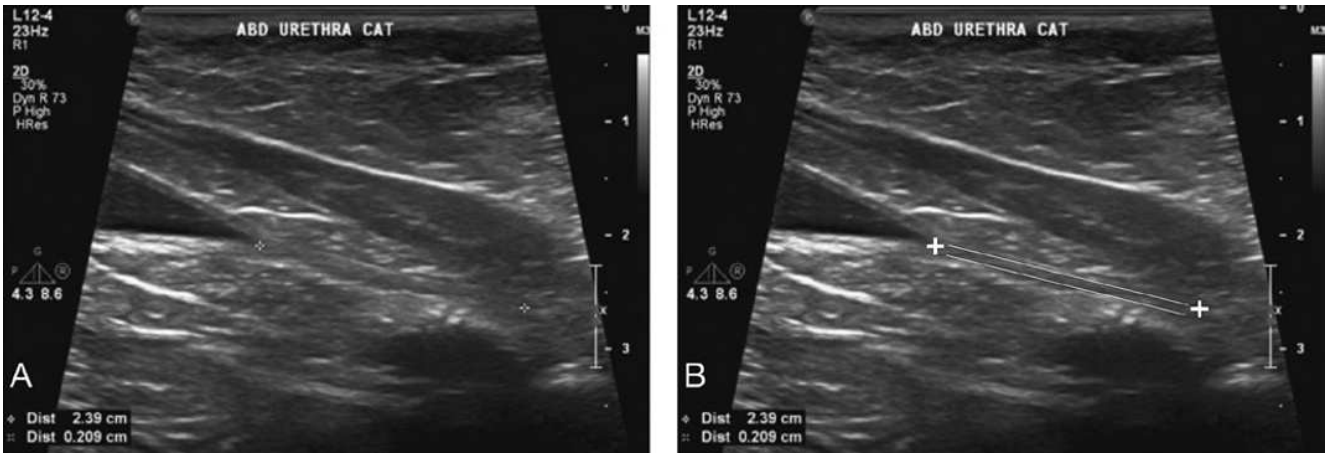


**Figure 39.15.** Feline urethra. A normal feline abdominal urethra is shown in B-mode (between the caliper markers) in (A) and outlined with (+) and (line) overlays in (B). Note the amount of urethra potentially examined during a POCUS urinary tract scan in the feline species. Source: Reproduced with permission from Dr Daniel Rodriguez, DVM, DACVR, Mexico City, Mexico.

adenocarcinoma; however, bacterial prostatitis, also rare, has been described (Dimitrov et al. 2010).

### Ovaries

The ovaries are superficial, round to oval, homogeneous in echogenicity, and located caudal and ventral to the caudal pole of each kidney (Figure 39.16). The size of the ovaries in dogs is more homogeneous and independent of weight compared to cats. One study showed an average canine ovarian size of 1.7 × 0.7 × 0.5 cm. The cat's ovaries are much smaller, and both canine and feline ovaries are best imaged with linear transducers, unless the patient is very large (Nyland and Mattoon 2015d).

### Uterus

The nongravid uterus is tubular, homogeneous in echotexture, with a lumen that is not readily seen and is differentiated from small intestine by lack of peristalsis and intraluminal gas, and absence of the layered appearance characteristics (Nyland and Mattoon 2015d). Uterine width varies from 3 to 5 mm in cats and 5 to 10 mm in dogs. If the uterine horn is superficial enough, and a linear transducer is used, the layers of the uterus are more evident, as in Figure 39.17. Further details regarding pathology of reproductive organs are beyond the scope of this chapter (see Section III).

## *Differences in Urine*

Canine urine should be homogeneously anechoic. If internal echoes are noted, the presence of active sediment should be suspected and urinalysis is necessary to characterize the type of sediment.

Regarding cats, the ability of the feline to concentrate urine is greater than the dog. As a result, cat urine is more commonly seen as partially echogenic, which could be a normal variation (floating sediment), and is not uncommonly due to floating fat droplets (Figure 39.18).

## AFAST Cysto-Colic View

### *Differences between Cats and Dogs*

The AFAST CC view is similar in both cats and dogs with no major differences other than those stated in the preceding paragraphs regarding the feline urethra and urine composition.

### *Estimating Urinary Bladder Volume*

When urinary bladder volume estimation is warranted, the formula is length × height × width (cm) × 0.625 = estimated urinary bladder volume (mL) (Lisciandro and Fosgate 2017) (Figure 39.19). If volume is calculated over time then urine output may be estimated noninvasively. The way in which to test the formula and become comfortable with its strengths and weaknesses is to perform your AFAST CC view urinary bladder measurements and then compare to the volume aspirated when placing urinary catheters.

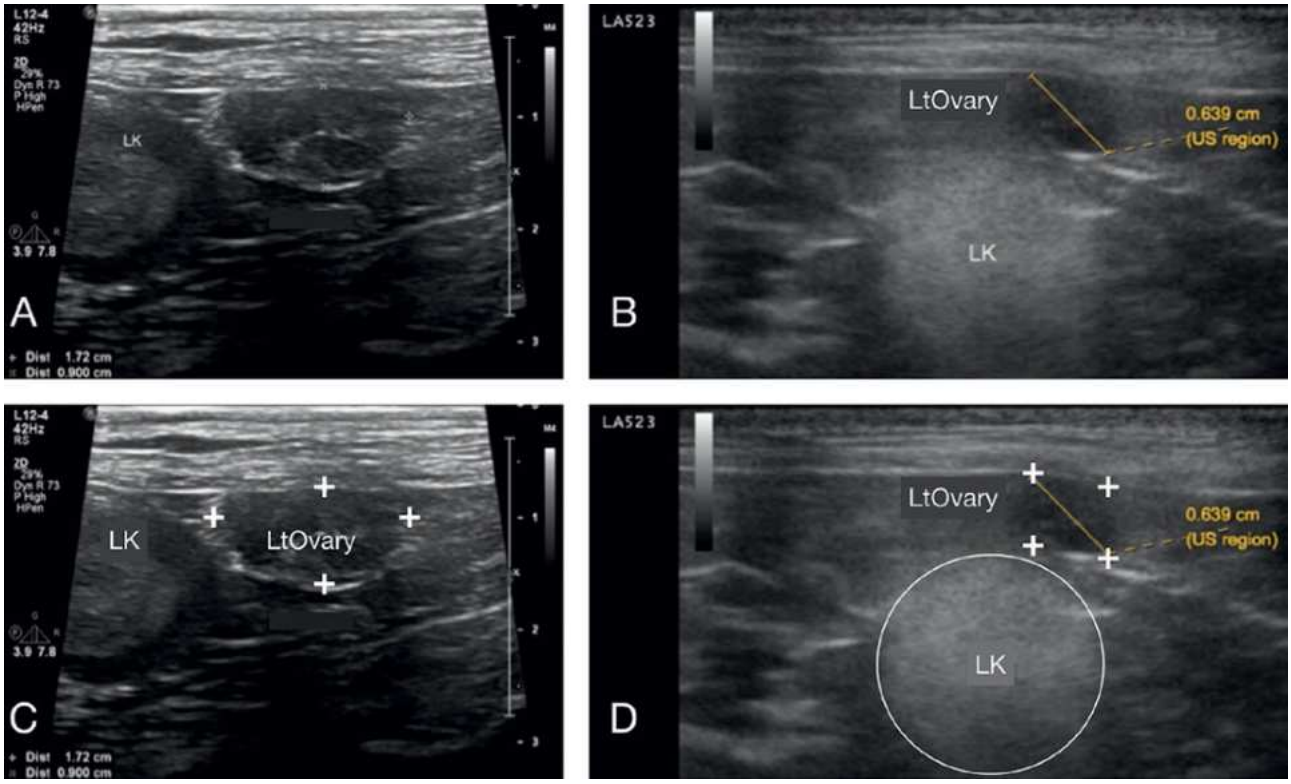


**Figure 39.16.** Feline and canine ovaries. (A) B-mode still image of the canine ovary of a normal cycling bitch (estrus a month prior to this image). The ovary (marked with calipers) is immediately caudal to the left kidney (LK). Compare to the image in (B) showing the ovary of a cat (queen) with endometrial hyperplasia. Note the smaller size (indicated with a line labeled as 0.639 cm) and the more rounded ovarian shape in the queen compared to the bitch. In (C) and (D) are the same images as (A) and (B), respectively, but with illustrative overlays. LK, left kidney; Lt Ovary, left ovary. Source: Reproduced with permission from Dr Daniel Rodriguez, DVM, DACVR, Mexico City, Mexico.

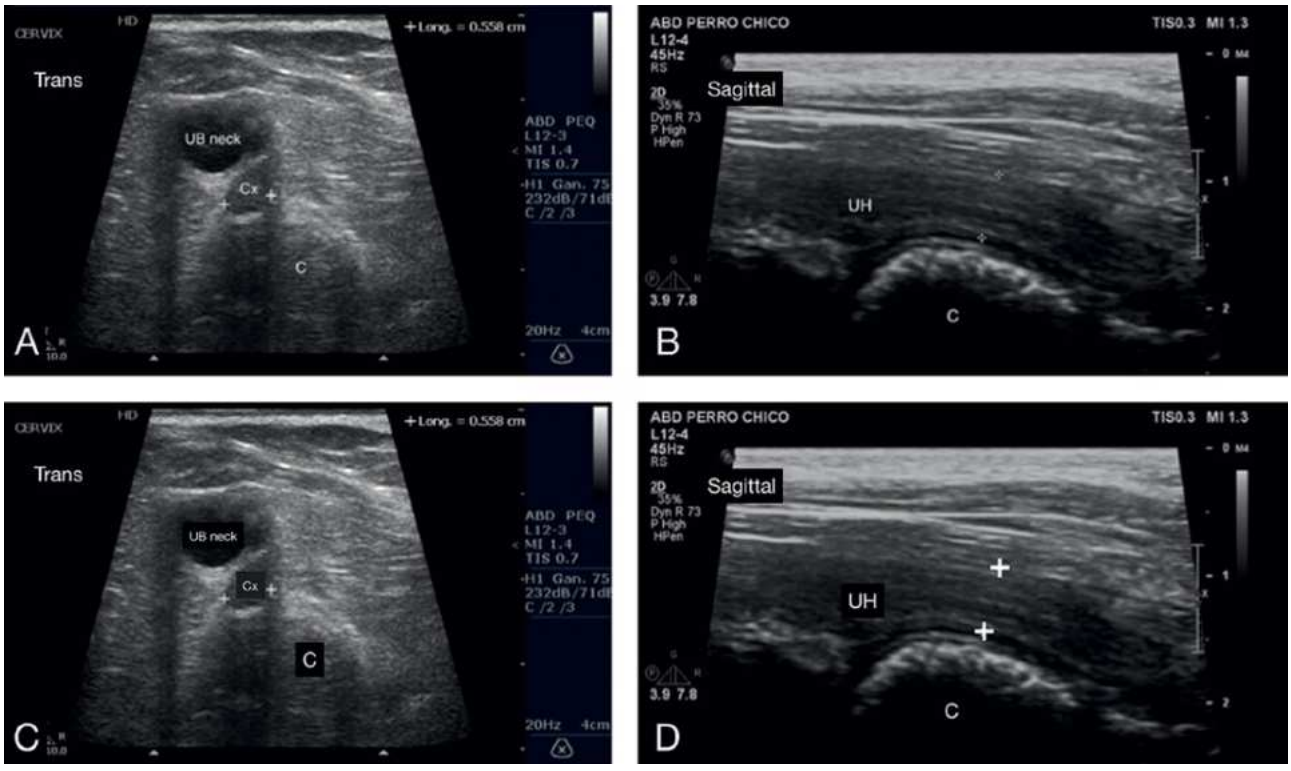


**Figure 39.17.** Uterus and cervix. (A) Transverse B-mode image of the cervix (Cx). Note the anatomical landmarks used to locate the cervix, the neck of the urinary bladder (UB neck), colon (C) and cervix (Cx) in between marked with calipers (+). (B) A long-axis (sagittal) B-mode image of a uterine horn (UH) showing the normal layering pattern. In this image the uterine horn is ventral to the colon (C). Note that the patient is being scanned in dorsal recumbency. (C,D) Labeled overlays corresponding to (A) and (B) Source: Reproduced with permission from Dr Daniel Rodriguez, DVM, DACVR, Mexico City, Mexico.

## Gastrointestinal Tract

### *Differences in Stomach*

In cats, the position of the stomach is quite different from that of the dog. Whereas the dog's antrum and pylorus are right-sided structures, in the cat they are located near midline. This can be better appreciated in radiographic ventrodorsal views of the abdomen, especially in cats with a normal amount of gas. This difference is very important for sonographers who will find it easier to locate the pyloric duodenal junction (PDJ) and duodenum along the midsagittal plane (Figure 39.20). The gastric submucosal layer in the cat can accumulate fat, and this intramural fat will appear distinctly hyperechoic in obese cats. It is important to recognize this difference from dogs and avoid misdiagnosis as an intramural abnormality. This layer of fat can be seen sonographically, radiographically, and on computed tomography (Heng et al. 2005).

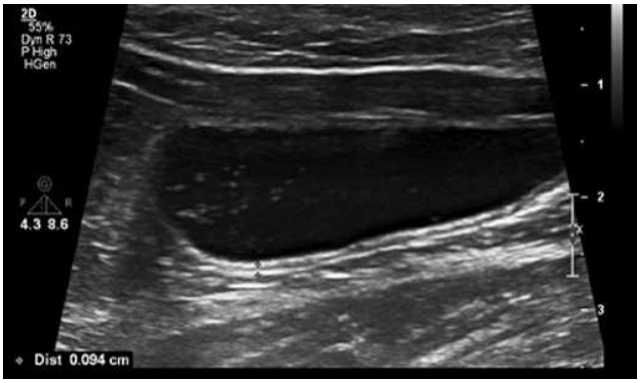


**Figure 39.18.** Lipid droplets in cat urine. Longitudinal (sagittal) image of the urinary bladder showing fat droplets in the urine as a normal finding in cats. Source: Reproduced with permission from Dr Daniel Rodriguez, DVM, DACVR, Mexico City, Mexico.

### *Differences in Pancreas*

The pancreas is one of those organs that can be difficult for the novice sonographer to identify. In order to find the pancreas, the ultrasonographer must rely on regional anatomy. The pancreas of both dogs and cats is usually medial to slightly dorsomedial to the descending duodenum. In the past, the pancreas was not as clearly seen as today with newer transducer technologies. The pancreas is isoechoic (same as) to slightly hypoechoic (darker) to the surrounding mesenteric fat. It is also located ventral to the prehepatic portal vein and this region of the pancreas corresponds to the pancreatic body. The right pancreatic lobe is larger than the left lobe in the dog and in the cat this is the opposite, the larger left pancreatic lobe predominates over the smaller right lobe.

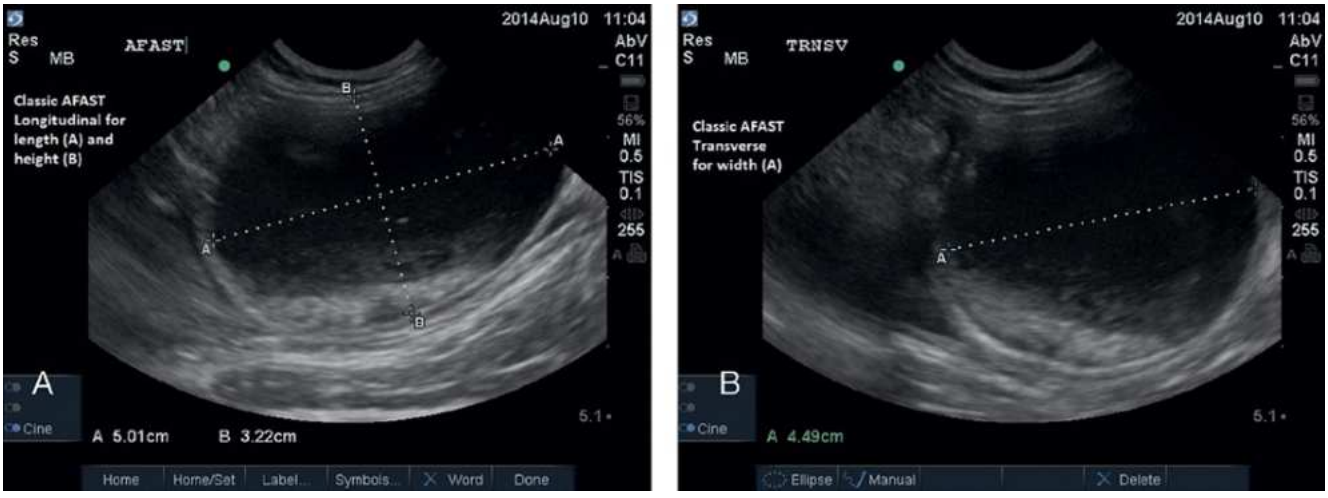


**Figure 39.19.** Urinary bladder volume estimation formula. How to acquire the measurements in a cat for estimating urinary bladder volume. In longitudinal, image the largest, most oval urinary bladder without extending into the trigone for length (L) and height (H) measurements as shown in the B-mode image in (A), Then, in transverse, rotate the probe 90° to the longitudinal plane and then slide the probe cranial and caudal for the largest, roundest, symmetrical circle or oval for width (W) measurements as shown in image (B) in the same cat. The formula is L × H × W (cm) × 0.625 = estimation of urinary bladder volume (mL) (Lisciandro and Fosgate 2017). Importantly, compression by probe pressure can distort the urinary bladder, leading to less accurate measurements. Source: Reproduced with permission from Dr Gregory Lisciandro, Hill Country Veterinary Specialists and FASTVet.com, Spicewood, TX.

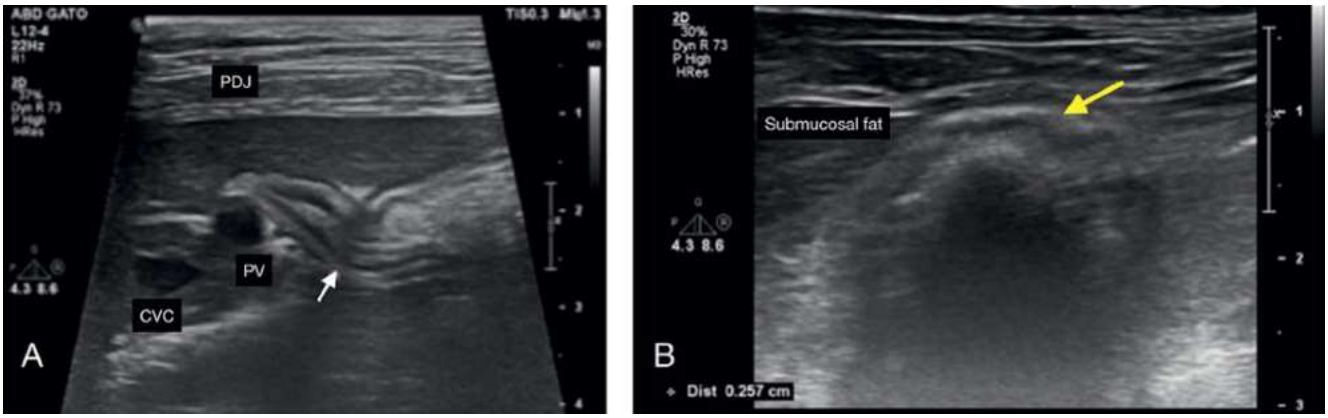


**Figure 39.20.** Feline stomach and pyloric duodenal junction. (A) The pyloric duodenal junction (PDJ) in the feline seen ventral (*arrow*) to the portal vein (PV) in the porta hepatis imaging from the right side intercostally (between ribs) using the caudal vena cava as an additional landmark (CVC). In the dog (not shown), the PDJ can be found similarly using the gallbladder neck as it approaches the porta hepatis. Note in (B) the hyperechoic submucosal layer due to fat accumulation in the cat (*arrow*). Source: Reproduced with permission from Dr Daniel Rodriguez, DVM, DACVR, Mexico City, Mexico.

In dogs, the size of the pancreas varies from 4 mm to 10 mm (Nyland and Mattoon 2015a). A landmark that is used by the author (DR) for both dogs and cats is to find the cranial pole of the left adrenal gland and the most caudal aspect of the left pancreatic lobe will be abutting it. The splenic vein also can be followed dorsally to the junction of the cranial mesenteric vein just before forming the prehepatic portal vein. The left pancreatic lobe will be ventral to this confluence of tributary veins. The pancreatic duct is difficult to visualize and it can be up to 1 mm diameter in normalcy.

In cats, the pancreas should be less than 1 cm (Nyland and Mattoon 2015a). The feline left pancreatic lobe can be found in a sagittal to sagittal oblique plane, caudal to the fundus of the stomach, dorsal to the spleen and cranial to the cranial pole of the left kidney, and is larger than the right pancreatic lobe (Figure 39.21). A landmark that is used by the author (DR) for both dogs and cats is to find the cranial pole of the left adrenal gland and the most caudal aspect of the left pancreatic lobe will be abutting it. The splenic vein also can be followed dorsally to the junction of the cranial mesenteric vein just before forming the prehepatic portal vein. The left pancreatic lobe will be ventral to this confluence of veins. The pancreatic duct diameter increases with age. The pancreatic duct can be up to 6 mm (Hecht et al. 2006).

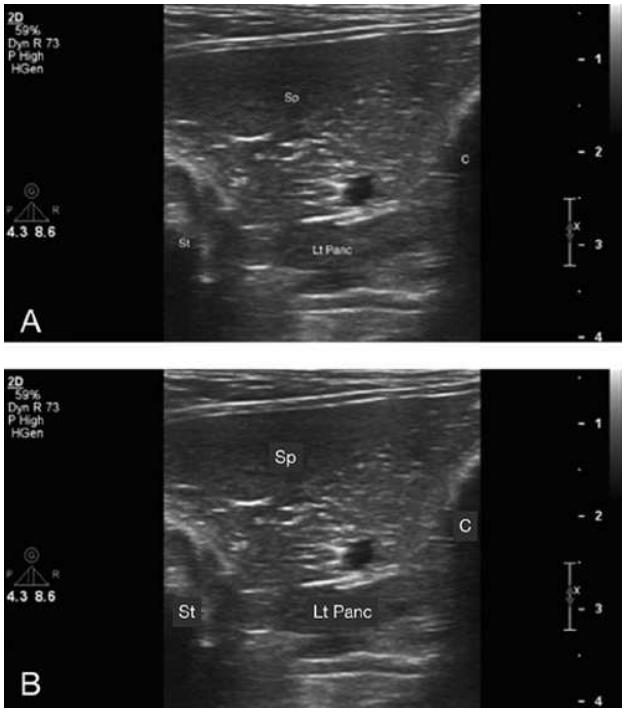


**Figure 39.21.** Feline pancreas. (A) Normal regional anatomy when locating the feline left pancreatic lobe with overlays in (B). Left pancreatic lobe in the middle, cranially the stomach (St), ventrally the spleen (Sp), and caudally the colon (C). Source: Reproduced with permission from Dr Daniel Rodriguez, DVM, DACVR, Mexico City, Mexico.

### *Differences in Small Intestine*

The small intestine in the cat and dog has five distinct layers (Figure 39.22). Extending from the outer surface, the serosa, muscularis, submucosa, mucosa, and lumen make up the ultrasonographic layering. In the cat, the wall thickness is more homogeneous relative to weight compared to the dog where weight-based intervals are applied to dogs.

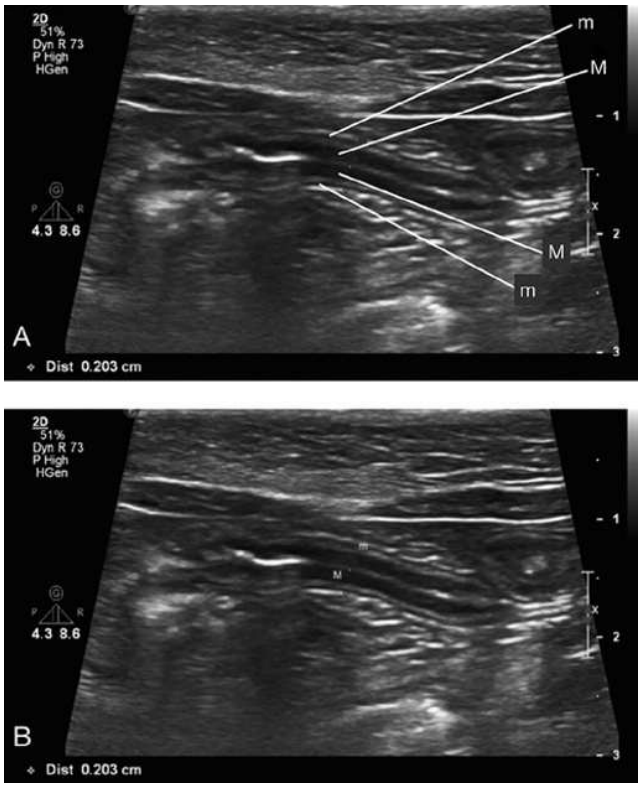


**Figure 39.22.** Small intestine. Normal longitudinal B-mode image of the small intestine in a cat labeled and unlabeled in (A) and (B), respectively. The mucosal layer (M) and muscularis layer (m). The jejunum of the cat normally measures <2.5 mm and the duodenum and ileum up to 3 mm. The muscularis layer and the mucosal layers are the hypoechoic (dark) layers. The author uses the mnemonic M&M, as in chocolate, to remind us that these both layers are hypoechoic. Source: Reproduced with permission from Dr Daniel Rodriguez, DVM, DACVR, Mexico City, Mexico.

The jejunum of the cat normally measures <2.5 mm and the duodenum and ileum up to 3 mm (Newell et al.1999; Goggin et al. 2000; Winter et al. 2014; di Donato et al. 2014). The muscularis layer (m) and the mucosal layers are the hypoechoic (dark) layers. The author uses the mnemonic M&M, as in chocolate, to remind us that both these layers are hypoechoic.

Intestinal layering is as follows from superficial to deep (see also Chapter 11).

- Serosal – hyperechoic (white)
- Muscularis – anechoic (black)
- Submucosal – hyperechoic (white)
- Mucosal (thickest) – anechoic (black)
- Mucosal-luminal interface – hyperechoic (white)

### *Differences in Ileocolic Junction*

In cats, the ileocolic junction region is easy to identify due to its unique appearance having a thicker and hyperechoic submucosa than small and large intestine. The ileum just prior to entering the colon in the transverse plane appears as a small, empty stomach or the classic "wagon wheel" appearance (Figure 39.23). In the author's experience (DR), the long-axis plane of the ileum can be confused with the duodenum by novice ultrasonographers for two possible reasons: because it is located medial to the right kidney in the right cranial abdomen, and because it is slightly thicker than other small bowel segments.

In dogs, the colon and cecum are typically gas filled. Thus, it is difficult to routinely see the canine ileocecocolic junction with the exception of an empty colon or a fluid-filled junction.

### *Differences in Large Intestine*

There are really no major differences between the colon of the dog and cat. The wall of the colon is thin and with faintly distinct layers, often best imaged using a high-frequency transducer (probe).

## AFAST Hepato-Renal and Spleno-Renal Umbilical View

### *Differences in Spleen and Small Intestine*

At the AFAST umbilical views (HRU and SRU), small intestine is commonly seen, but the spleen is variably seen at the level of the umbilicus and less reliably than in dogs. A midabdominal sweep may be necessary to locate the spleen. In most cases, a POCUS spleen exam is recommended following AFAST. Differences between the feline and canine spleen are described in more detail in the preceding paragraphs. As in the dog, when imaging in the transverse plane at the level of the umbilicus, the liver and stomach should not be in view in normalcy.

Small intestine will be imaged at the HRU view (right lateral recumbency, and the analogous SRU view when in left lateral recumbency). The AFAST sonographer can get used to eyeballing small intestinal wall thickness, peristalsis, and lumen diameter as a screening test to trigger therapeutic and diagnostic interventions. Little is known about the frequency of peristalsis in cats and the effects of fasting and anorexia.

## AFAST-Applied Abdominal Fluid Scoring System

The AFAST-applied abdominal fluid scoring system is a simple 0–4 scale (Lisciandro et al. 2009, 2015;

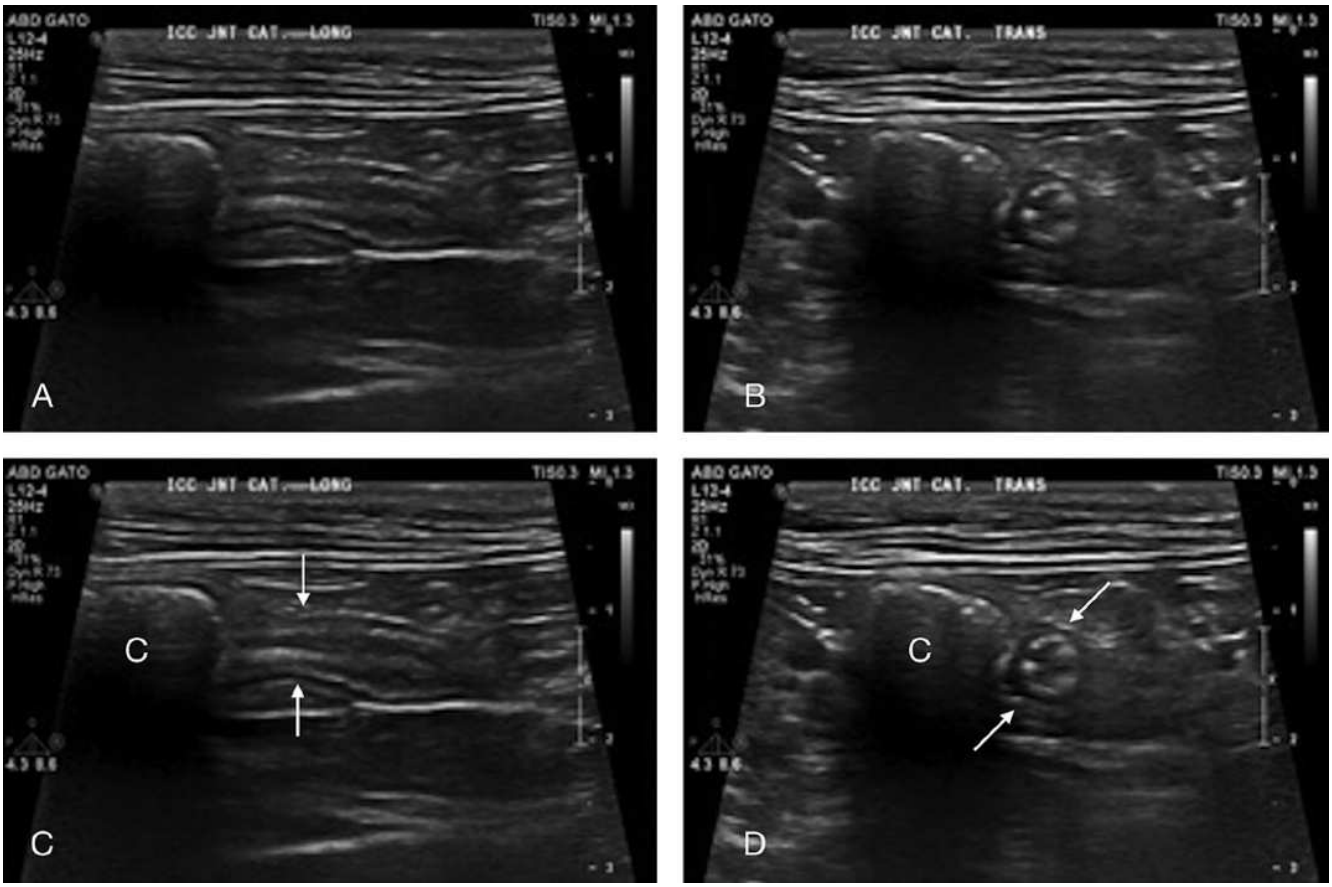


**Figure 39.23.** Feline ileocecal colic junction. The ileocecal colic junction has a distinct appearance in cats. The ileum has a prominent hyperechoic layer shown in longitudinal (sagittal) orientation in (A) unlabeled and (C) labeled (*arrows*) with its proximity near the colon (C). In transverse orientation (B) unlabeled and (D) labeled with arrows, the ileum just before entering the colon (C) resembles a small, empty stomach or the classic "wagon wheel" appearance. The dog lacks this ultrasonographic feature. Source: Reproduced with permission from Dr Daniel Rodriguez, DVM, DACVR, Mexico City, Mexico.

Lisciandro 2011, 2012, 2014a). The abdominal fluid score (AFS) is negative or 0 when no intraabdominal fluid is found at any of the four AFAST views; and then ranges from 1 to 4 depending on how many AFAST views are positive (Figure 39.24). We have revised the AFS to include the additional score of 1/2 to better semiquantitate volume and categorize as small-volume versus large-volume bleeder/effusion (Figure 39.25) (Lisciandro et al. 2015).

### *Modifications of the Abdominal Fluid Score*

The abdominal fluid scoring system has been modified by the author (GL) based on recent research in clinically normal cats (Lisciandro et al. 2015) by making smaller pockets of maximum dimensions and maximum widths of fluid stripes of free fluid of less than 5 mm (<5 mm) AFS of 1/2 rather than a full 1, while keeping the same AFS 1 and 2 (AFS <3) as major injury (or pathology in nontrauma), small-volume bleeder/effusion, and AFS 3 and 4 (AFS ≥3) as major injury (or pathology in nontrauma), large-volume bleeder/effusion (see Figure 39.25).

This is important because by categorizing the bleeding feline patient, AFS 1 and 2 (AFS <3) cats that remain AFS <3 on serial examinations will not become anemic whereas AFS 3 and 4 (AFS ≥3) will become anemic from their intraabdominal bleed. Depending on the subset of the feline patient, trauma (blunt and penetrating), postinterventional, and nontrauma, decisions regarding blood transfusion and exploratory surgery may be more expediently made (Table 39.2).

Although the use of abdominal radiographic serosal detail has not been compared to AFS in cats, as in dogs and humans, feline radiography would probably be a

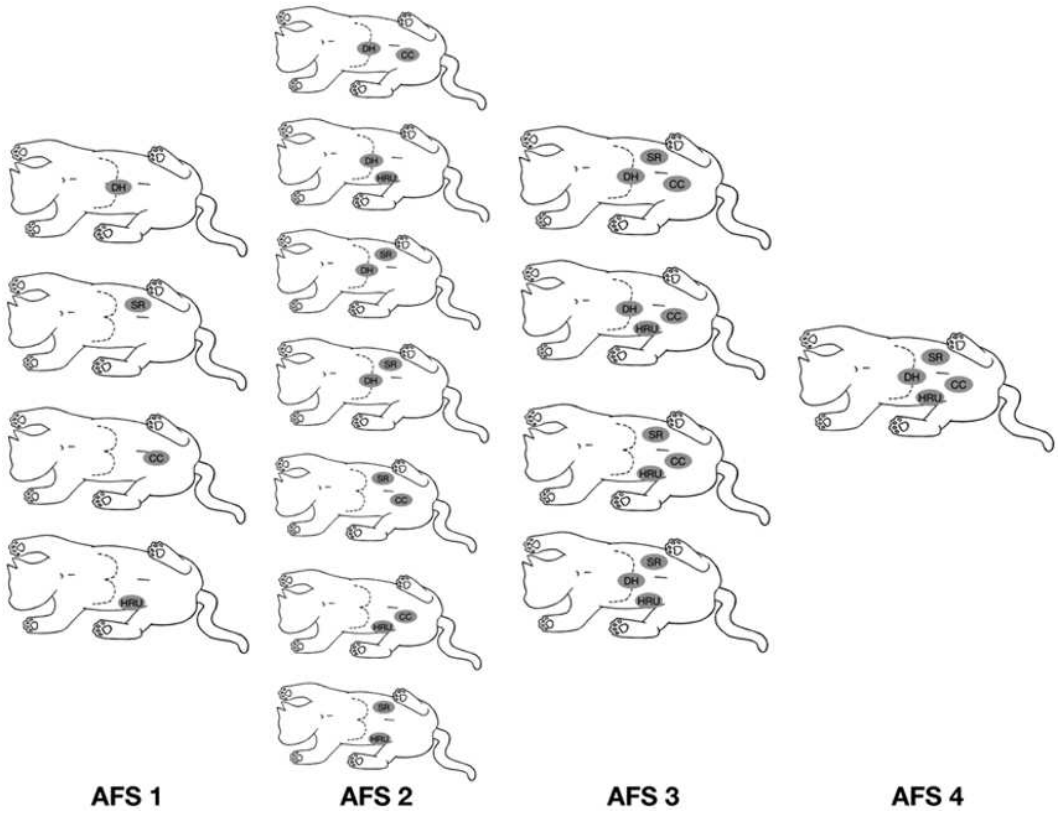


**Figure 39.24.** AFAST-applied fluid scoring system in a cat positioned in right lateral recumbency; left lateral recumbency (not shown) would be analogous. The AFS is calculated by totaling the number of positive views ranging from 0, negative at all AFAST views, to a maximum AFS of 4. Historically, AFS 1 is positive at any single view, AFS 2 positive at any combination of two views, AFS 3 any combination of three views, and AFS 4 positive at all four views. The HR5th and SR5th bonus views, depending on lateral recumbency, are not part of the fluid scoring system and are not shown. The AFS has been modified to include the additional score of 1/2 to better semiquantitate volume and better categorize patients as small-volume versus large-volume bleeder/effusion (see Figure 39.25). Source: Reproduced with permission from Dr Gregory Lisciandro, Hill Country Veterinary Specialists and FASTVet.com, Spicewood, TX. Illustration by Hannah M. Cole, Adkins, TX.

similarly unreliable test (Lisciandro et al. 2009; Lisciandro 2012). Not only is abdominal radiographic serosal detail unreliable for establishing the patient as fluid positive or fluid negative (binary "yes or no" question), but radiographic serosal detail cannot semiquantitate the volume of hemorrhage or other effusions (cannot predict the actual AFS) (Lisciandro et al. 2009; Lisciandro 2012). Thus, by applying an AFS to the feline patient, along with serial monitoring using AFAST, worsening (increasing AFS), resolving (decreasing AFS), or static (unchanged AFS) hemorrhagic or other effusions may be premised on evidence-based information.

### *Use of the AFS in Bleeding Felines*

The AFS system semiquantitates the volume and in bleeding cats allows rapidly categorization as a small-volume bleeder (AFS 1 and 2, AFS <3) versus a large-volume bleeder (AFS 3 and 4, AFS ≥3) on initial and serial exams (Figure 39.26). By categorizing the bleeding cat using AFS, expectations for the degree of anemia and decision making for blood transfusion(s) and/or exploratory surgery may be made with evidence-based information (see Figure 39.25) (Lisciandro et al. 2009; Lisciandro 2011, 2012, 2014a; Boysen and Lisciandro 2013).

Thus, generally speaking, felines with an AFS of 1 or 2 (<3) will not predictably become anemic if they remain an AFS of 1 or 2 over time (importance of serial exams). Therefore, if a feline is categorized as a major injury/pathology, small-volume bleeder AFS 1 or 2 (<3) and is anemic then there are only four major reasons for this: (1) the cat has preexisting anemia, (2) the cat is bleeding somewhere else (the importance of doing a full Global FAST), (3) the cat is hemodiluted

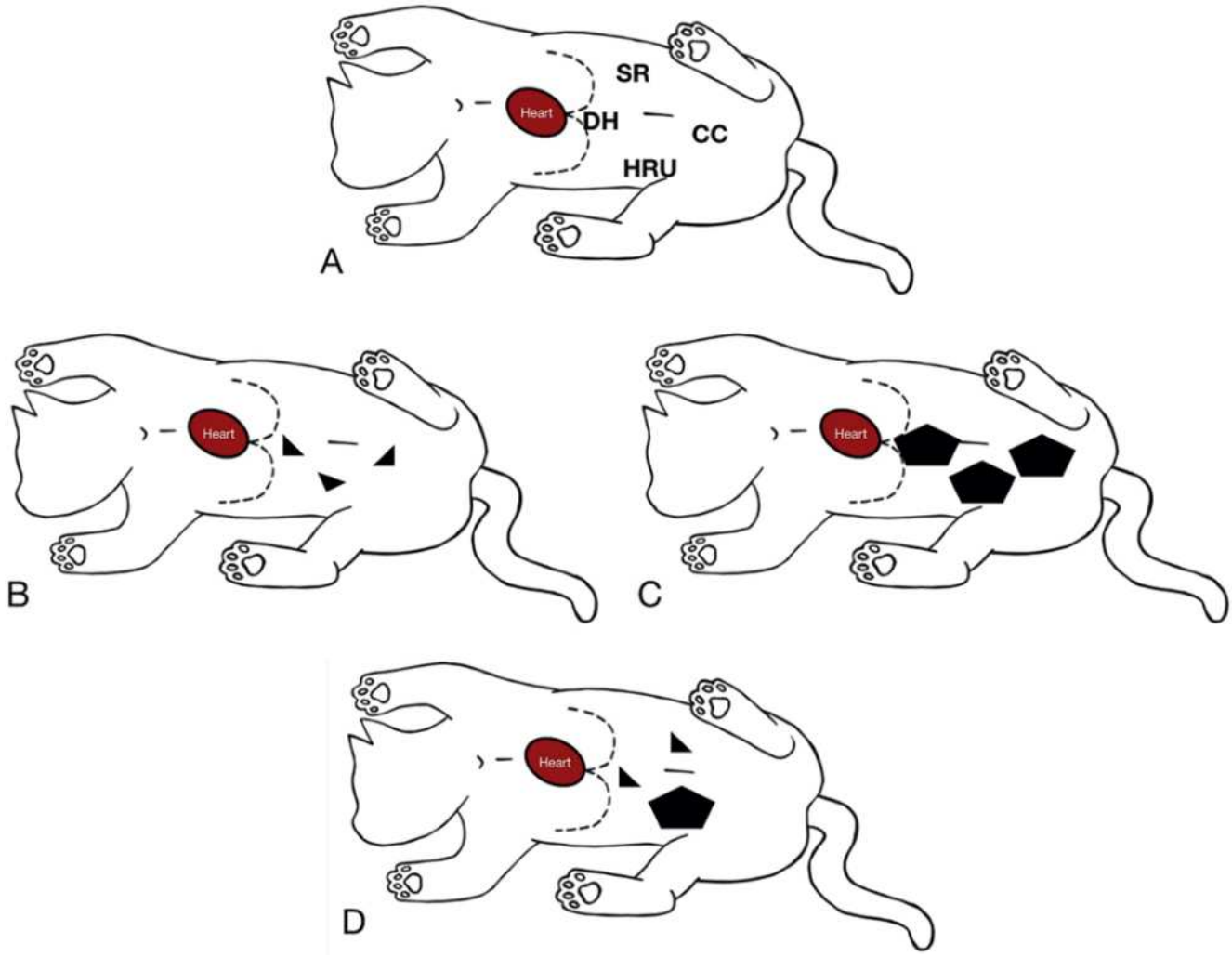


**Figure 39.25.** Modification of the feline AFAST-applied abdominal fluid score. Pockets of <5 mm are assigned a value of 1/2 rather than a full 1, which better semiquantitates the total intraabdominal volume and better categorizes small-volume versus large-volume bleeders/effusions shown in the top image (Lisciandro et al. 2015). In the bottom image, the 1/2 versus 1 is illustrated with examples. In (A) the AFAST and its respective views are shown. In (B) the feline scores 1/2 at three views, giving it a total AFS of 1 1/2 categorized as a small-volume bleeder/effusion. In (C) the feline has scores of 1 at three views, making its total AFS 3, categorized as a large-volume bleeder/effusion. In (D) there are two views scored as 1/2 and a single view scored as 1, making a total AFS of 2 categorized as a small-volume bleeder/effusion. Source: Reproduced with permission from Dr Gregory Lisciandro, Hill Country Veterinary Specialists and FASTVet.com, Spicewood, TX. Illustration by Hannah M. Cole, Adkins, TX.

(less common with graduated fluid therapy strategies), or (4) the cat's anemia is lab error. On the other hand, a feline with an AFS 3 or 4 (≥3) is categorized as major injury/pathology, large-volume bleeder and there is enough blood volume within the abdominal cavity to result in severe anemia requiring blood transfusion therapy.

In bleeding dogs, the AFS is better studied because dogs are more likely to survive large-volume bleeds because the canine spleen serves as a blood reservoir whereas the feline spleen does not. As a result and in addition to felines being much smaller, cats are less likely to survive large-volume bleeds (AFS 3 or 4, ≥3), whereas dogs routinely survive. Thus, a feline that has survived hit-by-car trauma with a large-volume effusion, especially when trauma was >8–24 hours, is much more likely to have a uroabdomen; and in nontrauma the most common cause is neoplasia (Mandell and Drobatz 1995; Lisciandro et al. 2009; Lisciandro 2011, 2012; Culp et al. 2010). The

**Table 39.2.**
Bleeding felines and decision making using the abdominal fluid score (AFS).

| Type of trauma | Major injury, small-volume bleeder (AFS 1, 2, <3) | Major injury, large-volume bleeder (AFS 3, 4, ≥3) |
|---|---|---|
| Blunt Trauma – Think Medical First<br>Blood rapidly defibrinates so is seen acutely as anechoic (black) triangles | • If stays AFS 1, 2 (<3) no blood transfusion necessary if only bleeding intraabdominally because do NOT expect anemia if only bleeding intraabdominally<br>• If stays AFS 1, 2 (<3) and becomes anemic with a packed cell volume (PCV) <25% rule out (1) another site of bleeding (retroperitoneal, pleural cavity, fracture site, externally), (2) hemodilution or (3) bleeding at another site by performing Global FAST and a good physical exam<br>*Expect when bleeding stops for the intraabdominal hemorrhage to resolve within 48 hours* | • If an AFS 3, 4 (≥3) or becomes AFS 3, 4 (≥3) then expect anemia to develop and use graduated fluid therapy (1/3 shock dose and repeat as fluid challenge needed)<br>• If becomes severely anemic PCV <25% generally needs a blood transfusion and less commonly surgery<br>*Expect when bleeding stops for the intraabdominal hemorrhage to resolve (AFS lessens to AFS 1 or 0) within 48 hours* |
| Penetrating Trauma – Think Surgical for Any Positive AFS<br>Blood from ripping, tearing, crushing is often clotted and thus often missed acutely during AFAST because clotted blood looks like adjacent soft tissue; however, in time blood clots will defibrinate and become visible during AFAST, so serial exams are key in cases in which you are unsure if medical vs surgical<br>Generally best to assume that it is a surgical problem with ANY positive in penetrating trauma | • Think Surgical for Any AFS Positive<br>• Combine with other clinical findings and surgical indications (hernia, free air, septic abdomen, refractory pain, etc.)<br>• Serial exams are key Even days later<br>• Sample fluid when accessible | • Think Surgical for Any AFS Positive<br>• Combine with other clinical findings and surgical indications (hernia, free air, septic abdomen, refractory pain, etc.)<br>• Serial exams are key Even days later<br>• Sample fluid when accessible |
| Postinterventional Trauma – Think Medical for AFS 1, 2 and Surgical for AFS 3, 4<br>Large-volume bleeding (AFS 3, 4, ≥3) is generally not going to stop without surgical correction<br>*Correct coagulopathy if present* | • If stays AFS 1, 2 (AFS <3) on serial exams, then generally NOT a surgical problem<br>• Do serial exams to make sure does not change score and become a large-volume bleeder (AFS 3, 4)<br>• Sample fluid when accessible<br>*Expect when bleeding stops for the intraabdominal hemorrhage to resolve within 48 hours* | • If an AFS 3, 4 (≥3) and not anemic, then generally it is still best to explore emergently and NOT wait (if you wait, you will likely have to blood transfuse your patient with its added extra cost and more patient surgical risk)<br>• If an AFS 3, 4 (≥3 and already anemic, transfuse as per patient assessment and explore emergently<br>• Sample fluid when accessible<br>*Expect when bleeding stops for the intraabdominal hemorrhage to resolve (AFS 1 or 0) within 48 hours* |

Source: Reproduced with permission from Dr Gregory Lisciandro, Hill Country Veterinary Specialists and FASTVet.com, Spicewood, TX.

nontrauma hemoabdomen feline warrants the Global FAST approach as a first-line test since neoplasia is the most common cause (Culp et al. 2010) (see Chapters 36 and 37).

### *Autotransfusion in Cats*

The mesothelial cells lining the peritoneal and retroperitoneal cavities and the pericardial sac are very efficient in defibrinating blood, resulting in free

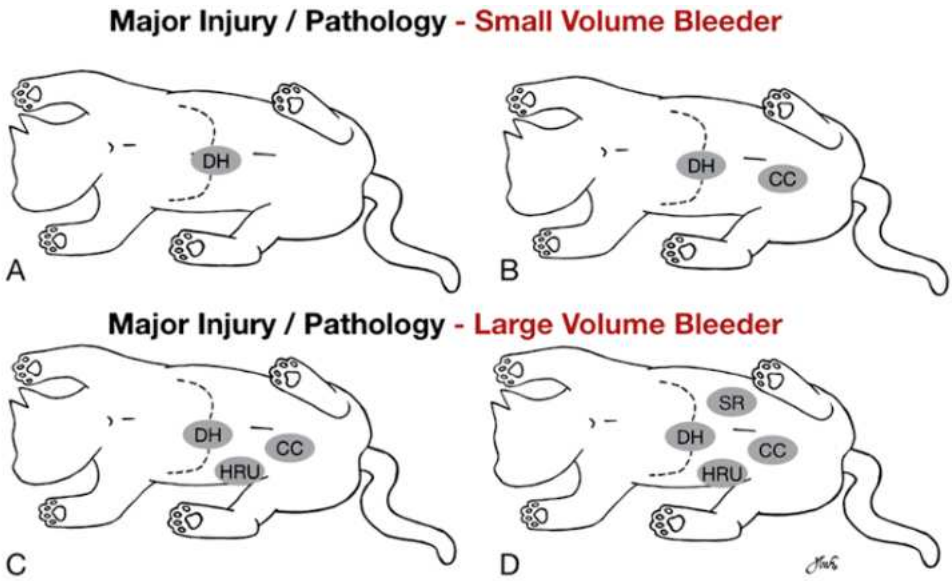


**Figure 39.26.** The AFAST-applied fluid scoring system helps by semiquantitating the volume of effusion within the abdominal cavity. In bleeding cats, as a general rule, AFS 1 and 2 (<3) that remain AFS 1 and 2 (<3) do not have enough blood to cause anemia as shown in (A) and (B). On the other hand, AFS 3 and 4 (≥3) cats do have enough blood in their abdominal cavity to anticipate anemia if anemia is not already present as shown in (C) and (D). AFS 1 and 2 (<3) are referred to as major injury (pathology), small-volume bleeder and AFS 3 and 4 (≥ 3) as major injury (pathology), large-volume bleeder. In nonhemorrhagic effusions, small-volume bleeder is replaced with small-volume effusion and large-volume bleeder with large-volume effusion. Source: Reproduced with permission from Dr Gregory Lisciandro, Hill Country Veterinary Specialists and FASTVet.com, Spicewood, TX. Illustration by Hannah M. Cole, Adkins, TX.

cavitary hemorrhage with few to no clots. Thus, importantly, there is no need to use anticoagulant when harvesting this blood, giving the attending clinician the option for autotransfusion with autologous blood in dogs and cats (Higgs et al. 2015; Robinson et al. 2016; Cole and Humm 2019). For autotransfusion, a blood filter is required to prevent thromboembolic complications from any small or occult clots within the harvested blood.

# Feline Thorax – TFAST and Vet BLUE

TFAST has become the staple for quick assessment of the heart, with three major echo views, the presence of pleural and pericardial effusion, and volume status view with the FAST DH view. The three TFAST echo views are performed at the right TFAST pericardial view and include the left ventricular short-axis view (LVSA, also called the mushroom view), the short-axis left atrial to aortic ratio (LA:Ao, called the "Mercedes-Benz view"), and the long-axis four-chamber view (LA4CV) for the right ventricular to left ventricular ratio (RV:LV) (Figure 39.27) (see also Figures 17.25, 17.26).

It is important to understand that left-sided congestive heart failure results in pulmonary edema and right-sided congestive heart failure in hepatic congestion. Thus, "Global FAST nonecho fallback views", Vet BLUE and the FAST DH view help minimize feline risk when echo views and/or radiographs cannot be safely performed (Lisciandro 2011, 2014a–d, 2019; Boysen and Lisciandro 2013; Lisciandro et al. 2016, 2017, 2018; Ward et al. 2017, 2018a,b).

## *Safe Positioning for Felines*

The saying that "death begins in radiology" in human medicine rings very true for the hemodynamically fragile and respiratory distressed feline. The axiom in human medicine is *never send a patient to radiology without a good physical examination and an EFAST exam* (analogous to our Global FAST approach). If you can place a stethoscope on your feline patient, you can place an ultrasound probe and most cats that are focusing on breathing will allow their forelegs to be placed on a roll of paper towels or a towel. The well-tolerated maneuver allows the ventral thoracic TFAST and Vet BLUE acoustic windows to be evaluated (TFAST echo views and assessment for presence and

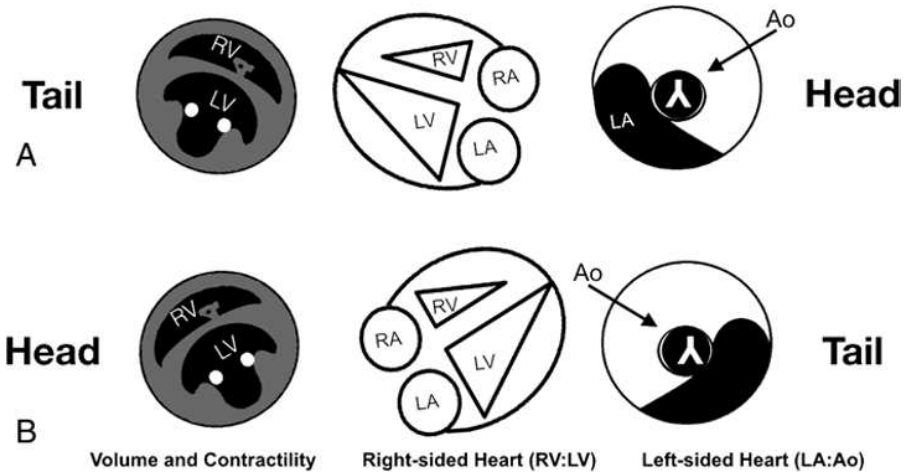


**Figure 39.27.** TFAST echo views expected normal ratios. Row (A) shows the views with the cardiac orientation in which the head and tail are reversed from all other imaging. Row (B) shows the same views, with the same orientation in which all other ultrasound is performed – the head to the left and tail to the right (same as radiography). Note that the orientation with head to the left and tail to the right is consistent with the orientation for all acoustic windows of AFAST, TFAST, and Vet BLUE – the Global FAST approach. The "eyeball method" is used for judging chamber sizes and their ratios and ventricular contractility without measurements. The "eyeball method" is more challenging in cats than in dogs because of the tight acoustic windows of the feline echo views due to the small size of the feline heart and faster heart rates. Freezing and rolling the cine ball to scroll through captured images of the heart will be necessary in most cats. The short-axis left ventricular view (LVSA) at the level of the chordae tendinae depicted by the two hyperechoic (white) dots is used for assessing both filling (volume status) and contractility. The long axis four-chamber view (LA4CV) screens for right-sided heart problems by the RV:LV. The short-axis view at the heart base where the "Mercedes-Benz sign" of the aorta is located screens for left-sided heart problems via the LA:Ao. Source: Reproduced with permission from Dr Gregory Lisciandro, Hill Country Veterinary Specialists and FASTVet.com, Spicewood, TX.

absence of pleural and pericardial effusion [PCS and DH views], plus obvious thoracic-related masses, and Vet BLUE) (Figure 39.28).

## Safer Acoustic Coupling Medium for Felines

The use of minimal isopropyl alcohol to wet and part the hair followed by alcohol-based hand sanitizer is a good option because the hand sanitizer lacks the noxious fumes, especially when cats are placed in oxygen cages, and is less noxious from the cold feeling when applied to skin (Figure 39.29). Moreover, minimal application of isopropyl alcohol is less likely to lower your patient's body temperature from its evaporative properties.

## Assessing Chamber Size (LVSA)

In cats, the heart is more challenging to image due to its small size and rounded shape compared to dogs. The cardiac planes are within a tight acoustic window and acquiring standard echo views differs by millimeters, so hand motion is much more subtle. Furthermore, the heart rate is generally much faster than dogs and hence evaluating the chambers, size, and ratios can be challenging without the use of cine loops. In other words, freeze and roll the cine ball to best evaluate the heart in most cats; in fact, in real time, judging cardiac chamber size and filling, the so-called "eyeball method," is more prone to error in cats. In contrast, most dogs, unless tachycardic, may be accurately evaluated in real time using the "eyeball method."

## Left Atrial to Aortic Ratio on Short Axis

When ruling out left-sided CHF, the ratio of diameters between the left atrium and aorta (LA:Ao) is measured or assessed visually by the "eyeball method" and most commonly in short axis (see Figure 39.27). The normal LA:Ao in cats should be <1.6:1 (versus <1.3:1 in dogs). Most often, the noncardiologist is looking for obvious increases in the LA:Ao (>2:1) in both cats and dogs. This measurement may be done using M-mode or B-mode. An increased LA:Ao and a positive Vet BLUE exam of ≥2 Volpicelli Strong Positive sites bilaterally in each hemithorax increase the probability for left-sided

**Figure 39.28.** Safe positioning for cats. In hemodynamically fragile or respiratory distressed cats, gently place a roll of paper towels or a towel under the forelegs as shown to better evaluate the gravity-dependent TFAST PCS and DH views. If minimal restraint is applied, your patient will likely focus on breathing, not panic, and in the majority of cases allow you to perform TFAST and Vet BLUE (and AFAST may be performed in standing or sternal until the patient is more stable to be placed in lateral recumbency). Source: Reproduced with permission from Dr Gregory Lisciandro, Hill Country Veterinary Specialists and FASTVet.com, Spicewood, TX.

congestive heart failure (Ward et al. 2017). Vet BLUE alone without the LA:Ao has the same high sensitivity and specificity for left-sided congestive heart failure as radiography and also serves as a rapid test to rule out left-sided CHF (Lisciandro et al. 2016, 2017, 2018; Ward et al. 2017, 2018b). See Chapters 22 and 23 and Figures 23.14, 23.17, and 36.17.

The reader should note that lung ultrasound, Vet BLUE, is the "Global FAST nonecho fallback view" when the TFAST echo view (quick peek LA:Ao) cannot be adequately imaged, especially in unstable, hemodynamically fragile, distressed cats. "Absent B-lines in All (Vet BLUE) Views" (ABAV) rules out left-sided CHF in cats with high sensitivity (96%) (Lisciandro et al. 2016) (Figure 39.30).

## *Left Ventricular Short-axis View for Volume Status and Contractility*

The left ventricular short-axis "mushroom view" for volume and contractility, fractional shortening percentage (FS%), is useful in cats, with some important differences from dogs (see Figures 17.25, 17.26, and 39.30). The view is often less reliable when judging in real time for the aforementioned reasons of the faster heart rate of felines making the left ventricular look thick and volume look deficient, and commonly results in assuming hypertrophic cardiomyopathy when in fact the cat is volume contracted (and empirical diuretic therapy potentially harmful). Pressing the freeze button and rolling the cine ball is the best way to estimate volume and contractility. Using Vet BLUE findings will give additional information regarding the presence or absence of alveolar-interstitial edema, and the degree by numbers of positive sites along with actual numbers of B-lines (Vet BLUE B-line scoring system; see Figures 23.14, 23.17, and 36.17).

The "Global FAST nonecho fallback view" for volume status is the FAST DH view and the characterization of the CVC and its associated hepatic veins. Hepatic veins should not be evident in normalcy when cats are imaged in lateral or standing/sternal positioning. The CVC is characterized as being flat with poor volume (hypovolemic CVC), FAT with too much volume (fluid-intolerant CVC due to high CVP) and right-sided heart failure/overload, or with a bounce (fluid-responsive CVC) (see Figures 7.12 and 39.30 and Table 7.6) (see Chapters 6, 7, 17–21, 26, 36, and 37).

The reader should note that the characterization of the CVC and its associated hepatic veins are the "Global FAST nonecho fallback views" when the TFAST echo view (LVSA) cannot be adequately imaged, especially in unstable, hemodynamically fragile, distressed cats.

## *Right Ventricular to Left Ventricular Ratio (RV:LV) on Long-axis Four-Chamber View*

With the feline heart being more rounded, and right-sided heart disease less common than in dogs and cats having higher heart rates, the right ventricular to left ventricular ratio (RV:LV) is more difficult to assess in real time (see Figure 39.27). Freeze and roll the cine ball to get a better idea of unremarkable versus abnormal. The "Global FAST nonecho fallback view" for right-sided CHF is characterizing the CVC and hepatic veins (see previous paragraph, Figure 7.12 and Table 7.6). The RV:LV is observed on the long-axis four-chamber view (see Figure 39.30).

The reader should note that the characterization of the CVC and its associated hepatic veins are the "Global FAST nonecho fallback views" when the TFAST echo view (LA4CV) cannot be adequately imaged, especially in unstable, hemodynamically fragile, distressed cats (see Figure 7.12 and Table 7.6).

**Figure 39.29.** Different options for coupling medium in cats. Acoustic coupling medium is important for maximizing image quality while minimizing noxious features to the patient. The author prefers a small amount of (A) isopropyl isopropyl alcohol to part the hair followed by hand sanitizer (B), being less noxious than the cold and fumes of alcohol; moreover, hand sanitizer wipes off more easily (and evaporates) when compared to (C) commercially available acoustic coupling gels. Check with the probe manufacturer to make sure that the coupling medium is approved for your probe. A squeeze bottle is less startling to your patient or, if a spray bottle is used, squeeze the trigger slowly with the spray head as close as possible to the patient's skin. Part the hair to get as close to the skin as possible. Placing the probe on a wetted mat of hair often makes for lots of air trapping and a poor image (see Figure 5.2). Source: Reproduced with permission from Dr Gregory Lisciandro, Hill Country Veterinary Specialists and FASTVet.com, Spicewood, TX.

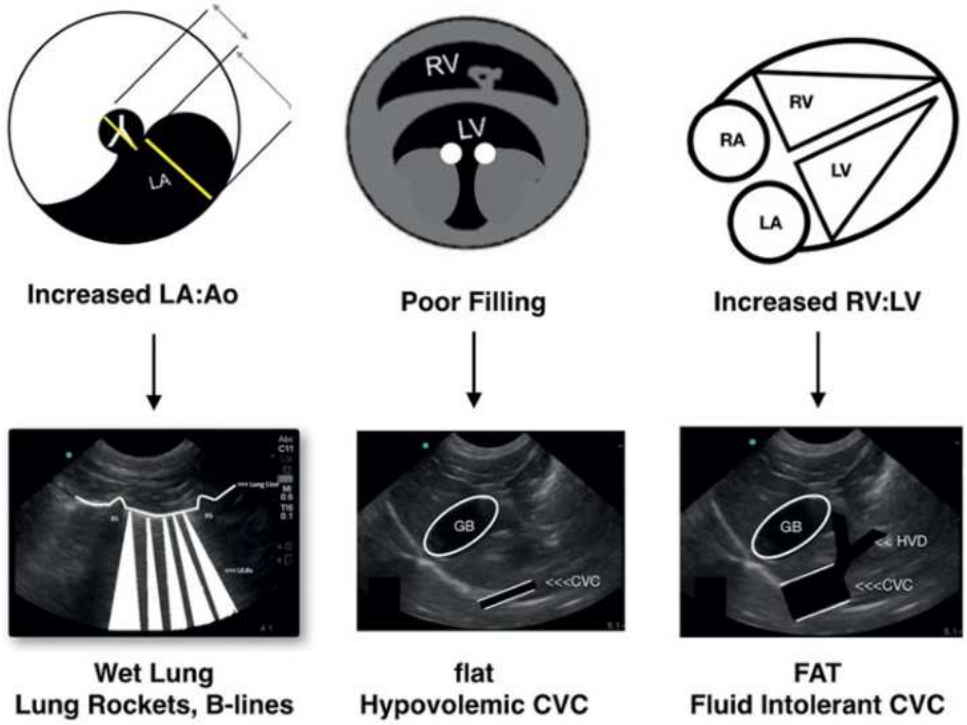


**Figure 39.30.** TFAST echo views and fallback views. TFAST echo views abnormal findings and their respective nonecho fallback views. Note the head is to the left and the tail to the right with the same orientation for a radiograph. Fallback views either double-check TFAST echo findings or are used when your patient is too unstable to get a TFAST echo view. The FAST DH view is used for CVC and hepatic venous characterization (unremarkable versus distended), which is helpful for volume status and right-sided congestive heart failure – volume overload. Vet BLUE images wet versus dry lung, the presence and absence of B-lines, for left-sided congestive heart failure – volume overload. Source: Reproduced with permission from Dr Gregory Lisciandro, Hill Country Veterinary Specialists and FASTVet.com, Spicewood, TX.

VetBooks.ir

### Differences in Echo Assessment

The major difference between cats and dogs primarily lies in image acquisition. The small size of the feline heart, its rapid rate, coupled with how tight the acoustic windows are for the various short- and long-axis views require very small hand movements. The "eyeball method" or gestalt approach, generally effective in dogs during real-time B-mode imaging, is more error prone in the majority of cats due to their more rapid heart rate and difficulty of holding the view of interest. The sonographer will need to learn how to freeze and roll the cine ball to accurately evaluate the feline heart and understand the use of "Global FAST nonecho fallback views" for the left and right heart for better clinical integration of information.

**Pearl:** The single most important TFAST echo view is the LA:Ao in short axis. If that is too risky, perform a Vet BLUE for two reasons: (1) left-sided CHF is rapidly ruled out in cats with absent B-lines all Vet BLUE views (ABAV), and (2) left-sided CHF is highly probable in cats with strong positive views (>3 or infinite B-lines) at two or more Vet BLUE views bilaterally (Ward et al. 2017). Don't jeopardize your feline patient trying to get the echo view(s) or a radiograph, but rather use the above strategy for an evidence-based working diagnosis, treat for CHF (or conversely asthma) and give the feline patient more time to stabilize (Ward et al. 2018b).

### Differences in the Sonographic Diagnosis and Causes of Pericardial Effusion

The accurate diagnosis of pericardial effusion in cats is similar to that in dogs (Lisciandro 2016). The tenets for accurately detecting pericardial effusion are as follows.

- See the heart in its entirety using the bright pericardium in the far-field as a landmark.
- One view is no view.
- Image toward the muscular apex of the heart using the FAST DH view and the TFAST right PCS view, thus minimizing mistaking the heart for free fluid (Lisciandro 2014a,b, 2016).
- Only the long-axis four-chamber view is an acceptable *single* view by knowing that the anatomy of the pericardium and the pericardial sac extends from one atrium around the muscular apex of the heart to the other atrium while identifying all four chambers, thus preventing mistaking a heart chamber for pericardial (or pleural) effusion (Lisciandro z2014a,b, 2016).

The most common cause of pericardial effusion in cats (~75%) is congestive heart failure, much different than in dogs (Davidson et al. 2008; Hall et al. 2007). In fact, in a recent feline study, pericardial effusion was 100% specific for feline CHF in cats enrolled at two different veterinary colleges (North Carolina State and Iowa State) (Ward et al. 2018a). In contrast to dogs, the feline heart is less reliably imaged via the FAST DH view, but when clinically relevant pericardial effusion is present, it will likely be observed via the FAST DH view. See Chapters 6, 7, 17–21 for more detail.

The accurate diagnosis of pleural effusion in cats is similar to that in dogs. The tenets for accurately detecting pleural effusion are as follows (Lisciandro 2014b, 2016).

- See the heart in its entirety using the bright pericardium in the far-field as a landmark.
- One view is no view – combine views.
- Image toward the muscular apex of the heart, FAST DH view, and TFAST right PCS view, minimizing mistaking the heart for free fluid as done for pericardial effusion.
- Perform the TFAST slide by recognizing the heart and then sliding caudally toward the diaphragm, followed by cranially toward the cervical region to observe for free fluid away from the heart.
- Only the long-axis four-chamber view is an acceptable *single* view by knowing that the anatomy of the pericardium and the pericardial sac extends from one atrium around the muscular apex of the heart to the other atrium while identifying all four chambers, thus preventing mistaking a heart chamber for pericardial (or pleural) effusion.

See Chapters 6, 7, 17–21 for more detail.

**Pearl:** Felines with pleural effusion and lung edema detected during TFAST and Vet BLUE, respectively, that have concurrent pericardial effusion of any degree very likely have CHF as their cause of distress (Ward et al. 2018a). Don't jeopardize your feline patient trying to get the echo view(s) or a radiograph, but rather use the above strategy for an evidence-based working diagnosis, treat for CHF (or conversely asthma) and give them time to stabilize.

### Differences in Detecting "Lung Sliding" and Pneumothorax during TFAST (Figure 39.31)

Regardless of the species, rapid shallow breathing is problematic for the detection of pneumothorax (PTX). For cats, mild sedation such as butorphanol, that may be given subcutaneously and is less likely to contribute to panting, is very helpful to slow the respiratory pattern through the alleviation of anxiety. Probe maneuvers that enhance "lung sliding" are placing the rib head in the center of the screen to scatter echoes ("one-eyed gator sign"), and fanning the probe from a 90° angle of insonation to a 75° angle to oblique the echoes (Lisciandro 2014b,c). In the author's experience (GL), spontaneously breathing cats with PTX have too much thoracic wall movement for M-mode to be effective (slowing the frame speed down is an important tip). The "lung point" should be sought in any suspect PTX feline and the TFAST PTX 1/3s Rule used for monitoring and decision making (Figure 39.32). See Chapters 17, 18, 22, and 23 for greater detail (Lisciandro et al. 2008; Lisciandro 2011; Boysen and Lisciandro 2013).

### Differences in Vet BLUE

Imaging of the lung is similar in cats and dogs. Expect all Vet BLUE views to be dry, "lung sliding" with A-lines, with uncommon B-lines in both adult and juvenile cats in normalcy (Lisciandro et al. 2017, 2018) (Figure 39.33). Moreover, the absence of B-lines during Vet BLUE (ABAV) in respiratory distressed cats (and dogs) effectively rules out left-sided CHF, sparing the patient the risk of restraint for an echocardiogram or thoracic radiography until they are more stable (Lisciandro et al. 2016, 2017; Ward et al. 2017). See Chapters 22 and 23 for greater detail.

### Differences in Applications of the Vet BLUE B-line Scoring System

Use of the Volpicelli Strong Positive Model, meaning that only a score of >3 or infinite B-lines is a "positive," works better for CHF in cats than dogs (see Figures 23.14, 23.17, and 36.17). In cats, Vet BLUE had the same sensitivity (87%) and specificity (89%) as thoracic radiography (Ward et al. 2017). However, regional disease as well as other "wet lung phenomena" must also be considered. In Texas, where one of the authors resides, fungal pneumonia caused by histoplasmosis has an overall Vet BLUE wet pattern (many B-lines) similar to that expected for feline CHF. Thus, the finding of the nodule sign is helpful for ruling in fungal granulomas (or neoplastic processes) that may otherwise be missed on thoracic radiography, especially when pleural effusion is present, or delayed, or missed depending on whether more advanced imaging is performed. Other inflammatory conditions may also mimic feline congestive heart failure using the Volpicelli Strong Positive Model, including parasitic pneumonias

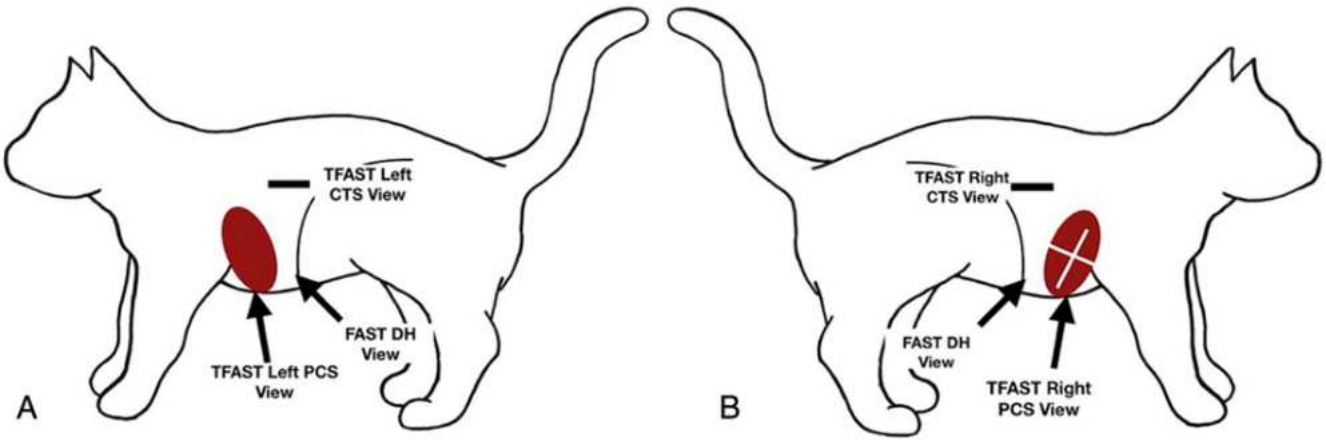


**Figure 39.31.** TFAST and its acoustic windows. TFAST is a five-view examination of the thorax that includes (A) left TFAST PCS view, left CTS view and DH view, and (B) right TFAST PCS view, right CTS view, and DH view. Learning the principle of staying on the "short-axis line" and "long-axis line" expedites becoming proficient with the TFAST echo views. Source: Reproduced with permission from Dr Gregory Lisciandro, Hill Country Veterinary Specialists and FASTVet.com, Spicewood, TX. Cat illustration by Hannah M. Cole, Adkins, TX.

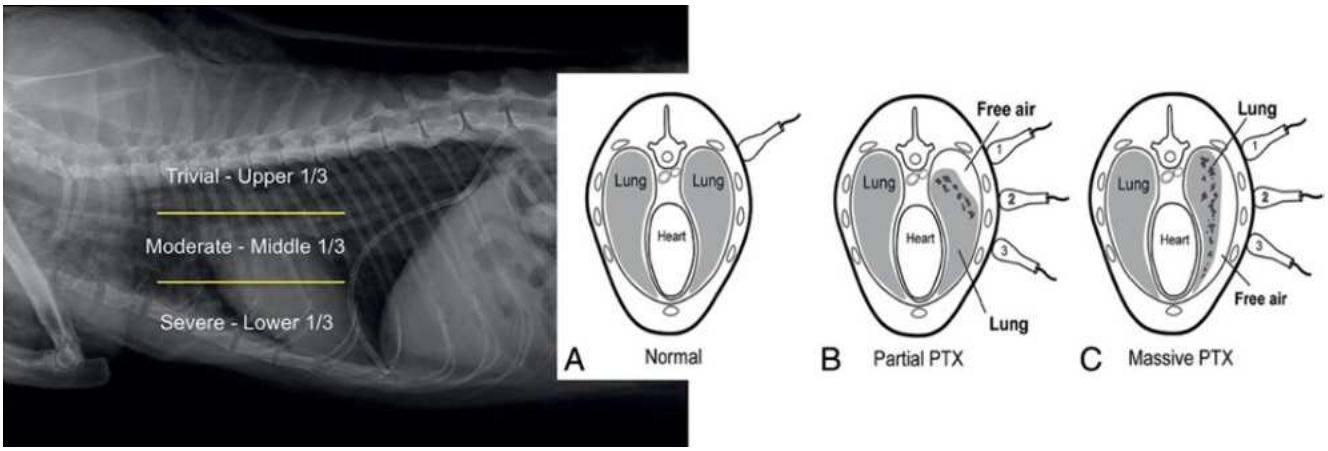


**Figure 39.32.** The "lung point" for semiquantitating and monitoring pneumothorax. The thoracic radiograph (note the cat has a thoracostomy tube in place) shows the thorax divided into thirds to show how the degree of pneumothorax (PTX) may be assessed and tracked. When PTX is present in the upper third, middle third or lower third it is characterized as trivial, moderate and severe, referred to as the TFAST PTX 1/3s Rule, along with clinical judgment. (A) No PTX. (B) PTX exists with a "lung point" in the middle third. (C) No "lung point" is found, making the PTX severe. Source: Reproduced with permission from Lisciandro (2011).

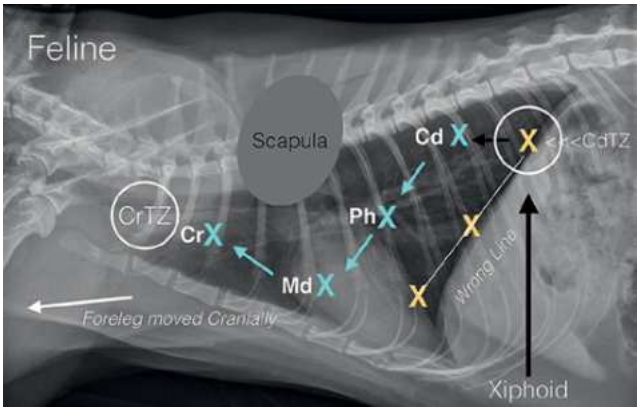


**Figure 39.33.** The feline Vet BLUE protocol. How to select the transthoracic Vet BLUE views by following the Vet BLUE line and its ninth acoustic window of the DH view. The nine Vet BLUE acoustic windows are the same for cats and dogs. The methodology is standardized and helps to avoid mistaking extreme margins of lungs, structures along the boundaries of lung, and abdominal structures for lung pathology. See Chapters 22 and 23 for greater detail. Cd, Caudodorsal lung region; Ph, Perihilar lung region; Md, Middle lung region; Cr, Cranial lung regions; CdTZ, caudodorsal transition zone; CrTZ, cranial transition zone. Source: Reproduced with permission from Dr Gregory Lisciandro, Hill Country Veterinary Specialists and FASTVet.com, Spicewood, TX.

(*Alurostrongylus abstrusus*, *Paragominus kellicotti*), feline anaphylaxis, diffuse hemorrhage, and other diffuse inflammatory conditions. See Chapters 22 and 23 for greater detail and Figures 23.14, 23.17, and 36.17.

# Performing Global FAST in a Cat

In our experience, the most efficient way to perform Global FAST in the cat is Vet BLUE-TFAST blend in standing, followed by AFAST in either lateral recumbency or the entire Global FAST in standing (Figure 39.34). AFAST in lateral or standing has identical acoustic windows and image acquisition with the respective target organs. If fluid negative during a standing or sternal AFAST, then there is likely no need to move to lateral for an abdominal fluid score (AFS). If AFAST is positive in standing or sternal, then when safe for the patient, move the cat to lateral recumbency, wait three minutes, then assign an AFS (see Chapters 6 and 7).

# Goal-Directed Templates

See Chapters 7, 18, 23, 36, and the Appendices.

# Pearls and Pitfalls, The Final Say

The sonographer using POCUS and FAST ultrasound needs to understand and acknowledge that cats are not small dogs and have important inherent differences sonographically (Table 39.3). These differences are important for proper interpretation of findings in the feline.

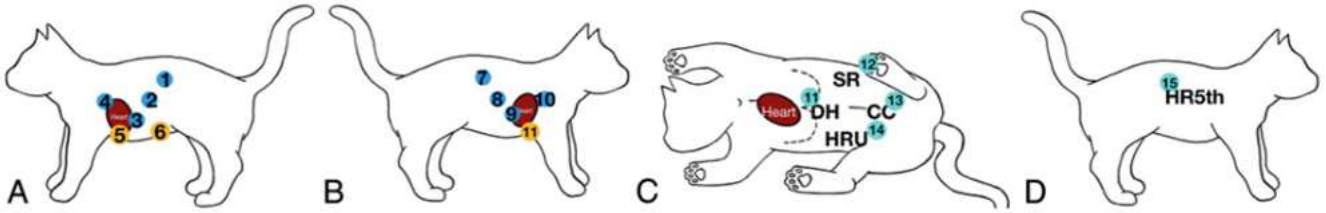


**Figure 39.34.** Efficiently performing Global FAST in the cat. The Global FAST format in the authors' recommended order. (A) Left Vet BLUE, left PCS view, DH view to (B) right Vet BLUE and right PCS view with echocardiographic views of the heart to (C) AFAST and its fluid scoring system and lastly (D) the AFAST HR5th bonus view. The AFAST may be performed with the same acoustic windows as in lateral recumbency in a standing feline especially when lateral restraint is risky. The AFAST-applied fluid scoring system is not valid in other than lateral recumbency, but when standing-sternal cats are negative (AFS 0) then fluid scoring in lateral is likely unnecessary. If a fragile cat is fluid positive then fluid may still be estimated, but a valid fluid score should wait until lateral recumbency is acceptably safe. Source: Reproduced with permission from Dr Gregory Lisciandro, Hill Country Veterinary Specialists and FASTVet.com, Spicewood, TX. Illustration by Hannah M. Cole, Adkins, TX.

**Table 39.3.**
Quick reference of normals and rules of thumb.

| Feline reference values | | Measurements |
|---|---|---|
| Stomach | Larger amount of fat in the submucosal layer. Pyloric duodenal junction located at midline and J-shaped | 1.7–3.6 mm (Newell et al. 1999; Goggin et al. 2000; Winter et al. 2014)<br>Obvious abnormal >6 mm |
| Duodenum | Ventral to right kidney. The cranial duodenal flexure is near the hepatic hilus using the portal vein as a reference. It lies ventral to it | 2.0–2.5 mm (Newell et al. 1999; Goggin et al. 2000; Winter et al. 2014; di Donato et al. 2014)<br>Obvious abnormal >4 mm |
| Small intestine | The jejunum is distinctly different with a prominent hyperechoic submucosal layer especially near the ileocecal junction (ICCJ). The ICCJ has a distinct appearance on a short-axis view. It resembles an empty miniature stomach, referred to as a "wagon wheel" appearance | Jejunum 2.0–2.5 mm (Newell et al. 1999; Goggin et al. 2000; Winter et al. 2014; di Donato et al. 2014)<br>Obvious abnormal >3 mm<br>Ileum 2.5–3.2 mm (Newell et al. 1999; Goggin et al. 2000; Winter et al. 2014; di Donato et al. 2014)<br>Obvious abnormal >4 mm |
| Pancreas | The left pancreatic lobe is larger and more prominent | Left pancreatic lobe ranges between 5 and 9 mm; right pancreatic lobe ranges between 3 and 6 mm (Nyland and Mattoon 2015a)<br>Obvious abnormal <1 cm<br>Feline pancreatic duct can be up to 6 mm (Hecht et al. 2006) |
| Liver | Adjacent often robust feline falciform fat can be confused with liver parenchyma if the depth is not set properly. The hepatic echogenicity pattern is otherwise similar to the dog | |
| Gallbladder | The common bile duct may be tortuous in normalcy in cats (and thus mistaken for pathology) | Common bile duct normally ≤4 mm; when >5 mm extrabiliary obstruction should be suspected (d'Anjou 2008b) |
| Spleen | | Normal is <10 mm in thickness and abnormal when >10 mm (Reese et al. 2013)<br>Obvious abnormal >10 mm |

(*Continued*)

**Table 39.3.**
(*Continued*)

| Feline reference values | | Measurements |
|---|---|---|
| Kidney | In obese cats, the cortex tends to be hyperechoic | Normal size<br>Length from 3 to 4.5 cm Width from 2.2 to 2.8 cm Height from 1.9 to 2.5 cm (Nickel et al. 1973; Walter et al. 1987; d'Anjou 2008a; Nevins et al. 2015)<br>Obvious abnormal: renomegaly >4.5 cm (sagittal plane)<br>Renal pelvis and pyelectasia:<br>the normal renal pelvis is collapsed, typically measuring less than 2 mm; normal renal pelvic dilation ranges from 1.5 to 2 mm with maximum height of 2.8 mm in cats (d'Anjou 2008a)<br>Obvious abnormal ≥3 mm |
| Urinary bladder | The contents are commonly echogenic from floating fat vacuoles | |
| Prostate | Rarely seen sonographically in neutered cats. In intact males, the prostate is small, ovoid, and hyperechoic. Prostatic disease is rare in cats | Ellipsoid formula: length × height × width × 0.524 (Nyland and Mattoon 2015b) |
| Uterus | The nongravid uterus is tubular, homogeneous in echotexture, with a lumen that is not readily seen and is differentiated from small intestine by lack of peristalsis, lack of intraluminal gas, and absence of the layered appearance (Mattoon 2015). Uterine width varies from 3 to 5 mm in cats and 5 to 10 mm in dogs | Uterine width varies from 3 to 5 mm in cats |
| AFAST-applied abdominal fluid score | Expect AFS 0 to 1/2 as not uncommonly adult and juvenile cats have a small linear stripe of free fluid along the diaphragm at the DH view | AFS <1/2–1 with maximum dimensions <3 mm (Lisciandro et al. 2015) |
| Caudal vena cava and hepatic veins | Similar to dogs | Hepatic veins are not obvious in normalcy; the CVC should fluctuate approximately 35–50% during respiratory cycles; maximum heights extrapolated from small dogs of <0.25 considered hypovolemic and >1.0 cm considered hypervolemic (FAT, right-sided volume overload) (Darnis et al. 2018) |
| Heart and TFAST echo views | Similar to dogs; however, because of normal faster heart rates the "eyeball method" is much less reliable so using the freeze function and rolling the cine ball to evaluate frame by frame is necessary for felines | LA:Ao <1.6:1 – the left atrium should be no more than ~1.6 times the size of the aorta; obvious abnormal LA:Ao >2:1 (Abbott and MacLean 2006)<br>RV:LV 1:3–4 – the right ventricle should be no more than 1/3 to 1/4 the size of the left ventricle; obvious abnormal 1:1 (Kittleson and Kienle 1998)<br>Fractional shortening ~30–50% (Kittleson and Kienle 1998) |
| Vet BLUE and expected numbers of B-lines | Similar to dogs | Expect absent B-lines all Vet BLUE views in cats and kittens >6 weeks of age (Lisciandro et al. 2017, 2018); approximately 12% of the time a *single* B-line at a *single* Vet BLUE transthoracic view is present |

Source: Reproduced with permission from Dr Gregory Lisciandro, Hill Country Veterinary Specialists and FASTVet.com, Spicewood, TX.

# References


Abbott JA, MacLean HN. 2006. Two-dimensional echocardiographic assessment of the feline left atrium. *J Vet Intern Med* 20:111–119.

Boysen SR, Lisciandro GR. 2013. The use of ultrasound in the emergency room (AFAST and TFAST). *Vet Clin North Am Small Anim Pract* 43(4):773–797.

Carlisle CH. 1977. Radiographic anatomy of the cat gallbladder. *Vet Radiol Ultrasound* 18:170–172.

Cole LP, Humm K. 2019. Twelve autologous blood transfusions in eight cats with hemoperitoenum. *J Feline Med Surg* 21:481–487.

Culp WT, Weisse C, Kellogg ME, et al. 2010. Spontaneous hemoperitoneum in cats: 65 cases (1994–2006). *J Am Vet Med Assoc* 236(9):978–982.

D'Anjou MA. 2008a. Kidneys and ureters. In: *Atlas of Small Animal Ultrasonography*, edited by Penninck D, d'Anjou MA. Ames: Blackwell Publishing, pp 351–357.

D'Anjou MA. 2008b. Liver. In: *Atlas of Small Animal Ultrasonography*, edited by Penninck D, d'Anjou MA. Ames: Blackwell Publishing, pp 243–247.

Darnis E, Boysen S, Merveille AC, et al. 2018. Establishment of reference values of the caudal vena cava by fast-ultrasonography through different views in healthy dogs. *J Vet Intern Med* 32(4):1308–1318.

Davidson BJ, Paling AC, Lahmers SL, et al. 2008. Disease association and clinical assessment of pericardial effusion. *J Am Anim Hosp* 44(1):5–9.

Di Donato P, Penninck D, Pietra M, et al. 2014. Ultrasonographic measurment of the relative thickness of intestinal wall layers in clinical healthy cats. *J Feline Med Surg* 16:333–339.

Dimitrov RP, Yonkova, Stamatova K. 2010. Comparative ultrasonographic study on prostate and bulbourethral glands of tomcat. *Bulg J Agric Sci* 16:521–525.

Ferrada P, Vanguri P, Anand RJ, et al. 2012a. Flat inferior cava: indicator of poor prognosis in trauma and acute care surgery patients. *Am Surg* 78(12):1396–1398.

Ferrada P, Anand RJ, Wheelan J, et al. 2012b. Qualitative assessment of the inferior vena cava: useful tool for the evaluation of fluid status in critically ill patients. *Am Surg* 78(4):468–470.

Goggin JM, Biller DS, Ward H, et al. 2000. Ultrasonographic measurement gastrointestinal wall thickness and the ultrasonographic appearance of the ileocolic region in healthy cats. *J Am Anim Hosp Assoc* 36:224–228.

Hall DJ, Shofer F, Meier CK, Sleeper MM. 2007. Pericardial effusion in cats: a retrospective study of clinical findings and outcome in 146 cats. *J Vet Intern Med* 21(5):1002–1007.

Harran N, d'Anjou MA, Dunn M, et al. 2011. Gallbladder sludge on ultrasound is predictive of increased liver enzymes and total bilirubin in cats. *Can Vet J* 52(9): 999–1003.

xHecht S, Penninck DG, Mahony OM, et al. 2006. Relationship of pancreatic duct dilation to age and clinical findings in cats. *Vet Radiol Ultrasound* 47:287–294.

Heng HG, Wrigley RH, Kraft SL, et al. 2005. Fat is responsible for an intramural radiolucent band in the feline stomach wall. *Vet Radiol Ultrasound* 46:54–56.

Higgs VA, Rudloff E, Kirby R, et al. 2015. Autologous blood transfusion in dogs with thoracic or abdominal hemorrhage: 25 cases. *J Vet Emerg Crit Care* 25(6):731–738.

Kittleson MD, Kienle RD (eds). 1998. *Small Animal Cardiovascular Medicine*. St Louis: Mosby, Table 6-2, p 104.

Lisciandro GR. 2011. Abdominal and thoracic focused assessment with sonography for trauma, triage, and monitoring in small animals. *J Vet Emerg Crit Care* 21(2):104–122.

Lisciandro GR. 2012. Evaluation of initial and serial combination focused assessment with sonography for trauma (CFAST) examination of the thorax (TFAST) and abdomen (AFAST) with the application of an abdominal fluid scoring system in 49 traumatized cats. *J Vet Emerg Crit Care* 22(S2):S11.

Lisciandro GR. 2014a. The Abdominal FAST$^3$ (AFAST$^3$) Exam. In: *Focused Ultrasound for the Small Animal Practitioner*, edited by Lisciandro GR. Ames: Wiley Blackwell, pp 17–43.

Lisciandro GR. 2014b. Thoracic FAST (TFAST). In: *Focused Ultrasound Techniques for the Small Animal Practitioner*, edited by Lisciandro GR. Ames: Wiley-Blackwell, pp 140–165.

Lisciandro GR. 2014c. The Vet BLUE lung Scan. In: *Focused Ultrasound for the Small Animal Practitioner*, edited by Lisciandro GR. Ames: Wiley Blackwell, pp 166–188.

Lisciandro GR. 2014d. Focused or COAST$^3$–Cardiopulmonary Resuscitation (CPR), Global FAST (GFAST) and the FAST-ABCDE Exam. In: *Focused Ultrasound Techniques for the Small Animal Practitioner*, edited by Lisciandro GR. Ames: Wiley-Blackwell, pp 269–285.

Lisciandro GR. 2016a. The use of the diaphragmatico-hepatic (DH) views of abdominal and thoracic focused assessment with sonography for triage (AFAST/TFAST) examinations for the detection of pericardial effusion in 24 dogs (2011–2012). *J Vet Emerg Crit Care* 26(1):125–131.

Lisciandro GR. 2016b. Abdominal FAST (AFAST)-detected hemorrhagic abdominal effusion in 11 dogs with acute collapse and gallbladder wall edema (halo sign) with presumed anaphylaxis. Abstract. *J Vet Emerg Crit Care* 26(S1):S8.

Lisciandro GR. 2019. The cardiac gallbladder: case series of 13 dogs and 1 cat with sonographically-detected gallbladder wall edema. *J Vet Emerg Crit Care* 26(S1):S8.

Lisciandro GR, Fosgate GT. 2017. Use of AFAST cysto-colic view urinary bladder measurements to estimate urinary bladder volume in dogs and cats. *J Vet Emerg Crit Care* 27(6):713–717.

Lisciandro GR, Lagutchik MS, Mann KA, et al. 2008. Accuracy of Focused Assessment with Sonography for Trauma (FAST) to detect pneumothorax in 145 dogs with blunt and penetrating trauma. *J Vet Emerg Crit Care* 18(3):258–269.

Lisciandro GR, Lagutchik MS, Mann KA, et al. 2009. Evaluation of an abdominal fluid scoring system determined using abdominal focused assessment with sonography for trauma in 101 dogs with motor vehicle trauma. *J Vet Emerg Crit Care* 19(5):426–437.

Lisciandro GR, Fosgate GT, Fulton RM. 2014. Frequency of ultrasound lung rockets using a regionally-based lung ultrasound examination named veterinary bedside lung ultrasound exam (Vet BLUE) in 98 dogs with normal thoracic radiographic lung findings. *Vet Radiol Ultrasound* 55(3):315–322.

Lisciandro GR, Fosgate GT, Romero LA, et al. 2015. Abdominal FAST (AFAST) and abdominal fluid scores in adult and juvenile cats. *J Vet Emerg Crit Care* 25(S1):S8.

Lisciandro G, Ward J, DeFrancesco T, et al. 2016. Absence of B-lines on lung ultrasound (Vet BLUE Protocol) to rule out left-sided congestive heart failure in 368 cats and dogs. *J Vet Emerg Crit Care* 26(S1):S8–9.

Lisciandro GR, Fulton RM, Fosgate GT, et al. 2017. Frequency of B-lines using a regionally-based lung ultrasound examination (the Vet BLUE protocol) in 49 cats with normal thoracic radiographical lung findings. *J Vet Emerg Crit Care* 27(3):267–277.

Lisciandro GR, Romero L, Fosgate GT. 2018. The frequency of B-Lines and other lung ultrasound artifacts during Vet BLUE in 91 healthy puppies and kittens. Abstract. *J Vet Emerg Crit Care* 28(S1):S16.

Mandell DC, Drobatz K. 1995. Feline hemoperitoneum 16 cases (1986–1993). *J Vet Emerg Crit Care* 5(2):93–97.

McMurray J, Boysen S, Chalhoub S. 2016. Focused assessment with sonography in nontraumatized dogs and cats in the emergency and critical care setting. *J Vet Emerg Crit Care* 26(1):64–73.

Moentk J, Biller DS. Bilobed gallbladder in a cat: ultrasonographic appearance. *Vet Radiol Ultrasound* 34:354–356.

Newell SM, Graham JP, Roberts GD, et al. 1999. Sonography of the normal feline gastrointestinal tract. *Vet Radiol Ultrasound* 40:40–43.

Nevins JR, Mai W, Thomas E. 2015. Associations between ultrasound and clinical findings in 87 cats with urethral obstruction. *Vet Radiol Ultrasound* 56(4):439–447.

Nickel R, Schummer A, Seiferle E, et al. 1973. Urogenital system. In: *The Viscera of the Domestic Mammals*, by Schummer A, Nickel R, Sack WO. Berlin: Verlin Paul Parcy, pp 291–293.

Nyland TC, Mattoon JS. 2015a. Pancreas. In: *Small Animal Diagnostic Ultrasound*, 3rd edition, edited by Matton JS, Nyland TG. St Louis: Elsevier Saunders, pp 438–467.

Nyland TC, Mattoon JS. 2015b. Prostate and testes. In: *Small Animal Diagnostic Ultrasound*, 3rd edition, edited by Mattoon JS, Nyland TG. St Louis: Elsevier Saunders, pp 608–633.

Nyland TC, Mattoon JS. 2015c. Spleen. In: *Small Animal Diagnostic Ultrasound*, 3rd edition, edited by Mattoon JS, Nyland TG. St Louis: Elsevier Saunders, pp 400–437.

Nyland TC, Mattoon JS. 2015d. Ovaries and Uterus. In: *Small Animal Diagnostic Ultrasound*, 3rd edition, edited by Mattoon JS, Nyland TG. St Louis: Elsevier Saunders, pp 634–654.

Nyland TG, Kantrowitz BM, Fisher P, et al. 1989. Ultrasonic determination of kidney volume in the dog. *Vet Radiol Ultrasound* 30:174–180.

Nyland TG, Mattoon JS, Herrgesell EJ, et al. 2002. Liver. In: Small Animal Diagnostic Ultrasound, *2nd edition, edited by Nyland TC, Mattoon JS*. Philadelphia: WB Saunders, pp 93–127.

Nyland TC, Widmer WR, Mattoon JS. 2015a. Urinary Tract. In: *Small Animal Diagnostic Ultrasound*, 3rd edition, edited by Mattoon JS, Nyland TG. St Louis: Elsevier Saunders, pp 557–607.

Nyland TC, Neelis DA, Mattoon JS. 2015b. Gastrointestinal Tract. In: *Small Animal Diagnostic Ultrasound*, 3rd edition, edited by Mattoon JS, Nyland TG. St Louis: Elsevier Saunders, pp 468–500.

Nyland TC, Moon Larson M, Mattoon JS. 2015c. Liver. In: Small Animal Diagnostic Ultrasound, *3rd edition, edited by Mattoon JS, Nyland TG*. St Louis: Elsevier Saunders, pp 332–399.

Quantz JE, Miles MS, Reed AL, et al. 2009. Elevation of alanine transaminase and gallbladderwall abnormalities as biomarkers of anaphylaxis in canine hypersensitivity patients. *J Vet Emerg Crit Care* 19(6):536–544.

Reese SH, Zekas LJ, Iazbik MC, et al. 2013. Effect of sevoflurane anesthesia and blood donation on the sonographic appearance of the spleen in 60 healthy cats. *Vet Radiol Ultrasound* 54(2):168–175.

Robinson DA, Kiefer K, Bassett R, et al. 2016. Autotransfusion in dogs using a 2-syringe technique. *J Vet Emerg Crit Care* 26(6):766–774.

Tsukagoshi T, Ohno K, Tsukamoto, et al. 2012. Decreased gallbladder emptying in dogs with biliary sludge or gallbladder mucocele. *Vet Radiol Ultrasound* 53:84–91.

Walter PA, Feeney DA, Johnston GR, et al. 1987. Feline renal ultrasonography: quantitative analyses of imaged anatomy. *Am J Vet Res* 48:596–599.

Ward JL, Lisciandro GR, Keene BW, et al. 2017. Accuracy of point-of-care lung ultrasonography for the diagnosis of cardiogenic pulmonary edema in dogs and cats with acute dyspnea. *J Am Vet Med Assoc* 250(6):666–675.

Ward JL, Lisciandro GR, Ware WA, et al. 2018a. Evaluation of point-of-care thoracic ultrasound combined with NT-proBNP for the diagnosis of congestive heart failure in cats with dyspnea. *J Vet Intern Med* 32(5):1530–1540.

Ward JL, Lisciandro GR, DeFrancesco TD. 2018b. Distribution of alveolar-interstitial syndrome in dogs and cats with respiratory distress assessed with lung ultrasound versus thoracic radiographs. *J Vet Emerg Crit Care* 28(5):415–428.

Winter MD, Londono L, Berry CR, et al. 2014. Ultrasonographic evaluation of relative gastrointestinal layer thickness in cats without clinical evidence of gastrointestinal tract disease. *J Feline Med Surg* 16:118–124.

# Further Reading

Ivančić M, Mai W. 2008. Qualitative and quantitative comparison of renal vs hepatic ultrasonographic intensity in healthy dogs. *Vet Radiol Ultrasound* 49:368–373.

Matheson JS, O'Brien RT, Delaney F. 2003. Tissue harmonic ultrasound for imaging normal abdominal organs in dogs and cats. *Vet Radiol Ultrasound* 44:205–208.

Ruth JD, Heng HG, Miller MA, Constable PD. 2013. Effect of anisotropy and spatial compound imaging on renal cortical echogenicity in dogs. *Vet Radiol Ultrasound* 54: 659–665.

Sisson DD, Knight DH, Helinski C, et al. 1991. Plasma taurine concentrations and M-mode echocardiographic measures in healthy cats and in cats with dilated cardiomyopathy. *J Vet Intern Med* 5:232–238.

CHAPTER FOURTY

# POCUS: Exotic Companion Mammals

Sara Gardhouse and Hugues Beaufrère

## Introduction

Point-of-care ultrasound (POCUS) of small mammal patients can provide important clinical information. The indications and principles in exotic companion mammals are similar to dogs and cats; however, this chapter will discuss more unique exotic companion mammal conditions that may be detected through POCUS. With advances in ultrasound technology, image quality has improved and its cost is more economical, making ultrasound an option for many exotic companion mammal patients. POCUS and FAST ultrasound of exotic companion mammals, as with dogs and cats, can help direct resuscitation strategies and diagnostic testing decisions and thus assist in emergency management during initial triage of these patients.

### What POCUS: Exotic Companion Mammals Can Do

- Diagnose free fluid in the abdomen.
- Allow for ultrasound-guided cystocentesis.
- Allow for the detection of urinary bladder abnormalities.
- Diagnose pleural effusion and guide thoracocentesis.
- Diagnose pericardial effusion and guide pericardiocentesis.
- Identify obvious abdominal masses and organomegaly.
- Identify obvious cardiac chamber enlargement.

### What POCUS: Exotic Companion Mammals Cannot Do

- Cannot ultrasonographically characterize free fluid, which requires sample acquisition and fluid analysis.
- Cannot replace proper training and experience.

### Indications

- Anorexia.
- Anemia.
- Acute abdomen.
- Suspicion of ascites, pleural effusion, or pericardial effusion.
- Further investigation of urinary tract abnormalities, such as hematuria, dysuria, stranguria, urine staining of the perineum, or history of cystolithiasis.
- Palpable abdominal mass or space-occupying lesion in the abdomen.
- Presence of vaginal discharge.
- Pregnancy diagnosis.
- Heart murmur, abnormal auscultation, or arrhythmias.
- Respiratory distress.

### Objectives

- Recognize basic abnormalities including obvious effusions and masses of the peritoneal and pleural cavities, retroperitoneal space, pericardial sac, and lung.

*Point-of-Care Ultrasound Techniques for the Small Animal Practitioner*, Second Edition. Edited by Gregory R. Lisciandro.
© 2021 John Wiley & Sons, Inc. Published 2021 by John Wiley & Sons, Inc.
Companion website: www.wiley.com/go/lisciandro/ultrasound2

- Understand some unique differences between exotic companion mammals and dogs and cats.
- Understand the limitations of POCUS and FAST ultrasound in exotic companion mammals.

# Anatomy

## Gastrointestinal Tracts

The anatomy of exotic companion mammals is generally similar to domestic carnivores with some important exceptions. Exotic companion mammal herbivores, particularly rabbits and hystricomorph rodents (i.e., guinea pigs, chinchillas), have a unique gastrointestinal system. Herbivorous hindgut fermenters have gastrointestinal tracts that are much larger than exotic companion carnivores, and when distended with gas as a result of ileus, these can hamper ultrasound imaging (ultrasound does not transmit through air). Moreover, their stomach is typically larger and never empty of ingesta in normalcy (solids, fluids, air). Furthermore, these herbivores also possess a large cecum, mainly located in the right abdomen in rabbits and in the central to left abdomen in guinea pigs. Unlike carnivores, rabbits have a gastrointestinal-associated lymphoid organ at their ileocecal junction, called the sacculus rotundus, which is sometimes visible and should not be confused with a mass. Occasionally, the blind end of their cecum is also visualized on ultrasound as thickened, finger-like projections, referred to as the vermiform appendix. It should be noted that ferrets do not have a cecum.

## Spleen

Rabbits have a very small spleen that is sometimes not visualized on a complete detailed abdominal ultrasound examination. Conversely, ferrets have a very large spleen that is easily detected on POCUS and AFAST ultrasound.

## Reproductive

Male guinea pigs have large paired seminal vesicles or vesicular glands that can be mistaken ultrasonographically for uterine horns.

# Patient Positioning and Probe Selection

Hair is generally not shaved but rather parted for maximal probe-to-skin contact with the use of 70% isopropyl alcohol and acoustic coupling gel. Keep in mind the size of the patient and amount of 70% isopropyl alcohol and acoustic coupling gel used because hypothermia can occur quickly, especially in unstable and critical patients. Clinical status should always be evaluated prior to any handling, degrees of restraint, and diagnostics being undertaken. Dyspneic or highly distressed exotic companion mammals often benefit from some degree of sedation and/or anesthesia prior to performing diagnostics, and supportive care principles should be implemented, such as flow-by oxygen. It is also important to have technical support from someone who is comfortable with exotic companion mammal restraint to decrease risk of injury to the patient, handler, and attending veterinarian. Positioning may range from the traditional dorsal recumbency in acceptably stable patients, as in Figure 40.1, to lateral recumbency and even standing (see Chapters 6, 7, 17, 18, 22, 23, 36, and 37).

**Figure 40.1.** Dorsal recumbency positioning in a ferret. Positioning of a ferret (*Mustela putorius furo*) for ultrasound examination of the abdomen. The ferret is sedated and receiving flow-by oxygen for the procedure. Note that the Global FAST approach is now being used in standing position for all three of its components, which may prove helpful in exotic companion mammals by lessening degrees of chemical restraint.

A curvilinear (microconvex) or linear transducer (probe) with a range of 5–10 MHz is often acceptable for larger patients such as rabbits and ferrets. However, a 7.5–8 MHz transducer (probe) for smaller patients is generally more useful. Higher frequency transducers (probes) provide better spatial resolution but will have less depth penetration in the patient (Fischetti 2012).

# Imaging the Normal Exotic Companion Mammal

Guidelines for POCUS and FAST ultrasound examinations, as well as complete detailed abdominal ultrasound and complete echocardiography, are generally analogous to those of the dog and cat with similar indications. However, the ferret gastrointestinal ultrasound examination often provides more diagnostic information and better image quality than the gas-filled abdomens of herbivorous rabbit and rodent patients (Fischetti 2012).

# POCUS-Detected Conditions

FAST ultrasound examinations are highly sensitive and specific for effusions and should be considered as good imaging modalities to rule in and rule out free fluid. On the other hand, soft tissue conditions are more user dependent and should be considered more as a rule-in test, triggering confirmatory imaging and testing.

The different exotic companion mammals and conditions that may be potentially recognized using POCUS and the Global FAST approach (AFAST, TFAST, and Vet BLUE) are described.

## *Ferrets*

### Urinary

Urolithiasis has become less common in ferrets due to improvements in husbandry and diet. However, urolithiasis should be considered in the differential diagnosis for any ferret that presents with stranguria and urinary tract signs (Pollock 2012). POCUS would be useful in rapidly ruling in cystolithiasis and soft tissue abnormalities of the urinary bladder as a cause of the ferret's presenting signs (Figure 40.2). A cystocentesis with ultrasound guidance can easily be performed in ferrets, providing a safer option over blind cystocentesis.

Another important differential for stranguria in the ferret is prostatic cysts, which often develop in association with adrenocortical disease. On POCUS, prostatic cysts often contain hypoechoic to anechoic (black) fluid. (Pollock, 2012) (Figure 40.3). Enlarged or irregular adrenal glands may also be detected or suspected via POCUS (Figure 40.4).

### Gastrointestinal and Hepatobiliary

Gastrointestinal foreign bodies in ferrets are typically not radiodense and thus are less obvious. Additionally, there may not be obvious radiographic signs of mechanical ileus compared to other domestic carnivores. Thus, ultrasonographic confirmation is often required prior to surgery and has been shown to be a more reliable test in dogs, when performed by skilled sonographers (Sharma et al. 2011). Indirect evidence of an obstruction and evidence of peritonitis may be recognized by general AFAST principles and the finding of distended loops of small intestine as well as plication may be noted (see Chapters 6, 7, and 12). Ascites

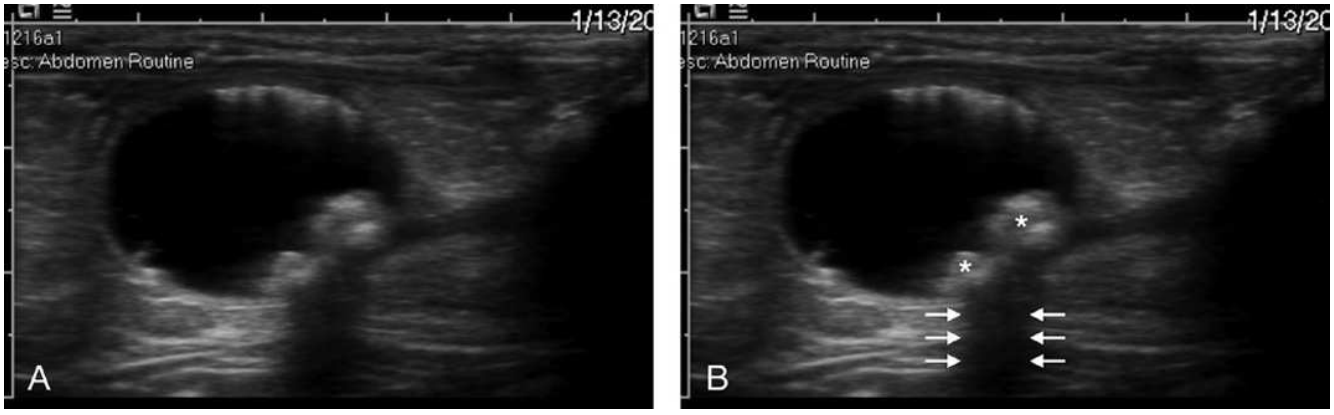


**Figure 40.2.** Bladder stones in a ferret. Ultrasound image of two cystoliths (marked with asterisks, *) within the urinary bladder of a ferret (*Mustela putorius furo*), unlabeled in (A) and labeled in (B). Note the hyperechoic proximal surface with clean acoustic shadowing through the far-field (*arrows*). Source: Image courtesy of Dr David Eshar, Manhattan, KS.

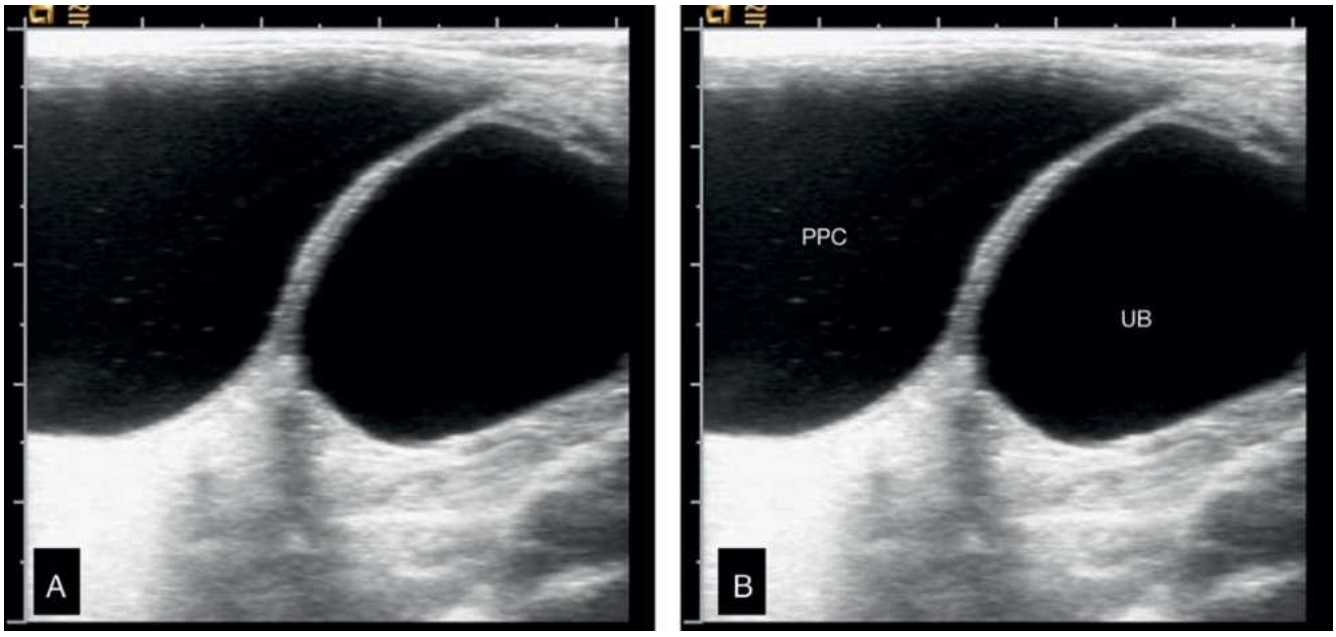


**Figure 40.3.** Paraprostatic cyst in a ferret. Ultrasound image of a paraprostatic cyst in a ferret (*Mustela putorius furo*), unlabeled in (A) and labeled in (B). The "double urinary bladder" finding is similar to that of dogs. UB, urinary bladder; PPC, paraprostatic cyst. Source: Image courtesy of Dr David Eshar, Manhattan, KS.

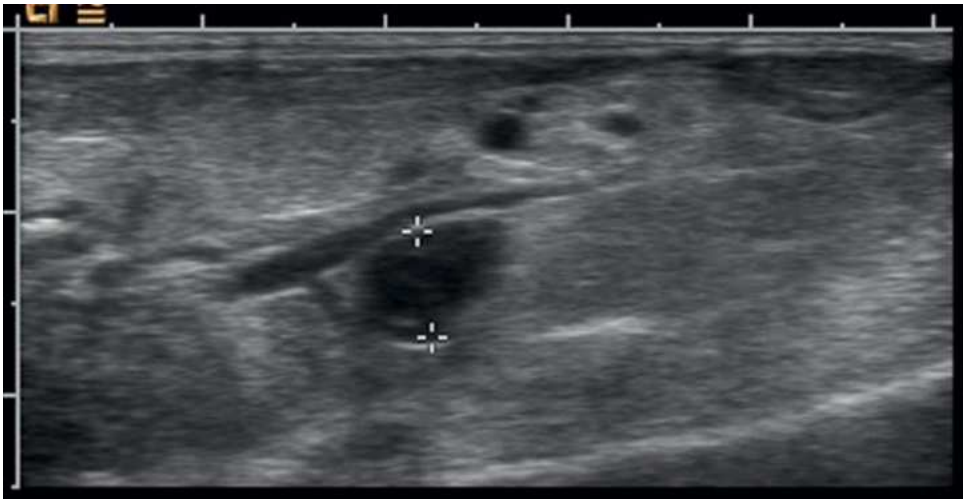

**Figure 40.4.** Adrenal mass in a ferret. Ultrasound image of an enlarged right adrenal gland in a ferret (*Mustela putorius furo*). The adrenal gland measures 0.59 cm in width and is outlined with calipers (+). Source: Image courtesy of Dr David Eshar, Manhattan, KS.

that is safely accessible allows for characterizing the fluid as septic or sterile, and thus expediting medical versus surgical management in many cases.

### Spleen

Splenomegaly is a very common clinical finding in most North American ferrets older than 1 year of age (Figure 40.5) (Morrisey and Draus 2012). Several conditions result in splenomegaly in ferrets, including extramedullary hematopoiesis (EMH) most commonly, as well as neoplasia (mainly lymphoma), hypersplenism, and splenic congestion. Typically, the EMH spleen has a uniform echogenicity compared to neoplasia, where the parenchyma appears mottled, similar to the "Swiss cheese" appearance in dogs (Morrisey and Draus 2012) (see Chapter 9). Some caution is required when evaluating the ferret spleen

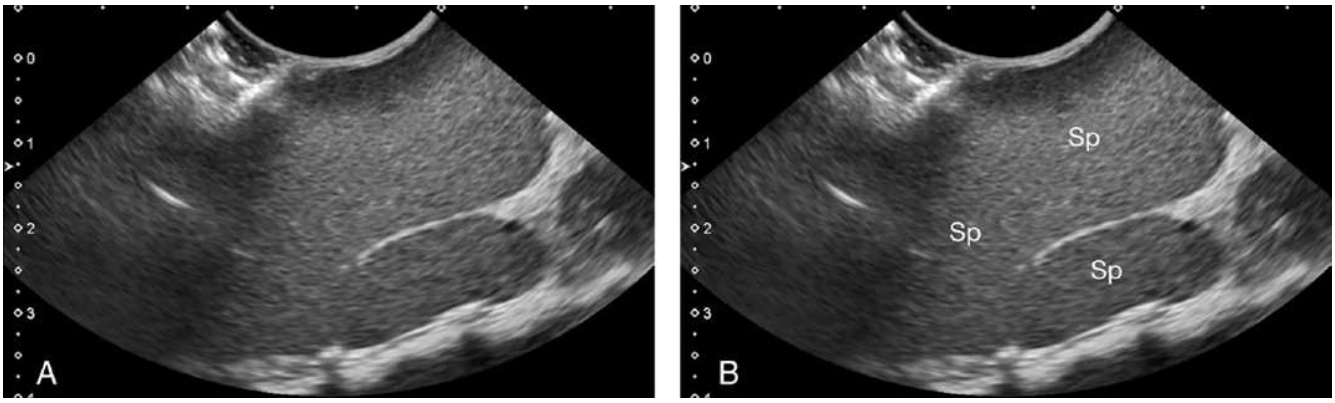


**Figure 40.5.** Splenomegaly in a ferret. Ultrasound image of the enlarged spleen of a ferret (*Mustela putorius furo*), unlabeled in (A) and labeled in (B). Note how the spleen is folded on itself. Sp, spleen.

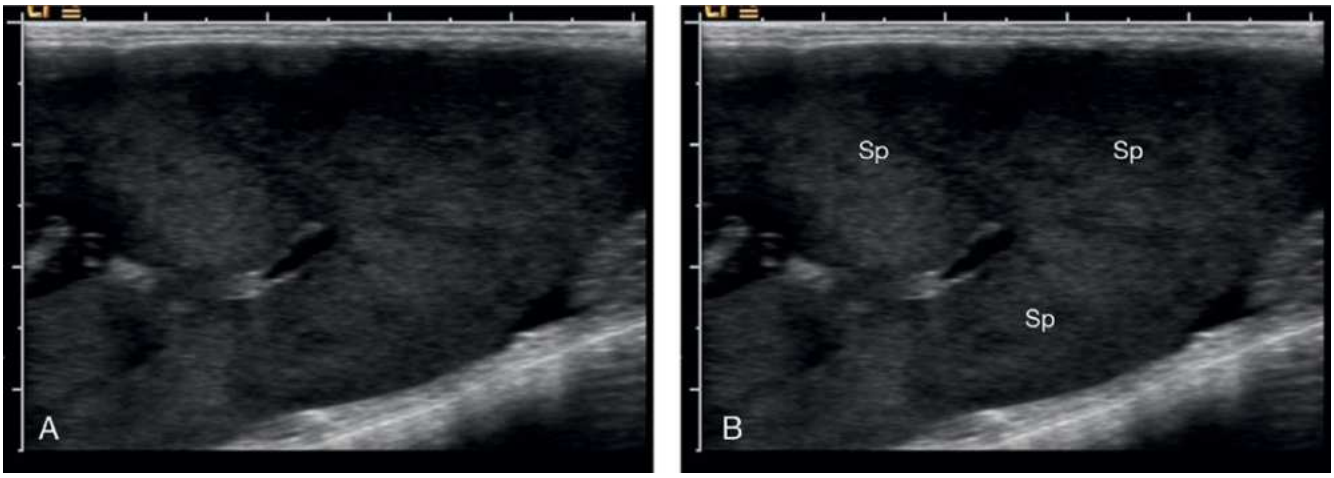


**Figure 40.6.** Splenic lymphoma in a ferret. Ultrasound image of a ferret (*Mustela putorius furo*) spleen diagnosed with lymphoma, unlabeled in (A) and labeled in (B). Note the mottled appearance, mixed echogenicity, of the spleen with rounded edges similar to the "Swiss cheese appearance" in dogs (see also Figure 9.14). Sp, spleen. Source: Image courtesy of Dr David Eshar, Manhattan, KS.

because small hypoechoic (dark) nodules and hypoechoic regions are common in EMH and can be confused with neoplastic nodules. As in POCUS spleen in dogs and cats, sampling and cytological evaluation are often required for a definitive diagnosis. Other conditions such as splenic torsion, splenic abscesses, and splenic ruptures are possible but quite rare (Morrisey and Draus 2012).

### Pancreas

A common ferret presentation is hypoglycemia due to pancreatic beta-islet cell tumors (Antinoff and Williams 2012). However, abdominal ultrasound has low sensitivity in detecting islet cell tumors, often due to the microscopic size the most of these tumors (Rosenthal and Wyre 2012). If sonographically detectable, these pancreatic beta-islet cell tumors are only recognized as small nodule(s) by skilled sonographers.

### Neoplasia

Ferrets with lymphoma commonly present with a mediastinal mass, thoracic lymphadenopathy, and/or pleural effusion, as well as enlargement of the spleen, liver, or kidneys (Antinoff and Williams 2012) (Figure 40.6). In these cases, POCUS or TFAST can be useful for diagnosis of pleural effusion, followed by ultrasound-guided thoracocentesis for sample acquisition and cytological evaluation. Moreover, ultrasound-guided aspiration of enlarged lymph node(s) is a common way of diagnosing lymphoma in ferrets (Figure 40.7).

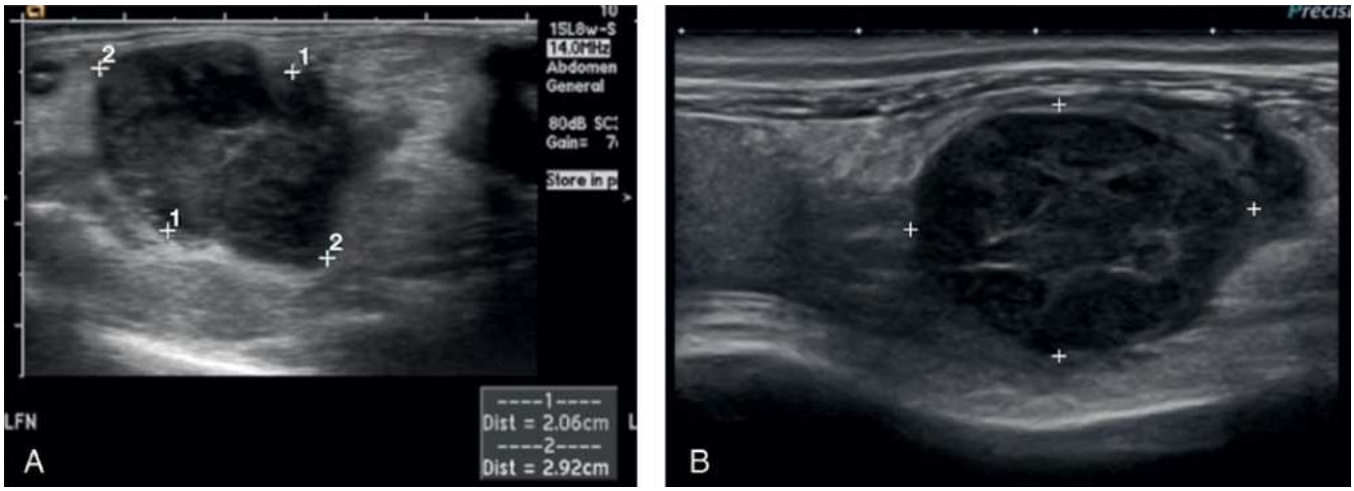


**Figure 40.7 Mesenteric lymph node in a ferret.** Two examples of enlarged mesenteric lymph nodes, cytologically diagnosed as lymphoma, detected during ultrasound examination of a ferret (*Mustela putorius furo*). Note each has a mottled appearance and lack of distinct borders. (A) measured with calipers (+) and (B) outlined with calipers (+). Source: Image courtesy of Dr David Eshar, Manhattan, KS.

### Other

Cavitary effusion, especially of the thorax, is relatively common in ferrets due to a variety of underlying causes, including cardiac disease. TFAST with basic echocardiography views can be helpful for expediting diagnosis through the finding of an enlarged left atrial to aortic ratio (LA:Ao) and alveolar-interstitial edema. Normal echocardiography measurements have been published in ferrets and the LA:Ao should be <1:1.3 (Vastenburg et al. 2004). TFAST provides a more thorough initial diagnostic evaluation in these cases over physical exam and auscultation alone when radiography and a complete echocardiogram are too risky or not immediately available (Figure 40.8; see also Figures 36.6 and 36.7) (see Chapters 17, 18–22, 23, 36 and 37).

## *Rabbits*

### Urinary

Rabbits have a unique calcium metabolism and as a result appear to have a high prevalence of urolithiasis when combined with other genetic and husbandry-related factors (Klaphake 2012). Rabbits have unregulated intestinal absorption of dietary calcium, which is excreted massively through the urine. Therefore, urinary "sludge" or slightly hyperechoic (bright) urine is a common finding in rabbits with high dietary calcium. Ultrasound can be useful to both detect discrete calculi in the urinary bladder and aid in collection of a urine sample via cystocentesis (Figure 40.9) (Klaphake and Paul-Murphy 2012). Cystocentesis in rabbits may be more challenging than other species because their bladder wall is somewhat flaccid and as a result the needle often indents the wall of the bladder without entering. Additionally, nonsedated rabbits may abruptly react to needle insertions, posing greater patient risk for iatrogenic urinary bladder trauma.

### Gastrointestinal and Hepatobiliary

Liver lobe torsion is not an uncommon problem in rabbits. Diagnosis of liver lobe torsion is best left to a skilled sonographer because the condition is surgically treated in a rabbit that may not be stable. If present,

**Figure 40.8.** *(Continued)* Note the crescent-shaped right ventricle that should not be mistaken for pleural or pericardial effusion (see Chapters 36 and 37). Correlating line drawing to the right. (B) Enlarged left atrium and left atrial to aortic ratio (LA:Ao) in a ferret with left-sided congestive heart failure. Its cardiogenic pulmonary edema may rapidly be recognized using Vet BLUE and observing "wet lung." Correlating image labeled with the sizes of the aorta and left atrium with a ratio much greater than 1:1.5. Correlating line drawing provided. (C) Left atrial enlargement on a long-axis four-chamber view. Correlating image labeled with the sizes of the aorta and left atrium with a ratio much greater than 1:1.5. The atria may also be compared and should be 1:1, outlined with circles. Note the left atrium is much larger than the right atrium. Correlating line drawing provided. (D) M-mode may be performed and is shown for the same ferret in short axis as in (B). RV, right ventricle; LV, left ventricle; RA, right atrium; LA, left atrium; Ao, aorta. Source: Images (B–D) courtesy of Dr Teresa DeFrancesco, Raleigh, NC.

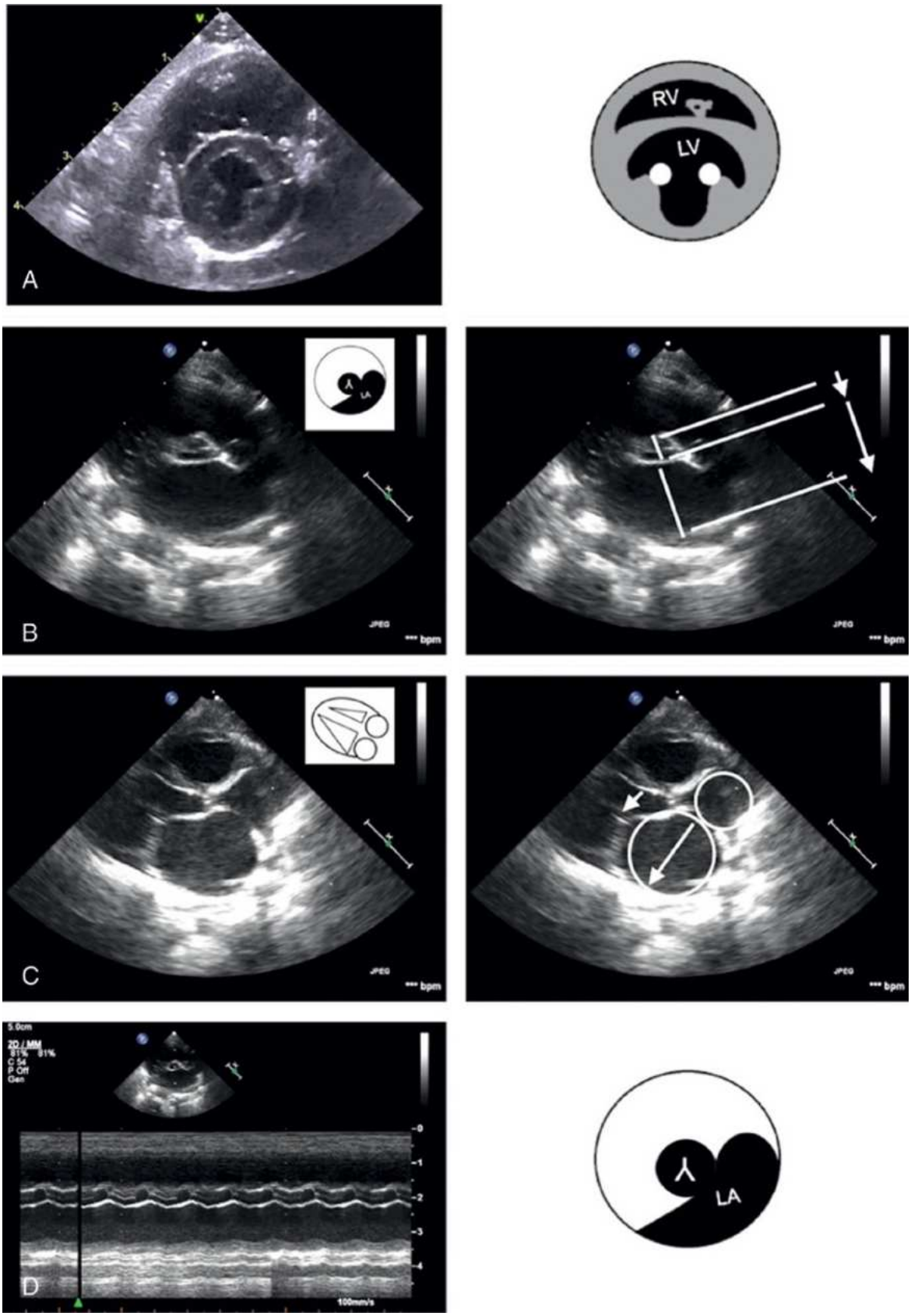


**Figure 40.8.** Cardiac images of a ferret. (A) Expected appearance of the short-axis left ventricular "mushroom view" of the heart of a ferret that has a similar appearance as expected in dogs and cats. From this short-axis view, volume and contractility (fractional shortening, FS%) may be estimated in real time using the "eyeball method" (see Chapters 19–21, 26, 36, and 37).

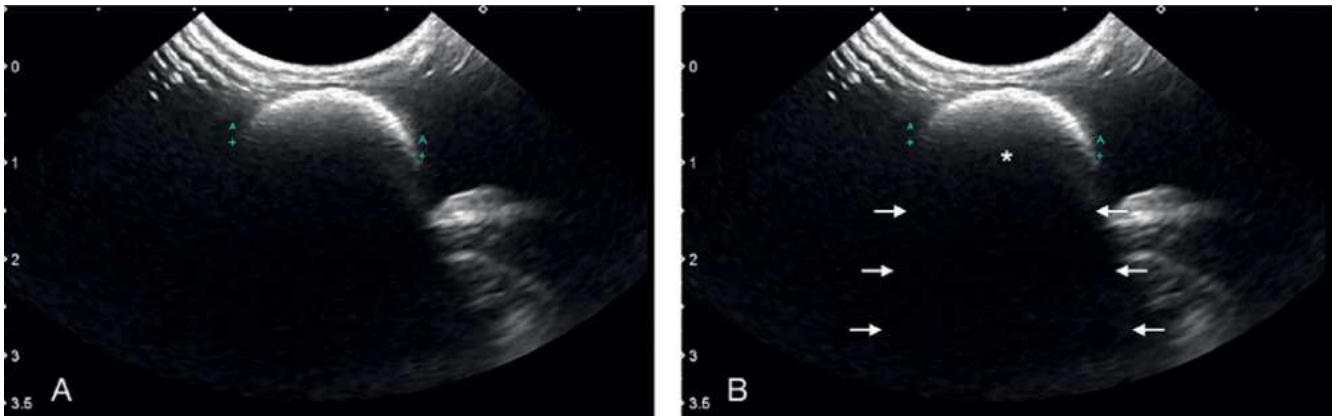


**Figure 40.9.** Bladder stone in a rabbit. Ultrasound image of a rabbit (*Oryctolagus cuniculus*) urinary bladder with a single urinary calculus, unlabeled in (A) and labeled in (B). Bladder stone labeled with an asterisk (*). Arrows show acoustic shadowing through the far-field.

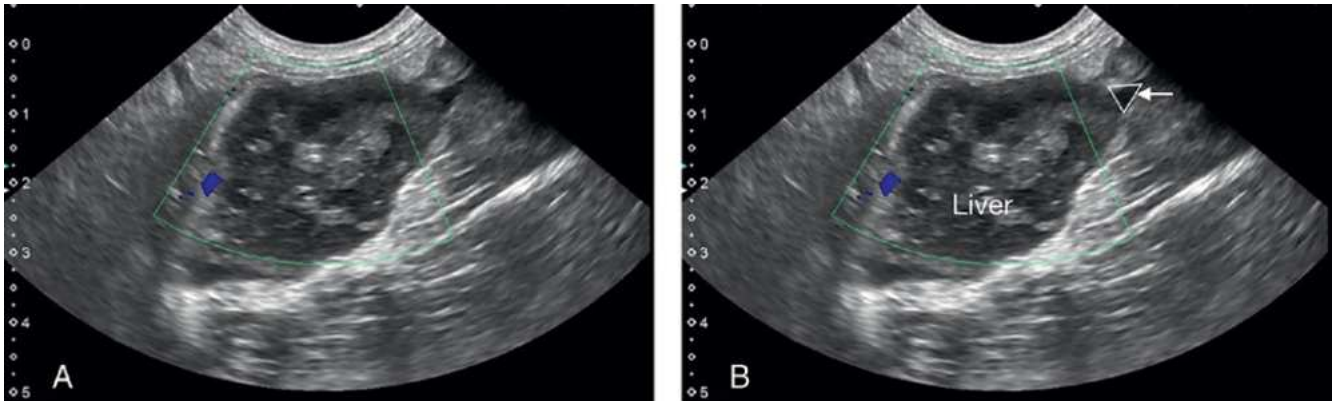


**Figure 40.10.** Liver lobe torsion in a rabbit. Ultrasound image of a liver lobe torsion in a rabbit (*Oryctolagus cuniculus*) with absence of blood flow on color flow Doppler, a hallmark for its sonographic diagnosis, unlabeled in (A) and labeled in (B). Note the small-volume peritoneal effusion marked with an arrow and a triangle.

there will be absence of blood flow in the affected liver lobe and typically mild to moderate free peritoneal fluid, characterized as a modified transudate (Figure 40.10). A complete, detailed abdominal ultrasound is typically the most sensitive test for diagnosing liver lobe torsion, which often requires an emergent lobectomy (Graham et al. 2014).

In young rabbits, hepatic coccidiosis is seen, and results in a very heterogeneous hyperechogenic (bright) liver parenchyma with hyperechogenic (bright) bile ducts and a hyperechogenic (bright white) gallbladder wall (Cam et al. 2008).

### Reproductive

Uterine adenocarcinoma is a common disease in intact female rabbits over the age of 4 years (Klaphake and Paul-Murphy 2012). Ultrasound imaging can assist in a diagnosis when a caudal abdominal soft tissue mass or uterine enlargement is palpable on physical examination (Figure 40.11) (Klaphake and Paul-Murphy 2012). In advanced stages of disease, enlarged abdominal lymph nodes, peritoneal and organ metastasis, or free abdominal fluid and combinations thereof may be detected. These masses are also frequently calcified (Kunzel et al. 2015). The Global FAST approach is a good way to rapidly stage the rabbit by surveying the remaining abdomen (AFAST), thorax (TFAST) and Vet BLUE (lung) (see Chapters 36 and 37 and Figure 36.20).

### Abscesses

Rabbits and some rodents have fairly thick inspissated exudate (more solid than liquid) that may not

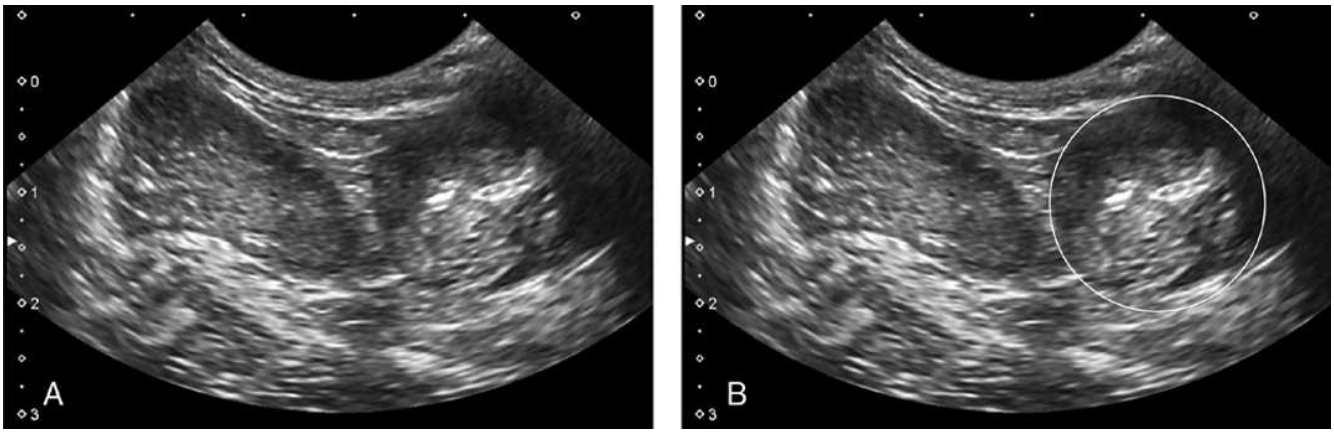


**Figure 40.11. Uterine adenocarcinoma in a rabbit.** Transverse ultrasound image of a rabbit (*Oryctolagus cuniculus*) with uterine adenocarcinoma, unlabeled in (A) and labeled in (B). Both uterine horns are dilated, but a mass can be visualized on one side, circled in (B). Use Global FAST to rapidly survey for evidence of disseminated disease (see Figure 36.20).

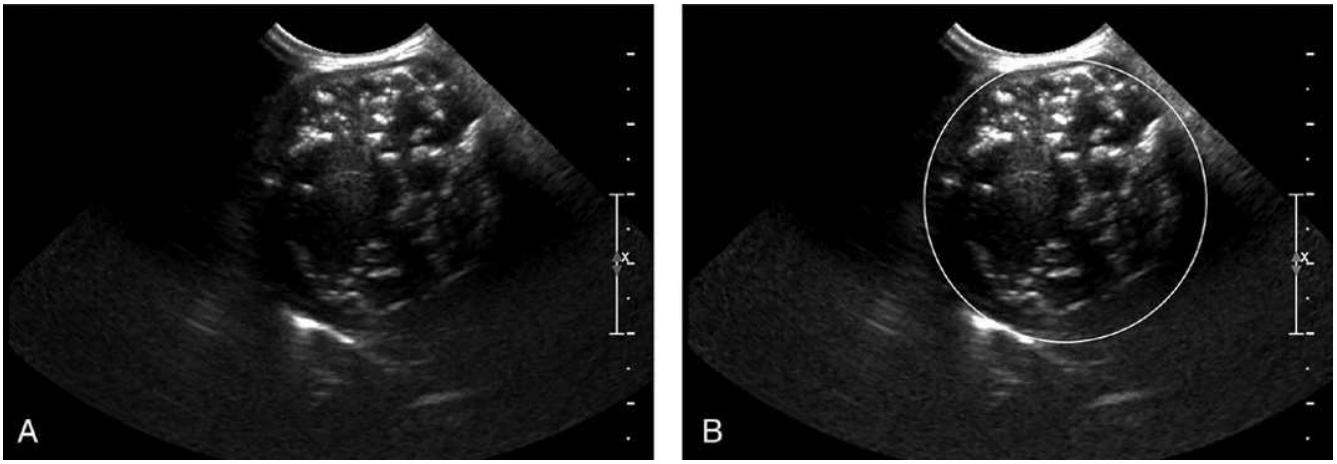


**Figure 40.12. Calcified midabdominal abscess in a rabbit.** Ultrasound image of a rabbit (*Oryctolagus cuniculus*) with a calcified abdominal abscess, unlabeled in (A) and labeled in (B). The midabdominal mass is circled in (B) and note the hyperechoic mineralized foci throughout the mass, which could be confused with intralesional air. Mineralized foci typically cleanly shadow through the far-field in contrast to intralesional gas that would dirty shadow. This can sometimes be difficult to differentiate sonographically; however, radiography serves as an adjunct confirmatory imaging modality.

have a liquid appearance on ultrasound. Thoracic and abdominal abscesses are not uncommon in rabbits (Figure 40.12). Use of color flow Doppler with ultrasound can be helpful to distinguish an abscess (absent blood flow) from a soft tissue mass, which is more likely to have positive blood flow (see Chapters 34 and 35).

Retrobulbar abscesses are a common sequela of periapical infection of the maxillary cheek teeth in rabbits. These rabbits typically present with unilateral exophthalmos without a history of trauma (Capello and Lennox 2012). A POCUS eye and associated tissues may be useful to demonstrate the purulent debris when a computed tomography (CT) scan is not available, not cost-effective, or too risky for the rabbit.

## *Guinea Pigs*

### Urinary

Guinea pigs commonly present for urolithiasis (Hawkins and Bishop 2012) and typically have a *single* large calculus. Ultrasonography can be useful to both

detect discrete calculi in the urinary bladder and assist in collection of a urine sample via cystocentesis.

### Reproductive

Another common presentation for guinea pigs is the presence of ovarian cysts in the female (Hawkins and Bishop 2012). Affected animals may or may not have associated clinical signs, but when present, are best diagnosed with the use of ultrasound (Hawkins and Bishop 2012). Ovarian cysts can be visualized sonographically dorsal to the kidney and contiguous with the ovary (Figure 40.13) (Beregi et al. 1999). The cysts are fluid filled and anechoic (black) with acoustic enhancement, allowing them to be easily distinguished from a mass (Beregi et al. 1999). Color flow Doppler may also be used for differentiation because cysts have no intracystic blood flow versus a mass. These cysts can be quite large, and an ultrasound-guided method may be used to drain large cysts, although recurrence of cystic fluid is common with this method of treatment.

## *Chinchillas*

### Reproductive

Pet chinchillas may present with pyometra and often have palpable uterine enlargement on physical examination (Mans and Donnelly 2012). Abdominal ultrasound is the preferred imaging technique for diagnosis of pyometra, with the uterus being fluid distended by various degrees of echogenicity from anechoic (black) to hyperechoic (bright) fluid (Figure 40.14).

## *Hamsters*

### Gastrointestinal and Hepatobiliary

Hepatic cystic disease is not an uncommon finding in hamsters (Brown and Donnelly 2012). The cysts are often diagnosed initially on palpation and verified with ultrasonography. They can be of multiple sizes and shapes (Figure 40.15; see also Figures 8.5, 8.6, and 8.9).

## *Hedgehogs*

### Reproductive

Various lesions of the uterus are common in African hedgehogs. Some of the most common uterine diseases include neoplasia, including adenosarcoma, endometrial stromal sarcomas, adenoleiomyosarcoma, and adenoleiomyoma (Mikaelian et al. 2004). Other common lesions include endometrial polyps, pyometra, and metritis (Figure 40.16) (Mikaelian et al. 2004; Ivy and Carpenter 2012).

### Neoplasia

Neoplasia is very common in African hedgehogs and a wide variety of both discrete tumors and disseminated neoplasms have been reported (Ivy and Carpenter 2012). An AFAST with its target organ approach or specific POCUS abdominal examinations can be useful to investigate the presence of a mass in a hedgehog. Use of the Global FAST approach for staging localized versus disseminated disease is a rapid add-on or initial approach (see Chapters 36 and 37).

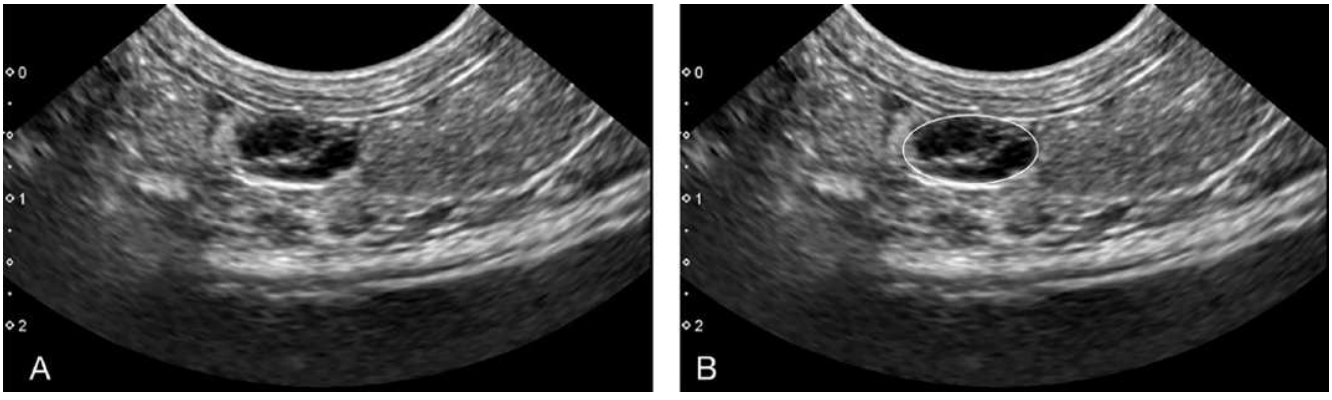


**Figure 40.13. Guinea pig ovarian cyst.** Ultrasound examination of a guinea pig (*Cavia porcellus*) with ovarian cysts, unlabeled in (A) and labeled with a oval in (B).

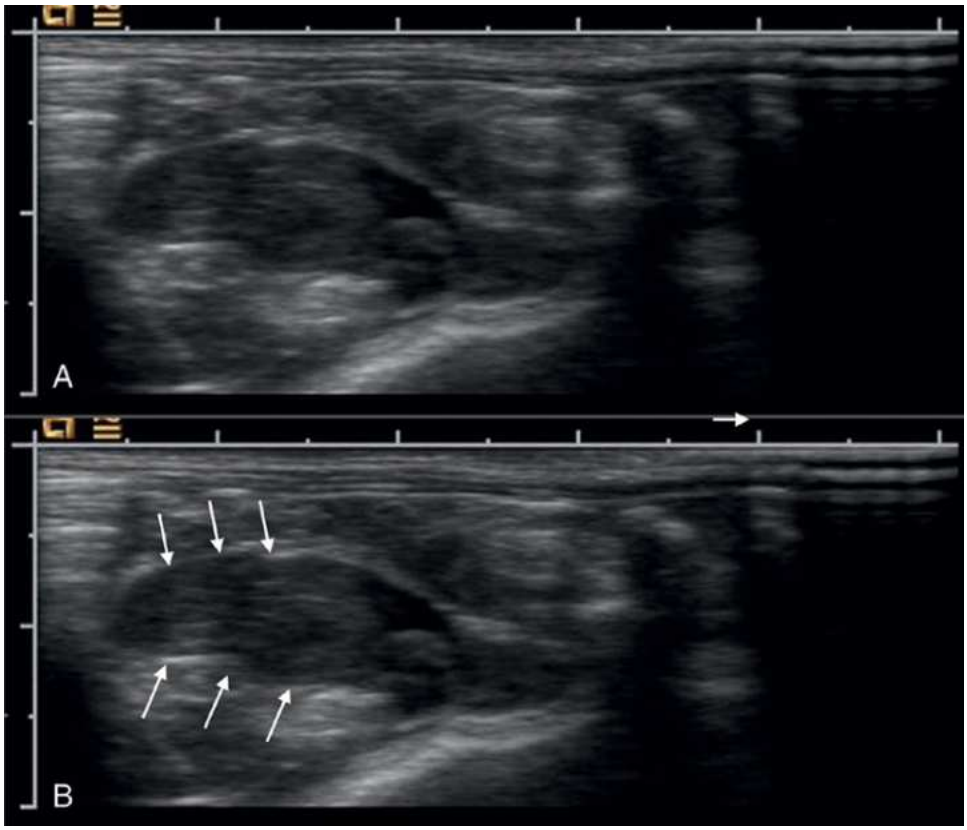


**Figure 40.14.** Pyometra in a chinchilla. Enlarged uterus in a chinchilla (*Chinchilla lanigera*) suspected to be an open pyometra, unlabeled in (A) and labeled in (B). The enlarged uterus is outlined with arrows. It is important to correlate physical examination findings with ultrasound findings. The presence of the urinary bladder is a helpful landmark and not shown in the image. Source: Image courtesy of Dr David Eshar, Manhattan, KS.

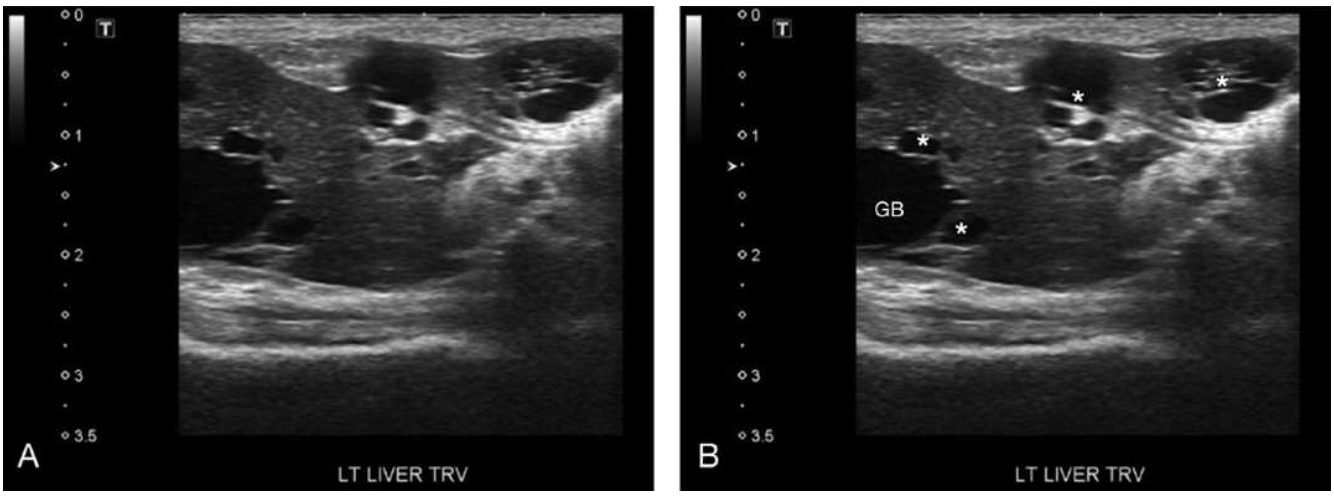


**Figure 40.15.** Hepatic cysts in a hamster. Ultrasound image of a hamster with multiple hepatic cysts, unlabeled in (A) and labeled in (B). The multiple hepatic cysts are labeled with asterisks (*). Color flow Doppler may be used to confirm the absence of blood flow typical of a cyst. Source: Image courtesy of Dr David Eshar, Manhattan, KS.

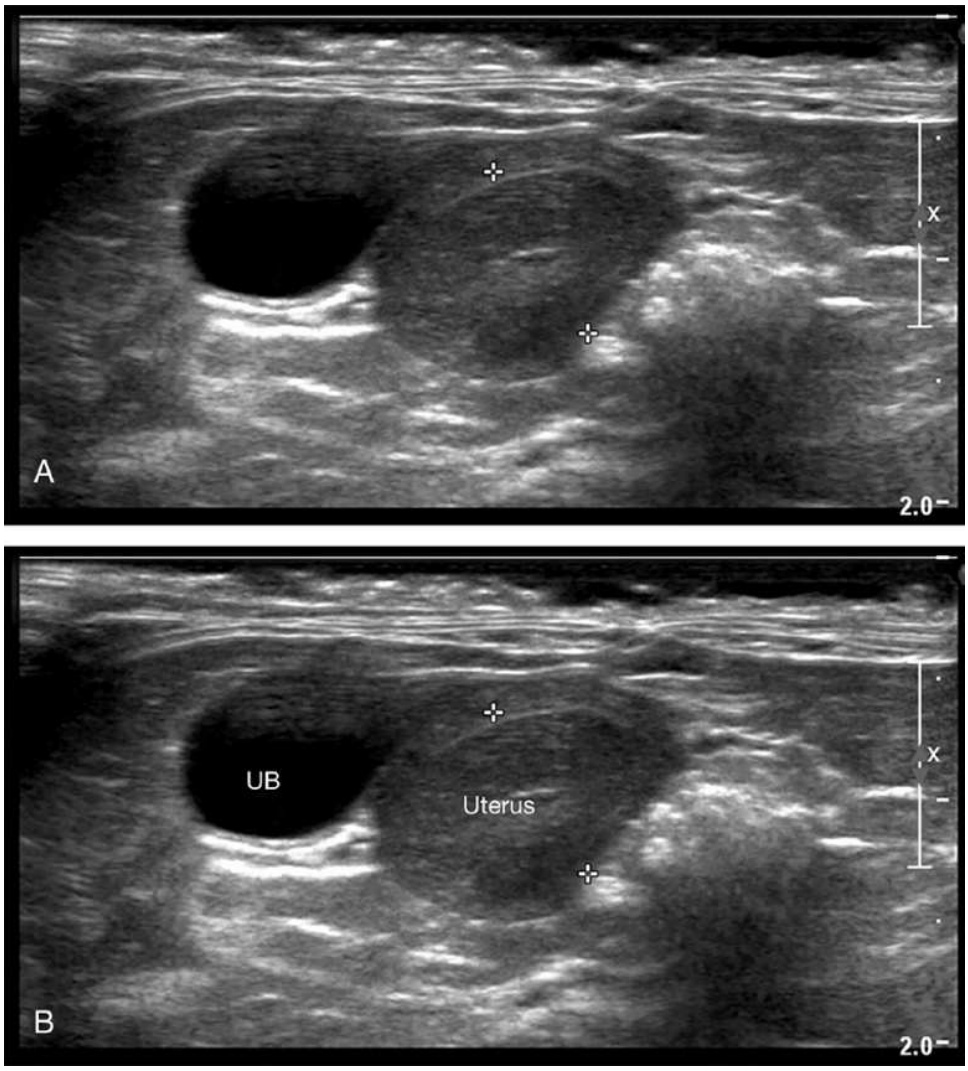


**Figure 40.16** **African pygmy hedgehog pyometra.** Ultrasound image of an African pygmy hedgehog (*Atelerix albiventris*) with pyometra, unlabeled in (A) and labeled in (B). The calipers (+) show the outer borders of the enlarged uterus. The presence of the urinary bladder (UB) serves as a landmark.

# Normal Reference Ranges for Various Exotic Companion Mammals

**Table 40.1.**
Ultrasound reference ranges[a] (some values may vary based on weight and distension).

| Site | Ferret (mm) | Rabbit (mm) | Chinchilla (mm) | Guinea pig (mm) | Rat (mm) | Hamster (mm) |
|---|---|---|---|---|---|---|
| Stomach wall | | 1±0.01[c] | | | | |
| Saccus cecus wall | | | | | 1.09±0.20[b] | |
| Fundus wall | | | | | 1.07±0.25[b] | |
| Pylorus wall | | 2.80±0.04[c] | | | 2.20±0.41[b] | |

**Table 40.1.**
(*Continued*)

| Site | Ferret (mm) | Rabbit (mm) | Chinchilla (mm) | Guinea pig (mm) | Rat (mm) | Hamster (mm) |
|---|---|---|---|---|---|---|
| Duodenum wall | | 1.9±0.04[c] | | | 1.54±0.21[b] | |
| Sacculus rotundus wall | | 2.2±0.06[c] | | | | |
| Cecum wall | | 0.8±0.1[c] | | | 0.89±0.13[b] | |
| Colon | | Spiral loop of ascending colon wall: 1.4±0.4[c] | | | | |
| | | Distal colon wall: 1.9±0.4[c] | | | | |
| Appendix wall | | 1.9±0.4[c] | | | | |
| Kidney | MALE<br>Length:<br>29.5 (27.0–32.0)<br>Width:<br>12.6 (12.0–13.0)<br>Height:<br>14.6 (11.0–17.0)<br>FEMALE<br>Length:<br>25.1 (22.0–27.0)<br>Width:<br>11.2 (9.0–12.0)<br>Height:<br>13.0 (12.0–16.0)[5] | Length:<br>L: 28.6±3.3<br>R: 28.7±3.4<br>Width:<br>L: 17.2±1.9<br>R: 16.2±1.7<br>Height:<br>L: 15.8±1.5<br>R: 16.6±1.4[c] | Length:<br>19.9 (17.8–22.4)<br>Width:<br>10.1 (8.3–12.2)<br>Medullary thickness:<br>2.4 (1.7–3.9)<br>Cortical thickness:<br>2.4 (1.7–3.3)<br>Pelvis length:<br>6.6 (4.9–8.0)<br>Pelvis width:<br>4.2 (3.1–5.2)[d] | Length: 20.3 (14.0–25.0)<br>Width:<br>13.9 (12.8–16.1)<br>Height: 15.0 (13.0–18.0)[f] | Length:<br>L:19.47±2.3<br>R: 19.45±2.18<br>Width:<br>L:10.74±1.1<br>R: 10.75±0.88<br>Height:<br>L:10.96±1.2<br>R: 11.04±1.00<br>Pelvis:<br>L:0.87±0.24<br>R:0.84±0.21[b] | Length:<br>13.6 (12.0–14.0)<br>Width:<br>7.2 (6.5–7.7)<br>Height:<br>7.8 (7.0–8.1)[f] |
| Urinary bladder | | | | | 0.73±0.13[b] | |
| Adrenals | Length:<br>L: 7.2±1.8<br>R: 7.6±1.8<br>Width:<br>L: 2.8±0.5<br>R: 2.6±0.4[e] | Length:<br>L: 3.4±0.8<br>R: 7.3±1.5<br>Width:<br>L: 3.8±1.1<br>R: 4.3±0.8[c] | Length:<br>L: 6.9 (5.2–8.7)<br>R: 9.9 (7.8–11.9)<br>Widest cross-section:<br>L: 2.4 (2–3.1)<br>R: 2.7 (2.4–3.9)[f] | Length: 15.4 (12.6–17.7)<br>Widest cross-section: 6.2 (4.3–8.4)[f] | L (DV): 3.41±0.49<br>R (DV): 3.07±0.36[b] | |
| Lymph node | | | | | | |
| Width | | | | | | |
| Length | | | | | 1.53±0.75<br>4.19±1.26[b] | |

[a]Note: to backcalculate 95% of the values, one should use mean ±2SD or mean±SEM$\sqrt{n}$ (SD, standard deviation, SEM, standard error of the mean).
[b]mean±SD.
[c]mean±SD.
[d]median and 2.5% to 97.5% percentiles.
[e]mean±SD.
[f]mean, range.
For further information, see Banzato et al. (2014, 2015), Ferrari et al. (2013), O'Brien et al. (1996), and Reese (2010).

# Pearls and Pitfalls, The Final Say

POCUS and the Global FAST approach have the potential to be advantageous imaging modalities for exotic companion mammal patients, being point-of-care and low impact with little patient restraint. These imaging strategies can help direct further diagnostic efforts and assist by "seeing" the problem(s) in emergency management of these patients.

Anatomy of these species is generally similar to dogs and cats with the exception of the more extensive

gas-filled gastrointestinal system of herbivorous rabbits and hystricomorph rodents (i.e., guinea pigs, chinchillas), which obscures and thus limits ultrasound imaging (ultrasound does not transit through air). Some of the more prevalent exotic companion mammal conditions that may be screened for using POCUS and FAST ultrasound have been described in this chapter. POCUS and FAST examinations have advantages over radiography being a rapid, point-of-care imaging tool that helps with further diagnostic and treatment decisions.

# References


Antinoff N, Williams BH. 2012. Neoplasia. In: *Ferrets, Rabbits, and Rodents: Clinical Medicine and Surgery*, 3rd edition, edited by Quesenberry KE, Carpenter JW. St Louis: Saunders, pp 103–121.

Banzato T, Bellini L, Contiero B, et al. 2014. Abdominal anatomic features and reference values determined by use of ultrasonography in healthy common rats (Rattus norvegicus). *Am J Vet Res* 75:67–76.

Banzato T, Bellini L, Contiero B, et al. 2015. Abdominal ultrasound features and reference values in 21 healthy rabbits. *Vet Rec* 176:101.

Beregi A, Zorn S, Felkai F. 1999. Ultrasonic diagnosis of ovarian cysts in 10 guinea pigs. *Vet Radiol Ultrasound* 40(1): 74–76.

Brown C, Donnelly TM. 2012. *Disease problems of small rodentsIn: Ferrets, Rabbits, and Rodents: Clinical Medicine and Surgery*, 3rd edition, edited by Quesenberry KE, Carpenter JW. St Louis: Saunders, pp 354–372.

Cam Y, Atasever A, Eraslan G, et al. 2008. Eimeria stiedae: experimental infection in rabbits and the effect of treatment with toltrazuril and ivermectin. *Exp Parasitol* 119:164–172.

Capello V, Lennox AM. 2012. Small mammal dentistry. In: *Ferrets, Rabbits, and Rodents: Clinical Medicine and Surgery*, 3rd edition, edited by Quesenberry KE, Carpenter JW. St Louis: Saunders, pp 452–471.

Ferrari M, Aparecida W, da Silva C, et al. 2013. Ultrasonographic features of the chinchilla (Chinchilla lanigera) kidney. *J Exot Pet Med* 22:393–395.

Fischetti AJ. 2012. Diagnostic imaging. In: *Ferrets, Rabbits, and Rodents: Clinical Medicine and Surgery*, 3rd edition, edited by Quesenberry KE, Carpenter JW. St Louis: Saunders, pp 502–510.

Graham JE, Orcutt CJ, Casale SA, et al. 2014. Liver lobe torsion in rabbits: 16 cases (2007–2012). *J Exo Pet Med* 23(3):258–265.

Hawkins MG, Bishop CR. 2012. Disease problems of guinea pigs. In: *Ferrets, Rabbits, and Rodents: Clinical Medicine and Surgery*, 3rd edition, edited by Quesenberry KE, Carpenter JW. St Louis: Saunders, pp 295–310.

Ivy E, Carpenter JW. 2012. African hedgehogs. In: *Ferrets, Rabbits, and Rodents: Clinical Medicine and Surgery*, 3rd edition, edited by Quesenberry KE, Carpenter JW. St Louis: Saunders, pp 411–427.

Klaphake E, Paul-Murphy J. 2012. Disorders of the reproductive and urinary systems. In: *Ferrets, Rabbits, and Rodents: Clinical Medicine and Surgery*, 3rd edition, edited by Quesenberry KE, Carpenter JW. St Louis: Saunders, pp 217–231.

Kunzel F, Grinninger P, Shibly S, et al. 2015. Uterine disorders in 50 pet rabbits. *J Am Anim Hosp Asso* 51(1):8–14.

Mans C, Donnelly TM. 2012. Disease problems of chinchillas. In: *Ferrets, Rabbits, and Rodents: Clinical Medicine and Surgery*, 3rd edition, edited by Quesenberry KE, Carpenter JW. St Louis: Saunders, pp 311–325.

Mikaelian I, Reavill DR, Practice A. 2004. Spontaneous proliferative lesions and tumors of the uterus of captive African hedgehogs (Atelerix albiventris). *J Zoo Wildl Med* 35(2): 216–220.

Morrisey JK, Draus MS. 2012. Cardiovascular and other diseases. In: *Ferrets, Rabbits, and Rodents: Clinical Medicine and Surgery*, 3rd edition, edited by Quesenberry KE, Carpenter JW. St Louis: Saunders, pp 62–77.

O'Brien RT, Paul-Murphy J, Dubielzig RR. 1996. Ultrasonography of adrenal glands in normal ferrets. *Vet Radiol Ultrasound* 37:445–448.

Pollock C. 2012. Disorders of the urinary and reproductive systems. In: *Ferrets, Rabbits, and Rodents: Clinical Medicine and Surgery*, 3rd edition, edited by Quesenberry KE, Carpenter JW. St Louis: Saunders, pp 46–61.

Reese S. 2010. Small mammals – abdomen. In: *Diagnostic Imaging of Exotic Pets*, edited by Krautwald-Junghanns M-E, Pees M, Reese S, Tully T. Hanover: Schlutersche, pp 230–236.

Rosenthal KL, Wyre NR. 2012. Endocrine diseases. In: *Ferrets, Rabbits, and Rodents: Clinical Medicine and Surgery*, 3rd edition, edited by Quesenberry KE, Carpenter JW. St Louis: Saunders, pp 86–102.

Sharma A, Thompson M, Scrivani P, et al. 2011. Comparison of radiography and ultrasonography for diagnosing small-intestinal mechanical obstruction in vomiting dogs. *Vet Radiol Ultrasound* 52(3):248–255.

Vastenburg M, Boroffka S, Shoemaker N. 2004. Echocardiographic measurements in clinically normal ferrets anesthetized with isoflurane. *Vet Radiol Ultrasound* 45(3):228–232.

CHAPTER FOURTY-ONE

# POCUS: Marine Mammals

Gregory R. Lisciandro, Jennifer M. Gambino, Debra P. Moore, and Enrique Yarto

Vetbooks.ir

## Introduction

The use of ultrasound has been applied to marine mammals because of the limitations of radiography that require transport and risk. Although not an exhaustive list of contributors to the body of imaging-related work in the field of marine mammals, much of the available literature has come from pioneering groups affiliated with the Navy Marine Mammal Program (NMMP); the National Marine Mammal Foundation; Sea World; Ocean Park (Hong Kong); the Brookfield Zoo, and Dolphin Quest. These institutions and affiliated experts have contributed substantially to the body of work and knowledge regarding the diagnostic imaging evaluations of marine mammals, including dolphins. The NMMP publications have included comparative computed tomography (CT) thoracic imaging to lung ultrasound using two different methods (Smith et al. 2012; Ivančić et al. 2014). They concluded that lung ultrasound was an effective means of cetacean pulmonary evaluation (Smith et al. 2012). The group also provided a full-body ultrasound approach of routine health assessment (of undisclosed frequency, e.g., annual versus semi-annual) for evaluation of the mixed population of dolphins within their collection (Smith et al. 2012).

Dr Enrique Yarto, MVZ, of Mexico City, and I (GL) met several years ago. We spoke about wildlife and zoo medicine, his area of special interest and expertise. Naturally, the subject of Global FAST came up as an extension of the physical exam for both wellness status assessment and preliminary minimally invasive illness evaluation in bottlenose dolphins (*Tursiops truncatus)*. Dr Yarto, familiar with several dolphin collections in Mexico, felt there was a need for advancing routine ultrasound use, especially because of the truncated time constraints typically inherent in sonographic evaluation of the cetacean species. In his experience, the use of ultrasound was primarily restricted to reproductive evaluation and pregnancy checks.

Numerous other marine mammal veterinarians across the various facilities use abdominal and thoracic ultrasound routinely for overall health assessments as in small animals. An abbreviated point-of-care ultrasound for the species is not described. Likely, most marine mammal veterinarians would like to increase their ultrasound proficiency and the translation of the Global FAST methodology offers an opportunity to do so in a standardized manner. Thus, we completed a prospective pilot study evaluating the Global FAST approach performed on a small population of 20 clinically normal bottlenose dolphins (*Tursiops truncatus*) (Yarto and Lisciandro 2017, unpublished data). A major objective included assessing proficiency at image acquisition of the target organs of the abdomen (AFAST) and thorax including heart and lung (TFAST, Vet BLUE).

We also compared a second lung ultrasound methodology, referred to as the zig-zag continuum approach, similar to one of the lung ultrasound examinations previously described (Smith et al. 2012), to our modified Vet BLUE protocol for dolphins (Yarto and Lisciandro 2017, unpublished data) (see Figure 41.23). Our preliminary findings show that Global FAST is effective in capturing its target organs and is easily learned. Similar to adult dogs, cats, puppies, and kittens over 6 weeks of age, "dry lung" artifacts, "lung sliding" and A-lines, predominate in dolphins as well

*Point-of-Care Ultrasound Techniques for the Small Animal Practitioner*, Second Edition. Edited by Gregory R. Lisciandro.
© 2021 John Wiley & Sons, Inc. Published 2021 by John Wiley & Sons, Inc.
Companion website: www.wiley.com/go/lisciandro/ultrasound2

(Lisciandro et al. 2014, 2017, 2018; Yarto and Lisciandro 2017, unpublished data). The use of Global FAST provides an unbiased set of data imaging points that may be recorded as part of general health screening and compared to future studies. Moreover, Global FAST provides a standardized and more abbreviated (shorter time duration) option for ultrasound image acquisition than traditional examinations from which images may be stored and forwarded to offsite telemedicine services, carrying the potential to improve marine mammal care.

### What POCUS: Marine Mammals Can Do

- Establish a Global FAST examination protocol with clear objectives of the abdomen and thorax including heart and lung.
- Provide a semi-annual to annual imaging assessment tool that can be recorded and compared to future serial health assessments with the potential for early detection of disease states and detrimental medical conditions.
- Provide a relatively noninvasive safe point-of-care imaging modality with minimal patient risk for recheck assessment during treatment of abdominal, thoracic, cardiac, and lung conditions.
- Create a rapid screening test for general health status that also provides a standardized set of imaging data points for clinically abnormal dolphins with the potential to "see" the problem list, and thus help dictate the diagnostic work-up and need for additional imaging procedures.
- Create a screening test for traumatic injury involving the abdominal and thoracic cavities, historically difficult to detect by physical examination alone (Dennison and Saviano 2018).
- Provide a standardized ultrasound examination format that may be forwarded to offsite telemedicine and specialty consulting services.

### What POCUS: Marine Mammals Cannot Do

- Cannot replace proper ultrasound training and expert knowledge of dolphin anatomy.
- Cannot replace a complete detailed abdominal ultrasound, complete detailed transthoracic or transesophageal echocardiogram, and noncardiac thoracic ultrasound examinations by a board-certified veterinary radiologist or marine mammal veterinarian with a high level of experience in medical care and ultrasonography.

### Indications

Serves as an extension of the physical exam for clinically normal and abnormal marine mammals for abdominal and thoracic conditions including the heart and lung for not only the detection of effusion(s) but also obvious target organ abnormalities within the abdomen and thorax.

### Objectives

- To understand basic anatomy of the dolphin (Figure 41.1).
- To provide a systematic, easy-to-perform, standardized and repeatable ultrasound examination that is achievable for the nonradiologist marine mammal veterinarian.
- To screen the abdominal cavity for the presence of peritoneal effusion and any obvious parenchymal lesions of abdominal target organs using AFAST and its five acoustic windows.
- To screen for pleural and pericardial effusion, for obvious cardiac problems, and volume status using TFAST, its echo views and volume status approach.
- To screen for pulmonary edema and other lung conditions using the nine transthoracic acoustic windows of Vet BLUE.
- To perform a standardized Global FAST with acceptable image acquisition for radiologist review.
- To understand that lateral positioning of dolphins is an option for Global FAST.
- To understand that avoiding (nonspontaneous) patient breath holding likely improves lung ultrasound evaluation and is likely safer for the patient.

## Equipment, Probe Type, and Settings

- Macroconvex probe of 2–5 MHz with up to 35 cm depth.
- Abdominal presets may be used for the entire Global FAST examination.
- No acoustic coupling gel needed if done in the water.
- Ultrasound machine.
  - Portable.
  - Laptop format.
  - Durable.
  - Machine – can withstand rough handling and transport.

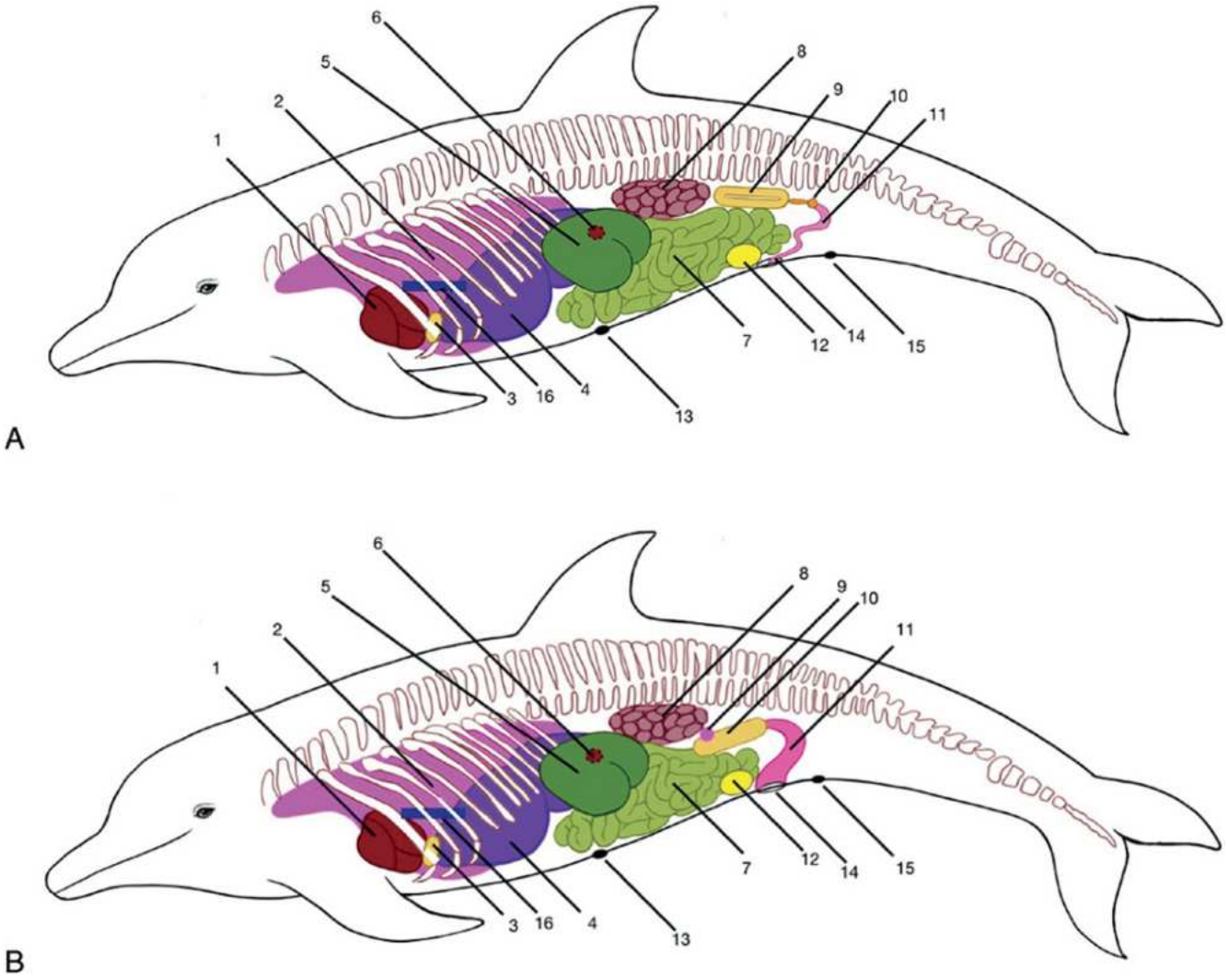


**Figure 41.1.** Basic dolphin anatomy. Basic anatomical features of the male and female bottlenose dolphin (*Tursiops truncatus*). (A) Male structures: 1) heart, 2) lung, 3) marginal lymph node, 4) liver, 5) gastric complex, 6) spleen, 7) small intestine, 8) left kidney, 9) testicle, 10) prostate, 11) penis, 12) urinary bladder, 13) umbilicus, 14) genital slit, 15) anus and 16) caudal vena cava. (B) Female structures: 1) heart, 2) lung, 3) marginal lymph node, 4) liver, 5) gastric complex, 6) spleen, 7) small intestine, 8) left kidney, 9) ovary, 10) uterus, 11) vagina, 12) urinary bladder, 13) umbilicus, 14) genital slit, 15) anus, and 16) caudal vena cava. Images are not drawn to scale. Note that the prostate, penis, anus, and vagina are not typically sonographically interrogated, and the mammary slits and glands are not shown. Source: Reproduced with permission from Dr Gregory Lisciandro, Hill Country Veterinary Specialists and FASTVet.com, Spicewood, TX. Illustration by Suji Park, Englewood Cliffs, NJ.

  - Probe – can withstand rough handling and transport.
  - Water-resistant keyboard available from some manufacturers.
  - Battery-powered for several hours.
- Electric cords are dangerous around water.
- Method for viewing the screen in bright outdoor environments.
- Ultrasound goggle viewing devices allow for viewing of the screen by the ultrasonographer in sunlight (Figure 41.2A).
- A head and screen/unit cover to shield sunlight and prevent splashing of salt water (e.g. large black felt or heavy knit cloth, towel, black garbage bag, umbrella, cardboard box) (Figure 41.2B,C).

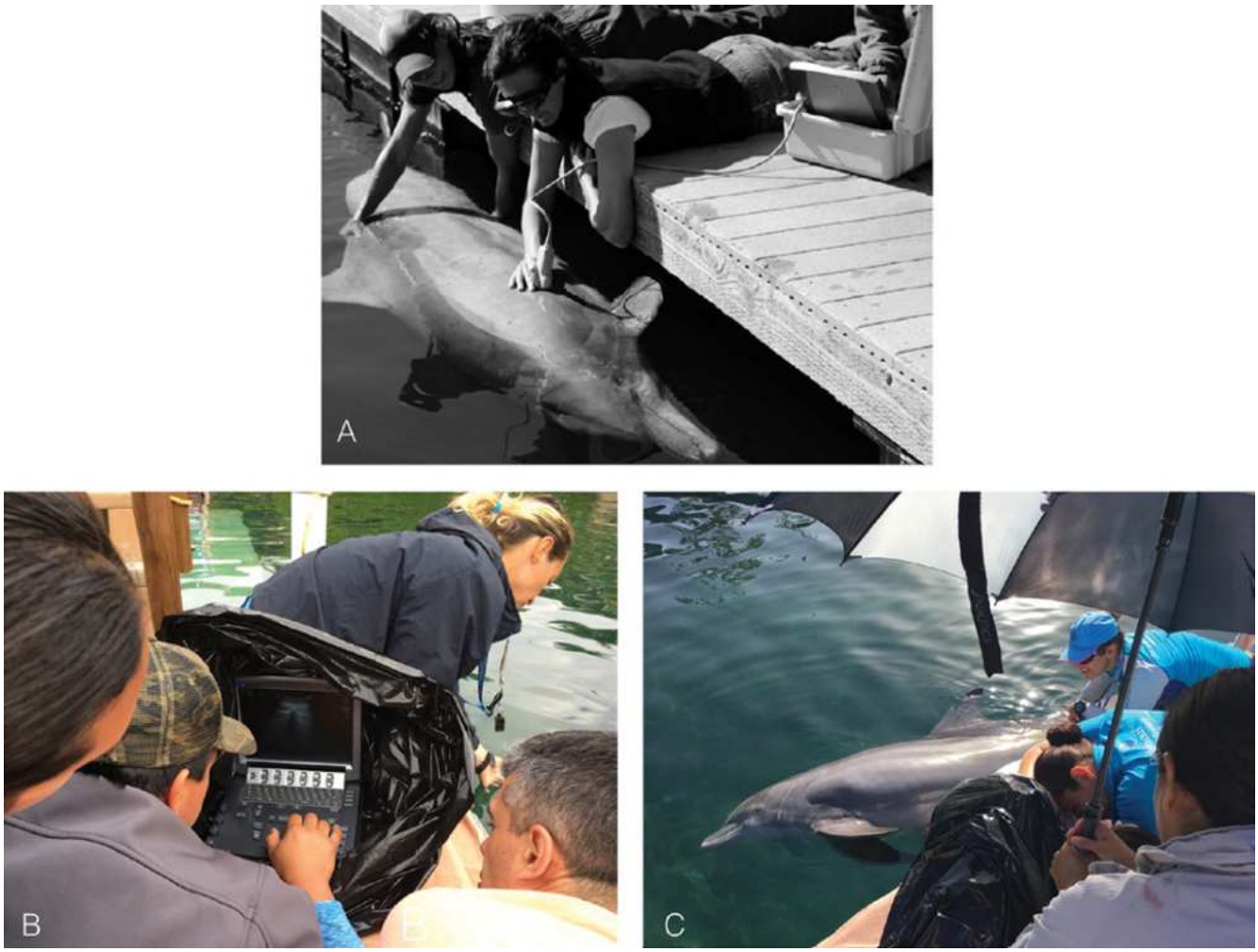


**Figure 41.2.** Viewing goggles, shading the screen, and machine set-up. (A) The use of viewing goggles available from some manufacturers allowing the sonographer to view the screen in real time. Source: Reproduced with permission from Smith et al. (2012). (B,C) How to scan without viewing goggles using a team of at least two, with the sonographer and an assistant whose job is image optimization and assisting the blinded sonographer. In bright environments the screen will need to be covered, using plastic (B), or shaded from sunlight, using an umbrella (C). A cover also protects the machine from salt water. The probe's cord must be long enough to reach the patient from wherever the machine is stationed. See also Figure 41.3C showing the sonographer and the second person working the machine and directing the image acquisition.

- Second sonographer or assistant on the dock or poolside who watches the screen, optimizes the image and directs the sonographer blinded to the ultrasound screen (Figure 41.3).
- Open water tank.

It is possible that some dolphins may react negatively to the harmonic sound waves arising from the probe. Most likely, this is due to a lack of conditioning to this specific acoustic stimulus as marine mammals are highly dependent on their acoustic sensory systems. It is also possible that the design of some concrete tank enclosures may enhance harmonic propagation.

## Environment, Machine, and Sonographer Location

Many factors must be considered when planning the ultrasound event (see Figures 41.2 and 41.3). Will the machine be next to the sonographer? Will a second sonographer be needed to direct from the deck or

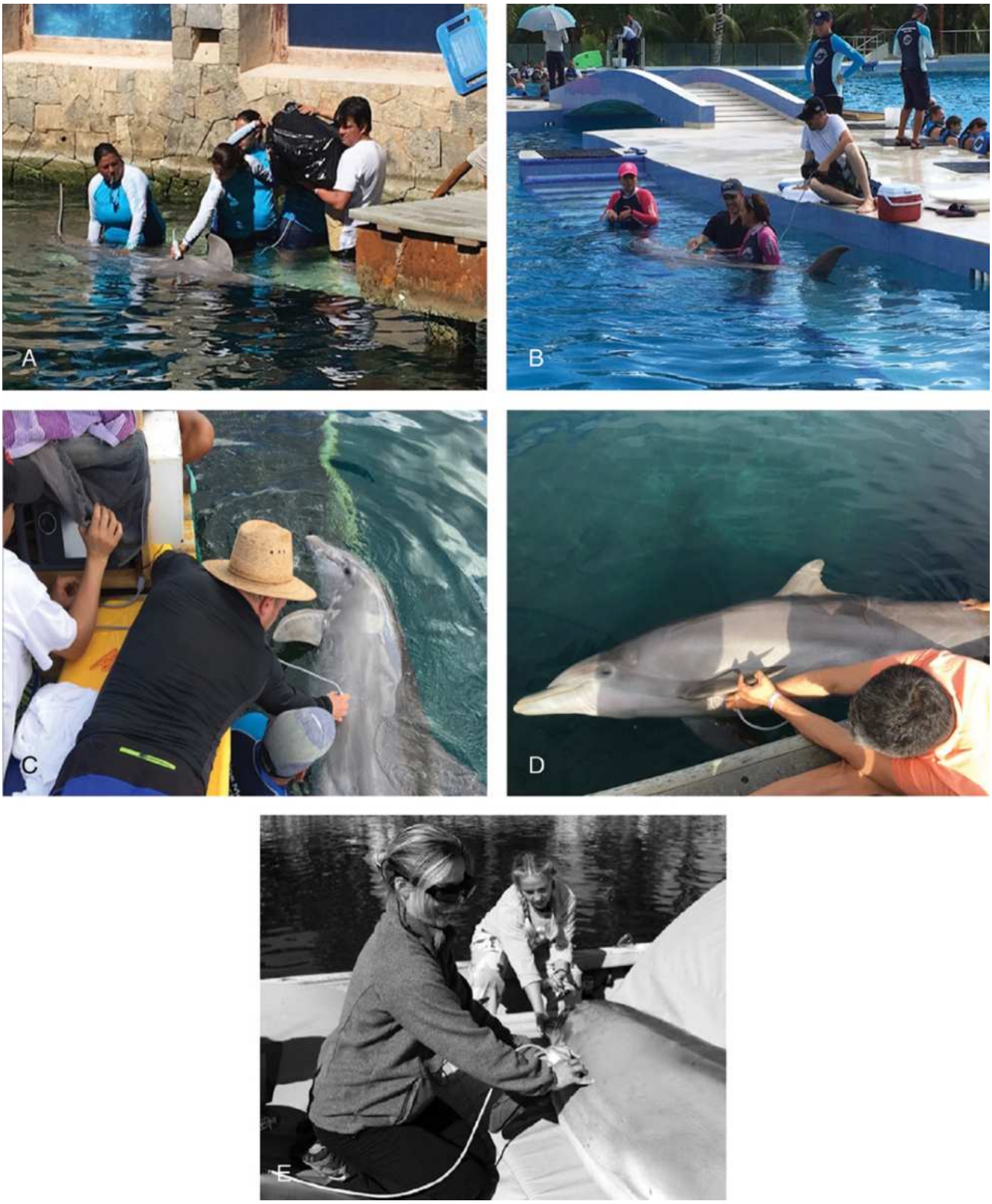


**Figure 41.3.** Different ways of scanning. Many environmental factors must be considered for efficient and successful scanning. The machine should be stationed away from water due to the risk of electrocution. In (A) the sonographer is in the water and can evaluate the screen in real time while scanning with a battery-operated ultrasound machine being held by an assistant, who is also standing in the water. In (B) the dolphins would not cooperate for ultrasound scanning and reacted negatively to the ultrasound probe placed on them. It is possible that reverberation or sound wave propagation within the construct of this specific concrete enclosure was problematic. However, lack of conditioning may have also played a role. In (C) the sonographer is on a low dock and an assistant, to the left of the picture, must direct the sonographer who is blinded to the ultrasound screen. In (D) the sonographer is also assisted by a second sonographer (not shown) as in (C). Note how the dolphin is stabilized by the sonographer holding the flipper with their nonprobe hand. In (E) ultrasound is performed out of water. Source: Reproduced with permission from Smith et al. (2012). Source for images (A–D): Reproduced with permission from Dr Gregory Lisciandro, Hill Country Veterinary Specialists and FASTVet.com, Spicewood, TX.

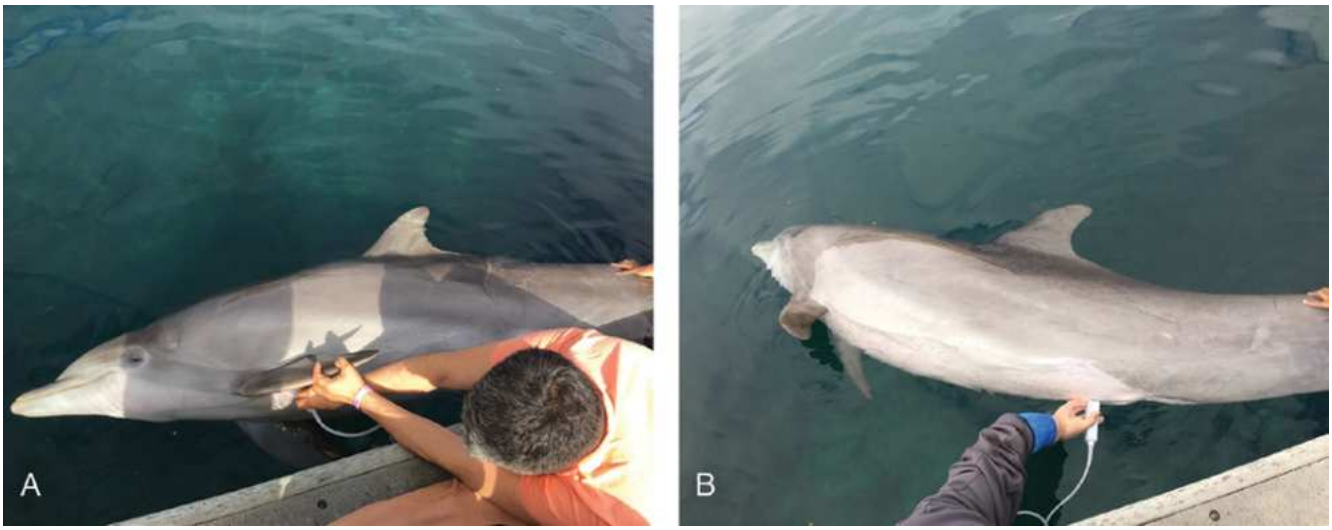


**Figure 41.4.** Comparison of a comfortable and a distressed dolphin. The dolphin in (A) is comfortable. Notice how the sonographer can gently restrain the dolphin by holding its pectoral fin, preventing the patient from drifting away. The trainer is positioned at the tail/fluke with their hand barely visible. In (B) the dolphin is beginning to show discomfort by arching and hyperextending its back. Distressed dolphins may also whistle or vocalize. When noticed (and ideally prior to its occurrence), the dolphin should be given a break from scanning. When signs of distress persist or appear imminent, the ultrasound study should be aborted. Source: Reproduced with permission from Dr Gregory Lisciandro, Hill Country Veterinary Specialists and FASTVet.com, Spicewood, TX.

nearby? The distance from the machine to the sonographer must also be considered since the probe's connection to the machine is also a limiting factor. The closer the machine is to the water, the more risk for damage to the machine if water is splashed. Only battery-powered ultrasound machines will be safe in the water environment since electric cords pose the serious risk of electrocution.

The actual environment and weather must be considered too. Is there a holding tank or will the event take place in an open water scenario with docks? Will the dolphin be scanned from a dock? If so, how elevated is the dock? Or will the sonographer be in the water with the dolphin? The authors have found that some dolphins might be uncomfortable with ultrasound initially and conditioning to the harmonics of the ultrasound probe is ideal. This may particularly be important when scanning wild dolphin populations where training the dolphins to be comfortable with diagnostic procedures and conditioning them to undergo sonography may not be possible. In the authors' opinion, conditioning is one of the most important factors for imaging success.

The dolphin trainer plays an integral role in the success of the sonographic assessment and communication is imperative. The sonographer must know where the trainer will be positioned and be familiar with the individual dolphin's personality. The trainer works in tandem to signal the sonographer as to when the ultrasound examination may be started and stopped or interrupted for any number of reasons, including dolphin breathing or allowing for a scan break including a brief swim or reward, and evaluating for signs of dolphin distress (Figure 41.4).

## Patient Positioning, Restraint, and Breathing

Sonographic evaluation of the dolphin in dorsal recumbency has been described but dorsal recumbency inherently presents some position-induced problems: uncomfortable/unsustainable positioning dependent on breath holding necessitating interruption of the ultrasound examination for breathing, and dorsal recumbency could be risky for the cardiovascular or respiratory-compromised dolphin (Figure 41.5). Spontaneous breathing is recommended for the following reasons: breath holding results in pulmonary overinflation which can obscure the heart, breath holding may be stressful and risky for those with respiratory disease or that are hemodynamically fragile, and dolphin breaks are less frequent (see Figure 41.5). Despite performing Global FAST using lateral positioning as in small animals, many dolphins will still breath hold naturally. The trainer will generally be at either the head or the fluke area of the

**Figure 41.5.** Lateral and dorsal recumbency. Many dolphins are trained to roll into dorsal recumbency. In (A) lateral positioning of the dolphin allows the animal to gently roll and lift its head to breathe then return to lateral recumbency for continued scanning. In (B) the blowhole is completely submerged and scanning time is more limited as longer breaks are needed for the dolphin to roll and breathe spontaneously, which in turn prolongs the ultrasound examination. The bottom line is that the ultrasound examination is going to take longer than a single breath hold. Source: Reproduced with permission from Dr Gregory Lisciandro, Hill Country Veterinary Specialists and FASTVet.com, Spicewood, TX.

dolphin. The sonographer can hold the pectoral fin to help keep the dolphin stable and still for scanning as well as for making small adjustments in the dolphin's position (with the help of the trainer).

### *Signs of Dolphin Stress*

So how does the stressed dolphin behave? Typically, the distressed dolphin may vocalize with a high pitch or frequent whistle or exhibit arch bending of the head and tail ventrally or laterally in the water (see Figure 41.4).

### *Dolphin Restraint and the Trainer*

Many dolphins have been trained to participate in their own healthcare assessment and working with the dolphin trainers helps establish clear training objectives to expedite ultrasound imaging.

## The Global FAST Examination

### *AFAST*

The acoustic windows of AFAST are named according to their target organs, similar to small animals but with some modifications (Figures 41.6 and 41.7). The target organ named AFAST views help the sonographer remember the objectives for image acquisition at each AFAST view, and remind the sonographer of the relevant anatomy.

The main objective for the sonographer is to quickly identify the target organs and capture them on cine clip images for review. Over time, the sonographer will gain proficiency in interpreting basic ultrasound findings and clinically integrating the information to direct diagnostic and therapeutic care, including additional or follow-up imaging and diagnostic procedures. With standardization of the AFAST acoustic windows, deviations from what is sonographically expected will help the sonographer begin to recognize abnormalities (Table 41.1).

Probe maneuvers are repetitive in their hand motion, similar to AFAST in small animals, with fanning, rocking and returning to the starting point primarily in a longitudinal scanning plane. Transverse plane (rotating the probe) is an add-on skill once the sonographer has become comfortable with the anatomy of each AFAST acoustic window.

The five AFAST acoustic windows have been modified from small animals (Lisciandro et al. 2009) and are summarized in Table 41.1. They are named as follows.

- Diaphragmatico-hepatic (DH) view
- Spleno-renal (SR) view
- Hepato-renal (HR) view
- Cysto-colic reproductive (CCR) view
- Umbilical (U) view

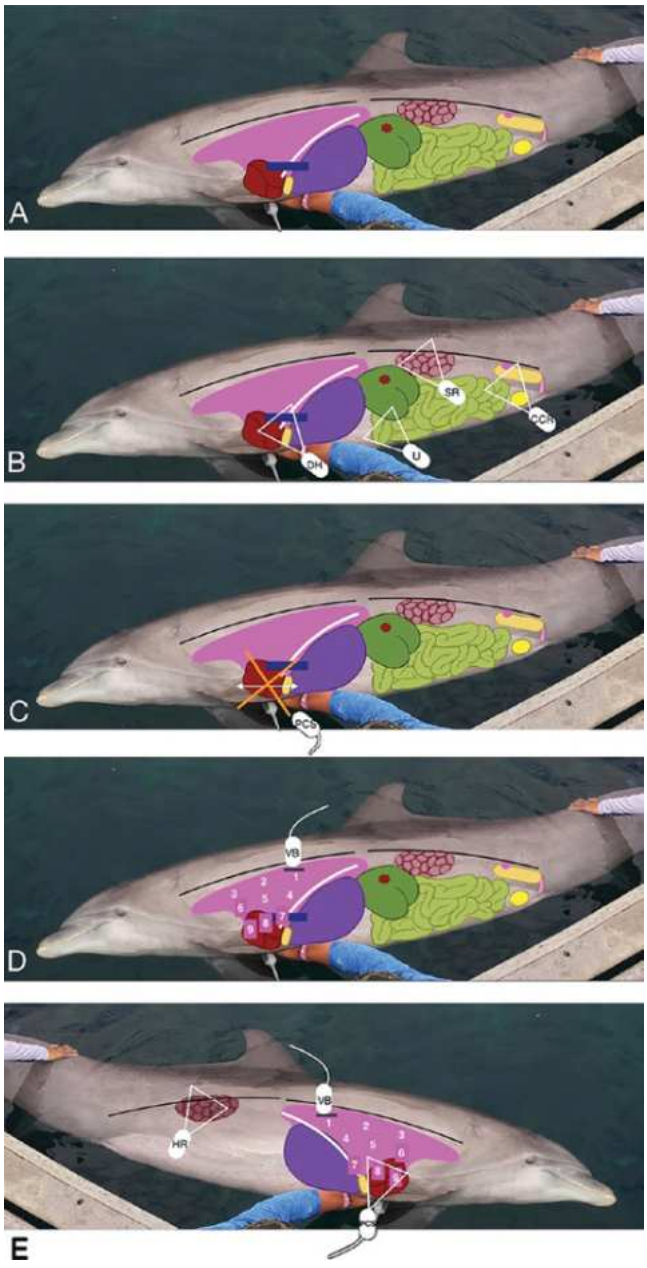


**Figure 41.6.** Overview of Global FAST on a female dolphin. In (A) simple line drawings overlay the important structures imaged during AFAST. In (B) the probes and their acoustic window (*triangles*) represent the approximate scanning region at each point of placement. Note the vagina is not routinely sonographically interrogated and the mammary slits and glands are not shown. In (C) the general position of the heart and probe placement for assessment are shown. (D) The nine acoustic left transthoracic windows of Vet BLUE. (E) The nine acoustic right transthoracic windows of Vet BLUE. The TFAST pericardial views may be performed from either right and left sides or both and transthoracic echocardiography is challenging especially with breath holding. Color coding and anatomical features match the line drawing in Figure 41.1. Source: Reproduced with permission from Dr Gregory Lisciandro, Hill Country Veterinary Specialists and FASTVet.com, Spicewood, TX. Illustration by Suji Park, Englewood Cliffs, NJ.

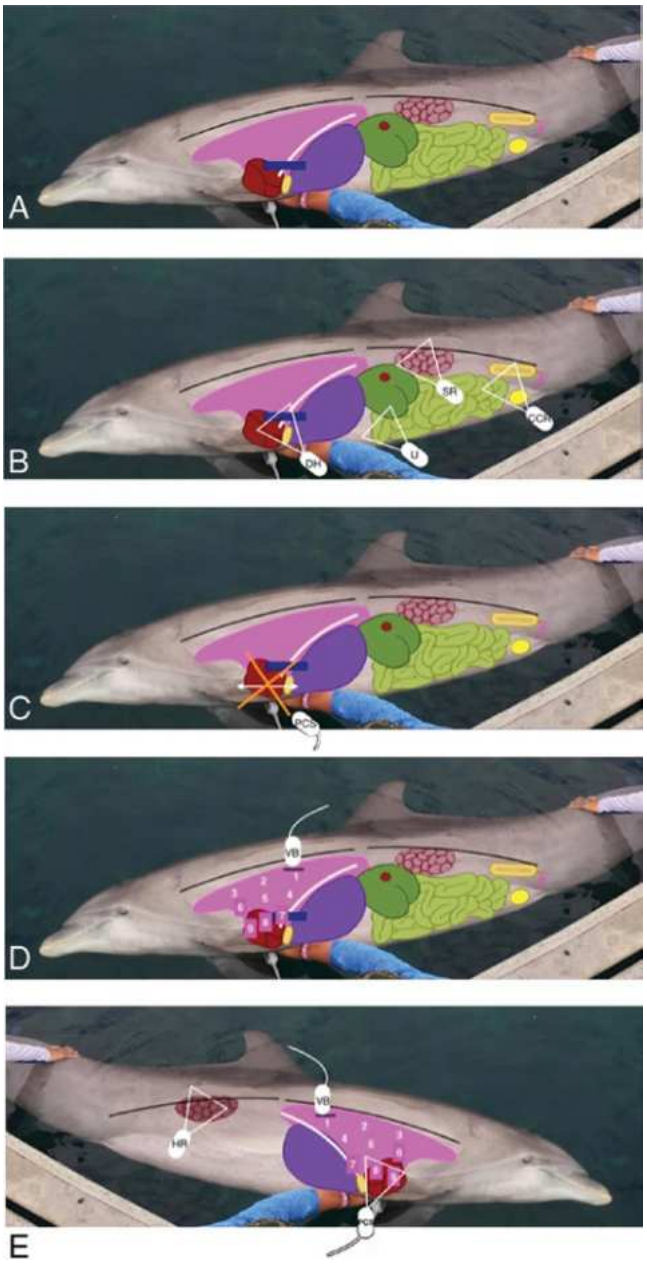


**Figure 41.7.** Overview of Global FAST on a male dolphin. In (A) simple line drawings overlay the important structures imaged during AFAST. In (B) the probe's acoustic window triangles represent the approximate scanning region at each point of placement. Note the prostate and penis are not routinely sonographically interrogated. In (C) the position of the heart is shown similarly with a probe. (D) The nine acoustic transthoracic windows of Vet BLUE. (E) The opposing Vet BLUE acoustic windows and final AFAST views. The TFAST pericardial views may be performed from either right and left sides or both and transthoracic echocardiography is challenging especially with breath holding. Color coding and anatomical features match the line drawing in Figure 41.1. Source: Reproduced with permission from Dr Gregory Lisciandro, Hill Country Veterinary Specialists and FASTVet.com, Spicewood, TX. Illustration by Suji Park, Englewood Cliffs, NJ.

**Table 41.1.**
Performing AFAST on dolphins.

| AFAST view or acoustic window | Target organs | External landmarks | Differs from dogs and cats |
|---|---|---|---|
| Diaphragmatico-hepatic view – right lateral | Liver, heart, caudal vena cava, dorsocaudal lung field along the diaphragm | Ventral midline immediately caudal to the xiphoid as in dogs and cats | The *normal* caudal vena cava and hepatic veins are large, distended and without dynamic changes with the cardiac and respiratory cycles compared to small animals and thus mimic what would be considered volume overload in small animals<br>Measurements for the marginal lymph node have been established as 5 × 2 × 2 cm in adults (Cowan and Smith 1999; Saviano 2013; Martony et al. 2017; Dennison and Saviano 2018) |
| Spleno-renal view – right lateral<br>Hepato-renal view – left lateral | Left kidney, spleen | Vertical line drawn from the caudal border of the dorsal fin ventrally to where it intersects with the hypaxial muscles | The kidneys are similar grossly in margination to bovine kidney due to hundreds of ~1 cm units called renules. The kidneys are quite large. Often, the ureter can be seen along the midcaudal aspect of the kidney. The spleen is similar to the bovine species as it is small (fist-like) and difficult to locate, but best imaged in this view from the right with the dolphin in left lateral recumbency. The stomach surrounds the spleen and digestive contents in the gastric complex can obscure evaluation. The ovaries may be identified caudomedial to the kidneys. In sexually immature females they are round and hypoechoic. In older females, they are isoechoic (or hyperechoic to that of younger females)<br>Splenic size established with diameter of 6–8 cm and 3.5–6 cm in *Tursiops truncatus* and *Tursiops aduncas*, respectively (Gili 2006; Dennison and Saviano 2018) |
| Cysto-colic reproductive view – right lateral | Urinary bladder, reproductive tract | Immediately craniodorsal to the rectum/genital slit | The testicles located craniodorsal to the genital slit are generally very large in sexually mature males and are easily identified by the echogenic linear rete testis (mediastinum or rete testis)<br>The ovaries are located craniodorsal to the genital slit caudal to the kidneys and hypo- to isoechoic (compared to liver) depending on the age and reproductive state. The vagina is not routinely imaged. Measurements of the ovaries have been determined in some dolphin species, 4.4 and 6.4 cm in nonlactating, nongravid *Tursiops truncatus/aduncas* and maximum diameter of preovulatory follicle 2.1 +/–0.5 cm (Brook et al. 2001; Dennison and Saviano 2018) |

(*Continued*)

**Table 41.1**
(*Continued*)

| AFAST view or acoustic window | Target organs | External landmarks | Differs from dogs and cats |
|---|---|---|---|
| Umbilical – either lateral | Small intestine, spleen, reproductive tract | Left dorsal along the larger curvature of the forestomach at the approximate level of the umbilicus | The spleen is located within the left dorsal abdomen and is relatively small compared to the dolphin size. The gastric complex gas and contents often obscure evaluation of the spleen. Gastrointestinal measurements have been established (Fiorucci et al. 2015; Dennison and Saviano 2018) |

*Note that AFAST scanning may begin on the left side and the views analogously performed. Moving to the opposing side allows reimaging at the DH, CCR and HRU (or SRU) views because they are generally accessible from either lateral positioning.*
*Source: Reproduced with permission from Dr Gregory Lisciandro, Hill Country Veterinary Specialists and FASTVet.com, Spicewood, TX.*

### Diaphragmatico-Hepatic View

The DH view target organs include the liver, diaphragm, caudal vena cava, heart, and lung along its pulmonary–diaphragmatic interface (Figures 41.8, 41.9, and 41.10).

- Place the probe immediately caudal to the xiphoid and direct the scan plane far cranially so that you can see simultaneously into the abdomen and thorax. The depth is usually between 20–30 cm for an adult. The probe is fanned through the liver in both lateral directions in the longitudinal plane.
- The (parietal and visceral) pleuroparenchymal junction is imaged through a relatively thick portion of blubber, typically 2–3 cm, depending on health status or seasonal changes of the individual.
- The probe is then rocked further cranially to find the "cardiac bump" created by the beating heart against the diaphragm (see Figures 41.8 and 41.9).
- The left and right marginal lymph nodes are found by fanning laterally along the cardiac apex from the midline and along the diaphragm (Figure 41.11; see also Figure 41.10).
- The pleural space and deep window into lung are observed for pleural and pericardial effusion, and lung lesions along the pulmonary–diaphragmatic interface, respectively.
- The caudal vena cava (CVC) is readily appreciated while fanning along the diaphragm.

#### *Questions Asked at the DH View*

- Is there free fluid in the abdominal cavity? In the author's experience, dolphins can have small to moderate volumes of peritoneal effusion in normalcy (Dr Eric Jensen, personal communication).
- What does the liver look like? Obvious masses or loss of homogeneous echogenicity?
- What does the marginal lymph node look like? And its size?
- What do the CVC and its associated hepatic veins look like?
- Is there fluid in the pericardial sac? In the author's experience, a small volume of pericardial effusion (<2–3 mm) can be present in otherwise apparently healthy individuals.
- Is there fluid in the pleural cavity?
- Are there any abnormalities along the pulmonary–diaphragmatic interface?
- Are any artifacts being mistaken for pathology?

#### *Comments*

The dolphin species does not have a gallbladder. The CVC traverses the diaphragm and then courses along the dorsal aspect of the liver and can be confused with free fluid. Interestingly, the hepatic venous system demonstrates prominent distension and branching in clinically normal dolphins, in contrast to dogs, cats and people, in which it would reflect an abnormally high central venous pressure (see Figures 36.8, 41.8F, and 41.9). Although the CVC is used as a marker of volume status in dogs and cats and the analogous inferior vena cava in people, the CVC in dolphins is impressively distended in the normal state (referred to as FAT; see Chapters 36 and 37). Moreover, the dolphin CVC lacks dynamic changes through the cardiac and respiratory cycles; however, most dolphins are breath holding during ultrasound examination, which likely contributes to their unique difference (Fahlman et al. 2015, 2019; Sklansky et al. 2006).

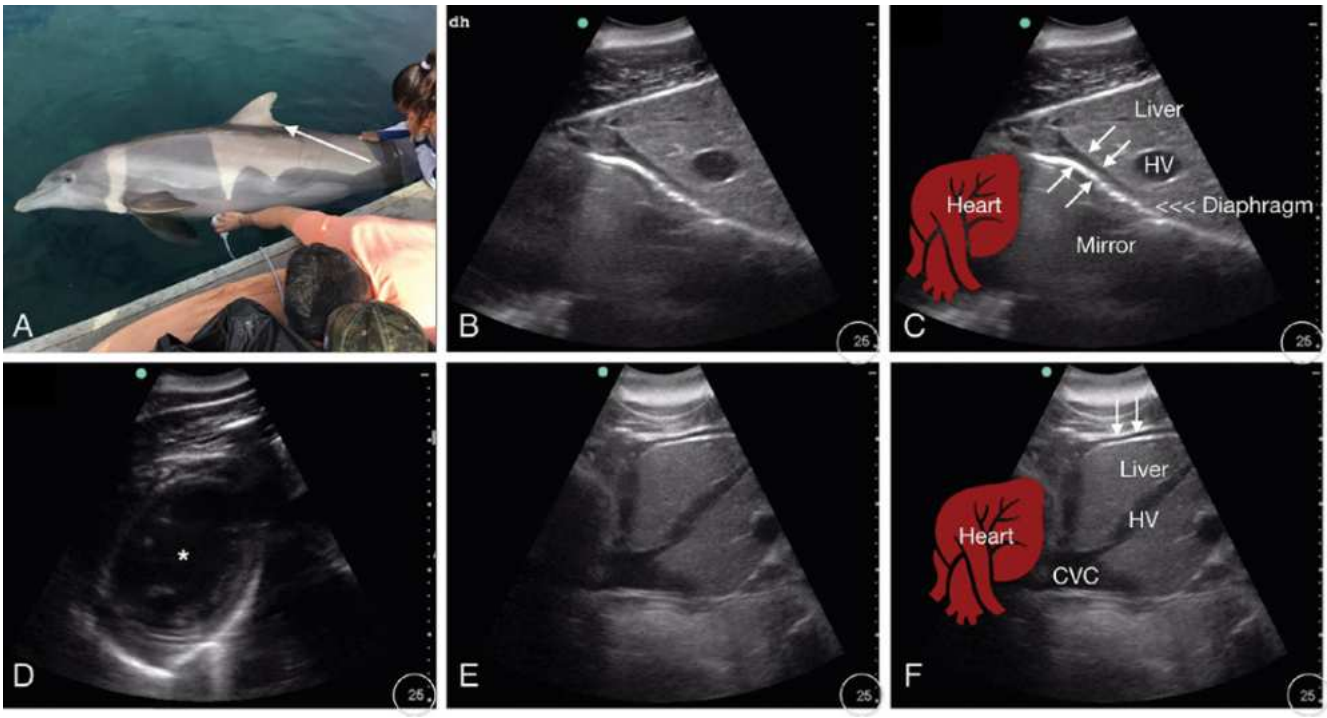


**Figure 41.8** The diaphragmatico-hepatic view. In (A) the probe is placed longitudinally, immediately caudal to the xiphoid and directed cranially toward the head (*arrow*). Though imaging can be evaluated in the longitudinal (sagittal) and transverse planes, all images are acquired in the longitudinal plane. (B,C) The same image unlabeled and labeled in which the diaphragm and liver are imaged with the probe placement shown in (A). Note there is enough depth to see past the diaphragm into the thorax (depth is set at 25 cm in this adult dolphin and is circled in the bottom right-hand corner of each image). There is a mirror image artifact of the liver common at this AFAST view because of the strong air interface of soft tissue and lung. The circular structure labeled HV represents a hepatic vein imaged obliquely. The dolphin species has no gallbladder. The arrows point out the small-volume ascites. In (D) the heart in its entirety is in view (marked by an asterisk, *). The apex of the heart is seen cranial to and immediately against the diaphragm, called the "cardiac bump," and may be evaluated for pericardial effusion, general contractility, and any other obvious soft tissue-associated abnormalities. The DH view may be the best cardiac window for dolphins without transesophageal echocardiography because of less air interference over transthoracic TFAST pericardial sites, which can be challenging. (E,F) The same images unlabeled and labeled in which the caudal vena cava (CVC) is routinely in view as it traverses the diaphragm. The hepatic venous branches that drain into the CVC are also readily identified within the hepatic parenchyma, labeled HV. The small volume of ascites is shown as an anechoic (black) stripe in the near-field in between the liver and the body wall and liver and diaphragm. Degrees of ascites, small to mild volumes, can be found in normalcy and thus must be placed into clinical context. This finding of ascites should be followed up with a serial examination to determine if it is increasing in quantity over time (Dr Eric Jensen, personal communication). The AFAST-applied abdominal fluid scoring system may make more sense of ascites in normalcy by recording volumes of ascites by assigning an abdominal fluid score (AFS 0–5), and which AFAST views are most commonly positive over subjective descriptors of trivial, mild, moderate, and severe. See Abdominal Fluid Scoring section. Source: Reproduced with permission from Dr Gregory Lisciandro, Hill Country Veterinary Specialists and FASTVet.com, Spicewood, TX.

Though the CVC is typically large (distended) in the normal state in dolphins, we are unsure whether or not any dynamic CVC changes occur with cardiovascular pathology or changes in volume status as occur in small animals and people (see Figure 41.9) (Nelson 2010; Ferrada et al. 2012a,b). For example, pericardial effusion, cardiac tamponade, and right-sided congestive heart failure in small animals result in a distended CVC with hepatic venous distension. Conversely, profound hypovolemia results in a small flat CVC (Ferrada et al. 2012a,b). Dolphin CVC hemodynamic alterations would be an area of future study but in the author's experience, there seems to be very little distensibility change during the cardiac cycle and manipulating the respiratory cycle to discourage breath holding (encourage spontaneous breathing) may not be possible (Yarto and Lisciandro 2017, unpublished data).

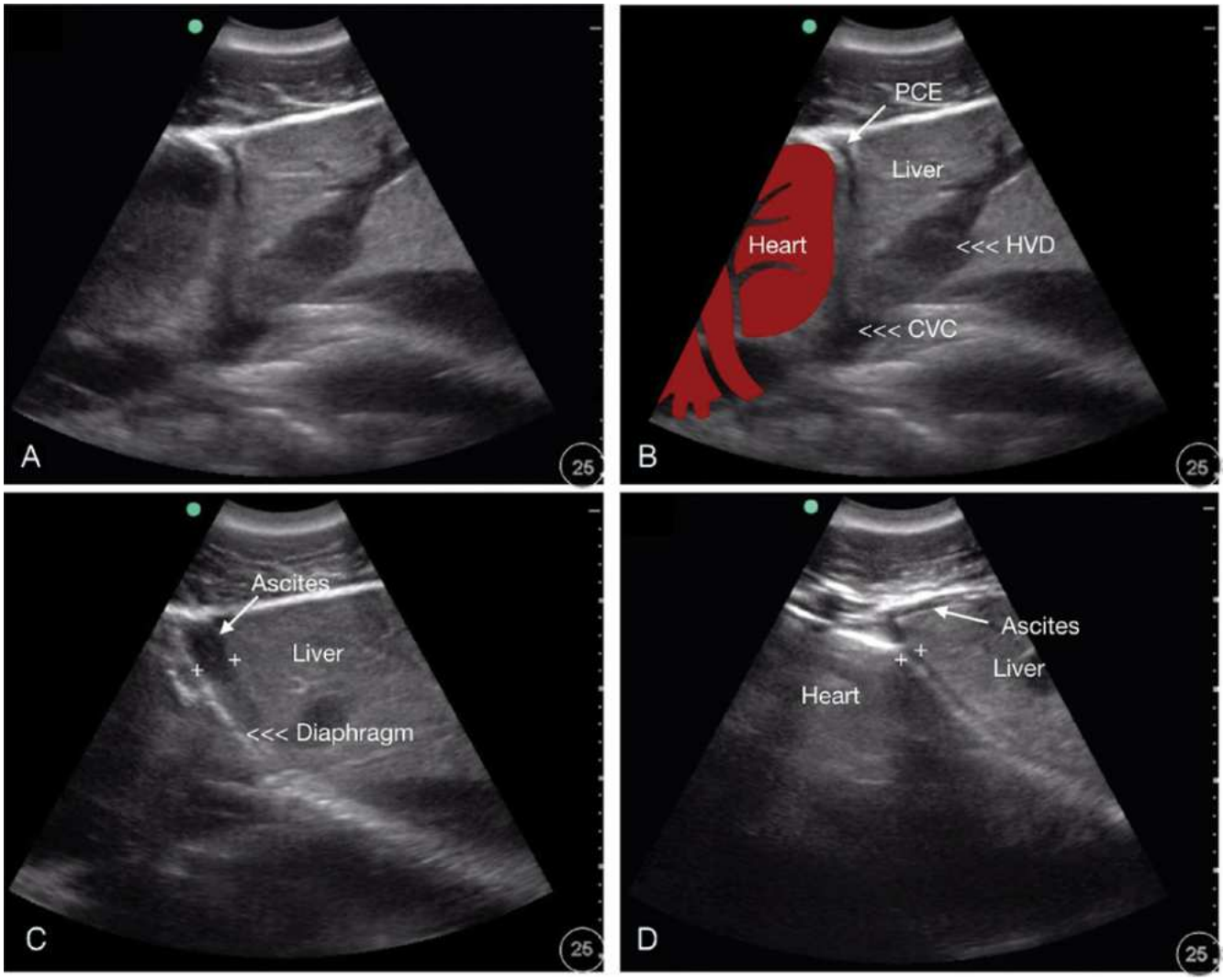


**Figure 41.9.** The caudal vena cava and hepatic venous system at the DH view. (A,B) The same images unlabeled and labeled of the DH view. Note the DH view shows how prominent and distended the caudal vena cava (CVC) and hepatic venous system (hepatic vein distension labeled HVD) are in a normal dolphin. Though the heart is difficult to fully evaluate via transthoracic sonography due to pulmonary air interference, the beating heart against the diaphragm, referred to as the "cardiac bump," is readily imaged and serves to screen for clinically relevant pericardial effusion (PCE, *arrow*), and possibly other cardiac abnormalities, including contractility. The small volume of PCE in this dolphin was of uncertain significance and etiology. In (C) there is ascites, indicated by calipers (+) and arrow, present along the liver and diaphragm. In (D) the arrow points out the smaller volume of ascites between the margin of the liver and diaphragm. The DH view is an ideal place to look for ascites due to the acoustic window provided by the liver. Depth is set at 25 cm and circled in the bottom right-hand corner in the images. HVD, hepatic venous distension; CVC, caudal vena cava; PCE, pericardial effusion. Source: Reproduced with permission from Dr Gregory Lisciandro, Hill Country Veterinary Specialists and FASTVet.com, Spicewood, TX.

Another interesting CVC factor to consider is patient positioning. In small animals, the pressure exerted by the abdominal organs is less in lateral and standing-sternal than dorsal recumbency, which affects hemodynamics and the character of the CVC and its associated hepatic venous system (Darnis et al. 2018). In dolphins, this may be less of a factor due to neutral buoyancy in the water.

### *Marginal Lymph Nodes*

The right and left marginal lymph nodes are sentinels for pulmonary diseases and their enlargement generally reflects significant disease (Martony et al. 2017). The marginal lymph nodes have established expected measurements in clinically normal dolphins (Martony et al. 2017) and the marginal lymph node may be

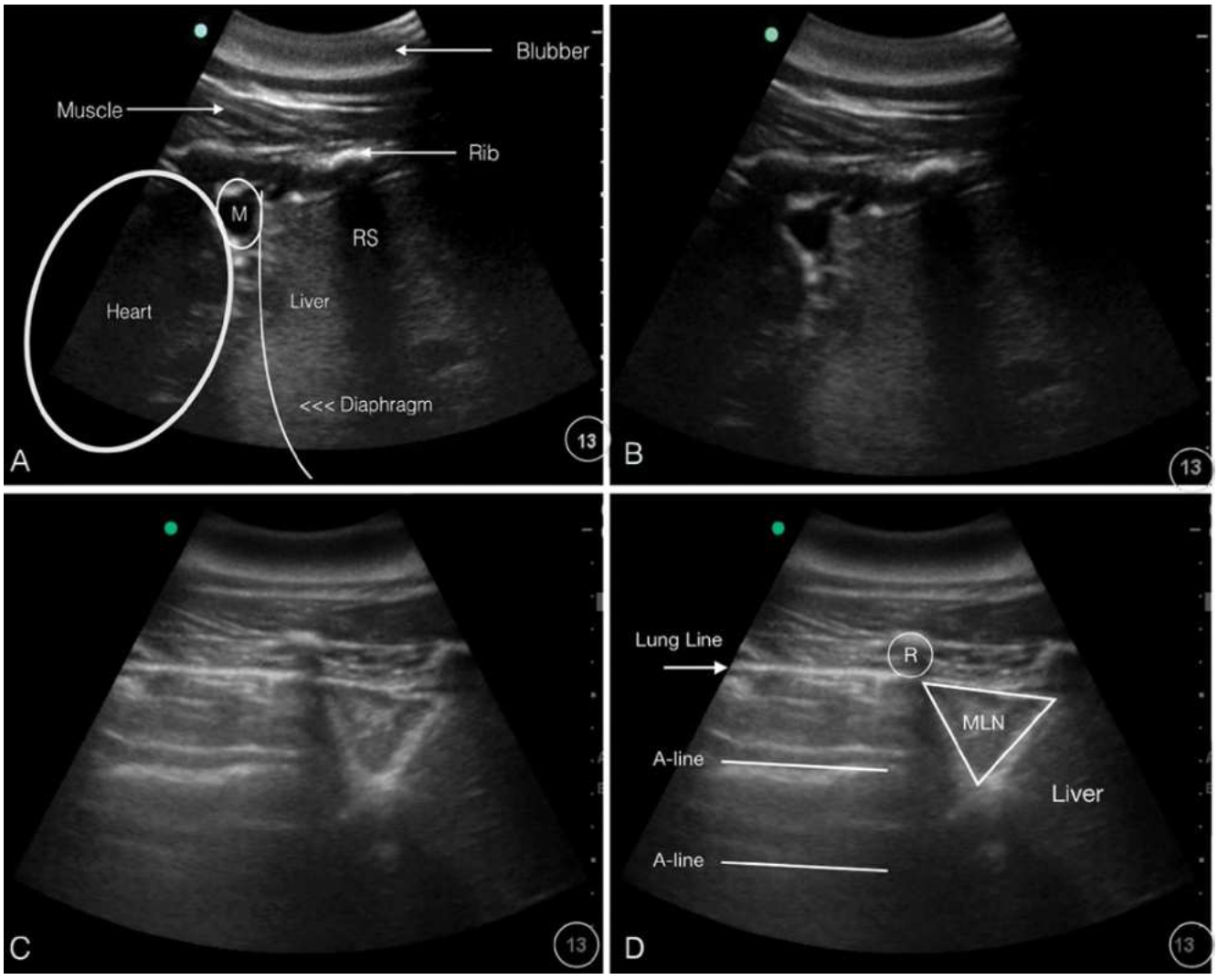


**Figure 41.10.** Marginal lymph nodes. (A,B) The same figure labeled and unlabeled. Imaging the left and right marginal lymph nodes is important due to their clinical relevance in certain disease states, particularly pneumonia (Martony et al. 2017). Note the heart against the diaphragm and in the cardiac-diaphragmatic recess is the marginal lymph node (M). The heart is outlined with the oval. (C,D) The same image unlabeled and labeled. The marginal lymph node is between the heart and diaphragm intimately associated with the caudal margin of the lung as shown in the still B-mode image. The "gator sign" is in view, with the rib, "lung line", and A-lines labeled. Depth is set at 13 cm (circled) and the marginal lymph node is classic in appearance. A triangular overlay points out the marginal lymph node. M, marginal lymph node in (A); MLN, marginal lymph node in (D); RS, rib shadow, R, rib. Source: Reproduced with permission from Dr Gregory Lisciandro, Hill Country Veterinary Specialists and FASTVet.com, Spicewood, TX.

reliably imaged via the FAST DH view and/or at point 7 of Vet BLUE as shown in Figures 41.10 and 41.11.

### *Confounders at the DH View*

The CVC and hepatic veins are prominent and markedly distended in normalcy, which can mimic ascites, and the hepatic veins appear oval and gallbladder-like (the dolphin species does not have a gallbladder) (Figure 41.12A; see also Figure 41.8B,C). Moreover, by rocking more toward the spine (versus far cranially), the sonographer then brings in gastric complex structures as shown in Figure 41.12A.

### Spleno-Renal and Hepato-Renal Views

The SR view is performed in right lateral positioning and the HR view in left lateral positioning (Figure 41.13).

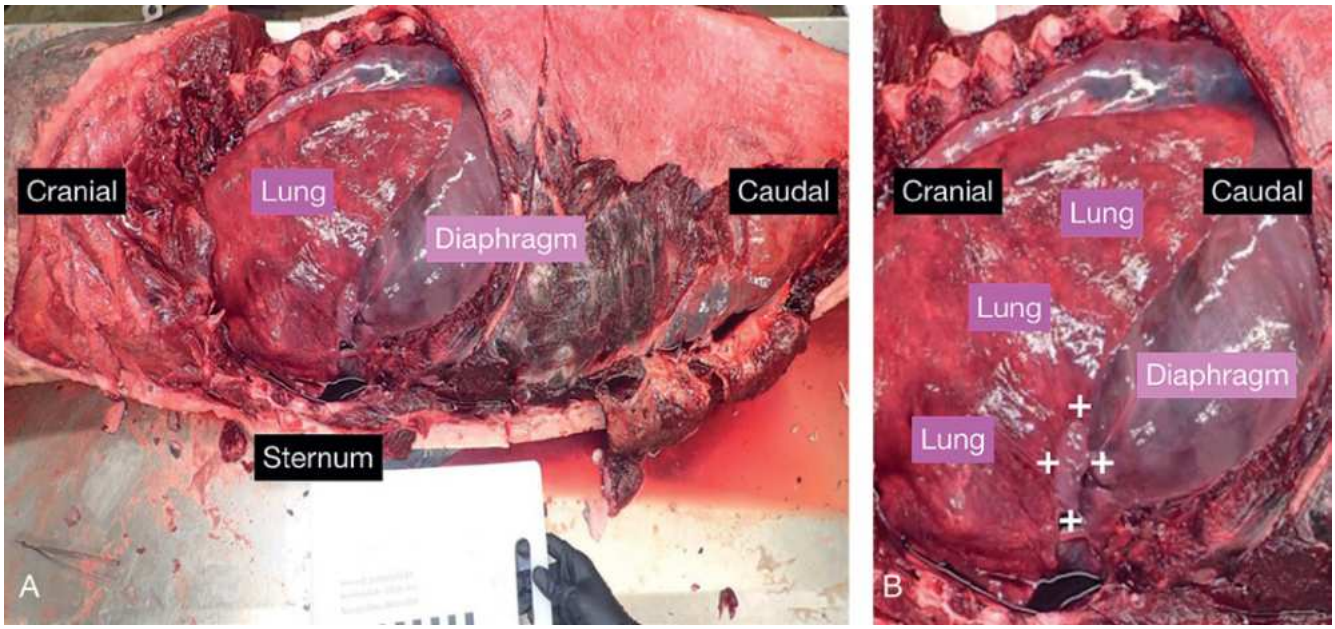


**Figure 41.11.** Marginal lymph nodes. (A) An overview of a necropsy showing the left marginal lymph node with the entire thorax, lung and diaphragm in view. Note the left sausage-shaped marginal lymph node that lies vertically at the caudal ventral lung margin in the cardiac-diaphragmatic recess. Lung and diaphragm are labeled. In (B) the region of interest is enlarged to show the left marginal lymph node, outlined in (+), and the nearby anatomy of the lung and diaphragm. The marginal lymph node is reliably imaged through the DH view as shown in Figure 41.10(A,B) and sliding dorsolateral from the xiphoid and over the pleural–peritoneal transition at Vet BLUE point 7 as in Figure 41.10(C,D). Source: Photo courtesy of the Institute for Marine Mammal Studies, Gulfport, MS.

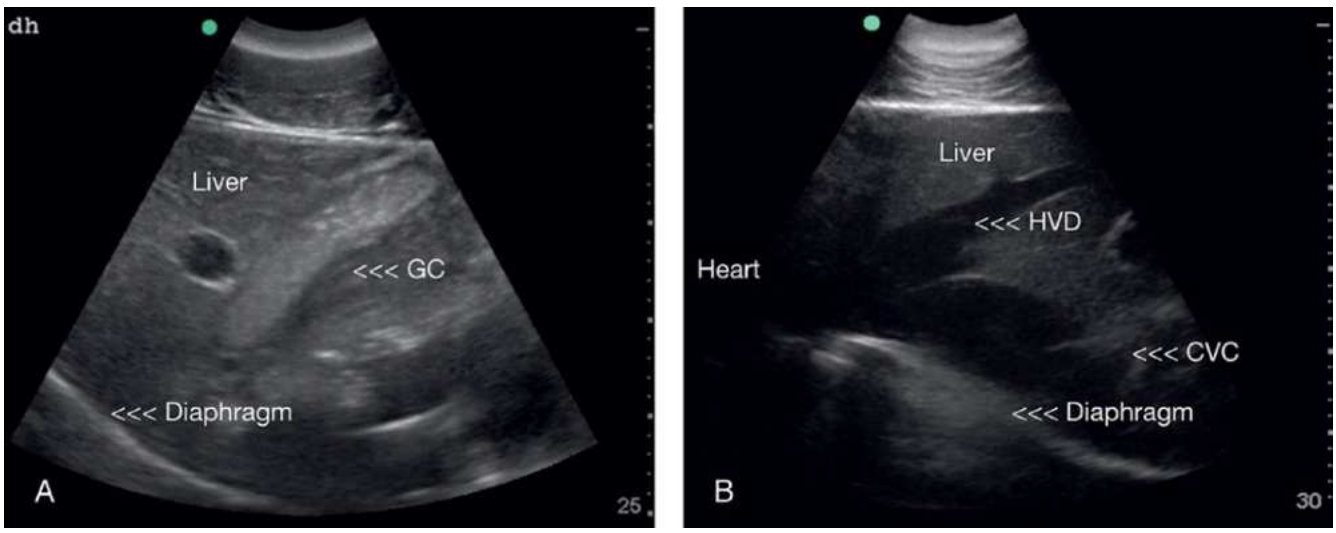


**Figure 41.12.** Confounders at the DH view. In (A) the gastric complex (GC) can appear echogenic (gray and tubular) and can be mistaken for parenchymal organs (although gastrointestinal peristalsis can help to distinguish). In (B) the CVC and its associated hepatic venous system are quite large. Note how the CVC courses along the far-field along the diaphragm and could be mistaken for ascites. GC, gastric complex; HVD, hepatic venous distension; CVC, caudal vena cava. Source: Reproduced with permission from Dr Gregory Lisciandro, Hill Country Veterinary Specialists and FASTVet.com, Spicewood, TX.

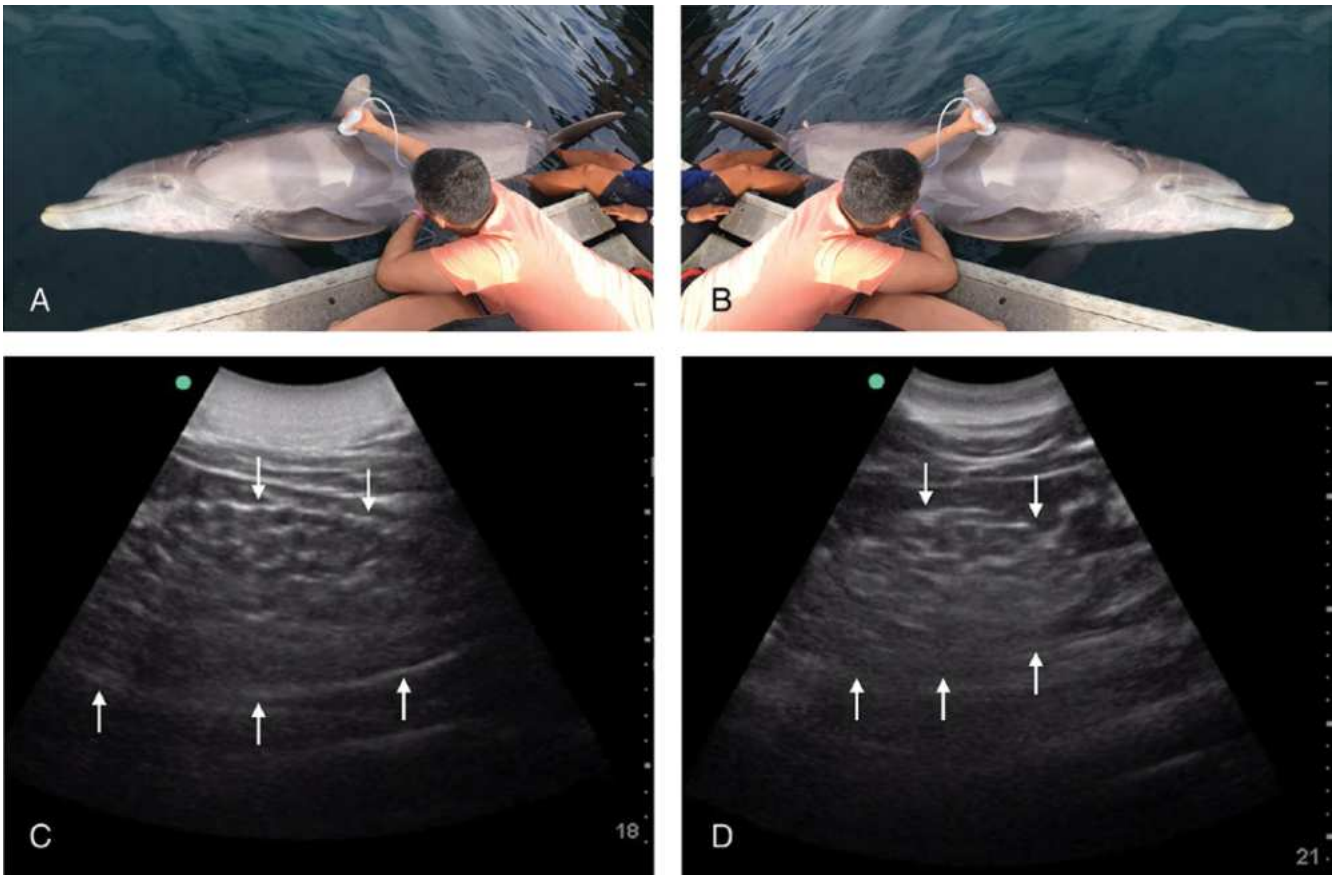


**Figure 41.13.** The spleno-renal and hepato-renal views. In (A) and (B) the external starting probe position is shown and in (C) and (D) the left and right kidney are shown. Sliding ventrally from the starting points brings the kidneys into view. Although subtle, the kidney is typically found just below the palpable hypaxial line ventral to slightly caudoventral to the middorsal fin. At this location, the probe is slid immediately along the hypaxial line while fanning until the kidney comes into view. The dolphin kidney can initially be difficult to recognize because its echo architecture is so dissimilar to dogs and cats. It has a lobulated bovine-like structure (or grape-like appearance), referred to as a reniculate kidney. The left and right kidney at the SR and HR views are imaged similarly. Source: Reproduced with permission from Dr Gregory Lisciandro, Hill Country Veterinary Specialists and FASTVet.com, Spicewood, TX.

However, the spleen may be imaged from the HR, SR (from left lateral recumbency) and Umbilical views, with SR view from left recumbency presenting the best acoustic window for visualization (see Figure 41.16). The expected target organs are the respective kidney, associated reproductive organs, spleen, and liver in small animals. In the dolphin, the respective kidneys and reproductive tract can be imaged at the SR and HR views. The spleen is a small organ not likely associated with extramedullary hematopoiesis in this species, and uncommonly associated with disease states such as lymphoma, trauma and splenic necrosis in association with *Brucella* sp. (Bossart et al. 1997; Cowan and Smith 1999; Jauniaux et al. 2010).

- Place the probe directly ventral to the caudal border of the dorsal fin. The hypaxial muscles may be thought of as the dorsal border of the abdominal body wall. Move the probe ventrally on the body wall, continuing to use the caudal border of the dorsal fin as your landmark until the multireniculated (multilobed) kidney is encountered (see Figure 41.13).
- On the left side, the left kidney should be fanned through in both directions longitudinally then rocked cranially for a view into the abdominal cavity (and in time the add-on skill of transverse orientation).
- On the right side, the right kidney should be fanned through in both directions longitudinally then rocked cranially for a view into the abdominal cavity (and in time the add-on skill of transverse orientation).
- The probe may also be directed ventrocaudal to the kidneys for reproductive organ imaging (see Figure 41.14).

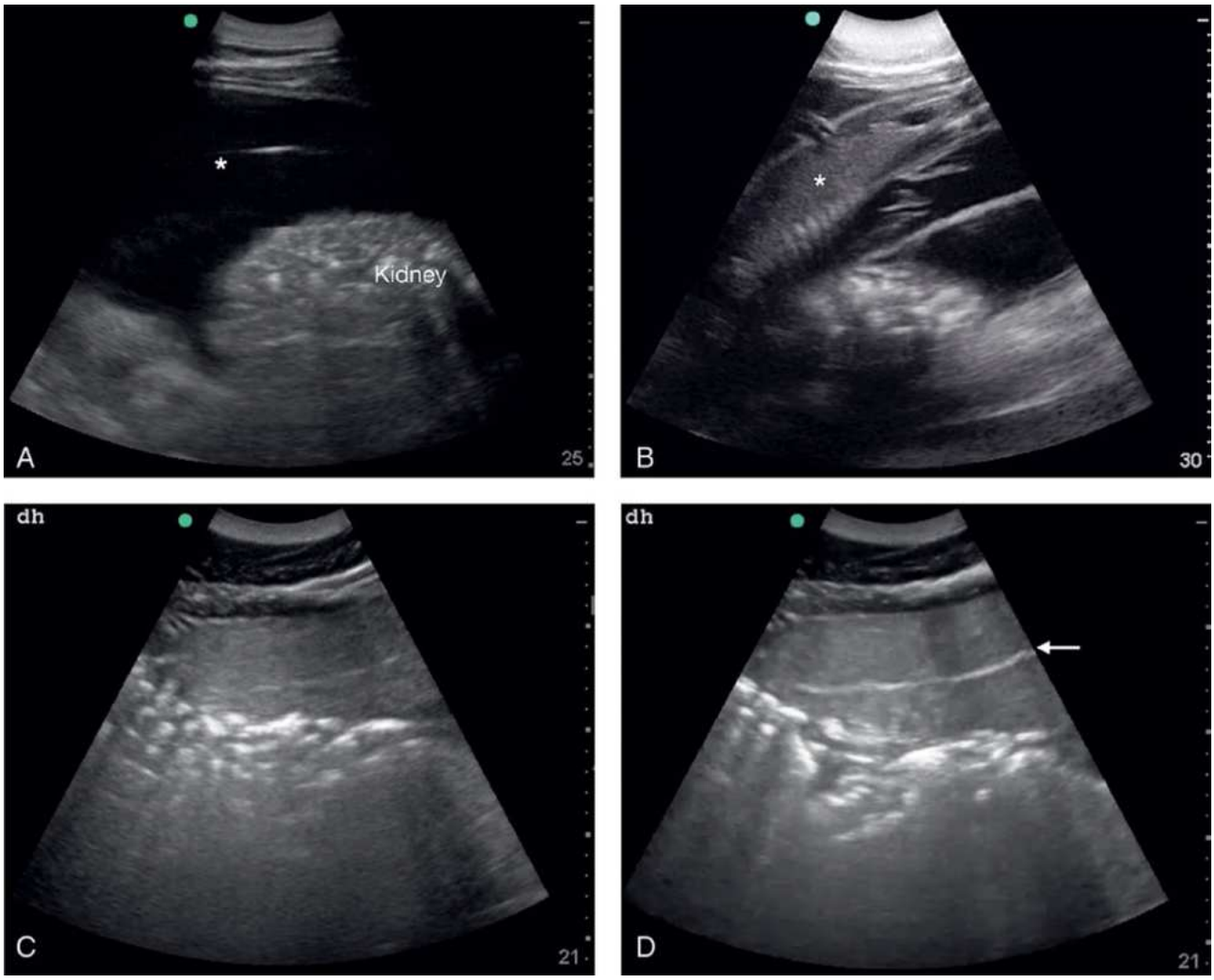


**Figure 41.14.** The spleno-renal and hepato-renal views and target organs. In (A) the grape-like appearance of the reniculate dolphin kidney is more evident with the surrounding fluid of the gravid uterus. In (B) the fetus is seen, marked (*). Notice the echogenic fetal ribs. The kidney is in the far-field and hyperechoic. In (C) the testicle is seen in close association with the kidney in a reproductively mature male. The far-field has gas-filled loops of small intestine. (D) Note the testicle with linear echogenic rete testis also referred to as the mediastinum testes, the testicular sonographic identifying landmark (*arrow*). The far-field has gas-filled loops of small intestine. Source: Reproduced with permission from Dr Gregory Lisciandro, Hill Country Veterinary Specialists and FASTVet.com, Spicewood, TX.

- A full forestomach or gas-filled stomach can interfere with clear visualization of the spleen.

### *Questions Asked at the SR and HR Views*

- Is there free fluid in the abdominal cavity?
- Is there any free fluid around the kidneys or the adjacent retroperitoneal space?
- What does the kidney look like? Are there any gas reverberations, comet-tailing artifacts (gas bubbles) or echogenic interphases with acoustic shadowing as can occur with intrarenule uric acid lithiasis (nephroliths) within the reniculi?
- Is the dolphin sexually mature? Are male or female reproductive structures apparent?
- Are any artifacts being mistaken for pathology?

### *Comments*

If fluid is detected only on the SR or HR views, and no other AFAST views, then the fluid is likely perinephric or retroperitoneal. If free fluid is seen at additional

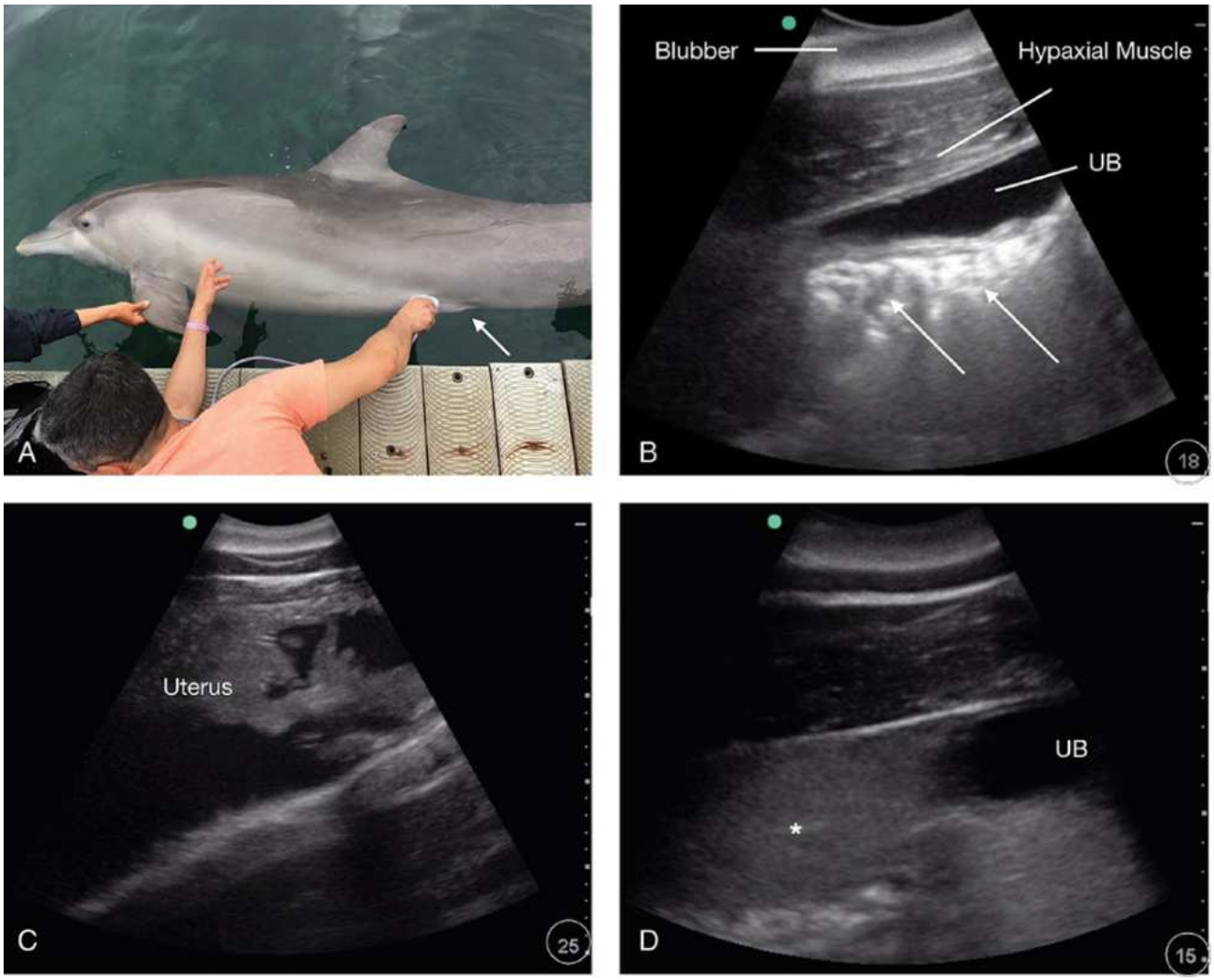


**Figure 41.15.** The cysto-colic reproductive view. In (A) the external location of the probe is shown just craniodorsal to the genital slit (*arrow*). The probe is fanned and an anechoic urine-filled urinary bladder is usually easy to image, as in (B). Notice the hyperechoic, gas-filled, small intestines located in the middle of the field that dirty shadow through the far-field having luminal air (*arrows*). Other landmarks are labeled including blubber and hypaxial muscles. The urinary bladder is labeled UB. Sex identification is readily apparent because a gravid uterus is evident (C). In (D) this male has large testicles (*asterisk*) seen just cranial to the urinary bladder (UB). By fanning through the testicle, the rete testis (not shown in this image) identifies the structure sonographically (see Figure 41.14D). Depth is between 15 and 25 cm and noted in the bottom right-hand corner of the images. Source: Reproduced with permission from Dr Gregory Lisciandro, Hill Country Veterinary Specialists and FASTVet.com, Spicewood, TX.

AFAST views then it is likely peritoneal in origin. Retroperitoneal fluid is not part of the abdominal fluid scoring system (see AFAST-applied Abdominal Fluid Scoring System section later). The gravid uterus will be seen at the SR view (Figure 41.14). In males, once the kidney is in view the probe can be slid caudoventral and the large intraperitoneal testicles will come into view. The landmark for the testicles is the hyperechoic (bright white) linear rete testes (see Figure 41.14D).

### Cysto-Colic Reproductive View

The target organs are the urinary bladder and associated reproductive organs (Figure 41.15).

- Place the probe cranial to the genital slit and slide or fan dorsally through the ventral body wall.
- When adequately distended, fan through the urinary bladder in both directions in the

longitudinal planes (and in time the add-on skill of transverse planes).
- Fan or rock cranially to evaluate the reproductive tract, which can then be followed in zigzag fashion cranially and caudally. The female ovarian tissue can be identified caudal to the kidneys. Depending on the degree of uterine distension, the uterus can be readily identified adjacent to the urinary bladder.

### *Questions Asked at the CCR View*

- Is there free fluid in the abdominal cavity? This is a frequent site of accumulation of small volumes of anechoic fluid likely of normal variation.
- What does the urinary bladder look like?
- For females – is the uterus imaged? Are there any abnormalities? Is the uterus fluid filled or gravid?
- For males – are the testicles imaged? Are there any abnormalities?
- Are any artifacts being mistaken for pathology?

### *Comments*

The gravid uterus will be seen at this view and the testicles immediately cranial especially obvious in sexually active males (hypertrophied testicles). The prostate, penis, and vagina are not routinely imaged. Differentiation between the bowel and uterine horn can be made through the observation of luminal gas and peristalsis in the intestinal tract, unlike the uterus.

## Umbilical View

- Place the probe at the umbilicus, which is easy to recognize externally (Figure 41.16).
- Fan longitudinally in both lateral directions and then rock cranially to capture the midabdominal structures.
- The umbilical view is the same from either right or left lateral recumbency but accessibility may be affected by the dolphin being more or less dorsolaterally positioned.
- The target organs found here in the dolphin include small intestine and the gastric complex (from cranial to caudal on the left, the fundic and forestomach and on the right, the pyloric stomach).
- Glimpses of the spleen can be imaged in this view but less reliably, as it is typically surrounded by the gastric complex which when air-filled obscures imaging.
- In females, the uterus may also be seen here, especially in pregnant dolphins.

### *Questions Asked at the Umbilical View*

- Is there free fluid in the abdominal cavity?
- What does the small intestine look like – motility, lesions?
- What does the spleen look like?
- For females – is the uterus imaged? Any abnormalities? Gravid?
- Are any artifacts being mistaken for pathology?

### *Comments*

It is easy to confuse the third gastric compartment (pyloric stomach) with the spleen. The spleen can lie ventrocaudal to the first gastric compartment (forestomach). Cine clips of this region are ideal for telemedicine evaluation by a radiologist or experienced marine mammal sonographer. Abnormalities of the fore, fundic, and pyloric stomachs are best reserved for an experienced radiologist or marine mammal sonographer. The gravid uterus may also be seen at this view, especially in late-term pregnancy.

## AFAST-Applied Fluid Scoring System

The AFAST-applied abdominal fluid scoring system may be calculated for peritoneal effusion, providing an objective number for recording in medical records and for tracking static, resolving or worsening ascites. The abdominal fluid score (AFS) ranges from 0 (negative all AFAST views) to 4 (positive all four AFAST views) in small animals (see Chapters 6 and 7) (Lisciandro et al. 2009). In dolphins, scoring of 1–5 may be more appropriate. Thus, an AFS of 1 is positive at any single view. An AFS of 2 is positive at any two views. An AFS of 3 and 4 is positive at any three or four views, respectively. A maximum AFS of 5 is positive at all five views. The terms trivial, mild, moderate, and severe in addition to the AFS may also be helpful for better semiquantifying ascites (Lisciandro et al. 2009, 2019; Lisciandro 2011). Regardless, the presence of mild anechoic peritoneal effusion can vary from one day to another and may be of little clinical relevance.

### *Modification in Abdominal Fluid Scoring*

Recently, the AFAST-applied AFS system was modified for dogs and cats to scoring smaller pockets as a 1/2 rather than a full 1 (Lisciandro et al. 2019). A similar scoring system may be helpful in dolphins in more specific quantifications of small volumes. For an animal as large as a dolphin, a fluid pocket with

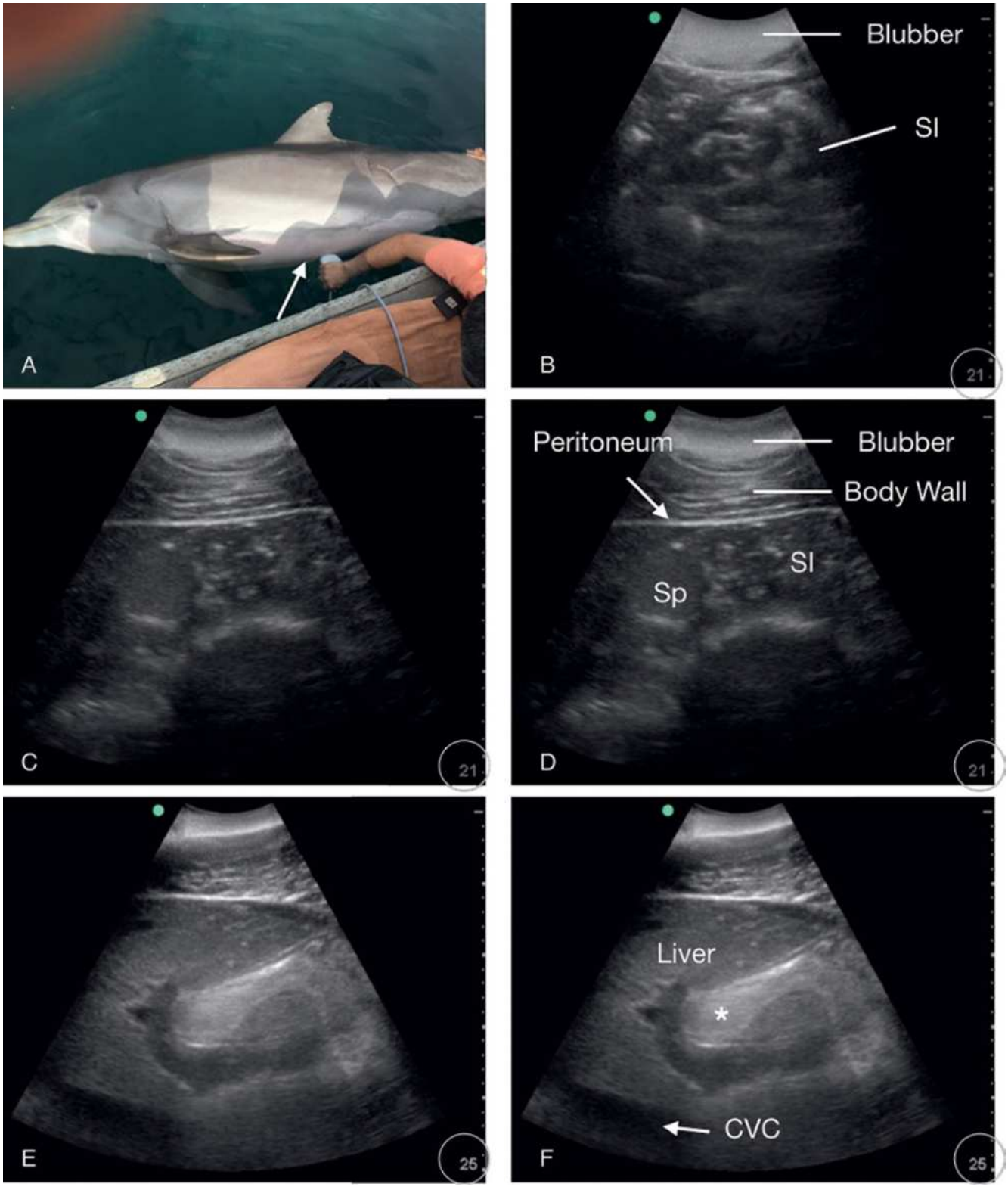


**Figure 41.16.** The umbilical view. In (A) the probe is placed in the region of the umbilicus (*arrow*), which is easy to identify. (B) The images show the small intestine. (C,D) Unlabeled and labeled images with intestinal tract and spleen. The spleen is the echogenic rounded structure left of center, labeled Sp. On a still image alone, it may be difficult to definitely determine whether or not this structure is the spleen. Evaluation for peristalsis on a cine clip can aid in differentiating the bowel from solid organs. Blubber, abdominal wall, and the peritoneum are additionally labeled. (E,F) The same unlabeled and labeled images with the liver and a portion of the gastric complex (*) which come into view when the probe is rocked cranially. Depth is circled in the bottom right-hand corner of each ultrasound image and ranges from 21 to 25 cm. CVC, caudal vena cava; Sp, spleen; SI, small intestine. Source: Reproduced with permission from Dr Gregory Lisciandro, Hill Country Veterinary Specialists and FASTVet.com, Spicewood, TX.

maximum dimensions of <2 cm can be scored as 1/2 and >4 cm as 1, as a starting point for this species. Caution is advised when interpreting the significance of ascites in this species as a small volume of effusion may be seen in apparently healthy individuals. Calculating and recording the AFS and where the dolphin is positive and negative and their positioning would likely serve as a useful tool of surveillance (see Chapters 6 and 7).

## TFAST

In small animals TFAST examination includes left and right pericardial site (PCS) views, left and right chest tube site (CTS) views, and the singly applied DH view (Lisciandro et al. 2008; Lisciandro 2016; McMurray et al. 2016). When applied to dolphins, the CTS views are eliminated and replaced by the Vet BLUE views when evaluated. The DH view is in fact part of AFAST, TFAST, and Vet BLUE. For pneumothorax (PTX), the highest point over the pleural cavity, analogous to the CTS view, would be imaged dependent on the dolphin's position (where free air in the pleural cavity would rise). In small animals, PCS views are used for pleural and pericardial effusion, any adjacent masses, and any obvious chamber enlargement, wall thickening or other abnormalities, including intracardiac masses. These transthoracic views seem to be more limited in the dolphin for cardiac evaluation because of their thoracic conformation and marked air interference from lung limiting the acoustic window. Dilated cardiomyopathy and right-sided congestive heart failure has been described (Lutmerding et al. 2015).

TFAST echo views are similar to those in small animals; however, the dolphin heart is very globoid in shape and much more difficult to image sonographically because of the barrel-shaped, somewhat bulldog-like conformation of the thoracic cavity (Sklansky et al. 2006). Further, air interference from breath holding can obscure cardiac assessment (Sklansky et al. 2006; Chetboul et al. 2012). During inspiration, dolphins aerate up to 95% of their lung capacity, which is significantly more than in terrestrial mammals, posing another challenging factor for TFAST evaluation (Fahlman et al. 2015).

- Find the heart, as in dogs and cats, by palpating with your nonprobe hand for the apical beat. Yes, despite their size, you can generally palpate their apical beat!
- Place the probe at the maximum intensity of the apical beat.
- Use the pectoral fin for stabilization of the probe and to prevent dolphin drifting.
- Theoretically, right parasternal short-axis views are performed for volume and contractility (fractional shortening, FS%).
- The right parasternal short-axis view for the left atrium:aorta ratio (LA:Ao) is performed to screen for left-sided problems (specifically left atrial enlargement).
- The "TFAST slide" as described in Chapters 17 and 18 may be applied to the dolphin by caudally sliding the probe into the "cardiac-diaphragmatic pouch" and then cranially into the "cardiac-cervical pouch" (see Figures 17.17 and 17.18).
- During the "TFAST slide" the probe may also be rotated to an orientation parallel to the ribs for an intercostal view detecting smaller volume pleural effusions that may not be obvious in perpendicular orientation (to the long axis of the ribs).

It takes repetition and practice to achieve proficiency in the TFAST echo views. Transesophageal echocardiography (TEE), when available, is the gold standard for cardiac evaluation in this species and has clear advantages over transthoracic echocardiography because it provides a better acoustic window. Specifically, TEE avoids the acoustic gas artifacts caused by surrounding lung interference (Sklansky et al. 2006). TEE is generally well tolerated by dolphins as a trained medical behavior, but is beyond the scope of this chapter (Sklansky et al. 2006).

### Questions Asked at TFAST

- Is there any pleural effusion?
- Is there any pericardial effusion?
- Are cardiac chamber ratios unremarkable or abnormal?
- Are there soft tissue masses in any cardiac chambers?
- Are there soft tissue masses in the pericardium or pleural cavity?
- Are any artifacts being mistaken for pathology?

### Detecting Pleural and Pericardial Effusion

The accurate diagnosis of pleural (PE) and pericardial (PCE) effusion depends on the same principles as in other species, including imaging the heart in its entirety (using the landmark of the hyperechoic pericardium in the far-field), and identifying its

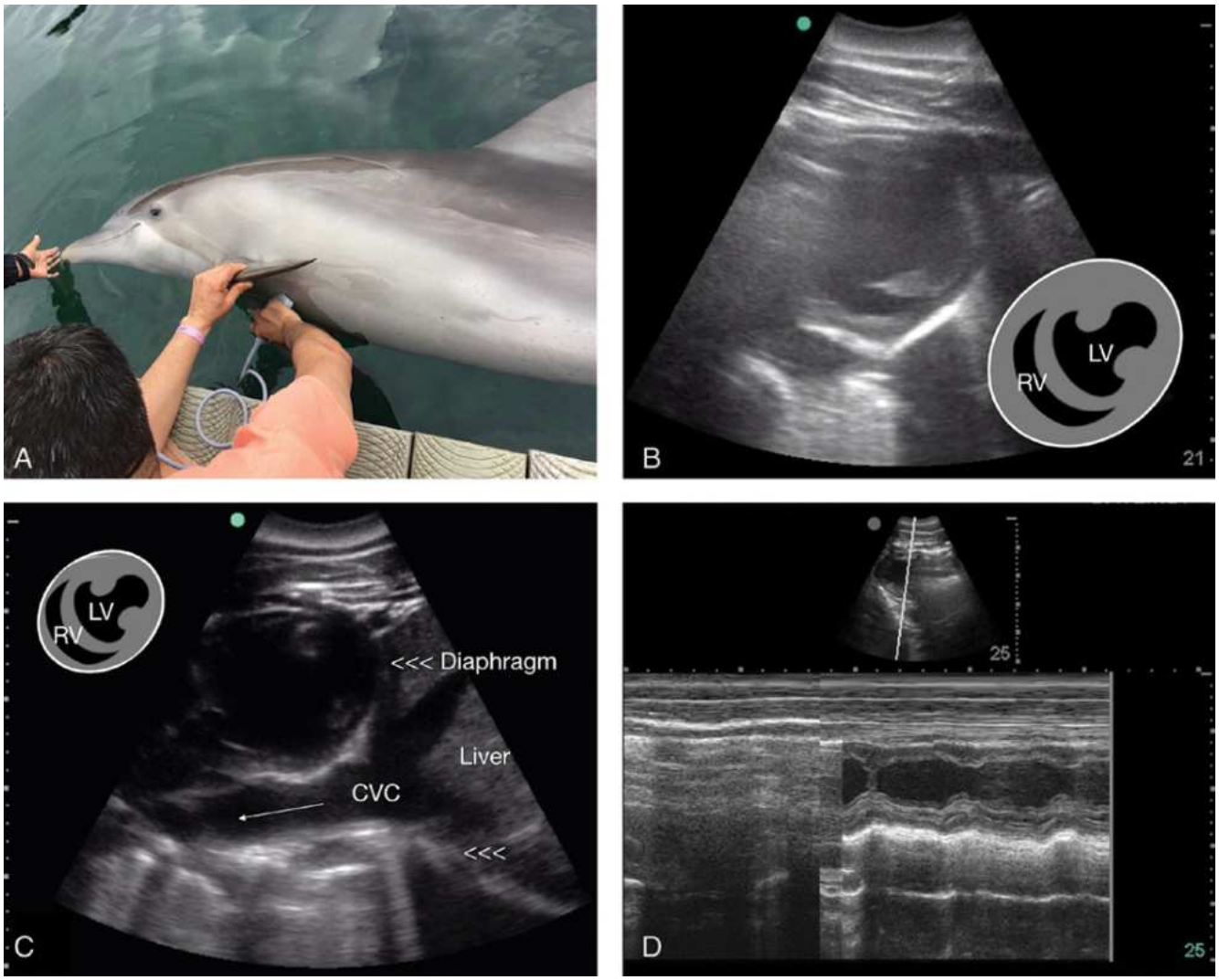


**Figure 41.17.** TFAST echo views. The acoustic windows for the TFAST echo views are challenging. The heart is very globoid. In (A) external probe positioning in between the pectoral flippers and holding the flipper for stability are shown. The scanning plane approximates the "short-axis line" and "long-axis line" of small animals (see Figures 17.22–26). This probe positioning allows for visualization of the right TFAST PCS short-axis views analogous to the right parasternal view of complete echocardiography. Images (B) and (C) are at the same approximate point on the patient with slight differences in fanning. In (B) the pericardium is seen in the far-field. In (C) note the CVC is large and anechoic (*arrow*) and should not be confused with pericardial effusion. Fanning at the apex and evaluation of the near-field can aid in further ruling out pericardial effusion. In (D) these views can be used to obtain M-mode images for echocardiogram evaluation. TFAST cardiac evaluation is used as a screening test by the "eyeball method" for assessing contractility (FS%), chamber sizes, chamber ratios, and evaluation for obvious structural abnormalities (masses, thrombi) (see Figures 17.21 and 36.7) (Ferrada et al. 2011; Atkinson et al. 2017). These assessments can then be used for future comparison in the same patient when images are stored and Global FAST findings recorded and help trigger the need for a complete detailed echocardiogram. Source: Reproduced with permission from Dr Gregory Lisciandro, Hill Country Veterinary Specialists and FASTVet.com, Spicewood, TX.

chambers and multiple views (one view is no view), especially directing the scanning plane toward the muscular apex of the heart so that heart chambers are not mistaken for either PE or PCE (see Table 18.6 and Figure 17.15).

### TFAST Echo Views and Using Global FAST Fallback Views

"Global FAST nonecho fallback views" are indirect ways to screen for left- and right-sided congestive heart failure *without* echo views (Figure 41.17) (see

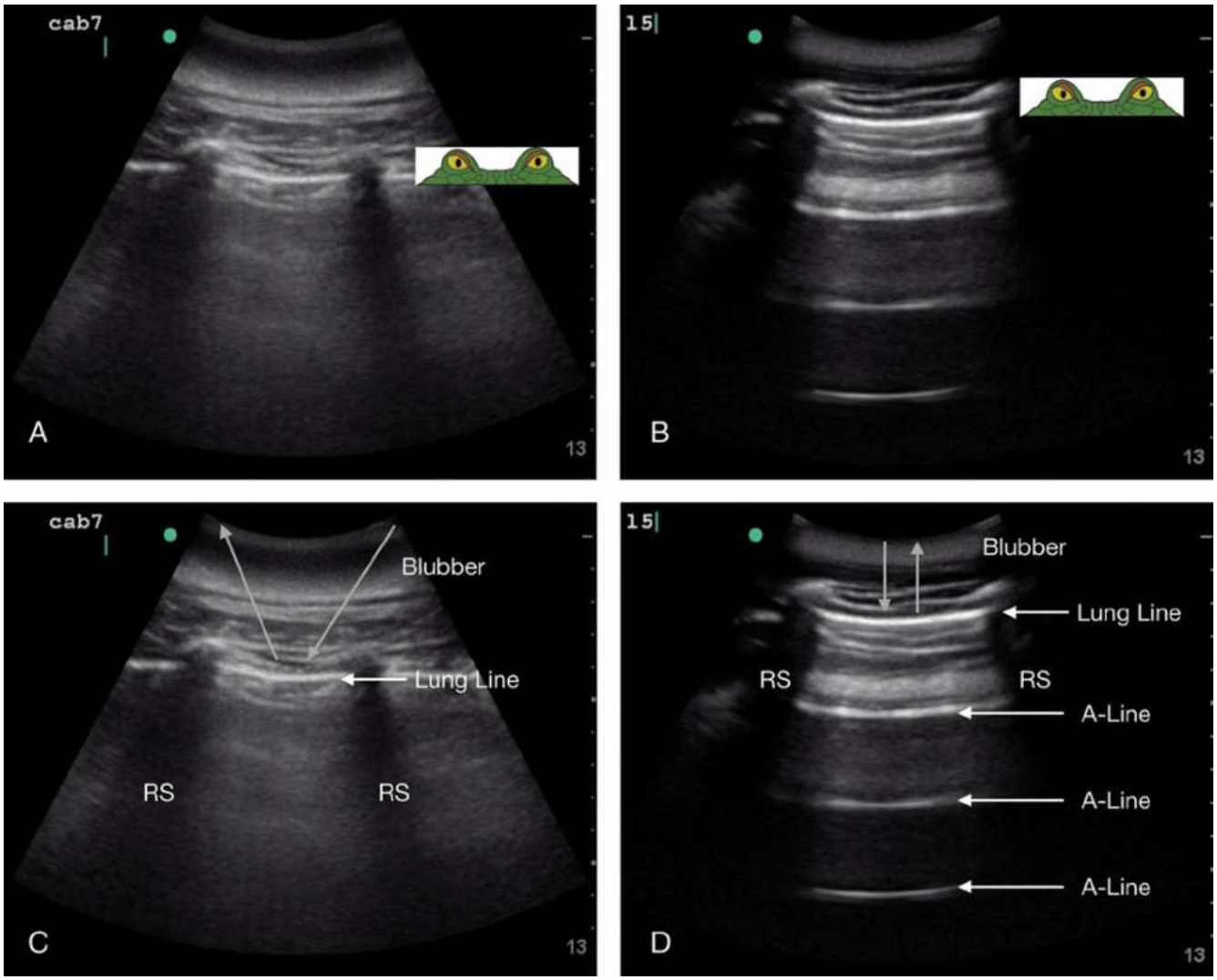


**Figure 41.18.** "Gator sign" orientation and angle of insonation. In the images in this chapter, the dolphin's head is always to the left and the tail (fluke) to the right of the screen. (A,B) Unlabeled images. (C,D) Labeled images. The "gator sign" orientation is the starting point for all lung ultrasound because it identifies the ribs, interposing intercostal space and the pulmonary–pleural interface. The two ribs (eyes) and intercostal space (bridge of the nose) are likened to an alligator partially submerged and looking at you (see cartoon) (Lisciandro et al. 2014). The air-related artifacts are much softer in (A) than in (B). This is due to the angle of insonation (see Chapters 22 and 23 and Figures 22.7 and 22.8). Arrows at the top of the images in (C) and (D) show the direction of the ultrasound beam. To best elicit the air reverberation artifacts of "dry lung" and pneumothorax when present, the beam should strike the "lung line" with an angle of insonation of 90° as in (D). Having the angle at 90° also best images for the other Vet BLUE signs of shred sign, tissue sign, nodule sign, and wedge sign. RS, rib shadow. Source: Reproduced with permission from Dr Gregory Lisciandro, Hill Country Veterinary Specialists and FASTVet.com, Spicewood, TX. Illustration by Suji Park, Englewood Cliffs, NJ.

Table 36.7). They are effective in people and small animals (Perera et al. 2010; Lisciandro 2011; Ferrada et al. 2012a,b; Lisciandro et al. 2014; Lichtenstein and Karakitsos 2012), but it is unknown if a similar strategy would be effective in dolphins, especially since marked distension of their CVC and hepatic veins without respirophasic variation is noted in normalcy in the author's experience.

Briefly, the "Global FAST nonecho fallback view" for left-sided congestive heart failure is the Vet BLUE evaluation because by definition, left-sided congestive heart failure requires the presence of pulmonary

edema (pulmonary congestion) or, in other words, the observation of B-lines on Vet BLUE (or lung ultrasound). Although B-lines are nonspecific and represent various forms of alveolar-interstitial edema, their absence rules out left-sided congestive heart failure (CHF) with high sensitivity in dogs, cats, and people (Lichtenstein et al. 2009; Lichtenstein and Karakitsos 2012; Lisciandro et al. 2014, 2016, 2017; Ward et al. 2017, Vezzosi et al. 2017).

The "Global FAST nonecho fallback view" for right-sided CHF is the FAST DH view, CVC, and hepatic venous characterization. By definition, right-sided CHF requires distension of CVC (FAT) and hepatic veins (hepatic venous congestion), referred to as the "tree trunk sign" (Lisciandro et al. 2014) (see Figure 36.8). Our preliminary findings are that the right-sided CHF "Global FAST nonecho fallback view" is likely unreliable in dolphins because the CVC is generally distended with little to no change in its dimensions (or collapsibility) during the cardiac and respiratory cycles (Yarto and Lisciandro 2017, unpublished data). Finding abnormalities during TFAST cardiac imaging can direct the need for more advanced imaging, including TEE and CT.

## Vet BLUE

### Lung Orientation: The "Gator Sign"

Vet BLUE is a regional lung ultrasound examination applied bilaterally with nine acoustic windows per hemithorax typically obtained at a depth of 11–13 cm. The Vet BLUE also includes the nontransthoracic DH view as a deeper window into lung along the pulmonary–diaphragmatic interface (see Figures 22.11, 22.12, 22.14, and 41.9). At each acoustic window, three intercostal spaces are evaluated with the probe positioned perpendicular to the long axis of the ribs to establish the "gator sign" as in small animals (Figure 41.18) (Lisciandro et al. 2014). The pulmonary–pleural interface (PPI) is identified by its linear hyperechoic appearance (Figures 41.18, 41.19, 41.20). Basic lung ultrasound signs are easily learned and include A-lines, "lung sliding," B-lines and then signs of varying degrees of consolidation – shred sign, tissue sign, nodule sign and wedge sign (see Figures 22.2 and 23.2–23.13). These artifacts, the six Vet BLUE lung ultrasound signs, plus signs of pneumothorax, as well as optimization of lung ultrasound imaging techniques, are detailed in Chapter 17, including the section Tricks of the Trade, and integration of Vet BLUE lung ultrasound signs in Chapters 22 and 23.

### Artifacts and Vet BLUE Lung Ultrasound Signs

#### *A-lines*

A-lines are equidistant horizontal lines that extend from, and are parallel to, the PPI in the absence of pleural space disease in the presence of normal aerated lung at its surface. "Lung sliding" (glide sign or gliding), the to and fro motion of lung with phases of respiration, distinguishes dry lung from pneumothorax in which "lung sliding" is absent. "A" stands for "air" is a good way to remember A-lines. The author refers to the finding of A-lines with "lung sliding" as "dry lung" or normal lung without pathology. "Lung sliding" will not be apparent when the patient is apneic (or breath holding). When scanning dolphins, breath holding is common and "lung sliding" may not be apparent for long periods of time during apnea. "Lung sliding" can be appreciated best when a rib is isolated at the center of the field of view, referred to as the "one-eyed gator sign" (see Figure 22.8). "Lung sliding" may also be appreciated when visualization and assessment are coordinated with prompted dolphin breath taking commanded by the trainer (see Figures 17.12 and 41.18).

#### *B-lines*

These are vertical lines that swing like a pendulum with inspiration and expiration that do not fade through the far-field while obliterating A-lines. B-lines have also been called ultrasound lung rockets (Lisciandro et al. 2014). B-lines most often represent forms of alveolar-interstitial edema but are nonspecific and thus when observed are referred to as alveolar-interstitial syndrome (AIS) (Lichtenstein et al. 1997; Volpicelli et al. 2006; Lisciandro et al. 2014, 2017; Ward et al. 2017, 2018). Less commonly, they represent fibrosis along the lung surface including senescent lung in people (Shyamsundar et al. 2013).

The B-line is created most often by fluid next to air on the outer surface of lung and the strong difference in acoustic impedance causes the artifact (Lichtenstein et al. 1997; Volpicelli et al. 2006). The author refers to the finding of B-lines as "wet lung" and numbers of B-lines are counted for a score using the Vet BLUE B-line scoring system (see Chapters 22 and 23). Briefly, the largest number over a single intercostal space representative of each Vet BLUE view is scored as 0 (negative), 1, 2, 3, >3, and infinity (when confluent and blended over the entire intercostal space) (see Figures 23.26, 36.17). In a recent study Vet BLUE detected alveolar-interstitial edema more frequently than three-view thoracic radiography in dogs and cats (Ward et al. 2018).

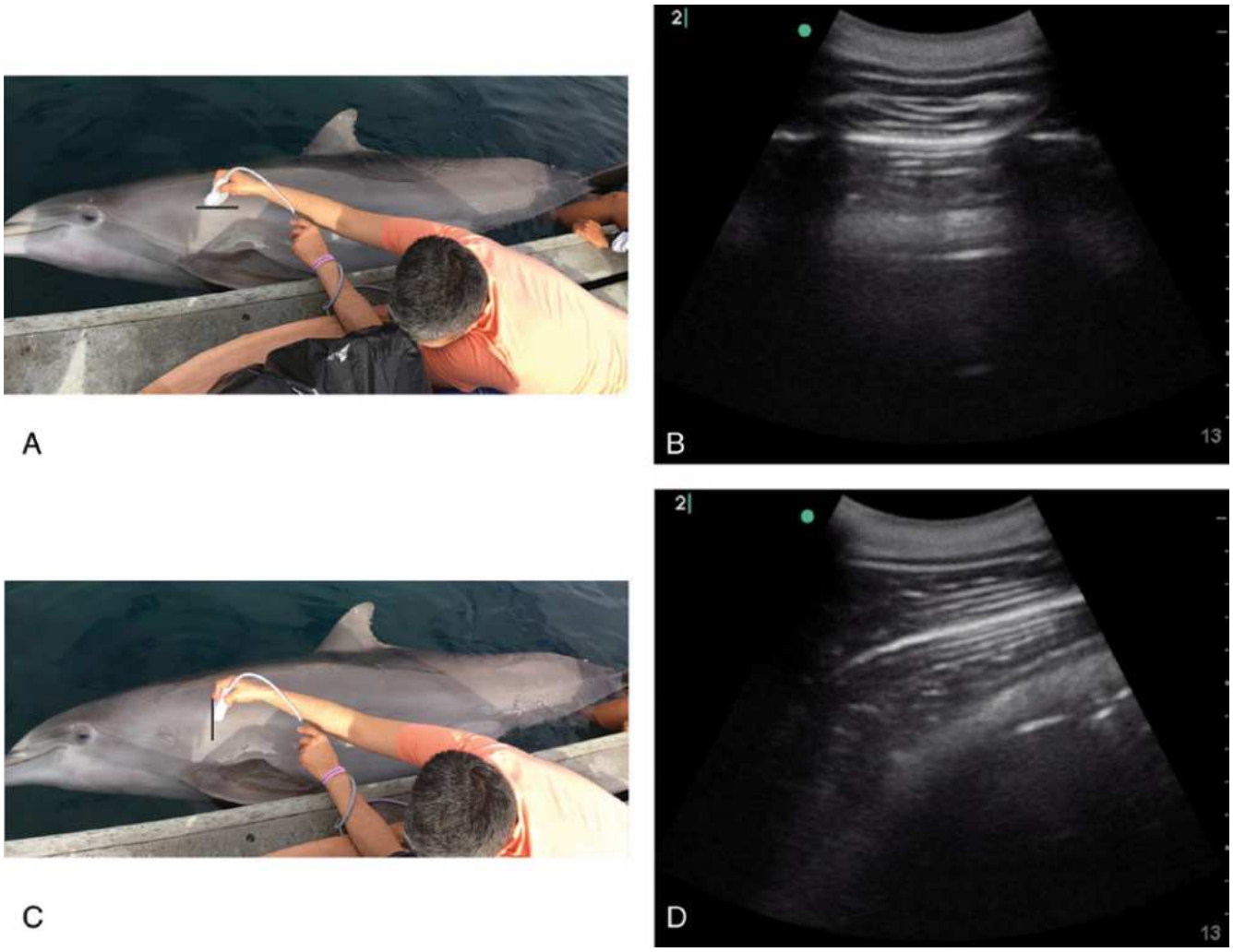


**Figure 41.19.** Probe orientation for lung. The sonographer is demonstrating Vet BLUE with two different probe orientations. The head is to the left and tail (fluke) to the right of the screen. The probe is started in longitudinal orientation to the patient or perpendicular to the long axis of the ribs (*horizontal black bar*) just caudal to the caudal border of the scapula (often palpated) as shown in (A) with the corresponding still image in (B) in which the "gator sign" is clearly seen. This assures the lung sonographer that they are accurately identifying the PPI and where the "lung line" is located. In (C) the probe is rotated parallel with the long axis of the ribs, which is a transverse orientation of lung (*vertical black bar*). In (D) notice how without the ribs for orientation, the "lung line" can be difficult to identify (*arrow*) and other hyperechoic lines may be mistaken for lung such as the scapula, fascial planes, and subcutaneous emphysema. The phases of respiration help identify the PPI and the "lung line" as does double-checking by rotating back to the "gator sign" orientation while following the hyperechoic line thought to be the "lung line." Vet BLUE imaging included both the longitudinal and transverse orientation at each intercostal space at each of the nine transthoracic views. Vet BLUE views were recorded on representative 10-second cine clips. See Figures 22.17 and 41.24. Source: Reproduced with permission from Dr Gregory Lisciandro, Hill Country Veterinary Specialists and FASTVet.com, Spicewood, TX.

### *Vet BLUE Lung Ultrasound Signs*

The Vet BLUE lung ultrasound signs are as follows and are described in detail in Chapters 22 and 23.

- *Shred sign*. Mildest form of alveolar lung disease that represents a peripheral air bronchogram (see Figure 23.8). With alveolar infiltrate, the ultrasound beam can penetrate and image into lung. In the abnormal state, the hypoechoic (or mildly, focally hepatized) lung tissue typically has inherent hyperechoic areas that represent air within larger bronchi.
- *Tissue sign*. More severe alveolar disease in which the airways are no longer aerated and the lung appears like liver (or spleen) which has been referred to as "hepatization" of lung (see Figure 23.9). The bronchi may be fluid filled or anechoic

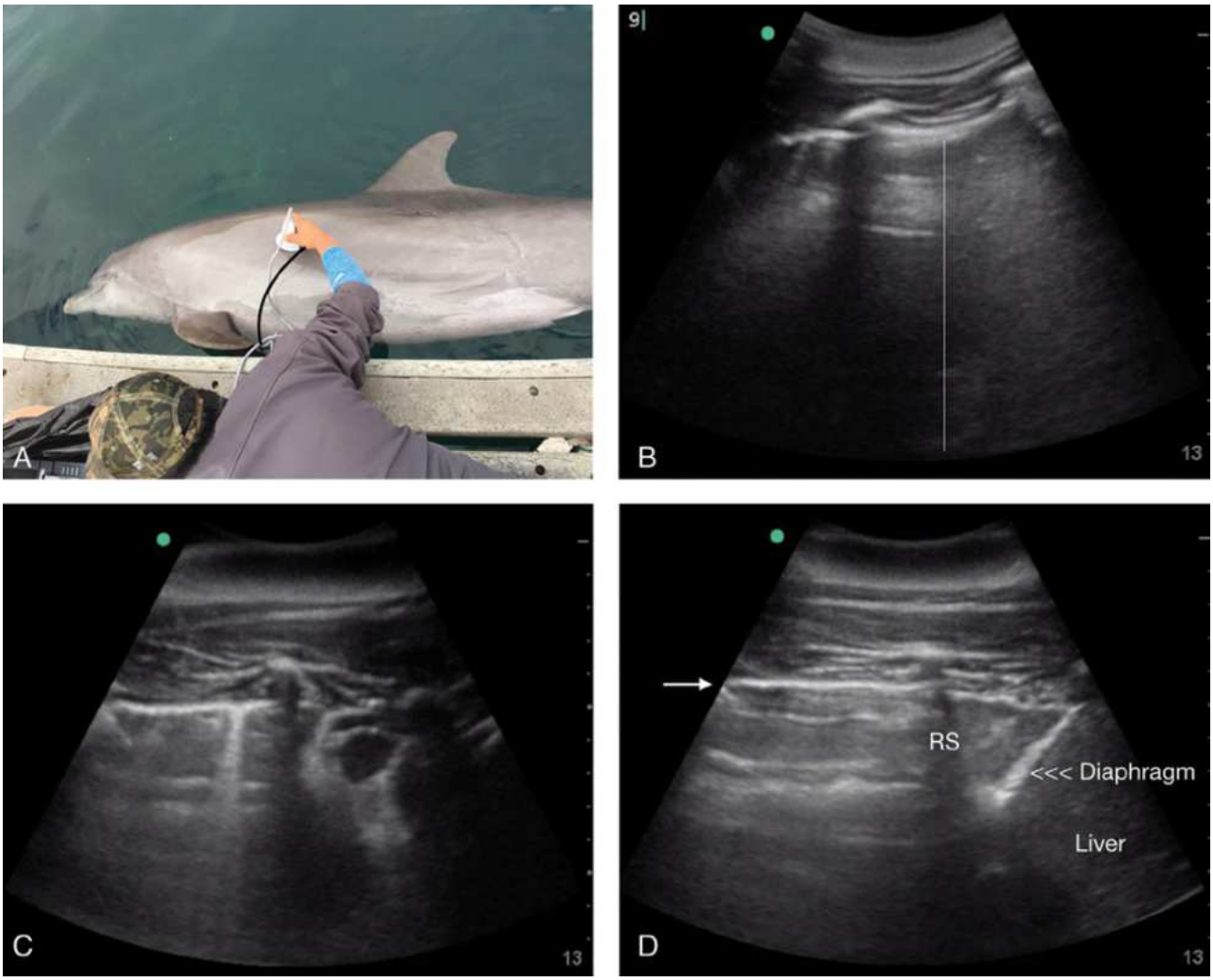


**Figure 41.20.** Transition zone of pleural and peritoneal cavities. The head of the dolphin is always to the left and the tail (fluke) to the right of the screen. This is very important for defining the pleural–peritoneal transition zone (PPTZ). PPTZ are encountered at Vet BLUE views 1, 4, and 7 and must be acknowledged by the sonographer to avoid mistaking abdominal structures for lung pathology. The "curtain sign" identifies this PPTZ created by the linear dirty shadowing of aerated lung over peritoneal structures (see also Figure 17.9) (Neelis et al. 2015). As lung slides to and fro during respiration, the aerated lung is like a curtain opening and closing. In (A) the sonographer is at acoustic window 1 (point 1) and is first locating the PPTZ. In (B) the vertical line overlay demonstrates aerated lung to the left of the line and peritoneal structures to its right. In (C) a B-line artifact (*vertical white streak*) is indicative of lung tissue, and to the right are the marginal lymph node and diaphragm. Few B-lines and comet-tail artifacts may be seen within the cranial and caudal ventral lung fields in the clinically normal dolphin especially the thinner extreme margins of lung. In (D) the lung (PPI) again is to the left with its hyperechoic "lung line" (*arrow*) and A-lines and the diaphragm and liver to the right. RS, rib shadow. See Chapters 22 and 23 for additional detail. Source: Reproduced with permission from Dr Gregory Lisciandro, Hill Country Veterinary Specialists and FASTVet.com, Spicewood, TX.

for which color flow Doppler interrogation can aid in the differentiation of these from vasculature.

- *Nodule sign*. Hypoechoic to anechoic oval or circular regions along the lung surface that have a hyperechoic far border (interphase circumferentially around the nodule at the junction with normal tissue). Pseudo B-lines often extend from them (see Figure 23.10).
- *Wedge sign*. A larger triangular shred sign or tissue sign at the lung margin that can aid in differentiating pulmonary infarction from thromboemboli which are typically smaller (see Figure 36.11).

VetBooks.ir

### Performing Vet BLUE Step by Step

Vet BLUE is performed similarly as in dogs and cats (and any other mammals) but there are nine acoustic windows per hemithorax (versus four in dogs and cats) (see Chapters 22 and 23, (Figures 41.6D,E, 41.7D,E, and 41.23) (Yarto and Lisciandro 2017, unpublished data).

- The caudodorsal transition zone (CdTZ) is located in the region directly dorsal to the xiphoid (see Figures 41.6D,E and 41.7D,E). The probe is placed perpendicular to the long axis of the ribs to identify the orientation for all lung ultrasound, called the "gator sign" (see Figure 41.18). This is the transition zone of the pleural and peritoneal cavities and is definitively identified by finding the "curtain sign" (see Chapter 17), where a linear distally oriented dirty shadow arises from left to right of the screen during a spontaneous breath and casts a dirty shadow over abdominal structures (see Figures 22.10 and 41.20) (Neelis et al. 2015). The other approach is to slide caudally and identify abdominal structures. From the abdominal structures, slide cranial until the "curtain sign" and the hyperechoic PPI or "lung line" are identified. Placing the probe too dorsal will reveal a pennate-like muscle pattern deep to the blubber with lack of a "lung line."
- From the CdTZ, slide 2–3 spaces cranial and this is Vet BLUE point 1.
- Evaluate point 1's intercostal space and then slide an intercostal space caudal, being aware you are moving toward the CdTZ. Survey that space by moving from the longitudinal to transverse orientation (rotating 90° and then returning to the "gator sign") before returning to point 1, then slide a space cranially, completing the evaluation of three intercostal spaces at point 1. This methodology is identically repeated at each transthoracic Vet BLUE view (see Figures 41.19. 41.20 and 41.23).
- The other eight Vet BLUE views are found by dividing the dolphin thorax into upper, middle, and lower thirds which are then divided into three points of evaluation horizontally across the regions (see Figures 41.6D,E and 41.7D,E).
- Slide cranially to point 2 in the upper third thoracic region then repeat sliding one intercostal space caudal and one cranial from your starting point 2 and within each intercostal space rotate 90° into the transverse plane and the return to the "gator sign" orientation.
- At point 3, you are moving toward the scapula; being a flat bone, it will have a hyperechcoic line similar to the PPI. Thus, it is important to pay attention as you slide the probe to point 3 and that your PPI line is continuous with that of point 2. Being careful to follow the PPI will avoid mistaking the scapular margin for lung tissue. Three intercostal spaces are again interrogated for lung ultrasound artifacts and signs.
- Points 4 and 7 in the middle third of the thorax are again in transition zones, referred to as pleural–peritoneal transition zones, and care must be taken not to mistake abdominal structures for lung pathology by repeating the same methodology as for point 1.
- Points 6 and 9 in the lower third of the thorax will be at the cranial borders of the thorax and as for point 3, care must be taken to ensure that bone is not mistaken for the PPI at point 6, and point 9 is *under* the pectoral fin (ventrally).
- Count numbers of B-lines at all Vet BLUE views and note comet-tails (small, triangular, echogenic reverberation artifacts arising from the PPI but failing to extend through the far-field as a B-line would). Comet-tail artifacts are not B-lines and should not generally be quantified by convention. See Chapters 22 and 23.
- The rule of thumb is that if you cannot clearly define the "gator sign" then you cannot be sure you are in fact imaging lung. The pectoral fin will need to be slightly extended to get a good image of the cranial lung region. It is not uncommon to have comet-tail artifacts and B-lines at the most ventral views bilaterally, thus these extremities of lung, where lung is thin, need to be interpreted cautiously.

## Pitfalls – Probe Positioning and Orientation

### *Longitudinal or Perpendicular to Ribs*

The "gator sign" orientation must be acquired with the probe held consistently perpendicular to the long axis of the ribs, what some sonographers would describe as a longitudinal orientation (parallel to the long axis [spine] of the patient's body) (see Figures 17.12, 41.18, and 41.19) (Lisciandro et al. 2014). Without clearly establishing the "gator sign" orientation, the PPI or "lung line" cannot be accurately located (Figures 41.21 and 41.22). There are two ways to describe the PPI. The first is where lung is directly juxtaposed to the intercostal space, preferred by the author and referred to as the "lung line." The second description is where parietal

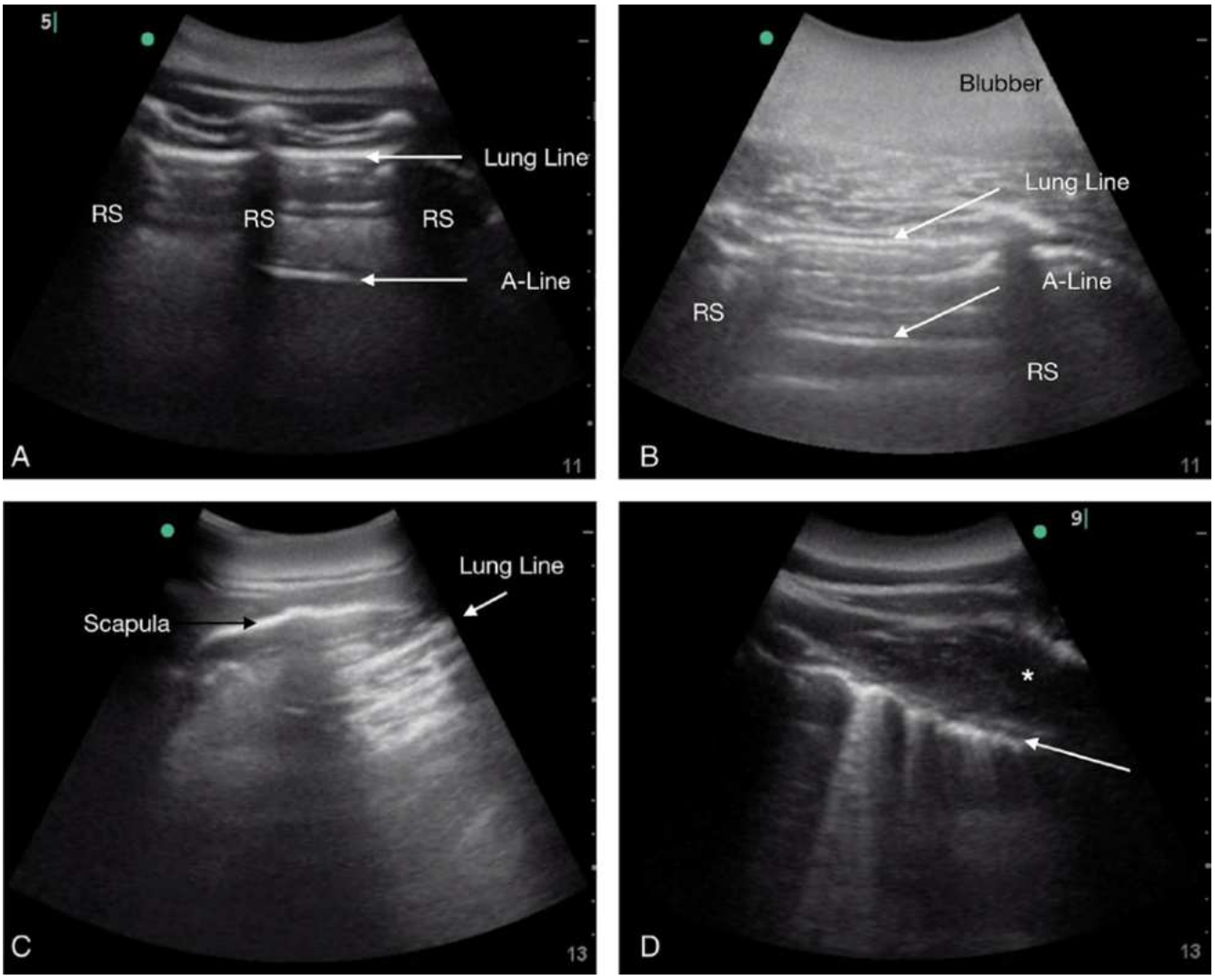


**Figure 41.21.** Pitfalls. In (A) is a nice image with adequate depth (11 cm) and proportionality to the image. A-lines are crisp and clear by angling the probe 90° to the lung surface. Compare to (B) in which the depth is too shallow (or decreased) for the patient and the near-field overgained (too bright), making it difficult to see the PPI or the "lung line." In (C) is a good example of how losing track of the "lung line" can lead to mistaking other structures for lung. The scapula, a flat bone, and its associated musculature are the cranial border for Vet BLUE points 3 and 6 (9 is ventral to the flipper). The scapula may be easily mistaken for lung surface. In (D) the sonographer should be able to recognize the pennate-like muscle appearance of the hypaxial musculature because it borders the thorax dorsally and cranially (see also Figure 22.17). Source: Reproduced with permission from Dr Gregory Lisciandro, Hill Country Veterinary Specialists and FASTVet.com, Spicewood, TX.

and visceral pleura are directly juxtaposed; however, in disease states, such as pleural effusion, there is often separation of the two pleura so the "lung line" is a better descriptor (see Figures 17.8, 17.9, and 17.12).

### *Transverse or Parallel to Ribs*

Some lung sonographers will advocate rotating the probe so that it is parallel to the long axis of the ribs, or in transverse orientation to the patient's long axis, and we have used this technique in the dolphin Vet BLUE examination. However, this can be a risky proposition because it is easy to lose sight of where the "lung line" is located (see Chapters 22 and 23 and Figure 41.18). The dorsocaudal margin of the scapula, subcutaneous emphysema, and even air in the stomach (in small animals), and fascial planes below the blubber can be easily mistaken for the lung surface. When moving to the transverse orientation of lung, the lung sonographer must always double-check by returning to the

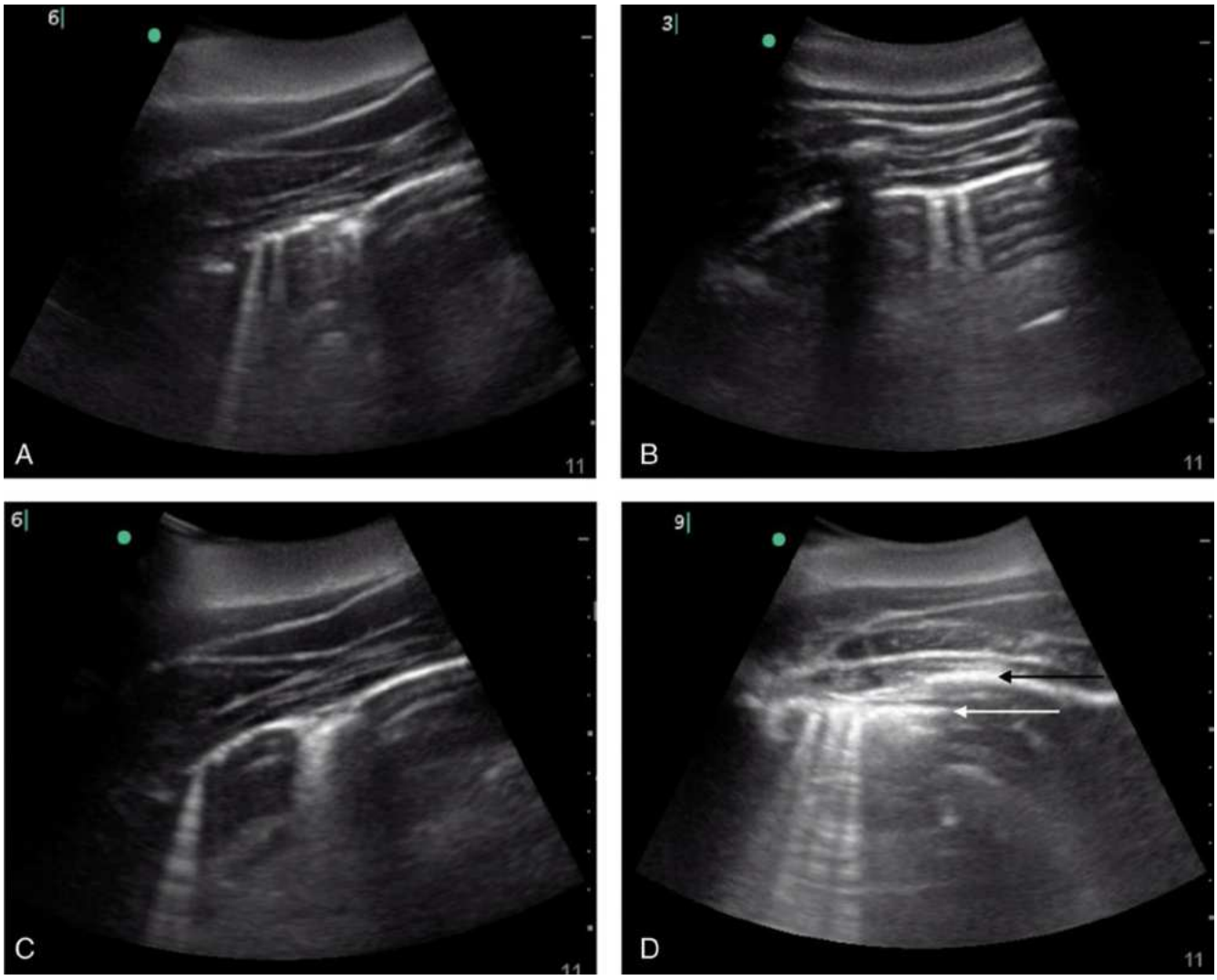


**Figure 41.22.** B-lines and comet-tail artifacts. B-lines are vertical hyperechoic streaks that swing like a pendulum during phases of respiration. Moreover, they do not fade and they obliterate A-lines. B-lines have also been called "ultrasound lung rockets" because of their streaky hyperechoic appearance from the "lung line" through the far-field. In breath holding, B-lines may be more difficult to recognize and count (score). Comet-tail artifacts are short and do not extend through the far-field. In images (A–D) you can see the difference between B-lines and comet-tail artifacts; however, B-lines may be dampened by breath-holding dolphins as in (B). B-lines and comet-tail artifacts are routinely seen at Vet BLUE points 7, 8, and 9 likely due to the least aerated character of the lung tissue in these locations because of some degree of atelectasis as the lungs in this location generally have less air volume and possibly greater compressibility. Source: Reproduced with permission from Dr Gregory Lisciandro, Hill Country Veterinary Specialists and FASTVet.com, Spicewood, TX.

"gator sign" orientation and reconfirming that the "lung line" is being accurately tracked (see Figures 41.18, 41.19, and 41.21).

## Comments

The zig-zag continuum (ZZC) is shown in Figure 41.23 along with comparison to Vet BLUE. The ZZC was evaluated in our study by recording 60-second clips of each hemithorax with similar ultrasound settings and depth proportions as Vet BLUE. We found that although effective as a screening test for obvious lung ultrasound artifacts and lung signs, the ZZC was problematic for the following reasons.

- The caudal, dorsal, ventral, and cranial borders of the pleural cavity must be known to avoid confusing border structures with lung pathology.

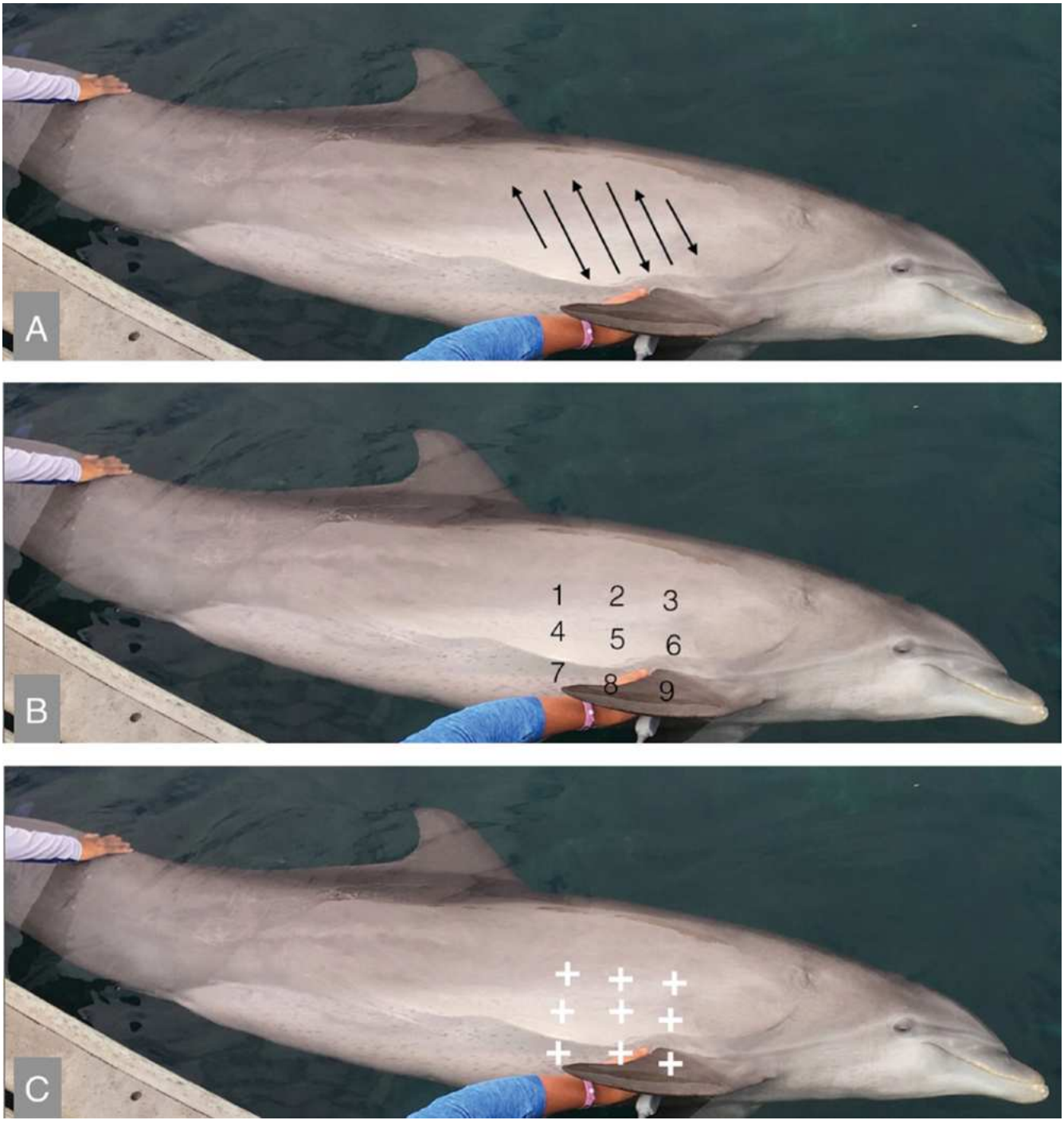


**Figure 41.23.** Comparison of the zig-zag continuum and Vet BLUE and how lung is imaged. (A) The zig-zag continuum with the probe slid through intercostal spaces. (B) The nine acoustic windows of Vet BLUE that include three intercostal spaces, one caudal and one cranial from the starting point (1–9). At each Vet BLUE view, the probe is held perpendicular to the long axis of the ribs and then rotated 90° and returned back to the starting point as illustrated by the crosses (+) as shown in (C). In this manner, lung at each intercostal space is interrogated in both imaging planes of longitudinal and transverse. The advantage of Vet BLUE is that pathology may be noted at each acoustic window and recorded in the medical record for future comparison. Source: Reproduced with permission from Dr Gregory Lisciandro, Hill Country Veterinary Specialists and FASTVet.com, Spicewood, TX.

- If the dolphin moved or needed a break, where do you restart the ZZC examination?
- Where were the lesions for recording purposes and for comparison on follow-up (serial) evaluations?

The advantage of the ZZC is that it may be a more comprehensive lung screening test. However, comparative studies are needed for further investigation of the efficacy of these techniques in identifying lung disease and providing a general lung overview. Vet BLUE likely provides nearly similar amounts of lung coverage and representation as the ZZC, with the distinct advantage of being able to record location of lung ultrasound findings for monitoring. Likely both formats would be included in a pulmonary assessment.

## Most Efficient Ways to Perform Global FAST

The Global FAST views are efficiently performed in the following manner, beginning with the easiest, quickest views and moving to the most time-consuming, challenging, and least reliable TFAST echo views, starting with the dolphin in right lateral positioning (Yarto and Lisciandro 2017, unpublished data).

- AFAST: DH to SR to CCR and then the umbilical view.
- Vet BLUE left views: points 1–9.
- TFAST: left PCS view for the left apical view and TFAST slide for pleural effusion followed by the right PCS view for short- and long-axis views and the TFAST slide for pleural effusion.

Position change from right lateral to left lateral.

- Vet BLUE right views: points 1–9.
- AFAST final HR view.

If starting in left lateral recumbency, analogously perform the blended AFAST-Vet BLUE TFAST and the right PCS view may be attempted when the dolphin is moved to right lateral if unsuccessful in left lateral. Findings should be documented on Goal-Directed Templates (Figure 41.24).

## Other POCUS – Venipuncture, Thyroids, Testicles, Eyes, and Fetus

POCUS can be used for venous puncture of the superficial caudal peduncular vein. This provides access for blood letting or phlebotomies, especially in cases of hemosiderosis. Placement of the animal in dorsal recumbency for sonographic purposes is time limited because the animal has to be turned frequently and repositioned for normal respiration (Kyung-Yeon et al. 2013).

The use of ultrasound for thyroid and testicular evaluation has been described (Brook 1997; Brook et al. 1991, 2000, 2019; Kot et al. 2012). Ocular ultrasound would follow similar principles to other species and is an effective imaging tool especially since the eye is a fluid-filled structure (Cartee et al. 1995; Brook et al. 2001; Dennison and Saviano 2018). Finally, fetal structures have been described in normalcy and in abnormal conditions not included in this chapter (Brook 1994; Brook et al. 2007; Jensen 1999; Stone et al. 1999; Sklansky et al. 2010).

## Global FAST Goal-Directed Template

Data must be recorded for it to be valuable. Moreover, the goal-directed template keeps the sonographer on task and objectives are clear to anyone looking over the report. Soft tissue abnormalities may be placed in the "Comments" section (see Figure 41.24).

## Pearls and Pitfalls, The Final Say

There is little widely accessible information regarding ultrasound use in marine mammals. This chapter serves as a standardized beginning from which sonographers can start building ultrasound skills and create global profiles as an extension of their physical exam for dolphins and other marine mammals. Much is unknown but in time, with more ultrasound use, conclusions may be better drawn on improving POCUS use in this fascinating species as well as other marine mammals.

## Acknowledgments

The authors would like to acknowledge the following experts for their contribution to the development of imaging assessment techniques and the depth of available literature on the topic of marine mammal imaging, without whom this work would not be possible: Fiona M. Brook, Sophie Denison, Marina Ivančić, William Van Bonn, Kelsey Seitz, L. R. Stone, Todd R. Robeck, Cynthia Smith, Eric Jensen, Pietro Saviano, and the late Warren "Sherm" Matthey. Additional resources from

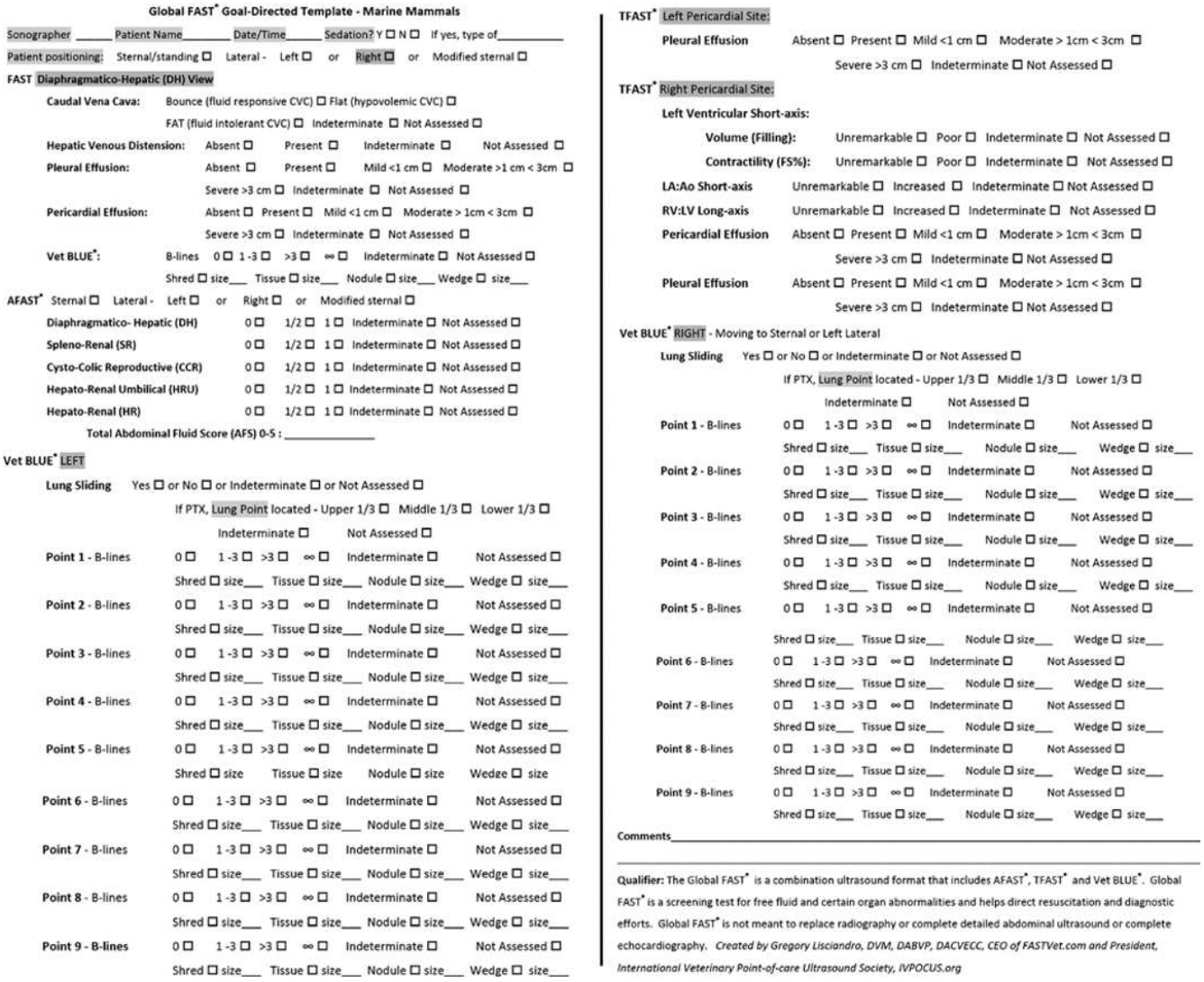

**Global FAST® Goal-Directed Template - Marine Mammals**

Sonographer _____ Patient Name_____ Date/Time_____ Sedation? Y ☐ N ☐ If yes, type of_____

Patient positioning: Sternal/standing ☐ Lateral - Left ☐ or Right ☐ or Modified sternal ☐

**FAST Diaphragmatico-Hepatic (DH) View**

Caudal Vena Cava: Bounce (fluid responsive CVC) ☐ Flat (hypovolemic CVC) ☐
FAT (fluid intolerant CVC) ☐ Indeterminate ☐ Not Assessed ☐

Hepatic Venous Distension: Absent ☐ Present ☐ Indeterminate ☐ Not Assessed ☐

Pleural Effusion: Absent ☐ Present ☐ Mild <1 cm ☐ Moderate >1 cm < 3cm ☐
Severe >3 cm ☐ Indeterminate ☐ Not Assessed ☐

Pericardial Effusion: Absent ☐ Present ☐ Mild <1 cm ☐ Moderate > 1cm < 3cm ☐
Severe >3 cm ☐ Indeterminate ☐ Not Assessed ☐

Vet BLUE®: B-lines 0 ☐ 1-3 ☐ >3 ☐ ∞ ☐ Indeterminate ☐ Not Assessed ☐
Shred ☐ size___ Tissue ☐ size___ Nodule ☐ size___ Wedge ☐ size___

**AFAST®** Sternal ☐ Lateral - Left ☐ or Right ☐ or Modified sternal ☐

Diaphragmatico- Hepatic (DH) 0 ☐ 1/2 ☐ 1 ☐ Indeterminate ☐ Not Assessed ☐

Spleno-Renal (SR) 0 ☐ 1/2 ☐ 1 ☐ Indeterminate ☐ Not Assessed ☐

Cysto-Colic Reproductive (CCR) 0 ☐ 1/2 ☐ 1 ☐ Indeterminate ☐ Not Assessed ☐

Hepato-Renal Umbilical (HRU) 0 ☐ 1/2 ☐ 1 ☐ Indeterminate ☐ Not Assessed ☐

Hepato-Renal (HR) 0 ☐ 1/2 ☐ 1 ☐ Indeterminate ☐ Not Assessed ☐

Total Abdominal Fluid Score (AFS) 0-5 : _____

**Vet BLUE® LEFT**

Lung Sliding Yes ☐ or No ☐ or Indeterminate ☐ or Not Assessed ☐
If PTX, Lung Point located - Upper 1/3 ☐ Middle 1/3 ☐ Lower 1/3 ☐
Indeterminate ☐ Not Assessed ☐

Point 1 - B-lines 0 ☐ 1-3 ☐ >3 ☐ ∞ ☐ Indeterminate ☐ Not Assessed ☐
Shred ☐ size___ Tissue ☐ size___ Nodule ☐ size___ Wedge ☐ size___

Point 2 - B-lines 0 ☐ 1-3 ☐ >3 ☐ ∞ ☐ Indeterminate ☐ Not Assessed ☐
Shred ☐ size___ Tissue ☐ size___ Nodule ☐ size___ Wedge ☐ size___

Point 3 - B-lines 0 ☐ 1-3 ☐ >3 ☐ ∞ ☐ Indeterminate ☐ Not Assessed ☐
Shred ☐ size___ Tissue ☐ size___ Nodule ☐ size___ Wedge ☐ size___

Point 4 - B-lines 0 ☐ 1-3 ☐ >3 ☐ ∞ ☐ Indeterminate ☐ Not Assessed ☐
Shred ☐ size___ Tissue ☐ size___ Nodule ☐ size___ Wedge ☐ size___

Point 5 - B-lines 0 ☐ 1-3 ☐ >3 ☐ ∞ ☐ Indeterminate ☐ Not Assessed ☐
Shred ☐ size Tissue ☐ size Nodule ☐ size Wedge ☐ size

Point 6 - B-lines 0 ☐ 1-3 ☐ >3 ☐ ∞ ☐ Indeterminate ☐ Not Assessed ☐
Shred ☐ size___ Tissue ☐ size___ Nodule ☐ size___ Wedge ☐ size___

Point 7 - B-lines 0 ☐ 1-3 ☐ >3 ☐ ∞ ☐ Indeterminate ☐ Not Assessed ☐
Shred ☐ size___ Tissue ☐ size___ Nodule ☐ size___ Wedge ☐ size___

Point 8 - B-lines 0 ☐ 1-3 ☐ >3 ☐ ∞ ☐ Indeterminate ☐ Not Assessed ☐
Shred ☐ size___ Tissue ☐ size___ Nodule ☐ size___ Wedge ☐ size___

Point 9 - B-lines 0 ☐ 1-3 ☐ >3 ☐ ∞ ☐ Indeterminate ☐ Not Assessed ☐
Shred ☐ size___ Tissue ☐ size___ Nodule ☐ size___ Wedge ☐ size___

**TFAST® Left Pericardial Site:**

Pleural Effusion Absent ☐ Present ☐ Mild <1 cm ☐ Moderate > 1cm < 3cm ☐
Severe >3 cm ☐ Indeterminate ☐ Not Assessed ☐

**TFAST® Right Pericardial Site:**

Left Ventricular Short-axis:

Volume (Filling): Unremarkable ☐ Poor ☐ Indeterminate ☐ Not Assessed ☐

Contractility (FS%): Unremarkable ☐ Poor ☐ Indeterminate ☐ Not Assessed ☐

LA:Ao Short-axis Unremarkable ☐ Increased ☐ Indeterminate ☐ Not Assessed ☐

RV:LV Long-axis Unremarkable ☐ Increased ☐ Indeterminate ☐ Not Assessed ☐

Pericardial Effusion Absent ☐ Present ☐ Mild <1 cm ☐ Moderate > 1cm < 3cm ☐
Severe >3 cm ☐ Indeterminate ☐ Not Assessed ☐

Pleural Effusion Absent ☐ Present ☐ Mild <1 cm ☐ Moderate > 1cm < 3cm ☐
Severe >3 cm ☐ Indeterminate ☐ Not Assessed ☐

**Vet BLUE® RIGHT** - Moving to Sternal or Left Lateral

Lung Sliding Yes ☐ or No ☐ or Indeterminate ☐ or Not Assessed ☐
If PTX, Lung Point located - Upper 1/3 ☐ Middle 1/3 ☐ Lower 1/3 ☐
Indeterminate ☐ Not Assessed ☐

Point 1 - B-lines 0 ☐ 1-3 ☐ >3 ☐ ∞ ☐ Indeterminate ☐ Not Assessed ☐
Shred ☐ size___ Tissue ☐ size___ Nodule ☐ size___ Wedge ☐ size___

Point 2 - B-lines 0 ☐ 1-3 ☐ >3 ☐ ∞ ☐ Indeterminate ☐ Not Assessed ☐
Shred ☐ size___ Tissue ☐ size___ Nodule ☐ size___ Wedge ☐ size___

Point 3 - B-lines 0 ☐ 1-3 ☐ >3 ☐ ∞ ☐ Indeterminate ☐ Not Assessed ☐
Shred ☐ size___ Tissue ☐ size___ Nodule ☐ size___ Wedge ☐ size___

Point 4 - B-lines 0 ☐ 1-3 ☐ >3 ☐ ∞ ☐ Indeterminate ☐ Not Assessed ☐
Shred ☐ size___ Tissue ☐ size___ Nodule ☐ size___ Wedge ☐ size___

Point 5 - B-lines 0 ☐ 1-3 ☐ >3 ☐ ∞ ☐ Indeterminate ☐ Not Assessed ☐
Shred ☐ size___ Tissue ☐ size___ Nodule ☐ size___ Wedge ☐ size___

Point 6 - B-lines 0 ☐ 1-3 ☐ >3 ☐ ∞ ☐ Indeterminate ☐ Not Assessed ☐
Shred ☐ size___ Tissue ☐ size___ Nodule ☐ size___ Wedge ☐ size___

Point 7 - B-lines 0 ☐ 1-3 ☐ >3 ☐ ∞ ☐ Indeterminate ☐ Not Assessed ☐
Shred ☐ size___ Tissue ☐ size___ Nodule ☐ size___ Wedge ☐ size___

Point 8 - B-lines 0 ☐ 1-3 ☐ >3 ☐ ∞ ☐ Indeterminate ☐ Not Assessed ☐
Shred ☐ size___ Tissue ☐ size___ Nodule ☐ size___ Wedge ☐ size___

Point 9 - B-lines 0 ☐ 1-3 ☐ >3 ☐ ∞ ☐ Indeterminate ☐ Not Assessed ☐
Shred ☐ size___ Tissue ☐ size___ Nodule ☐ size___ Wedge ☐ size___

Comments_____

**Qualifier:** The Global FAST® is a combination ultrasound format that includes AFAST®, TFAST® and Vet BLUE®. Global FAST® is a screening test for free fluid and certain organ abnormalities and helps direct resuscitation and diagnostic efforts. Global FAST® is not meant to replace radiography or complete detailed abdominal ultrasound or complete echocardiography. *Created by Gregory Lisciandro, DVM, DABVP, DACVECC, CEO of FASTVet.com and President, International Veterinary Point-of-care Ultrasound Society, IVPOCUS.org*

**Figure 41.24.** Example of a Global FAST goal-directed template for recording findings. Source: Reproduced with permission from Dr Gregory Lisciandro, Hill Country Veterinary Specialists and FASTVet.com, Spicewood, TX.

these experts and others on the topic of marine mammal imaging are interspersed throughout the references alphabetically. The dissected dolphin photo referenced in this chapter was authorized by the National Marine Fisheries Service through a Stranding Agreement with the Institute for Marine Mammal Studies.

# References


Atkinson P, Bowra J, Milne J, et al. 2017. International Federation for Emergency Medicine Consensus Statement: Sonography in hypotension and cardiac arrest (SHoC): An international consensus on the use of point of care ultrasound for undifferentiated hypotension and during cardiac arrest. *Can J Emerg Med* 19(6):459–470.

Bossart GD, Ewing R, Herron AJ, et al. 1997. Immunoblastic malignant lymphoma in dolphins: histologic, ultrastructural, and immunohistochemical features. *J Vet Diagn Invest* 9(4):454–458.

Brook FM. 1994. Ultrasound diagnosis of anencephaly in a bottlenose dolphin. *J Zoo Wildl Med* 25:569–573.

Brook FM. 1997. The use of diagnostic ultrasound in assessment of the reproductive status of the bottlenose dolphin, Tursiops aduncas, in captivity and applications in management of a controlled breeding programme. PhD dissertation, Hong Kong Polytechnic University, Kowloon, Hong Kong.

Brook FM, Chow DCMA, Schroeder JP. 1991. Ultrasound imaging of the reproductive tract of the male bottlenose dolphin. *Br J Radiol* 763:645.

Brook FM, Kinoshita R, Brown B, et al. 2000. Ultrasonographic imaging of the testis and epididymis of the bottlenose dolphin, Tursiops truncatus aduncus. *J Reprod Fertil* 119:233–240.

Brook F, van Bonn W, Jensen JD. 2001. Ultrasonography. In: *Handbook of Marine Mammal Medicine*, 2nd edition, edited by Dierauf L, Gulland F. Boca Raton: CRC Press, pp 593–618.

Brook F, Parraga TA, Alvaro MV, et al. 2007. Umbilical cord accidents and dolphin calf mortality. Proceedings of the 38th Annual Conference of the International Association for Aquatic Animal Medicine, Orlando, FL, USA.

Cartee RE, Brosemer K, Ridgeway SH. 1995. The eye of the bottlenose dolphin (Tursiops truncatus) evaluated by B mode ultrasonography. *J Zoo Wildl Med* 26:414–421.

Chetboul V, Lichtenberger J, Merlin M, et al. 2012. Within-day and between-day variability of transthoracic anatomic M-mode echocardiography in the bottlenose dolphin (Tursiops truncatus). *J Vet Cardiol* 14(4):511–518.

Cowan DF, Smith TL. 1999. Morphology of the lymphoid organs of the bottlenose dolphin, Tursiops truncatus. *J Anat* 194(4):505–517.

Darnis E, Boysen S, Merveille AC, et al. 2018. Establishment of references values of the caudal vena cava by fast-ultrasonography through different views in healthy dogs. *J Vet Intern Med* 32(4):1308–1318.

Dennison S, Saviano P. 2018. Diagnostic imaging. In: *CRC Handbook of Marine Mammal Medicine*, 3rd edition, edited by Gulland FMD, Dierauf LA, Whitman KL. Boca Raton: CRC Press, pp 537–551.

Fahlman A, Loring SH, Levine G, et al. 2015. Lung mechanisms and pulmonary function testing of cetaceans. *J Exp Biol* 218(13):2030–2038.

Fahlman A, Miedler S, Rocho-Levine J, et al. 2019. Re-evaluating the significance of the dive response during voluntary surface apneas in the bottlenose dolphin, Tursiops truncatus. *Sci Rep* 9(1): article no. 8613.

Ferrada P, Anand RJ, Whelan J, et al. 2011. Limited transthoracic echocardiogram: so easy any trauma attedning can do it. *J Trauma* 71(5):1327–1331.

Ferrada P, Vanguri P, Anand RJ, et al. 2012a. Flat inferior vena cava: indicator of poor prognosis in trauma and acute care surgery patients. *Am Surg* 78(12):1396–1398.

Ferrada P, Attand RJ, Whelan J, et al. 2012. 2012b. Qualitative assessment of the inferior vena cava: useful tool for the evaluation of volume status in criticall ill patients. *Am Surg* 78(4):468–470.

Fiorucci L, Garcia-Parraga D, Macrelli R, et al. 2015. Determination of the main reference values in ultrasound examination of the gastrointestinal tract in clinically healthy bottlensoe dolphins (Tursiops truncatus). *Aquat Mamm* 41:345–350.

Gili C. 2006. Esame autopico dei cetacei. In: *Tecnica Autopica e Diagnostica Cadaverica*, edited by Taccini E, Rossi G, Gili C. Rome: Poletto, pp 366–415.

Ivančić M, Solano M, Smith CR. 2014. Computed tomography and cross-sectional anatomy of the thorax of live bottlenose dolphin (Tursiops truncatus) cranial anatomy. *Anat Rec* 297:901–915.

Jauniaux TP, Brenez C, Fretin D, et al. 2010. Brucella ceti infection in harbor porpoise (Phocoena phocoena). *Emerg Infect Dis* 16(12):1966–1968.

Jensen E. 1999. Early embryonic loss. Proceedings of the Bottlenose Dolphin Reproductive Workshop, pp 273–278.

Kot BC, Ying MT, Brook FM, et al. 2012. Ultrasonographic assessment of the thyroid gland and adjacent anatomic structures in Indo-Pacific bottlenose dolphins (Tursiops aduncus). *Am J Vet Res* 73(11):1696–1706.

Kyung-Yeon E, Yong-Gu Y, Oh-Deog K. 2013. Modified endoscopic removal of foreign objects from the forestomach of a common bottlenose dolphin (Tursiops truncatus). *Pak Vet J* 33(2):251–253.

Lichtenstein D, Karakitsos D. 2012. Integrating lung ultrasound in the hemodynamic evaluation of acute circulatory failure (the fluid administration limited by lung sonography protocol). *J Crit Care* 27(5):533.

Lichtenstein D, Meziere G, Bideman P, et al. 1997. The comet-tail artifact. An ultrasound sign of alveolar-interstitial syndrome. *Am J Respir Crit Care Med* 156(5):1640–1646.

Lichtenstein D, Mezière G, Lagoueyte JF et al. 2009. A-lines and B-lines: lung ultrasonography as a bedside tool for predicting pulmonary artery occlusion pressure in the critically ill. *Chest* 136:1014–1020.

Lisciandro GR. 2011. Abdominal and thoracic focused assessment with sonography for trauma, triage and monitoring in small animals. *J Vet Emerg Crit Care* 21(2):104–122.

Lisciandro GR. 2016. The use of the diaphragmatico-hepatic (DH) views of the abdominal and thoracic focused assessment with sonography for triage (AFAST/TFAST) examinations for the detection of pericardial effusion in 24 dogs (2011–2012). *J Vet Emerg Crit Care* 26(1):125–131.

Lisciandro GR, Lagutchik MS, Mann KA, et al. 2008. Accuracy of Focused Assessment with Sonography for Trauma (TFAST) to detect pneumothorax in 145 dogs with blunt and penetrating trauma. *J Vet Emerg Crit Care* 18(3):258–269

Lisciandro GR, Lagutchik MS, Mann KA, et al. 2009. Evaluation of an abdominal fluid scoring (AFS) system determined using abdominal focused assessment with sonography for trauma (AFAST) in 101 dogs with motor vehicle trauma. *J Vet Emerg Crit Care* 19(5):426–437.

Lisciandro GR, Fosgate GT, Fulton RM. 2014. Frequency of ultrasound lung rockets using a regionally-based lung ultrasound examination named veterinary bedside lung ultrasound exam (Vet BLUE) in 98 dogs with normal thoracic radiographic lung findings. *Vet Radiol Ultrasound* 55(3):315–322.

Lisciandro GR, Ward JL, DeFrancesco TC, Mann KA. 2016. Absence of B-lines on lung ultrasound (Vet BLUE protocol) to rule out left-sided congestive heart failure in 368 cats and dogs. *J Vet Emerg Crit Care* 26(S1):S8.

Lisciandro GR, Fulton RM, Fosgate GT, Mann KA. 2017. Frequency of B-lines using a regionally-based lung ultrasound examination (the Vet BLUE protocol) in 49 cats with normal thoracic radiographical lung findings. *J Vet Emerg Crit Care* 27(3):267–277.

Lisciandro GR, Romero L, Fosgate GT. 2018. The frequency of B-Lines and other lung ultrasound artifacts during Vet BLUE in 91 healthy puppies and kittens. *J Vet Emerg Crit Care* 28(S1):S16.

Lisciandro GR, Fosgate GT, Romero LA, et al. 2019. The frequency and amount of free peritoneal fluid estimated using abdominal FAST-applied abdominal fluid scores in clinically normal adult and juvenile dogs. *J Vet Emerg Crit Care*, in press.

Lutmerding B, Huston S, Frank K, et al. 2015. Evidence of dilated cardiomyopathy and congestive heart failure in a geriatric bottlenose dolphin (Tursiops truncatus). Proceedings of the 46th Annual Conference for the International Aquatic Animal Medicine, Chicago, IL, USA.

Martony ME, Ivančić M, Gomez FM, et al. 2017. Establishing marginal lymph node ultrasonographic characteristics in healthy bottlenose dolphins (*Tursiops truncatus*). *J Zoo Wildlife Med* 48(4):961–971.

McMurray J, Boysen S, Chalhoub S. 2016. Focused assessment with sonography in nontraumatized dogs and cats in the emergency and critical care setting. *J Vet Emerg Crit Care* 26(1):64–73.

Neelis DA, Mattoon JS, Nyland TG. 2015. Thorax. In: *Small Animal Diagnostic Ultrasound*, edited by Mattoon JS, Nyland TG. Philadelphia: Elsevier Saunders, pp 188–216.

Nelson NC, Drost WT, Lerche P, et al. 2010. Noninvasive estimation of central venous pressure in anesthetized dogs by measurement of hepatic venous blood flow velocity and abdominal venous diameter. *Vet Radiol Ultrasound* 51(3):313–323.

Perera P, Mailhot T, Riley D, et al. 2010. The RUSH exam: Rapid Ultrasound in SHock in the evaluation of the critically ill. *Emerg Med Clin North Am* 28(1):29–56.

Saviano P. 2013. *Handbook of Ultrasonography in Dolphins, Abdomen Thorax & Eye*. Privately published, available as a Kindle Edition. www.amazon.com/gp/product/B00BRXUSPG?ref_=

Shyamsundar M, Attwood, B, Keating L, et al. 2013. Clinical review: The role of ultrasound in estimating extravascular lung water. *Crit Care* 17(5):237.

Sklansky M, Levine G, West N, et al. 2006. Transesophageal echocardiogaphic evaluation of the bottlenose dolphin (Tursiops truncatus). *J Zoo Wildlife Med* 37(4):454–463.

Sklansky M, Renner M, Clough P, et al. 2010. Fetal echocardiographic evaluation of the bottlenose dolphin (*Tursiops truncatus*). *J Zoo Wildl Med* 41(1):35–43.

Smith CR, Solano M, Lutmerding BA, et al. 2012. Pulmonary ultrasound findings in a bottlenose dolphin *Tursiops truncatus* population. *Dis Aquat Organisms* 101:243–255.

Stone LR, Johnson RL, Sweeney JC, et al. 1999. Fetal ultrasonography in dolphins with emphasis on gestational aging. In: *Zoo and Wild Animal Medicine, Current Therapy*, 4th edition, edited by Fowler ME, Miller RE. Philadelphia: WB Saunders, pp 501–506.

Vezzosi T, Mannucci A, Pistoresi F, et al. 2017. assessment of lung ultrasound b-lines in dogs with different stages of chronic valvular heart disease. *J Vet Intern Med* 31(3):700–704.

Volpicelli G, Mussa A, Garofalo G, et al. 2006. Bedside lung ultrasound in the assessment of alveolar-interstitial syndrome. *Am J Emerg Med* 24:689–696.

Ward JL, Lisciandro GR, Keene BW, et al. 2017. Accuracy of point-of-care lung ultrasonography for the diagnosis of cardiogenic pulmonary edema in dogs and cats with acute dyspnea. *J Am Vet Med Assoc* 250:666–675.

Ward JL, Lisciandro GR, DeFrancesco TC. 2018. Distribution of alveolar-interstitial syndrome in dyspneic veterinary patients assessed by lung ultrasound versus thoracic radiography. *J Vet Emerg Crit Care* 28(5):415–428.

# Further Reading

Davis DS, Templeton JW, Ficht TA, et al. 1990. *Brucella abortus* in captive bison. I. Serology, bacteriology, pathogenesis, and transmission to cattle. *J Wildlife Dis* 26:360–371.

Dicker SA, Lisciandro GR, Newell SM, et al. 2019. Diagnosis of pulmonary contusions with point-of-care lung ultrasonography and thoracic radiography compared to thoracic computed tomography in dogs with motor vehicle trauma: 29 cases (2017–2018). *J Vet Emerg Crit Care*, in press.

Jambrik Z, Monti S, Coppola V, et al. 2004. Usefulness of ultrasound lung comets as a nonradiologic sign of extravascular lung water. *Am J Cardiol* 93(10):1265–1270.

Miedler S, Fahlman A, Valls Torres M, et al. 2015. Evaluating cardiac physiology through echocardiography in bottlenose dolphins: using stroke volume and cardiac output to estimate systolic left ventricular function during rest and following exercise. *J Exp Biol* 218: 3604–3610.

Noren SR, Kendall T, Cuccurullo V, et al. 2012. The dive response redefined: underwater behavior influences cardiac variability in freely diving dolphins. *J Exp Biol* 215:2735–2741.

Robeck TR, McBain JF, Mathey S, et al. 1998. Ultrasonographic evaluation of the effects of exogenous gonadotropins on follicular recruitment and ovulation induction in the Atlantic bottlenose dolphin (Tursiops truncatus). *J Zoo Wildl Med* 29:6–13.

Robeck TR, Jensen E, Brook F, et al. 2000. Preliminary investigations into ovulation manipulation techniques in delphinids. Proceedings of Joint Meeting of the American

Association of Zoo Veterinarians and the International Association for Aquatic Animal Medicine, New Orleans, LA, pp 222–225.

Seitz KE, Smith CR, Marks SL, et al. 2016. Liver ultrasonography in dolphins: use of ultrasonography to establish a technique for hepatobiliary imaging and to evaluate metabolic disease-associated liver changes in bottlenose dolphins (Tursiops truncatus). *J Wildl Med* 47(4):1034–1043.

Stone LR. 1990. Diagnostic ultrasound in marine mammals. In: *CRC Handbook of Marine Mammal Medicine*, edited by Dierauf L. Boca Raton: CRC Press, pp 235–264.

Stone LR, Phillips B, Sweeney JC. 1994. Diagnostic ultrasound of the bottlenose dolphin. Abstract, Annual Proceedings of the American Association of Zoo Veterinarians, p 94.

Vientós-Plotts AI, Wiggen KE, Lisciandro GR, et al. 2019. The utility of point-of-care ultrasound non-echo right-sided cardiac markers as a screening test for moderate to severe pulmonary hypertension in dogs. *Vet J* 250:6–13.

Williamson P, Gales NJ, Lister S. 1990. Use of real-time B-mode ultrasound for pregnancy diagnosis and measurement of fetal growth rate in captive bottlenose dolphins (Tursiops truncatus). *J Reprod Fertil* 88:543–548.

CHAPTER FOURTY-TWO

# POCUS: Birds and Reptiles

Sara Gardhouse and Hugues Beaufrère

Vetbooks.ir

## Introduction

Ultrasound of the coelom is an important diagnostic tool in avian and reptile medicine (Fitzgerald and Beaufrère 2016). Point-of-care ultrasound (POCUS) can provide important and timely diagnostic information. Moreover, ultrasonography is a primary diagnostic imaging tool for the detection of soft tissue abnormalities including neoplasia, abscesses, and fluid (Schumacher and Toal 2001). Ultrasound has practical applications for the common presentation of coelomic distension, assisting in distinguishing between ascites, organomegaly, and an intracoelomic mass (Doneley 2016). Ultrasound can also be useful for differentiating between cystic and solid masses on the skin (Schumacher and Toal 2001). Additionally, POCUS can be useful for sex determination and evaluation of reproductive activity dependent on sexual cycle (females with follicular development) and actual sex. The male reproductive tract is commonly obscured by air sacs in birds, making sex determination more challenging since ultrasound does not transmit through air (Schumacher and Toal 2001).

With advances in ultrasound technology, image quality with smaller sized devices has improved tremendously, making ultrasound a practical everyday imaging option for both birds and reptiles (Hochleithner and Holland 2014). As in exotic companion mammals, a brief POCUS and Global FAST approach as part of the physical exam can help "see" the problem list and thus better direct diagnostic efforts and more accurately assist in emergency management of sauropsid (avian and reptilian) patients.

This chapter first addresses general POCUS principles in birds followed by reptiles.

## Avian

### What POCUS Birds Can Do

- Identify obvious cardiac abnormalities including chamber dilation, cardiomegaly, and pericardial effusion (Fitzgerald and Beaufrère 2016),
- Identify ascites (Fitzgerald and Beaufrère 2016).
- Identify organomegaly,
- Identify a mass,
- Recognize ocular abnormalities.

### What POCUS Birds Cannot Do

Organ visualization in the avian patient is limited due to the presence of their air sac system and the inability of ultrasound waves to penetrate the gas-filled air sacs (Helmer 2006).

- Cannot reliably image dorsally positioned organs such as the reproductive system and kidneys because of air sacs.
- Cannot reliably screen for reproductive disease because of air sacs, the dependency on reproductive stage, and the predominantly left-sided oviparous system in females.
- Cannot image for respiratory disease as in mammalian lungs.
- Cannot reliably gain a view into the coelom in many smaller species because of the small acoustic window.

*Point-of-Care Ultrasound Techniques for the Small Animal Practitioner*, Second Edition. Edited by Gregory R. Lisciandro.
© 2021 John Wiley & Sons, Inc. Published 2021 by John Wiley & Sons, Inc.
Companion website: www.wiley.com/go/lisciandro/ultrasound2

- Cannot reliably achieve a view of the heart, especially in smaller species because of the small acoustic window.

## Indications

- Suspicion of coelomic effusion based on physical examination and/or radiographic findings.
- Palpation of a coelomic mass on physical examination and/or radiographic findings.
- Coelomic distension with or without accompanying dyspnea.
- Suspicion of cardiomegaly based on radiographic findings.
- Ocular abnormalities or lack of vision undifferentiated via direct eye examination.

## Objectives

- Recognize the acoustic windows in birds.
- Diagnose coelomic effusion.
- Diagnose obvious coelomic organ abnormalities, including abdominal and cardiac.
- Diagnose pericardial effusion.
- Recognize basic pathology in birds involving their coelom and heart.
- Recognize the limitations of avian ultrasonography and their unique differences among different avian species and from mammals.

## Anatomy

### Lungs and Air Sacs

Avian anatomy differs markedly from mammalian with important consequences ultrasonographically (Figure 42.1). Of significant note, the respiratory system is inaccessible. The lower respiratory tract is composed of dorsally positioned and relatively incompressible lungs where the site of gas exchange is the parabronchial tissue and air capillaries and not alveoli, as in mammals. From the avian lungs, a complex and large air sac system composed of nine air sacs in most

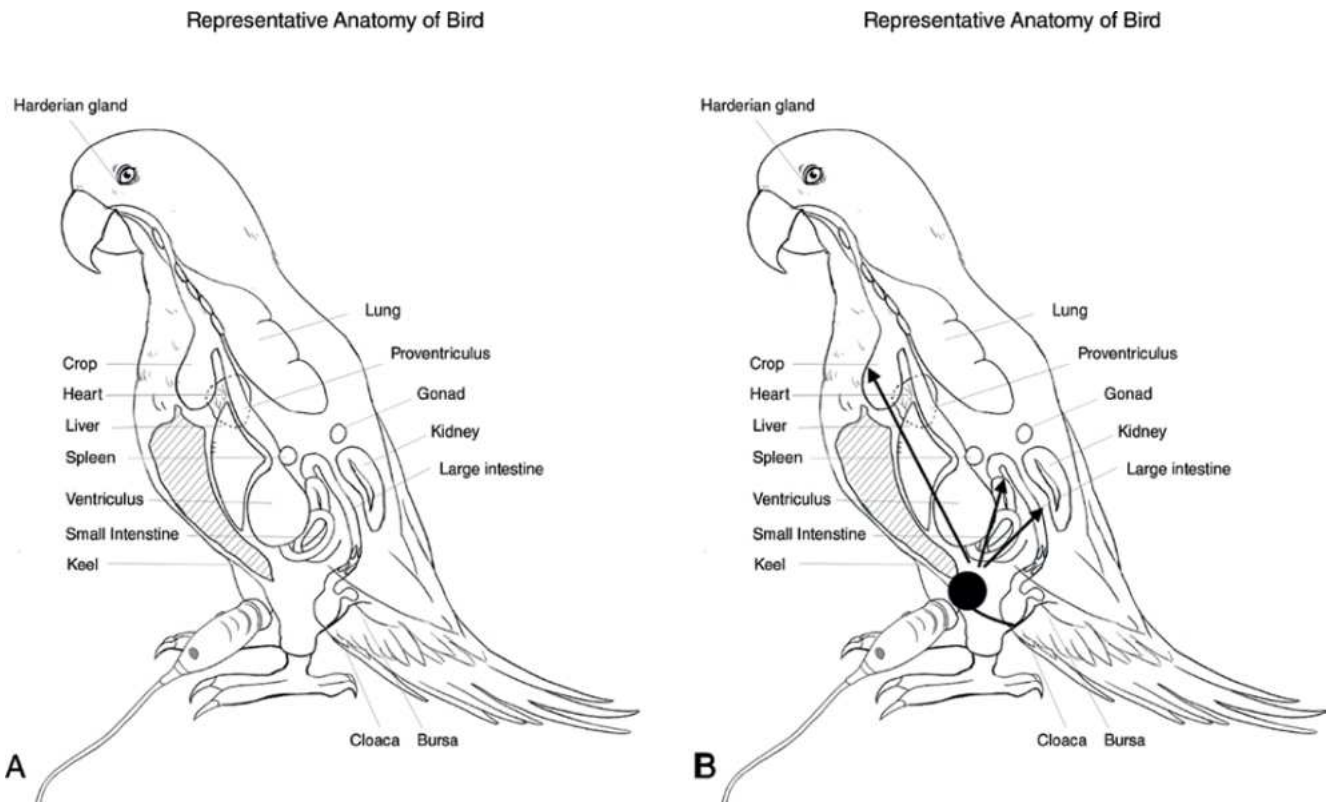


**Figure 42.1.** Simple line drawing of the most clinically relevant ultrasonographically accessible anatomy in a bird. The acoustic window used for the coelom and for echocardiography views is identical as shown in (A). The probe is placed between the legs (*black circle*) and directed cranially to image the liver and heart and directed more toward the spine for coelomic structures (*arrows*) as shown in (B). Source: Reproduced with permission of Dr Gregory Lisciandro, DVM, Hill Country Veterinary Specialists and FASTVet.com, Spicewood, TX. Illustration by Suji Park, sujisuji.com.

VetBooks.ir

birds is located throughout the entire body and between organs with a multitude of air sac diverticula. The avian lung-air sac system drastically reduces the acoustic windows for ultrasonographic examination of their coelom to a *single* median soft tissue window just caudal to the sternum. In addition, birds seldom have pleural effusion and the pleural cavities are not accessible to ultrasonographic examination, reducing the usefulness of TFAST-like examinations.

Furthermore, the avian coelom is divided into many subcavities, numbering seven in most birds, and divided by various septa that become apparent on ultrasonographic examination when cavitary effusions are present. Additionally, most organs have different ultrasonographic appearances in different species of birds and from mammals. For instance, the liver primarily has two lobes with a gallbladder in cockatoos and raptors, but not in parrots and pigeons. The stomach is divided into a glandular stomach (proventriculus) and a muscular stomach (ventriculus). The kidneys have three lobes that are typically not accessible by ultrasound when normal. Most female birds have only the left reproductive system and are oviparous. A basic knowledge of ultrasonographic anatomy, even for POCUS and Global FAST-like examinations, is essential for accurate avian ultrasonographic interpretation.

#### Coelomic

In addition, the anatomy, organ topography, and diseases vary among bird species because of their great biodiversity. For instance, sonographic examination of the coelom is relatively easy in chickens because the keel is much smaller and fenestrated compared to other avian species, providing a large acoustic window for ascites and organ changes to be detected. Moreover, chickens commonly present for coelomic distension caused by ascites and diseases of the reproductive system. On the other side of the spectrum, ultrasonographic examination is very difficult in passerines due to their small size and large keel, resulting in a very small acoustic window for imaging the coelom and its organs.

## Patient Positioning and Probe Selection

Feathers are parted for maximal probe-to-skin contact with the use of combinations of 70% isopropyl alcohol, alcohol-based hand sanitizer, and acoustic coupling gel. Keep in mind the size of the patient and amount of 70% isopropyl alcohol and acoustic coupling gel used because hypothermia can occur quickly, especially in unstable and critical patients. Clinical status should always be evaluated prior to any handling, degrees of restraint, and diagnostics being undertaken. Dyspneic or highly distressed birds often benefit from sedation and/or anesthesia prior to performing diagnostics and supportive care principles should be implemented, such as flow-by oxygen (Figure 42.2). It is also important to have technical support from someone who is comfortable with avian restraint to decrease risk of injury to the patient, handler, and attending veterinarian. Positioning may range from the traditional dorsal recumbency in acceptably stable patients to lateral recumbency and even standing, as for the bird in Figure 42.2.

Patients with coelomic distension, a common indication for POCUS or AFAST-like exam, often present with accompanying dyspnea. The stability of the patient should always be evaluated prior to any handling or diagnostics being undertaken, and the patient should always be stabilized as much as possible prior to restraint.

A 7.5–18 MHz transducer (probe) that has a small contact area (pediatric transducer) is preferred (Doneley 2016). The most common "acoustic windows" or views used for birds include:

- Ventromedian coelom, just caudal to the sternum (Doneley 2016) (see Figures 42.1 and 42.2).
- right lateral approach, just behind the last rib in some species such as pigeons and chickens and those with ascites (Doneley 2016).

## Imaging the Normal Coelom

Begin the POCUS coelomic exam with the bird in an upright position.

- Find the location of the ventromedial coelomic acoustic window.
- Part the feathers and expose areas with apterylae (featherless tracts) and judiciously apply a small amount of 70% isopropyl alcohol, alcohol-based hand sanitizer, and/or ultrasound coupling gel. Keep in mind the size of the patient and amount of coupling medium used, as hypothermia can occur quickly. Alcohol-based hand sanitizer is less noxious and less cooling than isopropyl alcohol, and wipes off more readily than acoustic coupling gel.
- Place the ultrasound probe in a longitudinal fashion on the ventral coelom.
- From the ventromedial coelomic approach, image the liver, ventriculus, active gonads, and heart (Helmer 2006; Doneley 2016) (see Figure 42.2). The

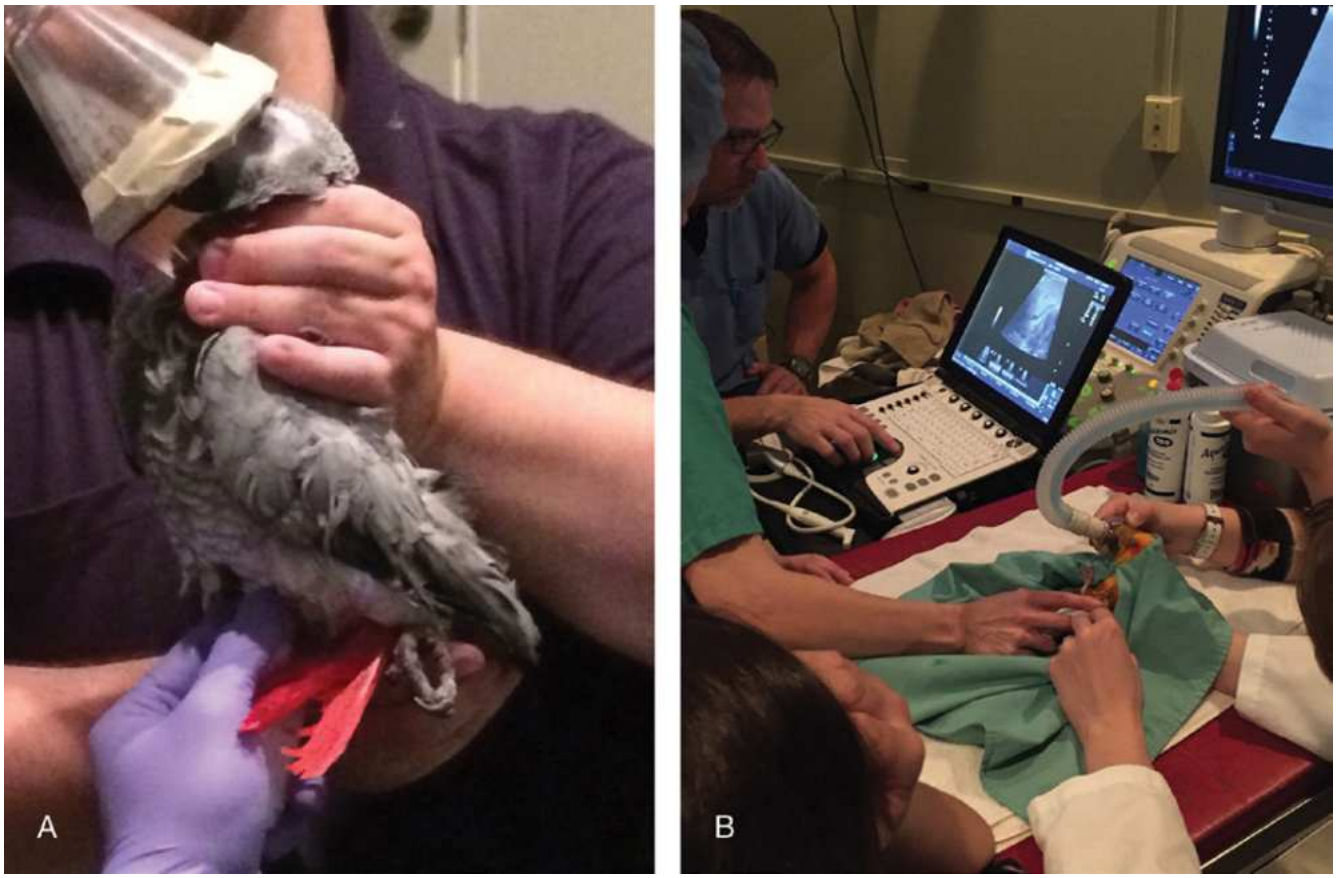


**Figure 42.2.** Probe placement and patient positioning. (A) Probe position in an upright Congo African gray parrot (*Psittacus erithacus erithacus*) receiving flow-by oxygen therapy via facemask. Dyspneic birds will benefit from flow-by oxygen during POCUS and FAST-like examinations. The bird should be held and positioned upright for low stress, especially with confirmed or suspected coelomic effusion. The probe is placed on the ventral coelom immediately caudal to the keel and directed cranially for the ventromedial coelomic acoustic window. (B) Ultrasound probe position in a sun conure (*Aratinga solstitialis*) receiving flow-by oxygen therapy via facemask; however, this more stable bird is being scanned in dorsal recumbency with some chemical restraint. The location of the acoustic window can vary with different species due to size and differences in musculoskeletal anatomy. Source: Image courtesy of Dr Miranda Sadar, Fort Collins, CO.

ventromedian coelomic acoustic window is variable and limited in smaller birds.

- Spleen, normal kidneys, and inactive gonads are often difficult or impossible to identify (Krautwald-Junghanns et al. 1991); however, the potential for recognition of obvious coelomic abnormalities and masses exists.

## *Conditions of the Coelom*

### Ascites

The presence of fluid in the coelom is easily recognizable to the most novice sonographer because of its anechoic and triangular appearance along with structures often wafting within the effusion (Figure 42.3). Positioning the bird upright allows free fluid to pocket in the gravity-dependent ventral coelomic regions and is much less stressful, especially in birds with compromised breathing. Exceptions include effusions that are compartmentalized to the hepatoperitoneal cavities. POCUS also assists in the collection of effusions for analysis (coelomocentesis) (see also Chapters 43 and 44). Following scanning of the coelom for fluid, the probe should be directed more cranial from the ventromedian approach to evaluate the liver and heart and for pericardial effusion (see Figures 42.1, 42.17, and 42.18). Pericardial effusion often accompanies coelomic effusion in birds.

**Pearl**: Keep the amount of time brief while the bird is in hand and the exam is under way, as often birds are dyspneic and stressed during restraint.

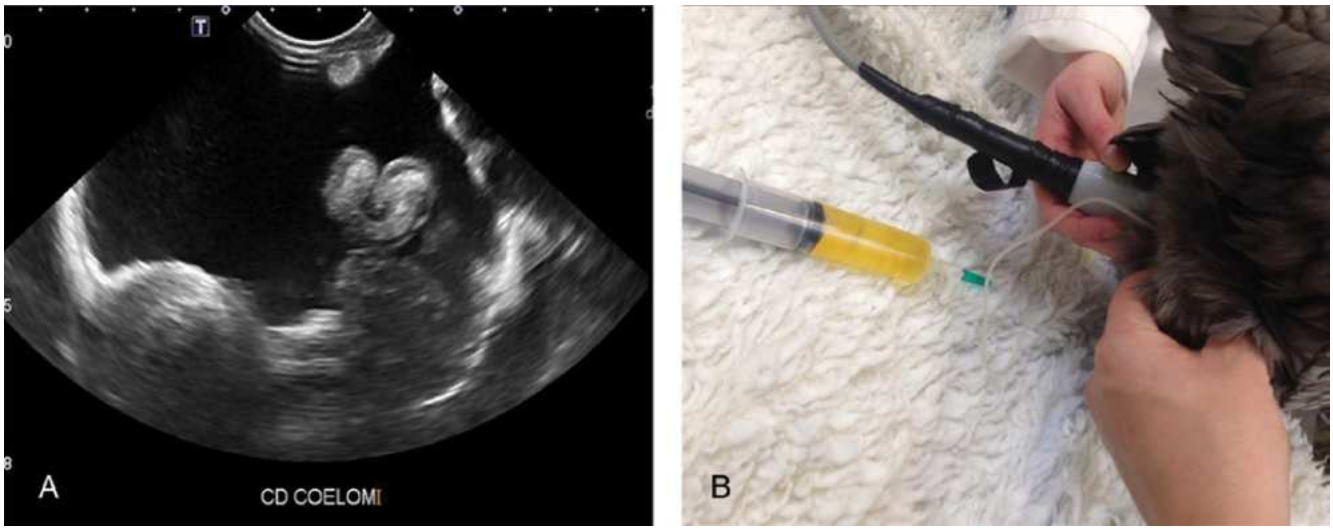


**Figure 42.3.** Ascites and coelomocentesis in a chicken. (A) The POCUS exam is used to identify free coelomic fluid. (B) Ceolomocentesis in shown on a chicken (*Gallus gallus domesticus*) and performed with ultrasound guidance. Coelomocentesis requires a butterfly catheter and syringe set up for sample collection. For larger volume removal, the use of a three-way stopcock can be beneficial.

**Pearl**: Often the sonographer cannot accurately differentiate many of the organs within the coelom; however, identification of free fluid is relatively easy and ultrasound can be used to help guide coelomocentesis and avoid complications of inadvertent puncture of nearby structures.

### Organomegaly and Masses

Hepatomegaly is most commonly diagnosed with the use of conventional radiographs, with evidence of the liver extending beyond the sternum caudally and beyond the acetabula laterally (Krautwald-Junghanns et al. 1991). POCUS may be used to verify the radiographic finding of an enlarged liver using the ventromedian coelomic acoustic window. A normal-sized avian liver ultrasonographically should have a characteristic coarse, homogeneous echotexture similar to a mammalian liver (Krautwald-Junghanns et al. 1991) (see Figure 42.6).

Large coelomic masses or granulomas may be identified quickly during POCUS. Masses and granulomas are typically of complex echogenicity, and appear very different from the sonographic appearance of a normal liver (Figure 42.4). Color flow Doppler is useful to demonstrate blood flow patterns that are helpful in differentiating a vascularized mass or a tumor from hypovascularized structures such as granulomas, ectopic uncalcified eggs, and oviductal impactions (see also Chapters 34 and 35).

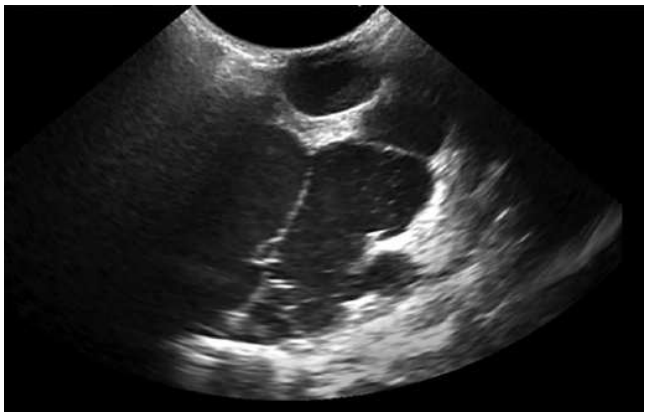

**Figure 42.4.** Cystic enlarged liver in a sun conure (*Aratinga solstitialis*). This bird presented with coelomic distension and on POCUS exam, marked abnormalities were detected in the liver, including cystic changes and hepatomegaly. The image shows a clear deviation from the expected normalcy of a homogeneous echogenicity to the liver capturing the abnormal sonographic finding for continued work-up and imaging.

### Reproductive

Ultrasonographic visualization of the gonads is only possible in sexually active female birds (Krautwald-Junghanns 2008). Active ovaries are characterized by the presence of follicles of different sizes representing various stages of development. An active oviduct is distinguishable due to the presence of eggs and the lack of contractility when differentiating from intestines,

which demonstrate contractility (Krautwald-Junghanns 2008). Cysts, neoplasia, salpingitis, and laminated eggs can be recognized with ultrasound (Figure 42.5).

### *Reproductive in Chickens*

Coelomic disease is a very common presenting complaint in pet chickens and most often reproductive in origin in the female. Ultrasound can be an extremely useful tool in assisting with diagnosis of common associated reproductive diseases such as free coelomic fluid (ascites), carcinomatosis, and forms of peritonitis (see Figures 42.3 and 42.5). Radiography in these same patients tends to lack coelomic detail and may be of limited use (Gingerich and Shaw 2014). Furthermore, ultrasound is the diagnostic tool of choice to help differentiate soft tissue opacities within the chicken coelom (Krautwald-Junghanns 2017). Egg yolk peritonitis is suspected by the presence of free fluid of heterogeneous echogenicity, with or without laminated eggs (Krautwald-Junghanns 2017). Definitive diagnosis can be obtained using ultrasound-guided fluid sampling and cytological evaluation. Concurrent salpingitis is suspected when the oviduct walls appear to be thickened (Helmer 2006). Oviductal impaction is also quite common and may take up the entire coelom.

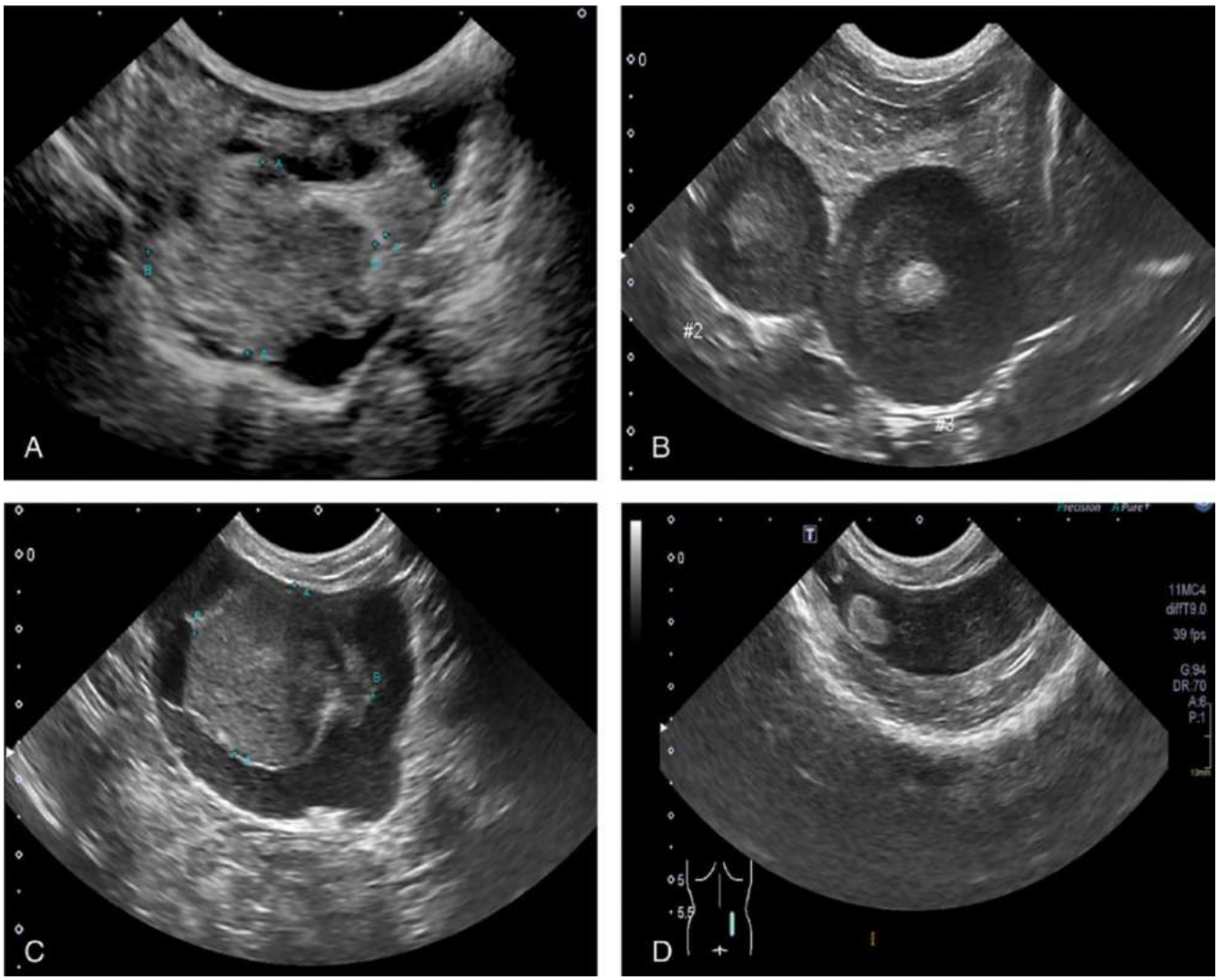


**Figure 42.5.** Findings involving the avian reproductive tract. (A) Image of an ovarian mass in a cockatiel (*Nymphicus hollandicus*). (B) Image of ovarian follicles in a chicken (*Gallus gallus domesticus*). The follicles are visualized as large, hypoechoic round structures. (C) Image with oviductal distension, fluid in the oviduct and the presence of an egg remnant. (D) An example of a fluid-filled oviduct from the chicken (*Gallus gallus domesticus*).

Oviductal impaction is easily identified through a POCUS or AFAST-like examination. The use of color flow Doppler helps differentiate a mass (positive blood flow) from cysts, abscesses, and granulomas (negative blood flow). Multiple small masses with or without ascites are typical of viral-induced neoplasia of chickens, such as avian leukosis virus and Marek's disease or carcinomatosis associated with ovarian adenocarcinoma.

## Cardiac Abnormalities

Often there is suspicion of cardiac disease based on physical examination findings, radiographs, or both. Detection of cardiomegaly on radiographs should prompt the clinician to perform a POCUS heart pending complete echocardiography. The heart is usually visualized cranial to the liver via the ventromedian coelomic acoustic window (see also anatomy Figure 42.1) (Helmer 2006). Cardiac chamber dilation and pericardial effusion can be diagnosed by a properly trained novice sonographer, although can be difficult in small patients with a small acoustic window (see Figure 42.2). Among the pathological conditions diagnosed, the most common abnormalities are pericardial effusion (Figure 42.6) and right ventricular dilation, both usually due to right-sided congestive heart failure (Krautwald-Junghanns 2017).

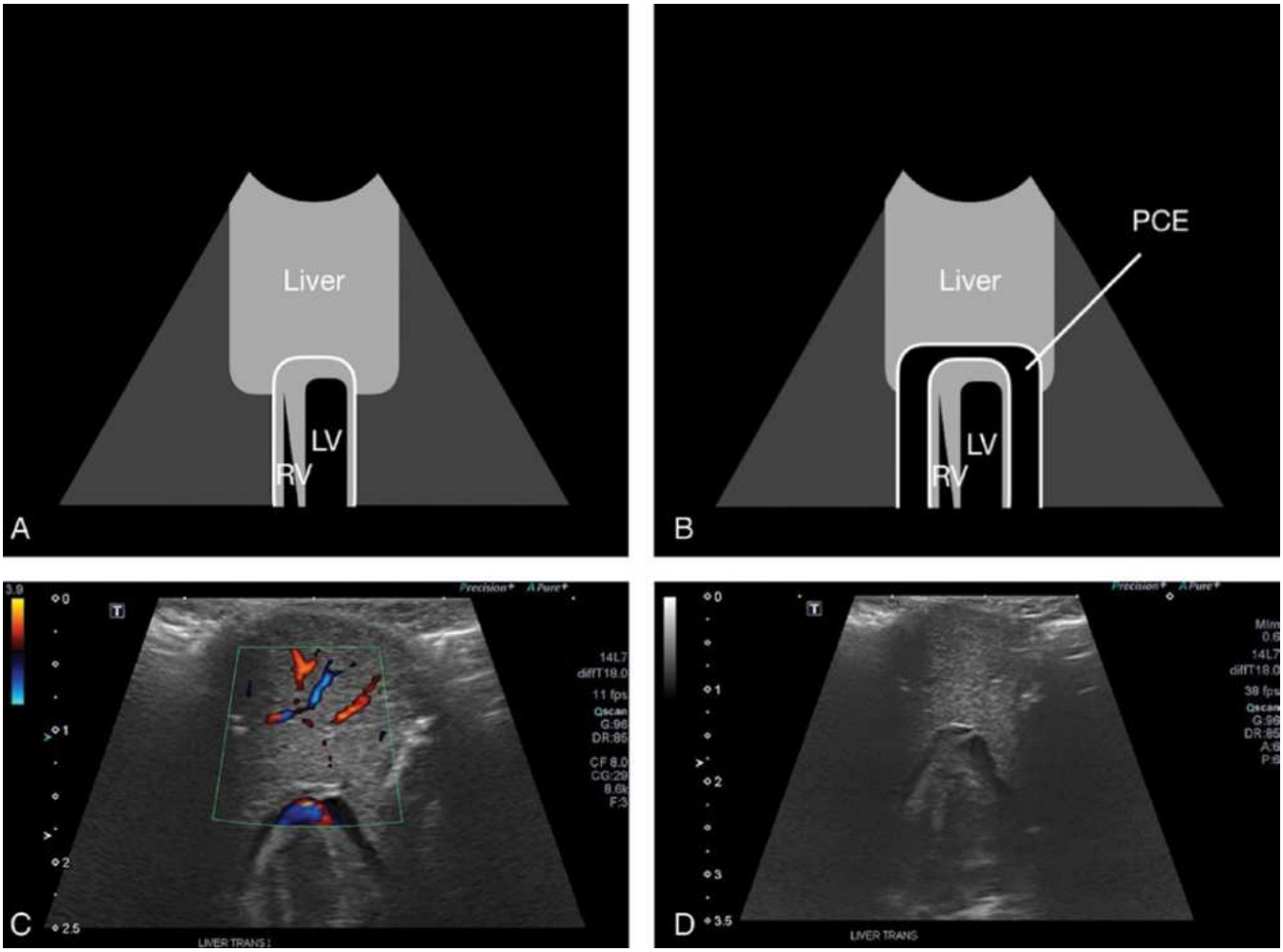


**Figure 42.6.** Pericardial effusion due to pericarditis in a sun conure (*Aratinga solstitialis*). (A,B) Line drawings showing the orientation when directing the probe toward the heart as in Figure 42.1. The liver is in the near-field and the heart in the far-field. There is no pericardial effusion in (A) but pericardial effusion is shown in (B). (C,D) Pericardial effusion in a sun conure due to pericarditis, shown with (C) and without (D) color flow Doppler. The colored pixels in the near-field are within the liver. LV, left ventricle; PCE, pericardial effusion; RV, right ventricle. Source: Image courtesy of Dr Miranda Sadar, Fort Collins, Colorado.

## Ocular Conditions

Being a fluid-filled structure, the eye is amenable to ultrasound and often overlooked. Special protective requirements are necessary for the acoustic coupling medium to prevent eye injury (see also Chapter 27) (Figure 42.7). In terms of rehabilitating wild birds that require vision for survival, POCUS of the eye could prove helpful as a screening test for the more novice sonographer. It is generally easy to perform and

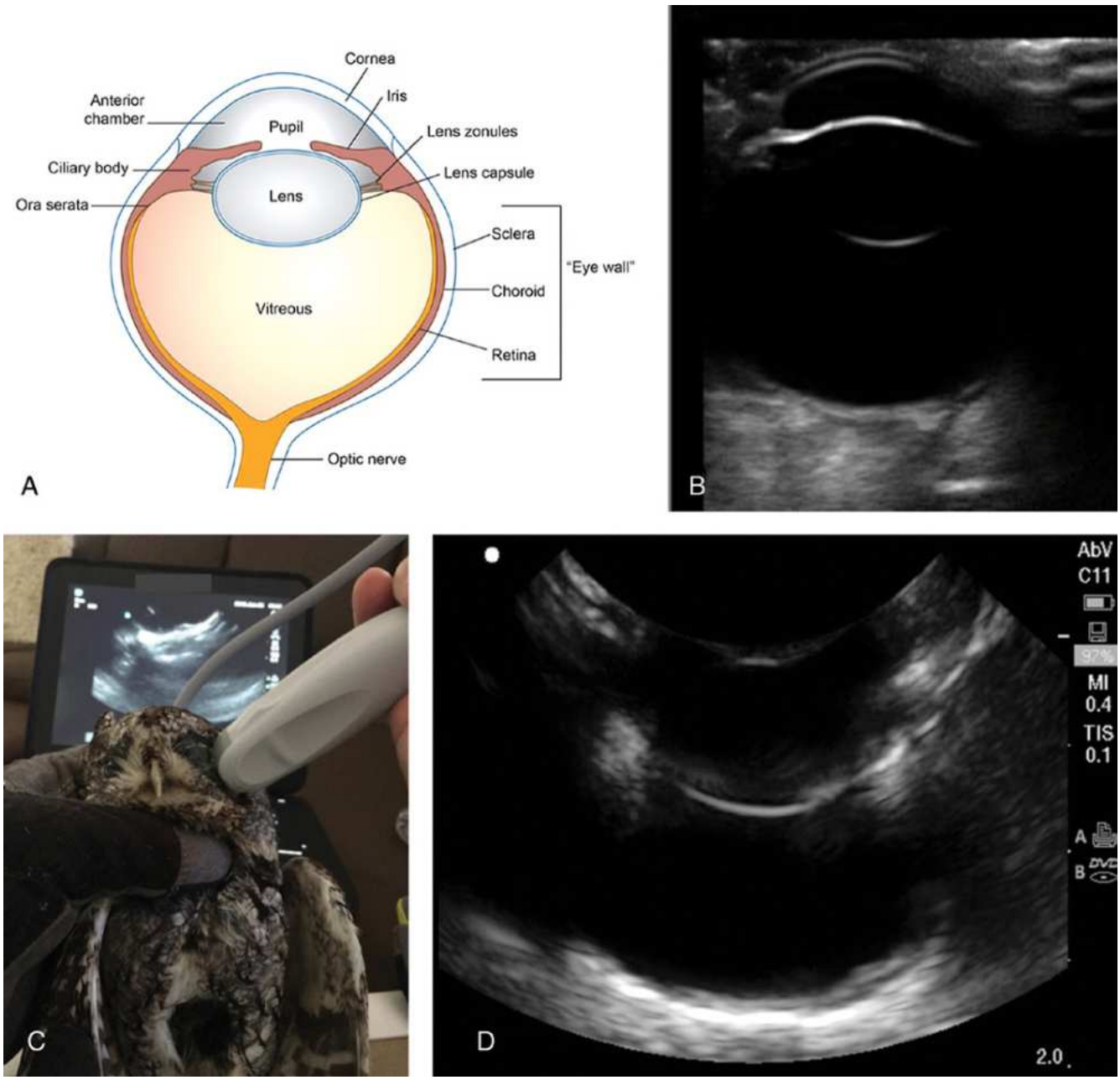


**Figure 42.7.** Screech owl POCUS eye. This Eastern screech owl (*Megascops asio*) was found on the side of the road, likely suffering from head trauma from an automobile strike. The POCUS eye with probe placement shown in (C) can provide important information regarding obvious lens luxation (anterior or posterior), intraocular hemorrhage and retinal detachments while at the same time documenting with an image. (A,B) Images from the POCUS eye chapter to correlate with the image in (D) in which the screech owl's eyes were unremarkable. As shown in (D), there is a normal lens position, normal anechoic anterior and posterior chambers, and normal smooth retina. Source: Reproduced with permission of Dr Gregory Lisciandro, DVM, Hill Country Veterinary Specialists and FASTVet.com, Spicewood, TX.

recognize basic ocular abnormalities such as lens luxations, retinal detachments, and intraocular hemorrhage as well as other intraocular abnormalities not apparent or questionable on direct examination. Moreover, images may be sent remotely to a veterinary ophthalmologist.

# Reptile

Successful application of ultrasonography in reptiles requires a good basic understanding of normal anatomy (Schumacher and Toal 2001). Reptile anatomy is heterogeneous among the different groups and some of these anatomical variations will be listed here.

Organ structure is typically simple with a two-lobed liver and a gallbladder that is uniquely caudal to the liver in snakes; a three-chambered reptilian heart; and usually a simple thoracoabdominal cavity. In some reptiles, the coelomic cavity is subdivided by septa, much like in birds. Specifically, tegus (group of lizard species) have a posthepatic septum located in the middle of the coelom (Figures 42.8, 42.9, and 42.10), monitor lizards and chelonians have a postpulmonary septum separating the pleural cavities from the rest of the coelom, and crocodilians have similar subdivisions to birds. The clinical relevance of these septa is the compartmentalization of free coelomic fluid, which can be anatomically useful when fluid is sonographically detected in more specific compartments. Lastly, some reptiles such as chameleons, skinks, and snakes have air sacs like birds, which consequently interfere with POCUS since ultrasound does not transmit through air.

The kidneys of some lizards are relatively caudal and retroperitoneal and thus located between the base of the tail and ventral to the cranial acetabular area. Not all reptiles have a urinary bladder. While snakes and crocodilians do not, chelonians (turtles and tortoises) and many lizards have a urinary bladder (Figure 42.11). Most reptile species are oviparous, but a few are viviparous such as boas, viperids, and some chameleons and skinks. Lizards have two large fat pads on the ventral coelom and rarely have any other foci of intracoelomic fat. The heart of most reptiles is in a cranial location at the level of the thoracic girdle (except in monitor lizards where it is more caudal) and thus echocardiography is not as easily accessed as in mammals (see Figures 42.8, 42.9, and 42.10).

## What POCUS Reptiles Can Do

- Diagnose ascites.
- Identify organomegaly (especially in snakes).
- Identify cystolithiasis and urolithiasis.
- Identify a mass or an abscess.
- Identify reproductive tract abnormalities.
- Identify reproductive stage in viviparous species.
- Sex squamates (types of lizards and snakes).
- Detect eye abnormalities.

## What POCUS Reptiles Cannot Do

- Cannot determine the type of free fluid.
- Cannot reliably detect diffuse parenchymal conditions.
- Cannot reliably detect lung and air sac pathology.
- Sexing is dependent on reproductive cycle, and is therefore not always possible.
- Account for wide species variation in anatomy.
- Cannot diagnose many specific cardiac abnormalities.

## Indications

- Suspicion of coelomic effusion based on physical examination or radiographic findings.
- Palpation of a coelomic mass on physical examination.
- Coelomic distension with or without accompanying dyspnea.
- Suspicion of reproductive tract abnormalities based on history and physical examination findings.
- Sexing in squamates.

## Objectives

- Recognize basic abnormalities that can be detected on ultrasound in reptile patients.
- Understand the wide anatomical diversity of reptiles.
- Understand the limitations of POCUS.

## Defining Species

*Squamates* are the largest order of reptiles, which includes snakes, lizards, and worm lizards. *Chelonians* includes turtles, terrapins, and tortoises.

## Patient Positioning and Probe Selection

The stability of the patient should always be evaluated prior to undertaking any handling or diagnostics. Most stable reptiles can be imaged with the use of manual restraint alone (Schumacher and Toal 2001), but forms of chemical restraint may be useful dependent on patient temperament and for more complete detailed

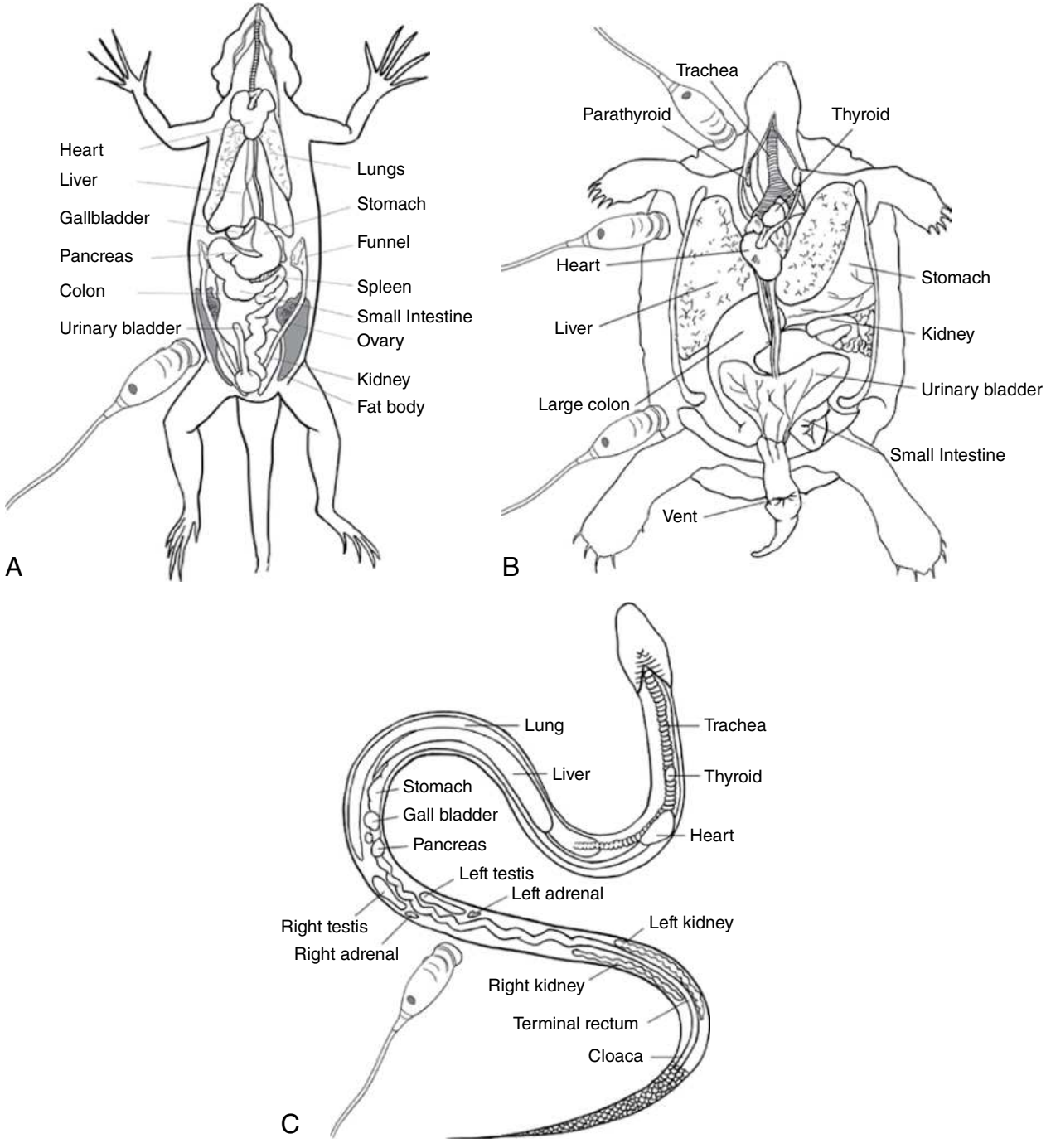


**Figure 42.8.** Line drawings showing clinically relevant anatomy and probe positioning. (A) A lizard. (B) Chelonians (turtles). (C) A snake. The anatomy is generalized to show basic structures and their relative locations, but can vary significantly depending on the species. Acoustic windows may be manipulated depending on the type of restraint, species, and body condition for lizards and snakes. In chelonians, the shell limits acoustic windows and the structures shown are primarily ventral because dorsal is the air-filled respiratory tract. The probe marker should always be directed toward the head in longitudinal planes. Source: Reproduced with permission of Dr Gregory Lisciandro, DVM, Hill Country Veterinary Specialists and FASTVet.com, Spicewood, TX. Illustration by Suji Park, sujisuji.com.

**Figure 42.9.** Various probe positions shown externally. (A) The coelomic ultrasound probe positioning in a tegu (*Tupinambus* sp.). The probe is placed at the cranial coelom to start and moved caudally for a complete examination. Of note, the probe approximates the FAST diaphragmatico-hepatic (DH) view. (B) Coelomic ultrasound probe positioning in a snake. The probe is placed just caudal to the head to start and moved caudally to allow for a complete examination. (C) The probe is placed in the axillary region of a bearded dragon (*Pogona vitticeps*) with its head and forelegs to the left of the image being held by the assistant's hands for an echocardiogram. The probe positioning, although far cranial, is analogous to the right parasternal view in small animals. Anatomy of most relevant structures is shown in Figure 42.8.

ultrasound examinations and ultrasound-guided procedures (see Figures 42.9 and 42.10). Respiratory-compromised and distressed patients require supportive care and stabilization and may benefit from sedation or anesthesia prior to performing POCUS.

Positioning of the patient depends on the species (Table 42.1); however, standing is now used in small animals and suggested for exotic companion mammals because dorsal recumbency is often stressful and risky. For species that cannot stand or lie flat such as squamates, lateral positioning provides another option over dorsal recumbency as well as support structures for getting under the patient (see Figures 42.9B and C, Chapters 37, 40 and 41).

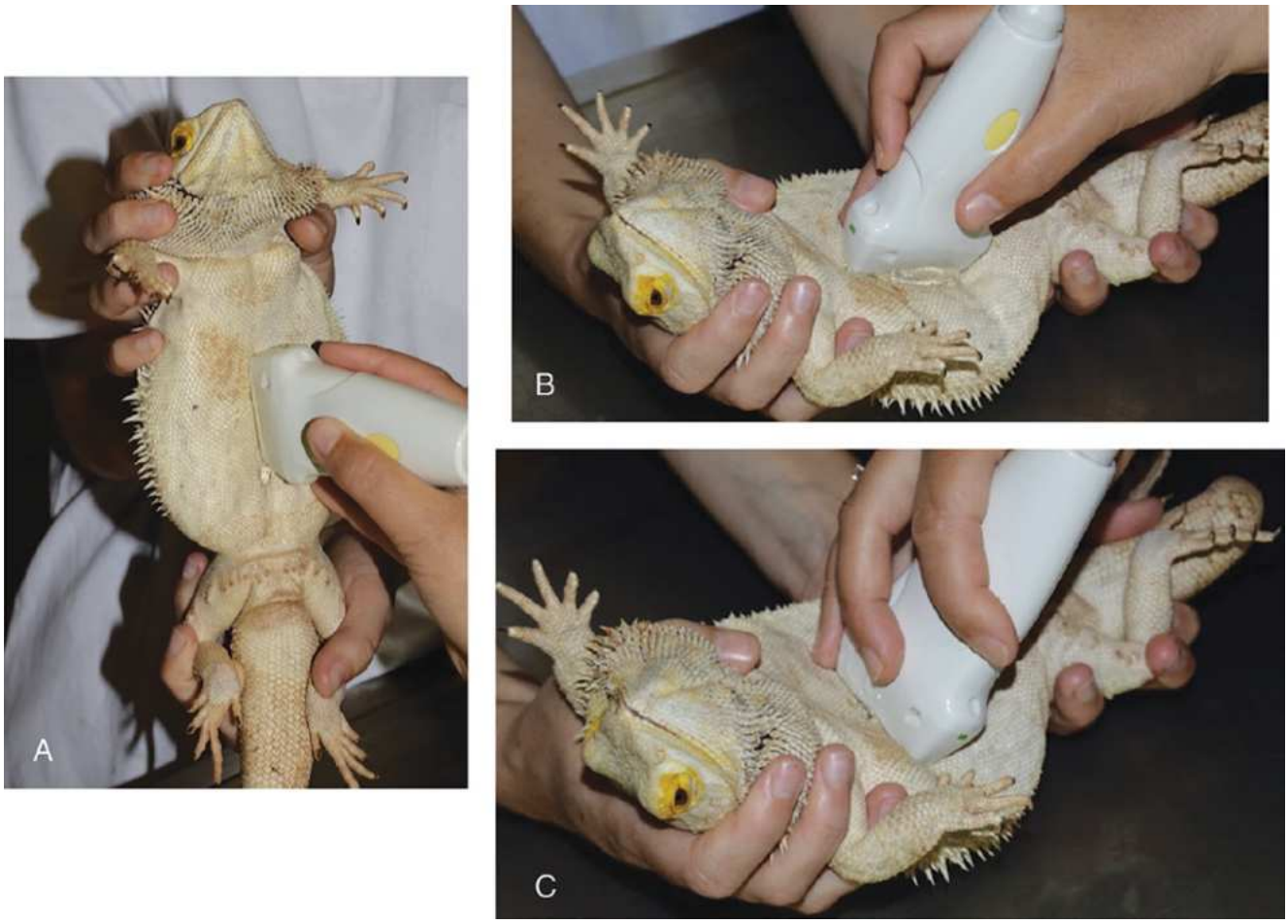


**Figure 42.10.** Orientation planes using a linear probe on a bearded dragon (*Pogona vitticeps*). (A,B) Longitudinal orientation is shown with two different forms of patient positioning using a linear probe. Upright positioning is used in (A) for weak patients. Dorsal positioning is shown in (B) in the same longitudinal plane while ultrasound is being performed. In (C) the linear probe is rotated to the left for the transverse imaging plane. Source: Reproduced with permission from Mader DR, Divers SJ. 2014. *Current Therapy in Reptile Medicine and Surgery*. St Louis: Elsevier Saunders.

A single transducer (probe) recommendation does not exist for reptiles due to the many different anatomical variations and body sizes encountered (Hochleithner and Holland 2014); however, some generalizations may be made. For smaller snakes and lizards, the use of a linear transducer (probe) is recommended (Hochleithner and Holland 2014). For chelonians (turtles and tortoises), a sector, also called phased array, transducer (probe) or curvilinear (microconvex) transducer (probe) with a small footprint is more useful due to their small acoustic windows located cranial and caudal to the thoracic limbs, and cranial to the pelvic limbs (prefemoral fossa) (see Figures 42.8, 42.9, and 42.10) (Hochleithner and Holland 2014). The frequency of the transducer (probe) selected is size dependent with higher frequency transducers for superior spatial resolution and detail but limited to shallow depths; therefore, these probes are recommended for smaller patients (Hochleithner and Holland 2014) (Table 42.2).

## Imaging the Normal Coelom

Begin the POCUS coelomic exam according to the species and its most accessible acoustic windows (see Figures 42.9 and 42.10).

- Place the probe in a longitudinal orientation on the ventral coelom of snakes and lizards.
- Place the probe cranial and caudal to the thoracic limbs and cranial to the pelvic limbs when imaging chelonians (turtles and tortoises).

**Figure 42.11.** Demonstration of the posthepatic septum in a tegu (*Tupinambus* sp.). The intraoperative image shows the posthepatic septum demonstrated by the arrows, located just caudal to the liver. The head of the tegu is towards the top of the image.

**Table 42.1.**
Reptile body positioning for POCUS (Hochleithner and Holland 2014).

| Reptile group | Position |
|---|---|
| Lizards | Dorsal<br>Upright |
| Snakes | Dorsal |
| Chelonians | Dorsal |

**Table 42.2.**
Transducer (probe) recommendations for reptile species (Hochleithner and Holland 2014).

| Reptile group | Transducer recommendations |
|---|---|
| Small lizards | 10–18 MHz |
| Larger lizards | 7.5–10 MHz |
| Giant tortoises | 2.5–5 MHz |

- The patient's scales can make imaging difficult, so to improve image quality use appropriate amounts and combinations of isopropyl alcohol, and acoustic coupling gel, working between the scales (Schumacher and Toal 2001). Alternatively, performing POCUS with the patient in a water bath can provide good imaging (Schumacher and Toal 2001), as is done with marine mammals, fish, and some amphibian species (see Chapter 41).
- Dependent on the acoustic window and area of interest, the probe is then moved cranially, caudally, and laterally, adhering to the rule of thumb of one probe maneuver at a time.
- In hard-shelled chelonians (turtles and tortoises), there are only three accessible acoustic windows. In soft-shelled chelonians, scanning through the plastron (ventral part of the shell) may be possible (Hochleithner and Holland 2014). These three acoustic windows are described below (see Figure 42.8)
  - The *first acoustic window* is located cranial to the forelimb beside the neck and allows for evaluation of the heart and liver.
  - The *second acoustic window* is located in the axillary region caudal to the forelimb and allows for evaluation of the heart and liver.
  - The *third acoustic window* is located in the inguinal region, referred to as the prefemoral fossa (cranial to the pelvic limb) and allows for evaluation of the intestines, urogenital tract, and bladder (Hochleithner and Holland 2014).

**Note:** Aquatic chelonian species generally have larger acoustic windows than terrestrial species.

**Pitfall:** An important consideration is the wide ultrasonographic variation of normal that is encountered within different reptile species. A common error is to misinterpret sonographically normal findings as abnormal when an unfamiliar species is examined (Hochleithner and Holland 2014).

**Pearl:** The skin and scales can cause significant artifact due to trapping of air between the scales, when attempting to ultrasound reptiles. Use of a shallow warm water bath when performing the POCUS examination can dramatically improve visualization (Hochleithner and Holland 2014).

## *Conditions of the Coelom*

### Distension

Enlargement of the coelom, due to a mass or fluid, and reproductive monitoring are the most common indications for POCUS and more complete ultrasound examinations in reptiles. With any coelomic distension, POCUS may be implemented to help determine obvious causes, such as ascites, cystic or solid tumor, granuloma/abscess, and herniation (Hochleithner and Holland 2014).

### Ascites

The presence of free fluid in the coelom is easily recognizable to the sonographer with minimal training because of its anechoic (black) triangulated appearance and wafting of intracoelomic structures, very different from coelomic imaging in the absence of ascites (see Figure 42.3).

**Pearl**: It may not be possible to accurately distinguish many of the organs within the coelom; however, sonographic identification of ascites is relatively easy. Moreover, ultrasound guidance may be used to help safely guide coelomocentesis (see Figure 42.3).

### Organomegaly and Masses

Suspected enlargement of organs and intracoelomic masses may be possible to detect ultrasonographically with minimal training, or at least recognize as different from expected normalcy. POCUS is especially useful in snakes where swellings along the body are common and related to a variety of coelomic organs. For example, gastrointestinal impaction, mainly due to ingestion of sand and substrate but also prey items, may be noticed in some lizards and snakes. On POCUS, such gastrointestinal impactions are imaged as heterogeneous echogenicity *without* vascularization on color flow Doppler (no flow) and strong shadowing, often triggering the need for radiography or computed tomography.

Hepatic lipidosis is also exceedingly common in a number of pet reptiles, especially bearded dragons (*Pogona vitticeps*). The liver is typically diffusely hyperechoic (bright) (Hernandez-Divers and Cooper 2001) (see Figure 42.16).

### Kidney and Urinary Bladder

Cystolithiasis and urolithiasis may also be suspected during POCUS, especially in higher risk species, such as the desert lizards (uromastyx, chuckwalla) and large tortoises. The same sonographic principles that are applied to mammalian species also apply to reptiles, with visualization of a hyperechoic near-field with clean acoustic shadowing (see Chapters 10, 11, and 40) (Figures 42.12 and 42.13). However, the reptilian kidney is much less accessible than mammalian kidneys due to the aforementioned differences in anatomy.

### Reproductive and Sexing

Ultrasound can be useful for determining the sex in some reptile species. The male hemipenes can be visualized in some species and are in fact calcified in normalcy in some monitor lizards (Figure 42.14) (Bucy et al. 2015). Additionally, seeing ovarian follicles is diagnostic for sexing the reptile as a female. Conversely, inactive female ovaries and male gonads are difficult to identify (Schumacher and Toal 2001) (Figure 42.15).

### Reproductive Conditions

Often reptiles present with various types of reproductive disease. The use of POCUS can help identify the presence of reproductive abnormalities. As previously mentioned, inactive female ovaries and male gonads are difficult to identify (Schumacher and Toal 2001); however, female reptiles commonly present with pre- or postovulatory stasis, which can be diagnosed ultrasonographically. Preovulatory follicles are hypoechoic (dark) compared to the more developed hyperechoic (bright) calcified shell of postovulatory

**Figure 42.12.** Large single bladder calculus in a uromastyx (*Uromastyx* sp.). Note the hyperechoic curved line caused by the ultrasonographically impenetrable urinary bladder calculus with clean shadowing through the far-field. A radiograph can confirm the suspicion if there is any question.

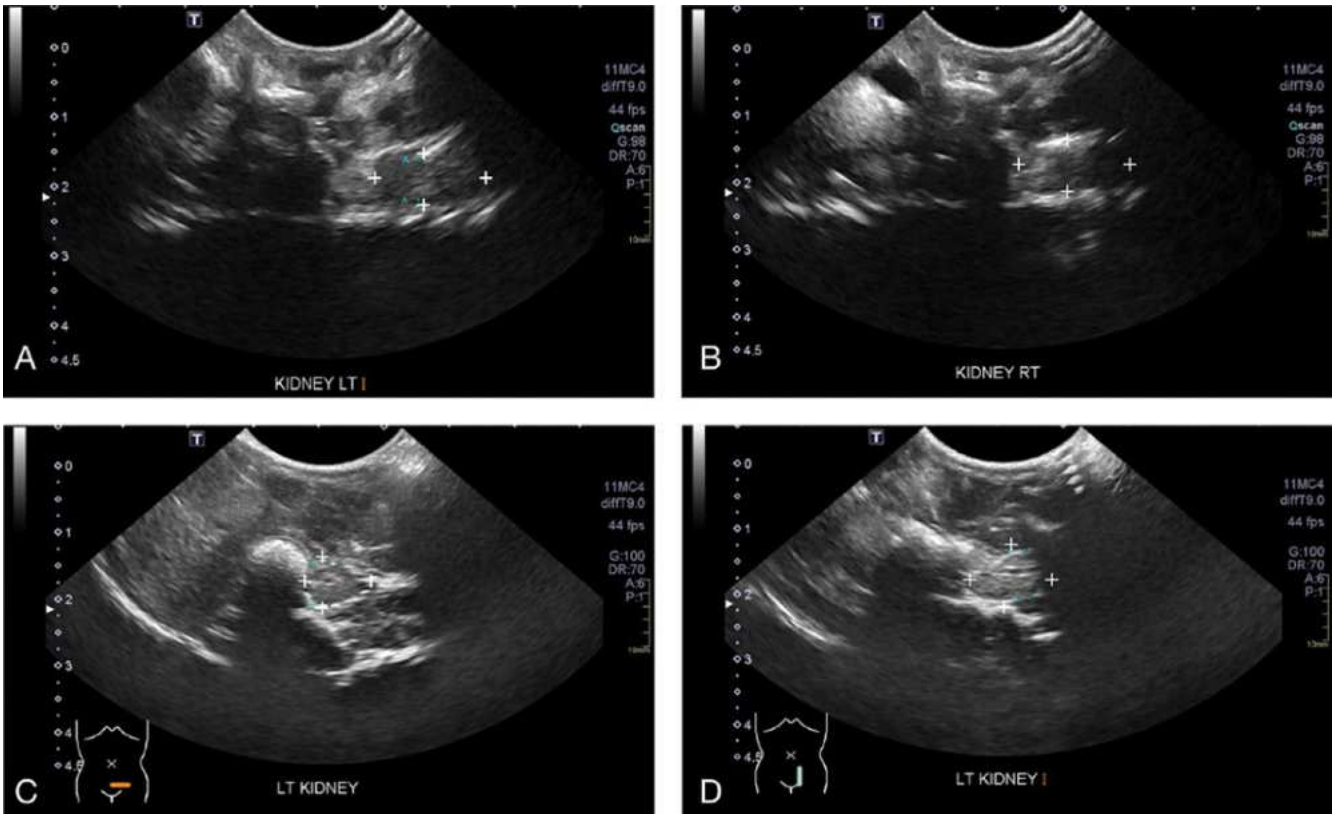


**Figure 42.13.** Kidneys in uromastyx and a bearded dragon. (A,B) The nondescript kidneys in a uromastyx left and right, respectively. (C,D) Two different images of the left kidney in a bearded dragon.

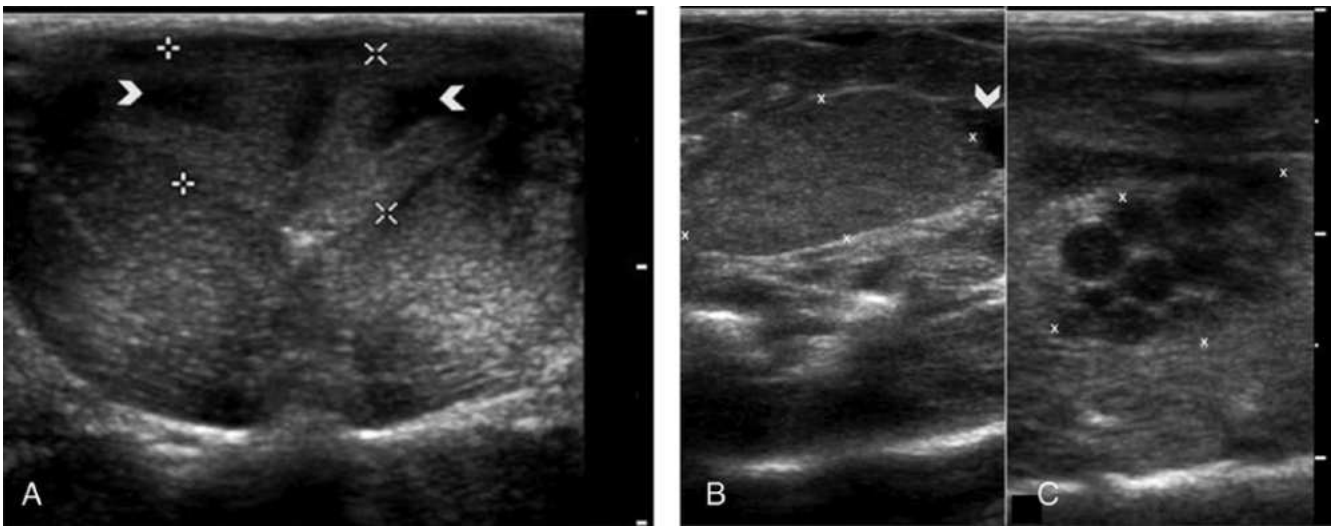


**Figure 42.14** Hemipenes, testicles, and ovaries in a bearded dragon (*Pogona vitticeps*). (A) Transverse ultrasonographic image of the hemipenes in a bearded dragon acquired with a 7–15 MHz linear transducer. The left side of the image is to the animal's right and the top of the image is ventral. The ventral and dorsal borders of the right hemipene (*crosses*) and the ventral and dorsal borders of the left hemipene (*X markers*) are indicated. There is a small pocket of fluid within the C-shaped hemipenes (*arrowhead*). (B) Sagittal ultrasonographic images of the right testis. A small amount of free coelomic fluid is evident (*arrowhead*). (C) The right ovary acquired with the same linear transducer as in (A). Margins of the testis and ovary are indicated (*X markers*). The left side of the image is cranial and the top of the image ventral. Source: Reproduced with permission Bucy et al. (2015).

follicles (Schumacher and Toal 2001). Preovulatory stasis may be differentiated from normal ovarian follicles. As the follicles remain unovulated, the echogenicity changes to a heterogeneous pattern with the surface of the follicles no longer smooth and well demarcated as is seen with normal follicles. Additionally, anechoic (black) fluid may be present around the follicles during stasis with the presence of echogenic free-floating particles indicative of inflammation. Lastly, and of note, ovarian follicles may be confused or difficult to differentiate from intestines and thus, peristalsis is helpful to distinguish ovarian follicles from the intestinal tract. Peristalsis is significantly affected by the species examined, diet, temperature, and many other factors, and should be a consideration when performing an ultrasound in reptiles.

Many female reptiles have large follicles that are not necessarily associated with reproductive disease (see Figure 42.15). Postovulatory stasis can also be differentiated from normal eggs by visualizing an irregular surface of the egg (versus expected normal smooth appearance) (see Figure 42.15) (Hochleithner and Holland 2014).

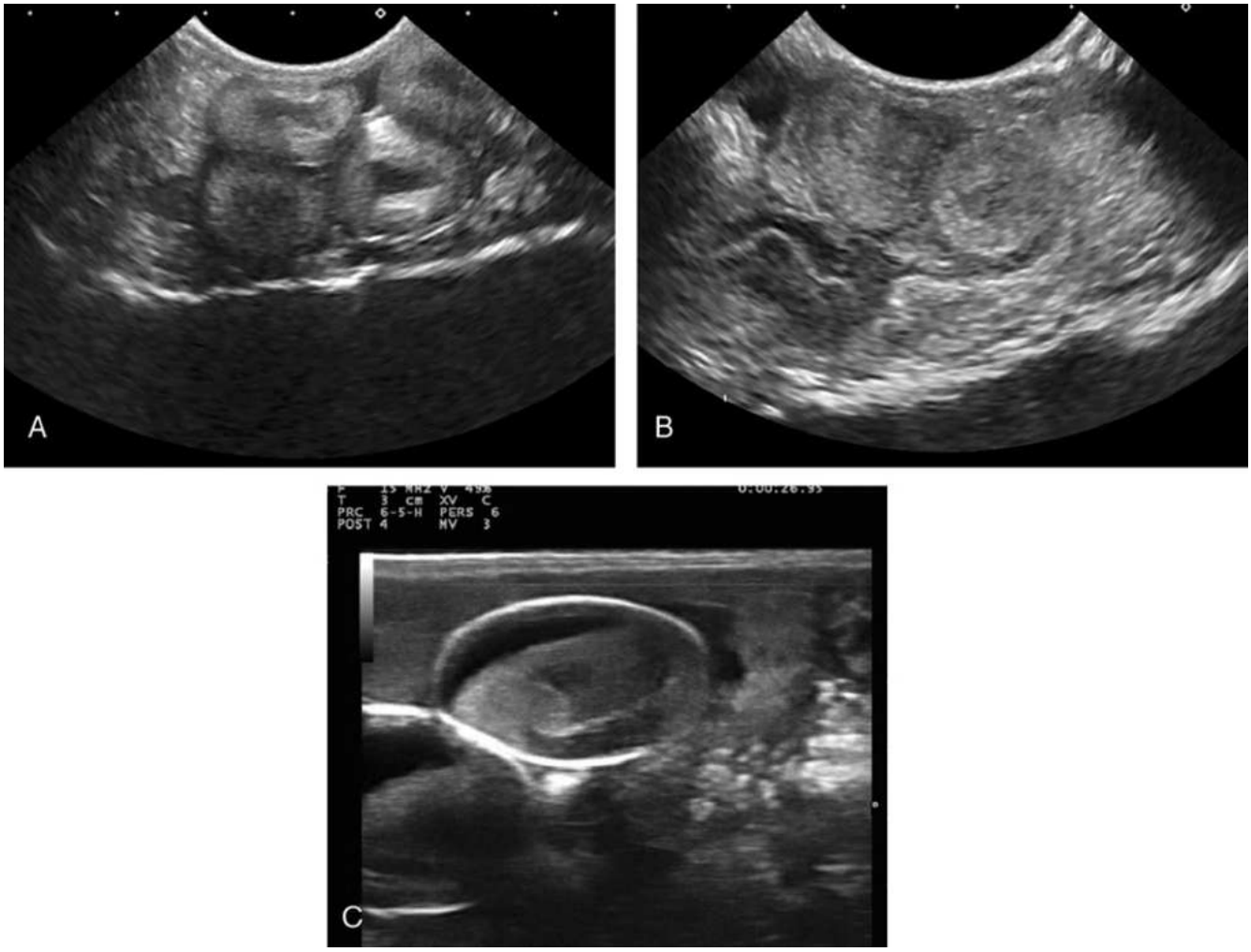


**Figure 42.15.** Follicles and eggs in a bearded dragon (*Pogona vitticeps*) and uromastyx (*Uromastyx* sp.). (A) Image of normal ovarian follicles in a uromastyx lizard. There is a small amount of free fluid in the upper right of the near-field, which can be a normal finding if anechoic. (B) Image of oophoritis in a bearded dragon with irregularly shaped follicles. There is a small amount of free fluid in the upper left of the near-field, which can be a normal finding if anechoic. (C) Sagittal plane of an egg in the bearded dragon. The hyperechoic oval structure is the shell, the hypoechoic part the albumin, and the rest of the content is the developing vitogenic mass, shortly before being oviposited. Source: Reproduced with permission from Mader DR, Divers SJ. 2014. *Current Therapy in Reptile Medicine and Surgery*. St Louis: Elsevier Saunders.

### Liver

The liver of reptile species other than chelonians (turtles and tortoises) is relatively simple to locate and image, and should be evaluated for size and the presence of parenchymal changes (Schumacher and Toal 2001). The sonographic expectation of the reptilian liver is one of homogeneous echogenicity; thus, the presence of masses (neoplasia, cysts, and abscesses) is often readily identified (Schumacher and Toal 2001) (Figure 42.16). A hyperechoic (bright) liver may be associated with hepatic lipidosis, which is common in a number of pet reptiles, especially bearded dragons (Hernandez-Divers and Cooper 2001).

## *Cardiac Abnormalities and Aneurysms*

Echocardiography is challenging in reptiles due to differences in anatomy from mammals, as well as a lack of available reference data (Schumacher and Toal 2001). Mild valvular regurgitation may be normal in many reptilian species; however, basic cardiac abnormalities may still be recognized, including obvious cardiac chamber enlargement and pericardial effusion, of which bearded dragons have a more frequent occurrence than other reptiles (Figures 42.17 and 42.18).

Vascular lesions and abnormalities are also possible. The caudal vena cava may be visualized subxiphoid as in dogs and cats and associated with the liver in similar imaging planes as the heart (see Figures 42.17 and 42.18). Several cases of aneurysms arising from the internal carotid or aorta have been reported in bearded dragons (Barten et al. 2006; Sweet et al. 2009; Finnburgh and Eshar 2018). Affected lizards usually present with a large fluctuant or firm swelling on the dorsolateral aspect of the neck (Barten et al. 2006). POCUS in these cases would be useful to demonstrate the presence of fluid within the mass along with acoustic enhancement through the far-field with variable blood flow on color flow Doppler.

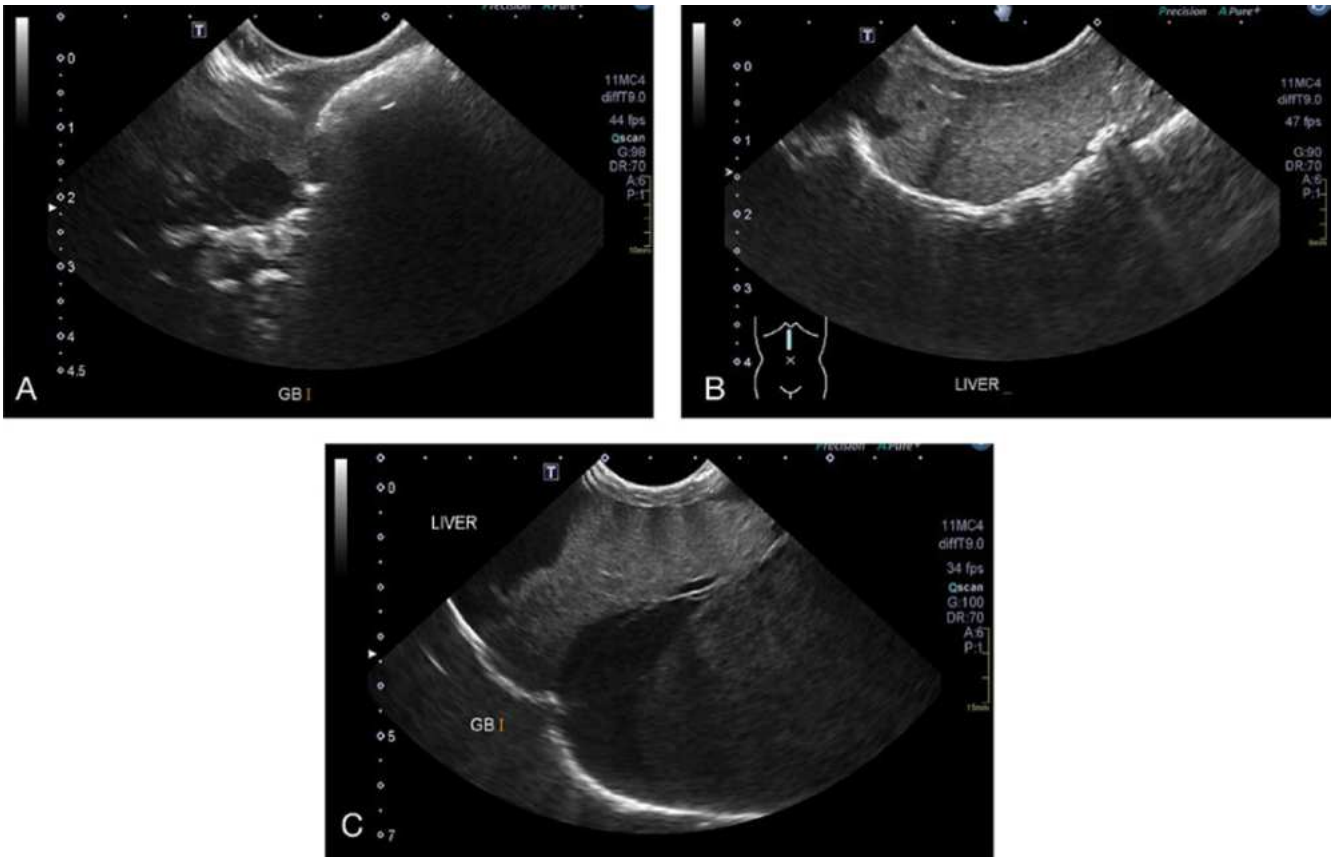


**Figure 42.16.** Gallbladder and liver in uromastyx (*Uromastyx* sp.), bearded dragon (*Pogona vitticeps*), and monitor lizard (*Varanus* sp.). (A) Image of the the gallbladder of a uromastyx. (B) Image of the homogeneous appearance of the liver of a bearded dragon. (C) Image of the liver and gallbladder of a monitor lizard (*Varanus* spp.).

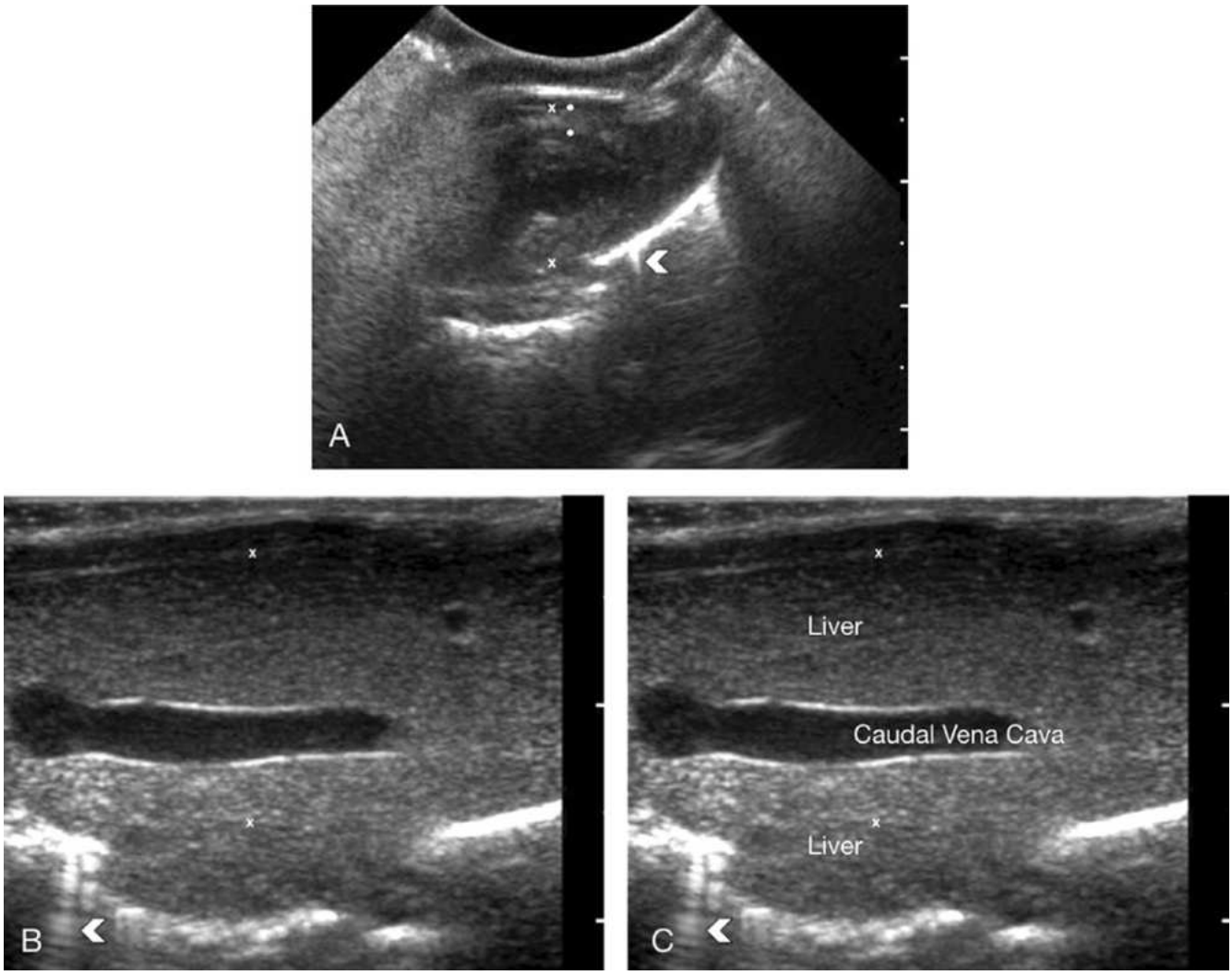


**Figure 42.17.** Cardiac and caudal vena cava imaging. (A) Sagittal ultrasonographic image of the cardiac ventricle of a bearded dragon (*Pogona vitticeps*) acquired with a 5–8 MHz curvilinear (microconvex) probe. The left side of the image is cranial and the top of the image is ventral. The cardiac muscle is isoechoic to the body wall with slightly coarse echo texture. Dorsal and ventral margins of the ventricle are indicated (*X markers*). The ventral ventricular wall is also shown (*circles*). A muscular septum is present within the ventricle, adjacent to the ventral ventricular wall. A small B-line artifact is evident in the aerated lung dorsal to the heart (*arrowhead*). (B) An oblique ultrasonographic image of the liver and intrahepatic portion of the caudal vena cava in a bearded dragon acquired with a 7–15 MHz linear probe placed over the right sides of the liver. The top of the image is ventral. The dorsal and ventral margins of the liver are indicated (*X markers*). Two B-line lung ultrasound artifacts are evident along the pulmonary–hepatic interface dorsal to the liver (*arrowhead*). (C) Same image as (B) but labeled with text identifying the caudal vena cava and the liver. Source: Reproduced with permission Bucy et al. (2015).

### *Ocular Conditions*

Being a fluid-filled structure, the eye is readily amenable to ultrasound and often overlooked. Special requirements are necessary for a safe corneal acoustic coupling medium to prevent iatrogenic eye injury (see also Chapter 27). POCUS eye is easy to perform and recognize basic ocular abnormalities such as lens luxations, retinal detachments, and intraocular hemorrhage (Figure 42.19). Other intraocular abnormalities can also be identified such as masses. POCUS eye would be a helpful diagnostic tool, especially in the rehabilitation of wild reptiles that require vision for survival.

## FAST Ultrasound in Birds and Reptiles

The combined AFAST, TFAST, and Vet BLUE examinations, called Global FAST, described in small animals could be applied to birds and reptiles with potentially less restraint

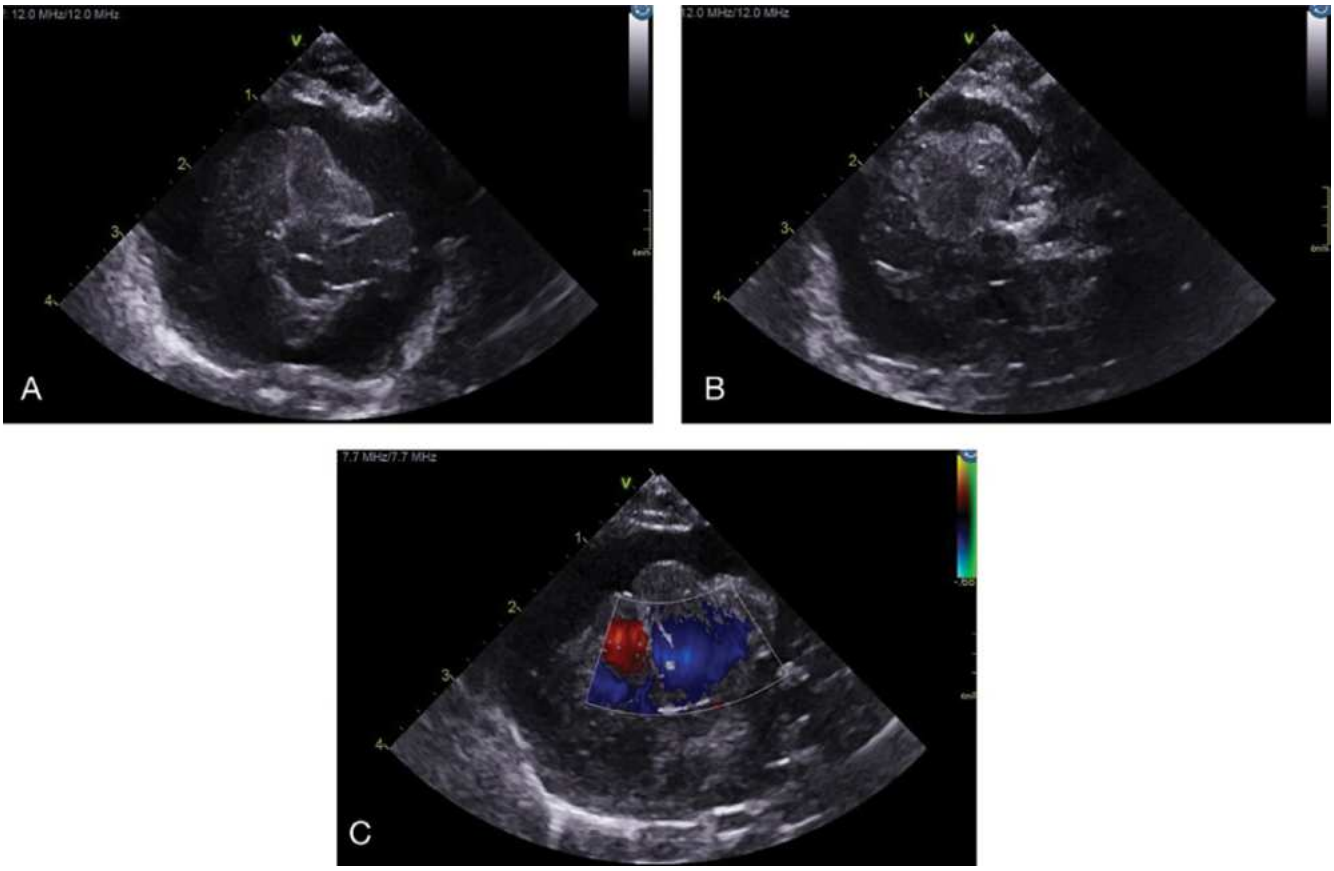


**Figure 42.18.** Pericardial effusion in a bearded dragon (*Pogona vitticeps*). Multiple views (A) through (C) of pericardial effusion using principles for small animals including seeing the heart in its entirety by having enough depth to see the bright pericardium in the far-field.

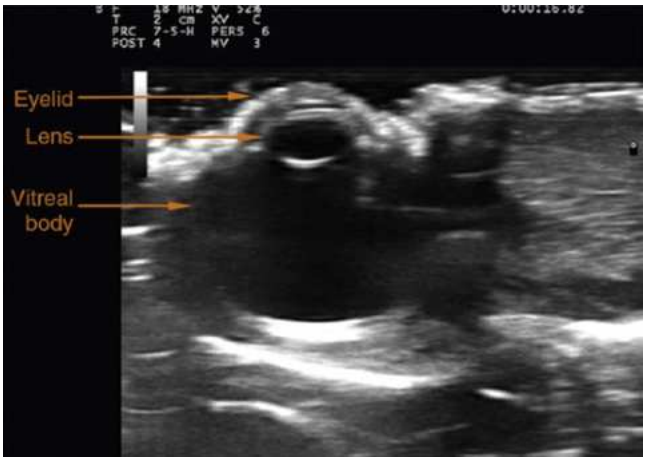


**Figure 42.19.** Ultrasound evaluation of the eye of a veiled chameleon (*Chamaeleo calyptratus*). The most superficial echogenic structure is the eyelid; the lens appears as an oval, anechoic structure with thin hyperechoic margins; the vitreal body is anechoic; and there is a round border to the fundus. Source: Reproduced with permission from Mader DR, Divers SJ. 2014. *Current Therapy in Reptile Medicine and Surgery*. St Louis: Elsevier Saunders.

and in lateral or upright positioning. Global FAST may be routinely used as an extension of the physical examination (see also Chapters 36 and 37) for a rapid survey for free fluid (ascites, pericardial effusion) and abnormalities of respective reptilian and avian target organs.

## Pearls and Pitfalls, The Final Say

POCUS has the potential to be an advantageous imaging modality for birds and reptiles by "seeing" the patient's problem list and thus helping direct further diagnostics, including triggering additional imaging. POCUS also potentially assists initial and emergency management of these often delicate patients without the restraint, delay, transport, and inherent risk of radiology or more complete ultrasound studies. The biggest challenge associated with POCUS imaging is the vast differences and variations in avian and reptilian anatomy compared to mammals. Additionally, the air sac system of birds (and some reptiles)

drastically reduces the acoustic windows for ultrasonographic examination of the coelom to a single ventromedian window just caudal to the sternum, prevents respiratory examination (Vet BLUE), and limits echocardiography (TFAST, POCUS heart).

However, coelomic distension is common and most nonspecialist veterinarians should be able to easily recognize ascites, pericardial effusion, fluid-related conditions (pregnancy, follicular development), intracoelomic masses (neoplasia, granulomas, and masses), and soft tissue abnormalities such as changes in hepatic parenchyma, urolithiasis, organomegaly, and follicular development. Additionally, ultrasound can be useful for sexing in some species. POCUS eye is also an easily learned skill for birds and reptiles.

Finally, standardized abbreviated ultrasound approaches have not been developed for birds and reptiles as in dogs and cats, and the future holds promise for future study and validity with more veterinarians incorporating the POCUS and FAST approach as a first-line imaging modality.

# References


Barten S, Wyneken J, Mader D, et al. 2006. Aneurysm in the dorsolateral neck of two bearded dragons (Pogona vitticeps). Association of Reptilian and Amphibian Veterinarians, Proceedings, Baltimore, MD, pp 43–44.

Bucy DS, Guzman DS, Zwingenberger AL. 2015. Ultrasonographic anatomy of bearded dragons (*Pogona vitticeps*). *J Am Vet Med Assoc* 246(8):868–876.

Doneley B. 2016. Ultrasound. In: *Avian Medicine and Surgery in Practice: Companion and Aviary Birds*, 2nd edition, edited by Doneley B. London: Mason Publishing, pp 104–105.

Finnburgh BM, Eshar D. 2018. Diagnostic challenge. *J Exot Pet Med* 27(2):123–125.

Fitzgerald B, Beaufrère H. 2016. *Cardiology. In: Current Therapy in Avian Medicine and Surgery*, edited by Speer BL. Amsterdam: Elsevier, p 297.

Gingerich E, Shaw D. 2014. Reproductive diseases. In: *Backyard Poultry Medicine and Surgery: A Guide for Veterinary Practitioners*, edited by Greenacre CB, Morishita TY. Hoboken: Wiley-Blackwell, pp 169–180.

Helmer P. 2006. Advances in diagnostic imaging. In: *Clinical Avian Medicine*, edited by Harrison G, Lightfoot T. Palm Beach: Spix Publishing, pp 653–658.

Hernandez-Divers SJ, Cooper JE. 2001. *Reptile hepatic lipidosis*. Association of Reptilian and Amphibian Veterinarians, Proceedings, Orlando, FL, pp 193–200.

Hochleithner C, Holland M. 2014. Ultrasonography. In: *Current Therapy in Reptile Medicine and Surgery*, edited by Mader DR, Divers SJ. St Louis: Saunders, pp 107–127.

Krautwald-Junghanns ME. 2008. Aids to diagnosis. In: *Essentials of Avian Medicine and Surgery*, edited by Coles BH. Hoboken: John Wiley and Sons, pp 98–101.

Krautwald-Junghanns ME. 2017. Radiography and ultrasonography in the backyard poultry and waterfowl patient. *J Avian Med Surg* 31(3):189–197.

Krautwald-Junghanns ME, Riedei U, Neumann W. 1991. *Diagnostic use of ultrasonography in birds*. Association of Avian Veterinarians, Proceedings, Chicago, IL, pp 269–275.

Schumacher T, Toal RL. 2001. Advanced radiography and ultrasonography in reptiles. *Semin Avian Exotic Pet Med* 10(4):162–168.

Sweet C, Linnetz E, Golden E, Mayer J. 2009. What is your diagnosis? *J Am Vet Med Assoc* 234(10):1259–1260.

SECTION IX

# Ultrasound-Guided Procedures

CHAPTER FOURTY-THREE

# POCUS: Ultrasound-Guided Procedures – Abdominocentesis, Thoracocentesis, and Pericardiocentesis

Søren R. Boysen

## Introduction

Ultrasound-guided interventional techniques are generally classified as indirect, free-hand and mechanical-guided.

With the indirect method, ultrasound is used to determine the location and depth of the target (usually fluid), and a needle trajectory is imagined but real-time ultrasound visualization of the needle during the procedure is not used. The indirect method is commonly used for pericardiocentesis, thoracocentesis, and abdominocentesis in veterinary patients.

With free-hand ultrasound-guided centesis, the location and depth of the target are determined and real-time ultrasound is used to visualize and help guide the needle tip into the desired target. The free-hand method is often preferred because it is less expensive (doesn't use commercially available needle guides) and allows greater flexibility in angling the needle and changing its location while entering cavities or tissues by using real-time ultrasound visualization for more precise aspiration or centesis (del Cura et al. 2010). In other words, this flexibility allows the attending clinician to move the needle/needle tip through different planes relative to the ultrasound beam, in contrast to the mechanical-guided ultrasound method.

With the mechanical ultrasound-guided system, a rigid ultrasound probe attachment is used to help guide the needle/needle tip into the target, be it a cavity or tissue, using real-time visualization. The attachment typically contains a slot for the needle, which fixes the needle track to the angle of the slot. The fixed path of the device ensures that the needle remains in the plane of the ultrasound beam and thus facilitates real-time ultrasound visualization of the needle/needle tip. On the other hand, the fixed path of the attachment has the disadvantage of limiting the number of needle/needle tip entry angles that may be utilized (del Cura et al. 2010).

## Pericardiocentesis

### *Introduction*

Pericardiocentesis is the aspiration of fluid from the pericardial space and is often performed for therapeutic and/or diagnostic purposes. Ultrasound is a rapid, sensitive, and noninvasive technique for the emergent detection of pericardial effusion with or without tamponade, concurrent pleural effusion, and the detection of underlying causes (masses, foreign

*Point-of-Care Ultrasound Techniques for the Small Animal Practitioner*, Second Edition. Edited by Gregory R. Lisciandro.
© 2021 John Wiley & Sons, Inc. Published 2021 by John Wiley & Sons, Inc.
Companion website: www.wiley.com/go/lisciandro/ultrasound2

bodies). In cardiovascularly stable cases of pericardial effusion without cardiac tamponade, emergent pericardiocentesis may be delayed until a thorough evaluation of the underlying cause is undertaken. Given pericardial effusion may occur secondary to coagulopathies, the patient's coagulation status or a toxin-induced coagulopathy (e.g., warfarin) should be considered prior to performing pericardiocentesis. When coagulopathy is present and pericardiocentesis is deemed necessary, the coagulopathy should ideally be corrected with rapid fresh frozen plasma (FFP) administration prior to performing pericardiocentesis (e.g., 8–10 mL/kg over 5–10 minutes, or at a slower rate dictated by the patient's cardiovascular status). If patients are agonal, life-saving pericardiocentesis is recommended prior to or concurrent with FFP transfusion.

## Ultrasound-guided versus Blind Pericardiocentesis

In veterinary medicine, pericardiocentesis is often performed blindly at the 5th–7th intercostal space, or using indirect ultrasound guidance. With indirect guidance, ultrasound is used to identify the preferred intercostal space, which is typically the deepest pericardial fluid pocket in the absence of surrounding vital structures (e.g., lung and heart), but the actual needle is *not* followed in real time. Another option is to use free-hand ultrasound-guided pericardiocentesis whereby the needle is tracked using real-time ultrasound guidance as it enters the pericardial space.

There are several studies in humans demonstrating reduced complications with free-hand ultrasound-guided pericardiocentesis compared to blind techniques (Callahan et al. 1985;Clarke and Cosgrove 1987; Taavitsainen et al. 1991; Tsang et al. 2002). Reported complications include ventricular or atrial penetration, coronary artery laceration, pneumothorax (PTX), dysrhythmias and inadvertent penetration of the diaphragm and abdominal organs (Clarke and Cosgrove 1987). Given anatomical differences in veterinary patients compared to humans, it is unknown if ultrasound-guided pericardiocentesis would result in fewer complications, although there are preliminary studies to suggest this may be the case in dogs (Celona et al. 2017). In cases of small-volume effusion causing tamponade, or compartmentalized fluid, free-hand ultrasound-guided pericardiocentesis may be particularly helpful. By direct visualization of structures and fluid, ultrasound-guided techniques should prove safer than blind techniques.

## Indications for Pericardiocentesis

Pericardiocentesis is indicated to remove fluid from the pericardial space, both for diagnostic and therapeutic purposes, and is the life-saving treatment of choice when cardiac tamponade is present.

**Pearl:** Leaving a small volume of pericardial effusion provides an acoustic window and helps with the detection of pericardial or heart-based masses if complete echocardiography is to be subsequently scheduled (Scansen 2011). However, in cardiovascularly unstable patients, pericardiocentesis must take precedence over complete echocardiography and sufficient pericardial fluid must be aspirated to ensure the patient is cardiovascularly stable.

## Scanning Technique for Pericardiocentesis

- Clip hair.
- Apply acoustic coupling gel or alcohol.
- Place the ultrasound probe between the fourth and fifth ribs on the right side of the patient at the level of the costochondral junction or alternately at the location of the strongest palpable heartbeat if the heart can be easily palpated.
- Move the ultrasound probe cranial and caudal 1–2 rib spaces and ventrally and dorsally 2–3 inches until the widest accumulation of pericardial fluid has been identified. Limit the survey to only several seconds in unstable patients.
- Dependent on patient stability, measure or approximate the distance from the skin to the pericardium and the greatest width (cm) of the pericardial effusion.

**Pearl:** Be familiar with the centimeter (cm) scale on your ultrasound machine, which is typically located on the right side of the screen, to rapidly approximate these measurements (Figure 43.1).

- Visualize the needle pericardiocentesis angle and trajectory path that allows safest penetration into the pericardial space (Figure 43.2A), which is usually over the site where the effusion is closest to the thoracic wall, thus minimizing lung trauma.

**Pearl:** Measurement of the pericardial effusion width prior to pericardiocentesis helps guide decisions regarding the depth the catheter needs to be inserted to enter the pericardial space and the distance between the pericardium and the heart.

- Measure the width of the pericardial effusion before and serially after pericardiocentesis to monitor for resolution or recurrence rates of the effusion. If pericardial effusion recurs, placement of an indwelling small-bore chest tube into the pericardial space allows recurrent pericardial effusion to be removed serially without the need to continually repeat the pericardiocentesis procedure (Figure 43.3).

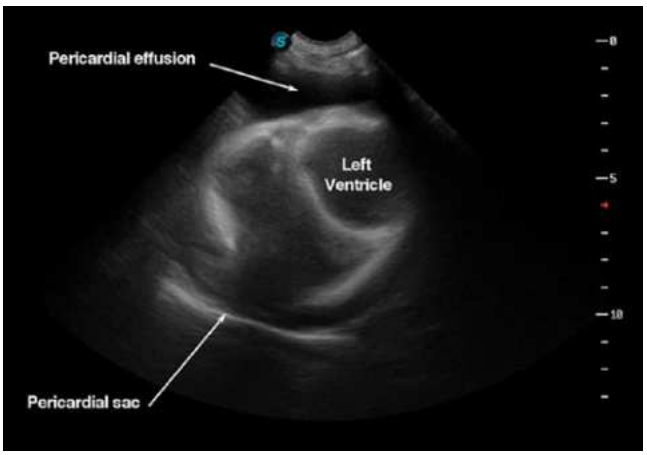


**Figure 43.1.** Left parasternal short-axis view of a dog with pericardial effusion. The centimeter (cm) scale is located on the right side of the screen and can be used to rapidly approximate measurements of pericardial depth.

## Materials Checklist for Pericardiocentesis

- Clippers and antimicrobial scrub.
- Sterile gloves.
- #11 scalpel blade.
- 14–16 gauge 2–6 inch over-the-needle or through-the -eedle catheter (Angiocath™, BD, Franklin Lakes, NJ) dependent on patient size. The author prefers over-the-needle catheters.
- Intravenous extension set.
- Three-way stopcock.
- 6, 12, 20, and 35 or 60 cc syringe.
- A receptacle for fluid collection (i.e., kidney bowl).
- Red (plain) and lavender (EDTA) topped tubes for collection of sterile fluid samples.
- Injectable lidocaine for local anesthesia and arrhythmia control.
- Electrocardiogram (ECG) monitor.
- Ultrasound machine with variable frequency curvilinear probes (a linear probe may be used in smaller animals).

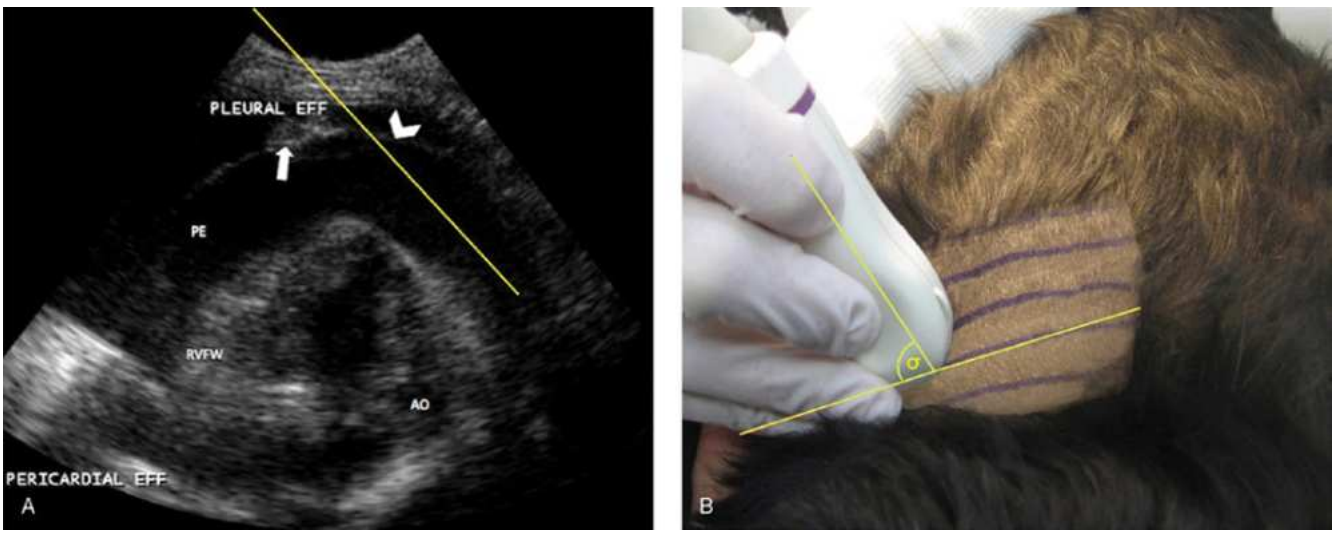


**Figure 43.2.** Indirect ultrasound-guided pericardiocentesis in a dog with pericardial and pleural effusion. (A) Right parasternal short-axis view at the level of the cardiac base of a 10-year-old female spayed miniature schnauzer with a history of idiopathic pericardial effusion (PE) of eight months' duration. In real time, the patient was in cardiac tamponade with secondary pleural effusion (denoted as PLEURAL EFF by the sonographer). Right ventricular free wall (RVFW) and aorta (AO). The arrowhead demonstrates the thin echogenic pericardium. A small amount of pericardial fat is seen (*arrow*). The image is labeled by the sonographer in the lower left-hand corner as pericardial effusion. The yellow line indicates the imaginary needle–pericardiocentesis trajectory path. A formal echocardiogram ruled out the macroscopic presence of cardiac neoplasia. The patient recovered well from a subsequently performed pericardial window. Source: Image courtesy of Dr Jennifer Gambino. (B) Probe-to-skin angle (σ) identifying the widest pericardial fluid accumulation, which also represents the imaginary needle–pericardiocentesis trajectory angle.

**Figure 43.3.** Free-hand ultrasound-guided probe orientation for pericardiocentesis. Place the ultrasound probe parallel to the ribs 1–3 cm below the determined pericardial site at an angle of approximately 60° to the skin. The catheter-to-skin angle is approximately 60° which creates a catheter-to-probe angle of approximately 60°.

**Pearl:** Preparing a pericardiocentesis kit in a large, clear bag along with the written list of inventory on a card saves invaluable time when emergent pericardiocentesis is needed and keeps the kit stocked.

## *Procedure for Performing Pericardiocentesis*

The pericardial space has historically been approached from the right side for anatomical reasons, including the minimization of left coronary artery laceration and lung trauma (cardiac notch). The procedure, however, may be successfully performed from the left side, although conversely, the left coronary artery (major heart artery) is more vulnerable and there is more lung (no window through the cardiac notch). The difference in right- versus left-sided approaches is a more important consideration in smaller effusions, with a right-sided approach considered safer.

- Place an intravenous (IV) catheter in case complications develop that may require IV volume expansion or the emergent control of arrhythmias using injectable medications.
- The patient may be given light sedation if needed. Opioids are generally safest because they are cardiovascularly sparing and may be reversed with naloxone.
- Connect the patient to an ECG continuous monitor as ventricular arrhythmias may occur if the catheter or stylet contacts the heart during the procedure.
- For right-sided pericardiocentesis, the patient is placed in sternal or left lateral recumbency.

**Pearl:** Some clinicians prefer to place the patient in right lateral recumbency on an echocardiography table and perform the procedure from the underside of the patient through the table's cut-out window because gravity assists in moving the heart, pericardium, and pericardial fluid closer to the thoracic wall while displacing the lung to either side of the heart.

- The procedure should be performed aseptically using sterile technique and sterile gloves.
- Clip hair and aseptically prep the skin on the right side of the thorax from the third to seventh intercostal spaces, extending 3–4 inches ventrally and dorsally from the costochondral junction.
- Confirm the pericardiocentesis site using ultrasound. This is typically the widest accumulation of fluid located near the fifth intercostal space at the costochondral junction. However, the optimal location may vary depending on the volume and where the widest accumulation of pericardial fluid exists (see Figure 43.2).
- Attach a 14–16 gauge, 2–6 inch over-the-needle catheter, depending on the size of patient, to an extension set, three-way stopcock, and 6, 12, 20, 35 or 60 cc syringe, dependent on patient size. Some clinicians prefer to use a smaller syringe (i.e., 10 cc) for the initial aspiration, which they set aside so that a sample of the pericardial effusion has been saved (see below for sample collection).
- One or two additional side-holes may be cut in larger bore catheters to improve drainage of the pericardial space. Care must be taken to preserve the integrity of the catheter, ensuring that the tip does not break off and remain within the pericardial sac.

**Pearl:** It is recommended to stagger and not to exceed 50% of the circumference of the catheter when making additional side-holes. Often, creating side-holes is *not* necessary.

- Apply a local lidocaine block at the pericardiocentesis site determined by ultrasound. Lidocaine should be infused into the subcutaneous space and intercostal muscles down to the level of the pleura.
- Make a small stab incision through the lidocaine-infiltrated skin using a #11 scalpel blade to facilitate advancing the pericardial catheter through the soft tissues.

**Pearl:** Making a stab incision through the skin helps prevent burring of the catheter and facilitates easier advancement of the catheter and stylet through the skin surface, subsequently allowing better catheter control.

- Place the ultrasound probe parallel to the ribs at the previously determined intercostal space noted to contain the widest accumulation of pericardial fluid.
- Gently rock and fan the probe back and forth to determine the safest imaginary needle trajectory path (see Figure 43.2).

At this time, either indirect or free-hand ultrasound-guided techniques can be used to complete the procedure. Follow the steps below depending on which of these two techniques is preferred.

### *Indirect Ultrasound-guided Pericardiocentesis*

1. Make a mental note of the site, angle, and imaginary needle–pericardiocentesis trajectory path to follow with the catheter and stylet.

**Pearl:** The stylet and catheter should be passed on the cranial side of the rib to avoid nerves and vessels on the caudal aspect of the ribs.

2. Using the angle determined by ultrasound (see Figure 43.2B), penetrate the skin and subcutaneous tissue with the catheter and stylet at the same angle.
3. Apply gentle negative pressure to the syringe when the stylet and catheter have been advanced into the subcutaneous tissues.
4. Continue to advance the catheter and stylet along the imaginary needle–pericardiocentesis trajectory path until fluid is noted within the hub of the stylet and extension tubing.
5. Continue to step 7.

### *Free-hand Ultrasound-guided Pericardiocentesis*

1. Slide the ultrasound probe 1–3 cm below the perceived site where the stylet and catheter will be advanced through the skin and subcutaneous tissues.
2. Fan the probe such that it will be at a 60–90° angle to the imaginary needle–pericardiocentesis trajectory path.

**Pearl:** If the desired imaginary needle–pericardiocentesis trajectory path is more perpendicular to the skin, the ultrasound probe-to-skin angle can be decreased, but image quality may diminish with decreased probe-to-skin contact.

3. Following the predetermined skin site and imaginary needle–pericardiocentesis trajectory path, advance the stylet and catheter through the skin into the subcutaneous tissues. The ultrasound probe should be at a 60–90° angle to the catheter and stylet (see Figure 43.3). The catheter and tip of the stylet should be visible within the subcutaneous tissues.
4. Apply gentle negative pressure to the syringe when the stylet and catheter have been advanced into the subcutaneous tissues.
5. Use real-time ultrasound guidance to advance both the stylet and catheter through the tissues until the catheter tip is seen to enter the pericardial space. Be sure to keep the stylet and catheter in plane with the ultrasound probe.

**Pearl:** The catheter tip may be easier to visualize if the bevel is directed towards the ultrasound probe (see Pearls and Pitfalls below).

6. Continue to step 7.

### *Completing Both the Indirect and Free-hand Ultrasound-guided Pericardiocentesis Techniques*

7. As the tip of the stylet enters the pericardial sac, fluid should be observed in the hub of the stylet and extension set. Pericardial fluid is typically dark red similar to venous blood.
8. Once the stylet has penetrated the pericardial space, advance the stylet and catheter another 2–4 mm to ensure the catheter, in addition to the

stylet, has entered the pericardial space. *Do not advance the sharp stylet any further*.

9. Advance the catheter off the sharp stylet and into the pericardial space. It is not always necessary to completely advance the catheter into the pericardial sac; however, it should be at least advanced a few centimeters to ensure that it is well seated within the pericardial sac along with all of the catheter's side-holes, if present.

**Pearl:** If sustained ventricular arrhythmias should occur during pericardial catheter advancement, retract the catheter slightly. If this fails to resolve the arrhythmia, administer a bolus (2 mg/kg) of lidocaine intravenously. Most ventricular arrhythmias are intermittent and self-limiting.

10. Once the catheter is seated within the pericardial sac, disconnect the extension set from the stylet, remove the stylet from the catheter, and reconnect the extension set to the catheter.
11. Drain fluid from the pericardial sac into an appropriate receptacle (i.e., kidney bowl) using the three-way stopcock and syringe.
12. Aseptically collect samples of the fluid into red (plain) and lavender (EDTA) topped tubes for further analysis. An additional red top tube sample should be collected to observe for clot formation because hemorrhagic pericardial effusions should typically not clot. If clotting is observed then fresh blood contamination should be suspected and the complication of aspiration of one of the cardiac chambers (most likely the right atrium) or coronary artery laceration may have occurred.

**Pearl:** Immediately filling and serially observing a red top tube filled with aspirated fluid helps ensure inadvertent puncture of a cardiac chamber has not occurred (pericardial effusion should not clot).

## Postpericardiocentesis Use of Ultrasound for Tracking (Monitoring)

- Following the procedure, reevaluate the pericardial sac ultrasonographically to be sure cardiac tamponade has resolved and note the presence and quantity of any residual pericardial fluid by caliper measurement (or approximated by using the scale on the right-hand side of the ultrasound screen) of the greatest width (cm).

**Pearl:** Leaving a small volume of pericardial effusion provides an acoustic window if complete echocardiography in search of a mass (neoplasia, foreign body, etc.) is to be performed subsequently.

- Repeat the ultrasound evaluation in 12–24 hours (or sooner as clinical course dictates) to look for reaccumulation of pericardial fluid. Remeasuring the width (cm) of pericardial effusion is helpful in determining if fluid is reaccumulating in the pericardial space.

**Pearl:** Some patients have concurrent pleural effusion present, which typically appears straw-colored and is often encountered as the catheter and stylet pass through the pleural space prior to entering the pericardial sac.

- If there are concerns for recurrence of pericardial effusion, a small-bore chest tube can be guided into the pericardial space using a guidewire Seldinger technique; a guidewire is passed through the 14–16 gauge pericardiocentesis catheter to enter the pericardial space prior to removal of the catheter. The small-bore chest tube is then passed into the pericardial space along the guidewire in a manner similar to placement of a small-bore Seldinger technique chest tube. Subsequently, intermittent aspirations can be performed as clinically indicated, usually every 4–6 hours, until the fluid return over a 24-hour period has decreased to less than 25 mL and follow-up two-dimensional echocardiographic assessment is satisfactory (Tsang et al. 2002**)** (Figure 43.4).

## Pearls and Pitfalls regarding Ultrasound-guided Pericardiocentesis

- Ultrasound-guided pericardiocentesis allows the operator to visualize the catheter tip as it traverses the pleural space, thus avoiding confusion of pleural with pericardial fluid when both are present (see Figure 43.2A).
- In patients with cardiac tamponade without respiratory distress, pericardiocentesis should take priority over evacuation of pleural fluid; the assistant should be instructed to release negative pressure on the syringe until the tip of the stylet is visualized within the pericardial space, at which point negative pressure is applied.

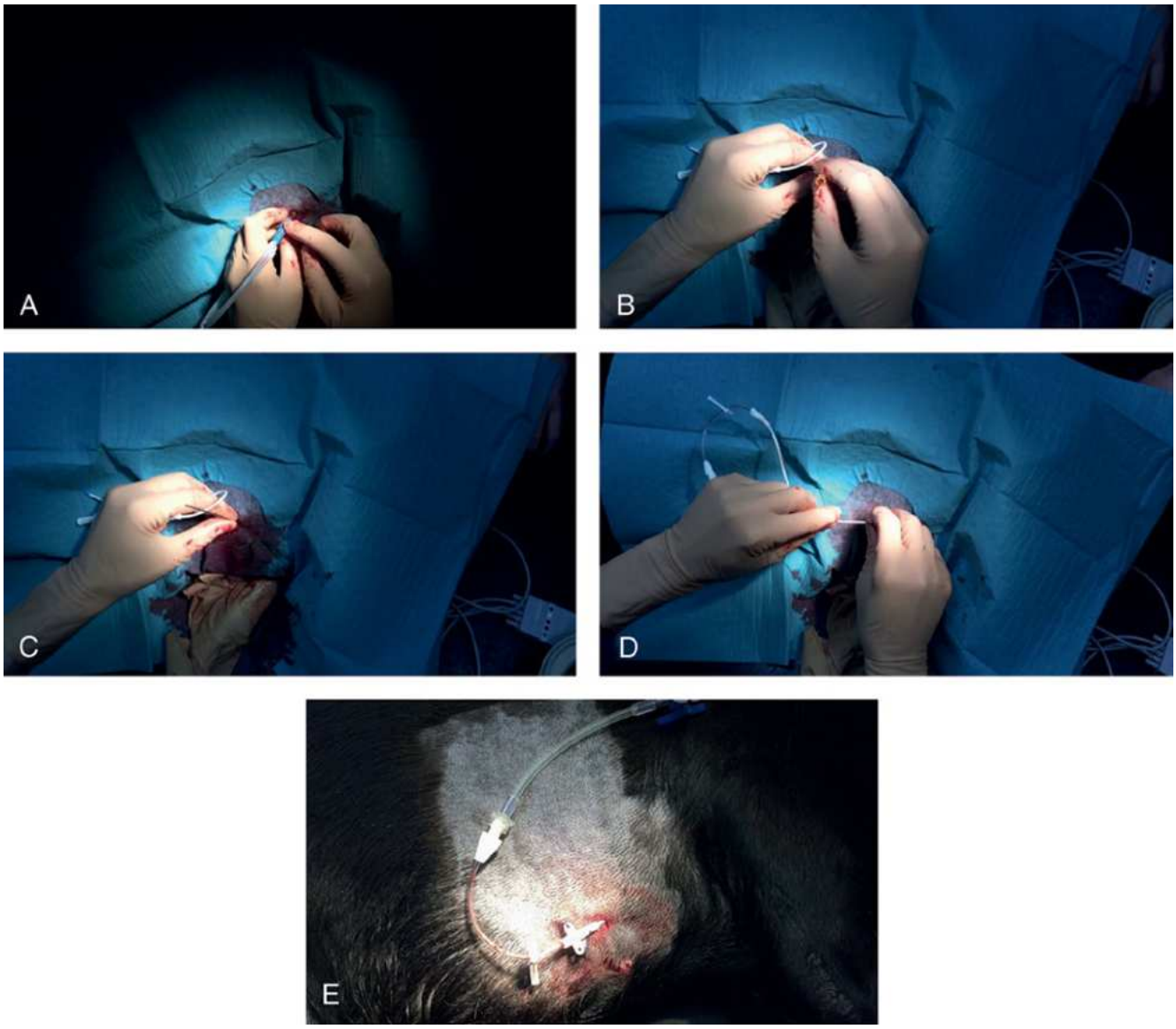


**Figure 43.4.** Seldinger technique used to place an indwelling small-bore chest tube into the pericardial space for repeated sampling as needed. (A) Following aspiration of pericardial fluid using a 14 gauge over-the-needle catheter, a guidewire can be connected to the catheter hub and advanced into the pericardial space. (B) Image of the guidewire and catheter after advancement of the guidewire into the pericardial space. (C) The catheter used to perform the initial pericardiocentesis is removed, leaving only the guidewire traversing the skin, pleural space and pericardial sac, with the guidewire tip located within the pericardial space. (D) The small-bore chest tube is advanced over the guidewire into the pericardial space. (E) Following placement of the chest tub,e the guidewire is removed and the chest tube can be sutured to the skin to allow repeated pericardial space aspiration as clinically indicated. Source: Reproduced with permission from Dr Bert Jan Reezigt, DVM, Sweden.

**Pearl:** Evaluation of the caudal vena cava (CVC) and any change in CVC diameter with the respiratory cycle can be evaluated to help decide if tamponade is present or not (see Chapters 17–21, 36 and 37).

- Patients that have clinically relevant pleural and pericardial effusions may have thoracocentesis and pericardiocentesis performed simultaneously.
- When continuous negative pressure is applied during catheter advancement in patients with pleural and pericardial effusions, the fluid will often

change in color from straw (typical pleural) to dark red (typical pericardial) as the catheter and stylet are advanced from the pleural space into the pericardial sac.

# Thoracocentesis

## Introduction

Thoracocentesis is a minimally invasive diagnostic or therapeutic procedure used to remove fluid or air from the pleural space. In the emergent veterinary patient with life-threatening pleural effusion or PTX, the objective is to remove pleural fluid/air and stabilize the patient as quickly as possible. Blind thoracocentesis is usually the method of choice in these circumstances.

In the more stable patient, ultrasound has the advantage of identifying the optimal puncture site, improving success rates, and, most importantly, minimizing the complications of the procedure (Nicolaou et al. 2007). Studies in human medicine have shown higher success rates for pleural effusions when using ultrasound-guided compared to blind thoracocentesis, and that following failed blind thoracocentesis attempts, ultrasound-guided thoracocentesis was successful in 88% of these patients (Weingardt et al. 1994). Complication rates with blind thoracocentesis in humans with pleural effusion vary from 20% to 50% and include PTX, inadvertent placement of the needle into the abdominal cavity across the diaphragm or into consolidated lung, or misplacement of the needle above fluid accumulations (Dewitz and Frazee 2003; Jones et al. 2003). Although complications are still possible with ultrasound guidance, rates in humans are reported to be lower when compared to blind techniques (Jones et al. 2003). For example, the incidence of postthoracocentesis PTX in humans with pleural effusion is reported to be 1.3–2.5% versus 4–30% for ultrasound-guided and blind techniques, respectively (Jones et al. 2003).

Despite the value of ultrasound in detecting PTX, given ultrasound does not image through air, there is little benefit in performing ultrasound-guided over blind thoracocentesis in cases of PTX (free air in pleural space). However, the glide sign, referred to as lung sliding in human medicine, should be assessed before and following thoracocentesis as the loss of a previously visible glide sign following thoracocentesis indicates iatrogenic PTX. In human medicine, the finding of a glide sign following thoracocentesis for PTX obviates the need for chest radiography to rule out PTX.

Pleural effusion must be differentiated from pericardial fluid and cardiac chambers as well as other intrathoracic structures including masses and intraabdominal structures in case of occult diaphragmatic herniation.

**Pearl:** Use multiple views including at least a single pericardial view and the diaphragmatico-hepatic (DH) view of FAST to help distinguish pleural effusion from pericardial effusion and cardiac chambers (see Chapters 17–21).

## Indications for Thoracocentesis

- To provide a therapeutic benefit whenever pleural effusion (fluid in the pleural space) or PTX (air in the pleural space) are present and causing respiratory compromise or distress.
- For diagnostic purposes to characterize pleural effusion.

## Contraindications to Thoracocentesis

- An uncooperative patient, although this can typically be managed with sedation/anesthesia.
- Severe coagulopathy, although this can typically be managed with blood products prior to thoracocentesis.
- A pleural effusion considered too small to be safely aspirated.

## Potential Complications of Thoracocentesis

- Pain (easily controlled with local blocks and systemic analgesia).
- Pneumothorax (probably more common with chronic long-standing pleural effusion).
- Reexpansion pulmonary edema (rare).
- Inadvertent lung, heart, liver or splenic puncture.
- Hemothorax from laceration of intercostal or other vessels (avoidable by performing centesis at the cranial rib margin).
- Infection (rare if aseptic technique is used).
- Subcutaneous emphysema (rare).
- A sheared-off catheter in the pleural space (ensure any added drainage holes are <50% of the catheter width and they occur on alternating staggered sides of the catheter if added).
- Subcutaneous hematoma (rare).

## Scanning for Pleural Effusion to Perform Thoracocentesis

The optimal puncture site is located by identifying the largest pocket of fluid superficial to the lung, and scanning throughout a full respiratory cycle. Scanning through a full respiratory cycle is recommended as structures such as the lung and/or diaphragm may enter and leave the ultrasonographic field of view during different phases of respiration. In addition to lung, other vital structures such as the heart and great vessels may lie in proximity to focal fluid accumulations, which can be avoided by direct visualization using ultrasound.

1. The ultrasound probe is placed on either side of the thorax, perpendicular to the ribs, and moved cranially and caudally over several intercostal spaces in the lower third of the thorax.
2. Following identification of the intercostal space containing the deepest fluid pocket, the ultrasound probe is then moved dorsally and ventrally at this site to further clarify the deepest fluid pocket.
3. Once this site has been identified, the ultrasound probe can once again be moved cranially and caudally to reconfirm the deepest fluid pocket and identify the presence of any obvious adjacent structures that should be avoided (heart, great vessels, lung, diaphragm, liver).

**Pearl:** The depth of the fluid pocket will help determine the chance of success because smaller fluid accumulations are more difficult to access.

4. A measurement of the depth of the fluid pocket should be made or easily approximated using the centimeter scale to the right of the ultrasound screen to help guide the length of needle or catheter insertion to safely use for thoracocentesis.

**Pearl:** Freeze the image to take an accurate caliper measurement (cm) from the skin surface to the desired location within the pleural fluid accumulation or approximate using the centimeter scale on the right side of the ultrasound screen.

5. The width of the pleural fluid may vary during the respiratory cycle and should be assessed with ultrasound to minimize complications and maximize success.

**Pearl:** Changing the ultrasound probe angle during the respiratory cycle and moving the needle tip away from aerated lung will help minimize lung puncture when pleural fluid depths change during the respiratory cycle (Lichtenstein et al. 1999).

## Materials Checklist for Thoracocentesis

- Clippers and antimicrobial scrub.
- An 18–22 gauge 1–2 inch butterfly needle, IV catheter or hypodermic needle.
- Intravenous extension set if using an IV catheter or hypodermic needle.
- Three-way stopcock.
- 10–60 mL syringe dependent on patient size and the amount of pleural effusion present.
- Receptacle for fluid collection (i.e., kidney bowl).
- Ultrasound machine and appropriate ultrasound probes.
- Sterile culturettes.
- Lidocaine for a local anesthetic block if elected.
- Sedation if needed.

**Pearl:** Preparing a thoracocentesis kit in a large, clear bag along with the written list of inventory on a card saves invaluable time when emergent thoracocentesis is needed and keeps the kit stocked.

## Procedure for Performing Thoracocentesis

- Thoracocentesis should be performed using aseptic technique.
- Any existing coagulopathies should ideally be corrected prior to performing the procedure unless the patient is in overt respiratory distress in which case urgent life-saving thoracocentesis should be performed.

**Pearl:** In cases of hemothorax, blood may be collected and autotransfused back to the patient using in-line filters or blood administration lines.

- Some sedation is generally beneficial to calm the patient, decrease the need for restraint, and lessen the work of breathing in respiratory compromised patients.
- A local anesthetic block using lidocaine may be given but is not usually necessary. If a local anesthetic is used, the skin, subcutaneous tissue, rib periosteum, intercostal muscles, and parietal pleura should be

infiltrated. Real-time ultrasonography using a high-frequency linear transducer can be used to identify structures and assist with infiltration.
- Patients may be placed in lateral or sternal recumbency depending on patient stability and clinician preference.

**Pearl:** Sternal recumbency is generally best for respiratory compromised patients because it is less stressful, allowing more comfortable breathing (versus lateral recumbency) and in the author's experience maximizes successful thoracocentesis.

1. With the assistance of ultrasound, look for the deepest pocket of fluid that is superficial to the lungs and not in proximity to vital structures such as the heart.
2. Use the location of the deepest fluid pocket to identify the side of the patient, the intercostal space, and how far ventrally or dorsally thoracocentesis may be performed.
3. Once the site of thoracocentesis has been identified, the skin should be clipped and aseptically prepped over this site. In cases of overt life-threatening distress, the hair can be parted and alcohol applied to the skin surface to allow for urgent thoracocentesis.

**Pearl:** Pressure atelectasis from pleural effusion follows pressure volume curves, thus clinical improvement can be substantial even if all fluid cannot be removed in difficult patients or circumstances.

4. Attach the three-way stopcock and syringe to the butterfly needle or attach an IV extension set, three-way stopcock and syringe to the hypodermic needle or stylet of the IV catheter depending on clinician preference.

The following technique will describe the use of a hypodermic needle attached to a three-way stopcock and IV extension set in both perpendicular and parallel ultrasound probe placement. When placed perpendicular to the ribs, the marker of the ultrasound probe is orientated cranially in standard fashion for the "gator sign" (see Chapters 17, 18, 22, and 23).

**Pearl:** To perform real-time ultrasound-guided thoracocentesis, the ultrasound probe may be orientated perpendicular to the ribs using the "gator sign" (Figure 43.5) or alternately parallel to the ribs.

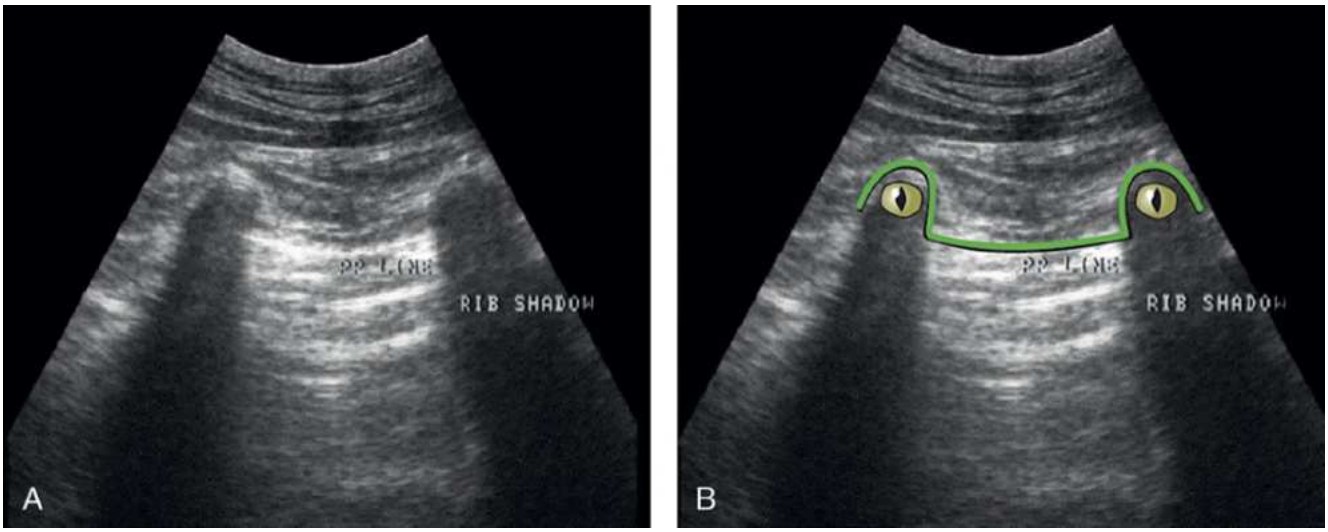


**Figure 43.5.** "Gator sign" orientation. When the probe is placed perpendicular (short-axis view of the needle) to the ribs, a classic "gator sign" image is formed as a result of the ribs (alligator's eyes) creating acoustic shadowing (rib shadow) on either side of the pleura (alligator's bridge of nose representing the intercostal space) at the site thoracocentesis is to be performed (see Chapters 17, 18, 22, and 23 for further details regarding the "gator sign"). (A) Unlabeled. (B) Labeled. Source: Reproduced with permission from Dr Greg Lisciandro, Hill Country Veterinary Specialists and FASTVet.com, Spicewood, TX.

### *Perpendicular Probe Placement Thoracocentesis*

Start by finding the "gator sign" orientation so that rib heads and the intercostals space are accurately identified (see Figure 43.5).

1. A 20–22 gauge needle attached to an IV extension set, three-way stopcock, and syringe is placed dorsal to the ultrasound probe at an angle of about 30° to the skin, bevel towards the ultrasound probe, starting about 1 cm dorsal to the probe.

**Pearl:** The needle will appear as a small white hyperechoic (bright white) dot when viewed in short axis (Figure 43.6A) with or without a ring-down artifact.

2. The needle should be inserted just caudal and dorsal to the center point of the ultrasound probe to avoid the nerves and vessels that run caudal to the ribs (Figure 43.6B). The orientation marker on the ultrasound probe is directed cranially.
3. As the needle is advanced through the skin, the needle tip will be visualized within the subcutaneous tissues.
4. An assistant can apply gentle negative pressure to the syringe at this time. As the needle is slowly advanced, the ultrasound probe is slid ventrally to follow the needle to the level of the parietal pleura. More specifically, using the dominant hand, the needle is slowly advanced through the subcutaneous tissues until the tip appears as a white dot on the ultrasound image. As soon as the tip of the needle is identified, advancement of the needle should be halted and held motionless. Using the nondominant hand, the ultrasound probe is then slowly moved ventrally off the needle tip until the tip is no longer visible within the ultrasound image. At this point, the probe is held stationary and the needle is again slowly advanced until the tip becomes visible in the ultrasound image. Once the tip is visualized, advancement of the needle is again halted and the procedure repeated until the tip of the needle can be seen advancing into the pleural space.

**Pearl:** The tip of the needle will typically indent the parietal pleura, which may be used to help orientate the ultrasound probe to better ultrasonographically locate the needle tip.

5. Once the needle tip is visible within the pleural space (see Figure 43.6A), fluid will be noted in the hub of the needle and IV extension set. To confirm the tip of the needle within the pleural fluid, the

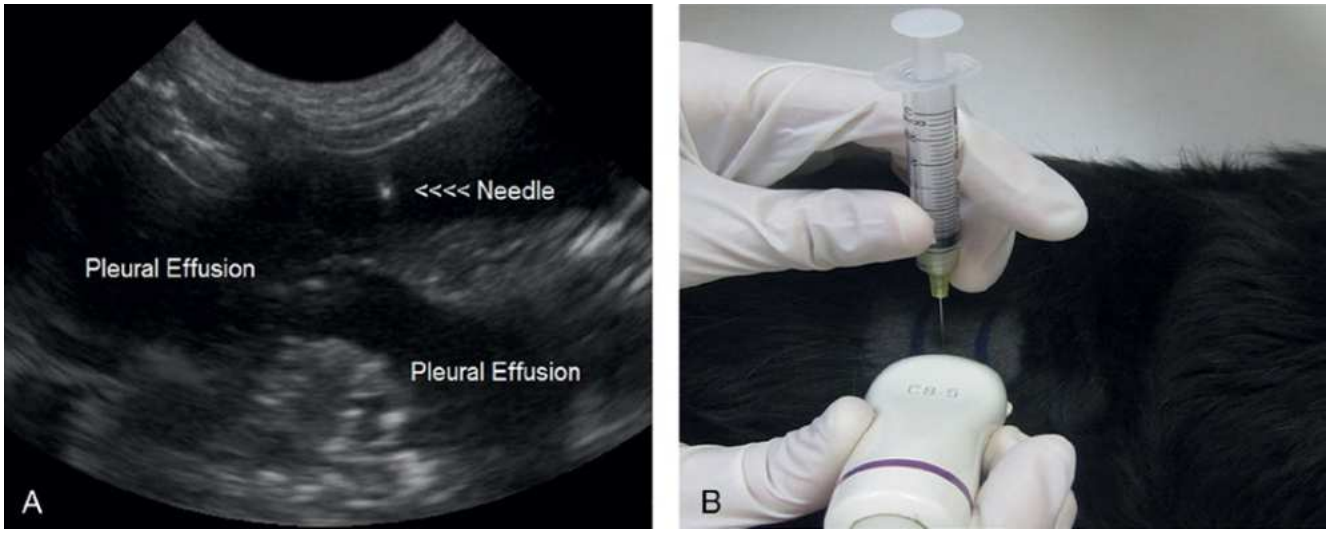


**Figure 43.6.** Free-hand ultrasound-guided thoracocentesis short axis. (A) The needle appears as a small white dot (*arrow*) on short-axis view. Source: Reproduced with permission from Dr Greg Lisciandro, Hill Country Veterinary Specialists and FASTVet.com, Spicewood, TX. (B) The ultrasound probe is placed at an angle of 90° to the skin, perpendicular to the ribs. The needle should be inserted at an angle of 30° to the skin (60° to the probe), just caudal and 1–2 cm dorsal to the center point of the probe, to avoid the nerves and vessels that run caudal to the ribs. The orientation marker on the probe is directed cranially.

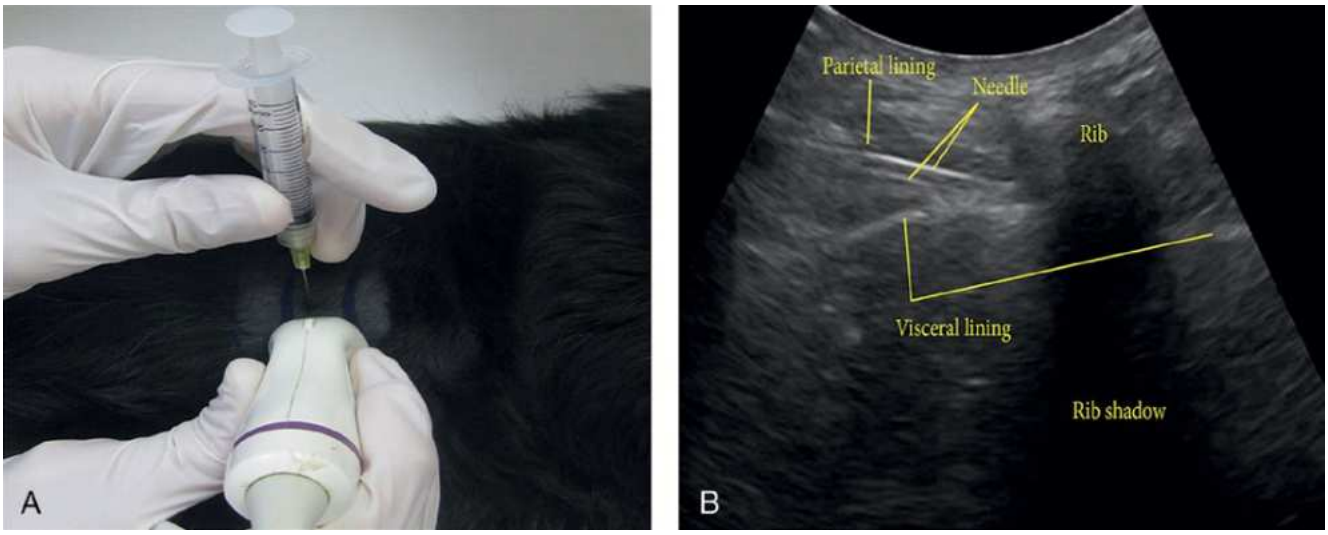


**Figure 43.7.** Free-hand ultrasound-guided thoracocentesis long axis. (A) The ultrasound probe is placed at 60° to the skin. The needle is orientated at 60° to the skin (60° to the probe) and should enter the thorax 1–2 cm dorsal to the probe with the bevel of the needle orientated towards the probe. (B) In the longitudinal plane, the needle appears as a long white structure between the pleura lining (parietal and visceral).

probe can be moved slightly proximal and distal to the needle. The needle tip will appear as a small white dot on short-axis view (see Figure 43.6A) with or without a ring-down artifact.

6. At this point, the needle can be angled ventrally so that it is lying against the thoracic wall with the bevel of the needle facing away from the thoracic wall.

**Pearl:** Take an accurate caliper measurement (cm) from the skin surface to the pleural line to help decide the length of needle required and/or the angle necessary to reach the pleural space. Alternatively, the depth can be approximated using the centimeter scale on the right side of the ultrasound screen.

### *Parallel Probe Placement Thoracocentesis*

1. When the ultrasound probe is placed parallel to the ribs (Figure 43.7A), care should be taken to avoid inserting the needle at the caudal rib margins as the nerves and vessels are located here. The needle should enter the center to caudal third of the intercostal space.
2. Ultrasonographically identify the widest fluid pocket (see above), which will be the site where the needle is inserted.
3. A 20–22 gauge hypodermic needle attached to an IV extension set, three-way stopcock, and syringe should enter the thorax at this site. The angle at which the needle enters the thorax will depend on the length of the needle relative to the width of the skin, subcutaneous tissues, and underlying muscles. A needle angle of 30–45° relative to the thoracic cage is often used but a 90° angle may be required in cases where the depth required to reach the pleural space is close to the length of the needle used.
4. Once the ideal centesis site is identified, orientate the ultrasound probe such that the orientation marker is directed dorsally and the probe is located just ventral to the site where the needle will be inserted.
5. The needle should enter the thorax 0.5 cm dorsal to the ultrasound probe with the bevel of the needle orientated towards the ultrasound probe (see Figure 43.7A). A lower needle angle will keep the needle more perpendicular to the ultrasound probe, increasing visualization of the needle/needle tip as it traverses the subcutaneous tissues and enters the pleural space, although the distance travelled by the needle to enter the pleural space will be longer (see Figure 43.7B). Alternatively, the tail of the ultrasound probe may be angled ventrally to orientate the probe more perpendicularly to the needle trajectory.
6. Once the needle/needle tip is seen to enter the subcutaneous space in real time, an assistant may apply gentle negative pressure while the needle

continues to be advanced through the intercostal muscles to the level of the pleura. The tip of the needle will typically indent the parietal pleura before piercing it and entering the pleural cavity.

7. As the needle tip is seen entering the pleural effusion, fluid should simultaneously enter the needle hub and extension set with the exception of viscous exudates. Now the needle should be angled ventrally towards the sternum so that it is lying against the thoracic wall with its bevel facing towards the pleural effusion and away from the thoracic wall.
8. In cases of a therapeutic thoracocentesis, aspiration of the pleural space should continue until negative pressure is established, as the patient allows.

Once fluid is obtained, samples should be collected into red (plain) and lavender (EDTA) topped tubes for diagnostic analysis. If a hemothorax (HTX) is suspected, a sample should be placed within a second red (plain) topped tube and checked after several minutes for clotting since most true noniatrogenic HTX will not clot. The sample should also be analyzed and the packed cell volume (PCV) compared to peripheral PCV for more definitive diagnosis of HTX. Clotting often indicates accidental aspiration of a vessel or a cardiac chamber.

**Pearl:** The diagnosis of HTX is made by a nonclotting sample with its PCV comparable to the peripheral PCV of the patient; it is very easy to visually overestimate the PCV by looking at a hemorrhagic sample – *always spin the fluid and measure the PCV*.

### Postthoracocentesis Use of Ultrasound for Tracking (Monitoring)

Ultrasound should be used post thoracocentesis for monitoring recurrence of the pleural effusion and any complications, including HTX and PTX. Measuring the widest aspect with the calipers or by approximation using the scale on the right-hand side of the screen provides more accurate assessments, especially if multiple veterinarians are involved in case management. As a general rule of thumb, stable postthoracocentesis cases should have TFAST and Vet Blue performed at least once fours hours post procedure (sooner if questionable or unstable) and then serially with time intervals determined by the patient's clinical course and the suspected condition (see Chapters 17, 18, 22, 23, 36, and 37).

**Pearl:** The use of ultrasound has been shown to be superior to chest auscultation and chest radiography in humans for pleural effusion, PTX, and many lung conditions (see Chapters 17, 18, 22, 23, 36, and 37).

## Abdominocentesis

### Introduction

Peritoneal effusion, also referred to as ascites, is always abnormal in mature dogs and cats; however, juvenile kittens and puppies may have small-volume effusions that are purely anechoic and considered normal (see Chapters 6, 7, and Section III). The process of aspirating or acquiring fluid from the peritoneal cavity is termed abdominocentesis. In general, veterinary patients with undifferentiated ascites should have their effusion characterized if acquisition may be safely performed at the attending veterinarian's discretion.

Although the complication rate with conventional blind abdominocentesis is low (0.9%) in humans, with hematoma formation being the most common complication, the morbidity associated with complications can be significant (Runyon 1986; Dewitz and Frazee 2003). False-positive results have been reported with accidental aspiration of abdominal organs such as the spleen or bowel, while false-negative results may be reported in cases where fluid is compartmentalized, present in small volumes, or the needle is entrapped within omentum or other intraabdominal organs (Bjorling et al. 1983; Crowe 1984; Walters 2003). The frequency of false-positive and -negative results can be reduced with real-time ultrasound-guided abdominocentesis; the trajectory path of the needle can be visualized throughout the procedure, allowing other abdominal organs to be visualized and avoided (Bard et al. 1986). Furthermore, ultrasound-guided abdominocentesis has a higher success rate when compared to blind abdominocentesis (Boysen et al. 2004; Lisciandro et al. 2009). This is especially true when there are small volumes of peritoneal fluid and when peritoneal fluid is compartmentalized (Nazeer et al. 2005; Patel et al. 2012).

### Indications for Abdominocentesis

- Characterization of ascites for diagnostic information.
- Characterization of ascites as being septic or sterile, with the former typically considered as life-threatening and an indication for emergent exploratory laparotomy.

- Therapeutic relief of symptoms such as respiratory compromise or distress or discomfort from large-volume ascites.

## Scanning Technique for Abdominocentesis

- The abdomen is quickly scanned, typically using the AFAST technique (see Chapter 6) to identify and localize fluid accumulations.
- In cases of suspected peritonitis based on physical examination and history, where a rapid AFAST scan is negative, additional emergency POCUS may be indicated (see Chapters 9 and 12). Using additional POCUS exams may help find otherwise occult small amounts of focal or localized ascites and any obvious intraabdominal abnormalities related to the effusion, such as hemoabdomen and splenic mass on POCUS spleen, peritonitis and mucocele on POCUS liver and gallbladder or peripancreatic fluid and pancreatic abnormalities on POCUS gastrointestinal and pancreas.

**Pearl:** AFAST should be performed after resuscitation and rehydration. As serial exams increase the sensitivity of FAST, repeat exams should generally be performed at least once four hours post admission in stable patients (sooner as clinical course dictates), and considered out to 12–24 hours.

## Materials Checklist for Abdominocentesis

- 20–22 gauge 1–2 inch hypodermic needles.
- Clippers for long-haired patients.
- Antimicrobial scrub and solution.
- Red (plain) and lavender (EDTA) topped tubes for sterile fluid collection.
- Sterile culturettes.
- 3 or 6 mL syringes.
- Ultrasound machine and appropriate ultrasound probe.

## Procedure to Perform Abdominocentesis

The following is a general overview regarding positioning, site preparation, and approximating needle length.

- Abdominocentesis may be performed with the animal in left or right lateral recumbency, dorsal recumbency or standing, depending on patient comfort and clinician preference.
- Abdominocentesis should be performed using aseptic technique.
- Free-hand ultrasound-guided abdominocentesis is typically preferred because it allows greater flexibility in choosing access sites and is not limited to a single plane.
- The abdomen should be rapidly scanned to identify the largest pocket of fluid, to ascertain the location of other abdominal organs in proximity to the fluid, and to help determine the possible cause of the abdominal fluid.
- The depth of the subcutaneous tissues and peritoneal fluid can be measured using the ultrasound machine's calipers or by approximating using the centimeter scale to the right of the screen to help ascertain the length of needle required, potentially improving patient safety.
- Once the largest fluid pocket has been identified, the abdominocentesis can be performed in longitudinal or transverse views.

The procedure for performing ultrasound-guided abdominocentesis is as follows.

1. Verify the location of the probe marker as it should be directed toward the head of the patient or to its right for longitudinal and transverse views, respectively, thus helping with orientation of the ultrasound probe relative to the needle.
2. For abdominocentesis in the longitudinal view, place the probe at a 60° angle to the skin with the ultrasound probe marker directed cranially (Figure 43.8).
3. Connect an 18–22 gauge hypodermic needle to a syringe.
4. Keeping the needle in plane to the ultrasound probe, angle the needle 30–50° to the skin and 1 cm from the side of the ultrasound probe with the probe marker (see Figure 43.8).
5. Point the bevel of the needle towards the ultrasound probe. Using real-time ultrasound-guided assistance, the tip of the needle can be visualized as it passes through the subcutaneous tissues and into the peritoneal cavity.

**Pearl:** If the needle is not visible ultrasonographically, the probe should be moved slightly to either side of the needle to try and visualize it. Rapid movement of the needle by advancing and retracting it a couple of millimeters may also help localize the needle as this will typically result in tissue movement in proximity to the needle.

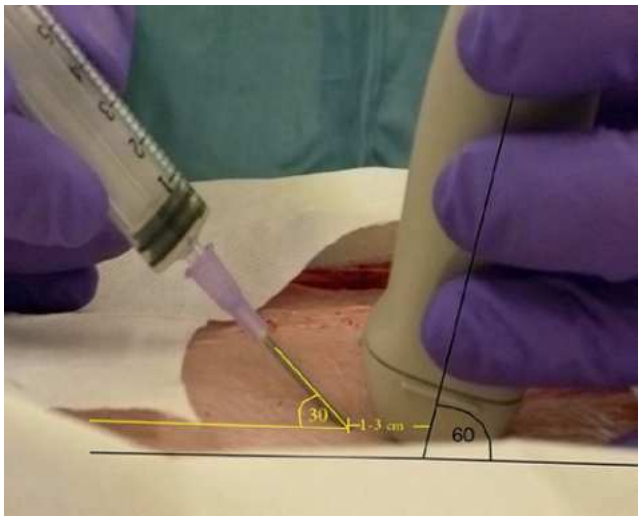


**Figure 43.8.** Free-hand ultrasound-guided abdominocentesis. The probe is positioned at an angle of 60° to the skin. Keeping the needle in plane to the ultrasound probe, angle the needle 30–60° to the skin (60–90° to the probe) 1–3 cm from the notched side of the probe.

6. Look for the tip of the needle as it often can be seen indenting the peritoneal lining before it enters the peritoneal cavity.

**Pearl:** The tip of the needle appears as a hyperechoic (bright) structure either as a dot or line with or without ring-down artifact (see Figures 43.6A, 43.7B).

7. Track the trajectory of the needle tip until it is lying within the peritoneal fluid to be aspirated (Figure 43.9).
8. Once the tip of the needle is confirmed to be in the desired location, gentle pressure should be applied to the syringe. The presence of fluid in the needle hub and syringe helps confirm proper location of the needle tip.
9. Release negative pressure on the syringe before withdrawing the needle from the peritoneal cavity.

**Pearl:** Alternately, the needle may be left open without an attached syringe and fluid acquired through capillary and gravitational flow.

10. Collect sterile samples of peritoneal fluid into sterile red (plain) and lavender (EDTA) topped tubes.

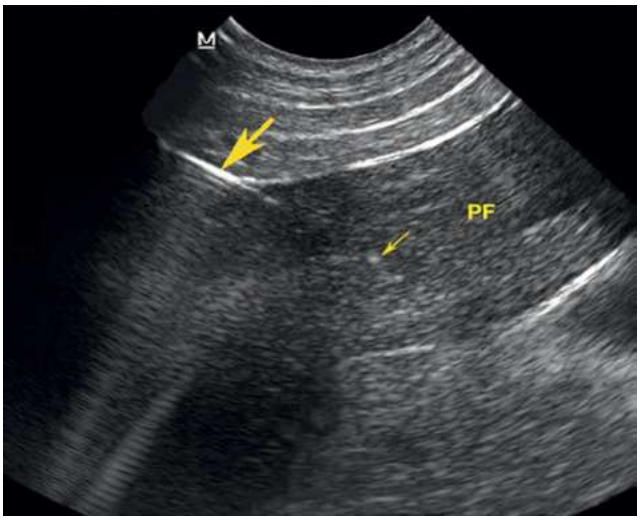


**Figure 43.9.** Free-hand ultrasound-guided abdominocentesis. The trajectory of the needle (*large arrow*) and needle tip (*small arrow*) should be tracked with ultrasound until it is lying within the peritoneal fluid (PF) to be aspirated. The peritoneal fluid in this patient is particulate and echogenic, suggestive of a cellular effusion such as an exudate or hemorrhage. A diagnosis of hemoabdomen was made based on evaluation of the aspirated abdominal fluid.

# Modified Ultrasound-guided Diagnostic Peritoneal Lavage

## *Ultrasound-guided versus Blind Diagnostic Peritoneal Lavage*

Diagnostic peritoneal lavage (DPL) has been advocated in cases of blunt and penetrating abdominal trauma, acute abdominal pain, and cases of suspected peritonitis when abdominocentesis has resulted in a negative tap (Walters 2003). Ultrasound has essentially replaced the need for DPL in most trauma patients. In humans, ultrasound has a similar sensitivity and specificity to DPL for diagnosing intraabdominal injury, but is less invasive, associated with fewer complications, and allows for collection of undiluted fluid samples via ultrasound-guided abdominocentesis even when the quantity of peritoneal fluid is very small (Tso et al. 1992; Singh et al. 1997).

However, ultrasound-guided abdominocentesis may not be feasible in clinical situations where peritoneal fluid is present in very small quantities, is walled off, or is located in proximity to vital organs. In these situations, DPL may still prove diagnostically useful. Unfortunately, complications and failure to obtain a fluid samples are common in veterinary and human patients undergoing traditional DPL. For these reasons, the author prefers to use a modified ultrasound -guided

diagnostic peritoneal lavage (MUG-DPL) technique, which is minimally invasive. Furthermore, MUG-DPL may reduce the complication rate while increasing the success rate of obtaining a fluid sample compared to blind traditional DPL techniques.

## Indications for MUG-DPL

The MUG-DPL technique is reserved for use in patients with acute abdominal pain or peritonitis with only small quantities of peritoneal fluid that cannot be aspirated by direct ultrasound-guided abdominocentesis, are unlikely to have advanced imaging, and samples of the fluid are urgently needed (and cannot wait for serial ultrasound exams).

In these patients, the quantity of peritoneal fluid is too small to tap or is located in proximity to vital organs that preclude direct ultrasound-guided abdominocentesis. By adding additional sterile fluid to the peritoneal cavity, it may be possible to identify and characterize small amounts of preexisting peritoneal fluid or inflammation.

**Pearl:** Serial AFAST examinations after resuscitation and rehydration will often detect larger and more accessible fluid pockets in cases of initially ultrasound-occult peritonitis.

**Pitfall**: MUG-DPL and traditional DPL will confound serial imaging because of the introduction of free fluid and possibly free air and should be delayed if the patient is stable and computed tomography (CT) or other imaging modalities are required.

## Scanning Technique for MUG-DPL

See scanning technique for abdominocentesis (this chapter) and Chapter 12.

## Ultrasonographic Findings

Findings are similar to abdominocentesis findings, although the quantity of fluid will be very small and/or localized to an area that is not easily accessible by direct ultrasound-guided abdominocentesis (Figure 43.10).

## Materials Checklist for MUG-DPL

- Ultrasound machine and probes.
- Sterile, warmed 0.9 % saline.

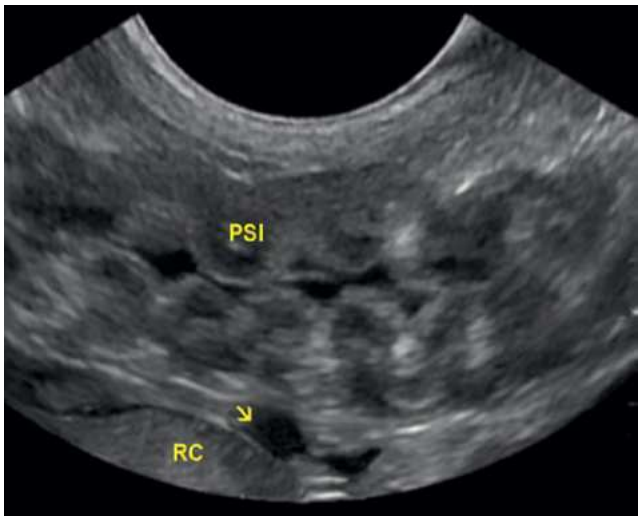


**Figure 43.10.** Indications for MUG-DPL. Small quantity of fluid (*arrow*) adjacent to plicated small intestine (PSI) and the renal cortex (RC) that is inaccessible to ultrasound-guided abdominocentesis due to the small quantity and its location.

- Intravenous fluid administration set.
- 16–22 gauge 1–4 inch over-the-needle catheters.
- Clippers.
- Antimicrobial scrub and solution.
- 3–6 mL syringes.
- Red (plain) and lavender (EDTA) topped tubes.
- Culturettes
- #11 scalpel blade
- Lidocaine for local anesthetic block if needed.

## Procedure to Perform MUG-DPL

The following is a general overview regarding positioning, site preparation, chemical restraint and local anesthesia, and approximating needle length.

- Aseptic technique should be used and coagulopathies should be ruled out or corrected prior to performing MUG-DPL.
- Sedation and/or local anesthetic blocks may be used to calm the patient, although it is not usually necessary unless large-bore catheters are used.
- The patient can be placed in left or right lateral or dorsal recumbency depending on patient comfort and clinician preference.
- Ultrasonography is used to localize small pockets of free abdominal fluid or areas of suspect focal peritonitis (see Chapter 12 on findings of focal peritonitis) that cannot be aspirated using ultrasound-guided techniques.

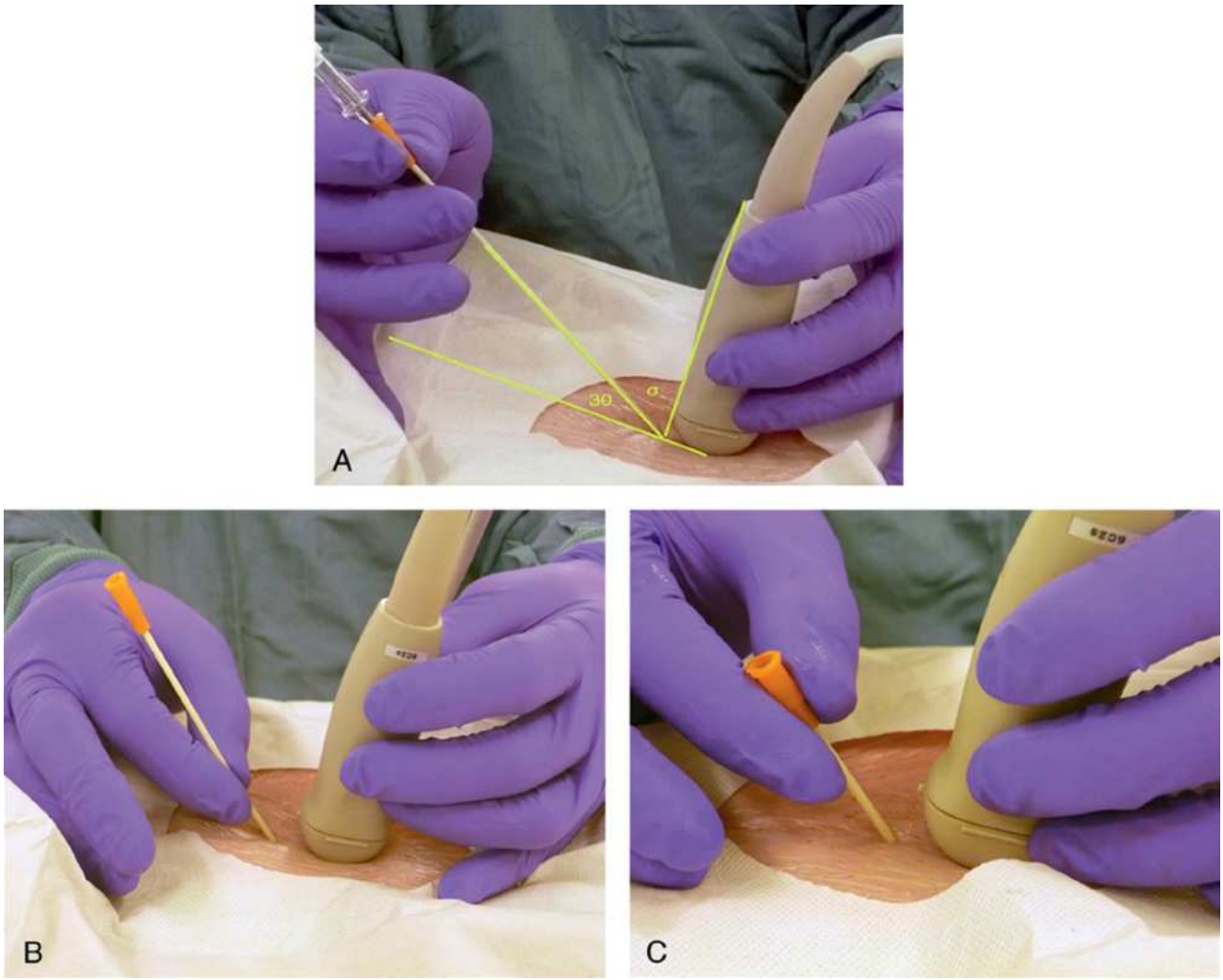


**Figure 43.11.** MUG-DPL procedure. (A) A 60° angle (σ) between the probe and catheter for placement of a 16 gauge 4 inch over-the-needle catheter and stylet into the peritoneal cavity. In this diagram, the probe is positioned at 90° to the skin and the catheter and stylet are placed at approximately 30° to the skin. (B) The catheter is advanced off the stylet and directed towards the identified focal fluid accumulation. (C) Final placement of the catheter prior to fluid administration.

The procedure for performing MUG-DPL is as follows.

1. The skin is clipped and aseptically prepped over the site where peritoneal fluid was noted with ultrasound.
2. Using a similar technique to performing abdominocentesis, free-hand ultrasound guidance is used to pass an over-the-needle catheter (16–20 gauge, 1–4 inch depending on the size of the patient and location of peritoneal fluid) and stylet into the peritoneal cavity towards the identified focal fluid accumulation, taking care to avoid abdominal organs (Figure 43.11A).
3. Additional side-holes may be made in the catheter although care should be taken not to damage the integrity of the catheter because it may break off, leaving the tip in the abdominal cavity.

**Pearl:** If 1–3 side-holes are added, it is recommended to stagger the holes and not to exceed 50% of the circumference of the catheter.

4. A small stab incision can be made into the skin of the abdomen using a #11 scalpel blade, but is not usually necessary unless a 16 gauge catheter or larger is used.

**Figure 43.12.** MUG-DPL fluid connection. A sterile bag of 0.9% warmed saline is connected to the catheter via an IV fluid administration set and approximately 3–5 mL/kg of saline is allowed to flow through the catheter via gravity.

**Figure 43.13.** MUG-DPL free-hand ultrasound-guided abdominocentesis. When sufficient fluid has been infused, the catheter is removed and a sample of fluid is directly aspirated from the area of interest using real-time ultrasound-guided abdominocentesis and a 20–22 gauge 1.5–2 inch hypodermic needle connected to a 3–6 mL syringe (see Abdominocentesis procedures).

5. Once the stylet and catheter tip are within the abdominal cavity, the catheter can be advanced off the stylet and directed as close to the area of interest as possible using real-time ultrasound guidance (Figure 43.11B). In some instances, it may be easier to reach the area of interest if the stylet is carefully advanced with the catheter.
6. Once the tip of the catheter is at the desired location, an IV extension set connected to a bag of warmed 0.9% saline solution is attached to the catheter (Figure 43.11C).
7. Approximately 3–5 mL/kg of sterile saline is allowed to flow through the catheter via gravity (Figure 43.12).

**Pearl:** The area of interest within the abdominal cavity can be monitored with real-time ultrasound as the sterile saline enters the abdomen to see if the infusate is reaching the site of interest.

8. If the infusate does not appear to reach the area of interest (no swirling of fluid or increase in size of the fluid pocket), or the size of the desired fluid pocket remains inaccessible via ultrasound-guided abdominocentesis, additional 3–5 mL/kg saline aliquots (up to 20 mL/kg) may be administered through the catheter via gravity until it becomes possible to obtain a sample of abdominal fluid that is continuous with the area of interest.
9. Monitor the patient for respiratory distress or discomfort when using larger quantities of sterile saline. Discontinue the infusion of fluid if discomfort or respiratory distress is noted.
10. If the fluid pocket is continuous between the area of interest and the catheter tip, as determined by real-time ultrasound, a sample can be directly aspirated via the catheter.

**Pearl:** To prevent excessive dilution and thus obtain a more representative sample of the site in question, the author often aspirates a sample of fluid from as close to the site of interest as possible *using a separate needle* and real-time ultrasound-guidance (see Abdominocentesis Procedure above and Figure 43.13).

11. Alternately, the infusion catheter is removed and a sample of fluid is directly aspirated from the area of interest using real-time ultrasound-guided abdominocentesis (see Ultrasound-guided Abdominocentesis) (see Figure 43.13). A 20–22 gauge, 1.5–2 inch hypodermic needle connected to a 3–6 mL syringe may be used. If the fluid is deeper than 2 inches, a spinal needle or the stylet from an intravenous catheter may be used with caution.

**Pearl:** If infusate does not appear to have reached the area of interest as determined by real-time ultrasound despite the maximum administration of 20 mL/kg, remove the catheter and reposition the patient by gently rolling from side to side. If necessary, reposition by standing or walking the patient while concurrently massaging and balloting the abdomen to help additionally redistribute the infused fluid.

12. Following the mixing of the infused fluid with preexisting free abdominal fluid or inflammation, ultrasonography is repeated and the opportunity to aspirate any visible fluid pockets (particularly those closest to the site of interest) with real-time ultrasound-guidance may be taken (see Figure 43.13). Fluid should be collected into red (plain) and lavender (EDTA) topped tubes and culturette for appropriate analysis.

# Pearls and Pitfalls, The Final Say

With the evolving use of ultrasound among non-radiologist physicians and veterinarians, the demand for newer technologies to improve the success of ultrasound-guided techniques has increased. Some final comments regarding ultrasound-guided techniques and improving needle visibility are briefly discussed here.

## *Factors Involving Needle Visualization*

Needle visualization is dependent on the complex interaction between the needle, the tissue type, and the degree of reflection of the ultrasound beam (McGahan 1986). The closer the echogenicity of the tissue is to the needle, the more difficult the needle is to visualize. Because fluid is anechoic, it provides a good contrast to the echogenicity of the needle, which often allows the needle or needle tip to be more readily visible within fluid-filled structures or spaces (McGahan 1986).

## *Needle Size*

In general, larger needles are easier to visualize ultrasonographically than smaller ones (Chapman et al. 2006). To improve visualization, several companies have created ultrasound needles that are scored or marked to provide a more intense reflection of ultrasound waves back to the probe, thus improving visualization of the needle (Figure 43.14).

**Figure 43.14.** Diagram of a notched needle to improve visualization. Several companies have created ultrasound needles that are scored or marked so that they will reflect more ultrasound waves back to the probe, improving visualization of the needle and accuracy of its placement.

## *Needle Bevel*

Pointing the bevel of the needle up towards the ultrasound beam has been reported to improve needle tip visualization by creating two echogenic foci at the needle tip as opposed to one (Bondestam 1992). The needle tip tends to be easier to visualize because it has an irregular surface as a result of the bevel being machine cut (Chapman et al. 2006). Moreover, the bevel is reported to be even more visually enhanced when the needle tip is within fluid.

## *Needle Angle*

The angle of the needle relative to the ultrasound beam also affects the ability to see the needle and its tip during ultrasound-guided centesis (Bradley 2001). Ultrasound waves reflected back from the needle or its tip will result in greater visibility of the needle during real-time imaging. The greatest number of ultrasound waves reflected back to the ultrasound probe occur when the needle is placed perpendicular to the probe. Unfortunately, most fluid-filled structures (with the exception of superficial vessels or lesions) are located too deeply to allow the needle to be passed in this manner. Experimentally, when aspirating deeper structures, the optimal needle/probe angle has been demonstrated to be 55–60° degrees (a needle–skin angle of 30° if the probe is perpendicular to the skin) with a distance between the needle insertion and probe of 2–3 cm (Bradley 2001).

## *Needle Movement*

Quick short 2–4 mm jabs of the needle facilitate visualization, as does rocking the ultrasound probe surface towards the needle. However, the benefit of rocking the probe will be lost if the skin–probe interface contact is diminished.

### Paying Attention to Needle and Probe

Looking at the ultrasound probe as well as the needle while performing free-hand ultrasound-guided procedures is helpful. For example, the needle should lie in the same plane as the ultrasound beam when using the longitudinal technique. To improve longitudinal visualization, the probe should be slowly moved above and below the longitudinal axis of the needle. As previously mentioned, it is helpful to also rapidly advance and withdraw the needle 2–4 mm as this creates visible movement of tissues adjacent to the needle. The probe angle can then be adjusted to attempt to maximize visualization at the site of tissue movement.

### Software Assistance

Finally, several companies have developed software (e.g., Sonix GPS, British Columbia, www.ultrasonix.com) that allows sensors within the ultrasound probe to track sensors placed within needles. These tracking systems allow predetermined trajectory tracks to be visualized on the screen and trace the needle outline as it is advanced through tissues, making exact location of the needle tip and needle much easier to see.

## References


Bard C, Lafortune M, Breton G. 1986. Ascites: ultrasound guidance or blind paracentesis? *Can Med Assoc J* 135(3):209–210.

Bjorling DE, Latimer KS, Rawlings CA, et al. 1983. Diagnostic peritoneal lavage before and after abdominal surgery in dogs. *Am J Vet Res* 44(5):816–820.

Bondestam S. 1992. The needle tip echo. *J Ultrasound Med* 11:253–256.

Boysen SR, Rozanski EA, Tidwell AS, et al. 2004. Evaluation of a focused assessment with sonography for trauma protocol to detect free abdominal fluid in dogs involved in motor vehicle accidents. *J Am Vet Med Assoc* 225(8):1198–1204,

Bradley MJ. 2001. An in-vitro study to understand successful free-hand ultrasound guided intervention. *Crit Radiol* 2001;56:495–498.

Callahan JA, Seward JB, Tajik AJ. 1985. Cardiac tamponade-pericardiocentesis directed by two-dimensional echocardiography. *Mayo Clin Proc* 60(5):344–347.

Celona B, Crino C, Guidice E, et al. 2017. Evaluation of pericardial effusion in dogs and successful treatment using a hemodialysis fistula needle: a retrospective study. *Top Compan Anim Med* 32(2):72–75.

Chapman GA, Johnson D, Bodenham AR. 2006. Visualization of needle position using ultrasonography. *Anaesthesia* 61:148–158.

Clarke DP, Cosgrove DO. 1987. Real-time ultrasound scanning in the planning and guidance of pericardiocentesis. *Clin Radiol* 38(2):119–122.

Crowe DT. 1984. Diagnostic abdominal paracentesis techniques: clinical evaluation in 129 dogs and cats. *J Am Anim Hosp Assoc* 20:223–230.

Del Cura JL, Zabala R, Corta C. 2010. US-guided interventional procedures: what a radiologist needs to know. *Radiologia* 52(3):198–207.

Dewitz A, Frazee B. 2003. Soft tissue applications. In: *Emergency Ultrasound*, edited by Ma OJ, Mateer J. New York: McGraw-Hill, pp 361–369.

Jones PW, Moyers JP, Rogers JT, et al. 2003. Ultrasound-guided thoracentesis: is it a safer method? *Chest* 123(2): 418–423.

Lichtenstein D, Hulot JS, Rabiller A, et al. 1999. Feasibility and safety of ultrasound-aided thoracentesis in mechanically ventilated patients. *Intensive Care Med* 25(9):955–958.

Lisciandro GR, Lagutchik MS, Mann KA, et al. 2009. Evaluation of an abdominal fluid scoring system determined using abdominal focused assessment with sonography for trauma in 101 dogs with motor vehicle trauma. *J Vet Emerg Crit Care* 19(5):426–437.

McGahan JP. 1986. Laboratory assessment of ultrasonographic needle and catheter visualization. *J Ultrasound Med* 5:373–377.

Nazeer SR, Dewbre H, Miller AH. 2005. Ultrasound-assisted paracentesis performed by emergency physicians vs. the traditional technique: a prospective, randomized study. *Am J Emerg Med* 23:363–367.

Nicolaou S, Talsky A, Khashoggi K, Venu V. 2007. Ultrasound guided interventional radiology in critical care. *Crit Care* 35(5):s186–s197.

Patel PA, Ernst FR, Gunnarsson CL. 2012. Evaluation of hospital complications and costs associated with using ultrasound guidance during abdominal paracentesis procedures. *J Med Econ* 15(1):1–7.

Runyon BA. 1986. Paracentesis of ascitic fluid. A safe procedure. *Arch Intern Med* 146(11):2259–2261.

Scansen BA. 2011. Interventional cardiology for the criticalist. *J Vet Emerg Crit Care* 21(2):123–136.

Singh G, Arya N, Safay R, et al. 1997. Role of ultrasonography in blunt abdominal trauma. *Injury* 28:667–670.

Taavitsainen M, Bondestam S, Mankinen P, et al. 1991. Ultrasound guidance for pericardiocentesis. *Acta Radiol* 32(1):9–11.

Tsang TS, Enriquez-Sarano M, Freeman WK, et al. 2002. Consecutive 1,127 therapeutic echocardiographically guided pericardiocentesis: clinical profile, practice patterns, and outcomes spanning 21 years. *Mayo Clin Proc* 77(5):429–436.

Tso P, Rodriguez A, Cooper C, et al. 1991. Sonography in blunt abdominal trauma: a preliminary progress report. *J Trauma* 33:39–44.

Walters JM. 2003. Lavage. *Clin Tech Sm Anim Pract* 18(1):32–38.

Weingardt JP, Guico RR, Nemcek AA Jr, et al. 1994 Ultrasound findings following failed, clinically directed thoracentesis. *J Clin Ultrasound* 22:419–426.

VetBooks.ir

# Further Reading

Brown D, Gaillot H. 2008. Heart. In: Atlas of Small Animal Ultrasonography, edited by Penninck D, d'Anjou MA. Ames: Blackwell Publishing, pp 151–208.

Field R. 2004. Ultrasound guided biopsies: tricks, needle tips, and other fine points. *Ultrasound Q* 20(3):91–99.

CHAPTER FOURTY-FOUR

# POCUS: Ultrasound-Guided Lung and Thoracic Sampling

Daniel Rodriguez

## Introduction

In order to feel comfortable performing an ultrasound-guided procedure, this chapter will discuss basic principles and artifacts that the sonographer should be aware of and specific transducer (probe) and needle positioning techniques to achieve the best results possible. There are many benefits associated with ultrasound-guided techniques, including improved target accuracy while minimizing complications using real-time monitoring when compared to blinded techniques (see also Chapters 24, 30–33, and 43). Ultrasound-guided procedures often provide a relatively quick way to obtain a diagnosis and at the same time avoid complications such as hemorrhage, pneumothorax, cardiac puncture, infection, etc. Furthermore, the use of color flow Doppler is important to avoid sampling masses of vascular origin or inadvertently puncturing large vessels or the heart, within the lesion itself or adjacent to it.

The use of ultrasound-guided procedures improves accuracy, is relatively quick in most instances, point-of-care without radiation exposure to the sonographer and procedure-associated healthcare worker(s), and patient, and is generally safe in experienced hands. The focus for this chapter is to describe the ultrasound-guided approach for peripheral lesions.

### *What POCUS: Ultrasound-Guided Lung and Thoracic Sampling Can Do*

- Facilitates the accurate sampling through visualization of the target of superficially located lesions involving the thoracic wall, mediastinum, pleural cavity, and lung.
- Acquires samples for histopathology and cytology and for culture and sensitivity.
- Expedites the diagnosis of different pneumonias, interstitial disease, and other forms of lower airway disease.
- May identify complications post sampling including pneumothorax, bleeding, pleural effusion, and congestive heart failure.

### *What POCUS: Ultrasound-Guided Lung and Thoracic Sampling Cannot Do*

- Sample lesions that are not superficial or are surrounded by air, making the lesions not ultrasonographically visible
- Replace proper training.

**Pearl:** If the targeted lesion is just beneath the lung surface on radiographs, the author usually places the patient in the same recumbency as the side of the lesion to create passive atelectasis for better lesion

*Point-of-Care Ultrasound Techniques for the Small Animal Practitioner*, Second Edition. Edited by Gregory R. Lisciandro.
© 2021 John Wiley & Sons, Inc. Published 2021 by John Wiley & Sons, Inc.
Companion website: www.wiley.com/go/lisciandro/ultrasound2

visualization. This maneuver may be successful if the distance between the targeted lesion to the lung surface is less than 0.5 cm.

### Indications

- Pneumonic processes that are ultrasonographically visible and accessible for sampling, thus directly targeted.
- Pneumonic processes nondiagnostic by bronchoalveolar lavage (BAL), endotracheal wash (ETW), and transtracheal wash (TTW).
- Sampling of small animals that are critically ill and hemodynamically fragile that pose excessive risk for a general anesthetic procedure, such as thoracotomy, thoracoscopy, and advanced imaging such as computed tomography (CT) and magnetic resonance imaging (MRI).
- Imaging pulmonary lesions undiagnosed or unrecognized via other procedures because lung ultrasound is extremely sensitive for lung surface pathology.

### Objectives

The objective is to obtain representative samples from thoracic and lung pathology in a safe and quick manner while avoiding complications and reducing the time and cost to get a diagnosis with other modalities of thoracic-related and lung pathology.

## Performing Ultrasound-Guided Lung and Thoracic Sampling

### Holding the Probe

Usually when doing a diagnostic ultrasound examination, the probe is held with the dominant hand; however, when performing ultrasound-guided procedures the nondominant hand is best used for holding the probe, while the dominant hand will be performing the procedure.

### Probe Orientation and Maneuvers

It is important to hold the probe firmly while doing the procedure without using excessive pressure that will not only fatigue your hand but also bother the patient, especially if only light sedation is used. The probe has a visible marker that will keep you properly oriented and also indicate the location relative to the probe where the needle is observed and guided. The probe can be maneuvered in four main ways: rotation, sliding, fanning, and rocking (see Chapter 4). These probe maneuvers will help you image the region of interest for nearby critical structures (fanning) and to center the target in the middle of the image (rocking) while creating a mental representation of the target in three dimensions. Knowledge of the regional anatomy is essential to optimize a successful ultrasound-guided procedure while minimizing complications and the reader is referred to a veterinary anatomy textbook and atlas.

### Relevant Artifacts

There are a few ultrasound artifacts of which the sonographer must be aware to accurately perform an ultrasound-guided procedure, and the reader is referred to Chapter 3 for more detail and illustrative examples.

#### Distal Acoustic Enhancement

This artifact occurs when the ultrasound beam encounters a fluid-filled structure or a structure that contains a homogeneous population of cells with a specific tissue component that will *not* attenuate the beam. The fluid-filled structure will appear anechoic or hypoechoic (darker) with a distal area of unattenuated beam that will appear hyperechoic (brighter) when compared to the surrounding tissue of attenuated ultrasound beam.

#### Reflection

This artifact creates generally a clean shadow beyond the reflector (needle) through the distal field of the image. The artifact is used to locate the metallic needle but will also be caused by bone and cartilage (ribs, sternum), and air (lung) because ultrasound does not transmit through these reflectors either.

#### Reverberation

This artifact occurs generally at the tip of the metallic needle (metallic reflector) or from adjacent structures like lung (air reflector) where the ultrasound beam reflects or bounces back to a second reflective surface several times before returning to the transducer (probe). As a result, multiple hyperechoic (bright white) lines are created that are evenly spaced beyond or deep into the reflector(s), referred to as ring-down

artifact or A-lines (air reverberation artifact). Air-filled lung, gas-filled gastrointestinal tract, and the metallic needle tip most commonly create examples of reverberation artifact.

#### Edge Shadowing

This artifact is a type of refraction that occurs along curved structures. When the ultrasound beam strikes the near-field edge of a curved structure such as the heart, end-on vessels or lymph nodes (intraabdominal examples include kidneys, stomach, gallbladder, and urinary bladder), the ultrasound beam redirects off the edge of the lesion, creating an anechoic shadow (black) that continues from the edge of the curved structure linearly through the far-field.

#### Mirror Artifact

Most commonly, the artifact is seen in the liver–diaphragm–aerated lung interface due to the curved shape of the diaphragm or the soft tissue–air interface of liver and lung with liver and gallbladder being mirrored, and in the far-field of the heart-lung interface with the heart being mirrored. As a result, a false representation or mirroring of the near-field structure will appear on the other side or past the reflector. The classic example involves the thorax and the liver–diaphragm–aerated lung interface in which the liver and gallbladder are mirrored on the thoracic side of or cranial to the diaphragm.

### *Optimizing Image Quality*

Optimizing image, using the "big four" features of focal zone, gain, frequency, and depth, should not be underestimated. Having a good image helps you better see the target and the ultrasound-guided needle, making for a safer procedure. First, position the focal zone (focus cursor and best to use a single focus cursor) across from the region of interest, and adjust the gain to best image the needle and target and its adjacent structures by first manipulating the time gain compensation (TGC) knobs, often featured on the right side of the machine as sliders, and then the overall gain knob. If the image is not acceptable, then next assess frequency. For instance, if the image is too dark, you may want to decrease your frequency to improve penetration. Frequency may be changed independently or through the machine's presets. Lastly, pay attention to depth and your centimeter scale for approximating distance and size(s) or structures. See Chapter 4 for more information on optimizing the image.

### *Optimizing Imaging and Tracking the Needle: In-Plane and Out-of-Plane*

There are two major ways of directing the needle using ultrasound guidance. The in-plane technique is most commonly used by the author. When using the in-plane technique, the needle and ultrasound beam are oriented in the same plane during the procedure from the needle insertion to its target. Careful orientation of the needle tip is important because if the angle of the needle with respect to the angle of the ultrasound beam is not ideal, the tip of the needle will be difficult to identify or not be seen. Optimizing the image must take into account the shape of the target and the angle of the needle to the ultrasound beam, which should be as close to perpendicular as possible. When using a linear probe with its rectangular shape, a shallow angle of about 20° with respect to the skin is required, whereas with a microconvex (curvilinear) probe, the needle angle often must approximate a 45° angle to create an ultrasound beam 90° to the needle (Figure 44.1). See subsequent comments in this chapter on probe types.

## Two Methods of Ultrasound Guidance: Free-hand and Using Probe Guides

### *Patient Preparation and Planning*

Thoracic radiographs are equally as important as the preparation and planning of the sampling procedure. Thoracic radiography not only will help choose the appropriate acoustic window for ultrasound imaging and the best target approach, but also help determine if the mass is close enough to the thoracic wall for ultrasound imaging, and what other structures are nearby, complementing your ultrasound imaging (Figure 44.2).

### *Skin Preparation*

The area to be sampled needs to be clipped and prepared aseptically. The supplies generally needed are shown in Figure 44.3. The need for sedation will depend on several factors and relies on clinical judgment:

- the area to be sampled
- the patient's demeanor
- the inherent risk of the procedure and what is being sampled

**Figure 44.1.** Free-hand sampling technique. (A) The cap of a hypodermic needle is used to create a small mark in the skin approximating the site of entrance of the needle. (B,C) Local anesthetic is deposited at the mark. This patient was nervous and intolerant of restraint so additionally had neuroleptanalgesia administered.

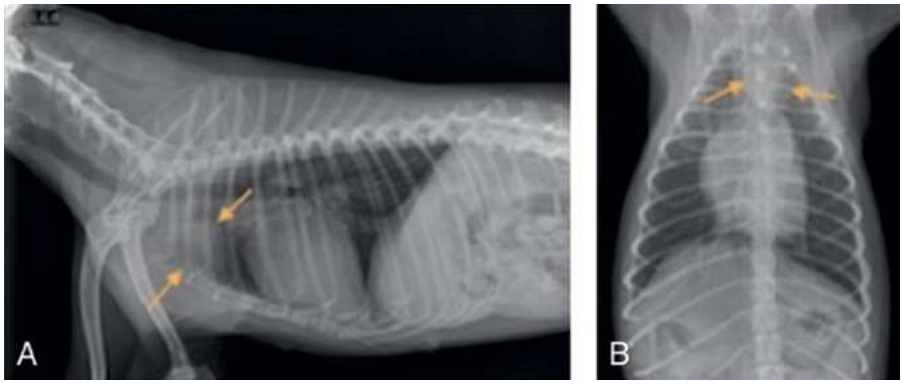


**Figure 44.2.** Cranial mediastinal mass radiographic assessment. Ultrasound combined with thoracic radiography as shown in (A) and (B) can locate the best approach to the target. Here, a left cranial thoracic approach appears to be best and the case was considered a good candidate for ultrasound-guided fine needle aspiration. Post procedure, a TFAST-Vet BLUE approach may be used to screen for complications including hemorrhage and pneumothorax along with use of the "lung point" (see Chapters 17, 18, 22, and 23).

- the type of ultrasound-guided procedure (fine needle aspirate or needle biopsy, versus core needle or Tru-Cut biopsy).

The use of coupling gel is not necessary and should be avoided to prevent contamination of the sample. Following aseptic technique of the skin, a small amount of 70% isopropyl alcohol is often sufficient for transient acoustic coupling of the probe.

## Probe Hygiene

The probe should be cleaned before the procedure according to manufacturer guidelines. If a core biopsy is to be taken, sterile technique including the probe is required to minimize infection. This may be done via two options: covering the probe with sterile gloves (see Chapter 24 for illustrative example) or use of commercially available sterile probe covers. Acoustic coupling gel (option 1) is needed between the probe and the glove-probe cover for transmission of ultrasound and optimization of image quality.

## Needle Selection

General considerations include the type and size of the targeted lesion(s). For instance, with small (<2 cm) cystic lesions, solid masses, vascularized lesions, or when lymphoma is suspected, fine needle aspiration (FNA) or needle biopsy is often adequate and safest

**Figure 44.3.** Fine needle aspiration set-up. Patient preparation and materials needed for a thoracic fine needle aspiration. (A) Sterile gloves, extension tube set, 22 gauge spinal needles, a few 3 and 5 cc syringes, microscope slides, and local anesthetic are generally the minimum materials needed. (B) The patient has been clipped and aseptically prepared for the procedure. (C) A Sharpie® maker may be used to designate the approximate needle entry site, indicated with an arrow.

using needles ranging from 20 to 25 gauge. The smaller needle gauges are often adequate for cyst aspiration and larger needle gauges for abscesses and solid lesions (20–22 gauge). Tissue core Tru-Cut biopsies generally include larger gauge needles (14–18 gauge). The use of larger gauge needles during core and Tru-Cut biopsies has been associated with an increased risk of complications such as hemorrhage (Haaga et al. 1983; Bigge et al. 2001). In the case of other thoracic sampling, ultrasound-guided techniques are used to sample pleural and pericardial fluid and lung, mediastinal and thoracic wall lesions that are superficial with an appropriate acoustic window of visualization, generally utilizing 20–22 gauge sizes.

The length of the needle necessary to acquire the ultrasound-guided sample must also be considered in addition to gauge. Either hypodermic needles or spinal needles are commonly used. The necessary needle length is best determined by the centimeter scale on the ultrasound image, or by taking measurements off thoracic radiographs, or both.

Additionally, the author attaches an extension tube to the needle to have more control during ultrasound guidance of the needle and prefers using the free-hand technique, especially if the target is smaller than 1.5 cm. Probe attachments that serve as needle and biopsy guides are commercially available. Probe guides are used more often by the author for ultrasound guidance to less superficial targets and while using spring-loaded Tru-Cut biopsy devices for masses >2.5 cm, keeping in mind that sampling complications are much higher (Parker et al. 1989).

## Probe Selection

For thoracic sampling, the author uses either a linear or microconvex (curvilinear) probe. The benefit of using a microconvex array is the ability to fit the probe head or its footprint in between the ribs. However, if the target is located in the cranial thorax, or predominantly ventral, or if sampling involves small pleural lesions, the author prefers a linear probe to better visualize the pleural surface, understanding

the drawback of its larger probe head necessitating orientation that minimizes rib shadowing.

## Chemical Restraint and Local Anesthetics

The use of local anesthetic is variable. The author generally prefers local anesthesia if several ultrasound-guided samples are anticipated. The delivery of local anesthesia can be more painful than the procedure itself; however, adding a 1:10 volume mixture of sodium bicarbonate can mitigate the acidity and stinging effect of lidocaine. An intravenous catheter is generally warranted for most patients and especially if a core Tru-Cut biopsy is undertaken, for two reasons: to deliver chemical restraint, and to deliver emergency drugs if necessary. In more difficult and risky cases, the use of a short-acting general inhalant anesthetic may be an appropriate choice (see Figure 44.3).

Commonly used drugs often considered solely or in safe combinations include ketamine hydrochloride, diazepam, dexmedetomidine, butorphanol, and intravenous propofol. Choosing the optimal protocol will depend on clinician preference and underlying medical conditions. The use of drugs that promote panting or splenomegaly should be avoided (if the target is abdominal). For tissue biopsies and some deep fine needle and needle biopsy procedures or fine needle and needle biopsy of lesions in critical areas, including lung lobe aspirates, the use of short-acting sedatives and anesthetic should be considered to minimize pain, patient movement, and panting. Panting is especially problematic from an imaging standpoint, since ultrasound does not transmit through air, and from a safety standpoint, when sampling lung.

## Lowering the Risk of Hemorrhage and Pneumothorax

The author considers four major parameters in assessing patient risk of bleeding:

- the target being sampled being superficial versus deep
- the needle size and type of sampling technique, such as fine needle aspiration (smaller gauge needle) beomg less risky than core or Tru-Cut biopsy (larger gauge needles)
- the coagulation profile of the patient
- the patient's respiratory and cardiovascular status.

The risk of postprocedure bleeding increases if the activated partial thromboplastin time (aPTT) and/or prothrombin time (PT) are increased and the platelet count is low (<50 000) (Bigge et al. 2001). Excessively elevated globulin levels should also be considered because of their effect on platelet function, which can be assessed point-of-care through buccal mucosal bleeding time (BMBT) assessment. Clinical judgment, patient history and profile, and risk–benefit assessment must always be considered.

In summary, fine needle aspirates of intrathoracic structures would be considered a low risk if the target is superficial, has low vascularity, and a smaller gauge needle is used (22–25 gauge) along with a good acoustic window of visualization and a stable, still, patient with an unremarkable coagulation profile. On the other hand, a target close to the heart, major vessels, and lung poses more risk and so does a fractious or moving patient and a limited acoustic window. Postprocedural point-of-care monitoring using a TFAST-Vet BLUE approach for detecting hemorrhage, developing effusions, and pneumothorax and the lung point is recommended for intrathoracic procedures. The TFAST-Vet BLUE approach should be performed immediately following the procedure and repeated again minimally four hours post procedure (sooner if status is questionable) (see Chapters 17, 18, 22, and 23).

## Lesion Identification

Usually, peripheral lung lesions have a mostly homogeneous to heterogeneous hypoechogenicity (darker) with hyperechoic reverberant foci extending past the lesion. The reverberant foci or horizontal A-lines commonly represent trapped air within the parenchyma or peripheral smaller airways. On many occasions, lung is consolidated having interstitial-alveolar edema with air within airways, the equivalent of finding air bronchograms on thoracic radiographs, and referred to as the shred sign (Figure 44.4). On other occasions, airways have luminal fluid and hyperechoic (bright white) walls indicating the presence of "fluid bronchograms" from consolidated lung tissue, resembling liver tissue, referred to sonographically as "hepatization of lung" when there is no air within the consolidation that has fluid bronchograms (Figure 44.5). This finding is referred to as the tissue sign (see Chapters 22 and 23 for more detailed information regarding lung ultrasound).

## Shape of Lesions

The dynamics of the peripheral, intrathoracic lesion can help to differentiate pulmonary from thoracic wall or pleural lesions (Figure 44.6). The pulmonary lesion

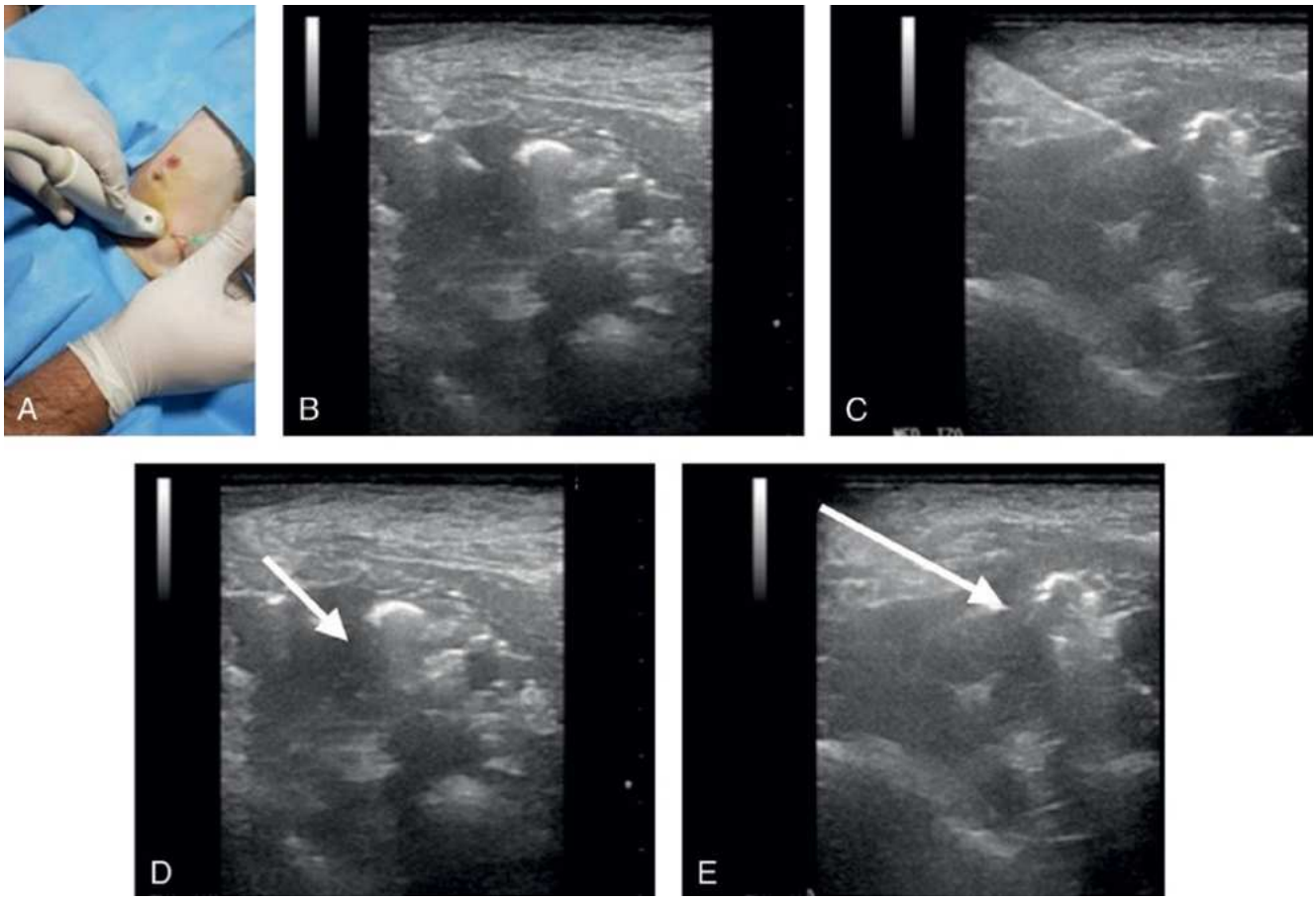


**Figure 44.4.** Sampling a lung lobe mass. (A) Showing the free-hand technique and the importance of the angle of insonation for optimal needle imaging in a patient with a lung lobe mass. (B) The angle is not 90° to the needle and thus the needle and its track are more difficult to visualize, in contrast to (C) in which the angle is more shallow (generally 20° from the skin surface with linear probes) to the target, showing much better visualization of the entire needle, which leads to more accurate and safe advancement and needle tracking. (D,E) The same images as (C) and (D) labeled with arrows overlaying the needle track.

will move with respiration whereas the thoracic wall-extrapleural lesion will not (see Figures 44.4–6). The extrapleural lesion will bulge into the pleural cavity from the parietal side of the thoracic wall, creating an extrapleural sign characterized by a well-demarcated, convex contour with tapering cranial and caudal edges.

## Lesion Size

Lesion size is also important. Smaller lesions (<1.5 cm) that are peripheral are more challenging to sample due to motion during respiration, and hence increase the risk for the development of postsampling pneumothorax (PTX). Also, the presence of underlying interstitial disease and bullae increases the risk for PTX. Sedation can be used with caution if the target is small to decrease panting as much as possible. In the author's practice, a set of thoracic radiographs are always included post FNA to document that the patient is free of PTX. Although more difficult to document PTX, ultrasound is likely a more sensitive test and a "lung point" strategy may be used to not only assess degree of PTX but also track worsening, static or resolving PTX (see Chapters 17 and 18). Ultrasound is also very sensitive and specific for pleural effusion.

## Slide Preparation for Sample Submission

Microscope slides should be clean and wiped with a soft tissue. There are two popular slide preparation techniques: the squash technique and the smear technique, just as if you were making a blood smear (Figure 44.7). When a core of tissue is obtained, the sample may be gently teased from the needle using a clean second needle and the tissue rolled over the slide

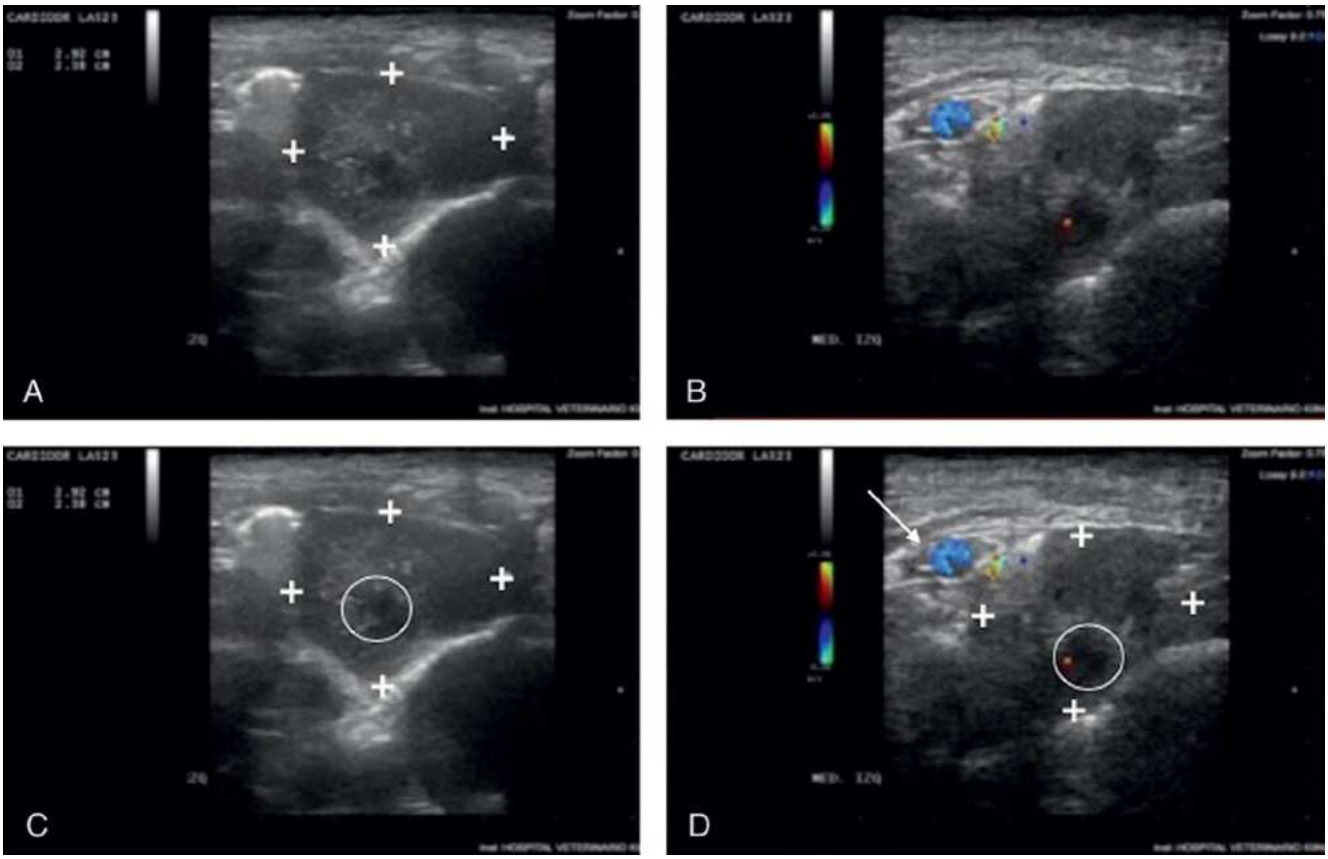


**Figure 44.5.** Cranial mediastinal mass and use of color flow Doppler. Thoracic mass shown in B-mode and with color flow Doppler. The mass in (A) is measured (calipers, +), helping to plan the ultrasound-guided procedure and the length and depth needed for successful sampling. Note the anechoic area in the center of the mass in the B-mode image, likely an area of central necrosis. (B) The use of color flow Doppler helps characterize the lesion and its blood supply. The importance of color flow Doppler is that it reveals the nearby vasculature that should be avoided during the procedure, minimizing the risk of postprocedure hemorrhage. (C,D) The same images as (A) and (B) with an overlay of a circle for the targeted lesion. The arrow points out the large vessel evident using color flow Doppler (blue pixels) that needs to be avoided to prevent postprocedure hemorrhage.

or imprinted in several areas on the slide (or both). To ensure that the collected sample is satisfactory, the author recommends performing in-house cytology to minimize the sending out of nondiagnostic samples.

## *Special Echogenic Enhanced Needles*

When performing ultrasound-guided interventions, visualization of the needle is important for accurate target sampling and needle tip positioning. We must remember that regular needles are only well visualized when the ultrasound beam hits the needle close to 90° (angle of insonation); thus, the lower this angle of insonation, the less visualization of the needle occurs. Coated needles that enhance ultrasound visualization (echogenic coatings) are commercially available and very helpful for successful ultrasound-guided procedures (Figure 44.8). The special echogenic coating may be a polyethersulfone and contain specially designed microbubbles. These microbubbles within the coating can be different sizes, ranging from 10 to 17 mm. Other types of echogenic needles have dimpled echogenic tips. The ideal needle would have the entire needle visible rather than only its tip, especially for small targets (<1.5 cm) that are adjacent to critical structures, where visualization of only the tip could increase the risk for bleeding or traumatizing adjacent more normal tissue.

Commercial 21 gauge echogenic needles are available with different features (Cook, Bloomington, IN)

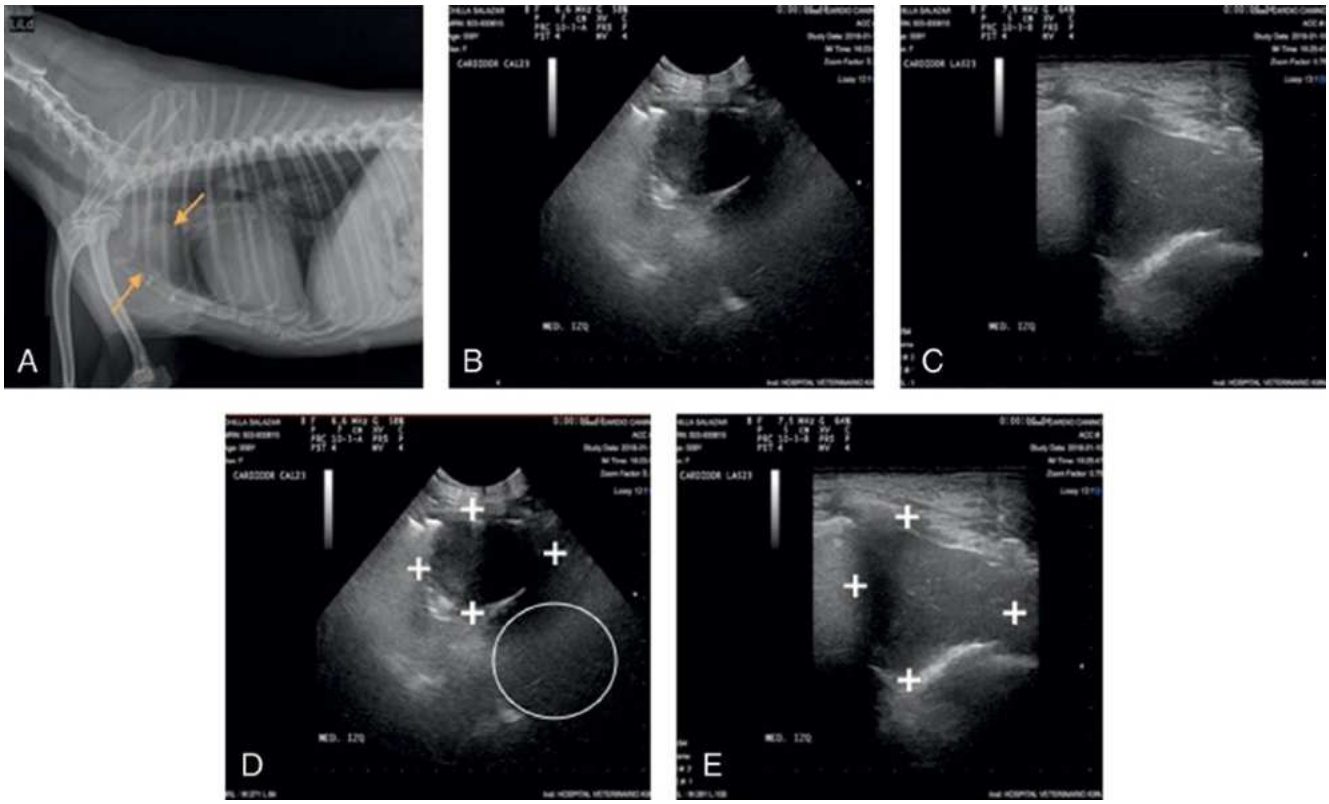


**Figure 44.6.** Sampling a cranial mediastinal mass. Cranial mediastinal mass shown radiographically with arrows in (A) and in B-mode ultrasonographically with a microconvex (curvilinear) probe in (B) and a linear probe in (C). Note in (B) the mirror image created by the curved soft tissue–air interface mimicking the erroneous presence of a second mass with a curvilinear probe, not as evident in (C) of the same mass using a linear probe. (D,E) The same images as (B) and (C) are labeled. The caliper (+) outlines the targeted mass in both (D) and (E). In (D) the mirror image "mass" is outlined with a circle overlay.

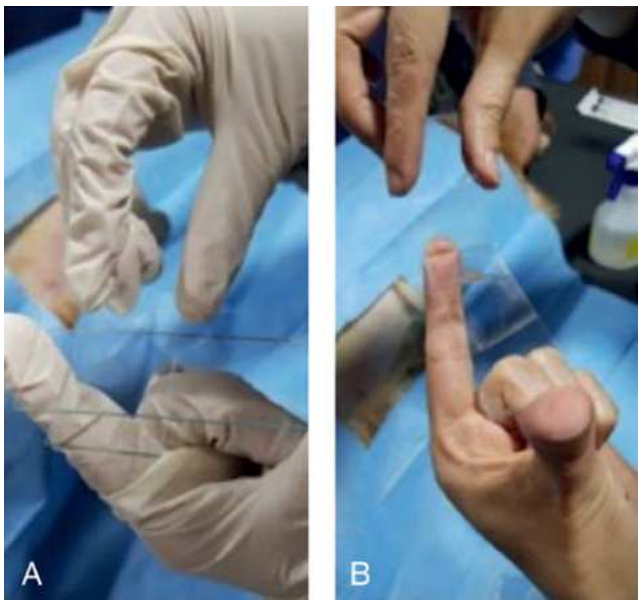


**Figure 44.7.** Slide preparation and the squash and smear techniques. (A) Squash technique. (B) Smear technique.

having a dimpled distal shaft (EchoTip®, Cook) or a standard smooth configuration coated with a thin polymeric film (Echo-Coat, STS Biopolymers, Henrietta, NY). Havel's (Cincinnati, OH) is another company with a wide array of echogenic needles including EchoStim®, EchoBlock® and AccuTarg®.

## *Special Needle Guides*

Previously in this chapter we described two methods of needle visualization, in-plane and out-of-plane (plus echogenic needles for optimal visualization), using the free-hand technique. A second method of needle positioning and guidance involves the use of mechanical guides attached to the probe. The benefit of these ultrasound guides is to increase accuracy and create a rigid linear track to deeper targets (>6 cm), situations in which the free-hand technique is more difficult for needle advancement, especially when using 22 gauge or smaller needles that may bend (during free-hand advancement).

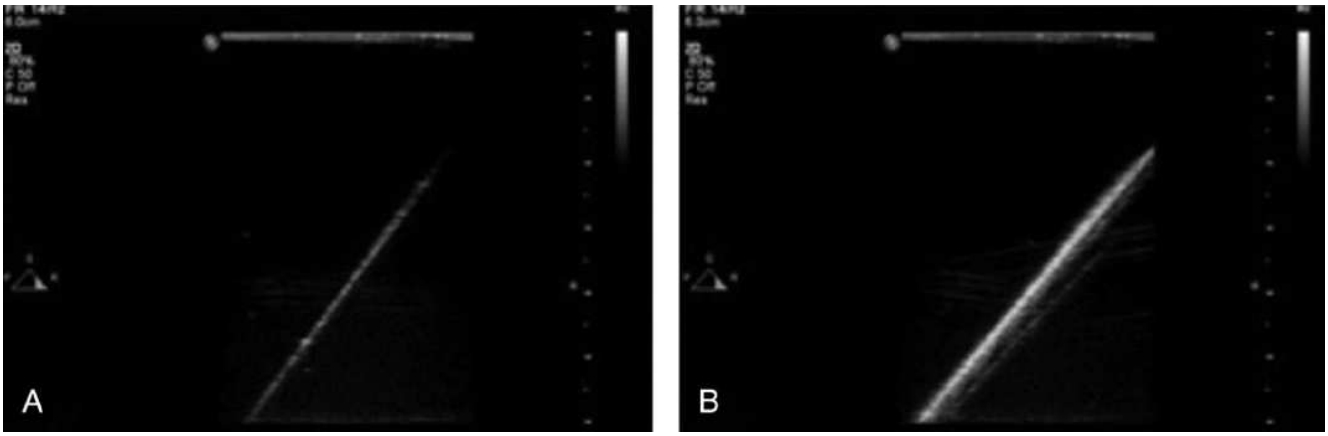


**Figure 44.8.** Echogenic needle. Conventional needle (A) versus (B) coated needle echogenicity characteristics using the same ultrasound parameters, phantom, and angulation. Note the marked difference in conspicuity between the two needles.

### *Ultrasound-Guided Biopsies*

The need for Tru-Cut biopsy is typically dictated by larger lesions (>3 cm). The Tru-Cut biopsy procedure inherently poses a higher risk than when using FNA and needle biopsy sampling techniques because of larger versus smaller needles (and spring-loaded devices). The use of spring-loaded biopsy guns is preferred over manual devices. The Bard® Magnum® reusable core biopsy instrument and MEDCORE automatic reusable biopsy guns are examples of these commercially available devices. When using spring-loaded guidance, ensuring that the needle does not travel beyond the limits of the lesion is imperative for patient safety. As in any ultrasound-guided procedure, the sampling should always avoid aerated tissue and large intralesional and extralesional vascular structures to prevent pneumothorax and hemorrhage. Generally, the risk of pneumothorax is low and self-limiting; however, close monitoring of respiratory rate and type of breathing pattern, and use of the TFAST-Vet BLUE approach are warranted.

## Building Skills on Phantoms

Practicing on phantoms before attempting ultrasound-guided procedures on your patient is important for the success of this skill. Several types of phantoms have been used historically in human medicine for the purpose of practicing ultrasound-guided procedures, including water-based, agar/gelatin-based, Blue Phantom™ (Sarasota, FL), and meat phantoms. A good phantom has the following features:

- provides echogenicity similar to real tissue
- readily available
- inexpensive
- can be reused
- provides tactile feedback
- will hold the needle in place
- does not generate needle tracks
- is not a potential health hazard (see chicken breast models, Chapter 24).

Blue Phantoms™ are commercially available but are prohibitively expensive for most institutions. The author recommends the use of phantoms made out of a mixture of gelatin and psyllium while using fluid-filled Penrose drains or linear balloons to function as a blood vessel(s) and grapes and cubed cheese as solid targets. Recipes for home-made phantoms are readily available on the internet.

## Pearls and Pitfalls, The Final Say

The skill of performing ultrasound-guided procedures is a challenge for all sonographers to take on since ultrasound can identify free fluid and parenychymal lesions, although sampling is necessary for definitive diagnosis.

### *Pitfalls – Most Common Errors*

- Not using the color flow Doppler feature to assess the vascularity of the targeted tissue or around the targeted tissue of interest can generate unnecessary patient risk for puncturing or lacerating large vessels or a heart chamber in the path of the needle.
- Losing awareness of the location of the ultrasound probe marker and needle orientation, and thus

having the tip of the needle entering in the wrong side of the field of view and then focusing on the opposite side while advancing the needle, resulting in error and possible misplacement into critical areas.
- Not inserting the needle exactly in the middle of the width of the probe's footprint, which leads to lack of accurate and optimal visualization of the needle.
- The angle of entrance at the skin surface with respect to the shape of the field of view is much less than 90° (not optimizing the angle of insonation).
- Inadvertently puncturing the probe's rubber footprint, which will lead to permanent damage.

# References

Bigge LA, Brown DJ, Penninck DG. 2001. Correlation between coagulation profile findings and bleeding complications after ultrasound-guided biopsies: 434 cases (1993–1996). *J Am Anim Hosp Assoc* 37:228–233.

Haaga JR, Puma JP, Bryan PJ, et al. 1983. Clinical comparison of small-and large-caliber cutting needles for biopsy. *Radiology* 146:665–667.

Parker SH, Hopper KD, Yakes WF, et al. 1989. Image-directed percutaneous biopsies with a biopsy gun. *Radiology* 171:663–669.

# Further Reading

Andriole JG, Haaga JR, Adams RB, et al. 1983. Biopsy needle characteristics assessed in the laboratory. *Radiology* 148:659–662.

Culp WC, McCowan TC, Goertzen TC, et al. 2000. Relative ultrasonographic echogenicity of standard, dimpled, and polymeric-coated needles. *J Vasc Intervent Radiol* 11(3):351–358.

Kim YH. 2016. Ultrasound phantoms to protect patients from novices. *Korean J Pain* 29(2):73–77.

Tang SJ, Vilmann AS, Saftoiu A, et al. 2016. EUS Needle Identification Comparison and Evaluation (NICE) study (with videos). *Gastrointest Endosc* 84(3):424–433.

Wood EF, O'Brien RT, Young KM. 1998. Ultrasound-guided fine-needle aspiration of focal parenchymal lesions of the lung in dogs and cats. *J Vet Intern Med* 12:338–342.

SECTION X

# Management

CHAPTER FOURTY-FIVE

# POCUS: Setting Up Successful POCUS and FAST Ultrasound Programs

Gregory R. Lisciandro

## Introduction

With the widespread use of ultrasound by nonradiologist veterinarians, it is important for the general practitioner, emergency clinician, or nonradiologist veterinarian to develop a structured ultrasound program for their practice or institution. This chapter tackles some of these issues through our own experiences over the past 15 years, with the author serving as an assistant and chief medical director for most of that time, and having a spouse being involved in specialty consulting and working as an internist at a referral practice.

The chapter will go over several tenets that are imperative for maximizing success for ultrasound skill proficiency as well as profit and generating income from this traditionally expensive technology that is becoming much more affordable.

### *What POCUS: Setting Up Successful POCUS and FAST Ultrasound Programs Can Do*

- Establish V-POCUS and Global FAST examinations with clear objectives.
- Maximize learning by detecting ultrasound strengths and weaknesses.
- Make use of the ultrasound machine accessible on multiple fronts from actual physical placement within the practice, to fee structure and coding, to replacement policies.
- Create accountability.
- Create quality control and performance measurement.
- Generate income by creating value to both the positive and negative examination.

### *What POCUS: Setting Up Successful POCUS and FAST Ultrasound Programs Cannot Do*

- Cannot replace proper training.
- Cannot replace a disciplined, standardized approach.

### *Indications*

Any practice or institution using POCUS and Global FAST as part of patient care.

*Point-of-Care Ultrasound Techniques for the Small Animal Practitioner*, Second Edition. Edited by Gregory R. Lisciandro.
© 2021 John Wiley & Sons, Inc. Published 2021 by John Wiley & Sons, Inc.
Companion website: www.wiley.com/go/lisciandro/ultrasound2

### Objectives

- To maximize success in your practice or institution's POCUS and Global FAST programs for proficiency and profit.
- For the reader to appreciate the following tenets for such success.
  - Proper training.
  - Accessibility physically and financially.
  - Communicating value to clients.
  - Goal-directed templates.
  - Quality control.
  - Celebrating your victories.

# Proper Training

### Standardized Methodology

There is no replacement for proper training and repetition through a systematic, standardized methodology. By applying POCUS and Global FAST in a systematic, standardized way, you will become proficient similar to how your skills developed during perfection of your physical exam.

### Where Should I Learn Ultrasound?

Good question. There are veterinary ultrasound companies that have been traditionally dedicated to ultrasound training and likely more that have made recent commitments to ultrasound education. Check with the ultrasound company from which you purchased your equipment. However, you should consider their ultrasound training model and what fits your practice's needs. At the time of writing, many companies begin with a basic complete abdominal ultrasound examination, basic echocardiography, or focused organ approaches. However, the case could be made that the nonradiologist veterinarian should learn the Global FAST approach as the initial format. However, a lack of clarity exists in terms of using FAST as a simple binary test of whether fluid is present or absent in the abdomen and thorax, also referred to as a "flash exam."

We encourage a format somewhere in between the complete abdominal and echocardiography study and the "flash exam" by learning AFAST and applying a fluid score and its target organ approach; TFAST and being able to recognize pleural and pericardial effusion, three major echo views, pneumothorax, lung pathology and volume status assessment through integration of the aforementioned; and Vet BLUE and its six lung ultrasound signs. The combination of these three FAST formats is referred to as Global FAST. A similar paradigm shift in ultrasound training is occurring in human medicine.

# Accessibility

### Accessible Machine

Your ultrasound machine must be placed in or in very close proximity to the area where all the action takes place in your practice or institution. The machine ideally should be turned on, booted up, and ready to go. Alternatively, have an ultrasound machine that may be readily moved to the patient with either a laptop format or a console on a stand with wheels. At the time of writing, hand-held ultrasound machines are now so portable the attending healthcare provide can carry the device with them to the patient.

What you want to avoid is (1) having your ultrasound machine stored in a closet down the hall in its original box that requires the box to be opened, the machine unpackaged and then transported to the area where it is to be used (followed, after its use, by being repackaged in its box, transported down the hall, and placed in the closet), or (2) placement of your machine in an inconvenient area of your practice, requiring extra effort to move the machine to the patient (in other words, having the machine in a "back area").

Inconvenience of physical accessibility contributes to lack of use of your ultrasound machine.

### Accessible Fees

The fee structure must be simple.

- Coding.
- Keep the initial fee general.
  - POCUS is a standard fee independent of the examination (or minimally varied).
  - Global FAST is a standard fee independent of how many of its components are performed.
- Include the serial exam.
- Bundle fees.

Over time, when your staff and clientele understand the importance of your ultrasound program, then fees can be modified and tailored to the practice and how its use of ultrasound has evolved.

#### Coding

Using codes that are easy to remember will help to ensure that the imaging is charged every time. Some

VetBooks.ir

electronic records now link the data or findings entry to the fee structure, saving time and freeing up resources since coding and entering fees take staff time that could be better spent on patient care. In any event, keep your coding system simple and minimal.

### Keeping the Initial Fee General

POCUS or Global FAST should be considered the same fee no matter what examination is performed. If you institute Global FAST for all patients as an extension of the physical exam, you strive for all its components every time – AFAST with a fluid score, TFAST, and Vet BLUE. If for some reason a component is not performed, the Global FAST fee is the same, and the data or findings entry states "indeterminate" or "not assessed." These entries should not be considered abject. We are well aware that patient risk if questionably stable or critical and staff safety enter the picture, limiting examination time. Patient body condition may also alter image quality; for example, a very obese patient may be difficult to image because of attenuation of the ultrasound beam through adipose tissue, a patient may be excessively large, exceeding the depth limits of your machine, subcutaneous air may be present, reflecting the ultrasound beam since ultrasound does not transmit through air, or a painful patient may preclude completing all the indicated acoustic windows. The argument could be made that possibly a POCUS of a soft tissue swelling during MSK evaluation should be a different fee from imaging the eye or brain; however, the hospital director should decide at least initially whether keeping the fee structure simple will contribute to more use and changing the hospital paradigm by encouraging habitual POCUS and Global FAST use through simple fee structures. The author suggests making Global FAST standard of care for all cases, with the POCUS examinations being an add-on.

### Bundling Fees

Bundle the Global FAST examination into triage examinations, rounds of hospitalized cases, preanesthetic testing, pre- and postprocedure evaluations, geriatric annual screening, and likely you may think of other "bundles" depending on the character of your practice. POCUS exams could be bundled depending on the patient subset. For example, eye problems could be bundled into the ocular work-up of a POCUS eye exam, and lameness into a POCUS MSK. However, the danger is that the eye problem could be fungal related, and a Global FAST examination would potentially detect pulmonary fungal granulomas that would otherwise be missed or delayed in their detection until disease is more advanced. The musculoskeletal problem could have other evidence-based information or comorbidities missed with Global FAST as part of the physical examination. Similar concerns regarding targeted and focused exams have been recently raised in human medicine (Narasimhan 2016).

#### *Bundle Global FAST into All Triaged Examinations*

Many clients will approve all that you think is necessary to ensure optimal care and expedite a diagnosis. A critical initial fee that includes physical examination, an intravenous catheter and the first liter of intravenous fluids, quick assessment blood testing, and Global FAST is a strategy that has been useful in our practices. Global FAST truly saves lives through expediting an evidence-based problem list and better directing resuscitation and diagnostic testing.

#### *Bundle Global FAST into Patient Rounds for All Hospitalized Cases*

Some practices make the fee so economical that the client does not require an explanation and it is accepted as standard of care within that institution. The push to do so with this strategy positively contributes to changing the practice culture, to use Global FAST as part of the physical exam.

#### *Bundle Global FAST into Your Preanesthetic Evaluation*

The idea came from a colleague, Dr Bruce Silverman, who has a special interest in veterinary ophthalmology. Dr Silverman is skilled in performing cataract and other ocular procedures. Several years ago during a Global FAST course I was teaching, I was curious as to why Dr Silverman would be learning Global FAST. His answer was intriguing. I paraphrase with his permission: "I am already doing ocular ultrasound. Most of my patients are geriatric, are diabetic, and may have significant occult comorbidities undetected by blood and urine testing and radiography if performed. I am going to perform Global FAST as part of their preanesthetic evaluation before I do my eye procedures." We adopted the Silverman strategy a few months later, and more recently this type of global approach preanesthetically is being proposed in human medicine.

VetBooks.ir

### *Bundle Global FAST into Pre- and Postprocedural Evaluation*

Pre- and postprocedural Global FAST uses screens for potentially life-threatening complications including bleeding, septic effusions, pneumothorax, aspiration pneumonia, pulmonary thromboembolism, and heart failure, to name a few examples. A board-certified radiologist raised his hand at one of my lectures a few years ago and stated that all practitioners should be using Global FAST on exit exams on same-day percutaneous procedures. We agree. A serial Global FAST should be standard postprocedural evaluation, having shown its superiority to physical exam, lab testing, and radiography for most complications.

### *Bundle Global FAST into Geriatric Annual Assessment*

In addition to a good physical exam, blood and urine testing, add Global FAST as a free fluid and soft tissue screening test of the abdomen, thorax, heart, and lung.

### *Bundle Fees with Complete Studies*

#### Global FAST + Complete Echocardiography

Make the fee similar to the others and explain to the client and referring veterinarian briefly and succinctly why both are indicated. You ordered complete echocardiography for your patient and waited on the radiographs due to cost of care. You feel like the complete echocardiography is adequate as your starting test and it is performed and rules out heart disease. However, the case had a splenic mass and an abdominal fluid score of 1–2, being a small-volume bleed. The liver was unremarkable and the lung surface had no nodule sign on Vet BLUE. You ordered the wrong test. Or this same patient had no significant heart disease causing its signs, but during Global FAST there are obvious lung nodules. You may have sent the patient home with the answer that no heart disease existed and instructed the client that we will begin with conservative therapy and continue the workup if the patient fails outpatient care. Or, the patient does have left-sided heart disease, and pre-echo you already know if the lung is wet or dry and any other Vet BLUE signs are present (left-sided congestive heart failure), what the caudal vena cava and its associated hepatic veins look like, if ascites is present (right-sided congestive heart failure), and if there are any comorbidities in the abdominal cavity *before* complete echocardiography.

#### Global FAST + Complete Abdominal Ultrasound

Make the fee similar to the others and explain to the client and referring veterinarian briefly and succinctly why both are indicated. As an example, an older dog was referred to me at a referral practice as the first-line evaluation. The dog was critical but stable. The signalment (older large-breed dog), physical exam, blood work, and radiographs prompted suspicion of an abdominal effusion and midabdominal mass. I could have passed on the Global FAST, but it is part of every physical exam. I explained to the owner that our next test after my evaluation would be a complete abdominal ultrasound by a board-certified radiologist. However, they would not look at the heart or lung surface and I would like to screen the abdominal cavity now, look for any obvious problems and confirm or refute the suspected abdominal effusion on the referral radiographs by "seeing" if fluid is present rather than suspecting. Moreover, if free fluid was present and safely accessible, I needed to sample and test it. "If your dog has a cancerous condition with disseminated disease, I am also screening for you before the expense of the complete study. There are two ultrasound examinations but the evaluations are different (as explained)."

The owner agreed. The dog had an AFAST with an abdominal fluid score of 4 (large-volume bleed/effusion), and no obvious masses or AFAST target organ conditions. TFAST showed no pleural or pericardial effusion, no pneumothorax, and unremarkable cardiac chambers, and Vet BLUE showed a normal "lung line" at all views. The fluid was sampled and tested in house with a packed cell volume (PCV) and total solids (TS) and brief cytology. The dog unexpectedly had a modified transudate, not the presumed hemoabdomen for which it was referred. I explained to the owner that the fluid was not a bleed but secondary to a splenic, hepatic or cardiac problem that required the complete study, that as far as I could tell, the condition was not widespread and I saw no evidence of cancer either localized or disseminated. The radiologist arrived and now my requirement was "The dog has a modified transudate, I need you to find for me why and what is the source." The case ended up being liver lobe torsion. The dog had a benign process that was surgical and successfully treated. The radiologist expediently provided me, the patient, and the client with a much better service. Global FAST did not replace the radiologist and with my training I would not have been able to make their diagnosis.

## *Replacements and Loaners*

Your ultrasound machine will hopefully become part of nearly every patient evaluation in your practice. When the machine malfunctions, you need a replacement or loaner within 24–48 hours; this point

VetBooks.ir

cannot be overemphasized. Make sure within your sales agreement that a replacement or loaner is provided within 24–48 hours. The frustration of waiting for completion of a repair over several weeks places you in the uncomfortable position of guessing or using less sensitive means to make decisions on inpatient and outpatient care, medical versus surgical conditions, with the daunting potential of sending your valued patient home not knowing if you missed a potentially catastrophic condition. Moreover, a potentially catastrophic condition that would have been easily detected using Global FAST.

# Communicating Value to Clients

## *The Spiel*

The spiel is imperative and will vary depending on patient subset and objectives of the POCUS and Global FAST examination. We advocate that Global FAST be part of every ultrasound study as the patient dictates because Global FAST provides an overall imaging patient picture and is part of your physical exam. The mindset is Global FAST first and POCUS as add-on ultrasound imaging.

### Example 1 – Trauma and Triage

"I am going to perform a FAST ultrasound examination on your pet, which includes a four-point scan of the abdomen looking for free fluid that could be from bleeding, infection or another cause. I will also be looking through major abdominal organs for any obvious pathology. I am not a radiologist or a cardiologist but I am trained to recognize many basic abnormalities of the liver, gallbladder, kidneys, urinary bladder, and spleen, and I will also look at the heart and lung surface and for any fluid around the lungs and in the heart sac. If there is free fluid that is safely accessible, may I have permission to use a needle about the same size as needles we use to vaccinate to sample that fluid? Ultrasound cannot tell what type of fluid is present without sampling. Your pet will not be shaved, and will have half the examination performed lying on their side and the other half standing (and many times the entire Global FAST standing). I will be back in about 15–20 minutes to let you know what I find. If you were triaged locally here in San Antonio, Texas, and went to the nearby medical center, the attending physician is likely going to perform a similar ultrasound evaluation on you because we know it is a very good screening test for major problems otherwise delayed or missed."

### Example 2 – Preanesthetic Testing

"I would like to perform a Global FAST on your pet before sedation/anesthesia to make sure that there are no obvious problems in their abdomen, heart, or along their lung surface. I am not a radiologist or cardiologist, but am trained to detect basic conditions in the abdomen, to look at basic views of the heart, and the lung surface. The examination, called a Global FAST, will be performed without shaving and with your pet on its side and then standing (or many times the entire Global FAST standing). It will take me about 15–20 minutes to perform and I will let you know my findings at that time."

### Example 3 – Hospitalized Cases

"We are performing Global FAST ultrasound as part of our physical exam on all hospitalized patients to better direct fluid therapy and potentially detect complications earlier within the abdomen and thorax, including your pet's heart and lung. By using this approach, we can often better detect internal bleeding, infection, vascular and heart problems, and aspiration pneumonia as well as other conditions, generally much sooner than without ultrasound."

### Example 4 – Pre and Post Procedure

"We are performing Global FAST ultrasound in patients having invasive procedures to better direct fluid therapy and potentially detect complications earlier by screening the abdomen and thorax, including your pet's heart and lung. By using this approach, we can often better detect internal bleeding, infection, vascular and heart problems, and aspiration pneumonia as well as other conditions, generally much sooner than without ultrasound."

### Example 5 – Geriatric Annual Evaluation

"We are making Global FAST ultrasound part of our annual geriatric profile because we know it is a good complement to our physical exam. On the physical exam, I can see the eyes, ears, oral cavity, and skin coat, but I cannot see internally. By using Global FAST, I can see within the abdomen and thorax conditions that may not be apparent on physical exam, blood and urine testing, and even radiography because X-ray is

limited to outlines and silhouettes." This spiel is used courtesy of Dr Mark Thompson, Dipl. ABVP, Brevard Animal Hospital, North Carolina.

#### Example 6 – POCUS of a targeted-organ

*POCUS eye* – "We are using a point-of-care eye exam to screen for any displacement of the lens, any intraocular or periorbital masses, and retinal detachments."

*POCUS MSK* – "We are going to apply ultrasound to the swelling to screen for any sign of infection, tumor, herniation, or foreign body."

The POCUS spiel will be dependent on the targeted organ and the clinical questions being answered.

### Addendums to the Spiel

- The use of Global FAST provides me with a soft tissue scan of the abdomen, heart, and lung.
- If you had trauma (or in nontrauma had weakness, low blood pressure) and you went to the medical center here in San Antonio, Texas, the attending physician is similarly going to use ultrasound to better assess you.
- The ultrasound probe is the new stethoscope. By using lung ultrasound, I can better screen for conditions requiring additional imaging, and better interpret my thoracic radiographs. You will soon see physicians using a similar approach.
- Radiography shows me outlines and silhouettes, whereas ultrasound shows me free fluid and soft tissue abnormalities.
- I am not a radiologist or cardiologist but have been trained to screen for problems otherwise missed or delayed by looking with ultrasound through the abdomen and thorax, including the heart and lung.

### Explaining Your Findings

#### Don't Undervalue a Negative Global FAST

"I did not see any signs of bleeding or infection in the abdominal cavity, thoracic cavity or heart sac. There were no obvious masses or organ conditions seen in the abdomen. Basic heart chamber ratios appeared normal. The lung surface was normal. I feel much better that we screened for any obvious conditions that could be potentially catastrophic."

#### Don't Fear a Positive Global FAST or POCUS Examination

You only have to recognize that something looks abnormal, which triggers more advanced imaging and gold standard testing. No matter what we do, no clinician is correct 100% of the time, and explaining that something appears suspect that requires x, y, and z for confirmation is better patient care than not looking. Sage advice – "You will miss more by not looking than not knowing."

## Use of Goal-Directed Templates

The importance of goal-directed templates cannot be overemphasized.

- Goal-directed templates establish clear objectives for your Global FAST and POCUS examinations.
- They will differ between practices and depending on what clinical questions are to be answered.
- They will evolve over time depending on skill set and types of cases seen at your practice.
- Goal-directed templates are best recorded following the order of the examination.
- Goal-directed templates allow measurement and evaluation of your program's performance, helping to develop diagnostic algorithms for different patient subsets within your practice.

### Establish Clear Objectives

Goal-directed templates should convey the Global FAST and POCUS examination goals to you, your practice, your colleagues, and your clients.

Examples are shown in Figures 45.1, 45.2, 45.3, and 45.4. See also Appendix I.

### Qualifiers for Your Templates

#### AFAST

The AFAST ultrasound examination is a screening test for the detection of free fluid and some types of organ pathology and conditions to better direct resuscitation and diagnostic testing. The AFAST examination is not intended to replace a complete abdominal ultrasound.

#### TFAST

The TFAST ultrasound examination is a screening test for the detection of free fluid around the lungs and within the heart sac, collapsed lung lobe(s), and some types of lung and heart pathology, to better direct resuscitation and diagnostic testing. The TFAST examination is not intended to replace complete echocardiography and thoracic radiography.

### Vet BLUE

The Vet BLUE ultrasound examination is a screening test for different types of lung pathology, including congestive heart failure, pneumonia, hemorrhage, lung contusions, and pulmonary thromboembolism, to better direct resuscitation and diagnostic testing. Vet BLUE can also detect nodules and different forms of lung consolidation. It is not meant to replace thoracic radiography.

### Global FAST

Global FAST ultrasound examination is a screening test for different types of abdominal, thoracic, heart, and lung pathology to better direct resuscitation and diagnostic testing. Global FAST is not meant to replace radiography, complete abdominal ultrasound, and complete echocardiography.

### POCUS of X, Y, or Z

These would be dictated by the system being examined and the clinical questions being answered. POCUS eye will differ from POCUS MSK that will differ from a POCUS avian examination.

## *You Must Record Your Findings*

If you don't record patient data, you cannot measure performance, and if you can't measure performance, you cannot properly evaluate your proficiency. By using goal-directed templates, skills can be evaluated, training can be improved to better maximize success, and deficiencies and strengths in your program recognized. Moreover, without recording the findings of your Global FAST and POCUS examinations, patient information is lost, likened to performing a physical examination without recording your findings.

The recording of findings for the patient's medical record must be logical and convenient. Reduce staff time by having a standard template within the medical record which limits free typing entries, or a hard copy template that is convenient by checking off boxes with limited need for writing in findings. Moreover, with a standardized entry system that mimics the order of image acquisition, findings are more readily remembered and entered.

**Template for AFAST®**

**Patient Positioning:**
Right Lateral ☐ Left Lateral ☐ Modified Sternal ☐ Standing ☐ Sternal ☐

**Gallbladder** unremarkable☐ abnormal ☐ indeterminate ☐ not assessed ☐
**Urinary Bladder** unremarkable☐ abnormal ☐ indeterminate ☐ not assessed ☐

**DH View**
Pleural Effusion absent ☐ present ☐ indeterminate ☐ not assessed ☐
Pericardial Effusion absent ☐ present ☐ indeterminate ☐ not assessed ☐

Caudal Vena Cava unremarkable (BOUNCE) ☐ small (flat) ☐ distended (FAT) ☐ indeterminate ☐ not assessed ☐
Hepatic Venous Distension unremarkable☐ distended ☐ indeterminate ☐ not assessed ☐

**AFAST Fluid Scoring**

| | | | |
|---|---|---|---|
| DH | 0 ☐ | 1/2 ☐ | 1 ☐ |
| SR/HR | 0 ☐ | 1/2 ☐ | 1 ☐ |
| CC | 0 ☐ | 1/2 ☐ | 1 ☐ |
| HR Umbilical | 0 ☐ | 1/2 ☐ | 1 ☐ |

**Total Abdominal Fluid Score (AFS) 0-4** = _____

**HR5th View** 0 ☐ 1/2☐ 1☐ *(not part of the AFS)*

**Focused Spleen** unremarkable☐ abnormal ☐ indeterminate ☐ not assessed ☐

**Comments** _____

**Qualifier:** The AFAST® exam is an ultrasound examination used as a screening test to detect the presence of free abdominal fluid (which is generally abnormal) as a screening test in order to better direct resuscitation efforts and diagnostic testing, detect complications, and manage critically ill patients. AFAST allows rapid but indirect assessment for evidence of major internal abdominal organ injury or disease. The AFAST exam is not intended to replace a complete detailed abdominal ultrasound of the abdomen.

**Figure 45.1.** Goal-directed template for AFAST. Source: Reproduced with permission from Dr Gregory Lisciandro, Hill Country Veterinary Specialists and FASTVet.com, Spicewood, TX.

## Template for TFAST®

**Pneumothorax?** Left CTS: absent ☐ present ☐ indeterminate ☐ not assessed ☐
Lung Point : upper 1/3 ☐ middle 1/3 ☐ lower 1/3 ☐ indeterminate ☐

Right CTS: absent ☐ present ☐ indeterminate ☐ not assessed ☐
Lung Point : upper 1/3 ☐ middle 1/3 ☐ lower 1/3 ☐ indeterminate ☐

**Pleural Effusion?** Left PCS: absent ☐ present ☐ indeterminate ☐ not assessed ☐
trivial < 5 mm ☐ mild < 1cm ☐ moderate >1 cm< 2 cm ☐ severe >2 cm ☐
Right PCS: absent ☐ present ☐ indeterminate ☐ not assessed ☐
trivial < 5 mm ☐ mild < 1cm ☐ moderate >1 cm< 2 cm ☐ severe >2 cm ☐

**Pericardial Effusion?** absent ☐ present ☐ indeterminate ☐ not assessed ☐
trivial < 5 mm ☐ mild < 1cm ☐ moderate >1 cm< 2 cm ☐ severe >2 cm ☐

**TFAST Echo Views**

**Right PCS** LVSA Volume - unremarkable☐ abnormal ☐
indeterminate ☐ not assessed ☐
LVSA Contractility (FS%) - unremarkable☐ abnormal ☐
indeterminate ☐ not assessed ☐
LA:Ao Ratio - unremarkable☐ abnormal ☐
indeterminate ☐ not assessed ☐
RV:LV Ratio - unremarkable☐ abnormal ☐
indeterminate ☐ not assessed ☐

Caudal Vena Cava unremarkable (BOUNCE) ☐ small (flat) ☐ distended (FAT) ☐
indeterminate ☐ not assessed ☐

Hepatic Venous Distension unremarkable☐ distended ☐
indeterminate ☐ not assessed ☐

**Comments** _____

**KEY: CTS** = chest tube site; **PCS** = pericardial sac; **LV** = left ventricle, **PTX** = pneumothorax, **LVSA**: left ventricular short-axis view, **LA:AO** aortic to left atrial ratio on short-axis view, **RVLV:** right ventricular to left ventricular ratio on long-axis view.

**Qualifier:** The TFAST® exam is an ultrasound examination used as a screening test to detect pleural and pericardial effusion, major thoracic wall, lung, and heart abnormalities as a screening test in order to better direct resuscitation efforts or manage hospitalized critically ill patients. TFAST exam is not intended to replace thoracic radiographs, or complete detailed echocardiography.

**Figure 45.2.** Goal-directed template for TFAST. Source: Reproduced with permission from Dr Gregory Lisciandro, Hill Country Veterinary Specialists and FASTVet.com, Spicewood, TX.

## Template for Vet BLUE®

**Ask Yourself?** Wet vs. Dry? Number of B-lines? Anything off the Lung Line? Are you mistaking abdominal contents for lung pathology?

**Left** **Cd** 0 ☐ 1-3 ☐ >3 ☐ ∞ ☐ Shred ☐ size__Tissue ☐ size__Nodule ☐ size__Wedge ☐ size___
OR indeterminate ☐ not assessed ☐
**Ph** 0 ☐ 1-3 ☐ >3 ☐ ∞ ☐ Shred ☐ size__Tissue ☐ size___Nodule ☐ size__Wedge ☐ size___
OR indeterminate ☐ not assessed ☐
**Md** 0 ☐ 1-3 ☐ >3 ☐ ∞ ☐ Shred ☐ size__Tissue ☐ size___Nodule ☐ size__Wedge ☐ size___
OR indeterminate ☐ not assessed ☐
**Cr** 0 ☐ 1-3 ☐ >3 ☐ ∞ ☐ Shred ☐ size__Tissue ☐ size__Nodule ☐ size___Wedge ☐ size___
OR indeterminate ☐ not assessed ☐

**Right** **Cd** 0 ☐ 1-3 ☐ >3 ☐ ∞ ☐ Shred ☐ size__Tissue ☐ size__Nodule ☐ size___Wedge ☐ size___
OR indeterminate ☐ not assessed ☐
**Ph** 0 ☐ 1-3 ☐ >3 ☐ ∞ ☐ Shred ☐ size__Tissue ☐ size__Nodule ☐ size___Wedge ☐ size___
OR indeterminate ☐ not assessed ☐
**Md** 0 ☐ 1-3 ☐ >3 ☐ ∞ ☐ Shred ☐ size__Tissue ☐ size___Nodule ☐ size___Wedge ☐ size___
OR indeterminate ☐ not assessed ☐
**Cr** 0 ☐ 1-3 ☐ >3 ☐ ∞ ☐ Shred ☐ size__Tissue ☐ size___Nodule ☐ size__Wedge ☐ size___
OR indeterminate ☐ not assessed ☐

**DH** 0 ☐ 1-3 ☐ >3 ☐ ∞ ☐ Shred ☐ size__Tissue ☐ size___Nodule ☐ size___Wedge ☐ size___
OR indeterminate ☐ not assessed ☐

**KEY: Cd:** Caudodorsal lung region; **Ph:** Perihilar lung region; **Md:** Middle lung region; **Cr:** Cranial lung region

**Comments**_____

**Qualifier:** The Vet BLUE® lung ultrasound exam is a screening test for many conditions that affect the lung surface such as heart failure, pneumonia, nodular disease and others. Vet BLUE helps characterize respiratory conditions as a screening test. Vet BLUE is not meant to replace thoracic radiography or computed tomography.

**Figure 45.3.** Goal-directed template for Vet BLUE. Source: Reproduced with permission from Dr Gregory Lisciandro, Hill Country Veterinary Specialists and FASTVet.com, Spicewood, TX.

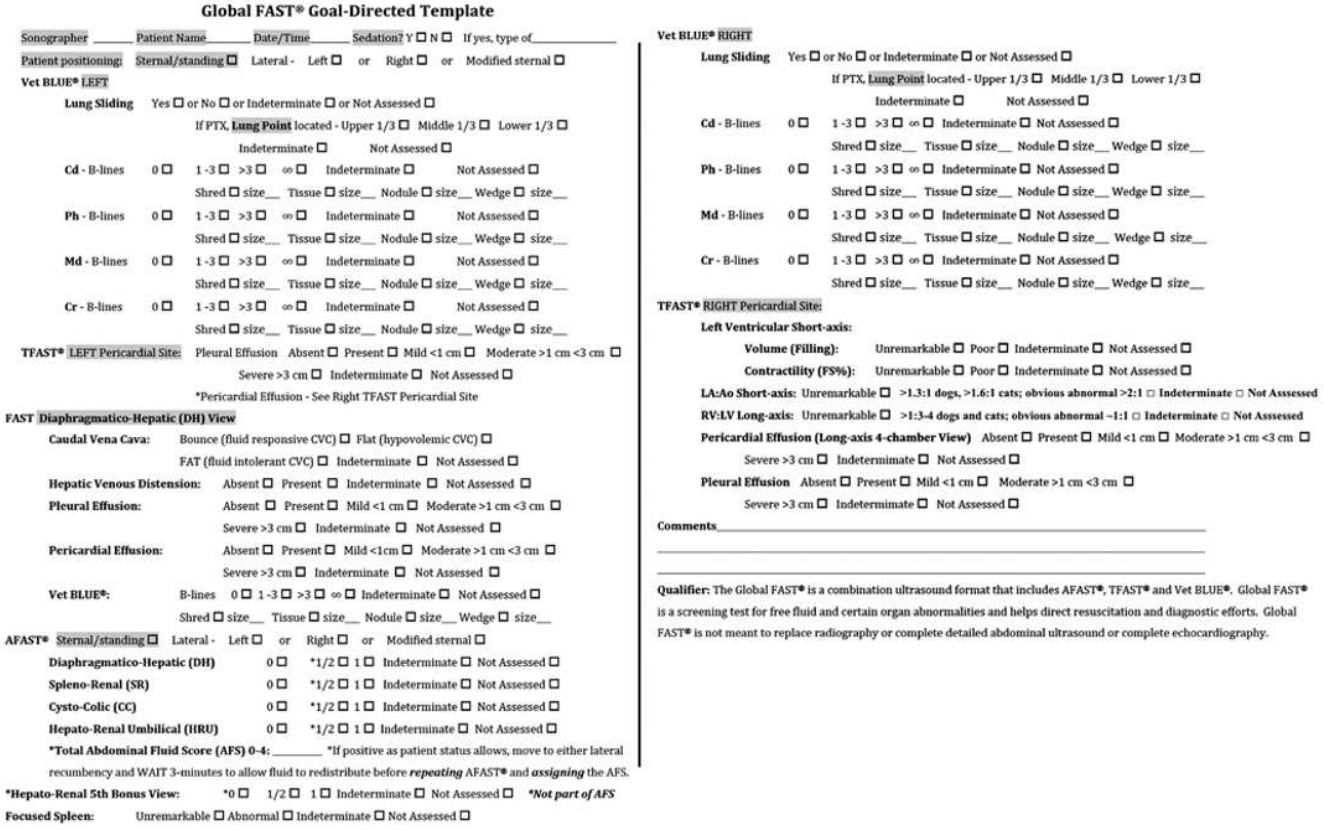

## Global FAST® Goal-Directed Template

Sonographer _____ Patient Name_____ Date/Time_____ Sedation? Y ☐ N ☐ If yes, type of_____

Patient positioning: Sternal/standing ☐ Lateral - Left ☐ or Right ☐ or Modified sternal ☐

**Vet BLUE® LEFT**

**Lung Sliding** Yes ☐ or No ☐ or Indeterminate ☐ or Not Assessed ☐

If PTX, **Lung Point** located - Upper 1/3 ☐ Middle 1/3 ☐ Lower 1/3 ☐

Indeterminate ☐ Not Assessed ☐

**Cd** - B-lines 0 ☐ 1 -3 ☐ >3 ☐ ∞ ☐ Indeterminate ☐ Not Assessed ☐

Shred ☐ size__ Tissue ☐ size__ Nodule ☐ size__ Wedge ☐ size__

**Ph** - B-lines 0 ☐ 1 -3 ☐ >3 ☐ ∞ ☐ Indeterminate ☐ Not Assessed ☐

Shred ☐ size__ Tissue ☐ size__ Nodule ☐ size__ Wedge ☐ size__

**Md** - B-lines 0 ☐ 1 -3 ☐ >3 ☐ ∞ ☐ Indeterminate ☐ Not Assessed ☐

Shred ☐ size__ Tissue ☐ size__ Nodule ☐ size__ Wedge ☐ size__

**Cr** - B-lines 0 ☐ 1 -3 ☐ >3 ☐ ∞ ☐ Indeterminate ☐ Not Assessed ☐

Shred ☐ size__ Tissue ☐ size__ Nodule ☐ size__ Wedge ☐ size__

**TFAST® LEFT Pericardial Site:** Pleural Effusion Absent ☐ Present ☐ Mild <1 cm ☐ Moderate >1 cm <3 cm ☐

Severe >3 cm ☐ Indeterminate ☐ Not Assessed ☐

*Pericardial Effusion - See Right TFAST Pericardial Site

**FAST Diaphragmatico-Hepatic (DH) View**

**Caudal Vena Cava:** Bounce (fluid responsive CVC) ☐ Flat (hypovolemic CVC) ☐

FAT (fluid intolerant CVC) ☐ Indeterminate ☐ Not Assessed ☐

**Hepatic Venous Distension:** Absent ☐ Present ☐ Indeterminate ☐ Not Assessed ☐

**Pleural Effusion:** Absent ☐ Present ☐ Mild <1 cm ☐ Moderate >1 cm <3 cm ☐

Severe >3 cm ☐ Indeterminate ☐ Not Assessed ☐

**Pericardial Effusion:** Absent ☐ Present ☐ Mild <1cm ☐ Moderate >1 cm <3 cm ☐

Severe >3 cm ☐ Indeterminate ☐ Not Assessed ☐

**Vet BLUE®:** B-lines 0 ☐ 1 -3 ☐ >3 ☐ ∞ ☐ Indeterminate ☐ Not Assessed ☐

Shred ☐ size__ Tissue ☐ size__ Nodule ☐ size__ Wedge ☐ size__

**AFAST®** Sternal/standing ☐ Lateral - Left ☐ or Right ☐ or Modified sternal ☐

**Diaphragmatico-Hepatic (DH)** 0 ☐ *1/2 ☐ 1 ☐ Indeterminate ☐ Not Assessed ☐

**Spleno-Renal (SR)** 0 ☐ *1/2 ☐ 1 ☐ Indeterminate ☐ Not Assessed ☐

**Cysto-Colic (CC)** 0 ☐ *1/2 ☐ 1 ☐ Indeterminate ☐ Not Assessed ☐

**Hepato-Renal Umbilical (HRU)** 0 ☐ *1/2 ☐ 1 ☐ Indeterminate ☐ Not Assessed ☐

***Total Abdominal Fluid Score (AFS) 0-4:** _____ *If positive as patient status allows, move to either lateral recumbency and WAIT 3-minutes to allow fluid to redistribute before ***repeating*** AFAST® and ***assigning*** the AFS.

***Hepato-Renal 5th Bonus View:** *0 ☐ 1/2 ☐ 1 ☐ Indeterminate ☐ Not Assessed ☐ ***Not part of AFS***

**Focused Spleen:** Unremarkable ☐ Abnormal ☐ Indeterminate ☐ Not Assessed ☐

**Vet BLUE® RIGHT**

**Lung Sliding** Yes ☐ or No ☐ or Indeterminate ☐ or Not Assessed ☐

If PTX, **Lung Point** located - Upper 1/3 ☐ Middle 1/3 ☐ Lower 1/3 ☐

Indeterminate ☐ Not Assessed ☐

**Cd** - B-lines 0 ☐ 1 -3 ☐ >3 ☐ ∞ ☐ Indeterminate ☐ Not Assessed ☐

Shred ☐ size__ Tissue ☐ size__ Nodule ☐ size__ Wedge ☐ size__

**Ph** - B-lines 0 ☐ 1 -3 ☐ >3 ☐ ∞ ☐ Indeterminate ☐ Not Assessed ☐

Shred ☐ size__ Tissue ☐ size__ Nodule ☐ size__ Wedge ☐ size__

**Md** - B-lines 0 ☐ 1 -3 ☐ >3 ☐ ∞ ☐ Indeterminate ☐ Not Assessed ☐

Shred ☐ size__ Tissue ☐ size__ Nodule ☐ size__ Wedge ☐ size__

**Cr** - B-lines 0 ☐ 1 -3 ☐ >3 ☐ ∞ ☐ Indeterminate ☐ Not Assessed ☐

Shred ☐ size__ Tissue ☐ size__ Nodule ☐ size__ Wedge ☐ size__

**TFAST® RIGHT Pericardial Site:**

**Left Ventricular Short-axis:**

**Volume (Filling):** Unremarkable ☐ Poor ☐ Indeterminate ☐ Not Assessed ☐

**Contractility (FS%):** Unremarkable ☐ Poor ☐ Indeterminate ☐ Not Assessed ☐

**LA:Ao Short-axis:** Unremarkable ☐ **>1.3:1 dogs, >1.6:1 cats; obvious abnormal >2:1 ☐ Indeterminate ☐ Not Asssessed**

**RV:LV Long-axis:** Unremarkable ☐ **>1:3-4 dogs and cats; obvious abnormal ~1:1 ☐ Indeterminate ☐ Not Asssessed**

**Pericardial Effusion (Long-axis 4-chamber View)** Absent ☐ Present ☐ Mild <1 cm ☐ Moderate >1 cm <3 cm ☐

Severe >3 cm ☐ Indeterminate ☐ Not Assessed ☐

**Pleural Effusion** Absent ☐ Present ☐ Mild <1 cm ☐ Moderate >1 cm <3 cm ☐

Severe >3 cm ☐ Indeterminate ☐ Not Assessed ☐

**Comments**_____

_____

_____

**Qualifier:** The Global FAST® is a combination ultrasound format that includes AFAST®, TFAST® and Vet BLUE®. Global FAST® is a screening test for free fluid and certain organ abnormalities and helps direct resuscitation and diagnostic efforts. Global FAST® is not meant to replace radiography or complete detailed abdominal ultrasound or complete echocardiography.

**Figure 45.4.** Goal-directed template for Global FAST. Source: Reproduced with permission from Dr Gregory Lisciandro, Hill Country Veterinary Specialists and FASTVet.com, Spicewood, TX.

### Recording and Archiving Images

See Quality Control section below.

# Quality Control

- Training individuals in house and offsite and encouraging professional staff to make Global FAST and, over time, POCUS specific for the character of the practice a core skill.
- Establishing a consensus within your practice for what the ultrasound program should be. Typically this evolves over time as skills are gained.
- Saving images for case review.
- Periodically reviewing the overall content of your ultrasound program and making adjustments accordingly.
- Establishing a Global FAST and POCUS director or point person to oversee your program.
- Communication with colleagues regarding your Global FAST and POCUS program, if your practice is a secondary or referral practice, and with clients so they are aware of your additional training and acumen in assessing their pets.

### Establishing a Program Director or Point Person

It is imperative for one individual within your practice to be specifically responsible for the implementation of the program.

- Should be properly trained through relative ultrasound courses with understanding not only of basic ultrasound principles but also of its limitations.
- Should be an effective communicator and motivator.
- Should be able to implement quality control with authority.

### Establishing a Consensus

Involve everyone who undertakes image acquisition, image interpretation, and other related in-house services in periodically (at least biannually) reviewing your Global FAST and POCUS program. Set out to discuss, determine or revise your program's objectives and goals, which will include reviewing your goal-directed templates for additions, subtractions, and revisions. These periodical reviews will also serve to assess strengths, weaknesses, need for additional training, and strategies to improve your program.

### Ensuring Quality Control and Periodical Reviews

Ideally, the program director or point person should institute a multitiered approach with each ultrasonographer, including (1) being trained with lectures and hands-on time, followed by (2) a minimum number of proctored exams (suggest 12–25), and then (3) periodic reviews of cases thereafter.

Periodic case reviews (suggest monthly at staff meetings) and overall program assessment (suggest biannually) are also imperative to ensure quality control in image acquisition and image interpretation through case discussions. As discussed within this chapter, the use of standardized goal-directed templates and saving of ultrasound images on all cases (routine and interesting) help pinpoint deficiencies and assist with training and reviews.

### Saving Images

#### Why Save Images?

Saving ultrasound images is important for three major reasons: 1) archives your patient's Global FAST and POCUS study, allows you to review studies to learn from them, and allows you to show great Global FAST and POCUS cases to your staff. Ideally, video clips are preferable over still images because more information is generally gained. However, the decision is complex and dependent on the resources and character of the practice as well as other factors unique to the practice and veterinary medicine regulations.

#### What Time Frame and How Long Should I Make the Video Clips?

We suggest as a starting point recording a six-second clip that is *prospective*; thus when you start the recording you know what image is being captured. In some instances, you may need to get two six-second clips at a view for various reasons. However, by including target organs and transition zones in your recordings, labeling is generally not needed unless the view is so abnormal that labeling is needed for clarity. Unlabeled or minimally labeled video clips present a more obvious representation during review than a still image.

### Labeling Images

When the studies are performed in a standardized protocol-driven manner, images do not need to be labeled. For example, if my study is an AFAST then I record the study from the DH to the SR to the CC to the HRU

view. If the AFAST target organ approach is used, the DH is apparent because the diaphragm, liver, gallbladder, "cardiac bump," and caudal vena cava are all in view. The SR view is evidenced by the left kidney and spleen, and so forth. When needed because of abnormalities or the captured video clip is not obvious, then label. Cardiac images are also obvious if the image acquired is acceptable. For Vet BLUE, the author always performs left to right and catches transition zone on the Caudodorsal view, the heart on the Middle view, and the thoracic inlet on the Cranial view. The Ph view lacks anything other than lung.

### *Reviewing Images*

Learning from stored images is extremely helpful, from looking through Global FAST views and focusing on a single artifact to see how that artifact is portrayed by your ultrasound machine, to reviewing Global FAST views after complete studies, to comparing to other imaging modalities for recognizing the strengths and limitations of your approach.

Saved images may also be presented to your staff, showing them how important implementation of Global FAST and POCUS was for care in specific patients, catching conditions otherwise missed, and ultimately streamlining and expediting care and saving lives. The use of this strategy carries the potential to build pride in patient care and push the staff to adopt this paradigm and culture change.

## Training Techniques

In addition to scanning on live volunteers, training may be performed on cadavers and phantoms that are commercially available as well as hand made. For example, the chicken breast model is very realistic for training to place central line intravenous catheters (see Figures 24.12, 24.13, and 24.14 and Chapter 24). Moreover, many hand-made phantom models have been described and some are listed in the Further Reading section of this chapter. There are several companies that provide ultrasound training, including the author's company FASTVet.com that provides both hands-on and online Global FAST and POCUS training.

## Pearls and Pitfalls, The Final Say

You can have all the information and be able to produce the best image acquisition possible, but if you cannot communicate that to the client, if you are unable to assign fair and affordable financial value to Global FAST and POCUS, if you are unable to record findings, if you are unable to review proficiency and identify the skill level of the practice, your Global FAST and POCUS program will likely fall short. Conversely, if you can make Global FAST and POCUS a new paradigm change in your practice, you will find a new rewarding dimension of patient care that provides renewed confidence in your practice of veterinary medicine.

## Reference

Narasimhan M, Koenig SJ, Mayo PH. 2016. A whole body approach to point of care ultrasound. *Chest* 150(4):772–776.

## Further Reading

Beaulieu Y, Laprise R, Drolet P, et al. 2015. Bedside ultrasound traimning using web-based e-learning and simulation early in the curriculum of resiodents. *Crit Ultrasound J* 7:1.

Bluthgen C, Sanabria S, Frauenfelder T, et al. 2017. Economical sponge phantom for teaching, understanding, and researching A- and B-line reverberation artifacts in lung ultrasound. *J Ultrasound Med* 36(10):2133–2142.

Brietkreutz R, Dutine M, Scheiermann P, et al. 2013. Thorax, trachea, and lung ultrasonography in emergency and critical care medicine: assessment of an objective strcutured training concept. *Emerg Med International* 2013:312758.

Butler KL, Chang Y, DeMoya M, et al. 2016. Needs assessment for a focused radiology curriculum in surgical residency: a multicenter study. *Am J Surg* 211:279–287.

Daly R, Planas JH, Edens MA. 2017. Adapting gel wax into an ultrasound-guided pericardiocentesis model at low cost. *West J Emerg Med* 18(1):114–116.

dell'Orto MC, Hempel D, Starzetz A, et al. 2013. Assessment of a low-cost ultrasound pericardiocentesis model. *Emerg Med International* 2013; 376415.

Do HH, Lee S. 2016. A low-cost training phantom for lung ultrasonography. *Chest* 150(6):1417–1419.

Ferrada P, Evans D, Parker S, et al. 2017. Limited echocardiogram examinations performed by intensivists: a surgeon-driven multidisciplinary program. *Am Surg* 83(1):78–81.

Ho AM, Critchley LA, Leung JY, et al. 2015. Introducing final-year medical students to pocket-sized ultrasound imaging: teaching transthoracic echocardiography on a 2-week anesthesia rotation. *Teach Learn Med* 27(3):307–313.

Hoppmann RA, Rao VV, Poston MB, et al. 2015. The evolution of an integrated ultrasound curriculum (iUSC) for medical students: 9-year experience. *Crit Ultrasound J* 7(1):18.

Kalivoda EJ, Sullivan A, Bunting L. 2019. A cost-effective, rapidly constructed simulation model for ultrasound-guided pericardiocentesis procedural training. *J Emerg Med* 56(1):74–79.

Kim YH. 2016. Ultrasound phantoms to protect patients from novices. *Korean J Pain* 29(2):73–77.

Lambert MJ, Jang T. 2014. Training and program development. In: *Emergency Ultrasound*, 3rd edition, edited by Ma OJ, Mateer JR, Reardon RF, Joing SA. New York: McGraw Hill, pp 1–14.

Lumb P, Karakitsos D (eds). 2015. Section X: Hola Logistics and The Ultrasound Experience/ Training/Credentialing. In: *Critical Care Ultrasound*. Philadelphia: Elsevier Saunders, pp 294–318.

Mackay FD, Zhou F, Lewis D, et al. 2018. Can you teach yourself point-of-care ultrasound to a level of clinical competency? Evaluation of a self-directed simulation-based training program. *Cureus* 10(9):e3320.

Maresky HS, Oikonomou A, Ali I, et al. 2019. Virtual reality and cardiac anatomy: exploring immersive three-dimensional cardiac imaging, a pilot study in undergraduate medical anatomy education. *Clin Anat* 32(2):238–243.

McGovern S, Thompson P. 2006. Setting up an emergency ultrasound service. In: Emergency Ultrasound Made Easy, edited by Bowra J, McLaughlin RE. Edinburgh: Churchill Livingstone Elsevier, pp 141–146.

Nordin AB, Sales S, Nielsen JW, et al. 2018. Standardized ultrasound templates for diagnosing appendicitis reduce annual imaging costs. *J Surg Res* 221:77–83.

Ostergaard ML, Nielson KR, Albrecht-Beste E, et al. 2018. Development of a reliable simulation-based test for diagnostic abdominal ultrasound with a pass/fail standard usable for mastery learning. *Eur Radiol* 28(1):51–57.

Piton G, Capellier G, Winiszewski H. 2018. Ultrasound-guided vessel puncture: calling for Pythagoras' help. *Crit Care* 22(1):292.

Sandefur K, Kondrashova T. 2018. Increasing self-awareness of medical students through the use of ultrasound. *J Am Osteopath Assoc* 118(3):190–198.

Situ-LaCasse EH, Amini R, Bain V, et al. 2019. Performance of ultrasound-guided peripheral nerve blocks by medical students after one-day training session. *Cureus* 11(1):e3911.

Soni NJ, Arntfield R, Kory P (eds). 2015. Section 10: Ultrasound Program Management. In: Point-of-Care Ultrasound. Philadelphia: Elsevier Saunders, pp 369–378.

Sultan SF, Iohom G, Shorten G. 2013. A novel phantom for teaching and learning ultrasound-guided needle manipulation. *J Med Ultrasound* 21:152–155.

APPENDIX I

# Goal-Directed Templates for Medical Records

## AFAST®

**Patient Positioning:**
**Right** lateral recumbency (right preferred) ☐
**Left** lateral recumbency ☐
**Modified lateral recumbency** ☐
**Standing** ☐
**Sternal** ☐

**Gallbladder:**
**Visualized – Yes** ☐ or **No** ☐
**Contour, lumen and wall** – normal ☐ **or** abnormal ☐
**Comments:** none ☐ **or** _____.
**Urinary Bladder:**
**Visualized – Yes** ☐ or **No** ☐
**Contour, lumen and wall** – normal ☐ **or** abnormal ☐
**Comments:** none ☐ **or** _____.

**Diaphragmatico-Hepatic (DH) view:**
**Pleural Effusion:**
**Absent** ☐
**Present** ☐ mild ☐ moderate ☐ severe ☐ greatest width ____cm.
**Indeterminate** ☐ **Not Assessed** ☐

**Pericardial Fluid:**
**Absent** ☐
**Present** ☐ mild ☐ moderate ☐ severe ☐ greatest width ____cm.
**Indeterminate** ☐ **Not Assessed** ☐

**Volume Status:**
**Caudal Vena Cava: Unremarkable** ☐ **or** fluid intolerant (FAT) ☐ **or** hypovolemic (flat) ☐ **or** indeterminate ☐ **or not assessed** ☐
**Hepatic Veins: Unremarkable** ☐ **or** distended (Tree Trunk Sign) ☐ **or indeterminate** ☐ **or not assessed** ☐

**Positive or Negative at the 4 views (0 negative, 1 positive)**

| | |
|---|---|
| Diaphragmatico-Hepatic **(DH)** View: | 0 or 1/2 or 1 |
| Spleno-Renal **(SR)** View: | 0 or 1/2 or 1 |
| Cysto-Colic **(CC)** View: | 0 or 1/2 or 1 |
| Hepato-Renal Umbilical **(HRU)** View: | 0 or 1/2 or 1 |

**Abdominal Fluid Score (AFS):** _____

HR5th Bonus View (not part of the AFS): 0 or 1/2 or 1

Focused Spleen: Unremarkable ☐ or _____ or Indeterminate ☐ Not Assessed ☐
**Comments:** None ☐ or _____ _____.
_____.

**AFAST®** is an ultrasound exam used to detect the presence of free abdominal fluid and other soft tissue conditions in order to better direct resuscitative and diagnostic efforts and patient care. The AFAST is not intended to replace a complete detailed abdominal ultrasound exam. Created by Gregory Lisciandro, DVM, DABVP, DACVECC, CEO of FASTVet.com and President, International Veterinary Point-of-care Ultrasound Society, IVPOCUS.org.

## POCUS – Liver and Gallbladder

**Gallbladder:**
***Bilobed?** Yes ☐ **or** No ☐ ***Bilobed** is a normal variation more common in cats.
**Degree of Gallbladder Filling:** small ☐ moderate ☐ large ☐

*Point-of-Care Ultrasound Techniques for the Small Animal Practitioner*, Second Edition. Edited by Gregory R. Lisciandro.
© 2021 John Wiley & Sons, Inc. Published 2021 by John Wiley & Sons, Inc.
Companion website: www.wiley.com/go/lisciandro/ultrasound2

VetBooks.ir

**Luminal Contents:**
**None** ☐
**Sediment** ☐ nonshadowing ☐ **or** shadowing ☐ **or** calculi ☐ **or** mucocele ☐
**Measurements of Any Calculi and Approximate Number:**_____.
**Wall Abnormalities (thickening):**
**None** ☐ **or** focal ☐ **or** multifocal ☐ **or** diffuse ☐ **or** mass effect ☐
**Location(s):** _____.
**Measurement(s):**_____.

**Normal Measurements of Gallbladder Wall (cats** <1 mm; **dogs** <3 mm; and **Normal Contents**: generally homogeneous anechoic bile although degrees of ***gallbladder sludge*** may be considered as clinically irrelevant or may indicate cholestasis based on the patient's clinical profile.

**Liver:**
**Overall Size (subjective,** radiography more sensitive evaluation**):**
**Unremarkable** ☐
***Enlarged (hepatomegaly** suggested by rounded edges and hepatic lobes [especially left side] extending past the costal arch**)** ☐ - moderate ☐ **or** severe ☐
*Abdominal radiography provides a more reliable assessment for hepatomegaly.
**Overall Liver Echogenicity:**
**Unremarkable** ☐
**Abnormal** ☐ – hyperechoic ☐ **or** hypoechoic ☐ or mixed echogenicity ☐ **and** focal ☐ **or** uniformly diffuse ☐ **or** multifocal/patchy ☐

**Normal Echogenicity Rule of Thumb:** The spleen (S) is more echogenic (hyperechoic) than the liver (Li) which is the same or slightly more echogenic (brighter) than the cortex of the kidney (CK), remembered as S > Li ≥ CK or "SLiCK." For the feline, hepatic echogenicity is often compared to the adjacent falciform fat and the feline liver should be isoechoic to slightly hyperechoic (brighter) to the falciform fat. The feline liver, spleen, and cortex of the kidney are isoechoic to one another.

**Nodule(s):**
**Absent** ☐
**Present** ☐ - single ☐ **or** multiple ☐
**Measurements & Approximate Number:**
_____.
**Echogenicity of Nodule(s):**
_____.
**Overall Clinical Impression & Comments:**
**Unremarkable** ☐ **or** _____.

**POCUS Liver & Gallbladder Examination** is a screening test designed to identify and characterize obvious soft tissue abnormalities and is not intended to replace a complete detailed abdominal ultrasound exam.

# POCUS Spleen

**Spleen:**
**Overall Size (dogs,** subjective**; cats, normal <10 mm thickness; and in cats the spleen is** never folded over unless it is enlarged [splenomegaly]**):**
**Unremarkable** ☐ or **Enlarged** ☐ - moderate ☐ **or** severe ☐
**Overall Splenic Echogenicity:**
**Unremarkable** ☐
**Abnormal** ☐ – hyperechoic ☐ **or** hypoechoic ☐ **and** focal ☐ **or** inhomogeneous/patchy ☐ **or** diffuse ☐ **or** lacy ☐

**Normal Echogenicity Rule of Thumb:** The spleen (S) is more echogenic (hyperechoic) than the liver (Li) which is the same or slightly more echogenic (brighter) than the cortex of the kidney (CK), remembered as S > Li ≥ CK or "SLiCK." For the feline, hepatic echogenicity is often compared to the adjacent falciform fat and the feline liver should be isoechoic to slightly hyperechoic (brighter) to the falciform fat. The feline liver, spleen, and cortex of the kidney are isoechoic to one another.

**Nodule(s):**
**Absent** ☐ or **Present** ☐ – single ☐ **or** multiple ☐
**Measurement(s):**_____**cm.**
**Echogenicity of Nodule(s):**_____.
**Overall Clinical Impression & Comments:**
**Unremarkable** ☐ **or** _____.

**POCUS Spleen Examination** is a screening test designed to identify and characterize obvious soft tissue abnormalities and is not intended to replace a complete detailed abdominal ultrasound exam.

# POCUS Kidney

**Kidney:**
**Overall Echogenicity:**
**Unremarkable** ☐
**Abnormal** ☐ – hyperechoic ☐ **or** hypoechoic ☐ **and** focal ☐ **or** multifocal/patchy ☐ **or** diffuse ☐

**Normal Echogenicity Rule of Thumb:** The spleen (S) is more echogenic (hyperechoic) than the liver (Li) which is the same or slightly more echogenic (brighter) than the cortex of the kidney (CK) remembered as the S > Li ≥ CK or "SLiCK." For the feline, hepatic echogenicity is often compared to the adjacent falciform fat and the feline liver should be isoechoic to slightly

hyperechoic (brighter) to the falciform fat. The feline liver, spleen, and cortex of the kidney are isoechoic to one another.

**Overall Corticomedullary Distinction (subjective):**
**Unremarkable** ☐ or **Abnormal (decreased)** ☐
**Normal Kidney Size (Cats** 3.0–4.4 cm; **Dogs** no established normal size ***so must compare sizes of*** left to right**):**
**Kidney - Measurement(s)(width × length):**
**Left (cm):** _____**×**_____**.**
**Right (cm):**_____**×**_____**.**
**Symmetrical** ☐ or **Asymmetrical** ☐
**Normal Renal Pelvis Size:** There is variability in both cats and dogs. The height is measured. Generally, normal in the cat is 1.5–2 mm with maximum height of 2.8 mm, and dogs 2–3 mm with a maximum height of 3.8 mm. A general rule of thumb is to consider the renal pelvis abnormal (pyelectasia) if it measures ≥3 mm cats and ≥4 mm dogs.
**Renal Pelvis - Measurement(s)(height):**
**Left (mm):** _____.
**Right (mm):** _____**.**
**Nodule(s):** absent ☐ **or** present ☐ **and** single ☐ **or** multiple ☐
**Measurement(s) & Approximate Numbers of Nodules:** _____
**Echogenicity of Nodules:**_____**.**
**Cysts(s):** absent ☐ **or** present ☐ **and** single ☐ **or** multiple ☐ **and location** cortical ☐ **or** corticomedullary ☐
**Measurement(s) & Approximate Numbers of Cysts:**_____**.**
**Retroperitineal Fluid:**
**Absent** ☐ or **Present** ☐ **and** trivial ☐ **or** mild ☐ **or** moderate ☐ **or** severe ☐
**Echogenicity of Retroperitoneal Fluid:** anechoic ☐ **or** hyperechoic ☐ **and** uniform? Yes ☐ **or** No ☐
**Measurement Greatest Width** _____cm.
**Perirenal or Subcapsular Fluid:**
**Absent** ☐ or **Present** ☐ **and** trivial ☐ **or** mild ☐ **or** moderate ☐ **or** severe ☐
**Echogenicity of Perirenal or Subcapsular Fluid:** anechoic ☐ **or** hyperechoic ☐ **and** uniform? Yes ☐ **or** No ☐
**Measurement Greatest Width** _____**cm.**
**Overall Clinical Impression & Comments:**
**Unremarkable** ☐ **or** _____.
**POCUS Kidney Examination** is a screening test designed to identify and characterize obvious soft tissue abnormalities and is not intended to replace a complete detailed abdominal ultrasound exam.

# POCUS Urinary Bladder

**Urinary Bladder:**
**Degree of Urinary Bladder Filling:** small ☐ **or** moderate ☐ **or** largely distended ☐
**Luminal contents:**
**None** ☐ or **Sediment** ☐ nonshadowing (nonmineralized) ☐ **or** shadowing (mineralized) ☐ **and** calculi ☐ **or** thrombus (blood clot) ☐
**Measurements of Any Calculi and Approximate Number:**
_____.
**Wall Abnormalities:** none ☐ focal ☐ multifocal ☐ diffuse ☐ **and** mass-like? Yes ☐
**or** No ☐ **and** polpypoid? Yes ☐ **or** No ☐
**Location(s):** _____**.**
**Measurement(s):** _____**mm.**
**Normal Measurements of Urinary Bladder Wall with Moderate Bladder Distension: Cats** 1.3–1.7 mm; **dogs** 1.4–2.3 mm but may be as thick as 3 mm in large dogs; **and normal contents:** anechoic urine in **dogs**; anechoic with or without fat droplets seen as ultrasonographic "sparkles" can be normal in **cats**.
**Overall Clinical Impression & Comments:**
**Unremarkable** ☐ **or** _____.
**POCUS Urinary Bladder Examination** is a screening test designed to identify and characterize obvious soft tissue abnormalities and is not intended to replace a complete detailed abdominal ultrasound exam.

## *POCUS Gastrointestinal & Pancreas*

**Stomach:**
**Visualized:** yes ☐ **or** no ☐
**Stomach Lumen:**
**Gas-filled** ☐ **or** fluid-filled ☐ **or** ingesta ☐ **and** shadowing **"dirty"** (gas and fluid, or possible foreign body) ☐ **or "clean"** (possible foreign body) ☐ **or** other ☐ _____.
**Wall:** unremarkable ☐ **or** abnormal ☐
**Normal Stomach Wall Thickness**: **Dogs** 3–5 mm, higher in some giant breeds; **cats** 2 mm interrugal (up to 4.4 mm if rugal fold is measured); **measured** from the hyperechoic outer serosal margin to inner mucosoluminal surface.
**Stomach Size (subjective):** unremarkable ☐ **or** obviously distended ☐ **or** indeterminate ☐
**General Stomach Overall Clinical Impression & Comments:**
**Unremarkable** ☐ **or** _____**.**

**Small Bowel:**

**Small Bowel Lumen:**

**Normal**, unremarkable ☐

**Abnormal** ☐ **and** gas-filled ☐ **or** fluid-filled ☐ **or** ingesta ☐ **and** shadowing **"dirty"** (gas and fluid, or possible foreign body) ☐ **or "clean"** (possible foreign body) ☐ **or** other ☐_____.

**Peristalsis Observed:** yes ☐ **or** no ☐ **or** indeterminate ☐ **and** normal ☐ **or** abnormal ☐ **or** indeterminate ☐

**Normal Peristalsis: Stomach** 4–5 contractions/minute; **small Bowel** 1–3 contractions/minute; **large Bowel** no movement; each counted over 3 minutes and averaged.

**Obvious Small Bowel Dilation (small bowel lumen distension of >1.5 cm, *measured from serosal surface to serosal surface*):**

**No** dilation ☐ **or Yes** dilation ☐ **and** focally ☐ **or** multifocally ☐ **or** diffusely ☐ **or** indeterminate ☐

**Small Bowel Wall Thickness** (**Normal** other than duodenum: **dogs** ≤4 mm; **cats** ≤2.5 mm, measured from the hyperechoic outer serosal margin to inner mucosoluminal surface):

**Normal** ☐ **or** abnormal ☐ **or** indeterminate ☐

**Small Bowel Wall Measurement(s):**

_____ (mm).

**Overall Clinical Impression & Comments Small Bowel:**

**Unremarkable** ☐ **or** _____.

**Pancreas:**

**Unremarkable (normally not easily observed)** ☐ **or** observed ☐

(**Dogs** right limb easier to identify and image; **cats** left limb easier to image)

**Measurement if Observed (length x width): _____×_____(cm).**

**Any Peripancreatic Abnormalities:**

**Fluid?** yes ☐ **or** no ☐ **and** greatest width_____(cm).

**Peripancreatic Structures:** unremarkable ☐ **or** hyperechoic (bright) ☐

**Overall Clinical Impression & Comments Pancreas:**

**Unremarkable** ☐ **or** _____.

**POCUS Gastrointestinal & Pancreas Examination** is a screening test designed to identify and characterize obvious soft tissue abnormalities and is not intended to replace a complete detailed abdominal ultrasound exam.

# POCUS Reproductive

**Male – Prostate, Testicles, Epididymis**

**Prostate:** unremarkable ☐ **or** abnormal ☐

**Symmetry of Lobes:** symmetrical ☐ **or** asymmetrical ☐

**Echogenicity: normal** (homogeneous **with the appearance of a hyperechoic "butterfly"** in the transverse plane) ☐ **or** hyperechoic ☐ **or** mixed echogenicity ☐ **or** hypoechoic ☐ **and** mineralized? – yes ☐ **or** no ☐

**Cysts:** parenchymal ☐ **or** paraprostatic ☐ **or** indeterminate ☐

**Nodule(s):** hyperechoic ☐ **or** mixed ☐ **or** hypoechoic ☐ **and** number and measurement(s)_____.

**Testicles:**

**Symmetry:** symmetrical ☐ **or** asymmetrical ☐ **or** *indeterminate (*retained and not accessible) ☐

***Right* Testicle Location:** scrotal ☐ **or** inguinal ☐ **or** intraabdominal ☐

***Right* Echogenicity: normal** (homogeneous with the **linear** hyperechoic mediastinum testes) ☐ **or** hyperechoic ☐ **or** hypoechoic ☐ **or** mixed ☐

***Right* Nodules: absent** ☐ **or** nodule(s) ☐ **with** measurement(s) and approximate number_____.

***Right* Measurement (length x width):** _____×_____cm.

***Right* Epididymis:** unremarkable ☐ **or** enlarged ☐ **with** fluid accumulation? yes ☐ **or** no ☐ **or** not evaluated ☐

***Left* Testicle – *repeat same format above*.**

**Overall Clinical Impression & Comments:**

**Unremarkable** ☐ **or** _____.

**POCUS Male Reproductive Examination** is a screening test designed to identify and characterize obvious soft tissue abnormalities and is not intended to replace a complete detailed abdominal ultrasound exam.

# Female – Uterus

**Uterus (present/absent):** unremarkable ☐ **or** abnormal ☐

**Uterine Fluid:** 0, 1, 2, 3, 4 (0 negative to 4 large amount)

**0 – No fluid** present, **normal.**

**1 – Mild fluid** present, minimal uterine distension.

**2 – Moderate fluid** and uterine distension.

**3 – Severe fluid** and uterine distension, consistent with closed pyometra. **Note:** The uterus should be considered fragile and at risk for rupture. Stabilize patient and proceed with directed medical or surgical care.

**4 – Uterine fluid** present ***with* free abdominal fluid** and may indicate uterine rupture and secondary peritonitis. Prompt surgery may be indicated based on remainder of clinical signs and patient status.

**POCUS Female Reproductive Examination** is a screening test designed to identify and characterize

obvious soft tissue abnormalities and is not intended to replace a complete detailed abdominal ultrasound exam.

# POCUS Reproductive Dystocia

**Fetuses:** present ☐ **or** absent ☐

**Fetal Heart Rate:** lowest ☐ _____ (bpm) **and** general impression ☐ _____ (bpm).

*Use both lowest HR obtained and overall general impression since variability can be remarkable, e.g., 1 dead and others alive.

**HR >180** – **Normal.**

**180 > HR > 160** – Early fetal stress, prompt intervention required.

**160 > HR > 140** – Moderate fetal stress, C-section warranted.

**HR <140** – Severe fetal stress, reduced fetal viability, immediate surgical intervention required.

**Fetal Development:**

**Small Bowel Evident:** yes ☐ **or** no ☐ – **Note:** small bowel development in normal layering and appearance indicates term or near term fetuses.

*Other ultrasonographic parameters for fetal development are not mentioned here but are available elsewhere.

**POCUS Dystocia Reproductive Examination** is a screening test designed to identify and characterize obvious soft tissue abnormalities and is not intended to replace a complete detailed abdominal ultrasound exam.

# TFAST®

KEY: CTS, chest tube site; PCS, pericardial site; LV, left ventricle, PTX, pneumothorax.

***Left CTS Glide Sign:**

**Present (Dry Lungs)** ☐ **-** no pneumothorax.

**Absent** – ☐ pneumothorax **– search for the** Lung Point.

**Lung Point –** upper 1/3 (trivial) ☐ **or** middle 1/3 (moderate to severe) ☐ **or** ventral 1/3 (severe) ☐ **or** indeterminate ☐

**Indeterminate** ☐ or **Not Assessed**

***Left CTS Lung Rockets:**

**Present (no PTX)** ☐ – alveolar-interstitial edema (i.e., edema, hemorrhage).

**Absent** ☐ **–** alveolar-interstitial edema (i.e., edema, hemorrhage).

**Indeterminate** ☐ or **Not Assessed**

***Left PCS View:**

**Absent** ☐ **-** no pleural **or** pericardial fluid.

**Present** ☐

**Pleural:** ☐ **–** mild ☐ **or** moderate ☐ **or** severe ☐; greatest width ___cm.

**Pericardial:** ☐ **–** mild ☐ **or** moderate ☐ **or** severe ☐; greatest width ___cm.

**Indeterminate** ☐ or **Not Assessed**

***Left CTS Step Sign:**

**Absent** ☐

**Present** ☐ **–** suggests thoracic wall, pleural space conditions, or *lung pathology.

***Characterize –** Shred sign, tissue sign, nodule sign, wedge sign

and **go to Vet BLUE.**

***Repeat same format for the Right side CTS and PCS views with the addition of cardiac assessment from the right PCS view:***

**LV filling on short-axis "mushroom view":**

**Adequate** ☐ – suggesting normovolemia.

**Inadequate** ☐ **–** suggesting hypovolemia.

**Indeterminate** ☐ or **Not Assessed**

**LV contractility on short-axis "mushroom view":**

**Adequate** ☐ – suggesting normovolemia.

**Inadequate** ☐ **–** suggesting dilated cardiomyopathy.

**Indeterminate** ☐ or **Not Assessed**

**LA:Ao ratio on short axis**

**Unremarkable** ☐

**Abnormal** ☐

**Indeterminate** ☐ or **Not Assessed**

**RV:LV ratio on long-axis**

**Unremarkable** ☐

**Abnormal** ☐

**Indeterminate** ☐ or **Not Assessed**

**Diaphragmatico-Hepatic (DH) View [free fluid]:**

**Absent** ☐ **–** no pericardial **or** pleural fluid

**Present** ☐

**Pericardial Effusion** ☐ **–** mild ☐ **or** moderate ☐ **or** severe ☐; greatest width _____cm.

**Pleural effusion** ☐ **–** mild ☐ **or** moderate ☐ **or** severe ☐; greatest width _____cm.

**Indeterminate** ☐ or **Not Assessed**

**Overall Clinical Impression & Comments:**

**Unremarkable** ☐ **or** _____.

**TFAST®** is an ultrasound exam used to help detect thoracic wall, lung, and pleural and pericardial space disease, soft tissue abnormalities of the heart, left-and right-sided cardiac abnormalities, and assess volume status in order to better direct resuscitative and diagnostic efforts and patient care. TFAST is not intended to replace thoracic radiographs or complete detailed echocardiography. Created by Gregory Lisciandro,

DVM, DABVP, DACVECC, CEO of FASTVet.com and President, International Veterinary Point-of-care Ultrasound Society, IVPOCUS.org.

# Vet BLUE® – Simple Version

KEY: VBLS, Vet BLUE; ULR, ultrasound lung rockets; Cd, caudodorsal lung region; Ph, perihilar lung region; Md, middle lung region; Cr, cranial lung region.

**Left VBLS (Cd, Ph, Md, Cr): X, X, X, X**
**Right VBLS (Cd, Ph, Md, Cr): Y, Y, Y, Y**
**DH: Z**

**Record Maximum B-lines over *a single* Intercostal Space at that respective Vet BLUE Lung Region:** 0, 1, 2, 3, >3, ∞ (infinity symbol)
**KEY:** 0, no ULRs; 1, single B-line; 2, two B-lines; 3, three B-lines; >3, more than three B-lines but still seen as individual B-lines; ∞ (infinity symbol), so many B-lines *that no longer can be counted individually* and cover the entire intercostal space.

**Add Notations after the Number of ULRs for Other Lung Findings Using Abbreviations: Shred Sign** (Sh), **Tissue Sign** (Ti), **Nodule(s) Sign** (Nd), **Wedge Sign** (Wdge)

***Always do in same order of lung regions then it really is a simple system for recording. Start left side and go as ordered in examples,*** *then* ***to right side,*** *then* ***finish with TFAST heart views when concurrently doing TFAST making it efficient and rapid.***

**Left (Cd *to* Ph *to* Md *to* Cr): X, X, X, X**
**Right (Cd *to* Ph *to* Md *to* Cr): X, X, X, X**
**DH: X**

**Example, Dry Lung or Absent B-lines All Views (ABAV):**
**Left (Cd, Ph, Md, Cr): 0, 0, 0, 0**
**Right (Cd, Ph, Md, Cr): 0, 0, 0, 0**
**DH: 0**

**Example, Wet Lung in caudodorsal and perihilar Vet BLUE lung regions supporting cardiogenic (left-sided congestive heart failure) and noncardiogenic pulmonary edema:**
**Left: >3, >3, 0, 0 or ∞, ∞, 0, 0**
**Right: >3, >3, 0, 0 or ∞, ∞, 0, 0**
**DH: >3**

**Example, Shred Sign, Tissue Sign supporting severe bacterial bronchopneumonia:**
**Left: 0, 0, 2 (Sh), >3(Ti)**
**Right: 0, 0, >3 (Sh), 0 (Ti)**
**DH: 0**

**Example, Nodule Sign:**
**Left: 0 (Nd), 0, 0, 0**
**Right: 0, 0, 0, 0**
**DH: 0**

**Example, Wedge Sign (Pulmonary Thromboembolism):**
**Left: ∞ Wdge, 0, 0, 0**
**Right**: **0, 0, 0, 0**
**DH: 0**

**Overall Clinical Impression & Comments:**
**Unremarkable ☐ or _____.**

**Vet BLUE®** is a lung examination used to help differentiate causes of respiratory distress, guide resuscitative and diagnostic efforts, monitor respiratory conditions and guide patient care. Vet BLUE is not intended to replace thoracic radiography or complete detailed echocardiography. Created by Gregory Lisciandro, DVM, DABVP, DACVECC, CEO of FASTVet.com and President, International Veterinary Point-of-care Ultrasound Society, IVPOCUS.org.

# Vet BLUE® – Detailed Version

**Ask Yourself:** Wet vs Dry? Number of B-lines? Anything off the Lung Line? Are you mistaking abdominal contents for lung pathology?

KEY: Sh, Shred Sign; Ti, Tissue Sign; Nd, Nodule; Wdge, Wedge; Cd, caudodorsal; Ph, perihilar; Md, middle; Cr, cranial.

**Left**
**Cd** 0 ☐ 1–3 ☐ >3 ☐ ∞ ☐
Sh ☐ Ti, ☐ Nd ☐ Wedge ☐ OR
indeterminate ☐ not assessed ☐
**Ph** 0 ☐ 1–3 ☐ >3 ☐ ∞ ☐
Sh ☐ Ti, ☐ Nd ☐ Wedge ☐ OR
indeterminate ☐ not assessed ☐
**Md** 0 ☐ 1–3 ☐ >3 ☐ ∞ ☐
Sh ☐ Ti, ☐ Nd ☐ Wedge ☐ OR
indeterminate ☐ not assessed ☐
**Cr** 0 ☐ 1–3 ☐ >3 ☐ ∞ ☐
Sh ☐ Ti, ☐ Nd ☐ Wedge ☐ OR
indeterminate ☐ not assessed ☐

Comments_____

**Right**
**Cd** 0 ☐ 1–3 ☐ >3 ☐ ∞ ☐
Sh ☐ Ti, ☐ Nd ☐ Wedge ☐ OR
indeterminate ☐ not assessed ☐
**Ph** 0 ☐ 1–3 ☐ >3 ☐ ∞ ☐
Sh ☐ Ti, ☐ Nd ☐ Wedge ☐ OR
indeterminate ☐ not assessed ☐
**Md** 0 ☐ 1–3 ☐ >3 ☐ ∞ ☐
Sh ☐ Ti, ☐ Nd ☐ Wedge ☐ OR
indeterminate ☐ not assessed ☐
**Cr** 0 ☐ 1–3 ☐ >3 ☐ ∞ ☐
Sh ☐ Ti, ☐ Nd ☐ Wedge ☐ OR
indeterminate ☐ not assessed ☐

Comments_____

**DH** 0 ☐ 1–3 ☐ >3 ☐ ∞ ☐
Sh ☐ Ti, ☐ Nd ☐ Wedge ☐ OR indeterminate ☐ not assessed ☐

Comments _____

Conclusion _____

**Qualifier:** The Vet BLUE lung ultrasound exam is a screening test for many conditions that affect the lung surface such as heart failure, pneumonia, nodular disease and others. Vet BLUE helps characterize respiratory conditions as a screening test. Vet BLUE is not meant to replace thoracic radiography or computed tomography. Created by Gregory Lisciandro, DVM, DABVP, DACVECC, CEO of FASTVet.com and President, International Veterinary Point-of-care Ultrasound Society, IVPOCUS.org.

# POCUS Echo (Heart)

Quantitative Assessment:

| Cardiac parameter | Measurement |
|---|---|
| LVEDD | |
| LVESD | |
| IVSD | |
| LVFWD | |
| Ao | |
| LA | |
| LA:Ao ratio | |
| FS% | |

**Quantitative Assessment:**

**Left Atrial Size:** small ☐ **or** normal ☐ **or** enlarged ☐ **or** indeterminate ☐ or not assessed

**Left Ventricular Size:** small ☐ **or** ☐ normal **or** enlarged ☐ **or** indeterminate ☐ or not assessed ☐

**Left Ventricular Function:** hypodynamic ☐ **or** normal ☐ **or** hyperdynamic ☐ **or** indeterminate ☐ or not assessed ☐

**Right Atrial Size:** small ☐ **or** normal ☐ **or** enlarged ☐ **or** indeterminate ☐ or not assessed ☐

**Right Ventricular Size:** small ☐ **or** normal ☐ **or** enlarged ☐ **or** indeterminate ☐ or not assessed ☐

**Pulmonary Artery Size:** small ☐ **or** normal ☐ **or** enlarged ☐ **or** indeterminate ☐ or not assessed ☐

**Pleural Effusion:** none ☐ **or** mild ☐ **or** moderate ☐ **or** severe ☐ **or** indeterminate ☐ or not assessed ☐

**Pericardial Effusion:** none ☐ **or** mild ☐ **or** moderate ☐ **or** severe ☐ **or** indeterminate ☐ or not assessed ☐

**Cardiac Tamponade Present:** no ☐ **or** yes ☐ **or** equivocal ☐ **or** indeterminate ☐ or not assessed ☐

**Cardiac Tumor Present:** no ☐ **or** yes ☐ **or** suspicious ☐ **or** indeterminate ☐ or not assessed ☐

**Caudal Vena Cava Size:** small ☐ **or** normal ☐ **or** enlarged ☐ **or** indeterminate ☐ or not assessed ☐

**Caudal Vena Cava Respiratory Fluctuations:** ☐ >50% **or** <50% ☐ **or** indeterminate ☐ or not assessed ☐

**Hepatic Venous Distension:** none ☐ **or** mild ☐ **or** moderate ☐ **or** severe ☐ **or** indeterminate ☐ or not assessed ☐

***Ascites:** none ☐ **or** mild ☐ **or** moderate ☐ **or** severe ☐ **or** indeterminate ☐ or not assessed ☐

***Note: The abdominal fluid scoring system (AFS) may be used for ascites.**

**Overall Clinical Impression & Comments:**

**Unremarkable** ☐ **or** _____.

**POCUS (Echo) Heart examination** is a screening test designed to identify and characterize obvious clinical conditions to better treat patients. POCUS Heart is not intended to replace complete detailed echocardiography or noncardiac thoracic ultrasound exam.

# POCUS Pediatrics

Suggest incorporating the listed POCUS abbreviated examinations in a format tailored to your practice's skill level.

# POCUS Eye

**Template for Ocular Ultrasound using Horizontal or Vertical Views Only**

**Cornea:**

**Shape, contour:** rounded and intact (normal) ☐ **or** abnormal ☐ (describe)_____ **or** indeterminate ☐ **or** not assessed ☐

**Anterior Chamber:**

**Depth:** shallow ☐ **or** normal ☐ **or** ☐ deep **or** indeterminate ☐

**Echogenicity (normal anechoic)**: unremarkable ☐ **or** abnormal ☐ (*describe) _____ **or** indeterminate ☐ **or** not assessed ☐

*If echogenic material in anterior chamber: location, size, shape, orientation, degree of mobility, degree of echogenicity.

**Iris:** flat (normal) ☐ **or** irregular ☐ and describe _____ **or** indeterminate ☐ **or** not assessed ☐

**Lens**:

**Location:** central lens capsules visible in normal location?

Yes ☐ **or** no ☐ _____ **or** indeterminate ☐ **or** notassessed ☐

**Contour:** central lens capsules have normal contour?

Yes ☐ **or** no ☐ _____ **or** indeterminate ☐ **or** notassessed ☐

**Lens Echogenicity:** lens material within capsules – hypoechoic ☐ **or** hyperechoic ☐ **or** indeterminate ☐ **or** not assessed ☐

**Vitreous Echogenicity:** unremarkable ☐ **or** abnormal ☐ **and** *describe _____ _____ **or** indeterminate ☐ **or** not assessed ☐

*If echogenic material in vitreous: location, size, shape, orientation, degree of mobility, degree of echogenicity _____.

***Cautious interpretation since clinically irrelevant conditions may be present in an echogenic vitreous.***

**Posterior Eye Wall:**

**Contour:** normal distinct contour ☐ **or** abnormal ☐ **and** describe _____ **or** indeterminate ☐ **or** not assessed ☐

**Retrobulbar Space:** hypoechoic extraocular muscle cone ☐ **or** n abnormal ☐ **and** describe _____ _____ **or** indeterminate ☐ **or** not assessed ☐

**Optic Nerve:** observed ☐ *and **width** if measured taken 3 mm from posterior eye wall*_____mm **or** indeterminate ☐ **or** not assessed ☐

**Optic Nerve Sheath Diameter (dogs only) Measured 3 mm Posterior to the Eye:** ≤2.7 mm considered normal; >3 mm considered abnormal suggesting increased intracranial pressure.

**Overall Clinical Impression & Comments:**

**Unremarkable** ☐ **or** ☐ _____.

**POCUS Eye Examination** is a screening test designed to identify and characterize obvious eye abnormalities to better treat patients. POCUS Eye is not intended to replace a complete ocular ultrasound performed by a specialist with advanced training.

# Vet FAST-ABCDE

**A: Airway (upper airway)**

**Laryngeal Movements:** unremarkable ☐ **or** abnormal ☐ **or** indeterminate ☐ **and** describe _____.

**Tracheal Integrity (scan larynx to thoracic inlet):** unremarkable ☐ **or** abnormal ☐ **or** indeterminate ☐ **or** not assessed ☐ **and** describe _____ _____.

**B: Breathing (lower airway)**

**Thoracic Wall Scan**

**C: Circulation**

**Thoracic Circulation**

**Focused ECHO Template**

**Abdominal Circulation**

**Major Abdominal Organs Injuries** – none ☐ **or** describe _____.

**D: Disability (screen for intracranial hypertension, eye conditions)**

**Optic Nerve Sheath Diameter (ONSD) Measured 3 mm Posterior to the Eye (normal** ≤2.7 mm; **abnormal** >3 mm suggesting increased intracranial pressure).

**ONSD Measurement** (if measured): _____ _____.

**Focused Eye Template (eye lesions, injury)**

**E: Exposure (listing any other relevant findings)**

**None** ☐ **or** describe _____.

**Overall Clinical Impression & Comments:**

**Unremarkable** ☐ **or** ☐ _____.

**VetFAST-ABCDE Examination** combines upper airway, abdominal, thoracic and lung ultrasound and POCUS Eye and ECHO for comprehensive patient evaluation. VetFAST-ABCDE is used for the rapid detection of potentially life-threatening thorax-related and lung, abdomen-related and retroperitoneal, upper airway, eye and heart problems or conditions in order to better direct resuscitative efforts and patient care. VetFAST-ABCDE is not intended to replace thoracic and abdominal radiographs or complete detailed echocardiography or complete detailed abdominal ultrasound.

# Global FAST® (GFAST℠)

**Use the AFAST®, TFAST®, and Vet BLUE® Templates and the Blended Global FAST® Template**

**Global FAST® Goal-Directed Template – RIGHT LATERAL**

Sonographer _____ Patient Name_____ Date/Time_____ Sedation? Y ☐ N ☐ If yes, type of_____

Patient positioning: Sternal/standing ☐ Lateral – Left ☐ or Right ☐ or Modified sternal ☐

**FAST DH**

Caudal Vena Cava: Bounce (fluid-responsive CVC) ☐ Flat (hypovolemic CVC) ☐

FAT (fluid-intolerant CVC) ☐ Indeterminate ☐ Not Assessed ☐

Hepatic Venous Distension: Absent ☐ Present ☐ Indeterminate ☐ Not Assessed ☐

Pleural Effusion (PE): Absent ☐ Present ☐ Mild <1 cm ☐ Moderate >1 cm <3 cm ☐ Severe >3 cm ☐ Indeterminate ☐ Not Assessed ☐

Pericardial Effusion (PCE): Absent ☐ Present ☐ Mild <1 cm ☐ Moderate >1 cm <3 cm ☐ Severe >3 cm ☐ Indeterminate ☐ Not Assessed ☐
Vet BLUE: B-lines 0 ☐ 1 –3 ☐ >3 ☐ ∞ ☐ Indeterminate ☐ Not Assessed ☐
Shred ☐ size____ Tissue ☐ size____ Nodule ☐ size____ Wedge ☐ size____

**AFAST®** Sternal/standing ☐ Lateral – Left ☐ or Right ☐ or Modified sternal ☐

**DH** 0 ☐ 1/2 ☐ 1 ☐ Indeterminate ☐ Not Assessed ☐
**SR** 0 ☐ 1/2 ☐ 1 ☐ Indeterminate ☐ Not Assessed ☐
**CC** 0 ☐ 1/2 ☐ 1 ☐ Indeterminate ☐ Not Assessed ☐
**HRU** 0 ☐ 1/2 ☐ 1 ☐ Indeterminate ☐ Not Assessed ☐

Total abdominal fluid score 0–4: _____
**Focused Spleen:** Unremarkable ☐ Abnormal ☐ Indeterminate ☐ Not Assessed ☐

**Vet BLUE®** LEFT

**Lung Sliding** Yes ☐ or No ☐ or Indeterminate ☐ or Not Assessed ☐
If PTX, Lung Point located – Upper 1/3 ☐ Middle 1/3 ☐ Lower 1/3 ☐ Indeterminate ☐ Not Assessed ☐

**Cd** B-lines 0 ☐ 1–3 ☐ >3 ☐ ∞ ☐ Indeterminate ☐ Not Assessed ☐ Shred ☐ size____ Tissue ☐ size____ Nodule ☐ size____ Wedge ☐ size____
**Ph** B-lines 0 ☐ 1–3 ☐ >3 ☐ ∞ ☐ Indeterminate ☐ Not Assessed ☐ Shred ☐ size____ Tissue ☐ size____ Nodule ☐ size____ Wedge ☐ size____
**Md** B-lines 0 ☐ 1–3 ☐ >3 ☐ ∞ ☐ Indeterminate ☐ Not Assessed ☐ Shred ☐ size____ Tissue ☐ size____ Nodule ☐ size____ Wedge ☐ size____
**Cr** B-lines 0 ☐ 1–3 ☐ >3 ☐ ∞ ☐ Indeterminate ☐ Not Assessed ☐ Shred ☐ size____ Tissue ☐ size____ Nodule ☐ size____ Wedge ☐ size____

**TFAST®** Left Pericardial Site: Pleural Effusion Absent ☐ Present ☐ Indetermimate ☐ Not Assessed ☐
**TFAST®** Right Pericardial Site:
**Contractility & Volume:**
Volume (LV Filling): Unremarkable ☐ Poor ☐ Indeterminate ☐ Not Assessed ☐
Contractility (LV FS%): Unremarkable ☐ Poor ☐ Indeterminate ☐ Not Assessed ☐
**LA:Ao Short-axis** Unremarkable ☐ Increased (>1:1.3 dogs, >1:1.6 cats) ☐ Indeterminate ☐ Not Assessed ☐
**RV:LV Long-axis** Unremarkable ☐ Increased (>1:1.3 dogs, >1:1.6 cats) ☐ Indeterminate ☐ Not Assessed ☐

**Vet BLUE®** RIGHT – Moving to Sternal or Standing or Left Lateral

**Lung Sliding** Yes ☐ or No ☐ or Indeterminate ☐ or Not Assessed ☐
If PTX, Lung Point located – Upper 1/3 ☐ Middle 1/3 ☐ Lower 1/3 ☐ Indeterminate ☐ Not Assessed ☐

**Cd** B-lines 0 ☐ 1–3 ☐ >3 ☐ ∞ ☐ Indeterminate ☐ Not Assessed ☐ Shred ☐ size____ Tissue ☐ size____ Nodule ☐ size____ Wedge ☐ size____
**Ph** B-lines 0 ☐ 1–3 ☐ >3 ☐ ∞ ☐ Indeterminate ☐ Not Assessed ☐ Shred ☐ size____ Tissue ☐ size____ Nodule ☐ size____ Wedge ☐ size____
**Md** B-lines 0 ☐ 1 –3 ☐ >3 ☐ ∞ ☐ Indeterminate ☐ Not Assessed ☐ Shred ☐ size____ Tissue ☐ size____ Nodule ☐ size____ Wedge ☐ size____
**Cr** B-lines 0 ☐ 1–3 ☐ >3 ☐ ∞ ☐ Indeterminate ☐ Not Assessed ☐ Shred ☐ size____ Tissue ☐ size____ Nodule ☐ size____ Wedge ☐ size____

**HR5th View:** *0 ☐ 1/2 ☐ 1 ☐ Indeterminate ☐ Not Assessed ☐ **Not part of AFS*

**Comments** _____
_____
_____
_____
_____

**Qualifier:** The Global FAST® is a combination ultrasound format that includes AFAST®, TFAST®, and Vet BLUE®. Global FAST is a screening test for free fluid and certain organ abnormalities and helps direct resuscitation and diagnostic efforts. Global FAST is not meant to replace radiography or complete detailed abdominal ultrasound or complete echocardiography.

Created by Gregory Lisciandro, DVM, DABVP, DACVECC, CEO of FASTVet.com and President, International Veterinary Point-of-care Ultrasound Society, IVPOCUS.org.

**Global FAST® Goal-Directed Template - STANDING**

Sonographer _____ Patient Name_____
Date/Time_____ Sedation? Y ☐ N ☐ If yes, type of_____
Patient positioning: Sternal/standing ☐ Lateral – Left ☐ or Right ☐ or Modified sternal ☐

**Vet BLUE®** LEFT

**Lung Sliding** Yes ☐ or No ☐ or Indeterminate ☐ or Not Assessed ☐
If PTX, Lung Point located - Upper 1/3 ☐ Middle 1/3 ☐ Lower 1/3 ☐ Indeterminate ☐ Not Assessed ☐

**Cd** B-lines 0 ☐ 1–3 ☐ >3 ☐ ∞ ☐ Indeterminate ☐
Not Assessed ☐ Shred ☐ size____ Tissue ☐ size____ Nodule ☐ size____ Wedge ☐ size____
**Ph** B-lines 0 ☐ 1–3 ☐ >3 ☐ ∞ ☐ Indeterminate ☐
Not Assessed ☐ Shred ☐ size____ Tissue ☐ size____ Nodule ☐ size____ Wedge ☐ size____
**Md** B-lines 0 ☐ 1–3 ☐ >3 ☐ ∞ ☐ Indeterminate ☐
Not Assessed ☐ Shred ☐ size____ Tissue ☐ size____ Nodule ☐ size____ Wedge ☐ size____
**Cr** B-lines 0 ☐ 1–3 ☐ >3 ☐ ∞ ☐ Indeterminate ☐
Not Assessed ☐ Shred ☐ size____ Tissue ☐ size____ Nodule ☐ size____ Wedge ☐ size____

**TFAST®** Left Pericardial Site: Pleural Effusion Absent ☐ Present ☐ Indeterminate ☐ Not Assessed ☐

**FAST DH**

Caudal Vena Cava: Bounce (fluid0responsive CVC) ☐ Flat (hypovolemic CVC) ☐
FAT (fluid-intolerant CVC) ☐ Indeterminate ☐ Not Assessed ☐
Hepatic Venous Distension: Absent ☐ Present ☐ Indeterminate ☐ Not Assessed ☐
Pleural Effusion (PE): Absent ☐ Present ☐ Mild <1 cm ☐ Moderate >1 cm <3 cm ☐
Severe >3 cm ☐ Indeterminate ☐ Not Assessed ☐
Pericardial Effusion (PCE): Absent ☐ Present ☐ Mild <1 cm ☐ Moderate >1 cm < 3 cm ☐ Severe >3 cm ☐ Indeterminate ☐ Not Assessed ☐
Vet BLUE: B-lines 0 ☐ 1–3 ☐ >3 ☐ ∞ ☐ Indeterminate ☐ Not Assessed ☐ Shred ☐ size____ Tissue ☐ size____ Nodule ☐ size____ Wedge ☐ size____

**AFAST®** Sternal/standing ☐ Lateral – Left ☐ or Right ☐ or Modified sternal ☐

**DH** 0 ☐ *1/2 ☐ 1 ☐ Indeterminate ☐ Not Assessed ☐
**SR** 0 ☐ *1/2 ☐ 1 ☐ Indeterminate ☐ Not Assessed ☐
**CC** 0 ☐ *1/2 ☐ 1 ☐ Indeterminate ☐ Not Assessed ☐
**HRU** 0 ☐ *1/2 ☐ 1 ☐ Indeterminate ☐ Not Assessed ☐

*Total abdominal fluid score 0–4: _____
*If negative then negative, but if positive must move to either lateral recumbency and WAIT 3 minutes to allow fluid to redistribute before ***repeating*** AFAST and ***assigning*** the AFS.

**Focused Spleen:** Unremarkable ☐ Abnormal ☐ Indeterminate ☐ Not Assessed ☐

**Vet BLUE®** RIGHT

**Lung Sliding** Yes ☐ or No ☐ or Indeterminate ☐ or Not Assessed ☐
If PTX, Lung Point located – Upper 1/3 ☐ Middle 1/3 ☐ Lower 1/3 ☐ Indeterminate ☐ Not Assessed ☐

**Cd** B-lines 0 ☐ 1–3 ☐ >3 ☐ ∞ ☐ Indeterminate ☐
Not Assessed ☐ Shred ☐ size____ Tissue ☐ size____ Nodule ☐ size____ Wedge ☐ size____
**Ph** B-lines 0 ☐ 1–3 ☐ >3 ☐ ∞ ☐ Indeterminate ☐
Not Assessed ☐ Shred ☐ size____ Tissue ☐ size____ Nodule ☐ size____ Wedge ☐ size____
**Md** B-lines 0 ☐ 1–3 ☐ >3 ☐ ∞ ☐ Indeterminate ☐
Not Assessed ☐ Shred ☐ size____ Tissue ☐ size____ Nodule ☐ size____ Wedge ☐ size____
**Cr** B-lines 0 ☐ 1–3 ☐ >3 ☐ ∞ ☐ Indeterminate ☐
Not Assessed ☐ Shred ☐ size____ Tissue ☐ size____ Nodule ☐ size____ Wedge ☐ size____

**TFAST®** Right Pericardial Site:

**Contractility & Volume:**

Volume (LV Filling): Unremarkable ☐ Poor ☐ Indeterminate ☐ Not Assessed ☐
Contractility (LV FS%): Unremarkable ☐ Poor ☐ Indeterminate ☐ Not Assessed ☐
**LA:Ao Short-axis** Unremarkable ☐ Increased (>1:1.3 dogs, >1:1.6 cats) ☐ Indeterminate ☐ Not Assessed ☐
**RV:LV Long-axis** Unremarkable ☐ Increased (>1:1.3 dogs, >1:1.6 cats) ☐ Indeterminate ☐ Not Assessed ☐

**HR5th View:** *0 ☐ 1/2 ☐ 1 ☐ Indeterminate ☐ Not Assessed ☐ **Not part of AFS*

**Comments** _____
_____
_____
_____
_____

**Qualifier:** The Global FAST® is a combination ultrasound format that includes AFAST®, TFAST®, and Vet BLUE®. Global FAST is a screening test for free fluid and certain organ abnormalities and helps direct resuscitation and diagnostic efforts. Global FAST is not meant to replace radiography or complete detailed abdominal ultrasound or complete echocardiography.

Created by Gregory Lisciandro, DVM, DABVP, DACVECC, CEO of FASTVet.com and President, International Veterinary Point-of-care Ultrasound Society, IVPOCUS.org.

See individual chapters for the respective references and also Appendix III Quick References of Normal Values and Rules of Thumb.

APPENDIX II

# Abbreviations, Terminology and Glossary

## Abbreviations and Acronyms

| | |
|---|---|
| **FAST:** | Focused assessment with sonography for trauma |
| **FAST³:** | Focused assessment with sonography for trauma, triage, and tracking (monitoring) |
| **GFAST:** | Global FAST |
| **AFAST:** | Abdominal focused assessment with sonography for trauma |
| **AFS:** | abdominal fluid score |
| **DH:** | diaphragmatico-hepatic |
| **SR:** | spleno-renal |
| **SRU:** | spleno-renal umbilical |
| **CC:** | cysto-colic |
| **HR:** | hepato-renal |
| **HRU:** | hepato-renal umbilical |
| **TFAST:** | Thoracic focused assessment with sonography for trauma |
| **PCS:** | pericardial site |
| **CTS:** | chest tube site |
| **DH:** | diaphragmatico-hepatic view |
| **PE:** | pleural effusion |
| **PCE:** | pericardial effusion |
| **PTX:** | pneumothorax |
| **SQE:** | subcutaneous emphysema |
| **ULRs:** | ultrasound lung rockets, same as B-lines |
| **B-lines:** | same as ULRs |
| **LA:** | left atrial |
| **Ao:** | atrial |
| **LA:Ao:** | left atrial to aortic ratio |
| **LV:** | left ventricular |
| **RV:** | right ventricular |
| **RV:LV:** | right ventricular to left ventricular ratio |
| **LVSA:** | left ventricular short-axis |
| **LA4CV:** | long-axis four-chamber view |
| **LA5CV:** | long-axis five-chamber view |
| **VetFAST-ABCDE:** | Veterinary FAST – Airway, Breathing, Circulation, Disability, Exposure |
| **Vet BLUE:** | veterinary brief lung ultrasound exam |
| **Cd:** | Caudodorsal lung region |
| **Ph:** | Perihilar lung region |
| **Md:** | Middle lung region |
| **Cr:** | Cranial lung region |
| **DH:** | diaphragmatico-hepatic view |
| **CdTZ:** | caudodorsal transition zone |
| **CrTZ:** | cranial transition zone |
| **PTX:** | pneumothorax |
| **ULRs:** | ultrasound lung rockets, same as B-lines |
| **B-lines:** | same as ULRs |
| **A-lines:** | air reverberation artifact |
| **Sh:** | shred sign |
| **Ti:** | tissue sign |
| **Nd:** | nodule(s) sign |
| **Wdge:** | wedge sign |
| **AIS:** | alveolar-interstitial syndrome |
| **ABAV:** | absent B-lines all (Vet BLUE) views |
| **SQE:** | subcutaneous emphysema |

### *Others*

| | |
|---|---|
| **ALI:** | acute lung injury |
| **ALS:** | advanced life support |
| **ARDS:** | acute respiratory distress syndrome |
| **AXR:** | abdominal radiographs |
| **CPA:** | cardiopulmonary arrest |
| **CPE:** | cardiogenic pulmonary edema |
| **CPR:** | cardiopulmonary resuscitation |
| **CT:** | computed tomography |

*Point-of-Care Ultrasound Techniques for the Small Animal Practitioner*, Second Edition. Edited by Gregory R. Lisciandro.
© 2021 John Wiley & Sons, Inc. Published 2021 by John Wiley & Sons, Inc.
Companion website: www.wiley.com/go/lisciandro/ultrasound2

**DCM:** dilated cardiomyopathy
**DPL:** diagnostic peritoneal lavage
**ECG:** electrocardiography
**FS:** fractional shortening
**GI:** gastrointestinal
**GIT:** gastrointestinal tract
**HCM:** hypertrophic cardiomyopathy
**IVS:** interventricular septum
**LAT:** left atrial tear
**LVFW:** left ventricular free wall
**MUG-DPL:** modified ultrasound-guided diagnostic peritoneal lavage
**MVD:** mitral valve disease
**NCPE:** noncardiogenic pulmonary edema
**PA:** pulmonary artery
**PEA:** pulseless electrical activity
**PHT:** pulmonary hypertension
**PTE:** pulmonary thromboembolism
**ROSC:** return of spontaneous circulation
**RVFW:** right ventricular free wall
**T³:** trauma, triage, and tracking (monitoring) applications of AFAST and TFAST
**TXR:** thoracic radiographic
**ZZC:** zig-zag continuum

# Terminology and Glossary

**1 view is no view:** Axiom from human medicine to combine views to make an accurate ultrasonographic assessment.

**2nd episode of anaphylaxis:** Describes the inflammatory products that are released into circulation following anaphylaxis contributing to complications including the acquired coagulopathy.

**4-quadrant approach:** Lung ultrasound examination in which the thorax is divided into four quadrants and then scanned cranial to caudal to cranial.

**Abdominal fluid scoring system:** The use of AFAST and numbers of positive views to assign an abdominal fluid score for ascites.

**Acoustic enhancement artifact:** Occurs with fluid-filled structures from which through the far-field beyond the scanning plane the structures are artifactually hyperechoic (brighter).

**AFAST-TFAST 48-hour rule:** Expect cavitary bleeding to resolve or nearly resolve within 48 hours once bleeding stops.

**A-lines:** Equidistant parallel lines that originate from a strong air–ultrasound interface representing air reverberation artifacts most commonly from normal aerated lung, pneumothorax, pneumoperitoneum, air-filled gastrointestinal tract and also through the far-field from the caudal vena cava at the FAST diaphragmatico-hepatic (DH) view.

**AFAST®:** Abdominal FAST protocol that is made up of targetorgan views rather than external locations as follows: diaphragmatico-hepatic view (DH), spleno-renal view (SR), cysto- colic view (CC), and hepato-renal umbilical view (HR).

**Alveolar-interstitial syndrome (AIS):** The presence of B-lines most commonly represents a variety of forms of alveolar-interstitial edema and thus is referred to as a syndrome.

**Anaphylactic gallbladder:** The presence of gallbladder intramural edema caused by anaphylaxis in dogs.

**B-lines:** Synonymous with ultrasound lung rockets (ULRs) that most commonly represent alveolar-interstitial edema at the lung surface. By definition, these are hyperechoic vertical artifacts that originate off the lung surface and extend through the far-field,obliterating A-lines while swinging like a pendulum in synchrony with inspiration and expiration.

**Bar code sign:** Term applied to the visual of pneumothorax during M-mode that is synonymous with the stratosphere sign.

**Batman:** Right TFAST pericardial short-axis descriptor of the heart at the level just ventral to the "mushroom view" and dorsal to the bull's eye.

**Bounce:** Term created by the author (GL) to describe the effect of the caudal vena cava when it has the normal dynamic changes in its height at the diaphragmatico-hepatic (DH) view.

**Boysen maneuver:** Term created by the author that describes the rotation of the probe parallel to the ribs in the cardiac-diaphragmatic pouch for the detection of pleural effusion.

**Bregmatic fontanelle:** Term used for the anterior fontanelle that is the largest fontanelle, open at birth, and closes with age (remains open in some dogs). It is located on the top of the skull at the junction of the sagittal, coronal, and frontal sutures.

**Bull's eye:** Right TFAST pericardial short-axis descriptor of the heart at the most ventral level to the sternum representing the muscular apex of the heart.

**Bull's eye sign:** The effect created at the right pericardial view when pericardial effusion is present around the muscular apex of the heart.

**C-line:** Line that is created by consolidated lung during lung ultrasound. Nomenclature is not universally accepted.

**Cardiac bump:** The effect created by the muscular apex of the heart (and the left ventricle) immediately

against the diaphragm that indents the diaphragm with each heart beat.

**Cardiac-cervical pouch:** The most gravity-dependent region in the pleural cavity immediately cranial to the heart, best imaged in the standing patient.

**Cardiac-diaphragmatic pouch:** The most gravity-dependent region in the pleural cavity between the heart and the diaphragm, best imaged in the standing patient.

**Cardiac gallbladder:** The presence of gallbladder intramural edema caused by pericardial effusion and right-sided heart failure including dilated cardiomyopathy in dogs.

**Caudodorsal transition zone:** The region of the interface of the pleural and peritoneal cavity identified by the presence of the curtain sign.

**Clean shadowing:** Shadowing that is created most often by bone and stone (calculi) that completely reflects the scanning plane, creating an anechoic shadow through the far-field.

**Comet-tail artifact:** The term used for partial hyperechoic lines that originate off the pulmonary–pleural interface and "lung Line" that do not extend through the far-field.

**Complete detailed abdominal ultrasound:** The term used for a complete abdominal ultrasound examination.

**Complete detailed echocardiography:** The term used for a complete echocardiogram examination.

**Curtain sign:** The term used when a linear border is created along the dirty shadowing created by lung moving to and fro over pleural effusion or abdominal structures at the transition zone of pleural and peritoneal cavities.

**Dirty shadowing:** Shadowing that is created most often by air-filled structures that partially reflects the scanning plane through the far-field, limiting accurate imaging beyond the reflective structure.

**Double lung point:** Term created in human medicine that describes the presence of two lung points most commonly seen when people (adults, children, and neonates) with pneumothorax are placed in supine positioning.

**Dry lung:** The presence of A-lines and lung sliding.

**E-line:** Line that is created by subcutaneous emphysema during lung ultrasound. Nomenclature is not universally accepted.

**Edge shadowing artifact:** Created off curved soft tissue surfaces in which an anechoic line extends off the curved surface through the far-field.

**Eyeball method:** Gestalt approach in which assessment is made of the heart and vena cava in which measurements are not performed – similar to eyeballing.

**Eyeballing:** Term use for the gestalt approach in which assessment is made of the heart and vena cava in which measurements are not performed – similar to eyeball method.

**False shred sign:** Created by the stomach, its wall, rugal folds, and ingesta that appear like consolidated lung.

**False tissue sign:** Created by the liver that appears like consolidated lung.

**False B-lines:** Created by the stomach and its ingesta that appear like alveolar-interstitial edema.

**FAT:** Term applied to the characterization of the distended caudal vena cava that represents an abnormally high central venous pressure.

**Flash exam:** Term applied to the general sweeping of the abdomen, thorax, and lung in which there is otherwise no defined acoustic window(s) in attempt to answer a single binary question of fluid positive or fluid negative (AFAST, TFAST) or B-lines positive or B-line negative (Vet BLUE).

**Flat:** Term applied to the characterization of the hypovolemic caudal vena cava that represents severe volume depletion.

**Fishmouth:** Right TFAST pericardial short-axis descriptor of the heart at the level just ventral to the Mercedes-Benz view and just above the windshield wipers where the mitral valves form an annulus.

**Focused ultrasound exams:** Term used for a targeted ultrasound examination.

**Gator sign:** The intercostal orientation for all lung ultrasound in which the probe is placed perpendicular to the long axis of the ribs, creating the image of a partially submerged alligator peering over the water at the sonographer, with the eyes as the ribs and the bridge of the nose as the intercostal space.

**Global FAST®:** The term used when AFAST, TFAST, and Vet BLUE are combined as a single ultrasound examination.

**Global FAST® approach:** The application of Global FAST to stage patients for localized versus disseminated disease and for assessing volume status dependent on the subset of patient.

**Globoid heart:** Descriptor of the generalized enlargement of heart that often accompanies chronic pericardial effusion.

**Hammerhead view:** Term applied to the left TFAST pericardial short-axis view and its most ventral level that includes the left and right ventricles.

**Helper hand:** Nonprobe hand that is used for palpation of external landmarks and the apical beat, and for moving skin and stabilizing the patient to optimize image quality.

**Hepatization:** Term describing the discontinuity of the expected linear continuity of the "lung line" along the intercostal space that represents complete lung consolidation without aeration – synonymous with the tissue sign.

**Kiwi fruit sign:** Term used to describe the appearance of a gallbladder mucocele.

**Knuckling the probe:** Term used for wrapping your probe hand around the top of the probe, providing a buttress or cushion against the thoracic wall when patients are in right lateral recumbency to acquire the right pericardial TFAST echo views.

**Line (lung) nomenclature:** A terminology system incorporating alphabetically created descriptive lines that include A-lines and B-lines as well as others that are not universally accepted for various lung ultrasound findings.

**Linear transducer:** Linear probe used for superior detail of smaller structures. The probe is also limited by depth and frequency.

**Long-axis (cardiac) line:** The scanning plane that is used for long-axis views of the heart from the right TFAST pericardial site view.

**Lung line:** Term used to describe the location of the lung surface most accurately in the presence of pleural space disease.

**Lung point:** The location where the lung recontacts the thoracic wall, the transition zone of pneumothorax and reopposition of lung against the thoracic wall, as evidenced by any presence of lung immediately against the thoracic wall, most commonly by lung sliding and B-lines; however, the lung pulse and other Vet BLUE lung ultrasound signs also determine where the lung point is located.

**Lung pulse:** Term for when lung sliding or B-lines are not in synchrony with inspiration and expiration but rather with each heart beat due to severely atelectatic or consolidated lun.

**Lung sliding:** The "to and fro" motion of the lung sliding in synchrony immediately adjacent to the intercostal space during inspiration and expiration – replaces the veterinary term "glide sign."

**Macroconvex transducer:** Used for examining the abdomen and thorax including heart and lung. Allows for deep imaging but limited by its large footprint (probe head).

**Mediastinum testis:** The linear hyperechoic landmark centered within the parenchyma of the testicle – synonymous with the term rete testis.

**Microconvex transducer:** Most durable and commonly used probe in small animal veterinary medicine because it can image the abdomen, thorax including heart and lung, as well as musculoskeletal, ocular and smaller parts. Limited by depth and midrange frequency.

**Mirror image artifact:** The duplication, partial and complete, of structures in the near-field immediately adjacent to a strong air interface. Most commonly occurs at the diaphragm but also can be seen at the cysto-colic view and the body wall and the heart off the pericardium in the far-field.

**MUG-DPL:** Modified ultrasound-guided diagnostic peritoneal lavage.

**Mushroom:** Right TFAST pericardial short-axis descriptor of the heart at the level where the chordae tendinae are attached to the left ventricular papillary muscles just ventral the mitral valves.

**Nodule sign:** Term created by the author that describes lung nodules along the pulmonary surface most commonly observed as a homogeneous relatively anechoic (or of low echogenicity) round to oval region at the lung surface with a hyperechoic border along its far side often associated with pseudo B-lines extending through the far-field.

**Nonecho fallback views:** Term applied by the author to describe the strategy to rule out left- and right-sided congestive heart failure without echocardiogram views.

**Nonecho fallback view for left-sided failure/volume overload:** Vet BLUE is used to assess for left-sided congestive heart failure with absent B-lines ruling out left-sided congestive heart failure.

**Nonecho fallback view for right-sided failure/volume overload:** The FAST diaphragmatico-hepatic (DH) view is used to assess for right-sided congestive heart failure with the absence of a distended (FAT) caudal vena cava and hepatic veins, the tree trunk sign, ruling out right-sided congestive heart failure.

**One-eyed gator sign:** A strategy developed by the author to enhance the observation of lung sliding by placing the rib in the center of the screen causing the echoes to scatter off reflective bone and then strike the lung line obliquely.

**Parking garage effect:** The poor ability to categorize the degree of pneumothorax in dogs and cats in lateral recumbency because of the small difference in height of the thorax.

**Parking garage–skyscraper concept:** The improved ability to categorize the degree of pneumothorax in dogs and cats in standing or sternal recumbency because of the much greater difference in height between the ventral and dorsal extremities of the pleural cavity when compared to lateral recumbency.

**Phased-array transducer:** Also called a sector transducer. This probe's greatest strength is for cardiac

imaging because of its small focal point that can send echoes in between ribs for superior echocardiography over other transducers. Probe may also be used for abdominal and lung imaging but our preliminary studies have shown it is likely not accurate for counting B-lines.

**Pouch:** Term that refers to the most gravity-dependent region in the abdomen and thorax where free fluid would accumulate.

**Power slide:** Term coined in human medicine for the documentation of lung sliding in people using power Doppler.

**Pneumothorax (PTX):** A-lines in the absence of lung sliding define pneumothorax.

**Probe hand:** The hand holding the probe.

**Pleural–peritoneal transition zone:** Another term describing more generally the transition zone of the pleural and peritoneal cavities identified by the "curtain sign."

**Pseudo-asystole:** Term used in human medicine to describe asystole refuted by echocardiogram by finding coordinated cardiac movement.

**Pseudo B-line:** Term used to describe B-lines associated with the gastric lumen and nodules.

**Pulmonary–diaphragmatic interface:** Term used to described the immediate proximity of lung against the diaphragm in the absence of pleural space disease.

**Pseudo-gastric B-lines:** Term used to describe B-lines created by fluid and air within the gastric lumen.

**Pulmonary–pleural line:** The location where lung is immediately against the intercostal space where the normal "to and fro" motion of lung sliding is observed along the thoracic wall – synonymous with pulmonary–pleural interface.

**Pulmonary–pleural interface:** The location where lung is immediately against the intercostal space where the normal "to and fro" motion of lung sliding is observed along the thoracic wall.

**Pseudo-PEA (pulseless electrical activity):** Term used in human medicine to describe pulseless electrical activity refuted by echocardiogram by finding coordinated cardiac movement.

**Racetrack sign:** Term applied to the finding of pericardial effusion rounding the muscular apex of the heart at the diaphragmatico-hepatic (DH) view.

**Rain sign:** Term applied to the visual of B-lines during M-mode.

**Rete testis:** The linear hyperechoic landmark centered within the parenchyma of the testicle – synonymous with the term mediastinum testis.

**Reverberation artifact:** Most commonly created by air and equidistant parallel lines that continue beyond the first encountered reflective surface referred to as A-lines with lung but can be seen with other air-filled structures.

**Reverse sliding sign:** Term applied to the effect of A-lines sliding opposite that of lung sliding at the caudal transition zone of pleural and peritoneal cavities described in dogs, with suspect validity.

**Rough pericardiocentesis:** Term used to describe opening the pericardial sac during pericardiocentesis to create a temporary pericardial window (should not be performed in patients with ruptured cardiac chambers).

**Satisfaction of search error:** Describes the situation in which a reporting radiologist fails to continue to search for subsequent abnormalities after identifying an initial one.

**Seashore sign:** Term applied to the visual of A-lines and lung sliding in M-mode.

**Seldinger technique:** A catheter insertion methodology that generally involves a step-wise progression of an over-the-needle temporary catheter, followed by a guidewire, followed by a dilator, and then the final catheter.

**Side-lobe artifact:** Fluid-associated artifact that can make fluid-filled lumens and structures, most commonly the gallbladder, urinary bladder, large vessels and eye, appear to contain sediment or luminal debris.

**Shimmy line:** Term created by the author that describes the Z-line.

**Short-axis (cardiac) line:** The scanning plane that is used for short-axis views of the heart from the right TFAST pericardial site view.

**Skyscraper effect:** The improved ability to categorize the degree of pneumothorax in dogs and cats in standing or sternal recumbency because of the much greater difference in height between the ventral and dorsal extremities of the pleural cavity when compared to lateral recumbency.

**Slice-thickness artifact:** Fluid-associated artifact that can make fluid-filled lumens and structures, most commonly the gallbladder, urinary bladder, large vessels and eye, appear to contain sediment or luminal debris or have false rents in their wall.

**Smiley face view:** Term applied to the left TFAST pericardial short-axis view that includes the left and right ventricles and right atrium and auricle immediately dorsal to the hammerhead view.

**Step sign:** Term that describes the deviation from the expected linear continuity of bone when fractured, lung with pathology such as consolidation, and lung that is displaced by thoracic wall trauma or pleural space disease.

**Stratosphere sign:** Term applied to the visualizing of pneumothorax during M-mode that is synonymous with the stratosphere sign.

**TFAST®:** Thoracic FAST protocol that includes bilaterally the left and right chest tube sites, left and right pericardial sites, and a single diaphragmatico-hepatic (DH) view.

**TFAST PTX 1/3s Rule:** Term developed by the author to assess the degree of pneumothorax as well as serving as a monitoring tool for tracking static, resolving, and worsening pneumothorax.

**TFAST slide:** Term used to described sliding the probe into the cardiac-diaphragmatic pouch and cardiac-cervical pouch.

**Tree trunk sign:** Term used by the author to describe hepatic venous distension.

**True asystole:** Term used in human medicine to describe asystole confirmed by echocardiogram.

**True PEA (pulseless electrical activity):** Term used in human medicine to describe pulseless electrical activity confirmed by echocardiogram.

**Twinkle artifact:** Term used to describe the use of color flow Doppler for the detection of small mineralizations (<5 mm) within the kidney that create a twinkle effect of colored pixels.

**Ultrasound lung rockets:** Synonymous with B-lines.

**Urinary bladder estimation formula:** Length × height × width measured in centimeters × 0.625 = volume estimation in milliliters.

**Urine output:** Urine produced over time divided by body weight.

**Vet BLUE®:** Lung ultrasound protocol that is a regional pattern-based approach that includes the transthoracic acoustic windows of the caudodorsal, perihilar, middle, and cranial lung regions and the diaphragmatico-hepatic (DH) view.

**Vet BLUE B-line lung contusion system:** The counting of maximum numbers of B-lines associated with each Vet BLUE acoustic window combined with numbers of positive Vet BLUE acoustic views.

**Vet BLUE lung ultrasound signs:** There are six described Vet BLUE lung ultrasound signs: dry lung, B-lines (wet lung), shred sign, tissue sign, nodule sign and wedge sign.

**Vet BLUE B-line scoring system:** The counting of maximum numbers of B-lines associated with each Vet BLUE acoustic window.

**Wagon wheel:** Ultrasonographic appearance of the ileocecal-colic junction in the cat.

**Wedge sign:** Term created by the author describing a triangulated shred sign in caudodorsal and perihilar lung regions that supports the presence of pulmonary thromboembolism.

**Shred sign:** Term created by the author describing the fractal discontinuity of the expected linear continuity of the lung line along the intercostal space that represents an air bronchogram.

**Tissue sign:** Term created by the author describing the discontinuity of the expected linear continuity of the lung line along the intercostal space that represents complete lung consolidation without aeration – synonymous with hepatization of lung.

**Wet lung:** The presence of B-lines (ultrasound lung rockets) that most commonly represent forms of alveolar-interstitial edema.

**Windshield wiper:** Right TFAST pericardial short-axis descriptor of the heart where the mitral valves are apparent just dorsal to the "mushroom view."

**Z-line:** Term for a lung ultrasound artifact that is not universally accepted that describes a vertical artifact that does not extend through the far-field, fades and has no synchrony with phases of respiration created by fascial planes of muscle in the near-field in the presence of dry lung.

**Zig-zag continuum approach:** A lung ultrasound examination in which the patient's thorax is scanned by moving dorsally and ventrally through intercostal sapces.

APPENDIX III

# Quick References of Normal Values and Rules of Thumb

This appendix includes selected highlights from the textbook chapters and is not meant to replace individual chapter content. It does provide some quick references including normal values, rules of thumb, and some charts and formulas. References may be found in the individual chapters as well as greater detail.

## AFAST®

- Free fluid is abnormal in *adult dogs and cats;* however, *puppies and kittens* can have *small quantities* of anechoic free fluid in normalcy with anechoic stripes and pockets of <3 mm in width and maximum dimensions, respectively, and generally no more than one or two positive AFAST views. The diaphragmatico-hepatic view is the most common positive view with anechoic stripes of maximum width <3 mm along the diaphragm and similar anechoic stripes of <3 mm may be found in sedated adult dogs and cats (Lisciandro et al. 2015, 2019).
- The abdominal fluid score (AFS) ranges from 0 (negative) to a maximum of 4 (positive all four AFAST sites). The AFS has been modified to include 0, 1/2, and 1 for scoring at each AFAST view dependent on the size of the fluid pocket with the same small-volume bleeder versus large-volume bleeder concept originally described.
- Small-volume bleeders, defined as dogs with an AFS <3, are *unlikely* to become anemic from their intraabdominal bleed.
- In a small-volume bleeder that is anemic there are four major causes: preexisting anemia, bleeding somewhere else, hemodilution, and lab error.
- Large-volume bleeders, defined as an AFS of ≥3, predictably become anemic from their intraabdominal bleed, and *approximately 20–25% of dogs will become severely anemic*, requiring blood transfusion(s) (Lisciandro et al. 2009).
- Large-volume bleeder hit-by-car dogs often need blood transfusion(s) but *uncommonly* exploratory laparotomy for control of their intraabdominal hemorrhage because bleeding *often* stops with medical management *without* surgery (Boysen et al. 2004; Lisciandro et al. 2009).
- Free intraabdominal fluid in hit-by-car trauma is reported in the veterinary literature to be hemoabdomen and uroabdomen at a frequency of ~98% to 2–3% of the time, respectively (Boysen et al. 2004; Simpson et al. 2009).
- The AFAST-applied abdominal fluid scoring system is applied similarly in cats, however, cats don't survive large volume bleeds as dogs (Lisciandro 2012).
- Packed cell volumes (PCV) as low as 3–5% from blood contamination can appear to be grossly bloody and mistaken for a cavitary bleed; thus, samples should always be spun (PCV) and measured for accurate patient assessment.
- Once bleeding stops, expect significant resorption of blood within 48 hours with minimal to resolved abdominal fluid scores, referred to as the AFAST-TFAST 48-hour rule.
- Large-volume bleeder postinterventional cases (postoperative laparotomy, laparoscopy, percutaneous biopsy procedures, etc.) that are *noncoagulopathic* may or may not need blood transfusion(s) depending on their current clinical status and degree of compensation. However, these cases

*Point-of-Care Ultrasound Techniques for the Small Animal Practitioner*, Second Edition. Edited by Gregory R. Lisciandro.
© 2021 John Wiley & Sons, Inc. Published 2021 by John Wiley & Sons, Inc.
Companion website: www.wiley.com/go/lisciandro/ultrasound2

*nearly always require exploratory surgery* to definitively control their intraabdominal bleeding, and delaying surgery on a large-volume bleeder commonly leads to more morbidity, complications, and expense because of progressive anemia.

- The large-volume bleeder versus small-volume bleeder concept applied to *nontraumatic*, noncoagulopathic cases (e.g., ruptured splenic mass) helps direct decision making regarding surgery ahead of overt decompensation in acute bleeds, i.e., large-volume bleeders even without anemia should be promptly explored and likely will need blood transfusion (autotransfusion is an option when a blood donor is not readily available and uncontaminated blood can be cleanly harvested).
- Small-volume bleeders without anemia *may be serially monitored* and *medically managed* as long as they remain small-volume bleeders.
- In small-volume bleeders that have significant anemia, a chronic process leading to anemia should be considered such as self-limiting intermittent low-grade bleeds or bone marrow disease.
- The large-volume bleeder versus small-volume bleeder concept applied to nontraumatic, coagulopathic cases, i.e., ruptured splenic mass, helps direct decision making regarding the need for blood transfusion(s) since compensated large-volume bleeders predictably become anemic in time.
- Pericardial and pleural effusion in the majority of cases can be diagnosed via the AFAST DH view. In one study, approximately 85% of clinically relevant pericardial effusion (and cardiac tamponade) was reportedly detected via the DH View (Lisciandro 2016a). *Always look into the thorax when performing the DH view*.
- The most common cause for pericardial effusion is neoplasia followed by idiopathic in the dog and is heart failure in cats (75%) (Stafford Johnson et al. 2004; Hall et al. 2007; McDonald et al. 2007). However, the presence of ascites (modified transudate) in dogs, that are also echo negative for a cardiac related mass, has a reported median survival of 605 days (versus 45 days without ascites).
- The gallbladder "halo sign" serves as a marker for canine anaphylaxis (Quantz et al. 2009; Lisciandro 2016; Lisciandro and Lisciandro 2019), referred to as an "anaphylactic gallbladder" by the author. The finding, however, is not pathognomonic and in acutely collapsed and weak dogs pericardial effusion and right-sided heart failure, including dilated cardiomyopathy, should be ruled out, with the gallbladder wall edema in these cases referred to as a "cardiac gallbladder" by the author (Lisciandro 2019).
- Always rule out pericardial effusion/cardiac tamponade when observing gallbladder wall edema by looking past the diaphragm for the "racetrack sign" and, in the absence of pericardial effusion, the right TFAST pericardial site views for dilated cardiomyopathy and right-sided heart enlargement (increased RV:LV). Although rare, cats may also develop the "cardiac gallbladder" (Lisciandro 2019).
- Sonographic striation representing gallbladder wall edema can occur in dogs with normal or equivocal abnormal gallbladder wall thickness (Quantz et al. 2009: Lisciandro and Lisciandro 2019).
- Integrating characterization of the caudal vena cava (CVC) can rapidly distinguish an "anaphylactic gallbladder" from a "cardiac gallbladder" through the finding of a flat, small CVC, versus a FAT distended CVC, respectively.
- Ascites (modified transudate) with an echo-negative study for a cardiac-related mass carries a better prognosis in cases of canine pericardial effusion with a reported median survival time of 605 days (versus 45 days without ascites) (Stafford Johnson et al. 2007).
- The urinary bladder volume may be estimated using the formula Length × Height × Width (cm) × 0.625 which provides an estimate in milliliters (Lisciandro and Fosgate 2017). Over time, the formula may be used serially to estimate urine output non-invasively.
- Normal residual urine after voiding in the dog is 0.2 mL/kg (Atalan et al. 1999).
- Both kidneys are often reliably imaged through the SR view in cats and some dogs.
- AFAST is superior to radiographic serosal detail in two major ways: it can both detect the presence or absence of free intraabdominal fluid and also semi-quantitate its volume over radiographic assessment that is unreliable (Lisciandro et al. 2009).
- AFAST carries the potential to detect soft tissue abnormalities missed radiographically.

Rule-outs for the finding of gallbladder wall edema in dogs and cats (Table 7.5)

| Condition | Expected characterization of the caudal vena cava (CVC) | Speculated pathophysiology |
|---|---|---|
| Canine anaphylaxis[a] | Flat, hypovolemic CVC, (see Table 7.6) | Massive histamine release resulting in acute marked hepatic venous congestion |
| Pericardial effusion[a] | FAT, distended, hypervolemic CVC, referred to as vena cava plethora in people (see Table 7.6) (Himelman et al. 1988) | Marked hepatic venous congestion from obstruction of blood flow to the right atrium |
| Right-sided congestive heart failure (dilated cardiomyopathy, pulmonary hypertension, tricuspid disease)[a] | FAT, distended, hypervolemic CVC, referred to as vena cava plethora in people (see Table 7.6) (Himelman et al. 1988) | Marked hepatic venous congestion from backflow of blood from the right atrium |
| Cholecystitis | Variable | Direct inflammation |
| Pancreatitis | Variable | Direct inflammation |
| Hypoproteinemia (third spacing) | Variable | Vascular leak |
| Immune-mediated hemolytic anemia | Variable (author experience) | Likely immune-mediated and volume overload, does not indicate anaphylaxis in many patients |
| Post transfusion[b] | Variable to FAT, hypervolemia (author experience) | Likely immune-mediated and volume overload, does not indicate anaphylaxis in many patients |

[a] Conditions that are most important to consider in the acute triage setting of acute collapse and weakness in a previously healthy patient (dog). FAT, flat, and bounce are defined in the text.
[b] Many posttransfusion cases develop gallbladder wall edema that is not anaphylaxis. Look at your patient and correlate its clinical profile with the finding of gallbladder wall edema for an accurate assessment.
Source: Reproduced with permission of Dr Gregory Lisciandro, Hill Country Veterinary Specialists and FASTVet.com, Spicewood, TX.

Reference values for the caudal vena cava (CVC) height measured in longitudinal at the subxiphoid[a] view in 126 healthy dogs, grouped into three body weight classes (Table 7.6)

| Size | Body weight (kg) | Expected CVC height measurement (cm) | CVC +/-2 standard deviations (cm) | Suggested CVC maximum height (cm) for a "flat" or hypovolemic, fluid-starved CVC | Suggested CVC maximum height (cm) for a "FAT" or fluid-intolerant CVC (high central venous pressure) |
|---|---|---|---|---|---|
| Small/Toy[b] | <9 kg | 0.55 | (0.23–0.86) | <0.25 | >1.0 |
| Medium | >9–15 kg | 0.85 | (0.32–1.38) | <0.35 | >1.5 |
| Large/Giant | >15 kg | 0.96 | (0.51–1.4) | <0.50 | >1.5 |

Data from the study by Darnis et al. (2018) and measurements created with permission by Lisciandro GR and Vientós-Plotts AI. These values are unproven but give some guidelines for veterinary clinicians to combine with the eyeball method – "bounce", "FAT," and "flat."
[a] The subxiphoid view is analogous to the FAST DH view and the CVC imaged in its longitudinal plane.
[b] Suggested starting point for felines while awaiting current research findings.

# Author's Treatment and Monitoring Guidelines for Canine Anaphylaxis (AX) in All AFAST Fluid-Positive Cases to Prevent and Treat AX-related Heparin-Induced Hemoabdomen

| | Intervention | Duration of activity | Comments |
|---|---|---|---|
| First line | | | |
| Intravenous (IV) fluids | 30–50 mL/kg IV repeated as needed | Short-acting | |
| Epinephrine (EPI) | Low dose 0.01 mg/kg – intramuscular (IM) or IV repeated as needed every 5–10 minutes; if fails injectable EPI then go to CRI | Ultra short-acting | Can use as a CRI starting at 0.05 μg/kg/min IV then increasing as needed based on blood pressure and taper off as soon as possible due to its side-effects |
| Second line | | | |
| *Dexamethasone Sodium phosphate (glucocorticoids) | 0.3 mg/kg IV | Long-acting | Repeat 12 hours post admission at 0.15 mg/kg if not able to take PO prednisone |
| *Potent arachidonic acid inflammatory pathway blocker (inhibiting phospholipase A2), histamine blocker, and inhibitor of mast cell degranulation | | | |
| Diphenhydramine (histamine-1 receptor blocker) | 2 mg/kg IM ONCE with maximum dose of 50 mg/dog | Intermediate | Avoid IV due to potential to initiate hypotension |
| Famotidine (histamine-2 receptor blocker) | 0.5 mg/kg IV or IM q12–24 hours (PO once if appropriate) | Intermediate to long-acting | Continue for 5–7 days while patient on steroids |
| *Prednisone | 0.25 mg/kg q12h for 3 days then 0.25 mg/kg q24h for 3 days | Long-acting | Tapering steroid regimen to prevent 2nd episode (wave) of inflammation that causes persistent coagulopathy |
| *Potent arachidonic acid inflammatory pathway blocker (inhibiting phospholipase A2), histamine blocker, and inhibitor of mast cell degranulation | | | |
| Fresh frozen plasma | Give if PT, aPTT *>25% over upper reference range* and repeat as needed<br>Delay if PT, aPTT *<25% over upper reference range* and recheck again in 4 hours and thereafter as needed depending on AFS and clinical course | Intermediate | Follow these cases with frequent PCV q2–4h plus serial AFAST and AFS scoring until you are confident that the coagulopathy and hemoabdomen are resolving |

| | AFAST | TFAST | Vet BLUE |
|---|---|---|---|
| Monitoring | | | |
| **Global FAST** – combining AFAST and AFS and its target organ approach, TFAST and Vet BLUE | **AFAST** and AFS and its target organ approach – on admission and then 4 hours post admission if stable and sooner if unstable<br>**AFAST** and **AFS** continued as part of daily patient rounds<br>*Expect dogs with resolved coagulopathy to have resolution of their AFS within 24–48 hours – decreasing to an AFS 1 or 0 (negative fluid score)* | **TFAST** for pleural and pericardial effusion, volume status and cardiac status<br>Left atrial to aortic ratio (LA:Ao), Global FAST nonecho fallback view is Vet BLUE for left-sided volume overload<br>Right ventricular to left ventricular ratio (RV:LV), Global FAST nonecho fallback view of the caudal vena cava and hepatic veins for right-sided volume overload | **Vet BLUE** for lung edema and other respiratory complications<br>*Expect lung to be dry in canine AX due to single insult unless complications!*<br>*Note massive envenomation has been reported to cause pulmonary edema* |

Source: Reproduced with permission from Dr Gregory Lisciandro, Hill Country Veterinary Specialists and FASTVet.com, Spicewood, TX.
aPTT, activated partial thromboplastin time; CRI, constant rate infusion; PCV, packed cell volume; PO, by mouth (*per os*); PT, prothrombin time.

# POCUS Liver and Gallbladder

- Liver assessment is subjective. Edges of the liver lobes should be sharply pointed. Rounded margins of liver lobes and hepatic extension (especially the left lobes) beyond the costal arch suggest enlargement. Abdominal radiography is more reliable for the determination of hepatomegaly.
- Target lesions: single target lesions have a high predictive value for malignancy. When multiple target lesions are seen, the positive predictive value of malignancy increases from 74% to 81% (Cuccovillo and Lamb 2002).
- Normal echogenicity rule of thumb: the spleen (S) is more echogenic (hyperechoic) than the liver (Li) which is the same or slightly more echogenic (brighter) than the cortex of the kidney (CK), remembered by the mnemonic "SLiCK." For the feline, hepatic echogenicity is often compared to the adjacent falciform fat and the feline liver should be isoechoic to slightly hyperechoic (brighter) to the falciform fat. The feline liver, spleen, and cortex of the kidney are isoechoic to one another.
- Gallbladder wall thickness is normally <1 mm in cats and <3 mm in dogs (Spaulding 1993; Hittmair et al. 2001; Quantz et al. 2009).
- Sonographic striation representing gallbladder wall edema can occur in dogs with normal or equivocal abnormal gallbladder wall thickness.
- Gallbladder luminal content is generally homogeneous anechoic bile although degrees of *gallbladder sludge* may be considered *as clinically irrelevant* or *may indicate cholestasis* based on the patient's clinical profile (Tsukagoshi et al. 2012).
- The gallbladder, being fluid filled, is subject to several artifacts including side-lobe, edge shadowing, and acoustic enhancement in the far-field; and the liver and gallbladder, being adjacent to the strong soft tissue–air interface between the diaphragm and the aerated lung, are subject to mirror image artifact.
- In cats, tortuosity of the bile duct can be a normal variation and a bile duct greater than 4 mm is considered to be consistent with extrahepatic biliary obstruction (d'Anjou 2008).

# POCUS Spleen

- Spleen size is subjective. A spleen that extends to a small or medium-sized urinary bladder is considered enlarged.
- Sonographic recognizing features of the spleen are its hyperechoic capsule and that its blood supply splits the capsule, unlike the liver.

- A folded spleen in a cat is always abnormal and indicates splenomegaly (Hecht 2008).
- Normal cat spleen thickness is <10 mm (Reese et al. 2012).
- Benign nodular hyperplasia usually consists of nodules that are of homogeneous echotexture, being either hypoechoic or hyperechoic.
- Splenic masses that deform the capsule of the spleen should always be considered a serious finding until proven otherwise.
- Splenic lymphoma has been characterized as a "Swiss cheese appearance" with increased echogenicity (brighter) in contrast to a splenic torsion that looks similar; however, the spleen has decreased echogenicity (darker).
- The "whale tail" appearance of the splenic vein that enters and then splits toward the head and tail of the spleen is a landmark for both dogs (more prominent) and cats.
- Target lesions: single target lesions have a high predictive value for malignancy. When multiple target lesions are seen, the positive predictive value of malignancy increases from 74% to 81% (Cuccovillo and Lamb 2002).
- Normal echogenicity rule of thumb: the spleen (S) is more echogenic (hyperechoic) than the liver (Li) which is the same or slightly more echogenic (brighter) than the cortex of the kidney (CK), remembered by the mnemonic "SLiCK." For the feline, hepatic echogenicity is often compared to the adjacent falciform fat and the feline liver should be isoechoic to slightly hyperechoic (brighter) to the falciform fat. The feline liver, spleen, and cortex of the kidney are isoechoic to one another.

# POCUS Kidney

- Normal kidney size for cats is generally considered to be 3.0–4.4 cm in length depending on the reference (Nickel et al. 1973; Walter et al. 1987).
- Normal kidney size in dogs is variable and depends on the size of the dog so assessment is generally subjective. Therefore, *assessment of symmetry and size between the two kidneys is particularly important in dogs* (d'Anjou 2008).
- Normal renal pelvis size (height in mm). Variability in both species. General rule of thumb is to consider abnormal if ≥3 mm cats and ≥4 mm dogs (normals: cat 1.5–2 mm with maximum of 2.8 mm; dogs 2–3 mm with a maximum of 3.8 mm) (d'Anjou et al. 2011).
- Perirenal fluid is not uncommon in cases of urinary obstruction and acute renal failure.
- Perirenal fluid and ascites have been reported to occur in feline urinary urethral obstruction that resolves in the great majority of cases without surgical intervention (and in dogs too, author experience) (Nevins et al. 2015).
- Normal echogenicity rule of thumb: the spleen (S) is more echogenic (hyperechoic) than the liver (Li) which is the same or slightly more echogenic (brighter) than the cortex of the kidney (CK), remembered by the mnemonic "SLiCK." For the feline, hepatic echogenicity is often compared to the adjacent falciform fat and the feline liver should be isoechoic to slightly hyperechoic (brighter) to the falciform fat. The feline liver, spleen, and cortex of the kidney are isoechoic to one another.

# POCUS Urinary Bladder

- The thickness of the urinary bladder wall varies depending on the degree of distension.
- Normal range for urinary bladder wall thickness in cats is 1.3–1.7 mm (Finn-Bodner et al. 1995; Nevins et al. 2015).
- Normal range for urinary bladder wall thickness in dogs is from 1.4 mm in moderately distended bladders to 2.3 mm in minimally distended bladders (Geisse et al. 1997). However, wall thickness in dogs has been reported to increase with body size, with heavier dogs having increased thickness by up to 1 mm or a maximum normal thickness of ≤3 mm (Geisse et al. 1997).
- The use of color flow Doppler potentially differentiates a thrombus (and artifact) from bladder masses by documenting whether pulsatile blood flow is present.
- Voiding urohydropulsion (VUH) guidelines are as follows (Defarges et al. 2013).
  - Female dogs (>2–kg) can typically void stones <3–4 mm.*
  - Female cats may be able to void stones <3 mm.*
  - Male dogs weighing 5–10 kg may be able to void stones <2–3 mm and male dogs >10 kg stones <3 mm.*
  - Male cats: *VUH is not recommended*.

  *The ease of passing a 9 French urinary catheter correlates with the successful voiding of 3 mm stones.
- The urinary bladder, being fluid filled, is subject to several artifacts including side-lobe, slice-thickness, edge shadowing, and acoustic enhancement in the far-field. Turning down the gain is a quick trick to eliminate slice-thickness and side-lobe artifacts that mimic sediment.

# POCUS Gastrointestinal and Pancreas

## Gastrointestinal

- Normal stomach wall thickness: dogs 3–5 mm (higher in some giant breeds); cats 2 mm interrugal (up to 4.4 mm if rugal fold is measured) (Nyland et al. 2002; Nyland and Mattoon 2015b). Measure from the hyperechoic outer serosal margin to the inner hyperechoic mucosoluminal surface.
- In dogs, the descending duodenal wall is *thicker* than other small intestinal segments and can normally measure up to 5 mm in large breed dogs (Newell et al. 1999). Measure from the hyperechoic outer serosal margin to the inner hyperechoic mucosoluminal surface.
- Small bowel wall measurements *other than the duodenum* of greater than 4 mm in dogs and 2.5 mm in cats would generally be considered as abnormally thickened (Newell et al. 1999). Measure from the hyperechoic outer serosal margin to the inner hyperechoic mucosoluminal surface.
- Use the mnemonic "the sun is bright and it's dark at midnight" to remember that layers starting with an "s" like the sun are bright (submucosa and serosa are hyperechoic [bright]), while layers starting with an "m" like midnight are dark (mucosa and muscular layer are hypoechoic [dark]) on the ultrasound image).
- Direct evidence of gastrointestinal foreign bodies. The majority of ultrasonographically detectable gastrointestinal foreign bodies typically involve a well-defined hyperechoic, hyperreflective acoustic interface with strong distal acoustic shadowing (Tidwell and Penninck 1992; Garcia et al. 2011).
- Linear foreign bodies: plication vs corrugation. The finding of bowel plication is *strongly suggestive* of a linear foreign body and should prompt careful evaluation of the intestine (longitudinal and transverse images) at sites where plication is seen (Tidwell and Penninck 1992; Garcia et al. 2011). Intestinal corrugation has also been associated with linear foreign bodies (Tidwell and Penninck 1992) but is *less specific* than plication.
- In differentiating "corrugated" from "plicated" bowel, overall direction of the intestine tends to appear straight with corrugated bowel (medical causes – enteritis/pancreatitis) in contrast to bunched or weaved with plicated bowel (surgical causes – linear foreign body).
- Indirect evidence of obstruction, such as a severely dilated jejunum with luminal dilation measuring greater than 1.5 cm, may highlight the need for a more extensive and complete abdominal ultrasonographic evaluation, abdominal radiographs or exploratory surgery. Measure from serosal to serosal surface.
- Determine the number of contractions per minute by recording the number of contractions over a three-minute period and average to get the number of contractions per minute (Penninck et al. 1989).
- The mean number of peristaltic contractions of the stomach and proximal duodenum is 4–5 contractions per minute (Penninck et al. 1989).
- The mean number of peristaltic contractions of the small intestine (jejunum) averages 1–3 contractions per minute (Penninck et al. 1989).
- The large bowel (colon) normally has no peristalsis.
- A generalized decrease in gastrointestinal motility is reported in small animals with functional and chronic mechanical ileus, whereas a generalized increase in motility is most commonly reported in cases of acute mechanical obstruction (Penninck 2008a). However, because of considerable overlap in motility, *motility alone does not indicate the need for surgery* (Sharma et al. 2011; Garcia et al. 2011).

## Pancreas

- *The right pancreatic limb* is generally easiest to image in dogs and is the more common lobe affected by pancreatitis (Hecht and Henry 2007; Nyland et al. 2002; Penninck 2008b).
- *The left pancreatic limb* is generally easiest to image in cats.
- Identification of the pancreas can be challenging for the novice sonographer because the pancreas is isoechoic to adjacent tissues. As a result, its identification commonly relies on the observance of its duct and vasculature.
- Historically, it has been thought that a *normal pancreas is generally not seen*; however, the normal pancreas is in fact frequently imaged with high-frequency transducers and newer machines.
- Pancreatitis is particularly common when corrugation of the duodenum is noted (Moon et al. 2003).
- Even in cases of severe acute pancreatitis, the sensitivity of ultrasound may only be 68% (Hess et al. 1998).

# POCUS Reproductive

- The mediastinum testis, also referred to as the rete testis, is a linear hyperechoic-identifying landmark of the testicle.
- The uterus appears as a tubular structure similar in size to small intestine and differentiated from small

intestine by lack of peristalsis, lack of expected intestinal layering and lack of luminal air.
- The uterine body is of medium, homogeneous echogenicity (shades of gray) and is easier to identify than the cervix, with both blending into each other sonographically.
- The uterine lumen lacks a central echogenic stripe in the normal anestrous bitch; however, in estrus a thin, echogenic (bright) stripe within the uterine lumen may be seen.
- Intraluminal uterine echogenicity can be the *same* (anechoic) between hydrometra and pyometra.
- Fetal heart rates and distress: HR > 180 – normal; 180 > HR > 160 – early fetal stress, prompt intervention required; 160 > HR > 140 – moderate fetal stress, C-section warranted next 2–3 hours; HR < 140 – severe fetal stress, reduced fetal viability, immediate surgical intervention required (Traas 2008). Note that variability exists in litters where a fetus may be severely distressed and another normal.
- M-mode provides a more accurate heart rate of the fetus; however, the "eyeball method" may also be used.
- Normal ultrasonographic layering of the small bowel in the fetus may be used as a guideline for full-term maturation of puppies and kittens (Mattoon and Nyland 2002).
- In anestrus, there is no uterine luminal fluid in normalcy; however, in estrus there may be a thin echogenic stripe also considered as a normal finding (Mattoon and Nyland 2002; Verstegen et al. 2008).
- Abdominal radiography is the most accurate way of determining the number of puppies or kittens in the litter (Davidson and Baker 2009). Avoid telling clients numbers in the litter using ultrasound because of its inaccuracy.

Fetal ultrasonographic maturation – canine

| Fetal structure | Days post luteinizing hormone surge |
|---|---|
| Gestational sac | 20 |
| Embryo | 23–25 |
| Cardiac activity | 23–25 |
| Yolk sac, U-shaped | 25–28 |
| Yolk sac, tubular | 27–31 |
| Fetal orientation (head and body) | 28 |
| Limb buds, fetal movement | 35 |
| Fetal skeleton | 33–39 |
| Stomach, urinary bladder | 35–39 |
| Lungs – hyperechoic to liver | 38–42 |
| Kidneys, eyes | 39–47 |
| Cardiac chambers | 40 |
| Intestines – layered appearance | 57–63 |

Source: Adapted from Mattoon and Nyland (2015).

Fetal ultrasonographic maturation – feline

| Fetal structure | Days post luteinizing hormone surge |
|---|---|
| Gestational sac – spherical shape | 10–11 |
| Gestational sac – lemon shape | 19–21 |
| Embryo | 23–25 |
| Cardiac activity | 16–18 |
| Yolk sac, tubular | 25–27 |
| Fetal orientation (head and body) | 24–27 |
| Limb buds, fetal movement | 30–34 |
| Fetal skeleton | 30–33 |
| Stomach, urinary bladder | 29–32 |
| Kidneys, eyes | 38–41 |
| Cardiac chambers | 48–50 |
| Intestines – layered appearance | 52–56 |

Source: Adapted from Zambelli et al. (2002).

# TFAST®

- A-lines with "lung sliding" rules out pneumothorax (PTX) and supports "dry lung" at the lung periphery (Lisciandro et al. 2008).
- B-lines *immediately* rule out PTX at that specific location on the thoracic wall and support "wet lung" at the lung periphery.
- "Wet lung" in trauma cases are lung contusions until proven otherwise (Lisciandro 2011; Dicker et al. 2019).
- A-lines without "lung sliding" with a "lung point" diagnose PTX (Lisciandro et al. 2008).
- The "lung pulse" is another finding in PTX in which "lung sliding" is in synchrony with the heartbeats rather than phases of respiration due to severely atelectatic or consolidated lung.
- Arguably, the best view for evaluating pleural and pericardial spaces is the diaphragmatico-hepatic (DH) view because of less air interference via the acoustic window of the liver and gallbladder (Reissig et al. 2011; Lisciandro 2016).
- The DH view is likely close to 100% sensitive and 100% specific in dogs with clinically relevant pericardial effusion via observation of the "racetrack sign" and is a good test in cats (Lisciandro 2014a,b, 2016).
- The TFAST right-sided cardiac markers include (1) the right ventricular to left ventricular ratio (RV:LV), (2) characterization of the caudal vena cava and hepatic veins, and (3) characterization of the gallbladder wall. The pulmonary artery to aortic ratio (PA:Ao) may also be used on right parasternal short-axis views. In right-sided failure, the following changes would be expected: an increased

RV:LV, a FAT distended caudal vena cava and hepatic venous distension ("tree trunk sign"), and gallbladder wall edema ("cardiac gallbladder") as well as a PA:Ao >1:1.

- The TFAST "mushroom view" is used to assess volume status and contractility in both dogs and cats. A fractional shortening (FS%) of <20% is diagnostic of poor systolic function and dilated cardiomyopathy.
- The right TFAST pericardial site view and the LA:Ao on short axis screen for left-sided heart strain/overload/failure and is obviously abnormal when the left atrium is twice the size of the aorta (LA:Ao >2:1). The "Global FAST nonecho fallback strategy" is the characterization of lung on Vet BLUE.
- The right TFAST pericardial site view and the RV:LV on long axis screen for right-sided strain/overload/failure and is obviously abnormal when the right ventricle is nearly the same size as the left ventricle (RV:LV ~1:1). The "Global FAST nonecho fallback strategy" is characterization of the caudal vena cava and hepatic veins at the FAST DH view.
- TFAST is used to screen for volume status via characterization of the caudal vena cava and its associated hepatic veins (combined with the short-axis left ventricular "mushroom view") expecting that neither would be distended unless right heart strain/overload/failure is present (Nelson et al. 2010).
- Ascites (modified transudate) with an echonegative study for a cardiac-related mass carries a better prognosis in canine pericardial effusion (Stafford Johnson et al. 2004).
- Heart failure is the most common cause of pericardial effusion in cats (Hall et al. 2007; Ward et al. 2018).
- Neoplasia and idiopathic are the most common causes of pericardial effusion in dogs (Stafford Johnson et al. 2004; Shaw and Rush 2007; MacDonald et al. 2009).

# Vet BLUE®

- A-lines with "lung sliding" referred to as "dry lung" (Lisciandro 2011; Lisciandro et al. 2014, 2017).
- B-lines, synonymous with ultrasound lung rockets, are referred to as "wet lung," representing most commonly forms of alveolar-interstitial edema that must be placed into clinical context and a regional pattern-based approach as with Vet BLUE (Lisciandro 2011, 2012; Lisciandro et al. 2014, 2017).
- The "step sign" and its subsets including the "shred sign," "tissue sign," nodule sign," and "wedge sign" represent forms of lung consolidation and infiltration (Lisciandro et al. 2009; Lichtenstein 2010; Lisciandro 2011, 2014; Hecht and Penninck 2015; Ward et al. 2017, 2019; Dicker et al. 2019).
- In normalcy, adult dogs and cats and puppies and kittens >6 weeks of age uncommonly have B-lines on Vet BLUE with no more than a single B-line sporadically at one and much less commonly two Vet Blue views (Lisciandro et al. 2018).
- B-lines in Caudodorsal and Perihilar lung regions or a widespread presence most commonly represent forms of cardiogenic pulmonary edema from left-sided congestive heart failure in acute respiratory distress; and integration of TFAST echo findings and Global FAST nonecho fallback views are key (Lisciandro et al. 2014, 2017; Ward et al. 2017).
- B-lines in Caudodorsal and Perihilar lung regions symmetrically support noncardiogenic pulmonary edema when placed into clinical context; and integration of TFAST echo findings and Global FAST nonecho fallback views are key.
- B-lines and "shred signs" in ventral gravity-dependent Middle and Cranial lung regions support bacterial and aspiration pneumonia in acute respiratory distress.
- "Wedge sign" in Caudodorsal and Perihilar lung regions supports the presence of pulmonary thromboembolism (Lisciandro 2013, unpublished data).
- B-lines are counted as 1, 2, 3, considered weak positives, and >3 when more than 3 but still recognized as individual B-lines, and ∞ (infinity) when lines are confluent over an entire intercostal space, as strong positives (Ward et al. 2017).
- Numbers of B-lines correlate with the degree of alveolar-interstitial edema on computed tomography (CT) in human lung and likely the same holds true for small animals (Volpicelli et al. 2006).
- "Absence of B-lines All (Vet BLUE) Views" effectively rules out left-sided congestive heart failure in dogs and cats with ~96% sensitivity (Lisciandro et al. 2016).
- B-lines in trauma patients represent lung contusions until proven otherwise (Soldati et al. 2006; Lisciandro 2011; Dicker et al. 2019).
- Expect no B-lines at all Vet BLUE views as a general rule in adult dogs and cats and puppies and kittens >6 weeks of age (Lisciandro et al. 2014, 2017, 2018).
- The more B-lines, the more alveolar-interstitial edema, and conversely lower scores represent less alveolar-interstitial edema. Thus, the strategy may be used to guide loop diuretic administration in left-sided congestive heart failure, monitor and guide therapy for other forms of lung edema, and score the severity of lung contusions (Lisciandro

et al. 2014, 2017; Rademacher et al. 2014; Vezzosi et al. 2017; Ward et al. 2017).
- Alveolar-interstitial edema is detected with higher frequency than with three-view thoracic radiography in dogs and cats, especially the cranial lung regions (Ward et al. 2018).
- Using the Volipicelli Strong Positive Model (having a severe alveolar-interstitial edema bias), left-sided congestive heart failure is detected with the same sensitivity and specificity as thoracic radiography in cats (Ward et al. 2017).
- Pulmonary nodules are detected in higher frequency than thoracic radiography in metastasis checks in dogs and cats (Kulhavy and Lisciandro 2015).
- Lung contusions are detected in higher frequency than three-view thoracic radiography in lung contusions, and Vet BLUE performs well when compared to CT (Dicker et al. 2019).

# POCUS Heart

- In normalcy, the left ventricle (LV) should be 3–4 times larger than the right ventricle (RV) in the right parasternal four-chamber view (3:1).
- Cats and left ventricular hypertrophy: feline interventricular septum (IVS) and left ventricular free wall (LVFW) thickness in diastole should be approximately 3–4 mm. LV wall thickness in diastole ≥6 mm is diagnostic for left ventricular hypertrophy.
- Pseudohypertrophy in cats: extreme hypovolemia causing "pseudohypertrophy" of the left ventricle can be misinterpreted as hypertrophic cardiomyopathy in the cat.
- If the RV is the same size as the LV, then severe right ventricular enlargement can be diagnosed (and its various rule-outs considered).
- In normalcy, the left and right atria are approximately the same size or 1:1 with a neutral (nondeviated) interatrial septum.
- In normalcy, the left atrium (LA) and aorta (Ao) in the short-axis right parasternal view should be nearly the same size (1:1).
- If the left atrium is more than 1.3 times the size of the aorta in dogs and 1.6 times in cats (LA:Ao >1.3:1 dogs, LA:Ao >1.6:1 cats) then the left atrium is enlarged, suggesting left-sided heart disease (Rishniw and Erb 2000; Abbott and Maclean 2006).
- Normal fractional shortening (FS%): in general, normal FS% is 28–45% in the dog and 30–50% in the cat.
- Abnormal fractional shortening: a FS% below 20% is suggestive of severe myocardial systolic failure and a FS% above 55% would be considered hyperdynamic LV function
- Causes of pericardial effusion in dogs and cats: neoplasia and idiopathic pericardial effusion are most common causes of PCE in dogs. Heart failure is the most common cause in cats.
- Left parasternal cranial view: allows for optimal visualization of the right heart, including the right auricle and tricuspid valve, and is the best view to visualize a small right auricular mass in a dog with pericardial effusion and cardiac tamponade.

Normal mean echocardiographic values (cm) in dogs

| BW(kg) | LVEDD | LVESD | IVSD | LVFWD | Ao | LA |
|---|---|---|---|---|---|---|
| 3 | 2.0 | 1.1 | 0.5 | 0.6 | 1.1 | 1.3 |
| 5 | 2.4 | 1.3 | 0.6 | 0.7 | 1.3 | 1.5 |
| 10 | 3.0 | 1.8 | 0.7 | 0.8 | 1.6 | 1.8 |
| 15 | 3.4 | 2.1 | 0.8 | 0.8 | 1.9 | 2.0 |
| 20 | 3.8 | 2.4 | 0.9 | 0.9 | 2.1 | 2.2 |
| 25 | 4.0 | 2.6 | 0.9 | 0.9 | 2.1 | 2.4 |
| 30 | 4.3 | 2.8 | 1.0 | 1.0 | 2.4 | 2.5 |
| 35 | 4.5 | 3.0 | 1.0 | 1.0 | 2.5 | 2.6 |
| 40 | 4.7 | 3.1 | 1.0 | 1.0 | 2.6 | 2.7 |
| 45 | 4.9 | 3.3 | 1.1 | 1.1 | 2.7 | 2.8 |
| 50 | 5.0 | 3.4 | 1.1 | 1.1 | 2.8 | 2.9 |

BW, body weight; LVEDD, left ventricular end-diastolic diameter; LVESD, left ventricular end-systolic diameter; IVSD, interventricular septal thickness in diastole; LVFWD, left ventricular free wall thickness in diastole; Ao, aortic diameter; LA, left atrial diameter.
Source: Reproduced with permission from Kittleson MD, Kienle RD. 1998. *Small Animal Cardiovascular Medicine*. St Louis: Mosby.

Normal ranges of echocardiographic values (cm) in cats

| Cardiac parameter | Normal range |
|---|---|
| LVEDD | 11.0–17.5 |
| LVESD | 0.40–1.0 |
| IVSD | 0.35–0.55 |
| LVFWD | 0.35–0.55 |
| Ao | 0.7–1.3 |
| LA | 0.9–1.4 |
| LA/Ao (sax 2D) | 0.9–1.4 |
| FS% | 33–66% |

LVEDD, left ventricular end-diastolic diameter; LVESD, left ventricular end-systolic diameter; IVSD, interventricular septal thickness in diastole; LVFWD, left ventricular free wall thickness in diastole; Ao, aortic diameter; LA, left atrial diameter; LA/Ao (sax 2D), ratio of left atrial and aortic diameter measured in short-axis view in two-dimensional echo; FS%, fractional shortening %.

### *Fractional Shortening Values (FS%)*

Keep in mind that normal FS% can vary by breed and loading (~volume status) conditions. In general, normal FS% is 28–45% in the dog and 30–50% in the cat. A FS% below 20% is suggestive of severe myocardial systolic failure and a FS% above 55% would be considered hyperdynamic LV function.

$$\left(\mathrm{FS\%} = \frac{\left[\mathrm{LV\ internal\ dimension\,(diastole)} - \mathrm{LVID\,(systole)}\right]}{\mathrm{LVID\,(diastole)}} \times 100\right)$$

# POCUS Caudal Vena Cava

Reference values using allometric scaling with body weight (BW) for the caudal vena cava (CVC) and aorta (Ao) in healthy dogs using different views (Darnis et al. 2018)

| View | Variable | Dimension | Formula |
|---|---|---|---|
| Hepatic view *B-mode* | $CVC_{min}$ | Area ($mm^2$) | $6.16 \times BW^{0.762}$ |
| | $CVC_{max}$ | Area ($mm^2$) | $7.24 \times BW^{0.787}$ |
| | $Ao_{max}$ | Diameter (mm) | $3.85 \times BW^{0.323}$ |
| Paralumbar view *B-mode* | $CVC_D$ | Diameter (mm) | $2.79 \times BW^{0.390}$ |
| | $Ao_D$ | Diameter (mm) | $3.49 \times BW^{0.328}$ |
| Paralumbar view *M-mode* | $CVC_D$ | Diameter (mm) | $2.53 \times BW^{0.419}$ |
| | $Ao_D$ | Diameter (mm) | $3.49 \times BW^{0.332}$ |

$CVC_{min}$ – minimal caudal vena cava area at the hepatic view.
$CVC_{max}$ – maximal caudal vena cava area at the hepatic view.
$Ao_{max}$ – maximal aortic diameter at the hepatic view.
$CVC_D$ – caudal vena cava diameter at the paralumbar view.
$Ao_D$ – aortic diameter at the paralumbar view.

# POCUS Pediatrics

- Juvenile puppies and kittens may have a small amount of anechoic (pure black) free intraabdominal fluid that may be considered normal, seen as generally anechoic stripes or small pockets at no more than two AFAST views that are <3 mm in maximum width and dimensions, respectively (Stander et al. 2010; Lisciandro et al. 2015, 2019; Romero et al. 2015).
- Expect puppies and kittens >6 weeks of age to have the same frequency of B-lines as found in adult dogs and cats, no more than 1–2 B-lines at a single Vet BLUE view in ~10% of studies (Lisciandro et al. 2018).

# POCUS Felines

Feline reference values

| | | Measurements |
|---|---|---|
| Stomach | Larger amount of fat in the submucosal layer. Pyloric duodenal junction located at midline and J-shaped | 1.7–3.6 mm (Newell et al. 1999; Goggin et al. 2000; Winter et al. 2014)<br>Obvious abnormal >6 mm |
| Duodenum | Ventral to right kidney. The cranial duodenal flexure is near the hepatic hilus using the portal vein as a reference. It lies ventral to it | 2.0–2.5 mm (Newell et al. 1999; Goggin et al. 2000; Winter et al. 2014; di Donato 2014)<br>Obvious abnormal >4 mm |
| Small intestine | The jejunum is distinctly different with a prominent hyperechoic submucosal layer especially near the ileocecal junction (ICCJ). The ICCJ has a distinct appearance on a short-axis view. It resembles an empty miniature stomach referred to as a "wagon wheel" appearance | Jejunum 2.0–2.5 mm (Newell 1999; Goggin 2000; Winter 2014; di Donato et al. 2014)<br>Obvious abnormal >3 mm<br>Ileum 2.5–3.2 mm (Newell et al. 1999; Goggin et al. 2000; Winter et al. 2014; di Donato et al. 2014)<br>Obvious abnormal >4 mm |
| Pancreas | The left pancreatic lobe is larger and more prominent | Left pancreatic lobe range 5–9 mm; right pancreatic lobe range 3–6 mm (Nyland and Mattoon 2015a)<br>Obvious abnormal <1 cm<br>Feline pancreatic duct can be up to 6 mm (Hecht et al. 2006) |

(*Continued*)

(Continued)

| | | Measurements |
|---|---|---|
| Liver | Adjacent often robust feline falciform fat can be confused with liver parenchyma if the depth is not set properly. The hepatic echogenicity pattern is otherwise similar to the dog | |
| Gallbladder | The common bile duct may be tortuous in normalcy in cats (and thus mistaken for pathology) | Common bile duct normally ≤4 mm; and when >5 mm extrabiliary obstruction should be suspected (d'Anjou 2008) |
| Spleen | | Normal is <10 mm in thickness and abnormal >10 mm (Reese et al. 2012)<br>Obvious abnormal >10 mm |
| Kidney | In obese cats, the cortex tends to be hyperechoic | Normal size:<br>Length 3–4.5 cm<br>Width 2.2–2.8 cm<br>Height 1.9–2.5 cm (Nickel et al. 1973; Walter et al. 1987; d'Anjou 2008b; Nevins et al. 2015)<br>Obvious abnormal: renomegaly >4.5–cm (sagittal plane)<br>Renal pelvis and pyelectasia:<br>the normal renal pelvis is collapsed, typically measuring less than 2 mm; normal renal pelvic dilation range1.5–2 mm with maximum height of 2.8 mm in cats (d'Anjou et al. 2011)<br>Obvious abnormal ≥3 mm |
| Urinary bladder | The contents are commonly echogenic from floating fat vacuoles | |
| Prostate | Rarely seen sonographically in neutered cats. In intact males, the prostate is small, ovoid and hyperechoic. Prostatic disease is rare in cats | Ellipsoid formula: length × height × width × 0.524 (Mattoon and Nyland 2015) |
| Uterus | The nongravid uterus is tubular, homogeneous in echotexture, with a lumen that is not readily seen and is differentiated from small intestine by lack of peristalsis, lack of intraluminal gas, and absence of the layered appearance characteristics (Mattoon and Nyland 2015). Uterine width varies from 3 to 5 mm in cats and 5 to 10 mm in dogs | Uterine width varies from 3 to 5 mm in cats |
| AFAST-applied abdominal fluid score (AFS) | Expect AFS 0 to 1/2 as not uncommonly adult and juvenile cats have a small linear stripe of free fluid along the diaphragm at the DH view | AFS <1/2–1 with maximum dimensions <3 mm (Lisciandro et al. 2015) |
| Caudal vena cava (CVC) and hepatic veins | Similar to dogs | Hepatic veins are not obvious in normalcy and the CVC should fluctuate approximately 35–50% during respiratory cycles; maximum heights extrapolated from small dogs of <0.25 considered hypovolemic and >0.9 cm considered hypervolemic (FAT, right-sided volume overload) (Darnis et al. 2018) |
| Heart and TFAST echo views | Similar to dogs; however, because of normal faster heart rates the "eyeball method" is much less reliable so using the freeze function and then rolling the cine ball to evaluate frame by frame is necessary for felines | LA:Ao <1.6:1 – the left atrium should be no more than ~1.6 times the size of the aorta; obvious abnormal >2:1 (Abbott and MacLean 2006)<br>RV:LV 1:3–4 – the right ventricle should be no more than 1/3–1/4 the size of the left ventricle; obvious abnormal 1:1 (Kittleson and Kienle 1998)<br>Fractional shortening ~30–50% (Kittleson and Kienle 1998) |

(Continued)

| | | Measurements |
|---|---|---|
| Vet BLUE and expected numbers of B-lines | Similar to dogs | Expect absent B-lines all Vet BLUE views in cats and kittens >6 weeks of age (Lisciandro et al. 2017, 2018); approximately 12% of the time a *single* B-line at a *single* Vet BLUE transthoracic view is present |

Source: Reproduced with permission of Dr Gregory Lisciandro, Hill Country Veterinary Specialists and FASTVet.com, Spicewood, TX.
LA, left atrium; Ao, aorta; RV, right ventricle; LV, left ventricle.

Characterization of the caudal vena cava (CVC) and hepatic veins for felines at FAST DH view

| | | | Clinical implications |
|---|---|---|---|
| Bounce – range of normovolemia | Fluid-responsive CVC | Change in CVC height ~35–50% with respiration; maximum height should be between 0.55 and 0.96 cm; combine the dynamic characterization (bounce, FAT, or flat) with maximum CVC DH view height (see Table 7.6), TFAST echo views and Vet BLUE lung for best integrative volume assessment | Safe to fluid challenge if the attending clinician feels the patient needs volume and lungs are dry on Vet BLUE |
| FAT – hypervolemia | Fluid-intolerant CVC | Minimal change in CVC height of <10% and the CVC is enlarged often with distended hepatic veins (tree trunk sign); CVC maximum height when >1.0–1.5 cm is considered FAT (see Table 7.6); combine the dynamic characterization (bounce, FAT, or flat) with maximum DH view height, TFAST echo views and Vet BLUE lung for best integrative volume assessment | The central venous pressure (CVP) is severely elevated and the right heart is volume overloaded; discontinue fluids and consider vasopressors if hypotensive; if normotensive reduce or stop intravenous fluid therapy; investigate the heart for pericardial effusion, enlarged right ventricle, and evidence of right-sided congestive failure, including ascites |
| Flat – hypovolemia | Hypovolemic CVC | Minimal change in CVC height of <10% and the CVC is small; CVC maximum DH view height when <0.25–0.45 cm is considered flat (see Table 7.6); combine the dynamic characterization (bounce, FAT, or flat) with maximum DH view height, TFAST echo views and Vet BLUE lung for best integrative volume assessment | The patient is severely volume depleted until proven otherwise; consider where the fluid loss is and evaluate with Global FAST for effusions in the peritoneal cavity, retroperitoneal space, pleural cavity and pericardial sac (plus lung edema using Vet BLUE) |

The CVC measurements were extrapolated by Lisciandro GR and Vientós-Plotts AI from small dog measurement data from the study by Darnis et al. 2018; thus, giving a starting point for feline CVC assessment (see Table 7.6). Use Global FAST to search for possible internal volume loss; and combine CVC information with TFAST echo views and the patient's Vet BLUE lung findings for best integrative patient assessment.
Source: Reproduced with permission of Dr Gregory Lisciandro, Hill Country Veterinary Specialists and FASTVet.com, Spicewood, TX.

# POCUS Exotic Companion Mammals

Normal reference ranges for various exotic companion animals[a]

| Site | Ferret (mm) | Rabbit (mm) | Chinchilla (mm) | Guinea pig (mm) | Rat (mm) | Hamster (mm) |
|---|---|---|---|---|---|---|
| Stomach wall | | 1±0.01[c] | | | | |
| Saccus cecus wall | | | | | 1.09±0.20[b] | |
| Fundus wall | | 2.80±0.04[c] | | | 1.07±0.25[b] | |
| Pylorus wall | | | | | 2.20±0.41[b] | |
| Duodenum wall | | 1.9±0.04[c] | | | 1.54±0.21[b] | |
| Sacculus rotundus wall | | 2.2±0.06[c] | | | | |
| Cecum wall | | 0.8±0.1[c] | | | 0.89±0.13[b] | |
| Colon | | Spiral loop of ascending colon wall: 1.4±0.4[c]<br>Distal colon wall: 1.9±0.4[c] | | | | |
| Appendix wall | | 1.9±0.4[c] | | | | |
| Kidney | MALE<br>Length: 29.5 (27.0–32.0)<br>Width: 12.6 (12.0–13.0)<br>Height: 14.6 (11.0–17.0)<br>FEMALE<br>Length: 25.1 (22.0–27.0)<br>Width: 11.2 (9.0–12.0)<br>Height: 13.0 (12.0–16.0)[5] | Length:<br>L: 28.6±3.3<br>R: 28.7±3.4<br>Width:<br>L: 17.2±1.9<br>R: 16.2±1.7<br>Height:<br>L: 15.8±1.5<br>R: 16.6±1.4[c] | Length: 19.9 (17.8–22.4)<br>Width: 10.1 (8.3–12.2)<br>Medullary thickness: 2.4 (1.7–3.9)<br>Cortical thickness: 2.4 (1.7–3.3)<br>Pelvis length: 6.6 (4.9–8.0)<br>Pelvis width: 4.2 (3.1–5.2)[d] | Length: 20.3 (14.0–25.0)<br>Width: 13.9 (12.8–16.1)<br>Height: 15.0 (13.0–18.0)[f] | Length:<br>L:19.47±2.3<br>R: 19.45±2.18<br>Width:<br>L:10.74±1.1<br>R: 10.75±0.88<br>Height:<br>L:10.96±1.2<br>R: 11.04±1.00<br>Pelvis:<br>L:0.87±0.24<br>R:0.84±0.21[b] | Length: 13.6 (12.0–14.0)<br>Width: 7.2 (6.5–7.7)<br>Height: 7.8 (7.0–8.1)[f] |
| Urinary bladder | | | | | 0.73±0.13[b] | |
| Adrenals | Length:<br>L: 7.2±1.8<br>R: 7.6±1.8<br>Width:<br>L: 2.8±0.5<br>R: 2.6±0.4[e] | Length:<br>L: 3.4±0.8<br>R: 7.3±1.5<br>Width:<br>L: 3.8±1.1<br>R: 4.3±0.8[c] | Length:<br>L: 6.9 (5.2–8.7)<br>R: 9.9 (7.8–11.9)<br>Widest cross-section:<br>L: 2.4 (2–3.1)<br>R: 2.7 (2.4–3.9)[f] | Length: 15.4 (12.6–17.7)<br>Widest cross-section: 6.2 (4.3–8.4)[f] | L (DV): 3.41±0.49<br>R (DV): 3.07±0.36[b] | |
| Lymph node | | | | | 1.53±0.75 | |
| Width | | | | | 4.19±1.26[b] | |
| Length | | | | | | |

[a] Note: to backcalculate 95% of the values, one should use mean ±2SD or mean±SEM$\sqrt{n}$ (SD, standard deviation, SEM, standard error of the mean).
[b] mean±SD.
[c] mean±SD.
[d] median and 2.5% to 97.5% percentiles.
[e] mean±SD.
[f] mean, range.

# VetFAST-ABCDE Exam

- Used to confirm endotracheal placement by direct visualization of the cranial cervical region.
- Used to survey cervical injury and abnormalities including tracheal lacerations and laryngeal dysfunction.
- Optic nerve sheath diameter (ONSD) measured 3 mm from the posterior eye should be ≤3 mm in dogs. Normal for cats is unknown. Values >3 mm may correlate with intracranial hypertension (Armenise 2012; Armenise et al. 2019).

# POCUS Marine Mammals

- Breath holding (apnea) limits observation of "lung sliding" until the dolphin takes a breath.
- Arching (and vocalizing) is a sign of distress in dolphins during ultrasound examination.
- Water environments make it mandatory to have battery-powered ultrasound units to prevent electrocution.
- Water environments make it mandatory to have screen covers or goggles for viewing the ultrasound image.
- Dolphins have small-volume ascites in normalcy. Expect a positive AFAST for many dolphins that must be placed into clinical context, fluid scored and recorded, and the examination repeated.
- The dolphin kidney is bovine-like and multireniculated (multilobulated), looking very different from the sonographic character of a canine or feline kidney.
- TFAST echo views are more challenging due to breath holding and the barrel-chested conformation of the dolphin. Transesophageal echocardiography provides much better studies (Chetboul et al. 2012; Sklansky et al. 2006; Sklansky et al. 2010).
- The caudal vena cava and hepatic veins in dolphins are robust (hugely distended) in normalcy and appear like right-sided volume overload in other species.
- The "gator sign" orientation for lung is the same as for all other mammalian species.
- Vet BLUE differs in dolphins having nine acoustic windows bilaterally on each hemithorax and lung is interrogated in longitudinal and transverse planes by gently rotating the probe from the starting "gator sign" position to 90° and returning to the "gator sign."
- Expect "dry lung" artifacts to predominate in dolphins, as expected in other mammalian lung (Yarto and Lisciandro 2017, unpublished data).
- The Vet BLUE B-line scoring system and visual lung language are applied to dolphins the same as in small animals (Yarto and Lisciandro 2017, unpublished data; Lisciandro et al. 2014, 2017, 2018; Ward et al. 2017, 2019).
- The marginal lymph nodes are markers for pulmonary disease in dolphins and should be imaged on every Global FAST (Smith et al. 2012).
- The marginal lymph nodes have published expected normal measurement (Martony et al. 2017).

# Global FAST®

Caudal vena cava absolute maximum height measurements at the FAST DH view in the longitudinal plane for dogs relative to body weight

| | Body weight | Suggested CVC maximum height (cm) for a "flat" or hypovolemic CVC (low CVP)[a] | Suggested CVC maximum height (cm) for a "FAT" or fluid-intolerant CVC (high CVP)[a] |
|---|---|---|---|
| Small/Toy[b] | <9 kg | <0.25 | >1.0 |
| Medium | >9 kg but <15–kg | <0.35 | >1.5 |
| Large | >15 kg | <0.50 | >1.5 |

[a] From the study by Darnis et al. (2018). Modified with permission by Lisciandro GR and Vientós-Plotts AI.
[b] Use the Small/Toy values for felines until further guidelines are available.
CVC, caudal vena cava; CVP, central venous pressure; cm, centimeters; kg, kilograms.

Characterization of the caudal vena cava (CVC) and hepatic veins for canines at the FAST DH view

| | | | Clinical implications |
|---|---|---|---|
| Bounce – range of normovolemia | Fluid-responsive CVC | Change in CVC height ~35–50% with respiration; maximum height should be 0.55–0.96 cm; combine the dynamic characterization (bounce, FAT, or flat) with maximum CVC DH view height (see Table 7.6), TFAST echo views and Vet BLUE lung for best integrative volume assessment | Safe to fluid challenge if the attending clinician feels the patient needs volume and lungs are dry on Vet BLUE |
| FAT – hypervolemia | Fluid-intolerant CVC | Minimal change in CVC height of <10% and the CVC is enlarged often with distended hepatic veins (tree trunk sign); CVC maximum height >1.0 cm for dogs <9 kg and >1.5 cm for dogs >9 kg is considered FAT (see Table 7.6); combine the dynamic characterization (bounce, FAT, or flat) with maximum DH view height, TFAST echo views and Vet BLUE lung for best integrative volume assessment | The central venous pressure (CVP) is severely elevated and the right heart is volume overloaded; discontinue fluids and consider vasopressors if hypotensive; if normotensive reduce or stop intravenous fluid therapy; investigate the heart for pericardial effusion, enlarged right ventricle, and evidence of right-sided congestive failure including ascites |
| Flat – hypovolemia | Hypovolemic CVC | Minimal change in CVC height of <10% and the CVC is small; CVC maximum DH view height <0.25 cm in dogs <9 kg, <0.35 cm in dogs >9 kg and <15 kg, and <0.5 cm in dogs >15 kg is considered flat (see Table 7.6); combine the dynamic characterization (bounce, FAT, or flat) with maximum DH view height, TFAST echo views and Vet BLUE lung for best integrative volume assessment | The patient is severely volume depleted until proven otherwise; consider where the fluid loss is and evaluate with Global FAST for effusions in the peritoneal cavity, retroperitoneal space, pleural cavity and pericardial sac (plus lung edema using Vet BLUE) |

The caudal vena cava measurements were extrapolated by Lisciandro GR and Vientós-Plotts AI from dog measurements provided by Darnis et al. 2018.
Use Global FAST to search for possible internal volume loss and combine CVC information with TFAST echo views and the patient's Vet BLUE lung findings for best integrative patient assessment.
Source: Reproduced with permission from Dr Gregory Lisciandro, Hill Country Veterinary Specialists and FASTVet.com, Spicewood, TX.

Using the author's TFAST PTX 1/3s Rule for location of the "lung point" to categorize the degree of pneumothorax (PTX)

| | Degree of PTX |
|---|---|
| Upper third of thorax | Trivial PTX – expect mild if any clinical signs |
| Middle third of thorax | Moderate PTX – expect increased respiratory effort |
| Lower third of thorax | Severe PTX – expect overt respiratory distress |
| Not found along thorax | Indeterminate study or most severe form of PTX – look at your patient's respiratory effort! |

Source: Reproduced with permission from Dr Gregory Lisciandro, Hill Country Veterinary Specialists and FASTVet.com, Spicewood, TX.

Accurate TFAST diagnosis of pericardial and pleural effusion

| Imaging strategies | FAST DH view | TFAST PCS view | Thoracic radiography | Gold standard |
|---|---|---|---|---|
| Pericardial effusion (PCE) | | | | |
| (1) Image toward the muscular apex of the heart where no heart chambers that can be mistaken for free fluid | Racetrack sign | Bull's eye sign | Unreliable test for PCE and for cardiac tamponade | Ultrasound and computed tomography (CT) |
| (2) Long-axis four-chamber view where all four chambers are identified is the only echo view for diagnosis | Enlarged left atrium supports left atrial tear in the mitral valve disease dog | TFAST right PCS view Long-axis four-chamber view | | |
| (3) Image the heart in its entirety using the hyperechoic pericardium in the far-field as a landmark | | | | |
| Pleural effusion | | | | |
| (1) Image the heart in its entirety using the hyperechoic pericardium in the far-field as a landmark | Anechoic triangulations | TFAST right and left PCS Anechoic triangulations | Good test | Debatable between ultrasound, CT, and thoracoscopy |
| (2) Image toward the muscular apex of the heart where no heart chambers that can be mistaken for free fluid | | | | |

Source: Reproduced with permission from Dr Gregory Lisciandro, Hill Country Veterinary Specialists and FASTVet.com, Spicewood, TX.

Ruling out your Hs and Ts. Use of the Global FAST approach for rapidly ruling out and ruling in the Hs and Ts in patients nearing cardiopulmonary arrest (CPA) and during cardiopulmonary resuscitation (CPR). Hs and Ts are rapidly evaluated for by physical exam, vital signs, venous (or arterial) blood gas, and the Global FAST approach

| The Hs | The Ts |
|---|---|
| Hypothermia | Tension pneumothorax (PTX) (TFAST and "lung point") |
| Hypotension/hypovolemia (AFAST, TFAST, Vet BLUE, cavitary bleeds and effusions)[a] | Trauma, hemorrhage (AFAST and abdominal fluid scoring system, TFAST, Vet BLUE, cavitary bleeds) |
| Hyperkalemia, hypokalemia[b] | Thromboembolism (pulmonary thromboembolism) (TFAST, Vet BLUE) |
| Hypoglycemia | Tamponade, (pericardial effusion) (TFAST, FAST DH view) |
| Hydrogen ion (acidosis) | Toxin, canine anaphylaxis (FAST DH view) |
| Hypocontractility (dilated cardiomyopathy) (TFAST) | |
| Hypertension (pulmonary hypertension, heartworm disease/caval syndrome) (TFAST) | |

Source: Reproduced with permission from Dr Gregory Lisciandro, Hill Country Veterinary Specialists and FASTVet.com, Spicewood, TX. Modified by the author for veterinary medicine from AHA CPR Guidelines (Neumar et al. 2010; Andrus 2015).

[a] AFAST, TFAST, Vet BLUE, to search for cavitary bleeds and effusions and alveolar-interstitial syndrome.

[b] AFAST, target organ approach for urinary obstruction including findings of large urinary bladder, distended urethra, dilated ureters, and renal pelvic dilation.

# References and Further Reading

VetBooks.ir

## AFAST®


Atalan G, Barr FJ, Holt PE. 1999. Frequency of urination and ultrasonographic estimation of residual urine in normal and dysuric dogs. *Res Vet Sci* 67(3):295–299.

Boysen SR, Lisciandro GR. 2013. The use of ultrasound in the emergency room (AFAST and TFAST). *Vet Clin North Am Small Anim Pract* 43(4):773–797.

Boysen SR, Rozanski EA, Tidwell AS, et al. 2004. Evaluation of a focused assessment with sonography for trauma protocol to detect free abdominal fluid in dogs involved in motor vehicle accidents. *J Am Vet Med Assoc* 225(8): 1198–1204.

Darnis E, Boysen S, Merveille AC, et al. 2018. Establishment of references values of the caudal vena cava by fast-ultrasonography through different views in healthy dogs. *J Vet Intern Med* 32(4):1308–1318.

Hall DJ, Schofer F, Meier KC, et al. 2007. Pericardial effusion in cats: a retrospective study of clinical findings and outcome in 146 cats. *J Vet Intern Med* 21:1002–1007.

Himelman RB, Kircher B, Rockey DC, et al. 1988. Inferior vena cava plethora with blunted respiratory response: a sensitive echocardiographic sign of cardiac tamoponade. *J Am Coll Cardiol* 12(6):1470–1477.

Lisciandro GR. 2011. Abdominal and thoracic focused assessment with sonography for trauma, triage, and monitoring in small animals. *J Vet Emerg Crit Care* 21(2): 104–122.

Lisciandro GR. 2012. Evaluation of initial and serial combination focused assessment with sonography for trauma (CFAST) examinations of the thorax (TFAST) and abdomen (AFAST) with the application of an abdominal fluid scoring system in 49 traumatized cats. *J Vet Emerg Crit Care* 22(S2):11.

Lisciandro GR. 2016a. The use of the diaphragmaticohepatic (DH) views of the abdominal and thoracic focused assessment with sonography for triage (AFAST/TFAST) examinations for the detection of pericardial effusion in 24 dogs (2011-2012). *J Vet Emerg Crit Care* 26(1):125–131.

Lisciandro GR. 2016b. Abdominal FAST (AFAST)-detected hemorrhagic abdominal effusion in 11 dogs with acute collapse and gallbladder wall edema (halo sign) with presumed anaphylaxis. *J Vet Emerg Crit Care* 26(S1):S8.

Lisciandro GR. 2019. The cardiac gallbladder: case series of 13 dogs and 1 cat with sonographically detected gallbladder wall edema. *J Vet Emerg Crit Care* 29(S1):S24.

Lisciandro GR, Fosgate GT. 2017. Use of AFAST cysto-colic view urinary bladder measurements to estimate urinary bladder volume in dogs and cats. *J Vet Emerg Crit Care* 27(6):713–717.

Lisciandro GR, Lisciandro SC. 2019. Sonographic changes of the gallbladder associated with anaphylaxis in dogs. *J Vet Emerg Crit Care* 29(2):214–215.

Lisciandro GR, Lagutchik MS, Mann KA, et al. 2009. Evaluation of an abdominal fluid scoring system determined using abdominal focused assessment with sonography for trauma in 101 dogs with motor vehicle trauma. *J Vet Emerg Crit Care* 19(5):426–437.

Lisciandro GR, Fosgate GT, Romero LA, Bridgeman CH. 2015. Abdominal FAST (AFAST) and abdominal fluid scores in adult and juvenile cats. *J Vet Emerg Crit Care* 25(S1):S8.

Lisciandro GR, Fosgate GT, Romero LA, et al. 2019. The expected frequency and amount of free peritoneal fluid estimated using the abdominal FAST-applied abdominal fluid scores in clinically normal adult and juvenile dogs. *J Vet Emerg Crit Care*, in press.

MacDonald KA, Cagney O, Magne ML. 2009. Echocardiographic and clinicopathologic characterization of pericardial effusion in dogs: 107 cases (1985–2006). *J Am Vet Med Assoc* 235(12):1456–1461.

McMurray J, Boysen S, Chalhoub S. 2016. Focused assessment with sonography in nontraumatized dogs and cats in the emergency and critical care setting. *J Vet Emerg Crit Care* 26(1):64–73.

Quantz JE, Miles MS, Reed AL, et al. 2009. Elevation of alanine transaminase and gallbladder wall abnormalities as biomarkers of anaphylaxis in canine hypersensitivity patients. *J Vet Emerg Crit Care* 19(6):536–544.

Simpson SA, Syring R, Otto CM. 2009. Severe blunt trauma in dogs: 235 cases (1997–2003). *J Vet Emerg Crit Care* 19(6):588–602.

Stafford Johnson M, Martin M, Binns S, et al. 2004. A retrospective study of clinical findings, treatment and outcome in 143 dogs with pericardial effusion. *J Small Anim Pract* 45(11):546–552.


## POCUS Liver and Gallbladder


Cuccovillo A, Lamb CR. 2002. Cellular features of sonographic target lesions of the liver and spleen in 21 dogs and a cat. *Vet Radiol Ultrasound* 43(3):275–278.

d'Anjou MA. 2008. Liver. In: *Atlas of Small Animal Ultrasonography*, edited by Penninck D, D'anjou MA. Ames: Blackwell Publishing, pp 243–247.

Hittmair KM, Vielgrader HD, Loupal G. 2001. Ultrasonographic gallbladder wall thickness in cats. *Vet Radiol Ultrasound* 42:149–155.

Quantz JE, Miles MS, Reed AL, et al. 2009. Elevation of alanine transaminase and gallbladder wall abnormalities as biomarkers of anaphylaxis in canine hypersensitivity patients. *J Vet Emerg Crit Care* 19(6):536–544.

Spaulding KA. 1993. Ultrasound corner: gallbladder wall thickness. *Vet Radiol Ultrasound* 34:270–272.

Tsukagoshi T, Ohno K, Tsukamoto A, et al. 2012. Decreased gallbladder emptying in dogs with biliary sludge or gallbladder mucocele. *Vet Radiol Ultrasound* 53(1):84–91.

## POCUS Spleen

Cuccovillo A, Lamb CR. 2002. Cellular features of sonographic target lesions of the liver and spleen in 21 dogs and a cat. *Vet Radiol Ultrasound* 43(3):275–278.

Hecht S. 2008. Spleen. In: *Atlas of Small Animal Ultrasonography*, edited by Penninck D, d'Anjou M. Ames: Blackwell Publishing, pp 263–280.

Reese SH, Zekas LJ, Iazbik MC, et al. 2013. Effect of sevoflurane anesthesia and blood donation on the sonographic appearance of the spleen in 60 healthy cats. *Vet Radiol Ultrasound* 54(2):168–175.

## POCUS Kidney

d'Anjou MA. 2008. Kidneys and Ureters. In: *Atlas of Small Animal Ultrasonography*, edited by Penninck D, d'Anjou M. Ames: Blackwell Publishing, pp 339–364.

d'Anjou MA, Bédard A, Dunn ME. 2011. Clinical significance of renal pelvic dilatation on ultrasound in dogs and cats. *Vet Radiol Ultrasound* 52(1):88–94.

Nevins JR, Mai W, Thomas E. 2015. Association between ultrasound and clinical findings in 87 cats with urethral obstruction. *Vet Radiol Ultrasound* 56(4):439–447.

Nickel R, Schummer A, Seiferle E, et al. 1973. Urogenital system. In: *The Viscera of Domestic Mammals*, edited by Schummer A, Nickel R, Sack WO. Berlin: Paul Parcy, pp 291–293.

Walter PA, Feeney DA, Johnston GR, Fletcher TF. 1987. Feline renal ultrasonography: quantitative analyses of imaged anatomy. *Am J Vet Res* 48:596–599.

## POCUS Urinary Bladder

Defarges A, Dunn M, Berent AC. 2013. New alternatives for minimally invasive management of uroliths: lower urinary tract uroliths. *Compendium* 35(1):E1.

Finn-Bodner ST. 1995. The urinary bladder. In: *Practical Veterinary Ultrasound*, edited by Cartee RE. Baltimore: Williams and Wilkins, pp 200–235.

Geisse AL, Lowry JE, Schaefer DJ, Smith CW. 1997. Sonographic evaluation of the urinary bladder wall thickness in normal dogs. *Vet Radiol Ultrasound* 38:132–137.

## POCUS Gastrointestinal and Pancreas

Garcia DA, Froes TR, Vilani OC, et al. 2011. Ultrasonography of small intestinal obstructions: a contemporary approach. *J Small Anim Pract* 52:484–490.

Hecht S, Henry G. 2007. Sonographic evaluation of the normal and abnormal pancreas. *Clin Tech Small Anim Pract* 22:115–121.

Hess RS, Saunders HM, van Winkle TJ, et al. 1998. Clinical, clinicopathological, radiographic and ultrasonographic abnormalities in dogs with fatal acute pancreatitis: 70 cases (1986–1985). *J Am Vet Med Assoc* 213:665–670.

Moon M, Biller D, Armburst L. 2003. Ultrasonographic appearance and etiology of corrugated small intestine. *Vet Radiol Ultrasound* 44(2):199–203.

Newell SM, Graham JP, Roberts GD, et al. 1999. Sonography of the normal feline gastrointestinal tract. *Vet Radiol Ultrasound* 40(1):40–43.

Nyland TG, Mattoon JS. 2015a. Pancreas. In: *Small Animal Diagnostic Ultrasound*, 3rd edition, edited by Nyland TG, Mattoon JS. St. Louis: Elsevier Saunders, pp 438–467.

Nyland TG, Mattoon JS. 2015b. Gastrointestinal Tract. In: *Small Animal Diagnostic Ultrasound*, 3rd edition, edited by Nyland TG, Mattoon JS. St. Louis: Elsevier Saunders, pp 468–500.

Nyland TG, Mattoon JS, Herrgesell EJ, et al. 2002. Pancreas. In: *Small Animal Diagnostic Ultrasound*, 2nd edition, edited by Nyland TG, Mattoon JS. Philadelphia: WB Saunders, pp 144–157.

Penninck D. 2008a. Gastrointestinal tract. In: *Atlas of Small Animal Ultrasonography*, edited by Penninck D, d'Anjou MA. Ames: Blackwell Publishing, pp 281–318.

Penninck D. 2008b. Pancreas. In: *Atlas of Small Animal Ultrasonography*, edited by Penninck D, d'Anjou MA. Ames: Blackwell Publishing, pp 319–338.

Penninck D, Nyland T, Fisher P, et al. 1989. Ultrasonography of the normal canine gastrointestinal tract. *Vet Radiol* 30(6):272–276.

Sharma A, Thompson M, Scrivani P, et al. 2011. Comparison of radiography and ultrasonography for diagnosing small-intestinal mechanical obstruction in vomiting dogs. *Vet Radiol Ultrasound* 52(3):248–255.

Tidwell AS, Penninck DG. 1992. Ultrasonography of gastrointestinal foreign bodies. *Vet Radiol Ultrasound* 2(33) 160–169.

## POCUS Reproductive

Davidson A, Baker T. 2009. Reproductive ultrasound in the bitch and queen. *Top Compan Anim Med* 24(2):55–63.

Mattoon J, Nyland T. 2002. Ovaries and uterus. In: *Small Animal Diagnostic Ultrasound*, 2nd edition, edited by Nyland TG, Mattoon JS. Philadelphia: WB Saunders, pp 231–249.

Mattoon JS, Nyland TG. 2015. Ovaries and Uterus. In: *Small Animal Diagnostic Ultrasound*, 3rd edition, edited by Nyland TG, Mattoon JS. St. Louis: Elsevier Saunders, pp 634–654.

Traas AM. 2008. Surgical management of canine and feline dystocia. *Theriogenology* 40:337–342.

Verstegen J, Dhaliwal G, Verstegen-Onclin K. 2008. Mucometra, cystic endometrial hyperplasia, and pyometra in the bitch: advances in treatment and assessment of future reproductive success. *Theriogenology* 70:364–374.

Zambelli D, Caneppele B, Bassi S, et al. 2002. Ultrasound aspects of fetal and extrafetal structures in pregnant cats. *J Feline Med Surg* 4:95–106.

## TFAST®

Dicker SA, Lisciandro GR, Newell SM, et al. 2019. Diagnosis of pulmonary contusions with point-of-care lung ultrasonography and thoracic radiography compared to thoracic computed tomography in dogs with motor vehicle trauma: 29 cases (2017–2018). *J Vet Emerg Crit Care*, in press.

Hall DJ, Shofer F, Meier CK, Sleeper MM. 2007. Pericardial effusion in cats: a retrospective study of clinical findings and outcome in 146 cats. *J Vet Intern Med* 21(5):1002–1007.

Lisciandro GR. 2011. Abdominal and thoracic focused assessment with sonography for trauma, triage, and monitoring in small animals. *J Vet Emerg Crit Care* 21(2):104–122.

Lisciandro GR. 2014a. The Abdominal FAST$^3$ (AFAST$^3$) Exam. In: *Focused Ultrasound for the Small Animal Practitioner*, edited by Lisciandro GR. Ames: Wiley Blackwell, pp 17–43.

Lisciandro GR. 2014b. The Thoracic FAST$^3$ (TFAST$^3$) Exam. In: *Focused Ultrasound for the Small Animal Practitioner*, edited by Lisciandro GR. Ames: Wiley Blackwell, pp 140–165.

Lisciandro GR. 2016. The use of the diaphragmatico-hepatic (DH) views of the abdominal and thoracic focused assessment with sonography for triage (AFAST/TFAST) examinations for the detection of pericardial effusion in 24 dogs (2011–2012). *J Vet Emerg Crit Care* 26(1):125–131.

Lisciandro GR, Lagutchik MS, Mann KA, et al. 2008. Evaluation of a thoracic focused assessment with sonography for trauma (TFAST) protocol to detect pneumothorax and concurrent thoracic injury in 145 traumatized dogs. *J Vet Emerg Crit Care* 18(3):258–269.

MacDonald KA, Cagney O, Magne ML. 2009. Echocardiographic and clinicopathologic characterization of pericardial effusion in dogs: 107 cases (1985–2006). *J Am Vet Med Assoc* 235(12):1456–1461.

Nelson NC, Drost WT, Lerche P, et al. 2010. Noninvasive estimation of central venous pressure in anesthetized dogs by measurement of hepatic venous blood flow velocity and abdominal venous diameter. *Vet Radiol Ultrasound* 51(3):313–323.

Reissig A, Copetti R, Kroegel C. 2011. Current role of emergency ultrasound of the chest. *Crit Care Med* 39(5):1–8.

Shaw SP, Rush JE. 2007. Canine pericardial effusion: pathophysiology and cause. *Compend Contin Educ Vet* 29(7):400–403.

Ward JL, Lisciandro GR, DeFrancesco TD, et al. 2018. Evaluation of point-of-care thoracic ultrasound and NT-proBNP for the diagnosis of congestive heart failure in cats with respiratory distress. *J Vet Intern Med* 32(5):1530–1540.

## Vet BLUE®

Dicker SA, Lisciandro GR, Newell SM, et al. 2019. Diagnosis of pulmonary contusions with point-of-care lung ultrasonography and thoracic radiography compared to thoracic computed tomography in dogs with motor vehicle trauma: 29 cases (2017–2018). *J Vet Emerg Crit Care*, in press.

Hecht S, Penninck D. 2015. Thorax. In: *Atlas of Small Animal Ultrasonography*, 2nd edition, edited by Penninck D, d'Anjou M. Ames: Wiley Blackwell, pp 81–110.

Kulhavy DA, Lisciandro GR. 2015. Use of a lung ultrasound examination called Vet BLUE to screen for metastatic lung nodules in the emergency room. *J Vet Emerg Crit Care* 25(S1):S14.

Lichtenstein D. 2010. Should lung ultrasonography be more widely used in the assessment of acute respiratory disease? *Expert Rev Respir Med* 4(5):533–538.

Lisciandro GR. 2011. Abdominal and thoracic focused assessment with sonography for trauma, triage and monitoring in small animals. *J Vet Emerg Crit Care* 21(2):104–122.

Lisciandro GR. 2012. Comparison of Vet BLUE to thoracic radiography – 432 cases (2010–2012). Unpublished data.

Lisciandro GR. 2013. The Vet BLUE wedge sign for detecting pulmonary thromboembolism: case series of 6 dogs. Unpublished data.

Lisciandro GR. 2014. The Vet BLUE lung scan. 2014. In: *Focused Ultrasound for the Small Animal Practitioner*, edited by Lisciandro GR. Ames: Wiley Blackwell, pp 166–188.

Lisciandro GR, Fosgate GT, Fulton RM. 2014. Frequency of ultrasound lung rockets using a regionally-based lung ultrasound examination named veterinary bedside lung ultrasound exam (Vet BLUE) in 98 dogs with normal thoracic radiographic lung findings. *Vet Radiol Ultrasound* 55(3):315–322.

Lisciandro GR, Ward JL, DeFrancesco TC, Mann KA. 2016. Absence of B-lines on lung ultrasound (Vet BLUE protocol) to rule out left-sided congestive heart failure in 368 cats and dogs. *J Vet Emerg Crit Care* 26(S1):S8.

Lisciandro GR, Fulton RM, Fosgate GT, Mann KA. 2017. Frequency of B-lines using a regionally-based lung ultrasound examination (the Vet BLUE protocol) in 49 cats with normal thoracic radiographical lung findings. *J Vet Emerg Crit Care* 27(3):267–277.

Lisciandro GR, Romero L, Fosgate GT. 2018. The frequency of B-Lines and other lung ultrasound artifacts during Vet BLUE in 91 healthy puppies and kittens. *J Vet Emerg Crit Care* 28(S1):S16.

Rademacher N, Pariaut R, Pate J, et al. 2014. Transthoracic lung ultrasound in normal dogs and dogs with cardiogenic pulmonary edema: a pilot study. *Vet Radiol Ultrasound* 55(4):447–452.

Soldati G, Testa A, Silva FR, et al. 2006. Chest ultrasonography in lung contusions. *Chest* 130(2): 533–538.

Vezzosi T, Mannucci A, Pistoresi F, et al. 2017. Assessment of lung ultrasound B-Lines in dogs with different stages of chronic valvular heart disease. *J Vet Intern Med* 31(3):700–704.

Volpicelli G, Mussa A, Garofalo G, et al. 2006. Bedside lung ultrasound in the assessment of alveolar-interstitial syndrome. *Am J Emerg Med* 24:689–696.

Ward JL, Lisciandro GR, Keene BW, et al. 2017. Accuracy of point-of-care lung ultrasonography for the diagnosis of cardiogenic pulmonary edema in dogs and cats with acute dyspnea. *J Am Vet Med Assoc* 250:666–675.

Ward JL, Lisciandro GR, DeFrancesco TC. 2018. Distribution of alveolar-interstitial syndrome in dyspneic veterinary patients assessed by lung ultrasound versus thoracic radiography. *J Vet Emerg Crit Care* 28(5):415–428.

Ward JL, Lisciandro GR, Ware WA, et al. 2019. Lung ultrasound findings in 100 dogs with various etiologies of cough. *J Am Vet Med Assoc* 255(5):574–583.

## *POCUS Heart*

Abbott JA, MacLean HN. 2006. Two-dimensional echocardiographic assessment of the feline left atrium. *J Vet Intern Med* 20:111–119.

Darnis E, Boysen S, Merveille AC, et al. 2018. Establishment of references values of the caudal vena cava by fast-ultrasonography through different views in healthy dogs. *J Vet Intern Med* 32(4):1308–1318.

Rishniw M, Erb HN. 2000. Evaluation of four 2-dimensional echocardiographic methods of assessing left atrial size in dogs. *J Vet Intern Med* 14:429–435.

## *POCUS* Pediatrics

Lisciandro GR, Fosgate GT, Romero LA, Bridgeman CH. 2015. Abdominal FAST (AFAST) and abdominal fluid scores in adult and juvenile cats. *J Vet Emerg Crit Care* 25(S1):S8.

Lisciandro GR, Romero L, Fosgate GT. 2018. The frequency of B-Lines and other lung ultrasound artifacts during Vet BLUE in 91 healthy puppies and kittens. *J Vet Emerg Crit Care* 28(S1):S16.

Lisciandro GR, Fosgate GT, Romero LA, et al. 2019. The expected frequency and amount of free peritoneal fluid estimated using the abdominal FAST-applied abdominal fluid scores in clinically normal adult and juvenile dogs. *J Vet Emerg Crit Care*, in press.

Romero LA, Lisciandro GR, Fosgate GT, Bridgeman CH. 2015. Abdominal FAST (AFAST) and abdominal fluid scores in adult and juvenile dogs. *J Vet Emerg Crit Care* 25(S1):S7–S8.

Stander N, Wagner WM, Goddard A, et al. 2010. Normal canine pediatric gastrointestinal ultrasonography. *Vet Radiol Ultrasound* 51(1):75–78.

## *POCUS Felines*

Abbott JA, MacLean HN. 2006. Two-dimensional echocardiographic assessment of the feline left atrium. *J Vet Intern Med* 20:111–119.

D'Anjou MA. 2008a. Liver. In: *Atlas of Small Animal Ultrasonography*, edited by Penninck D, d'Anjou MA. Ames: Blackwell Publishing, pp 243–247.

D'Anjou MA. 2008b. Kidneys and ureters. In: *Atlas of Small Animal Ultrasonography*, edited by Penninck D, d'Anjou MA. Ames: Blackwell Publishing, pp 351–357.

D'Anjou MA, Bédard A, Dunn ME. 2011. Clinical significance of renal pelvic dilatation on ultrasound in dogs and cats. *Vet Radiol Ultrasound* 52(1):88–94.

Darnis E, Boysen S, Merveille AC, et al. 2018. Establishment of references values of the caudal vena cava by fast-ultrasonography through different views in healthy dogs. *J Vet Intern Med* 32(4):1308–1318.

Di Donato P, Penninck D, Pietra M, et al. 2014. Ultrasonographic measurment of the relative thickness of intestinal wall layers in clinical healthy cats. *J Feline Med Surg* 16:333–339.

Goggin JM, Biller DS, Ward H, et al. 2000. Ultrasonographic measurement gastrointestinal wall thickness and the ultrasonographic appearance of the ileocolic region in healthy cats. *J Am Anim Hosp Assoc* 36:224–228.

Hecht S, Penninck DG, Mahony OM, et al. 2006. Relationship of pancreatic duct dilation to age and clinical findings in cats. *Vet Radiol Ultrasound* 47:287–294.

Kittleson MD, Kienle RD. 1998. *Small Animal Cardiovascular Medicine*. St Louis: Mosby, Table 6-2, p 104.

Lisciandro GR, Fulton RM, Fosgate GT, Mann KA. 2017. Frequency of B-lines using a regionally-based lung ultrasound examination (the Vet BLUE protocol) in 49 cats with normal thoracic radiographical lung findings. *J Vet Emerg Crit Care* 27(3):267–277.

Lisciandro GR, Romero L, Fosgate GT. 2018. The frequency of B-Lines and other lung ultrasound artifacts during Vet BLUE in 91 healthy puppies and kittens. *J Vet Emerg Crit Care* 28(S1):S16.

Mattoon J, Nyland T. 2002. Ovaries and uterus. In: *Small Animal Diagnostic Ultrasound*, 2nd edition, edited by Nyland T, Mattoon J. Philadelphia: WB Saunders, pp 231–249.

Mattoon JS, Nyland TG. 2015a. Ovaries and uterus. In: *Small Animal Diagnostic Ultrasound*, 3rd edition, edited by Nyland TG, Mattoon JS. St. Louis: Elsevier Saunders, pp 634–654.

Mattoon JS, Nyland TG. 2015b. Prostate and testes. In: *Small Animal Diagnostic Ultrasound*, 3rd edition, edited by Nyland TG, Mattoon JS. St. Louis: Elsevier Saunders, pp 608–633.

Nevins JR, Mai W, Thomas E. 2015. Associations between ultrasound and clinical findings in 87 cats with urethral obstruction. *Vet Radiol Ultrasound* 56(4):439–447.

Newell SM, Graham JP, Roberts GD, et al. 1999. Sonography of the normal feline gastrointestinal tract. *Vet Radiol Ultrasound* 40:40–43.

Nickel R, Schummer A, Seiferle E, et al. 1973. Urogenital system. In: *The Viscera of the Domestic Mammals*, by Schummer A, Nickel R, Sack WO. Berlin: Paul Parcy, pp 291–293.

Nyland TC, Mattoon JS. 2015. Pancreas. In: *Small Animal Diagnostic Ultrasound*, 3rd edition, edited by Matton JS, Nyland TG. St Louis: Elsevier Saunders, pp 438–467.

Reese SH, Zekas LJ, Iazbik MC, et al. 2013. Effect of sevoflurane anesthesia and blood donation on the sonographic appearance of the spleen in 60 healthy cats. *Vet Radiol Ultrasound* 54(2):168–175.

Walter PA, Feeney DA, Johnston GR, et al. 1987. Feline renal ultrasonography: quantitative analyses of imaged anatomy. *Am J Vet Res* 48:596–599.

Winter MD, Londono L, Berry CR, et al. 2014. Ultrasonographic evaluation of relative gastrointestinal layer thickness in cats without clinical evidence of gastrointestinal tract disease. *J Feline Med Surg* 16:118–124.

## POCUS Exotic Companion Mammals

Banzato T, Bellini L, Contiero B, et al. 2014. Abdominal anatomic features and reference values determined by use of ultrasonography in healthy common rats (Rattus norvegicus). *Am J Vet Res* 75:67–76.

Banzato T, Bellini L, Contiero B, et al. 2015. Abdominal ultrasound features and reference values in 21 healthy rabbits. *Vet Rec* 176:101.

Ferrari M, Aparecida W, da Silva C, et al. 2013. Ultrasonographic features of the Chinchilla (Chinchilla lanigera) kidney. *J Exot Pet Med* 22:393–395.

O'Brien RT, Paul-Murphy J, Dubielzig RR. 1996. Ultrasonography of adrenal glands in normal ferrets. *Vet Radiol Ultrasound* 37:399–491.

## VetFAST-ABCDE Exam

Armenise A, Ricciardi M, Giannuzzi AP, et al. 2012. Ultrasonographic measure of the optic nerve sheath in canine patients with signs of raised intracranial pressure. A preliminary study. Abstract. *J Vet Emerg Crit Care* 22(S2):S20.

Armenise A, Boysen RS, Rudloff E, et al. 2019. Veterinary-focused assessment with sonography for trauma-airway, breathing, circulation, disability and exposure: a prospective observational study in 64 canine trauma patients. *J Small Anim Pract* 60(3):173–182.

## POCUS Marine Mammals

Chetboul V, Lichtenberger J, Merlin M, et al. 2012. Within-day and between-day variability of transthoracic anatomic M-mode echocardiography in the bottlenose dolphin (Tursiops truncatus). *J Vet Cardiol* 14(4):511–518.

Martony ME, Ivančić M, Gomez FM, et al. 2017. Establishing marginal lymph node ultrasonographic characteristics in healthy bottlenose dolphins (*Tursiops truncatus*). *J Zoo Wildlife Med* 48(4):961–971.

Sklansky M, Levine G, West N, et al. 2006. Transesophageal echocardiogaphic evaluation of the bottlenose dolphin (Tursiops truncatus). *J Zoo Wild Med* 37(4):454–463.

Sklansky M, Renner M, Clough P, et al. 2010. Fetal echocardiographic evaluation of the bottlenose dolphin (*Tursiops truncatus*). *J Zoo Wildl Med* 41(1):35–43.

Smith CR, Solano M, Lutmerding BA, et al. 2012. Pulmonary ultrasound findings in a bottlenose dolphin *Tursiops truncatus* population. *Dis Aquatic Org* 101:242–255.

## Global FAST®

Andrus P. 2015. Cardiac arrest. In: *Point-of-Care Ultrasound*. edited by Soni N, Arntfield R, Kory P. Philadelphia: Elsevier Saunders, pp 359–365.

Darnis E, Boysen S, Merveille AC, et al. 2018. Establishment of references values of the caudal vena cava by fast-ultrasonography through different views in healthy dogs. *J Vet Intern Med* 32(4):1308–1318.

Neumar RW, Otto CW, Link MS, et al. 2010. Part 8: Adult advanced cardiovascular life support: 2010 American Heart Association guidelines for cardiopulmonary resuscitation and emergency cardiovascular care. *Circulation* 122:S729–S767.

# Index


ABAV. *See* Absent B-lines all (Vet BLUE) views
ABCDE. *See* VetFAST-ABCDE
Abdomen
  drying of, 123
  thorax compared to, 337
Abdominal abscess, rabbits, 823
Abdominal breathing, cats, 494, 496
Abdominal circulation, 761–762, 766
Abdominal disorders, pediatric POCUS, 271, 279–286
Abdominal FAST (AFAST)
  abbreviations and terminology, 62–63
  clinical integration
    AFS calculation and use, 113–121, 124–125
    blunt and penetrating trauma, 121–128
    canine anaphylaxis, 61–62, 108, 127, 129–136
    capabilities, 111–112
    dehydrated and hypovolemic patients, 127–128
    documentation using goal-directed templates, 142–143, 933
    indications, 113
    limitations, 112–113
    nonhemorrhagic effusions, 126–127
    objectives, 113
    pearls and pitfalls, 142
    pericardial effusion, 136–140
    postinterventional exit exam, 125–126
    quick references of normal values and rules of thumb, 142, 144, 951–955
    target organ approach for soft tissue screening, 140–141
    urinary bladder volume estimation, 140–141, 793, 795
  clinical questions answered, 60, 112
  definition, 4
  depth settings, 33
  efficiency, 695
  FAST compared to, 58–60
  feline
    AFS, 797–802
    CC view, 793, 795
    DH view, 781–786
    gastrointestinal tract, 795–798
    HRU and SRU views, 797
    image acquisition, 778
    kidney, 788–791
    liver and gallbladder, 778–783
    spleen, 786–788, 797
    SR and HR views, 791–792
    urinary bladder, urine, urethra, and reproductive structures, 792–795
  Flash exam *versus*, 4
  Global FAST *versus*, 687
  goal-directed templates, 926–927
  historical development and studies, 57–58
  image acquisition
    acoustic windows overview, 69–70, 72
    capabilities, 61
    cats, 778
    CC view performance, 91–100
    DH view, 699–701
    DH view performance, 73–84
    documentation using goal-directed templates, 106, 933
    HR5th and SR5th bonus view performance, 102, 104–106
    HRU and SRU view performance, 97, 99–104
    image quality optimization, 64
    indications, 64
    limitations, 61, 63
    objectives, 64
    patient positioning, 65–71
    pearls and pitfalls, 106
    probe preferences, 64
    probe–skin contact optimization, 64
    quick references of normal values and rules of thumb, 106–108, 951–955
    serial repetition, 57–58, 84, 91, 97, 102, 106, 117, 119, 122–123, 127–128, 164
    SR and HR view performance, 84–91
    ultrasound settings, 64
  leaks and plugs, 705–706
  maneuvers for, 693
  marine mammal POCUS, 829
    abdominal fluid scoring, 846–847
    cysto-colic reproductive view, 837, 845–846



*Point-of-Care Ultrasound Techniques for the Small Animal Practitioner*, Second Edition. Edited by Gregory R. Lisciandro.


© 2021 John Wiley & Sons, Inc. Published 2021 by John Wiley & Sons, Inc.


Companion website: www.wiley.com/go/lisciandro/ultrasound2

Abdominal FAST (AFAST) (*cont'd*)
diaphragmatico-hepatic view, 837–842
efficiency, 858
hepato-renal view, 837, 841, 843–845
overview of, 835–838
spleno-renal view, 837, 841, 843–845
umbilical view, 838, 846
patient positioning, 692–696
patient staging
hemoabdomen, 712
pericardial effusion, 715–716
urinary bladder mass, 715
with POCUS abdominal exams, 149
with POCUS dystocia exam, 265
with POCUS gastrointestinal tract and pancreas, 225–226
with POCUS kidney exam, 189, 207
with POCUS liver and gallbladder exams, 169–170
with POCUS reproductive exam, 247, 255
with POCUS spleen exam, 173, 186–187
with POCUS urinary bladder exam, 221–222
probe and helper hand placement, 41–42, 44
probe maneuvering, 43, 70–73
with TFAST, 297–298
with TFAST echo views, 382–383
trouble-shooting algorithm for poor, 49–52
Abdominal fluid score (AFS), 57–59, 61, 63
AFAST views included in, 69–70, 101
ascites, 707
calculation of, 113–114
canine anaphylaxis, 131–136
cats, 63, 106–108, 797–802
dehydrated and hypovolemic patients, 127–128
dolphins, 846, 848
hemoabdomen application, 115–121, 124–125
large-volume bleeder, 114–117, 124
management guidelines and decision making using, 118–121
modification using maximum dimensions, 114–116, 124
nonhemorrhagic effusions, 126–127
patient position, 695–696
with POCUS dystocia exam, 265
with POCUS gastrointestinal tract and pancreas, 225–226
with POCUS kidney exam, 189, 207
with POCUS liver and gallbladder exams, 169–170
with POCUS spleen exam, 173, 186–187
with POCUS urinary bladder exam, 221–222
postinterventional exit exam, 125–126
quick references of normal values and rules of thumb, 106–108, 142, 144, 951
retroperitoneal fluid exclusion, 87
serial AFAST monitoring, 117, 119, 127–128
small-volume bleeder, 114–117, 119, 124
sources and location of bleeding, 124–125
Abdominal presets, 303, 319–320, 428, 430–433
Abdominal radiograph
AFAST acoustic window correlation, 72
litter size, 262, 268, 270
penetrating trauma, 122
serial AFAST compared to, 128
serosal detail, 57
Abdominal scan, pediatric POCUS, 272–279
Abdominal wall block, 630
Abdominal wall injury, 657–660
Abdominocentesis
fluid characterization, 102
indications, 897–898
scanning technique for, 898
ultrasound-guided
introduction, 897
materials checklist, 898
procedure, 898–899
Abscess
hepatic, 156–157, 159
prostatic, 250
rabbits, 822–823
scrotal, 253–254
splenic, 179–180
ultrasonographic appearance, 654–655
Absent B-lines all (Vet BLUE) views (ABAV), 481, 485–486
Absorption, sound waves, 13
Accessibility, 922–925
Achilles tendon rupture, 673, 679
Acoustic coupling gel, 36
AFAST, 64
air trapping elimination, 40–41
POCUS eye, 555–556, 558
TFAST, 303
Vet BLUE, 427
Acoustic coupling medium, cats, 803, 805
Acoustic enhancement
AFAST
CC view, 93, 96
DH view, 79, 81–82
bones and joints POCUS, 666
fluid-filled structures, 17–18
hepatic cysts, 158
liver and gallbladder POCUS, 156
ultrasound-guided lung and thoracic sampling, 908
Acoustic impedance, 13
Acoustic shadowing
bones and joints POCUS, 666
gastrointestinal foreign bodies, 233–235, 280–281
nephroliths, 200, 203
urinary bladder sediment, 221–222
uroliths, 214, 219–220
Acoustic windows. *See also specific views*
AFAST, 69–70, 72
brachial plexus block
axillary approach, 614–615
paravertebral approach, 611–612
subscalene approach, 613
chelonians, 872, 875
intrathecal approach, 643–644
neuroaxial nerve block
lumbosacral area, 639–641
thoracolumbar area, 641
pelvic nerve block
inguinal region, 623–625
sublumbar region, 621–622
RUMM block, 616–618
TCDUS, 597
TCUS, 580, 597
TFAST, 300–301, 332
Acute Hemorrhagic diarrhea syndrome (AHDS), 704. *See also* Hemorrhagic gastroenteritis syndrome (HGE)
Acute kidney injury (AKI), 207
Adenocarcinoma
prostatic, 717–718
uterine, rabbits, 822–823
Adrenal glands
mass, ferrets, 817–818
pediatric POCUS, 274, 276–278
SR view on AFAST, 86–87
Advanced life support (ALS)
Global FAST
capabilities, 730–731
hyperkalemia, 736–737
hypertension–pulmonary hypertension, 737–739

hypocontractility–dilated cardiomyopathy, 736–738
hypotension/hypovolemia, 734, 736
indications, 731
limitations, 731
objectives, 731
patient management, 751
pearls and pitfalls, 751
tamponade–pericardial effusion, 741, 744–746
tension pneumothorax, 740–741
thromboembolism–pulmonary thromboembolism, 741, 744–745
toxin–canine anaphylaxis, 745, 748–749
trauma–hemorrhage, 741–742
VetFAST-ABCDE, 759, 771–772
AFAST. *See* Abdominal FAST
AFAST-focused spleen, 106–107, 121, 136
AFAST-TFAST 48-hour rule, 123
AFS. *See* Abdominal fluid score
Air. *See also* Pneumothorax
abdominal, 281, 283
acoustic impedance, 13
artifacts, 15–16, 18–22
TFAST, 306–308, 313, 339, 341, 344
Vet BLUE, 431–432, 449–452, 462–466, 468–471, 850–851
attenuation, 13
echogenicity, 5–7
intraluminal, 233–234
nongravity dependent nature, 299, 344–345, 347–348
pneumoperitoneum, 235–239
sound waves velocity through, 12–13
thorax compared to abdomen, 337
Air bronchogram, 462–463, 466, 474–475
Air sacs, 864–865
Air trapping, 40–41
Airway
ultrasound skills, 757
VetFAST-ABCDE
abnormal findings, 758
assessment, 759–762
Global FAST *versus*, 767–769
AIS. *See* Alveolar-interstitial syndrome
AKI. *See* Acute kidney injury
Alcohol. *See* Isopropyl alcohol
Alcohol-based hand sanitizer
AFAST, 64
air trapping elimination, 40–41
cats, 803, 805
TFAST, 303
Vet BLUE, 427
A-lines, 6, 19–20
TFAST
image acquisition, 306–308, 313
pneumothorax diagnosis, 339, 341, 344, 354
Vet BLUE
image acquisition, 431–432, 449–452
marine mammal POCUS, 850–851
visual lung language, 462–466, 468–471
Allometric scaling formulas, CVC POCUS, 548
ALS. *See* Advanced life support
Alveolar-interstitial syndrome (AIS), 341, 705
B-line scoring systems, 470–474, 710
Vet BLUE, 449–450, 462–466, 468–474
A-mode, 33
Amplitude, sound wave, 13
Anaphylactic gallbladder, AFAST findings, 61–62, 108
CVC characterization with, 130–132
sonographic striation in gallbladder wall edema, 127, 129–132
Anaphylaxis. *See* Canine anaphylaxis
Anechoic, definition, 5–7
Anechoic anterior chamber, 559–560
Anechoic triangulations, 4
Anemia
AFAST anticipation, 61, 115–117, 119–121
intrapelvic bleeding, 125–126
Anesthesia. *See also* Forelimb nerve block; Pelvic limb nerve block
Global FAST, 719–720
lung and thoracic sampling, ultrasound-guided, 911–912
MRI, 579
POCUS eye, 556–557
preanesthetic evaluation, 494–495
thoracocentesis, 893
Aneurysms, reptile POCUS, 879–881
Angle, needle, 903
Angle of insonation, 29–32
TFAST, 308, 312, 314
Vet BLUE, 431–433, 436–437
Angle of reflection, sound waves, 13
Anisotropy artifacts, bones and joints POCUS, 666–667
anterior chamber opacities, 555
Anterior lens luxation, 562–565
Anticoagulant rodenticide toxicosis, 198
Antihistamines, canine anaphylaxis, 132–135
Aorta
abnormalities with, 699
anatomy, 531
FCU, 393–394, 396, 398, 400
pediatric POCUS, 276, 278
SR view on AFAST, 85–87, 90
Aortic body tumor, 409–411
Aortic thrombosis (AT), 537
Aphakic crescent, 566
Arcuate vessels, kidney POCUS, 191, 193
Arterial catheterization
capabilities, 512
femoral
anatomy, 520–521
equipment, 520
orientation, 521–523
patient preparation, 521
procedure, 520
indications, 513
limitations, 512
objectives, 513
pearls and pitfalls, 526–527
peripheral vessels, 512
practice phantom for, 524–526
training advancements, 512
transverse *versus* longitudinal orientation, 524
ultrasound guidance for, 512
Arterial thromboembolism (ATE), 537. *See also* Thromboembolism
Artifacts, 7. *See also specific artifacts*
AFAST
CC view, 91-100
DH view, 79–82
focused spleen, 106, 107
HRU view, 97–104
HR5th and SR5th bonus view,102, 104–106
SR view, 87, 89–90
air, 15–16, 18–22
TFAST, 306–308, 313, 339, 341, 344
Vet BLUE, 431–432, 449–452, 462–466, 468–471, 850–851
of attenuation, 15–18
bones and joints POCUS, 666–667
common locations, 52–53
liver and gallbladder POCUS, 156, 170–171
of multiple echoes, 22–23
summary of common, 23
TFAST
air, 306–308, 313, 339, 341, 344
PCS view, 330
ultrasound-guided lung and thoracic sampling, 908–909
urinary bladder POCUS, 211–216, 219, 221–222
of velocity or propagation, 18–22
Vet BLUE, 459, 462–471
marine mammal POCUS, 850–853, 856

Ascites
abdominal fluid score, 707
abdominocentesis, 897
AFAST AFS system in, 126
birds, 866–867
ferrets, 817–818
pediatric POCUS, 279–280, 286
pericardial effusion, 137–139, 364–365
reptiles, 876
Aspiration, 655
lung, 502–504
Aspiration pneumonia, 485, 489, 500–501
Asteroid hyalosis, 571
AT. *See* Aortic thrombosis
ATE. *See* Arterial thromboembolism
Attenuation
artifacts of, 15–18
sound waves, 13
Autotransfusion, cats, 801–802
Avian POCUS. *See* Bird POCUS
Axillary approach, brachial plexus block, 609–610, 613–615

Bacterial pneumonia, 485, 489, 500–501
Bandwidth, probe, 37
Bar code sign. *See* Stratosphere sign
Batman sign, 323–328
Beam direction, 46, 51
Bearded dragons, 876–878
Benign neoplastic masses, 658, 660
Benign nodular hyperplasia. *See* Nodular hyperplasia
Benign prostatic hypertrophy (BPH), 250
Bevel, needle, 903
Biceps injuries, 673, 678–679
Bile duct tortuosity, 167, 169
Biliary cysts, 158
Biliary obstruction, liver and gallbladder POCUS, 155, 167, 169
Biliary peritonitis, 164, 167–169
Biliary sludge/sediment, 22–23, 53, 155, 164, 166, 779–781
Biliary system
cat, 779, 782
DH view on AFAST, 82–83
liver and gallbladder POCUS, 155–156, 167, 169
Biliary tract distension, 167, 169
Biopsies, ultrasound-guided, 916
Bird POCUS
anatomy, 864–865
applications, 863
capabilities, 863
cardiac abnormalities, 869
coelom
conditions, 866–869
normal, 865–866
Global FAST, 880–881
indications, 864
limitations, 863–864
objectives, 864
ocular conditions, 870–871
patient positioning, 865–866
pearls and pitfalls, 881–882
probe selection, 865
Birth, difficult. *See* Dystocia
Bladder stones, 93, 98–99, 214–215, 219–220, 290–291
B-line scoring systems
Vet BLUE, 341–342, 450, 452–453, 470–473, 709–711, 807–808
Volpicelli Strong Positive model, 472–474
B-lines, 21–22
AFAST, DH view, 81–82
alveolar-interstitial edema, 341, 705
scoring system, 470–474, 710
Vet BLUE, 449–450, 462
pneumoperitoneum, 237–238
pseudo, 17, 21, 342–343, 447, 462, 467, 475–476, 485–486
TFAST, 305
pneumothorax diagnosis, 339, 341–342, 354
Vet BLUE
B-line counting, 470–473
comet-tail artifact *versus*, 474
diffusely wet lung conditions, 486, 490
image acquisition, 449–452
loop diuretic usage, 483–484, 488
lung contusion severity score, 491–492, 710–711
marine mammal POCUS, 851, 856
scoring system, 341–342, 450, 452–453, 470–473, 709–711, 807–808
visual lung language, 462–466, 468–471
VetFAST-ABCDE, 758
Blood clots. *See* Thrombus
Blood transfusion
AFS-informed, 59
canine anaphylaxis, 133–134
Blunt trauma (BT)
AFAST application to, 121–128
AFS-based decision making, 118–119
pediatric patients, 280
B-mode, 33–34
characteristic image shapes of probes, 28–29
Bone
acoustic impedance, 13
artifacts, 15–16, 20–21
attenuation, 13
echogenicity, 5–7
normal findings, 668
POCUS
abnormal findings, 669–674
artifact minimization, 666–667
capabilities, 663–664
clipping hair and coupling medium, 664–665
indications, 664
limitations, 664
normal findings, 667–671
objectives, 664
pearls and pitfalls, 680
probe types, 665
settings, 666
stand-off pads, 665–666
transducer orientation, 667–668
sound waves velocity through, 12–13
tumors, 670, 674–676
ultrasonographic appearance, 650
Bounce CVC, 63, 130–132, 136–138, 362, 365, 376, 699–701, 703, 735
Bowel movements, fetal stress, 268
Bowel perforation
pediatric POCUS, 281, 283
POCUS GIT, 226–227, 235, 238
BPH. *See* Benign prostatic hypertrophy
Brachial plexus
anatomy of, 610
block of
axillary approach, 609–610, 613–615
paravertebral approach, 609–612
subscalene approach, 609–613
Brain. *See also* Transcranial Doppler ultrasonography; Transcranial ultrasonography; Traumatic brain injury
acoustic windows
rostral, 580, 589–592, 597–598
suboccipital, 580, 587–588, 598, 600
temporal, 580–586, 598–599
anatomy of, 582–592
vascular, 598, 601–602
imaging of, 579
pathology of
encephalitis, 600, 602–603, 606
hydrocephaly, 599–600, 605–606
strokes, 600, 606
planes
dorsal, 588, 598–599
dorsal caudal, 581–584
dorsal cranial, 584–587
sagittal, 587, 589–590, 597–598, 600
transverse, 590–592, 597–598, 600

POCUS of
capabilities, 579, 596
functions of, 579
indications for, 580, 596
limitations, 579, 596
mechanism of, 580–582
objectives, 580, 596
parenchyma, 598, 601
pearls and pitfalls, 592, 603
probe type for, 580, 597
technique for, 581–582, 597–602
vasculature, 598, 601–602
ventricular system evaluation, 579–580, 590–592
Breathing
marine mammal POCUS, 834–835
ultrasound skills, 757
VetFAST-ABCDE
abnormal findings, 758
assessment, 759–760, 762–764
Global FAST *versus*, 769
Brucellosis, 252–253
BT. *See* Blunt trauma
Bulging eye, 553, 557
Bull's eye sign, 235, 237, 323–328, 359, 362–363, 734, 743, 745–747
Bundling fees, 923–924
Buphthalmos, 557, 566, 573–574
Bupivacaine, 611, 613–614, 616, 621, 623–624, 626–627, 631–632, 634
Butorphanol, TFAST, 314, 351
Butterfly pattern, prostate, 249

Cageside organ assessment with sonography for trauma (COAST), POCUS replacement of, 3
CAH. *See* Chronic active hepatitis
Calcification
prostatic, 250–251
renal, 200, 203
Calculi
gallbladder, 164, 167
renal, 200, 203
urinary bladder, 93, 98–99, 214–215, 219–220, 290–291
Callus formation, 671, 673–674
Calvaria, 583
Canine anaphylaxis
AFAST use in, 61–62, 108
CVC characterization, 130–132
heparin-induced hemoabdomen, 131–136
large-volume bleeders/effusions, 133–135
pathogenesis, 135
small-volume bleeders/effusions, 131–134
sonographic striation in gallbladder wall edema, 127, 129–132
therapy, 135–136
liver and gallbladder POCUS, 165
second episode of, 135
toxin, 745, 748–749
Cardiac abnormalities
bird POCUS, 869
reptile POCUS, 879–881
Cardiac bump, 63
AFAST, 75, 78–79, 136–138
TFAST, 330–332
Cardiac chamber rupture, 366
Cardiac evaluation, TFAST echo views, 378–383, 939
Cardiac gallbladder, 61–62, 108, 131–132, 137, 366, 368–369, 685–686, 699, 703, 784–786
Cardiac ladder, TFAST PCS views, 323–329
Cardiac mass, 139–140, 378–382, 408–411
Cardiac presets, 300, 302, 320, 391
Cardiac tamponade
AFAST, 136–138
cardiac neoplasia, 408–411
definition, 361, 364
dolphins, 839
liver and gallbladder POCUS, 165
pericardiocentesis for, 886
TFAST, 361–366, 368–369, 376
Cardiac ultrasound. *See* Focused cardiac ultrasound
Cardiac valves, FCU, 398–399
Cardiac views
ferrets, 820–821
long-axis, 43–44
patient monitoring, 698–699
short-axis, 43–44
patient monitoring, 698
Cardiac-cervical pouch, 318–320
Cardiac-diaphragmatic pouch, 318–320
Cardiogenic shock, 690, 750
Cardiologist studies, definition, 4
Cardiomegaly, 869
Cardiopulmonary arrest (CPA)
FCU, 414
Global FAST, 730
VetFAST-ABCDE, 758–759
Cardiopulmonary resuscitation (CPR)
Global FAST
capabilities, 730–731
hyperkalemia, 736–737
hypertension–pulmonary hypertension, 737–739
hypocontractility–dilated cardiomyopathy, 736–738
hypotension/hypovolemia, 734, 736
indications, 731
limitations, 731
objectives, 731
pearls and pitfalls, 751
tamponade–pericardial effusion, 741, 744–746
tension pneumothorax, 740–741
thromboembolism–pulmonary thromboembolism, 741, 744–745
toxin–canine anaphylaxis, 745, 748–749
trauma–hemorrhage, 741–742
PEA, pulseless electrical activity, 729–730
VetFAST-ABCDE, 758, 771–772
Cartilage, normal findings, 669, 671
Castrated male
marked, 247–248
prostate findings, 249–250
Cataract, 556
Catheter, central venous jugular, 514
Catheterization. *See* Arterial catheterization; Central venous catheterization
Cats. *See also* Feline POCUS
acoustic coupling medium, 803, 805
AFS use in, 63, 106–108, 797–802
bile duct tortuosity, 167, 169
cardiac bump, 75
cardiac gallbladder, 108
concurrent pleural and pericardial effusion, 375–376
falciform fat, 779-780
FCU for respiratory distress, 389–390
hemoabdomen, 93, 124
large-volume bleeders, 124, 799–802
normal kidney size, 194–195, 208, 788–790
normal mean echocardiographic values, 398
patient positioning, 802–804
pericardial effusion, 495–496
pleural effusion, 494–497
pneumothorax, 807
small-volume bleeders, 124, 799–802
spleen, liver, and kidney echogenicity, 153, 170, 175–176
SR view of kidneys in, 87, 89
urinary bladder wall thickness, 212–213, 223
uroabdomen *versus* hemoabdomen probability, 93
Vet BLUE, 494–497, 807–808
Caudal vena cava (CVC)
AFAST
characterization, 61–63, 108, 130–132, 136–138

Caudal vena cava (CVC) (*cont'd*)
DH view, 75–76, 78–80, 83–84, 136–138, 699–701
SR view, 85–87, 90
target organ approach, 141
anatomy, 531
assessment
DH view, 702–706
eyeball method, 702, 705
location, 702, 704
cat, 779, 781–782, 784
dolphins, 838–842
FCU, 389, 397, 399–400, 411–413
liver and gallbladder POCUS, 154
pediatric POCUS, 276, 278
POCUS
allometric scaling formulas, 548
application, 541
capabilities, 541–542
finding integration, 548
fluid therapy, 687
Global FAST *versus*, 687
indications, 542
intercostal view, 543–546
limitations, 542
methods, 542–544
objectives, 542
paralumbar view, 544, 546–548
pearls and pitfalls, 549
probe, 542
quick references of normal values and rules of thumb, 961
reptiles, 879–881
settings, 542
subxiphoid view, 543–545
volume status comparison, 548–549
TFAST, 734–736
characterization, 361–362, 364–365, 376
image acquisition, 300–301, 330–332
thrombosis, 532–534
VetFAST-ABCDE, 766–767
Caudodorsal (Cd) lung region
location, 434–435, 438–441
order, 441, 443–444
Vet BLUE step by step, 445–447
Caudodorsal transition zone (CdTZ), 305, 309–311, 434–435, 438–439, 444–445, 477–478
Caval syndrome
FCU, 411–412
TFAST, 378–382
Vet BLUE, 477
Cavitary effusion
birds, 865
ferrets, 820–821
nonhemorrhagic, 126–127
Cavitary hemorrhage
AFS application to, 115–119, 124–125
blunt trauma, 118–119
clotted blood, 121–122
harvest of, 123
large-volume bleeders, 116–117, 124
management guidelines and decision making, 118–121
nontraumatic, 121
penetrating trauma, 118–119
postinterventional trauma, 119–121
serial AFAST monitoring of, 117, 119
small-volume bleeders, 115–117, 119, 124–125
sources and location of bleeding, 124–125
time to resolution, 123
CC pouch, 91–100
CC view. *See* Cysto-colic view
CCR view. *See* Cysto-colic reproductive view
Cd lung region. *See* Caudodorsal lung region
CdTZ. *See* Caudodorsal transition zone
CEH-pyometra. *See* Cystic endometrial hyperplasia pyometra
Cellulitis, ultrasonographic appearance, 651–652
Centimeter scale, 48–50
Central venous catheterization
capabilities, 512
indications, 513
jugular
anatomy, 515
catheter selection, 514
dynamic technique, 514–515
line length, 514
longitudinal orientation, 517, 519–520
orientation, 515–517
patient preparation, 515
probe, 513
short temporary, 520
skill development, 515
static technique, 514
transverse orientation, 516–519
limitations, 512
objectives, 513
pearls and pitfalls, 526–527
peripheral vessels, 512
practice phantom for, 524–526
training advancements, 512
transverse *versus* longitudinal orientation, 524
ultrasound guidance for, 511
Central venous thrombosis, 532, 534
Cerebellar tentorium, 583
Cerebellum, 583–584, 587–588, 592
Cerebral arterial circle, 598, 601–602
Cerebral hemispheres, 584–585
Cerebral mantle thickness, 596
Cerebrovascular accident (CVA), 600, 606
Cervix
feline AFAST, 793–794
reproductive POCUS, 257
Chameleons, 871
*Chelonians*, 871
Chelonians, acoustic windows, 872, 875
Chemical damage, probe heads, 35–36
Chemodectoma, 409–411
Chest tube site (CTS) view
lung findings
A-lines without lung sliding in pneumothorax diagnosis, 344, 354
lung point in pneumothorax diagnosis, semiquantification, and monitoring, 344–351
missed pneumothorax diagnosis, 351
M-mode and power Doppler pneumothorax detection, 351–354
pleural effusion, 357
pseudo pleural effusion, 343–344
step sign, 354, 357–358
subcutaneous emphysema, 353–356
summary of major, 354, 357
TFAST advantages, 357–358
wet *versus* dry, 339, 341–344, 354
TFAST image acquisition, 300–301
gator sign, 305–313, 353, 355–356
lateral recumbency, 303–304, 306, 311, 313–314
lung sliding, 305, 308–315
pearls and pitfalls, 333
probe positioning and orientation, 308, 313
pulmonary-pleural interface and lung line imaging, 306–308, 311–315
standing, 306
subcutaneous emphysema and fat, 308–309
ultrasound settings, 305, 308, 311–312
CHF. *See* Congestive heart failure
Chicken breast phantom, 524–526
Chinchillas, 824–827
quick references of normal values and rules of thumb, 964
Choked dog, 494
Cholangiohepatitis, liver and gallbladder POCUS, 162–163
Cholecystitis, gallbladder wall edema
AFAST, 127, 130
POCUS, 164–165

Cholelithiasis
biliary tract, 169
gallbladder, 164, 167
Cholestasis, liver and gallbladder POCUS, 155
Chordae tendineae rupture, 404–405
Choroidal melanocytoma, 570
Chronic active hepatitis (CAH), liver and gallbladder POCUS, 162–163
Ciliary body, 560
Cine ball, 51–52, 320
Circulation
ultrasound skills, 757
VetFAST-ABCDE
abnormal findings, 758
assessment, 760–762, 765–767
Global FAST *versus*, 769
Clean shadowing, 6, 15–16
Client communication, 925–926
C-lines, 477–481
Clotted blood, AFAST detection, 121–122
Cloudy eye, 553–556
Coagulopathy, anaphylaxis-acquired, 135
COAST. *See* Cageside organ assessment with sonography for trauma
Coding, 922–923
Codman's triangle, 670
Coelom
birds
conditions, 866–869
normal, 865–866
reptiles
anatomy, 871–872
conditions, 876–879
normal, 873–875
Colon
AFAST
CC view, 91, 93
SR view, 86–89
feline AFAST, 798
liver and gallbladder POCUS, 151
POCUS, reproductive, 257–258
urinary bladder POCUS, 211, 214, 219
Color flow Doppler, 34
abscess, 655
cellulitis, 651–652
coelom, /869
epidural and intrathecal injection, 644–645
jugular catheterization, 516
vascular POCUS, 530–531
Combo FAST, 297
Comet-tail artifact, 474, 479, 482. *See also* B-lines
Common bile duct
cat, 779, 782
liver and gallbladder POCUS, 155
Complete detailed abdominal ultrasound, definition, 4
Complete detailed echocardiography, definition, 4
Computed tomography (CT)
AFAST correlation, 72
tumor detection, 579
Vet BLUE compared to, 425, 462, 476–477, 491–493
Congenital anomalies, 271, 281
herniation, 284–286
patent urachus, 290, 292
portosystemic shunts, 286–288
renal, 287–289
urogenital ectopia, 288–290
Congestive heart failure (CHF)
AFAST
AFS system, 126
CVC characterization, 131–132
dolphins, 839
gallbladder wall edema, 127, 130
screening, 61–62, 108
FCU, 407–409, 411–413
feline AFAST, 784–786
four-quadrant approach, 451, 453–454
left-sided, 470–473, 481–482, 485, 487, 494, 496, 699, 701
Vet BLUE monitoring, 497–498
mitral valve disease, 404–405
right-sided, 699
TFAST, 371, 382–383
gallbladder wall edema, 366, 368–369
Vet BLUE, 470–473, 481–482, 485, 487, 494, 496–498
Console machines, 36
Consolidation, lung, 462–467, 474–476
Contractility
FCU, 398
feline TFAST, 804
Contusion, pulmonary. *See* Pulmonary contusions
Cornea, 559–561
Corneal edema, 554, 562, 566, 569
Corneal opacity, 554
Corneal pigmentation, 554
Corneal scarring, 554
Corrugated small bowel, 233, 235–236, 240
Coupling medium. *See* Acoustic coupling gel
CPA. *See* Cardiopulmonary arrest
CPR. *See* Cardiopulmonary resuscitation
Cr lung region. *See* Cranial lung region
Cranial (Cr) lung region, 434
location, 437, 440–442
order, 441, 443–444
Vet BLUE step by step, 445–446
Cranial transition zone (CrTZ), 437, 442, 444–445
Crump factor, prevention, 58, 84, 117, 120
Cryptorchidism, 247, 251–252, 291–292
CT. *See* Computed tomography
CTS view. *See* Chest tube site view
Curtain sign, 305, 310, 319, 330, 344, 346, 435, 439, 444, 478
Curvilinear probes, 36–37
image shapes, 28–29
Vet BLUE, 428, 430
CVA. *See* Cerebrovascular accident
CVC. *See* Caudal vena cava
Cystic calculi, 93, 98–99, 200, 203, 214–215, 219–220, 290–291
Cystic endometrial hyperplasia (CEH)-pyometra, 259–261
Cystitis
CC view on AFAST, 99
pediatric POCUS, 290–291
urinary bladder POCUS, 215–217
Cystocentesis
ferrets, 817
rabbits, 820
Cysto-colic reproductive (CCR) view, AFAST image acquisition, marine mammal POCUS, 837, 845–846
Cysto-colic (CC) view
abdominal radiograph and CT correlation, 72
AFAST image acquisition, 92
artifacts, 93, 96
clinical questions investigated, 91
false negatives, 97
false positives, 93, 96
left lateral recumbency, 67–68
modified lateral-sternal recumbency, 69–70
probe maneuvering, 73
right lateral recumbency, 65–66, 72
typical negatives, 94
typical positives, 93, 95
urinary bladder abnormalities, 97–100
AFAST order of performance, 69–70
feline AFAST, 793, 795
urinary bladder volume estimation, 140–141, 793, 795
Cystolithiasis, reptiles, 876
Cysts
biliary, 158
hepatic, 156–158
hamsters, 824–825

Cysts (*cont'd*)
ovarian, 824
paraprostatic, 250
prostatic, 250
ferrets, 817–818
renal, 199–201
retrobulbar, 574
uveal, 569

Data recording and documentation. *See* Documentation and recording
DCM. *See* Dilated cardiomyopathy
Deep venous thrombosis (DVT), 535–536
Dehydrated patients, AFAST and AFS in, 127–128
Depth
POCUS eye settings, 555
recommended settings, 32–33
TFAST, 33, 305, 311, 319, 330
trouble-shooting algorithm for poor images, 49–51
Vet BLUE, 428, 430, 433, 435
Dermis, 650
DH view. *See* Diaphragmatico-hepatic view
Diagnostic peritoneal lavage (DPL). *See also* Modified ultrasound-guided diagnostic peritoneal lavage
ultrasound-guided *versus*, 899–900
Diagnostic studies, definition, 4
Diaphragm, 13
AFAST
DH view, 75–81, 83, 136–138, 699–701
HR5th and SR5th views, 105
cat, 781, 783
liver and gallbladder POCUS, 150, 152–154
mirror artifact at, 18–19, 53, 443
TFAST, 330–332
Diaphragmatic herniation
congenital, 285
liver and gallbladder POCUS, 152–153, 156
TFAST, 377–379
traumatic, 286
Diaphragmatico-hepatic (DH) view
abdominal radiograph and CT correlation, 72
AFAST image acquisition, 74–76, 78
artifacts, 79–82
clinical questions investigated, 73
false positives, 82–84
left lateral recumbency, 67–68
marine mammal POCUS, 837–842
modified lateral-sternal recumbency, 69–70
probe maneuvering, 71
right lateral recumbency, 65–66, 72
typical positives, 77, 79
AFAST order of performance, 69–70
caudal vena cava, 702–706
deep lung lesions, 140
feline AFAST, 781–786
Global FAST, 694–695, 732
right-sided cardiac markers, 699
pericardial effusion, 75, 136–140, 358–359, 362–363, 376
pleural effusion, 370
TFAST
clinical relevance, 358–359, 362–363, 370, 376–378
image acquisition, 300–301, 303–304, 330–332
thoracic radiograph correlation, 136–137
Vet BLUE
clinical integration, 477, 479
image acquisition, 434, 438, 440–441, 443, 445
Diastolic dysfunction, 758
Diffuse bladder wall thickening, 215–216
Diffuse parenchymal disease
kidney, 195–196
liver, 160–163
spleen, 184–185
Dilated cardiomyopathy (DCM), 736–738
AFAST, gallbladder wall edema, 127, 130
FCU, 406–407
TFAST, 378–382
*Dirofilaria immitis*. *See* Caval syndrome
Dirty shadowing, 6, 15–16
AFAST
CC view, 91, 93
SR view, 85, 87, 89
Disability
ultrasound skills, 757
VetFAST-ABCDE
abnormal findings, 758
assessment, 762–766, 768
Global FAST *versus*, 769–770
Distal thigh region, saphenous nerve block, 623–625
Distension, reptiles, 876
Distributive shock, 690, 750
Diuresis, pyelectasia with, 201–202, 204
Diuretics, B-line scoring, 711
Documentation and recording, 5, 34–35, 926–930
AFAST, 106, 142–143, 933
dystocia POCUS, 937
echo cardiac evaluation, 939
eye POCUS, 939–940
gastrointestinal and pancreas POCUS, 935–936
Global FAST, 720–722, 751, 927, 929, 940–943
kidney POCUS, 934–935
liver and gallbladder POCUS, 933–934
marine mammal POCUS, 858–859
pediatric POCUS, 939
reproductive POCUS, 936–937
spleen POCUS, 934
TFAST, 333, 383–384, 937–938
urinary bladder POCUS, 935
Vet BLUE, 455, 499–504, 938–939
VetFAST-ABCDE, 940
Dogs
AFAST development for, 57–58
AFS norms in, 106–108
anaphylactic, 61–62, 108
CVC characterization, 130–132
heparin-induced hemoabdomen, 131–136, 165
large-volume bleeders/effusions, 133–135
pathogenesis, 135
small-volume bleeders/effusions, 131–134
sonographic striation in gallbladder wall edema, 127, 129–132
therapy, 135–136
comparison of FAST and AFAST in, 58–60
concurrent pleural and pericardial effusion, 375
congestive heart failure screening, 61–62, 108
normal kidney size, 195, 208
normal mean echocardiographic values, 398
spleen, liver, and kidney echogenicity, 153, 170, 175–176
TFAST development for, 297
urinary bladder wall thickness, 213, 223
uroabdomen, 92–93
Vet BLUE, 494–495, 500, 502
Dolphin. *See* Marine mammal POCUS
Doppler, 34. *See also* Transcranial Doppler ultrasonography
pneumothorax detection, 351–354
Doppler velocimetry parameters, 595–596
Dorsal plane, 26
brain POCUS, 580
suboccipital acoustic window, 588
temporal acoustic window, 581–587, 598–599

Dorsal recumbency
AFAST, 68–69, 71
Global FAST, 695–696
pediatric POCUS, 272
POCUS exams
gastrointestinal and pancreas, 227–229
kidney, 190
liver and gallbladder, 150
reproductive, 249, 256–258
spleen, 174
urinary bladder, 212
TFAST, 302–303
Vet BLUE, 428
Dorsoventral dimension of lateral ventricle, 596
Dorsoventral percentage, 596
Dorzolamide, 564, 567
Double curtain sign, 344
Double lung point, 305, 313–314, 344, 348
Double rim effect, 61–62, 127, 129–132, 164–165, 784–786
Double trachea sign, 758
Double tract sign, 759
DPL. *See* Diagnostic peritoneal lavage
Drainage, 655
Drifting, 41–42, 447
Dry lung, 339, 341–344, 354
Vet BLUE
conditions, 481, 483, 485–486
image acquisition, 449–452
visual lung language, 462–466, 468–471
wet lung *versus*, 339, 341–344, 354, 462–466, 699, 701
Duodenum
normal thickness, 242
pediatric POCUS, 272, 277
peristalsis, 238-240
POCUS gastrointestinal tract and pancreas, 228–230, 234
Dura mater, 583–584, 589
Dural sac collapse, epidural injection, 645
DVT. *See* Deep venous thrombosis
Dynamic air bronchogram, 474
Dyscoria, 569–570
Dystocia POCUS
AFAST add-on, 265
capabilities, 265
fetal maturation imaging, 266–268
fetal stress monitoring, 266, 268–270
goal-directed templates, 937
indications and objectives, 265
limitations, 265
pearls and pitfalls, 269
quick references of normal values and rules of thumb, 270
serial repetition, 269
Dystrophic mineralization, renal, 200, 203

Echo table, 392
Echo views, TFAST
cardiac evaluation, 378–383, 939
cats, 802–803, 806
with Global FAST, 382–383
image acquisition, 317, 321–329
pericardial effusion diagnosis, 359–363
with Vet BLUE, 382–383, 490–491
Echoes
artifacts of multiple, 22–23
physical assumptions about, 15
Echogenicity
degrees of, 5–7
kidney, 151, 153, 170, 175–176, 191, 193–196, 274, 789–790
liver, 151–154, 161–163, 170, 175–176, 191, 194–195, 273–274, 778–780
pancreas, 229–230
small intestine, 232
spleen, 151, 153, 170, 175–177, 179–181, 184–185, 191, 193–195, 274, 786–788
urine, 213
Ectopia, urogenital, 288–290
Edema. *See also* B-lines
gallbladder wall, 127, 129–132, 164–165, 366, 368–369, 720, 784–786
pulmonary, 341, 462, 705
B-line scoring systems, 470–474, 710
noncardiogenic, 484, 488, 490
Vet BLUE, 449–450, 462–466, 468–474, 484, 488
ultrasonographic appearance, 651–652
Edge shadowing, 16–17, 53
AFAST
CC view, 17
DH view, 82
SR view, 89–90
hepatic cysts, 158
liver and gallbladder POCUS, 156
TFAST, PCS view, 330
ultrasound-guided lung and thoracic sampling, 909
EFAST
definition, 3–4
TFAST *versus*, 688–689
Egg yolk peritonitis, 868
Ehrlichiosis, 179
Electronic probes, 36
E-lines, 353, 479–481
EMH. *See* Extramedullary hematopoiesis
Emphysematous cystitis, 215–216
Encephalic structures, 582–583, 587–591
Encephalitis, 600, 602–603, 606
Endocarditis, 405–406
Endotracheal placement confirmation, 759, 761
Enhanced peritoneal stripe sign (EPSS), 236–237, 239
Enteric agenesis, 281–282
Enteric duplication, 281
Enteric parasites, 284
Enteric thrombus, 285
Epidermis, 650
Epididymitis, 251–253
Epidural approach
neuroaxial nerve block, 641–643
ultrasound signs of, 644–645
Epidural hematoma, 598, 603
Epidural space enlargement, epidural injection, 645
Epinephrine, canine anaphylaxis, 133–134
Epitheliotropic lymphoma, 658
EPSS. *See* Enhanced peritoneal stripe sign
Esophagus, 769
Estrus, 259–260, 262
Ethylene glycol toxicosis, kidney POCUS, 195–196
EVLW. *See* Extravascular lung water
Exit exam, AFAST, 125–126
Exophthalmos, 557, 573–575
Exotic companion mammals POCUS
anatomy
gastrointestinal tracts, 816
reproductive, 816
spleen, 816
capabilities, 815
conditions
chinchillas, 824–825
ferrets, 817–820
guinea pigs, 823–824
hamsters, 824–825
hedgehogs, 824, 826
rabbits, 820–823
imaging, 817
indications, 815
limitations, 815
objectives, 815–816
patient positioning, 816
pearls and pitfalls, 827–828
probe, 817
quick references of normal values and rules of thumb, 964
reference ranges for, 826–827

Exposure
ultrasound skills, 757
VetFAST-ABCDE
abnormal findings, 758
assessment, 766
Global FAST *versus*, 770
Extrahepatic biliary obstruction
liver and gallbladder POCUS, 155, 167, 169
pancreatitis, 241
Extrahepatic shunts, congenital, 286–287
Extramedullary hematopoiesis (EMH)
ferrets, 818–819
POCUS spleen, 178, 184
Extravascular lung water (EVLW), B-line scoring, 710
Eye
abnormal findings in
anterior lens luxation, 562–565
bird, 870–871
globe rupture, 575–578
intraocular hemorrhage, 571–573
intraocular masses, 569–571
normal eye, 559–562
posterior lens luxation, 566–567
reptiles, 880–881
retinal detachment, 567–569
suspected retrobulbar masses/exophthalmos, 573–578
bulging, 553, 557
cloudy, 553–556
normal ultrasonographic findings in, 559–562
opaque, 553–556
POCUS
functions, 553
goal-directed templates, 939–940
indications, 553–557, 562
limitations, 553
marine mammal, 858
method for, 556–559
objectives, 554
overview, 553
pearls and pitfalls, 578
preparation, 555–556
ultrasound settings for, 554–555
preparation, 555–556
traumatized, 554

Falciform fat, 150, 152–153, 779–780
Fan, rock cranially, and return probe maneuver, 43, 70–73
Fanning probe maneuver, 30–31, 46
Fascia, 650
FAST. *See* Focused assessment with sonography for trauma
FAST-ABCDE, 757. *See also* VetFAST-ABCDE
Fat
falciform, 150, 152–153, 779–780
heart, 396
pericardial, 330
TFAST, 308–309, 354
Vet BLUE, 448–449
FAT CVC, 61–63, 130–132, 136–138, 361–362, 364–365, 376, 699–701, 703, 735
FCU. *See* Focused cardiac ultrasound
Fee structure, 922–924
Feline POCUS
AFAST
AFS, 797–802
CC view, 793, 795
DH view, 781–786
falciform fat, 779-780
gastrointestinal tract, 795–798
HR5th and SR5th bonus views, 102, 104–106
HRU and SRU views, 797
image acquisition, 778
kidney, 788–791
liver and gallbladder, 778–783
spleen, 786–788, 797
SR and HR views, 791–792
urinary bladder, urine, urethra, and reproductive structures, 792–795
capabilities, 777
Global FAST, 808–809
indications, 777
limitations, 777
objectives, 777
pearls and pitfalls, 808
quick references of normal values and rules of thumb, 809–810, 961–963
TFAST
acoustic coupling medium, 803, 805
echo views, 802–803, 806
LA:Ao, 803–805
lung sliding and pneumothorax, 807
LVSA view, 803–804
patient positioning, 802–804
pericardial effusion, 806
RV:LV, 804
Vet BLUE, 807–808
Femoral arterial catheterization
anatomy, 520–521
equipment, 520
orientation, 521–523
patient preparation, 521
procedure, 520
Femoral artery and vein
CC view on AFAST, 92, 100
inguinal region, 623
Femoral nerve
inguinal region block, 620, 622–623
psoas compartment block, 620–622
Femoral triangle, 623
Ferrets
cavitary effusion, 820–821
gastrointestinal conditions, 817–818
hepatobiliary conditions, 817–818
neoplasia, 819–820
pancreas conditions, 819
quick references of normal values and rules of thumb, 964
reference ranges for, 826–827
spleen
anatomy, 816
conditions, 818–819
urinary conditions, 817
Fetal maturation, 266–268
Fetal stress, 266, 268–270
Fetal structures, 262, 266–268
Fibrin, 555–556
Fishmouth sign, 323–328
Flash exam, 4, 374–376, 685–687
Flat CVC, 61–63, 130–132, 699–701, 703, 735
Flat detachment, 568
Fluid
acoustic impedance, 13
attenuation, 13
echogenicity, 5–7
free cavitary, 4
gravity dependent nature, 299
sound waves velocity through, 12–13
Fluid responsiveness, FCU, 389
Fluid scoring systems. *See* Abdominal fluid score
Fluid therapy
AFS-informed administration strategy, 59
Global FAST, 687
Vet BLUE monitoring, 491
VetFAST-ABCDE, 766
Fluid-filled structures, artifacts, 16–18
Fluid-intolerant CVC, 63, 130–132, 361–362, 364–365
Fluid-responsive CVC, 63, 130–132
Fluid-starved CVC, 63, 130–132
Focus cursor, 48
TFAST, 320
trouble-shooting algorithm for poor images, 50–51
Vet BLUE, 430, 435
Focus position and number, recommended settings, 32–33

Focused assessment with sonography for trauma (FAST). *See also* Abdominal FAST; Global FAST; Thoracic FAST
AFAST compared to, 58–60
AFAST development from, 57–58
artifacts, 7, 15–23
basic physical principles, 11–14
definition, 3–4
degrees of echogenicity, 5–7
documentation of findings, 5, 34–35
Flash exam *versus*, 4
goal-directed templates, 5
image features, 25–28
image optimization, 32–33
modes, 33–34
presets, 33, 39
probe maneuvers, 28–32, 43, 46, 48, 70–73
program
accessibility, 922–925
capabilities, 921
communicating value to clients, 925–926
goal-directed templates, 926–930
indications, 921
limitations, 921
objectives, 922
pearls and pitfalls, 931
proper training, 922
quality control, 930–931
training techniques, 931
screen orientation, 7–8
technological advancements, 34
Focused cardiac ultrasound (FCU), 3, 704
cardiac abnormalities
capabilities, 403
cardiac neoplasia, 408–411
cardiopulmonary arrest, 414
great vessel abnormalities, 411–413
indications, 404
limitations, 403–404
myocardial diseases, 406–409
objectives, 404
pearls and pitfalls, 414
quick references of normal values and rules of thumb, 414, 960–961
valvular heart diseases, 404–406
diagnostic value, 389–390
image acquisition
capabilities, 390
indications, 390
left parasternal window, 394–396, 399
limitations, 390
objectives, 390–391
patient positioning and preparation, 391–392
pearls and pitfalls, 400
probe preferences, 391
quick references of normal values and rules of thumb, 400, 960–961
right parasternal window, 392–399
subcostal window, 395, 397, 399–400
ultrasound settings, 391
pericardiocentesis, 417–424
pleural effusion, 389–391, 398, 417–424
Fontanelles, 582
Footprint, probe, 36
Foreign bodies
gastrointestinal
ferrets, 817
pediatric POCUS, 280–282
POCUS gastrointestinal and pancreas, 226–227, 233–237, 240
ultrasonographic appearance, 655–656
Foreleg, extension, 44–45
Forelimb nerve block
approaches to
axillary, 609–610, 613–615
paravertebral, 609–612
subscalene, 609–613
brachial plexus anatomy, 610
capabilities, 609
indications for, 609
limitations, 609
materials for, 610
objectives, 609
pearls and pitfalls, 617–618
probe type for, 610
radial, ulnar, median, and musculocutaneous, 609, 614–618
Four-quadrant approach, Vet BLUE comparison to, 451, 453–454
Fractional shortening (FS), 321, 323, 379–380, 399, 406, 961
Fracture, 669–672
Free cavitary fluid, 4
Free fluid. *See also* Intraabdominal fluid; Pericardial effusion; Peritoneal effusion; Pleural effusion; Retroperitoneal fluid
AFAST detection, 57–61, 107–108
CC view, 92–96
DH view, 75–77, 79, 82–84
HR5th and SR5th views, 105–106
HRU view, 97, 99, 101–103
SR view, 87–91
time to bleeding resolution, 123
clotted blood *versus*, 121–122
thorax compared to abdomen, 337
Frequency
POCUS eye settings, 554–555
probe, 37
range used in ultrasound, 12
recommended settings, 32–33
trouble-shooting algorithm for poor images, 49–50
Frontal lobe, 581–582, 584–585
FS. *See* Fractional shortening
Functional ileus, POCUS gastrointestinal tract and pancreas, 226–227, 238–240
Fungal granulomas, 500–503
Fur
parted, 40–41, 64, 427
shaved, 303–304

Gain
color flow Doppler, 34
recommended settings, 32–33
TFAST, 305, 311, 315, 319
trouble-shooting algorithm for poor images, 49–52
Vet BLUE, 430, 435
Gallbladder
AFAST target organ approach, 141
anaphylactic AFAST findings, 61–62, 108
CVC characterization with, 130–132
sonographic striation in gallbladder wall edema, 127, 129–132
cardiac, 61–62, 108, 131–132, 137, 366, 368–369, 685–686, 699, 703, 784–786
DH view on AFAST, 74–77, 79, 81–83
feline AFAST, 778–783
luminal abnormalities, 164, 166–168
mirror artifact at, 53
mucocele, 164, 166, 168
pediatric POCUS, 272–273
POCUS, goal-directed templates, 933–934
POCUS examination
abnormal findings, 164–169
AFAST and Global FAST add-on, 169–170
artifacts, 156, 170–171
capabilities, 149
goals, 149, 156
image acquisition, 150–153
indications, 150
limitations, 149
normal findings, 151–156
objectives, 150
pearls and pitfalls, 170
quick references of normal values and rules of thumb, 170–171, 955
ultrasound settings and patient positioning, 150

Gallbladder (*cont'd*)
reptiles, 871–872
rupture, 164, 166–169
sludge/sediment, 22–23, 53, 155, 164, 166, 779–781
stones, 164, 167
TFAST, image acquisition, 300–301, 330–332
Vet BLUE, 447
wall edema, 127, 129–132, 164–165, 366, 368–369, 720, 784–786
Gas, intraluminal, 233–234
Gastric pseudo B-lines, 342–343
Gastroenterocolitis, 281, 283
Gastrointestinal impaction, 876
Gastrointestinal tract (GIT). *See also specific organs*
AFAST
CC view, 98
dolphins, 846–847
HRU view, 102
conditions
ferrets, 817–818
rabbits, 820, 822
reptiles, 876
exotic companion mammals, 816
feline AFAST, 795–798
foreign bodies, 226–227, 233–237, 240, 280–282
inguinal hernia and, 658
intussusception, 234–235, 237, 283–284
kidney POCUS, 190
motility, 226–227, 238–240
obstruction, 226–227, 233–234, 280–282
pediatric disorders, 279–286
perforation, 226–227, 235, 238, 281, 283
POCUS
abnormal findings, 233–240
accuracy, sensitivity, and specificity, 225–226
AFAST add-on, 225–226
capabilities, 226
goal-directed templates, 935–936
indications, 226–227
limitations, 226
normal findings, 232, 234
objectives, 227
patient positioning and probe selection, 227–228
pearls and pitfalls, 241–242
quick references of normal values and rules of thumb, 242–243, 957
scanning technique, 228–229
Gastroschisis, 285
Gator sign
TFAST, 301, 305–313, 353, 355–356
ultrasound-guided thoracocentesis, 894–895
Vet BLUE, 430–432, 434–435, 445, 447–449, 461, 850–854
Genitourinary disorders. *See also* Reproductive POCUS
pediatric POCUS, 287–292
Gestational vesicles, 262
GIT. *See* Gastrointestinal tract
Glaucoma, 565–566, 569, 571
Glide sign, 892. *See also* Lung sliding
Global FAST, 39, 61, 113, 297–298, 383, 461
anesthesia, 719–720
birds and reptiles, 880–881
canine anaphylaxis, 133–136
cardiac gallbladder, 685–686
case examples
malignant melanoma, 718–719
prostatic adenocarcinoma, 717–718
rat, 719
cats, 808–809
comments on, 750
data points with, 685–686
efficiency, 695
geriatric health screening, 720
goal-directed templates, 720–722, 751, 927, 929, 940–943
hemoabdomen, 685–686
Hs and Ts, 730
hyperkalemia, 736–737
hypertension–pulmonary hypertension, 737–739
hypocontractility–dilated cardiomyopathy, 736–738
hypotension/hypovolemia, 734, 736
tamponade–pericardial effusion, 741, 744–746
tension pneumothorax, 740–741
thromboembolism–pulmonary thromboembolism, 741, 744–745
toxin–canine anaphylaxis, 745, 748–749
trauma–hemorrhage, 741–742
image acquisition, optimization, 692, 731
image acquisition mistakes, 40–52
image interpretation mistakes, 52–53
image saving, 720–722, 750–751
integration of gallbladder wall edema and CVC characterization, 131–132
leaks and plugs, 706–707
maneuvers for, 693
marine mammal POCUS, 829–830
AFAST, 835–848
efficiency, 858
goal-directed template, 858
pearls and pitfalls, 858
pitfalls, 854–858
TFAST, 836, 848–851
Vet BLUE, 836, 851–854
monitoring tools
AFS for ascites, 707
pericardial effusion, 707–708
pleural effusion, 707
pneumothorax estimation, 708–709
urine output estimation, 707–708
Vet BLUE B-line scoring system, 709–711
nonecho fallback view, 698–702, 850–851
echocardiography, 698
left-sided heart problems, 698–702
right-sided heart problems, 699–701
nonhemorrhagic effusions, 126–127
patient monitoring, 687
capabilities, 691
component integration, 696
limitations, 691
pearls and pitfalls, 723
volume loss, 704–706
volume status, 696–704
patient positioning, 692–696, 732–734
patient staging
canine bladder masses, 713–715
canine hemoabdomen, 711–713
canine pericardial effusion, 715–716
capabilities, 691
decision making, 689
feline bladder masses, 715
feline hemoabdomen, 713
feline pericardial effusion, 716–717
limitations, 691
localized *versus* disseminated disease, 687, 711–712
neoplastic lesions, 687, 689
pearls and pitfalls, 723
with POCUS abdominal exams, 149
with POCUS gastrointestinal tract and pancreas, 226
with POCUS kidney exam, 189, 207
with POCUS liver and gallbladder exams, 169–170
with POCUS reproductive exam, 247, 255
with POCUS spleen exam, 173, 186–187
with POCUS urinary bladder exam, 221–222
probe preference, 692, 731
probe–skin contact, 692, 731
probe–skin contact mistakes, 44–48, 51

pulmonary thromboembolism, 719
quick references of normal values and rules of thumb, 965–967
renal failure, 719
RUSH exam *versus*, 688–689, 697, 749
settings, 692, 731
shock, ALS, CPR
capabilities, 730–731
indications, 731
limitations, 731
objectives, 731
patient management, 751
pearls and pitfalls, 751
rapid assessment, 749–750
screening, 729–730, 743, 750
with TFAST echo views, 382–383
trouble-shooting algorithm, 49–51
ultrasound machine mistakes, 48–52
urinary obstruction, 719
vascular POCUS and, 529
with Vet BLUE, 490–491
VetFAST-ABCDE *versus*, 767–770
volume status, 687, 690
Globe rupture, 575–578
Glucocorticoids, canine anaphylaxis, 132–135
GME. *See* Granulomatous meningoencephalitis
Goal-directed templates, 5
AFAST, 106, 142–143, 933
dystocia POCUS, 937
echo cardiac evaluation, 939
eye POCUS, 939–940
gastrointestinal tract and pancreas POCUS, 935–936
Global FAST, 720–722, 751, 927, 929, 940–943
kidney POCUS, 934–935
liver and gallbladder POCUS, 933–934
marine mammal POCUS, 858–859
pediatric POCUS, 939
reproductive POCUS, 936–937
spleen POCUS, 934
TFAST findings, 333, 383–384, 937–938
urinary bladder POCUS, 935
use of, 926–930
Vet BLUE, 455, 499–504, 938–939
VetFAST-ABCDE, 940
Granuloma, fungal, 500–503
Granulomas, 867
Granulomatous meningoencephalitis (GME), 600, 602–603, 606
Great vessels
AFAST, SR view, 85–87, 90
FCU abnormalities, 411–413
Guinea pigs, 823–824, 826–827
quick references of normal values and rules of thumb, 964

Hair
parted, 40–41, 64, 427
shaved, 303–304
Halo sign
gallbladder, 61–62, 127, 129–132, 164–165, 784–786
kidney, 195–196
Hammerhead sign, 301, 317–319, 328–329
Hamsters, 824–827
quick references of normal values and rules of thumb, 964
Hand-held machines, 36
Hands, placement, 41–42, 44, 51
HCM. *See* Hypertrophic cardiomyopathy
Head
fetal, 267–268
patient positioning, 41–43
Heart. *See also* Focused cardiac ultrasound
AFAST
DH view, 75–76, 78–79, 136–138
target organ approach, 141
cat, 781, 783
left-sided problems, 699–702
mass, 139–140, 378–382, 408–411
mirror artifact at, 53
POCUS
fluid therapy, 687
Global Fast *versus*, 687
preanesthetic evaluation, 494–495
reptiles, 871–872
right-sided problems, 699–701
TFAST, 337
anatomy, 358–359
echo view cardiac evaluation, 378–383, 939
image acquisition, 300–301
PCS view, 315–330
pericardial effusion diagnosis, 358–363
pitfalls of imaging, 376
pleural effusion diagnosis, 370–371, 376
Heart failure. *See also* Congestive heart failure
FCU, 389–390, 403–404
Heart rate, fetal, 266, 268–270
Heartworms
FCU, 411–412
TFAST, 378–382
Vet BLUE, 477
Hedgehogs, 824, 826
Helper hand, 41–42, 44
Hemangiosarcoma (HSA), 660
cardiac, 409–411
hepatic, 159
kidney, 197
splenic, 180–181, 183
Hematoma
epidural and subdural, 598, 603
hepatic, 157–158
retroperitoneal, 198
scrotal, 253–254
splenic, 179, 182
ultrasonographic appearance, 653, 670
Hemoabdomen
AFAST detection of, 57–59
AFS application to, 115–121, 124–125
blunt trauma, 118–119
canine anaphylaxis-related heparin-induced, 131–136, 165
cats, 93, 124
clotted blood, 121–122
Global FAST, 685–686
harvest of, 123
management guidelines and decision making, 118–121
nontraumatic, 121
pediatric patients, 280
penetrating trauma, 118–119
postinterventional trauma, 119–121
sources and location of bleeding, 124–125
staging
canine, 711–713
feline, 713
time to bleeding resolution, 123
Hemorrhage. *See also* Cavitary hemorrhage
intraocular, 571–573
intraparenchymal, 598, 604
intrapelvic bleeding, 125–126
intraventricular, 598, 603
lung and thoracic sampling, ultrasound-guided, 912
retroperitoneal, 197
splenic, 173
trauma, 741–742, 758
Hemorrhagic gastroenteritis syndrome (HGE), 704. *See also* Acute hemorrhagic diarrhea syndrome (AHDS)
Hemothorax (HTX), thoracocentesis, 897
Heparin-induced hemoabdomen, canine anaphylaxis-related, 131–136, 165
Hepatic abscess, 156–157, 159
Hepatic coccidiosis, rabbits, 822

Hepatic cysts, 156–158
hamsters, 824–825
Hepatic hematomas, 157–158
Hepatic lipidosis, 876
liver and gallbladder POCUS, 162–163
Hepatic neoplasia, 158–161
Hepatic nodular disease, 156–157
Hepatic parenchyma, POCUS examination
abnormal findings, 160–163
normal findings, 151–153
Hepatic veins
cat, 779, 781, 784
DH view on AFAST, 82, 84, 699–704
dolphins, 841–842
eyeball method assessment, 702, 705
FCU, 399–400
liver and gallbladder POCUS, 151, 154–156, 161–163
pediatric POCUS, 272–273
TFAST, characterization, 361–362, 364–365
thrombosis, 532–534
VetFAST-ABCDE, 766
Hepatic venous congestion
causes, 127, 129–132, 137
liver and gallbladder POCUS, 154, 162–163
TFAST, 361–362, 364
Hepatic venous distension
AFAST, 61, 80
FCU, 399–400
liver and gallbladder POCUS, 163
TFAST, 361–362, 364
Hepatitis, liver and gallbladder POCUS, 162–163
Hepatization of lung, 462–464, 467, 474–476
Hepatobiliary conditions
ferrets, 817–818
rabbits, 820, 822
Hepatocellular adenoma/carcinoma, 158–159, 161
Hepatomegaly, birds, 867
Hepato-renal umbilical (HRU) view
abdominal radiograph and CT correlation, 72
AFAST image acquisition, 99–100
clinical questions investigated, 97
false negatives, 102
false positives, 102, 104
modified lateral-sternal recumbency, 69–70
probe maneuvering, 73
right lateral recumbency, 65–66, 72
typical negatives, 101
typical positives, 101–103
AFAST order of performance, 69–70
feline AFAST, 797
Hepato-renal (HR) view
AFAST image acquisition, 85–86
artifacts, 87, 89–90
clinical questions investigated, 84
false negatives, 91
false positives, 90–91
left lateral recumbency, 67–68
marine mammal POCUS, 837, 841, 843–845
order of performance, 69–70
typical positives, 87–88
AFAST order of performance, 69–70
feline AFAST, 791–792
Herbivores, gastrointestinal tract, 816
Hernia, 657–660
Herniation
congenital, 284–286
diaphragmatic, 152–153, 156, 285–286, 377–379
peritoneal pericardial, 152–153
into scrotum, 253
HGE. *See* Hemorrhagic gastroenteritis syndrome
Hiatal hernias, congenital, 286
High-resolution ultrasound (HRUS), ocular, 554
Hindlimb nerve block. *See* Pelvic limb nerve block
Histamine-2 receptor blockers, canine anaphylaxis, 132–135
Histoplasmosis, 181
Horizontal probe position, POCUS eye, 558
HR view. *See* Hepato-renal view
HR5th bonus view
AFAST image acquisition, 104
clinical questions investigated, 102
false negatives, 106
false positives, 106
kidney investigations, 97, 101
modified lateral-sternal recumbency, 69–70
probe maneuvering, 73
right lateral recumbency, 65–66, 72
typical positives, 105
AFAST order of performance, 69–70
HRU pouch, 97, 100
HRU view. *See* Hepato-renal umbilical view
HRUS. *See* High-resolution ultrasound
Hs and Ts, Global FAST, 730
hyperkalemia, 736–737
hypertension–pulmonary hypertension, 737–739
hypocontractility–dilated cardiomyopathy, 736–738
hypotension/hypovolemia, 734, 736
tamponade–pericardial effusion, 741, 744–746
tension pneumothorax, 740–741
thromboembolism–pulmonary thromboembolism, 741, 744–745
toxin–canine anaphylaxis, 745, 748–749
trauma–hemorrhage, 741–742
HSA. *See* Hemangiosarcoma
HTX. *See* Hemothorax
Hydrocele, 254
Hydrocephalus, pediatric patients, 289
Hydronephrosis, 202–205
pediatric patients, 289–290
Hymenoptera species envenomation, heparin-induced hemoabdomen, 131–136, 165
Hyperechogenicity, definition, 5–7
Hyperkalemia, 736–737
Hypertension. *See* Pulmonary hypertension
Hypertrophic cardiomyopathy (HCM), 378
FCU, 407–409
Hypervolemia, 548, 701
Hyphema, 555, 567, 569, 571–572, 575–576
Hypocontractility–dilated cardiomyopathy, 736–738
Hypoechogenicity, definition, 5–7
Hypoglycemia, ferrets, 819
Hypoproteinemia, AFAST, gallbladder wall edema, 127, 130
Hypopyon, 555
Hypotension, 734, 736
Hypothermia, pediatric patients, 273
Hypovolemia, 734, 736
Hypovolemic CVC, 63, 130–132, 701
Hypovolemic patients, AFAST and AFS in, 127–128
Hypovolemic shock, 690, 750

Ice pick mode, 34
ICP. *See* Intracranial pressure
IE. *See* Infectious endocarditis
Ileocolic junction, feline AFAST, 797–798
Ileus, POCUS gastrointestinal tract and pancreas, 226–227, 238–240
I-lines, 479, 482
Iliopsoas muscle, 673, 678
Image acquisition
AFAST

capabilities, 61
cats, 778
CC view, 91–100
DH view, 73–84
documentation of findings, 106, 933
HR5th and SR5th bonus view, 102, 104–106
HRU and SRU view, 97, 99–104
image quality optimization, 64
indications, 64
limitations, 61, 63
objectives, 64
patient positioning, 65–71
pearls and pitfalls, 106
probe preferences, 64
probe–skin contact optimization, 64
quick references of normal values and rules of thumb, 106–108, 951–955
serial repetition of, 57–58, 84, 91, 97, 102, 106, 117, 119, 122–123, 127–128
SR and HR view, 84–91
ultrasound settings, 64
views overview, 69–70, 72
common mistakes, 40–52
data recording, 5, 34–35
FCU
capabilities, 390
indications, 390
left parasternal window, 394–396, 399
limitations, 390
objectives, 390–391
patient positioning and preparation, 391–392
pearls and pitfalls, 400
probe preferences, 391
quick references of normal values and rules of thumb, 400, 960–961
right parasternal window, 392–399
subcostal window, 395, 397, 399–400
ultrasound settings, 391
features, 25–28
fetus, 266–268
modes, 33–34
optimization, 32–33
Global FAST, 692, 731
TFAST CTS view, 305–314
ultrasound-guided lung and thoracic sampling, 909
POCUS
gastrointestinal tract, 228–229
kidney, 190–192
liver and gallbladder, 150–153
pancreas, 228–231
pediatric, 272–279
spleen, 174–175
urinary bladder, 212–213
presets, 33, 39
probe maneuvers, 28–32, 43, 46, 48, 70–73
reproductive POCUS
female, 256–259
male, 249, 251
TFAST
acoustic windows overview and summary, 300–301, 332
capabilities, 298
CTS view performance, 305–315
DH view performance, 330–332
documentation using goal-directed templates, 333
indications, 299
light dimming, 305
limitations, 298–299
machine positioning, 302
objectives, 299
patient positioning, 300–304, 306, 311, 313–314
patient preparation, 303
patient shaving, 303–304
PCS view performance, 315–330
pearls and pitfalls, 333
probe preferences, 300
quick references of normal values and rules of thumb, 333–334, 958–959
screen orientation, 300, 302
ultrasound settings, 300, 305, 308, 311–312, 315, 319–320, 330
trouble-shooting algorithm for poor, 49–51
Vet BLUE
acoustic window names and locations, 429, 433–443
acoustic window order, 441–444
capabilities, 426
DH view, 434, 438, 440–441, 443
documentation using goal-directed templates, 455
indications, 426
limitations, 426
lung line optimization, 431, 433, 435–437
lung orientation, 430–432, 434
objectives, 426–427
patient positioning, 428–429
patient preparation, 427–428
pearls and pitfalls, 455
probe orientation, 430–431, 434
probe preferences, 428, 430
quick references of normal values and rules of thumb, 456, 959–960
step by step performance, 445–447
transthoracic views, 434–442
trouble shooting, 447–450
ultrasound settings, 428, 430–433, 435
Image orientation, 7–8, 26–28, 41–43, 300, 302, 330, 430–432, 434
Image saving, Global FAST, 720–722, 750–751
Imaging planes, 7–8, 25–26, 41–43
Immune-mediated hemolytic anemia, AFAST, gallbladder wall edema, 127, 130
*In utero* imaging
fetal maturation, 266–268
fetal stress, 266, 268–270
Infarction
kidney, 205–206
lung, 536–537
Global FAST, 719, 741, 744–745
Vet BLUE, 462–464, 467, 475, 477
splenic, 182, 186, 280
Infectious disease
bacterial cystitis, 215–216
bacterial pneumonia, 485, 489, 500–501
brucellosis, 252–253
diffusely wet lung, 486, 490
pediatric patients, 271, 281, 283–284, 290–291
POCUS spleen, 177, 179, 181, 184
Infectious endocarditis (IE), 405–406
Infiltrative processes, kidney, 200, 202
Inflammatory disease, POCUS spleen, 184
Inguinal hernia, 658–660
congenital, 285–286
Inguinal region, femoral nerve block, 620, 622–623
Intercostal block, 629–630, 632–633
Intercostal view, CVC POCUS, 543–546
Interlobar vessels, kidney POCUS, 191, 193
International Veterinary Point-of-Care Ultrasound Society, 37
Intestinal intussusception, 234–235, 237
Intestinal obstruction
pediatric POCUS, 280–282
POCUS gastrointestinal tract, 226–227, 233–234
Intestines. *See* Gastrointestinal tract
Intraabdominal fluid. *See also* Abdominal fluid score
AFAST detection, 57–61, 106–108
CC view, 92–96
DH view, 75–77, 79, 82–84

Intraabdominal fluid (*cont'd*)
HR5th and SR5th bonus views, 102, 104–106
HRU view, 97, 99, 101–103
SR view, 87–91
clotted blood, 121–122
harvest of, 123
lavage fluid resorption, 123
Intracardiac masses, 378–382
Intracranial mass lesion, 599, 605
Intracranial pressure (ICP)
mass lesion and, 599, 605
resistive index and, 595
Intrahepatic bile ducts, liver and gallbladder POCUS, 155–156
Intrahepatic shunts, congenital, 286–288
Intraluminal gas, 233–234
Intraocular hemorrhage, 571–573
Intraocular masses, 569–571
Intraparenchymal hemorrhage, 598, 604
Intrapelvic bleeding, AFAST limitations, 125–126
Intraperitoneal gas, POCUS gastrointestinal and pancreas, 235–239
Intrathecal approach
neuroaxial nerve block, 643–644
ultrasound signs of, 644–645
Intravenous fluid resuscitation, AFS-informed, 59
Intraventricular hemorrhage, 598, 603
Intussusception, 234–235, 237, 283–284
Ipsilateral phrenic nerve, 613
Iris, 559–561, 570
Iris adhesions, 556
Islet cell tumors, 819
Isoechoic, definition, 5–6
Isopropyl alcohol
AFAST, 64
air trapping elimination, 40–41
cats, 803, 805
probe head damage, 35–36
TFAST, 303
Vet BLUE, 427

Joint
normal findings, 668
POCUS
abnormal findings, 669–674
artifact minimization, 666–667
capabilities, 663–664
clipping hair and coupling medium, 664–665
indications, 664
limitations, 664
normal findings, 667–671
objectives, 664
pearls and pitfalls, 680
probe types, 665
settings, 666
stand-off pads, 665–666
transducer orientation, 667–668
Jugular catheterization
anatomy, 515
catheter selection, 514
dynamic technique, 514–515
line length, 514
longitudinal orientation, 517, 519–520
orientation, 515–517
patient preparation, 515
probe, 513
short temporary, 520
skill development, 515
static technique, 514
transverse orientation, 516–519

Kerley B-lines, 474
Kidney
AFAST
dolphins, 843–844
HR5th and SR5th views, 97, 101–102, 104–105
penetrating trauma, 122–123
SR view of left, 84–91
SR view of right, 87, 89
target organ approach, 141
anatomy, 192–194
capsule, 192, 194
cortex, 192–194
cysts, 199–201
echogenicity, 151, 153, 170, 175–176, 191, 193–196, 274, 789–790
feline AFAST, 788–791
fetal, 266
hydronephrosis, 202–205
image planes, 26
infarcts, 205–206
infiltrative processes, 200, 202
location, 791
mass lesions, 196–198
medulla, 192–194
pediatric POCUS, 274–277, 287–291
perirenal fluid, 192, 206–207
POCUS
abnormal findings, 195–207
AFAST and Global FAST add-on, 189, 207
capabilities, 189
goal-directed templates, 934–935
image acquisition, 190–192
indications, 190
limitations, 189
normal findings, 192–195
objectives, 190
patient positioning and probe selection, 190
patient preparation, 190
pearls and pitfalls, 208
quick references of normal values and rules of thumb, 208, 956
POCUS gastrointestinal and pancreas, 229–230
pyelectasia, 194, 200–202, 204
renal pelvis, 192–194, 200–202, 204, 274–275
reptiles, 871–872, 876
retroperitoneal fluid, 192, 197–198, 206–207
size and symmetry, 194–195, 208, 788–790
Kidney stones, 200, 203

LA. *See* Left atrium
LA4CV. *See* Long-axis four-chamber view
LA5CV. *See* Long-axis five-chamber view
LA:Ao. *See* Left atrial to aortic ratio
Labeling, ultrasound images, 35
Lagophthalmos, 575
Large-volume bleeder/effusion
AFS system, 114–117, 124
anemia in, 116–117
canine anaphylaxis, 133–135
cats, 124, 799–802
modified AFS system, 115–116
nonhemorrhagic effusions, 126–127
postinterventional trauma, 119, 121
Laryngeal masses, 758
Laryngeal paralysis, 758
Larynx, assessment, 759–760
LAT. *See* Left atrial tear/rupture
Lateral probe position
marine mammal POCUS, 841–843
POCUS eye, 558–559
Lateral recumbency
AFAST, 65–70, 72
FCU, 391–392
Global FAST, 693–695, 732
POCUS
gastrointestinal and pancreas, 228
kidney, 190–192
reproductive, 251
TFAST, 302–304, 306, 311, 313–314, 320–321
Lateral ventricular height, 596
Lavage fluid, resorption of, 123
L-CHF. *See* Left-sided congestive heart failure
Left atrial enlargement, FCU, 389, 393

Left atrial tear/rupture (LAT), 366–367, 378–382, 404–405
Left atrial thrombus, 408–409
Left atrial to aortic ratio (LA:Ao), 321, 323, 379–380, 394, 803–805
Left atrium (LA), FCU, 393–396, 398, 400
Left heart strain/overload/failure, TFAST, 321, 378–382
Left lateral (LL) recumbency
  AFAST, 65–70
  POCUS exams, kidney, 190–192
  POCUS gastrointestinal and pancreas, 228
Left parasternal window, FCU image acquisition, 394–396
  apical and cranial views, 399
Left ventricle (LV)
  FCU, 393–400
  TFAST, 317–318, 324–329
Left ventricular failure, FCU, 406–407
Left ventricular hypertrophy, FCU, 407–409
Left ventricular outflow tract (LVOT), 699
  FCU, 394, 396–398
  TFAST, 321, 323, 327, 329–330
Left ventricular short-axis (LVSA) view, 321, 323, 379–380, 698, 803–804
Left-sided congestive heart failure (L-CHF), 470–473, 481–482, 485, 487, 494, 496, 699, 701
  Vet BLUE monitoring, 497–498
Lens, 560
  anterior lens luxation, 562–565
  capsule, 560–561
  posterior lens luxation, 566–567
  subluxation, 569
  zonules, 560, 566
Levobupivacaine, 611, 613–614, 616, 621, 623–624, 626–627, 631–632, 634
Ligament, normal findings, 668–669
Light dimming
  TFAST, 305
  Vet BLUE, 428
Linear anechoic stripes, SR view on AFAST, 90
Linear gastrointestinal foreign bodies, 233–237, 240, 280–282
Linear probes, 36–37
  image shapes, 28–29
Lipomas, 658, 660
Litter size, 262, 268, 270
Liver
  AFAST
    DH view, 75–77, 79, 81–82
    dolphins, 843–844
    HR5th and SR5th views, 102, 104–105
    HRU view, 97
    target organ approach, 141
  birds, 865
  capsule, 176
  echogenicity, 151–154, 161–163, 170, 175–176, 191, 194–195, 273–274, 778–780
  FCU, 397, 399–400
  feline AFAST, 778–782
  fetal, 266
  kidney POCUS, 191–192
  masses, 156–161, 170
  parenchymal disease, 160–163
  pediatric POCUS, 272–274, 280, 286–288
  POCUS
    abnormal findings, 156–163, 167–169
    AFAST and Global FAST add-on, 169–170
    artifacts, 156, 170–171
    capabilities, 149
    goal-directed templates, 933–934
    goals, 149, 156
    image acquisition, 150–153
    indications, 150
    limitations, 149
    normal findings, 151–156
    objectives, 150
    pearls and pitfalls, 170
    quick references of normal values and rules of thumb, 170–171, 955
    ultrasound settings and patient positioning, 150
  reptiles, 871–872, 879
  Vet BLUE, 447
Liver lobe torsion, rabbits, 820, 822
LL recumbency. *See* Left lateral recumbency
Long bone fracture, 673
Long-axis cardiac views, 43–44
  patient monitoring, 698–699
  TFAST PCS views, 318, 321–323, 326–330
  VetFAST-ABCDE, 765
Long-axis five-chamber view (LA5CV), 380, 399
Long-axis four-chamber view (LA4CV), 321, 323, 327, 359, 361, 380, 399, 698–699, 804
Longitudinal plane and orientation, 7–8, 26–28, 41–43
  AFAST, 70–73
  catheterization
    femoral arterial, 521–523
    jugular, 517, 519–520
    transverse *versus*, 524
  caudal vena cava POCUS
    paralumbar view, 544, 546–548
    subxiphoid view, 543–545
  lumbosacral area, 638–639
  TFAST, 308, 313
  thoracolumbar area, 640–641
  vascular POCUS, slice-thickness artifact, 531–532
  Vet BLUE, 430–432, 434
    marine mammal POCUS, 850, 852, 854–856
Loop diuretic usage, B-line guidance, 483–484, 488
LSA. *See* Lymphosarcoma
Lumbar plexus
  anatomy, 620
  psoas compartment, 621–622
Lumbosacral area
  epidural approach, 642–643
  longitudinal scan of, 638–639
  transverse scan of, 640
Lumbosacral trunk block, 625–626
Lung. *See also* Veterinary bedside lung ultrasound exam
  AFAST
    deep lesions, 140
    DH view, 75–76, 79, 81–82, 140
    target organ approach, 141
  alveolar-interstitial syndrome, 341, 705
    B-line scoring, 470–474, 710
    Vet BLUE, 449–450, 462–466, 468–474
  anatomy, birds, 864–865
  aspiration, 502–504
  atelectasis, 720
  boundaries, 447–448
  centrally located disease, 461
  consolidation, 462–467, 474–476
  contusion, 339, 341–342, 354, 462, 705
    B-line severity score, 491–492, 710–711
    comparative imaging, 491–493
  dry
    TFAST, 339, 341–344, 354
    Vet BLUE, 449–452, 462–466, 468–471, 481, 483, 485–486
    wet lung findings *versus*, 339, 341–344, 354, 462–466, 699, 701
  fibrosis, 462, 470–471
  hepatization, 462–464, 467, 474–476
  infarction, 536–537

Lung (*cont'd*)
Global FAST, 719, 741, 744–745
Vet BLUE, 462–464, 467, 475, 477
marine mammal POCUS
artifacts, 850–851
orientation, 850–853
signs, 852–854
wet lung *versus* dry lung findings, 699, 701
masses and nodular disease, 377, 462–464, 467, 475–477, 485–486
aspiration, 502–504
fungal granuloma, 500–503
identification, 912, 914
shape, 912–913, 915
size, 913
Vet BLUE monitoring, 498
normal, 456, 462–463, 470, 959–960
old dog, 500, 502
pressure atelectatic, 497
TFAST, 337
advantages, 357–358
A-lines without lung sliding in pneumothorax diagnosis, 344, 354
false negatives, 351
false positives, 351
image acquisition, 305–315
lung point in pneumothorax diagnosis, semiquantification, and monitoring, 344–351
missed pneumothorax diagnosis, 351
M-mode and power Doppler pneumothorax detection, 351–354
pleural effusion on CTS view, 357
subcutaneous emphysema, 353–356
wet *versus* dry lung findings, 339, 341–344, 354
wet
dry lung *versus*, 339, 341–344, 354, 462–466, 699, 701
TFAST, 339, 341–344, 354
Vet BLUE, 449–452, 462–466, 468–474, 481–491, 710
Lung and thoracic sampling, ultrasound-guided
artifacts, 908–909
biopsies, 916
capabilities, 907
chemical restraint and local anesthetics, 911–912
echogenic enhanced needles, 914–916
hemorrhage and pneumothorax risk, 912
image quality optimization, 909
indications, 908
lesion identification, 912, 914
lesion shape, 912–913, 915
lesion size, 913
limitations, 907–908
needle guides, 915
needle selection, 910–911
needle tracking, 909–910
objectives, 908
patient preparation and planning, 909–910
pearls and pitfalls, 916–917
phantom skill building, 916
probe holding, 908
probe hygiene, 910
probe orientation and maneuvers, 908
probe selection, 911–912
skin preparation, 909–911
slide preparation, 913–915
Lung injury, TFAST, 297
Lung line
TFAST
image acquisition, 306–308, 311–315
pneumothorax diagnosis, 339, 341
Vet BLUE, 426, 430, 432, 434, 445, 447–449, 461
optimization, 431, 433, 435–437
pleural effusion in cats, 496–497
Lung point, 708–709, 749, 759–760, 763
image acquisition, 305, 313–315
pneumothorax
diagnostic algorithm, 349
lung pulse, 346–347
lung sliding with, 345–346
patient positioning effects, 344–345, 347–348
sensitivity improvement, 345–346
TFAST PTX 1/3s rule for semiquantification and monitoring, 347–351
Vet BLUE, 441
Lung pulse, 346–347
Lung sliding
feline TFAST, 807
pseudo, 343
TFAST
image acquisition, 305, 308–315
M-mode and power Doppler, 351–354
pneumothorax diagnosis, 339, 341, 344–346, 351–354
Vet BLUE
image acquisition, 430–431, 433, 435–437, 441, 449–452
visual lung language, 462–466, 468–471
Lung ultrasound (LUS), 459. *See also* Veterinary brief lung ultrasound exam
considerations and limitations, 461–462
six signs, 347, 349, 449–452, 462–467, 474–479
LUS. *See* Lung ultrasound
LV. *See* Left ventricle
LVOT. *See* Left ventricular outflow tract
LVSA view. *See* Left ventricular short-axis view
Lymph nodes
abdominal, pediatric POCUS, 276
dolphin, 840–841
mesenteric, pediatric POCUS, 277–279
Lymphoma
cardiac, 409–411
epitheliotropic, 658
ferrets, 819–820
Lymphosarcoma (LSA)
liver, 159, 162–163
renal, 200, 202
splenic, 179–180, 183–184, 186

Magnetic resonance imaging (MRI), for brain imaging, 579
Malignant melanoma, 718–719
Malignant neoplastic masses, 658, 660
Mammary glands, reproductive POCUS, 262–263
Mandibular salivary gland, 650–651
sialadenitis, 655–656
sialocele, 656–657
Marine mammal POCUS
AFAST, 829
abdominal fluid scoring, 846–847
cysto-colic reproductive view, 837, 845–846
diaphragmatico-hepatic view, 837–842
hepato-renal view, 837, 841, 843–845
overview of, 835–838
spleno-renal view, 837, 841, 843–845
umbilical view, 838, 846
capabilities, 830
development of, 829–830
efficiency, 858
environment, machine and sonographer location, 832–834
equipment, 830–833
goal-directed template, 858–859
indications, 830
limitations, 830
objectives, 830–831
ocular, 858
patient positioning, restraint, and breathing, 834–835
pearls and pitfalls, 858–859
probe, 830–833

quick references of normal values and rules of thumb, 965
settings, 830–833
testicular evaluation, 858
TFAST, 829, 836
echo views and fallback views, 849–851
pleural and pericardial effusion, 848–849
questions, 848
views, 848
thyroid evaluation, 858
venipuncture, 858
Vet BLUE, 829
artifacts, 850–851
longitudinal orientation, 850, 852, 854–856
lung orientation, 850–853
lung signs, 852–853
performance, 836, 854
transverse orientation, 850, 852, 855–856
zig-zag continuum, 856–858
Maropitant, 135
Mass lesions. *See also* Splenic mass
adrenal glands, ferrets, 817–818
birds, 867–869
bone, 670, 674–676
cardiac, 139–140, 378–382, 408–411
computed tomography (CT) detection, 579
hedgehogs, 824
intracranial, lesion, 599, 605
intraocular, 569–571
Islet cell, 819
kidney, 196–198
laryngeal, 758
liver, 156–161, 170
lung, 377, 462–464, 467, 475–477, 485–486
aspiration, 502–504
fungal granuloma, 500–503
identification, 912, 914
shape, 912–913, 915
size, 913
Vet BLUE monitoring, 498
midabdominal, 102, 104, 156, 170
muscle, 679, 681
pleural cavity, 377
reptiles, 876
retrobulbar, 573–578
urinary bladder, 93, 99, 215, 217–219, 713–715
Mass sign. *See* Nodule sign
Mast cell tumors, 658
liver, 160, 162–163
splenic, 181, 184
Md lung region. *See* Middle lung region
Mechanical probes, 36
Median nerve
anatomy, 615
block, 616–617
scanning, 618
Median plane, 26
Medical records, 5, 34–35. *See also* Documentation and recording
Medulla oblongata, 587–589, 592
Medullary rim sign, 194–196
Melanocytoma
choroidal, 570
uveal, 569
Melanoma
malignant, 718–719
ultrasonographic appearance, 658
uveal, 569
Meninges, 583–584
Mercedes-Benz sign, 323–328, 734, 738, 743
Mesenchymal tumors, liver, 159
Mesothelioma, 409–410
Metabolic disorders, pediatric POCUS, 286–289
Metal, artifacts, 20–21
Metastatic neoplasia
liver, 159–161
splenic, 181, 183–184
Methazolamide, 564, 567
Methodology, standardized, 922
Microconvex probes. *See* Curvilinear probes
Midabdominal masses
HRU view on AFAST, 102, 104
origin of, 156, 170
Middle (Md) lung region, 434
location, 437, 440–441
order, 441, 443–444
Vet BLUE step by step, 445–447
Mirror image artifacts, 18–19, 53, 443
AFAST
CC view, 93, 96
DH view, 79, 81
SR view, 89
liver and gallbladder POCUS, 156
TFAST, PCS view, 330
ultrasound-guided lung and thoracic sampling, 909
Mitral valve, FCU, 398–399
Mitral valve disease (MVD)
FCU, 404–405
preanesthetic evaluation, 494–495
M-mode, 34
fetal heart rate determination, 268–269
heart, 394, 396, 398, 400
pneumothorax detection, 351–354
Modified lateral-sternal recumbency
AFAST, 66, 69–70
TFAST, 302–304
Modified ultrasound-guided diagnostic peritoneal lavage (MUG-DPL)
blind *versus*, 899–900
findings, 900
indications, 900
materials checklist, 900
procedure, 900–903
scanning technique, 900
Monitor lizards, 871, 876
Monro–Kellie Doctrine, 599
Movement, needle, 903
MRI. *See* Magnetic resonance imaging
MSK. *See* Musculoskeletal system
Mucocele, gallbladder, 164, 166, 168
MUG-DPL. *See* Modified ultrasound-guided diagnostic peritoneal lavage
Multiple echoes, 22–23
Muscle
atrophy, 678–680
injuries, 671, 673, 677
masses, 679, 681
normal findings, 650, 668
Musculocutaneous nerve
anatomy, 615
block, 616–617
scanning, 618
Musculoskeletal (MSK) system
bones and joints POCUS
abnormal findings, 669–681
artifact minimization, 666–667
capabilities, 663–664
equipment, 664–666
indications, 664
limitations, 664
normal findings, 667–671
objectives, 664
pearls and pitfalls, 680
settings, 666
transducer orientation, 667–668
soft tissue POCUS
abdominal wall injury, 657–658
capabilities, 647
common structures, 650–651
equipment, 648
hernia, 657–658
indications, 648
lesions, 651–657
limitations, 647–648
method, 649
nerves, 669
neoplasia, 658, 660
objectives, 648
patient preparation, 649

Musculoskeletal (MSK) system (*cont'd*)
pearls and pitfalls, 659, 661
settings, 648–649
Mushroom sign, 323–328, 734, 736–739, 743, 747
MVD. *See* Mitral valve disease
Myelolipoma, splenic, 179, 182

Narcotic sedation, pediatric patients, 272
NCPE. *See* Noncardiogenic pulmonary edema
Needle
echogenic enhanced, 914–916
guides, 915
probe head damage, 35–36, 517–518
selection, lung and thoracic sampling, ultrasound-guided, 910–911
visualization, 903–904
ultrasound-guided lung and thoracic sampling, 909–910
Neoplastic lesions
bone, 670, 674–676
cardiac, 408–411
ferrets, 819–820
Global FAST staging, 687, 689
hedgehogs, 824, 826
hepatic, 158–161
mammary gland, 262–263
prostate findings, 249–251
splenic, 179–184
superficial structures, 658, 660
testicular, 253
urinary bladder, 215, 217–219
NeoPolyDex, 567, 570, 572
Nephroblastoma, 197
Nephroliths, 200, 203
Nerve, normal findings, 668–670
honeycomb appearance, 669
onion ring appearance, 669
Nerve block. *See* Forelimb nerve block; Neuroaxial nerve blocks; Pelvic limb nerve block; Trunk nerve block
Neuritis, 678–680
Neuroaxial nerve blocks
approaches
epidural, 641–643
intrathecal, 643–644
lumbosacral, 637–640, 642–643
sacrococcygeal, 637–638
thoracolumbar, 637–638, 640–643
ultrasound signs of, 644–645
capabilities, 637
indications, 637
limitations, 637
longitudinal scan, lumbosacral area, 638–639
objectives, 637
pearls and pitfalls, 645
transverse scan, lumbosacral area, 640
Neutered patients
marked, 247–248, 255–256
postoperative mounting, 262
prostate findings, 249–250
stump pyometra, 261
Nodular hyperplasia
hepatic, 156–157
splenic, 178–180, 182, 184
Nodule. *See* Mass
Nodule pseudo B-lines, 342–343
Nodule sign, 345, 462–464, 467, 475–477, 485–486, 853
Noncardiogenic pulmonary edema (NCPE), 484, 488, 490
Nonecho fallback view, 850–851
ascites, 699
echocardiography, 698
left-sided heart problems, 699–702
right-sided heart problems, 699–701
Nonhemorrhagic effusions, AFAST and AFS in, 126–127
Nontraumatic hemoabdomen, 121
Nostril flaring, cats, 494, 496

Obesity
TFAST, 308–309, 354
Vet BLUE, 448–449
Obstructive shock, 690, 750
cardiac tamponade, 136–138, 165, 361–362, 364–365
Occipital lobe, 581–582, 584–585, 592
Ocular opacities, 556
Ocular ultrasonography. *See* Eye
Off-axis artifacts, bones and joints POCUS, 666–667
Omphalocele, 284–285
One-eyed gator, 308, 312, 314–315, 355–356
Opaque eye, 553
anterior chamber, 555
corneal opacity, 554
ocular opacities, 556
Optic nerve, 561, 571
Optic nerve sheath, 561–562
VetFAST-ABCDE, 758, 762–766, 768
Orbital ligament probe positioning, 558–559
Orchitis, 251–253
Organomegaly
birds, 867
reptiles, 876
Orientation
image, 7–8, 26–28, 41–43, 300, 302, 330
probe markers, 28–29, 46–47
Osteochondrosis, 671
Osteomyelitis, 670, 674–676
Osteosarcoma, 674–675
Ovariohysterectomy
postoperative bleeding, 125
stump pyometra, 261
Ovary
cysts, guinea pigs, 824
feline AFAST, 793–794
reproductive POCUS, 256–257
reptiles, 876–878
Oviductal impaction, 868–869
Ovulatory follicles, 876–878
Oxytocin injection, 269

Packed cell volume (PCV), canine anaphylaxis monitoring, 134
Pancreas
conditions, ferrets, 819
echogenicity, 229–230
feline AFAST, 795–796
pediatric POCUS, 273–274, 277–278
POCUS
abnormal findings, 241
accuracy, sensitivity, and specificity, 225–226
AFAST add-on, 225–226
capabilities, 226
goal-directed templates, 935–936
indications, 226–227
limitations, 226
normal findings, 232
objectives, 227
patient positioning and probe selection, 228
pearls and pitfalls, 241–242
quick references of normal values and rules of thumb, 243, 957
scanning technique, 228–231
Pancreatic duct, POCUS gastrointestinal and pancreas, 229–231
Pancreaticoduodenal vessels
pediatric POCUS, 278
POCUS gastrointestinal and pancreas, 229–231
Pancreatitis
AFAST, gallbladder wall edema, 127, 130
AFAST AFS system in, 126
POCUS gastrointestinal and pancreas, 226–227, 229–231, 236, 241
Pantoprazole, 135
Parallel probe placement thoracocentesis, 896–897
Paralumbar view, CVC POCUS, 544, 546–548
Paramedian plane, 7–8, 26

Paraprostatic cysts, 250
Parasacral space, lumbosacral trunk, 626
Parasites, enteric, 284
Paravertebral approach
  brachial plexus block, 609–612
  thoracic wall block, 630–632
Parenchyma, TCUS of, 583, 587, 598, 601
Parenchymal disease
  kidney, 195–196
  liver, 160–163
  spleen, 184–185
Parenchymal injury, splenic, 179
Parietal lobe, 582–584, 586
Parking garage effect, pneumothorax, 344–345, 347–348
Parotid salivary gland, 650
  sialadenitis, 655–656
Parturition, difficult. *See* Dystocia
Passive splenic congestion, 184
Patent urachus, 290, 292
Patient monitoring
  Global FAST, 687
    AFS for ascites, 707
    capabilities, 691
    component integration, 696
    limitations, 691
    pericardial effusion, 707–708
    pleural effusion, 707
    pneumothorax estimation, 708–709
    urine output estimation, 707–708
    Vet BLUE B-line scoring system, 709–711
    volume loss, 704–706
    volume status, 696–704
  ultrasound-guided pericardiocentesis, 890–891
  ultrasound-guided thoracocentesis, 897
Patient positioning
  abdominal fluid score, 695–696
  AFAST, 65–71
  cats, 802–804
  FCU, 391–392
  Global FAST, 692–696, 732–734
  pneumothorax, 344–345, 347–348
  POCUS examination
    bird, 865–866
    exotic companion mammals, 816
    eye, 557–558
    femoral arterial catheterization, 521
    forelimb nerve block, 611–612
    gastrointestinal tract, 227–228
    kidney, 190
    liver and gallbladder, 150
    marine mammal, 834–835
    neuroaxial nerve block, 639–644
    pancreas, 228
    pediatric, 272
    pelvic limb nerve block, 621–622, 624, 626–627
    reptile, 871, 873–875
    soft tissue, 649
    spleen, 174
    trunk nerve block, 631, 633–634
    urinary bladder, 212
  reproductive POCUS, 249, 256–258
  TFAST, 300–304, 306, 311, 313–314
  Vet BLUE, 428–429
  VetFAST-ABCDE, 759
Patient staging, Global FAST
  canine bladder masses, 713–715
  canine hemoabdomen, 711–713
  canine pericardial effusion, 715–716
  capabilities, 691
  decision making, 689
  feline bladder masses, 715
  feline hemoabdomen, 713
  feline pericardial effusion, 716–717
  limitations, 691
  localized *versus* disseminated disease, 687
  neoplastic lesions, 687, 689
Paw handling, 44–45
PCE. *See* Pericardial effusion
PCS view. *See* Pericardial site view
PCV. *See* Packed cell volume
PDI. *See* Power Doppler imaging
PE. *See* Pleural effusion
PEA. *See* Pulseless electrical activity
Pediatric POCUS
  abdominal disorders, 271, 279–286
  capabilities, 271
  equipment, 271–272
  genitourinary disorders, 287–292
  goal-directed templates, 939
  image acquisition, 272–279
  indications and objectives, 271
  limitations, 271
  metabolic conditions, 286–289
  patient preparation, 272–273
  pearls and pitfalls, 292
  quick references of normal values and rules of thumb, 961
  serial examinations, 273
PEH. *See* Pseudoplacentational endometrial hyperplasia
Pelvic limb nerve block
  capabilities, 619
  femoral nerve
    inguinal region, 620, 622–623
    psoas compartment, 620–622
  indications, 619–620
  limitations, 619
  lumbar plexus anatomy, 620
  materials for, 620
  objectives, 619–620
  pearls and pitfalls, 628
  sacral plexus anatomy, 624
  saphenous nerve, in distal thigh region, 623–625
  sciatic nerve
    lateral thigh region, 626–627
    lumbosacral trunk, 624–626
Penetrating trauma (PT)
  AFAST application to, 121–128
  AFS-based decision making, 118–119
  serial AFAST monitoring of, 122–123
Penile spines, 247–248
Perforation, gastrointestinal
  pediatric POCUS, 281, 283
  POCUS gastrointestinal and pancreas, 226–227, 235, 238
Pericardial effusion (PCE)
  AFAST, 60–61, 63
    CVC characterization, 131
    DH view, 75, 136–140
    gallbladder wall edema, 127, 130
    marine mammals, 839
  ascites in, 137–139
  cardiac neoplasia, 408–411
  cats, 495–496
  causes, 138–139
  chronic *versus* acute, 365
  clinical signs and signalment, 139
  concurrent pleural effusion, 375–376
  FCU, 389–391, 398
  Global FAST, 741, 744–746
  liver and gallbladder POCUS, 165
  pericardiocentesis for, 886–887
  POCUS
    birds, 866, 869
    reptiles, 879–881
  prevalence, 138
  recognition of acute, 139–140
  staging
    canine, 715–716
    feline, 716–717
  TFAST
    cardiac chamber rupture, 366
    cardiac tamponade, 361–366, 368–369, 376
    definitive characterization with sampling, 376–377
    estimation, 707–708
    gallbladder wall edema, 366, 368–369
    image acquisition, 297–300, 315–320, 324–329, 337–338
    left atrial tear/rupture, 366–367
    marine mammals, 839
    pleural effusion *versus*, 358, 369–371

Pericardial effusion (PCE) (*cont'd*)
radiography compared to, 368–369
rules for accurate diagnosis, 359–363, 377
view preference, 358–359
VetFAST-ABCDE, 758
Pericardial fat, 330
Pericardial site (PCS) view
echo view cardiac evaluation, 378–383, 939
pericardial effusion diagnosis, 359–363
pleural effusion, 370
TFAST image acquisition, 300–301, 315–316
anatomy, 330
artifacts, 330
echo views, 317, 321–329
lateral recumbency, 303–304, 320–321
left view, 316–319, 328–330
optimization, 319–322
pearls and pitfalls, 333
pitfalls, 330
right view, 316, 319–330
Pericardiocentesis
cardiac tamponade, 136–138, 165, 365–366
FCU, 417–424
indications for, 886
skill of, 140
ultrasound-guided
blind *versus*, 886
completion of, 889–890
free-hand, 889
indirect, 889
introduction, 885–886
materials checklist for, 887
monitoring of, 890–891
pearls and pitfalls, 890–892
procedure for, 888–889
scanning technique for, 886–888
Perihilar (Ph) lung region, 434
location, 437, 440–441
order, 441, 443–444
Vet BLUE step by step, 445–447
Perinephric pseudocysts, 200–201
Peripheral nerve block. *See* Forelimb nerve block; Pelvic limb nerve block; Trunk nerve block
Peripheral vessels, 512
Perirenal fluid, kidney POCUS, 192, 206–207
Peristaltic contractions, 238–239, 242
Peritoneal effusion. *See also* Ascites; Intraabdominal fluid
pediatric patients, 279–280
POCUS gastrointestinal and pancreas, 226–227, 235
Peritoneal pericardial hernia, 152–153
Peritonitis
abdominocentesis, 898
AFAST evaluation, 63, 164, 167, 225–226
egg yolk, 868
ferrets, 817
gallbladder rupture, 164, 167–169
pediatric patients, 279–280
POCUS gastrointestinal and pancreas, 225–227, 235–239
Perpendicular probe placement thoracocentesis, 894–896
Ph lung region. *See* Perihilar lung region
Phased-array probes, 36–37
image shapes, 28–29
Pheochromocytoma, 198
Phrenic nerve, 613
Phrenicoabdominal vein, pediatric POCUS, 274
PHT. *See* Pulmonary hypertension
Physics, basic ultrasound, 11–14
Pia mater, 589
Piezoelectric effect, 12
Planes
brain POCUS, 580
dorsal, 588, 598–599
dorsal caudal, 581–584
dorsal cranial, 584–587
sagittal, 587, 589–590, 597–598, 600
transverse, 590–592, 597–598, 600
imaging, 7–8, 25–26, 41–43
Pleural cavity
masses, 377
TFAST, 337
CTS view, 305–315
Vet BLUE outside of, 447–449
Pleural effusion (PE)
AFAST, 60–61
DH view, 75
cats, 494–497
concurrent pericardial effusion, 375–376
FCU, 389–391, 398, 417–424
measurement and monitoring, 376
pericardiocentesis for, 886–887
pseudo, 343–344
radiography, 371, 375–376
scanning for, 893
TFAST, 297–300, 337–338
CTS view, 357
definitive characterization with sampling, 376–377
estimation, 707
image acquisition, 300–301
lung point, 345
marine mammals, 848–849
PCS view, 316–320, 324–330
pericardial effusion *versus*, 358, 369–371
pitfalls of imaging, 376
POCUS thoracic or flash approach compared to, 374–376
rules for accurate diagnosis, 371, 377
TFAST slide use, 370–374
thoracocentesis, 892–893
VetFAST-ABCDE, 758
Plicated small bowel, 233, 235–236, 240
Pneumonia, Vet BLUE, 469, 474, 485, 489, 500–501
Pneumoperitoneum, POCUS gastrointestinal and pancreas, 235–239
Pneumothorax (PTX)
AFAST, DH view, 75, 79
feline TFAST, 807
four-quadrant approach, 451, 453–454
Global FAST, 708–709
lung and thoracic sampling, ultrasound-guided, 912
tension, 740–741, 758
TFAST, 297–300, 337–338
advantages, 357–358
A-lines with lung sliding, 339, 341, 354
A-lines without lung sliding, 344, 354
B-lines, 339, 341–342, 354
CTS view acquisition, 305–306, 313–314
diagnostic algorithm, 349
false negatives, 351
false positives, 351
lung point diagnosis, semiquantification, and monitoring, 344–351
missed diagnosis, 351
M-mode and power Doppler detection, 351–354
patient positioning effects, 344–345, 347–348
pseudo B-lines, 342–343
pseudo lung sliding, 343
subcutaneous emphysema confounding, 353–356
thoracocentesis for, 892
Vet BLUE, 441, 449, 462, 465–466, 468–469
VetFAST-ABCDE, 759–760, 763
Point-of-care ultrasound (POCUS). *See also* Focused assessment with sonography for trauma; Veterinary brief lung ultrasound exam
artifacts, 7, 15–23

basic physical principles, 11–14
definition, 3
degrees of echogenicity, 5–7
documentation of findings, 5, 34–35
goal-directed templates, 5
image acquisition mistakes, 40–52
image features, 25–28
image interpretation mistakes, 52–53
image optimization, 32–33
modes, 33–34
presets, 33, 39
probe maneuvers, 28–32, 43, 46, 48, 70–73
probe–skin contact mistakes, 44–48, 51
program
accessibility, 922–925
capabilities, 921
communicating value to clients, 925–926
goal-directed templates, 926–930
indications, 921
limitations, 921
objectives, 922
pearls and pitfalls, 931
proper training, 922
quality control, 930–931
training techniques, 931
screen orientation, 7–8
technological advancements, 34
terminology updates, 3–5
trouble-shooting algorithm, 49–51
ultrasound machine mistakes, 48–52
Pollakiuria, 290
Polycystic kidney disease, 199–201
Polypoid cystitis, 215, 217
Polyps, urinary bladder, 215, 217
Pons, 587–589
Porta hepatis anatomy, 531
Portable machines, 36
Portal vein
anatomy, 531
DH view on AFAST, 82, 84
FCU, 400
liver and gallbladder POCUS, 151, 154, 161–163
pediatric POCUS, 272–273
POCUS gastrointestinal and pancreas, 229
thrombosis, 534–535
Portosystemic shunts, congenital, 286–288
Positive pressure ventilation (PPV), pneumothorax, 345
Post transfusion gallbladder wall edema, 127, 130
Posterior eye wall, 560
Posterior lens luxation, 566–567
Postinterventional exit exam, AFAST, 125–126
Postinterventional trauma, AFS-based decision making, 119–121
Postoperative ileus, 239–240
Power Doppler imaging (PDI), 34
pneumothorax detection, 351–354
Power slide, 353
PPI. *See* Pulmonary-pleural interface
PPV. *See* Positive pressure ventilation
Preanesthetic evaluation, 494–495
Preanesthetic test, 719–720
Pregnancy, 262
fetal stress, 266, 268–270
*in utero* fetal maturation, 266–268
Presets, 391
global recommendations, 39
options available, 33
TFAST, 300, 302–303, 319–320
Vet BLUE, 428, 430–433
Pressure atelectatic lung, 497
Pressure/compression probe maneuver, 31–32, 46
PRF. *See* Pulse repetition frequency
Probe hand, 41–42, 44, 51
Probe pressure artifact, 93, 96
Probes
AFAST recommendations, 64
air trapping, 40–41
care of, 35–36
central venous jugular catheterization, 513
characteristic image shapes, 28–29
curvilinear, 28–29, 36–37, 428, 430
damage to, 517–518
external location of, 45–46
FCU, 391
femoral arterial catheterization, 520
forelimb nerve block, 610
Global FAST, 692, 731
Global FAST recommendations, 39
intrathecal approach, 643
linear, 28–29, 36–37
lumbosacral area, 638
lung and thoracic sampling, ultrasound-guided, 910–912
maneuvers, 28–32, 43, 46, 48, 70–73
pelvic limb nerve block
distal thigh region, 623
inguinal region, 622
lateral thigh region, 626
lumbosacral trunk, 625
psoas compartment, 621
POCUS recommendations
bird, 865
bones and joints, 665
caudal vena cava, 542
exotic companion mammals, 817
gastrointestinal tract, 227–228
kidney, 190
marine mammal, 830–833
pancreas, 228
pediatric, 271–272
reproductive, 256
reptile, 874
soft tissue, 648
spleen, 174
urinary bladder, 212
vascular, 530
VetFAST-ABCDE, 759
reference markers, 28–29, 46–47
selection of, 36–37
single crystal, 34
TCDUS, 597
TCUS, 555, 557–559, 580, 597
TFAST, 300
CTS view, 308, 313
PCS view, 320–322
transmitter and receiver functions, 11–12
trunk nerve block
intercostal, 632
paravertebral approach, 630
transversus abdominis plane, 633
Vet BLUE, 428, 430–431, 434
Probe–skin contact
AFAST optimization, 64
common mistakes, 44–48, 51
Global FAST optimization, 692, 731
TFAST optimization, 303–304
Processor, 11–12
Propagation, artifacts of, 18–22
Prostate
feline AFAST, 792–793
pediatric POCUS, 276–277
reproductive POCUS, 249–251, 254
urinary bladder POCUS, 212
Prostatic adenocarcinoma, Global FAST, 717–718
Prostatic cysts, 250
ferrets, 817–818
Prostatitis, 250
Pseudo B-lines, 17, 21, 342–343, 447, 462, 467, 475–476, 485–486
Pseudo lung sliding, 343
Pseudo pleural effusion, 343–344
Pseudo shred sign, 447
Pseudo step sign, 305, 310
Pseudo tissue sign, 447
Pseudocysts, perinephric, 200–201
Pseudoplacentational endometrial hyperplasia (PEH), 261
Pseudopregnancy, 262
Psoas compartment, femoral nerve block, 620–622
PT. *See* Penetrating trauma

PTE. *See* Pulmonary thromboembolism
PTX. *See* Pneumothorax
Pulmonary artery, FCU, 393, 396
Pulmonary contusions, 339, 341–342, 354, 462
  B-line severity score, 491–492, 710–711
  comparative imaging, 491–493
Pulmonary disease. *See* Lung
Pulmonary edema, 341, 462, 705. *See also* B-lines
  B-line scoring systems, 470–474, 710
  noncardiogenic, 484, 488, 490
  Vet BLUE, 449–450, 462–466, 468–474, 484, 488
Pulmonary fibrosis, 462, 470–471
Pulmonary hypertension (PHT), 737–739
  AFAST, gallbladder wall edema, 127, 130
  FCU, 411–412
  TFAST, 378–382
  Vet BLUE monitoring, 498
Pulmonary thromboembolism (PTE), 536–537
  Global FAST, 719, 741, 744–745
  Vet BLUE, 462–464, 467, 475, 477, 486
Pulmonary-pleural interface (PPI)
  TFAST
    image acquisition, 306–308, 311–315
    pneumothorax diagnosis, 339, 341
  Vet BLUE, 426, 430, 432, 434, 445, 447–449, 461, 851–854
    optimization, 431, 433, 435–437
    pleural effusion in cats, 496–497
Pulse repetition frequency (PRF), color flow Doppler, 34
Pulseless electrical activity (PEA), 729–730
Pyelectasia, 194, 200–202, 204
Pyelonephritis, 201–202, 204
  pediatric POCUS, 289–291
Pyloric stomach, 846
Pylorus
  pediatric POCUS, 280–281
  POCUS gastrointestinal and pancreas, 228, 233
Pyometra, 259–261
  chinchillas, 824–825
  hedgehogs, 824, 826
  HRU view on AFAST, 104
Pyothorax, 371

Quality control, 930–931

Rabbit ear sign, 101–102
Rabbits
  abscesses, 822–823
  gastrointestinal conditions, 820, 822
  hepatobiliary conditions, 820, 822
  quick references of normal values and rules of thumb, 964
  reference ranges for, 826–827
  reproductive conditions, 822–823
  spleen anatomy, 816
  urinary conditions, 820, 822
Racetrack sign, 63, 75, 136–137, 359, 362–363, 368–370
Radial, ulnar, median, musculocutaneous nerve block (RUMM)
  anatomy for, 615
  application, 614
  indications for, 609
Radial nerve
  anatomy, 615–616
  block, 615–616
  scanning, 617
Radiography. *See also* Abdominal radiograph; Thoracic radiograph
  ultrasonography compared to, 26–28
Radiologist studies, 4
Rain sign, 351–352, 354
Rapid Ultrasound in Shock (RUSH) exam
  Global FAST *versus*, 688–689, 697, 749
  volume assessment, 690
Rat
  Global FAST, 719
  quick references of normal values and rules of thumb, 964
Recording. *See* Documentation and recording
Reference markers, probe orientation, 28–29, 46–47
Reflection
  artifacts of strong, 15–16, 18–22
  sound waves, 13
  ultrasound-guided lung and thoracic sampling, 908
Rehydration, repeat AFAST after, 127–128
Renal adenocarcinoma, 197
Renal agenesis, 287
Renal artery and vein, AFAST, SR view, 85–87
Renal calcification, 200, 203
Renal carcinoma, 200
Renal cortex, 192–194
Renal cysts, 199–201
Renal dysplasia, 287–289
Renal failure, 719
Renal infarcts, 205–206
Renal injury, serial AFAST monitoring of, 122–123
Renal masses, 196–198
Renal medulla, 192–194
Renal pelvic fat, 193
Renal pelvis
  anatomy, 192–194
  dilation, 194, 200–202, 204, 274–275
Renal vein thrombosis, 535
Reproductive POCUS
  female
    AFAST and Global FAST add-on, 255
    anatomy, 256
    capabilities, 255
    goal-directed templates, 936–937
    image acquisition, 256–259
    indications, 255–256
    limitations, 251
    mammary gland findings, 262–263
    objectives, 256
    ovarian findings, 256–257
    patient positioning and probe selection, 256
    pearls and pitfalls, 263
    quick references of normal values and rules of thumb, 263, 957–958
    uterine findings, 256–262
  male
    AFAST and Global FAST add-on, 247
    capabilities, 247
    goal-directed templates, 936
    image acquisition, 249, 251
    indications, 248
    limitations, 247
    objectives, 248
    pearls and pitfalls, 254
    prostate findings, 249–251, 254
    quick references of normal values and rules of thumb, 254, 957–958
    scrotum and testicle findings, 251–254
Reproductive tract
  birds, 865, 867–869
  conditions
    guinea pigs, 824
    hedgehogs, 824, 826
    rabbits, 822–823
  dolphins, 845–846
  exotic companion mammals, 816
  feline AFAST, 792–795
  female, 255–256
  male anatomy, 247–248
  pediatric patients, 276–277, 287–292
  reptiles, 876–878
Reptile POCUS
  anatomy, 871–872
  applications, 863
  capabilities, 871

cardiac abnormalities and aneurysms, 879–881
coelom
conditions, 876–879
normal, 873–875
Global Fast, 880–881
indications, 871
limitations, 871
objectives, 871
ocular conditions, 880–881
patient positioning, 871, 873–875
pearls and pitfalls, 881–882
probe selection, 874
Resistive index (RI)
encephalitis, 603, 606
hydrocephaly, 600, 605–606
intracranial pressure and, 595
Respiratory distress
cats, 494, 496
FCU, 389–390, 404–405
Vet BLUE
dry lung conditions, 481, 483, 485–486
pattern-based pattern approach overview, 479, 481, 483–484
wet lung conditions, 481–491
Restraint
lung and thoracic sampling, ultrasound-guided, 911–912
marine mammal POCUS, 834–835
for POCUS eye, 557
Resuscitation, repeat AFAST after, 127–128
Retinal detachment, 567–569, 571, 577
Retrobulbar abscess, rabbits, 823
Retrobulbar masses, 573–578
Retrobulbar probe position, 558–559
Retroperitoneal fluid
AFAST
detection, 60–61
SR view, 87, 90–91
kidney POCUS, 192, 197–198, 206–207
Retroperitoneal space, AFAST, SR view, 84–91
Return of spontaneous circulation (ROSC), 758
Reverberation artifact, 19–20. *See also* A-lines
AFAST, CC view, 93
bones and joints POCUS, 666
intraluminal gas, 233–234
pneumoperitoneum, 237–239
ultrasound-guided lung and thoracic sampling, 908–909
urinary bladder POCUS, 212, 214, 216
Reverse curtain sign, 344
Reverse piezoelectric effect, 12
Reverse sliding sign, 344
RI. *See* Resistive index
Rib fracture, 676
Right atrial enlargement, FCU, 389
Right atrium
FCU, 395, 398–400
TFAST, 318
Right heart strain/overload/failure, TFAST, 321, 328, 378–382
Right lateral (RL) recumbency
AFAST, 65–66, 69, 72
POCUS gastrointestinal and pancreas, 228
TFAST, 302–303, 320–321
Right parasternal window, FCU image acquisition, 392–394
long-axis views, 396–399
short-axis views, 395–396
Right ventricle (RV)
FCU, 395, 397–400
TFAST, 317–318, 324–329
Right ventricular hypertrophy, FCU, 411–412
Right ventricular to left ventricular ratio (RV:LV), 321, 323, 327–328, 804
Right-sided cardiac markers (RSCM), 699
Ring sign, 235, 237
Ring-down artifact. *See* B-lines
RL recumbency. *See* Right lateral recumbency
Rocking probe maneuver, 30–31, 46
Ropivacaine, 611, 613–614, 616, 621, 623–624, 626–627, 631–632, 634
ROSC. *See* Return of spontaneous circulation
Rostral acoustic window
brain POCUS, 580–581
sagittal plane, 589–590, 597–598, 600
transverse plane, 590–592, 597
TCDUS, 598, 601–602
Rotating probe maneuver, 30–31, 46
RSCM. *See* Right-sided cardiac markers
RUMM. *See* Radial, ulnar, median, musculocutaneous nerve block
RUSH exam. *See* Rapid Ultrasound in Shock exam
RV. *See* Right ventricle
RV:LV. *See* Right ventricular to left ventricular ratio

Sacculus rotundus, 816
Sacral plexus, anatomy of, 624
Sagittal plane and orientation, 7–8, 26–27, 41–43
AFAST, 70–73
rostral acoustic window, 589–590, 597–598
suboccipital acoustic window, 587, 598, 600
Salivary gland, 650–651
sialadenitis, 655–656
sialocele, 656–657
Salpingitis, 868
Saphenous nerve block, in distal thigh region, 623–625
Scanning planes, 7–8, 25–26, 41–43
Scapula fracture, 676
Scatter, sound waves, 13
Sciatic nerve block
lateral thigh region, 626–627
lumbosacral trunk region, 624–626
Scleral rupture, 571
Screen
image orientation, 7–8, 26–28, 41–43, 300, 302, 330
position, 41–42, 302, 428
Scrotal swelling, 247, 253–254
Scrotum, reproductive POCUS, 251–254
Seashore sign, 351–352, 354
Sector probes. *See* Phased-array probes
Sedation
pediatric patients, 272
for POCUS eye, 556–557
TFAST, 314, 351
thoracocentesis, 893
Sediment
artifacts mimicking, 22–23, 53
gallbladder, 22–23, 53, 155, 164, 166, 779–781
urinary bladder, 22–23, 53, 93, 96, 221–222
Seizure disorders, pediatric patients, 286, 289
Seldinger technique, pericardiocentesis, 890–891
Semimembranosus muscle, 677
Sepsis, peritonitis, 225–227, 235–239, 279–280
Seroma, 652–653
Shadowing. *See* Acoustic shadowing; Clean shadowing; Dirty shadowing; Edge shadowing
Shaved patients, 303–304
Shimmy line, 342–343, 479–481
Shock
cardiogenic, 690, 750
distributive, 690, 750
Global FAST
capabilities, 730–731
hyperkalemia, 736–737
hypertension–pulmonary hypertension, 737–739
hypocontractility–dilated cardiomyopathy, 736–738

Shock (*cont'd*)
hypotension/hypovolemia, 734, 736
indications, 731
limitations, 731
objectives, 731
pearls and pitfalls, 751
rapid assessment, 749–750
screening, 729–730, 743, 750
tamponade–pericardial effusion, 741, 744–746
tension pneumothorax, 740–741
thromboembolism–pulmonary thromboembolism, 741, 744–745
toxin–canine anaphylaxis, 745, 748–749
trauma–hemorrhage, 741–742
hypovolemic, 690, 750
obstructive, 690, 750
VetFAST-ABCDE, 759, 771–772
Short-axis cardiac views, 43–44
patient monitoring, 698
TFAST PCS views, 318, 321–329
VetFAST-ABCDE, 765
Shred sign, 345–346, 462–463, 466, 474–475, 852
Sialadenitis, ultrasonographic appearance, 655–656
Sialocele, ultrasonographic appearance, 656–657
Side-lobe artifact, 22–23, 53
AFAST
CC view, 93
DH view, 82
bones and joints POCUS, 666–667
liver and gallbladder POCUS, 156
TFAST, PCS view, 330
urinary bladder POCUS, 221–222
Sightline, patient and ultrasound screen in, 41–42, 302, 428
Single crystal probes, 34
Skin. *See* Probe–skin contact
Skinks, 871
Skull imaging, 672
Skyscraper effect, pneumothorax, 344–345, 347–348
Slice-thickness artifact, 22–23, 52–53
AFAST
CC view, 93, 96
DH view, 82
liver and gallbladder POCUS, 156
POCUS, vascular, 531–532
TFAST, PCS view, 330
urinary bladder POCUS, 221–222
SLiCK mnemonic, 153, 170, 175, 194–195, 274
Sliding probe maneuver, 31, 46
Sludge
artifacts mimicking, 22–23, 53
gallbladder, 22–23, 53, 155, 164, 166, 779–781
Small intestine
AFAST
dolphins, 846–847
HRU view, 97, 99–103
SR view, 86, 90
corrugation, 233, 235–236, 240
echogenicity, 232
feline AFAST, 796–797
fetal, 266–267
normal measurements, 242
normal POCUS findings, 232, 234
pediatric POCUS, 277–279
plication, 233, 235–236, 240
urinary bladder POCUS, 211
Small mammals. *See* Exotic companion mammals
Small-volume bleeder/effusion
AFS system, 114–117, 119, 124
anemia in, 115–117
canine anaphylaxis, 131–134
cats, 124, 799–802
modified AFS system, 115–116
nonhemorrhagic effusions, 126–127
postinterventional trauma, 119–121
serial AFAST monitoring of, 117, 119, 127–128
sources and location of bleeding, 124–125
Smartphone applications, 34
Smiley face sign, 301, 317–319, 329
Snakes, 871
Snow globe effect, sediment, 22–23, 221–222
Soft tissue sarcoma, 658
Soft tissues
acoustic impedance, 13
AFAST target organ approach, 140–141
attenuation, 13
degrees of echogenicity, 5–7
Global FAST, 706–707
POCUS of
abdominal wall injury, 657–658
capabilities, 647
common structures, 650–651
equipment, 648
hernia, 657–658
indications, 648
lesions, 651–657
limitations, 647–648
method, 649
neoplasia, 658, 660
objectives, 648
patient preparation, 649
pearls and pitfalls, 659, 661
settings, 648–649
sound waves velocities through, 12–13
Vet BLUE, 448–449
Software assistance, needle visualization, 904
Sound flux, 13
Sound waves, 11
absorption, scatter, and reflection, 13
acoustic impedance, 13
assumptions about echoes, 15
attenuation, 13
frequency ranges, 12
velocity, 12–13
Spayed patients
marked, 255–256
postoperative mounting, 262
stump pyometra, 261
Sperm granuloma, 253–254
Spinal cord, 589
Spine, sonoanatomy, 637–639
Spleen
AFAST
dolphins, 843–844, 846–847
HRU view, 97, 100–103
SR view, 84–91
target organ approach, 141
AFAST-focused, 106–107, 121, 136
capsule, 176
conditions, ferrets, 818–819
echogenicity
abnormal, 177, 179–181, 184–185, 193
normal, 151, 153, 170, 175–176, 191, 193–195, 274, 786–788
exotic companion mammals, 816
feline AFAST, 786–788, 797
kidney POCUS, 190–192
mass, 106–107
pediatric POCUS, 273–275, 280
POCUS
abnormal findings, 176–186
AFAST and Global FAST add-on, 173, 186–187
capabilities, 173
goal-directed templates, 934
image acquisition, 174–175
indications, 173
limitations, 173
normal findings, 174–177
objectives, 174
patient positioning and probe selection, 174
pearls and pitfalls, 187
quick references of normal values and rules of thumb, 187–188, 955–956

size
enlargement, 177–181
normal, 174–175
Splenic hemorrhage, 173
Splenic infarction, 182, 186, 280
Splenic mass
AFAST, 106–107, 121, 136
POCUS liver and gallbladder, 156, 160
POCUS spleen, 176–184
Splenic torsion, 177, 184–185
Splenic vein
pediatric POCUS, 274
POCUS, 174–176, 185–186
Splenic venous thrombosis (SVT), 533–534
Splenomegaly
ferrets, 818–819
POCUS, 177–181
Spleno-renal umbilical (SRU) view
AFAST image acquisition, 99–100
clinical questions investigated, 97
false negatives, 102
false positives, 102, 104
left lateral recumbency, 67–68
probe maneuvering, 73
typical negatives, 101
typical positives, 101–103
AFAST order of performance, 69–70
feline AFAST, 797
Spleno-renal (SR) view
abdominal radiograph and computed tomography (CT) correlation, 72
AFAST image acquisition, 85–86
artifacts, 87, 89–90
clinical questions investigated, 84
false negatives, 91
false positives, 90–91
marine mammal POCUS, 837, 841, 843–845
modified lateral-sternal recumbency, 69–70
probe maneuvering, 71, 73
right lateral recumbency, 65–66, 72
typical positives, 87–88
AFAST order of performance, 69–70
feline AFAST, 791–792
SQE. *See* Subcutaneous emphysema
*Squamates*, 871
Squamous cell carcinoma, 658
SR view. *See* Spleno-renal view
SR5th bonus view
AFAST image acquisition, 104
clinical questions investigated, 102
false negatives, 106
false positives, 106
kidney investigations, 97, 101
left lateral recumbency, 67–68
probe maneuvering, 73
typical positives, 105
AFAST order of performance, 69–70
SRU view. *See* Spleno-renal umbilical view
Standing positioning
AFAST, 66–68, 105
Global FAST, 692–693, 695, 733–734
TFAST, 300–302, 306
Vet BLUE, 428–429
Static air bronchogram, 474
Step sign, 305, 310, 669–670
lung findings, 354, 357–358
fracture, 672-675
Sterilization. *See* Neutered patients
Sternal positioning. *See also* Standing positioning
FCU, 391–392
Global FAST, 695, 733–734
Stomach
AFAST
DH view, 83–84
HRU view, 97, 102
SR view, 85–89
birds, 865
feline AFAST, 795–796
liver and gallbladder POCUS, 151
normal wall thickness, 242
pediatric POCUS, 272
POCUS gastrointestinal and pancreas, 228, 233
Vet BLUE, 447
Stone
acoustic impedance, 13
artifacts, 15–16
attenuation, 13
echogenicity, 5–7
sound waves velocity through, 12–13
Stratosphere sign, 351–352, 354
Stress, dolphin, 835
Stroke, 600, 606
Stump pyometra, 261
Subarachnoid space, 589
Subcostal window, FCU image acquisition, 395, 397, 399–400
Subcutaneous emphysema (SQE)
E-lines, 479–481
TFAST, 308–309, 353–356
Vet BLUE, 447–450
Subcutaneous tissue, normal findings, 669
Subdural hematoma, 598, 603
Sublingual salivary gland, 650–651
sialadenitis, 655–656
sialocele, 656–657
Suboccipital acoustic windows
brain POCUS, 580, 597
dorsal plane, 588
sagittal plane, 587, 598, 600
transverse plane, 598, 600
TCDUS, 598, 601–602
Subscalene approach, brachial plexus block, 609–613
Subxiphoid view, CVC POCUS, 543–545
Suppurative splenitis, 181
Supraspinatus injuries, 673, 678
Suprasylvian groove, 581–582, 585
Surgical sterilization. *See* Neutered patients
SVT. *See* Splenic venous thrombosis
Sweeping probe maneuver, 32, 46
Systolic dysfunction, 758

T³. *See* Trauma, Triage, and Tracking
Tail, patient positioning, 41–43
Tamponade–pericardial effusion, 741, 744–746, 758
TAP. *See* Transversus abdominis plane block
Target lesions
liver, 160–161, 170
splenic, 181, 183–184
Target organ approach, AFAST, 140–141
TBI. *See* Traumatic brain injury
TCC. *See* Transitional cell carcinoma
TCDUS. *See* Transcranial Doppler ultrasonography
TCUS. *See* Transcranial ultrasonography
Tegus, 871
Temporal acoustic windows
brain POCUS, 580, 597
dorsal caudal plane, 581–584
dorsal cranial plane, 584–587
dorsal plane, 581, 598–599
TCDUS, 598, 601–602
Temporal lobe, 581–587
Tendon
injuries, 673, 678–679
normal findings, 668
Tension pneumothorax, 740–741, 758
Testicles
marine mammal POCUS, 858
pediatric POCUS, 276–277, 291–292
reproductive POCUS, 251–254
reptiles, 876–877
Testicular torsion, 253
Testicular tumors, 253
TFAST. *See* Thoracic FAST
TFAST PTX 1/3s rule, 347–351

TFAST slide, 301, 318–320, 330
pleural effusion diagnosis, 370–374
TGC. *See* Time gain compensation
Thigh, CC view on AFAST, 92, 100
Third spacing, AFAST, gallbladder wall edema, 127, 130
Thoracic abscess, rabbits, 823
Thoracic circulation, 760–761, 765
Thoracic FAST (TFAST)
acoustic windows
challenges, 337
clinical utility, 332
overview and summary, 300–301, 332
with AFAST, 297–298
cardiac imaging, 43–44, 698–699
caudal vena cava characterization, 734–736
clinical integration, 300
capabilities, 337–338
CTS view lung and pneumothorax findings, 339–358
DH view findings, 377–378
diaphragmatic herniation, 377–379
documentation using goal-directed templates, 383–384, 937–938
echo view cardiac evaluation, 378–383, 939
indications, 338
limitations, 338
objectives, 338–339
pearls and pitfalls, 384
pericardial effusion findings, 358–369, 377
pleural cavity masses, 377
pleural effusion findings, 369–377
quick references of normal values and rules of thumb, 383, 958–959
clinical questions answered, 299–300, 340
definition, 4
depth settings, 33, 305, 311, 319, 330
EFAST *versus*, 688–689
efficiency, 695
fallback views, 695, 697
feline
acoustic coupling medium, 803, 805
echo views, 802–803, 806
LA:Ao, 803–805
lung sliding and pneumothorax, 807
LVSA view, 803–804
patient positioning, 802–804
pericardial effusion, 806
RV:LV, 804
Flash exam *versus*, 4
goal-directed templates, 926, 928
historical development and studies, 297
image acquisition
acoustic windows overview and summary, 300–301, 332
capabilities, 298
CTS view performance, 305–315
DH view performance, 330–332
documentation using goal-directed templates, 333
indications, 299
light dimming, 305
limitations, 298–299
machine positioning, 302
objectives, 299
patient positioning, 300–304, 306, 311, 313–314
patient preparation, 303
patient shaving, 303–304
PCS view performance, 315–330
pearls and pitfalls, 333
probe preferences, 300
quick references of normal values and rules of thumb, 333–334, 958–959
screen orientation, 300, 302
ultrasound settings, 300, 305, 308, 311–312, 315, 319–320, 330
leaks and plugs, 705–706
maneuvers for, 693
marine mammal POCUS, 829, 836
efficiency, 858
pleural and pericardial effusion, 848–849
questions, 848
views, 848
patient positioning, 692–696
patient staging
hemoabdomen, 712
pericardial effusion, 716
urinary bladder mass, 715
pericardial effusion, 136–137, 707–708
pleural effusion, 707
probe and helper hand functions, 41–42, 44
short-axis and long-axis view recommendations, 43–44
trouble-shooting algorithm for poor images, 49–52
Thoracic paravertebral block, 629–632
Thoracic radiograph (TXR)
AFAST acoustic window correlation, 136–137
pericardial effusion, 368–369
pleural effusion, 371, 375–376
Vet BLUE compared to, 425, 462, 476–477, 491–493, 499–500
Thoracic sampling, ultrasound-guided. *See* Lung and thoracic sampling, ultrasound-guided
Thoracic spinal nerves, 630–631
Thoracic wall block, 630
Thoracocentesis
complications, 892
contraindications, 892
indications, 892
pleural effusion scanning, 893
ultrasound-guided
introduction, 892
materials checklist for, 893
monitoring, 897
parallel probe placement, 896–897
perpendicular probe placement, 894–896
procedure, 893–894
Thoracolumbar area
epidural approach, 642–643
longitudinal scan, 640–641
Thorax, abdomen compared to, 337
Thromboembolism
arterial, 537
pulmonary, 536–537, 719, 741, 744–745
Thrombosis
aortic, 537
caudal vena cava, 532–534
central venous, 532, 534
deep venous, 535–536
hepatic vein, 532–534
portal vein, 534–535
renal vein, 535
splenic venous, 533–534
Thrombus
enteric, 285
left atrial, 408–409
splenic, 185–186
urinary bladder, 93, 99, 217, 220–222, 706
Thyroid evaluation, marine mammal POCUS, 858
Time gain compensation (TGC), 33
trouble-shooting algorithm for poor images, 49–52
Timolol, 564, 567
Tissue sign, 345–346, 462–463, 467, 474–476, 852–853
Tissues
acoustic impedance, 13
attenuation, 13
degrees of echogenicity, 5–7
sound waves velocities through, 12–13
Torsion
splenic, 177, 184–185
testicular, 253
uterine, 261–262

Toxic hepatopathies, 163
Toxin–canine anaphylaxis, 745, 748–749
Tracheal abnormalities, 758
Tracheal collapse, 758–759, 762
Tracheal dislocation, 758
Tracheal injury, 769
Training, 922, 931
Transcranial Doppler ultrasonography (TCDUS)
  acoustic windows for, 597
  capabilities, 595–596
  development of, 595
  encephalitis, 603, 606
  hydrocephaly, 600, 605–606
  indications for, 596
  limitations, 596
  objectives, 596
  pearls and pitfalls, 603
  probe type for, 597
  stroke, 600, 606
  technique for, 598, 601–602
Transcranial ultrasonography (TCUS)
  acoustic windows for, 597
    rostral, 580, 589–592
    suboccipital, 580, 587–588
    temporal, 580–586
  anatomy, 582–592
  capabilities, 579, 596
  echo views
    cardiac evaluation, 378–383, 939
    cats, 802–803, 806
    with Global FAST, 382–383
    image acquisition, 317, 321–329
    pericardial effusion diagnosis, 359–363
    with Vet BLUE, 382–383, 490–491
  functions of, 579
  indications for, 580, 596
  limitations, 579, 596
  mechanism of, 580–582
  objectives, 580, 596
  parenchyma, 598, 601
  pearls and pitfalls, 592, 603
  pediatric patients, 286, 289
  planes, 580
    dorsal, 588, 598–599
    dorsal caudal, 581–584
    dorsal cranial, 584–587
    sagittal, 587–590, 597–598, 600
    transverse, 590–592, 597–598, 600
  probe type for, 580, 597
  technique for, 581–582, 597–602
  ventricular system evaluation, 579–580, 590–592
Transducer. *See* Probes
Transitional cell carcinoma (TCC), bladder, 215, 217–219
Transmission, sound, 11–14
Transthoracic views, Vet BLUE, image acquisition, 434–442
Transverse plane and orientation, 7–8, 25–28, 41–43
  catheterization
    femoral arterial, 521–523
    jugular, 516–519
    longitudinal *versus*, 524
  CVC POCUS
    intercostal view, 543–546
    paralumbar view, 544, 546–548
  lumbosacral area, 640
  rostral acoustic window, 590–592, 597
  suboccipital acoustic window, 598, 600
  TFAST, 308
  vascular POCUS, slice-thickness artifact, 531–532
  Vet BLUE, 430–431, 434
    marine mammal POCUS, 850, 852, 855–856
Transversus abdominis plane (TAP) block, 629–630, 633–635
Trauma, Triage, and Tracking ($T^3$), 3, 766
Traumatic brain injury (TBI)
  evaluation of, 595
  sonographic features of, 598–599, 603–605
  TCDUS for, 595–596
Traumatic diaphragmatic herniation, 286
Traumatized eye, 554
Tree trunk sign, 61, 63, 80, 132, 361, 364, 699, 704
Tricuspid valve, FCU, 398–399
Tricuspid valvular disease, AFAST, gallbladder wall edema, 127, 130
Truncal nerves, 630–631
Trunk nerve block
  approaches, 629
    intercostal, 632–633
    thoracic paravertebral, 629–632
    transversus abdominis plane, 633–635
  capabilities, 629
  indications, 629
  limitations, 629
  objectives, 629–630
  pearls and pitfalls, 634–635
Tumors. *See* Mass lesions
Tunica albuginea, 251
Twinkle artifact, 200, 203, 215, 219
TXR. *See* Thoracic radiograph

Ulnar nerve
  anatomy, 615
  block, 616–617
  scanning, 618
Ultrasound
  artifacts, 7, 15–23
  basic physics, 11–14
  biomicroscopy, ocular, 554
  image features, 25–28
  image optimization, 32–33
  modes, 33–34
  probe maneuvers, 28–32, 43, 46, 48, 70–73
  radiography compared to, 26–28
  technological advancements, 34
Ultrasound gel. *See* Acoustic coupling gel
Ultrasound lung rockets. *See* B-lines
Ultrasound machine
  care of, 35–36
  common mistakes, 48–52
  pediatric POCUS, 271–272
  physical assumptions, 15
  presets, 33, 39
  probe and processor functions, 11–12
  screen position, 41–42, 302, 428
  selection of, 36–37
  settings, 32–34
    AFAST, 64
    FCU, 391
    Global FAST, 692, 731
    marine mammal POCUS, 830–833
    POCUS bone, 666
    POCUS CVC, 542
    POCUS eye, 554–555
    POCUS gallbladder, 150
    POCUS joint, 666
    POCUS liver, 150
    POCUS soft tissues, 648–649
    TFAST, 300, 305, 308, 311–312, 315, 319–320, 330
    Vet BLUE, 428, 430–433, 435
    VetFAST-ABCDE, 759
  smartphone applications, 34
  trouble-shooting algorithm for poor images, 49–51
Ultrasound-guided procedures, 885, 907. *See also* Lung and thoracic sampling, ultrasound-guided
  abdominocentesis
    indications, 897–898
    introduction, 897
    materials checklist, 898
    procedure, 898–899
    scanning technique for, 898
  biopsies, 916
  modified ultrasound-guided diagnostic peritoneal lavage
    blind *versus*, 899–900
    findings, 900
    indications, 900

Ultrasound-guided procedures (*cont'd*)
materials checklist, 900
procedure, 900–903
scanning technique, 900
pearls and pitfalls, 903–904
pericardiocentesis
blind *versus*, 886
completion of, 889–890
free-hand, 889
indications for, 886
indirect, 889
introduction, 885–886
materials checklist for, 887
monitoring of, 890–891
pearls and pitfalls, 890–892
procedure for, 888–889
scanning technique for, 886–888
thoracocentesis
complications, 892
contraindications, 892
indications, 892
introduction, 892
materials checklist for, 893
monitoring, 897
parallel probe placement, 896–897
perpendicular probe placement, 894–896
pleural effusion scanning, 893
procedure, 893–894
Umbilical hernias, 285–286
Urachus, patent, 290, 292
Ureter
feline AFAST, 791–792
kidney POCUS, 194
pediatric POCUS, 288–290
urinary bladder POCUS, 213–214, 217–218
Ureteral obstruction, 202–205
Ureteral papilla, 213–214
Ureterocele, 290
Urethra
feline AFAST, 792–795
pediatric POCUS, 276
urinary bladder POCUS, 211–212, 217–218
Urinary bladder
AFAST
assessment, 59–61
CC view, 91–100
dolphins, 845–846
serial exams, 117, 119
target organ approach, 141
volume estimation, 140–141, 793, 795
calculi, 93, 98–99, 214–215, 219–220, 290–291
feline AFAST, 792–795
ferrets, 817
Global FAST, 707–708
inguinal hernia and, 658
intraluminal abnormalities, 219–222
mass, 93, 99, 215, 217–219
canine, 713–715
feline, 715
mirror artifact at, 53
pediatric POCUS, 276, 288–292
POCUS
abnormal findings, 215–222
AFAST and Global FAST add-on, 221–222
artifacts, 211–216, 219, 221–222
capabilities, 211
goal-directed templates, 935
image acquisition, 212–213
indications, 211
limitations, 211
normal findings, 212–214
objectives, 211–212
patient positioning and probe selection, 212
pearls and pitfalls, 223
quick references of normal values and rules of thumb, 223, 956
reproductive, 249, 256–258
reptiles, 871–872, 876
sediment, 22–23, 53, 93, 96, 221–222
thrombi, 93, 99, 706
thrombus, 93, 99, 217, 220–222
wall abnormalities, 215–219
Urinary conditions
ferrets, 817
guinea pigs, 823–824
obstruction, 719
rabbits, 820, 822
Urinary disorders, pediatric POCUS, 287–292
Urinary tract infection, 290–291
Urinary tract obstruction, 202–205
Urine
feline AFAST, 792–795
urinary bladder POCUS, 213
Urine output, AFAST estimation, 59–61, 63, 91–92, 140–141, 793, 795
Uroabdomen, AFAST detection, 92–93
Urogenital ectopia, 288–290
Urolithiasis, 93, 98–99, 200, 203, 214–215, 219–220, 290–291
ferrets, 817
guinea pigs, 823–824
rabbits, 820, 822
reptiles, 876
Urothelial carcinoma. *See* Transitional cell carcinoma
Uterine adenocarcinoma, rabbits, 822–823
Uterine torsion, 261–262
Uterus
dolphins, 846–847
feline AFAST, 793–794
HRU view on AFAST, 102, 104
lesions, hedgehogs, 824, 826
pediatric POCUS, 276–277
reproductive POCUS, 256–262
Uveal cysts, 569
Uveal melanocytoma, 569
Uveal melanoma, 569
Uveitis, 566–567, 569, 572

V trough, 41–42, 44, 447
Vaginal discharge, 259–260
Valvular heart disease
FCU, 404–406
preanesthetic evaluation, 494–495
TFAST, 378–382
Vasculature. *See also* Arterial catheterization; Central venous catheterization
anatomy
brain, 598, 601–602
femoral artery, 520–521
jugular vein, 515
POCUS
capabilities, 529
color Doppler, 530–531
Global FAST and, 529
indications, 529–530
limitations, 529
objectives, 530
patient preparation, 530
pearls and pitfalls, 537, 539
porta hepatis anatomy, 531
probe, 530
technique, 530–531
thromboembolism, 532–537
vessel orientation and slice-thickness artifact, 531–532
TCDUS of, 598, 601–602
Velocity
artifacts of, 18–22
sound waves, 12–13
Venipuncture, marine mammal POCUS, 858
Venous catheterization. *See* Central venous catheterization
Venous thromboembolism. *See* Thromboembolism
Ventral complex, 638–639
Ventricle-hemisphere ratio, 596
Ventricle-mantle ratio, 596
Ventricular system

guidelines for measurement of, 595–596
TCUS evaluation, 579–580, 590–592
Ventriculomegaly, 592, 599–600, 605–606
Vertebrobasilar system, 598, 601–602
Vertical probe position, POCUS eye, 558
Veterinary brief lung ultrasound exam (Vet BLUE)
with AFAST and TFAST, 297–298
alveolar-interstitial syndrome, 705
artifacts, 459, 462–471
marine mammal POCUS, 850–853, 856
B-line scoring system, 341–342, 450, 452–453, 470–473, 709–711, 807–808
canine anaphylaxis, 134–135
cats, 494–497, 807–808
clinical integration
B-line counting, 470–473
capabilities, 459–460
cat examples, 494–497
congestive heart failure and volume overload monitoring, 497–498
documentation using goal-directed templates, 499–504, 938–939
dog examples, 494–495
dry lung conditions, 481, 483, 485–486
false negatives, 492
false positives, 492, 494
fluid therapy monitoring, 491
future, 499
important considerations, 461–462
indications, 460–461
limitations, 460–462, 492, 494
line nomenclature, 477–482
lung contusions, 491–493
nodular disease monitoring, 498
objectives, 461
pattern-based pattern approach overview, 479, 481, 483–484
pearls and pitfalls, 504–505
pneumonia monitoring, 498
pulmonary hypertension monitoring, 498
quick references of normal values and rules of thumb, 505, 959–960
six lung ultrasound signs, 462–467, 474–479
visual lung language, 462–471
Volpicelli Strong Positive model, 472–474
wet lung conditions, 481–491
clinical questions answered, 427, 460
comparative imaging, 425, 462, 476–477, 491–493, 499–500
comparison to other protocols, 450
four-quadrant approach, 451, 453–454
Zigzag Intercostal Continuum, 453–455
deep lung lesions, 140
efficiency, 695
Flash exam *versus*, 4
focus cursor awareness, 48
Global FAST *versus*, 687
goal-directed templates, 927–928
image acquisition
acoustic window names and locations, 429, 433–443
acoustic window order, 441–444
capabilities, 426
DH view, 434, 438, 440–441, 443
documentation using goal-directed templates, 455
indications, 426
limitations, 426
lung line optimization, 431, 433, 435–437
lung orientation, 430–432, 434
objectives, 426–427
patient positioning, 428–429
patient preparation, 427–428
pearls and pitfalls, 455
probe orientation, 430–431, 434
probe preferences, 428, 430
quick references of normal values and rules of thumb, 456, 959–960
step by step performance, 445–447
transthoracic views, 434–442
trouble shooting, 447–450
ultrasound settings, 428, 430–433, 435
maneuvers for, 693
marine mammal POCUS, 829
artifacts, 850–851
efficiency, 858
longitudinal orientation, 850, 852, 854–856
lung orientation, 850–853
lung signs, 852–853
performance, 836, 854
transverse orientation, 850, 852, 855–856
zig-zag continuum, 856–858
patient positioning, 692–696
patient staging
hemoabdomen, 712
pericardial effusion, 716
urinary bladder mass, 715
probe and helper hand functions, 41–42, 44
probe drifting, 41–42, 447
sensitivity and specificity, 425–426, 462
six lung ultrasound signs, 347, 349, 449–452, 462–467, 474–479
staging patients, 687
TFAST CTS extension, 338, 430
with TFAST echo views, 382–383, 490–491
trouble-shooting algorithm for poor images, 49–52
wet lung *versus* dry lung, 462–466, 699, 701
Veterinary POCUS (V-POCUS), definition, 3
VetFAST-ABCDE
abnormal findings, 758, 766
airway
assessment, 759–762
Global FAST *versus*, 767–769
breathing
assessment, 759–760, 762–764
Global FAST *versus*, 769
capabilities, 758
circulation
assessment, 760–762, 765–767
Global FAST *versus*, 769
development, 757
disability
assessment, 762–766, 768
Global FAST *versus*, 769–770
exposure
assessment, 766
Global FAST *versus*, 770
goal-directed templates, 940
indications, 758
limitations, 758
objectives, 759
patient positioning, 759
pearls and pitfalls, 772
probe preferences, 759
quick references of normal values and rules of thumb, 965
settings, 759
shock, CPR, ALS, 771–772
Visualization
needle, 903–904
ultrasound beam, 46, 51
Vitreous body, 560
Voiding urohydropulsion (VUH), 219, 223
Volpicelli Strong Positive (VSP) model, 472–474
Volume loss, Global FAST, 704–706
Volume overload, 497–498
Volume responsiveness, FCU, 411–413

Volume status
AFAST, 60–61
FCU, 389
feline TFAST, 804
Global FAST
ascites, 699
assessment, 687, 690
clarity, rapidity, standardization, 698
CVC evaluation, 702–704
nonecho fallback views, 698
nonecho fallback views for left-sided heart problems, 699–702
nonecho fallback views for right-sided heart problems, 699–701
patient monitoring, 696–697
TFAST cardiac imaging, 698–699
TFAST, 382–383
V-POCUS. *See* Veterinary POCUS
VSP model. *See* Volpicelli Strong Positive model
VUH. *See* Voiding urohydropulsion

Wall filter setting, color flow Doppler, 34
Warfarin toxicosis, 198
Warming devices, 273
Wedge sign, 345, 462–463, 467, 475, 477, 853
Wet lung, 339, 341–344, 354
dry lung *versus*, 339, 341–344, 354, 462–466, 699, 701
Vet BLUE
B-line scoring systems, 470–474, 710
conditions, 481–491
image acquisition, 449–452
visual lung language, 462–466, 468–471
Windshield wipers sign, 323–328

Zig-zag continuum (ZZC), 829, 856–858
Zigzag Intercostal Continuum (ZZIC), 453–455
Z-lines, 342–343, 479–481
Zygomatic salivary gland, 651, 655–656
ZZC. *See* Zig-zag continuum
ZZIC. *See* Zigzag Intercostal Continuum

# WILEY END USER LICENSE AGREEMENT

Go to www.wiley.com/go/eula to access Wiley's ebook EULA.

Vetbooks.ir